

SIMULTANEOUS MULTIELEMENT ATOMIC-EMISSION SPECTROMETRY WITH A CHARGE-INJECTION DEVICE DETECTOR

G. R. SIMS and M. B. DENTON

Department of Chemistry, University of Arizona, Tucson, AZ 85721, U.S.A.

(Received 8 August 1988. Accepted 16 January 1989)

Summary—Simultaneous multielement atomic-emission spectrometry with a charge-injection device (CID) as a multichannel optical detector is described. The system used in this study employs a standard commercial D.C. plasma source, a modified echelle spectrometer, and a special digital camera system that uses a two-dimensional CID array sensor. A description of the modified spectrometer is given along with performance results. Computer algorithms for acquiring and analyzing spectral information are described. Detection limits for several elements are determined simultaneously. Results of simultaneous determination of several elements in an NBS standard reference material (SRM 1643A) are given. These results indicate that the CID detector is capable of reasonably good accuracy and high sensitivity in the simultaneous determination of several elements in complex samples.

Inductively coupled plasma and direct current plasma atomic-emission spectrometry (AES) have become two of the most widely accepted techniques for elemental determinations. These emission sources are excellent for this application, providing the high excitation energy necessary for high emission intensity and low chemical interference. For accurate determinations with atomic-emission spectrometry, the spectral line for the determination of a given element must often be chosen with due consideration of possible spectral interferences from other components of the sample. It is also highly desirable to be able to determine several elements in a sample simultaneously in order to conserve both sample and laboratory resources. Ultimately, the ideal spectroscopic system helps to guide the analyst in the selection of the optimum spectral lines for a given sample, and then rapidly and simultaneously determines the desired elements.

The ideal situation for simultaneous multielement AES would be the capability to make simultaneous measurements at all wavelengths from the near infrared to the ultraviolet with high spectral resolution. Some of the advantages to this approach are that both analytical line and background information are simultaneously obtained, and the relative intensities of several emission lines for a given element can be checked to determine whether any spectral interferences are present. Another important

benefit is that weak ionic or non-resonance transition lines may be used to quantify species at high concentrations, thereby minimizing analysis time.

It is also desirable that the detector for simultaneous AES be an integrating detector. With this capability, transient signals, such as those encountered when using electrothermal atomization or monitoring chromatographic effluents are detected in an optimum fashion.

For many years, interest has been focused on using one of a variety of multichannel imaging detectors, originally developed for television applications, for simultaneous multielement AES. A variety of devices, both of tube type and solid state, have been investigated for potential use for this application, but none has been found to be completely suitable, for one or more of a number of reasons. To be generally suitable for most spectroscopic applications, a detector must have good quantum efficiency over a wide spectral range, low readout noise, dynamic range in excess of six orders of magnitude, direct electronic readout, a large number of resolution elements, no cross-talk or blooming among individual detector elements, and no readout lag, and also be economically feasible to acquire and operate.

Tube-type imaging detectors, principally various types of vidicons, intensified vidicons, and the image dissector, have been evaluated by a number of investigators.¹⁻⁶ The vidicons and

intensified vidicons suffer from limited dynamic range, blooming, cross-talk, and a variety of other problems. Good single-element detection limits have been reported for an image dissector, but high background caused by stray electrons emitted from regions of the photocathode other than the one being monitored is a problem.² This background is especially severe when samples containing a large number of elements at high concentrations are being analyzed.

In recent years, several solid-state linear and imaging detectors have been developed and employed as multichannel spectroscopic detectors. Among these are the photodiode array,⁷ the charge-coupled device,⁸ and the charge-injection device (CID). Each of these devices has characteristics which make it the superior detector for specific applications. For AES, the CID is a superior choice because of its good quantum efficiency over a wide dynamic range, resistance to charge blooming, and the high effective dynamic range and low readout noise made possible through the use of its unique readout mode.⁹

Charge-injection device

The CID is a two-dimensional array of optical detectors (pixels) constructed by using metal-oxide semiconductor integrated-circuit technology. The principles of operation of this device and its electro-optical characteristics have been described elsewhere.⁸⁻¹⁰ The CID has been demonstrated to have high sensitivity from ultraviolet to near infrared wavelengths, good linearity over a wide dynamic range, low dark current (when operated at liquid-nitrogen temperature), and freedom from readout lag. The geometry of the CID prevents spill-over of charge from saturated pixels into adjacent pixels (charge blooming). Though the CID does suffer from two related forms of signal cross-talk, termed row-column cross-talk and column-column cross-talk, the effect is understood and is easily removed.¹⁰ In addition, a very small hysteresis effect has been observed, arising from interactions of the accumulated charge with energy levels between the conduction and valence bands which occur at the silicon-silicon dioxide interface.¹⁰

The CID can be operated in a unique readout mode that uses the intra-cell charge-transfer method of charge-sensing in a reversible manner, which allows nondestructive quantification of accumulated charge. This capability, called nondestructive readout (NDRO), is especially

useful in reducing the effective temporal readout noise and increasing the effective dynamic range for the CID.^{9,11} The NDRO capability allows use of variable integration times for different spectroscopic features within a single exposure. This means that the moderately high dynamic range of the raw spectrum (ratio of the charge capacity of the pixels to the temporal readout noise) can be expanded to over 10^7 by changing the integration times for different pixels within a single exposure. This is in contrast to other solid-state detectors which must make multiple exposures to increase the dynamic range synthetically.

The ability to access pixels rapidly in a pseudo-random manner is an additional important property of the CID. This permits data-acquisition from pixels of interest without having to read or purge the charge from pixels containing no useful information. All pixels may be simultaneously accessed in order to clear charge simultaneously from all pixels. By combination of pseudo-random access with NDRO, a particular spectral feature may be dynamically monitored while an integration is proceeding. This gives the capability of allowing an integration to proceed only as long as necessary to yield a desired signal-to-noise ratio.

Optical systems for imaging detectors

Electronic imaging detectors such as vidicons, image dissectors, and CIDs are only available in a limited size, with restricted spatial resolution. This means that optimum use of the available detector elements must be made. Optical dispersion in two dimensions is preferable to the one-dimensional dispersion provided by traditional spectrometers. An echelle grating spectrometer using either an echellette grating or a prism for cross-dispersion is the optical approach most widely used for imaging detectors. The echelle spectrometer not only has format advantages, but also exhibits high dispersion and resolution, and limits most grating stray light to a single order, making it ideal for the complex and intense spectra encountered in AES.

Previous results and scope of the present work

We have previously reported single-element detection limits for species with emission wavelengths ranging from the near infrared (K at 766.49 nm) to the ultraviolet (Zn at 202.55 nm). These results were obtained with the CID camera system used in this work and an unmodified

SpectraMetrics SpectraSpan III Spectrometer.¹¹ The detection limits for the CID system were superior to those obtained with photomultiplier tube (PMT) detection for near infrared wavelengths, approximately equal to them for visible region wavelengths, and somewhat inferior in the ultraviolet. In the worst case, the CID camera system gave a detection limit that was poorer by a factor of 13 than the literature value obtained with a PMT detector. This difference in performance for CID and PMT detectors is attributed to the relatively greater quantum efficiency of the CID in the near infrared and lower relative quantum efficiency in the ultraviolet.

In this paper, we address the issues of sensitivity and accuracy for simultaneous multi-element determinations, on a type of sample that may be routinely encountered, done with the CID detector and a modified spectrometer. The spectrometer was modified to allow observation of a larger spectral range than was previously allowed, but even with these modifications only a few analytically useful spectral lines can be simultaneously viewed. There are several analytical emission lines for several elements between 310 and 470 nm, so a portion of this wavelength range was selected for this evaluation.

EXPERIMENTAL

Apparatus

The CID used in this work was a General Electric CID11B normally used in an RS170 format video camera that supports only normal video output. Because this camera does not support many of the capabilities of the CID, new camera electronics optimized for atomic spectroscopy were designed and constructed at the University of Arizona. This system consists of a sensor head cooled with liquid nitrogen, a high-speed digital camera controller, and a host computer. Table 1 summarizes the optoelectronic characteristics of the CID11B sensor

as operated in the UA/CID11B camera system as previously reported.⁹

The UA/CID11B camera system supports the many capabilities of the CID11B detector, including NDRO, pseudo-random pixel access, simultaneous clearing of all pixels, readout of any arbitrary subarray size and position, and the operation of an optical shutter. In addition, the charge level of all pixels of the array can be truncated to a preset level which prevents severe column-column cross-talk.¹⁰ The CID is cooled with liquid nitrogen by contact with a copper cold finger, in order to eliminate thermal charge-generation. Intensity data are digitized to 12 bits precision. Readout time for a single pixel is 30 μ sec; the maximum latency in accessing a pixel is 90 μ sec. The camera has already been described in further detail.^{9,11}

The host computer system is a PDP11/23 with standard peripherals, including graphics terminal, mass storage devices, printer, and plotter. The language used for software development is CONVERS V3.1; a FORTH-like threaded code interpretive compiler language developed in these laboratories. Details of the host system have been published elsewhere.⁹

The spectrometer used in these studies is a modified commercial echelle spectrometer (SpectraMetrics model SpectraSpan III, SpectraMetrics Inc., Andover, MD). Figure 1 shows top and side views of the configuration of the optical elements in the modified spectrometer. A description of each optical element is given in Table 2.

The primary modifications to the commercial echelle spectrometer consisted of replacing the collimating mirror with an off-axis section of a parabolic mirror and replacing the focusing mirror with a shorter focal length spherical mirror. The mounts for the grating and prism were not modified, but the apparatus used in the stock instrument to position the grating in the horizontal and vertical axis was removed and replaced by simple adjusting screws. A laboratory-constructed mount was used for the focusing mirror. This mount was attached to a precision translation stage (Newport model 420, Newport Corporation, Fountain Valley, CA) to permit accurate focusing. The stock mount was used for the collimating mirror.

The focusing mirror was tilted so as to locate the center of the focal plane 5.8 cm above the horizontal optical plane of the spectrometer. This avoids vignetting of any optical paths by the camera head cryostat. The CID is oriented

Table 1. Summary of CID11B characteristics

<i>Pixel format:</i>	244 (horizontal) \times 248 (vertical)
<i>Pixel size:</i>	47 μ m (horizontal) \times 35 μ m (vertical)
<i>Read noise:</i>	630 charge carriers/read 156 carriers with 36 NDROs
<i>Dark current:</i>	4.6 \times 10 ⁶ carriers sec at 296 K undetectable at 77 K
<i>Full well:</i>	2.3 \times 10 ⁶ carriers
<i>Raw spectrum</i>	2600:1 with 1 readout
<i>dynamic range:</i>	10500:1 with 36 NDROs
<i>Spectral range:</i>	200–1000 nm

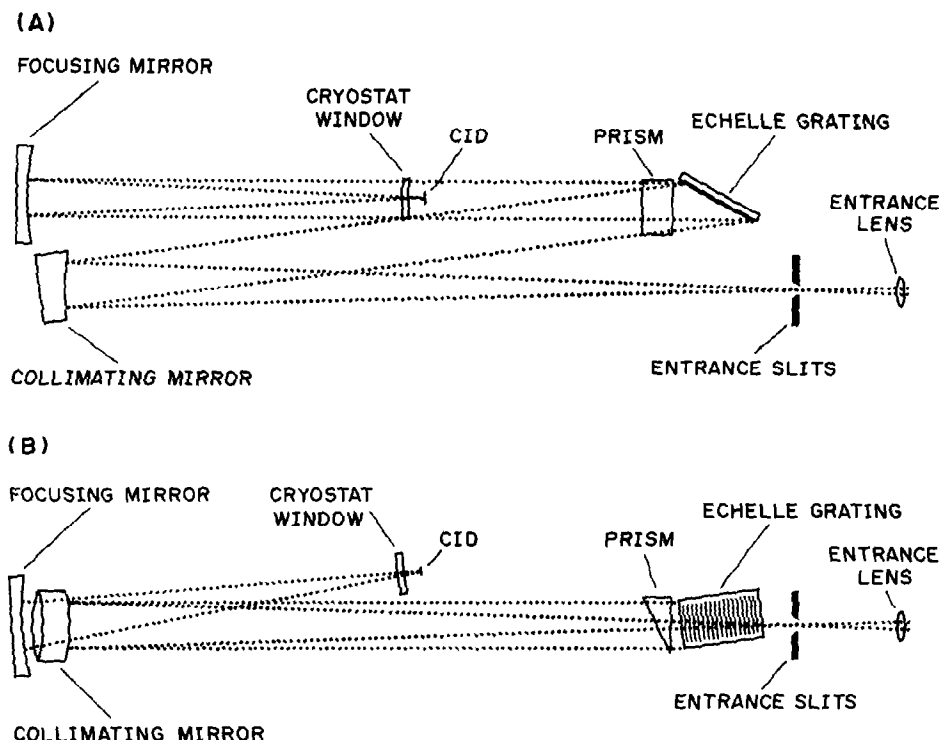


Fig. 1. Top (A) and side (B) views of the optical configuration for the modified echelle spectrometer. The dotted lines represent the optical path through the spectrometer.

in the cryostat so that the long axis (axis with 248 pixels, 1.17 cm length) of the sensor is in the direction of grating dispersion.

The stock spectrometer cover was replaced with one of similar construction but tall enough to accommodate the height of the cryostat. Removable hatches on the cover allowed access to fill the camera head cryostat with liquid nitrogen and to adjust the grating angles. The internal surfaces of the cover were insulated with 1-in. thick polystyrene foam and the entire

spectrometer and camera head was thermally regulated to $30 \pm 0.5^\circ$ by a strip heater, proportional temperature controller, and recirculating fan mounted on the spectrometer base within the cover. This not only stabilized the mechanical components of the spectrometer, but also the sensitive analog components in the camera head.

An electric shutter (Ilex No. 1, Ilex Co., Rochester, NY) was mounted on the spectrometer and used to control the exposure time for the CID camera. It was located between the input lens and the input slits. The shutter was controlled by the computer through a parallel interface module (Model DRV11J, Digital Equipment Corp., Maynard, MA).

Two red-light emitting diodes (LEDs) were attached to the sides of the focusing mirror mount and pointed towards the CID. These LEDs were used to illuminate the CID in order to introduce a bias charge (see next section). They were turned on and off under computer control through the parallel interface module discussed in the previous paragraph.

The DC plasma source and nebulizer were SpectraMetrics SpectraJet III, operated in accordance with the manufacturer's suggested settings.

Table 2. Echelle spectrometer components

<i>Focusing mirror:</i>	42 cm focal length, f 4.1 spherical mirror.
<i>Collimating mirror:</i>	75 cm focal length, f 13 off-axis parabola. Section taken 10.2 cm off center axis of a 35.6 cm blank.
<i>Cryostat window:</i>	fused-silica window 0.64 cm thick, 4.3 cm diameter. The two planar surfaces are angled at 1.5° with respect to each other. Window is coated with an MgF_2 antireflection coating optimized for 400–900 nm wavelength range.
<i>Order-sorting prism:</i>	fused-silica 30° Littrow prism taken from a commercial spectrometer.
<i>Echelle grating:</i>	79 groove/mm, $63^\circ 26'$ blaze grating with a groove length of 5.6 cm and a ruled width of 12.8 cm, taken from a commercial spectrometer.
<i>Entrance slits:</i>	Adjustable in the horizontal direction to 25, 50, 100, 200 and 500 μm and in the vertical direction to 100, 200, 300 and 500 μm . Taken from a commercial spectrometer.
<i>Entrance lens:</i>	30 cm focal length, f 13 fused-silica lens taken from a commercial spectrometer.

Reagents

Standards (1000 $\mu\text{g/ml}$) for detection limit studies were made in 5% v/v nitric acid, from spectroscopic grade metals (Cr, Cu, Fe, Ni), metal carbonate (Pb), ACS grade nitric acid, and distilled demineralized water. Standards for the NBS standard reference material analysis were plasma-grade standards purchased from Spex Industries (Metuchen, NJ). All dilutions of primary standards were made with 5% v/v nitric acid.

DATA-ACQUISITION AND ANALYSIS ALGORITHMS

The CID11B as operated in the UA/CID11B camera system has the capability to read sub-arrays of pixels of any size in a pseudo-random manner. This capability is used to read only those pixels that contain spectroscopic information of interest. The approach used for data acquisition is to take sequentially the coordinates of spectral lines from a database, nondestructively read a subarray at the location of the line to determine the signal intensity, then nondestructively read a subarray several times until an adequate signal is reached. The intensities of the spectral lines are checked constantly, in the order of their placement in the database, while the integration is proceeding. The checking process continues until either the integration produces an adequate signal, or integration has proceeded for a preset maximum period, typically 2 min. At this point, any spectral lines that did not produce the threshold integration are read several times and the data-acquisition process is terminated.

When data are acquired as part of an analysis, a 10×3 pixel subarray, called a "spectral window", is used. This permits reading both the spectral line intensity and character of the background. When a spectral line is checked for intensity, a smaller 3×3 pixel subarray, called an "examination window", is used. This causes the intensity check to proceed faster than if the spectral window is used.

The coordinates of analytical spectral lines are determined manually and put into a master database. The coordinates are computed and stored relative to a position-reference spectral line. The barium line at 381.978 nm was used as this position reference. The location of the position-reference line is updated before each analysis session by nebulizing a barium nitrate solution and determining the exact position of

the maximum emission intensity. If the barium line is found to have moved more than 2 pixels in any direction since the last update, the relative locations of all analytical lines in the database are re-established by nebulizing a solution consisting of a mixture of each element being determined, and determining the position of maximum intensity for each analytical line. The updated coordinates are then used to update the database for future use.

The CID must be prepared for an exposure by precharging it with a "bias charge" of at least 6.73×10^5 photoelectrons in order for it to give a linear response function.⁹ The spectrometer contains light-emitting diodes (LEDs) which are under computer control for this purpose. The LEDs are positioned to illuminate the entire array uniformly. The bias charge is introduced in a program loop under computer control. In this procedure, a 10×10 pixel subarray near the center of the array is established, the entire array is cleared of charge, then a loop is entered in which the LEDs are flashed on and off for 1 msec and the subarray is read. The subarray data are averaged, and if the result is greater than or equal to the required bias signal, the process is terminated. Otherwise, the flash-and-read loop is repeated.

Once the CID is precharged, the exact bias signal for each pixel to be used in the analysis must be determined. This not only establishes an exact baseline for each pixel, but also eliminates the effect of shot noise from the bias charge.^{9,11} To read the bias signal for each spectral window, the relative coordinates of the spectral lines used in the analysis are read from a disk file, then absolute coordinates are determined from the most recent update of the barium calibration line coordinates. All analytical lines are then given an "active" status, meaning that analysis for those lines has not been completed. Next, a loop is entered in which the spectral window coordinates for a line are computed, the pixels in that window are read repeatedly, and the data are summed in a data array. This is repeated for each line of the database. The pixel data are stored as a negative number so that when the same pixels are again read after the integration is complete, the new data can simply be summed in the array. This expedites the data-acquisition process during a time-critical step.

The algorithm used to collect analytical data during the integration is shown in Fig. 2. An exposure is started while the solution under

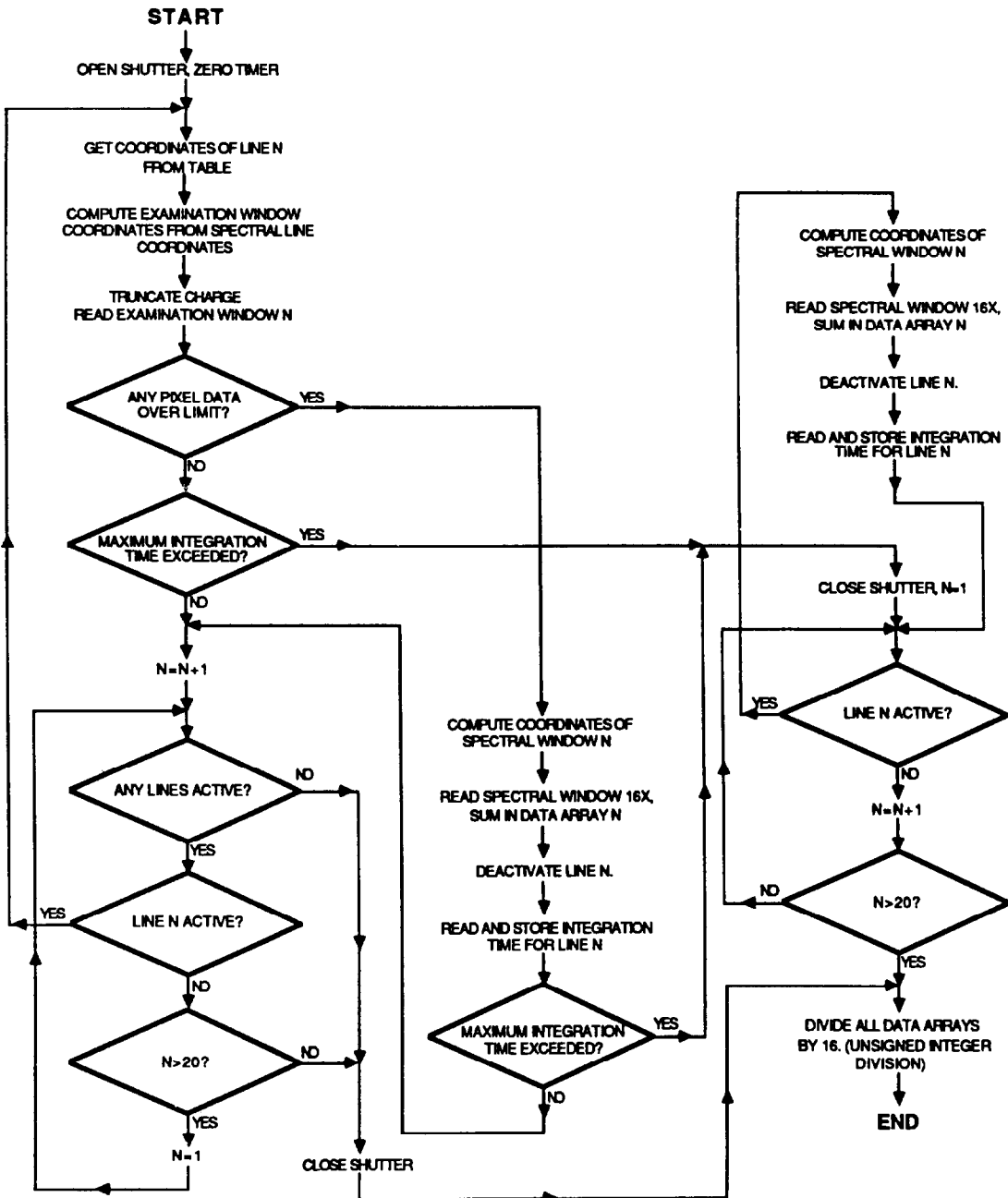


Fig. 2. Flow chart for the main data-acquisition routine. Spectral lines are checked periodically until either the integrated intensity is near to exceeding the capacity of the CID, or until a maximum time has elapsed.

analysis is being nebulized into the plasma source. A computer-controlled clock with 1 msec resolution is reset to zero and the shutter is opened. An indefinite loop is then entered where the examination window for each line is read in sequential order until either the data from one window indicate that a preset threshold has been exceeded or the elapsed time has exceeded a preset maximum. If the data read from one window exceed the threshold, that

means that the charge capacity of pixels in that window has nearly been reached, and thus integration for that line should be terminated. Charge truncation is then executed to ensure that there is no interference from column-column cross-talk.⁹ Next, the spectral window is read repeatedly and the data are summed in the same array as the previous bias data. The elapsed time is then read and stored, and the status of that line is changed to "inactive,"

meaning it will no longer be checked during this analysis run. If the elapsed time exceeds a preset maximum, the shutter is closed and the spectral windows of all remaining active lines are read, and the elapsed time is recorded in the same fashion as described above.

Once the exposure is complete, the data sum for each spectral window is divided by the number of readings used. Summation of the spectral data with the negative bias data effectively performs bias subtraction.

Reduction of the collected data takes two general forms, depending on the type of analysis being performed. If the profile of a spectral line and its associated background are to be determined, computations involving cross-talk corrections and pixel sensitivity variations are performed.¹⁰ If the nature of an analytical line is to be determined but not the background information, an analysis can be made on a blank solution, followed by another analysis of a sample solution. The data from a spectral window of the blank can then be subtracted on a pixel-by-pixel basis from the data from the spectral window of the sample. As a result, a spectral line which is not observable in a sample because of a high complex background can be made apparent.

Figure 3 illustrates this point. Figure 3A is a 2-min integration of a spectral window at the 352.454 nm nickel line. The sample solution contained 0.080 $\mu\text{g/ml}$ nickel. Figure 3B is an identical integration of a blank solution. Figure 3C is the result of subtracting the data of Fig. 3B from those of 3A. Note the change in vertical scale between Fig. 3A and 3C. The irregular nature of the background at this wavelength completely obscures the nickel emission unless the blank subtraction is performed.

Data reduction is straightforward if the only information required is relative intensity as a function of concentration. The procedure normally used involves summing data from pixels located at the spectral line position and subtracting data from pixels at the wings of the line for background correction. A 3×3 pixel group at the center of the spectral window is typically used as the "signal" pixels from which data are summed and normalized. Two groups of pixels on both sides of the signal pixels are summed and normalized as the background. The background groups are 1 (horizontal) \times 3 (vertical) and are typically located at equal horizontal spacings from the center of the analytical emission line. Optimum spacing is chosen for

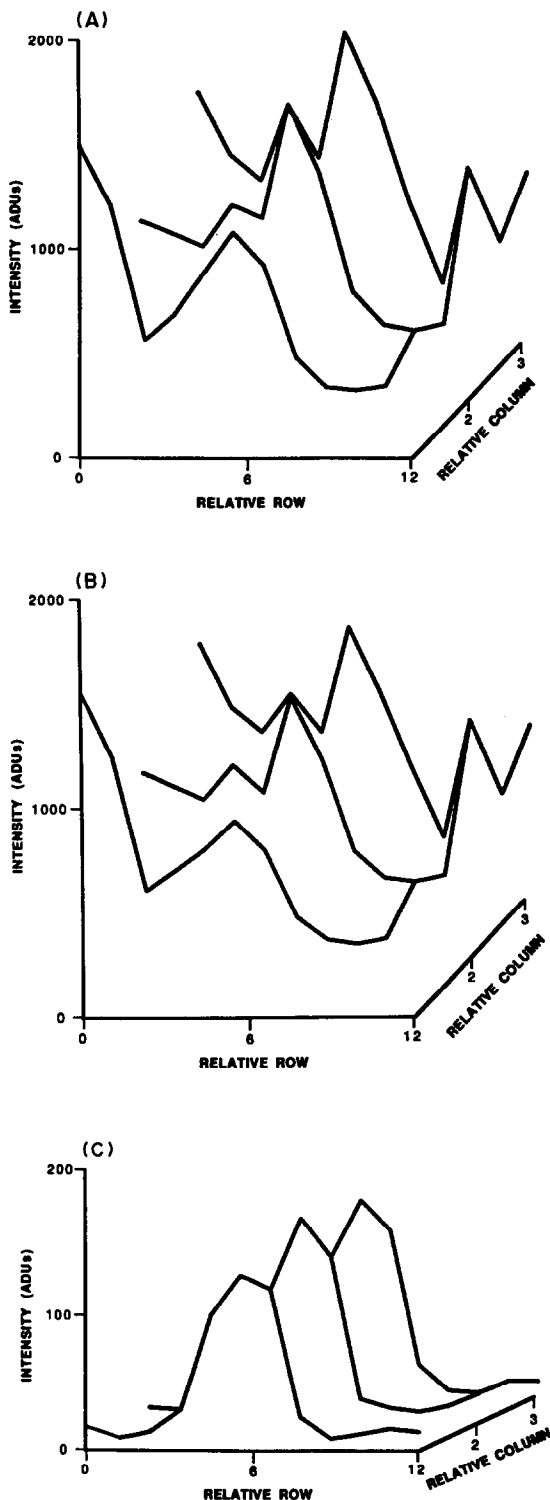


Fig. 3. (A) Readout of a spectral window located at the nickel 352.454 nm emission line. A nickel solution containing 0.08 $\mu\text{g/ml}$ was nebulized into the plasma source. The high irregular background has obscured the spectral line. ADV = arbitrary data unit. (B) Readout of the same spectral window as in (A). A blank solution was nebulized. Note the similarity between this and (A). (C) Subtraction of the data in (B) from the data in (A). The nickel 352.454 nm spectral line is now clearly visible.

different spectrometer entrance-slit widths. A spacing of plus and minus three pixels is normally used for 100 μm slits.

When this type of data-reduction is employed, all measurements are relative, thus no cross-talk or sensitivity variation corrections are made. Only column-column cross-talk has the potential of causing an error in this measurement and this is controlled in the data-collection algorithm by charge truncation. All results discussed in the remainder of this paper were performed by this straightforward relative measurement algorithm.

RESULTS AND DISCUSSION

Modified echelle spectrometer optical characteristics

The most significant change in the optical system of the stock spectrometer is the change in the focusing mirror. The substitution of the shorter focal length mirror reduces both the slit image size and the linear dispersion by a factor of 1.78. This permits a greater spectral range to be simultaneously viewed with the CID than is permitted with the stock focusing mirror.

Figure 4 illustrates the spectrometer output format and typical CID spectral coverage. Grating orders 42–77, covering the range from 542 to 291 nm, are shown in this figure. Note that the vertical scale in this figure has been greatly expanded to permit wavelengths to be listed on each order. The rectangle drawn illustrates one spectral range that can be simultaneously observed with the CID. This “observation window” can be relocated to new wavelengths by changing the orientation of the echelle grating in the manner employed in the commercial spectrometer.

The reciprocal linear dispersion of the modified spectrometer ranges from 0.00291 nm/pixel at 400 nm to 0.01175 nm/pixel at 800 nm. Dispersion and resolution are illustrated by Fig. 5. This is a plot of relative intensity *vs.* pixel number on a CID row illuminated with the mercury 313 nm doublet. A low-pressure mercury pen lamp (Pen-Ray model SC-1 with model SCT-1 power supply, Ultra-Violet Products Inc., San Gabriel, CA.) was used as the light source. The entrance slits were set to 25 μm horizontal, 300 μm vertical. The more intense line is 313.155 nm, the less intense 313.183 nm; a difference of 0.028 nm. The separation of these lines is 164 μm , or 3.5 pixels. Note the nearly baseline resolution of the doublet.

Figure 6 illustrates the effect of slit width on resolution and throughput. A mercury pen lamp was again utilized as the light source. The emission line studied was the mercury 546.1 nm line. The entrance slit height was set to 300 μm and the slit width varied from 100 μm (Fig. 6A), to 50 μm (6B) and 25 μm (6C). For each spectrum, the echelle grating rotation was adjusted so that the spectral line peak was centered on one pixel. Otherwise, identical exposure times and other conditions were used.

In the switch from 25 μm to 100 μm slit width, the intensity of illumination of the central pixel increased by a factor of 1.5, while the intensity of the adjacent two pixels increased by a factor of 5. This indicates that significant improvement in resolution can be obtained with the smaller slit settings, without a major compromise in optical throughput.

The instruction manual for the SpectraSpan III spectrometer lists a “practical resolution” which is a factor of 12.4 smaller than the linear dispersion at a given wavelength when 25 μm exit slits are used. For the unmodified spectrometer, this value is 0.005 nm resolution at 200 nm (grating order 112) and 0.020 nm resolution at 800 nm (grating order 28). At 313 nm, the practical resolution is expected to be approximately 0.0086 nm. Although no criterion for “practical resolution” is given, it could be interpreted as being the point at which two adjacent spectral lines of Gaussian profile can be discriminated.

The value for practical resolution suggested by the spectrometer manual is far below the theoretical resolving power of the echelle grating. The reason for this is probably optical aberrations in the commercial optical system. The aberrations can be largely attributed to the spherical collimation and focusing mirrors. The modified spectrometer employs an off-axis parabolic mirror for the collimator, thus diminishing aberrations from this element. A spherical mirror was retained for the focusing mirror, as a parabolic mirror would suffer from comatic aberrations at the edges of the field of view that far exceed the spherical aberration.

Because the modified spectrometer has an image quality sufficient to put nearly all the energy into the width of a single pixel when 25 μm entrance slits are used, the “practical resolution” can be considered to be the Nyquist limit of 2 pixels. This is equal to 0.0058 nm at 400 nm and 0.0235 nm at 800 nm. This is nearly the same as the commercial spectrometer

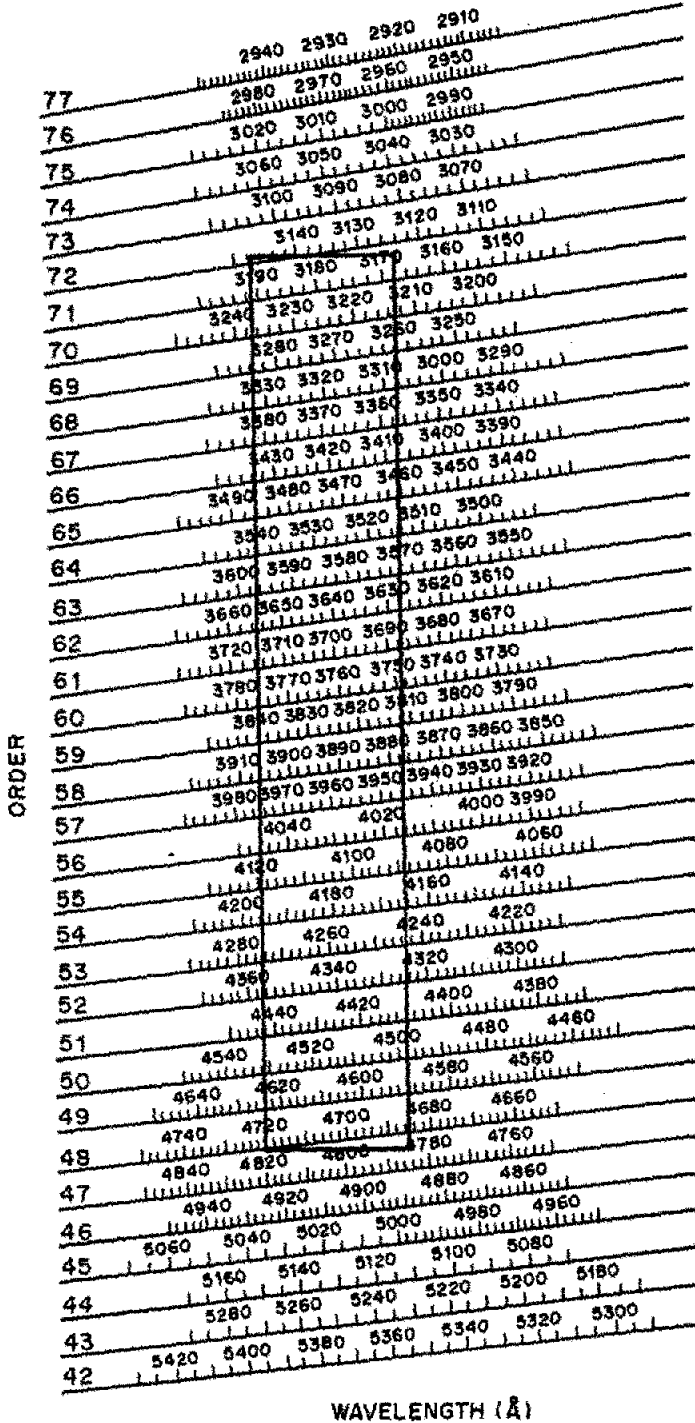


Fig. 4. Spectral output format of the modified echelle spectrometer. The rectangle represents a typical spectral range that can be simultaneously examined with the CID camera.

configuration, with twice the linear dispersion. This improvement can be attributed to the parabolic collimating mirror and the configuration of the focusing mirror, which causes most of the comatic aberration to be perpendicular to the direction of grating dispersion rather than parallel to it as is the case with the stock spectrometer.

System linearity and dynamic range

Previous work has demonstrated that the UA/CID11B camera system is highly linear over a wide dynamic range. The raw spectral dynamic range is greater than 6000:1 when readout noise is reduced by use of 16 non-destructive repeated readings.⁹

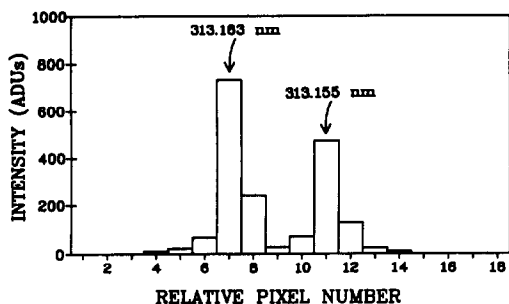


Fig. 5. Plot demonstrating dispersion and resolution of the modified echelle spectrometer. The mercury doublet with emission lines at 313.183 and 313.155 nm is shown.

Approximately 2 msec are required to read one examination window and decide whether the maximum charge threshold has been exceeded. Approximately 60 msec are required to read a spectral window 15 times, store the data,

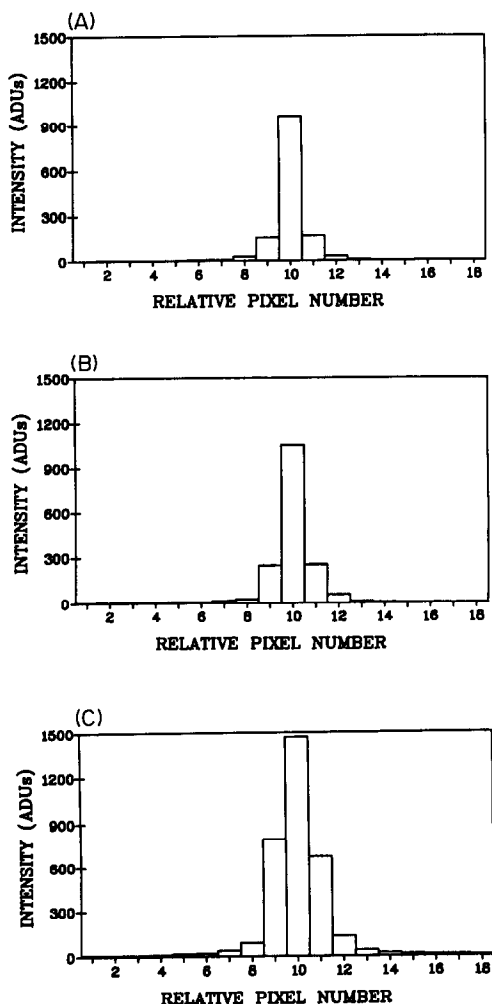


Fig. 6. Plots demonstrating the effect of entrance-slit width on the resolution and throughput for the modified echelle spectrometer. Slit widths are 100 μm (A), 50 μm (B), and 25 μm (C).

and record the elapsed time. During an analysis in which 10 spectral lines are used, each spectral line is checked every 20 msec. In the event that one spectral line must be read out during a check loop, up to 80 msec may elapse before a line is rechecked. If the maximum integration time allowed is 2 min, the minimum extension of the CID raw spectrum dynamic range is by a factor of $120/0.08$ or 1500. Under these conditions, the CID system will have a composite dynamic range of 9×10^6 . Note that the dynamic range will be even wider if it is not necessary to read out a line during a check loop or if longer integration times are allowed. The maximum achievable composite dynamic range is dictated by the number of analytical lines used and the composition of the sample.

The single-element dynamic range of several spectral lines was determined experimentally by analyzing solutions of various elements over the range from 0.003 to 10000 $\mu\text{g/ml}$. Results for the simultaneous analysis of three spectral lines of magnesium are given in Fig. 7. Shown are plots of relative signal for the 279.553 nm ion line (open circles), the 285.213 nm atomic line (triangles), and a third line believed to be the nonresonant line at 279.806 nm (closed circles). It should be noted that both the atomic and ionic line responses are linear over a wide range, with indications of self-absorption at concentrations above 100 $\mu\text{g/ml}$. This is consistent with results obtained with photomultiplier tube detectors.¹² The weak nonresonance line shows no self-absorption and gives linear results up to 7000 $\mu\text{g/ml}$. Results obtained for emission lines of other elements are similar and indicate that the composite dynamic range of the UA/CID11B camera system is more than sufficient for typical analytical applications. The widely different linear ranges exhibited by these

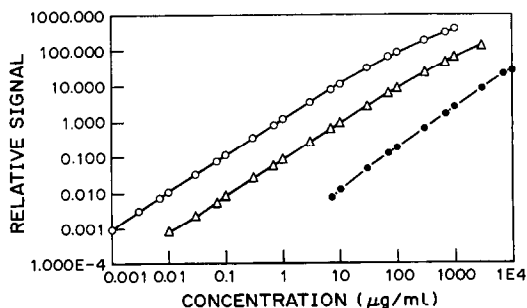


Fig. 7. Graph showing the high dynamic range of analytical signals for several spectral lines of magnesium. The wavelengths for these lines are 279.553 nm (open circles), 285.213 nm (triangles), and 279.806 nm (closed circles).

Table 3. Multiple element detection limits

Element	Wavelength, nm	Detection limit, $\mu\text{g/ml}$	
		This study*	Theoretical†
Ca	396.847	0.002	
Ca	443.496	0.127	
Cr	435.235	0.021	0.023
Cr	357.869	0.018	0.017
Cu	327.396	0.013	0.012
Cu	324.754		
Fe	358.120	0.103	0.108
Fe	382.043	0.324	
Ni	352.454	0.028	
Ni	341.476	0.007	
Pb	363.995	0.109	

*Detection limit for this study is defined as the concentration which gives a signal equal to 3 times the standard deviation of a blank solution.

†Estimated theoretical detection limit based on the numbers of signal and background photoelectrons detected by the CID.

three emission lines of magnesium also demonstrate the importance of the capability to monitor many emission lines for an element, even those that are not normally used as analytical lines.

Simultaneous multielement detection limits

Detection limits for several spectral lines of 6 elements were simultaneously determined; the results are listed in Table 3. The values listed are computed according to the IUPAC recommendation of the concentration needed to give a signal equal to three times the standard deviation of a blank solution. The standard deviation of the blank was determined from 20 trials. The detection limits of each line were determined in three different instances and the results averaged. In each instance, the instrumental conditions were the same: the maximum integration time was 2 min; entrance slits were set to 300 μm vertical and 100 μm horizontal. The plasma position and settings were not optimized for any one element but were set to best overall conditions. Nitric acid (5% v/v) was used for the blank.

A detection limit of 0.010 $\mu\text{g/ml}$ has been previously reported¹³ for the 341.476 nm emission line for nickel, obtained with an unmodified SpectraSpan III system using PMT detection under conditions quite similar to those reported in this work. This compares favorably with the 0.007 $\mu\text{g/ml}$ detection limit found in this work. Two significant differences exist in how these two values were determined. In the cited value, 10-sec integrations of the PMT signal were used and the detection limit was calculated as a signal equal to twice the standard

deviation of a blank solution. In this work, a 120-sec integration time was used and the detection limit was calculated as a signal equal to three times the standard deviation of a blank solution. These results reinforce the previously reported conclusions that the CID detector can perform approximately the same as PMT detectors in terms of sensitivity in this wavelength region.¹¹

Theoretical detection limits for some lines were calculated as the concentration of analyte necessary to produce a signal (in photoelectrons) equal to three times the shot noise from the background radiation. The background shot noise was calculated as the square root of the mean background intensity. These theoretical values are also listed in Table 3. Note that they approximate the experimentally determined detection limits, which indicates that the detection limits obtained are controlled primarily by the background intensity. This implies that detection limits can be improved only by increasing the total number of photons detected.

Accuracy

The accuracy of the CID camera system was evaluated by simultaneous determination of several elements in an NBS standard reference material (SRM 1643a: trace elements in water). The method of standard additions was used. Aliquots of the standard reference material were spiked with increments of a solution consisting of a mixture of all the elements being determined. Spectrometer slit settings were 300 μm height and 100 μm width. Maximum integration time was 2 min. The raw data were processed by subtracting the averaged background from the signal and dividing by the integration time. No cross-talk or pixel sensitivity variation corrections were made.

Plots of relative intensity as a function of concentration are shown for several representative emission lines in Fig. 8. The experimentally determined values, the equivalent standard deviations for each analytical line, and the NBS certified values are listed in Table 4. Note that the levels determined for all lines are near or below the detection limits for the instrument. All experimental values fall within one standard deviation of the certified values, with the exception of results for the chromium 357.869 nm line. The accuracy of the determination using this line was affected by a relatively strong emission line of iron at 358.120 nm. The rising background to the chromium line, caused by the

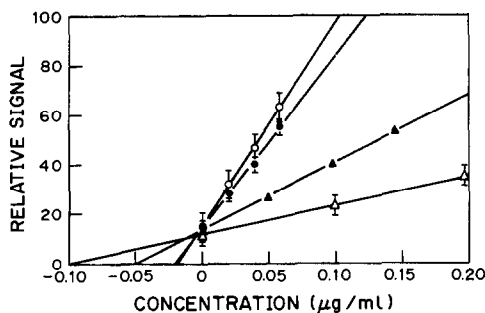


Fig. 8. Signal vs. concentration plots for several spectral lines used in the multielement, multiwavelength analysis of a standard reference material. The elements and wavelengths are: Fe 358.120 nm (open triangles), Ni 341.476 nm (open circles), Cr 435.235 nm (open triangles), and Cu 327.396 nm (closed circles).

incremental addition of iron, resulted in an underestimation of the emission signal for the chromium additions, which in turn led to an overestimation of the chromium concentration.

The erroneous results for this one spectral line illustrate the value of simultaneously monitoring several spectral lines for each element. Because the result from the two spectral lines used in the determination of chromium do not correlate, it is obvious that a problem exists. Once the problem is traced to a spectral interference, the erroneous result can be discounted with good cause.

CONCLUSIONS

The results described in this paper clearly demonstrate that the CID is a unique detector highly suitable for simultaneous multielement atomic-emission spectrometry. The system described is shown to have excellent sensitivity, dynamic range, accuracy, and precision, while having the advantages of flexible multielement

and multiwavelength capability. The problems encountered when using other types of multi-channel detectors for this application, such as uncorrectable cross-talk, blooming, limited spectral range, and high noise, do not arise with the CID.

One significant limitation exhibited by the system described in this work is that only a limited portion of the total desired spectral range can be simultaneously viewed. Any desired wavelength can be examined by adjusting the orientation of the echelle grating, but this is inconvenient and prevents the full advantage of this approach from being realized. A CID detector with higher spatial resolution combined with improved optical systems is necessary to cover a wider spectral range and maintain adequate spectral resolution. A system using the newer, higher resolution CID17B detector combined with a new generation echelle system has been designed to meet these problems.¹⁴ The CID17 also has higher quantum efficiency in the ultraviolet; thus better detection limits are expected for many analytical lines. With these improvements in detector resolution and performance, almost the entire spectral range encountered in atomic emission spectrometry can be simultaneously monitored without adjusting the dispersion optics.

With this capability, a system can be conceived that will approach the optimum system for simultaneous AES described in the introduction. Such a system will provide rapid intelligent qualitative and semiquantitative analysis of samples without significant operator intervention and will help the analyst design optimum methods for quantification, avoiding various interferences that could give rise to erroneous results in a diverse range of sample types.

Acknowledgements—This research was partially supported by the Office of Naval Research and SmithKline Beckman.

Table 4. Analysis results for SRM 1643a

Element	Wavelength, nm	Certified value, µg/ml	Experimental value, µg/ml
Cr	435.235	0.0186	0.0183 ± 0.0065
Cr	357.869	0.0186	0.0292 ± 0.0065
Cu	327.396	0.0219	0.0202 ± 0.0042
Fe	358.120	0.099	0.099 ± 0.026
Fe	382.043	0.099	0.130 ± 0.11
Ni	352.454	0.049	0.0504 ± 0.0091
Ni	341.476	0.049	0.0491 ± 0.0022

Notes:

- (1) Error values shown for experimental values are equal to one standard deviation.
- (2) The determination of chromium at the 357.869 nm line was affected by interference from an iron emission line.

REFERENCES

1. H. L. Felkel, Jr. and H. L. Pardue, *Anal. Chem.*, 1978, **50**, 602.
2. *Idem*, *Clin. Chem.*, 1978, **24**, 602.
3. A. Gustavsson and F. Ingram, *Spectrochim. Acta*, 1979, **34B**, 31.
4. D. L. Wood, A. B. Dargis and D. L. Nash, *Appl. Spectrosc.*, 1975, **29**, 310.
5. N. Furuta, C. W. McLeod, H. Haraguchi and K. Fuwa, *ibid.*, 1980, **34**, 211.
6. H. L. Felkel, Jr. and H. L. Pardue, *Anal. Chem.*, 1977, **49**, 1112.

7. Y. Talmi and K. W. Busch, in *Multichannel Image Detectors*, Y. Talmi (ed.), Vol. 2, Chap. 1. American Chemical Society, Washington D.C., 1983.
8. M. B. Denton, H. A. Lewis and G. R. Sims, in *Multichannel Image Detectors*, Y. Talmi (ed.), Vol. 2, Chap. 6. American Chemical Society, Washington D.C., 1983.
9. G. R. Sims and M. B. Denton, *J. Opt. Eng.*, 1987, **26**, 1008.
10. *Idem, ibid.*, 1987, **26**, 999.
11. *Idem*, in *Multichannel Image Detectors* Y. Talmi (ed.), Vol. 2, Chap. 5. American Chemical Society, Washington D.C., 1983.
12. R. K. Skogerboe and I. T. Urasa, *Appl. Spectrosc.*, 1978, **32**, 527.
13. G. W. Johnson, H. E. Taylor and R. K. Skogerboe, *Spectrochim. Acta*, 1979, **34B**, 197.
14. R. S. Pomeroy, J. V. Sweedler and M. B. Denton, *Talanta*, 1990, **37**, 15.

CHARGE-INJECTION DEVICE DETECTION FOR IMPROVED PERFORMANCE IN ATOMIC-EMISSION SPECTROSCOPY

ROBERT S. POMEROY, JONATHAN V. SWEDLER and M. BONNER DENTON
Department of Chemistry, University of Arizona, Tucson, AZ 85721, U.S.A.

(Received 25 July 1988. Accepted 29 November 1988)

Summary—Studies into the use of simultaneous multiwavelength detection over a broad wavelength region (220–520 nm) demonstrate the power and flexibility offered by a charge-injection device for detection in atomic-emission spectrometry. An echelle monochromator and a charge-injection device utilizing the General Electric CID17B array detector are used in conjunction with a direct current plasma source to perform multi-line analysis for Mg, Sr, Fe, Dy, Ho and Yb, increasing the sensitivity and limits of detection. By monitoring the 341-nm OH band and background Ar emission lines, changes in the nebulization and excitation conditions are easily detected. The presence of an organic matrix component not present in the standards is detected by observing the C(I) emission at 247.8 nm. These diagnostic tools can be combined with the use of an internal standard to obtain a reliability not previously available in automated AES instrumentation.

The detector most often used for atomic-emission spectrometry (AES) is currently the photomultiplier tube (PMT).¹ The PMT is an extremely sensitive, wide dynamic range detector. Before the dominance of PMT-equipped instrumentation, AES systems often used photographic emulsions. The use of photographic film allowed the integration and simultaneous determination of emission lines over a wide spectral region. However, the difficulty in quantification, and the narrow dynamic range of film contributed to the replacement of film by photomultiplier tubes. The recent appearance of two-dimensional detectors with formats large enough to supply the number of resolution elements required in AES, with a sensitivity and dynamic range matching or exceeding those of the PMT has prompted several studies into replacing the PMT with these new detectors. The detector used in these studies, the charge-injection device (CID), has a number of characteristics which make it well suited to AES.^{2,3} This paper describes an approach to AES with CID detection that greatly increases the flexibility and diagnostic ability of AES.

The CID is a solid-state silicon detector with a two-dimensional rectangular array format. The CID used in these studies, the CID17B, is composed of a 244 × 388 array of detector elements. The detector integrates signal information much like photographic film. After a desired integration period, the detector is read,

and the charge information at each individual detector element is proportional to the amount of light striking that element. When properly operated and cooled, the CID has a negligible dark current (<0.08 photoelectron/sec). For a dark current of this level, many months are required before the device is saturated solely by the dark current. In addition, the quantum efficiency of the detector is extremely high compared to the photocathode materials used in PMTs.²

The CID detector has several other characteristics which make it particularly well suited for AES compared to other solid-state array detectors. Of prime importance to AES, CIDs are extremely resistant to the phenomenon called charge blooming. Blooming is the process in which excess photogenerated charge from a detector element exposed to a bright spectral feature spills into nearby detector elements, obscuring adjacent spectral features. In addition, the CID architecture allows random access to any detector element, permitting an individual detector element to be interrogated without reading all of the other elements. Lastly, the CID readout process can be nondestructive, so an individual detector element can be interrogated during the course of an exposure, to monitor the accumulation of integrated signal without affecting the integration process. By utilizing the nondestructive readout and selective interrogation in a process called random

access integration (RAI), the system interrogates each detector element to determine the level of photogenerated signal during the course of each analysis.³⁻⁶ No prior knowledge is needed regarding line intensity, because the system determines the intensity during the course of the analysis. Background is measured simultaneously on both sides of the line, allowing a variety of sophisticated background correction algorithms to be used. The interested reader is referred to several recent descriptions of the architecture, operating methods and spectroscopic performance of CIDs.²⁻⁹

In this study, several new capabilities of the AES system that are made possible by using a CID detector are investigated. Simultaneous multi-line analysis allows the choice of the most appropriate lines for analysis. Determining which lines will be most analytically useful depends on such things as the composition of the sample (the concentration of each analyte as well as of the potentially interfering species), the solvent, and the plasma background. The use of multiple lines from a particular element can be used to improve the overall analysis in a number of ways. The linear dynamic range can be increased by using the most sensitive lines for low concentrations of the analyte and less sensitive lines for higher concentrations. The limit of detection (defined here as 3 times the standard deviation of the blank) can be improved by

summing the signal from multiple lines. This summing of the signals can result in increases in the sensitivity (slope of the calibration curve). Various improved diagnostic procedures are demonstrated, including monitoring and quantifying the presence of an organic matrix component and detecting changes in nebulization and excitation conditions by monitoring OH and Ar emission features in the background. Employing such methods increases the reliability of the analytical results by alerting the user to potential problems. Utilizing an internal standard, along with judicious choice of analyte and internal standard emission lines, is shown to greatly increase the analytical performance of the system and provide a means of semiquantitative analysis.

EXPERIMENTAL

An echelle spectrometer (Fig. 1) equipped with a GE CID17B array detector (388×244) is used.^{4,8,11} The block diagram of the system is shown in Fig. 2. The source is a three-electrode direct current plasma (ARL, Sunland, CA). Stock solutions were prepared from $\text{Mg}(\text{NO}_3)_2 \cdot 6\text{H}_2\text{O}$, $\text{Sr}(\text{NO}_3)_2$, $\text{LuCl}_3 \cdot 6\text{H}_2\text{O}$ and high-purity Fe, Cr and Al wire. All solutions were diluted with 5% v/v nitric acid (Mallinckrodt). All glassware was soaked for a minimum of 24 hr in a bath of 0.1M EDTA and stored

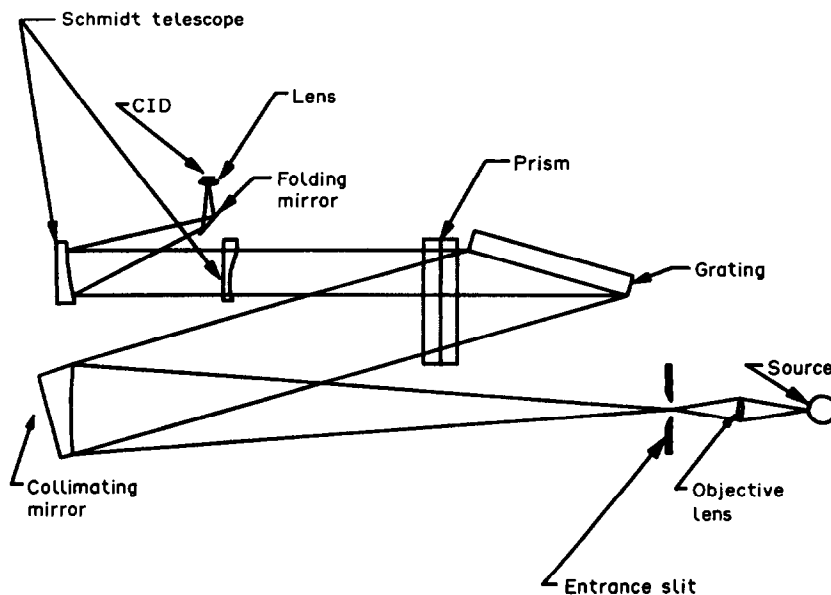


Fig. 1. Optical diagram of the echelle spectrometer designed for use with CID detection. A focal plane image covering the wavelength range from 225 to 515 nm is created in an area of 6.5×8.7 mm, compatible with the General Electric CID17 detector.

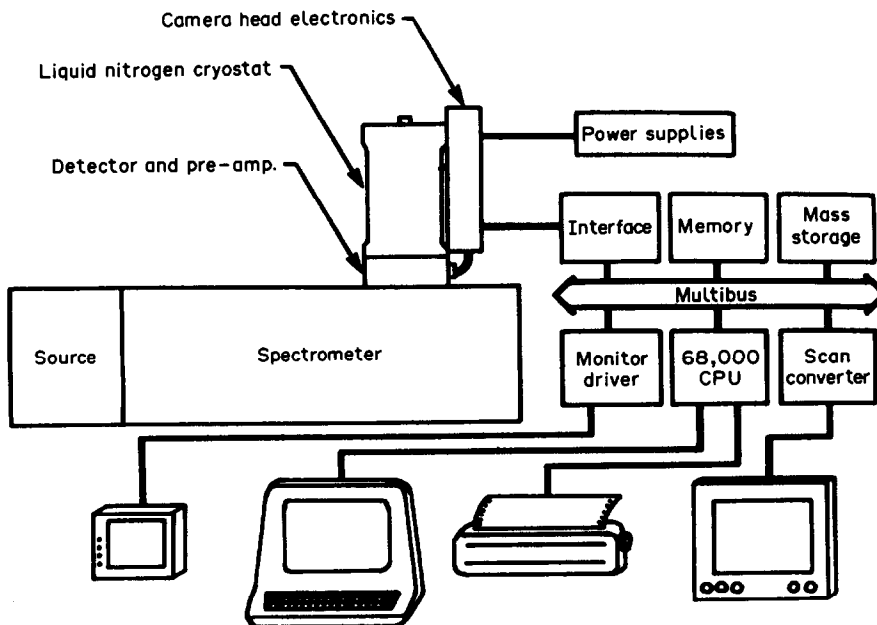


Fig. 2. Schematic diagram of the CID17 AES system. Array detector operation is provided by a Photometrics Ltd (Tucson, AZ) camera controller which receives instructions from the host Motorola 68,000 based computer.

with 5% v/v nitric acid. The spectroscopic reference blank in all cases was 5% v/v nitric acid. The organic diluent in the organic matrix study was 95% ethanol (Mallinckrodt).

RESULTS AND DISCUSSION

Multi-line analysis

Multi-line analysis can be used to monitor for the presence of chemical and spectral interferences. As examples, the presence of easily ionized elements can significantly alter plasma conditions and the 385.8 nm Ni(I) line can interfere with the commonly used 386.0 nm Fe(I) line. Multi-line analysis can be employed to confirm the validity of the results. If the values obtained from different lines are in good agreement, averaging all the values results in increased precision. If a discrepancy in the results from the individual lines exists, examination of changes in the background may indicate a decrease in the excitation energy of the plasma. In this case, more reliable results are obtained from low-lying neutral ground-state transitions. If no such trend is apparent, the discrepancy may be due to spectral or chemical interferences. By display of the entire spectrum and comparison of the locations of the spectral lines with a spectral library of element lines, qualitative elemental identification is obtained. Employment of appropriate multi-line pattern-

recognition routines can be used to confirm the presence of spectral and chemical interferences and allow appropriate lines to be used to arrive at a valid result.

The results of summing multiple lines for Fe, Mg, Sr, Dy, Ho, and Yb are shown in Table 1. One example of a summed working curve for Fe is shown in Fig. 3. Summing the line intensities from three Fe lines increases the sensitivity by 90% and halves the limit of detection (LOD). The Fe lines selected are reasonably equivalent in terms of their analytical sensitivity, with similar single-line LODs. This is necessary when working at the detection limit because less sensitive lines make little or no contribution to improving the summed-line working curve at the detection limit of the more sensitive lines. However, the less sensitive lines can be used to extend the linear dynamic range. The LOD is inversely proportional to the square root of the number of lines used, when all the summed lines are equivalent and the noise sources of the lines are uncorrelated. Many noise sources for each spectral line are independent from line to line. For example, background shot noise from each line is independent. However, overall system noises such as fluctuations in power supply to the DCP, or nebulizer instability are, to a large extent, correlated for all spectral lines; in this case, summing multiple spectral lines in a determination does not lead to great improvements

in sensitivity. Because a "square root" improvement in the limit of detection is observed in these investigations as the number of summed lines is increased, the dominant noise source for these spectral lines at these low levels is uncorrelated among the different spectral lines.

System diagnostics

Emission bands from OH and Ar are present during every analysis with the system used. Normally, this background emission is subtracted, leaving only the spectrum of analytical interest. Subtraction of the background is valid only if there is little or no change in any of the experimental parameters between the measurement of the sample and the blank. With careful monitoring of the background and comparison of the background between sample and blank, the user can be alerted to changes in the system status and appropriate action can be initiated, such as ignoring that result or re-running the analysis under more appropriate conditions.

One such area concerns changes in nebulization. In order to simulate nebulizer problems, the nebulization rate was varied by increasing the pump rate. This can affect the analytical results in several ways. Increasing the rate of sample introduction provides more analyte to the plasma and consequently increases the emission signal. On the other hand, increasing the sample introduction rate increases the solvent load, which can cool the plasma, thereby decreasing the emission signal. To determine the effect of solvent load on the excitation conditions, a mixture of 5% methane in argon was used as the nebulizer gas. This provides a constant amount of carbon to the plasma, independent

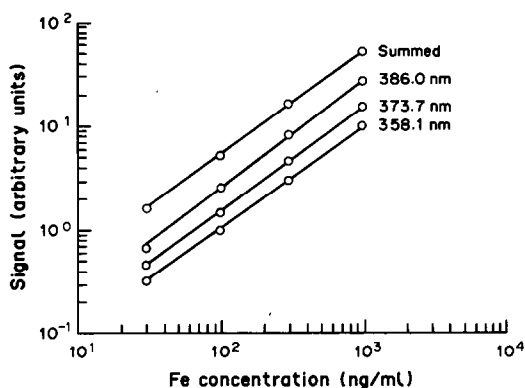


Fig. 3. Comparison of the summed and individual working curves for three iron spectral lines—358.1, 373.7 and 386.0 nm.

of the sample pump rate. The pump rate of the peristaltic pump which delivers sample to the nebulizer was varied over the range from 0.5 to >2 ml/min. The carbon emission was monitored as a function of the pump rate, and observed to decrease by only about 6% as the pump rate was increased from 0.5 to about 2.6 ml/min (Fig. 4). If the excitation conditions for the analyte behave in a similar fashion, then mass transport of the analyte into the plasma is the most important consideration over this range of pump rates. A linear relationship is obtained between pump rate and the OH emission at 341 nm. Because changes in nebulization rate outside this range are unlikely, monitoring the OH emission allows the nebulizer performance to be followed during the analysis. When the differences in OH emission from one analysis to the next exceeds a threshold value, the user is alerted.

Table 1. Improvement in LOD and sensitivity by summing multiple lines

Element and wavelengths	No of lines summed	LOD for summed lines, ng/ml	Improvement in LOD,* %	Increase in sensitivity, %
Mg 279.6, 280.3, 285.2 nm	3	0.1	60	110
Fe 358.1, 373.7, 386.0 nm	3	7	50	90
Sr 421.6, 460.7 nm	2	8	30	50
Dy 364.5, 353.2 nm	2	8	30	95
Ho 345.6, 379.7, 389.1 nm	3	2	35	70
Yb 369.4, 398.8 nm	2	0.3	25	50

*Multiple-line LOD expressed as a fraction of single-line LOD.

As previously mentioned, atom and ion lines from argon are present in every plasma spectrum obtained. Because changes in the excitation conditions affecting the emission of the analyte species also effect the argon emission spectrum, the plasma excitation conditions can be monitored during every analysis. The presence of easily ionized elements (EIEs) can enhance the atom line emission from the analyte, particularly the emission from the alkali and alkaline-earth metals in the DCP. Thus, the presence of EIEs in the sample but not in the standards can lead to erroneous results. Figure 5 shows the argon atom and argon ion emission and their ratio as a function of EIE concentration (the EIE in this case is Na). The results are consistent with the changes expected in the ionization equilibrium on increase in the number of electrons in the plasma; thus atom emission is enhanced and ion emission is suppressed. By monitoring of the argon emission, any changes in the excitation conditions are detected during the course of each analysis.

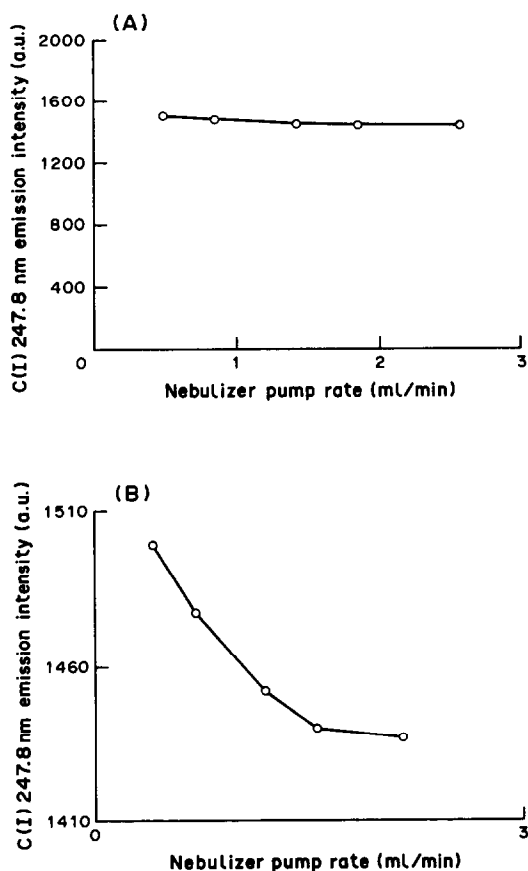


Fig. 4. Effect of increasing solvent load on the plasma, for C(I) 247.8 nm emission.

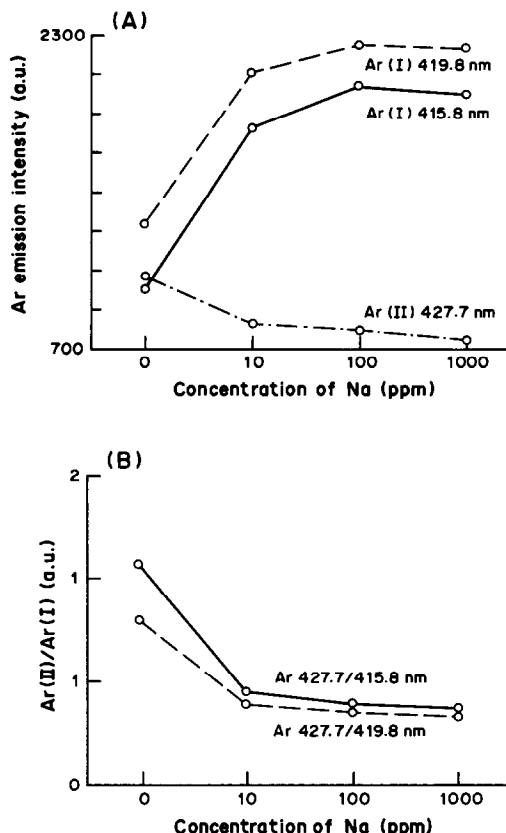


Fig. 5. (A) Effect of EIE on plasma excitation conditions, monitored by following behavior of the argon background. (B) Data from (A) redisplayed as ratio of Ar (I) to Ar(II). This ratio is more sensitive to initial changes than is either Ar(I) or Ar(II) emission alone.

Internal standards

Many of the difficulties in nebulization and excitation can be overcome by the use of appropriate internal standards and the judicious choice of internal standard emission lines. Ideally, an intensity ratio of the analyte emission line and an internal standard line works best if these lines have similar ionization and excitation characteristics. Because the analytically important lines include both ionic and atomic transitions occurring over a wide wavelength range, the internal standard should have many atomic and ionic emission lines throughout the wavelength region of interest but not cause spectral interference problems. Lutetium was chosen for these studies because it is not commonly found in samples to be analyzed, is rarely of analytical interest, has intense emission lines throughout the observation region of the system, and is an effective ionization buffer.

To determine the effectiveness of Lu as an internal standard, the response of five representative elements was recorded, for various

nebulization rates. The results obtained with a 100 ppm Lu internal standard are shown in Table 2. The use of the line ratios almost completely compensates for the nebulization changes and provides an excellent means of internal standardization in a wide variety of applications.

Another potentially useful aspect of employing internal standards is the development of an automated semiquantitative analysis scheme for all elements present in the sample. Linear working curves for all elements investigated are obtained by proper choice of analyte and internal standard lines. Each of the analyte to internal standard emission intensity ratios was measured 15 times over the course of several weeks. The variation in the ratios for a set of

Table 2. Comparison of change in emission intensity and line ratio due to changes in nebulization

Line	Change, %	Change ratio,* %
Mg(I) 285 nm	6	0.5
Sr(I) 461 nm	12	0.8
Ni(I) 349 nm	7	3.0
Cr(I) 359 nm	12	1.0
Al(I) 403 nm	6	0.1

*Ratio to change in Lu(I) 328 nm line.

test elements (Al, Mg, Ni, Cu and Sr) was less than 30%, indicating that by simply spiking the sample with the Lu standard, semiquantitative results can be simultaneously obtained *without the need for concentration standards*, by use of previously determined working curves of the intensity ratio of the analyte line to internal standard line.

Presence of organic matrix components

The presence of volatile organic solvents has been observed to cause instability in the plasma source,^{12,13} solvent loading of the plasma, increased analyte emission and strong background emission (C₂, CH, CN). A working curve of carbon emission intensity *vs.* % ethanol shows that monitoring the carbon atomic C(I) 247.8 nm line allows detection and quantification of carbon from ethanol present at relatively high levels, from <1 to >95%. The effect of changes in % ethanol present for three lines of Mg is shown in Fig. 6. The two ion lines (279.5 and 280.2 nm), the strongest and most often used emission lines of Mg, show larger changes in emission intensity as a function of % ethanol than does the Mg(I) 285.2 nm line. Thus, when the presence of an ethanol matrix component is detected during the course of analysis by monitoring the carbon emission intensity, the most reliable results are obtained, without further sample preparation, by using the Mg 285.2 nm line. Similarly, Fe and Sr emissions are affected by the presence of the organic matrix component. Unfortunately, no one line from either element gives an acceptable answer without further standard preparation (error <20%).

These studies demonstrate that during the analysis of an unknown sample, a change in the solvent can easily be brought to the spectroscopist's attention. In certain instances, the appropriate lines can be used to minimize the errors introduced by the solvent changes, without additional sample preparation or recalibration. Even in cases where appropriate line

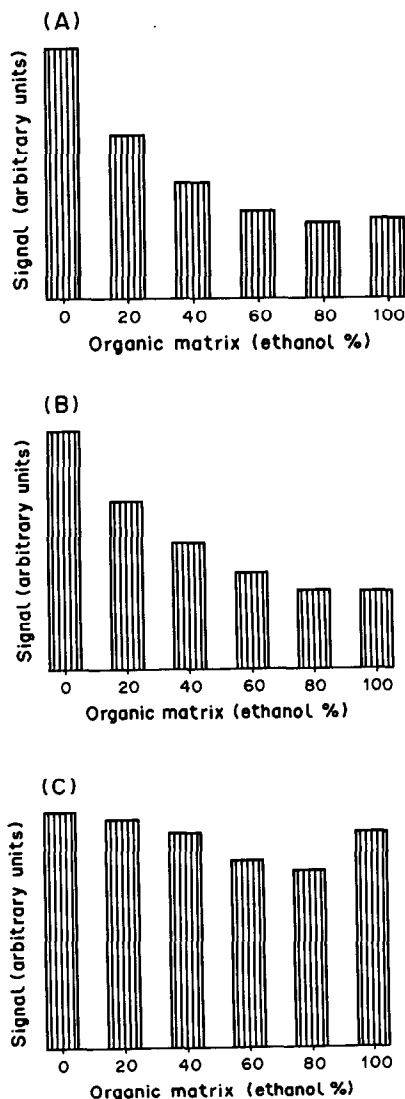


Fig. 6. Dependence of Mg lines on ethanol content of sample: (A) 279 nm; (B) 280 nm; (C) 285 nm.

selection does not allow accurate results, notifying the operator prevents erroneous results from being accepted as correct and directs the analyst to provide more appropriate calibration standards or additional sample preparation.

CONCLUSIONS

Atomic-emission spectroscopy is one of the most widely used techniques for elemental analysis. A large demand exists for the commercial market to provide automated instrumentation for quality control, and research and development. In quality control applications where a great deal of prior knowledge exists concerning a sample, the current technology, such as direct readers, has been successful in providing acceptable precision and sensitivity. However, in analyses where there is little prior knowledge about the sample, current commercial systems can easily fail to provide proper analysis, owing to their limited spectral data interrogation.

Use of a properly configured array-detector echelle spectrograph provides adequate resolution for AES with *simultaneous* detection. Examining and using the large amounts of spectral information generated with this system does not require additional analysis time. This is in contrast to scanning systems where monitoring background or additional spectral lines can lead to an increase in analysis time and a loss in sensitivity because the original spectral line is not being examined during other measurements. Because of the simultaneous nature of CID detection, the system generates information which can deal with a large compositional variation in samples.¹⁴

The examples of multi-line analysis, determination of the presence of organic matrix components, and system diagnostics, serve to demonstrate that the CID17 echelle system is capable of addressing the important analytical question: how valid are the data obtained in any given analysis? Modern automated instrumentation arrives at answers; however, the ability of most analytical instrumentation to determine the validity of an answer is usually limited. The CID/echelle system is able to monitor for several possible error conditions associated with an unknown sample, and either take appro-

priate action and/or alert the user. Great strides in the development of expert systems are potentially realized by using the large amount of data generated during the course of each analysis, as active feedback to correct the system response as necessary. Only a few of the techniques to improve the reliability of AES have been demonstrated. The full potential of this technology will require the development of sophisticated software which extracts analytical information from the large amount of spectral information available. The studies reported here demonstrate the promise of simultaneous multiwavelength for AES.

Acknowledgements—The authors gratefully acknowledge the work of Dr. Robert Bilhorn of Eastman Kodak (Rochester, NY) and Dr. Gary Sims of Photometrics Ltd (Tucson, AZ) on developing CID-AES systems. This work has been partially funded by SmithKline Beckman, the Office of Naval Research, the Analytical Technologies Division of Eastman Kodak, and the Analytical Division of the American Chemical Society Summer Fellowship sponsored by the Society of the Analytical Chemists of Pittsburgh.

REFERENCES

1. P. W. M. Boumans, *Inductively Coupled Plasma Emission Spectroscopy, Part 1—Methodology, Instrumentation, and Performance*, Wiley, New York, 1987.
2. J. V. Sweedler, R. B. Bilhorn, P. M. Epperson, G. R. Sims and M. B. Denton, *Anal. Chem.*, 1988, **60**, 282A.
3. R. B. Bilhorn, J. V. Sweedler, P. M. Epperson and M. B. Denton, *Appl. Spectrosc.*, 1987, **41**, 1114.
4. R. B. Bilhorn, *Ph.D. Dissertation*, University of Arizona, 1987.
5. G. R. Sims and M. B. Denton, *J. Opt. Eng.*, 1987, **26**, 1008.
6. *Idem*, in *Multichannel Image Detectors*, Y. Talmi (ed.), Vol. 2, Chap. 5. American Chemical Society, Washington D.C., 1983.
7. M. B. Denton, H. A. Lewis and G. R. Sims, in *Multichannel Image Detectors*, Y. Talmi (ed.), Vol. 2, Chap. 6. American Chemical Society, Washington D.C. 1983.
8. R. B. Bilhorn, P. M. Epperson, J. V. Sweedler and M. B. Denton, *Appl. Spectrosc.*, 1987, **41**, 1125.
9. P. M. Epperson, J. V. Sweedler, R. B. Bilhorn, G. R. Sims and M. B. Denton, *Anal. Chem.*, 1988, **60**, 327A.
10. P. N. Keliher and C. C. Wohlers, *ibid.*, 1976, **48**, 333A.
11. R. B. Bilhorn and M. B. Denton, *Appl. Spectrosc.*, 1989, **43**, 1.
12. P. N. Keliher and W. J. Boyko, in *Recent Advances in Analytical Spectroscopy*, K. Fuwa (ed.), Pergamon Press, New York, 1982.
13. D. D. Nygaard and J. J. Sotera, *Appl. Spectrosc.*, 1987, **41**, 703.
14. M. B. Denton, *Analyst*, 1987, **112**, 347.

USE OF A SPECTRALLY SEGMENTED PHOTODIODE-ARRAY SPECTROMETER FOR INDUCTIVELY COUPLED PLASMA ATOMIC-EMISSION SPECTROSCOPY

EXAMINATION OF PROCEDURES FOR THE EVALUATION OF DETECTION LIMITS

K. R. BRUSHWYLER, N. FURUTA* and G. M. HIEFTJE†

Department of Chemistry, Indiana University, Bloomington, IN 47405, U.S.A.

(Received 3 January 1989. Accepted 7 April 1989)

Summary—The utility of a spectrally segmented photodiode array spectrometer was examined by using inductively coupled plasma atomic-emission spectrometry (ICP–AES). The spectrometer used in this study is capable of high resolution (reciprocal linear dispersion of approximately 0.08 nm/mm at 300 nm) over a wide spectral range (190–415 nm). The effect of using spectral peak areas instead of peak heights as a signal definition was examined by using the emission signals from 10 molybdenum lines obtained with various photodiode-array integration periods. In addition, a procedure to determine the detection limits obtainable with such a spectrometer is proposed. It was found that a signal definition involving a summation over a range of 5 pixels offered the best signal-to-noise ratio when the noise was defined as the standard deviation of the residual values from the line fitted to the sideband background level. A detection limit of 6 ng/ml was determined in this way for molybdenum. The multichannel capability of the spectrometer was found to permit continuous background correction, thereby reducing errors caused by low-frequency noise or plasma drift. The linearity of response was found to extend over three orders of magnitude with use of a single integration period. However, by use of different integration periods, the linear range of the detector could be extended to at least four orders of magnitude. The precision (RSD) of the spectrometer for a molybdenum concentration of 0.5 $\mu\text{g/ml}$ was found to be about 3–4% for molybdenum peaks where the background emission was relatively low.

Multichannel detectors such as vidicon tubes, linear photodiode arrays, and charge-transfer devices have been evaluated as detection systems for inductively coupled plasma atomic-emission spectrometry (ICP–AES).^{1–4} Spectrometers which utilize solid-state multichannel detectors are generally considered to be less sensitive to ultraviolet light than are those using photomultiplier-tubes and to suffer from either poor spectral resolution or limited spectral range. However, with the rapid development of solid-state technology, the sensitivity of linear photodiode arrays has improved dramatically. Recently, a spectrally segmented photodiode-array spectrometer (Plasmarray[®], LECO Corporation) has been made commercially available for ICP–AES.^{5–7} The unique optical arrangement of the spectrometer enables the simul-

taneous measurement of a number of emission lines over a wide spectral range (190–415 nm) with a high degree of spectral resolution. The spectrometer is easily reconfigured for examination of different sets of spectral lines. As such, it is in essence a field-reprogrammable direct-reading spectrometer.^{5–7} In the present study, several different definitions of noise and signal were examined, in order to establish realistic detection limits obtainable with the spectrometer. A total of ten molybdenum lines were measured. Because of the number and variety of molybdenum spectral lines that were investigated, the findings of this study can be extended to any spectral line when due consideration has been given to the definition of both the signal and the noise.

EXPERIMENTAL

Instrumentation

The linear photodiode-array spectrometer used in this study has been discussed thoroughly

*On leave from The National Institute for Environmental Studies, 16–2 Onogawa, Tsukuba, Ibaraki 305, Japan.

†Author for correspondence.

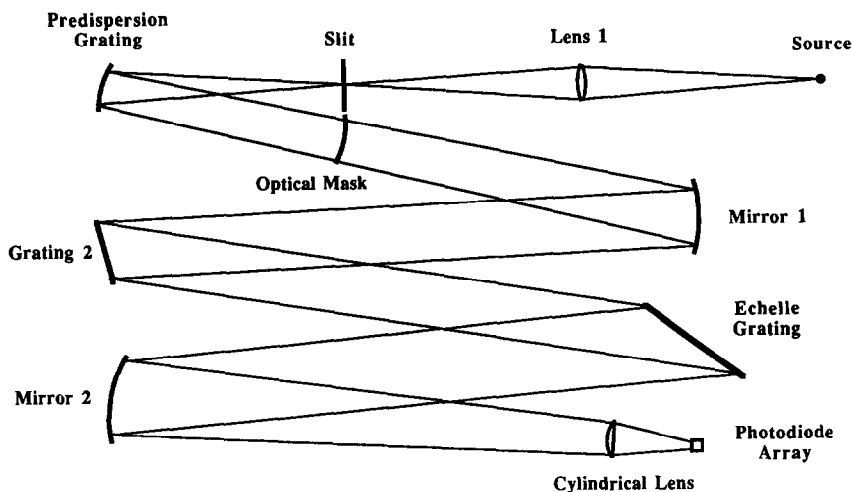


Fig. 1. Schematic diagram of the Plasmarray spectrometer.

in earlier papers⁵⁻⁷ and will be described only briefly here. The optical system is shown schematically in Fig. 1. The unique combination of wide spectral range and high resolution offered by this arrangement is derived from the combined use of three optical elements: a predispersion grating, an optical mask, and an echelle grating. The source (an ICP was used in this study) is imaged by lens 1 onto a low-resolution (590 grooves/mm) predispersion grating. The resulting dispersed light falls upon a demountable mask which has slots cut in it at positions corresponding to the elemental spectral lines of interest. The masks are designed and fabricated for specific sets of analytical lines and are readily interchanged. Light which is passed by slots in the optical mask is recollimated by mirror 1, "un-dispersed" by grating 2, and is then incident on an echelle grating (31.6 grooves/mm, 63.5° blaze angle) for final dispersion onto the photodiode array. The lack of a cross-dispersing element results in a spectrum at

the photodiode array which represents the union of many orders from the echelle grating. Accordingly, the spectral display is unconventional, but elemental lines can be identified either by empirical calibration or computer modeling.⁵⁻⁷

The mask used in this study was cut specifically for ten molybdenum spectral lines and contained ten slots. Table 1 relates the labeled spectral peak numbers in Fig. 2(d) with the type of emission (*i.e.*, ionic or atomic), the actual peak wavelengths, the grating order in which the dispersed spectral line falls, the reciprocal linear dispersion at the location of incidence on the photodiode array, and the measured resolution calculated as full width at half maximum. Figure 2 shows a series of spectra obtained with this mask. Spectrum (a) is a typical dark-current signal from the photodiode array. Spectrum (b) is a blank signal obtained from the continuous nebulization of water into an inductively coupled plasma. The dark-current signal shown in

Table 1. Peak specifications for peaks 1-10 (see Fig. 2)

Peak number*	Spectral line	Wavelength, nm	Echelle order	Dispersion, pm/mm	Resolution, † pm
1	Mo I	386.411	147	106.7	8.6
2	Mo II	287.151	198	79.2	8.8
3	Mo II	281.615	202	77.6	9.0
4	Mo II	277.540	205	76.5	8.1
5	Mo II	284.823	200	78.4	8.4
6	Mo I	379.825	150	104.5	10.0
7	Mo II	390.296	146	107.4	9.4
8	Mo II	263.876	216	72.6	7.6
9	Mo II	292.339	195	80.4	9.1
10	Mo I	313.259	182	86.2	9.7

*Peak numbers refer to designations on the spectrum in Fig. 2(d).

†Calculated as full width at half maximum.

spectrum (a) has been subtracted from the signal obtained for the blank. Spectrum (c) is a dark-current-subtracted spectrum showing the signal obtained from a 5 $\mu\text{g/ml}$ solution of molybdenum. Spectrum (d) is the signal obtained by subtracting (b) from spectrum (c).

Operating parameters

The observation height in the ICP was fixed at 20 mm above the load coil, on the basis of visual observation of the emission from a 1000 $\mu\text{g/ml}$ solution of yttrium. Signal-to-noise ratios for the analytical lines of molybdenum were optimized by changing independently the plasma input power and the carrier-gas flow-rate. The emission spectra obtained under optimal conditions for (a) atomic emission and (b) ionic emission are shown in Fig. 3. The optimal conditions for atomic emission were an ICP power of 1.1 kW and a carrier (central) gas flow-rate of 1.0 l./min. Throughout this study, the ICP was operated under conditions optimized for ionic emission, listed in Table 2.

Experimental procedure

Because of the unconventional spectral presentation at the photodiode array, it is essential to define carefully both signal and noise in order to assign realistic detection limits. Three different methods of determining noise were evaluated. First, a conventional approach was taken in which noise was defined as the standard deviation of ten independent measurements of a blank solution, at the spectral location of interest. For this definition of the detection limit, the effect of integrating both the signal and the background over different numbers of pixels was examined. For a given determination, the number of pixels used to compute both the signal and the background area was equal. Each spectral line was examined for signal definitions covering a range from 1 to 13 pixels, centered at the peak of the line (*i.e.*, peak ± 0 pixels, peak ± 1 pixel, peak ± 2 pixels, . . . , peak ± 6 pixels). This procedure is illustrated in Fig. 4(a) and (b), where signal and background definitions covering a five-pixel range are shown. For each of these definitions, four different

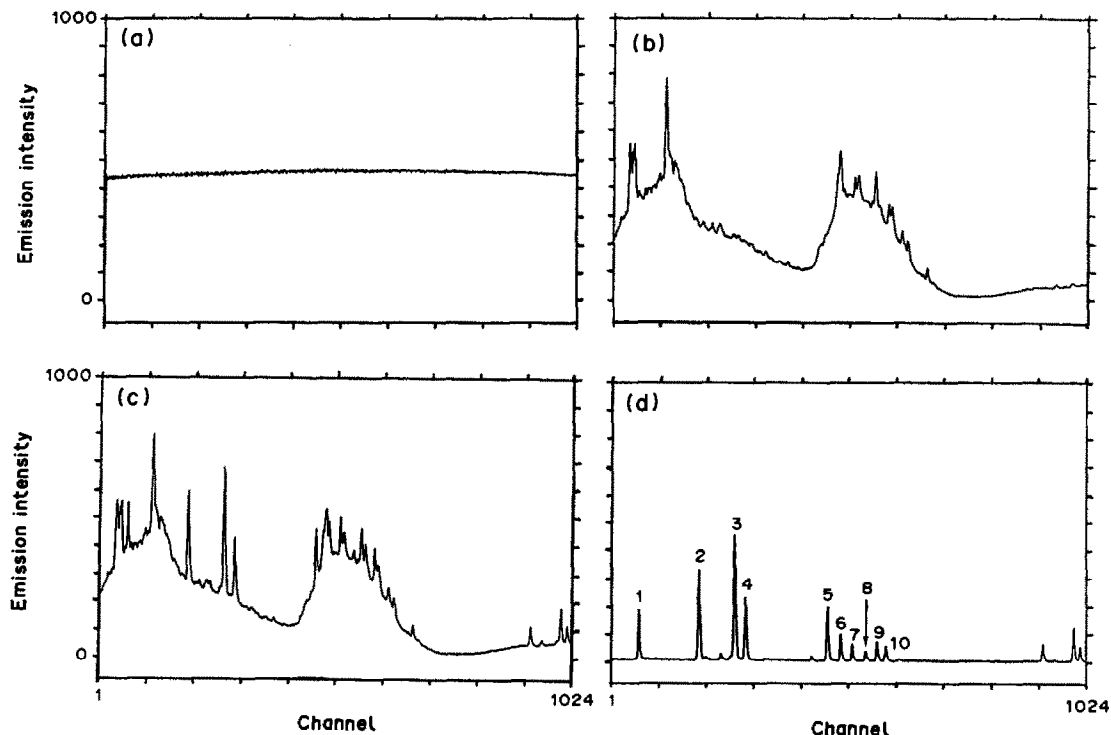


Fig. 2. Spectra obtained from the photodiode array, 10-sec integration, vertical scales are identical for all spectra: (a) dark current; (b) dark-current-subtracted blank spectrum; (c) dark-current-subtracted sample spectrum from 5 $\mu\text{g/ml}$ molybdenum solution; (d) blank-subtracted Mo spectrum [spectrum (c) - spectrum (b)].

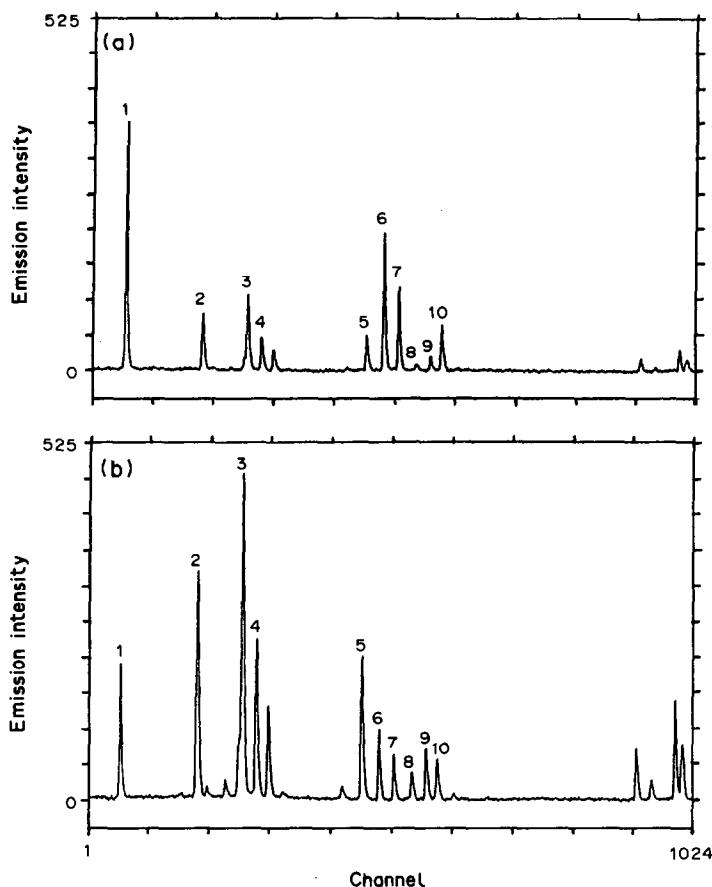


Fig. 3. Spectra obtained under optimized operating conditions for (a) atomic emission and (b) ionic emission. Optimized conditions for atomic emission: plasma forward power, 1.1 kW; sample delivery rate, 1.0 ml/min. All other parameters were the same as the optimized conditions for ionic emission, listed in Table 2. Spectral lines are identified in Table 1; peaks 1, 6, and 10 arise from the neutral atom, while all other numbered peaks correspond to Mo ion lines.

photodiode array integration times were examined: 10, 30, 50, and 100 sec. From the definition of S (signal) and N (noise), the detection limit, DL, for analyte x was defined in the conventional manner:

$$DL = 3(\sigma/S)[x] \quad (1)$$

where σ is the standard deviation of the 10 blank measurements, and S is the average signal magnitude of 10 sample injections having an analyte concentration $[x]$. In addition to providing information regarding detection limits, these data helped to evaluate the precision of the technique. For this latter portion of the study, a concentration of $0.5 \mu\text{g/ml}$ molybdenum was used.

A second definition of noise involved utilizing the multichannel capability of the spectrometer to monitor simultaneously the signal and the neighbouring background. By this method [see

Fig. 4(c)], selected regions on each side of a spectral line could be defined as the background. A total of six pixels were used to define the background region. During data processing,

Table 2. Instrumental parameters optimized for Mo II emission

Plasma forward power	1.9 kW
Gas flow-rates	
Outer	16.0 l./min
Intermediate	0.5 l./min
Inner (carrier)	0.9 l./min
Sample delivery rate	1.6 ml/min
Observation height	20 mm above the load coil
Magnification of ICP image	1
Prepolychromator	
Entrance slit width	25 μm
Entrance slit height	5 mm
Photodiode array detector (1024 channels)	
Temperature	-40°C

a best-fit line was established for these background regions. This best-fit line represents the average baseline above which the actual signal was determined. The noise was then defined as the standard deviation of the residuals between the best-fit line and the values at individual pixels. The signal was defined as the difference between the best-fit line and the actual value of a particular pixel. Once again, the effect of using different pixel ranges, from 1 to 13 pixels, as an integrated signal value was examined.

The third method for defining noise was more empirical but practical in nature and was used as a standard against which the other definitions could be evaluated. This method [see Fig. 4(d)] involved determining a peak-to-trough value for the noise neighboring each spectral line, and taking this as equal to 5σ . The noise was evaluated in the region of signal levels which

were not more than about 10 times the detection limit. The standard definition of the detection limit [equation (1)] was then used to ascertain a detection-limit value. In essence, these empirical detection limits indicate the concentration at which a signal peak begins to disappear in the baseline noise and serve as a convenient *de facto* standard.

The software required for data processing was supplied with the spectrometer. Solutions of 0.01, 0.05, 0.1, 0.5, 1, 5, 10, 50, and 100 $\mu\text{g}/\text{ml}$ molybdenum were used to obtain data for detection limits, linearity, and dynamic range. Detection limits calculated on the basis of the sideband-noise definition represent the average of those obtained from solutions having a molybdenum concentration within one or two orders of magnitude of the determined detection limit.

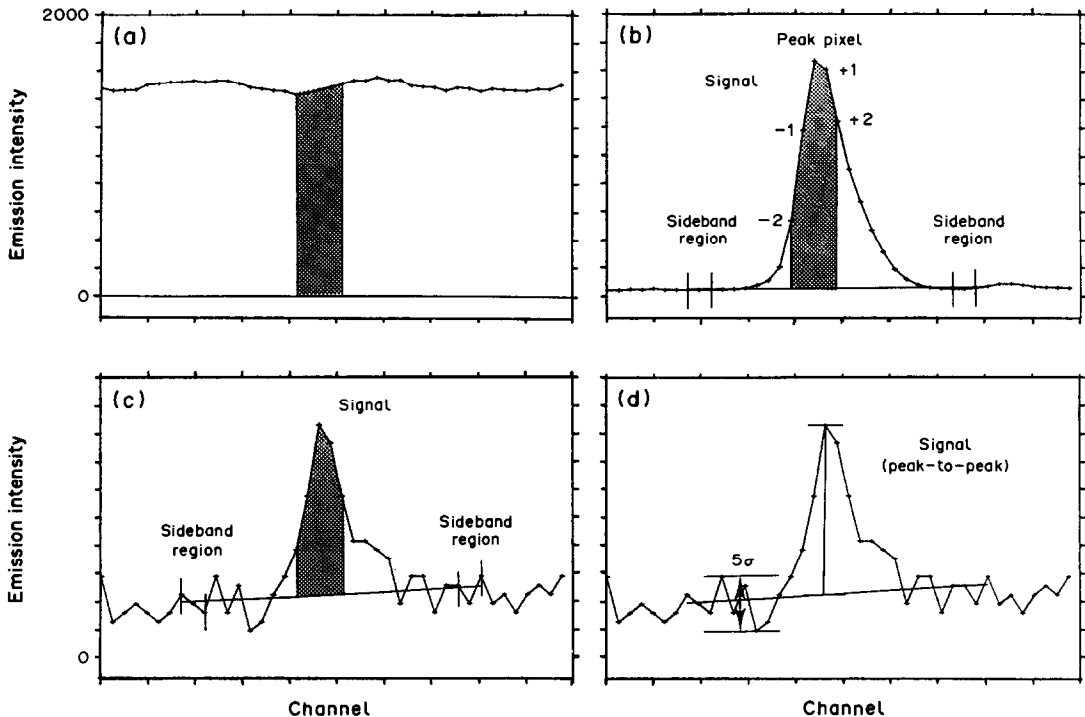


Fig. 4. Signal definitions. (a) Dark-current-subtracted blank trace illustrating the procedure for obtaining noise for the background-based detection limit. The noise was defined as the standard deviation of the peak areas obtained for 10 blank determinations. The number of pixels integrated for the total signal was varied. (b) Blank-subtracted peak illustrating the procedure for defining the signal for the background-based detection limit. A best-fit line was obtained from selected regions in the sideband background. The signal was defined as the summation of the difference values between the signal and the best-fit line. The number of pixels integrated for the total signal was varied. (c) Blank-subtracted peak illustrating the procedure for defining the signal and noise for the sideband-based detection limit. The noise was defined as the standard deviation of the pixel values in the defined sideband regions. The signal was defined in the same manner as in (b). (d) Blank-subtracted peak illustrating the procedure for defining the signal and noise for the empirically-based detection limit. The peak-to-trough pixel values of the surrounding sideband regions were defined as being equal to 5σ . The signal was defined as the peak height above a best-fit line which was obtained from the surrounding sideband regions.

Reagents

A 1000 $\mu\text{g/ml}$ standard stock solution of molybdenum (Aldrich) was used for preparation of the dilute molybdenum solutions used in this study. The stock solution was prepared by the manufacturer by dissolving ammonium heptamolybdate tetrahydrate in water, and was appropriately diluted with distilled and demineralized water and stored in precleaned polypropylene containers (Nalgene).

RESULTS

Detection limits

In the foregoing discussion, the noise was taken simply as the standard deviation of the residuals of the sideband pixels, σ . However, if the background noise is random, *i.e.*, normally

distributed, the standard deviation of the sum of n pixels should be $\sigma n^{1/2}$; that is, because the noise on individual pixels is random, the individual variances (σ^2) are additive. Accordingly, if the peak signal area, A , is obtained as a summation of n pixels, the proper sideband noise to employ in assigning a detection limit is $\sigma n^{1/2}$. Therefore

$$DL_{(\text{side})} = [\text{Mo}](3\sigma/A)n^{1/2} \quad (2)$$

where $[\text{Mo}]$ is the concentration of molybdenum resulting in the defined signal peak area A .

The consistency in the detection limits that are based upon sideband noise (see Tables 3 and 4) for peak areas covering 3–13 pixels is an indication of the general applicability of this sideband definition of the detection limit. In every case, the use of a single pixel for the

Table 3. Detection limits (ng/ml) for peaks 1–4

No. of pixels* (n)	Detection limit											
	Peak 1 Mo I (386.411)			Peak 2 Mo II (287.151)			Peak 3 Mo II (281.615)			Peak 4 Mo II (277.540)		
	Emp.†	Backg.§	Side‡	Emp.	Backg.	Side	Emp.	Backg.	Side	Emp.	Backg.	Side
10-sec integration												
1	91	164	98	28	61	39	26	52	20	68	112	42
3		116	66		49	25		49	13		54	27
5		125	67		60	22		54	11		65	25
7		158	71		70	23		56	12		62	26
9		206	76		74	24		66	12		92	26
11		221	82		83	25		68	13		98	28
13		245	87		94	26		79	14		89	29
30-sec integration												
1	62	47	50	19	36	18	24	33	22	29	47	33
3		40	36		40	12		23	14		44	21
5		56	36		48	11		26	13		59	20
7		79	38		56	11		26	13		69	20
9		74	41		62	11		32	13		80	21
11		93	44		72	12		37	14		97	22
13		110	46		79	13		41	15		114	24
50-sec integration												
1	43	88	41	11	35	19	7	26	14	16	27	27
3		93	29		35	13		27	9		24	17
5		115	29		44	12		29	8		36	16
7		133	31		49	12		33	8		39	16
9		154	33		56	12		33	9		44	17
11		163	35		63	13		37	9		48	18
13		173	37		65	14		39	10		52	19
100-sec integration												
1	33	138	31	12	32	10	7	21	11	18	34	14
3		173	21		36	6		23	7		35	9
5		219	22		42	6		24	6		41	8
7		282	23		47	6		25	7		49	9
9		334	25		51	6		27	7		61	9
11		320	26		54	7		30	7		77	10
13		250	27		61	7		32	8		90	10

*Number of pixels used in determining both signal integral and blank (background) noise.

†Empirical detection limit.

§Background-based detection limit.

‡Sideband-based detection limit.

determination of the sideband detection limit results in a value significantly different from the value obtained by using 3–13 pixels.

The detection limits obtained for peaks 1–4 and peaks 5–10 (see peak designations in Table 1) are listed in Tables 3 and 4, respectively. Figures 5 and 6 show examples of the signals obtained with different integration periods for peaks 1–4 and for peaks 5–10. No empirical detection limits are given in Table 4 for those peaks (*i.e.*, peaks 5, 6, 8 and 9) which were neighbored by interfering spectral lines, since the empirical detection limit obtained in such a situation would be unrealistically high.

The results compiled in Tables 3 and 4 show that detection limits based upon the normalized sideband noise are more consistent with the empirical values than are those based upon the background noise. For example, detection limits based upon background noise tend to increase

as the number of pixels used in the peak definition is raised. Additionally, for peaks 1, 7 and 10, as the integration time is increased from 10 to 100 sec, the background-based detection limit increases whereas the empirical detection limit is lowered. Significantly, peaks 1, 7 and 10 all appear at positions on the photodiode array that are dominated by strong background emission [see Fig. 4(c)]. The consistency of detection limits obtained by using the sideband definition of noise when the background emission is high, indicates the importance of the multiplex advantage offered by the photodiode-array spectrometer.

Detection limits for all three signal definitions tend to improve for peaks 1, 2, 3, 4, 7 and 10 as the integration time is raised from 10 to 100 sec. However, significant improvements in both the empirical and the background-based definitions are not observed as the integration time is

Table 4. Detection limits (*ng/ml*) for peaks 5–10 (designations as in Table 3)

No. of pixels (<i>n</i>)	Detection limit														
	Peak 5 Mo II (284.823)		Peak 6 Mo I (379.825)		Peak 7 Mo II (390.296)		Peak 8 Mo II (263.876)		Peak 9 Mo II (292.339)		Peak 10 Mo I (313.259)				
	Backg.	Side	Backg.	Side	Emp.	Backg.	Side	Backg.	Side	Backg.	Side	Emp.	Backg.	Side	
10-sec integration															
1	145	104	147	217	154	267	306	572	358	281	368	204	507	191	
3	97	66	145	146		347	208	458	225	275	230		456	122	
5	85	59	199	141		302	203	497	199	326	211		411	111	
7	94	60	228	148		344	212	523	200	351	215		462	111	
9	102	63	221	159		436	225	647	212	416	228		481	115	
11	95	67	256	171		524	240	808	228	451	246		665	122	
13	108	72	309	183		590	255	864	243	560	267		774	130	
30-sec integration															
1	66	35	239	124	74	486	108	363	168	238	168	121	416	182	
3	59	23	200	86		458	76	310	105	201	105		336	121	
5	75	21	186	83		480	76	363	96	216	98		300	109	
7	88	21	170	86		527	80	385	98	232	100		312	109	
9	98	22	153	90		567	85	475	103	262	105		384	112	
11	113	24	198	95		616	90	557	109	263	111		453	118	
13	131	25	222	101		731	95	669	116	280	119		533	125	
50-sec integration															
1	57	19	149	51	68	327	60	187	246	147	187	57	403	101	
3	51	12	198	35		345	43	194	158	142	121		300	65	
5	59	11	196	34		279	42	220	145	154	112		237	59	
7	66	12	179	36		298	45	284	149	163	115		227	59	
9	81	12	280	38		311	47	331	158	189	122		243	61	
11	93	13	392	40		345	50	384	169	223	130		265	64	
13	104	14	427	42		403	53	441	180	279	138		303	68	
100-sec integration															
1	62	39	514	119	46	635	50	264	306	326	290	50	941	88	
3	64	25	364	80		705	34	316	195	245	183		840	56	
5	71	24	127	78		720	33	420	180	167	166		730	51	
7	84	24	571	84		661	35	525	186	235	169		679	52	
9	93	26	1334	92		659	37	576	196	478	181		779	54	
11	103	28	2021	100		843	39	627	207	814	193		953	57	
13	119	31	2268	108		1113	41	731	220	1277	208		1085	60	

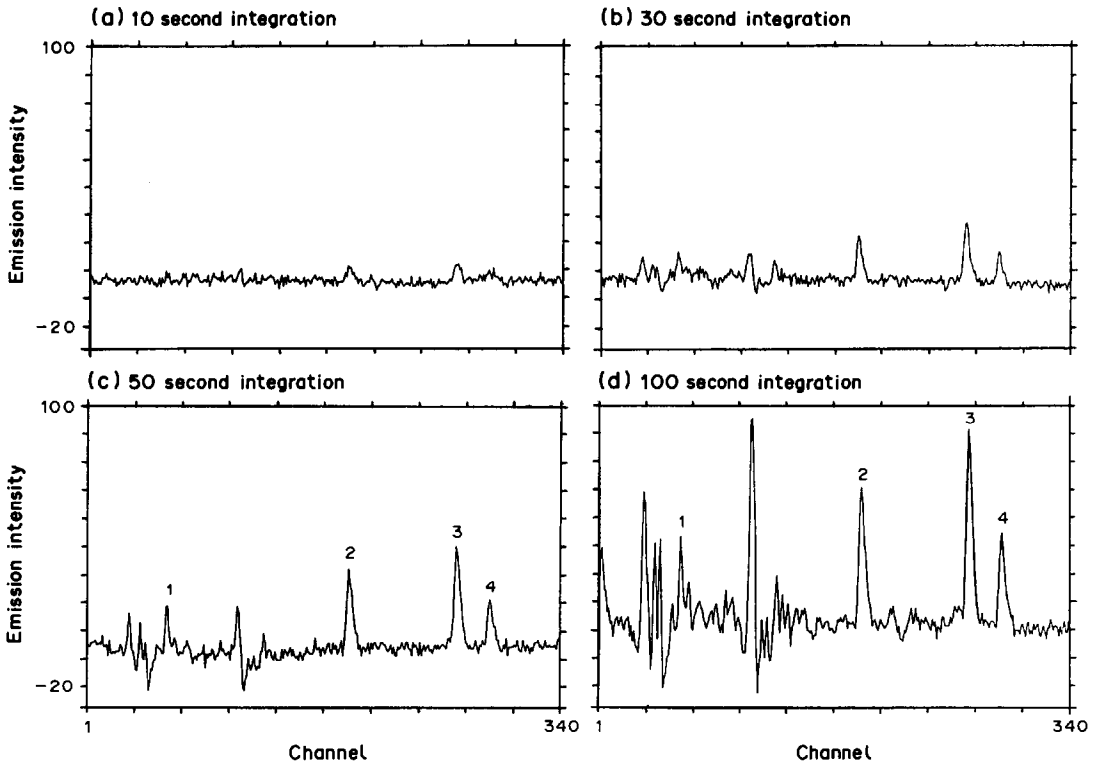


Fig. 5. Spectra obtained for peaks 1-4 by using signal-integration periods of (a) 10 sec, (b) 30 sec, (c) 50 sec and (d) 100 sec. The molybdenum concentration was 100 ng/ml.

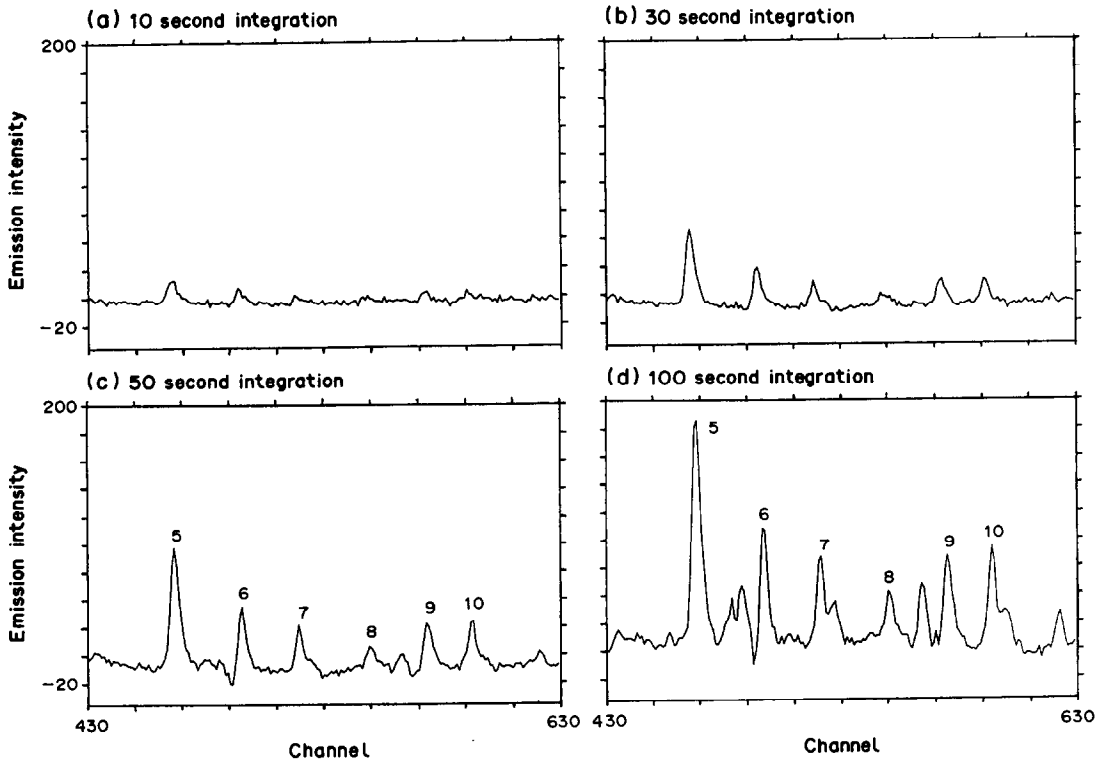


Fig. 6. Spectra obtained for peaks 5-10 with signal integration periods of (a) 10 sec, (b) 30 sec, (c) 50 sec and (d) 100 sec. The molybdenum concentration was 500 ng/ml.

Table 5. Linearity and linear dynamic range of blank-corrected peak areas obtained from five pixels

Integration time, sec	Peak 2		Peak 3		Peak 4	
	10	100	10	100	10	100
Linear dynamic range, $\mu\text{g/ml}$	0.05–100	0.01–10	0.05–100	0.01–10	0.5–100	0.05–10
Slope $\pm \sigma$	263.6 ± 0.8	2347 ± 4	396.0 ± 0.5	3437 ± 8	184.0 ± 0.6	1590 ± 2
y-intercept $\pm \sigma$	-40 ± 30	10 ± 20	-40 ± 20	-20 ± 30	-40.0 ± 30	0 ± 10
Correlation coefficient, r	1.000	1.000	1.000	1.000	1.000	1.000

increased from 50 to 100 sec. This result indicates that the dominant source of noise at integration periods longer than 50 sec is probably source flicker.

Consistently, the best values for sideband-based detection limits are derived for peak integrals obtained from five pixels. Similar results have been published elsewhere.⁸ Because of the number, spectral range, and the variety (ionic and atomic) of peaks used in this study, we feel that this conclusion can be generalized to include peaks from other elements, even under circumstances in which the signal is in a region dominated by background emission.

Linearity and dynamic range

Table 5 shows the results obtained for linearity and dynamic range for peaks 2–4. Similar results were obtained for peaks 1 and 5–10. The fact that the slopes reported for the 100-sec integration period differ from the slopes reported for the 10-sec integration period by a factor other than 10 indicates that the instrument response is slightly different for these two integration periods. The linear dynamic range when a single integration time is used is approximately three orders of magnitude. If integration periods of 10 and 100 sec are both used, the dynamic range of the instrument covers an additional order of magnitude. However, accuracy is best when the instrument is calibrated individually for each integration period.

Precision

Table 6 shows the precision of the instrument for all 10 peaks at a molybdenum concentration of 0.5 $\mu\text{g/ml}$. The values were obtained with a 50-sec integration time and are based on a peak definition of 5 pixels. Sideband baseline correction was used. The data were collected over a period of 1.5 hr. The reported precision for peaks 2–4 (3–4%) is significantly better than that for peaks 1 and 5 (8%) and peaks 6–10 (14–20%). The deterioration in precision for peak 1 and for peaks 5–10 can be attributed to the complex background emission observed

in these regions of the photodiode array (see Fig. 2 and 6).

DISCUSSION

The ability of a multichannel spectrometer to monitor simultaneously both the signal and the sideband background offers the capability to correct for low-frequency fluctuations in background emission. In this sense, such a spectrometer offers a distinct advantage over single-channel photomultiplier-based systems.

When detection limits are determined with a multichannel spectrometer, the best definition of noise involves measuring the pixel-to-pixel fluctuations in background on each side of the spectral line. The signal definition which empirically provides the highest signal-to-noise ratio is derived from integrating a range of five pixels centered at the spectral peak. If such a peak area is employed, the noise must be normalized by a factor of $n^{1/2}$ where n is the number of pixels (five, here) in the peak-area definition. This definition of noise results in detection limits which are similar to those obtained by empirical methods.

The linearity of the spectrometer response extends over three orders of magnitude when a single integration period of 100 sec is used, but can be extended to at least four orders of magnitude by use of additional integration times. However, when multiple integration periods are employed, each period must be calibrated independently.

Table 6. Precision for a signal definition of 5 pixels

Peak number	Wavelength, nm	Precision (%R.S.D.)
1	386.411	7.8
2	287.151	4.0
3	281.615	2.7
4	277.540	3.8
5	284.823	7.6
6	379.825	17.0
7	390.296	14.3
8	263.876	15.2
9	292.339	14.0
10	313.259	19.6

The precision attainable is dependent on the level of background emission; in instances where the background emission is relatively low, a precision of about 3–4% can be expected for an integration period of 50 sec (for 0.5 $\mu\text{g/ml}$ Mo).

Acknowledgements—Financial support by LECO Corporation, the National Science Foundation through grant CHE87-22639, and by the Office of Naval Research is gratefully acknowledged. One of the authors (N.F.) wishes to thank the Science and Technology Foundation of Shimadzu for the grant of a travel fellowship. The authors are grateful to Dr. Scott W. McGeorge for his assistance in the preparation of software used in this study. In addition, the authors acknowledge the contributions of Dr. Gary Horlick

during several discussions pertaining to photodiode-array detectors.

REFERENCES

1. N. G. Howell and G. H. Morrison, *Anal. Chem.*, 1977, **49**, 106.
2. Y. Talmi, *Appl. Spectrosc.*, 1982, **36**, 1.
3. P. M. Epperson, J. V. Sweedler, R. B. Bilhorn, G. R. Sims and M. B. Denton, *Anal. Chem.*, 1988, **60**, 327A.
4. Y. Talmi and R. W. Simpson, *Appl. Opt.*, 1980, **19**, 1401.
5. S. W. McGeorge, *Spectroscopy*, 1987, **2**, No. 4, 106.
6. G. M. Levy, A. Quaglia, R. E. Lazure and S. W. McGeorge, *Spectrochim. Acta*, 1987, **42B**, 106.
7. V. Karanossios and G. Horlick, *Appl. Spectrosc.*, 1986, **40**, 106.
8. E. D. Salin and G. Horlick, *Anal. Chem.*, 1980, **52**, 1578.

SELECTION OF SPECTRAL WINDOWS FOR PLASMA ATOMIC-EMISSION SPECTROMETRY

D. P. WEBB and E. D. SALIN*

Department of Chemistry, McGill University, 801 Sherbrooke St. W., Montreal, P.Q. H3A 2K6, Canada

(Received 13 September 1988. Accepted 13 February 1989)

Summary—A program has been developed to evaluate the number of spectral windows required to perform elemental analysis by ICP-AES, given a certain spectral window width. The data indicate that photodiode array systems (sequential slew scan) with as few as 7 or 8 acquisitions (windows) might be viable. With smaller windows, approaching in size those used by direct-reading spectrometers, it appears that conventionally designed spectrometers with photomultiplier tube detectors could use between 29 and 37 windows to determine 59 elements. This indicates that a general purpose direct-reading spectrometer may be feasible.

We have discussed elsewhere the performance of linear photodiode arrays with respect to their potential for atomic-emission spectrometry.¹⁻⁴ Though linear arrays continue to increase in size, there is no indication that this simple format, so well suited to simple grating systems, will reach a length and pixel count sufficient for plasma emission spectrometry with a single device. This is unfortunate, because these devices can provide simultaneous background spectral information which can be of enormous value, particularly when primitive (one and two point) spectral stripping schemes will fail. We have often wondered how a slew scanning (multiwindow) system might perform. Our previous work² indicated that photodiode arrays (PDAs) can give performance comparable to that of systems based on photomultiplier tube (PMT) detectors, although longer integration times may be necessary for unintensified systems. The real questions seem to be (1) how many windows would be needed and (2) how wide should these windows be? Certainly the combined concerns of window width and number of pixel elements required would dictate the length and consequently the cost of the system.

We recently acquired a direct-reading spectrometer equipped with a refractor plate for background correction purposes. The spectral window accessed by this system varies with wavelength, but is approximately 0.18 nm. We investigated the possibility of using a conventional system of this type for multielement

analysis within a given window. Our hope was that a scanning capability combined with a judicious choice of compromise windows might allow the manufacture of systems designed to solve specific problems with a significant reduction in the number of "channels" (exit-slit assemblies). Alternatively, a conventional multi-channel spectrometer with broad applicability could be developed. Compared with a PDA-based system, the spectral windows used in photomultiplier-based systems are of course much smaller, though the methodology of investigation is the same. We report below the results of an investigation of spectral windows for both types of instrument.

EXPERIMENTAL

We set about this investigation by using the PROLOG language. PROLOG is a logic-based language and well suited to questions such as "How many 20 nm windows are needed to cover the best lines of elements X, Y and Z?". In addition to its logic-based orientation, it has inherent database-management facilities which were useful in the program development. We used a compiler version of PROLOG, Turbo PROLOG, rather than the more common interpreter form, because of the speed advantage expected from a compiled program. We utilized a somewhat modified version of the atomic spectral line database published by Winge *et al.*⁵ as well as information provided by P. W. J. M. Boumans.⁶ Though the database may not be as complete as some versions, it was quite adequate for the limited searching that we had

*Author to whom correspondence should be addressed.

Table 1. List of elements used

Ag	Al	As	AU	B	Ba	Be	Bi	C	Ca	Cd
Ce	Co	Cr	Cu	Fe	Ga	Ge	Hg	In	Li	Mg
Mn	Mo	Nb	Ni	P	Pb	Pt	Sb	Se	Si	Sn
Sr	Ta	Te	Th	Ti	Tl	U	V	W	Zn	Zr

in mind. A program called Windows-I was developed initially to investigate this problem. The program was provided with several sets of elements randomly selected from the list in Table 1. The program was also provided with a Degradation Factor² and a Window Width (in nm). All these parameters were read in from a file to allow convenient batch processing. Several of the parameters will be discussed in more detail below.

When initiated, the program reads in the selected set of elements. The Degradation Factor is used to extract the analytical lines of the various elements into the line set. It simply delineates the maximum level of detection limit degradation allowed during the line selection process.² For example, with a Degradation Factor (DF) of 3 and an element for which the best line has a detection limit (DL) of 1 ng/ml, all the element's lines with detection limits of $DL \cdot DF = 3$ ng/ml or less would be read into the database. For simplicity, in our experiments, the same Degradation Factor has been applied to all elements in the set.

After the full database has been read in and pruned as described above, the window selection procedure begins. The time required for a given computation depends on both the number

of lines (variable, depending on the DF) and the number of elements. The relationship of the two factors can be estimated by examining the times in Table 2 for various numbers of lines and windows. All computation times reported were based on times obtained by using a 10 MHz 80286 CPU system with zero wait state memory. When computations were done on other 8088 or 80286 CPU machines the values were corrected for the speed difference, based on a calibration program run on both machines. When the element set consisted of 15 or more elements, the search time became excessive. In several cases we simply were not able to get data values even though we ran the search continuously for 7 days.

Windows-I utilizes a method of search for which PROLOG is particularly well configured. This is a "breadth first" method. It will search first for any combination of lines which will satisfy the requirements in a single window. Then it will try two windows, then three . . . *etc.* The search strategy utilized by Windows-I is exhaustive and so ensures that the best solution at any number of windows, if one exists, is found.

As the data in Table 2 indicate, processing time becomes excessive for Windows-I when

Table 2. List of times (sec) for Windows-I and Windows-II

	Windows-I	Windows-II
5 elements, 10 nm, DF3	2.5×10^1	8.9×10^0
10 elements, 10 nm, DF3	5.7×10^3	3.2×10^1
15 elements, 10 nm, DF3	N/A	1.1×10^2
20 elements, 10 nm, DF3	N/A	2.2×10^2
25 elements, 10 nm, DF3	N/A	3.9×10^2
30 elements, 10 nm, DF3	N/A	6.6×10^2
5 elements, 10 nm, DF10	2.1×10^1	2.2×10^1
10 elements, 10 nm, DF10	4.7×10^3	8.6×10^1
15 elements, 10 nm, DF10	N/A	2.5×10^2
20 elements, 10 nm, DF10	N/A	5.0×10^2
25 elements, 10 nm, DF10	N/A	7.9×10^2
30 elements, 10 nm, DF10	N/A	1.4×10^3
5 elements, 20 nm, DF3	1.7×10^1	1.1×10^1
10 elements, 20 nm, DF3	8.8×10^2	2.8×10^1
15 elements, 20 nm, DF3	1.8×10^4	1.1×10^2
20 elements, 20 nm, DF3	N/A	2.0×10^2
25 elements, 20 nm, DF3	N/A	3.7×10^2
30 elements, 20 nm, DF3	N/A	7.1×10^2
5 elements, 20 nm, DF10	3.4×10^1	2.2×10^1
10 elements, 20 nm, DF10	7.6×10^2	8.1×10^1
15 elements, 20 nm, DF10	4.4×10^4	2.4×10^2
20 elements, 20 nm, DF10	N/A	4.7×10^2
25 elements, 20 nm, DF10	N/A	8.5×10^2
30 elements, 20 nm, DF10	N/A	1.6×10^3

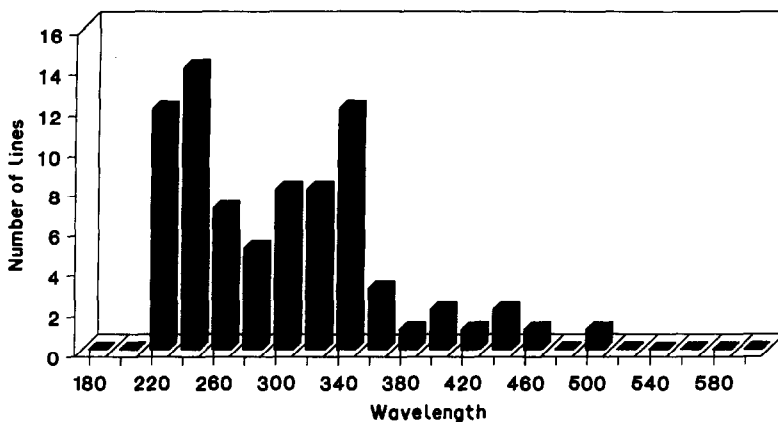


Fig. 1. Lines for elements in Table I with detection limits less than 10 ng/ml.

larger data sets are involved. These times are obviously unacceptable for operation in real time. To overcome this problem a second program called Windows-II was developed, which we called the heuristic program, because it used an intelligent search strategy rather than the brute force, "test all possible combinations", approach used by Windows-I.

The histogram in Fig. 1 indicates that the vast majority of the lines we would be interested in fall in a narrow spectral range (200–360 nm). This suggested to us that an efficient and acceptable, but not necessarily perfect, solution to the window selection problem might be found by simply selecting windows based on the number of elements (elemental lines) which each window eliminated from the list of elements. In other words, whichever spectral window contains the most elements becomes the first window. The second window is the one which finds the most elements remaining in the line set . . . etc. This

is the approach used by Windows-II. This algorithm is well suited to a recursive approach and encouraged us in our decision to use PROLOG again for Windows-II.

RESULTS AND DISCUSSION

As the data in Table 2 indicate, the scheme used in Windows-II is much faster; indeed, it seems to be fast enough to be implemented on a fast microcomputer for real time operation of a windowed slew scan system. It must be kept in mind that there are at least two common 32-bit CPUs (80386 and 68030) now used in microcomputers, which operate at 25 MHz. Data from Windows-I and Windows-II are plotted together in Figs. 2–5. The lower set of data has been slightly offset to the right to allow the error bars to be seen. The data from Windows-I runs are limited to very small data sets, because of the computation time required.

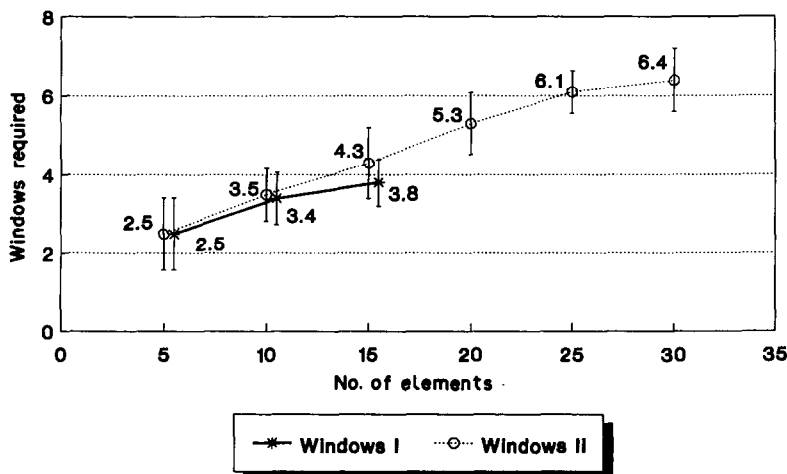


Fig. 2. Number of 20 nm windows needed with DF of 3. In Figs. 2–5 the error bars represent one standard deviation.

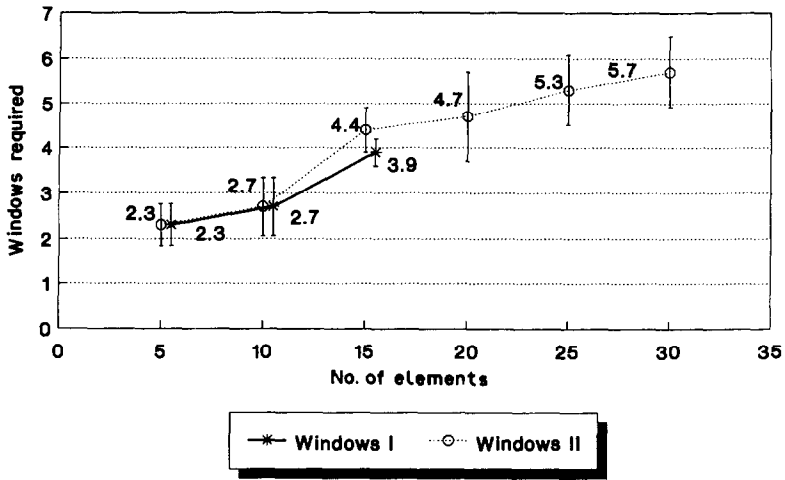


Fig. 3. Number of 20 nm windows needed with DF of 10.

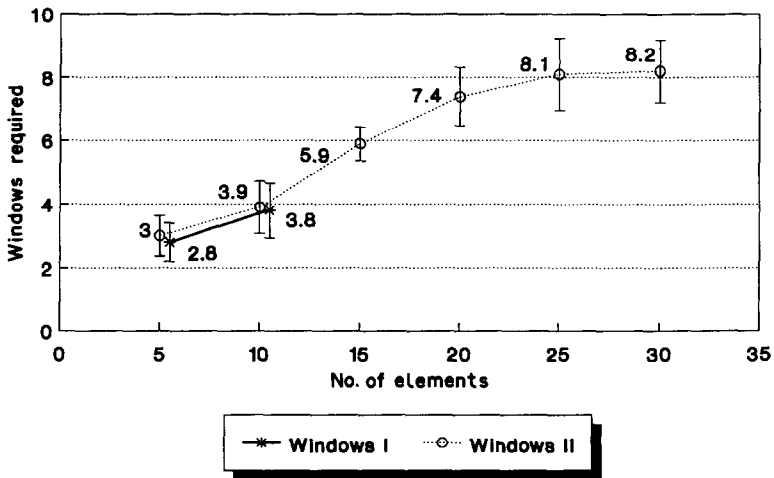


Fig. 4. Number of 10 nm windows needed with DF of 3.

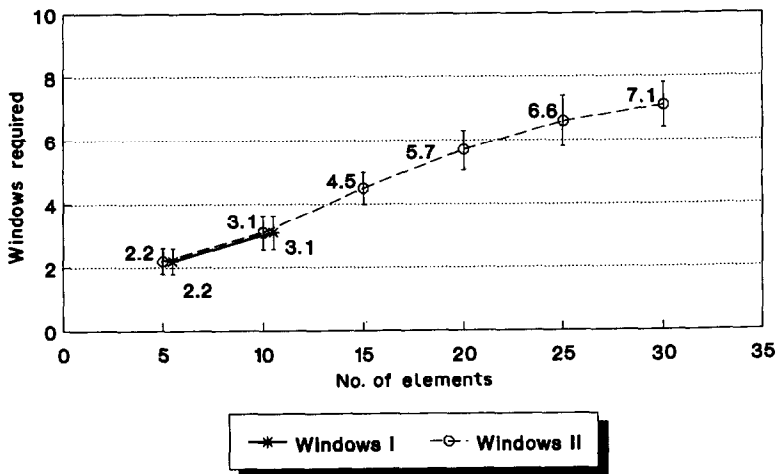


Fig. 5. Number of 10 nm windows needed with DF of 10.

It is encouraging to note that the data provided by Windows-II runs are very similar or identical to those of Windows-I, indicating that our heuristic approach was good. The reader should keep in mind that Windows-I always finds the best solution. Windows-II uses a faster approach which will find a solution, but not necessarily the best.

As the data in Figs. 2-5 indicate, the number of windows required does not always increase linearly as the number of elements increases; however, it certainly has linear characteristics up to 25 elements. As would be expected, the lines/window ratio increases as the DF increases, simply because more lines become available, thereby enhancing the probability of solving the problem with fewer windows. We found the comparison between the data in Figs. 2 and 3 to be particularly interesting. With a 1000-element linear array, there would be a spacing of 0.02 nm between element lines. There appears to be little advantage in using a Degradation Factor of 10. A Degradation Factor of 3 would allow most 30-element spectral analysis problems to be solved with 7 windows. By the use of a rapid scanning drive system and assuming that 10-sec integrations would be adequate, over half the analyses could be completed in about 70 sec. If the resolution must be doubled, then the data in Figs. 4 and 5 become applicable. Even in this situation, almost half of the problems can be solved with 8 windows.

To obtain similar quality data (with similar information for background correction) in the region of a single spectral line with a direct-reading spectrometer specifically configured for those elements might reasonably take from 30 to 60 sec if 60 spectral positions (0.03 nm between positions) were used with 0.5 or 1 sec integration at each position. It should be noted that the 60 positions and 0.18 nm window are typical of our spectrometer system. The time required for a conventional scanning system to cover 30 elements could then be estimated at 900 sec. If almost zero translation time and only 10 sec per element are assumed, the time spent would still be 300 sec. A scanning windowed system would offer flexibility in wavelength selection and would appear to have some advantage with respect to throughput at moderate to high light levels. It is probable, however, that an unintensified photodiode array operated in a typical linear dispersion system will not have a sufficient flux to allow use of 10 sec integration

times for low light levels in the shorter wavelength regions of the spectrum.²

This brings forth the question, "What can conventional multichannel PMT-based systems with spectrum shifters do?" The Windows-II program was used for all this work, so superior solutions may be possible. The window width was set to three different values, 1.8, 0.4 and 0.18 nm. A 0.4 nm window is used in a modified Jarrell Ash system⁷ which drives the galvanometer through a larger angle. The value of 0.18 nm is provided by the normal Jarrell Ash software on the Model 61 system. The wider 1.8 nm spectral coverage is possible with the same system by simply placing a thicker refractor plate in the system. Using only the 1.8 nm windows and a variety of 30 element sets, with a Degradation Factor of 3, it is possible to determine 30 elements in an average of 13.4 windows (standard deviation 1.2). The maximum number of windows found necessary was 16. If a Degradation Factor of 10 can be accepted, the average number of windows required is 10.9, with a standard deviation of 1.2. The maximum found necessary was 13. The question then arises, "How many windows are needed to cover all the elements?" In this case we consulted several experts about elements that were monitored for environmental impact or used in common industrial processes. We arrived at a list of 59 elements. The elements added to our original database (Table 1) are listed in Table 3. The complete data set for number of windows is listed in Table 4. The data indicate that as few as 17 windows are needed to solve this problem with a Degradation Factor of 10, or 21 with a Degradation Factor of 3. Major line overlaps will not be a problem in our determination because the closest major analytical lines in any of the windows were those of As (228.812 nm) and Cd (228.802 nm). We have been able to resolve this overlap on our

Table 3. List of additional elements

Cs	Gd	Ho	Ir	K	La	Na	Os
Pd	Rb	Re	Rh	Sc	Sm	Y	

Table 4. Number of windows required for 59 elements

Window width, nm	No. of windows	
	DF3	DF10
1.8	21	17
0.4	34	26
0.18	37	29

system by using the technique of multiple linear regressions.⁸

These computations suggest to us that it should be possible to build a general purpose 59-element system that would satisfy the needs of many users. We have not in our work considered the spectral overlaps that can occur from minor lines of major elements in the matrix, a factor which might increase the number of windows, nor have we considered the use of the second order, which might reduce the number of windows by causing a given spectral line to appear in two places on the focal plane.

REFERENCES

1. S. W. McGeorge and E. D. Salin, *Anal. Chem.*, 1985, **57**, 2740.
2. *Idem*, *Spectrochim. Acta*, 1985, **40B**, 435.
3. *Idem*, *ibid.*, 1986, **41B**, 327.
4. *Idem*, *ibid.*, 1983, **38B**, 633.
5. R. K. Winge, V. J. Peterson and V. A. Fassel, *Appl. Spectrosc.*, 1979, **33**, 206.
6. P. W. J. M. Boumans, Personal communication giving 450 major lines, 1986.
7. G. Legere, Technical Services Laboratory, Toronto, Ontario, Canada, Personal communication, 1988.
8. L. Gervais and E. D. Salin, Atomic spectral deconvolution by multiple linear regression, in preparation.

A FACTOR ANALYSIS APPROACH TO OPTIMIZED LINE SELECTION IN INDUCTIVELY COUPLED PLASMA ATOMIC-EMISSION SPECTROMETRY

D. F. WIRSZ and M. W. BLADES*

Department of Chemistry, University of British Columbia, Vancouver,
British Columbia V6T 1Y6, Canada

(Received 1 February 1989. Accepted 17 April 1989)

Summary—The best analytical line for determination of a specified analyte is selected from a set of lines on the basis of the least interference in a particular sample matrix, by several cycles of mathematical analysis. Unsuitable lines are rejected in the first few cycles, the best lines being retained until last. A multivariate analysis after each cycle provides an updated estimate of the analyte concentration. This process is performed without reference to spectral tables.

Inductively-coupled plasma optical-emission spectrometry (ICP-OES) provides a wealth of spectral emission lines for each element, allowing great flexibility in the choice of analytical lines. The spectral tables of Boumans¹ list over 750 potential spectral lines which can be used for elemental analysis. Traditional ICP-OES instruments (sequential slew scanning and simultaneous direct readers) typically utilize only one analytical line for each element to be determined. Choosing an appropriate set of lines for multielement determinations can be very complex. The intensity of an emission line relative to background noise determines the detection limit, but the utility of a particular line for an analyte may also be affected by partial or complete spectral overlap by lines of concomitant elements. Many of these overlaps or coincidences have been documented in line tables such as those of Boumans, but even the most comprehensive tables do not list all the lines of all the elements. Further, the degree of overlap depends on the spectrometer bandpass and to a lesser degree the plasma operating conditions. Thus each new analytical problem requires an *ad hoc* solution, by so-called "methods development". In this process various options for the choice of analysis lines are studied and, presumably, the optimum set of lines is found. This procedure includes the collection of spectral scans for all the potentially useful lines, from single-element standards and

standard reference materials with a composition similar to the prospective sample. Useful lines are chosen on the basis of their sensitivity and relative freedom from spectral interferences. For direct-reading multichannel spectrometers this line set is then "hardware programmed" into the instrument, and the instrument then becomes more or less specialized to solve that problem. For sequential slew-scanning spectrometers, the line set is "software programmed" and consequently the instrument is more flexible, solving a wider variety of problems, although at the cost of slower data-acquisition. Sequential spectrometers may also allow selection of an alternative line when there is a spectral line overlap with the chosen analysis line. However, even when sequential spectrometers are used it is too time-consuming to examine all the potential choices, for all lines, for all samples.

In recent years there have been many reports on the use of multiplex spectrometers for ICP-OES.²⁻⁷ Multiplex spectrometers are capable of simultaneously acquiring a window of spectral information, thus combining the flexibility of a sequential system with the speed of a direct reader. The two most common multiplex approaches are through the use of Fourier transform spectrometers (FTS)²⁻⁴ and instruments based on optoelectronic image sensors.⁵⁻⁷ The key feature of multiplex spectrometers is their ability to collect multiple wavelength data, so that in principle the spectrum includes all of the information about the analyte line, interferences, and background,

*To whom correspondence should be addressed.

provided by the ICP. Two different approaches can be taken to utilization of this spectral information for analytical determinations. First, since several lines are available for each analyte, all, or selected lines, may be used to construct the calibration curve. Secondly, the utility of each of the analytical lines in the spectral window can be rapidly assessed with respect to sensitivity and relative freedom from interferences to enable choice of the optimum lines for each element in each individual sample. Through the application of factor analysis and related techniques developed in this laboratory, this selection process can be simplified. Furthermore, this method does not require that the identity of interferents be known.

EXPERIMENTAL

Instrumentation and computer hardware

An inductively coupled plasma unit manufactured by Plasma-Therm Inc. (Kreeseon, NJ) was used, consisting of an HFP-2500E rf generator, an AMN-2500E automatic matching network, and an APCS-1 automatic power control unit. A Sherritt-Gordon (Fort Saskatchewan, AB) MAK-200 cross-flow nebulizer running at 200 psig was used for sample introduction. A plano-convex fused-silica lens with a focal length of 150 mm produced a 1:1 image of the plasma on the entrance slit of the monochromator. A Schoeffel-McPherson (Acton, MA) Model 2061, 1 m Czerny-Turner monochromator with a Model AH-3264 1200 line/mm holographic grating provided dispersion onto a Reticon (Sunnyvale, CA) Model RL-4096/20 linear photodiode array. The 4096 detecting elements of the array covered a wavelength range of approximately 45.0 nm, giving a resolution of 0.04 nm when a 60 μ m entrance slit was used. The array was cooled to -15° with a Melcor (Trenton, NJ) Model CP14-71-10L Peltier cooler mounted on the back of the array. Read-out of the array was performed with a Reticon Model RL-4096S-3 evaluation board interfaced with an R. C. Electronics (Santa Barbara, CA) Model ISC-16 A/D converter card installed in a Telex (Tulsa, OK) Model 1280 PC-AT computer. A complete software package written in Turbo Pascal was used for data acquisition, screen display, plotting and other specialized applications. This program also contained routines for dynamic range enhancement.⁸ Spectra were stored on 5 $\frac{1}{4}$ in. floppy disks, and transferred to the campus computer

Table 1. Wavelengths of analyte lines used

Element	Diode number	Wavelength, nm	Atom (I) or ion (II) line	
Fe	146	364.784	I	
	286	363.146	I	
	395	361.877	I	
	480	360.886	I	
	717	358.120	I	
	812	357.010	I	
	852	356.538	I	
	1491	349.058	I	
	1620	347.545	I	
	1916	344.061	I	
	Co	818	356.938	I
		1156	352.981	I
		1357	350.632	I
1391		350.228	I	
1632		347.402	I	
1807		345.350	I	
1844		344.917	I	
1892		344.364	I	
2158		341.234	I	
2219		340.512	I	
Cr		510	360.533	I
	612	359.349	I	
	738	357.869	I	
	1979	343.331	II	
	2069	342.274	II	
	2188	340.876	II	
	2235	340.332	II	
	2535	336.805	II	
	2601	336.030	II	
	2616	335.850	II	
La	167	364.542	II	
	309	362.883	II	
	2425	338.091	II	
	2464	337.633	II	
	2735	334.456	II	
	2795	333.749	II	
	3087	330.311	II	
	3405	326.567	II	
3543	324.935	II		
3579	324.513	II		

system. All programs used for post-collection processing were written in APL for ease of programming and modification of source code.

Preparation of analyte solutions

Standard aqueous solutions were prepared from the nitrates for Co, Cu, Ni and La (all 500 ppm), and Cr (375 ppm). The sulfates were used for Fe (2000 ppm) and Mn (500 ppm). A number of mixtures were prepared with combinations of these elements, with Co at 100 ppm, Cu, Mn, Fe and La at 50 ppm, and Cr at 37.5 ppm. The results reported in this paper are for the most complex mixture, containing all seven components.

Identification of analyte lines

The wavelengths of each of the analyte lines used in this paper are given in Table 1. Lines are henceforth referred to by diode number. The

photodiode array was calibrated by matching photodiode array intensity maxima with tabulated wavelengths for each of the ten Fe Lines.⁹ A second order polynomial fit gave the relationship between diode number and wavelength. The wavelength obtained from the polynomial fit was in all cases within 0.005 nm of the tabulated wavelength. For all other lines (10 each for Co, Cr and La) wavelengths were assigned by locating the line closest to the predicted wavelength. In all cases the assignments were unambiguous. As the methods applied in this paper are designed to indicate interferences without the need for wavelength tables, the wavelengths of interferent lines have not been tabulated.

THEORY

A general description of factor analysis is given, followed by a more detailed discussion of the line-selection algorithms. The details of the mathematical operations behind each step may be found in any of several excellent books. Particularly recommended is the book by Malinowski and Howery.¹⁰

Factor analysis

Initially, the data are entered into a two-dimensional matrix. The number of rows (M) corresponds to the number of detecting elements used, and the number of columns (N) to the number of spectra. A covariance matrix is generated by multiplying the transpose of the initial matrix by the matrix itself. This covariance matrix (now $N \times N$) is subjected to an eigenvector analysis. The resulting eigenvalues and eigenvectors are stored for later reference.

Eigenvalues and eigenvectors

The spectrum of any element can be thought of as a vector in multidimensional space. Since the line intensities and wavelengths are different for each element, the vector representing the spectrum of each element will point in a characteristic and unique direction in this multidimensional space. Thus the number of dimensions spanned by the data set will reflect the number of elements present. In a data set where the number of elements is not known, the variance of the data set can be described by the way the data are spanned by a series of orthogonal vectors. The number of orthogonal vectors required to span the data set in multidimensional space will equal the number of elements. These

orthogonal vectors are called eigenvectors. The first eigenvector is derived by finding the direction in which the highest variance is spanned in multidimensional space. The second eigenvector is then restrained to being orthogonal to the first, but may be rotated in any of the other directions to span the greatest of the remaining variances. Subsequent eigenvectors are obtained by continuing this process. The eigenvalues give a measure of the magnitude of the variance spanned by each eigenvector. The first eigenvector spans the largest variance, and will have the greatest eigenvalue. Subsequent eigenvalues are of decreasing magnitude. The eigenvalues commonly exhibit a sudden drop when all the variance due to the number of components has been spanned, which corresponds to the number of elements present. The remaining, much smaller, variance is normally due to random noise.

Determination of the number of factors

Ideally, there will be an obvious difference in magnitude between the eigenvectors which represent real factors (large eigenvalues) and the remaining eigenvectors which represent only random noise (small eigenvalues). The data matrix can then be reconstructed within experimental error by using only these first few eigenvectors. The selection of an appropriate number of eigenvectors for reconstruction of the data matrix is equivalent to the determination of the number of factors, and thus the number of elements. This determination of the number of factors can be complex, requiring the evaluation of not just one but a number of indicator functions.¹¹⁻¹⁴ As an additional benefit of this approach, the rejection of the eigenvectors that are due to noise leads to a reduction in the overall noise in the data matrix.

When the correct number of eigenvectors is chosen, they define a subspace containing all the data points (within experimental error). If too few factors are chosen, the data matrix will be poorly reconstructed, since significant information pertaining to the real components (in one or more of the eigenvectors) has been left out. In multidimensional space, some of the data points will lie significantly outside the defined subspace. If too many factors are chosen, the data will be satisfactorily reproduced, but will not have the optimum amount of noise removed. In practice, the partition between those significant eigenvectors due to real factors, and the less significant eigenvectors

due to noise, can be indistinct. For this reason, a number of parameters and associated indicator functions¹⁰⁻¹² are examined, such as a ratio of successive eigenvalues, which can be useful in separating the total number of real factors in a data set from those factors due to noise.

After the eigenvalues and eigenvectors have been calculated, the real, imbedded and extracted errors are computed for each possible number of components from 1 to $N - 1$. Real error is an estimate of the total error present in the data matrix. Extracted error is that portion of the error which is removed by reconstructing the data matrix with just the first N' eigenvectors (where $1 \leq N' < N$), and imbedded error is that portion of the error which remains in the data matrix even after reconstruction. All these indicators reach a relatively constant value when the correct number of components is reached. A second means of determining the number of factors is given by the indicator function (IND),^{11,12} which is derived from the real error. The correct number of factors is characterized by a minimum in this function. Another indicator is a ratio (RATIO) of successive values of the eigenvectors.¹³ This indicator shows a peak at the correct number of factors. A consensus of these indicator functions must be considered when deciding upon the number of factors present in a particular set of data.

In this paper, regardless of the actual number of components, the data may be reproduced by two factors, since only a standard spectrum (in practice, several, virtually identical spectra) and a sample spectrum are present in the data matrix. Thus the factor analysis finds only two factors. In the original co-ordinate system in multidimensional space, these factors can be represented by a spectrum for the standard, and a spectrum for the sample. In a new co-ordinate system, the two dimensions are spanned by a factor for the element of interest, and a factor for a linear combination of all interferences present in the sample spectrum.

In more general applications of factor analysis, the identity of the elements present may not be known. Once the number of factors has been determined, the elemental spectra to which the eigenvectors correspond must be found. This identification is accomplished by target factor analysis.

Target factor analysis

In target factor analysis, a target test vector is first selected as a likely candidate to represent

one of the factors. This test vector will usually be the spectrum of a single element. The test indicates whether the chosen spectrum is in fact present in the data set. Several target tests are applied. When more than one component must be identified, more than one successful test vector will be found. After completion of the target testing, the number of successful test vectors should equal the previously determined number of components. An understanding of this process is helped by considering the eigenvectors generated at the beginning of the analysis.

The eigenvectors define a subspace in the multidimensional space of the original M intensity measurements. Any vector which is to successfully describe the real spectrum of the component must lie in this subspace within experimental error. A target test gives an evaluation of the goodness of fit of the test vector to the subspace. In a multielement determination, target factor analysis is continued until the number of test vectors found that have a satisfactory fit to the subspace is sufficient to account for the total number of factors determined to be present. If all the factors, each representing a different element, cannot be successfully identified, the remaining dimensionality of the subspace may be spanned by generating residual vectors. These residual vectors are orthogonal to each other and to each of the successful test vectors.

In this paper, the data matrix contains several spectra of the element of interest, thus the target test for the one element of interest must be successful. The most useful information obtained in this case is not the confirmation of the presence of an element, but the generation of a residual vector from the variance *not* covered by that element. In the cases considered in this paper, the subspaces are simply two-dimensional planes, where one factor corresponds to the element of interest, and the other factor is a single residual vector generated to be orthogonal to the first factor. The vectors representing all the spectra in the original data matrix are projected onto the factors (real and residual) found by this method. The projection along each factor axis gives the concentration of the element represented by that factor axis.

This approach may be easily adapted to the determination of several elements simultaneously. The sample vector is projected onto several factor axes in a higher dimensional space, with one factor axis for each of the

elements desired and one for a residual spectrum. Such a determination would follow steps analogous to those outlined here for a single-element determination, but is not exemplified in this paper.

Algorithms for line selection

Initial selection of suitable diodes for further analysis. A preliminary analysis may be made with a data matrix (Fig. 1) containing diodes representing all the analyte lines (above a threshold) in the spectral window. However, this leads to the selection of a different number of diodes for each determination, which depends on the threshold chosen, the number of lines above the threshold, and their relative intensity for each element within the spectral window. Thus, the selection of an element with many intense lines within the window will lead to an initial matrix containing more diodes than that for an element with only a few intense lines within the window. The number of diodes chosen will depend on the concentration of the standard solution used, higher concentrations resulting in more diodes yielding signals above the threshold. The number of diodes chosen for each line will also vary since a more intense line will have a wider base, and will cover a larger number of diodes (Fig. 2). The results from these factor analysis procedures may be biased by the presence of a few elements with very intense lines, at the expense of other elements. For an individual element, the more intense lines dominate because a larger number of diodes is selected, and this again could lead to an undesirable bias.

In an attempt to avoid these problems, a different method was adopted for the choice of

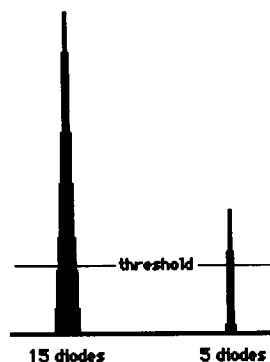


Fig. 2. The number of diodes above a chosen threshold for a line will vary with the intensity and width of the peak.

the initial number of diodes. Regardless of the element to be examined, only the ten most intense lines for that element in the spectral window are selected, and for each line the five diodes covering the greatest intensity are chosen. These fifty diodes are the only ones retained for further processing.

The data are entered into a matrix where each column contains the spectral intensities for a single spectrum, at the fifty selected photodiodes in the array. Since the same fifty diodes are chosen for all spectra, each row in this data matrix contains the measured intensity at the same diode for different spectra (Fig. 1). Ten standard spectra of the element of interest are contained in the matrix. A single spectrum of the sample to be analyzed is also included in the matrix. A single spectrum is chosen to facilitate illustration of the methods in use, but any number of sample spectra could be accommodated. In addition, the spectra of standard reference materials could also be included as an internal check.

The first cycle of factor analysis. A factor analysis, with target tests for the single element of interest, is performed as specified previously, and a residual vector is generated. This residual vector is used as a first approximation to the actual spectrum of an interferent in the sample matrix. If more than one interferent is present in the sample, but only a single residual vector is generated, the residual vector will be an approximation to some linear combination of the spectra of all interferents. The residual vector defines a line in multidimensional space, but the direction must be chosen (from the two possibilities) to be positive. This ensures that the lines in the residual spectrum represent positive spectral intensities, as required in further stages of the data manipulation. If the sum of all

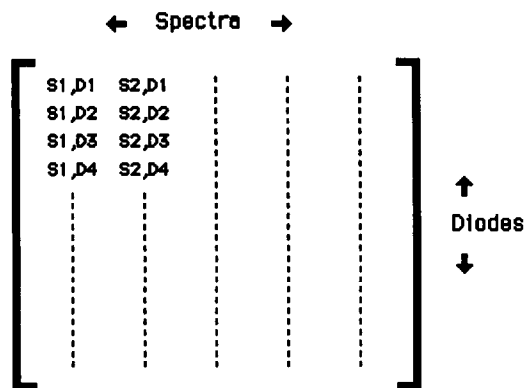


Fig. 1. The structure of a typical data matrix. Each entry represents an intensity measured at a specific diode (e.g., D3), for a specific sample spectrum (e.g., S2).

intensities is not positive, the entire residual spectrum is inverted (multiplication by -1).

The residual is not an exact representation of the interferent spectrum, but only a mathematical approximation which fits the variance of the data. It is not uncommon for a few negative lines to appear along with a majority of positive lines in a residual spectrum (Fig. 3). A non-negative restriction must be applied, and this is done by setting all negative values in the residual to zero. A second factor analysis is then done, and two factors are found. The first target vector is the standard spectrum, as before, and the second target vector is the non-negative residual spectrum. This generates a row matrix containing reconstructed spectra for the analyte and the residual, and a column matrix proportional to the concentrations of each in the sample. Multiplication by a previously entered standard concentration yields an estimate of the actual analyte concentration in the sample.

Subsequent cycles of factor analysis. The next steps involve a cyclic process, where the most interfered-with line is rejected, and a factor analysis as described previously is applied to the remaining diodes.

The most interfered-with line is determined by examining the residual. The signals of all five of the diodes corresponding to each line are summed, giving a residual spectrum as seen in Fig. 3. The line with the largest value in the residual is rejected by removing all intensity information for the corresponding diodes from the data matrix. The factor analysis of the remaining data generates another residual spectrum, along with an updated estimate of the analyte concentration. This process is continued

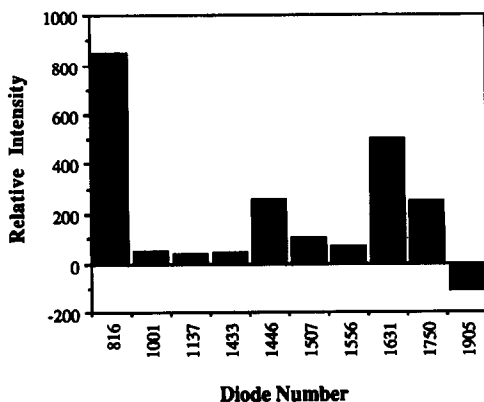


Fig. 3. A typical residual spectrum. Each of the ten bars represents a prediction of the sum of all interferent intensities over five diodes.

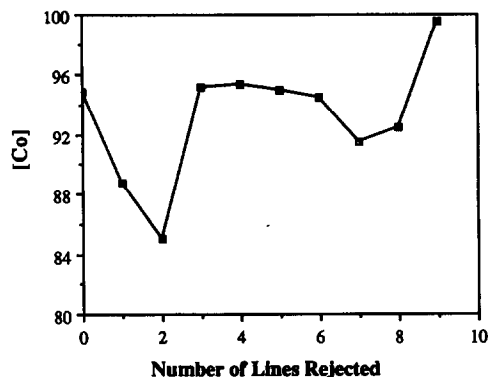


Fig. 4. As each line is sequentially rejected, the concentration of Co (in ppm) is recalculated in a multivariate analysis using the remaining lines.

until all lines have been rejected, one by one, and the best line remains.

Three options are available as variations of this approach to analysis.

(1) The last line retained may be taken as the best line.

(2) The line with the best signal/interference (target/residual) ratio may be used in a single-line determination.

(3) Once the first few lines have been rejected, most of the lines containing major interferences have been successfully removed. The factor analysis using the remaining lines gives a multi-line analysis, which in many cases may be preferred to a single-line determination.

The results from these different approaches will be compared in the discussion section.

RESULTS AND DISCUSSION

Owing to the volume of data available for analysis, considerable compression into a more suitable form for presentation is required. A number of graphs have been generated, illustrating the methods described above and the progress made during each cycle of the analysis. Many figures portray spectra as bar-graphs, where each bar represents the summed intensity of all the five diodes used for each line. Both real spectra (initial data) and residual spectra (generated by the program) are represented in this manner. The units of intensity for real spectra are derived directly from the read-out of the photodiode array. These real spectra are normalized to the same scale to give an equivalent dynamic range enhanced spectrum⁸ at an integration time of 64 units (corresponding

to approximately 0.57 sec). The units of intensity for residual spectra are arbitrary.

Several determinations for different elements will be examined, and graphs illustrating the methods described in this paper will be discussed.

Determination of cobalt in the presence of interferences

A sample was prepared from the standards, containing Co as the analyte (100 ppm), and La, Cu, Ni, Fe, Mn (all 50 ppm) and Cr (37.5 ppm) as interferences.

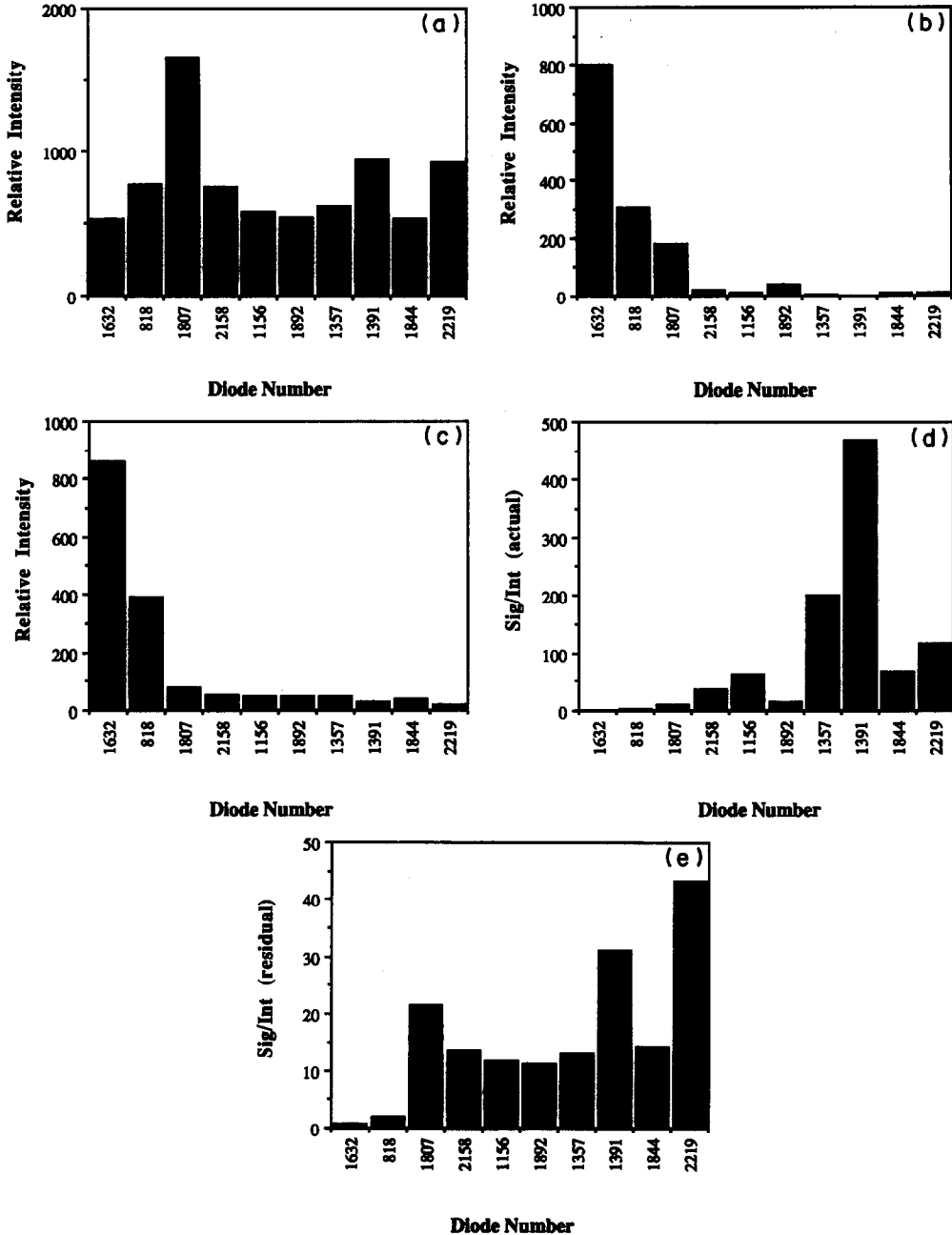


Fig. 5. (a) The ten most intense lines for the spectrum of Co in the region of 340 nm. Each of the ten bars represents the sum of the five diodes with the greatest intensity for each line. (b) The actual sum of all interferent intensities for the ten Co lines. (c) An estimate of the sum of all interferent intensities for the ten Co lines, as obtained from the residual spectrum. (d) The ratio of the signal (Co spectrum) to the actual sum of the interferents. (e) The ratio of the signal (Co spectrum) to the estimated sum of the interferents, obtained from the residual spectrum.

Figure 4 is a plot of the calculated concentration of Co as a function of the number of lines rejected, for a sample containing Cu, Mn, Cr, Ni, Fe and La as interferences. The first point represents the result of a multivariate determination for which all analyte lines are retained (none rejected), so that all interferences are still present. Subsequent points represent the result of a multivariate determination with one, two, or more lines removed from the data set. Lines are removed sequentially on the basis of interference, as indicated in the residual spectrum. For all points, a single residual spectrum is incorporated into the fit to account for the contribution from the unidentified interferences.

In a case where the data are fitted to a single parameter representing the Co spectrum, a large error due to unquantified interferences would be expected. Although the presence of interferences is known, their precise effect on the measured intensity of each line is not. The residual spectrum provides a first approximation to the interferent spectrum. The inclusion of a residual spectrum in the fit produces a better fit for Co by allowing for the variance due to the presence of an interferent. In other words, the incorporation of a residual spectrum which models the interferences provides an improvement over the representation of a two-component system by only a single Co spectrum.

The result obtained for the concentration of Co when a residual is incorporated into the determination is reasonably close to the actual value (100 ppm), even though the interferences have not yet been removed (Fig. 4). Following the first cycle, the line with the largest indicated interference is removed from the data set, and another analysis is performed. The calculated concentration drifts considerably over the first few cycles, depending on how well the residual and the Co standard fit the sample spectrum. As the lines with major interferences are removed, the concentration of Co tends towards a consistent value (Fig. 4).

The interpretation of these graphs is complicated by the scatter in the points, an indication of noise in the determination. Each point on this graph represents the result of a full multivariate determination using all remaining lines after each cycle of factor analysis. Each cycle yields an improvement in the fit for Co as lines with interferences are removed, and less interfered-with lines are retained. However, each subsequent cycle of analysis also uses fewer

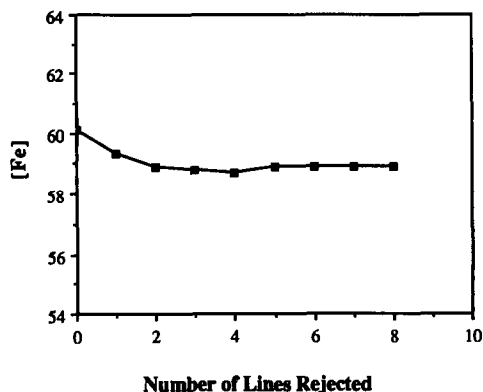


Fig. 6. As each line is sequentially rejected, the concentration of Fe (in ppm) is recalculated in a multivariate analysis using the remaining lines.

lines, and therefore less information, for the determination.

The last line retained may not be the strongest line of the ten lines chosen. For the photodiode array used for this paper, the read-out noise is high and the signal-to-noise ratio decreases with decreasing line intensity, so an analysis with a weak line would be expected to give a less precise value for Co concentration.

The optimum result for a multi-line determination of Co is likely to be a balance between the removal of most of the interferences, and the removal of the useful analytical lines in the same process. Our experience in dealing with simultaneous analyses of 1–4 analytes in the presence of 1–5 interferences is that an optimum probably exists somewhere in the middle between these two extremes. The most interfered-with lines must be removed from the data matrix to yield an improved result, but too many lines should not be removed, since this results in a decrease in analytical information for the determination.

Figure 5a is a plot of the spectrum of 100 ppm Co, with a vertical bar representing the sum of the signals from 5 diodes for each line. The diode numbers listed on the horizontal axis refer to the position of the line on the photodiode array, and appear in the order in which they are rejected, from left to right. All the Co lines initially chosen are reasonably intense, and the most intense line at diode 1807 is roughly three times as intense as the weakest line at diode 1844. Therefore, the removal of any one line from the data matrix should not remove a large percentage of the useful analytical information. The question arises as to how many lines need to be removed before all the major interferences may be considered as removed.

Figure 5b is a plot of the actual sum of all the interferences present. Normally the identity of the interferences would not be known, so a graph such as this would not be available. Since the compositions of the samples in this study are precisely known, the progress of the method can be followed and evaluated. The lines with the

largest interference are removed first, and after the first three lines at diodes 1632, 818, and 1807 are removed, contributions from interferences are small.

The residual spectrum models the spectrum of the interferences. Figure 5c gives an estimate of the sum of all the contributing interferences as

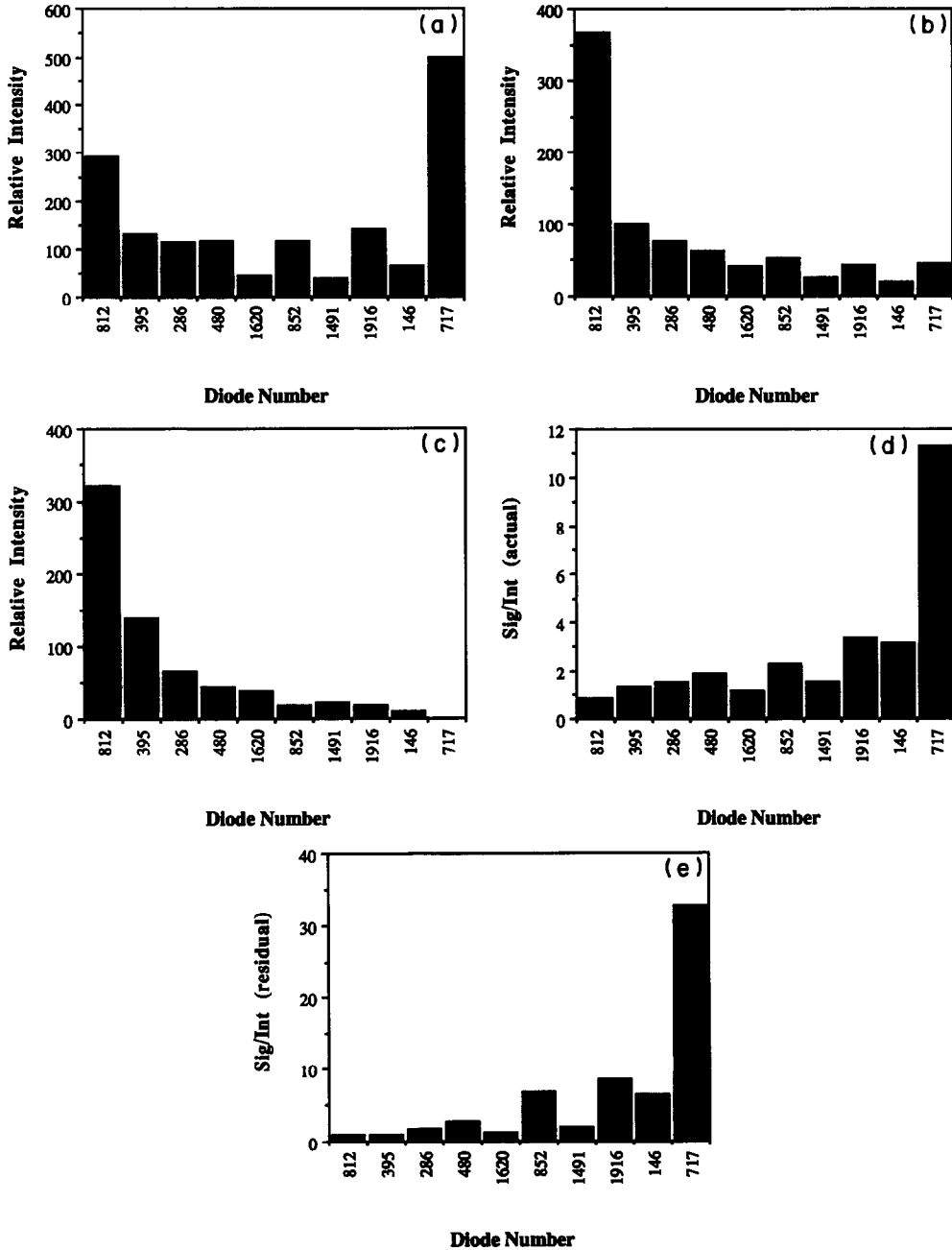


Fig. 7. (a) The ten most intense lines for the spectrum of Fe in the region of 340 nm. Each of the ten bars represents the sum of the five diodes with the greatest intensity for each line. (b) The actual sum of all interferent intensities for the ten Fe lines. (c) An estimate of the sum of all interferent intensities for the ten Fe lines, as obtained from the residual spectrum. (d) The ratio of the signal (Fe spectrum) to the actual sum of the interferences. (e) The ratio of the signal (Fe spectrum) to the estimated sum of the interferences, obtained from the residual spectrum.

obtained in a residual spectrum from the factor analysis. The agreement between the actual interferences and the residual is good, with the first two rejected lines, at diodes 1632 and 818, clearly indicated. This graph was generated without knowledge of the identity of the interferences, or even the number of interferences present. The close match of the residual to the actual interferences shows that the residual vector can be a reliable indicator of the relative degree of interference for each analytical line. The residual spectrum does not indicate that the line at diode 1807 suffers from severe interference, but it does rank it correctly as the third most interfered-with of the lines, and as such it is the third line to be rejected. The rejection process may then be expected to continue, with the identification of subsequent interferences and the rejection of lines in roughly their order of severity of interference.

Figure 5d is a plot of the actual signal/interference ratio for the determination of Co in the presence of several interferences. This ratio is obtained by dividing the signals for the analyte (Fig. 5a) by the summed signals for the interferences (Fig. 5b). Such a graph would not normally be available since knowledge of the actual spectrum of the interferences is required.

Figure 5e is a plot of the signal/residual ratio, generated by dividing the analyte signals by the residual signals. The information for this graph may be obtained without any knowledge of the nature of the interferences. Examination of this graph suggests that the line with the least interference is the last one retained (at diode 2219), showing that the order of rejection is related to the amount of interference, leaving the best line for last. The second least interfered-with line in this graph is the one at diode 1391. Thus, on the basis of the residual spectra generated, two lines are suggested, the best at diode 2219, and a close second at diode 1391.

A comparison of Fig. 5d with Fig. 5e reveals that the second best line on the basis of signal/interference ratio (at diode 1391) is a good choice. Therefore, the method was successful in identifying the most useful lines to use for an analysis.

Two approaches may be taken in the interpretation of these data. The last line retained may be taken as the best line, as suggested in the first option in the Theory section. Alternatively, the line with the highest signal/interference ratio (target/residual ratio) may be taken as the best

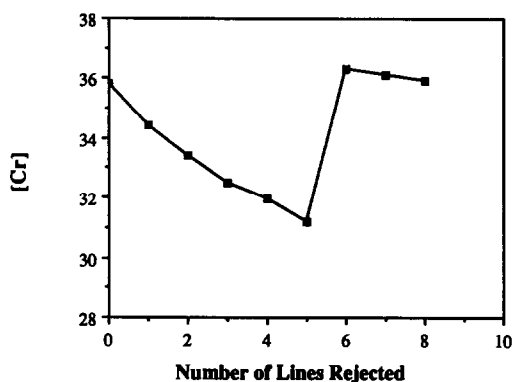


Fig. 8. As each line is sequentially rejected, the concentration of Cr (in ppm) is recalculated in a multivariate analysis using the remaining lines.

line, as mentioned as the second option. As a third option, some intermediate multi-line result may be taken, but in this paper the focus is on the selection of a single line. This third option is not discussed here, but will be explored more fully in the future.

In the determination of Co, the same line is indicated by both the first two options. The line suggested was not the best according to the actual signal/interference ratio, but was nevertheless a reasonable choice. Further examination of analyses for other elements will show that when both options do not select the same line, either line suggested is generally a good choice.

Determination of iron in the presence of interferences

A sample was prepared from the standards, containing Fe as the analyte (50 ppm), and La, Cu, Ni, Mn (all 50 ppm), Co (100 ppm) and Cr (37.5 ppm) as interferences.

Figures 6 and 7 are a set of graphs which outline the determination of Fe in the presence of Co, Cu, Mn, Cr, Ni and La as interferences. These graphs may be interpreted in a manner similar to that used for the analogous graphs presented for the determination of Co. In this case there is one major interference at diode 812, which is removed in the first cycle (Figs. 7b and 7c). The best line, by either option, is the last line retained, at diode 717, as seen in Figs. 7d and 7e. In this case, the line chosen is also the best line by several other criteria, having the best actual signal/interference ratio (Fig. 7a), and the greatest intensity of the Fe lines used in this analysis. The selection of the most intense line is thus justified in this case.

There is at least one severe interference at diode 812, but it is easily detected. A number of less severe interferences at the remaining diodes are sequentially eliminated, leaving a clear choice of diode 717 for the best line. The calculated concentrations of Fe are systematically higher

than the actual concentrations in the sample. This is due to slight hydrolysis in the 2000 ppm Fe standard (which was treated differently from the samples). The resulting lower concentration in the standard gives a systematically higher apparent concentration in the sample mixture.

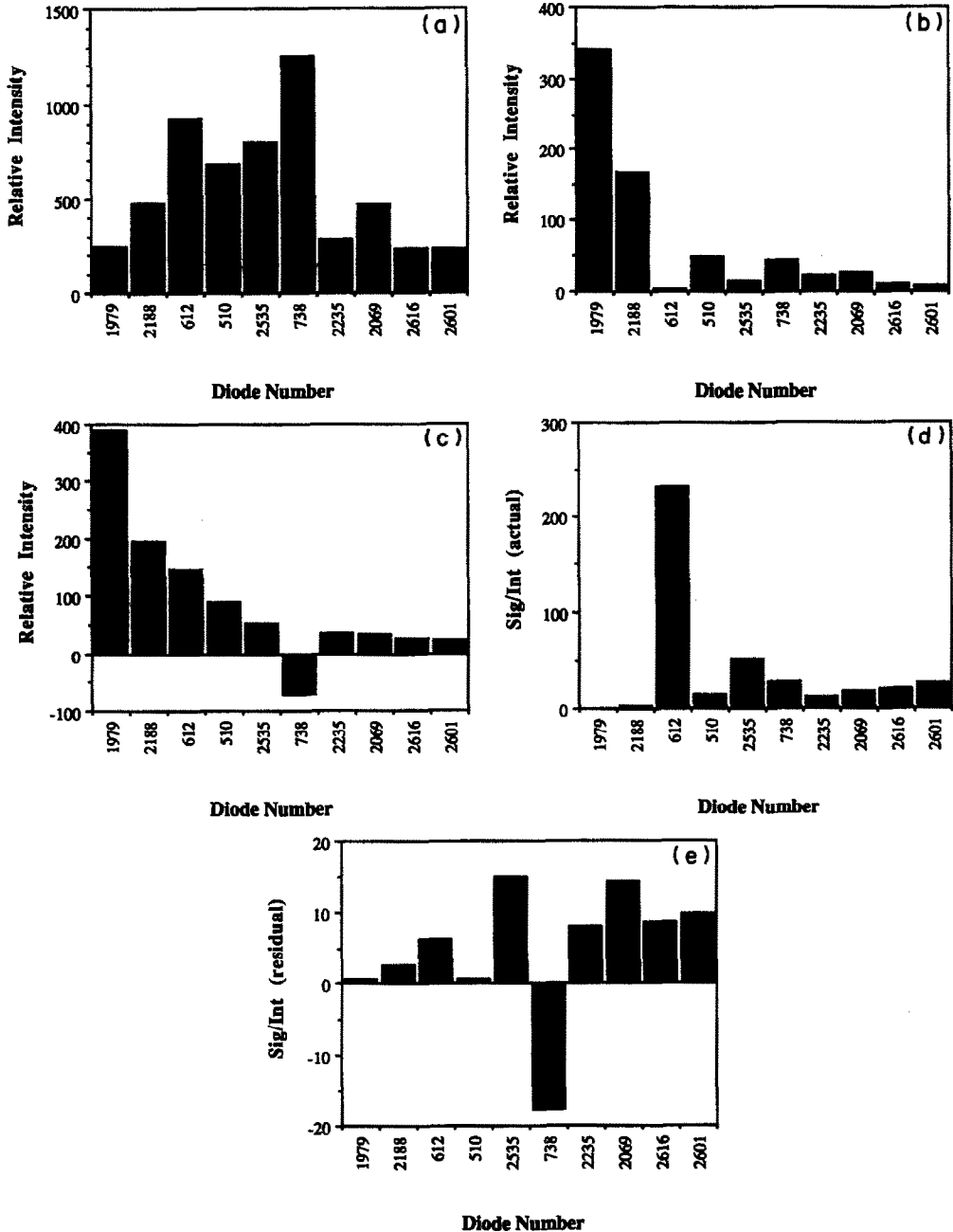


Fig. 9. (a) The ten most intense lines for the spectrum of Cr in the region of 340 nm. Each of the ten bars represents the sum of the five diodes with the greatest intensity for each line. (b) The actual sum of all interferent intensities for the ten Cr lines. (c) An estimate of the sum of all interferent intensities for the ten Cr lines, as obtained from the residual spectrum. (d) The ratio of the signal (Cr spectrum) to the actual sum of the interferents. (e) The ratio of the signal (Cr spectrum) to the estimated sum of the interferents, obtained from the residual spectrum.

Determination of chromium in the presence of interferences

A sample was prepared from the standards, containing Cr as the analyte (37.5 ppm), and La, Cu, Ni, Fe, Mn (all 50 ppm) and Co (100 ppm) as interferences.

Figures 8 and 9 show graphs for the determination of Cr in the presence of several interferences. Examination of these graphs yields some differences from the first two cases studied. In the plot of estimated Cr concentration *vs.* number of cycles (Fig. 8), there is a sudden jump between the fifth and sixth line rejected. Thereafter the value seems to be stable. In Fig. 9d, the highest signal to interference ratio is for the line centered at diode 612, yet this line is rejected early, in the third cycle. In Fig. 9c, there is a negative intensity in the residual for the line at diode 738, which seems to be responsible for the sudden jump in concentration in Fig. 8. Such a negative intensity can be explained by a poor overall fit of the target spectrum (Cr) and residual to the data. With the exception of this line, the method performs as expected, picking the best line (based on signal/interferent ratio) from the remaining four lines. The problem lies in the fact that the two best lines, at diodes 612 and 2535, are rejected before the line at diode 738. In an attempt to understand this problem better, an additional indicator to track the progress of the analysis was used. If the contributions to the residual are small, as is the case when a fit to the target is very close, the mean value of the residual would be expected to be small, as would the standard deviation of the residual. In Fig. 10, both of these values are plotted as a function of the

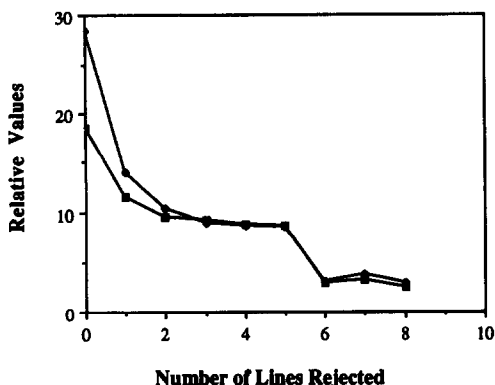


Fig. 10. The residual mean (—■—) and the residual standard deviation (—◆—) (determination of Cr) can be seen to drop as the lines with the worst interferences are sequentially rejected.

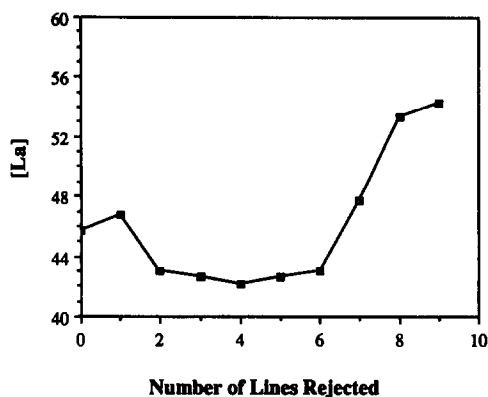


Fig. 11. As each line is sequentially rejected, the concentration of La (in ppm) is recalculated in a multivariate analysis using the remaining lines.

number of lines rejected. The large drop over the first two cycles corresponds to the rejection of the lines at diodes 1979 and 2188, which both have major interferences (Fig. 9b). These interferences are also noted in the residual (Fig. 9d). One remaining major interference is seen at diode 510, and it is expected that this line would be rejected next. However, the next line rejected is at diode 612, which is the best line on the basis of signal to interferent intensity. This is accompanied by a minimal drop in the residual mean and standard deviation (Fig. 10). The next line to be rejected is at diode 510, as would be expected from the actual sum of the interferences (Fig. 9b), but this produces no significant drop in the residual mean and standard deviation. In fact the mean and standard deviation do not drop until the line at diode 738 is removed.

In the analyses for Co and Fe, the ten lines chosen for each were all atom lines. Of the ten lines chosen for Cr, seven are ion lines, and three are atom lines. The atom lines appear at diodes 510, 612 and 738. There is a strong possibility that the anomalous behavior of Cr in this analysis is related to the mixture of atom and ion lines for a single element in the multivariate analysis. All ion-line intensities are well correlated since they are produced by the same species. The atom lines should be similarly well correlated. A shift in the ion to atom equilibrium will, however, affect the relative intensities of atom lines relative to ion lines, so the correlation between ion-line and atom-line intensities will be lower. Such an effect would cause a factor analysis to give a poorer fit in a one-factor determination. Thus the elemental spectrum would be better represented by two

factors, one for the atom spectrum and one for the ion spectrum. This was not done for these data since it would represent a "two-element" simultaneous determination (the Cr atom and Cr ion being treated as two independent

"elements"), and this paper deals only with single-element determinations. Multielement simultaneous determinations and the effect of ion and atom lines will be covered in a future paper.

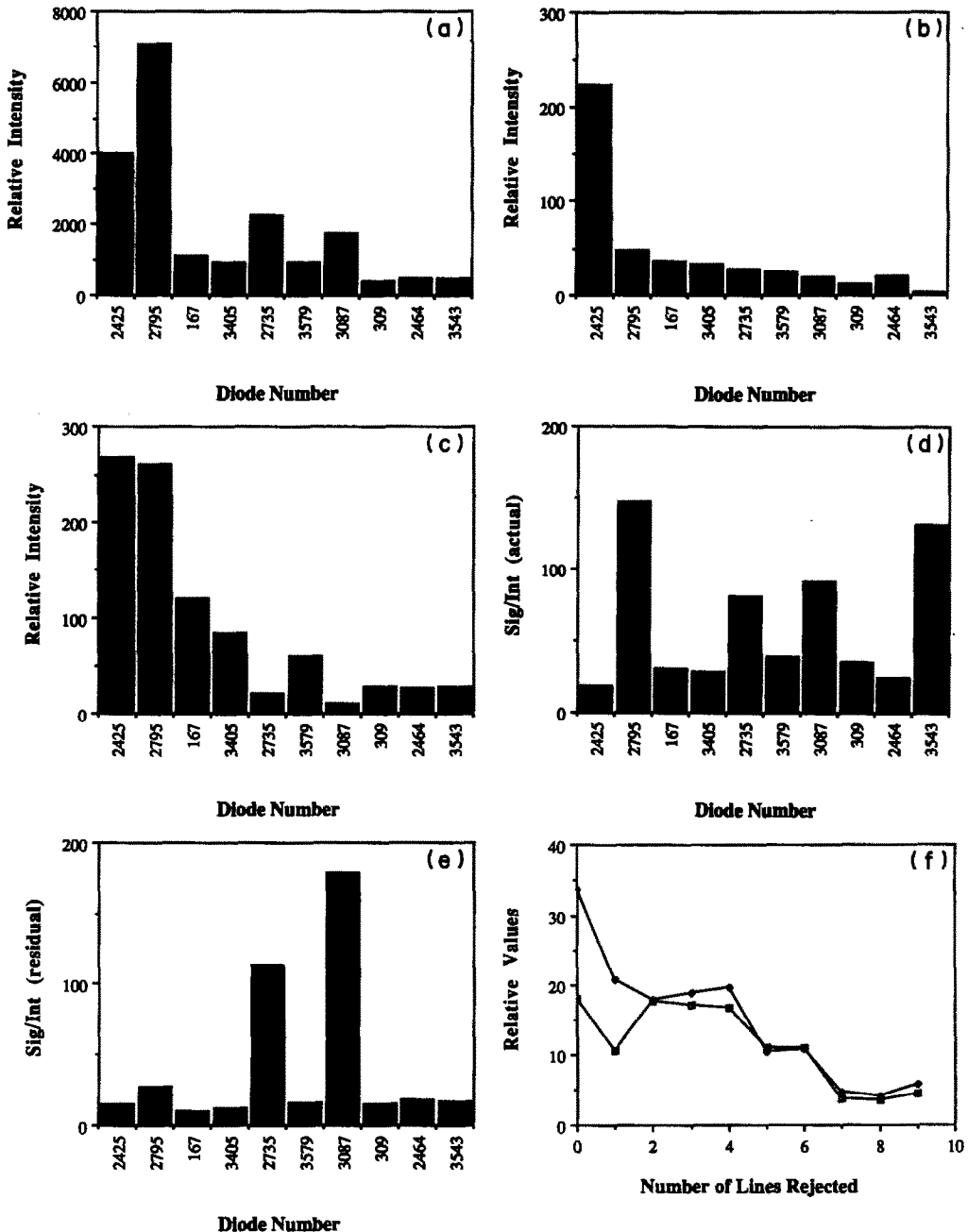


Fig. 12. (a) The ten most intense lines for the spectrum of La in the region of 340 nm. Each of the ten bars represents the sum of the five diodes with the greatest intensity for each line. (b) The actual sum of all interferent intensities for the ten La lines. (c) An estimate of the sum of all interferent intensities for the ten La lines, as obtained from the residual spectrum. (d) The ratio of the signal (La spectrum) to the actual sum of the interferents. (e) The ratio of the signal (La spectrum) to the estimated sum of the interferents, obtained from the residual spectrum. (f) The residual mean (\square) and the residual standard deviation (\blacklozenge) (determination of La) can be seen to drop as the lines with the worst interferences are sequentially rejected.

Determination of lanthanum in the presence of interferences

A sample was prepared from the standards, containing La as the analyte (50 ppm), and Cu, Ni, Fe, Mn (all 50 ppm), Cr (37.5 ppm) and Co (100 ppm) as interferences.

A set of graphs for the determination of La in the presence of several interferences is given in Figs. 11 and 12. In this case there is one major interference, which is removed in the first cycle, and a number of less severe interferences, which are removed successively. The line finally chosen, at diode 3543, is a reasonable choice, being the second best on the basis of the actual signal/interference ratio (Fig. 12d), and within 20% of equalling the best line at diode 2795. In this case, the best line, as suggested by the last retained line at diode 3543, is not the same as the line suggested by the target/residual ratio (Fig. 12e). The target/residual ratio suggests two other lines, at diode 3087, with a close second at diode 2735. These are the third and fourth best lines on the basis of the actual signal/interference ratios (Fig. 12d). Any of these three lines is quite acceptable for a single-line determination of La. In that sense the method was successful in identifying a suitable line. However, another likely candidate at diode 2795 was passed over. These four lines are all within a factor of two for signal/interference ratio (Fig. 12d), and the line at diode 2795 is the third choice when target/residual ratio is considered. These lines being so close in signal/interference ratio, it is to be expected that there would be some randomness in the order of choice. On the basis of absolute intensity, the line at diode 2795 is the best choice, but the interferences are also greater, so the ratio of signal to interference is probably a better measure of analytical utility.

The ten lines used in the analysis of La were all ion lines, and the analysis behaved as expected. This further supports the hypothesis that the Cr results are affected by the use of a mixture of atom and ion lines. For the determination of Co, Cr and La, the difference between actual and calculated concentrations when all

the interferences have been removed is due to the high noise level of the array itself, which is soon to be replaced by a newer, much quieter array.

CONCLUSION

A method has been described for selecting a suitable line for analysis when there are several lines available, some of which may suffer from spectral interferences. The method is best suited to multiplex spectrometers which provide a window of spectral information. In most cases a suitable line is correctly identified. As no knowledge of the identity of the interferent(s) is required, this method has an advantage over other methods which must make use of spectral tables. The errors arising from the noise level of the array, and hydrolysis of the iron standard, can be rectified, and do not affect the validity of the multivariate methods used. These methods should be particularly useful for the selection of suitable analytical lines for a complex sample with untabulated interferences.

REFERENCES

1. P. W. J. M. Boumans, *Line Coincidence Tables for Inductively Coupled Plasma Atomic Emission Spectrometry*, Pergamon Press, Oxford, 1980.
2. E. A. Stubbley and G. Horlick, *Appl. Spectrosc.*, 1985, **39**, 800.
3. *Idem, ibid.*, 1985, **39**, 805.
4. R. C. L. Ng and G. Horlick, *ibid.*, 1985, **39**, 834.
5. V. Karanassios and G. Horlick, *ibid.*, 1986, **40**, 813.
6. Y. Talmi (ed.), *Multichannel Image Sensors*, Vol. 2, American Chemical Society, Washington D.C., 1983.
7. G. M. Levy, A. Quaglia, R. E. Lazure and S. W. McGeorge, *Spectrochim. Acta*, 1987, **42B**, 341.
8. D. F. Wirsz, R. J. Browne and M. W. Blades, *Appl. Spectrosc.*, 1987, **41**, 1383.
9. C. H. Corliss and W. R. Bozman, *Experimental Transition Probabilities for Spectral Lines of Seventy Elements*, NBS Monograph 53, U.S. Government Printing Office, Washington D.C., 1962.
10. E. R. Malinowski and D. G. Howery, *Factor Analysis in Chemistry*, Wiley, New York, 1980.
11. E. R. Malinowski, *Anal. Chem.*, 1977, **49**, 606.
12. *Idem, ibid.*, 1977, **49**, 612.
13. D. F. Wirsz and M. W. Blades, *ibid.*, 1986, **58**, 51.
14. *Idem, J. Anal. At. Spectrom.*, 1988, **3**, 363.

SELECTIVE MULTIPLEX ADVANTAGE WITH AN ELECTRO-OPTIC HADAMARD TRANSFORM SPECTROMETER FOR MULTIELEMENTAL ATOMIC EMISSION

DAVID C. TILOTTA*, ROBERT C. FRY and WILLIAM G. FATELEY

Department of Chemistry, Willard Hall, Kansas State University, Manhattan, KS 66506, U.S.A.

(Received 31 May 1988. Accepted 15 December 1988)

Summary—A liquid-crystal spatial light-modulator Hadamard transform spectrometer is adapted for multielemental atomic spectrochemical analysis. The flame emissions of alkali metals are studied as a preliminary example. The multiplex *disadvantage* normally plaguing application of Hadamard and Fourier transform methods to atomic analysis is circumvented. Permanent electro-optic "closure" of certain Hadamard mask slits (corresponding to intense major element emissions) improves the signal-to-noise ratio (SNR) of the remaining trace element emissions. This approach to SNR enhancement of weaker spectral features by blocking known intense features is called the *selective* multiplex advantage. A problem with the contrast ratio (relative transmissions of the transparent and opaque states) of the liquid-crystal Hadamard mask has been identified in terms of "optical leakage". This produces an offset in the Hadamard encodegram, and leads to concentration-dependent baseline-offset effects in the transformed spectrum. A mathematical correction procedure was devised and evaluated experimentally.

The current state-of-the-art in simultaneous multielemental atomic-emission spectroscopy generally relies on multichannel photomultiplier "direct-reading" systems, photodiode array detectors, and Fourier transform spectrometers (FTS). The first two detection systems rely on dispersion of the radiation followed by detection of discrete wavelengths by separate detectors, and the third system multiplexes the radiation onto a single detector.

Multichannel photomultiplier "direct-readers" are sensitive and exhibit wide dynamic ranges, but they are also expensive and monitor only a few selected wavelengths while ignoring most of the useful spectrum of a sample. Photodiode arrays, on the other hand, utilize more of the spectrum but are often not very sensitive because of low gain, and have limited dynamic range within a single exposure. Photodiode array sensitivity can be increased by image intensification, but only at a considerable increase in cost, loss in resolution and impairment of the upper limit of the dynamic range. Denton and co-workers are currently experimenting with low noise, unity gain, charge-coupled (CCD) and charge-injection (CID) cameras as

multielement detectors for dispersive spectroscopic analysis,^{1,2} but a system is not yet commercially available for routine chemical analysis.

In contrast to dispersive methods, the Fourier transform spectrometer employs a single detector which can be selected for high gain and good sensitivity in the ultraviolet-visible region. However, atomic-emission FTS is widely known for the multiplex *disadvantage* which occurs when photon noise from intense *major element* emissions (e.g., lines of Ar, Fe, Ca, Mg) is distributed throughout the atomic spectrum. This "major element" noise can obscure emissions from minor and trace sample components in steel (e.g., B, C, Cr, Ni) or ultratrace elements found in complex samples of biological, environmental or geological origin (e.g., Hg, As, Se, Pb). A similar multiplex disadvantage, encountered in the form of "Rayleigh line noise", leads to extreme optical filtering requirements in FT-Raman experiments.³

Horlick *et al.*⁴ have also pointed out that the saturation limits of the detector, preamplifier, and/or analog-to-digital converter can impose further restrictions on the intra-spectral dynamic range of FTS applications in atomic analysis. In practice, this means that the overall detector and readout system gain must be

*Present address: Department of Chemistry, Baylor University, Waco, TX 76798, U.S.A.

reduced to keep the strongest major element and plasma background lines within the working range.

In a previous report involving a mechanical moving-mask Hadamard transform spectrometer, Plankey *et al.*⁵ showed that the multiplex disadvantages and intra-spectral dynamic range problems encountered in FTS also hinder the application of conventional Hadamard transform spectrometry (HTS) to atomic spectral analysis.

The present paper will explore the potential of a new liquid-crystal spatial light-modulator (LC-SLM) Hadamard transform spectrometer^{6,7} for creating a *selective* multiplex advantage. This development raises the possibility of eliminating "major element" noise and dynamic range limitations plaguing earlier FTS and HTS atomic emission and fluorescence instruments. A liquid crystal electro-optic encoding mask located at the intermediate focal plane of a conventional subtractive double polychromator is used to selectively modulate polychromatic radiation onto a single detector.

The LC-SLM Hadamard transform spectrometer, by virtue of its electronically programmable multi-slit array, is used in this study as a simultaneous multiwavelength detector for atomic-emission spectroscopy. The electro-optic Hadamard encoding mask can function as a tunable optical filter by "closing" selected slits for the duration of the data-acquisition period. By removal of certain wavelength components (*i.e.*, intense major element emissions), the noise associated with those components will also be removed. If this radiation never impinges on the detector, the shot-noise contribution from the detector will also not be as significant. The option of pseudo-permanent closure of selected encoding slits is referred to as selective multiplexing. The selective multiplex advantage in LC-SLM HTS is an instrumental advantage which provides HTS with a unique means of selectively implementing the multiplex gain advantage found in ultraviolet-visible FTS.⁸

This paper will explore the application of LC-SLM HTS to simultaneous, multielement atomic analysis using the flame atomic-emissions from selected alkali metals as a preliminary example. Li, K, Rb and Cs were chosen for this study, because of the overlap of their red/near-infrared emission lines with the response curve of the instrument. The selective multiplex advantage is investigated, and a

method is presented for compensating optical leakage of the LC-SLM encoding mask.

THEORY

Optical leakage of the LC-SLM mask

The LC-SLM is not a perfect Hadamard encoding mask, *i.e.*, the liquid-crystal encoding slits transmit significantly less than 100% of the radiation when switched open and more than 0% of the radiation when switched closed. The transmission of the present encoding mask has an average value of 23% in its transparent state and 9% in its opaque state for the red/near-infrared region.⁶ These transmission characteristics were reported to be reasonably independent of wavelength in this region.

The HTS encodegrams are distorted as a result of the imperfect transmission characteristics of the LC-SLM mask. Encodegram distortion arises principally from known characteristics of the polarizers in this spectral region,⁶ and is further complicated because both optical defects occur in all channels at some time within a single scan. Because the LC-SLM is used to modulate the polychromatic radiation, these optical transmission defects result in poorer optical modulation of the radiation than if the instrument were fitted with a "perfect" Hadamard encoding mask. An analogy of poor optical modulation in HTS would be poor fringe visibility in FTS.

The defective opaque state causes two major problems. Its undesirable influence on the signal to noise ratio has been previously discussed.⁹ A further problem of the "leaky" opaque state involves a baseline offset which varies with the total incident-light level. For example, the baseline value will increase with increasing analyte concentration, and for that matter with increasing concentration of any emitting species in the sample or flame. The baseline offset appears first in the encodegram, and is carried through the Hadamard transformation to the final spectrum as well.

Specifically, distortion from the LC-SLM mask results because the Nelson-Fredman¹⁰ fast Hadamard transform algorithm used in this spectrometer requires a coding basis set of +1s (completely open slits) and 0s (completely closed slits). Of course, an imperfect Hadamard encoding mask does not have either completely open or closed slits. Therefore, the requirement of +1s and 0s for a basis set is violated. If the Nelson-Fredman fast Hadamard transform is

used with an imperfect encoding mask (the LC-SLM), then the violation shows up as a baseline offset (generally, to more positive values) for the actual intensity values of the spectral resolution elements (*i.e.*, the discrete wavelength intervals) in a given spectrum. Since the amount of light leakage through the opaque state of the LC-SLM encoding mask is a function of both the transmission of the opaque state of the mask and the total light intensity impinging upon the mask, the amount of baseline shift for a fixed wavelength region depends upon the source intensity. Therefore, in order to make quantitative inter-spectral comparisons when using the Nelson-Fredman fast Hadamard transform, the baseline offset must be removed from each spectrum.

One method of correcting the encodegram for the leakage offset (the method used in this study) is to determine the offset of the encodegram by direct measurement. Since the amount of the offset is the same for each point in the encodegram, it can be subtracted directly. Transforming the corrected encodegram will then yield a spectrum with no artificial baseline offset.

A minor consequence of performing this offset subtraction in the Hadamard domain is a constant mathematical attenuation of the overall system gain. This component of the optical leakage effect will *not* vary with the incident light level. This attenuation is similar to that obtained by placing a neutral density filter in the optical path of the radiation for all samples and calibration standards. It will change the absolute intensity scale, but will not alter any spectral comparisons made on the basis of relative intensity.

EXPERIMENTAL

Apparatus

The circular capillary-head, premixed air-acetylene burner of Aldous *et al.*¹¹ was used with a Perkin-Elmer atomic-absorption spray chamber and nebulizer. The optics, electronic data system, and liquid-crystal encoding mask of the previous 127-channel LC-SLM HT spectrometer^{6,7} were used with the following modifications. Two 830 groove/mm plane diffraction gratings, blazed for 950 nm in the first order, were employed in the 1-m subtractive double polychromator. A Hoya 25A long-pass red filter (588 nm wavelength cut-off) was used for order sorting. The detector was a room-temperature

silicon photodiode (Hamamatsu Model S1337-16BQ) operated in the photovoltaic mode.

Reagents

All emission experiments were performed with a 3000 ppm Cs ionization suppressant prepared from Aldrich high-purity CsCl (99.9995%). Calibration standards were diluted from 1000 ppm K and Rb salt stock solutions (Aldrich gold label, original salt purity 99.99% each) and 10,000 ppm Li salt stock solution (Inorganic Ventures, Inc., ICP grade LiCl).

Experimental conditions

Fuel-lean flame stoichiometry was employed for all measurements, and the burner sheath-gas was omitted. The flame was imaged at unity magnification onto the 100- μ m wide entrance slit by a biconvex 10-cm focal length glass lens. The emission signals were observed over a 1.3 cm vertical section centered at a height of 1.5 cm above the burner top.

A total of 127 individual exposure periods comprised a single encodegram of 15 sec overall duration. Each 118 msec exposure period consisted of a 106 msec "wait" delay followed immediately by a 12 msec data-accumulation sequence. The wait delay allows the mask encodement pattern to stabilize after liquid-crystal energization. The 12 msec data-accumulation sequence, which has been previously described,⁶ is required to minimize intensity fluctuations due to the liquid-crystal cell multiplex drivers. Upon Hadamard transformation, each encodegram yields a spectral scan.

Procedure

The spectral region from 738 to 835 nm was simultaneously monitored. With the near-infrared diffraction gratings used in this study, the LC-SLM HT spectrometer had an effective resolution of 1.4 nm.

The leakage offset of the encodegram was determined by electronically disconnecting the modulator circuit and acquiring one additional encodegram under the same conditions as the actual spectrum was acquired (*i.e.*, aspirating the sample into the flame). Since the modulator circuit was disconnected and the source was of the same intensity, the mask was continually in its off state for 127 separate measurements. Therefore, the data-acquisition system measured the offset voltage from the detector circuit 127 times. These 127 measurements were then used to obtain an average leakage-offset signal. This

average leakage signal was then subtracted from each data point in the encodegram and yielded the leakage-offset corrected encodegram. The leakage-offset corrected encodegram was then transformed by use of the Nelson–Fredman fast Hadamard transform.

RESULTS AND DISCUSSION

The LC–SLM Hadamard multiplex advantage

The LC–SLM Hadamard transform spectrometer, owing to its programmable multi-slit encoding mask, can be operated in several data-acquisition modes. One such operating mode corresponds to a single-slit scanning mode that simulates a conventional scanning monochromator. For this mode, the encoding elements of the mask are electronically closed and then opened, one at a time, in stepwise fashion. To

a first approximation, this sequential scanning of the spectrum would be equivalent to a discrete-wavelength monochromator scan attenuated by the opacity of the encoding mask in its optically open state.

Of course, programming the LC–SLM encoding mask with the Hadamard code presents another means of collecting spectral information. Because the Hadamard transform encoding method requires $(N + 1)/2$ encoding slits to transmit their spectral information per encodegram (where N is the total number of measurements),¹² the Hadamard data-collection algorithm multiplexes the optical information onto the single detector.

The spectra in Fig. 1 illustrate the improvement in the SNR when the LC–SLM spectrometer is operated in the Hadamard multiplex mode, compared with the single-slit monochromator mode. Both spectra were acquired in

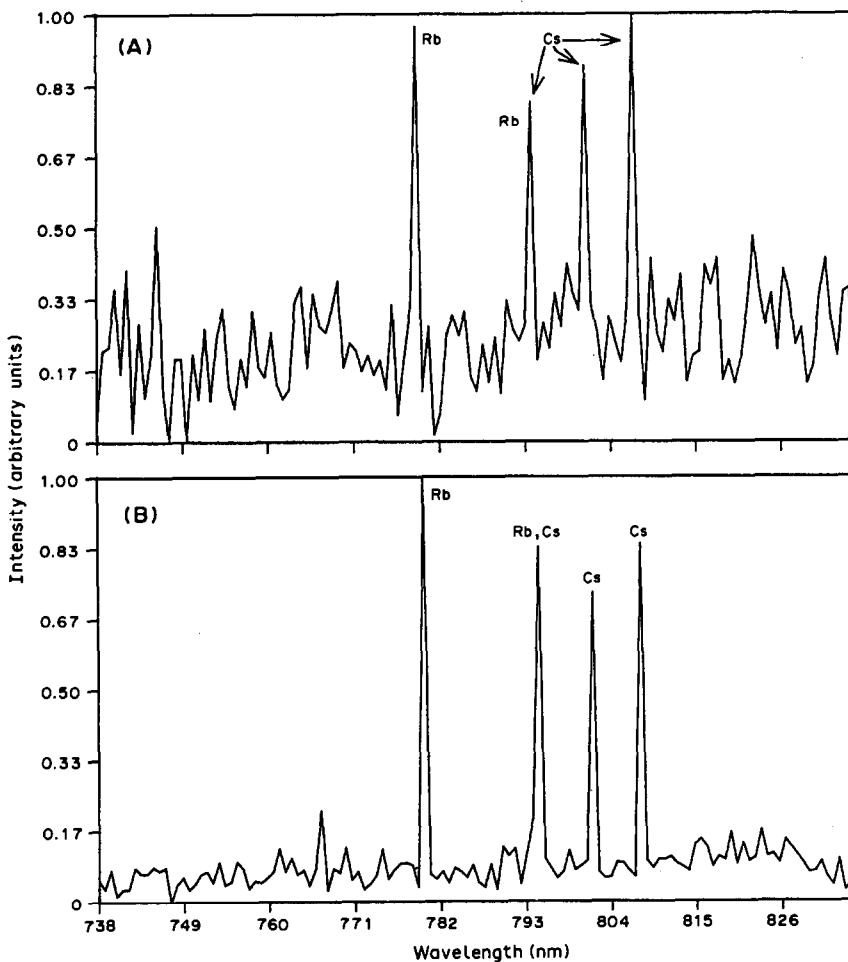


Fig. 1. Spectra of some near-infrared flame atomic-emission lines of rubidium and cesium. (A) A single-slit mask scan, monochromator simulation mode. (B) A single Hadamard multiplex scan. Spectral acquisition time 15 sec.

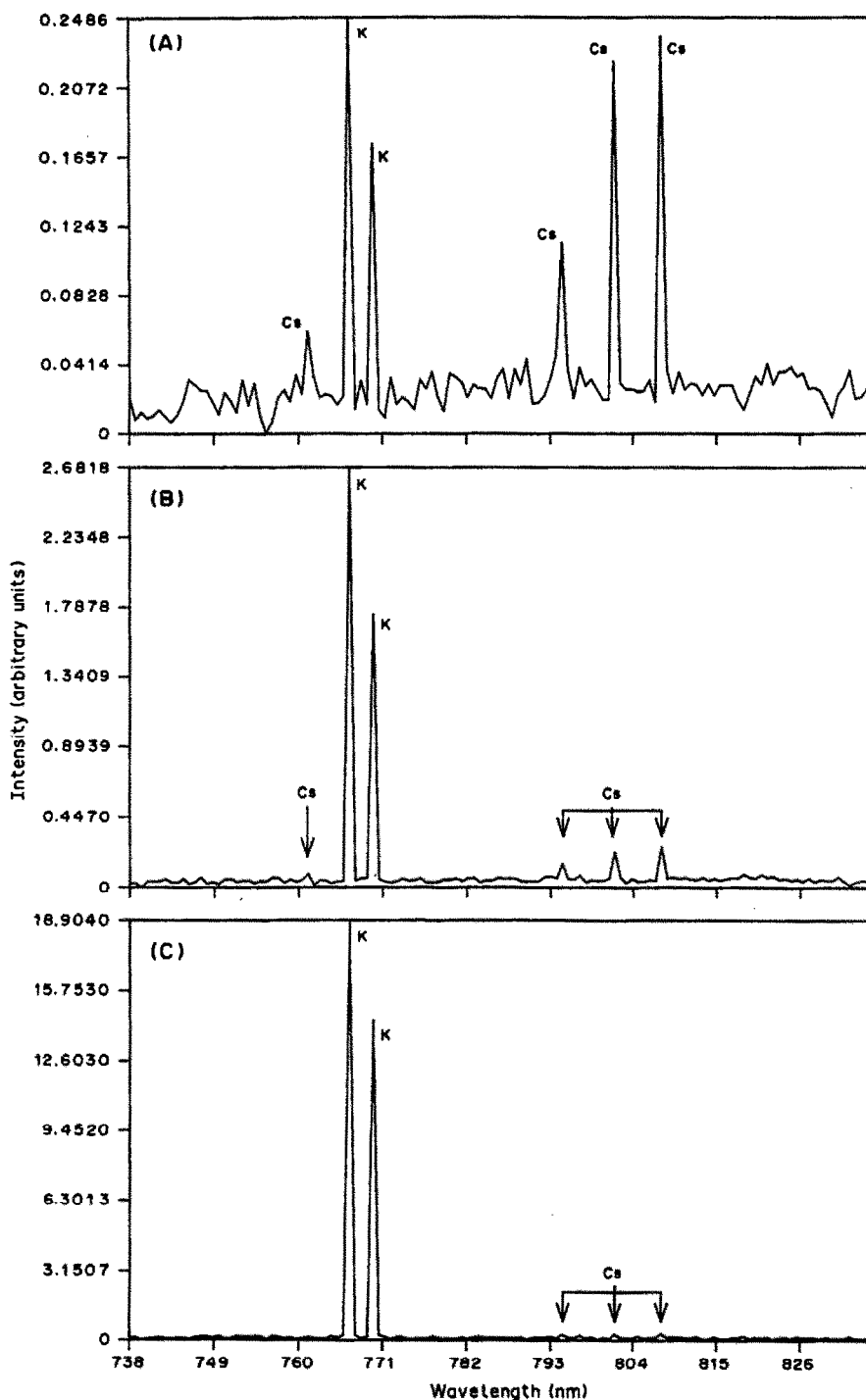


Fig. 2. Representative spectra used in obtaining the calibration curve for potassium: (A) 0.050 ppm K solution, (B) 1 ppm K solution, (C) 10 ppm K solution. It should be noted that the ordinates in each of these spectra have been expanded to full scale for the most intense emission line in each window. All solutions contained 3000 ppm Cs as ionization suppressant.

the same time period and were obtained by aspirating 100 ppb Rb in a 3000 ppm Cs ionization suppressant into the air-acetylene flame. The spectrum in Fig. 1A results when the instrument is operated in the monochromator simula-

tion mode and the SNR (measured for the principal line of Rb at 780 nm) is 3. When the instrument is treated as a Hadamard transform spectrometer, where the encoding mask multiplexes the spectral information, the spectrum in

Fig. 1B is obtained. This spectrum has an SNR of 12, an improvement by a factor of 4 compared to the spectrum in Fig. 1A.

It can be observed that the three weak Cs lines at 794, 802 and 808 nm have different intensities in Fig. 1A compared to those in Fig. 1B. This result is simply due to the noise in Fig. 1A.

Hadamard multiplexing the data, *i.e.*, opening more than one encoding slit per data measurement, increases the total amount of light impinging upon the detector. Therefore, the detector responds to a larger incident light flux. Although a photon detector was used in this study, it is clear that under these circumstances, the Hadamard transform method produces spectra with better SNRs than if the instrument is treated in the single-slit monochromator simulation mode.

Calibration curves

To test the fidelity of the leakage-offset correction procedure and the overall linearity of the LC-SLM HTS, calibration curves were prepared for K and Rb with the 766 and 780 nm lines, respectively. Each of the points on the calibration curves was obtained from the co-addition of three complete Hadamard data scans. Figure 2 is representative of the spectra used in system calibration. The spectra in Fig. 2A, 2B and 2C were obtained by aspirating K standards having concentrations of 0.05, 1 and 10 ppm, respectively. The calibration curves for K and Rb are shown in Fig. 3 and were obtained over the concentration range 0.02–10 ppm.

Uncompensated opaque-state leakage of the LC-SLM encoding mask would have shown up as increased baseline values in Fig. 2C (compared with 2B and 2A, respectively), and as upward curvature in the plots of Fig. 3. Neither of these phenomena is apparent from the figures. This implies that all significant leakage-

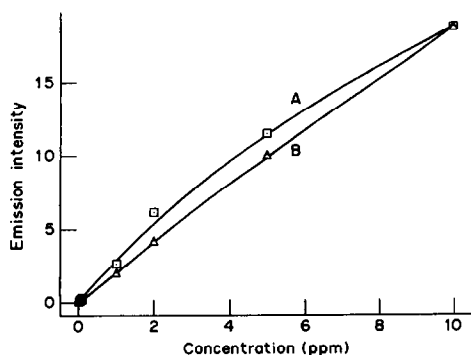


Fig. 3. Emission calibration curves for (A) K and (B) Rb.

offset has been removed by the correction procedure.

The curves in Fig. 3 display the kind of linearity and self-absorption effects normally observed in conventional flame emission analysis. The detection limits for K and Rb with this system were found to be 10 and 20 ppb, respectively. The overall system performance is similar to that of conventional flame photometry, with the added advantage of simultaneous, multi-element determination.

Selective multiplexing

The stationary LC-SLM encoding mask, by virtue of its electronically programmable encoding "slits", can function as a tunable optical notch filter. Specifically, this tunability arises because any of the encoding slits in the mask can be turned off during the entire data-acquisition period. If the intensity and noise contribution of the radiation that is impinging upon that encoding slit is never included with the multiplexed data, then the shot-noise contribution, and the noise due to that resolution element, will also not be included. By reduction of the noise components in the multiplexed data, the overall SNR of the transformed spectrum will be improved. This improved SNR results in a better intra-spectral dynamic range. Of course, improvements in both the SNR and the dynamic range of a spectrum can be useful in atomic-emission spectroscopy for the determination of trace or ultratrace elements in the presence of intense major element emissions.

The degree of this selective multiplex advantage will be governed by (1) the intensity of each of the spectral resolution elements in the spectral observation window, (2) the total amount of noise present in each of the resolution elements, and (3) the optical leakage of the encoding mask in its opaque optical state. Factors (1) and (3) will determine the SNR improvements due to shot-noise reduction, and factors (2) and (3) will minimize source-noise contributions to the SNR. Figure 4 illustrates the selective multiplex advantage of LC-SLM HTS.

The spectra in Fig. 4 were obtained by aspirating a solution containing 1 ppm K, 0.1 ppm Rb, 500 ppm Li, and 3000 ppm Cs. (It should be noted that the lithium and cesium lines which appear in this spectral window are not the major analytical lines for these elements.) The ordinates of the spectra in Fig. 4, which have been labeled in arbitrary units, have been expanded by a factor of 49. It should be noted that the

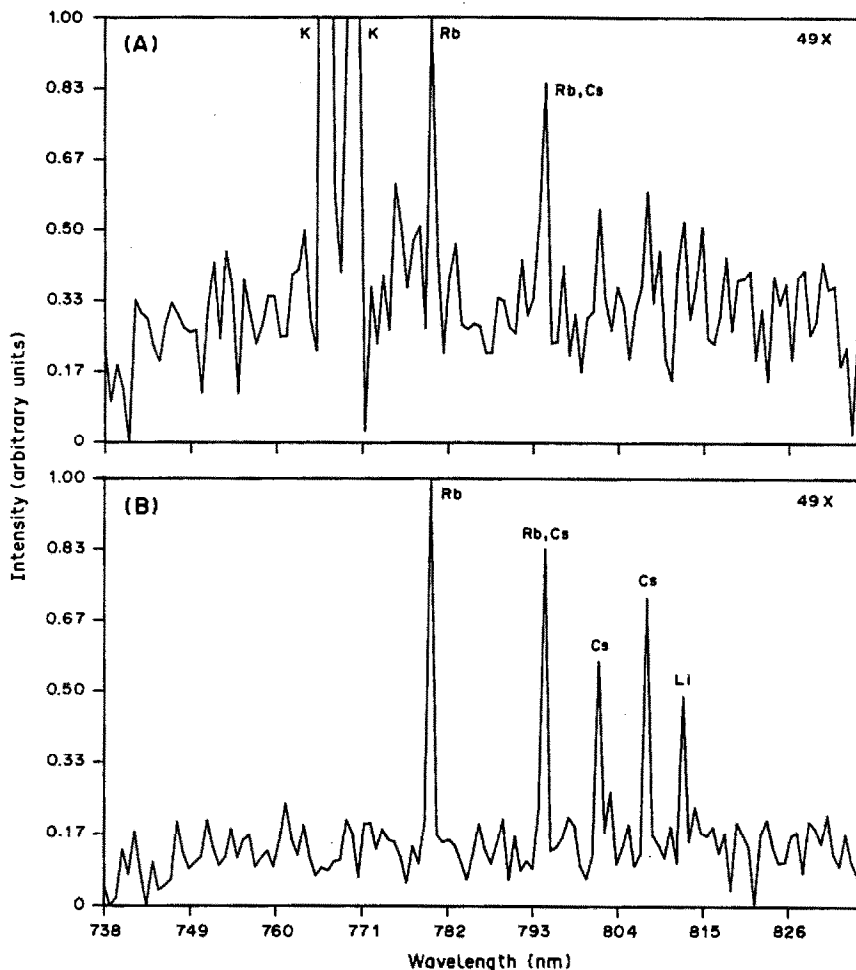


Fig. 4. Spectra illustrating the selective multiplex advantage in LC-SLM HTS. (A) A Hadamard multiplex scan of a solution containing 1 ppm K, 0.1 ppm Rb, 500 ppm Li and 3000 ppm Cs. (B) A Hadamard selective multiplex scan (both K lines excluded) of a solution containing 1 ppm K, 0.1 ppm Rb, 500 ppm Li and 3000 ppm Cs.

potassium lines at 766 and 770 nm are off-scale. The SNR of the spectrum in Fig. 4A, for the 780 nm Rb line, is about 2 and is determined principally by the noise associated with the significantly more intense potassium lines.

When the selective multiplexing procedure is invoked, the spectrum in Fig. 4B results. This spectrum was obtained by closing the LC-SLM encoding mask slits corresponding to the potassium lines for the duration of the data-acquisition. The data-acquisition times for both spectra in Fig. 4A and 4B were identical. Note that the SNR of the 780 nm Rb line is now 6 and has been improved by a factor of 3 owing to the optical elimination of the more intense K lines. Note also that the weak Li emission line at 813 nm, which was completely buried in the baseline noise in Fig. 4A, is readily observed in Fig. 4B.

CONCLUSIONS

LC-SLM HTS has been shown to function as a viable detection system for flame atomic-emission spectroscopy. A simple procedure for correcting encodegrams for encoding mask imperfections has been demonstrated. Although LC-SLM HTS is a multiplexing technique, the electronically programmable electro-optic encoding mask can be used to circumvent two problems due to multiplexing: the multiplex disadvantage due to source instability and the shot-noise generation by photon-type detectors.

Acknowledgements—The authors would like to thank Dr. Richard Browner of the Georgia Institute of Technology for the loan of the capillary-head burner. This contribution was prepared with the support of the Environmental Protection Agency, grant 5007291 (Dr. Billy Fairless, Scientific Officer) and the Phillips Petroleum Corporation in the form of a

fellowship for D. C. Tilotta. This work was taken from the Ph.D. dissertation of D. C. Tilotta¹³ and was presented in part at the 1988 Pittsburg Conference on Analytical Chemistry and Applied Spectroscopy, New Orleans, LA, paper number 1058.

REFERENCES

1. J. V. Sweedler, R. B. Bilhorn, P. M. Epperson, G. R. Sims and M. B. Denton, *Anal. Chem.*, 1988, **60**, 282A.
2. J. V. Sweedler, P. M. Epperson, R. B. Bilhorn, G. R. Sims and M. B. Denton, *ibid.*, 1988, **60**, 327A.
3. D. B. Chase, *J. Am. Chem. Soc.*, 1986, **108**, 7485.
4. G. Horlick, R. H. Hall and W. K. Yuen, in *Fourier Transform Infrared Spectroscopy*, Vol. 3, J. R. Ferraro and L. J. Basile (eds.), pp. 37-81. Academic Press, New York, 1982.
5. F. W. Plankey, T. H. Glenn, L. P. Hart and J. D. Winefordner, *Anal. Chem.*, 1974, **46**, 1000.
6. D. C. Tilotta, R. M. Hammaker and W. G. Fateley, *Appl. Spectrosc.*, 1987, **41**, 727.
7. D. C. Tilotta, R. D. Freeman and W. G. Fateley, *ibid.*, 1987, **41**, 1287.
8. T. Hirschfeld, *ibid.*, 1976, **30**, 68.
9. D. C. Tilotta, R. M. Hammaker and W. G. Fateley, *Appl. Opt.*, 1987, **26**, 4285.
10. E. D. Nelson and M. L. Fredman, *J. Opt. Soc. Am.*, 1970, **60**, 1664.
11. R. M. Aldous, R. F. Browner, R. M. Dagnall and T. S. West, *Anal. Chem.*, 1970, **42**, 939.
12. M. Harwit and N. J. A. Sloane, *Hadamard Transform Optics*, p. 18. Academic Press, New York, 1979.
13. D. C. Tilotta, *Ph.D. Dissertation*, Kansas State University, 1988.

THEORETICAL MULTIPLEX GAIN IN A UV/VIS HADAMARD TRANSFORM SPECTROMETER UTILIZING A UNIFORMLY IMPERFECT ENCODING MASK

DAVID C. TILOTTA

Department of Chemistry, Baylor University, Waco, TX 76798, U.S.A.

(Received 4 May 1989. Accepted 23 June 1989)

Summary—The effect of a uniformly imperfect (non-ideal) encoding mask on the signal-to-noise ratio improvement in a Hadamard transform spectrometer utilizing photon detection is theoretically studied. General equations are developed for the calculation of the multiplex gain (the Fellgett advantage) under conditions of limitation by shot noise and source-fluctuation noise. It is shown that for both cases, the multiplex gain depends on the transmission properties of the encoding mask, the UV/VIS spectrum impinging upon the mask, and the multiplex size, N . It is demonstrated that a uniformly imperfect encoding mask allows sufficient multiplex gain, and that photon-detection in Hadamard transform spectrometry can have advantages in some spectroscopic applications. In addition, comparisons are made between the multiplex gain advantages present in UV/VIS FTS and those present in UV/VIS HTS.

Recent developments in optics have spurred a renewed interest in UV/VIS (ultraviolet/visible) Hadamard transform spectrometry.¹⁻⁴ Though sharing some similarities with Fourier transform spectrometry (FTS), Hadamard transform spectrometry (HTS) relies on a multi-slit masking array to modulate optical radiation. The multi-slit array, which can be fabricated from either a movable mechanical mask or a stationary mask of electro-optical switches, selects dispersed radiation for detection according to Hadamard mathematics. An appropriate optical system focuses the Hadamard-selected radiation onto a single detector. Thus, the encoding mask multiplexes the radiation.

A major goal in the application of the Hadamard transform multiplexing method to spectral analysis is the improvement in the signal-to-noise ratio (SNR) of a spectrum over the SNR which could have been obtained with a conventional scanning dispersive instrument under the same conditions. Fundamental to achieving this goal is the assumption that the only source of noise in the spectrometric system is the detector (and detection electronics) and that this noise is independent of the light intensity of the source. This assumption is generally valid in the infrared, and therefore the use of Hadamard transform spectrometers has led to substantial improvements in SNRs.⁵⁻⁷

In the UV/VIS spectral region, however, two additional sources of noise are often encoun-

tered: shot noise (also referred to as quantum noise) and source-fluctuation noise (also called proportional, low frequency, scintillation, flicker, or $1/f$ noise). The magnitudes of both of these noises increase with the intensity of the light source, and therefore can degrade the SNR of a spectrum when multiplexing is performed.

Shot noise, which obeys Poisson statistics, can arise from either quantum detectors or optical radiation sources. Quantum detectors (or photon detectors, *e.g.*, photoconductor cells or photomultiplier tubes) rely on the direct interaction of the incident photon flux and the electrons in some photoresponsive material. The noise output of a photon detector is caused by the statistical fluctuation of the electrons. Photon shot noise on the other hand, is generated from light sources and is caused by the statistical fluctuation in the photon generation rate. However, regardless of the cause, shot noise is proportional to the square root of the incident light intensity and can be represented by⁸

$$i_p = (I_k 2em \Delta f)^{1/2} \quad (1)$$

where i_p is the shot-noise contribution to the standard deviation of the mean detector current, e is the charge on the electron, I_k is the detector current (which is assumed to be directly proportional to the light intensity), m is the gain, and Δf is the noise bandwidth (generally assumed to be 1 Hz).

Source-fluctuation noise is a multiplicative noise and originates primarily from analyte and background flicker, *i.e.*, the noise is carried by the signal. Source-fluctuation noise is directly proportional to the total light intensity:⁹

$$i_f = KI_k [\ln(f_u/f_l)] \quad (2)$$

where i_f is the fluctuation-noise contribution to the standard deviation of the mean detector current, K is the fractional fluctuation constant expressed as the ratio of the fluctuation-noise power to the signal power, I_k is the detector current (which is assumed to be directly proportional to the light intensity), and f_u and f_l are the upper and lower frequencies, respectively, of the noise bandpass.

Shot noise and source-fluctuation noise seemingly violate the premise of HTS (and for that matter of any multiplexing technique), since the noise of the spectrometric system increases with increasing light intensity. Equations (1) and (2) imply that the process of Hadamard multiplexing, in contradistinction to measuring the spectral resolution elements separately, increases the noise component of a spectrum rather than reducing it. (A spectral resolution element is defined as a short wavelength-interval of radiation.)

The multiplex (Fellgett) advantage of Fourier transform spectrometry (FTS) has been shown to be proportional to the square root of the number of spectral resolution elements impinging upon the detector, $(N^{1/2})/E$, where E is an efficiency factor which can be greater than or equal to unity.¹⁰⁻¹⁷ If a photon detector is used in continuum source FTS (conventional UV/VIS molecular-absorption spectroscopy, for example),¹⁸ the multiplex advantage of the FTS may nearly offset the shot-noise disadvantage of the detector. In addition, it has been shown that under some circumstances, such as emission spectroscopy where the spectral power density is low, a type of multiplex advantage can be gained in utilizing photon detection in FTS.^{9,17,19,20} Hirschfeld^{17,19} termed this multiplex advantage the multiplex gain, or the distributive Fellgett advantage. For measurements limited by source-fluctuation noise, it has been shown that a multiplex disadvantage exists because of the distributive nature of the Fourier transform.¹⁷

Previous workers^{9,21-24} have shown that under some circumstances, a multiplex gain advantage can be obtained in a UV/VIS Hadamard transform spectrometer by utilizing a perfect encod-

ing mask of completely open and completely closed encoding elements. In HTS utilizing a single, uniformly imperfect encoding mask, *i.e.*, a mask which, owing to its method of operation, imparts a constant, wavelength-independent attenuation to the incident radiation (such as a liquid-crystal spatial light modulator), it has been proposed that a multiplex advantage can exist if thermal detection is used.²⁵

This paper presents an examination of the effect of shot noise and source-fluctuation noise on the SNR in a Hadamard transform spectrometer utilizing a single, uniformly imperfect encoding mask. General equations are developed which demonstrate the change in the SNR of a spectrum when Hadamard multiplexing is performed rather than acquiring the spectrum on an ideal scanning dispersive instrument. It is shown that under many spectral circumstances, multiplex gain advantages can exist, and that these multiplex gains are similar to the multiplex gain advantages present in FTS.

THEORY

Assumptions

To examine the effect of Hadamard multiplexing on the SNR improvement in a spectrometer equipped with a photon-type detector and a single uniformly imperfect encoding mask, it is convenient to make several assumptions.

1. Diffraction of the radiation by the mask is negligible.
2. Although the error in a given measurement obeys Poisson statistics, for large average values, *i.e.*, significant light intensity, the Poisson distribution of the error is approximated by a normal distribution. Thus, the error in a given measurement, e , can have associated with it a normal variance. This is expressed by using the expected-value notation:

$$E(e^2) = s^2$$

3. Dark-current detector noise can be considered insignificant.
4. With the exception of the encoding mask, the ideal scanning spectrometer utilizes the same optical components as the HTS, and thus both have equal luminosity-resolving power (LR) products. However, for the ideal scanning spectrometer, the encoding mask in the HTS is replaced with a single perfect (*i.e.*, with 100% transmission) exit slit having the same physical

dimensions as a single encoding element in the HTS encoding mask.

5. The same detector is used in both the Hadamard transform spectrometer and the ideal scanning dispersive spectrometer.

6. The errors in different measurements, e and e' , are uncorrelated (unbiased):

$$E(ee') = 0$$

7. The average value of the error is zero:

$$E(e) = 0$$

8. The number of multiplexed spectral resolution elements, N , is equal to the number of discrete measurements performed with the ideal scanning dispersive spectrometer. Further, N is large enough for the approximations

$$N \approx (N + 1) \approx (N - 1)$$

to be valid.

9. The time required for N Hadamard multiplex measurements and N discrete scanning measurements is the same.

General considerations

The improvement in the root-mean-square signal-to-noise ratio due to multiplexing, $(\text{SNR}_{\text{rms}})_{\text{imp}}$, in comparison to measuring the resolution elements separately on an ideal scanning dispersive spectrometer, is given by²⁵

$$(\text{SNR}_{\text{rms}})_{\text{imp}} = (s_i^2/\epsilon)^{1/2} \quad (3)$$

where s_i^2 is the variance in the measurement of the resolution elements on the ideal scanning spectrometer and ϵ is the average mean-square error incurred from the multiplex measurement of the spectral resolution elements.

If a Hadamard data multiplexing procedure is employed to measure the spectral resolution elements then

$$\epsilon = (s_m^2/N)\text{Trace}(\mathbf{W}^T\mathbf{W})^{-1} \quad (4)$$

where s_m^2 is the variance (noise) in the measurements obtained from the Hadamard multiplexing procedure, N is the total number of spectral resolution elements multiplexed, \mathbf{W} is the Hadamard encoding matrix (weighing matrix), and \mathbf{W}^T is the transpose of the Hadamard encoding matrix.

For the general case of a Hadamard transform spectrometer utilizing a single uniformly imperfect encoding mask, it has been shown that the average mean-square error incurred

from the multiplexing process is well approximated by²⁵

$$\epsilon = [s_m^2/(\Delta T)^2](4/N) \quad (5)$$

where $\Delta T = T_1 - T_0$, T_1 being a fractional term representing the average transmission of the encoding mask in its transparent state, and T_0 a fractional term representing the average transmission of the encoding mask in its opaque state.

A general equation for the effect of Hadamard multiplexing on noise reduction can be found by substituting equation (5) into equation (3):

$$(\text{SNR}_{\text{rms}})_{\text{imp}} = [(s_i^2/s_m^2)(\Delta T^2 N/4)]^{1/2} \quad (6)$$

For the case of source-independent detector noise, such as that typically encountered in the infrared spectral region, $s_i^2 = s_m^2$, and equation (6) simplifies to:²⁵

$$(\text{SNR}_{\text{rms}})_{\text{imp}} = \Delta T(\sqrt{N}/2) \quad (7)$$

However, equation (7) explicitly assumes the detector noise output is constant and independent of the intensity of the light source. As stated previously, the magnitudes of both the shot noise and the source-fluctuation noise depend upon the light intensity. Thus, $s_i^2 \neq s_m^2$ for measurements limited by either shot noise or source-fluctuation noise, since during the Hadamard multiplexing procedure, where groups of spectral resolution elements are measured, the detector operates under a larger irradiance than if the spectral resolution elements are measured separately. In order to determine the effects of Hadamard multiplexing on noise reduction in the shot-noise and fluctuation-noise regimes, the variances in equation (6) must be examined at both noise limits.

Shot-noise variance in Hadamard multiplexing

From equation (1), the variance of the detector output signal is proportional to the light intensity impinging upon the detector. For a given Hadamard encodement pattern obtained from an S-matrix, $(N + 1)/2$ mask elements transmit their spectral information and are attenuated by T_1 , and $(N - 1)/2$ mask elements block (do not transmit) their spectral information and are attenuated by T_0 .^{25,26} Since it is assumed that N is large, both $(N + 1)/2$ and $(N - 1)/2$ can be replaced by $N/2$. Thus for each detector measurement of light intensity in Hadamard multiplexing, approximately one-half of the spectral resolution elements are

attenuated by T_1 and the other half are attenuated by T_0 .

For any of the N measurements of light intensity in a Hadamard transform spectrometer utilizing a uniformly imperfect encoding mask, the light intensity impinging upon the detector for each measurement will be given by:

$$I_{H,i} = T_1 \sum_{j=1}^{N/2} I_j + T_0 \sum_{k=1}^{N/2} I_k \quad \text{for } i = 1, \dots, N \quad (8)$$

where $I_{H,i}$ is the light intensity of the i th detector measurement by Hadamard multiplexing, I_j is the light intensity incident on the j th transmissive mask element, and I_k is the light intensity incident on the k th opaque mask element. For all encodement patterns (*i.e.*, i values), the $N/2$ values of I_j and the $N/2$ values of I_k are drawn from the group of N light intensities incident on the N resolution elements of the mask, I_l (with $l = 1, \dots, N$). Each encodement then has a different collection of $N/2$ of the N values of I_l that are incident on transmissive mask elements (to give $N/2$ values of I_j in the sum over j) and $N/2$ values of I_l that are incident on opaque mask elements (to give $N/2$ values of I_k in the sum over k). Therefore, the indices j and k in equation (8) are a function of i . However, as will be illustrated, knowledge of the exact nature of j and k is unnecessary.

In order to simplify the analysis, it is useful to consider the average light intensity impinging upon the detector for all Hadamard encodement measurements, I'_H . This simplification is readily justified, owing to the pseudo-random nature of the Hadamard code (that is, each measurement of intensity, $I_{H,i}$, is a pseudo-random combination of the individual spectral resolution elements).²⁷ Therefore, it can be assumed that the measurements of light intensity are not significantly different from one another.

The average light intensity for all Hadamard encodement measurements can be defined as:

$$I'_H = 1/N \sum_{i=1}^N I_{H,i} \quad (9)$$

and can be rewritten by the use of equation (8) as:

$$I'_H = 1/N \sum_{i=1}^N \left[T_1 \sum_{j=1}^{N/2} I_j + T_0 \sum_{k=1}^{N/2} I_k \right] \quad (10)$$

The grand sum in equation (10) represents the sum of the measurements for all N . Since each spectral resolution element (I_l) appears $N/2$ times in the sum over j and $N/2$ times in the sum over k for an entire Hadamard multiplex

encodement of N total measurements, equation (10) can be rewritten as:

$$I'_H = 1/N \left[(N/2)T_1 \sum_{l=1}^N I_l + (N/2)T_0 \sum_{l=1}^N I_l \right] \quad (11)$$

The two summations over l in equation (11) represent the sum of the intensities of all the spectral resolution elements in the spectrum. Thus, both sums can be replaced by

$$P = \sum_{l=1}^N I_l \quad (12)$$

Finally, the average light intensity impinging upon the detector for the encodement patterns of a Hadamard transform multiplex data acquisition can be obtained by substituting equation (12) into equation (11):

$$I'_{H,i} = (P/2)(T_1 + T_0) \quad (13)$$

The shot-noise variance in the signal of the Hadamard multiplex measurement, $s_{m,p}^2$, is obtained by substituting equation (13) into equation (1), and then squaring the result:

$$s_{m,p}^2 = i_{p,H}^2 = (P/2)(T_1 + T_0)2em\Delta f \quad (14)$$

It is interesting to note that this variance is constant for a given spectrum. Thus, $s_{m,p}^2$ is fundamentally similar to s_i^2 , with the exception of its origin.

Source-fluctuation variance in Hadamard multiplexing

The variance of the source-fluctuation noise is given by the square of equation (2). Similarly to the evaluation of the shot-noise variance discussed in the preceding section, it is necessary to determine the light signal impinging upon the detector during Hadamard multiplexing in order to evaluate the source-fluctuation variance. However, since the intensity of each spectral resolution element is randomly modulated by fluctuation noise, the total variance in the detector output, i_f^2 from equation (2), will be a linear sum of the individual variances of the intensities of each of the spectral resolution elements selected by the Hadamard code (assuming the variances are statistically independent).

For source-fluctuation noise-limited measurements, the variance in the detector output for each of the N light intensity measurements in a Hadamard transform spectrometer utilizing a

uniformly imperfect encoding mask will be given by:

$$s_{m,f,i}^2 = i_{f,i}^2 = [\ln(f_u/f_i)]^2 \left[T_i^2 \sum_{j=1}^{N/2} (K_j I_j)^2 + T_0^2 \sum_{k=1}^{N/2} (K_k I_k)^2 \right] \quad \text{for } i = 1, \dots, N \quad (15)$$

where $i_{f,i}^2 (= s_{m,f,i}^2)$ is the fluctuation variance in the detector output of the i th measurement of light intensity by Hadamard multiplexing, K_j and K_k are the fractional fluctuation constants for the light intensity impinging upon the j th open mask element and the k th opaque mask element, respectively, and the other terms have the same definitions as in the previous section.

Although equation (15) is an explicit expression for the evaluation of the source-fluctuation variance for each of the light measurements performed during a Hadamard multiplex data acquisition, it is mathematically cumbersome to evaluate. A more useful expression can be obtained, and one that provides more insight into the effect of multiplexing source-fluctuation noise, if it is assumed that the intensity of each spectral resolution element is modulated by the same time-correlated fractional fluctuation constant. This is equivalent to saying that the variances in the individual measurements are statistically dependent, and that the change in light signal intensity (due to fluctuation) with respect to time is the same for all spectral resolution elements (and is independent of wavelength):

$$\frac{dI_{1,f}}{dt} = \frac{dI_{2,f}}{dt} = \dots = \frac{dI_{N,f}}{dt} \quad (16)$$

where $dI_{1,f}$, $dI_{2,f}$, and $dI_{N,f}$ are the changes in the intensities of spectral resolution elements 1, 2, and N , respectively, due to fluctuation, and dt is the time increment.

The assumption stated by equation (16) is readily justifiable for emissions arising from similar electronic transitions and/or the same excitation source (e.g., atomic-emission and Raman spectroscopy), background and analyte flicker due to nebulization effects in atomic-emission and atomic-absorption spectroscopy, background flicker from the same excitation source, etc.⁹

The consequence of equation (16) is that the fluctuation variance in the light intensity for any

of the N measurements in a Hadamard transform spectrometer utilizing a uniformly imperfect encoding mask can be written as a product of the total light intensity and the fractional fluctuation constant as:

$$s_{m,f,i}^2 = [\ln(f_u/f_i)]^2 K^2 \left[T_i \sum_{j=1}^{N/2} I_j + T_0 \sum_{k=1}^{N/2} I_k \right]^2 \quad \text{for } i = 1, \dots, N \quad (17)$$

Furthermore, by use of equation (8), equation (17) can be rewritten as:

$$s_{m,f,i}^2 = [\ln(f_u/f_i)]^2 K^2 [I_{H,i}]^2 \quad (18)$$

Then, similarly to the discussion in the preceding section, it can be shown in a straightforward manner that the source-fluctuation variance in the average light intensity impinging upon the detector for the Hadamard multiplex measurements is given by:

$$s_{m,f}^2 = [\ln(f_u/f_i)]^2 K^2 (P/2)^2 (T_i + T_0)^2 \quad (19)$$

Shot-noise variance in a scanning dispersive spectrometer

The signal impinging upon the detector in a scanning dispersive spectrometer, I_{ss} , has associated with it a shot-noise variance given by equation (1) as:

$$s_p^2 = I_{ss} 2em \Delta f \quad (20)$$

Source-fluctuation variance in a scanning dispersive spectrometer

The signal impinging upon the detector in a scanning dispersive spectrometer, I_{ss} , has associated with it a source-fluctuation variance given by equation (2) as:

$$s_f^2 = [\ln(f_u/f_i)]^2 K^2 I_{ss}^2 \quad (21)$$

RESULTS AND DISCUSSION

Shot-noise limited measurements

The improvement in the root-mean-square signal-to-noise ratio due to Hadamard multiplexing limited by shot-noise, $(\text{SNR}_{\text{rms}})_{\text{imp,p}}$, can be obtained by substituting equations (14) and (20) into equation (6), and is, after simplification and rearrangement:

$$(\text{SNR}_{\text{rms}})_{\text{imp,p}} = \frac{(T_i - T_0)}{\sqrt{T_i + T_0}} \sqrt{\frac{N}{2}} \sqrt{\frac{I_{ss}}{P}} \quad (22)$$

The right-hand side of equation (22) has been arranged into the product of three distinct factors. The first factor represents the contribution

Table 1. Shot-noise limited signal-to-noise ratio improvements, in comparison to a scanning dispersive spectrometer, expressed as $(P/I_{ss})^{1/2}(\text{SNR}_{\text{rms}})_{\text{imp}}$ for selected values of N , T_i and T_0

$T_i - T_0$	$\sqrt{T_i + T_0}^*$	$N = 15$	$N = 63$	$N = 255$	$N = 1023$	$N = 4095$
1.0	1.00	2.74	5.61	11.3	22.6	45.2
0.9	1.05	2.35	4.81	9.68	19.4	38.8
	0.949	2.60	5.32	10.7	21.4	42.9
0.8	1.10	1.99	4.08	8.21	16.4	32.9
	0.894	2.45	5.02	10.1	20.2	40.5
0.7	1.14	1.68	3.45	6.93	13.9	27.8
	0.837	2.29	4.69	9.44	18.9	37.8
0.6	1.18	1.39	2.85	5.74	11.5	23.0
	0.775	2.12	4.35	8.74	17.5	35.0
0.5	1.23	1.11	2.28	4.59	9.19	18.4
	0.707	1.94	3.97	8.00	16.0	32.0
0.4	1.27	0.863	1.77	3.56	7.12	14.3
	0.632	1.73	3.55	7.15	14.3	28.6
0.3	1.30	0.632	1.30	2.61	5.22	10.4
	0.548	1.50	3.07	6.18	12.4	24.8
0.2	1.34	0.409	0.838	1.69	3.38	6.75
	0.447	1.23	2.51	5.05	10.1	20.2
0.1	1.38	0.198	0.407	0.818	1.64	3.28
	0.316	0.866	1.78	3.57	7.16	14.3
0.0	1.41	0.00	0.00	0.00	0.00	0.00
	0.00	0.00	0.00	0.00	0.00	0.00

*The first value in this column corresponds to T_0 large (i.e., $T_i = 1.00$, $T_0 = 1 - \Delta T$). The second value in this column corresponds to T_0 small (i.e., $T_0 = 0.00$, $T_i + T_0 = T_i - T_0$).

to the multiplex gain from the encoding mask, the second reflects the change in the signal-to-noise ratio improvement due to the number of multiplexed spectral resolution elements, and the third describes the spectrum impinging upon the mask.

Table 1 lists the signal-to-noise ratio improvements obtained with a variety of mask imperfections (T_i and T_0) and number of spectral resolution elements multiplexed (N). The SNR improvements have been expressed as the product of $(\text{SNR}_{\text{rms}})_{\text{imp,p}}$ and $(P/I_{ss})^{1/2}$ since the actual SNR improvement is spectrum-dependent (*vide infra*).

The spectral dependence of the multiplex gain. The third factor in equation (22) shows that

$$(\text{SNR}_{\text{rms}})_{\text{imp,p}} \propto (I_{ss}/P)^{1/2} \quad (23)$$

Thus, the signal-to-noise ratio improvement for a shot-noise limited spectrum depends upon the square root of the ratio of the intensity of the spectral resolution element sought to the sum of the intensities of all spectral resolution elements. This result is consistent with a model described earlier in a slightly modified form,²¹ and explicitly implies that the SNR improvement afforded by Hadamard multiplexing depends inversely upon the square root of the total intensity [equation (12)] of the spectrum. Thus, the SNR improvement would be expected to be greater

for spectra with few strong resolution elements, such as Raman spectroscopy (provided the more intense Rayleigh line is removed and the detector dark-current noise is not a substantial portion of the signal) and atomic-emission spectroscopy. The signal-to-noise ratio improvement would be expected to be less for spectra with many intense resolution elements, such as molecular-absorption spectroscopy in the UV/VIS.

It should be borne in mind, however, that equation (23) is not the only contributor to the SNR improvement, and that the stationary nature of an electro-optic encoding mask allows spectral co-addition to improve the SNR further. Also, the selective multiplex advantage¹ can be used to reduce P by eliminating unnecessary spectral resolution elements and further improve the SNR.

In addition to the power factor, the SNR improvement also depends upon the intensity of the spectral resolution sought, I_{ss} . A given spectrum may be expected to have spectral resolution elements with widely varied intensity values. Thus, the SNR improvement will not be constant for all resolution elements in the spectrum and will tend to be greater for intense resolution elements. It should be noted that the $(\text{SNR}_{\text{rms}})_{\text{imp}}$ with thermal detection is approximately independent of the spectrum impinging upon the mask.²⁵

The multiplex gain as a function of the encoding mask. The dependence of the SNR improvement on the encoding mask, for shot-noise limited detection [equation (22)], is similar to the dependence encountered with thermal detection [equation (7)]. In both cases the SNR improvement is directly proportional to the difference in the two optical states of the encoding mask, ΔT . The major difference between the two cases, however, is the term $\sqrt{T_1 + T_0}$ in the denominator. The effect of the optical defects in the encoding mask when photon detection is used also depends upon their sum, since

$$(\text{SNR}_{\text{rms}})_{\text{imp}, p} \propto \frac{(T_1 - T_0)}{\sqrt{T_1 + T_0}} \quad (24)$$

Table 1 shows the SNR improvements obtained with uniformly imperfect encoding masks possessing a variety of defects. It shows that for all values of N , T_1 and T_0 , the SNR improvement is less if the encoding mask possesses a small difference in its two optical states and/or a large transmittance in its "off" optical state (large T_0). The latter result is not surprising because the shot-noise component will increase as the encoding (multiplexing) efficiency decreases.

The multiplex gain as a function of the multiplex size. Table 1 shows that as the number of multiplexed spectral resolution elements increases, the SNR improvement increases. This result for the case of shot-noise limited HTS is similar to the result predicted for thermal detection HTS, differing from it only by a factor of $1/\sqrt{2}$. Provided the power of the spectrum, P , does not increase with N , which can be true for both Raman and atomic-emission spectroscopy, increasing the multiplex size should improve the SNR.

Ideal cases. In the limit of an ideal encoding mask, where $T_1 = 1.00$ and $T_0 = 0.00$, equation (22) simplifies to

$$(\text{SNR}_{\text{rms}})_{\text{imp}, p} = \sqrt{\frac{NI_{\text{ss}}}{2P}} \quad (25)$$

This equation is similar to a form derived earlier by Larson *et al.*²¹ for the case of a perfect Hadamard encoding mask. The only difference between the two equations (N instead of $N + 1$) is minor and arises because N is assumed to be large in this paper.

As stated in the introduction, Hirschfeld showed that a multiplex gain exists in UV/VIS

FTS with shot-noise limited detection. Since P/N represents the intensity of the mean spectral resolution element, the ideal multiplex gain in HTS, represented by equation (25), differs by a factor of $1/\sqrt{2}$ from the multiplex gain in UV/VIS FTS. However, none of the equations presented in this paper takes into account the optical throughput or relative spectrometer efficiencies of FTS or HTS.

Small T_0 . If $T_0 \ll T_1$, then equation (22) can be written as

$$(\text{SNR}_{\text{rms}})_{\text{imp}} = \sqrt{T_1 \frac{NI_{\text{ss}}}{2P}} \quad (26)$$

Equation (26) shows the SNR improvement will be approximately proportional to the square root of the transmission of the encoding mask in its "on" optical state. The SNR improvement in thermal detection HTS with an imperfect mask, on the same assumption, is proportional to T_1 . Thus, since $T_1 < 1$, $\sqrt{T_1} > T_1$, and the effect of the encoding mask on the SNR improvement for photon detection is less severe than for thermal detection HTS.

Measurements limited by source-fluctuation noise

The improvement in the SNR by Hadamard multiplexing limited by source-fluctuation noise, $(\text{SNR}_{\text{rms}})_{\text{imp}, f}$, can be obtained by substituting equations (19) and (21) into equation (6), and is, after simplification and rearranging:

$$(\text{SNR}_{\text{rms}})_{\text{imp}, f} = \left(\frac{T_1 - T_0}{T_1 + T_0} \right) \sqrt{N} \left(\frac{I_{\text{ss}}}{P} \right) \quad (27)$$

where the terms have the same definitions as before. Note that equation (27) has been arranged into a product of three separate factors.

Table 2 lists the signal-to-noise ratio improvements obtained with a variety of mask imperfections (T_1 and T_0) and number of spectral resolution elements multiplexed (N). The SNR improvements in Table 2 have been expressed as a product of $(\text{SNR}_{\text{rms}})_{\text{imp}, f}$ and P/I_{ss} since the SNR improvement will be spectrum-dependent.

The spectral dependence of the multiplex gain. The third factor in equation (27) shows that

$$(\text{SNR}_{\text{rms}})_{\text{imp}, f} \propto I_{\text{ss}}/P \quad (28)$$

In contrast to the SNR improvements expected in the shot-noise limited regime, the SNR improvements obtained by Hadamard multiplexing limited by source-fluctuation noise depend upon the ratio of the intensity of the line sought to the sum of the intensities of all

Table 2. Source-fluctuation noise limited signal-to-noise ratio improvements, in comparison to a scanning dispersive spectrometer, expressed as (P/I_{ss}) $(\text{SNR}_{\text{rms}})_{\text{imp}}$ for selected values of N , T_1 and T_0

$T_1 - T_0$	$T_1 + T_0^*$	$N = 15$	$N = 63$	$N = 255$	$N = 1023$	$N = 4095$
1.0	1.00	3.87	7.94	16.0	32.0	64.0
0.9	1.10	3.17	6.50	13.1	26.2	52.4
0.8	1.20	2.58	5.29	10.6	21.3	42.7
0.7	1.30	2.09	4.27	8.60	17.2	34.5
0.6	1.40	1.66	3.40	6.84	13.7	27.4
0.5	1.50	1.29	2.65	5.32	10.7	21.3
0.4	1.60	0.968	1.98	3.99	8.00	16.0
0.3	1.70	0.683	1.40	2.82	5.64	11.3
0.2	1.80	0.430	0.882	1.77	3.55	7.11
0.1	1.90	0.204	0.418	0.840	1.68	3.37
0.0	2.00	0.00	0.00	0.00	0.00	0.00

*The entries in this column correspond to $(T_1 + T_0) = 1.00 + [1.00 - \Delta T]$.

spectral resolution elements. Thus, the signal-to-noise ratio improvement would be greater for spectra with few intense resolution elements, and smaller for spectra with many intense resolution elements.

Equation (27) has important implications in emission spectroscopy, and gives rise to the so-called "multiplex disadvantage" present in Hadamard transform spectrometry (however, it should be pointed out that all multiplexing methods, where combinations of spectral resolution elements are measured simultaneously on the same detector, exhibit a multiplex disadvantage). Under source-fluctuation noise conditions, the noise in the spectrum due to the flicker of the resolution elements is distributed throughout the entire spectrum, principally through the P -factor, and degrades the SNR improvement for the whole spectrum. In fact, if a spectrum contains N intense spectral resolution elements, it is straightforward to show with equation (27) that the multiplex advantage will be proportional to $1/\sqrt{N}$ and thus a multiplex disadvantage. However, it should be noted that the selective multiplex advantage, previously demonstrated,¹ can be used to reduce P by eliminating unnecessary spectral resolution elements, and further improve the SNR.

In addition to depending upon the total power of the spectrum, P , the SNR improvement also depends upon the intensity of the spectral resolution element sought, I_{ss} . Thus, if a spectrum contains one or more very intense lines which have a greater fluctuation-noise component than shot-noise component, the SNR improvement will be acceptable for those lines, but appreciably degraded for other lines in the spectrum. For example, if the Rayleigh line (and its fluctuation noise) is included in the multiplexed data acquired from a Raman

experiment, I_{ss}/P will be of the order of 10^{-3} for any of the Raman bands (assuming the total integrated intensity of the Raman-scattered radiation is negligible in comparison to the intensity of the Rayleigh-scattered radiation). Assuming an ideal encoding mask of completely open and closed encoding slits, equation (27) predicts that at least 10^6 resolution elements would need to be multiplexed in order to attain a SNR improvement of unity for the Raman bands.

The multiplex gain as a function of the encoding mask and multiplex size. The dependence of the SNR improvement on the encoding mask for detection limited by source-fluctuation noise is similar to that of improvements obtained for detection limited by photon noise:

$$(\text{SNR}_{\text{rms}})_{\text{imp},f} \propto \left(\frac{T_1 - T_0}{T_1 + T_0} \right) \quad (29)$$

Table 2 shows the SNR improvements obtained with uniformly imperfect encoding masks possessing a variety of defects. As the defect in the opaque state of the encoding mask becomes larger, the SNR improvement becomes smaller, due to multiplex coding inefficiency.

In addition, Table 2 shows that the SNR improvement increases as the multiplex size increases. This result is similar to the shot-noise limited case, differing from it only by a factor of $1/\sqrt{2}$.

Ideal cases. In the limit of an ideal encoding mask, where $T_1 = 1.00$ and $T_0 = 0.00$, equation (27) simplifies to:

$$(\text{SNR}_{\text{rms}})_{\text{imp},f} = \frac{\sqrt{N} I_{ss}}{P} \quad (30)$$

It is interesting to note that the ideal multiplex gain in UV/VIS HTS limited by source-fluctuation noise is nearly equivalent to that of UV/VIS FTS.¹⁷

If $T_0 \ll T_i$, then equation (27) will again be approximately equal to equation (30). This implies that under conditions of limitation by source-fluctuation noise, there is little difference between a UV/VIS Hadamard transform spectrometer utilizing an imperfect mask and a UV/VIS HTS with a perfect encoding mask. This is a reasonable implication because the magnitude of the fluctuation noise is proportional to the signal: when the source intensity is reduced, the noise is also reduced.

CONCLUSIONS

The effect of a non-ideal encoding mask on the signal-to-noise ratio improvement in UV/VIS Hadamard transform spectrometry has been theoretically examined. It has been shown that a multiplex gain advantage can exist under shot-noise limitations for an HTS utilizing a non-ideal encoding mask and a photon detector. The shot-noise multiplex gain depends upon the spectrum impinging upon the encoding mask, the multiplex size, and the transmission parameters of the encoding mask. Under limitations by source-fluctuation noise, Hadamard multiplexing with a uniformly imperfect encoding mask provides some multiplex gain, but can lead to a multiplex disadvantage due to the distribution properties of the Hadamard transform. Both multiplex gains are similar to the multiplex gain advantages present in UV/VIS FTS.

A uniformly imperfect encoding mask affects the SNR improvement in a UV/VIS spectrum in proportion to ΔT and in inverse proportion to $(T_i + T_0)^{1/2}$ for shot-noise limited spectra and to $T_i + T_0$ for spectra limited by source-fluctuation noise. The multiplex gain in UV/VIS HTS under both shot-noise and source-fluctuation noise limitations will be greater for spectra with few intense spectral resolution elements and smaller for spectra with many intense resolution elements. Finally, for some spectroscopic

applications, the SNR improvement can be increased by increasing the multiplex size, as well as using the selective multiplex procedure to reduce the total spectral power.

REFERENCES

1. D. C. Tilotta, R. C. Fry and W. G. Fateley, *Talanta*, 1990, **37**, 53.
2. D. C. Tilotta, R. D. Freeman and W. G. Fateley, *Appl. Spectrosc.*, 1987, **41**, 1287.
3. F. K. Fotiou and M. D. Morris, *ibid.*, 1986, **40**, 704.
4. P. J. Treado and M. D. Morris, *ibid.*, 1989, **43**, 190.
5. J. A. Decker, *Appl. Opt.*, 1971, **10**, 510.
6. P. Hansen and J. Strong, *ibid.*, 1972, **11**, 502.
7. R. D. Swift, R. B. Wattson, J. A. Decker, Jr., R. Paganetti and M. Harwit, *ibid.*, 1972, **11**, 1596.
8. W. Schottky, *Ann. Phys.*, 1918, **57**, 541.
9. J. D. Winefordner, R. Avni, T. L. Chester, J. J. Fitzgerald, L. P. Hart, D. J. Johnson and F. W. Plankey, *Spectrochim. Acta*, 1976, **31B**, 1.
10. P. B. Fellgett, *J. Phys. Radium*, 1958, **19**, 187.
11. R. R. Treffers, *Appl. Opt.*, 1977, **16**, 3103.
12. A. G. Marshall and M. B. Comisarow, *Anal. Chem.*, 1975, **47**, 491A.
13. T. L. Chester, J. J. Fitzgerald and J. D. Winefordner, *ibid.*, 1976, **48**, 779.
14. M. H. Tai and M. Harwit, *Appl. Opt.*, 1976, **15**, 2664.
15. T. Hirschfeld, *ibid.*, 1977, **16**, 3070.
16. M. Harwit and M. H. Tai, *ibid.*, 1977, **16**, 3071.
17. T. Hirschfeld, in *Fourier Transform Infrared Spectroscopy*, Vol. 2, J. R. Ferraro and L. J. Basile (eds.), p. 193. Academic Press, New York, 1979.
18. M. R. Click, B. T. Jones, B. W. Smith and J. D. Winefordner, *Appl. Spectrosc.*, 1989, **43**, 342.
19. T. Hirschfeld, *ibid.*, 1976, **30**, 68.
20. A. S. Filler, *J. Opt. Soc. Am.*, 1973, **63**, 589.
21. N. M. Larson, R. Crosman and Y. Talmi, *Appl. Opt.*, 1974, **13**, 2662.
22. Y. Talmi, R. Crosman and N. M. Larson, *Anal. Chem.*, 1976, **48**, 326.
23. F. W. Plankey, T. H. Glenn, L. P. Hart and J. D. Winefordner, *ibid.*, 1974, **46**, 1000.
24. M. J. Keir, J. B. Dawson and D. J. Ellis, *Spectrochim. Acta*, 1977, **32B**, 59.
25. D. C. Tilotta, R. M. Hammaker and W. G. Fateley, *Appl. Opt.*, 1987, **26**, 4285.
26. E. D. Nelson and M. L. Fredman, *J. Opt. Soc. Am.*, 1970, **60**, 1664.
27. P. Horowitz and W. Hill, *The Art of Electronics*, p. 438. Cambridge University Press, Cambridge, 1984.

TWO-DIMENSIONAL MULTIPLE ENTRANCE-SLIT VIDICON SPECTROMETER FOR SIMULTANEOUS MULTIELEMENT ANALYSIS

MARIANNA A. BUSCH*, KENNETH W. BUSCH and BETSY B. MALLOY
Department of Chemistry, Baylor University, Waco, TX 76798-7348, U.S.A.

(Received 29 March 1989. Accepted 3 May 1989)

Summary—A new type of wavelength dispersion system for use with a multichannel detector has been developed for simultaneous multielement analysis. The system employs a monochromator with fixed grating position, and incident angle varied by horizontal displacement of the entrance slits. The overlapping spectral windows which result can be arranged to produce a composite spectrum having minimal interference from emissions by other sample constituents. Entrance slits may also be displaced vertically to create a two-dimensional system in which spectra are stacked one above the other and scanned by use of a multi-raster scanning pattern. A number of optical and performance characteristics of the system are evaluated in both the one- and two-dimensional modes, and the system is applied to the determination of Ca, Na and K in blood serum and to the determination of the exchangeable cations Ca, Na, Li and K in clay. The advantages of this system for simultaneous multielement analysis are discussed.

The need for analytical systems capable of providing quantitative information on many elements in a sample simultaneously has led analytical spectroscopists to develop a variety of novel and ingenious detection systems.¹ In reviewing this field, Busch and Malloy² have shown that the evolution of these detection systems has proceeded along two principal lines, one based on dispersive systems and the other based on multiplex techniques. While multiplex techniques, such as Fourier³ and Hadamard⁴ transform methods, rely on simultaneous transmission of coded information from more than one spectral resolution element along the same channel (and must be decoded to retrieve the individual intensities), in the dispersive systems the signals to be resolved are separated in either a temporal or spatial manner and their magnitudes are measured individually.

Multielement dispersive systems which rely on spatial separation all have at least one feature in common—multiple detection elements which are separated from each other in space. Although the photographic plate⁵ may be considered the original spatial detector, more modern spatial devices employ electronically-based detection systems such as the photomultiplier (used in the direct-reading spectrometer⁶) and

various solid-state array detectors, including silicon vidicons,⁷ silicon intensified target (SIT) vidicons,⁷ secondary-electron conduction (SEC) tubes,⁸ linear photodiode arrays⁹ and charge-transfer devices.¹⁰⁻¹²

Because of the way in which their detection elements are arranged, some spatial detectors have the potential for operation in either a one- or a two-dimensional mode. In the one-dimensional mode, a single dispersive device is used to spread out the spectral information in the form of a single band of information. However, since each detector consists of a finite number of detection elements, one-dimensional systems are based on a window concept,¹³ requiring a compromise between resolution and wavelength coverage. Two-dimensional dispersive systems, such as the echelle spectrometer,¹⁴ avoid the limited wavelength coverage associated with one-dimensional systems, by dividing the dispersed spectral information into "window-length" segments, and stacking these segments under one another like the printed lines of a book. Other approaches which have been used to ameliorate the compromise conditions involving resolution and wavelength coverage include the use of overlapping orders¹⁵ and multiple entrance slits.^{2,7,16}

In the multiple entrance-slit spectrometer (MESS),¹⁷ an ordinary one-dimensional dispersion system is employed with a series of

*Author to whom correspondence should be addressed.

regularly spaced entrance slits arranged in the focal plane of the entrance port, while the detector is mounted in the focal plane of the exit port. The system may be visualized as the reverse of a direct-reading spectrometer, *i.e.*, instead of using a single entrance slit and multiple exit slits, the one-dimensional MESS uses a linear arrangement of multiple entrance slits and a single detector. Unlike the direct reader, however, in which resolution is determined by how closely the multiple exit slits can be placed in the exit focal plane, the resolution of a spectrometer employing multiple entrance slits is determined by the entrance-slit width, the reciprocal linear dispersion of the optical system, and the size and spacing of the individual elements in the spatial detector. Entrance-slit position is, in fact, not at all related to resolution, but instead controls the spectral regions, or windows, imaged on the detector. Since each entrance slit focuses a different spectral region onto the multichannel detector, a composite of overlapping spectra is produced. Fiber-optic light guides are used to convey the radiation from the source to the individual slits, and can be "plugged in" (like a telephone switchboard) in front of any desired entrance slit in order to produce overlapping spectra with a maximum number of analyte lines and a minimum amount of line coincidence.

In a closely related system,^{18,19} narrow wavelength regions of the spectrum are preselected by a low-resolution predispersion system and a slotted mask in the focal plane of the predisperser. Wavelengths transmitted by this mask are recombined, collimated, directed to an echelle grating, and finally focused onto a linear photodiode array detector. Because of the high dispersion produced by the echelle grating, spectral interference within any given order is minimal.

In the one-dimensional MESS system described by Busch *et al.*¹⁶ a grating spectrometer with a reciprocal linear dispersion of 3.2 nm/mm was used to focus five 40-nm segments of dispersed radiation simultaneously onto a 13-mm SIT vidicon detector target. Because the vidicon system employed in this previous study scanned the target in a single-raster pattern, the 29 multiple entrance slits were arranged in a 12-cm horizontal row so that any wavelength within a range of 384 nm could be imaged at the detector with adequate resolution. With this system, widely separated lines of Mn (403.0 nm), Cr (425.4 nm), Sr (460.7 nm), Ba (553.6

nm) and Li (670.7 nm), normally requiring a 267.8-nm window, were obtained as a composite spectrum by plugging five fiber-optic light guides simultaneously into a suitable arrangement of entrance slits. Detection limits ($S/N = 2$) for these five elements were degraded by a factor of about 400 compared to the best values reported in the literature,²⁰ but were still below 1 ppm. Although these detection limits are quite adequate for many samples, this preliminary report did not include the analysis of any real samples.

Several potential difficulties may arise when different segments of a spectrum are overlapped on the detector in this manner. (1) An increase in baseline noise can result from the combined effect of source flicker noise originating from independent variations in the spectral background of each overlapped spectral segment. (2) Detector saturation can occur at lower signal intensities, owing to the elevated background level present when several spectral regions are superimposed. (3) If several segments of a spectrum are overlapped, various lines may be found to accidentally overlap each other. Although accidental overlap can be easily remedied by altering the position of one or more of the entrance slits, the overlap may be totally unsuspected, as in the analysis of a sample containing an element for which many secondary lines are excited.

This paper describes an alternative arrangement to the one-dimensional MESS system—a dispersion system where the spectral information is presented in a two-dimensional format, allowing the spectral segments to be imaged in a series of strips, one above the other.^{21,22} The spectral information in these strips, or tracks, is read off the vidicon target by a multiple-raster scan pattern. This two-dimensional arrangement will be evaluated, and application of the system to the analysis of real samples in both single-raster and multiple-raster modes will be presented.

EXPERIMENTAL

Vidicon spectrometer

The experimental facilities used in this study are similar to those employed previously,¹⁶ with the following exceptions. An Option 8 two-dimensional scan pattern card (Princeton Applied Research Corporation, Princeton, NJ) was added to the 1205 A Optical Multichannel Analyzer (OMA), and, except where indicated,

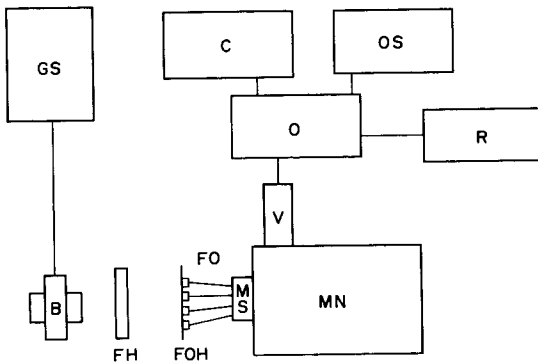


Fig. 1. Schematic diagram of the multiple entrance-slit spectrometer. Gas supply and controls (GS); burner (B); filter holder (FH); fiber-optic lens holder (FOH); multiple entrance-slit array (MS); monochromator (MN); SIT vidicon (V); optical multichannel analyzer (O); chart recorder (C); oscilloscope (O); digital readout (R).

higher quality fiber optics (Welch Allyn Industrial Products Division, Skaneateles Falls, NY) were substituted for those employed in the previous study. For transmission of visible radiation, PVC-sheathed 0.062 in. diameter glass bundles were used. These bundles, which have a

numerical aperture of 0.66 (85°), were made from individual fibers (diameter 0.0022 in.). For transmission of both ultraviolet and visible radiation, 2 mm diameter quartz bundles, composed of 100 μm diameter strands and clad with fluorocarbon resin, were used. These bundles transmit radiation over the wavelength range 200–1300 nm. Figure 1 shows a schematic diagram of the basic instrumental configuration used in this study.

A new multiple entrance-slit assembly, shown in Fig. 2, was constructed. This assembly was similar to the one described previously,¹⁶ except that a series of 6 horizontal rows of 29 holes was employed, instead of a single row of 22 holes. Each row was numbered sequentially from top to bottom, and the holes in each horizontal row were numbered sequentially from left to right, giving each hole a unique row-column coordinate in the two-dimensional array.

Because the brass ferrules on the two types of fiber optics employed were of different diameter, two rows of 0.16 in. diameter holes and four rows of 0.125 in. diameter holes were employed. These diameters allowed the entire shank of the

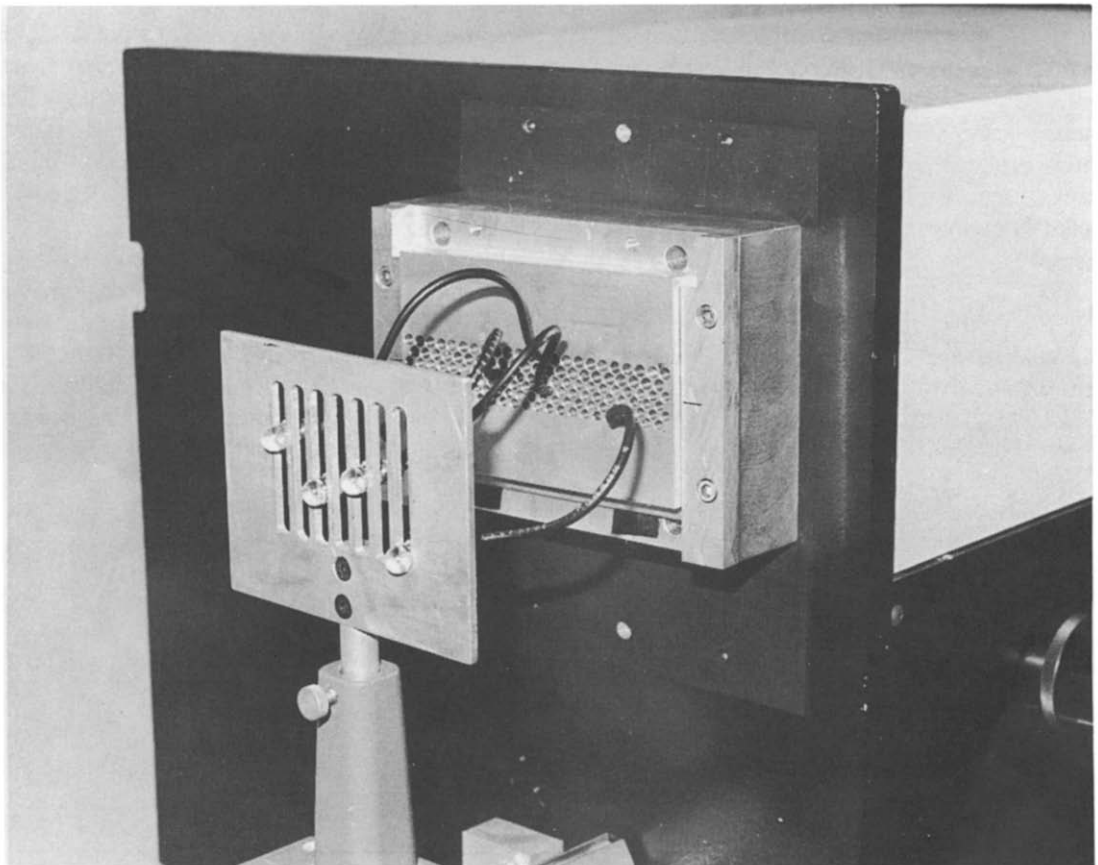


Fig. 2. Fiber-optic system showing input lenses and two-dimensional switchboard entrance-slit array.

ferrule to be inserted into the hole. The thickness of the plate was such that the end of the fiber optic was flush with the back of the plate when the ferrule was completely inserted into the hole. The holes were staggered between adjacent rows to permit smaller vertical separation between the horizontal rows. Razor-blade edges, taped to the back of the plate, were used to form the entrance slits. A series of vertical slots placed between the flame and the multiple entrance-slit array (Fig. 2) allows each fiber-optic light guide to be adjusted to monitor the sampling zone of the flame which gives the optimum signal for the analyte lines in a particular spectral window.

The present system can be operated in either a one- or a two-dimensional mode. For one-dimensional operation, single-raster scanning was employed, and the fiber-optic light guides were all inserted into holes in the same row of the multiple slit array. For two-dimensional operation, multiple-raster scanning was employed, and the fiber-optic light guides were inserted into holes having different row coordinates. Multiple-raster scanning with the Option 8 two-dimensional scan pattern card is accomplished by a reduction in the line-scan amplitude, proportional to the number of tracks desired. A second waveform is applied to the vertical deflection coils, which steps the scan to a new track every 32.8 msec. Total scan time for the entire target is 32.8 msec times the number of tracks used. Any individual track may be selected for observation, or accumulation into memory.

One-dimensional operation

Blood serum analysis. Freeze-dried blood serum standards (General Diagnostics Versatol,

Rupp and Bowman, Inc., Dallas TX) were reconstituted as directed by the manufacturer. Two serum concentrations were used as calibration standards, and a third analyzed serum sample was used as an unknown.

Serum standards and the unknown were each diluted prior to analysis. To 0.5 ml of reconstituted serum was added 1.0 ml of a diluent containing 45 ppm Li as an internal standard and 10500 ppm Cs as an ionization buffer. This dilution resulted in final concentrations of 30 ppm Li and 7000 ppm Cs.

Diluted samples were introduced into a nitrous oxide/acetylene flame by a sample injection system described earlier.¹³ The 50- μ l serum samples were injected by syringe into the injection port and transported to the burner by a carrier solution consisting of 1:4 v/v 2-propanol/water mixture. Table 1 gives the analytical conditions used in the determination.

To arrange the composite spectrum, the monochromator was adjusted for the middle of the wavelength range needed for the analysis, and the appropriate entrance-slit positions were chosen after the monochromator was set. With the single-raster scan pattern used for this analysis, it was found that 600 accumulation cycles were necessary to integrate all the signal from one injection of serum. Accumulation in memory A of the OMA was begun immediately after the sample was injected. Background correction was accomplished by accumulating the signal from carrier solution alone for 600 accumulation cycles, in memory B.

Influence of overlapping spectra on S/N. To determine the influence of overlapping spectra on *S/N* during one-dimensional operation of the MESS system, the change in *S/N* of a spectral line was monitored while the intensity

Table 1. Analytical conditions for blood serum analysis*

Element	Function	Wavelength, <i>nm</i>	Hole number	Filter	Observation height, <i>cm</i>
Ca	analyte	422.7	1	430 nm bandpass	1.1
Na	analyte	589.0	11	589.6 nm bandpass, 0.9 absorbance neutral density	1.1
Li	internal standard	670.7	14	none	1.1
K	analyte	766.5	21	none	1.1

*Acetylene flow-rate 6.2 l./min; nitrous oxide flow-rate 9.5 l./min; fiber optic light guides 10.3 cm from burner.

of a second line in an overlapping window was varied. In the first experiment, the Li 670.7 nm line from a hollow-cathode lamp at a current of 20 mA was overlapped with a window containing the Hg 546.0 nm line from a pen lamp. The intensity of the Li line was held constant while the intensity of the Hg line was increased by means of a series of neutral density filters. At each Hg intensity, the spectrum was accumulated for 20 cycles, and the S/N for Li was calculated. To determine the influence of overlapping spectra on S/N under flame conditions, the signal produced by 0.1 ppm Na (589.6 nm, air/acetylene flame) was overlapped with the Hg 546.0 nm window, and the S/N of the Na line was calculated for different Hg intensities.

Two-dimensional operation

Clay extract analysis. Exchangeable Ca, Na, Li and K were determined for a series of clay samples after extraction according to the procedure described by Chhabra *et al.*²³ Clay samples (0.5 g) were equilibrated for 4 hr with 25 ml of an extractant solution which was 0.1M in thiourea and ammonium acetate and 0.01M in silver nitrate. During the equilibration period, the extraction mixtures were agitated every 30 min. After equilibration, the clay was filtered off on Whatman No. 2 filter paper, and 5 ml of 10000 ppm Cs solution was added to the filtrate, which was then diluted accurately to 50 ml with distilled water prior to analysis. Diluted samples were aspirated directly into a nitrous oxide/acetylene flame by using a Varian Techtron AA-6, 5-cm slot burner–nebulizer assembly, and the signals were accumulated for 100 cycles.

Multielement standards were prepared from reagent-grade chemicals and were diluted with the extraction solution to match the background composition of the standards and samples. The

standard solutions also contained 1000 ppm Cs as an ionization buffer.

Clay analyses were conducted with a multiple-raster format consisting of four tracks. The analysis line for each element (Ca, Na, Li and K) was imaged on a separate track. Table 2 gives the analytical conditions used in the determination.

Since no standards were available for testing the accuracy of the determination, recovery experiments^{24,25} were used for this purpose. Five clay samples were extracted in duplicate, the solutions resulting from both extractions were combined, and the extract was diluted as described above. After analysis of these extracts, the samples were spiked with various amounts of Ca, Na, Li and K, approximately equal to the amounts initially present. The spiked samples were then analyzed.

Detection limits. Multielement detection limits under clay analysis conditions were determined by using two solution concentrations near the detection limit to construct a calibration curve from which the concentration corresponding to an S/N of 3 could be estimated. Each measurement was accumulated for 100 cycles, and each detection limit was determined as the average of 5 measurements.

Single-element detection limits were determined in the same manner, with aqueous solutions containing 1000 ppm Cs as an ionization buffer. Experimental parameters common to all single-element detection-limit determinations include a 3-mm observation height in the flame, a nitrous oxide flow-rate of 9.5 l./min, an acetylene flow rate of 6.5 l./min, and a distance of 9.7 cm between burner and fiber-optic light guide. Plastic (Crofon) fiber bundles (Edmond Scientific, Barrington, NJ) consisting of sixty-four 0.01 in. diameter fibers in a polyethylene

Table 2. Analytical conditions for clay extract analyses*

Element	Wavelength, nm	Row number	Hole number	Filter	Observation height, cm
Ca	422.7	1	1	430 nm	4.3
Na	589.0	2	11	589.6 nm bandpass, 0.3 absorbance neutral density	3.0
Li	670.7	3	16	none	3.0
K	766.5	4	23	none	3.0

*Acetylene flow-rate 6.3 l./min; nitrous oxide flow-rate 9.5 l./min; fiber-optic light guides 10.3 cm from burner.

jacket were employed for the transmission of visible radiation, and quartz bundles (Welch Allyn, Inc.) were employed for the transmission of ultraviolet radiation.

RESULTS AND DISCUSSION

Multiple-track spectra

Figure 3 shows a photograph (obtained by using the MESS system operating in the two-dimensional mode) of a multiple track spectrum of the neon lines emitted by a hollow-cathode lamp. Three entrance slits were employed, each having a different row co-ordinate in the 6×29 array of holes shown in Fig. 2.

To achieve vertical separation between tracks, the two-dimensional MESS takes advantage of the stigmatic nature of the Czerny–Turner dispersion system, which focuses in both the horizontal and vertical directions. Thus, for a fixed grating position, the locus of an entrance slit image in the exit focal plane depends not only

on the wavelength of the incident radiation, but also on the vertical displacement of the entrance slit from the optical axis of the Czerny–Turner mirror system. Entrance slits vertically displaced above the optical axis of the mirror system will focus at a similar displacement below the optical axis in the exit focal plane. Conversely, entrance slits located below the optical axis will produce spectral tracks above the optical axis in the exit focal plane.

Optical characteristics of the system

Vertical cross-talk. A potential difficulty which could be associated with the two-dimensional MESS is the appearance of a spurious signal on a track, caused by the presence of a very intense signal on an adjacent track. This vertical cross-talk could result from blooming on the target or be due to optical aberrations in the system causing the light beam to spread in the vertical dimension as it passes through the monochromator.

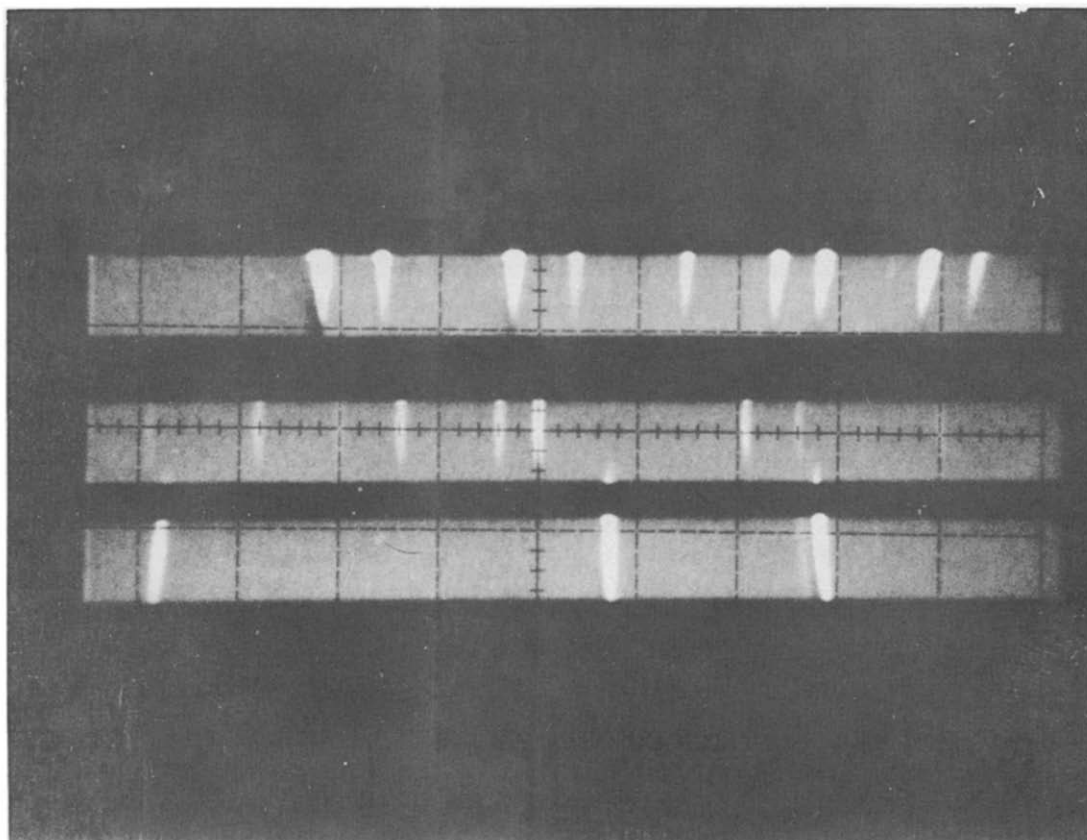


Fig. 3. Spectrum of neon lines emitted by a hollow-cathode lamp, obtained with the multiple entrance-slit spectrometer operating in the two-dimensional mode. Spectrum obtained by using three entrance slits, each having a different row co-ordinate, and the detector operating in a multi-raster scanning pattern. Reprinted with permission from K. W. Busch and L. D. Benton, *Anal. Chem.*, 1983, **55**, 445A. Copyright 1983, American Chemical Society.

To evaluate the potential severity of this effect, the vertical cross-talk between two adjacent tracks was monitored by observing the signal produced in one track when the mercury 546.0 nm line was imaged on the adjacent track. The percentage of vertical cross-talk, defined as

$$C = 100(S_d/S_i) \quad (1)$$

where S_d is the signal on the non-illuminated track and S_i is the signal on the illuminated track, was measured as a function of S_i . The intensity of the mercury line on the target was increased in a known manner by removal of a series of neutral density filters from the light-path. Since the absorbance of the filters was known, the relative intensity in the illuminated track was known. This relative intensity was used to calculate the effective S_i , even though the actual signal from the vidicon could not be monitored at the higher intensities because it would be beyond the range of the A/D converter in the OMA. S_d was taken as the signal relative to adjacent background in the non-illuminated track in the channel where the vertical cross-talk from the mercury line was expected. S_d was taken as zero when the ratio of the signal to adjacent rms background was less than 3.

Vertical cross-talk was evaluated for the particular vertical separation between adjacent rows of holes in the multiple entrance-slit assembly shown in Fig. 2. With this configuration, each spectral track was approximately 1 mm high in the exit focal plane, and there was approximately 1 mm separation between tracks. With this vertical separation between adjacent tracks, cross-talk was found to be negligible until the Hg intensity reached 3.4×10^6 counts. At this intensity, the signal in the dark track measured 76 counts, resulting in a vertical cross-talk of 0.002%.

Stray light. The stray light level is an important characteristic of any spectrometric system. The presence of stray light, which originates from the dispersive system as a result of scatter from optical components or walls, is revealed by an elevation of the background level. The presence of stray light in the system was monitored as a function of the incident intensity by measuring the average background level in a non-illuminated track while the mercury 546.0 nm line was imaged on an adjacent track. The mercury line intensity was varied in a known manner with neutral density filters, and the effective digital signal was calculated from this information for those intensities which exceeded

the capabilities of the OMA. Figure 4 shows the variation in the stray light level as a function of incident intensity. Since the percentage of stray light, defined as

$$L = 100(I_s/I_0) \quad (2)$$

where I_s is the stray light intensity and I_0 is the incident intensity, was of the order of 0.12%, baffles were installed in the monochromator, as shown in Fig. 5, in an effort to reduce the stray light level. The baffles were placed to reduce the possibility that light could escape from the desired path in the monochromator and reach the detector without being dispersed by the grating. Figure 4 shows the effect of the baffles on the stray light level. Although the baffles do not eliminate stray light, they do reduce the background level by 200 counts or more.

Resolution and vignetting. For a system with a triangular slit function, two lines will be theoretically completely resolved if they are separated by at least twice the spectral bandwidth of the system. Thus, the spectral bandwidth, which is equivalent to the width of an isolated spectral line at half the maximum intensity, is a measure of the resolution of the system. For an ideal system with a triangular slit function, the half-intensity bandwidth should equal half the peak width at the baseline.

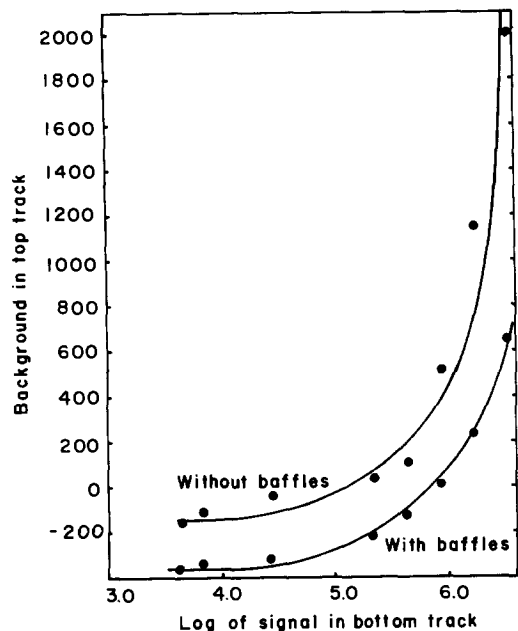


Fig. 4. Effect of baffles on stray light. Points on the graph represent the average background level in a non-illuminated (top) track as a function of the intensity of the Hg 546.0-nm line in the adjacent (bottom) track. Position of the baffles is shown in Fig. 5.

Figure 6 shows the variation in peak width (in channels), peak height, and peak area at various positions across the target with a three-track system. A $25\ \mu\text{m}$ wide entrance slit was used to image the mercury 546.0 nm line onto the detector at various positions across the target, and the signal was accumulated for 100 cycles in each case. The line was moved across the target by varying the grating angle.

The peak width is a measure of the spectral bandwidth of the system at that location on the target and is therefore an indication of the resolution of the system at this point. Peak height and peak area are both indicative of the total intensity striking the target at the various positions. It can be seen from Fig. 6 that all three responses are degraded near the edges of the target. The reduction in resolution toward the edges of the target arises from two potential sources: (1) degradation in detector resolution at the edges of the target, owing to pin-cushion distortion in the SIT by the electrostatically focused image intensifier section, and (2) degradation in resolution at the edges of the target because the focal plane of the monochromator is curved but the detector surface is flat. Of the two sources of broadening, pin-cushion distortion with the SIT is the major cause of loss in resolution at the target edges.²

Figure 6 also reveals a loss in intensity at the edges of the target owing to vignetting in the system. Since the Spex 0.5 m monochromator is being used in the reverse of the way in which it was intended,¹⁶ the smaller collimating mirror is being used in this system as the focusing mirror. Since this mirror is not very wide, some vignetting undoubtedly occurs at this point in the system. Another potential source of vignetting, which was not measured in this experiment,

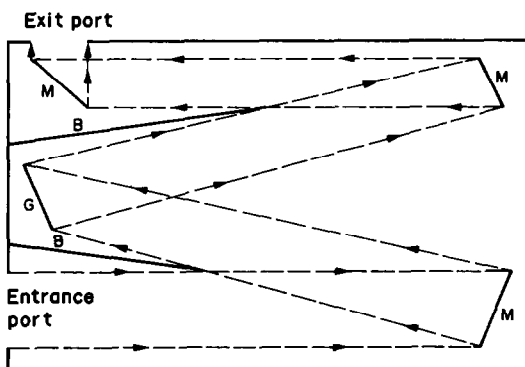


Fig. 5. Schematic diagram of the Czerny-Turner monochromator, showing placement of baffles. Mirror (M); grating (G); baffle (B).

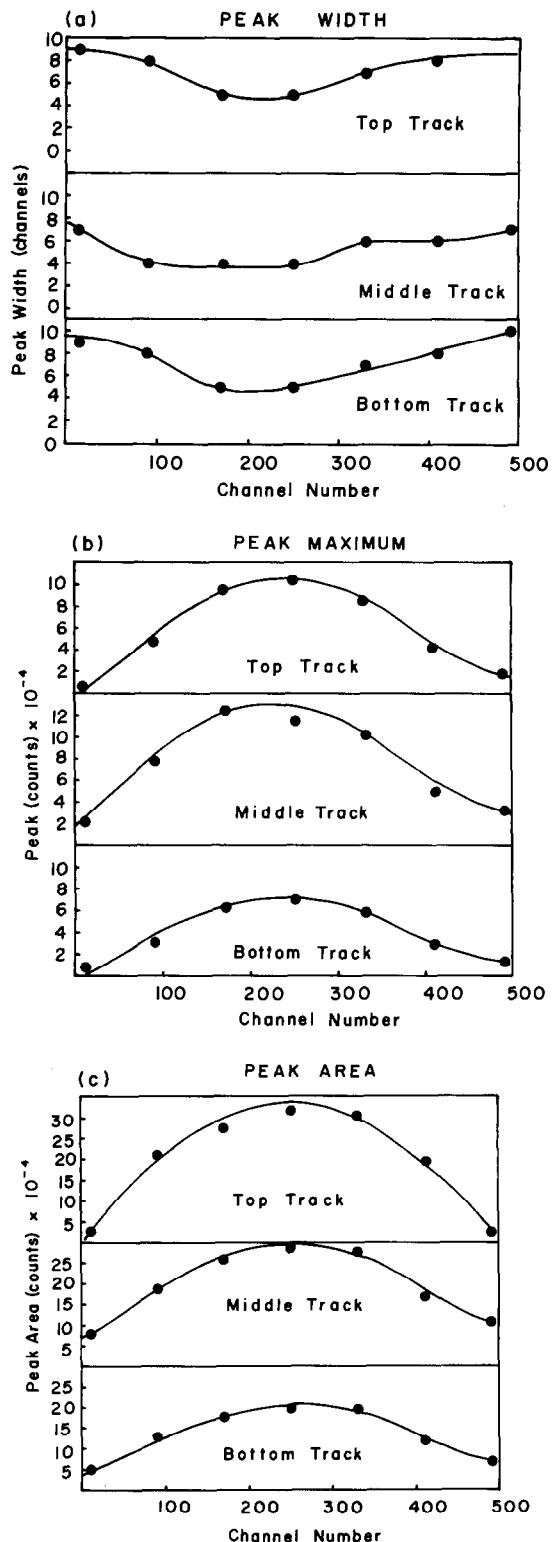


Fig. 6. Variation in resolution and signal intensity across the SIT vidicon target for a two-dimensional multiple entrance-slit spectrometer employing three tracks. Each point represents the signal parameter associated with the Hg 546.0 nm line, accumulated for 100 accumulation cycles. (a) Peak width vs. channel number; (b) peak height vs. channel number; (c) peak area vs. channel number.

might occur for entrance slits at the extreme ends of a horizontal row in the multiple entrance-slit assembly. If the collimating mirror is unable to intercept enough radiation from these slits to fill the grating, an attenuation in intensity will be observed for spectral segments originating from these extreme entrance slits.

Performance characteristics of the system

Linearity. Linearity of response was evaluated near the center of the target in three tracks, by using the mercury 546.0 nm line emitted from a pen lamp, and its attenuation by a series of neutral density absorbance filters. The background-corrected signal corresponding to 20 accumulations was obtained with each filter. The mercury line intensity was varied from an intensity giving a signal just below system overload to an intensity giving a value of 3 for the ratio of signal to rms of adjacent background. Figure 7 shows a plot of the logarithm of the relative signal *vs.* filter absorbance, the relative signal being the intensity ratio of the signal to the most intense signal in the track.

The variation of signal current with incident intensity for a vidicon tube is determined by the value of γ in the following transfer equation,²⁶

$$i_s = KI^\gamma \quad (3)$$

where i_s is the signal current, K is a proportionality constant, I is the intensity incident on the tube target, and γ is a constant characteristic of the tube. Typical gamma values for various electro-optic devices vary from about 0.5 to 1.0, depending on the particular photosensitive layer

employed in the tube.²⁶ Although a one-to-one correspondence between signal output and light input will exist regardless of the actual value of gamma, there will be true linearity of response only for electro-optic devices with a gamma of unity. Starting with equation (3), it is easy to show that

$$\log(N/N_{\max}) = -\gamma A \quad (4)$$

where N is the signal level (in counts), N_{\max} is the signal level with no filter in the path, and A is the absorbance of the neutral density filter. The least-squares slope for all three lines in Fig. 7 was found to be -0.9 , which indicates a gamma value of 0.9 for the SIT tube. Since the expected value for gamma for an SIT vidicon is normally 1, the low measured value reported here may indicate a lag problem with the tube used in this study.

S/N performance in single-track and multi-track modes. To compare the signal-to-noise (S/N) performance of the system under different target interrogation scan patterns, the S/N of the sodium 589 nm line was measured as the scanning pattern on the target was varied from single-raster to six-raster scanning. For this experiment, the multiple entrance-slit assembly was replaced by a conventional straight entrance slit, with its height adjusted to 2 cm so that the spectrum was imaged over the entire vertical dimension of the target.

The points plotted in Fig. 8 show the measured S/N produced when a solution containing 0.01 ppm sodium was aspirated into an air/acetylene flame under different scanning

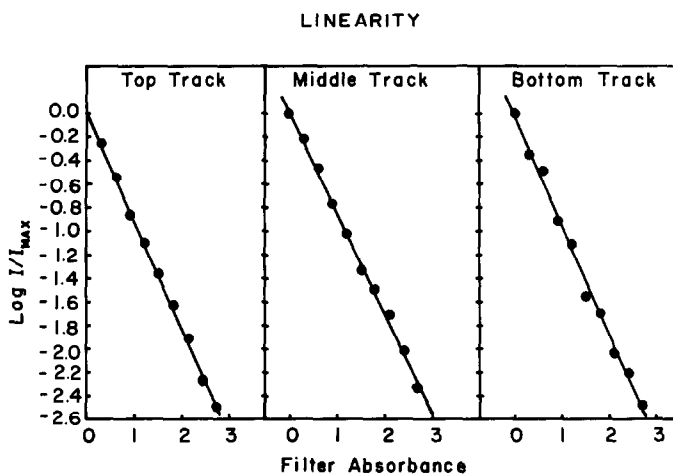


Fig. 7. Linearity of target response for a two-dimensional multiple entrance-slit spectrometer employing three tracks. Each point represents the background-corrected signal associated with the Hg 546.0 nm line imaged near the center of the target. Twenty accumulations were made with each filter in place.

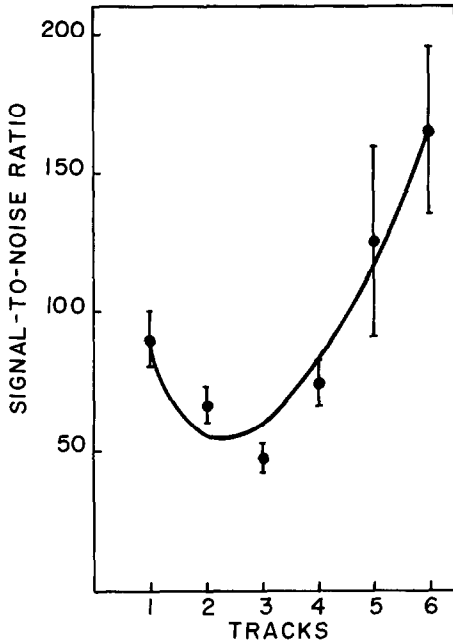


Fig. 8. Influence of the number of tracks on signal-to-noise ratio. The points represent the S/N of the 589.0 nm Na line as a function of the number of tracks employed by the two-dimensional multiple entrance-slit spectrometer. Bars represent one standard deviation. The full line is a plot of equation (5) for $k_1 = 90$, $k_2 = 5$, and $n =$ the number of tracks.

conditions. S/N measurements in the multi-raster mode correspond to the S/N observed from one of the multiple tracks.

The observed variation in S/N can be shown to follow an empirical equation of the following form reasonably well,

$$(S/N)_n = (k_1/n) + k_2 n(n-1) \quad (5)$$

where $(S/N)_n$ is the signal-to-noise ratio for n tracks, and k_1 and k_2 are constants. The full line in Fig. 8 is a plot of equation (5) with $k_1 = 90$ and $k_2 = 5$. This functional dependence of S/N can be qualitatively rationalized as a combination of three factors. (1) As the number of tracks increases, the track height decreases, decreasing the number of pixels available for detection of the radiation. This factor causes the S/N to vary inversely with the number of tracks. (2) As the number of tracks increases, the integration period between successive passes of the electron beam over an individual track increases. This factor causes the S/N to increase directly with the increased integration time. The increase in the integration time varies as $(n-1)$. (3) As the track height decreases, the dwell time of the electron beam on the individual pixels increases. This occurs because the electron beam

does not have to cover as large a vertical deflection during the channel scan period of $64 \mu\text{sec}$. The result is a more complete erasure of the charge developed on the target during the integration period, causing the S/N to increase directly with the number of tracks employed.

One-dimensional MESS operation

Blood serum analysis. Figure 9 shows the spectrum obtained with the system in the single-raster mode for a $50\text{-}\mu\text{l}$ injection of blood serum. Although in this case the same results could have been obtained by using only one horizontal row in the two-dimensional array shown in Fig. 2, the original entrance plate¹⁶ with a single row of 22 holes placed 5 mm apart was employed as the linear multiple entrance-slit array. Four fiber-optic light guides were used to transmit radiation to four appropriately

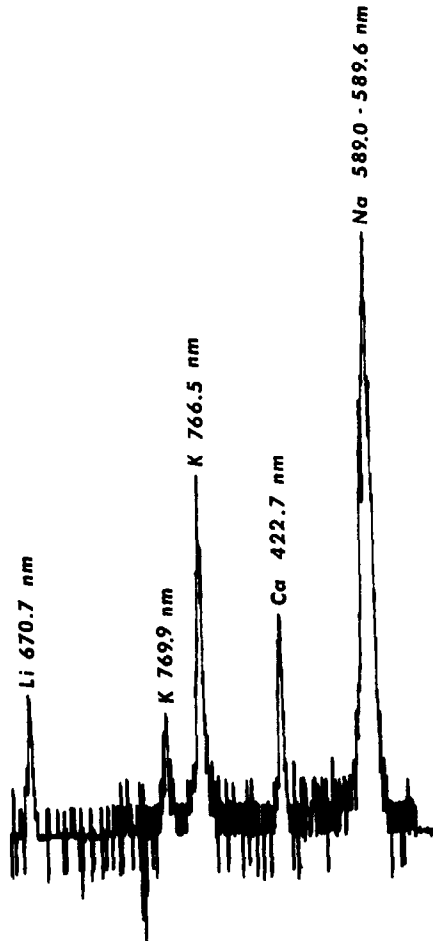


Fig. 9. Spectrum of blood serum, obtained with the one-dimensional multiple entrance-slit spectrometer. The spectrum is a composite of four spectral windows, each window containing one element of interest.

placed entrance slits so that the primary resonance line of each element was simultaneously imaged on the target. Table 1 shows the analytical conditions employed in the determination. Filters were used to modify different regions of the spectrum individually so that the system was not overloaded.

As pointed out previously,¹⁶ one of the advantages of the MESS is its ability to vary the intensity of each line individually. This feature has been utilized in this determination of blood serum to modify individually the intensities originating from the sodium and calcium fiber optics. A 589.6 nm narrow bandpass filter and a 0.9 absorbance neutral density filter were placed in front of the fiber optic monitoring the sodium region of the spectrum, to reduce the sodium intensity to a point where the system was not overloaded. At the same time, a 430 nm narrow bandpass filter, transmitting the calcium line, was placed in front of the fiber optic monitoring the calcium region of the spectrum, to reduce the high flame background from the nitrous oxide/acetylene flame.

Results of the serum analysis, performed in the one-dimensional mode, are given in Table 3. The values given are the averages from 10 injections for each standard and sample.

Table 4 shows a comparison of blood serum results obtained by the one-dimensional MESS system with those obtained by use of several other simultaneous multichannel spectrometers. Several points of comparison should be noted. (1) Of the vidicon systems, only the one-dimensional MESS is able to monitor the primary lines of all pertinent elements simultaneously in the first order. (2) No sacrifice in resolution is necessary to include lithium as an internal standard in the MESS system. (3) For those systems which were analyzed for accuracy and precision, MESS has the worst average precision (11%), but the best average accuracy (0.9%). The lack of precision is probably due to two factors: the use of an internal standard, and the sample introduction system.

Internal standardization depends on taking the ratio of the signals for two different elements, the internal standard and the analyte. Since the internal standard is not viewed in the same place in the flame as the analyte line, both signals vary completely independently, and the variation in their ratio is greater than the variation in either signal separately. Thus, while internal standardization improves the accuracy of the determination, it degrades the precision.

The sample introduction system used in this study is an injection method; hence, the signal incident on the detector increases and then decreases during the accumulation time. Since a steady-state signal is never achieved during the measurement time, the advantages of signal averaging are lost and precision is degraded below that of a steady-state measurement.

Influence of overlapping spectra on S/N. In one-dimensional MESS operation, composite spectra are produced by focusing more than one signal on the same detector element. Depending on the noise characteristics of the system, multiplexing could result in deterioration of the S/N of the composite spectrum. Therefore, an additional factor which should be considered in evaluating the one-dimensional MESS system is the effect of overlapping windows on the S/N of the analyte line.

Table 5 shows the results of evaluation of the overlap of two windows, one containing the Li 670.7 nm line from a hollow-cathode lamp and the other containing the Hg 546.0 nm line from a pen lamp. Although the Hg signal was varied from one tenth of that required for detector overload to 90 times the overload value, the S/N for Li remained constant even with Hg signals well above the overload condition.

Table 6 shows the results of evaluation of the overlap of two windows, one containing the Na 589.6 nm line produced by aspirating a 0.1 ppm solution of Na into an air/acetylene flame and the other containing the Hg 546.0 nm line from a pen lamp. Although increased Hg

Table 3. Results of serum analysis

Element*	Result†	"True" value	Relative std. devn., %	Relative error, %
Ca	10.5 mg/dl	10.3 mg/dl	11	1.9
Na	142 meq/l.	141 meq/l.	12	0.7
K	5.1 meq/l.	5.1 meq/l.	11	0

*Analytical conditions given in Table 1; Li used as internal standard.

†Average of 10 determinations.

Table 4. Comparison of serum analyses

Method	Wavelength, <i>nm</i>	Resolution, <i>nm/mm</i>	Dilution	Sample size, μ l	Relative std. devn., %	Relative error, %	Reference
Time multiplex multiple grating	Ca 422.7	varies with grating	1:100	not given	Ca 3.0	not given	28
	Na 589.5				Na 0.2		
	Li 670.7*						
	K 766.0				K 0.1		
Programmed scanning monochromator	Ca 422.7	not given	1:25	not given	Ca 1-2	not given	29
	Na 330.3				Na 2-3		
	Li 670.7				Li 1-2		
	K 404.4				K 3-5		
Vidicon, one window	Ca 422.7†	3.2	none	200	Ca 1.7	Ca 1.1	15
	Na 819.5				Na 0.64	Na 1.4	
	K 404.4†				K 1.4	K 1.2	
Vidicon, one window	Ca 422.7	5.6	none	25	Ca 2.2	Ca 0.9	30
	Na 819.5				Na 2.8	Na 1.2	
	Li 670.7				Li 1.6	Li 0.4	
	K 766.5				K 1.4	K 1.6	
1-D MESS	Ca 422.7	3.2	1:2	50	Ca 11	Ca 1.9	§
	Na 589.0				Na 12	Na 0.7	
	Li 670.8*						
	K 766.5				K 11	K 0	

*Internal standard.

†Second order.

§This work.

intensity does raise the background levels, there is no significant decrease in the S/N of the Na line, even under detector overload conditions.

In practice, signals would rarely be allowed to overload the detector, since intensities in multi-element samples can be adjusted through the use of filters, selection of alternative analyte lines, or adjustment of solution concentrations. Hence, it can be concluded that little or no loss in S/N would arise in one-dimensional MESS operation as a result of the overlap of several spectral windows, provided the analyte lines are well-resolved and are overlapped only by signals resulting from relatively weak background emis-

sion. The case of overlap of analyte lines with relatively strong background emission was not considered, since such situations could mostly be avoided either by moving the fiber-optic light guides and selecting an alternative arrangement of entrance slits or by operating the MESS in a two-dimensional mode. Of course, interference by intense flame bands or spectral lines in the same wavelength region as the analyte line could not be eliminated in this manner, but would still be amenable to removal by spectral stripping.²⁷ However, under shot-noise-limited conditions, the presence of intense flame bands in the overlapped spectra would be expected to produce a multiplex disadvantage since the shot noise which results cannot be removed by spectral stripping.

Table 5. Evaluation of effect of spectral overlap on S/N (no flame)

Mercury signal,* <i>counts</i>	Filter absorbance	Li†, S/N
90 × overload	0	6.7
46 × overload	0.3	14.4
23 × overload	0.6	16.2
11 × overload	0.9	17.5
7.2×10^4	1.2	17.3
3.6×10^4	1.5	17.3
1.8×10^4	1.8	19.5
9.0×10^3	2.1	17.4
5.4×10^3	2.4	17.2
3.2×10^3	2.7	17.1
1.6×10^3	3.0	18.5

*546.0 nm.

†670.7 nm.

Table 6. Evaluation of spectral overlap on S/N under flame conditions

Mercury signal,* <i>counts</i>	Filter absorbance	Na†, S/N §	Na background, <i>counts</i>
overload	0.3	17.3 ± 4.3	266
overload	0.9	18.5 ± 4.9	107
5.2×10^4	1.5	15.7 ± 4.9	55
2.4×10^4	2.1	21.3 ± 3.3	8
6.8×10^3	2.7	20.8 ± 5.3	4
0	—	16.0 ± 4.0	-4

*546.0 nm.

†589.6 nm.

§Average of 10 measurements.

Two-dimensional MESS operation

Clay extract analysis. Figure 10 shows the spectrum obtained for the system in the multiple-raster mode when clay extract was aspirated directly into the flame by a nebulizer assembly. An entrance plate with 5 rows of 22 holes, the holes placed 5 mm apart, was employed as the multiple entrance-slit array. Four fiber-optic light guides were used to transmit radiation to four appropriately placed entrance slits so that four spectral segments, each containing a primary resonance line of one of the four analytes, were simultaneously imaged on the target, one under the other. Table 2 shows the analytical conditions employed in the determination. Filters were used for individual modification of different regions of the spectrum so that the system was not overloaded.

Table 7 gives the results obtained for the determination of four exchangeable cations in

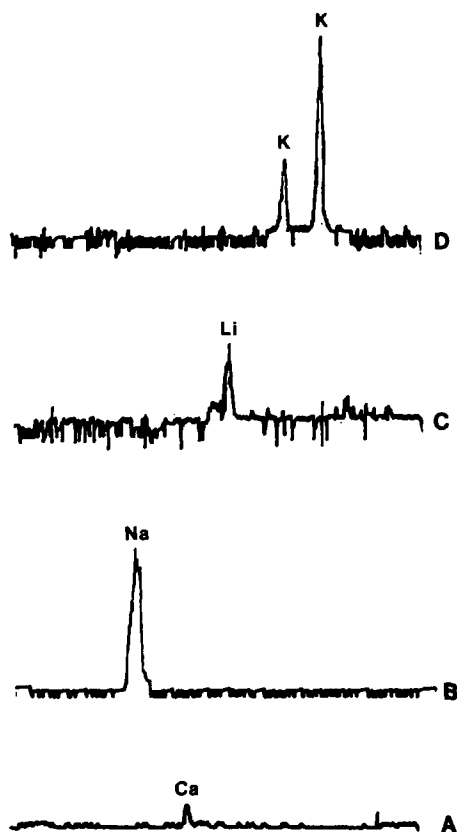


Fig. 10. Spectrum of clay extract, obtained with the two-dimensional multiple entrance-slit spectrometer. Four separate tracks (A–D) are used to monitor four different spectral windows, each window containing one element of interest. Track A, 422.7 nm Ca line; B, 589.0 nm Na line; C, 670.7 nm Li line; D, 769.9 and 766.5 nm K doublet. Signals in tracks A and B are amplified by a factor of ten relative to those in tracks C and D.

Table 7. Results of clay analyses*

Sample	Concentration found, meq/g†			
	Ca	Na	Li	K
1A	0.33	0.025	0.00016	0.0082
2A	0.075	0.013	0.00012	0.0087
3A	0.19	0.010	0.000048	0.015
4A	0.20	0.014	0.000053	0.012
5A	0.044	0.011	0.000076	0.0046

*Analytical conditions given in Table 2.

†Average of 5 determinations.

five different clay samples, by the extraction procedure of Chhabra *et al.*²³ Although it is clear from the results that the five clay samples showed widely different levels of extractable Ca, Na, Li and K, it is impossible to assess the accuracy of these results by using only the information contained in Table 7.

Since no reference standard clay was available to check the accuracy of these determinations, a series of recovery experiments^{24,25} was conducted. Table 8 shows the results of these recovery experiments on the combined extracts resulting from two extractions of each of the five clay samples. It should be noted that spiking the extract solutions excluded the bias of the extraction procedure from the variation in recovery.

If the analyses reported in Table 7 were completely accurate, spiking the extracts with known amounts of the extractable cations should have given recoveries (Table 8) of 100%. The overall average recovery for all four elements was in fact 98.5%, a value which is quite good. However, it is also clear from the individual recoveries that the results for calcium and potassium tended to be somewhat high, and those for sodium and lithium somewhat low. These results suggest that, on average, the slopes of the calibration curves for calcium and potassium were lower than they should have been, while for sodium and lithium, the opposite was true. For calcium, the high recoveries seem to be concentration-dependent (see Tables 7 and 8), the clays containing lesser amounts of exchangeable Ca giving higher recoveries. For potassium, recoveries greater than 100% were obtained regardless of the amount of exchangeable K present in the clay. By contrast, low recoveries were obtained for sodium, regardless of the level of exchangeable Na ions present.

While it is clear that some small bias exists in the determination of these four ions in clay extracts, the errors involved are small and are common to any flame analysis procedure. Thus, the errors are not a result of using the multiple

Table 8. Results of recovery experiments*

Sample No.	Ca			Na			Li			K		
	Expected, ppm	Found, ppm	Recovery, %	Expected, ppm	Found, ppm	Recovery, %	Expected, ppm	Found, ppm	Recovery, %	Expected, ppm	Found, ppm	Recovery, %
1B	127	107	84	4.4	4.2	95	0.031	0.031	100	5.2	5.4	104
2B	27	31	115	4.9	4.5	92	0.028	0.025	88	5.4	5.6	104
3B	68	68	100	4.4	3.9	89	0.013	0.013	100	9.8	10	102
4B	71	71	100	5.2	4.8	92	0.014	0.013	93	8.6	9.4	109
5B	17	19	113	4.5	4.2	93	0.015	0.014	93	3.8	4.0	105
Average recovery %			102 ± 12			92 ± 2			95 ± 5			105 ± 3

*Analytical conditions given in Table 2.

entrance-slit spectrometer, but arise in the flame source itself as a result of matrix effects encountered with real samples.

Detection limits. Table 9 gives the multielement detection limits obtained for Ca, Li, Na and K under the clay-analysis conditions with the two-dimensional MESS system. As might be expected, two of these detection limits are significantly degraded relative to those obtained with an SIT vidicon in a single-raster mode, for single-element aqueous solutions²⁰ (also shown in Table 9 for comparison). Several factors undoubtedly contribute to these differences in detection limits, including attenuation of the signal by the fiber-optic light guides, the decreased number of pixels available to monitor a particular line when multiple tracks are employed, alteration in flame conditions resulting from the presence of additional ions and organic solvents in the multielement clay sample, and the use of filters in the case of Ca and Na (the two elements most strongly affected). Nevertheless, in spite of the poorer detection limits, the two-dimensional MESS system is still quite adequate for the determination of trace elements in real samples.

Detection limits possible for two-dimensional MESS operation with single-element aqueous solutions are shown in Table 10. Except for Cu, Al and Fe, all measurements were made by use of fiber-optic light guides composed of plastic (Crofon) bundles with a light-gathering lens attached to the end of the fiber closest to the flame. The effects of the lens, and composition and length of the fiber-optic light guide on detection limits for Ca are shown in Table 11. As can be seen from these data, the detection limits are improved by using shorter lengths of the quartz-fiber optic and omitting the light-gathering lens.

CONCLUSIONS

For performing multielement analyses, the MESS switchboard system allows the spectro-

Table 9. Detection limits for clay analysis conditions*

Element	Detection limit, ppm
Ca	0.17
Na	0.0051
Li	0.00064
K	0.056

*Analytical conditions given in Table 2.

Table 10. Single-element detection limits (D.L.) for the two-dimensional MESS system

Element	Wavelength, <i>nm</i>	Track*	Hole number	D.L. for MESS,† <i>ppm</i>	D.L. for SIT,§ <i>ppm</i>
Ba	553.6‡	1	16	0.14	0.001
Ca	422.7‡	3	5	0.022	0.0001
Cr	425.4‡	3	5	0.18	0.002
Li	670.7‡	2	25	0.014	0.00001
Na	589.0‡	2	18	0.0078	0.0002
Sr	460.7‡	3	9	0.055	0.0002
Mn	403.0‡	3	5	0.10	0.003
Cu	324.7 #	1	4	0.62	—
Al	396.2 #	1	4	0.034	0.01
Fe	386.0 #	1	4	0.08	0.01

‡This work; average of 5 determinations.

*Since spectral images are inverted, fiber-optic light guides positioned in row 4 give spectra which appear on track 1, *etc.*

†12-mm plastic (Crofon) fiber-optic light guide.

§Reference 20.

12-mm UV fiber-optic light guide.

scopist the freedom to arrange various combinations of elements in the most efficient manner on a detector target of limited size. For detectors which permit a two-dimensional scan pattern, the two-dimensional multiple entrance-slit array offers maximum flexibility. When only one horizontal row of slits is used, various combinations of fiber-optic light guides can be plugged into the entrance plate to build up a composite spectrum such that the analytical wavelengths of interest are imaged simultaneously on the detector with minimum interference from emissions by other sample constituents. Since all slits are active simultaneously, the composite spectrum is simultaneously integrated, allowing the system to be used in situations limited by source fluctuation noise or shot noise situations, or even with time-varying sources. Although the composite spectrum may not be arranged in order of increasing wavelength, all that is necessary for the analysis is to know which detector channels are associated with a particular analyte line. Use of only one track in the slit array also permits the detector to be operated in a single-raster mode, allowing maximum utilization of the detector in the vertical direction and thereby maximizing the sensitivity of the system.

Bystroff *et al.*³¹ have developed a statistical model, based on Poisson statistics, which predicts that even when the number of chemical elements in a multielement sample exceeds 25, the chances are good that all can be determined in a single measurement with a 1000-element linear array detector. However, in those cases where overlap of analyte lines

cannot be avoided, the multielement analysis can still be performed by operating the MESS system in a two-dimensional mode. For two-dimensional operation, windows with overlapping analyte lines can be plugged into different rows of entrance slits, the detector is operated in a multiple-raster mode, and the spectral regions are stacked one above the other.

A possible disadvantage with two-dimensional operation is a trade-off in sensitivity. The larger the number of tracks employed, the smaller the number of vertical detector elements which can be utilized for a particular spectral line in a given window. Loss in sensitivity can be minimized, however, by minimizing the number of tracks required for each multielement analysis. This is readily accomplished with the two-dimensional MESS system by plugging more than one fiber-optic light guide into each horizontal row of slits and maximizing the number of analytically useful lines observed in each track. An example where such an arrangement might be beneficial is a multielement sample in which the wavelengths of interest are spread out over a wide spectral region. In such a case, one track might be used to monitor a single window in the short-wavelength end of the spectrum, where

Table 11. Influence of system parameters on Ca 422.7 nm detection limit

Fiber optic composition	Lens	Fiber length, <i>mm</i>	Detection limit, <i>ppm</i>
Plastic	Yes	12	0.022
Plastic	No	12	0.0053
Quartz	No	12	0.0031
Quartz	No	60	0.017

lines are closely spaced and the potential for overlap in a composite spectrum is relatively high. A second track could then be used to monitor a composite spectrum consisting of many windows in the long-wavelength end of the spectrum, where the lines are less dense and the potential for overlap in a composite spectrum is relatively low.

Another important advantage of the MESS switchboard is the ability to modify the intensities of various spectral features to avoid target saturation and blooming. Since typically each chemical element (or at most 2 or 3 chemical elements) will be monitored by an individual fiber-optic light guide, individual adjustment of the intensities transmitted by each light guide can be achieved in a number of ways. For example, a variable neutral density filter can be used to attenuate the line or lines transmitted by a particular fiber-optic light guide, without simultaneously attenuating the radiation transmitted by other light guides. Alternatively, the size of the entrance slits can be individually adjusted to alter the intensity of lines in a particular window without affecting the intensity of lines present in other spectral windows. Finally, very intense lines can simply be moved off the detector target by moving the light guide to a new position in the entrance slit array and selecting a weaker analytical line. Additional light guide parameters which can be individually varied include observation height in the flame, the length of the light guide, and the composition of the fiber-optic material.

It should be emphasized that the MESS system described in this study is only a prototype, and a number of design changes would undoubtedly result in significant improvement in the detection limits reported here. For example, an updated system would employ UV-transmitting fiber-optic light guides, a more sophisticated entrance-slit array (i.e., a curved focal plane with regularly spaced, adjustable entrance slits), a concave grating spectrometer, and a charge-coupled device as detector. Even without these improvements, the general utility of the system is apparent, and the potential for application to real multielement samples has been demonstrated.

Acknowledgements—The authors would like to thank Mr. Clyde Moorehead of the Baylor University machine shop for assistance in fabricating the multiple entrance-slit array and fiber-optic lens holder, and Mr. George Harris of the Baylor Geology Department for assistance with the clay

analyses. Financial support from the American Petroleum Research Fund, administered by the American Chemical Society, and from the Robert A. Welch Foundation, Houston, Texas, is gratefully acknowledged. Special thanks are due to Baylor University for support in the form of summer sabbaticals for two of the authors, M. and K. Busch.

REFERENCES

1. K. W. Busch and M. A. Busch, *Multielement Detection Systems for Spectrochemical Analysis*, Wiley, New York, 1989.
2. K. W. Busch and B. Malloy, in *Multichannel Image Detectors*, Y. Talmi (ed.), pp. 27–58. American Chemical Society, Washington, D.C., 1979.
3. G. Horlick, R. H. Hall and W. K. Yuen, in *Fourier Transform Infrared Spectroscopy*, Vol. 3, J. R. Ferraro and L. J. Basile (eds.), pp. 37–81. Academic Press, New York, 1982.
4. D. Tilotta, R. C. Fry and W. G. Fateley, *Talanta*, 1990, **37**, 53.
5. G. R. Harrison, R. C. Lord and J. R. Loofbourow, *Practical Spectroscopy*, Prentice-Hall, Englewood Cliffs, NJ, 1948.
6. M. F. Hasler and H. W. Dietert, *J. Opt. Soc. Am.*, 1944, **34**, 751.
7. K. W. Busch and L. D. Benton, *Anal. Chem.*, 1983, **55**, 445A.
8. Y. Talmi, *ibid.*, 1975, **47**, 658A and 697A.
9. G. Horlick, *Appl. Spectrosc.*, 1976, **30**, 113.
10. P. M. Epperson, J. V. Sweedler, R. B. Bilhorn, G. R. Sims and M. B. Denton, *Anal. Chem.*, 1988, **60**, 327A.
11. G. R. Sims and M. B. Denton, *Talanta*, 1990, **37**, 1.
12. R. S. Pomeroy, J. V. Sweedler and M. B. Denton, *Talanta*, 1990, **37**, 15.
13. K. W. Busch, N. G. Howell and G. H. Morrison, *Anal. Chem.*, 1974, **46**, 575.
14. P. N. Keliher and C. C. Wohlers, *ibid.*, 1976, **48**, 333A.
15. K. W. Busch, N. G. Howell and G. H. Morrison, *ibid.*, 1974, **46**, 1231.
16. K. W. Busch, B. Malloy and Y. Talmi, *ibid.*, 1979, **51**, 670.
17. K. W. Busch, 1983, *U.S. Patent*, No. 4,375,919.
18. V. Karanassios and G. Horlick, *Appl. Spectrosc.*, 1986, **40**, 813.
19. K. R. Brushwyler, N. Furuta and G. M. Hieftje, *Talanta*, 1990, **37**, 23.
20. N. G. Howell and G. H. Morrison, *Anal. Chem.*, 1974, **49**, 106.
21. K. W. Busch, 1985, *U.S. Patent*, No. 4,494,872.
22. Y. Talmi, 1981, *U.S. Patent*, No. 4,259,014.
23. R. Chhabra, J. Pleyzier and A. Cremers, *Proc. Intern. Clay Conf.* 1975, p. 439; *Chem. Abstr.*, 1976, **85**, 176043k.
24. R. M. Dagnall, G. F. Kirkbright, T. S. West and R. Wood, *Anal. Chem.*, 1971, **43**, 1765.
25. *Handbook for Analytical Quality Control in Water and Wastewater Laboratories*, Chapter 6, pp. 6–3, 6–4. Analytical Quality Control Laboratory, National Environmental Research Center, Cincinnati, OH, 1972.

26. R. E. Johnson, *Application of RCA Silicon Diode Array Target Vidicons, RCA Camera Tube Application Note, AN-4623*.
27. K. W. Busch, N. G. Howell and G. H. Morrison, *Anal. Chem.*, 1974, **46**, 2074.
28. A. Johansson and L. E. Nilsson, *Spectrochim. Acta*, 1976, **31B**, 419.
29. R. W. Spillman and H. V. Malmstadt, *Anal. Chem.*, 1976, **48**, 303.
30. N. G. Howell, J. D. Ganjei and G. H. Morrison, *ibid.*, 1976, **48**, 319.
31. R. Bystroff, T. Hirschfeld and J. Pesek, *Pittsburgh Conference on Analytical Chemistry and Applied Spectroscopy*, 1980, paper No. 338.

DESIGN AND EVALUATION OF A NEW PROGRAMMED-SCAN SPECTROMETER FOR MULTIELEMENT DETERMINATIONS BY ATOMIC EMISSION

KENNETH W. BUSCH*, MARIANNA A. BUSCH and LARRY D. BENTON†

Department of Chemistry, Baylor University, Waco, TX 76798, U.S.A.

(Received 29 March 1989. Accepted 21 April 1989)

Summary—A new type of programmed-scan monochromator that employs a multiple entrance-slit dispersion system with stationary dispersion optics has been assembled and tested. The instrument uses an optical multiplexer, connected to the multiple entrance-slit spectrometer (MESS) by means of fiber-optic light guides, to illuminate up to eight entrance slits sequentially. A single high-sensitivity relatively inexpensive photomultiplier tube is used as the detector. A microcomputer interfaced with the detector is used to acquire data at a rate of approximately 4 sec per element and to control the optical multiplexer. Detection limits obtained from atomic emission measurements with an acetylene/air flame excitation source are reported for lithium, sodium, calcium, barium and strontium. The influence of signal averaging and sampling rate on system performance has been studied, and it was found that the delay time had essentially no influence on the measured signal-to-noise ratio.

The development of multielement detection systems for spectrochemical analysis has been an active area of research since the introduction of the direct-reading spectrometer by Hasler and Dietert¹ in 1944. Since that time, a wide variety of approaches to the development of electronic alternatives to photographic detection have been taken, and these are discussed in the monograph by Busch and Busch.² Broadly speaking, these approaches can be divided into two major types: transform-based systems, *i.e.*, those which employ either Fourier^{3,4} or Hadamard^{5,6} transform techniques, and non-transform systems. Non-transform systems can be further classified as either parallel (spatial) or sequential (temporal), depending on the manner in which the spectral information is encoded.

With the advent of solid-state array detectors such as the photodiode array and charge-coupled array detectors, various research groups have sought ways to employ these sensors for multielement determinations by atomic spectrometry. The approaches which have been developed include the use of array detectors in conjunction with echelle spectrometers,⁷⁻⁹ with modified dispersion systems,¹⁰ and with multiple

entrance-slit spectrometers.¹¹⁻¹⁵ These systems can be classified as parallel multichannel devices, and the object of all of these designs is to image as much spectral information as possible on the limited sensor area without loss of information from spectral overlap.

The second type of non-transform spectrometer for multielement analysis employs a single detector and encodes spectral information in the time domain. These systems include dispersive instruments such as rapid scanning monochromators^{16,17} and programmed (or slew scan) monochromators,^{18,19} as well as non-dispersive systems such as spectrometers which use rotating filter systems, and atomic-fluorescence systems which pulse excitation sources sequentially to encode signals from different elements.²⁰⁻²²

All sequential instruments attempt to transmit information about several elements over the same transmission channel. To accomplish this task, signals from various elements (*i.e.*, at various wavelengths) are staggered in time prior to transmission. Because of the sequential nature of data acquisition with these spectrometers, they fall into the category of sampled-data systems. From an information theory standpoint, an advantage of the sequential transmission of data is that the signal from each element has the full use of the transmission channel bandwidth. However, because

*Author to whom correspondence should be addressed.

†Current Address: Hercules Aerospace Division, McGregor, TX 76657, U.S.A.

high-speed transmission of information requires the electronics to have a wide frequency-response bandwidth, a compromise must be found between the speed of data acquisition and immunity from photon shot noise and Johnson noise present in the radiation field under observation.²³ In addition, for systems with a constant scan period, the sampling time for each analytical wavelength decreases as the number of spectral resolution elements in a spectral sweep increases.

All single-detector spectrometers developed to date suffer from various disadvantages. Rotating filter systems, for example, have limited spectral resolution, while rapid scanning monochromators, which scan entire spectral regions, are basically inefficient because much of the information they acquire is for wavelengths of no analytical interest. In addition, the signal-to-noise ratio obtained with rapid scanning monochromators decreases as the scan speed is increased. Although pulsed-source atomic-fluorescence instruments have good wavelength stability, they suffer from interference from source scattering in certain sample matrices.

Perhaps the most serious problem encountered with programmed scanning monochromators used for atomic-emission measurements, however, is the need for high wavelength reproducibility because of the narrow linewidth of atomic lines. It can be shown² for a typical Czerny–Turner monochromator that the change in wavelength with grating rotation can be estimated by

$$d\lambda/dr = (d/m)[\cos a + \cos b]\cos r \quad (1)$$

where λ is the wavelength, d is the grating constant, m is the spectral order, a and b are constants for the given optical layout (see Fig. 1), and r is the angle of rotation of the grating. For a typical system with a 1200 groove/mm grating, where a and b are approximately equal (about 10°), and r is less than 30° , the change in grating angle corresponding to an atomic linewidth (say, 0.001 nm) is about 6×10^{-7} radians or 3×10^{-5} degrees in the first order. Such tolerances in grating rotation are difficult to achieve mechanically because of hysteresis in the grating drive, and mechanical wear of parts with time.

To overcome the wavelength reproducibility problems often encountered with programmed scanned spectrometers for atomic emission, a new type of instrument with stationary dispersion optics that employs a multiple entrance-slit

dispersion system in conjunction with a single photomultiplier detector was assembled and tested. This system is based on the multiple entrance-slit spectrometer design developed by Busch and co-workers¹¹⁻¹³ but uses a single photomultiplier rather than a more expensive array detector. While it was clear from previous work that the multiple entrance-slit approach showed promise as a dispersion system for array detectors,¹³ its potential with a non-imaging detector such as a photomultiplier detector had not been evaluated. The relatively low cost, wide dynamic range, and high sensitivity of the photomultiplier all suggested that a multiple entrance-slit spectrometer using a photomultiplier was worth developing and evaluating.

EXPERIMENTAL

Instrumentation

Figure 1 shows a schematic diagram of the optical system of the instrument, which consists of an acetylene/air flame source and a predispersion optical system connected to the multiple entrance-slit spectrometer by means of fiber-optic light guides. Figure 2 shows a schematic diagram of the signal-processing path used in the instrument. The computer-controlled data-acquisition system processes the signal from the photomultiplier and also controls the predispersion optical system.

Source. The flame emission source used to evaluate the performance of the spectrometer was a Varian Techtron AA-6 nebulizer/burner (Varian Instruments, Palo Alto, CA) fitted with a custom-built, one-piece Méker burner head machined from stainless steel. Premixed fuel and oxidant gases emerged from a circular array of 1/16 in. (1.6 mm) holes in the burner head to give an acetylene/air flame approximately 15 cm tall with a diameter of 2.5 cm.

Predispersion optical system. The predispersion optics, used for sequentially encoding the spectral information, consisted of a laboratory-constructed optical multiplexer, shown in Fig. 3, connected to the multiple entrance-slit spectrometer by means of an array of eight non-coherent fiber-optic light guides. The optical multiplexer, or optiplexer, which focused the image of the source on successive fiber-optic light guides (Fig. 1), consisted of a 4.5 in. (11.4 cm) diameter aluminum tubular housing which supported two mirrors, a shutter arrangement, and a computer-controlled stepping motor. The array of eight fiber-optic light guides

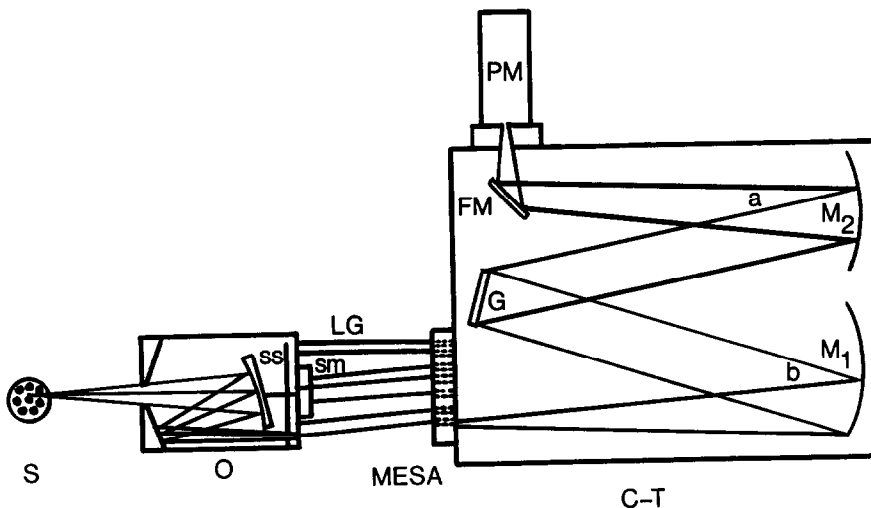


Fig. 1. Schematic diagram of the optical system used in the instrument. S, flame source; O, optical multiplexer; ss, scanning shutter disk; sm, stepper motor; LG, fiber-optic light guide; MESA, multiple entrance-slit assembly; C-T, Czerny-Turner monochromator; M₁, collimating mirror; M₂, focusing mirror; G, diffraction grating; FM, folding mirror; PM, photomultiplier tube.

was arranged around the periphery of the back plate of the optiplexer.

An Airpax Model K82701-P1 (North American Philips Control Corp., Cheshire, CT) unipolar stepper motor with a step angle of 7.5° (48 steps per revolution) was used to control the position of the rotating inner mirror and the shutter disk. A front-surfaced concave mirror (Oriel, Stamford, CT) with a focal length of 8 cm was used as the rotating inner mirror. One end of each of the eight metal-sheathed non-coherent glass fiber-optic light guides (Schott Optical Glass, Duryea, PA) was plugged into the back plate of the optiplexer so that the light guides were spaced equally around the outer circumference of the back plate (*i.e.*, every 45°). The other end of each light guide was plugged into the multiple entrance-slit plate of the MESS. A switching arrangement attached to the

shaft of the inner mirror was used to determine the home position of the rotating mirror.

Multiple entrance slit spectrometer (MESS). The dispersion system of the MESS consisted of a 0.5-m Czerny-Turner monochromator (Spex Industries, Metuchen, NJ, Model 1870) equipped with a 600 groove/mm diffraction grating blazed for 500 nm. A multiple entrance-slit array plate, shown in Fig. 4, was fabricated from aluminum and attached at what was normally the exit focal plane of the monochromator. Each entrance slit was manually adjustable and located in the entrance focal plane to pass the desired analytical lines through the exit slit of the monochromator.

The aluminum multiple entrance-slit plate was mounted in the entrance focal plane of the system with a specially designed bracket, and holes were drilled in the plate to permit the

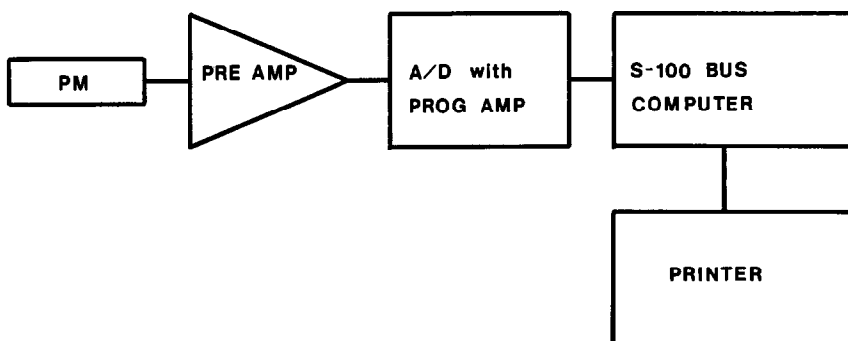


Fig. 2. Schematic diagram showing the signal-processing path used in the instrument.

fiber-optic light guides from the optiplexer to be plugged into the plate at locations corresponding to desired analytical lines. The positions of the apertures were calculated from an arbitrary wavelength chosen as the center wavelength for the group of analytical lines under consideration. The location of each analytical wavelength from the center of the plate was determined by using the reciprocal linear dispersion of the instrument (3.2 nm/mm).

A 13-stage photomultiplier (Thorn EMI Gencom, Fairfield, NJ, Model 6256B) with an S-20 spectral response was used as the detector. The high-voltage power supply for the photomultiplier was a Hewlett-Packard (Berkeley Heights, NJ) model 6516A power supply operated at 1 kV.

Signal-processing electronics. The signal from the photomultiplier tube was buffered and amplified by one of the four amplifiers of an RCA SK9173 quad operational amplifier, as shown in Fig. 5a. An RC low-pass filter with 0.1 sec time-constant was added to the output of the amplifier to reduce high-frequency noise in the signal. The bipolar power supply for the amplifier was constructed with 7815 and 7915 three-terminal voltage regulators, as shown in Fig. 5b.

The conditioned analog signal from the low-pass filter was made the input to a California Data Corporation (Newbury Park, CA) analog-to-digital converter (ADC) board (Model AD-100) with a programmable amplifier having a gain from 1 to 1024 and an ADC with a

resolution of 12 bits. The board used a Burr-Brown SDM856 analog-to-digital converter with a sampling rate of 29 kHz, and had a maximum linearity error of $\pm 0.048\%$ of full scale range. A Burr-Brown 3606 digitally-controlled programmable gain amplifier with a maximum inaccuracy of $\pm 0.02\%$ of the signal was used to provide variable gains. The 3 dB response of the amplifier at a gain of 1 was 100 kHz. With gains from 32 to 128, the frequency-response bandwidth was 40 kHz, and for gains from 256 to 1024, the bandwidth decreased to 10 kHz. The slew rate of the amplifier for a gain of 1 was 0.5 V/ μ sec.

Data-acquisition and control circuitry. Data-acquisition, processing, and instrument control were all accomplished with a California Computer Systems (Sunnyvale, CA) microcomputer having an IEEE-696 (S-100) bus structure. The central processing unit of the microcomputer was a Zilog Z-80 operating at a clock speed of 4 kHz. The system had 64 kbyte of random access memory (RAM) and operated under CP/M version 2.2 from Digital Research (Pacific Grove, CA). Mass storage was accomplished with two double-sided double-density 8-in. disk drives capable of storing 2.4 megabytes of data.

The optiplexer mirror and shutter positions were controlled by means of a model MC100 stepper motor controller board from Snow Micro Systems, Inc. (Fairfax, VA). The board provided for the control of two stepper motors from the IEEE-696 bus, and allowed control of

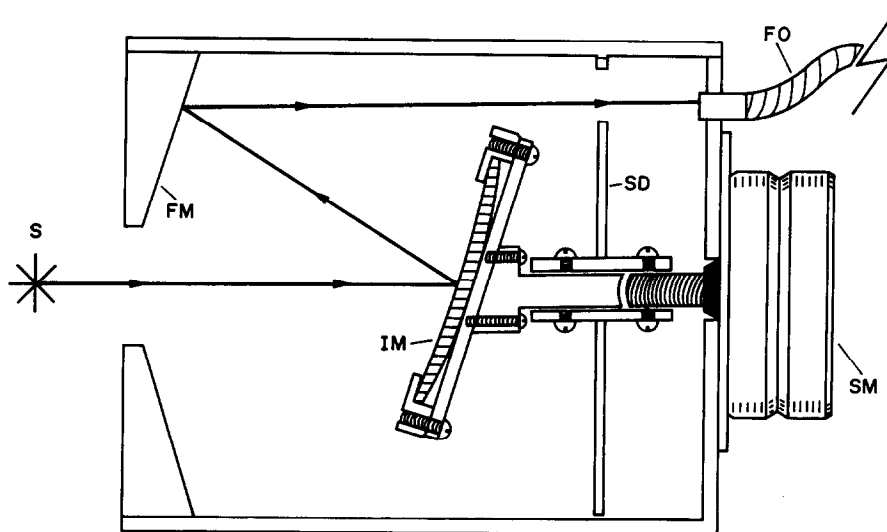


Fig. 3. Schematic diagram of the optical multiplexer. S, emission source; FM, front mirror; IM, rotating inner mirror; SD, rotating shutter disk; FO, fiber-optic light guide; SM, stepper motor. Only the central ray is shown. Both the central and extreme rays are shown in Fig. 1.

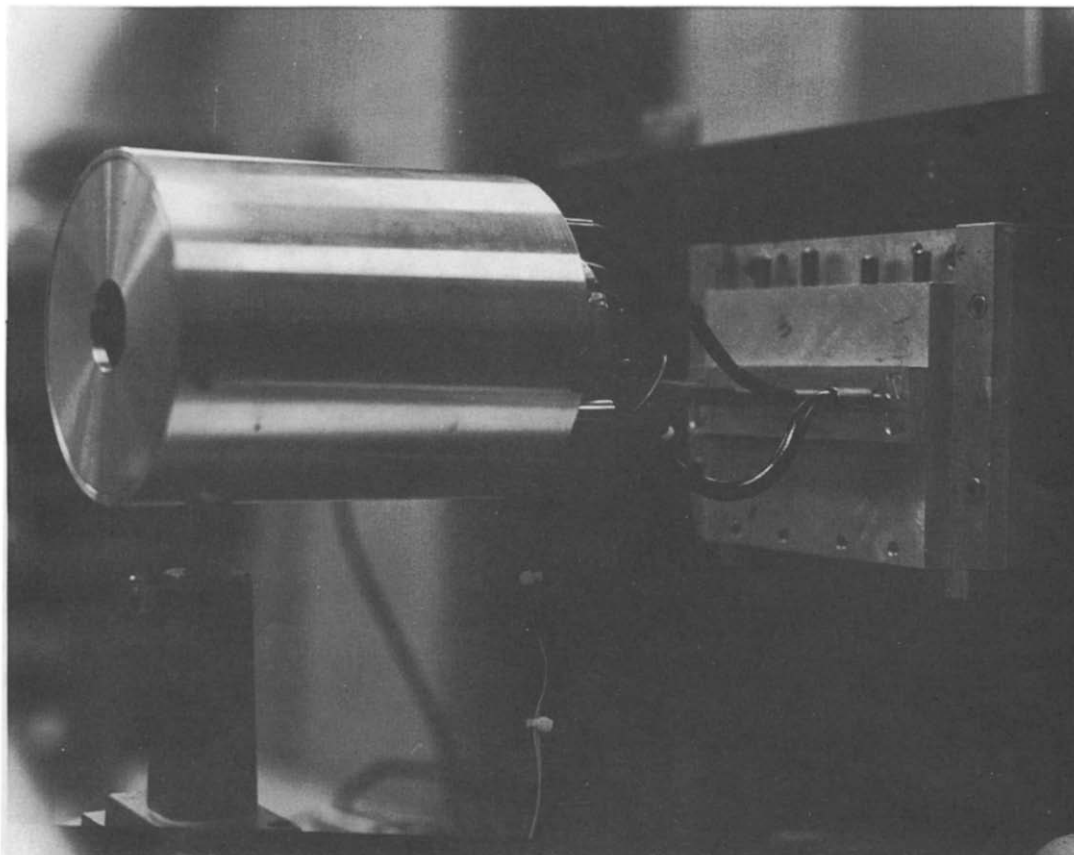


Fig. 4. Photograph showing the optical multiplexer, fiber-optic light guides, and multiple entrance-slit assembly mounted on the Czerny-Turner monochromator.

the motor stepping rate, motor direction, and extent of rotation (*i.e.*, number of steps). The board also provided for feedback from the stepper motor by means of two four-bit parallel ports.

Procedure

Solutions. All solutions were prepared with analytical-grade reagents and triply demineralized water. Stock solutions of lithium, strontium, barium, and calcium containing 1000 ppm of the metal ion were prepared by dissolving the dry carbonates in hydrochloric acid and diluting the solutions in standard flasks. A 1000 ppm stock solution of sodium was prepared directly from dried reagent-grade sodium chloride. The appropriate amount of a 10000 ppm cesium chloride solution was added to all multielement standards as an ionization buffer, to give a final cesium concentration of 1000 ppm.

Three multielement standards were prepared from the stock solutions described above. Standard A contained 6.88, 15.32, 9.81, 9.45 and 9.82 ppm respectively, of lithium, strontium,

barium, sodium and calcium. The concentrations in standard B were half those in standard A, and those in standard C were a tenth of those in A.

Analytical conditions. Spectrometer operating conditions were kept as constant as possible to permit intercomparisons between different data sets. Fuel and oxidant flow-rates to the burner were maintained with Brooks Instruments rotameters (Emerson Electric Co., Hatfield, PA). An acetylene flow-rate of 1.8 l./min and an air flow-rate of 8 l./min were used throughout. The photomultiplier voltage was kept at 1000 V. The buffer amplifier was set for a gain of 200 with a 0.1 sec time-constant low-pass filter on the output. All samples were introduced into the flame by conventional pneumatic nebulization.

RESULTS AND DISCUSSION

Principle of operation

Multiple entrance-slit spectrometer. The operation of the multiple entrance-slit spectrometer

(MESS) can best be understood in terms of the principle of reverse optics, which states that, for any optical system, if light rays passing through the system from the entrance aperture to the exit aperture are reversed, they must retrace their original paths. To apply this principle to spectroscopy, consider a conventional direct-reading spectrometer with a single entrance slit and multiple exit slits located in the exit focal plane at locations corresponding to particular analytical lines. If this system is used in the reverse fashion, the principle of reverse optics requires that, if a particular exit slit is illuminated with light of its own particular analytical wavelength, this radiation must travel through the dispersion system and emerge from the entrance slit. Therefore, if a series of slits is placed in one of the two conjugate focal planes of the dispersion system at locations determined by the grating equation for desired analytical lines, then when these slits are irradiated by light from the source, each will transmit radiation of its own analytical wavelength through the spectrometer, with each such beam converging at a single exit slit located in the other conjugate focal plane.

In the system developed in this laboratory, a Czerny–Turner monochromator, designed to give a wide, unvignetted, flat exit focal plane,

Table 1. Configuration of multiple entrance-slit plate

Hole number	Emitting species	Analytical wavelength, nm
1	Ca I	422.7
2	Cs I	455.5
3	Sr I	460.7
4	MgOH	507.4
5	CaOH	547.5*
6	Ba I	553.5
7	Na I	589.6
8	Li I	670.8

*This wavelength corresponds to the steep short-wavelength side of the CaOH emission band and was selected to test the wavelength reproducibility of the instrument.

was selected and used in the reverse fashion (*i.e.*, what was normally the exit focal plane was used as the entrance focal plane). With this arrangement, the entrance focal plane of the MESS was 114 mm wide, and corresponded to a wavelength range of 365.8 nm in the first order with a grating giving a reciprocal linear dispersion of 3.2 nm/mm.

Table 1 shows the analytical wavelengths corresponding to the eight entrance-slit positions used in this study. Since the purpose of the study was to demonstrate the feasibility of

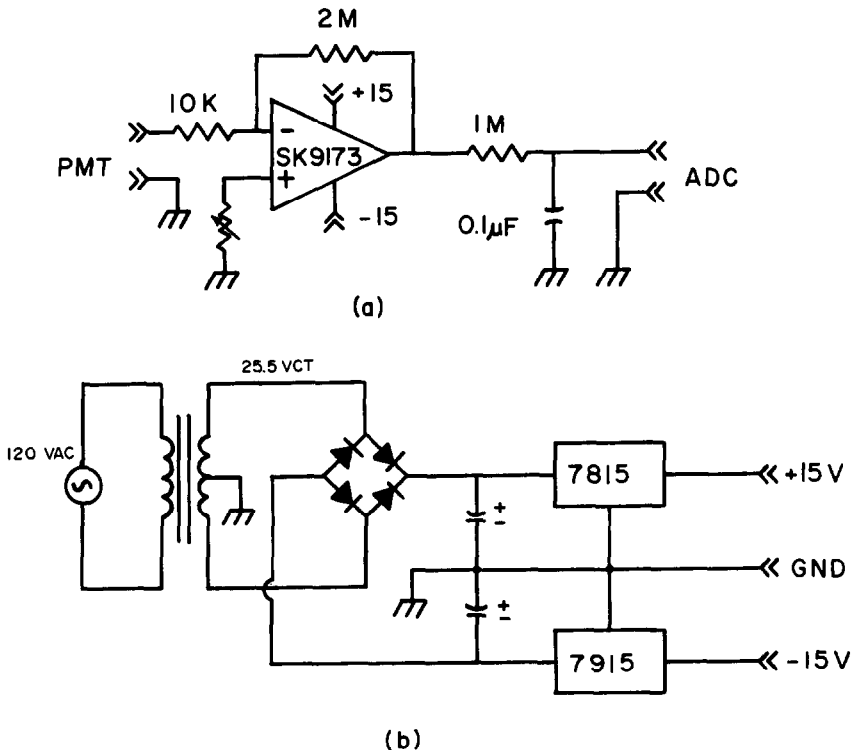


Fig. 5. Signal processing electronics: (a) preamplifier circuit; (b) bipolar power supply for operational amplifier.

the optical system rather than demonstrate a particular analytical application, the multiple entrance-slit plate was configured for elements which would be easily excited in the acetylene/air flame used as the atomic-emission excitation source.

Predispersion optics. In order for the MESS to operate as described above, only one entrance slit in the array can be illuminated at any given time. In addition, since the array of entrance slits is spread out across the entrance-slit plate, some means must be used to illuminate each entrance slit successively and in a uniform manner.

These conditions were satisfied with the optical multiplexer or optiplexer shown schematically in Figs. 1 and 3. In operation, light entering the aperture in the front mirror of the optiplexer strikes a front-surfaced concave inner mirror oriented at an angle to the optical axis of the optiplexer. Light reflected from the inner mirror strikes the polished conical aluminum surface of the interior front plate of the optiplexer, which acts as the second mirror, directing the radiation toward the circular array of light guides at the back of the optiplexer. Since the optical axes of the two mirrors are parallel, the effect of this arrangement is to displace the radiation spatially toward the outer perimeter of the back plate of the optiplexer. A shutter disk with a single opening was attached to the shaft of the stepper motor so that it rotated as the inner mirror rotated. The purpose of the shutter disk was to prevent scattered light from accidentally striking fiber-optic light guides not being accessed by the inner mirror. Each fiber-optic light guide in the array could be illuminated by the source by rotation of the inner mirror of the optiplexer.

Compared with other programmed scanned monochromators, a major advantage of the spectrometer described in this paper is the fact that the *dispersion optics are stationary*. As a result, wavelength registration problems commonly encountered with other slew-scan systems are avoided. Since undispersed radiation is directed through the predispersion optics, any instability in the optical alignment of the optiplexer (*i.e.*, the extent of rotation of the inner mirror) does not affect wavelength stability. Instead, variations in the optical alignment of the optiplexer result in intensity variations in the undispersed radiation incident on the fiber-optic light guides. Since the tolerances involved in directing the relatively wide beam of undis-

persed radiation onto a fiber-optic light guide are much less stringent than those involved in precisely rotating a diffraction grating so as to image an atomic spectral line reproducibly on an exit slit, the overall reproducibility of the MESS is expected to be greater than that of scanning systems which move the dispersion optics.

The optiplexer/MESS has other important advantages compared with conventional programmed scanning spectrometers. Since individual analytical wavelengths are accessed by rotating the inner mirror in the optiplexer, the time required to jump from one analytical wavelength to another is independent of the wavelength separation between lines. In addition, the order of interrogation of the various analytical wavelengths is not dependent on the wavelength (as would be true for a programmed scanned system which would jump from one wavelength to another in either ascending or descending order), but may be varied at will by simply rearranging the order in which the fiber-optic light guides are plugged into the system.

Finally, it should be mentioned that the optiplexer/MESS is potentially a flexible multielement detection system. Flexibility is a design goal that is frequently cited in papers discussing various multielement detection systems. It is frequently stated, for example, that a disadvantage of direct-reading spectrometers is their lack of flexibility in their ability to monitor different combinations of elements. Conceptually, this is not a problem with the MESS. If a more sophisticated multiple entrance-slit plate could be fabricated, it should be possible to make a plate which would be capable of accessing a large number of elements (*i.e.*, analytical wavelengths). Because of the switchboard nature of the system,^{12,13} various combinations of elements could be determined with the system simply by plugging the fiber optics into prelocated apertures. Those apertures not in use would be blocked with opaque plugs.

One of the important realities in multielement determinations by atomic spectroscopy is the need for a wide dynamic range in the detection system. This need arises because the emission intensities associated with analytical lines of major, minor, and trace elements vary over some orders of magnitude. The already large dynamic range of the photomultiplier detector used with the optiplexer/MESS can be increased further to accommodate the range of emission

intensities encountered in multielement determinations, by four methods: (1) by varying the integration time for different elements; (2) by varying the slit-widths employed for different elements; (3) by varying the photomultiplier voltage used with different elements; (4) by varying the amplifier gain used for different elements.

Because the optiplexer/MESS is under computer control, signal averaging at individual analytical wavelengths is possible for lengths of time that can be varied to suit the particular emission intensity. Because each entrance slit is independently adjustable, a wide range of intensities can be monitored with this instrument by opening or closing selected entrance slits to increase or decrease the amount of light striking the detector. In addition, amplifier gain and/or photomultiplier voltage can be adjusted to different preselected levels for each element in a scan during the time when the stepper motor is rotating the inner mirror to the next wavelength.

Data-acquisition and system control. A micro-computer is essential to the operation of the spectrometer, not only because of the large amounts of data collected during an analysis but also to control the rotation of the inner mirror of the optiplexer. The software that controls the system was written in a structured dialect of Basic (Cbasic version 1.4 by Digital Research) and performs four basic functions. Figure 6 shows the program flowchart used to run the instrument. The first function of the program is to control the location of the rotating mirror in the optiplexer. The second is to set the programmable gain of the amplifier on the analog-to-digital converter board by means of an autoranging routine. The third function is to collect time-integrated spectral data and time-integrated background data. After collection, the sum of the background counts in a given channel is subtracted from the sum of the signal accumulated in that channel. Finally, the noise is calculated as the standard deviation of the background, and the background-corrected signal-to-noise ratio is calculated.

The use of autoranging to set the gain of the programmable amplifier on the ADC board enhances the versatility of the instrument by reducing operator interaction and allowing the signal from each element to be amplified to the mid-range of the ADCs (*i.e.*, 2048 out of the maximum possible digital output of 4095 for a 12-bit ADC). In operation, as the subroutine

runs, it first defines a starting gain for the ADC board. A trial signal is then read and compared with a window of values set by the routine. If the signal value is too small, the gain is multiplied by two. If it is too large, the gain is divided by two. After this is done, a second trial signal is taken and the process is repeated until the signal falls within the window of permissible values. If the gain is set above 1024 or below 1, the routine prints a warning message to alert the operator that the system is not functioning properly.

Another subroutine maintains complete control over the stepper motor, controlling the number of steps taken, the rate of rotation, and the direction that the motor turns. Home position for the rotating mirror is determined by means of a microswitch coupled to the shaft of the stepper motor. In operation, the subroutine directs the optiplexer to locate home position, delay for half a second, and then find it again. This technique of seeking the home position twice was found to be necessary to avoid positional errors of the rotating mirror. When the inner mirror is rotated to the next fiber-optic position (one-eighth of a complete rotation, or six steps), a delay of at least 1 sec is introduced by the program to allow the electronics in the detection section of the instrument to settle to their correct value. The delay also allows the stepper motor to recover from any overshoot ("hunting") and lock into position.

System performance

Fiber-optic light guides. The transmission properties of the fiber-optic light guides used in this study were determined by mounting light guides with a specially designed holder in the sample compartment of a Varian Superscan 3 spectrometer. Transmission through the fiber-optic light guides was measured with respect to air as the reference over the wavelength interval from 700 to 350 nm at a scan-rate of 200 nm/min. These studies revealed that the transmission of the fiber-optic light guides was constant over the wavelength range from 475 to 700 nm. Attenuation of transmission was observed to begin gradually at 475 nm and continued to 375 nm. At 375 nm, the transmission dropped sharply and cut-off occurred at 365 nm.

This test confirms that the fiber-optic light guides used in this study were adequate for use in the visible portion of the spectrum (*i.e.*, for the analytical wavelengths shown in Table 1), although the analytical lines for Ca, Cs and Sr

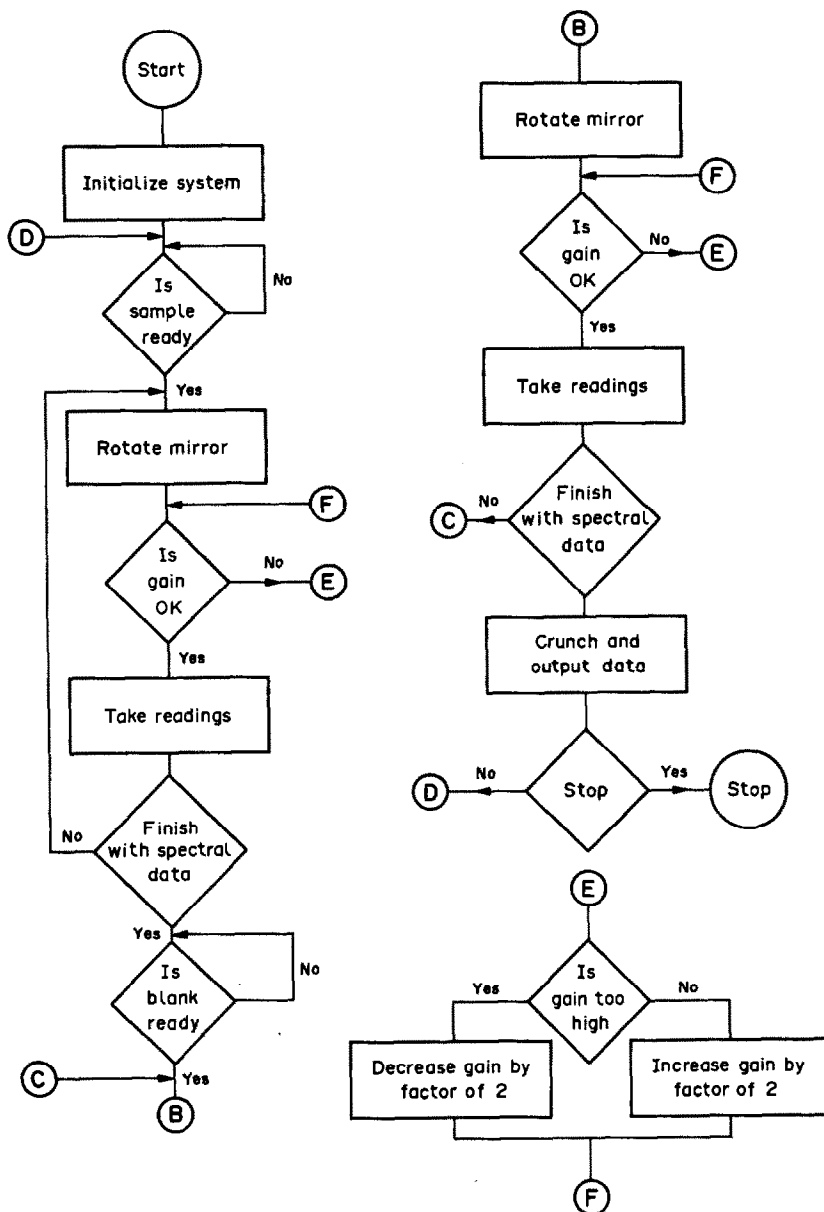


Fig. 6. Flowchart of program used to run the instrument.

would be affected to some extent. To be completely satisfactory for real analytical determinations, however, any multielement detection system must have adequate response in the ultraviolet. One of the limitations of the optplexer instrument in its current stage of development, therefore, is a lack of short-wavelength response. UV-transmitting fiber-optic light guides are available, however, and further development of the optplexer would involve their use.

Multiple entrance-slit plate. One of the essential components affecting the performance of the MESS system is the multiple entrance-slit

plate. A key factor in fabricating the plate is the accurate placement of the individual entrance apertures. To determine the extent of misalignment of the individual entrance apertures in the multiple entrance-slit plate, a sodium solution was aspirated into the flame, the grating was rotated to give a maximum signal with the sodium entrance slit, and the wavelength setting on the monochromator was noted. The process was repeated by aspirating samples of each of the other elements in turn and noting the amounts by which the wavelength setting on the monochromator must be varied to maximize the signals for the other atomic lines. This

wavelength variation was converted into a linear error in the position of the entrance apertures by dividing it by the reciprocal linear dispersion.

Table 2 shows the results of these measurements for three wavelengths across the plate. Errors in the precise location of the entrance apertures were corrected by careful positioning of the entrance slits. Since each fiber-optic light guide had a diameter of 3 mm, errors in wavelength of up to 9.6 nm could be corrected by this means although large corrections resulted in severe light attenuation as a result of the circular cross-section of the light guides.

Although the accurate positioning of the holes for the light guides in the multiple entrance-slit plate is a matter of careful machining and can easily be accomplished, a good slit design is much more difficult to implement. Figures 7 and 8 show two slit designs used in this study. In Fig. 7, front views of the entrance-slit plates are shown, each plate having either eight (7a) or four (7b) holes for the fiber-optic light guides. In Fig. 8, the back of each plate is shown (the side facing inside the monochromator). In the first design (Fig. 8a), the multiple entrance-slit plate used eight fixed slits of various widths held in place with set screws. In the second design (Fig. 8b), the multiple entrance-slit plate used four adjustable slits designed to monitor Na (589.6 nm), Li (670.7 nm), K (766.5 nm), and Ca (422.7 nm in 2nd order). The slits in both designs were somewhat crude, resulting in loss of resolution, difficulty in positioning, and excessive light losses.

One possible means of producing an improved multiple entrance-slit plate would be to use a photographic mask for the entrance-slit array. Such a mask could be made by exposing a photographic plate to the atomic lines desired and etching slits into the material by photoresist etching methods. Another alternative would be to use specially designed light guides with one end made rectangular with a high length-to-width ratio, which would partially simulate the function of an entrance slit.

The effect of using the monochromator in the reverse fashion with the multiple entrance-slit

plate (Fig. 1) was investigated photographically by centering a sheet of photographic paper at the position of the collimating mirror (*i.e.*, the camera mirror when the instrument is used in the conventional manner). Photographic sheets were exposed by passing light from a tungsten lamp through the optiplexer, a fiber-optic light guide, and the entrance-slit plate. Exposures were made with apertures from the short wavelength side of the plate, the center of the plate, and the long wavelength side of the plate. After development, the aperture of the mirror mask was drawn on the sheet, and the relationship between the light pattern produced by the entrance-slit plate and the aperture of the mirror could be assessed.

These studies revealed that, although the collimating mirror was filled with light regardless of the aperture used, a large quantity of light from the entrance slit plate missed the mirror. Most of the mismatch in light-beam position occurred in the horizontal plane with very little difference observed in the vertical position of the light-beam with respect to the mirror center. Part of this mismatch was believed to result from the manner in which the entrance-slit plate was fabricated. Ideally, the entrance-slit array should lie on the curved focal plane of the collimating mirror. With the present prototype system, however, the flat entrance-slit plate is tangential to the curved focal plane at the position where the exit slit would normally be located. This slight difference in position and angle is sufficient to shift the center of the light-beam produced by the light guide, away from the center of the mirror. It also decreases the resolution of the system at the extreme edges of the wavelength window since the slit image for these wavelengths is slightly out of focus.

The variation in the signal with respect to input position on the entrance plate was measured by monitoring the intensity of the green line (546.7 nm) from a mercury pen lamp for each aperture of the multiple entrance-slit plate. This was accomplished by removing the photomultiplier and manually rotating the grating until the green line could be observed at the exit slit. The detector was reattached and the signal was maximized by rotating the grating. The process was repeated for each entrance aperture in the plate. The signal was taken as the average of 1000 digitized samples. Table 2 shows that, with the exception of the two apertures which were displaced vertically from the rest, there was little dependence of the signal on

Table 2. Extent of misalignment in multiple entrance-slit plate

Element	Wavelength, nm	Misalignment, nm	Linear error, mm
Li	670.7	8.5	2.7 (right)
Ba	553.5	0.25	0.08 (left)
Sr	460.7	0.38	0.11 (left)

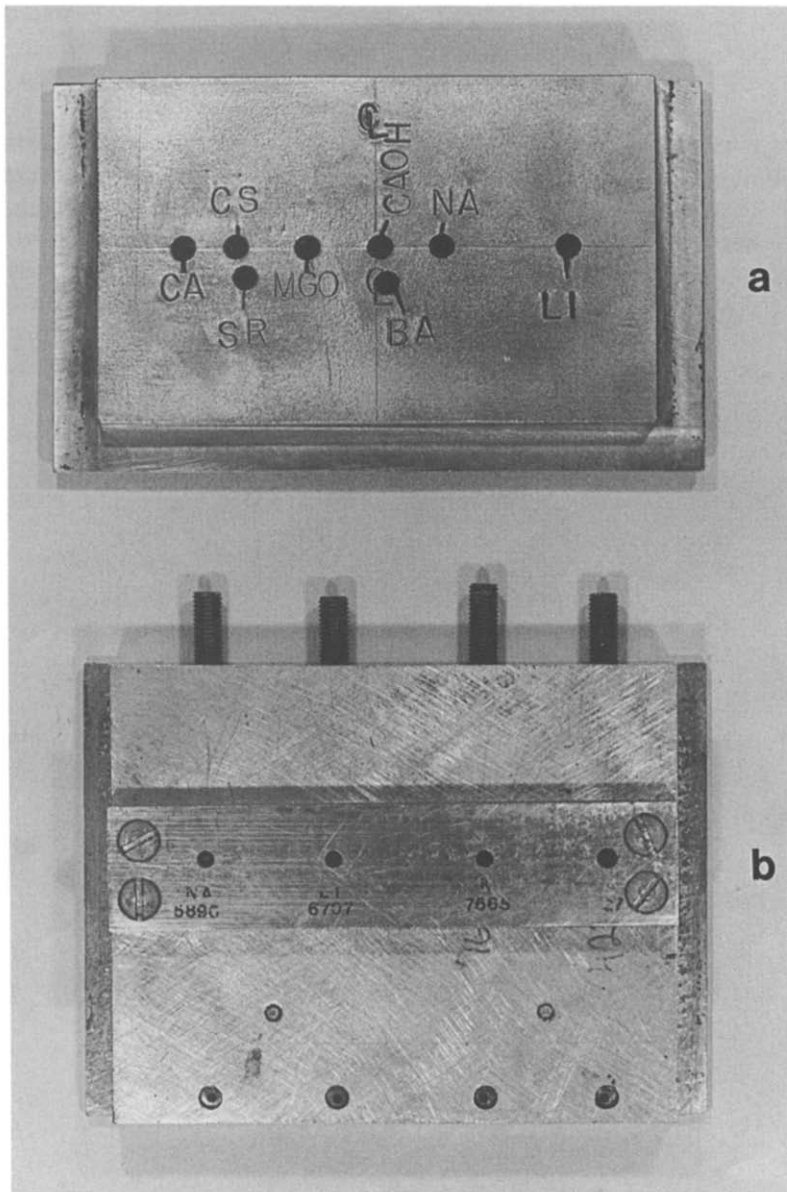


Fig. 7. Photograph showing the front of two multiple entrance-slit designs: (a) eight holes for fiber-optic light guides, (b) four holes for fiber-optic light guides.

the position of the light guide in the entrance focal plane. This lack of variation was due to the wide emergence angle of the fiber-optic light guide rather than to ideal plate design. Regardless of the position of the light guide on the multiple entrance-slit plate, the light-beam from the light guide emerged with a sufficiently large solid angle to fill the collimating mirror.

Detection limit studies. Detection limits were determined by linear extrapolation of signal-to-noise ratio *vs.* concentration plots to the origin. The detection limit was taken as a signal-to-noise (rms) ratio of 3. Table 4 shows the detection limits obtained with the system when the

spectrometer was programmed to acquire 15 measurements of flame background and 15 sample measurements. The signal was taken as the difference between the sample intensity and the flame background intensity. The signal-to-noise ratio was calculated by dividing the average signal by the standard deviation of the signal. It can be seen from the table that all detection limits except that for barium are in the low ppm range. The detection limits for strontium and barium are both poorer because the apertures for these were displaced vertically, thereby reducing the input light flux from these slits (see Table 3). In addition, the detection limit for

barium is further affected adversely by the presence of the CaOH molecular band which overlaps the barium emission line at 553.5 nm. This spectral interference is well known,²⁴ and produces an anomalously large variation in the barium signal because the line falls on the steep edge of the calcium band emission.

The effect of sampling time on the detection limit for lithium was determined by measuring the detection limit as a function of the number of data points collected by the spectrometer. Figure 9 shows the results of this study which follows typical signal-averaging behavior. On

the basis of this study, the collection of 15 data points by the instrument was deemed to provide the best compromise detection limit for the smallest observation time.

Actually, the length of observation required can be varied from element to element with the MESS system and can be used to advantage in multielement determinations where one element is present in large amount while others are present in very small quantities. With the system, the operator can program the instrument to spend just enough time on major elements to measure their presence to some predetermined

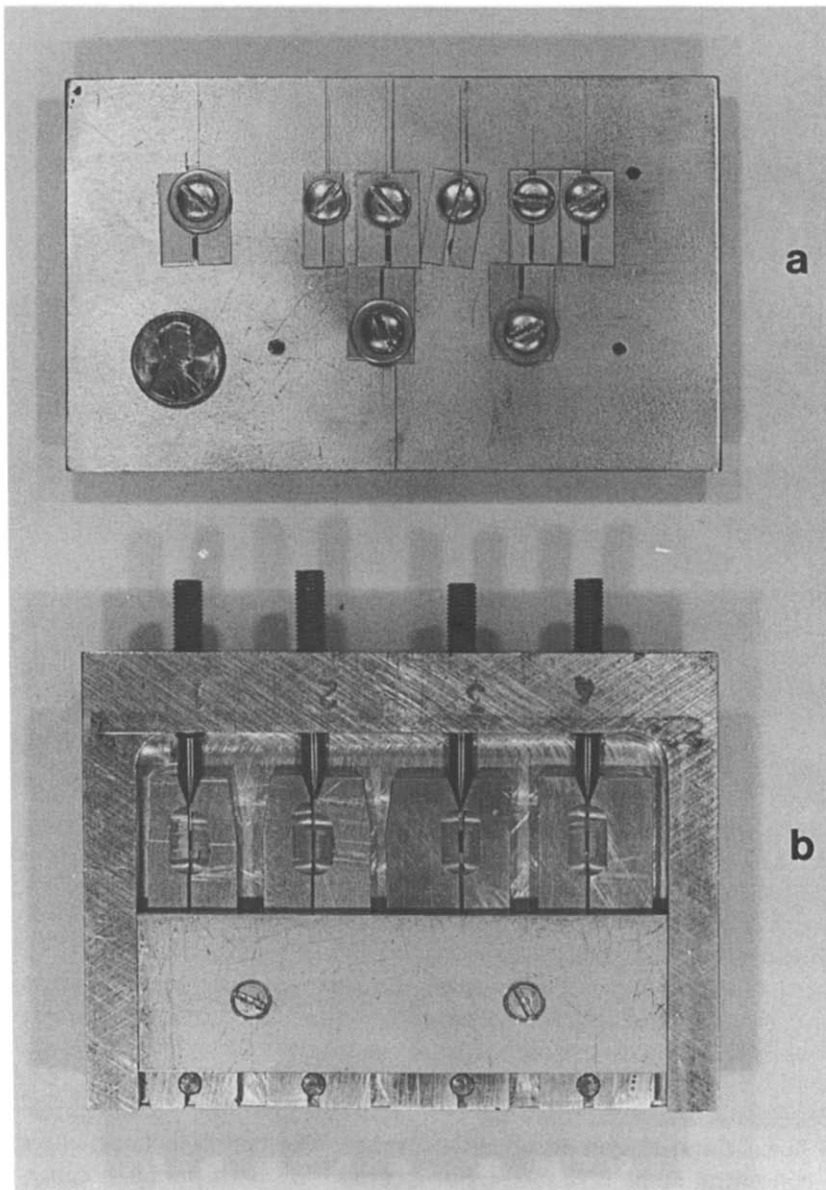


Fig. 8. Photograph showing the back (side facing inside the monochromator) of the two multiple entrance-slit designs in Fig. 7: (a) fixed slit arrangement for eight entrance slits, (b) multiple entrance-slit plate with four adjustable entrance slits.

Table 3. Variation of input flux across the multiple entrance-slit plate

Hole number	Wavelength, nm	Signal, counts
1	422.7	1658
2	455.5	1666
3	460.7	512*
4	507.4	1665
5	547.5	1661
6	553.5	473*
7	589.6	1662
8	670.8	1675

*Aperture hole was displaced vertically, resulting in low reading.

precision, and spending correspondingly more time on elements present in minute quantities.

The decrease in detection limit for lithium with increasing observation time, shown in Fig. 9, raised the issue of whether the signal-to-noise ratio was affected by the sampling rate of the spectrometer. To answer this question, a fixed number of readings was collected with a variable delay between each reading, for three elements. A fixed delay of 0.5 sec after the optplexer accessed a channel was programmed to allow the RC low-pass filter time to reach equilibrium (*i.e.*, 5 time constants). After the filter had been given time to equilibrate, readings were taken at timed intervals (delay time). The results of this study, shown in Table 5 for calcium, strontium and lithium, reveal that there is essentially no influence of delay time on the measured signal-to-noise ratio. This suggests that high-frequency noise components predominate over source-fluctuation noise for the flame. Since noise is a random phenomenon, the particular instant of signal sampling is not important, although the number of readings and the frequency of sampling affect the characterization of the noise. Increasing the length of time spent sampling the probe area of the flame permits a more detailed characterization of lower frequency noise. Since increasing delay time did not significantly change the signal-to-noise ratios observed, the influence of low-frequency noise components was believed to be small.

Table 4. Detection limits obtained with the spectrometer

Element	Emitting species	Wavelength, nm	Detection limit, ppm
Li	Li I	670.7	0.91
Na	Na I	589.6	0.41
Ca	CaOH	547.5	0.69
Ba	Ba I	553.5	213
Sr	Sr I	460.7	6.4

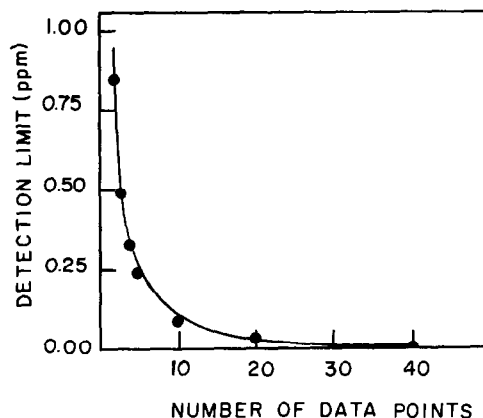


Fig. 9. Influence of signal averaging on detection limit for lithium.

CONCLUSIONS

The instrument described in this paper is only a prototype assembled to test the feasibility of developing a programmed-scan monochromator with stationary dispersion optics for high wavelength stability, with an ordinary photomultiplier used as the detector. The optplexer/MESS approach was shown to be feasible for atomic lines in the visible region of the spectrum. The major limitations of the instrument at its current stage of development are the short-wavelength transmission properties of the light guides used with the optplexer (current fiber optics set the lower wavelength limit at 370 nm) and the need for a more sophisticated entrance-slit plate. Although the resolving power of the instrument is adequate for certain flame applications, at the present stage of development it is certainly not adequate for use with spectrally rich sources such as the induction coupled plasma.

Although the optplexer/MESS system may seem like nothing more than a direct-reading spectrometer used backwards, it is actually easier to fabricate and align the multiple entrance-slit spectrometer because it is easier to place an

Table 5. Influence of delay time between data points on the signal-to-noise ratio

Delay time, sec	Signal-to-noise ratio		
	Ca*	Sr†	Li‡
0	17.97‡	29.82‡	54.01‡
0.5	18.33	29.90	54.10
1.0	17.95	31.00	54.18
2.0	18.47	31.57	54.22
4.0	17.87	31.52	54.08

*4.91 ppm.

†7.66 ppm.

‡3.44 ppm.

‡Computed from 15 measurements.

array of fiber-optic light guides close together in the entrance focal plane than it is to place an array of detectors together in the exit focal plane. The optiplexer/MESS system is also simpler than a conventional direct-reading spectrometer because only a single detector is required. However, because only one detector is employed, the multiple entrance-slit system described here is useful only for stable sources because source drift contributes to limiting the overall precision of the measurement in sampled-data instruments.

Finally, it should be mentioned that a modification of the instrument could be envisioned which would permit the system to be used in a Hadamard mode (for those situations where multiplexing may be advantageous). By using electronically controlled shutters at each of the entrance slits, combinations of analytical wavelengths could be made to strike the detector. By limiting the wavelengths included in the transform only to analytical wavelengths of interest (instead of the complete spectrum) and by modifying the relative intensities of the lines (by adjusting the slit-widths), some of the multiplex disadvantages observed with conventional transform instruments may be reduced.

Acknowledgements—This work was supported by Baylor University Research Grants 033-S80-URC, 011-S83-URC, and 089-F81-URC. The authors would like to express their appreciation to Milton Luedke of the Baylor Chemistry/Physics Machine Shop for fabricating specialized parts for the instrument. Two of the authors (KWB and MAB) would like to thank Baylor University for a summer sabbatical to provide the time needed to prepare this paper for publication. This work was taken from the Master's Thesis of Larry D. Benton, portions of which were presented at the 12th Annual Meeting of the Federation of Analytical Chemistry and Spectroscopy Societies, 29 September–4 October 1985, Philadelphia, Pennsylvania.

REFERENCES

1. M. F. Hasler and H. W. Dietert, *J. Opt. Soc. Am.*, 1944, **34**, 751.
2. K. W. Busch and M. A. Busch, *Multielement Detection Systems for Spectrochemical Analysis*, Wiley, New York, 1989.
3. G. Horlick, R. H. Hall and W. K. Yuen, in *Fourier Transform Infrared Spectroscopy*, Vol. 3, J. R. Ferraro and L. J. Basile (eds.), pp. 37–81. Academic Press, New York, 1982.
4. P. R. Griffiths and J. A. de Haseth, *Fourier Transform Infrared Spectrometry*, pp. 520–535. Wiley, New York, 1986.
5. D. Tilotta and W. G. Fateley, *Spectroscopy*, 1988, **3**, 14.
6. D. C. Tilotta, R. C. Fry and W. G. Fateley, *Talanta*, 1990, **37**, 53.
7. J. V. Sweedler, R. B. Bilhorn, P. M. Epperson, G. R. Sims and M. B. Denton, *Anal. Chem.*, 1988, **60**, 282A.
8. P. M. Epperson, J. V. Sweedler, R. B. Bilhorn, G. R. Sims and M. B. Denton, *ibid.*, 1988, **60**, 327A.
9. G. R. Sims and M. B. Denton, in *Multichannel Image Detectors*, Vol. 2, Y. Talmi (ed.), pp. 117–132. American Chemical Society, Washington, D.C., 1983.
10. R. M. Hoffman and H. L. Pardue, *Anal. Chem.*, 1979, **51**, 1267.
11. K. W. Busch and B. B. Malloy, in *Multichannel Image Detectors*, Y. Talmi (ed.), Chapter 2. American Chemical Society, Washington, D.C., 1979.
12. K. W. Busch, B. B. Malloy and Y. Talmi, *Anal. Chem.*, 1979, **51**, 670.
13. M. A. Busch, K. W. Busch and B. B. Malloy, *Talanta*, 1990, **37**, 71.
14. V. Karanassios and G. Horlick, *Appl. Spectrosc.*, 1986, **40**, 813.
15. K. R. Brushwyler, N. Furuta and G. M. Hieftje, *Talanta*, 1990, **37**, 23.
16. R. M. Dagnall, G. F. Kirkbright, T. S. West and R. Wood, *Anal. Chem.*, 1971, **43**, 1765.
17. *Idem*, *Analyst*, 1972, **97**, 245.
18. E. Cordos and H. V. Malmstadt, *Anal. Chem.*, 1973, **45**, 425.
19. H. V. Malmstadt and E. Cordos, *Am. Lab.*, 1972, **4**, No. 8, 35.
20. D. G. Mitchell and A. Johansson, *Spectrochim. Acta*, 1970, **25B**, 175.
21. *Idem*, *ibid.*, 1971, **26B**, 677.
22. E. F. Palmero, A. Montaser and S. R. Crouch, *Anal. Chem.*, 1974, **46**, 2155.
23. S. W. McGeorge and E. D. Salin, *Spectrochim. Acta*, 1985, **40B**, 447.
24. K. W. Busch, N. G. Howell and G. H. Morrison, *Anal. Chem.*, 1974, **46**, 2074.

STATISTICAL EVALUATION OF THE PERFORMANCE OF A NEW PROGRAMMED-SCAN MONOCHROMATOR FOR MULTIELEMENT DETERMINATIONS BY ATOMIC EMISSION

KENNETH W. BUSCH*, MARIANNA A. BUSCH and LARRY D. BENTON†

Department of Chemistry, Baylor University, Waco, TX 76798, U.S.A.

(Received 28 March 1989. Accepted 9 May 1989)

Summary—The reproducibility of a programmed-scan monochromator with stationary dispersion optics was evaluated by means of analysis of variance (ANOVA). The spectrometer used an optical multiplexer coupled with glass-fiber optic light-guides to a multiple entrance-slit spectrometer employing a photomultiplier as the detector. With this spectrometer, 15 emission intensity measurements at the lithium resonance line wavelength (670.7 nm) were collected for five rotations of the optiplexer mirror under four different emission situations: flame background emission at 670.7 nm, lithium emission from an acetylene-air flame in the absence of an ionization buffer, lithium emission from an acetylene-air flame in the presence of an ionization buffer, and tungsten lamp emission at 670.7 nm. For all four situations, the ANOVA results showed that instrumental changes which occurred during mirror rotation in the optiplexer were a significant source of signal variation compared with factors not associated with mirror rotation, *i.e.*, photon shot noise, source fluctuation noise, and electronic drift. The actual magnitude of the signal variability introduced during mirror rotation, however, was found to be quite small, producing an average relative standard deviation of only 0.76% for the signal.

Busch and co-workers¹⁻³ have described a new programmed-scan monochromator with stationary dispersion optics which promises to provide the high wavelength stability necessary for accessing atomic lines reproducibly. The system, described in detail in the preceding paper of this issue,¹ uses an optical multiplexer coupled by means of fiber-optic light-guides to a multiple entrance-slit spectrometer (MESS)⁴⁻⁶ employing a photomultiplier detector. Although still in the prototype stage of development, and limited at present by a lack of short-wavelength transmission in the fiber-optic light-guides used with the optiplexer, the instrument has a number of features which offer potential advantages for multielement determinations by atomic spectroscopy. These include (1) an inexpensive detector having high sensitivity and wide dynamic range, (2) stationary optics, resulting in good wavelength stability, (3) a fixed scan-time between wavelengths, regardless of wavelength separation between lines, (4) the capability for individual optimization, during the time period of mirror rotation, for elements with different

spectrochemical properties, and (5) ease of addition to existing spectrometers.

A key question regarding the performance of the optiplexer/MESS system is the effect of rotation of the inner mirror of the optiplexer on signal reproducibility. Although the wavelength stability of the instrument is expected to be quite high because the dispersion optics are stationary, intensity variations can result if the rotating inner mirror does not image the source reproducibly on the light guides from scan to scan. To assess the effect of the mirror movement and other instrument parameters on system reproducibility, a series of statistical studies was conducted, each involving five optiplexer scans (mirror rotations). During each scan, the intensity of the emission signal at 670.7 nm was determined as an average of 15 measurements. Analysis of variance (ANOVA) was then used to determine whether significant differences existed between the averaged data sets for the five mirror rotations.

THEORY

Suppose that the intensity of a spectral line is determined as an average of n measurements, the mirror in the optiplexer is rotated and

*Author to whom correspondence should be addressed.

†Present address: Hercules Aerospace Division, McGregor, TX 76657, U.S.A.

returned to its original position, and the intensity of the same spectral line is redetermined as the average of a second set of n measurements. The whole process is then repeated to obtain a total of N averaged intensities, each average resulting from n intensity measurements. Clearly, if no statistical difference exists between the N data sets, their means should be the same. However, variations within each data set (due to factors such as source noise and differences in sampling) generally make it difficult to tell from simple inspection whether the N means are really the same or significantly different. ANOVA is a statistical procedure for comparing the variation between the N data sets (spectrometer scans or mirror rotations) with the variation within individual data sets (the n intensity measurements for a given scan) to determine whether the mirror rotation has significantly affected the measurement.⁷⁻⁹

For this statistical procedure, we use the variance, V , as a measure of data variability. Variance is defined as the sum of the squares (SS) of the deviations of k individual data from the data mean, \bar{X} ,

$$V = \frac{\sum_i (x_i - \bar{X})^2}{(k - 1)} = \frac{SS}{DF} \quad (1)$$

where x_i is the value of the i th individual data value and $(k - 1)$ is the number of degrees of freedom (DF) associated with the measurements.

Suppose we wish to determine the variability of signal measurement between N scans as a variance, V_B , on the basis of only one measurement for each scan. Since variance is an additive property, V_B may be considered as the sum of two independent contributions, $V_B = V_S + V_E$. The term V_S represents the "variance between," *i.e.*, the true variance due to causes which are independent of V_E and associated only with mirror rotation. The term V_E represents the "variance within", *i.e.*, the variance in intensity measurements which is not associated with mirror rotation (factors such as photon shot noise, flame source drift, nebulizer drift, and electronic drift). Because V_E is unrelated to differences between scans, it is sometimes called the error term. Since V_S cannot be measured directly, V_E is the error associated with estimating V_S from V_B .

To improve the accuracy of our estimate of the variance between scans, we can determine V_B as the mean of n replicate observations. Since

the error term, V_E , is evenly distributed about the central value of each scan, it does not accumulate in the same way as the variation due to the difference between scans, V_S . Therefore, the effect of increasing the number of observations within a scan is to increase the accuracy of the determination of V_S and reduce the variance due to experimental error to V_E/n . The total variance resulting from mirror rotation, V_B , is then calculated from equation (2):

$$V_B = V_S + V_E/n \quad (2)$$

Equation (2) shows that as the number of measurements, n , increases, V_E/n approaches zero and V_B approaches V_S , the true variance associated only with mirror rotation.

In terms of equation (2), V_S is given by

$$V_S = (nV_B - V_E)/n \quad (3)$$

If mirror rotation does not affect the intensity measurements, then V_S is actually zero, and any observed difference between nV_B and V_E is due only to inaccuracies in the estimates of these quantities. This null hypothesis (*i.e.*, $V_S = 0$) can be tested by means of an F -test or variance ratio test.

The F -ratio is given by

$$F = nV_B/V_E \quad (4)$$

and is designed to determine whether the variance between groups (the N scans) is really greater than the variance within a group (the n intensity measurements within each scan). In practice, only estimates of the true values of nV_B and V_E can be calculated because the sampled populations n are finite. Therefore, the F -test can only determine whether the variances are different with a certain preselected probability (*i.e.*, confidence level). If the calculated F -ratio exceeds the critical value listed in the statistical table for the desired confidence level, it means that a significant difference exists between nV_B and V_E and, according to equation (3), V_S is not equal to zero. If V_S is not zero, then rotating the mirror does have a statistically significant effect on the intensity measurements obtained with the spectrometer.

From the discussion above, it is clear that two variances must be determined in order to perform an ANOVA study. As shown in equation (1), these variances can be generated conveniently in the form of sums of squares (SS). For any given set of data, three sums of squares can be determined: the "sum of squares within" (SSW) which is related to V_E , the "sum of

squares between" (SSB) which is related to nV_B , and the total sum of squares (SST). The sum of squares within is given by

$$SSW = \sum_i \sum_j (x_{ij} - \bar{X}_i)^2 = \sum_i s_i^2 \quad (5)$$

where x_{ij} is any individual intensity measurement j belonging to the i th scan, and \bar{X}_i is the mean of the i th scan. The sum of squares between is given by

$$SSB = \sum_i n_i (\bar{X}_i - \bar{X})^2 \quad (6)$$

where \bar{X}_i is the mean of the i th scan, \bar{X} is the grand mean of all the $N \times n$ measurements, and n_i is the number of values in the i th scan. The total sum of squares is given by

$$SST = \sum_i \sum_j (x_{ij} - \bar{X})^2 \quad (7)$$

where the terms are as defined above. From equations (5)–(7), it is clear that

$$SST = SSB + SSW \quad (8)$$

and knowledge of any two sums permits the calculation of the third.

The sum of squares within (SSW) and the sum of squares between (SSB) may be converted into their corresponding variances V_E and nV_B , respectively, by dividing each by the appropriate number of degrees of freedom (DF), where the total degrees of freedom (DFT) is the sum of the degrees of freedom between scans (DFB) and the degrees of freedom within scans (DFW),

$$DFT = DFB + DFW \quad (9)$$

Since the total variance is fixed when the last intensity measurement is taken, the total number of degrees of freedom, DFT, is $(nN - 1)$, where nN is the total number of measurements (75 in this case). Since SSB is the sum of squares for the individual scans, its value is fixed when the last scan is completed. If there are N scans, SSB will have $DFB = (N - 1)$ degrees of freedom. Finally, since SSW is computed from the sums of the individual intensity measurements minus the mean of the intensity measurements for that scan [equation (5)], and since each mean is fixed by the last intensity measurement made for that scan, there are $DFW = (nN - N)$ or $N(n - 1)$ degrees of freedom associated with SSW. Thus

$$V_E = SSW / (nN - N) \quad (10)$$

and

$$nV_B = SSB / (N - 1) \quad (11)$$

EXPERIMENTAL

The optiplexer/multiple entrance-slit spectrometer used in these studies has already been described.¹ The data acquisition program was modified to output the raw data acquired from the analog-to-digital converter (ADC) board in the microcomputer. All ANOVA studies were conducted by acquiring 15 measurements before rotating the inner mirror by a complete revolution (*i.e.*, back to the same fiber-optic light-guide). The process was repeated five times and corresponded to five wavelength scans in the multielement mode. The photomultiplier voltage was maintained at 1000 V. When the air-acetylene flame was employed, the fuel flow was maintained at 1.8 l./min and the oxidant flow at 8 l./min.

RESULTS AND DISCUSSION

Before discussing the results of the ANOVA studies, it is worthwhile to discuss the requirements which must be satisfied in order for the analysis of variance to be valid.⁷⁻⁹ The first requirement is that the intensity measurements have a normal distribution. The second, referred to as homogeneity of variance, is that the variances within each of the N scans must be the same. The final requirement is that there must be no bias in the data, *i.e.*, that all $n \times N$ measurements are randomly and independently drawn from the same population.

Of these three requirements, the one most frequently violated in an ANOVA study is homogeneity of variance. Proof of homogeneity of variance can be established by two statistical tests, the Cochran test⁸ and the Bartlett test.⁷ Since the same number of intensity measurements was made for each scan, the Cochran test may be used and was selected because of the ease of computation.

The Cochran test statistic (C) is designed to test whether one of the variances in the N scans is much larger than the rest and is calculated from

$$C = \text{largest } s_j^2 / SSW \quad (12)$$

where s_j^2 is the largest sum of squares obtained within a particular scan, and SSW is the sum of squares obtained within all scans [equation (5)]. The hypothesis of equal variances is rejected if the computed value for the Cochran statistic exceeds the tabulated value,⁸ which is selected on the basis of the desired confidence level.

By and large, the other two requirements for the validity of an analysis of variance are satisfied in the present study. Although, strictly speaking, the photon shot noise is expected to follow a Poisson distribution, this distribution approaches a normal distribution as the photon flux increases. Since the ADC board of the instrument samples the signal periodically with a fixed interval between measurements, it is not likely that any bias was introduced at this stage in selecting the data.

Analysis of variance studies

The reproducibility of the instrument was first evaluated by aspirating a solution containing only lithium into the flame and rotating the inner mirror with the stepper motor five times. After each rotation, 15 intensity measurements were acquired by the system and stored in memory. Table 1 shows the intensity measurements that were collected and the analysis of variance table prepared from the raw data. From the data in Table 1, the calculated F -ratio is 78.2 (see Table 7). Since the critical F -ratio at the 99% confidence level for the appropriate number of degrees of freedom for this study is slightly less than 3.65,⁷ the null hypothesis for this experiment must be rejected. A check of homogeneity of variance was performed with the Cochran test and revealed that the variances satisfied this requirement at the 99% confidence level (Table 7).

Table 1. Signal (counts at 670.7 nm) obtained with unbuffered lithium standard

Scan 1	Scan 2	Scan 3	Scan 4	Scan 5
273.0	277.5	277.7	277.5	277.7
272.2	277.5	277.5	277.7	277.7
272.0	277.7	277.2	277.7	279.0
272.5	277.0	277.7	279.0	277.7
273.7	277.5	277.7	279.7	277.7
273.2	277.7	275.5	279.7	277.7
273.7	277.7	275.7	279.7	279.7
273.7	277.7	276.5	279.5	281.0
273.7	277.7	279.2	279.7	280.5
273.0	278.5	280.5	279.7	281.7
271.7	278.5	280.0	279.7	281.7
271.7	277.5	280.0	281.0	281.7
271.2	277.0	280.5	279.7	281.7
271.7	277.5	280.5	279.7	281.0
271.2	277.5	280.0	279.7	281.5

Source of variation	Sum of squares	Degrees of freedom	Variance
Between scans	513.2	4	128.3
Within a scan	114.7	70	1.64

Table 2. Signal (counts at 670.7 nm) obtained with buffered lithium standard

Scan 1	Scan 2	Scan 3	Scan 4	Scan 5
285.0	281.25	277.75	281.5	281.75
285.5	281.7	277.7	281.7	281.7
285.2	281.7	277.7	281.7	281.7
281.7	281.7	279.7	281.7	281.5
281.7	281.7	281.7	281.7	279.7
281.7	281.7	281.7	281.7	279.7
281.7	281.7	279.7	281.5	279.7
281.7	283.7	279.7	279.7	281.7
281.7	283.7	277.7	281.2	281.7
283.7	281.7	279.7	281.7	281.7
285.5	279.7	281.7	281.5	281.7
285.2	279.7	283.7	281.5	281.7
285.2	281.7	285.7	281.7	281.7
285.2	281.5	285.7	281.5	281.7
285.7	279.7	285.7	281.7	281.7

Source of variation	Sum of squares	Degrees of freedom	Variance
Between scans	72.90	4	18.22
Within a scan	202.9	70	2.90

To see whether the variability between scans in the first experiment could be attributed to long-term instability of the flame rather than to mirror rotation in the optiplexer, a second ANOVA study was conducted with a multielement solution containing sodium, calcium, barium and strontium, plus 1000 ppm of cesium as an ionization buffer. The purpose of the ionization buffer was to improve the uniformity of the emission profile for the lithium signal by reducing the ionization of the lithium atoms and decreasing the dependence of the lithium signal on observation height in the flame.¹⁰ The results obtained by use of the buffered solution are shown in Table 2 along with the analysis of variance table prepared from the raw data. The calculated F -ratio was found to be 6.28 (Table 7), still greater than the critical value at the 99% confidence level, but much less than the F -ratio obtained when lithium was aspirated without the ionization buffer present. A check on the homogeneity of variance by the Cochran test revealed that at the 99% confidence level, the variances obtained for the five scans were just at the point of being inhomogeneous (Table 7).

A third ANOVA study was conducted by monitoring the flame background at 670.7 nm without aspirating anything into the flame. This experiment eliminated the lithium emission as a source of variability between scans. Table 3 shows the intensity measurements obtained in this experiment, and the ANOVA table prepared from the raw data. The calculated F -ratio

Table 3. Flame background signal (counts at 670.7 nm)

Scan 1	Scan 2	Scan 3	Scan 4	Scan 5
16.94	16.94	16.94	16.56	16.56
16.94	17.44	17.37	16.56	16.56
16.44	16.94	16.94	16.62	16.62
16.44	16.94	16.94	16.69	16.69
16.44	16.94	16.87	16.69	16.69
16.94	16.94	16.87	16.69	16.69
16.94	16.94	16.87	16.62	16.69
16.44	16.94	16.87	16.62	16.56
16.44	16.94	16.87	16.62	16.56
16.94	16.94	16.87	16.69	16.62
16.94	17.44	16.87	16.69	16.69
16.44	16.44	16.87	16.69	16.69
16.44	16.44	16.87	16.62	16.69
16.44	16.44	16.87	16.62	16.69
16.44	16.44	16.87	16.62	16.69
16.44	16.94	16.87	16.56	16.69

Table 4. Signal (counts) obtained with tungsten lamp, monitored at 670.7 nm

Scan 1	Scan 2	Scan 3	Scan 4	Scan 5
67.75	65.75	67.50	65.75	67.50
67.50	65.75	65.75	67.75	66.25
67.75	65.00	65.75	67.75	66.00
67.50	65.50	65.75	67.75	66.50
67.50	67.50	65.50	67.75	66.50
67.50	65.50	67.75	67.75	66.50
67.50	65.75	67.50	67.50	65.75
67.50	65.50	67.75	67.50	65.75
67.75	65.75	65.75	67.75	66.00
67.50	65.50	67.75	67.50	65.75
67.50	67.50	67.50	67.50	66.00
66.50	67.50	67.75	67.50	66.25
67.75	66.50	67.50	65.50	65.75
67.50	67.50	67.50	65.50	64.75
67.50	66.50	65.75	65.50	65.50

Source of variation	Sum of squares	Degrees of freedom	Variance
Between scans	1.337	4	0.3342
Within a scan	2.441	70	0.0349

Source of variation	Sum of squares	Degrees of freedom	Variance
Between scans	22.13	4	5.53
Within a scan	43.61	70	0.62

was 9.57, again indicating variability between scans. A check of the homogeneity of variance by the Cochran test showed that the variances obtained from the five scans were clearly homogeneous at the 99% confidence level (Table 7).

At the outset of this study it had been assumed that photon shot noise would be much greater than any variations associated with the instrument, because the dispersion optics were stationary. However, the ANOVA studies for all of the first three experiments using the flame source indicated that the variance associated with mirror movement was statistically significant. To determine whether the observed variation was really due to the optiplexer spectrometer or to long-term drift in the flame, it was decided to conduct a fourth ANOVA study with use of a more stable emission source.

The fourth ANOVA study was conducted with a tungsten-lamp source in place of the flame and monitoring the tungsten-lamp intensity at 670.7 nm by using the lithium channel of the optiplexer. Table 4 shows the intensity measurements obtained for this experiment and the ANOVA table prepared from the raw data. The calculated F -ratio was 8.92, again indicating a variability between scans which was comparable to that obtained for the flame background and buffered lithium emission. A check for homogeneity of variance by the Cochran test showed that the variances obtained for the five scans were clearly homogeneous at the 99% confidence level (Table 7).

The ANOVA results obtained with the tungsten lamp suggested that the variation observed between scans must actually be due to the optiplexer spectrometer itself, not to source instability. Two potential sources of variation within the optiplexer were identified: (1) instability of image formation at the light guide, owing to variation in mirror repositioning, and (2) signal variations resulting from software gain adjustments on the ADC board. Two final ANOVA studies were conducted to determine whether either of these two effects might contribute to the variability of measurements observed between scans.

To examine the role of image formation on system reproducibility, a series of signal measurements (Table 5) was obtained with the optiplexer set at 670.7 nm, but with no source of any kind present. Even though no emission source was present and the mirror could no longer image a signal on the fiber optic, the ANOVA results (Table 5) reveal a calculated F -ratio of 24.0, indicating a significant variation between scans. A check of the homogeneity of variance by the Cochran test showed that the variances obtained for this experiment were clearly homogeneous at the 99% confidence level (Table 7).

In the final experiment, an ANOVA study was conducted with the high voltage to the photomultiplier turned off (Table 6). With this arrangement, the only possible source of variation left would have to be associated with the

Table 5. Signal (counts at 670.7 nm) obtained without flame

Scan 1	Scan 2	Scan 3	Scan 4	Scan 5
16.75	16.37	16.31	16.19	16.19
16.50	16.37	16.31	16.19	16.19
16.31	16.37	16.18	16.19	16.19
16.37	16.37	16.18	16.19	16.31
16.37	16.37	16.18	16.19	16.25
16.37	16.37	16.18	16.06	16.25
16.37	16.31	16.31	16.19	16.19
16.31	16.37	16.31	16.19	16.19
16.25	16.37	16.31	16.19	16.19
16.25	16.37	16.19	16.19	16.19
16.31	16.37	16.19	16.19	16.25
16.37	16.37	16.19	16.06	16.37
16.37	16.37	16.31	16.19	16.19
16.31	16.37	16.31	16.19	16.19
16.25	16.37	16.19	16.19	16.19

Source of variation	Sum of squares	Degrees of freedom	Variance
Between scans	0.4833	4	0.1208
Within a scan	0.3526	70	0.005037

stability of the electronics used for signal processing. The ANOVA results reveal a calculated *F*-ratio of 13.8, indicating a significant variation between scans. A check of the homogeneity of variance by the Cochran test showed that the variances obtained for this experiment were clearly homogeneous at the 99% confidence level (Table 7). Though long-term drift in the preamplifier circuit could not be ruled out, a more likely source of variation between scans would be the amplifier gain adjustment, on the ADC board, which occurs between mirror

Table 6. Output (counts at 670.7 nm) of ADC board with photomultiplier high voltage off

Scan 1	Scan 2	Scan 3	Scan 4	Scan 5
15.69	15.81	15.94	15.94	15.81
15.69	15.81	15.94	15.94	15.94
15.81	15.81	15.94	15.94	15.75
15.81	15.81	15.94	15.94	15.81
15.81	15.69	15.94	15.94	15.87
15.75	15.75	15.94	15.94	15.87
15.69	15.81	15.94	15.87	15.87
15.75	15.81	15.94	16.44	15.81
15.81	15.81	15.94	15.87	15.75
15.81	15.81	15.94	15.75	15.87
15.81	15.69	15.94	15.87	15.81
15.81	15.75	15.94	15.94	15.87
15.69	15.81	15.94	15.94	15.94
15.69	15.81	15.94	15.75	15.81
15.81	15.81	15.94	15.81	15.75

Source of variation	Sum of squares	Degrees of freedom	Variance
Between scans	0.3750	4	0.09375
Within a scan	0.4766	70	0.006808

rotations. This potential instrumental variability was felt to be more a probable source of variation because it is definitely correlated with mirror rotation.

Interpretation of results

Influence of mirror rotation on instrument stability. The purpose of this study was to answer two important questions regarding the performance of the optiplexer/multiple entrance-slit spectrometer. (1) Does mirror rotation influence the reproducibility of the signal from the spectrometer? (2) If mirror rotation does influence the signal reproducibility, what is the extent and source of the variability introduced?

The results of the statistical analysis of the data clearly show that, in all cases, the changes which occur during the rotation of the optiplexer mirror do result in a statistically significant variation in the signal at the 99% confidence level. This means that the signal variation which occurs during mirror rotation is significantly greater than that observed for photon shot noise, short-term source-fluctuation noise (*i.e.*, source drift and nebulizer drift), short-term electronic drift (photomultiplier power supply fluctuations and amplifier drift), and other sources of variability which are not correlated with mirror movement.

The influence of mirror rotation was essentially the same, regardless of whether a line source (buffered lithium emission from the flame) or a continuum source (tungsten lamp) was used. Since the dispersion optics are stationary within the instrument, the signal variation observed between rotations cannot be a result of wavelength instability, but must result either from inability of the inner mirror to access the individual light guides reproducibly, or from some other instrumental parameter such as the amplifier gain adjustment which varies along with mirror rotation, or from a combination of both.

The influence of mirror rotation in the optiplexer on signal reproducibility should be most severe for a source with a non-uniform intensity profile. With such a source, even small variations in imaging the source onto the light guide could produce large signal variations, owing to changes in the source zone sampled. This interpretation is in line with the magnitude of the first four *F*-ratios shown in Table 7. The most significant influence of mirror rotation was observed when an unbuffered lithium solution was aspirated into the flame. This source should

Table 7. Summary of analysis of variance results

Test run	Variance within*	Variance between†	Calculated F -ratio‡	Calculated Cochran C ‡
Unbuffered Li	1.64	128.3	78.2	0.467
Buffered Li	2.90	18.22	6.28	0.489
Flame background	0.0349	0.334	9.57	0.294
Tungsten lamp	0.623	5.53	8.92	0.329
HV on, no source	0.00504	0.121	24.0	0.335
PMT HV off	0.00681	0.0938	13.8	0.242

* V_E , equation (10).† nV_B , equation (11).‡Critical F -ratio = 3.65 at 99% confidence level.‡Critical C value = 0.488 at 99% confidence level.

have the most pronounced non-uniform intensity profile because of ionization effects in the flame. In contrast, the F -ratios obtained for the flame background and buffered lithium solution were similar to those obtained for the tungsten lamp.

The results obtained without the flame and with the high voltage to the photomultiplier turned off, however, suggest that irreproducibility of image formation on the light guides of the optoplexer may not be the sole cause of the observed signal variation between mirror rotations. Even with no signal from the photomultiplier, the offset of the electronics showed a significant variation between rotations of the mirror. Since there is no direct link between preamplifier offset and mirror rotation, the most likely cause of the observed variations between mirror rotations is variability in the gain adjustment step which takes place between mirror rotations.

Extent of variability introduced by mirror rotation. Inspection of the analysis of variance tables (Tables 1–4) permits an estimation of the variability introduced in the signal during mirror rotation (*i.e.*, V_S). As indicated by equation (3), the variance between scans, V_S , is determined by the difference between the weighted variance observed between scans, nV_B , and the variance within scans, V_E , divided by n , the

number of intensity measurements associated with each scan.

Table 8 shows the values obtained for V_S , the standard deviation of the signal as a result of mirror rotation, and the relative standard deviation, due to mirror rotation, of the signal, for all six experiments. It should be re-emphasized that the values for V_S reported in Table 8 are only estimates. Since V_S is a function of the difference between two variances (one based on 4 degrees of freedom and the other based on 70 degrees of freedom), the estimate of the variance between scans is subject to larger errors than the estimate for the variance within scans, V_E . Nevertheless, the average relative standard deviation in the observed signal, due to rotation of the mirror for the four experiments conducted with a light source, was only 0.76%. Thus, although parameters associated with the rotation of the mirror were found to be a significant source of variability in the signal, compared with various forms of drift, the relative magnitude of the signal variation introduced during mirror rotation itself is quite small.

CONCLUSIONS

This study has demonstrated the power of statistical analysis in evaluating the performance of new instruments and suggests that

Table 8. Estimated signal* variability during rotation of optoplexer

Test run	$V_S \dagger \pm V_E/n \S$	Standard deviation	Average signal	Rel. standard deviation, %
Unbuffered Li	8.44 ± 0.11	2.91 ± 0.33	277.6	1.0 ± 0.1
Buffered Li	1.02 ± 0.19	1.01 ± 0.44	281.9	0.36 ± 0.16
Flame background	0.0199 ± 0.0023	0.141 ± 0.048	16.75	0.84 ± 0.29
Tungsten lamp	0.327 ± 0.042	0.572 ± 0.204	66.73	0.86 ± 0.31
HV on, no source	0.008 ± 0.0003	0.089 ± 0.018	16.26	0.55 ± 0.11
PMT HV off	0.006 ± 0.0005	0.077 ± 0.021	15.85	0.49 ± 0.13

*Counts at 670.7 nm.

†Estimate of variance due to mirror rotation, equation (3).

§Error in the estimate of the variance due to mirror rotation, equation (2).

greater use should be made of statistical methods in instrumental development. For example, when this study was undertaken, it was thought that because of the high wavelength stability of the instrument, photon shot noise and nebulizer drift would be the major sources of variability in the signal. Indeed, casual inspection of the data in Tables 1–6 might lead to this conclusion. Careful statistical analysis of the data, however, leads to quite a different conclusion. While simple analysis of variance can point out where differences exist between treatment groups, even more powerful statistical analyses such as multiple linear regression studies can be used to identify the causes actually responsible for the treatment group differences, as well as their magnitude. Such information can be vital for improving the performance of prototype systems during instrumental development.

ANOVA studies conducted with the optiplexer/multiple entrance-slit spectrometer have shown that variations in instrumental parameters which occur during mirror rotation in the optiplexer are a significant source of signal variation, compared with photon shot noise, source-fluctuation noise, and electronic drift. Although wavelength reproducibility is ensured by the use of stationary dispersion optics, significant signal variations do occur during rotation of the inner mirror of the optiplexer.

Two sources of variability which might affect the performance of the instrument, and are correlated with mirror movement, are the irreproducibility in illuminating the fiber-optic light-guides, and variability introduced by the amplifier gain adjustment step between mirror rotations. When a spectral source was used, the results showed that the most significant effect of mirror rotation occurred with an unbuffered lithium solution, suggesting that emission sources with non-uniform intensity profiles increase the need for reproducibility in source-imaging on the light guides. If this is true, some means of image defocusing at the light guides of the optiplexer could result in better reproducibility. One way to accomplish this would be to place a diffuser screen in the opening in the shutter disk. Clearly, the autoranging gain

adjustment step which takes place between mirror rotations needs to be studied in more detail to determine its effect on signal variability and to see whether other more stable alternatives exist for gain adjustment.

Even though the instrumental changes that occurred during mirror rotation were found to be a significant source of signal variation in the prototype instrument, compared with other sources of variability, the actual magnitude of the variation introduced during mirror rotation was quite small. The average relative standard deviation introduced in the signal during mirror rotation was found to be only 0.76%.

Acknowledgements—This work was supported by Baylor University Research Grants 033-S80-URC, 011-S83-URC, and 089-F81-URC. The authors would like to express their appreciation to Milton Luedke of the Baylor Chemistry/Physics Machine Shop for fabricating specialized parts for the instrument. Two of the authors (KWB and MAB) would like to thank Baylor University for a summer sabbatical to provide the time needed to prepare this paper for publication. This work was taken from the Master's Thesis of Larry D. Benton, portions of which were presented at the 12th Annual Meeting of the Federation of Analytical Chemistry and Spectroscopy Societies, 29 September–4 October 1985, Philadelphia, Pennsylvania.

REFERENCES

1. K. W. Busch, M. A. Busch and L. D. Benton, *Talanta*, 1990, **37**, 89.
2. K. W. Busch and L. D. Benton, *12th Annual Meeting of the Federation of Analytical Chemistry and Spectroscopy Societies*, Philadelphia (1985), Paper No. 73.
3. *Idem*, *Anal. Chem.*, 1983, **55**, 445A.
4. K. W. Busch and B. B. Malloy, in *Multichannel Image Detectors*, Y. Talmi (ed.), pp. 27–58, American Chemical Society, Washington D.C. 1979.
5. K. W. Busch, B. B. Malloy and Y. Talmi, *Anal. Chem.*, 1979, **51**, 670.
6. M. A. Busch, K. W. Busch and B. B. Malloy, *Talanta*, 1990, **37**, 71.
7. O. L. Davies, *Statistical Methods in Research and Production*, 1st Ed., Chapter 5. Oliver and Boyd, London, 1949.
8. W. J. Dixon and F. J. Massey, Jr., *Introduction to Statistical Analysis*, Chapter 10. McGraw-Hill, New York, 1957.
9. M. A. Sharaf, D. L. Illman and B. R. Kowalski, *Chemometrics*, Wiley, Chapter 2. New York, 1986.
10. R. Herrmann and C. T. J. Alkemade, *Chemical Analysis by Flame Photometry*, pp. 35–36, 299. Wiley, New York, 1963.

RAPID SCREENING OF POLYCYCLIC AROMATIC HYDROCARBONS AND FINGERPRINTING OF ENVIRONMENTAL MATERIALS BY LASER-EXCITED FLUORESCENCE SPECTROMETRY*

A. MELLONE, BENJAMIN W. SMITH and J. D. WINEFORDNER†

Department of Chemistry, University of Florida, Gainesville, FL 32611, U.S.A.

(Received 17 May 1988. Revised 18 October 1988. Accepted 25 October 1988)

Summary—Laser-excited fluorescence of aromatic molecular vapors in a graphite furnace has been used as a rapid screening method for polycyclic aromatic hydrocarbons (PAHs) in various sample types and as a fingerprinting technique for crude oils, petroleum products and particulate matter. The simplicity and speed of the method indicate that it will be a useful method for PAH screening.

Many polycyclic aromatic hydrocarbons (PAHs) are classified as EPA priority pollutants because they are known or suspected carcinogens. The two main sources of PAHs in the environment arise from incomplete combustion of fossil fuels for energy production and from incomplete combustion of refuse. Interest in carcinogenic compounds led to the development of many gas and liquid chromatographic techniques for determination of specific compounds in such samples as crude oils, petroleum products, diesel particulates and urban dust.¹ These methods generally involve elaborate extraction and fractionation schemes prior to analysis.

Recently, several groups have reported the use of electrothermal atomizers for the study of the ultraviolet absorption of molecular vapors. Tittarelli *et al.*² found that by monitoring ultraviolet absorption at 190 nm as a crude oil sample was vaporized at temperatures from 140 to 900°, spectral fingerprints characteristic of the samples could be rapidly obtained. In later work,³ a photodiode array was used to monitor absorption in the wavelength range 190–355 nm. Plotting the sequential spectra produced a three-dimensional plot characteristic of the sample vaporized. These representations were also used as a fingerprint for the sample, and had more distinguishing characteristics than the earlier two-dimensional plots. Absorption of ultraviolet light by vapors produced in a graphite furnace has also been used to charac-

terize pollutants in water and sediments and as a fingerprinting technique for various oils, petroleum products and soaps.⁴ The high temperatures obtained with a graphite furnace facilitated the direct analysis of heavy oils, resinous materials and other complex samples often too difficult for analysis by gas chromatographic techniques.

In this work, a novel system involving laser-induced fluorescence of PAHs in a graphite furnace was investigated as a screening method for PAHs and as a fingerprinting technique for environmental samples and other complex mixtures. Direct analysis of crude oil, petroleum products and solid materials was accomplished without sample pretreatment.

EXPERIMENTAL

A block diagram of the experimental system is shown in Fig. 1. The laser used was an He–Cd continuous wave laser (Model 4210N, Liconix, 1390 Borregas Ave., Sunnyvale, CA 94089) with a maximum output of 6 mW at 325 nm. The laser beam passed through a 1.5 mm hole drilled through a polished aluminum off-axis parabolic mirror before passing lengthwise through the inside of the graphite tube.

The graphite furnace was from an atomic-absorption spectrometric system (Model CTF555, Instrumentation Laboratories, Thermo Jarrell Ash, 590 Lincoln St., Waltham, MA 02254). The controller had adjustments for six temperature settings and allowed selection of the ramp rate between the six stages. The furnace was set

*Research supported by DOE-DE-AS05-78OR06022.

†Author to whom all correspondence should be sent.

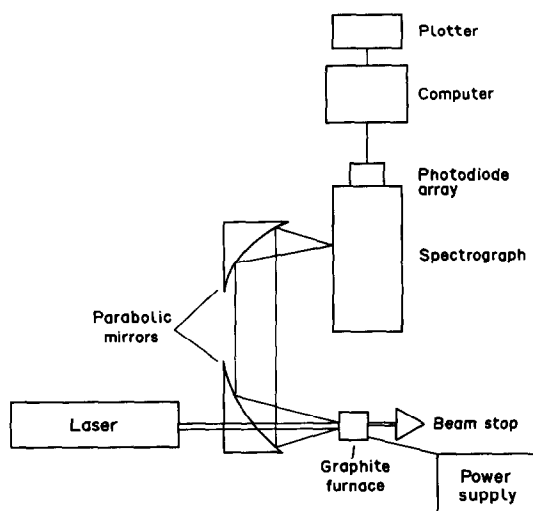


Fig. 1. Schematic diagram of experimental system.

to heat slowly from room temperature to 50° over 1 min to dry the sample, then linearly from 50 to 500° over approximately 2 min as fluorescence spectra were collected. The furnace was contained in a small enclosed housing which allowed volatilization of the sample in an inert environment of argon. The housing also contained a thermocouple in contact with the graphite tube to monitor the temperature.

The fluorescence was collected at 180° relative to the laser excitation. The cone of fluorescent light leaving the graphite tube was collimated by an off-axis parabolic mirror. About 0.3% of the signal was lost by light escaping back through the 1.5 mm hole. The collimated light was focused on the entrance slit of the spectrograph by a second off-axis parabolic mirror.

The flat field spectrograph (Instruments SA, Inc., 173 Essex Ave., Metuchen, NJ 08840) had a dispersion of 24 nm/mm, a focal length of 0.2 m and a spectral range of 200–800 nm. A 1024 pixel intensified diode array (Model TN 6100, Tracor Northern, 2551 West Beltline Highway, Middleton, WI 53562) was mounted on the spectrograph with a laboratory-constructed flange which held the array in the focal plane. The diode array head contained a Peltier effect thermoelectric cooler capable of cooling the head to -20° , which reduced the dark current. A dedicated computer controlled the acquisition, storage, processing and output of data. Generally, the array was exposed for 2 sec before data were read and stored. Spectra were displayed on the screen and stored after automatic subtraction of a pre-stored background spectrum. Additional software called Quadra (Tracor Northern) allowed for the generation, scaling and plotting of three-dimensional representations of fluorescence intensity *vs.* wavelength *vs.* scan number of sequentially accumulated spectra. Scan number was correlated to time and therefore furnace temperature.

RESULTS AND DISCUSSION

To determine the sensitivity of the system, analytical calibration curves were prepared by placing 100 μ l of standard solutions in methanol, ranging from 100 to 0.1 μ g/ml, into the graphite furnace. A drying cycle was employed to evaporate the solvent. The appearance time of the sample has been found to depend linearly on the boiling point of the compound.⁵ Figure 2 shows

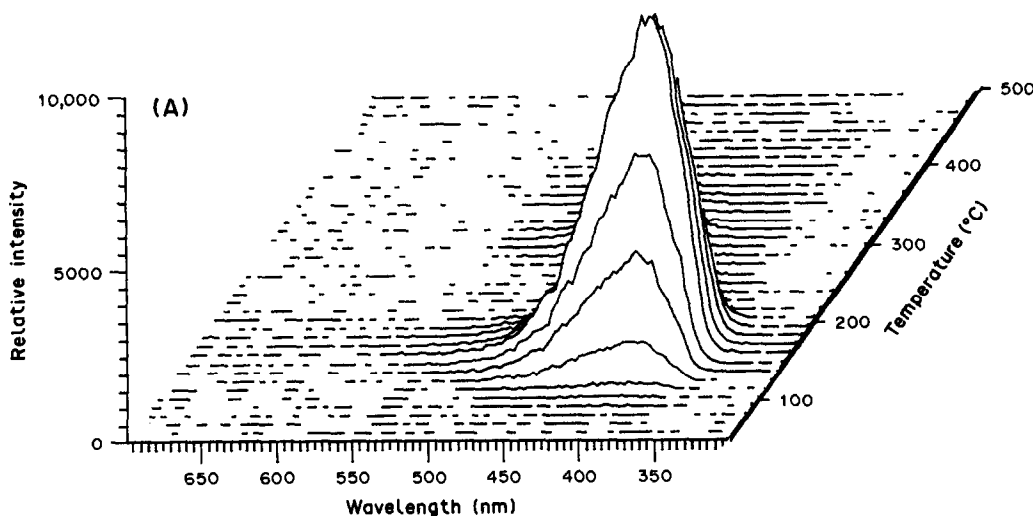


Fig. 2(A). *Caption opposite.*

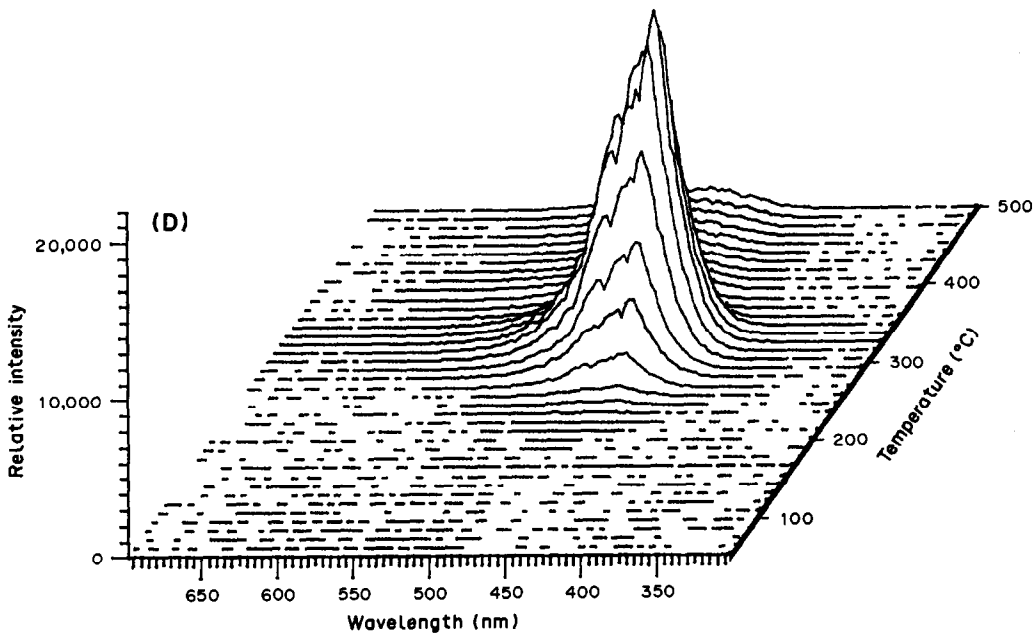
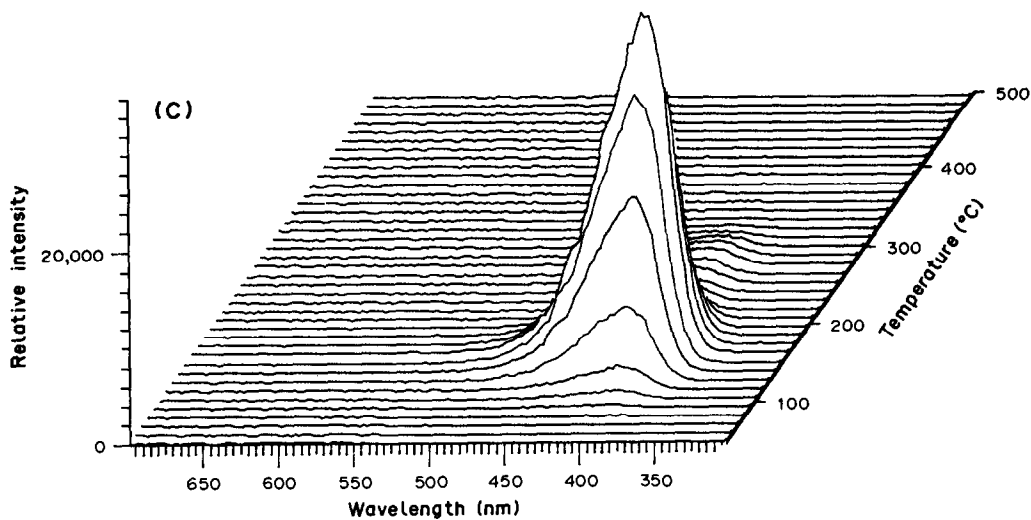
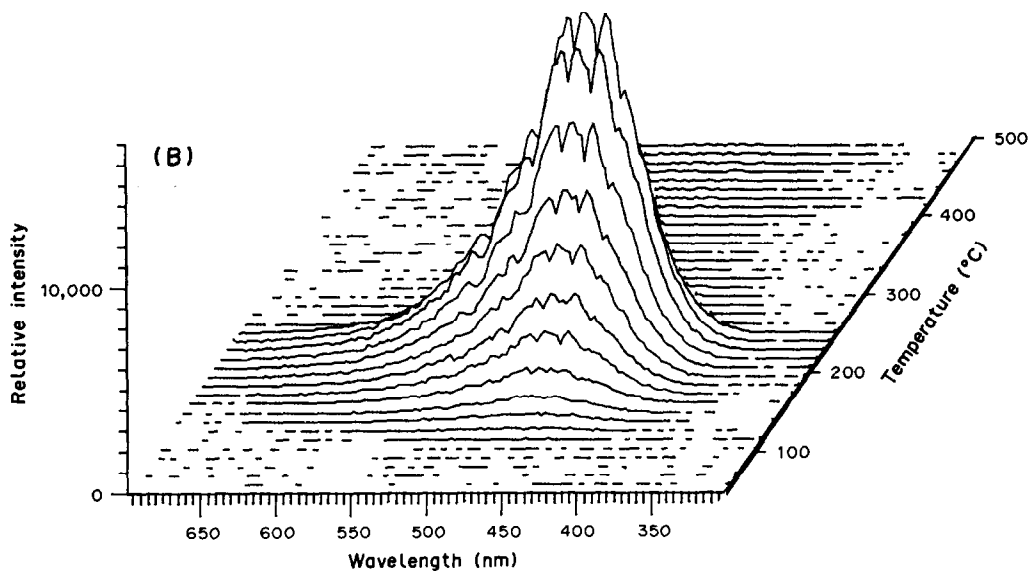


Fig. 2(B-D).

Fig. 2. Vaporization cycles of (A) anthracene, (B) benzo(*b*)fluoranthene, (C) pyrene and (D) coronene.

Table 1. Limits of detection (LOD) obtained by laser fluorescence spectrometry of vaporized polycyclic aromatic hydrocarbons

PAH	LOD, ng	Linear dynamic range*	Slope†
Pyrene	34	3	0.99
Benzo(<i>b</i>)fluoranthene	47	3	1.04
Benzo(<i>a</i>)pyrene	73	>3	1.04
Coronene	79	>3	0.97
Anthracene	103	>3	1.03
Fluoranthene	138	>2	1.01

*Orders of magnitude.

†Slope of log-log calibration curve.

typical vaporization cycles for several standards. The temperature ramp rates were chosen to give a compromise between the increased sensitivity obtained with fast ramp rates and the increased thermal resolution from use of slower ramp rates. Small variations in ramp rates have very little effect on the appearance of the three-dimensional plot. Since all plots have the same temperature scale, the ramp rate simply affects the number of spectra that can be taken during the vaporization cycle, assuming that the scan-rate remains unchanged. For instance, the plot of a standard vaporized at a 30% greater ramp rate would appear the same if the number of scans displayed was reduced from 55 to 39.

For preparation of calibration curves, spectral information is collected and stored in a slightly different form. The software allows the user to define a spectral region of interest. This region is chosen to correspond to the fluorescence peak of a particular compound. As the sample vaporizes, only the area above the base-

line of the region of interest is stored. A representation of the peak area of the fluorescence peak *vs.* time is plotted as a histogram. The area under the histogram peak is proportional to the volume under the peak in the three-dimensional representation, but required much less computer memory. For the six compounds for which standard curves were prepared, the log-log plots are linear over three or more orders of magnitude. The limits of detection (LODs) are calculated as three times the standard deviation of the blank measurement, divided by the slope of the analytical calibration curve (counts/ng). The slopes of the analytical calibration curves, the linear dynamic ranges and the LODs for the six PAHs are shown in Table 1. The major limitation to lower LODs is the high standard deviation of the blank measurement. Uncertainty in the background subtraction causes the low concentration points to deviate from the linear calibration curve. At higher concentrations, the curves bend over, especially for strongly absorbing compounds, owing to pre-filter, post-filter and self-absorption effects. Also, the furnace emission interferes with compounds fluorescing at longer wavelengths and/or vaporizing at higher temperatures. These detection limits are about 10 times higher than those reported for previous work in this laboratory by Kirsch.⁶ However, Kirsch⁶ used more powerful lasers and the fluorescence collection angle was not limited by baffles in the graphite tube housing. In addition, averaging pixels produced a higher signal to noise ratio at

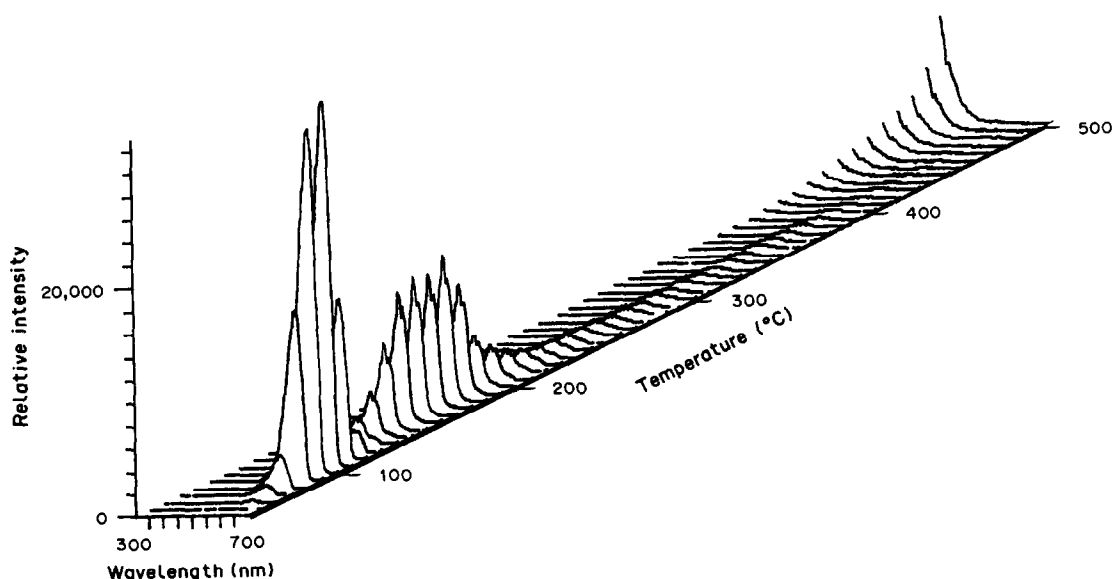


Fig. 3. Vaporization cycle of a standard mixture of anthracene and perylene, showing the thermal resolution of two PAHs.

the expense of spectral resolution. The detection limits obtained in this work are comparable to the approximate determination limits reported by Shekiri and Skogerboe⁵ for absorbance measurements of PAH vapors. If we calculate our detection limits with the same criteria as

Shekiri and Skogerboe,⁵ then our detection limits will be lower by a factor of 3–5 than those shown in Table 1.

To demonstrate the thermal resolution of the system, standard mixtures were vaporized. Figure 3 shows the thermal resolution of two

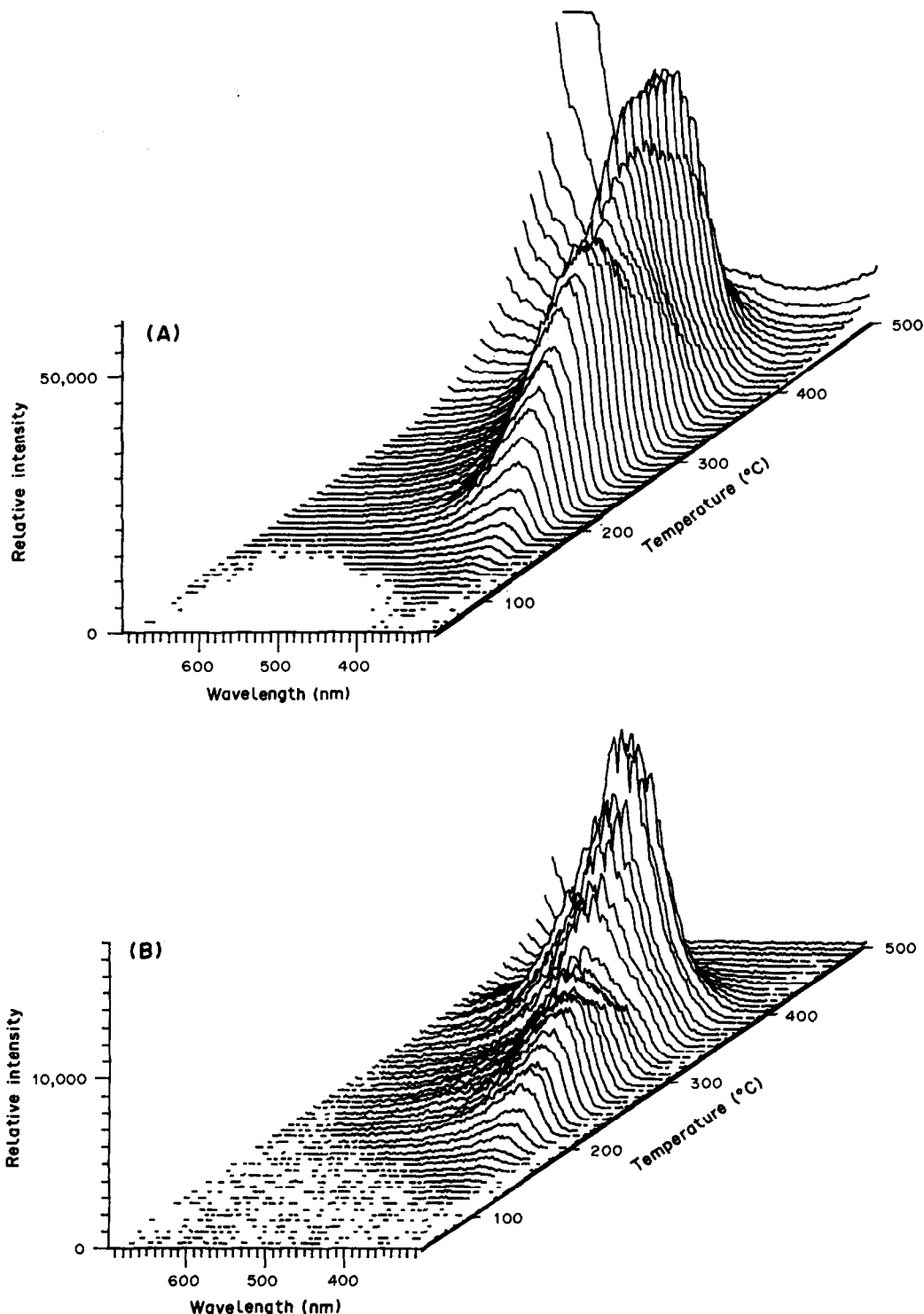


Fig. 4(A) and (B). See p. 118 for caption.

PAHs. The standard compounds evolved over about a 25 sec or 145° interval. In the thermal dimension, the FWHM for most of the compounds tested is about 9 sec, or about 50°. Since the PAHs fail to undergo sharp vaporization transitions into the vapor phase, the thermal resolution capabilities are limited. The highest number of compounds thermally resolved is three. On average, vapor phase PAH spectra

exhibit peak widths of 60–90 nm FWHM. This lack of sharp features and the limited thermal resolution preclude the identification of individual components of a complex mixture. It also seems likely that components in a sample matrix will vaporize at slightly different temperatures than the pure materials do, further complicating the extraction of qualitative information. Finally, to demonstrate the fingerprinting

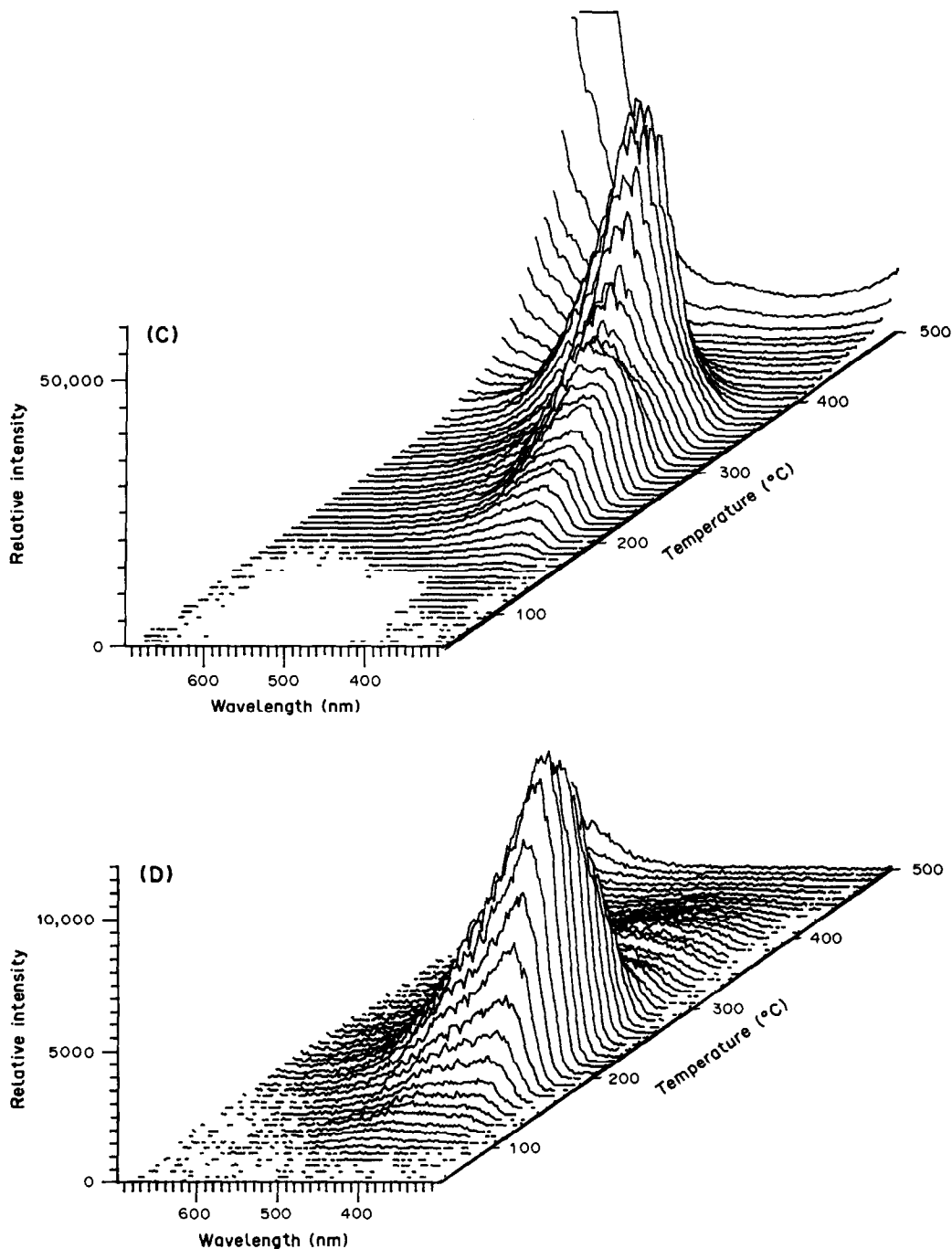


Fig. 4(C) and (D). See p. 118 for caption.

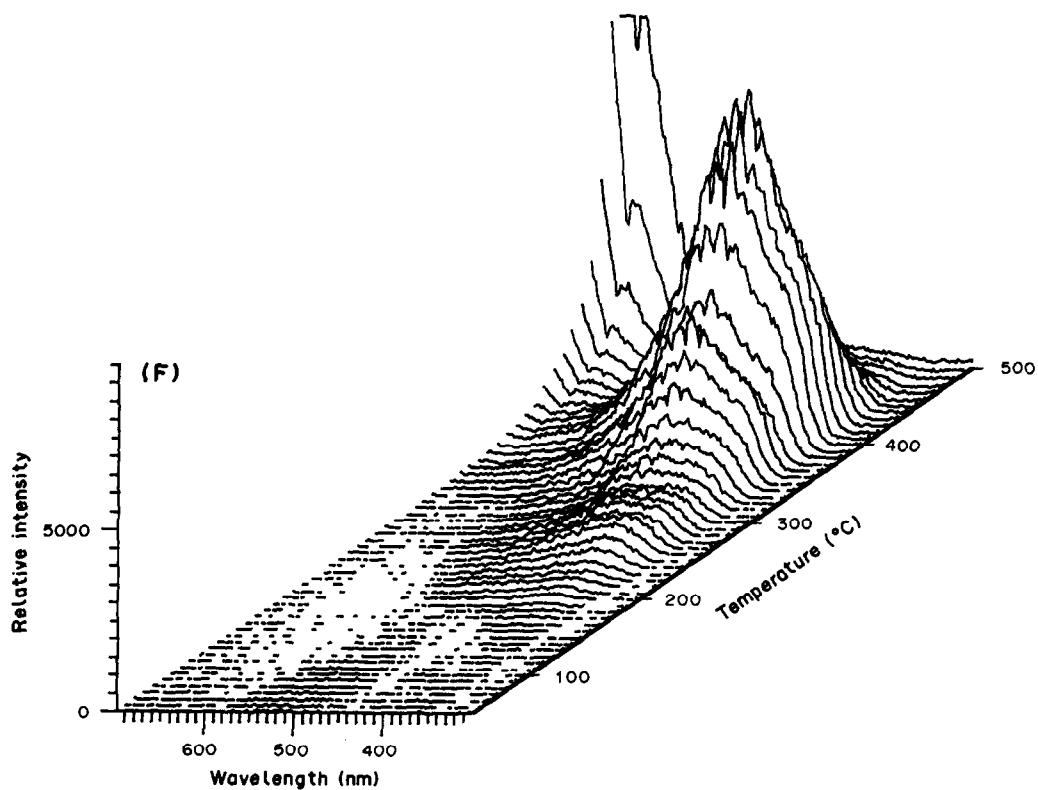
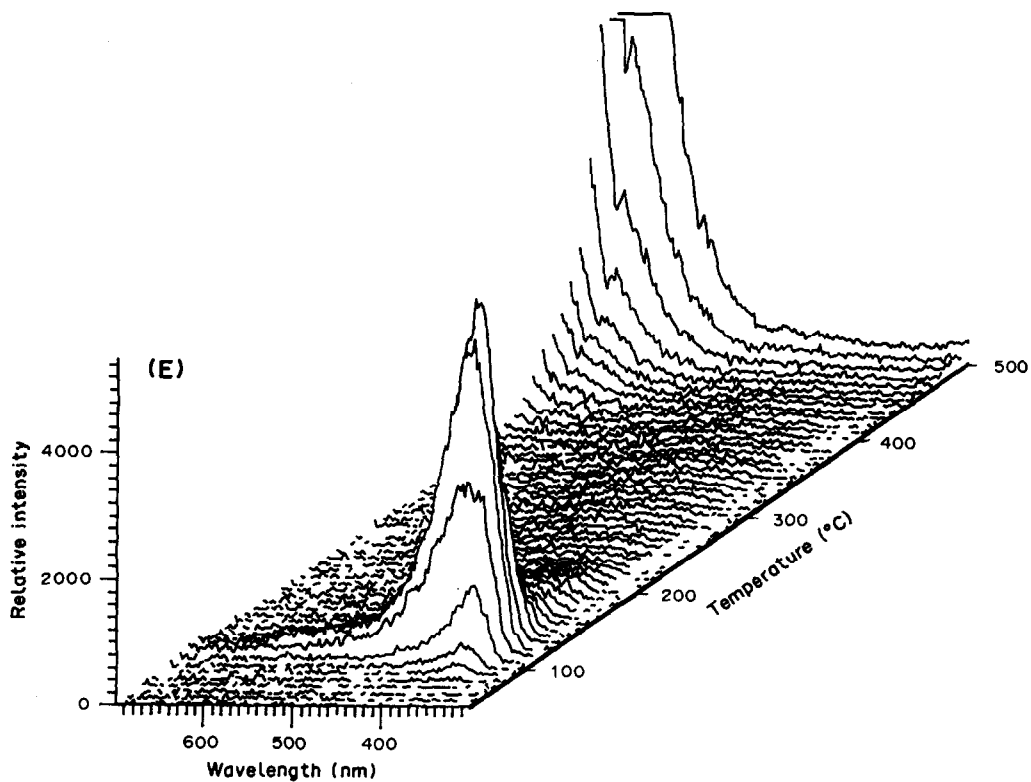


Fig. 4(E) and (F). See p. 118 for caption.

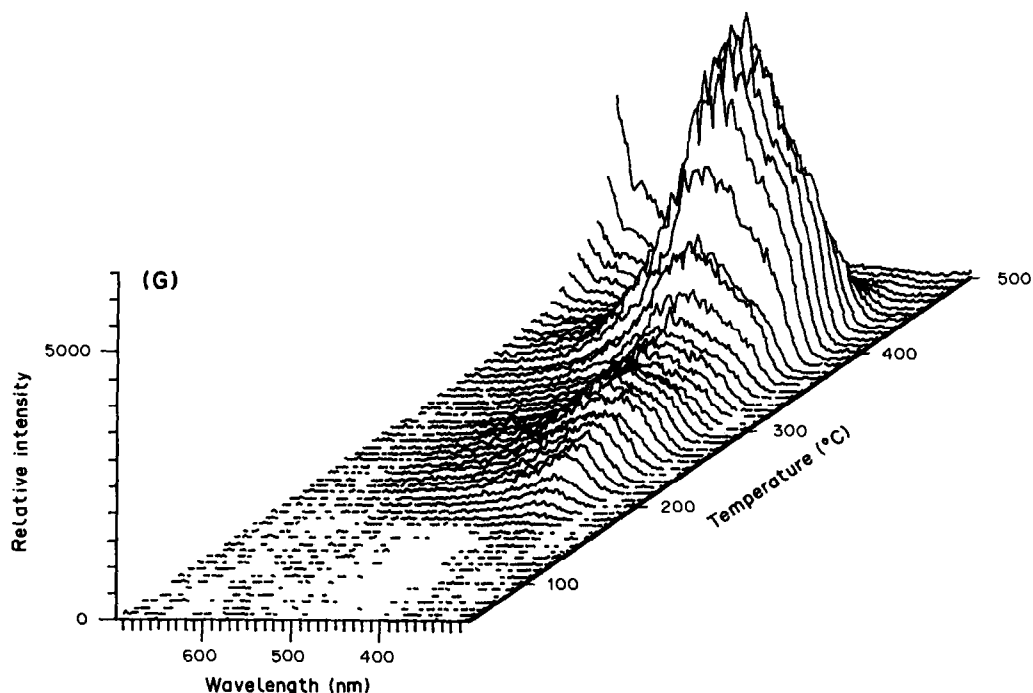


Fig. 4(G).

Fig. 4. Vaporization cycles of (A) Kirkuk crude oil, (B) SRM 1582 crude oil, (C) ES Sider crude oil, (D) SRM 1580 shale oil, (E) regular gasoline, (F) SRM 1649 urban dust and (G) SRM 1648 urban dust.

capability of the system, three samples of crude oil, three samples of particulate matter and several types of petroleum products were analyzed. The resulting three-dimensional plots all contain distinguishing features. Samples producing similar plots can be differentiated by the relative intensities or peak widths of the various features. Figure 4 shows plots obtained from the vaporization of some of these samples.

Future work in this laboratory will be focused on adapting a pulsed laser and gated photodiode array to increase the signal to noise ratio and gain added selectivity, based on the fluorescence lifetime of vaporized species. Additional work is planned to investigate matrix, absorption and pyrolysis effects which contribute to the appearance time of the various components.

Acknowledgements—We would like to thank Mark Glick for help with the computers.

REFERENCES

1. M. L. Lee, M. V. Novotny and K. D. Bartle, *Analytical Chemistry of Polycyclic Aromatic Hydrocarbons*, Academic Press, New York, 1981.
2. P. Tittarelli, L. T. Baldassari and T. Zerlia, *Anal. Chem.*, 1981, **53**, 1708.
3. P. Tittarelli, R. Lancia and T. Zerlia, *ibid.*, 1985, **57**, 2005.
4. K. C. Thompson and K. Wagstaff, *Analyst*, 1979, **104**, 668.
5. J. M. Shekero, R. K. Skogerboe and H. E. Taylor, *Environ. Sci. Technol.*, 1988, **22**, 338.
6. B. Kirsch and J. D. Winefordner, *Anal. Chem.*, 1987, **59**, 1874.

SIMULTANEOUS MULTIELEMENT ATOMIC-ABSORPTION ANALYSIS OF BIOLOGICAL MATERIALS

NANCY J. MILLER-IHLI

U.S.D.A., Nutrient Composition Laboratory, Beltsville, MD 20705, U.S.A.

(Received 7 April 1989. Accepted 15 May 1989)

Summary—A prototype multielement atomic-absorption spectrometer (SIMAAC) consisting of a continuum source and an echelle polychromator modified for wavelength modulation, has been used to determine several elements in a variety of biological materials. Analyses have been done with flame atomization as well as graphite furnace atomization. Compromise atomization conditions do not significantly limit the accuracy or precision. Analytical results for a variety of samples are reported.

Atomic-absorption spectrometry (AAS) has gained widespread acceptance since it was first introduced in the late 1950s. AAS is acknowledged as being a straightforward atomic spectroscopic technique with relatively few interferences and has widely been used for trace metal analysis. Several atomic spectroscopic techniques have been commercially developed for multielement analyses but until recently, only sequential multielement AAS systems were commercially available. In 1979 Harnly *et al.*¹ described a prototype simultaneous multielement AAS system based on the continuum source system first described by Zander *et al.*² This spectrometer is referred to as the SIMAAC system (Simultaneous Multielement Atomics Absorption Spectrometer with a Continuum Source). The SIMAAC system consists of an echelle polychromator modified for wavelength modulation, a continuum light source, a flame or graphite furnace atomizer, and a minicomputer for data acquisition and manipulation. A block diagram of the system is shown in Fig. 1. This spectrometer, with its simple optical configuration, has several unique features and offers some capabilities which exceed those provided by conventional single-element line-source AAS (AAL).¹ SIMAAC features simultaneous determination of up to 16 elements by use of a multielement exit cassette with the echelle polychromator. In addition, simultaneous multielement detection limits similar to those obtainable with line-source AAS are yielded for those elements measured at wavelengths longer than 270 nm. Wavelength modulation provides double beam,

background-corrected absorbances as well as extended analytical ranges covering 5–7 orders of magnitude of concentration for each element. This facilitates the simultaneous determination of multiple elements, the concentration of which may differ by a factor of 1000 or more. Computer control of the SIMAAC system provides high speed (18 kHz) intensity-data acquisition as well as controlling the wavelength modulation. All intensity data from the 16 channels are stored, absorbances are computed, and all data processing, calibration, statistical review of the data, and presentation of data in the form of a final report are done by the computer. Although fairly complex, the software associated with the system is quite flexible and can also facilitate furnace emission measurements and atomic-absorption spectra measurements.

When evaluating SIMAAC as a multielement system, it is often compared with inductively coupled plasma atomic-emission spectrometry (ICP–AES) and inductively coupled plasma mass spectrometry (ICP–MS), most often with the former. SIMAAC GFAAS detection limits are superior to ICP–AES detection limits and sample volume requirements are much smaller, typically 5–25 μ l. ICP–AES direct reading polychromator systems are typically capable of determining more elements simultaneously than the sixteen which SIMAAC can simultaneously detect.³ Generally, multielement AAS is more susceptible to chemical interferences, and ICP–AES to spectral interferences. SIMAAC GFAAS detection limits are in many instances comparable to ICP–MS detection limits. ICP–MS has the advantage of being more

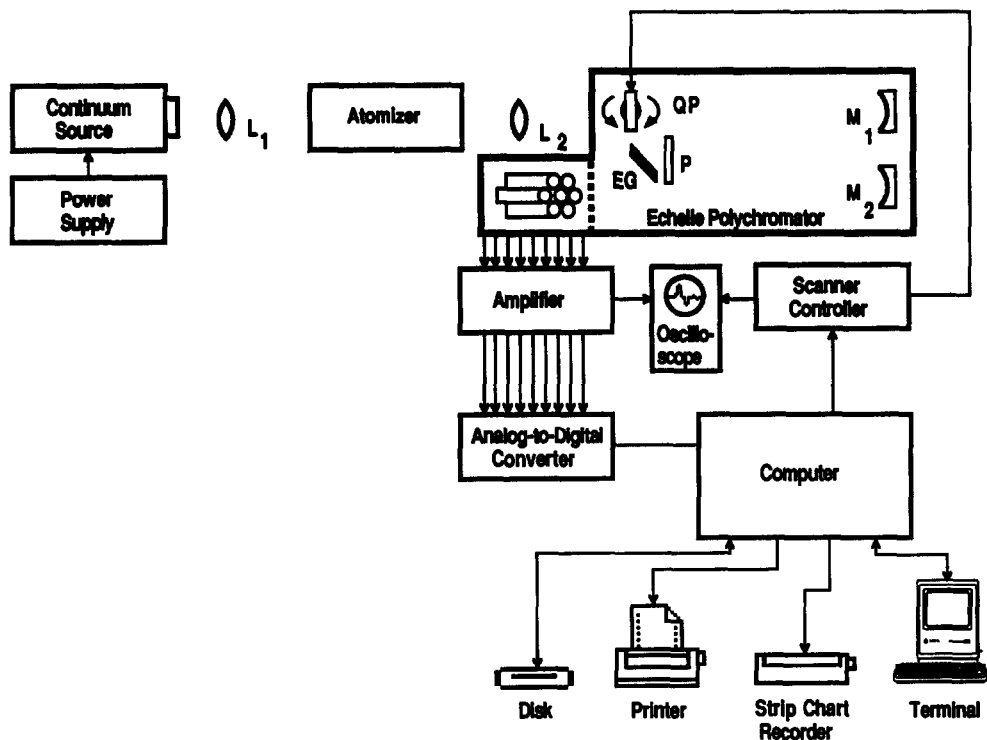


Fig. 1. Block diagram of the SIMAAC system. (L_1 and L_2 are lenses; QP is a quartz refractor plate, M_1 and M_2 are mirrors; EG is the echelle grating; P is the order-sorting prism).

suitable for the determination of refractory elements than is AAS, but is susceptible to interferences from polyatomic ions when analyzing complex biological samples.⁴

The SIMAAC system was developed jointly by Tom O'Haver of the University of Maryland and the Nutrient Composition Laboratory of the U.S. Department of Agriculture. Several researchers have been involved in the development, characterization, and optimization of this system over the last decade, providing hardware, software, and analytical applications expertise.⁵⁻²⁶ Although research continues on future hardware and software modifications which may be implemented, the system has been used in the same basic configuration for routine multielement applications for the past 8 years. Both flame analyses and graphite furnace analyses have been done with this system. Applications have ranged from semi-quantitative determinations of metalloenzymes to determine molar ratios, to high-accuracy trace metal determinations for the characterization of commercial reference materials. The author's experience with some multielement methods and resultant analytical applications data obtained by using the SIMAAC system are discussed here.

EXPERIMENTAL

SIMAAC

The data presented in this work were obtained with the SIMAAC prototype multielement AAS system.¹ The system has five main components: the continuum source, the atomizer, the echelle polychromator, the wavelength modulation hardware and the signal-processing electronics. The continuum source is a 300-W Cermax lamp (ILC Technology, Sunnyvale, CA). Either a flame or a graphite furnace atomizer can be used with the system (see Fig. 1). Flame AAS data were obtained by using either a conventional air-acetylene flame or a nitrous oxide enriched air-acetylene flame. Graphite furnace AAS (GFAAS) data were obtained with an HGA 500 graphite furnace equipped with an AS-40 autosampler (Perkin-Elmer Corp., Norwalk, CT). The echelle polychromator is a Spectraspan III (Beckman Instrument Co.) with photomultiplier tubes as detectors. Wavelength modulation is accomplished with a quartz plate mounted on a galvanometer inside the entrance slit and driven by a scanner controller (General Scanning, Watertown, Mass). Photomultiplier tube currents are amplified by a preamplifier

and converted into a voltage by a preamplifier circuit and the outputs are multiplexed by the computer. Voltages are digitized by the analog-to-digital converter of the computer and stored for future data processing. The PDP 11/34 computer (Digital Equipment Corp., Maynard, Mass.) provides control of the wavelength modulation, and is responsible for acquisition of intensity data, computation of absorbances, file maintenance of analytical data and experimental conditions, analytical calibration with non-linear calibration algorithms, and printing of the final report summaries.

Elements and wavelengths

Elements were selected for determination by means of the multielement cassette of the echelle on the basis of their potential interest in the context of nutrition and food composition. The elements (and measurement wavelengths) are: Al (309.3 nm), Ca (422.7 nm), Co (240.7 nm), Cr (357.9 nm), Cu (324.7 nm), Fe (248.3 nm), K (404.4 nm), Mg (285.2 nm), Mn (279.5 nm), Mo (313.3 nm), Na (589.6 nm), Ni (232.0 nm), Pb (283.3 nm), Sn (224.6 nm), V (318.5 nm) and Zn (213.9 nm).

In most cases, the most sensitive resonance lines are utilized, but a less sensitive line has been employed for potassium, which is often present at high concentrations in samples analyzed with this system.

Air-acetylene flame conditions

Compromise conditions have been established for the simultaneous determination of 8 elements (Co, Cr, Cu, Fe, K, Mn, Na, and Zn). Acceptable Ca and Mg recoveries are obtained after dilution of the sample with 0.5% lanthanum solution. The optimum conditions include an air-acetylene flow-ratio of 4.2 (air flow 10.8 l./min; acetylene flow 2.6 l./min) and a viewing height in the flame of 1.5 mm.⁵ These conditions provide accuracies of $100 \pm 5\%$ and precisions of 5% relative standard deviation (RSD) for the analysis of reference materials of various compositions. These conditions were used for all air-acetylene flame analyses reported in this work.

Nitrous oxide enriched air-acetylene flame

Normal air-acetylene flames do not provide sufficiently high flame temperatures to dissociate some of the stable compounds formed by Mg and Ca. Nitrous oxide may be added to an air-acetylene flame (60% N₂O) to increase the

flame temperature, allowing the simultaneous determination of Ca, Cu, Fe, K, Mg, Mn, Na, and Zn.⁶ With a 60% N₂O-enriched air-acetylene flame, accuracies of $100 \pm 11\%$ were achieved for the simultaneous determination of these 8 elements.⁶ The nitrous oxide enriched flame is more turbulent, providing precisions which are a factor of 2-3 poorer than those obtainable with a normal air-acetylene flame. All nitrous oxide enriched air-acetylene flame data were obtained at a viewing height of 9 mm in the flame. An ionization suppressant was added (1000 µg/ml Cs) to both samples and standards to prevent low recoveries for potassium.

Graphite furnace conditions

Simultaneous multielement furnace analyses were done under compromise atomization conditions which are summarized in Table 1.⁷ A char temperature of 500° was selected to avoid pre-atomization losses of Pb and Zn. The compromise atomization temperature of 2700° was selected to ensure complete atomization of refractory elements such as Mo and V. All determinations utilized a 20-µl injection volume. Argon was used as the purge gas, at the default flow-rate of 300 ml/min. All determinations were done with platform atomization and peak area measurements were used for quantification.

Calibration standards

Multielement calibration standards were made with multielement stock solutions from Spex Industries (Metuchen, NJ). The standards had a final nitric acid concentration of 5% v/v, obtained by addition of nitric acid purified by sub-boiling (isopiestic) distillation (Seastar Chemicals, Seattle, WA). Nine standards were made for flame analyses, covering 4 orders of magnitude of concentration (0.1, 0.5, 1.0, 5.0, 10.0, 50.0, 100 and 500 µg/ml Mn, Zn, Cu, Co, Cr; 1.0, 5.0, 10.0, 50.0, 100, 500, 1000 and

Table 1. GFAAS program for simultaneous multielement determinations*

	Temperature, °C	Ramp, sec	Hold, sec
Dry	170	20	30
Char	500	20	30
Atomize†	2700	0	10
Clean-out	2700	1	5
Cool down	20	1	10

*Platform atomization.

†Argon flow, 20 ml/min during atomization.

5000 $\mu\text{g/ml}$ Ca, Fe, K, Mg, and Na). Standards for nitrous oxide enriched air-acetylene flame work contained 1000 $\mu\text{g/ml}$ cesium as an ionization suppressant. The 10,000 $\mu\text{g/ml}$ Cs stock solution was prepared from Suprapur cesium chloride (EM Laboratories, Darmstadt, F.R.G.).

Sample preparation

Most samples were prepared by wet-ashing with a nitric acid/hydrogen peroxide mixture. This low-temperature procedure is suitable for biological sample preparation for large studies. Biological fluids such as serum and urine were decomposed by a dry-ashing procedure, the samples being heated in a muffle furnace at 480° overnight. Nitric acid purified by sub-boiling distillation, and Ultrex (J. T. Baker, Phillipsburg, NJ) or Perone (DuPont, Wilmington, DE) hydrogen peroxide were used for all sample preparation work.

RESULTS AND DISCUSSION

Air-acetylene flame analyses

Flame analysis methods were validated initially by analyzing a number of reference materials. From the large number of total multielement determinations done, it has been found that accuracies of $100 \pm 5\text{--}15\%$ can generally be obtained.⁸ Flame applications over the past 8 years have ranged from single-sample analysis to studies involving hundreds of samples. Sample throughput for large studies has been as high as 90 samples (or 720 determinations) per day. One large study recently completed dealt with the analysis of chicken samples obtained for a nationwide study at USDA. As part of the quality control (QC) program for this study, a chicken QC material was developed in-house and characterized. Table 2 contains data resulting from the characterization of this

Table 2. Analytical data for a chicken control material (C21-1916), flame results

Element	Concentration, $\mu\text{g/g}$, dry weight	
	SIMAAC results*	Line-source AAS results†
Cu	0.85 ± 0.15	1.15 ± 0.28
Zn	22.6 ± 2.4	24.2 ± 1.5
Na	1806 ± 326	1963 ± 52
K	13819 ± 968	14005 ± 472
Mg	1285 ± 264	1092 ± 40
Fe	12.3 ± 3.3	15.9 ± 2.2
Ca	313 ± 54	265 ± 29

*Uncertainties represent ± 1 standard deviation ($n = 9$).

†Uncertainties represent 95% confidence intervals ($n = 15$).

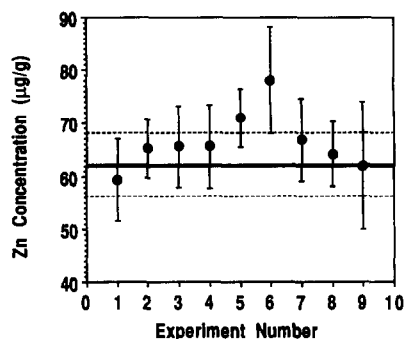


Fig. 2. Quality-control chart for Zn determined in NBS SRM1572 Tomato Leaves. Data obtained over 9 experiments spanning a 5-month period. The solid line represents the mean certified Zn value and the dotted lines represent the uncertainties quoted in the certificate. (Certified value: $62 \pm 6 \mu\text{g/g}$ Zn.)

chicken QC material (C21-1916) for 7 elements. The SIMAAC multielement analytical data are compared with conventional single-element AAS (AAL) data obtained under specific optimized analytical conditions. Review of the data shows good agreement between the SIMAAC and AAL values. Uncertainties for the SIMAAC Na, K, and Mg data reflect the decrease in the slope of the analytical calibration curve at high concentrations for these elements, leading to larger concentration uncertainties. This material and several NBS standard reference materials (SRMs) were analysed during the course of the study (5 months) to ensure that accurate results were being reported. Trace element results from this study indicated that Fe and Zn were present in much higher concentrations in dark meat than in light meat and that there was no significant difference in trace metal concentrations as a function of the brands analyzed.

A collaborative study with a scientist from the Plant Stress Laboratory of USDA was made, in which peanut leaf samples were analyzed to evaluate the effect of metals added to the soil on the trace metal levels in peanut leaves. More than 2000 peanut leaf samples were analyzed in duplicate over the course of the study. A peanut-leaf control material was prepared and characterized for 7 elements (Mn, Zn, Fe, Cu, Mg, Ca, K) and repeatedly analyzed throughout the course of the study, along with NBS SRM1572 Tomato Leaves. A QC chart for Zn determinations in the Tomato Leaves control material is shown in Fig. 2. Here, Zn data for 9 experiments for the study (spanning a 5 month period) are shown. Use of Tomato Leaves as a QC material showed significantly high Zn values

Table 3. Peanut-leaf control material reference values

Element	Concentration, $\mu\text{g/g}$, as received*
Mn	84.8 ± 4.0
Zn	42.6 ± 6.5
Fe	135 ± 20
Cu	12.6 ± 1.0
Mg	0.97 ± 0.08
Ca	2.18 ± 0.24
K	1.12 ± 0.12

*Uncertainties represent 95% confidence intervals ($n = 15$).

for experiments 5 and 6, indicating a possible problem and resulting in these experiments being repeated. These and similar data for the elements determined indicate that analytical accuracy is not adversely affected by the compromise flame atomization conditions. Reference values for the peanut-leaf control material developed for the study are shown in Table 3.

Multielement analysis capabilities of the SIMAAC system have proven useful in the characterization of a number of reference materials, including Mixed Diet RM8431.⁹ This material was prepared by USDA and is marketed by the National Bureau of Standards. Flame analyses were done to quantify levels of Cu, Zn, Mn, Na, K, Mg, Fe, and Ca in this freeze-dried diet material. Supplemental data from 9 additional laboratories, using a total of 10 different analytical methods, contributed to the reference values for this material.⁹ The SIMAAC flame data as well as the reference values for Mixed Diet RM8431 are given in Table 4. Good agreement is seen between the SIMAAC data (mean \pm standard deviation) and the reference values.

Nitrous oxide enriched air-acetylene flame analyses

Simultaneous determination of Mg and Ca with the other elements routinely determined requires a hotter flame for analysis. Typical Ca results obtained by using standard multielement conditions with an air-acetylene flame are compared with results obtained by using a 60% nitrous oxide enriched air-acetylene flame, in

Table 4. Flame results for diet reference material RM8431

Element	Concentration, $\mu\text{g/g}$, dry weight	
	SIMAAC results*	Reference values†
Cu	3.30 ± 0.15	3.36 ± 0.33
Zn	16.0 ± 0.8	17.0 ± 0.6
Mn	7.76 ± 0.31	8.12 ± 0.31
Na	3607 ± 410	3120 ± 160
K	9158 ± 350	7900 ± 420
Mg	760 ± 100	650 ± 40
Fe	36.8 ± 1.9	37.0 ± 2.6
Ca	2259 ± 306	1940 ± 140

*Uncertainties represent ± 1 standard deviation ($n = 5$).

†Uncertainties represent 95% confidence intervals.

Table 5. Clearly, low Ca values are seen for most of the reference materials analyzed with a conventional air-acetylene flame. The nitrous oxide enriched flame permits the simultaneous determination of all the elements of interest. Larger uncertainties are reported for Tomato Leaves and Spinach Leaves because these sample digests contained high Ca concentrations corresponding to a region of decreased slope and the calibration curve. Results from the simultaneous determination of 8 elements in NBS SRM 1577 Bovine Liver are shown in Table 6. The average accuracy was $100 \pm 6\%$ for the 8 elements determined simultaneously, based on the mean certified values for this material.

Graphite furnace AAS analyses

The full potential of multielement AAS determinations can only be realized when a graphite furnace is selected as the atomization device. Multielement GFAAS provides sub-ng/ml detection limits with μl -sized samples⁷ but can also tolerate fairly high analyte concentrations by using the extended range capabilities of the SIMAAC system. Results from the analysis of dry-ashed SRM 2670 Toxic Elements in Freeze-Dried Urine (elevated level) are given in Table 7. Simultaneous multielement GFAAS results for 5 elements compare favorably (average accuracy $100 \pm 4\%$) with the mean certified values for this material.

Table 5. Flame results for Ca concentrations in reference materials*

Material	Concentration, $\mu\text{g/g}$, dry weight		
	Air-acetylene	Enriched	Certified value
Wheat flour	65.7 ± 5.8	198 ± 8	190 ± 10
Rice flour	35.7 ± 5.3	145 ± 3	140 ± 20
Bovine liver	43.1 ± 5.8	113 ± 4	124 ± 6
Tomato leaves	—	30365 ± 1339	30000 ± 300
Spinach	12300 ± 1100	12829 ± 310	13500 ± 300

*Uncertainties represent ± 1 standard deviation ($n = 3-5$).

Table 6. Nitrous oxide enriched air-acetylene flame results for Bovine Liver SRM 1577

Element	Concentration, $\mu\text{g/g}$, dry weight	
	SIMAAC results*	Certified value
Mn	9.68 \pm 2.34	10.3 \pm 1.0
Zn	125 \pm 13	130 \pm 13
Fe	233 \pm 12	268 \pm 8
Cu	187 \pm 5	193 \pm 10
Mg	598 \pm 24	604 \pm 9
Ca	113 \pm 4	124 \pm 6
Na	2682 \pm 145	2430 \pm 130
K	9262 \pm 424	9700 \pm 600

*Uncertainties represent ± 1 standard deviation ($n = 5$).

Its multielement capabilities and small sample-size requirements make SIMAAC well suited for GFAAS analyses of biological fluids which may only be available in limited quantities. Recently, SIMAAC data were provided for the characterization of a protein reference solution prepared by Dr. Gordon Fell at the Royal Infirmary in Glasgow, Scotland.⁴ This material is used for quality control purposes for clinical analyses. Simultaneous multielement analytical data obtained by using the SIMAAC system are compared with the ranges of data obtained by experts using atomic-absorption spectrometry, ICP-AES, and ICP-MS, in Table 8. The range of SIMAAC results compares favorably with the ranges of results obtained by the other techniques.

Several years ago Dr. Susan Lewis developed several methods for multielement determinations in blood serum with the SIMAAC system. Of particular interest were the GFAAS methods developed.^{10,11} The first method permits the determination of Fe, Cu, and Zn in 25 μl of serum and the second method was developed to facilitate the determination of Al, Co, Cr, Mn, Mo, Ni, and V in blood serum after dry-ashing of 2 ml of lyophilized serum and dilution to a final volume of 0.5 ml. These methods were used to assist in the characterization of Bovine Serum reference material (RM8419) produced at USDA and sold by the

Table 7. GFAAS results for toxic elements in freeze-dried urine SRM 2670

Element	Concentration, $\mu\text{g/g}$, dry weight	
	SIMAAC results*	Certified values
Cu	331 \pm 33	370 \pm 30
Pb	98 \pm 12	109 \pm 4
Cr	86 \pm 7	85 \pm 6
Ni	294 \pm 23	(300)
Cd	84 \pm 6	88 \pm 3

*Uncertainties represent ± 1 standard deviation ($n = 3$).

Table 8. GFAAS results for plasma protein solutions

Element	Range of concentrations, ng/ml	
	SIMAAC	Reference values*
Al	320-360	330-420
Cr	100-160	120-150
Cu	160-220	180-280
Mn	200-400	160-250

*Based on data from AAS, ICP-AES, and ICP-MS.

National Bureau of Standards.¹² As a result of the success with this material, a second bovine serum material was developed as a standard reference material (SRM1598) and SIMAAC characterization data were requested. The first serum control material was run as a QC material for the characterization study and analytical data for 5 elements (Mn, Cr, Co, Mo, and Al) for both RM8419 and SRM1598 are listed in Table 9. The SRM1598 data are those which were reported to NBS in the characterization of that material. Co determinations were somewhat variable, so a range was reported rather than a mean \pm standard deviation. The certified values and uncertainties were determined subsequently and include reference data from a variety of methods and analysts.

Graphite furnace slurry analyses

Clearly, conventional sample preparation procedures provide a satisfactory means of sample decomposition for multielement GFAAS analyses. Additional benefits with regard to time saving and avoidance of sample contamination may be realized by eliminating this tedious sample preparation step and analyzing solids directly. Solid samples prepared as slurries may be introduced into the graphite furnace directly by conventional liquid sample delivery techniques, and extensive treatment of the samples is thus avoided.¹³ Slurry data thus obtained for the simultaneous multielement analyses of NBS SRM1568 Rice Flour appear in Table 10. A slurry of 10 mg of material in 5 ml of 5% v/v nitric acid containing 0.04% Triton X-100 was prepared. The slurry sample was mixed by ultrasonic agitation until the time that the autosampler withdrew an aliquot for injection into the graphite furnace. The SIMAAC data compare favorably with the certified values (average accuracy $100 \pm 11\%$ based on the mean certified value). These and similar data for a variety of reference materials and biological and botanical materials suggest that this technique shows a great deal of promise.

Table 9. GFAAS results for bovine serum materials

Material	Element	Concentration, ng/ml	
		SIMAAC result*	Reference/certified value
Bovine Serum SRM1598	Mn	3.56 ± 0.41	3.89 ± 0.33
	Cr	0.23 ± 0.06	0.14 ± 0.08
	Co	0.6-1.6	1.28 ± 0.19
	Mo	10.9 ± 2.9	11.8 ± 1.1
	Al	3.14 ± 0.89	3.8 ± 0.9
Bovine Serum RM8419	Mn	2.12 ± 0.18	2.6 ± 0.5
	Cr	0.34 ± 0.04	0.30 ± 0.05
	Co	0.8-2.4	1.2 ± 0.3
	Mo	13.7 ± 3.2	16 ± 4
	Al	8.04 ± 0.30	13 ± 5

*Uncertainties represent ±1 standard deviation (n = 5).

Table 10. Slurry GFAAS results for NBS SRM 1568 Rice Flour

Element	Concentration, µg/g, dry weight	
	SIMAAC result*	Certified value
Mn	17.0 ± 1.1	20.1 ± 0.4
Zn	17.0 ± 3.4	19.4 ± 1.0
Fe	9.5 ± 0.2	8.7 ± 0.6
Cu	1.9 ± 0.2	2.2 ± 0.3
Ca	133 ± 6	140 ± 20

*Uncertainties represent ±1 standard deviation (n = 3).

CONCLUSIONS

The SIMAAC system, with its simple optical configuration, is a versatile analytical tool allowing rapid and convenient multielement determination of up to 16 elements. Good background correction capability and the extended range provided by the wavelength modulation are very desirable features of the system. Sub-ng/ml detection limits can be obtained with µl samples when graphite furnace atomization is employed. A large number of applications have been made with both flame and graphite furnace atomization under compromise conditions, with minimal effect on the accuracy and precision. Sample matrices analyzed range from biological fluids to coals and sediments. The rapid multielement analysis capabilities of this system make it well suited for the evaluation of new methods such as the GFAAS slurry analysis techniques.

Acknowledgement—The author would like to acknowledge the assistance of Mrs. F. E. Greene and recognize all of those individuals who have contributed to the success of the SIMAAC system, providing expertise for both instrumentation development and methods development, laying the foundation for the successful applications which have been achieved with this instrument. Those persons include Dr. Thomas O'Haver, Dr. James Harnly, Dr. Andrew Zander, Dr. Peter Keliher, Dr. Jerry Messman, Dr. Wayne Wolf, Mrs. Jean Kane, and Dr. Susan Lewis.

REFERENCES

1. J. M. Harnly, T. C. O'Haver, B. Golden and W. R. Wolf, *Anal. Chem.*, 1979, **51**, 2007.
2. A. T. Zander, T. C. O'Haver and P. M. Keliher, *ibid.*, 1976, **48**, 1166.
3. J. M. Harnly, *ibid.*, 1968, **58**, 933A.
4. D. B. Lyon, G. S. Fell, R. C. Hutton and A. N. Eaton, *J. Anal. At. Spectrom.*, 1988, **3**, 265.
5. J. M. Harnly, J. S. Kane and N. J. Miller-Ihli, *Appl. Spectrosc.*, 1982, **36**, 637.
6. N. J. Miller-Ihli, *Anal. Chem.*, 1985, **57**, 2892.
7. J. M. Harnly, N. J. Miller-Ihli and T. C. O'Haver, *Spectrochim. Acta*, 1984, **39B**, 305.
8. T. C. O'Haver, *Analyst*, 1984, **109**, 211.
9. N. J. Miller-Ihli and W. R. Wolf, *Anal. Chem.*, 1986, **58**, 3225.
10. S. A. Lewis, T. C. O'Haver and J. M. Harnly, *ibid.*, 1984, **56**, 1651.
11. *Idem*, *ibid.*, 1985, **57**, 2.
12. C. Veillon, S. A. Lewis, K. Y. Patterson, W. R. Wolf, J. M. Harnly, J. Versieck, L. Vanballenberghe, R. Cornelis and T. C. O'Haver, *ibid.*, 1985, **57**, 2106.
13. N. J. Miller-Ihli, *J. Anal. At. Spectrom.*, 1988, **3**, 73.
14. J. M. Harnly and T. C. O'Haver, *Anal. Chem.*, 1981, **53**, 1291.
15. J. M. Harnly, *ibid.*, 1982, **54**, 876.
16. *Idem*, *ibid.*, 1982, **54**, 1043.
17. J. M. Harnly, N. J. Miller-Ihli and T. C. O'Haver, *J. Autom. Chem.*, 1982, **4**, 54.
18. J. S. Kane and J. M. Harnly, *Anal. Chim. Acta*, 1982, **139**, 297.
19. N. J. Miller-Ihli, T. C. O'Haver and J. M. Harnly, *Anal. Chem.*, 1982, **54**, 799.
20. N. J. Miller-Ihli, T. C. O'Haver and J. M. Harnly, *Appl. Spectrosc.*, 1983, **37**, 429.
21. J. D. Messman, M. S. Epstein, T. C. Rains and T. C. O'Haver, *Anal. Chem.*, 1983, **55**, 1055.
22. J. M. Harnly and J. S. Kane, *ibid.*, 1984, **56**, 48.
23. N. J. Miller-Ihli, T. C. O'Haver and J. M. Harnly, *ibid.*, 1984, **56**, 176.
24. J. M. Harnly, *ibid.*, 1984, **56**, 895.
25. N. J. Miller-Ihli, T. C. O'Haver and J. M. Harnly, *Spectrochim. Acta*, 1984, **39B**, 1603.
26. E. W. Herbert and N. J. Miller-Ihli, *Am. Bee J.*, 1987, **127**, 367.

CHARACTERIZATION AND OPTIMIZATION OF HPIC FOR ON-LINE PRECONCENTRATION OF TRACE METALS WITH DETECTION BY ICP-MASS SPECTROMETRY

D. W. BOOMER, M. J. POWELL* and J. HIPFNER

Ontario Ministry of the Environment, Inorganic Trace Contaminants Section, 125 Resources Rd.,
Rexdale, Ontario M9W 5L1, Canada

(Received 4 May 1989. Accepted 12 June 1989)

Summary—The objective of this study was to investigate the feasibility of using a commercially available cation-exchange column for trace metal preconcentration. In addition, the advantages of interfacing the column to a highly sensitive element-selective detector were examined. A high-performance ion-chromatograph (HPIC) with a high-pressure pump and valve system was used to aid loading and delivery of the mobile phase. An inductively coupled plasma mass spectrometer combination (ICP-MS) was used as a detection device, with interfacing by means of a small diameter liquid-transport tube. The performance of the HPIC/ICP-MS combination was optimized by varying the concentration and flow-rate of two eluents (nitric acid and hydrochloric acid). The effects of varying the sample pH were assessed and the column capacity was determined by "breakthrough" tests. The elements copper, cadmium, mercury and lead were studied; the detection capability was dependent upon the sample volume loaded onto the column. The accuracy of the method was assessed by analysis of an "in house" reference standard.

The Ontario Ministry of the Environment conducts many environmental studies which require information regarding the metal content of different sample matrices. An example of this is the acidic precipitation in Ontario study (APIOS). Many of these samples contain trace concentrations of elements that are of key importance to the project but are below the detection capability of the conventional ultratrace metal determination methods based on ICP-MS. In particular, the levels of Cd and In are below the detection capability of the instrumental technique for many typical sample events.¹ Other studies that require ultratrace metal determination in different matrices include long-range transport of air particulates, and metal contamination of freshwater invertebrates and of surface and ground waters.²⁻⁴ The preliminary work reported in this paper will be the basis for developing an analytical method to support some or all of these studies.

Ion-exchange columns have long been used for preconcentration for trace metal determination.⁵⁻⁷ Commercial cation-columns specifically designed for use in high-performance ion-chromatography (HPIC) systems are in use.⁸ Though most of the applications involve

separation of the common transition metals, some work has been done with concentrator columns.⁹

Commercially available HPIC systems generally use photometric or conductimetric detection to determine analytes in the eluate. These detectors provide a non-specific, universal response for various analytes. Single-element detectors have an advantage over non-specific detectors for the determination of individual analytes in the eluate from a chromatographic column. These techniques include colorimetry,^{10,11} atomic-absorption spectrophotometry (AAS)^{12,13} and graphite-furnace atomic-absorption spectrophotometry (GFAAS).¹⁴ GFAAS provides superior detection limits but sample throughput is limited by the discrete sample-introduction system.

Multielement detectors have the advantage of being specific as well as more sensitive than traditional single-element detectors. The use of multielement detectors can eliminate chromatographic interference caused by co-eluted peaks of different elements.¹⁵ Systems that use multielement detectors to measure elements in an eluate include atomic-fluorescence spectrometry (AFS),¹⁶ inductively coupled plasma atomic-emission spectrometry (ICP-AES)^{17,18} and direct current plasma atomic-emission spectrometry (DCP-AES).^{19,20}

*Author for correspondence.

Work in HPLC/ICP-AES has advanced to the point where temperature gradients are being employed in reversed-phase liquid chromatography to solve some of the elution problems for sulphur and silicon compounds in order to achieve better detection limits.²¹

Inductively coupled plasma mass spectrometry (ICP-MS) is a relatively new technique for elemental analysis; its operation and performance have been described elsewhere.^{22,23}

In the work described here an ICP-MS system was used as the detector for analytes eluted from a resin-based short IC cation guard-column. The advantages offered by the ICP-MS system include excellent detection limits, very fast sequential multielemental detection capability and the ability to measure isotope ratios in eluting peaks. Other workers have used ICP-MS as a detector in chromatographic separation and speciation studies,^{24,25} and off-line in studies of preconcentration, with use of the isotope dilution and standard addition techniques.^{26,27} Gel filtration has also been used recently for sample preparation in interference studies.²⁸

Maximum preconcentration is achieved when the analytes are removed from the column as rapidly as possible. Well defined, narrow analyte peak-widths are required since the ICP-MS system uses peak-height measurements to determine concentrations. Peak-area measurements can be made, but calculations must then be done off-line, with external software. Short retention times also permit higher sample throughput. Since all analytes from a previous sample must be removed from the column before a new sample is loaded, the retention times dictate the sample analysis rate.

Copper, cadmium, mercury and lead were chosen as test analytes because of their significance in many environmental studies. They are also representative of a mass range that is scanned frequently.

Interfacing of an HPIC with ICP-MS has been studied by other workers. Dean *et al.*²⁹ stated that the number of theoretical plates, an indication of column efficiency and retention time, was not affected significantly by changes in the size of the liquid-transport tube. On the other hand, Whaley *et al.*³⁰ conducted extensive work on the flow and transport characteristics of an HPLC coupled to ICP-AES and found that the distance between the column and nebulizer should be as short as possible. It seems logical to minimize dispersion throughout the system. The major contributor to dispersion in

an ICP is the spray chamber but this is a fixed variable. Large connection lines will cause additional dispersion. However, this potential problem can be minimized by keeping the distance between the column and nebulizer as short as possible by using a small-bore connection tube.

This work describes the general characteristics of the HPIC/ICP-MS system and the optimization of chromatographic conditions for the cation guard column for concentration and elution of metal ions. The final objective of the study is to demonstrate significant elemental preconcentration.

EXPERIMENTAL

Apparatus

An Eldex model 264-100 dual-piston high-pressure pump was used in this study. Two Rheodyne six-port syringe-loading manual sample injector valves (model 7125) were employed to load the sample onto the column. The syringe-loading ports were modified to permit continuous sample flow rather than single injections. This allowed the sample-loading and elution to be performed in a semi-automated mode. Switching from loading to injection was done manually.

The column used for these studies was a Dionex Ionpac cation guard cartridge, model HPIC-CS5. Information on the physical and chemical make-up of the ion-exchange resin is a commercial secret. The column and the sample-introduction system of the ICP-MS were connected with 90 cm of 0.58 mm bore polyethylene tube (Clay Adams Inc.). The operating conditions for the ICP and the mass spectrometer were optimized for precision and detecting power prior to connection to the HPIC (Table 1).

Reagents

The eluents for this study were prepared from Sea-Star ultrapure nitric and hydrochloric acids (Sea-Star Chemicals, Sydney, British Columbia, Canada). The analyte contamination levels in the concentrated nitric acid were listed as 0.020 ng/ml Cu, 0.005 ng/ml Cd and 0.04 ng/ml Pb. The analyte contamination levels in the concentrated hydrochloric acid were 0.050 ng/ml Cu, 0.020 ng/ml Cd and 0.50 ng/ml Pb. There were no assay listings for Hg in either acid. The stock metal standard solutions (1000 µg/l.) were prepared from either Fisher

Table 1. Spectrometer description and operating conditions

Instrument		
ICP-MS System	Perkin-Elmer/Sciex Elan model 250	
ICP	Plasma Therm Co. model 2500	
Sample introduction	Meinhard C-3 nebulizer Scott-type spray chamber Fassel-type torch with extension for interface compatibility	
Software	Beta copy of version 11.0	
Operating conditions		
ICP	Forward power	1100 W
	Coolant flow-rate	12 l./min
	Auxiliary flow-rate	0.8 l./min
	Nebulizer flow-rate	1.6 l./min
	Nebulizer back pressure	45 psig
	Viewing height	20 mm above load coil
Ion lens	P	-11.97 V (d.c.)
	B	+3.55 V (d.c.)
	S2	+17.00 V (d.c.)
	E1	-10.11 V (d.c.)
Operating pressure	1st stage	10 ⁻³ mmHg
	2nd stage	3.5 × 10 ⁻⁵ mmHg
Measurement parameters	low resolution	
	sequential mode; 3 points per peak, 0.5 sec measurement time	
Isotopes scanned	63Cu, 114Cd, 208Pb, 202Hg	

or BDH reagent grade materials. The sodium hydroxide used was BDH analytical reagent grade. Doubly distilled demineralized water (DDW) was prepared by passing distilled water through a Barnstead Nanopure-II system, and collecting it in batches.

RESULTS AND DISCUSSION

Column capacity

Since information on the column packing material and dimensions was not available, the column capacity was determined experimentally. Solutions containing 10 µg/ml of each element of interest were passed through the column at a flow-rate of 2.0 ml/min. "Breakthrough" was indicated by the continuously monitored analyte signal increasing significantly above background. Table 2 displays the column capacity results. The theoretical column capacity is expected to be similar for all four elements. Differences in flow-rates, concentrations of standards, analyte contamination of the eluent, and column packing/analyte inter-

action can result in experimental differences of column capacity for each element.

Cadmium, copper and lead were eluted quickly, with sharp peaks, but the mercury peak had a long tail, showing a significant background signal for 15–20 min after the peak maximum had appeared. This was attributed to a memory effect, the mercury being adsorbed on the system components and then slowly leached. Figure 1 shows a multielement scan produced by using the sequential scanning mode of the ICP-MS with 5% v/v nitric acid as eluent and a multielement solution containing 10 ng/ml of each analyte. Note the substantial tail on the Hg peak, indicative of a memory effect.

Effects of eluent strength on retention time

The removal of cations from cation columns is dependent on the acidity of the eluent. In general, the higher the acid concentration, the shorter the retention time.³¹ As mentioned earlier, rapid removal of the analyte "plug" from the column is desirable. A series of experiments was conducted to determine the effects of eluent strength on retention time, with various concentrations of nitric and hydrochloric acids.

A multielement solution of copper, cadmium and lead, each at a concentration of 10 ng/ml, was used for this experiment. The pH of this solution (2.8) was rather low because of preservation of the stock solution with nitric acid. The solution was pumped through the column until 200 ng of each element had been loaded, then the elements were eluted with nitric acid at concentrations varied from 0.05 to 10% v/v. The set of experiments was then repeated with hydrochloric acid as the eluent.

Figure 2 shows a profile of retention time *vs.* nitric acid concentration for Cu, Cd and Pb. The retention time decreases rapidly with increasing acid concentration up to about 3%, and then more gradually. The profile for Hg is similar (Fig. 3). Figures 4 and 5 show the results for use of hydrochloric acid as eluent. The curves exhibit the same general trends, with a decrease in retention time with increasing acid concentration, but the time resolution of the elements is better than that with nitric acid, at all but the highest acid concentrations, suggesting that hydrochloric acid may be preferable for methods requiring separation rather than preconcentration.

Nitric acid was preferred for the present work because it generally gave lower retention times for all the elements studied. Because of the

Table 2. Column capacity

Element	Breakthrough time, min	Capacity, µeq
Cu	38	6.0
Cd	70	6.3
Hg	88	5.7
Pb	126	6.1

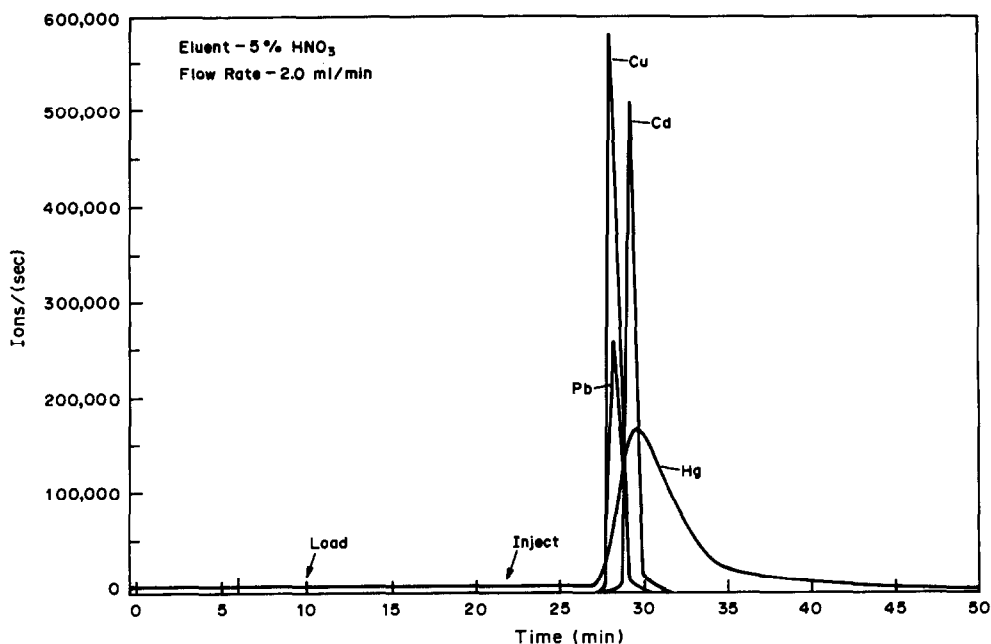


Fig. 1. Scan of a multi-element solution eluted from the cation column after passage of a solution containing 10 ng/ml of each element, for 11 min at 2 ml/min.

significantly longer retention times and poor peak resolution for mercury, no further experiments were done with it.

Limitations on eluent strength

With the ICP-MS system, the acid concentrations of the sample entering the spray chamber should be kept as low as practicable because high concentrations of acid degrade the nickel sampling orifice, resulting in imprecision of the signal.³²

In addition, spectral interferences appear, owing to the combination of H, N and O atoms with metal ions in the plasma. Since the nitric acid is a good source of these elements, the acid concentration becomes a limiting factor. Tan

and Horlick have done extensive work documenting the spectral interferences caused by nitric acid solutions.³³ A further reason for limiting the concentration of the acid in the eluent is that there are detectable levels of analyte contamination in the acid, which will degrade the detection limits. Also, high concentrations of acid ($>6M$) will cause the column resin to shrink, resulting in a diminished diffusion velocity of ions in the resin bed. This will result in longer retention times for the analytes.³¹

On the basis of these considerations and the experimental results discussed above, the eluent concentration of 5% v/v nitric acid chosen was a good compromise.

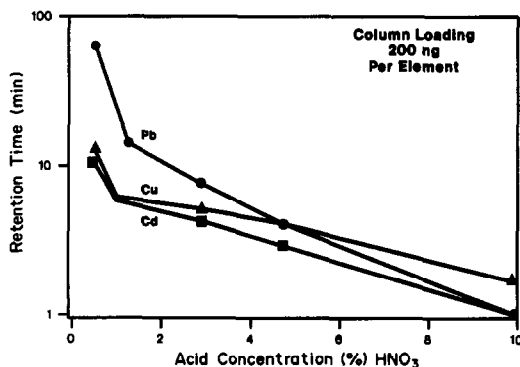


Fig. 2. The effect of varying the concentration of nitric acid as eluent on the retention time for Cu, Cd and Pb.

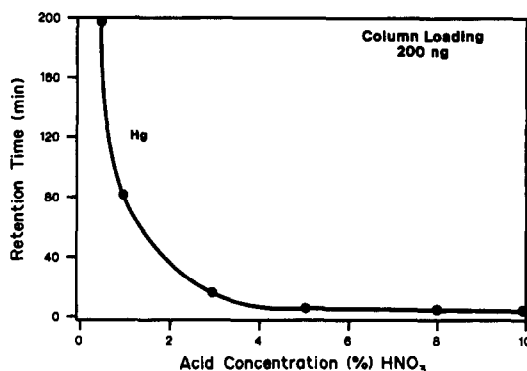


Fig. 3. The effect of varying the concentration of nitric acid as eluent on the retention time for Hg.

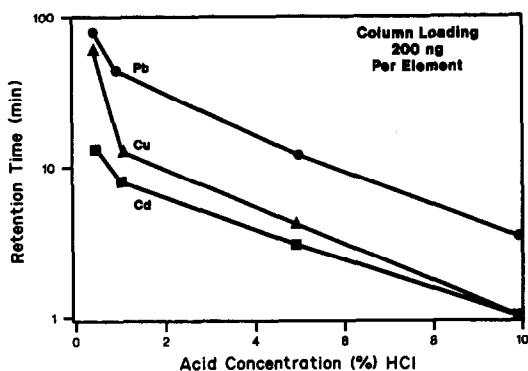


Fig. 4. The effect of varying the concentration of hydrochloric acid as eluent on the retention time for Cu, Cd and Pb.

Effects of flow-rate on retention and response times

The piston pump delivers both the sample loading stream and the elution acid stream. Monitoring the elution profiles of analytes while changing the flow-rate through the piston pump allows determination of the effects of flow-rate on retention and response times. In these experiments we have defined the response time as the time elapsed from the beginning of the loading sequence to the initial response of the detector to the eluted analyte.

Pump flow-rates were adjusted by mechanical movement of the micrometer scaled stop-rod which controlled the length of piston travel. Flow-rates for the experiment were 0.5, 1.0, 2.0, 3.5 and 5.0 ml/min. The pump setting for each flow-rate was determined experimentally by collecting the eluent from the column for 1 min and measuring its volume. The maximum flow-rate with this pump was found to be 5 ml/min. Retention and response times were determined by monitoring the profile produced for each

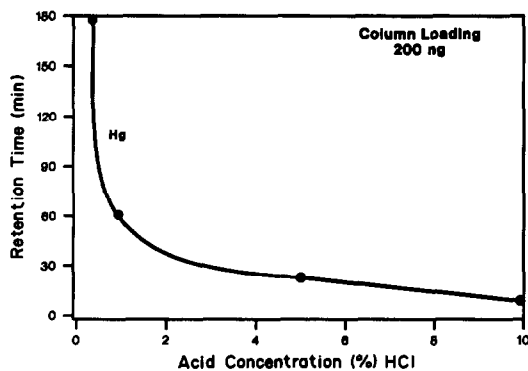


Fig. 5. The effect of varying the concentration of hydrochloric acid as eluent on the retention time for Hg.

analyte. The retention and response times were found to be similar for all three elements, so plots for one analyte will be given. A solution of 10 ng/ml Cu was pumped to produce a column loading of 200 ng of Cu, the loading time being adjusted according to the flow-rate setting, e.g., to 40 min at the 0.5 ml/min flow-rate. Figure 6 shows the retention and response times as functions of flow-rate. As expected, the retention time decreases as the pump flow-rate is increased. It levels off at flow-rates above 3.0 ml/min. The response time decreases more rapidly as the flow-rate is increased. At a flow-rate greater than 2.0 ml/min, the response time is constant at approximately 2.0 min. A flow-rate of 3.5 ml/min was chosen as optimum.

Higher flow-rates degrade the precision of the analyte signal from the ICP-MS, because the flow-rate exceeds the optimum input rate for the nebulizer. Increased pumping speed may also cause imprecise movements of the piston, resulting in irregular flow-rates.

Effects of sample pH on retention time and instrument response

Samples submitted to the laboratory may vary in pH. Any analytical method chosen for sample analysis must ensure that variations in the sample pH will not bias the accuracy of the results.

The acidity or alkalinity of a sample will affect the complex equilibrium of the column.³⁴ It is necessary to establish a "working pH range" that will have minimal effect on instrument response and retention time. This will eliminate the need for any sample pH adjustment, which would not only be time-consuming but could also be a significant source of contamination.

Six sample solutions with pH values of 11.5, 9.5, 7.4, 4.7, 3.0 and 1.6 were prepared with

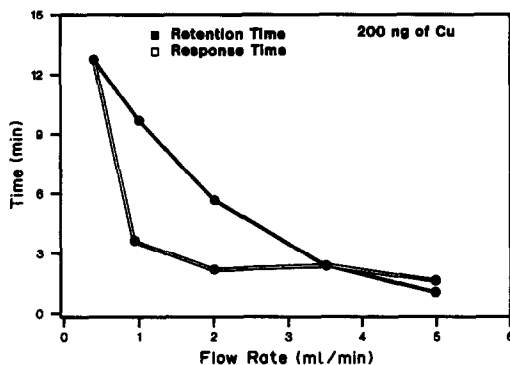


Fig. 6. Effect of flow-rate on retention and response time.

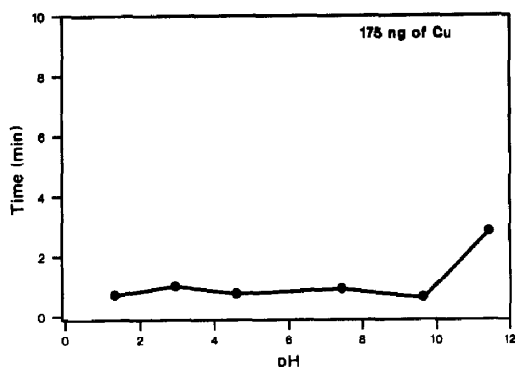


Fig. 7. Effect of pH on retention time for Cu.

analyte concentrations of 10 ng/ml each of Cu, Cd and Pb. The pH was adjusted with nitric acid and sodium hydroxide solution. Each of the six solutions was loaded onto the column at a flow-rate of 3.5 ml/min for 5 min, giving an analyte loading of 175 ng for each element, and 5% v/v nitric acid was used as the eluent. The instrumental responses for each analyte at the different pH levels were measured and retention times were determined.

Figure 7 depicts a plot of the retention time for Cu as a function of sample pH. Insignificant variation in retention time was observed over the range of pH from 1.6 to 9.5. At pH >9.5 the retention time increased, probably because of precipitation of metal hydroxides on the column.

Figure 8 displays the Cu signal response *vs.* sample pH. Unlike the relatively flat retention time curve, this profile exhibits a decreased signal at low pH and an increased one at high pH, with a constant response between pH 4 and 9. This means that any sample with a pH falling in this range can be loaded onto the column, eluted and analysed, with minimal bias in the result. The lower limit could be extended to

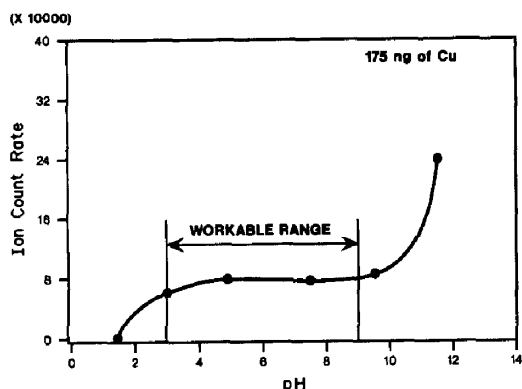


Fig. 8. Effect of pH on ion count-rate of an analyte solution

Table 3.

Element	Mean count ($n = 10$), ions/sec	Standard deviation ions/sec	RSD, %
Cu	106,666	9456	8.8
Cd	71,617	4067	5.6
Pb	362,880	16,849	4.6

pH 3 without much loss of accuracy. Copper was used as a representative element since all three elements gave similar profiles.

Recovery studies

To confirm that all the analyte was recovered from the column with each elution, the relationship of the peak area for a steady-state nebulized sample to the peak area for a preconcentrated sample was monitored. The recoveries calculated for Cu, Cd and Pb were 105, 104 and 111% respectively.

Precision

Precision was measured by loading a solution containing 10 ng/ml of Cu, Cd and Pb onto the column at a flow-rate of 3.5 ml/min for 5.0 min, giving a 175 ng loading per element. The results are given in Table 3.

Detection limits

The detection limit was determined by loading 20 ml of DDW as a blank and 20 ml of an aqueous 10 ng/ml standard onto the column, eluting with 5% v/v nitric acid and measuring the ion count-rates for the blank and standard. Ten replicates were run, and the detection limit was calculated as the sample concentration corresponding to a signal that was three times the standard deviation of the blank. The values found are given in Table 4. A comparison with the detection limits obtained for direct nebulization suggests that the HPIC detection limit (with a 20-ml sample) is lower by a factor of 10–17. Theoretically, the detection limits can be further lowered by increasing the loading on the column. For example, loading 40 ml of sample should result in halving the detection limits. The

Table 4. Detection limit comparison

Element	Detection limit, ng/l.	
	Direct nebulization	HPIC*
Cu	20	2
Cd	50	3
Pb	35	2

*Based on a 20-ml sample.

validity of this assumption will be tested in future investigations.

High-purity blanks are necessary for ultra-trace metal determinations. As seen above, the laboratory DDW is adequate for measurements at ng/l. levels, but for pg/l. levels the water would contain sufficient contaminant to reduce the detection power of the method.

Laboratory DDW can be purified by passing it through the HPIC column and collecting the effluent. As the capacity of the cation column used in this study is high, a substantial amount of water can be ultrapurified by this method. If this water is used for the blanks, serial dilution of standards and preparation of the eluent, the blank count-rates will be reduced and thus the detection power increased.

Figure 9 depicts the peaks obtained for Cu, by analysing 100 ml of a blank re-purified as described above, and a 100-pg/l. standard obtained by serial dilution with the re-purified water. As can be seen, there is a significant difference between the count-rates for the standard and the blank.

Accuracy

The accuracy of the method was examined by using a Ministry of the Environment (MOE) control reference sample, used in a documented method for ultratrace determination of metals in acid precipitation samples.¹ Table 5 shows a comparison of accuracy between the conventional method and HPIC/ICP-MS. The measured values are within 10% of the accepted values for the MOE control reference. It was expected that the technique would be as accurate as the data indicate, with this reference material, since it is a relatively clean matrix.

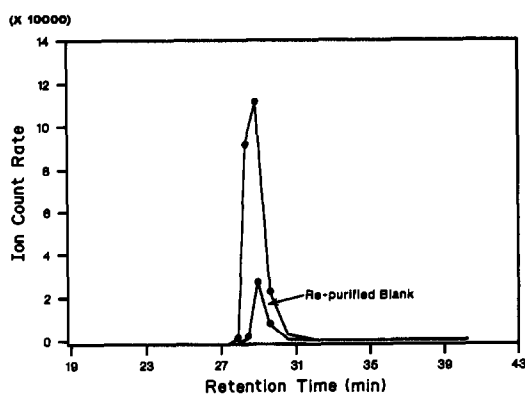


Fig. 9. Ion count-rate for a 100 pg/l. Cu standard solution and a re-purified blank (100 ml; concentration on the column and elution with 5% v/v nitric acid).

Table 5. Accuracy of the HPIC method with Ministry of the Environment Reference Standard (MOE-CHK5)*

Element	Expected value, ng/ml	Observed value, † ng/ml
Cu	5.73 ± 0.29	6.03 ± 0.48
Cd	5.23 ± 0.26	5.77 ± 0.29
Pb	5.10 ± 0.25	4.75 ± 0.33

*This material is an "in house" reference standard used as an instrument control for the determination of trace elements in acid precipitation.¹

†Concentrations are based on use of a 10-ml aliquot of sample.

Matrices containing higher levels of dissolved solids may cause some chemical interferences.

CONCLUSIONS

Use of ICP-MS detector with its advantages of excellent detection power and simultaneous multielement detection, has resulted in development of a successful HPIC/ICP-MS technique for on-line preconcentration. The Dionex CS5 column has been shown to be capable of concentrating up to 6 μ eq of analyte before being overloaded. The optimum eluent strength for the determination of Cu, Cd and Pb has been established as 5% v/v nitric acid, used at a flow-rate of 3.5 ml/min.

Characterization of the Dionex CS5 column has shown that samples with a pH range of 3-9 can be successfully analyzed by this technique. Knowledge of the column capacity and retention times permits automation of off-line performance of the preconcentration step, allowing the ICP-MS system to be used for other analyses while fractionated samples are being prepared. Mercury gives a peak with prolonged tailing, so peak-area rather than peak-height measurements must be used, and the analysis time is practically doubled.

Hydrochloric acid has better separation capability than nitric acid and is a potential eluent for future studies.

REFERENCES

1. Analytical Methods Documentation, Ontario Ministry of the Environment, *Trace Metal Analyses of Acid Precipitation*, 1987, Document 00678.
2. F. Hopper, D. W. Boomer and M. J. Powell, A.S.C. Conference, Toronto, Ontario, Canada, 1988, *ICP-MS Isotope Ratio Identification of Atmospheric Emissions of Metals*.
3. N. Yan, G. Makie and D. W. Boomer, *Sci. Total Environ.*, 1990 in the press.

4. P. G. S. Campbell and P. M. Stokes, *Can. J. Fish Aquat. Sci.*, 1985, **42**, 2034.
5. E. Abrahamczik, *Mikrochemie Mikrochim. Acta*, 1938, **25**, 228.
6. J. P. R. Riches, *Nature*, 1946, **158**, 96.
7. B. Kahn and S. A. Reynolds, *J. Am. Water Works Assoc.*, 1958, **50**, 613.
8. *Technical Note 10R*, Dionex Corporation, August 1983.
9. *Application Note 51*, Dionex Corporation, February 1985.
10. J. Shida, S. Kakizaki, Y. Hozumi, A. Itoh and T. S. Matuso, *Bull. Chem. Soc. Japan*, 1983, **56**, 633.
11. D. L. Johnson, *Sci. Technol.*, 1971, **5**, 411.
12. A. Taylor and A. A. Brown, *Analyst*, 1983, **108**, 1159.
13. D. Chakraborti, W. R. A. De Jonghe, W. E. Van Mol, R. J. A. Van Cleuvenbergen and F. C. Adams, *Anal. Chem.*, 1984, **56**, 2692.
14. R. A. Stockton and K. J. Irgolic, *Int. J. Environ. Anal. Chem.*, 1979, **6**, 313.
15. J. J. Thompson and R. S. Houk, *Anal. Chem.*, 1986, **58**, 2541.
16. D. D. Siemer, P. Koteel, D. T. Haworth, W. J. Taraszewski and S. R. Lawson, *ibid.*, 1979, **51**, 575.
17. M. Morita, T. Uehiro and K. Fuwa, *ibid.*, 1981, **53**, 1806.
18. K. J. Irgolic, R. A. Stockton and D. Chakraborti, *Spectrochim. Acta*, 1983, **38B**, 437.
19. P. C. Uden, B. D. Quimby, R. M. Barnes and W. G. Elliot, *Anal. Chim. Acta*, 1978, **101**, 99.
20. P. E. Gardiner, P. Bratter, V. E. Negretti and G. Schulze, *Spectrochim. Acta*, 1983, **38B**, 427.
21. W. R. Briggs and J. C. Fetzer, *Anal. Chem.*, 1989, **61**, 236.
22. D. J. Douglas and R. S. Houk, *Prog. Anal. At. Spectrosc.*, 1985, **8**, 1.
23. R. S. Houk, V. A. Fassel, G. D. Flesch, H. J. Svec, A. L. Gray and C. E. Taylor, *Anal. Chem.*, 1980, **52**, 2283.
24. J. J. Thompson and R. S. Houk, *ibid.*, 1986, **58**, 2541.
25. M. R. Plantz, J. S. Fritz, F. G. Smith and R. S. Houk, *ibid.*, 1989, **61**, 149.
26. J. W. McLaren, A. P. Mykytiuk, S. N. Willie and S. S. Berman, *ibid.*, 1985, **57**, 2907.
27. J. W. McLaren, D. Beauchemin and S. S. Berman, *J. Anal. At. Spectrom.*, 1987, **2**, 277.
28. T. D. B. Lyon, G. S. Fell, R. C. Hutton and A. N. Eaton, *ibid.*, 1988, **3**, 601.
29. J. R. Dean, M. Seumas, L. Ebdon, H. M. Crews and R. C. Massey, *ibid.*, 1987, **2**, 607.
30. B. S. Whaley, K. R. Snable and R. F. Browner, *Anal. Chem.*, 1982, **54**, 162.
31. O. Samuelson, *Ion Exchange Separations in Analytical Chemistry*, 2nd Ed., Wiley, New York, 1963.
32. G. M. Hieftje and G. H. Vickers, *Anal. Chim. Acta*, 1989, **216**, 1.
33. S. H. Tan and G. Horlick, *Appl. Spectrosc.*, 1986, **40**, 445-460.
34. E. R. Tompkins, J. X. Kyme and W. E. Cohn, *J. Am. Chem. Soc.*, 1947, **69**, 2769.

COMPARISON OF INSTRUMENTAL NEUTRON ACTIVATION ANALYSIS OF GEOLOGICAL MATERIALS WITH OTHER MULTIELEMENT TECHNIQUES

G. E. M. HALL, G. F. BONHAM-CARTER, A. I. MACLAURIN and S. B. BALLANTYNE
Geological Survey of Canada, Ottawa, Ontario K1A 0E8, Canada*

(Received 16 February 1989. Accepted 17 March 1989)

Summary—Results obtained for 12 elements in approximately 1600 rocks by instrumental neutron activation analysis (INAA) are compared with those obtained by ICP emission spectrometry (ICP-ES), XRF, and atomic-absorption spectrometry (AAS). Sample duplicates and two controls are used to evaluate the precision of the methods investigated. Application of a method (Maximum Likelihood Functional Relationship) to determine and quantify rotational and translational bias is demonstrated. The elements Na, Fe, Ba, Co, Cr, La, Ni and Rb can be determined in rocks by INAA with sufficient sensitivity and precision, whereas the determination of Ag, Yb, Zn and Zr suffers from inadequate sensitivity. Good agreement is seen in the results for Na (by INAA, ICP-ES and XRF) and Ag (INAA and AAS). A significant positive bias (13% or less) is evident in the comparison of results by INAA and ICP-ES or XRF for Cr, Ba, Ni and Fe over a wide range of concentration. A similar trend, though less significant, is observed for the elements Yb, Rb, La and Co; the upper limit of concentration for satisfactory determination is within a decade of the highest detection limit for these elements. Rotational and translational bias is evident for Zn in the comparison of data obtained by INAA and ICP-ES, the results by INAA being appreciably lower above about 400 ppm Zn.

Since the advent of high-resolution germanium detectors in the 1960s, instrumental neutron activation analysis (INAA) has played a major role in the determination of trace elements in silicate rocks.¹ This technique has been particularly well suited to the direct determination of rare-earth elements and refractory metals such as Hf, Ta, Th and U, as evidenced by the large amount of data reported in the characterization of geochemical standard reference materials.²⁻⁶ Renewed interest in exploration for deposits of Au and the platinum group elements (PGEs) in the 1980s led to the widespread application of this technique in the analysis of rocks, soils and stream or lake sediments. While sensitivity for Au and its pathfinder elements (*e.g.*, As, Sb, Se) is adequate by INAA, prior separation and preconcentration are necessary in the determination of PGEs.⁷ Features such as the unrivalled simplicity of INAA, its low detection limit of about 5 ng/g for Au, and the ability to analyse sample weights greater than 1 g (usually 1–30 g) have encouraged the growth of commercial laboratories using nuclear reactor facilities. The ease of handling sample weights in excess of 5 g

has been particularly beneficial in the determination of Au, where the well-known “nugget” effect⁸ creates uncertainty when inadequate sampling sizes are used. In recent years, “packages” have been developed by these INAA laboratories, designed to provide the geochemist with additional data to be used in identifying rock type, alteration processes and pathfinder elements. Thus, as many as 33 elements are determined along with Au for only a fractional increase in the cost. The non-destructive nature of this technique, together with its cost-effectiveness, have resulted in its adoption in large-scale regional reconnaissance surveys in countries such as the U.S.A. and Canada.⁹ The Geological Survey of Canada (GSC) is currently applying this technique to the analysis of large numbers of archived samples, primarily for Au, but information on the concentrations of other elements is proving valuable.

The objective of this work was to compare results obtained by INAA with those obtained by other established techniques such as wavelength-dispersive X-ray fluorescence (XRF), inductively-coupled plasma emission spectrometry (ICP-ES) and atomic-absorption spectrometry (AAS). The data sets used in this

*GSC contribution 10189.

evaluation are not ideal, in that the main objective of the original programme was to support a follow-up geochemical interpretation study and not to compare analytical methods. The choice of elements needed by the geochemist in this investigation dictated the use of various "packages" employing the techniques of INAA, ICP-ES, XRF and AAS. The elements determined in the INAA "packages" which are also common to the other three are those under study here, namely Na, Fe, Ba, Ag, Co, Cr, La, Ni, Rb, Yb, Zn and Zr. Some elements in the INAA suite, such as Cd, Hg, Ir, Te and Sn, have detection limits which are too high for geochemical exploration purposes; ideally, such limits should be at or below natural abundance levels in the medium analysed.

Data for about 1600 rocks, analysed over a two-year period, have been collated for this comparison. The samples have widely varying matrices, largely unweathered, from felsic to basic in nature and ranging from "background" granites to ore-grade drill-core rocks high in chromites or sulphides. Samples were crushed, ground and ball-milled to less than 200 mesh (74 μm) at the GSC, split into two groups and analysed at several production-oriented laboratories. In evaluating the results obtained, it should be borne in mind that these laboratories are employing methods designed to be cost-effective and efficient for as many elements as possible, and hence compromises have been effected. This is not a comparison of methods each optimized for sensitivity and selectivity. Therefore, results may be degraded not solely by the errors inherent in each method but also by the presence of heterogeneity in the samples, possible sample mix-up, and errors in the reporting of data by the laboratories. The precision of the methods and bias between them are evaluated for the 12 elements according to methods described later. Absolute accuracy is more difficult to assess, as in-house control samples rather than international standard reference materials were used because large amounts of sample material were required. This study is a comparison of data produced by using production-oriented methods or "analytical systems" as designed and implemented by the respective laboratories. Hence, the conclusions to be drawn are valid with respect to the "systems" employed but may not be relevant in other comparisons involving laboratories using similar techniques but different overall methods.

EXPERIMENTAL

The INAA data were obtained under contract with Becquerel Laboratories of Mississauga, Ontario, Canada; all other results were reported by the Analytical Chemistry Laboratories of the GSC. Samples were usually sorted into batches of similar geology, varying in number from about 30 to 150 and split into two sets for analysis at GSC and contract laboratories. Two control samples were inserted at regular intervals (usually 1 in 20) and numbered in sequence with the rock samples, and were to be used to measure the precision of the analytical methods. Samples were also split, following preparation, to form a set of "blind duplicates" or replicates which would yield information not only on the precision of the methods used but also on the degree of homogeneity of each element in the various sample types. Both controls and blind duplicates were designed to be "unknowns" in each suite of samples.

INAA

Samples, weighing between 5 and 10 g, were encapsulated in snap-cap polyethylene vials, 3.5 cm in diameter and 1 cm in height. A flux monitor (proprietary) was attached to each vial and then shrink-wrapped to ensure sample integrity. Some commercial laboratories use nichrome or iron wires inserted in a batch of vials to monitor the change in flux density with distance from the core. Samples were stacked in bundles and irradiated for approximately 20 min at the McMaster Nuclear Reactor (Hamilton, Ontario) in a neutron flux of 4×10^{12} n.cm⁻².sec⁻¹. Cadmium shielding was employed to permit activation by epithermal rather than thermal neutrons, as this type of irradiation with energy above 0.5 eV enhances sensitivity of Au, the element around which the "package" was designed. After a seven-day decay period, the gamma-ray spectra were acquired by use of co-axial germanium detectors and a Nuclear Data multichannel analyser system optimized for high count-rate applications and incorporating a Westphal-type dead-time correction. The resolution of the Ge detector is 1.8 keV (FWHM) at the 1.333 MeV peak of ⁶⁰Co. Samples were mounted on an automatic changing-wheel and counted for 15 min at a distance of approximately 1 cm from the detector.

The nuclear data relevant to the elements under discussion are shown in Table 1. If there are two or more interference-free peaks avail-

Table 1. Nuclear data for the 12 elements under study: all nuclear reactions are (n, γ) except for $^{58}\text{Ni}(n, p)^{58}\text{Co}$

Parent nuclide	Isotopic abundance, %	Radionuclide	Gamma-ray, keV	Half-life	Interferences
^{23}Na	100	^{24}Na	1368.5 2754.1	15.0 hr	Sb
^{58}Fe	0.31	^{59}Fe	1099.2 1291.6	44.6 d	Ni, Co, Ta
^{130}Ba	0.11	^{131}Ba	496.3	11.7 d	U fission
^{109}Ag	48.2	$^{110\text{m}}\text{Ag}$	884.7	252 d	
^{59}Co	100	^{60}Co	1173.2 1332.5	5.27 y	Ni
^{50}Cr	4.35	^{51}Cr	320.0	27.7 d	Lu, Nd, Fe
^{139}La	99.9	^{140}La	487.0 1596.5	40.2 hr	U fission
^{58}Ni	68.3	^{58}Co	810.8	70.8 d	
^{85}Rb	72.2	^{86}Rb	1076.6	18.8 d	
^{174}Yb	31.6	^{175}Yb	396.3	4.19 d	Th
^{64}Zn	48.6	^{65}Zn	1115.5	244 d	Sc, Eu, Tb, Ta
^{94}Zr	17.4	^{95}Zr	756.7	65.5 d	U fission

able for quantification of an isotope, results are averaged. Where gamma-rays produced by an interfering radionuclide cannot be resolved from the analyte peak (e.g., 1120.52 keV from ^{46}Sc and 1115.52 keV from ^{65}Zn), inter-element corrections are made. Similarly, when a significant proportion of the activity measured occurs from the fission of U within the sample and not just from the activation of the analyte, as can be the case for Ba, La and Zr, corrections are computed by quantifying the amount of U in the sample. Hence, net peak areas are derived; this laboratory does not currently employ peak deconvolution programs. Calibrations are performed with USGS, NBS and IAEA standard reference materials, supplemented where necessary by synthetic solutions spiked on known matrices such as SiO_2 . Results are corrected for weight differences between samples, exponential decay of activity neutron-flux gradient and variations in counting geometry. A laboratory control sample is analysed at a frequency of 1 in 20 to check for errors. Changes in the routing procedure, such as an increase in decay period, counting time or detector distance, are made when samples abnormally high in trace elements are encountered. When this occurs, for example when heavy mineral concentrates or ore-grade materials are analysed, precision is often degraded for elements at low levels, and hence detection limits are raised. In this study, some samples contained ore-grade concentrations of Au, Ag, Zn, Cu, Ba and Sb.

ICP-ES/AAS

The elements Na, Fe, Ba, Co, Cr, La, Ni, Yb and Zr were determined by ICP-ES. Silver was

determined by AAS. The methods used are similar to those described in the handbook by Thompson and Walsh.¹⁰ A Jobin-Yvon Model 48 simultaneous ICP atomic-emission spectrometer incorporating a holographic 2400 grooves/mm grating was used. Details of the instrumentation and operating conditions are given in Table 2. The AA spectrometer employed in analysis for Ag was the Varian Model 475; standard conditions with background correction at the 328.1 nm Ag line were used.

Two sample digestion procedures were employed: fusion for major and minor elements (Na, Fe, Ba) and acid attack combined with a fusion for trace elements (Ag, Co, Cr, La, Ni, Yb, Zn). The former involves fusion of a 0.5-g sample with 1.5 g of a 3:1 w/w mixture of lithium metaborate and lithium tetraborate at 900°. The melt is dissolved in 250 ml of 4% v/v nitric acid containing 10 ml of 0.8% EDTA solution to stabilize elements such as Ba in solution. The dissolution procedure for the trace elements consists of an acid attack on 1 g of sample with an $\text{HF}/\text{HNO}_3/\text{HCl}/\text{HClO}_4$ mixture and evaporation to dryness followed by dissolution in 10% v/v hydrochloric acid. Any residue remaining is filtered off, then fused with 0.5 g of lithium metaborate and the cooled melt is dissolved in 10% v/v hydrochloric acid. Again, EDTA is added as a complexing agent and the two hydrochloric acid solutions are combined and diluted accurately to a total volume of 100 ml. Hence, the solution for trace element analysis is five times as concentrated as the solution for determination of major elements.

Calibration is done with a combination of USGS and CANMET standard reference mate-

Table 2. Hardware and operating conditions used in analysis by ICP-ES

RF generator	2.5 kW, frequency 27.12 MHz	
Nebulizer	Meinhard "C" concentric glass	
Spray chamber	Scott-type	
Torch	JY demountable HF resistant	
RF power	1.2 kW	
Plasma Ar flow-rate	13 l./min	
Auxiliary Ar flow-rate	0.2 l./min	
Sheath Ar flow-rate	0.3 l./min	
Solution uptake rate	1.7 ml/min	
Integration time	10 sec, 3 measurements each	
Spectral lines		
Element	Wavelength, <i>nm</i>	Spectral interferences
Na	588.9	
Fe	261.1	
Ba	233.5	
Co	228.6	Ti, Fe, Mg
Cr	267.7	Fe, Mg, Mn
La	233.7	Ti, Mn
Ni	231.6	Fe, Mg, Mn, Ba
Yb	328.9	Ti, Fe
Zn	213.8	Al, Fe

rials and synthetic solutions made by spiking blanks for each procedure. Three 10-sec integrations of the ICP signal are made and inter-element corrections calculated where necessary (Table 2).

XRF

The elements Na, Fe, Ba, Rb and Zr were determined by XRF. The sequential Philips PW 1404 wavelength-dispersive spectrometer was employed. The side-window Rh tube was operated at 40–60 kV and 50–75 mA and the analysing crystals were LiF (200) (for Fe, Ba, Rb, Zr) and PX-1 (for Na). X-Ray intensities were measured with a scintillation detector at the 2θ goniometer positions corresponding to the respective K_α (Na, Fe, Rb, Zr) and L_α (Ba) lines.

Glass discs were prepared by fusing 1 g of sample with a mixture comprising 5 g of $\text{Li}_2\text{B}_4\text{O}_7$, 0.3 g of LiF, 0.5 g of NH_4NO_3 and 0.3 g of NH_4I at about 1000° for 20 min in a Claisse-type fluxer, after which the melt was poured into a 95% Pt–5% Au alloy mold. Calibration was done with duplicate samples of 26 standard reference materials. Corrections for interference effects were based on the LaChance–Traill model; an iteration process employing a 22×22 matrix was applied. Further details of the method are given elsewhere.^{11–13}

Data presentation and statistical analysis

The principal goal of the data analysis was to ascertain whether bias exists between different methods of determination. The simplest way to achieve this is to examine x – y scatter plots, where x refers to method 1 and y to method 2; in the absence of bias, data points should fall symmetrically about the 45° line, corresponding to the equation $y = x$. In the presence of a linear bias, the point will fall about some other line, $y = \alpha + \beta x$, where α is the intercept and β is the slope. Statistical characterization of bias involves the estimation of α and β ; if $\alpha \neq 0$, a translational bias is suspected and if $\beta \neq 1$, a rotational bias is suspected.

Conventional least-squares fitting to minimize $\Sigma(y - \alpha - \beta x)^2$ is unsuitable, because different lines are determined according to whether y is regressed on x , or x on y , and both methods involve measurement error which varies with concentration. Ripley and Thompson¹⁴ have proposed a new technique, using the Maximum Likelihood Functional Relationship (MLFR), to overcome these problems. The MLFR expresses the theoretical relationship between methods as a straight line, but the same line is obtained when x and y are reversed. The method combines the advantages of a reduced major-axis correlation, with the ability to consider the measurement errors for both x and y

at each point. The MLFR method uses weights, w_i , for the $i = 1, 2 \dots n$ sample points. In ordinary weighted regression the weights are often assumed to be inversely proportional to the variance of the dependent variable, $w_i = 1/\text{var}(y_i)$. For MLFR, the expression for the weights involves the variances for both x and y : $w_i = 1/[\text{var}(x_i) + \beta^2 \text{var}(y_i)]$. Because β appears in this expression, and is one of the unknowns, a non-linear method of solution is required. For each sample, x , $\text{var}(x)$, y , and $\text{var}(y)$ must be available for the MLFR line to be calculated. When $\text{var}(x)$ and $\text{var}(y)$ are constant, the MLFR line is the same as the reduced major axis correlation.

Ideally, each sample would be split into at least four, so that duplicate determinations could be used to estimate measurement errors for both methods with each sample. In practical situations this may be too costly, and estimates of error can be substituted for measured errors.

For many analytical systems, the relationship $\sigma_c = \sigma_0 + kc$ has been shown to be an appropriate model for measurement error, where σ_c is the standard deviation of measurement at concentration c , σ_0 is the standard deviation at "zero" concentration and k is a constant.¹⁵ Analytical variation is often given in terms of precision, P_c , which is normally taken to be twice the relative standard deviation (rsd), $P_c = 2\sigma_c/c$. Combining these two expressions gives $P_c = 2\sigma_0/c + 2k$, from which it can be seen that the precision approaches $2k$ at high concentrations. (P_c must be multiplied by 100 if it is to be expressed as a percentage).

Thompson and Howarth¹⁵ show that blind duplicates (sample splits, not field duplicates) inserted randomly in a batch of samples provide an excellent method for estimating analytical error. Their method involves plotting the absolute difference *vs.* the mean for each duplicate pair, where the absolute difference is used as an estimate of the standard deviation of measurement, and the mean is used as an estimate of average concentration. They show that a robust method of fitting a line to these points provides reasonable estimates of σ_0 and k . However, when fewer than 50 duplicates are available they suggest using a graphical control chart to verify an assumed level of precision.

Because of the relatively small number of blind duplicates, the control chart method is employed here. This allows a rough estimate of precision, which in turn is used to calculate the measurement errors for fitting the MLFR line.

The blind-duplicate control charts illustrated here are log-log plots, and include two control lines. These are both 95th percentile lines for the selected precision. The precision is specified only as $2k$, and the intercept is assumed to be zero for these charts, *i.e.*, zero error at zero concentration. The 95th percentile for a particular precision is an upper confidence line, above which no more than 5% of the points should lie if that level of precision is to be accepted, and assuming that the errors are Gaussian. For small numbers of points, tables of the binomial distribution can be used to calculate the exact probability that M out of N points will fall above the 95% percentile.¹⁵ The approach taken in this paper has been to plot a series of 95% percentile lines, corresponding to 5, 10, 20, 30, 40, 50, 60, 70, 80, 90 and 100% precision, using the expressions given by Fletcher,¹⁶ on each blind duplicate graph. After rejecting any obvious "fliers" that appear to be due to errors such as sample mix-up, two of these lines are selected and retained. Two pairs of samples which appear to be mismatches are identified by "stars" in the control charts. The 95% percentile line separating *roughly* 5% of the points on its upper side is chosen as an approximate guide to the precision. For comparison, the 95% percentile for a much lower precision is also illustrated, as the "sandwich" between the pair of lines assists a graphical appraisal. Note that in this paper, the two control lines both represent 95% percentiles for two different precision specifications, whereas in reference 15 two control lines for two different percentiles (90th, 99th) are illustrated at the *same* precision specification. Also note that when duplicate results are identical, the points are plotted at the lowest level of the logarithmic y -axis on the graphs.

In estimating bias between methods by MLFR, a range of precision specifications for each method was tested experimentally to evaluate the sensitivity of the value of α and β and their standard errors to different values of precision. In general, the values of α and β varied little even with quite large changes in precision, whereas their standard errors increased with increasing precision. Thus, if the precision is improperly specified, the slope and intercept of the MLFR line are not much affected, but the tests of significance for $\alpha = 0$, $\beta = 1$ can be affected. For most of the cases reported here, the test $\beta = 1$ could be rejected with confidence for a wide range of precision specification, whereas the test $\alpha = 0$ could normally not be

rejected. The exceptions are discussed in the results section.

Note that for all the bias calculations, values at or below the detection limit were omitted from the MLFR calculations, although the points are plotted. For some elements, an upper bracket was also imposed for line-fitting, as discussed in the text. Where INAA values are reported as below the detection limit, they have been multiplied by 5/8. This has not affected any calculations but the points are then evident on the plots. The values computed for α and β in the MLFR line are shown, together with the number of data points, in the figures (Figs. 1–12).

RESULTS AND DISCUSSION

The detection limits established by the laboratories are given in Table 3, together with each element's average crustal abundance. These limits are regarded as being the lowest concentrations which can be distinguished from procedural blanks in applying the methods as used by the laboratories. Many factors contribute to the variation associated with an analytical method or system, such as the instrumental precision, the quality of reagents used, the environment, the analyst, the presence of interferences, and the procedures employed for calibration and blank correction. These are in addition to the variance associated with the representativeness of the sample or its degree of heterogeneity; in this study this variance should be minimal for the INAA, for which relatively large sample weights are taken (5–10 g). The detection limits shown for Na and Ba determi-

nation by XRF are probably unusually high, owing to the particular configuration of the spectrometer (*e.g.*, the Rh tube is insensitive for Ba). Similarly, epithermal irradiation is less sensitive than thermal irradiation for Fe and Yb, hence commercial laboratories employing the latter technique report superior detection limits of 0.02% for Fe (*cf.* 0.2%) and 0.2 ppm for Yb (*cf.* 2 ppm). However, the detection limits for Ni and Rb are significantly better by epithermal irradiation, at 20 ppm (*cf.* 200 ppm) and 5 ppm (*cf.* 30 ppm), respectively.

Results for the two sediment control samples, SS04 and SS06, are shown in Table 4. Sample SS04 was analysed about 26 times by each of the methods indicated, but SS06 was inserted more frequently, to give a total of 78 separate analyses. It is customary at the GSC to determine major and minor elements in predominantly silicate or carbonate matrices by XRF and to select other samples, high in S for example (greater than 1 or 2%), for analysis by ICP–ES. Therefore, these sediments, composed mainly of fine silt and clays, were analysed for Na, Fe and Ba by XRF. Some elemental concentrations determined by XRF or ICP–ES were reported as being below the stated detection limits.

Sodium

Results for Na determined by INAA are compared with those by ICP–ES and XRF in Figs. 1a and 1b, respectively. The correlation of both methods with INAA is excellent; $y = 0.94x$ for ICP–ES *vs.* INAA and $y = 0.98x$ for XRF *vs.* INAA. The MLFR lines are not significantly different from the 45° lines shown on the graphs. In both data sets some 'fliers' exist, where, for

Table 3. Detection limits reported by the production laboratories for the 12 elements under study: values in ppm ($\mu\text{g/g}$) unless noted otherwise

Element	Detection limit			Average crustal abundance ¹⁷
	INAA	ICP–ES	XRF	
Na	0.02%	0.07%	0.37%	2.5%
Fe	0.2%	0.06%	0.07%	4.7%
Ba	50	20	20	425
Ag	2	2*		0.07
Co	5	5		25
Cr	20	10		100
La	2	10		30
Ni	20	10		75
Rb	5		20	90
Yb	2	0.5		3
Zn	100	5		70
Zr	200		20	165

*Determined by AAS, in the solution analysed by ICP–ES for the trace elements Co, Cr, La, Ni, Yb and Zn.

Table 4. Results of analysis by INAA, ICP-ES and XRF for the control samples, SS04 and SS06: brackets indicate: in the median column, the number of separate analyses; and in the mean column, the coefficient of variation

Element	SS04						SS06					
	INAA		ICP-ES		XRF		INAA		ICP-ES		XRF	
	median	mean \pm SD	median	mean \pm SD	median	mean \pm SD	median	mean \pm SD	median	mean \pm SD	median	mean \pm SD
Na	2.07 (25)	2.14 \pm 0.19 (8.9%)	2.0	2.00 \pm 0.16 (8.0%)	2.02 (77)	2.04 \pm 0.14 (6.9%)	1.78 (78)	2.00 \pm 0.16 (8.0%)	2.02 (77)	2.04 \pm 0.14 (6.9%)	1.78 (78)	1.81 \pm 0.10 (5.5%)
Fe	2.80 (25)	2.82 \pm 0.18 (6.4%)	2.52 (26)	2.48 \pm 0.19 (7.7%)	6.10 (77)	6.10 \pm 0.39 (6.4%)	5.39 (78)	2.52 (26)	6.10 (77)	6.10 \pm 0.39 (6.4%)	5.39 (78)	5.34 \pm 0.19 (3.6%)
Ba	1600 (25)	1583 \pm 221 (14.0%)	1330 (26)	1290 \pm 151 (11.7%)	850 (77)	858 \pm 64 (7.4%)	738 (78)	1330 (26)	850 (77)	858 \pm 64 (7.4%)	738 (78)	752 \pm 42 (5.5%)
Ag*	<2 (25)	<2	2.0 (6)	4.8 \pm 7.5 (156%)	<2 (77)	<2	1.0 (6)	2.1 \pm 2.4 (114%)	1.0 (6)	<2	2.1 \pm 2.4 (114%)	
Co	15 (25)	15 \pm 2 (13.3%)	16 (26)	16 \pm 1 (6.3%)	47 (77)	48 \pm 4 (8.3%)	40 (74)	16 (26)	47 (77)	48 \pm 4 (8.3%)	40 (74)	40 \pm 3 (7.5%)
Cr	170 (25)	167 \pm 27 (16.2%)	140 (26)	134 \pm 18 (6.2%)	520 (77)	529 \pm 41 (7.8%)	390 (74)	140 (26)	520 (77)	529 \pm 41 (7.8%)	390 (74)	377 \pm 48 (12.7%)
La	22 (25)	21 \pm 2 (9.5%)	19 (26)	18 \pm 3 (16.7%)	37 (77)	37 \pm 3 (8.1%)	32 (74)	19 (26)	37 (77)	37 \pm 3 (8.1%)	32 (74)	31 \pm 3 (9.7%)
Ni	45 (25)	46 \pm 10 (21.7%)	40 (26)	41 \pm 12 (30.0%)	340 (77)	342 \pm 27 (7.9%)	310 (73)	40 (26)	340 (77)	342 \pm 27 (7.9%)	310 (73)	312 \pm 16 (5.1%)
Rb	54 (25)	53 \pm 8 (15.1%)	50 (26)	51 \pm 4 (7.8%)	140 (77)	146 \pm 11 (7.5%)	114 (78)	50 (26)	140 (77)	146 \pm 11 (7.5%)	114 (78)	115 \pm 9 (7.8%)
Yb	1.3 (25)	1.6 \pm 0.3 (18.8%)	1.6 (26)	1.5 \pm 0.2 (13.3%)	5.0 (77)	4.9 \pm 0.6 (12.2%)	3.9 (74)	1.6 (26)	5.0 (77)	4.9 \pm 0.6 (12.2%)	3.9 (74)	3.8 \pm 0.4 (10.5%)
Zn	120 (25)	122 \pm 23 (18.8%)	62 (26)	62 \pm 8 (12.9%)	190 (77)	196 \pm 37 (18.9%)	150 (74)	62 (26)	190 (77)	196 \pm 37 (18.9%)	150 (74)	154 \pm 10 (6.5%)
Zr	290 (25)	308 \pm 100 (32.5%)	250 (26)	242 \pm 25 (10.3%)	340 (77)	326 \pm 164 (50.3%)	170 (78)	250 (26)	340 (77)	326 \pm 164 (50.3%)	170 (78)	185 \pm 31 (16.8%)

SD = standard deviation.

*Ag was determined by AAS, in the solution analysed by ICP-ES for the other trace elements.

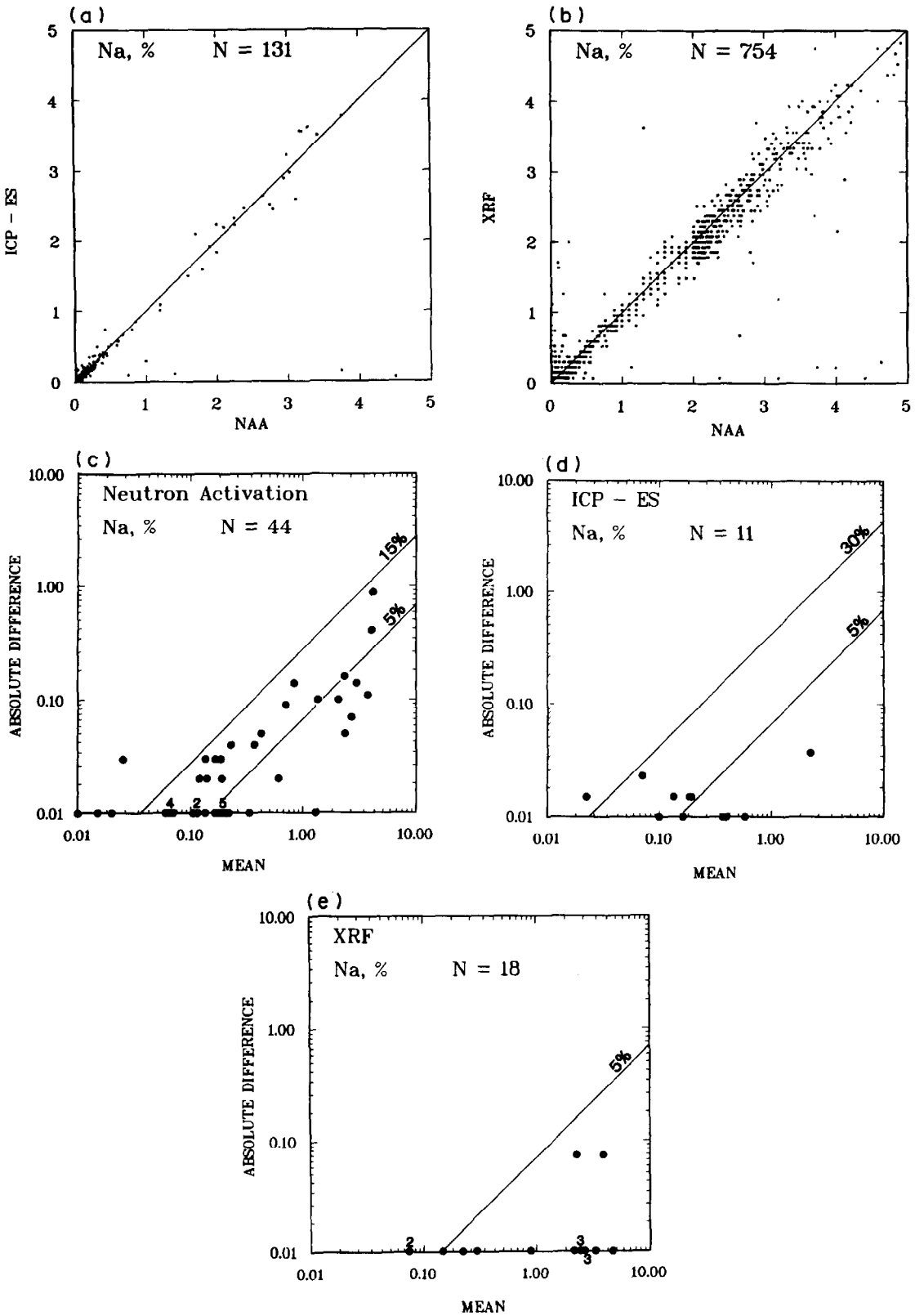


Fig. 1. (a) Comparison of results by ICP-ES and INAA for Na. (b) Comparison of results by XRF and INAA for Na. (c) Control chart of duplicate pairs in the determination of Na by INAA. (d) Control chart of duplicate pairs in the determination of Na by ICP-ES. (e) Control chart of duplicate pairs in the determination of Na by XRF.

example, the Na content is estimated to be in the range 1–5% by INAA but near the detection limit by ICP–ES or XRF.

In examining the control charts (Figs. 1c, d, e) illustrating the data for the blind duplicates, it is apparent that the precision is best for XRF and can be expected to be better than 5% at the 95% confidence level. Indeed, 16 of the 18 pairs show no measurable difference in Na content. Precision, in the range 0.02–10.0% Na, can be expected to be better than 15% by INAA, with results for 18 out of 44 pairs agreeing exactly. Performance for Na by ICP–ES appears to be inferior to that of the other two methods; however, only 11 sets of duplicates were analysed. Data obtained for the control samples, SS04 and SS06, by INAA and XRF indicate only slightly superior precision by XRF (Table 4). Here the precision (twice the *rsd*) is in the range 11–16% by XRF and 14–18% by INAA, showing more similarity between the two methods than is demonstrated by the agreement between duplicates. The mean values for the controls agree within the ranges set by the standard deviations, again indicating a lack of bias for Na between INAA and XRF. The data do not support the widely different detection limits established by the laboratories where the XRF limit is the poorest, 0.4% Na (Table 3).

Iron

Results for Fe are significantly higher by INAA than by either ICP–ES or XRF, the slopes of the MLFR lines being 0.86 ± 0.03 and 0.94 ± 0.01 , respectively (Figs. 2a, 2b). There are relatively few “fliers” in both data sets, considering the large number of samples analysed (179 + 1083). As the other two methods show a similar trend, though of different magnitude, to that of INAA, it is concluded that there is a problem with accuracy in determination of this element by INAA and this is likely to be due to an error in the construction of the calibration curve. The data for the control samples (Table 4) further exemplify this high bias of as much as 16% (for SS04) by INAA compared for XRF.

Precision for Fe by ICP–ES and XRF appears to be comparable (Figs. 2d, 2e), at 10% or better in the range 1–10% Fe. However, analysis by INAA is less reproducible and the upper limit for precision is about 15%. This finding is confirmed by the data for SS06 (Table 4). However, the precision obtained by XRF for SS04 is worse than that predicted by the dupli-

cates and is comparable to that for INAA, in the range 13–15%.

Barium

A high bias is evident in the determination of barium by INAA, as shown in Figs. 3a and 3b, where the slopes of the MLFR lines comparing ICP–ES and XRF with this technique are both very significant and essentially equal to 0.88. Similarly, the mean values for Ba in SS04 and SS06 are significantly higher by INAA (1583 and 858 ppm, respectively) compared to XRF (1290 and 752 ppm, respectively). It is thought that a poor calibration exists in the determination of Ba by INAA at this laboratory, as the other two methods exhibit identical behaviour, and it would be very unlikely that both would be equally affected by interferences.

The worst precision is shown by INAA (Figs. 3c–3e), about half the results for the blind duplicates falling between 5 and 50% in the wide range of 20–30000 ppm Ba content. Though the upper limits of precision by ICP–ES and XRF are 20 and 30%, respectively, most of the points lie at below 5%. The precision for control samples conforms to the pattern shown by the duplicates in analysis by INAA and XRF (Table 4).

Silver

Results for Ag by AAS correlate well with those by INAA; the values of 0.94 and 0.97 for the intercept and slope of the MLFR line are not significant (Fig. 4a). There is a substantial amount of scatter, however, showing higher results by AAS at low Ag contents (<20 ppm) and the opposite trend at levels of Ag between 20 and 150 ppm. The precision is difficult to estimate, as nearly half (21) of the duplicates analysed by INAA were below the detection limit of 2 ppm; however, it can be expected to be considerably better than 50% at Ag concentrations from 2 ppm to >1000 ppm (Fig. 4b). Analysis by AAS should yield precisions between 5 and 60% (Fig. 4c), essentially equivalent to INAA. The two control samples did not contain detectable quantities of Ag but the noisy data obtained by the AAS method (Table 4) indicate that a detection limit of 1 ppm is somewhat optimistic. This is confirmed by results for a third control sample, SS03, where results by AAS yielded a strongly skewed distribution with mean and standard deviation of 5.6 ± 7.2 ppm ($n = 7$) and all eight results by INAA were below the detection limit of 2 ppm.

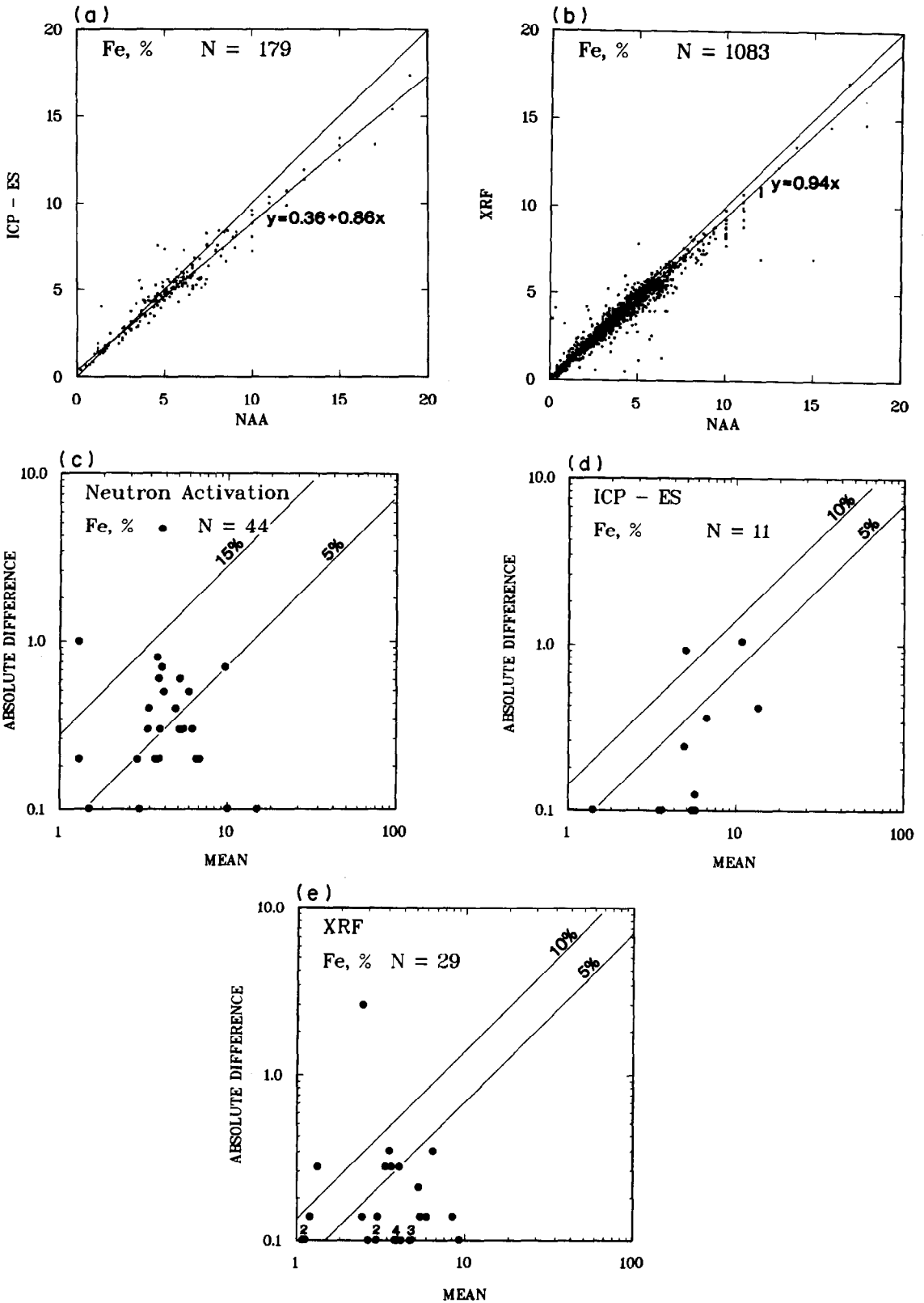


Fig. 2. (a) Comparison of results by ICP-ES and INAA for Fe. (b) Comparison of results by XRF and INAA for Fe. (c) Control chart of duplicate pairs in the determination of Fe by INAA. (d) Control chart of duplicate pairs in the determination of Fe by ICP-ES. (e) Control chart of duplicate pairs in the determination of Fe by XRF.

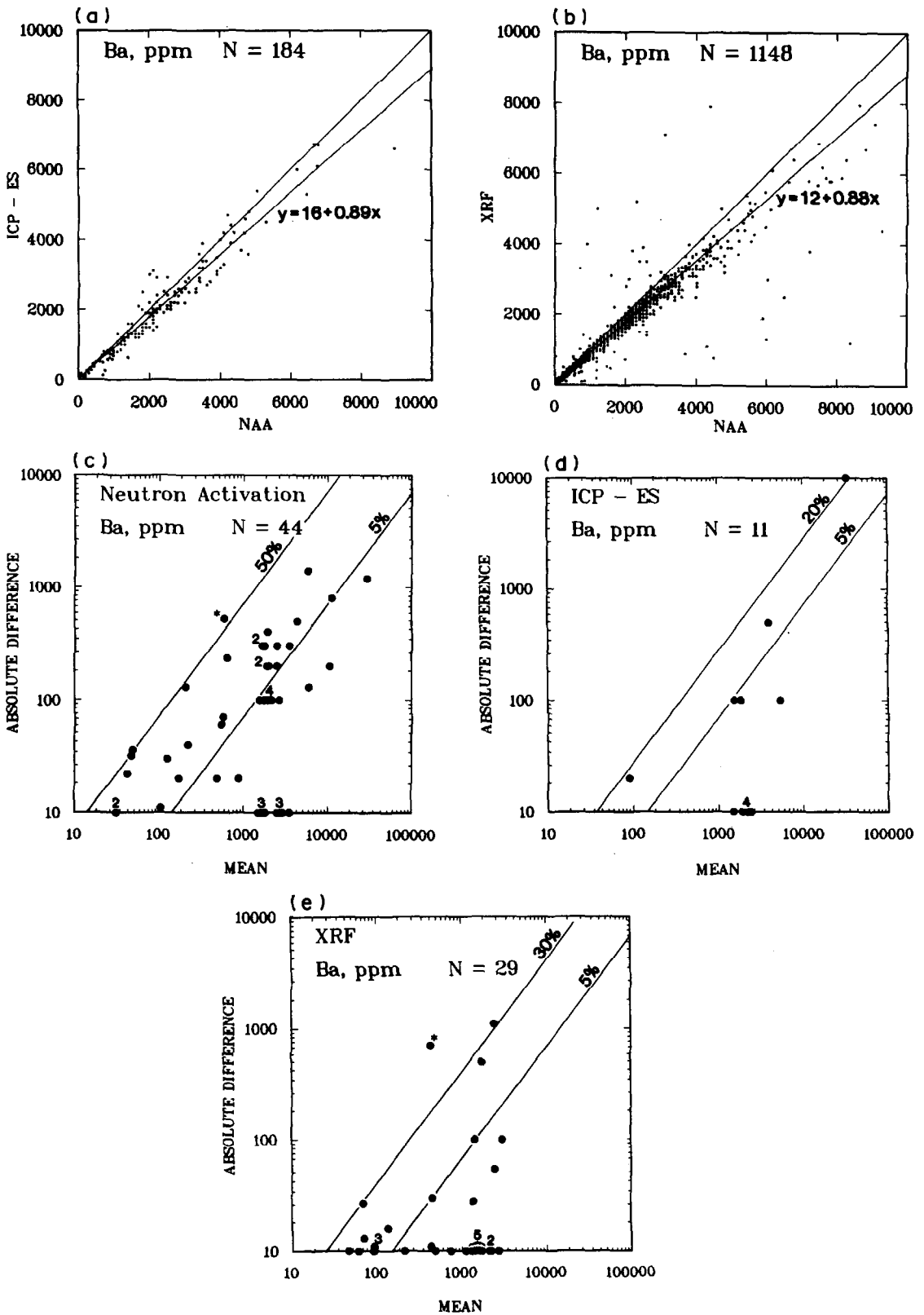


Fig. 3. (a) Comparison of results by ICP-ES and INAA for Ba. (b) Comparison of results by XRF and INAA for Ba. (c) Control chart of duplicate pairs in the determination of Ba by INAA. (d) Control chart of duplicate pairs in the determination of Ba by ICP-ES. (e) Control chart of duplicate pairs in the determination of Ba by XRF.

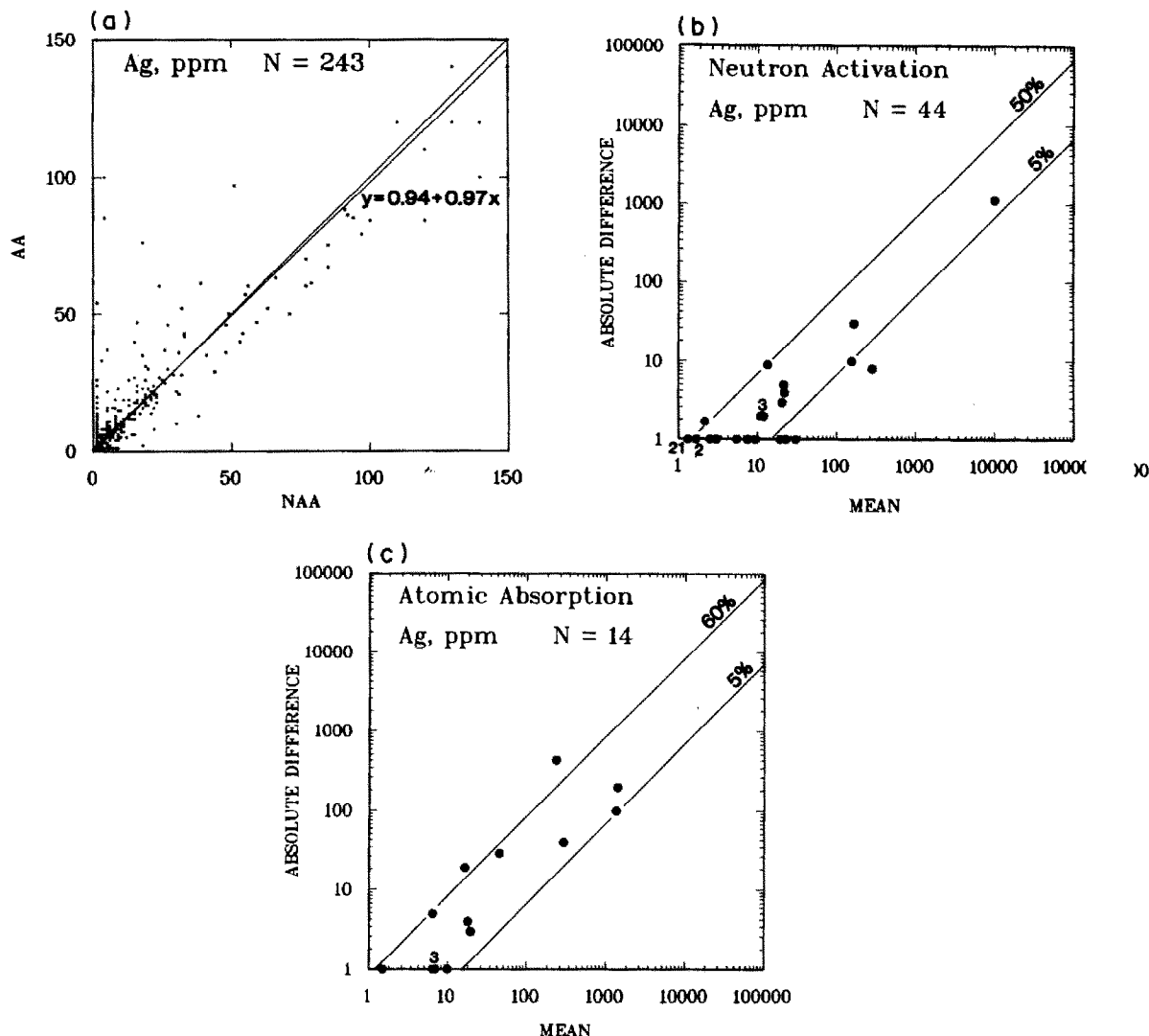


Fig. 4. (a) Comparison of results by AAS and INAA for Ag. (b) Control chart of duplicate pairs in the determination of Ag by INAA. (c) Control chart of duplicate pairs in the determination of Ag by AAS.

Cobalt

Unlike most of the other MFLR lines, that for Co was fitted not over the entire concentration range shown in Fig. 5a but rather between 5 and 50 ppm Co. This was done to exclude those points showing a linear relationship parallel to the 45° line but displaced towards the y-axis. These points correspond to ultramafic rocks high in Ni (> 1000 ppm) and Cr (> 1000 ppm), elements which degrade detection of Co by INAA and therefore raise the detection limits proportionately from 5 ppm to over 100 ppm. Hence, setting values reported as "less than" to five-eighths of the associated detection limit, can result in such an erroneous pattern. Both the intercept (2.4) and slope (0.92) of the plot of ICP-ES vs. INAA data are significant. Thus the

ICP-ES results tend to be high at or below about 30 ppm Co, and above this level the INAA results are higher. This relationship is shown by the control samples, where ICP-ES yields a slightly higher mean for SS04 at 16 ppm Co, but the INAA mean is higher for SS06, at 48 ppm compared to 40 ppm Co (Table 4).

About half of the duplicate pairs show virtually identical results by INAA, whereas the remainder exhibit absolute differences consistent with precision levels of about 5–20% (Fig. 5b). A misleading estimation of the precision associated with the ICP-ES method is given by three or four pairs showing exceptionally poor agreement; the majority of the points exhibit the same pattern as those for INAA (Fig. 5c). This is confirmed by the control data

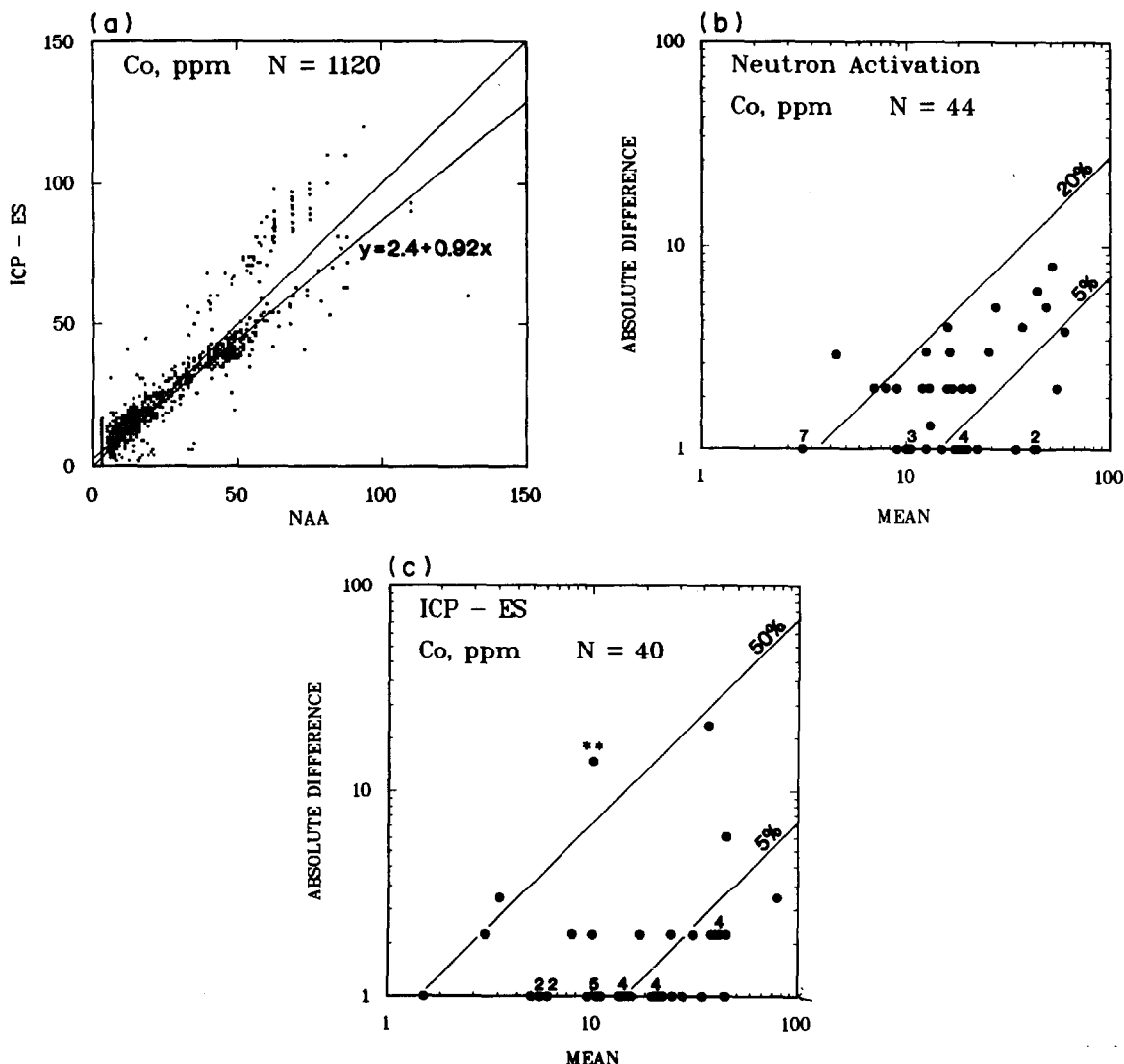


Fig. 5. (a) Comparison of results by ICP-ES and INAA for Co. (b) Control chart of duplicate pairs in the determination of Co by INAA. (c) Control chart of duplicate pairs in the determination of Co by ICP-ES.

for Co (Table 4) and by the identical detection limits established by both laboratories.

Chromium

There is considerable scatter, especially at higher levels (>1000 ppm), in the plot of ICP-ES vs. INAA results for Cr (Fig. 6a). However, the slope of 0.80 is significant with a standard error of about 0.02. The distribution of chromite in rocks can be heterogeneous, but a fairly even spread of points on either side of the 45° line would be expected if this were the cause of the noise. The lack of agreement between the INAA and ICP-ES results is evidenced by the control samples where values by the former method are about 21% and 33% higher (Table 4).

The precision of both methods appears comparable, consistent with 5 and 30–40% for the blind duplicates (Figs. 6b, 6c). The precision for the control samples ranges from 12 to 32% with INAA showing superior reproducibility for SS06 and the reverse for SS04.

Lanthanum

A significant bias is seen in the MLFR line for La in the comparison of ICP-ES and INAA data (Fig. 7a), producing a slope of 0.83 ± 0.02 . There is a considerable degree of scatter, especially towards the x-axis, which is caused by high and varying detection limits (2–400 ppm) for samples with higher Au (>1 ppm), Sb (>3000 ppm) and As (>3000 ppm). Such samples were not used in the computation of the

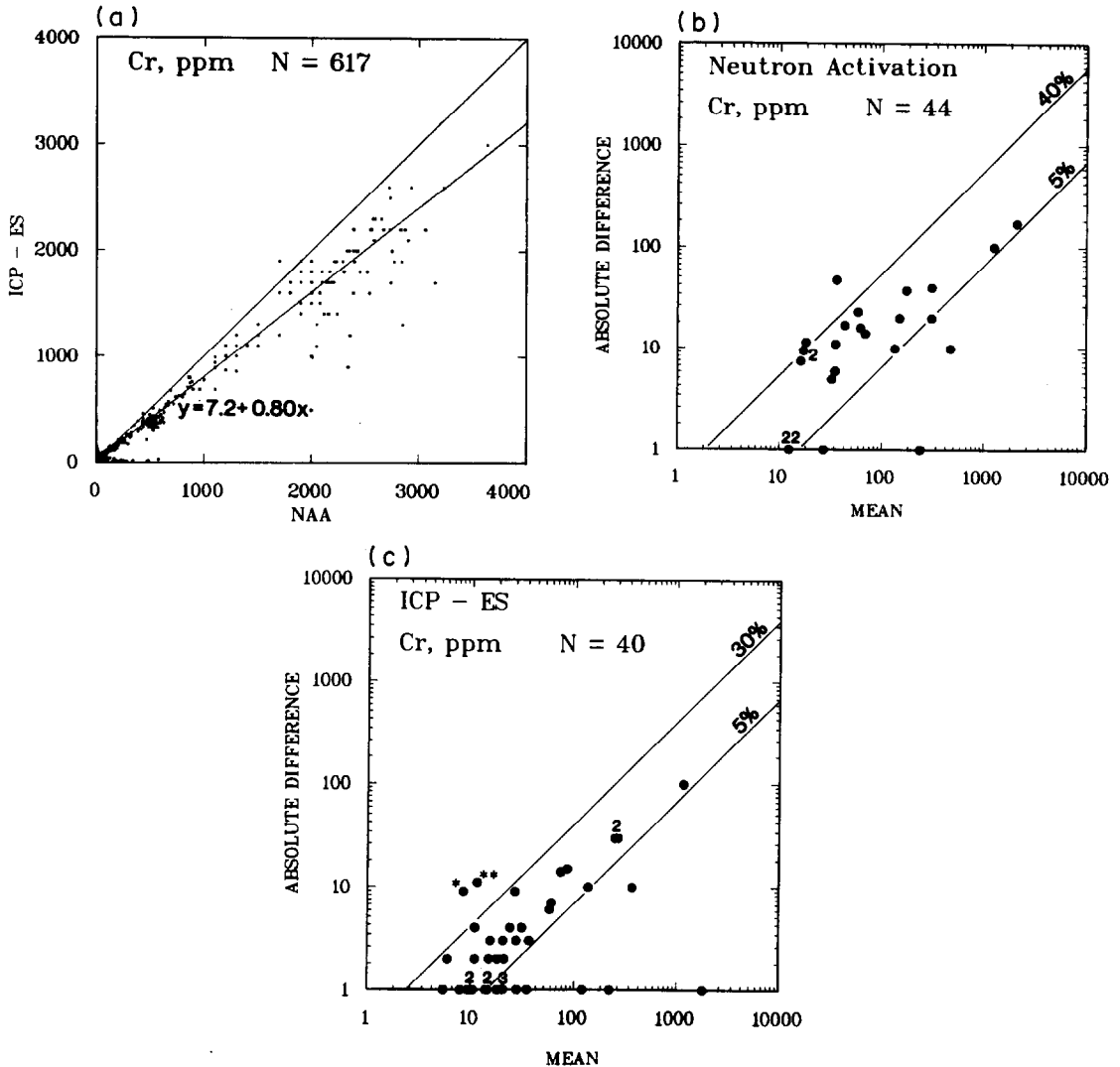


Fig. 6. (a) Comparison of results by ICP-ES and INAA for Cr. (b) Control chart of duplicate pairs in the determination of Cr by INAA. (c) Control chart of duplicate pairs in the determination of Cr by ICP-ES.

MLFR line. The results for the controls obey the predicted behavior where the value by ICP-ES is 84–85% of that by INAA.

The upper limit of the precision for La by ICP-ES is slightly inferior to that by INAA, at 30% (Figs. 7b, 7c). However, most of the duplicate results agree extremely well for both methods (note the density of points on the x -axis) indicating that a value considerably lower than 30% is likely. It is interesting to note that the same eight duplicate samples show precision in the 5–30% range on both graphs, suggesting that this is a heterogeneity effect. Virtually identical precision is obtained by both methods in the analysis of SS06, but results for SS04 by ICP-ES are considerably less reproducible than

those by INAA (Table 4). These data suggest that the detection limit of 10 ppm reported by the ICP-ES laboratory (Table 3) is pessimistic and should be similar to that by INAA.

Nickel

Bias also exists in the comparison of ICP-ES and INAA results for Ni, the slope of the MLFR line being 0.90 ± 0.02 (Fig. 8a). Similarly, the mean values obtained by ICP-ES for the control samples are 89–91% of the concentrations by INAA (Table 4).

More than half the results for the blind duplicates fall below the detection limit of 20 ppm Ni by INAA. However, the control charts (Figs. 8b, 8c) for the pairs by both

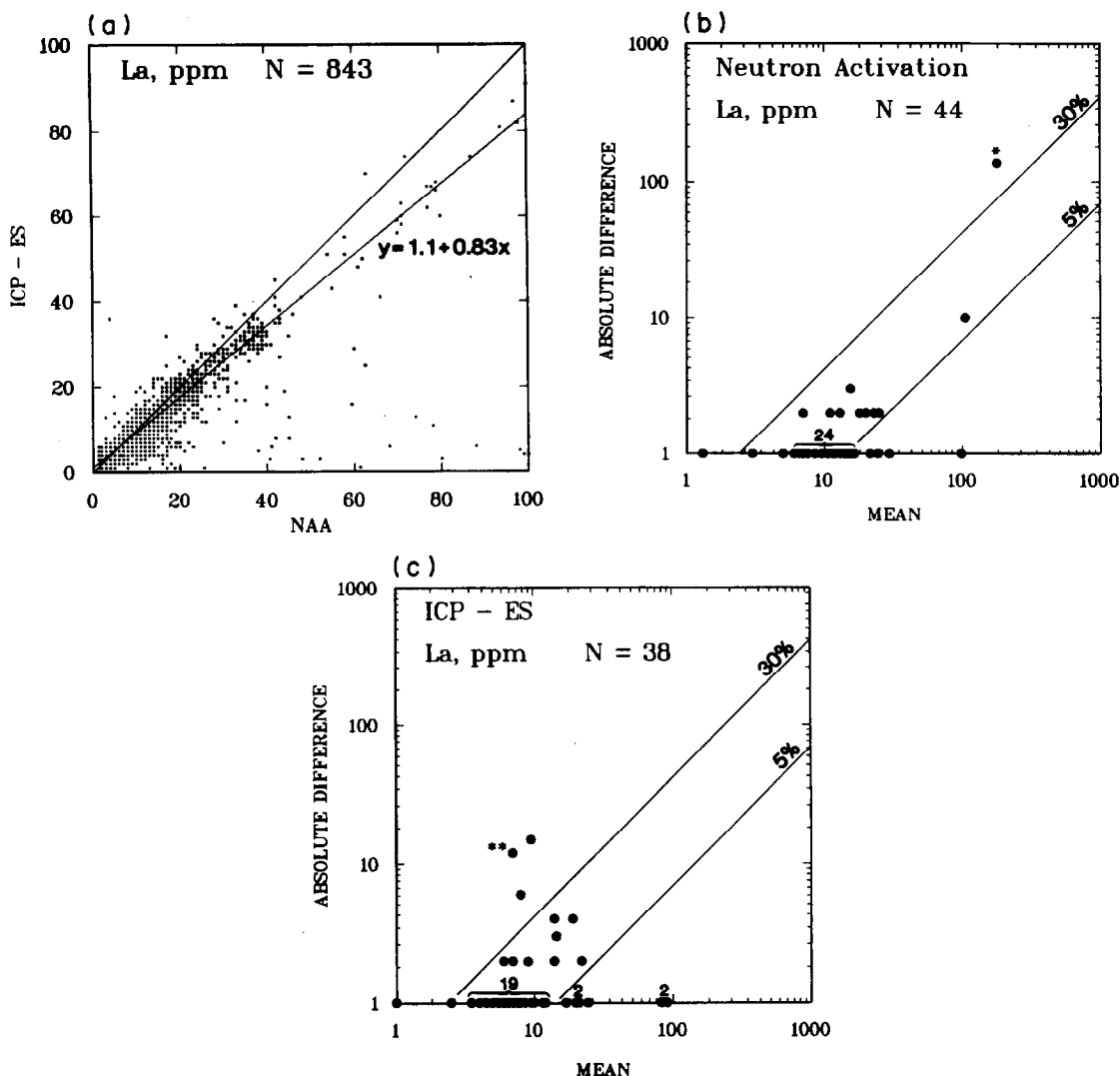


Fig. 7. (a) Comparison of results by ICP-ES and INAA for La. (b) Control chart of duplicate pairs in the determination of La by INAA. (c) Control chart of duplicate pairs in the determination of La by ICP-ES.

methods are very similar, indicating an upper limit of precision of about 30% in the range 10–1000 ppm Ni. The data for SS06 obey this rule (Table 4), but poor precision of about 45–60% is obtained by both methods for SS04 at about 45 ppm Ni. This may be due to the concentration of Ni in SS04 being only 2–4 times that of the detection limit, or to a moderate heterogeneity effect which seems evident in this sample.

Rubidium

Values between 30 and 300 ppm Rb were used in the estimation of the MLFR line (XRF *vs.* INAA) in order to eliminate the effect of scatter towards the y -axis shown in Fig. 9a. This noisy set of data was derived from two batches of

ultramafic rocks, but it was not possible to correlate the high XRF results with the above average concentrations of Cr, Fe, Ni, As or Au in these suites. However, these are the same samples for which the detection limits were higher in the INAA method for Co and it is possible that high levels of Cr *etc.* lead to a higher background in XRF. Although the XRF laboratory reports Rb down to 0 ppm, a detection limit of 20 ppm (*cf.* 5 ppm by INAA) is suggested (Table 3). Again, bias between the methods based on XRF and INAA is evident in Fig. 9a, the intercept being significant at 0.82. The mean results by INAA for the control samples are also higher than those by XRF (53 *vs.* 51 ppm for SS04 and 146 *vs.* 115 ppm for SS06).

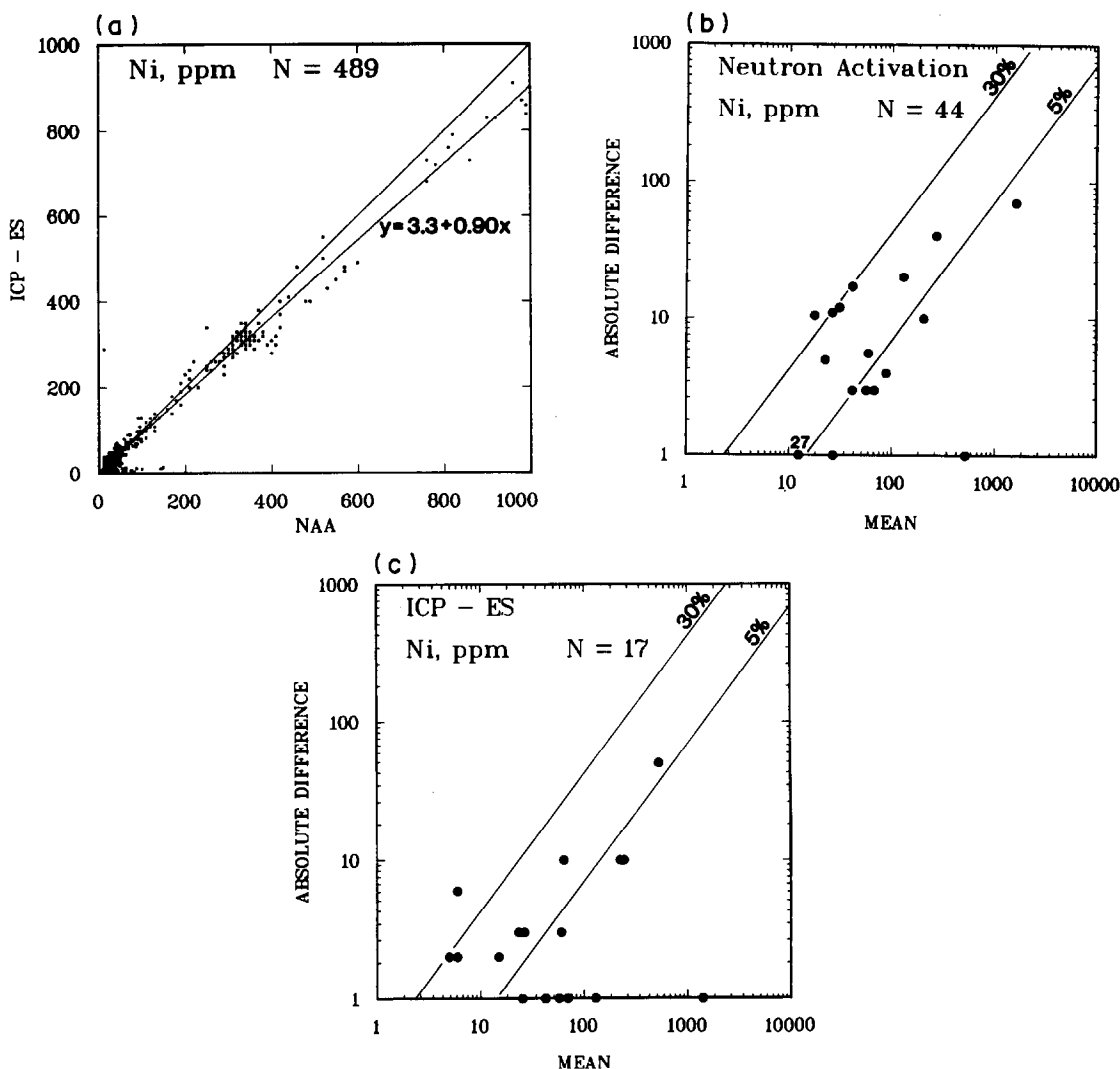


Fig. 8. (a) Comparison of results by ICP-ES and INAA for Ni. (b) Control chart of duplicate pairs in the determination of Ni by INAA. (c) Control chart of duplicate pairs in the determination of Ni by ICP-ES.

The precision of both methods is similar. More than half the duplicate pairs exhibit precision better than 5%, and most of the remainder fall between 5 and 40–60% in precision (Figs. 9b, 9c). The control samples behave accordingly, with essentially the same *rsd* (8%) by both methods for SS06 and a higher standard deviation for SS04, which has an Rb concentration of about 52 ppm, closer to the detection limit (Table 4).

Ytterbium

As in the case of La, the plot of results for Yb by ICP-ES *vs.* INAA shows scatter along the *x*-axis (Fig. 10a). This is caused by elevated detection limits for samples very high in Au

(>1 ppm) and Sb (>1000 ppm). However, elimination of these points in the computation of the MLFR line still results in a bias towards high INAA results ($y = 0.80x$). This is confirmed by the mean results for SS06 (4.9 ppm *vs.* 3.8 ppm by ICP-ES), although the results for SS04 are identical (Table 4).

The upper limit of precision by both methods appears to be 40% (Figs. 10b, 10c) but few samples contain Yb at concentrations much above the detection limits of 0.5 and 2 ppm. Remarkably good reproducibility is shown in the replicate data for the control samples which are low in Yb concentration (Table 4). This suggests that the detection limit for Yb by INAA could be lowered to equal that by ICP-ES, *viz.* 0.5 ppm.

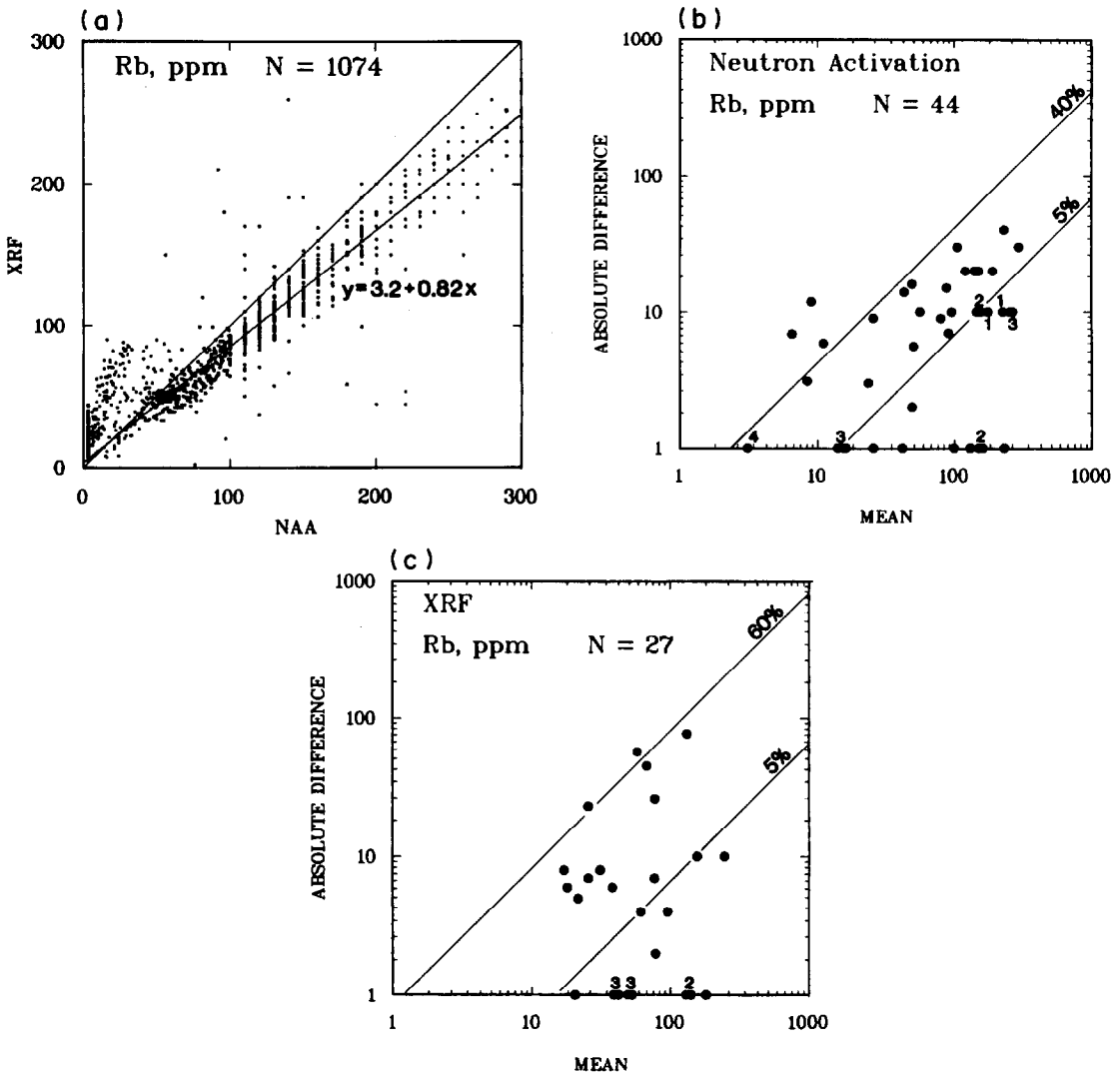


Fig. 9. (a) Comparison of results by XRF and INAA for Rb. (b) Control chart of duplicate pairs in the determination of Rb by INAA. (c) Control chart of duplicate pairs in the determination of Rb by XRF.

Zinc

The comparison of methods based on ICP-ES and INAA for Zn differs from that for the other 11 elements. It is evident in Fig. 11a that there is a bias towards high INAA results at low levels of Zn, which is reversed dramatically at about 400 ppm Zn. Rotational and translational effects are present. If the relationship $y = -83 + 1.2x$ is used to predict the ICP-ES results for SS04 and SS06 (Table 4), the values for Zn are computed to be 63 and 152 ppm, respectively, which agree well with the mean results of 62 ($n = 26$) and 154 ppm ($n = 74$). The conformity of fit to this MLFR line at such low levels of Zn suggests that the

real detection limit for Zn by INAA is in fact much better than the 100 ppm reported and that the calibration in this region should be investigated.

The control chart for duplicate results by ICP-ES shows only modest improvement in precision over that for INAA (Figs. 11b, 11c), with about half the points falling between the 5 and 30% lines, compared to the corresponding limits of 5 and 40% by INAA. This is not consistent with the large disparity in the stated detection limits of 5 and 100 ppm Zn, respectively. The control samples show a greater spread in the precision of the two methods, to be expected near the 100 ppm Zn concentration (Table 4).

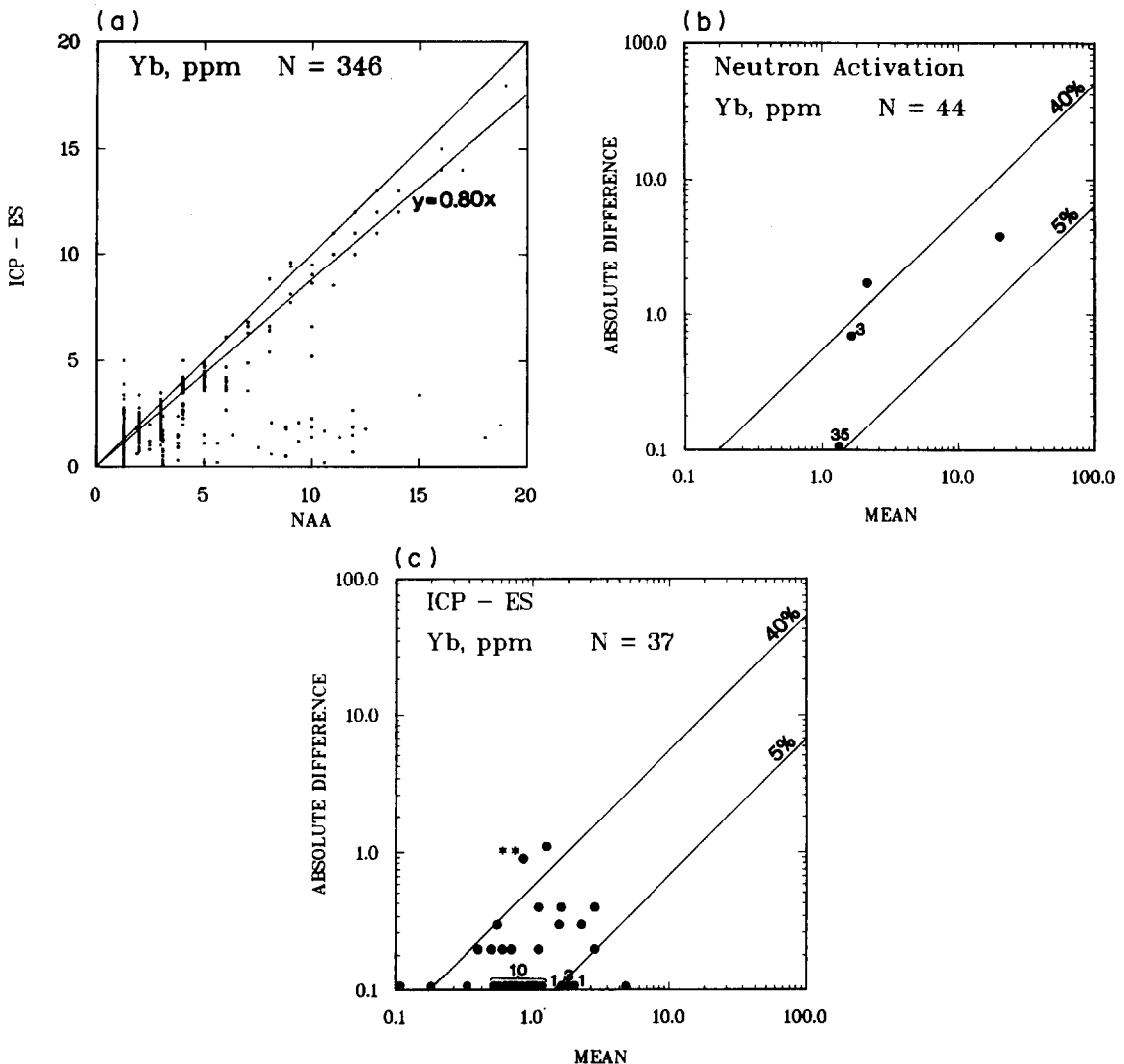


Fig. 10. Comparison of results by ICP-ES and INAA for Yb. (b) Control chart of duplicate pairs in the determination of Yb by INAA. (c) Control chart of duplicate pairs in the determination of Yb by ICP-ES.

Zirconium

There is no apparent relationship between the results obtained by XRF and those obtained by INAA in the determination of Zr between 200 and 1000 ppm (Fig. 12a), where the detection limits differ by an order of magnitude (Table 3). Scatter would have been predicted on both sides of the 45° line rather than on only the one. The mean results for the control samples (Table 4) agree within the wide limits set by the standard deviations. Most of the duplicates have Zr concentrations below the detection limit by INAA (Fig. 12b). However, the XRF results appear to have good reproducibility, the majority of points on the control chart (Fig. 12c) falling below the 5% line and most of the remainder below the 10% precision line.

It is unlikely that these disparities in results between INAA and ICP-ES for the elements Fe, Ba, Co, Cr, La, Ni, and Yb are caused by inadequate dissolution of the samples in the latter technique. Both major and trace element decompositions are regarded as "total". Acid decomposition alone, with the HF/HClO₄/HNO₃ mixture, is inefficient for minerals such as chromites, spinels and zircons, but in the ICP-ES method used here, any residue is decomposed by fusion with LiBO₂. The probability of inter-element interferences causing enhancements in the INAA method or suppressions in the ICP-ES method is low for those elements such as Co and Ni where there is an absence of scatter about the MLFR line (Figs. 5a, 8a). The samples analysed represent a wide range of major and minor elemental concentra-

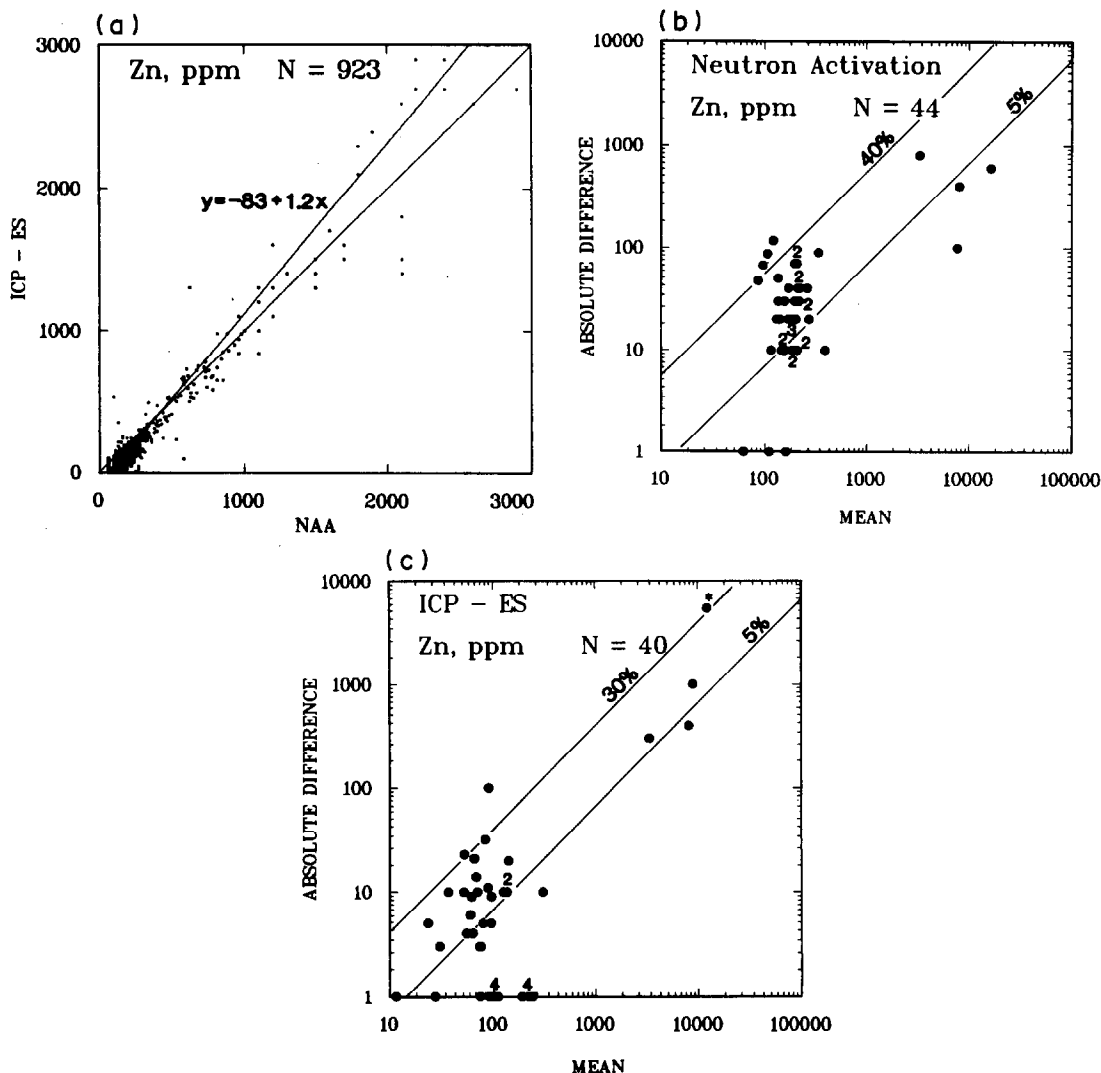


Fig. 11. (a) Comparison of results by ICP-ES and INAA for Zn. (b) Control chart of duplicate pairs in the determination of Zn by INAA. (c) Control chart of duplicate pairs in the determination of Zn by ICP-ES.

tions. The degree of fit to the MLFR line for Cr is less tight and the presence of interferences, shown by rotational and translational effects, is suggested (Fig. 6a). Though the bias in results for the elements La and Yb is large (slopes of 0.83 and 0.80, respectively), the maximum concentration under investigation is only ten times the highest detection limit and hence uncertainty is to be expected (Figs. 7a, 10a). The bias may be suggestive of slightly inadequate background correction in the INAA method at low levels of La and Yb. The XRF data for Ba support the contention that the high bias in the INAA results is caused by calibration error. However, agreement between the XRF and INAA ($y = 0.94x$) results for Fe is better than that shown between ICP-ES and INAA, indi-

cating that the high bias in the INAA is not serious (Figs. 2a, 2b). The slope of the MLFR line for XRF *vs.* INAA for Rb is significant, but there is considerable scatter in this narrow range close to the detection limit of 20 ppm by XRF (Fig. 9a). Rotational and translational effects in the comparison of results for Zn by ICP-ES and INAA (Fig. 11a) are highly significant; the behaviour predicted by using the MLFR relationship is exact for the control samples. International reference materials well documented for Zn over a wide concentration range are required to identify the source(s) of the disagreement.

Another evaluation¹⁸ of multielement neutron activation analysis in geochemical exploration, as applied to lake sediments, has found the

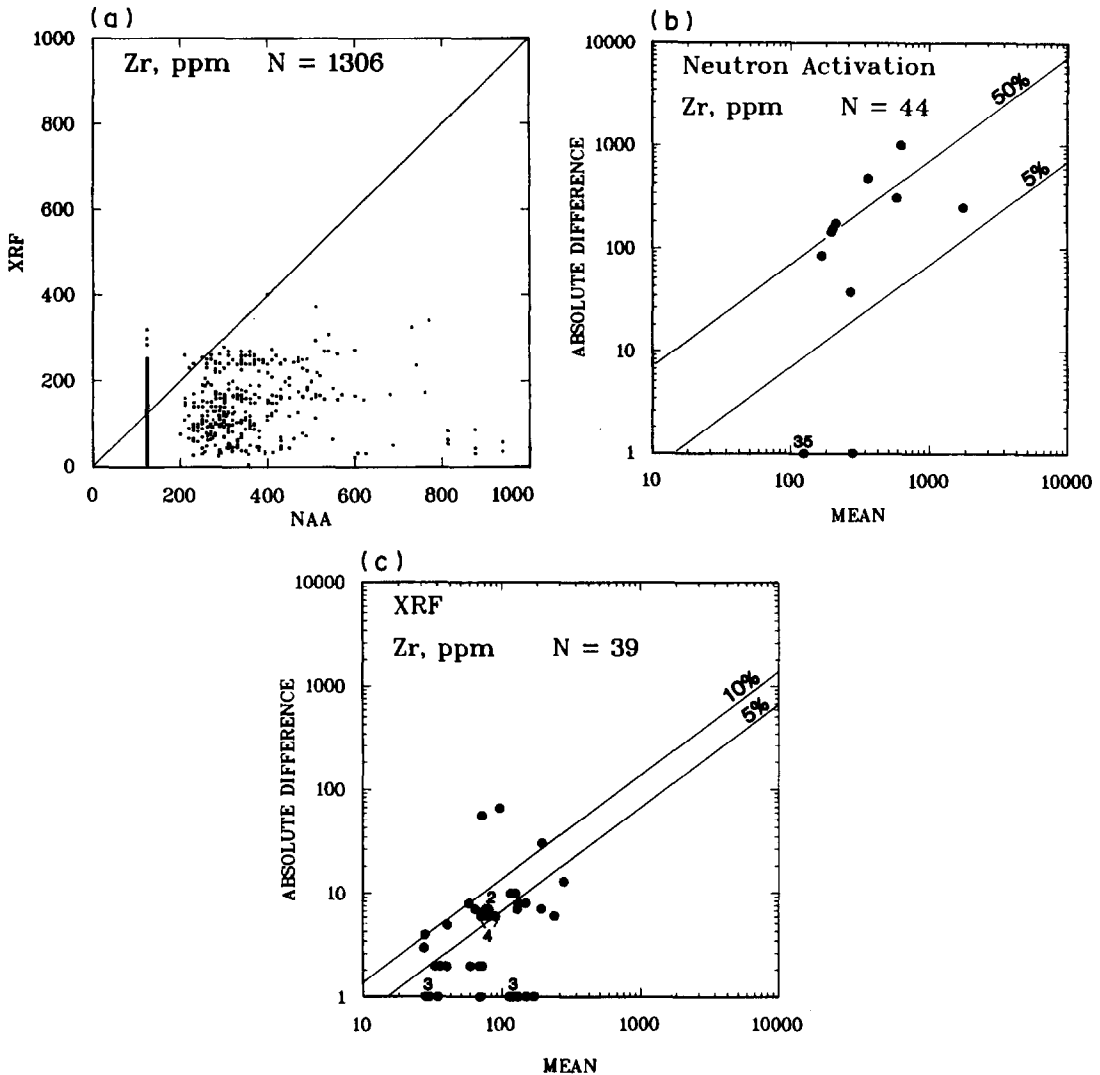


Fig. 12. (a) Comparison of results by XRF and INAA for Zr. (b) Control chart of duplicate pairs in the determination of Zr by INAA. (c) Control chart of duplicate pairs in the determination of Zr by XRF.

method capable of providing good-quality useful data for 18 elements, including Fe, Ba, Co, La, Rb and Yb; detection limits for Cr, Ni, Zn and Zr were too high relative to the elemental abundances in this medium. An accurate assessment of bias was not made, though comparison was made with other methods based on ICP-ES and AAS, for about 1500 sediments.

CONCLUSIONS

The elements Na, Fe, Ba, Co, Cr, La, Ni and Rb can be determined in rocks by epithermal INAA with adequate sensitivity and reproducibility for application in geochemical studies. Control charts for duplicate samples indicate that the precision by INAA can be expected to

be moderately inferior for Fe, Ba and Cr, compared to the ICP-ES method, and for Na, Fe and Ba compared to the wavelength-dispersive XRF method. Equal or slightly superior precision by INAA was in evidence for Na, Co, La and Ni compared to that achieved by the ICP-ES method and for Rb compared to the XRF method. Inadequate sensitivity was found for the determination of Ag, Yb, Zn and Zr in rocks by INAA. The data suggest that though the detection limit of 200 ppm for Zr may be optimistic, the limits for Zn and Yb could actually be lower than those (100 and 2 ppm respectively) reported by the laboratory.

Results for Na by the INAA method agree well with those by the XRF and ICP-ES methods. Similarly, bias was not in evidence in

the comparison of INAA and AAS methods for Ag. Application of the MLFR technique indicated positive bias of INAA compared to ICP-ES and XRF for the elements Cr, Yb, Rb, La, Ba, Ni, Fe and Co, listed in order of decreasing severity of bias. However, since most of the data points for Yb, Rb, La and Co were within a decade of one of the detection limits, such a bias of 108–120% is neither surprising nor serious. However, bias between the methods for Cr, Ba, Ni and Fe has major implications when data sets incorporating various analytical methods are merged for interpretive studies. The two independent sets of results for Ba and Fe by XRF and ICP-ES methods strongly support the belief that the INAA method gives high results, rather than the contention that the other two methods are producing results which are systematically low. The significant rotational and translational effects evident for Zn in the comparison of results obtained by INAA and ICP-ES require further investigation. This is the only element for which lower results can be expected at high concentration levels by INAA than by ICP-ES. Replicate data for the two sediment control samples universally confirm the predictions made by application of the MLFR technique and conform to the precision specifications outlined by the control charts for duplicate samples.

In view of the numerous errors and sources of variance possible in the application of the production-oriented methods in this investigation, the precision demonstrated by the results is good. The biases shown for Fe, Ba, Cr, Ni and Zn warrant further investigation of the accuracy, by analysis of international standard reference materials. Such biases may be related to the calibration strategies adopted by the laboratories and may not reflect differences inherent in the analytical techniques themselves. The

advantages of simplicity, ease of automation, minimal sample preparation or treatment, flexibility in sample size, non-destructive nature of the technique and cost-effectiveness ensure an increasing application of INAA in geochemical programmes.

Acknowledgements—The authors are grateful to Craig Stuart of Becquerel Laboratories for information and discussion and thank members of the Analytical Chemistry Laboratories, GSC, for their assistance and I. R. Jonasson for critical review of this manuscript. The computer program for the MLFR calculations was obtained from Professor B. R. Ripley, University of Strathclyde.

REFERENCES

1. P. J. Potts, *A Handbook of Silicate Rock Analysis*, p. 399. Blackie, New York, 1987.
2. H. A. van der Sloot and J. Zonderhuis, *Geostd. Newsl.*, 1979, **3**, 185.
3. E. S. Gladney and D. R. Perrin, *ibid.*, 1981, **5**, 113.
4. M. Geisler, *ibid.*, 1985, **9**, 19.
5. Y.-J. Zhang, X.-B. Li and L.-S. Song, *ibid.*, 1986, **10**, 61.
6. P. J. Potts and N. W. Rogers, *ibid.*, 1986, **10**, 121.
7. G. E. M. Hall and G. F. Bonham-Carter, *J. Geochem. Explor.*, 1988, **30**, 255.
8. H. E. Clifton, R. E. Hunter, F. J. Swanson and R. L. Phillips, *U.S. Geol. Surv. Prof. Paper*, 625-C, 1969.
9. J. A. Plant, M. Hale and J. Ridgeway, *Trans. Inst. Metall.*, 1988, **97**, B116.
10. M. Thompson and J. N. Walsh, *Handbook of Inductively Coupled Plasma Spectrometry*, Blackie, New York, 1988.
11. R. M. Rousseau, *X-Ray Spectrom.*, 1984, **13**, 115.
12. *Idem*, *ibid.*, 1984, **13**, 121.
13. R. M. Rousseau and M. Bouchard, *ibid.*, 1986, **15**, 207.
14. B. R. Ripley and M. Thompson, *Analyst*, 1987, **112**, 377.
15. M. Thompson and R. J. Howarth, *J. Geochem. Explor.*, 1978, **9**, 23.
16. W. K. Fletcher, *Analytical Methods in Geochemical Prospecting*, p. 32. Elsevier, New York, 1981.
17. A. A. Levinson, *Introduction to Exploration Geochemistry*, p. 43. Applied Publishing, Calgary, 1974.
18. P. H. Davenport, *Curr. Res., Newfoundland Dept. of Mines*, 1988, No. 88-1, 403.

UPDATING A VINTAGE ICP ATOMIC-EMISSION SPECTROMETER

ROBERT I. BOTTO

Exxon Research and Engineering Company, Baytown Specialty Products, P.O. Box 4255,
Baytown, TX 77522, U.S.A.

(Received 15 June 1989. Accepted 12 July 1989)

Summary—The Analytical Research Laboratory at Exxon Research and Engineering Company in Baytown, Texas acquired one of the first inductively coupled plasma atomic-emission spectrometer (ICP-AES) systems in the petroleum industry in early 1976. During the next ten years, extensive hardware and software improvements were made to increase flexibility and maintain state-of-the-art performance. In 1987 the purchase of a new ICP-AES was considered but postponed in favor of renovation/modernization of the vintage instrument. A factor in the decision was a reorganization of the laboratory that year, which significantly altered its analytical needs. This paper details the construction of a combination simultaneous/sequential ICP-AES system, using as a foundation the 13-year old polychromator. The new system is meeting the needs of the new analytical laboratory, chartered to provide analytical problem-solving services for the Exxon Baytown Refinery/Chemical Plant complex and affiliates throughout the Exxon circuit.

The Analytical Research Laboratory of Exxon Research and Engineering Company in Baytown, Texas ordered a Jarrell Ash Plasma AtomComp 90-975 in late 1975. This inductively coupled plasma atomic-emission spectrometer (ICP-AES) consisted of a 24-channel 0.75-m polychromator interfaced to a 2-kW, 27-MHz inductively coupled plasma (ICP) source. A Digital Equipment Corporation PDP 8/m computer and a teletypewriter completed the system, which cost \$62,000. At the time of purchase, the analytical research laboratory was responding to the needs of a rapidly expanding synthetic fuels research program. Justification for the purchase was based on increasing workload of samples of a variety of complex materials (coal, shale, ash, coal liquids, shale oils, process water, metals, deposits, *etc.*) and increased emphasis on multielemental analysis, particularly for environmentally important elements.

The instrument was installed in May 1976, and was one of the first in the petroleum industry. Detection limit specifications negotiated with the manufacturer were not met during the first few months, owing to the poor sensitivity obtained with the split-flow atomic absorption-type nebulizer initially supplied (Table 1). Development of the cross-flow nebulizer improved the sensitivity for all elements, and met specifications. Improvement in the argon-flow control and optimization of the plasma/poly-

chromator resulted in still lower detection limits. Description of these improvements is given in the literature.^{1,2} By 1980, measured detection limits compared well with those in published compilations.^{3,4}

During the first 5 years the workload for the ICP-AES increased rapidly and the cost per sample analyzed decreased. A study performed at the end of 1980 revealed accumulated savings exceeding one million dollars, based on the cost differential between ICP-AES and alternative methods.⁵ The polychromator array was expanded to include environmentally important elements and low sensitivity lines for abundant elements. Methods were developed for obtaining accurate and reproducible corrections for spectral interferences.^{1,6}

Increasing need for accurate determination of environmentally important elements in coal, coal fly-ash, shale, sludge and other complex materials justified the addition of a high-resolution echelle spectrometer (SpectraSpan IIIB) in 1981. The echelle spectrometer was mounted on an optical table to the right of the ICP source unit so that the plasma could be viewed by both spectrometers simultaneously.⁷ The combination of higher resolution and the ability to choose optimum positions for off-line background corrections resulted in 70-97% reduction in spectral interferences affecting 10 important elements. This was accomplished

Table 1. ICPES polychromator detection limits for aqueous solution*

Element	Wavelength, nm	Specification, October '75	AA nebulizer, July '76	Cross-flow nebulizer, January '77	Optimization with Cu/Mn, April '77	Background correction, November '78	Mass flow control aerosol carrier, February '80	Renovated polychromator, January '89
Ag	338.289	—	—	—	—	0.002	0.0053	0.004
Al	308.215	0.03	0.125	0.034	0.015	0.018	0.011	0.0092
As	193.759	0.08	0.72	0.073	0.09	0.064	0.017	0.037
B	249.773	—	—	—	—	0.017	0.0012	0.0048
Ba	455.403	0.001	0.001	0.0003	0.0002	0.0003	0.0002	0.0002
Be	234.861	—	—	—	—	0.0012	0.0007	0.0002
Ca	393.366	0.002	0.064	0.0022	0.002	0.003	0.0003	0.0001
Cd	214.438	—	—	0.0099	0.005	0.0075	0.0051	0.0058
Co	228.616	0.005	0.005	0.0089	0.004	0.0066	0.0052	0.002
Cr	357.869	0.003	0.016	0.0098	0.007	0.0027	0.0029	0.007
Cu	324.754	0.004	0.004	0.0006	0.0008	0.0006	0.0004	0.0006
Fe	259.94	0.005	0.044	0.0022	0.003	0.0019	0.0017	0.0026
K	766.49	4	—	0.092	0.02	0.027	0.016	0.21
Li	670.784	—	—	—	—	—	0.0005	0.0008
Mg	279.553	0.001	0.033	0.0007	0.001	0.0003	0.0003	0.0001
Mn	257.61	0.005	0.002	0.0004	0.0004	0.0005	0.0003	0.0004
Mo	202.03	0.007	0.013	0.0092	0.01	0.019	0.0047	0.0036
Na	588.995	0.004	0.083	0.0023	0.002	0.0022	0.0008	0.0026
Ni	341.476	0.009	0.03	0.0081	0.006	0.0098	0.013	0.011†
P	214.914	0.08	0.11	0.86	0.14	0.059	0.044	0.034
Pb	220.353	0.02	0.062	0.046	0.03	0.027	0.013	0.0094
Pt	265.945	—	—	—	—	0.045	0.076	0.061
Sb	231.147	—	—	—	—	0.09	0.023	0.011†
Se	196.09	0.06	0.25	—	0.02	0.079	0.023	0.017
Si	288.158	0.03	0.011	0.021	0.013	0.027	0.0037	0.0066
Sn	189.989	0.012	0.15	0.049	0.026	0.02	0.014	0.011
Sr	407.771	—	—	—	—	—	0.0001	0.0002
Ti	334.941	0.001	0.012	0.001	0.0008	0.001	0.0011	0.0008
Tl	377.572	—	—	—	—	0.034	0.034	0.03
U	367.007	—	—	—	—	0.052	0.025	0.087
V	292.402	0.002	0.006	0.0073	0.006	0.013	0.0091	0.0052
W	207.911	—	—	—	—	—	0.06	0.068
Zn	206.2	0.01	0.005	0.015	0.016	0.0036	0.0016	0.0018

*Concentration equivalent to a signal that is twice the standard deviation of the blank (10 exposures, 10 sec at peak).

†Line changes, Ni to 231.604 nm; Sb to 206.833 nm.

with little or no loss in sensitivity (Table 2). Both multichannel spectrometers were operated simultaneously, resulting in a dual polychromator ICP-AES system.

Figure 1 shows the ICP-AES system as it was operated from 1981 to 1988. One-way communication was provided between the two data terminals and a Hewlett-Packard HP-1000

Table 2. Dual polychromator ICP-AES system (1981)

Jarrell Ash AtomComp 750		SpectraSpan III B	
Type:	0.75 m Paschen-Runge	Type:	0.75 m Czerny-Turner
Grating:	2400 grooves/mm, ruled, reciprocal linear dispersion 0.54 nm/mm, 270 nm blaze	Grating:	echelle, reciprocal linear dispersion 0.1 nm/mm (300 nm, 75th order)
Resolution:	0.03 nm (first order)	Resolution:	0.005 nm-0.02 nm
Array:	41 channels for 33 elements	Array:	10 channels for 10 elements plus single element capability either side of line, variable distance from line.
Background correction:	0.04 nm on high wavelength side of line	Background correction:	
Detection limits ($\mu\text{g/ml}$) for elements common to both spectrometers			
Element	Wavelength, nm	AtomComp 750	SpectraSpan III B
As	193.759	0.025	0.080
Be	234.861	0.0014	0.0003
Cd	214.438	0.008	0.009
Mo	202.030	0.007	0.013
Pb	220.353	0.014	0.035
Se	196.090	0.040	0.070
Tl	377.572	0.040	0.070
Ni	341.476	0.016	
	231.604		0.005
Sb	231.147	0.030	
	206.833		0.040
U	367.007	0.050	
	409.014	0.080	

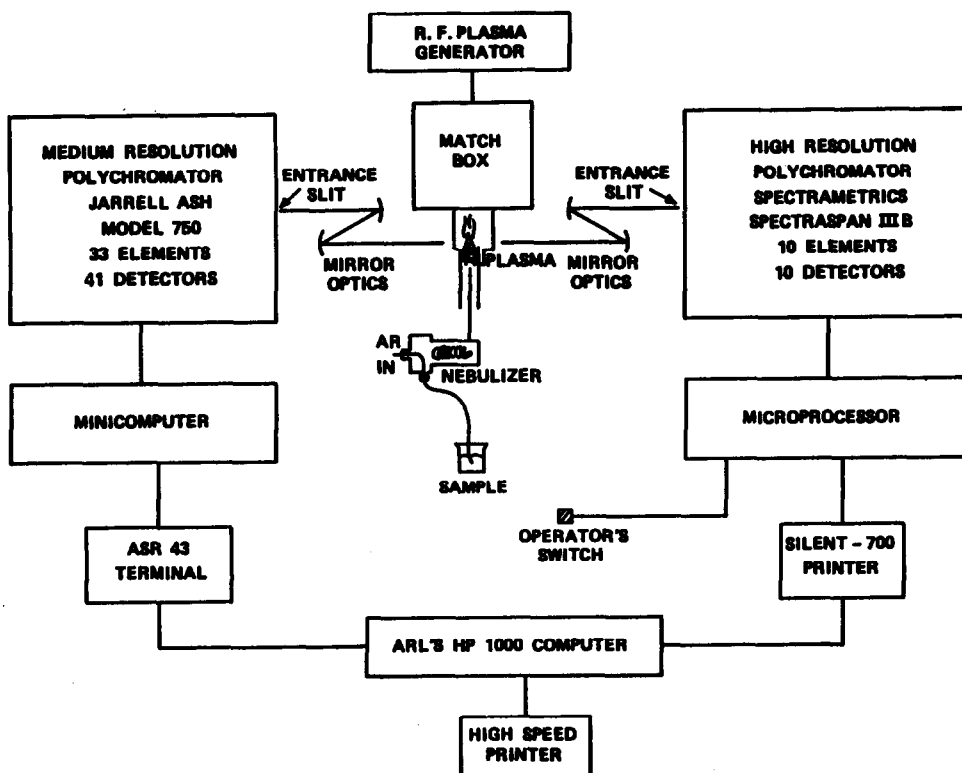


Fig. 1. Dual spectrometer ICP-AES system as configured 1981-1988. The high-resolution echelle polychromator was turned with its back to the operator, making it necessary to wire the sample analysis switch to the ASR 43 console.

computer. Data were collected from both spectrometers simultaneously and combined into one file per run. Reagent-blank correction, dilution, and spectral interference corrections were performed by the HP-1000 and a report was generated for each sample analyzed. Provision was made for entering values for elements found to be at high concentrations and redetermined by subsequent dilution and repeat analysis. Interference corrections were performed on the basis of the value entered; thus accurate analyses for major, minor and trace concentrations were included on a single printout.

By 1988 the Analytical Research Laboratory had analyzed a large number of samples, performing 2.3 million elemental determinations by ICP-AES. A program of long-term spectrometer performance monitoring and maintenance included the following.

(1) Every 6–12 months all optical surfaces were examined for fogging and cleaned/replaced as necessary. All photomultiplier tube windows were cleaned and exit-slit alignments were checked and reprofiled as necessary. Weak photomultiplier tubes and defective parts were replaced.

(2) Every 2–3 years a “major overhaul” included the items above plus replacement of gas-handling apparatus, R.F. load coil and impedance matching electronics (isolation capacitors, *etc.*).

The program of long-term maintenance combined with daily optimization performed by using the Cu/Mn intensity ratio was effective in maintaining long-term performance.⁸ No irreversible changes in sensitivity were noted for the polychromator from 1980 to 1988. The sensitivity of the echelle spectrometer was degraded by a factor of two during this period, by fogging of the transfer optics.

In 1986 the purchase of a new ICP-AES system was considered for the following reasons.

(1) The AtomComp 750 was over 10 years old, and needed major renovation.

(2) The PDP 8/m computer/disk drive and the echelle spectrometer were becoming unreliable and expensive to service.

(3) The calculation programs on the HP-1000 computer were written in BASIC. A need existed to shut down the BASIC interpreter on the system. Rewriting these in FORTRAN would have been expensive and time-consuming.

A market survey conducted in 1987 pointed out several instruments that would have met or exceeded specifications for sensitivity, selectivity and precision. However, none possessed software capable of performing the calculations currently performed for full matrix correction for spectral interferences and correction for interferences with elements determined after dilution. The same year the Analytical Research Laboratory was reduced in size and reorganized concurrently with the relocation of the Synthetic Fuels Research Laboratory. The reorganized laboratory, Baytown Specialty Products Analytical, remained in Baytown to serve the needs of the Exxon Baytown complex for problem solving and non-routine analysis. The amount and character of the ICP-AES workload changed, resulting in a lighter but steady workload with even more variety of sample types—alloys, catalysts, corrosion deposits, process waters, petroleum products, *etc.*, and continued need for flexibility to determine special elements, and greater emphasis on rapid, reliable service for plant control/troubleshooting.

In mid-1987 Thermo Jarrell Ash Corporation announced the availability of an IBM PC/AT microcomputer upgrade/replacement for the PDP 8 series computers. The software supplied with this system included multi-position background correction and improved capability for spectral interference corrections. The decision was made to purchase this upgrade together with a sequential spectrometer at a cost less than half that of a new combination simultaneous/sequential ICP-AES system. Plans were made for a complete renovation of the vintage polychromator and interfacing of the sequential spectrometer. Data transfer to the HP-1000 and new software to compensate for limitations in the vendor software were required.

The remainder of this paper details the construction and performance of an ICP-AES system for the 1990s.

SYSTEM HARDWARE

In addition to the “major overhaul” items mentioned above, the light baffling for each polychromator exit-slit assembly was disassembled and reassembled with fresh light-proof tape. The old tape had dried and become embrittled, breaking free and partially blocking the light-path more than once during the past few years. All optical surfaces, except the grating and the exit-slit refractor plates were replaced.

Refractor plates were cleaned and electronic connections inside the spectrometer housing were cleaned and checked. The optics were aligned and the exit-slits reprofiled. Two spectral-line changes were made (footnote, Table 1).

The PDP 8/m computer, disk drive and teletypewriter were replaced with an IBM PC/AT microcomputer with 640 kB RAM, 30 MB hard disk drive, 1:2 MB floppy drive and graphics printer. The spectrometer control interface was made through the original "spectrum shifter" refractor plate servo driver. It was necessary to install a thicker refractor plate to accommodate the ± 1 nm spectral displacement range capability of the vendor's "ThermoSPEC" software.

The decommissioned echelle polychromator was removed and the table it rested on was lowered to allow the sequential spectrometer to view the plasma from the same direction, and on a level with it. Optical transfer was accomplished with a 76 mm diameter MgF₂-coated quartz projection lens (75 mm focal length, Thermo Jarrell Ash #006542) positioned 90 mm from the plasma observation zone and 450 mm from the sequential spectrometer entrance

Table 3. Sequential spectrometer

Type:	Crossed Czerny-Turner
Focal length:	0.75 m
Grating:	2400 grooves/mm, galvanic drive
Wavelength range:	190-265 nm (second order) 265-535 nm (first order)
Linear dispersion:	0.5 nm/mm (first order) 0.25 nm/mm (second order)
Resolution:	0.018 nm (first order) 0.009 nm (second order)
Step size:	0.001 nm (first order) 0.0005 nm (second order)
Slit size:	Width, 0.025 mm Height, 3 mm
Temperature control:	35 \pm 0.05°
Photomultipliers:	Hamamatsu R427, R300

slit (image magnification 5:1). The lens was attached to an xyz positioning device on an optical track built within the ICP source housing. A laser was used to align the light-path from the plasma through the spectrometer.

The sequential spectrometer specifications are given in Table 3. Operating software for this spectrometer resides in an Apple IIe computer having a dual floppy disk and a separate graphics printer. The configuration of the dual spectrometer ICP-AES system is shown in Fig. 2.

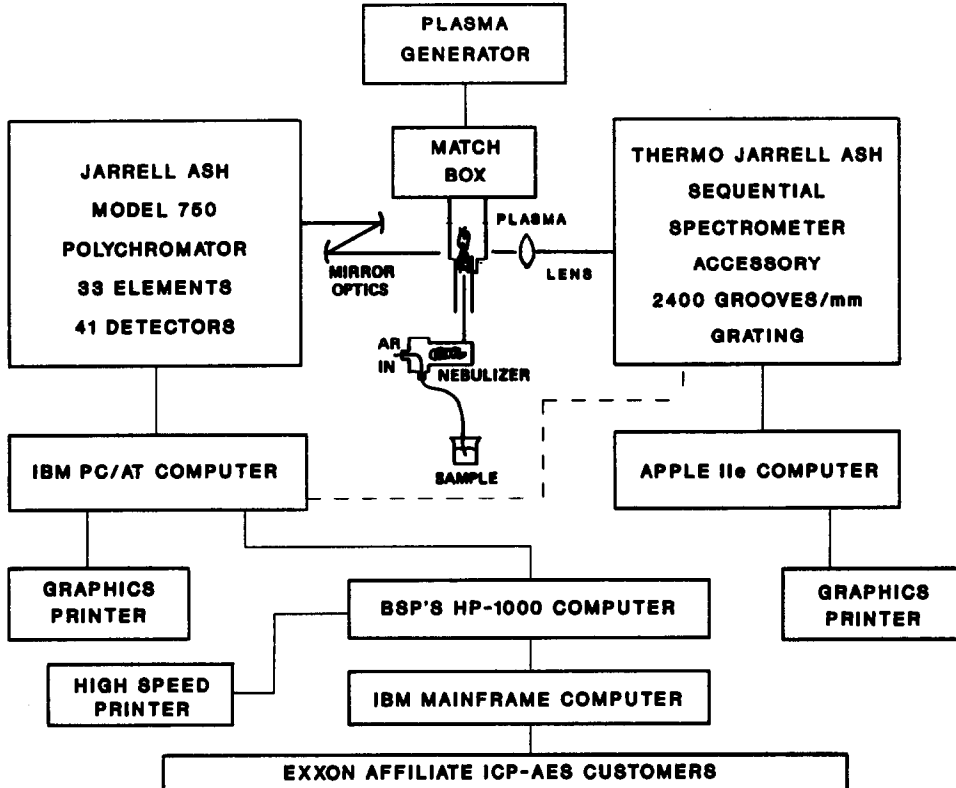


Fig. 2. Present configuration of the dual spectrometer ICP-AES system. IBM software will soon operate the sequential spectrometer, eliminating the need for the Apple IIe computer.

DATA TRANSFER/SOFTWARE

The ThermoSPEC software lacks the capability of correcting an analysis for high concentrations by use of subsequent dilution and repeat analysis. To overcome this limitation data are transferred in batch mode from the IBM PC/AT to the HP-1000 computer. The transfer is accomplished in two stages. The IBM ENABLE program is used to select and transfer completed sample analyses from the ThermoSPEC data base to a floppy disk. The IBM PC/AT then becomes a terminal of the HP-1000, using "Reflection 7" run from DOS. Data on the floppy disk are read into files for processing on the HP-1000.

Fortran software was written for the HP-1000 to accomplish the following tasks.

(1) To produce a custom-formatted printout of each analysis with organizational heading, sample description, customer identification, sample dilution factor, units, date and time analyzed. Customer and sample description are obtained automatically by interaction with the Laboratory Information Management System (Beckman LAO "Lab Manager"). The operator provides only a six-digit analytical sample number as each sample is analyzed.

(2) To identify samples giving results outside the linear calibration range ("out of range" values). A bold warning is provided at the top of the report and upper limit concentrations are printed.

(3) To permit the operator to enter corrected values for "out of range" elements and perform incremental interference corrections for concentrations entered to replace out of range data. Comprehensive spectral interference corrections performed by the IBM computer are valid and complete if no determinations performed are out of range.

(4) To provide diagnostic information for each determination, including the standard deviation for replicate exposures, detection limits (corrected for dilution) for elements not detected, and notation for elements determined at concentrations within a factor of 5 times the detection limit.

A later version of the software will include diagnostics indicating the relative amount of interference correction performed for each determination, as offered with the BASIC programs.⁸ In the near future ICP-AES customers throughout Exxon will be able to receive

analysis reports electronically over a data-link with an IBM mainframe computer.

PERFORMANCE

After the reconditioning of the polychromator hardware and optics, optimum positions were chosen for background correction, and detection limits were determined with several values of the Cu/Mn intensity ratio.¹ The value of the Cu/Mn ratio selected as the best compromise yielded the detection limits shown in the furthest right column of Table 1. Except for potassium, the optimum detection limits measured 9 years apart are comparable. The detection limit for potassium was degraded when the adjustable cross-flow nebulizer was replaced with a fixed cross-flow nebulizer, both operated without an aerosol baffle within the Scott spray chamber. The adjustable cross-flow nebulizer could be "tuned" to produce an aerosol droplet size distribution favoring larger droplets and increasing sensitivity for the alkali metals. The fixed cross-flow nebulizer has the advantage of greater convenience and reliability.

Criteria for evaluation of the performance of the sequential spectrometer are as follows.

(1) Resolution—should be adequate for the determination of trace elements in complex materials where spectral interferences compromise the accuracy of data produced by the polychromator.

(2) Sensitivity—should be comparable to that of the polychromator. Sensitivity at wavelengths shorter than 200 nm should not be degraded significantly by the optical components, as they are with the echelle spectrometer.

(3) Precision—should not be degraded significantly by error in resetting wavelengths.

The resolving power of the sequential spectrometer is significantly better than that of the polychromator, and equivalent to the resolution of the echelle spectrometer as used in routine operations. Figure 3 shows a comparison of wavelength scans obtained for a solution of 1:100 Be:Fe at Be(I) 234.861 nm. Figure 4 shows a scan in the same wavelength region performed with the echelle spectrometer, for a solution having the same Be:Fe ratio. The sequential spectrometer scan (Fig. 3, scan B) reveals at least 5 Fe lines, with a single Be line marked by the cursor. Expansion of the central portion of this scan (scan C) shows

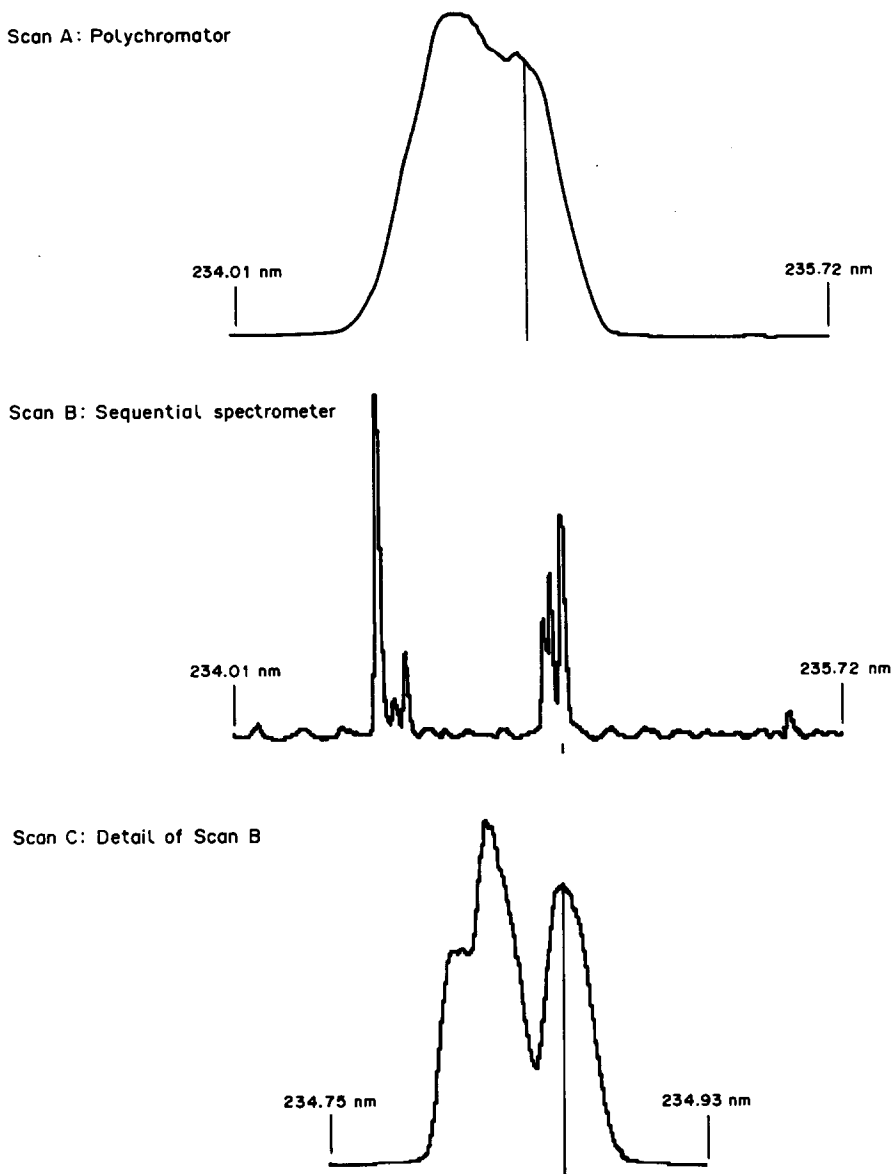


Fig. 3. Wavelength scans centered at Be (I) 234.861 nm, performed with an aqueous solution of Be ($1 \mu\text{g/ml}$) and Fe ($100 \mu\text{g/ml}$). Scan A: polychromator scan in first order. Scan B: sequential spectrometer scan in second order. Scan C: sequential spectrometer scan showing resolution of Be line from nearby Fe lines.

nearly complete resolution of an iron line at 234.830 nm from the Be line. Complete baseline separation of these lines is achieved by the echelle spectrometer with optimum slit sizes (Fig. 4). This resolution is often compromised in routine operations because of the necessity of using larger slit sizes to increase sensitivity. The slit sizes used for the scans in Fig. 3 are those employed routinely. The wavelength mismatch between scans A and B probably indicates calibration error in the polychromator scan. Comparison of scans A and B emphasizes that the sequential spectrometer should be

used each time an important trace element determination is affected by spectral interferences.

A comparison of sensitivity and precision for the polychromator and the sequential spectrometer is shown in Table 4. The sensitivity of the two spectrometers is approximately equal throughout the wavelength range of the sequential spectrometer. The sequential spectrometer does not exhibit as much loss in sensitivity as the echelle spectrometer at 190–200 nm, even though the interior of both spectrometers was nitrogen-purged. Short-term precision was

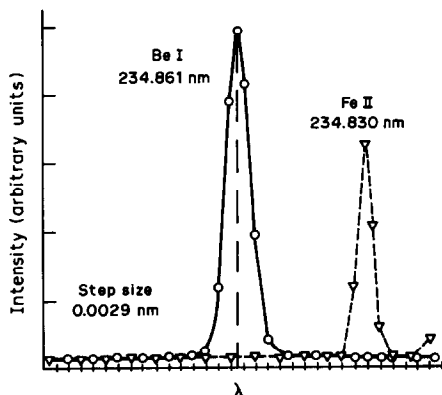


Fig. 4. Direct current plasma echelle spectrometer wavelength scan showing the complete resolution of Fe (II) (1000 $\mu\text{g/ml}$) and Be (I) (10 $\mu\text{g/ml}$). (Reproduced from R. Botto, *Spectrochim. Acta*, 1983, **38B**, 129, by permission. Copyright 1983, Pergamon Press, Oxford.)

measured at concentrations approximately 20 and 1000 times the detection limit. Except for Mo, the precision at low concentrations is the same, within a factor of two, for both spectrometers. The results are approximately the same at the higher concentrations. The high precision obtained for resetting the wavelength by the galvanic grating drive in the sequential spectrometer yields analytical precision on a par with that of a fixed grating/detector system. Values for short-term and day-to-day precision of wavelength resetting are in Table 5. The day-to-day precision values were determined without grating drive recalibration, by using the Hg lamp as reference. Thermostatic control of the sequential spectrometer minimizes analytical calibration drift due to wavelength change. Early experience has shown that long-term calibration drift is similar for both spectrometers and related mainly to changes in the source/sample delivery system.

A reduction in spectral interferences for the polychromator was achieved by the use of flexible background corrections (1 or 2 positions, variable distance from peak wavelength). Some important examples are shown in Table 6. The line change for Ni was made to avoid a Zr interference even more troublesome than those listed elsewhere.⁷

CONCLUSIONS

A high-performance dual spectrometer ICP-AES system was built by renovating a 13-year old polychromator and interfacing it with a high-resolution scanning sequential spectrometer. The cost of the entire project was

Table 4. Sensitivity and precision comparison: polychromator vs. sequential spectrometer

Element	Wavelength, nm	Detection limits†, 2σ , mg/l.		Precision at low concn., σ , mg/l.		Precision at higher concn., σ , mg/l.	
		Polychromator	Sequential	Polychromator	Sequential	Polychromator	Sequential
As	193.759	0.037	0.048	1.0	0.036	50.0	0.66
Ba	455.403	0.0002	0.0002	0.05	0.0007	1.0	0.026
Be	234.861	0.0002	0.0004	0.01	0.0003	1.0	0.0041
Cd	214.438	0.0058	0.0050	0.1	0.0029	10.0	0.033
Cr	357.869	0.0070	0.0062	0.2	0.0052	10.0	0.35
Mo	202.030	0.0036	0.0088	0.2	0.0039	10.0	0.12
Ni	231.604	0.011	0.011	0.2	0.0133	10.0	0.18
Pb	220.353	0.0094	0.0062	0.2	0.0072	10.0	0.12
Sb	206.833	0.011	0.038	1.0	0.019	50.0	0.64
Se	196.060	0.017	0.056	1.0	0.016	50.0	0.85

*Ten exposures, 10 sec duration, one background correction point.

†Concentration equal to a signal that is twice the standard deviation of the blank.

Table 5. Wavelength repeatability of sequential spectrometer, nm*

Element	Literature wavelength, nm	Measured wavelength, nm	Short-term precision (σ)	Day-to-day precision (σ)
As	193.759	193.736	0.00070	0.0105
Cd	214.438	214.449	0.00086	0.0170
Be	234.861	234.957	0.00101	0.0195
V	292.402	292.431	0.00239	0.0127
Cr	357.869	357.968	0.00138	0.0168
Ba	455.403	455.533	0.00078	0.0292

*Data from 10 replicate measurements performed on 7 different days over 13 day period.

Table 6. Reduction of spectral interferences by flexible background correction

Element	Peak wavelength, nm	Old background wavelength, nm	New background wavelength(s), nm	Interfering element	Interference reduction, %	Source of interference
As	193.759 ($\times 2$)	193.779 ($\times 2$)	193.455, 194.118 ($\times 2$)	Al	95	Background increased at lower wavelength
Cd	214.438	214.478	213.831	Ni	>98	Broadened Ni line at 214.518 nm
Mo	202.030	202.070	201.423	Fe	>98	Fe (II) 202.070 nm
P	214.914 ($\times 2$)	214.934 ($\times 2$)	215.273 ($\times 2$)	V	84	V (II) 214.939 nm
Pb	220.353	220.393	220.105	Cr	93	Cr (II) 220.386 nm
Pb	220.353	220.393	220.105	Fe	87	Fe 220.348 nm
Se	196.090	196.130	195.842	Fe	>98	Fe (I) 196.123 nm
Se	196.090	196.130	195.842	Mo	>98	Mo 196.127 nm
Tl	377.572	377.612	378.290	Ti	94	Ti (II) 377.604 nm

considerably less than half the cost of a new system having comparable features. The performances of the updated polychromator and the sequential spectrometer are comparable in terms of sensitivity and precision. The higher resolution of the scanning spectrometer provides for accurate determination of trace elements in complex materials where spectral interferences abound. Enhanced by custom software and computer network links, the life of a vintage ICP-AES system should be extendable to the turn of the century.

Acknowledgements—The author is grateful for the technical assistance provided by C. P. (Skip) Carter. Mary C. Benham prepared the manuscript for publication.

REFERENCES

1. R. I. Botto, in *Developments in Atomic Spectrochemical Analysis*, R. M. Barnes (ed.), p. 141. Heyden, Philadelphia, 1981.
2. *Idem*, *op. cit.*, p. 506.
3. R. K. Winge, V. J. Peterson and V. A. Fassell, *Inductively Coupled Plasma-Atomic Emission Spectroscopy: Prominent Lines*, EPA-600/4-79-017, March 1979, NTIS Springfield, VA.
4. R. K. Winge, V. A. Fassel, V. J. Peterson and M. A. Floyd, *Inductively Coupled Plasma-Atomic Emission Spectroscopy: An Atlas of Spectral Information*, Elsevier, New York, 1985.
5. R. I. Botto, *Jarrell Ash Plasma Newslett.*, 1981, **4**, No. 2, 7.
6. *Idem*, *Anal. Chem.*, 1982, **54**, 1654.
7. *Idem*, *Spectrochim. Acta*, 1983, **38B**, 129.
8. *Idem*, *ibid.*, 1984, **39B**, 95.

IMPROVEMENT OF THE SMETS METHOD IN ELECTROTHERMAL ATOMIC-ABSORPTION SPECTROMETRY

YAN XIUPING*

Department of Chemistry, Taizhou Teachers College, Linnai, Zhejiang Province,
People's Republic of China

LIN TIEZHENG and LIU ZHIJUN

Dalian Institute of Chemical Physics, Academia Sinica, 129 Street, Dalian,
People's Republic of China

(Received 9 March 1987. Revised 9 July 1989. Accepted 16 August 1989)

Summary—The Smets method, which is frequently used to obtain the rate constant of atom formation in the gas phase, has been improved. The assumption of first-order kinetics for atom formation and the steady-state approximation appearing in the previous models are avoided, so the non-linearity in the Arrhenius plots can be eliminated. The reasons for this non-linearity are discussed.

A number of methods have been developed for determining the kinetic parameters of atom formation in electrothermal atomic-absorption spectrometry.¹⁻¹⁰ Among these methods, the Smets method² and the Sturgeon and Chakrobari method³ are frequently used to study the atomization mechanism.¹¹⁻¹⁵ The experimental conditions in the Smets method are similar to actual analytical conditions,¹⁵ so this method can be regarded as a better one for determining the kinetic parameters for atom formation. However, the Arrhenius plots obtained by the Smets method often curve toward the abscissa at higher temperatures. This makes the method suitable only for the initial part of the absorbance signal, and sets a limit for obtaining kinetic information about atom formation over a wider range of temperature.

The present study was undertaken to solve the non-linearity problem in the Arrhenius plots and to discuss the reasons for the phenomenon.

EXPERIMENTAL

A Perkin-Elmer 5000 atomic-absorption spectrometer equipped with an HGA-500 furnace and an Atomic Spectroscopy Data System 10 was used. A model AS-40 autosampler was used to inject the test solutions into the furnace. The absorbance-time data could be collected at

0.02-sec intervals and stored on a diskette by the Data System 10. The temperature-time characteristics of the graphite furnace were obtained with an optical pyrometer, and a Perkin-Elmer standard pyrolytic graphite tube was used throughout the experimental work. A typical absorbance signal profile is shown in Fig. 1.

All chemicals used were of the highest purity commercially available. Atomic-absorbance measurements were made at 232.0 nm by use of a nickel hollow-cathode lamp and at 670.8 nm with a lithium hollow-cathode lamp. High-purity argon (99.99%) was used as the purge gas.

RESULTS AND DISCUSSION

Improvement of the Smets method

Smets has described a method for determining the rate constant for atom formation. The rate of change of the number of atoms in the optical pathway, dn/dt , is given as the difference between the rate formation, R_{form} , and the rate of dissipation, R_{diss} :

$$dn/dt = R_{\text{form}} - R_{\text{diss}} \quad (1)$$

Assuming that the processes of formation and dissipation follow first-order kinetics, equation (1) is rewritten as

$$dn/dt = k_1N - k_2n \quad (2)$$

where k_1 and k_2 are the rate constants of formation and dissipation, respectively, and N is

*Author for correspondence.

the number of metal atoms left on the tube surface. The initial number of atoms, N_0 , is given by

$$N_0 = \frac{1}{\beta} \int_0^{\infty} R_{\text{form}} dt \quad (3)$$

where β is the atomization efficiency. The number of atoms ($N_0 - N$) vaporized during the time t is equal to

$$\frac{1}{\beta} \int_0^t R_{\text{form}} dt.$$

Integration of equation (2) from $t = 0$ to $t = \infty$ gives

$$\int_0^{\infty} R_{\text{form}} dt = \int_0^{\infty} R_{\text{diss}} dt \quad (4)$$

and using the steady-state approximation results in

$$k_1 = \frac{k_2 A}{\langle k_2 \rangle \int_0^{\infty} A dt - \langle k_2 \rangle \int_0^t A dt} \quad (5)$$

or

$$k_1 = \frac{1}{\beta} \frac{A}{\int_0^{\infty} A dt} \quad (6)$$

where

$$\langle k_2 \rangle = \int_0^{\infty} k_2 dt / \int_0^{\infty} n dt,$$

$$\langle k_2 \rangle = \int_0^t k_2 n dt / \int_0^t n dt,$$

A is the absorbance, and β is arbitrarily set equal to 1.

In fact, from equation (2) to equation (6), it has been assumed that the number of atoms ($N_0 - N$) vaporized is equal to that

$$\left(\int_0^t k_2 n dt \right)$$

removed during the time t . However, to be more exact, the number of atoms vaporized ($N_0 - N$) should be expressed as

$$N_0 - N = \int_0^t k_2 n dt + n \quad (7)$$

whence

$$N = p \left(k_2 \int_0^{\infty} A dt - A \right) \quad (8)$$

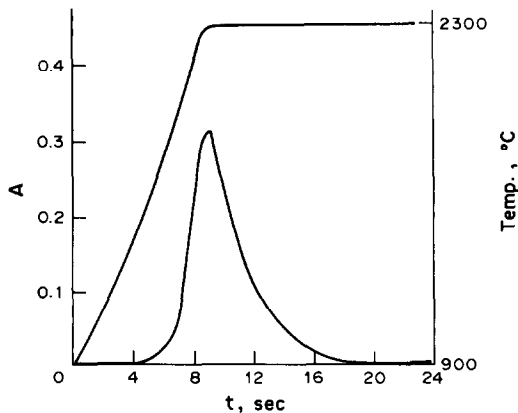


Fig. 1. Typical absorbance signal profile. Conditions: 0.1 ng Li/HNO₃, ashing temperature 900°, atomization temperature 2300° (8-sec ramp), no internal gas-flow.

where p is the proportionality constant between the absorbance and the number of gaseous analyte atoms. Although p is slightly temperature-dependent, it is generally assumed to remain unchanged.^{5,6,16,17} If the formation of gaseous atoms is an x th order kinetic process, the rate of formation R_{form} can be written as

$$R_{\text{form}} = -\frac{dN}{dt} = k_1 N^x = k_0 N^x e^{-E_a/RT} \quad (9)$$

where k_0 and E_a are the frequency factor and activation energy for atom formation, respectively, and R is the gas constant. If the heating rate is $\alpha = dT/dt$, then

$$-\frac{d \left(k_2 \int_t^{\infty} A dt - A \right)}{\left(k_2 \int_t^{\infty} A dt - A \right)^x} = k_0 p^{x-1} \alpha^{-1} e^{-E_a/RT} dT. \quad (10)$$

According to Coats and Redfern,¹⁸ equation (10) becomes

$$\ln Y = -E_a/RT + \ln [k_0 p^{x-1} R (1 - 2RT/E_a) / \alpha E_a] \quad (11)$$

where

$$\ln Y = \ln \left\{ \left[\ln \left[k_2 \int_0^{\infty} A dt / \left(k_2 \int_t^{\infty} A dt - A \right) \right] \right] / T^2 \right\} \quad \text{for } x = 1 \quad (12)$$

and

$$\ln Y = \ln \left\{ \frac{\left(k_2 \int_t^\infty A \, dt - A \right)^{1-x} - \left(k_2 \int_0^\infty A \, dt \right)^{1-x}}{T^2(x-1)} \right\}$$

for $x \neq 1$ (13)

Thus, a plot of $\ln Y$ vs. $1/T$ should result in a straight line with slope $-E_a/R$ for the correct value of x , since it may be shown that for most values of E_a and the temperature range over which reactions generally occur, the second term on the right-hand side of equation (11) is practically constant.¹⁸

Consideration of atom dissipation

Before calculating E_a by using equations (11) and (12) or (11) and (13), we should obtain the value of k_2 . The atom loss from the furnace is the resultant of element-specific removal processes such as element recombination in the gas phase, and three different transport processes—diffusion, expansion and convection.¹⁹ Of these factors, diffusion is the dominant removal process.^{17,19,20} Assuming that atom formation is negligibly small during the decay portion of the signal, many workers^{6,8,16,20} have successfully obtained the k_2 value from the decay portion of the signal by plotting the logarithm of the absorbance vs. time. In this work, we calculated k_2 in the same way. To eliminate the influence of convection on atom loss, we conducted the experiments with and without a low internal gas

flow at the atomization stages. The expulsion of atom vapour caused no problem when only small quantities of metals, typically in the ng range, were introduced into the furnace.^{14,17,21} The temperature-dependence of k_2 can be treated as negligible, as proved by Chung.⁶

The $\ln A$ vs. t plots for calculating k_2 values are shown in Fig. 2. Except for the initial parts these plots exhibit good linearity. This suggests that the later part of the signal is solely determined by the dissipation process. However, the initial bend in the curve observed indicates that atomization is not complete near to the absorbance maximum. To minimize any influence of atom formation, the data used to calculate k_2 values were chosen from the period 0.6–1.8 sec after the absorbance maximum.

Arrhenius plots

It is well known that the Arrhenius plots obtained by the Smets method [equation (6)] often bend towards the abscissa at higher temperatures.^{2,6,11,12,15} A few workers have dealt with this problem. L'vov *et al.*^{12,22} took the bending of the Arrhenius plots as a common phenomenon in ETAAS and developed a macrokinetic theory of sample vaporization which was based on consideration of the distribution of a sample, and surface diffusion in the condensed phase. An analysis of mathematical models describing the vaporization process for the cases of a sample distributed in a porous bulk and over the vaporizer surface revealed several regions. The vaporization rate in these regions depends in different ways on the vaporization rate and diffusion coefficient of the sample in the condensed phase. Thus, they successfully predicted and explained the appearance of breaks and inflections in the Arrhenius plots. However, the assumption in the Smets method that the sample is distributed over the surface in a monolayer is contrary to the major prerequisite of the macrokinetic theory. Guerrieri *et al.*¹⁰ also theoretically predicted the sigmoid shape of the Arrhenius plots. According to this model,¹⁰ atomization is assumed to be a reversible release process in which heterogeneous equilibrium is established between a monolayer or submonolayer surface film and a small interfacial region in the gas phase. A single binding energy is assumed to characterize all analyte atoms on the surface. Frech *et al.*¹¹ suggested that equation (6) holds if the rate constant of atom loss is larger than that of atom formation. Since the rate of atom formation (but not the rate of atom

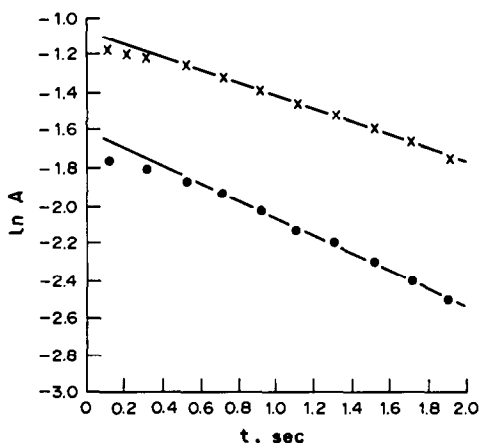


Fig. 2. Plots of $\ln A$ vs. t for Li (x) and Ni (●); $t = 0$ at the absorbance maximum. Conditions for Li as in Fig. 1. Conditions for Ni: 0.1 ng Ni/HNO₃, ashing temperature 700°, atomization temperature 2300° (8-sec ramp), internal gas-flow 50 ml/min.

loss) increases exponentially with temperature, this condition might not be fulfilled at higher temperatures, and that would be one reason for the bending of the Arrhenius plots at higher temperatures. Chung⁶ considered the bending of the Arrhenius plots to be a result of underestimation of the removal effect in the Smets model, in which the peak area was used to estimate it. Smets² tentatively attributed the high-temperature decrease in experimental activation energy to an increased contribution of diffused atoms to the atomization.

The bending of the Arrhenius plots may be an unavoidable fact which depends on the nature of the vaporization. Another possibility should be noted, however, namely that the bending of the Arrhenius plots perhaps results from some errors in the Smets model itself. Any unreasonable assumptions in the Smets model might be responsible for the bending of the Arrhenius plots. First-order kinetics for atom formation, and monolayer surface coverage over the entire furnace area, were assumed in the Smets model and in other models.²⁻¹⁰ However, it is possible that the dependence of the release rate on surface coverage is of some order other than unity, and permits fractional surface coverages. Holcombe *et al.*²³ used the Monte Carlo method to simulate the atomization of Ag in a graphite furnace and found it to be a nearly zero-order process. By using equations (11) and (12) or (13), the kinetic order and activation energy for atom formation can be obtained. Figures 3 and 4 show near zero-order kinetics for the atomization of lithium and near first-order for nickel. In addition, a steady-state approximation was used in the Smets model, but this approximation is valid only for the maximum of the signal. Thus the k_1 value calculated by using

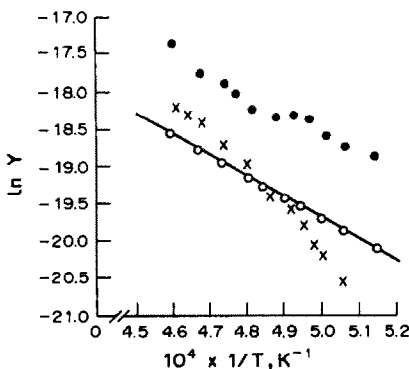


Fig. 3. Plots of $\ln Y$ vs. $1/T$ for Li at different x values: 0(\circ), 1(\bullet) and 2(\times). Conditions as for Fig. 1.

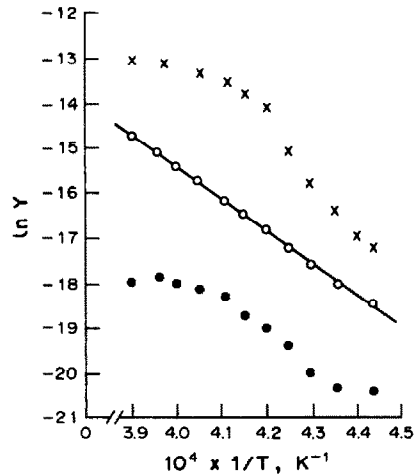


Fig. 4. Plots of $\ln Y$ vs. $1/T$ for Ni at different x values: 0(\bullet), 1(\circ), and 2(\times). Conditions as for Fig. 2.

equation (6) might be different from the actual value. The Arrhenius plots obtained by the Smets method and by equation (11) are shown in Fig. 5. It can be seen that the Arrhenius plot obtained by use of equation (11) is linear over a wider temperature range than does that obtained by the Smets method, which bends towards the abscissa at higher temperatures.

Akman *et al.*⁵ proposed another method for determining the rate constant of atom formation. According to this model, it is assumed that atoms are not removed from the system at the very beginning of the signal ($t \ll$ residence time) and therefore, the second term on the right-hand of equation (1) is neglected. For a constantly increasing temperature, it is assumed that the rate of atom formation is a linear function of time, and that the sample is com-

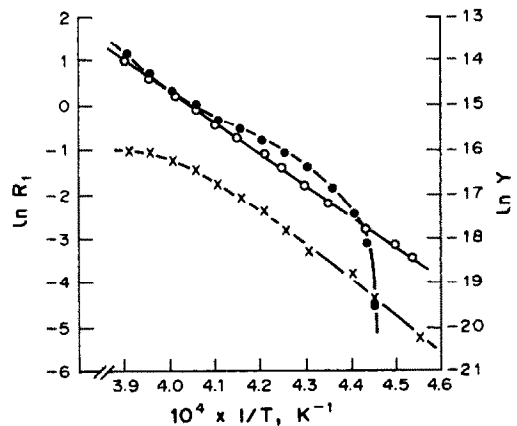


Fig. 5. Arrhenius plots obtained by the Smets method (\times), Akman method (\bullet) and the present method (\circ). Conditions as for Fig. 4.

pletely atomized in a period τ_1 , defined as the time from the beginning of atomization to the maximum of the signal, and for atom formation the following equations are derived:

$$R_{\text{form}} = \frac{2N_0}{\tau_1^2} t = k_1 N \quad (14)$$

$$k_1 = \frac{2t}{\tau_1^2 - t^2} \quad (15)$$

The Arrhenius plot obtained by the Akman method [equation (15)] is also shown in Fig. 4. The sigmoid shape of the Arrhenius plots obtained by the Akman method is obvious. Thus, it is difficult to extract meaningful information about atom formation, from the Akman method.⁵ As mentioned above, the sigmoid shape of the Arrhenius plots was predicted by L'vov *et al.*^{12,22} and Guerrieri *et al.*,¹⁰ their results suggesting that the sigmoid shape of the Arrhenius plots resulted from the nature of the vaporization. However, an unreasonable assumption in the Akman model may be the cause of the sigmoid shape. First, we can check the assumption that the removal of atoms can be neglected. At the beginning of the signal this may be valid, but at later stages, the removal of atoms cannot be neglected, because there is an increase in the number of gaseous analyte atoms. It can be seen that neglecting the removal of atoms could result in the sigmoid shape. However, it is unnecessary to assume that the initial removal of atoms from the furnace can be neglected, since equation (15) is correct in the absence of this assumption. From equation (14), the number of atoms unatomized is given by

$$N \int_t^{\tau_1} R_{\text{form}} dt = \frac{N_0}{\tau_1^2} (\tau_1^2 - t^2) \quad (16)$$

and combining equation (14) with equation (16) yields equation (15). Therefore, the sigmoid shape of the Arrhenius plots cannot be attributed to this assumption. Secondly, we can check the assumption that the rate of atom formation is a linear function of time. Since the number of unatomized atoms N decreases with increase in time, while the rate constant of atom formation k_1 increases with time (as the temperature increases), the rate of atom formation R_{form} should have a maximum with the change in time. Therefore, it is impossible that the rate of atom formation should be a linear function

of time during the atomization, and the assumption is therefore false and might result in the sigmoid shape of the Arrhenius plots obtained by the Akman method.

CONCLUSION

It is shown that certain assumptions which were made in the previous methods for determining the kinetic parameters for atom formation (and may not be valid under all conditions) might result in the non-linear phenomenon observed in the Arrhenius plots. To avoid this non-linearity and to study atomization processes further, it is necessary to develop more correct methods for obtaining the kinetic parameters for atom formation.

REFERENCES

1. C. W. Fuller, *Analyst*, 1974, **99**, 739.
2. B. Smets, *Spectrochim. Acta*, 1980, **35B**, 33.
3. R. E. Sturgeon and C. L. Chakrabarti, *Prog. Anal. Atom. Spectrosc.*, 1978, **1**, 5.
4. S. L. Paveri-Fontana, G. Tessari and G. Torsi, *Anal. Chem.*, 1974, **46**, 1032.
5. S. Akman, Ö. Genc, A. R. Özduval and T. Balkis, *Spectrochim. Acta*, 1980, **35B**, 373.
6. Chung Chan-Huan, *Anal. Chem.*, 1984, **56**, 2714.
7. D. A. Katskov, *Zh. Prikl. Spektrosk.*, 1979, **30**, 612.
8. C. L. Chakrabarti, C. C. Wan, R. J. Teskey, S. B. Chang, H. A. Hamed and P. C. Bertels, *Spectrochim. Acta*, 1981, **36B**, 427.
9. S. Nakamura, *J. Anal. Atom. Spectrom.*, 1986, **1**, 227.
10. A. Guerrieri, L. Lampugnani and G. Tessari, *Spectrochim. Acta*, 1984, **39B**, 193.
11. W. Frech, N. G. Zhou and E. Lundberg, *ibid.*, 1982, **37B**, 691.
12. B. V. L'vov, P. A. Bayunov and G. N. Ryabchuk, *ibid.*, 1981, **36B**, 397.
13. O. Vyskočilová, V. Sychra and D. Koliňová, *Anal. Chim. Acta*, 1979, **105**, 271.
14. M. Suzuki, K. Ohta, T. Yamakita and T. Katsuno, *Spectrochim. Acta*, 1981, **36B**, 679.
15. P. A. Bayunov, A. S. Savin and B. V. L'vov, *At. Spectrosc.*, 1982, **3**, 161.
16. S. Akman, Ö. Genc and T. Balkis, *Spectrochim. Acta*, 1981, **36B**, 1121.
17. B. V. L'vov, *Atomic Spectrochemical Analysis*, Hilger, London, 1970.
18. A. W. Coats and J. P. Redfern, *Nature*, 1964, **201**, 68.
19. W. M. G. T. van den Broek and L. de Galan, *Anal. Chem.*, 1977, **49**, 2176.
20. R. E. Sturgeon and C. L. Chakrabarti, *ibid.*, 1977, **49**, 1100.
21. J. P. Matousek, *Spectrochim. Acta*, 1984, **39B**, 205.
22. B. V. L'vov and P. A. Bayunov, *Zh. Analit. Khim.*, 1985, **40**, 614.
23. J. A. Holcombe, G. D. Rayson and N. Akerlind, Jr., *Spectrochim. Acta*, 1982, **37B**, 319.

DETERMINATION OF TELLURIUM IN ORES, CONCENTRATES AND RELATED MATERIALS BY GRAPHITE-FURNACE ATOMIC-ABSORPTION SPECTROMETRY AFTER SEPARATIONS BY IRON COLLECTION AND XANTHATE EXTRACTION*

ELSIE M. DONALDSON and MAUREEN E. LEAVER

Mineral Sciences Laboratories, Canada Centre for Mineral and Energy Technology,
Department of Energy, Mines and Resources, Ottawa, Canada

(Received 30 May 1989. Accepted 19 July 1989)

Summary—A method for determining $\sim 0.01 \mu\text{g/g}$ or more of tellurium in ores, concentrates, rocks, soils and sediments is described. After sample decomposition and evaporation of the solution to incipient dryness, tellurium is separated from $> 300 \mu\text{g}$ of copper by co-precipitation with hydrous ferric oxide from an ammoniacal medium and the precipitate is dissolved in $10M$ hydrochloric acid. Alternatively, for samples containing $\leq 300 \mu\text{g}$ of copper, the salts are dissolved in $10M$ hydrochloric acid. Tellurium in the resultant solutions is reduced to the quadrivalent state by heating and separated from iron, lead and various other elements by a single cyclohexane extraction of its xanthate complex from $\sim 9.5M$ hydrochloric acid in the presence of thiosemicarbazide as a complexing agent for copper. After washing with $10M$ hydrochloric acid followed by water to remove residual iron, chloride and soluble salts, tellurium is stripped from the extract with $16M$ nitric acid and finally determined, in a 2% v/v nitric acid medium, by graphite-furnace atomic-absorption spectrometry at 214.3 nm in the presence of nickel as matrix modifier. Small amounts of gold and palladium, which are partly co-extracted as xanthates if the iron-collection step is omitted, do not interfere. Co-extraction of arsenic is avoided by volatilizing it as the bromide during the decomposition step. The method is directly applicable, without the co-precipitation step, to most rocks, soils and sediments.

Because of the shortage of available reference ores and related materials with certified tellurium contents, the accurate determination of trace and μg -amounts of tellurium in these materials, particularly in copper, lead and zinc concentrates, is of importance in CANMET's certified reference materials project (CCRMP). Since the inception of this project in the early 1970s, only one recent reference material, copper concentrate CCU-1a, has been certified (with rather wide confidence limits) for tellurium, while approximate values for information purposes have been provided for an earlier copper concentrate, CCU-1, and for lead and zinc concentrates, CPB-1 and CZN-1, containing $< 1 \mu\text{g/g}$ of tellurium. During the interlaboratory certification programmes, these copper concentrates were analysed for tellurium by a spectrophotometric method based on measurement of the chloroform extract of the tellurium(IV) hexabromide-diantipyrilmethane ion-association complex, after separation of

tellurium from copper by co-precipitation with iron(III), followed by its separation from the iron, and lead and other co-precipitated elements by chloroform extraction as the xanthate from $\sim 12M$ hydrochloric acid.¹ However, this method was not applicable to the lead and zinc concentrates because of their low tellurium content. Consequently, in this earlier work an attempt was made to utilize a more sensitive flameless (carbon rod) atomic-absorption (AAS) finish, involving manual sample solution injection, for small amounts of tellurium, but this work was discontinued because of the poor reproducibility obtained. In recent years, numerous graphite-furnace (GFAAS) and some flame AAS methods for tellurium have been based on its separation from matrix elements by extraction, usually into methyl isobutyl ketone, of the tellurium(IV) chloro- and bromo-complexes from hydrochloric²⁻⁶ and hydrobromic acid^{7,8} media, and several very recent methods involve the extraction of the trioctylmethylammonium (TOMA)-iodide ion-association complex.⁹⁻¹¹ However, most of these extraction

*Crown Copyright reserved.

procedures, particularly of the chloro- and iodo-complexes, are not too selective, because many other elements, notably iron(III) in the chloro-complex procedure and copper, lead and zinc in the TOMA-iodide procedure, are co-extracted under the same conditions. The bromo-complex extraction procedure is more selective because the co-extraction of iron(III) can be largely prevented by reduction with ascorbic acid, but the extraction of tellurium is not quantitative in the presence of > 50 mg of iron. Consequently, to minimize error, it is necessary to extract the calibration solutions—to which iron must be added—regardless of whether the extract or an aqueous strip solution is used for the GFAAS measurement. Owing to the relatively high selectivity of the xanthate extraction procedure described previously,¹ and the recent acquisition of more sophisticated graphite-furnace instrumentation, equipped with an automatic sampling device, it was considered that the earlier xanthate extraction-flameless AAS approach might merit further investigation, particularly if quantitative extraction of the tellurium complex could be achieved in one extraction step into a solvent of specific gravity < 1 .^{12,13} This would simplify and shorten the extraction procedure, and facilitate washing of the extract to remove entrained salts and reduce the concentration of some co-extracted elements.

In the proposed method, tellurium is separated from ≤ 300 μg of copper and from iron(III), lead, zinc and various other matrix elements by a single cyclohexane extraction of its xanthate complex from $\sim 9.5M$ hydrochloric acid in the presence of thiosemicarbazide as a complexing agent for copper. After washing to remove residual iron and soluble salts, tellurium is stripped from the extract with $16M$ nitric acid and determined by GFAAS in a 2% v/v nitric acid medium in the presence of nickel as matrix modifier. For samples containing > 300 μg of copper, the preliminary separation of tellurium from copper by co-precipitation with hydrous ferric oxide is necessary.

EXPERIMENTAL

Apparatus

A Perkin-Elmer model 5000 atomic-absorption spectrometer, an HGA-400 graphite-furnace, an AS-40 autosampler, and a Data System 10 equipped with HGA graphics and data-collection software, were used, with a tellurium hollow-cathode lamp operated at 7 mA. The 214.3 nm resonance line was used with a spectral band-pass of 0.7 nm. Pyrolytically-coated graphite tubes with solid pyrolytic graphite platforms were employed, and 20- μl aliquots of the appropriate solutions, containing 0.01% nickel as matrix modifier, were injected. Measurements were made in the peak-area mode without background correction. The instrumental conditions for the dry, char and atomization steps are given in Table 1.

Reagents

Standard tellurium solution, 100 $\mu\text{g}/\text{ml}$. Dissolve 0.1251 g of pure tellurium dioxide by heating gently with 50 ml of concentrated nitric acid. Cool, transfer the solution to a 1-litre standard flask and dilute to volume with water. Prepare a 1- $\mu\text{g}/\text{ml}$ working solution in $\sim 2\%$ v/v nitric acid by appropriate dilution of the stock solution. The diluted solution is stable for at least 2 weeks.

Nickel solution, 10 mg/ml. Dissolve 1 g of high-purity nickel metal by heating gently with ~ 20 ml of water containing 3 ml of concentrated nitric acid. Cool and dilute to 100 ml with water.

Iron(III) solution, ~ 20 mg/ml. Dissolve 48 g of ferric chloride hexahydrate by heating gently with ~ 400 ml of water containing 25 ml of concentrated hydrochloric acid. Cool and dilute to ~ 500 ml with water.

Thiosemicarbazide solution, 4% in 5M hydrochloric acid. Prepare a sufficient volume of solution, fresh as required, by warming the reagent with equal volumes of water and $10M$ hydrochloric acid. Cool and filter the solution through Whatman No. 541 filter paper.

Table 1. Instrumental conditions for the determination of tellurium

Step function	1 Dry	2 Char	3 Char	4 Atomize	5 Clean
Temperature, °C	110	300	900	2300	2600
Ramp time, sec	10	5	5	0	1
Hold time, sec	20	10	20	5	1
Internal argon flow, ml/min	300	300	300	0	300
Read, sec	—	—	—	-1	—
Base-line, sec	—	—	—	-2	—

Potassium ethylxanthate solution, 20%. Prepare fresh as required.

Ammonia solution, 2% v/v. Store in a plastic bottle.

Hydrochloric acid, 10M.

Hydrochloric acid, 10% v/v.

Sulphuric acid, 50% v/v.

Cyclohexane. Analytical-reagent grade.

Doubly demineralized water was used throughout and all acids employed were analytical-reagent grade.

Calibration solutions

Prepare 0.01-, 0.02-, 0.03-, 0.04-, 0.05- and 0.06- $\mu\text{g}/\text{ml}$ tellurium solutions by adding 0.5, 1, 1.5, 2, 2.5 and 3 ml, respectively, of 1- $\mu\text{g}/\text{ml}$ standard tellurium solution to 50-ml standard borosilicate glass flasks containing 1 ml of concentrated nitric acid and 500 μl of 10-mg/ml nickel solution. Dilute each solution to volume with water. Prepare a blank calibration solution in a similar manner. These solutions are stable for at least 2 weeks.

Procedures

Copper $\leq 300 \mu\text{g}$ and iron $\leq 250 \text{mg}$. Transfer up to 1 g of powdered sample (Note 1), containing up to $\sim 20 \mu\text{g}$ of tellurium, to a 250-ml Teflon beaker. Add ~ 5 ml of water and 0.5 g of sodium chlorate (Note 2), then cover the beaker with a watch-glass and add 10 ml of concentrated nitric acid followed by 10 ml of concentrated perchloric acid. Heat the solution until the evolution of oxides of nitrogen ceases, then allow it to cool to room temperature, remove the cover and wash down the sides of the beaker with water. Add 10 ml of concentrated hydrofluoric acid and carefully evaporate the solution to fumes of perchloric acid. Cool, wash down the sides of the beaker with water again, then add 5 ml of concentrated hydrobromic acid (Note 3) and carefully evaporate the solution to ~ 3 ml. Cool, add 2 ml of water and 30 ml of concentrated hydrochloric acid, cover and heat the solution at $95\text{--}100^\circ$ in a hot water-bath for ~ 30 min to reduce tellurium(VI) to tellurium(IV), then cool to room temperature. Run a blank through the whole procedure.

If the sample contains $\leq 2 \mu\text{g}$ of tellurium, transfer the solution to a 125-ml separating funnel, marked at 50 ml, using 10M hydrochloric acid contained in a plastic squeeze-type wash-bottle to wash the beaker (Note 4).

If the sample contains $> 2 \mu\text{g}$ of tellurium, transfer the solution to a 100-ml standard flask,

using 10M hydrochloric acid to wash the beaker. Dilute the solution to volume with 10M hydrochloric acid, allow it to stand until any insoluble material has settled (Note 5), then transfer a suitable aliquot (5–50 ml), containing up to $\sim 2 \mu\text{g}$ of tellurium, to a separating funnel and dilute to the mark with 10M hydrochloric acid.

Add 5 ml of 4% thiosemicarbazide solution to the resulting solution, mix, allow the solution to stand for 10 min, then add 15 ml of cyclohexane and 1 ml of freshly prepared 20% potassium ethyl xanthate solution (Note 6) and shake the mixture for 2 min. Allow the layers to separate (Note 7), then drain off and discard the aqueous phase. Wash the extract by shaking it for ~ 30 sec with 5 ml of 10M hydrochloric acid, drain off the acid phase, then wash it twice in a similar manner with 5-ml portions of water to remove sodium salts. Add 5 ml of concentrated nitric acid to the extract, stopper the funnel tightly and shake it for 10 min with a wrist-action shaker. Allow the layers to separate (Note 8), then drain the acid layer into a 100-ml beaker and wash the stem of the funnel with water. Wash the extract twice by shaking it for ~ 15 sec each time with 5-ml portions of water and add the washings to the beaker. Wash the stem of the funnel with water each time and collect these washings in the beaker.

Add 1 ml of 50% v/v sulphuric acid and 500 μl of concentrated perchloric acid to the resulting blank and sample solutions, then add 50 μl (*i.e.*, 500 μg of nickel) of 10-mg/ml nickel solution to the blank solution. Depending on the expected tellurium content, add sufficient nickel solution to the sample solution so that 50 μl will be present for each 5 ml of final solution (Note 9), then cover the beakers and carefully evaporate the solutions to copious fumes of perchloric acid. Cool, remove the covers and evaporate the solutions to dryness. Cool, wash down the sides of the beakers with water and evaporate the solutions to dryness again to ensure the complete removal of sulphuric acid. Cool, add 100 μl of concentrated nitric acid and ~ 2 ml of water to the beaker containing the blank. Add sufficient concentrated nitric acid (Note 9) to the beaker containing the sample so that the final solution will be 2% v/v in nitric acid, then add $\sim 2\text{--}10$ ml of water, depending on the volume of the final solution. Heat both solutions gently to dissolve the salts and, if necessary, use a rubber-tipped glass rod to dislodge any salts adhering to the

bottom of the beaker. Cool the solutions to room temperature, then transfer the blank solution to a 5-ml standard flask. Transfer the sample solution to a standard flask of appropriate size (5–50 ml). Dilute both solutions to volume with water and mix.

Measure the integrated absorbance of the sample and blank solutions under the conditions described under "Apparatus" and in Table 1 (Note 10). Determine the tellurium concentrations of the solutions by reference to peak-area values obtained concurrently for the calibration solutions. Calculate the tellurium content of the solutions (in ng or μg) and correct the result obtained for the sample solution by subtracting that obtained for the blank solution.

Copper > 300 μg –50 mg. After sample decomposition (Note 11) and evaporation of the solution to ~ 3 ml as described above, add ~ 100 ml of water, 5 ml of concentrated hydrochloric acid and, if necessary, sufficient 20-mg/ml iron(III) solution so that ~ 80 mg of iron will be present (Note 12), then heat to dissolve the soluble salts. Run a blank, with ~ 80 mg of iron(III) added, through the whole procedure.

Add sufficient concentrated ammonia solution to the resulting solution to precipitate iron as the hydrous oxide, then add 5 ml in excess, cover, and heat the solution to boiling point to coagulate the precipitate. Allow this to settle, then filter (Whatman No. 541 paper) the solution while hot and wash the beaker twice with 2% ammonia solution added from a wash-bottle. Wash the paper and precipitate three times with 2% ammonia solution. Discard the filtrate.

If the sample contains ≤ 5 mg of copper (Note 13), wash the paper and precipitate once with water to remove ammonium salts, then place the original beaker under the funnel and dissolve the precipitate with 10M hydrochloric acid added from a plastic squeeze-type wash-bottle. Wash the paper three times with the acid solution, then discard the paper (Note 14). Cover the beaker, place it in a hot water-bath and proceed with the reduction, the dilution of the solution to 100 ml with 10M hydrochloric acid, if necessary, and the extraction and determination of tellurium as described above.

If the sample contains > 5 mg of copper (Note 11), dissolve the precipitate back into the beaker with hot 10% v/v hydrochloric acid, added from a wash-bottle, and wash the paper three times with the acid solution, then once

with water to remove most of the excess of acid. Reprecipitate the iron, filter the solution through the original filter paper, wash the beaker, paper and precipitate as described above, then dissolve the precipitate with 10M hydrochloric acid and proceed with the reduction and determination of tellurium as described above.

Notes

1. The recommended limits of copper and iron apply only if the whole sample solution is taken for extraction. For samples of high tellurium content, in which the solution is diluted to 100 ml and an aliquot is taken for extraction, the amount of copper and iron in the aliquot should not exceed these limits. However, if the iron content of the solution or aliquot taken for extraction is ≤ 100 mg, up to 500 μg of copper can be present during the extraction. The Teflon beakers used for sample decomposition and the glass beakers used for the strip solutions should be cleaned with hot ($\sim 30\%$) hydrochloric acid followed by washing with doubly demineralized water before use.

2. The addition of more sodium chlorate than this is not recommended, because too much sodium chloride would be formed during the extraction step and could interfere with the separation of the layers and/or clog the separating funnel.

3. Hydrobromic acid can be omitted if the arsenic, antimony and tin contents of the sample are low.

4. The total volume of the solution should not exceed ~ 60 ml. A small amount of insoluble material present at this stage will not usually interfere with the extraction of tellurium unless it interferes with the separation of the layers. Moderate amounts can be removed by filtering the solution into the separating funnel, using Whatman No. 541 or 42 (Note 5) paper, or preferably glass-fibre paper, and then washing the beaker and paper with 10M hydrochloric acid. However, the solution should be warmed first to ensure the dissolution of any soluble salts that may have crystallized on standing.

5. Insoluble material can be removed more quickly, if desired, by centrifuging a suitable portion of the solution or filtering it through a dry filter paper. Whatman No. 42 paper is recommended if fine precipitates such as barium and strontium sulphates are present.

6. Because of the rapid decomposition of xanthate in acidic solutions, xanthate solution

should only be added to two solutions at a time, followed by immediate extraction of the complex. For health reasons, all operations involving xanthate should be performed in a fume-hood, and an automatic pipette or one equipped with a suction bulb should be used for dispensing the solution. The aqueous phase after extraction, and any remaining xanthate solution, should be treated with concentrated nitric acid and boiled vigorously to destroy the xanthate before disposal of the solution.¹⁴

7. If sodium chloride or precipitates such as barium and strontium sulphates clog the separating funnel, stopper the funnel tightly, open the stop-cock and unplug it with an aluminium or preferably platinum wire. Any sodium chloride or other water-soluble salts remaining at this stage, or after the 10M hydrochloric acid wash of the extract, will be removed by the two succeeding water washes.

8. If the acid phase is not clear because of the presence of barium and/or strontium sulphates, add ~5 ml of water to dilute the acid and filter (Whatman 9 cm No. 42 paper) the solution and the succeeding strip solutions into the beaker. A simple and practical way to do this is to use a short-stemmed plastic funnel (60-mm diameter) supported on the beaker by a 70-mm diameter circle of thin flat plastic with a hole in the centre for the stem of the funnel.

9. For final sample solution volumes of 5, 10, 25 or 50 ml, add 50, 100, 250 or 500 μ l of nickel solution, respectively. The corresponding volumes of concentrated nitric acid to be added in the subsequent part of the procedure are 100, 200, 500 or 1000 μ l.

10. If dilution of the sample solution is necessary, dilute a suitable aliquot directly in the autosampler cup with the blank calibration solution.

11. Samples containing more than 50 mg of copper can be used if the tellurium content is relatively high and a small aliquot of the solution obtained after a double hydrous ferric oxide separation is used for extraction. For the copper concentrates shown in Table 2, 400-mg samples were employed and 10-ml aliquots of the solutions obtained after a double iron separation, followed by dissolution of the precipitate and dilution of the solutions to 100 ml with 10M hydrochloric acid, were taken for the determination of tellurium.

12. Samples containing more than ~150 mg of iron are not recommended, because the filtration step may become unduly slow and

more copper will be retained in the hydrous ferric oxide precipitate.

13. If the copper content of the sample is not known and the filtrate is definitely or even slightly blue, a second precipitation should be performed. In cases of doubt, a double precipitation is strongly recommended.

14. The volume of the solution should not exceed ~40 ml. It is not necessary to remove all of the yellow iron colour from the filter paper.

RESULTS AND DISCUSSION

Nickel as matrix modifier

Nickel,¹⁵ palladium¹⁶ and mixtures of palladium and magnesium,¹¹ copper and magnesium,¹⁰ and nickel and copper⁹ have been recommended as matrix modifiers for the GFAAS determination of tellurium. In this work, both nickel and palladium (as nitrates) were investigated by use of platform-atomization of tellurium from 2% v/v nitric acid solutions. Figure 1 (a) and (b), in which the simultaneous peak-height and peak-area measurements are plotted, show that under these conditions nickel is a better modifier for tellurium than palladium is, and that the appropriate maximum charring temperature in the presence of nickel is ~1100°. This agrees with earlier work¹⁵ in which a maximum temperature of ~1200° is reported. Erratic results, which were most noticeable for the integrated absorbance measurements, were obtained in the presence of palladium. With nickel as modifier, the integrated absorbance values were relatively constant and well-defined peaks were obtained at char temperatures up to 1100°. In these tests, the nickel solution was added directly to the tellurium solution during preparation, which ensured that a homogeneous mixture was injected into the furnace, but the palladium solution was injected separately in 5- μ l portions. Further tests with nickel showed that its effect is constant from ~1 to at least 8 μ g, and in subsequent work 2 μ g were used per 20- μ l aliquot of injected solution. This corresponds to a concentration of 0.01% nickel in the sample and calibration solutions.

Separation of tellurium by extraction as the xanthate

Preliminary tests to determine whether tellurium could be quantitatively extracted as the xanthate in a single extraction into a solvent of specific gravity <1 from \geq 9M hydrochloric

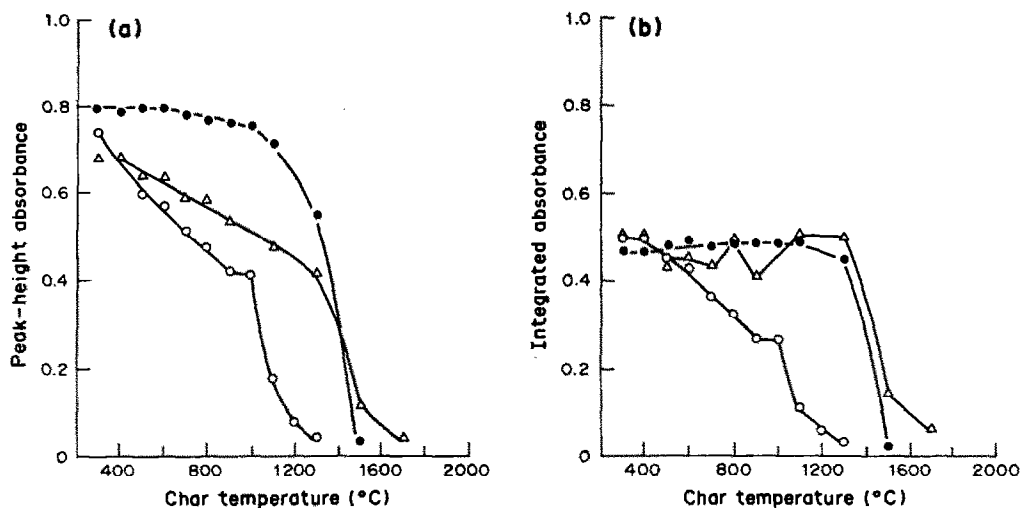


Fig. 1. Effect of char temperature and matrix modifier on the peak-height (a) and integrated absorbance (b) for tellurium. Te taken, 20 μ l of 0.1 μ g/ml solution in 2% v/v HNO_3 ; \circ , in the absence of a modifier; \bullet , in the presence of 2 μ g of nickel; \triangle , in the presence of 2 μ g of palladium.

acid were performed with cyclohexane under essentially the same conditions used recently for the extraction of arsenic xanthate.^{12,13} These tests showed that under such conditions up to at least 5 μ g of tellurium can be completely extracted into 15 ml of cyclohexane from up to at least 60 ml of solution. As reported earlier,¹ tellurium must be in the quadrivalent state for the extraction step. In the absence of iron(III), the reduction can readily be accomplished by heating $\geq 7M$ hydrochloric acid solutions of tellurium at $\sim 100^\circ$ for ~ 10 – 15 min. In its presence, heating for ~ 30 min is recommended.¹

Stripping and GFAAS determination of tellurium

As found earlier for arsenic,¹² the tellurium xanthate complex can be readily stripped from the cyclohexane extract by shaking it for ~ 10 min with ~ 5 ml of concentrated nitric acid. No attempt was made to determine tellurium by direct injection of the extract into the furnace, because of the high sulphur-compound content resulting from the co-extraction of the excess of xanthate.¹² In this work, the sulphuric acid produced during the stripping process, by nitric acid oxidation of the xanthate, is readily removed by evaporating the solution to dryness in the presence of perchloric acid as oxidant for any organic material present. The addition of the required volume of nickel modifier solution to the strip solution before the evaporation step is recommended, to prevent the possible formation of insoluble tellurium oxy-compounds. Peak-area measurement was chosen for this

work because peak-height measurements yielded low and erratic results for tellurium after treatment of the strip solutions as described above. Deuterium-arc background correction was found unnecessary.

Effect of copper plus iron on the extraction of tellurium

Previous work¹ showed that neither copper(II) nor iron(III) alone interferes with the extraction of tellurium as the xanthate, but that the extraction is either prevented or severely inhibited when both are present. This necessitated the separation of tellurium from copper by co-precipitation with iron(III) from an ammoniacal medium. In the present work, where only one extraction is performed, this effect is even more serious. The reason for this behaviour is not known. However, tests have shown that, at low levels of copper, this interference can be eliminated or minimized by complexing the copper with thiosemicarbazide (thiourea is ineffective as a complexing agent for copper at high hydrochloric acid concentration). Figure 2 (a) shows that in the absence of thiosemicarbazide more than ~ 50 μ g of copper in the presence of 100 mg of iron(III) will cause a low result for tellurium, but up to ~ 500 μ g can be tolerated under the same conditions in the presence of 200 mg of thiosemicarbazide. Figure 2 (b) shows that, for the same amount of thiosemicarbazide, up to ~ 250 mg of iron(III) can be present at the 300- μ g copper level, but more than ~ 100 mg cannot be tolerated in the presence of 500 μ g of copper. Further work showed

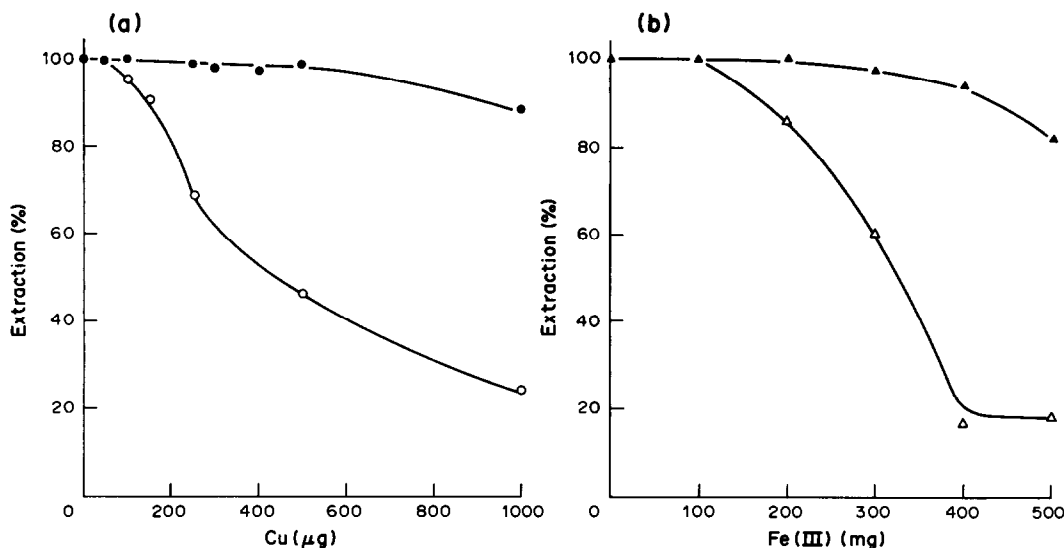


Fig. 2. Effect of copper plus iron on the extraction of tellurium. (a) Te taken, 2 μg ; Fe(III) taken, 100 mg; \circ , in the absence of thiosemicarbazide; \bullet , in the presence of 200 mg of thiosemicarbazide. (b) Te taken, 2 μg ; thiosemicarbazide taken, 200 mg; \triangle , in the presence of 500 μg of Cu; \blacktriangle , in the presence of 300 μg of Cu.

that tellurium can be completely extracted from solutions containing 300 mg of iron(III) and 500 μg of copper if the amount of thiosemicarbazide is doubled, but the addition of more than 200 mg, as recommended in this work, would not usually be necessary, because 1-g samples of most ordinary rocks, soils and sediments do not often contain more than $\sim 300 \mu\text{g}$ of copper and 250 mg of iron. Consequently, most of these materials can be analysed directly without prior separation of the tellurium from copper by co-precipitation with iron. However, for samples containing larger amounts of copper, either a single or double co-precipitation is required, depending on the amount present. Under the precipitation and washing conditions used in this work, ~ 260 and $370 \mu\text{g}$ of copper were retained in the precipitate, from initial 5- and 10-mg levels, respectively, after a single co-precipitation with 100 mg of iron, and ~ 36 and $73 \mu\text{g}$ were retained after a double co-precipitation. Consequently, a single co-precipitation step is recommended for samples containing 300 μg –5 mg of copper, while a double co-precipitation is recommended for 5–50 mg of copper. At higher levels of copper a third co-precipitation step would be required.

Effect of other ions

Under the acid conditions ($\sim 9.5M$ hydrochloric acid) used for the extraction of tellurium, arsenic(III) is completely co-extracted as the xanthate, gold(III) and palladium(II) are

largely co-extracted and platinum(IV) is slightly co-extracted.^{12,17} Selenium(IV) is also quantitatively extracted, but is completely removed from the strip solution by volatilization, presumably as the dioxide, when the solution is evaporated to dryness in the presence of sulphuric acid. Interference from arsenic, if this is present in large amounts, can be readily avoided by volatilizing the bromide in the presence of perchloric acid during the sample decomposition step. Tin and antimony are also removed under these conditions. Gold, platinum and palladium are completely separated from tellurium during the iron(III) co-precipitation step. However, even if this step is omitted, the amounts of these elements in ores, concentrates, rocks and related materials would not interfere in the determination of tellurium by GFAAS. Up to at least 20 μg of these elements per ml will not cause significant error in the result. Washing the extract with 10M hydrochloric acid removes small amounts of co-extracted platinum, antimony and molybdenum,^{12,17} and residual iron and other elements that may be mechanically entrained in the extract. Washing with water removes residual hydrochloric acid and sodium chloride, and other water-soluble salts that may have precipitated in the highly acidic sample solution before or during the extraction step. Sodium and potassium, if present in the final solution, will cause a high result for tellurium.

In the direct method, in which the co-precipitation step is omitted, large amounts of

insoluble material may interfere during the extraction step by preventing the complete separation of the layers. If this occurs, the use of a smaller sample is recommended, if feasible, or tellurium can first be separated from the insoluble material and some matrix elements by co-precipitation with iron. Any barium and strontium sulphates present during the extraction step are partly removed with the aqueous phase. The remaining precipitate adhering to the inside of the funnel and mechanically entrained in the extract will be retained in the strip solution but this can readily be removed by filtration before the solution is evaporated to dryness.

Applications

Table 2 shows that the mean results obtained for tellurium in the CCRMP copper concentrates are in excellent agreement with the certified values, and with previous results obtained in this laboratory during the respective inter-laboratory certification programmes by the iron collection/xanthate extraction/tellurium hexabromide-diantipyrilmethane spectrophotometric method¹ mentioned earlier. Those obtained for the zinc and lead concentrates, CZN-1 and CPB-1, are in good agreement with the values given for information purposes, which are the means of only 1 and 3 sets of data, respectively, obtained during the certification programmes. For the copper concentrates, a double iron(III) co-precipitation step was used to separate tellurium from copper, and a single step for the lead and zinc concentrates. The results obtained for the CCRMP soils, for some United States Geological Survey (USGS) muds and shales and for the National Bureau of Standards (NBS) river sediment 1645 are in good agreement with other reported values, while those obtained for the USGS GXR series of samples agree reasonably well with the mean of other reported values. These means were calculated from absolute values only, with exclusion of any gross outliers. The result obtained for NBS 1646 is considerably lower than the value given for information only, which according to NBS is not the result of a definitive method or of two or more independent analytical methods. No other tellurium value for this material was found in the literature. Except for GXR-4, all the soils, rocks and sediments shown in Table 2 were analysed directly, without the iron co-precipitation step, with use of either the whole solution or a

suitable aliquot (for GXR-1) for the extraction. Because of the large amount of insoluble material present in solutions of some of the GXR samples (GXR-2, -5 and -6), 0.4–0.5-g subsamples of these materials were taken. In addition, because of their high barium and, in some cases, strontium contents, the strip solutions were filtered to remove barium and strontium sulphate before the evaporation step. Each of the individual results obtained for all the reference materials was the mean of 3 or 4 GFAAS runs, each including a single peak-area measurement. The tellurium concentration was calculated by the linear regression least-squares method from peak-area data obtained for each run for tellurium calibration solutions covering the linear response range of 0–0.06 $\mu\text{g/ml}$.

The proposed method can easily be modified to include a hydride-generation (HGAAS) atomic-absorption finish if desired. In this case, omit the addition of nickel solution and sulphuric acid to the strip solution, add ~ 3 ml of concentrated perchloric acid, cover the beaker, evaporate the solution to fumes of perchloric acid, then reflux it vigorously for ~ 30 min. Remove the cover and, if necessary, evaporate the solution to ~ 1 ml (not to dryness). Add 4 ml of water and 7.5 ml of concentrated hydrochloric acid, cover the beaker, heat the solution to the boiling-point on a hot-plate, then boil it gently for ~ 10 – 15 min to reduce tellurium. Cool the resulting solution to room temperature, transfer it to a standard flask of appropriate size (≥ 25 ml), add sufficient concentrated hydrochloric acid, if necessary, for the final concentration to be $\sim 30\%$ v/v, then dilute to volume with water and determine tellurium by the HGAAS method, using appropriate tellurium(IV) solutions in 30% v/v hydrochloric acid for calibration. It should be emphasized that this alternative procedure has been designed for determining tellurium by continuous hydride-generation with the vapour-generation accessory employed previously in this laboratory for the determination of arsenic.¹³ Modification of the final volume or final acid concentration might be necessary for other HGAAS systems. This hydride-generation method is not recommended for most ores, rocks and related materials, unless the iron co-precipitation procedure is first employed to separate tellurium from palladium and gold, because even μg -amounts of these elements interfere seriously in the determination of tellurium by HGAAS. Some preliminary work has

Table 2. Determination of tellurium in CCRMP and other reference concentrates and related materials

Sample*	Nominal Fe and Cu content		Tellurium, µg/g			Mean of other values
	Fe, %	Cu, µg/g†	Certified value	This work‡	Other reported values	
CCU-1 Copper concentrate	30.9	24.7%	19 ± 8§	18.2 ± 0.8 (4)	19.1 ± 1.0 #	
CCU-1a Copper concentrate	30.5	26.8%	31 ± 5	30.6 ± 0.7	29.5 ± 0.6 #	
CPB-1 Lead concentrate	8.4	0.25%	0.7 ± 0.3§	0.53 ± 0.05		
CZN-1 Zinc concentrate	10.9	0.14%	0.2§	0.18 ± 0.01		
SO-1 Regosolic soil	6.0	61	—	0.035 ± 0.004	0.040 ¹¹	
SO-2 Podzolic soil	5.6	7	—	0.013 ± 0.003	<0.02 ¹¹	
SO-3 Calcareous C Horizon soil	1.5	17	—	0.011 ± 0.006	<0.02 ¹¹	
SO-4 Chernozemic A Horizon soil	2.4	22	—	0.028 ± 0.009	0.030 ¹²	
USGS GXR-1 Jasperoid	24.7	1070	—	15.7 ± 0.0	8.7, 9.3, ⁸ 19/20, ¹⁸ 12.0, ⁹ 16.1,19.0, ¹⁹ 12 ¹¹	13.8 ± 4.4
USGS GXR-2 Soil	1.9	70	—	0.51 ± 0.06 (4)	0.88, ⁷ 0.83, ⁸ <2.5, ¹⁸ 3.3,0.49, ¹⁹ 0.35 ¹¹	0.64 ± 0.26 [¶]
USGS GXR-3 Fe-Mn-W-rich hot spring deposit	18.6	10.7	—	0.006 ± 0.003	0.009, ⁷ <0.1, ⁸ <2.5, ¹⁸ 0.11,0.01, ¹⁹ <0.02 ¹¹	0.009 ± 0.001 [¶]
USGS GXR-4 Porphyry copper mill heads	3.0	6400	—	0.93 ± 0.06	1.0, ⁷ 0.92, ⁸ <2.5, ¹⁸ 1.6, ⁹ 1.15,0.74, ¹⁹ 0.80 ¹¹	1.04 ± 0.31
USGS GXR-5 Soil	3.2	340	—	0.041 ± 0.015 (5)	<0.1, ⁸ <2.5, ¹⁸ 0.15,0.04, ¹⁹ 0.03 ¹¹	0.035 ± 0.007 [¶]
USGS GXR-6 Soil	5.6	62	—	0.046 ± 0.013 (5)	0.016, ⁷ <0.1, ⁸ <2.5, ¹⁸ 0.08,0.07, ¹⁹ 0.02 ¹¹	0.046 ± 0.033
USGS MAG-1 Marine mud	4.9	30	—	0.063 ± 0.005	0.066 ²⁰	
USGS SCo-1 Cody shale	3.6	28.7	—	0.073 ± 0.005	0.077 ²⁰	
USGS SGR-1 Green River shale	2.1	66	—	0.24 ± 0.00	0.248 ²⁰	
NBS 1645 River sediment	11.3	109	—	4.53 ± 0.22	4.60 ²⁰	
NBS 1646 Estuarine sediment	3.4	18	0.5§	0.037 ± 0.002		

*CCRMP reference materials except where indicated otherwise. Nominal compositions are given in references 18, 21, 22 and 23.

†Results shown are in µg/g unless otherwise indicated.

‡Mean and standard deviation for 3 values except where indicated otherwise in parentheses.

§Value given for information only (not certified).

Mean value and standard deviation obtained for CCU-1 (n = 10) and CCU-1a (n = 5) by the senior author during the certification programmes, by a spectrophotometric method.

¶Gross outlier excluded in calculation of mean.

shown that tellurium can be selectively stripped from the extract and completely separated from up to at least 100 μg of co-extracted palladium, and almost completely separated from the same amount of gold, by shaking the extract for ~ 30 min (or possibly less) with 25–35% v/v nitric acid. However, the GFAAS finish is quicker and more advantageous than the HGAAS finish because small amounts of co-extracted palladium and gold do not interfere and a second reduction step is not necessary.

Because selenium(IV) is completely co-extracted as the xanthate under the conditions used for the extraction of tellurium, it is also possible to determine selenium by HGAAS, particularly by the direct xanthate extraction method (no co-precipitation step) if some precautions are taken to avoid loss of selenium. In this case the omission of hydrobromic acid and the addition of ~ 10 mg of nickel during the decomposition step is recommended,²¹ and the initial reduction of selenium and tellurium in ~ 30 ml of 7M hydrochloric acid, by heating as described in the proposed method, is recommended to avoid possible loss of selenium by volatilization as the chloride. For the determination, after dilution of the solution to ~ 50 ml in a separating funnel with concentrated hydrochloric acid, proceed with the addition of thiosemicarbazide solution, the extraction and the ultimate stripping of the extract as described in the proposed method. Treat the strip solution as described above for tellurium but add sufficient 10-mg/ml nickel solution for the final solution to contain ~ 4 μg of nickel per ml, then proceed with the evaporation of the solution, the refluxing and reduction steps and the subsequent determination of selenium by HGAAS, and calibration with selenium(IV) solutions containing the same concentration of nickel. However, this method for selenium has the same disadvantages as the HGAAS method for tellurium, because gold and palladium also interfere in the generation of selenium hydride. In addition, 25–30% v/v nitric acid cannot be used to strip selenium selectively from the extract, because it is only partly stripped under these conditions. Although the co-precipitation step can be used to separate selenium from gold and palladium, the selenium must first be reduced to the quadrivalent state because selenium(VI) is not co-precipitated with iron(III). Furthermore, the precipitate must be washed with water because selenium is lost to the filtrate if the precipitate is washed with dilute ammonia sol-

ution. Under these conditions, more copper is retained in the precipitate, which, if tellurium is being determined at the same time, can lead to incomplete extraction of tellurium if the sample contains an appreciable amount of copper. Some additional work has shown that copper(II) and iron(III) in admixture also inhibit the extraction of selenium as the xanthate under the conditions used in this work. However, in the case of selenium, thiosemicarbazide is much more effective in preventing this interference. In the presence of 200 mg of thiosemicarbazide, as recommended in this method, and 100 mg of iron(III), complete extraction of selenium was obtained in one extraction from 9.5M hydrochloric acid containing $\sim 2\%$ v/v sulphuric acid and up to at least 10 mg of copper. This suggests that an HGAAS method based on the extraction of selenium(IV) xanthate under these conditions might be extremely useful for the analysis of materials that do not contain gold and palladium. The determination of selenium by GFAAS after xanthate extraction is not recommended, because of the high sulphate content of the strip solution resulting from the nitric acid oxidation of the co-extracted excess of xanthate.¹²

In the proposed method, the detection limit, calculated as three times the standard deviation of the reagent blank, based on a 1-g sample taken through the extraction step and a final volume of 5 ml, is ~ 8 ng of tellurium per g of sample. The sensitivity (or characteristic mass) is ~ 16 pg for 0.0044 integrated absorbance. In this work the reagent blank varied from ~ 0 to 6 ng of tellurium.

REFERENCES

1. E. M. Donaldson, *Talanta*, 1976, **23**, 823.
2. R. D. Beaty and O. K. Manuel, *Chem. Geol.*, 1973, **12**, 155.
3. R. D. Beaty, *At. Abs. Newsl.*, 1974, **13**, 38.
4. I. I. Nazarenko, G. E. Kalenchuk and I. V. Kislova, *J. Anal. Chem. USSR*, 1976, **31**, 426.
5. G. P. Sighinolfi, A. M. Santos and G. Martinelli, *Talanta*, 1979, **26**, 143.
6. W. A. Maher, *Anal. Lett.*, 1984, **17**, 979.
7. T. T. Chao, R. F. Sanzalone and A. E. Hubert, *Anal. Chim. Acta*, 1978, **96**, 251.
8. A. E. Hubert and T. T. Chao, *Talanta*, 1985, **32**, 568.
9. J. R. Clark, *J. Anal. At. Spectrom.*, 1986, **1**, 301.
10. I. Rubeska, B. Ebarvia, E. Macalalad, D. Ravis and N. Roque, *Analyst*, 1987, **112**, 27.
11. B. Ebarvia, E. Macalalad, N. Roque and I. Rubeska, *J. Anal. At. Spectrom.*, 1988, **3**, 199.

12. E. M. Donaldson, *Talanta*, 1988, **35**, 47.
13. *Idem*, *ibid.*, 1988, **35**, 297.
14. E. M. Donaldson and E. Mark, *ibid.*, 1982, **29**, 663.
15. R. D. Ediger, *At. Abs. Newsl.*, 1975, **14**, 127.
16. L. M. Voth-Beach and D. E. Shrader, *Spectroscopy*, 1986, **1**, 49.
17. E. M. Donaldson, *Talanta*, 1976, **23**, 411.
18. A. R. Date and D. Hutchison, *Spectrochim. Acta*, 1986, **41B**, 175.
19. B. F. Arbogast, D. E. Detra and G. Vantrump, *U.S. Dept. Interior Geol. Surv. Open-file Report* 87-436, 1987.
20. R. D. Loss, K. J. R. Rosman and J. R. DeLaeter, *Geostds. Newsl.*, 1983, **7**, 321.
21. E. M. Donaldson, *Talanta*, 1988, **35**, 633.
22. E. S. Gladney and C. E. Burns, *Geostds. Newsl.*, 1984, **8**, 119.
23. E. S. Gladney and I. Roelandts, *ibid.*, 1988, **12**, 253.

DETERMINATION OF BROMINE, CHLORINE, SULPHUR AND PHOSPHORUS IN PEAT BY X-RAY FLUORESCENCE SPECTROMETRY COMBINED WITH SINGLE-ELEMENT AND MULTI-ELEMENT STANDARD ADDITION

MARIT ANDERSSON* and ÅKE OLIN

Department of Analytical Chemistry, Uppsala University, P.O. Box 531, S-751 21 Uppsala, Sweden

(Received 24 April 1989. Revised 19 June 1989. Accepted 28 June 1989)

Summary—Bromine (20–40 ppm), chlorine (200–500 ppm), sulphur (0.2–3%) and phosphorus (300–1000 ppm) in peat have been determined by X-ray fluorescence spectrometry (XRFS) combined with the standard-addition method. Chlorine, sulphur and phosphorus have also been determined by other methods and agreement between the results is good. Theoretical calculations based on the Sherman equation were made to validate the linearity of the standard-addition curves. A multi-element standard-addition technique has been tested with addition of all elements at the same time. The results for chlorine were high but after correction for the difference in attenuation coefficient between the sample and added compound the results agreed with those from single-element standard addition.

XRFS is used to determine elements in solid samples directly. This is a considerable advantage, especially for volatile elements, which may be partly lost during the dissolution step often needed with other methods. On the other hand, the XRFS technique has several disadvantages, the most important being strong interelement effects on the analytical signal. The influence of the matrix can be overcome in a variety of ways, including the use of a closely matched standard. Empirical influence-coefficients have been used for many years^{1,2} to correct absorption-enhancement effects of elements which co-exist with the analyte in the specimen matrix. More recently³ these influence-coefficients have been calculated from the fundamental equation of XRF spectrometry derived by Sherman⁴ and in common use in fundamental parameter corrections.⁵ The successful application of the various correction methods generally requires measurement of all the components in the sample.

For partial analysis, methods based on mathematical corrections for interelement effects are less suitable and comparative methods are used. An external standard can be employed but this requires that the sample composition should lie within rather narrow limits, so that the samples and standard can be kept well matched. In many cases this technique cannot be used, because no standards are available.

For single-element determinations in samples where matrix effects are present, the standard-addition method is frequently employed in instrumental analysis. In XRFS this method is seldom used, owing to the difficulties connected with making standard additions to solid samples. Also, the pronounced interelement effects in XRFS, which lead to non-linear analytical functions, restrict the method to the determination of analytes present at low concentration.^{6,7} Non-linear analytical functions have been used^{8,9} but require an increased number of additions, because of the increased number of parameters in the analytical function.

This paper describes a method for making standard additions to plant material. It has been used for the determination of bromine, chlorine, sulphur and phosphorus in peat. Single-element as well as multi-element determinations have been made by using single and multi-element standard additions, respectively. The linearity of the standard-addition functions has been investigated by theoretical calculations based on the Sherman equation. An approximate method correcting for interelement effects in multi-element standard addition has also been studied.

EXPERIMENTAL

Peat samples

Seven peat samples of different origin were analysed. The samples were dried in an air

*Author for correspondence.

stream at 110° in an oven, ground and homogenized in a mixer, then allowed to equilibrate with the laboratory atmosphere and thereafter kept in plastic bags. The moisture content was 7–12% in the air-equilibrated samples, the actual figures being somewhat dependent on the season. It was found that wetted peat dried in an oven for 16–20 hr at 110° reaches a “dry weight” reproducible to 0.5%. All analytical results are reported with respect to a dry weight thus obtained.

Chemicals

The stock solutions of bromide, chloride, sulphate and phosphate were prepared from salts of *pro analysi* quality dried at 110°. Solutions for single-element or multi-element standard additions were made from the stock solutions by dilution. The distilled water used in the preparations was filtered through a Milli-Q system. The salts used were: NaBr, LiCl, Li₂SO₄, NaH₂PO₄.

XRFS measurements

The XRFS measurements were performed with a Philips PW 1410 spectrometer equipped with a scandium/molybdenum dual anode X-ray tube and a PW 1710 processor. The K_α lines were measured in vacuum and the sample was spun during measurement. The background was measured on both sides of the analytical line with equal counting times for peak and background intensities. The instrumental settings are given in Table 1. The measurement series—background 1, peak, background 2—was repeated three times in order to reveal spurious peaks in the count rate. Thus in general, averages of three measurements at each peak and background position were used to calculate the net intensity. Instrument stability was checked by measurement of tungsten or sulphur standards at regular intervals. No drift corrections were needed.

Sample preparation for the XRFS measurements

Single-element determinations. Samples (3.00 g) of the peat were weighed into each of five Teflon containers holding two steel balls (diam. 11 mm). One ml of ethanol was added to wet the samples followed by 0–3.00 ml of the appropriate standard solution (NaBr 100.1 μg/ml, LiCl 1.156 mg/ml, Li₂SO₄ 18.02 mg/ml, NaH₂PO₄ 7.00 mg/ml). One ml of water was added to the sample which did not receive a standard addition. The samples were dried at 110° for at least 17 hr. They were allowed to cool for 1 hr in a desiccator and weighed to obtain the dry weight of the peat after correction for the added material. The containers were shaken for 5 min in a Braun “Mikro-dismembrator II” (West Germany) to mix the samples. Briquettes were prepared by transferring 2.50 g of the mixed sample to a die. The surface was smoothed and 1 g of cellulose powder added to act as a backing. The die was subjected to a pressure of 130 MPa for 1 min. The briquettes may be covered by a mylar film to protect the interior of the spectrometer from dust or cracking briquettes. This precaution was not used in the determination of phosphorus since the film (Du Pont de Nemours International SA, Geneva, Mylar C, 3.5 μm) yielded a high blank value. The mechanical stability of the briquettes is very good, and no cracking occurred during the measurement of several hundred discs.

Multi-element determinations. The briquettes for the multi-element determinations were prepared as above, with the exception that only one addition (of 1.00 ml) of the mixed standard (NaBr 200.8 μg/ml, LiCl 1.539 mg/ml, Li₂SO₄ 36.03 mg/ml, NaH₂PO₄ 13.97 mg/ml) was made.

Non-XRFS determinations

Bromine. Bromine was determined by neutron activation analysis (Studsvik AB, Nyköping, Sweden).

Table 1. Instrumental settings for X-ray fluorescence measurements

Parameter	Element			
	Br	Cl	S	P
Tube voltage, <i>kV</i>	80	60	60	60
Tube current, <i>mA</i>	30	45	45	45
Crystal	LIF*(200)	PE†	PE	PE
Counter	S + F‡	F	F	F
Measuring time, <i>sec</i>	40	20	20	40

*Lithium fluoride.

†Pentaerythritol.

‡S = scintillation, F = gas flow proportional detector.

Chlorine. Chlorine was determined by the mercury(II) thiocyanate-iron method¹⁰ after combustion of the sample (50 mg) in a Schöniger oxygen-flask (500 ml) and absorption in 5 ml of Milli-Q-filtered water. The results were corrected for bromine, as measured by XRFs.

Phosphorus. A 100-mg sample was decomposed by heating with an acid mixture (HNO₃:H₂SO₄:HClO₄ 47:25:12 v/v) in a Kjeldahl flask until a ring of condensing sulphuric acid was formed in the neck of the flask. After dilution and filtration, the phosphorus was determined by the molybdenum blue method.¹¹

Sulphur. Sulphur was determined with a Leco SC-32 sulphur analyser (Mikro Kemi AB, Uppsala, Sweden).

CALCULATIONS

Primary fluorescence intensities (relative) were calculated from the Sherman equation. Most parameters were taken from the NBSGSC program.¹² The mass-absorption coefficients were calculated from the equation and data of Tinh and Leroux.¹³ The tube spectrum was generated by the method and data of Pella *et al.*¹⁴ and the distribution of the molybdenum radiation was modified by filtering through a thin scandium film. This approach was taken since an experimental spectrum for the radiation from the tube was not available. It is expected to overestimate the contribution from molybdenum to the spectrum since it does not compensate for the absorption of incoming electrons by the scandium. Since the calculation of fluorescence intensities of the light elements showed that the contribution from excitation by molybdenum radiation was small, the procedure used is probably justified in this case, although we have no experimental proof. The program was written in Microsoft Quick BASIC.

RESULTS AND DISCUSSION

When standard additions are made, weight B of a component containing the analyte at concentration C_0 is added to a sample weight A containing the analyte at the unknown concentration C_x ; C_0 and C_x are expressed as weight fractions. The fluorescence intensity of the analytical line, I , can be expressed as^{9,15}

$$I = \frac{Q}{\mu_A^*} \left[\frac{C_x + xC_0}{1 + x(\mu_B^*/\mu_A^*)} \right] \quad (1)$$

provided enhancement effects are absent. This is usually the case for biological materials, which have a light element matrix. In equation (1) Q is a proportionality constant that is dependent on the analyte considered and the instrumentation used, x is the ratio B/A , and μ_A^* and μ_B^* are the effective mass-attenuation coefficients¹⁵ of the original sample and the added compound, respectively.

The standard addition curve, $y(=I) = f(x)$, is non-linear because of the term $x(\mu_B^*/\mu_A^*)$ in the denominator of equation (1). Thus a linear standard addition curve will only be obtained for small analyte concentrations, since the additions (x) can then be kept small and hence $x(\mu_B^*/\mu_A^*) \ll 1$. Further, μ_B^* should be as small as possible. In the present study this was accomplished by using lithium salts whenever possible. The influence of the term $x(\mu_B^*/\mu_A^*)$ on the linearity of the standard-addition curve is brought out by Fig. 1. The curves were calculated from equation (1), but in order to simplify the calculations C_x was set equal to zero and a normalized intensity was calculated from

$$I' = I \frac{\mu_A^*}{QC_0} = \frac{x}{1 + x(\mu_B^*/\mu_A^*)} \quad (2)$$

It can be seen that for $\mu_B^* > \mu_A^*$, which is always the case for organic materials, the non-linearity becomes pronounced for larger additions (x). For a real sample, C_x will, of course, be non-zero. This will change the shape of the curves somewhat and determine the range of x needed for the standard additions. However, the conclusions about the influence of the term $x(\mu_B^*/\mu_A^*)$ on the linearity of the standard addition curve remain the same.

In the single-element determinations four standard additions were made, the last being

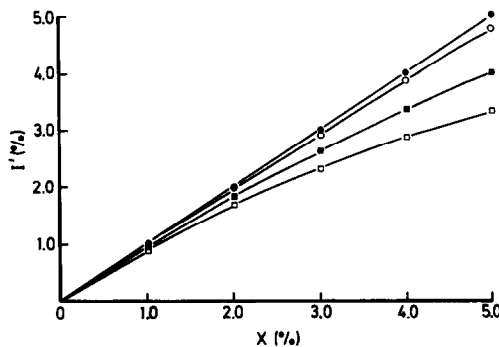


Fig. 1. The influence of the ratio μ_B^*/μ_A^* on the linearity of the standard-addition curve according to equation (2). ● $\mu_B^*/\mu_A^* = 0.1$; ○ $\mu_B^*/\mu_A^* = 1.0$; ■ $\mu_B^*/\mu_A^* = 5.0$; □ $\mu_B^*/\mu_A^* = 10.0$.

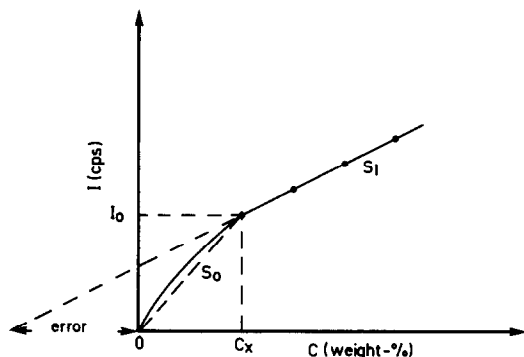


Fig. 2. Hypothetical analytical calibration curve for the analyte in the matrix. The slope obtained from the standard additions (●) is S_1 . If this slope differs from S_0 an erroneous result will be obtained for the analyte concentration, C_x .

about twice the analyte concentration in the sample. The addition of 1 ml of ethanol to the sample prior to the aqueous standard greatly improved the dispersion of the latter into the sample. No difference in the analytical signal was observed when various volumes containing the same amount of the standard were added.

In the standard-addition method the analyte concentration, C_x , is usually found from the intercept on the x -axis of the straight line fitted to the data pairs, $x; y (=I)$. This approach thus neglects the normally unknown term $x(\mu_B^*/\mu_A^*)$, cf. equation (1). We have used $y = I(1 + x)$ rather than $y = I$, since this is a better approximation of the correct value of y , namely $y = I[1 + x(\mu_B^*/\mu_A^*)]$, because $\mu_B^* > \mu_A^*$.⁹ A full correction cannot be made, since μ_A^* and μ_B^* are unknown. The correlation coefficient was greater than 0.999, which indicates that the influence of the term $x(\mu_B^*/\mu_A^*)$ should be small in the range of x used. This conclusion was further corroborated by the theoretical calculations described below.

The analytical results are given in Table 2 under the heading "SA". The values refer to determinations done on different days and

indicate that the reproducibility is better than 2–3%. The precision in the determination of chloride is somewhat worse (mean 2.1%) than for the other elements (mean 1.2%). We ascribe this to contamination, since introduction of a regime aimed at reducing the contamination risk significantly improved the reproducibility.

The results from the determinations with XRFS and the other methods are compared in Table 3. For sulphur and phosphorus the agreement between methods is satisfactory, considering that the uncertainty in the determinations with the Leco sulphur analyser is 0.01–0.02% absolute. The chemical chlorine determination is less precise, owing to problems with homogeneity, since only 50-mg samples could be taken. For sample No. 2 it was not even possible to obtain results concordant within 25%. No systematic differences appear between the XRFS data and those obtained by the other methods. No method was available to us for the determination of bromine at the concentration level present in peat. A determination of bromine in sample No. 7 by NAA yielded 12.3 ppm.

The standard-addition method is based on the assumption of linearity between analytical signal and concentration. In essence the intensities from the samples spiked with standard are used to calculate the (mean) sensitivity in the concentration range covered by the additions. An erroneous result will be obtained if this sensitivity differs appreciably from the sensitivity in the range from zero analyte concentration to that in the sample. This is shown in an exaggerated fashion by the curve in Fig. 2, which is the calibration function for the analyte in the matrix. Only if the sensitivity, S_0 , defined by

$$S_0 = \frac{I_0}{C_x} \quad (3)$$

Table 2. Results from the determination of Br, Cl, S and P in peat by XRFS and single-element (SA) or multi-element (MA) standard additions, expressed on a dry weight basis

Sample	Br, ppm		Cl, ppm		S, %		P, ppm	
	SA	MA	SA	MA	SA	MA	SA	MA
1	32.5; 32.1	33.3	262; 267	290* 270†	0.302; 0.301	0.321	855; 847	870
2	35.6; 35.9	34.6	307; 294	314 298	0.322; 0.317	0.321	779; 776	773
3	37.2; 37.2	36.4	516; 497	535 514	2.88; 2.90	3.01	797; 797	800
4	32.3; 32.8	35.6	344; 350	380 355	0.378; 0.376	0.387	1060; 1030	1010
5	15.7; 15.8	16.8	196; 200	217 203	0.308; 0.308	0.319	303; 296	304
6	20.0; 20.3	21.2	313; 315	346 320	0.228; 0.229	0.231	454; 457	464
7	14.5; 15.1	17.4	291; 289	316 304	0.163; 0.169	0.171	425; 426	415

*Uncorrected.

†Corrected.

Table 3. Comparison between results obtained with XRFs and other methods (OM)

Sample	Cl, ppm			S, %			P, ppm		
	XRFS	OM	Δ , %	XRFS	OM	Δ , %	XRFS	OM	Δ , %
1	265	263	0.8	0.301	0.335	-11	850	847	0.4
2	300	—	—	0.320	0.295	8.1	778	788	-1.3
3	507	527	-3.9	2.89	2.84	1.6	797	778	2.4
4	347	385	-10	0.377	0.39	-3.4	1045	1023	2.1
5	198	222	-11	0.308	0.32	-3.8	300	280	6.9
6	314	351	-11	0.229	0.245	-6.8	456	466	-2.2
7	290	275	5.3	0.166	0.155	6.7	426	394	7.8

Mean values are used, Δ is the relative difference between XRFS and OM.

equals the slope of the calibration curve in the standard-addition range, will a correct result be obtained. Since the calibration curves may be non-linear, *cf.* equation (1), for the elements present at the highest concentrations, sulphur and phosphorus, theoretical calculations were made to find out whether our results could have been affected by this type of error.

Two peat samples, Nos. 2 and 4, were subjected to elemental analysis (SGAB, Luleå, Sweden). With the matrix known, relative sensitivities defined as

$$S_{\text{rel}} = \frac{I_{\text{rel}}}{C} \quad (4)$$

were obtained from the Sherman equation as a function of the analyte concentration, C . When S_{rel} starts to change appreciably with C , a curvature of the calibration curve is indicated. A more sensitive measure of a changing slope is obtained by calculating the differential relative sensitivity defined by

$$S_{\text{diff}} = \left(\frac{\partial I_{\text{rel}}}{\partial C} \right)_c \quad (5)$$

The expression for S_{diff} is derived in Appendix 1. S_{diff} will approach S_{rel} at low values of C , equation (A1.4). Because the additions made for bromine were very small, calculations were performed only for the other elements, which were assumed to be excited by only the scandium radiation, since calculations indicated that the contribution from molybdenum was less than 10%.

The calculations showed that the greatest change in S_{diff} occurred for sulphur. The changes in S_{diff} over the range from the composition of the original sample to the composition of the last standard addition was 1% and the difference between S_{diff} and S_0 was less than 2%. Hence evaluation of the analytical result from a linear standard-addition curve was justified.

The standard-addition method is not well suited for routine analysis of solid samples, because of the time-consuming sample preparation. The analytical throughput can be increased by making additions of a multi-element standard and by the use of only one addition. With this technique, however, an increased imprecision can be expected not only from a statistically less well defined standard-addition curve but also from increased matrix effects.

We have tested the single-addition multi-element approach by determination of the four analytes simultaneously. The size of the standard additions was chosen so that the imprecision in the result from the counting statistics did not exceed 1%. The error arising from counting statistics was estimated by an expression derived by Vos and Hubaux,¹⁶ modified to apply to our measurements. The results of the determinations are entered in Table 2 under the heading "MA".

For bromine, sulphur and phosphorus the agreement between the two standard-addition techniques is satisfactory. The standard deviation estimated from replicates was, however, three times the standard deviation expected from counting statistics alone. The systematic deviation of about 5–10% for chlorine is most likely due to interference from sulphur (and phosphorus) in the chlorine determination.

A correction for matrix effects on the chlorine determination was calculated from equation (A2.5) in Appendix 2. No peat standards were available. Therefore the two peat samples (Nos. 2 and 4) that had been subjected to complete analysis were used as standards in the evaluation of the others. The applicability of the concept of an equivalent wavelength, λ_e , was tested as follows. The mineral composition and the ash content of a peat specimen were allowed to vary within wide ranges, then λ_e was calculated as described in Appendix 2 for each composition, from the scandium excitation

spectrum (the contribution from molybdenum excitation can be neglected). In all instances λ_e was found to be close to the wavelength of the ScK_α characteristic line. Hence $\lambda_e = 3.03\text{\AA}$ was used in the applications of equation (A2.5).

The corrected results for chlorine, entered in Table 2, show good agreement with the results obtained by the single-element multiple standard additions. The two standards lead to consistent results. We can thus conclude that XRFS combined with the use of single addition of a multi-element standard could be used as an efficient analytical technique if proper heed is paid to matrix effects. It should also be pointed out that use of a simple ratio to a standard yields erroneous results, since the sensitivities changed by a factor of almost two between the samples investigated here.

Acknowledgements—Thanks are due to Pertti Knuutila for performing the XRFS measurements and to Erik Forsman for making the non-XRFS determinations of chlorine.

REFERENCES

1. R. Tertian and F. Claisse, *Principles of Quantitative X-Ray Fluorescence Analysis*, p. 131. Heyden, London, 1982.
2. G. R. Lachance and R. J. Traill, *Can. Spectrosc.*, 1966, **11**, 43.
3. R. Rousseau and F. Claisse, *X-Ray Spectrom.*, 1974, **3**, 31.
4. J. Sherman, *Spectrochim. Acta*, 1955, **7**, 283.
5. J. W. Criss and L. S. Birks, *Anal. Chem.*, 1968, **40**, 1080.
6. W. J. Campbell and H. F. Carl, *ibid.*, 1954, **26**, 800.
7. N. Pind, *Talanta*, 1984, **31**, 1118.
8. P. B. De Groot, *Adv. X-Ray Anal.*, 1983, **26**, 395.
9. M. Andersson, C. Ericzon and Å. Olin, *Talanta*, 1988, **35**, 337.
10. T. M. Florence and Y. J. Farrar, *Anal. Chim. Acta*, 1971, **54**, 373.
11. J. Murphy and J. P. Riley, *ibid.*, 1962, **27**, 31.
12. G. Y. Tao, P. A. Pella and R. M. Rousseau, *NBSGSC-A FORTRAN Program for Quantitative X-ray fluorescence Analysis*, NBS Technical Note 1213, 1985.
13. T. P. Thin and J. Leroux, *X-Ray Spectrom.*, 1979, **8**, 85.
14. P. A. Pella, L. Feng and J. A. Small, *ibid.*, 1985, **14**, 125.
15. R. Tertian and F. Claisse, *Principles of Quantitative X-Ray Fluorescence Analysis*, p. 71. Heyden, London, 1982.
16. G. Vos and A. Hubaux, *Spectrochim. Acta*, 1969, **24B**, 545.
17. Z. H. Kalman and L. Heller, *Anal. Chem.*, 1962, **34**, 946.
18. R. Tertian, *Spectrochim. Acta*, 1972, **27B**, 159.

APPENDIX 1

The primary fluorescence intensity, I , of an analyte can be evaluated from

$$I = QC\Sigma \frac{\mu(\lambda)J(\lambda)\Delta\lambda}{\mu_a^*(\lambda)} = QC\Sigma\Delta I(\lambda) \quad (\text{A1.1})$$

where Q is a constant of proportionality, C is the concentration of the analyte, $\mu(\lambda)$ is the mass-attenuation coefficient of the analyte, $\mu_a^*(\lambda)$ is the effective mass-attenuation coefficient of the sample and $J(\lambda)$ is the intensity of the tube spectrum within the wavelength interval $\Delta\lambda$. The sum is taken from the short-wavelength end of the spectrum to the absorption edge of the analytical line.

The average sensitivity (S_0) in the concentration interval from 0 to C is obtained from equation (A1.1) as

$$S_0 = \frac{I}{C} = Q\Sigma\Delta I(\lambda) \quad (\text{A1.2})$$

The differential sensitivity of the analyte in the matrix is defined by

$$S_{\text{diff}} = \left(\frac{\partial I}{\partial C} \right)_c \quad (\text{A1.3})$$

Differentiation of equation (A1.1) yields

$$S_{\text{diff}} = Q\Sigma\Delta I(\lambda)(=S_0) + QC \frac{\partial}{\partial C} \Sigma\Delta I(\lambda) \quad (\text{A1.4})$$

Consider the sample as composed of x parts of standard (B), containing the analyte at concentration C_0 and $(1-x)$ parts of sample (A) with analyte concentration C_x . Then

$$\mu_a^*(\lambda) = (1-x)\mu_a^*(\lambda) + x\mu_b^*(\lambda); \quad \frac{d\mu_a^*(\lambda)}{dx} = \mu_b^*(\lambda) - \mu_a^*(\lambda) \quad (\text{A1.5})$$

$$C = xC_0 + (1-x)C_x; \quad \frac{dC}{dx} = C_0 - C_x \approx C_0 \quad (\text{A1.6})$$

From the definition of $\Delta I(\lambda)$ we get

$$\frac{\partial \Delta I(\lambda)}{\partial C} = -\frac{\mu(\lambda)J(\lambda)\Delta\lambda}{[\mu_a^*(\lambda)]^2} \left[\frac{\partial \mu_a^*(\lambda)}{\partial C} \right] \quad (\text{A1.7})$$

and from equations (A1.5) and (A1.6)

$$\frac{\partial \mu_a^*(\lambda)}{\partial C} = \frac{\mu_b^*(\lambda) - \mu_a^*(\lambda)}{C_0} \quad (\text{A1.8})$$

Combining equations (A1.4), (A1.7) and (A1.8) we obtain

$$S_{\text{diff}} = Q\Sigma \frac{\mu(\lambda)J(\lambda)\Delta\lambda}{\mu_a^*(\lambda)} \left\{ 1 + \frac{C[\mu_b^*(\lambda) - \mu_a^*(\lambda)]}{C_0\mu_a^*(\lambda)} \right\} \quad (\text{A1.9})$$

APPENDIX 2

The following treatment assumes a mono-energetic excitation source or the existence of an equivalent wavelength in the case of a continuous excitation spectrum. The sample (A) and the standard (B) contain the analyte at concentrations C_x and C_0 , respectively. Sample and standard are mixed in proportions $1-x$ and x . The intensity of a fluorescence line can be written

$$I_1 = Q \frac{C_x}{\mu_a^*} \quad (\text{A2.1})$$

for the original sample and

$$I_2 = Q \frac{(1-x)C_x + xC_0}{(1-x)\mu_a^* + x\mu_b^*} \quad (\text{A2.2})$$

after the standard addition. Eliminating Q between the equations and denoting $x C_0$ by ΔC we obtain

$$C_x = \frac{\Delta C}{\frac{I_2}{I_1} \left[1 + x \left(\frac{\mu_B^*}{\mu_A^*} - 1 \right) \right] - (1 - x)} \quad (\text{A2.3})$$

In this equation, ΔC , I_1 and I_2 are known or measured quantities; μ_B^* can be calculated from the known composition of the standard and the μ -values at the appropriate wavelength. However, μ_A^* remains unknown, so a matrix-corrected C_x cannot be calculated directly. By measuring the intensity from a standard sample of known total composition, μ_A^* can be estimated from

$$\mu_A^* = \mu_{stand}^* \frac{I_{stand} C_x}{I_1 C_{stand}} \quad (\text{A2.4})$$

and a calculated value of μ_{stand}^* . Equations (A2.3) and A2.4 yield

$$C_x = \frac{\Delta C - x C_{stand} \frac{\mu_B^* I_2}{\mu_{stand}^* I_{stand}}}{(1 - x) \left(\frac{I_2}{I_1} - 1 \right)} \quad (\text{A2.5})$$

for the concentration of the analyte.

Continuous excitation radiation was used in the present investigation. The equivalent wavelength, λ_e , was found by first calculating an equivalent effective mass-attenuation coefficient,^{17,18} μ_e^* , from

$$\mu_e^* = \frac{\int \mu(\lambda) J(\lambda) d\lambda}{\int \frac{\mu(\lambda)}{\mu_e^*(\lambda)} J(\lambda) d\lambda} \quad (\text{A2.6})$$

For notations, see Appendix 1. Then $\mu_e^*(\lambda)$ was calculated as a function of wavelength for monochromatic excitation. At λ_e , $\mu_e^*(\lambda)$ equals μ_e^* .

DETERMINATION OF SUBMICROGRAM AMOUNTS OF GALLIUM BY ION-EXCHANGER FLUORIMETRY

DETERMINATION OF GALLIUM IN NATURAL WATERS

F. CAPITAN, A. NAVALON, J. L. VILCHEZ and L. F. CAPITAN-VALLVEY*

Department of Analytical Chemistry, University of Granada, 18071-Granada, Spain

(Received 16 May 1988. Revised 7 August 1989. Accepted 16 August 1989)

Summary—A method for microdetermination of gallium at ng/ml level has been developed, based on ion-exchanger fluorimetry. The gallium reacts with salicylidene-*o*-aminophenol to give a highly fluorescent complex, which is fixed on a dextran-type cationic resin. The fluorescence of the resin, packed in a 1-mm silica cell, is measured directly with a solid-surface attachment. The range of concentration of the method is 2.0–10.0 ng/ml, the RSD 1.3% and the detection limit 0.3 ng/ml. The method has been applied to the determination of gallium in natural waters. The gallium content found in tap water was higher than that in raw water. This is related to the use of commercial aluminium salts in the water-treatment plant.

Scanning of fluorescence emitted from solid surfaces has been widely used in the direct assay of organic substances held on such surfaces, such as paper chromatograms, thin-layer chromatoplates, KBr disks, electrophoresis strips, and silicone rubber pads.¹⁻³

The solid-surface fluorescence technique has been used as a detector system in planar chromatography or electrophoresis, or as a simple reagentless system for analysis. It has been applied in environmental research, especially on air pollution,^{4,5} forensic science, *e.g.*, in questioned-document work,⁶ pesticide analysis by thin-layer chromatography,^{1,7} with previous derivatization in some cases,⁸ and biochemistry and clinical chemistry for determination of enzymes, substrates, activators and inhibitors.³

Our aim is to combine the measurement of solid-surface fluorescence with use of a solid, *e.g.*, an ion-exchanger resin, to preconcentrate the analyte, made fluorescent by use of an appropriate reagent. To the best of our knowledge this technique has so far been used only once, for preconcentration of aluminium from dilute solution by use of an azo dye immobilized on silica.⁹

This approach, named by us ion-exchanger fluorimetry (IEF), can be potentially useful for the analysis of very dilute solutions, as in water analysis. Furthermore the fluorescence measured is the diffuse transmitted fluorescence,

which increases the signal intensity, compared to that in the diffuse reflected fluorescence methods. This is due to the fact that at the 1 mm thickness used, the dextran-type resin employed is more translucent than the silica gel or alumina more generally employed.

A related technique is the solid phase spectrophotometry devised by Yoshimura,¹⁰ and called ion-exchanger photometry, that measures directly the absorbance of a resin that contains the analyte fixed as a coloured chromogenic species.

One advantage of IEF methods is their simplicity, since it is not necessary to immobilize a reagent on an insoluble substrate. The reagents are added to the sample and the fluorescent species are collected on the resin, which is then transferred to a 1-mm silica cell and measured without previous drying. Other advantages are decreased interferences and increased sensitivity (because this is a function of the sample volume). Hence, we can design methods tailored to the problem in hand.

Here we propose a new method for determination of gallium by the IEF method. Reports on the antitumour activity of gallium,¹¹ its use as a tumour-scanning agent,¹² as well as other studies on the pharmacokinetics and toxicity of gallium^{13,14} suggest there is a need for sensitive and reliable methods for its determination.

Salicylidene-*o*-aminophenol (SOAPh), a known Schiff's base fluorimetric reagent for gallium,^{15,16} can be employed for IEF determination of gallium in natural waters.

*Author for correspondence.

Surprisingly, the gallium content found in tap water by us is ten times higher than that in raw water. This can be related to the use of commercial aluminium salts as flocculants in the water treatment.

EXPERIMENTAL

Reagents

Ion-exchanger. To avoid contamination, the Sephadex SP C-25 cation-exchange resin in the sodium form is used without previous treatment.

Salicylidene-o-aminophenol (SOAPh, 2-hydroxyaniline-N-salicylidene). Synthesized by condensation of salicylaldehyde with *o*-aminophenol by heating at 100° for 30 min,¹⁷ purified by repeated recrystallization from ethanol and dried at room temperature over silica gel (yield 77%; m.p. 184.5–185°). Its purity was checked by TLC. The reagent was characterized by its infrared and ¹H-NMR spectra and elemental analysis (required for C₁₃H₁₁O₂N: C, 73.24%; H, 5.16%; N, 6.57%; found: C, 73.1%; H, 5.01%; N, 6.4%). Used as a 0.1% solution in absolute ethanol; the solution is stable for at least 1 week.

Standard gallium(III) stock solution, 1.0 mg/ml. Prepared from Ga(NO₃)₃·8H₂O in 0.1M nitric acid and standardized titrimetrically with EDTA (Xylenol Orange as indicator); diluted further with doubly-distilled water as required.

Buffer solutions. Prepared from monochloroacetic acid, acetic acid and ammonia.¹⁵

Unless otherwise stated, the reagents were of analytical grade.

Apparatus

All fluorimetric measurements were performed with an LS 5 Perkin-Elmer spectrofluorimeter provided with a Quantic Rhodamine 101 counter to correct the excitation spectra, a Hamamatsu R928 photomultiplier, a Houston Omnigraphic X-Y recorder, a variable-angle solid-surface accessory, designed and constructed by us, and a Braun Melsungen Thermomix 1441 thermostat. A set of fluorescent polymer samples was used daily to adjust the spectrofluorimeter and compensate for changes in source intensity. A Crison 501 digital pH-meter with calomel and glass electrodes, and an Agitaser 2000 rotating agitator were also used.

Fluorescence measurements

The mixture of Sephadex, sample solution and reagent was shaken mechanically in a polyethylene bottle. The resin beads were filtered off under suction and packed together with a small volume of solution into a 1-mm silica cell by means of a pipette. The relative fluorescence intensity (RFI) measured was the diffuse fluorescence transmitted through the resin at the unirradiated face of the cell. The optimal angle between the plane of the cell and the excitation beam was 45° in all cases.

Procedures

Basic procedure. A 500-ml water sample containing 1.0–5.0 µg of Ga(III) was transferred to a 1-litre polyethylene bottle, and 2 ml of pH 4.70 buffer solution,¹⁵ 5 ml of 0.1% SOAPh solution and 100 mg of Sephadex SP C-25 resin were added. The mixture was shaken mechanically for 20 min. Afterwards, the resin beads were collected by filtration under suction and with the aid of a pipette were packed into a 1-mm cell together with a small volume of the filtrate. A blank solution containing all the reagents but no gallium was prepared and treated in the same way as the sample. The intensity of fluorescence (at 20.0 ± 0.5°) for the sample and blank was measured at λ_{em} = 515 nm (with λ_{ex} = 405 nm) 20 min after loading of the samples. A calibration graph was constructed in the same way, with Ga(III) solutions of known concentration.

Procedure for tap water. To a 500-ml water sample in a 1-litre polyethylene bottle, 2 ml of pH 4.70 buffer solution,¹⁵ 7 ml of 0.1 g/l. sodium tetrafluoroborate solution, 5 ml of 0.1% SOAPh solution and 100 mg of Sephadex SP C-25 resin were added. The mixture was shaken mechanically for 20 min, and the subsequent steps were as in the basic procedure. The standard-addition method was used for calibration.

Procedure for raw water. To a 6000-ml water sample in a 15-litre polyethylene container, 24 ml of pH 4.70 buffer solution,¹⁵ 24 ml of 0.1 g/l. sodium tetrafluoroborate solution, 60 ml of 0.1% SOAPh solution and 100 mg of Sephadex SP C-25 resin were added. The mixture was shaken mechanically for 60 min, and the analysis continued as for tap water. The standard-addition method was used for calibration.

Treatment of sample. Natural waters (preserved by addition of 0.25 ml of concentrated nitric acid per litre) were filtered through a 0.45-µm membrane filter (Millipore) into a polyethylene container carefully cleaned with

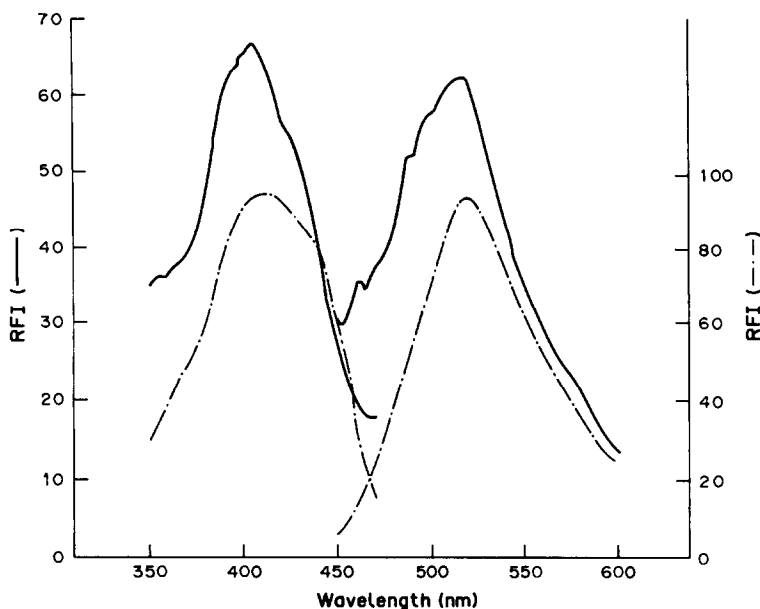


Fig. 1. Fluorescence spectra of SOAph-Ga(III) complex. (—) resin phase: [SOAph] $9.4 \times 10^{-5} M$; [Ga(III)] $2.9 \times 10^{-7} M$; pH = 4.00; 100 mg of Sephadex SP C-25; 500-ml sample; stirring time 15 min; λ_{exc} 405 nm; λ_{em} 515 nm; $f_s = 0.4$, slit_{exc} = slit_{em} = 2.5 nm; T $20.0 \pm 0.5^\circ$. (---) solution: [SOAph] $1.6 \times 10^{-4} M$; [Ga(III)] $2.9 \times 10^{-5} M$; pH 4.00; λ_{exc} 410 nm; λ_{em} 515 nm; $f_s = 0.7$; slit_{exc} = slit_{em} = 2.5 nm; T $20.0 \pm 0.5^\circ$; ethanol 20%, (f_s = sensitivity factor).

nitric acid. The pH of an aliquot of the water was adjusted to 4–5 with sodium hydroxide solution immediately before analysis.

RESULTS AND DISCUSSION

Excitation and emission spectra of the resin and solution

Salicylidene-*o*-aminophenol reacts with Ga(III) to give a fluorescent 1:1 chelate at pH 4.¹⁶ In the presence of Sephadex cation-exchanger, the complex is sorbed on the resin, so is probably cationic since it is not fixed by an anionic resin. An SP C-25 dextran-type resin is recommended, as it gives less background fluorescence.

The peak wavelengths (515 nm) in the emission spectra of the SOAph-Ga(III) system are identical for the immobilized and solvated systems (Fig. 1). The similarities in the emission spectra of the immobilized and solvated systems suggest that the complex is relatively insensitive to its environment. The maxima of the excitation spectra of the two systems differ. The maximum is at 410 nm for the solution and 405 nm for the resin phase. On the other hand, the most noticeable differences between the fluorescence spectra are the better resolution of the resin phase spectra, and the smaller peak

width of the spectra of the solution system. The opposite is observed in the fixation of aluminium chelates on silica gel.⁹

From the half-life of the excited state of the complex in the solid phase at different temperatures, we infer that the luminescence process is fluorescence ($\tau < 5 \mu\text{sec}$).

Optimization of variables

Dependence on pH. First, we chose a buffer solution from those proposed in the literature on this system in solution. The ammonium acetate/hydrochloric acid buffer¹⁶ cannot be used, because it alters the resin. The monochloroacetic acid, acetic acid and ammonia mixture¹⁵ was found to give the best results. The optimum pH value, adjusted with this buffer, for the formation and fixation of the species falls in the narrow range 4.60–4.80 (Fig. 2). At pH values below 3.5 or above 5.5 the complex is not fixed on the resin. We should point out that the optimum pH for use of the resin phase is higher than that for use of the solution system (4.0).

The fluorescence is independent of ionic strength (μ), adjusted with the buffer solution, up to 7.5×10^{-3} . Above this value there is a decrease in the fluorescence according to the equation $\text{RFI} = 0.56\mu^{3/4}$ ($r = 0.992$). This effect could be due to increased competition of

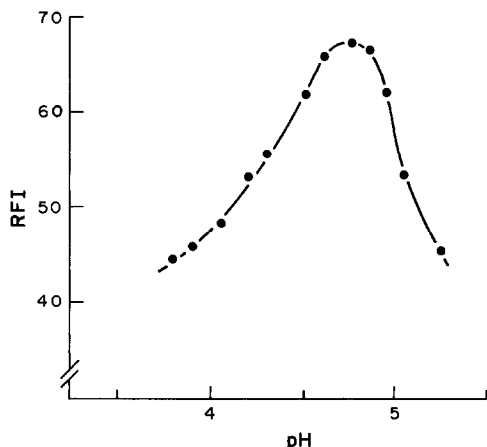


Fig. 2. Influence of pH on RFI. [SOAph] $9.4 \times 10^{-5} M$; [Ga(III)] $2.9 \times 10^{-7} M$; 100 mg of Sephadex SP C-25; 500-ml sample; stirring time 15 min; λ_{exc} 405 nm; λ_{em} 515 nm; $f_s = 0.4$; slit_{exc} = slit_{em} = 2.5 nm; $T = 20.05 \pm 0.5^\circ$.

hydrogen and ammonium ions with the complex for ionic sites on the resin, or to deactivation of excited SOAph in the resin.

SOAph concentration. The dependence of the RFI on SOAph concentration (Fig. 3) can be described by the equation $RFI = 177.7 + 11.5 \ln[SOAph]$ ($r = 0.996$). As optimum SOAph concentration we chose $4.7 \times 10^{-5} M$. For maximum fluorescence intensity the [SOAph]/[Ga(III)] ratio must be at least 160.

Influence of temperature. The ion-exchange process is independent of temperature in the range 10–60°, the RFI being measured at 20° (Fig. 4). On the other hand the RFI decreases when the temperature of measurement increases, but this effect is completely reversible. The decreases in RFI are 2% at 25°, 9% at 40° and 25% at 60°. This effect can be explained as

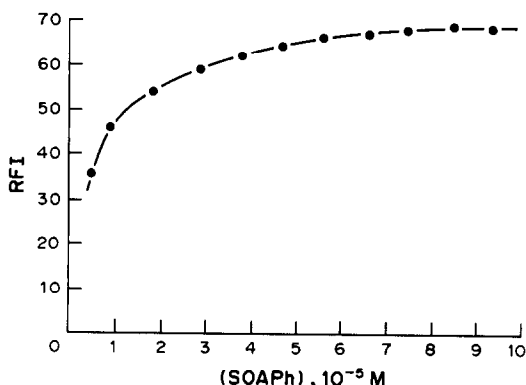


Fig. 3. Effect of SOAph concentration on RFI. [Ga(III)] $2.9 \times 10^{-7} M$; [SOAph] from 4.7×10^{-6} to $9.4 \times 10^{-5} M$; pH 4.70; 100 mg of Sephadex SP C-25; 500-ml sample; stirring time 15 min; λ_{exc} 405 nm; λ_{em} 515 nm; f_s 0.4; slit_{exc} = slit_{em} = 2.5 nm; $T = 20.0 \pm 0.5^\circ$.

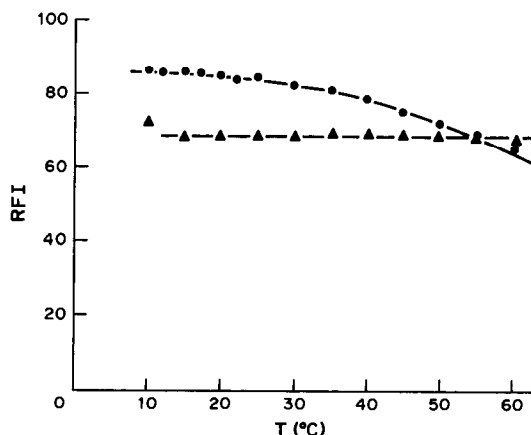


Fig. 4. Influence of temperature. (●): On RFI (ion-exchange at 20°). (▲): On ion-exchange process (RFI measured at 20°). [SOAph] $9.4 \times 10^{-5} M$; [Ga(III)] $5.8 \times 10^{-7} M$; pH 4.70; 100 mg of Sephadex SP C-25; 500-ml sample; stirring time 15 min; λ_{exc} = 405 nm; λ_{em} = 515 nm; $f_s = 0.3$; slit_{exc} = slit_{em} = 2.5 nm.

due to internal conversion processes as the temperature increases, facilitating non-radiative deactivation of the excited singlet state, because the intersystem crossing deactivation is nearly independent of temperature.¹⁸ All other measurements reported here were made at $20.0 \pm 0.5^\circ$.

Other experimental conditions. The stirring time necessary for maximum RFI development is 20 min for a 500-ml sample and 60 min for a 6000-ml sample. As the use of a large amount of the resin lowers the RFI, for all measurements we used the optimum amount needed to fill the cell and make handling convenient, *viz.* 100 mg. The RFI of the immobilized complex decreased slightly in the first 20 min, and then was constant for at least 3 hr.

Volume effect on the sensitivity. In ion-exchanger fluorimetry the sensitivity should be increased if a larger amount of sample solution is taken for equilibrium with the solid. The increase in sensitivity can be estimated by measuring the RFI of Sephadex equilibrated with different volumes of solutions containing the same concentration of Ga(III) and proportional amounts of the other reagents. Figure 5 shows the increase of fluorescence signal with sample volume. The shape of the graph suggests a Langmuir-type isotherm, as is observed in some ion-exchanger photometry studies.¹⁹

Calibration and precision

The calibration graphs for standards treated by the procedure described above were linear over the concentration range 2.0–10.0 $\mu g/l$.

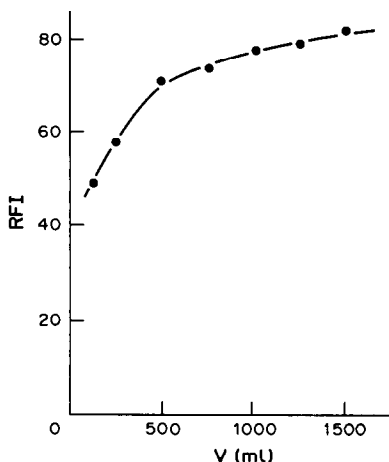


Fig. 5. Influence of the sample volume on RFI. [SOAPH] $4.7 \times 10^{-5} M$; [Ga(III)] $2.9 \times 10^{-7} M$; pH 4.70; 100 mg of Sephadex SP C-25; sample volume from 100 to 1500 ml; stirring time 20 min; λ_{exc} 405 nm; λ_{em} 515 nm; f_s 0.4; $slit_{exc} = slit_{em} = 2.5$ nm; $T = 20.0 \pm 0.5^\circ$.

gallium for 500-ml samples. The equation $RFI = 2.68C$ ($r = 0.999$) was found for this range of concentrations, where C is the concentration of gallium ($\mu g/l.$) in the sample solution.

The reproducibility of the proposed method and of the packing of the resin into the 1-mm cell was found by use of 500-ml sample solutions with a gallium concentration of $8 \mu g/l.$ For 10 determinations the relative standard deviation (RSD) was 1.3%; 10 measurements for replicate packing of the resin gave an RSD of 1.5%. It seems that the packing of the resin makes a major contribution to the overall error.

Sensitivity and detection limit

The method reported here is substantially more sensitive than the solution methods using SOAPH as reagent. A calibration graph for the determination of Ga(III) with SOAPH in solution, by the method of Dagnall *et al.*¹⁵ but under our experimental conditions, gave the equation $RFI = 0.1 + 0.04C$ ($r = 0.999$), so the new method is 67 times more sensitive.

The standard deviation of the background fluorescence measured for 10 determinations of the blank was 0.3 RFI units for 500-ml samples. The IUPAC detection limit is therefore $0.3 \mu g/l.$ Ga(III) and the determination limit $1.1 \mu g/l.$

The method is compared in Table 1 with chelate formation methods described in the literature for fluorimetric determination of Ga(III). For comparison purposes we have chosen those methods which in our opinion could be considered as among the most sensitive devised so far.

Effect of foreign ions

A systematic study was made of the effect of foreign ions on the determination of $8 \mu g/l.$ Ga(III). A 100-fold w/w ratio of potentially interfering ion to gallium was first tested and, if interference occurred, the ratio was reduced progressively until interference ceased. Higher ratios were not tested. The tolerance level is defined as the amount of foreign ion that produces an error equal to $\pm 5\%$ in determination

Table 1. Methods for the fluorimetric determination of gallium(III)

Reagent	Detection limit*	
	$\mu g/l.$	Reference
2-Hydroxy-5-methylbenzaldehyde-4-aminoantipyrine	0.1	21
1,5-Bis(salicylidene) thiocarbohydrazon†	0.1	22
Salicylidene- <i>o</i> -aminophenol—IEF	0.3	This paper
4-(5-Chloro-2-hydroxyphenylazo)resorcinol†	0.5	23
4-Amino-2,4-dihydroxybenzil-2,3-dimethyl-1-phenyl-5-pyrazolone	1	24
Dodecyl-lumogallion	1	25
Hexyl-lumogallion†	1	26
8-Hydroxyquinaldin†	1	27
Lumogallion†	1	28
Pyridine-2-aldehyde 2-furoylhydrazone	1	29
Resorcyldene-4-aminoantipyrine	1	30
4-Salicylideneaminoantipyrine	1	31
Benzyl 2-pyridyl ketone 2-pyridylhydrazone	1.4	32
Rhodamine B + Cl ⁻ §	20	33
Rhodamine 6G + Cl ⁻ §	3	33
<i>o</i> -(Salicylideneamino)-2-hydroxybenzene sulphonic acid	2	34
<i>N</i> -Salicylidene-2-hydroxy-5-sulphoaniline	2	35
3,5,7,4'-Tetrahydroxyflavone	2	36
1,5-Bis(salicylidene) thiocarbohydrazon	2	37

*Or minimum concentration used for calibration.

†Extraction procedure.

§Ternary complex and extraction procedure.

Table 2. Effect of foreign ions on the determination of 8 $\mu\text{g/l.}$ gallium

Foreign ion or species	Tolerance, $\mu\text{g/l.}$
Ag, K, Na, Tl(I), Ba, Be, Ca, Cd, Cu(II), Hg(II), Mg, Mn, Ni, Co, Pd, Sr, Zn, As(III), B, Bi, Eu(III), In, La, Sb(III), Y, Ce(IV), Ge, Se(IV), Th, Mo, W, NO_3^- , NO_2^- , SO_4^{2-} , Cl^- , PO_4^{3-}	> 800
BF_4^-	710
Cr(III)	670
Fe(III)	240
F^-	140
Cr(VI)	90
Al(III)	4

of the analyte. The results are summarized in Table 2.

To apply this system to determination of Ga(III) in natural waters, we studied the interference of the ions commonly found in water. The relative errors found in the determination of 8 $\mu\text{g/l.}$ gallium were 8% for SO_4^{2-} (20 mg/l.), 2% for NO_3^- (2 mg/l.), 11% for Cl^- (10 mg/l.), 26% for Ca^{2+} (36 mg/l.), 20% for Mg^{2+} (12 mg/l.). In all cases the interference was manifested as a reduction in calibration slope, necessitating determination by the standard-addition method.

The most serious interference is that of Al^{3+} , however. Better tolerances for it can be accomplished by two methods. The first uses the different effect of temperature on the two systems, *e.g.*, the RFI of the aluminium complex is decreased (by 78% at 50°) more than that of the gallium complex (16% at 50°), and moreover the change in RFI is fully reversible for the gallium complex on cooling, but not for the aluminium complex.³⁸

In practice we take advantage of both features, packing the analyte-loaded resin in the 1-mm cell and heating it for 15 min in a water-bath at 70°, then cooling it to 20° for measurement of the RFI. By this method, a fivefold increase in tolerance to Al(III) is obtained (20 $\mu\text{g/l.}$ instead of 4 $\mu\text{g/l.}$).

The second system for eliminating the interference of Al^{3+} uses sodium tetrafluoroborate as masking agent.²⁰ The optimum amount needed is a function of the aluminium content, because the masking agent itself interferes (see Table 2). For an aluminium level of 200 $\mu\text{g/l.}$ a 7-fold weight ratio is needed and for 20 $\mu\text{g/l.}$ a 20-fold ratio.

Determination of gallium in tap and natural waters

The method was applied to the determination of gallium in water samples by the standard-

addition method. As representative samples we selected tap water and raw water from Granada town supplies (Spain). The sample volume was a function of the gallium content: 500 ml for the tap water samples and 6000 ml for the raw water. The loss of sensitivity by the matrix effect can be evaluated from the ratio of the slopes of the standard calibration graph and the standard-additions calibration graph (9 in this case). The use of a high volume of sample increases the sensitivity. The experimental sensitivity ratio, calculated from the ratio of the slopes of the standard-additions calibration graphs for the two volumes used, is 6.7.

Before the gallium determination we established the aluminium content in the waters by AAS, in order to select the amount of BF_4^- necessary. The average (\pm standard deviation, five determinations) gallium found was 63.0 ± 0.9 $\mu\text{g/l.}$ for the tap water and 6.5 ± 0.2 $\mu\text{g/l.}$ for the raw water from a nearly natural supply (Quentar dam).

To check the accuracy of the proposed method, we used the water samples for a recovery study. The recoveries of 20.0, 30.0 and 40.0 $\mu\text{g/l.}$ gallium added to 500 ml portions of the tap water were 96.5, 102.3 and 101.0% respectively, and for 4.0, 6.0 and 8.0 $\mu\text{g/l.}$ added to 6000 ml portions of raw water, 95.5, 98.2 and 101.8% respectively.

The gallium content of the Granada town tap water is surprisingly high compared with the raw water supplied to the town. To establish the source of the gallium we have analysed all the chemicals used in the Granada water treatment plant. Only the commercial aluminium salts used as flocculants contained gallium. To analyse these salts we first established the aluminium content by AAS and then determined the gallium. The results obtained were: aluminium sulphate 4.34% Al and 0.048% Ga; aluminium chloride, 9.53% Al and 0.047% Ga; aluminium chlorosulphate, 5.13% Al and

0.035% Ga. This implies that the flocculation with commercial aluminium salts increases the gallium content in tap water.

It is interesting that the Al/Ga ratio (w/w) in the tap water (2.86) is practically the same as the ratio (2.92) in the raw water. In view of the Al/Ga ratio in the flocculating agents, this means that in the water treatment relatively more gallium than aluminium is extracted from the chemicals used.

The high content of gallium found in the tap water would justify the gallium concentration in human urine in Tokyo found by Nakamura *et al.*³⁹ (48 $\mu\text{g/l.}$), since gallium is readily excreted from the human body.¹⁴

Acknowledgement—This research was supported by the Comisión Asesora de Investigación Científica y Técnica (CAICYT) of Spain (Project No. 3082/83).

REFERENCES

- R. J. Hurtubise, *Solid Surface Luminescence Analysis: Theory, Instrumentation, Applications*, Dekker, New York, 1981.
- Idem*, *Trace Analysis by Luminescence Spectroscopy*, in *Trace Analysis: Spectroscopic Methods for Molecules*, G. D. Christian and J. B. Callis (eds.), Wiley, New York, 1986.
- G. G. Guilbault, *Photochem. Photobiol.*, 1977, **25**, 403.
- E. Sawicki, *Talanta*, 1969, **16**, 1231.
- C. R. Sawicki and E. Sawicki, in *Progress in Thin Layer Chromatography and Related Methods*, Vol. III, Chapter 6, A. Niederwieser and G. Pataki (eds.), Ann Arbor Science, Ann Arbor, 1972.
- E. P. Gibson, *J. Forensic Sci.*, 1977, **22**, 680.
- J. F. Lawrence and R. W. Frei, *J. Chromatog.*, 1974, **98**, 253.
- J. G. Zakrevsky and V. N. Mallet, *ibid.*, 1977, **132**, 315.
- M. A. Ditzler, G. Doherty, S. Sieber and R. Allston, *Anal. Chim. Acta*, 1982, **142**, 305.
- K. Yoshimura, H. Waki and S. Ohashi, *Talanta*, 1976, **23**, 449.
- M. M. Hart and R. H. Adamson, *Proc. Natl. Acad. Sci. USA*, 1980, **68**, 1623.
- P. B. Hoffer, C. Bekerman and R. E. Henkin (eds.), *Gallium-67 Imaging*, Wiley, New York, 1978.
- R. A. Newman, A. R. Brody and I. H. Krakoff, *Cancer*, 1979, **44**, 1728.
- D. P. Kelsen, N. Alcock, S. Yeh, J. Brown and C. Young, *ibid.*, 1980, **46**, 2009.
- R. M. Dagnall, R. Smith and T. S. West, *Chem. Ind. London*, 1965, **34**, 1499.
- K. Morishige, *Anal. Chim. Acta*, 1980, **121**, 301.
- D. C. Freeman and C. E. White, *J. Am. Chem. Soc.*, 1956, **78**, 2678.
- D. M. Hercules, *Fluorescence and Phosphorescence Analysis: Principles and Applications*, Interscience, New York, 1966.
- K. Yoshimura, M. Ishii and T. Tarutani, *Anal. Chem.*, 1986, **58**, 591.
- V. Patrovský, *Chem. Listy*, 1954, **48**, 537.
- A. T. Pilipenko and A. I. Volkova, *Ukr. Khim. Zh.*, 1977, **43**, 536.
- N. Scott, D. E. Carter and Q. Fernando, *Anal. Chem.*, 1987, **59**, 888.
- L. Ngog Thu, R. M. Dranitskaya and V. A. Nazarenko, *Ukr. Khim. Zh.*, 1968, **34**, 186.
- A. T. Tashkodzhaev, L. E. Zel'tser, Sh. T. Talipov and Kh. Khikmatov, *Zh. Vses. Khim. Obshch. D. I. Mendeleeva*, 1976, **21**, 114.
- K. Kenyu, H. Houichi and I. Nobuhiko, *Bunseki Kagaku*, 1977, **26**, 246.
- K. Kina, K. Shiraiishi and N. Ishibashi, *ibid.*, 1976, **25**, 501.
- T. Shigematsu, *ibid.*, 1958, **7**, 787.
- T. Imasaka, T. Harada and N. Ishibashi, *Anal. Chim. Acta*, 1981, **129**, 195.
- E. Requena, J. J. Laserna, A. Navas and F. García-Sánchez, *Analyst*, 1983, **108**, 933.
- A. T. Tashkodzhaev, L. E. Zel'tser, Sh. T. Talipov and Kh. Khikmatov, *Zavodsk. Lab.*, 1975, **41**, 281.
- Sh. T. Talipov, A. T. Tashkodzhaev, L. E. Zel'tser and Kh. Khikmatov, *Otkr. Izobret, Prom. Obraztsy, Tovarnye Znaki*, 1972, **15**, 1109.
- J. J. Laserna, A. Navas and F. García-Sánchez, *Anal. Chim. Acta*, 1980, **121**, 295.
- A. P. Golovina, S. M. Sapezhinskaya and V. K. Runov, *Tezisy tret'ei usesoyuznoi konferentsii po analiticheskoi khimii, Minsk, 1979*, Vol. 1, p. 262, quoted in *Zavodsk. Lab.*, 1981, **47**, No. 1, 17.
- K. Morishige, *J. Inorg. Nucl. Chem.*, 1978, **40**, 843.
- Idem*, *Anal. Chim. Acta*, 1974, **72**, 295.
- Z. T. Maksimycheva, Sh. T. Talipov, Z. P. Pakudina and S. Sadykov, *Izv. Vyssh. Ucheb. Zaved. Khim. Khim. Tekhnol.*, 1974, **17**, 348.
- E. Ureña, A. García de Torres, J. M. Cano-Pavón and J. L. Gómez-Ariza, *Anal. Chem.*, 1985, **57**, 2309.
- M. J. Blanch, *Tesis Licenciatura*, Pub. Univ. Granada, 1986.
- K. Nakamura, M. Fujimori, H. Tsuchiya and H. Orii, *Anal. Chim. Acta*, 1982, **138**, 129.

BEHAVIOUR OF DIFFERENT ELUENTS AND STABILIZING AGENTS IN THE DETERMINATION OF SULPHITE IN WATER BY ION-CHROMATOGRAPHY

L. CAMPANELLA, M. MAJONE and R. POCCHI

Department of Chemistry, University "La Sapienza", Rome, Italy

(Received 31 January 1989. Revised 20 July 1989. Accepted 10 August 1989)

Summary—Ion-chromatography has been used for the determination of sulphite in water. The eluents were solutions of Na_2CO_3 (1.1mM)– NaHCO_3 (1.4mM) or NaHCO_3 (1.0mM)–formaldehyde (0.2% w/w), and formaldehyde, glycerol or fructose was used as stabilizing agent. With the first eluent, fructose or glycerol can be used to stabilize samples against sulphite oxidation, but formaldehyde affects the peak height. On the other hand, formaldehyde can stabilize sulphite in the presence of Fe(III), whereas glycerol and fructose can not. If Fe(III) is present, the second eluent is used and sulphite is eluted directly as hydroxymethanesulphonate; formaldehyde will not then affect the peak height. This eluent allows a good peak separation and is suitable for the sulphite concentration range 0.1–12.0 mg/l.

The determination of sulphite in natural and waste water by ion-chromatography has been proposed by several authors as an alternative to the classical iodometric¹ or pararosaniline² methods. Much of the work^{3–7} was concerned mainly with the chromatographic aspects of sulphite elution, with little emphasis on quantification. As shown in Table 1, there was a prevalence of classical carbonate-based alkaline eluents.

However, determination of sulphite is quite difficult because of rapid oxidation of sulphite by dissolved oxygen. Aging of sulphite standard solutions shows direct proportionality between decrease in the sulphite peak and increase in the sulphate peak.⁴ Oxidation of sulphite can be avoided by adding formaldehyde to the solution⁸ to form an addition compound (hydroxymethanesulphonate), which is stable in slightly acid media, but quickly hydrolyses in alkaline media to give the starting compounds.⁹ This feature is utilized in the ion-chromatography methods since formation of the addition compound stabilizes the sample, but the compound can be hydrolysed by the alkaline eluent during the analytical run. Lindgren *et al.*¹⁰ showed that the apparent elution times for the addition compound and sulphite are the same when eluents with $\text{pH} > 10.7$ are used.

However, when formaldehyde is used to stabilize sulphite in an unknown sample, a severe drawback is that the formaldehyde/sulphite molar ratio strongly affects both the

height and area of the sulphite peak. Lindgren *et al.*¹⁰ studied several other compounds (particularly fructose and glycerol), which were effective in stabilizing sulphite when used in higher molar ratios than that for formaldehyde, without any effect on the sulphite peak. However, their experiments were not extended to the very high molar ratios necessary in the case of unknown samples.

Furthermore, little information is at present available on the effectiveness of these stabilizing agents when heavy metals are present. It has long been known^{11,12} that heavy metals (such as iron, copper, cobalt, manganese, lead) catalyse sulphite oxidation in water. Hansen *et al.*¹³ showed that sulphite oxidation is significant in the presence of iron or copper and also in formaldehyde-stabilized sulphite solutions, owing to almost concurrent hydrolysis and metal-catalysed oxidation during passage of the solution through the chromatograph. They concluded that ion-chromatography is not suitable for sulphite determination, but their tests were generally performed at high sulphite concentration levels (over 20 mg/l.). It seems that the effect is less important at lower concentrations.

To eliminate sulphite oxidation during the analysis and/or to overcome problems due to use of an incorrect concentration of stabilizing agent, the use of eluents which do not decompose the stable addition compound should be of interest. Dasgupta *et al.*⁵ proposed potassium

hydrogen phthalate as an acid eluent but it gave a poor chromatographic performance. As an alternative, Dasgupta¹⁴ studied the use of a very weak eluent (NaHCO_3 at 1.0mM concentration, with 0.2% of formaldehyde), to avoid hydrolysis of hydroxymethanesulphonate in the separation column. He also pointed out the disadvantages of this eluent, *viz.* strongly retained anions are eluted only after a long time or not at all, the eluent baseline can increase owing to oxidation of formaldehyde to formic acid, and the column deteriorates quickly, probably because of a Schiff-base reaction of formaldehyde with the quaternary ammonium exchange sites. However, the eluent has still been recently proposed¹⁵ and used with good results in a field study.¹⁶

Thus, in spite of the promise of ion-chromatography for determining sulphite, an accurate procedure has not yet been defined and more research on the sample stabilization and chromatographic analysis is required. To explore these two aspects we have studied the behaviour of different stabilizing agents under different conditions, particularly in the presence of metals, together with the behaviour of different eluents, both with and without the chosen stabilizing agent.

EXPERIMENTAL

The ion-chromatograph used was a Dionex model 2000i, equipped with a conductivity detector, HPIC-AG4 and HPIC-AS4 separation columns and an AFS fibre suppressor. The recorder was a Leeds and Northrup model Speedomax XL 681A.

The eluents were an NaHCO_3 (1.4mM)– Na_2CO_3 (1.1mM) solution (delivered at 2.0 ml/min) or an NaHCO_3 (1.0mM)–formaldehyde (0.2% w/w) solution (at flow rates ranging from 0.5 to 4.0 ml/min, usually 2.0 ml/min). The

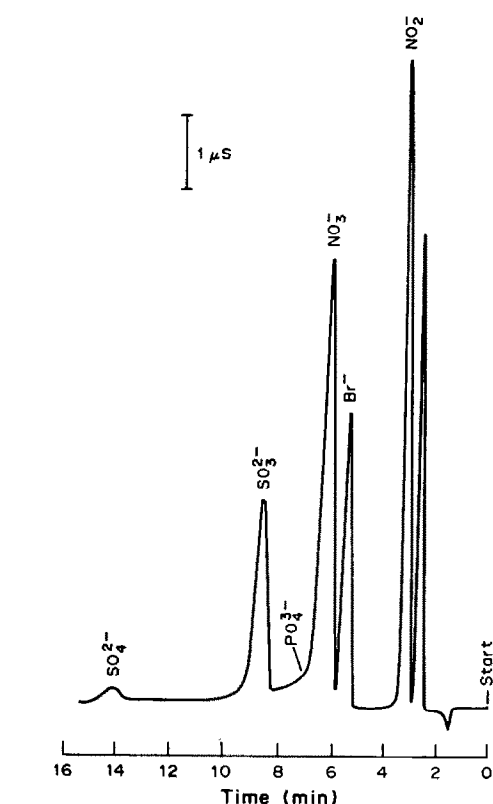


Fig. 1. Typical chromatogram of a solution containing sulphite, bromide, nitrate, nitrite and phosphate (each 10 mg/l.). Eluent Na_2CO_3 (1.1mM) and NaHCO_3 (1.4mM); flow-rate 2.0 ml/min; injection volume 100 μl .

suppression solution was 0.012M sulphuric acid. All reactants were analytical grade.

A fresh solution of anhydrous sodium sulphite (1 g/l.) was prepared daily in distilled water. Working sulphite solutions were obtained by diluting mixtures of this solution and the chosen stabilizing agent solution (formaldehyde, glycerol or fructose) with dilute hydrochloric acid (pH 4.3.). Final sulphite concentrations ranged from 0.1 to 12 mg/l. (normally ≈ 5 mg/l.) and the stabilizing agent/

Table 1. Proposed eluents for sulphite determination by ion-chromatography

Composition	Flow-rate, ml/min	Reference
5.0mM Na_2CO_3 –4.0mM NaOH	1.7	3
3.0mM NaHCO_3 –2.4mM Na_2CO_3	2.3	4
1.0mM KH phthalate	2.3	5
4.8mM NaHCO_3 –4.7mM Na_2CO_3	3.4	6
15.0mM H_2PO_4^- (pH 4.8)	2.0	7
0.7mM Na_2CO_3 –0.7mM <i>p</i> -cyanophenol (pH 11.4 with NaOH)	3.1	8
3.0mM NaHCO_3 –2.4mM Na_2CO_3	1.9	10
3.5mM Na_2CO_3 –2.6mM NaOH	2.4	13
1.0mM NaHCO_3 –0.2% w/w HCHO	2.3	14

sulphite molar ratio ranged from 1 to 10^4 . For calibration purposes, a standard sulphite solution (5 mg/l.) was prepared daily from sodium hydroxymethanesulphonate and analysed: corrections for any variations in the instrumental sensitivity were then made. In some cases other anions (acetate, bromide, fluoride, nitrite, nitrate, phosphate and sulphate) or metals (iron, manganese, aluminum, lead and copper) were also added to the working solutions.

RESULTS AND DISCUSSION

Eluents

The chromatographic behaviour of sulphite and hydroxymethanesulphonate with the two different eluents was studied.

A typical chromatogram obtained with the $\text{NaHCO}_3/\text{Na}_2\text{CO}_3$ eluent is shown in Fig. 1. The sulphite peak is well separated and all anions are eluted after 15 min. From tests performed at different weight ratios of other anions to sulphite, it was found that the phosphate and nitrite peaks partially overlapped the sulphite peak for weight ratios of $>10:1$ and $>100:1$, respectively. Other anions tested do not interfere at the 100:1 weight ratio. Phosphate interference can be overcome by using an Na_2CO_3 (3.5mM)– NaOH (3.1mM) eluent, which elutes phosphate very slowly.¹⁷

A good sulphite separation can also be obtained with the formaldehyde/ NaHCO_3 eluent. A typical chromatogram obtained with this eluent at 3.5 ml/min flow-rate is shown in Fig. 2. At this high flow-rate a short analysis time is possible without significant loss of resolution. No peak overlap has been found at weight ratios of anions tested to sulphite $>100:1$. However, elution of nitrate takes more than 15 min, and sulphate and phosphate are not eluted at all.

Stabilizing agents

Table 2 shows the stabilizing effect of various compounds. Glycerol is almost as effective as formaldehyde. Fructose must be present in molar ratio of 100–1000 to sulphite to maintain oxidation at less than 5% per day, but at higher concentrations is less effective. However, this effect was due to a slow pH increase and could be prevented by adequate buffering. A similar pH effect was observed for glycerol.

The presence of heavy metals (commonly present in natural and waste water) completely changes the situation. Table 3 shows that

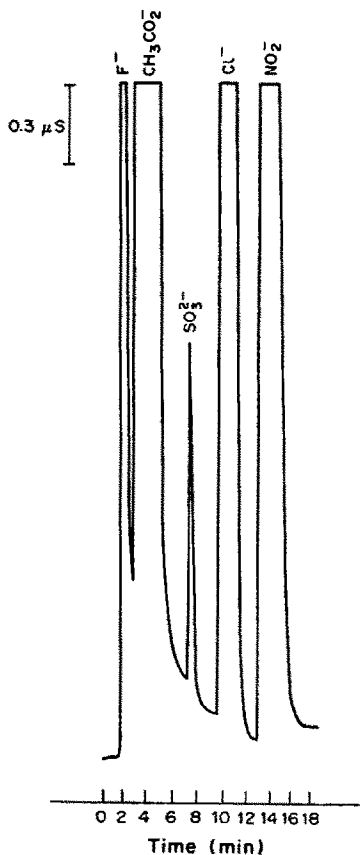


Fig. 2. Typical chromatogram of a solution of sulphite (10 mg/l., from hydroxymethanesulphonate), bromide, nitrate, nitrite and phosphate (each 500 mg/l.). Eluent NaHCO_3 (1.0mM) and HCHO (0.2% w/w); flow-rate 3.5 ml/min; injection volume 100 μl .

Fe(III) , at molar ratio 1:10 with respect to the sulphite, induces in fructose-stabilized solutions a sulphite peak decrease of about 80% in a few hours. Combining stabilization with fructose with other procedures, such as purging with nitrogen and storage in the dark and cold, does not decrease the rate of oxidation. Immediate injection of freshly prepared samples shows no significant differences between samples with or without iron present, *i.e.*, most of the oxidation takes place in the storage medium. Other metals have less (manganese) or no effect. Glycerol behaves like fructose whereas formaldehyde slows the oxidation to less than 10% per day. Table 4 shows that formaldehyde can stabilize sulphite, even at only 1:1 molar ratio, when iron is present at the mg/l. level.

Lindgren *et al.*¹⁰ showed that when an $\text{NaHCO}_3/\text{Na}_2\text{CO}_3$ eluent is used, the sulphite peak height is strongly affected by excess of formaldehyde, the amount of which cannot be foreseen when there is no prior knowledge of the

Table 2. Sulphite stabilization: peak height (relative to initial value = 100) as a function of the stabilizing agent and of the excess used: sulphite concentration 5 mg/l., initial pH 4.2 (*indicates buffered pH), eluent Na₂CO₃ (1.4mM)–NaHCO₃ (1.1mM), flow-rate 2 ml/min

Stabilizing agent	Stabilizing agent/sulphite, molar ratio	Relative peak height		
		4 hr	24 hr	48 hr
Fructose	1	98.2	89.3	81.5
	10	98.4	88.3	80.3
	100	100.0	96.0	91.8
	1000	100.0	98.8	92.7
	10000	99.7	91.8	85.3
	10000*	99.2	100.6	90.4
Glycerol	1	98.7	95.4	93.7
	10	97.8	98.0	94.9
	100	99.6	99.2	99.2
	1000	99.0	100.4	98.1
	10000	98.3	62.8	13.3
	10000*	101.8	101.2	102.5
Formaldehyde	1	99.7	97.9	97.6
	10	94.7	96.0	104.1
	100	97.0	99.9	93.0
	1000	97.6	92.5	93.5

Table 3. Sulphite stabilization in the presence of metals: peak height (relative to initial value = 100) as a function of the stabilizing agent and the metal ion: sulphite concentration 5 mg/l., pH 4.2, metal/sulphite molar ratio 1:10, eluent Na₂CO₃ (1.4mM)–NaHCO₃ (1.1mM), flow-rate 2 ml/min

Stabilizing agent	Stabilizing agent/sulphite, molar ratio	Metal	Relative peak height		
			4 hr	24 hr	48 hr
Fructose	1000	None	99.6	97.2	92.8
		Pb(II)	98.2	94.7	90.5
		Al(III)	95.6	96.6	93.0
		Cu(II)	98.2	95.6	92.9
		Mn(II)	94.1	85.8	81.4
		Fe(II)	22.1	18.5	16.4
		None	95.5	97.8	95.5
Glycerol	1000	Mn(II)	100.0	98.7	93.4
		Fe(III)	18.2	7.9	6.3
		None	100.0	102.0	96.8
Formaldehyde	1	Mn(II)	101.2	100.6	92.3
		Fe(III)	100.3	95.2	85.6
		None	100.0	102.0	96.8

Table 4. Sulphite stabilization with formaldehyde in the presence of iron: peak height (relative to initial value = 100) as a function of the formaldehyde/sulphite and iron/sulphite molar ratios: sulphite concentration 5 mg/l., pH 4.2, eluent Na₂CO₃ (1.4mM)–NaHCO₃ (1.1mM), flow-rate 2 ml/min

Formaldehyde/sulphite molar ratio	Iron(III)/sulphite molar ratio	Relative peak height		
		4 hr	24 hr	48 hr
1	1:10	103.0	99.3	92.1
1	1:4	101.1	96.4	92.6
1	1:2	100.6	96.4	92.1
1	1:1	100.0	95.8	92.1
10	1:10	103.0	103.4	102.3
10	1:4	100.0	99.4	97.2
10	1:2	101.1	98.8	96.7
10	1:1	100.6	98.2	91.6

composition of the sample. Our experiments confirmed that the sulphite peak is stable when glycerol and fructose are used, even at very high molar ratios. Excess of formaldehyde does not interfere when the formaldehyde-containing eluent is used, because the formaldehyde-sulphite addition compound is directly eluted.

From these observations it would seem that if no iron or manganese is present, fructose and particularly glycerol may be used effectively over a wide concentration range without any effect on the sulphite peak. On the other hand, if these metals are present, both formaldehyde and the formaldehyde-containing eluent have to be used. As the second case seems to be more common, it has been examined thoroughly.

Formaldehyde-containing eluent and sulphite determination

From our experiments, the eluent appears to be stable for at least two weeks, the baseline remaining at $15.9 \pm 0.8 \mu\text{S}$ with no drift to higher values. Column efficiency decreases regularly and a 10% decrease is observed over ≈ 60 hr, *i.e.*, about 300 assays. No recovery of efficiency is obtained by washing the column with the $\text{Na}_2\text{CO}_3/\text{NaHCO}_3$ eluent.

The peak height is a linear function of sulphite concentration from 0.1 to 12 mg/l. Replicate determinations on different days always resulted in correlation coefficients >0.999 . The sensitivity is $\approx 0.27 \mu\text{S.l.mg}^{-1}$ and is reproducible.

CONCLUSIONS

Stabilization of sulphite in the sample is very important if accurate determination is to be achieved. Good stabilization can be obtained with fructose (at high molar excess) or glycerol only if iron(III) or manganese(II) is not present in the sample. In that case, the chromatographic analysis with the traditional alkaline NaHCO_3 - Na_2CO_3 eluent is not affected by the stabilizing agent/sulphite molar ratio.

If these metals are present, however, formaldehyde can be used with good results at a molar ratio of 1:1 to sulphite. The amount of formaldehyde needed to give this molar ratio when added to stabilize an unknown sample cannot be accurately predicted, and this has a marked effect on the peak height if the

NaHCO_3 - Na_2CO_3 eluent is used. However this problem does not arise when the formaldehyde-containing eluent is used.

Certain advantages are associated with this eluent. Sulphite is eluted as hydroxymethanesulphonate and is well separated from most common anions even when these are present at high concentrations. High flow-rates (up to 3.5 ml/min) result in short analysis times with no loss of resolution. Chloride, fluoride, acetate, nitrite and nitrate can be determined together with sulphite in about 15 min, but phosphate and sulphate are not eluted at all.

The eluent gives a stable and low baseline even when a week old, and column degradation seems to be slow.

Peak height is linearly correlated to sulphite concentration, with a high correlation coefficient in the range 0.1–12 mg/l., thus allowing determination of sulphite with good sensitivity and accuracy and a low limit of detection.

REFERENCES

1. *ASTM Book of Standards*, Part 23, Method D1339-67, ASTM, Philadelphia, 1970.
2. P. W. West and G. C. Gaeke, *Anal. Chem.*, 1956, **28**, 1816.
3. T. S. Stevens, V. T. Turkelson and W. R. Albe, *ibid.*, 1977, **49**, 1176.
4. N. P. Barkley, G. L. Contner and M. Malanchuk, in *Ion Chromatographic Analysis of Environmental Pollutants*, J. D. Mulik and E. Sawicki (eds.), p. 115. Ann Arbor Science, Ann Arbor, 1979.
5. P. K. Dasgupta, K. DeCesare and J. C. Ullrey, *Anal. Chem.*, 1980, **52**, 1912.
6. T. Sunden, M. Lindgren, A. Cedergren and D. D. Siemer, *ibid.*, 1983, **55**, 2.
7. R. G. Gerritse and J. A. Adeney, *J. Chromatog.*, 1985, **347**, 419.
8. C. O. Moses, D. K. Nordstrom and A. L. Mills, *Talanta*, 1984, **31**, 331.
9. S. D. Boyce and M. Hoffmann, *J. Phys. Chem.*, 1984, **88**, 4740.
10. M. Lindgren, A. Cedergren and J. Lindberg, *Anal. Chim. Acta*, 1982, **141**, 279.
11. E. C. Fuller and R. H. Crist, *J. Am. Chem. Soc.*, 1941, **63**, 1644.
12. R. D. Srivastava, A. F. McMillan and I. J. Harris, *Can. J. Chem. Eng.*, 1968, **46**, 181.
13. L. D. Hansen, B. E. Richter, D. K. Rollins, J. D. Lamb and D. J. Eatough, *Anal. Chem.*, 1979, **51**, 633.
14. P. K. Dasgupta, *Atmos. Environ.*, 1982, **16**, 1265.
15. J. M. McCormick and L. M. Dixon, *J. Chromatog.*, 1985, **322**, 478.
16. D. M. Davies and J. P. Ivey, *Anal. Chim. Acta*, 1987, **194**, 275.
17. N. Grados, L. Campanella, E. Cardarelli and M. Majone, *Metodi Anal Acque*, 1986, **6**, No. 4, 37.

A MODIFIED METHOD FOR THE DETERMINATION OF METHYLMERCURY BY GAS CHROMATOGRAPHY

M. HORVAT and A. R. BYRNE

"J. Stefan" Institute, "E. Kardelj" University, Ljubljana, Yugoslavia

K. MAY

Institute of Applied Physical Chemistry, Nuclear Research Centre, Julich, Federal Republic of Germany

(Received 7 January 1989. Revised 7 July 1989. Accepted 7 August 1989)

Summary—A simple modification of the Westöö extraction procedure for methylmercury and its determination by gas chromatography (GC) is presented. The cysteine clean-up step has been modified, with use of cysteine-impregnated paper instead of cysteine solution. Methylmercury bromide is extracted from the sample into toluene and is selectively adsorbed on the cysteine paper. Interfering compounds are washed from the paper with toluene. The isolated methylmercury is set free with sulphuric acid containing bromide, extracted into benzene and determined by GC. The modification of the extraction procedure results in good recovery and reproducibility for various biological and environmental samples, good sensitivity with a detection limit of 0.1 ng/g, avoidance of difficulties arising from emulsion formation, cleaner chromatograms, and faster analysis. It is particularly suitable for determination of low levels of MeHg.

Determination of methylmercury (MeHg) by gas chromatography (GC) is still preferable to indirect methods for total organic mercury determination by cold vapour atomic-absorption spectrometry (CV-AAS), mainly because MeHg is measured directly, not after conversion into inorganic mercury. This is particularly important when samples with different levels of MeHg have to be analysed. Nevertheless, in the case of very low concentrations of MeHg (sediments, soils, algae, *etc.*) none of the analytical techniques for MeHg can guarantee accuracy, and results should be treated critically. Unfortunately, standard reference materials (SRMs) are available only for total mercury, and not for MeHg, and therefore accuracy for MeHg determination has to be established by inter-laboratory comparisons, standard-addition experiments and comparisons of the results of at least two and preferably more analytical techniques. Such a study was recently published,¹ in which four different analytical methods for MeHg were compared.

At present, the method used in most laboratories is based on an extraction procedure for MeHg originally devised by Gage² and later modified by Westöö.³ Modifications to the Westöö procedure have been reported and reviewed.^{4,5} They are based on addition of acid (hydrochloric, hydrobromic or hydriodic) to a

homogenized sample, extraction of the MeHg halide into an organic solvent (benzene or toluene), purification by stripping with a thiol compound (cysteine, glutathione) or thio-sulphate, and re-extraction into benzene. The MeHg is then determined by GC with various detection systems (electron-capture, atomic-absorption, mass spectrometry, microwave emission spectrometry). The main difficulties are the formation of emulsions (often persistent) during the extraction or stripping and loss of volatile MeHg.

The method mainly used for routine analysis in our laboratory is based on volatilization of MeHgCN or MeHgCl, which is released from the sample and captured on cysteine-impregnated paper in a microdiffusion cell.^{6,7} The main drawback is the lower recovery with increasing weight of sample. In an attempt to overcome this problem, a new distillation procedure has recently been developed.¹

In the present work, aimed at simplifying a modified Westöö procedure which has been used in our laboratory mainly for samples such as sediments and soils, the cysteine clean-up step has been improved. The original use of a cysteine solution has been replaced by use of cysteine-impregnated paper as in the volatilization technique.⁶ The results obtained by the new and the older modified Westöö procedures and

some other isolation techniques have been compared.

EXPERIMENTAL

Reagents

L(+)-Cysteine hydrochloride solution (1%). Prepared daily in 20% sodium citrate solution.

Sulphuric acid (2M) saturated with cupric sulphate.

Potassium bromide, 4M.

Hydrochloric acid, 4M.

Mercuric chloride, saturated solution in benzene.

Benzene and toluene. Chromatographic grade (Merck).

Methylmercury and ethylmercury standard solutions (1 mg/ml). Dissolve 116.3 mg of CH_3HgCl or 115.4 mg of $\text{C}_2\text{H}_5\text{HgCl}$ (Merck) in 100 ml of toluene. Make working standard solutions by appropriate dilution with benzene to cover the range 0.02–0.10 ng/ μl .

Methylmercury and ethylmercury standard aqueous solutions. Dissolve the same amounts of CH_3HgCl and $\text{C}_2\text{H}_5\text{HgCl}$ as above in 1–2 ml of acetone and dilute to 100 ml with 0.1M hydrochloric acid. The stock and working standard solutions have to be kept in darkness to prevent decomposition of MeHg by ultraviolet light.

All chemicals and solvents should be of highest purity. Benzene is a better extractant than toluene for MeHg and is also cleaner, but because of its toxicity is used only for the final stage in the extraction procedure when small volumes are involved, and for the final dilutions in preparation of working standard

solutions. All operations with benzene were conducted under a well ventilated hood.

Apparatus and materials

Gas chromatograph. A Hewlett Packard model 5890 instrument connected to an HP 3390 A integrator was used, with an electron-capture detector (^{63}Ni radioactive source). The chromatographic conditions were as follows.

Column temperature: 160°

Injector temperature: 190°

Detector temperature: 280°

Carrier gas, N_2 : flow-rate 60 ml/min

Glass columns. Length 1.6 m, inner diameter 2 mm, packed with 5% DEGS-PS on Supelcoport 100–120 mesh, commercially available from Supelco.

Pyrex test-tubes with ground stoppers (Fig. 1).

Filter papers. A narrow strip 2 mm in width, cut from the circumference of a circular filter paper (Schleicher and Schüll, No. 589³, 7 cm diameter), is saturated with cysteine solution and dried at room temperature in an acid-free atmosphere, just before use. It is inserted as a spiral into the extraction tube.

Methods

Two approaches for isolation of MeHg are presented schematically in Scheme 1. Various approaches to homogenization may be used. The choice depends mainly on the sample type. Fresh samples (fish, mussels, algae) are homogenized in a stainless-steel homogenizer (SORVALL omni-mixer). A hair sample is cut into small fragments with scissors, then washed with acetone and three times with water–acetone

1–3 g of fresh sample (0.1–1.5 g of dry sample) + 2 ml of H_2SO_4 saturated with CuSO_4 + 2 ml of KBr solution + 3 ml of toluene in test-tube "a", Fig. 1. Equilibrate for 10 min, centrifuge for 5 min at 6000 rpm. Repeat the extraction with 2 ml of toluene and transfer the toluene phases quantitatively.

Shake toluene phase + 1 ml of cysteine solution in test-tube "b", Fig. 1. Centrifuge at 6000 rpm. Transfer the aqueous phase quantitatively. Repeat the extraction with cysteine.

Shake toluene phase + cysteine paper in test-tube "b", Fig. 1, for 10 min. Decant organic phase and wash the cysteine paper with three 5-ml portions of toluene. Dry the paper.

Shake aqueous phase + 1 ml of KBr solution + 1 ml of H_2SO_4 + 0.5–1.0 ml of benzene, in test-tube "c", Fig. 1. Centrifuge.

Transfer the paper into test-tube "c", Fig. 1, and add 0.1 ml of HBr + 0.1 ml of H_2SO_4 + 0.2–1.0 ml of benzene. Equilibrate, centrifuge.

Transfer the benzene phase into test-tube "c", Fig. 1.

Inject 1–5 μl of the organic phase into GC column

Scheme 1. Flow-chart of the extraction methods for methylmercury determination.

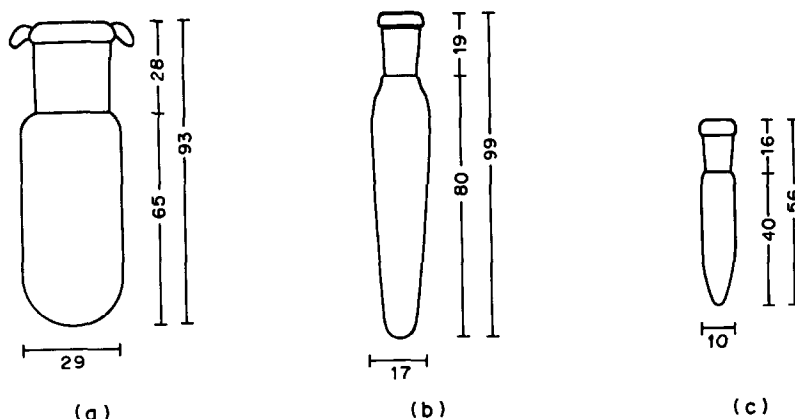


Fig. 1. Test tubes for extraction of methylmercury: (a) 25 ml, (b) 9 ml, (c) 1 ml.

mixture and then decomposed with 7.5M sodium hydroxide at 90° in a closed test-tube (Fig. 1, "a"). This approach has been used in our laboratory as a reference method for human hair analysis for assessing exposure and possible health hazards due to seafood consumption in the Mediterranean.^{8,9} Alkaline decomposition (with addition of cysteine to stabilize MeHg), as proposed by some authors,¹⁰ may be successfully used for other fresh biological samples.

Another possibility is acid extraction of MeHg from the sample by hydrochloric acid, as used in the method devised by May *et al.*¹¹ for subsequent ion-exchange separation and CV-AAS determination of MeHg after conversion into inorganic mercury. Ten ml of 6M hydrochloric acid are added to the sample and the mixture is left overnight in darkness. More than 90% of the MeHg is released into the acid. All the extract, or an aliquot, can be taken for subsequent extraction and GC determination, by the procedure presented in Scheme 1.

Alkaline decomposition and acid extraction serve two purposes: first to release MeHg from the binding sites in the sample, which makes further extraction more effective, and secondly, to homogenize a large amount of sample, from which only a small aliquot is taken for analysis.

RESULTS AND DISCUSSION

To release MeHg bound in a tissue, some acid must be added. Many workers use hydrochloric acid. In our method the use of potassium bromide and sulphuric acid saturated with cupric sulphate is advantageous, mainly because MeHgBr has a higher partition coefficient,¹² and the Cu(II) promotes release of MeHg bound to sulphur. This is especially important when sedi-

ments or other samples containing sulphide compounds are to be analysed. Addition of Cu(II) was found to have no effect in the analysis of biological samples, however.

The first extraction step is repeated at least once, especially when there is difficulty in separation of the aqueous and organic phases. The organic phases are transferred as quantitatively as possible. The recovery at this stage is usually more than 90% (as shown by recovery experiments with spiked samples), depending mainly on the type and amount of sample. When larger amounts of sample are taken, the volumes of the reagents have to be optimized. It is very important to transfer only clear organic phase. MeHg is extracted into aqueous cysteine solution only at neutral pH. Any emulsion present in the organic phase significantly affects the partition of MeHg into cysteine solution or its trapping on cysteine paper. Centrifugation at 6000 rpm effectively breaks any emulsion in the toluene phase after the initial extraction.

The main difficulty when using cysteine solution for back-extraction is emulsion formation, which is very persistent with certain types of sample and may cause losses during equilibration and transfer. This difficulty can be avoided by using cysteine impregnated paper as described above.

Table 1 shows the influence of the dimensions of the filter paper and the volume of the toluene extract on the recovery of MeHg and EtHg. The shape of the paper does not significantly affect the recovery, nor does the amount of cysteine on the paper (use of 1% or 5% cysteine solution for the impregnation gave the same results). The volume of toluene used is critical however. Repeating the extraction with toluene would be expected to maximize the amount of methylmercury extracted, but experiments with 3 + 2 ml,

Table 1. Effect of the size of the cysteine paper and the volume of the toluene phase on the recovery of MeHg and EtHg

Paper size	Volume of the toluene phase, ml					
	5		8		10	
	MeHg	EtHg	MeHg	EtHg	MeHg	EtHg
0.5 × 8 cm*	98 ± 5	83 ± 3	85 ± 2	80 ± 3	82 ± 4	74 ± 3
0.5 × 4 cm*	90 ± 5	75 ± 5	82 ± 4	81 ± 2	80 ± 5	75 ± 2
0.2 × 21 cm†	96 ± 2	91 ± 2	84 ± 2	79 ± 4	80 ± 1	70 ± 1

Results are given as mean value (ng MeHg found ± std. devn. of three determinations). 100 ng of MeHg and EtHg in aqueous solutions were added to acidified algae before toluene extraction.

*Rectangular strip.

†A narrow strip cut from a filter circle (diameter = 7 cm).

3 + 3 + 2 ml and 3 + 3 + 2 + 2 ml of toluene gave diminishing recoveries in the stripping of the combined extracts with the cysteine paper, as shown in Table 1. This is presumably a consequence of the lower concentration of methylmercury as the extract volume is increased. The optimal recovery is obtained with 3 + 2 ml toluene. After washing with toluene, the cysteine paper is dried carefully, especially when small volumes of benzene are used in the final extraction step.

The final extraction step may influence the results, by incomplete extraction of MeHg from the paper into the organic phase. Depending on the amount of MeHg expected in the sample, the cysteine paper is transferred to a specially designed tube of appropriate volume (b or c in Fig. 1), where the MeHg is extracted into a defined volume of benzene. Partition of MeHg between the benzene and the acid solution depends mainly on the phase-volume ratio as shown in Fig. 2. It is evident that extraction of MeHgBr gives better recoveries than does extraction of MeHgCl. In practical terms, the cysteine paper has to be completely wetted by the acid solution. With the narrow strip of paper (0.2 × 21 cm), a minimum of 0.1 ml of acid solution is required to release MeHg from the paper. Extraction into 0.1 ml of benzene in a 1-ml test-tube gives lower and irreproducible results; although use of a specially designed microextractor⁶ results in very good recovery (>90%), it is time-consuming, and it is simpler to employ larger volumes of reagents. The philosophy is not to use as small a volume as possible, but to optimize the volume ratio of the reagents in order to reach the required sensitivity for the sample analysed. Thus 0.2 ml of benzene is the minimum volume for MeHg extraction. The operational limit of quantification when cysteine paper is used in an extraction

tube (3 g sample, 0.2 ml benzene extract, 5 µl injection) is about 0.1 ng/g.

The last step is to chromatograph alternate injections of sample and standard solutions. In general, the chromatograms are very clean and do not present any problems in evaluation of the results. Peak overlap can occur when MeHg from a large weight of sample is back-extracted with cysteine solution. All such interfering peaks disappear when the cysteine paper is used, as shown in the chromatograms in Fig. 3. Using silica gel or florasil to remove impurities, as suggested by some authors,¹³ gave irreproducible and lower results.

When peaks begin to tail, the performance of the column should be restored by injection of

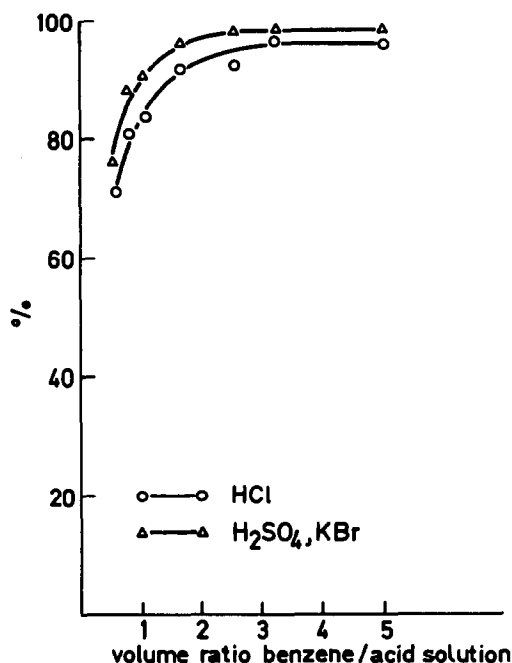


Fig. 2. Effect of the volume ratio (benzene/acid solution) on the recovery of MeHg from cysteine paper.

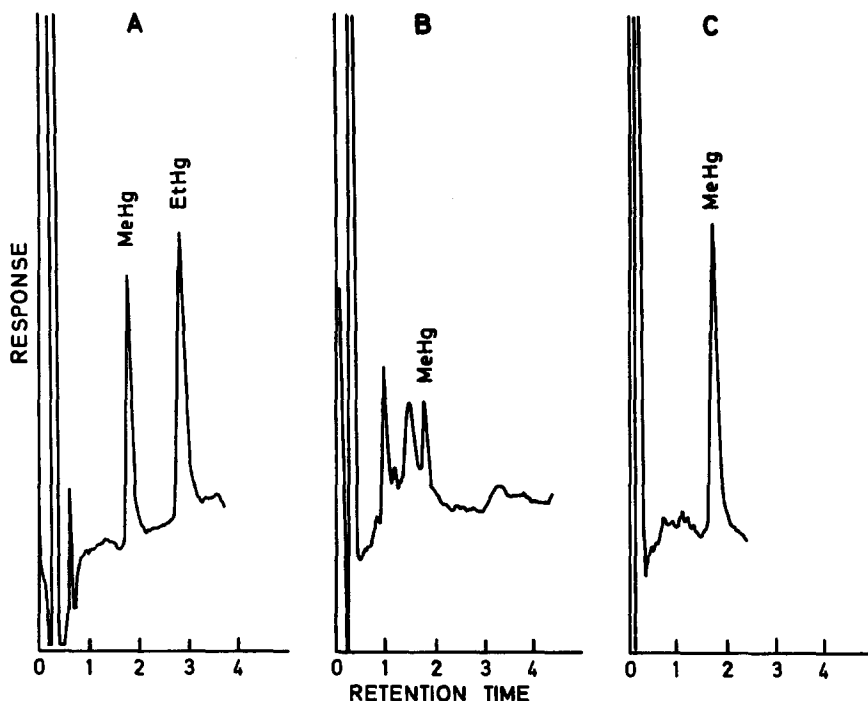


Fig. 3. Typical chromatograms for (A) 1 μ l injection of a standard solution of 0.05 μ g MeHg/ml and 0.05 μ g EtHg/ml in benzene, (B) 1 μ l from 0.5 ml of the final benzene extract from fresh algae sample with a concentration of 0.4 ng MeHg/g, with use of cysteine solution, (C) 1 μ l from 0.2 ml of the final benzene extract of the same sample as for (B), with use of cysteine paper.

5 μ l of a saturated solution of mercuric chloride in benzene.^{1,14} After 2 hr it is then possible to continue taking chromatograms.

Some results obtained for various kinds of sample and concentration levels by using different isolation and final measurement techniques are presented in Table 2. The results show that consistent values were obtained for these materials, indicating satisfactory recoveries.

In addition to this comparative approach, standard-addition experiments were also used to estimate the recoveries, though MeHg added to the sample is not entirely equivalent to that bound in the sample. Most materials gave high and consistent recoveries, but the sediment samples were problematic. The reproducibility for unspiked replicate determinations was satisfactory ($\pm 5\%$), but recoveries of MeHg added

Table 2. Comparison of the results for various matrices, obtained by different approaches to MeHg determination: results for MeHg are given as ng of Hg per g of sample

Sample	Extraction		Distillation ¹	Ion-exchange ¹
	Cyst. solution	Cyst. paper	GC/CV-AAS	CV-AAS
KFA, Fish Standard 1981	247 \pm 6 (6)	250 \pm 7 (3)	261 \pm 5 (3)	253 \pm 4 (4)
KFA, Fresh mussel 182-21	7.0 \pm 0.7 (3)	10.9 \pm 0.8 (2)	7.2 \pm 0.5 (4)	9.3 \pm 0.5 (2)
KFA, Fresh algae 182-11	0.25 \pm 0.08 (2)	0.27 \pm 0.05 (4)	0.18 \pm 0.00 (2)	0.21 \pm 0.01 (2)
183-11	1.30 \pm 0.16 (2)	1.21 \pm 0.20 (3)	0.70 \pm 0.07 (3)	0.90 \pm 0.05 (2)
185-11	0.22 \pm 0.07 (2)	0.32 \pm 0.02 (4)	0.26 \pm 0.04 (2)	0.28 \pm 0.02 (2)
NIES, No. 9 Sargasso	5.65 \pm 0.02 (2)	4.80 \pm 0.20 (3)	5.70 \pm 0.17 (2)	5.04 \pm 0.74 (2)
Kastela Bay sediment				
polluted area	42 \pm 1 (3)	33 \pm 4 (4)	39 \pm 11 (4)	
BCR, Hair sample	528 \pm 18 (3)	553 \pm 12	591 \pm 31 (3)	610 \pm 21 (3)

Number in parentheses is the number of determinations; quoted variation is one standard deviation.

to the sediment varied from 25 to 80%. Probably the MeHg added reacts in contact with sediment (decomposition or adsorption). When the spike is added to the acid extract of the sediment (*i.e.*, with no solid phase present) the reproducibility is much better. This is an example of a well known difficulty in speciation work with insoluble materials; the recovery is very often difficult or impossible to estimate. In such cases it is very difficult to establish an accurate value; comparison of the results obtained by different isolation techniques may be the best way to approach the problem of the accuracy of MeHg determination in sediments.

This should be done for all matrices analysed in a given laboratory. If agreement is reached between the results, these samples may serve as laboratory reference materials for a particular matrix. The results obtained for these samples should be a measure of the accuracy achieved in the series of analyses.

To summarize, the modified extraction technique using cysteine paper offers several advantages over the conventional approach. As well as being simpler manipulatively, and avoiding the problems of emulsion formation, it results in cleaner chromatograms. It represents a real improvement for determination of MeHg at low levels in environmental samples.

Acknowledgement—We are grateful for support through the German–Yugoslav Bilateral Scientific Cooperation Agreement, via the project “Reference materials and methods in environmental and biological research”, administered by the International Bureau, Kernforschungsanlage, Julich, and through the Research Community of Slovenia.

REFERENCES

1. M. Horvat, K. May, M. Stoeppler and A. R. Byrne, *Appl. Organometall. Chem.*, 1988, **2**, 850.
2. J. C. Gage, *Analyst*, 1961, **86**, 457.
3. G. Westöð, *Acta Chem. Scand.*, 1968, **22**, 2277.
4. J. A. Rodriguez-Vazquez, *Talanta*, 1978, **25**, 299.
5. K. Sumino, *Heavy Metals in the Aquatic Environment, A Supplement to Progress in Water Technology*, P. A. Krenkel (ed.), p. 35. Pergamon Press, Oxford, 1975.
6. V. Zelenko and L. Kosta, *Talanta*, 1973, **20**, 115.
7. I. Gvardjancic, L. Kosta and V. Zelenko, *Zh. Analit. Khim.*, 1978, **32**, 812.
8. M. Dermelj, M. Horvat, A. R. Byrne and P. Stegnar, *Chemosphere*, 1987, **16**, 877.
9. WHO/FAO/UNEP, *Consultation Meeting on Health Effects of Methyl Mercury in the Mediterranean Area*, Athens, September 1986, Document ICP/CEH 054(S), WHO Regional Office for Europe, Copenhagen.
10. C. J. Cappon and J. C. Smith, *Anal. Chem.*, 1980, **52**, 1529.
11. K. May, M. Stoeppler and K. Reisinger, *Toxicol. Environ. Chem.*, 1987, **13**, 153.
12. J. A. Ealy and W. D. Shuts, *Anal. Chim. Acta*, 1973, **64**, 235.
13. J. E. Longbottom, R. C. Dressman and J. J. Lichtenberg, *J. Assoc. Off. Anal. Chemists*, 1973, **56**, 1297.
14. J. E. Reilly, *J. Chromatog.*, 1982, **238**, 433.

ELECTROCHEMICAL BEHAVIOR OF MARCELLOMYCIN AT LIPID-MODIFIED CARBON-PASTE ELECTRODES

OLIVIER CHASTEL, JEAN-MICHEL KAUFFMANN and GASTON J. PATRIARCHE

Institut de Pharmacie, Université Libre de Bruxelles, Campus Plaine, CP 205/6, Boulevard du Triomphe,
1050 Bruxelles, Belgium

GARY D. CHRISTIAN

Department of Chemistry, BG-10, University of Washington, Seattle, WA 98185, U.S.A.

(Received 18 April 1989. Revised 29 June 1989. Accepted 10 July 1989)

Summary—A lipid-modified carbon-paste electrode is prepared by mixing phospholipids with the carbon-paste matrix. The resulting electrodes have polar head-groups which allow interactions with positively charged drugs and improved preconcentration/extraction steps. The accumulation of the antitumor drug, marcellomycin, is enhanced in the presence of lipids, giving an 8-fold enhancement of current. The electrode response has been optimized with respect to paste composition, nature of the lipid, pH, temperature, and stirring time. A mechanism for marcellomycin accumulation is proposed, based on electrochemical and UV-visible spectrometric measurements as a function of pH. The electrode response is linearly related to the marcellomycin concentration within the range 1×10^{-8} – 6×10^{-6} M. Known amounts of marcellomycin added to a urine sample diluted sixfold with water have been measured by use of the medium-exchange technique.

In earlier work we reported on a new phospholipid-modified glassy-carbon electrode for the measurement of the glycoside marcellomycin¹ and other compounds which are known to interact with phospholipids.² We have recently investigated the use of a carbon-paste electrode modified with fatty acids, in a study of the electrochemical oxidation of the phenothiazine compound promethazine.³ Carbon paste, owing to its mechanical and electrochemical properties, is ideally suited as the matrix material. By mixing the lipid with the organic liquid (Nujol) used to make the carbon paste, an electrode can be prepared which retains the properties of the carbon paste and has at its surface the functional groups of the lipids. In this paper we report investigation of the electrochemical behaviour of phospholipid-modified carbon-paste electrodes (LMCPE) by studying the preconcentration and oxidation of marcellomycin as a model compound (Fig. 1).

Marcellomycin, which belongs to the anthracycline family, has been characterized both pharmacologically^{4,5} and electrochemically.⁶ The anthracycline molecules are known to interact strongly with phospholipids constituting living cell membranes, and particularly with cardiolipin (diphosphatidylglycerol).^{7,8} The electrochemical oxidation occurs at the hydro-

quinone part of the molecule by a 2-electron 2-proton transfer.⁶ In our previous work on lipid-modified glassy-carbon electrodes,^{1,2} we reported the tendency of the molecule to accumulate in the lipid layer, which resulted in a fourfold increase in the oxidation signal. The present electrode has improved long-term stability and enhanced sensitivity for marcellomycin.

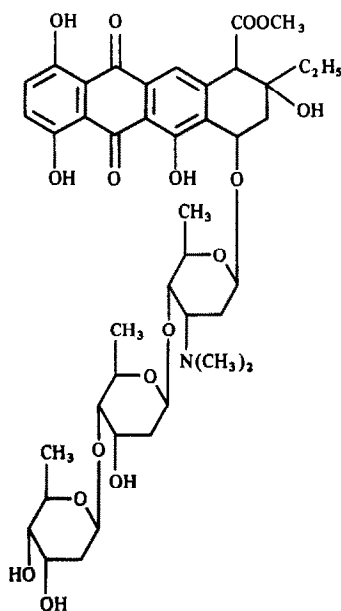


Fig. 1. Structure of marcellomycin.

EXPERIMENTAL

Apparatus

Voltammetric measurements were made with a BAS CV 27 instrument connected to a Hewlett Packard 7090 A recorder. A three-electrode cell containing the carbon-paste working electrode, a platinum wire as counter-electrode and a saturated calomel electrode (SCE) as reference was used throughout the study. The temperature of the cell was controlled with a thermostatic bath (Haake F, $\pm 0.1^\circ$).

The Metrohm EA 267 carbon-paste electrode (geometric area 0.50 cm^2) was made with a paste (CP-Met) made of graphite and liquid paraffin (Metrohm EA 207c). Three other pastes (from Bioanalytical Systems, West Lafayette, IN) were utilized for comparison: CP-W (graphite + ceresin wax), CP-O (graphite + paraffin oil) and CP-S (graphite + silicone grease). The ratio of graphite to binder was not listed by the manufacturers. Comparative experiments between the different electrodes were made by using home-made electrodes with a geometric surface area of 0.07 cm^2 .

The pH of the solutions was measured with a Tacussel 80 pH-meter. UV-visible spectra were recorded with a Shimadzu-UV 160 spectrophotometer.

Reagents

All reagents were of analytical grade. Marcellomycin was furnished by Bristol Meyers (Brussels), and was used without further purification. The triply distilled water used to prepare solutions was stored in polyethylene bottles. Buffer solutions ($0.1M$) were prepared from sodium hydrogen phosphate (Merck p.a.) and the pH was adjusted with dilute hydrochloric acid or sodium hydroxide solution. The lipids used were from Sigma: L- α -phosphatidylcholine (PC); asolectin (ASO) extracted from soybean, and containing 18% of PC, based on choline determination, along with other lipids to mimic a membrane; cardiolipin (CL); phosphatidyl-ethanolamine (PEA).

Electrode preparation and procedure

The modified carbon-paste electrode was prepared by thoroughly mixing the Metrohm carbon paste with the lipid in the appropriate ratio in a mortar in the presence of a minimum amount of chloroform, and allowing the solvent to evaporate overnight. Marcellomycin determi-

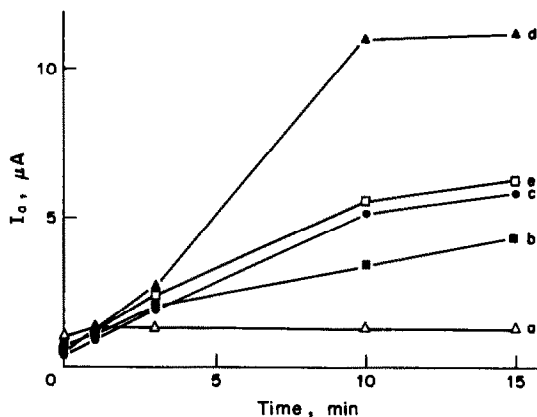


Fig. 2. Electrode response I_a (μA) as a function of accumulation time for different paste compositions (home-made electrodes). a, CP-Met; b, CP-Met + 1% ASO; c, CP-Met + 3% ASO; d, CP-Met + 5% ASO; e, CP-Met + 10% ASO. Phosphate buffer pH 7.0; 37° ; marcellomycin $5 \times 10^{-5} M$.

nation consists of accumulating the molecule at the electrode surface by stirring the analyte at ~ 200 rpm with a magnetic stirring bar, with no potential applied (open circuit), then recording the voltamperogram from 0.0 to +1.0 V vs. SCE at a scan-rate of 10 mV/sec.

In medium-exchange experiments, the analyte is accumulated at the electrode from the sample solution (*e.g.*, urine), then the electrode is removed, rinsed with water, and transferred to the electrolyte solution used for the electrochemical oxidation step.

RESULTS AND DISCUSSION

The oxidation of marcellomycin ($5 \times 10^{-5} M$) was investigated at both the CPE and the LMCPE at pH 7.0 and $37.0 \pm 0.1^\circ$. In Table 1 are reported the characteristics of the oxidation

Table 1. Electrochemical characteristics of marcellomycin oxidation peaks (marcellomycin $5 \times 10^{-5} M$, pH 7.0, accumulation times 0 and 10 min, 37°)

Electrode	Peak current, μA		Peak potential, V		Peak shape, mV
	$I_{p(0)}$	$I_{p(10)}$	$E_{p(0)}$	$E_{p(10)}$	$E_p - E_{p/2}$
CP-Met	1.0	1.3	0.45	0.45	40
CP-W	1.3	2.3	0.45	0.45	60
CP-O	1.4	2.5	0.41	0.41	40
CP-S	1.2	1.9	0.40	0.40	30
CP-PEA*	0.9	6.8	0.50	0.47	70
CP-PC*	1.4	7.2	0.42	0.42	50
CP-ASO*	0.6	10.8	0.53	0.45	60
CP-CL*	2.0	18.9	0.52	0.51	90

*Prepared with CP-Met paste and 5% of phospholipid.

peaks, E_p , recorded without accumulation ($I_{p(0)}$) and after 10 min of accumulation ($I_{p(10)}$). With the non-modified electrodes, the results clearly indicate different behaviour, depending on the carbon paste utilized. The intensity of the response as well as the efficiency of preconcentration are higher with CP-W, CP-O and CP-S than CP-Met. In terms of peak shape ($E_p - E_{p/2}$) and ease of oxidation (E_p), the CP-S electrode exhibits the least positive peak potential and the highest reaction rate. Differences between carbon pastes in the oxidation of organic compounds have also been reported by others.^{10,11} They can be related to differences in the amount and nature of the graphite as well as in the nature of the organic binder. Since it gave comparatively lower background currents within the positive potential range, the CP-Met paste was selected for preparation of the lipid-modified electrodes. As reported in Table 1, the responses observed are significantly different, depending on the nature of the lipid. In direct recording (zero accumulation time), the oxidation peak of marcellomycin is shifted toward positive potentials when the lipid-modified electrodes are used (except with the CP-PC electrode) owing to a less rapid electrode process, as shown by higher values of $E_p - E_{p/2}$. The intensity of the response is decreased with the CP-Met-ASO electrode but is of comparable magnitude with the CP-Met-PEA electrode and is increased with the CP-Met-CL and CP-Met-PC electrodes. From these results, we may suggest that a rapid accumulation process occurs at the last two electrodes and that the shift in potential may be a consequence of the interaction between the lipid and marcellomycin.

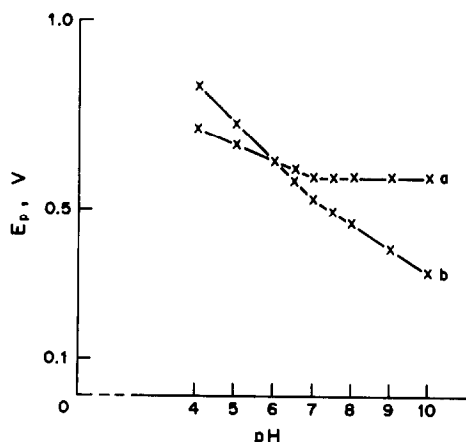


Fig. 3. Peak potential evolution as a function of pH. Marcellomycin $5 \times 10^{-5} M$; a, CP-Met; b, CP-Met + 5% ASO; $t_{acc} = 10$ min; $37^\circ C$.

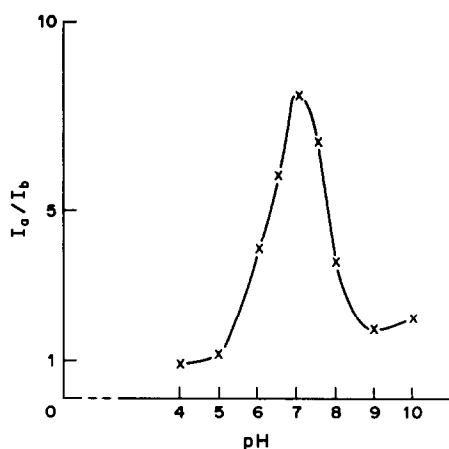


Fig. 4. Relative electrode response as a function of pH. Marcellomycin $5 \times 10^{-5} M$; $t_{acc} = 10$ min; $37^\circ C$; CP-Met + 5% ASO. I_a , peak current at LMCPE, with accumulation; I_b , peak current at CP-Met, with no accumulation.

This association occurs at the protonated amino group of the drug and the ionized phosphate site of the phospholipids,⁸ giving a less favorable orientation of the electroactive hydroquinone moiety.

Accumulation of the analyte occurs to a greater extent when the solution is stirred, possibly by penetration of the drug into the paste.¹¹ This results in a continuous increase in peak current intensity with accumulation time and a more facile oxidation of the molecule after accumulation (10 min). The magnitude of accumulation increases according to the lipid used, in the order PEA < PC < ASO < CL, in accordance with results previously reported for the lipid-modified glassy-carbon electrode.^{1,2} Studies with the mixed lipid carbon-paste electrode (CP-Met-ASO) were made, to give a closer approach to modeling a biomembrane.

Effect of quantity of lipid

Accumulation of marcellomycin ($5 \times 10^{-5} M$) from aqueous solution at pH 7.0 and $37^\circ C$ was performed by stirring for times ranging from 1 to 15 min and with 1–10% of asolectin in the paste (Fig. 2). At the CPE the response remains small, even with stirring for up to 15 min. In the presence of lipid, the oxidation current is clearly improved, with a maximum response for a paste containing 5% asolectin. Higher lipid contents give no further increase in accumulation but rather a decreasing response (Fig. 2, curve e). This can be related to destruction of the mechanical integrity of the paste because of a swelling phenomenon.¹² For all the paste compositions tested, a similar trend in response is observed,

with a progressive increase with up to 10 min stirring, and a levelling off of the curve (but continuous increase) for longer stirring periods. With optimum accumulation conditions (10 min and 5% of each lipid), the current is increased by as much as eightfold over that in the absence of lipid.

The effect of medium-exchange on the extent of preconcentration was studied. Under optimum conditions, 56% of the amount of analyte accumulated was lost when the electrode was transferred from the test solution into the blank electrolyte (pH 7.0) used for the voltammetry.

Effect of solution pH

Measurements were performed on $5 \times 10^{-5} M$ marcellomycin solutions in the pH range 4–10 at 37°. At the CPE the intensity of the oxidation current was independent of the pH and the accumulation of marcellomycin was small over the entire pH range studied. The peak potential as a function of pH was examined for the LMCPE and CPE, with accumulation for 10 min. At the CPE (Fig. 3, curve a), the peak potential decreases linearly with increasing pH up to 7.0 (slope 40 mV/pH), then remained unchanged with further pH increase, indicating an electrode process which is not regulated by proton transfer. At the LMCPE two linear portions intersecting at pH 7.0 were observed, with a slope of 200 mV/pH for the first part and 70 mV/pH for the second (Fig. 3, curve b); these unusually high slopes suggest a complex electrode process with a possible effect at the polar phosphate groups of the lipids. The pH of the solution also has a marked effect on the preconcentration step, as shown by the ratio of response at the LMCPE to the response at the CPE, with stirring for 10 min (Fig. 4). The response ratio reaches a sharp maximum at pH 7.0, and at pH values lower than 5 or higher than 9 essentially no accumulation occurs.

Spectrophotometric measurements of $1 \times 10^{-5} M$ solutions of marcellomycin at various pH values between 6.0 and 9.0 were made in order to obtain information about the electronic structure of the anthraquinone portion of the molecule.¹³ Below pH 7.0, the spectrum exhibits one absorption peak at 490 nm, and at pH 7.0 a small new peak appears at 590 nm. The latter peak increases with increasing pH, while the main peak at 490 nm progressively decreases. The formation of the new peak at 590 nm can be ascribed to the appearance of the ionized form of the phenolic portion of the molecule, in accordance with the literature.¹⁴

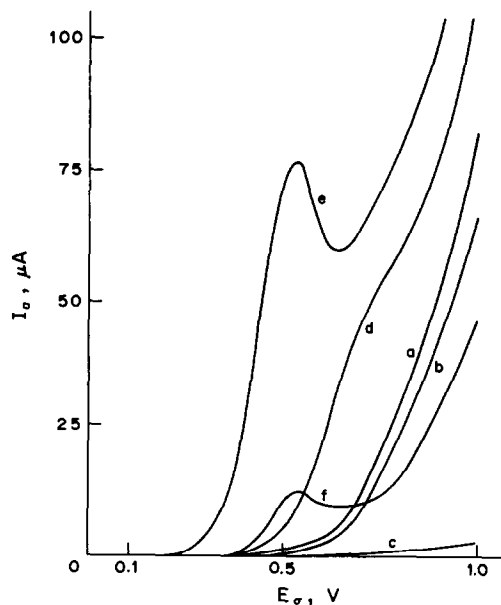


Fig. 5. Voltammetric oxidation curves of $5 \times 10^{-5} M$ marcellomycin in sixfold diluted urine at the CP-Met + 5% ASO electrode: a, urine; b, urine + $t_{acc} = 10$ min; c, urine + $t_{acc} = 10$ min + medium-exchange; d, urine + marcellomycin; e, urine + marcellomycin + $t_{acc} = 10$ min; f, urine + marcellomycin + $t_{acc} = 10$ min + medium-exchange.

Taking into account the electrochemical results as a function of pH, the spectroscopic data, and the fact that the electrode surface bears a negative charge over the whole pH range investigated (pK_a of the phosphate group is between 1 and 2), we may suggest the following electrode processes. At the CPE, the first segment of the pH response curve (Fig. 3, curve a) corresponds to the oxidation of the analyte molecule in the non-ionized form and the proton transfer controls the electrode process, while for the ionized form of the molecule at pH above 7, E_p is independent of pH. At the LMCPE at pH < 7, the amount of lipid ionized is low and interaction with the positively charged marcellomycin is therefore also low (Fig. 4). With increase in pH, the interaction is higher but at pH above 7.0 decrease in response is observed, which may be related to electrostatic repulsion between the negatively charged lipids and the ionized phenol groups of the analyte molecule.

Effect of temperature, and analytical performance

Accumulation of marcellomycin from a $5 \times 10^{-5} M$ aqueous solution at pH 7 was performed at 20 and 37° (accumulation time

10 min, 5% lipid). At 37°, the current is as much as 40% greater than that at 20°. The reproducibility of the response was determined (7 trials). The average voltammetric peak height was 3.19 μA with a coefficient of variation of 2.1%. A linear response was obtained for concentrations from $5 \times 10^{-6} M$ down to the detection limit of $1 \times 10^{-8} M$ ($S/N = 3$), with a correlation coefficient of 0.9997.

Measurement of marcellomycin in urine

At the CPE the direct measurement of marcellomycin in urine diluted sixfold with water is disturbed by the oxidation of uric acid which occurs at the same potential. However, if the medium-exchange technique is applied at pH 7.0, the resulting electrode response is too slight to be of analytical significance.

In contrast, quantitative measurement of relatively high concentrations of marcellomycin is possible with the LMCPE (Fig. 5). The oxidation of uric acid (urate) is shifted to more positive potentials (curves a and b), while the oxidation of marcellomycin is still observed (curves d and e). With the medium-exchange technique (curve f) the peak corresponding to marcellomycin is depressed, but well separated from the potential limit, thus giving improved response. The peak current varies linearly with concentration between 5×10^{-6} and $1 \times 10^{-4} M$ in the sixfold diluted urine, with a correlation coefficient of 0.9993. The coefficient of variation calculated for six measurements at a marcellomycin concentration of $5 \times 10^{-5} M$, with medium-exchange, is similar to that without medium-exchange, namely 4.0%.

CONCLUSION

Modification of the carbon-paste electrode with lipids offers a new type of electrode exhibiting long term stability and possessing the functional polar head-groups of the constituent lipids. With respect to interaction with marcel-

lomycin, the sharp maximum response observed at pH 7.0 is of particular biological significance, since strong anthracyclin-phospholipid complexes have been shown to be responsible for the anthracyclin cardiotoxicity.⁸

The proposed electrode gives valuable qualitative and quantitative information with respect to drug analysis and drug-membrane interactions. The ease and rapidity of electrode preparation and renewal constitute definite advantages over more sophisticated techniques used to study the drug-phospholipid interaction.

Acknowledgements—Bristol Meyers (Brussels) graciously provided the marcellomycin. Thanks are expressed to le Fonds National de la Recherche Scientifique (FNRS Belgium) for help to G.J.P. and to the SPPS (Belgium Politic Research, A.R.C.) Contract No. 86/91-89.

REFERENCES

1. O. Chastel, J.-M. Kauffmann, G. J. Patriarche and G. D. Christian, *Anal. Chem.*, 1989, **61**, 170.
2. O. Chastel, V. Lopez, J.-M. Kauffmann and G. J. Patriarche, *Analisis*, 1990, in the press.
3. M. Khodari, J.-M. Kauffmann, G. J. Patriarche and M. A. Chandour, *Electroanalysis*, 1990, in the press.
4. R. B. Weiss, G. Sarosy, K. Clagett-Carr, M. Russo and B. Leyland-Jones, *Cancer Chemoth. Pharmacol.*, 1986, **18**, 185.
5. S. K. Carter, *ibid.*, 1980, **4**, 5.
6. F. Mebsout, J.-M. Kauffmann and G. J. Patriarche, *Analisis*, 1987, **15**, 243.
7. E. Goormaghtigh, P. Chatelain, J. Caspers and J.-M. Ruyschaert, *Biochim. Biophys. Acta*, 1980, **597**, 1.
8. E. Goormaghtigh and J.-M. Ruyschaert, *Colloids and Surface*, 1984, **10**, 239.
9. J. Wang, B. Deshmukh and M. Bonakdar, *J. Electroanal. Chem.*, 1985, **194**, 339.
10. F. N. Albahadily and H. A. Mottola, *Anal. Chem.*, 1987, **59**, 958.
11. J. Wang and B. A. Freiha, *ibid.*, 1984, **56**, 849.
12. L. L. M. van Deenen (ed.) *Progress in the Chemistry of Fats and Other Lipids*, Vol. 8, Part 1, Pergamon Press, Oxford, 1965.
13. E. Goormaghtigh, *Ph.D. Thesis*. Université Libre de Bruxelles, Belgium, 1983.
14. M. S. El Ezaby, T. M. Salem, A. H. Zewail and R. J. Issa, *J. Chem. Soc. (B)*, 1970, **7**, 1293.

AN INVESTIGATION INTO THE DETERMINATION OF STABILITY CONSTANTS OF METAL COMPLEXES BY CONVOLUTION–DECONVOLUTION CYCLIC VOLTAMMETRY

GARETH M. BARNARD, TERRY BODDINGTON, JAN E. GREGOR, LESLIE D. PETTIT*
and NORMAN TAYLOR

School of Chemistry, The University, Leeds, LS2 9JT, England

(Received 28 February 1989. Revised 10 May 1989. Accepted 7 June 1989)

Summary—A technique is described for calculating stability constants of metal–ligand complexes from convolution–deconvolution voltammetry. Semi-integration of the cyclic voltammetric currents with respect to time allows calculation of $E_{1/2}$ values in a manner comparable to the use in polarography of the Heyrovský–Ilkovič equation. The technique described also allows determination of the ratio of the diffusion coefficients of the free and complexed metal ions and provides a second check of the stoichiometry. A reliable route to the metal–complex stability constants by the equations of Lingane and DeFord and Hume is therefore obtained. Advantages of this technique compared with the use of polarography, differential pulse polarography and pH titrations are discussed, with the complexes formed by cadmium with glycine, alanine, valine and aspartic acid as examples.

Stability constants for labile systems may be calculated from polarographic experiments provided that the half-wave potential ($E_{1/2}$) of the metal ion can be measured as a function of the free ligand concentration. Consider the simple reduction of a metal ion, A:



If, in the absence of completion, the rate of electron exchange in reaction (1) is fast relative to the voltage scan-rate (*i.e.*, there is electrochemical reversibility) then the polarographic currents, i , at fixed sampling time adhere to the Heyrovský–Ilkovič equation:¹

$$E = E_{1/2} + \frac{RT}{nF} \ln \left(\frac{i_d - i}{i} \right)$$

where i_d = the limiting diffusion current, and E , $E_{1/2}$, R , T and F have their usual significance. From this test for electrochemical reversibility, $E_{1/2}$ is readily found since $E = E_{1/2}$ at $i_d/2$. It also lies at the steepest point of a plot of i vs. E . When the metal is co-ordinated to a ligand to form a system of labile complexes, the basic shape of the polarographic wave is undisturbed but $E_{1/2}$ is shifted, usually to a more negative value. The wave is, however, reduced in size by an amount dependent on the relative diffusion

coefficients of the free metal ions and the complexed species. There is a quantitative relationship between the shift in $E_{1/2}$ and the stability constants of the complexes formed. For a single complex ML_j this relationship is:

$$\Delta E_{1/2} = \frac{2.303RT}{nF} (\log \beta_j + j \log [L]) \quad (2)$$

where β_j is the overall stability constant, $[ML_j]/[M][L]^j$, charges being omitted for simplicity. Hence, a plot of $\Delta E_{1/2}$ as a function of $\log [L]$ yields a straight line from which j and β_j can be calculated as described originally by Lingane.² When several labile complexes are formed in a stepwise manner, a rather similar treatment yields the various stability constants (see later).³

Major problems inherent in the use of polarographic techniques are the difficulty in measuring the polarographic currents, so that the correct value for $E_{1/2}$ may be calculated, and the fact that relatively few metal ions can be reduced with sufficiently fast rates of electron transfer for the Heyrovský–Ilkovič equation to be valid. The second problem can be relieved to a large extent by using cyclic voltammetry, since the necessary $E_{1/2}$ values can still be obtained reliably when electron transfer rates are insufficient to conform to the requirements of the Heyrovský–Ilkovič equation. The first problem

*Author for correspondence.

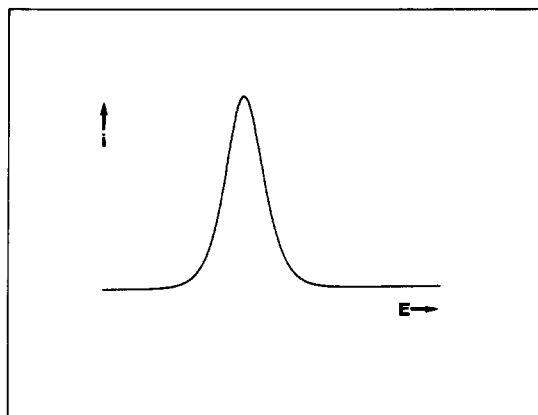


Fig. 1. Typical differential-pulse polarogram.

can be partly overcome by pulse techniques, *e.g.*, in differential-pulse polarography which gives a peak similar to that shown in Fig. 1. In the simplest case, with fast electron transfer, the peak of the differential-pulse plot at the limiting small pulse amplitude is symmetrical (Fig. 1) with the maximum corresponding to $E_{1/2}$. However, in practice, this peak can be unsymmetrical and the true value for $E_{1/2}$ then corresponds more closely to that value for E which divides the peak into two equal areas.

A further disadvantage of all polarographic experiments is that the net process represented by equation (1) occurs only during reduction, and with the dropping mercury electrode only a single measurement of the current response is made for each mercury drop. This does not allow study of the mechanistic scheme in any detail. For example, electrochemical reversibility of the process is not fully tested, particularly in differential-pulse experiments, where a suitable test would necessitate investigating the whole of the peak.

In cyclic voltammetry with a hanging mercury drop, the mercury and reference electrodes are subjected to a potential difference which cycles from a starting value at which the current flow is initially zero, up to a preset maximum and back again. The current flowing between the drop and a counter-electrode is recorded as a function of the potential difference between the drop and a reference electrode. Hence both the anodic and cathodic waves are recorded. In the absence of voltage-drop effects due to the resistance of the cell (see below), the two peaks should, in the case of fast electron transfer, be separated by $2.218 RT/nF$ mV (*e.g.*, $56.5/n$ mV at 298 K)⁴ when the switching potential is well beyond the value of E_p (the potential

difference corresponding to the peak current). The potential at the mid-point between the forward and reverse current peaks corresponds closely to $E_{1/2}$, as shown in Fig. 2(a). When the electrode process is not completely electrochemically reversible, the peak separation will begin to increase and the value for $E_{1/2}$ will only approximate to the average of the peak potentials.⁵ These relationships for the peak potentials can be used as a test for electrochemical reversibility but, at the limit, they suffer from the disadvantage of involving only the two datum points of E_p for the forward and backward regions of the sweep. In addition, as the scan rate is increased the peak potentials will shift as electrochemical irreversibility becomes evident, which can give errors of 10 mV or more in $E_{1/2}$.⁶

A better method for calculating $E_{1/2}$ by use of voltammetry is to use a transformation of the current rather than the actual current values. In many cases a suitable transformation is a convolution of the current with an inverse square-root function of time, the semi-integral $I_1(t)$, defined by the expression:

$$I_1(t) = \int_0^t \frac{i(u)}{\sqrt{\pi(t-u)}} du \quad (3)$$

where $i(u)$ is the current at time u and t is the total elapsed time.^{7,8} In the case of electron-transfer processes, including fast complexation, the Heyrovský-Ilkovič equation may now be used as for polarographic data, but with convolutions of the current replacing the polarographic current, with the notable advantage that all experimental data (from the forward and backward sweeps) are utilized. In the case of fast electron transfer, the convolution I_1 as a function of E for the reverse wave is an exact overlay of that of the forward sweep [see Fig. 2(b)] and hence provides a good test of the electron-transfer kinetics. Moreover, the overlay is independent of the shape of the voltage sweep and the sweep rate and thus provides, for a series of experiments, a route to $E_{1/2}$ similar to that using polarographic data. The derivative dI_1/dE in the case of fast electron transfer thus consists of two mirror-image peaks with maximum amplitude at $E_{1/2}$ and a half-width of $(2RT/nF) \ln[(\sqrt{2}+1)/(\sqrt{2}-1)]$ mV, *i.e.*, $3.526 RT/nF$, which is $90.53/n$ mV at 298 K, see Fig. 2(c). The peak response is similar to that of differential-pulse polarography at the limit of small pulses, and of a.c. polarography and voltammetry. In the case of slower electron transfer, the mean

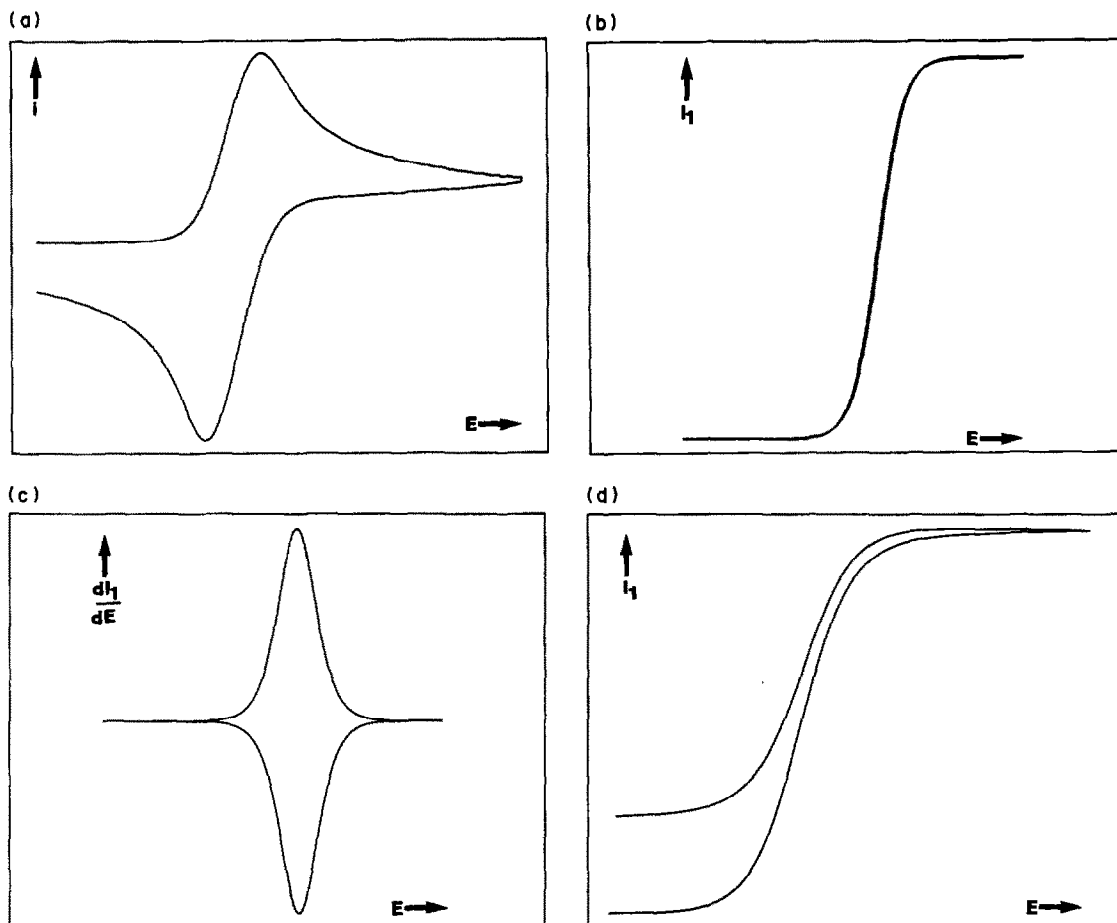


Fig. 2. (a) A typical cyclic voltammogram, (b) the I_1 convolution of (a) for the case of fast electron transfer; (c) the derivative dI_1/dE of (b) for fast electron transfer; (d) the I_1 convolution of (a) for the case of further chemical reaction of the products.

value of these peak potentials corresponds approximately to $E_{1/2}$. Numerical techniques for calculating stability constants from I_1 convolutions are outlined in the theory section below.

There are other advantages in this convolution-deconvolution approach compared with the use of differential-pulse polarography, in addition to the use of the entire sets of potential/current/time data in the assessment of the electrochemical reversibility and $E_{1/2}$ of the electrode process. Cyclic voltammograms can be collected quickly with use of a single drop, so the response is similar to that of a planar electrode, and all the data can be treated in a matter of seconds by a computer-based data-acquisition system.⁹⁻¹¹ Clearly, the calculations involved would be impractical without suitable dedicated computing facilities. Additionally, if high-resistance electrolytes are encountered, the addition of a species known to exhibit fast electron transfer will allow "software compensation" of the potential axes through the

function I_1 or dI_1/dE . In these cases I_1 for example, gives an exact overlay only if the potential axis is appropriately corrected. This "adjusted" potential axis is then usable for other studies in the same electrolyte system and allows $E_{1/2}$ values to be more accurately assessed.

In this work, the semi-integral function I_1 equation (3), has been applied to the measurement of the stepwise stability constants of the complexes of Cd^{2+} with a number of amino-acids (HL). Under normal circumstances the species CdL , CdL_2 and CdL_3 (charges omitted for simplicity) are to be expected, with the possibility of complexes such as $[\text{CdL}_4]$ (*i.e.*, with one or more ligands co-ordinating in unidentate mode) at very high ligand concentrations.

From pH titrations, stability constants of complexes such as CdL_3 are difficult to evaluate accurately. A degree of formation of more than 20% is necessary for reliable measurements and,

to reach this level, high pH values (pH well above $\log K_{HL}$) and high $[L]:[Cd^{2+}]$ ratios are necessary. At high pH, measurements are dependent on the value chosen for K_w , on electrode sensitivity, and on possible contamination with carbon dioxide. The requirements of high pH and high $[L]:[Cd^{2+}]$ are both contrary to requirements for high precision in the measurement of stability constants. Thus β_3 cannot be determined with high accuracy.

By use of voltammetry, $[L]:[Cd^{2+}]$ ratios of 100:1 or more can be employed (provided that constant ionic strengths are maintained) and measurements at high pH ($>1 + \log k_{HL}$) are comparatively insensitive to small errors in measurement of pH. We therefore report the results of measurements performed by pH titrations, cyclic voltammetry and differential-pulse polarography for determination of the stability constants of Cd^{2+} complexes with glycine, alanine, valine and aspartic acid.

EXPERIMENTAL

pH studies

Stability constants for H^+ and Cd^{2+} complexes were calculated from titrations at 25° with a Metrohm automatic burette. Changes in pH were followed by using a glass electrode calibrated with perchloric acid to give H^+ concentrations. All solutions were of ionic strength $0.10M$ (KNO_3) and the amino-acid concentrations were 0.003 – $0.01M$. Calculations were made with the aid of the computer program SUPERQUAD.¹² In all cases, duplicate or triplicate titrations were performed, at L:Cd ratios of up to 5:1. The standard deviations quoted were computed by SUPERQUAD and refer to random errors only. Hence they overestimate the real precision of the results (see discussion section, below).

Cyclic voltammetry

This utilized an E G & G static mercury drop electrode, model 303A, coupled to an E G & G Model 362CV-1 Cyclic Voltammetry system incorporating the CONDECON 300 software. Data were collected, stored and manipulated with the E G & G CONDECON 300 software. Two computer systems were used, a Galaxy Gemini and an Amstrad 1640, both with mathematics co-processors. Operating conditions of the potentiostat were: scan rate, 0.2 V/sec; initial potential, -0.4 V; final potential,

-1.0 V; current range $100 \mu A$ FSD. The reference electrode was double jacketed with $1M$ potassium nitrate to protect the inner Vycor frit from damage by alkaline solutions.

The pH of solutions containing Cd^{2+} (0.0005 – $0.001M$ in $0.1M$ potassium nitrate) and ligand (up to $0.4M$) was adjusted to a precise value (around 10.3) by the addition of sodium hydroxide. Solutions were deoxygenated for 16 min before data were recorded.

Differential-pulse polarography

An E G & G 303A stand, with a dropping mercury electrode, was coupled with an E G & G model 364 polarographic analyser. Operating conditions on the potentiostat were: scan rate, 2 mV/sec; initial potential, -0.4 V; final potential, -1.0 V; current range, $100 \mu A$ FSD. Data were recorded on a chart recorder and the solutions were of composition similar to those used in the cyclic voltammetry.

THEORY

Numerical basis of calculation from cyclic voltammetry

During the recording of the voltamperograms electron-transfer processes cause the concentrations of electroactive species at the electrodes to differ from those originally present in the bulk solutions. The concentration profiles thus change with time, and distance, x , from the electrode. For simple electron-transfer processes, the reactant concentrations [for reaction (1)] at planar electrodes (C_A^* and C_B^*) are related to the bulk concentrations (C_A^b , C_B^b ; note that if there is only one initial reactant, $C_B^b = 0$) by the following expressions where D_A and D_B are the diffusion coefficients of A and B:

$$D_A \frac{\partial C_A^*}{\partial x} + D_B \frac{\partial C_B^*}{\partial x} = 0$$

(conservation of mass) (4)

$$D_A \frac{\partial C_A^*}{\partial x} = \frac{-i}{nFa}$$

(conservation of charge) (5)

(where a is the surface area of the electrode)

$$\frac{\partial C_A}{\partial t} = D_A \frac{\partial^2 C_A}{\partial x^2} \text{ etc.}$$

(Fick's second law)⁷ (6)

From Laplace transformations of relationships (4)–(6) and of the boundary conditions remote from the electrode, it follows that:

$$C_A^b - C_A^* = I_1/nFa \sqrt{D_A}$$

and

$$C_B^* = I_1 nFa \sqrt{D_B}$$

where I_1 is defined by equation (3).

Hence, if D_A and D_B are known, C_A^* and C_B^* can be calculated from I_1 or *vice versa*, quite irrespective of the rate of electron transfer, form of voltage sweep and the voltage sweep rate.

The limiting value, I_L , “well past” the wave, is related to the various parameters of the system by equation (7), again provided that the sweep rate is high enough for the electrode system to approximate to planarity.^{8,13,14}

$$I_L = naFC_A^b \sqrt{D_A} \quad (7)$$

It should be noted that when B decomposes chemically, the I_1 convolution depends on E and on the time-scale of the experiment. However, I_L is still related to C_A^b by equation (7) and provides a route between the diffusion coefficient, D_A , and the concentration of A.

In the case of fast electron transfer, application of the Nernst equation to the species A and B gives the relationship:

$$(E - E_0) = (RT/nF) \times \ln[(I_L - I_1)/I_1 \sqrt{D_A/D_B}] \quad (8)$$

and since $E_{1/2} = E^0 + (RT/nF) \ln \sqrt{D_A/D_B}$, we have an alternative expression in terms of $E_{1/2}$, equivalent to the Heyrovský–Ilkovič equation as applied to the original polarographic experiment.

$$E = E_{1/2} + \frac{RT}{nF} \ln[(I_L - I_1)/I_1] \quad (9)$$

Hence I_1 is a function of potential only and is equal to $0.5 I_L$ at $E_{1/2}$, so $E_{1/2}$ can be calculated.

The arguments above show how $E_{1/2}$ can be measured precisely, under a variety of conditions, from cyclic voltammetry data. Since the form of the cyclic voltamperogram is not influenced by the presence of labile complexes, the values for $E_{1/2}$ can now be used in the calculation of stability constants of chemically labile complexes.

For the equilibrium between a metal ion and ligand:



$$\beta_j = [ML_j]/[M][L]^j$$

$$\beta_j [L]^j = [ML_j]/[M] = (I_L - I_1)/I_1.$$

Hence

$$\begin{aligned} \Delta E_{1/2} &= E_{1/2}(\text{complex}) - E_{1/2}(\text{metal}) \\ &= (RT/nF) \ln(\beta_j [L]^j) \\ &\quad + (RT/nF) \ln \sqrt{(D_{\text{complex}}/D_{\text{metal}})} \end{aligned}$$

where D_{complex} is an effective diffusion coefficient of the metal ion in the presence of ligand (it is a function of ligand concentration).

For the stepwise formation of a series of complexes ($j = 0 \dots N$)

$$\begin{aligned} \Delta E_{1/2} &= (RT/nF) \ln \left(\sum_0^N \beta_j [L]^j \right) \\ &\quad + (RT/nF) \ln \sqrt{(D_{\text{complex}}/D_{\text{metal}})} \quad (10) \end{aligned}$$

Rearrangement gives

$$\begin{aligned} (nF \Delta E_{1/2} / RT) \ln \sqrt{(D_{\text{complex}}/D_{\text{metal}})} \\ = \ln \left(\sum_0^N \beta_j [L]^j \right) \end{aligned}$$

which gives

$$\epsilon/\rho = 1 + \beta_1 [L] + \beta_2 [L]^2 + \dots \quad (11)$$

where $\epsilon = \exp(nF \Delta E_{1/2} / RT)$ and ρ is the experimental quantity defined by

$$\rho = \sqrt{(D_{\text{complex}}/D_{\text{metal}})} = I_L(\text{complex})/I_L(\text{metal}).$$

Here $I_L(\text{complex})$ is the observed limiting convoluted current (in the presence of the ligand) and $I_L(\text{metal})$ is the value of I_L that would be observed for the same total metal concentration in the absence of ligand.

Thus a plot of $\ln[L]$ against $\ln(\epsilon/\rho - 1)$ will give a segmented curve composed of overlapping straight lines with slopes of j and intercepts (on extrapolation) corresponding to $\ln \beta_j$. Alternatively equation (11) can be treated mathematically to allow a computer-based calculation of all the β values. A non-linear least-squares analysis, which compares values for ϵ/ρ calculated from experimental data ($\Delta E_{1/2}$ and I_L) with values for ϵ/ρ calculated from equation (11) (β_j and $[L]$) for given values of $[L]$, is used. If it is known that the complex ML is present in only negligible amounts (e.g., at high $[L]$ and pH)

then the polynomial may be reduced in order to give:

$$\frac{(\epsilon/\rho) - 1 - \beta_1[L]}{[L]^2} = \beta_2 + \beta_3[L] + \dots \quad (12)$$

Least-squares analysis now involves the term on the left-hand side of this equation. For the case when ML_3 is the highest complex (as with many Cd^{2+} -amino-acid complexes) this equation reduces to a straight line with intercept β_2 and slope β_3 .

This approach differs from the Lingane approach² in allowing for decreases in current (*i.e.*, a shrinkage of the calculated curve) as a result of the differences between the diffusion coefficients of the free solvated metal ion and the complexed metal species (*i.e.*, ρ generally less than 1).

The effect of the ionic background used for the cyclic voltammetric experiments, and of charging currents *etc.*, can be compensated for by software subtraction of the background. The voltage drop due to internal resistance of the cell creates a problem, since it distorts the form of the voltage wave as applied at the electrode and hence directly influences the shape of the cyclic voltamperogram. Experimentally this can be diminished by adjustment at the potentiostat or by software compensation of the collected voltage data. The latter approach was used here; the R_u value is adjusted until the mid-point of the I_1 convolution of the anodic wave is exactly superimposed on that for the cathodic wave [see

Fig. 2(b)] when electron transfer is known to be fast (*i.e.*, for an electrochemically reversible system). The potential differences between the mercury drop and the reference electrode are then adjusted according to $E_{\text{new}} = E_{\text{old}} - iR_u$, where R_u is the non-compensated resistance of the electrolyte between the mercury drop and the reference electrode. The sweep rate can then be increased until superimposition of the two waves of the I_1 convolution is no longer possible, thus fixing the maximum sweep rate consistent with electrochemical reversibility.

If the convolution cannot be made to give exact superimposition [*e.g.*, as in Fig. 2(d)], even at slow sweep rates (*i.e.*, fast electron-transfer conditions), then an incorrect mechanistic scheme has been envisaged. For example, a subsequent irreversible chemical process results in an I_1 value which fails to give an exact overlay, as demonstrated in Fig. 2(d).

RESULTS AND DISCUSSION

The protonation constants and Cd^{2+} -complex stability constants calculated for glycine (Gly), alanine (Ala), valine (Val) and aspartic acid (Asp) are presented in Table 1. These ligands were selected because the first three form a series of simple bidentate amino-acids, expected to form the *N, O*-bonded complexes $[CdL]$, $[CdL_2]$ and possibly $[CdL_3]$, whereas Asp is a potentially terdentate ligand and so expected to form only the *N, O, O*-bonded complexes $[CdL]$ and $[CdL_2]$.

Table 1. Formation constants* ($\log \beta_i$ values) for H^+ and Cd^{2+} complexes, determined from pH titrations, cyclic voltammetry and differential-pulse polarography, at 25° and $I = 0.10M KNO_3$

Ion	Ligand	Technique†	$\log \beta_1$	$\log \beta_2$	$\log \beta_3$
H^+	Gly	pot	9.62 (1)	12.29 (1)	
	Ala	pot	9.82 (1)	12.24 (1)	
	Val	pot	9.62 (1)	12.00 (1)	
	Asp	pot	9.64 (1)	13.41 (1)	15.77 (1)
Cd^{2+}	Gly	pot	4.24 (1)	7.85 (1)	—
		cv	—	7.74 (5)	9.25 (6)
	Ala	pot	4.00 (1)	7.40 (1)	—
		cv	—	7.20 (6)	8.96 (3)
		dpp	—	7.1 (1)	9.36 (2)
	Val	pot	3.69 (1)	6.86 (1)	—
		cv	—	6.78 (4)	8.83 (4)
	Asp	pot	4.68 (1)	8.04 (1)	—
		cv	—	8.1 (1)	—

*Standard deviations (sigma values) are given in parentheses and relate to the last decimal place. They refer to random errors *only* and hence reflect the precision of the results rather than the absolute accuracy. An estimate of 0.05–0.1 for the absolute accuracy for both cv and pH titrations of Cd^{2+} complexes appears reasonable.

†Pot = pH titrations, cv = cyclic voltammetry (0.2 V/sec), dpp = differential-pulse polarography.

Potentiometry

Protonation constants were calculated from pH titration data for use in calculation of the free-ligand concentrations required in calculations based on voltammetric data. The $\log K_{HL}$ values calculated for the series Gly, Ala, Val do not follow the expected trend but are entirely compatible with values reported in the literature. A critical evaluation of the vast body of literature values, measured under the same conditions as used here, gives mean values of 9.61, 9.75 and 9.58 respectively,¹⁵ very close to the values given in Table 1.

Stability constants for the complexes with Cd^{2+} were calculated from pH titrations but the degree of formation of the complexes was, of necessity, low. For reasonable precision the degree of formation of a complexed species should be greater than 20%. In practice, the precision of calculated constants also drops rapidly as the L:M ratio increases, making 6:1 the highest practical ratio. High pH values are to be avoided in potentiometry, firstly because at $\text{pH} > 9$ metal hydrolysis may occur if, as a result of weak complexation, there is still a significant amount of free metal ion in solution. For Ala and Val a total ligand concentration of 0.01M is required in titration with 1M sodium hydroxide to form significant concentrations of CdL and CdL_2 before metal hydrolysis occurs. Secondly, accurate pH measurements are difficult to make at pH above 10, because of the effects of electrode liquid-junction potentials, changing ionic strength and the value used for K_w . Stability constants for complexes formed at $\text{pH} > 10$ are very sensitive to slight changes in pH, especially if the ligand is still undergoing deprotonation reactions at high pH, as is the case for many amino-acids. Because of these constraints, complexes higher than CdL_2 cannot

be detected reliably, so only the species CdL and CdL_2 could be assigned meaningful stability constants. This is demonstrated in Fig. 3(a) which shows species distribution curves for 3:1 Ala:Cd ($C_{\text{Cd}} = 0.001M$) mixtures. With Asp, tris-complexes are not to be expected; hence an earlier potentiometric study¹⁶ which reports a constant for CdL_3 must be questioned.

Cyclic voltammetry

Use of the theory discussed above for the determination of stability constants relies on the assumption that the complexes formed in solution are labile. Only if labile chemical equilibria exist will the shift in half-wave potential be related to the stability constant as defined by equation (10). However, the definition of lability is dependent on the mode of polarography/voltammetry used. It is the *time-scale of measurement* that is the important factor in defining which species in solution will be classed as labile with reference to a transient technique such as differential-pulse polarography or cyclic voltammetry.

For a pulsed technique (*e.g.*, differential-pulse polarography) the time-scale of the experiment can be taken as the duration of the applied pulses before the current is sampled, plus the mean of each sampling interval.¹⁷ For cyclic voltammetry, where continuous electrolysis occurs on a single mercury drop in an unstirred solution, the time-scale of the experiment is the total sweep time.

A labile equilibrium can then be defined as an equilibrium where the amount of ligand exchanged is large in the time-scale of the experiment. Here large means much greater than the amounts of material moved by diffusional processes or converted by electron exchange in the same time interval. The current will differ from

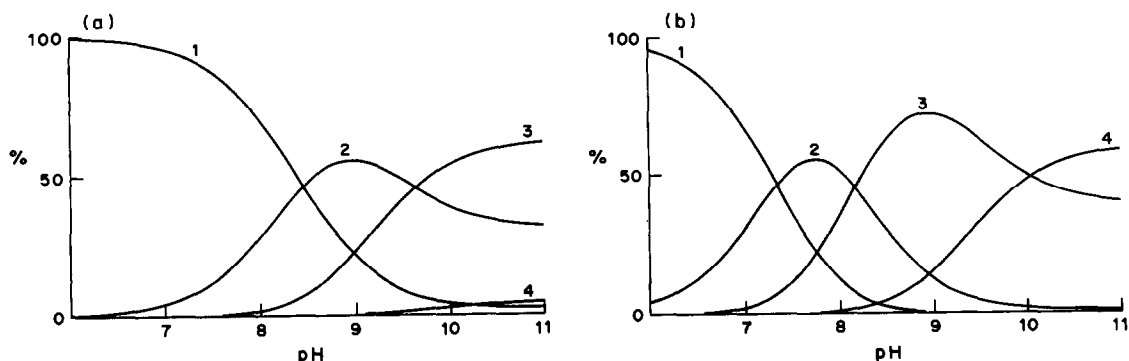


Fig. 3. Species distribution curves for (a) 3:1 and (b) 30:1 Ala: Cd^{2+} ratios (total Cd = 0.001M); 1 = Cd^{2+} , 2 = CdL , 3 = CdL_2 , 4 = CdL_3 .

that for the simple solvated metal ion, only because of the difference between the diffusion coefficients of the metal ion and the complex. The half-wave potential will be shifted, and this shift can be related to the stability constant.

If the lability within the time-scale of the experiment is not large, a kinetic effect is observed. Depending on the extent of the kinetic effect, the current at a given time will vary between zero and the current for the simple solvated ion. At the extreme limit (non-labile equilibria) no exchange occurs and the current is proportional to the concentration of non-complexed metal ion, as defined by the stability constant for a given pH and the total concentrations of ligand and metal. The half-wave potential is that of the simple metal ion.

For the ligand series Gly, Ala, Val and Asp, complexation was studied at a precise pH value between 9.75 and 10.5. As the ligand concentration increased, the cyclic voltammetric wave was observed to shift in a negative direction relative to $E_{1/2}$ for the free metal, and the limiting current (i_d) and limiting convoluted current (I_L) decreased slightly, relative to the free metal i_d and I_L values (Fig. 4). This is indicative of formation of a labile complex. The decrease in current was shown to be the result of dilution and the difference in the diffusion coefficients of the free solvated metal and the complexed metal species, rather than the result of a kinetic effect. The Heyrovský-Ilkovič relationship held true for both free metal (*i.e.*, in the absence of ligand, or for metal-ligand solutions at low pH) and complexed metal solutions, at the scan rates used. Plots of $\ln[(I_L - I_1)/I_1]$ vs. E yielded straight lines with slopes equal to

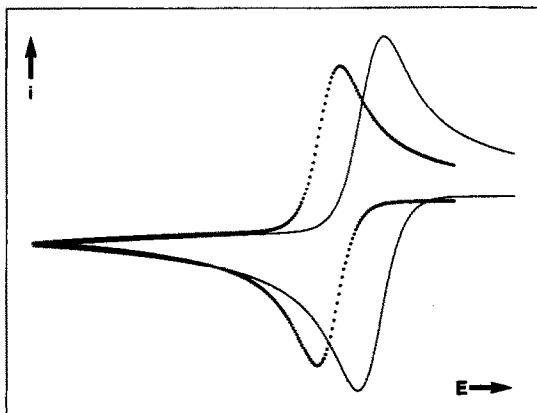


Fig. 4. Cyclic voltamperograms for the Cd^{2+} -Ala system: (—) free metal ion (pH 4), (....) complexed species at pH 10.

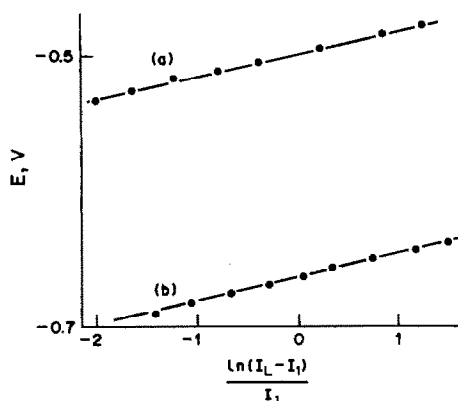


Fig. 5. Heyrovský-Ilkovič plot, $\ln[(I_L - I_1)/I_1]$ vs. E , for (a) free Cd^{2+} and (b) Cd-Ala complexes,

RT/nF ($n = 2$) and intercepts equal to $E_{1/2}$ (Fig. 5).

Over the pH range 9.75–10.5 and with a large L:Cd ratio no CdL complex exists [Fig. 3(b)] so the reduced polynomial [equation (12)] can be applied to calculate β_2 and β_3 . The straight line plot for the Cd^{2+} -Ala system is shown in Fig. 6, in which the results are a combination of datum points recorded by two different instrumental arrangements, at several pH values, and hence demonstrate the absolute reproducibility (as distinct from precision) of the technique.

The species distribution curves for the equilibrium between Cd^{2+} and Ala are shown in Fig. 3 where β_2 and β_3 are taken from the cyclic voltammetric studies and β_1 from the potentiometric work. Typical concentrations and ratios are shown for (a) potentiometry, L:Cd = 3:1, and (b) cyclic voltammetry, L:Cd = 30:1, with $C_{\text{Cd}} = 0.001M$. It can be seen that for a 3:1 L:Cd ratio the maximum concentration of the tris complex is 5%, demonstrating why reliable values for β_3 cannot be calculated. However, with a 30:1 ratio (as in cyclic voltammetry) 60% of the metal exists as the tris complex, which allows accurate calculation of β_3 .

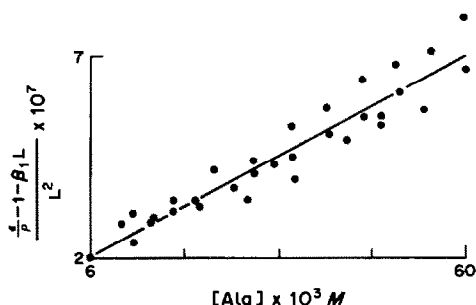


Fig. 6. Plot of the reduced polynomial [equation (12)] vs. free ligand concentration for the Cd-Ala system, with data combined from two different instrumental arrangements.

Thus constants calculated for the Cd^{2+} -Ala system were independent of scan rate over the range 0.05–0.2 V/sec, justifying the use of a scan rate of 0.2 V/sec throughout this work. To render complexes labile the scan rate must be slow enough to allow ligand exchange within the time-scale of the experiment. The slower the scan rate the more likely a complex is to be classed as labile. However, there is a lower limit to the scan rate. At very slow scan rates, convection currents can be set up, resulting in the migration of reactants to the mercury drop no longer being controlled by diffusion.

For Gly at concentrations greater than 0.05M the results indicated the presence of a fourth complex, most likely CdL_4 . Equation (12) was no longer satisfied as a first-order polynomial, and a second-order polynomial (*i.e.*, with CdL_2 , CdL_3 and CdL_4) improved the numerical fit to the experimental data. Inclusion of a mixed hydroxy species (*e.g.*, $\text{Cd}_2\text{L}_2\text{H}_{-2}$) was considered. Although this seemed to be a reasonable species for the conditions arising in potentiometry (L:M < 6:1), the large excess of ligand in the cyclic voltammetric experiment makes it unlikely that hydroxy species would form. Defining β_4 is hindered by the changes in ionic strength that arise as $[\text{L}^-]$ is increased (the background electrolyte is 0.1M potassium nitrate). However, an approximate value of 10.5 was calculated for $\log \beta_4$. It can be assumed that this species has two ligands giving bidentate co-ordination, and two giving unidentate binding.

For Asp, there was no evidence to support the formation of a CdL_3 complex at pH up to 10.5 and 50:1 L:Cd ratios. A plot of $\ln[\text{L}]$ vs. $\ln(\epsilon/\rho - 1)$ yielded a straight line with slope 2.00 ± 0.03 (co-ordination number) and intercept of 18.7, *i.e.*, $\log \beta_2 = 8.1 \pm 0.1$ {equation (11) with no CdL , or $\ln(\epsilon/\rho - 1) = \ln \beta_2 + 2\ln[\text{L}]$ }.

Differential pulse polarography

The differential-pulse polarographic technique, in which a pulsed voltage wave is applied and current sampling is employed (both modifications of the original d.c. polarographic technique), was used to determine stability constants for the Cd^{2+} -Ala system. Although the constants calculated by this technique (Table 1) are comparable with those calculated by convolution-deconvolution cyclic voltammetry, the experiment is more time-consuming and more dependent on the state of the mercury electrode.

Unlike cyclic voltammetry, polarography uses a dropping mercury electrode (dme). This requires good electrode behaviour for some 300 sec (*ca.* 300 mercury drops), the duration of the experiment. This is very dependent on the quality of the mercury used, and the slightest discontinuity in the mercury flow means that the experiment has to be repeated. In contrast with cyclic voltammetry an equilibrium system can be completely analysed with very many fewer mercury drops than in a single dme run. For the differential-pulse polarography, all polarograms were recorded on a chart recorder and current/voltage data were read by eye.

Comparison of results

The only constants which can usefully be compared are those for the CdL_2 species, for the reasons outlined above. Results given in Table 1 show agreement to be reasonably good, the logarithmic values varying by at most 0.2. This is within the range of systematic errors of both techniques since, for example, in potentiometry an error of $\pm 1\%$ in alkali concentration has the effect of changing $\log \beta_1$ by 0.02 and $\log \beta_2$ by 0.03. An uncertainty in $\log \beta_{\text{HL}}$ of ± 0.03 has the effect of changing $\log \beta_1$ by only 0.02 but changes $\log \beta_2$ by almost 0.1 because the ligand is undergoing a deprotonation reaction over the pH range in which ML_2 is forming. For cyclic voltammetry, an error of 1 mV $\Delta E_{1/2}$ would translate to a change of about 0.1 in $\log \beta_1$.

One study reported for Gly and Ala in the literature compares results from potentiometry with those from differential-pulse polarography (at 25° and 0.7M NaClO_4).¹⁸ Although reasonable agreement was reported, the species CdL_3 was rejected, although its presence would be expected from the L:Cd ratios used. There are no literature values for comparison of the complexes of Cd^{2+} with the series of ligands Gly, Ala, Val.

CONCLUSIONS

In many ways the techniques of pH titration and cyclic voltammetry are complementary. The first is certainly the simpler to perform and the experimental data are easier to treat mathematically, but the second has distinct advantages when very high ligand:metal ratios are used and when the complexes are comparatively weak. These conditions are frequently found in biological systems, pollution studies, natural waters *etc.*, and cyclic voltammetry can give

meaningful answers when pH titrations are of limited use. Cyclic voltammetry as a method for determining stability constants thus complements the pH technique, allowing study of equilibrium regions that are inaccessible by potentiometry.

Acknowledgements—We would like to thank Mr. D. Mills for assistance in the early stages of this investigation and the SERC for financial support.

REFERENCES

1. J. Heyrovský and D. Ilkovič, *Collection Czech. Chem. Commun.*, 1935, **7**, 198.
2. J. J. Lingane, *Chem. Rev.*, 1941, **29**, 1.
3. D. D. DeFord and D. N. Hume, *J. Am. Chem. Soc.*, 1951, **73**, 5321.
4. A. J. Bard and L. R. Faulkner, *Electrochemical Methods*, Wiley, New York, 1980.
5. R. S. Nicholson and I. Shain, *Anal. Chem.*, 1964, **36**, 706.
6. G. A. Mabbott, *J. Chem. Educ.*, 1983, **60**, 697.
7. K. B. Oldham, *Anal. Chem.*, 1972, **44**, 196, 1121.
8. J. C. Imbeaux and J. M. Savéant, *J. Electroanal. Chem.*, 1973, **44**, 169.
9. A. Blagg, S. W. Carr, G. R. Cooper, I. D. Dobson, J. B. Gill, D. C. Goodall, B. L. Shaw, N. Taylor and T. Boddington, *J. Chem. Soc., Dalton Trans.*, 1985, 1213.
10. I. D. Dobson, N. Taylor and L. R. H. Tipping, in *Electrochemistry, Sensors and Analysis*, pp. 61–75. Elsevier, Amsterdam, 1986.
11. J. B. Gill, M. Hall and N. Taylor, *Electrochim. Acta*, 1988, **33**, 891.
12. P. Gans, A. Sabatini and A. Vacca, *J. Chem. Soc., Dalton Trans.*, 1985, 1195.
13. A. M. Bond, *Modern Polarographic Methods in Analytical Chemistry*, pp. 311–313, Dekker, New York, 1980.
14. C. P. Andrieux, L. Nadjo and J. M. Savéant, *J. Electroanal. Chem.*, 1970, **26**, 147.
15. A. Gergely, T. Kiss and I. Sovago, *Pure Appl. Chem.*, to be published.
16. R. Kamari, C. P. S. Chandel and C. M. Gupta, *Indian J. Chem.*, 1986, **25A**, 877.
17. W. Davison, *J. Electroanal. Chem.*, 1978, **87**, 395.
18. M. L. S. Simões Gonçalves and M. M. Correia Dos Santos, *ibid.*, 1985, **187**, 333.

COMPARATIVE STUDY OF IBMK AND DIBK AS EXTRACTION SOLVENTS IN STRONGLY ACIDIC MEDIA: EXTRACTION BEHAVIOUR AND KINETIC STABILITY OF $\text{Cu}(\text{PCD})_2$ IN THESE SOLVENTS

MASAHIKO MURAKAMI and TAKEO TAKADA

Department of Chemistry, College of Science, Rikkyo (St. Paul's) University, Nishi-Ikebukuro,
Toshima-ku, Tokyo 171, Japan

(Received 14 October 1987. Revised 28 July 1989. Accepted 5 August 1989)

Summary—The use of di-isobutyl ketone (DIBK) and isobutyl methyl ketone (IBMK) as the solvent for extraction of copper(II) from strongly acidic media (0.01–8*M* hydrochloric acid) with ammonium 1-pyrrolidinecarbodithioate has been studied. In contrast to IBMK, the volume of the DIBK extract remains the same, irrespective of the acidity of the aqueous phase. A certain amount of free acid is transferred into both solvents, and affects the kinetic stability of the chelate extracted; the free acid can be completely removed by washing the extract with water, and partly by filtering it through a dry filter paper. However, the chelate extracted into DIBK exhibits excellent stability without such treatment, since the amount of free acid in DIBK is much smaller than that in IBMK. When DIBK is used, the copper chelate can be quantitatively extracted as long as the extraction is done from acidic media.

Solvent extraction of metal chelates is used for increasing the sensitivity of atomic-absorption spectrophotometry (AAS). Isobutyl methyl ketone (IBMK) is widely used as the organic solvent for this purpose, since it gives good extraction of metal chelates and burns with a clear, steady flame. However, its mutual solubility with water is relatively large, and this can often be a problem in an analysis. Various workers¹⁻³ have reported that the decrease in the IBMK phase volume because of its partial dissolution in the aqueous phase leads to a higher absorbance signal than that expected from the initial organic/aqueous phase-volume ratio.

We have already reported on the extraction of Cu(II) from highly acidic solution (0.01–8*M* hydrochloric acid) into IBMK with ammonium 1-pyrrolidinecarbodithioate (APCD).^{4,5} From 4*M* hydrochloric acid the copper chelate could be extracted quantitatively provided a large excess of reagent was used, but it was observed that the absorbance for the same amount of Cu(II) increased when the acidity was increased. Further, with use of 8*M* acid, a significant amount of IBMK was dissolved in the aqueous phase and caused an abnormally high absorbance reading although extraction of the chelate was incomplete. In addition, we observed that decomposition of the chelate was

suppressed by washing or filtering the separated extract. This indicates that the acid which is dissolved in the organic phase during the extraction (and can be removed by these treatments) affects the kinetic stability of the extracted metal chelate. Therefore these effects make IBMK less suitable for extraction of metal chelates from highly acidic media.

In the work described in this paper, we studied the use of di-isobutyl ketone (DIBK) as an alternative to IBMK. DIBK is far less soluble than IBMK in water (IBMK 1.7% w/w, DIBK 0.043% w/w at 25°).⁶ Correspondingly the solubility of water is 1.9% w/w in IBMK but only 0.4% w/w in DIBK. Moreover, DIBK is as useful as IBMK in extraction–AAS analysis.⁸⁻¹⁰ We have therefore investigated the extraction of the Cu(II)–APCD complex into DIBK from various concentrations of hydrochloric acid, and the relative suitability of DIBK and IBMK as solvents for extraction from strongly acidic media.

EXPERIMENTAL

Reagents

All chemicals used were of reagent grade. Water was redistilled in all-glass apparatus. Stock copper solution, 1000 $\mu\text{g/ml}$, was prepared from 99.99% pure copper metal, and its

acidity was adjusted to 0.01*M* hydrochloric acid; the solution was diluted 100-fold with water to give the 10- μ g/ml working solution. APCD solution (1.5×10^{-2} *M*) was prepared by dissolving 0.13 g of ammonium 1-pyrrolidine-carbodithioate in 50 ml of water containing 0.5 ml of 0.1*M* ammonia solution, and stored in a refrigerator; it was stable for at least 1 month. All solvents were used without further purification.

Procedure

Extraction. A 20-ml portion of hydrochloric acid of the desired concentration, and 2.5 ml of 10- μ g/ml copper solution were transferred to a 100-ml separatory funnel, and 10 ml of DIBK and 2.5 ml of APCD solution were added. The mixture was mechanically shaken vigorously. The absorbance of the DIBK phase at 435 nm was measured in a 10-mm silica cell against DIBK as reference. To improve the accuracy of the absorbance measurement, immediately after the aqueous phase had been withdrawn the organic phase was washed by mechanical shaking with 25 ml of water for 300 sec, and the absorbance was then measured.

Potentiometric titration of free acid in the solvent. The titration and titrant preparation were performed as described by ASTM.¹¹ A 25-ml portion of hydrochloric acid of the desired concentration and 10 ml of IBMK or DIBK were transferred to a 100-ml separatory funnel, and the mixture was mechanically shaken vigorously for 30 sec. After standing for 300 sec, 5–9 ml of the upper phase and 30 ml of isopropyl alcohol were transferred to a 100-ml beaker and the mixture was titrated with 0.1*M* potassium hydroxide solution in isopropyl alcohol, and the end-point was detected by use of a glass and Ag/AgCl electrode system.

RESULTS AND DISCUSSION

Extraction of Cu(II)–APCD chelate

To optimize the conditions of Cu(II)–APCD extraction into DIBK, the shaking time and reagent concentration needed for quantitative extraction from 0.01–8*M* hydrochloric acid were studied. The amount of copper left in the aqueous phase was also checked by flame atomic-absorption spectrometry to estimate the degree of copper chelate extraction.

Shaking time. The shaking time needed for completing the extraction of copper chelate was examined with 1.6×10^{-3} *M* APCD (100-fold

reagent:copper molar ratio). From 0.01–6*M* acid, the copper chelate could be extracted quantitatively by shaking for 60 sec or more, and the absorbance was found not to decrease even with a shaking period of 20 min. On the other hand, from the 8*M* acid, the extraction with 1.6×10^{-3} *M* APCD was incomplete whatever the shaking time. However, when 7.5×10^{-3} *M* APCD (500-fold ratio to copper) was used, the copper chelate was completely extracted in 60–300 sec of shaking, but with longer shaking the absorbance began to decrease. Hence, in our later studies shaking times of 300 and 120 sec were used for extraction from 0.01–6*M* and 8*M* hydrochloric acid, respectively.

APCD concentration. The concentration of reagent needed for complete extraction of the copper chelate was also examined. As previously reported,⁵ this increased as the acidity was increased; the APCD concentration needed for complete extraction of the copper chelate was 6.5×10^{-5} *M* (4-fold ratio to copper) from 0.01–4*M* acid, 3.1×10^{-4} *M* (20-fold) for 6*M* and 2.4×10^{-3} *M* (150-fold) for 8*M* acid.

The concentration needed for complete extraction into DIBK is lower than that for extraction into IBMK under the same conditions; in the IBMK system, 1.0×10^{-5} *M* (6-fold) APCD was needed for the 4*M* acid, and for 8*M*, complete extraction was not observed even with 1.6×10^{-2} *M* (1000-fold) APCD.⁵ This indicates that the decomposition of reagent and chelate during the shaking period is less in the DIBK system than in the IBMK system.

Change in volume and absorbance of extract

Previously, we observed that when the copper chelate was extracted from 8*M* hydrochloric acid, a significant amount of IBMK was dissolved in the aqueous phase and this caused an abnormally high absorbance reading for the IBMK extract.⁵ The absorbance and volume were measured for DIBK and IBMK extracts containing a constant amount of copper chelate, as a function of the acidity of the aqueous phase.

Table 1 shows that the volume of the IBMK extract decreases (and the absorbance increases) with increase in the acidity of the aqueous phase, but the product of the volume and absorbance is practically constant for the extracts from 0.01–6*M* hydrochloric acid. At still higher acid concentration the decrease in volume of the IBMK extract rapidly becomes more

Table 1. Effect of acidity on organic phase volume (V) and absorbance (A) of extract

Acidity, M	DIBK		IBMK	
	A	V, ml	A	V, ml
0.01	0.545	9.93	0.570	9.60
2	0.547	9.95	0.579	9.40
4	0.543	9.90	0.587	9.10
6	0.541	9.92	0.613	8.52
8	0.545	9.95	—	4.68

Cu^{2+} 3.93×10^{-7} mole, shaking time 300 sec,
 [APCD] $1.5 \times 10^{-2}M$ for 0.01–4M acid,
 $3.0 \times 10^{-2}M$ for 6 and 8M acid, aqueous
 phase 25 ml, organic phase 10 ml.

marked until the system becomes completely miscible at 10M acid concentration.

In contrast, the volume and absorbance of the DIBK extract did not change over the whole range of acidity. This shows that in the IBMK extraction, the copper chelate is "concentrated" by the decrease in volume of the organic phase during the extraction.

Kinetic stability of the extract

As stated earlier,⁵ the kinetic stability of the copper chelate is highly dependent on the concentration of reagent added, and the decomposition of the chelate is suppressed by filtering the extract through a dry filter paper and washing it with water. Hence, the kinetic stability of the chelate extracted from hydrochloric acid into IBMK and DIBK was studied with various APCD concentrations and treatments of the extract. The stability was determined by measuring the change in absorbance at 435 nm with time, throughout the period the sample was kept in the spectrophotometer. The temperature of the sample was kept constant at 25° by means of a water-jacketed cell holder and circulation of water at constant temperature; timing was started when the reagent was added to the mixture.

Figure 1 shows the results for the DIBK system. Characteristically, the absorbance is constant for a certain time and then suddenly drops; this behaviour is similar to that of the IBMK system. Table 2 gives the time ($t_{1/2}$) needed for the absorbance of the extract to decrease to half its original value. The kinetic stability of the copper chelate is dependent on the concentration of APCD added, the treatment of the extract, and the kind of solvent. The chelate is much more stable in DIBK than in IBMK: under the same conditions. With $1.5 \times 10^{-3}M$ APCD, the absorbance of the

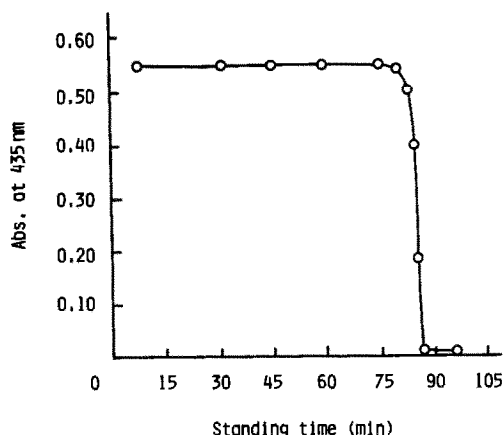


Fig. 1. Kinetic stability of $Cu(PCD)_2$ extracted from 4M HCl into DIBK: $[Cu(II)]$ $1.5 \times 10^{-3}M$; [APCD] $1.5 \times 10^{-4}M$.

DIBK extract was constant for 48 hr, whereas $t_{1/2}$ for the IBMK extract was only 40 min. Even with 8M acid, a $t_{1/2}$ of 40 min was obtained for the DIBK system with $7.5 \times 10^{-3}M$ APCD, and if the extract was washed with water the absorbance did not vary over a 24-hr period.

The washing and filtration contribute to stabilizing the extract, but the DIBK extract is sufficiently stable without these treatments if a large enough excess of APCD (about 10-fold or more, relative to copper) is added. These findings suggest that the decomposition of the copper chelate is due to free acid in the organic phase, so the concentration of this free acid was determined.

Table 3 shows that the amount of free acid in IBMK is considerably larger (by a factor of 5–10) than that in DIBK under the same conditions, and that a large part of it can be removed by filtering. No acid could be detected in either solvent after washing with water. The results suggest that the free acid is partly transferred by dissolution in the organic phase

 Table 2. Half-life ($t_{1/2}$) for $Cu(II)$ -PCD chelate extracted from 4M HCl

[APCD], M	$t_{1/2}$	
	DIBK	IBMK
Without washing		
7.0×10^{-5}	25.0 min	11.5 min
1.5×10^{-4}	86.0 min	29.0 min
1.5×10^{-3}	> 48 hr	40.0 min
1.5×10^{-2}	> 48 hr	85.0 min
With washing or filtration		
1.5×10^{-4}	> 24 hr	88.0 min
1.5×10^{-3}	> 48 hr	> 24 hr

$[Cu^{2+}]$ $1.5 \times 10^{-3}M$, shaking time 300 sec.

Table 3. Free acid dissolved in DIBK and IBMK

Acidity, M	Concn. of free HCl, M			
	DIBK		IBMK	
	With filtn.	Without filtn.	With filtn.	Without filtn.
8	9.78×10^{-3}	3.19×10^{-2}	1.00×10^{-1}	1.82×10^{-1}
6	1.01×10^{-3}	3.80×10^{-3}	7.59×10^{-3}	2.24×10^{-2}
4	3.16×10^{-5}	4.33×10^{-4}	6.88×10^{-4}	4.81×10^{-3}

(especially for the 8M acid system, where there will be an appreciable vapour pressure of hydrogen chloride) and partly by suspension of fine droplets of the aqueous phase. It is noted that the extracts containing almost the same concentration of free acid exhibit almost the same half-life; for example, when the chelate is extracted from 4M HCl with 1.5×10^{-4} M APCD, the half-lives for "DIBK without filtration" and "IBMK with filtration" are 86 and 44 min respectively (see Table 2), and the concentrations of free acid are 4.3×10^{-4} and 6.88×10^{-4} M, respectively (Table 3).

From these results, the rate of decomposition of the chelate is primarily related to the solubility of the free acid in the organic solvent.

CONCLUSIONS

When DIBK is used as the extracting solvent for Cu(PCD)₂, the system is practically unaffected by the acidity of the aqueous phase, and for practical purposes, pH adjustments are not required for the extraction, as long as this is done from acidic media. The calibration graph for determination of copper by APCD/DIBK extraction from 0.01–8M acid does not vary with the acidity, and the kinetic stability of the extract is sufficient for use of the whole range of acidity, without the necessity of washing the extract. Thus, this system permits rapid anal-

ysis, since a solid sample can be dissolved in concentrated hydrochloric acid and the copper extracted directly without further treatment of the sample, such as evaporation of the acid and pH adjustment.

However, Cu(PCD)₂ chelate extracted into DIBK exhibits decomposition behaviour similar to that of an IBMK extract, and the kinetic stability of the chelate is dependent on the concentration of APCD added, and a proper combination of the reaction conditions is needed to confer "robustness" on the system.

REFERENCES

1. D. C. Munro, *Appl. Spectrosc.*, 1968, **22**, 119.
2. R. R. Brooks, B. J. Presley and I. R. Kaplan, *Talanta*, 1967, **14**, 809.
3. R. J. Everson and H. E. Parker, *Anal. Chem.*, 1974, **46**, 2040.
4. T. Takada, *Talanta*, 1982, **29**, 799.
5. M. Murakami and T. Takada, *ibid.*, 1985, **32**, 513.
6. P. M. Ginnings, D. Plonk and E. Carter, *J. Am. Chem. Soc.*, 1940, **62**, 1923.
7. F. S. Stross, C. M. Gable and G. C. Rounds, *ibid.*, 1947, **69**, 1629.
8. J. H. Culp, R. L. Windham and R. D. Whealy, *ibid.*, 1971, **43**, 1321.
9. Y. Nagafuchi and K. Fukamachi, *Bunseki Kagaku*, 1980, **29**, T98.
10. C. H. Branch and D. Huchison, *Analyst*, 1986, **111**, 231.
11. American Society for Testing Materials, *ASTM Standards on Petroleum Products and Lubricants*, D664-81, p. 90.

COMPARISON OF ALGORITHMS FOR ERROR-COMPENSATED KINETIC DETERMINATIONS WITHOUT PRIOR KNOWLEDGE OF REACTION ORDERS OR RATE CONSTANTS

JAN A. LARSSON and HARRY L. PARDUE

Department of Chemistry, Purdue University, West Lafayette, IN 47907, U.S.A.

(Received 16 June 1989. Accepted 31 July 1989)

Summary—This paper describes the evaluation of algorithms written for error-compensated kinetic determinations, that do not need prior knowledge of reaction orders or rate constants. Results are reported for the quantification of acetoacetate in aqueous solution and urine. In addition to examination by nonlinear and linearized versions of the proposed new algorithms, the kinetic data were processed by a first-order model for comparison purposes. All the models yielded linear relationships between computed absorbance change and concentration; the new algorithms yield virtually identical results that represent better fits to the kinetic data than those obtained with the first-order model. The ability of the new algorithms to detect errors in the models is briefly discussed.

Several recent reports have reviewed a variety of approaches for error-compensated kinetic determinations.¹⁻⁴ Most of these approaches reported to date require prior knowledge of the exact mathematical model for the kinetic process on which the determination is based. Two recent papers have described two versions of a general approach that requires no prior knowledge of either the rate constant or the reaction order, except that the order should not be zero^{5,6} or unity.⁶

Because these two approaches do not require prior knowledge of reaction order and are applicable to both fractional and integral orders, they are more versatile than other approaches that are applicable only to integral orders.^{1-4,7} To date, these new methods have been evaluated only with simulated data.^{5,6} Although the simulated data had the advantage that they permitted the approaches to be evaluated for a wide range of well-defined conditions, they did not demonstrate the utility of the methods for any real situation. This paper describes evaluation of these new methods for a reaction system that is not easily described by an ideal kinetic model.

The example involves quantification of acetoacetate based on its reaction with glycine and nitrosopentacyanoferrate(III) (nitroprusside). This is a multistep reaction⁸ that produces an unstable product that decays gradually to a colorless product. The progress of the reaction

is monitored by means of the unstable product, which absorbs light at 540 nm.

EXPERIMENTAL

Data collected in an earlier study⁸ were used. The data (bottom of p. 440 in the paper⁸ cited) were obtained by first incubating acetoacetate samples with glycine until equilibrium was reached, then adding nitroprusside and monitoring the absorbance change at 540 nm. The data were obtained from nine runs for each of four aqueous standards and four urine samples containing acetoacetate at 0.47, 1.89, 3.78 and 4.25mM concentration. Samples and reagents were mixed in a centrifugal system that permitted all the samples in each group to be processed simultaneously in order to reduce any effects of instrumental variables. The data processed consisted of 95 absorbance *vs.* time values collected at between 10 and 301 sec for each sample. In addition to treatment by the nonlinear⁵ and linearized⁶ models, the data were also processed by a first-order model⁹ for comparison purposes.

The study included experimental and simulated data for interference-free systems, and also with first-order interferences superimposed on them. The latter data were included to test the ability of the algorithms to produce information that might be useful for error diagnosis. The interference-free simulated data were for total

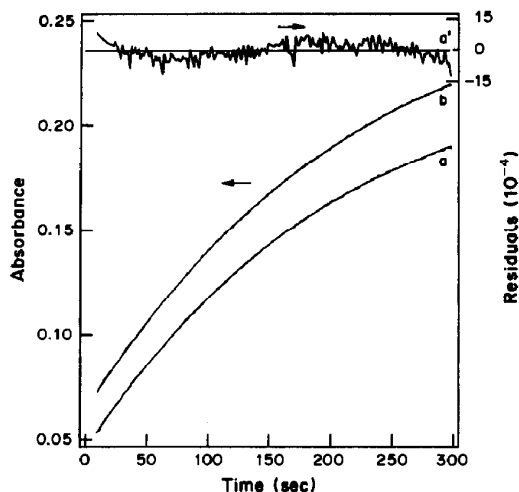


Fig. 1. Response curves for acetoacetate (0.47mM) in aqueous solution (a) and urine (b) with superimposed fit of first-order model: a', residuals for curve a.

absorbance changes (ΔA_{∞}) of 0.1–0.9 and rate constant and reaction order of 0.02 sec^{-1} and 1.25, respectively. The interference data superimposed on the simulated data were for first-order processes ($n = 1.00$) with a rate constant of 0.0100 sec^{-1} and total signal changes of 0.10 and 0.20 added to data with total absorbance changes of 0.7 and 0.2, respectively. Interference signals corresponding to a first-order process with $k = 0.020 \text{ sec}^{-1}$ and a total absorbance change of 0.050 were added to all nine of the data sets for two aqueous samples that contained acetoacetate at the 1.89 and 4.25mM level and had average total absorbance changes of 0.7 and 1.66, respectively. These data with superimposed interferences were processed only with the nonlinear model.⁵

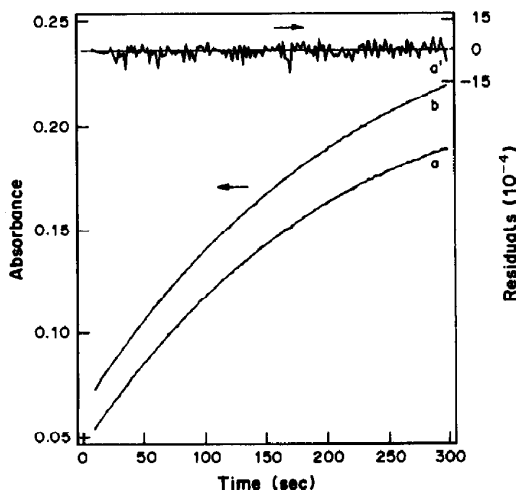


Fig. 2. Response curves as in Fig. 1 but with n th-order fit.

RESULTS AND DISCUSSION

Unless stated otherwise, uncertainties are reported as the standard deviation.

Comparison of methods

Figures 1 and 2 show experimental and fitted data for 0.47mM level acetoacetate in aqueous solution (a) and urine (b). Although the first-order fits in Fig. 1 appear to be completely superimposed on the experimental data, the residuals at the top of the plot exhibit systematic deviations about zero. On the other hand, the results in Fig. 2 for the nonlinear fit to an n th order model not only show a fitted curve superimposed on the experimental data, but also show residuals that are distributed more randomly about zero. Even at this lowest concentration of acetoacetate, the n th-order model appears to give better fits to the data than the first-order model. For higher acetoacetate concentrations, the n th-order model continues to give good fits to the data, but the first-order model tends to predict larger values of absorbance change than are observed experimentally, probably because the decomposition of the colored product causes the absorbance change to be less than it would be for a true first-order process.⁸

These differences are reflected in calibration plots. Although plots of computed absorbance changes *vs.* concentration are linear for both the aqueous and urine systems with both models, the slopes are higher for the first-order model than for the n th-order model. These and other effects are illustrated by the least-squares parameters in Table 1, which also contains the values obtained for the linearized n th-order model.⁶

As noted above, the most significant difference among the results is in the slopes. Whereas the two n th-order models yield very similar slopes, the first-order model gives substantially larger slopes because at longer times the fitted data are higher than the experimental data. Intercepts, standard errors of the estimates and correlation coefficients are very similar for the three models; the mean square due to pure error (MSPE)¹⁰ is somewhat higher for the first-order model than for the others. However, it is difficult to judge whether this difference is significant, because the variances of the absorbance changes for the lowest and highest concentrations (1.2×10^{-5} and 1.2×10^{-3}) bracket the MSPE values in Table 1.

Table 1. Least-squares statistics for fits of computed absorbance change vs. acetoacetate concentration; nine runs at each of four concentrations (0.5–4.25mM)

Medium	Slope (SD), l./mmole	Intercept (SD) absorbance	Std. error absorbance	Correlation coefficient	MSPE absorbance ²
Nonlinear, n th-order model					
Aqueous	0.399 (0.0027)	-0.032 (0.0082)	0.025	0.9992	4.4×10^{-4}
Urine	0.380 (0.0024)	-0.0002 (0.0071)	0.022	0.9993	2.8×10^{-4}
Linearized n th-order model					
Aqueous	0.396 (0.0028)	-0.032 (0.0087)	0.026	0.9991	4.8×10^{-4}
Urine	0.379 (0.0025)	-0.0009 (0.0075)	0.023	0.9993	3.0×10^{-4}
First-order model					
Aqueous	0.453 (0.0027)	-0.029 (0.0082)	0.025	0.9994	5.6×10^{-4}
Urine	0.436 (0.0024)	-0.004 (0.0073)	0.022	0.9995	3.5×10^{-4}

The most significant observations are that the nonlinear n th-order model gives a better fit to the data throughout the concentration range than does the first-order model and there is excellent agreement between the results obtained by the two n th-order models.

Error diagnostics

Data with and without first-order interference added were used to evaluate different possibilities for detecting errors in the model; the nonlinear n th-order model was used for all these studies.

Although it was very difficult to detect visually any differences between the experimental and fitted curves obtained with or without interference added, the computed residuals exhibited substantive differences as illustrated by Fig. 3. Thus, a "runs" test, which involves the number of times the residuals cross the zero line,¹⁰ would give significantly different results for evaluation of these two sets of samples (with and without an error in the model).

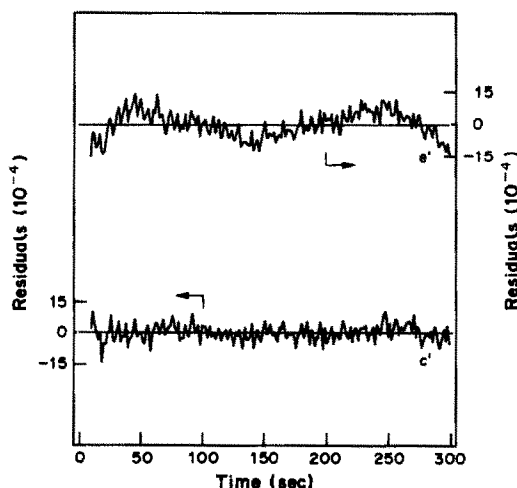


Fig. 3. Residuals for n th-order fit to data for acetoacetate (4.25mM) without (c') and with (e') first-order interference.

On the basis of these results, it was thought that the standard error of the estimate (*i.e.*, the square root of the residual mean square), which is a quantitative measure of the magnitude of the residuals, might be a useful error diagnostic. However, plots of the standard error vs. concentration had no distinguishing features to indicate the type and magnitudes of model-error evaluated here.

If sufficient experience has been gained with a system for it to be known what values of rate constant and reaction order are expected for normal variations, then deviations from these expected values might be used as indicators of possible problems. Figure 4 shows computed values of reaction orders and rate constants for aqueous and spiked urine samples with and without first-order interference added. It can be seen that the computed values of the reaction orders (\circ , \times) and rate constants (Δ , $+$) for aqueous and urine samples without

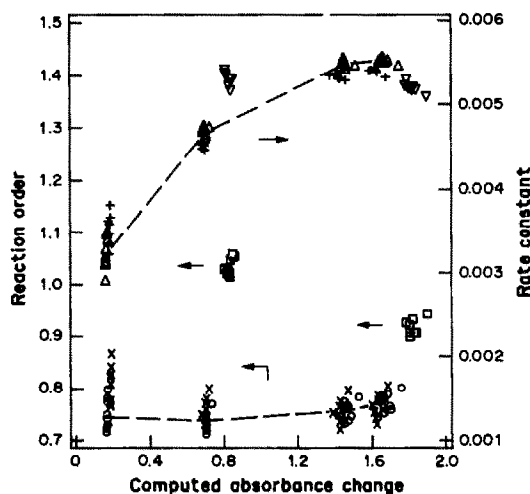


Fig. 4. Computed values of reaction order (\circ , \times , \square) and rate constants ($+$, Δ , ∇) in aqueous (\circ , Δ , \square , ∇) and urine (\times , $+$) matrices without (\circ , \times , Δ , $+$) and with (\square , ∇) first-order interference. Acetoacetate concentrations (mM): 0.47, 1.89, 3.78, 4.25.

added interference follow similar patterns, represented by the dashed lines. Although the two clusters of values of rate constants (∇) for the two groups of samples with interference added are somewhat removed from the general pattern of the samples without interference, the differences are so small that the rate constants would not be a useful error diagnostic in this case. On the other hand, the two clusters of values for reaction order (\square) are very different from the expected trend. These results suggest that the computed values of reaction order are more dependent on the type of model-error considered here than are those of the rate constants.

The results were somewhat different and slightly reversed for the simulated data. Because both the rate constant and reaction order were quantified with much better precision, both could be used as error diagnostics. However, differences in the values with and without interference added were larger for the rate constants than for the reaction orders; also, the two clusters of rate constants were on the same side of zero, whereas the two clusters of reaction orders were on opposite sides.

More extensive work with this and other types of model-errors is needed to determine more definitively which parameters (or their combinations) are most useful as diagnostics of model-error. However, these results support earlier conclusions⁹ that the parameters

obtained by the multipoint curve-fitting methods may be useful for error diagnostics, and that these newer algorithms^{5,6} extend the error-identification capabilities by providing the reaction order in addition to the rate constant that was used earlier⁹ as an error diagnostic.

The results reported here indicate that both the nonlinear⁵ and linearized⁶ models are useful for error-compensated kinetic determinations with nonideal reactions.

Acknowledgements—This work was supported in part by Grant No. GM 13326-21 from the National Institutes of Health, and in part by Grant No. CHE-8319014 from the National Science Foundation.

REFERENCES

1. R. C. Harris and E. Hultman, *Clin. Chem.*, 1983, **29**, 2079.
2. P. D. Wentzell and S. R. Crouch, *Anal. Chem.*, 1986, **58**, 2855.
3. H. A. Mottola, *Kinetic Aspects of Analytical Chemistry*, Wiley, New York, 1988.
4. H. L. Pardue, *Anal. Chim. Acta*, 1989, **216**, 69.
5. J. A. Larsson and H. L. Pardue, *ibid.*, 1989, **224**, 289.
6. *Idem*, *Anal. Chem.*, 1989, **61**, 1949.
7. I. B. C. Matheson, *Anal. Inst.*, 1987, **16**, 345.
8. I. Laios, D. M. Fast and H. L. Pardue, *Anal. Chim. Acta*, 1986, **180**, 429.
9. G. E. Mieling, H. L. Pardue, J. E. Thompson and R. A. Smith, *Clin. Chem.*, 1979, **25**, 1581.
10. N. Draper and H. Smith, *Applied Regression Analysis*, 2nd Ed, Wiley, New York, 1981.

SPECTROPHOTOMETRIC METHODS FOR THE DETERMINATION OF MANGANESE

BARRY CHISWELL and GUY RAUCHLE

Department of Chemistry, University of Queensland, St. Lucia, Qld. 4067, Australia

MARK PASCOE

Brisbane City Council Laboratories, Donaldson Road, Rocklea, Qld. 4106, Australia

(Received 27 May 1987. Revised 9 August 1989. Accepted 18 August 1989)

Summary—A comprehensive and critical review of the available spectrophotometric methods for the determination of manganese is presented. Details are given of a wide range of direct colour-forming reactions of manganese with organic ligands, which have been claimed to be of use in analysis for the metal. The use of the very sensitive kinetic methods of analysis is also discussed. It is found that there is a paucity of reliable detail concerning the general applicability of most methods to manganese determination and that there is even less detail on the comparative value of different methods for determination of the metal in particular types of matrix.

Technological developments in the latter part of this century have placed an increasing demand on chemists to produce analytical techniques which are cheap (in terms of outlay and running costs), reliable, rapid, simple to operate, accurate, sensitive, amenable to automation, and use of portable equipment. Photometric methods are therefore particularly attractive. This review is an attempt to assess critically the spectrophotometric methods currently available for the determination of manganese. This task is not easy, for though authors usually justify their work in terms of specific application(s), they more rarely make an objective comparison of it with other methods.

Marczenko¹ has commented that the major colorimetric methods for determining manganese are the permanganate, formaldoxime and pyridylazonaphthol methods, and listed many of the other organic reagents that have been used. The oxidation of manganese to permanganate by such reagents as bismuthate, periodate and persulphate, and the measurement of the absorbance of the 528 nm charge-transfer band of permanganate has long been used as a standard method for manganese determination. The method is basically suitable for determinations in the mg/l. range and is fully discussed by Marczenko. However, its sensitivity can be increased by the use of derivative spectrometry.^{2,2a} This review will concern itself almost entirely with spectrophotometric methods that use organic colour-forming reagents.

Snell and Snell³ reported the use of four colorimetric methods based on reactions of organic molecules with various oxidation states of manganese (Table 1), but of these only the formaldoxime method has found much use; Snell and Snell commented that the methods are either less sensitive or selective than the permanganate methods or have poor reproducibility. Cheng and Bray⁴ reported on the possible analytical applications of 1-(2'-pyridylazo)-2-naphthol, and Pollard *et al.*⁵ reported methods for the photometric determination of Co, Pb, and U with 4-(2'-pyridylazo)resorcinol. The successful application of these two dyes as sensitive reagents for the determination of a wide variety of metal ions was responsible, at least in part, for the interest during the mid-1960s in research directed towards developing improved colorimetric reagents.

As well as yielding precise and accurate results, an organic reagent for the colorimetric determination of a particular metal should form a complex with it that

- (i) has a high molar absorptivity, *i.e.*, gives high sensitivity;
- (ii) has a spectrum significantly different from that of the reagent, *i.e.*, gives a high spectral contrast;
- (iii) gives high selectivity.

Multidentate organic ligands are most likely to possess such properties.

Table 1. Colorimetric methods for manganese determination recommended by Snell and Snell³ in 1959

Reagent	Comments
Formaloxime	Forms an Mn(II) or Mn(III) complex*
<i>o</i> -Tolidine	Oxidized by Mn(III) and MnO ₄ ⁻
Benzidine	Oxidized by MnO ₄ ⁻
<i>N,N</i> -Diethyl- <i>p</i> -phenylenediamine	Oxidized by MnO ₄ ⁻

*Also reported to form an Mn(IV) complex (see oximes section in text).

Sensitivity is often described in terms of the molar absorptivity, (ϵ , units $l \cdot \text{mole}^{-1} \cdot \text{cm}^{-1}$)[†] of the metal–ligand complex. Savvin⁶ suggested the following criteria for describing the sensitivity:

- low sensitivity, $\epsilon < 2 \times 10^4$;
- moderate sensitivity, $\epsilon = 2\text{--}6 \times 10^4$;
- high sensitivity, $\epsilon > 6 \times 10^4$.

It is generally stated⁷ that the molar absorptivity will not exceed approximately 10^5 . Transitions giving an absorptivity of this magnitude are generally $\pi \rightarrow \pi^*$ or $n \rightarrow \pi^*$ and are associated with highly conjugated systems or, in the latter case, with systems containing hetero-atoms having non-bonding electrons. As the extent of conjugation increases, the energy difference between the lower and upper electronic states decreases, and a red-shift occurs in the spectrum; this decrease in excitation energy also results in a transition becoming more allowed. A common property of sensitive reagents, therefore, is that they have extensive conjugation. In developing new reagents, a common strategy for achieving this conjugation is the use of an azo group to link two aromatic systems. This tactic has a two-fold advantage since the azo group can also act as a complexation site.

Other ways of specifying sensitivity are as the specific absorptivity⁸ or the Sandell sensitivity (SS),⁹ both methods give the sensitivity in terms of mass of analyte per unit volume of solution. Such an approach is perhaps more convenient than using molar absorptivities as a basis of

comparison, since analytical results are usually expressed as weight/volume concentrations, but both quantities are readily calculated from the molar absorptivity. Specific absorptivity is defined as the absorbance of a 1-mg/l. analyte solution in a cell with a path-length of 1 cm, whereas the Sandell sensitivity is the concentration of analyte (in $\mu\text{g/ml}$) which will give an absorbance of 0.001 in a cell of path-length 1 cm, and is expressed as $\mu\text{g/cm}^2$.

Contrast is a measure of the extent of red-shift produced by complexation. It is defined as the difference in wavelength ($\Delta\lambda_{\text{max}}$) between the absorption maxima for the complex and the reagent, under the same conditions. A reagent is described as having high contrast when $\Delta\lambda_{\text{max}}$ is $> 80 \text{ nm}$,⁶ such descriptions, however, should take into account the broadness of the peaks concerned. The contrast may be increased by the introduction of appropriate substituent groups into the reagent⁶ or a judicious choice of solvent (mixed solvent systems have also been investigated as a means of increasing sensitivity by making complex formation more favourable¹⁰).

Typical spectrophotometric reagents contain at least one acidic complexing group, which forms a bond with the metal ion by replacement of the proton. The contrast in such cases can be approximated as the difference between the λ_{max} values for the dissociated and undissociated forms of the free ligand (particularly for ROH groups)¹¹ since metal–ligand bond formation has only a second-order effect on the absorbance, depending on the charge and polarizability of the metal. Solvents that increase the acidity of the reagent molecule are known to have a contrast-enhancing effect. The solvents dimethylformamide (DMF) and dimethylsulphoxide (DMSO) (both strong proton-acceptors) have been employed for this reason.⁶

Selectivity of complexation by a ligand has two aspects.

(a) The inherent selectivity of the reagent. This depends on (i) the ability of the reagent to complex the analyte preferentially, and (ii) the spectral differences between the various metal complexes formed by the reagent. The second of these factors is the more problematic, since the metal complexes usually absorb in a similar wavelength region (Table 2). Development of selective reagents for Mn is particularly difficult because Mn(II) complexes are less stable than other transition metal complexes of the same reagent and Mn(II) has no marked stereochem-

[†]For economy of space, the units will be omitted in the rest of the text.

Table 2. λ_{max} values for some metal-PAN complexes

Metal	λ_{max} , nm	Solvent
Mn(II)	575	CHCl ₃
Ni(II)	560	iso-C ₃ H ₁₁ OH
Ni(II)	575	CHCl ₃
Cd(II)	555	CHCl ₃
Hg(II)	560	CHCl ₃
Zn(II)	555	iso-C ₃ H ₁₁ OH
Rh(III)	598	CHCl ₃
Cu(II)	564	CHCl ₃
Fe(III)	775	CHCl ₃
Pd(II)	620/678	CHCl ₃
Co(III)	590/640	CHCl ₃

ical co-ordination preferences. An exception to this is constituted by the porphines, which have relatively high selectivity for Mn as a result of the geometry of the chelating sites. However, efforts to design multidentate reagents with a specific cavity size for accommodation of one particular metal ion have not been very successful. It appears that the complexity of structure found in metal-protein complexes is required for the desired selectivity to be achieved by this procedure.

(b) Selectivity achieved by sequestration of interfering metals. Iron is generally the most serious interferent in determination of manganese, partly because it will react competitively with most reagents for manganese, and partly because it will usually be present at much higher concentration than the manganese.

The sequestration of the interfering metals may be chemical ("masking" by formation of more stable complexes with other reagents) or physical (selective separation of either the interferent or the analyte by volatilization, extraction, precipitation, co-precipitation, flotation, chromatography, ion-exchange).

Both the sensitivity and the contrast may be enhanced by use of ternary complexes in which a charged metal complex forms an ion-association species with a non-chelating oppositely charged reagent.¹² When both the reagent and the ligand are extensively conjugated, a single conjugated system may be formed, which will result in a red-shift for the relevant transition and a possible increase in absorptivity. The selectivity is also often greater than that for the simple binary complex.

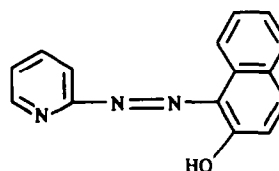
Ternary systems are generally classified according to the acid/base character of the chromophore, which is generally an organic dye. When an acidic organic dye is used, a neutral ligand is required. The ion-associate formed

may be extracted or determined in the aqueous phase if it is water-soluble. An acidic dye may also be used to form an anionic complex with the metal, in which case a cationic surfactant such as a cetyltrimethylammonium or cetylpyridinium salt is used to provide the counter-ion for forming the ion-associate with the complex, and the product is dissolved in the surfactant micelles.

AZO REAGENTS

The azo dyes are the largest single class of potential reagents for colorimetric analysis. The compounds used are usually terdentate ligands with phenolic groups and/or nitrogen atoms in aromatic heterocycles or amines as the donors. Sometimes, *e.g.*, in the bis-azo-chromotropic acid derivatives, the azo group does not function as a donor group, but serves only to increase the conjugation of the system and hence improve its sensitivity. A major feature of azo dye metal complexes is their insolubility. Many workers have attempted to overcome this by adding "solubilizing" groups (non-chelating hydroxy or sulphonic acid groups). The selectivity of the azo dyes is generally poor in the absence of a masking agent, presumably because the geometry of the chelate is practically independent of the nature of the metal ion.

The most widely used azo dye is 1-(2'-pyridyl-azo)-2-naphthol (PAN, 1), synthesized by Tschitschibabin.¹³ Studies by Liu¹⁴ of PAN-metal complexes prompted Cheng and Bray⁴ to study use of the dye for analytical purposes. PAN has since been developed as a photometric reagent (with or without extraction) and as a complexometric indicator for a wide variety of metal ions.¹⁵ Its rather poor selectivity can be improved by pH control and use of masking agents. Shibata has reviewed its use for spectrophotometric determination of a number of metals,¹⁶ and it has been used for the determination of manganese in mining effluent,¹⁷ ground water¹⁸ and high-purity group V and group VI metals.¹⁹ It has also been used for simultaneous



determination of Te, Ni, Cu, Zn and Mn in aluminium and magnesium alloys.²⁰

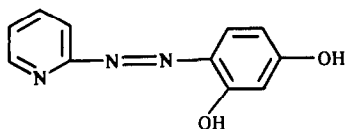
Initially, chloroform¹⁹ or diethyl ether¹⁶ was used to extract the Mn-PAN complex from a basic solution (pH 9.2). Donaldson and Inman¹⁹ reported $\epsilon = 4.8 \times 10^4$ at 562 nm, with interference from cobalt and zinc, but this could be prevented by masking with cyanide. The extraction can be avoided by solubilizing the PAN-metal complex with a mixed solvent system²¹ or surfactants.²²

The last of these studies led to development of a specific method for manganese, using Triton X-100, a non-ionic surfactant, to solubilize the PAN complex. Goto *et al.*¹⁸ reported the molar absorptivity at pH 9.2 to be 4.4×10^4 at 562 nm, with Beer's law obeyed up to 2 mg/l. Iron, cadmium, cobalt and nickel were masked with cyanide and triethanolamine. A significant feature of this method is that it can easily be adapted for automatic analysis, and it has been applied, with minimal modification, to the analysis of potable water, with apparatus originally designed for the formaldoxime method. Though this method is far superior to the formaldoxime method, difficulties are experienced with manganese concentrations below about 100 $\mu\text{g/l}$. because of overlap of the ligand peak ($\lambda_{\text{max}} = 470$ nm; $\epsilon = 1.2 \times 10^4$) with the peak for the complex, which may occur as a shoulder on the ligand peak.^{23,24}

A number of sulphonated PAN derivatives have been investigated with the aim of producing a suitable water-soluble complex, but only 1-(2'-pyridylazo)-2-naphthol-7-sulphonic acid and 2-(2'-pyridylazo)-1-naphthol-4-sulphonic acid produce any significant colour reaction with manganese,²⁵ and no use of these reagents for determination of manganese has been reported.

In an attempt to find more sensitive reagents Shibata *et al.* prepared 1-(5'-bromo-2'-pyridylazo)-2-naphthol²⁶ and its 5'-chloro analogue,²⁷ which give manganese complexes having ϵ values of $\sim 7 \times 10^4$, but neither reagent seems to have been exploited for determination of manganese.

4-(2'-Pyridylazo)resorcinol (PAR, **2**), another of the dyes prepared by Tschitschibabin,¹³ was



2

studied as a complexing agent by Liu.¹⁴ Although it is less selective than PAN, its water solubility and greater sensitivity have led to PAR being used for the spectrophotometric determination of a large number of metal ions, at wavelengths between 495 and 550 nm (except for palladium). As selective solvent extraction methods are not applicable, the use of PAR instead of PAN requires more involved schemes for the separation or masking of interfering ions.²⁸

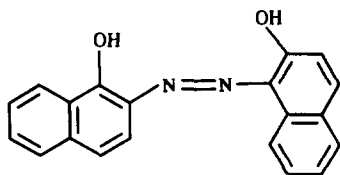
Yotosuyanagi *et al.*²⁹ and Ueda *et al.*³⁰ independently reported the use of PAR for the spectrophotometric determination of manganese. It has been used for the determination of manganese in steel^{31,32} and water (both potable and industrial).^{29,33} It has also been employed for the automatic detection and spectrophotometric determination of metals, including manganese, after separation by liquid chromatography.^{34,35}

Various values of range and sensitivity have been reported for the PAR-manganese complex; Ahrlund and Herman,³⁶ in an attempt to duplicate previous work,^{29-31,37} found the molar absorptivity to be 7.8×10^4 at 500 nm in borate buffer at pH 10, with Beer's law obeyed over the range 0.1-1.1 mg/l.

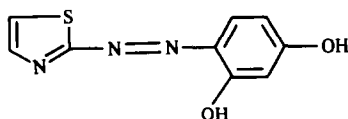
Many cations and anions, including Cr, Ni, Cu, Mg, Cd, Zn, Pb, Fe, Al, oxalate, phosphate, citrate, ascorbate,³⁷ V, U, and EDTA³¹ interfere; iron appears to provide the most serious interference. Methods have been discussed by various authors for overcoming these interferences.^{29-31,36}

Although PAR was originally favoured over PAN because of the greater water solubility of its metal complexes, the studies by Watanabe²² on solubilization of PAN complexes make this no longer a significant factor to be considered when comparing the two reagents.

The successful application of PAN and PAR as sensitive colorimetric reagents for a wide variety of metals led to widespread interest in developing new azo dyes as analytical reagents. The thiazolylazo analogues soon followed, and the analytical applications of a large number of them were investigated.^{11,38-49} Shibata *et al.* suggested that these reagents are generally less suitable than the pyridylazo compounds,³⁸ and only 1-(2'-thiazolylazo)-2-naphthol (TAN, **3**), and 4-(2'-thiazolylazo)resorcinol (TAR, **4**) have been developed to yield methods for the spectrophotometric determination of manganese. Rudometkina *et al.*¹⁰ reported the effect of



3



4

different solvents on the absorbance of the Mn-TAR complex. More recently Gaokar and Eshwar⁵⁰ have described a spectrophotometric determination of manganese with TAR at pH 8.8 (borate buffer) in aqueous solution containing 20% v/v *tert*-butyl alcohol, claiming that the alcohol increases the absorptivity by preventing hydrolysis of the Mn-O bond formed between the metal and one of the hydroxyl groups of the dye. The complex obeys Beer's law over the range 0.04–1.4 $\mu\text{g/l}$. ($\epsilon = 4.2 \times 10^4$). Severe interference from Co(II), Zn(II), Cd(II) and Pb(II) was reported but the method was described as suitable for determination of manganese in alloy steel, after ether extraction of iron, and addition of cyanide as masking agent.

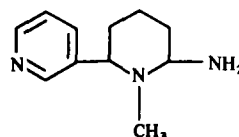
Analytical applications of 1-(2'-thiazolylazo)-2-naphthol were first suggested by Nakagawa and Wada,⁵¹ who reported that TAN formed complexes with a number of metal ions, including Mn(II), and that these complexes were extractable into chloroform. These authors noted that TAN gave similar sensitivity to PAN, but was more selective. Grzegorzolka⁵² extracted the Mn-TAN complex into chloroform and reported the Beer's law range as 0.1–1.3 mg/l. ($\epsilon = 3.8 \times 10^4$). The reagent has also been applied to the simultaneous determination of manganese and zinc in tap water by a method based on the difference in the rate of exchange of the two TAN complexes with EDTA.⁵³ The method is described as free from interferences and the reaction is done in aqueous solution, with Triton X-100 present to solubilize the metal complexes.

To increase the sensitivity, variations of the 2-pyridylazo type of ligand have been prepared in which groups that extend the ligand conjugation are included. Of these, 2-(5'-bromo-2'-

pyridylazo)-5-dimethylaminophenol has been described as one of the most sensitive of the pyridylazo dyes.⁵⁴ It reacts with a number of metals, including manganese. The diethyl analogue, 5-Br-PADAP, shows similar sensitivity ($\epsilon = 1.06 \times 10^5$) and has been used by Zhu and co-workers for the determination of manganese.^{55–57} It has also been used in conjunction with Chrome Azurol S.^{57a} With the use of masking agents, the technique shows few serious interferences. An aqueous ethanolic medium has been employed to improve the solubility of the metal complex,⁵⁶ and surfactants can be used to increase the sensitivity.^{57b} The reagent has been used to determine water-soluble manganese in a number of soil types,^{56,57} and as a metal indicator for tissue staining.⁵⁸ Zhang *et al.*⁵⁹ have used 2-(3',5'-dichloropyridylazo)-5-diethylaminophenol in the presence of a non-ionic surfactant.

Shibata *et al.*³⁸ prepared fifteen azo derivatives of 3-dimethylaminophenol, of which twelve gave colour reactions with manganese. The reagents were rather unselective, but the pyridylazo derivatives all exhibited large redshifts (110–120 nm) on complexation, and high molar absorptivities ($\sim 10^5$), characteristic of dyes having an amino group *para* to the azo group.

Even more complex variations of the pyridylazo reagent are found in the use of anabasine azo derivatives formed by the diazotization of 6-amino-*N*-methylanabasine (5).^{60–67} The *n*-heptylresorcinol derivative⁶¹ forms an extractable manganese complex which obeys Beer's law over a wide concentration range. Podlipskaya *et al.* reported a method using the azotol derivative.⁶⁸ The β -naphthol derivative reacts with cobalt in strongly acidic solution, with interference by low levels of manganese⁶³ and might be usable for determination of the latter. The 6'-aminohydroxyphenylazo derivative⁶⁵ has been used for the determination of manganese in duralumin, the complex being water-soluble and having a molar absorptivity of 7.57×10^4 . Talipov and co-workers have reported a number of derivatives^{66,67} which ap-



5

pear to form water-soluble complexes with manganese and which may be worth considering as analytical reagents.

Many other azo compounds have been proposed as possible colorimetric reagents for the determination of manganese. Thus 2-(2'-pyridylazo)-4-methylphenol is described⁶⁹ as being preferable to both PAN and PAR, and 2,7-bis(4'-carboxyphenylazo)chromotropic acid gives an intense colour ($\epsilon = 1.5 \times 10^5$) with manganese,⁷⁰ which can be determined after extraction into chloroform.⁷¹ Both ammonium 2-(2'-lepidylazo)-1-naphthol-4-sulphonate⁷² and Solochrome Black T⁷³ have been used as titrimetric indicators for manganese. 2-(1'-Carboxyphenylazo)-7-(4'-sulphophenylazo)-chromotropic acid,⁷⁰ 5-[(1'-oxo-4'-pyridyl)azo]-8-hydroxyquinoline⁷⁴ and 7-(benzeneazo)-8-hydroxyquinoline-5-sulphonic acid⁷⁵ all give colour reactions which can be used for manganese determinations, while there appears to be a similar potential in the use of the naphthalene-based reagents Acid Chrome Blue Black,⁷⁶ Fast Navy Blue 2R⁷⁷ and 1-(1',2',4'-triazolyl-3'-azo)-2-naphthol.⁷⁸ 2,4-Dinitrophenylazopyrocatechol has been used to determine manganese over the range 0.08–1.70 mg/l. by formation of an ion-associate with 1,10-phenanthroline,⁷⁹ bathophenanthroline⁸⁰ or 2,2'-bipyridyl.⁸¹ This method is somewhat cumbersome, as it requires an extraction step, and appears to offer little

advantage over the use of PAN and its derivatives. Khimduchlorophosphonazo-I has recently been reported as a reagent for manganese.⁸²

Various other azo compounds^{83–100} have been shown to yield colour reactions with manganese, but their usefulness as colorimetric reagents has not been assessed.

In summary, it would seem that TAR is more sensitive than TAN, PAR and PAN, but that lack of selectivity can be a major problem in its use. TAN appears to be more selective than PAN, but both reagents suffer solubility problems which can be best avoided by use of surfactants rather than extraction. The best of these reagents for the colorimetric determination of manganese appears to be 5-Br-PADAP, and this reagent should be studied more intensively.

OXIMES

Oximes, particularly the dioximes, have found wide application as analytical reagents. Marczenko¹² suggests that they form the most selective class of reagent, being commonly employed to effect analytical separations and they have been applied as spectrophotometric reagents for a variety of metal ions.¹⁰² Several methods using oxime reagents for the determination of manganese have been reported (Table 3),

Table 3. Oximes used for colorimetric determination of manganese

Reagent	Comments	Reference
Salicylaldoxime	Extracted with n-butanol	103
	In presence of H ₂ O ₂	104
	Simultaneous determination of Fe and Mn	105
3,5-Dichloro-2-hydroxyacetophenone oxime	Spot test	106
5-Chloro-2,4-dihydroxypropiophenone oxime	Range 1–6 mg/l.	107
Diphenylsuccinimide monoxime	Range up to 14 mg/l.	108
Biacetyl oxime thiosemicarbazone	Detection limit 0.1 mg/l.	109
Biacetylmonoxime phenylthiosemicarbazone	In aqueous solution or after selective extraction into amyl alcohol. Range 2–12 mg/l.	110
2,6-Pyridinediacetaldoxime	Range 0.1–10 mg/l.	111
Phthalimide dioxime [1,3-bis(hydroxyimino)isoindoline]	Sensitive to 0.1 mg/l.	112
Succinimide dioxime [1,3-bis(hydroxyimino)pyrrolidine]	Sensitive to 0.01 mg/l.	112
4(5)-Imidazolealdoxime	Range 0.8–8.0 mg/l. Interferences given.	113
Formaldoxime	Complex with Mn(IV). Range 0–3 µg/ml.	101
	For up to 5 µg/ml. Concentration on Amberlite IR-120 for <0.02 µg/ml	114
	Interference by Fe is removed by EDTA	115
	Flow-injection analysis	116
	Silicate rock analysis	117

but apart from formaldoxime¹ the reagents are generally insensitive, being suitable only for determinations in the mg/l. range. A number of other oximes have been reported¹¹⁸⁻¹²⁷ to yield colours with manganese and may be of analytical potential.

The formaldoxime method, though not recognized as a standard method, has been frequently used as an alternative to the permanganate method because it is substantially more sensitive ($\epsilon = 1.12 \times 10^4$ at $\lambda_{\max} = 455$ nm) and less time-consuming. The manganese to formaldoxime ratio of the brown-red complex is said to be 1:6,¹⁰¹ and its stability is remarkable, the colour reaction being unaffected by tartrate, oxalate, phosphate, pyrophosphate, sulphide, cyanide or EDTA.¹ However, the coloured complex gradually decomposes with time.¹²⁸ Complexes of formaldoxime with iron and manganese were first described by Denigès¹²⁹ in 1932, and the first use for the determination of manganese was reported by Sideris,^{130,131} who used sodium cyanide to mask the serious interference caused by iron. EDTA has also been used for the purpose.¹¹⁵ Since the initial development of the method, several improvements¹³²⁻¹³⁵ have been suggested and it has been applied to analysis of natural water,^{114,115,133,136-138} plant material,¹³⁸⁻¹⁴⁰ biomaterials,¹⁴¹ ores and rocks,^{116,117,142} and soils.¹⁴³ The nature of the method also makes it particularly amenable to automation,^{115,116,134,138,144,145} and for use in simple test procedures.¹²⁸ Its sensitivity is, however, insufficient for determinations below 100 $\mu\text{g/l.}$ unless preconcentration¹¹⁴ is used.

PORPHINES

These reagents give high sensitivity and are selective towards a limited number of metal ions, because of the rigid geometry of the reagent complexing sites.

Ishii *et al.*^{146,147} investigated the analytical applications of a number of substituted porphines, and found a major drawback in the slow rates of complexation. This, however, was overcome by using a substitution reaction, in which a metal ion such as Cd(II), Hg(II) or Pb(II) is displaced from the porphine ring and replaced by the analyte.¹⁴⁶ This technique has since been developed for the determination of manganese with the cadmium- $\alpha,\beta,\gamma,\delta$ -tetrakis-(4'-carboxyphenyl)porphine complex.¹⁴⁷ The method is reported to be suitable for the determination of manganese in the range 25-560 $\mu\text{g/l.}$ ($\epsilon =$

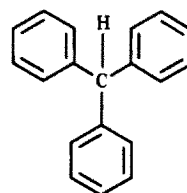
1.0×10^5 at 469 nm) with few serious interferences. It has been successfully applied to the determination of manganese in tea leaves.¹⁴⁷ The free reagent has also been used in an HPLC determination of manganese,¹⁴⁸ and $\alpha,\beta,\gamma,\delta$ -tetrakis(4'-trimethylammoniumphenyl)porphine has been used in a fourth-derivative spectrophotometric method.¹⁴⁹

The free 4-sulphophenyl derivative shows similar sensitivity and has been employed directly for the determination of manganese in ores and steel, as the water-soluble associate formed with cetyltrimethylammonium bromide.¹⁵⁰ The cadmium complex of the 4-trimethylammoniumphenyl derivative has also been successfully applied to the determination of manganese.¹⁵¹

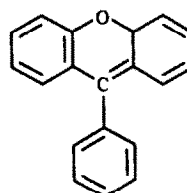
Work in our laboratories, on the automatic continuous monitoring of manganese levels in raw waters from storage dams, has shown that these porphine ligands are very sensitive, yield good contrast and are highly selective for manganese. The sensitivity may be enhanced by measurement of the second derivative of the spectrum.¹⁵²

TRIPHENYLMETHANE, XANTHENE AND ANTHRAQUINONE REAGENTS

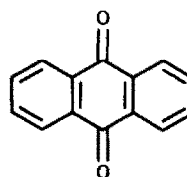
Dyes based on a triphenylmethane (6), xanthene (7), or anthroquinone (8) skeleton have



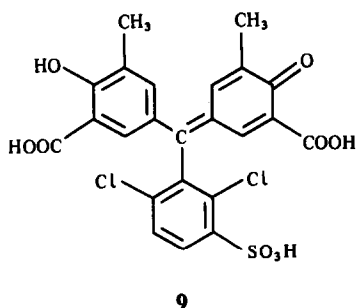
6



7



8



found widespread application as acid–base and complexometric indicators. Their application as photometric reagents is therefore not surprising. Some of the dyes investigated are listed in Table 4, and several have been applied to the determination of manganese with some success, particularly as ternary or ion-association complexes, with consequent increased selectivity and sensitivity. Some of the reagents of these types are discussed in detail below.

Chrome Azurol S (9) reacts with several metal ions to form soluble complexes. The dye contains two identical bidentate potential chelating sites, but their geometric relation precludes both sites from interacting with a single metal ion. This leads to the possibility of observing a number of chelate species in solution.¹⁶³ Horiuchi and Nishida¹⁶⁴ reported a method with an optimum range of 0.72–12 mg/l., the complex having an apparent molar absorptivity of 3.1×10^3 , but numerous transition metal cations

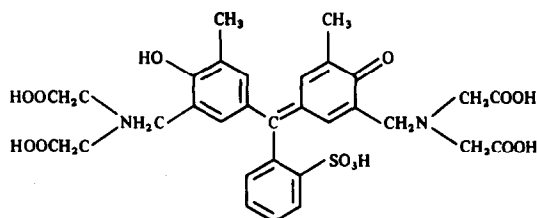
interfered. Oktavec *et al.*¹⁶⁵ reported the use of the reagent for the spectrophotometric determination of a mixture of metals (including manganese) after initial separation on a Dowex-1 ion-exchange column. The manganese was determined in aqueous pyridine solution, probably as the ion-associate formed with the Mn–pyridine complex. Oktavec *et al.* measured the absorbance at 610 nm, and Horiuchi and Nishida used 555 nm. An increase in the wavelength of the absorption maximum could be attributed to formation of the ion-associate.

More recently, Li¹⁶⁶ has reported a method based on a quaternary system which uses 1,10-phenanthroline, Chrome Azurol S and the surfactant cetyltrimethylammonium bromide (CTAB) for the determination of manganese. The maximum absorptivity is 8.0×10^4 at 635 nm (an even longer wavelength than that reported by Oktavec *et al.*). The only serious interference resulted from rare-earth metals. The method was applied to the analysis of steel and aluminium alloys with satisfactory results. Eriochrome Azurol B has been used^{166a} in combination with 2,2'-bipyridyl and CTAB for determination of manganese in steel and cobalt sulphate; again there was interference by lanthanides. These papers clearly show the advantages offered by mixed ligand systems, in terms of both selectivity and sensitivity.

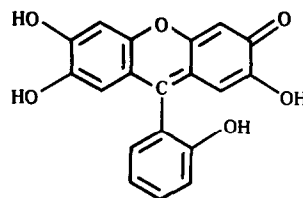
Table 4. Triphenylmethane, xanthese and anthraquinone reagents used to determine manganese

Reagents	Comments	Reference
<i>Triphenylmethanes</i>		
<i>o</i> -Hydroxyhydroquinonephthalein	Determined as the ternary complex with zephiramine*. Applied to potable and waste waters	153
Methylthymol Blue	With the surfactants cetylpyridinium bromide and CTAB. Shows increased sensitivity for Mn Comparison with other techniques	154 155
<i>Anthraquinones</i>		
Anthrapurpurin complexone (1,2,7-trihydroxy-3-methylamino-anthraquinone- <i>N,N</i> -diacetic acid)	Recommended range 1–7 mg/l.	156
Alizarin complexone	Range 1–10 mg/l.	157 158
<i>Xanthenes</i>		
Rhodamine 6G	Extraction (into benzene) of the ion-associate formed with the Mn(II)–5,7-dichloro-8-hydroxyquinoline complex, $\epsilon = 7 \times 10^4$	159
Tetraiodofluorescein	Ion-associate with Mn–phen complex. Extracted with EtOAc. $\epsilon = 1.05 \times 10^5$	160
Phenylfluorone	As the ternary complex with CTAB. $\epsilon = 8 \times 10^4$	161
<i>n</i> -Butyl xanthate	Extraction with CHCl_3 . $\epsilon = 5.5 \times 10^3$	162

*Zephiramine = tetradecyldimethylbenzylammonium chloride.



10



12

Xylenol Orange (10) is a triphenylmethane reagent which is closely related to Methylthymol Blue. Otomo¹⁶⁷ used it as a photometric reagent for Fe, Ni, Mn, Cu and Co but the method is unselective since the reagent is a metallochromic indicator. Cabrera-Martin *et al.*¹⁶⁸ used it for the determination of manganese in a number of natural matrices such as rocks, water and sera, masking interfering cations with fluoride. Manganese forms complexes with Xylenol Orange in 1:1 or 1:2 ratio which obey Beer's law in the ranges 0.0–1.6 and 1.6–4.2 mg/l., respectively. The reagent has also been used in a catalytic method.¹⁶⁹

Bromopyrogallol Red (11) is an acidic xanthene dye structurally related to phenylfluorone. Cheng *et al.*¹⁷⁰ have detailed the history of this reagent, including its use as a complexometric indicator for the determination of manganese.^{171,172}

Rudzitis *et al.*¹⁷³ reported the formation of an extractable ion-pair formed between the manganese complex and diphenylguanidine. The method, however, was developed for determination of aluminium, with n-butanol as extractant. More recently Xu *et al.*¹⁷⁴ investigated the colour reactions of Bromopyrogallol Red in the presence of several surfactants and suggested a method for determination of manganese.

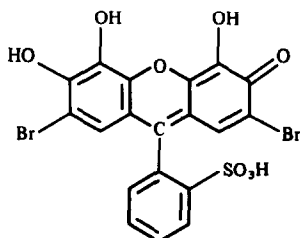
9-Salicylfluorone (12) is a significant reagent for the colorimetric determination of manganese because of the comparative study made by Tataev and Anisimova¹⁵⁵ (one of the few

papers of this type found). They studied the possible analytical applications of PAR, Xylenol Orange, Methylthymol Blue (13) and 9-salicylfluorone for the determination of manganese and found that the last two reagents formed complexes with molar absorptivities of 2.06×10^4 and 8.0×10^4 , respectively, and that PAR was the most selective of the reagents studied. In the light of their results there appears no good reason to suggest that the other reagents should replace PAR. However, phenylfluorone¹⁷⁵ and *o*-nitrophenylfluorone¹⁷⁶ have recently been investigated in quaternary systems involving hexadecyltrimethylammonium bromide and an emulsifier, with good results.

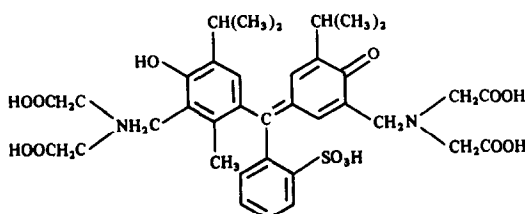
Colour reactions with manganese or manganese complexes have been reported^{177–188} for a much wider range of triphenylmethane, anthraquinone and xanthene reagents than those noted above, but none has been investigated for quantitative use.

OTHER REAGENTS

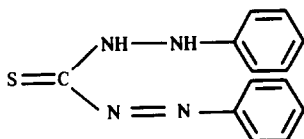
Many other organic compounds have been studied as possible colour reagents for manganese determination. In particular, dithizone (diphenylthiocarbazon, 14)¹⁸⁹ and related carbazones have been widely studied (Table 5), as have hydroxamic acid derivatives (Table 6) and a large assortment of other reagents (Table 7). The general applicability of these methods has not been worked out and it is hard to assess



11



13



14

which may be promising methods for manganese in a specific matrix.

Colour-forming reactions with various carbazones,^{250,251} hydroxamic acids²⁵²⁻²⁵⁴ and other reagents²⁵⁵⁻²⁸⁸ have been noted in the literature, but no analytical details were made available in the abstracts consulted.

KINETIC METHODS

There is a dogma in analytical chemistry that determinations should be based on systems at equilibrium or those which can go to completion stoichiometrically.²⁸⁹ In other branches of chemistry, kinetics has been recognized as being relatively important, but in analytical chemistry has been of little import, except where a reaction is slow to reach equilibrium, *e.g.*, in relation to an end-point indicator reaction, or in considering the effect of possible competing side-reactions.²⁹⁰ However, where a relationship exists between a change of a property of a system with time and the amount of a component in the system, there exists a means by which the amount of substance can be measured quantitatively. Although the possibility of employing

such methods of analysis has long been recognized (*e.g.*, the cerium-arsenic reaction was proposed by Sandell and Kolthoff in 1934 as a method for determining osmium and iodide by monitoring their catalytic effect²⁹¹), until recently analytical chemists have considered the use of dynamic methods as little more than an academic novelty. Interest in their use has been stimulated by the development of the continuous-flow methods of analysis, in which non-equilibrium conditions are generally used.²⁹²⁻²⁹³

Kinetic methods potentially offer advantages of increased sensitivity and selectivity and, with the developing needs of analytical chemistry in the area of trace analysis, such methods have found increasing application. These methods may be subdivided into three groups:⁷

- (1) non-catalytic methods;
- (2) catalytic methods—determination of a catalyst or activator/inhibitor;
- (3) enzymatic methods—determination of enzyme, substrate or activator/inhibitor; an example of this is the horseradish peroxidase (HRP) method,²⁹⁴ in which manganese is determined as a result of its ability to activate the enzyme HRP.

For the determination of Mn, there is no significant difference between the last two techniques. The papers reviewed here, with the exception of the HRP method, deal exclusively with methods of type (2).

The catalytic reaction may be monitored directly or indirectly (where the product of a

Table 5. Analyses for manganese with dithizone and related compounds

Reagents	Comments	Reference
Diphenylthiocarbazon (dithizone)	Ternary complex with pyridine, extracted with CHCl ₃ ; $\epsilon = 5.7 \times 10^4$	190 191
	Extracted into CHCl ₃ as ternary complex with phenanthroline; $\epsilon = 4.6 \times 10^4$; applied to spring waters and carbonate rocks	192
Di- β -naphthylthiocarbazon	Unstable complex with Mn	193
1,5-Di(4'-sulphophenyl)thiocarbazon		194
Diphenylcarbazon	Extraction with benzene; applied to blood samples	195
	Assay and study of extractive behaviour	196
Substituted 1,5-diphenylcarbazones	<i>p</i> -Nitro substitution in either the 1- or the 5-phenyl group; ϵ values for Mn are low	197
Bipyridylglyoxal bis(4-phenyl-3-thiosemicarbazone)	Complex obeys Beer's law over the range 0.2-1.2 mg/l.	198
4,4'-Diphenylthiosemicarbazones of 1,2-diketones	A number of analogous compounds were investigated and found to produce extractable (into EtOAc) complexes with several metals, including Mn. ϵ values for the complexes were $1.0-2.3 \times 10^4$	199
2-Oximinocyclohexanone thiosemicarbazone	Applied to analysis of iron ore	200

Table 6. Analysis for manganese with hydroxamic acid derivatives

Reagent	Comments	Reference
<i>p</i> -Methoxybenzothiohydroxamic acid	Mn(III) complex extracted with CHCl ₃ ; $\epsilon = 1.25 \times 10^4$	201 202
	Original assay	203
	Isophthalidihydroxamic acid	Extracted into toluene-Adogen 464* solution; range 1-7 mg/l., $\epsilon = 8.5 \times 10^3$
Benzohydroxamic acid	Method without extraction. Range 3-9 mg/l.	205
	Detailed study of complex	206
Dipicolinedihydroxamic acid	In water or aqueous DMF as solvent; $\epsilon = 3.6 \times 10^3$; for Mn in alloys	207
	Extracted in benzene-Adogen 464* solution; $\epsilon = 4.1 \times 10^3$; range 0.5-5 mg/l.	208
Potassium hydrogen phthalomonohydroxamate	Extracted in DMF; range 1-17 mg/l.	209
<i>o</i> -Aminobenzohydroxamic acid	$\epsilon = 3.7 \times 10^3$; range 1-17 mg/l.	210
<i>p</i> -Methoxybenzothiohydroxamic acid	After selective extraction; $\epsilon = 1.06 \times 10^4$; applied to determination in several salts	211
Salicylhydroxamic acid	Extracted into toluene as a ternary complex with adogen 464*; for steel; range 0.3-7 mg/l.	212
5,5'-Dithiodi(salicylohydroxamic acid)	Fe(III), Ti(IV), Cu(II) and V(V) interfere at $> 2 \mu\text{g/ml}$.	213

*Adogen 464 = trioctylmethylammonium chloride.

subsequent chemical reaction is the indicator substance), by such techniques as photometry, fluorimetry, chemiluminescence, potentiometry (e.g., the use of the perchlorate ion-selective electrode for monitoring the manganese-catalysed oxidation of triethanolamine by periodate²⁹⁵), conductometry, thermometric methods (Alfimova²⁹⁶ reported a method for the determination of manganese with thermometry to monitor the decomposition of hydrogen peroxide), or by traditional wet methods of analysis. Chemiluminescence techniques are potentially very sensitive,²⁹⁷ but require the use of a spectrophotometer modified for making the measurements. When continuous monitoring is required, an instrument can be dedicated to the specific analysis.

Weisz²⁹⁸ has written a general review on the application of catalysed reactions in analytical chemistry, in which he explains the associated theory and a number of methods employed to monitor indicator reactions. The reviews by Müller⁷ and Mottola²⁹⁰ take a more detailed approach to the subject, and two recent books are useful.^{299,300} Bontchev and Aleksiev³⁰¹ have studied the use of ligands to activate catalysed reactions—nitrogen-containing ligands, particularly phenanthroline, are commonly employed to enhance the catalytic effect of the metal and improve the sensitivity of the method. Little

attempt has been made in any of the work on kinetic methods of analysis for manganese to compare methods for a given analytical situation. Only Pérez-Bendito and co-workers,³⁰²⁻³⁰⁴ appear to have considered this need, and have studied the relative merits of methods based on 2-hydroxybenzaldehyde thiosemicarbazone and 2-hydroxynaphthaldehyde thiosemicarbazone for the determination of manganese in food-stuffs. They found that the latter reagent was more selective and could be used over a wider range of manganese concentrations (Table 8). It should be noted that the operative range for many of the kinetic methods is very narrow.

Table 8 contains a summary of catalytic methods for the determination of manganese by use of a photometric method to follow the indicator reaction. A number of other catalytic systems have been proposed,³⁷⁶⁻³⁹⁴ but seem to offer no advantages over the best of those listed in Table 8. The types of catalysed reactions used are potentially very selective. Interferences may be masked by conventional means, as positively interfering ions have a similar catalytic effect to the analyte. In this case masking agents, by virtue of their ability to complex an interfering metal ion selectively, can inhibit or remove the catalytic activity of the interferent.

Separation techniques may be used prior to determination, (e.g., selective extraction, ion-

Table 7. Miscellaneous colorimetric methods for the determination of manganese

Reagent	Comments	Reference
Pyridine-2-aldehyde-2'-pyridylhydrazone	Mn complex extractable with CHCl ₃ ; $\epsilon = 5.71 \times 10^4$	214
Pentamethylenedithiocarbamate	After extraction into benzene	215
Diethyldithiocarbamate	Mn in food products	216
	Increased sensitivity by using UV spectrum	217
1,5-bis(2-Hydroxy-5-sulphophenyl)-3-acetylformazan	$\epsilon = 1.3 \times 10^4$	218, 219
Benzamidrazone	Sensitivity 0.3 mg/l. in 75% alcohol solution	220
Methyliminodimethylenephosphonic acid	Determination of both Mn and Zn	221
Diantiprylmethane	Mn in enamels and dyes	222
Determination as [Mn(CN) ₆] ⁴⁻	Range 3–50 mg/l., not linear	223
Gluconic acid	Range 9–47 mg/l., interferences are given	224
	Mn in garnet	225
Thenoyltrifluoroacetone	Separation and analysis of mixtures of Ce and Mn by extraction and back extraction	226
Thiothenoyltrifluoroacetone	Extraction with CCl ₄ ; interferences are given; range 1.25–20 mg/l.	227
	Mn extracted into xylene in the presence of phenanthroline; $\epsilon = 3.58 \times 10^4$; applied to Mn in Al and Al alloys	228
Triethanolamine	Range 2–45 mg/l. (long-path cell); applied to sea-water	229, 230
<i>N,N</i> -bis(2-Hydroxy-5-sulphophenyl)- <i>C</i> -cyanoformazan	$\epsilon = 1.5 \times 10^4$	231
<i>N</i> -Hydroxy- <i>N</i> -phenyl- <i>N'</i> -benzylbenzamide hydrochloride	$\epsilon = 5.3 \times 10^3$	232
1-Benzylbenzimidazolyl-5-phenylformazan (or the corresponding <i>p</i> -nitrophenylformazan)	Method for extraction and analysis of a mixture of Cd, Zn, Cu and Mn	233
Pyrophosphate	Range 50–1000 mg/l., Mn in ores <i>etc.</i>	234
Thiocyanate	Range 0.2–2 mg/l. $\epsilon = 3.6 \times 10^5$; extract with tribenzylamine	235
<i>N</i> -Hydroxy- <i>N,N'</i> -diaryl-substituted- <i>p</i> -toluamides	A number of compounds were synthesized and found to have molar absorptivities in the range $5.2\text{--}7.5 \times 10^3$; suggested for Mn in the range 1.6–10 mg/l.	236
<i>N</i> -Hydroxy- <i>N-m</i> -tolyl- <i>N'</i> -(2,3-dimethyl)phenylbenzamide hydrochloride	In alcohol solution	237
<i>N,N',N''</i> -Trihydroxytrimethylenetriamine	$\epsilon = 1.6 \times 10^4$	238
(<i>p</i> -Aminophenyl)thioacetic acid		239
<i>N,N,N',N'</i> -Tetrakis(2-hydroxypropyl)ethylenediamine	Range 2–100 mg/l. Applied to four NBS metal samples	240
	Applied to soils	241, 242
EDTA	Determined as the Mn(III) complex; range 4–170 mg/l.	243
Binazine	After extraction with CHCl ₃ ; range 0.2–15 mg/l., applied to sea-waters	244
Tetraphenylarsonium chloride	Range 0.1–5.0 mg/l., applied to high-purity CaCO ₃	245
Dibenzoylmethane/piperidine	Mn in cast iron; the ternary complex is extracted into CHCl ₃	246
Eriochrome Black T	Range up to 10 ng/ml. Decrease in indicator absorbance is measured at 611 nm	246a
8-Mercaptoquinoline	Mn in a mixture of metals after extraction into CHCl ₃	247
2-Aceto-1-naphthol- <i>N</i> -salicyl hydrazone	Extraction with DMF	248
Cacotheline	As spot test and for photometric determination	249
8-Hydroxyquinoline/Aliquat 336	Extraction; $\epsilon = 2.2 \times 10^4$	249a

Table 8. Kinetic methods used to analyse for manganese

Reagent	Range	Comments	Reference
2,3-Diketogulonate	4–30 mg/l.	Mn(II) activates the oxidation of DGA by horseradish peroxidase. The H ₂ O ₂ produced is determined with <i>p</i> -hydroxyphenylacetic acid as a fluorophore ³⁰⁵	294
Luminol	≈0.005–5 μg/l.	Using H ₂ O ₂ as the oxidant and a mixture of 1,10-phenanthroline and Na citrate to activate the reaction and improve selectivity; detection by luminescence	306, 307
	0.01–10 mg/l.	The luminescence is observed in a carbonate buffer solution in the absence of the activators used above. The interference of several ions is masked by use of cyanide	308
		Using Na bismuthate	309
	1–5000 μg/l.	By luminescence; used for Mn in minerals and polluted waters Electrolytic preconcentration. Fixed-time luminescence (H ₂ O ₂) method	310 311
Leucomalachite Green	≈1–15 μg/l.	Using periodate to oxidize the leuco base to Malachite Green. For Mn in human serum	312
		Semiautomatic analysis at sea, but not sensitive enough for studying open-ocean Mn distribution	313
Malachite Green (C.I. Basic Green 4)	>5 μg/l.	Using periodate as the oxidant and nitrilotriacetic acid as activator	314
	5–100 μg/l.	Using periodate. Interferences from Fe and Al are masked with F ⁻ . Used for Mn in HF, HNO ₃ and high-purity silicon	315
	70–200 μg/l.	Using periodate	316
	70–200 μg/l.	Using periodate. Fe and Al masked with EDTA	317
	5–200 μg/l.	Using periodate	318
	2–200 ng	Using periodate	319
	Up to 7 ng	Peroxide as oxidant, flow-injection analysis	319a
	0.4–5.0 μg/l.	Periodate as oxidant, nitrilotriacetic acid as activator	320
		Mn in marine sediments	321
	0.03–2 ng	Flow-injection analysis, periodate as oxidant	322
		Flow-injection analysis, periodate as oxidant	323
	0.1–15 ng/ml	Stopped-flow: periodate as oxidant, nitrilotriacetic acid as activator	323a
	<i>o</i> -Dianisidine	Sensitivity 0.2 μg/l.	Using periodate. Tartrates, citrates, oxalates and Fe(II) interfere. For Mn in natural waters
Sensitivity 0.1 μg/l.		Using periodate. Applied to Mn in clays	325
		A study of the reaction	326
Sensitivity 80 μg/l.		A comparison with a number of other aromatic amines	327
2–10 μg/l.		Using H ₂ O ₂ as the oxidant in an aqueous DMF medium	328
Sensitivity 0.5 μg/l.		Using H ₂ O ₂ as oxidant and 1,10-phenanthroline as activator	329
<i>o</i> -Dianisidine + tiron		0.2–1 ng/ml	H ₂ O ₂ as oxidant, 1,10-phenanthroline as activator, absorbance measured at 440 nm after 0.5 and 2 min.

continued overleaf

Table 8—*continued*

Reagent	Range	Comments	Reference
Succinimidedioxime	2–12 $\mu\text{g/l.}$	By autoxidation; Pd interferes	331
	50–1300 $\mu\text{g/l.}$	Fe(III) and Co(II) interfere; other interferences are masked with EDTA. Mn in foodstuffs	332
<i>p</i> -Fuchsin leuco base	Sensitivity 2 $\mu\text{g/l.}$	Using periodate as oxidant and nitrilotriacetic acid as activator. Mn in products for fibre optics	333
		Using <i>N</i> -phosphonomethyliminodiacetic acid as activator	334
Indigosulphonates mono- di- tetra-	1–10 $\mu\text{g/l.}$	Using H_2O_2 as oxidant. Many ions are tolerated in large excess	335
Thymol Blue		Periodate as oxidant	336
3-Hydroxypyridinaldehyde azine	0.4–0.9 $\mu\text{g/l.}$	Tolerances are given for interfering ions. H_2O_2 is used as the oxidant	337
3-Hydroxypyridinaldehyde thiosemi-carbazone	5–50 $\mu\text{g/l.}$	Fe(III) interferes but can be masked. H_2O_2 is used as the oxidant	337
Acetylacetone	5–500 $\mu\text{g/l.}$	Periodate as the oxidant. Mn in natural waters	338
Alizarin S	0.3–56 $\mu\text{g/l.}$	H_2O_2 as the oxidant	339
Pyrocatechuic acid	0–40 $\mu\text{g/l.}$	H_2O_2 as the oxidant. Co interferes seriously. Fe(III) and Cr(III) interfere in >10- and 20-fold amounts, respectively	340
5-(2'-Hydroxy-3'-sulpho-5'-chlorophenylazo)barbituric acid	Sensitivity 6 $\mu\text{g/l.}$	Using H_2O_2 as oxidant and ethylenediamine as activator. Interferences were studied	341
I^-	0.5–40 $\mu\text{g/l.}$	Oxidation of I^- by periodate is catalysed by the 1,10-phenanthroline complex of Mn and is followed by measuring the absorbance of the starch-iodine complex	342
Na carminate	Sensitivity 0.12 $\mu\text{g/l.}$	Oxidation by H_2O_2 . Interferences are given	343
Hydroxy Naphthol Blue	0–5 $\mu\text{g/l.}$ Sensitivity 0.01 $\mu\text{g/l.}$	H_2O_2 as the oxidant. Fe(III) interferes	344
Lumomagneson	Sensitivity 0.44 $\mu\text{g/l.}$	H_2O_2 as the oxidant. Highly selective	345
Indigo Carmine	≈ 0.3 –1.6 $\mu\text{g/l.}$	Mn determined as the complex with 1,10-phenanthroline, with H_2O_2 as the oxidant. Interferences are given	346
Nitrosin Yellow	0.06–6.02 $\mu\text{g/l.}$	Using H_2O_2 as the oxidant and 1,10-phenanthroline as activator. Interferences are given, but none is serious	347
Purpurin	14–160 ng/l.	Using ethylenediamine as an activator and H_2O_2 as the oxidant. Mn in hair	348
Tropacolin 0002	0.1–12.3 $\mu\text{g/l.}$	Oxidation by H_2O_2 with 1,10-phenanthroline as activator	349
Na diphenylamine sulphonate		Oxidation by peroxocapric acid. 2,2'-Bipyridyl and 1,10-phenanthroline act as activators and stabilize the Mn(II)	350
NaH_2PO_2	10–100 $\mu\text{g/l.}$	Using periodate as the oxidant and nitrilotriacetic acid as activator. For Mn in natural and potable waters	351
	0.05–5 $\mu\text{g/l.}$	Stopped-flow reverse flow-injection analysis. Periodate as oxidant, nitrilotriacetic acid as activator. Trace Mn in water samples	352
	0.2–9 $\mu\text{g/l.}$	Periodate as oxidant, nitrilotriacetic acid as activator. Co interferes. Used for polluted water samples	352a

continued opposite

Table 8—continued

Reagent	Range	Comments	Reference
Sulphanilic acid	50–500 $\mu\text{g/l}$.	Using periodate as the oxidant	353
	0.5–5 $\mu\text{g/l}$.	As above, using 1,10-phenanthroline as an activator. Fe interferes in a 10-fold amount. Shows better selectivity than the method above	354
1-Amino-8-naphthol-3,6-disulphonic acid	Sensitivity 0.5 $\mu\text{g/l}$.	Using ethylenediamine as an activator and H_2O_2 as the oxidant	355
Sb(III)	0.5–50 $\mu\text{g/l}$.	Using periodate as the oxidant and nitrilotriacetic acid as an activator. Used for Mn in non-ferrous alloys	356
Lucigenin	Sensitivity 1–2 $\mu\text{g/l}$.	Mn has a catalytic affect on the luminescence of lucigenin in the presence of H_2O_2	357 358
	<i>N,N</i> -Diethylaniline	Sensitivity 0.5 $\mu\text{g/l}$.	Using periodate. For Mn in blood and other tissues
10–80 ng/l .		For Mn in natural waters	360
0.1–1.0 ng/ml		Periodate as oxidant. Flow-injection analysis of sea-water	360a
2-Hydroxybenzaldehyde thiosemicarbazone	2–9 $\mu\text{g/l}$.	Using H_2O_2 as the oxidant. Detection by fluorescence. For Mn in a variety of foodstuffs. Interferences are given	302
		Variation of the method above to give simultaneous determination of Mn(II) and Fe(III)	303
2-Hydroxynaphthaldehyde thiosemicarbazone	0.75–50 $\mu\text{g/l}$.	Method similar to that above but the reagent is more selective. For Mn in wine and other foodstuffs	304
Eriochrome Black T	Sensitivity 0.05 $\mu\text{g/l}$.	Using H_2O_2 as the oxidant	361
Eriochrome Blue Black R	Up to 1.6 pg/l .	H_2O_2 as oxidant at pH 9.8	361a
Pyrocatechol Violet	Sensitivity 0.12 $\mu\text{g/l}$.	Using ethylenediamine as an activator and H_2O_2 as the oxidant. Most ions tolerated in 1000-fold ratio. Fe(III) is tolerated in 10-fold ratio	362
Azorubin S	5.5–33 $\mu\text{g/l}$.	Using H_2O_2 as the oxidant. Mo and W may interfere	363
	0.44–1.76 $\mu\text{g/l}$.	Determination made in 30% v/v acetone	364
Acid Blue 45 (Na 1,5-dihydroxy-4,8-diaminoanthraquinone-2,6-disulphonic acid)	4–25 $\mu\text{g/l}$.	Using H_2O_2 as the oxidant. Cu(II) interferes. Adapted as indicator for EDTA titration	365, 366
	6–22 $\mu\text{g/l}$.	Atmospheric oxidation. For Mn in potable water and industrial fumes	367
Salicylaldehyde guanylhydrazone	8–80 ng/ml	H_2O_2 as oxidant. EDTA interferes seriously. Used for natural waters, cement, basic slag, iron ore and lead concentrate	368
		H_2O_2 as oxidant. Simultaneous determination of Mn and Zn	369
Xylenol Orange	0.25–2.5 ng/ml	H_2O_2 as oxidant, 1,10-phenanthroline as activator	370
Bromophenol Blue	0.6–40 ng/ml	Periodate as oxidant, 1,10-phenanthroline as activator. Used for analysis of tea and Al alloy	371
Pyrogallol Red	Sensitivity 18 pg/ml	H_2O_2 as oxidant, 2,2'-bipyridyl as activator. Analysis of well water	372
Xylene Cyanol FF	2–11 ng/ml	Periodate as oxidant, 1,10-phenanthroline as indicator. Food analysis	373
3-(2'-Hydroxyphenylazo)-pyridine-2,6-diol	0.5–9 ng/ml	H_2O_2 as oxidant. EDTA and Sn(II) interfere. Analysis of coffee, rice, beer and tap water	374
3,4-Dihydroxybenzoic acid	1–11 ng/ml	Continuous-flow detection after ion-exchange separation. H_2O_2 as oxidant	375

Table 9. Determination of manganese after initial oxidation to permanganate

Reagent	Range	Comments	Reference
Oxine-5-sulphonic acid	2.5–2500 $\mu\text{g/l}$.	By fluorescence, persulphate and AgNO_3 as the oxidant	395
6-Methoxy-2-methylthio-4-pyrimidine carboxylic acid	2–60 $\mu\text{g/ml}$	Permanganate reduced to manganate in alkaline medium	396
8-Aminoquinoline	12–550 $\mu\text{g/l}$.	Oxidized with bismuthate	397
Ethylenebis(triphenylphosphonium) bromide	0–120 μg	Extraction of permanganate	398
	Up to 25 $\mu\text{g/ml}$	Flow-injection analysis	399
Trimethylenebis(triphenylphosphonium) bromide	0–120 μg	Extraction of permanganate	400

chromotography or precipitation) either to pre-concentrate the analyte or to remove or reduce the level of interfering species. Differential rate methods, which assume that the rates for the analyte-catalysed and interference-catalysed reactions are different, may also be used to counter the effect of interfering species.

Reactions of permanganate

Finally, Table 9 lists a few methods of determination of permanganate.

CONCLUSIONS

This work has comprehensively reviewed the literature on colorimetric methods for the determination of manganese up to about mid-1989. It is evident that there has been a major problem in categorizing the information in a systematic fashion. Part of this problem stems from the widespread use of trade and trivial names for colorimetric reagents. One apparent solution would be for editors to insist upon the use of systematic nomenclature, but given the structure of some of the reagents, this may not produce the clarification sought. Two practices of great value would be the inclusion of a structural formula and of all known trade and trivial names, as well as the systematic name of the reagent. The second requirement would certainly simplify computer searches of the literature.

The growth in interest in the use of organic colorimetric reagents in the 1960s led several authors, including Belcher⁴⁰¹ and Wilson,⁴⁰² to call for collation of the data being reported. A selectivity index, as a basis for assessing the usefulness of a reagent, was proposed. In attempting to prepare reagents that are either more sensitive or selective in their action, most authors do not undertake the detailed analysis of the effect of changing functional groups on

the organic ligand. This contrasts markedly with work in inorganic co-ordination chemistry, where many authors have been able to correlate the co-ordinating abilities and stereochemistries of metal-multidentate ligand compounds with ligand substituent changes. Savvin's⁶ approach is of relevance here.

We now have a large number of colorimetric reagents for the determination of manganese and much more work on the comparative usefulness of such methods in specific analytical situations is required. Work in our laboratories is currently aimed at assessing why a number of common colorimetric methods for the determination of manganese in natural waters yield consistently different results.

Acknowledgements—The authors acknowledge financial support for their work from the Queensland Department of Local Government and general support from Brisbane City Council, Queensland.

Addendum—Further details of colour reactions of various reagents with manganese, contained in the references 38–48, 69–81, 83–100, 118–127, 177–188, 252–254 and 255–288 have been put into tabular form. Although this material is not published here, copies are available from the authors.

REFERENCES

1. Z. Marczenko, *Separation and Spectrophometric Determination of Elements*, Horwood, Chichester, 1986.
2. C. Jiang and Z. Li, *Fenxi Shijianshi*, 1988, 7, No. 10, 59; *Anal. Abstr.*, 1989, 51, 4827.
- 2a. S. Kuš and Z. Marczenko, *Talanta*, 1989, 36, 1139.
3. F. D. Snell and C. T. Snell, *Colorimetric Methods of Analysis*, 3rd Ed., Vol. 2, pp. 390–399; Vol. 2A, pp. 306–311. Van Nostrand, Princeton, 1959.
4. K. L. Cheng and R. H. Bray, *Anal. Chem.*, 1955, 27, 782.
5. F. H. Pollard, P. Hanson and W. J. Geary, *Anal. Chim. Acta*, 1959, 20, 26.
6. S. B. Savvin, *CRC Crit. Rev. Anal. Chem.*, 1979, 8, 55.
7. H. Müller, *ibid.*, 1982, 13, 313.
8. G. H. Ayres and B. D. Narang, *Anal. Chim. Acta*, 1961, 24, 241.

9. E. B. Sandell, *Colorimetric Determination of Traces of Metals*, 3rd Ed., pp. 83–84. Interscience, New York, 1959.
10. T. F. Rudometkina, V. M. Ivanov and A. I. Busev, *Zh. Analit. Khim.*, 1977, **32**, 1674; *Chem. Abstr.*, 1978, **88**, 130050u.
11. *Idem*, *Russ. J. Inorg. Chem.* 1977, **22**, 77.
12. Z. Marczenko, *CRC Crit. Rev. Anal. Chem.*, 1981, **11**, 195.
13. A. E. Tschitschibabin, *J. Russ. Phys. Chem. Soc.*, 1918, **50**, 513; *Chem. Abstr.*, 1924, **18**, 1496.
14. J. Liu, *Ph. D. Thesis*, University of Illinois, 1951.
15. K. L. Cheng, K. Ueno and T. Imamura, *Handbook of Organic Analytical Reagents*, p. 185. CRC Press, Boca Raton, 1982.
16. S. Shibata, *Anal. Chim. Acta*, 1961, **25**, 348.
17. K. Nakagawa, T. Ogata, K. Haraguchi and S. Ito, *Bunseki Kagaku*, 1981, **30**, 149; *Chem. Abstr.*, 1981, **95**, 54132z.
18. K. Goto, S. Taguchi, Y. Fukue, K. Ohta and H. Watanabe, *Talanta*, 1977, **24**, 725.
19. E. Donaldson and W. Inman, *ibid.*, 1966, **13**, 489.
20. I. G. Per'kov, G. V. Artsebashev, A. V. Drozd and G. G. Syrova, *Zh. Analit. Khim.*, 1987, **42**, 1951.
21. K. L. Cheng and B. L. Goydich, *Anal. Chim. Acta*, 1966, **34**, 156.
22. H. Watanabe, *Talanta*, 1974, **21**, 295.
23. K. O'Halloran, *Honours Thesis*, University of Queensland, 1986.
24. B. Chiswell, M. Bin Mokhtar and K. O'Halloran, *Proc. 9th Austr. Symp. Anal. Chem.*, 1987, 806.
25. K. Ohshita, H. Wada and G. Nakagawa, *Anal. Chim. Acta*, 1982, **140**, 291.
26. S. Shibata, K. Goto and E. Kamata, *ibid.*, 1969, **45**, 279.
27. S. Shibata, M. Furukawa, E. Kamata and K. Goto, *ibid.*, 1970, **50**, 439.
28. R. G. Anderson and G. Nickless, *Analyst*, 1967, **92**, 207.
29. T. Yoytsuyanagi, K. Goto, M. Nagayama and K. Aomura, *Bunseki Kagaku*, 1969, **18**, 477; *Chem. Abstr.*, 1969, **71**, 56313n.
30. K. Ueda, Y. Yamamoto and S. Ueda, *Nippon Kagaku Zasshi*, 1969, **90**, 903; *Chem. Abstr.*, 1969, **71**, 119327t.
31. S. G. Nagarkar and M. C. Eshwar, *Chem. Era*, 1975, **11**, 1; *Chem. Abstr.*, 1976, **84**, 115451z.
32. D. Nonova and B. Evtimova, *Talanta*, 1973, **20**, 1347.
33. T. Watase, *Kyushu Yakugakkai Kaiho*, 1979, No. 33, 111; *Chem. Abstr.*, 1980, **92**, 185593m.
34. W. Wang, Y. Chen and M. Wu, *Analyst*, 1984, **109**, 281.
35. J. R. Jezorek and H. Freiser, *Anal. Chem.*, 1979, **51**, 373.
36. S. Ahrland and R. Herman, *ibid.*, 1975, **47**, 2422.
37. O. A. Tataev and L. G. Anisimova, *Zh. Analit. Khim.*, 1971, **26**, 184; *Chem. Abstr.*, 1971, **74**, 119769a.
38. S. Shibata, M. Furukawa and K. Toei, *Anal. Chim. Acta*, 1973, **66**, 397.
39. H. R. Hovind, *Analyst*, 1975, **100**, 769.
40. J. Minczewski and K. Kasiura, *Chem. Anal. (Warsaw)*, 1965, **10**, 21; *Chem. Abstr.*, 1965, **63**, 17109h.
41. C. Sanchez-Pedreno, *Quim. Anal.*, 1977, **31**, 249; *Chem. Abstr.*, 1978, **89**, 118418h.
42. A. T. Pilipenko, A. E. Parkhomenko and S. D. Isaev, *Ukr. Khim. Zh.*, 1976, **42**, 741; *Chem. Abstr.*, 1977, **86**, 64925p.
43. V. Gonzalez Diaz, C. Sanchez-Pedreno and F. Garcia Montelongo, *Quim. Anal.*, 1974, **28**, 211; *Chem. Abstr.*, 1975, **82**, 67668k.
44. C. Sanchez-Pedreno, F. Garcia Montelongo and V. Gonzalez Diaz, *An. Quim.*, 1975, **71**, 79; *Chem. Abstr.*, 1975, **83**, 187799w.
45. F. Garcia Montelongo and R. Perez Oimos, *ibid.*, 1977, **73**, 1136; *Chem. Abstr.*, 1978, **89**, 172956v.
46. J. Gao, T. Chen, G. Gu, X. Liu, F. Hui and Y. Huang, *Huaxue Shiji*, 1984, **6**, 199; *Chem. Abstr.*, 1984, **101**, 221500u.
47. T. Tanaka, K. Hiro and A. Kawahara, *Osaka Kogyo Gijutsu Shikensho Kiho*, 1980, **31**, 251; *Chem. Abstr.*, 1981, **94**, 14926g.
48. T. F. Rudometkina, V. M. Ivanov and A. I. Busev, *Org. Reagenty Anal. Khim., Tezisy Dokl. Vses. Konf.*, 4, 1976, **2**, 74; *Chem. Abstr.*, 1978, **88**, 66448a.
49. T. Rudometkina, V. M. Ivanov and A. I. Busev, *Zh. Analit. Khim.*, 1977, **32**, 446; *Chem. Abstr.*, 1977, **87**, 15380u.
50. U. G. Gaokar and M. C. Eshwar, *Mikrochim. Acta*, 1982 **II**, 247.
51. G. Nakagawa and H. Wada, *Nippon Kagaku Zasshi*, 1962, **83**, 1185; *Chem. Abstr.*, 1963, **59**, 9289d.
52. E. Grzegorzolka, *Chem. Anal. (Warsaw)*, 1977, **22**, 303; *Chem. Abstr.*, 1977, **87**, 193129b.
53. K. Haraguchi, K. Nakagawa, T. Ogata and S. Ito, *Bunseki Kagaku*, 1980, **29**, 809; *Chem. Abstr.*, 1981, **94**, 57480b.
54. S. Shibata and M. Furukawa, *ibid.*, 1974, **23**, 1412.
55. F. Wei, P. Qu and Y. Zhu, *Fen Hsi Hua Hsueh*, 1981, **9**, 345; *Chem. Abstr.*, 1981, **95**, 231307h.
56. X.-C. Qiu, Y.-S. Zhang and Y.-Q. Zhu, *Soil Science*, 1984, **138**, 432.
57. *Idem*, *Chem. Anal. (Warsaw)*, 1985, **30**, 127.
- 57a. J. Li, C. Xi and H. Shi, *Fenxi Huaxue*, 1987, **15**, 131; *Anal. Abstr.*, 1987, **49**, 11A50.
- 57b. C. Chen, *Lihua Jianyan Huaxue Fence*, 1987, **23**, 26; *Anal. Abstr.*, 1988, **50**, 2B142.
58. Y. Sumi, T. Inoue, T. Muraki and T. Suzuki, *Stain Technol.*, 1983, **58**, 325.
59. G. Zhang, B. Liu and Y. Hu, *Fenxi Huaxue*, 1987, **15**, 142; *Anal. Abstr.*, 1987, **49**, 11B230.
60. V. S. Podgornova and T. B. Amirkhanova, *Nauchn. Tr., Tashkentsk. Gos. Univ.*, 1964, No. 263, 77; *Chem. Abstr.*, 1965, **63**, 17108h.
61. I. P. Shesterova, N. F. Kostylev, Sh. T. Talipov and R. Kh. Dzhiyanbaeva, *Uzb. Khim. Zh.*, 1966, **10**, No. 6, 7; *Chem. Abstr.*, 1967, **66**, 72068p.
62. S. E. Podlipskaya, R. Kh. Dzhiyanbaeva and Sh. T. Talipov, *Nauchn. Tr. Tashkent. Gos. Univ.*, 1967, No. 288, 87. *Chem. Abstr.*, 1968, **68**, 106053p.
63. L. F. Chaprasova, Sh. T. Talipov and R. Kh. Dzhiyanbaeva, *ibid.*, 1967, No. 284, 42; *Chem. Abstr.*, 1968, **69**, 92630f.
64. N. G. Kagramanova, Sh. T. Talipov and R. Kh. Dzhiyanbaeva, *ibid.*, 1968, No. 323, 11; *Chem. Abstr.*, 1970, **72**, 96255x.
65. *Idem*, *ibid.*, 1968, No. 323, 28; *Chem. Abstr.*, 1970, **72**, 96356f.
66. Sh. T. Sharipova, R. K. Dzhiyanbaeva and Sh. T. Talipov, *ibid.*, 1968, No. 323, 39; *Chem. Abstr.*, 1970, **72**, 96261w, 139227j.
67. N. G. Kagramanova, Sh. T. Talipov and R. Kh. Dzhiyanbaeva, *Izv. Akad. Nauk Kaz. SSR, Ser. Khim.*, 1969, **19**, 14; *Chem. Abstr.*, 1969, **71**, 56314p.

68. S. E. Podlipskaya, R. K. Dzhiyanbaeva and S. T. Talipov, *Nauch. Tr. Tashkent. Gos. Univ.*, 1972, No. 419, 57; *Chem. Abstr.*, 1973, 79, 121549a.
69. G. Nakagawa and H. Wada, *Nippon Kagaku Zasshi*, 1962, 83, 1098; *Chem. Abstr.*, 1963, 59, 12143d.
70. S. B. Savvin, T. V. Petrova and T. G. Dzherayan, *Zh. Analit. Khim.*, 1975, 30, 2092; *Chem. Abstr.*, 1976, 85, 153380d.
71. *Idem, ibid.*, 1978, 33, 516; *Chem. Abstr.*, 1978, 89, 70204f.
72. R. C. Chadha, B. S. Garg and R. P. Singh, *Proc. Indian Natl. Sci. Acad., Part A*, 1979, 45, 20; *Chem. Abstr.*, 1979, 91, 185994x.
73. T. S. West, *Complexometry*, 3rd Ed., p. 194. BDH Chemicals, Poole, 1969.
74. G. M. Pisichenko and V. D. Ponomarev, *Org. Reagenty Anal. Khim., Tezisy Dokl. Vses. Konf.*, 4th, 1976, 2, 136; *Chem. Abstr.*, 1978, 88, 15420c.
75. T. F. Rudometkina, V. M. Ivanov and A. I. Busev, *Zh. Analit. Khim.*, 1977, 32, 669; *Chem. Abstr.*, 1977, 87, 173531y.
76. G. A. Butenko, A. S. Grzhegorzhevskii and V. P. Korzh, *Vop. Khim. Khim. Tekhnol.*, 1973, No. 28, 60; *Chem. Abstr.*, 1974, 80, 43712c.
77. A. A. Abd El-Raheem, M. Z. El-Sabban and M. M. Dokhana, *Z. Anal. Chem.*, 1962, 188, 96.
78. J. C. Palomar and C. N. de la Puerta, *Afinidad*, 1982, 39, 44; *Chem. Abstr.*, 1982, 96, 228154w.
79. I. K. Guseinov and S. A. Zeinalova, *Azerb. Khim. Zh.*, 1980, No. 2, 130; *Chem. Abstr.*, 1981, 94, 149606a.
80. I. K. Guseinov, S. A. Zeinalova, M. O. Gumbatov and N. B. Agaev, *U.S.S.R. SU* 929,569, 1982; *Chem. Abstr.*, 1982, 97, 155586x.
81. S. A. Zeinalova, I. K. Guseinov and N. Kh. Rustamov, *Zh. Analit. Khim.*, 1983, 38, 241; *Chem. Abstr.*, 1983, 98, 172181z.
82. Y. Zhang and L. Xiang, *Lihua Jianyan Huaxue Fence*, 1988, 24, 54; *Anal. Abstr.*, 1988, 50, 10B207.
83. S. Zereba, *Ann. Univ. Mariae Curie-Skłodowska, Sect. AA: Chem.*, 1980, 35, 73; *Chem. Abstr.*, 1983, 99, 132847k.
84. P. Tarin and M. Blanco, *An. Quim., Ser. B*, 1982, 78, 257; *Chem. Abstr.*, 1983, 98, 10775u.
85. M. Suchánek, H. Činátlová and L. Šůcha, *Sb. Vys. Šk. Chem.-Technol. Praze, Anal. Chem.*, 1977, H12, 119; *Chem. Abstr.*, 1979, 90, 47797p.
86. C. Woodward and H. Freiser, *Talanta*, 1973, 20, 417.
87. J. Cacho and C. Nerin, *Anal. Chim. Acta*, 1981, 131, 271.
88. H. Činátlová, L. Šůcha and M. Suchánek, *Sb. Vys. Šk. Chem.-Technol. Praze, Anal. Chem.*, 1974, H10, 75; *Chem. Abstr.*, 1975, 82, 67667j.
89. M. Suchánek and L. Šůcha, *ibid.*, 1974, H10, 39; *Chem. Abstr.*, 1975, 82, 79958t.
90. H. Činátlová and L. Šůcha, *ibid.*, 1977, H12, 105; *Chem. Abstr.*, 1979, 90, 47796n.
91. O. Puente, *Biol. Soc. Quim. Peru*, 1962, 28, 78; *Chem. Abstr.*, 1964, 61, 13844b.
92. N. T. Turakhanova and S. T. Tallipov, *Uzb. Khim. Zh.*, 1982, No. 3, 21; *Chem. Abstr.*, 1982, 97, 229247m.
93. A. T. Pilipenko, V. Demchenko and P. F. Ol'khovich, *Ukr. Khim. Zh.* 1973, 39, 601; *Chem. Abstr.*, 1974, 80, 55503y.
94. T. V. Petrova, S. B. Savvin and T. G. Dzherayan, *Zh. Analit. Khim.*, 1973, 28, 1888; *Chem. Abstr.*, 1974, 80, 77922m.
95. S. K. Datta, *Chemist-Analyst*, 1961, 50, 104; *Chem. Abstr.*, 1962, 56, 9386i.
96. Y. L. Mehta, B. S. Garg and R. P. Singh, *Curr. Sci.*, 1974, 43, 11; *Chem. Abstr.*, 1974, 80, 77938w.
97. M. Furukawa and S. Shibata, *Anal. Chim. Acta*, 1982, 140, 301.
98. V. P. Zhivopistsev, I. S. Kalmykova and L. P. Pyatosin, *Uch. Zap., Permsk. Gos. Univ.*, 1963, 25, 108; *Chem. Abstr.*, 1964, 61, 1236f.
99. T. V. Petrova and T. G. Dzherayan, *Org. Reagenty Anal. Khim., Tezisy Dokl. Vses. Konf.*, 4th, 1976, 1, 16; *Chem. Abstr.*, 1977, 87, 145265w.
100. A. A. Nemodruk, I. M. Gibalo and O. K. Kleimenova, *Zh. Analit. Khim.*, 1977, 32, 457; *Chem. Abstr.*, 1977, 87, 47606p.
101. Z. Marczenko, *Anal. Chim. Acta*, 1964, 31, 224.
102. R. B. Singh, B. S. Garg and R. P. Singh, *Talanta*, 1979, 26, 425.
103. P. B. S. Reddy and S. B. Rao, *Curr. Sci.*, 1978, 47, 84; *Chem. Abstr.*, 1978, 89, 35998w.
104. C. Chang, Y. Liu and H. Wu, *Fen Hsi Hua Hsueh*, 1979, 7, 165; *Chem. Abstr.*, 1980, 92, 140062w.
105. P. B. S. Reddy and B. Rao, *Acta Cienc. Indica, Ser. Chem.*, 1981, 7, 100; *Chem. Abstr.*, 1982, 97, 48885x.
106. K. Lal, S. R. Malhotra and R. P. Katyal, *J. Inst. Chem. (India)*, 1981, 53, 13; *Chem. Abstr.*, 1981, 94, 184914w.
107. J. Singh, K. N. Sharma, U. K. Jetley, S. N. Rastogi and G. S. Bhuee, *Chem. Era*, 1982, 18, 218; *Chem. Abstr.*, 1983, 99, 98456v.
108. C. Mongay, E. Rodriguez, F. Borrull and V. Cerdá, *Anal. Quim., Ser. B*, 1982, 78, 247; *Chem. Abstr.*, 1983, 98, 46045v.
109. Z. Holzbecher and J. Ježek, *Sb. Vys. Šk. Chem.-Technol. Praze, Anal. Chem.*, 1967, 1, 53; *Chem. Abstr.*, 1970, 73, 10393b.
110. J. M. Cano Pavon, J. C. Jimenez Sanchez and F. Pino, *Anal. Chim. Acta*, 1975, 75, 335.
111. H. Hartkamp, *Angew. Chem.*, 1960, 72, 349; *Chem. Abstr.*, 1962, 56, 13540b.
112. F. Buscarons and J. Abello, *Anales Real Soc. Espan. Fis. Quim. (Madrid) Ser. B.*, 1962, 58, 591; *Chem. Abstr.*, 1963, 58, 9611h.
113. C. F. Pereira and J. G. Gomez, *Anal. Lett.*, 1985, 18, 2219; *Chem. Abstr.*, 1986, 104, 122133g.
114. M. Kastelan-Macan, S. Cerjan-Stefanovic, M. Pavlinic and F. Kapor, *Kem. Ind.*, 1987, 36, 113; *Anal. Abstr.*, 1987, 49, 10H58.
115. D. J. Hydes, *Anal. Chim. Acta*, 1987, 199, 221.
116. K. Oguma, K. Nishiyama and R. Kuroda, *Anal. Sci.*, 1987, 3, 251.
117. R. Kuroda, Y. Matsuzawa and K. Oguma, *Z. Anal. Chem.*, 1987, 326, 156.
118. S. G. Kadarmandalgi, *J. Chem. Educ.*, 1964, 41, 437.
119. K. Burger and I. Egyed, *Magy. Kem. Folyoirat*, 1965, 71, 143; *Chem. Abstr.*, 1965, 63, 2364h.
120. F. Buscarons and R. Mena, *Anales Real Soc. Espan. Fis. Quim (Madrid) Ser. B*, 1961, 57, 495; *Chem. Abstr.*, 1962, 57, 14413i.
121. V. Armeanu, D. Camboli and C. Iancu, *Rev. Chim. (Bucharest)*, 1958, 9, 218; *Chem. Abstr.*, 1959, 53, 5966e.
122. V. Armeanu and D. Camboli, *ibid.*, 1959, 10, 529; *Chem. Abstr.*, 1962, 57, 9191i.
123. F. Buscarons and H. Iturriaga, *An. Real Soc. Espan. Fis. Quim., Ser. B*, 1967, 63, 95; *Chem. Abstr.*, 1967, 67, 28944t.

124. F. Buscarons and E. Caralt, *Inform. Quim. Anal.*, 1973, **27**, 138; *Chem. Abstr.*, 1974, **80**, 22280v.
125. N. D. Tambat and R. N. Merchant, *J. Indian Chem. Soc.*, 1968, **45**, 517; *Chem. Abstr.*, 1968, **69**, 92633j.
126. M. Jimenez Ruedas and M. Hernandez Lopez, *Afinidad*, 1979, **36**, 240; *Chem. Abstr.*, 1979, **91**, 116838n.
127. A. Mantecon, V. Cadiz and V. Cerdá, *ibid.*, 1981, **38**, 137; *Chem. Abstr.*, 1981, **95**, 125431j.
128. *Aquaquant Test Kit Information*, Merck, Darmstadt.
129. G. Denigés, *Compt. Rend.*, 1932, **194**, 895.
130. C. P. Sideris, *Ind. Eng. Chem., Anal. Ed.*, 1937, **9**, 445.
131. *Idem, ibid.*, 1940, **12**, 307.
132. M. I. Abdullah, *Anal. Chim. Acta*, 1968, **40**, 526.
133. K. Goto, T. Komatsu and T. Furukawa, *ibid.*, 1962, **27**, 331.
134. A. Henriksen, *Analyst*, 1966, **91**, 647.
135. Z. Marczenko and K. Kasiura, *Chem. Anal. (Warsaw)*, 1965, **10**, 449.
136. T. A. Dick, *Manganese Raw Potable Water Spectrophotometry (Using Formaldoxime)*, HMSO, London, 1977; *Chem. Abstr.*, 1979, **90**, 28789w.
137. P. B. Armstrong, W. B. Lyons and H. E. Gaudette, *Estuaries*, 1979, **2**, 198.
138. M. F. Giné, E. A. G. Zagatto and H. Bergamin Filho, *Analyst*, 1979, **104**, 371.
139. E. G. Bradfield, *ibid.*, 1957, **82**, 254.
140. J. Ch. van Schouwensburg and I. Walinga, *Neth. J. Arg. Sci.*, 1966, **14**, 131; *Chem. Abstr.*, 1967, **66**, 62547e.
141. B.-Z. Yan, Y.-F. Qin and X.-G. Zeng, *Ssu-ch'uan I Hsueh Yuan Hsueh Pao*, 1981, **12**, 68; *Chem. Abstr.*, 1981, **95**, 111183t.
142. J. Adam, *Hutn. Listy*, 1973, **28**, 592.
143. A. D. Golobov, *Pochowedenie*, 1965, **3**, 89.
144. J. Crowther, *Anal. Chem.*, 1978, **50**, 1041.
145. B. Compton, D. R. Blaisdell and G. J. Dorosh, *Advan. Automat. Anal., Technicon Int. Congr.*, 1969, **2**, 163; *Chem. Abstr.*, 1970, **72**, 12495t.
146. H. Ishii, H. Koh and K. Sato, *Nippon Kagaku Kaishi*, 1980, 1919; *Chem. Abstr.*, 1981, **94**, 76125f.
147. H. Ishii, H. Koh and K. Satoh, *Anal. Chim. Acta*, 1982, **136**, 347.
148. S. Igarashi, A. Obara, H. Adachi and T. Yatsuyanagi, *Bunseki Kagaku*, 1986, **35**, 829; *Anal. Abstr.*, 1987, **49**, 2B14.
149. R. Lin, *Fenxi Huaxue*, 1987, **15**, 318; *Anal. Abstr.*, 1988, **50**, 1B220.
150. H. Li and M. Tu, *ibid.*, 1984, **12**, 695; *Chem. Abstr.*, 1985, **102**, 55255s.
151. M. Xu, Z. Pan, N. Xie and S. He, *Wuhan Daxue Xuebao, Ziran Kexueban*, 1985, *Anal. Chem. Spec. Ed.* **51**; *Chem. Abstr.*, 1986, **104**, 218217p.
152. H. Ishii, *Kenkyu Hokoku—Asahi Garasu Kogyo Gijutsu Shoreikai*, 1980, **37**, 339; *Chem. Abstr.*, 1981, **95**, 49012f.
153. I. Mori, Y. Fujita, K. Sakaguchi and S. Kitano, *Bunseki Kagaku*, 1982, **31**, E239; *Chem. Abstr.*, 1982, **97**, 119729n.
154. C. Vekhande and K. N. Munshi, *J. Indian Chem. Soc.*, 1973, **50**, 384; *Chem. Abstr.*, 1974, **80**, 66381h.
155. O. A. Tataev and L. G. Anisimova, *Zh. Analit. Khim.*, 1971, **26**, 184; *Chem. Abstr.*, 1971, **74**, 119769a.
156. F. Capitan, M. Roman and A. Guiraum, *An. Quim.*, 1971, **67**, 147; *Chem. Abstr.*, 1971, **74**, 150841s.
157. *Idem, Quim. Ind. (Madrid)*, 1971, **17**, 15; *Chem. Abstr.*, 1971, **75**, 58318z.
158. N. B. El-Assy, A. M. Dessouki, N. E. Amin and F. A. Ahmed, *Ann. Chim. (Rome)*, 1982, **72**, 173; *Chem. Abstr.*, 1982, **97**, 48839k.
159. J. Minczewski, J. Chwastowska and E. Lachowicz, *Chem. Anal. (Warsaw)*, 1973, **18**, 199; *Chem. Abstr.*, 1973, **79**, 73293p.
160. S. Hoshi and S. Inoue, *Bunseki Kagaku*, 1983, **32**, 287; *Chem. Abstr.*, 1983, **99**, 15674r.
161. C. Zhan, *Huaxue Shijie*, 1982, **23**, 237; *Chem. Abstr.*, 1984, **100**, 114116f.
162. Y. Sasaki, *Anal. Chim. Acta*, 1982, **138**, 419.
163. K. L. Cheng, K. Ueno and T. Imamura, *Handbook of Organic Analytical Reagents*, p. 53. CRC, Boca Raton, 1982.
164. Y. Horiuchi and H. Nishida, *Iwate Daigaku Kogakubu Kenkyu Hokoku*, 1967, **20**, 35; *Chem. Abstr.*, 1968, **69**, 40966a.
165. D. Oktavec, O. Liška and S. Kudela, *Zb. Pr. Chemickotechnol. Fak. SVST (Slov. Vys. Sk. Tech.)*, 1971, **81**; *Chem. Abstr.*, 1973, **78**, 131664c.
166. Z. Li, *Fenxi Huaxue*, 1985, **13**, 96; *Chem. Abstr.*, 1985, **102**, 214308e.
- 166a. D. Cheng and Z. Li, *Fenxi Huaxue*, 1987, **15**, 308; *Chem. Abstr.*, 1987, **107**, 189871b.
167. M. Otomo, *Bunseki Kagaku*, 1965, **14**, 45; *Chem. Abstr.*, 1965, **62**, 15414h.
168. A. Cabrera-Martin, J. L. Peral-Fernandez, C. R. Moreno Villalba and F. Burriel-Marti, *Inform. Quim. Anal.*, 1973, **27**, 110; *Chem. Abstr.*, 1974, **80**, 43685w.
169. Z. Zheng and Q. Zheng, *Huaxue Shiji*, 1988, **10**, 75; *Anal. Abstr.*, 1989, **51**, 1B152.
170. K. L. Cheng, K. Ueno and T. Imamura, *Handbook of Organic Analytical Reagents*, p. 45. CRC, Boca Raton, 1982.
171. A. Jeničková, V. Suk and M. Malát, *Chem. Listy*, 1956, **50**, 760.
172. *Idem, Collection Czech. Chem. Commun.*, 1956, **21**, 1257.
173. I. Rudzitis, L. Čermáková, K. Nedomová and M. Malát, *Chem. Anal. (Warsaw)*, 1981, **26**, 1045.
174. Q. Xu, Z. Zhou and Z. Yin, *Fenxi Huaxue*, 1985, **13**, 170; *Chem. Abstr.*, 1985, **103**, 204989j.
175. Z. Li and C. Li, *Fenxi Shiyanshi*, 1986, **5**, 61; *Anal. Abstr.*, 1987, **49**, 3B163.
176. M. Ding, D. Xia, F. Wang and Y. He, *Huaxue Shiji*, 1987, **9**, 260; *Anal. Abstr.*, 1988, **50**, 6-B168.
177. K. Vytřas and J. Vytřasová, *Chem. Zvesti*, 1974, **28**, 779; *Chem. Abstr.*, 1975, **83**, 21423u.
178. K. Vytřas, V. Mach and M. Malcová, *Chem. Zvesti*, 1976, **30**, 648. *Chem. Abstr.*, 1977, **87**, 94858g.
179. M. M. Tananaiko and L. I. Gorenshtein, *Ukr. Khim. Zh.*, 1977, **43**, 1319; *Chem. Abstr.*, 1978, **89**, 35925v.
180. N. L. Shestidesyatnaya, L. I. Kotelyanskaya and N. M. Milyaeva, *Org. Reagenty Anal. Khim., Tezisy Dokl. Vses. Konf.*, 4th, 1976, **2**, 5; *Chem. Abstr.*, 1977, **87**, 177045r.
181. R. Yu, Z. Zhang and Z. Zhang, *Talanta*, 1984, **31**, 1121.
182. S. C. Shrivastava and A. K. Mukherji, *Anal. Chim. Acta*, 1964, **30**, 495.
183. P. Sun and C. Liu, *Hua Hsueh*, 1971, No. 2, 47; *Chem. Abstr.*, 1972, **76**, 67650z.
184. F. Capitan, M. Roman and F. Garcia-Sanchez, *Inform. Quim. Anal.*, 1973, **27**, 7; *Chem. Abstr.*, 1973, **79**, 111354u.

185. *Idem, ibid.*, 1973, **27**, 1; *Chem. Abstr.*, 1973, **79**, 111355v.
186. F. Capitan, M. Roman and E. Alvarez-Manzaneda, *ibid.*, 1973, **27**, 291; *Chem. Abstr.*, 1974, **80**, 140794p.
187. F. Capitan and M. Roman, *ibid.*, 1967, **21**, 208; *Chem. Abstr.*, 1968, **69**, 80066b.
188. D. N. Lisitsyna and D. P. Shcherbov, *Zh. Analit. Khim.*, 1973, **28**, 1203; *Chem. Abstr.*, 1973, **79**, 111383c.
189. H. M. N. H. Irving, *CRC Crit. Rev. Anal. Chem.*, 1980, **8**, 321.
190. Z. Marczenko and M. Mojski, *Anal. Chim. Acta*, 1971, **54**, 469.
191. *Idem, Chem. Anal. (Warsaw)*, 1971, **16**, 865.
192. H. Akaiwa, H. Kawamoto and S. Kogure, *Bunseki Kagaku*, 1979, **28**, 498; *Chem. Abstr.*, 1979, **91**, 203736w.
193. R. J. DuBois and S. B. Knight, *Anal. Chem.*, 1964, **36**, 1316.
194. S. Zhang, F. Tang, F. Yang and F. Liu, *Huaxue Shiji*, 1982, **4**, 335; *Chem. Abstr.*, 1983, **99**, 15640b.
195. D. Soldatovic and G. Farah, *Arh. Farm.*, 1974, **24**, 129; *Chem. Abstr.*, 1975, **82**, 135186d.
196. S. Balt and E. Van Dalen, *Anal. Chim. Acta*, 1962, **27**, 188.
197. N. Czech, B. Friese and F. Umland, *ibid.*, 1980, **121**, 275.
198. A. G. Asuero and M. Gonzalez-Balairon, *Microchem. J.*, 1980, **25**, 14.
199. U. Niederschulte and K. Ballschmiter, *Z. Anal. Chem.*, 1972, **261**, 191.
200. F. Salinas, J. C. Jimenez Sanchez and T. Galeano Diaz, *Microchem. J.*, 1987, **36**, 285.
201. Z. Skorko-Trybula and B. Debska, *Chem. Anal. (Warsaw)*, 1968, **13**, 557; *Chem. Abstr.*, 1969, **70**, 25385n.
202. Z. Skorko-Trybula, *ibid.*, 1967, **12**, 815.
203. Z. Skorko-Trybula and J. Minczewski, *ibid.*, 1964, **9**, 397; *Chem. Abstr.*, 1964, **61**, 7698c.
204. F. Salinas, M. Jimenez-Arrabal and M. C. Mahedero, *Anal. Lett.*, 1983, **16**, 1449.
205. F. Salinas and M. Jimenez-Arrabal, *Microchem. J.*, 1985, **31**, 113.
206. Z. Ksandr, *Collection Czech. Chem. Commun.*, 1962, **27**, 31; *Chem. Abstr.*, 1962, **57**, 1841f.
207. D. O. Miller and J. H. Yoe, *Talanta*, 1960, **7**, 107.
208. F. Salinas, R. Forteza and J. G. March, *Quim. Anal. (Barcelona)*, 1983, **2**, 283; *Chem. Abstr.*, 1985, **102**, 142416p.
209. F. Salinas, J. M. Estela and R. Forteza, *Afinidad*, 1983, **40**, 359; *Chem. Abstr.*, 1983, **99**, 186538d.
210. F. Salinas, M. Llinas and J. M. Estela, *Quim. Anal. (Barcelona)*, 1983, **2**, 38; *Chem. Abstr.*, 1985, **102**, 124740k.
211. Z. Skorko-Trybula, *Pr. Nauk. Politech. Warsz.*, *Chem.*, 1973, **8**, 101; *Chem. Abstr.*, 1975, **83**, 71070x.
212. F. Salinas and J. G. March, *Quim. Anal. (Barcelona)*, 1984, **3**, 11; *Chem. Abstr.*, 1985, **102**, 159644j.
213. J. L. Martinez-Vidal, J. Gonzalez-Parra and F. Salinas, *Microchem. J.*, 1988, **37**, 241.
214. M. A. Quddus and C. F. Bell, *Anal. Chim. Acta*, 1968, **42**, 503.
215. P. Dostál, J. Čermák and J. Kartous, *Collection Czech. Chem. Commun.*, 1968, **33**, 1539; *Chem. Abstr.*, 1968, **68**, 111060t.
216. L. Caton, M. Melinte and O. Mitoseriu, *Lucr. Stiint., Inst. Politeh. Galati*, 1970, **4**, 101; *Chem. Abstr.*, 1972, **77**, 138416m.
217. V. N. Podchainova and L. N. Ushkova, *Dostizh. Razvit. Nov. Metodov Khim. Anal.*, 1974, **18**; *Chem. Abstr.*, 1977, **86**, 100316b.
218. V. M. Fofanova and V. Malevannyi, *Tr. Inst. Khim., Ural. Nauchn. Tsentr. Akad. Nauk. SSSR*, 1974, **30**, 88; *Chem. Abstr.*, 1976, **85**, 13350u.
219. V. A. Malevannyi and I. A. Shikhova, *Tezisy Dokl. Nauchno-Tekh. Konf. "Khim. Primen. Formazonov" 2nd*, 1974, **24**; *Chem. Abstr.*, 1977, **87**, 15481c.
220. R. Pelova and A. Toleva, *Nauchni Tr. Plodivski Univ.*, 1974, **12**, 29; *Chem. Abstr.*, 1975, **83**, 85826k.
221. M. C. L. Pazos, A. B. Barrera and F. B. Martinez, *Acta Quim. Compostelana*, 1982, **6**, 1, *Chem. Abstr.*, 1983, **99**, 98320w.
222. V. S. Romanova, *Tr. Ural'sk. NII Chern. Met.*, 1974, No. 21, 100; *Chem. Abstr.*, 1975, **83**, 165795q.
223. J. Meditsch and S. Santos, *Rev. Quim. Ind. (Rio de Janeiro)*, 1970, **39**, No. 461, 13; *Chem. Abstr.*, 1971, **74**, 119686w.
224. G. Branas Miguez, *Acta Cient. Compostelana*, 1966, **6**, 21; *Chem. Abstr.*, 1970, **73**, 126568s.
225. F. Bermejo and G. Branas, *Mikrochim. Acta*, 1971, 489.
226. H. Onishi and Y. Toita, *Bunseki Kagaku*, 1972, **21**, 756; *Chem. Abstr.*, 1973, **78**, 37655d.
227. K. R. Solanke and S. M. Khopkar, *Z. Anal. Chem.*, 1975, **275**, 286.
228. M. Deguchi and S. Hayakawa, *Bunseki Kagaku*, 1982, **31**, 612; *Chem. Abstr.*, 1983, **98**, 10795a.
229. H. A. Flaschka, S. McClure and J. V. Hornstein, *Anal. Lett.*, 1978, **11**, 383.
230. H. A. Flaschka and J. V. Hornstein, *Anal. Chim. Acta*, 1978, **100**, 469.
231. M. Furukawa, S. Sasaki, K. Goto, E. Kamata, R. Nakashima and S. Shibata, *Nagoya Kogyo Gijutsu Shikensho Hokoku*, 1968, **17**, 161; *Chem. Abstr.*, 1969, **71**, 9299c.
232. K. K. Deb and R. K. Mishra, *J. Indian Chem. Soc.*, 1978, **55**, 289. *Chem. Abstr.*, 1978, **89**, 122616p.
233. R. I. Oglobina, L. V. Kholevinskaya and L. N. Emel'yanova, *O.S.S.R. Patent*, SU 1.033,939, 1983; *Chem. Abstr.*, 1983, **99**, 168730f.
234. J. Knoeck and H. Diehl, *Talanta*, 1967, **14**, 1083.
235. K. Khan and M. Amin, *Pak. J. Sci. Ind. Res.*, 1984, **27**, 263; *Chem. Abstr.*, 1985, **102**, 71980e.
236. K. S. Patel and R. K. Mishra, *J. Indian Chem. Soc.*, 1978, **55**, 773; *Chem. Abstr.*, 1979, **90**, 33464r.
237. P. K. Sharma, H. Mohabey and R. K. Mishra, *Acta Cienc. Indica, Ser. Chem.*, 1982, **8**, 198; *Chem. Abstr.*, 1983, **98**, 113391v.
238. M. Kajiwara and K. Goto, *Nippon Kagaku Zasshi*, 1964, **85**, 539; *Chem. Abstr.*, 1965, **62**, 1072h.
239. F. Bermejo-Martinez and E. Mendez-Doménech, *Z. Anal. Chem.*, 1969, **247**, 53.
240. L. Pike and J. Yoe, *Anal. Chim. Acta*, 1964, **31**, 318.
241. S. S. Khanna, M. L. Manchanda and S. L. Chopra, *J. Indian Soc. Soil Sci.*, 1968, **16**, 193; *Chem. Abstr.*, 1969, **70**, 56719d.
242. L. Pike, *Univ. Microfilms (Ann Arbor, Mich.) Order No. 64-12*, 406; *Chem. Abstr.*, 1965, **62**, 12433f.
243. V. A. Rad'ko and E. M. Yakimets, *Tr. Ural'sk. Politekhn. Inst.*, 1963, No. 130, 62; *Chem. Abstr.*, 1964, **60**, 12653b.

244. H. Sikorska-Tomicka, *Chem. Anal. (Warsaw)*, 1977, **22**, 761; *Chem. Abstr.*, 1978, **88**, 176880t.
245. M. L. Richardson, *Analyst*, 1962, **87**, 435.
246. S. S. Khalikov and V. A. Alekseevskii, *Fiz.-Khim. Issled. Sint. Prir. Soedin.*, 1982, **42**, *Chem. Abstr.*, 1983, **99**, 1511235a.
- 246a. C. Li and Z. Li, *Fenxi Huaxue*, 1986, **14**, 682; *Anal. Abstr.*, 1987, **49**, 6B164.
247. S. V. Kharkover and M. Z. Kharkover, *Gig. Sanit.*, 1973, No. 11, 107; *Chem. Abstr.*, 1974, **80**, 148707h.
248. M. A. Khattab, G. El-Enany and M. E. Soliman, *Pak. J. Sci. Ind. Res.*, 1984, **27**, 81; *Chem. Abstr.*, 1985, **102**, 89155z.
249. N. K. Murthy and Y. P. Rao, *Z. Anal. Chem.*, 1975, **275**, 204; 1976, **282**, 141.
- 249a. S. K. Menon, Y. K. Agrawal and M. N. Desai, *Talanta*, 1989, **36**, 675.
250. I. R. Rusina, *Chem. Zvesti*, 1961, **15**, 869; *Chem. Abstr.*, 1963, **58**, 1895d.
251. R. Craciuneanu and E. Florean, *Rev. Chim. (Bucharest)*, 1976, **27**, 622; *Chem. Abstr.*, 1977, **86**, 83125u.
252. F. Salinas, J. Cantalops and J. M. Estela, *Quim. Anal. (Barcelona)*, 1983, **2**, 96; *Chem. Abstr.*, 1985, **102**, 142414m.
253. S. P. Bhargava and N. C. Sogani, *J. Inst. Chem., Calcutta*, 1971, **43**, 172; *Chem. Abstr.*, 1972, **76**, 80556t.
254. R. F. Zagrebina, *Tr. Molodykh. Uch. Saratov. Univ. Vyp. Khim.*, 1973, No. 2, 138; *Chem. Abstr.*, 1973, **79**, 61150b.
255. W. Ch'i, S. Chang and M. Hsu, *Hua Hsueh Hsueh Pao*, 1965, **31**, 179; *Chem. Abstr.*, 1965, **63**, 3599d.
256. T. Hata and T. Uno, *Bull. Chem. Soc. Japan*, 1972, **45**, 477.
257. W. Beyer and R. D. Ott, *Mikrochim. Acta*, 1965, 1131.
258. A. B. Sakla, A. A. Helmy, W. Beyer and F. E. Harhash, *Talanta*, 1979, **26**, 519.
259. D. De Filippo and C. Preti, *Atti Soc. Nat. Mat. Modena*, 1964, **95**, 48; *Chem. Abstr.*, 1966, **64**, 1328h.
260. A. Garcia De Torres, M. Valcárcel and F. Pino, *Talanta*, 1973, **20**, 919.
261. E. Fernandez Gomez, F. Vila Brion and J. Areses Trapote, *Quim. Anal.*, 1976, **30**, 271; *Chem. Abstr.*, 1977, **87**, 126563a.
262. J. Rius, C. Mongay and V. Cerdá, *Afinidad*, 1981, **38**, 235; *Chem. Abstr.*, 1981, **95**, 143425q.
263. F. Capitan, M. Jimenez Ruedas and T. Prieto, *ibid.*, 1981, **38**, 261; *Chem. Abstr.*, 1981, **95**, 143426r.
264. S. Vincente-Perez, A. Cabrera-Martin and F. Gomis-Medina, *Quim. Anal.*, 1976, **30**, 381; *Chem. Abstr.*, 1977, **87**, 161071k.
265. V. E. Kononenko, V. M. Chuishchev and R. O. Kochkanyan, *Zavodsk. Lab.*, 1975, **41**, 1186; *Chem. Abstr.*, 1976, **84**, 144166r.
266. E. Jansons and S. Berzina, *Uch. Zap. Latv. Univ.*, 1970; No. 177, 107. *Chem. Abstr.*, 1972, **77**, 139706t.
267. P. Heizmann and K. Ballschmiter, *Z. Anal. Chem.*, 1972, **259**, 110.
268. M. Garcia-Vargas, J. M. Bautista and P. De Toro, *Microchem. J.*, 1981, **26**, 557.
269. R. Pietsch, *Mikrochim. Acta*, 1959, 854.
270. A. Cabrera-Martin and S. Rubio Barroso, *Quim. Anal.*, 1977, **31**, 295; *Chem. Abstr.*, 1978, **89**, 84114p.
271. F. Buscarons and J. Canela, *Anal. Chim. Acta*, 1973, **67**, 349.
272. A. Gonzalez-Portal, F. Bermejo-Martinez and C. Baluja-Santos, *Microchem. J.*, 1982, **27**, 357.
273. L. Erdey and I. Buzás, *Mikrochim. Acta*, 1962, 340.
274. F. Capitan, F. Salinas and L. F. Capitan-Vallvey, *Bull. Soc. Chim. France*, 1979, 1.35.
275. J. Doležal and E. Štulíková, *Z. Anal. Chem.*, 1969, **244**, 316.
276. E. Casassas and F. Buscarons, *Chim. Anal. Paris*, 1962, **44**, 20; *Chem. Abstr.*, 1962, **56**, 12294i.
277. P. B. Berrera, A. G. Sanchez and F. B. Martinez, *Acta Quim. Compostelana*, 1983, **7**, 29; *Chem. Abstr.*, 1984, **101**, 182780p.
278. M. M. Tananaiko, T. I. Vysotskaya and N. A. Chernobrovkina, *Vestn. Kiev. Un-ta. Khimiya*, 1984, No. 25. 36. *Chem. Abstr.*, 1985, **102**, 197059e.
279. Y. Ujihira and E. Niki, *Nippon Kagaku Zasshi*, 1966, **87**, 620; *Chem. Abstr.*, 1966, **65**, 11335e.
280. J. Danuch and F. Buscarons, *Analisis*, 1973, **2**, 510; *Chem. Abstr.*, 1973, **79**, 73178e.
281. V. Zatka, J. Holzbecher and D. E. Ryan, *Anal. Chim. Acta*, 1971, **55**, 273.
282. S. Bilinski and D. Misiuna, *Ann. Univ. Mariae Curie-Skłodowska, Sect. D*, 1970, **25**, 405; *Chem. Abstr.*, 1972, **76**, 148408d.
283. A. Izquierdo, J. Guasch and J. Miquel, *An. Quim., Ser. B*, 1984, **80**, 382, *Chem. Abstr.*, 1985, **102**, 71833j.
284. A. Izquierdo, J. Gausch and M. P. Callao, *Quim. Anal. (Barcelona)*, 1983, **2**, 174; *Chem. Abstr.*, 1985, **102**, 124703a.
285. S. K. Datta and S. N. Saha, *Mikrochim. Acta*, 1961, 361.
286. S. K. Datta and P. Ghose, *Naturwissenschaften*, 1958, **45**, 515; *Chem. Abstr.*, 1959, **53**, 8910h.
287. F. B. Rieg, J. M. Calatayud and M. C. Garcia Alvarez-Coque, *Afinidad*, 1980, **37**, 137; *Chem. Abstr.*, 1981, **94**, 24347k.
288. J. H. Mendez, F. B. Rieg, J. M. Calatayud and M. C. P. Marti, *ibid.*, 1978, **35**, 345; *Chem. Abstr.*, 1979, **90**, 96930k.
289. D. A. Skoog and D. M. West, *Fundamentals of Analytical Chemistry*, 3rd Ed., p. 22. Holt, Rinehart and Winston, San Francisco, 1976.
290. H. A. Mottola, *CRC Crit. Rev. Anal. Chem.*, 1975, **4**, 229.
291. E. B. Sandell and I. M. Kolthoff, *J. Am. Chem. Soc.*, 1934, **56**, 12426.
292. J. Růžička and E. L. Hansen, *Flow-Injection Analysis*, 2nd Ed., Wiley, New York, 1988.
293. M. Valcárcel and M. D. Luque de Castro, *Flow-Injection Analysis: Principles and Applications*, Horwood, Chichester, 1987.
294. V. L. Biddle and E. L. Wehry, *Anal. Chem.*, 1978, **50**, 867.
295. C. E. Efstathiou and T. P. Hadjiioannou, *Anal. Chem.*, 1977, **49**, 414.
296. L. D. Alfimova, *Deposited Doc.*, 1977, VINITI 3432-77, 23; *Chem. Abstr.*, 1979, **90**, 132248e.
297. D. B. Paul, *Talanta*, 1978, **28**, 377.
298. H. Weisz, *Angew. Chem. Eng. Ed.*, 1976, **15**, 150.
299. H. Mottola, *Kinetic Aspects of Analytical Chemistry*, Wiley-Interscience, New York, 1988.
300. D. Pérez-Bendito and M. Silva, *Kinetic Methods in Analytical Chemistry*, Horwood, Chichester, 1988.
301. P. R. Bontchev and A. A. Aleksiev, *Teor. Eksp. Khim.*, 1973, **9**, 191; *Chem. Abstr.*, 1973, **79**, 70576x.

302. A. Moreno, M. Silva, D. Pérez-Bendito and M. Valcárcel, *Talanta*, 1983, **30**, 107.
303. *Idem*, *Anal. Chim. Acta*, 1984, **159**, 319.
304. D. Pérez-Bendito, J. Peinado and F. Toribio, *Analyst*, 1984, **109**, 1297.
305. G. A. Guilbault, S. S. Kuan and K. J. Brignac, *Anal. Chim. Acta*, 1969, **47**, 503.
306. I. E. Kalinichenko, *Ukr. Khim. Zh.*, 1969, **35**, 755; *Chem. Abstr.*, 1969, **71**, 119328u.
307. *Idem*, U.S.S.R. Patent 252,712, 1969; *Chem. Abstr.*, 1970, **72**, 62527x.
308. J. L. Burguera and A. Townshend, *Talanta*, 1981, **28**, 731.
309. L. A. Pilipenko, L. I. Dubovenko and N. A. Ol'shevskaya, *Vestn. Kiev. Un-ta. Khimiya*, 1984, No. 25, 50. *Chem. Abstr.*, 1985, **102**, 178309v.
310. Z. Zheng and Z. Wang, *Fenxi Huaxue*, 1985, **13**, 510; *Chem. Abstr.*, 1986, **104**, 56013q.
311. E. Nakayama, K. Isshiki, Y. Sohrin and K. Karatani, *Anal. Chem.*, 1989, **61**, 1392.
312. A. A. Fernandez, C. Sobel and S. L. Jacobs, *ibid.*, 1963, **35**, 1721.
313. J. Olafsson, *Sci. Total Environ.*, 1986, **49**, 101.
314. H. A. Mottola and C. R. Harrison, *Talanta*, 1971, **18**, 683.
315. T. Fukasawa and Y. Takeshi, *Bunseki Kagaku*, 1973, **22**, 168; *Chem. Abstr.*, 1973, **79**, 26813y.
316. H. Weisz and K. Rothmaier, *Anal. Chim. Acta*, 1975, **80**, 351.
317. Z. Liu and Y. Hu, *Huaxue Shijie*, 1983, **24**, 45; *Chem. Abstr.*, 1983, **99**, 186518x.
318. T. Fukasawa, S. Kawakubo and M. Mochizuki, *Bunseki Kagaku*, 1983, **32**, 669; *Chem. Abstr.*, 1984, **100**, 44554w.
319. T. Fukasawa, M. Iwatsuki, S. Kawakubo and M. Mochizuki, *Mikiochim. Acta*, 1986 III, 71.
- 319a. C. Zhang, S. Kawakubo and T. Fukasawa, *Anal. Chim. Acta*, 1989, **217**, 23.
320. Z. Wang, Z. Zheng and X. Hu, *Fenxi Huaxue*, 1987, **15**, 145; *Anal. Abstr.*, 1987, **49**, 11H80.
321. H. Zhao, *Fenxi Shiyanshi*, 1986, **5**, No. 12, 61; *Anal. Abstr.*, 1987, **49**, 10H57.
322. S. Kawakubo, T. Fukasawa, M. Iwatsuki and T. Fukasawa, *J. Flow Inject. Anal.*, 1988, **5**, 14.
323. C. Zhang, S. Kawakubo and T. Fukosawa, *Anal. Chim. Acta*, 1989, **217**, 23.
- 323a. M. Quintero, M. Silva and D. Pérez-Bendito, *Talanta*, 1989, **36**, 1091.
324. I. F. Dolmanova, N. T. Yatsimirskaya, V. P. Poddubienko and V. M. Peshkova, *Zh. Analit. Khim.*, 1971, **26**, 1540; *Chem. Abstr.*, 1971, **75**, 147493v.
325. I. I. Alekseeva and Z. P. Davydova, *ibid.*, 1971, **26**, 1786; *Chem. Abstr.*, 1972, **76**, 41694s.
326. I. F. Dolmanova, N. T. Yatsimirskaya and V. M. Peshkova, *Kinet. Katal.*, 1972, **13**, 678; *Chem. Abstr.*, 1972, **77**, 100452g.
327. *Idem*, *Zh. Analit. Khim.*, 1973, **28**, 112; *Chem. Abstr.*, 1973, **78**, 154529b.
328. I. F. Dolmanova, G. A. Zolotova and M. A. Ratina, *ibid.*, 1978, **33**, 1356; *Chem. Abstr.*, 1978, **89**, 190358f.
329. I. F. Dolmanova and N. M. Ushakova, *Vestn. Mosk. Univ. Ser. 2, Khim.*, 1978, **19**, 369; *Chem. Abstr.*, 1978, **89**, 190377m.
330. N. M. Ushakova and I. F. Dollmanova, *Vestn. Mosk. Univ. Ser. 2, Khim.*, 1987, **28**, 466; *Anal. Abstr.*, 1988, **50**, 4B135.
331. F. Grases, R. Forteza, J. G. March and V. Creda, *Anal. Chim. Acta*, 1983, **155**, 299.
332. S. Maspoeh, M. Blanco and V. Cerdá, *Analyst*, 1986, **111**, 69.
333. S. U. Kreingol'd, L. I. Sosenkova and I. M. Nelen, *Khim. Prom-st., Ser. Reakt. Osobo Chist. Veshchestva*, 1980, No. 1, 46; *Chem. Abstr.*, 1980, **93**, 178866v.
334. S. U. Kreingol'd, L. I. Sosenkova, G. S. Petrova and I. M. Nelen, U.S.S.R. Patent, 715,998, 1980; *Chem. Abstr.*, 1980, **93**, 60535h.
335. A. Sychev, V. G. Isak and U. Pfannmeller, *Izv. Akad. Nauk Mold. SSR, Ser. Biol. Khim. Nauk*, 1979, **4**, 88; *Chem. Abstr.*, 1980, **92**, 68967a.
336. P. Bartkus, A. Nauekaitis and E. Jasinskiene, *LietTSR Aukstuju Mokyklu Mokslo Darbai. Chemija ir Chem. Technol., Nauch. Tr. Vyssh. Ucheb. Zavedenii LitSSR. Khimiya i Khim. Tekhnol.*, 1975, **15**; *Chem. Abstr.*, 1976, **85**, 28237m.
337. J. Vazquez Ruiz, A. Garcia de Torres and J. M. Cano-Pavon, *Talanta*, 1984, **31**, 29.
338. D. P. Nikolelis and T. P. Hadjiioannou, *Anal. Chim. Acta*, 1978, **97**, 111.
339. T. J. Janjic, G. A. Milovanovic and M. B. Celap, *Anal. Chem.*, 1970, **42**, 27.
340. T. Yamane and Y. Nozawa, *Bunseki Kagaku*, 1984, **33**, 652; *Chem. Abstr.*, 1985, **102**, 142390a.
341. P. Bartkus and E. Jasinskiene, *Liet. TSR Aukst. Mokyklu Mokslo Darb., Chem. Chem. Technol.*, 1970, **11**, 83; *Chem. Abstr.*, 1972, **76**, 10039c.
342. Ya. D. Tiginyanu and V. I. Oprya, *Zh. Analit. Khim.*, 1973, **28**, 2206; *Chem. Abstr.*, 1974, **80**, 90879x.
343. P. Bartkus and E. Jaskinskiene, *Liet. TSR Aukst. Mokyklu Mokslo Darb., Chem. Chem. Technol.*, 1970, **11**, 25; *Chem. Abstr.*, 1971, **75**, 29628v.
344. T. Yamane and T. Fukasawa, *Bunseki Kagaku*, 1977, **26**, 300; *Chem. Abstr.*, 1978, **88**, 68533y.
345. A. Ya. Sychev, V. G. Isak and U. Pfannmeller, *Zh. Analit. Khim.*, 1978, **33**, 1351; *Chem. Abstr.*, 1978, **89**, 190357e.
346. A. Ya. Sychev and Ya. D. Tiginyanu, *ibid.*, 1969, **24**, 1842; *Chem. Abstr.*, 1970, **72**, 74432a.
347. P. Bartkus, *Nauchn. Konf. Khim.-Anal. Pribalt. Resp. B. SSR, Tezisy Dokl., Ist*, 1974, 193; *Chem. Abstr.*, 1977, **86**, 83146b.
348. P. Bartkus and A. Nauekaitis, *ibid.*, 1974, 190; *Chem. Abstr.*, 1977, **86**, 83145a.
349. P. Bartkus and D. Daugirdiene, *ibid.*, 1974, 187; *Chem. Abstr.*, 1977, **86**, 83144z.
350. Ya. P. Skorobogatyi, V. K. Zinchuk and R. F. Markovskaya, *Ukr. Khim. Zh.* 1984, **50**, 742; *Chem. Abstr.*, 1984, **101**, 182933r.
351. D. P. Nikolelis and T. P. Hadjiioannou, *Analyst*, 1977, **102**, 591.
352. Y. Yuan, Y. Wang and K. Qu, *Fenxi Huaxue*, 1988, **16**, 315; *Anal. Abstr.*, 1988, **50**, 10H82.
- 352a. Z. Wang and Z. Zheng, *ibid.*, 1986, **14**, 467; *Anal. Abstr.*, 1987, **49**, 3H61.
353. A. Aleksiev and K. Mutafchiev, *Anal. Lett.*, 1983, **16**, 769.
354. *Idem*, *Mikrochim. Acta*, 1985 II, 115.
355. S. U. Kreingol'd and V. I. Martsokha, *Fiz.-Khim. Metody Anal.*, 1976, **1**, 51; *Chem. Abstr.*, 1978, **88**, 83073s.
356. D.P. Nikolelis and T. P. Hadjiioannou, *Anal. Chem.*, 1978, **50**, 205.

357. L. I. Dubovenko and A. P. Tovmasyan, *Zh. Analit. Khim.*, 1970, **25**, 940; *Chem. Abstr.*, 1970, **73**, 94342v.
358. L. I. Dubovenko, A. P. Tovmasyain and N. F. Evtushenko, *Visn. Kiiiv. Univ., Ser. Khim.*, 1971, **12**, 38; *Chem. Abstr.*, 1974, **80**, 150583h.
359. S. P. Srivastava, K. P. Pandya and S. H. Zaidi, *Analyst*, 1969, **94**, 823.
360. K. Hirayama and N. Unohara, *Bunseki Kagaku*, 1984, **33**, E517; *Chem. Abstr.*, 1985, **102**, 71894e.
- 360a. I. Ya, Kolotyrkina, L. K. Shpigun and Yu. A. Zolotov, *Zh. Analit. Khim.*, 1988, **43**, 284.
361. A. B. Blank and A. Y. Voronkova, *Zavodsk. Lab.*, 1965, **31**, 1299; *Chem. Abstr.*, 1966, **64**, 8920d.
- 361a. Z. Zhang, *Huaxue Shiji*, 1989, **11**, 4; *Anal. Abstr.*, 1989, **51**, 8B107.
362. P. Bartkus, S. Kalesnikaite, L. Siaurukaite and E. Jasinskiene, *Liet. TSR Aukst. Mokyklu Mokslo Darb., Chem. Chem. Technol.*, 1967, **8**, 37; *Chem. Abstr.*, 1969, **70**, 43762n.
363. M. A. Sekheta, G. A. Milovanović and T. J. Janjić, *Mikrochim. Acta*, 1978 **I**, 297.
364. G. A. Milovanović, L. Trifković and T. J. Janjić, *Glas. Hem. Drus. Beograd*, 1981, **46**, 285; *Chem. Abstr.*, 1982, **96**, 14739s.
365. S. Abe, K. Takahashi and T. Matsuo, *Anal. Chim. Acta*, 1975, **80**, 135.
366. S. Abe and K. Takahashi, *Bunseki Kagaku*, 1974, **23**, 1326; *Chem. Abstr.*, 1975, **82**, 164411d.
367. A. Navas and F. S. Rojas, *Talanta*, 1984, **31**, 1075.
368. F. Salinas, J. J. Berzas Nevado and P. Valiente, *ibid.*, 1987, **34**, 321.
369. E. Klaventis, *Analisis*, 1989, **17**, 136.
370. Z. Zheng and Q. Zheng, *Huaxue Shiji*, 1988, **10**, 75; *Anal. Abstr.*, 1989, **51**, 1B152.
371. Z. Zhang and B. Li, *Fenxi Huaxue*, 1988, **16**, 334; *Anal. Abstr.*, 1988, **50**, 10B206.
372. G. Chen, *ibid.*, 1987, **15**, 920; *Anal. Abstr.*, 1988, **50**, 5B149.
373. Z. Yang, L. Huang and Y. Gao, *Gaodeng Xuexiao Huaxue Xuebao*, 1988, **9**, 82; *Anal. Abstr.*, 1988, **50**, 12F9.
374. P. Tarin and M. Blanco, *Analyst*, 1988, **113**, 433.
375. T. Yamane, *Anal. Sci.*, 1986, **2**, 191.
376. E. A. Morgen, N. A. Vlasov and L. A. Kozhemyakina, *Zh. Analit. Khim.*, 1972, **27**, 2064; *Chem. Abstr.*, 1973, **78**, 52175r.
377. S. Hiraoka, T. Shinonaga, T. Aso and D. Yamamoto, *Bunseki Kagaku*, 1984, **33**, 496; *Chem. Abstr.*, 1985, **102**, 16674h.
378. R. Belcher, S. M. T. Hasani and A. Townshend, *Egypt. J. Chem. (Spec. Issue)*, 1973, **131**; *Chem. Abstr.*, 1975, **83**, 90284.
379. A. Sugii, K. Harada and K. Kitahara, *Chem. Pharm. Bull.*, 1975, **23**, 2376.
380. D. Pérez-Bendito and M. Valcárcel, *Anal. Chim. Acta*, 1977, **94**, 405.
381. R. Yu, G. Zeng and R. Lin, *Huaxue Xuebao*, 1983, **41**, 960; *Chem. Abstr.*, 1983, **99**, 205236x.
382. A. V. Terletskaia, N. M. Lukovskaya and N. L. Anatienco, *Zh. Analit. Khim.*, 1979, **34**, 1460; *Chem. Abstr.*, 1980, **92**, 14787y.
- 382a. A. Navas and F. S. Rojas, *Talanta*, 1984, **31**, 437.
383. M. Gallego, M. Silva and M. Valcárcel, *Talanta*, 1984, **31**, 1075.
384. M. A. Koupparis and M. I. Karayannis, *Anal. Chim. Acta*, 1982, **138**, 303.
385. M. P. Babkin, *Zh. Analit. Khim.*, 1962, **17**, 256; *Chem. Abstr.*, 1962, **57**, 1536h.
386. A. A. Alexiev and K. L. Mutaftchiev, *Mikrochim. Acta*, 1982 **I**, 441.
387. I. F. Dolmanova, V. P. Poddubienko and V. M. Peshkova, *Zh. Analit. Khim.*, 1970, **25**, 2146; *Chem. Abstr.*, 1971, **74**, 60526p.
388. C. Sanchez-Pedreño, F. Sierra and L. C. Martinez, *Inform. Quim. Anal.*, 1970, **24**, 39; *Chem. Abstr.*, 1970, **73**, 72733w.
389. C. Sanchez-Pedreño and J. J. Arias, *ibid.*, 1974, **28**, 184; *Chem. Abstr.*, 1975, **82**, 67787y.
390. S. Nakono, A. Ohata and T. Kawashima, *Mikrochim. Acta*, 1985 **II**, 273.
391. M. H. Córdoba, P. Viñas and C. Sanchez-Pedreño, *Talanta*, 1986, **33**, 135.
392. D. Yamamoto, S. Hiraoka and T. Shinonaga, *Meiji Daigaku Nodakubu Kenkyu Hokoku*, 1985, No. 68, 91; *Chem. Abstr.*, 1986, **104**, 84709q.
393. L. T. Gvelesiani, V. K. Akimov and G. D. Supatashvili, *Zavodsk. Lab.*, 1985, **51**, No. 11, 10; *Chem. Abstr.*, 1986, **104**, 81153t.
394. H. P. Henriques, L. Hainberger and H. Grupe, *Mikrochim. Acta*, 1971, 807.
395. B. K. Pal and D. E. Ryan, *Anal. Chim. Acta*, 1969, **47**, 35.
396. O. K. Chung and C. E. Meloan, *Anal. Chem.*, 1967, **39**, 525.
397. V. K. Gustin and T. R. Sweet, *ibid.*, 1964, **36**, 1674.
398. D. T. Burns and D. Chimpalee, *Anal. Chim. Acta*, 1987, **199**, 241.
399. D. T. Burns, N. Chimpalee, M. Harriott and G. M. McKillen, *ibid.*, 1989, **217**, 183.
400. D. T. Burns, D. Chimpalee and N. Chimpalee, *Z. Anal. Chem.*, 1988, **332**, 453.
401. R. Belcher, *Talanta*, 1976, **23**, 883.
402. A. L. Wilson, *ibid.*, 1965, **12**, 701.

FIELD AND LABORATORY DETERMINATION OF A POLY(VINYL/VINYLDENE CHLORIDE) ADDITIVE IN BRICK MORTAR

STEPHEN L. LAW, JAMES H. NEWMAN and FRANCIS L. PTAK

Gascoyne Laboratories, Inc., 2101 Van Deman St., Holabird Industrial Park, Baltimore,
MD 21224-6697, U.S.A.

(Received 1 March 1989. Revised 5 July 1989. Accepted 15 August 1989)

Summary—A polymerized vinyl/vinylidene chloride additive, used in brick mortar during the 60s and 70s, is detected at the building site by the field method, which employs a commercially available chloride test strip. The field test results can then be verified by the laboratory methods. In one method, total chlorine in the mortar is determined by an oxygen-bomb method and the additive chloride is determined by difference after water-soluble chlorides have been determined on a separate sample. In the second method, the polymerized additive is extracted directly from the mortar with tetrahydrofuran (THF). The difference in weight before and after extraction of the additive gives the weight of additive in the mortar. Evaporation of the THF from the extract leaves a thin film of the polymer, which gives an infrared "fingerprint" spectrum characteristic of the additive polymer.

A Saran latex additive was used to strengthen the mortar in the construction of prefabricated brick masonry panels and single-course brick walls from about 1965 until possibly as recently as 1980. Initially the principal ingredient of the additive was polymerized vinyl chloride¹ until regulatory restrictions required the replacement of vinyl chloride with vinylidene chloride. The additive was used to increase the strength and hardness of the mortar.

Four gallons of the additive were mixed with each bag of cement and aggregate used to prepare a 2.5–3 ft³ batch of mortar. The additive is estimated to comprise approximately 4% by weight of the total batch of mortar, when used according to the manufacturer's instructions.

Though all the chlorine in poly(vinyl chloride) and poly(vinylidene chloride) is organically bound and therefore non-corrosive, the additive has become the subject of concern. Expansion of corroding metal inserts in mortars containing the additive is causing brick panels to crack, resulting in costly replacement. It is suspected that this corrosion may be induced by chloride, and that the chloride has been liberated from the additive.

Regardless of origin, water-soluble chlorides in mortar will cause corrosion of certain metal inserts under suitable environmental conditions. To help building owners delineate the problem, a method has been developed for use at the

building sites to determine the chloride content in brick mortars, both as the vinyl/vinylidene chloride polymer and as water-soluble chlorides. The field results can then be verified by the laboratory tests developed.

EXPERIMENTAL

Reference mortars

Additive-free reference mortar. Mortar was taken from glass bricks removed from Northwestern High School, Hyattsville, MD. It was estimated that the mortar had been prepared in 1967. Approximately 1.4 kg of it was ground with a mortar and pestle and passed through a U.S. Standard Testing Sieve No. 16 (ASTM-E-11 Specification) giving particles less than 1.18 mm in diameter. This is approximately the particle size expected from the use of an electric drill and masonry bit in sampling mortar in buildings. This stock material was mixed thoroughly and riffle-split into portions for accurate determination of chlorine content. The water-soluble chloride was found to be $0.015 \pm 0.001\%$. No additive was found in this mortar.

A 300-g split of the Northwestern High School (NW) mortar was slurried with an aqueous solution containing 3 g of sodium chloride and evaporated to dryness at 105° to prepare a reference mortar containing

Oxygen bomb method for total chlorine

Reagents. Reagent grade chemicals are used in all tests. A 0.5M sodium carbonate solution is prepared. The oxygen used for the combustion in the oxygen bomb should be free from combustible matter; oxygen manufactured from liquid air, guaranteed to be greater than 99.5% pure, will meet this requirement. Refined "white oil" (also known as "mineral oil"), chlorine-free, is used.

Apparatus. The oxygen bomb conforms to ASTM specifications.²

Procedure. Weigh into the bomb capsule, to the nearest 0.1 mg, about 1 g of thoroughly mixed air-dried mortar sample. Add a volume of white oil approximately equal to the volume of mortar sample. Stir the mixture with a short length of quartz rod and leave the rod in the sample cup during the combustion. Place the capsule containing the sample and white oil in the capsule holder. Connect a length of firing wire (~100 mm) to the ignition terminals so that it is in contact with the sample.

Spray 10–20 ml of the 0.5M sodium carbonate into the bomb, wetting the entire internal surface of the bomb (0.02M potassium hydroxide or sodium hydroxide may be used instead of the sodium carbonate solution). Assemble the bomb.

Admit oxygen into the bomb slowly, to avoid blowing the sample from the capsule, until a pressure of 30 atm is reached. The weight of mortar sample and the oxygen pressure in the bomb must not exceed the bomb manufacturer's recommendations. Recommended practice³ for safe use of the bomb should be followed at all times.

There is a tendency for chloride to adhere to the bomb walls, especially if the bomb is pitted or has been used previously to determine high levels of chlorine. Unless the bomb is thoroughly cleaned before use, the blanks may have values in excess of the true value.

Immerse the bomb in a cold water-bath, connect it to the firing circuit, and close the circuit to ignite the sample. Allow the bomb to stand in the water-bath for not less than 10 min after firing. Remove the bomb from the water-bath, invert the bomb and shake it for about 10 min. Release the pressure at a slow, uniform rate so that the pressure is reduced to atmospheric in not less than 1 min. Open the bomb and examine the inside for traces of unburned oil or sooty deposits. If any are found, discard

the determination and thoroughly wash all parts of the bomb interior before using it again. If no unburned oil or sooty deposit is present, rinse the interior of the bomb, the sample capsule, and the interior surface of the bomb cover with a fine jet of hot water and collect the contents and washings in a beaker or flask. Filter off the solids and dilute the filtrate to a known volume, as described below for water-soluble chlorides. Determine total chloride by titration with mercuric nitrate to a diphenylcarbazone endpoint,⁴ the Volhard method,⁵ a potentiometric method,⁵ or some other reliable standard method.

Determination of water-soluble chlorides

Weigh to the nearest 0.1 mg about 5 g of thoroughly mixed, air-dried mortar sample. Transfer it into a 500-ml beaker and add 100 ml of water. Stir for 30 min to ensure thorough wetting of the sample. Decant the supernatant liquid through a fast qualitative filter paper, collecting the filtrate in a beaker. Repeat the extraction twice more, each time using 100 ml of water and pooling the filtrates. After the third extraction, wash the sample thoroughly with 100 ml of water, adding the washings to the pooled filtrates. The weight of sample used can be adjusted when higher or lower concentrations of water-soluble chlorides are expected. Also, when high concentrations of chlorides are expected, dilute the extraction solution to volume in a suitable size of standard flask and continue the analysis with an appropriate size of aliquot. Determine the chloride by one of the methods listed above for total chloride determination.

Determination of additive chloride

The content of organically-bound, or additive, chlorine is calculated by difference, from the total chlorine found by oxygen bomb method and the water-soluble chloride determined as just described. The presence of over 0.5% organically-bound chlorine in brick mortar indicates the presence of the poly(vinyl/polyvinylidene chloride) additive. It is assumed that no other source of water-insoluble, organically bound chloride would be present in brick mortar at a concentration this high. For irrefutable evidence of the presence of the additive, the following infrared method may be used.

Table 1. Quantab vs. laboratory results

Mortar*	Mean water-soluble Cl ⁻ , %		Total Cl, %
	Quantab	Laboratory	
NW stock	0.014	0.015	0.015
0.5% Cl ⁻	0.53	0.52	0.52
1.0% Cl ⁻	0.97	1.0	1.0
2.9% Cl ⁻	2.7	2.85	2.85
CS-2	0.10	0.05	1.2
MT-1	0.22	0.22	2.0
MT-2	0.73	0.77	2.3
MT-3	0.48	0.52	1.8
MT-4	0.49	0.53	1.6

*NW = Northwestern, CS = Cedar Square, MT = Monocacy Towers.

Infrared method for poly(vinyl/polyvinylidene chloride) in mortar

Reagents. Tetrahydrofuran (THF), reagent grade (may be stabilized with 0.1% hydroquinone, which can be removed by adsorption on alumina before use of the THF).

Apparatus. The infrared spectrophotometer should have a resolving power of 0.02 μm or better at 12 μm . The spectral region from 2.5 (4000 cm^{-1}) to 15 μm (667 cm^{-1}) is used. A centrifuge or a Baker-10 extraction system is used.

Separation of additive. Weigh to ± 0.1 mg approximately 5 g of fine particle-size mortar sample and put it in a 50-ml beaker. Add 10 ml of THF (previously passed through a 150 \times 12.7 mm diameter alumina adsorption column to remove hydroquinone) and stir for about 20 min. Wash the contents of the beaker quantitatively into a tared 50-ml centrifuge tube with 10 ml of THF, swirl to mix, and centrifuge for 30 min. Decant the solution for infrared analysis. Wash the residue remaining in the tared centrifuge tube with 20 ml of THF and centrifuge again for 30 min. Decant the solution. Repeat the operation. Dry the tared centrifuge tube, containing the residue, in an oven at 110° for 1 hr, cool and weigh.

Alternatively, a Baker-10 extraction system may be used. Preweighed 6-ml disposable filtration columns with dual 20 μm frits and approximately 1-g samples were used to obtain the data for this report. The system was used without vacuum suction, so that there would be longer contact time with the extractant for the initial 10 ml extraction with THF. Washing with 10-ml portions of THF was then conducted with suction and the sample was dried at 110° for 1 hr, cooled, and weighed.

The additive content in the mortar is calculated as follows: Additive, % = (sample wt. - wt. of residue) \times 100/sample wt.

Infrared spectrum. The major portion of any poly(vinyl/polyvinylidene chloride) extracted is in the first decanted THF solution. Evaporate a few ml of the solution a few drops at a time on a microscope slide. When the resultant film is dry, peel it from the microscope slide and dry it in a vacuum desiccator or vacuum oven to reduce spectral interference by the solvents. A number of films may be prepared from each sample in order to obtain one of suitable quality and thickness. Mount the film in the infrared spectrophotometer and record its spectrum from 2.5 to 15 μm .

Bands at 7.0 μm (1429 cm^{-1}) and 9.3 μm (1075 cm^{-1}), characteristic of a vinyl/vinylidene chloride polymer, and at 5.7 μm (1754 cm^{-1}), are observed in the infrared spectrum of the additive. The presence of the latex film itself, as well as the spectral bands at these positions, provide positive proof of additive being present.

RESULTS AND DISCUSSION

Field method

Quantab vs. laboratory results. Table 1 shows a comparison of results obtained with Quantab Chloride Titrator strips and laboratory analyses for water-soluble chlorides only. The calibration table supplied by the manufacturer was used to obtain the Quantab results. However, it is recommended that each new batch of Quantab Titrators be recalibrated. The results in Table 1 are within $\pm 10\%$ of the laboratory analyses in every case. The Quantab results were obtained by taking an accurately weighed portion of mortar (~ 1 g) and shaking it for 1 min with 5 ml of demineralized water in a stoppered 125 \times 16 mm test-tube. The Quantab Titrator strip was placed directly in the solution in the test-tube with no prior filtration. In no case was the capillary tube clogged by the fine mortar particles, which allowed omission of a filtration step.

Table 2. Quantab reproducibility and time taken for test

Mortar	Quantab Titrator	Time to reach blue signal	Quantab reading	Water-soluble Cl ⁻ , %	Average (±std. devn.) Cl ⁻ , %
MT-1	A	7 min 18 sec	3.7	0.218	0.218 ± 0.010
	B	7 min 20 sec	3.8	0.227	
	C	7 min 4 sec	3.6	0.210	
MT-2	A	7 min 29 sec	6.9	0.734	0.726 ± 0.014
	B	6 min 58 sec	6.9	0.734	
	C	7 min 40 sec	6.8	0.711	
MT-3	A	7 min 33 sec	5.7	0.464	0.479 ± 0.019
	B	7 min 22 sec	5.9	0.496	
	C	7 min 35 sec	5.8	0.477	

Reproducibility. Table 2 shows the reproducibility of the Quantab determinations, obtained by use of separate Quantab Titrators for the same solution; three MT mortar samples were used. The relative standard deviation (calculated by range method) was better than 5% in all three cases.

Time taken for test. Also shown in Table 2 is the time elapsed from the introduction of the Quantab Titrator into the solution being tested until the completion signal strip at the top is triggered to change from yellow to dark blue. The times ranged from 6 min 58 sec to 7 min 40 sec in this series of tests. For field use, if the completion signal has not been triggered within 12 min, it can be assumed that the capillary opening was at least partially sealed during manufacture or has otherwise become clogged, and a new Quantab Titrator is needed. A more common problem in the field is premature triggering of the completion signal by water entering through the side of the titrator at either end of the yellow moisture indicator strip. Care must be taken to keep this portion of the titrator free from water. After the completion signal has been triggered, the titrator strip should be left in the solution for an additional 2 min to ensure saturation of the capillary.

Thermal breakdown of additive. As can be seen in Table 1, the total chlorine in the MT and CS mortars is up to an order of magnitude greater than the amount of water-soluble chloride. The non-soluble chlorine is a part of the additive

polymer. An attempt was made to prepare a mortar containing only the additive and no water-soluble chlorides, by water-leaching all the soluble chlorides. However, it was found that drying at 105° releases more water-soluble chlorides. Successive leaching and drying of the same sample resulted in additional water-soluble chloride after each drying. This can only be attributed to gradual decomposition of the polymer. To prepare a mortar containing only polymer-bound chlorine, the mortar was air-dried at room temperature after the initial leaching of water-soluble chlorides. With room-temperature drying, no additional water-soluble chlorides were detected.

Because of the release of chlorides from the additive by heat, a step was included in the field method to heat the mortar sample prior to water extraction. A cigarette-lighter flame held for half a minute or more to the bottom of the test tube adequately releases the chlorides from the polymer. A visible darkening of the mortar from charring of the poly(vinyl/polyvinylidene chloride) is noticed when additive-containing mortars are heated.

Table 3 gives a comparison of Quantab titrator strip results for heated and unheated mortars. The increase in water-soluble chlorides after the additive-containing mortars, CS and MT, have been heated is around an order of magnitude. The NW mortar, which contains no additive, showed no increase in water-soluble chlorides on heating.

Table 3. Additive detection after cigarette-lighter heating

Mortar	Chloride detected, %		
	No heating (water-soluble Cl ⁻ only)	After heating (1 min) (total chloride)	Additive chloride (by difference)
CS-1	0.13	2.9	2.8
CS-2	0.10	1.2	1.1
CS-3	0.10	2.6	2.5
MT-3	0.46	2.3	1.8
NW-1	0.018	0.016	0.0

Table 4. Total, water-soluble, and additive chlorides in mortars

Mortar	Chloride, %		
	Oxygen bomb (total)	Water-soluble	Additive
MT-1	2.0	0.22	1.8
MT-2	2.3	0.77	1.5
MT-3	1.8	0.52	1.3
MT-4	1.6	0.53	1.1
CS-2	1.2	0.05	1.1
NW	0.015	0.015	0.0
0.5% Cl ⁻	0.52	0.52	0.0
1.0% Cl ⁻	1.0	1.0	0.0
2.9% Cl ⁻	2.9	2.9	0.0

Polymer chloride vs. water-soluble chloride. To obtain an estimate of only the poly(vinyl/polyvinylidene)-bound chloride in a mortar sample, two splits of the sample are used. One portion is heated to free all chlorides in the polymer for Quantab determination of total chlorides; and the other is not heated, allowing detection of only the water-soluble chlorides. As seen in Table 3, the difference between the two results gives an estimate of the additive chloride.

Interferences. Because of the alkalinity of brick mortars, a blackening of the silver dichromate in the initial portion of the capillary column will often be noticed in strips showing a negative test for chlorides. This is caused by the formation of the dark brown to blackish hydrated silver oxide. If chlorides are present, the white silver chloride is formed preferentially, so the alkalinity does not interfere with the test. This was verified by tests with 0.1M sodium hydroxide containing added chloride. Consultation of the solubility products for selected silver compounds reveals that significant concentrations of free bromide, iodide, sulfide and thiocyanate ions in solution can be expected to interfere. Sulfates and carbonates will not, as was verified by experimentation. Aluminates were also tested and found not to interfere.

Any significant exposure of the strips to direct sunlight was found to result in reduction of the silver ions in the silver dichromate to elemental silver. Humidity affects only the completion strip, rendering it useless.

Laboratory methods

Table 4 gives the results obtained from additive-containing MT and CS mortars, and from the non-additive mortar and the chloride-spiked mortars by using the oxygen bomb method and the water-soluble chloride method. The amount of additive chloride in the mortars was found by difference.

The reproducibility of the water-soluble chloride method was found to be 10% relative standard deviation for the NW sample ($0.0147 \pm 0.0014\%$). For the oxygen bomb method, the relative standard deviation was 7% for MT-4 ($1.55 \pm 0.11\%$), and 8% for CS-2 ($1.20 \pm 0.09\%$).

Figure 1 shows the infrared spectra of the THF extracts from a mortar containing no additive (NW-1, spectrum A) and from a mortar containing the additive (CS-2, spectrum B). In the absence of the additive, the characteristic spectral peaks at $9.3 \mu\text{m}$ (1075 cm^{-1}), $7.0 \mu\text{m}$ (1429 cm^{-1}) and $5.7 \mu\text{m}$ (1754 cm^{-1}) are not observed (spectrum A). The CS-2 spectrum (B), however, contains the three distinguishing peaks, clearly identifying the presence of the additive.

Weighing of the additive extracted by THF from sample MT-2 gave a value of $2.9 \pm 0.3\%$ (relative standard deviation 10%). The chlorine content of vinylidene chloride is 73.1%. If the extracted additive is poly(vinylidene chloride), the corresponding chlorine in MT-2 is calculated to be 2.1%. This result does not agree very well with the 1.5% additive chlorine found by difference between the total (oxygen-bomb) chlorine and water-soluble chloride, as shown in Table 3. A quick test of the solubility of sodium chloride in THF established that the water-soluble chlorides in the mortar are, indeed, not soluble in THF.

The chlorine content of vinyl chloride is 56.8%. If this factor is used, the amount of chlorine in the MT-2 additive extracted by THF is 1.6%, in good agreement with the 1.5% additive chlorine found by difference. The building from which the MT-2 sample was taken was completed in 1973. Prior to the environmental regulations restricting its use in October 1974, poly(vinyl chloride) was the principal ingredient in the mortar additive.

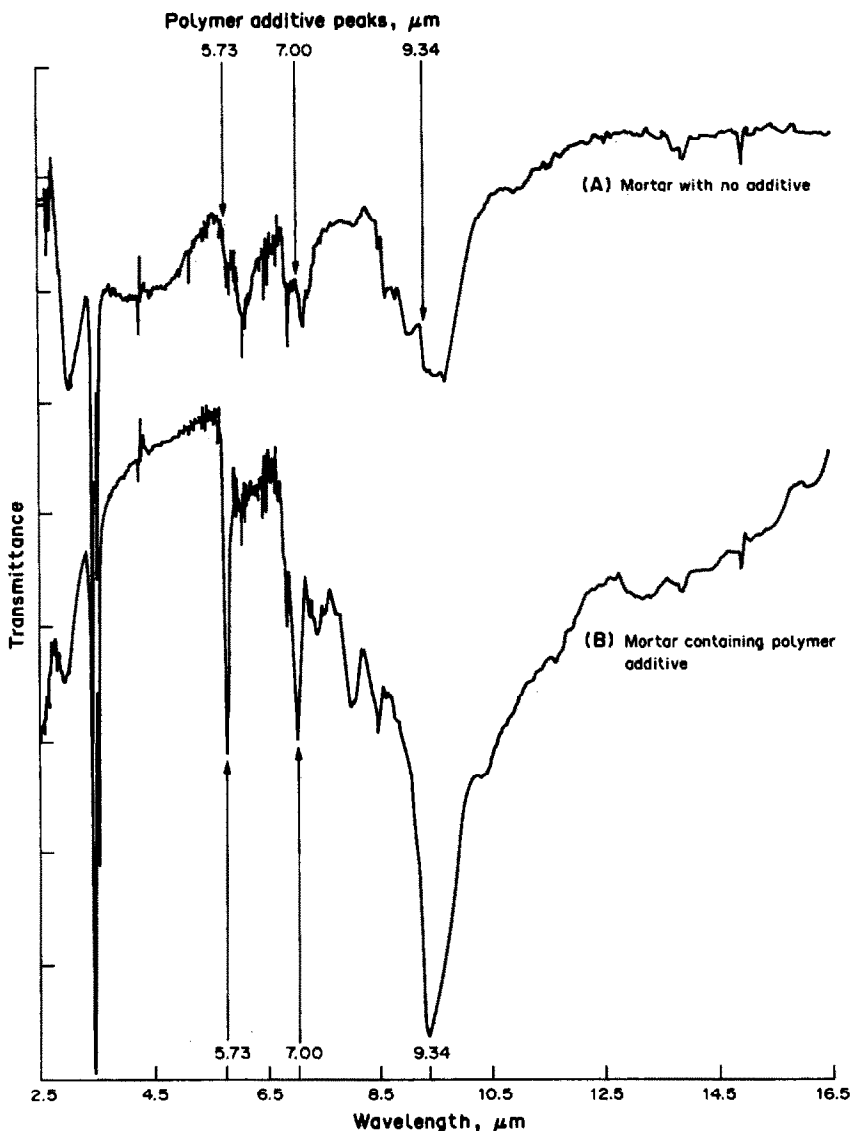


Fig. 1. Infrared spectra of THF extracts from mortars.

Poly(vinyl chloride) can also be seen to be present in the CS-2 mortar. By the Baker-10 extraction system method described above, the content of THF-extracted additive was found to be $2.05 \pm 0.08\%$. Multiplication by the poly(vinylidene chloride) factor of 0.731 will give 1.50% additive chlorine, whereas use of the poly(vinyl chloride) factor of 0.568 gives 1.16% additive chlorine. The amount found by the difference method was 1.15%, rounded to 1.1% in Table 3. Again, good agreement is seen if poly(vinyl chloride) is the predominant polymer present. The building from which the CS mortar was taken was completed in 1974, and would also have been

built with use of the poly(vinyl chloride) additive.

Acknowledgement—Funding support for this research was provided under Purchase Order No. DU100P87 987 by the U.S. Department of Housing and Urban Development.

REFERENCES

1. J. Peters, R. D. Van Dell, R. D. Fash and L. F. Lamoria, *U.S. Patent*, No. 4,086,201, 1965.
2. *Annual Book of ASTM Standards*, Vol. 5.05, Standard D 2015 and Standard D 3286, 1986.
3. *Ibid.*, Vol. 14.02, Standard E 144, 1986.
4. U.S. Environmental Protection Agency, *Methods for Chemical Analysis of Water and Wastes*, EPA-600/4-79-020, Method 325.3, 1979.
5. *Annual Book of ASTM Standards*, Vol. 11.04, Standard E 776-81, 1986.

TITRIMETRIC METHODS FOR THE DETERMINATION OF VITAMIN C IN SOME PHARMACEUTICAL PREPARATIONS BY USE OF TWO *N*-BROMOIMIDES

K. GIRISH KUMAR and P. INDRASENAN*

Department of Chemistry, University of Kerala, Trivandrum 695 034, India

(Received 21 December 1988. Revised 17 March 1989. Accepted 21 August 1989)

Summary—Potentiometric and visual end-point titrations with *N*-bromophthalimide and *N*-bromosaccharin are proposed for the determination of vitamin C in various pharmaceutical preparations. These methods are simpler than the existing methods for the purpose.

Vitamin C (ascorbic acid) preparations may consist of the pure compound or its mixtures with other vitamins. The methods available for their analysis include titration with iodine,¹ *N*-bromosuccinimide,² chloramine-T,³ chloranil⁴ and 2,6-dichlorophenolindophenol,⁵ and methods using cupric salt⁶ and ceric ammonium sulphate.⁷ Recently, we have recommended use of *N*-bromophthalimide (NBP) and *N*-bromosaccharin (NBSA) for the determination of some sulphur drugs and carbohydrates, on account of their stability and reactivity.⁸⁻¹¹ We now report their use for analysis of vitamin C preparations.

EXPERIMENTAL

Apparatus

A Toshniwal titration potentiometer type CL 06A fitted with a "null meter" detector, magnetic stirrer, a smooth platinum indicator electrode and an aqueous saturated calomel reference electrode was used for direct potentiometric titrations.

Reagents

NBP and NBSA were prepared by brominating phthalimide and saccharin, respectively. Their standard solutions (~0.01M) were prepared in anhydrous acetic acid and were kept in amber-coloured bottles as reported earlier.^{10,11} The vitamin C preparations were obtained from the local market. A known weight (~0.5 g) of each preparation was dissolved in water (tablets are powdered first), and any residue was filtered

off on a Whatman No. 41 filter paper and washed with water 5 or 6 times, the filtrate and washings being collected in a 250-ml standard flask and made up to the mark with water. A standard solution of pure vitamin C (~0.5 g in 250 ml) was also prepared. The concentrations of these solutions were checked by the iodimetric method.¹ For visual end-point titrations, aqueous Quinoline Yellow solution (0.1%) was used as the indicator.¹²

Procedures

Potentiometric titration. A known volume (5–15 ml) of vitamin C solution was titrated with NBP or NBSA added from a microburette. The potential after each addition was measured after stirring the solution for a few seconds. Towards the end-point the titrant was added in 0.1 ml portions and the solution was stirred for 30 sec for steady potentials to be obtained. The titration was continued until there was no significant change in potential on further addition of the oxidant. The equivalence points were calculated graphically.¹²

Visual end-point titrations. Two drops of indicator were added to a known volume (5–15 ml) of vitamin C solution, which was then titrated with NBP or NBSA added from a microburette until the indicator became colourless.

The amount (*W*) of vitamin C is calculated from the following equation.

$$W = 176.1MV \text{ mg}$$

where *W* is the amount of vitamin C present in the sample titrated, *M* the molarity of the NBP (or NBSA) solution, and *V* the volume of titrant used.

*Author for correspondence.

Table 1. Direct potentiometric titrations with *N*-bromophthalimide and *N*-bromosaccharin*

Tablet/syrup	Maker's specification, mg/tablet or mg/ml	NBP		NBSA	
		Found, mg/tablet or mg/ml	C.V., %	Found, mg/tablet or mg/ml	C.V., %
Chevicee	500	499	0.8	497	0.3
Celin	500	500	0.2	502	0.4
Redoxon	500	504	0.1	502	0.2
Ceecon Drops	100	98	0.3	99	0.4
Sorvicin Drops	100	101	0.8	97	0.5
Sukcee Drops	100	97	1.0	95	0.6
Abdec Drops	100	83	0.3	82	0.1
Becosules	150	150	0.9	149	0.9
Basiton Forte	150	165	0.4	155	1.0

*Averages of 10 replicates; C.V. = coefficient of variation.

RESULTS AND DISCUSSION

The results are presented in Tables 1 and 2. During the titration, ascorbic acid is oxidized to dehydroascorbic acid by NBP and NBSA, which are reduced to phthalimide and saccharin, respectively, as reported earlier.^{10,11}

Direct potentiometric titrations were successful for all the vitamin C preparations studied, with both NBP and NBSA, but direct visual end-point titrations were possible only for six of the preparations and were unsuccessful for Abdec drops, Basiton Forte and Becosules because these are coloured. The results show that all four methods are reasonably accurate and precise. The potential jump is high (~300 mV) and electrode equilibration rapid (<30 sec). The colour change at the end-point (yellow to colourless) is very distinct.

Validation was done with two typical samples, Celin and Redoxon, for both NBP and NBSA, by determining the recovery of known amounts of added vitamin C (~4–10 mg). The recoveries were 99.1–100.5% (Celin) and 98.7–100.8% (Redoxon) for NBP titration,

and 98.3–100.9% (Celin) and 98.6–100.7% (Redoxon) for NBSA. The effect of vitamins B₂, B₆ and B₁₂, which are usually found in vitamin C preparations was also studied, and they were found not to interfere in determination of 8 mg of vitamin C when present in 1.5–4.5 mg amounts. However, in similar experiments substances such as cysteine and glutamic acid were found to interfere, causing high results. Tablet excipients such as starch, lactose, calcium and magnesium stearates and talc do not interfere.

The proposed methods have some advantages over existing methods for the analysis of vitamin C preparations. All four are direct titrations without addition of auxiliary agents (unlike the chloramine-T method³). The indicator used for visual end-point detection is reversible, so over-titration can be corrected by back-titration with ascorbic acid, in contrast to the chloramine-T method in which an irreversible indicator is used.³ The proposed methods can be used for the determination of vitamin C in certain multivitamin preparations without prior separation.

Table 2. Direct titrations (visual end-point) with *N*-bromophthalimide and *N*-bromosaccharin*

Tablet/syrup	Maker's specification, mg/tablet or mg/ml	NBP		NBSA		Comparison method†	
		Found, mg/tablet or mg/ml	C.V., %	Found, mg/tablet or mg/ml	C.V., %	Found, mg/tablet or mg/ml	C.V., %
Chevicee	500	498	0.9	497	1.1	498	1.2
Celin	500	501	0.1	503	0.1	503	0.6
Redoxon	500	503	0.9	501	0.7	498	0.8
Ceecon Drops	100	99	1.1	99	0.8	95	1.4
Sorvicin Drops	100	100	1.8	101	1.7	98	1.4
Sukcee Drops	100	96	0.6	97	1.4	94	1.4

*Average of 10 replicates.

†Iodimetric method.

Acknowledgement—The authors are grateful to the State Committee on Science, Technology and Environment, Government of Kerala, Trivandrum for financial support for the work.

REFERENCES

1. *British Pharmacopoeia 1953*, p. 56. H.M. Stationery Office, London, 1953.
2. M. Z. Barakat, M. F. Abdel-Wahab and M. M. El-Sadar, *Anal. Chem.*, 1955, **27**, 536.
3. K. K. Verma and A. K. Gulati, *ibid.*, 1980, **52**, 2236.
4. K. K. Verma, A. Jain and R. Rawat, *J. Assoc. Off. Anal. Chem.*, 1984, **67**, 262.
5. *Official Methods of Analysis*, 12th Ed., p. 839. AOAC, Arlington, 1975.
6. M. Z. Barakat, S. K. Shehab, N. Darwish and El-Zoheiry, *Anal. Biochem.*, 1973, **53**, 245.
7. *British Pharmacopoeia 1973*, p. 36. H.M. Stationery Office, London, 1973.
8. K. G. Kumar, C. Mohanadas and P. Indrasenan, *Talanta*, 1988, **35**, 651.
9. K. G. Kumar and P. Indrasenan, *Analyst*, 1988, **113**, 1369.
10. C. Mohanadas and P. Indrasenan, *Indian J. Chem.*, 1987, **26A**, 55.
11. *Idem*, *Intern. J. Food Sci. Technol.*, 1987, **22**, 339.
12. A. I. Vogel, *A Text Book of Quantitative Inorganic Analysis*, 3rd Ed., p. 384, Longmans, London, 1961.

SOFTWARE SURVEY SECTION

Software package TAL-007/89

NOTEBOOK II V.3.02

Contributor: Pat Burke, University of Colorado, CBC424, Chem. Eng., Boulder, Co 80309, U.S.A. Tel. 303-492-7471.

Brief description: NOTEBOOK II is a database system for storing and retrieving text such as bibliographies and research and lab notes on a personal computer. It will store, edit, interrogate, sort on any character string for any field, form logical subsets/views, print (to disc or hardcopy) the database or a logical subset in any format you specify. The default maximum record size of 20000 characters may be expanded to 50000. Database size is limited only by disc space. May import information from most word-processors and many databases and programs. It handles foreign characters with ASCII character codes. You may place up to 36 foreign characters within the regular alphabet so that they will properly sort/re-order. Separate CONVERT utility will download records from online databases in your format. Separate BIBLIOGRAPHY utility compares citations in a manuscript with the database and constructs a bibliography of all entries cited. It offers exceptional value for money.

Potential users: scientists, students, teachers, smaller abstract services.

Fields of interest: bibliographic data storage and retrieval.

This utility program has been developed for the IBM-PC and compatibles, and was written in C, to run under MS-DOS 2 or 3. It is available on 5.25 or 3.5-inch discs. The memory required is 256K.

Distributed by Pro/Tem Software Inc., 814 Tolman Drive, Stanford, CA 94305, USA. Tel. 415-947-1000.

The machine requires 2 floppy drives, or 1 floppy and a hard disc. The program is user-friendly and self-documenting, but with extensive external documentation also. The source code is not available. The program is fully operational; it has been share-used for two years, and is in use at 10000 sites. The contributor is willing to deal with enquiries.

Software package TAL-006/89

Fig-P

Contributor: BIOSOFT, 22 Hills Road, Cambridge CB2 1JP.

Brief description: Fig.P is a scientific graphics program for the preparation of artist-quality graphs and diagrams. Data can be entered direct from laboratory instruments, or from spreadsheet files. Statistical methods are included, together with many curve-fitting methods. Labelling can be in any size and direction, with boxes, error bars, lines, arrows, text and symbols, including Greek characters. True superscripts and subscripts can be used. Colour is available on screen, and can be printed on appropriate printers, plotters, and slides. Figures can be exported as disc files for incorporation in word-processor documents.

Potential users: all scientists.

Fields of interest: any science.

This program has been developed for IBM PC, PS2 and compatibles, with CGA, HGA, EGA, EGA-mono, MCGA or VGA. The memory required is 512K minimum, and a hard disc is also required. Output is to HP plotters, HP LaserJets, PCL

compatible laser printers, IBM and Epson dot-matrix printers, HPGL compatible film recorders, SCODL format Matrix film recorders, CGM format (ANSI standard), EPS format (Postscript including colour).

Distributed by BIOSOFT. Tel. 0223 68622. Price £250.

The program is exceptionally user-friendly, with context-sensitive help. Intuitive menus are appropriate to scientists and their assistants.

ANALYTICAL APPLICATIONS OF SOME FLOTATION TECHNIQUES—A REVIEW

M CABALLERO, R CELA* and J A PEREZ-BUSTAMANTE

Department of Analytical Chemistry, Faculty of Sciences, University of Cadiz, Spain

(Received 10 August 1987 Revised 10 July 1989 Accepted 28 July 1989)

Summary—A review is given of the principles and more recent applications of foam flotation

Separation techniques based on use of adsorptive bubbles (flotation techniques) have received a great deal of attention in chemical engineering, but have awakened less interest in analytical chemistry. Flotation techniques were first used to obtain mineral concentrates or selective separation of them.

In chemical engineering, these techniques began to expand in the 1960s and today have many applications in industry, to separate toxic substances, suspended solids, micro-organisms, *etc* from residual, industrial, sea and drinkable waters. These techniques turned out to be very simple compared with classical separation methods such as liquid-liquid extraction, ion-exchange, co-precipitation *etc*. They allow the handling of large volumes of sample, and present considerable saving in reagents, time and energy. Their analytical applications started to be studied in the middle 1970s, especially in the U.S.A., U.S.S.R. and Japan. Sometimes, this makes it difficult to achieve a readily accessible bibliography. On the other hand, the U.S.A. papers are basically in chemical engineering.

Discussions of these techniques as methods of separation and/or preconcentration are not yet available in analytical chemistry textbooks and they are scarcely found even as monographs and reviews. The monograph edited by Lemlich¹ presents a general treatment of all these techniques, as well as their development up to 1972. There are also some very specialized monographs, such as Sebba's on ionic flotation,² and another more recently by Clarke and Wilson³ that discusses the theory and applications of foam separations. Some books on separation methods contain chapters dealing more or less

extensively⁴⁻⁶ with the general or particular aspects of these techniques.

The most outstanding recent reviews are those by Clarke and Wilson,⁷ and by Hiraide and Mizuike.^{8,9} The first is a very complete review of books, reviews, theories and models of separation by flotation, including a section on metal and organic compound separations. The last two reviews consider flotation techniques from an analytical chemistry perspective, especially precipitation and ion flotation of organic and inorganic species; unfortunately, the Russian work is largely ignored.

At the present time flotation studies on most of the elements are known (Fig. 1) as well as on a large number of different species, therefore, in the present review the analytical applications of precipitate flotation are included, as well as ion flotation and solvent sublation, covering the last few years (from about 1980). Furthermore, a description of the techniques, and the theoretical foundations of precipitate flotation and solvent sublation are included, because these are the most interesting in analytical chemistry.

DESCRIPTION AND CLASSIFICATION OF THE TECHNIQUES

Lemlich¹ proposed the term "Adsubble Techniques", based on a contraction of "adsorptive bubbles". There are a number of separation methods, based on differences in surface tension, in which dispersed solids, precipitates, colloids and dissolved substances are adsorbed on an ascending gas stream, and thus separated from the liquid mass where they were initially. This separation is due to the ability of some species to orient themselves in the air-water interface, and the adsorption on the bubble surfaces is due to the presence of certain functional groups. The substances to be separated

*Author for correspondence

H																		He
Li	Be											B	C	N	O	F	Ne	
Na	Mg											Al	Si	P	S	Cl	Ar	
K	Ca	Sc	Ti	V	Cr	Mn	Fe	Co	Ni	Cu	Zn	Ga	Ge	As	Se	Br	Kr	
Rb	Sr	Y	Zr	Nb	Mo	Tc	Ru	Rh	Pd	Ag	Cd	In	Sn	Sb	Te	I	Xe	
Cs	Ba	La	Hf	Ta	W	Re	Os	Ir	Pt	Au	Hg	Tl	Pb	Bi	Po	At	Rn	
Fr	Ra	Ac																

Ce	Pr	Nd	Pm	Sm	Eu	Gd	Tb	Dy	Ho	Er	Tm	Yb	Lu
Th	Pa	U	Np	Pu	Am	Cm	Bk	Cf	Es	Fm	Md	Nb	Lw

Fig 1 The elements within the shaded area are those with ions amenable to separation by flotation techniques

by means of these techniques must either already possess these groups or be given them by addition of some surfactant agent

Karger *et al*¹⁰ classified these techniques in two large groups based on foam formation (Table 1) Later, Pinfold¹¹ suggested they should be classified according to the adsorption mechanism, depending on the flotation of particles, ions and molecules

Obviously this second option is more logical, but in practice the classification by Karger *et al* continues to be the more widely accepted. According to it, in the first group (non-foaming techniques) the bubble fractionation technique¹² must be included, which can be used for the separation of the solution components by adsorption on the bubbles of an ascending gas stream, leading to an enrichment of the surface-active substances in the upper zone of the column. This is the simplest "adsorbable technique" and also the least used in practice. It is mainly applied to the separation and/or pre-concentration of surfactants at low concentrations. Obviously, in this case it is not necessary to add a foaming agent. In practice, these phenomena and fractionation processes

could occur by accidental bubble formation, as in the liberation of gas during a chemical reaction, and this can give rise to separations of surface-active substances

The technique known as solvent sublation was initially proposed by Sebba² as an option for ion flotation, if excessively copious foam formation occurred. The main difference from the other techniques is that the substances adsorbed on the ascending bubbles, once they arrive in the column upper zone, find a different layer of solvent, immiscible with the liquid from which we wish to separate them. This immiscible liquid collects the substances (sublates) which arrive at the interface, and this produces the separation of these substances.

The "adsorbable techniques" with foam formation are divided into two large groups: foam fractionation and flotation.

Foam fractionation consists in the separation of dissolved substances which possess a lyophobic group or (in which case they are called colligends) can be made sufficiently surface active by combination with surfactant agents (collectors) by chelate formation, ionic bonding or any other kind of union, the resulting

Table 1 Classification of the flotation techniques according to Karger *et al*¹⁰

Non-foaming techniques	{	Solvent sublation
		Bubble fractionation
Foam separation	{	Foam fractionation
	{	Flotation
		{
		Macroflotation
		Microflotation
		Precipitate flotation
		Ionic flotation

surface-active substances being adsorbed on the surface of the bubbles ascending through the liquid mass

Flotation techniques can be divided, in turn, into four large groups

I—*Macroflotation* An example is mineral flotation, a widespread and intensively studied technique used in the mining industry for obtaining mineral concentrates and eliminating impurities.

II—*Microflotation* Flotation of micro-particles such as colloids, micro-organisms. The analyte may be adsorbed on a charged colloidal species generated to act as a carrier, and the colloid may be floated by addition of a surfactant, as in precipitate flotation

III—*Precipitate flotation* Separation of substances by precipitation and gas streaming, in which bubbles are adsorbed on the precipitate, floating it up to the liquid surface. It is possible to consider two kinds of precipitate flotation

- (a) Precipitate flotation of the first kind. The surfactant does not itself form an insoluble compound with the species to be separated, but helps it to reach the surface of the liquid mass when it is precipitated with some other reagent. This has been used in two different ways. In some cases the ion to be separated is precipitated, and in other cases, is co-precipitated with an excess of some other precipitate or colloid, and then the combined floc is floated. This last technique has been the most used, and is probably the one exhibiting greatest analytical interest. Sheiham and Pinfold¹³ named it co-flotation.
- (b) Precipitate flotation of the second kind. Here the addition of a surfactant is not necessary, because a hydrophobic substance is formed from two hydrophilic ones.

IV—*Ion flotation* This was introduced by Sebba,^{2,14} and is the separation of ions in solution that are not surface-active, by addition of surfactants (collectors), and the subsequent passage of a gas stream to produce a foam containing a solid compound of the surfactant with the species of interest. Normally the collector is an ion with opposite charge to the colligend, but any suitable type of chemical union can be used.

Some related techniques are "laminae column foaming"¹⁵ and "booster bubble fractionation"¹⁶. The first technique is a flotation process of

laminar type, by means of a continuous chain of wall-to-wall bubbles rising up the column. The second uses volatile organic compounds, together with the gas bubbles, in solutions with a low concentration of active substance, causing foam formation and subsequent separation, this may be quicker than the classic flotation technique, and improves the selectivity.

The "adsorptive droplet techniques"¹⁷ are similar to these techniques but, instead of gas bubbles, droplets of immiscible liquid are added.

In "solvent sublation" a water-insoluble organic solvent is floated on top of the column to extract neutral species from the foam.

Finally, it should be mentioned that the term "spectrophotometric-flotation", although apparently related to those above, is different because there is no gas bubbling, and therefore it cannot be considered as an "adsorbable technique". It is based on the fact that some ion-pairs are not soluble in polar organic solvents, and when an aqueous phase is shaken with an organic solvent, a precipitate originates in the interface or on the extraction funnel walls. Once both phases have been separated the precipitate is dissolved in an appropriate solvent, and the corresponding measurements are made by spectrophotometry. This technique was introduced by Marczenko *et al*¹⁸.

INSTRUMENTATION

There are no instruments on the market for these techniques, and because of the simplicity of the necessary devices, these are tailored according to the task in hand. However, all flotation set-ups include several common basic devices.

- Gas generating source. This can be a small air compressor or gas cylinder. Air is the gas most commonly used, however there are works that report use of nitrogen, helium or argon.
- Regulator system for controlling pressure and gas flow (needle valves, *etc.*).
- Gas washing flask. Its purpose is to saturate the gas with water or other suitable solvent, to avoid any change in the volume of the system. In some cases it is used to eliminate carbon dioxide from the system to avoid undesirable reactions in the column.
- Flowmeter. This is for measuring the gas flow-rate through the column, normally a soap-bubble flowmeter is used.

—Column. Glass is generally used, but plastic columns are also used. The size and form are based on the system needs, but there is always a sintered-glass plate at the bottom with adequate porosity (usually G3 or G4). The gas passing through this porous plate produces the small ascending bubbles which generate the foam

Auxiliary equipment, varying from case to case, may include peristaltic pumps (generally used for continuous operation), magnetic stir-

rers, devices for collection of the foam and precipitate (foam suction sets, polyethylene laminae on the walls of the column to keep the precipitate attached; shielding and safety devices for work with radioactive substances, *etc.*), lateral taps (to allow monitoring the kinetics of the process, to discharge the liquid at the end of the process, or as an outlet for effluent in continuous flow operation), and a thermometer.

Figure 2 show some of the devices reported. A typical solvent sublation column is illustrated in the paper by Womack *et al.*²⁸

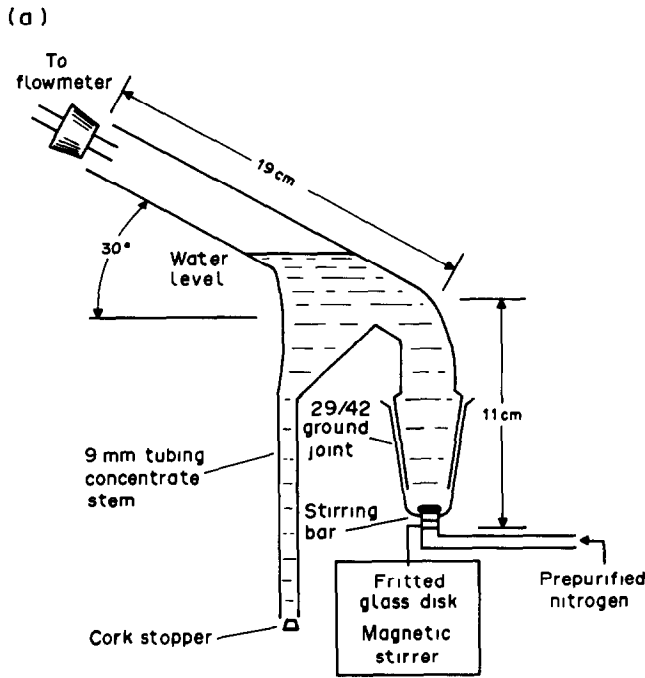


Fig 2(a)

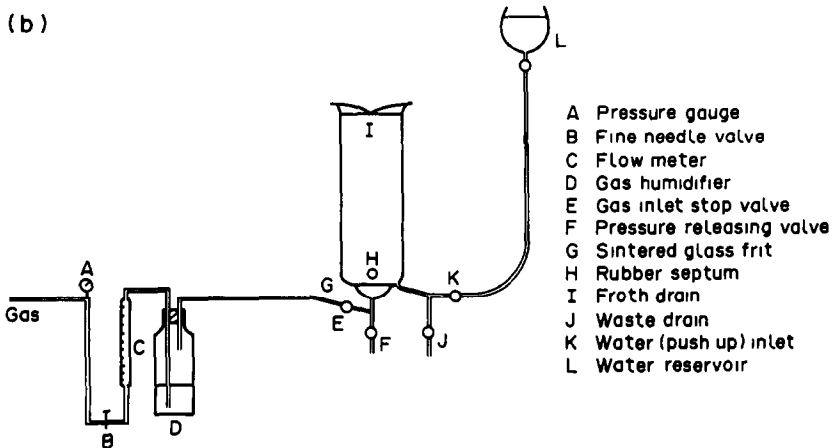
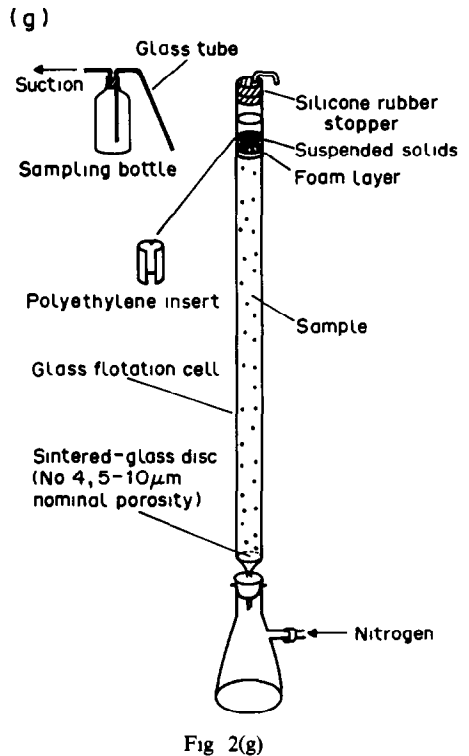
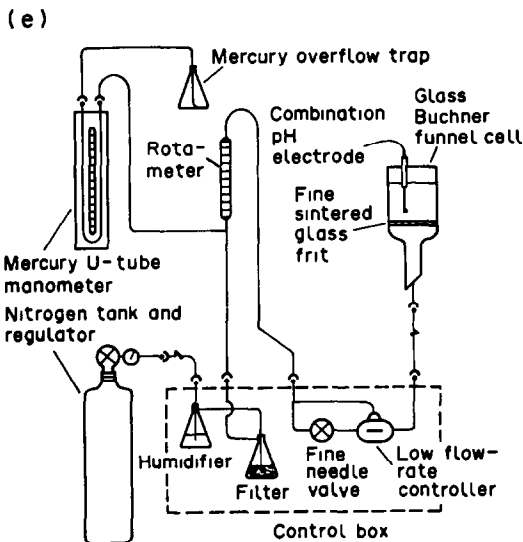
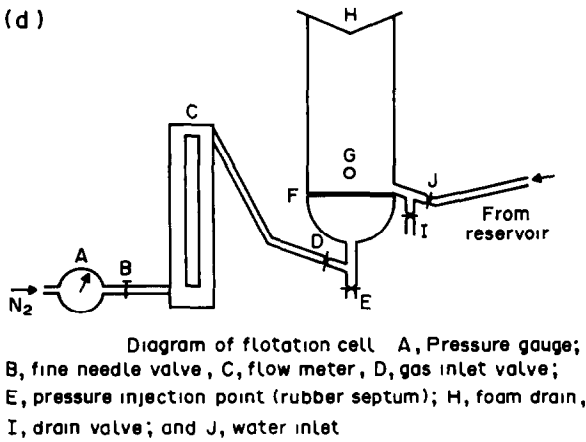
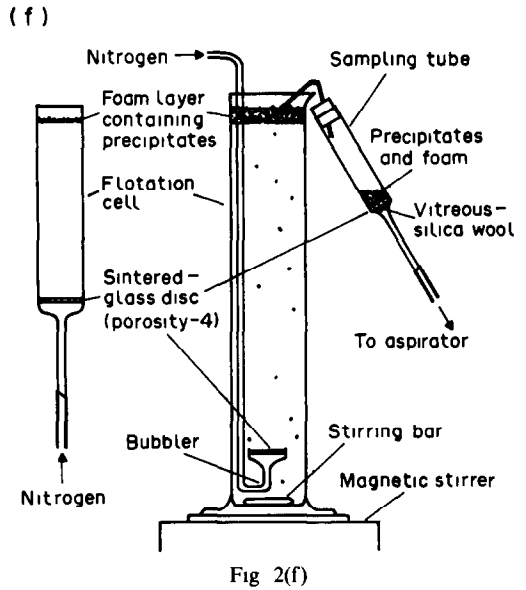
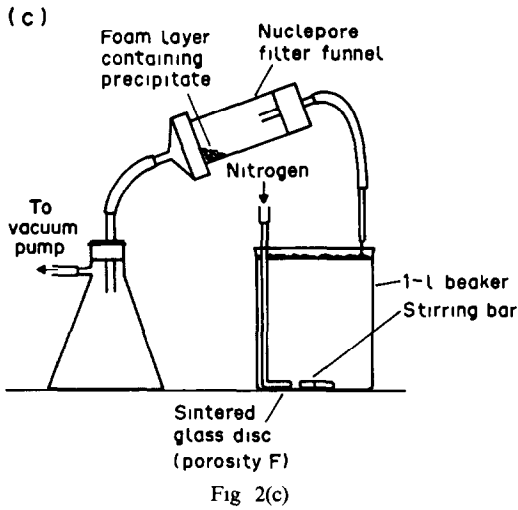


Fig 2(b)



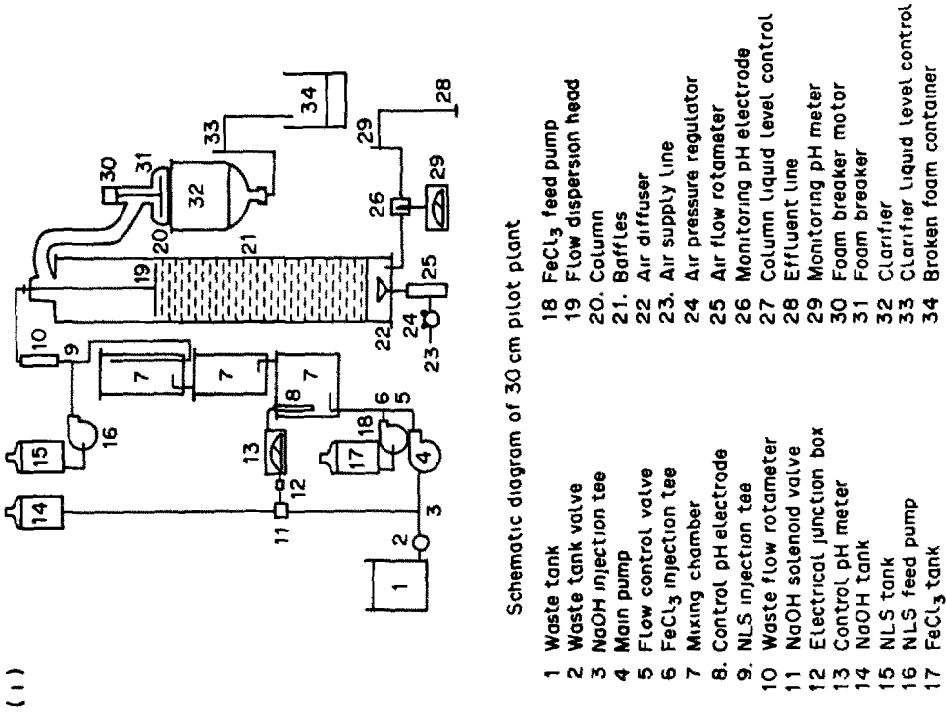


Fig 2(i)

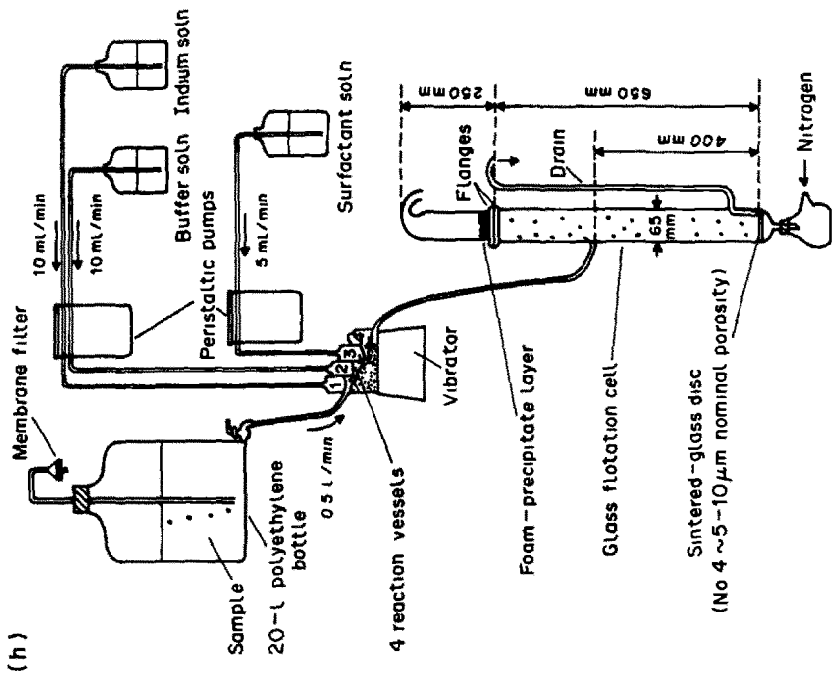
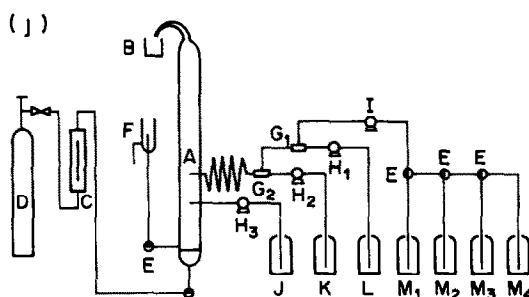


Fig 2(h)



(A) Separation tube; (B) foam collector (containing 5 ml of 1-propanol); (C) flow meter; (D) nitrogen cylinder, (E) three-way cock; (F) effluent drain, (G_1, G_2) mixing chambers, (H_1, H_2, H_3) plunger pumps; (I) diaphragm pump, (J) surfactant solution (1% SLS) reservoir; (K) 1% NEDA solution reservoir, (L) 2% ABSA solution reservoir, (M_1, M_2, M_3, M_4) sample reservoirs. The coil between G_2 and A is 8 m long.

Fig 2(j)

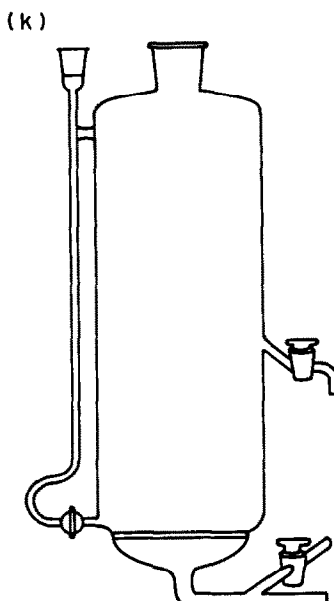


Fig 2(k)

Fig 2 Some examples of flotation apparatus. Reproduced, with permission, from (a) reference 19, p 158, by courtesy of Marcel Dekker, Inc., (b) reference 20, p 507, by courtesy of Marcel Dekker, Inc., (c) R S S Murthy and D E Ryan, *Anal Chem*, 1983, **55**, 682, copyright 1983, American Chemical Society, (d) W J Williams and A H Gillam, *Analyst*, 1978, **103**, 1239, copyright 1978, Royal Society of Chemistry, (e) reference 23, p 358, by courtesy of Marcel Dekker, Inc., (f), (g) reference 6, by courtesy of Springer-Verlag, Heidelberg, (h) reference 24, copyright 1983, Elsevier Science Publishers, (i) reference 25, p 606, courtesy of Marcel Dekker, Inc., (j) reference 26, copyright 1982, Elsevier Science Publishers, (k) reference 27, p 621, by courtesy of Marcel Dekker, Inc.

PARAMETERS AFFECTING THE FLOTATION PROCESSES

Several factors influence the processes: some affect the solution and others are operational factors. Some of the first group are of basic importance for all the flotation techniques (e.g.,

colligend and collector concentrations and their relationship, pH and ionic strength); others are important for particular techniques (for example, the induction time). The operational variables include gas flow-rate, porosity of the sintered-glass plate, average bubble size, and the column geometry.

Collector and colligend concentration

If the collector concentration is too low, there will not be enough colligend-collector product (ion-pair, complex, adsorption compound, *etc.*) formed, so not all of the colligend will be separated by adsorption on the gas bubbles.

On the other hand, if too high a concentration of collector is present, although ion separation is favoured, the excess of collector will compete for sites in the bubble surface, and may even form micelles if its CMC (critical micelle concentration) is reached. In all cases undesirable effects on the flotation process are observed. As a rule, to achieve a complete separation in ion flotation and solvent sublation, it is necessary to have a collector concentration in excess over the stoichiometric amount. In precipitate flotation the collector concentration has to be large enough to form a foam that is stable and persistent enough to keep the precipitate suspended; this is not related to the sublate stoichiometry.

The colligend concentration is related to the collector, and it may be necessary to use different concentrations with different techniques. For example, in precipitate flotation, the relationship between the amounts of colligend and precipitate has to be considered, as well as the precipitate solubility, to avoid redispersion of the precipitate into the bulk solution.

pH of the solution

The most critical variable for all the techniques is the pH of the solution, since it will determine the sign and magnitude of the charges on the surface and some of the ionic species involved in the process. Variation of pH can produce colligend charge variations by hydrolysis or by formation of other complexes that can produce colligends, precipitates and changes in the collector behaviour. In ion and precipitate flotation, the pH has an influence on foam stability.

Ionic strength

The influence of the ionic strength of the medium varies from technique to technique, probably because of the different effects that take place in the adsorption process on the interface responsible for the separation. Usually, an increase in the ionic strength will decrease the effectiveness of separation, probably because of competition between the colligend and the other ions for the collector. Since

surfactant adsorption in the gas-liquid interface is increased with increasing ionic strength, foam-type separations are improved when the ionic strength is increased, unless the surfactant concentration reaches the CMC. In precipitate flotation of the first kind and in ion flotation the effectiveness of separation usually decreases when the ionic strength of the medium is increased, owing to competition by the foreign ions for the collector, on the other hand, the surfactant will float more quickly. Finally, in precipitate flotation, increasing the ionic strength will increase the solubility of the precipitate. However, the addition of foreign ions could produce changes in the nature of the colligend, thus enabling separations which would not be possible otherwise. For instance, the addition of certain ions may give rise to formation of complexes with opposite charge to that expected, changing the behaviour of the surfactant, and consequently give rise to an effective separation.

Induction time

The duration of agitation of the sample before it is transferred to the flotation cell could have a positive influence on the separation. This is the case for precipitate flotation, because the longer the time, the bigger the particles formed in the precipitation or co-precipitation reaction. Nevertheless some workers^{1,29} advise not to use an induction period, but to add the surfactant at the beginning of the flotation or even stepwise during the flotation process. This factor is important in connection with optimization of the process, though less so than the flow-rate, pH, and ionic strength of the medium.

Temperature

The effect of temperature varies according to the particular system. Thus in some cases an increase of temperature has no effect on ion flotation, whereas in others it may have positive or negative effects. In precipitate flotation a temperature increase has a positive effect due to its influence on the size of the particles formed. On the other hand it will also increase the solubility of the precipitate and the instability of the foam, giving rise to partial dissolution of the precipitate and insufficient foam consistency to hold up the precipitate. Increase or decrease in the separation yield as the temperature increases can be explained as due to collector adsorption being a temperature-dependent physical or chemisorption process. Since this parameter has

an important and variable influence on the flotation process, it is very interesting to study each particular case, especially for large temperature variations.

Presence of ethanol

Addition of small quantities of ethanol (or any other substance for the same purpose) to the solution has several functions, such as avoiding micelle formation and decreasing bubble size, which will improve the separation. However, large quantities of ethanol could give rise to foam breakage (too quick coalescence) or cause no foam at all to form. Most of the collectors are added in ethanolic solution, because of their low solubility in aqueous solutions. Usually it is not necessary to add more ethanol than that added with the collector, but this has to be decided from the results obtained for each case.

Gas flow-rate

One of the most important parameters is the gas flow-rate, which depends on the technique to be used, the quantity of sample, and the porosity of the sintered-glass plate fitted in the column. When fine-porosity plates are used the flow-rates are lower and the separation yield increases with the flow-rate, a mild turbulence being produced, causing precipitate redispersion. Thus fine-porosity plates are used in ion flotation and solvent sublation, with low flow-rate to avoid fluctuation of the organic layer or turbulence near the foam layer. In precipitate flotation sintered-glass plates of higher porosity are used together with higher gas flows, in order to maintain a consistent foam that supports the precipitate, thus avoiding its re-entry into solution in cases characterized by slow kinetics.

Sintered-glass plate porosity and bubble size

The sintered-glass plate porosity and the bubble size are usually very closely related to the gas flow-rate. Normally, it is better to use small and uniform bubbles, because the gas-liquid interface surface is increased.

Column form and size

The column form, size and arrangement influence the efficiency of the process. There are some works in the literature proving that the cross-section, capacity,³⁰ and inclination from the vertical³¹ have an influence on the sublate recovery.

PRECIPITATE FLOTATION AND SOLVENT SUBLATION MECHANISMS

Precipitate flotation

There are currently several physical models available to explain precipitate separation by flotation; those most often used are based on coulombic attraction (the Gouy-Chapman double-layer) and on the contact angle (for mineral flotation).

Both models are complementary and valid, as shown in the theoretical developments published by Wilson and co-workers³²⁻⁵⁰ since 1974, in which they have been trying to predict and justify the influence that some variables have on the flotation process, introducing successive modifications and considerations in both models, and reporting experimental results to support their arguments.

Coulombic attraction model. Jaycock and Ottewill⁵¹ observed that in a colloidal dispersion of silver iodides initially exhibiting a negative electrophoretic mobility, the charge was first neutralized and eventually became positive when HEDABr (see surfactants abbreviation key on p 292) was added. They explained that in this phenomenon the polar groups of the surfactant are linked to the charged particle surface by electrostatic forces, forming a single layer, but if all the surface charges are neutralized the zeta potential becomes zero, and if a second layer of surfactant molecules is adsorbed, held by van der Waals forces, this would give rise to an increase of the zeta potential, even up to positive values.

DeVivo and Karger⁵² started from this model and took into account that the zeta potential will be related to the surface charge, and will depend not only on the type and concentration of the surfactant but also on the presence of electrolytes and the quantity of particles present. They studied the correlation between potential, ionic strength and particle size with the purpose of evaluating the influence of these variables on the flotation process. From experimental results on flotation of kaolin and montmorillonite with HEDABr, they proved that addition of electrolytes produced a decrease in the initial zeta potential and a loss of efficiency in the flotation process, therefore, in principle, an inverse relation is expected to exist between the aggregate sizes and the degree of flotation. However, this result disagreed with that published by Rubin and Lackey⁵³ to the effect that flotation of *Bacillus cereus* is considerably better

when it is coagulated with alum. Taking into account the work of Spargo and Pinfold²⁷ on the influence of bubble size, DeVivo and Karger⁵² found that this difference arose from the use of smaller bubble sizes and smaller flow-rate by Rubin and Lackey. To prove this they examined the clay separation with sintered-glass plates of lower porosity, and obtained much better results with coagulated species.

Thus the bubble size can affect the capacity of the particle-surfactant species to become attached to the bubbles, and consequently the effectiveness of flotation. When plates of higher porosity are used, bubbles of the same size as the particles, or even bigger, are formed; therefore, the attachment of more than one bubble to a particle will be less likely, and the particles' capacity to float will be consequently reduced. Using smaller bubbles will increase the probability of union of more than one bubble with an aggregate, and therefore increase flotation separation. The bubble size also has an influence on the stability of the foam,⁵⁴ foam obtained with big bubbles is usually less stable.

Just before the work of DeVivo and Karger⁵² was published, a paper by Jorné and Rubin⁵⁵ appeared in which they applied the Gouy-Chapman theory of the double electric layer to predict the distribution of species by foam fractionation, taking into account the sizes and charges of the species. They found that the experimental results agreed with the theoretical model.

Wilson and Wilson, in the first work of their series tried to apply the Gouy-Chapman theory to justify the fact, already very well known, that increasing the ionic strength causes a decrease in flotation efficiency. By means of a series of calculations, they determined the free energy responsible for the attraction forces between the precipitate particles and the surfactant film. Using a computer simulation program, they calculated the variation of the free energy with ionic strength, concluding that these values were in good agreement with those expected from the influence of ionic strength.

Later, Huang and Wilson³³ studied the equilibrium of separation of the precipitate from the liquid mass. Starting from the Gouy-Chapman model they studied the effect of several factors on the kinetics and equilibrium of precipitate flotation. Starting from a 1-cm² film surface area and thickness L , they calculated the variation of the colloid concentration with time and distance from the film, as a function of the solution

potential, which itself is influenced by the distance, ionic strength, dielectric constant and temperature. The results of this model indicated that the migration of the colloids must be extraordinarily fast, so the equilibrium between the precipitate particles in the boundary layer and the inner part of the foam should be the process-controlling factor.

Wilson and Wilson also studied the influence of ionic strength, charge and floc size on the flotation process, taking into account the floc volume.³⁴ A first study on the attachment of surfactant film to colloids, in agreement with a simple model, allowed them to obtain expressions in accordance with the experimental results, that increasing precipitate floc size decreases the process efficiency. With a model based on the Gouy-Chapman theory, they studied the electrostatic attraction between the charged surfactant surface and the flocs, in terms of electrolyte concentration and dielectric constant of the medium. This last model was found to furnish results similar to those obtained with the simple one, but was more precise.

Wilson³⁶ calculated the adsorption isotherms by using three different approximations, taking into account the finite volume of the flocs and the ions responsible for the ionic atmosphere. With any of these models there is a decrease in the adsorption isotherms when the ionic strength and temperature increase (in the last model to only a slight degree), but there is only very small influence of the ion size.

Wilson, using methods from statistical mechanical studies of non-ideal gases, calculated the adsorption isotherm, taking into account the attractions and repulsions produced between the flocs.³⁷ He developed four models to calculate the isotherms, and studied the influence of ionic strength, temperature, *etc* on them, obtaining slightly different isotherms according to the approximations used, especially when the floc size is large. All these models predict a more or less marked decrease in the adsorption when the ionic strength increases, whereas the temperature has a much less marked effect.

According to the data published by Riddick,⁵⁶ some colloids with negative zeta potential produced an even smaller zeta potential when small quantities of electrolytes were added, and this might cause some colloids to float more efficiently. On this basis, Clarke *et al*³⁹ studied the effect produced by different variables on the zeta potential, and on ion adsorption by flocs. They applied it to the adsorption of different

anions, and the effect of glycerine (by means of the possibility of iron-complex formation) on the flotation of $\text{Fe}(\text{OH})_3$ with NaLS. According to the Gouy–Chapman model and taking as a basis the effect of electric potential, they calculated the influence of the adsorbed ion and the temperature at different electrolyte concentrations, observing that larger differences appeared when low electrolyte concentrations were considered.

The contact angle model. For mineral flotation Fuerstenau and Healy⁵⁷ proposed a model in which the surfactant polar tail is directly adsorbed on the solid surface. At sufficiently high concentrations, the surfactant hydrocarbon tail presents a rather hydrophobic surface to be attached to the bubble, this allowing the flotation. In this model, hemimicelle formation on the solid surface has a special interest; it occurs when there is a high enough concentration of the surfactant, and is caused by the van der Waals forces between the surfactant hydrocarbon chains. Therefore, the larger the surfactant chain the smaller the surfactant concentration required to produce the flotation. The same phenomenon explains the rapid increase observed in flotation when the surfactant concentration is increased.

Fowler and Guggenheim⁵⁸ described a method for the approximate calculation of adsorption isotherms, with models similar to those later proposed by Fuerstenau and Healy. Wilson used these approximations for the isotherm calculation, taking into account the electric potential in the vicinity of the solid surface.³⁸ From the results obtained it was concluded that a temperature increase will increase the surfactant concentration necessary to form the hemimicelle, and an increase of the ionic strength will decrease the quantity of surfactant agent needed.

Wilson and Kennedy, using the same model, studied the effect of an increase in the surfactant concentration on hemimicelle formation.⁴⁰ In this case, there will be a situation in which the formation of a second layer over the first will change the character of the particle, making it hydrophilic, and consequently no separation will take place. From a theoretical analysis of this adsorption phenomenon on the first layer, the effects of the ionic strength, length of the hydrocarbon chain, temperature *etc.* were inferred. The results obtained are as expected; an ionic strength increase will bring about a decrease in the flotation effectiveness. An

increment in the carbon chain length generates an increment of the van der Waals forces and, facilitates the formation of a second layer, which blocks the flotation. Therefore, it is necessary to take special care when the concentration of long-chain surfactants is increased.

With the same model Kiefer and Wilson studied the effects (on the adsorption isotherms) of the coulombic repulsions of the surfactant ionic heads, and the van der Waals attractions in the hydrocarbon chains.⁴²

In the last works of the series Wilson and co-workers undertook the calculation of isotherms for surfactant mixtures.^{46,48,50} The results obtained⁴⁶ show that the isotherms can vary widely, depending on the factors to be considered; it was therefore suggested that for industrial use these isotherms should be calculated to economise in use of expensive surfactants.⁴⁰

Solvent sublation

According to Sebba² the separation mechanism in the solvent sublation technique is very simple. As the gas bubbles pass through the liquid mass they collect the colligend–collector species, which is then transferred to the organic phase on the upper surface of the liquid mass.

Later, Karger's group and associates made a series of studies and deduced a much more complex mechanism.^{27,59–63} The bubbles are enriched in the material when they are passing through the aqueous medium. When they arrive at the liquid–liquid interface they are not able to overcome the interfacial tension immediately. Also, some bubbles coalesce before passing through the interface. It is expected that repulsions between the bubbles, deriving from the zeta potentials, would result in a slow bubble coalescence process. Consequently, a relatively stationary bubble layer is formed under the liquid–liquid interface; the liquid trapped in this layer is protected from the turbulence of the ascending bubbles in the aqueous phase.

When the coalescing bubbles are moving through the liquid–liquid interface, they carry away a small quantity of the liquid contained in the aforementioned interfacial region, although its amount is much less than the quantity of liquid trapped in some other bubble flotation techniques. The collector and colligend (sublate) that go to the organic phase dissolve in it quickly, while the accompanying water returns to the aqueous phase as small drops once the bubbles are broken down. All these are

experimental phenomena readily observed in the laboratory.

In Karger's hypothesis it is accepted that probably an equilibrium is established between the drops of aqueous phase and the organic phase, although for volume-ratio reasons it is logical to accept that the quantity of sublimate dissolved in the small water drops returning to the aqueous mass must be very small. Moreover, this sublimate does not itself return to the aqueous mass but to the intermediate stationary interface

On the basis of this model it is obvious that an equilibrium between the aqueous mass and organic phase is not established, and therefore it is easy to deduce that there are fundamental differences between solvent sublimation and liquid-liquid extraction. This distinction was pointed out by Pinfold and co-workers.^{61,63}

The studies of Karger's group, whose fundamental conclusions have just been summarized, gave a better qualitative approximation to the separation mechanism that controls solvent sublimation. In fact, they allow rational justification of most of the experimental phenomena associated with this technique. Nevertheless they were not translated into a mathematical model suitable for a theoretical and predictive treatment of these phenomena. This has been remedied, however, by Wilson's group, since 1981.^{28,30,64-68} In this series of papers, the equations that constitute the theoretical model are deduced in full detail and have been submitted to continuous refinement by the authors. For that reason, here only the most outstanding results from the conceptual point of view and the final formulae will be summarized as a basis for the discussion.

In practice, Wilson's model did not accept Karger's hypothesis, because it was considered that the experimental results contradict it.

Two contributions by Karger and co-workers point to the fact that the separation velocity decreases considerably as the process deviates further from first-order kinetics.^{59,62} These authors interpret this phenomenon as derived from progressive dissolution and saturation of the organic solvent in the aqueous mass, giving rise to a second equilibrium competitive with the fundamental one of the separation at the interface. Wilson and co-workers showed the error of this working hypothesis by using presaturated aqueous phases in the organic solvent, observing that a sharp change in the sublimation during the process is also produced under these conditions. Obviously there were some other

limiting factors involved in the rate of mass transfer. These time-dependent factors must be taken into account when a mathematical model with predictive capacity is to be developed.

The Wilson group has developed different models which are initially based on the adsorption of volatile compounds on a stream of bubbles. In these models the rate-limiting step is the mass transfer of solute from the solution to the air-water interface. The next approximation was the consideration of non-volatile compounds, taking into account the Langmuir isotherm of adsorption in the air-water interface, as well as the mass transfer throughout the bubble limiting layer. Finally models were developed for single or multiple stage columns controlled by an equilibrium or a mass transfer process.

The first work of the series dealt with the solvent sublimation of 1,1,1-trichloroethane and developed a mathematical model for processes of this kind involving surface-active and volatile compounds.⁶⁴ Later the effects of some variables, such as the air flow-rate and the addition of a salt, on the solvent sublimation of two ion-pairs (Methylene Blue-tetradecylsulphate and Methyl Orange-hexadecyltrimethylammonium) were studied.²⁸

In the case of separation by solvent sublimation of molecular, surfactant and volatile substances the rate of transfer is given by

$$\frac{dm_b}{dt} = 4\pi r^2 k \left[\frac{4}{3}\pi r^3 K_w c_w + \frac{4\pi r^2 \Gamma_m}{(1 + c_{1/2}/c_w)} - m_b \right] / \frac{4}{3}\pi r^3 \quad (1)$$

where

- t = time elapsed after bubble formation
- m_b = moles of solute associated with a bubble
- r = bubble radius
- k = mass transfer rate coefficient (cm/sec)
- K_w = Henry's law constant for the solute in water, ($= c_{vap}/c_{water}$ at equilibrium)
- c_w = solute concentration in the aqueous phase
- Γ_m = Langmuir's isotherm parameter (saturation concentration of the solute in the air-water interface)
- $c_{1/2}$ = Langmuir isotherm parameter (concentration in the aqueous phase at which the surface concentration is $\frac{1}{2} \Gamma_m$)

In equation (1) it is assumed that the axial diffusion in the column is large enough to

warrant considering the column liquid phase as a single well-mixed pool. The bubble radius is kept constant all along its ascending path in the column. Furthermore, mass transfer to the bubble is proportional to the difference between the solute mass associated with the bubble, and that which could be associated with it assuming that the bubble was in equilibrium with the surrounding liquid mass.

The solute mass separated from the aqueous phase by a bubble, if we accept that c_w does not change during the time necessary to allow a bubble to pass through the liquid mass, is obtained by integrating equation (1)

$$m_{b(\text{out})} = \frac{4\pi r^3}{3} \left[K_w c_w + \frac{3\Gamma_m}{r(1 + c_{1/2}/c_w)} \right] \times \left[1 - \exp\left(-\frac{3kh_w}{ru_w}\right) \right] \quad (2)$$

where

h_w = aqueous column height

u_w = bubble ascension velocity (which is a function of the density and viscosity of the aqueous phase)

Taking into account the volume of air introduced into the column as bubbles, the following equation is obtained

$$V_w \frac{dc_w}{dt} = -N_b \frac{4\pi r^3}{3} \left[1 - \exp\left(-\frac{3kh_w}{ru_w}\right) \right] \times \left[K_w c_w + \frac{3\Gamma_m}{r(1 + c_{1/2}/c_w)} \right] \quad (3)$$

where

V_w = aqueous phase volume

N_b = number of bubbles introduced into the aqueous phase per second

t = time elapsed from the beginning of the process (sec)

If the solute is a non-volatile species, equation (3) is simplified to

$$\frac{dc_w}{dt} = -A(1 + c_{1/2}/c_w) \quad (4)$$

where A incorporates a group of constant factors. By integration the following equation is obtained

$$c_w(t) - c_w(0) + c_{1/2}[\ln c_w(t)/c_w(0)] = -At \quad (5)$$

When $\ln c_w(t)/c_w(0)$ was plotted *vs.* t , Womack *et al.*²⁸ obtained plots that were in disagreement with the experimental results for the Methylene Blue-tetradecylsulphate pair, and it was necessary to consider the value of the

mass transfer coefficient (k). To do this, the diffusion of solute through the boundary layer around the air bubbles had to be taken into account.

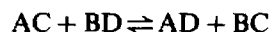
Starting from this conclusion and from the calculations of the solute chemical potential, they obtained the expression

$$K = r\lambda_1/3 \quad (6)$$

where λ_1 is a time constant associated with the diffusion process and r is the bubble radius. This is thus a limiting factor of the separation rate, that causes the formation of curves similar to those obtained experimentally.

Let us assume that formation of ion-pairs between the solute (ionizable) and the surfactant gives rise to the sublute that has to be separated, assuming that the surface concentrations of the surface-active species are given by linear isotherms.

We can assume the establishment of the following equilibrium in solution



$$K_e = \frac{[AD][BC]}{[AC][BD]} \quad (7)$$

where

A = surfactant anionic agent

B = solute anion

C = solute cation

D = surfactant cationic agent

AC = sublute (ion-pair)

AD = non-dissociated surfactant

The species AC and AD are surfactants and will compete for the gas bubbles. The anion B cannot be separated by means of solvent substitution, so

$$[BC] + [BD] = [B] = \text{constant} \quad (8)$$

Furthermore, there is only one possible way for the solute cation to be separated from the solution, so

$$\frac{d}{dt} ([AC] + [BC]) = -K_{AC}[AC] \quad (9)$$

where K_{AC} is the mass transfer rate parameter for AC.

In contrast, the surfactant can be separated in two ways:

$$\frac{d}{dt} ([AC] + [AD]) = -K_{AC}[AC] - K_{AD}[AD] \quad (10)$$

The K parameters depend on the bubble radii, the gas flow-rate, the volume and height of the aqueous phase, and the rising velocity of the bubbles.

Therefore we have four equations for the four unknowns. This system is conveniently solved,²⁸ yielding the expression:

$$K_e = \frac{([AD]_0 - [AC])([BC]_0 - [AC])}{[AC]([BD]_0 + [AC])} \quad (11)$$

where the subscript zero indicates the initial nominal concentration

Equation (11) is arrived at from equation (10) by choosing the root of this equation that conforms to all the following conditions $[AC] \geq 0$; $[AD] = ([AD]_0 - [AC]) \geq 0$, $[BC] = ([BC]_0 - [AC]) \geq 0$ and $[BD] = [BD]_0 + [AC]$

From these initial values the differential equations (8) and (9) can be solved, yielding expressions to calculate the curves of the separation kinetics during the process

On studying the effect of the equilibrium constant shown in equation (7) on dissociation of the ion-pair, it was observed that when this increases, the sublate separation velocity decreases. In this case, the theoretical curves are similar to the experimental ones

At the same time it was observed that decreasing the surfactant concentration would be expected to give a lower yield and separation velocity, in accordance with the experimental results. Finally, the effect was examined of adding salts, which would obviously displace the formation equilibrium of the ion-pair and, therefore, cause a serious loss of efficiency when the technique is applied to brines or sea-waters

This theoretical treatment accounts very well for the experimental behaviour of the technique, with the exception that in practice the rates of removal early in a run are much higher than those predicted by the model. Womack *et al.* accounted for these differences by considering the occurrence of secondary ionic equilibria²⁸

Because one of the most useful characteristics of the technique is the possibility of working with large volumes of sample, there is an obvious interest in obtaining theoretical treatment of systems working in the continuous flow mode. This technique should be useful in chemical analysis (avoiding the use of large experimental devices, increasing the sensitivity of determinations by means of greater preconcentration factors, *etc.*) as well as in chemical engineering (treatment of large quantities of

water). Wilson and Valsaraj have suggested a quick and efficient algorithm for the treatment of this situation, taking into account that the axial dispersion is not great enough, in a continuous feed regimen of the column, to guarantee homogeneity.³⁰

This model allows design and adjustment of the device in the continuous operation mode, which is of obvious interest industrially, and this mode of operation could also be used in some analytical work.

In a later work,⁶⁵ these authors developed another theoretical model that allows the calculation of the adsorption isotherm, at the air-water interface, of the compounds of interest when they are intrinsically hydrophobic. In this way it is possible to predict the applicability of this method for the removal of as yet unstudied compounds

ANALYTICAL APPLICATIONS

Bearing in mind all the techniques discussed, the most interesting ones, from the analytical point of view, are precipitate flotation, ion flotation and solvent sublation, therefore the bibliographic review will be restricted to these.

Precipitate flotation

Precipitate flotation is the most interesting technique, analytically. Co-flotation has a very special interest within precipitate flotation, voluminous metal hydroxides and organic reagents have been used as co-precipitating agents in this kind of process, however, during the period that we are considering, metal hydroxides are practically the only ones used, especially ferric hydroxide, as shown in Tables 2 and 3. On the other hand, multi-elemental separations have also been developed during this period (Table 3), these had not received much attention previously. Co-flotation, compared with centrifugation and co-precipitation, presents several advantages

- (1) It allows for the use of very large volumes of sample, thus increasing the preconcentration factor
- (2) It is quicker and more convenient, because the other techniques require more time, also separation of voluminous precipitates is difficult
- (3) It eliminates the difficulties associated with separation of colloidal precipitates.

Table 2 Precipitate flotation single-element separations

Species	Sample medium	Co-precipitant or precipitated compound	Surfactants	Observations	Reference
Ag	Sea-water	PbS (colloid)	SA	AAS	69
As	Sea-water, pH 8-9 Natural waters Geothermal fluids, pH 6.5	Fe(OH) ₃	NaO NaO NaLS + LACl NaLS + NaO	AAS, hydride generation Idem Idem AAS, hydride generation (detrn limit 0.6 ng/ml)	70 71 72 73
Bi	Water, pH 4	Fe(OH) ₃	NaLS or NaE + HTABr	AAS	74
Cd	Waste waters River and tap water, pH 9.1 Water	Fe(OH) ₃ or Al(OH) ₃ Zr(OH) ₄ Ti(OH) ₄ , Zr(OH) ₄	NaO BACl, NaO NaDBS	AAS, electrothermal atomization Detn limit 20 ng/ml, recoveries > 97%	75 76
Co	Waste waters Sea-water, pH 8.5-9	In(OH) ₃ Fe(OH) ₃ + Al(OH) ₃ In(OH) ₃	NaLS NaLS + NaO	pH 9 Liquid scintillation	77 78
Cr	Natural and waste waters pH 4.5-6 Al(OH) ₃ , pH 5.5-7.5 Prior reduction with Fe(II) Waste waters. Prior reduction with Fe(II), pH 4.5-7	Fe(OH) ₃ or Al(OH) ₃ Fe(OH) ₃ Fe(OH) ₃	NaLS NaLS	Spectrophotometric detn	79
Cs	Waste waters from radiochemical processes	CuFe(CN) ₆	NaLS or HTMABr	pH 5-8 Continuous spectrophotometric detn	79 25
Cu	Aqueous solutions of high and low salinity	Fe(OH) ₃ , Al(OH) ₃ La(OH) ₃ , Sn(OH) ₂ Th(OH) ₄	NaDBS, NaO HDBI	AAS Experimental parameter study and influence of the nature of co-precipitant and surfactant	81
Cu	Aqueous solutions pH > 7 pH 7.5-11	Fe(OH) ₃ Fe(OH) ₃ Fe(OH) ₃	NaO NaLP + TX100 or HTMABr LDC	AAS Development of simplex optimization procedure AAS Study of the influence of different species (anionic) AAS Study of the influence of several ions	82 83 77
Hg		Fe(OH) ₃ or Al(OH) ₃	NaLS, NaE, HTMABr	Study of the influence of several factors in the separation	84
Mn	pH > 9	Fe(OH) ₃	NaLP + TX100	AAS Study of the influence of several anionic species	83
Mo	Sea-water, natural waters	Fe(OH) ₃	HTMABr + ODA	ODA not necessary for natural waters	85

continued overleaf

Table 2—*continued*

Species	Sample medium	Co-precipitant or precipitated compound	Surfactants	Observations	Reference
Pb	Waste waters	Fe(OH) ₃	NaLS	Separation and recovery of Pb Study of the variables affecting lead separation	86
	Pilot plant, pH 6–7	Fe(OH) ₃	NaLS		87
	Aqueous solutions	Fe(OH) ₃ or Al(OH) ₃	HTMABr, NaE NaLS		88
Sb	Natural waters, pH 4.0	Fe(OH) ₃	NaLS + NaO	AAS, hydride generation	89
	Sea-water, pH 4.0	Fe(OH) ₃	NaLS + NaO		AAS, hydride generation
Sc	Aqueous solutions pH 6–9 (NaO), pH > 10 (HTMABr)	Fe(OH) ₃	NaO or HTMABr	Spectrophotometric detn with Arsenazo III, or GFAAS NaO shows better results	91
Sc	Sea-water, pH 4.0	Fe(OH) ₃	NaLS	AAS, hydride generation	92
Sn	Natural and manne waters, pH 4.0	Fe(OH) ₃	NaLS	AAS, hydride generation	93
	Water	Fe(OH) ₃ or Al(OH) ₃	NaLS		Recoveries > 99.8%
Tc	Water and sea-water, pH 8–9	Fe(OH) ₃	NaLS	AAS, hydride generation	95
Zn	Water pH >> 7	Fe(OH) ₃	NaLP + TX100	AAS Study of the influence of several anionic species	83
Phosphate	Waste waters	Al(OH) ₃	NaN	Phosphate separation	96

Table 3 Precipitate flotation multi-elemental separations

Species	Sample medium	Co-precipitant or precipitated compound	Surfactants	Observations	Reference
Ag, Au	Aqueous solutions	$\text{Sn}(\text{OH})_2$	Succinon, octandiol	AAS	97
As, Cd, Co, Cu, Hg, Mo, Sb, Sn, Te, Ti, U, V, W	Synthetic sea-water, pH = $f(\text{species})$	$\text{Fe}(\text{OH})_3$ + $\text{Fe}(\text{APDC})$	$\text{NaLS} + \text{NaO}$	Activation	98
As, Ge, Sb, Sn	High salinity solutions, pH 5.5	$\text{Fe}(\text{OH})_3$	NaLS	AAS, hydride generation	99
As, Mo, Se, U, V, W	Sea-water, pH 5.7	$\text{Fe}(\text{OH})_3$	NaLS	Activation	21
Bi, Sb, Sn	Water, pH 9.1	$\text{Zr}(\text{OH})_4$	NaO	AAS, hydride generation	100
Cd, Co, Cr, Cu, Fe, Mn, Ni, Pb, Zn	Sea-water, pH 9.5	$\text{Al}(\text{OH})_3$	NaO	AAS	101
Cd, Co, Cr, Cu, Mn, Ni, Pb	Water water and sea-water, pH 9.5	$\text{In}(\text{OH})_3$	$\text{NaO} + \text{NaLS}$	ICP Idem but continuous technique for separation	102 24
Cd, Co, Cu	Sea-water, pH 9.5-9.9	$\text{Fe}(\text{OH})_3$	$\text{SA} + \text{NaLS}$	AAS	103
Cd, Co, Cu, Ni	High salinity solutions, sea-water	Phenolphthalein or 2-naphthol	ODA	Flame AAS Cd, Co, Ni > 90% yield, Cu lower	104
Cd, Co, Cu, Zn	High and low salinity aqueous solutions	$\text{Fe}(\text{OH})_3$, $\text{Al}(\text{OH})_3$, $\text{Th}(\text{OH})_4$	HTMABr	AAS Study of influence of sample salinity on separation and recoveries	105
Cd, Cr, Cu, Hg, Pb, Zn	High ionic strength (μ) solutions	$\text{Fe}(\text{OH})_3$ or $\text{Al}(\text{OH})_3$ (colloids)	NaLS	Efficiency decreases with increasing μ , can compensate with Al, Mg, Zn as activators	106
Cd, Pb	Water, pH 8-10	$\text{Fe}(\text{OH})_3$ or $\text{Al}(\text{OH})_3$	NaDBS	AAS	107
Co, Cu, Mn, Ni	Water Mn nodules	$\text{Fe}(\text{OH})_3$ or $\text{Al}(\text{OH})_3$ (colloid)	Fatty acid, sodium salts HCILA	AAS AAS Quantitative recovery Cu at pH > 6, Co, Mn, Ni at pH 9	108 109
Co, Cu, Mn, Ni, Zn	Lixiviates from ferromanganese nodules, pH 8-10	$\text{Fe}(\text{OH})_3$ + $\text{Mn}(\text{OH})_2$	HCILA or HTMACI + TX100	AAS The lixiviates and the residual liquors are analysed	110
Co, Cu, Ni	Water, pH 9.1	$\text{Zr}(\text{OH})_4$	NaO	AAS, electrothermal atomization	111
Cr, Cu, Zn	Waste waters, pH 7-7.6	$\text{Fe}(\text{OH})_3$	NaLS	AAS Pilot plant studies on the separation of these elements from waste waters	112
PAHs	Water	CH_2Cl_2	TX100	Maximum recovery at pH 3-4	113

Precipitate flotation of the first kind has received much less attention, nevertheless it has been used with organic and inorganic species in development of single and multi-element separations (Table 4) and presents, in contrast to precipitate separation, the same advantages as does co-flotation with respect to co-precipitation.

Ion flotation

This technique and precipitate flotation are the most used, and have particularly been developed in the U.S.S.R., as shown in Tables 5 and 6. Usually, the ions to be separated are in complex form and bound to a surfactant of appropriate charge. Ion flotation has been used in connection with both single and multi-elemental separation schemes (Tables 5 and 6).

On comparing ion flotation with precipitate flotation techniques, it can be said that the former have several disadvantages. They are slower, and give lower preconcentration factors. Also it requires destruction of the surfactant in the foam, so more care is needed than in precipitate flotation.

Solvent sublation

Solvent sublation, in comparison with ion flotation, has an advantage in that it allows analysis of the organic phase directly, and it is not necessary to destroy the foam (which is not always a very easy task).

Solvent sublation has practical and theoretical advantages over liquid-liquid extraction, although most of the reasoning and practical knowledge and experience in solvent extraction could be applied to develop efficient solvent sublation procedures. In liquid-liquid extraction the quantity of substance transferred from one phase to another is determined and limited by an equilibrium constant. In contrast, equilibrium in solvent sublation is only established in the aqueous-organic interface. This interface can be kept motionless when the flow-rates are low enough. Except when saturation of the organic phase occurs, the quantity of sublimate collected by the organic layer is independent of its volume because no equilibrium is established in the overall system, and the passage of a sublimate into the organic phase through the interface is a process forced by the gas stream, not a spontaneous distribution process related to the relative solubility of the sublimate in the two phases. Further advantages over solvent extraction arise from the absence of formation of

emulsions, because the interface remains practically immobile, and the possibility of handling large volumes of samples. On the other hand, in solvent extraction the equilibrium is reached quickly. Moreover, in solvent sublation it is necessary to have a close control of the gas flow-rate and bubble size to obtain good separation and reproducibility in the results.

In spite of the advantages mentioned above, together with the possibility of its use as an alternative to ion flotation and extraction, solvent sublation has so far not been used for the separation and determination of trace metals (see Table 7). Nevertheless, theoretical studies on the separation process mechanism for organic species^{28,64-68} confirm the advantages that the technique presents for the determination of a number of important organic pollutants. It is therefore very likely that in the next few years this technique will attract much closer attention from analytical chemists.

SURFACTANTS ABBREVIATION KEY

Cationic Surfactants

Quaternary ammonium salts

ABDACl	Alkylbenzyltrimethylammonium chloride
ATACl	Alkyltrimethylammonium chloride
BACl	Benzalkonium chloride
BDDABr	Benzyltrimethylammonium bromide
CTAB	Cetyltrimethylammonium bromide
DPCl	Dodecyltrimethylammonium chloride
HDMABr	Hexadecyltrimethylammonium bromide
HPBr	Hexadecylpyridinium bromide
HPCl	Hexadecylpyridinium chloride
HTBABr	Hexadecyltributylammonium bromide
HTEABr	Hexadecyltriethylammonium bromide
HTMABr	Hexadecyltrimethylammonium bromide
HTMACl	Hexadecyltrimethylammonium chloride
HTPABr	Hexadecyltripropylammonium bromide
LACl	Laurylammonium chloride
LDC	Ammonium lauryldithiocarbamate
STACl	Stearyltrimethylammonium chloride
TACl	Trimethylammonium chloride
TCMACl	Tricaprylmethylammonium chloride
TDBACl	Tetradecyldimethylbenzylammonium chloride (zephiramine)

Amines

ANP-2	Aliphatic amine hydrochlorides
HA	Hexadecylamine
HCILA	Laurylamine hydrochloride
HCILD	Lauroyldiethylenetriamine hydrochloride
LA	Laurylamine
ODA	Octadecylamine
SA	Stearylamine
TDEDAHCl	Tridodecylethylenediamine hydrochloride
TEA	Triethanolamine
TOA	Trioctylamine

Table 4 Precipitate flotation of the first kind

Species	Sample medium	Precipitate nature	Surfactants	Observations	Reference
Al	Waste water	Hydroxide			114
Cd	Water, pH 10	Hydroxide	NaLS	Polarography	115
Cd, Cu	Cyanide solutions	Ferrocyanide	NaO	Separation of copper from cadmium	116
Co	Waste waters, pH 11	Hydroxide	NaLS	Recovery of Co in the waste water effluent	77
		Hydroxide	HTMABr	Study of the influence of addition of several salts	117
Co, Cu, Mn, Ni	Cu, pH > 7.5 Ni, Co, Mn, pH 9	LIX 65, LIX 63 compounds	HTMABr + TX100	AAS Study of the effect of addition of different salts and comparison with the use of NaLS	118
Co, Cu, Zn	Aqueous solutions Zn and Cu, pH 10 Co and Cu, pH 12.3	Hydroxide	NaDBS BDDABr		119
Cu	pH 7.5-9.5	Hydroxide	NaLP + TX100	AAS Study of the influence of several ions	83
Fe, In, Ni, Sb, Sn, Ti, Zr		Hydroxide	BACl, NaO NaDBS		76
Hg	Waste water	Colloidal Hg	KM	Bentonite addition	120
	Waste water	Colloidal Hg	aliphatic amines		121
	Waste water	Colloidal Hg	KP, KS		122
	Waste water	Colloidal Hg and Hg oxide	KA		123
Mg	Aqueous solutions, pH 11.5 High salinity media	Hydroxide	NaLS KO	Study of the influence of several salts	124
Mn	pH 8.5-10	Hydroxide	NaLP + TX100	AAS Study of the influence of several ions	83
U	Sulphuric acid pH 2.2-2.3 pH variable	Oxinate	TOA + ANP-2		126
		Oxinate	HTMABr, NaLS	Spectrophotometry with Tiron or Arsenazo	127
Zn	pH 9.5-10	Hydroxide	NaDBS		128
	pH 9	Hydroxide	NaLP + TX100	AAS Study of the influence of several ions	83

Table 5 Ion flotation single-element separations

Species	Sample medium	Surfactants	Observations	Reference
Ag	Sea-water, pH 2	SA	AAS	69
Cd	Natural waters, pH 6-8	TEA	AAS, 20-200 ng/ml	129
	Water	NaLS and NaL	Polarography	130
Co	Thiocyanate, iodide	HTMABr	Studies on the effectiveness of several surfactants	131
	Cyanide media	HPCl and NaDBS	Flotations in media containing different species	132
	CoCl ₂ , 4.3 × 10 ⁻⁴ M	Collected with finely dispersed solid solution of saturated aliphatic acids in paraffin	Radiochemical determination Maximum recovery at pH 10-10.5 Based on electrocoagulation of Co(OH) ₂	133
Cr	Cr(VI)	HDABr	Spectrophotometry with sensitivities around the ng/ml level	134
	Cr(III)-diphenylcarbazide, 1M sulphuric acid	NaLS	Spectrophotometry	135
Cu	Waste waters from mining industry	LA and SA	Studies of the feasibility of copper separation	136
	Butyl xanthate ppt	HTMABr	Concentration factor 100	137
Fe	Waste waters from mining and electroplating industries	TCMACl	Separation of ferrocyanide, ferricyanide and cyanide	138
Hf	Cyanide media pH 4-10	NaLS	Spectrophotometry	139
	1,10-Phenanthroline	NaLS or HTMABr	Studies of the separation and flotation mechanism	140
Hg	Waste waters from radiochemical processes	TDEDHCl	Recoveries 80-92%	141
	Chloride media, 1.5M, pH 6-8	Primary aliphatic amines	Studies on the separation and IR spectra	142
	Thiocyanate media, pH 3.0 and 9-10.5	HL	Studies on the separation mechanism	143
	KCl medium, 1.5M, pH 5.1	Aliphatic amines	Studies on the influence of different variables affecting the separation process	144
	Chloride media, 0.25M, pH 6	KO	Spectrophotometry	145
	Nitrate media, pH 5-8.5	LA + HL	Spectrophotometry	146
Mo	Sea-water	HPCl	Separation and study of several parameters	147
Nb	Bromopyrogallol Red	Amines and quaternary ammonium salts	Recoveries around 87%	148
	pH 5-9	HDMABr	Spectrophotometry	149
Ni	KCl 0.05M, pH 5	NaLS	Idem but using a continuous technique for the flotation process	150
	Natural waters, HCl 0.012M, <i>p</i> -amino benzenesulphonamide and <i>N</i> -1-naphthylethylenediamine	NaLS		26

continued opposite

Table 5—continued

Species	Sample medium	Surfactants	Observations	Reference
NO_3^-	Idem	NaLS	Idem, but prior reduction of nitrate with Zn	151
Pb	Waste waters Waste waters, pH 7.0	KL, KTD, KPD, KP K ethyl xanthate	Optimization studies of the separation conditions in each case	152 153
S	Waters, Methylene Blue formation	NaLS	Spectrophotometry	154
Ta	pH 0.5–1.5 and 5–9	ATACl, ABDACl and ANP-2	Studies on the effect of different variables	155
U	Carbonate media, pH 5–6 Sea-water, pH 5 or lower Sea-water, pH 5–6 Phosphoric acid media Sea-water, pH 3.5	HPBr Amidozimes Stearox-6 + HS Anionic organophosphorus cpds Arsenazo III + TDBACl	Studies on the effect of different variables Studies on the recovery Spectrophotometry with Arsenazo III Studies on the separation mechanism and recoveries Studies on the influence of several parameters Spectrophotometry	156 157 158 159 160, 161
Zn	HCl, 2M pH 10	HDMABr KC	Studies on the separation mechanism and kinetics	162 163
Zr	$\text{UO}_2(\text{NO}_3)_2$	NaLS, Na decylsulphate, Na tetradecylsulphate	Surface properties of precipitate studied by electrophoresis	164
31 ions	HCl/HNO ₃	Cetylpyridinium chloride	Flotation in mixed acids more efficient than in HCl alone	164a

Table 6 Ionic flotation, multielemental separations

Species	Sample medium	Surfactants	Observations	Reference
Ag, Au, Cd, Co, Cr, Hg, In, Mn, Pd, Pt, Zn	Cyanide and chloride media	Alkyl + alkylsulphonates	Studies on the mechanism, separation order, kinetics and recoveries of each species	165
Ag, Co, Cu, Fe, Hg, In, Pt, Zn	Thiocyanate media	HPCl, HTMACl, TDBACl	Studies on the feasibility of separations between elements as a function of pH and surfactant nature	166
Al, Bi, Co, Cu, Fe, Ga, In, Pb, Zn	pH 6–6.3 (Al, Ga, Fe, In, Bi) pH 6–9 (Co, Ni, Cu, Zn, Pb)	<i>N</i> -Stearoyl-L-glutamic acid	Detn. of the sublate stoichiometry and studies on possible separations between elements	167
Al, Ga, In	Halide and hydroxy complexes, halo-acid and basic media Idem	HPCl + STACl	Structural detn. of the sublates (IR) Optimization of the separation	168
Au, Cd, Hg, Zn	Acidic solutions, $1.0 \times 10^{-5}M$	HPCl, NaLS and quaternary ammonium salts HTMACl	Gallium is separated in 7M HCl medium	169
Au, Hg, Pd, Pt	Medium HBr	HPCl, TDBACl, HTMACl	Foam fractionation	170
Au, Ir, Pd, Pt	Chloride media	Quaternary ammonium salts	Separation of the group	171
Au, Pd, Pt	Medium HCl, 3M	HPCl, TDBACl, HTMACl	Radiochemical detn. Separation from Rh, Ir and Ru	172 173

continued overleaf

Table 6—*continued*

Species	Sample medium	Surfactants	Observations	Reference
Cd, As	Medium phosphoric acid, 1.7M	Diethylphosphate	Study of the influence of several parameters on the separation process	174
Cd, Co	Thiocyanate media	HTMABr	Study of the effect of different alcohols in the process Spectrophotometric detn	175
Cd, Co, Cu, Fe, Ni, Zn	1,10-Phenanthroline	NaLS	AAS	176
Cd, Pb, Sb, Sn	Medium HBr	HPCI, TDBACI, HTMACI	Studies of the feasibility of separations	177
Cd, Zn	APDC	DPCI	Study of separations	178
Cu, Fe, Ga		β -Diketones	Study of the effectiveness of several β -diketones AAS detn Comparative study with solvent extraction methods	179
Cu, Mo, U, Zn	Waste water pH 3-8 (Mo, U) pH 5-7 (Cu, Zn)	Amines (Mo, U) ethyl xanthate or butyl xanthate (Cu, Zn)		180
Cu, Pb, Zn	pH 4.5	KL	Studies of the kinetics and possible separation schemes	181
Hg, Pb		KL + KS (Pb) KS, KM, KP (Hg) HC, HTD, HM (Pb) HTD, KP, KS (Hg)	Optimization of the flotation process	182
Ir, Pt	Medium HCl, 0.1M	Quaternary ammonium salts (best results with HTBABr HTPABr, HTEABr, HTMABr)	Studies on optimization and feasibility of separation	183
Ir, Rh	Chloride media, pH 2	Idem	Study of the feasibility of the separation as a function of the surfactant nature	184
Mo, W	pH 6-10 (Mo) (chloride and sulphate media) pH 4 (W) (Waste waters) Waste waters Mo pH 7 W pH 4	HClHA LA, HA, SA LA, HA, SA LA, HA, SA	Hydroxylamine must be added to reduce Ir(III) Radiochemical detn Rh detd by spectrophotometry Separation from Fe and Cu Study of the effect of different amines	185 186 187
Sc, Gd, Y	(Sc) pH 4.8, (Gd) pH 6.8 (Y) pH 6.9	Fatty acids	Studies of the influence of pH and other parameters	188
Th, La	Chloride media (La) pH 5	HPBr + ANP-2	Studies on the optimization of pH values and recoveries	189
U, Th	Waste waters, sulphate media pH 0.5-4.0	Primary aliphatic amines	Study of the separation mechanism Uranium separation and recovery	190 191
V, Mo	pH 8-10	HCILDT	Separation of V Mo remains in the solution	192
V, W		Primary amines	Study of the influence of several added salts and other experimental parameters	193
Zr, Nb	Oxalic acid media	NaLS	Niobium is masked with hydrogen peroxide Study of the separation	194

Table 7 Solvent sublation (inorganic compounds)

Species	Medium solvent	Surfactants	Observations	Reference
Cr, Cu, U	LIX 64N (Cu) DEHPA + TOA (U, Cr)	NaDBS	Studies with different organic solvents	195
Co	Chloride and cyanide media	HPCI + NaDBS	Radiochemical detn Study of the influence of several added salts results with ion flotation are given Solvent sublation results are better	132
Cu	pH 6-6.4, NaDDTC isoamyl alcohol		Spectrophotometry	196
	Dithizone/MIBK	NaLS	EDTA and tartrate are used as masking agents	197
Fe	3-(2-Pyridyl)-5,6-diphenyl-1,2,4-triazine complex	NaLS	Spectrophotometry	198
Ir, Rh	Butyl acetate	Quaternary ammonium salts	Comparison with ion flotation techniques	185

Anionic surfactants

HC	Decanoic acid
HE	Stearic acid
HL	Lauric acid
HM	Myristic acid
HDBI	Heptadecylbenzylimidazole
HTD	Tridecanoic acid
KA	Potassium abietate
KC	Potassium caprate
KL	Potassium laurate
KM	Potassium myristate
KO	Potassium oleate
KP	Potassium palmitate
KPD	Potassium pentadecanoate
KS	Potassium stearate
KTD	Potassium tridecanoate
NaDBS	Sodium dodecylbenzenesulphonate
NaE	Sodium stearate
NaL	Sodium laurate
NaLP	Sodium laurylphosphate
NaLS	Sodium laurylsulphate
NaN	Sodium naphthenate
NaO	Sodium oleate

Non-ionic surfactants

TX100	Triton X-100
-------	--------------

REFERENCES

- 1 R Lemlich (ed), *Adsorptive Bubble Separation Techniques*, Academic Press, New York, 1972
- 2 F Sebba, *Ion Flotation*, Elsevier, Amsterdam, 1962
- 3 A N Clarke and D J Wilson, *Foam Flotation Theory and Applications*, Dekker, New York, 1983
- 4 B L Karger, L R Snyder and C Horvath, *Adsorptive Bubble Separation Process*, in *An Introduction to Separation Science*, Wiley, New York, 1973
- 5 P Somasundaran, *Separation Using Foaming Techniques*, in *New Developments in Separation Techniques*, Dekker, New York, 1976, *Sep Purif Methods*, 1972, **1**, 117
- 6 A Mizuike, *Flotation*, Chapter 10 in *Enrichment Techniques for Inorganic Trace Analysis*, Springer-Verlag, Heidelberg, 1983
- 7 A N Clarke and D J Wilson, *Sep Purif Methods*, 1978, **7**, 55
- 8 M Hiraide and A Mizuike, *Rev Anal Chem*, 1982, **6**, 151
- 9 A Mizuike and M Hiraide, *Pure Appl Chem*, 1982, **54**, 1956
- 10 B L Karger, R B Grieves, R Lemlich, A J Rubin and F Sebba, *Sep Sci*, 1967, **2**, 401
- 11 T A Pinfeld, *ibid*, 1970, **5**, 379
- 12 D C Dorman and R Lemlich, *Nature*, 1962, **207**, 145
- 13 I Shetham and T A Pinfeld, *J Appl Chem*, 1962, **18**, 217
- 14 F Sebba, *Nature*, 1959, **184**, 1062
- 15 K Maas, *Sep Sci*, 1969, **4**, 69
- 16 *Idem, ibid*, 1969, **4**, 457
- 17 R Lemlich, *Ind Eng Chem*, 1968, **60**, 16
- 18 Z Marczenko, *Mikrochim Acta*, 1977 **11**, 651
- 19 P Somasundaran, *Sep Purif Methods*, 1972, **1**, 117
- 20 Y S Kim and H Zeitlin, *Sep Sci*, 1917, **6**, 505
- 21 R S S Murthy and D E Ryan, *Anal Chem*, 1983, **55**, 682

- 22 W J Williams and A H Gillam, *Analyst*, 1978, **103**, 1239
- 23 A J Rubin and W L Lapp, *Sep Sci*, 1971, **6**, 357
- 24 A Mizuike, M Hiraide and K Mizuno, *Anal Chim Acta*, 1983, **148**, 305
- 25 S-D Huang and D J Wilson, *Sep Sci Technol* 1984, **19**, 603
- 26 M Aoyama, T Hobo and S Suzuki, *Anal Chim Acta*, 1982, **141**, 427
- 27 P E Spargo and T A Pinfold, *Sep Sci*, 1970, **5**, 619
- 28 J A Womack, J C Lichter and D J Wilson, *Sep Sci Technol*, 1982, **17**, 897
- 29 C Mizutani and H Zeitlin, *Sep Sci*, 1973, **8**, 185
- 30 D J Wilson and K T Valsaraj, *Sep Sci Technol*, 1982, **17**, 1387
- 31 E Valdes-Krieg, *AIChE J*, 1975, **21**, 400
- 32 J W Wilson and D J Wilson, *Sep Sci*, 1974, **9**, 381
- 33 S-D Huang and D J Wilson, *ibid*, 1975, **10**, 407
- 34 J W Wilson and D J Wilson, *ibid*, 1976, **11**, 89
- 35 J W Wilson, D J Wilson and J H Clarke, *ibid*, 1976, **11**, 223
- 36 D J Wilson, *ibid*, 1976, **11**, 391
- 37 *Idem*, *ibid*, 1977, **12**, 231
- 38 *Idem*, *ibid*, 1977, **12**, 447
- 39 A N Clarke, D J Wilson and J H Clarke, *Sep Sci Technol*, 1978, **13**, 573
- 40 D J Wilson and R M Kennedy, *ibid*, 1979, **14**, 319
- 41 B L Currin, R M Kennedy, A N Clarke and D J Wilson, *ibid*, 1979, **14**, 669
- 42 J E Kiefer and D J Wilson, *ibid*, 1980, **15**, 57
- 43 R M Moffatt and D J Wilson, *ibid*, 1980, **15**, 1339
- 44 J M Brown and D J Wilson, *ibid*, 1981, **16**, 773
- 45 J E Kiefer, P C Sundareswaran and D J Wilson, *ibid*, 1982, **17**, 561
- 46 D J Wilson, *ibid*, 1982, **17**, 1219
- 47 P C Sundareswaran and D J Wilson, *ibid*, 1983, **18**, 555
- 48 D J Wilson, *ibid*, 1983, **18**, 657
- 49 W Abraham, T M Harris and D J Wilson, *ibid*, 1984, **19**, 389
- 50 M Sarker, M Bettler and D J Wilson, *ibid*, 1987, **22**, 47
- 51 M J Jaycock and R H Ottewill, *Inst Mining Met*, 1963, **72**, 497
- 52 D G DeVivo and B L Karger, *Sep Sci*, 1970, **5**, 145
- 53 A J Rubin and S C Lackey, *J Am Water Works Assoc*, 1968, **60**, 1156
- 54 J J Bikerman, *Foams Theory and Industrial Applications*, Reinhold, New York, 1953
- 55 J Jorné and E Rubin, *Sep Sci*, 1969, **4**, 133
- 56 T M Riddick, *Control of Colloid Stability through Zeta Potential*, Zet-Meter, New York, 1968
- 57 D W Fuerstenau and T W Healy, in *Adsorptive Bubble Separation Techniques*, R Lemlich (ed), p 91 Academic Press, New York, 1972
- 58 R H Fowler and E A Guggenheim, *Statistical Thermodynamics*, Cambridge University Press, Cambridge, 1952
- 59 B L Karger, *Solvent Sublation*, Chapter 8 in *Adsorptive Bubble Separation Techniques*, R Lemlich (ed), Academic Press, New York, 1972
- 60 J Elhanan and B L Karger, *Anal Chem*, 1969, **41**, 671
- 61 T A Pinfold and E J Mahne, *J Appl Chem*, 1969, **19**, 188
- 62 B L Karger, T A Pinfold and S E Palmer, *Sep Sci*, 1970, **5**, 603
- 63 I Sheiham and T A Pinfold, *ibid*, 1972, **7**, 43
- 64 T Lionel, D J Wilson and D E Pearson, *Sep Sci Technol*, 1981, **16**, 907
- 65 K T Valsaraj and D J Wilson, *Colloids Surf*, 1983, **8**, 203
- 66 S-D Huang, K T Valsaraj and D J Wilson, *Sep Sci Technol*, 1983, **18**, 941
- 67 K Tamamushi and D J Wilson, *ibid*, 1985, **19**, 1013
- 68 L K Foltz, K N Carter, Jr and D J Wilson, *Sep Sci Technol*, 1986, **21**, 57
- 69 N Rothstein and H Zeitlin, *Anal Lett*, 1976, **9**, 461
- 70 S Nakashima, *Bunseki Kagaku*, 1979, **28**, 561
- 71 S Nakashima and M Yagi, *ibid*, 1984, **33**, T1
- 72 E H DeCarlo and D M Thomas, *Environ Sci Technol*, 1985, **19**, 538
- 73 S Nakashima, *Z Anal Chem*, 1980, **303**, 10
- 74 L-F Wu, R-C Kuo and S-D Huang, *J Chem Chem Soc*, 1980, **27**, 165, *Chem Abstr*, 1981, **95**, 48473v
- 75 S Nakashima and M Yagi, *Anal Chim Acta*, 1983, **147**, 213
- 76 M Hiraide and A Mizuike, *Bunseki Kagaku*, 1980, **29**, 84
- 77 J-Y Gau and S-D Huang, *Chieh Mien K'o Hsueh*, 1984, **24**, 2, *Chem Abstr*, 1985, **102**, 10162t
- 78 M Hiraide, K Sakurai and A Mizuike, *Anal Chem*, 1984, **56**, 2861
- 79 S-D Huang, C-F Fann and H-S Hsieh, *J Colloid Interface Sci*, 1982, **89**, 504
- 80 M Aziz, K Shakir and K Benyamin, *Radioact Waste Management Nucl Fuel Cycle*, 1986, **7**, 335
- 81 R Cela and J A Pérez-Bustamante, *Afinidad*, 1982, **39**, 124
- 82 M Caballero, R Cela and J A Pérez-Bustamante, *Sep Sci Technol*, 1986, **21**, 39
- 83 N A Mumallah and D J Wilson, *ibid*, 1981, **16**, 213
- 84 L-F Wu, Y-F Chiu and S-D Huang, *Ying Yung Chieh Mien Hua Hsueh*, 1980, **7**, 2, *Chem Abstr*, 1980, **93**, 225148z
- 85 J D Hidalgo, M A Gomez, M Caballero, R Cela and J A Pérez-Bustamante, *Talanta*, 1988, **35**, 301
- 86 M A Slapik, E L Thackston and D J Wilson, *Proc Ind Waste Conf*, 1980, **35**, 694
- 87 E L Thackston, D J Wilson, J S Hanson and D L Miller, *J Water Pollut Control Fed*, 1980, **52**, 317
- 88 Y-F Chiu and S-D Huang, *Ying Yung Chieh Mien Hua Hsueh*, 1979, **6**, 2, *Chem Abstr*, 1980, **92**, 204009u
- 89 S Nakashima, *Bull Chem Soc Japan*, 1981, **54**, 291
- 90 S Nakashima and M Yagi, *Z Anal Chem*, 1983, **314**, 155
- 91 S Liang, Y Zhong and Z Wang, *ibid*, 1984, **318**, 19
- 92 S Nakashima, *Anal Chem*, 1979, **51**, 654
- 93 *Idem*, *Bull Chem Soc Japan*, 1979, **52**, 1844
- 94 T F Ferng, J J Tzuoo and S D Huang, *Ying Yung Chieh Mien Hua Hsueh*, 1982, **17**, 2, *Chem Abstr*, 1983, **98**, 57702v
- 95 S Nakashima and M Yagi, *Anal Chim Acta*, 1984, **157**, 187
- 96 T Tomotaka and K Yoshio, *Oita Kogyo Daigaku Kogai Kenkyusho Ho*, 1980, **3**, 19, *Chem Abstr*, 1980, **93**, 79130u
- 97 U Dietze, J Braun and H-J Peter, *Z Anal Chem* 1985, **322**, 7

- 98 X Feng and D. E. Ryan, *Anal. Chim. Acta*, 1984, **162**, 47
99. E. H. DeCarlo, H. Zeitlin and Q. Fernando, *Anal. Chem.*, 1981, **53**, 1104
- 100 S Nakashima and M Yagi, *Bunseki Kagaku*, 1982, **31**, E431
- 101 M Hiraide, Y Yoshida and A Mizuike, *Anal Chim Acta*, 1976, **81**, 185
- 102 M Hiraide, T Ito, M Baba, H Kawaguchi and A Mizuike, *Anal Chem*, 1980, **52**, 804
- 103 L M Cabezón, M Caballero, R Cela and J A Pérez-Bustamante, *Talanta*, 1984, **31**, 597
- 104 M Caballero, R Lopez, R Cela and J A Pérez-Bustamante, *Anal Chim Acta*, 1987, **196**, 287
- 105 L M Cabezón, R Cela and J A Pérez-Bustamante, *Afinidad*, 1983, **40**, 144
- 106 S-D Huang, T P Wu, C-H Ling, G-L Sheu, C-C Wu and M-H Cheng, *J Colloid Interface Sci*, 198, **124**, 666
- 107 S M Nemets, A K Charykov and Yu I Turkin, *Vestn Leningr Univ, Fiz, Khim*, 1983, No 4, 65, *Chem Abstr*, 1984, **100**, 55060h
- 108 S M Nemets, Yu I Turkin and V L Zueva, *Tr Gl Geofiz Obs um A I Voeikova*, 1985, **495**, 136, *Chem Abstr*, 1986, **104**, 135118f
- 109 E H DeCarlo, H Zeitlin and Q Fernando, *Anal Chem*, 1982, **54**, 898
- 110 E H DeCarlo, B D Bleasdel, H Zeitlin and Q Fernando, *Sep Sci Technol*, 1982, **17**, 1205
- 111 S Nakashima and M Yagi, *Anal Lett*, 1984, **17**, 1693
- 112 G T McIntyre, J J Rodriguez, E L Thackston and D J Wilson, *Report*, 1981 W82-06708 OWRT-A-064-TENN (I) Order No PB82-256827, *Chem Abstr*, 1983, **98**, 77619q
- 113 Xu Bo-xing and Fang Yu-zhi, *Talanta*, 1988, **35**, 891
- 114 A Yu Chikin and G D Rusetskaya, *Obogashch Rud, Irkutsk*, 1979, **93**; *Chem Abstr*, 1980, **92**, 134740z
- 115 K Jurkiewicz, *Sep Sci Technol*, 1985, **19**, 1051
- 116 Y Nakahiro, *Fine Part Process Proc, Int Symp*, 1980, **2**, 1810
- 117 K Jurkiewicz, *J Colloid Interface Sci*, 1986, **112**, 229
- 118 N A-K Mumallah and D J Wilson, *Sep Sci Technol*, 1980, **15**, 1753
- 119 W A Charewicz and S Basak, *Fizykokhym Probl Mineralurgu*, 1982, **14**, 43, *Chem Abstr*, 1983, **99**, 8698y
- 120 L D Skrylev, S K Babinets, V V Kostik and A N Purich, *Izv Vyssh Uchebn Zaved, Khim i Khim Tekhnol*, 1985, **28**, 63, *Chem Abstr*, 1985, **103**, 146588q
- 121 L D Skrylev, S K Babinets and A N Purich, *Zh Prikl Khim*, 1982, **55**, 2375, *Chem Abstr*, 1983, **98**, 38226q
- 122 *Idem, ibid*, 1985, **58**, 913, *Chem Abstr*, 1985, **103**, 41986n
- 123 *Idem, Khim Tekhnol Vody*, 1986, **8**, 77
- 124 T Inoue, T Shiba and S Takiuchi, *Sogo Shikensho Nenpo*, 1980, **39**, 185, *Chem Abstr*, 1981, **94**, 49638u
- 125 M Maksimovic and S Rozga, *Kem Ind*, 1985, **34**, 743, *Chem Abstr*, 1986, **104**, 92713b
- 126 L D Skrylev and V Menchuk, *Izv Vyss Uchebn Zaved, Tsvetn Metall*, 1985, No 5, 100, *Chem Abstr*, 1986, **104**, 54056g
- 127 K Shakir, K Benyamin and M Aziz, *Can J Chem*, 1984, **62**, 51
- 128 K. H. Suh and M. G. Lee, *Pusan Susan Taehak Yongu Pogo, Chayon Kwahak*, 1984, **24**, 107; *Chem Abstr*, 1985, **103**, 43104z
- 129 S M Nemets, P F Svistov and Yu I Turkin, *Probl. Sovrem Anal Khim* 1983, **4**, 104, *Chem Abstr.*, 1984, **100**, 73654j
- 130 K Jurkiewicz, *Sep Sci Technol*, 1985, **19**, 1039
- 131 *Idem, ibid*, 1985, **20**, 179
- 132 W Walkowiak, *J Chem Technol Biotechnol*, 1980, **30**, 611
- 133 L D Skrylev, V V Kostik, A N Purich and G F Os'machko, *Izv Vyssh Uchebn Zaved Isvetn Metall*, 1988, No 1, 2, *Chem Abstr*, 1988, **109**, 96447u
- 134 M Aoyama, T Hobo and S Suzuki, *Bunseki Kagaku*, 1981, **30**, 224
- 135 *Idem, Anal Chim Acta*, 1981, **129**, 237
- 136 L Stoica, I Jitaru, M Dinculescu, M Georgescu, A German and A Lupu, *Rev Chum (Bucharest)*, 1980, **31**, 454, *Chem Abstr*, 1980, **93**, 153735p
- 137 T Hobo, Y Sudo, S Suzuki and S Araki, *Bunseki Kagaku*, 1978, **27**, 104
- 138 R O Busch, D J Spottiswood and G W Lower, *J Water Control Fed*, 1980, **52**, 2925
- 139 K Yamada, M Aoyama, T Hobo and S Suzuki, *Bunseki Kagaku*, 1985, **33**, 99
- 140 D M Downey, C N Narick and T A Cohen, *J Radioanal Nucl Chem*, 1985, **91**, 259
- 141 A Dimov and E Prodanov, *Wiss Z Tech Hochsch "Carl Schorlemmer" Leuna-Merseburg*, 1982, **24**, 485, *Chem Abstr*, 1983, **98**, 149085n
- 142 L D Skrylev, L M Bulygina and L A Sin'kova, *Khim Tekhnol Vody*, 1982, **4**, 514, *Chem Abstr*, 1983, **98**, 113097d
- 143 K Volke, G Para, J Pawlikowska-Czubak and H Neubert, *Colloid Polym Sci*, 1984, **262**, 245
- 144 L D Skrylev, L M Lopatenko and L A Sin'kova, *Izv Vyssh Uchebn Zaved, Khim i Khim Tekhnol*, 1985, **28**, 58, *Chem Abstr*, 1985, **103**, 226316q
- 145 *Idem, Izv Vyssh Uchebn Zaved, Tsvetn Metall*, 1985, No 3, 8, *Chem Abstr*, 1985, **103**, 90800h
- 146 G Para, K Volke, A Pomianowski and J Pawlikowska-Czubak, *Colloid Polym Sci*, 1986, **264**, 260
- 147 I Yu Andreeva, L I Lebedeva and O L Drapchinskaya, *J Anal Chem USSR*, 1985, **40**, 564, *Zh Analit Khim*, 1985, **40**, 694
- 148 L I Ushakova, V G Berezyuk and A M Kasimov, *Zh Prikl Khim*, 1983, **56**, 758, *Chem Abstr*, 1983, **99**, 28402a
- 149 C W McDonald and J Jaganathan, *Microchem J*, 1982, **27**, 240
- 150 M Aoyama, T Hobo and S Suzuki, *Bunseki Kagaku*, 1982, **31**, E99
- 151 *Idem, ibid*, 1982, **31**, E163
- 152 L D Skrylev, L M Lopatenko and L A Sin'kova, *Khim Tekhnol Vody*, 1985, **7**, 14, *Chem Abstr*, 1985, **103**, 128511e
- 153 *Idem, Izv Vyssh Uchebn Zaved Tsvetn Metall*, 1984, No 6, 3, *Chem Abstr*, 1985, **102**, 207024f
- 154 M Aoyama, T Hobo and S Suzuki, *Bunseki Kagaku*, 1982, **31**, E7
- 155 L I Ushakova, V G Berezyuk and A F Man'shin, *Kompleksn, Ispol'z Miner Syr'ya*, 1983, No 1, 67, *Chem Abstr*, 1983, **98**, 219491t

- 156 S N Pavlenko, I A Legenchenko and V V Menchuk, *Zh. Prikl. Khim.*, 1983, **56**, 1049, *Chem Abstr.*, 1983, **99**, 74462t
- 157 Y Koide, H Takamoto, K Matsukawa and K Yamada, *Bull Chem Soc. Japan*, 1983, **56**, 3364
- 158 A A Bezborodov and S V Lyashenko, *Dopov Akad Nauk Ukr RSR, Ser B Geol, Khim, Biol Nauki*, 1983, No 6, 3, *Chem Abstr.*, 1983, **99**, 143700h
- 159 E Jdid, P Blazy and J Bessière, *Trans-Inst Min Metall, Sect C*, 1985, C179
- 160 K Sekine and H Onishi, *Anal Chim Acta*, 1972, **62**, 468
- 161 K Sekine, *Mikrochim Acta*, 1975 I, 313
- 162 C W McDonald and O A Ogunkeye, *Microchem J.*, 1981, **26**, 80
- 163 I A Legenchenko, L A Sin'kova and E A Kovrik, *Zh Prikl Khim.*, 1984, **57**, 458, *Chem Abstr.*, 1984, **100**, 142842h
- 164 P Bernasconi, J E Poirier, G Bouzat, P Blazy, J Bessiere and R Durand, *Ind J Miner Process.*, 1988, **23**, 243
- 164a D Hualing and H Zhude, *Talanta*, 1989, **36**, 633
- 165 W Walkowiak, *Pr Nauk Inst Chem Nierog Metal Pierwiasikow Rzaadkich Politech Wroclaw*, 1985, **53**, 54, *Chem Abstr.*, 1986, **104**, 72267f
- 166 T Nozaki, K Kato, K Okamura, Y Soma, N Ikuta and N Mise, *Bunseki Kagaku*, 1983, **32**, 479
- 167 T Nozaki and T Nagano, *ibid.*, 1984, **33**, 618
- 168 V V Sviridov, *Kompleksn Ispol z Miner Sir'ya*, 1983, No 6, 25, *Chem Abstr.*, 1983, **99**, 143725v
- 169 V V Sviridov, G I Mal'tsev and L D Skrylev, *Deposited Doc.*, 1983, VINITI 51187-83, 10, *Chem Abstr.*, 1985, **102**, 29169x
- 170 W Walkowiak, D Bhattacharyya and R B Grieves, *Anal Chem.*, 1976, **48**, 975
- 171 T Nozaki, M Maeno, R Higaki, S Kamisaka and O Kamei, *Bunseki Kagaku*, 1985, **34**, 58
- 172 E W Berg and D M Downey, *Anal Chim Acta*, 1980, **120**, 237
- 173 T Nozaki, M Takahashi, T Kaneko, K Matsuoka, K Okamura and Y Soma, *Bunseki Kagaku*, 1982, **31**, 353
- 174 J Bessière, M Bruant, E A Jdid and P Blazy, *Int J Miner Process.*, 1986, **16**, 63
- 175 K Jurkiewicz, *Sep Sci Technol.*, 1986, **21**, 209
- 176 T Hobo, K Yamada and S Suzuki, *Anal Sci.*, 1986, **2**, 361
- 177 T Nozaki, K Kato, M Uchida, M Doi, N Mise and Y Soma, *Bunseki Kagaku*, 1983, **32**, 145
- 178 Y Kato, *Japan Tokkyo Koho*, JP 61 17,770; *Chem Abstr.*, 1986, **105**, 230397a
- 179 Y Koide, S Kitaoka and K. Yamada, *Bull Chem Soc Japan*, 1985, **58**, 2456
- 180 E Jude, *Rom 71647 (Cl CO2Cl/40)* 20 Feb 1980 Appl. 74757 12 May 1973, *Chem Abstr.*, 1981, **94**, 178659a
- 181 L D Skrylev, L A Sin'kova, L M Lopatenko and D M Erimu, *Zh Prikl Khim.*, 1986, **59**, 2318; *Chem Abstr.*, 1987, **106**, 9010t
- 182 L D Skrylev, L A Sin'kova and L M Lopatenko, *ibid.*, 1985, **58**, 1624, *Chem Abstr.*, 1985, **103**, 90798p
- 183 L D Skrylev, L M Lopatenko and L A Sin'kova, *Izv Vyssh Uchebn Zaved, Tsvetn Metall.*, 1986, No 3, 9, *Chem Abstr.*, 1986, **105**, 137486u
- 184 E W Berg and D M Downey, *Anal Chim Acta*, 1981, **123**, 1
- 185 *Idem, ibid.*, 1980, **121**, 239
- 186 I Johannes and R Koch, *Eesti NSV Tead, Akad Toim Keem.*, 1984, **33**, 127, *Chem Abstr.*, 1984, **101**, 76617f
- 187 L D Skrylev, S N Pavlenko and V F Sazonova, *Izv Vyssh Uchebn Zaved, Tsvetn Metall.*, 1986, No 1, 28, *Chem Abstr.*, 1986, **104**, 228088m
- 188 *Idem, Izv Vyssh Uchebn Zaved, Gorn Zh.*, 1986, No 6, 108, *Chem Abstr.*, 1986, **105**, 118650b
- 189 L D Skrylev and V F Sazonova, *Izv Vyssh Uchebn Zaved, Tsvetn Metall.*, 1980, No 3, 24, *Chem Abstr.*, 1980, **93**, 117939z
- 190 L D Skrylev, S N Pavlenko and V F Sazonova, *ibid.*, 1983, No 2, 71, *Chem Abstr.*, 1983, **98**, 219514c
- 191 L D Skrylev, V V Menchuk, V F Sazonova and I M Minaev, *ibid.*, 1981, No 2, 66, *Chem Abstr.*, 1981, **95**, 28331u
- 192 M Izumi, M Sato, S Shoji and K. Oikawa, *Japan Kokai Tokkyo Koho*, 79,109,100, *Chem Abstr.*, 1980, **93**, 29770g
- 193 L D Skrylev, V V Kostyuk and A N Purich, *Zh Prikl Khim.*, 1984, **57**, 930, *Chem Abstr.*, 1984, **101**, 11766j
- 194 D M Downey and C L McLaughlin, *Radiochim Acta.*, 1983, **33**, 91
- 195 H Takeuchi, K Takahashi, M Mizutani and S Hibi, *Nippon Kagaku Kaishi*, 1984, 161, *Chem Abstr.*, 1984, **101**, 134726
- 196 H Dong and X Yue, *Fenxi Huaxue*, 1986, **14**, 569, *Chem Abstr.*, 1986, **105**, 217991v
- 197 J Cervera, R Cela and J A Pérez-Bustamante, *Analyst*, 1982, **107**, 1425
- 198 K Kotsuji, K Kameyama, M Arakawa and S Hayashi, *Bunseki Kagaku*, 1977, **26**, 475, *Anal Abstr.*, 1978, **34**, 3B156

HPLC ANALYSIS OF ANTIOXIDANTS

C. GROSSET, D. CANTIN, A. VILLET and J. ALARY

Laboratoire de Chimie Analytique et Bromatologie, U.F.R. de Pharmacie de Grenoble, Domaine de la Merci, 38700 La Tronche, France

(Received 21 December 1988 Revised 10 August 1989 Accepted 22 August 1989)

Summary—Qualitative and quantitative HPLC methods are described for the analysis of mixtures of twelve antioxidants. For identification of the components present, gradient elution with a convex profile from 35.65 v/v water-methanol to pure methanol is used, on a Waters 5 μm C₁₈ Resolve column, with an ultraviolet detector. Propyl gallate and methyl *p*-hydroxybenzoate cannot be separated, however. For quantitative analysis, with ultraviolet and electrochemical detectors in series, the 35.65 water-methanol mixture or pure methanol is used as the eluent, under isocratic conditions, with lithium perchlorate as supporting electrolyte. An applied potential ranging from +0.8 to +1.7 V allows detection of all the antioxidants tested. Both modes of detection are very sensitive, with limits of detection as low as 61 pg (UV, methyl *p*-hydroxybenzoate) and 360 pg (electrochemistry, butylhydroxyanisole).

The technological and economic requirements of the pharmaceutical and food industries have intensified the use of antioxidants.¹ In France the use of these additives is subject to regulations which define the permitted compounds and their concentration limits. As a consequence there is a need for analytical control of products that are prone to oxidation, to verify the absence of prohibited antioxidants and to determine any permitted ones present.

We are interested in the authorized antioxidants. L(+)-ascorbic acid (AA), ascorbyl palmitate (AP), DL- α -tocopherol (α T), butylhydroxytoluene (BHT), butylhydroxyanisole (BHA), propyl gallate (PG), octyl gallate (OG) and dodecyl gallate (DG). We have also studied the analytical behaviour of nordihydroguaiaretic acid (NDGA), an antioxidant that is forbidden in France but permitted in certain EEC countries, and of the methyl, ethyl and propyl esters of *p*-hydroxybenzoic acid (MHB, EHB and PHB, respectively) which are conservation agents often used in conjunction with the antioxidants listed above (and able to interfere in their determination).

The determination of antioxidants is difficult partly because they are used at low concentration and often dispersed in a complex matrix, and partly because the chemical similarity of some of these compounds may result in mutual interference when a mixture of them is present.

In an earlier work, a method of identifying these compounds by "nanochromatography" on thin layers of silica gel and reversed-phase

RP₁₈ was proposed.² Since the reversed-phase system gave the better performance, we decided to adapt it for an HPLC separation. There are already numerous such systems available for the purpose,³⁻¹⁰ but they are generally concerned with mixtures of only a few of these antioxidants. Ultraviolet spectrometry has generally been used for detection in analysis for these compounds by HPLC,³⁻¹⁰ but electrochemical detection can also be used for the phenolic antioxidants.¹¹ The optimal conditions for determination of each antioxidant have been studied by both methods. For the electrochemical method a preliminary study by anodic voltammetry is necessary. Only Kitada *et al.*¹² and Masoud and Cha¹³ seem to have used both methods in series, and then only for BHA and BHT.

EXPERIMENTAL

Apparatus

A Waters liquid-phase chromatograph equipped with two M₅₁₀ pumps operating at constant rate was used with a Waters M₆₈₀ gradient elution programme, a 20- μl injection loop, a Shimadzu SPD-6 AV ultraviolet detector set at 280 nm and 0.8 absorbance full scale, and a Shimadzu CR-3 A integrating recorder (speed 5 mm/min). A 15 cm \times 3.9 mm Waters 5 μm C₁₈ Resolve column was used, with elution at room temperature by a 35.65 v/v water-methanol mixture (adjusted to pH 5.5 with 0.01% phosphoric acid) at 0.8 ml/min for 6 min, then a convex gradient (profile No. 2) to pure

methanol in 9 min (at 0.8 ml/min) and finally pure methanol at 1.5 ml/min for 5 min.

For electrochemical detection a Tacussel DELC detector was used, comprised of a DEL 1 electrochemical cell with solid electrodes for thin-layer work, together with a PRG-DEL amperometric unit consisting of a potentiostat and current-measurement and attenuation circuits. A pyrolytic glassy-carbon working electrode, an Ag/AgCl (saturated KCl/AgCl) reference electrode and a platinum disc auxiliary electrode were used. The dead volume was 0.2 μ l.

The electrochemical detector was placed after the ultraviolet detector and connected to a potentiometric recorder (speed 5 mm/min).

Reagents

The reference compounds were obtained from Merck (AA), Sigma (DL- α T) and Fluka (for the rest), and used to prepare 0.01M solutions in methanol (Prolabo "Rectapur"). When protected from light and kept in a cold-room, these solutions were stable for about 24 hr, except for the ascorbic acid solution, which had to be freshly prepared before use. The solutions were diluted as required, with eluent previously adjusted to pH 5.5 to ensure that the compounds were all in undissociated form.

Eluents

The use of electrochemical detection necessitated the addition of lithium perchlorate, at 0.01M concentration, to the eluents, two of which were used. A, 0.01M lithium perchlorate in water-methanol, 35.65 v/v, pH 5.5, and B, 0.01M lithium perchlorate in methanol, pH 5.5.

Detection conditions

For determination by ultraviolet detection, each compound was measured (peak-area method) at its wavelength of maximum absorption. For electrochemical detection, the hydrodynamic voltamperograms were recorded with increasing potential applied to the working electrode until a peak of maximal intensity was obtained (Fig. 1). The peak height was used for the determination, since it was as accurate as the peak area, and more convenient.

RESULTS AND DISCUSSION

Qualitative analysis

The chromatogram obtained by ultraviolet detection for the mixture of all twelve compounds is shown in Fig. 2. All are well separated except for the PG-MHB pair. The values of the retention (t_R and k') and separation (α and R_S) parameters confirm that the separation obtained is qualitatively satisfactory. The k' values range between 1 and 15, and those of α and R_S are all greater than 1, except for the pair that is not separated. The retention times are given in the caption to Fig. 2. Ascorbic acid is well separated from the other antioxidants, but is not retained by the stationary phase.

The repeatability and reproducibility were determined with a mixture of all twelve antioxidants, with or without an internal standard (0.05% acenaphthene solution in methanol, t_R 12.03 min) and were calculated as the coefficients of variation of the absolute and relative retention times of the compounds. Good results were obtained, the repeatability being

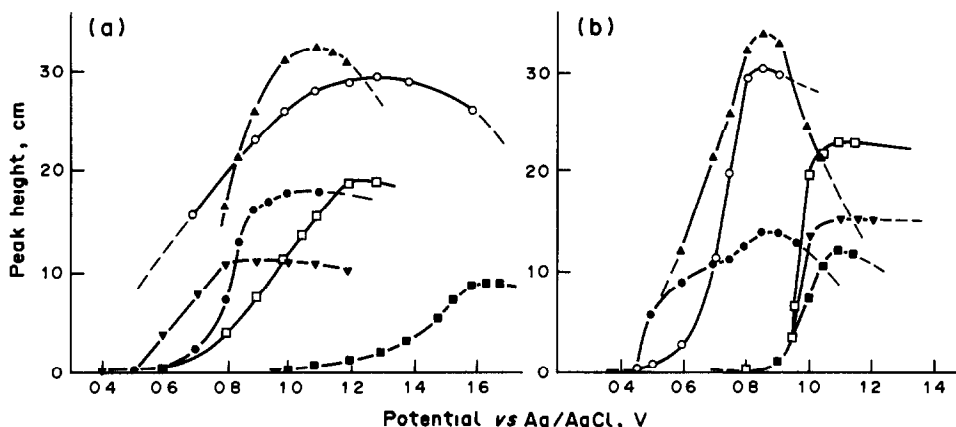


Fig. 1 Hydrodynamic voltamperograms obtained under the conditions for calibration. Detector sensitivity settings are given in parentheses: (a) PG, $2 \times 10^{-5}M$ (0.25 nA/cm), ● OG, $2 \times 10^{-5}M$ (0.25 nA/cm), □ DG, $2 \times 10^{-5}M$ (0.25 nA/cm), ▲ BHA, $10^{-5}M$ (0.125 nA/cm), ■ BHT, $10^{-5}M$ (0.50 nA/cm), ○ α T, $1.6 \times 10^{-5}M$ (0.05 nA/cm) (b) ▲ AA, $10^{-4}M$, ● AP, $10^{-3}M$, ■ MHB, $10^{-3}M$, ▼ EHB, $10^{-4}M$, □ PHB, $10^{-4}M$, ○ NDGA, $7 \times 10^{-5}M$ (all 0.25 nA/cm).

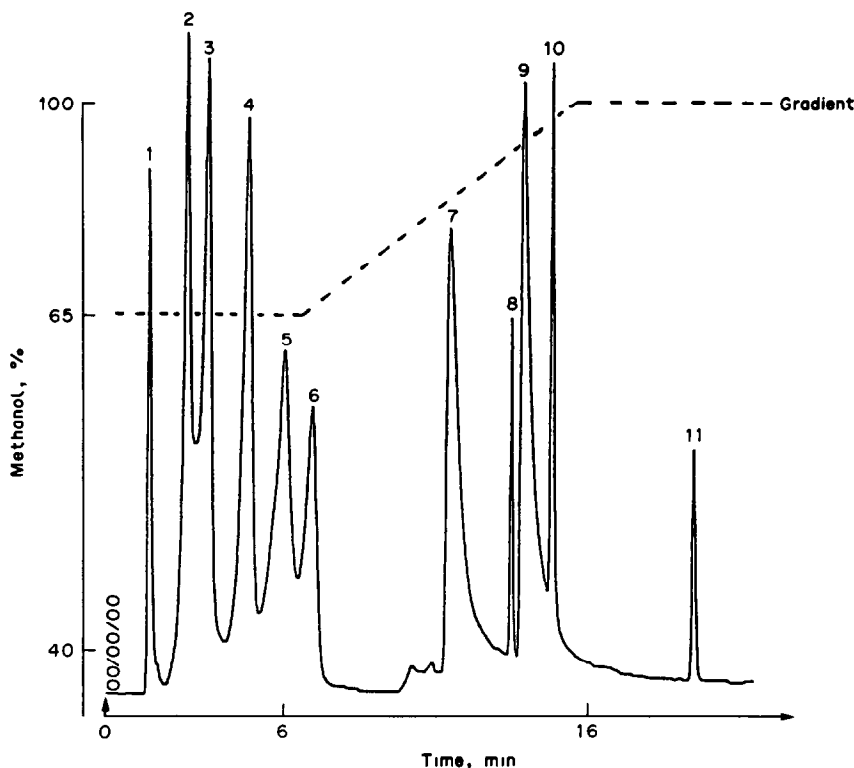


Fig 2 Chromatographic separation of the 12 antioxidants, on a $5 \mu\text{m}$ C_{18} resolve column with a 35:65 v/v water-methanol eluent (pH 5.5) for 6 min, followed by a convex gradient to pure methanol in the next 9 min, both at a flow-rate of 0.8 ml/min, then elution with methanol at 1.5 ml/min for 5 min. Detection at 280 nm. Peaks and retention times (min): 1, AA (1.28), 2, PG-MHB (2.51), 3, EHB (3.21), 4, PHB (4.54), 5, NDGA (5.71), 6, BHA (6.63), 7, OG (10.96), 8, BHT (12.98), 9, DG (13.36), 10, AP (14.36), 11, αT (18.51).

between 0.1 and 2.4% and the reproducibility between 0.1 and 3.2%. Use of the internal standard improved the precision.

The method permits rapid identification of eleven antioxidants in a mixture. In practice, such complicated mixtures would never be met, and only one, or at most a mixture of two or three, of the compounds would be encountered. It is therefore quite easy to adapt the system for quantitative use.

Quantitative analysis

The twelve compounds studied can all be detected by both methods. The electrochemical studies showed that they gave well defined waves, except for the gallate and *p*-hydroxybenzoate esters, which exhibited adsorption and film formation on the electrode. It appears that the ester group is responsible for this, as substitution of methyl, methoxy or *tert*-butyl groups at positions 2 and/or 4 causes these phenomena to disappear. It should be noted, however, that these adsorption effects are not incompatible with use of the electrochemical detection.

For each antioxidant a calibration graph was obtained under the conditions listed in Table 1. The range of molar concentrations studied was chosen so that both modes of detection could be used. Each series was run on the same day, without repolishing of the electrode.

The performance characteristics¹⁴ of the method for each of the twelve compounds are given in Table 2. The linearity of calibration is very good for both detection modes: the coefficients of variation are between 0.3 and 3.1%. The limit of detection is taken as the concentration equivalent to a signal equal to three times the standard deviation of the blank,¹⁵ measured at the maximum sensitivity of the detector (0.001 absorbance full scale, or 0.5–2 nA).

For most of the antioxidants studied, the ultraviolet detection gives better sensitivity than the electrochemical detection, except for PG and NDGA, for which the detection limits are the same by both techniques. Figure 3 compares the limits of detection obtained for PHB by both methods.

Table 1 Conditions for calibration plots (established with $5 \times 10^{-4}M$ antioxidant)

Antioxidant	Eluent	Flow-rate, ml/min	λ , nm	$E_{1/2}^*$, V vs SCE	E , V vs Ag/AgCl	t_R , min
AA	A	0.6	249	0.50	0.85	1.6
PG	A	1.2	274	0.40	0.80	1.8
MHB	A	1	256	0.80	1.10	1.9
EHB	A	1.2	256	0.85	1.10	2.2
PHB	A	1.2	256	0.85	1.10	3.5
NDGA	A	1.2	282	0.45	0.85	4.2
BHA	B	0.5	288	0.68	1.10	2.8
OG	B	1.3	274	0.50	0.95	1.1
BHT	B	0.5	276	1.05	1.70	3.5
DG	B	1.3	274	0.55	1.20	1.5
AP	B	1	248	0.45†	0.85	1.9
α T	B	2	291	0.50†	1.20	4.3

Eluent A 0.01M LiClO₄ in water-methanol, 35:65 v/v, pH 5.5

Eluent B 0.01M LiClO₄ in methanol, pH 5.5

Glassy-carbon working electrode

*Supporting electrolyte 0.01M K₂HPO₄-methanol (1:1), pH 5.7

†Supporting electrolyte 0.01M K₂HPO₄-methanol (1:3), pH 5.7

Comparison of the limits of detection with those reported in the literature, allowing for the difference in conditions used, between one author and another, shows that our values obtained by ultraviolet detection are lower than those found by others, and those obtained by electrochemical detection are lower than those reported by Kitada *et al.*,¹² Masoud and Cha,¹³ and King *et al.*¹⁶

Practical application

As already said, there will generally be not

more than three of the compounds present simultaneously, so they can first be identified by means of the qualitative system, and then determined under the optimal conditions (flow-rate of eluent for use under isocratic conditions, wavelength, applied potential, *etc.*) for the particular combination present. If a gradient elution must be used, then only ultraviolet detection should be used.

It should be noted that the range of electroactivity of the classical eluents does not allow electrochemical detection of BHT. However,

Table 2 Performance characteristics

Antioxidant	Linearity range, M	Regression equation	Correlation coefficient	Coefficient of variation, %	Detection limits, μ g
AA	$1 \times 10^{-4} - 1 \times 10^{-5}$	$Y = 162.2X - 245.7$ $Y' = 0.170X - 0.981$	0.9999 0.9999	2.0 2.4	176 3.52×10^3
PG	$2 \times 10^{-5} - 2 \times 10^{-6}$	$Y = 93.0X + 82.3$ $Y' = 0.277X + 0.225$	0.9993 0.9998	1.9 2.9	4.24×10^3 4.24×10^3
MHB	$1 \times 10^{-4} - 1 \times 10^{-5}$	$Y = 208.4X + 80.9$ $Y' = 0.0601X + 0.519$	0.9999 0.9999	0.3 2.2	61 6.08×10^3
EHB	$1 \times 10^{-4} - 1 \times 10^{-5}$	$Y = 152.1X + 227.7$ $Y' = 0.0755X - 0.658$	0.9999 0.9999	0.5 1.9	66 6.64×10^3
PHB	$1 \times 10^{-4} - 1 \times 10^{-5}$	$Y = 169.5X + 609.2$ $Y' = 0.110X - 0.546$	0.9999 0.9999	0.6 1.3	72 3.600×10^3
NDGA	$7 \times 10^{-5} - 7 \times 10^{-6}$	$Y = 60.830X - 155.9$ $Y' = 0.216X - 0.133$	0.9998 0.9999	2.4 3.1	1.21×10^3 1.21×10^3
BHA	$1 \times 10^{-5} - 1 \times 10^{-6}$	$Y = 124.1X + 15.55$ $Y' = 1.622X + 0.172$	0.9999 0.9999	1.0 1.5	180 360
OG	$2 \times 10^{-5} - 2 \times 10^{-6}$	$Y = 117.8X - 68.6$ $Y' = 0.424X + 0.180$	0.9999 0.9999	1.2 0.3	282 2.82×10^3
BHT	$1 \times 10^{-5} - 1 \times 10^{-6}$	$Y = 461.1X - 52.7$ $Y' = 0.442X + 0.150$	0.9999 0.9999	0.4 1.6	440 2.20×10^3
DG	$2 \times 10^{-5} - 2 \times 10^{-6}$	$Y = 98.6X - 69.9$ $Y' = 0.465X - 0.795$	0.9996 0.9999	1.7 1.9	676 3.38×10^3
AP	$1 \times 10^{-5} - 2 \times 10^{-6}$	$Y = 96.3X + 49.5$ $Y' = 0.678X + 1.742$	0.9998 0.9995	1.3 2.0	828 1.66×10^3
α T	$1.6 \times 10^{-5} - 2 \times 10^{-6}$	$Y = 15.1X - 33.2$ $Y' = 0.880X - 1.642$	0.9998 0.9999	1.6 1.7	3.45×10^3 4.31×10^3

X = amount injected, μ mole

Y = peak area (ultraviolet detector), mm ,

Y' = peak area (electrochemical detector), mm^2

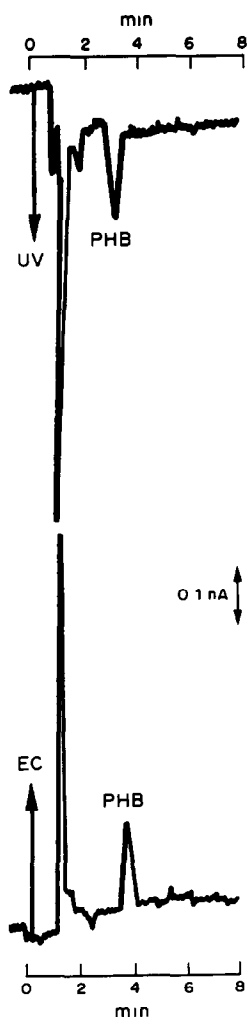


Fig 3 Limits of detection for PHB by ultraviolet detection (72 pg) and electrochemical detection (3.6 ng). Water-methanol 35:65 v/v, pH 5.5, 0.01M LiClO₄ at 1.2 ml/min, $\lambda = 256$ nm (0.001 absorbance full scale), $E = +1.1$ V (vs Ag/AgCl)

eluent B is usable up to +1.8 V, permitting determination of BHT. Figure 4 shows that at a potential of +1.7 V with this eluent, the baseline drift is very small. As far as we know, a potential as high as this is never normally needed in practice¹⁷⁻¹⁹

Conclusions

Electrochemical detection is a very useful complement to ultraviolet detection in the analysis of mixtures which pose interference problems that cannot be resolved spectrally. It is also sensitive enough for routine analysis.

The detection limits obtained for the antioxidants studied are well below the concentrations permitted for use in preservation of food and drugs. The reliability and selectivity of the tech-

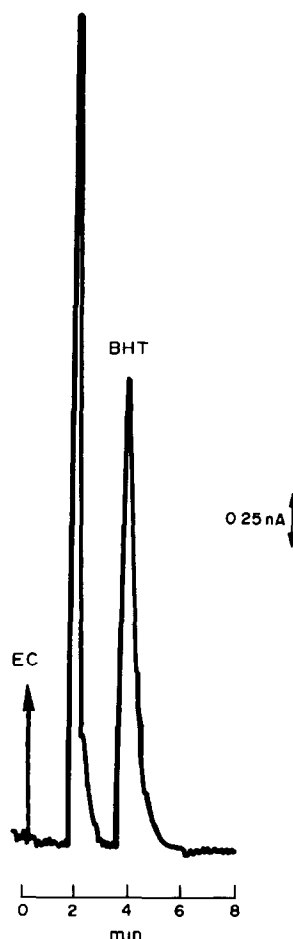


Fig 4 Electrochemical detection of BHT (44 ng). $E = +1.7$ V (vs Ag/AgCl), methanol, pH 5.5, 0.01M LiClO₄, at 0.5 ml/min

nique make it applicable for control of antioxidants in a wide variety of samples, but the operating conditions should be adjusted to be optimal for the problem in hand.

REFERENCES

- 1 J. Alary and C. Grosset, *Bull. Trav. Soc. Pharm. Lyon*, 1982, **26**, 80
- 2 J. Alary, C. Grosset and A. Coeur, *Ann. Pharm. Fr.*, 1982, **40**, 301
- 3 A. W. Archer, *Anal. Chim. Acta*, 1981, **128**, 235
- 4 R. Galensa, *Z. Lebensm. Unters. Forsch.*, 1984, **178**, 475
- 5 R. Galensa and F. I. Schafers, *Dtsch. Lebensm. Rundsch.*, 1982, **78**, 258
- 6 C. E. Graciani, *Grasas Aceites (Seville)*, 1975, **26**, 150
- 7 K. J. Hammond, *J. Assoc. Publ. Analysts*, 1978, **16**, 17
- 8 B. D. Page, *J. Assoc. Off. Anal. Chem.*, 1979, **62**, 1239
- 9 *Idem, ibid.*, 1983, **66**, 727
- 10 F. M. Pujol and S. Lopez, *Circ. Farm.*, 1984, **42**, 3
- 11 B. Fleet and C. J. Little, *J. Chromatog. Sci.*, 1974, **12**, 747

- 12 Y Kitada, Y Ueda, M Yamamoto, K Shinomiya and H Nakazawa, *J Liq Chromotog* 1958, **8**, 47
- 13 A N Masoud and Y N Cha, *JHRC & CC*, 1982, **5**, 299
- 14 D Lecompte, *STP Pharma*, 1986, No 2, 843
- 15 Analytical Methods Committee, *Analyst*, 1987, **112**, 199
- 16 W P King, K T Joseph and P T Kissinger, *J Assoc Off Anal Chem*, 1980, **63**, 137
- 17 G E Hayes and D E Hillman, *J Chromatog*, 1985, **322**, 376
- 18 P Leroy, V Leyendecker, A Nicolas and C Garret, *Ann Fals Exp Chim*, 1986, **79**, 283
- 19 K Štulík and V Pacáková, *CRC Crit Rev Anal Chem*, 1984, **14**, 297

INVESTIGATION OF MATERIALS FOR MAKING A CARBON-SUPPORT ZINC-SELECTIVE ELECTRODE

M J ROCHELEAU and W C PURDY*

Department of Chemistry, McGill University, Montreal, Quebec, Canada H3A 2K6

(Received 15 July 1989 Revised 1 September 1989 Accepted 28 September 1989)

Summary—The usefulness of zinc orthophosphate and zinc mercuric thiocyanate to make a carbon-support electrode responsive to zinc was investigated. The best results were obtained with zinc orthophosphate, which produced a Nernstian response to zinc in the concentration range from 10^{-5} to $10^{-2}M$. The electrode response was lowered by the formation of acidic oxides on the surface of the electrode. Different ways of minimizing this problem are discussed. Interference effects from copper(II) ($K_{Zn}^{pot} = 1.0$), cadmium ($K_{Zn}^{pot} = 8.9$) and lead ($K_{Zn}^{pot} = 10$) were observed.

In the field of ion-selective electrodes, there have been only a few reports of zinc(II)-selective electrodes.¹⁻¹⁰ Those based on ion-exchangers or chelates¹⁻⁶ gave poor selectivity and therefore suffered strong interference effects. Zinc solid-state electrodes based on zinc sulfide, telluride or selenide⁷⁻⁹ were found to be of limited usefulness, owing to their lack of stability and selectivity. Similarly, a "Selectrode" impregnated with a tetracyanoethylene polymer containing zinc showed limited sensitivity towards zinc, and long response time.¹⁰

In light of the poor selectivity displayed by organic ion-exchangers and chelating agents for zinc ions, the usefulness of some insoluble inorganic materials for the determination of zinc was considered. Zinc orthophosphate and zinc mercuric thiocyanate, which are both more stable than zinc sulfide, telluride or selenide on exposure to light and air, were therefore selected. A carbon-support electrode was used, since its simple and robust construction allows easy renewal of the ion-sensitive surface. It is therefore especially well suited for testing new materials.

THEORY

In the early seventies, Růžička and Lamm¹¹ introduced a new type of solid-state electrode based on a solid carbon support, they named this solid-state electrode a "Selectrode". They found that insoluble compounds, such as silver

halides and metal sulfides, could be applied directly to the carbon surface to yield an ion-selective electrode which behaves similarly to an electrode of the second kind. The response of such an electrode can be described by the Nernst equation for metal cations, M^{n+} . At 25° the potential E , in mV, is given by

$$E = \text{constant} + \frac{59}{n} \log a_M$$

where a_M is the activity of the metal ion.

The sensitivity and limit of detection of this type of electrode depend on the composition and purity of the electroactive material employed and can reach the limits imposed by the solubility product of the electroactive compound. The presence of certain species may cause potential drifts because of changes in the membrane surface when these species enter the solid phase. The effect on the behavior of the electrode can be predicted by calculating the free-energies of formation of the compounds which can be formed from the interfering ions.¹²

The standard free-energy of formation of $M_m X_n$ in the reaction



is given by

$$\Delta G_f^\circ = -RT \ln K_{sp}$$

where R is the gas constant, T the absolute temperature, and K_{sp} the solubility product of the compound. That is, the standard free energy of formation is a logarithmic function of the solubility product of the material formed.

*Author for correspondence

EXPERIMENTAL

Apparatus and materials

Potentiometric measurements were made with a Fisher Accumet Model 805MP pH/ion meter A Servogor 120 recorder (BBC Goerz Metrawatt) was used to monitor potential drifts. All potential measurements were made with reference to a saturated calomel electrode (SCE). The solutions were maintained at 25° with a Heto Type 623 thermostatic bath (Heto, Denmark).

Graphite powder (ultra "F" purity) and spectrographic grade 6-mm thick graphite rods (available from Ultra-Carbon, Bay City, Michigan) were used. Zinc orthophosphate, $Zn_3(PO_4)_2 \cdot 4H_2O$, can be easily prepared by mixing appropriate volumes of solutions of $ZnSO_4 \cdot 7H_2O$ and $Na_2HPO_4 \cdot 2H_2O$ at the boiling point¹³. The crystalline precipitate which forms immediately is analytically pure and loses two molecules of water of crystallization when dried at 100°. Zinc mercuric thiocyanate, $ZnHg(SCN)_4$, was prepared by the reaction of a zinc salt with ammonium mercuric thiocyanate (prepared by mixing of mercuric chloride and ammonium thiocyanate solutions in stoichiometric ratio),¹⁴ and was dried for an hour at 100° before use.

Construction of the electrodes

Spectrographic graphite electrode. A 10-cm long graphite rod was cleaned by soaking overnight in 6M hydrochloric acid, and dried in an oven at 120° for an hour. A metal spring was fitted over one end of the rod to make the electrical connection (Fig. 1a). The graphite rod and connector were then inserted into a length of heat-shrink tubing and sealed into it with PVC at the other end to prevent seepage of test solution. The bare tip was cleaned and roughened with sandpaper, then coated with electroactive material by applying and rubbing in the dry powder. The thin layer of material was hand-polished on a hot (100°) stainless-steel surface. The graphite was made hydrophobic by impregnation with carbon tetrachloride. Mixtures of electroactive materials were prepared by mixing the powders with a mortar and pestle.

Carbon-paste electrodes. Carbon pastes were obtained by mixing the graphite powder and paraffin oil in the ratio 5:1 w/v or the graphite powder and paraffin wax in the ratio 3:1 w/w. The ion-selective pastes were prepared by mixing the carbon paste and the electroactive

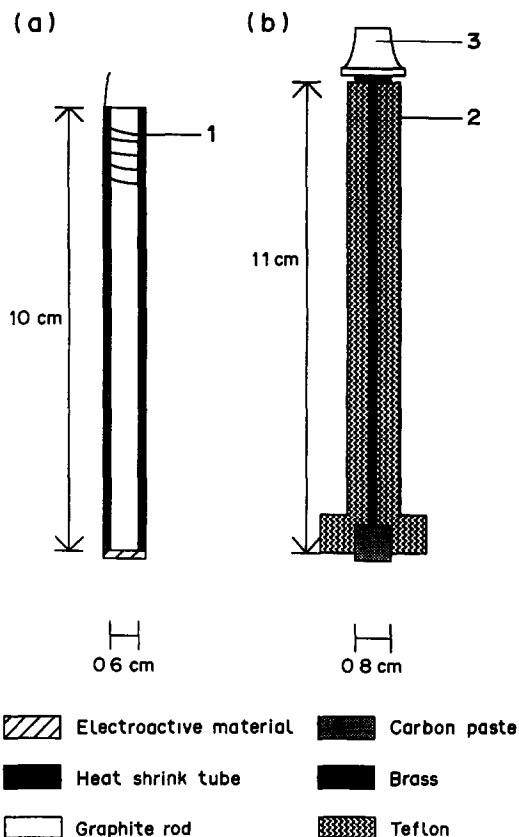


Fig 1 (a) Graphite electrode. The graphite rod is inserted in a poly(vinyl chloride) heat shrink tube. The electroactive material is coated at the tip of the electrode and the electrical contact is effected with a metal wire spring (1). (b) Carbon paste electrode. The activated carbon paste is packed in the well of the Adams pool electrode. The body (2) of the electrode is made of Teflon and contact between the paste and the connection jack (3) is made by a brass rod.

materials in 70:30 ratio. The active carbon paste was packed in the well of an Adams pool electrode (Fig. 1b) and a smooth surface was obtained by polishing on a piece of filter paper.

Calibration

Calibration graphs were obtained for unbuffered solutions containing zinc in concentrations ranging from 10^{-6} to $10^{-1}M$. The ionic strength was set at 0.1M with potassium nitrate or sodium chloride solution. The electrodes thus prepared were also tested as sensors in zinc solutions prepared in distilled demineralized water.

RESULTS AND DISCUSSION

Graphite conditioning

The graphite support acts as the conductive inert body of the electrode and it should not play any other part in establishment of the

measured potentials. Graphite is well-known for its non-ideal and poorly reproducible pH-sensitivity and memory effects, reflected by irreproducibility of measurements. It was found here that graphite exhibits pH-sensitivity because of the presence of chemisorbed oxygen on its surface¹⁵ This problem must then be overcome because of the requirement for inertness of the graphite body Růžicka and Lamm¹¹ proposed dealing with this problem by making the graphite hydrophobic by impregnation with hydrocarbons or using a carbon/Teflon mixture¹⁵ (which is unfortunately not easily available commercially) Materials such as poly(vinyl chloride) and paraffin wax can also be used for this purpose.

East and Da Silva¹⁶ demonstrated that hydrophobized spectro-grade graphite is still responsive to pH and proposed the use of the Williamson synthesis, known as an irreversible route to ethers, to modify the acidic carboxyl groups found at the graphite surface, and thus reduce the pH-sensitivity of the graphite support. This simple synthesis consists of the reduction of the acidic groups at the graphite surface with lithium aluminium hydride and methylation of the reduced groups with dimethyl sulphate The procedure is quite effective and the graphite body was found insensitive to the pH of the test solution in the range 4–10.

Choice of electroactive materials

The solid electroactive materials should have the following properties. low solubility in water ($pK_{sp} > 6$), ion-exchange at selective functional groups, and sufficient conductivity. Zinc orthophosphate and zinc mercuric thiocyanate were therefore selected for this study

Response characteristics of the graphite electrode coated with zinc orthophosphate

The electrode coated with zinc orthophosphate showed a linear response to zinc activity in the concentration range from 10^{-5} to $10^{-2}M$, with a Nernstian slope of 28.9 ± 0.8 mV/decade (Fig. 2a) A delay of 60 sec was required to attain a steady-state potential reading. A limit of detection of $5.5 \times 10^{-6}M$ was obtained, which compares favorably with the limits of detection of the zinc selective electrodes previously reported¹⁻¹⁰

The use of 0.1M potassium nitrate or sodium chloride to maintain constant ionic strength decreased the limit of detection. A significant downward potential shift was observed when

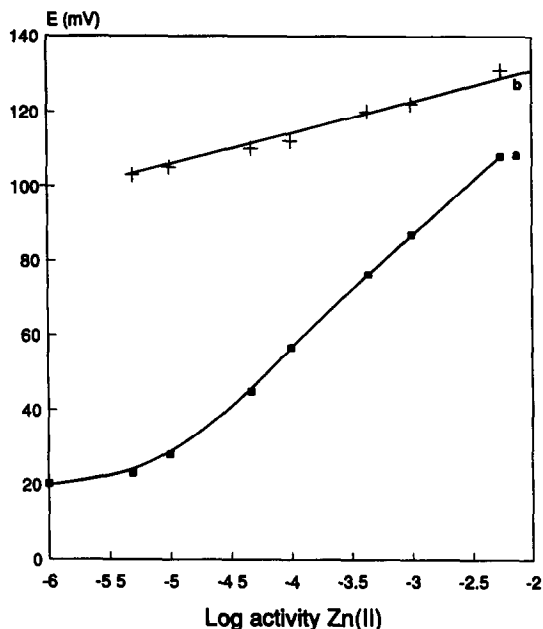


Fig 2 (a) Response of the zinc orthophosphate graphite electrode The straight-line portion has a slope of 29 mV/decade (b) Response of the same electrode after exposure to an acidic solution (at pH 3.0) of zinc (1mM)

sodium chloride was used, because zinc can form soluble complexes with chloride, which would reduce the zinc activity in solution.¹⁷

After a few days of storage (dry or in solution), the electrode showed a strong shift in potential of about 100 mV and reduced response. Brief exposure to moderately acidic solutions (pH < 3) or solutions of strong oxidants resulted in a similar shift in potential readings and a decrease in sensitivity (Fig. 2b) It was concluded that these discrepancies were due to the slow formation of acidic oxides at the electrode surface, which is known to be catalysed in acidic and oxidant solutions.¹⁴ These acidic groups are responsible for the pH-sensitivity of the electrode and reduce the sensitivity of the electrode towards zinc

The pH-sensitivity of the electrode can be minimized by hydrophobization with paraffin wax or poly(vinyl chloride), and the use of the Williamson synthesis to modify the acidic groups at the graphite surface. However, such pretreatments significantly reduce the electrode response to zinc, because of the increased impedance of the membrane.

Since it was observed that a graphite electrode impregnated with carbon tetrachloride and activated with silver sulfide had lower sensitivity to pH, mixtures of different ratios of zinc orthophosphate and silver sulfide (1:1, 3:1 and 9:1 w/w) were used to coat a graphite electrode. The

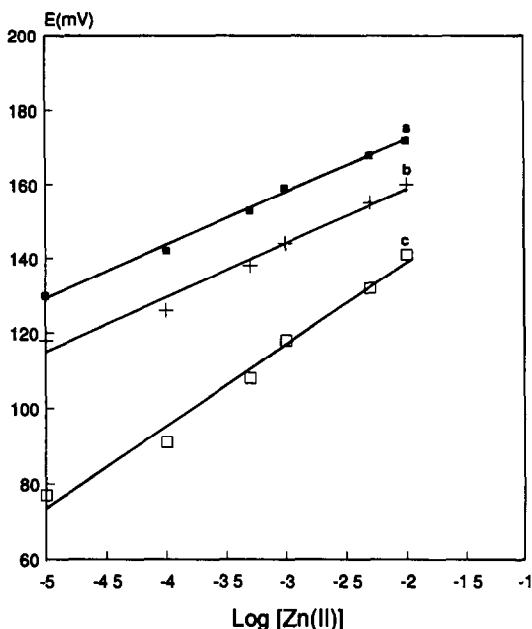


Fig 3 Response of the graphite electrode based on zinc orthophosphate and silver sulfide (a) 1:1 mixture (slope = 15 mV/decade), (b) 3:1 (slope = 17 mV/decade), (c) 9:1 (slope = 25 mV/decade)

use of silver sulfide also increases the conductivity of the membrane. The electrodes coated with the 1:1 and 3:1 mixtures had a low sensitivity to zinc. Better sensitivity was obtained with the graphite electrode coated with the 9:1 mixture (Fig. 3). The use of a mixture of zinc orthophosphate and silver sulfide helps to improve the stability of the electrode over a period of a few weeks, but frequent calibration of the electrode is still required, to compensate for the drifts observed.

Interestingly, the metathesis of most potentially interfering ions with zinc orthophosphate is not thermodynamically favorable (Table 1). This suggested that determination of

Table 1 Solubility products and values of free energy of formation of some orthophosphates

Species	Orthophosphates	Solubility product*	ΔG_f° , kcal/mole
Zn(II)	$Zn_3(PO_4)_2$	9.0×10^{-31}	43.7
Li(I)	Li_3PO_4	3.2×10^{-19}	25.2
Na(I)		(soluble)	
K(I)		(soluble)	
Mg(II)	$Mg_3(PO_4)_2$	1×10^{-23}	31.4
Ca(II)	$Ca_3(PO_4)_2$	2.0×10^{-29}	39.2
Ba(II)	$Ba_3(PO_4)_2$	3.4×10^{-23}	30.7
Cu(II)	$Cu_3(PO_4)_2$	1.3×10^{-37}	50.3
Cd(II)	$Cd_3(PO_4)_2$	2.5×10^{-33}	44.5
Pb(II)	$Pb_3(PO_4)_2$	8.0×10^{-43}	57.4
Ag(I)	Ag_3PO_4	1.4×10^{-16}	21.6

*From *Lange's Handbook of Chemistry*, 13th Ed., McGraw-Hill, New York, 1985, pp 5-7

Table 2 Selectivity coefficients for the zinc orthophosphate carbon-support electrode

Interfering cations	Selectivity coefficients
Li(I)	$< 1 \times 10^{-4}$
Na(I)	$< 1 \times 10^{-4}$
Mg(II)	0.072
Ca(II)	0.032
Ba(II)	0.21
Cu(II)	1.0
Cd(II)	8.9
Pb(II)	10

*Determined by the fixed interference method ([interferent] = 1 mM) and 0.1M KNO_3 was used in the salt bridge

zinc with this electrode would not significantly suffer from interferences. As predicted, the presence of alkali-metal and alkaline-earth metal ions did not significantly affect the electrode response (Table 2). However, the presence of some transition metals was found to interfere more significantly than expected. The presence of silver gave rise to very strong interference effects, particularly if a mixture of zinc orthophosphate and silver sulfide was used.

The selectivity of this electrode can be favorably compared to that of the zinc-selective electrodes based on ion-exchangers and chelating agents previously reported,^{1-6,10} which demonstrated poor selectivity in the presence of some alkaline-earth metal ions such as calcium.⁶ However, we observed a selectivity pattern similar to the one observed for other zinc solid-state electrodes,⁷⁻⁹ and the interferences caused by copper, cadmium, lead and silver still remain a problem.

Response characteristics of the graphite electrode coated with zinc mercuric thiocyanate

The zinc mercuric thiocyanate carbon-support electrode gave a limited linear response to zinc in the concentration range from 10^{-3} to $10^{-2}M$, with a sub-Nernstian slope of 23 mV/decade. The limit of detection ($2.5 \times 10^{-4}M$) was imposed by the solubility of zinc mercuric thiocyanate (Table 3).

Table 3 Limits of detection of the electrodes studied

Coating materials	pZn*	pD†
$Zn_3(PO_4)_2 \cdot 2H_2O$	6.7	5.3
$ZnHg(SCN_4)$	3.3	3.6

*Calculated from the solubility product of the activating material

†D = detection limit (mole/l)

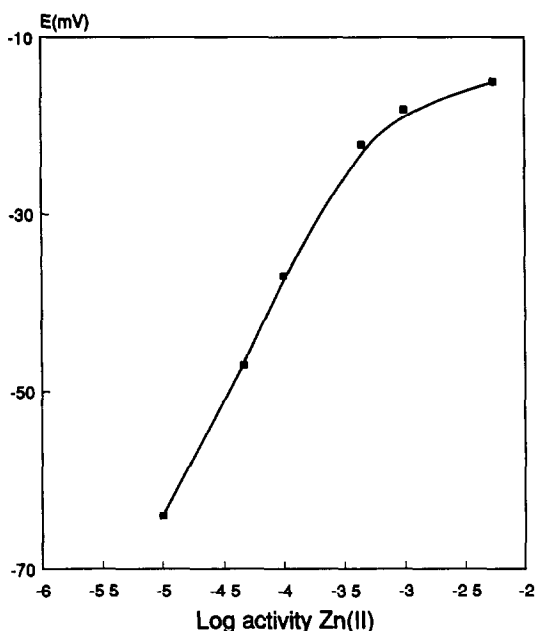


Fig 4 Response of the zinc orthophosphate carbon-paste electrode. The straight-line portion has a slope of 26 mV/decade

No significant potential shift was caused by storage.

Response characteristics of carbon-paste electrodes

The carbon-paste electrode was proposed as a useful alternative to the "Selectrode", to ease surface problems.¹⁸ However, the carbon paste must be sufficiently compressed to limit the formation of cracks at the electrode surface because of swelling. These cracks usually occur after prolonged pretreatment in solution, so this may seriously impair the electrode life.

The zinc orthophosphate carbon-paste electrode made with either paraffin wax or paraffin oil as a mulling agent showed a linear response at low zinc activity, which leveled off at concentrations above $1 \times 10^{-3} M$ (Fig. 4). According to the theory of the potentiometric response of ion-selective membrane electrodes, a Nernstian cation response is obtained only if the fluxes of all the anions within the membrane are minimized. An anion response can be observed in the presence of oil-soluble anions in the sample, owing to their significant extraction by the membrane at high concentrations.¹⁹ Of course, this response to co-ions seriously impairs the response to cations, as was observed in the present case.

Pretreatment with demineralized water or very dilute solutions of zinc nitrate or zinc sulfate is necessary to ensure sufficient membrane conductivity and to obtain a stable response. However, prolonged pretreatments cause the membrane to swell, followed by the formation of pores, which increases the non-selective mobility of ions in the membrane. This is confirmed by the total loss of selectivity exhibited when certain other cations are present in the test solutions. These carbon-paste electrodes for zinc are therefore of limited use.

Acknowledgement—The authors are indebted to the Natural Sciences and Engineering Research Council of Canada for financial support of this work

REFERENCES

- O A Lebedeva and E Jansons, *Latv PSR Zinat Akad Vestis, Kim Ser*, 1987, **4**, 483, *Chem Abstr*, 1987, **107**, 189732g
- A Viksna, E Jansons, S Pastare and A Klajse, *Otkrytiya, Izobret*, 1986, **15**, 154, *Chem Abstr*, 1986, **105**, 71788k
- A G Rodichev, T P Ushangishvili, V A Dolidze and V G Krunchak, *ibid*, 1986, **8**, 263, *Chem Abstr*, 1986, **104**, 218326y
- U Fiedler-Linnersund and K M Bhatti, *Anal Chim Acta*, 1979, **111**, 57
- M Uchida, E Ikeda, I Ohba and T Kashima, *Kyoryutsu Yakka Daigaku Kenkyu Nempo*, 1978, **23**, 19, *Chem Abstr*, 1979, **91**, 44573x
- L Gorton and U Fiedler, *Anal Chim Acta*, 1977, **90**, 233
- S Zhang, *Zhongguo Kexue Jishu Daxue Xuebao*, 1982, **12**, 124, *Chem Abstr*, 1983, **98**, 136652v
- A F Zhukov, A V Vishnyakov, Ya L Kharif, Yu I Urusov, F K Volynets, E I Ryzhikov and A V Gordievskii, *Zh Analit Khim*, 1975, **30**, 1761, *Chem Abstr*, 1976, **84**, 97045p
- H Hirata and K Higashiyama, *Talanta*, 1972, **19**, 391
- M Sharp, *Anal Chim Acta*, 1975, **76**, 165
- J Růžicka and C G Lamm, *ibid*, 1971, **53**, 206
- V M Jovanović and M S Jovanović, *ibid*, 1985, **176**, 285
- F Wagenecht and R Juza, in *Handbook of Preparative Inorganic Chemistry*, G Brauer (ed), 2nd Ed, Vol 2, p 1081 Academic Press, New York, 1965
- F D Snell and C L Hilton (eds), *Encyclopedia of Industrial Chemical Analysis*, Vol 5, p 148 Interscience, New York, 1967
- J Růžicka, C G Lamm and J Chr Tjell, *Anal Chim Acta*, 1972, **62**, 15
- G A East and I A Da Silva, *ibid*, 1983, **148**, 41
- G Scibona, F Orlandini and P R Danesi, *J Inorg Nucl Chem*, 1966, **28**, 1313
- Š. Mesarić and E A M F Dahmen, *Anal Chim Acta*, 1973, **64**, 431
- J H Boles and R P Buck, *Anal Chem*, 1973, **45**, 2057

POTENTIOMETRIC FLOW-INJECTION DETERMINATION OF IODIDE AND IODINE

DAVID E DAVEY, DENNIS E. MULCAHY and GREGORY R. O'CONNELL

School of Chemical Technology, S A Institute of Technology, P O Box 1, Ingle Farm, South Australia, 5098

(Received 9 August 1988 Revised 4 July 1989 Accepted 29 September 1989)

Summary—A potentiometric flow-injection system is described, in which iodide in the concentration range 10^{-6} – $10^{-1}M$ may be determined at rates of up to 360 samples/hr at a flow-rate of 17.8 ml/min. Iodine, after on-line reduction to iodide with 0.1M sodium metabisulphite, can also be determined, with a throughput of 60 samples/hr for 10^{-5} – $10^{-3}M$ iodine. Analyses of two pharmaceutical preparations for iodide and iodine are reported, and the results are in reasonable agreement with titrimetric values.

There are three reports in the literature, on measurements made with iodide electrodes in FIA. Trojanowicz and Matuszewski¹ used a sensor prepared by electro-deposition of silver iodide on silver, and noted that adsorption at the surface of the electrode led to significant reductions in the limit of detection. Trojanowicz *et al.*² described a flow manifold in which a similarly prepared silver iodide electrode was used to determine chlorine in tap water by monitoring changes in the equilibrium between iodide and iodine. Müller³ employed a differential detector cell comprising two flow-through solid-state iodide sensors, to determine iodide, cyanide, tungsten(VI) and molybdenum(VI). After separation on an appropriate anion-exchange column, chloride, bromide and thiocyanate were also determined.

In the present study, a commercially available homogeneous membrane iodide-selective electrode⁴ was calibrated over a much wider concentration range than those previously reported, with emphasis on the effect of pH on the response characteristics. The feasibility of determining iodine by use of a mild reductant solution was also assessed. The flow system was then used to determine iodide and iodine in two pharmaceutical preparations, the results being compared with those obtained by argentimetric and iodometric titrimetry.

EXPERIMENTAL

Apparatus

The flow-injection manifold and detector cell used are depicted in Fig. 1. A Gilson Minipuls

2 peristaltic pump was used with Tygon pump tubes, and the components of the system were linked by a network of polypropylene connectors and 0.5-mm i.d. PTFE tubing.

The sampling device was a Rheodyne 5041 4-way rotary valve driven by a Festo DSN-10-25P pneumatic actuator. A 110- μ l sample loop was found to provide the best combination of response time and sensitivity. The unit was activated by a Rheodyne 7163 solenoid unit and all switching sequences were controlled by an

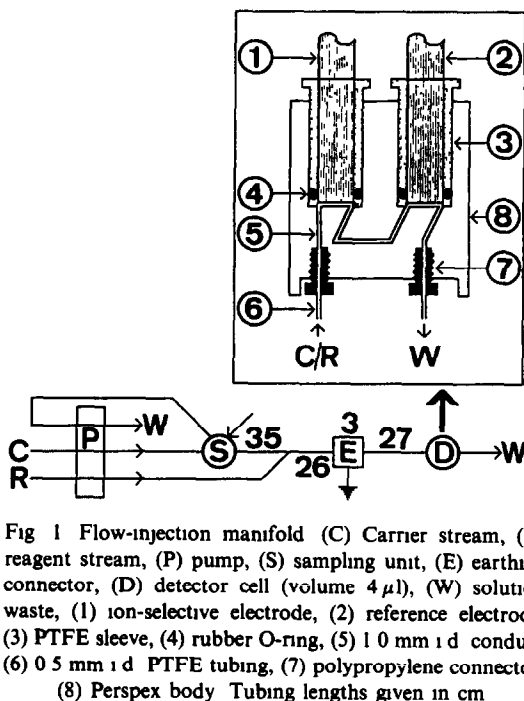


Fig 1 Flow-injection manifold (C) Carrier stream, (R) reagent stream, (P) pump, (S) sampling unit, (E) earthing connector, (D) detector cell (volume 4 μ l), (W) solution waste, (1) ion-selective electrode, (2) reference electrode, (3) PTFE sleeve, (4) rubber O-ring, (5) 1.0 mm i.d. conduit, (6) 0.5 mm i.d. PTFE tubing, (7) polypropylene connector, (8) Perspex body. Tubing lengths given in cm.

MC6802 microprocessor-based Datum timer (Gammatron, Pooraka, S.A)

An Orion 94-06A AgI/Ag₂S electrode was used with a 90-02 double-junction reference electrode filled with Orion internal (90-00-02) and external (90-00-03) solutions. All potentiometric measurements were made with an Orion 701A digital pH/mV-meter connected to an MFE 2115M variable-scan pen-recorder through a home-made offset unit⁵

Reagents

Iodide standards and carrier solutions were prepared from analytical grade potassium iodide; the carrier stream for all studies reported here was made at least $10^{-6}M$ in iodide to minimize baseline drift.^{1,6} Electrostatic noise in the flow system was suppressed by use of a 0.1M potassium chloride reagent stream unless otherwise stated.

For the study of pH effects, the iodide standards and carriers were mixed with equivalent volumes of buffers prepared from analytical grade potassium tetroxalate (pH 2.15), laboratory-reagent grade potassium hydrogen phthalate (pH 4.02), analytical grade potassium hydrogen and dihydrogen phosphates (pH 6.82), and analytical grade sodium tetraborate (pH 8.92).⁷

A 0.05M iodine stock solution was made by dissolving 12.7 g of resublimed iodine in a solution of 20 g of potassium iodide in 30 ml of conductivity water, and diluting the solution to 1 litre.⁸ Analytical grade sodium metabisulphite and sodium thiosulphate, and laboratory-reagent grade ascorbic acid were assessed as reductants for use in the iodine determination.

Argentimetric titrations were performed with 4',5'-di-iodo-2',7'-dimethylfluorescein solution in 70% ethanol as adsorption indicator⁹ "Iotect" indicator (May and Baker) was used in titrations of iodine with thiosulphate.

Pharmaceutical preparations

The pharmaceuticals analysed were "Betadine" antiseptic (Faulding, Thebarton, S.A.), an ethanolic solution of povidone-iodine complex, and "Iodine Colourless BPC34" (Chem-Mart, Thebarton, S.A.), a solution of ammonium iodide in ethanol. To minimize the effects of the organic solvent on the electrode response¹⁰ and of the sample viscosity on dispersion within the flow manifold,¹¹ both preparations were diluted by a factor of 10^4 with conductivity water.

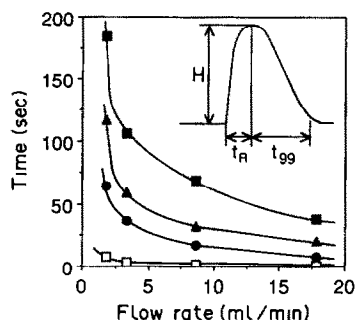


Fig. 2. Effect of carrier stream iodide level and total flow-rate (Q) on response time (t_R) and 99% baseline recovery time (t_{99}) for an injected iodide standard (concentration 1000 times that of the carrier iodide concentration) (■) t_{99} for $10^{-6}M$, (▲) $10^{-5}M$ and (●) $10^{-4}M$ KI carrier streams, (□) t_R for all three carriers Reagent stream 0.1M KCl throughout

RESULTS AND DISCUSSION

Calibration with iodide standards

The Orion electrode exhibited Nernstian response over a wide concentration range, the limit of linearity depending solely on the iodide concentration in the carrier. This behaviour has been discussed at length elsewhere.¹ For standards injected into a $10^{-6}M$ potassium iodide carrier/0.1M potassium chloride reagent stream, the lower limit of linearity was $5 \times 10^{-6}M$, below the $2 \times 10^{-5}M$ reported by Trojanowicz and Matuszewski for their home-made iodide sensor.¹ The sample throughput of 360/hr was attained with full return to baseline between peaks, and excellent peak-height repeatability, at a flow-rate of 17.8 ml/min through the detector cell. Alexander and Seegopaul¹² achieved the same sampling rate with an air-segmented continuous-flow system, but observed about 1% carry-over between successive standards.

Effect of flow-rate and iodide concentration in the carrier

The electrode response characteristics are summarized in Fig. 2. For standards injected into a given carrier stream, both the response time (t_R) and the time for 99% return to baseline (t_{99}) were found to decrease as the flow-rate was increased, the peak-height remaining essentially constant. Increasing the iodide level in the carrier reduced t_{99} significantly, but did not affect t_R , and the peak-height was enhanced by about 17% when the carrier iodide level was increased from 10^{-6} to $10^{-4}M$.

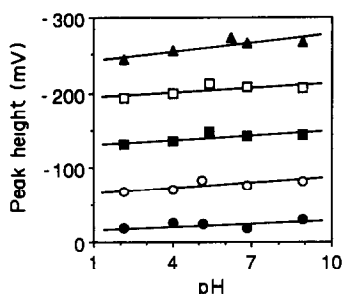


Fig 3 Effect of pH buffers on electrode calibration in iodide standards (●) $5 \times 10^{-6}M$, (○) $5 \times 10^{-5}M$, (■) $5 \times 10^{-4}M$, (□) $5 \times 10^{-3}M$ and (▲) $5 \times 10^{-2}M$ KI standards injected into $10^{-6}M$ KI carrier/ $0.1M$ KCl reagent stream

In contrast to previous experience with fluoride electrodes,^{6,13} polishing the AgI/Ag₂S membrane with an alumina slurry did not seem to affect its performance to a marked degree, but proved invaluable in restoring sensor response after contact of the membrane with thiosulphate

Effect of pH on iodide calibration

The influence of pH on the calibration is summarized in Fig. 3. Increasing the pH shifted the baseline potential, the peak potentials remaining constant within experimental error. Peak height was therefore reduced and, hence, sensitivity decreased in the buffered systems. The sensor gave close to Nernstian response (60 ± 2 mV/decade) in all buffers for the concentration range of standards investigated. Response and recovery times were also similar for both unbuffered and buffered systems, but an increase in baseline noise was detected for the pH 8.92 carrier stream.

Choice of reductant for iodine determination

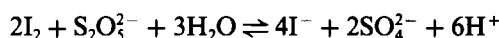
The iodide electrode can be applied to the determination of iodine provided that the determinand is first reduced to iodide. In steady-state procedures, the reductant is added some time before the measurement is made. Preliminary studies revealed that $0.1M$ solutions of ascorbic acid, sodium thiosulphate and sodium metabisulphite rapidly decolourized iodine solutions, suggesting that on-line addition of such reagents in FIA might prove successful

Each reductant was tested by injecting it into a $10^{-6}M$ carrier potassium iodide that was then merged with the $0.1M$ potassium chloride reagent stream. Thiosulphate yielded a considerably greater electrode response than that ex-

pected on the basis of the steady-state selectivity coefficient.¹⁴ Ascorbic acid gave much smaller signals than thiosulphate, but was subsequently rejected on account of the excessive baseline noise generated when it was used instead of potassium chloride in the reagent stream. In contrast, the iodide electrode showed negligible response to metabisulphite, and when this was used as the reagent stream in the flow-injection manifold, a concentration of $0.1M$ gave the best results in terms of reductive ability, speed of electrode response and reduction in electrostatic noise.

Calibration with iodine standards

The reduction of iodine by metabisulphite may be expressed by



To determine the extent of on-line reduction possible, iodine and iodide standards were injected into a $10^{-6}M$ potassium iodide carrier, which was then merged with a $0.1M$ sodium metabisulphite reagent stream. From peak-height data for the iodide standards, a calibration plot was constructed and used to interpret the calibration data for the iodine standards. The calibration plot gave the total iodide concentration detected as I^- by the electrode ($[I^-]_T$). The effective molar concentration of iodine determined by the flow-injection method was then calculated from

$$[I_2] = \frac{[I^-]_T - [I^-]_B}{2}$$

where $[I^-]_B$ is the iodide concentration arising from the use of potassium iodide in preparation of the iodine stock solution. The iodine concentrations thus obtained were compared with those derived by titration of the $5 \times 10^{-3}M$ iodine solution with iodate-standardized thiosulphate⁸ and are reported as percentage recoveries in Table 1. On-line reduction to iodide with

Table 1 Determination of iodine in standards after reduction with $0.1M$ Na₂S₂O₅

Iodine found by titration, M	Iodine found by FIA after reduction, M	Recovery, %
4.93×10^{-6}	2.68×10^{-6}	54
9.85×10^{-6}	8.30×10^{-6}	84
4.93×10^{-5}	4.43×10^{-5}	90
9.85×10^{-5}	9.29×10^{-5}	94
4.93×10^{-4}	4.93×10^{-4}	100
9.85×10^{-4}	9.77×10^{-4}	99
4.93×10^{-3}	4.93×10^{-3}	100

Table 2 Determination of iodide and iodine in pharmaceuticals

Experiment*	Determinand	Potentiometric FIA	Titrimetry	Nominal value
1	I ⁻	0.238 ± 0.014	0.2344 ± 0.0006†	0.225§
2	I ₂	0.042 ± 0.001	0.0403 ± 0.0004‡	0.0395
3	Free I ⁻ /I ₃ ⁻	0.072 ± 0.002	Not determined	

*1, Iodine Colourless BPC34, 0.1M KCl reagent stream, 2, Betadine antiseptic, 0.1M Na₂S₂O₃ reagent stream, 3, Betadine antiseptic, 0.1M KCl reagent stream

†Determination of iodide by titration with 0.1000M silver nitrate, by use of 4',5'-di-iodo-2',7'-dimethylfluorescein as adsorption indicator

‡Determination of iodine by titration with 0.1031M sodium thiosulphate (Iotect indicator)

§From description of Decolourized Iodine Solution BPC34 given by Wade¹⁶

||From manufacturer's claim

metabisulphite was thus analytically acceptable, the poor recovery for iodine concentrations below 10⁻⁵M setting the lower limit for use of the method.

When a 0.1M potassium chloride reagent stream was used, the recovery of iodine was very poor. The value of 38% recorded for the most dilute standard may be attributed to the electrode responding to the tri-iodide ion.

The characteristics of the peaks obtained for the iodine standards were similar to those for iodide, with the same *t_R* values within experimental error, but the *t₉₉* times were on average about 15% longer. A flow-rate of 8.6 ml/min permitted a sample throughput of 60/hr. Higher analysis rates would be possible with increased flow-rate or level of iodide in the carrier, or reduction in the sample volume injected.

Determination of iodide and iodine in pharmaceuticals

Aliquots of the 0.1 ml/l. solutions of Iodine Colourless BPC34 and Betadine were added to equivalent volumes of selected iodide standards, then injected into a 10⁻⁶M potassium iodide carrier, which merged with either 0.1M potassium chloride or 0.1M sodium metabisulphite downstream of the sampling unit. The data linearization technique devised by Rix *et al*¹⁵ was used for obtaining concentrations from the standard additions; the values derived from both the slope and intercept equations showed good correlation. Similar processing was used for the peak heights obtained for the Betadine solution. The results (Table 2) show reasonable agreement with those obtained by titrimetry.

Acknowledgements—The authors thank Messrs G Marsson, K Randell, P Stumbury and S Sweeney for technical support. G R O'Connell is grateful to S A I T for the award of a postgraduate scholarship.

REFERENCES

- 1 M Trojanowicz and W Matuszewski, *Anal Chim Acta*, 1982, **138**, 71
- 2 M Trojanowicz, W Matuszewski and A Hulanicki, *ibid*, 1982, **136**, 85
- 3 H Muller, in E Pungor (ed.) *Modern Trends in Analytical Chemistry, Part A Electrochemical Detection in Flow-Analysis*, pp 353–356 Elsevier, Amsterdam, 1984
- 4 M S Frant, J H Riseman and J W Ross, Jr., *US Patent* 3563874, 1971
- 5 D E Davey, D E Mulcahy and G R O'Connell, *J Chem Educ*, in the press
- 6 *Idem*, *Anal Lett*, 1986, **19**, 1387
- 7 A I Vogel, J Bassett, R C Denney, G H Jeffery and J Mendham (eds.), *Vogel's Textbook of Quantitative Inorganic Chemistry*, 4th Ed., pp 587–588 Longmans, London, 1978
- 8 *Idem*, *op cit*, pp 375–379
- 9 *Idem*, *op cit*, p 339
- 10 J F Coetzee and M W Martin, *Anal Chem*, 1980, **52**, 2412
- 11 D Betteridge, W C Cheng, E L Dagless, P David, T B Goad, D R Deans, D A Newton and T B Pierce, *Analyst*, 1983, **108**, 1
- 12 P W Alexander and P Seegopaul, *Anal Chem*, 1980, **52**, 2403
- 13 W J van Oort and E J J M van Eerd, *Anal Chim Acta*, 1983, **155**, 21
- 14 E Pungor, K Tóth and A Hrabéczy-Páll, *Pure Appl Chem*, 1971, **51**, 1915
- 15 C J Rix, A M Bond and J D Smith, *Anal Chem*, 1976, **48**, 1236
- 16 A Wade (ed.), *Martindale—The Extra Pharmacopoeia*, 27th Ed., p 826 Pharmaceutical Press, London, 1977

DETERMINATION OF TRACE AMOUNTS OF THORIUM BY ELECTROANALYTICAL TECHNIQUES

GIAN-ANTONIO MAZZOCCHIN and SALVATORE DANIELE

Department of Physical Chemistry, University of Venice, Calle Larga S Marta, 2137, 30123 Venice, Italy

LIGIA MARIA MORETTO*

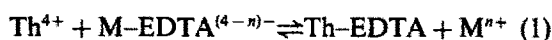
University of Caxias do Sul, Brazil

(Received 25 May 1989 Revised 26 July 1989 Accepted 20 August 1989)

Summary—Trace amounts of thorium have been determined in the presence of uranyl nitrate and ammonium diuranate (as interferents) by cyclic voltammetry, differential-pulse polarography, differential-pulse voltammetry, square-wave voltammetry and anodic-stripping voltammetry. The determination is based on the substitution of thorium for copper, lead and cadmium in their EDTA complexes and voltammetric measurement of the displaced metal ion. The detection limits ranged between 2×10^{-7} and $1 \times 10^{-6} M$ (r.s.d. 2–7%) for solutions free from the uranium compounds, and between 8×10^{-7} and $5 \times 10^{-6} M$ (r.s.d. 3–5%) in the presence of the uranium compounds at concentrations up to about 1000 times that of thorium. The detection limits depend on both the particular technique and the EDTA complex employed. Anodic-stripping voltammetry gave detection limits of 8×10^{-8} and $10^{-7} M$ in the absence and presence of uranium respectively.

Thorium is an important element in nuclear technology and several analytical techniques have been employed for its determination. Neutron activation,¹ mass spectrometry² and X-ray fluorescence spectrometry³ provide sensitive measurements at trace level, but require costly instrumentation. Polarographic techniques, which are less expensive, are not suitable for direct determination of thorium in aqueous solution, because the reduction wave of Th^{4+} is masked by the large hydrogen-evolution background current. However, trace amounts of Th^{4+} have been detected by adsorptive stripping voltammetry,^{4,5} since thorium forms polarographically active chelates with several organic ligands, and by use of the catalytically induced reduction wave obtained in the presence of lithium nitrate.⁶ Direct amperometric titrations of Th^{4+} by complex-formation, with indication of the end-point by following the anodic dissolution wave of mercury from a DME in the presence of an excess of ligand, have also been described.^{7–9} By this procedure with normal pulse polarography a detection limit of $3 \times 10^{-7} M$ with a relative standard deviation (r.s.d.) of 8% has been achieved.⁷

An alternative, simple, approach based on the displacement reaction between thorium ions and some M-EDTA complexes (M = Cu, Bi, Pb and Cd) allows the evaluation of thorium by monitoring the free metal ion released from the M-EDTA complex



Potentiometric methods^{10,11} have been used for this purpose, but are not very sensitive. A method based on chronopotentiometric stripping analysis gave a detection limit of the order of $10^{-7} M$, but only with a preconcentration time as long as 1 hr.¹² Most of these papers give little information on the analytical procedure itself. Nowadays, sensitive voltammetric methods can reach detection limits for M^{n+} at least as low as those above,¹³ but have not been tested for this application.

In the present work the approach based on the exchange reaction (1) is used for determining Th^{4+} by linear-sweep voltammetry (LSV), differential-pulse polarography (DPP), differential-pulse voltammetry (DPV), square-wave voltammetry (SWV) and anodic-stripping voltammetry (ASV). The method is then used for determining small amounts of thorium in a matrix containing high levels of uranyl nitrate and ammonium diuranate as interferents, a

*Present address Institute of Nuclear Energy Research (IPEN), Av. Lineu Prestes, 2242, São Paulo, Brazil

situation that can be encountered in the production of nuclear-grade uranium products from monazite sand, in which care is devoted to the decontamination from thorium,¹⁴ and in the determination of thorium in bulk ores. In this regard, it has been verified that the polarographic and amperometric methods cited above can tolerate a 5–20-fold molar ratio of uranium(VI) to thorium^{4,7,9}

EXPERIMENTAL

Chemicals

Thorium nitrate was kindly supplied by the Istituto di Chimica e Tecnologia dei radioelementi del CNR, Padova, Italy. Ammonium diuranate was prepared from uranyl nitrate and concentrated aqueous ammonia solution.¹⁵ The other chemicals were of reagent-grade quality. Stock solutions of the cations and of disodium dihydrogen ethylenediaminetetraacetate ($\text{Na}_2\text{H}_2\text{EDTA}$) ($10^{-3}M$) were prepared by dissolving the salts in doubly distilled water. Acetate buffer stock solutions ($0.1M$) of pH 4.5 were prepared from sodium acetate and acetic acid diluted with doubly-distilled water and were used as the background electrolyte throughout.

Nitrogen (99.99% pure) was used to remove oxygen from the test solutions before voltammetric measurement.

Apparatus

Function generation and data acquisition were performed by a PAR 273 potentiostat in conjunction with an Olivetti M24 minicomputer for linear-sweep, cyclic, square-wave and anodic-stripping voltammetry. An Amel 472 multipolarographic unit was used to perform differential-pulse polarography and voltammetry. A PAR 303 static mercury electrode was used in the three-electrode working cell for LSV, CV, SW, DPV and ASV measurements and the Amel 460 dropping mercury electrode (with mechanical control of the drop-time) for differential-pulse polarographic measurements. Either SCE or Ag/AgCl reference electrodes were used.

Procedure

Before each set of measurements, the acetate buffer solutions were checked for metal impurities able to bind EDTA, by back-titrating $10 \mu\text{l}$ of $10^{-4}M$ EDTA (added to 10 ml of acetate

buffer) with $10^{-5}M$ cadmium nitrate, with end-point detection by DPV. The metal impurities never exceeded $10^{-7}M$.

Calibration graphs relevant to reaction (1) were obtained as follows. The M-EDTA complexes were prepared from equimolar amounts of $\text{Na}_2\text{H}_2\text{EDTA}$ and $\text{M}(\text{NO}_3)_2$ ($M = \text{Cu}, \text{Pb}$ and Cd) diluted to 10 ml. Next, stepwise additions of $\sim 10^{-4}M$ thorium nitrate were made (until the Th^{4+} was equimolar with the M-EDTA). To allow attainment of equilibrium (1), a 15-min delay was allowed after each addition of thorium before the voltamperogram was recorded. Longer delay-times were also tried, in order to verify whether reaction (1) had reached equilibrium; to speed up reaction (1) the solutions were also heated at about $60\text{--}70^\circ$ under an infrared lamp for 5 min.

The detection limits in the absence of uranium compounds were obtained from simulated samples containing different amounts of thorium nitrate diluted to 10 ml with buffer solution. To these were added appropriate volumes of $10^{-4}M$ M-EDTA, giving concentrations of the complexes between 5×10^{-7} and $10^{-6}M$. The solutions were heated for 5 min, cooled to room temperature and then transferred to the voltammetric cell. This procedure was also applied for determining the detection limits in the presence of uranium compounds, the only difference being the addition of uranyl nitrate or ammonium diuranate and the use of $10^{-6}M$ M-EDTA throughout.

For evaluating the peak currents relevant to the free M^{n+} concentrations, a computer-based procedure was used to subtract the background currents. This method was particularly effective for measurements made with uranium compounds present.

The experimental parameters characterizing each voltammetric technique (*i.e.*, scan-rate for CV, step-height, drop-time, frequency *etc.* for the pulsed techniques) were properly optimized in order to reach the best conditions with respect to sensitivity and resolution.

RESULTS AND DISCUSSION

The effectiveness of the exchange method depends on both the ratio of the stability constants of the Th-EDTA and M-EDTA complexes and the rate of attainment of equilibrium (1). The choice of M and the experimental conditions such as pH are of fundamental importance. In addition, because

the method ultimately consists in the determination of the free M^{n+} , the concentration of M^{n+} arising from dissociation of the M-EDTA complex will affect the detection limit of the method.

The metal ions considered in this work were Cu^{2+} , Pb^{2+} and Cd^{2+} because their reduction potentials are not too negative (whereas the voltammetric signals for zinc, for instance, can be obscured to some extent by signals for hydrogen evolution) and the ratios of the stability constants of their EDTA complexes to that of the Th-EDTA complex enable reaction (1) to proceed quantitatively¹⁶ The pH was maintained at 4.5 by acetate buffer solutions in order to ensure adequate stability of the complexes and a good rate of the displacement reaction (1). At higher pH values thorium can form hydroxo-complexes, whereas at lower pH the dissociation of M-EDTA increases, causing a loss of sensitivity in the measurements. The concentration of M^{n+} arising from dissociation of the M-EDTA complex also depends on the M-EDTA concentration, as can be inferred from simple stoichiometric considerations. In particular, for M-EDTA concentrations of the order of $10^{-4}M$ (except for Cd-EDTA) the expected free M^{n+} concentrations should be below $10^{-8}M$, which is not detectable even with the more sensitive DPP, DPV and SWV techniques. The experimental voltamperograms revealed, however, that the concentration of free M^{n+} from dissociation of M-EDTA sometimes exceeded $10^{-5}M$. The residual M^{n+} evaluated by DPV ranged between 10^{-7} and $10^{-6}M$ for Pb^{2+} and Cu^{2+} and between $3 \times 10^{-7}M$ and $2 \times 10^{-6}M$ for Cd^{2+} for M-EDTA concentrations between 10^{-5} and $10^{-4}M$. The high values may be partly due to the difficulty of ensuring exactly equimolar metal/EDTA ratios at very low concentrations. Also, the conditional stability constants may be lower than those usually reported,¹⁷ in agreement with conclusions drawn from stripping voltammetric measurements.^{18,19} High background levels of M^{n+} can be avoided by an appropriate choice of M-EDTA concentration. For instance, concentrations of M-EDTA between 5×10^{-7} and $10^{-6}M$ did not produce any appreciable DPV or SWV reduction peak for M^{n+} .

To establish the range of linearity obtained by use of reaction (1), a series of measurements was made in which increasing amounts of Th^{4+} were added to buffer solutions containing different amounts of the M-EDTA complexes. Linear

Table 1 Correlation coefficients of calibration graphs (r) and fraction (%) of total M^{n+} displaced in reaction (1) when $[Th^{4+}]$ added is equal to $[M-EDTA]$

Complex	$10^{-4}M$ M-EDTA		$10^{-5}M$ M-EDTA	
	r	M^{n+} displaced, %	r	M^{n+} displaced, %
Cu-EDTA	0.987	40	0.989	65
Pb-EDTA	0.991	70	0.990	85
Cd-EDTA	0.992	85	0.993	95

relationships between M^{n+} released and Th^{4+} added were obtained, whatever the initial M-EDTA concentration, but the slopes of the lines depended on the initial M-EDTA concentration, the delay between adding thorium and running the voltamperogram, and the amount of Th^{4+} added in each step. This behaviour occurred with all the voltammetric techniques employed. Table 1 shows typical correlation coefficients for the relationships and the average fraction of M^{n+} released when the Th^{4+} added was equimolar with the M-EDTA taken.

The fractions released were calculated by comparing the peak currents for the M^{n+} released, with those for M^{n+} standards in the same buffer solution, as shown in Fig. 1.

An improvement in the release of M^{n+} was obtained in all cases by increasing the delay time or heating the solution after each addition of Th^{4+} . This effect can be rationalized by taking into account the formation of hydroxo-complexes of thorium, which can either slow down reaction (1) or be adsorbed on the mercury electrode and causing poisoning effects.¹² The higher the initial M-EDTA concentration, the greater the volume of Th^{4+} solution added in each step, this causes larger

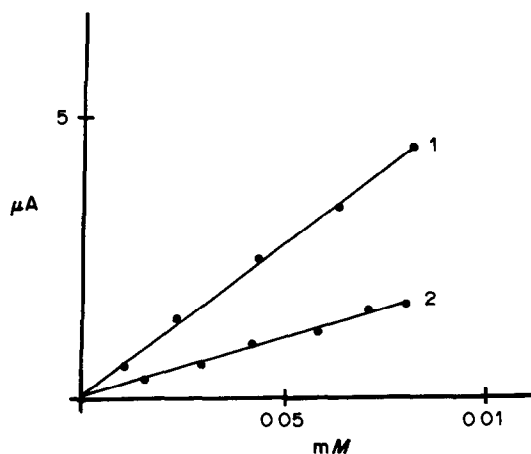


Fig. 1 Differential-pulse peak currents plotted as a function of (1) concentration of Cu^{2+} and (2) concentration of Th^{4+} displacing Cu^{2+} from $0.1mM$ Cu-EDTA

Table 2 Detection limits (DL) and relative standard deviations (r s d, 5 replicates) for different technique and M-EDTA combinations

Complex	Technique											
	LSV			DPP			DPV			SWV		
	[M-EDTA], μM	DL, μM	r s d, %	[M-EDTA], μM	DL, μM	r s d, %	[M-EDTA], μM	DL, μM	r s d, %	[M-EDTA], μM	DL, μM	r s d, %
Cu-EDTA	2.0	1.0	7	1.0	0.6	5	0.5	0.4	5	0.5	0.5	6
Pb-EDTA	2.0	0.9	6	1.0	0.3	4	0.5	0.2	3	0.5	0.2	4
Cd-EDTA	2.0	0.9	6	1.0	0.3	3	0.5	0.2	2	0.5	0.2	2

amounts of hydroxo-complexes to be added, and hence greater effect on reaction (1) or an increase in undesirable effects at the surface of the mercury electrode.

The detection limits reported in Table 2 were found by making standard additions of Th^{4+} to solutions containing M-EDTA complexes at concentrations between 5×10^{-7} and 10^{-6}M , depending on the voltammetric technique employed. The detection limit was taken as the concentration of Th^{4+} corresponding to a peak current for M^{n+} that was three times the standard deviation of the peak current for a blank solution.

The results show that the use of Cd-EDTA and DPV or SWV gives the most sensitive measurements. The precision of the method for concentrations of the order of the detection limits are reported in Table 2. Table 2 also shows that the detection limits and relative standard deviations for DPP, DPV and SWV are better than those for direct titrimetry with normal pulse polarographic detection.⁷

Determination of Th^{4+} in the presence of uranyl nitrate and ammonium diuranate

The electrochemical behaviour of U(VI) in aqueous solution is characterized by a rather complex mechanism in which the first electrochemical step is coupled with homogeneous chemical reactions leading to products which undergo further electrochemical steps.²⁰ Figure 2 shows the cyclic voltamperograms obtained for (a) uranyl nitrate and (b) ammonium diuranate in pH-4.5 acetate buffer. The two voltamperograms differ in the position of the second reduction peak and the reversibility of the first process. Because the voltamperogram for uranyl nitrate is the more complex, attempts were made to simplify it by varying the scan-rate (the chemical reactions associated with the electron transfers are not very fast, so it is thus possible to mask their effects). The effect of increased scan-rate on the reduction process of uranyl nitrate is shown in (c) in Fig 2. The reduction is characterized by one reversible wave at about $-0.4\text{ V vs. Ag/AgCl}$ (at the same potential as the first wave for ammonium diuranate). Under these conditions the potential region free from interference is much wider, and for both cases the use of equilibrium (1) for the determination of Th^{4+} is practicable with the copper and cadmium EDTA complexes, whereas Pb-EDTA is not useful because the free Pb^{2+} wave coincides with the first wave for the uranium compounds.

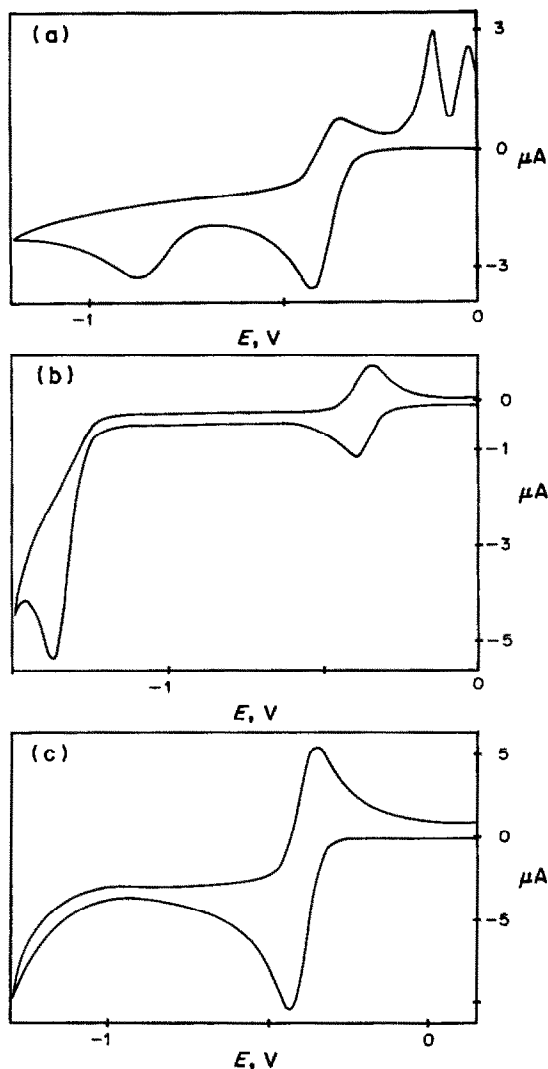


Fig 2 Cyclic voltamperograms recorded for 0.1 M aqueous acetate buffer solutions containing (a) 2 mM $\text{UO}_2(\text{NO}_3)_2$, scan-rate 100 mV/sec, (b) 2.3 mM $(\text{NH}_4)_2\text{U}_2\text{O}_7$, scan-rate 100 mV/sec and (c) 2 mM $\text{UO}_2(\text{NO}_3)_2$, scan-rate 1.5 V/sec

Preliminary experiments were performed to ascertain whether interferences arose from interaction between the uranyl and M-EDTA systems. For this purpose, 10^{-3} M solutions of the uranium compounds in pH-4.5 acetate buffer were added to Cu^{2+} , Cd^{2+} or EDTA solutions in the concentration range 10^{-5} – 10^{-4} M. The peak-heights for both Cu^{2+} and Cd^{2+} increased linearly with concentration with correlation coefficients of 0.982 and 0.988, respectively (these are averages of the values obtained with the different voltammetric techniques). However, the copper peak became broader, and the cadmium peak appeared as a shoulder on the uranyl peak (Fig 3)

The pulsed techniques gave good resolution between peaks. The EDTA added did not affect the uranyl reduction, though formation of a UO_2 -EDTA complex could not be excluded. Since in the determination of Th^{4+} the EDTA is added as a metal complex, the possibility of displacement of the metal ion by uranyl was also studied. The addition of 10^{-4} M Cu-EDTA or Cd-EDTA to 10^{-3} M solutions of uranyl nitrate or ammonium diuranate revealed only small waves due to the reduction of free Cu^{2+} and Cd^{2+} , similar to those obtained in the absence of the uranium compounds. This indicates that the metals are preferentially bound to the EDTA, in agreement with the lower conditional stability constant for UO_2 -EDTA¹⁶

Calibration graphs for thorium in the presence of the uranium compounds were satisfactorily linear, with correlation coefficients of 0.989, 0.969 and 0.983 for cadmium and 0.986, 0.980 and 0.981 for copper, determined by SWV, LSV and DPP, respectively, but the slopes were lower than those obtained in the absence of uranium. The average fractions of M^{n+} released were about 60 and 40% for cadmium and copper, respectively. Typical voltamperograms are shown in Fig 4.

Table 3 shows the detection limits obtained for thorium with the different techniques, for uranium to thorium concentration ratios of about 1000. For lower ratios, the detection limits ranged between those in Tables 2 and 3 for each M^{n+} and voltammetric technique combination, and for higher ratios the detection limits are higher than those in Table 3, being 10^{-4} M or more for 0.1 M uranium. These tables indicate that it is possible to make precise measurements of less than micromolar levels of thorium in the presence of up to a thousandfold molar ratio of uranium compounds by DPP, DPV and SWV. CV (the least sensitive technique used) also gives good results, although the precision is less satisfactory.

Table 4 shows typical results for the determination of Th^{4+} in the presence of uranium compounds in synthetic samples.

If the results in Tables 3 and 4 are considered in the context of industrial practice, e.g., for finished nuclear-grade uranium products, where the recommended²¹ maximum thorium impurity is $10 \mu\text{g/g}$,²¹ the selectivity is inadequate. Nevertheless the proposed procedure is the best amongst those described for evaluating thorium in presence of a large excess of uranyl ion^{4,5,7,9}. Hence, a separation step would be required if the

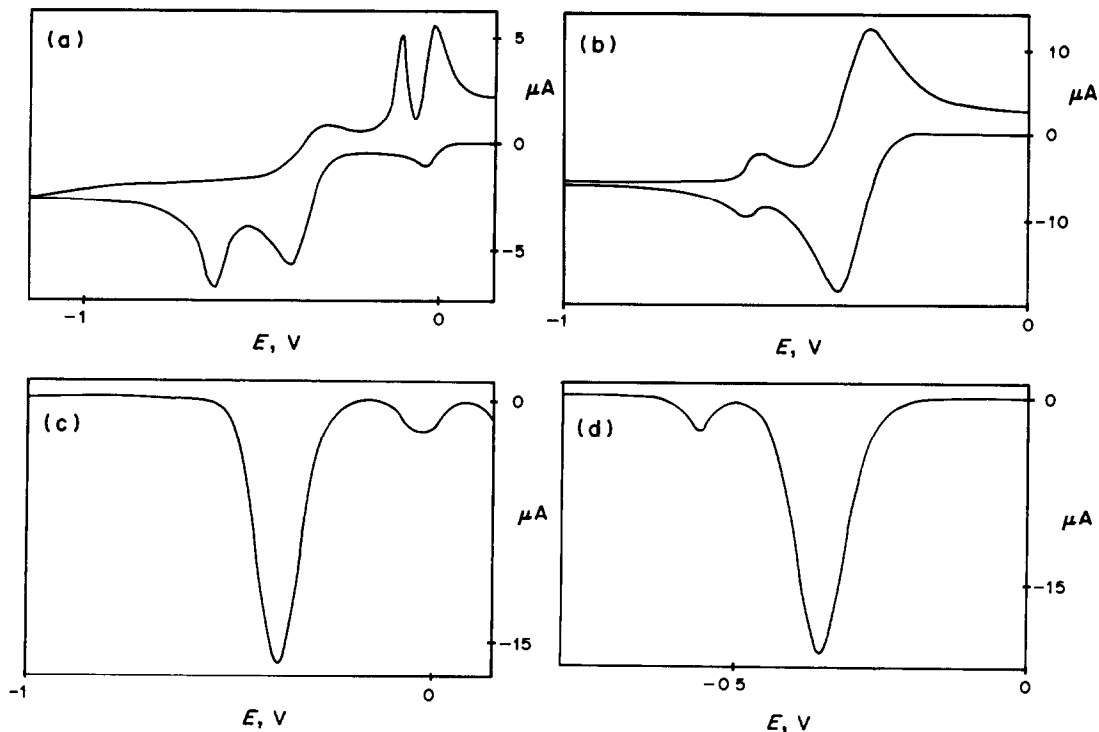


Fig 3 Voltamperograms recorded for 0.1M acetate buffer solutions (a) CV of 1.5mM $\text{UO}_2(\text{NO}_3)_2$ and 0.1mM $\text{Cu}(\text{NO}_3)_2$, scan-rate 100 mV/sec, (b) CV of 1.7mM $\text{UO}_2(\text{NO}_3)_2$ and 0.1mM $\text{Cd}(\text{NO}_3)_2$, scan-rate 1.5 V/sec, (c) SWV as for (a), step height 3 mV, pulse amplitude 50 mV, frequency 37 Hz, (d) SWV as for (b), step height 3 mV, pulse amplitude 25 mV, frequency 75 Hz

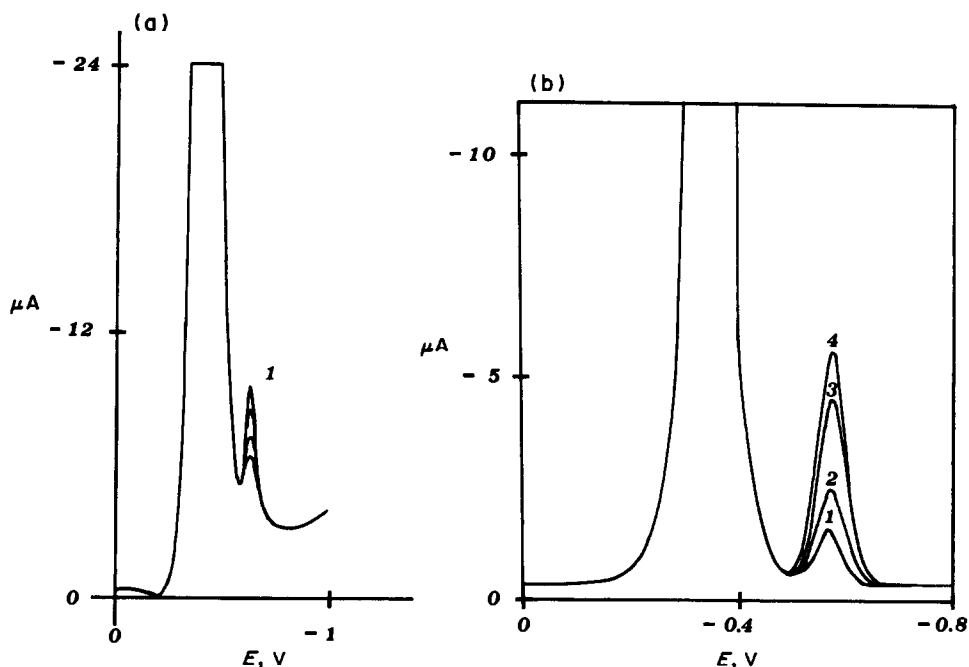


Fig 4 Sequence of voltamperograms for acetate buffer solutions initially containing 1mM $(\text{UO}_2)_2\text{NO}_3$ and 0.01mM Cd-EDTA (a) DPP four stepwise additions of 10 μl of 1mM $\text{Th}(\text{NO}_3)_4$, scan-rate 5 mV/sec, drop-time 1 sec, pulse height 20 mV, (b) SWV stepwise additions of (1, 2, 4) 10 μl and (3) 20 μl of 1mM $\text{Th}(\text{NO}_3)_4$, step height 3 mV, pulse amplitude 25 mV, frequency 75 Hz

Table 3 Detection limits (DL) and relative standard deviations (r s d, 5 replicates) for Th⁴⁺ in the presence of 1mM uranyl nitrate or for the different technique and M-EDTA combinations

Complex	Techniques							
	LSV		DPP		DPV		SWV	
	DL, μM	r s d, %	DL, μM	r s d, %	DL, μM	r s d, %	DL, μM	r s d, %
Cu-EDTA	6.0	5	2.1	4	1.2	4	2.3	4
Cd-EDTA	5.0	4	0.9	3	0.8	2	0.8	3

uranium concentration is more than 1mM. It must be remarked, however, that such steps are common in other methods for determining thorium²³

Use of the stripping approach

Anodic stripping has been tried for monitoring the free Mⁿ⁺ released in reaction (1). This technique, in principle, gives higher sensitivity for electroactive species able to give amalgams, whilst excluding interference from those which do not. This is just the case under investigation, in that the uranium reduction products are not soluble in mercury, whereas the EDTA complexes used are those of typical heavy metal determined by stripping analysis.

Measurement of solutions containing Pb-EDTA or Cd-EDTA but no uranium provided poorly reproducible results when Th(NO₃)₄ was added to obtain calibration graphs for reaction (1). For instance, for a solution containing 5 × 10⁻⁷M Pb-EDTA, to which 2 × 10⁻⁷M thorium nitrate was added, which should result in a free Pb²⁺ concentration of about 2 × 10⁻⁷M, six replicate DPV stripping peaks recorded after preconcentration for 1 min at -0.8 V in stirred solution gave an r.s.d. of about 16%, which is far higher than the typical values of 6-12% found for ASV at these concentration levels²². The stripping voltammetric peaks were less reproducible, the longer the preconcentration time, in agreement with the conclusion drawn about adsorption effects caused by thorium hydroxo-complexes. To minimize these effects, the measurements were made after preconcentration in quiescent

solution for almost zero time. These conditions were realized by use of cyclic DPV [see Fig. 5(b)], so that mass transport during the preconcentration time occurred only by diffusion to the electrode surface and not by convection. This implies a current decaying as a function of time according to the Cottrell equation²³ and therefore a high current can be established only for a short time.

This procedure was used for preparing calibration graphs relevant to reaction (1). The correlation coefficients of the calibration lines were 0.921 and 0.910 for cadmium and lead, respectively. The detection limits determined were about 8 × 10⁻⁸M for Cd²⁺ and 10⁻⁷M for Pb²⁺. The relative standard deviations were about 6% for both cations. These results are quite satisfactory when compared with others,¹² the detection limits are slightly lower and the measurement can be performed in a few minutes instead of an hour.

Stripping measurements performed on buffer solutions containing 10⁻³M uranyl nitrate or ammonium diuranate did not show any oxidation process occurring in the potential region between -1.0 and -0.3 V, but measurements on solutions containing both Cd²⁺ and either of the uranium compounds showed the peak for oxidation of cadmium metal [Fig. 5(b)]. This peak had poor reproducibility, however (r.s.d. of about 15% for 2 × 10⁻⁷M Cd²⁺). The reproducibility was even worse when Th⁴⁺ was added in order to prepare calibrations for reaction (1), the best results were again obtained by using very short preconcentration times.

Table 4 Determination of Th⁴⁺ in synthetic samples containing uranium compounds

Complex	[M-EDTA], μM	Technique	Uranium compound and concn, mM	Correlation coefficient	Th ⁴⁺ found*, μM	Th ⁴⁺ taken, μM	Error, %
Cd-EDTA	17.15	SWV	(NH ₄) ₂ U ₂ O ₇ , 1.10	0.998	2.31	2.23	3.7
Cd-EDTA	47.61	LSV	UO ₂ (NO ₃) ₂ , 0.98	0.999	5.36	5.37	-0.1
Cu-EDTA	55.11	SWV	UO ₂ (NO ₃) ₂ , 0.89	0.997	8.38	8.39	-0.2
Cd-EDTA	25.21	DPP	UO ₂ (NO ₃) ₂ , 0.99	0.989	4.60	4.75	-3.2

*Mean of five replicate measurements

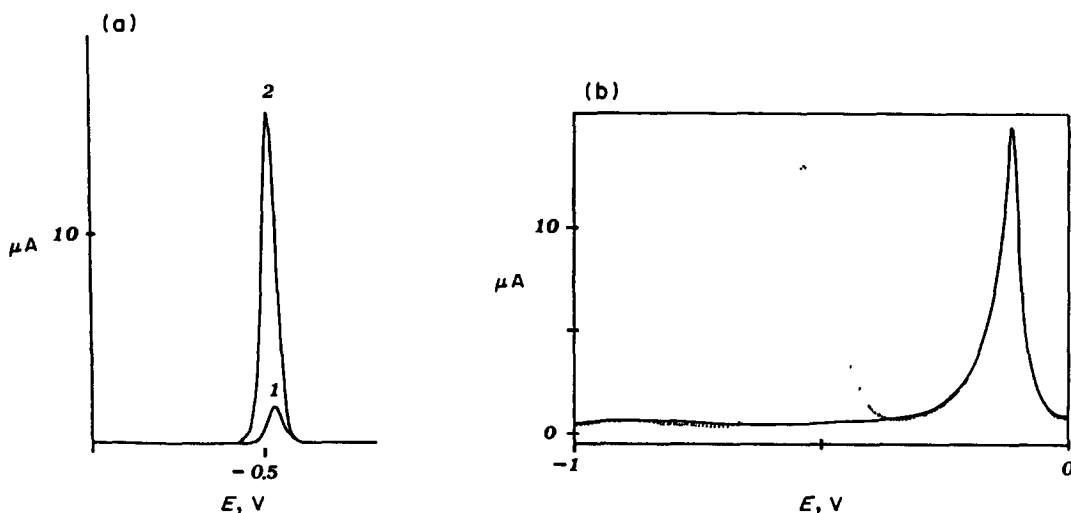


Fig 5 (a) Cyclic DPV of acetate buffer solution containing 0.01 mM $\text{Pb}(\text{NO}_3)_2$ (1) direct scan, (2) reverse scan, scan-rate 5 mV/sec, pulse height 25 mV (b) SWASV of acetate buffer solutions containing (—) 1 mM $\text{UO}_2(\text{NO}_3)_2$, (---) 1 mM $\text{UO}_2(\text{NO}_3)_2$ and 0.001 mM $\text{Cd}(\text{NO}_3)_2$ Electrolysis for 30 sec at -1.00 V, step height 3 mV, pulse amplitude 25 mV, frequency 75 Hz

The presence of uranium compounds did not allow use of the cyclic wave-form as above, because stirring during the preconcentration step was necessary to enhance the flux of the uranium products away from the electrode surface, since these would otherwise have severely interfered with the metal stripping process. However, interference still arose to some extent when cadmium concentrations below $5 \times 10^{-7} M$ were measured. The detection limit in these conditions was about $10^{-7} M$, with an r.s.d. of about 15%.

Comparison of these results with those reported in the previous section shows that the stripping approach improves the detection limits sufficiently for about 100 μg of thorium per g of uranium to be determined, but the reproducibility of the measurements is poorer.

Acknowledgements—The authors thank Mr D Rudello for his skilful experimental assistance. The Institute of Chemistry and Technology of Radioelements of CNR, Padova, and financial aid from the Italian National Research Council and the Ministry of Public Education are gratefully acknowledged.

REFERENCES

- 1 C-A Huh and M P Bacon, *Anal Chem*, 1985, **57**, 2138
- 2 L W Green, N L Elliot and T H Longhurst, *ibid*, 1983, **55**, 2394
- 3 I Roelandts, *ibid*, 1983, **55**, 1637
- 4 Z Zhao, X Cai, P Li and H Yaung, *Talanta*, 1986, **33**, 623
- 5 J Wang and J Zadeu, *Anal Chim Acta*, 1986, **188**, 187
- 6 P Szefer, *Z Anal Chem*, 1977, **287**, 46
- 7 J W Dieker, W E van der Linden and G den Boef, *Talanta*, 1977, **24**, 321
- 8 C L Sharma and P K Jain, *ibid*, 1977, **24**, 754
- 9 C L Sharma and R S Arya, *ibid*, 1979, **26**, 577
- 10 E W Baumann and R M Wallace, *Anal Chem*, 1969, **41**, 2072
- 11 E W Baumann, *Anal Chim Acta*, 1982, **138**, 391
- 12 J Adam, *Talanta*, 1982, **29**, 939
- 13 A M Bond, *Modern Polarographic Methods in Analytical Chemistry*, Dekker, New York, 1980
- 14 A Abrao, *Inorg Chim Acta*, 1987, **140**, 207
- 15 V Urbánek, V Šára and J Moravec, *J Inorg Nucl Chem*, 1979, **41**, 537
- 16 A E Martell and R M Smith, *Critical Stability Constants*, Vol 1, Plenum Press, New York, 1974
- 17 A Ringbom, *Complexation in Analytical Chemistry*, Interscience, New York, 1963
- 18 M S Shuman and G P Woodward, *Anal Chem*, 1973, **45**, 2032
- 19 J R Tuschall and P L Brezonik, *ibid*, 1981, **53**, 1986
- 20 I M Kolthoff, W E Harris and G Matsuyama, *J Am Chem Soc*, 1944, **66**, 1782
- 21 ANSI/ASTM Standard C776-79, in *Annual Book of ASTM Standards, Part 45, Nuclear Standards*, American Society for Testing and Materials, Philadelphia, 1982
- 22 T M Florence, *J Electroanal Chem*, 1970, **27**, 273
- 23 A J Bard and L R Faulkner, *Electrochemical Methods*, p 143, Wiley, New York, 1980

INDIRECT POLAROGRAPHIC DETERMINATION OF ARSENIC

E BARRADO, Y CASTRILLEJO, E DEL REAL, R PARDO and P. SANCHEZ BATANERO

Departamento de Química Analítica, Facultad de Ciencias, Universidad de Valladolid,
47005, Valladolid, Spain

(Received 9 December 1987 Revised 5 October 1989 Accepted 19 October 1989)

Summary—A method for determination of arsenic(V) in the range between 1×10^{-7} and $1.2 \times 10^{-6} M$ has been developed. These levels are reached by means of the multiplication factor yielded by use of 12-molybdoarsenic acid and the great sensitivity of polarographic determination of the Mo(VI) in the heteropoly acid. The procedure has been successfully applied to determination of arsenic in copper alloys, after selective extraction of phosphorus.

The toxic character of arsenic makes its determination at trace level important. Many procedures have been proposed, but preconcentration and/or isolation of the arsenic is frequently needed.¹ Some polarographic methods have been described, but mainly for determining As(III), because it is difficult to reduce As(V) at the mercury electrode.²

In the method proposed here, the As(V) is electrochemically determined by an indirect method in which the 12-fold multiplicative effect given by forming arsenomolybdic acid (AMA) and determining the molybdenum in it is used, analogously to some spectrophotometric methods.³⁻⁶ The sensitivity is further increased by using the polarographic peak resulting from the catalytic reduction of H_2O_2 in the presence of the Mo(VI) arising from the heteropoly acid.⁷ In this way, a DC-polarography procedure with a detection limit of $5.9 \mu g/l$ is obtained. Its usefulness has been established by the analysis of certified samples, after elimination of the interference of phosphorus by selective extraction of phosphomolybdic acid (PMA) with ethyl acetate.⁸

EXPERIMENTAL

Apparatus

This was described earlier.⁸

Standard arsenic solution, 0.01M

Dissolve 1.895 g of sodium monohydrogen arsenate in 1 litre of demineralized water; prepare and store the solution in polythene ware. Prepare working solutions by appropriate dilution.

Procedures

Determination of arsenic. Transfer 2 ml of 2% ammonium paramolybdate solution, 0.75 ml of 5M sulphuric acid and a known volume of sample (or standard) containing arsenic(V) into a 100-ml separating funnel, and dilute to 25 ml with demineralized water. After 20 min add 10 ml of n-butanol, shake the mixture for 3 min and then separate the organic phase. Wash this with two 10-ml portions of 0.8M sulphuric acid to remove the excess of free Mo(VI). Strip the arsenomolybdic acid with 25 ml of 1M sodium hydroxide. Adjust this solution to pH 4.0 with 4M sulphuric acid, add 5 ml more of this acid, and 10 ml of 0.2M hydrogen peroxide, and finally dilute to volume in a 100-ml standard flask with demineralized water. Transfer a portion of this solution into the polarographic cell and run a DC-polarogram between 0.40 and 0.00 V (*vs* SCE). Deaeration is not required, but the temperature must be kept constant ($25 \pm 0.1^\circ$). Measure the current at 0.20 V, and by comparison with a calibration line obtained under the same conditions, determine the As(V) concentration.

Analysis of copper-based alloy. Weigh accurately a 0.5-g sample of alloy and dissolve it in nitric acid (1 + 1). If dissolution is not complete, add a few drops of concentrated nitric acid and, if necessary, one or two drops of concentrated hydrochloric acid, boil carefully to expel nitrous fumes, cool, and dilute to volume in a 100-ml standard flask with water. Take an aliquot of this solution and adjust its pH to about 4 with sodium hydroxide solution. Transfer in this order, 2 ml of 2% ammonium paramolybdate

solution, 1 ml of 5M sulphuric acid and the aliquot of sample into a separating funnel and dilute to 25 ml with demineralized water. After 20 min, add 1 ml of 5M sulphuric acid and 10 ml of ethyl acetate. Shake the funnel for 3 min, then let it stand for 15 min. Discard the organic phase containing the MPA. Neutralize the aqueous phase with sodium hydroxide, then add enough sulphuric acid to give a concentration of 0.15M, extract the arsenomolybdic acid with n-butanol and complete the analysis as described above.

RESULTS AND DISCUSSION

The complete procedure involves (a) formation of AMA from arsenic(V) and excess of molybdate, (b) selective extraction of AMA, (c) washing the organic extract to eliminate the co-extracted isopolymolybdate species, and (d) stripping of molybdenum(VI) from the AMA for polarographic determination.

Step (d) has already been described and optimized,⁸ so the experimental conditions to be optimized are those of steps (a), (b) and (c). Formation of AMA depends not only on the acid concentration but also on the Mo/As ratio. Figure 1 shows that when the molybdate concentration is increased, the acidity range over which the highest current ($\Delta i = i_{\text{sample}} - i_{\text{blank}}$) is obtained is extended to higher acidity. Figure 2 shows the relative response surface, as a function of the molybdenum(VI) concentration and the acidity. $\Delta i/i_{\text{blank}}$ was chosen as the analytical response for optimization because our main purpose was to find a procedure giving both

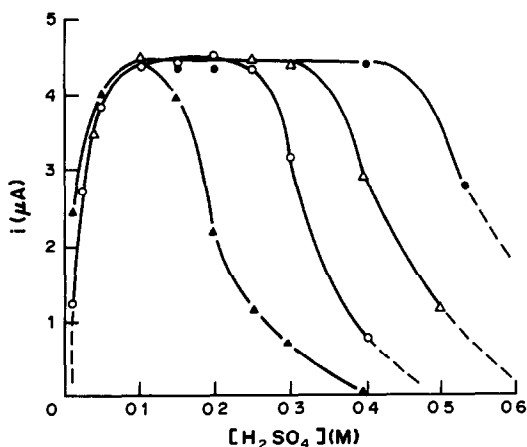


Fig 1 Effect of the sulphuric acid and molybdate concentrations on the catalytic intensity. Volume of 2% ammonium paramolybdate solution added: $\blacktriangle = 1$ ml, $\circ = 2$ ml, $\triangle = 3$ ml, $\bullet = 4$ ml, $\square = 5$ ml.

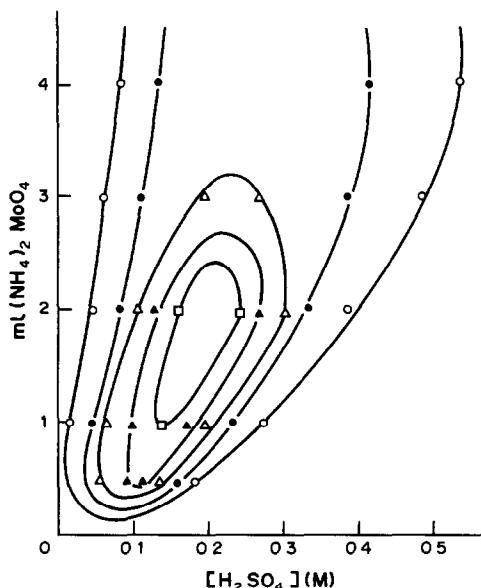


Fig 2 Surface response shown as a contour map $[\text{As(V)}] = 5 \times 10^{-7} \text{M}$. $\Delta i/i_{\text{blank}}$: \circ 0.4, \bullet 0.8, \triangle 1.2, \blacktriangle 1.6, \square 1.7.

high precision and low detection limit, *i.e.*, Δi must be large and i_{blank} small. Figure 1 shows that the molybdenum(VI) and sulphuric acid concentrations in the recommended procedure are within the optimum zone, and no further optimization is needed.

For the extraction, we have tested the systems recommended as most suitable for AMA,^{4,5,9,10} ranging from alcohols, such as n-butanol, through ketones such as MIBK, to mixtures, such as diethyl ether-n-butanol. Of those examined, n-butanol was chosen because it gives the best results under the experimental conditions of the proposed method.

On the other hand, since some free Mo(VI) is extracted together with AMA, the organic phase must be washed with an appropriate liquid. Sulphuric acid was chosen because the heteropoly acid is not stripped by an acidic medium⁵ and this acid does not introduce any new ions which might interfere in later steps. The results show that the efficiency of the washing step is the same over the concentration range 0.1–0.8M sulphuric acid. To find the optimum number of washings, a 10-ml portion of organic phase was treated with several 10-ml portions of 0.8M sulphuric acid and the Mo(VI) transferred to the aqueous phase was measured polarographically. The results indicate that the Mo(VI) is almost completely removed in two washings. The heteropoly acid is decomposed and stripped with 1M sodium hydroxide, as explained above.

Under the optimal conditions, the linear range of calibration is from $1 \times 10^{-7}M$ ($7.5 \mu\text{g/l.}$) to $1.20 \times 10^{-6}M$ ($90 \mu\text{g/l.}$) The sensitivity is $8.95 \text{ A.l.mole}^{-1}$, and the detection limit $6.0 \mu\text{g/l}$

Na, K, Mg, Co, Al, Fe, Zn, Cd, NO_3^- and SO_4^{2-} do not interfere. Silicon, phosphorus and germanium produce a positive error because of co-extraction of the corresponding heteropoly acids. The allowed tolerance limits, expressed as the interferent/arsenic ratio, are 0.15 for phosphate, 3 for silicate and 0.2 for germanate, for an As(V) concentration of $5.0 \times 10^{-7}M$

Analytical applications

When the recommended procedure was applied to copper alloys, some of the results obtained were too high. This was found to be due to phosphorus in the samples. This problem was eliminated by selective extraction of PMA with ethyl acetate.⁸ Other possible interferents were present at the level lower than the tolerance limits. The certified values of arsenic in the

samples were 0.0080% and 0.0041%. The results obtained were $0.0084 \pm 0.0004\%$ and $0.0042 \pm 0.0007\%$, respectively (means of 5 determinations, 95% confidence level).

Acknowledgement—This work was supported by a grant from the CAICYT (3123/83), Ministerio de Educación y Ciencia (Spain)

REFERENCES

- 1 J. L. Webb, *Enzyme and Metabolic Inhibitors*, Vol. 3, Chapter 6, Academic Press, New York, 1966
- 2 I. M. Kolthoff and J. J. Lingane, *Polarography*, Interscience, New York, 1952
- 3 S. A. Morosanova and N. B. Rozhmanova, *Zh Analit Khim*, 1981, **36**, 1541
- 4 S. Motomizu, T. Wakimoto and K. Tokei, *Analyst*, 1983, **108**, 944
- 5 Y. Yamamoto, T. Kumamaru, Y. Hayashi, M. Kanke and A. Matsui, *Talanta*, 1972, **19**, 1633
- 6 A. S. Khan and A. Chow, *ibid.*, 1984, **31**, 304
- 7 I. M. Kolthoff and E. P. Parry, *J. Am. Chem. Soc.*, 1951, **73**, 5315
- 8 R. Pardo, E. Barrado, Y. Castrillejo and P. Sánchez Batanero, *Talanta*, 1983, **30**, 655
- 9 R. S. Danchuk and D. F. Boltz, *Anal. Lett.*, 1968, **1**, 347
- 10 C. Wadelin and M. G. Mellon, *Analyst*, 1952, **77**, 708

SPECTROPHOTOMETRIC DETERMINATION OF PALLADIUM WITH SULFOCHLOROPHENOLAZORHODANINE BY FLOW INJECTION

PAUL M. SHIUNDU, PETER D. WENTZELL and ADRIAN P. WADE*

Laboratory for Automated Chemical Analysis, Department of Chemistry, University of British Columbia,
Vancouver, B.C., Canada V6T 1Y6

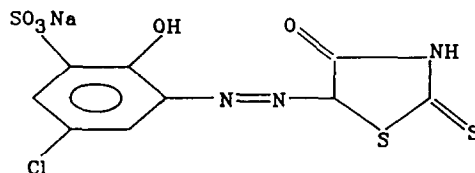
(Received 11 May 1989; Revised 11 July 1989; Accepted 26 July 1989)

Summary—Sulfochlorophenolazorhodanine (as its sodium salt) has been used in the automated development of a sensitive flow-injection procedure for the spectrophotometric determination of palladium. The resulting method has high sample throughput, good precision, and low consumption of both sample and reagents. The optimum pH for the reaction is 5.0 and the response is constant at pH between 4.7 and 5.3. The sensitivity (calibration slope) of the procedure is 4.4×10^3 l./mole. The linear dynamic range is 0.045–30.0 µg/ml. The sample throughput is at least 120/hr. An automated procedure for optimization of analytical variables is described and a two-variable response surface for the system is given. Interference studies on 19 metal ions show that the method has good selectivity.

Until recently, little attention has been given to development of flow-injection procedures for palladium. This is somewhat surprising in view of the commercial value and wide use of this element in catalysts and alloys. Traditional manual methods for palladium determination have used spectrophotometric methods with liquid-liquid extraction,¹⁻⁴ precipitation by reagents such as dimethylglyoxime,⁵ and atomic-absorption spectrometry.⁶ For flow-injection analysis, direct colorimetric methods are preferred because of their simplicity. Haj-Hussein and Christian⁷ reported a direct colorimetric flow-injection method which provided reasonable selectivity, and Sakai and Ohno⁸ have recently reported a method with greater sensitivity. No other flow-injection methods for palladium have been found in the literature.

Savvin and Guereva⁹ reported that a number of azo compounds based on rhodanine and thiorhodanine may be used as highly sensitive and selective reagents for the spectrophotometric determination of noble metals. The reaction times cited for maximum color development were typically several hours. It was thought that acceptable analytical sensitivity might be obtained with shorter reaction times if the highly repeatable timing of flow-injection systems was employed. Of particular interest was

sulfochlorophenolazorhodanine (SCPAR), the structure of which is shown below. This was reported to form a palladium complex with a very high molar absorptivity (1.2×10^5 l./mole⁻¹.cm⁻¹ at very high acidity, 5.0×10^4 in 1M hydrochloric acid). This paper reports further investigation of this system and development of a flow-injection method for palladium, based on use of this reagent.



Simplex optimization is a useful means of rapidly optimizing chemical and flow conditions in flow-injection systems.¹⁰ Though this approach rapidly locates an optimum, it gives little information about the nature of the response surface.¹¹ Mapping response surfaces by performing multiple experiments in a regular pattern such as a square or triangular lattice allows better characterization of complete systems. It provides the experimentalist with evidence of the stability and therefore experimental repeatability of the analytical method, but at the expense of more experiments and perhaps less information about the region of the optimum. This has been discussed elsewhere.¹²

*Author for correspondence

Automated flow-injection analyzers have much to offer analytical chemistry.¹³ In particular, they facilitate automated development of analytical methods by appropriate control of injection/stream-switching valves and variable-speed pumps. Such systems achieve their full potential only when a high degree of computer control is employed. This allows for "soft automation" whereby the function of the analyzer is in part specified through software, and thus may be modified in real-time. Simplex optimization can be implemented on automated hardware to facilitate method development without assistance by the operator.^{10,13}

In this work we have used both automated simplex optimization and automated response-surface mapping to help characterize the Pd(II)-SCPAR system

EXPERIMENTAL

Reagents

A stock solution of palladium(II) ($1.00 \times 10^{-3} M$) was prepared by dissolving palladium(II) chloride (Alfa, Danvers, MA), in 0.01 M hydrochloric acid. Sample solutions were prepared by appropriate dilution. Solutions of metal ions for the interference studies were made from the nitrates of copper(II), nickel(II), lead(II), aluminum(III), mercury(II), bismuth(II), silver(I), cobalt(II), rhodium(III), the chlorides of iron(II), iron(III), platinum(IV), ruthenium(III), zinc(II), iridium(III), cadmium(II), tin(II), gold(III), and manganese(II) sulfate. Analytical-reagent grade salts were used, except for the platinum(IV) solution, which was prepared by dissolution of platinum wire in *aqua regia*.

A universal buffer solution¹⁴ (pH 2.0) was prepared for the automated optimization and batch method experiments. Buffer solutions at various pH values above this were then obtained by addition of appropriate volumes of 0.2 M sodium hydroxide.

Synthesis of SCPAR (sodium salt)

Synthesis of the sodium salt of SCPAR (Na-SCPAR) employed a diazotization step followed by a coupling reaction. First, 11 g of 2-amino-4-chlorophenolsulfonic acid (ACPS) (ATK Inc., Tokyo, Japan) were dissolved in 100 ml of distilled water. About 20 ml of concentrated hydrochloric acid were added and the reaction mixture was cooled in an ice-bath before addition of 3.45 g of sodium nitrite. The mixture was then stirred constantly while about

40 ml of water were gradually added over a period of 1 hr. After standing for another hour at 0°, the mixture was neutralized by addition of 2.5 g of sodium acetate.

The coupling reaction was then performed by adding a solution containing 6.7 g of rhodanine (Aldrich, Milwaukee, WI) in 150 ml of 1 M sodium hydroxide to the reaction mixture, which was then kept in an ice-bath for 1 hr, with the pH maintained between 7 and 9 by addition of small amounts of either dilute sodium hydroxide solution or hydrochloric acid. Concentrated hydrochloric acid was then added dropwise until a pH of about 3 was obtained. The precipitate formed was filtered off and washed with small amounts of cold water, and then purified. First, it was dissolved in about 200 ml of water and about 3 g of sodium carbonate were added. The insoluble residue which remained was discarded. The filtrate was acidified with a few drops of 6 M hydrochloric acid to precipitate the purified product, which was then filtered off, washed with cold distilled water, and dried in air. The product was a red-orange powder, yield about 10 g (54%).

A portion of the isolated product was further purified by preparative column chromatography. Na-SCPAR was separated from a minor amount of residual ACPS on a silica-gel column with a mobile phase consisting of 5% methanol and 1% acetic acid in diethyl ether. For this, a $9.44 \times 10^{-4} M$ Na-SCPAR stock solution was prepared by dissolving 0.3676 g of the purified reagent in 1 litre of 0.01 M hydrochloric acid. Our own elemental analysis results, and the work by Savvin and Guereva,⁹ indicated some difficulty in purifying the SCPAR reagent.

Apparatus

A diode-array spectrophotometer (Hewlett Packard 8452A) with a standard 1-cm fused-silica cell was used for absorption measurements. For the flow-injection studies, a 30- μ l 1-cm pathlength fused-silica flow-cell was used. The pH of reaction mixtures was determined with a laboratory pH meter (Fisher Scientific) and a flow-through electrode cell designed in our laboratory.

The automated flow-injection analyzer used was based on a design reported previously,¹³ and will be discussed in detail elsewhere. Its key units include a custom-built 5-channel peristaltic pump unit, two high-precision peristaltic pumps (Alitea USA, Seattle, WA), and an injection valve unit incorporating three

6-port air-driven solenoid-actuated injection valves (Rheodyne 5020P, Cotati, CA) each equipped with a 70- μl sample loop. All units were controlled by a computer compatible with an IBM PC-AT. Polytetrafluoroethylene (PTFE) tubing (0.5 mm i.d.) was used throughout

Software

The Flow Injection Development and Optimization (FIDO) software used for the optimization and response-surface mapping experiments was written in our laboratory in Microsoft QuickBASIC[®] version 4.0, as was the code used for nonlinear curve fitting, factor analysis, and other data-processing tasks. The optimization algorithm used was the composite modified simplex method^{15,16} Response-surface plots were generated by a commercial scientific graphics program (SURFER[®] version 3.0, Golden Software, Golden, CO)

Procedures

Kinetic studies. To establish the effect of pH on the rate of the Pd(II)/Na-SCPAR reaction, both manual and stopped-flow studies were made. For the initial manual experiments, a 5.00-ml aliquot of $1.00 \times 10^{-4} M$ palladium was added to a mixture containing 15.00 ml of buffer solution and 5.00 ml of $9.44 \times 10^{-4} M$ Na-SCPAR. After thorough mixing, an appropriate volume was transferred to the cell of the spectrophotometer. Absorbance measurements were initiated 30 sec after the start of the reaction and acquired at 30-sec intervals for a period of 600 sec, over the wavelength range 300–750 nm. The pH range 2–11 was examined in this manner.

Once the optimum reaction pH was identified, stopped-flow experiments were conducted to determine the kinetic parameters. Buffered streams of Na-SCPAR ($3.78 \times 10^{-4} M$) and palladium (10^{-5} – $10^{-4} M$) were merged at a mixing T-piece and directed to the flow-cell through a 4-cm length of tubing. Pumps were run at maximum speed to transport the reaction mixture to the cell and then stopped to allow the kinetic measurements. Absorbance measurements at 488 nm were made at 1-sec intervals for a period of 200 sec after the pumps were stopped.

Automated optimization. The flow-injection configuration used for the automated simplex optimization experiments is shown in Fig 1a. The reagent stream, R, consisted of Na-SCPAR merged with distilled water to give a total flow-rate of 0.50 ml/min and a maximum Na-SCPAR concentration of $9.44 \times 10^{-4} M$

The buffer stream, B, was allowed to vary in pH during the automated optimization, but was kept at a constant flow-rate of 0.50 ml/min. The carrier stream was maintained at a fixed flow-rate of 1 ml/min and merged with the other two streams to give a total flow-rate of 2.00 ml/min at the detector. This ensured a constant sample residence time in the system. Separate pumps were used for each solution. The configuration chosen merges the sample with the reagent stream rather than directly injecting the sample into it. This is to preclude precipitation within the injection valve under adverse experimental conditions. During the automated simplex optimization process, the flow-rates of the Na-SCPAR, sodium hydroxide and buffer streams were automatically adjusted so as to attain wide variation in Na-SCPAR concentration and pH.

For each experiment, the required flow-rates were established, and the system was allowed to equilibrate. Once a steady baseline was obtained, a 70- μl sample of $1.0 \times 10^{-4} M$ palladium was injected into the carrier stream. Absorbances were measured at 488 nm. The pH of the reaction mixture was measured in a

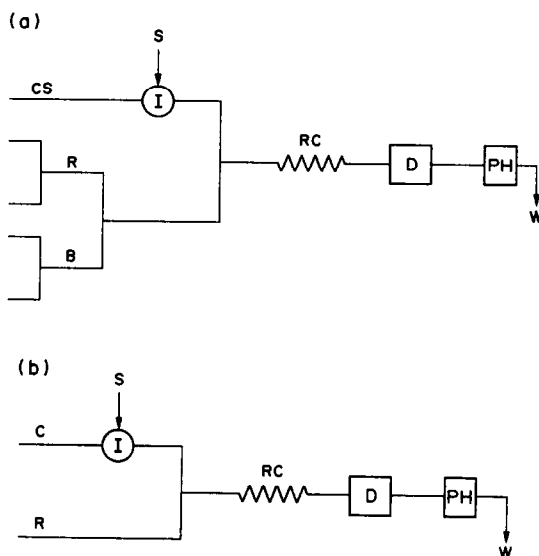


Fig 1 (a) Flow-injection manifold used for automated optimization and response-surface mapping studies, comprised of aqueous carrier stream (CS), injection valve with 70- μl loop (I), sample in 1mM HCl (S), 0.2M NaOH and universal buffer at pH 2.0 (B), 0.94mM Na-SCPAR and distilled water (R), reaction coil (RC), spectrophotometer (D), and pH-electrode cell (PH). Stream goes to waste (W). (b) Flow-injection manifold used for the calibration and interference studies, comprised of buffer carrier stream (C), injection valve with 70- μl loop (I), sample in 1mM HCl (S), premixed $9.44 \times 10^{-4} M$ Na-SCPAR reagent stream, buffered to pH 5.0 (R), reaction coil (RC), spectrophotometer (D), and pH-electrode cell (PH). Stream goes to waste (W).

simple flow-through cell situated after the detector

Several simplex optimizations were performed to establish the optimum reaction-coil length. Coil lengths of 50, 75, 100, 125 and 150 cm were used.

Once the optimum conditions were established, they were implemented on a simpler flow-injection system (Fig. 1b) which was used for both routine analysis and the interference studies. Such routine analyses can be done with a simple flow-injection system comprising one pump, two pump tubes and a single injection valve.

RESULTS AND DISCUSSION

Effect of pH on Na-SCPAR

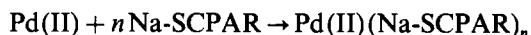
The absorption spectra of Na-SCPAR at various pH values are shown in Fig. 2. In strongly acidic media, absorption maxima occur at 306 and 420 nm. The band at 306 nm undergoes a red-shift and an increase in amplitude as the pH increases to ~ 7 , and there is a decrease in the absorbance at 420 nm. Under alkaline conditions, the absorption band at 420 nm shifts to longer wavelengths with increasing pH, but the amplitude does not change appreciably. These pH effects may be attributed to protonation of basic groups, deprotonation of acidic groups, and/or various tautomeric processes.

The reagent is unstable in strong alkali, and at above pH 11 decomposition of the reagent follows zero-order kinetics, the rate increasing with pH. Figure 3 shows the change in Na-SCPAR absorbance at pH 12.6, as a function of time.

Effect of pH on complexation

The nature of the reagent in solution strongly influences its ability to form metal complexes. The reaction of Na-SCPAR with some noble metals, such as palladium, and some base metals, such as copper, zinc and iron, is known to be highly pH-dependent.⁹ Experimental results indicate that acidic conditions are optimum for palladium, and little reaction occurs under basic conditions. Any products formed under alkaline conditions decompose rapidly.

The kinetics of the reaction was investigated at the optimum pH under pseudo-first-order conditions with Na-SCPAR in excess. If the reaction is expressed as



the reaction rate can be written as

$$\text{Rate} = k'[\text{Pd(II)}] \quad (1)$$

where k' is the pseudo-first-order rate constant.

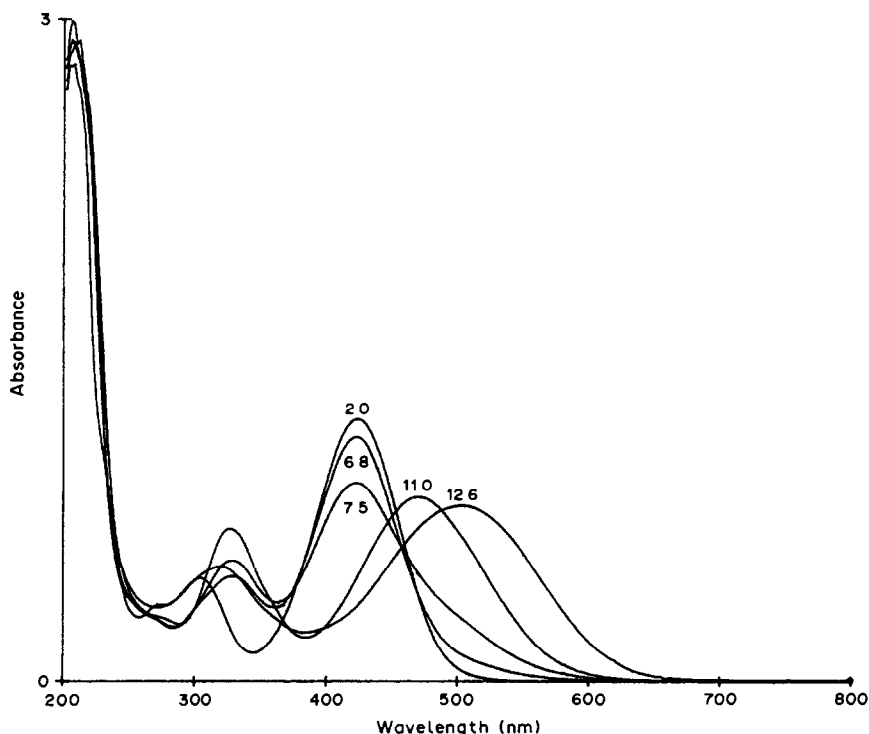


Fig. 2 Absorption spectra of Na-SCPAR at pH 2.0, 6.8, 7.5, 11.0 and 12.6

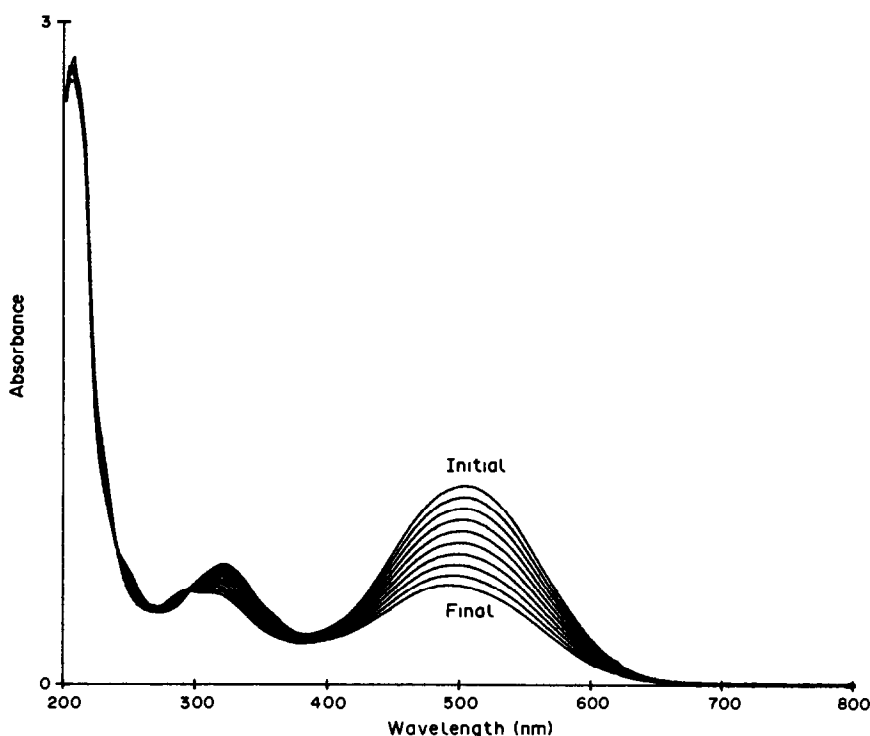


Fig 3 Absorbance of Na-SCPAR at pH 12.6, showing instability. Measurements taken at 30-sec intervals from 30 sec after mixing ("initial") to 300 sec ("final"). The zero-order rate constant for the decomposition is $1.7 \times 10^{-3} \text{ sec}^{-1}$.

A nonlinear curve-fitting program was used to extract the pseudo-first-order rate constant from the stopped-flow data. The equation fitted to the data was

$$A_t = A[1 - \exp(-k't)] + Bt + C \quad (2)$$

where A_t is the absorbance at time t , A is the final solution absorbance due to the product, B is a linear-drift term, and C is a constant background term. The linear-drift term was needed to account for thermal effects on the solution in the cell, since the cell was not kept at constant temperature. This term was generally very small. Figure 4 shows a typical fit of the model to the data. Good fits were obtained for each of the solutions tested. The pseudo-first-order rate constant returned by the fitting routine was about $0.11 \pm 0.01 \text{ sec}^{-1}$ at room temperature for 0.378 mM Na-SCPAR. The final equilibrium absorbance due to the product did not change for Na-SCPAR concentrations within the range $0.19\text{--}0.76 \text{ mM}$, indicating that the equilibrium lies well to the right.

The reaction rate is much higher under the mildly acidic conditions used here than under the strongly acidic conditions used previously.⁹ Reaction rates measured in this study indicate

the reaction is essentially finished in less than 60 sec. The maximum absorbance is found at 488 nm rather than the 520 nm reported⁹ earlier.

The pseudo-first-order rate constant was also found to be largely independent of Na-SCPAR concentration in the range used, indicating that the reaction does not have a simple single-step mechanism. Treatment of the kinetic curves by factor analysis¹⁷ indicated that a minimum of two components made sufficient contributions to the observed absorbance-time behavior. It may reasonably be presumed that these are the

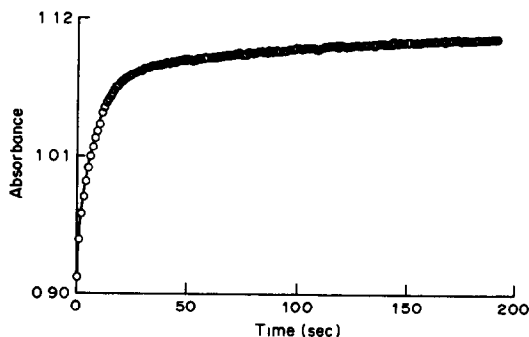


Fig 4 Fit of a pseudo-first-order reaction model (solid line) to data collected for the reaction between Na-SCPAR and Pd(II) at pH 5.0

Table 1 Optimization of coil length for Na-SCPAR/Pd(II) reaction

Coil length, cm	Maximum absorbance	Relative performance, %
50	0.451	78.6
75	0.574	100.0
100	0.513	89.4
125	0.448	78.0
150	0.428	74.6

Na-SCPAR reagent and the complex. However it should be noted that this algorithm is unable to differentiate between the effect of a single component and a fast equilibrium.

Automated optimization of the flow-injection system

The optimum pH and reagent concentration for the flow-injection determination of palladium with Na-SCPAR were automatically established by simplex optimization and response-surface mapping. An average of 30 experiments was performed during the automated optimization procedure, with four replicate runs for each experiment. Optimum performance was achieved in just under 2 hr. For the automated response-surface mapping, a factorial design consisting of 64 experiments with four replicates of each was used. These experiments took about 4 hr to complete.

As shown in Fig. 1a, the pumps for all streams were arranged to give a fixed total flow-rate of 2.00 ml/min. The reagent stream consisted of $9.44 \times 10^{-4} M$ Na-SCPAR coupled with a distilled-water stream so that while the relative flow-rates of the two streams could change, the total flow-rate of the reagent stream remained at 0.50 ml/min. In this way, the Na-

SCPAR concentration could be changed without grossly affecting the total flow-rate. Likewise the buffer stream consisted of 0.2M sodium hydroxide coupled with the pH-2 universal buffer stream. The precision with which the individual flow-rates were matched so as to maintain a constant total was good but was limited by the pump stepper-motor drivers.¹³ Calibration data for the pump-tube flow-rates, obtained at the start of the procedure, were assumed to hold throughout its duration.

The initial automated simplex optimization showed that the optimum Na-SCPAR flow-rate was in the range 0.42–0.50 ml/min. This is as expected, since the greatest amount of product should be formed when the Na-SCPAR concentration is at its maximum value. This study established that the optimum flow-rate range for the sodium hydroxide stream was 0.125–0.150 ml/min, which corresponds to pH 4.70–5.30. This is consistent with the earlier studies of pH effects.

The effect of reaction-coil length on the sensitivity of the system was determined by performing the automated optimization experiments with several different coil lengths. Optimum performance was observed with a reaction-coil length of 75 cm. Both longer and shorter coil lengths resulted in decreased absorbance, as shown in Table 1. This can be readily explained by the interaction of reaction kinetics and physical dispersion.¹⁸

The three-dimensional response-surface plot and contour map shown in Fig. 5 indicates how the Na-SCPAR and sodium hydroxide flow-rates affect the system performance. The Na-SCPAR flow-rates correspond to Na-SCPAR

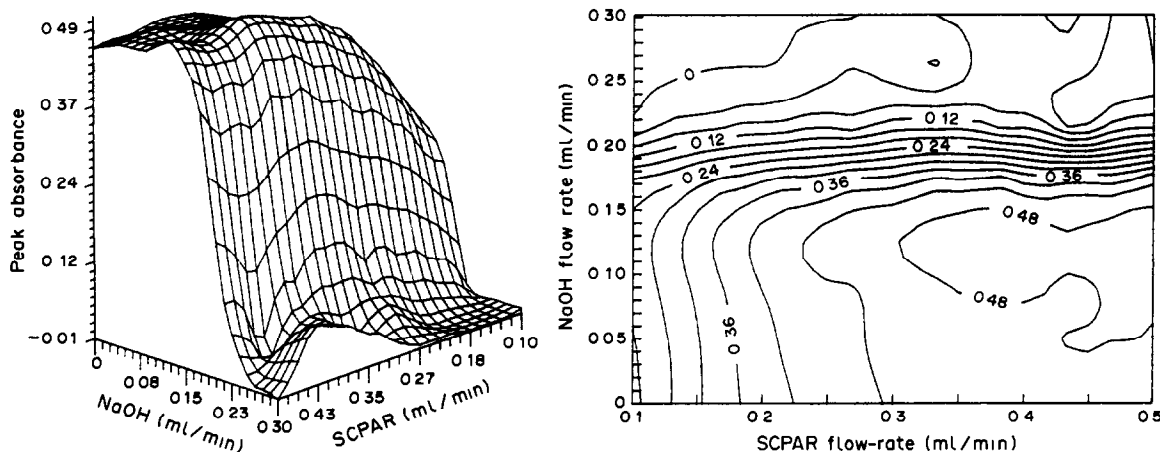


Fig. 5 The Na-SCPAR-Pd(II) response surface shown as a three-dimensional projection and its corresponding contour map. Response is the peak absorbance at 488 nm, and the NaOH and Na-SCPAR flow-rates are in ml/min.

Table 2 Metal ions interfering in the determination of palladium

Ion	Sensitivity*	λ_{max} , † nm
Rh(III)	0.27	482
Au(III)	0.25	348, 498
Cu(II)	0.24§	520
Pt(IV)	0.22	488
Ag(I)	0.18	500
Pb(II)	0.15	294, 472
Fe(II)	0.09	474
Ir(III)	0.08	496
Al(III)	0.07	490
Zn(II)	0.05	334, 520

*Sensitivity relative to that for an equal concentration of Pd(II)

†For reaction mixture at pH 5

§Can be effectively masked with $10^{-3}M$ EDTA

concentrations of 0.19–0.94 mM in the reagent stream. The sodium hydroxide flow-rates correspond to a pH range of approximately 3.0–11.0. The optimum conditions indicated by this plot are in good agreement with other results obtained in this study. The plateau region found by the automated response-surface mapping indicated that the method developed was stable. Experimental conditions in this region of the response surface are recommended for routine analysis.

Interferences

The effects of various concentrations of other metal ions on the determination of 10 $\mu\text{g/ml}$ palladium was examined for this system. Cobalt(II), iron(III), nickel(II), tin(II), ruthenium(III), manganese(II), cadmium(II) and mercury(I) did not interfere at the optimum pH even when present at a level of 0.01 M, i.e., one hundred times the palladium concentration. Interaction of these metal ions with Na-SCPAR

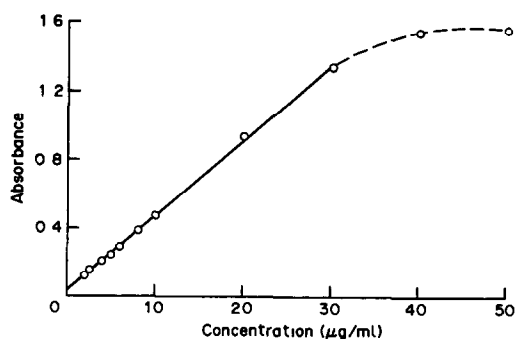


Fig. 6 Calibration curve for palladium determination. The solid line represents the linear dynamic range.

under alkaline conditions has been reported.⁹ Table 2 lists a number of metal ions that interfere. Also listed are the sensitivities for these ions relative to palladium, and the wavelength maxima observed in the spectra of their complexes. Most of these ions give complexes having maximum absorbance at a wavelength different from that for palladium, and thus further selectivity should be achievable by use of multi-wavelength measurements.⁷

Analytical performance

For routine analysis, the flow-injection geometry shown in Fig. 1b was employed. The calibration graph obtained with this apparatus (Fig. 6) was linear up to a palladium concentration of 30 $\mu\text{g/ml}$ with a sensitivity (slope) of 0.04 ml/ μg . The non-zero intercept observed in the calibration plot results from a refractive index effect due to the injection of the palladium standard into the buffer stream. The detection limit with this system was 0.04 $\mu\text{g/ml}$.

The apparent molar absorptivity obtained for the SCPAR–Pd(II) complex was 4.28×10^4

Table 3 Comparison of detection limits, dynamic ranges and interferences in this work and the other flow-injection methods for palladium determination

Method	Reference	Detection limit, $\mu\text{g/ml}$	Linear dynamic range, $\mu\text{g/ml}$	Interferences
EDTA/Pd	7	Not given	9–180	[Os(IV), Ru(III), Pt(IV), Rh(III), Ir(III), Ir(IV)]*
5-Br-PSAA/Pd	8	0.002	0.01–0.10	Cu(II)†, Fe(II)†, Co(III)§, Ni(II)§, Pt(VI)§, Os(VIII)§, Ru(II)§, W(VI)†§
Na-SCPAR/Pd	This work	0.045	0.045–30	See text

*0.02–1.5 mg permissible weight giving less than 5% error in determination of 1 mg of palladium

†Tolerated up to 1–10 mg/l when $10^{-3}M$ EDTA is added to carrier stream to mask interferences

§Tolerated up to 1–5 mg/l in determination of 0.1 mg/l palladium

$\text{l. mole}^{-1} \cdot \text{cm}^{-1}$, lower than the values obtained by Savvin and Guereva.⁹ The sample throughput rate was 120/hr. In the unlikely event that even higher sampling rates are needed, an increase in flow rate and/or a decrease in reaction coil length would increase this, at the expense of sensitivity.

Table 3 compares the detection limits, linear dynamic ranges and interfering metal ions cited for the other two flow-injection methods^{7,8} for palladium with those of the present procedure.

Conclusion

Na-SCPAR is a sensitive and moderately selective reagent for the spectrophotometric determination of palladium(II). The results from manual pH studies, and automated response-surface mapping and simplex optimization experiments, show good agreement. The apparatus employed is simple and allows the rapid determination of palladium without an extraction step. Additional advantages of this analytical method are those generic to flow injection, and include relatively inexpensive equipment, high precision, high sample throughput, and low sample and reagent consumption.

REFERENCES

- 1 V Michaylova, B Evtimova and D Nonova, *Anal Chim Acta*, 1988, **207**, 373
- 2 F Kai, Y Sakanashi, S Satoh and S Uchikawa, *Anal Lett*, 1983, **16**, 1013
- 3 Z Marczenko and M Jarosz, *Talanta*, 1981, **28**, 561
- 4 K Watanabe and M Hojatie, *Anal Chim Acta*, 1988, **218**, 111
- 5 W M MacNevin and O H Knege, *Anal Chem*, 1954, **26**, 1768
- 6 R Lockyer and G E Hames, *Analyst*, 1959, **84**, 385
- 7 A T Haj-Hussein and G D Christian, *ibid*, 1986, **111**, 65
- 8 T Sakai and N Ohno, *Anal Chim Acta*, 1988, **214**, 271
- 9 S B Savvin and R F Guereva, *Talanta*, 1987, **34**, 87
- 10 D Betteridge, T J Sly, A P Wade and J E W Tillman, *Anal Chem*, 1983, **55**, 1292
- 11 P D Wentzell, A P Wade and S R Crouch, *ibid*, 1988, **60**, 905
- 12 G E P Box, *Biometrics*, 1954, **10**, 16
- 13 D Betteridge, T J Sly, A P Wade and D G Porter, *Anal Chem*, 1986, **58**, 2258
- 14 D D Perrin and B Dempsey, *Buffers for pH and Metal Ion Control*, p 48 Chapman & Hall, London, 1974
- 15 D Betteridge, A G Howard and A P Wade, *Talanta*, 1985, **32**, 709
- 16 *Idem*, *ibid*, 1985, **32**, 723
- 17 E R Malinowski and D G Howery, *Factor Analysis in Chemistry*, Wiley, New York, 1980
- 18 J Růžicka and E H Hansen, *Flow Injection Analysis*, 2nd Ed, Wiley, New York, 1988

DIRECT SPECTROPHOTOMETRIC DETERMINATION OF Nd AND Er IN MIXED RARE EARTHS WITH 8-HYDROXYQUINOLINE-5-SULPHONIC ACID AND CETYLPYRIDINIUM CHLORIDE

SHI-FU ZHOU and NAI-XING WANG

Department of Chemistry, Shandong University, Jinan, Shandong, People's Republic of China

(Received 30 June 1988 Revised 12 September 1989 Accepted 29 September 1989)

Summary—Neodymium and erbium can form stable ternary complexes with 8-hydroxyquinoline-5-sulphonic acid and cetylpyridinium chloride, but a photometric method based on this does not give high enough sensitivity and is subject to interference by cerium. Use of the third derivative spectra, however, eliminates the interference by cerium and increases the sensitivity.

Many kinds of ternary rare-earth complexes have been reported, but few of them can enhance the amplitude of the absorption bands for the $4f$ electron transitions, and thus be useful for the determinations of individual rare earth elements.¹⁻⁶ Neodymium and erbium have been found to form ternary complexes with 8-hydroxyquinoline-5-sulphonic acid and cetylpyridinium chloride which have a molar absorptivity higher than that of the free ions or the binary complexes. On this basis a method has been developed for determining these two rare-earth elements in mixtures of lanthanides by means of the third derivative spectra. The method has good selectivity and accuracy, but the sensitivity is rather low.

EXPERIMENTAL

Apparatus

A Shimadzu UV-3000 double-beam spectrophotometer was used.

Reagents

Standard solutions of La, Ce, Pr, Nd, Sm, Eu, Ho, Er and Y were prepared from the pure oxides (Johnson Matthey).

Solutions of 8-hydroxyquinoline-5-sulphonic acid (HQS, 0.100M), cetylpyridinium chloride (CPC, 0.200M) and poly(vinyl alcohol) (PVA, 2%) were prepared.

Analytical-reagent grade chemicals were used whenever possible.

Procedure

Transfer a known volume of lanthanide solu-

tion to a 25-ml standard flask, add 1.00 ml of 8-hydroxyquinoline-5-sulphonic acid solution, 1.00 ml of cetylpyridinium chloride solution, 1.0 ml of poly(vinyl alcohol) solution and 8.0 ml of 1M hexamine buffer solution (pH 6.5), dilute to the mark with distilled water and mix. Record the third-derivative spectrum against a reagent blank as reference, using 4-cm cells.

RESULTS AND DISCUSSION

The absorption spectra of Nd^{3+} , Er^{3+} and binary and ternary complexes formed with HQS and CPC at pH 6.5 are shown in Figs 1 and 2.

The difference between curves 2 and 3 in the spectra shows an increase in sensitivity when the binary complex is converted into the ternary complex. As the characteristic peaks of the binary and ternary complexes are at almost the same wavelength as those of the free ions, it can be concluded that the sensitivity is increased as a result of the ligands affecting the co-ordination field. The molar absorptivities are shown in Table 1.

The experimental conditions were optimized by varying one of them at a time, and the values thus selected are those given in the procedure. To allow for consumption of the reagents by other lanthanides in analysis of mixtures, the amounts recommended in the procedure are about 10 times that necessary for the sum of the lanthanides present.

Generally, turbidity or even precipitation can occur to some extent in solutions containing cationic surfactants at low temperature. Precipitation occurred at temperatures below 15° in the

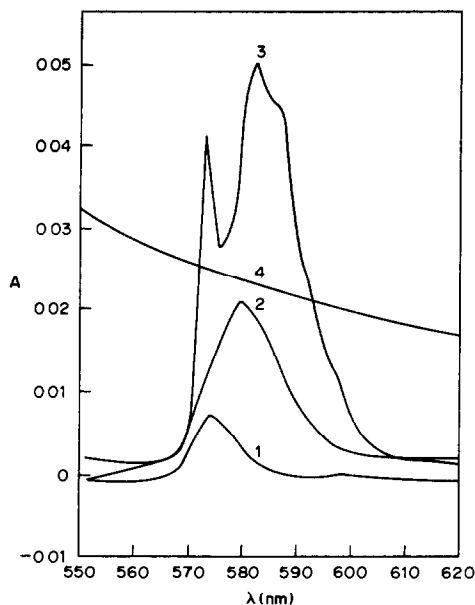


Fig 1 Absorption spectra of neodymium and its binary and ternary complexes $[Nd] = 3.0 \times 10^{-4}M$, $[HQS] = 3.0 \times 10^{-3}M$, $[CPC] = 3.0 \times 10^{-2}M$ 1, Nd^{3+} , 2, $Nd^{3+} + HQS$, 3 $Nd^{3+} + HQS + CPC$, 4, $HQS + CPC$, 1 and 4, water as reference, 2 and 3, reagent blank as reference

reaction mixtures described here, so PVA was added to prevent it. The spectra of the solutions with PVA added are almost the same as those without PVA except for a slight chromic shift,

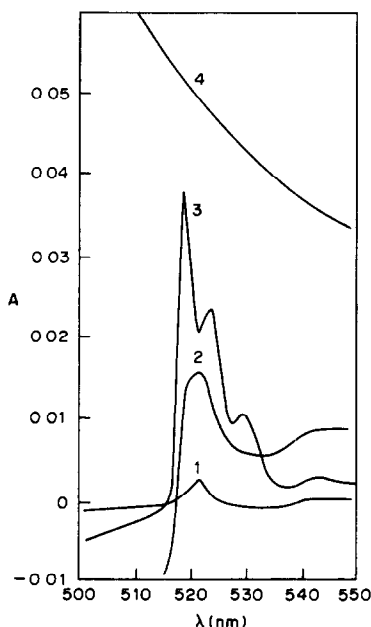


Fig 2 Absorption spectra of erbium and its binary and ternary complexes $[Er] = 3.0 \times 10^{-4}M$, $[HQS] = 3.0 \times 10^{-3}M$, $[CPC] = 3.0 \times 10^{-2}M$ 1, Er^{3+} , 2, $Er^{3+} + HQS$, 3, $Er^{3+} + HQS + CPC$, 4, $HQS + CPC$, 1 and 4, water as reference, 2 and 3, reagent blank as reference

Table 1 Molar absorptivities of the Nd and Er species in the different systems

System	λ_{max}, nm	$\epsilon, l\ mole^{-1}\ cm^{-1}$
Nd^{3+}	575	6.4
$Nd^{3+}-HQS$	581	15.9
$Nd^{3+}-HQS-CPC$	583	40.3
Er^{3+}	523	2.4
$Er^{3+}-HQS$	523	14.5
$Er^{3+}-HQS-CPC$	520	31.3

so the addition of PVA appears to have no significant effect on the original reaction. The ternary complexes form rapidly and the absorbances are stable for at least 7 hr.

The interference of the other lanthanides tested is shown in Fig 3, only cerium shows serious interference.

Use of the derivative spectra both eliminates the interference of Ce and Ho, and increases the sensitivities for Nd and Er (Fig. 4). The oxidation state of the cerium is immaterial. In the range from 500 to 620 nm, La, Pr, Sm, Ce(III or IV), Eu, Ho and Y produce only a constant signal in the third-derivative spectrum, so cause no interference. The characteristic peaks of Nd are free from interference, and can be used to determine Nd directly. The difference in amplitude of the peak at 576.8 nm and the trough at 573 nm is recommended for the calculation. The

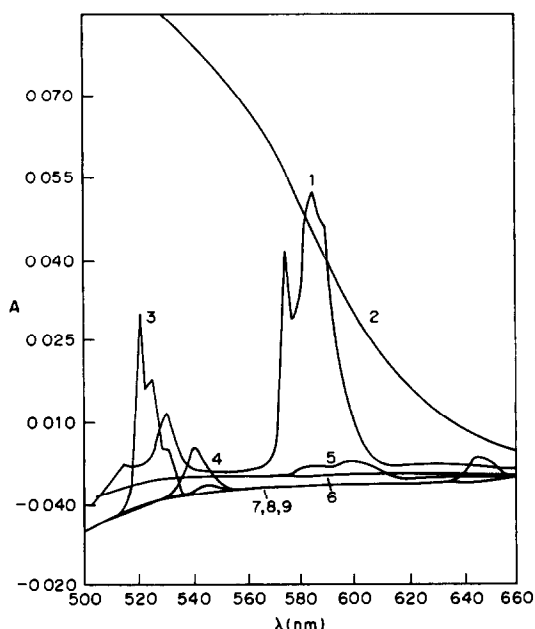


Fig 3 Absorption spectra of other lanthanide (Ln) ternary complexes (pH 6.5) $[HQS] = 3.0 \times 10^{-3}M$, $[CPC] = 3.0 \times 10^{-2}M$ $[Ln] (10^{-4}M)$ 1, Nd (3.0), 2, Ce (1.0), 3, Er (2.9), 4, Ho (2.4), 5, Pr (3.0), 6, La (2.7), 7, Eu (2.5), 8, Sm (2.2), 9, Y (2.5) Reagent blank as reference

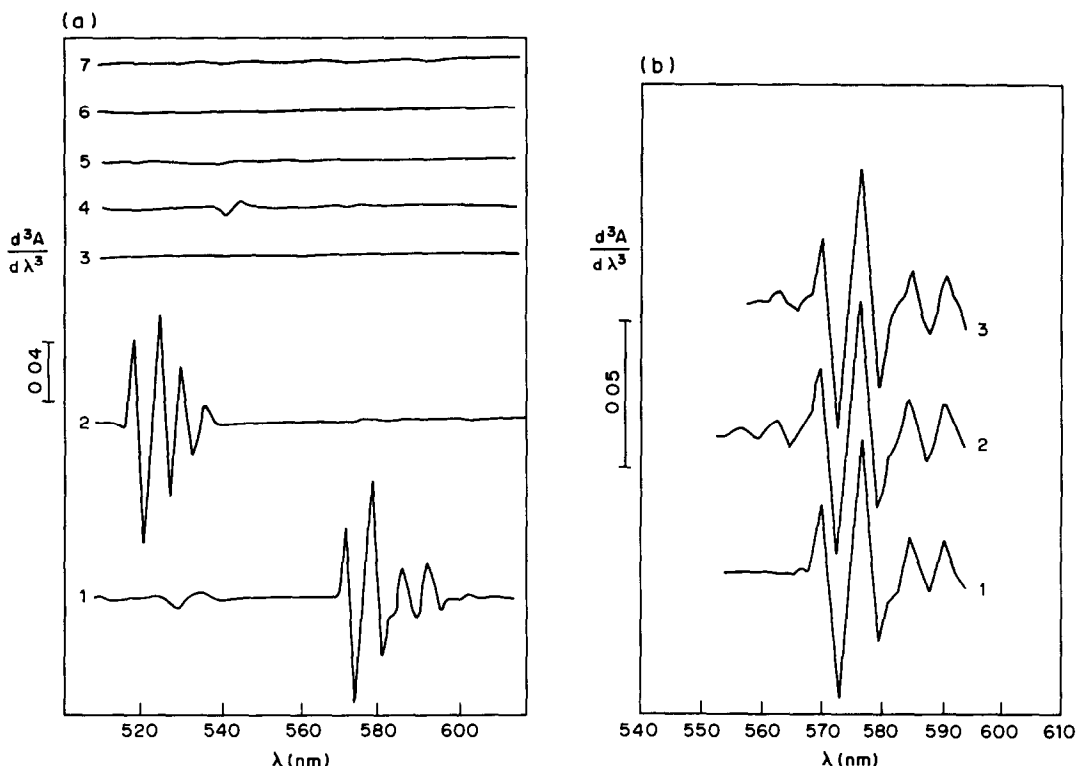


Fig 4 Derivative spectra of the ternary complexes (pH 6.5) (a) $[HQS] = 1.5 \times 10^{-3} M$, $[CPC] = 1.0 \times 10^{-2} M$, $\Delta\lambda = 3.5$ mm, bandpass = 0.25 nm $[Ln] (10^{-4} M)$ 1, Nd (1.5), 2, Er (1.5), 3, Pr (1.2), 4, Ho (1.2), 5, Sm (1.1), 6, Eu (1.5), 7, Ce (2.1), reagent blank as reference (b) $[HQS] = 1.2 \times 10^{-3} M$, $[CPC] = 1.5 \times 10^{-3} M$ $[Ln] (10^{-4} M)$ 1, Nd (1.0), 2, Nd (1.0) + Ce(III) (1.0), 3, Nd (1.0) + Ce(IV) (1.0)

characteristic peak of Er is subject to slight interference from Nd, and when both are present, a correction must be applied by means of a factor obtained by measurement of a standard neodymium solution at the two wavelengths concerned:

$$f^{Nd} = A_{522.5}^{Nd} / A_{576.8}^{Nd}$$

$$(A_{522.5}^{Er})_{corrected} = (A_{522.5}^{Er+Nd})_{measured} - (A_{576.8}^{Nd})_{measured} \times f^{Nd}$$

The calibration graphs are linear over the range 0–25 $\mu\text{g/ml}$ for Nd and 0–30 $\mu\text{g/ml}$ for Er (in the final solution), and the sensitivity is 7 times higher for Nd and 9 times for Er than in the normal method.

Because the third derivative is in direct ratio to the concentration of the ternary complex but not of its components, it may be used to determine the composition of the ternary complex. The molar ratio method showed the lanthanide:ligand:surfactant ratio to be 1.4.5. If the lanthanide(III) ion has a co-ordination number of 8, then the fourth ligand is presumably bound without loss of a proton from the hydroxyl group (pK for loss of this proton is 8.5 at 0.1M ionic strength), and in that case the ternary species would carry a single positive charge (5 positive charges from the cetylpyridinium ions, 4 negative charges from the sulphonate groups). The ternary species was found to be retained by a cation-exchange resin but not by an anion-exchanger, supporting this view.

Table 2 Compositions of synthetic samples ($Ln_2O_3\%$)

Sample	La_2O_3	CeO_2	Pr_6O_{11}	Nd_2O_3	Sm_2O_3	Eu_2O_3	Ho_2O_3	Ey_2O_3	Y_2O_3
1	31.28	20.88	3.77	11.84	1.64	1.95	17.97	6.73	3.94
2	1.85	3.62	10.91	3.43	1.89	1.13	30.58	7.79	38.80

Table 3 Results for synthetic samples

		Nd ₂ O ₃	Er ₂ O ₃
Sample 1	Present, %	11.84	6.73
	Found, %	11.41	6.68
Sample 2	Present, %	3.43	7.79
	Found, %	3.55	7.90

To test the utility of the method, two synthetic samples were prepared (Table 2) and analysed. The results are listed in Table 3.

*From Baotou Rare Earths Academy, China. The composition is CeO₂ 49.21%, La₂O₃ 27.11%, Pr₆O₁₁ 5.18%, Nd₂O₃ 16.75%, Sm₂O₃ 1.29%, heavier rare-earth and Y oxides 1.09%.

A reference sample* was also analysed for Nd, and the three values obtained were 15.94, 16.05 and 16.08%, which compare reasonably well with the certified value (16.75%).

REFERENCES

- 1 T. Taketatsu and C. V. Banks, *Anal. Chem.*, 1966, **38**, 1524.
- 2 L. I. Kononenko and T. P. Piontkovskaya, *Zh. Analit. Khim.*, 1969, **24**, 379.
- 3 L. I. Kononenko, M. A. Tishchenko and V. N. Drobyazko, *ibid.*, 1971, **26**, 729.
- 4 Gao Jin-Zhang, Kang Jing-wan and Bi Guang-Bi, *Acta Chim. Sin.*, 1979, **24**, 1119.
- 5 Kang Jing-wan, Chen Ru-Yao and Bi Guang-Bi, *ibid.*, 1984, **42**, 921.
- 6 Zhou-Shi Fu and Wang Nai-Xing, *Fenxi Huaxue*, 1987, **11**, 1041.

SPECTROPHOTOMETRIC STUDY AND ANALYTICAL APPLICATIONS OF LANTHANIDE-KOJIC ACID COMPLEXES

DIRECT DETERMINATION OF Nd, Ho AND Er IN MIXTURES OF RARE EARTHS

SHI-FU ZHOU and ZHONG LI

Department of Chemistry, Shandong University, Jinan, Shandong, People's Republic of China

(Received 8 April 1987 Revised 17 August 1989 Accepted 29 September 1989)

Summary—The complexes of the rare-earth metals with kojic acid in weakly alkaline solution are reported. The characteristic absorbances of neodymium, holmium and erbium can be increased by factors of 4.3, 11.0 and 6.4 respectively, compared with those of the chlorides. The third-derivative spectra have been used to eliminate the interference of Ce, La and Y, and the sensitivities are again increased, by a factor of 6–9.

There has always been interest in the determination of individual rare-earth metals in their mixtures. In the last two decades, however, almost no new reagents for the purpose have been reported. Several earlier reagents, such as dibenzoylmethane,^{1,2} 1-phenyl-3-methyl-4-benzoylpyrazol-5-one,^{3,4} thenoyltrifluoroacetone^{5,6} and disodium 1,2-dihydroxybenzene-3,5-disulphonate,^{7,8} are still used. It appears that tri-ethylhexyl phosphate,⁹ suggested by Zakı *et al.* cannot be used for determining individual rare-earth elements. We have discovered that kojic acid [5-hydroxy-2-(hydroxymethyl)-4H-pyran-4-one] can form stable complexes with rare-earth metals in weakly alkaline solution. In the absorption spectra, the peaks of Nd, Ho and Er in the visible region are enhanced, the absorbances at λ_{\max} being increased by factors of 4.3, 11.0 and 6.4 respectively, compared with those of the chlorides. However, the sensitivities are still rather low for general use. Therefore their derivative spectra have been studied and use of the third derivative spectra has been found to increase the sensitivity considerably and eliminate the interference of Ce, La and Y. A new method for Nd, Ho and Er has been based on this and used for analysis of two synthetic samples and one routine sample. The results obtained are quite satisfactory.

EXPERIMENTAL

Apparatus

Shimadzu recording spectrophotometers,

models UV-240 and UV-3000 were used. For the third-derivative spectra the band-pass used was 1 nm, $\Delta\lambda$ 0.3 nm, scan speed 50 nm/min.

Reagents

Standard solutions of rare-earth metals. Prepared from the pure oxides (Johnson Matthey) and mixed as required.

Kojic acid solution, 0.150M. All other reagents used were of analytical grade.

Procedure

Transfer the sample solution containing less than 0.15 mmole of rare-earth metal ions, to a 25-ml standard flask, add 10 ml of 0.150M kojic acid and 5 ml of 0.1M ammonia-ammonium chloride buffer (pH 9.2), dilute to the mark with water and mix. Record the absorption spectrum or its derivative with water (or a reagent blank) as reference.

RESULTS AND DISCUSSION

The absorption spectra of kojic acid at various pH values (Fig. 1) and the kojic acid complexes of Nd, Ho and Er (Figs. 2–4) were recorded. The variation of the absorbance of the complexes as a function of pH is shown in Fig. 5. Figure 1 shows that pH has hardly any effect on the absorption spectrum of kojic acid at wavelengths > 500 nm, whereas Fig. 5 shows that pH has a considerable effect on the absorbances of the complexes. Since precipitation

would occur at $\text{pH} > 10.5$, a pH of 9.2 was chosen for measurements. The molar absorptivities calculated for the Nd, Ho and Er complexes were 28.0, 41.5 and 20.8 $\text{l. mole}^{-1} \cdot \text{cm}^{-1}$, respectively, which are 4.3, 11.0 and 6.4 times greater than those for the chlorides.

Figure 6 shows the effect of the amount of reagent. In view of this, the amount of kojic acid used in the determinations was always at least 10 times that of the lanthanides. Variation of the amount of buffer solution between 2 and 10 ml had no effect on the absorbance of the complexes. The complexes formed quickly and were stable for more than 6 hr.

From Fig. 7 it is evident that the interference of Ce(III) and Ce(IV) must be eliminated to allow the determination of individual lanthanides in a mixed system. A chemical separation is tedious, whereas use of the derivative

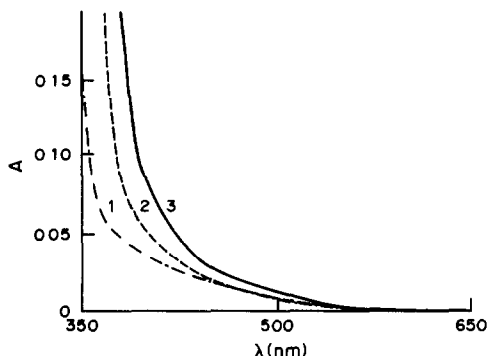


Fig 1 Absorption spectra of kojic acid ($6.00 \times 10^{-2} M$) at various pH values. 4-cm cell, water as reference, pH 1—4.50, 2—6.30, 3—9.20

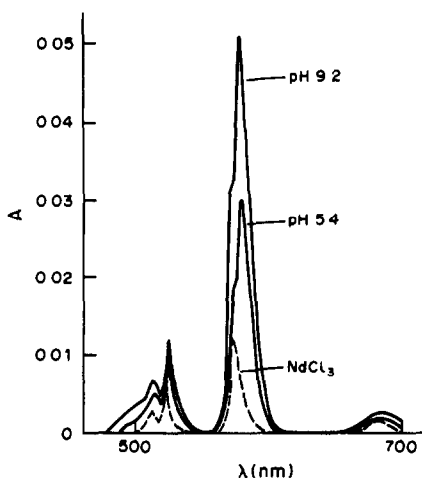


Fig 2 Absorption spectra of Nd-kojic acid complexes (pH 9.2 and 5.4) Nd $4.46 \times 10^{-4} M$, kojic acid $1.15 \times 10^{-2} M$, 4-cm cell, reagent blank as reference

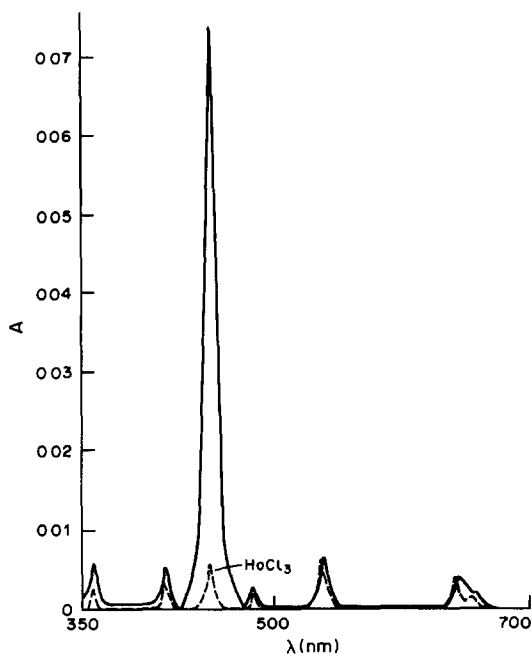


Fig 3 Absorption spectra of Ho-kojic acid complexes at pH 9.2 Ho $3.83 \times 10^{-4} M$, kojic acid $1.15 \times 10^{-2} M$, 4-cm cell, reagent blank as reference

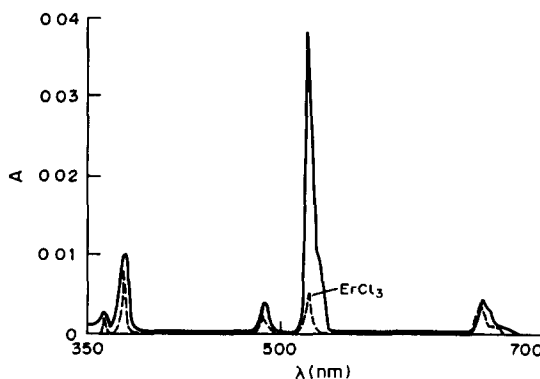


Fig 4 Absorption spectra of Er-kojic acid complexes at pH 9.2 Er $4.62 \times 10^{-4} M$, kojic acid $1.15 \times 10^{-2} M$, 4-cm cell, reagent blank as reference

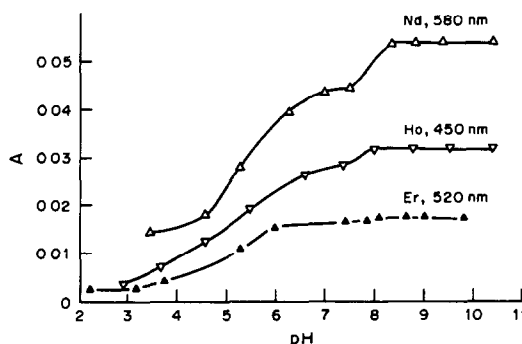


Fig 5 Variation of absorbance at λ_{max} as a function of pH Nd $4.4 \times 10^{-4} M$, Ho $1.92 \times 10^{-4} M$, Er $2.31 \times 10^{-4} M$, kojic acid $1.15 \times 10^{-2} M$, 4-cm cell, reagent blank as reference

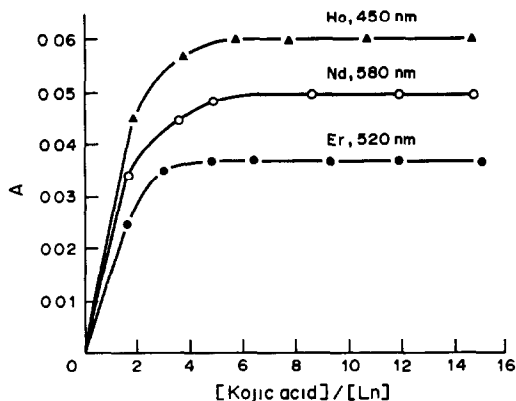


Fig 6 Effect of the amount of reagent Nd $4.46 \times 10^{-4}M$, Ho $3.83 \times 10^{-4}M$, Er $4.62 \times 10^{-4}M$, kojic acid $0.075M$, 4-cm cell, pH 9.2, reagent blank as reference

spectra is not only simple, but also improves the sensitivity. We have investigated the 1st–4th derivative spectra, and selected the third-derivative spectra since they gave the highest sensitivities. Figure 8 shows the third derivative spectra

Because the ordinary spectra of Ce(III) and Ce(IV) (Fig 7) are smooth curves, their third derivative spectra have no peaks from 400 to 700 nm, like those of La and Y. Therefore, these elements cause no interference. The characteristic peaks of Nd are free from interference from the other lanthanides and can be used to determine Nd directly. We use the sum of the peak height at 585 nm and the depth of the trough at 580 nm for the determination. The characteristic peaks of Ho and Er are subject to interference by Pr and Nd respectively. To find

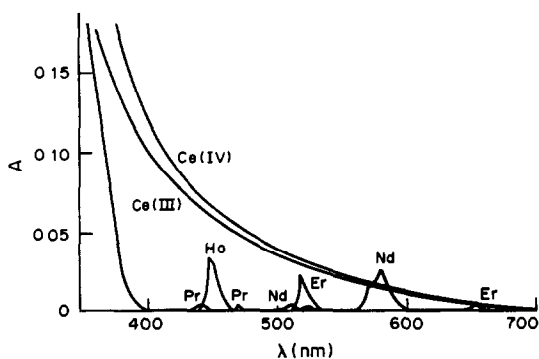


Fig 7 Absorption spectra of lanthanide-kojic acid complexes at pH 9.2 Kojic acid $1.15 \times 10^{-2}M$, Nd $2.229 \times 10^{-4}M$, Pr $2.35 \times 10^{-4}M$, Sm $2.08 \times 10^{-4}M$, Ho $1.92 \times 10^{-4}M$, Er $2.31 \times 10^{-4}M$, Eu $2.51 \times 10^{-4}M$, Ce $1.65 \times 10^{-4}M$, Ce(III) $1.71 \times 10^{-4}M$, La $3.81 \times 10^{-4}M$, Y $4.03 \times 10^{-4}M$, 4-cm cell, pH 9.2, water as reference

a means of removing this interference, we have measured several sets of spectra of solutions in which Ho and Pr, or Er and Nd, were both present (Fig. 9).

As shown in Fig. 9, the Ho peak at 454 nm is free from Pr interference, so its height can be used to calculate the Ho content. Both characteristic peaks of Er are subject to interference by Nd, but that with the trough at 524 nm is very slight, and the height of this peak may be used to calculate the Er content when that is greater than that of Nd. If the Nd content is more than that of Er, a correction coefficient (f^{Nd}) derived from a standard solution of Nd must be applied:

$$f^{Nd} = A_{524}^{Nd} / A_{585}^{Nd}$$

$$(A_{524}^{Er})_{corrected} = (A_{524}^{Er+Nd})_{measured} - (A_{585}^{Nd})_{measured} \times f^{Nd}$$

The calibration graphs are linear up to ~ 0.11 mg/ml for Nd_2O_3 and ~ 0.19 mg/ml for Ho_2O_3 and Er_2O_3 . The sensitivities for Nd, Ho and Er are 6, 7 and 9.5 times greater than those of the ordinary method.

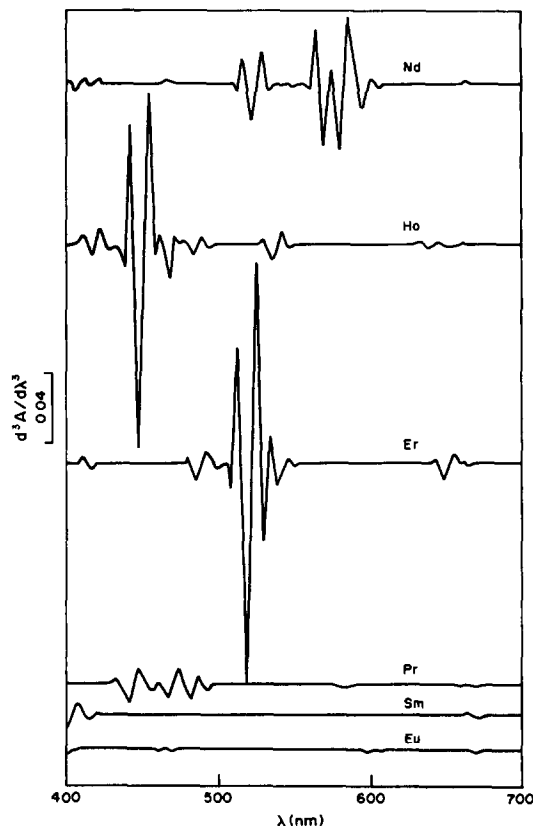


Fig 8 Derivative spectra of the rare-earth-kojic acid complexes Kojic acid $1.40 \times 10^{-2}M$, pH 9.2, 1-cm cell, Nd $4.46 \times 10^{-4}M$, Ho $2.88 \times 10^{-4}M$, Er $5.78 \times 10^{-4}M$, Pr $2.35 \times 10^{-4}M$, Sm $2.08 \times 10^{-4}M$, Eu $2.51 \times 10^{-4}M$

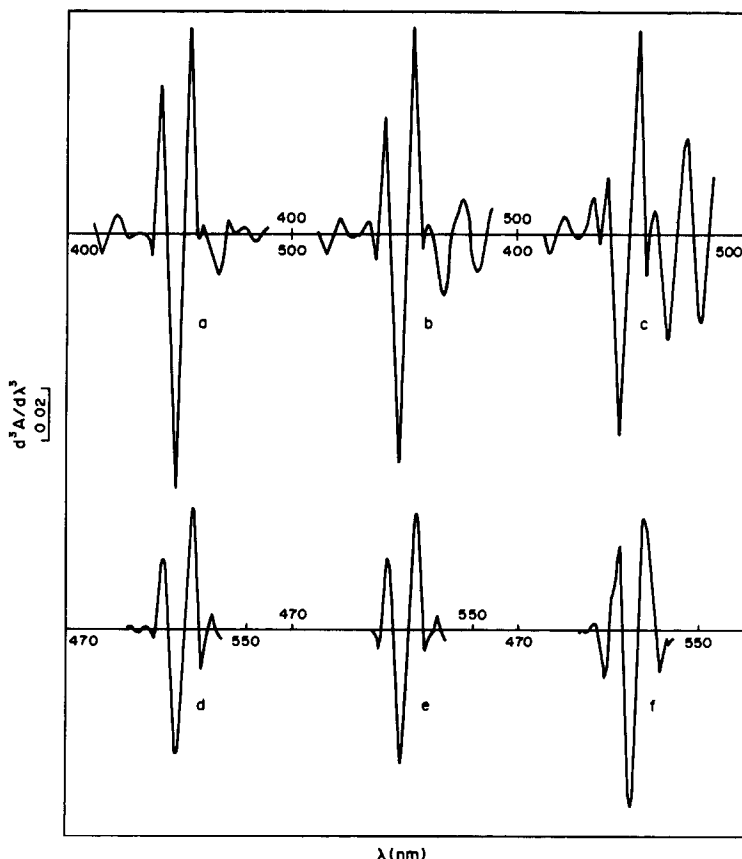


Fig 9 Interference of Pr with Ho and Nd with Er Kojic acid $1.40 \times 10^{-2}M$, pH 9.2, 1-cm cell. Curves a—Ho ($2.40 \times 10^{-4}M$), b—Ho ($2.40 \times 10^{-4}M$), Pr ($2.35 \times 10^{-4}M$), c—Ho ($2.40 \times 10^{-4}M$), Pr ($1.28 \times 10^{-3}M$), d—Er ($2.31 \times 10^{-4}M$), e—Er ($2.31 \times 10^{-4}M$), Nd ($2.23 \times 10^{-4}M$), f—Er ($2.31 \times 10^{-4}M$), Nd ($1.21 \times 10^{-3}M$)

Table 1 Compositions of synthetic samples (Ln_2O_3 , %)

Sample	La_2O_3	CeO_2	Pr_6O_{11}	Nd_2O_3	Sm_2O_3	Eu_2O_3	Ho_2O_3	Er_2O_3	Y_2O_3
I	23.02	51.03	4.93	14.40	1.48	0.21	1.08	2.50	1.35
II	1.50	8.42	11.53	2.05	2.76	1.60	3.50	7.50	61.14

Table 2 Results for synthetic samples (5 replicates, 25-mg samples)

		Nd_2O_3	Ho_2O_3	Er_2O_3
Sample I	Taken, %	14.40	1.08	2.50
	Found \pm std. devn, %	14.5 ± 0.1	1.10 ± 0.02	$2.56 \pm 0.04^*$
Sample II	Taken, %	2.05	3.50	7.50
	Found \pm std. devn, %	2.08 ± 0.03	3.47 ± 0.03	7.43 ± 0.05

The amounts of the two samples weighed out are 25 mg

*Corrected for Nd interference

In order to test the applicability of the method, two synthetic samples were prepared (Table 1) and analysed. The results are listed in Table 2, which shows that the relative errors of

*From Baotou Rare Earth Academy, China. The composition was CeO_2 49.21%, La_2O_3 27.11%, Pr_6O_{11} 5.18%, Nd_2O_3 16.75%, Sm_2O_3 1.29%, heavier rare-earth and Y oxides 1.09%

the method are below 3%. In addition, the amount of Nd in a reference material* was determined. The value found was 17.06% and the certified value was 16.75% (relative error 1.8%). The relative standard deviation (5 determinations) was 1.7%. This shows that the accuracy and precision of the method are reasonably satisfactory.

REFERENCES

- 1 L. I. Kononenko, M. A. Tishchenko and V. N. Drobyazko, *Zh Analit Khim*, 1971, **26**, 729
- 2 Yang Zhen-xi, *Fenxi Huaxue*, 1975, **3**, 133
- 3 I. R. Efimov and A. K. Nurtaeva, *Zh Analit Khim*, 1977, **32**, 1735
- 4 Kang Jing-wan, Chen Ru-yao and Bai Guang-bi, *Acta Chim Sin*, 1984, **42**, 921
- 5 T. Taketatsu and C. V. Banks, *Anal Chem*, 1966, **38**, 1524
- 6 Ren Ying, Liu Zhou-jing and Zhou Hong-ping, *Fenxi Huaxue*, 1985, **13**, 6
- 7 T. Taketatsu and N. Toriumi, *Talanta*, 1970, **17**, 465
- 8 Ren Ying and Zhang Pei-xun, *Acta Chim Sin*, 1986, **44**, 920
- 9 M. T. M. Zaki, A. F. Shouky and M. B. Hafez, *Analyst*, 1983, **108**, 531

A NEW SPECTROPHOTOMETRIC METHOD FOR QUANTITATIVE MULTICOMPONENT ANALYSIS RESOLUTION OF MIXTURES OF SALICYLIC AND SALICYLURIC ACIDS

F. SALINAS, J. J. BERZAS NEVADO and A. ESPINOSA MANSILLA

Department of Analytical Chemistry, University of Extremadura, 06071 Badajoz, Spain

(Received 29 December 1988; Revised 16 August 1989; Accepted 29 September 1989)

Summary—A new spectrophotometric method for resolving binary mixtures is proposed. The method is based on use of the first derivative of the ratios of spectra. The absorption spectrum of the mixture is obtained and the amplitudes at appropriate wavelengths are divided by the corresponding amplitudes in the absorption spectrum of a standard solution of one of the components, and the first derivative of the ratio spectrum is obtained. The concentration of the other component is then determined from a calibration graph. The method has been applied for resolving binary mixtures of salicylic and salicyluric acids. Calibration graphs for 2.6–52 ppm salicylic acid and for 2.1–42 ppm salicyluric acid were established by measuring the analytical signals at the maximum at 241.5 nm (for salicylic acid) and from the peak at 258 nm to the trough at 247 nm (for salicyluric acid) in the first derivative ratio spectra.

New methods for the simultaneous determination of two or more compounds in the same sample, without previous chemical separation, are always of interest. Derivative spectrophotometry offers greater selectivity than does normal spectrophotometry,^{1,2} because it decreases spectral overlap and allows better resolution. Mixtures of compounds with highly overlapped spectra have been resolved by using a multicomponent analysis program.^{3,4} Recently, Blanco *et al.*^{5,6} reported a method for treating the results, called multi-wavelength linear regression analysis (MLRA) and applied it to the determination of Fe(II) and Fe(III) with a mixture of 1,10-phenanthroline and sulphosalicylic acid as reagents, and use of a diode-array detector in flow-injection analysis. In effect, the method was based on use of each component in turn as a reference standard. The approach taken has now been extended. The method has been applied to the simultaneous determination of salicylic acid and salicyluric acid, which have strongly overlapped spectra. The results obtained are compared with those obtained by the method of Blanco *et al.*

THEORY

Consider a mixture of two compounds M and N. If Beer's law is obeyed for both compounds over the whole wavelength range used and the

path-length is 1 cm, the absorption spectrum of the mixture is defined by the equation

$$A_{m,\lambda_i} = \epsilon_{M,\lambda_i} C_M + \epsilon_{N,\lambda_i} C_N \quad (1)$$

where A_{m,λ_i} is the absorbance of the mixture at wavelength λ_i , ϵ_{M,λ_i} and ϵ_{N,λ_i} are the molar absorptivities of M and N at wavelength λ_i , and C_M and C_N are the concentrations of M and N.

If equation (1) is divided by the corresponding equation for the spectrum of a standard solution of M (concentration C_M^0), the following equation can be written:

$$\frac{A_{m,\lambda_i}}{\epsilon_{M,\lambda_i} C_M^0} = \frac{C_M}{C_M^0} + \frac{\epsilon_{N,\lambda_i} C_N}{\epsilon_{M,\lambda_i} C_M^0} \quad (2)$$

which can be simplified to

$$\frac{A_{m,\lambda_i}}{\epsilon_{M,\lambda_i}} = C_M + C_N \frac{\epsilon_{N,\lambda_i}}{\epsilon_{M,\lambda_i}} \quad (3)$$

By plotting $A_{m,\lambda_i}/\epsilon_{M,\lambda_i}$ as a function of $\epsilon_{N,\lambda_i}/\epsilon_{M,\lambda_i}$, a straight line is obtained. The intercept of the straight line provides the value of C_M and the slope of the straight line is C_N .

To obtain the ratio $\epsilon_{N,\lambda_i}/\epsilon_{M,\lambda_i}$ at each wavelength, the absorption spectra of equimolar standard solutions of N and M are measured and the absorbance ratio at each wavelength is calculated. This is the basis of the method of Blanco *et al.*

A new method can be developed from this for determining N in the presence of M, by using

the first derivative of equation (2)

$$\frac{d}{d\lambda} \left(\frac{A_{m,\lambda}}{\epsilon_{m,\lambda} C_M^0} \right) = \left(\frac{C_N}{C_M^0} \right) \frac{d}{d\lambda} \left(\frac{\epsilon_{N,\lambda}}{\epsilon_{M,\lambda}} \right) \quad (4)$$

Equation (4) indicates that the "derivative ratio spectrum" of the mixture is dependent only on the values of C_N and C_M^0 and is independent of the value of C_M in the mixture

A calibration graph is obtained by recording and storing the spectra of solutions of pure N at different concentrations, and the spectrum of a solution of pure M, of concentration C_M^0 . The amplitudes for N are then divided, wavelength by wavelength, by the corresponding amplitudes for M; the program "Data Leader" is used for this purpose.

The "ratio spectra" thus obtained are then differentiated with respect to wavelength and the derivative values for a given wavelength are plotted against C_N to give a calibration graph. Application of the method to the sample containing both M and N, and use of the calibration graph, will then give the value of C_N in the mixture. M can be determined by an analogous procedure. When molar concentrations are not used, the molar absorptivity, ϵ , is replaced by a proportionality constant K .

If the concentration of the standard (the divisor) is increased or decreased, the resulting first derivative values are proportionately decreased or increased, respectively, although the maxima and minima remain at the same wavelengths. In consequence the ratio of the slopes of two calibration graphs must be equal to the inverse of the concentration ratio of the divisors.

Accuracy and precision of the method

Accuracy and precision, in the spectrophotometric resolution of a binary mixture, depend on the spectra of the compounds and the treatment of the data. In general, when the spectra of the two compounds are very different, the resolution of the mixture requires only a simple mathematical treatment of the data obtained at two wavelengths, but mixtures of compounds having highly overlapped spectra yield poor results and other mathematical treatments are required, such as derivative spectrophotometry.⁷

In the proposed method, overlap of the spectra in a certain region is actually desirable, because in division of one spectrum by another, the error increases when one of the absorbances approaches zero

EXPERIMENTAL

Reagents

Salicylic acid was obtained from Merck and salicylic acid from Aldrich. Ammonia/ammonium chloride buffer solution (pH 10) was made from analytical-reagent grade reagents

Apparatus

A Beckman DU-50 spectrophotometer connected to an IBM PC-XT fitted with Beckman Data Leader Software and an Olivetti DM 282 printer was used for all the measurements and treatment of data.

Procedure

Samples were prepared in 25-ml standard flasks, and contained 2.6–52 ppm of salicylic acid and/or 2.1–42 ppm of salicylic acid and 2 ml of buffer solution, and were diluted with water to the mark. The absorption spectra were recorded and stored in the IBM PC-XT

For determining salicylic acid, the stored spectra of the mixtures were divided by a standard spectrum of salicylic acid. The ratio spectra thus obtained were smoothed through the use of 15 experimental points and the first derivatives calculated with $\Delta\lambda = 8$ nm were recorded. The concentration of the salicylic acid was proportional to the amplitude of the minimum at 269 nm or the maximum at 241.5 nm.

For salicylic acid, the corresponding procedure was used. The concentration of the salicylic acid was proportional to the amplitude from the peak at 345 nm to the trough at 337 nm or the corresponding amplitude at wavelengths 258 and 247 nm

RESULTS AND DISCUSSION

Figure 1 shows the absorption spectra of salicylic and salicylic acids. We selected this pair of acids because salicylates are used for a variety of medical applications and because salicylic acid is the main metabolite of salicylic acid⁸ and a variety of methods have been proposed for resolving their mixtures.^{9–13} Also, the spectra of salicylic and salicylic acids overlap sufficiently to demonstrate the resolving power of the proposed methodology

Figure 2 shows the ratio spectra of different salicylic acid standards (spectra divided by the spectrum of a 26 ppm salicylic acid solution) and their first derivatives. The first-derivative amplitudes at a given wavelength are propor-

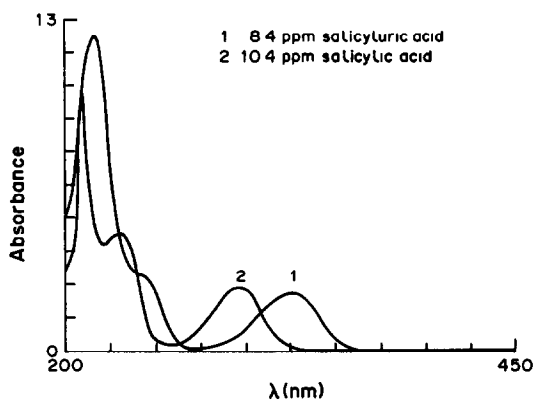


Fig 1 Absorption spectra of salicylic acid and salicyluric acid

tional to the salicylic acid concentration. The concentration of the salicyluric acid (divisor) can be increased or decreased in at least the range 4–21 ppm.

For calibration graphs, two derivative values were selected, at 269 and 241.5 nm, corresponding to a minimum and a maximum respectively. Figure 3 shows the resulting calibration graphs

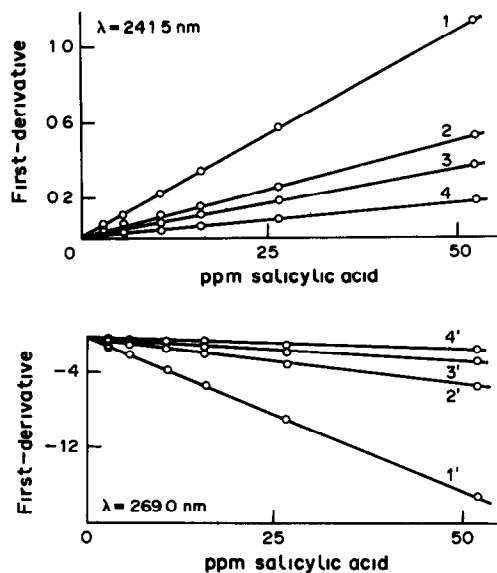


Fig 3 Calibration graphs of salicylic acid (SA) for different salicyluric acid (divisor) concentrations, measured at 241.5 and 269 nm SU 1 and 1' (4.2 ppm SU), 2 and 2' (8.4 ppm), 3 and 3' (12.6 ppm); 4 and 4' (21.0 ppm)

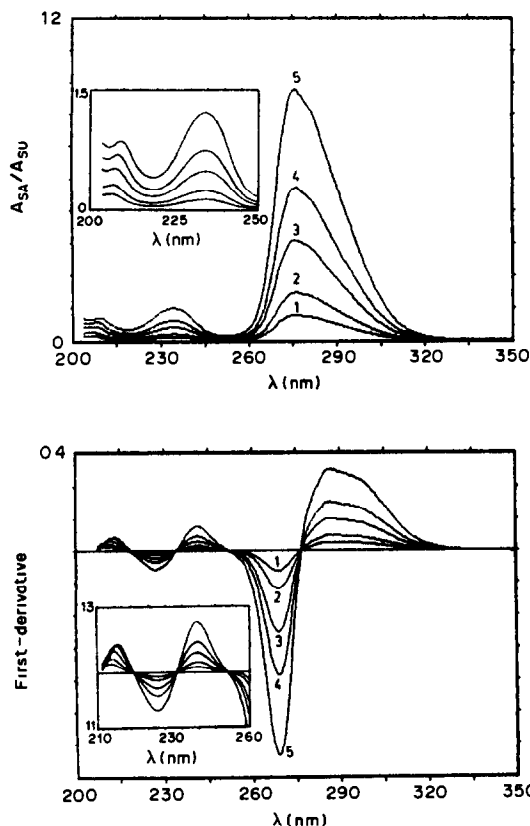


Fig 2 Ratio spectra and first derivatives for different concentrations of salicylic acid (SA), when salicyluric acid (SU) (divisor) was 26 ppm SA 1 (2.6 ppm), 2 (5.2 ppm), 3 (10.4 ppm), 4 (16.6 ppm) and 5 (26.0 ppm)

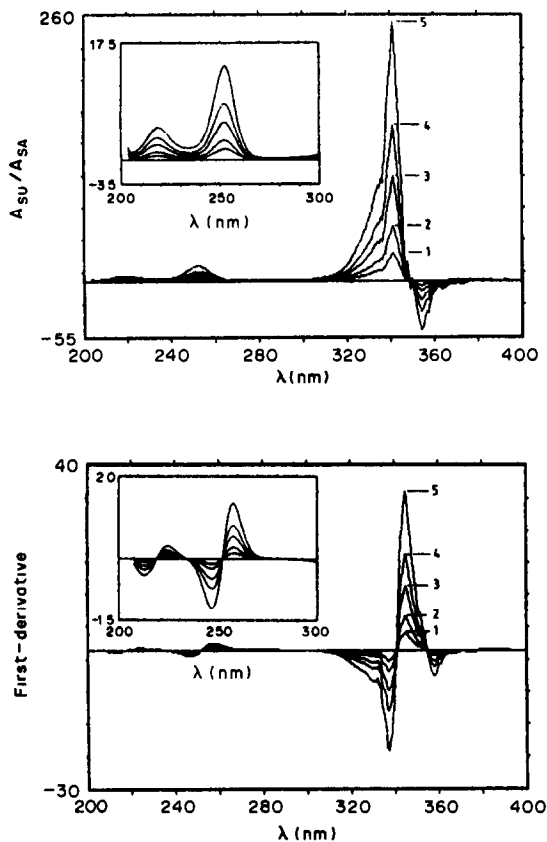


Fig 4 Ratio spectra and first derivatives for different concentrations of salicyluric acid (SU) when salicylic acid (divisor) was 12.6 ppm SU 1 (2.1 ppm), 2 (4.2 ppm), 3 (8.4 ppm), 4 (12.6 ppm) and 5 (21.0 ppm)

Table 1 Statistical data for calibration graphs in the determination of salicylic and salicyluric acids

Divisor, ppm			Standard deviation			
SA	SU	Range, ppm	Equations	Slope	Intercept	Regression coefficient
—	2 1	2 6–52	$Y = 0.0063 + 0.0381X$	4.21×10^{-4}	0.0061	0.9998
—	4 2	2 6–52	$Y = 0.0032 + 0.0195X$	2.16×10^{-4}	0.0032	0.9998
—	8 4	2 6–52	$Y = 0.0016 + 0.0097X$	1.08×10^{-4}	0.0016	0.9998
—	12 6	2 6–52	$Y = 0.0011 + 0.0064X$	0.71×10^{-4}	0.0010	0.9998
—	21 0	2 6–52	$Y = 0.0006 + 0.0038X$	0.42×10^{-4}	0.0006	0.9998
2 6	—	2 1–42	$Y = 0.0490 + 0.6389X$	6.88×10^{-4}	0.0081	1.0000
5 2	—	2 1–42	$Y = 0.0253 + 0.3163X$	3.01×10^{-4}	0.0044	1.0000
10 4	—	2 1–42	$Y = 0.0121 + 0.1484X$	2.22×10^{-4}	0.0026	1.0000
15 6	—	2 1–42	$Y = 0.0082 + 0.1002X$	1.51×10^{-4}	0.0018	1.0000
26 0	—	2 1–42	$Y = 0.0046 + 0.0573X$	0.84×10^{-4}	0.0009	1.0000

obtained for salicylic acid, and different salicyluric acid (divisor) concentrations.

For determining the other component (salicyluric acid) an analogous procedure was followed. Figure 4 shows the divided spectra of different standards of salicyluric acid and their first derivatives. Calibration graphs were ob-

tained by measuring at 345/337 or 258/247 nm, and gave straight lines for 2.1–42.0 ppm salicyluric acid

Table 1 summarizes the statistical data for the different calibration graphs of salicylic and salicyluric acids, obtained by using different divisor concentrations and by measuring at 241.5 nm

Table 2 Influence of divisor concentration in the determination of salicylic (SA) and salicyluric (SU) acids

Divisor salicylic acid, $\mu\text{g/ml}$	Mixture 2 1 (SA SU)			Mixture 1 2 (SA SU)			Mixture 1 4 (SA SU)		
	SU added, $\mu\text{g/ml}$	SU found, $\mu\text{g/ml}$	Recovery, %	SU added, $\mu\text{g/ml}$	SU found, $\mu\text{g/ml}$	Recovery, %	SU added, $\mu\text{g/ml}$	SU found, $\mu\text{g/ml}$	Recovery, %
2 6	4 20	4 00	95	25 20	25 32	100	42 00	41 39	98
5 2	4 20	4 07	97	25 20	25 19	100	42 00	41 37	98
10 4	4 20	4 02	96	25 20	25 20	100	42 00	41 45	99
15 6	4 20	4 02	96	25 20	25 20	100	42 00	41 45	99
26 0	4 20	4 00	95	25 20	25 23	100	42 00	41 25	98

Divisor salicyluric acid, $\mu\text{g/ml}$	SA added, SA found, Recovery, %			SA added, SA found, Recovery, %			SA added, SA found, Recovery, %		
	$\mu\text{g/ml}$	$\mu\text{g/ml}$	%	$\mu\text{g/ml}$	$\mu\text{g/ml}$	%	$\mu\text{g/ml}$	$\mu\text{g/ml}$	%
2 1	10 40	10 60	102	10 40	11 58	111	10 40	11 96	115
4.2	10 40	10 53	101	10 40	11 01	106	10 40	11 02	106
8 4	10 40	10 50	101	10 40	10 74	103	10 40	10 57	102
12 6	10 40	10 47	101	10 40	10 53	101	10 40	10 23	98
21 0	10 40	10 43	100	10 40	10 43	100	10 40	10 04	96

Table 3 Results obtained for different mixtures by using the proposed method

Composition of mixture, ppm		12 6 ppm SU (divisor)		15 6 ppm SA (divisor)	
		Measured at 241 5 nm		Measured at 258/247 nm	
SA	SU	SA found, ppm	Recovery, %	SU found, ppm	Recovery, %
10.40	4 20	10 50	101	4 07	97
10 40	8 40	10 50	101	8 28	98
10 40	16 80	10 50	101	16 53	98
10 40	25 20	10 74	103	25 19	100
10 40	42 00	10 57	102	41 37	98
5 20	21 10	4 96	95	2 22	106
5 20	4 20	4 96	95	4 19	100
5 20	8 40	4 98	96	8 38	100
5 20	12 60	5 05	97	12 59	100
5 20	21 00	5 13	99	21 01	100
26 00	2 10	25 72	99	2 26	108
26 00	4 20	25 95	100	4 33	103
26 00	4 20	25 95	99	8 51	101
26 00	12 60	25 79	99	12 73	101
26 00	21 00	25 87	99	21 15	101

Table 4 Results obtained for different mixtures by the Blanco *et al* method

Mixture composition, ppm		SU (divisor)				SA (divisor)			
		Found*, ppm		Recovery, %		Found*, ppm		Recovery, %	
SA	SU	SA	SU	SA	SU	SA	SU	SA	SU
10 40	4 20	9 70	4 03	93	96	10 33	4 16	99	99
10 40	8 40	9 95	8 19	96	97	10 08	8 06	97	96
10 40	16 80	10 71	16 63	103	99	10 46	16 13	100	96
10 40	25 20	12 60	24 32	121	96	10 33	25 20	99	100
10 40	42 00	—	—	—	—	10 33	41 96	99	100

*Data obtained by using 10 wavelengths in the range 270–350 nm

for salicylic acid and at 258/247 nm for salicylic acid. In all cases, the linear regression coefficients were higher than 0.9998.

Several binary mixtures of salicylic and salicylic acids were prepared and resolved by the proposed method. We first tested the method by using different divisor concentrations, and the results are summarized in Table 2. Similar results were obtained for all samples examined and in consequence we selected 12.6 ppm salicylic acid and 15.6 ppm salicylic acid as suitable values of the divisor concentrations for obtaining the ratio spectra. By use of these values, different binary mixtures were resolved and the results obtained are summarized in Table 3. In all cases recovery values between 95 and 108% were obtained.

Table 4 shows the results obtained for the same mixtures by the method of Blanco *et al*.

CONCLUSIONS

The method described permits the resolution of binary mixtures of compounds having overlapping spectra and gives results comparable to those obtained with the method of Blanco *et al*.

The method can be developed further for the resolution of ternary mixtures by use of higher order derivative equations.

REFERENCES

- 1 T C O'Haver and G L Green, *Anal Chem*, 1976, **48**, 312
- 2 P Levillain and D Fompeydie, *Analyst*, 1986, **14**, 1
- 3 Y R Tahboud and H L Pardue, *Anal Chem*, 1985, **57**, 38
- 4 D T Rossi and H L Pardue, *Anal Chim Acta*, 1985, **175**, 153
- 5 M Blanco, J Gene, H Iturruga, S Maspocho and J Riba, *Talanta*, 1987, **34**, 987
- 6 M Blanco, J Coello, H Iturruga and S Maspocho, *Técnicas de Laboratorio*, 1988, **XII**, 198
- 7 F Sánchez Rojas, C Bosch Ojeda and J M Cano Pavón, *Talanta*, 1988, **35**, 753
- 8 A J Cummings, B K Martin and R Renton, *J Pharmacol Chemother*, 1966, **26**, 461
- 9 D Schacter and J G Manis, *J Clin Invest*, 1958, **37**, 800
- 10 M A Chirigos and S J Udenfriend, *J Lab Clin Med*, 1959, **54**, 769
- 11 C J Umberger and F F Fiorese, *Clin Chem*, 1963, **9**, 91
- 12 M Rowland and S Riegelman, *J Pharm Sci*, 1987, **56**, 717
- 13 A Muñoz de la Peña, F Salinas and I Durán Merás, *Anal Chem*, 1988, **60**, 2493

A SIMPLE SPECTROPHOTOMETRIC DETERMINATION OF SOME CHLOROBENZOQUINONES WITH MORPHOLINE, THIOMORPHOLINE AND PIPERAZINE

U MURALIKRISHNA, K SURENDRA BABU and M KRISHNAMURTHY

Chemistry Department, Andhra University P G E Centre, Nuzvid 521 201, India

(Received 20 July 1988, Revised 7 November 1988 Accepted 22 August 1989)

Summary—A spectrophotometric method for the determination of 2,5-dichloro-, 2,6-dichloro- and 2,3,5,6-tetrachloro-1,4-benzoquinones is based on the yellow products of their reaction with morpholine, thiomorpholine and piperazine in chloroform

Chloro-substituted 1,4-benzoquinones have been used as analytical reagents¹⁻³ and oxidants.⁴ Some general methods have been suggested by Cheronis and Ma⁵ and Berger and Rieker⁶ for the determination of quinones. Coulometric titrations with electrogenerated vanadium(III)⁷ and titanium(III)⁸ have been applied only for the estimation of semimicro quantities of tetrachloro-1,4-benzoquinone.

Electron donor-acceptor interactions are often used for determination of the acceptors and donors concerned. Chloro-1,4-benzoquinones are good π -acceptors because of the negative inductive effect of the substituent and can be used for determination of piperazine¹ and morpholine,² as donors. We have now examined the use of these two compounds and thiomorpholine for the photometric determination of three chloro-1,4-benzoquinones

EXPERIMENTAL

Reagents

Morpholine (Fluka) and thiomorpholine (EGA, FRG) were purified by distillation from potassium hydroxide, and piperazine (Fluka) was recrystallized from cyclohexane. Tetrachloro-1,4-benzoquinone (Merck) and 2,5- and 2,6-dichloro-1,4-benzoquinones (Bio-organics, India) were recrystallized thrice from acetone. Chloroform (Glaxo, spectroscopy grade) was further purified by a standard method.⁹ All other chemicals used were of sufficient purity

Apparatus

A Carl Zeiss Spekol spectrophotometer was used with a pair of optically matched stoppered fused-silica cells of 1 cm path length

Procedure

Stock solutions of the quinones ($5 \times 10^{-4} M$) and 0.1 M solutions of morpholine, thiomorpholine and piperazine were prepared in chloroform. A volume of quinone solution ranging from 0.3 to 1.5 ml was placed in a test-tube along with 2 ml of reagent solution and 5-8 ml of chloroform, and the mixture was heated at about 50° on a water-bath for about 10 min, cooled, transferred to a 10-ml standard flask and diluted to the mark with chloroform. The absorbance of the yellow solution was measured against a solvent blank at the wavelength of maximum absorption (listed in Table 1). The calibration plots thus obtained were used in the analysis of unknown samples by the same procedure.

RESULTS AND DISCUSSION

Chemical reaction

Morpholine, thiomorpholine and piperazine are known to be twin-site *n*-donors. The molecular interaction of this type of base with quinones leads to the formation of complexes, the stability and transformation of which generally depend on the reaction conditions used and the characteristics of the donor and acceptor. For the systems examined here, the molar ratio of the reactants seems to be critical.

If the quinone is in excess (acceptor to donor ratio ≥ 1) the complex formed is stable. In spite of the presence of two donation sites on the donor, the stoichiometry of the complexes is found to be 1:1. The complexes are useful for determination of the base¹⁻³

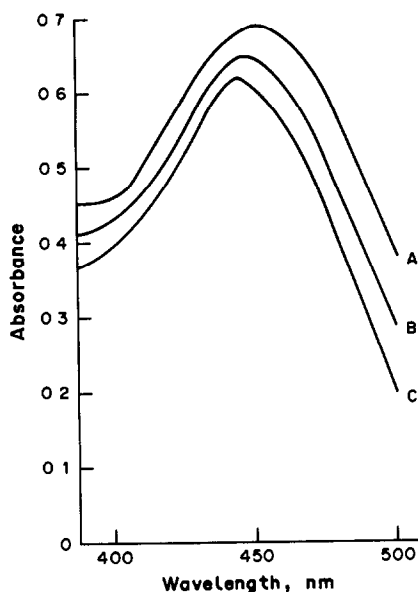


Fig 1 Absorption spectra of the products formed by tetrachloro-1,4-benzoquinone ($6 \times 10^{-5}M$) with $3 \times 10^{-3}M$ piperazine (A), thiomorpholine (B) and morpholine (C)

In contrast, if the donor is in excess (acceptor to donor ratio < 1) the complex is rapidly transformed into a disubstituted product^{10,11} since the haloquinones are very reactive^{12,13} and two of the halogen atoms are generally replaceable by amino groups, if the concentration of amine is sufficiently high. The final products thus formed are now considered as a means of determining quinones.

Absorption spectra

1,4-Benzoquinones generally have a very intense $\pi-\pi^*$ absorption band in the ultraviolet region.⁶ A medium $\pi-\pi^*$ band and a much weaker absorption due to the $n-\pi^*$ transition can also be observed. Table 1 lists the wave-

Table 1 Optical characteristics of benzoquinones and their products in chloroform medium

1,4-Benzoquinone	Absorption maxima, nm (log ϵ^*)			
	Parent	Product with PZ	Product with TML	Product with ML
2,5-Dichloro	276 (4.24)	387 (4.08)	381 (4.07)	380 (4.06)
2,6-Dichloro	278 (4.26)	409 (4.06)	387 (4.05)	384 (4.04)
Tetrachloro	293 (4.41)	448 (4.07)	445 (4.05)	442 (4.04)

* ϵ = molar absorptivity, l mole⁻¹ cm⁻¹

PZ, piperazine, TML, thiomorpholine and ML, morpholine

Table 2 Analytical data for the spectrophotometric determination of benzoquinones

Reagent	Beer's law range, $\mu\text{g/ml}$	Coefficient of variation, $n = 8$, %
<i>2,5-Dichloro-1,4-benzoquinone</i>		
Piperazine	2-12	1.0
Thiomorpholine	2-14	0.7
Morpholine	2-15	0.8
<i>2,6-Dichloro-1,4-benzoquinone</i>		
Piperazine	2-13	0.9
Thiomorpholine	2-15	0.9
Morpholine	2-15	0.6
<i>Tetrachloro-1,4-benzoquinone</i>		
Piperazine	2-15	0.8
Thiomorpholine	2-17	1.0
Morpholine	2-18	0.8

lengths of maximal absorption of the quinones listed and of their products with the three reagents. Replacing the electron-withdrawing chloro group with an electron-donating amino group results in a large red-shift into the visible region accompanied by a slight decrease in molar absorptivity. The absorption spectra of the tetrachloro-1,4-benzoquinone products are shown in Fig 1.

Effect of reagent concentration

The proposed method tolerates a wide variation in the reagent concentration, from 4×10^{-4} to $8 \times 10^{-2}M$. A reagent concentration of not less than $10^{-3}M$ gives rapid conversion of the di- or tetrachlorobenzoquinone into the corresponding diaminoquinone.

Effect of temperature

With about 50-fold excess of the reagent, the reaction is completed in 25-30 min with tetrachloro-1,4-benzoquinone and in 60 min with the dichlorobenzoquinones at room temperature. Heating accelerates the conversion and is recommended for minimizing the analysis time. The determination ranges and sensitivities are not affected by the heating.

Stability of the colour

Maximum absorbance of the products is reached in less than 10 min with heating at 50° , and the absorbance remains constant for at least 12 hr if the solution is protected from light and kept in a stoppered vessel.

Analytical data

The Beer's law ranges and the precision are listed in Table 2

Interferences

1,4-Benzoquinone interferes at all concentrations, but methyl-, 2,6-dimethyl-, 2-methyl-5-isopropyl- and tetramethyl-1,4-benzoquinones and benzoquinone-4-chlorimide do not interfere up to 25-fold molar ratio to analyte

Acknowledgement—One of the authors (KSB) is thankful to the UGC, New Delhi, for the award of a fellowship under the FIP programme and to the management of SVRM College, Nagaram, for secondment

REFERENCES

- 1 U Muralikrishna, M Krishnamurthy and N S Rao, *Analyst*, 1984, **109**, 1277
- 2 U Muralikrishna, M Krishnamurthy and Y V S K Seshasayi, *Indian J Chem*, 1983, **22A**, 904
- 3 M Krishnamurthy and U Muralikrishna, *Indian Drugs*, 1985, **22**, 171, *Microchem J*, 1985, **31**, 210
- 4 H D Becker, in S Patai (ed), *The Chemistry of Quinonoid Compounds*, p 335 Wiley, London, 1974
- 5 N D Cheronis and T S Ma, *Organic Functional Group Analysis by Micro and Semimicro Methods*, p 212 Wiley, New York, 1964
- 6 St Berger and A Rieker, in S Patai (ed), *The Chemistry of Quinonoid Compounds*, p 163 Wiley, London, 1974
- 7 A I Kostromin, I F Addullin and P K Agasyan, *Zh Analit Khim*, 1981, **36**, 681
- 8 J C Viré, M Chateau-Gosselin and G J Patriarche, *Mikrochim Acta*, 1981 **I**, 227
- 9 A I Vogel, *A Text-book of Practical Organic Chemistry* p 176 E L B S, London, 1968
- 10 U Muralikrishna, Y V S K Seshasayi and M Krishnamurthy, *J Indian Chem Soc*, 1983, **60**, 447, 1048, 1987, **64**, 665
- 11 M Krishnamurthy, K S Babu and U Muralikrishna, *Indian J Chem*, 1988, **27A**, 669
- 12 D Buckley, H B Henbest and P Slade, *J Chem Soc*, 1957, 4891
- 13 U Muralikrishna and M Krishnamurthy, *Spectrochim Acta*, 1984, **40A**, 65

ANALYTICAL DATA

STUDIES ON HYDROLYTIC POLYMERIZATION OF RARE-EARTH METAL IONS—V

HYDROLYTIC POLYMERIZATION OF Dy^{3+}

QINHUI LUO*, MENGCHANG SHEN, YI DING, XINLU BAO and ANBANG DAI

Coordination Chemistry Institute, Nanjing University, Nanjing, People's Republic of China

(Received 20 March 1989 Revised 23 August 1989 Accepted 29 September 1989)

Summary—The hydrolytic polymerization of Dy^{3+} was determined by the equilibrium-pH method. The concentration of Dy^{3+} was varied from 0.1 to 0.6 M. The composition and hydrolysis constants of the Dy^{3+} hydrolysis products were obtained by a graphical method and then refined by computer fitting and *pq* analysis. The results show that the species in the Dy^{3+} solution are $[Dy(OH)]^{2+}$, $[Dy_2(OH)_2]^{4+}$ and $[Dy_3(OH)_3]^{6+}$, but the last of these is a minor species. The behaviour of Dy^{3+} is the same as that of Er^{3+} and Yb^{3+} but different from that of the medium lanthanide ions Sm^{3+} , Eu^{3+} and Gd^{3+} .

Hydrolytic polymerization of the lanthanide ions is closely related to the separation and determination of the lanthanide elements, treatment of nuclear fuel and environmental protection, and has been extensively studied.¹⁻¹⁵ The lanthanide ions have not yet all been studied, so the regularity of their hydrolysis is still not clear. The light lanthanide ions have been studied more than the heavy ones, and although Dy^{3+} is an important lanthanide ion, no detailed studies on its state in solution have been reported. We have tried to study the regularity of hydrolysis of the lanthanide ions and have made systematic studies of Pr^{3+} ,¹⁶ Sm^{3+} ,¹⁷ Eu^{3+} ,¹⁸ Gd^{3+} ,¹⁸ and Yb^{3+} and Er^{3+} .¹⁹ We discovered that the hydrolytic polymerization of lanthanide ions is not an instantaneous process, so we studied it by the equilibrium-pH method. In the present paper, we first estimated the hydrolysis model of Dy^{3+} by a graphical method and then used computer fitting and *pq* analysis²⁰ to screen possible species one by one, and thus studied the state in solution in detail and obtained the hydrolysis constants. The results showed that the main hydrolysis products of Dy^{3+} may be expressed as $[Dy(OH)]_n^{2n+}$, with $n = 1, 2, 3$. These are different from the hydrolysis products of the medium lanthanide ions Sm^{3+} , Eu^{3+} and Gd^{3+} which we have studied, but the same as

those of Er^{3+} and Yb^{3+} , perhaps because the 4f orbitals of the heavy lanthanide ions are all at least singly occupied.

EXPERIMENTAL

Reagents

Dysprosium sesquioxide, purity 99.95%, Yaolung Chemicals Factory, sodium nitrate, analytical grade, recrystallized twice from redistilled water, sodium hydroxide, analytical grade, treated by the method of Powell *et al.*²¹ All other chemicals used were analytical grade.

Instrumentation

A Corning pH-meter, equipped with a Corning glass-Ag/AgCl combination electrode, precision ± 0.1 mV. Data were calculated by the program LEMIT^{22,23} on a Honeywell DPS 8/49 computer.

Procedure

A known weight of Dy_2O_3 was dissolved in nitric acid, and the Dy determined by EDTA titration. The excess of nitric acid in the solution was determined by titration with CO_2 -free sodium hydroxide solution. Solutions with 0.100, 0.200, 0.400 and 0.600 M $Dy(NO_3)_3$ concentration were prepared, enough sodium nitrate was added to make the nitrate concentration of all solutions 2.0 M, and the pH

*Author for correspondence

Table 1 Typical data for log h and Z (NaOH concentration 0.03325M)

$B = 0.200M, V = 50.00 \text{ ml}, H_0 = 2.85 \times 10^{-5}M$				$B = 0.600M, V = 25.00 \text{ ml}, H_0 = 8.55 \times 10^{-5}M$			
$V_{\text{NaOH}}, \text{ ml}$	$E, \text{ mV}$	$-\log h$	$10^3 \times Z$	$V_{\text{NaOH}}, \text{ ml}$	$E, \text{ mV}$	$-\log h$	$10^3 \times Z$
0.100	131.6	5.180	0.223	0.160	137.2	5.086	0.226
0.200	118.4	5.404	0.542	0.320	130.8	5.194	0.578
0.400	107.5	5.588	1.20	0.600	119.1	5.392	1.19
0.700	94.8	5.803	2.19	1.100	110.6	5.535	2.30
1.000	89.8	5.887	3.19	1.600	104.4	5.640	3.41
1.400	84.4	5.978	4.52	2.200	97.5	5.757	4.74
1.900	80.0	6.053	6.18	2.900	95.1	5.797	6.29
2.400	78.2	6.083	7.84	3.600	92.0	5.850	7.84
2.800	76.7	6.109	9.17	4.300	90.4	5.877	9.39
3.200	75.2	6.134	10.50	5.100	87.7	5.923	11.16

was then adjusted by adding standard sodium hydroxide until precipitation just began. The solutions were then diluted to a preselected volume and stored in polythene bottles at 25° in a nitrogen atmosphere. The potential, E , of the solutions (in a nitrogen atmosphere) was measured at $25 \pm 0.01^\circ$ at intervals of several hours until equilibrium was thought to have been established, i.e., when the successive measurements of E did not differ by more than 0.5 mV. The relationship between the equilibrium potential E (in mV) and the hydrogen-ion molar concentration h can be written in the form²⁴

$$E = E_0 + E_j + 59.15 \log h$$

where E_0 is a constant, different for each type of cell, and E_j is the liquid-junction potential, which is an approximately linear function of h . To determine $E_0 + E_j$, a 2M sodium nitrate solution with a known concentration of nitric acid was prepared, and titrated with sodium hydroxide solution, and the measured potential E was plotted against the hydrogen-ion concentration calculated from the volume of titrant added and the nitric acid concentration. For our system, we obtained the empirical equation

$$E = 438.08 + 59.16 \log h \quad (1)$$

Determination of hydrolysis products by the graphical method^{1,2,17}

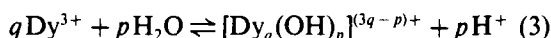
The average number (Z) of hydroxyl groups bound to each Dy^{3+} ion was calculated by means of equation (2), with h obtained by use of equation (1)

$$Z = (h + M_{\text{OH}} - H_0)/B \quad (2)$$

where M_{OH} denotes the molar concentration of the added sodium hydroxide, H_0 denotes the nitric acid concentration in the $\text{Dy}(\text{NO}_3)_3$ solution before addition of the sodium hydroxide, and B denotes the total concentration of Dy^{3+} .

Typical data are shown in Table 1. Figure 1 shows a plot of Z vs. $-\log h$ for solutions with different Dy^{3+} concentrations.

The family of curves in Fig. 1 implies that Dy^{3+} is hydrolysed and partly polymerized at a given Dy^{3+} concentration and acidity according to the equation



The equilibrium constant is

$$\beta_{pq} = [\text{Dy}_q(\text{OH})_p] h^p / b^q \quad (4)$$

where b denotes the equilibrium concentration of Dy^{3+} , the charges of species are omitted for simplicity.

From Fig. 1 it is seen that the Z values are small in the experimental pH region but the total concentration of Dy^{3+} is comparatively high, so we have

$$BZ = \sum_p \sum_q p \beta_{pq} B^q / h^p = \sum_p p K_p / h^p \quad (5)$$

where

$$K_p = \sum_q \beta_{pq} B^q \quad (6)$$

K_p is a homo-ligand constant concerned with

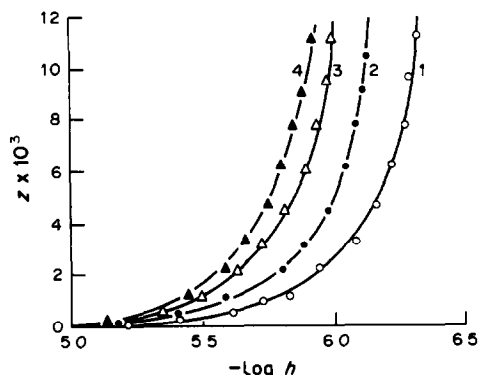


Fig. 1 Plot of Z vs. $-\log h$. B 1, 0.1M, 2, 0.2M, 3, 0.4M, 4, 0.6M

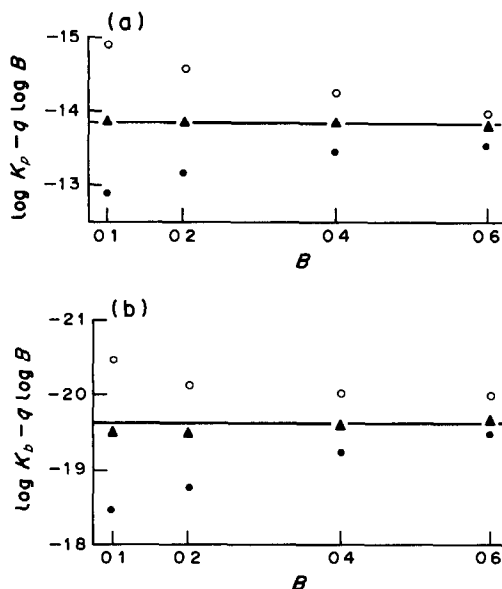


Fig 2 Plot of $(\log K_p - q \log B)$ vs B (a) $p = 2$, (b) $p = 3$, \circ , $q = 2$, \blacktriangle , $q = 3$, \bullet , $q = 4$

the concentration of the metal ion and the values of p .

Experimental curves were obtained by plotting BZ vs. $-\log h$ values in Table 1 and were fitted with normalized curves for assumed numbers of hydroxyl groups. Species with $p = 2$ existed over the widest pH region, so $[\text{Dy}_q(\text{OH})_2]^{(3q-2)+}$ species are predominant. Although species with $p = 1$ and $p = 3$ existed in a narrower pH region than those with $p = 2$, they also fitted well. Existence of species with $p = 5$ could not be confirmed because there were not many fitting points. K_p values were obtained by fitting.

Only one kind of species existed in certain pH regions, because of the low degree of hydrolysis of Dy^{3+} , so we have

$$\log K_p - q \log B = \log \beta_{pq} \quad (7)$$

When $(\log K_p - q \log B)$ is plotted vs. B for various q values, only the line with the correct q value will be parallel to the abscissa, and thus correct q and β_{pq} values can be obtained. Very good fitting was obtained for $p = q = 1$, $p = q = 2$ and $p = q = 3$, but it was difficult to establish a fit for $p = 5$, $q = 3$, so the computer

q	$p=1$	$p=2$	$p=3$	$p=4$	$p=5$
5	+ 54 22 (-6 96)	+ 40 60 (-13 12)	+ 38 04 (-19 18)	+ 38 50 (-25 20)	+ 40 00 (-31 21)
4	+ 43 67 (-7 21)	+ 28 36 (-13 35)	+ 24 52 (-19 41)	+ 24 18 (-25 44)	+ 25 77 (-31 46)
3	+ 29 90 (-7 45)	+ 12 70 (-13 59)	+ 8 80 (-19 66)	+ 12 60 (-25 72)	+ 31 60 (-31 80)
2	+ 14 10 (-7 71)	+ 0 44 (-13 87)	+ 15 70 (-20 01)	+ 67 10 (-26 23)	+ 133 50 (-32 63)
1	+ 20 00 (-8 05)	+ 56 50 (-14 38)	+ 124 00 (-20 82)	+ 167 00 (-27 36)	+ 184 00 (-33 90)

Fig 3 U and $\log \beta$ values for $[\text{Dy}_q(\text{OH})_p]^{(3q-p)+}$

was used to screen possible species. Some of the fitting results are presented in Fig 2.

Because only one kind of species predominates in solution, we have $Z = p\beta_{pq}B^{q-1}/h^p$, so by plotting Z vs. $1/h^p$ and extrapolation, β_{pq} is also obtained. The β_{pq} values obtained by the two methods are summarized in Table 2.

Computer fitting^{20,22,23}

Each experimental point should satisfy the following general equations

$$T_{H_i} = \sum_{j=1}^{NK} p_j \beta_{p,q_j} b_i^{q_j} / h_i^{p_j} + h_i \quad (8)$$

$$T_{M_i} = \sum_{j=1}^{NK} q_j \beta_{p,q_j} b_i^{q_j} / h_i^{p_j} + b_i \quad (9)$$

where i ($i = 1, 2, \dots, N$) denotes the ordinal number of the experimental points, j ($j = 1, 2, \dots, NK$) denotes the ordinal number of the complexes, T_{H_i} and T_{M_i} denote respectively the total acidity and total Dy^{3+} concentration corresponding to the i th experimental point. First, estimates of the β values, the hydrolysis constants of the complexes, are input, then equations (8) and (9) are solved iteratively by Newton-Raphson successive approximation to obtain h_i and b_i , and next the T_{H_i} values are calculated by equation (8) to give $T_{H_i}^{\text{calc}}$. The error-square sum, U , for a given β value is calculated by using $T_{H_i}^{\text{calc}}$ and the corresponding experimental value $T_{H_i}^{\text{exp}}$.

$$U = \sum_{i=1}^N (T_{H_i}^{\text{calc}} - T_{H_i}^{\text{exp}})^2 \quad (10)$$

Table 2 Hydrolysis constants of Dy^{3+} , at 25°C, in 2M NO_3^- medium (σ = standard deviation)

Method	$\log(\beta_{11} \pm 3\sigma)$	$\log(\beta_{22} \pm 3\sigma)$	$\log(\beta_{33} \pm 3\sigma)$
Homo-ligand constant	-8.55 ± 0.11	-13.88 ± 0.08	-19.60 ± 0.35
Extrapolation	-8.48 ± 0.17	-13.90 ± 0.07	-19.54 ± 0.38
Computer-fitting	-8.63 ± 0.24	-13.88 ± 0.05	-19.53 ± 0.45

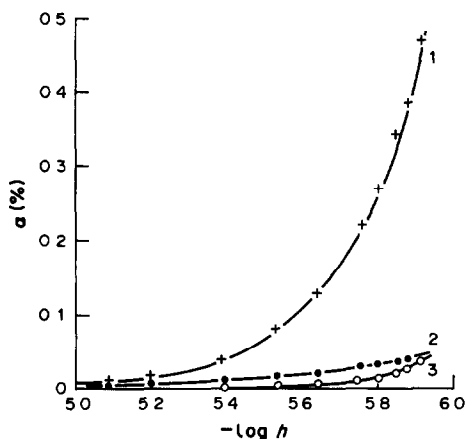


Fig 4 Distribution plot ($B = 0.4M$) for 1, $[Dy_2(OH)_2]^{4+}$, 2, $[Dy(OH)]^{2+}$, 3, $[Dy_3(OH)_3]^{6+}$

First it is assumed that only one kind of complex exists in the solution, and the U values are calculated by equation (10), with p and q changed one by one, and the calculated U and $\log \beta$ values are displayed as a function of p and q as shown in Fig. 3, where the values of $10^6 \times U$ and $\log \beta$ (in brackets) corresponding to given p and q values are displayed for $[Dy_q(OH)_p]^{(3q-p)+}$

From Fig. 3 it is seen that U is least for (p, q) equal to (2,2) and (3,3). Combining these species one by one with species (1,1), (2,3), (4,3) and others with rather small U values gives $\log U = -6.6606$ for the species combination (1,1), (2,2) and (3,3), and this is the lowest U value. When (5,3) is added to the combination system or substituted for (3,3), divergence is obtained, so (5,3) is eliminated and the combination of (1,1), (2,2), (3,3) is the most probable model. It also has the least Hamilton R -factor (0.422×10^{-3}), which again implies that it is the best model. The $\log(\beta \pm 3\sigma)$ values obtained are presented in Table 2.

An F -test showed that the results obtained by the three methods are not significantly different (90% confidence limits) and are all acceptable. From Table 2 it is seen that $\log \beta_{22}$ has the lowest value, and from the graphical fitting that species (2,2) exists in the widest acidity region and is therefore the major species. Species (3,3) exists only in a comparatively high basicity region and in small amounts, so is the minor species.

A distribution plot of the species in solution as a function of $-\log h$ is shown in Fig. 4.

By comparing the values for Dy^{3+} species in Table 2 and those for Er^{3+} and Yb^{3+} reported

in previous papers¹⁰⁻¹³ it is seen that the three representatives of heavy lanthanide ions behave in the same way and may be expressed as $[Ln(OH)]_n^{n+}$, $Ln = Dy^{3+}, Er^{3+}, Yb^{3+}$, $n = 1, 2, 3$. Earlier papers^{8,9} reported that the major hydrolytic products of Sm^{3+} , Eu^{3+} and Gd^{3+} are $[Ln(OH)]^{2+}$ and $(Ln[Ln(OH)_2]_n)^{(3+n)+}$, $n = 1, 2, 3$, which are different from those of the heavy lanthanide ions. This may be due to the fact that the $4f$ orbitals of Dy^{3+} , Er^{3+} and Yb^{3+} , being more than half-full, decrease the ionic radii still further, so the hydroxylation number and degree of polymerization also decrease.

The values reported are conditional constants, since they will be affected by any formation of nitrate complexes of Dy^{3+} .

REFERENCES

- 1 G Biedermann and L Ciavatta, *Acta Chem Scand*, 1961, **15**, 1347
- 2 G Biedermann and L Newmann, *Arkiv Kemi*, 1964, **22**, 303
- 3 K A Burkov, E A Bus'ko and I V Pichugina, *Russ J Inorg Chem*, 1982, **27**, 643
- 4 K A Burkov, L S Lilich and Nguyen Din Ngo, *ibid*, 1973, **18**, 1513
- 5 K A Burkov, E A Bus'ko, L S Lilich and Nguyen Din Ngo, *Izvest Vyssh Ucheb Zaved SSSR, Khim i Khim Tekhnol*, 1983, **26**, 771
- 6 K A Burkov, L S Lilich and Nguyen Din Ngo, *ibid*, 1975, **18**, 181
- 7 Nguyen Din Ngo and K A Burkov, *Russ J Inorg Chem*, 1974, **19**, 1249
- 8 L N Usherenko and N A Skorik, *ibid*, 1972, **17**, 2918
- 9 T Amaya, H Kakihana and M Maeda, *Bull Chem Soc Japan*, 1973, **46**, 1720
- 10 J Kragten and L G Decnop-Weever, *Talanta*, 1979, **26**, 1105
- 11 *Idem, ibid*, 1980, **27**, 1047
- 12 *Idem, ibid*, 1983, **30**, 131
- 13 *Idem, ibid*, 1982, **29**, 219
- 14 L Ciavatta, M M Iuliano and R Porto, *Polyhedron*, 1987, **6**, 1283
- 15 N A Kostromina and Yu B Badaev, *Ukr Khim Zh*, 1986, **52**, 793
- 16 Qinhui Luo, Mengchang Shen and Yi Ding, *J Nanjing University (Nat Sci)*, 1983, 429
- 17 Qinhui Luo, Mengchang Shen, Yi Ding and Zhongdui Chen, *Acta Chim Sinica*, 1983, **41**, 1115
- 18 Qinhui Luo, Yi Ding and Mengchang Shen, *Chem J Chinese Universities*, 1985, **6**, 201
- 19 Qinhui Luo, Yi Ding, Mengchang Shen, *J Chinese Rare Earth Soc*, 1988, **6**, 73
- 20 L Petterson, I Andersson, L Lyhamn and N Ingrn, in E Hogfeldt (ed), *Coordination Chemistry in Solution*, p 116. Berlingska Bostyrkeriet, Lund, 1972
- 21 J E Powell and M A Hiller, *J Chem Educ*, 1957, **34**, 330
- 22 Qinhui Luo, Mengchang Shen, Yi Ding, Qingyun Tu and Anbang Dai, *Acta Chim Sinica*, 1986, **44**, 568
- 23 *Idem, ibid*, (English edition), 1987, No 2, 144
- 24 S Hietanen, *Acta Chem Scand*, 1954, **8**, 1628

ANNOTATION

KINETIC EVIDENCE FOR A CHARGE-TRANSFER MECHANISM IN THE INTERACTION OF AMMONIA WITH 2,4-DINITROPHENYLHYDRAZINE IN DIMETHYLSULPHOXIDE

PUSHKIN M. QURESHI, SANT BAHADUR SINGH and S. IQBAL. M. KAMOONPURI
Department of Chemistry, Aligarh Muslim University, Aligarh-202001, India

I A KHAN

Department of Chemistry, Gaya College, Gaya, Bihar, India

(Received 27 January 1988 Revised 16 August 1989 Accepted 30 September 1989)

Summary—Kinetic evidence is adduced to show that charge-transfer is involved in the interaction of ammonia with 2,4-dinitrophenylhydrazine in dimethylsulphoxide. The charge-transfer mechanism is further confirmed by the linear relation between the ionization potential and molar absorptivity of the complex for three aliphatic amines.

The colours produced when an aliphatic amine is added to a solution of a polynitro-aromatic compound have been explained as due to various interactions,¹ and even to all of them occurring almost simultaneously. Orvik and Bunnett² supported the view that the colours are due to formation of anionic sigma-complexes. This view was confirmed by the studies of Fyfe *et al.*^{3,4} Though this interpretation may hold for this particular system, it is not necessarily applicable to all aliphatic amine/polynitro-aromatic systems. It is known⁵ that in non-polar solvents such as cyclohexane and in polar aprotic solvents such as dimethylsulphoxide (DMSO), tertiary aliphatic amines form charge-transfer complexes with 1,3,5-trinitrobenzene. Though charge-transfer complexes have been postulated for the corresponding reactions with other aliphatic amines and ammonia, conclusive evidence is largely lacking. Since in the systems in question there is an electron donor and an electron acceptor, the possibility seems attractive. We have scanned a number of polynitro-aromatic compounds and found one⁶ for which kinetic and other data showed the presence of charge-transfer in its reaction with aliphatic amines. This reagent (2,4-dinitrophenylhydrazine) has been used in DMSO for the determination of aliphatic amines in the ppm range, and the product was postulated as an anionic sigma-complex formed by deprotona-

tion of the hydrazine. In retrospect, it seems possible that charge-transfer forces might also play a role in such reactions. Some of the implications are reported in this study, which is an extension of the earlier work.⁶

We have studied spectrophotometrically the reaction of ammonia with 2,4-dinitrophenylhydrazine (DNPH) to give 6-nitro-1-hydroxy-1,2,3-benzotriazole.⁷ As far as we are aware there has been no previous kinetic or spectrophotometric study of this reaction.

EXPERIMENTAL

Reagents

The DNPH was a Merck Guaranteed Reagent, the ammonia solution was B.D.H. AnalaR quality, the ethylamine and n-butylamine were B.D.H. Laboratory reagent grade and the DMSO was a Baker Analyzed Reagent.

Procedure

The rate of colour development was monitored at 640 nm and constant temperature.

RESULTS AND DISCUSSION

Solutions of ammonia and DNPH in DMSO immediately generate a green colour (λ_{\max} 640 nm) when mixed. The immediate generation of colour is indicative of charge-transfer. The

colour is stable when the reactant ratio $[\text{NH}_3]/[\text{DNPH}]$ is ≤ 1

A Job plot indicated formation of a 1:1 complex. Most charge-transfer complexes have 1:1 stoichiometry, whereas the anionic sigma-complexes formed between polynitro-aromatic compounds and aliphatic amines have a stoichiometry of 1:2. However, a Job plot gives only the stoichiometry and cannot distinguish between charge-transfer, deprotonation or other reaction mechanisms

When a large excess of ammonia is present, decomposition takes place, as further irreversible chemical reactions proceed. The kinetics of decomposition in the presence of a large excess of ammonia (to ensure pseudo first-order conditions) was determined spectrophotometrically by monitoring the coloured product at 640 nm. Good first-order plots were obtained. However, the pseudo first-order rate constant was dependent on the initial concentrations of both reactants. On going from $2 \times 10^{-4} M$ to $4 \times 10^{-4} M$ DNPH with the ammonia concentration held constant at 0.1M, the pseudo first-order rate constant at 50° changed by 28%, and on going from 2×10^{-2} to $8 \times 10^{-2} M$ ammonia the pseudo first-order rate constant changed by 33%. These changes are far too great to be attributable to experimental error. Similar variation of the rate constant with the concentration of the reactants was found by Ross and Kuntz⁸ for the reaction of aniline and 2,4-dinitrochlorobenzene, and was shown to be due to charge-transfer.

When the pseudo first-order rate constants were plotted against the initial concentration of ammonia (present in large excess) a straight line with slope b and a large and reproducible positive intercept a was obtained. The kinetic equation thus takes the form

$$k_{\text{obs}} = a + b[\text{NH}_3]$$

This led us to believe that there are two interactions. We next investigated this behaviour at three different temperatures, and the three intercepts were taken as rate constants for the first process, and the three slopes as rate constants for the second process. We then computed the thermodynamic activation parameters. We were surprised to find that $-\Delta H^*$ for the first process is only 3.17 ± 0.30 kcal/mole, which is too low for breakage of a normal

covalent bond. (The decomposition of α -complexes with so low a value of $-\Delta H^*$ is not known). When this value is taken together with a $-\Delta S^*$ value of 28.5 ± 0.9 cal. mole⁻¹ deg⁻¹ it can well be accepted that the first interaction is due to charge-transfer. The value of $-\Delta H^*$ for the second process is 10.33 ± 0.15 kcal/mole, and with $-\Delta S^* = 44.8 \pm 1.4$ cal mole⁻¹ deg⁻¹ can be attributed to a breakage of a covalent bond. The validity of these values obtained from the intercepts is supported by the excellent linearity of the plot of $\ln a$ vs. the inverse of the temperature.

The molar absorptivities found for the complexes formed by ammonia and the amines are much lower than those expected for anionic sigma-complexes and are much nearer to those observed for charge-transfer complexes.¹

The possibility of charge-transfer in such systems has often been dismissed on the grounds that there is no linear dependence of the frequency of the charge-transfer band ν_{CT} with ionization potential of the aliphatic amine. There seems no theoretical justification for expecting such linearity,⁹ but there is a theoretical justification to expect that the molar absorptivity (ϵ) decreases with increasing ionization potential of the donor.¹⁰ Hence ϵ should vary with the donor, whereas for anionic sigma-complexes ϵ is effectively constant for interaction of all donors with the same acceptor.¹ We found a plot of ϵ vs. the ionization potentials of the donors was linear, with negative slope as expected for a charge-transfer system.

REFERENCES

- 1 E Buncel, A R Norris and K E Russell, *Q Rev*, 1968, **22**, 123
- 2 J A Orvik and J F Bunnett, *J Am Chem Soc*, 1970, **92**, 2417
- 3 C A Fyfe, S W H Damji and A Koll, *ibid*, 1979, **101**, 951
- 4 *Idem*, *ibid*, 1979, **101**, 956
- 5 M J Strauss, *Chem Rev*, 1970, **70**, 667
- 6 M Qureshi, S A Nabi, I A Khan and P M Qureshi, *Talanta*, 1982, **29**, 757
- 7 A K Macbeth and J R Price, *J Chem Soc*, 1934, 1637
- 8 S D Ross and I Kuntz, *J Am Chem Soc*, 1954, **76**, 3000
- 9 R Foster, *Organic Charge Transfer Complexes*, p 46 Academic Press, New York, 1969
- 10 B Dodson, R Foster, A A S Bright, M I Foreman and J Gorton, *J Chem Soc*, B, 1971, 1283

ELEMENTAL ANALYSIS OF HIGH-PURITY SOLIDS BY MASS SPECTROMETRY

R. GIJBELS

University of Antwerp (UIA), Department of Chemistry, B-2610 Antwerp-Wilrijk, Belgium

(Received 15 March 1988. Revised 30 August 1989. Accepted 7 October 1989)

Summary—The applications of mass spectrometry in the determination of trace elements in some of the high-purity solid materials used in modern technology are reviewed.

One of the areas of current interest in materials science is the development of high-purity materials; different classes of purity are indicated by a number of nines (N), *e.g.*, 5 N (signifying 99.999%), meaning that the total trace element content is about 10 ppm (10 $\mu\text{g/g}$). Even at low levels, impurities perturb the basic lattice of a solid: a different oxidation state creates a perturbed electrical field, a different magnetic moment produces a perturbed magnetic field and a different ionic or atomic radius results in a perturbed elastic field. Hence, the migration of “particles” (phonons, electrons, holes, interstitials, vacancies, *etc.*) through the solid will be influenced by scattering or trapping phenomena. Trace elements can thus have a decisive influence on the physical properties of materials, *e.g.*, electrical conductivity, optical characteristics, or mechanical strength. One of the aims of materials research is to change the physical properties either by lowering the trace element content in a material, *e.g.*, by refining (as in semiconductor production), or doping with specific trace elements to achieve certain properties. The greatest progress has been made in semiconductor technology, where extreme purification of silicon down to a total trace content of *ca.* 1 ng/g, and controlled doping with trace elements (*e.g.*, B, P, As, Sb in Si) is the basis of the production of electronic devices with specific properties.

In large-scale production of metals, the total trace content is usually high and less well controlled. With the increasing demands for particular mechanical and other properties, greater purification and controlled doping with trace elements to achieve a specific microstructure will become more important.¹ Very low contents of alpha-emitters (uranium,

thorium) are required in the aluminium used for metallization of integrated circuits, and high-purity metals are obviously required for the production of compound semiconductor materials, such as gallium arsenide, or cadmium mercury telluride.

Similar developments are taking place for ceramic materials, especially in the production of wear-resistant coatings on metals by deposition from the gas phase. In such materials nucleation, grain growth, surface morphology and the mechanical properties are all strongly influenced by trace elements.¹

This new technology can only be developed if suitable means for quality control are available, such as methods for trace and ultra-trace analysis, both in bulk and with spatial resolution (surfaces, interfaces, micro-domains). Recent developments in atomic spectrometry methods for trace element determination in general have been reviewed by Broekaert and Tölg.² The present paper will be focused on mass spectrometry methods, which have several interesting features for inorganic analysis: mass spectrometry is the only universal multielement method, which allows the determination of all elements and their isotopes in both solids and liquids; its detection limits for virtually all elements are low; it can be more easily applied than other spectroscopic techniques as an absolute method, because the analyte atoms produce the analytical signal themselves, and their amount is not deduced from emitted or absorbed radiation; the spectra are simple compared to the line-rich spectra often found in optical emission spectrometry. The resolving power of conventional mass spectrometers is sufficient to separate all isotope signals, although expensive instruments are required to

eliminate interferences from molecules and polyatomic cluster ions.

For many industrial problems direct analysis of the solid is preferred because the problems of contamination and losses are much smaller than those arising in wet chemical separations or enrichment techniques. We will therefore emphasize multielement bulk trace analysis of solids by mass spectrometry; some attention will also be paid to determination of the spatial distribution of trace elements, since contaminants, for instance, often reside at the surface, or are segregated at interfaces or in inclusions. Electron probe X-ray microanalysis and Auger electron spectroscopy are the standard techniques, but both are limited by their poor detection power. Mass spectrometric techniques are more sensitive by several orders of magnitude, and SIMS in particular is playing an increasingly important role in solving technical problems.

Mass spectrometric analysis is based on the ionization of atoms or molecules in an ion source, separation of the ions in a mass analyser according to the mass-to-charge ratio (m/z), and the detection and recording of the mass spectrum. The location of the mass lines provides a qualitative analysis, and their intensity, mostly measured relative to that of the matrix element or a suitable internal standard, gives a quantitative analysis.

SPARK-SOURCE MASS SPECTROMETRY (SSMS)

Principle

For determination of the elemental composition of a solid by mass spectrometry, its crystal and molecular structure must be destroyed, *i.e.*, the substance must be atomized, and then its atoms ionized. In the spark ion source this is achieved by applying in a vacuum, a high-frequency (*ca.* 1 MHz) potential difference of 20–100 kV between the electrodes, one or both of which must be prepared from the sample material. The following picture can be presented of the phenomena occurring in the spark ion source. Breakdown of the vacuum gap takes place and a plasma cloud is formed quickly (in 5–10 nsec) between the electrodes; it is a small (initial radius 15–50 μm), but rather dense (initial density 10^{18} – 10^{19} particles/ cm^3) and hot (initial temperature 5–20 eV, *i.e.*, up to 2×10^5 K) cloud.³

During expansion of the plasma, extensive recombination occurs and more than 99.9% of the ions will be transformed into neutral

particles, which are not detected by the mass spectrometer. The remaining ions are accelerated in the expanding plasma by a hydrodynamic mechanism or in a “self-consistent field”³ and acquire such high and dissimilar energies that double-focusing mass spectrometers are required. In spite of this recombination, the overall degree of ionization of the plasma is still sufficiently high (0.1%) for absolute detection limits of 10^{-10} – 10^{-12} g to be reached. The analysis is usually based on singly charged cations, but multiply charged ions can also be detected, especially for the matrix elements. Most commercially produced instruments contain a Dempster’s spark source or a triggered d.c. arc source and a Mattauch–Herzog mass analyser. An ion-sensitive emulsion (a “photoplate”) serves as a detector as well as a recording system. The lay-out of a typical instrument is shown in Fig. 1. A comprehensive treatment of the spark-source mass spectrometric technique can be found in the monograph edited by Ahearn,⁴ and reviews by Bacon and Ure⁵ and Ramendik *et al.*³

Spark-source mass spectrometry is one of the most efficient methods for multielement analysis of solids. It allows simultaneous detection of nearly all elements with high specificity, is applicable to major, minor and trace elements down to concentrations of about 10^{-7} – 10^{-6} atom%, and requires only simple sample preparation, typically without any chemical pretreatment, except for insulators, which must be powdered and mixed with a suitable conductor such as graphite. Surface contamination, *e.g.*, from machining of the electrodes, can largely be eliminated by pre-sparking before the actual analysis.

Hannay and Ahearn⁶ used SSMS as early as the 1950s for the direct “panoramic” analysis of semiconductor samples, such as silicon. The technology for manufacturing high-purity silicon and germanium is now well developed, but there is a need for characterizing a variety of new materials for the microelectronics industry, based on high-purity Ga, As, Se, Te, Cd, In and their combinations: GaAs, CdHgTe, InP, *etc.* Although other analytical techniques may be suitable for determining selected impurities at the ng/g level—perhaps with better reproducibility—SSMS is unsurpassed when it comes to obtaining a general view, covering the whole periodic table (including elements such as C, N, O, Cl and P), at such low levels and without previous knowledge of composition.

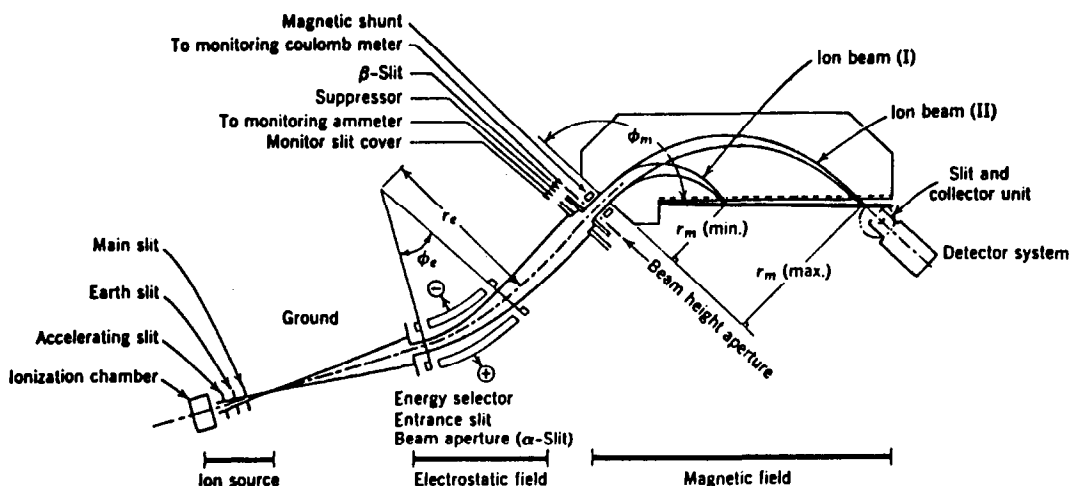


Fig. 1. Double-focusing mass spectrometer with Mattauch-Herzog geometry, used in SSMS.

Sensitivity and mass resolving power

For trace analysis, high sensitivity is a primary requirement. Table 1 shows the low detection limits of SSMS for various materials of interest to the microelectronics industry.⁷ High sensitivity can be obtained by applying high acceleration voltages (higher detection efficiency

for both photoplate and electron multiplier detectors), and by using a spherical instead of a cylindrical electrostatic sector (z -focusing). A high vacuum will reduce spectral background and when light elements such as C, O, N, are to be determined, cryo-pumping is essential. The instrument should be designed to minimize

Table 1. Detection limits (10^{-4} atom %) of SSMS for the analysis of some materials used in the microelectronics industry (reprinted from reference 7 by permission of the copyright holders, Royal Society of Chemistry)

Element	Ga	GaAs	Ge	Si	Element	Ga	GaAs	Ge	Si
Li	0.001	0.005	0.01	0.003	Zr	0.007	0.01	0.02	0.006
Be	0.001	0.01	0.01	0.01	Nb	0.004	0.003	0.01	0.003
B	0.001	0.001	0.002	0.003	Mo	0.02	0.02	0.03	0.01
F	0.002	0.003	0.003	0.003	Ru	0.01	0.02	0.01	0.01
Na	0.02	1	0.01	0.01	Rh	0.003	0.03	0.005	0.003
Mg	0.002	0.03	0.2	0.01	Pd	0.01	0.02	0.01	0.01
Al	0.002	0.003	0.01	0.01	Ag	0.007	0.006	0.01	0.006
Si	0.002	0.01	0.01	n.a.	Cd	0.01	0.02	0.003	0.03
P	0.002	0.003	0.01	—	In	0.004	0.005	0.001	0.03
S	0.002	0.05	0.05	0.05	Sn	0.01	0.01	0.003	0.003
Cl	0.003	0.003	—	0.01	Sb	0.007	0.006	0.002	0.002
K	0.002	0.01	0.01	0.01	Te	0.01	0.01	0.003	0.003
Ca	0.002	0.01	0.01	0.01	I	0.004	0.003	0.001	0.001
Se	0.002	0.003	0.01	0.01	Cs	0.004	0.003	0.001	0.001
Ti	0.003	0.005	0.02	0.01	Ba	0.04	0.02	—	0.002
V	0.003	0.003	0.01	0.01	La	0.04	0.003	0.1	0.001
Cr	0.003	0.01	0.002	0.01	Hf	0.02	0.01	—	0.003
Mn	0.003	0.003	0.1	1	Ta	—	0.3	0.03	0.03
Fe	0.003	0.002	0.1	0.03	W	0.03	0.004	0.003	0.003
Co	0.002	0.001	0.1	0.1	Re	0.008	0.002	0.002	0.002
Ni	0.004	0.01	0.1	0.05	Os	0.01	0.003	0.002	0.002
Cu	0.004	0.002	0.2	0.005	Ir	0.008	0.002	—	0.002
Zn	0.006	0.002	0.2	0.005	Pt	0.02	0.003	0.003	0.003
Ga	n.a.	n.a.	1	0.006	Au	0.02	0.001	0.001	0.01
Ge	0.009	0.3	n.a.	0.01	Hg	0.02	0.004	0.003	0.01
As	0.003	n.a.	1	0.003	Tl	0.007	0.005	0.003	0.001
Se	0.006	0.2	1	0.006	Pb	0.01	0.002	0.01	0.002
Br	0.006	0.06	—	0.006	Bi	0.02	0.003	0.01	0.001
Rb	0.02	0.05	0.01	—	Th	0.006	0.001	0.001	0.001
Sr	0.01	0.01	0.01	0.3	U	0.006	0.001	0.001	0.001
Y	0.003	0.003	0.01	0.02					

n.a. = not applicable.

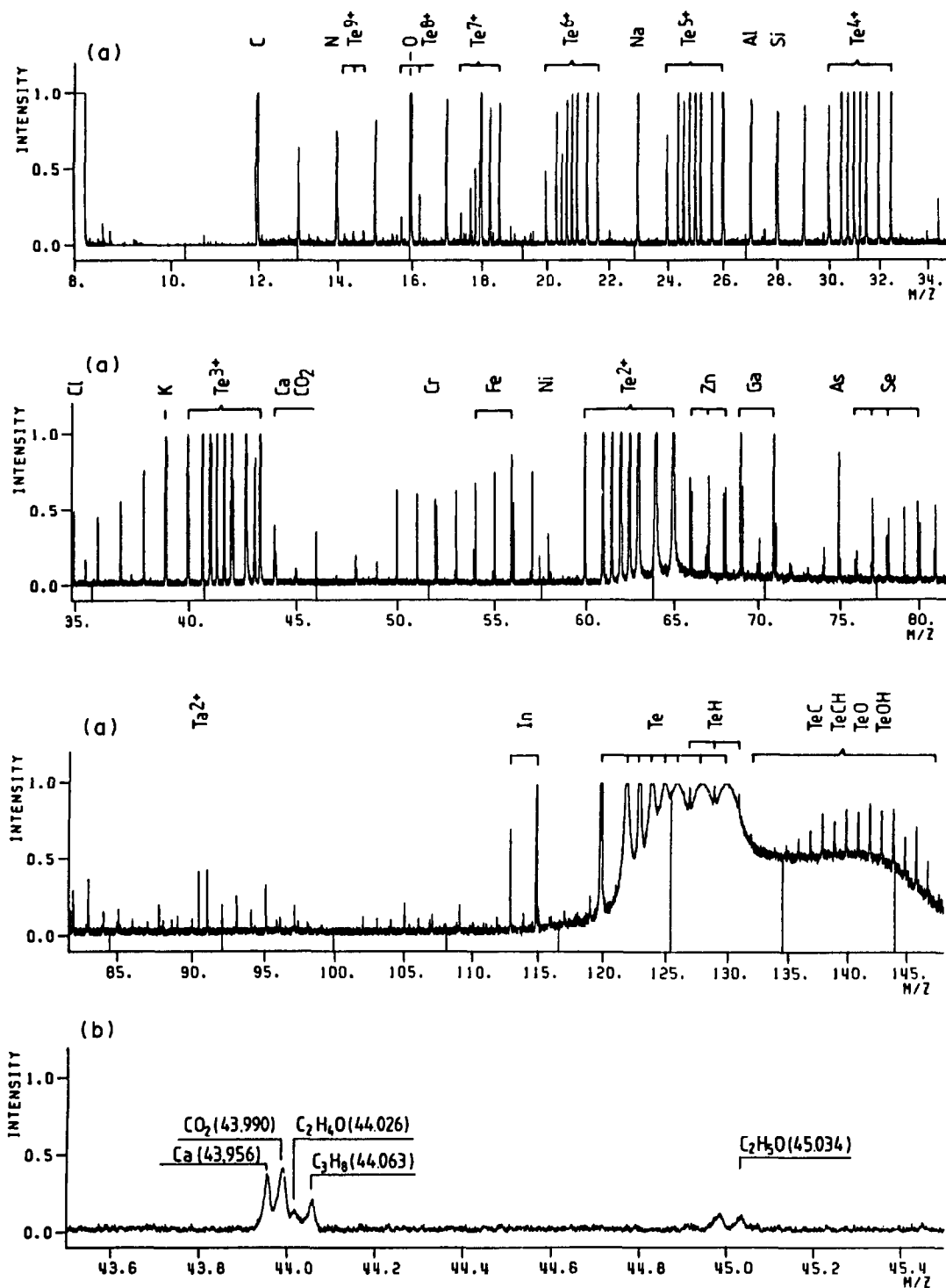


Fig. 2. Spark-source mass spectrum of a high-purity tellurium sample (exposure 545 nC), recorded on a photoplate.⁹ (a) Mass range m/z 8–148. (b) Mass range m/z 43.5–45.5 (detail). Note the fogging (enhanced background) at the high mass side of the matrix lines, due to the emission of secondary ions from the emulsion, which are reflected back to the plate by the magnetic analyser (*cf.* Fig. 1).

photoplate fogging (alternatively the plate can be cut out at the matrix line) or electron multiplier background current. At the same time, high mass resolution must be available to avoid

misinterpretation of the spectrum because of spectral interference from multiply charged ions (especially matrix ions), charge-exchange ions, molecular (polymer and compound) ions, and

background (hydrocarbon and residual gas) ions, with the lines for the atomic impurity ions (usually singly charged) normally used for analysis. This requirement means that electrical detection cannot be used. However, by computer-controlled magnetic step-scanning, Dale⁸ was able to reach a resolving power of 3000 and a detection limit of 5×10^{-7} atom%.

The lines due to hydrocarbons are usually well resolved from those of analytical interest (*e.g.*, Fig. 2b), but in a tellurium matrix elements such as Mg, P, Cu, and I are completely lost because of interference by multiply and singly charged matrix ions (Fig. 2a); the $^{40}\text{Ca}^+$ and $^{41}\text{K}^+$ lines are completely obscured by $^{120}\text{Te}^{3+}$ and $^{123}\text{Te}^{3+}$, but those for the isotopes $^{39}\text{K}^+$ and $^{44}\text{Ca}^+$ are free from interference (Fig. 2b). Other elements detected in the tellurium sample were: N, O, Na, Al, Si, S, Cl, Cr, Mn, Fe, Ni, Zn, Ga, Ge, As, Se; the In and C were due to memory effects from previous analyses. The following elements were below the limit of detection: Li, Be, B, F, Sc, Ti, V, Co, Br, Rb (1–5 ng/g), P, Rh (5–10 ng/g), Mg, Nb, Mo, Pd, Ag, Cd, Sn, Sb, La, Pr, Eu, Tb, Ho, Er, Tm, Lu, W, Re, Os, Pt, Hg, Tl, Pb, Bi, Th, U (10–50 ng/g), Ba, Ce, Sm, Gd, Dy, Yb, Hf, Au (50–100 ng/g).

Quantification

For quantitative analysis, the photoplate blackenings must be converted into ion intensities, and the characteristics of the emulsion taken into account. If comparison with a similar sample of known composition is possible, relatively accurate concentrations can be obtained. Such standards are, however, seldom available for high-purity materials; sometimes a 4 N sample, which has been characterized by AAS, for instance, can be used as a standard for its 5 or 6 N analogue.

If such a standard is not available, it is still useful if at least one element in the unknown sample can be determined by an independent method. All other impurities can then be related to this "internal standard", by using appropriate relative sensitivity factors (RSF); if the latter are not known, they are usually set equal to 1, which makes the analytical results uncertain by a factor of about 3 (except for the alkali and alkaline-earth metals, for which the sensitivity is usually significantly higher), as is known from experience with many types of matrices.

The impurities can also be related to the matrix element, but because of the limited dynamic range of the ion-sensitive emulsion,

graded exposures are normally applied to cover major, minor, trace and ultratrace elements (15 exposures in steps of a factor of 10 cover 7 orders of magnitude, *e.g.*, from 10^6 to $0.1 \mu\text{g/g}$).

Relative sensitivity factors

Many efforts have been devoted to predicting RSFs from various physicochemical properties of the elements and the matrix element of interest, *e.g.*, the melting or boiling point, heat of sublimation, ionization potential or cross section, *etc.* Some recent proposals were made by Opausky,¹⁰ Vieth¹¹ and Ramendik.¹² According to Verlinden *et al.*¹³ RSFs of metals are related to modifications in the surface composition of the electrodes during sparking. The spatial distributions of a number of elements in the sparked surface of some metals (iron, copper and aluminium) were measured by secondary-ion mass spectrometry (Fig. 3). The surface composition of the sparked electrodes is seen to differ from that of the bulk. The ratio F_x of the secondary ion intensities in the sparked surface and in the bulk of the electrodes, both normalized to the corresponding signal of Fe^+ , agreed quite well with RSFs which were experimentally determined by SSMS with Fe as the internal standard, for using well-known standard reference materials.¹³

This observation suggests that differences in RSFs are, at least to some extent, caused by various processes which occur in the electrode surface during sparking (melting, oxidation, segregation, selective vaporization, fractional condensation). In the case of iron and copper matrices, the data suggest that the redistribution of impurities is related to the solid-liquid phase change at the electrode surface during sparking.¹⁴

Precision and accuracy

If reliable and homogeneous standard reference materials are available, quantitative analysis with an error of less than 10–20% is possible: deviations of less than 5% from independent analyses were observed in the concentration range 10^{-5} –1% in the case of metals and alloys.¹⁵ Even for a completely error-free analytical method, the relative standard deviation $R(\%)$ of an analysis will not be zero, because of sample heterogeneity: R is inversely proportional to the square root of the analytical sample weight w :

$$R(\%) = 100 \sqrt{K_s/w}$$

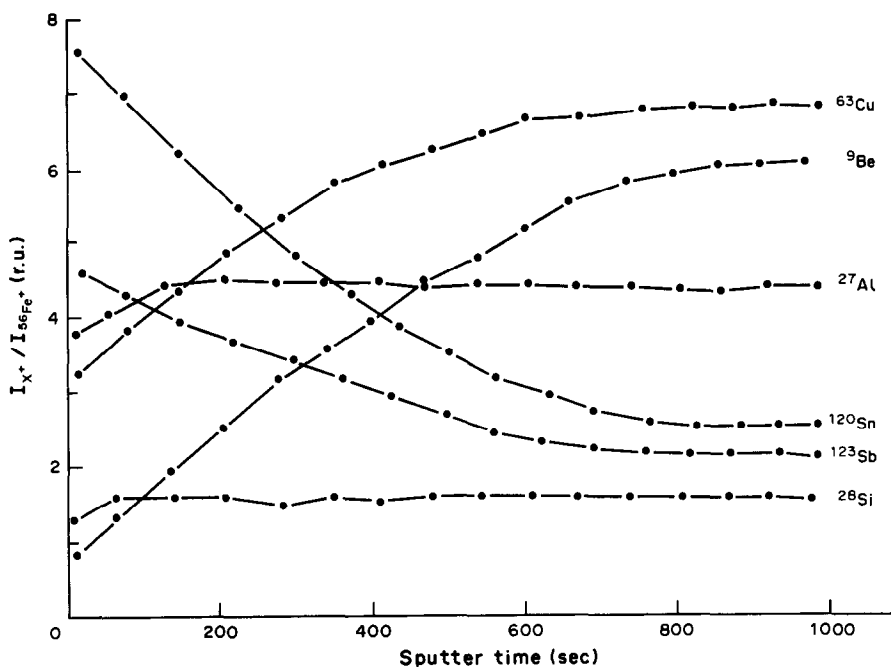


Fig. 3. In-depth distribution of some elements at the surface of sparked Cu and CuBe electrodes, measured by SIMS. (Reproduced by permission, from J. Verlinden, K. Swenters and R. Gijbels, *Anal. Chem.*, 1985, **57**, 131. Copyright 1985, American Chemical Society.)

where K_s is the "sampling constant".¹⁶ This effect is illustrated in Fig. 4 for the determination of Mn in gold at the 40 ng/g level by SSMS, with electrical detection.¹⁷

Localized analysis

Since the spark transfers energy to a small volume of the specimen, SSMS can be used

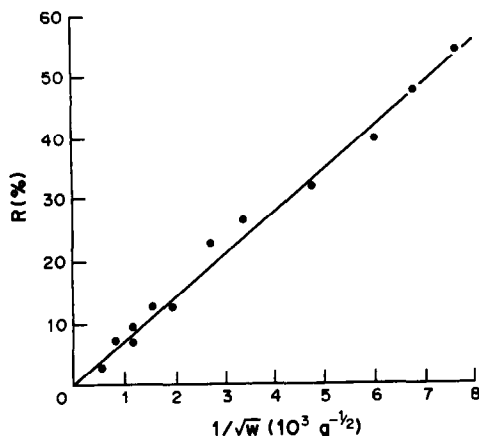


Fig. 4. Sampling error R (*i.e.*, total error minus analytical error) for determination of manganese in gold wire at the 40 ng/g level, by SSMS with electrical detection in the magnetic peak-switching mode. The analytical sample weight w was varied over more than 2 orders of magnitude, mainly by selecting different spark parameters (breakdown voltage). (Reproduced from reference 17 by courtesy of the copyright holders, JEOL).

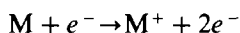
for localized analysis, although this is a less frequently used application. The lateral resolution, with a sharp counter-electrode, is *ca.* 10–100 μm (single shot). Multielement analysis of surface contaminants (information depth $< 1 \mu\text{m}$) is possible by scanning the sample under a counter-electrode, and integrating the whole mass spectrum with a photoplate. For more details, see Gijbels *et al.*,¹⁷ Ramendik *et al.*³ and Verlinden *et al.*⁷

GLOW DISCHARGE MASS SPECTROMETRY (GDMS)

Principle

As shown above, the high-voltage vacuum spark exhibits high sensitivity, broad applicability and relatively few interferences, but its ion yield is erratic and has a wide energy spread. In recent years, the glow discharge (GD) has been developed as a more stable, low-energy alternative ion source. The GD is a simple two-electrode device filled with a noble gas to a pressure of about 0.1–10 mmHg.¹⁸ A few hundred volts applied across the electrodes causes breakdown of the gas and formation of ions, electrons and other species that make the GD useful in analytical chemistry. Only two plasma zones need concern us here: the cathode dark space over which nearly all of the discharge

voltage drop takes place, and the negative glow, which is an essentially field-free region and tends to fill much of the remaining discharge volume in the case of small analytical sources. Positive gas ions (e.g., Ar^+) are accelerated across the field established in the cathode dark space and collide with the cathode surface (sample), releasing a variety of secondary particles required to maintain the discharge.¹⁹ The sample is thus atomized by a process called sputtering; positive ions are returned to the surface by the cathode dark space field, but the neutral species diffuse into the negative glow region. Glow discharge analytical methods are based on the utilization of this large sputtered neutral population. The glow discharge is a collision-rich environment: the sputtered atoms can be ionized by electron and Penning (metastable impact) ionization:¹⁸



and



The ions formed can be extracted into a mass spectrometer, by a differential pumping system to eliminate the argon gas of the discharge. It is conceivable that some mass fractionation occurs at this stage. The GD mass spectra arise primarily from singly charged atomic ions, although certain molecular ions do appear in lower abundances, e.g., MAr^+ , M_2^+ , MO^+ . Glow discharge sputter yields and ionization efficiencies are rather uniform, producing generally similar relative sensitivity factors (see below), which is a desirable feature for quantitative analysis without standard reference materials, and comparable with other forms of "sputtered neutral mass spectrometry" (see below) and also with SSMS.

The most versatile source configuration is probably the pin source, which uses a spring clip or pin-vice type mount adaptable to samples ranging from thin wires to rods. The disc ion source may be preferable for materials that are easily cut into discs, and for insulators after pelleting with a conducting powder.²⁰

Most of the reported work on GDMS has been done with quadrupoles^{20,21} which make it possible to design simple inexpensive instruments with low sampling voltages and high ion transmission, particularly in the lower mass ranges: the weakness of the quadrupoles is their low mass resolution. When suitable interfacing

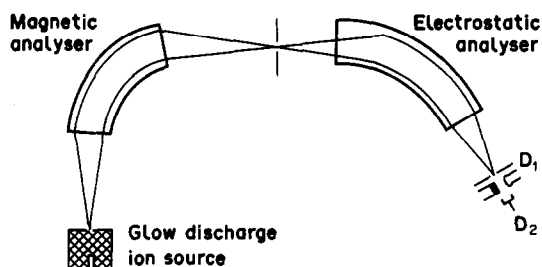


Fig. 5. Schematic diagram of a double-focusing mass spectrometer with inverse Nier-Johnson geometry, used in the VG 9000 GDMS.

is employed, the mass spectra obtained have a low background signal from clusters,²¹ and the detection limits appear to be in the $\mu\text{g/g}$ range. The only commercial instrument (VG 9000) has a double-focusing (inverse Nier-Johnson) mass spectrometer (see Fig. 5), allowing high mass resolution, typically *ca.* 4000, but at additional expense, of course, which we feel is justified when analysing high-purity materials. The manufacturer²² claims detection limits in the ng/g range, which is similar to that for SSMS. The mass spectrometer design does not allow simultaneous detection of all elements; data accumulation has to be done sequentially, for preselected m/z values; a high dynamic range detection system ($1-10^9$) is available which allows measurement of major and ultratrace components in a single measuring sequence.

Applications, sensitivity and mass resolving power

GDMS appears to be a useful technique for elemental analysis of solids. Studies to date show the following useful features:²⁰ direct analysis of metals and alloys; analysis of insulators after compacting with a graphite or metal matrix; response to both metallic and non-metallic elements; minimal matrix effects; ng/g detection limits obtainable; sensitivities generally similar for most elements; isotopic information is obtained; the mass spectra are much simpler than optical emission spectra; the sample can be cleaned by sputtering before the actual analysis.

SSMS also has most of these features, but there are some differences: the spark source gives a higher abundance of multiply charged ions, which precludes the determination of some elements, even if a high mass resolving power is available, e.g., Mg, P and Cu in tellurium (see above); on the other hand, glow discharge mass spectra contain large peaks from the discharge gas, such as Ar^+ and MAr^+ (argides), an example being $^{56}\text{Fe}^{40}\text{Ar}^+$, which interferes with

$^{96}\text{Mo}^+$ in the case of a steel matrix. The glow discharge is more stable, however, and requires less attention than the spark.

Most applications reported to date deal with the analysis of metals and alloys, semiconductor materials and oxides (after mixing and pelleting with a conducting powder). Some examples²³ will be discussed below. Ultrapure aluminium is used extensively in the semiconductor industry for connections and contact pads in integrated circuits, and in the manufacture of multi-component semiconductors such as GaAlAs. Typical impurities of interest include high-mobility elements (Li, Na, K), first row transition metals (Ti, V, Cr, Cu, Co, Ni, Zn), alloying components (Si and Cu), radioactive elements (alpha-emitters U and Th) and any potential contaminants arising from the production process. High mass resolution (> 5000) is required in the determination of potassium, to separate $^{39}\text{K}^+$ from $^{38}\text{ArH}^+$ ($^{40}\text{K}^+$ and $^{41}\text{K}^+$ are swamped by the $^{40}\text{Ar}^+$ and $^{40}\text{ArH}^+$ signals), see Fig. 6. Detection limits in the ng/g range have been achieved for uranium and thorium. Figure 7 shows the mass spectrum at $m/z = 238$; the result (17 ng/g U) was in agreement with that obtained by neutron activation analysis. For the analysis of low-melting materials, such as gallium, cooling of the cell with liquid nitrogen has been used. A similar approach is customary in SSMS⁷ and has also been described for SIMS.²⁴

Its stability makes the glow discharge useful for precise determination of major components. Table 2 shows concentrations of Si in an Al-1% Si alloy.

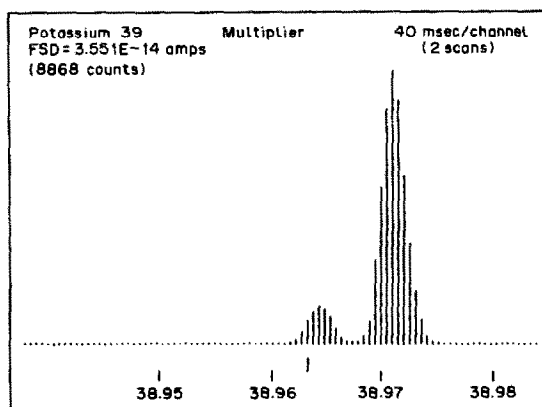


Fig. 6. High-resolution ($M/\Delta M \sim 6000$) GD mass spectrum of aluminium at nominal m/z 39, showing the $^{38}\text{ArH}^+$ peak to the right of the $^{39}\text{K}^+$ peak. (Reproduced from reference 23 by courtesy of VG Isotopes Ltd., Winsford, U.K.)

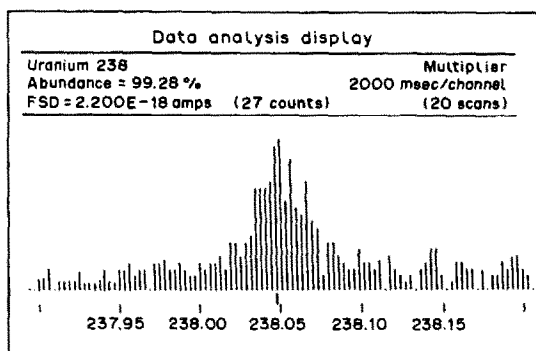


Fig. 7. GD mass spectrum of aluminium at m/z 238. The ^{238}U concentration is 17 ng/g. (Reproduced from reference 23 by courtesy of VG Isotopes Ltd., Winsford, U.K.)

Quantification and relative sensitivity factors

The concentration of an element can be directly derived from the ratio of the ion-beam current to that for a matrix isotope. More accurate results are obviously obtained by using relative sensitivity factors, usually defined as the number by which the raw data must be divided to obtain the correct concentration. These appear to vary over a range of about 0.2–3 (e.g., ~ 2 –3 for Ti, Zr, Nb; ~ 1 for Fe, Mo, Co; ~ 0.6 for Pb, Si; ~ 0.2 for Cu, Zn, C, P, S), but systematic data for different matrices are not yet readily available. So far, no pronounced matrix effects are apparent. It is also to be expected that the RSF values will depend on the instrument used. Some data reported at a recent "Open forum discussion" in Antwerp are shown in Table 3. The situation is reminiscent of that in SSMS,²⁵ but no rationalization of the data has yet been reported.

Precision and accuracy

Because of the stable nature of the glow discharge, the precision is quite good, at least for homogeneous samples. For heterogeneously distributed elements, the same remark holds as for SSMS: the sampling error should be inversely proportional to the square root of the analytical sample weight (see above). There do

Table 2. Major component analysis of Al-1% Si alloy by GDMS (reproduced from reference 23 by courtesy of VG Isotopes Ltd., Winsford, U.K.)

Isotope	Run 1	2	3	4	Mean
^{28}Si	1.15	1.16	1.20	1.16	1.168
^{29}Si	1.16	1.26	1.20	1.19	1.20
^{30}Si	1.27	1.35	1.22	1.23	1.26

Table 3. Relative sensitivity factors, obtained by analysing NBS SRM 1261A steel with different glow discharge mass spectrometers²⁵

Element	A	B	C	D	Certified concentration, $\mu\text{g/g}$
B	1.72	0.19	0.64	3.8	5
C	0.21	0.13	0.16	0.21	3900
Al	1.21	0.42	0.62	0.80	200
Si	0.51	0.34	0.96	0.42	2280
P	0.09	0.26	0.19	0.23	160
S	0.13	0.29	0.19	0.35	150
Ti	1.58	1.30	2.43	2.41	200
V	1.47	1.20	1.90	1.84	110
Cr	1.11	0.53	0.52	0.37	6900
Mn	1.29	0.73	0.76	0.57	6700
Fe	= 1.00	= 1.00	= 1.00	= 1.00	
Co	0.77	0.87	0.84	0.82	320
Ni	0.69	0.95	0.43	0.48	20000
Cu	0.76	0.35	0.18	0.13	420
As	0.18	0.58	0.12	0.16	170
Se	0.64	0.61	0.17	0.30	40
Zr	0.54	1.59	1.55	1.56	90
Nb	1.72	1.84	1.41	1.35	220
Mo	1.67	1.52	0.97	1.02	1900
Ag		0.48	0.22	0.17	4
Sn	1.44	0.74	0.39	0.30	100
Sb	0.95	0.42	0.19	0.15	42
Te	1.03	0.74	0.20	0.20	6
La	1.33	0.79	1.17	1.75	4.2
Ce	1.66	0.64	1.43	2.29	14
Ta	1.56	1.20	—	0.70	210
W	1.31	1.11	0.75	0.54	170
Pb	—	—	0.28	0.25	0.25
Bi	0.87	0.35	0.17	0.13	4

A: quadrupole mass analyser (University of Virginia).

B: quadrupole mass analyser (ISAS, Dortmund).

C: double-focusing GDMS, VG 9000 (C. Evans & Associates, Redwood City).

D: double-focusing GDMS, VG 9000 (VG Isotopes, Ltd, Winsford).

not seem to have been any systematic studies on sample consumption in the GD ion source, so no further comment can be made.

Localized analysis

In contrast to the spark ion source, in GD the energy transfer to the sample is not localized, so lateral element distribution cannot be studied. It appears from some preliminary studies, however, that depth profiling and thin layer analysis are both possible if a flat cell geometry is used.^{26,27}

SPUTTERED NEUTRALS MASS SPECTROMETRY (SNMS)

There have been several attempts to use post-ionized sputtered particles in mass spectrometry.²⁸ The sputtering has been achieved by means of ion beams and also by ions originating from a plasma in front of the sample (see also

GDMS, above) and the post-ionization has been realized by interaction of the sputtered neutral species with excited atoms (as in GDMS), electrons or photons.

Hot electron-gas SNMS was developed by Oechsner²⁹ in an experimental arrangement applying the same low-pressure high-frequency plasma (10^{-5} – 10^{-3} mbar noble gas) to generate energetic ions for sample surface sputtering as well as low-energy electrons for post-ionization of the sputtered neutral species. Electron-beam post-ionization of sputtered particles has been reported, and high sensitivities have been obtained.³⁰

Post-ionization of sputtered particles by a laser beam can be realized either by single-photon resonance ionization³¹ or by multiphoton non-resonance ionization.³² If it is assumed that most of the particles emitted from the sample surface are neutral, the calibration of SNMS is much simpler than SIMS (see below). If the cross sections for the post-ionization process are relatively uniform, any sample can be analysed quantitatively by SNMS, provided the emitted secondary ions, the distribution of sputtered atoms between different molecular species, and changes in energy and angular distribution of the neutral species emitted when different matrices are used, and so on, are neglected.²⁸

SNMS is a rapidly developing technique. One commercial instrument (INA 3, Leybold-Heraeus GmbH, Köln) has three operating modes: direct bombardment (the same low-pressure high-frequency noble-gas plasma is used to sputter the sample and to provide electrons for post-ionization of the sputtered neutral species); separate bombardment (an ion gun is used to bombard the sample with primary ions, and the neutral species released are ionized in the surrounding plasma). The ion gun and quadrupole detection system used in SNMS can also be used for SIMS analysis (without plasma).

SNMS can be used for quantitative depth profiling, with good resolution, of metals, alloys and semiconductors, but also for quantitative bulk analysis of metals and alloys, without significant matrix effects. Detection limits in the $\mu\text{g/g}$ range have been reported.³³ Some relative sensitivity factors for a standard reference material (stainless steel) are shown in Table 4,³³ they appear to be rather similar, the highest being less than 5 times the lowest.

One of the unique features of SNMS is the ease of analysis of insulators. Whereas SSMS,

Table 4. Relative sensitivity factors, obtained by analysing a standard reference stainless-steel sample by SNMS (reproduced from reference 33, by courtesy of Leybold-Heraeus GmbH)

Element	Bulk concentration, atom %	RSF, D_{Fe}/D_x
Fe	69.08	1
C	0.206	2.64
Si	1.37	0.60
Mn	1.82	1.18
P	0.058	0.92
S	0.005	1.25
Cr	18.71	1.11
Mo	0.11	1.76
Ni	8.54	1.71
N	0.098	2.28
Al	0.006	0.5

GDMS and SIMS are handicapped by electrical charging effects, which have to be overcome by special electron-flooding devices (in SIMS) or by mixing the sample with a conductor, SNMS makes use of the self-compensating plasma/sample interaction. This feature is of considerable interest in the study of ceramics, for instance.

SECONDARY ION MASS SPECTROMETRY (SIMS)

Principle

SIMS is based on the ejection of charged atomic and molecular species (secondary ions) from the surface of a solid under heavy-particle bombardment (usually with primary ions, sometimes neutral atoms). Most of the secondary ions originate from the uppermost atomic layers of the bombarded surface, so that SIMS is very often used for surface analysis. The secondary ions can be separated by different types of mass analysers: quadrupole, magnetic, time-of-flight, *etc.* The mass spectra contain not only atomic ions, but also many polyatomic cluster ions, *e.g.*, for an aluminium sample under Ar^+ bombardment Na^+ , K^+ , Al^+ , Al_2^+ , Al_3^+ , AlO^+ , $AlOH^+$, but multiply charged ions such as Al^{2+} , Al^{3+} are not very abundant. Ions of electro-negative elements can more easily be observed in the negative ion spectrum, *e.g.*, O^- , O_2^- , AlO^- , AlO_2^- , Cl^- , OH^- .

By scanning of a finely focused primary ion beam over the sample surface, information about the lateral surface distribution of the secondary ion emission can be obtained, which can in principle be converted into a lateral element distribution.

The ion bombardment results in erosion of the surface. In so-called dynamic SIMS conditions, the removal rate is of the order of a monolayer per second, and depth profiling of element concentration can be achieved with high sensitivity (in favourable cases down to the ng/g range). Dynamic SIMS with a focused scanning ion-beam allows a three-dimensional analysis of the sample.

The possibility of performing localized microanalysis with SIMS in its various forms is of course very important, but this aspect will not be further discussed here. Reference may be made to the very comprehensive monograph by Benninghoven *et al.*²⁸ The possibility of using SIMS for quantitative bulk analysis will, however, briefly be dealt with.

Sensitivity

SIMS is a very sensitive technique (10^{-7} – 10^{-2} atom %) and can thus be used for ultratrace and trace analysis. As an example, some typical detection limits are given in Table 5. It can be seen that the sensitivities vary widely from element to element (by 5 orders of magnitude). It is clear that for the highest sensitivities to be obtained, a mass spectrometer with high transmission should be used. Comparative studies have shown that a magnetic instrument, such as the Cameca IMS-3f/4f, is the most suitable for the purpose.

Quantification

Even if mass spectral interferences, from polyatomic cluster ions for instance, can be excluded, quantitative elemental analysis by SIMS is not an easy task, because of the dependence of the relative and absolute secondary ion

Table 5. Detection limits in GaAs for SIMS (reproduced from reference 28, p. 792, by permission of the copyright holders, John Wiley & Sons, Inc.)

Element	Ion detected	Detection limit	
		10^{-4} atom %	atoms/cm ³
H	$^1H^+$	10 ²	5×10^{18}
Bc	$^9Be^+$	0.002	8×10^{13}
B	$^{11}B^+$	0.01	5×10^{14}
Al	$^{27}Al^+$	0.008	4×10^{14}
Si	$^{28}Si^+$	0.008	4×10^{14}
S	$^{32}S^-$	1	5×10^{16}
Cr	$^{52}Cr^+$	0.001	4×10^{13}
Mn	$^{55}Mn^+$	0.001	4×10^{13}
Fe	$^{56}Fe^+$	0.002	7×10^{13}
Cu	$^{63}Cu^+$	0.02	1×10^{15}
Zn	$^{64}Zn^+$	0.1	5×10^{15}
Ge	$^{74}Ge^+$	0.2	1×10^{16}
Sn	$^{120}Sn^+$	0.1	5×10^{15}

yields on matrix effects, surface coverage with reactive elements (*e.g.*, oxygen), background pressure in the sample environment, effect of the crystallographic orientation relative to the primary and secondary ion beams, angular effects, mass-dependent transmission of the mass spectrometer, energy band-pass of the mass spectrometer, *etc.*²⁸

Calibration curves are sometimes used for quantitative analysis, but then the standards should differ as little as possible in composition from the sample to be analysed, and the ion intensities should be measured under identical experimental conditions.

Methods have been described for the construction of a calibration curve by use of ion-implanted samples, *e.g.*, by Leta and Morrison,³⁴ but this approach requires the availability of an ion implanter and is not applicable to all elements of interest.

Another approach is to work with relative sensitivity factors, and standard reference materials. However, such materials are not easy to come by, or, in the case of high-purity materials, are not available at all. In addition, it is not straightforward to transfer experimental RSFs obtained for one instrument to use with another, although progress is being made in this area, and a prescribed procedure for "tuning" the SIMS instruments must be strictly followed.^{35,36} The RSFs for different elements usually depend in a different way on the state of the sample surface during ion bombardment, *e.g.*, they change as a function of partial oxygen pressure. It is comparatively easy to determine experimentally the dependence of a set of RSFs on a particular internal indicator which is representative of the oxidation state of the analysed surface (see Fig. 8), and can be derived from the mass spectrum of the unknown sample; for example, the matrix ion species ratio (MISR) $^{112}\text{Fe}_2^+ / ^{54}\text{Fe}^+$ for steel, decreases with the partial oxygen pressure in the ion source. The MISR approach has been shown to yield lower analytical errors (5–20% relative) than either the straightforward RSF method, or the different versions of LTE models (see below).

In the absence of any standard reference materials, quantification algorithms based on physical models of the ion emission process can be utilized,²⁸ The empirically observed exponential dependence of positive secondary ion yields on the first ionization potential (E_i) of the corresponding element has led to the assumption of some type of thermodynamic

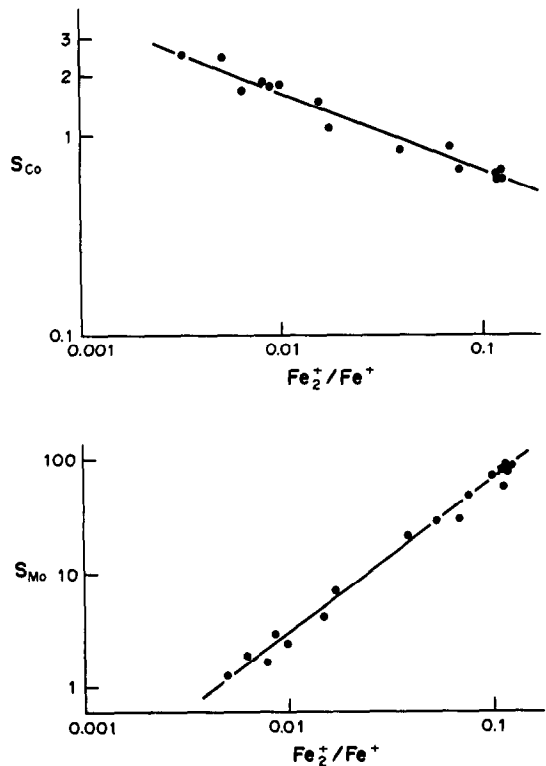


Fig. 8. Relative sensitivity factors for SIMS analysis of Co and Mo in steel as a function of the matrix-ion species ratio $\text{Fe}_2^+/\text{Fe}^+$.

equilibrium (complete, local or partial) of the sputtered ions with their surroundings. For the reaction



the equilibrium volume concentrations n_+ (for M^+), n_e (for e^-) and n (for M) are given by the Saha–Eggert equation.³⁸

$$\frac{n_+ n_e}{n} \approx \frac{2Z_+(T)}{Z(T)} \left(\frac{2\pi m_e kT}{h^2} \right)^{3/2} \exp \left(-\frac{E_i - \Delta E}{kT_i} \right)$$

where $Z_+(T)$ and $Z(T)$ are the partition functions for M^+ and M respectively, E_i is the first ionization potential of M and ΔE is the decrease in ionization potential caused by Coulombic interaction between the particles. This implies that the n_+/n ratios for different elements depend on the "ionization temperature" T_i and the electron density n_e . A semilog plot of normalized secondary ion intensities *vs.* E_i is then a straight line, the slope of which mainly depends on T_i . If two elements with known atomic concentrations and sufficiently different ionization potentials can be found in the sample (*e.g.*, major or minor elements, which can be determined by a reliable analytical

technique, e.g., electron probe X-ray micro-analysis), values for the fitting parameters T_i and n_e , can be obtained from the Saha-Eggert equation and used to estimate the relative sensitivities for other elements from their ionization energies. For a more detailed discussion, reference may be made to the monograph on SIMS by Benninghoven *et al.*²⁸

As already mentioned, even for an error-free method the relative standard deviation of an analysis will not be zero, because of sample heterogeneity. In the case of SIMS, Scilla and Morrison³⁹ have derived an expression for the sampling error E_s for a particular element in a given matrix:

$$E_s = K/a^{1/2}$$

where K (μm) is the sampling constant, which is determined solely by the heterogeneity of the sample with respect to the element of interest, and a (μm^2) is the area sampled. In some cases, an element can be so heterogeneously distributed in a sample, that results from as many as 100 different sampling areas might have to be averaged in order to reduce the sampling error to an acceptable level. It is clear that this sampling problem is more severe for SIMS than for SSMS analysis, for instance, because of the much lower sample consumption in the former case. In fact, SIMS, especially in the ion microprobe version, is mostly applied just to reveal differences in concentration between different positions on or in a solid sample.

LASER MASS SPECTROMETRY

A laser pulse (usually from an Nd:YAG laser) can be used to evaporate and ionize material from a solid, for subsequent mass analysis. There are two commercial instruments—LAMMA (Leybold-Heraeus, GmbH, Köln) and LIMA (Cambridge Mass Spectrometers Ltd.)—that emphasize the microprobe aspect; they are equipped with time-of-flight mass spectrometers for obtaining a complete mass spectrum from a single shot, and can work in either the transmission or reflection mode. A good idea of the range of applications of these laser microprobe mass spectrometers can be obtained from the proceedings of the 3rd Laser Microprobe Mass Spectrometer Workshop at the University of Antwerp (August 1986), or from some recent reviews.^{40,41} This type of equipment is useful for particle characterization and sensitive local microanalysis in a more

general sense, but is not used for bulk trace element analysis of high-purity solids.

The double-focusing laser mass spectrometer (Mattauch-Herzog geometry) described by Jansen and Witmer⁴² can be used for the semi-quantitative bulk analysis of solids and powders without the aid of standards. The samples may be either conductive or insulating, but should not be completely transparent to the laser radiation (1060 nm wavelength). The detection limit is about 10 ng/g for bulk analysis, with a consumption of about 100 μg of material, and about 0.1% for microanalysis. The relative standard deviation is about 20% and the result of a single analysis may range from half to twice the true value if no standards are used, and be within $\pm 20\%$ of the true value when standards are employed. Microanalysis is possible with a crater diameter of ~ 20 μm and a depth of ~ 0.1 μm . The system can perform thin-film and profile analysis with a depth resolution of ~ 0.1 μm .

It is of interest to note that the intensity ratio of singly-charged to multiply-charged ions can be influenced by varying the energy of the laser

Table 6. Analysis of NBS SRM 1235 zirconium by laser mass spectrometry (Nd:YAG laser, power density *ca.* 10^9 W/cm², pulse repetition rate 10 kHz) (reprinted from Dietze and Becker,⁴⁵ by permission of the copyright holders, Springer Verlag, Heidelberg)

Element	Concentration,*		RSF†
	$\mu\text{g/g}$	NBS value, $\mu\text{g/g}$	
Na	270	—	—
Mg	8	—	—
Al	(810)§	105	(7.7)
Si	96	95	1.01
P	42	44	0.95
S	46	—	—
Cl	9	—	—
K	(1000)§	—	—
Ca	70	—	—
Ti	230	90	2.55
V	90	10	9.0
Cr	340	60	5.66
Mn	26	25	1.04
Cu	44	80	0.55
Fe	930	850	1.09
Co	20	20	1.00
Ni	70	65	1.08
Nb	210	200	1.05
Mo	38	40	0.95
Sn	25	25	1.00
Hf	52	95	0.55
Ta	70	280	0.25
W	14	50	0.28

*The element concentrations, except Hf, are not yet certified by the National Bureau of Standards, Washington D.C.

†Relative sensitivity factor.

§Contamination possible.

Table 7. Comparison of mass spectrometry methods for elemental analysis of solids with some commercially available instruments

	SSMS	GDMS	SNMS	SIMS
Ion source	RF vacuum spark (triggered dc arc)	triggered dc discharge in Ar, Ne, <i>etc.</i>	HF low-pressure plasma in Ar, <i>etc.</i>	ion bombardment (Ar ⁺ , O ₂ ⁺ , Cs ⁺)
Mass spectrometer (mass resoln.)	double-focusing Mattauch-Herzog geometry (~4000)	double-focusing inverse Nier-Johnson geometry (~4000)	quadrupole (1 amu)	double-focusing (500-10000)
Manufacturer	Jeol (JMS 01-BM2)	VG (VG-9000)	Leybold-Heraeus (INA-3)	Cameca (3f/4f)
Detector	electron multiplier; ion-sensitive emulsion (whole spectrum simultaneously)	Daly and Faraday cup (masses sequentially)	electron multiplier (mass scan)	electron multiplier and Faraday cup; microchannel plate (ion image) (masses sequentially)
Quantity of sample	0.5 g	0.5 g	0.5 g	0.5 g
Sample form	bar or flat (with counter-electrode)	pin or flat	flat	flat
Metals and semiconductors	yes	yes	yes	yes
Insulators	after mixing with conductor and pelleting possible	after mixing with conductor and pelleting possible	directly	charge compensation (electron gun)
Cryo-cooling of sample	possible	possible	—	possible
Information on bulk-analysis	yes	yes	yes	(yes)
Surface layer/depth profiling	difficult	yes in principle	yes	yes
Lateral resolution	~ 100 μm (with counter-electrode)	—	—	0.2-100 μm
Elemental coverage and relative sensitivity factors	large coverage, small range of RSFs	large coverage, small range of RSFs	large coverage, small range of RSFs	large coverage, wide range of RSFs
Dynamic range	limited by photoplates (graded exposures)	very wide	wide	wide
Sensitivity	~ ng/g	~ ng/g	< μg/g	ng/g (not all elements)
Speed of analysis*	slow	fast	fast	moderate
Main M.S. interference	multiply charged ions	"argides", dimers	"argides", dimers	polyatomic ions
Ease of analysis	requires skilled interpretation	good	good	requires skilled operation

*Speed of analysis is also influenced by memory effects from previous analyses.

beam and the repetition frequency of the laser pulses. The intensity ratio of atomic to cluster ions is reported to be higher than with the radiofrequency spark source. These attractive features have led several other laboratories to mount a laser on existing double-focusing instruments, but it appears not always to be easy to realize a straightforward ion-optical coupling of the ionization chamber to the mass spectrometer.⁴³

This problem has been tackled and the literature reviewed by Dietze and Becker.⁴⁴ Table 6 gives some analytical results obtained for a zirconium sample by the same authors.⁴⁵ For exposures of 100 nC, detection limits of *ca.* 10 ng/g were obtained. The authors developed an

ion-optical system with excellent characteristics, as appears from the reported quality of the mass lines; a mass resolution of ~10⁴ was reached and there was no problem in determining Nb (*m/z* = 93) in the middle of the Zr matrix lines.

CONCLUSION

Although there are other mass spectrometric techniques for the analysis of solid samples, such as laser ablation coupled to inductively-coupled plasma mass spectrometry, we have limited ourselves here to surveying those which are now well developed. A comparison of some characteristics of a few commercially available systems is presented in Table 7.

REFERENCES

1. M. Grasserbauer, P. Wilhartitz and G. Stinger, *Mikrochim. Acta*, 1983 **III**, 467.
2. J. A. C. Broekaert and G. Tölg, *Z. Anal. Chem.*, 1987, **326**, 495.
3. G. Ramendik, J. Verlinden and R. Gijbels, *Spark Source Mass Spectrometry*, in *Inorganic Mass Spectrometry*, F. Adams, R. Gijbels and R. Van Grieken (eds.), Wiley, New York, 1988.
4. A. J. Ahearn (ed.), *Trace Analysis by Mass Spectrometry*, Academic Press, New York, 1972.
5. J. R. Bacon and A. M. Ure, *Analyst*, 1984, **109**, 1229.
6. N. B. Hannay and A. J. Ahearn, *Anal. Chem.*, 1954, **26**, 1056.
7. J. Verlinden, R. Gijbels and F. Adams, *J. Anal. Atom. Spectrom.*, 1986, **1**, 411.
8. L. S. Dale, I. Liepa, P. S. Rendell and R. N. Whittom, *Anal. Chem.*, 1981, **53**, 2288.
9. Xiande Liu, *Ph.D. Thesis*, University of Antwerp, 1986.
10. I. Opauszky and I. Nyary, Report KFKI-1981-09, Budapest, 1981.
11. W. Vieth, Private communication.
12. G. I. Ramendik, B. M. Mauzon, D. A. Tyurin, N. E. Benyaev and A. A. Komleva, *Talanta*, 1987, **34**, 61.
13. J. Verlinden, K. Swenters and R. Gijbels, *Anal. Chem.*, 1985, **57**, 131.
14. K. Swenters, J. Verlinden, P. Bernard and R. Gijbels, *Intern. J. Mass Spectrom. Ion Proc.*, 1986, **71**, 85.
15. E. Van Hoye, F. Adams and R. Gijbels, *Talanta*, 1976, **23**, 789.
16. C. O. Ingamells and P. Switzer, *Talanta*, 1973, **20**, 547.
17. R. Gijbels, J. Verlinden and K. Swenters, *Jeol News*, 1984, **20A**, No. 2, 5.
18. B. Chapman, *Glow Discharge Processes*, Wiley, New York, 1980.
19. W. W. Harrison, *Glow Discharge Mass Spectrometry in Inorganic Mass Spectrometry*, F. Adams, R. Gijbels and R. Van Grieken (eds.), Wiley, New York, 1988.
20. W. W. Harrison, K. R. Hess, R. K. Marcus and F. L. King, *Anal. Chem.*, 1986, **58**, 341A.
21. N. Jakubowski, D. Stüwer and G. Tölg, *Intern. J. Mass Spectrom. Ion Proc.*, 1986, **71**, 183.
22. P. J. Goddard, M. T. MacPherson and R. Ware, *European Design & Production*, March 1985 (reprinted by VG Isotopes Ltd.).
23. *Technical Information*, No. GD-011, VG Isotopes Ltd., Winsford, U.K.
24. M. T. Bernius, S. Chandra and G. H. Morrison, *Rev. Sci. Instrum.* 1985, **86**, 1347.
25. W. W. Harrison, *Open Forum Discussion on Elemental Analysis of Solids by Mass Spectrometry*, 10th Intern. Symp. Microchem. Techniques, Antwerp, August 1986.
26. M. Hecq, A. Hecq and M. Fontignies, *Anal. Chim. Acta*, 1983, **155**, 191.
27. *Technical Information*, No. 02-717, VG Isotopes Ltd, Winsford, U.K.
28. A. Benninghoven, F. G. Rüdener and W. H. Werner, *Secondary Ion Mass Spectrometry: Basic Concepts, Instrumental Aspects, Applications and Trends*, Wiley, New York, 1987.
29. H. Oechsner, in *Topics in Current Physics*, Vol. 37, *Thin Film and Depth Profile Analysis*, H. Oechsner (ed.), Springer-Verlag, Berlin, 1984.
30. P. Sander, U. Kaiser, R. Jede, D. Lipinski, O. Ganschow and A. Benninghoven, *J. Vac. Sci. Technol.*, 1985, **A3**, 1946.
31. D. M. Gruen, M. J. Pellin, C. E. Young and M. H. Mendelsohn, *Phys. Scripta*, 1983, **T6**, 42.
32. C. H. Becker and K. T. Gillen, *Anal. Chem.*, 1984, **56**, 1671.
33. *Technical Information*, No. 190-52.00.2, Leybold-Heraeus GmbH, Köln.
34. D. P. Leta and G. H. Morrison, *Anal. Chem.*, 1980, **52**, 514.
35. F. Rüdener, W. Steiger, M. Riedel, H. E. Beske, H. Holzbrecher, H. Düsterhöft, M. Gericke, C. E. Richter, M. Rieth, M. Trapp, J. Giber, A. Solyom, H. Mai and G. Stinger, *Anal. Chem.*, 1985, **57**, 1636.
36. M. Riedel, F. Rüdener, W. Steiger, M. Gericke, C. E. Richter, M. Trapp, H. Düsterhöft, M. Kröher, H. Mai, S. Oswald, R. Voigtmann, A. Lodding, H. E. Beske, H. Holzbrecher, J. Giber, A. Solyom, F. Michiels, F. Adams and R. Gijbels, *XXX Hungarian Conf. on Spectroscopy*, Debrecen, 24-28 August 1987.
37. J. D. Ganjei, D. P. Leta and G. H. Morrison, *Anal. Chem.*, 1978, **50**, 285.
38. Reference 28, p. 311.
39. G. J. Scilla and G. H. Morrison, *Anal. Chem.*, 1977, **49**, 1529.
40. E. Michiels, L. Van Vaeck and R. Gijbels, *Scanning Electron Microsc.*, 1984 **III**, 1111.
41. A. Verbueken, F. Bruynseels, R. Van Grieken and F. Adams, *Laser Microprobe Mass Spectrometry*, in *Inorganic Mass Spectrometry*, F. Adams, R. Gijbels and R. Van Grieken (eds.), Wiley, New York, 1988.
42. J. A. J. Jansen and A. W. Witmer, *Spectrochim. Acta*, 1982, **37B**, 483.
43. *Arbeitsreffen Funkenmassenspektrometrie*, Freiburg (1987), Eindhoven (1986), Jülich (1985), Antwerp (1984).
44. H. J. Dietze and S. Becker, *Beiträge zur Laserionisations-Massenspektroskopie, ZfI-Mitteilungen*, No. 101, Leipzig, 1985.
45. H. J. Dietze and S. Becker, *Z. Anal. Chem.*, 1985, **321**, 490.

A COMPARISON OF PULSED AMPEROMETRIC DETECTION AND CONDUCTIVITY DETECTION OF UNDERIVATIZED AMINO-ACIDS IN LIQUID CHROMATOGRAPHY

LAWRENCE E. WELCH*

Department of Chemistry, Knox College, Galesburg, IL 61401-4999, U.S.A.

WILLIAM R. LACOURSE, DAVID A. MEAD, JR.† and DENNIS C. JOHNSON

Department of Chemistry, Iowa State University, Ames, IA 50011, U.S.A.

(Received 26 July 1989. Accepted 1 September 1989)

Summary—Pulsed amperometric detection (PAD) in tandem with conductivity detection (CD) has been applied to the direct detection of amino-acids by liquid chromatography. Although sensitive, PAD has a limited linear range of response. Sequential use of conductimetric detection and then PAD extends the dynamic range of amino-acid determination.

Recent progress in amino-acid determination can be attributed to technological advances in liquid chromatography (LC) and chromatographic detectors. Cation-exchange stationary phases¹ have long been the standard for LC separations of amino-acids, and the use of anion-exchange separations² is more recent. Numerous pre-column derivatization schemes produce adducts that can be separated by reversed-phase stationary phases.³ Post-column derivatization is employed in most ion-exchange methods to overcome the lack of response of traditional LC detectors towards amino-acids. Alternatively, "indirect" methods can be used.⁴ Direct and sensitive amino-acid detection without a derivatization step is a desirable further alternative to traditional methods.

Pulsed amperometric detection^{5,6} uses a triple-step potential waveform to combine amperometric detection with alternating anodic and cathodic polarizations to clean and reactivate the electrode surface. This waveform exploits the surface-catalyzed oxidation of the amine group, activated by the transient formation of surface oxides on noble metals. Use of pulsed amperometric detection following liquid chromatography has gained prominence as a selective and sensitive technique for the determination of alcohols, polyalcohols, carbo-

hydrates,⁷⁻¹⁰ amino-alkanols,¹¹ many inorganic and organic sulfur-containing compounds¹² and amino-acids.¹³ Although sensitive, amino-acid determinations by use of PAD exhibit a limited linear response range.

Conductimetric detection has been utilized successfully in ion-chromatography for the determination of inorganic and organic ions.¹⁴⁻¹⁶ Suppressed CD of amino-acids has been shown to be feasible in work on alternative ion-chromatographic eluents,¹⁷ but no amino-acid separations were attempted. Recently, Johnson *et al.* applied unsuppressed CD in tandem with PAD for carbohydrate determinations.¹⁸ The dual detection provided linear calibration over a wide dynamic range.

This paper compares the application of PAD and CD to the simple, direct determination of amino-acids by isocratic chromatography. No suppressor columns were used with the CD system. In addition, CD was applied before PAD, to provide a non-destructive method of extending the linear range of amino-acid determination.

EXPERIMENTAL

Reagents

All solutions were prepared from reagent grade chemicals. Amino-acid standards were obtained from Aldrich Co. (Milwaukee, WI), Fisher Scientific Co. (Springfield, NJ), and

*Author for correspondence.

†Commonwealth Edison, Maywood, IL 66046, U.S.A.

Pierce (Rockford, IL). L-Lysine and Amino Acid Complex dietary supplements were obtained from American Dietary Laboratories (Pasadena, CA). Water was purified either in a MILLI-Q system (Millipore Corp., Milford, MA) or a Barnstead NANOpure II system (Newton, MA), followed by filtration (0.2 μm).

Apparatus

Chromatographic separations were performed with an AS-6 anion-exchange column preceded by an AG-6 guard column in an isocratic liquid chromatography system (Dionex Corp., Sunnyvale, CA). All mobile phases were filtered with 0.45 μm Nylon-66 filters (Rainin Corp., Woburn, MA) and a solvent filtration kit (Millipore) before use. The injection volume was 50 μl .

PAD was performed with the Model PAD-2 electrochemical detector (Dionex) with home-made gold and platinum flow-through cells.¹⁹ A saturated calomel reference electrode and a platinum wire counter-electrode were used. Conductimetric detection was done with the CD module from a Model-10 Ion Chromatograph (Dionex). For tandem CD and PAD experiments, the detector cells were placed in series, with the conductivity detector cell first.

Procedure

Calibration data were plotted as $\log[(A_p - a)/bC]$ vs. \log concentration,²⁰ where A_p is the peak area, C the analyte concentration and a and b are the intercept and slope obtained from modified regression analysis²¹ of the linear region of a plot of A_p vs. C . Accordingly, for data which fall exactly on the regression line, $\log[(A_p - a)/bC] = 0.0$. This plotting scheme has several advantages over the traditional plotting of A_p vs. C , as follows: relative deviations from the regression line are quantitatively depicted throughout the concentration range, the upper (and lower) limits of linearity are readily apparent, and calibration data for two or more detection techniques can be compared easily on the same relative scale.

RESULTS AND DISCUSSION

Pulsed amperometric detection

Pulsed amperometric detection for amino-acids at gold electrodes in basic solutions was successful when a three-step potential waveform was used. The anodic current was sampled for 16.7 msec following a 540 msec delay at 0.5 V.

This detection step was followed by an anodic potential pulse to 1.05 V for 180 msec and then a cathodic pulse to -0.55 V for 240 msec. The anodic detection mechanism for lysine is believed to be electrocatalytic, requiring simultaneous formation of a surface oxide.¹³ All other essential amino-acids display electrochemical behavior nearly identical to that of lysine.

Chromatography

For glycine, pK_a of the carboxyl group is 2.35 and pK_a of the amine group is 9.778.²² Other amino-acid pK_a values are similar to these.²³ The traditional zwitterion form of glycine observed under neutral conditions is not present in the basic chromatographic eluents used in this work. At high pH the amine group is deprotonated, resulting in an anionic form suitable for separation by anion-exchange chromatography. Sodium hydroxide solution was used as an eluent since it provided the necessary high pH as well as serving as an excellent electrolyte for the electrochemical detector.

Two dietary supplement pills were analyzed to illustrate the application of PAD to amino-acids. The contents of an L-lysine capsule were dissolved, and the solution was diluted and an aliquot injected without further pretreatment, along with a series of standards. The lysine content was found to be within 6% of the nominal value (625 mg). The contents of a capsule of Amino Acid Complex were analyzed in a similar manner: the chromatogram (with PAD) is shown in Fig. 1. No sample pretreatment was applied other than dissolution.

The dissolution of atmospheric carbon dioxide in the sodium hydroxide eluent proved problematic when CD was used. A similar problem was encountered during CD of carbohydrates,¹⁸ which was solved by using barium hydroxide instead of sodium hydroxide. Barium hydroxide proved to be the eluent of choice for amino-acids as well, and concentrations of 1–5mM gave the best results.

Conductimetric detection

The applicability of CD for amino-acids is due to the difference between the limiting equivalent ionic conductances (LEIC) of the eluting anion and the analyte anion. Hydroxide ions have a very high LEIC (198 $\mu\text{hmo}\cdot\text{cm}^2$),²⁴ whereas the values for amino-acid anions are much lower.¹⁷ The elution of the anion of an amino-acid, with simultaneous sorption of OH^- , results in a decrease in CD response to

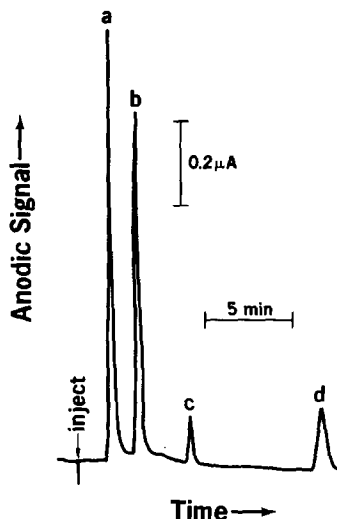


Fig. 1. Chromatogram for Amino Acid Complex. Conditions: contents of a single capsule diluted to 5 l., 50- μ l injection, eluent 50mM NaOH at 1.0 ml/min, pulsed amperometric detection. Peaks: (a) arginine, (b) lysine, (c) leucine, (d) phenylalanine.

give a "negative" peak. The separation of a mixture of lysine, methionine, asparagine and glycine is shown in Fig. 2.

Analytical response

The calibration data for lysine obtained by PAD and CD are shown in Fig. 3. The PAD response for lysine was linear (intercept 1.77 μ C, slope = $6.79 \times 10^4 \mu$ C.l.mole⁻¹, $S_y = 1.6 \times 10^{-3}$) over nearly one decade, with significant deviation from linearity for concentrations greater than 0.110mM. The CD response was linear (intercept = -0.872

μ mho.sec, slope $2.71 \times 10^5 \mu$ mho.sec.l.mole⁻¹, $S_y = 0.0002 \times 10^5$) throughout the range 0.1–10mM studied, with a higher limit of linearity (LOL) but a poorer limit of detection (LOD), compared to PAD. The two detectors used in tandem offer linear detection over more than three decades of concentration.

The estimated limit of detection ($S/N = 3$) for lysine by PAD at a gold electrode was 200 ng/ml (10 ng, 70 pmole). Response for other primary amino-acids was between 0.3 and 3 times that for lysine. The secondary amino-acids, hydroxyproline and proline, also gave reasonable PAD detection limits (3 and 4 μ M respectively). The limit of detection for lysine by CD was 2 μ g/ml (100 ng, 700 pmole). The coupling of PAD at a platinum electrode and CD has been shown to work satisfactorily as well, but this system was not studied extensively.

The long-term stability of the PAD response was confirmed by injecting a lysine solution every hour for 6 hr. The responses showed only a 1.3% relative standard deviation over this time span.

CONCLUSION

The determination of underivatized amino-acids by anion-exchange separation with pulsed amperometric detection is direct, sensitive and simple, with detection limits superior to those obtained by spectrophotometric detection of ninhydrin adducts. PAD is much more sensitive than CD but has a response which deviates from linearity for concentrations above ca. 0.1mM. Use of the two detectors in tandem can give a

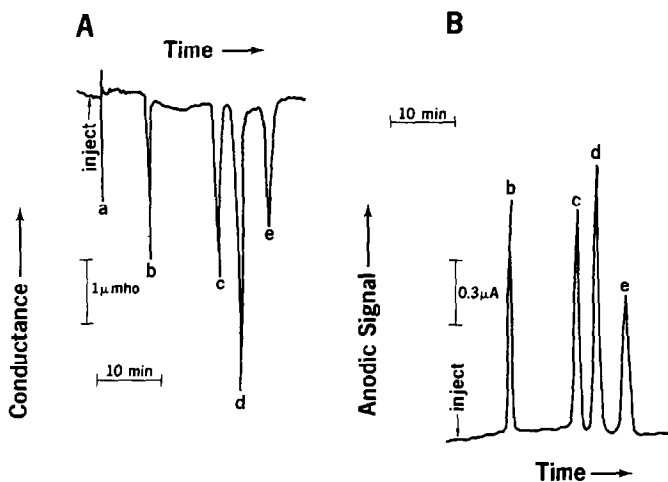


Fig. 2. Sequential chromatograms obtained by CD and PAD. Conditions: eluent 2.0mM Ba(OH)₂ at 1.0 ml/min. Detection: (A) conductivity, (B) pulsed amperometry. Peaks: (a) sample matrix, (b) 2.2 μ g of lysine, (c) 2.8 μ g of methionine, (d) 2.5 μ g of asparagine, (e) 2.9 μ g of glycine.

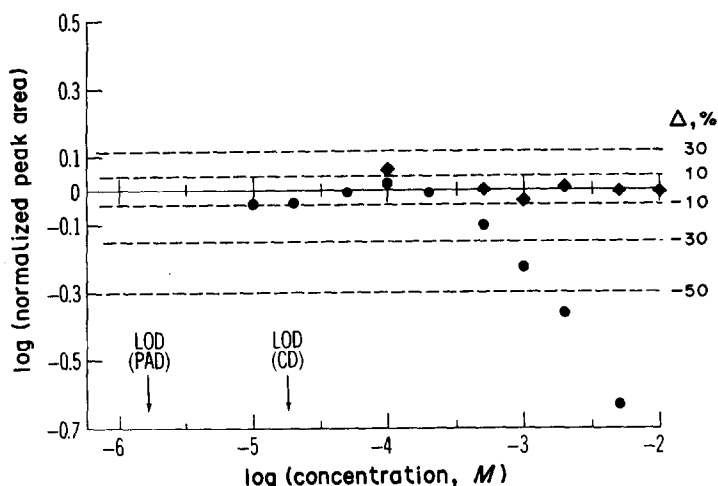


Fig. 3. Calibration plots for lysine. Conditions: eluent 2.0M Ba(OH)₂ at 1.0 ml/min. ◆ Conductivity detection, ● pulsed amperometric detection. The solid horizontal line represents $\log[(A_p - a)/bC] = 0$. The parallel dashed lines delineate relative errors (Δ) of 10, 30 and 50%.

combined linear dynamic range of *ca.* three decades for lysine.

Acknowledgement—This research was supported by a grant from Dionex Corp., Sunnyvale, CA.

REFERENCES

- G. Ogden and P. Foldi, *LC-GC*, 1987, **5**, 28.
- J. A. Polta and D. C. Johnson, *J. Liq. Chromatog.*, 1983, **6**, 1727.
- D. W. Hill, F. H. Walters, T. D. Wilson and J. D. Stuart, *Anal. Chem.*, 1979, **51**, 1338.
- W. G. Kuhr and E. S. Yeung, *ibid.*, 1988, **60**, 1832.
- S. Hughes, P. L. Meschi and D. C. Johnson, *Anal. Chim. Acta*, 1981, **132**, 1.
- J. A. Polta, *Ph.D. Dissertation*, Iowa State University, 1985.
- S. Hughes and D. C. Johnson, *Anal. Chim. Acta*, 1981, **132**, 11.
- P. Edwards and K. K. Haak, *Am. Lab.*, 1983, **15**, No. 4, 78.
- R. D. Rocklin and C. A. Pohl, *J. Liq. Chromatog.*, 1983, **6**, 1577.
- D. C. Johnson, *Nature*, 1986, **321**, 451.
- W. R. LaCourse, W. A. Jackson and D. C. Johnson, *Anal. Chem.*, submitted for publication.
- D. C. Johnson and T. Z. Polta, *Chromatog. Forum*, 1986, **1**, 37.
- L. E. Welch, W. R. LaCourse, D. A. Mead, Jr., D. C. Johnson and T. Hu, *Anal. Chem.*, 1989, **61**, 555.
- H. Small, T. Stevens and W. Bauman, *ibid.*, 1975, **47**, 1801.
- D. Gjerde, J. S. Fritz and G. J. Schmuckler, *J. Chromatog.*, 1979, **186**, 509.
- J. S. Fritz and K. Tanaka, *ibid.*, 1987, **409**, 271.
- O. A. Shpigun, L. N. Voloshik and Yu. A. Zolotov, *Anal. Sci.*, 1985, **1**, 335.
- L. E. Welch, D. A. Mead and D. C. Johnson, *Anal. Chim. Acta*, 1988, **204**, 323.
- T. Z. Polta, *Ph.D. Dissertation*, Iowa State University, 1986.
- D. C. Johnson, *Anal. Chim. Acta*, 1988, **204**, 1.
- M. Naturella, *Experimental Statistics*, pp. 6–19. NBS, Washington, DC, 1963.
- L. G. Hargis, *Analytical Chemistry*, Prentice-Hall, Englewood Cliffs, NJ, 1988.
- A. Martell and R. Smith, *Critical Stability Constants*, Vol. 3, Plenum Press, New York, 1977.
- R. C. Weast (ed.), *Handbook of Chemistry and Physics*, 65th Ed., CRC Press, Boca Raton, FL, 1984–5.

LIQUID CHROMATOGRAPHY OF LANTHANIDE CHELATES OF 1-(*p*-NITROPHENYL)ETHYLENEDIAMINE-*N,N,N',N'*- TETRA-ACETIC ACID

ORLANDO MULERO, DAVID A. NELSON, VERNON S. ARCHER*,
GREGORY MIKNIS, JAMES R. BECKETT and HOWARD L. MCLEAN
Department of Chemistry, University of Wyoming, Laramie, WY 82071, USA

(Received 18 May 1989. Revised 10 August 1989. Accepted 17 August 1989)

Summary—Preparation of the chelating agent, 1-(*p*-nitrophenyl)ethylenediamine-*N,N,N',N'*-tetra-acetic acid (*p*-nitrophenylEDTA), is described in detail. Separation of *p*-nitrophenylEDTA chelates of ytterbium(III), erbium(III), dysprosium(III) and europium(III) has been achieved by reversed-phase ion-pair liquid chromatography. With spectrophotometric detection at 254 nm, linear responses over about four orders of magnitude were achieved with detection limits ($S/N = 2$) of about 0.5 pmole.

During the past decade, a number of investigators have applied modern liquid chromatographic methods to the separation of ionic metal chelates. Much of this work involved application of the ion-chromatographic technique proposed by Small *et al.*¹ Sevenich and Fritz² used ion-chromatography, with a conductivity detector, to separate a number of bivalent metal ions and trivalent lanthanide cations. Their method required the use of various complexing eluents. Gjerde and Fritz³ have reviewed the field of ion-chromatography in a recent monograph. An extensive review of the application of high-performance liquid chromatography (HPLC) to metal chelate separations has been published by O'Laughlin.⁴

Trace metal determinations with HPLC have often depended on the utilization of chelating agents with strongly absorbing chromophores for spectrophotometric detection. Roston⁵ has used 4-(2-pyridylazo)resorcinol (PAR) as a pre-column chelating agent for the determination of Cu^{2+} , Co^{2+} , Ni^{2+} and Fe^{2+} by reversed-phase liquid chromatography (RPLC) with both fixed-wavelength (254 nm) ultraviolet absorption and oxidative thin-layer amperometric detection. Knight *et al.*⁶ have utilized post-column chelation with PAR or 3,6-*bis*[(*o*-arsenophenyl)azo]-4,5-dihydroxy-2,7-naphthalenedisulfonic acid (Arsenazo III) for the spectrophotometric detection of the lanthanides after separation by dynamic ion-exchange chromatography. Götze

and Bialkowski⁷ have described the preliminary separation of the EDTA chelates of erbium, dysprosium and europium by ion-pair chromatography.

The chelating agent 1-(*p*-nitrophenyl)ethylenediamine-*N,N,N',N'*-tetra-acetic acid (*p*-nitrophenylEDTA) forms complexes with a wide variety of metal ions of interest in trace analysis.^{8,9} These chelates absorb strongly in the ultraviolet region, with molar absorptivities $> 8000 \text{ l. mole}^{-1} \text{ cm}^{-1}$ at 254 nm, the wavelength used in many fixed-wavelength liquid-chromatography detectors. The desirable spectroscopic properties of these chelates, combined with their high stabilities, make *p*-nitrophenylEDTA an excellent pre-column chelating agent for HPLC separation and determination of metal ions. In this paper, we describe the preparation of this reagent and the preparation and separation of some representative lanthanide chelates by reversed-phase ion-pair liquid chromatography (RIPC). The separation and highly sensitive detection of these four chemically similar chelates serves as a model to illustrate the utility of this analytical reagent.

EXPERIMENTAL

Apparatus

Liquid chromatographic separations were performed with a Waters Associates Model ALC 204 liquid chromatograph equipped with a Model 6000A liquid-chromatography pump, a Rheodyne Model 7125 sample injection valve with a 20- μl injection loop, and a Model 440

*Author for correspondence.

UV detector (254 nm). The detector output was monitored by use of a strip-chart recorder at a chart speed of 30 cm/hr.

Ultraviolet spectra were obtained with a Cary 2300 spectrophotometer. Nuclear magnetic resonance spectra were obtained for D₂O solutions with *tert*-butyl deuterio-alcohol as the internal reference, with a Jeol FX270 FT-NMR spectrometer.

Reagents

The solvents used for chromatography were J. T. Baker HPLC-grade water and methanol. Rare-earth metal oxides with the purities indicated in brackets were obtained from Research Chemicals, Phoenix, Arizona: Yb₂O₃ (99.99%), Er₂O₃ (99.999%), Dy₂O₃ (99.999%) and Eu₂O₃ (99.99%).

The ion-pairing reagent used was Waters Associates PIC-A[®] (Regular), which provided tetrabutylammonium ion at specified concentrations when appropriately diluted with HPLC-grade water.

Other chemicals used were of ACS reagent-grade purity.

Preparation of *p*-nitrophenylEDTA

Nitric acid (90%, 50 ml) was transferred into a 100-ml 3-necked flask fitted with an overhead stirrer. This was cooled in a salt-ice bath and maintained at a temperature between 0 and -5°C. A thermometer was placed inside the flask to monitor the temperature of the nitration mixture. Phenylethylenediaminetetra-acetic acid (phenylEDTA) (10.0 g, 0.03 mole) was added in small portions over a period of ~2 hr so that the temperature did not rise above 0°. After addition of all the phenylEDTA, the reaction mixture was stirred for 5 hr at 0°, and then poured over 250 g of ice. The reaction mixture was adjusted to pH 1.3 by addition of 50% aqueous sodium hydroxide solution and allowed to stand for 24 hr in a refrigerator at 10°. A light yellow product crystallized and was collected by filtration with a sintered-glass funnel. The mother liquor from this filtration was concentrated on a rotary evaporator to ~100 ml. The pH of this concentrate was 2.4. On standing for 24 hr at 10° some sodium nitrate crystals separated and were removed by filtration. The pH of the filtrate was adjusted to 1.2 with 6*M* hydrochloric acid. After standing for 24 hr at 10°, crystals of *p*-nitrophenylEDTA formed and were collected by filtration (0.90 g). The filtrate was reduced to 50 ml, adjusted to

pH 1.2, and cooled for 24 hr at 10°, and another crop of product (1.30 g) was collected. The original light yellow product was suspended in 100 ml of water and 50% sodium hydroxide solution was added dropwise until dissolution was complete. The solution was then adjusted to pH 1.2 with 6*M* hydrochloric acid and allowed to stand for 24 hr at 10°, then the precipitated product (1.4 g) was collected. Concentration of the mother liquor to 50 ml, adjustment to pH 1.2 and cooling as described above yielded an additional 1.0 g of product. The yield of *p*-nitrophenylEDTA at this point was 4.6 g. The melting point (uncorrected) of *p*-nitrophenylEDTA was 174–176°. Nuclear magnetic resonance was used to confirm the absence of the *meta*-isomer.

Preparation of lanthanide chelates of *p*-nitrophenylEDTA

Lanthanide perchlorate stock solutions (0.20*M*) were prepared by dissolving 0.010 mole of high-purity rare-earth metal oxide (M₂O₃) in 20 ml of 9.1*M* perchloric acid and diluting to 100 ml. About 0.51 g (1.1 mmole) of *p*-nitrophenylEDTA dihydrate was mixed with a slight excess of the lanthanide perchlorate stock solution and 10 ml of demineralized water. After adjustment of the pH of the mixture to about 7 with 7*M* sodium hydroxide, the volume was reduced to about 5 ml by heating on a hotwater-bath, and absolute ethanol was added until the solution became cloudy. After standing overnight in a refrigerator at 10°, the precipitate was removed by filtration. The product was recrystallized from aqueous ethanol, dried for two days at room temperature in the air, and subsequently dried and stored in a desiccator over anhydrous calcium sulfate.

Ytterbium(III) chelate. Ytterbium(III) perchlorate solution (1.29 mmole) and 1.15 mmole of *p*-nitrophenylEDTA dihydrate were used. The yield was 0.766 g (98%) of the sodium salt. Na[Yb(C₁₆H₁₅O₁₀N₃)]·4H₂O requires C 28.36%; H 3.42%. Analysis gave: C 28.3%; H 3.5%.

Erbium(III) chelate. Erbium(III) perchlorate solution (1.12 mmole) and 1.12 mmole of *p*-nitrophenylEDTA dihydrate were used. The yield was 0.654 g (99%) of the sodium salt. Na[Er(C₁₆H₁₅O₁₀N₃)]·3H₂O requires C 29.40%; H 3.24%. Analysis gave: C 29.2%; H 3.2%.

Dysprosium(III) chelate. Dysprosium(III) perchlorate solution (1.24 mmole) and 1.12 mmole of *p*-nitrophenylEDTA dihydrate were used. The yield was 0.744 g (97%) of the sodium

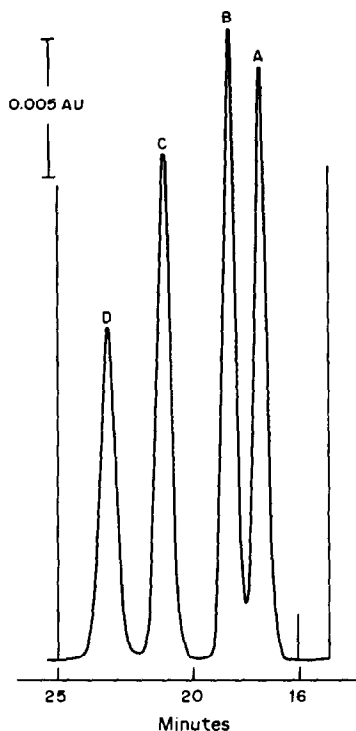


Fig. 1. HPLC chromatogram of *p*-nitrophenylEDTA chelates with ultraviolet detection at 254 nm: peaks for ytterbium(III) chelate (A), erbium(III) chelate (B), dysprosium(III) chelate (C) and europium(III) chelate (D). A 0.6- μ l aliquot of an aqueous solution containing each chelate at $3 \times 10^{-3}M$ concentration was injected. Mobile phase: methanol-water (21:79 v/v), 0.0025M PIC-A[®] (Regular), pH 6.5 at a flow-rate of 1.0 ml/min. Column: IBM Instruments Octadecyl (C18) column (4.5×150 mm, 5 μ m particle size).

salt. Na[Dy(C₁₆H₁₅O₁₀N₃)] \cdot 5H₂O requires C 28.06%, H 3.68%. Analysis gave C 28.0%; H 3.3%.

Europium(III) chelate. Europium(III) perchlorate solution (1.24 mmoles) and 1.12 mmoles of *p*-nitrophenylEDTA dihydrate were used. The yield was 0.726 g (99%) of the sodium salt. Na[Eu(C₁₆H₁₅O₁₀N₃)] \cdot 4H₂O requires C 29.28%; H 3.53%, Analysis gave C 28.9%; H 3.4%.

Liquid chromatography

Stock solutions of the chelates ($3 \times 10^{-3}M$ and $5 \times 10^{-3}M$) were prepared in HPLC-grade water. These solutions were stable indefinitely when stored in the dark. The stock solutions were further diluted with HPLC-grade water as required.

The mobile phase used was prepared by diluting 790 ml of 0.0025M PIC-A[®] (adjusted to

pH 6.5 with 85% phosphoric acid) to 1000 ml with HPLC-grade methanol. Separations were achieved with an IBM Instruments Octadecyl (C18) column (4.6×150 mm, 5 μ m particle size) with a mobile phase flow-rate of 1.0 ml/min.

RESULTS AND DISCUSSION

The *p*-nitrophenylEDTA was prepared by nitration of phenylEDTA with 90% nitric acid at 0°. The phenylEDTA was prepared by the method of Okaku *et al.*¹⁰ as modified by Beckett.⁸ Nitration of phenylEDTA is a more direct procedure than the previous synthesis of *p*-nitrophenylEDTA described by Sundberg¹¹ and modified by Beckett,⁸ and gives a higher yield. Some *meta*-isomer is formed during the nitration. Fortunately, under the conditions described for the preparation, the *para*-isomer crystallizes in preference to the *meta*-isomer. The *para*-isomer is reasonably soluble at pH above 2.4, but begins to separate from aqueous solution at pH below 1.5. The procedure given allows the isolation of a good yield of *p*-nitrophenylEDTA. In all cases, the purity of the product was monitored by proton nuclear magnetic resonance spectrometry. The *para*-isomer shows an aromatic AA'BB' pattern centered at $\delta = 7.8$ ppm. The presence of the *meta*-isomer is shown by the appearance of a complex peak at $\delta = \sim 7.4$ ppm. Pure *m*-nitrophenylEDTA was not isolated.

Figure 1 shows the HPLC separation achieved under the conditions described, with injection of 0.6 μ l of a solution containing $3.0 \times 10^{-3}M$ ytterbium(III) chelate, $3.1 \times 10^{-3}M$ erbium(III) chelate, $2.9 \times 10^{-3}M$ dysprosium(III) chelate and $3.0 \times 10^{-3}M$ europium(III) chelate. This chromatogram shows that these four very similar anionic chelates are easily separated under isocratic conditions with tetrabutylammonium ion as the ion-pairing reagent. Chromatograms of mixtures prepared from 5-month old stock solutions (stored in the dark) of the chelates were essentially equivalent to those obtained by using freshly prepared

Table 1. Ultraviolet spectral data for aqueous *p*-nitrophenylEDTA chelates solutions

	λ_{\max} , nm	Molar absorptivity, $l \cdot mole^{-1} \cdot cm^{-1}$
Ytterbium(III)	270	9.72×10^3
Erbium(III)	270	9.67×10^3
Dysprosium(III)	268	1.27×10^4
Europium(III)	269	9.42×10^3

stock solutions. This indicates that these chelates are highly stable in aqueous solution.

The *p*-nitrophenylEDTA chelates gave detector responses at 254 nm that were linear over about four orders of magnitude, *viz.* from 1 to 2×10^4 pmole or about 0.2–4000 ng of the rare-earth metal. The detection limit ($S/N = 2$) for the ytterbium chelate was ~ 0.5 pmole when the mobile phase was adjusted to give a retention time of 10 min. The mobile phase was $5 \times 10^{-4} M$ tetrabutylammonium ion in a water-methanol mixture (72:28 v/v, pH 6.4). All the chelates exhibited very similar ultraviolet spectra, with absorption maxima at about 270 nm and molar absorptivities of about 10^4 l.mole⁻¹.cm⁻¹ (Table 1). The detector signal would therefore be enhanced somewhat if a variable-wavelength detector set at 270 nm rather than 254 nm were used.

The chromatographic separation of the four rare-earth chelates prepared in this study illustrates the potential utility of *p*-nitrophenylEDTA as a pre-column derivatizing agent for lanthanide determination by HPLC. Although Knight *et al.*⁶ achieved very good separations of the lanthanides, our preliminary results indicate detection limits about an order of magnitude lower than theirs. In addition, our separation does not involve the relative complexity of a post-column reaction detection system. The ion-pair chromatographic separation of EDTA chelates of three lanthanides

reported by Götze and Bialkowski⁷ gives less complete resolution than that obtained by our procedure.

In conclusion, *p*-nitrophenylEDTA appears to have great potential as a pre-column chelating agent for liquid chromatography of a wide variety of different metal ions. The high stabilities and molar absorptivities of these complexes, in combination with the high resolution of modern reversed-phase columns, make trace metal determinations by HPLC an attractive alternative to many of the spectroscopic methods commonly used.

REFERENCES

1. H. Small, T. S. Stevens and W. C. Bauman, *Anal. Chem.*, 1975, **47**, 1801.
2. G. J. Sevenich and J. S. Fritz, *ibid.*, 1983, **55**, 12.
3. D. T. Gjerde and J. S. Fritz, *Ion Chromatography*, 2nd Ed., Hüthig Verlag, Heidelberg, 1987.
4. J. W. O'Laughlin, *J. Liq. Chromatog.*, 1984, **7**(S-1), 127.
5. D. A. Roston, *Anal. Chem.*, 1984, **56**, 241.
6. C. H. Knight, R. M. Cassidy, B. M. Recoskie and L. W. Green, *ibid.*, 1984, **56**, 474.
7. H. J. Götze and D. Bialkowski, *Z. Anal. Chem.*, 1985, **320**, 370.
8. J. R. Beckett, Jr., *Ph. D. Dissertation*, University of Wyoming, Laramie, Wyoming, 1978.
9. H. L. Mclean, *Ph.D. Dissertation*, University of Wyoming, Laramie, Wyoming, 1988.
10. N. Okaku, K. Toyoda, Y. Moriguchi and K. Ueno, *Bull. Chem. Soc. Japan*, 1967, **40**, 2326.
11. M. W. Sundberg, *Ph.D. Dissertation*, Stanford University, Order No. 74-6559, University Microfilms, Ann Arbor, Michigan, 1973.

SIMULTANEOUS DETERMINATION OF GALLIUM AND ALUMINIUM IN BIOLOGICAL SAMPLES BY CONVENTIONAL LUMINESCENCE AND DERIVATIVE SYNCHRONOUS FLUORESCENCE SPECTROMETRY

J. M. CANO PAVON*, A. GARCIA DE TORRES and M. E. UREÑA POZO

Department of Analytical Chemistry, Faculty of Sciences, University of Málaga, 29071 Málaga, Spain

(Received 27 January 1988. Revised 25 September 1989. Accepted 6 October 1989)

Summary—The simultaneous determination of gallium and aluminium by using conventional fluorimetry and derivative synchronous fluorescence spectrometry has been studied. These determinations are based on the formation of fluorescent complexes of gallium and aluminium with salicylaldehyde carbohydrazone (SACH). In the conventional method, two samples are analysed under different analytical conditions, and the results are evaluated by solving a system of two simultaneous equations. In the derivative synchronous method (at pH = 2.6, in an ethanol–water medium containing 72% of ethanol), the following conditions are used: a constant wavelength difference of 20 nm between the monochromator settings, a time-constant of 1.5 sec, a scan-speed of 120 nm/min, and a derivative wavelength difference of 10 nm; gallium can be determined in the range 7–38 ng/ml, and aluminium between 6 and 45 ng/ml. The synchronous method shows more advantages, and has been used in the determination of both metal ions in diverse biological samples (animal tissues and human serum) with good results.

In recent years, determination of gallium and aluminium at ng/ml levels in water, biological fluids and other materials has aroused considerable interest, though for different reasons. Analysis for traces of gallium is required for studying the physiological distribution of this element in biological systems; such studies are becoming interesting because some gallium compounds have exhibited antitumour activity,¹⁻³ but at certain levels gallium shows appreciable toxicity. Several methods for determination of gallium, involving the use of neutron-activation analysis,⁴ atomic-absorption spectrometry,⁵ atomic-emission spectrometry⁶ and fluorimetry⁷⁻¹⁰ have been described.

On the other hand, although aluminium was considered in the past to be a non-toxic element, in recent years the aetiology of various clinical disorders manifest in patients with renal failure has been attributed to aluminium intoxication. The adverse effects of aluminium were most dramatically demonstrated in patients suffering dialysis dementia.^{11,12} Aluminium toxicity is also associated with osteodystrophy,¹³ anaemia,¹⁴ gastrointestinal symptoms¹⁵ and possibly cardio-toxicity;¹⁶ the most important source of aluminium in the patients appears to be the

water used for dilution of the dialysis solution.¹⁷ In general, graphite-furnace atomic-absorption spectrometry has been used for the determination of aluminium in waters.¹⁸⁻²¹

Synchronous fluorimetry has been described as a method of improving the selectivity of conventional luminescence spectrometry by taking full advantage of the ability to vary both the excitation and emission wavelengths during an analysis. In this method, the excitation and emission monochromators are scanned simultaneously and synchronously so that a constant wavelength difference is maintained between them.²² The use of derivative synchronous fluorescence spectrometry was first applied primarily in the analysis of organic compounds,²³ although it can also be used for inorganic mixtures.

This paper describes the use of conventional fluorimetry and second-derivative synchronous fluorescence spectrometry for the simultaneous determination of gallium and aluminium. This determination is based on the fluorogenic reactions of gallium and aluminium with salicylaldehyde carbohydrazone (SACH). The results obtained show that both methods can be used for the simple, rapid, sensitive and selective determination of both elements in a wide variety of samples.

*Author for correspondence.

EXPERIMENTAL

Apparatus

This work was performed on a Perkin-Elmer fluorescence spectrophotometer, model MPF-43 A, equipped with a xenon lamp, excitation and emission monochromators, R-777 photomultiplier, Perkin-Elmer 023 recorder, and a differential corrected-spectra unit (Perkin-Elmer DSCV-2) between the signal output and the record input (by means of this unit, it is possible to generate second-derivative spectra at different wavelength increments).

A Crison Digit-501 pH-meter was used for the pH measurements (throughout this paper pH is used to denote the pH-meter reading and not the negative logarithm of the actual concentration of hydrogen ions in the solution).

Reagents

Materials of analytical-reagent grade or better were used whenever available, and distilled and demineralized water was used throughout.

Solutions of gallium (0.997 g/l.) and aluminium (0.665 g/l.) were standardized by EDTA titration. Working solutions were prepared by suitable dilution.

A $10^{-3}M$ solution of salicylaldehyde carbohydrazone (SACH) in ethanol was used (prepared daily); the reagent was synthesized as previously described²⁴ and characterized by elemental analysis and infrared and NMR spectroscopy.

Hydrochloric acid-potassium chloride "buffer" solution of pH 1.9 was prepared by mixing 50 ml of 0.2M potassium chloride and 13.3 ml of 0.2M hydrochloric acid and diluting to 200 ml with demineralized water.

Buffer of pH 2.6 was prepared by mixing 33 ml of 0.2M hydrochloric acid with 50 ml of 0.2M potassium hydrogen phthalate and diluting to 200 ml with demineralized water.

Determination of gallium and aluminium by conventional fluorimetry

An aliquot containing 156–950 ng of gallium and 250–1500 ng of aluminium was placed in a 25-ml standard flask, 7 ml of $1 \times 10^{-3}M$ SACH, 7 ml of ethanol and 4 ml of the pH 1.9 solution were added and the solution was made up to the mark with distilled water. The fluorescence intensity (I_A) was measured with an excitation wavelength of 360 nm and an emission wavelength of 450 nm.

A similar aliquot was placed in a 25-ml standard flask, and the same volumes of SACH

solution and ethanol as before were added, and 4 ml of pH 2.6 buffer solution. The mixture was diluted to the mark with demineralized water, and the fluorescence intensity (I_B) was measured with excitation and emission wavelengths of 360 and 440 nm, respectively.

With the I_A and I_B values two simultaneous equations can be established (as described under Results and Discussion). It is necessary to construct calibration graphs for gallium and aluminium separately under each set of fluorimetric conditions (450 and 440 nm emission wavelengths) and to calculate the four slopes.

Determination of gallium and aluminium by second-derivative synchronous fluorimetry

A sample containing 190–950 ng of gallium and 150–1125 ng of aluminium was placed in a 25-ml standard flask, 10 ml of $1 \times 10^{-3}M$ SACH, 8 ml of ethanol and 5 ml of pH 1.9 solution were added, and the solution was made up to the mark with demineralized water. The second-derivative synchronous fluorescence spectrum was recorded by scanning both monochromators together, with a 20 nm constant difference between their wavelengths, a time-constant of 1.5 sec, a scan-speed of 120 nm/min, and a derivative wavelength interval of 10 nm. The excitation monochromator was scanned from 300 to 500 nm, and the emission monochromator from 320 to 520 nm. Peak-to-trough measurements were made in the range 445–470 nm for Al(III) and 405–425 nm for the sum of Al(III) and Ga(III) (the peak-to-trough distances were measured in arbitrary units on the recorder chart) as shown in Fig. 3. The concentration of gallium was obtained by difference.

The fluorescence intensities of these derivative signals are directly related to the concentration of each ion, the concentration of which is determined from the calibration graphs.

Determination of gallium and aluminium in biological samples

Biological samples (0.01–1 g) were digested with a mixture of concentrated nitric acid (10 ml) and 30% hydrogen peroxide (3 ml) in a reflux apparatus. If the material was incompletely decomposed, more nitric acid and hydrogen peroxide were added and the mixture was reheated until a clear solution was obtained. After digestion, samples were evaporated to small volume, neutralized with sodium hydroxide, and finally diluted with demineralized water

to volume in a 10–50 ml standard flask. A suitable aliquot of this sample solution was pipetted and the gallium and aluminium were determined by the procedure above.

For gallium and aluminium in blood serum a 3-ml portion of the serum was placed in a 10-ml conical centrifuge tube and, with mixing after each addition, 3 ml of 2*M* hydrochloric acid and 0.8–1 ml of 40% trichloroacetic acid solution were added. The mixture was stirred vigorously with a glass rod for about 45 sec and then centrifuged for 10–20 min at 3000 rpm. A suitable aliquot of the supernatant fluid was pipetted, and the aluminium and gallium content was determined by the procedure above by the method of standard additions or by use of calibration graphs and the two simultaneous equations.

RESULTS AND DISCUSSION

Gallium forms a colourless complex with SACH; the complex exhibits weak absorption in the same region as the reagent alone, but has an intense blue fluorescence, with maximal emission at 450 nm (excitation at 360 nm) (Fig. 1). The reaction is performed at pH 2.4–3.1, in aqueous ethanol medium (60% v/v ethanol). The detection limit is 0.5 ng/ml and the range of application is 1.5–60 ng/ml.

SACH also reacts instantaneously with aluminium to form a complex which has intense fluorescence, with maximum emission at 440 nm (excitation at 362 nm) (Fig. 1). The reaction is done at pH 3.3–3.8 in aqueous ethanol medium (60% v/v ethanol). The detection limit is 1 ng/ml, and the range of application 3–90 ng/ml.

Simultaneous determination by conventional fluorimetry

The simultaneous determination of Ga(III) and Al(III) with SACH by the classical fluorescence technique can be achieved by measurements of the fluorescence due to both complexes under the optimal experimental conditions for each. Thus, two series of samples (A_1 , A_2) are prepared at pH 2.6, and another two (B_1 , B_2) at pH 3.5. In series A_1 and B_1 (both without aluminium), the concentration of gallium is varied over the range 1.5–60 ng/ml, and in series A_2 and B_2 (both without gallium) the concentration of aluminium is varied in the range 3–90 ng/ml. In the four series, 7 ml of $1 \times 10^{-3}M$ SACH 7 ml of ethanol and 4 ml of the appropriate buffer solution are added to each sample, and the solutions are diluted to volume in 25-ml standard flasks. The fluorescence intensities are directly related to the concentration of the corresponding metal ion; calibration graphs are

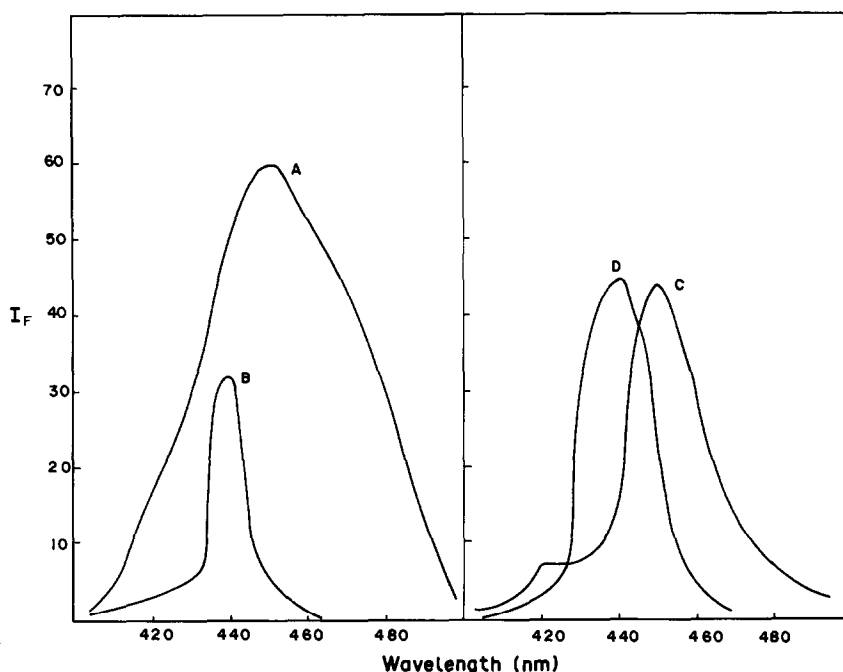


Fig. 1. Emission spectra of the gallium (A at pH 2.6, C at pH 3.7) and aluminium (B at pH 2.6, D at pH 3.7) complexes. Concentration of each ion is 30 ng/ml.

Table 1. Simultaneous determination of gallium and aluminium by conventional fluorimetry

Sample	Ga:Al, w/w	Taken, ng/ml		Ga found, ng/ml	Al found, ng/ml
		Ga	Al		
1	1:1	6.3	6.4	6.1	7.0
2	1:2	6.3	13.0	6.4	14.0
3	1:3	6.3	19.0	6.3	20.0
4	1:4	6.3	25.5	6.0	25.5
5	1:5	6.3	32.0	5.8	33.3
6	1:6	6.3	38.0	5.6	40.0
7	1:1	10.0	10.0	9.0	12.0
8	2:1	20.0	10.0	20.7	9.0
9	3:1	30.0	10.0	28.0	9.7
10	4:1	40.0	10.0	36.0	12.0
11	5:1	50.0	10.0	47.0	9.3
12	6:1	60.0	10.0	—	—

constructed from the results, and the slopes of the four graphs are calculated. From these results, two simultaneous equations are established; in our work these were:

$$I_A = 0.897 [\text{Ga(III)}] + 0.610 [\text{Al(III)}]$$

$$I_B = 0.880 [\text{Ga(III)}] + 0.720 [\text{Al(III)}]$$

I_A and I_B being the fluorescence intensities measured at 450 and 440 nm, respectively (λ_{ex} 360 nm in both cases), and [Ga] and [Al] the unknown concentrations. Obviously, these equations, as well as those obtained by use of

the synchronous technique, depend on the instrument used and the experimental variables, and must be established in each case, according to the procedure described. The concentrations of gallium and aluminium can be obtained by solving both equations. These equations are valid because the fluorescence intensities of the complexes are additive for the stated ranges.

Results obtained for the determination of gallium and aluminium in samples with Ga:Al ratios from 1/6 to 6 are shown in Table 1. They indicate that the method is satisfactory. The relative standard deviations found were 5.4% for gallium and 4.0% for aluminium.

Simultaneous determination by second-derivative synchronous fluorimetry

Figure 2 shows the individual second-derivative synchronous fluorescence spectra of the gallium and aluminium complexes and their mixtures (the concentrations were 7.5 ng/ml for gallium and 20 ng/ml for aluminium in all cases). The distance *ab* between the maximum at 445 nm and the minimum at 470 nm is proportional to the concentration of aluminium and independent of gallium concentration. The distance *cd* between the maximum at 400 nm and the minimum at 420 nm is proportional to the

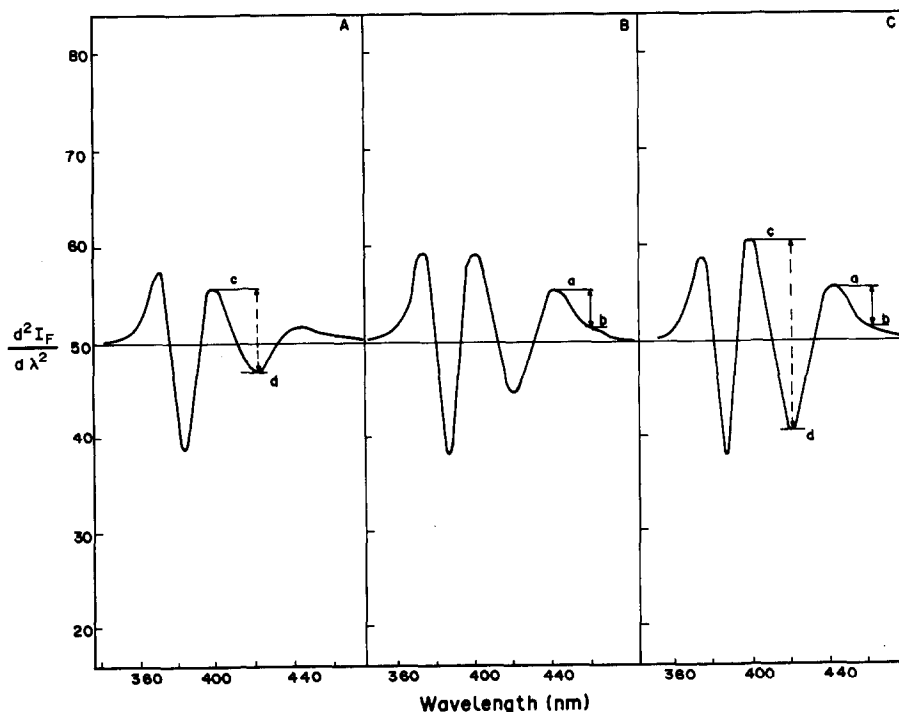


Fig. 2. Second-derivative synchronous fluorescence spectra for the gallium (A) and aluminium (B) complexes and for their mixture (C) at $\Delta\lambda = 20$ nm, $\Delta\lambda' = 10$ nm, time-constant 1.5 sec, scan speed 120 nm/min, and pH 2.6. Concentrations are 7.5 ng/ml for gallium and 20 ng/ml for aluminium.

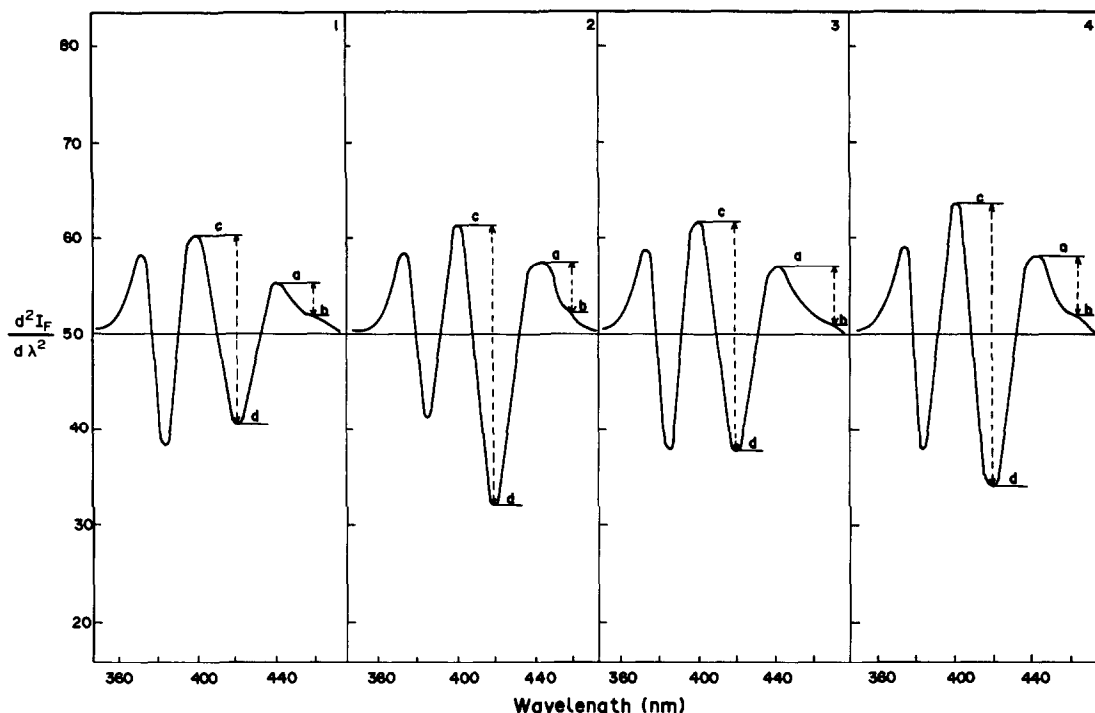


Fig. 3. Second-derivative fluorescence spectra of gallium and aluminium. (1) Ga, 10 ng/ml; Al, 10 ng/ml. (2) Ga, 20 ng/ml; Al, 25 ng/ml. (3) Ga, 5 ng/ml; Al, 30 ng/ml. (4) Ga, 20 ng/ml; Al, 30 ng/ml.

sum of the concentrations of both metal ions. As a general example, Fig. 3 shows the second-derivative synchronous fluorescence spectra of a series of mixtures containing different concentrations of gallium and aluminium.

The most important parameter in the simultaneous analysis of mixtures by this technique is the selection of the optimum wavelength difference between the monochromator settings ($\Delta\lambda$). For selection of the appropriate value, various second-derivative synchronous fluorescence spectra at different $\Delta\lambda$ values between 10 and 60 nm were recorded. $\Delta\lambda = 20$ nm was selected as the optimum value. The optimal bandpass was found to be 10 nm for both slits.

For recording the second-derivative spectra, three derivative wavelength intervals (2, 5 and 10 nm) were employed. The maximum response was obtained with the 10 nm interval.

Time-constants of 0.3, 1.5 and 3.0 sec were used in order to study the effect of the spectrofluorimeter response; a value of 1.5 sec was selected. A scan-speed of 120 nm/min was found to be convenient.

The optimum pH range is slightly different for each ion; however, the response function for the resolution of a gallium-aluminium mixture is maximum at an apparent pH of 2.6. A hydrochloric acid-potassium chloride mixture

(pH 1.9) was selected, since the volume of ethanol added in the preparation of the solutions increased the pH by 0.7.

Increasing the ionic strength produced no significant changes in the fluorescence. The response function remained constant when there was more than a 36-fold molar excess of SACH. Therefore, 10 ml of $1 \times 10^{-3}M$ SACH in a final volume of 25 ml is sufficient.

The optimum amount of ethanol in the final solution was found to be 60–80% v/v; a medium containing 72% ethanol was selected. In this medium the response remains constant for at least 2 hr. There is no temperature effect in the range 10–50°. All measurements were made at 25°.

Several procedures are available for quantitative evaluation of second-derivative synchronous spectra, and a detailed survey of these procedures, including a description of possible errors, has been given by O'Haver and Green.²⁵ In the present work, for the determination of aluminium the amplitude between the maximum centred at 445 nm and the shoulder at 470 nm was selected because the experimental values obtained in this way are related to the aluminium concentration more linearly than those obtained from other possible constructions. The calibration graph prepared by plot-

Table 2. Determination of aluminium and gallium in synthetic mixtures

Ga taken, ng/ml	Al taken, ng/ml	Distance ab, mm	Distance cd, mm	Ga found, ng/ml	Al found, ng/ml
3	25	13	55	4	25
5	30	14	61	6	28
4	20	11	49	3	20
10	10	8	49	12	11
20	30	14	76	20	28
20	4	5	52	22	4
30	5	5	58	28	4
35	4	5	62	32	4
40	5	6	72	38	7

ting the derivative signal against the aluminium concentration gives a straight line. The equation obtained for this graph in our work was

$$M_1 = 0.380 [\text{Al(III)}] + 3.4$$

where M_1 is the derivative signal height, in mm, and the aluminium concentration is in $\mu\text{g/ml}$. A negative deviation from linearity was observed at higher aluminium concentrations.

Gallium cannot be determined directly because the presence of aluminium modifies the derivative signals corresponding to gallium. For this reason, the gallium has to be determined by difference. For this purpose we use the distance cd (Fig. 3). From our calibration graphs obtained for both metal ions, the following equation was deduced for the signal height M_2 (in mm) and the concentrations in $\mu\text{g/ml}$:

$$M_2 = 1.050 [\text{Ga(III)}] + 1.074[\text{Al(III)}] + 24.5$$

The analysis of samples containing various concentrations of the two ions is feasible over the concentration ranges 7–38 ng/ml Ga(III) (relative standard deviation 2.8%) and 6–45 ng/ml Al(III) (relative standard deviation 3.5%). The detection limit is 1 ng/ml for gallium and 2 ng/ml for aluminium.

Some results obtained for analysis of various mixtures are shown in Table 2.

Interferences

The selectivity of the derivative synchronous method was investigated by determination of gallium and aluminium at the 20 ng/ml level in the presence of various amounts of other ions. The tolerance limits, defined as the concentration causing a deviation of less than $\pm 5\%$ in the analytical response, are listed in Table 3. The tolerance level for certain metal ions can be increased by addition of iodide, citrate, thiosulphate and ascorbic acid.

Applications

To evaluate its effectiveness, the recommended synchronous derivative procedure for the simultaneous determination of gallium and aluminium was applied to a variety of samples, including aquatic plants, aquatic moss, olive leaves, human blood serum, bovine liver, kidney and brain.

In the analysis of the biological samples (except blood serum), a preliminary step is the destruction of the organic matter. Of the various methods tested, the most adequate is the proce-

Table 3. Tolerance ratios for various ions in the simultaneous determination of gallium (20 ng/ml) and aluminium (20 ng/ml)

Tolerance ratios	Foreign ion without masking agent	Foreign ion with masking agent	Masking agent, $\mu\text{g/ml}$
5000	Na(I), K(I), Pb(II), Cd(II), Sr(II), Ca(II), Ba(II), Mg(II), Cr(III), Tl(I), Cl^- , NO_3^- , I^- , NO_2^- , Br^- , dimethylglyoxime, phthalate, ascorbic acid		
4000	Se(IV), W(VI)		
3000	CO_3^{2-}		
2500	BrO_3^- , IO_3^- , ClO_3^- , IO_4^-		
2000	Bi(III), Co(II), Sb(III), V(V), thiourea, $\text{S}_2\text{O}_3^{2-}$		
1500		Ag(I)	I^- , 100
1200	As(V)	Zn(II)	Citrate, 0.4
1000	Tartrate, arsenite, Ni(II)	Fe(III)	Ascorbic acid, 100
		Hg(II)	I^- , 100
500		Cu(II)	$\text{S}_2\text{O}_3^{2-}$, 40
60	Zn(II)		
25	Y(III)		
20	Citrate		
5	PO_4^{3-}		

Table 4. Determination of gallium and aluminium in biological samples

Sample	Ga, ng/ml		Al, ng/ml	
	Added	Found	Added	Found
Aquatic plant	10.4	9.4	—	42.0
	20.0	19.0	10.0	51.0
Aquatic moss	10.0	10.0	—	15.0
	8.0	8.0	15.0	30.0
Olive leaves	10.0	10.0	—	10.0
	20.0	22.0	10.0	21.0
Blood serum 1	5.0	5.4	—	5.0
	5.0	4.0	10.0	14.0
Blood serum 2	5.0	5.0	—	2.5
	5.0	4.0	5.8	8.0
Blood serum 3	5.0	5.0	—	—
	10.0	10.0	5.0	5.0
Blood serum 4	10.0	10.0	—	—
	5.0	5.4	5.0	5.0
Blood serum 5	10.0	9.5	11.0	10.0
Blood serum 6	15.0	14.0	20.0	19.0
Blood serum 7	10.0	9.0	10.0	9.2
Blood serum 8	20.0	18.0	12.0	11.4
Bovine liver	10.0	11.0	—	12.5
	10.0	9.5	15.0	27.0
Kidney	10.0	11.0	—	15.0
	15.0	18.0	—	18.0
Brains	15.0	15.4	—	17.6
	10.0	11.0	5.0	23.0

ture described by Bajo *et al.*,²⁶ in which a mixture of concentrated nitric acid and hydrogen peroxide is used. Blood serum can be analysed without mineralization; protein is removed by means of trichloroacetic acid and centrifugation; gallium and aluminium are measured in the supernatant liquid.

Results obtained in these analyses are given in Table 4.

Acknowledgement—The authors thank the Comision Asesora de Investigacion Cientifica y Técnica (Project PB87-0711) for supporting this study.

REFERENCES

1. M. M. Hart and R. H. Adamson, *Proc. Natl. Acad. Sci. U.S.A.*, 1971, **68**, 1623.

2. R. C. Hayes, *J. Nucl. Med.*, 1970, **18**, 740.
3. R. A. Zweidinger and R. L. Barnett, *Anal. Chem.*, 1973, **45**, 1565.
4. K. Nakamura, M. Fujimori and H. Tsuchiya, *Anal. Chim. Acta*, 1982, **138**, 129.
5. J. C. Yu and C. M. Wai, *Anal. Chem.*, 1984, **56**, 1689.
6. S. Caroli, A. Alimonti, P. Delle Femmine and S. K. Shukla, *Anal. Chim. Acta*, 1982, **136**, 225.
7. N. B. Lebed and R. P. Pantaler, *Zh. Analit. Khim.*, 1965, **20**, 59.
8. L. S. Bark and A. Rixon, *Anal. Chim. Acta*, 1969, **45**, 425.
9. A. Lypka and A. Chow, *ibid.*, 1972, **60**, 65.
10. M. E. Ureña Pozo, A. García de Torres, J. M. Cano Pavón and J. L. Gómez-Ariza, *Anal. Chem.*, 1985, **57**, 2309.
11. G. Dunea and S. D. Mahurkar, *N. Engl. J. Med.*, 1978, **88**, 502.
12. A. M. Davison, H. Oli, G. S. Walker and A. M. Lewins, *Lancet*, 1982, ii, 785.
13. M. R. Wills, *Clin. Chem.*, 1985, **31**, 5.
14. I. Fernández Soto, M. T. Allende, M. C. Diaz de Greña, M. Machos, B. Diaz López and J. B. Cannata, *Nefrologia*, 1986, **6**, 71.
15. S. Siderman and D. Manor, *Nephron*, 1982, **31**, 71.
16. S. P. Andreoli, J. M. Bergstein and D. J. Sherrard, *N. Engl. J. Med.*, 1984, **310**, 1079.
17. C. Rodriguez Suarez, M. Serrano, R. Rodriguez Roza, V. Peral and J. B. Cannata, *Nefrologia*, 1986, **6**, 75.
18. I. S. Parkinson, M. K. Ward and D. N. S. Kerr, *Clin. Chim. Acta*, 1982, **125**, 125.
19. D. C. Manning and W. Slavin, *Appl. Spectrosc.*, 1983, **37**, 1.
20. J. M. Cano Pavón, M. L. Trujillo and A. García de Torres, *Anal. Chim. Acta*, 1980, **117**, 319.
21. M. Salgado Ordoñez, A. García de Torres and J. M. Cano Pavón, *Talanta*, 1985, **32**, 887.
22. J. B. F. Lloyd, *Analyst*, 1980, **105**, 97.
23. P. John and I. Soutar, *Anal. Chem.*, 1976, **48**, 520.
24. M. T. Montaña, J. L. Gómez-Ariza and A. García de Torres, *An. Quim.*, 1984, **80B**, 129.
25. T. C. O'Haver and G. L. Green, *Anal. Chem.*, 1976, **48**, 312.
26. S. Bajo, U. Suter and B. Aeschliman, *Anal. Chim. Acta*, 1983, **149**, 321.

A NEW CHEMILUMINESCENCE SYSTEM FOR DETERMINATION OF COBALT

LU MINGGANG, LU XIAOHU and YIN FANG

Department of Applied Chemistry, China University of Science and Technology, Hefei,
People's Republic of China

(Received 26 September 1988. Revised 27 May 1989. Accepted 7 October 1989)

Summary—The chemiluminescence of the reaction of tartaric acid with hydrogen peroxide in the presence of Co(II) in alkaline buffer media has been examined. The maximum emission wavelength is 460 nm. The kinetic curve of the chemiluminescence system has been modelled with a computer, and the reaction conditions have been optimized. Foreign ions, such as Fe(II), Cr(III) and Mn(II), interfere when present in more than 10-fold ratio to Co(II), but several ions can be tolerated when present in higher ratios to Co(II). The concentration range of linear response is from 3.5×10^{-9} to 2.0×10^{-6} g/ml, and the detection limit is 4×10^{-11} g/ml. The procedure has been satisfactorily applied to determine trace cobalt in human blood serum.

In comparison with other kinetic determination methods, chemiluminescence (CL) analysis is rapid, sensitive and does not require expensive instruments. Some CL methods for cobalt determination have been reported, but many metals interfere (Table 1).

Marino *et al.* have reported a determination of cobalt with the lophine CL system after ion-exchange separation of the cobalt,⁵ but the CL system itself has poor selectivity. In recent years, therefore, a search has been made for more selective CL systems^{6,7}

Tartaric acid has been observed to give chemiluminescence when treated with hydrogen peroxide in alkaline medium. Several metal ions were found to enhance the reaction, Co(II) giving by far the largest effect. The reaction has now been adopted for determination of trace cobalt.

EXPERIMENTAL

Apparatus

CL meter, Model YHF-1 (made in China), including photomultiplier tube, fused-silica

reaction cell, and a flat-bed recorder. The reaction cell is cylindrical with inlet tubes at opposite sides. The bottom of the cell (diameter 2.2 cm) faces the photomultiplier tube. A model wp₄ optical spectrum analyser (made in Hefei) was also used.

Reagents

Standard cobalt solution, 1.0 mg/ml. Prepared by dissolving the required weight of analytical grade Co(NO₃)₂ in the requisite volume of redistilled water, and diluted further as required.

Tartaric acid solution, 1.0M.

Hydrogen peroxide solution, 0.097M. Further diluted as required.

Buffer solution 0.1M NaHCO₃-0.1M Na₂CO₃. Adjusted to pH 10.4.

Procedure

Clean and dry the reaction cell, then inject 2 ml of 1.0M tartaric acid, 1 ml of 0.097M hydrogen peroxide and 1 ml of Co(II) test solution through one side-tube, start recording

Table 1. Reported CL methods for Co(II) determination

System	Detection limit, ng/ml	Interferences	Reference
Lucigenin + H ₂ O ₂ + KOH + Co	1.4	Tl, Fe, Ni, Ag, Bi, Cu, Cr, Os, Ce, Mn, Pb	1
Luminol + H ₂ O ₂ + KOH + Co	0.01	Al, Sn, Pb, Bi, Cr, Fe, Cu, Zn, Ag, Mn, Ce	2
Gallic acid + H ₂ O ₂ + NaOH + Co	0.4	Pb, Cu, Ag, Mn	3
Pyrogallol + NaHCO ₃ + Co	0.5	Ca, Mg, Mn, Fe	4

the signal, and 30 sec later inject 1 ml of buffer solution through the other side-tube. Measure the peak height of the recorded kinetic curve of the CL reaction. Drain the cell through a side-tube.

RESULTS AND DISCUSSION

The CL reaction

A mixture of tartaric acid and hydrogen peroxide in alkaline solution, with Co(II) as catalyst, emits light, which reaches maximum intensity 2 sec after injection of the alkaline buffer. In a further 3 sec the light intensity falls to 50% of the maximum. Various buffer solutions such as 0.1M NaHCO₃-0.1M Na₂CO₃ (pH 10.4), 0.1M NH₄Cl-0.1M NH₃ (pH 10.1), and 0.1M H₃BO₃-0.1M KOH (pH 10.3) were tested, and the first of these gave the highest emission intensity.

The decay curve (Fig. 1) of the CL system was analysed by computer, and corresponded to $I(t) = Ae^{-kt}$ where k is the decay constant (sec⁻¹), t is time (sec) and A is a constant related to the quantum efficiency, concentration of Co(II), and the apparatus parameters. The value of k was found to be 0.38 sec⁻¹.

Optimization of conditions

Figure 2 illustrates the results from the study of optimization of the tartaric acid and hydrogen peroxide concentrations. The tartaric acid and peroxide concentrations selected were $1.0 \times 10^{-3}M$ and $1.9 \times 10^{-3}M$ respectively. Figure 3 illustrates the effect of the acidity of the Co(II) solution; pH 6 was chosen as optimal. The chemiluminescence spectrum of the tartaric

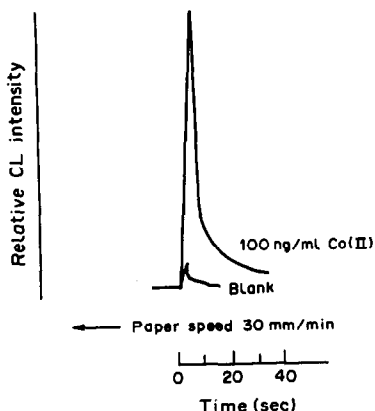


Fig. 1. Kinetic curve of tartaric acid CL light emission.

acid-H₂O₂-Co(II) system obtained under the selected conditions is shown in Fig. 4.

Calibration and detection limit

Figure 5 shows that the light intensity is directly proportional to Co(II) concentration from 3.5×10^{-9} to 2.0×10^{-6} g/ml. The detection limit is 4×10^{-11} g/ml, defined as the concentration corresponding to the mean background signal plus twice its standard deviation.

Interferences

An extensive interference study gave the results shown in Table 2. Although Fe(II), Fe(III), Cr(III) and Mn(II) interfere when present at greater than 10-fold w/w ratio to Co(II), they can be screened with $1.0 \times 10^{-3}M$ sodium citrate, which does not affect the CL intensity.

Determination of cobalt in human serum

Of the elements present in human blood

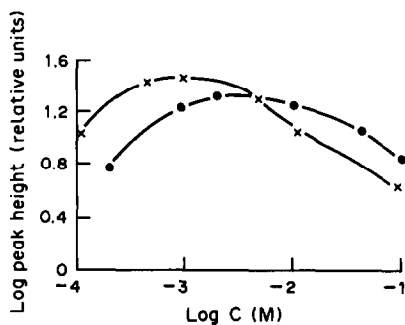


Fig. 2. Tartaric acid optimization (x). Initial conditions: [H₂O₂] = $2.0 \times 10^{-3}M$, [Co(II)] = 2.0×10^{-7} g/ml, 0.1M NaHCO₃-0.1M Na₂CO₃, pH = 10.4. H₂O₂ concentration optimization (●). Initial conditions: [tartaric acid] = $1.0 \times 10^{-3}M$, [Co(II)] = 2.0×10^{-7} g/ml, 0.1M NaHCO₃-0.1M Na₂CO₃, pH = 10.4. No blank signal was detected.

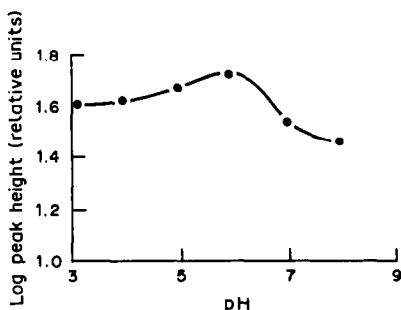


Fig. 3. Chemiluminescence intensity as a function of pH of the Co(II) solution. Initial conditions: [tartaric acid] = $1.0 \times 10^{-3}M$, [H₂O₂] = $1.9 \times 10^{-3}M$, Co(II) = 2.0×10^{-7} g/ml, 0.1M NaHCO₃-0.1M Na₂CO₃, pH = 10.4.

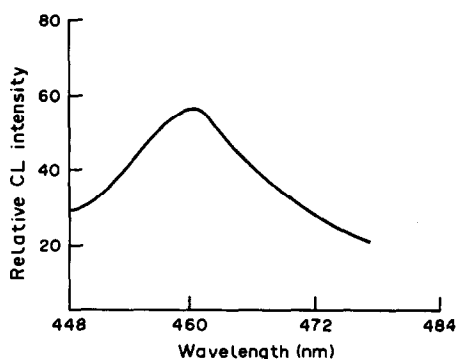


Fig. 4. Chemiluminescence spectrum.

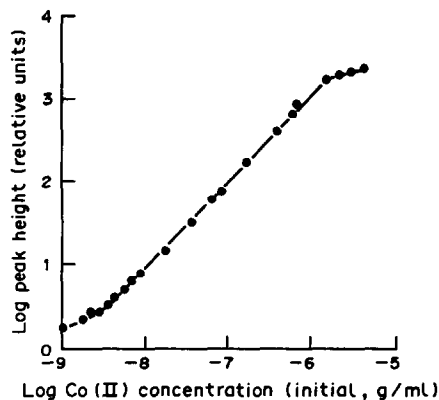


Fig. 5. Calibration curve for Co(II).

Table 2. Effect of foreign ions on the determinations of 10.0 ng of cobalt

Foreign ion	Added, μg	Co found, ng	Foreign ion	Added, ng	Co found, ng
Cd(II)	5.0	9.9	Cu(II)	0.6	10.7
Hg(II)	5.0	10.5	Pt(IV)	1.0	11.0
Ni(II)	4.0	10.6	Ba(II)	1.0	9.7
Zn(II)	5.0	10.5	Mg(II)	5.0	9.1
Au(III)	2.0	9.0	Ca(II)	1.0	10.0
Ag(I)	5.0	9.5	Mo(VI)	1.0	8.9
Al(III)	10.0	10.5	Mn(II)	0.10	9.4
Pb(II)	6.0	10.7	Fe(III)	1.0	9.8
Fe(II)*	1.0	10.4	Cr(III)	0.40	10.5
ClO_3^-	10.0	10.4	PO_4^{3-}	10.0	8.9
SO_4^{2-}	25	10.8	F^-	9.5	10.5
Cl^-	180	10.1	Br^-	100	10.4
I^-	130	10.2	Citrate	$1 \times 10^{-3}M$	9.7

*In presence of $1.0 \times 10^{-3}M$ sodium citrate as masking reagent.

Table 3. Determination of cobalt in human serum (mean of five determinations)

Sample	[Co] found, $\mu\text{g/ml}$		Coefficient of variation, %	Co added, $\mu\text{g/ml}$	Co recovered, $\mu\text{g/ml}$	
	This method	AAS			$\mu\text{g/ml}$	%
A	0.53	0.52	5.1	0.50	0.46	92
B	1.03	0.98	2.3	0.50	0.53	106
C	0.51	0.51	8.5	0.50	0.47	94

serum, iron and copper may interfere in the determination of cobalt, so sodium citrate should be used to screen them. The sample is wet-ashed by heating 0.5 ml of serum with 5 ml of concentrated nitric acid in a beaker on a controlled hot-plate until nearly dry, then adding 5 ml of concentrated perchloric acid, heating until all white fumes have disappeared, and then making up to volume in a 50-ml standard flask. A known volume of this solution is pipetted into a 10-ml standard flask, 1 ml of $1.0 \times 10^{-2}M$ sodium citrate is added, the pH is adjusted to 6 with sulphuric acid, and the solution is diluted to volume with redistilled

water, and analysed as already described. Typical results are shown in Table 3.

REFERENCES

1. L. I. Dubovenko and N. V. Beloshitskii, *J. Anal. Chem. USSR*, 1974, **29**, 85.
2. V. Nau and T. A. Nieman, *Anal. Chem.*, 1979, **51**, 424.
3. S. Stieg and T. A. Nieman, *ibid.*, 1977, **49**, 1322.
4. R. J. Miller and J. D. Ingle, Jr., *Talanta*, 1982, **29**, 303.
5. D. F. Marino and J. D. Ingle, Jr., *Anal. Chem.*, 1981, **53**, 292.
6. F. Zhang, G. Chen and H. Chen, *Fenxi Huaxue*, 1985, **13**, 266; *Chem. Abstr.*, 1985, **103**, 152880v.
7. M. Ling, M. Lu, N. Tao, H. Cui, X. Lu and F. Yin, *ibid.*, 1986, **14**, 941; *Chem. Abstr.*, 1987, **106**, 152422j.

LABILE METAL CONTENT OF SEDIMENTS—FRACTIONATION SCHEME BASED ON ION-EXCHANGE RESINS

JANECE SLAVEK, PAMELA WALLER and WILLIAM F. PICKERING

Department of Chemistry, University of Newcastle, N.S.W. 2308, Australia

(Received 26 June 1989. Revised 12 September 1989. Accepted 4 October 1989)

Summary—The labile metal content of sediments can be evaluated by equilibrating sediment suspensions with ion-exchange resins. By use of a sequence of strong-acid and weak-acid cation-exchangers (H^+ - and Na^+ -form) and chelating resins, extraction can be performed at pH values ranging from 2 to 10. The results allow the total metal content to be subdivided into seven categories designated as (i) low-pH labile, (ii) weak-acid labile, (iii) exchangeable and readily desorbed at sediment-suspension pH, (iv) weak-base labile, (v) high-pH labile, (vi) non-labile soluble forms and (vii) detrital metal content. The sediment suspensions are mixed overnight with the different types of exchanger (held in porous containers) and the cations transferred from the sediment are subsequently back-extracted from the resins into 0.05M EDTA (pH 7.5). The EDTA extracts are analysed for Cu, Pb, Zn, Cd, Ca, Mg, Fe and Al. Analysis of the aqueous phase left in contact with the sediment residue gives the amount of non-labile species released. Eighteen sediments, containing various levels of metal contamination, and an effluent dam sludge have been examined by this technique. All the exchangers released Ca and Mg from the sediments, and the H^+ -form exchangers also released Fe and Al. Some of the Fe, Al and to a lesser extent Zn released by the sediment/exchanger interactions was present as non-labile "soluble" species. The advantages and limitations of this "labile metal" fractionation scheme have been considered.

As indicated in review articles,¹⁻³ in the past two decades many research groups have proposed schemes for division of the total metal content of soils or sediments into fractions which may reflect the "availability", "bonding mode" or "matrix component association pattern" of an element of interest. The major analytical approach has involved judicious use of chemical extraction solutions, applied in sequence. However, views still differ on the most appropriate reagents and sequencing pattern.

In one proposal⁴ the fractionation scheme included metal distribution into a strong-acid cation-exchanger and in a later study⁵ agitation of lacustrine sediments with an excess of H^+ -form exchanger was used to remove the carbonate-phase fractions. The possibility of using different types of exchanger in metal lability studies has been investigated more recently.^{6,7} The favourable aspects of such a scheme include: (i) the ability of the exchange process to distinguish between labile and non-labile forms of the metal content, (ii) minimization of re-adsorption of displaced metal ions on the matrix, because the equilibrium levels of metal ion are low, and (iii) transfer to exchange resins may simulate natural processes

(e.g., uptake by roots) more closely than does direct chemical attack. On the other hand, agitation of a sparingly soluble compound with exchanger materials can lead to total dissolution^{8,9} of the compound, and dissolution of the more soluble components of sediments by this process may saturate so many exchange sites that total transfer of labile metal may not occur. Metal ion transfer requires release of soluble metal species from the soil or sediment, diffusion of this species to the exchanger and finally uptake of the cation at the functional-group sites.

The degree of bi- or trivalent cation release from sediments can be strongly influenced by the system-pH. For example, the H^+ present in low-pH systems can promote displacement of loosely sorbed surface species, cause dissociation of weak complexes and aid release of chemisorbed material by attacking matrix components such as carbonate minerals. At higher pH, in the presence of particulate matter, the released metal ion can be re-sorbed as a hydroxy species¹⁰ unless present as stable complex ion. The equilibrium pH of exchanger/sediment systems is determined by the nature of the functional group and the counter-ion (which can be

modified by interaction with the base content of the sediment). With sulphonate exchange-group resins, the affinity of metal ions for the group sites is nominally independent of pH, but with weak-acid exchangers (*e.g.*, with $-\text{COOH}$ functional groups) the relative affinity of cations for exchange sites is pH-dependent. Weak-acid exchangers also preferentially sorb cations present as salts of weak acids, because proton-displacement from the functional group is promoted by interaction with the basic anion, *e.g.*, $2\text{RCOOH} + \text{MgCO}_3 \rightarrow (\text{RCOO})_2\text{Mg} + \text{H}_2\text{CO}_3$.

Theory suggests that the introduction of different types of exchanger material (to yield a different system pH and/or cation affinity) should allow sub-division of the total metal content of a sediment/soil into a number of categories, as outlined in Fig. 1. Not all of

these categories may be present in a given sample. Preliminary studies^{6,7} indicated that a fractionation scheme of this type could be developed by refinement of the experimental approach initially tested. These predictions have now been examined, by use of sediments drawn from a polluted tidal creek and a contaminated estuary, and the results are given here. To test the wider applicability of the technique, an effluent-dam sludge has also been analysed.

EXPERIMENTAL

Analytical techniques

A Varian® AA 875 atomic-absorption spectrometer was used to determine the heavy metal and matrix element contents of the various test solutions, with an air-acetylene flame for the

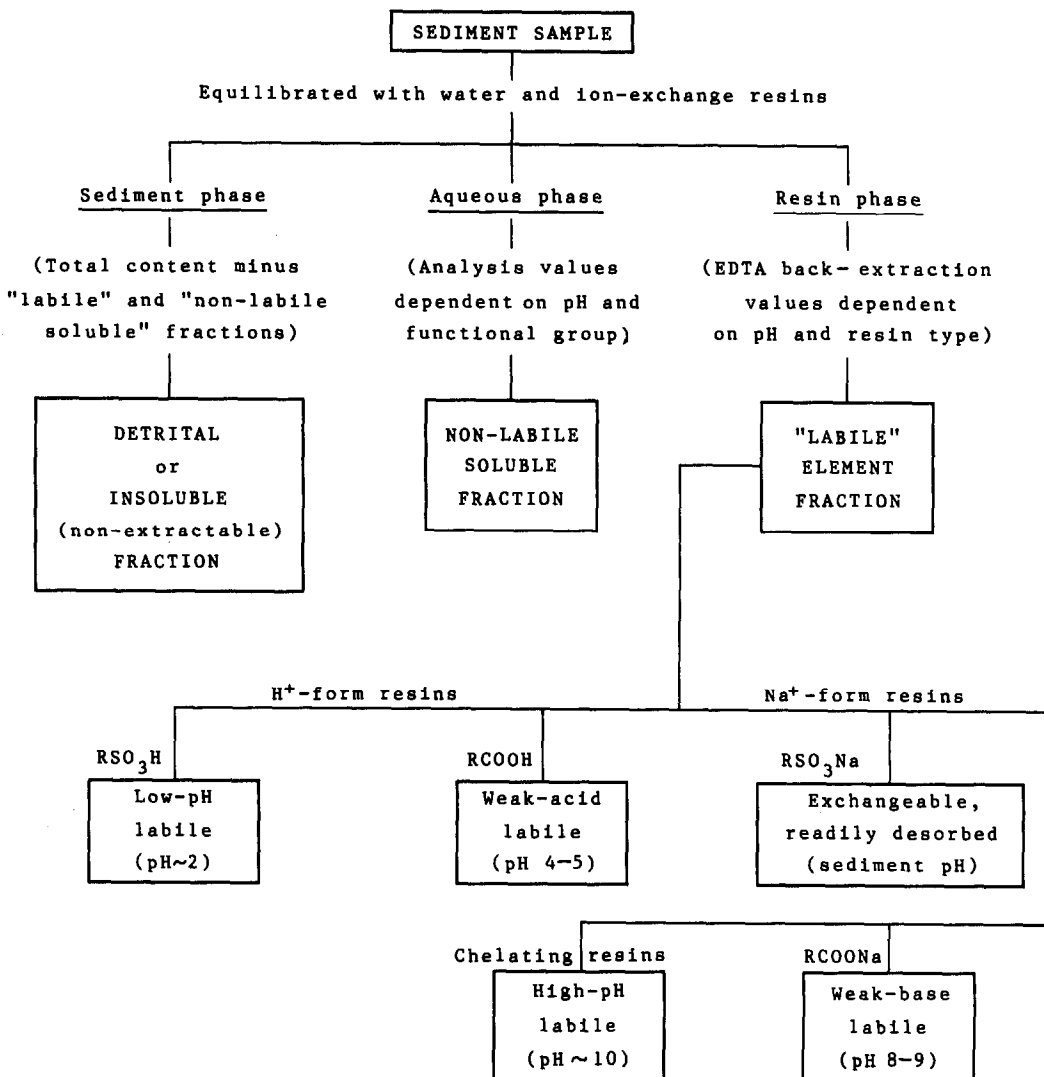


Fig. 1

Pb, Cu, Cd, Zn, Mg and Fe measurements and a nitrous oxide-acetylene flame for Ca and Al measurements. The calibration solutions (prepared by dilution of B.D.H. AAS standards) were made 0.05M in EDTA (pH 7.5) when appropriate. A Hanna Instruments digital meter (model 8521) was used for pH measurements.

Sediment samples

Most of the waterway sediments used in the investigation were drawn from a local tidal creek fed by an urban wastewater system. These accumulated muds are contaminated by industrial run-off and dumped rubbish (e.g., galvanized sheeting and old lead batteries). Five sites were sampled by an independent group, at three different positions in the profile. Three mildly polluted samples, drawn from a polluted estuary in another state, yielded results similar to those for the local sediments. The total levels of Cu, Pb and Zn present (listed in Tables 2 and 3) ranged from 20 to 150 $\mu\text{g/g}$ (Cu), 60 to 750 $\mu\text{g/g}$ (Pb) and 0.13 to 2.4 mg/g (Zn). Fe contents varied between 10 and 40 mg/g; Ca between 3 and 14 mg/g; Mg between 2 and 8 mg/g and Mn between 150 and 550 $\mu\text{g/g}$. Cd (10 $\mu\text{g/g}$) was found in only two samples. Although eighteen sediment samples were studied, only a representative group of ten is included in Tables 2 and 3.

For comparison, a metal-rich sludge was included in the study. This sludge was drawn from an acid/smelter waste entrapment dam. The total element analysis for this material was Mg (5.8%), Ca (4.1%), Fe (3.7%), Zn (2.9%), Pb (2.5%), Al (1.3%), Cu (2.8 mg/g) and Cd (1.5 mg/g). All samples were kindly made available by the Sulfide Corporation, Boolaroo.

Cation-exchange materials

Two sulphonated-polystyrene cation-exchanger resins (Amberlite-IR 120 and Zerolit 225) and two carboxylated polymer materials (Amberlite IRC-50 and Zerolit 236) were prepared in both H^+ - and Na^+ -forms. Two chelating resins, possessing either iminodiacetate (Chelex 100) or aminophosphonate (Duolite C46) functional groups, were used in the Na^+ -form supplied.

For the fractionation tests, a fixed weight of resin (500 mg) was weighed into "cages" made from 2–3 cm lengths of thin rigid plastic tubing (~ 1 cm i.d.) enclosed at both ends by ~ 100 -mesh polyester cloth, which was held in place with plastic rings. (Earlier studies^{6,7} demonstrated that the weight of resin taken should at least equal the weight of sediment used.)

Back-extraction of multivalent cations held on resins

A range of chemical solutions was tested for extracting the metal ions sorbed on the exchanger resins. The most satisfactory proved to be 0.05M EDTA (pH 7.5), which consistently retrieved $> 95\%$ of exchanger-bound heavy metal in a single back-extraction step. The distribution ratios for Ca and Mg were not so favourable and at high alkaline-earth metal levels a minimum of two extractions was required.

Other reagents worked well in restricted conditions. For example, Zn, Cu, Pb and Cd were quantitatively displaced from sulphonated resins by an acetate buffer solution and by a sodium citrate solution. Oxalate buffer effectively displaced Zn and Cu from the strong-acid exchangers. None of these reagents, however, proved capable of retrieving high proportions of the metal ion held by carboxylated polymer resins (in a single extraction step). Retrieval of metal ions by use of mineral acids in batch operations was not quantitative.

"Labile metal" exchange studies

The experimental approach was a refined version of that proposed previously.⁶ Sediment samples (0.5 g) were placed in 30-ml plastic vials together with 25 ml of water and in each sediment suspension was placed a resin cage containing 0.5 g of air-dried exchanger. Each vial was capped and its contents equilibrated overnight in an end-over-end mixer. The cage was then raised (with tweezers) to allow the internal aqueous phase to drain back into the sediment vial, and was then removed and washed with a stream of water to displace any adhering solids. The washed cages were placed in fresh vials, together with 25 ml of 0.05M EDTA (pH 7.5). Overnight mixing (to extract cations sorbed on the resin) was followed by analysis of the EDTA extract by AAS for Pb, Cu, Cd, Zn, Ca, Mg, Fe and Al content. After draining, the resins in the cages were extracted with a second 25-ml portion of the EDTA solution in order to assess the effectiveness of the first extraction.

The sediment suspensions left in the original vials were centrifuged and the supernatant liquids analysed for the same group of elements. The AAS technique measured the total element content left in the aqueous solution phase, *i.e.*, the sum of all unsorbed metal species, such

as non-labile metal complexes and metal-rich colloidal particles. The EDTA-extract values, on the other hand, reflected the labile content (under specified conditions) since only hydrated cations (derived from soluble salts or labile complexes) were taken up by the resin exchangers.

The pH of each resin/sediment suspension was measured after removal of the cage.

Precision of measurement

The analytical technique involves many stages and is prone to error at each, yet the reproducibility of the results equalled that found in earlier selective chemical extraction studies. Each sediment/exchanger system was analysed in triplicate and for most combinations the spread of results was normally within $\pm 10\%$ of the mean. Repeat studies generally yielded similar mean values. The mean values obtained with different brands of exchanger with the same functional groups were often quite close (within 10%), but there were exceptions (noted in Tables 2 and 3). Such differences were most marked in the matrix element determinations and in many studies on Ca, Mg, Fe and Al the means obtained with Amberlite and Zerolit materials differed considerably from the overall average (*e.g.*, by 25%). In recognition of this high degree of variability, matrix element results are reported only as ranges (Table 4). Contributing to this variance were experimental factors such as migration of fine sediment particles through the resin cage mesh and entrapment of particles in the mesh or under the plastic rings. Migration through the mesh was only visibly detectable for non-sediment samples (*e.g.*, calcine and dam sludge), but effective washing of the cloth

membranes proved difficult with a number of sediment samples. In such cases replacement with a fresh cloth disc eliminated any error resulting from entrapped particles. Moving the plastic rings to a new position facilitated removal of particles trapped under them. The heterogeneity of the samples also contributed to the variance, as shown by an occasional "wild" result attributable to inclusion of an element-rich fragment in the particular sub-sample. Blank studies with sediment absent failed to detect any errors attributable to metal contamination from the reagents, resins or cages.

RESULTS AND DISCUSSION

pH of exchanger/sediment suspensions

Aqueous suspensions of the various sediments were all alkaline (Table 1) and the pH values altered very little when Na⁺-form sulphonate exchangers (RSO₃Na) were added. The introduction of Na⁺-form carboxylate exchangers (RCOONa) tended to increase the system pH. The addition of H⁺-form weak-acid exchanger (RCOOH) reduced the system pH to 4–5.5, reflecting the buffering effect of partial proton removal by salts of weak acids and other basic sediment components. The two brands of weak-acid exchanger interacted to different extents with the sediments (see the RCOOH and RCOONa columns in Table 1). When H⁺-form sulphonate resins (RSO₃H) were added, the equilibrium pH ranged from 2.2 to 3.0. The addition of the very basic Na⁺-form chelating resins raised the pH of all sediment suspensions to around 10.0 and at this pH most systems developed a tan to brown colour (attributed to

Table 1. System pH in exchange resin/sediment suspensions (0.5 g of sediment, 0.5 g of resin, 25 ml of water)

Sediment No.	Exchanger type					
	RSO ₃ H* A/Z	RCOOH* A/Z	RSO ₃ Na†	RCOONa* A/Z	Chelex 100	Duolite C46
1	2.2/2.7	5.4/5.0	7.6	7.8/8.8	10.3	10.1
2	2.5	4.9/4.3	7.4	7.7/9.2	10.1	9.9
3	2.4	5.3/4.6	8.1	7.8/8.7	10.2	10.1
4	2.3	5.4/5.5	7.2	7.7	9.9	9.8
5	2.4	5.2/4.6	7.9	7.7/9.2	10.3	10.2
6	2.9	4.8/4.5	7.4	7.6/9.2	10.6	10.4
7	2.2	5.2/4.5	7.8	7.5/9.3	10.3	10.2
8	2.4	4.6/4.0	8.1	7.4/9.6	10.6	10.2
9	2.5/2.2	4.6/4.0	7.2	7.4/8.9	10.0	9.8
10	2.7/3.0	4.5/4.1	7.4	7.7/9.6	10.8	10.5

*When the mean values obtained with the Amberlite (A) and Zerolit (AZ) brands of exchanger were significantly different, both are given; otherwise a composite mean is quoted.

†These values were similar to those for the suspension alone.

Table 2. Zinc species distribution in sediment samples

Sample No.	Total content*	Labile Zn					Non-labile (soluble) Zn					
		RSO ₃ H†	RCOOH†	RSO ₃ Na†	RCOONa†	Chelex 100	Duolite C46	RSO ₃ H	RCOOH	RSO ₃ Na	RCOONa	Chel Na§
1	2390	1315	1090	300	395	773	637	120	105	90	90	95
2	1950	1385	1045	700	275	693	547	65	195	45	60	40
3	1550	1080	930	95	210	567	350	15	120	35	45	50
4	1390	1345	835	355	235	635	450	25	95	70	40	55
5	1025	850	635	120	120	450	260	90	90	60	55	50
6	680	495	240	200	60	260	153	n.d.	60	20	50	35
7	590	415	245	20	40	207	98	n.d.	30	50	45	60
8	460	390	170	35	100	170	100	n.d.	60	60	90	75
9	225	150	90	20	25	75	40	n.d.	15	30	35	35
10	130	100	70	50	25	50	25	n.d.	15	20	20	20

*Detrital values can be obtained by subtracting the labile plus non-labile (soluble) RSO₃H values from the total Zn content.

†Means of results for both Amberlite (A) and Zeolite (Z) exchangers.

§Mean for Chelex 100 and Duolite CH6.

organic matter). By using resins of different types it was thus possible to examine "lability" over the pH range 2-10.

Trefry and Metz¹¹ used chemical buffer systems to examine metal-ion release within different pH ranges and in some respects the ion-exchange study may be regarded as a modification of their fractionation scheme. The exchanger approach has the advantage, however, of allowing distinction between labile and non-labile released forms.

As shown in Tables 2 and 3, metal-ion release was greatest at low pH (as expected) and passed through a minimum at normal suspension pH (*i.e.*, that when RSO₃Na was used). The amount transferred to the chelating resins (pH 10) was sometimes greater, though generally less, than the intermediate values found in pH 4-5 systems (interpretation is complicated by the lower affinity of some metal ions, *e.g.*, Pb and Zn, for the aminophosphonate functional groups). A pH < 7 was required for release of labile Fe and Al (Table 4), but transfer of Ca and Mg was little affected by system pH. Non-labile forms of Fe, Al and Zn were released from the sediment over a wide range of pH (Tables 2 and 5).

The results shown in Tables 2-5 arose from a combination of pH and exchanger dissolution effects, modified by cation affinity for different functional groups, specific chemical behaviour (*e.g.*, formation of oxyanions of Zn and Al at high pH) and the relative stability of any organometallic complexes present.

Distribution patterns of metals in sediments

Zinc. The distribution of Zn between the various categories, for ten of the sediments tested, is summarized in Table 2 (the values obtained with different brands of exchanger have been averaged, even though in many cases the means differed by more than 10%).

The "low-pH labile" Zn contents for the sediments were relatively high (300-1400 µg/g) and represented 55-85% of the total zinc. With many sediments, over a fifth of this "low-pH labile" value could be assigned as "exchangeable and/or readily desorbed" (see RSO₃Na values); with the other sediments the exchangeable fraction was > 10% of the RSO₃H value. The weak-acid resins (RCOOH) also extracted significant amounts (~20%) of the total zinc content, which suggests that much of the zinc in the sediment was present as the salt of a weak acid.

Table 3. Distribution of lead and copper in sediment samples ($\mu\text{g/g}$), based on transfer to ion-exchange resins (n.d. = not detected, tr = trace)

Sediment No.	Total content	Labile					Non-labile	
		RSO ₃ H† A/Z	RCOOH† A/Z	RSO ₃ Na† A/Z	RCOONa† A/Z	Chel Na§ C/D	RCOONa	Chel Na
<i>Lead</i>								
1	750	340	240/295	30	45	115/113	20	25
2	405	205	115/175	tr	n.d.	40/30		tr
3	440	175	80/165	tr	n.d.	25/tr		tr
4	650	445	195/300	22	25/tr	77/35	20	37
5	530	125	110/155	32/tr	40/20	55/tr		tr
6	130	75	50	tr	n.d.	38/tr		tr
7	250	125	37/60	tr	n.d.	32/tr	15	28
8	300	155	100/68	20	25	60/tr	35	30
9	65	55	tr/30	tr	n.d.	25/n.d.		tr
10	60	20	32/25	tr	n.d.	25/n.d.		
<i>Copper</i>								
1	150	75/55	25	n.d.	n.d.	30		17
2	135	65	17	n.d.	n.d.	20		12
3	103	35	tr	n.d.	n.d.	20		12
4	125	65	n.d.	n.d.	n.d.	25		15
5	125	50/37	20	n.d.	n.d.	30/12		10
6	55	45/37	n.d.	n.d.	n.d.	20/10		10
7	145	82/97	17	n.d.	n.d.	40/20		25
8	75	70/57	tr	n.d.	n.d.	30/15		15
9	95	62/52	10	n.d.	n.d.	30/15		21
10	20	20	n.d.	n.d.	n.d.	17/tr		tr

*Detrital values can be obtained by subtracting the RSO₃H values from the total content.

†Means of triplicate results obtained with Amberlite (A) and Zerotit (Z) exchangers; the overall mean is quoted when the A and Z means differ by $\leq 10\%$.

§Means for Chelex 100 (C) and Duolite C46 (D); overall mean when C and D values differ by $\leq 10\%$.

The differences in labile contents found by using the RSO₃Na and RCOONa exchangers can be attributed in most cases (*i.e.*, where the values obtained with RCOONa were higher) to the formation at the higher pH of a more labile complex ion. This interpretation is consistent with the "high-pH labile" content ($\sim 30\%$ of the total) found with the chelating resins. Tetrahydrozincate ion formation and dissolution of zinc humates would have contributed to the pH-10 labile values. Three sediments, however, released more Zn into the RSO₃Na resin than

Table 4. Matrix dissolution: transfer of elements from sediments to exchangers after overnight mixing of equal quantities of resin and sediment

Element	Range, <i>mg/g</i>	Sediment Nos.				
		RSO ₃ H	RCOOH	RSO ₃ Na	RCOONa	Chel Na
Al	0-0.5	—	8	1-10	1-10	1-10
	0.6-1.5	—	2, 3, 5-7, 9, 10	—	—	—
	1.6-2.5	1, 3, 5, 6, 8, 10	1, 4	—	—	—
	2.6-4.0	7, 9, 2	—	—	—	—
	5.0-6.0	4	—	—	—	—
Fe	0-0.5	—	1, 2, 6, 8-10	1-10	1-10	1-10
	0.6-1.5	4-6	3-5, 7	—	—	—
	1.6-3.0	1, 3, 7-9	—	—	—	—
Mg	0.5-1.5	2, 6, 10	2, 6, 8-10	6, 10	2, 6, 10	2, 6, 10
	1.6-2.5	1, 3, 5, 7-9	1, 3-5, 7	1-3, 5, 8	1, 3-5, 7-9	1, 3, 5, 8
	2.6-3.5	—	—	4, 7, 9	—	4, 7, 9
	3.6-4.5	4	—	—	—	—
Ca	1.0-1.9	—	6-10	8	—	—
	2.0-2.9	7-9	2, 5	6, 10	6, 8, 10	—
	3.0-3.9	10	1, 3	1, 2, 4, 5, 7, 9	1, 4, 5, 7, 9	1, 8, 10
	4.0-5.5	2, 3, 5, 6	4	3	2, 3	2, 3, 5-7, 9
	6.0-7.4	1	—	—	—	4
	7.5-9.5	4	—	—	—	—

Table 5. Levels of species left in the aqueous phase after equilibration with exchange resin (mg per g of sediment): means of results for different brands of exchanger

Sediment No.	Iron					Aluminium				
	RSO ₃ H	RCOOH	RSO ₃ Na	RCOONa	Chel Na	RSO ₃ H	RCOOH	RSO ₃ Na	RCOONa	Chel Na
1	0.81	0.07	0.51	0.44	0.58	0.73	0.27	1.92	2.37	2.84
2	0.17	0.10	0.17	0.18	0.21	0.53	0.28	0.79	1.23	1.29
3	1.00	0.06	0.35	0.32	0.35	0.60	0.18	1.04	1.16	1.89
4	0.26	0.29	0.65	0.66		0.52	0.50	1.63	1.19	
5	0.95	0.06	0.31	0.35		0.68	0.17	1.26	1.96	
6	0.11	0.23	0.22	0.29	0.32	0.29	0.47	1.47	1.47	1.54
7	0.16	0.21	1.00	1.20	2.10	0.14	1.33	4.55	6.2	8.41
8	0.68	0.36	1.28	1.38		0.16	2.35	3.94	8.5	
9	0.12	0.35	1.12	1.29		0.17	2.21	4.68	10	
10	0.88	0.21	0.25	0.41		0.58	0.72	2.65	2.8	

Range	Calcium		Magnesium	
	Resin	Sediment Nos.	Resin	Sediment Nos.
0.01-0.02	Chel Na RCOOH	2, 3, 6-8, 10	Chel Na	1-3, 5, 6, 10
0.03-0.05	Chel Na RCOOH	8	Chel Na RCOOH	7-9, 4
0.06-0.10	RCOOH	1, 4, 5, 9	RCOOH	6, 10
0.11-0.15	RCOOH	7, 9, 10	RCOOH	2, 8, 9
	RCOOH	1, 4-6	RCOOH	1, 4, 7
	RCOOH	2, 3	RCOOH	3, 5

was found with the RCOONa materials, a result which implies that these samples contained more simple zinc salts.

The existence of a soluble non-labile fraction supports the idea of the formation of soluble zinc complexes, but detection of zinc ions in the aqueous phase can also be attributed to incomplete cation-exchange, *i.e.*, cations released from the matrix may have successfully competed for exchange sites. An interference study recently completed⁷ has shown that this is most likely to occur with weak-acid resins, since these materials take up Ca more readily than Zn. With sulphonated resins, it was found that solution Ca levels had to exceed 300 mg/l. before Zn uptake was significantly affected. In the current sediment study, Ca solution levels were well below this limit and competition for RSO_3^- sites was discarded as an explanation for the observed aqueous phase Zn levels. To support this view, it was noted that though matrix dissolution was greatest at low pH, the amount of "non-labile" Zn was least in the low-pH systems (in fact, half of the RSO_3H values were below the detection limit).

Up to 10% of the total zinc was found in the aqueous phase, the highest values usually being detected when the sediments were equilibrated with the weak-acid resins (RCOOH). This zinc may be a mixture of species, some soluble (*e.g.*, zinc humate and tetrahydrozincate ion) and some insoluble but of very small particle size (*e.g.*, basic zinc carbonate).

Lead. The Pb distribution pattern for ten of the sediments tested is shown in Table 3. A third of the samples contained small amounts (<8% of total content) of Pb which was labile at near the suspension pH (*i.e.*, when the RSO_3Na and RCOONa resins were used). This fraction may be described as "exchangeable or readily desorbed" lead ion, or it can be attributed to dissolution of a sparingly soluble salt (*e.g.*, PbSO_4). The marginally higher values observed by use of RCOONa exchangers and the significant amounts of labile (and non-labile) Pb found at pH 10 suggests that some Pb present can react to form the plumbite ion, while another portion is probably associated with organic matter. About 25–35% of the total Pb content was transferred to the RCOOH resins, which suggests that all the sediments contained this proportion of "weak-acid" lead salts. Around half of the total Pb was transferred to the strong-acid resins (RSO_3H) and this "low-

pH labile" fraction is considered to contain Pb released during dissolution of sparingly soluble salts (*e.g.*, PbSO_4 , PbCO_3) in addition to displaced chemisorbed Pb (*e.g.*, that associated with hydrous oxide surfaces). The affinity of Pb for the amorphous hydrous oxide of Fe has been reported¹³ to exceed that of other metal ions and alkaline-earth metal cations.

Copper. Distribution of the total Cu content of the sediments between fraction types is also shown in Table 3. No labile copper was detected at suspension pH (*i.e.*, with RSO_3Na and RCOONa resins) and no non-sorbed/non-labile Cu was detected at pH < 9. At pH 10, significant amounts of Cu became labile and this has been attributed to Cu initially associated with organic matter. It has been noted¹² that humic substances contain a sizeable portion of the Cu, Mo and Zn found in sediments. Only half the samples transferred Cu at pH 4–5 (*i.e.*, to RCOOH resins) but it can be proposed that when this did occur, the Cu was initially present as the salt of a weak acid (*e.g.*, CuCO_3 , Cu humate). Most of the copper present, however, appears to be chemisorbed and thus displaceable by proton attack (*e.g.*, it is associated with carbonate minerals or hydrous oxides of Fe and Al). The RSO_3H values indicate that the "low-pH labile" fraction varied from 30 to 100% of the total, while 20–35% was "high-pH labile" (Chel Na resin).

Cadmium. Cd was not detected in most of the sediments tested, partly because of the low total level of Cd present (10 $\mu\text{g/g}$ or less). With the high-pH chelating resins, 5 $\mu\text{g/g}$ labile Cd was found in sediments 2 and 5, and also in four samples not reported in the tables.

Matrix dissolution—release of Ca, Mg, Fe and Al

The degree of matrix dissolution induced by the introduction of ion-exchangers is indicated in Table 4. The matrix cations were released from the sediment particles through proton attack (low-pH systems) and through disturbance of solubility equilibria arising from the withdrawal of cations from the aqueous phase. For the release of Fe and Al the presence of free protons was required, but for Ca and Mg cation-abstraction by the exchangers appeared to be dominant (since Na^+ -form exchangers caused nearly as much release of alkaline-earth metal cations as the H^+ -form materials did). About half of the total Ca and Mg content of the sediment samples was taken up by the

exchangers, but the fraction of Fe and Al released as exchangeable cations was much smaller and probably arose from acid-soluble material of fairly recent origin (*e.g.*, amorphous hydrous oxides or weak-acid salts).

The amount of Ca, Mg, Fe or Al transferred to the resins varied with the type of functional group, system pH and brand of exchanger. The uptakes reported in Table 4 did not exceed the exchange capacity of any resin material used, which suggests that factors other than availability of exchange sites were operative, for example, exchange equilibria effects (*e.g.*, competition from released counter-ions) and solubility effects (*e.g.*, low equilibrium cation values due to accumulation of anion from the sparingly soluble component). In spite of such limitations, the matrix element data allow sediments to be placed in categories based on Ca, Mg, Fe and Al "availability".

Significant amounts of Fe and Al were detected in the aqueous phase after equilibration with the exchanger materials. Half the sediments did not release non-labile Fe or Al to the chelating resin exchangers, but with other functional groups present every sediment released non-exchangeable Fe and Al (Table 5). The Al values were highest in alkaline media, but Fe values varied randomly with pH. The chemical species responsible for these readings could range from dispersed colloids to stable oxyanions or organometallic complexes.

Small amounts of non-sorbed Ca and Mg were detected in some sediment studies, generally when the chelating resins (high pH) or exchangers with carboxylate functional groups were used (Table 5).

Dam sludge studies

The chemical composition of this material was vastly different from that of normal sediments, being very rich in alkaline-earth metal species arising from the occasional addition of baked lime, lime slurry and/or limestone to the dam in order to neutralize sulphuric acid waste inputs. The sludge suspension had a pH of 9.2 and contained enough free base to neutralize all protons introduced with H⁺-form exchangers.

The "labile" metal contents determined by the ion-exchange fractionation scheme are summarized in Table 6. The labile Zn and Pb contents were much higher than the values found in the sediment studies, but each was still only a small fraction of the total. In contrast, most of the Cd content of the sludge was transferred to the weak-acid exchangers (~1.44 mg/g), with lesser amounts going to other exchanger types (RSO₃H, 0.44 mg/g; RCOONa, 0.15 mg/g). The higher values for labile Cd, Pb and Zn obtained with RCOOH resins in the sludge systems imply that these elements were present in this material as salts of weak acids. Transfer of matrix elements (Mg, Ca and Al) was also higher with this form of exchanger, hence the greater metal transfer could not be attributed to less competition for sites.

With the heavy metal and matrix element determinations there was often poor correlation between the values obtained by using different brands of exchanger (Table 6, columns A and Z), partly because of fine sample components passing through the fabric filters.

Interaction between H⁺-form exchangers and the matrix released large amounts of Ca

Table 6. Amounts of heavy-metal ions and matrix-component cations (mg/g) sorbed on equilibration of 0.5 g of effluent waste-dam sludge with 0.5 g of Amberlite (A) and Zerolit (Z) resins

Element	RSO ₃ H		RCOOH		RCOONa		RSO ₃ Na		Total content, mg/g
	A	Z	A	Z	A	Z	A	Z	
Cu	0.01	0.01	0.01	0.02	0.01	0.02	0.02	0.01	2.8
Cd	0.47	0.40	1.40	1.48	0.20	0.09	0.03	0.02	1.5
Pb	0.95	0.60	2.80	5.00	1.23	1.55	0.44	0.31	32
Zn	6.95	5.10	12.20	16.95	0.60	0.39	0.50	0.36	28.5
Fe	1.00	0.80	0.50	1.05	0.14	0.11	0.44	0.35	39.0
Al	0.18	0.07	0.54	1.97	0.05	0.05	0.21	0.07	43.7
Ca	24.5	23.0	26.9	32.1	16.0	20.9	9.6	9.1	40.7
Mg	18.0	23.4	26.9	32.5	14.0	16.0	11.0	9.6	41.4
Amounts left in aqueous phase (mg per g of sludge)									
Zn	0.6		0.2		—		—		
Ca	~6		3.6-4.5		0.03-0.05		0.11-0.15		
Mg	~5		~12		0.03-0.08		0.19-0.30		
Cd	0.3		—		—		—		
Al	0.15		—		—		—		

and Mg that were not subsequently sorbed by the exchanger sites (bottom of Table 6). The amount released exceeded the exchange capacity of the resin added and the high levels of aqueous phase Ca and Mg partially inhibited uptake of Cd and Zn ions released from the sludge sample.

In future studies of lime-rich sediments a higher ratio of exchanger to sediment weights should be used (*e.g.*, 2:1) but despite the limitations, the exchanger fractionation technique clearly delineates between labile metal contents and total contents.

CONCLUSIONS

It has been shown that the metal content of sediments can be subdivided into a number of operationally defined categories through equilibration with exchange materials of different types. Each category defines the lability of the element within a given pH range and partially distinguishes between chemical forms (*e.g.*, RCOOH preference for salts of weak acids).

This form of element content "fractionation" is quite important if the premise is accepted that it is the "labile" fractions which are most readily available for plant uptake or leaching. It can be asserted that the ion-exchange technique is more selective than direct reagent attack since it allows distinction between "labile" cations and non-labile species (*e.g.*, the Zn results given in Table 2) and should be less prone to losses by re-adsorption. The precision of the ion-exchange procedure is no worse than the variance found in earlier selective reagent studies. The sensitivity in both approaches is limited by the measuring technique used (AAS) and for the experimental conditions used in this study the detection limits were 25 $\mu\text{g/g}$ (Pb), 20 $\mu\text{g/g}$ (Cu), 10 $\mu\text{g/g}$ (Zn) and 5 $\mu\text{g/g}$ (Cd).

A single extraction of the isolated resin phase with 0.05M EDTA (pH 7.5) retrieves 95–100% of the transferred metal ion and therefore, in routine studies a second extraction step is unnecessary. However, if matrix-element transfer values are required, two extractions are sometimes essential.

There are some obvious disadvantages associated with the ion-exchange fractionation procedure. It can be more time-consuming than direct chemical extraction and matrix attack can be greater than with salt solutions. The

exchanger sequence also does not specifically define the possible effect of reducing conditions on metal release, *i.e.*, the amount likely to be released from Fe and Mn surfaces in anaerobic conditions, but this could be remedied by adding hydroxylamine (or another reducing agent) to RSO_3H /sediment suspensions prior to equilibration. Such a modification could prove unnecessary, since it appears that the RSO_3H alone will attack the hydrous oxides of most recent origin, and so should release the bulk of sorbed metal ion present in this phase.

With chemical reactant fractionations the responses vary with the reagents selected; with exchanger studies it was found that some "labile" values varied with the brand of exchanger. Accordingly, users of the exchange technique will need to standardize procedures and specify particular exchanger brands or the exchange properties (*e.g.*, exchange capacity, degree of cross-linking). Variations in the initial counter-ion used (*e.g.*, substituting Ca^{2+} for Na^+) or addition of complementary chemicals (*e.g.*, fluoride to complex Fe and Al) could increase the versatility and usefulness of the exchanger fractionation procedure.

Acknowledgement—This project was supported by the Australian Research Committee and the financial assistance received is gratefully acknowledged.

REFERENCES

1. U. Förstner, *Z. Anal. Chem.*, 1983, **316**, 604.
2. W. F. Pickering, *CRC Crit. Rev. Anal. Chem.*, 1981, **12**, 233.
3. *Idem*, *Ore Geol. Rev.*, 1985, **1**, 83.
4. S. R. Patchineelam, *Dissertation*, University of Heidelberg, 1975.
5. R. Deurer, U. Förstner and G. Schmolz, *Geochim. Cosmochim. Acta*, 1978, **42**, 425.
6. A. Beveridge, P. Waller and W. F. Pickering, *Talanta*, 1989, **36**, 535.
7. *Idem, ibid.*, 1989, **36**, 1217.
8. F. Helfferich, *Ion Exchange*, pp. 226–229, 295–299. McGraw-Hill, New York, 1962.
9. W. Riemann III and H. F. Walton, *Ion Exchange in Analytical Chemistry*, pp. 36–46, 79–85. Pergamon Press, Oxford, 1970.
10. H. Farrah and W. F. Pickering, *Aust. J. Chem.*, 1978, **31**, 1501.
11. J. H. Trefry and S. Metz, *Anal. Chem.*, 1984, **56**, 745.
12. A. Nissenbaum and D. J. Swaine, *Geochim. Cosmochim. Acta*, 1976, **40**, 809.
13. D. G. Kinniburgh, M. L. Jackson and J. K. Syers, *Soil Sci. Soc. Am. J.*, 1976, **40**, 796.

SORPTION OF ORGANIC DYES BY POLYURETHANE FOAM

A. CHOW, W. BRANAGH and J. CHANCE

Department of Chemistry, University of Manitoba, Winnipeg, Manitoba, Canada R3T 2N2

(Received 9 July 1989. Revised 20 September 1989. Accepted 3 October 1989)

Summary—The sorption of fifty-nine organic dyes, indicators and stains by polyester and polyether-type polyurethane foams was investigated by use of aqueous solutions and powdered foam material. Comparisons were made with sorption from 50% methanol solutions for some dyes and also with solvent extractions done with diethyl ether or ethyl acetate for several dyes. The R_f values for the dyes run on cellulose TLC plates in water or a mixed solvent mobile phase were compared to the distribution coefficients with polyurethane foam. The relationship between the structure of the test substances and their sorption is discussed.

Polyurethane foams have been employed in many separation and preconcentration studies since they were first used in analytical chemistry by Bowen in 1970.¹ Both organic and inorganic species can be sorbed by polyurethane, as reviewed by Moody and Thomas² and Braun *et al.*³ Solvent extraction was initially considered to be the major mechanism in this type of sorption, but work by Hamon *et al.*⁴ has shown that it cannot explain the high sorption of several inorganic complex anions such as those containing cobalt or palladium. Instead, a "cation chelation" mechanism has been described which accounts for the much greater sorption by the polyether-type of polyurethane than that by the polyester-type. The main consideration in this mechanism is the presence of a helix of inwardly directed oxygen atoms in the poly(ethylene oxide) molecule, which gives it a crown-ether type of configuration. The similarity to crown ethers is shown by the enhanced sorption of hydrophobic anions in the presence of various univalent and bivalent cations. Polyester-type foam shows no enhanced effect for different cations and in general appears to behave simply as a solid solvent-extractant. Schumack and Chow⁵ have shown that even the sorption of organic species is affected by the type of polyurethane foam used, and that some hydrogen-bonding occurs, especially with polyether-type foams.

Several organic compounds have been loaded onto polyurethane foam to act as chelating agents for various metal ions.³ In most cases these compounds have been dissolved in an

organic solvent or plasticizer and held on the foam either in the plasticizer or as an insoluble dispersed solid. Some compounds such as dithizone and dimethylglyoxime are soluble in the foam itself. Methylene Blue and Crystal Violet have been used on polyether-type polyurethane⁶ to concentrate alkylbenzene sulphonate for determination, but polyethylene, polystyrene, poly(vinyl chloride) and polyester-type polyurethane were found unsuitable. Although there have been studies of the sorption of several organic compounds it is clear that no mechanism has been proposed that will completely explain the variation in sorption behavior reported. The wide range of organic dyes available was considered to offer a valuable means of probing the sorption mechanism of polyurethane foams. Preliminary trials with a variety of dyes and indicators showed that many of these are sorbed by polyurethane foam, so a larger range of dyes, indicators and biological stains was chosen for further investigation of the problem.

EXPERIMENTAL

Apparatus

All absorbance readings and spectra were obtained with a Hewlett-Packard Model 8452A diode-array spectrophotometer or a Varian Series 634 spectrophotometer. A Fisher Accumet Model 825MP pH-meter was used. Sample solutions were shaken with a Burrell wrist-action shaker.

Reagents

All chemicals used were of reagent grade and water was purified by reverse osmosis and a Barnsted Nanopure II™ system before use. The dyes were obtained mainly from a Biological Stain Kit, BS-100, prepared by Chem Service Inc., West Chester, Pennsylvania as part of their Chem Supply system. A few indicators and dyes from a variety of regular chemical companies were used to expand the range of compounds tested. All the compounds tested were used without further purification.

Polyether-type polyurethane foam was obtained from a local department store and polyester-type polyurethane was obtained as diSPo™ plugs from Canlab, Winnipeg, Canada. No information was available concerning the formulation or primary manufacturer of either material. Several cleaning methods were evaluated before a procedure was found that consistently gave satisfactory results. The residual imprecision in the results was presumably partly due to materials in the foam that were not removed by the cleaning.

Procedure

Both foam types were washed in separate batches, of several pieces of foam. First, the foam was repeatedly squeezed in a large quantity of 1M hydrochloric acid in a plastic cylinder during a period of 5 hr and then left in the acid for a further 48 hr. The foam was then freed from acid by repeatedly squeezing it in each of several changes of clean water during 48 hr. After removal of as much water as possible by squeezing, the foam was refluxed with acetone in a large Soxhlet extraction apparatus for 6 hr, then after as much acetone as possible had been removed by squeezing, the foam was air-dried and stored in brown glass jars.

To make the foam sample as uniform as possible, the foam pieces were ground to a coarse powder by freezing them in liquid nitrogen and grinding them in a stainless-steel container on a Waring™ blender to pass a 16-mesh sieve. Any pieces of unground foam were discarded. Powdered polyurethane foam and the parent material should act similarly and have the same distribution coefficient; the major difference is that the finer material will reach equilibrium more quickly.

Dye solutions were prepared shortly before use by weighing accurately about 5 mg of the dye, dissolving it in water and diluting to

volume in a 250-ml standard flask. Occasionally the dye mixture was allowed to stand overnight to ensure that dissolution was complete.

The sorption was tested by adding 10 ml of dye solution by pipet to a 20-ml screw-top vial together with approximately 0.1 g of foam, capping the vial, shaking it for 6 hr in the automatic shaker, then filtering the solution through a Whatman No. 541 filter paper.

The sorption was judged by means of two parameters, the percentage of dyestuff sorbed (E) and the distribution coefficient (D):

$$E = 100(C_0 - C_{eq})/C_0; \quad D = (VE)/W(100 - E)$$

where C_0 = initial molar concentration of solution, C_{eq} = concentration of solution after sorption, V = volume of solution (l.), W = mass of foam (kg).

The distribution coefficient (l./kg) is the ratio of the concentration of dye in the foam to the concentration in solution and should become constant once the sorption process has reached equilibrium.

DISCUSSION

This study involved a wide variety of stains, indicators and dyes and their sorption on either polyether or polyester-type polyurethane foam. The sorption efficiency was markedly different for many of the compounds tested, as shown in Table 1. Several general and specific points for discussion arise from the results in Tables 1–3.

One of the possible mechanisms of sorption by polyurethane foam which has found some general acceptance^{2,3} is a simple solvent extraction mechanism. Schumack and Chow⁵ found support for this mechanism in the sorption of aromatic organic compounds. The present study also provides some support for it. When polyurethane foams were exposed to a solution of dye containing lithium chloride or potassium chloride, the sorption increased for both polyether and polyester foams. This suggests that the dye was forced into the less polar organic foam phase by addition of the salt, *i.e.*, "salted out". By comparing the dyes of the triphenylmethane series (marked TPM in Table 1), it can be seen that as the molecule becomes more polar the sorption decreases. The more non-polar triphenylmethane dyes all lack sulphonate groups and all have large distribution coefficients for polyether and polyester respectively [Ethyl Violet (1800, 9400); Victoria Blue R (750, 2500); Gentian Violet (790, 8500);

Table 1. Dye sorption coefficients and TLC data

Dyes	Structural information	$D, l./kg$		TLC	
		Polyether	Polyester	R_f in H ₂ O	R_f in mixed solvent†
Acridine Orange Basic	C	150	72	0.00	1.00
Alizarin Yellow R	A; 1(N=N)	230	60	0.29	0.97
Auramine O	C	29	100	0.01	1.00
Brilliant Green	C; TPM	640	800	0.04	1.00
Brilliant Yellow	A; 2(N=N); 2(NaSO ₃)	74	16	0.04§	0.45
Bromocresol Purple	A	9500	400	0.75	0.99
Clayton Yellow	A; 2(NaSO ₃)	76	33	0.12	0.35
Congo Red	A; 2(N=N); 2(NaSO ₃)	110	29	0.02	0.09
Eosin Y	A	410	81	0.07§	1.00
Eriochrome Blue Black R	A; 1(N=N); 1(NaSO ₃)	710	220	0.07	0.86
Eriochrome Black A	A; 1(N=N); 1(NaSO ₃)	4100	510	n.d.	n.d.
Eriochrome Red B	A; 1(NaSO ₃)	170	53	0.15	0.86
Ethyl Violet	C; TPM	1800	9400	0.00	1.00
Fluorescein	A	400	540	0.04	1.00
Fuchsin Basic	C; TPM	150	2000	0.01	1.00
Gentian Violet	C; TPM	790	8500	0.01	1.00
Hematoxylin	A	47	49	0.31§	0.95§
Janus Green B	C; 1(N=N)	210	5400	0.00	1.00
Malachite Green	C; TPM	320	970	0.05	1.00
Martius Yellow	A	190	69	0.50	0.95
Mentanil Yellow Orange MNO	A; 1(N=N); 1(NaSO ₃)	430	580	0.32	0.96
Methylene Blue	C	99	160	0.01	0.56
Methyl Orange	A; 1(N=N); 1(NaSO ₃)	74	19	0.62	0.81
Mordant Black 11	A; 1(N=N); 1(NaSO ₃)	200	350	0.00	0.70
Neutral Red	C	120	170	0.00	1.00
New Methylene Blue	C	89	170	0.02	0.56§
Orange IV	A; 1(N=N); 1(NaSO ₃)	400	1100	0.24	0.88
Orange II	A; 1(N=N); 1(NaSO ₃)	86	31	0.55	0.82
Phloxine	A	110	36	0.08	0.96
Primulin Yellow	A; 1(NaSO ₃)	150	72	0.00	0.22
Rhodamine B	C	980	1600	0.03	1.00
Rosaniline HCl	C; TPM	420	2200	0.01	1.00
Safranin O	C	64	240	0.01	1.00
Toluidine Blue D	C	110	140	0.01	0.99
Tropaeolin O	A; 1(N=N); 1(NaSO ₃)	61	16	0.65§	0.77
Victoria Blue R	C; TPM	750	2500	0.00	1.00
Amaranth	A; 1(N=N); 3(NaSO ₃)	1.3	0.2	0.94§	0.07
Amido Naphthol Red G	A; 1(N=N); 2(NaSO ₃)	3.7	0.4	0.93	0.20
Aniline Blue Black	A; 2(N=N); 2(NaSO ₃)	11	5.5	0.57	0.35
Aniline Yellow	N; 1(N=N)	4.1	1.5	0.97	0.23
Biebrich Scarlet	A; 2(N=N); 2(NaSO ₃)	34	20	0.44	n.d.§
Bordeaux Red	A; 1(N=N); 2(NaSO ₃)	5.0	15	0.78	0.40
Chicago Blue	A; 1(N=N); 2(NaSO ₃)	7.2	8.3	0.06	0.00
Fuchsin acid	A; TPM; 3(NaSO ₃)	43	12	1.00	0.21
Fast Green FCT	A; TPM; 3(NaSO ₃)	2.1	0.8	1.00	0.53
Indigo Carmine	A; 3(NaSO ₃)	7.4	3.6	0.82	0.10
Light Green SF	A; TPM; 3(NaSO ₃)	6.0	2.7	0.99	0.48
Mordant Blue 29	A; TPM; 1(NaSO ₃)	30	49	0.93	0.89
Naphthol Yellow S	A; 1(NaSO ₃)	59	17	0.95	0.47
Orange G	A; 1(N=N); 3(NaSO ₃)	2.1	0.2	0.99	0.48
Patent Blue	A; TPM; 2(NaSO ₃)	20	13	0.90	0.75
Ponceau 3R	A; 1(N=N); 2(NaSO ₃)	8.0	4.9	0.82	0.40
Ponceau S	A; 2(N=N); 4(NaSO ₃)	0.5	0.5	0.96	0.06
Tartrazine	A; 1(N=N); 2(NaSO ₃)	0	0	0.97	0.08§
Trypan Blue	A; 2(N=N); 4(NaSO ₃)	6.6	5.3	0.28	0.01
Wool Green S	A; TPM; 2(NaSO ₃)	42	23	0.94	0.58
Xylene Cyanol FF	A; TPM; 2(NaSO ₃)	15	1.9	0.94	0.75§
Alizarin Red S	A	160	90	0.77	0.58
Picric acid	A	260	150	0.95	0.74

*A, anionic dye; C, cationic dye; N, neutral dye; TPM, triphenylmethane dye; N=N, phenyl-N=N-phenyl moiety.

†n-Butanol-ethanol-water (50:15:10 v/v).

§TLC shows more than one band.

Each sorption experiment was run for 6 hr with 0.1 g of powdered foam and 10 ml of test solution; n.d. = not determined.

Table 2. Sorption from water and from 50% methanol*

Dye	Water medium, <i>D</i> , l./kg		50% Methanol medium, <i>D</i> , l./kg	
	Polyether	Polyester	Polyether	Polyester
Bordeaux Red	5.0	15	19	14
Ethyl Violet	1800	9400	28	190
Gentian Violet	800	8500	23	67
Mordant Black 11	200	350	650	1400
Naphthol Yellow S	59	17	20	20
Picric Acid	260	150	240	130
Patent Blue	20	13	53	12
Rosaniline HCl	420	2200	20	33
Victoria Blue R	750	2500	30	170

*Dye solutions (10 ml) were shaken for 6 hr with 0.1 g of powdered foam.

Malachite Green (320, 970); Fuchsin Basic (150, 2000); Rosaniline HCl (420, 2200)] whereas the more polar triphenylmethane dyes all have sulphonate groups and much smaller distribution coefficients [Light Green SF (6.0, 2.7); Fast Green FCT (2.1, 0.8); Patent Blue (20, 13); Wool Green S (42, 23); Xylene Cyanole FF (15, 1.9); Fuchsin Acid (43, 12); Mordant Blue 29 (30, 49)]. The sorption of the more polar dyes decreases in general as the number of sulphonate groups, and thus the polarity, increases. Although these results support a solvent extraction mechanism, there are some inconsistencies. For example, Gentian Violet, although more polar than Victoria Blue R, is much more strongly sorbed on polyester foam. Also, as a group, the more non-polar triphenylmethane dyes are more highly sorbed by polyester than by polyether-type polyurethane foam, which is opposite to the effect expected, since the polyester foam is more polar⁴ and should show less affinity for non-polar dyes. In addition, the more polar triphenylmethane dyes appear to be somewhat better sorbed by polyether than by polyester foam.

Additional support for a solvent extraction mechanism is shown in Table 2, for dyes sorbed from water and from 50% aqueous methanol solution, by both polyester and polyether foams. The non-polar dyes (Ethyl Violet, Gentian Violet, Rosaniline HCl and Victoria Blue

R, which are all triphenylmethane dyes with no sulphonate or other polar groups) showed a significant decrease in sorption from the methanol solution, indicating the increased affinity of these dyes for the more non-polar solution. For the more polar dyes containing polar groups such as SO₃, NO₂, or OH, the sorption remained approximately the same from both solutions, except for Mordant Black 11, which showed a large increase in sorption from the methanol solution. This increase is consistent with a solvent extraction mechanism with the dye being less soluble in the more non-polar solution, but since Mordant Black 11 has a polarity similar to the other more polar dyes in Table 2, there is no obvious reason for only this dye showing an increase in sorption from the methanol solution.

It can also be considered whether or not the foam is analogous to the corresponding liquid solvent, assuming ethyl acetate to be equivalent to the polyester and diethyl ether to the polyether in terms of sorption ability. Although this would not be completely true because the polyurethanes are not completely homogeneous materials, whereas the liquid extractants are, a reasonable comparison is still possible since the effect of an ether or an ester should play a major role and the helical form of the poly(ethylene oxide) in the polyether foam apparently⁴ plays an integral role in the mechanism for the

Table 3. Comparison of sorption by foam, with solvent extraction

Dye	Foam sorption, <i>D</i> , l./kg		Solvent extraction, <i>D</i>	
	Polyether	Polyester	Diethyl ether	Ethyl acetate
Bordeaux Red	5.0	15	0	0
Eosin Y	410	81	*	5.1
Ethyl Violet	1800	9400	0.1	0.2
Mentanyl Yellow Orange MNO	430	580	0	0
New Methylene Blue	89	170	0.1	0.1
Rhodamine B	980	1600	11.3	33.0
Tartrazine	0	0	0.1	0.1

*100% extraction.

sorption of several species. A difference in the rate of sorption should be the only major difference, with the liquid solvent-extraction reaching equilibrium quite rapidly, owing to the better contact between the phases. Dyes with various efficiencies of sorption by foam were tested for efficiency of solvent extraction. A 10-ml portion of the aqueous dye solution was shaken for 2 min with 10 ml of either diethyl ether or ethyl acetate, then the absorbance of the aqueous solution was compared with the original value and the distribution coefficient was calculated. The results are given in Table 3. Dyes that were sorbed poorly by the foam (Tartrazine and Bordeaux Red) were also poorly extracted by either solvent. However, New Methylene Blue and Mentanil Yellow Orange MNO, which are reasonably well sorbed by the foams, were found to be barely extracted by either liquid solvent. Ethyl Violet has a very high distribution coefficient with foam but is only slightly extracted by the solvents, whereas Rhodamine B has medium sorption by the foams and the highest extraction into the liquid solvents, of all the dyes tested. Therefore these results do not support the hypothesis of a simple solvent extraction mechanism.

In normal solvent extraction, D values range from 20 to 1000. The occurrence, in foam sorption, of D values exceeding 1000 suggests that some sort of ion-exchange process might be operative. A possible mechanism for the sorption of anionic species is the cation chelation mechanism previously reported.⁴ If this mechanism were predominant for the sorption of dyes, then "anionic" dyes (*i.e.*, those capable of acid dissociation) would be sorbed more efficiently in the presence of potassium and lithium salts than from pure water. Also, as noted by Hamon *et al.*,⁴ the presence of the potassium ion should facilitate sorption more than the lithium ion does, owing to the better fit of this ion into the central cavity of the oxygen-rich helix in the polyether foam. The sequence of selectivity expected⁷ is that found with an 18-crown-6, *i.e.*, $\text{Li}^+ < \text{Na}^+ < \text{Cs}^+ < \text{Rb}^+ < \text{K}^+ \approx \text{NH}_4^+$. Bromocresol Purple, a dye with two hydroxyl groups, was found to be sorbed better from 0.02M potassium chloride than from 0.02M lithium chloride and better from both than from water.

Classifying the dyes according to the scheme given by Gurr,⁸ we found that generally cationic dyes are sorbed better by polyester than by polyether foam, while anionic dyes are better

sorbed by polyether foam. This latter observation is consistent with the cation chelation mechanism but does not by itself explain why one dye is more efficiently sorbed than another by the same foam type. Any specific sorption efficiency must be based on the structure, geometry and properties of the particular dye.

To classify the various dyes according to polarity, they were chromatographed on a cellulose TLC plate, with either water or a mixture of *n*-butanol-ethanol-water (50:15:10) as the mobile phase; the results are shown in Table 1. The use of water as the mobile phase gave results which generally mimicked the foam-water sorption system. The dyes that are sorbed best by polyurethane foam had low R_f values, *i.e.*, were highly partitioned into cellulose, and conversely, dyes that are poorly sorbed had R_f values that approached 1.00. In the mixed-solvent mobile phase, the opposite occurred; dyes that were sorbed poorly by the foam had low R_f values and dyes that showed high sorption had high R_f values. In general, if the R_f value in the mixed solvent was greater than that in water, the foam distribution coefficient was found to be greater than 30-40. If the magnitudes of the R_f values were in the opposite order to this, the foam distribution coefficient would be less than 40. In Table 1 the dyestuffs are classified into these two groups (and listed in alphabetical order) except for the two compounds at the end, which do not fit the general observation. From these results it is apparent that the polarity of the dye plays a major role in its sorption by polyurethane foams. This conclusion is supported by the lack of correlation between the distribution coefficients for the polyurethane also shown in Table 1 and the presence of specific functional groups such as NO_2 , OH , $\text{C}=\text{O}$, COOH/COONa , $\text{SO}_3\text{H}/\text{SO}_3\text{Na}$ or $-\text{N}=\text{N}-$. Thus it appears that the polarity of the dye molecule is more important than the presence of any particular functional group.

The lack of reproducibility in the sorption experiments created some difficulties in these studies. Originally cylindrical plugs of foam were used, but to improve the precision, later experiments used the homogenized, powdered foam. This technique improved the reproducibility for five parallel experiments to better than $\pm 10\%$ for both foam types. Although considerable efforts were made to improve the precision still further, they were unsuccessful. Some of the inconsistency may be due to the dyes, which

were assumed to be pure enough to be used without additional purification. Thin-layer chromatography later indicated the presence of two or more species of varying relative concentrations for ten of the dyes, as indicated in Table 1. In any case the dye solutions themselves were homogeneous and any impurities should be the same in each sample of the individual dye, which would permit this study to be useful. Some dyes were found to be unstable in aqueous solution and thus are not reported here.

All the dye solutions used were very dilute, ranging from 10^{-4} to $10^{-5}M$. These low concentrations increase the difficulty of the experiments as there was some evidence of adhesion of the dye to vessel surfaces, including that of the spectrophotometric cells; this causes interfering losses of dye from solution and necessitates a strict cleaning regime for the cells, with dilute acid. In addition, many of the dyes are indicators and therefore pH-sensitive, especially in dilute solution. Because some of the dyes were sorbed at a pH within their transition range, a slight change in pH during the sorption would have considerably more effect on the results than it would with Alizarin or picric acid, which have transition ranges outside those used for the sorption.

The rate and duration of sorption was also studied for many of the dyes in Table 1, with aqueous solutions. Trials of 10, 30 and 60 min and 3, 6, 12 and 24 hr showed that the sorption increased for up to 24 hr for some dyes, although in most cases no significant changes occurred after 3 hr. During these times there were no appreciable changes in the pH of the sample solutions. No significant trends relating dye structure and sorption time required were observed.

The sorption of dyes by polyurethane foams shows some support for both the solvent extrac-

tion and cation chelation mechanisms and cannot be explained solely by either. The polyurethane foam available is not a pure material and usually contains a variety of reagents and additives to enhance its commercial use. Although considerable care was taken to remove any loosely-held organic and inorganic substances, the resulting product must still be considered to have somewhat uncertain structure and composition. Fortunately, for most species the sorption is consistent and the major mechanisms for the process can be examined by a variety of techniques. Further work is still necessary to clarify why different mechanisms can predominate, or to develop an overall mechanism. If the sorption process can be clarified for organic compounds, developments could be made more easily in the useful applications of polyurethane foams.

Acknowledgements—The authors wish to acknowledge the financial support of the University of Manitoba, the Province of Manitoba CareerStart program and the Natural Sciences and Engineering Research Council of Canada. They also acknowledge the valuable assistance of Dr. D. M. McKinnon in discussions of dye structures.

REFERENCES

1. H. J. M. Bowen, *J. Chem. Soc. A*, 1970, 1082.
2. G. J. Moody and J. D. R. Thomas, *Chromatographic Separation and Extraction with Foamed Plastics and Rubbers*, Vol. 21, Dekker, New York, 1982.
3. T. Braun, J. D. Navratil and A. B. Farag, *Polyurethane Foam Sorbents in Separation Science*, CRC Press, Boca Raton, 1985.
4. R. F. Hamon, A. S. Khan and A. Chow, *Talanta*, 1982, **29**, 313.
5. L. Schumack and A. Chow, *ibid.*, 1987, **34**, 957.
6. T. Tanaka, K. Hiroy and A. Kawahara, *Bunseki Kagaku*, 1973, **22**, 523.
7. J. J. Christensen, D. J. Eatough and R. M. Izatt, *Chem. Rev.*, 1974, **74**, 351.
8. E. Gurr, *Synthetic Dyes in Biology, Medicine and Chemistry*, Academic Press, London, 1971.

THE RAMESES ALGORITHM FOR MULTIPLE EQUILIBRIA—II

SOME FURTHER DEVELOPMENTS

B. W. DARVELL and V. W.-H. LEUNG

Dental Materials Science Unit, University of Hong Kong, Prince Philip Dental Hospital,
34 Hospital Road, Hong Kong

(Received 12 June 1989. Accepted 25 October 1989)

Summary—The algorithm RAMESES has been made more efficient by incorporation of additional procedures: to extrapolate to the next point by an exact polynomial of any desired order, to control the gain on the adjustment of each independent species, and to optimize the initial guess. The need to consider electroneutrality is emphasized, and some problems with convergence criteria and synthetic test systems are discussed. Some conditions for objective algorithm testing are proposed.

Recently, we reported¹ the development of the algorithm RAMESES, a rapid algorithm for solution of multiple equilibrium systems. This procedure offered some advantages over previously published routines in that the structure of the program was simple, the algebraic basis being particularly clear in matrix terms, and that a number of problems noted with other procedures simply did not arise.

Having gained some experience of the application of RAMESES, we report some procedures now incorporated which enhance performance. The notation will be that of the earlier report, and the equations therein are referred to by the prefix "1.". Some results are presented to illustrate these additions, and tests using previously described examples are reported.

TERMINOLOGY

In some published work there is a labelling convention which may present some confusion in that it contains an element of illogicality, *viz.* only complexes are termed "species".^{2,3} In the present work, as before,¹ the term species refers to any and all possible types of entity in solution, thus including uncomplexed ions or molecules. "Components" are taken as being chemical entities, without regard to sign of charge, from which all species are considered to be formed. Thus, Al^{3+} , AlOH^{2+} , H^+ , and H_2O are all "species"; whereas $[\text{Al}]$, $[\text{H}]$, and $[\text{OH}]$, are the corresponding components. Like-

wise, the use of imaginary species such as " AlH_{-3} "^{2,3} to represent " $\text{Al}(\text{OH})_3$ " is an unnecessary complication (despite an algebraic equivalence), with potential for error. It certainly does not add to the clarity of exposition of examples.

FORWARD EXTRAPOLATION

For simplicity, the initial guess for vector \mathbf{X}_A in equation (1.1) for all but the first point of a scan in one variable of a system was taken as the value of that vector in the previous solution, a common procedure.⁴⁻⁶ Clearly, there is some scope for refinement of this, and an extrapolation to the next point based on more than one previous value is a logical way to utilize the information contained in those values.

De Robertis *et al.*² claimed to have done this in their equation (6) for a second-order extrapolation. Unfortunately, incorporation of this in RAMESES gave no improvement whatsoever in the run time for the program, even if the extrapolation were done in terms of vector \mathbf{P}_A , the logarithmic form of \mathbf{X}_A . This might have been expected to be more effective, because the logarithmic concentrations of many species change nearly linearly over large regions of a scan. However, the algebraic basis of their equation is not clear, and no source was cited. Nevertheless, from first principles, it is easy to write down the series of polynomial equations for equally spaced points, needed to predict the next point in the sequence. Indicating by a

negative subscript how far back in the sequence from the desired point the previous solution lies, we have for the predicted logarithmic concentration p_0 :

Order,

$$\begin{array}{l}
 b \\
 0 \quad p_0 = 0 \\
 1 \quad p_0 = p_{-1} \\
 2 \quad p_0 = 2p_{-1} - p_{-2} \\
 3 \quad p_0 = 3p_{-1} - 3p_{-2} + p_{-3} \\
 4 \quad p_0 = 4p_{-1} - 6p_{-2} + 4p_{-3} - p_{-4} \\
 5 \quad p_0 = 5p_{-1} - 10p_{-2} + 10p_{-3} - 5p_{-4} + p_{-5}
 \end{array}
 \left. \vphantom{\begin{array}{l} b \\ 0 \\ 1 \\ 2 \\ 3 \\ 4 \\ 5 \end{array}} \right\} (1)$$

and so on (the zero on the right-hand side of the zero-order equation must be read as "no information" rather than a "guess" of zero, which would of course give an all-zero result). The coefficients are those of the expansion of $(1-a)^b = 0$, *i.e.*, binomial, where b is the order of the extrapolation, that is, the number of points used for the prediction. Such extrapolation is exact for a curvature of degree $(b-1)$ with $b \geq 2$, and therefore gives prediction errors of order h^{b-1} if h is the stepping interval. Most benefit is expected when d^2p/dh^2 is large; conversely, no deterioration in performance should result when $d^2p/dh^2 \rightarrow 0$, although the calculation may be redundant for an extrapolation equation of order $b > 2$.

On the other hand, since the polynomials above are exact, the accuracy of the predicted point is dependent on the accuracy of the points used for its estimation. In general, a tolerance $\epsilon > \sim h^{b-1}$ implies wasted effort in the extrapolation. In other words, the expectation might be that the optimum order is given by an equation such as:

$$b = \frac{\log \epsilon}{\log h} + 1 \quad (2)$$

Despite the obvious advantage of such a prediction strategy, it is nevertheless important to optimize the algorithm for the zero-order "blind" calculation, that is, when only a guess can be made for the elements of the initial \mathbf{X}_A , because in the absence of prior information the overall calculation speed with extrapolation may depend primarily on that guess. The robustness of an algorithm will in part be measured by its ability to handle such blind calculations. Equally, the optimization of the initial guess requires attention, but this clearly must be a general procedure and not one which depends on any kind of special knowledge of the system, otherwise there would be a rever-

sion to the preparatory exploration previously discommended.¹

Some algorithms have employed the total concentrations as the initial guesses for the uncomplexed species:⁴⁻⁶

$$\mathbf{X}_{A(1)} = \mathbf{T} \quad (3)$$

It is easy to see that all dependent species concentrations thus calculated must be high, so the initial evaluation of \mathbf{S} [equation (1.12)] is also high. This overshoot may be extremely large, and require drastic correlation at the next iteration, with the possibility of initial instability, and this has been observed in some tests of RAMESES. Here, no formal initial guess was required,¹ because of the lack of sensitivity to this variation. COMPLX⁷ also used arbitrary input, but no comment was made.

OSCILLATION

The kernel of the RAMESES algorithm is the solution of the r dependent, linear simultaneous equations [equation (1.7)], whence the errors in the component total are calculated, and the next guess for \mathbf{X}_A is refined. Although this is not easy to visualize in detail, it is clearly possible that a correction may result in an overshoot, which in turn leads to a correction back to the original estimate. Such oscillation depends on the particular concentrations of components at the time, and the exact values of the K values used, and in principle can arise whatever value is used for the damping factor f [equation (1.14)], and with any estimation procedure. Essentially, such behaviour is a property of the (arbitrary) rule used for the next estimate. Changing the rule changes the region for that behaviour. Some systems have been observed to contain regions where such oscillation leads to many hundreds of iterations being required for a solution, even of moderate accuracy. Inspection showed that such nearly-stable oscillating solutions of equation (1.7) could readily be destabilized and made to converge on a proper solution by perturbing any of the oscillating elements of \mathbf{X}_A . In addition, many systems, in converging rapidly to a proper solution, do so by oscillating, albeit in a highly damped manner, and possibly only for one or a few of the elements of \mathbf{X}_A .

This observation provides the opportunity for dynamic optimization of the factor f [equation (1.14)] previously suggested and its introduction for controlling the effect of each other element of \mathbf{F} [equation (1.16)]. Thus, since a change of

direction of approach to a required component total T_i implies overshoot, as above, and therefore that the corresponding F_{ii} [equation (1.13)] departs from unity by too great an amount, we introduce the (diagonal) gain matrix, \mathbf{G} ($t \times t$). This matrix is set initially equal to the identity matrix, \mathbf{I} , and an element is adjusted downwards whenever an over- or undershoot occurs in the corresponding component total. Then equation (1.16) becomes:

$$\mathbf{X}_{A(n+1)} = [\mathbf{G}(\mathbf{F} - \mathbf{I}) + \mathbf{I}]\mathbf{X}_{A(n)} \quad (4)$$

[\mathbf{F} must be preserved as defined in equation (1.13) in order that the tolerance test of equation (1.15) can be performed properly.] The adjustments in the elements of \mathbf{G} must necessarily be arbitrary, and the gain increment g needs to be chosen so that

$$G_{ii(n+1)} = G_{ii(n)}(1 - g) \quad (5a)$$

when a change of direction occurs. Equally, when a change of direction does not occur, the gain can safely be increased:

$$G_{ii(n+1)} = G_{ii(n)}(1 + g) \quad (5b)$$

This then has the effect of tending to cause oscillation if it is not already occurring, but always ensures that on average a more appropriate G_{ii} is adopted.

The following symbolic program fragment illustrates the implementation of these ideas. $Xa2$ is the estimated independent vector from the previous operation, Xa is the present vector, and SGN is the BASIC function for returning the algebraic sign of an expression:

```
FOR i = 1 TO r
  xsign2(i) = xsign1(i)
  xsign1(i) = SGN(Xa(i) - Xa2(i))
  IF xsign1(i) < > xsign2(i) THEN
    Xa(i) = (Xa(i) + Xa2(i))/2
    G(ii) = G(ii) * (1-g)
  ELSE
    G(ii) = G(ii) * (1 + g)
  END IF
NEXT i
```

Clearly, this can only be applied after the third iteration. It is designed to be sensitive only to the oscillating elements, as any more general procedure tends to retard convergence by upsetting well-behaved elements. This procedure permits the abandonment of the less efficient conditional adjustment represented by equations (1.17)–(1.19).

\mathbf{G} may be viewed as reflecting the perturbation sensitivity of each element X_A . Thus, if h is not too large, it might be expected that the values of G_{ii} would be good approximations to the values needed for the next point to be evaluated, thus improving the convergence efficiency, particularly if forward extrapolation is used.

TOLERANCE

The convergence of RAMESES was tested¹ by the condition:

$$|F_{ii} - 1| < \epsilon, \quad \text{all } i \quad (6)$$

COGS⁴ used the perhaps more exact, but essentially equivalent

$$\left| \frac{T_i - S_i}{T_i} \right| < \epsilon, \quad \text{all } i \quad (7)$$

(in the present notation). Both of these ensure accuracy by requiring that any error greater than the tolerance forces a further iteration, no matter how well the other concentrations have been determined.

As well as a form equivalent to (7), HALTAFALL⁸ had an option to set a tolerance on each individual total:

$$|T_i - S_i| < \epsilon_i, \quad \text{all } i \quad (8)$$

This seems to require prior knowledge, in some sense, of the importance of a component; it is therefore considered an impractical general criterion.

EQUIL,⁶ the unrelated EQUIL,⁹ and MULTIREACTIONEQUILIBRIUM¹⁰ all required that all concentration shifts be less than the specified tolerance:

$$\left| \frac{X_{i(n)} - X_{i(n-1)}}{X_{i(n)}} \right| < \epsilon, \quad \text{all } i \quad (9)$$

This perhaps places too much reliance on the rate of convergence being proportional to the actual error, a property which seems not to have been demonstrated. However, COMPLX⁷ and COGSNR⁵ employed a criterion of the form:

$$\sum_i^r \left| \frac{X_{Ai(n)} - X_{Ai(n-1)}}{X_{Ai(n)}} \right| < \epsilon \quad (10)$$

which allows, say, one large error if the remainder are very small. Clearly, if this is not tested for, the results for the set of dependent species could be greatly misleading.

Taking this a stage further, the routine ESTIME³ used:

$$\frac{\sum(T_i - S_i)^2}{\sum T_i^2} \leq \epsilon \quad (11)$$

Clearly, in the presence of a large concentration of one component, for which the calculated total error may even be zero, any other error is correspondingly diluted in its effect on the summation. The errors in all related species concentrations will be nearly proportional to one another, and therefore potentially highly misleading. Indeed, any non-interacting background species required for charge balance or ionic strength adjustment (where relevant) would automatically suppress errors unless special precautions were built in.

It is thought that conditions (6) and (7) are intrinsically more reliable criteria for convergence, even though more iterations for a given solution are required, as they set maximum permissible proportional errors for all species simultaneously.

CHARGE BALANCE

An important aspect of the solution of an equilibrium system is electroneutrality, which should be self-evident. It was incorporated in RAMESES [in equations (1.10) and (1.14)] as an integral part of the procedure. It is surely somewhat negligent to omit such detail in the consideration of a scan of, say, pH, if the means of achieving that scan is ignored. If for no other reason, this check is demanded by the need to know whether a certain combination of concentrations can exist, yet we find no mention of this consideration in most published procedures. Thus, ES4EC,² ESTIME,³ COGS,⁴ COGSNR,⁵ EQUIL,⁶ and HALTAFALL,⁸ all fail even to mention charge, although this would not affect their ability (in principle) to return correct answers for all species other than the one scanned (other limitations have already been reported¹). COMPLEX⁷ is the only other reported routine known to take electroneutrality into account, but it, too, has weaknesses.¹

For the relatively simple problem of the distribution of species in an analytically determined system, which therefore exists *de facto*, such a consideration may not seem to matter. Yet the calculation of the distribution depends, ultimately, on the activity of each species, which in turn is a function of the ionic strength of the medium. If, as has been found in some scans

performed with RAMESES and should be apparent from elementary estimates, large concentrations of the "free" ion are necessary for charge balance, then non-negligible effects of ionic strength must be present, and therefore severe interference with the calculated concentrations. Conversely, a charge excess of the same sign as the charge of the free species categorically implies non-existence.

There is however a different type of problem in which charge balance cannot be ignored; that is, when the notionally "titrant" free species is involved in the equilibria of the system (typically in the case of weak acids or bases, but in general where any complex is formed). Plainly, it is impossible to ignore charge balance in this circumstance as there is no other information available to determine the solution of the problem. Indeed, solubility-product work may demand such an approach.

There are, then, classes of problem important to solution chemistry (and other equilibria, by extension) which may not be tackled correctly by most existing algorithms. We can only conclude that it is, at best, dangerous to ignore the condition of electroneutrality; at worst, such algorithms would be unserviceable.

Given, then, that it is possible to establish non-existence of a system on electroneutrality grounds, it is necessary to test for this condition. RAMESES achieves this very simply by setting a lower limit to the concentration of the "free" species (X_j), such as $10^{-25}M$, after a minimum number of iterations, say 10. This causes an exit from the main algorithm, having set a flag to indicate the condition of non-existence. The boundary for the physically possible region is thus readily identified without resorting to "timeout" or error trap routines as a matter of course.

With the introduction of the oscillation control mentioned above, an improvement can be made to the charge-balance calculation: the two-column matrix \mathbf{Q} [equation (1.9)] is replaced by the equivalent vector \mathbf{Q} ($s \times 1$) where:

$$Q_i = z_i \quad (12)$$

z being the sign and charge of the species as before. Then, the charge error Δ is given by:

$$\Delta = \mathbf{X}^T \mathbf{Q} \quad (13)$$

so equation (1.14) becomes:

$$F_{ij} = \left\{ 1 - \frac{\Delta}{X_{Aj} z_j} \right\} \quad (14)$$

where j designates the "free" species being used for charge balance. This is less conservative than before, but the use of the dynamic gain factor G_{jj} as in equation (3) provides the necessary control.

GAS EQUILIBRATION

In some closed systems, the (total) concentrations of dissolved gases may be predetermined, and consequent species distributions found directly from the existing algorithm. However, when the system is to be equilibrated with a gas or gas mixture, the system is in effect open, with fixed partial pressures. An example of such a system is saliva in contact with expired air, where the equilibria involving CO_2 are particularly important in buffering.

In RAMESES, it is then simply a matter of requiring that the partial pressure of the dissolved gas (which must equal the partial pressure in the equilibrated atmosphere) remain constant, by setting the corresponding element of \mathbf{F} to 1 instead of to the correction factor implied by equation (1.13). This is achieved by testing a flag at that point to make the appropriate decision.

ZERO CONCENTRATIONS

A minor programming matter, but one of considerable importance in practical applications, especially for interactive use on "personal" computers, is that of handling zero concentrations. As required for linearization of the equilibrium equations, the calculations are done in terms of logarithmic concentrations [equation (1.5)] and log zero (which is $-\infty$) cannot be defined on the computer. However, by replacement of zero by the smallest possible positive machine number, EPS, such that the machine's versions of $\log_{10}(\text{EPS})$ and of 10 raised to the power of $\log_{10}(\text{EPS})$ [see equation (1.8)] both return allowable values, the calculation may proceed without detriment to the accuracy of the required concentrations (the machine would have to have a peculiarly small dynamic range for this to be otherwise). However, it is obvious that a calculated $\log(\text{concentration})$ may still be less than $\log_{10}(\text{EPS})$, so that taking the antilog returns a (true) machine zero. This condition is readily trapped for the next iteration by using EPS in the conversion expression, thus (in BASIC):

$$\text{Pa}(i) = \text{LGT}(\text{Xa}(i) + \text{EPS})$$

The effect of including a component can thus be readily tested by switching its presence "on" and "off" without having to redefine the system.

TESTING

The language used for comparative work was QuickBasic V4.0 (Microsoft Corp., Redmond, WA, USA), running in the development environment, *i.e.*, uncompiled, on an 80286/80287 machine (AST Premium 286, AST Research Inc., Irvine, CA, USA) running at 10 MHz. Results were displayed graphically on an EGA colour monitor, from which a graphics-screen dump to printer could be made. The distribution diagrams given here were redrawn from such prints.

A series of preliminary tests of RAMESES were conducted to examine the effect of varying the initial guess. The form used was:

$$X_{A_i(1)} = aT_i, \quad \text{all } i \neq k \quad (15)$$

where k corresponded to the scanning species (such as H^+), over the range of a from 1 to 10^{-25} . The general effect was to decrease execution time as a was decreased, with erratic behaviour at large values, but levelling off at a minimum for $a < \sim 10^{-15}$. An arbitrary choice of $a = 10^{-20}$ was made. No problems have been detected in its general use.

The gain increment g [equations (5a) and (5b)] was tested over the range 0.01–0.25 during development of the present procedures. As might be expected, small values were relatively inefficient in that the rate of adjustment was slower, and large values led to a risk of instability. Over the range 0.025–0.15 there was little more than random variation in timing, or of maximum or minimum numbers of iterations. The RAMESES algorithm is thus essentially insensitive to such variation, and the value $g = 0.05$ was adopted for further work.

A series of tests was made to find whether in equations 5(a) and 5(b) the gain and damping could be separately optimized. The outcome was that the same value of g should be used in both cases.

Previously,¹ it was suggested that the elements of \mathbf{F} be given a default value of 0.01 or 0.001, when the calculated value was negative. The effect of this lower limit was examined. The conclusion was that no practical problems arise from setting very low values; indeed, running was appreciably faster the smaller the value adopted, down to about 10^{-15} , below which the

levelled out. Again, an arbitrary choice of 10^{-20} was adopted as a practical working value. No upper limit for the elements of F has been found necessary so far.

Considerable effort has been expended in comparison of the speed of computations of the present kind as a function of machine, language, machine precision, and whether or not the program was compiled and by what compiler.³ This seems to be a somewhat fruitless pursuit, as developments in programming languages, compilers, and especially processors occur regularly and with great frequency. Clock speeds in particular are rising at impressive rates. In a sense, the speed at which a calculation can be made depends primarily on the user's access to a fast machine. Attention would perhaps be better directed to making an algorithm reliable, robust and efficient, and its implementation, the program, reflect these properties. The importance of such ideas has been amply stated,¹¹ and motivates the present development work.

EXAMPLES

To test RAMESES, and in particular the effect of the oscillation detector and the forward extrapolation procedures, several systems were used. As has been argued,³ there is a need for a standard test system which would enable the comparison of algorithms. Accordingly, the proposed synthetic system ESTIME,³ and four earlier examples (Systems I-IV)² were used for direct comparisons with RAMESES. In each case, however, because of the use of the ES4EC algorithm in the earlier work,^{2,3} no charge information was then reported. This provides no

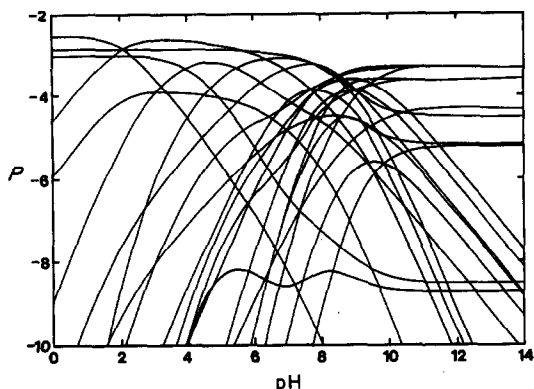


Fig. 1. Log (concentration), P , vs. pH for the synthetic system ESTIME, condition a. Background "NaCl" omitted. Some species do not appear, because their concentrations are too low; identifications are omitted as the system is of no intrinsic value.

great difficulty for real systems, as the species are clearly identifiable, but for synthetic systems arbitrary arrangements have to be made. Further, in each system a nominal non-interacting ionic background has to be added (e.g., Na^+ , Cl^-) in order that the implicit "titration" of the required pH scan be performed in RAMESES. This implies that each system thus tested is larger by 2 species, and therefore involves a little more computation, although without affecting the other species in any way.

In testing these examples, the following were considered:

(i) run time vs. order of extrapolation for tolerances of 10^{-10} – 10^{-3} ;

(ii) run time vs. tolerance at zero-order extrapolation (i.e., no extrapolation);

(iii) number of iterations vs. pH for the zero-order extrapolation.

For (ii) and (iii), G was reset equal to I at each step. The species distribution diagrams were also examined. For the extrapolation order tests, the following procedure was necessary: for k points already evaluated, when the required b was > 1 and $k < b$, then a temporary $b^* = k$ was used for extrapolation in order to utilize continuously the full information available at each stage.

ESTIME

Containing two principal metals and one ligand in 35 equilibria, this was believed to be a representative system.³ The species distribution diagram is given in Fig. 1, and the results of the three tests are shown in Figs. 2–4. Some other results for all five suggested conditions (in order, a – e) are given in Table 1.

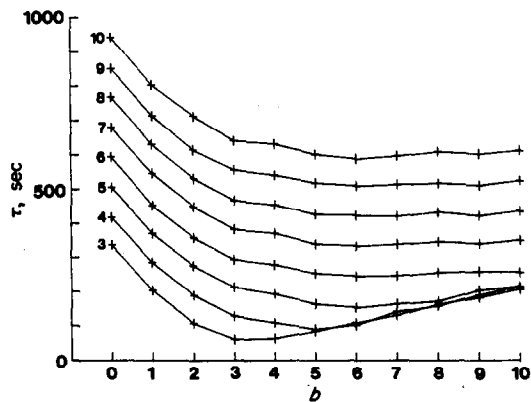


Fig. 2. Run time, τ , vs. extrapolation order, b ; $-\log \epsilon = 3$ – 10 (ϵ = tolerance), for the system ESTIME, condition a. pH: 2.0–9.75, step 0.25.

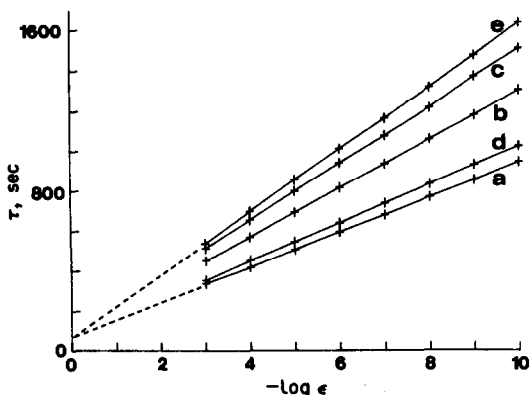


Fig. 3. τ vs. $-\log \epsilon$ for the five test conditions proposed for the system ESTIME: $b = 0$. pH: 2.0-9.75, step 0.25.

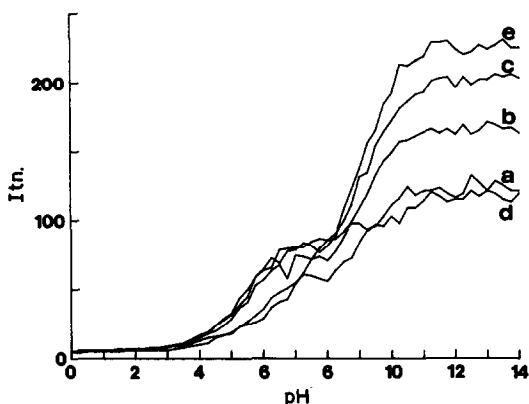


Fig. 4. Number of iterations required for solution (Itn.) vs. pH for the five test conditions proposed for ESTIME; $b = 0$.

System I

Dealing only with the hydrolysis of aluminium, this system was thought² to offer various problems that would test the robustness of algorithms. The distribution diagram is given in

Table 1. Some illustrative results for the test systems discussed, running in RAMESSES. pH: 0-14, step 0.25, $b = 0$, $-\log \epsilon = 3$

System	τ , sec	Iterations			
		Max.	Min.	Mean	
ESTIME	a	815.7	132	4	59.0
	b	1092.1	171	5	79.2
	c	1287.4	206	5	93.4
	d	817.8	121	5	59.2
	e	1403.3	231	5	101.9
I	a	11.9	9	2	3.0
	b	11.9	9	2	3.0
	c	22.1	5	4	5.0
II	475.1	111	5	72.7	
III	429.6	8	5	7.4	
IV	80.8	5	5	5	

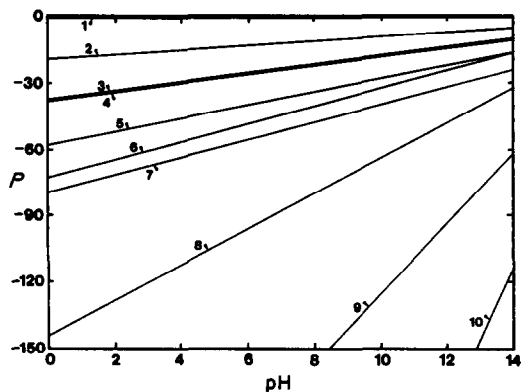


Fig. 5. P vs. pH for System I, the hydrolysis of aluminium, total $[Al] = 3.7 \times 10^{-5} M$ (condition a). Background "NaCl" omitted. Key: 1. $[Al^{3+}]$, 2. $[AlOH^{2+}]$, 3. $[Al(OH)_2^+]$, 4. $[Al(OH)_3]$, 5. $[Al(OH)_4^-]$, 6. $[Al_2(OH)_2^{4+}]$, 7. $[Al_3(OH)_4^{5+}]$, 8. $[Al_4(OH)_6^{8+}]$, 9. $[Al_7(OH)_{16}^{13+}]$, 10. $[Al_{13}(OH)_{32}^{17+}]$.

Fig. 5, and the results of test (i) in Fig. 6. Only the first of the three conditions suggested² was used, because the differences between them (in order, a-c) were insignificant (Table 1).

System II

This involved K^+ , Cu^{2+} and Ni^{2+} with citrate in 18 equilibria for one set of total concentrations. With both polynuclear and mixed complexes present, this system contains enough interaction between species for it to pose a reasonable challenge to the algorithm. The distribution diagram is given in Fig. 7. Run-time test (i) results are given in Fig. 8, test (iii) results in Fig. 9.

System III

In comparing 75 equilibria for a mixture of 10 organic acids and three metals, this system

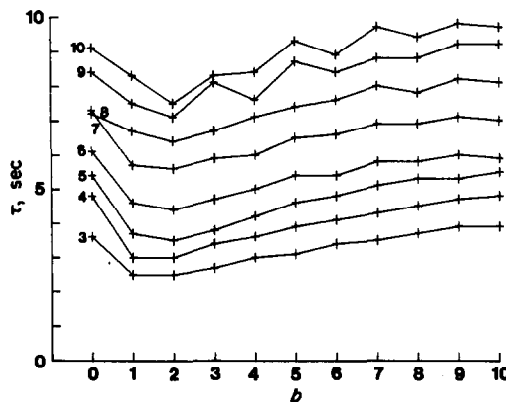


Fig. 6. τ vs. b , $-\log \epsilon = 3-10$, for System I, total $[Al] = 3.7 \times 10^{-5} M$. Machine-timer rounding errors give apparent conflict at $-\log \epsilon = 7$ and 8 , $b = 0$.

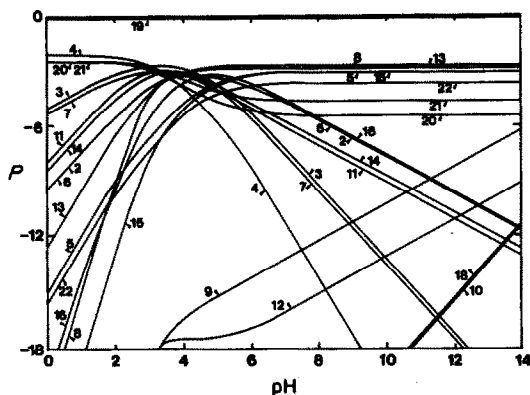


Fig. 7. P vs. pH for System II, $K^+/Cu^{2+}/Ni^{2+}/citrate^{3-}$. Key: species numbers as in original report,² plus: 19, $[K^+]$; 20, $[Cu^{2+}]$; 21, $[Ni^{2+}]$; 22, $[citrate^{3-}]$.

offered the challenge of size. A partial distribution diagram is given in Fig. 10, and test (i) timing results in Fig. 11. Between five and eight iterations were needed for solution over the pH range 0–14 at $b = 0$.

System IV

This was another synthetic system, dealing with the hydrolysis of 6 metals, 35 equilibria, and involving polynuclear species. The distribution diagram is given in Fig. 12, and the test (i) result in Fig. 13. For $b = 0$, five iterations were uniformly required for solution over the pH range 0–14.

DISCUSSION

None of the test systems above caused any problem with RAMESES. In terms of run time, τ , ESTIME was the most difficult to solve but this was not unreasonable, given the obvious high degree of interaction between species. Even so, it is apparent from Fig. 4 that the difficulty

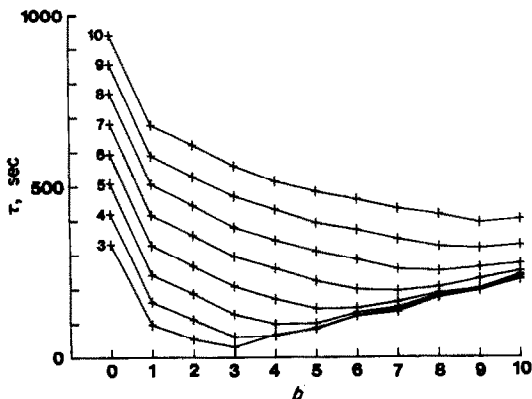


Fig. 8. τ vs. b , $-\log \epsilon = 3-10$, for System II; pH: 3.0–9.0, step 0.15.

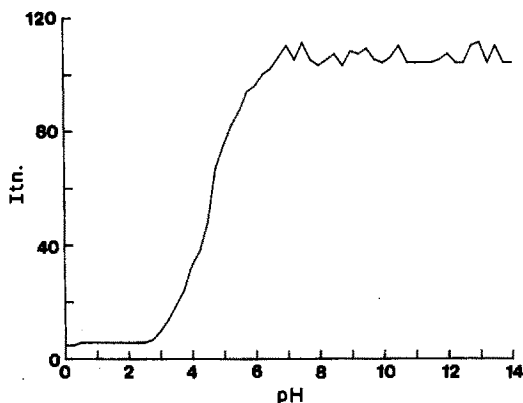


Fig. 9. Itn. vs. pH for System II; $b = 0$.

arises only at high pH, mostly beyond the range previously tested,³ but dependent on the actual (relative) component concentrations.

Also, run time depended linearly on \log (tolerance) (Fig. 3), *i.e.*, each further digit of precision required the same increment in τ , with little “overhead” as judged from the extrapolation to the (meaningless) $\epsilon = 1$. (Very erratic results were obtained in tests for $\epsilon \gg 10^{-3}$, as might be expected, but see below.)

This relationship, of τ and $\log \epsilon$, also applied generally to each system tested, and for each value of b (but with some variation, as discussed below). The variation of τ with ϵ seems not to have been considered previously. It is therefore proposed that reports of such algorithm testing specifically include a description of the relationship between τ and ϵ .

The form of tolerance criterion previously used for ESTIME,³ equation (11), was tested

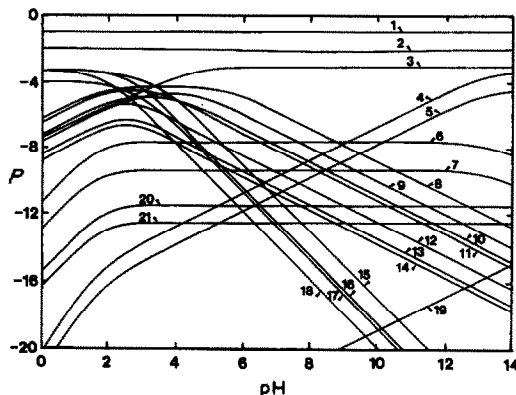


Fig. 10. P vs. pH for selected species for System III. Background “NaCl” omitted. Key: 1. $[K^+]$, 2. $[Ca^{2+}]$, 3. $[ac^-]$, 4. $[his^-]$, 5. $[CaHis^+]$, 6. $[HHis]$, 7. $[CaHHis^{2+}]$, 8. $[KHmale]$, 9. $[NaHmala]$, 10. $[CaHtart^+]$, 11. $[CaHoda^+]$, 12. $[Hsucc^-]$, 13. $[NaHsucc]$, 14. $[CaHsucc^+]$, 15. $[H_2 tart]$, 16. $[H_2 succ]$, 17. $[H_2 oda]$, 18. $[H_3 his^{3+}]$, 19. $[CaOH^+]$, 20. $[gly^-]$, 21. $[Cagly^+]$ (abbreviations as reported²).

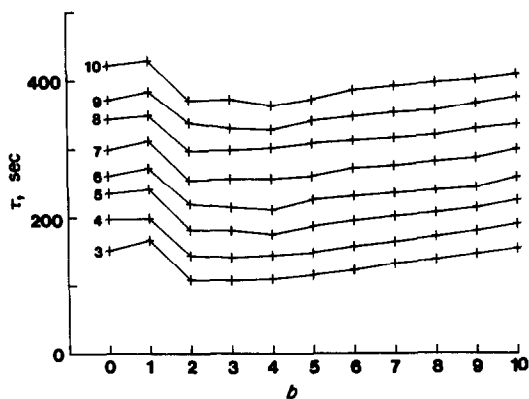


Fig. 11. τ vs. b , $-\log \epsilon = 3-10$, for System III; $\text{pH} = 1.0-10.5$, step 0.5.

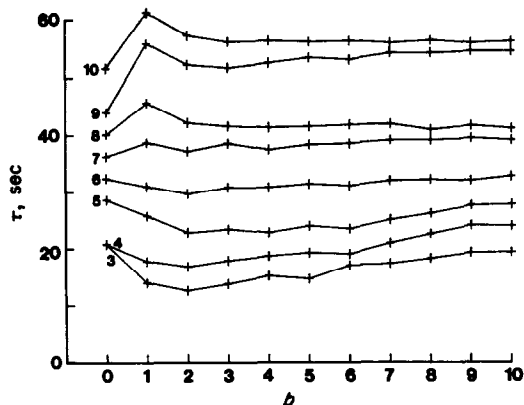


Fig. 13. τ vs. b , $-\log \epsilon = 3-10$, for System IV; $\text{pH} = 3.5-10.0$, step 0.5.

now for condition a with a limit of 10^{-7} (as used before³), with $1M \text{Cl}^-$ added. The run time for $\text{pH} 0-14$ (step 0.25), $b = 0$, was 660 sec, the maximum, minimum, and mean number of iterations being 101, 2, and 46.9 respectively. On comparing this with the data in Table 1, and noting the form of Fig. 3, it is clear that the criterion is both weak and unreliable, and gives a false sense of algorithm speed. For this reason, the timing results obtained before^{2,3} cannot be properly interpreted, despite the efforts then made to define rules for comparison.³ The proper inclusion of charge balance now increases the difficulty.

A particular and rather strange property of the ESTIME system was the "titration" curve represented by the total of $[\text{Na}^+]$ required for charge balance: it showed a local maximum for two of the conditions, c and e (Fig. 14). Although this was not a large feature, it does seem to indicate that the system is physically unrealistic. The charge numbers chosen for the

uncomplexed metals and the ligand were each 2; this set was optimal in the sense of avoiding what seemed to be inappropriately large charges of, for example, ± 7 , for some species, when what might otherwise be thought to be a reasonable charge number of 3 was introduced for one or more of these. That the effect was not due to calculation errors was shown by the persistence of the feature at very small tolerance ($\epsilon = 10^{-8}$).

This effect appears to imply that for a certain range of compositions, three distinct pH values may be exhibited. If such a system were to exist, it would seem to challenge some basic tenets of solution chemistry. It may be concluded that there are subtle dangers in "synthetic" problems of this kind. However, a bigger problem would be that when the pH was to be determined, a single-value solution would not be possible under some circumstances. The algorithm would fail, but only because of the design of the test system.

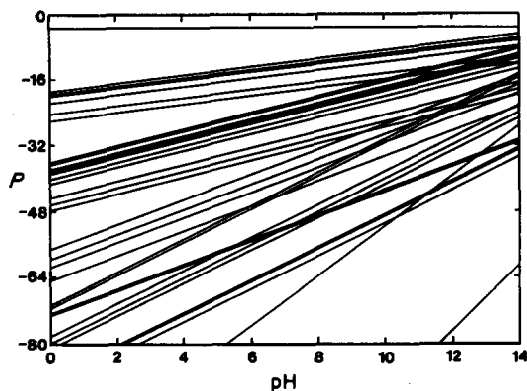


Fig. 12. P vs. pH for synthetic System IV. Background "NaCl" omitted. Identifications omitted as the system is of no intrinsic value.

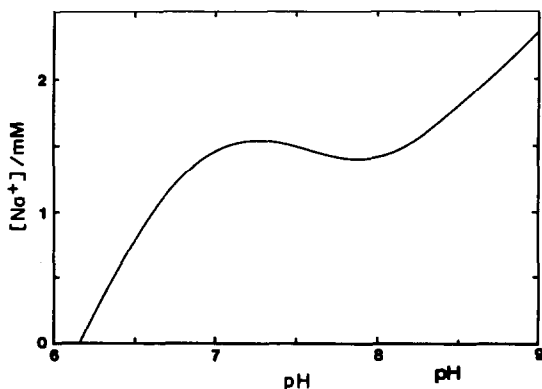


Fig. 14. Calculated titration curve for ESTIME system, condition e (arbitrary zero).

The solution of System I is essentially trivial, as is apparent from the distribution diagram (Fig. 5). The elementary direct calculation would yield a proportional error of less than 10^{-4} in all species, at the worst, at pH 14. It is therefore somewhat peculiar that algorithms EQUIL⁶ and COMICS⁴ (which used COGS) were reported to have failed.² Nevertheless, though it can be problematic for such procedures, it provides a good vindication of the RAMESES algorithm, notwithstanding the fact that the majority of species are essentially non-existent over the entire range of pH.

System II was also reported² to have failed with the algorithm COMICS,⁴ but ran without difficulty now. However, the species distribution diagram for it (Fig. 7) bears only some similarities to that previously published (Fig. 2 in de Robertis *et al.*²), the discrepancies being substantial for a number of species. For example, $[\text{Cu}_2(\text{cit})_2\text{OH}^{3-}]$ (species 9, $\log \beta = 11.9$)² at about pH 4.3 was given as accounting for about 30% of the citrate. The present result for this species is about 10^{-10} % of the total citrate. This may be compared with species 8, $[\text{Cu}_2(\text{cit})_2^-]$ ($\log \beta = 15.28$), for which the corresponding amount of citrate is about 3% of the total. It does not seem possible, given the β values, for these species to have these relative proportions at that pH. The situation for species 10, $[\text{Ca}_2(\text{cit})_2\text{OH}_2^{4-}]$ ($\log \beta = 6.66$), is even worse. Hence, it is apparent that the previous result cannot be correct. No reason for the error can be surmised with the available information, but clearly ES4EC² must be carefully re-examined to remove whatever bug has caused this problem. No attempt has been made to do that now.

System III presented no difficulties, despite its size. The distribution diagram (Fig. 10) shows the results for only a selection of species, as the similarities in the β values gave many sets of superimposed and parallel lines. All types of behaviour are illustrated, however. That size alone is not *per se* a challenge for RAMESES is illustrated by the very few iterations required for solution (Table 1), far fewer than for System II.

System IV is also an essentially trivial problem as there is negligible interaction between species.

The forward extrapolation procedure was of most benefit when a large number of iterations was required for solution (ESTIME and System II, Figs. 2 and 8). The tendency for τ to decrease with increasing b is clearest for System II, and the minimum very nearly keeps step with

b , as expected. This effect is still present for the ESTIME system, but is rather weak for $-\log \epsilon > \sim 5$. For $b \gg -\log \epsilon$, the benefit of extrapolation is offset by the lever effect of the errors in the p_i used for the calculation, and limiting values for τ are observed.

For Systems III and IV, the first-order extrapolation could give timings worse than $b = 0$: this emphasizes the greater efficiency of the adopted rule of $\mathbf{X}_{A_i(1)} \rightarrow 0$ [equation (15)] than even "reasonable" guesses, on average. For the trivial systems, I and IV, there was negligible benefit, if any, from employing $b > 2$, as predicted.

Overall, if a single value of b is to be chosen, most benefit is obtained with $b = 3$, given that there is in general little point in using $-\log \epsilon > \sim 4$, as this is the typical limit of precision of the equilibrium constants. Equally, for the more difficult systems, such as ESTIME and System II, there is a clear benefit in using larger values of b for the extrapolation. Even so, and notwithstanding the improvements that can be obtained by forward extrapolation, the better test of an algorithm is the zero-order calculation.

It may be noted that the pH ranges previously employed^{2,3} for the test systems described above were variable, with the limits having no obvious significance. In view of the absence of physical reasons (declared or deducible) for those limits, such as those dictated by fixing the concentrations of background species and the identity of the "free" species, the systems were re-examined for the pH range 0–14 in order to cover better the possible chemical gamut (Table 1). The timing results presented are only illustrative (being peculiar to the particular machine, language, and so on, of the implementation), but the iteration results are a more general measure of performance, both in the sense of efficiency discussed above and for comparison between systems. However, it is suggested that any algorithm needs to be demonstrated to function over all possible conditions. As can be seen from Figs. 4 and 9, RAMESES was successful in dealing with this increased range.

If objective testing of equilibrium algorithms is valuable, as we believe, a number of guidelines for it should be followed.

(i) Range—pH 0–14 (or more, if the system warrants it) or the equivalent for any other relevant variable; the region of the distribution

diagram in which the solution lies has a major bearing on the outcome.

(ii) Order— $b = 0$; a well-behaved procedure should be able to handle any starting conditions successfully.

(iii) Tolerance test—the worst case should be used rather than any average; interpretation is otherwise difficult, and results unreliable.

(iv) Tests should be made of (a) number of iterations *vs.* pH [for example, see (i) above]; (b) τ *vs.* ϵ ; (c) τ *vs.* b for a given ϵ .

The specification of an algorithm for this kind of work should include electroneutrality as a condition. Figures 1–4 represent typical results of the minimum tests and conditions listed above. More work is required to identify a suitable general test-system or range of systems. Sheer size is not relevant, but synthetic systems must be designed with great care if they are to be valid. RAMESES, meanwhile, has demonstrated speed, robustness, and precision.

Acknowledgements—Part of this work was done in partial fulfilment of the degree of Ph.D. for one of us (V.W.-H.L.) at, and supported by, the Faculty of Dentistry, University

of Hong Kong. We are grateful to the referees for helpful remarks in refining this report.

REFERENCES

1. V. W.-H. Leung, B. W. Darvell and A. P.-C. Chan, *Talanta*, 1988, **35**, 713.
2. A. de Robertis, C. de Stefano and S. Sammartano, *Anal. Chim. Acta*, 1986, **191**, 385.
3. C. de Stefano, P. Princi, C. Rigano and S. Sammartano, *Comput. Chem.*, 1988, **12**, 305.
4. D. D. Perrin and I. G. Sayce, *Talanta*, 1967, **14**, 833.
5. I. G. Sayce, *ibid.*, 1968, **15**, 1397.
6. Ting-Po I. and G. H. Nancollas, *Anal. Chem.*, 1972, **44**, 1940.
7. K. J. Johnson, *Numerical Methods in Chemistry*, p. 226. Dekker, New York, 1980.
8. N. Ingrì, W. Kakolowicz, L. G. Sillén and B. Warnqvist, *Talanta*, 1967, **14**, 1261; *errata*, 1968, **15**, No. 3, ix.
9. M. Bos and H. Q. J. Meershoek, *Anal. Chim. Acta*, 1972, **61**, 185.
10. P. Benedek and F. Olti, *Computer-Aided Chemical Thermodynamics of Gases and Liquids*, Wiley, New York, 1985.
11. W. J. Cody, *Lect. Notes. Math.*, 1975, 506.

Note. In the first paper¹ of this series, reference 12 was inadvertently omitted; it would have been the same as reference 5 above.

THE RAMESES ALGORITHM FOR MULTIPLE EQUILIBRIA—III

ACCELERATION AND STANDARDIZED FORMATION CONSTANTS (RAMESES II)

V. W.-H. LEUNG and B. W. DARVELL

Dental Materials Science Unit, University of Hong Kong, Prince Philip Dental Hospital,
 34 Hospital Road, Hong Kong

(Received 26 June 1989. Accepted 25 October 1989)

Summary—By the use of a matrix-algebra identity, the algorithm RAMESES for solution of systems of equilibrium equations may be modified to reduce both computer storage requirements and execution time. As a result, standardized formation constants and solubility products are found. This may facilitate compilation of such data in uniform style. An illustrative example is given.

The algorithm RAMESES for the solution of multiple equilibrium systems has already been reported¹ and certain aspects of its programming made more efficient.² In referring to the first report,¹ equation numbers will be identified by the prefix "1".

The importance of work on computational methods for speciation problems has recently been emphasized,³ but as has been pointed out,⁴ there have been difficulties in minimizing the two principal variables of the computation process: storage requirements for the coefficient matrix, C , and the execution time, τ . These appear to make conflicting demands on the programming, and require some decision to be made regarding computational strategy.⁴ That such a decision requires prior knowledge or an arbitrary rule is an unfortunate aspect, but either way the solution is not very elegant. We report now an algebraic identity which simultaneously minimizes both variables for RAMESES in its current implementation, and which provides two useful side-results: the calculation of standardized formation constants, and an extension to solubility products. An illustrative example is given.

NUMERICAL METHOD

The solution of the equilibrium equations to determine the logarithmic concentrations of the r dependent species is given by equations (1.6) and (1.7), *i.e.*,

$$P_B = C_B^{-1}(L - C_A P_A) \quad (1)$$

This may be expanded to give

$$P_B = C_B^{-1}L - (C_B^{-1}C_A)P_A \quad (2)$$

Multiplying through by C'_B gives

$$C'_B P_B = C'_B(C_B^{-1}L) - C'_B(C_B^{-1}C_A)P_A \quad (3)$$

but if $C'_B = C'_B^{-1} = I$, *i.e.*, if the equations are those of direct formation from the independent species, corresponding to

$$L'_i = \log(\beta_i) \quad (4)$$

where the transformed matrices are denoted by the prime, we would have:

$$I P_B = I(L') - I(C'_A)P_A \quad (5)$$

which is identically

$$P_B = L' - C'_A P_A \quad (6)$$

when

$$L' = C_B^{-1}L \quad (7)$$

and

$$C'_A = C_B^{-1}C_A \quad (8)$$

With the exception of the previous¹ conventional treatment of OH^- and H^+ ,

$$C'_A \equiv -M_B \quad (9)$$

where, by reference to equation (1.11),

$$M = \begin{bmatrix} M_A \\ M_B \end{bmatrix} \quad (10)$$

and the matrix M_A ($t \times t$) is

$$M_A = I \quad (11)$$

The independent species may be chosen to be identified with the corresponding uncomplexed species, although from the algebra this is not a necessary condition, merely one of logical convenience.

SOLUBILITY PRODUCTS

By use of the matrix notation, the ion products for a given set of expected solids may be simply written. Now, let us construct a multiplicity matrix \mathbf{N} ($s \times u$) for the u solids to be tested. Then, if the logarithmic solubility products are held in \mathbf{H} ($u \times 1$), and \mathbf{P} is the logarithmic concentration vector

$$\mathbf{P} = \begin{bmatrix} \mathbf{P}_A \\ \mathbf{P}_B \end{bmatrix} \quad (12)$$

[see equations (1.5) and (1.7)], inspection of the elements of \mathbf{W} ($u \times 1$)

$$\mathbf{W} = \mathbf{H} - \mathbf{N}^T \mathbf{P} \quad (13)$$

indicates whether any solubility product has been exceeded. In this manner, it is of no consequence how the solubility product is expressed.

The solubility product data may be transformed in an exactly similar manner to the equilibrium constants above. We construct the augmented coefficient matrices, denoted by the asterisk, \mathbf{C}_A^* [$(r+u) \times r$], \mathbf{C}_B^* [$(r+u) \times (r+u)$] and $\log K$ vector \mathbf{L}^* ($r+u \times 1$) as follows:

$$\mathbf{C}_A^* = \begin{bmatrix} \mathbf{C}_A \\ \mathbf{N}_A \end{bmatrix} \quad (14)$$

$$\mathbf{C}_B^* = \begin{bmatrix} \mathbf{C}_B & 0 \\ \mathbf{N}_B & \pm \mathbf{I} \end{bmatrix} \quad (15)$$

$$\mathbf{L}^* = \begin{bmatrix} \mathbf{L} \\ \mathbf{H} \end{bmatrix} \quad (16)$$

where in \mathbf{C}_B^* the upper right matrix is null, *i.e.*, empty, and the sign ambivalence of the lower right submatrix reflects the possibility of use of either solubility products (negative sign) or their inverse, the solid "formation" constants (positive sign), (or, indeed, any mixture of these).

It follows immediately from equations (7) and (8) that

$$\mathbf{C}_A^{*'} = \mathbf{C}_B^{*-1} \mathbf{C}_A^* \quad (17)$$

and

$$\mathbf{L}^{*'} = \mathbf{C}_B^{*-1} \mathbf{L}^* \quad (18)$$

However, we may note that

$$\begin{bmatrix} \mathbf{C}_B & 0 \\ & \pm \mathbf{I} \end{bmatrix}^{-1} = \begin{bmatrix} \mathbf{C}_B^{-1} & 0 \\ & \pm \mathbf{I} \end{bmatrix} \quad (19)$$

irrespective of the contents of the lower left submatrix. Therefore, since

$$\mathbf{C}_B^{*-1} \cdot \begin{bmatrix} \mathbf{L} \\ \mathbf{H} \end{bmatrix} = \begin{bmatrix} \mathbf{L}' \\ \mathbf{H}' \end{bmatrix} \quad (20)$$

and

$$\mathbf{C}_B^{*-1} \cdot \begin{bmatrix} \mathbf{C}_A \\ \mathbf{N}_A \end{bmatrix} = \begin{bmatrix} \mathbf{C}_A' \\ \mathbf{N}_A' \end{bmatrix} \quad (21)$$

if $\mathbf{C}_B \equiv \mathbf{I}$, that is, \mathbf{L}' and \mathbf{C}_A' are already known from equations (7) and (8), then

$$\begin{bmatrix} \mathbf{I} & 0 \\ \mathbf{N}_B & \pm \mathbf{I} \end{bmatrix}^{-1} = \begin{bmatrix} \mathbf{I} & 0 \\ & \pm \mathbf{I} \end{bmatrix} \quad (22)$$

i.e., \mathbf{N}_B is left unchanged. Therefore

$$\mathbf{H}' = [\mathbf{N}_B \pm \mathbf{I}] \cdot \begin{bmatrix} \mathbf{L}' \\ \mathbf{H} \end{bmatrix} \quad (23)$$

and

$$\mathbf{N}_A' = [\mathbf{N}_B \pm \mathbf{I}] \cdot \begin{bmatrix} \mathbf{C}_A' \\ \mathbf{N}_A \end{bmatrix} \quad (24)$$

In other words, when the solution equilibrium equations are already in the β form, the solubility data may be similarly recalculated without having to resort to a further matrix inversion. Equation (13) may therefore be replaced by

$$\mathbf{W} = \mathbf{H}' - \mathbf{N}_A'^T \mathbf{P}_A \quad (25)$$

for determining whether any solid should form, so that the size of the required matrix multiplication is substantially reduced, which is most beneficial when the system is large, and few solids are to be considered.

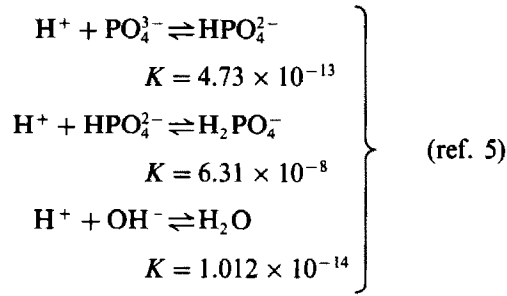
EXAMPLES

A number of test systems have been run previously to examine the efficiency of an implementation of RAMESES.² These same systems have now been re-run to find out how much computational acceleration equation (6) would provide (the details of these systems have already been given²). The results are given in Table 1. The gain is relatively modest for small, simple systems such as System I, but substantial when a larger number of iterations at each point is required, more than doubling the speed for System III.

Table 1. Timing comparisons for some test systems with RAMESES and RAMESES II (pH 0-14, step 0.25; $b = 0$; $-\log \epsilon = 3$).

System	Run time, τ , sec		
	RAMESES	RAMESES II	
ESTIME	a	815.7	428.5
	b	1092.1	578.2
	c	1287.4	686.8
	d	817.8	433.2
	e	1403.3	742.0
I	a	11.9	10.9
	b	11.9	10.9
	c	22.1	16.7
II		475.1	354.2
III		429.6	182.6
IV		80.8	51.4

The aqueous calcium phosphate system is used as an example of the use of equations (17) and (18), and the problem of the comparison of reported solubility products for hydroxyapatite is treated. The following are taken as representative values.



$$\frac{[\text{Ca}^{2+}]^5[\text{HPO}_4^{2-}]^3}{[\text{H}^+]^4} = 7.24 \times 10^{-4} \quad \text{(ref. 6)}$$

$$\frac{[\text{Ca}^{2+}]^5[\text{PO}_4^{3-}]^3[\text{OH}^-]}{=} = 4.7 \times 10^{-59} \quad \text{(ref. 7)}$$

$$\frac{[\text{Ca}^{2+}]^{10}[\text{H}_2\text{PO}_4^-]^6[\text{OH}^-]^2}{[\text{H}^+]^{12}} = 4.0 \times 10^3 \quad \text{(ref. 8)}$$

The input data are as follows:

$$\mathbf{L} = \begin{bmatrix} -12.325 \\ -7.200 \\ -13.995 \end{bmatrix}$$

$$\mathbf{H} = \begin{bmatrix} -3.140 \\ -58.328 \\ -3.602 \end{bmatrix}$$

$$\mathbf{X}_A = \begin{bmatrix} \text{Ca}^{2+} \\ \text{PO}_4^{3-} \\ \text{H}^+ \end{bmatrix}$$

$$\mathbf{X}_B = \begin{bmatrix} \text{OH}^- \\ \text{H}_2\text{PO}_4^- \\ \text{HPO}_4^{2-} \end{bmatrix}$$

$$\mathbf{C}_A = \begin{bmatrix} 0 & 1 & 1 \\ 0 & 0 & 1 \\ 0 & 0 & 1 \end{bmatrix}$$

$$\mathbf{C}_B = \begin{bmatrix} 0 & 0 & -1 \\ 0 & -1 & 1 \\ 1 & 0 & 0 \end{bmatrix}$$

$$\mathbf{N}_A = \begin{bmatrix} 5 & 0 & -4 \\ 5 & 3 & 0 \\ 10 & 0 & -12 \end{bmatrix}$$

$$\mathbf{N}_B = \begin{bmatrix} 0 & 0 & 3 \\ 1 & 0 & 0 \\ 2 & 6 & 0 \end{bmatrix}$$

so that

$$\mathbf{C}_B^* = \left[\begin{array}{ccc|ccc} 0 & 0 & -1 & 0 & 0 & 0 \\ 0 & -1 & 1 & 0 & 0 & 0 \\ 1 & 0 & 0 & 0 & 0 & 0 \\ \hline 0 & 0 & 3 & -1 & 0 & 0 \\ 1 & 0 & 0 & 0 & -1 & 0 \\ 2 & 6 & 0 & 0 & 0 & -1 \end{array} \right]$$

Then,

$$\mathbf{C}_B^{*-1} = \left[\begin{array}{ccc|ccc} 0 & 0 & -1 & 0 & 0 & 0 \\ -1 & -1 & 0 & 0 & 0 & 0 \\ -1 & 0 & 0 & 0 & 0 & 0 \\ \hline -3 & 0 & 0 & -1 & 0 & 0 \\ 0 & 0 & 1 & 0 & -1 & 0 \\ -6 & -6 & 2 & 0 & 0 & -1 \end{array} \right]$$

and

$$\mathbf{L}^{*'} = \begin{bmatrix} -13.995 \\ 19.525 \\ 12.325 \\ \hline 40.116 \\ 44.333 \\ 85.559 \end{bmatrix}$$

$$C_A^{*'} = \begin{bmatrix} 0 & 0 & 1 \\ 0 & -1 & -2 \\ 0 & -1 & -1 \\ \hline -5 & -3 & 1 \\ -5 & -3 & 1 \\ -10 & -6 & 2 \end{bmatrix}$$

Equations (23) and (24) may be readily confirmed as yielding the lower half of $L^{*'}$ and $C_A^{*'}$ respectively.

An important point to notice is that the order of the L_i' in L' is that of the species in X_B , because these are now formation constants in the β sense.

Then, given that the third solubility product was expressed in terms of the unit cell formula, *i.e.*, twice that of the others, either the coefficients in N_B (but not $\pm I$) may be adjusted, by division by 2, or the resultant $\log \beta$ values can be treated similarly. We thus find that the quoted K_{sp} values for hydroxyapatite are discrepant, with a range of some 4 orders of magnitude.

DISCUSSION

In terms of computation, once L' and C_A' have been found, C_B^{-1} can be erased, as the matrix multiplication corresponding to equation (1.7) is not then required. Thus, for large systems, the storage requirements may be substantially reduced because C_B and C_B^{-1} are now reduced to temporary matrices, but more significantly the time-consuming multiplication of the very sparse matrix C_B^{-1} is eliminated from the iterative procedure altogether. In addition, the entry of the data for the multiplicity matrix M is obviated, as this is now directly calculable for any choice of independent species.

For extremely large systems, of course, the problems of storage space still remain for the inversion of C . It is, however, beyond the scope of the present report to deal with such a purely machine-dependent programming problem: solutions are to be found in standard libraries of matrix routines. However, if the equations are already all expressed in terms of β values, the procedures represented by equations (7) and (8), as well as the inversion of C , are unnecessary, and both space and time are further reduced. In addition, formation constants may be found in more manageable groups by using the above

procedures, and the full system assembled subsequently, when the inversion routine may again be bypassed.

In this context, it is noteworthy that a number of reported procedures seem to rely on the use of solution-species β formation constants^{3,9-12} as input. In fact, given the confused presentation of such data in the literature, with association, dissociation, stepwise, and more complicated forms being used, such procedures would ordinarily require much preparatory work to calculate, essentially manually, each input constant if not immediately available. In contrast, the RAMESES algorithm¹ has no restriction on input format; all manner of reaction statement styles can be accommodated by the algebra, so long as due notice is taken of the signs of the coefficients which represent the reactions. Systems may therefore be assembled from several sources without the need for prior conversion into a standardized format, with obvious advantages. The present development does not alter or diminish those advantages, but rather adds to them.

The algebra above may be employed directly and deliberately for the computation of standardized formation constants and the inter-conversion of the many different kinds of expression (according to how the components are defined). It would also facilitate the routine compilation and organization of such data in a standardized format, a move long overdue in our view, despite recognition of the need for it,¹³ although the labour involved may be excessive. It would seem that a convention needs to be formally adopted. We offer this point for consideration, suggesting that these constants primarily be in terms of free ions or non-dissociable component molecules only, and using $[H^+]^{-1}$ in place of $[OH^-]$ (noting that this implies that $[H^+]$ would appear as a divisor in the equilibrium statement, and not that the species composition itself would be represented as being formed by the abstraction of hydrogen ions, when this is physically unrealistic²).

In like manner, we are of the opinion that the same should be done in respect of the solubility product, a term which does not adequately reflect its definition, and which is defined indeed in a sense opposite to its intended function and already described as illogical.¹⁴ It should, perhaps, and more informatively, be called the saturation product. Thus, we incline to the view that the conditions for the formation of a solid are of primary interest in the majority of

circumstances and therefore that the relevant K should be defined by:

$$K = \frac{\{\text{solid}\}}{\prod \{\text{component } i\}} \quad (26)$$

where the numerator is the conventional unit activity. This makes K a formation constant, in line with that of solution species, as outlined above. The value of such an approach and definition has already been discussed.^{13,14}

The RAMESES algorithm has thus been extended in its scope to determine standardized formation constants, both for solution species and solids, whilst substantially accelerating the calculation of species distribution diagrams and the checking of solubility limits. This extended algorithm we have named RAMESES II. The fact that these extensions can be expressed in succinct matrix—algebra terms maintains the procedural clarity of the original algorithm, which again may offer some benefits in the teaching of the subject of equilibria.

Acknowledgement—Part of this work was done in partial fulfilment of the degree of Ph.D. for one of us (V.W.-H.L.) at, and supported by, the Faculty of Dentistry, University of Hong Kong.

REFERENCES

1. V. W.-H. Leung, B. W. Darvell and A. P.-C. Chan, *Talanta*, 1988, **35**, 713.
2. B. W. Darvell and V. W.-H. Leung, *ibid.*, 1990, **37**, 413.
3. J. R. Duffield and D. R. Williams, *Chem. Brit.*, 1989, **25**, 375.
4. A. de Robertis, C. de Stefano and S. Sammartano, *Anal. Chim. Acta*, 1986, **191**, 385.
5. E. Högfeldt, *Stability Constants of Metal-Ion Complexes, Part A, Inorganic Ligands*, Pergamon Press, Oxford, 1982.
6. Y. Ericsson, *Acta Odont. Scand.* 1949, **8**, Suppl. 3, 67.
7. G. H. Nancollas, in *Environmental Phosphorus Handbook*, E. J. Griffith (ed.), Chap. 2, Wiley, New York, 1973.
8. P. Vieillard and Y. Tardy, *Environmental Phosphorus Handbook*, E. J. Griffith (ed.), Chap 4, Wiley, New York, 1973.
9. K. J. Johnson, *Numerical Methods in Chemistry*, p. 226. Dekker, New York, 1980.
10. D. D. Perrin and I. G. Sayce, *Talanta*, 1967, **14**, 833.
11. I. G. Sayce, *ibid.*, 1968, **15**, 1397.
12. C. de Stefano, P. Princi, C. Rigano and S. Sammartano, *Comput. Chem.*, 1988, **12**, 305.
13. D. Dyrssen, D. Jagner and F. Wengelin, *Computer Calculation of Ionic Equilibria and Titration Procedures*, p. 38. Almqvist & Wiksell, Stockholm, 1968.
14. R. A. Chalmers, *Aspects of Analytical Chemistry*, Chap. 2, Oliver & Boyd, Edinburgh, 1968.

SOLVENT EXTRACTION BEHAVIOUR OF LANTHANUM(III), CERIUM(III), EUROPIUM(III), THORIUM(IV) AND URANIUM(VI) WITH 3-PHENYL-4-BENZOYL-5-ISOXAZOLONE

A. JYOTHI and G. N. RAO

Department of Chemistry, Indian Institute of Technology, New Delhi-110016, India

(Received 24 September 1988. Revised 10 August 1989. Accepted 31 October 1989)

Summary—The extraction behaviour of La(III), Ce(III), Eu(III), Th(IV) and U(VI) with 3-phenyl-4-benzoyl-5-isoxazolone (HPBI) in chloroform has been studied. The mechanism of extraction and the species extracted have been identified. Extraction constants for each system have been calculated. The system has been used to separate Th(IV) from U(VI) and from La(III), Ce(III) and Eu(III). A comparison of the extraction constants with those for the 1-phenyl-3-methyl-4-benzoyl-5-pyrazolone (HPMBP) and thenoyltrifluoroacetone (HTTA) systems indicates that HPBI extracts these metal species better than HPMBP and HTTA do.

β -Diketones, especially thenoyltrifluoroacetone (HTTA),¹ have been used extensively for the extraction of various metals. Acylpyrazolones have also been found effective for the efficient extraction of lanthanides,^{2,3} actinides^{4,5} and other metals.⁶⁻¹⁰ Recently, we have reported the extraction of manganese(II), iron(II), cobalt(II), nickel(II), zinc(II), cadmium(II) and lead(II) with 3-phenyl-4-benzoyl-5-isoxazolone (HPBI) in chloroform. HPBI is a new chelating ligand in which the β -diketone moiety is fused to the heterocyclic ring. These studies are now extended to the extraction of lanthanum(III), cerium(III), europium(III), thorium(IV) and uranium(VI). Deposits of thorium and uranium are generally associated with the rare earths. It is therefore of technological interest to make a comparative study of the solvent extraction behaviour of lanthanides and actinides so as to develop an efficient procedure for their separation and purification. In common with other β -diketones (e.g. HTTA) HPBI exists in keto and enol forms (Fig. 1). The presence of an enolic peak at $\sim\delta$ 12 ppm relative to that

of TMS in the proton magnetic resonance (PMR) spectrum of HPBI in deuteriochloroform (CDCl_3) confirms the existence of the enolic form.¹² Solid complexes of these metals with HPBI have also been isolated, and characterized by elemental analysis, and infrared and PMR spectral studies.¹² The effectiveness of HPBI in the separation of metals has also been described.

EXPERIMENTAL

Reagents

HPBI was prepared according to the method of Korte and Storiko¹³ from 3-phenyl-5-isoxazolone and benzoic anhydride and the purity was checked by elemental analysis. Analytical reagent grade chloroform was used as the solvent for extraction. Stock solutions were prepared from spectrally pure metal oxides or nitrates and were standardized by titration with EDTA or gravimetrically. The stock solutions were diluted to 30 ppm (lanthanum, cerium, europium), 20 ppm (thorium) and 50 ppm (uranium) for the extraction studies. The pH was

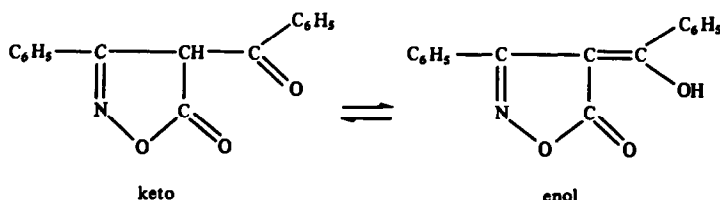


Fig. 1. The enol and keto forms of 3-phenyl-4-benzoyl-5-isoxazolone.

adjusted in the range 1–3 by appropriate addition of 1M hydrochloric acid, the ionic strength being kept constant by addition of 1M potassium chloride. For the pH range 3–6, acetic acid–sodium acetate buffers were used, with ionic strength maintained constant with potassium nitrate. All the other reagents used were of analytical reagent grade.

Apparatus

All experiments were done at $25 \pm 1^\circ$. An Elico L1-120 digital pH-meter with a compatible glass–calomel electrode assembly was used. Absorbances were measured with a Unicam SP-500 visible spectrophotometer. For extractions, 60-ml stoppered bottles and a mechanical shaker were used.

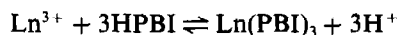
Procedure

Ten ml of aqueous phase containing an aliquot of metal solution, 5 ml of buffer solution and 1 ml of 1M potassium nitrate were shaken with an equal volume of 0.01M HPBI solution in chloroform for 1 hr. Previous studies had shown that this period is sufficient for establishing equilibrium. The organic phase was then separated and the equilibrium pH of the aqueous phase measured. The concentration of

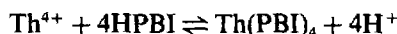
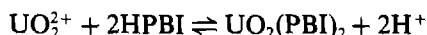
metal ion in the aqueous phase was determined spectrophotometrically with Alizarin Red-S¹⁴ for lanthanum, cerium(III) and europium(III), thoron¹⁵ for thorium and dibenzoylmethane¹⁶ for uranium(VI). Preliminary experiments established that the Alizarin Red-S reaction is very sensitive to pH, so it was necessary to destroy the acetate, the presence of which made it difficult to attain the desired pH. Five ml of the aqueous phase were heated with perchloric acid until fumes were evolved, to destroy the acetate. The residue was dissolved in distilled water and the metal determined with Alizarin Red-S.¹⁴ In some cases the organic phase was stripped with 2M nitric acid and the metal content determined. The results were used for calculating the distribution ratio, K_d .

RESULTS AND DISCUSSION

The extraction of lanthanum, cerium(III), europium(III), thorium and uranium(VI) with 0.01M HPBI in chloroform was studied as a function of pH. The results are shown in Fig. 2. The degree of extraction was found to increase with pH and became almost quantitative near the pH at which the metal ion hydrolyses. Plots of $\log K_d$ vs. pH at constant ligand concentration gave straight lines with slopes of around two for uranium(VI), three for lanthanum, cerium(III) and europium(III), and four for thorium. Similar slopes were obtained for plots of $\log K_d$ vs. $\log [\text{HPBI}]$ at constant pH. Hence the extraction systems can be represented as



for Ln = La, Ce, Eu, and



Hence,

$$\log K_{\text{ex}} = \log K_d - n\text{pH} - n\log[\text{HPBI}]_{\text{org}}$$

where K_{ex} is the extraction constant and $n = 2, 3$ and 4 for the uranium(VI), Ln(III) and Th(IV) systems, respectively. The values found for $\log K_{\text{ex}}$ are given in Table 1. Comparison of the values with those for the corresponding 1-phenyl-3-methyl-4-benzoyl-5-pyrazolone (HPMBP) and thenoyltrifluoroacetone (HTTA) systems (Table 1) indicates the superiority of HPBI, which is attributed to the lower pK_a value

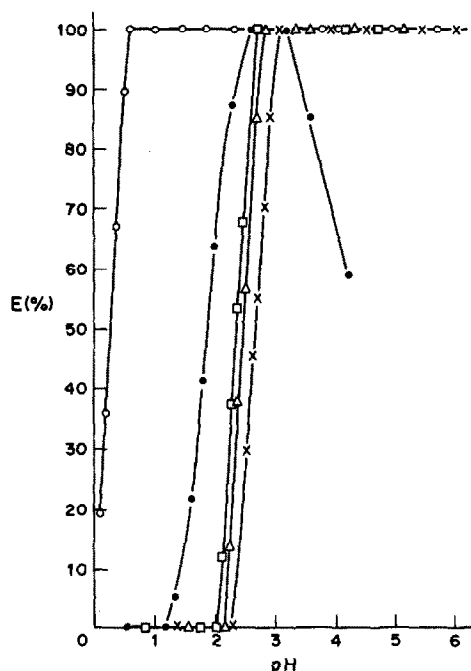


Fig. 2. Plots of degree of extraction(% E) vs. pH. \circ = Th(IV), 20 ppm; \bullet = $\text{UO}_2(\text{II})$, 50 ppm; \square = Eu(II), 30 ppm; \times = La(III), 30 ppm; \triangle = Ce(III), 30 ppm; 0.01M HPBI in chloroform.

Table 1. Comparison of log K_{ex} values of metal-HPBI, metal-HPMBP and metal-HTTA systems

Metal ion	Ligand		
	HPBI*	HPMBP ^{2,4}	HTTA ^{1,17,18}
La(III)	-1.95	-7.28	-9.90
Ce(III)	-1.20	-6.71	-9.60
Eu(III)	-1.05	-5.33	-8.99
Th(IV)	+6.92	-1.00	+1.00
U(VI)	+0.35	-1.15	-2.40

*Present work. Estimated uncertainty in the value is ± 0.1 . All results are mean values of three determinations.

of this reagent¹⁹ (1.14) compared with that of HTTA¹ (6.23) and HPMBP²⁰ (4.10).

Separations

HPBI extracts lanthanum, cerium(III) and europium(III) quantitatively at pH 3.0–6.0, uranium(VI) at pH 2.5–3.2, and thorium at pH 0.5–6. Hence it should be possible to separate thorium easily from the other four metals, in a single extraction at pH 0.5–1.0.

The extraction of uranium decreases rapidly with increase in pH above 3.2 (Fig. 2) whereas that of lanthanum, cerium and europium does not. At pH 6 there is still 25% extraction of uranium, but this could presumably be dealt with by three or four washes of the organic phase with acetate buffer of pH 6, which should remove practically all the uranium from the organic phase.

Acknowledgement—The financial assistance provided by the Council of Scientific and Industrial Research, New Delhi, India, is gratefully acknowledged.

REFERENCES

1. Y. Marcus and A. S. Kertes, *Ion Exchange and Solvent Extraction of Metal Complexes*, Wiley-Interscience, New York, 1967.
2. A. Roy and K. Nag, *J. Inorg. Nucl. Chem.*, 1978, **40**, 331.
3. Z. Kolařík, *ibid.*, 1971, **33**, 1135.
4. H. C. Arora and G. N. Rao, *Indian J. Chem.*, 1982, **21A**, 335.
5. F. T. Coronel, St. Mareva and N. Yordanov, *Talanta*, 1982, **29**, 119.
6. O. Navrátil and B. S. Jensen, *J. Radioanal. Chem.*, 1970, **5**, 313.
7. Yu. A. Zolotov and V. G. Lambrev, *Zh. Analit. Khim.*, 1965, **20**, 659.
8. G. N. Rao and H. C. Arora, *J. Inorg. Nucl. Chem.*, 1977, **39**, 2057.
9. Y. Akama, K. Sato, M. Ukaji, T. Kawata and M. Kajitani, *Polyhedron*, 1985, **4**, 59.
10. Y. Akama, K. Sato, H. Yokota and T. Nakai, *Talanta*, 1986, **33**, 288.
11. A. Jyothi and G. N. Rao, *Chem. Scr.*, 1987, **27**, 367.
12. *Idem*, *Synth. React. Inorg. Metal-Org. Chem.*, 1988, **18**, 487.
13. F. Korte and K. Störko, *Chem. Ber.*, 1961, **94**, 1956.
14. R. W. Rinehart, *Anal. Chem.*, 1954, **26**, 1820.
15. A. Mayer and G. Bradshaw, *Analyst*, 1952, **77**, 154.
16. J. H. Yoe, F. Will, III and R. A. Black, *Anal. Chem.*, 1953, **25**, 1200.
17. A. M. Poskanzer and B. M. Foreman, *J. Inorg. Nucl. Chem.*, 1961, **16**, 323.
18. T. Sekine and D. Dyrssen, *ibid.*, 1967, **29**, 1457.
19. R. H. Wiley, A. Quilico, G. Speroni, L. C. Behr and R. C. McKee, *The Chemistry of Heterocyclic Compounds*, p. 1430. Interscience, New York, 1962.
20. N. T. Sizonenko and Yu. A. Zolotov, *Zh. Analit. Khim.*, 1969, **24**, 1305.
21. Yu. A. Zolotov, *Extraction of Chelate Compounds*, p. 26. Humphrey, Ann Arbor, Michigan, 1970.

HIGHLY SENSITIVE SPECTROPHOTOMETRIC MICRODETERMINATION OF SULPHOXIDES

W. CIESIELSKI, W. JĘDRZEJEWSKI and Z. H. KUDZIN*

Institute of Chemistry, University of Łódź, Narutowicza 68, Łódź 90-136, Poland

J. DRABOWICZ

Centre of Molecular and Macromolecular Studies, Polish Academy of Sciences, Department of Organic Sulphur Compounds, 90-362 Łódź, Sienkiewicza 112, Poland

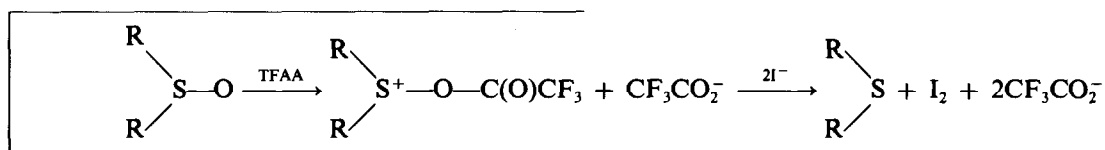
(Received 22 December 1988. Revised 5 October 1989. Accepted 31 October 1989)

Summary—The reaction of sulphoxides with trifluoroacetic anhydride and iodide in acetone medium to produce iodine, which can be used for their titrimetric determination, has been adapted for spectrophotometric determination of sub- μ mole amounts of sulphoxides.

Sulphoxides can be successfully applied as starting materials in organic synthesis, and also play a significant role in industrial chemistry.^{1,2} Some sulphoxides have also received much attention because of their biological activity.^{3,4} For this reason, their isolation and determination, which have long been investigated,^{5,6} are still of interest in the analytical chemistry of sulphur. Most of the procedures are based on reduction,⁷⁻¹² oxidation¹³⁻¹⁶ or neutralization titrations,^{17,18} and thus are most suitable for the determination of sulphoxides at higher concentrations. The more sensitive methods developed recently are either spectrophotometric or based on the formation of chelate-type derivatives.

for spectrophotometric determination of some sulphoxides. Sulphoxides can also be determined by reduction with leuco-compounds derived from tryptophan and glyoxylic acid,²² or *p*-dimethylaminobenzaldehyde,²³ to form strongly absorbing dyes.

A few sulphoxides have also been determined chromatographically, some aliphatic ones by gas chromatography²⁴ and others by high-pressure liquid chromatography with post-column derivatization with hexachloroplatinate.²⁵ Recently we reported²⁶ a sensitive method of sulphoxide determination, based on the use of trifluoroacetic anhydride/iodide (TFAA-I) reagent,²⁷ followed by titration of the iodine formed:



In contrast to the simple aliphatic sulphoxides, which are characterized by low molar absorptivity in the 200–240 nm region, derivatives which contain unsaturated groups have much stronger absorption in this region.¹⁹ Strongly absorbing compounds are also formed by complexation between the sulphinyl oxygen atom and transition metal ions, and can be used for the spectrophotometric determination of some sulphoxides. Thus, complex formation with iron(III) ($\lambda = 410 \text{ nm}$)²⁰ and aquopentacyanoferrate(II) ($\lambda = 658 \text{ nm}$)²¹ have been used

The sensitivity of this method is limited by the method of iodine determination and a spectrophotometric finish would enhance it.

EXPERIMENTAL

Reagents

Dimethylsulphoxide (DMSO, Aldrich) was standardized by the permanganate method,¹³ and the other sulphoxides were prepared according to Drabowicz *et al.*²⁸ and were all of the purity previously reported. They were used as 0.1M solutions in anhydrous acetone and

*Author to whom correspondence should be addressed.

diluted as required, just before use. Trifluoroacetic anhydride (Aldrich) was used as a 0.5M solution in anhydrous acetone, prepared immediately before use. Acetone was refluxed over phosphorus pentoxide and stored over molecular sieve 3A. Sodium iodide (Aldrich) was dried under vacuum over phosphorus pentoxide, and used as a 0.5M solution in anhydrous acetone.

Procedure

For calibration, known amounts of sulphoxide (20–1000 μl of $5 \times 10^{-4}\text{M}$ solution in acetone) are transferred into 10-ml standard flasks and 1 ml of the 0.5M sodium iodide and 100 μl of the 0.5M TFAA solutions (in acetone) are added to each, and the mixtures are diluted with acetone to the mark. After 2 min, the absorbances at 362 nm are measured in fused-silica cuvettes (5-cm path-length for 10–50 of sulphoxide, 1-cm path-length for 50–500 nmole) at 20°, against acetone. A reagent blank is similarly prepared and measured. The absorbances are corrected for the reagent blank and plotted against amount of sulphoxide taken. The calibration graph is used for interpretation of the absorbances of sample solutions similarly prepared.

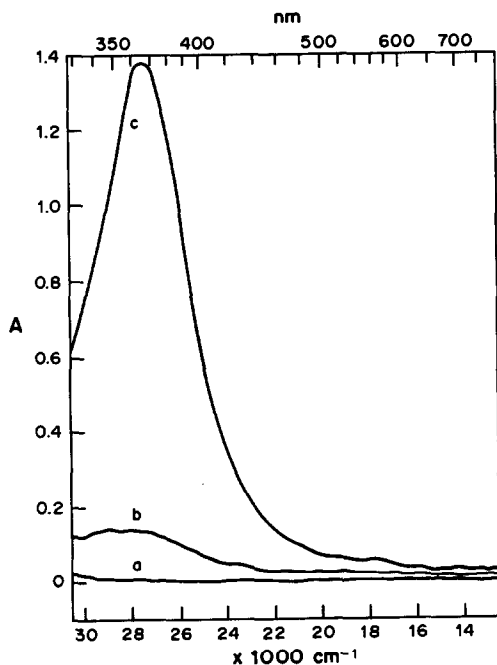


Fig. 1. Absorption spectra of sulphoxides (a), TFAA-I reagent (b) and reaction mixture of TFAA-I and sulphoxide (c): 2 min reaction time, 25°, 1-cm cuvettes; a, 500 nmole of DMSO or DPSO in acetone; b, standard solution of TFAA-I in acetone (without sulphoxide); c, standard reaction mixture containing 500 nmole of DPSO (in 10 ml of acetone).

RESULTS AND DISCUSSION

The relatively high molar absorptivity of iodine in acetone solution ($\epsilon = 2.5 \times 10^4 \text{ l. mole}^{-1} \cdot \text{cm}^{-1}$ at 362 nm) allows the determination of 10–500 nmole of sulphoxide. In principle, the reaction of TFAA and iodide with sulphoxides requires a 1:2 molar ratio of these two reagents. For determination of μmole amounts of sulphoxides we used a minimum of a fourfold molar ratio of TFAA and a 2.5-fold molar ratio of sodium iodide to sulphoxide.²⁶

In the present procedure a 100-fold molar ratio of TFAA and 1000-fold molar ratio of sodium iodide to sulphoxide are used. This high excess of iodide leads to a strong increase in the absorbance, apparently because of formation of the tri-iodide anion ($\text{I}_2 + \text{I}^- \rightleftharpoons \text{I}_3^-$) which has a higher molar absorptivity (Fig. 2). Such a high iodide:sulphoxide ratio, however, results in some oxidation of the excess of iodide (Fig. 1), which necessitates a reagent blank measurement.

Examination of the release of iodine as a function of time showed that reduction of the sulphoxide is completed in a few seconds, after mixing of the solutions, and is followed by a slow increase in the iodine level because of oxidation of the iodide excess (the absorbance

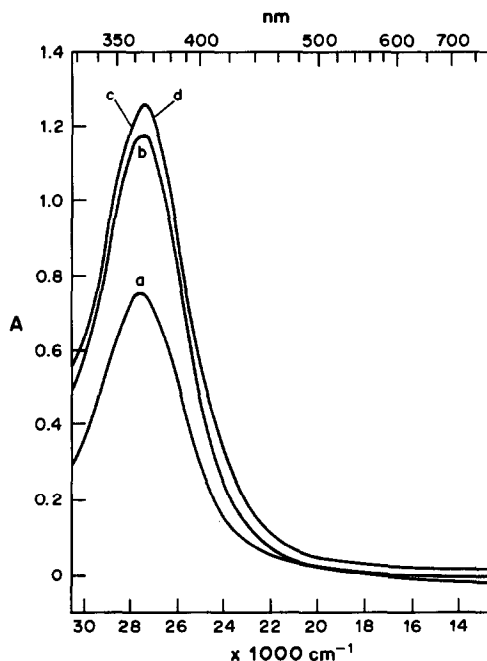


Fig. 2. Influence of the excess of sodium iodide on the absorbance of 500 nmole of iodine in (a) 10 ml of acetone, and in 10 ml of acetone solutions of sodium iodide [(b) 0.01M, (c) 0.05M, (d) 0.1M].

Table 1. Spectrophotometric determination of sulphoxides (1-cm cuvettes, 362 nm, 6 determinations)

R ¹ —S(O)—R ²		Taken, nmole	Found, nmole	Relative std. devn., %
R ¹	R ²			
CH ₃	CH ₃	50	48	4.4
		100	99	1.9
		200	206	2.4
		300	300	1.8
		400	399	1.3
		500	502	1.4
n-C ₄ H ₉	n-C ₄ H ₉	50	51	4.5
		100	101	4.0
		200	195	3.0
		300	298	2.7
		400	392	2.7
		500	492	2.3
C ₆ H ₅	C ₆ H ₅	50	50.5	4.1
		100	99	4.1
		200	204	2.1
		300	295	2.2
		400	405	2.5
		500	497	1.0
C ₆ H ₅	<i>p</i> -CH ₃ —C ₆ H ₄	50	48	4.8
		100	102	3.6
		200	200	2.7
		300	304	2.4
		400	395	2.6
		500	492	2.0
PhCH ₂	PhCH ₂	50	49	5.0
		100	102	4.2
		200	197	3.0
		300	295	3.4
		400	404	2.6
		500	502	2.2
CH ₃ [†]	CH ₃ [†]	10	10.5	9.0
		20	19.5	6.2
		31	31	4.0
		40	41	2.6
		50	49	2.8

*5-cm cuvettes.

increases by 0.02–0.03 in 20 min). For this reason the reagent blank is run separately and its absorbance is subtracted from that for the sulphoxide determinations. The very low molar absorptivity of dialkyl or diaryl sulphides and sulphoxides in acetone, in the wavelength region of interest (Fig. 1), practically eliminates the need for additional correction for the presence of these species. The method is not affected by the presence of sulphides and sulphones. Thus, the determination of diphenyl sulphoxide (500 nmole) alone, or in a mixture with 500 nmole of diphenyl sulphide or diphenyl sulphone, always gave consistent results.

Acknowledgements—This project was financially supported by the Polish Academy of Sciences within the project CPBP 01.13, and the National Committee of Chemistry. The authors thank Professor M. Milolajczyk for his interest in the work and for helpful discussions.

REFERENCES

1. T. Durst, in *Comprehensive Organic Chemistry*, D. N. Jones (ed.), Vol. 3, p. 121. Pergamon Press, Oxford, 1979.
2. *Idem*, *Special Periodical Reports, Organic Compounds of Sulphur, Selenium and Tellurium*, Vols. 1–6, Chemical Society, London, 1970–1986.
3. A. Kjaer, *Tetrahedron*, 1974, **30**, 1551.
4. R. L. Whistler, *Carbohydrates, Nucleotides, Nucleosides*, 1979, **16**, 199.
5. M. R. F. Ashworth, in *Determination of Sulphur-containing Groups*, Vol. 1, p. 30. Academic Press, New York, 1972.
6. J. H. Karchmer, *The Analytical Chemistry of Sulfur and its Compounds*, Part II, Chap. 11, Wiley-Interscience, New York, 1972.
7. E. Glynn, *Analyst*, 1947, **72**, 248.
8. D. Barnard and K. R. Hargrave, *Anal. Chim. Acta*, 1951, **5**, 536.
9. R. R. Legault and K. Groves, *Anal. Chem.*, 1957, **29**, 1495.
10. E. N. Karaulova and G. D. Galpern, *Zh. Obshch. Khim.*, 1959, **29**, 3033.

11. F. Jančík and J. Körbl, *Cesk. Farm.*, 1962, **11**, 305.
12. S. Allenmark, *Acta Chem. Scand.*, 1966, **20**, 910.
13. J. Gopalakrishnan and C. C. Patel, *Inorg. Chim. Acta*, 1967, **1**, 165.
14. V. V. Savant, J. Gopalakrishnan and C. C. Patel, *Z. Anal. Chem.*, 1968, **238**, 273.
15. T. B. Douglas, *Talanta*, 1968, **15**, 704.
16. Rangaswamy, H. S. Yathirajar and D. S. Mahadevappa, *Indian J. Chem.*, 1979, **17A**, 602.
17. D. C. Wimer, *Anal. Chem.*, 1958, **30**, 2060.
18. C. A. Streuli, *ibid.*, 1958, **30**, 997.
19. C. C. Price and S. Oae, *Sulfur Bonding*, Ronald, New York, 1962.
20. Z. Dizdar and Z. Idjaković, *Talanta*, 1972, **19**, 1217.
21. H. E. Toma, E. Giesbrecht and J. M. Malin, *An. Acad. Bras. Cienc.*, 1976, **48**, 41; *Anal. Abstr.*, 1978, **34**, 3B99.
22. A. P. Safronov, *Zh. Analit. Khim.*, 1963, **18**, 548.
23. F. Vláčil and D. K. Huynh, *Collection Czech. Chem. Commun.*, 1979, **44**, 1908.
24. A. M. Awwad and T. M. Sarkissian, *J. Chromatog. Sci.* 1977, **15**, 487.
25. M. Horiuchi, H. Takashina, K. Fujimura and T. Iso, *Yakugaku Zasshi*, 1986, **106**, 1028; *Chem. Abstr.*, 1987, **106**, 131139g.
26. W. Ciesielski, J. Drabowicz, W. Jędrzejewski, Z. H. Kudzin and R. Skowroński, *Talanta*, 1988, **35**, 969.
27. J. Drabowicz and S. Oae, *Synthesis*, 1977, 404.
28. J. Drabowicz, W. Midura and M. Mikołajczyk, *ibid.*, 1979, 39.

SPECTROPHOTOMETRIC DETERMINATION OF SELENIUM(IV) WITH 5,5-DIMETHYL-1,3-CYCLOHEXANEDIONE

MARIO E. BODINI*, JORGE PARDO and VERÓNICA ARANCIBIA

Facultad de Química, Pontificia Universidad Católica de Chile, Casilla 6177, Santiago, Chile

(Received 8 November 1988. Revised 6 October 1989. Accepted 31 October 1989)

Summary—5,5-Dimethyl-1,3-cyclohexanedione (dimedone) reacts in acid aqueous solution with selenium(IV) to give a benzoxaselenol which has an absorption maximum at 313 nm with a molar absorptivity of $4.00 \times 10^3 \text{ l. mole}^{-1} \cdot \text{cm}^{-1}$. The compound is extractable into chloroform, to give a solution with an absorption maximum at 300 nm with a molar absorptivity of $3.77 \times 10^3 \text{ l. mole}^{-1} \cdot \text{cm}^{-1}$. The calibration graph is linear up to 30 ppm selenium, with a detection limit of 0.1 ppm in the final solutions. Of the various other ions tested, only iron(III) interferes at all concentrations but the addition of 1000 ppm fluoride will mask 50 ppm Fe^{3+} . The method has good reproducibility, with a relative standard deviation of 1.0% for pure solutions. The method has been applied to the analysis of fire-refined copper.

Although many methods exist for the determination of selenium, its spectrophotometric determination is still very interesting because of its sensitivity and the simplicity of the procedure. The most frequently utilized of these methods are based on the reaction of Se(IV) with an aromatic *o*-diamine, in which a heterocyclic compound called a piaszelenol is formed and measured.¹⁻⁴ However, these methods have the disadvantage that the reagents are highly toxic and the results do not have high reproducibility. Kamaya *et al.*⁵ recently reported a new method based on the reaction with ferrocene, which is indicative of continuous research in this area.

Stamm and Gosrau⁶ reported that selenium dioxide reacts with 5,5-dimethyl-1,3-cyclohexanedione (dimedone), in methanol, to yield a yellow compound with an absorption maximum in the ultraviolet region. The characteristics of this compound make it attractive as the basis for an alternative spectrophotometric method for determination of selenium, in which a toxic aromatic *o*-diamine is not involved.

Laitalainen⁷ has determined the structure of this yellow compound (benzoxaselenol) which is formed by the mechanism shown in Scheme 1. This structure is in good agreement with that reported by Still and Kutney for the sulphur analogue.⁸

The main goal of the present work was to establish the conditions in which this reaction

can be used for analytical purposes, and its performance characteristics. The procedure developed has been applied to the analysis of fire-refined copper for selenium.

EXPERIMENTAL

Reagents

A dimedone stock solution (2.5 g/l) was prepared in 0.25M phosphate buffer (pH 2.0), saturated with nitrogen and stored in the refrigerator. It did not decompose appreciably for two weeks.

The standard selenium(IV) solution was prepared by diluting the contents of a Merck "Titrisol" ampoule (containing 1000 mg of Se) to 500 ml with doubly distilled water. The 250-ppm stock solutions of selenium(IV) were prepared by dilution of this solution. Class A volumetric glassware was used for this purpose.

All other chemicals used were reagent grade.

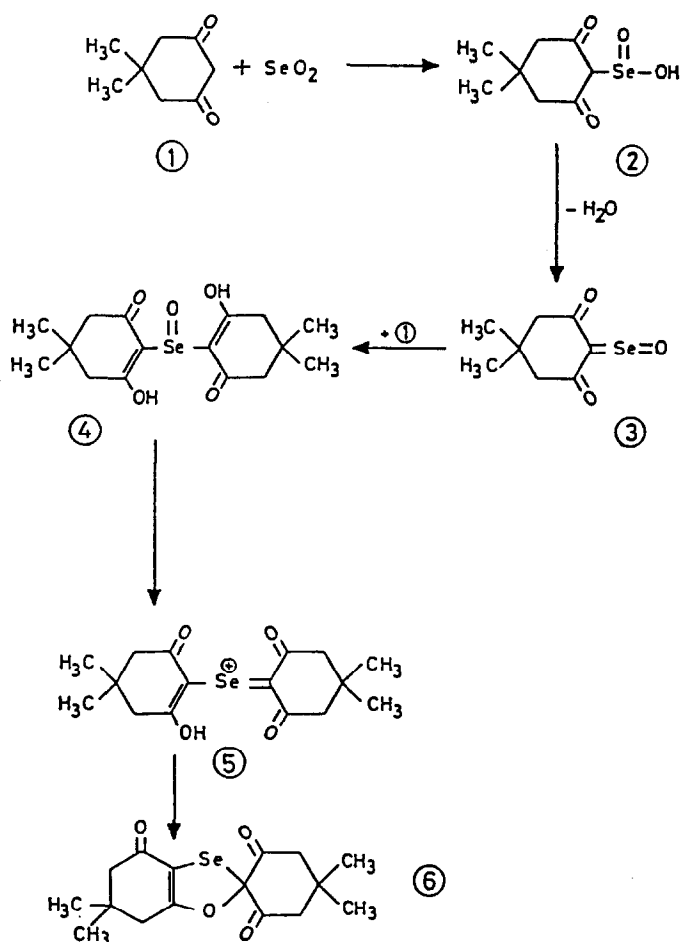
Apparatus

The spectrophotometric measurements were made with a Beckman Model ACTA CV spectrophotometer, and 1-cm fused-silica cells.

Determination of selenium in fire-refined copper

Dissolve approximately 4 g of the cleaned sample (accurately weighed) in concentrated nitric acid (approx. 25 ml) and heat until the solution is evaporated almost to dryness. Take up the cooled residue in water, dilute the solution to about 100 ml and adjust it to pH 2.0

*Author for correspondence.



with solid sodium hydroxide. Add 0.02M potassium permanganate until a slight excess is present. Boil the solution and then add filter-paper pulp to eliminate the excess of permanganate. Filter off the pulp and concentrate the filtrate to 50 ml, then add 25 ml of a mixture of concentrated sulphuric acid, concentrated nitric acid and water (10:7:25 v/v). Electrolyse the resulting solution with two platinum electrodes at a current of 2 A and applied voltage of 2.5 V. After the electrolysis is finished (it takes 2.5 hr to deposit all the copper) concentrate the solution to 25 ml and then add 8 ml of concentrated hydrochloric acid. Reflux the solution until starch-paper does not give a positive reaction in the vapour. Concentrate the solution to approximately 20 ml, adjust to pH 2 and dilute to volume in a 25-ml standard flask. Take an aliquot of 5 ml of this solution, add 2 ml of the $8 \times 10^{-3}M$ stock solution of dimedone and dilute to 10 ml with phosphate buffer (pH 2). Heat the solution for 60 min at 90° , then cool, adjust the pH to 6.0 with sodium hydroxide, and

add 1 ml of 0.1M EDTA and 1 ml of 1000 ppm sodium fluoride solution. Extract the benzoxaselenol with 6 ml of chloroform and measure the absorbance at 300 nm, against a blank made by extracting 2 ml of dimedone solution plus 3 ml of phosphate buffer and 5 ml of water with 6 ml of chloroform.

RESULTS AND DISCUSSION

The spectra of benzoxaselenol in aqueous medium and in chloroform are shown in Fig. 1. In aqueous medium there is an absorption maximum at 313 nm with a molar absorptivity of $4.00 \times 10^3 \text{ l. mole}^{-1} \text{ cm}^{-1}$. The chloroform solution has an absorption maximum at around 300 nm and the molar absorptivity is $3.77 \times 10^3 \text{ l. mole}^{-1} \text{ cm}^{-1}$.

To determine the optimum temperature for the reaction in water, three solutions were prepared, with pH adjusted to 2.0 and containing 2000 ppm dimedone and 15 ppm Se(IV), and their temperatures were fixed at 40, 60, 75 and

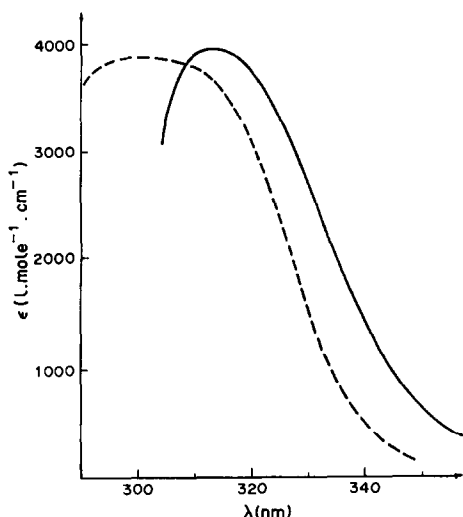


Fig. 1. Absorption spectra of benzoxaselenol in CHCl_3 (---) and in aqueous solution (—).

90° . The absorbance of each system was monitored at 313 nm as a function of time and the results are illustrated in Fig. 2. From the results we conclude that the optimum temperature for the reaction is 90° , since the reaction is then fastest.

The optimum pH was established with solutions containing the amounts of dimedone and Se(IV) used in the temperature study, adjusted to pH 1.2, 2.2, 2.7, 3.0, 5.0, 7.0 and 9.0, and heated at 90° . Figure 3 shows the dependence of the absorbance at 313 nm on time at pH 1.2, 2.2, 2.7 and 3.0. At pH 5.0 or higher no colour development is observed. As its pK_a value is 5.22,⁹ dimedone is increasingly dissociated with increase in pH, and this presumably accounts for the lack of reaction at $\text{pH} \geq 5$.

It was also observed, however, that after heating for 2 hr a pink precipitate, which appeared to be elemental selenium, was formed and the pH of the solution had gone down to 1.0. From the mechanism of the reaction between dimedone and selenium(IV) we can see

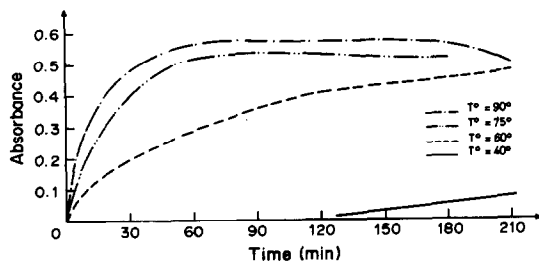


Fig. 2. Time dependence of the absorbance at 313 nm at different temperatures. Dimedone 2000 ppm, Se(IV) 15 ppm, pH 2.

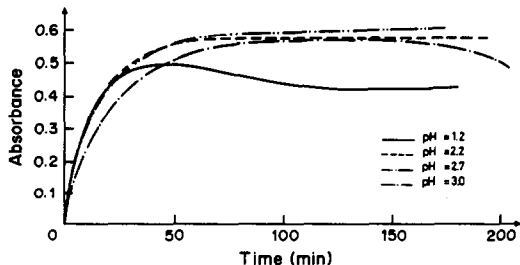


Fig. 3. Time dependence of the absorbance at 313 nm at different pH values. Dimedone 2000 ppm, Se(IV) 15 ppm, temperature 90° .

that the intermediate steps generate protons, which decrease the pH of the solution. Apparently, under these conditions the reaction product decomposes. Therefore, a buffer solution must be used to ensure quantitative transformation of selenium into the benzoxaselenol. In our case we chose the 0.1M phosphate buffer of $\text{pH} = 2$.

The optimal conditions for the reaction were established by a self-directing optimization method¹⁰ for the three variables studied (pH, temperature and time). It was found that pH 2.2 and heating at 80° for 50 min gave the best results. However, on the basis of Figs. 2 and 3 it was decided to use heating in a water-bath at 90° for 60 min.

Figure 4 shows the dependence of the absorbance at 313 nm, under the best practical working conditions, on the mole-ratio of dimedone to Se(IV), measured against a blank solution containing the same concentration of dimedone as the sample solution. The reaction is complete at a mole-ratio of 80 or more, so a large excess of dimedone is necessary.

The calibration graph obtained under the recommended conditions is linear up to 30 ppm of selenium and the molar absorptivity at 300 nm is $3.77 \times 10^3 \text{ l. mole}^{-1} \cdot \text{cm}^{-1}$. The detection limit is 0.1 ppm of Se. A reproducibility study gave a relative standard deviation of

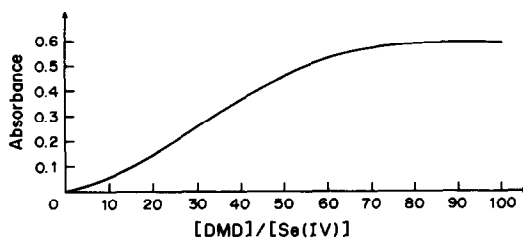


Fig. 4. Dependence of the absorbance at 313 nm with mole ratio of dimedone to Se(IV). Se(IV) $1.9 \times 10^{-4} \text{ M}$ (15 ppm), pH 2, temperature 90° , reaction time 50 min.

Table 1. Determination of selenium in fire-refined copper (five replicates)

Sample	Proposed method		<i>o</i> -Phenylenediamine method ³	
	Se, ppm	rsd, %	Se, ppm	rsd, %
A	13.2	5.7	13.6	3.0
B	14.3	6.1	14.7	2.9

1.0% in a series of 15 determinations on pure solutions containing 15 ppm of selenium.

Of the ions normally present in the samples of interest, it has been found that Cu²⁺ (50 ppm), Pb²⁺ (50 ppm), Te⁴⁺ (50 ppm), Mn²⁺ (50 ppm), Ni²⁺ (100 ppm), Ag⁺ (10 ppm), As³⁺ (500 ppm), Sb³⁺ (20 ppm), SO₄²⁻ (200 ppm), NO₃⁻ (200 ppm), Cl⁻ (200 ppm) and F⁻ (2000 ppm) do not interfere when present at the levels shown in brackets. Fe³⁺ interferes at any concentration, but up to 50 ppm can be masked by fluoride (1000 ppm).

Determination of selenium in fire-refined copper

The proposed method was used to determine trace amounts of selenium in copper metal. Prior separation of selenite from copper(II) was necessary and the method of total electrolysis was employed.

The results (Table 1) showed good agreement with those found by the *o*-phenylenediamine method.³ Five independent copper samples were analysed by both methods. The rsd appears higher than that for pure solutions, because the results refer to 2 ppm selenium in the final

solution for the copper analysis, compared with 15 ppm for the test on pure solutions, *i.e.*, the standard deviations are similar (~0.2 ppm). The rsd for the proposed method is higher than that of the comparison method because the latter method has a much higher sensitivity.

Acknowledgement—This work was supported by the Dirección de Investigación (DIUC) of the Pontificia Universidad Católica de Chile.

REFERENCES

1. J. Hoste, *Anal. Chim. Acta*, 1948, **2**, 402.
2. J. Hoste and J. Gillis, *ibid.*, 1955, **12**, 158.
3. H. Ariyoshi, M. Kuniwa and M. Toei, *Talanta*, 1960, **5**, 112.
4. M. Bodini and O. Alzamora, *ibid.*, 1983, **30**, 409.
5. M. Tamaya, T. Murakami and E. Ishii, *ibid.*, 1987, **34**, 664.
6. H. Stamm and K. Gossrau, *Ber.*, 1933, **66**, 1558.
7. T. Laitalainen, *J. Chem. Soc., Perkin Trans. I*, 1983, 333.
8. I. W. J. Still and G. W. Kutney, *J. Org. Chem.*, 1981, **46**, 4911.
9. R. P. Bell and R. R. Robinson, *Trans. Faraday Soc.*, 1961, **57**, 965.
10. C. Hendrix, *CHEMTECH*, 1980, **10**, 488.

EXTRACTION AND SPECTROPHOTOMETRIC DETERMINATION OF COBALT WITH DITHIZONE

MARTIN V. DAWSON and SAMUEL J. LYLE

Department of Chemistry, King Fahd University of Petroleum and Minerals, Dhahran 31261, Kingdom of Saudi Arabia

(Received 1 November 1988. Revised 11 October 1989. Accepted 31 October 1989)

Summary—Cobalt(II) in acetate-tartrate buffer (pH 6.0–7.3) is extracted quantitatively as cobalt(III) dithizonate with excess of dithizone in CCl_4 . The molar absorptivity in the CCl_4 phase is 4.6×10^4 l. mole⁻¹. cm⁻¹ at the absorption maximum 550 nm. The calibration graph is linear for 1–10 μg of cobalt in 10 ml of CCl_4 when excess of dithizone is removed by back-extraction with 0.01M aqueous ammonia. Most interferences can be overcome by (a) initial extraction with dithizone at pH 1.3, (b) selective back-extraction into hydrochloric acid (pH 1 to 2), (c) oxidation of iron and tin to iron(III) and tin(IV) and addition of fluoride to complex the former, and (d) selective reaction of nickel dithizonate with 1,10-phenanthroline in the CCl_4 phase followed by back-extraction of nickel into 0.1M acid. The method has been applied to determination of cobalt in a copper-nickel-zinc alloy and a nimonic alloy.

Cobalt(II) reacts with dithizone (H_2Dz) in carbon tetrachloride to give, depending on the conditions used, cobalt(II) or cobalt(III) dithizonate, of which the latter is particularly stable towards dilute mineral acid and has a large molar absorptivity at its absorption maximum. However, this reaction appears only to have been used for the separation and concentration of cobalt from a variety of samples, notably silicate rocks, soils, plant material and fertilizers,² and more recently in separation from other metal dithizonates by high-performance liquid chromatography^{3,4} and thin-layer chromatography.⁵ In this paper it is shown that cobalt(III) dithizonate is readily produced, has good stoichiometry, photometric stability and sensitivity and can be separated from other dithizonates at comparable concentrations by masking and selective extraction procedures. It is recommended for spectrophotometric determination of cobalt at minor and trace levels, and its use for analysis of two standard alloys is described.

EXPERIMENTAL

Reagents

Dithizone (BDH, Poole, England), other reagents, and the solvents used were of analytical reagent grade. All aqueous solutions were prepared in demineralized water. For use in measurement of molar absorptivity the dithizone was purified as described by Sandell and Onishi.⁶ For spectrophotometric determinations and molar-ratio studies, the reagent was used as

received; 10^{-3}M stock solutions in carbon tetrachloride were prepared fresh every few days and stored in the dark at 4°.

Standard solutions of metal ions were prepared in very dilute nitric acid. For quantitative analysis the buffer used was 0.5M sodium acetate/0.1M sodium tartrate adjusted to pH 6.8 ± 0.5 with acetic acid. For molar-ratio studies 0.5M sodium acetate buffers adjusted to pH values from 6.0 to 7.0 with acetic acid were prepared. Before use the buffers were shaken with 10^{-4}M dithizone in carbon tetrachloride to remove traces of any extractable metals present.

Apparatus

A Bausch and Lomb Spectronic 20 spectrophotometer was used for determinations and molar-ratio studies, and spectra and absorbance data for calculation of molar absorptivity were obtained with a Varian Cary-2390 spectrophotometer.

Calibration and determination in the absence of interferences

A standard solution or a sample (5–25 ml of aqueous solution containing 1–10 μg of cobalt in pH-6.8 \pm 0.5 buffer) was shaken with 10.0 ml of 10^{-3}M dithizone solution in carbon tetrachloride for 20 min. Excess of dithizone was removed from the organic phase by shaking with two 10-ml portions of 0.01M ammonia solution and the absorbance of the organic phase was measured in a 1-cm cell at 550 nm

against a blank prepared by similar treatment of demineralized water.

Analysis of alloys

N.B.S. Standard 157A. About 1 g was accurately weighed and dissolved in the minimum of 8M nitric acid. The solution was diluted to 100 ml with water, 1 g of urea was added and the copper electro-deposited at 2 A and 3 V on a platinum electrode. The electrolyte solution was then evaporated to about 75 ml, transferred to a 100-ml standard flask with water and diluted to volume. A 10.0-ml portion was made strongly alkaline in a centrifuge tube with 10M sodium hydroxide. The supernatant liquid was removed after centrifugation and the precipitate washed with two 5-ml portions of 10M sodium hydroxide and then two 20-ml portions of water, with centrifugation between washes. The precipitate was dissolved in 5 ml of 10M hydrochloric acid, and run through a column 1 cm in diameter, containing 15 g of Dowex-1 × 8, 50–100 mesh, anion-exchange resin conditioned with 10M hydrochloric acid. The column was washed with 50 ml of the same acid, the eluate being discarded. Cobalt was then eluted with 60 ml of 3.5M hydrochloric acid at a flow-rate of 4 ml/min. Five ml of 16M nitric acid were added to this eluate and the solution was evaporated nearly to dryness. The residue was taken up in water and diluted to volume in a 20-ml standard flask. A 5.0-ml portion was adjusted to about pH 1.5 with sodium hydroxide and extracted with 10 ml of $10^{-3}M$ dithizone and then 10 ml of carbon tetrachloride. The extracts were discarded, the aqueous phase was adjusted to about pH 4.5 with sodium hydroxide and an equal volume of buffer (pH 6.8 ± 0.5) and 0.5 g of potassium fluoride were added. The solution was then shaken for 20 min with 10.0 ml of $10^{-3}M$ dithizone. Next, about 10 mg of 1,10-phenanthroline was dissolved in the extract, which was then shaken for 1 min with 10 ml of 0.1M hydrochloric acid. The aqueous phase was discarded and the organic phase was shaken for 1 min each time with two 10-ml portions of 0.01M ammonia solution and the absorbance of organic phase was measured at 550 nm against an organic phase prepared by extracting 10.0 ml of $10^{-3}M$ dithizone with two 10-ml portions of 0.01M aqueous ammonia.

Nimonic 901 alloy

About 0.1 g of sample was accurately weighed and dissolved in the minimum volume of a 1:1

v/v mixture of concentrated hydrochloric and nitric acids. The surplus nitric acid was removed by evaporation of the solution nearly to dryness, addition of 5 ml of concentrated hydrochloric acid, and repetition of the evaporation. The residue was taken up in 10 ml of 8M hydrochloric acid and this solution was extracted with 10-ml portions of diethyl ether until a colourless extract was obtained. The aqueous phase was evaporated nearly to dryness and the residue was taken up in 10 ml of 10M hydrochloric acid and transferred to the Dowex-1 × 8 anion-exchange column, conditioned as above. The column was washed with 75 ml of 10M hydrochloric acid, the eluate being discarded, and then cobalt was eluted with 50 ml of 3.5M hydrochloric acid. The eluate was evaporated to a low bulk and then diluted to volume with water in a 200-ml standard flask. A 5.0-ml portion of this solution was then analysed as described for the N.B.S. alloy.

RESULTS AND DISCUSSION

When a solution of cobalt(II) buffered at pH 6–7 is extracted with dithizone solution in carbon tetrachloride and the extract is freed from excess of dithizone, the spectrum of the extract has a single broad absorption peak with a maximum at 550 nm. The mean molar absorptivity found from four determinations was $4.6 \times 10^4 \text{ l. mole}^{-1} \text{ cm}^{-1}$, which is similar to the value $4.88 \times 10^4 \text{ l. mole}^{-1} \text{ cm}^{-1}$ at 550 nm reported⁷ for a chloroform extract. The reaction with dithizone is relatively slow, but once formed the complex has good stability to light; for a solution kept in a stoppered flask on the laboratory bench the absorbance remained constant for 3 days at 23° and for at least 2 weeks in the dark at 4°.

Duncan and Thomas⁸ reported that radiometric titration of dithizone in carbon tetrachloride with aqueous cobalt(II) solution in acetate buffer at pH 6.5–7.3 gave a cobalt:dithizone ratio of 1:3 at the equivalence point. A subsequent detailed study¹ confirmed the presence of cobalt(III). An earlier photometric study⁹ with acetate medium at pH 6.0 had given a ratio of 1:2 for the complex. In the course of the present work 5 photometric measurements gave a ratio of $1:3.01 \pm 0.05$, irrespective of the presence of a reducing agent introduced into the organic phase (sulphur dioxide) or the aqueous phase (hydroxylamine or ascorbic acid), provided the pH of the latter

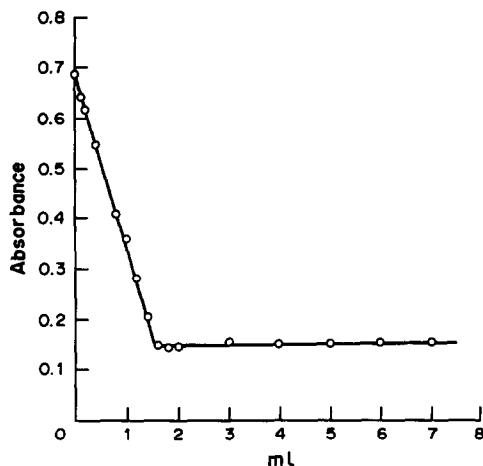


Fig. 1. Absorbance of the CCl_4 phase at 620 nm, after equilibration, vs. volume of $1.70 \times 10^{-5}M$ cobalt(II) initially in the aqueous phase. Each phase 4.00 ml; initial dithizone concentration $2.10 \times 10^{-5}M$. Aqueous phase $0.25M$ acetate buffer, pH 7.0.

phase remained in the range 6.0–7.3. A typical set of data is presented in Fig. 1. It appears that aerial oxidation of the cobalt(II) occurs in the system, probably at the liquid interface or the container wall.

The stability of the $\text{Co}(\text{HDz})_3$ complex in carbon tetrachloride towards various aqueous solutions was examined by shaking together equal volumes of the phases for 15 min at maximum rate on a mechanical shaker. The results are presented in Table 1. None of the aqueous phases examined (pH range 1.3–10.6) affected the absorbance, but contact with $0.01M$ sodium hydroxide for 15 min produced a slight decrease. Acetate, tartrate or citrate, at the specified concentrations, were without effect. However, cobalt is not extracted efficiently from $0.01M$ aqueous ammonia by dithizone in carbon tetrachloride, probably because of formation of $\text{Co}(\text{NH}_3)_6^{3+}$. Copper(II), palladium(II), silver, mercury(II) and bismuth are selectively removed⁶ by extraction of the dithizonate complexes at pH 1.3. Zinc, cadmium, thallium(I) and lead(II) would accompany cobalt in extraction at pH 6.0–7.3 but can readily be removed by back-extraction into dilute hydrochloric acid (pH 1–2). Some iron(II) and tin(II) would also be extracted along with cobalt into the organic phase and if present, should first be oxidized to iron(III) and tin(IV).

Table 1. Stability of $\text{Co}(\text{HDz})_3$ in CCl_4 on vigorous mixing with various aqueous solutions for 15 min

Aqueous phase	pH	Absorbance at 550 nm
Water	6.1	0.424
Hydrochloric acid	1.3	0.423
Hydrochloric acid	2.6	0.425
$0.5M$ Acetate + $0.1M$ tartrate	6.3–7.3	0.425
$0.1M$ Sodium citrate	8.7	0.424
$0.01M$ Aqueous ammonia	9.6	0.424
$0.1M$ Aqueous ammonia	10.6	0.423
$0.01M$ Sodium hydroxide	—	0.415

It was observed in the course of the present work that the oxidation of dithizone by iron(III) is prevented by the presence of fluoride in the aqueous phase. Nickel(II) is efficiently, but somewhat slowly, extracted along with the cobalt, as $\text{Ni}(\text{HDz})_2$. Treatment of the $\text{Ni}(\text{DHZ})_2$ extract with heterocyclic bases results in the formation of ternary complexes,^{10,11} with a change of colour; 1,10-phenanthroline is convenient for this purpose. However, conversion by equilibration with 1,10-phenanthroline in aqueous solution is slow, requiring 30 min at pH 1.3 with $0.002M$ base.¹² In the present work it was found that direct addition of solid 1,10-phenanthroline to the extract produced a nearly instantaneous reaction. Furthermore, the resulting ternary complex, $\text{Ni}(\text{HDz})_2 \cdot \text{phen}$, is rapidly destroyed with transfer of the nickel to the aqueous phase, when the organic phase is shaken for about 1 min with 0.01 – $0.1M$ hydrochloric acid; there is no effect on the $\text{Co}(\text{HDz})_3$. The interference of at least $100 \mu\text{g}$ of nickel, iron(III), tin(IV), zinc, cadmium, lead or thallium(I) can be overcome as described above. The only slow phase transfer is that of the cobalt; the other transfers are accomplished within 1 min by manual shaking in a separating funnel.

Linear calibration curves over the range 1–10 μg of cobalt were obtained, and for 5.0 μg of cobalt extracted into 10.0 ml of carbon tetrachloride the coefficient of variation was 1.6% for 10 measurements. Removal of the excess of dithizone allows a simple spectrophotometer to be used, with a reasonable calibration range.

The method was applied to the determination of cobalt in two alloys, the compositions of which are presented in Table 2. For analysis of

Table 2. Compositions of the alloys (%); averages for (a) 7 and (b) 8 participating laboratories

(a) N.B.S. 157A	Cu	Zn	Ni	Mn	Fe	Pb	Sn	Co	P		
	58.61	29.09	11.82	0.174	0.174	0.034	0.021	0.022	0.009		
(b) B.A.S. 387	Ni	Fe	Cr	Mo	Ti	Si	Al	Co	Mn	Cu	C
	41.9	36.0	12.46	5.83	2.95	0.28	0.24	0.21	0.08	0.032	0.030

the N.B.S. standard the copper was removed by electro-deposition, most of the zinc as tetrahydrozincate when the heavy metal hydroxides were precipitated, and the nickel (with some zinc) by elution with 10M hydrochloric acid from a strong-base anion-exchanger. Any remaining traces of these elements, along with other potentially interfering species, were rendered harmless by masking reactions or removed by selective extraction. Values of 0.19, 0.18 and 0.22% were obtained. Most of the iron was removed from the B.A.S. mimonic alloy by extraction into diethyl ether from 6–8M hydrochloric acid. Thereafter the treatment followed that of the N.B.S. alloy. Three determinations gave 0.026, 0.025 and 0.021%. These values were all within the ranges reported by the collaborating standardization laboratories and used to deduce the average compositions recorded in Table 2.

Probably the most widely used spectrophotometric methods for cobalt are those based on the red tris-complex formed by cobalt(III) with nitroso-R-salt (disodium 1-nitroso-2-hydroxynaphthalene-3,6-disulphonate) and the blue tetrathiocyanatocobaltate(II) complex. Though the former has good tolerance for many metals, that for nickel and chromium is limited and for analysis of the two alloys described here, separation of these elements would be necessary. The thiocyanate method has better tolerance for the elements present in these samples but lacks sufficient sensitivity.¹³ Dithizone and nitroso-R-salt have comparable sensitivities for cobalt, but nitroso compounds are not particularly stable even in the solid, and may not be available in sufficiently pure form for analytical purposes; their purification can be time-consuming.¹⁴ Thus the choice of reagent could depend on availability and quality.

Dithizone has been used to separate cobalt and other metal ions from soil,^{15,16} plant material,¹⁶ fertilizers¹⁶ and silicate rocks,¹⁷ with photometric^{16,17} or titrimetric¹⁵ determination after destruction of the dithizonates. The procedures described here permit direct determination of cobalt in the dithizone extract.

REFERENCES

1. J. F. Duncan and F. G. Thomas, *J. Chem. Soc.*, 1960, 2814.
2. A. K. De, S. M. Khopkar and R. A. Chalmers, *Solvent Extraction of Metals*, Van Nostrand Reinhold, London, 1970.
3. K. Ohashi, S. Iwai and M. Horiguchi, *Bunseki Kagaku*, 1982, **31**, E285.
4. E. B. Edward-Inatimi, *J. Chromatog.*, 1983, **256**, 253.
5. P. Bruno, M. Caselli, F. Fracassi and A. Traini, *Anal. Lett.*, 1984, **17**, 397.
6. E. B. Sandell and H. Onishi, *Colorimetric Determination of Traces of Metals*, 4th Ed., Part I, Wiley, New York, 1978.
7. W. Kemula, A. Janowski and T. Ganko, *Rocz. Chem.*, 1972, **46**, 1235; *Chem. Abstr.*, **77**, 159598.
8. J. F. Duncan and F. G. Thomas, *J. Inorg. Nucl. Chem.*, 1957, **4**, 376.
9. S. Miyakawa and T. Uemura, *Bull. Chem. Soc. Japan*, 1951, **24**, 25.
10. K. S. Math, K. S. Bhatki and H. Freiser, *Talanta*, 1969, **16**, 412.
11. K. S. Math and H. Freiser, *Anal. Chem.*, 1969, **41**, 1682.
12. H. Akaiwa, H. Kawamoto and M. Konishi, *Bunseki Kagaku*, 1979, **28**, 690.
13. R. S. Young, *Chemical Analysis in Extractive Metallurgy*, Griffin, London, 1971.
14. J. M. Dale and C. V. Banks, in I. M. Kolthoff and P. J. Elving (eds.), *Treatise on Analytical Chemistry*, Part II, Vol. 2, Interscience, New York, 1962.
15. P. L. Hibbard, *Ind. Eng. Chem., Anal. Ed.*, 1938, **10**, 615.
16. R. Gallego, W. B. Deijns and J. H. Feldmeijer, *Rec. Trav. Chim.*, 1952, **71**, 987.
17. R. E. Stanton, A. J. McDonald and I. Carmichael, *Analyst*, 1962, **87**, 134.

STABILITY OF REDUCED MOLYBDOSILICIC ACIDS

JAN MIGDALSKI and ZYGMUNT KOWALSKI

Academy of Mining and Metallurgy in Kraków, Institute of Materials Science, Al. Mickiewicza 30,
30-059 Kraków, Poland

(Received 19 June 1987. Revised 10 October 1989. Accepted 31 October 1989)

Summary—The effect of reduction on the stability of molybdosilicic acids (MSA) has been investigated. It has been found that when two or more of the 12 Mo(VI) atoms in α or β -MSA are reduced to Mo(V), the products are stable in alkaline medium. Also, β -MSA reduced to this extent is stable at higher temperature and is not transformed into α -MSA. Solutions in which the apparent degree of reduction is less than 2 Mo(V) per MSA ion should be treated as a mixture of unreduced MSA and MSA reduced exactly to 2 Mo(V) per MSA ion. A mixture of unreduced MSA and MSA reduced to contain 4 Mo(V) per MSA ion is not a stable system. The yellow unreduced MSA is reduced by the reduced form to give the product with 2 Mo(V) per MSA ion. The consequences for determining silicon as MSA are given, as well as a method of obtaining pure β -MSA from a mixture of α -MSA and β -MSA.

The yellow forms of α - and β -molybdosilicic acids are easily electrochemically or chemically reduced. The reduced forms are blue, which is characteristic of Mo(V)/Mo(VI) mixed oxidation-state compounds. All four forms find application for spectrophotometric determination of traces of silicon. The literature is extensive and many aspects of the systems have been discussed, including methods of reducing the molybdosilicic acids (MSA),¹⁻⁷ the chemical properties of the reduced acids,³⁻⁶ methods of formation of the acids,^{1,8-10} polarography and voltammetry of MSA,^{1,3-6,11-19} analytical applications,^{9,20-29} and automatic methods of determination of silica as MSA.³⁰⁻³³ From the observations made by Sen and Chatterjee³ it follows that reduced MSA is stable in alkaline medium, whereas the unreduced acid is not. Much new information about reduced MSA has been supplied by Massart and co-workers.^{5,6} Examination of the system has been undertaken to find the reason for the limited reproducibility of the methods utilizing reduced MSA. This limited reproducibility remains even when the synthesis and reduction conditions recommended by the various authors are maintained. The positive results obtained when using reduced MSA and alkaline medium³³ encouraged us to extend our work. We had made some observations about the stability of MSAs in alkaline media, which partly contradicted those made by Massart and co-workers,^{5,6} and this led us to continue the work.

EXPERIMENTAL

Solutions were prepared from reagent grade chemicals. Molybdosilicic acid (MSA) was prepared by acidifying a solution containing molybdate and silicate. α -MSA was made by acidifying to pH 1 and then boiling the solution. For β -MSA, ethanol was added before acidifying and the solution was not heated. To prepare a solid MSA, excess of perchloric acid was added to precipitate it. Solid samples of MSA (α and β) were used to prepare the stock solutions. Voltammetric curves for yellow α -MSA or β -MSA, recorded by the DC technique with a platinum microelectrode, show three cathodic two-electron waves (the recorded wave currents are negative). It is assumed that each wave corresponds to the reduction of two Mo(VI) atoms to Mo(V) in an MSA molecule. The yellow MSA can be reduced chemically or electrochemically by bulk electrolysis. In this experiment only electrochemical reduction was applied.

If, as a result, six of the twelve Mo(VI) atoms present in a molecule of MSA are reduced to Mo(V), then a voltammetric curve with three two-electron anodic waves can be obtained for the product (the recorded wave currents are positive). If the voltammetric curves for a reduced MSA have only one anodic wave (Fig. 1b) or two anodic waves, this is regarded as due to two or four Mo(VI) atoms (as the case may be) having been reduced to Mo(V), representing 2/12 or 4/12 of the total number of

molybdenum atoms in the molecule. The degrees of reduction of the MSA are thus equal to 2/12, 4/12 or 6/12 (this last for the case of three anodic waves). If the first wave is not fully anodic, but of anodic-cathodic nature, then the description of the situation in the solution becomes more complex. This situation will be explained later on. The average number of Mo(V) atoms per MSA molecule, referred to throughout this paper as n , can be determined from the voltammetric curve by calculating the ratio of the anodic current of the first wave, I_{a1} , to the limiting current of this wave, I_{L1} . This ratio assumes values ranging from 0 (for yellow, unreduced MSA) to 1 (for a fully anodic wave). Accordingly, the average number of Mo(V) atoms per MSA molecule, n , assumes values from 0 to 2 (it need not be an integer). Similar considerations can be applied when the first wave is fully anodic, but the second is of anodic-cathodic nature, or when two successive waves are both fully anodic, and the third is anodic-cathodic. According to the proposed definition, n is given by:

$$n = 2(I_{a1}/I_{L1} + I_{a2}/I_{L2} + I_{a3}/I_{L3})$$

and may assume values in the range 0–6. The symbols I_{a1} , I_{a2} , I_{a3} denote the anodic currents for the first, second and third waves, respectively, and I_{L1} , I_{L2} , I_{L3} indicate the limiting currents for the three waves. The DC voltammetric curves obtained with a platinum electrode allow the progress of MSA reduction to be followed and also allow the α - and β -forms of MSA to be distinguished. For example, in 0.1M hydrochloric acid medium, the half-wave potentials, $E_{1/2}$ for the three waves are +0.27, +0.13 and -0.06 V for α -MSA, but +0.33, +0.24 and -0.18 V for β -MSA. The appearance of only three waves on the voltammetric curve is evidence that only one form is present in the solution. Voltammetric curves with more than three waves indicate a mixture of both forms and in this case measurement of the limiting currents of the waves makes it possible to determine the α - and β -forms. In what follows, the values of n will be given in brackets, followed by α and β outside the brackets to indicate the form of MSA. Figure 1 illustrates the method of determining n from the voltammetric curves. Attempts to record the voltammetric curves in alkaline media with a platinum electrode did not give satisfactory results. In such cases the dropping mercury electrode (DME) was applied. It should be added that

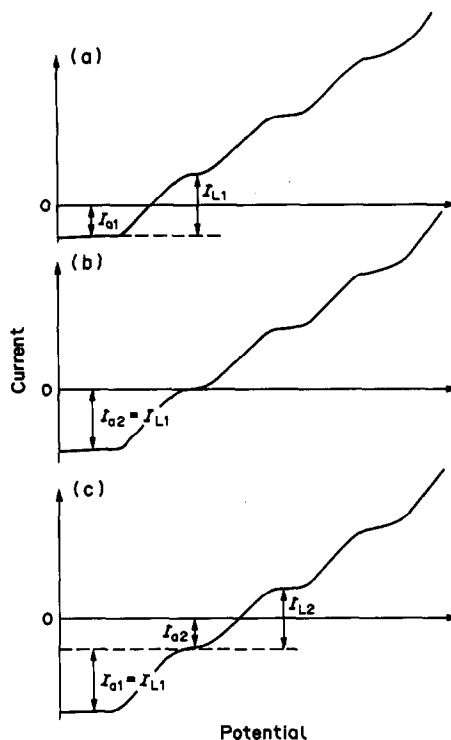


Fig. 1. Illustration of the method of determining the degree of reduction of α - or β -MSA by the DC technique with a rotating platinum electrode. Degrees of reduction: 1/12—curve a; 2/12—curve b; 3/12—curve c.

the DME cannot be used in acidic media, as mercury is oxidized by yellow MSA. In our further experiments, two types of working electrode were used: (a) a rotating platinum electrode (area 0.0014 cm², rotation at 1200 rpm); (b) a DME (flow-rate = 1.816 mg/sec, drop time = 5.11 sec).

DC Tast polarography was mostly used. To determine small amounts of MSA, derivative pulse polarography, DPP, was applied. It should be mentioned here that the DPP curves, being derivative curves, do not allow determination of the degree of reduction, as they do not distinguish between anodic and cathodic currents.

Relation between the degree of reduction of α -MSA and its stability

A large sample of yellow α -MSA was reduced stepwise, and after each step the degree of reduction was determined by voltammetry with a rotating platinum electrode. When the degree of reduction had been determined, a small sample was taken, alkalinized to pH 11, and after a few minutes the α -MSA not decomposed after alkalinization was measured by DPP with the DME. This experiment was repeated 7 times.

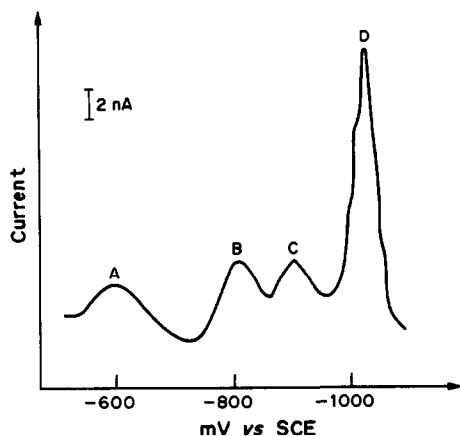


Fig. 2. DPP polarogram (DME) of an alkaline solution of reduced α -MSA.

Figure 2 shows the DPP polarogram of MSA, and Fig. 3 illustrates the dependence between a particular peak current and the degree of reduction of α -MSA in alkaline medium. The peak currents are proportional to the concentrations of the depolarizers, in this case the reduced α -MSA species, since the yellow unreduced α -MSA is decomposed in this medium (pH 11). In the first reduction stages the peak currents increase proportionally to the degree of reduction of MSA. When the degree of reduction

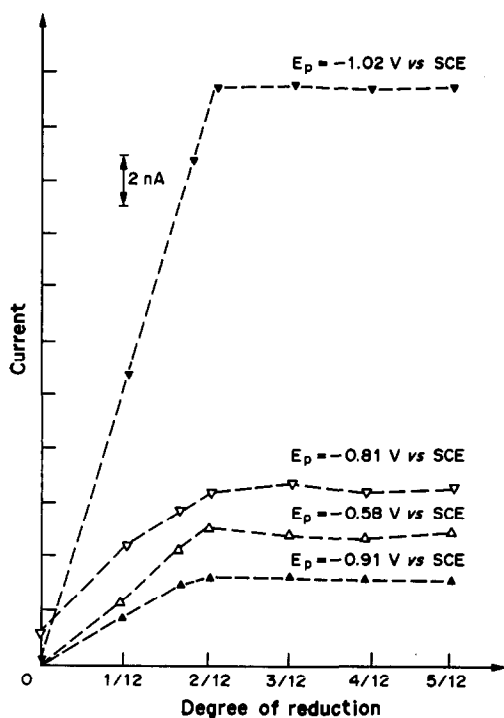


Fig. 3. Height of the DPP peaks of residual α -MSA after alkalization of a sample, as a function of degree reduction of α -MSA (for explanation see text).

exceeds 2/12, no further increase of the peak currents is observed. This can be explained as follows: (1) α -MSA reduced to at least the degree 2/12 is stable in alkaline medium, and (2) α -MSA reduced to less than the degree 2/12 is partly decomposed in this medium.

The relations in Fig. 3 show that the content of non-decomposed α -MSA (after alkalization of the solution) is directly proportional to the degree of reduction of α -MSA. To determine the degree of reduction of the α -MSA that remained undecomposed by the alkalization, the solutions were re-acidified and analysed voltammetrically with a platinum electrode and the DC Tast technique. Two aliquots of a solution containing α -MSA reduced to the degree 1/12 were taken. In the first only the ionic strength was corrected. The second sample was alkalized to pH 11 and acidified again to the initial pH value. Both solutions were then examined by DC Tast voltammetry. The curves recorded are shown in Fig. 4. In the alkalized solution the MSA content decreased by half, with α -MSA reduced exactly to the degree 2/12 remaining undecomposed in the solution. This is evidence that α -MSA with a 1/12 degree of reduction is a mixture of unreduced α -MSA and α -MSA reduced to the degree 2/12.

This conclusion concerning the stability of α -MSA is contrary to the data obtained by Massart and co-workers,^{5,6} who believed that only α -MSA reduced to the degree 4/12 is stable in alkaline medium. The same authors believe

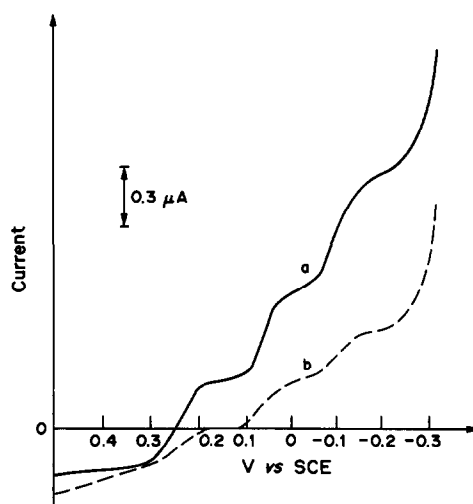


Fig. 4. DC voltammetric curves (rotating platinum electrode) for solutions obtained from identical samples of α -MSA, reduced to a degree of 1/12: a—non-alkalized $2 \times 10^{-3} M$ reference solution of α -MSA; b—test solution, initially alkalized to pH 11 and then acidified to pH 1.

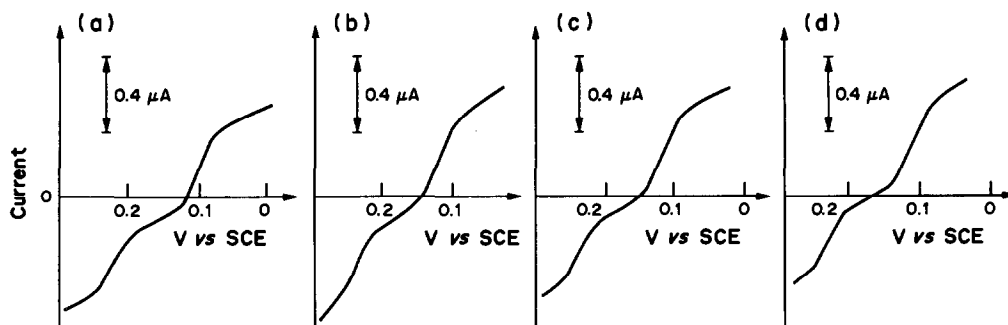


Fig. 5. DC voltammetric curves (rotating platinum electrode) for an α -MSA solution reduced to somewhat above the degree 2/12: non-alkalized $2 \times 10^{-5}M$ reference solution of α MSA, curve (a) and the same solution initially alkalinized to pH 11 and re-acidified to pH 1 after (b) 10 min, (c) 2 hr, (d) 24 hr.

that over a period of time α -MSA reduced to the degree 2/12 becomes decomposed in an alkaline medium according to two different mechanisms, depending on the pH. The products of the decomposition are said to be α -MSA reduced to the degree 4/12, molybdate and silicate. To resolve this question, reduced and alkalinized α -MSA was observed for a few hours. The parameter measured was the concentration of α -MSA after re-acidification of the solution. The degree of reduction of α -MSA in the solutions was a little greater than 2/12. Aliquots of the α -MSA solution were placed in measuring vessels filled with argon, then alkalinized to pH 11 with sodium hydroxide solution, and the vessels were tightly closed. The solutions were re-acidified after various intervals of time and analysed voltammetrically. The reference sample was an aliquot which had not been alkalinized, but was adjusted to the same ionic strength as the other aliquots by addition of sodium chloride and hydrochloric acid. To check that MSA was not re-formed after the alkalinization and re-acidification, the voltammetric measurement was repeated after repetition of the alkalinization and acidification of the

sample of yellow, unreduced α -MSA. Figure 5 illustrates the successive stages of this experiment for the reference solution and for test solutions re-acidified 10 min, 2 hr, and 24 hr after alkalinization. All the curves show a very similar content of α -MSA reduced to somewhat above a degree of 2/12. This confirms the conclusion that α -MSA reduced to such a degree is stable in alkaline medium (pH 11). The experiment was repeated with the solutions in contact with oxygen. Figure 6 shows the results for the reference solution and for test solutions left in contact with oxygen for 15 min and 1 hr between alkalinization and re-acidification. The curves show that the concentration of α -MSA reduced to a degree of 2/12 decreases on increased contact of the solution with oxygen, indicating chemical oxidation of the reduced α -MSA.

Relation between the degree of reduction of β -MSA and its stability

Analogous measurements to those for α -MSA indicated that β -MSA reduced to a degree of 2/12 or more is also stable in alkaline medium. Measurements of the stability, in alka-

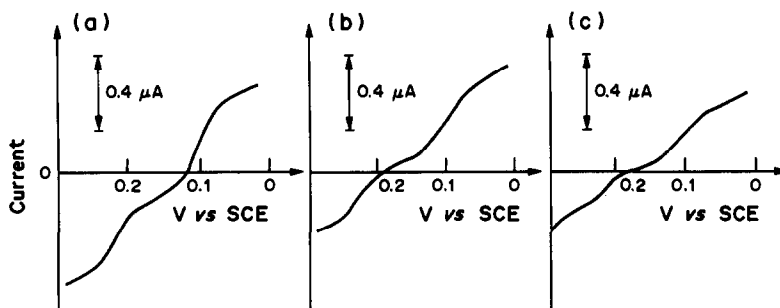


Fig. 6. DC voltammetric curves (rotating platinum electrode) for α -MSA solutions reduced to somewhat above the degree 2/12: $2 \times 10^{-5}M$ non-alkalized reference solution of α -MSA curve (a), and the same solution initially alkalinized to pH 11 and re-acidified to pH 1 after (b) 15 min, (c) 1 hr. The solutions for curves (b) and (c) were left in contact with air after alkalinization.

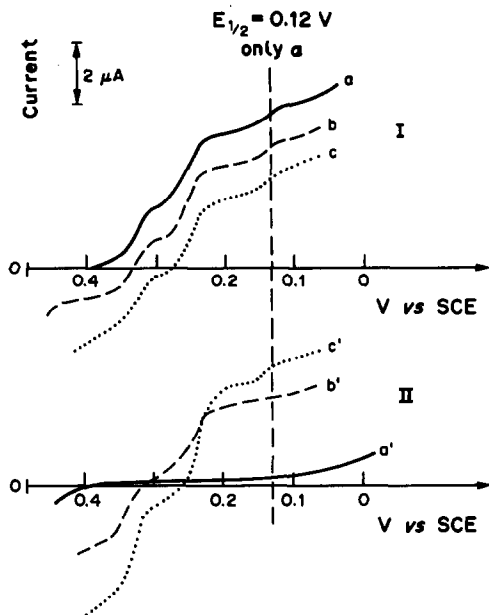


Fig. 7. DC voltammetric curves (rotating platinum electrode) for $1.5 \times 10^{-4} M$ solutions of β -MSA: a, non-reduced; b, reduced to the degree 1.2/12; c, reduced to the degree 2.3/12. The curves a', b', c' correspond to the samples of solutions a, b, c after alkalization to pH 11 and re-acidification to pH 1.

line medium, of β -MSA reduced to a degree of less than 2/12 gave the results shown in Fig. 7 and in Table 1. Figure 7 shows the voltammetric curves for reduced samples of β -MSA which were to be alkalized and acidified. The degrees of reduction of the β -MSA for the various steps of the experiment are listed in Table 1. They increased from 0 to 2.8/12. Figure 7(I) shows that all the solutions of the reduced acids contained chiefly β -MSA and some α -MSA. All these solutions were then alkalized to pH 11 and re-acidified to pH 1, and their voltammetric curves were recorded, Fig. 7(II). These curves show that on alkalization, (1) non-reduced β -MSA is decomposed; (2) β -MSA reduced to

a degree of 2/12 or more remains as β -MSA; (3) β -MSA reduced to below a degree of 2/12 undergoes partial decomposition, and only β -MSA reduced exactly to a degree of 2/12 remains. The quantitative results from this experiment (Table 1) show that β -MSA reduced to a degree of 2/12 or more gives a constant height of the first wave. The proportionality of the height of the first wave to degrees of reduction below 2/12, together with the fact that after these solutions have again been alkalized and acidified, β -MSA reduced exactly to a degree of 2/12 remains in the solutions, proves that these, similarly to those of α -MSA, are mixtures of non-reduced β -MSA and β -MSA reduced to a degree of 2/12. From Fig. 7 an additional conclusion can be drawn, concerning the possibility of obtaining pure β -MSA from a mixture with α -MSA. It is well known that in practice such mixtures always arise because of spontaneous transformation of the β - into the α -form of non-reduced MSA. Since the difference in the half-wave potentials of the first waves of α -MSA and β -MSA is about 60 mV at pH 1, and β -MSA is the stronger oxidant, it is possible to reduce β -MSA electrochemically to a degree of 2/12, without reducing α -MSA, if the experiment is done carefully enough. The non-reduced α -MSA can then be decomposed by alkalization, as demonstrated by curve b' in Fig. 7.

Unreduced β -MSA is completely transformed into α -MSA by boiling the solution for a few minutes. The effect of the degree of reduction of the β -MSA on the stability on boiling was therefore investigated. Solutions containing β -MSA reduced to a definite degree were heated at boiling point for about 30 min. After cooling, the solutions were analysed voltammetrically. The curves obtained are shown in Fig. 8. Curves a and a' show the effect of heating unreduced β -MSA. Curves e

Table 1. Stability of β -MSA in an alkaline medium as a function of the degree of reduction

Initial solution of β -MSA ($1.5 \times 10^{-4} M$) in 0.1M HCl		Solutions obtained by alkalization and re-acidification of initial solution	
Degree of reduction of β -MSA	$E_{1/2}$ values of the first wave, V vs. SCE	$E_{1/2}$ values of the first wave, V vs. SCE	Height of the first wave, μA
0	+0.32	—	0
0.9/12	+0.32	+0.32	2.55
1.2/12	+0.31	+0.32	3.50
1.6/12	+0.32	+0.33	4.40
2.3/12	+0.31	+0.32	5.50
2.8/12	+0.32	+0.32	5.50

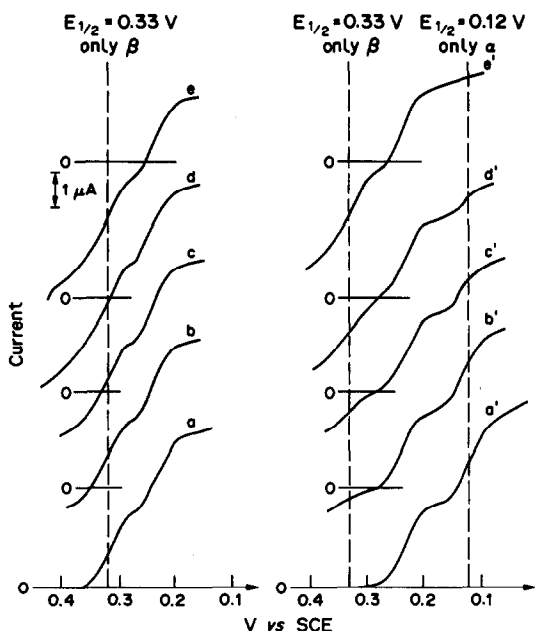


Fig. 8. DC voltammetric curves (rotating platinum electrode) for $2 \times 10^{-4}M$ solutions of β -MSA: a, non-reduced; b, reduced to the degree 0.3/12; c, reduced to the degree 0.8/12; d, reduced to the degree 1.3/12; e, reduced to the degree 2.3/12. Curves a', b', c', d', e' correspond to samples of solutions a, b, c, d, e cooled after previous heating to boiling.

and e' show that β -MSA reduced to at least the degree 2/12 is not transformed into α -MSA on boiling. Curves b', c' and d' are characteristic of a mixture of α -MSA and β -MSA. The concentration of β -MSA reduced exactly to a degree of 2/12 in this mixture is determined from the first anodic wave, the half-wave potential of which is +0.33 V (*vs.* SCE). The limiting current of this wave increases proportionally with increasing degree of reduction of β -MSA, as shown by comparison with curves b, c and d. This confirms the conclusion already drawn that β -MSA with an apparent degree of reduction less than 2/12 is a mixture of β -MSA reduced exactly to the degree 2/12 and unreduced β -MSA. Thus this experiment confirms the similarity of the results for α -MSA and β -MSA, and it is obvious that heating a solution of β -MSA that is reduced to less than a degree of 2/12 will not result in a pure solution of the corresponding reduced α -MSA, a fact that may lead to error in spectrophotometric determination of silicon (industrial samples are often contaminated with a reducing agent). Massart and co-workers^{5,6} reported that the decomposition of β -MSA reduced to the degree 2/12 in acidic medium results in a mixture of unreduced β -MSA and

β -MSA reduced to the degree 4/12. They also reported that α -MSA behaves similarly (but in alkaline medium), which implies that a mixture of unreduced MSA and MSA reduced to a degree of 4/12 is stable. As this opinion is contrary to ours, some further experiments were performed. The solutions were prepared by dissolving solid unreduced α -MSA or β -MSA in 0.1M hydrochloric acid, and were divided into two parts. In one the MSA was reduced to the degree of 4/12. A volume V_1 of this reduced solution was mixed with volume V_2 of the unreduced solution, in a ratio V_1/V_2 that would give an apparently reduced MSA solution. In the mixed solution, no unreduced α -MSA was found by alkalization and re-acidification of the solution, which leads to the conclusion that yellow α -MSA (0)_x is chemically reduced by α -MSA (4)_x to a degree of at least 2/12.

In an analogous experiment with β -MSA, no unreduced β -MSA was found in the mixture of reduced and unreduced forms, and no transformation of β -MSA into α -MSA on boiling for 30 min was found either, as shown by the half-wave potentials and limiting currents.

Conclusions

- (1) α -MSA and β -MSA reduced to a degree of 2/12 or more are stable compounds in alkaline solutions.
- (2) β -MSA reduced to a degree of 2/12 or more is not transformed into α -MSA when heated.
- (3) α -MSA and β -MSA solutions with an apparent degree of reduction less than 2/12 should be treated as mixtures of unreduced MSA and MSA reduced exactly to a degree of 2/12.
- (4) Mixtures of unreduced MSA and MSA reduced to a degree of 4/12 are not stable systems, the unreduced MSA being reduced to a degree of 2/12.

These four points have some consequences for determination of silicon as silicomolybdate, as follows.

- (1) For determination of silicon as reduced MSA in alkaline medium (pH > 8), the MSA must be reduced to a degree of 2/12 or more.

- (2) Pure α -MSA cannot be obtained by heating a solution containing a mixture of unreduced β -MSA and β -MSA reduced to a degree of 2/12.

- (3) For spectrophotometric determination of silicon as reduced MSA in the presence of excess of molybdate, it is best to alkalinize the solution before measurement, since doing so will decompose any reduced isopolymolybdates, without

affecting the MSA reduced to a degree of 2/12 or more.

(4) In alkaline medium reduced MSA is oxidized by air and the oxidized MSA is then decomposed. Hence such solutions must be protected from atmospheric air.

REFERENCES

1. J. D. H. Strickland, *J. Am. Chem. Soc.*, 1952, **74**, 868, 872.
2. L. G. Hargis, *Anal. Chem.*, 1970, **42**, 1497.
3. B. P. Sen and S. N. Chatterjee, *ibid.*, 1966, **38**, 536.
4. R. Massart and G. Herve, *Rev. Chim. Min.*, 1968, **5**, 501.
5. R. Massart, *Ann. Chim. (Paris)*, 1969, **4**, 285, 365, 441.
6. J. P. Launay, R. Massart and P. Souchay, *J. Less-Common Metals*, 1974, **36**, 139.
7. V. W. Truesdale and C. J. Smith, *Analyst*, 1975, **100**, 203, 797; 1977, **102**, 73; 1979, **104**, 897.
8. R. A. Chalmers and A. G. Sinclair, *Anal. Chim. Acta*, 1965, **33**, 384.
9. T. Škerlak, *Bull. Soc. Chim. Rep. Populare Bosnie et Herzégovine*, 1956, **5**, 27, 43; *Chem. Abstr.*, 1957, **51**, 12747b.
10. T. Škerlak and B. Skundric, *Glasnik Društva Hemicara Tehnol. N.R. Bosne-Hercegovine*, 1960, **9**, 19; *Chem. Abstr.*, 1962, **57**, 5384c.
11. W. Kemula and S. Rosołowski, *Rocz. Chem.*, 1962, **36**, 1417.
12. R. Massart and P. Souchay, *Compt. Rend.*, 1963, **257**, 1297.
13. R. Massart, *Ann. Chim. (Paris)*, 1968, **3**, 507.
14. Z. Kowalski, *Zeszyty Naukowe AGH, Ceramika*, 1971, No. 20.
15. F. Umland, F. Pottkamp and F. Alt, *Z. Anorg. Allg. Chem.*, 1973, **395**, 320.
16. L. D. Paklerova and S. V. Lugovoi, *Zh. Fiz. Khim.*, 1976, **50**, 2892.
17. S. V. Lugovoi and L. D. Paklerova, *Zh. Neorgan. Khim.*, 1977, **22**, 1550.
18. A. C. Barbosa and F. A. Tourinho, *Anal. Lett.*, 1984, **17**, 957.
19. A. C. Barbosa and P. A. Tourinho, *ibid.*, 1984, **17**, 2159.
20. A. Ringbom, P. E. Ahlers and S. Sittonen, *Anal. Chim. Acta*, 1959, **20**, 78.
21. V. Kratochvil, *Chem. Listy*, 1965, **59**, 672.
22. R. A. Chalmers and A. G. Sinclair, *Anal. Chim. Acta*, 1966, **34**, 412.
23. Y. Kakita and H. Goto, *Talanta*, 1967, **14**, 543.
24. A. A. Nemodruk and E. V. Bezrogova, *Zh. Analit. Khim.*, 1970, **25**, 1587.
25. J. D. Ingle, Jr. and S. R. Crouch, *Anal. Chem.*, 1971, **43**, 7.
26. K. Kato, *Anal. Chim. Acta*, 1976, **82**, 400.
27. A. G. Fogg and A. A. Osakwe, *Anal. Lett.*, 1976, **9**, 23.
28. *Idem*, *Talanta*, 1978, **25**, 226.
29. A. G. Fogg and N. K. Bsebsu, *ibid.*, 1981, **28**, 473.
30. A. L. Wilson, *Analyst*, 1965, **90**, 270.
31. P. G. Brewer and J. P. Riley, *Anal. Chim. Acta*, 1966, **35**, 544.
32. V. W. Truesdale and C. J. Smith, *Analyst*, 1976, **101**, 19.
33. Z. Kowalski, J. Migdalski and E. Kolder, *Chem. Anal. (Warsaw)*, 1976, **21**, 655.
34. T. Moeller, *Inorganic Chemistry*, Wiley, New York, 1952.

A NEW DESIGN OF LEAD AMALGAM/LEAD SULPHATE ELECTRODE FOR POTENTIOMETRIC MEASUREMENT OF SULPHATE

P. LUTS, J. L. C. VANHEES, J. H. E. YPERMAN,
J. M. A. MULLENS and L. C. VAN POUCKE*

Inorganic and Physical Chemistry, Limburgs Universitair Centrum, Universitaire Campus,
B-3610 Diepenbeek, Belgium

(Received 8 April 1989. Revised 21 July 1989. Accepted 15 September 1989)

Summary—A new lead amalgam/lead sulphate electrode has been developed which is easy to handle and can be used in a simple measuring cell. Its electrochemical characteristics have been tested in two different cell systems. The potentials obtained were very stable, and reproducible within ± 0.04 mV. The electrode exhibited a Nernstian response to sulphate and its calculated standard potential (-350.68 ± 0.13 mV) agreed very closely with that recorded in the literature.

For determination of the stability constants of sulphato-complexes of metal ions it is very useful to measure the concentration of the free ligand. Despite the remarkable improvement of ion selective electrodes (ISEs) in the last few decades, no satisfactory electrode is available for the determination of sulphate.

Of the various kinds of sulphate electrodes reported in the literature,¹⁻⁶ amalgam electrodes are still preferred for precise electromotive-force (emf) measurements of ions in solution, because of their high accuracy and selectivity.^{7,8} A thorough study of the conditions necessary for precise emf measurements with lead amalgam/lead sulphate electrodes was made by Bray,⁹ who drew the following conclusions: (i) oxygen must be excluded from the cell to prevent the formation of oxide layers on the surface of the amalgam; (ii) a definite crystalline form of lead sulphate is necessary; (iii) equilibrium between the solid lead sulphate and the solution is best established before the electrode is made up; (iv) the use of two-phase amalgams is essential if the activity of the lead in the amalgam phase is to be invariant.¹⁰ To fulfil conditions (i)–(iv), complicated measuring vessels were used in earlier investigations¹¹⁻¹³ of lead amalgam/lead sulphate electrodes.

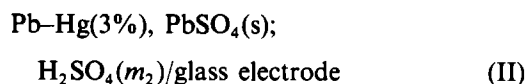
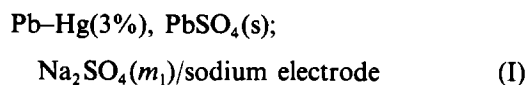
Ohtaki⁷ described suitable apparatus for the preparation of amalgam electrodes, and this has been used in our laboratory for the preparation of an indium amalgam electrode which shows

excellent electrochemical behaviour.^{14,15} However, this design cannot be used for the present purpose, because of the need for a lead sulphate layer above the metal amalgam. Therefore, a particular design and method of construction of a lead amalgam lead/sulphate electrode for precise potentiometric measurements in a simple measuring cell have been developed.

EXPERIMENTAL

Electrodes and apparatus

All measurements were made in a box thermostatically controlled at $25.0 \pm 0.2^\circ$. The double-walled glass cell was independently kept at $25.00 \pm 0.02^\circ$. Before and during the experiment, nitrogen was bubbled through and over the solution. A magnetic stirrer was used. The electrode potentials were measured with a Keithley 197 digital voltmeter equipped with an operational amplifier (Analog Devices AD515LH) to create a high-impedance input for the measuring circuit. The sulphate electrode construction is illustrated in Fig. 1a. A platinum wire contact, Φ , with a purity of 99.99%, is used to avoid the formation of other metal amalgams. The electrochemical behaviour of this sulphate electrode was investigated with the following cells:



*To whom correspondence should be addressed.

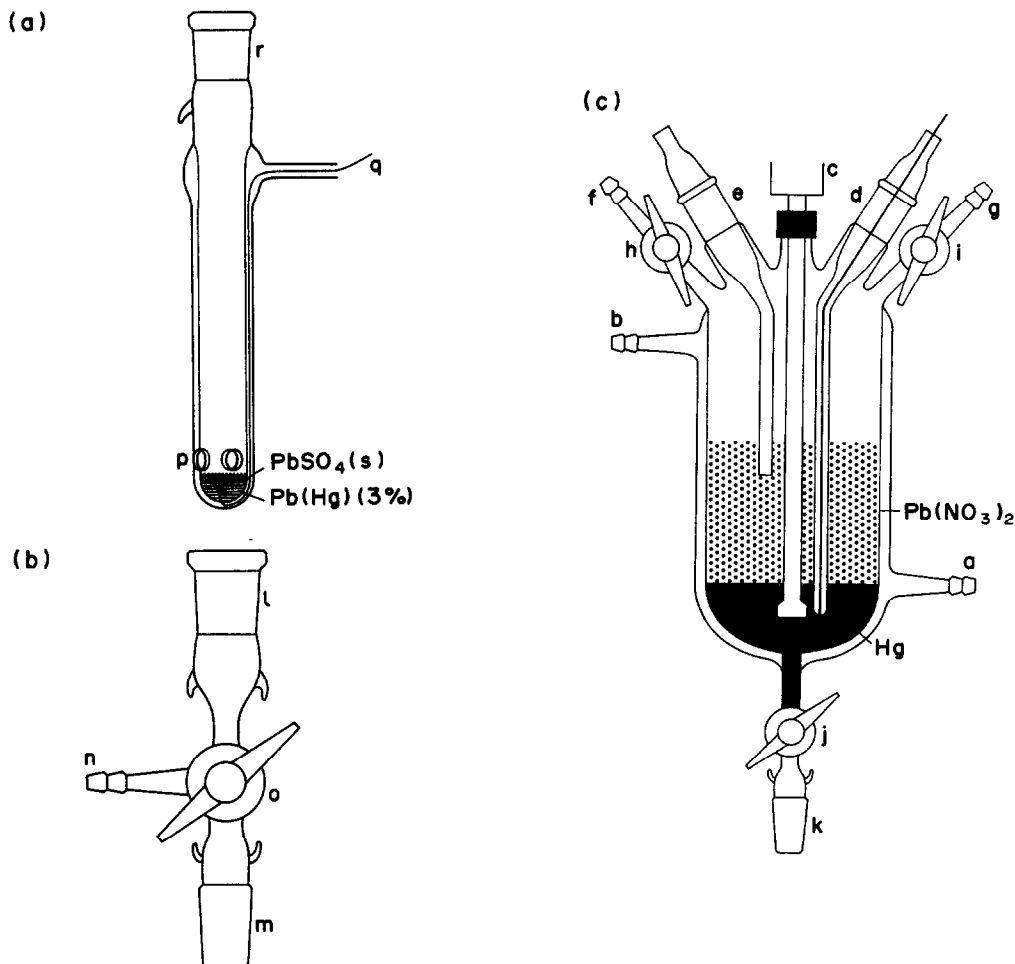


Fig. 1

An Ingold sodium-sensitive glass electrode (Type 10 205 3064) was used. Proton activities were determined with an Ingold glass electrode (LOT 271.TT.S7). The standard potentials and Nernstian responses of the pH and sodium electrodes were determined with cells (III) and (IV):

Ag, AgCl(s);

NaCl (m_3)/sodium electrode (III)

Ag, AgCl(s); HCl (m_4)/glass electrode (IV)

The silver-silver chloride electrodes were made by procedures analogous to those given by Ives and Janz¹ for the thermal electrolytic type. Bias potentials between different electrodes were less than 0.02 mV and changed by less than 0.01 mV over periods of several days.

Densities of solutions were measured with an Anton Paar digital density meter (Modules 60, 602 and 602M) with a precision of ± 0.00002 g/ml.

Reagents

Lead sulphate was prepared by adding 0.4M sodium sulphate solution in stoichiometric proportion to a solution of lead nitrate. The precipitate was washed repeatedly by decantation and stored under water. High-quality mercury was obtained as described elsewhere.¹³ Merck Titrisol 0.1M hydrochloric acid was used. Merck Titrisol 0.005 and 0.05M sulphuric acid solutions were prepared and further diluted with doubly distilled water as required. All other chemicals used were of analytical grade.

Preparation of lead amalgam

An amalgam containing about 3% w/w lead was prepared electrolytically after unsuccessful attempts to obtain satisfactory amalgams from etched granular lead and purified mercury. The cathode compartment is shown in Fig. 1c. A 3% w/w lead amalgam separates into two phases at 25° but coalesces to a single phase when heated to above 80°,¹⁰ allowing homogeneous transfer.

During electrolysis the mechanical stirrer ensures the formation of a homogeneous amalgam. Electrical contact is made by the platinum electrode *d* and the liquid junction *e* to the anode compartment, which consists of a vessel filled with 1*m* nitric acid and containing a large platinum electrode. The liquid junction is made by applying a vacuum at an inverted Y-connection between the compartments. To avoid syphoning of the solution between the two compartments, care is taken to ensure that both levels are the same. The cathode compartment contains 200 g of mercury and twice as much 1*m* lead nitrate as that required for the electrolysis, so that the concentration of lead ions is always in vast excess relative to any impurity, thereby reducing the possibility of discharging foreign cations in the later stages of the electrolysis. A current of 0.07 A is required for about 24 hr to give an amalgam of the desired composition. During the electrolysis the amalgam is not susceptible to oxidation, but once the applied potential is removed, precautions are necessary; 15 min before the electrolysis is complete, the cathode compartment is flushed with oxygen-free nitrogen through the inlet and outlet tubes *f* and *g*. Subsequently, while a vigorous stream of nitrogen flows into the cathode compartment at *f* and out at *g*, the anode compartment is disconnected and the stirrer and platinum electrode are removed from the cathode compartment and replaced by stoppers. Finally, taps *h* and *i* are closed, while a positive pressure of nitrogen is maintained. Amalgams prepared in this manner can be stored for about two weeks. A very sensitive indication of oxidation of the amalgam is its adhesion to glass.⁷

Sulphate electrode preparation

The electrode body is immersed in the cell solution, passing through a fitting on the sealed titration vessel containing the test solution (Fig. 1a), which is freed from oxygen by passage of nitrogen through it for 30 min before introduction of the lead amalgam. As soon as sufficient oxygen-free solution can enter the electrode body through the three holes *p* (Fig. 1a), the cathode compartment is attached to the electrode by means of the simple transfer apparatus shown in Fig. 1b (connections *k-l* and *m-r*). This connector allows transfer of the amalgam without oxidation. While the amalgam is heated to about 80° by the water jacket, a balloon connected to the outlet tube *g* compensates the pressure difference, and a vigorous

stream of nitrogen is passed through the system by the route *n-o-(l)-m-r-p*. When all traces of the solid phase HgPb₂ have disappeared, part of the amalgam is allowed into the electrode body by turning tap *j*, under continuous nitrogen flow. In this manner the amalgam is transferred into an oxygen-free solution in the sulphate electrode, and the cathode compartment and transfer apparatus can then be removed. Finally, lead sulphate is brought into the electrode through *r* to form a thin layer. Direct contact between the amalgam and the atmosphere is prevented by the oxygen-free solution in the titration vessel. During all these manipulations a continuous nitrogen flow is maintained through the test solution.

RESULTS AND DISCUSSION

In the first stage, the electrochemical characteristics of the lead amalgam/lead sulphate electrode were investigated with cell (I). The Nernst equation for this cell is:

$$E_1 = E_{\text{Na}^+}^0 - E_{\text{SO}_4^{2-}}^0 + (RT/2F) \times \ln[(m_{\text{Na}^+})^2 (\gamma_{\text{Na}^+})^2 m_{\text{SO}_4^{2-}} \gamma_{\text{SO}_4^{2-}}] \quad (1)$$

With $m_{\text{Na}^+} = 2m_1$, $m_{\text{SO}_4^{2-}} = m_1$ and $\gamma_{\pm} = \gamma_1 = [(\gamma_{\text{Na}^+})^2 \gamma_{\text{SO}_4^{2-}}]^{1/3}$ equation (1) becomes:

$$E_1 = E_{\text{Na}^+}^0 - E_{\text{SO}_4^{2-}}^0 + (RT/2F) \ln 4 + (3RT/2F) \ln(m_1 \gamma_1) \quad (2)$$

During preliminary experiments the effects of controllable variables were examined. A change in stirring rate, the thickness of the lead sulphate layer and the depth of immersion of the electrodes in the solution did not affect the cell potential. The effect of bubbling nitrogen through the solutions was more critical. A vigorous stream of nitrogen increases the evaporation of the solution, but slow bubbling increases the risk of oxidation. Thus the nitrogen flow-rate must be adapted to the experimental conditions (e.g., equilibration time, stirring rate, cell construction). The most significant factor in obtaining stable and reproducible potentials was the need to clean the platinum wire *q* thoroughly before each preparation of the lead amalgam. Both concentrated nitric acid and *aqua regia* had to be used in the cleaning, probably because of the formation of platinum amalgam at higher temperatures.¹⁰ With all these conditions fulfilled, emf values stable and reproducible within ± 0.04 mV could be

obtained after an equilibration time of 1 hr and maintained for at least 3 hr.

To evaluate the standard potential and the response of the sulphate electrode by use of cell (I), knowledge of E^0 of the sodium electrode was required. This potential was obtained by titration of 20 ml of 0.1002*m* sodium chloride (density 1.00116 ± 0.00002 g/ml) with 20 ml of water (density 0.9970429 g/ml) in cell (III), with emf readings taken at 12 titration points. The equation for the cell potential is:

$$E_{\text{III}} = E_{\text{Na}^+}^0 - E_{\text{Ag,AgCl}}^0 + (2RT/F) \ln(m_3 \gamma_3) \quad (3)$$

$E_{\text{Ag,AgCl}}^0$ is 222.34 ± 0.01 mV at 25° .^{16,17} The molality m_3 after each addition could be calculated from the density of the initial solution. To obtain the mean activity coefficients γ_3 for an arbitrary molality m_3 , Pitzer's equation^{18,19} was used:

$$\ln \gamma_{\text{MX}} = |z_{\text{M}} z_{\text{X}}| f^\gamma + m(2v_{\text{M}} v_{\text{X}}/v) B^\gamma + m^2 [(2/v)(v_{\text{M}} v_{\text{X}})^{3/2}] C^\gamma \quad (4)$$

where f^γ , B^γ and C^γ are given by the equations:

$$f^\gamma = -A^\phi \{ [I^{1/2}/(1 + bI^{1/2})] + (2/b) \ln(1 + bI^{1/2}) \} \quad (5)$$

$$B^\gamma = 2\beta_{\text{MX}}^0 + (2/\alpha^2 I) \beta_{\text{MX}}^1 \times [1 - (1 + \alpha I^{1/2} - \alpha^2 I/2) e^{-\alpha I^{1/2}}] \quad (6)$$

$$C^\gamma = 3C_{\text{MX}}^\phi/2 \quad (7)$$

In these equations m is the molality of the electrolyte, v_{M} and v_{X} are the numbers of M and X ions in the formula and z_{M} and z_{X} the charge numbers of M and X; $v = v_{\text{M}} + v_{\text{X}}$, and $I = 1/2 \sum m_i z_i^2$ is the ionic strength. A^ϕ is the Debye-Hückel osmotic coefficient and is given by:

$$A^\phi = (1/3) (2\pi N_0 d_w / 1000)^{1/2} (e^2 / DkT)^{3/2} \quad (8)$$

where N_0 is Avogadro's number, d_w the density of water, D the dielectric constant of water at absolute temperature T , k the Boltzmann constant and e the electronic charge. The value of A^ϕ at 25° is 0.392. The two parameters β_{MX}^0 and β_{MX}^1 define the second virial coefficient and C_{MX}^ϕ

defines the third virial coefficient. For the parameters b and α , the values 1.2 and 2.0 respectively were selected.¹⁸ The parameters β_{MX}^0 , β_{MX}^1 and C_{MX}^ϕ for various single electrolytes are tabulated in the literature^{19,20} for concentrations up to 6*m*. In this investigation, the ion interaction parameters for the electrolytes NaCl, HCl and Na₂SO₄ were evaluated in a small dilute concentration range. A computer program was developed in our research group to fit equation (4) to the experimental activity coefficient data¹⁶ at 25° . In this program, the function $U = \sum (1/\sigma_i^2) (\ln \gamma_i^{\text{exp}} - \ln \gamma_i^{\text{calc}})^2$ is minimized, where $1/\sigma_i^2$ is a weighting factor. Occasionally, in the past, particular weights have been given to various data in obtaining best values of the parameters, e.g., 1 for $0 < I < 4$, and $(4/I)^2$ for $I > 4$.¹⁸ In our calculations $\sigma_i^2 = [d(\ln \gamma_{\text{MX}})/dm]^2 \sigma_m^2$ is used. Since σ_i is solely dependent on m , the value for σ_m can be chosen arbitrarily.

$$d(\ln \gamma_{\text{MX}})/dm = |z_{\text{M}} z_{\text{X}}| f^{*\gamma} + (2v_{\text{M}} v_{\text{X}}/v) B^{*\gamma} + m(2v_{\text{M}} v_{\text{X}}/v) B^{*\gamma} + 2m[(2/v)(v_{\text{M}} v_{\text{X}})^{3/2}] C^\gamma \quad (9)$$

where

$$f^{*\gamma} = -A^\phi I^{1/2} \{ 1/[2m(1 + bI^{1/2})^2] + 1/[m(1 + bI^{1/2})] \} \quad (10)$$

$$B^{*\gamma} = (-2\beta_{\text{MX}}^1/\alpha^2 I m) \times [1 - (1 + \alpha I^{1/2} + \alpha^2 I/2 - \alpha^3 I^{3/2}/4) e^{-\alpha I^{1/2}}] \quad (11)$$

In all the calculations, the third virial coefficient can be omitted since this term is not required for low concentrations. The results for the electrolytes NaCl, HCl and Na₂SO₄ are given in Table 1.

The standard potential of the sodium electrode used was determined just before the experiments with the sulphate electrode in cell (I) by plotting and extrapolating the curve of E vs. $\log(m_3 \gamma_3)$. The results are given in Table 2. The slopes obtained at 25° are Nernstian. An E^0

Table 1. Parameters of the Pitzer equation for the electrolytes NaCl, HCl and Na₂SO₄

Electrolyte	β_{MX}^0	β_{MX}^1	Concentration range	Maximum deviation ($\gamma^{\text{exp}} - \gamma^{\text{calc}}$)*
NaCl	0.01752	0.3846	$0 < m < 0.1$	0.0004
HCl	0.2103	0.2945	$0 < m < 0.1$	0.0010
Na ₂ SO ₄	0.02557	1.0628	$0 < m < 0.5$	0.0003

*For γ^{exp} see Robinson and Stokes.¹⁶

Table 2. Standard potential and Nernstian behaviour of the cells used

Slope	E^0_{cell}, mV		Cell No.
86.82 ± 0.09	704.63 ± 0.08	$E^0_{\text{SO}_4^{2-}} = -350.73 \pm 0.13 \text{ mV}$	I
88.64 ± 0.02	973.15 ± 0.04	$E^0_{\text{SO}_4^{2-}} = -350.63 \pm 0.13 \text{ mV}$	II
117.86 ± 0.03	113.75 ± 0.04	$E^0_{\text{Na}^+} = 336.09 \pm 0.05 \text{ mV}$	III
118.41 ± 0.06	400.18 ± 0.08	$E^0_{\text{GE}} = 622.52 \pm 0.09 \text{ mV}$	IV

value of $336.09 \pm 0.05 \text{ mV}$ was obtained for the sodium electrode by means of a linear least-squares fit.

Immediately after these experiments, the sodium-sensitive glass electrode was used in cell (I) for the titration of 20 ml of 0.5033*m* sodium sulphate (density $1.05772 \pm 0.00002 \text{ g/ml}$) with water. After each addition, m_1 and γ_1 were calculated by the same procedure as for the calculation of m_3 and γ_3 . The results of the linear least-squares analysis of the curve plotted for E vs. $\log(m_1\gamma_1)$ are given in Table 2. The standard potential obtained for the sulphate electrode ($-350.73 \pm 0.13 \text{ mV}$) is in good agreement with published values (Table 3).

To test the reproducibility of preparation of the lead amalgam/lead sulphate electrode, a batch method was used with cell (II) and seven sulphuric acid concentrations of 0.04985, 0.02501, 0.009999, 0.007499, 0.004972, 0.002499 and 0.0009998*m*. To ensure reliable and reproducible emf values, all solutions were measured twice with a freshly prepared electrode. The standard potential of the glass electrode was determined before and after these experiments, by titration of 40 ml of 0.09950*m* hydrochloric acid (density = $0.99885 \pm 0.00002 \text{ g/ml}$) with water in cell (IV) and by using the same evaluation procedure as described above. The results are summarized in Table 2. Various assumptions, models, extrapolation methods and corrections for the solubility of lead sulphate can be used in the calculation of the E^0 value and the response slope of the sulphate electrode.^{12, 13, 21}

The dependence of the solubility, S , of lead sulphate on sulphuric acid concentration²²⁻²⁴ was taken into account by means of a polynomial regression analysis of a plot of S vs. $\ln m_2$. These corrections were not necessary for cell (I) since the solubility of lead sulphate in the sodium sulphate solutions investigated was negligible.²⁵ To calculate the mean activity coefficients, γ_2 , for the seven sulphuric acid solutions, the parameters β^0_{MX} and β^1_{MX} in Pitzer's equation were optimized with respect to experimental γ_2 values.^{16, 26} However, no minimum was observed. An extended Pitzer equation is necessary for the sulphuric acid system, where not only ionic interactions but also an association equilibrium must be taken into account.^{18, 27} To avoid an extra experimental parameter (*i.e.*, the second dissociation constant of sulphuric acid) equation (12) was optimized with respect to experimental γ_2 -values:

$$\begin{aligned} \ln \gamma_{\text{MX}} + |z_{\text{M}}z_{\text{X}}| A^{\phi} I^{1/2} / (1 + bI^{1/2}) \\ = DI^{1/4} + EI^{1/2} + FI^{3/4} + GI + H \quad (12) \end{aligned}$$

The parameters D , E , F , G and H were obtained by a polynomial regression analysis of the function $\ln \gamma_{\text{MX}} + |z_{\text{M}}z_{\text{X}}| A^{\phi} I^{1/2} / (1 + bI^{1/2})$ vs. $I^{1/4}$. With the same procedure as described above for the calculation of the E^0 value of an electrode together with corrections for the solubility of lead sulphate, very satisfactory results were obtained, as shown in Table 2.

The experimental slopes are Nernstian and the calculated standard potential is in excellent

Table 3. Literature values for the standard potential of the lead amalgam/lead sulphate electrode

Cell	$E^0_{\text{SO}_4^{2-}}, mV$	References
Pt, H ₂ ; H ₂ SO ₄ (<i>m</i>); PbSO ₄ (s), Pb-Hg	-350.52	12
Pt, H ₂ ; H ₂ SO ₄ (<i>m</i>); PbSO ₄ (s), Pb-Hg	-351.3 ± 0.3	20
Pt, H ₂ ; H ₂ SO ₄ (<i>m</i>); PbSO ₄ (s), Pb-Hg	-351.75 to -352.80	27
Pt, H ₂ ; H ₂ SO ₄ (<i>m</i>); PbSO ₄ (s), Pb-Hg	-352.17	11
Ca ²⁺ -ISE//CaSO ₄ (<i>m</i>); PbSO ₄ (s), Pb-Hg	-352.6 ± 0.4	28
{ Zn-Hg; ZnX ₂ (<i>m</i>); AgX, Ag X = Cl, Br Zn-Hg; ZnSO ₄ (<i>m</i>); PbSO ₄ (s), Pb-Hg	-349.4 to -350.2	19, 29, 30
{ Zn-Hg; ZnSO ₄ (<i>m</i>); PbSO ₄ (s), Pb-Hg $E^0_{\text{Zn-Hg}} = 762.80 \text{ mV}$	-350.49	13
Pb-Hg(3%), PbSO ₄ (s); Na ₂ SO ₄ (<i>m</i>)/sodium electrode	-350.73 ± 0.13	This work
Pb-Hg(3%), PbSO ₄ (s); H ₂ SO ₄ (<i>m</i>)/glass electrode	-350.63 ± 0.13	This work

agreement with the literature values, summarized in Table 3. These results indicate that the lead amalgam/lead sulphate electrode, prepared as described, behaves correctly.

CONCLUSIONS

A new lead amalgam/lead sulphate electrode which exhibits good electrochemical behaviour has been developed. Its main advantage is that the severe precautions necessary to obtain a satisfactory lead amalgam/lead sulphate electrode can be achieved with a simple measuring system. The availability of a satisfactory electrode for the determination of the sulphate ion is very useful in several applications, *e.g.*, determination of the stability constants of sulphato-complexes of metal ions.

Acknowledgement—The authors are indebted to the I.W.O.N.L., Belgium for financial support.

REFERENCES

1. D. J. G. Ives and G. J. Janz, *Reference Electrodes, Theory and Practice*, Chapter 8, Academic Press, New York, 1961.
2. K. Nagy and T. A. Fjeldly, *Talanta*, 1979, **26**, 811.
3. W. Misniakiewicz and K. Raszka, in *Ion-selective Electrodes*, E. Pungor and I. Buzas, p. 467. Elsevier, Amsterdam, 1978.
4. M. S. Mohan and G. A. Rechnitz, *Anal. Chem.*, 1973, **45**, 1323.
5. T. Cserfalvi and G. G. Guilbault, *Anal. Chim. Acta*, 1976, **84**, 259.
6. E. W. Baumann, *ibid.*, 1978, **99**, 247.
7. H. Ohtaki, M. Tsurumi and T. Kawai, *Anal. Chem.*, 1977, **49**, 190.
8. H. P. Bennetto and A. R. Willmott, *Q. Rev. Chem. Soc.*, 1971, **25**, 501.
9. U. B. Bray, *J. Am. Chem. Soc.*, 1927, **49**, 2372.
10. M. Hansen and K. Anderko, *Constitution of Binary Alloys*, 2nd Ed., p. 829. McGraw-Hill, New York, 1958.
11. G. M. S. Baumstark, *Dissertation*, The Catholic University of America, 1932.
12. J. Shrawder and I. A. Cowperthwaite, *J. Am. Chem. Soc.*, 1934, **56**, 2340.
13. J. C. Rasaiah, *Dissertation*, University of Pittsburgh, 1965.
14. J. L. C. Vanhees, J. P. François and L. C. Van Poucke, *J. Phys. Chem.*, 1981, **85**, 1713.
15. J. L. C. Vanhees, J. P. François, J. M. A. Mullens, J. H. E. Yperman and L. C. Van Poucke, *ibid.*, 1985, **89**, 2661.
16. R. A. Robinson and R. H. Stokes, *Electrolyte Solutions*, 2nd Ed., Butterworths, London, 1959.
17. R. G. Bates and V. E. Bower, *J. Res. Natl. Bur. Stds.*, 1954, **53**, 283.
18. R. M. Pytkowicz, *Activity Coefficients in Electrolyte Solutions*, Vol. 1, CRC Press, Boca Raton, 1979.
19. K. S. Pitzer and G. Mayorga, *J. Phys. Chem.*, 1973, **77**, 2300.
20. H. T. Kim and J. Frederick, *J. Chem. Eng. Data*, 1988, **33**, 177.
21. K. S. Pitzer, *J. Phys. Chem.*, 1976, **80**, 2863.
22. M. Huybrechts and H. Ramelot, *Bull. Soc. Chim. Belg.*, 1927, **36**, 239.
23. R. B. Purdum and H. A. Rutherford, *J. Am. Chem. Soc.*, 1933, **55**, 3221.
24. D. N. Craig and G. W. Vinal, *J. Res. Natl. Bur. Stds.*, 1939, **22**, 55.
25. M. Huybrechts and N. A. De Langeron, *Bull. Soc. Chim. Belg.*, 1929, **38**, 43.
26. H. S. Harned and B. B. Owen, *The Physical Chemistry of Electrolyte Solutions*, 3rd Ed., Reinhold, New York, 1958.
27. K. S. Pitzer, R. N. Roy and L. F. Silvester, *J. Am. Chem. Soc.*, 1977, **99**, 4930.
28. T. H. Lilley and C. C. Briggs, *Electrochim. Acta*, 1975, **20**, 257.
29. K. S. Pitzer, *J. Phys. Chem.*, 1973, **77**, 268.
30. *Idem*, *J. Chem. Soc., Faraday Trans. II*, 1972, **68**, 101.

H⁺-SELECTIVE ELECTRODES BASED ON NEUTRAL CARRIERS: SPECIFIC FEATURES IN BEHAVIOUR AND QUANTITATIVE DESCRIPTION OF THE ELECTRODE RESPONSE

V. V. EGOROV and YA. F. LUSHCHIK

Institute for Physico-Chemical Problems, Byelorussian State University, Minsk, USSR

(Received 18 January 1989. Revised 24 August 1989. Accepted 29 September 1989)

Summary—The influence has been studied of the membrane and solution composition on the response of H⁺-ISEs with plasticized polymer and liquid membranes based on the neutral carriers *N,N*-dioctylaniline and tridecylamine in association with trioctyloxybenzene sulphonic acid. It is shown that the extraction processes at the membrane/solution interface exert the main effect on the response limits by inducing essential changes in the activity of potential-determining ions in the membrane. At low pH, the amine extraction of acids followed by neutralization (free amines binding in ion-pairs) is the relevant process, while at high pH it is the extraction of metal cations with amine salts of a lipophilic acid, with the consequent displacement of amine from the salts. Equations are suggested to represent the interphase potential of the H⁺-ISE membranes with allowance for these extraction processes. The experimental electrode responses of both liquid and polymer membranes are shown to be well described by the equations for the interphase potential, thus indicating its dominant contribution to the membrane potential.

The first H⁺-ion selective electrodes based on ionophores¹⁻⁴ have already exhibited a number of advantages over the traditional glass H⁺-electrodes, including low resistance (with consequent advantages for miniaturization), safe handling, and promising applications in some aggressive media. Therefore, although H⁺-ISEs based on ionophores are characterized by much lower selectivity and narrower response ranges than glass electrodes, their applications in medical and biological studies, where they have most advantages over glass H⁺-ion selective electrodes, are still increasing. Various compounds have been studied as carriers of hydrogen ions, mainly aliphatic and heterocyclic amines and their derivatives,²⁻⁸ but also other sufficiently strong organic bases that can form a complex cation with a proton, *e.g.*, hexabutylphosphotriamide.⁹

Simon⁶ has shown for such electrodes that deviations from the ideal proton-response in the acidic region are caused by protonation of the membrane ionophore, while in the alkaline region metal cations interfere. The ISE response range (dynamic interval) depends mainly on the basicity of the carrier. Since Simon did not study in detail the effect of membrane/solution interface extraction on the form of the electrode response, his conclusions were basically qualita-

tive. Moreover, the mechanisms of the interfering effect of metal cations in alkaline media remains unclear.

The present work is aimed at developing a quantitative description of the potential of amine carrier-based H⁺-ISEs, allowing for membrane/solution extraction processes. The validity of this approach is supported by experimental measurements showing the electrode responses of the membranes to be well approximated by the boundary potential equations with regard to the extraction processes at the membrane/solution interface. Neglecting the contribution of the diffusion potential, which is difficult to allow for because of the mobility differences and activity gradients of charged components in the membrane, is, therefore, justifiable in these cases, although this may not always be so.

EXPERIMENTAL

Reagents

N,N-Dioctylaniline (DOA) and tridecylamine (TDA) of analytical grade were further purified¹⁰ and trioctyloxybenzene sulphonic acid (TOBS) was synthesized with a purity $\geq 97\%$ for use as the electroactive components in the

Table 1. Compositions of H⁺-ISE membranes used

Membrane	Membrane composition (the content of electroactive material is given in mole/kg or mole/l., other components in % w/w or v/v)								
	DOA	TDA	TOBS	PVC	DOP	1-BN	THP	Carbon tetrachloride	Nitrobenzene
I	0.050	—	—	24.5	73.6	—	—	—	—
II	0.050	—	0.026	24.2	72.6	—	—	—	—
III	—	0.050	0.026	24.1	72.3	—	—	—	—
IV	0.029	—	0.010	24.7	73.9	—	—	—	—
V	0.050	—	0.026	24.2	—	72.6	—	—	—
VI	—	0.050	0.026	24.1	—	72.3	—	—	—
VII	0.015	—	0.010	24.8	—	—	74.2	—	—
VIII	0.010	—	0.010	24.8	74.4	—	—	—	—
IX	0.012	—	0.010	24.8	74.3	—	—	—	—
X	—	0.029	0.010	24.6	73.6	—	—	—	—
XI	0.015	—	0.010	24.8	—	74.2	—	—	—
XII	—	0.001	0.0005	—	—	—	—	90	10

membranes. Poly(vinyl chloride) (PVC) PZh-S-70 was used as the membrane matrix and was dissolved in commercial grade cyclohexanone that had previously been distilled. Dioctyl phthalate (DOP), trihexylphosphate (THP) and 1-bromonaphthalene (1-BN) of commercial grade, nitrobenzene of analytical grade and carbon tetrachloride of reagent grade were used as membrane plasticizers or solvents. DOP and THP were purified by acid treatment¹¹ and 1-BN was distilled. The membranes prepared from these components are summarized in Table 1.

Distilled water solutions of electrolytes were made from boric, acetic, phosphoric, hydrofluoric, hydrochloric and perchloric acids as well as sodium, potassium, rubidium and caesium chlorides, sodium thiocyanate and bromide, sodium hydroxide and silver nitrate. These electrolytes were of at least analytical reagent grade.

Preparation of samples

The ISE membranes were produced conventionally.¹² The buffer solutions for pH between 1.8 and 12.0 were made by mixing acetic, phosphoric and boric acids and sodium hydroxide.¹³ The same mixtures were employed to prepare buffered solutions of sodium chloride, sodium thiocyanate and other salts. Hydrochloric acid was used to adjust solutions to pH < 1.8.

Estimation of extraction equilibrium constants

The extraction equilibrium constants, equations (7) and (18) below, were measured at 293 ± 1 K. In determining the extraction constants of hydrobromic and thiocyanic acids, the initial TDA concentration in the organic phase was 0.01M, the sodium thiocyanate concentration was 0.01M and the sodium bromide con-

centration ranged from 0.01 to 0.1M. The aqueous phase pH was adjusted with universal buffer mixture solutions in the range 1.8–7.0. The equilibrium concentrations of either bromide and thiocyanate in the aqueous and organic phases or of free amine in the organic phase were measured, depending on the extraction range. The anions were measured by potentiometric titration with silver nitrate in 1-propanol. Free TDA concentrations were measured by potentiometric titration with hydrochloric acid solution in acetic acid. The equilibrium concentrations of the other components were determined by difference. The extraction constants were calculated from the formula:

$$K_{\text{ex}}^a = \frac{\bar{C}_{\text{AmH}^+\text{X}^-}}{\bar{C}_{\text{Am}} C_{\text{X}^-} a_{\text{H}^+}} \quad (1)$$

where $\bar{C}_{\text{AmH}^+\text{X}^-}$ and \bar{C}_{Am} are the equilibrium concentrations of the ion-associate and free amine in the organic phase and a_{H^+} and C_{X^-} are the hydrogen-ion activity and the acid anion concentration, respectively.

In assessing the extraction constants of sodium ions, the initial concentrations of TDA and DOA in the organic phase ranged from 0.011 to 0.015M, that of TOBS was 0.010M and the sodium bromide concentration in the aqueous phase ranged between 0.1 and 0.065M. When equilibrium had been achieved, the organic phase was separated and the sodium ions were re-extracted with an equal volume of 0.1M hydrochloric acid. The sodium concentration in this aqueous phase was measured with a PFM-U4.2 flame photometer. The extraction constants were estimated from the formula

$$K_{\text{ex}}^b = \frac{\bar{C}_{\text{M}_e^+\text{R}^-} \bar{C}_{\text{Am}}}{C_{\text{AmH}^+\text{R}^-} C_{\text{M}_e^+} a_{\text{OH}^-}} \quad (2)$$

where $\bar{C}_{M^+R^-}$ is the concentration of the ion-associate of the metal cation with the TOBS anion, $\bar{C}_{AmH^+R^-}$ is the concentration of the protonated amine ion-associate with the TOBS anion and a_{OH^-} and C_{M^+} are the hydroxide ion activity and metal ion concentration, respectively.

Potentiometric measurements

Potentiometric measurements were performed with an EV-74 universal ionometer operated as a millivoltmeter. The pH-values of aqueous solutions were measured with an ESP-43-07 glass electrode and an EVL-IMZ silver-silver chloride reference electrode. Measurements were made at 293 ± 1 K with the cell

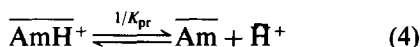
Ag, AgCl	KCl (sat.)	Sample solution	Membrane	Reference solution; buffer (pH 7.0 or 2.7), 0.1M NaCl	AgCl, Ag
----------	---------------	--------------------	----------	---	----------

RESULTS AND DISCUSSION

For the membranes under consideration, the potential is due to selective transfer of hydrogen ions from the sample solution to the membrane phase by means of an amine or other organic base:



Here and elsewhere, a bar indicates the membrane phase. The complex cation \bar{AmH}^+ is in equilibrium with free amine and hydrogen ions:

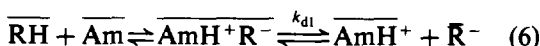


where K_{pr} is the amine protonation constant in the membrane phase.

According to the expression

$$E = E^0 + \frac{RT}{F} \ln \frac{a_{H^+}}{\bar{a}_{H^+}} \quad (5)$$

the proton-response will be ideal provided the activity of hydrogen ions in the membrane is constant. The latter condition is achieved by stabilizing the concentration of alkylammonium cations \bar{C}_{AmH^+} by adding a lipophilic acid RH in less than the amount equivalent to the amine in the membrane. An amine salt is thereby produced which partly dissociates into \bar{AmH}^+ and \bar{R}^- in the membrane:



where K_{d1} is the dissociation constant of the ion-pair $\bar{AmH}^+ \bar{R}^-$.

It is seen from Fig. 1 that inclusion of a subequivalent quantity of TOBS in the DOA-based membrane results in a Nernst slope for the proton-response and extends the electrode response range to a lower pH. Moreover, the TOBS-modified membrane has more stable potentials. Therefore, despite some reduction in sensitivity to H^+ at high pH, the advantages of the TOBS-modified membrane are greater than its shortcomings. Similar results were obtained for H^+ -selective membranes based on other neutral carriers and plasticizers as well as for liquid membranes.

The data in Figs 2 and 3 show that the upper response limit of the H^+ -ISE is strongly dependent on the nature of the anions in the test solution, on the neutral carrier and on the anion concentration. This parameter is also greatly affected by the solvent (plasticizer) and the amine:TOBS concentration ratio.

As noted above, protonation of the ionophore in the membrane is mainly responsible for the deviation of the proton-response of these H^+ -ISEs in acidic media.⁶ In this case, the extraction of acids from the test solution into the membrane phase is described by the equation

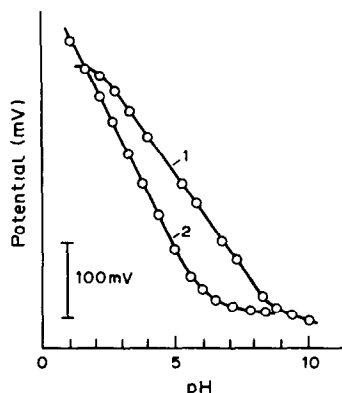
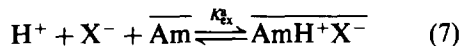


Fig. 1. TOBS effect on the DOA-based H^+ -ISE response in universal buffer solutions: (1) membrane I, without TOBS; (2) membrane II, with TOBS (compositions of the membranes are in Table 1).

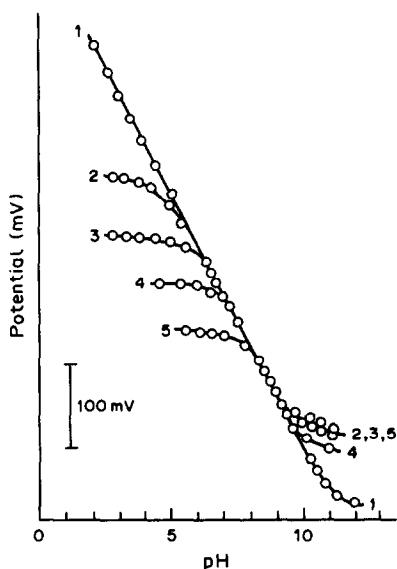


Fig. 2. Effect of nature and concentration of the anion on the TDA-based H^+ -ISE response (membrane III) in universal buffer solutions: (1) no background electrolyte, (2) 1.0M NaCl, (3) 1.0M NaBr, (4) 0.1M NaSCN and (5) 1.0M NaSCN.

where K_{ex}^a is the extraction constant of the ion-pair. The salt generated is partly dissociated into ions:



As a result, the concentration of the complex cation AmH^+ in the membrane layer adjacent to the test solution increases, while that of the free amine decreases, resulting, in accordance with equation (4), in the increasing activity of hydrogen ions in the membrane and, eventually, in distortion of the proton-response.

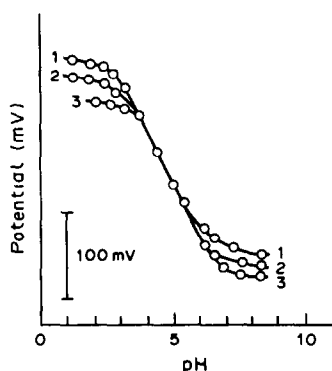


Fig. 3. Effect of plasticizer nature and Am:TOBS ratio on the upper response limit of H^+ -ISEs based on DOA in buffer solutions with 0.1M NaSCN: (1) DOP, Am:TOBS = 1.9:1 (membrane II); (2), DOP, Am:TOBS = 2.9:1 (membrane IV); (3) 1-BN, Am:TOBS = 1.9:1 (membrane V).

It is worth noting here that the formalism suggested by Morf^{14,15} for a quantitative description of the extraction effect on the membrane potential of cation-selective ISEs based on neutral carriers, which assumed complete ionic dissociation in the membrane phase, cannot directly be applied to H^+ -ISEs based on amine-type neutral carriers, because amine salts in the low dielectric constant media of ordinary ISE membranes mainly exist as non-associates. If the concentration of ions in such membranes can be neglected in comparison with the concentration of the ion-associates, the mass balance for the amine is

$$\overline{C}_{Am}^{tot} = \overline{C}_{AmH^+R^-} + \overline{C}_{AmH^+X^-} + \overline{C}_{Am} \quad (9)$$

where \overline{C}_{Am}^{tot} is the total concentration for all forms of the amine in the membrane, and $\overline{C}_{AmH^+R^-}$ is the concentration of the ion-pair of the complex alkylammonium cation with the lipophilic anion R^- introduced into the membrane. In the case considered, virtually all of the lipophilic acid HR introduced into the membrane is bound with amine as an ion-pair and so to a first approximation, $\overline{C}_{AmH^+R^-} = \overline{C}_R^{tot}$.

Subject to the condition of ideal behaviour of membrane components, from equations (7) and (9) we obtain the following expression for the concentration of the ion-pair AmH^+X^- extracted into the membrane:

$$\overline{C}_{AmH^+X^-} = \frac{K_{ex}^a (\overline{C}_{Am}^{tot} - \overline{C}_R^{tot}) a_{H^+} a_{X^-}}{1 + K_{ex}^a a_{H^+} a_{X^-}} \quad (10)$$

The concentrations of the free anions R^- and X^- in the membrane are

$$\overline{C}_{R^-} = \frac{\overline{C}_R^{tot} K_{d1}}{\overline{C}_{AmH^+}} \quad (11)$$

$$\overline{C}_{X^-} = \frac{\overline{C}_{AmH^+X^-} K_{d2}}{\overline{C}_{AmH^+}} \quad (12)$$

Since the concentration of free hydrogen ions in the membrane is much less than the concentration of alkylammonium cations AmH^+ , the electroneutrality condition is

$$\overline{C}_{AmH^+} = \overline{C}_{R^-} + \overline{C}_{X^-} \quad (13)$$

Combining (11), (12) and (13), we obtain

$$\overline{C}_{AmH^+} = \sqrt{\overline{C}_R^{tot} K_{d1} + \overline{C}_{AmH^+X^-} K_{d2}} \quad (14)$$

Taking into account that dissociation constants of ion-pairs depend only slightly on the nature of the anion, being mainly a function of the dielectric constant of the solvent,¹⁶ the following

approximation can be made: $K_{d_1} \approx K_{d_2} = K_d$. Then equation (14) becomes:

$$\bar{C}_{AmH^+} = \sqrt{(\bar{C}_R^{tot} + \bar{C}_{AmH^+X^-}) K_d} \quad (14')$$

In accordance with equation (4), the concentration of free hydrogen ions in the membrane is:

$$\bar{C}_{H^+} = \frac{\bar{C}_{AmH^+}}{\bar{C}_{Am} K_{pr}} \quad (15)$$

Substituting (10) and (14') into (15) yields the following expression for the hydrogen-ion concentration:

$$\bar{C}_{H^+} = \frac{\sqrt{\bar{C}_R^{tot} K_d}}{K_{pr}(\bar{C}_{Am}^{tot} - \bar{C}_R^{tot})} \times \sqrt{\left(1 + \frac{\bar{C}_{Am}^{tot}}{\bar{C}_R^{tot}}\right) K_{ex}^a a_{H^+} + a_{X^-} + \frac{\bar{C}_{Am}^{tot}}{\bar{C}_R^{tot}} (K_{ex}^a)^2 a_{H^+}^2 + a_{X^-}^2 + 1} \quad (16)$$

Equations (6) and (15) can be used to show that the first factor in equation (16) is the initial concentration of hydrogen ions in the membrane, $\bar{C}_{H^+}^0$.

Substituting \bar{C}_{H^+} from equation (16) into equation (5) and combining $\ln \bar{C}_{H^+}^0$ and the constants with E^0 (to give $E^{0'}$), we arrive at the membrane potential equation allowing for acid extraction from the sample solution

$$E = E^{0'} + \frac{RT}{F} \ln a_{H^+} - \frac{RT}{2F} \ln \left[\left(1 + \frac{\bar{C}_{Am}^{tot}}{\bar{C}_R^{tot}}\right) K_{ex}^a a_{H^+} + a_{X^-} + \frac{\bar{C}_{Am}^{tot}}{\bar{C}_R^{tot}} (K_{ex}^a)^2 a_{H^+}^2 + a_{X^-}^2 + 1 \right] \quad (17)$$

Analysis of equation (17) implies that when extraction is insignificant and the first two terms inside the square brackets can be neglected, the second logarithmic term will be zero and an ideal proton-response is obtained. As the degree of extraction increases, the slope of the function E vs. $\log a_{H^+}$ decreases until sensitivity to the hydrogen-ion is completely lost (when the second term inside the square brackets is predominant and measurements are performed at constant extracted anion concentration, a_{X^-}). For measurements in solutions of varied acid concentration when the acid itself can be extracted into the membrane ($a_{H^+} = a_{X^-}$), the curve E vs. $\log a_{H^+}$ can pass through a maximum, and a negative slope appears at high concentrations (Fig. 4). Equation (17) implies that the amine-extraction constant of the acid,

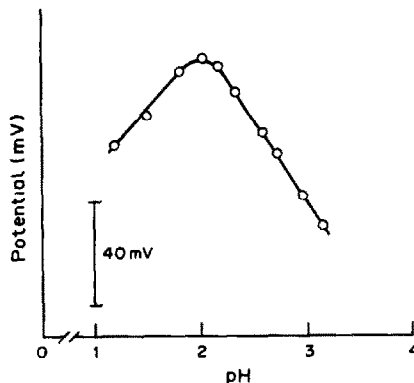


Fig. 4. H^+ -ISE response in hydrofluoric acid solutions (membrane II).

which is strongly dependent on the amine extracting power and the nature of the anions in the test solution, is the main factor responsible for the upper limit of the proton-response. To compare the extractability of different anions, their hydration energies can be used.¹⁷ The extracting power of amines is, to a first approximation, proportional to their protonation constants or those of their lower homologues, in water. For instance, the pK_a values of triethylamine and N,N -diethylaniline are 10.87 and 6.56, respectively¹⁸ and the upper response limits of the ISEs based on their corresponding higher homologues are some 5 orders of magnitude different, other conditions being equal (Figs. 2 and 3).

According to equation (17), interference by extraction should decrease as the lipophilic acid concentration in the membrane increases, which is confirmed by the experimental results (Fig. 3). However, the relationship $\bar{C}_R^{tot} < \bar{C}_{Am}^{tot}$ restricts the use of this factor to shift the upper response limit of the H^+ -ISE to a lower pH, because violation of it results in the loss of membrane selectivity for hydrogen ions.

Because measuring extraction constants for polymer membranes involves great difficulties, the constants of acid extraction with amine solutions in pure plasticizers have been used to evaluate the adequacy of equation (17). Results of extraction experiments are given in Table 2. It has been assumed that a comparatively inert polymer matrix, constituting 25% of the total membrane mass does not significantly affect the extraction constant. The data in Fig. 5 show quite satisfactory agreement between the experimental and theoretical E vs. $\log a_{H^+}$ functions, thus supporting the assumptions above.

Table 2. Extraction equilibrium constants

Solvent	Electroactive substance	Extracted acid	K_{ex}^a	Extracted alkali	K'_{ex}
1-BN	TDA + TOBS	HSCN	2.0×10^8	—	—
1-BN	TDA + TOBS	HBr	2.0×10^6	—	—
CCl ₄ + nitrobenzene (9:1 v/v)	TDA + TOBS	HBr	4.2×10^5	—	—
1-BN	TDA + TOBS	—	—	NaOH	12
1-BN	DOA + TOBS	—	—	NaOH	1.5×10^5

H^+ -ISE function at high pH

In contrast to the upper limit of the H^+ -ISE function, the lower limit is independent of the

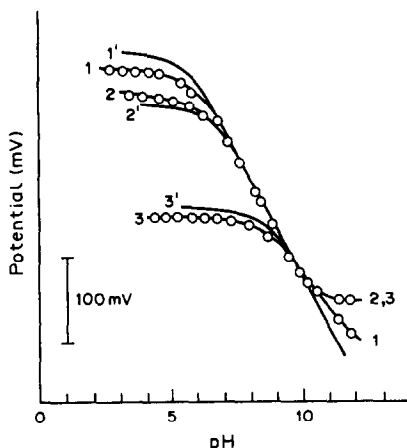
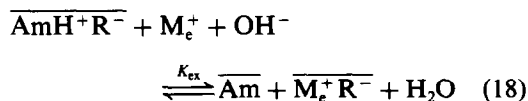


Fig. 5. Theoretical and experimental response of TDA-based H^+ -ISE (membrane VI): (1)–(3) experimental curves in buffer solutions containing backgrounds of $1.0 \times 10^{-3} M$ NaSCN, $1.0 M$ NaBr and $1.0 M$ NaSCN, respectively; (1')–(3'), theoretical curves in the same solutions, calculated by equation (17) with $K_{ex}^a(\text{HSCN}) = 2.0 \times 10^8$ and $K_{ex}^a(\text{HBr}) = 2.0 \times 10^6$.

form of the anions in the test solution and is determined by the nature and concentration of interfering cations (Fig. 6). The non-ideality of the electrode response is apparently the same as for other ISEs based on neutral carriers. In fact, however, the deviation of the H^+ -ISE response obeys a specific mechanism, which is peculiar to these electrodes and requires a special consideration. Indeed, displacement of the analyte ion from the carrier complex by interfering ions, which depends on the relationship between the corresponding extraction and complexing constants, cannot be responsible for the loss of the proton-response, because the amine protonation constants (which are formally similar to complex stability constants) are rather high and amines do not typically form complexes with alkali-metal cations.

The experimental results can be accounted for by the extraction process:



At fairly high pH, amines, being comparatively

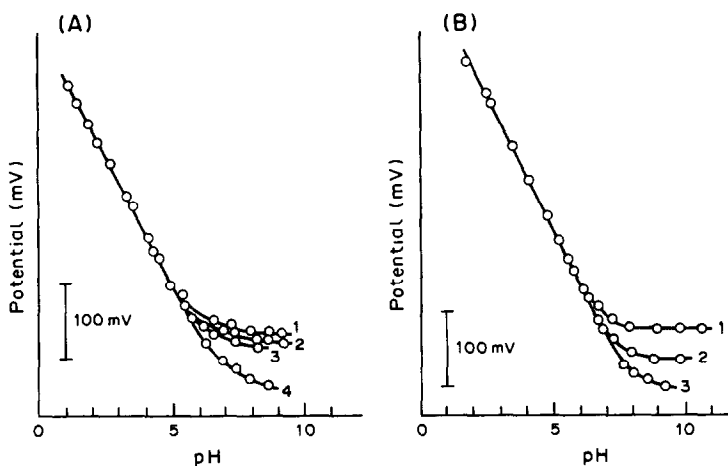


Fig. 6. Effect of the $0.1 M$ electrolyte (A) and dilution of buffer solution (B) on the lower response limit of DOA-based H^+ -ISEs (membrane IV). A: (1) CsCl, (2) RbCl, (3) KCl and (4) NaCl; B: (1) initial buffer mixture, (2) diluted 1:10, (3) diluted 1:100.

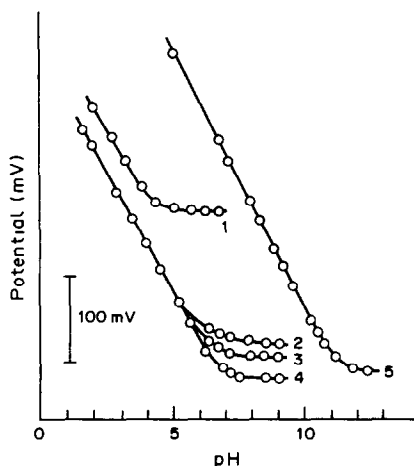


Fig. 7. Effect of the plasticizer nature, neutral carrier and Am:TOBS ratio on the H^+ -ISE lower response limit: (1) THP, DOA (membrane VII); (2)–(4) DOP with DOA:TOBS = 1:1 (membrane VIII), 1.2:1 (membrane IX) and 2.9:1 (membrane IV), respectively, (5) DOP, TDA (membrane X).

weak bases, are replaced in the lipophilic acid salts by metal ions. The concentration of molecular amine in the membrane is thereby increased, while the concentrations of the protonated amine AmH^+ and the hydrogen ion in equilibrium with it decrease, thus causing non-Nernstian electrode response at high pH.

Naturally, the extent of the extraction process depends on the extractability of the metal cations and the basicity of the amines. As shown above, the basicity of TDA is more than 4 orders of magnitude larger than that of DOA, so the lower response limit of the TDA-based ISE is shifted to the alkaline region by about 4 pH units (Fig. 7). The strong dependence of the lower limit of the H^+ -ISE function on the solvating power of plasticizers (THP and DOP) relative to metal cations further supports the suggested mechanism of deviation from ideal behaviour, implying the absence of appreciable interaction of metal cations with the neutral carrier in the membrane phase. As the amine:lipophilic acid ratio in the membrane increases, the lower H^+ -ISE response limit naturally shifts to higher pH owing to the decreased degree of extraction, described by equation (18). Thus, the suggested model logically accounts for the dependence of the change in the lower H^+ -ISE response limit on the membrane and test solution compositions. The equation for evaluating the effect of foreign cations on the H^+ -ISE potential can be obtained from the approximations above, assuming also equality of the

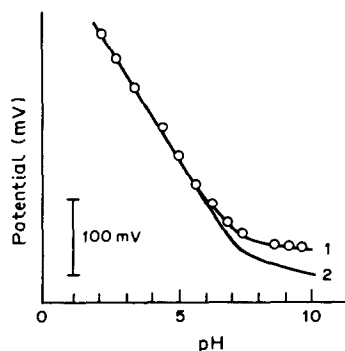


Fig. 8. Responses of DOA-based H^+ -ISE (membrane XI) in solutions of dilute (1:100) buffer mixture, containing 0.1M NaCl background: (1) experimental; (2) calculated from equation (25) with $K'_{ex(NaCl)} = 1.5 \times 10^5$.

dissociation constants of the ion-pairs $M_c^+R^-$ and AmH^+R^- . With these assumptions, the following relationships hold:

$$\bar{C}_{M_c^+R^-} = \bar{C}_R^{tot} - \bar{C}_{AmH^+R^-} \quad (19)$$

$$\bar{C}_{Am} = \bar{C}_{Am}^{tot} - \bar{C}_{AmH^+R^-} \quad (20)$$

$$\bar{C}_{AmH^+} = \frac{\bar{C}_{AmH^+R^-} \sqrt{K_d}}{\sqrt{\bar{C}_R^{tot}}} \quad (21)$$

where all the lipophilic acid in the membrane (\bar{C}_R^{tot}) is bound in the ion-pairs $M_c^+R^-$ and AmH^+R^- and K_d is the dissociation constant of these ion-pairs. Equation (18) implies that

$$\bar{C}_{AmH^+R^-} = \frac{\bar{C}_{M_c^+R^-} \bar{C}_{Am}}{K'_{ex} a_{M_c^+} a_{OH^-}} \quad (22)$$

where $K'_{ex} = K_{ex}/55.55$ (with allowance for C_{H_2O} in the aqueous phase).

Substituting equations (19) and (20) into (22) and solving for $\bar{C}_{AmH^+R^-}$ gives

$$\bar{C}_{AmH^+R^-} = \frac{1}{2}(\bar{C}_R^{tot} + \bar{C}_{Am}^{tot} + Ex) - \sqrt{\frac{(\bar{C}_R^{tot} + \bar{C}_{Am}^{tot} + Ex)^2}{4} - \bar{C}_R^{tot} \bar{C}_{Am}^{tot}} \quad (23)$$

where $Ex (= K'_{ex} a_{M_c^+} a_{OH^-})$ characterizes the extraction effect on the membrane composition.

Substituting equation (23) into (21) and (15) and taking \bar{C}_{Am} from equation (20), we arrive at the equation which describes the concentration of free hydrogen ions in the membrane, with

allowance for extraction [equation (18)]:

$$\bar{C}_{H^+} = \bar{C}_{H^+}^0 \frac{\bar{C}_{Am}^{tot} - \bar{C}_R^{tot}}{\bar{C}_R^{tot}} \times \frac{\frac{1}{2}(\bar{C}_R^{tot} + \bar{C}_{Am}^{tot} + Ex) - \sqrt{\frac{(\bar{C}_R^{tot} + \bar{C}_{Am}^{tot} + Ex)^2}{4} - \bar{C}_R^{tot} \bar{C}_{Am}^{tot}}}{\bar{C}_{Am}^{tot} - \frac{1}{2}(\bar{C}_R^{tot} + \bar{C}_{Am}^{tot} + Ex) + \sqrt{\frac{(\bar{C}_R^{tot} + \bar{C}_{Am}^{tot} + Ex)^2}{4} - \bar{C}_R^{tot} \bar{C}_{Am}^{tot}}} \quad (24)$$

where $\bar{C}_{H^+}^0$ is the initial concentration of hydrogen ions in the membrane (without extraction) as given by the first factor in equation (16).

Substituting equation (24) into equation (5) and again including $\ln \bar{C}_{H^+}$ and the constants with E^0 , gives the following equation for the lower branch of the E vs. $\log a_{H^+}$ curve:

$$E = E^{0'} + \frac{RT}{F} \ln a_{H^+} + \frac{RT}{F} \ln \frac{\bar{C}_R^{tot}}{\bar{C}_{Am}^{tot} - \bar{C}_R^{tot}} - \frac{RT}{F} \ln \frac{\frac{1}{2}(\bar{C}_R^{tot} + \bar{C}_{Am}^{tot} + Ex) - \sqrt{\frac{(\bar{C}_{Am}^{tot} - \bar{C}_R^{tot})^2}{4} + \frac{1}{2}Ex \left(\frac{Ex}{2} + \bar{C}_R^{tot} + \bar{C}_{Am}^{tot} \right)}}{\frac{1}{2}(\bar{C}_{Am}^{tot} - \bar{C}_R^{tot} - Ex) + \sqrt{\frac{(\bar{C}_{Am}^{tot} - \bar{C}_R^{tot})^2}{4} + \frac{1}{2}Ex \left(\frac{Ex}{2} + \bar{C}_R^{tot} + \bar{C}_{Am}^{tot} \right)}} \quad (25)$$

$$E = E^{0'} + \frac{RT}{F} \ln a_{H^+} - \frac{RT}{2F} \ln \left[\left(1 + \frac{\bar{C}_{Am}^{tot}}{\bar{C}_R^{tot}} \right) K_{ex}^a a_{H^+} a_{X^-} + \frac{\bar{C}_{Am}^{tot}}{\bar{C}_R^{tot}} (K_{ex}^a)^2 a_{H^+}^2 a_{X^-}^2 + 1 \right] + \frac{RT}{F} \ln \frac{\bar{C}_R^{tot}}{\bar{C}_{Am}^{tot} - \bar{C}_R^{tot}} - \frac{RT}{F} \ln \frac{\frac{1}{2}(\bar{C}_R^{tot} + \bar{C}_{Am}^{tot} + Ex) - \sqrt{\frac{(\bar{C}_{Am}^{tot} - \bar{C}_R^{tot})^2}{4} + \frac{1}{2}Ex \left(\frac{Ex}{2} + \bar{C}_R^{tot} + \bar{C}_{Am}^{tot} \right)}}{\frac{1}{2}(\bar{C}_{Am}^{tot} - \bar{C}_R^{tot} - Ex) + \sqrt{\frac{(\bar{C}_{Am}^{tot} - \bar{C}_R^{tot})^2}{4} + \frac{1}{2}Ex \left(\frac{Ex}{2} + \bar{C}_R^{tot} + \bar{C}_{Am}^{tot} \right)}} \quad (26)$$

Analysis of equation (25) shows that when Ex is negligible, the second and the third logarithmic terms cancel, resulting in Nernstian response. Figure 8 compares the theoretical and experimental E vs. pH curves for a PVC-membrane plasticized with 1-BN and containing DOA as neutral carrier. The value of K'_{ex} was calculated for pure 1-BN.

The satisfactory agreement between the experimental and theoretical curves proves the predominant contribution of the extraction process described by equation (18) to the loss (at high pH) of the proton-response of H^+ -ISEs

based on neutral carriers. Because the effects of the two types of extraction are manifest at opposite ends of the pH range, where their interdependence is impossible, equations (17) and (25) may be combined into a generalized equation for the proton-response of an H^+ -ISE over the entire pH range [equation (26)].

The good agreement in Fig. 9 between the experimental E vs. pH curve and that calculated by equation (26) for a liquid membrane containing TDA as the neutral carrier supports the considerations presented.

CONCLUSIONS

Extraction processes at the membrane-test solution interface, by causing changes in the concentration of hydrogen ions in the membrane, are mainly responsible for the restrictions

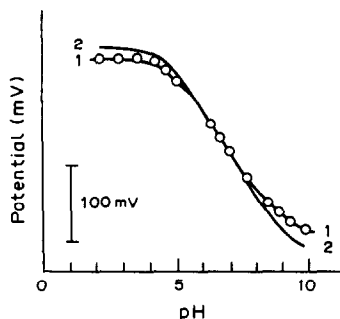


Fig. 9. Responses of TDA-based H^+ -ISE (membrane XII) in solutions of buffer mixture containing 0.1M NaBr background: (1) experimental; (2) calculated from equation (26) with $K_{ex(HBr)}^a = 4.2 \times 10^5$ and $K'_{ex(NaBr)} = 12$.

on the response range of H^+ -ISEs based on neutral amine-type carriers. In acidic media the extraction of ion-associates of anions with protonated amines is the operative factor, whereas in alkaline media, it is the extraction of metal cations by amine salts of lipophilic acids. The degree of extraction is strongly dependent on the composition of both the membrane and the test solution. Among the membrane components, the greatest effect on the extraction processes and, hence, on the response range of H^+ -ISEs is exerted by the nature (primarily the basicity) of the amine used as the neutral carrier. The solvating power of the plasticizer and the amine:lipophilic acid concentration ratio in the membrane have less pronounced, but still significant, influence.

It should be noted that the proposed approach yields good results only when the potential-determining reaction is solely specified by the electroactive substance introduced into the membrane. In a number of cases, however, the presence of electroactive impurities in the membrane polymer or plasticizer can lead to alternative mechanisms of charge transfer through the membrane. In addition, the inter-phase processes can sometimes be controlled by kinetic as well as equilibrium factors. In this connection, approaches that take into account the role of all the substances capable of charge transfer^{19,20} and those including kinetic factors²¹⁻²⁷ seem to be very promising.

We hope that these results add to the understanding of the mechanism of the relationship between the dynamic range of H^+ -ISEs and

amine basicity described by Simon⁶ and will stimulate further purposeful search for membrane compositions giving a required response range.

REFERENCES

1. R. L. Coon, N. C. J. Lai and J. P. Kampine, *J. Appl. Physiol.*, 1976, **40**, 625.
2. D. Erne, D. Ammann and W. Simon, *Chimia*, 1979, **33**, 88.
3. D. Ammann, F. Lanter, R. A. Steiner, P. Schulthess, Y. Shijo and W. Simon, *Anal. Chem.*, 1981, **53**, 2267.
4. D. Erne, K. V. Schenker, D. Ammann, E. Pretsch and W. Simon, *Chimia*, 1981, **35**, 178.
5. C. Hongbo, E. H. Hansen and J. Růžička, *Anal. Chim. Acta*, 1985, **169**, 209.
6. U. Oesch, Z. Brzózka, A. Xu, B. Rusterholz, G. Suter, H. V. Pham, D. H. Weiti, D. Ammann, E. Pretsch and W. Simon, *Anal. Chem.*, 1986, **58**, 2285.
7. G. L. Starobinets, V. V. Egorov and Ya. F. Lushchik, *Zh. Analit. Khim.*, 1986, **41**, 1030.
8. H.-L. Wu and R.-Q. Yu, *Talanta*, 1987, **34**, 577.
9. K. N. Mikhel'son, O. V. Mukhacheva, V. M. Lutov, V. Ya. Semenii and A. N. Khutsishvili, *USSR Author Cert.*, N 1326977, IB, 1987, N 28.
10. S. M. Leshchev, E. M. Rakhmanko, E. V. Vorobieva and G. L. Starobinets, *USSR Author Cert.*, N 1027151, IB, 1983, N 25.
11. T. M. Alkhashivili, N. V. Astakhova, V. V. Egorov, Z. F. Kirpichnikova, L. V. Koleshko, E. M. Rakhmanko, G. L. Starobinets, Yu. M. Tarasova and A. N. Khutsishvili, *USSR Author Cert.*, N 1310401, IB, 1987, N 18.
12. K. Cammann, *Das Arbeiten mit ionenselektiven Elektroden*, Springer, Berlin, 1979.
13. Yu. Yu. Lurie, *Handbook of Analytical Chemistry*, Khimiya, Moscow, 1979.
14. W. E. Morf, G. Kahr and W. Simon, *Anal. Lett.*, 1974, **7**, 9.
15. W. E. Morf and W. Simon, in *Ion-Selective Electrodes in Analytical Chemistry*, Vol. 1, H. Freiser (ed.), p. 211. Plenum Press, New York, 1978.
16. K. S. Krasnov, *Radiochemistry*, 1963, **5**, 222.
17. K. P. Mishchenko and A. A. Ravdel (eds.) *A Handbook of Physico-Chemical Quantities*, Khimiya, Moscow, 1967.
18. A. Albert and E. Serjeant, *Ionization Constants of Acids and Bases*, Chapman & Hall, London, 1964.
19. S. Kihara and Z. Yoshida, *Talanta*, 1984, **31**, 789.
20. T. Kakiuchi and M. Senda, *Bull. Chem. Soc. Japan*, 1984, **57**, 1801.
21. K. Cammann, *Anal. Chem.*, 1978, **50**, 936.
22. J. Koryta, *Anal. Chim. Acta*, 1979, **111**, 1.
23. T. Fujinaga, *Phil. Trans. R. Soc.*, 1982, **305A**, 631.
24. J. Koryta, *Ion-Selective Electrode Rev.*, 1983, **5**, 131.
25. K. Cammann and G. A. Rechnitz, in *Ion-Selective Electrodes*, **4**, p. 35. Akadémiai Kiadó, Budapest, 1985.
26. R. D. Armstrong, *J. Electroanal. Chem.*, 1988, **245**, 113.
27. Sheng-Luo Xie and K. Cammann, *ibid.*, 1988, **245**, 117.

THIN-LAYER CHROMATOGRAPHY/LIQUID SECONDARY ION MASS SPECTROMETRY IN THE DETERMINATION OF MAJOR BILE SALTS IN DOG BILE

JOCELYN C. DUNPHY and KENNETH L. BUSCH*

School of Chemistry and Biochemistry, Georgia Institute of Technology, Atlanta, GA 30332, U.S.A.

(Received 19 June 1989. Revised 6 September 1989. Accepted 3 October 1989)

Summary—Positive and negative ion liquid-state secondary-ion mass spectrometry (LSIMS) was applied to several bile acids and bile salts and their spectra were measured directly from the surface of silica gel thin-layer chromatograms. Such spectra were identical to the LSIMS spectra of the pure compound at the same concentration. Three-dimensional ion images were obtained of a model mixture of cholic, chenodeoxycholic and lithocholic acids in both the positive and negative ion modes. A sample of dog bile was prepared, and the bile acids extracted from it were separated by high-performance TLC; TLC/LSIMS spectra were obtained for sodium taurocholate and sodium taurochenodeoxycholate/taurodeoxycholate, the predominant bile salts present. Quantitative estimates of the analytes were obtained by monitoring the ion intensity for the sample spot and a standard spot that had been developed in parallel on the same TLC plate. The concentration of sodium taurocholate in the bile of this particular dog was found to be 38 mg/ml.

The clinical analysis of bile acids is common in the diagnosis of certain liver or intestinal disorders, and bile acid assays have also been used for probing the complex pathways of cholesterol metabolism. Traditional methods for such analyses involve one or more sample clean-up steps by extraction or chromatography, followed by detection and identification by mass spectrometry. For many years, gas chromatography/mass spectrometry (GC/MS) has been the method of choice, although this requires that the bile acid be derivatized in order to make it sufficiently volatile for the chromatography.¹⁻³ The simplest derivative is the bile acid methyl ester, but protection of the hydroxyl groups through acetylation, trifluoroacetylation or trimethylsilylation is often also considered necessary. Under certain conditions, the conjugated bile acids, often present in clinical samples in much larger amounts than the free bile acids themselves, must be hydrolyzed prior to analysis.

With the advent of particle-induced desorption ionization for mass spectrometry, other methods for bile acid analysis have been reported. The advantage of liquid-state secondary-ion mass spectrometry (LSIMS) and fast atom bombardment (FAB) over conventional electron ionization in GC/MS is that the

mass spectra can be obtained without volatilization of the sample, and derivatization is not required. In most cases, a preliminary separation step prior to mass spectral identification is still recommended. In a series of papers, Whitney and co-workers have developed a method including a solid-phase Sep-Pak C₁₈ extraction, followed by radial compression HPLC and finally LSIMS.⁴⁻⁷ Thanks to the lack of fragmentation in the mass spectra, complex mixtures can be analyzed directly by LSIMS, especially in the negative ion mode, in which molecular ions such as (M - H)⁻ are of large relative abundance. Ito *et al.* have developed the direct coupling of a microbore liquid chromatography (LC) column with an LSIMS ionization source for the analysis of bile acids.⁸ Tomer *et al.* have used daughter-ion MS/MS following LSIMS ionization to differentiate individual isobaric bile acids in a complex mixture.⁹ Finally, an instrument designed to obtain LSIMS mass spectral data directly from thin-layer chromatograms has been used for bile acid analysis.¹⁰

Traditional detection methods for TLC involve staining, charring, fluorescence, or densitometry. Mass spectrometry provides additional sensitivity and selectivity, and an instrument for the direct two-dimensional analysis of developed thin-layer chromatograms with an LSIMS ionization source has been described.^{11,12}

*To whom correspondence should be addressed.

In this system, the point of focus of the primary particle beam on the xy surface of the chromatogram is also the point of secondary ion extraction into the quadrupole mass analyzer. The TLC plate is moved with an xy manipulator stage to bring the sample spots to the point of focus. Secondary ions are sputtered from the chromatogram by suitable irradiation of the analyte held in a glassy semi-liquid matrix.¹³ Spatial profiles for distribution of organic ions in the xy plane are generated by moving the manipulator in the x and y directions while monitoring abundances of the selected ions. Three-dimensional images for organic ions on the surface of the chromatogram are produced by plotting the ion intensity as a function of the x and y coordinates. In addition, a complete mass spectrum can be measured for each point in the chromatogram. Imaging of sample spots within chromatograms by use of LSIMS has been reported for mixtures of phenothiazine drugs,¹⁴ small peptides¹⁵ and natural products.¹⁶

There are several parts to the present study. First, the positive and negative ion LSIMS spectra of discrete samples of several bile acids and salts are recorded and interpreted. Next, the conditions necessary to minimize differences between the spectra of the individual compounds and those on developed and spotted TLC plates are explored. In particular, the effects of concentration of the bile acid in the solvent are delineated with respect to the competitive formation of $(M + H)^+$ and $(M + Na)^+$ ions. Clinical samples of dog bile are prepared and separated, and the mass spectra of the individual sample spots recorded. The advantages of recording three-dimensional ion images from the TLC plate are discussed. Finally, quantitative estimates for the concentration of bile salts in dog bile are made by comparing signal levels for the sample spots with those for a standard developed on the same TLC plate.

EXPERIMENTAL

Reagents

Cholic, chenodeoxycholic and lithocholic acids were purchased from Aldrich Chemical Co. and the taurine-conjugated bile salts from Sigma Chemical Co. Solvents used for TLC development were obtained from Mallinckrodt and Aldrich. Matrices for the LSIMS experiments (glycerol, threitol and sorbitol) were obtained from Aldrich and used as received.

Samples of dog bile were obtained from an experimental animal.

Instrumentation

Standard positive and negative ion SIMS spectra of each bile acid or salt were obtained by depositing ~ 1 mg of acid or salt into approximately $30 \mu\text{l}$ of glycerol on the tip of the direct insertion probe. Mass spectra were measured with a modified Extrel C-50 quadrupole mass spectrometer. The primary beam consisted of cesium ions from a commercial cesium ion gun (Phrasor Scientific) or argon atoms from an FAB gun (Ion Tech, Ltd.). Each gun was mounted on a vacuum flange at an angle of 45° to the sample. The primary ion current (6 keV Cs^+ ; 8 kV Ar) was maintained at approximately $1\text{--}2 \mu\text{A}$ at the surface. Mass spectra were recorded with a home-built microcomputer using modified ASYST software,¹⁷ which also generated the three-dimensional images by standard plotting routines. In some cases, spectra were recorded directly on an xy recorder.

Mass spectra from TLC plates were obtained as follows. The spot on the TLC plate, containing approximately $20 \mu\text{g}$ of bile acid, was cut out and affixed with double-sided adhesive cellophane tape to the tip of the direct insertion probe. Ten μl of glycerol were applied to cover the spot and the probe was inserted into the mass spectrometer source.

For the initial experiments on spatially-resolved images, $10\text{--}20 \mu\text{g}$ of a bile acid or its salt (in ethanol solution) were spotted onto a silica TLC plate in the relative positions established by the chromatography experiments discussed below. For the dog bile sample, images were acquired from a developed chromatogram. A thin layer (~ 0.5 mm thick) corresponding to $8 \mu\text{l}$ of molten sorbitol or threitol was applied with a microspatula or micropipette to each area of the plate containing a bile acid or salt, and the plate was then positioned on the platform inside the source of the mass spectrometer. The platform was heated to maintain the matrix near its melting point during the imaging experiment. The sample was moved either manually with an xyz manipulator, or, in later work, with perpendicular piezoelectric translator stages from Burleigh Instruments. Images were obtained by using the gallium primary ion beam from a liquid ion gun (FEI), also mounted on the chromatography/LSIMS instrument. The gallium gun was used to collect images because of its small beam diameter. Better spatial

resolution is therefore possible than with the cesium ion gun or the argon FAB gun. The gallium gun was operated at 5 kV beam voltage, approximately 2.0 kV lens voltage (variable), -1.5 kV suppressor voltage, 11 kV extractor voltage and 5 μ A emission current. Under these operating conditions and with a 5-cm working distance, the primary beam diameter is calculated to be 0.8 μ m. The FAB gun was used to collect the image (shown later, Fig. 4) from the dog bile sample, with the beam diameter reduced to 0.4 mm by a small aperture. Spatial resolution for the grids shown for the images reported here was 0.5 mm except for the dog bile sample, for which it was 0.4 mm. Each point shown on the image represents the average of 200 scans across the ion of interest. Although not needed in these experiments, higher spatial resolution (to 1 μ m with the Burleigh piezoelectric translator stages) can be achieved for applications in which the chromatography does not sufficiently separate the analytes.

Thin-layer chromatography

Mixtures of free bile acids were separated on aluminum-backed silica TLC plates (0.2 mm, EM Science) with the solvent system iso-octane, ethyl acetate, acetic acid (10:10:2 v/v).¹⁰ The R_f values were cholic acid, 0.16; chenodeoxycholic acid, 0.40; lithocholic acid, 0.71. The dog-bile extract and standard mixture of common conjugated bile salts were both chromatographed on 100- μ m silica gel HPTLC plates with the solvent system n-butanol, acetic acid, water (40:10:10 v/v).¹⁸ Taurocholate, the more polar of the two, has an R_f value of 0.40, taurochenodeoxycholate an R_f value of 0.52 and taurodeoxycholate an R_f value of 0.52. Before chromatography, samples of dog bile were extracted with ethanol by use of C₁₈ Sep-Pak cartridges, in a procedure similar to that developed by Whitney and Thaler.¹⁹

Quantitative estimates

Quantitative estimates were obtained by scanning across the region on the TLC plate containing both the standard and the sample in separate lanes. The sample and standard were spotted with a Camag Linomat IV bander in 5-mm long bands 1 mm in width, and the chromatogram was developed over a length of 5 cm with the n-butanol, acetic acid, water solvent system. About 4 μ l of threitol were applied to each spot as the extraction matrix and the plate was inserted into the mass spectrometer chamber.

The platform temperature was held just below the melting point of threitol (70–73°) throughout the experiment to keep the previously molten threitol in a tacky state. Scans were performed at 0.2-mm steps in the y direction with a motion of 50 μ m/sec in the x direction and a scan-rate of 10 amu/sec across a 14 amu range encompassing the molecular ion in the negative ion mode. An argon FAB gun was used with a beam-limiting aperture which reduced the diameter of the beam to approximately 0.4 mm. Relative intensities of sample and standard as a function of distance were recorded with an xy recorder.

RESULTS AND DISCUSSION

The liquid-state SIMS and FAB mass spectra of the various bile acids and salts, including those in this study, have been documented by Whitney and Burlingame.⁶ The present work confirms their results. In general, LSIMS spectra of the free acids show $(M - H)^-$ as the predominant ion in the negative ion mode. In the positive ion mode, the $(M + H)^+$ ions are of low abundance and fragment ions corresponding to successive losses of water are dominant. Lithocholic acid, however, does not provide any abundant ions in the positive ion FAB mass spectrum. If excess of sodium in the form of sodium chloride is added to the matrix, sodium adduct ions, $(M + Na)^+$, are formed. The bile acid sodium salts yield predominantly the $(M - Na)^-$ ion in the negative ion mode, and $(M + Na)^+$ and $(M + H)^+$ in the positive ion mode. Small ions corresponding to losses of water are also sometimes observed.

The spectra of the bile acids and salts obtained directly from the TLC surface are similar to those of the individual compounds in a glycerol matrix. A slight increase in background noise is observed, as less sample is available for ionization and detection. Protons and sodium ions compete for the bile salt anion, as discussed in greater detail in the section on dog bile analysis.

The plate containing the bile acids and salts was not analyzed further after the LSIMS analysis, but there appeared to be no evidence of destructive processes induced by the primary beam bombardment. The mass spectra did not change appreciably with exposure time even during the longer periods needed to obtain the three-dimensional images. In addition, experiments performed on other systems in this

laboratory show that a single spot can generate identical images in repeated analyses even when these are taken at intervals of days. We calculate that tens of picograms of sample are consumed per second during a typical TLC/LSIMS experiment and are confident, therefore, that with the ng- μ g quantities of sample material on typical TLC plates, there is sufficient material left in the extraction matrix or the silica gel to make further analyses possible, if desired.

The absolute sensitivity in the mass spectra of the conjugated salts studied is approximately 6 times higher for the base peak $[(M - Na)^-]$ in the negative ion mode than for the base peak $[(M + Na)^+]$ in the positive ion mode. Detection limits for each salt in the negative ion mode were estimated by measuring those for sodium taurocholate. In the TLC/LSIMS experiment, 100 ng or so will suffice to give a full negative ion mass spectrum, stable for 30 min. Since it takes only about 30 sec to record the mass spectrum, detection limits of about 1 ng are indicated. However, for the imaging experiments described below, 1 μ g is usually required, owing to the longer time currently required to make the measurements needed to compile a complete image by manual operation. The high sensitivity of the negative ion LSIMS mode for bile acids, along with the reliable molecular weight information provided, with little or no

obscuring fragmentation, makes this the preferred analytical mode. However, the ability to measure both positive and negative ion mass spectra from the same sample spot aids in sample identification.

Imaging analysis

Imaging spectral measurements obtained by using TLC/LSIMS provide unique characteristics in the study of bile acids, including free choice of order of access to sample spots, variable spatial resolution and integration, and preservation of the chromatogram along with the complete spectral information from the mass spectrum itself. Figure 1 shows the three-dimensional positive ion image of a model mixture of cholic, chenodeoxycholic and lithocholic acids separated by TLC. For this image, the plate was treated with sodium chloride after development, allowing lithocholic acid to be detected by means of the $(M + 2Na - H)^+$ ion peak at m/z 421. By movement of the sample in successive 0.5-mm steps in the x direction, with the y value kept constant, and monitoring the appropriate ion for each acid (cholic acid, m/z 355; chenodeoxycholic acid, m/z 357; lithocholic acid, m/z 421), the spatially-resolved image was measured. The procedure was repeated with the y value changed until an entire image was obtained.

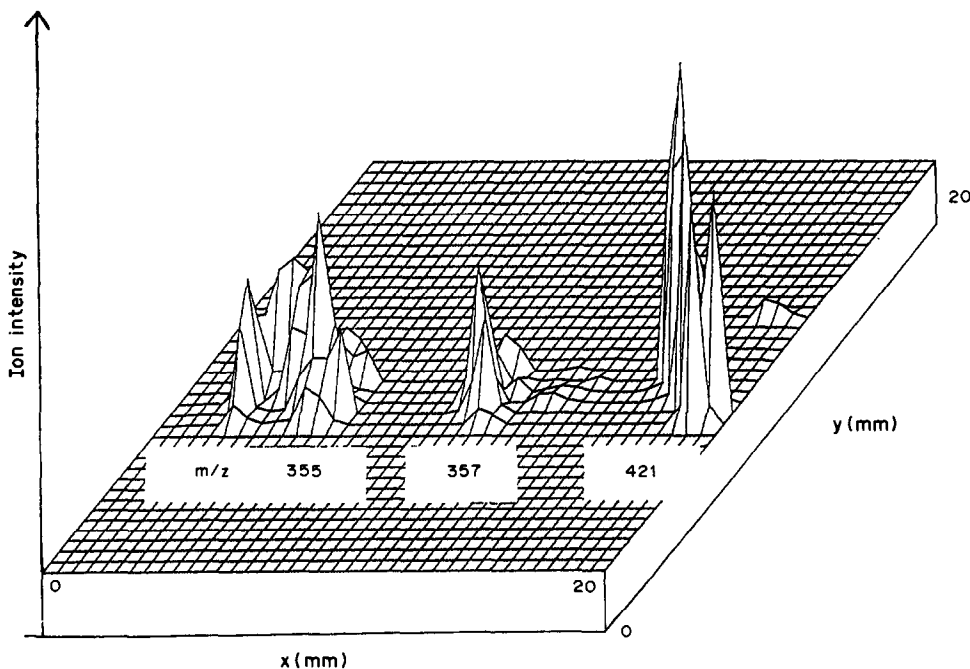


Fig. 1. Three-dimensional positive ion image of a TLC plate containing cholic, chenodeoxycholic and lithocholic acids.

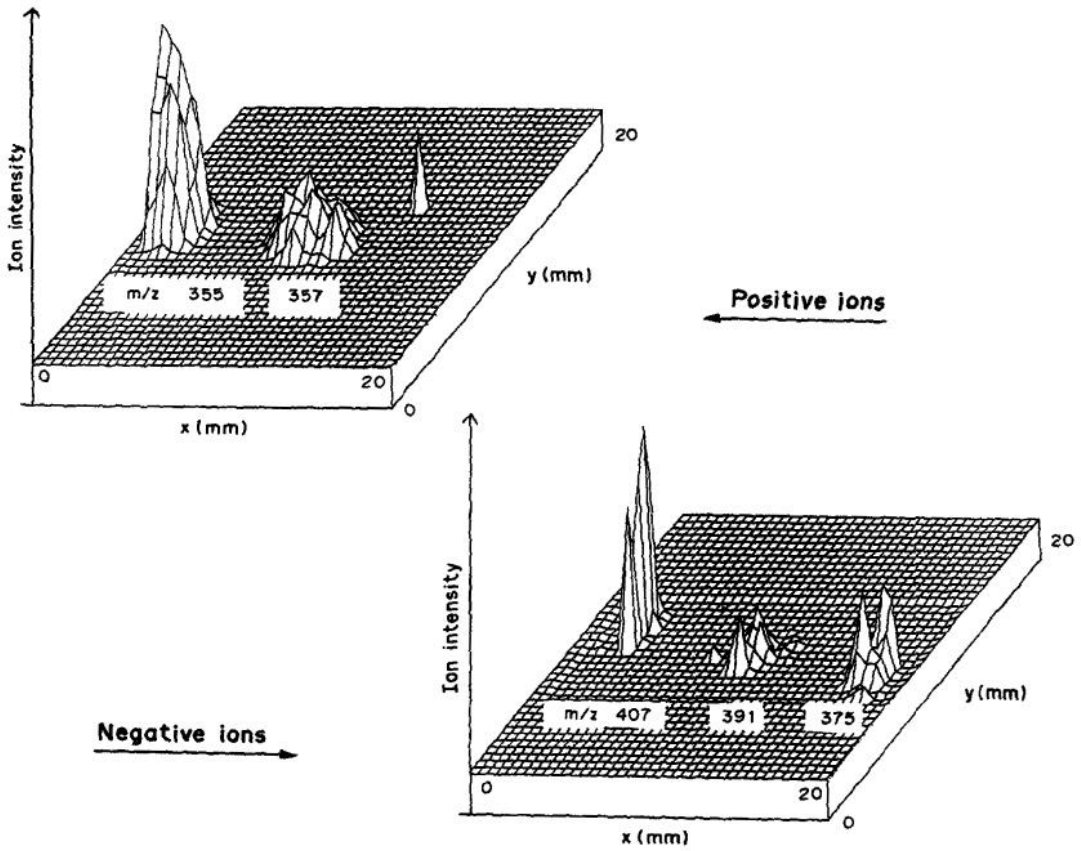


Fig. 2. Comparison of the positive ion and negative ion images of a TLC plate containing cholic, chenodeoxycholic and lithocholic acids.

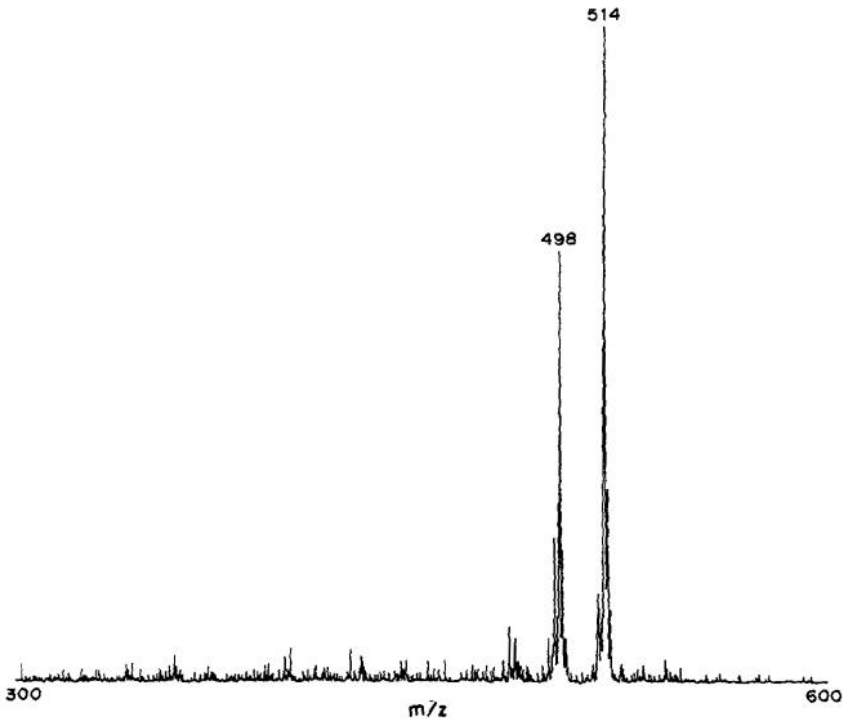


Fig. 3. Negative ion LSIMS spectrum of dog bile extract.

The figure shows that the spots are completely resolved, and signal-to-noise ratios are excellent for the ions monitored.

The ability to correlate positive and negative ion spatial images is demonstrated in Fig. 2. The acids separated are cholic, chenodeoxycholic and lithocholic. The negative ion image was obtained first by monitoring the $(M - H)^-$ ions for each acid. In this experiment the positive ion image shows no signal for lithocholic acid as the TLC plate in this case was not treated with sodium chloride. The positive ion/negative ion correlation experiment is useful when two bile acids are unresolved by the TLC and give the same ion in one of the two modes. Measurement of the ions in the other mode would allow an unambiguous identification.

Dog bile analysis

In the mass spectral analysis of the dog bile sample several experiments were performed. The first measured the negative ion LSIMS mass spectrum of the unchromatographed bile extract (Fig. 3). From the combination of the data in this spectrum with R_f data from subsequent TLC experiments on a similar extract, the major bile salts present were found to be sodium taurocholate and either or both of the dihydroxy taurine-conjugated isomers. The heaviest ions in the spectrum, at m/z 514 and 498, correspond to the $(M - Na)^-$ ions of sodium taurocholate and sodium taurochenodeoxycholate/taurodeoxycholate, respectively. These salts are chromatographed with the *n*-butanol, acetic acid, water solvent system. As noted above, the dihydroxy isomers are not

resolved. Another spot was located at a lower R_f value, but since the spot was colored, the compound was presumed to be a bile pigment. No ions above background were seen for this compound, and we assume, therefore, that either the amount present is small enough not to be detected in the pure extract or on the developed TLC plate, or the compound is not amenable to LSIMS ionization. Figure 4 is the three-dimensional image in the negative ion mode showing two distinct spots corresponding to the bile salts present. The ion at m/z 514 was monitored to locate sodium taurocholate, and that at m/z 498 for the taurochenodeoxycholate/taurodeoxycholate mixture.

Mass spectra of these salts taken directly from the TLC spot (for the developed dog bile sample) are given in Figs. 5 and 6. The negative ion spectra are identical to the standard spectra discussed above. However, in the positive ion mode, the $(M + H)^+$ ion in the TLC/LSIMS experiment is greatly enhanced relative to the $(M + Na)^+$ ion, and successive losses of water from it are seen. Further experiments established that the difference in the TLC/LSIMS spectrum is due to the standard spectrum being measured for a relatively high concentration of bile salt in glycerol, whereas in the TLC/LSIMS experiment a total of only $\sim 10 \mu\text{g}$ of salt was present, which was then extracted into $10 \mu\text{l}$ of glycerol. It was found that when standard spectra were taken for concentrations of the bile salt in glycerol ranging from 1.5 to $9.5 \mu\text{g}/\mu\text{l}$, the $(M + H)^+/(M + Na)^+$ ratio decreased with increase in sample concentration from 0.38 to $7.2 \mu\text{g}/\text{ml}$. This phenomenon is interpretable in

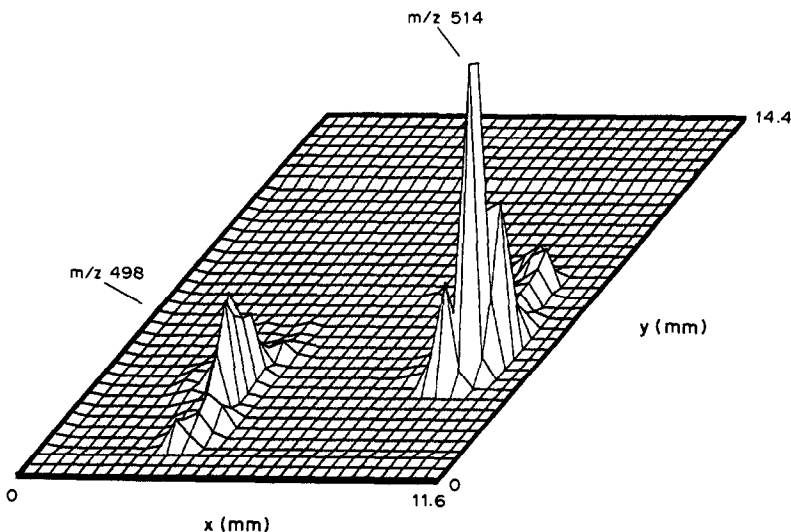


Fig. 4. Three-dimensional negative ion image of bile salts present in dog bile, contained on a TLC plate.

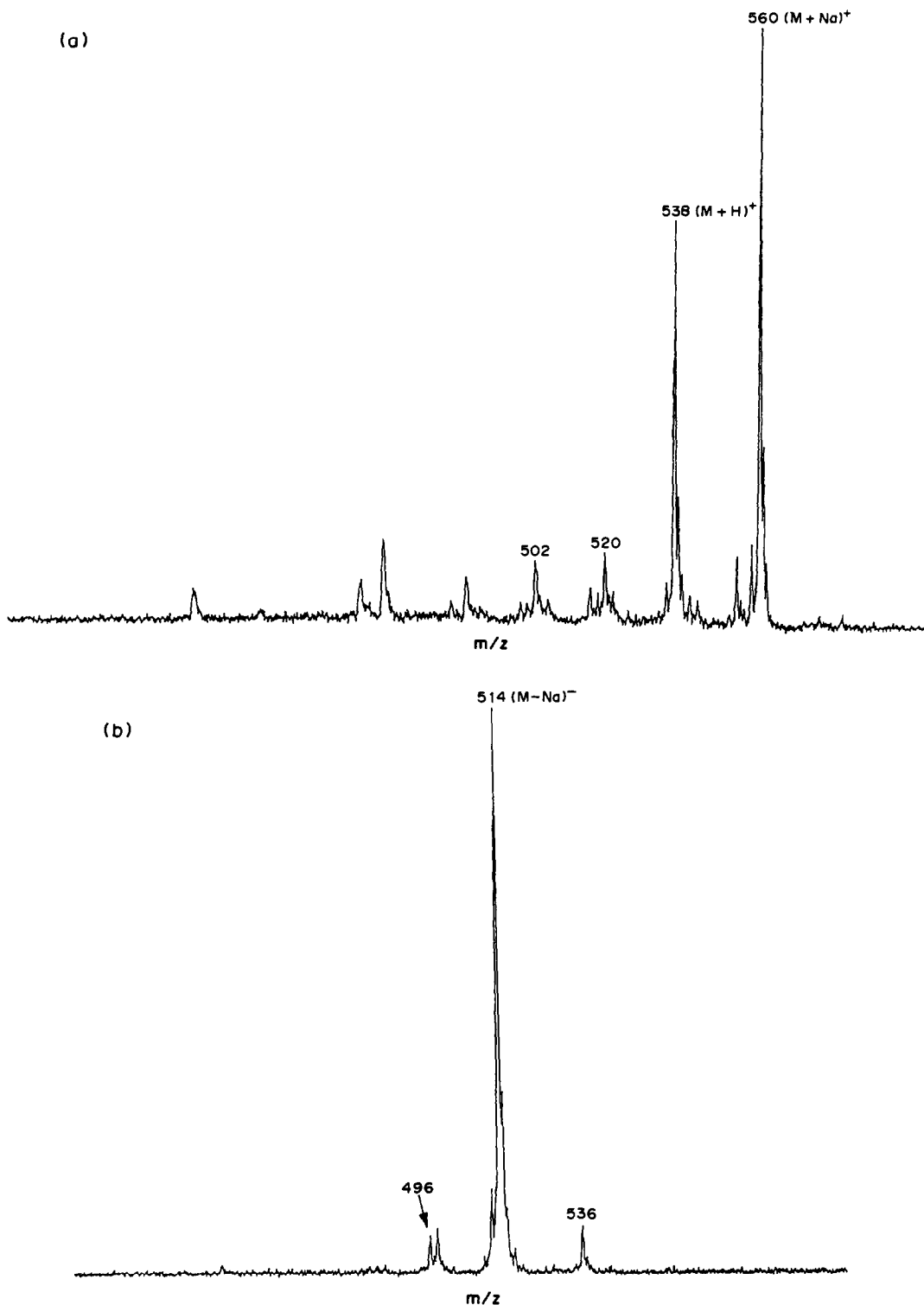


Fig. 5. (a) Positive ion LSIMS spectrum of sodium taurocholate obtained directly from the TLC plate, with glycerol as extraction matrix. (b) Negative ion LSIMS spectrum of sodium taurocholate obtained directly from the TLC plate.

terms of a competition between sodium ions and protons (presumably from the matrix) for the bile salt anion. Higher bile salt concentrations favor formation of $(M + Na)^+$. The fact that

the sodium ion concentration is the crucial variable was determined by the following experiment. Ten μg of bile salt were deposited on a silica TLC plate and 10 μl of glycerol,

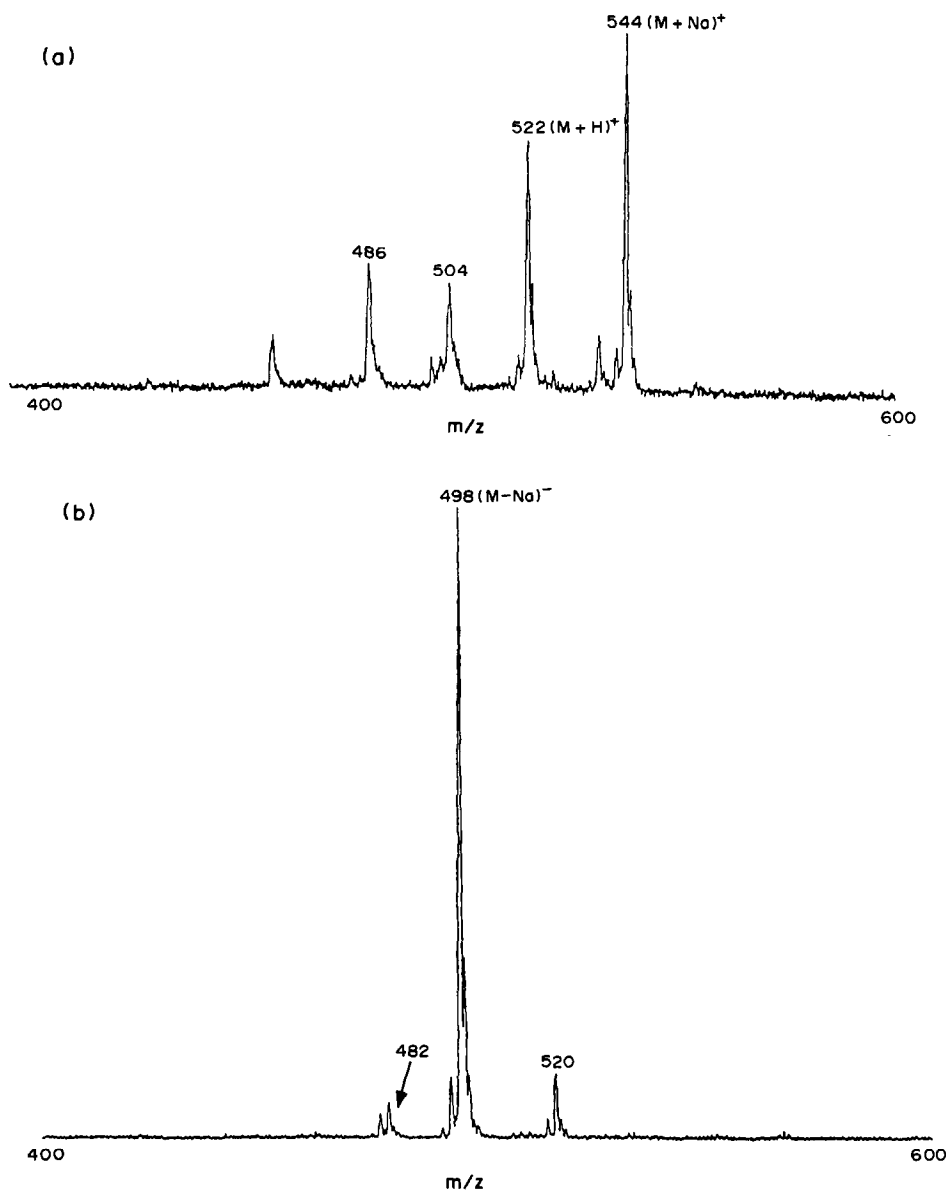


Fig. 6. (a) Positive ion LSIMS spectrum of TLC spot corresponding to the dihydroxy isomeric bile salts present in dog bile. (b) Negative ion LSIMS spectrum of the TLC spot corresponding to the dihydroxy isomeric bile salts present in dog bile.

doped with an excess (1 mg) of sodium chloride, were applied over the spot as the extraction matrix. The resulting spectrum was identical to that for the standard bile salt at higher concentration in glycerol, rather than the usual TLC/LSIMS spectrum, in which there is a high relative abundance of $(M + H)^+$ ion. The amount of bile salt was not altered; only the sodium ion concentration was changed.

It should be noted that TLC plates contain an unknown amount of adventitious sodium, and in favorable cases this sodium may contribute to the formation of the $(M + Na)^+$ ion. In our

experience, this level of sodium does not significantly increase the relative abundance of the sodium-cationized molecular ion. Only addition of a large excess of sodium to the plate itself (as in the case of lithocholic acid) or to the matrix (as in the experiments described above) will alter the spectrum. The addition of excess of sodium does not appear to reduce the overall sensitivity of the bile salt detection; in fact, it may improve the detection limits if the analyte prefers to attach a sodium ion rather than a proton, or other alkali-metal cation. Even at high concentrations ($10 \mu\text{g}/\mu\text{l}$), where the available protons from the glycerol matrix outnumber the sodium

ions, the $(M + Na)^+$ ion still dominates, giving evidence that the bile salts do prefer to act in this way. The sodium levels in LSIMS and FAB analyses of these compounds should be brought to a known and reproducible value.

Quantitative estimates

For quantification studies, the intensities of the appropriate ion $[(M - H)^-]$ of sodium taurocholate were measured and summed for a total of 26 scans for sample and standard. It should be noted that a similar experiment for taurodeoxycholate/taurochenodeoxycholate would only yield the total concentration of the dihydroxy isomers and not values for each salt, since the two salts are not resolved by the chromatography. Figure 7 shows a typical scan across the center of the spots corresponding to the sample and standard. The total signal intensity (in arbitrary units) is 7506.5 for the standard and 11327.0 for the sample. Simple proportion was used to determine the amount of taurocholate on the plate, for the dog bile sample. The standard spot corresponded to 12.5 μg of taurocholate, so the sample content was 19 μg . This amount in a total spotted volume of 5 μl corresponds to 7.6 mg in the total volume of dog bile extract, 2.0 ml. Since 0.2 ml of dog bile was extracted, if the extraction efficiency was 100%, the concentration of sodium taurocholate in the dog bile was 38 mg/ml. Two more trials with additional plates containing the same amount of standard and the same bile extract yielded values of 21 and 46 mg/ml.

The factors limiting precision are generally associated with the matrix and its application to the surface of the chromatogram. Specific concerns are the amount of matrix sorbed into the thin layer, compared with the amount remaining above the layer surface, the completeness and evenness of coverage of the spot, and the temperature gradients that may form within each spot, causing sputtering conditions to change with time. In addition, since each quantitative trial required 30–45 min to complete, such variables may be expected to become more difficult to control. The chromatography/LSIMS instrument is currently being automated with respect to sample movement and data acquisition, and an automated imaging experiment should take less than 5 min to complete, greatly reducing the uncertainties involved. Clearly, an internal standard (an isotopically-labelled bile salt mixed and developed with the sample) would provide more accurate quantification. However, an internal standard would reduce the linear dynamic range of quantification simply because it would compete with the analyte for the surface of the liquid matrix. Since the bile salts possess surfactant properties, the calibration curve levels off at higher concentrations and this will occur at lower concentrations because the analyte and standard both interact with the liquid matrix surface in the same manner. This phenomenon is characteristic of LSIMS ionization in general and is not specific to TLC/LSIMS.

TLC/LSIMS is effective in providing qualitative and semi-quantitative information about mixtures of bile acids. TLC is a quick, reliable and inexpensive separation method utilized in a variety of analytical screening applications. The need for a compound-specific detector for TLC is met by LSIMS. An additional advantage of TLC/LSIMS is the ability to screen for a particular compound in multiple samples on the same TLC plate. For example, a patient with a particular enterohepatic disorder may be tested for bile salt concentrations at different times to test the effectiveness of a particular drug. The samples may all be developed on the same TLC plate and the relative concentrations of a particular salt determined without the risk of other matrix component effects normally present when a mixture is analyzed directly by LSIMS. LSIMS can also be used as a semi-quantitative tool for the determination of analytes on TLC plates. The concept demonstrated here is analogous to densitometry, except that

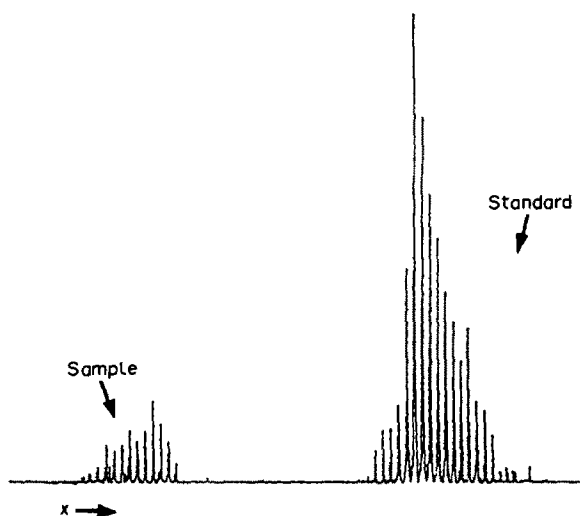


Fig. 7. One-dimensional spatial profile of sample spot and adjacent standard spot on TLC plate: ion intensities of a series of these scans are summed and compared for quantitative purposes.

directly determining the mass spectrum for each component makes more specific information available.

One drawback of TLC/LSIMS is the lack of separating power of conventional TLC plates for positional isomers. We have seen that the dihydroxy isomers of bile acids are not efficiently separated, even by HPTLC. Positional isomers of tri- and monohydroxy bile acid salts, which must also be determined in certain clinical applications, suffer from this problem as well. However, when coupled with tandem mass spectrometry (MS/MS), which has been shown to successfully distinguish the bile acid dihydroxy isomers,²⁰ TLC-MS/MS should be able to provide the additional "separation" not provided by TLC alone. Poorly separated isomers cannot be distinguished in this way by their conventional LSIMS spectra, which are identical. However, overlapping spots containing compounds that are not isobaric can be distinguished by means of LSIMS data taken at several different spatial locations. Once the spatial boundaries of each compound present are determined, quantification can proceed by the methods described.

Acknowledgements—This work was supported by the National Institutes of Health (R01 GM36454-01) and the National Science Foundation (DMB 85-14983) to KLB at Indiana University. The authors would also like to thank Dr. John Watkins of the Department of Pharmacology at the Indiana University School of Medicine for the dog bile samples, and Dr. G. C. DiDonato of the Squibb Institute for helpful discussions.

REFERENCES

1. J. Sjovall, P. Eneroth and R. Ryhage, in *The Bile Acids*, Vol. 1, P. G. Nair and D. Kritchevsky (eds.), pp. 209–248. Plenum Press, New York, 1971.
2. M. Tohma, H. Takeshita, R. Mahara and T. Kurosawa, *J. Chromatog.*, 1987, **421**, 9.
3. J. Sjovall, *Adv. Steroid Anal.*, 1984, **23**, 359.
4. J. O. Whitney, S. Lewis, K. M. Straub, M. M. Thaler and A. L. Burlingame, *Koenshu-Iyo Masu Kenkyukai*, 1981, **6**, 33.
5. J. O. Whitney, *Adv. Steroid Anal.*, 1984, **23**, 375.
6. J. O. Whitney and A. L. Burlingame, *Koenshu-Iyo Masu Kenkyukai*, 1982, **7**, 3.
7. J. O. Whitney, V. Ling, D. Grunberger, M. M. Thaler and A. L. Burlingame, *ibid.*, 1983, **8**, 47.
8. Y. Ito, T. Takeuchi, D. Ishii, M. Goto and T. Mizuno, *J. Chromatog.*, 1986, **358**, 201.
9. K. B. Tomer, N. J. Jensen, M. L. Gross and J. O. Whitney, *Biomed. Environ. Mass Spectrom.*, 1986, **13**, 265.
10. J. Tamura, S. Sakamoto and E. Kubota, *Analisis*, 1988, **16**, No. 6, LXIV.
11. J. W. Fiola, G. C. DiDonato and K. L. Busch, *Rev. Sci. Instrum.*, 1986, **57**, 2294.
12. K. L. Busch, *Trends Anal. Chem.*, 1987, **6**, No. 4, 95.
13. G. C. DiDonato and K. L. Busch, *Anal. Chem.*, 1986, **58**, 3231.
14. M. S. Stanley and K. L. Busch, *Anal. Chim. Acta*, 1987, **194**, 199.
15. J. C. Dunphy and K. L. Busch, *Biomed. Environ. Mass Spectrom.*, 1988, **17**, 405.
16. S. J. Doherty, S. M. Brown and K. L. Busch, *Abstracts of the Pittsburgh Conference, Atlanta*, 1989, No. 403.
17. R. A. Flurer and K. L. Busch, *Anal. Instrum.*, 1988, **17**, 255.
18. J. Sjovall, P. Eneroth and R. Ryhage, in *The Bile Acids*, Vol. 1, P. G. Nair and D. Kritchevsky (eds.), pp. 144–145, Plenum Press, New York, 1971.
19. J. O. Whitney and M. M. Thaler, *J. Liq. Chromatog.*, 1980, **3**, 545.
20. J. G. Liehr, E. E. Kingston and J. H. Beynon, *Biomed. Mass Spectrom.*, 1985, **12**, No. 3, 95.

HPLC DETERMINATION OF NIRIDAZOLE

NAWAL A. EL-RABBAT, HASSAN H. FARAG, MICHAEL E. EL-KOMMOS
and IBRAHIM H. REFAAT

Pharmaceutical Chemistry Department, Faculty of Pharmacy, Assiut University, Assiut, Egypt

(Received 3 August 1988. Revised 19 November 1989. Accepted 25 November 1989)

Summary—A high-performance liquid chromatographic method has been developed for the determination of niridazole in bulk form and in pharmaceutical dosage form. A reversed-phase system, based on an octadecylsilane-bonded stationary phase and a 60:40 v/v methanol/water mobile phase, is used. The detector response at 370 nm is linearly related to the amount injected, over a wide range. The method is sensitive, simple, rapid and precise.

Niridazole, 1-(5-nitrothiazol-2-yl)imidazolidin-2-one, is a schistosomicide¹ which is particularly active against *Schistosoma haematobium*² and *Schistosoma japonicum*.³ It is also used in the treatment of amoebiasis, guinea-worm infections² and dracontiasis.⁴ Niridazole is also a valuable immunosuppressive agent.⁵⁻⁸

Niridazole is widely used in countries where schistosomiasis is epidemic, but is not included in any pharmacopoeia. A gas-liquid chromatographic method is available for its determination⁹ but the retention time is 27.8 min. Niridazole in urine and serum has also been assayed by high-performance liquid chromatography (HPLC).¹⁰ In the present work, HPLC is used for the determination of the drug in tablets and in bulk form. The method is as accurate and precise as the fluorimetric method reported earlier,¹¹ but simpler.

EXPERIMENTAL

Materials

Pharmaceutical grade niridazole (CIBA) and was used as the working standard. Ambilhar tablets each containing 500 mg of niridazole were used. Methanol (HPLC grade) and methanolic solutions in water (redistilled deionized), were subjected to filtration and degassing before use.

Apparatus

An SP 1750 spectrophotometer with an AR 55 linear recorder and an SP 1805 program controller (all from Pye Unicam), was used for scanning the absorption spectrum of niridazole. The chromatograph used consisted of a DuPont

chromatographic pump, a column oven, an ultraviolet spectrophotometer and a computing integrator. The detector was set at 370 nm and 0.005 absorbance full scale. The recorder used was a Servogor 310, chart-speed 5 mm/min. A 25 cm × 4.6 mm column of Zorbax ODS (particle size 10 μm) was used, at 35°. The mobile phase was made by diluting 60 ml of methanol to 100 ml with doubly-distilled demineralized water, and was used at a flow-rate of 1 ml/min.

Calibration graph

A stock solution of niridazole was made by dissolving 25 mg of the pure compound (accurately weighed) in 50 ml of methanol by gentle heating, cooling, and diluting to volume with mobile phase in a 100-ml standard flask.

The stock solution of niridazole was quantitatively diluted stepwise to give the following series of concentrations: 0.25, 0.50, 1.00, 2.00 and 4.00 ng/50 μl; a 50-μl aliquot of each solution was injected into the column and the heights and integrated areas of the HPLC peaks were measured.

Assay of tablets

Twenty tablets were accurately weighed and finely powdered. An amount of the powder equivalent to about 25 mg of pure niridazole was weighed accurately and heated gently with 25.0 ml of methanol, and the solution was filtered. One ml of the yellow filtrate was diluted accurately with mobile phase to 100.0 ml, and 0.1 ml of this solution was diluted with the same solvent to 250 ml. Six 50-μl portions of this sample solution were injected, and the content

Table 1. Effect of mobile phase composition on niridazole retention

Mobile phase	t_R , min	k'
CH ₃ OH/H ₂ O (40:60)	6.3	1.423
CH ₃ OH/H ₂ O (60:40)	4.4	0.692
CH ₃ OH/H ₂ O (75:25)	3.5	0.346
CH ₃ OH/H ₂ O (90:10)	3.0	0.154
Absolute methanol	2.8	0.077

of the drug in the tablets was calculated from the mean peak height.

RESULTS AND DISCUSSION

The separation of a wide range of chemical types with an octadecylsilane (ODS) stationary phase with a methanol-water mobile phase has been reported.¹² The optimum mobile phase composition was found to be methanol/water (60:40), which gives the best compromise between capacity factor (k' -value) and band-broadening (Table 1). The number of theoretical plates was calculated to be 1936.

The wavelength for detection was selected from the absorption spectrum of a solution of niridazole in the eluent (Fig. 1). This spectrum has two absorption maxima, that at 370 nm having about twice the amplitude of that at 242 nm. As little as 0.1 ng of niridazole could be detected at 370 nm (signal-to-noise ratio 3.0).

It was found that peak-height measurement gave more precise and accurate results than peak-area measurement did, the correlation

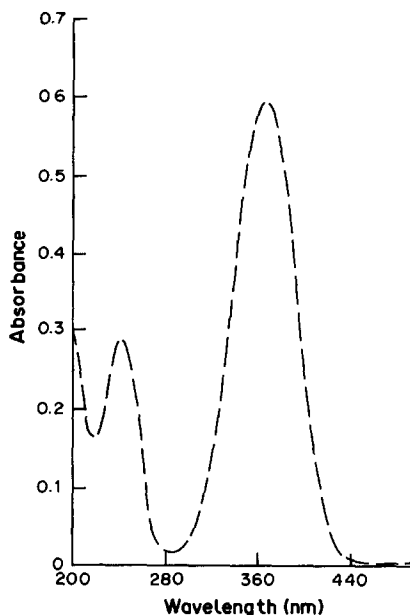


Fig. 1. Absorption spectrum of niridazole in 60:40 v/v methanol/water mixture.

Table 2. Mean and relative standard deviation of 10 replicate determinations of niridazole

Variable	Mean	RSD, %
Retention time	4.465 min	0.2
Peak-height	4.71 cm	1.2
Peak-area	4780 mV . sec	1.8

Table 3. Assay of 500-mg Ambilhar tablets (mean of 6 injections, and relative standard deviation)

Sample	HPLC method		Fluorometric method	
	Found, mg	RSD, %	Found, mg	RSD, %
1	496	0.9	497	1.3
2	478	1.2	480	1.4
3	487	0.9	486	1.0

coefficients for the regression equations for 6 injections of each of the standard solutions containing niridazole in the linearity range 0.25–4.00 ng in 50 μ l being 0.999 for the peak-heights and 0.978 for the peak-areas.

The reproducibility data from 10 replicate injections of a methanol/water (60:40) solution containing 2.0 ng of niridazole per 50 μ l are given in Table 2.

Table 3 gives the results obtained for determination of niridazole in pharmaceutical dosage form; they agree well with those obtained by a fluorimetric method.¹¹

The proposed procedure is simple and suitable for quality-control analysis of both the bulk drug and tablets. The method offers higher sensitivity and specificity than direct ultraviolet spectrophotometry does and is much faster than the gas chromatographic method. It is also simpler than the fluorimetric method¹¹ which involves evaporation of an alcohol solution of niridazole to dryness and heating of the residue with malonic acid and acetic anhydride before dilution and measurement.

REFERENCES

1. A. A. Mahmoud, *N. Engl. J. Med.*, 1977, **297**, 1329.
2. *Martindale's Extra Pharmacopoeia*, 28th Ed., J. E. F. Reynolds and A. B. Prasad (eds.), Pharmaceutical Press, London, 1982.
3. *Anon., Med. Lett.*, 1982, **24**, 7.
4. G. Raffier, *Am. N.Y. Acad. Sci.*, 1969, **160**, 720.
5. J. R. Salaman, M. Bird, A. M. Godfrey, B. M. Jones, D. Millar and J. J. Miller, *Transplant. Proc.*, 1977, **9**, 989.
6. *Idem, Transplantation*, 1977, **23**, 29.
7. B. M. Jones, M. Bird, M. Howells, D. Millar, J. J. Miller, S. Reeves and J. R. Salaman, *ibid.*, 1978, **24**, 134.
8. S. V. Lucas, J. C. Daniels, R. D. Schubert, J. M. Simpson, A. A. R. Mahmoud, K. S. Warren, J. R. David and L. T. Webster, *J. Immunol.*, 1977, **118**, 418.

9. J. J. Miller and R. J. Oake, *J. Chromatog.*, 1977, **131**, 442.
10. J. J. Miller, B. M. Jones, P. R. Massey and J. R. Salaman, *ibid.*, 1978, **147**, 507.
11. I. H. Refaat, M. E. El-Kommos, H. H. Farag and N. A. El-Rabbat, *Bull. Pharm. Sci. Assiut Univ.*, 1987, **10**, 85.
12. P. J. Twitchett and A. C. Moffat, *J. Chromatog.*, 1975, **111**, 149.

SEPARATION OF SOME PLATINUM METAL 8-HYDROXYQUINOLINATES BY NORMAL PHASE HIGH-PERFORMANCE LIQUID CHROMATOGRAPHY

I. P. ALIMARIN✠, E. M. BASOVA, A. YU. MALYKHIN and T. A. BOL'SHOVA

Department of Chemistry, M.V. Lomonosov Moscow State University, Leninskie Gory, Moscow, USSR

(Received 12 October 1988. Revised 11 September 1989. Accepted 7 October 1989)

Summary—The method of normal phase high-performance liquid chromatography has been applied to the separation and determination of Pd(II), Pt(II), Rh(III), Ir(IV), Ru(III) and Os(IV) as chelates with 8-hydroxyquinoline on a 62 × 2 mm column packed with Silasorb 600 5 μm silica gel by elution with methylene chloride-isopropyl alcohol mixture (97:3 v/v). The detection limits (ng per 5 μl), were Pd 0.3, Pt 1.0, Rh 1.0, Ir 5.0, Ru 1.5, Os 25. The separation time was 12 min at a flow-rate of 0.1 ml/min.

High-performance liquid chromatography (HPLC) is currently widely applied to quantitative analysis of mixtures of organic compounds, especially in trace analysis. HPLC sometimes has advantages over other instrumental methods of analysis, for example, atomic-absorption spectroscopy, voltammetry, in terms of sensitivity, selectivity and rapid sequential determination of several elements in the same sample; moreover, in this particular case the preparation of samples for analysis is simplified and the time required is less, which is of special importance in routine analysis of large numbers of samples. The most widespread inorganic application of HPLC is the separation and determination of metals in the form of chelates, with spectrophotometric detection.^{1,2}

A successful solution to one of the most complicated problems of analytical chemistry, viz. use of a single sample for determination of several platinum metals within a group, seems to be possible only with the use of chromatographic methods, among which HPLC appears to be the most effective, sensitive and fast.³ Various organic reagents have been used to separate platinum metals by HPLC: β-diketones, 1-(2-pyridylazo)-2-naphthol, 1-hydroxy-2-pyridinethione, β-ketoimines, 8-hydroxyquinoline, dithiocarbamates and others.³ Of great importance in quantitative analysis is 8-hydroxyquinoline, which simultaneously forms stable neutral chelates with all platinum metals, but only one publication on their separ-

ation is available in the literature.⁴ It describes the determination of Ru, Rh and Ir with detection limits of 5 ng by normal phase HPLC with chloroform-tetrahydrofuran (THF) mixture (6:4 v/v) as the mobile phase. However, the 8-hydroxyquinolates of Pt and Pd were eluted together, as a single peak which could not be completely separated from the ruthenium chelate peak. The authors also failed to separate the osmium and ruthenium 8-hydroxyquinolates.

The present work was devoted to study of the retention of all six platinum metals as their hydroxyquinolates, and the choice of conditions for their separation and determination by normal phase HPLC.

EXPERIMENTAL

The work was done with a Milichrom micro-column chromatograph equipped with a spectrophotometric detector (range 190–360 nm). A stainless-steel column (62 × 2 mm) was packed with Silasorb 600 silica gel (average particle diameter 5 μm). The detection wavelength was 254 nm. The flow-rate of the mobile phase was 0.1 ml/min. Aliquots (5 or 10 μl) of chloroform solutions of the chelates were injected into the column. The chelates were made as follows. A known volume of metal salt solution containing 16–150 μg of the metal (or 140–500 μg of mixed metals) was placed in a graduated 20-ml test-tube (fitted with a stopper) and diluted to 10 ml with pH 4.8 acetate buffer, and 30 mg of solid 8-hydroxyquinoline was added. The mixture

✠Deceased 17 December 1989.

was heated for 2 hr in a water-bath at 90°, then cooled and shaken for 1–2 min with 2 ml of chloroform. The excess of 8-hydroxyquinoline also passes into the organic phase, and must be removed, since it absorbs light of the wavelength used for detection, and is also strongly adsorbed on silica gel, which results in overlap of the reagent peak with the peaks of some of the chelates when there is a small excess, and a drift of the baseline when there is a large excess. The excess of 8-hydroxyquinoline was removed by shaking the chloroform phase with two 15-ml portions of 0.1M sodium hydroxide.

The following characteristics were used to describe the chromatographic behaviour of chelates: the retention volume (V'_R) corrected for the dead volume of the column (the retention volume of CCl_4 , a non-retained component), the capacity factor (k'), the relative retention (α), the resolution (R_S) of two adjacent peaks and the number of theoretical plates⁵ (N).

RESULTS AND DISCUSSION

Choice of the mobile phase

The mixtures of chloroform and THF usually used for the separation of metal 8-hydroxyquinolinates are not sufficiently selective for the platinum metals.⁴ Also, cyclic ethers are readily oxidized by atmospheric oxygen to yield peroxides which, in turn, can oxidize certain components of the mixtures to be separated and absorb light in the ultraviolet. When ultraviolet detectors are used, these solvents should be purified by passage through a column of an adsorbent,⁶ as well as by distillation (with strict adherence to the safety rules). 2-Propanol seems to be a more promising modifier for the mobile phase in adsorption chromatography, but it may contain traces of water, which would rather strongly affect the chromatographic properties of the analytes, and could decrease the reproducibility of separation. It is known that the greater the solubility of water in the eluent, the less the effect of the water content on the value of k' .⁵ The solubility of water in non-polar and weakly polar solvents is least in aliphatic hydrocarbons and greatest in chloroform and methylene chloride.⁵ Hence, in elution with aliphatic hydrocarbons the water content in the eluent has the maximum effect on the separation, and in elution with chloroform or methylene chloride the effect is minimal.

Thus, for separation of the platinum metal 8-hydroxyquinolinates, we used binary mixtures of chloroform or methylene chloride with 2-propanol, controlling the eluting power of the mobile phase by changing the 2-propanol content from 2 to 5% v/v. Before use, the column was washed with the eluent for 15 min to establish equilibrium with the adsorbent. The dependence of the basic chromatographic parameters, characterizing the separation process, on the 2-propanol content in the mobile phase is given in Table 1. It is seen that an increase in the polar additive concentration in both mobile phases decreases the retention of all the chelates, the peaks become narrower (the number of theoretical plates increases), but the resolution of neighbouring peaks deteriorates. At best, five elements, Pd, Pt, Rh, Ir and Ru, can be simultaneously determined by elution with the chloroform/2-propanol mixture (98:2). The chromatogram is shown in Fig. 1. The peaks for the Pd and Os chelates are poorly resolved, and these two elements cannot be determined when present together.

The peaks of all six chelates are well separated ($R_S \geq 1.5$) by use of methylene chloride containing 2–3% v/v 2-propanol for elution. Since HPLC aims to attain optimal rather than maximum separation, in other words, maximal separation in the shortest time, the methylene chloride/2-propanol mixture (97:3) was chosen as the mobile phase for further development of the analytical procedure. Pd, Pt, Rh, Ir, Ru, Os could be separated within 12 min (Fig. 2). The use of mobile phases containing less 2-propanol results in longer separation times, deterioration of peak shapes (dilution) and consequently lower sensitivity of determination. All five metals, Pd (or Pt), Rh, Ir, Ru and Os, are separated in 6 min with the methylene chloride/2-propanol mixture (95:5) as eluent (Fig. 3).

Retention mechanism

It should be noted that the elution of each of the chelates examined results in only one peak. According to the literature,⁷ 8-hydroxyquinoline reacts with Pd and Pt to form ML_2 complexes, whereas with Rh, Ir, Ru and Os it gives ML_3 species. However, it is reported by Fedorova *et al.*⁸ that a thin-layer chromatography (TLC) study of ruthenium(III) 8-hydroxyquinolate solutions (with 19:1 chloroform/ethanol mixture as eluent) has shown that when the chromatograms are overloaded, then in addition to the green zone corresponding to the

Table 1. Dependence of the chromatographic parameters of the platinum metal 8-hydroxyquinolinates on the nature and composition of the mobile phase

Mobile phase	2-Propanol content in the mobile phase, % v/v																			
	2					3					4					5				
Element	V_R	k'	N	α	R_S	V_R	k'	N	α	R_S	V_R	k'	N	α	R_S	V_R	k'	N	α	R_S
Chloroform/ 2-propanol	Pt	52	0.36	2140	—	—	0.29	2300	—	—	35	0.24	2590	—	—	33	0.23	3340	—	—
	Pd	66	0.45	5200	1.25	1.19	0.34	5750	1.17	0.72	39	0.27	6130	1.12	0.44	35	0.24	6410	1.04	0.15
	Os	82	0.56	2150	1.24	0.97	0.39	2070	1.15	0.42	47	0.32	2120	1.04	0.10	36	0.25	2350	1.04	0.09
	Ru	130	0.89	890	1.59	1.30	0.59	1090	1.51	1.03	73	0.50	1300	1.56	1.07	53	0.36	1340	1.44	0.74
	Ir	224	1.53	1800	1.72	2.69	1.08	1800	1.83	2.49	121	0.83	1330	1.66	1.64	91	0.62	1900	1.72	1.74
Rh	334	2.29	1600	1.49	2.30	1.56	1760	1.44	1.95	174	1.19	2050	1.43	1.85	129	0.88	23.00	1.42	1.66	
Methylene chloride/ 2-propanol	Pt	107	0.73	6180	—	—	0.53	6220	—	—	58	0.40	6200	—	—	44	0.30	5800	—	—
	Pd	162	1.11	2300	1.51	2.51	0.75	2450	1.41	1.54	70	0.48	2560	1.21	0.71	50	0.34	2550	1.14	0.39
	Os	349	2.39	1210	2.15	4.10	1.63	1380	2.17	3.10	128	0.88	1420	1.83	2.01	78	0.53	1730	1.56	1.29
	Ru	648	4.44	1450	1.86	4.20	2.96	1650	1.81	3.40	230	1.58	1430	1.80	2.57	138	0.94	1270	1.77	1.88
	Ir	893	6.12	810	1.38	2.90	4.48	960	1.52	2.17	334	2.29	890	1.45	1.61	202	1.38	1130	1.47	1.56
Rh	1400	9.57	1130	1.57	3.10	6.81	1280	1.52	2.67	504	3.45	1210	1.51	2.28	308	2.11	1220	1.53	2.05	

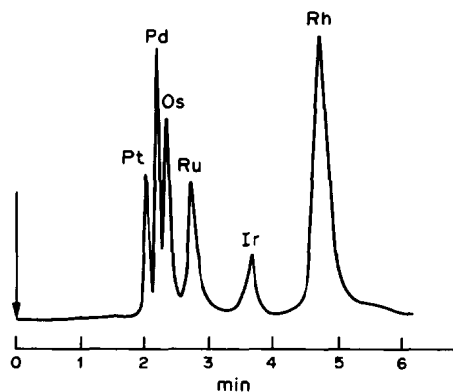


Fig. 1. Chromatogram of platinum metal 8-hydroxyquinolinates with the chloroform/2-propanol mixture (98:2) as eluent. Chromatographic conditions: column 62×2 mm, stationary phase Silasorb 600 ($5 \mu\text{m}$), flow-rate 0.1 ml/min, detection at 254 nm.

ruthenium tris-chelate, the major component, three other chromatographic zones of characteristic shape and colour can be detected, and probably correspond to other complexes of ruthenium with 8-hydroxyquinoline. These authors proposed a scheme of interaction with ruthenium(III), which in the initial solutions is in the form of various chloro and aquo-chloro complexes with 8-hydroxyquinoline. The additional TLC zones are small in area and have low intensity; that is, their ruthenium content is a few magnitudes of order lower than that of the main zone. According to the authors, these

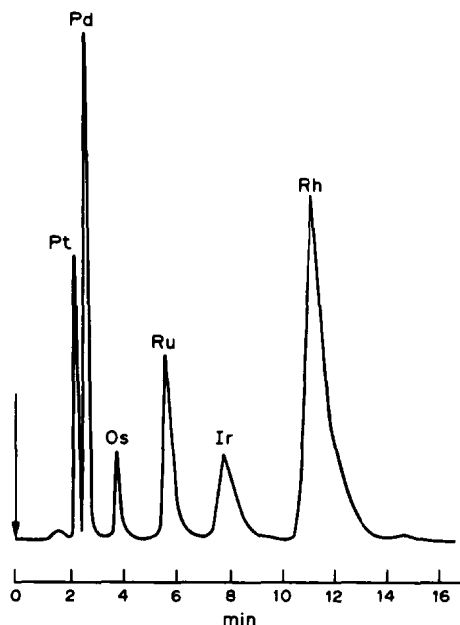


Fig. 2. Chromatogram of platinum metal 8-hydroxyquinolinates with the methylene chloride/2-propanol mixture (97:3) as eluent. Chromatographic conditions similar to those for Fig. 1.

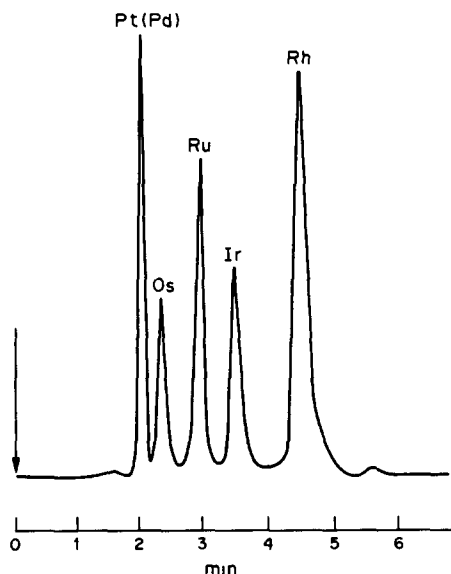


Fig. 3. Chromatogram of platinum metal 8-hydroxyquinolinates with the methylene chloride/2-propanol mixture (95:5) as eluent. Chromatographic conditions similar to those for Fig. 1.

zones can correspond to the monochelate, and the *cis*- and *trans*-isomers of the bischelate with 8-hydroxyquinoline. Similar results were obtained for rhodium 8-hydroxyquinolate.⁹ In our work the concentration of the chelates is one magnitude of order lower than that used by Fedorova *et al.*,⁸ and the fraction of these three species of the ruthenium and rhodium chelates appears negligible, or at least the detector is not

sensitive enough for their detection. Consequently, the chromatograms obtained exhibited only one peak, corresponding to the tris-chelate, the principal form of the complex.

As seen from Figs. 1–3, the chelates are eluted in the order (of retention times) Pt < Pd < Os < Ru < Ir < Rh, which is independent of the nature and composition of the mobile phase. For the pairs of elements in the same groups of the Periodic Table (Pt–Pd, Ir–Rh, Os–Ru) the elution order of the chelates correlates with the decrease in electronegativity (1.44–1.39, 1.55–1.45 and 1.52–1.42, respectively).¹⁰ The chelates are retained on silica gel by hydrogen bonding of a ligand donor atom (most likely the oxygen atom) with the surface silanol groups.¹¹ A decrease in the electronegativity of the elements should increase their effective charge, the electron density on the donor atom of the ligand and, therefore, the adsorption capacity of the chelates, as observed experimentally (Fig. 2).

Plots of $\log k'$ vs. $\log X_s$, where X_s is the mole fraction of the polar component of the binary mobile phase, were prepared for both types of eluent and all the platinum metals (Fig. 4). The slopes of the plots are equal to the number of bonds formed by the chelates with the silica gel (Table 2).¹² According to the data in Table 2, the chelates should be eluted by the chloroform/2-propanol mixture in the order Pt < Pd < Ru < Ir < Rh, and by the methylene chloride/2-propanol mixture in the order Pt < Pd < Os <

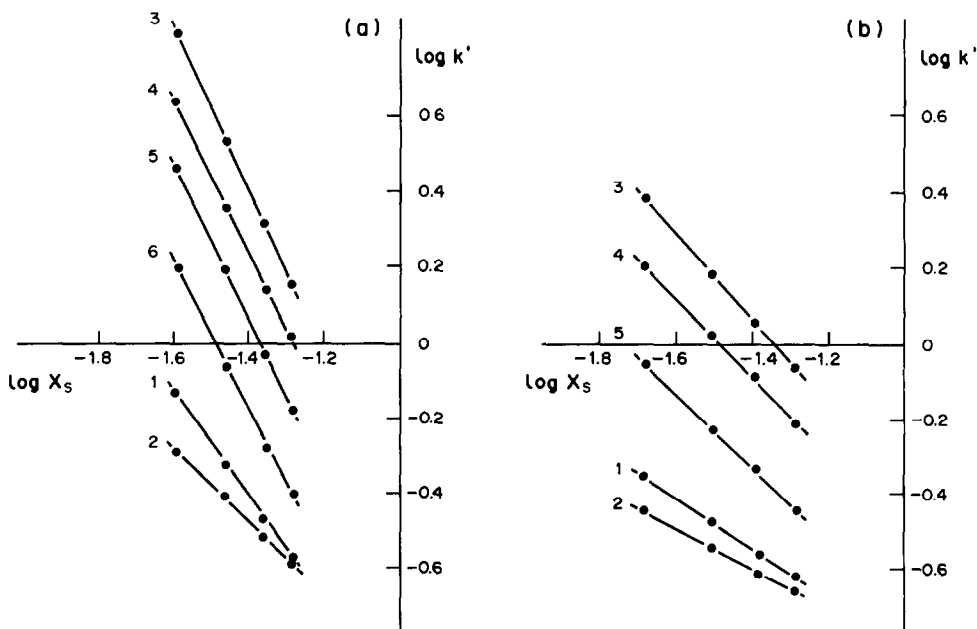


Fig. 4. The dependence of $\log k'$ on $\log X_s$ for 8-hydroxyquinolinates of Pd (1), Pt (2), Rh (3), Ir (4), Ru (5) and Os (6). Mobile phase: (a)—methylene chloride/2-propanol; (b)—chloroform/2-propanol.

Table 2. The number of bonds formed by platinum metal 8-hydroxyquinolates with silica gel ($n = 4$, $P = 0.95$)

Mobile phase	Pd	Pt	Rh	Ir	Ru	Os
Chloroform/2-propanol	0.7 ± 0.1	0.5 ± 0.2	1.1 ± 0.2	1.0 ± 0.2	0.9 ± 0.4	—
Methylene chloride/ 2-propanol	1.5 ± 0.2	1.0 ± 0.2	2.2 ± 0.1	2.1 ± 0.5	2.1 ± 0.3	2.0 ± 0.4

Table 3. Analytical characteristics of the procedure for the simultaneous determination of platinum metals by HPLC: mobile phase methylene chloride/2-propanol (97:3); calibration equation $y = bx$, where y is the peak height in mm and x is the metal concentration in ng per $5 \mu\text{l}$ of sample

Element	b	Range of calibration graph linearity, ng	Detection limit, ng
Pd	3.51 ± 0.02	1–300	0.3
Pt	1.00 ± 0.03	3–300	1.0
Rh	1.02 ± 0.02	3–300	1.0
Ir	0.22 ± 0.01	15–300	5.0
Ru	0.73 ± 0.02	3–300	1.5
Os	0.78 ± 0.05	50–200	25

$\text{Ru} = \text{Ir} < \text{Rh}$, which is observed experimentally (Figs. 1 and 2).

The methylene chloride/2-propanol (97:3) mobile phase was used to develop a procedure for simultaneous determination of all the platinum metals. As seen from Fig. 2, all the peaks are sharp, Gaussian and completely resolved, and therefore can be quantified by measurement

of the peak heights. Some characteristics of the procedure developed are given in Table 3. The detection limits are calculated for a signal/noise ratio of 2. Calibration graphs are linear over a wide concentration range (two orders of magnitudes for all six metals except osmium). For osmium the calibration is non-linear in the low concentration range, probably because of decomposition of the chelate in the course of the chromatography. Table 4 gives the results of determination of the platinum metals in synthetic mixtures. The relative standard deviations are about 3–4% except for osmium, for which the poor linearity results in an rsd of about 8%. The procedure developed allows the simultaneous determination of all six platinum metals in one aliquot of solution, in 12 min, with detection limits of 0.3–25 ng. The procedure can be recommended for the determination of platinum metals in technological solutions, concentrates, alloys and catalysts.

REFERENCES

Table 4. Determination of platinum metals in synthetic mixtures ($n = 5$; $P = 0.95$; $5 \mu\text{l}$ injection)

Central ion	Added, ng	Found, ng	rsd, %
Pt(II)	50	46 ± 2	4
Pd(II)	30	31 ± 2	4
Os(IV)	150	157 ± 13	7
Ir(IV)	150	147 ± 4	3
Ru(III)	50	47 ± 2	3
Rh(III)	88	91 ± 2	3
Pt(II)	15	15.3 ± 0.3	3
Pd(II)	25	23 ± 2	5
Os(IV)	75	68 ± 6	7
Ir(IV)	25	24 ± 2	4
Rh(III)	44	43 ± 2	3
Ru(III)	75	79 ± 4	4
Pt(II)	12	11.4 ± 0.7	4
Pd(II)	8	7.5 ± 0.2	3
Os(IV)	62	59 ± 6	8
Ir(IV)	10	9.7 ± 0.5	3
Ru(II)	38	41 ± 3	6
Rh(III)	10	8.6 ± 0.6	5

1. A. R. Timerbaev, O. M. Petrukhin and Yu. A. Zolotov, *Zh. Analit. Khim.*, 1981, **36**, 1160.
2. G. Schwedt, *Chromatographic Methods in Inorganic Analysis*, Hüthig, Heidelberg, 1981.
3. I. P. Alimarin, E. M. Basova, T. A. Bol'shova and V. M. Ivanov, *Zh. Analit. Khim.*, 1986, **41**, 5.
4. B. Wenclawiak and F. Bickmann, *Bunseki Kagaku*, 1984, **33**, E67.
5. H. Engelhardt, *Hochdruck-flüssigkeits Chromatographie*, Springer, Heidelberg, 1977.
6. E. L. Styskin, L. B. Itsekson and E. V. Braude, *Prakticheskaya vysokoeffektivnaya zhidkostnaya khromatografia*, Khimiya, Moscow, 1986.
7. B. Wenclawiak and M. Flemming, *Z. Anal. Chem.*, 1987, **326**, 551.
8. T. D. Fedorova, L. V. Znobishcheva and A. G. Kir'yanova, *Izv. SO Akad. Nauk SSSR*, 1987, **2**, 95.
9. A. B. Benediktov and A. V. Belyaev, *Koord. Khim.*, 1984, **10**, 1516.
10. A. J. Gordon and R. A. Ford, *The Chemist's Companion*, Wiley, New York, 1972.
11. A. R. Timerbaev, O. M. Petrukhin and Yu. A. Zolotov, *Zh. Analit. Khim.*, 1982, **37**, 1360.
12. E. Soczewinski and W. Golkiewicz, *Chromatographia*, 1973, **6**, 269.

CHELATING POLYMERS AND RELATED SUPPORTS FOR SEPARATION AND PRECONCENTRATION OF TRACE METALS

C. KANTIPULY, S. KATRAGADDA, A. CHOW* and H. D. GESSER

Department of Chemistry, University of Manitoba, Winnipeg, Manitoba, Canada R3T 2N2

(Received 16 September 1988. Revised 15 July 1989. Accepted 19 October 1989)

Summary—This review is concerned mainly with the applications of chelating polymeric resins for the separation and concentration of trace metals from oceans, rivers, streams and other natural systems. Commercially available resins, specially prepared polymers and a selection of other sorbents are described and their uses outlined. Special emphasis is placed on the preconcentration of uranium from sea-water.

Metal ions and their chemical compounds find their way into ocean waters from streams, rivers and weathering of rocks, minerals, ores and soils. In addition, significant contribution is possible from all avenues of human endeavour, ranging from large industrial enterprises to home activities. A thorough understanding and characterization of ocean water calls for an accurate determination of trace elements and their species.

The chemical speciation of these elements is primarily determined by complexes formed by inorganic anions (OH^- , Cl^- , CO_3^{2-} , HPO_4^{2-} , SO_4^{2-} , F^- , etc.) and organic complexing agents such as carboxylic, humic and fulvic acids. In this connection, trace elements are defined here as those elements that are present in ocean waters at concentrations less than 1 ppm (1 $\mu\text{g}/\text{ml}$) and are difficult to determine directly by instrumental methods, mainly because of the high salt content in these waters.

Accurate analysis of ocean waters, especially at trace levels, is one of the most difficult and complicated analytical tasks, because the oceans contain very many of the naturally occurring elements and radioactive isotopes. The current interest of analytical chemists in the constituents of ocean waters emphasizes determination at ppm levels or below, with special attention to monitoring of radionuclides. Despite their low concentrations, these latter constituents are of interest because they are both geochemically and biologically "reactive". The analyst is presented with a difficult task by the increasingly rigorous requirements of versatility, specificity,

sensitivity and accuracy in the analyses. During the past three decades rapid development of electronic instrumentation has created powerful analytical tools for trace-element determination. However, these tools can give erroneous results for ocean-water samples because of matrix effects, if the limitations of the devices go unheeded. Kantipuly and Westland, in their recent review,¹ made evident the matrix effects involved and the importance of separation chemistry in instrumental methods such as neutron-activation analysis, plasma-source emission and mass spectrometry, X-ray fluorescence spectrometry, atomic absorption and spectrophotometric methods. To obtain reliable data, the best course is to separate the analytes of interest from the matrix constituents and determine them in the isolated state. This results in greater sensitivity, but calls for elegant separation and concentration techniques involving chelating resins and ion-exchange resins. There have been several reviews²⁻⁸ dealing with chelating polymers in separation and preconcentration methods. The purpose of this review is to document various practical chelating polymers available for preconcentration and separation of trace metals and radionuclides from natural water systems.

CHELATING POLYMERS: GENERAL PROPERTIES

The chemistry underlying the use of ion-exchange and chelating polymers for the separation and preconcentration of trace elements is reasonably well understood^{9,10} and progress today is mainly in improving the

*To whom reprint requests should be addressed.

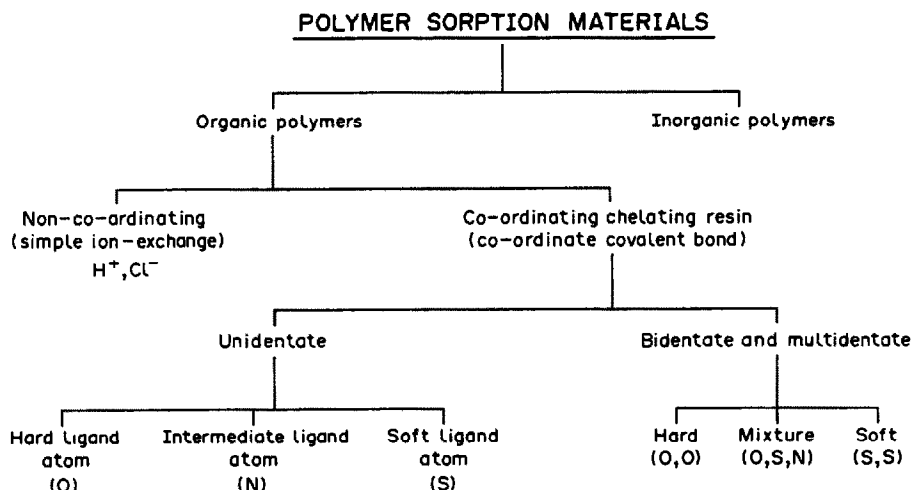


Fig. 1

specificity of the resins and the techniques of application. The analytical application of chelating polymers depend on many factors. Normally a metal ion exists in ocean water as a hydrated ion or as a complex species in association with various anions, with little or no tendency to transfer to a chelating polymer. To convert a metal ion into an extractable species its charge must be neutralized and some or all of its water of hydration replaced. The nature of the metal species is therefore of fundamental importance in extraction systems. Most significant is the nature of the functional group and/or donor atom capable of forming complexes with the metal ions in solution, and it is logical to classify chelating polymers on this basis. Also, for simplicity, it is desirable to classify chelating polymers according to Fig. 1. This method of classification is not meant to imply that these systems are mutually exclusive. Indeed, some polymers can belong to more than one class, depending on experimental conditions.

Functional groups

The functional group atoms capable of forming chelate rings usually include oxygen, nitrogen and sulphur. Nitrogen can be present in a primary, secondary or tertiary amine, nitro, nitroso, azo, diazo, nitrile, amide and other groups. Oxygen is usually in the form of phenolic, carbonyl, carboxylic, hydroxyl, ether, phosphoryl and some other groups. Sulphur is in the form of thiol, thioether, thiocarbamate, disulphide groups *etc.*

These groups can be introduced into the polymer by chemical transformation of the matrix or by the synthesis of sorbents from

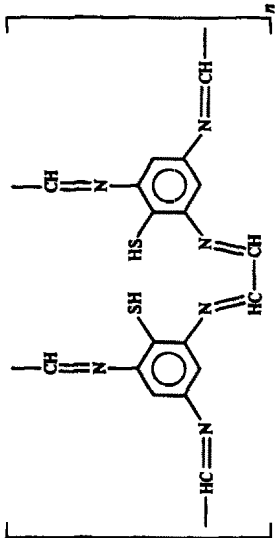
monomeric ligands. The insertion of suitable specific functional groups into the polymeric matrix makes them capable of reacting with metal ions or metal species under certain favorable conditions, to form chelate rings. The selective concentration and separation of elements from natural water systems depends both on elemental speciation and the chelating properties of the polymer. Examples of chelating groups and their application for selective pre-concentration of inorganic elements were recently reviewed by Myasoedova and Savvin,² but these authors did not include an important class of commercially available chelating resins, namely the Chelite, Duolite and Amborane series of resins. However, Schwochau³ has documented the application of some of these resins for the extraction of metals from sea-water and these form the basis of Table 1. It is interesting to note that an entire section of his review was devoted to the extraction of uranium from sea-water, and the data are included in Table 2. It is the prime objective of the present review to document the available chelating polymers and their various applications comprehensively. Special emphasis is placed on the extraction of uranium from sea-water, because of the increasing attention it has received over the past two decades.

Selection of chelating polymers

Synthetic chelating polymers have almost entirely displaced inorganic ion-exchange polymers, with a few exceptions such as metal phosphates (zirconium and stannic phosphates) and some oxides (MnO_2 , Al_2O_3 , SiO_2 gel, *etc.*).

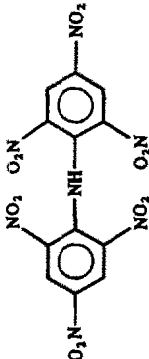
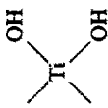
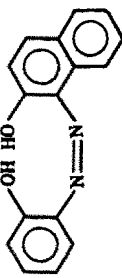
Table 1. Extracting systems used for metal separation from natural water systems (after Schwochau,³ by permission of the copyright holders, Springer Verlag, Heidelberg)

System and active group	Metal ions	Remarks	References
Chelex-100, Dowex A-1 $\begin{array}{c} \text{CH}_2\text{COOH} \\ \\ -\text{CH}_2-\text{N} \\ \\ \text{CH}_2\text{COOH} \end{array}$	Sc, V, Cr, Mn, Fe, Co, Ni, Cu, Zn, Y, Mo, Ag, Cd, In, lanthanides, W, Re, Pb, Bi, Th, U, Al, Sn, Ti	Cation elution with dilute mineral acids, anion elution with 4M ammonia solution	11-18 19-23
Retardant 11-A8 -CH ₂ COOH -CH ₂ N ⁺ (CH ₃) ₃ Cl ⁻ Amberlite CG400 -CH ₂ N ⁺ (CH ₃) ₃ SCN ⁻	Li	Concentration factor of 30 in the ethyl alcohol eluent	24
Poly(tetraethylenepentamine)-polyurea resin	Ti, Co	Sorption after complexation with SCN ⁻ Elution with 2M mineral acids	25, 26
Poly(glyoxaltriiminophenol)	Ni, Cu, Zn	Nearly quantitative recovery at natural pH of sea-water	27
Poly(glyoxaltriiminothiophenol)	Cu, U	Separation at natural pH of sea-water; elution with dilute mineral acids	28,29
	Au	Separation at natural pH of sea-water; elution with dilute mineral acids	29
Hydrous aluminium oxide $\begin{array}{c} \text{OH} \\ \\ -\text{Al} \\ \\ \text{OH} \end{array}$	Li	Elution with boiling water; maximal concentration factor 46 in the eluate	30, 31



Continued overleaf

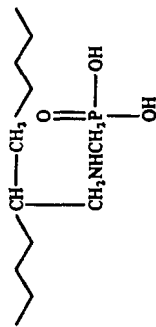
Table 1—Continued

System and active group	Metal ions	Remarks	References
Dipicrylamine 	K	Precipitation of the potassium salt elution of K ⁺ with mineral acids	32-34
Zirconium phosphate	K	Potassium capacity 25 mg/g	35
Hydrous titanium oxide 	Na, Mg, Al, Ca, V, Cr, Mn, Fe, Ni, Cu, Sr, Ba, U	Sorption at natural pH of sea-water; elution with dilute mineral acids; selective elution of U with 2M (NH ₄) ₂ CO ₃	36, 37
Hyphan on cellulose or polystyrene 	Fe, Ni, Cu, Zn, Pb, U	Almost complete separation; elution with 1M HCl	38-40
Thiazoline on polystyrene	Hg	Extraction at pH 1; complete elution with 0.1M HCl containing 5% thiourea	41
8-Hydroxyquinoline on C ₁₈ -bonded silica gel	Mn, Fe, Co, Ni, Cu, Zn, Cd	Concentration factors 50-100 in methanol eluate	42
1-Nitroso-2-naphthol-3,6-disulphonate	Co	Elution with titanium(III) chloride	43
4-(2-Thiazolyazo)resorcinol	Co	Elution with methanol-chloroform (1:1) mixture	44
Duolite CS-100 (carboxylic acid and phenolic hydroxyl groups)	¹³⁷ Cs, ⁹⁰ Sr	Alkaline low-level radioactive wastes	45

46

U

Polyallylamine phosphonic acid



Sumichela Q-10
(vinyl polymer with dithiocarbamate)

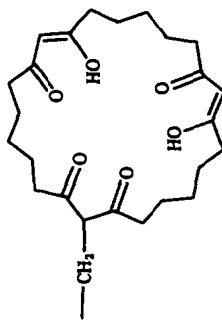
ALM-125
(dithiocarbamate)

MnO₂-impregnated fibre filter

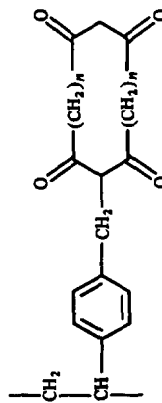
2,5-Dimercapto-1,3,4-thiadiazole loaded on silica gel (DMT-SG)

Mercapto-modified silica

Polystyrene-bound hexaketone



Polystyrene-bound tetraketones



47

Hg

Hg

²³⁸Pu,²³⁹,²⁴⁰Pu

Bi

Zn²⁺, Cd²⁺, Cu⁺, Pb²⁺

U

Sea-water

Preconcentration of trace amounts of Bi(III) from water samples; eluted with 0.05M EDTA

Elution with 3M nitric acid

Sea-water

53

Cu²⁺, Ni²⁺, Co²⁺

Table 1—Continued

System and active group	Metal ions	Remarks	References
Polystyrene-bound 1,3-diketone	UO_2^{2+} , Cu^{2+} , Ni^{2+} , Fe^{3+}	Sea-water buffered at pH 5.6; elution with 1M HCl	54
Ethylenediaminetriacetic acid on porous glass	Cu, Zn, Pb		55
<i>p</i> -Dimethylaminobenzylidenerhodamine on silica gel	Pd, Ag, Au	Quantitative retention from acidified sea-water; elution with 0.1M HCl containing thiourea	56
Chitin	Co, Sb, Au, Hg	Sorption at pH 7	57
Chitosan	Co, Zn, Cu, Mo, Pd, Sb, Cs, Ir, Au, Hg, U	Sorption at pH 7	57
Amidoxime $\begin{array}{c} N-OH \\ \\ C \\ \\ NH_2 \end{array}$	Na, Mg, Ca, V, Fe, Cu, Sr, Ba, Au, U	Sorption at natural pH of sea-water; elution with dilute mineral acids; uranium capacity > 3600 ppm	37, 58, 59
Dithiocarbamate cellulose derivative	Cu, Cd, Hg, Pb, U	Sea and tap water	60
Poly(maleic anhydride)	Pb	Tap water	61
<i>Flotation systems:</i> Iron(III) hydroxide + sodium dodecylsulphate	V, Mo, U	More than 80% recovery at the appropriate pH	62–64
Iron(III) hydroxide + dodecylamine	Cu, Zn	More than 90% recovery at pH 7.6	64, 65
Lead sulphide + stearylamine	Ag	Almost quantitative separation at pH 2	66
2-Mercaptobenzothiazole co-precipitate without surfactant	Ag	More than 95% recovery at pH 1	67
Cadmium sulphide + octadecyltrimethylammonium chloride	Hg	Quantitative separation at pH 1	68
<i>Complexing agents/organic solvents:</i> Ammonium pyrrolidone dithiocarbamate/methyl isobutyl ketone, chloroform or Freon TF	V, Cr, Mn, Fe, Co, Ni Cu, Zn, Cd, Pb	Extraction at pH 3–5	69–73
4-Benzoyl-3-methyl-1-phenyl-5-pyrazolone/isoamyl alcohol or methyl isobutyl ketone	Cu, Mo	Extraction of Cu at pH 7, Mo extraction at pH 1–3	74, 75

Table 2. Uranium loading of selected inorganic, organic, and biological sorbents in natural sea-water with a uranium concentration of about $3.3 \mu\text{g/l}$; the loadings refer to the dry sorbent or its metal content (reproduced from Schwochau³ by permission of the copyright holders, Springer Verlag, Heidelberg)

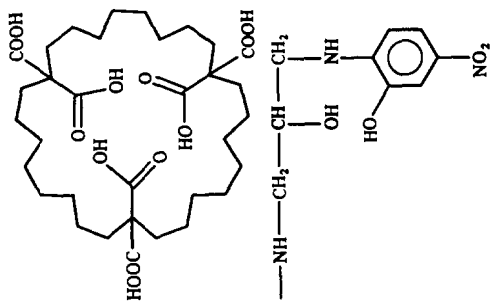
Sorbent	Functional group	Uranium loading	References
<i>Inorganic:</i>			
Hydrous aluminium oxide	$\begin{array}{c} \text{OH} \\ \\ \text{---Al---} \\ \\ \text{OH} \end{array}$	61 $\mu\text{g/g Al}$	76
Hydrous iron(III) oxide	$\begin{array}{c} \text{OH} \\ \\ \text{---Fe---} \\ \\ \text{OH} \end{array}$	60 $\mu\text{g/g Fe}$	76
Silica gel	$\begin{array}{c} \text{OH} \\ \\ \text{---Si---} \\ \\ \text{OH} \end{array}$	27 $\mu\text{g/g sorbent}$	77
Hydrous lanthanum oxide	$\begin{array}{c} \text{OH} \\ \\ \text{---La---} \\ \\ \text{OH} \end{array}$	38 $\mu\text{g/g La}$	76
Hydrous titanium oxide	$\begin{array}{c} \text{OH} \\ \\ \text{---Ti---} \\ \\ \text{OH} \end{array}$	550 $\mu\text{g/g Ti}$ 200 $\mu\text{g/g sorbent}$	36, 78
Hydrous titanium oxide (freshly precipitated)	—	1550 $\mu\text{g/g Ti}$	79
Basic zinc carbonate	—	540 $\mu\text{g/g Zn}$	76
Hydrous tin oxide	$\begin{array}{c} \text{OH} \\ \\ \text{---Sn---} \\ \\ \text{OH} \end{array}$	17 $\mu\text{g/g Sn}$	76

Continued overleaf

Table 2—Continued

Sorbent	Functional group	Uranium loading	References
Hydrous zirconium oxide		13 $\mu\text{g/g}$ Zr	76
<i>Organic:</i> Polystyrene-methylene phosphonic acid	$-\text{CH}_2\text{PO}(\text{OH})_2$	24 $\mu\text{g/g}$ sorbent	76
Resorcinolarsonic acid/formaldehyde copolymer	$-\text{AsO}(\text{OH})_2$	1112 $\mu\text{g/g}$ sorbent	76
Duolite ES 467	$-\text{CH}_2-\text{NH}-\text{CH}_2-\text{PO}_3\text{Na}_2$	45 $\mu\text{g/g}$ sorbent	79
Duolite ES 346		3600 $\mu\text{g/g}$ sorbent	37, 59
Poly(acrylamidoxime)			
Oxamidoxime-terephthalic acid chloride condensation polymer (fibres)		240 $\mu\text{g/g}$ sorbent	80
Poly(glyoxaltriaminophenol)		45 $\mu\text{g/g}$ sorbent	77
Hypkan on cellulose		80 $\mu\text{g/g}$ sorbent	81

Macrocyclic hexacarboxylic acid
on polystyrene



70 $\mu\text{g/g}$ sorbent

82

Macrocyclouimide resin S08

930 $\mu\text{g/g}$ sorbent

83

Biological:
Halimeda opuntia (green alga)
Laurencia papillosa (red alga)
Dicliyoita divaricata (brown alga)
Oscillatoria spec (blue-green alga)
Phytoplankton (North Pacific Ocean)
Zooplankton (North Pacific Ocean)
Chitosan phosphate

1.85 $\mu\text{g/g}$ sorbent

84

0.66 $\mu\text{g/g}$ sorbent

84

2.14 $\mu\text{g/g}$ sorbent

84

2.00 $\mu\text{g/g}$ sorbent

85

0.86 $\mu\text{g/g}$ sorbent

86

0.31 $\mu\text{g/g}$ sorbent

86

2.60 $\mu\text{g/g}$ sorbent

87

Conventionally, the resin materials can be classified into three main divisions: (a) cation-exchangers, (b) anion-exchangers, and (c) chelating polymeric resins. These can further be subdivided into strong, weak, or intermediate types, depending on the functional group.

The choice of an effective chelating resin and its value in analytical method development is dictated by the physicochemical properties of the resin materials. These are the acid-base properties of the metal species and the resin materials, and the polarizability, selectivity, sorptive capacity, kinetic and stability characteristics of the resin. Chelating polymers usually contain polyfunctional groups. In view of the complex nature of sea-water, selection of the proper chelating polymeric material for a specific suite of trace metals is of most importance. Akaiwa and Kawamoto⁸⁸ have discussed the advantage of having a synergic agent on a chelating resin to improve the sensitivity and separation of trace metals. The distribution coefficient of the analyte of interest should differ from that of the matrix constituents in the sea-water by several orders of magnitude. One of the rules of selection is based on the concept of hard and soft acids and bases.^{89,90} The functional groups in the chelating polymer materials usually act as bases; oxygen-containing functional groups are hard and sulphur-containing groups soft. Functional groups with a basic nitrogen atom have an intermediate character. Two aspects of extraction of uranium from sea-water have to be considered: analytical reproducibility and commercial recovery. These are not necessarily incompatible, though they may have different requirements as regards capacity, cost, re-use, *etc.* Since uranium acts as a hard acid, chelating polymers having oxygen-containing functional groups can be used to extract uranium from sea-water. Also, it is reasonable to use sulphur-containing functional-group materials for soft acids such as the precious metals, Hg, Ag, *etc.* Although this guide is highly useful in practical selection and synthesis of chelating polymers, it should be borne in mind that there is a substantial difference in the stability of complexes formed by metal ions with macromolecular and low molecular-weight functional ligands. This is primarily caused by the polymeric structure for the resin material.

The kinetic characteristics of a chelating polymer are of considerable importance and depend

on the nature and properties of the polymeric matrix and the degree of cross-linkage. Whereas in the ordinary type of exchanger the exchange processes are more rapid and controlled mainly by diffusion, those in a chelating exchanger are slower and controlled either by a particle-diffusion mechanism or by a second-order chemical reaction. For complexation or sorption to occur, it is not sufficient that surface functional groups are present; they must also be accessible for the chelation of the metal ion without steric hindrance. Thus within chelating resin particles, many surface functional groups may remain inactive in complexation because equilibrium cannot be attained.

On comparing the kinetic properties of different chelating sorbents, it quickly becomes obvious that the sorbents with the best characteristics are those based on hydrophilic macroporous co-polymers and cellulose, or on fibrous materials. Sorbents based on synthetic fibers are successfully used for various purposes. Recently, a new type of chelating sorbent has been proposed, made of fine fibrous materials with a porous structure which holds very fine particles (up to several μm) of chelating sorbents.^{91,92} These sorbents have high selectivity and excellent kinetic properties, *i.e.*, the time needed to reach equilibrium is only a few minutes.

SOME NOVEL CHELATING POLYMERS

Iminodiacetic acid resin

Among the earliest chelating resins to be studied were analogues of EDTA, *viz.* Dowex A-1, Chelex-100 and Chelex-20. The uses of Chelex resins have been well documented^{93,94} and these resins continue to be useful in a wide variety of systems. Some of the metals extracted from sea-water and other systems with Chelex-100 and Dowex A-1 are listed in Table 1.

Boniforti *et al.*¹¹ compared five methods for the preconcentration of trace metals (Mn, Fe, Co, Zn, Ni, Cu and Cr) from sea-water: (a) retention on Chelex-100, (b) APDC/8-quinolinol complexation followed by extraction with 4-methyl-2-pentanone, (c) APDC/8-quinolinol complexation followed by extraction with Freon-113, (d) co-precipitation with $\text{Mg}(\text{OH})_2$, and (e) co-precipitation with $\text{Fe}(\text{OH})_2$. They reported that (a) gave the best recovery for Mn, Fe, Co, Zn, Ni and Cu, whereas preconcentration of only Cr(III) and Cr(VI) was achieved by

co-precipitation with iron(II) hydroxide. Van Berkel *et al.*¹² and Paulson¹³ studied in detail the effects of flow-rate and pretreatment on the extraction of trace metals from estuarine coastal sea-water and artificial sea-water.

In an interesting paper, Chiba *et al.*¹⁶ examined the effect of using a magnetic field during the extraction of metal ions by Dowex A-1. They reported an increase of 1-6% in the amount sorbed per unit mass of resin. Sasaoka *et al.* used a chelating filter paper ("Expapier F-2", 2-hydroxypropyliminodiacetic acid loaded on cellulose fiber) to preconcentrate and separate thorium from monazite.¹⁷ They also used this chelating paper¹⁸ to preconcentrate and separate Sc(III) and Zr(IV) from Fe(III) and Al(III). The pH-dependence of the extractions was used to develop a separation scheme. Various matrices or resins⁹⁵⁻⁹⁷ containing aminoacetic acid or iminodiacetic acid have been synthesized, mainly to improve the physical and chemical stability.

Porous chelating polymers

Kaczvinsky *et al.*⁹⁸ have described the synthesis of porous phenol-formaldehyde polymers containing iminodiacetic acid. The porosity was introduced by the addition of a finely divided solid material ("template") that was insoluble under the reaction conditions, and was removed by dissolution after the polymerization was complete. Silica gel, carbonates and various other salts were used as templates. Resins containing different phenols were synthesized and their effectiveness for the removal of radioactive cesium and strontium from alkaline concentrated sodium salt solutions was examined. These solutions typify the soluble nuclear waste obtained from the defence industry.

Poly(β -diketone) resins

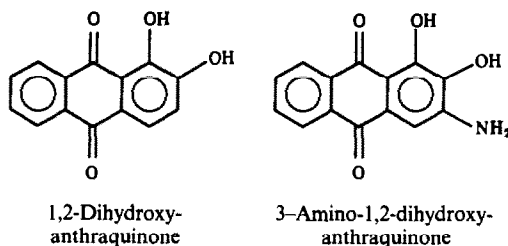
A water-soluble poly(β -diketone) chelating resin has been prepared by the controlled oxidation of poly(vinyl alcohol) (PVA) with chromic acid.⁹⁹ This polymer forms stable complexes with bivalent and trivalent cations, such as Co^{2+} , Cu^{2+} , Mn^{2+} , Ni^{2+} , Fe^{2+} , Au^{3+} and UO_2^{2+} and removes them completely from dilute aqueous solution. The ions may be recovered quantitatively from the resin complex by elution with dilute aqueous acid and it is claimed that the resin is re-usable. We have attempted to synthesize this material by oxidizing PVA (m.w.

1.15×10^5), but though the product was fairly effective in extracting uranium from synthetic sea-water, it crumbled in column operation, and its stability was poor. However, if supported on a durable material, this resin may be suitable for extracting uranium and trace metals from sea-water.

Tabushi *et al.*¹⁰⁰ have described the preparation of a macrocyclic hexaketone (tris- β -diketone) and cyclic tetraketone (bis- β -diketone) which were effective in extracting UO_2^{2+} selectively. The hexaketone was subsequently bonded to a polystyrene resin,⁵² to give a product that was highly selective for extracting UO_2^{2+} from sea-water. Similar cyclic bis- β -diketone resins were synthesized⁵³ and shown to extract Cu^{2+} , Ni^{2+} and Co^{2+} . Djamali and Lieser⁵⁴ have synthesized a resin with a 1,3-diketone as anchor group, by treating aminopolystyrene with diketene; the product was shown to extract UO_2^{2+} , Cu^{2+} , Ni^{2+} and Fe^{3+} .

Immobilized polyhydroxyanthraquinones

Nine polyhydroxyanthraquinones and two polyhydroxynaphthoquinones have been screened to determine which have the greatest ability to accumulate uranium.¹⁰¹ 1,2-Dihydroxyanthraquinone and 3-amino-1,2-dihydroxyanthraquinone have extremely high accumulation abilities, and to improve their adsorption characteristics have been immobilized by coupling with diazotized aminopolystyrene.

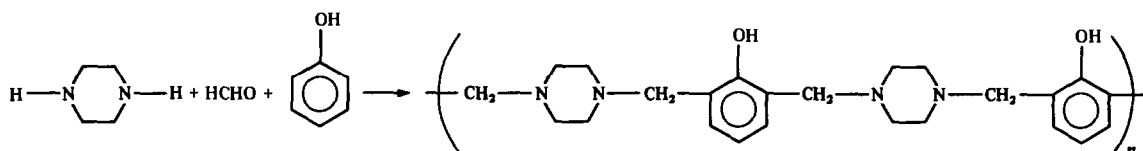


The immobilized 1,2-dihydroxyanthraquinone had the most favorable features, such as high selectivity, rapid sorption rate, and applicability in both column and batch methods. The authors examined the selective sorption of heavy metal ions from a solution containing $4 \times 10^{-5} M$ Mn^{2+} , Co^{2+} , Ni^{2+} , Cu^{2+} , Zn^{2+} , Cd^{2+} and UO_2^{2+} at pH 5. The relative order of magnitude of metal sorption appeared to be $\text{UO}_2^{2+} > \text{Cu}^{2+} \gg \text{Ni}^{2+} > \text{Cd}^{2+}$, Co^{2+} , $\text{Zn}^{2+} > \text{Mn}^{2+}$. The

sorbent takes up far larger amounts of uranyl and copper ions than of other metal ions, and can recover uranium almost quantitatively from natural sea-water. Almost all the uranium extracted could be desorbed in 1M hydrochloric acid, and the ability of resin to extract uranium from sea-water was found not to be decreased after 10 such sorption-desorption cycles, showing good mechanical properties.

Sirorez-Cu

This copper-selective polymer has been prepared by the reaction of phenol, formaldehyde and piperazine under neutral Mannich-reaction conditions to give the product shown below.^{102,103}

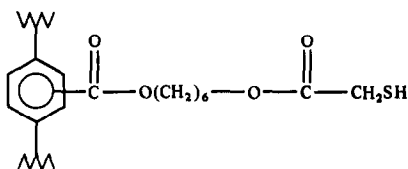


This polymer was found to chelate Cu^{2+} ions selectively, with capacities of up to 2.4 mmole/g, over a pH range of 3–10.5. Alkali and alkaline earth metal ions are not chelated or retained at any practical pH values.

Other metal ions studied in selectivity tests included Zn^{2+} , Sn^{2+} , Ag^+ , Hg_2^{2+} , Fe^{2+} and Fe^{3+} . None of these ions except Fe^{3+} was chelated by the resin at pH 7. The authors claimed that "Sirorez-Cu" can be used as a normal ion-exchanger, the only restricting factor being the slow physical breakdown of the resin particles on prolonged use. Similar resins, "Sirorez-Fe" and "Duolite A-7", have been used as a means of selectively separating Fe^{3+} from univalent and multivalent metal ions by extraction.¹⁰⁴

HTG-4 resin

This resin has a hexylthioglycollate group attached to an XAD-4 polymer matrix through an ester linkage¹⁰⁵ as shown below:

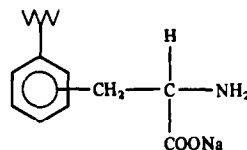


The authors claimed that HTG-4 is highly selective for Ag^+ , Hg^{2+} , Bi^{3+} and Au^{3+} in acidic aqueous solution. The first three metal ions were sequentially eluted with increasing concentra-

tions (0.5–6M) of hydrochloric acid and Au^{3+} was eluted with thiourea solution.

Phenylalanine resin

This polystyrene-based macroreticular resin containing phenylalanine groups was synthesized by Sugii *et al.*¹⁰⁶

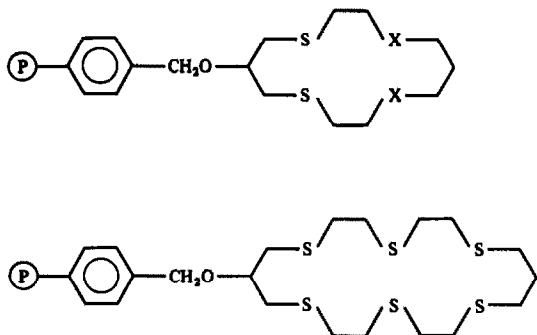


It showed high selectivity for Hg^{2+} and Cu^{2+}

in the pH region 2–3. The authors examined the sorption of copper in detail, with the intention of using the resin analytically. The important characteristics of the resin were fast equilibration, high selectivity and small volume change between its hydrogen-form and metal-forms. These features enable it to be applied for the rapid concentration of trace amounts of copper in the presence of large amounts of diverse metal ions. The authors also suggested use of the resin for determination of copper in sea-water and for separation of copper from cobalt and nickel.

Macrocylic polythioethers

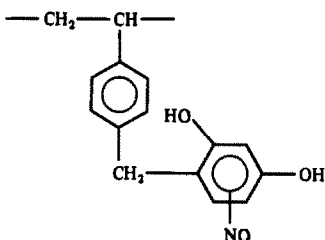
Polymer-supported macrocylic polythioethers¹⁰⁷ have been prepared from chloromethylated polystyrene resins and 14- or 20-membered polythioethers carrying a hydroxyl group, which were synthesized by reaction of the corresponding dithiols with 1,3-dichloro-2-propanol. The polymer-supported polythioethers were found to be highly efficient sorbents for Ag^+ , moderately effective for Cu^{2+} , but less effective for Cd^{2+} . Ag^+ or Cu^{2+} could be removed from the polymer-supported macrocylic polythioethers, which could be re-used without a significant decrease in binding ability.



(P) = polymer support ; X = S or O

Chelating resins with a nitrosoresorcinol group

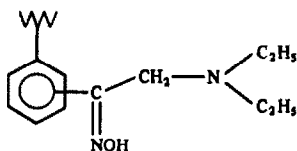
A macroreticular polystyrene-based chelating resin with nitrosoresorcinol as functional group was synthesized by Sugii and Ogawa.¹⁰⁸



The resin shows selectivity for Cu^{2+} , Fe^{3+} and Co^{2+} . The sorption behaviour of Co^{2+} was examined in detail, with the intention of using the resin analytically. Fe^{3+} and Co^{2+} were separated on a column by stepwise elution with oxalic acid and hydrochloric acid respectively.

Chelating resin containing an oxime group

Sugii *et al.*¹⁰⁹ synthesized a macroreticular polystyrene-based chelating resin with oxime and diethylamino functional groups. The resin was stable in acid and alkaline solutions.

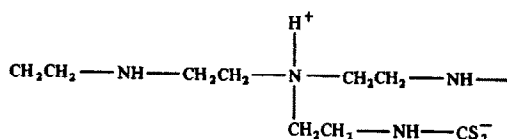


The resin had higher selectivity for Cu^{2+} than for other metal ions tested and the time required for 50% uptake of copper from 0.03M copper nitrate was 15 min. The highest capacity for Cu^{2+} was 2.0 mmole/g at pH 6.0. In a

column operation, copper was quantitatively recovered by elution with 1M hydrochloric acid and the resin could be re-used. The presence of neutral salts such as sodium chloride or sodium nitrate (0.5M) did not affect the sorption of Cu^{2+} .

Poly(iminoethylene)dithiocarbamate co-polymer

This was prepared by substitution of CS_2 at the primary and secondary amino groups of poly(iminoethylene).¹¹⁰

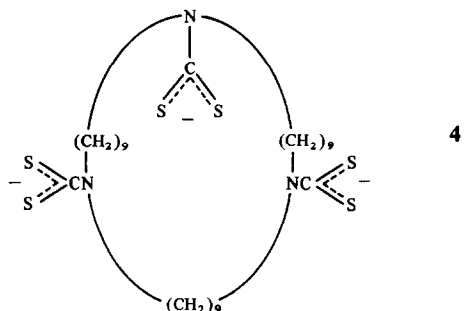
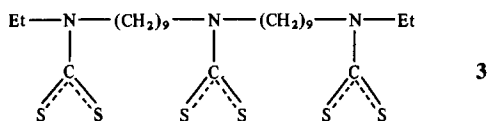
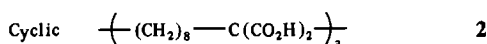
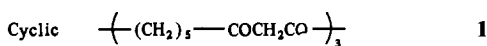


The binding of the transition metal ions VO^{2+} , Fe^{2+} , Fe^{3+} , Co^{2+} , Co^{3+} , Ni^{2+} and Cu^{2+} was investigated by uptake studies and physical measurements. The metal ions may be bound by both the dithiocarbamate and amino groups of the co-polymer. Factors such as the binding sites and stereochemistry of the co-polymer, which determine the relative uptake of the metal ions, were discussed. Binding to nitrogen (in addition to binding to sulphur) increased in the order $\text{Fe}^{2+} < \text{Ni}^{2+} < \text{Cu}^{2+}$ and accounted for the metal ion uptake by the co-polymer increasing in the same order.

A similar resin was characterized by Horváth and Barnes,¹¹¹ who reported that the presence of SCN^- reduced the capacity of the resin for Cu^{2+} , Co^{2+} and Fe^{3+} . King and Fritz¹¹² studied complexation of metal ions with sodium bis(2-hydroxyethyl)dithiocarbamate to form neutral complexes. Different XAD resins were then used for the preconcentration of these complexes. The metal ions that are completely retained on the XAD-4 resin at all pH values between 1.0 and 10.0 are Bi^{3+} , Co^{2+} , Cu^{2+} , Pb^{2+} , Hg^{2+} , Tl^+ and Sn^{2+} . Wagner *et al.*¹¹³ synthesized cross-linked polystyrene-dithiocarbamate polymers and then studied their uptake of heavy metals from water.

Tris(dithiocarbamate)

Tabushi *et al.*¹¹⁴ synthesized a linear tris(dithiocarbamate) specific for the extraction of uranium from dilute carbonate solutions.



Strong ligands specific for a given metal ion have generally been designed by considering (a) the size-fitting factor, (b) the nature of the ligand-metal interaction, and (c) the orientation in the binding. These authors have designed and synthesized several uranophiles, **1**, **2**, **3** and **4**, which are specific for the uptake of uranyl ions. In particular, O⁻ or S⁻ groups were introduced into the ligands, since the formation of U-O⁻ or U-S⁻ bonds is generally favored. It is of interest that molecule **4** showed a unique macrocyclic effect which unexpectedly led to slow rate-determining U-S⁻ bond formation. This finding prompted the design of uranophiles capable of rapid U-ligand bond formation together with satisfactorily high stability constants. The same authors also reported the successful "kinetic design" of a new type of uranophile, **3**, having high values of both the formation rates and stability constants. It was observed that the macrocyclic uranophile **4** showed a much slower exchange rate than the monomeric uranophile Et₂(NCS)₂⁻, in spite of the fact that it forms a much more stable uranyl complex. This unexpectedly slow carbonate ligand exchange by **4** is due to the S_N2 type mechanism, in which the specific "topological requirement" for macrocyclic binding is important, whereas the fast S_N1 type mechanism was observed for carbonate exchange by Et₂(NCS)₂⁻.

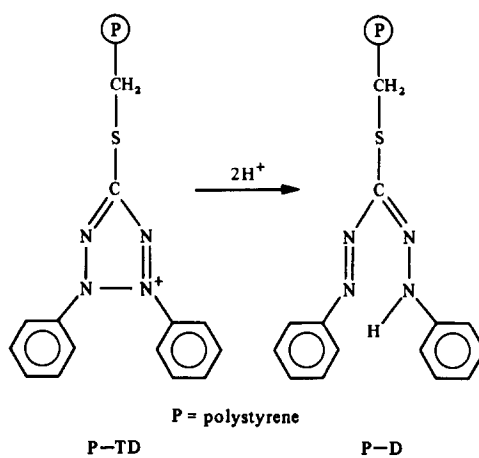
On this basis, it was predicted that fast uranyl binding might be achieved by avoiding such a restricted transition state, while maintaining the

high stability constant by using intramolecular terdentate ligands. A linear tris(dithiocarbamate) should satisfy both requirements.

Compound **3** binds UO₂²⁺ strongly and may be useful for extracting it from sea-water in a rapid ocean current.

Ion-exchange resins with S-bonded dithizone

This novel type of anion-exchanger was synthesized by Grote and Kettrup.¹¹⁵ The exchanger P-TD, based on polystyrene (P), contained S-bonded dehydrodithizone and reduction of this product yielded the chelating resin, P-D, characterized by S-bonded dithizone groups.

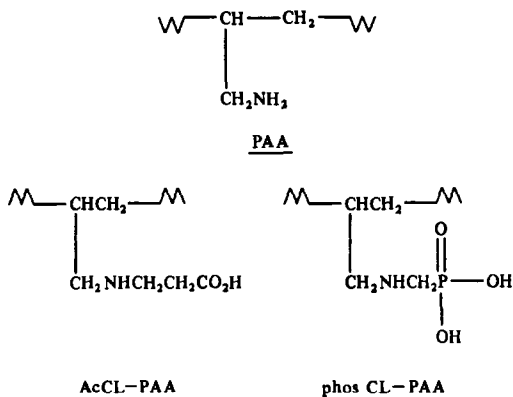


Each sorbent was loaded batchwise with precious metals, singly or in combination, and then treated with excess of various extracting agents. Strong retention of some metals and instability during the loading and elution stages were found with the P-D resin, but selective separation of palladium and gold from accompanying metals was possible. The P-TD resin has superior properties. Pd and Pt, loaded individually, were desorbed quantitatively by thiourea, but co-extracted Ir(IV) completely inhibited their elution. The regeneration of P-TD by a special sequence of eluents was utilized for selective chromatographic separation of Pd, Pt, Os, Au and (with restrictions) Ir from each other and also from large amounts of base metals and salts.

Poly(allylamine)

The chelating properties of poly(allylamine), PAA, for Ni²⁺, Cu²⁺, Zn²⁺, Cd²⁺ and UO₂²⁺ have been examined quantitatively. Three resins for recovery of uranium from sea-water were

studied; cross-linked PAA (CL-PAA), PAA modified by acrylic acid, and cross-linked (AcCL-PAA), and CL-PAA modified with phosphorous acid and formaldehyde (phos CL-PAA).⁴⁶



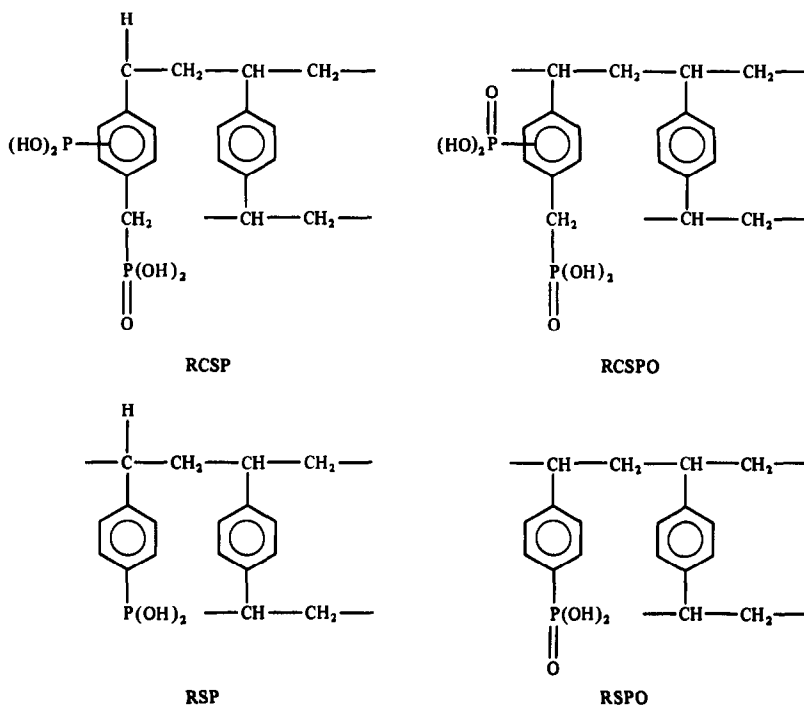
The last resin (phos CL-PAA) showed the highest sorption for uranium, *viz.* 500 mg of resin recovered 12.9 mg of uranium from 5 litres of sea-water at 25° within 24 hr, which corresponds to 78% of the uranium in the original sea-water.

Other nitrogen-containing polymers, such as those of pyridine, have been well documented. It has been shown that poly(4-vinylpyridine) can bind Co^{2+} ,¹¹⁶ as well as

Ni^{2+} , Cu^{2+} and Zn^{2+} .¹¹⁷ A summary of their uses in separation and concentration of metal ions has been given by Sugii *et al.*¹¹⁸ More varied pyridine resins have recently been used for the extraction of Cu^{2+} in the presence of Zn^{2+} .¹¹⁹

Macroreticular chelating resins containing phosphorus

Marhol and co-workers^{120,121} have described the preparation and extraction properties of several phosphorus-containing resins, which were treated as ion-exchangers. Manecke *et al.*¹²² synthesized a polymer containing a methylphosphonic acid anchor group and studied its ability to bind Cu^{2+} , Zn^{2+} , Ni^{2+} and Mg^{2+} . A polystyrene-divinylbenzene tributyl phosphate resin has been used for the extraction chromatography of U, Pu, Np, Nb, Ru, Rh, and Am.¹²³ Akio and Yoshiaki¹²⁴ synthesized a chelate resin containing methylene phosphonate groups. They reported that this resin was selective for extracting uranium from sea-water. Macroreticular chelating resins (RSP, RSPO, RCSP and RCSP) containing dihydroxyphosphino and/or phosphono groups were prepared and their sorption capacity for UO_2^{2+} and the recovery of uranium from sea-water were investigated by Egawa *et al.*¹²⁵



The order of recovery of uranium from sea-water with these four resins was RC-SPO ~ RCSP > RSPO > RSP. The sorption of uranium was affected not only by the chemical structure but also by the physical structure of the resins. Uranium was eluted with 0.25–1M sodium carbonate or bicarbonate in batch and column methods. The average recovery of uranium from sea-water with the Na⁺-form and H⁺-form RCSP in 10 recycles were 84.9% and 90.5% respectively when 20 litres of sea-water were passed through the column (resin 4 cm³, 50 × 10 mm) at 60 bed-volumes per hr. RCSP had a high physical stability and resistance to acid and alkali. Since RCSP exhibited high sorption capacity, high sorption rate of uranium from sea-water, and high chemical stability and physical stability, it should be an excellent resin for recovery of uranium from sea-water.

For recovery of uranium from sea-water by a column method, the resin must have a high sorption rate. The sorption of UO₂²⁺ with RCSP having various degrees of cross-linking was investigated. The resins were identified as RSP-10, RCSP-5, RCSP-10, *etc.* The authors claimed that RSP-10 and RSPO-10 exhibited lower recovery than RCSP-10 for uranium from sea-water. RSP-10 exhibited the lowest recovery because RSP has only one pK_a value, which is low. RCSP-10 exhibited higher recovery than RSP-10 because RCSP has phosphono groups bound to methylene groups, and these can easily form a chelate with UO₂²⁺ because of their high flexibility.

Both the H⁺-form and Na⁺-form of RCSP-10 were used to recover UO₂²⁺ from sea-water, and the sorption–elution cycle was repeated 10 times. Although H⁺-form RCSP gave higher recovery of uranium from sea-water, the Na⁺-form RCSP was more favourable for the recovery of uranium, because after the uranium had been eluted and the resin washed with water or sea-water, the resin could be re-used immediately. Furthermore, the sorption capacity for UO₂²⁺ was claimed not to decrease even after treatment of the resin with 1M sodium hydroxide or hydrochloric acid at 60° for 24 hr, showing the resin had high resistance to acid and alkali.

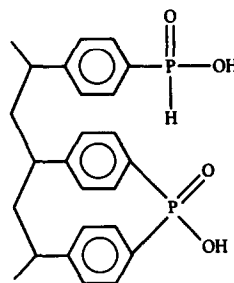
Bifunctional ion-exchange/co-ordination resins

Alexandratos *et al.*¹²⁶ have recently synthesized bifunctional resins that complex metal ions by both ion-exchange and co-ordination.

These resins are a class of polymer-supported bifunctional complexing agents for specific metal-ion extraction by a dual mechanism. The synthesis of new bifunctional ion-exchange co-ordination resins containing phosphonic acid ligands for ion-exchange and either phosphonate ester or amine ligands for co-ordination to the metal ion is described in Schemes I and II.

Initial extraction studies with these resins were focused on complexation of americium from 4M nitric acid and varying amounts of sodium nitrate at different pH values.

The phosphonic acid resins (I) have been studied¹²⁷ for the extraction of europium, thorium, uranium, americium and plutonium from acid nitrate media as a function of acid concentration and ionic strength.



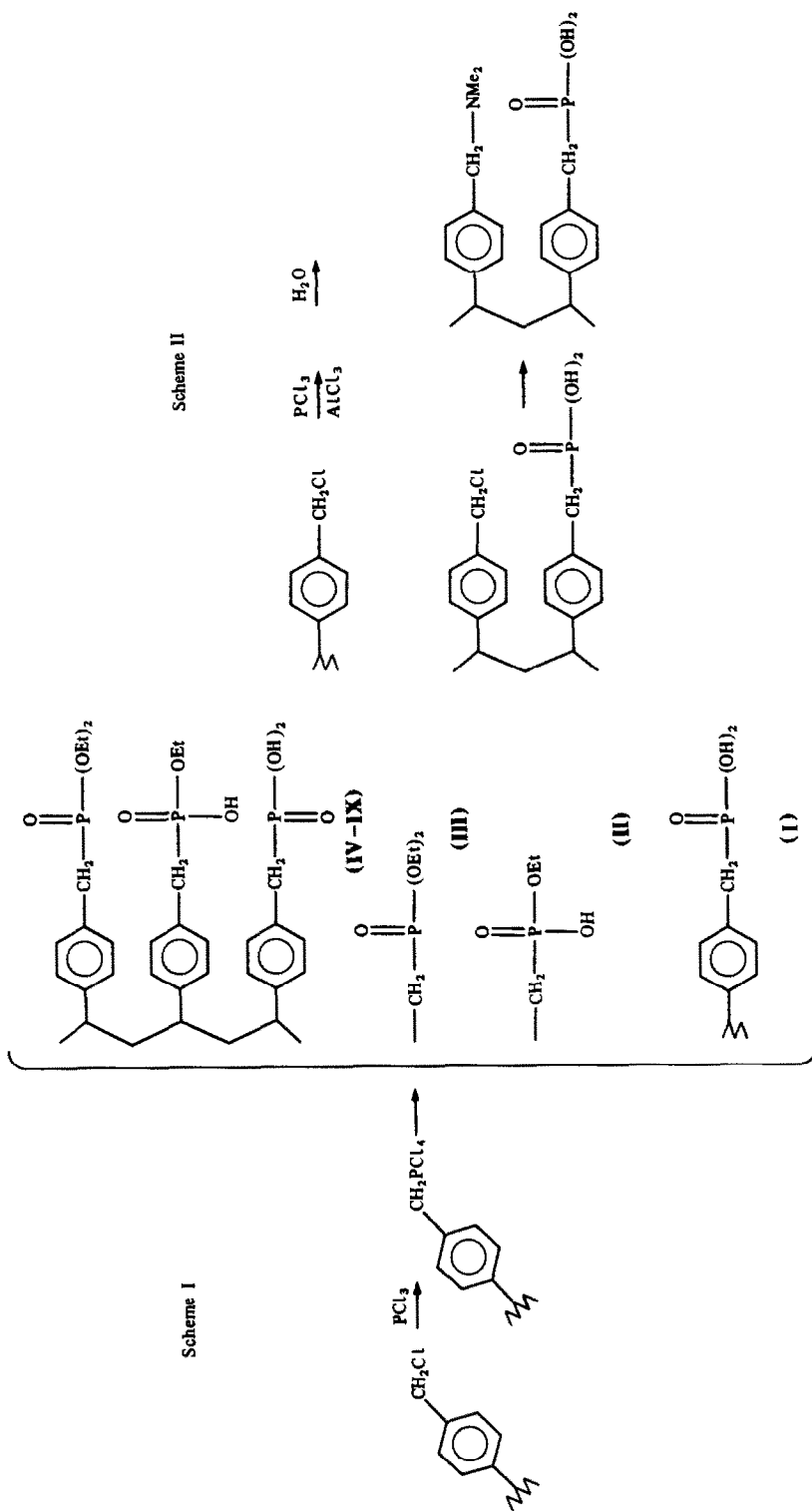
(I)

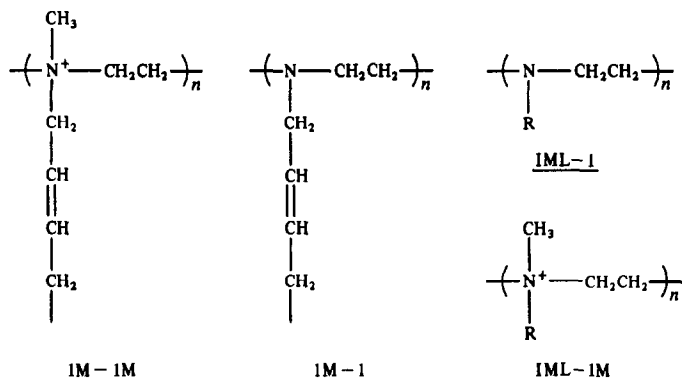
The phosphonic acid resins show better extraction than the sulphonic acid resins for these ions, especially from more acid solution (4M nitric acid), owing to the superior co-ordination ability of the phosphoryl oxygen atom. The resins also exhibit a higher selectivity, relative to sodium, for the ions tested. Under conditions where sulphonic resins absorb 85% of the plutonium in solution, the phosphonic acid resins absorb 99.7%.

Polyethyleneimine-supported resins

Resins with retention properties for Cu²⁺ and UO₂²⁺ have been synthesized by cross-linking of polyethyleneimine with 1,4-dibromo-2-butene and subsequent alkylation with dimethyl sulphate.¹²⁸

That paper reported the synthesis of the resins and their retention properties for Cu²⁺, UO₂²⁺, Fe²⁺ and Fe³⁺. The resin 1M-1 did not retain copper appreciably at pH < 1. However, at pH 2–4 it retained 94% of the copper added. The resin 1M-1M did not extract copper



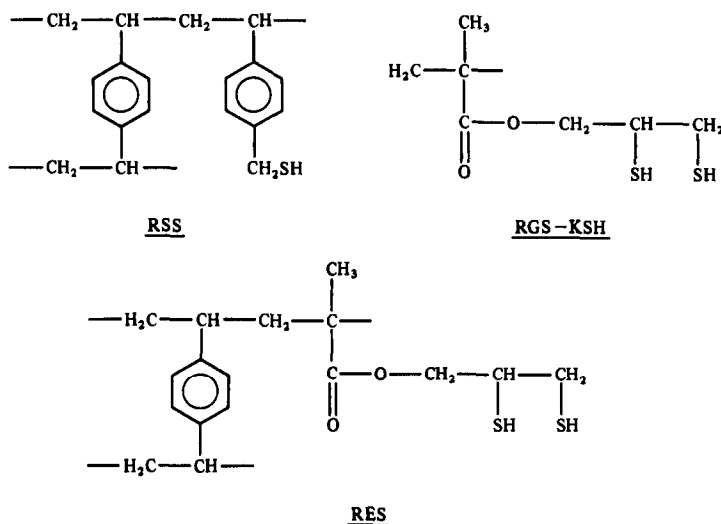


between pH 0 and 4 but selectively retained 44.8–99.9% of the uranium present. Also, this resin had a greater maximum capacity for uranium (3.2 meq/g) than did IM-1 (2.8 meq/g). According to these results the resins retain copper and uranium by different mechanisms. Usually copper is retained by ion-exchange and possibly by chelate ring formation; uranium was apparently held by adduct formation with the protonated tertiary amine group. Rivas and co-workers have also synthesized several other resin materials,^{129–131} by

were stable up to 140°. From 140 to 300°, ILM-1 loses 60% by weight. Resin IML-1M shows better thermal stability, does not lose weight until 200°, and loses 83% by weight at 400°.

Chelating resins containing mercapto groups

Egawa *et al.*¹³² have synthesized certain chelating resins containing mercapto functional groups, as shown below.



cross-linkage of polyethyleneimine with 1,4-dibromo-2-butene, 1,9-dibromononane and 1,10-dibromodecane, and subsequent alkylation with dimethylsulphate. The influence of pH on the retention, maximum load capacity and elution was studied for Cu^{2+} , UO_2^{2+} , Fe^{2+} and Fe^{3+} . The morphology of the resin materials was examined by scanning electron microscopy and the thermal stability by TGA. All the resins

Removal and recovery of arsenic from a geothermal-power waste solution with three macroreticular chelating resins containing mercapto groups were investigated. The resin (RES) prepared from 2,3-epithiopropyl methacrylate-divinylbenzene co-polymer beads, exhibited high affinity for arsenic(III) and high resistance to hot water. Arsenic(III) in aqueous solution was favourably sorbed on the RES when a sodium arsenite solution (pH 6.2) containing 3 mg/ml arsenic(III) was passed through

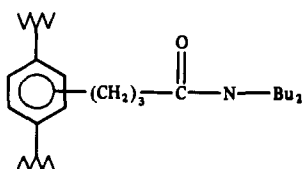
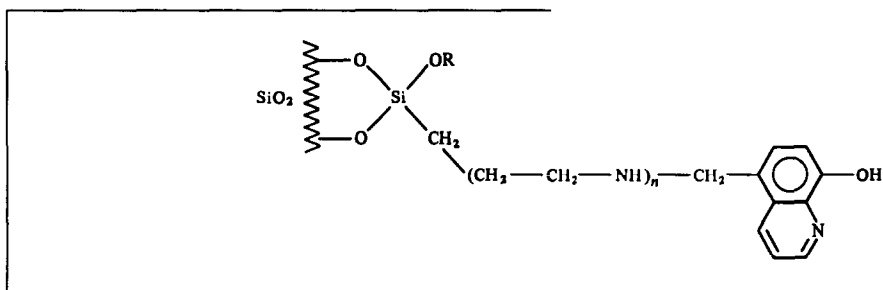
an RES column at 15 bed-volumes per hr. The arsenic(III) was eluted with 2M sodium hydroxide containing 5% sodium hydrogen sulphide. Sorption/elution cycling was found to be satisfactory. The RES also exhibited high sorption ability for arsenic(III) in the geothermal-power waste solution.

Since this waste solution contains large amounts of Na^+ , Ca^{2+} , Mg^{2+} , Li^+ and K^+ , the sorption of arsenic(III) on RES was tested in the presence of sodium chloride and calcium chloride, and found not to be influenced by 10–40 mg/ml Na^+ or Ca^{2+} .

Volkan *et al.*⁵¹ modified silica gel by incorporation of mercapto chelating groups, and used it to preconcentrate Zn^{2+} , Cu^{2+} and Pb^{2+} from sea-water, obtaining 90–95% recovery. Egawa *et al.*¹³³ used chelating resins containing epithio groups to determine methylmercury in sea-water. Methylmercury can be selectively eluted with 4M hydrochloric acid containing 0.5 mg/l. sodium thiosulphate, leaving inorganic mercury on the resin.

Chelating amide resin

Synthetic routes for the incorporation of a tertiary aliphatic amide group in a macroporous polystyrene–divinylbenzene resin have been discussed.¹³⁴



The amide resin retains UO_2^{2+} , Th^{4+} and Zr^{4+} selectively from aqueous solution at pH 3.0. A liquid chromatographic separation scheme using the resin was developed and quantitative results were obtained for uranium in synthetic and actual samples and for thorium in synthetic samples. Au^{3+} and Pd^{2+} were selectively retained by the resin from aqueous

solutions containing hydrochloric acid. The capacity of the resin for gold was 1.7 mmole/g. Many resins that are selective for gold(III) cause its partial reduction, perhaps to the metal. This does not occur nearly so readily on the amide resin, although the yellow band corresponding to the gold(III) on the resin column does turn black if left for a long period; however, this can easily be removed by elution with cyanide and the resin can be used for many sorption and elution cycles.

Immobilized 8-hydroxyquinoline

Simple methods for the immobilization of 8-hydroxyquinoline on silica have been described.^{135,136} The suitability of the immobilized quinolinol for trace enrichment has been tested for Cu^{2+} , Ni^{2+} , Co^{2+} , Fe^{3+} , Cr^{3+} , Mn^{2+} , Zn^{2+} , Cd^{2+} , Pb^{2+} and Hg^{2+} in the pH range from 4 to 6. The metal uptake capacities were found to range from 0.2 to 0.7 mmole/g and the distribution ratios from 1×10^3 to 9×10^4 . McLaren *et al.*¹³⁷ have employed 8-hydroxyquinoline immobilized on silica for preconcentration of trace metals (Mn, Co, Ni, Cu, Zn, Cd, Pb, Cr and Cd) from sea-water samples, with the final determination performed by inductively-coupled argon plasma–mass spectrometry (ICAP–MS).

The work has recently been extended by using ICP–MS for samples concentrated by chelation with 8-hydroxyquinoline immobilized on silica.¹³⁸ The effect of the silica support on the capacity of the chelation system has been studied.¹³⁹ The synthesis and characteristics of nine chelating groups immobilized on silica have been described and their use in metal-ion separation by liquid chromatography was evaluated.¹⁴⁰ The use of macroporous resins (XAD-4 and XAD-7) impregnated with 7-dodecyl-8-quinolinol for the preconcentration of trace metals from sea-water has also been evaluated.¹⁴⁴ The bonding of 8-hydroxyquinoline to

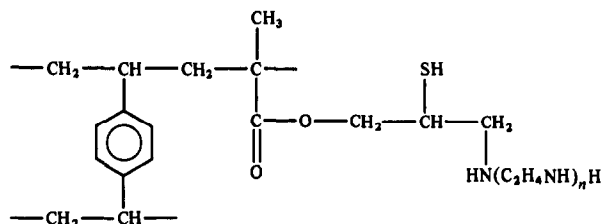
glycidyl methacrylate gel,¹⁴² epoxide "separon"¹⁴³ and styrene-ethylene dimethacrylate copolymer¹⁴⁴ has been studied for the uptake of Cu^{2+} . The preconcentration and complexation properties of poly-(7-acetyl-8-hydroxyquinoline-5-aldehyde) chelating polymer have been described.¹⁴⁵ The rate of attainment of equilibrium was established for UO_2^{2+} , Fe^{3+} , Zn^{2+} , Cu^{2+} and Mn^{2+} . Different chelating agents immobilized on glass have been compared with Chelex 100 for the preconcentration of Cu^{2+} ,¹⁴⁶ and the 8-hydroxyquinoline material was found the most suitable for preconcentration work.

Modified silica gel with 3-(1-imidazolyl)propyl groups

Silica gel modified with 3-(1-imidazolyl)propyl groups and packed in a glass column has been used to sorb and preconcentrate metal ions from ethanol solutions.¹⁴⁷ Elution was done with 0.1M hydrochloric acid and ethanol/water mixture (15:85 v/v). The modified silica was used for preconcentrating metal ions (Cu, Ni, Fe, Zn and Cd) from commercial ethanol, normally used as engine fuel. The method was suitable for determining these metals at low $\mu\text{g/l.}$ levels.

Chelating resins containing polyethylene polyamine side-chains and mercapto groups

Macroreticular chelating resins containing both polyethylene polyamine side-chains and mercapto groups have been prepared by the reaction of 2,3-epithiopropyl methacrylate-divinylbenzene macroreticular co-polymer beads with polyethylene polyamine.¹⁴⁸ The sorption behaviour of metal ions on the resins was then investigated.

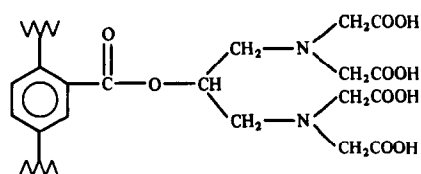


The macroreticular co-polymer beads could effectively be aminated by treatment with polyethylene polyamine in an organic solvent (benzene or tetrahydrofuran) or in the absence of organic solvent at 80 or 100° for 1 hr. It was found that the sorption capacity of the resins for metal ions is affected not only by the ion-

exchange capacity of the resins but also by their porosity. Hg^{2+} , Ag^{+} and Cu^{2+} were effectively sorbed by the resins even at $\text{pH} < 3$, whereas Co^{2+} , Ni^{2+} and Cd^{2+} were sorbed at $\text{pH} > 3$, Mn^{2+} at $\text{pH} > 7$ and Ca^{2+} at $\text{pH} > 8$. The results suggest that these metal ions can be effectively separated by varying the pH of the loading solution and of the eluent. The metal ions sorbed on the resins could easily be eluted with dilute mineral acid with or without thiourea present.

Propylenediaminetetra-acetic acid resin

Moyers and Fritz¹⁴⁹ have synthesized a new chelating resin (PDTA-4) containing propylenediaminetetra-acetic acid functional groups attached to a carboxylic acid divinylbenzene resin by an esterification reaction.



The resin was found to retain multivalent metal cations at $\text{pH} \geq 3$. It retained Cu^{2+} , UO_2^{2+} , Th^{4+} and Zr^{4+} from more acidic solutions. A scheme was given for clean, rapid chromatographic separation of the last three elements from each other. The resin was claimed to retain quantitatively a number of trace elements from simulated sea-water, and the results are given in Table 3.

A macrocyclic hexacarboxylic acid resin⁸² has been used to remove uranium from sea-water in a batch process. The rate of complexation

appears to be too slow for column use. Takeda *et al.*¹⁵⁰ have synthesized a number of chelating resins with aminopolyacetic acid moieties such as iminodiacetic acid, ethylenediaminetetraacetic acid and diethylenetriaminetetraacetic acid. A chromatographic gel coupled to

Table 3. Recovery of trace elements from spiked sea-water; sorbent propylenediaminetetra-acetic acid resin (reproduced by permission from E. M. Moyers and J. S. Fritz, *Anal. Chem.*, 1977, 49, 418; copyright 1977, American Chemical Society)

Ion added	Added	Recovered, %	Eluent
Cr(III)	100 Ci	83.1 ± 0.7	2.0M HCl
Fe(III)	25 Ci	94.4 ± 0.2	2.0M HCl
Mn(II)	25 Ci	102.0 ± 0.6	2.0M HCl
U(VI)	0.5 ppm	98.5 ± 0.2	0.1M HCl
Zn(II)	25 Ci	102.8 ± 0.4	2.0M HCl

carboxymethyl(imino)-bis(ethylenitrilo)tetra-acetic acid (DTPA) has been used to extract Cu^{2+} from sea-water with high selectivity.¹⁵¹

SELECTED COMMERCIAL RESINS

A few selected commercially available chelating resins suitable for extracting uranium and other trace metals from sea-water are listed in Table 4. The donor atoms listed are those which may be covalently bound to the metal ions or metal species in solution. Duolite resins could be used in solving problems of water and process-liquid treatment, but also for many applications in the pharmaceutical, food, nuclear and hydrometallurgic industries and environmental protection. The principal application of these chelating resins is in removing calcium and magnesium from the brine feed for chloralkali cells. Duolite ES467 is capable of reducing the concentration of Ca^{2+} and Mg^{2+} to a few $\mu\text{g/l.}$, as required for the membrane cells.¹⁵² The Chelite series resins have complex-forming chemical configurations fixed to a porous matrix. They can specifically retain and remove

various multivalent cations from solutions. Furthermore, they have ion-exchange properties, so it is necessary to equilibrate the resins with the matrix solution before use, to avoid changes in the overall ionic composition of the liquid phase. At INCO's Port Colborne refinery in Canada,¹⁵³ trace amounts of nickel and copper are removed by use of picolylamine (2-aminomethylpyridine) resin (XF54195).

Duolite CS-100

This is a granular weak-acid cation-exchange resin containing both carboxylic acid and phenolic functional groups. It has a rigid macroporous structure which is unusually resistant to attrition. The swelling of this resin is much less than that of most weak-acid cation-exchangers and very little resin breakdown is encountered in acid-base cycling. Phenolic resins are more resistant than polystyrene exchangers to radiation. Duolite CS-100 has unusually high selectivity for ^{137}Cs , ^{90}Sr and some multivalent cations, and thus is suitable for the effective treatment of alkaline low-level radioactive waste solutions. This high degree of selectivity may suggest other uses for this resin. The presence of the phenolic group increases the selectivity for caesium by a factor of 10–100. This very weakly acidic group is activated at $\text{pH} > 9$. This resin has been particularly useful in the selective removal of ^{137}Cs and ^{90}Sr from alkaline low-level radioactive wastes. This process, originally developed at the Oak Ridge National Laboratory,⁴⁵ consists of precipitation with alkali to remove suspended solids and hardness, removal of sludge, then

Table 4. Commercial chelating resins

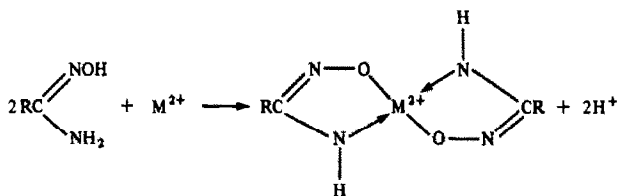
Trade name	Functional group	Nature of functional group	Donor atoms	Company
Chelex-100	$\text{CH}_2\text{N}(\text{CH}_2\text{CO}_2\text{H})_2$	Iminodiacetate	N, O, O	Bio-rad
Duolite ES-466	$\text{CH}_2\text{N}(\text{CH}_2\text{CO}_2\text{H})_2$	Iminodiacetate	N, O, O	Duolite
Not named		8-Hydroxyquinoline	N, O	Seakem
Duolite ES-467	$\text{CH}_2\text{NCH}_2\text{PO}(\text{OH})_2$	Aminophosphonic acid	N, O, O	Duolite
Chelite-P	$\text{CH}_2\text{NCH}_2\text{PO}(\text{OH})_2$	Aminophosphonic acid	N, O, O	Duolite
Duolite ES-465	—SH	Mercapto	S	Duolite
Chelite-S	—SH	Mercapto	S	Duolite
Duolite ES-346	$\text{H}_2\text{N}-\overset{\text{O}}{\parallel}{\text{C}}-\text{N}-\text{OH}$	Polyacrylate with amidoxime	O, N	Duolite
Chelite-N	$\text{H}_2\text{N}-\overset{\text{O}}{\parallel}{\text{C}}-\text{N}-\text{OH}$	Macroporous polymer with amidoxime	O, N	Duolite
MISSO ALM	NCS_2H	Dithiocarbamic acid	N, S, S	Nippon Soda
KRUPTOFIX 22IB	Cryptand	Cryptand	N, O	Parish
CR20	$\text{CH}_2\text{N}(\text{CH}_2\text{CH}_2\text{N})_n-\text{H}$	Polyamine	N	Mitsubishi
XFS4195	$\text{—CH}_2\text{N}-\overset{\text{R}}{\text{C}}\text{H}-\text{C}_5\text{H}_5\text{N}$	Weak base	N, N	Dow Chemicals
Amborane 345	$\text{P}-\text{BH}_3$	Amine-borane	—	Rohm and Haas
Amborane 355				

filtration through a column of Duolite CS-100 to remove residual radionuclides. The resin is regenerated with dilute nitric, hydrochloric or sulphuric acid. According to published reports, this integrated approach of scavenging precipitation/ion-exchange removes more than 99.9% of the caesium and strontium, leaving levels well below the maximum permissible concentration of these radionuclides.

Duolite ES-346, Duolite CS-346 and Chelite-N

All these resin materials are cross-linked copolymers in spherical form containing amidoxime groups, $-\text{C}(\text{NH}_2)=\text{NOH}$. The resin also contains a small proportion of hydroxamic acid groups which function in the higher pH ranges. Because of their three-dimensional cross-linked structure, these resins are insoluble in common organic and aqueous solvents. They offer a number of possibilities for the separation and isolation of trace metals from various matrices, including sea-water.^{58,154} The amidoxime group forms strong complexes with a wide variety of metal ions such as Cu^{2+} , Au^{3+} , Ru^{3+} , V^{2+} , V^{3+} , VO^{2+} , VO_2^+ , UO_2^{2+} , Fe^{3+} , Mo^{6+} , Th^{4+} , Cd^{2+} , Cr^{3+} , Pu^{4+} , Ag^+ , Hg^{2+} , Sb^{3+} , Pb^{2+} *etc.*¹⁵⁵ It does not form chelates with alkali and alkaline-earth metal ions. The resin can be employed for removal of unwanted ions such as copper and iron from water or other polar solvents, and for the recovery of trace amounts of valuable materials (such as noble metals) from metal-finishing wastes. Also, a resin containing an amidoxime functional group has been employed to recover gallium from Bayer liquor,¹⁵⁶ and a similar resin to preconcentrate vanadium.¹⁵⁷

A possible chelation mechanism for the complexation is:



Since the resin contains a weak-base functional group, the chelation and ion-exchange capacity depends on the pH. Regeneration with mineral acid converts the weak-base function into its protonated form. If it is not neutralized, this conjugate acid will dissociate in the succeeding loading cycle and may depress the pH below the point of optimum chelation. In such cases the

resin should be buffered to a suitable pH following acid regeneration.

Owing to the immense worldwide interest during the last two decades in the extraction of uranium from sea-water there have been many papers dealing with this problem. Amidoxime-containing sorbents have shown to be usable for the purpose, and this has prompted a number of papers mainly dedicated to synthesis of these materials.

Egawa *et al.*^{158,159} prepared a macroreticular chelating resin containing amidoxime by reacting acrylonitrile-divinylbenzene co-polymer beads with hydroxylamine. They reported an average recovery of 82.9% in the extraction of uranium from sea-water.

A number of polyacrylamidoxime resins made from various co-polymers of acrylonitrile and cross-linking agents¹⁶⁰ have been synthesized and tested for the extraction of uranium.

Recently, Egawa *et al.*¹⁶¹ have synthesized macroreticular chelating resins (RNH) containing amidoxime groups, with various degrees of cross-linking obtained by using various amounts of ethyleneglycol dimethacrylate (1G), dimethyleneglycol dimethacrylate (2G), triethyleneglycol dimethacrylate (3G), tetraethyleneglycol dimethacrylate (4G) and enneaethyleneglycol dimethacrylate (9G) as cross-linking reagents. The effect of cross-linking reagents on the pore structure, ion-exchange capacity, swelling ratio, and sorption ability for uranium(VI) in sea-water by RNH was investigated.

In similar work, chelating resins containing amidoxime groups were synthesized from alkyl-methacrylate, acrylonitrile-divinylbenzene-alkylacrylate, or vinylpyridine co-polymer beads. A resin containing acrylonitrile divinyl-

benzene-methyl acrylate proved to be the most effective for the sorption of uranium from sea-water. To improve the flow-rate through the column and the mechanical stability of the resin, various fibres carrying amidoxime groups were synthesized. Commercial acrylonitrile fibres were treated with hydroxylamine in

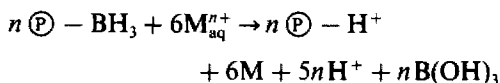
methanol to give the required acrylonitrile amidoxime fibres.¹⁶⁰ Fibres were also made by radiation-induced graft polymerization of acrylonitrile onto polymeric fibres, followed by amidoximation.¹⁶³⁻¹⁶⁵

Duolite GT-73, Duolite ES-465 and Chelite-S

All three resins have a thiol functional group, with minor quantities of sulphonic acid groups, and are bound to a macroporous cross-linked polystyrene matrix. It has long been recognized that the mercury-sulphur bond is very strong, and in fact, thiols are also called mercaptans, from the Latin *mercurium captans*, "seizing mercury". The thiol groups in these resins give them a very high selectivity for mercury, and also a high tendency to bind metal ions such as copper, silver, cadmium and lead, the selectivity sequence is $\text{Hg} > \text{Ag} > \text{Cu} > \text{Pb} > \text{Cd} > \text{Ni} > \text{Co} > \text{Fe} > \text{Ca} > \text{Na}$. In the early 1970s, AKZO Chemicals Co. of the Netherlands developed a process for the removal of mercury with Duolite GT-73, which has been well documented in the literature.¹⁶⁶⁻¹⁶⁸

Amborane™-345

This resin material offers a convenient means for metal recovery. Amborane-345 is a highly porous, solid polymeric amine-borane reducing agent.¹⁶⁹ Amborane-345 has reducing power comparable to that of monomeric amine-boranes, but it offers greater stability, selectivity and processing advantages for precious metal recovery and reduction. Amborane-345 is acrylic-based and is supplied as spherical particles usable in column or batch type operations. It removes the metal ions from solution by reduction, concentrating the reduced metal within the highly porous matrix of the bead. Amborane-345 has a wide operational pH range of 1-10, and a high capacity of 2 g of precious metal per g of dry resin. Unlike ion-exchange resins, where mass action and equilibria effects often limit the removal of low concentrations of ions from solution, the reductive mechanism of this resin permits the complete removal of the reduced species even at low levels. The stoichiometry of the metal ion reduction is as follows:



The effective capacity of Amborane-345 is influenced by temperature and pH. The hydrolytic

stability is excellent at room temperature and pH 7. At elevated temperature and lower pH, the capacity of the resin decreases.

Certain non-precious metal ions such as ionic species of mercury (including methylmercury), arsenic, antimony and bismuth can be reduced by the resin. Amborane-345 can also be employed for selective removal and recovery of precious metals from process or waste streams.

Koster reported the use of an active chelating resin (containing two resonating amino groups on a bound carbon) for the separation of noble metals.¹⁷⁰ Myasoedova *et al.*¹⁷¹ have described the properties of some new chelating sorbents (Polyorgs™) for the selective concentration of noble metals. Yasuda and Yamauchi¹⁷² have examined the extraction ability of Amberlite IRA-743, Diaion CRB 02, Duolite ES-371 and Uniselec UR-3500 for the recovery of boron from brines. The use of chelating sorbents has not been limited to synthetic resins. Many natural products have been evaluated, including tree bark, wool, cotton and onion skin.¹⁷³

In our own laboratory, various chelating polymers have been evaluated for the extraction and determination of uranium, zinc, chromium, copper, lead, silver, manganese, cerium, zirconium and nickel in synthetic sea-water and freshwater. The chelating polymers tested were Chelite-P, Chelite-N, Duolite ES-467, Duolite ES-346, suitably immobilized 8-hydroxyquinoline and Chelex-100. The effects of flow-rate, pH and temperature on the extraction efficiency were investigated. The selectivity and stability of these materials were adequate for preconcentration of trace metals from synthetic sea-water and freshwater. The results will be published separately.

CONCLUSION

Chelating polymer resin materials are mainly used in analytical, industrial and radiochemical laboratories, but only to a limited extent in solving environmental problems. Metal pollution of the environment poses unique problems. Predominantly, metal pollution originates with trace contamination in waters and soil systems. The behavior of trace metals in the environment is primarily determined by the specific forms (speciation) of the metals rather than by their bulk concentration. Since metals are not subject to biodegradation, for practical purposes they have infinite lifetimes. The most promising way to decontaminate aqueous systems such as

wastewater treatment sludges and recover the trace metals from them is by employing specific chelating resin materials. Although almost all common chelating polymers are non-selective, research efforts are being directed to synthesize selective chelating polymers with high physical and chemical stability, for metal extraction. These chelating polymers can also play a vital role in environmental monitoring of toxic trace metals.

It is difficult to make a critical evaluation of the usefulness of the various chelating resins, because of the limited published application of the resins specifically synthesized for uranium or other metal extraction. Presumably the commercial availability of several successful sorbents, as indicated by the large number of papers published, combined with the cost and difficulty of production, has prevented the commercial development of many materials which may have been shown to have good applicability in laboratory tests.

A survey of the recent literature (1983–88) on three commercially available chelating resins gives some indication of their relevant suitability and use in the extraction of uranium from sea-water. There were only two references each to Chelex-100^{14,174} and phosphonic acid,^{175,176} but 43 to amidoxime.^{154,161,162,164,177–216} Japanese workers, in particular, have shown considerable interest in this resin and only 6 of these 43 contributions were not from Japan. Amidoxime resins were shown to take up uranium rapidly from solution and to have stronger preference for uranium and several other metal ions than for alkali and alkaline-earth metal ions. Other advantages include cheapness, good physical and chemical stability in sea-water, and (depending on the method of preparation) a high loading capacity. Another major factor affecting the number of recent publications is that the longer availability of Chelex-100 has served to diminish the number of new applications of this material, although it is still widely used. It is obvious that in other specific applications the relative suitability would probably be different.

The procedures based on chelating polymers seem to offer unexplored opportunities that may deserve the attention of scientists concerned with environmental pollution abatement in general, and decontamination to remove hazardous species. Preconcentration with chelating sorbents improves the sensitivity and reliability of determination of elements in a wide variety of

samples, including natural waters, geological, biological and industrial materials.

Acknowledgement—This work was financially supported by the Natural Sciences and Engineering Research Council of Canada.

REFERENCES

1. C. J. Kantipuly and A. D. Westland, *Talanta*, 1988, **35**, 1.
2. G. V. Myasoedova and S. B. Savvin, *Crit. Rev. Anal. Chem.*, 1986, **17**, 1.
3. K. Schwochau, *Top. Curr. Chem.*, 1984, **124**, 91.
4. K. S. Massie, *Elsevier Oceanogr. Ser.*, 1980, **24B**, 569.
5. G. V. Myasoedova and S. B. Savvin, *Zh. Analit. Khim.*, 1982, **37**, 499.
6. A. Chow and H. D. Gesser, *Hazard Assess. Chem.*, 1981, **1**, 17.
7. R. S. S. Murthy, J. Holzbecher and D. E. Ryan, *Rev. Anal. Chem.*, 1982, **6**, 113.
8. P. MacCarthy, R. W. Klusman and J. A. Rice, *Anal. Chem.*, 1987, **59**, 308R.
9. G. Schmuckler, *Talanta*, 1963, **10**, 745.
10. *Idem, ibid.*, 1965, **12**, 281.
11. R. Boniforti, R. Ferraroli, P. Frigieri, D. Heltai and G. Queirazza, *Anal. Chim. Acta*, 1984, **162**, 33.
12. W. W. Van Berkel, A. W. Overbosch, G. Feenstra and F. J. M. J. Maesson, *J. Anal. At. Spectrom.*, 1988, **3**, 249.
13. A. J. Paulson, *Anal. Chem.*, 1986, **58**, 183.
14. P. Pakalns, *Anal. Chim. Acta*, 1980, **120**, 289.
15. R. R. Greenberg and H. M. Kingston, *Anal. Chem.*, 1983, **55**, 1160.
16. A. Chiba, S. Ichiishi, H. Kanda and T. Ogawa, *Nippon Kagaku Kaishi*, 1987, 2481.
17. N. Sasaoka, K. Morishige, T. Shigematsu, Y. Nishikawa and T. Matsumoto, *Bunseki Kagaku*, 1987, **36**, 261.
18. *Idem, ibid.*, 1987, **36**, 722.
19. J. P. Riley and D. Taylor, *Anal. Chim. Acta*, 1968, **40**, 479.
20. H. M. Kingston, I. L. Barnes, T. J. Brady, T. C. Rains and M. A. Champ, *Anal. Chem.*, 1978, **50**, 2064.
21. T. M. Florence and G. E. Batley, *Talanta*, 1975, **22**, 201.
22. M. I. Abdullah, O. A. El-Rayis and J. P. Riley, *Anal. Chim. Acta*, 1976, **84**, 363.
23. J. N. Mathur and P. K. Khopkar, *Solvent Ext. Ion Exch.*, 1985, **3**, 753.
24. Y. Koyanaka and Y. Yasuda, *Suiyo Kaishi*, 1977, **18**, 523.
25. T. Kiriya, M. Haraguchi and R. Kuroda, *Z. Anal. Chem.*, 1981, **307**, 352.
26. T. Kiriya and R. Kuroda, *ibid.*, 1977, **288**, 354.
27. D. E. Leyden, T. A. Patterson and J. J. Alberts, *Anal. Chem.*, 1975, **47**, 733.
28. E. Bayer and H. Fiedler, *Angew. Chem.*, 1960, **72**, 921.
29. E. Bayer, *ibid.*, 1964, **76**, 76; *Intern. Ed.*, 1964, **3**, 325.
30. T. Kitamura and H. Wada, *Japan Patent*, 7674999, 1976; *Chem. Abstr.*, 1977, **86**, 6868m.
31. K. Ooi, H. Wada, T. Kitamura, S. Katoh and K. Sugasaki, *Rep. Gov. Ind. Res. Inst. Shikoku*, 1980, **6**, 12.

32. J. Kjelland, *German Patents*, 691366, 1940; 704545, 715199, 715200, 1941; *Chem. Abstr.*, 1941, **35**, 4164²; 1942, **36**, 1446²; 1944, **48**, 2171⁸.
33. H. Isobe and T. Shimamoto, *Japan Patent*, 2271, 1959; *Chem. Abstr.*, 1959, **53**, 17451d.
34. A. Skogseid, *Norwegian Patent*, 83579, 1954; *Chem. Abstr.*, 1954, **48**, 11015f.
35. H. Matsushita and T. Takayanagi, *Nippon Kaisui Gakkaishi*, 1972, **25**, No. 136, 269.
36. N. J. Keen, *J. Brit. Nucl. Energy Soc.*, 1968, **7**, 178.
37. K. Schwochau, L. Astheimer, H. J. Schenk and E. G. Witte, *Chem. Ztg.*, 1983, **107**, 177.
38. K. H. Lieser and B. Gleitsmann, *Z. Anal. Chem.*, 1982, **313**, 203.
39. *Idem, ibid.*, 1982, **313**, 289.
40. M. Förster and K. H. Lieser, *ibid.*, 1981, **309**, 177.
41. A. Sugii, N. Ogawa and H. Hashizume, *Talanta*, 1980, **27**, 627.
42. R. E. Sturgeon, S. S. Berman and S. N. Willie, *ibid.*, 1982, **29**, 167.
43. R. Stella, M. T. G. Valentini and L. Maggi, *Anal. Chem.*, 1985, **57**, 1941.
44. K. Isshiki and E. Nakayama, *ibid.*, 1987, **59**, 291.
45. *Oak Ridge National Laboratory Repts.*, 3036, TM-5, 3322, 3349, 3863.
46. S. Kobayashi, M. Tokunoh, T. Saegusa and F. Mashio, *Macromolecules*, 1985, **18**, 2357.
47. K. Minagawa, Y. Takizawa and I. Kifune, *Anal. Chim. Acta*, 1980, **115**, 103.
48. E. Yamagami, S. Tateishi and A. Hashimoto, *Analyst*, 1980, **105**, 491.
49. D. R. Mann, L. D. Surprenant and S. A. Casso, *Nucl. Instrum. Methods*, 1984, **223**, 235.
50. K. Terada, K. Matsumoto and Y. Nanao, *Anal. Sci.*, 1985, **1**, 145.
51. M. Volkan, O. Y. Ataman and A. G. Howard, *Analyst*, 1987, **112**, 1409.
52. I. Tabushi, Y. Kobuke and T. Nishiya, *Nature*, 1979, **280**, 665.
53. Y. Ito and T. Saegusa, *J. Macromol. Sci. Chem.*, 1979, **A13**, 303.
54. M. G. Djamali and K. H. Lieser, *Ang. Makromol. Chem.*, 1983, **116**, 195.
55. M. M. Guedes de Mota, M. A. Jonker and B. Griepink, *Z. Anal. Chem.*, 1979, **296**, 345.
56. K. Terada, K. Morimoto and T. Kiba, *Anal. Chim. Acta*, 1980, **116**, 127.
57. R. A. A. Muzzarelli and O. Tubertini, *Talanta*, 1969, **16**, 1571.
58. L. Astheimer, H. J. Schenk, E. G. Witte and K. Schwochau, *Sep. Sci. Technol.*, 1983, **18**, 307.
59. K. Schwochau, L. Astheimer, H. J. Schenk and E. G. Witte, *Z. Naturforsch.*, 1982, **37b**, 214.
60. R. S. S. Murthy and D. E. Ryan, *Anal. Chim. Acta*, 1982, **140**, 163.
61. S. J. De Mora and R. M. Harrison, *ibid.*, 1983, **153**, 307.
62. M. Hagadone and H. Zeitlin, *ibid.*, 1976, **86**, 289.
63. Y. S. Kim and H. Zeitlin, *Sep. Sci.*, 1971, **6**, 505.
64. *Idem, Chem. Commun.*, 1971, 672.
65. *Idem, Sep. Sci.*, 1972, **7**, 1.
66. N. Rothstein and H. Zeitlin, *Anal. Lett.*, 1976, **9**, 461.
67. H. Hiraide and A. Mizuike, *Bull. Chem. Soc. Japan*, 1975, **48**, 3753.
68. D. Joyce and H. Zeitlin, *Anal. Chim. Acta*, 1974, **69**, 27.
69. Y. Kusaka, H. Tsuji, Y. Tamari, T. Sagawa, S. Ohmori, S. Imai and T. Ozaki, *J. Radioanal. Chem.*, 1977, **37**, 917.
70. Y. Kubo, N. Nakazawa and M. Sato, *Sekiyu Gakkaishi*, 1973, **16**, 588.
71. R. E. Sturgeon, S. S. Berman, A. Desaulniers and D. S. Russell, *Talanta*, 1980, **27**, 85.
72. L. G. Danielsson, B. Magnusson and S. Westerlund, *Anal. Chim. Acta*, 1978, **98**, 47.
73. K. Kremling and H. Petersen, *ibid.*, 1974, **70**, 35.
74. Y. Akama, T. Nakai and F. Kawamura, *Nippon Kaisui Gakkaishi*, 1979, **33**, 120; *Chem. Abstr.*, 1980, **92**, 64405t.
75. *Idem, ibid.*, 1979, **33**, No. 183, 180. E.
76. R. V. Davies, J. Kennedy, J. W. A. Peckett, B. K. Robinson and R. J. W. Streeton, *U.K. At. Energy Auth. Res. Group Rep.*, AERE-R-5024, 1965.
77. K. Schwochau, L. Astheimer and H. L. Schenk, *26th IUPAC Congress, Tokyo*, 4-10 Sept. 1977.
78. H. Yamashita, Y. Ozawa, F. Nakajima and T. Murata, *Bull. Chem. Soc. Japan*, 1980, **53**, 3050.
79. N. Ogata, *Nippon Kaisui Gakkaishi*, 1971, **24**, No. 131, 197; *Chem. Abstr.*, 1971, **75**, 112744a.
80. H. Tani, H. Nakayama and F. Sakamoto, *Japan Patent*, 1975, 75134911; *Chem. Abstr.*, 1976, **84**, 93286v.
81. P. Burba and K. H. Lieser, *Z. Anal. Chem.*, 1977, **286**, 191.
82. I. Tabushi, Y. Kobuke, K. Ando, M. Kishimoto and E. Ohara, *J. Am. Chem. Soc.*, 1980, **102**, 5947.
83. Y. F. Chen, *Nippon Kaisui Gakkaishi*, 1981, **36**, No. 193, 24; *Chem. Abstr.*, 1981 **95**, 151495c.
84. D. N. Edgington, S. A. Gordon, M. M. Thommes and L. R. Almodovar, *Limnol. Oceanog.*, 1970, **15**, 945.
85. K. Schwochau, L. Astheimer and H. J. Schenk, *Rep. Julich-1415*, 1977.
86. Y. Miyake, Y. Sugimura and M. Mayeda, *Nippon Kaiyo Gakkaishi*, 1970, **26**, 123.
87. T. Sakaguchi, A. Nakajima and T. Horikoshi, *Nippon Nogei Kagaku Kaishi*, 1979, **53**, 211.
88. H. Akaiwa and H. Kawamoto, *Rev. Anal. Chem.*, 1982, **6**, 65.
89. O. M. Petrukhin, *Zh. Neorgan. Khim.*, 1979, **24**, 3155.
90. R. G. Pearson, *J. Am. Chem. Soc.*, 1963, **85**, 3533.
91. O. P. Shvoeva, G. P. Kuchava, G. V. Myasoedova, S. B. Savvin, L. N. Bannykh, N. G. Zhukova, O. N. Grishina and M. S. Mezhirov, *Zh. Analit. Khim.*, 1985, **40**, 1606.
92. S. B. Savvin and G. V. Myasoedova, *2nd USSR-Japan Joint Symp. Anal. Chem. Moscow*, 1-10 July, 1984, p. 155.
93. Bio-Rad Laboratories Bulletin 2024, 1981.
94. Bio-Rad Laboratories Bulletin 1224, 1986.
95. W. G. Mitchell and M. M. Jones, *J. Inorg. Nucl. Chem.*, 1978, **40**, 199.
96. T. Yoshioka, *Bull. Chem. Soc. Japan*, 1985, **58**, 2618.
97. E. Oikawa and K. Ohtomo, *React. Polym. Ion Exch., Sorbents*, 1988, **8**, 17.
98. J. R. Kaczvinsky, Jr., J. S. Fritz, D. D. Walker and M. A. Ebra, *J. Radioanal. Nucl. Chem.*, 1985, **91**, 349.
99. S. Marmor and G. Kidane, *Polym. Bull. (Berlin)*, 1978, **1**, 239.
100. I. Tabushi, Y. Kobuke and T. Nishiya, *Tetrahedron Lett.*, 1979, **37**, 3515.
101. T. Sakaguchi and A. Nakajima, *Sep. Sci. Technol.*, 1986, **21**, 519.

102. J. H. Hodgkin and R. Eibl, *React. Polym. Ion Exch., Sorbents*, 1985, **3**, 83.
103. J. H. Hodgkin, *Chem. Ind. London*, 1979, 153.
104. J. H. Hodgkin and R. Eibl, *React. Polym., Ion Exch., Sorbents*, 1986, **4**, 285.
105. E. M. Moyers and J. S. Fritz, *Anal. Chem.*, 1976, **48**, 1117.
106. A. Sugii, N. Ogawa and I. Katayama, *Talanta*, 1982, **29**, 263.
107. M. Tomoi, O. Abe, N. Takasu and H. Kakiuchi, *Makromol. Chem.*, 1983, **184**, 2431.
108. A. Sugii and N. Ogawa, *Talanta*, 1979, **26**, 970.
109. A. Sugii, N. Ogawa and H. Hashizume, *ibid.*, 1979, **26**, 189.
110. P. C. H. Mitchell and M. G. Taylor, *Polyhedron*, 1982, **1**, 225.
111. Zs. Horváth and R. M. Barnes, *Anal. Chem.*, 1986, **58**, 725.
112. J. N. King and J. S. Fritz, *ibid.*, 1985, **57**, 1016.
113. C. K. Wagner, G. Hall, B. Riegel, J. D. Virgilio, V. Kamath and G. Germann, *J. Appl. Polym. Sci.*, 1986, **31**, 1797.
114. I. Tabushi, A. Yoshizawa and H. Mizuno, *J. Am. Chem. Soc.*, 1985, **107**, 4585.
115. M. Grote and A. Kettrup, *Anal. Chim. Acta*, 1985, **175**, 239.
116. R. Bedetti, V. Caranchio and E. Cernia, *Polymer Lett.*, 1975, **13**, 329.
117. N. H. Agnew, *J. Polym. Sci. Chem. Ed.*, 1976, **14**, 2819.
118. A. Sugu, N. Ogawa, Y. Iinuma and H. Yamamura, *Talanta*, 1981, **28**, 551.
119. D. Lindsay, D. Sherrington, J. Greig and R. Hancock, *J. Chem. Soc., Chem. Commun.* 1987, 1270.
120. M. Marhol, *Z. Anal. Chem.*, 1967, **231**, 265.
121. M. Marhol, H. Beranova and K. L. Cheng, *J. Radioanal. Chem.*, 1974, **21**, 177.
122. G. Manecke, K. Stockhausen and P. Gergs, *Makromol. Chem.*, 1969, **128**, 229.
123. J. Schoer and W. Ochsenfeld, *Angew. Makromol. Chem.*, 1982, **109/110**, 215.
124. S. Akio and E. Yoshiaki, *U.S. Patent*, 4414183, 1983; *European Patent Appl.* 37655, 1981; *Chem. Abstr.*, 1982, **96**, 36216w.
125. H. Egawa, T. Nonaka and M. Ikarai, *J. Appl. Polym. Sci.*, 1984, **29**, 2045.
126. S. D. Alexandratos, D. R. Quillen and M. E. Bates, *Macromolecules*, 1987, **20**, 1191.
127. S. D. Alexandratos, D. R. Quillen and W. J. McDowell, *Sep. Sci. Technol.*, 1987, **22**, 983.
128. B. L. Rivas, H. A. Maturana, I. M. Perich and U. Angne, *Polym. Bull. (Berlin)*, 1985, **14**, 239.
129. *Idem*, *ibid.*, 1986, **15**, 121.
130. B. L. Rivas, H. A. Maturana, J. Bartulin, R. E. Catalan and I. M. Perich, *ibid.*, 1986, **16**, 299.
131. B. L. Rivas, H. A. Maturana, U. Angne, R. E. Catalan and I. M. Perich, *ibid.*, 1986, **16**, 305.
132. H. Egawa, T. Nonaka and H. Maeda, *Sep. Sci. Technol.*, 1985, **20**, 653.
133. H. Egawa, T. Kuroda and N. Shiraiishi, *Nippon Kagaku Kaishi*, 1982, 685.
134. G. M. Orf and J. S. Fritz, *Anal. Chem.*, 1978, **50**, 1328.
135. M. Lührmann, N. Stelter and A. Kettrup, *Z. Anal. Chem.*, 1985, **322**, 47.
136. R. E. Sturgeon, S. S. Berman, S. N. Willie and J. A. H. Desaulniers, *Anal. Chem.*, 1981, **53**, 2337.
137. J. W. McLaren, A. P. Mykytiuk, S. N. Willie and S. S. Berman, *ibid.*, 1985, **57**, 2907.
138. D. Beauchemin, J. W. McLaren, A. P. Mykytiuk and S. S. Berman, *ibid.*, 1987, **59**, 778.
139. M. A. Marshall and H. A. Mottola, *ibid.*, 1983, **55**, 2089.
140. K. H. Faltynski and J. R. Jezorek, *Chromatographia*, 1986, **22**, 5.
141. K. Isshiki, F. Tsuji and T. Kuwamoto, *Anal. Chem.*, 1987, **59**, 2491.
142. K. Janák and J. Janák, *Collection Czech. Chem. Commun.*, 1986, **51**, 643.
143. *Idem*, *ibid.*, 1986, **51**, 650.
144. *Idem*, *ibid.*, 1986, **51**, 657.
145. H. S. Patel, *Angew. Makromol. Chem.*, 1986, **139**, 17.
146. D. K. Ryan and J. H. Weber, *Talanta*, 1985, **32**, 859.
147. J. C. Moreira and Y. Gushikem, *Anal. Chim. Acta*, 1985, **176**, 263.
148. H. Egawa and T. Nonaka, *J. Appl. Polym. Sci.*, 1986, **31**, 1677.
149. E. M. Moyers and J. S. Fritz, *Anal. Chem.*, 1977, **49**, 418.
150. K. Takeda, M. Akiyama and T. Yamamizu, *React. Polym., Ion Exch., Sorbents*, 1985, **4**, 11.
151. C. H. Culberson, Y. J. Liang, T. M. Church and R. H. Wood, *Anal. Chim. Acta*, 1982, **139**, 373.
152. J. J. Wolff, *Ion-Exchange and Solvent Extraction, Symposium, Oslo*, 1982 Paper IV/62-IV/74.
153. R. R. Grinstead, *J. Met.*, 1979, **31**, 13.
154. K. H. Lieser, M. Erboj and B. Thybusch, *Angew. Makromol. Chem.*, 1987, **152**, 169.
155. Diamond Sharmrock *Duolite CS346*, Technical Sheet, Ohio, U.S.A.
156. Y. Kataoke, M. Matsuda, H. Yoshitake and Y. Hirose, *U.S. Patent*, 4468374, 1984.
157. H. Egawa, T. Nonaka, S. Matsumoto and M. Nakayama, *Isr. J. Chem.*, 1985, **26**, 56.
158. H. Egawa, H. Harada and T. Nonaka, *Nippon Kagaku Kaishi*, 1980, 1767.
159. H. Egawa, H. Harada and T. Shuto, *ibid.*, 1980, 1773.
160. K. Sugasaka, S. Katoh, N. Takai, H. Takahashi and Y. Umezawa, *Sep. Sci. Technol.*, 1981, **16**, 971.
161. H. Egawa, M. Nakayama, T. Nonaka and E. Sugihara, *J. Appl. Polym. Sci.*, 1987, **33**, 1993.
162. H. Egawa, M. Nakayama, T. Nonaka, H. Yamamoto and K. Uemura, *ibid.*, 1987, **34**, 1557.
163. H. Omichi, A. Katakai, T. Sugo and J. Okamoto, *Sep. Sci. Technol.*, 1986, **21**, 563.
164. H. Omichi, A. Katakai, T. Sugo, J. Okamoto, S. Katoh, K. Sakane, K. Sugasaka and T. Itagaki, *ibid.*, 1987, **22**, 1313.
165. T. Hori, S. Furusaki, T. Sugo and J. Okamoto, *Nippon Kagaku Kaishi*, 1987, 1071.
166. M. D. Rosenzweig, *Chem. Eng.*, 1975, **82**, 60.
167. G. J. De Jong and C. J. N. Rekers, *J. Chromatog.*, 1974, **102**, 443.
168. *Akzo Zout Chemie, Technical Literature*, The Akzo Imac TMR Process for the Removal of Mercury from Waste Water.
169. Rohm and Haas, *Amborane TM 345 Reductive Resin, Tech. Rep.*, DIC-79-2, 1979.
170. G. Koster and G. Schmuckler, *Anal. Chim. Acta*, 1967, **38**, 179.
171. G. V. Myasoedova, I. I. Antol'skaya and S. B. Savvin, *Talanta*, 1985, **32**, 1105.

172. S. Yasuda and H. Yamauchi, *Nippon Kagaku Kaishi*, 1987, 752.
173. P. Kumar and S. S. Dara, *J. Polym. Sci. Polym. Chem. Ed.*, 1981, **19**, 397.
174. A. Hirose, *J. Radioanal. Chem.*, 1978, **46**, 211.
175. Kumamoto University, *Japanese Patent*, No. 58/186436; *Chem. Abstr.*, **100**, 89381d.
176. K. Ueda, Y. Sato, O. Yoshimura and Y. Yamamoto, *Analyst*, 1988, **113**, 773.
177. N. Takagi, T. Hirotsu and S. Kato, *Japan Patent*, 63/248440, 1988; *Chem. Abstr.*, 1989, **110**, 215567r.
178. *Idem, ibid.*, 63/248439, 1988; *Chem. Abstr.*, 1989, **110**, 215566q.
179. *Idem, ibid.*, 63/248438, 1988; *Chem. Abstr.*, 1989, **110**, 195640d.
180. H. Omichi, A. Katakai and J. Okamoto, *Sep. Sci. Technol.*, 1988, **23**, 2445.
181. T. Hori, K. Saito, S. Furusaki, T. Sugo and J. Okamoto, *Nippon Kagaku Kaishi*, 1988, 1607.
182. H. Omichi, A. Katakai and J. Okamoto, *Sep. Sci. Technol.*, 1988, **23**, 1133.
183. T. Hirotsu, K. Shunsaku, K. Sagasaka, N. Takai, M. Seno and T. Itagaki, *J. Appl. Polym. Sci.*, 1988, **36**, 1741.
184. M. Nakayama, K. Uemura, T. Nonaka and H. Egawa, *ibid.*, 1988, **36**, 1617.
185. Y. Kobuke, *Hyomen*, 1988, **26**, 461; *Chem. Abstr.*, 1988, **109**, 234546d.
186. K. Sakane and S. Katoh, *Shikoku Kogyo Gijutsu Shikensho Hokoku*, 1988, **19**, 98; *Chem. Abstr.*, 1988, **109**, 215664z.
187. T. Shiotsuka, K. Onoe and S. Mochizuki, *Nippon Kaisui Gakkaishi*, 1988, **42**, 15; *Chem. Abstr.*, 1988, **109**, 194307t.
188. K. Uezu, K. Saito, T. Hori, S. Furusaki, T. Sugo and J. Okamoto, *Nihon Genshiryoku Gakkaishi*, 1988, **30**, 359; *Chem. Abstr.*, 1988, **109**, 194306s.
189. H. Egawa and S. Furusaki, *ibid.*, 1987, **29**, 1079; *Chem. Abstr.*, 1988, **108**, 208122x.
190. D. W. Jun, S. K. Choi and J. S. Hong, *Han'guk Somyu Konghakhoechi*, 1987, **24**, 519; *Chem. Abstr.*, 1988, **108**, 190301t.
191. K. Saito, K. Uezu, T. Hori, S. Furusaki, T. Sugo and J. Okamoto, *AIChE J.*, 1988, **34**, 411.
192. T. Hirotsu, S. Kato, K. Sugasaka, N. Takai, M. Seno and T. Itagaki, *Sep. Sci. Technol.*, 1987, **23**, 49.
193. T. Hori, K. Saito, S. Furusaki, T. Sugo and J. Okamoto, *Kagaku Kogaku Ronbunshu*, 1987, **13**, 795; *Chem. Abstr.*, 1988, **108**, 24977y.
194. T. Hirotsu, N. Takagi, S. Katoh, K. Sugasaka, N. Takai, M. Seno and T. Itagaki, *Sep. Sci. Technol.*, 1978, **22**, 2217.
195. K. Saito, T. Hori, S. Furusaki, T. Sugo and J. Okamoto, *Ind. Eng. Chem. Res.*, 1987, **26**, 1977.
196. T. Hirotsu, S. Katoh, K. Sugasaka, N. Takai, M. Seno and T. Itagaki, *ibid.*, 1987, **26**, 1970.
197. M. Morita, M. Higuchi and I. Sakata, *J. Appl. Polym. Sci.*, 1978, **34**, 1013.
198. T. Hirotsu, S. Katoh, T. Sugasaka, N. Takai, M. Seno and T. Itagaki, *Sep. Sci. Technol.*, 1987, **22**, 1725.
199. M. Suzuki, T. Fujii, S. Tanaka, T. Itagaki and S. Kato, *Proc. Eng. Found. Conf. Fundam. Adsorpt.*, 1986. A. I. Liapis (ed.) p. 537. Engineering Foundation, New York, 1987; *Chem. Abstr.*, 1987, **107**, 100265m.
200. K. Saito, Y. Tanji, S. Furusaki, T. Sugo and J. Okamoto, *Chemeca 85: Innovation Process Resour. Ind., Aust. Chem. Eng. Conf.*, 1985, 145; *Chem. Abstr.*, 1987, **106**, 180290h.
201. M. Suzuki, S. Kato and K. Itagaki, *Japan Patent*, 61/219719, 1986; *Chem. Abstr.*, 1987, **106**, 145806j.
202. K. Nakajima, K. Kono, K. Miyasaka, M. Komatsu, S. Fujii and J. Tabuchi, *ibid.*, 61/157344, 1986; *Chem. Abstr.*, 1986, **105**, 227901e.
203. I. Hagiwara and T. Kamaishi, *ibid.*, 61/54237, 1986; *Chem. Abstr.*, 1986, **105**, 198950n.
204. N. Takagi, T. Hirotsu, S. Katoh, K. Sugasaka, N. Takai, H. Takahashi and T. Itagaki, *Nippon Kaisui Gakkaishi*, 1986, **40**, No. 223, 3; *Chem. Abstr.*, 1986, **105**, 195021z.
205. T. Hirotsu, S. Katoh, K. Sugasaka, M. Seno and T. Itagaki, *J. Chem. Soc., Dalton Trans.*, 1986, 1983.
206. M. Zhuang and S. Cai, *Haiyang Xuebao*, 1985, **7**, 778; *Chem. Abstr.*, 1986, **104**, 228092h.
207. T. Hirotsu, S. Kato, N. Takagi, S. Takai, K. Itagaki, E. Ochi and J. Watanabe, *Japan Patent*, 60/210532, 1985; *Chem. Abstr.*, 1986, **104**, 92799j.
208. H. Omichi, A. Katakai, T. Sugo and J. Okamoto, *Sep. Sci. Technol.*, 1986, **21**, 299.
209. N. Takai, *Kagaku Kyoiku*, 1982, **31**, 342; *Chem. Abstr.*, 1986, **104**, 8643y.
210. B. Zheng, S. Cai, M. Zhuang and L. Jiang, *Haiyang Xuebao*, 1985, **7**, 34; *Chem. Abstr.*, 1985, **103**, 200471m.
211. H. Omichi, A. Katakai, T. Sugo and J. Okamoto, *Sep. Sci. Technol.*, 1985, **20**, 163.
212. Sumitomo Chemical Co., *Japan Patent*, 59/123540, 1984; *Chem. Abstr.*, 1984, **101**, 214509a.
213. A. Sasaki, Y. Echigo, M. Yamao, Y. Suematsu, T. Ishikura, T. Hirotsu, S. Katoh and K. Sugasaka, *Nippon Kaisui Gakkaishi*, 1984, **37**, No. 210, 341; *Chem. Abstr.*, 1984, **101**, 76683z.
214. Hitachi Ltd., *Japan Patent*, 58/166934, 1983; *Chem. Abstr.*, 1984, **100**, 93278t.
215. Y. Koide, H. Takamoto, K. Matsukawa and K. Yamada, *Bull. Chem. Soc. Japan*, 1983, **56**, 3364.
216. F. Vernon and T. Shah, *React. Polym., Ion Exch., Sorbents*, 1983, **1**, 301.

USE OF MATRIX-MODIFIERS IN ATOMIC-ABSORPTION DETERMINATION OF CHROMIUM IN ARGILLITES

E. KLAOS* and V. ODINETS

Institute of Chemistry, Estonian Academy of Sciences, Tallinn, Estonian SSR, USSR

(Received 24 January 1989. Revised 19 October 1989. Accepted 31 October 1989)

Summary—The direct atomic-absorption determination of chromium in argillites, without preliminary concentration and separation, has been studied. A map of selective flame zones for determining Cr in argillites has been designed. An express method for determining Cr in Estonian argillites has been suggested.

Atomic-absorption spectrometry is one of the best methods for determining chromium in argillites. Two types of flame are usually used for this purpose—nitrous oxide-acetylene and air-acetylene. With the first, the determination is affected by the oxidation state of the chromium,¹ as well as by interferences from Al, Fe, La, Ti, V, Mo, W and other elements. These interferences depend on the observation height above the burner, the chromium oxidation state, the concentration of the interfering elements, and the nature and concentration of the acids in the solution.²

Determination in the air-acetylene flame is also subject to interferences and is useful only for solutions with relatively simple composition, unless the standard-addition technique is used.

In reducing flames the influence of acids and such elements as Al, Co, Fe, Mn, Mo, Ni, Ti and V is observed,³ and the effect depends on the chromium oxidation state.⁴ Prior reduction of Cr(VI) to Cr(III) in the samples and standards (with hydrogen peroxide in hydrochloric acid medium) is recommended. For determination of chromium in particular matrices, by AAS with the air-acetylene flame, 1–2% NH₄Cl solution,¹ 1% NH₄HF₂ + 0.2% Na₂SO₄ solution,⁶ 0.025M sodium dodecyl sulphate⁷ and other additives are recommended. However, none of these eliminates the influence of the argillite matrix (consisting of 10–20% organic matter, 20–40% clay minerals and 50–55% aleurite).

We have investigated various matrix-modifiers to develop a completely matrix-independent method, requiring use of only

pure analyte solution (plus matrix-modifier) for calibration.

EXPERIMENTAL

Apparatus

A Pye Unicam SP-1900 spectrophotometer with a three-slot burner was used.

Reagents

All reagents were of analytical grade. The standard solutions of chromium were prepared according to Price.⁸ The potassium thiocyanate solution (10%) was prepared by dissolving the required amount in demineralized water, and the dodecylamine hydrochloride solution (2%) was prepared in ethanol. Argillite solutions were prepared by heating a 1-g sample with 20 ml of concentrated hydrofluoric acid, 10 ml of concentrated perchloric acid and 6 ml of concentrated nitric acid in a platinum dish until perchloric acid fumes were evolved, then cooling, rinsing down with a little demineralized water, heating again until perchloric acid was completely removed, cooling, taking up the residue with 40 ml of hydrochloric acid (1 + 1), and finally diluting to volume in a 100-ml standard flask with demineralized water.

Procedure

Aliquots of the argillite and additive solutions were placed in a 25-ml standard flask and diluted to the mark with demineralized water. Calibration solutions were matched with sample solutions in acid and additive contents. The solutions were aspirated into the air-acetylene flame and the atomic absorption was measured under the conditions given in Table 1 for

*To whom correspondence should be addressed.

Table 1. Instrumental conditions for determination of Cr without additives

Wavelength, nm	357.9
Slit-width, mm	0.4
Observation height, cm	0.8
Air flow, l./min	7
Acetylene flow, l./min	1.4
Lamp current, mA	8
Integration period, sec	4

samples without additives and in Table 2 for samples with additives.

RESULTS AND DISCUSSION

Flame composition and observation height

Changing the acetylene flow-rate from 1.0 to 1.8 l./min, at constant air flow-rate, resulted in an approximately fivefold increase in the chromium absorbance (Fig. 1). The maximum absorbance was obtained with an acetylene flow-rate of 1.8 l./min, air flow-rate of 7.0 l./min and an observation height, in the flame, of 5 mm, presumably because these conditions corresponded to the optimal carbon to oxygen ratio in the flame. Molybdenum displayed similar behaviour. Though these conditions, which correspond roughly to the acetylene flow-rate of 1.0–1.2 l./min and air flow-rate of 5 l./min recommended by Pye Unicam, gave the highest sensitivity, the chromium signal was subject to matrix effects when Estonian argillites were analysed. We therefore investigated the dependence of the apparent chromium concentration found for a particular argillite (with calibration by means of pure chromium solutions), on the flame composition and observation height

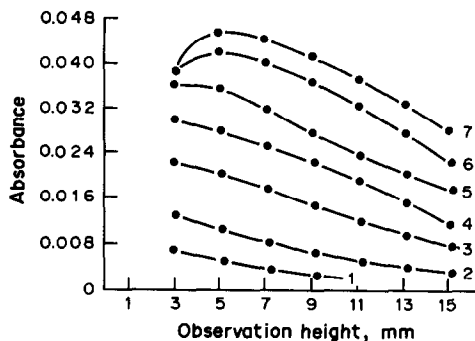


Fig. 1. Dependence of Cr absorbance on observation height and flame composition. Acetylene flow-rate (l./min): 1.0 (1), 1.2 (2), 1.4 (3), 1.5 (4), 1.6 (5), 1.7 (6), 1.8 (7). Air flow-rate 7.0 l./min.

above the burner (Fig. 2). The argillite solution contained no chemical additives. The shaded area in Fig. 2 corresponds to the confidence interval of the true chromium concentration, determined by the standard-addition method and confirmed by neutron-activation analysis.⁹

As can be seen from Fig. 2, the apparent chromium concentration found in the argillite solution strongly depends on which flame zone and composition are chosen for measurements, and the direct determination of chromium, *i.e.*, without preliminary separation, in the argillite solution leads to a systematic positive relative error ranging from 20 to 100% under the conditions examined, as can be seen in Table 3.

Effects of additives

The experiments just described were repeated with the addition of two spectroscopic buffers, which in our opinion are potentially useful for

Table 2. Instrumental conditions for the determination of Cr in argillites in the presence of additives (air flow-rate 7 l./min)

Additive	Characteristic Cr concentration, $\mu\text{g/ml}$	Acetylene flow-rate, l./min	Observation height, mm
Dodecylamine hydrochloride	0.07	1.7	9
	0.08	1.7	11
Potassium thiocyanate	0.07	1.6	5
	0.08	1.5	2
	0.08	1.6	7
		1.7	11
	0.10	1.5	8
	0.20	1.3	4
	0.3	1.2	8
Potassium thiocyanate + perchloric acid	0.07	1.6	4–5
	0.08	1.6	7
	0.08	1.7	11
	0.10	1.5	8
	0.20	1.35	7
	0.3	1.20	8

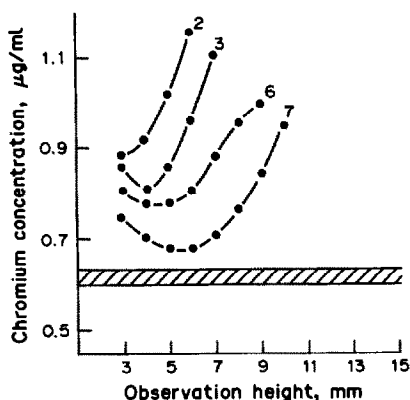


Fig. 2. Dependence of the Cr contents detected in argillite solution on observation height and flame composition (curve marking as in Fig. 1) in the absence of additives. The shaded area denotes the true Cr concentration (here and in Figs. 3–5).

use with Estonian argillites, *viz.* dodecylamine hydrochloride⁷ and potassium thiocyanate.⁹ In the presence of the first of these, the pattern of the relationship of the signal to the parameter varied changes sharply (Fig. 3), and this is obviously associated with a change in the aerosol generation mechanism and reactions in the flame. To illustrate this, the apparent chromium values found were plotted as functions of both observation height and acetylene flow-rate at constant air flow-rate (Fig. 3A).

In Fig. 3B the same data were plotted in a different way, with the observation heights corresponding to the upper and lower confidence limits for the true chromium concentration for each acetylene flow-rate being plotted as points. It was then assumed that this set of observation heights would change linearly with change in flow-rate, and the points were accordingly joined by straight lines. The shaded area bounded by these lines was taken as delineating "correct" combination of observation height and acetylene flow-rate. In addition, contours were drawn through points corresponding to equal characteristic concentrations of chromium. Even minor changes in the combination of observation height and flow-rate strongly affect the accuracy and precision of the chromium determination. For example, at an acetylene flow-rate of 1.5–1.6 l./min and observation height of 6–11 mm the error ranges from –8 to +24%. Overlap of the characteristic concentration contour with the "correct combination" zone indicates the flame zone and composition with which chromium can be determined without preliminary separation, and with maximum

precision, sensitivity and economy in acetylene. For dodecylamine hydrochloride as additive the most sensitive and selective conditions are 1.7 l./min acetylene flow-rate and 8 mm observation height. Under conditions for which the characteristic concentration is greater than 0.15 µg/ml, no determination at all is possible. Potassium thiocyanate, first used by us as a matrix modifier for Mo,⁹ and later for V,¹⁰ also proved effective for Cr. The corresponding diagrams for argillite solutions containing potassium thiocyanate as additive (Fig. 4) show this to be more effective than dodecylamine hydrochloride.

The efficiency of potassium thiocyanate in the air–acetylene flame is attributed to the change in the reaction products in the analytical zone, the formation of CN and NH radicals, and the decrease in the carbon effect.

It is interesting that in the fuel-lean flame (see Fig. 4) at an acetylene flow-rate of 1.2–1.6 l./min there are two selective zones. Also, it is only at the two extremes of this range that the selective zone exists over an appreciable length of the flame (4–8 mm at 1.2 l./min, 4–11 mm at 1.6 l./min). This is presumably due to variations in the atomization mechanism of argillite particles in the flame. At the two critical flow-rates (1.2 and 1.6 l./min) a radical atomization mechanism predominates and the presence of potassium thiocyanate affects the whole of the inner flame zone. At 1.3–1.5 l./min acetylene flow-rate it is effective only in the central zone of the inner cone and in the secondary reaction zone (*i.e.*, at 4 and 8 mm), where the temperature is nearly maximal for a given gas mixture. It is probably a thermal reaction mechanism that prevails here. For determination, an acetylene flow of 1.3 l./min and observation height of 4 mm, or a flow-rate of 1.7 l./min and height of 11 mm are optimal, the latter permitting determination of chromium at a concentration of 0.08 µg/ml.

Thus, in a certain flame zone the addition of potassium thiocyanate allows direct determination of chromium with higher accuracy than that attainable with dodecylamine hydrochloride as additive. The addition of perchloric acid has been recommended because the chromium oxidation state affects the absorption signal.¹¹ In the flame zone diagram obtained with argillite solutions containing both potassium thiocyanate and perchloric acid (Fig. 5), it is seen that the selective zone widens, giving a wide range of combinations of observation heights

Table 3. Determination of Cr without using additives

Sample	Cr in sample solution, $\mu\text{g/ml}$	Cr added, $\mu\text{g/ml}$	Observation height above burner, mm	C_2H_2 flow-rates, l./min	Added Cr found, $\mu\text{g/ml}$	Apparent recovery of Cr added, %
Argillite 1	0.65	0.5	5	1.2	0.84	168
				1.4	0.69	138
				1.6	0.64	128
			7	1.2	—	—
				1.4	0.90	180
				1.6	0.69	138
			9	1.2	—	—
				1.4	—	—
				1.6	0.81	162
Argillite 2	0.38	0.4	5	1.2	0.66	165
				1.4	0.55	137
				1.6	0.52	130
			7	1.2	—	—
				1.4	0.70	175
				1.6	0.57	142
			9	1.2	—	—
				1.4	—	—
				1.6	0.62	155
Mineral fraction	0.78	0.8	5	1.2	1.16	145
				1.4	0.89	111
				1.6	0.92	115
			7	1.2	—	—
				1.4	1.12	140
				1.6	1.07	134
			9	1.2	—	—
				1.4	—	—
				1.6	1.09	136
Organic fraction	1.56	1.50	5	1.2	2.29	153
				1.4	1.75	117
				1.6	1.71	114
			7	1.2	—	—
				1.4	2.28	152
				1.6	2.08	139
			9	1.2	—	—
				1.4	—	—
				1.6	2.13	142

from 4.5 to 8.5 mm with acetylene flow-rates of 1.2–1.8 l./min. In this case, a reliable determination of chromium is possible at characteristic concentrations of 0.07–0.2 $\mu\text{g/ml}$. The determination is practically independent of choice of flame composition and observation height. Thus, in the presence of potassium thiocyanate, perchloric acid increases not only the sensitivity of the chromium determination but also the selectivity. This is presumably because perchloric acid favours the oxidation of chromium to volatile chromyl chloride and volatilization

predominates over reduction by the graphite. The presence of chromium in lower oxidation states promotes rapid reduction to non-volatile products, even in the solid aerosol particles. Moreover, in the presence of Cr^{3+} and other refractory elements in low-oxidation states in the aerosol, part of the potassium thiocyanate is used for complex formation and part for the formation of CN and NH radicals. The presence of perchloric acid considerably increases the efficiency of the potassium thiocyanate buffer, probably because formation of chromium(VI),

Argillite + dodecylamine hydrochloride (0.2%)

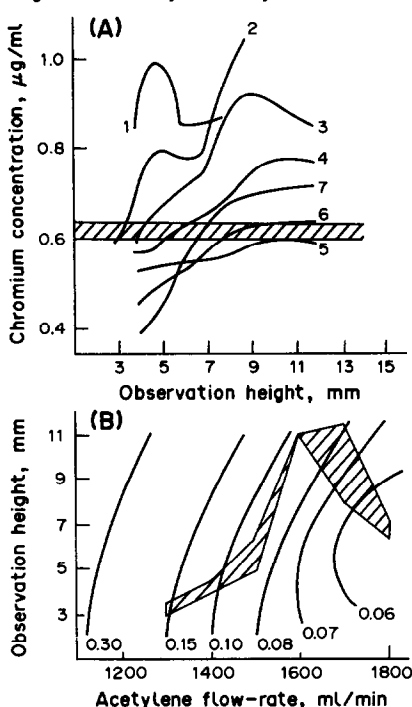


Fig. 3. The Cr contents detected in argillite solution (A), and the map of selective zones (B) in the air-acetylene flame, in the presence of dodecylamine hydrochloride (0.2%). Acetylene flow-rate (l./min): 1.2 (1), 1.3 (2), 1.4 (3), 1.5 (4), 1.6 (5), 1.7 (6), 1.8 (7) (here and in Figs. 4 and 5).

Argillite + KCNS + HClO₄

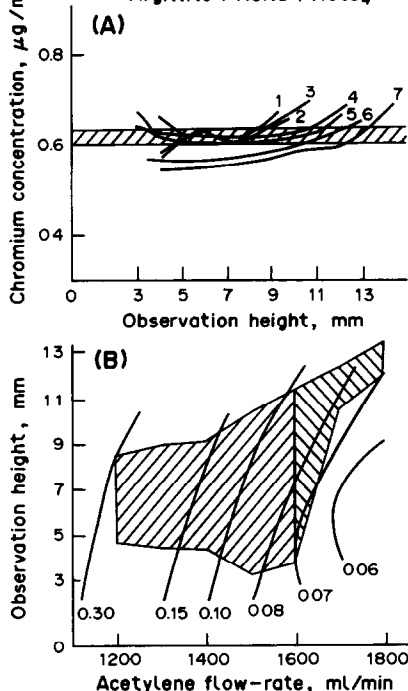


Fig. 5. The Cr contents detected in argillite solution (A), and the map of selective zones (B) in the air-acetylene flame, in the presence of potassium thiocyanate (0.4%) and perchloric acid (0.3%).

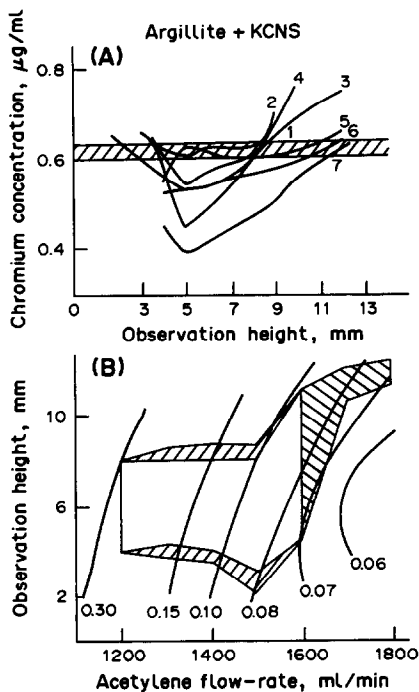


Fig. 4. The Cr contents detected in argillite solution (A), and the map of selective zones (B) in the air-acetylene flame, in the presence of potassium thiocyanate (0.4%).

which does not form thiocyanate complexes, frees all the buffer for formation of CN and NH radicals. However, as shown above, with a proper choice of the flame zone and composition, potassium thiocyanate can be used alone as the additive, without perchloric acid.

Figures 3-5 show that the selective zones change their boundaries according to the type of modifier used. It should be stressed, however, that the absence of a selective effect under the most sensitive instrumental conditions does not necessarily mean that the modifier has no selectivity at all, but only that a set of conditions under which it can act effectively as a matrix modifier has not yet been found.

Thus, a thorough study of flame zones, construction of the zone map and elucidation of an analytical zone with its help, permit chromium determination over a wide concentration range with high sensitivity, speed and reliability. Neither separation of the chromium nor matrix-matching of the standard and sample solutions is necessary. The results of chromium determination in some oil-shale samples and their fractions by the method developed are shown in Tables 3-6.

Table 4. Determination of Cr in the presence of 0.2% dodecylamine hydrochloride (air flow-rate 7 l./min)

Sample	Cr in sample solution, $\mu\text{g/ml}$	Cr added, $\mu\text{g/ml}$	Observation height above burner, mm	C_2H_2 flow-rates, l./min	Added Cr found, $\mu\text{g/ml}$	Apparent recovery of Cr added, %
Argillite 1	0.65	0.50	5	1.2	0.81	162
				1.4	0.56	112
				1.6	0.45	90
			7	1.2	0.64	128
				1.4	0.59	118
				1.6	0.46	92
			9	1.2	0.67	134
				1.4	0.73	146
				1.6	0.49	98
Argillite 2	0.38	0.40	5	1.2	0.62	155
				1.4	0.43	107
				1.6	0.33	82
			7	1.2	0.51	127
				1.4	0.49	122
				1.6	0.36	90
			9	1.2	0.53	132
				1.4	0.62	155
				1.6	0.38	95
Mineral fraction	0.78	0.80	5	1.2	1.20	150
				1.4	0.85	106
				1.6	0.71	89
			7	1.2	1.00	125
				1.4	0.91	114
				1.6	0.74	92
			9	1.2	1.08	135
				1.4	1.16	145
				1.6	0.76	95
Organic fraction	1.56	1.50	5	1.2	2.34	156
				1.4	1.59	106
				1.6	1.27	85
			7	1.2	1.89	126
				1.4	1.72	115
				1.6	1.33	87
			9	1.2	1.98	132
				1.4	2.24	149
				1.6	1.47	98

Table 5. Determination of Cr in the presence of 0.4% KSCN (air flow-rate 7 l./min)

Sample	Cr in sample solution, $\mu\text{g/ml}$	Cr added, $\mu\text{g/ml}$	Observation height above burner, mm	C_2H_2 flow-rates, l./min	Added Cr found, $\mu\text{g/ml}$	Apparent recovery of Cr added, %
Argillite 1	0.65	0.50	5	1.2	0.49	98
				1.4	0.40	80
				1.6	0.51	102
			7	1.2	0.51	102
				1.4	0.44	88
				1.6	0.49	98
			9	1.2	0.52	104
				1.4	0.54	108
				1.6	0.49	98
Argillite 2	0.38	0.40	5	1.2	0.39	97
				1.4	0.31	77
				1.6	0.42	105
			7	1.2	0.41	102
				1.4	0.35	87
				1.6	0.40	100
			9	1.2	0.40	100
				1.4	0.42	105
				1.6	0.38	95
Mineral fraction	0.78	0.80	5	1.2	0.78	97
				1.4	0.64	80
				1.6	0.83	104
			7	1.2	0.82	102
				1.4	0.70	87
				1.6	0.81	101
			9	1.2	0.81	101
				1.4	0.88	110
				1.6	0.79	99
Organic fraction	1.56	1.50	5	1.2	1.48	99
				1.4	1.14	76
				1.6	1.53	102
			7	1.2	1.53	102
				1.4	1.32	88
				1.6	1.50	100
			9	1.2	1.54	103
				1.4	1.59	106
				1.6	1.48	99

Table 6. Determination of Cr in the presence of 0.4% KSCN + 0.3% HClO₄ (air flow-rate 7 l./min)

Sample	Cr in sample solution, $\mu\text{g/ml}$	Cr added, $\mu\text{g/ml}$	Observation height above burner, mm	C ₂ H ₂ flow-rates, l./min	Added Cr found, $\mu\text{g/ml}$	Apparent recovery of Cr added, %
Argilite 1	0.65	0.50	5	1.2	0.50	100
				1.4	0.51	102
				1.6	0.50	100
			7	1.2	0.49	98
				1.4	0.51	102
				1.6	0.51	102
			9	1.2	0.53	106
				1.4	0.52	104
				1.6	0.50	100
Argillite 2	0.38	0.40	5	1.2	0.41	102
				1.4	0.39	97
				1.6	0.41	102
			7	1.2	0.40	100
				1.4	0.40	100
				1.6	0.39	97
			9	1.2	0.42	105
				1.4	0.41	102
				1.6	0.39	97
Mineral fraction	0.78	0.80	5	1.2	0.82	102
				1.4	0.83	104
				1.6	0.83	104
			7	1.2	0.82	102
				1.4	0.79	99
				1.6	0.80	100
			9	1.2	0.84	105
				1.4	0.83	104
				1.6	0.79	99
Organic fraction	1.56	1.50	5	1.2	1.52	101
				1.4	1.52	101
				1.6	1.53	102
			7	1.2	1.54	103
				1.4	1.51	101
				1.6	1.50	100
			9	1.2	1.56	104
				1.4	1.54	103
				1.6	1.48	99

REFERENCES

- H. C. Green, *Analyst*, 1975, **100**, 640.
- J. Y. Marks and G. G. Welcher, *Anal. Chem.*, 1970, **42**, 1033.
- J. M. Ottaway, D. T. Coker and B. Singleton, *Talanta*, 1973, **20**, 927.
- M. Yanagisawa, M. Suzuki and T. Takeuchi, *Anal. Chim. Acta*, 1970, **52**, 386.
- J. A. Hurlbut and C. D. Chriswell, *Anal. Chem.*, 1971, **43**, 465.
- A. Purushottam, P. P. Naidu and S. S. Lal, *Talanta*, 1972, **19**, 1193.
- M. Kodama, S. Shimizu, M. Sato and T. Tominaga, *Anal. Lett.*, 1977, **10**, 591.
- W. I. Price, *Analytical Atomic Absorption Spectrometry*, Heyden, London, 1972.
- E. Klaos and V. M. Odinets, *Otkerytiya, Tzobret*, 1985, No. 6, 134; *USSR Patent* SUR 1140015; *Chem. Abstr.*, 1985, **102**, 214364v.
- G. F. Kirkbright and T. S. West, *Appl. Optics*, 1968, **7**, 1305.
- L. Pelekis, Z. Pelekis, I. Taure, O. Kirret and E. Rajavee, *Izv. AN ESSR. Khim.*, 1985, **34**, 161. Eesti NSV Tead. Akad. Toim., Keem.

HETEROCYCLIC DITHIOPHOSPHATES AS ANALYTICAL REAGENTS

INDIRECT EXTRACTION-SPECTROPHOTOMETRIC DETERMINATION OF SILVER IN COPPER CONCENTRATES AND ORES

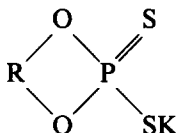
D. ATANASSOVA and A. N. SHISHKOV

Plovdiv University "Paissii Hilendarski", Department of Analytical Chemistry, 4000 Plovdiv, Bulgaria

(Received 22 March 1989. Revised 29 July 1989. Accepted 14 November 1989)

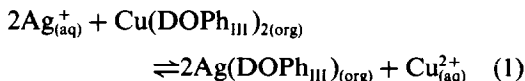
Summary—The proposed method is based on the exchange reaction between the complex of copper(II) with 4,7-dimethyl-2-thiol-2-thion-1,3,2-dioxophosphorinane (DOPh_{III}) in toluene and an aqueous solution of silver(I). The decrease in the absorbance of the Cu(DOPh_{III})₂ solution is proportional to the silver(I) concentration for 5–90 µg of silver in 5 ml of toluene extract and 5–30 µg in 10 ml of toluene extract. The method is applied to the determination of silver in copper concentrates and ores.

The heterocyclic dithiophosphates of general formula



where R is CH₂CH₂CH₂ (DOPh_I) CH(CH₃)CH₂CH₂(DOPh_{II}) or CH(CH₃)CH₂CH₂CH₂(CH₃)(DOPh_{III}) are reagents utilized for the direct spectrophotometric determination of copper¹ and molybdenum.² A study of the interaction of copper(II) with various dithiophosphates was reported in a previous paper¹. These complexes are coloured, and less stable than the corresponding colourless complexes of silver(I).³

The present paper describes a new method for determination of silver, based on the exchange reaction



EXPERIMENTAL

Reagents

DOPh_{III} was synthesized as described elsewhere.⁴ Its purity was checked by thin-layer chromatography. Aqueous 0.01M solutions of the reagent were prepared.

Standard silver solution, 1000 µg/ml, was prepared from high-purity silver nitrate and diluted to give a 5 µg/ml working solution.

Toluene (*pro analysi* grade) was treated with concentrated sulphuric acid, washed with distilled water until acid-free (pH-paper), dried with anhydrous sodium sulphate for 24 hr, and finally distilled. The purified toluene was stored in dark glass bottles and was stable for some months.

Copper(II)–DOPh_{III} solution in toluene was made as follows. Dissolve 0.9828 g of pure CuSO₄·5H₂O in distilled water, add 10 ml of 6M sulphuric acid and dilute accurately to 250 ml with distilled water; 1 ml contains 1000 µg of Cu(II). Take 25 ml of this solution, acidify it with 10 ml of sulphuric acid (1 + 2), add 30 ml of 1 × 10⁻²M aqueous solution of DOPh_{III} and leave it for 15 min. Extract with 150 ml of toluene. Leave the phases to separate then wash the organic layer with three portions of 100 ml of copper(II) solution (1000 µg/ml) and three portions of 500 ml of distilled water. The toluene extract should not contain any excess of DOPh_{III}. It is checked for traces of DOPh_{III} as follows. Shake 5 ml of the toluene solution with 10 ml of aqueous phase (5 ml of 1000-µg/ml copper solution + 1 ml of perchloric acid + 4 ml of water) for 3 min. The absorbances of the initial and treated toluene layers should not differ. Washing of the toluene extract is continued until it gives a negative reaction for free DOPh_{III}, then the extract is filtered through a fine filter paper, dried with anhydrous sodium sulphate and stored in a dark bottle. The solution is stable for more than 5 months.

All other reagents used were of analytical-reagent grade and were not purified further.

Procedures

Calibration graph. Pipette 1.0, 3.0, 5.0, 10.0 and 15.0 ml of the 5 $\mu\text{g/ml}$ silver solution into 100-ml separating funnels. To each add 5 ml of concentrated perchloric acid and dilute to 50 ml with distilled water, then add 5 ml of $\text{Cu}(\text{DOPh}_{\text{III}})_2$ solution in toluene and shake the mixtures for 2 min. Centrifuge (or let stand for 45 min) to separate the layers. Filter the organic layer through a filter paper previously impregnated with toluene. Measure the absorbance at 420 nm in a 1-cm cell against toluene. Plot the calibration graph.

Analysis of copper concentrate. Weigh 1.0 g of the concentrate into a 150-ml conical flask. Add 10 ml of nitric acid (1 + 1), cover the flask with a watch glass, and heat on a hot-plate until evolution of nitrogen oxides ceases. Remove the watch glass and evaporate almost to dryness. If the samples are to be analysed for gold, repeat the evaporation step, with 15 ml of *aqua regia*. Add 20 ml of concentrated perchloric acid and heat until the volume has decreased to 8–10 ml, cool, wash down the walls of the flask with water, and heat until fumes of perchloric acid are evolved. Cool, dilute with 20–30 ml of distilled water and filter through a double filter paper into a 100-ml standard flask. Wash the conical flask and residue with 6 portions of distilled water. Dilute the filtrate and washings to volume and analyse 50 ml of the solution as described above for the calibration graph.

Analysis of copper ore. Weigh 4 g of the ore into a beaker and add 16 ml of *aqua regia*. Evaporate on a hot-plate almost to dryness then add a few ml of concentrated hydrochloric acid and evaporate again (repeat this step twice more). Finally add 20 ml of perchloric acid and proceed as for analysis of copper concentrate, except that the filtrate and washings should be diluted to 50 ml, and the total volume extracted with $\text{Cu}(\text{DOPh}_{\text{III}})_2$ solution.

RESULTS AND DISCUSSION

Extraction of the silver complex

When an aqueous solution of silver and a toluene solution of $\text{Cu}(\text{DOPh}_{\text{III}})_2$ (silver and copper in stoichiometric ratio) was shaken for 1 min, the toluene layer became colourless, indicating that silver completely replaced the

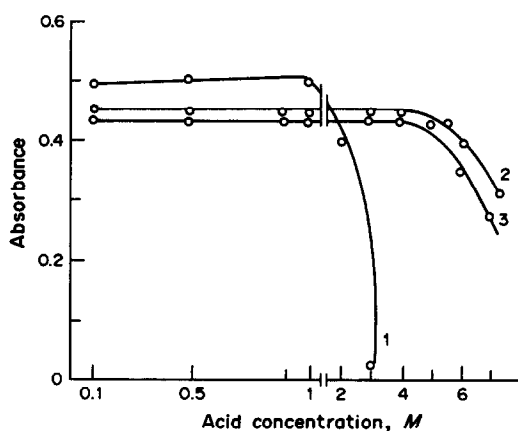


Fig. 1. Plot of absorbance vs. acid concentration: (1) HNO_3 , (2) H_2SO_4 , (3) HClO_4 .

copper in the complex [see reaction (1)]. In all further experiments the phases were shaken for 2 min.

The effect of mineral acid concentration on the exchange reaction (1) was studied by acidifying 10 ml of 5 $\mu\text{g/ml}$ silver solution, diluting to 20 ml with water, shaking the solution with 5 ml of $\text{Cu}(\text{DOPh}_{\text{III}})_2$ solution for 2 min, then measuring the absorbance of the organic layer as described above. Plots of the absorbance vs. acid concentration (Fig. 1) show that the reaction occurs in 0.1–1.0M nitric acid, 0.1–4M sulphuric acid and 0.1–4M perchloric acid. At concentrations above 1M, nitric acid causes destruction of the $\text{Cu}(\text{DOPh}_{\text{III}})_2$. The exchange reaction can also be done in 0.8–1.5M hydrochloric acid, but in 2M hydrochloric acid it is strongly hindered, and does not occur when the acid concentration is above 3.5M.

A study of the effect of changing $V_{\text{org}}:V_{\text{aq}}$ showed that at ratios of up to 1:50 the replacement of Cu(II) and Ag(I) was not affected, making preconcentration of silver possible.

The plot of absorbance vs. silver concentration was linear in the range 5–90 μg of silver in 5 ml of toluene extract and 5–130 μg of Ag in 10 ml of extract.

The effect of various ions that commonly occur with silver in natural samples was studied by analysing model solutions containing 50 μg of Ag. Up to 80 mg of iron(III), 100 mg of copper(II), magnesium(II), calcium(II), strontium(II), barium(II), zinc(II), cadmium(II), aluminium(III), chromium(III), nickel(II), molybdenum(VI), tungsten(VI), manganese(II), uranium(VI), cobalt(II), 70 mg of rhenium(VII), 40 mg of tin, 15 mg of lead(II), 5 mg of antimony(III), 1 mg of platinum(II) and

Table 1. Determination of silver in reference standard samples and copper concentrates (6 replicates, probability 0.95)

Sample	Silver,* g/ton				
	Certified value	By fire-assay method	By AAS method	This work	
				Lab. 1	Lab. 2
MDK-1	11	—	—	11.1 ± 0.3	—
MDK-2	17	—	—	17.1 ± 0.3	—
MDK-3	23	—	—	23.0 ± 0.3	—
Cu concentrate 1	—	21.2	21.2	21.1 ± 1.5	26.4 ± 2.0
Cu concentrate 2	—	22.6 ± 2.7	24.2 ± 3.0	24.9 ± 1.6	25.6 ± 2.0
Cu concentrate 3	—	20.9 ± 2.5	22.3 ± 3.8	22.6 ± 2.8	29.3 ± 3.1
Cu concentrate 4	—	18.9 ± 3.8	21.9 ± 3.3	22.0 ± 3.1	26.2 ± 0.8

*According to the Bulgarian Standard Method,⁶ the tolerable differences between parallel determinations are ≤ 5 g/ton for the 10–20 g/ton range, and ≤ 7 g/ton for the 20–40 g/ton range.

arsenic(III), 0.5 mg of selenium(VI) and tellurium(VI), 0.5 mg of selenium(IV) and tellurium(IV), 0.25 mg of bismuth(III), palladium(II) and gold(II) and 100 mg of sulphate and 25 mg of nitrate will not interfere in the determination of silver by the proposed method. More than ~ 0.25 mg of bismuth(III), gold(III), palladium(II) and 0.5 mg of selenium(IV), selenium(VI), tellurium(IV) and tellurium(VI) will cause a positive error. Fluoride, thiocyanate, thiosulphate and mercury(II) interfere with the exchange reaction.

The proposed reaction was applied to the analysis of reference standard samples of silver in metal matrices. The results are shown in Table 1.

APPLICATIONS

Silver in copper concentrate is usually determined by fire assay or atomic-absorption spectrometry.⁶ The fire assay is slow and requires special equipment and a skilled operator. The precision is poor. The second method gives better precision but an expensive piece of equipment is needed. Of the spectrophotometric methods available, those based on dithizone and rhodanine⁵ are suitable for determination of traces of silver and compete favourably with the fire-assay method. However, the rhodanine method is inapplicable to copper concentrates⁵ and the dithizone method suffers from serious matrix interference⁵.

Four industrial samples were analysed by the proposed method. The results are shown in Table 1. They are compared with data from the fire-assay and atomic-absorption spectrometric determination.⁶ The results agree very well. The chi-square values ($P = 0.95$, $n = 6$) calculated for concentrates 2 and 3 are 2.41 and 0.958, respectively. The critical values for $\chi^2(P, f)$ are 7.81 ($P = 0.95$) and 11.3 ($P = 0.99$).⁷

Six industrial samples of copper ores were analysed by the proposed method. The results were in good agreement with those of semi-quantitative spectral analyses.

The proposed indirect extraction–spectrophotometric method is advantageous for determination of traces of silver in copper concentrates and ores and competes favourably with the classical fire-assay analysis.

REFERENCES

1. D. Atanassova, A. N. Shishkov and N. D. Jordanov. Submitted to *Talanta*.
2. A. N. Shishkov and D. Atanassova, *Commun. Dept. Chem. Bulg. Acad. Sci.*, 1984, **17**, 340.
3. *Idem*, *Ditiofosfati i tekhnii disulfidi kato analitichni reagenti*, Bulletin No. 342/89, Central Scientific Technical Library, Sofia, pp. 1–114.
4. D. Atanassova and A. N. Shishkov. *Commun. Dept. Chem. Bulg. Acad. Sci.*, 1989, **22**, 131.
5. G. Charlot, *Metody analiticheskoi khimii*, p. 1008. Khimia, Moskva, Leningrad, 1965.
6. *Bulgarian Standard Method*, 8792–83.
7. K. Doerffel, *Statistik in der analytischen Chemie*, VEB Deutscher Verlag für Grundstoffindustrie, Leipzig, 1984.

AN IMPROVED SPECTROPHOTOMETRIC METHOD FOR THE DETERMINATION OF SILVER WITH 5-[*p*-(DIMETHYLAMINO)BENZYLIDENE]RHODANINE*

ZHOU NAN†, ZHOU MIN and HE CHUN-XIANG

Shanghai Research Institute of Materials, MMBEI, Shanghai, People's Republic of China

JU ZHAO-QIANG and LIN LI-FEN

The Third Factory of Shanghai Reagent Chemicals, Shanghai, People's Republic of China

(Received 15 June 1989. Revised 22 October 1989. Accepted 30 October 1989)

Summary—The proposed spectrophotometric determination of Ag^+ with 5-[*p*-(dimethylamino)benzylidene]rhodanine has the following improvements: (1) more effective control of pH; (2) use of poly(vinyl alcohol)-200 as the protective colloid to enhance the molar absorptivity to $3.5 \times 10^4 \text{ l. mole}^{-1} \text{ cm}^{-1}$ and to lengthen the period of stable absorbance to 50 min; (3) use of lactic and hydrofluoric acids as maskants to improve the selectivity. Beer's law is obeyed over the range 10–40 μg of Ag. The standard deviation is 0.39 μg of Ag ($n = 14$).

5-[*p*-(Dimethylamino)benzylidene]rhodanine (DMABR) is well known as a spectrophotometric reagent for silver,¹ but the nature of the reaction product is not yet fully understood,² and the reaction characteristics reported vary from author to author. Hence the system needs further study. In this paper an improved procedure is proposed, with use of a purified reagent.

EXPERIMENTAL

Reagents

Analytical-reagent grade chemicals were used unless otherwise specified, and demineralized water was used for preparation of reagents and for dilutions.

Nitric acid, chloride-free. The concentrated acid and a 50-fold dilution with water were used.

Poly(vinyl alcohol)-200 solution, 0.5%.

Lactic acid, (1 + 1).

DMABR solution, 0.02% in acetone.

Standard silver solution, 20 $\mu\text{g}/\text{ml}$. Freshly prepared by dilution of a 1.00 mg/ml solution in 1M nitric acid.

Calibration graph

Pipette 0.5, 1.0, 1.5 and 2.0 ml portions of standard silver solution into four separate 50-ml standard flasks. To each add 25 ml of water, 1 drop of 2,4-dinitrophenol indicator, and saturated sodium bicarbonate solution dropwise until the yellow colour appears, then add 15 ml of nitric acid (1 + 49), 4.0 ml of poly(vinyl alcohol)-200 solution and 2.50 ml of DMABR solution by pipette. Dilute to volume with water and mix. Let stand for 15 min, then measure the absorbance at 470 nm against a reagent blank, with 3-cm cells. Plot absorbance *vs.* μg of silver to construct the calibration graph.

Procedure

Pipette an appropriate volume of analyte solution (in *ca.* 1M nitric acid), containing 10–40 μg of silver, into a 50-ml standard flask, and proceed as for calibration.

RESULTS AND DISCUSSION

The following modifications are made to the earlier procedures. The chosen pH (1.1 ± 0.1) is lower than that used previously, *viz.* 1.8,²⁻⁴ 3.0,⁵ and 9.3.⁶ In this spectrophotometric system the DMABR species HL and H_2L^+ , and the silver complexes AgL and AgL_2^- , all co-exist and their molar absorptivities at the specified wavelength

*This work was financially supported by the Chinese TDMI Science Foundation, Project No. 87J51203, and presented at the 2nd National Symposium on Analysis of Noble Metals in 1988.

†Author for correspondence. Present address: 99 Handan Road, 200433, Shanghai, People's Republic of China.

(*vide infra*) differ, so any change in pH would affect the distribution pattern of the ligand and complex species, respectively, thus affecting simultaneously the absorbances of the sample and blank solutions. It was found, however, that the net absorbance of the sample solution remains virtually constant over the pH range 1.0–1.2.

Poly(vinyl alcohol)-200 is used as a protective colloid to sensitize the reaction and stabilize the predominating reaction product, which is in linear polymerized form.² The period of constant absorbance is thus lengthened to at least 50 min instead of 15–30,³ or 20–30,⁷ reported earlier. The optimum amount is 4 ml of 0.5% solution. In these respects the poly(vinyl alcohol) is superior to gum arabic,² starch,⁴ gelatin,⁴ sucrose,⁸ or organic solvents such as ethanol.^{3,4}

Rigid control of pH is realized by first adding saturated sodium bicarbonate solution dropwise to the analyte solution (25 ± 5 ml, in *ca.* 1M nitric acid) until appearance of the yellow colour of 2,4-dinitrophenol (added as indicator), then between 14 and 20 ml of nitric acid (1 + 49) is added. After dilution of this solution to 50 ml, the pH does not differ by more than 0.02, irrespective of the volume of acid (in the specified range) that has been added. This technique would seem much better than evaporating to dryness,¹⁰ which is time-consuming and could cause loss of silver by adsorption on the vessel wall, or use of a sulphate buffer,⁸ which would decrease the absorbance and also precipitate any Pb(II), Ba(II) and Sr(II) present, which are themselves non-interferents.

Less DMABR (purified) is used, to reduce the blank; its final concentration in the spectrophotometric system is 10 $\mu\text{g/ml}$. The solution would be turbid in the presence of 15 $\mu\text{g/ml}$ DMABR, and the absorbance would be lowered if a 5 $\mu\text{g/ml}$ concentration were used. A 0.02% solution in acetone is used, since the optimum amount of acetone is 2.5 ml.

Hydrofluoric and lactic acids are added to prevent hydrolysis, olation or oxolation of metal ions during the pH adjustment.

The absorption maximum of Ag-DMABR (470 nm) is taken as the wavelength for determination, despite the closeness of the absorption maximum of DMABR (480 nm), since at this wavelength the net absorbance is the largest between 400 and 580 nm, even though the reagent blank is quite appreciable.

These modifications give the proposed method some special features. The sensitivity

Table 1. Effect of diverse ligands and cations on determination of 21.4 μg of silver

	Added		Ag found, μg
	mg	ml	
Lactic acid (1 + 1)		0.1	22.0
HF		0.15	22.1
Na tartrate	10.0		20.5
Cu(II)	10.0*		22.2
Sn(IV)	4.60*		21.2
Pb(II)	4.50*		21.6
Ni(II)	0.050*		21.0
In(III)	0.150		20.6
Zn(II)	1.65*		20.5
Fe(III)	0.076*		21.4
Sb(III)	0.024*		21.4
W(VI)	10.0*		32.2†

*Plus 0.1 ml of lactic acid (1 + 1) and 0.05 ml of HF.
†42.8 μg of Ag taken

is increased, the molar absorptivity of 3.5×10^4 l.mole⁻¹.cm⁻¹ being much higher than the values reported earlier (2×10^4 ,² or 2.32×10^4 ,⁸). The true value would be 3.8×10^4 l.mole⁻¹.cm⁻¹ if a correction for the overcompensation of the blank is made by the method of Kroll and Elin.¹¹ The blank overcompensates because the amount of free DMABR left in the sample solution is always less than that in the blank, and the molar absorptivity of DMABR at 470 nm is 3.4×10^3 l.mole⁻¹.cm⁻¹.

The upper limit of determination is 40 μg of silver. Beer's law is obeyed over the range of 10–40 μg and the standard deviation is 0.39 μg ($n = 14$). The method is more selective, as the reaction takes place in a more acidic medium and in the presence of complexing agents. Considerable amounts of Cu(II), Sn(IV) and Pb(II) are tolerable (Table 1), but anions that form insoluble silver salts, *e.g.*, tungstate, molybdate, vanadate, will still interfere.

A mixture of hydrofluoric acid and nitric acid may be used for sample dissolution if necessary.

Application

The proposed method is suitable for direct determination of 0.25–1.0% of silver in copper,

Table 2. Analysis of simulated samples

Sample composition, %	Ag found, %	
	AAS method*	Proposed method
Cu 90.7; Sn 8.23; Ag 1.07	1.06	1.08
Sn 98.9; Ag 1.07	1.03	1.06
Sn 99.5; Ag 0.43	0.43	0.43
Pb 99.2; Sb 0.25; Ag 0.50	0.48	0.49

*Measured at 328.1 nm.

tin and lead alloys, with a coefficient of variation varying from 1.0 to 3.9%. It is more convenient to use than the dithizone and Cu-DDTC methods, which require a solvent extraction. Simulated samples were prepared by mixing solutions of the high-purity metals and analyzed by both the proposed and AAS methods. Some examples are given in Table 2.

Acknowledgement—Grateful thanks are due to all members of SRIM's Directorate for permission to publish this paper.

REFERENCES

1. F. Feigl, *Z. Anal. Chem.*, 1928, **74**, 380.
2. Z. Marczenko, *Spectrophotometric Determination of Elements*, pp. 494, 495. Horwood, Chichester, 1976.
3. R. Borissova, M. Koeva and E. Topalova, *Talanta*, 1975, **22**, 791.
4. E. B. Sandell, *Colorimetric Determination of Traces of Metals*, 3rd Ed., pp. 806–811. Interscience, New York, 1959.
5. E. S. Dicker and E. A. Johnson, *Analyst*, 1957, **82**, 285.
6. M. Castagna and J. Chauveau, *Bull. Soc. Chim. France*, 1961, 1165.
7. R. Doicheva and M. Koeva, *Ann. L'Ecole Supérieure Chim. Industrielle, Sofia*, 1968, **15**, 255.
8. G. C. B. Cave and D. N. Hume, *Anal. Chem.*, 1952, **24**, 1503.
9. Zhou Nan, Yu Ren-qing, Yao Xu-zhang and Lu Zhi-ren, *Talanta*, 1985, **32**, 1125.
10. N. V. Markova and T. V. Yakubtseva, *Tr. Tsent. Nauch. Issled. Gornorazved. Inst. Tsvet., Redk. Blagorod. Metal.*, 1971, **97**, 175.
11. M. H. Kroll and R. J. Elin, *Clin. Chem.*, 1985, **31**, 462.

DETERMINATION OF 1,3-BIS(4-HYDROXYIMINOMETHYLPYRIDINIUM)- PROPANE DICHLORIDE (TMB-4) WITH Pd(II)

Z. KORIČANAC, K. KARLJKOVIĆ-RAJIĆ and B. STANKOVIĆ

Institute of Inorganic and Analytical Chemistry, Faculty of Pharmacy, University of Belgrade,
11000 Belgrade, dr Subotića 8, Yugoslavia

(Received 4 November 1988. Revised 27 October 1989. Accepted 14 November 1989)

Summary—The colour reaction of TMB-4 and palladium(II) chloride has been investigated. The optimum reaction conditions, spectral characteristics, stability constant and composition of the yellow water-soluble complex have been established. A new spectrophotometric method is proposed for microdetermination of TMB-4.

It is generally accepted that the best therapeutic or prophylactic approach to the problem of exposure to highly toxic organophosphorus compounds is the application of atropine in combination with oximes that act as cholinesterase re-activators. Among the mono- and bis-pyridinium oximes, only PAM-2, obidoxime and TMB-4 are used in standard therapy.^{1,2} Smerić *et al.*³ have proposed use of the aminopentacyanoferrate(II) (AmPF) and nitrosylpentacyanoferrate (NP) anions as reagents for spectrophotometric determination of TMB-4 by formation complex, and Karas-Gašparec and Weber have studied the reaction of TMB-4 with the aquapentacyanoferrate(II) (AqPF) anion.⁴ Vashek determined TMB-4 by a spectrophotometric method based on the modified Zinke-Koning reaction, and in the same paper described the polarographic determination of TMB-4.⁵

In earlier work we developed spectrophotometric methods for the determination of quinolinium oximes⁶ and obidoxime chloride in water and injection solutions⁷ with palladium(II) chloride as reagent. We have now extended this to determination of TMB-4.

EXPERIMENTAL

Reagents

TMB-4, 1,3-bis(4-hydroxyiminomethylpyridinium)propane dichloride (purity > 99.5%) was synthesized in the Laboratory of Organic Chemistry, Bosnalijek, Sarajevo. All other chemicals were of analytical-grade purity (Merck). Redistilled water was used throughout.

A freshly prepared $2 \times 10^{-3}M$ aqueous solution of pure TMB-4 was used as the stock solution; it was stable for several days. Palladium(II) chloride standard solution ($2.08 \times 10^{-2}M$) was prepared by dissolving the requisite amount of the compound in distilled water containing 0.60 ml of concentrated hydrochloric acid, with warming on a water-bath, then cooling and diluting to volume with water in a 250-ml standard flask. The solution was standardized gravimetrically with dimethylglyoxime,⁸ and diluted as required.

Britton-Robinson buffer solutions⁹ covering the pH range 3.3–7.03 were prepared. The pH 6.05 buffer was prepared by mixing 100 ml of a mixture of phosphoric, boric and acetic acids (each 0.04M) with 42.5 ml of 0.20M sodium hydroxide and 1.45 ml of 2M potassium chloride. The ionic strength of the final solution for determination was kept constant at 0.50M by addition by 2M potassium chloride solution.

Apparatus

A Pye Unicam SP-6-500 spectrophotometer and a Varian Super Scan TM-3 spectrophotometer were used, with 10-mm fused-silica cells. A Radiometer PHM-62 pH-meter, calibrated with appropriate standard buffer solutions, was used.

Procedure for calibration (Method A)

Potassium chloride solution (2M, 2.25 ml) and palladium(II) chloride solution ($5 \times 10^{-3}M$, 1.0 ml) were placed in a 10-ml standard flask and a portion (0.05–1.0 ml) of $2 \times 10^{-4}M$ TMB-4 was added, followed by 5.00 ml of

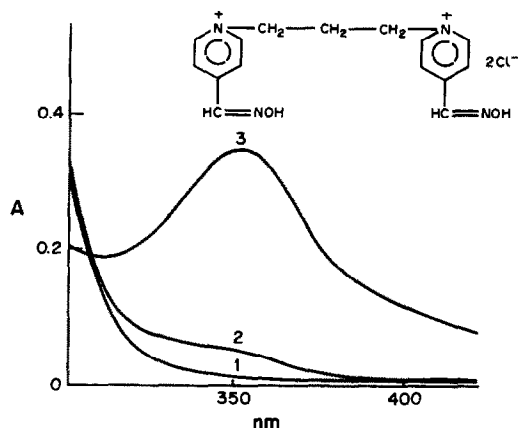


Fig. 1. Absorption spectra of TMB-4 (curve 1); palladium(II) chloride (curve 2); and complex (curve 3): $c_{\text{TMB-4}} = 1 \times 10^{-5} M$; $c_{\text{Pd(II)}} = 1 \times 10^{-4} M$; pH = 6.05; $\mu = 0.5$.

pH 6.05 buffer, and the solution was diluted to volume with water. The absorbance at 350 nm was measured after 10 min, against a reagent blank.

Procedure for calibration (Method B)

A portion (0.05–0.8 ml) of $2 \times 10^{-4} M$ TMB-4 was placed in a 10-ml standard flask, 1.0 ml of 0.1M hydrochloric acid was added, and the solution was diluted to volume with water. The absorbance at 280 nm was measured against a reagent blank.

RESULTS AND DISCUSSION

Absorption spectra

The reaction between TMB-4 and Pd(II) chloride in Britton–Robinson buffer solution in the pH range 3.30–7.03 was studied. The spectra of the solutions containing the water-soluble yellow complex of TMB-4 with Pd(II) were recorded over the wavelength range 300–450 nm. The complex gave a sharp absorption peak at 350 nm (Fig. 1, curve 3), where the absorbance of Pd(II) was low (curve 2) and that of TMB-4 negligible (curve 1). Since the reagent absorbed at the wavelength of maximum absorbance of the complex, all measurements were performed against a reagent blank.

Reaction conditions

The complex is produced only at pH above about 4 and is quantitative at pH 6–7 (Fig. 2). The shape of the spectra is independent of pH, indicating the formation of only one type of complex under these conditions. A Britton–Robinson buffer of pH 6.05 was used to provide the working pH. At this pH at least a tenfold

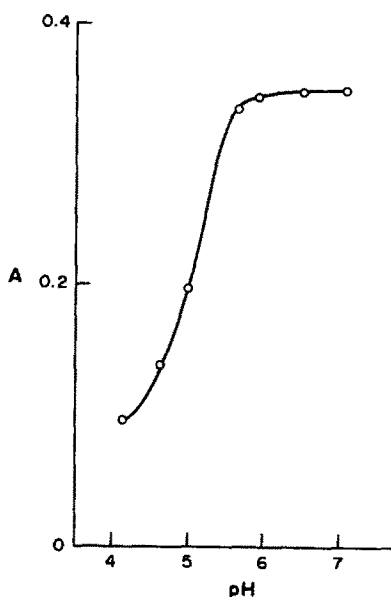


Fig. 2. Dependence of the absorbance on pH for the TMB-4-Pd(II) complex at $\lambda_{\text{max}} = 350 \text{ nm}$: $c_{\text{TMB-4}} = 1 \times 10^{-5} M$; $c_{\text{Pd(II)}} = 1 \times 10^{-4} M$; $\mu = 0.5$.

molar ratio of reagent to analyte is necessary for maximum complex formation.

It was found that increasing the ionic strength in the range 0.25–0.75 decreases the absorbance of the complex. On the other hand, at ionic strength (μ) lower than 0.5 the colour fades with time, particularly at $\mu < 0.25$. Hence an ionic strength of 0.5 was selected. Under these conditions the colour takes 10 min for full development, and is then stable for at least 2 hr. At higher ionic strength the absorbance is lower than at $\mu = 0.5$, but is still stable for > 2 hr.

Physicochemical properties of the TMB-4-Pd(II) complex

The composition of the complex was established by the continuous-variations method,^{10,11} the molar-ratio method,¹² the Bent and French method¹³ and Nash's method.¹⁴ All four methods showed that a 1:1 complex was formed.

To determine the conditional stability constant (K'), we used the methods of Sommer,¹⁵ Asmus¹⁶ and Nash¹⁴ and Job's method with non-equimolar solutions. The mean values of $\log K'$ obtained by the first three methods, 5.18, 5.23 and 5.13 respectively, were in good agreement. For the results obtained by the Sommer method the relative standard deviation was 0.2% (15 replicates).

Beer's law and sensitivity

Under the optimum conditions described above, the calibration graph for method A was

Table 1. Spectrophotometric determination of TMB-4

Taken, μM	Method A (λ 350 nm)			Method B (λ 280 nm)		
	3	5	10	3	5	10
\bar{x} , μM	3.03	4.97	9.92	2.94	4.95	9.85
x_{\min} , μM	2.92	4.89	9.83	2.86	4.79	9.77
x_{\max} , μM	3.17	5.07	10.05	3.11	5.04	10.05
SD*, μM	0.09	0.05	0.09	0.0798	0.07	0.08
RSD, %	3.0	1.0	0.9	2.7	1.4	0.8
Calculated t -value	0.004	0.736	1.878			
Tabulated t -value ($t_{20,0.05}$)		2.086				

*Inter-assay standard deviation ($n = 11$).

a straight line over the range 1–20 μM ; the molar absorptivity was $3.07 \times 10^4 \text{ l. mole}^{-1} \cdot \text{cm}^{-1}$. The detection limit was found to be 0.357 $\mu\text{g/ml}$.

For method B the linear range was 1–16 μM and the molar absorptivity was $4.05 \times 10^4 \text{ l. mole}^{-1} \cdot \text{cm}^{-1}$.

Precision and accuracy

Table 1 shows the comparison of results obtained by the two methods; both methods gave results with a similar relative standard deviation. *Student's t*-test showed no significant difference between the means obtained by these methods.

The proposed method is suitable for rapid determination of TMB-4. The relative standard deviation varies over the range 3.0–0.9% ($N = 11$) for TMB-4 concentrations of 3–10 μM .

REFERENCES

- Z. Binenfeld and V. Vojvodić, *Forsvars Medicin*, 1974, **10**, 114.
- N. Engelhard and W. D. Erdmann, *Arzneim.-Forsch.*, 1964, **14**, 870.
- Z. Smerić, V. Hankonyi and V. Karas-Gašparec, *Acta Pharm. Jugosl.*, 1977, **27**, 97.
- V. Karas-Gašparec and K. Weber, *Z. Phys. Chem. Leipzig*, 1968, **237**, 235.
- J. Vashek, *Cesk. Farm.*, 1952, **11**, 464.
- K. Karljiković, B. Stanković and Z. Binenfeld, *Mikrochim. Acta*, 1985 **II**, 195.
- K. Karljiković-Rajić, B. Stanković and Z. Binenfeld, *J. Pharm. Biomed. Anal.*, 1987, **5**, 141.
- A. Vogel, *Quantitative Inorganic Analysis*, 3rd Ed., p. 445. Longmans, London, 1961.
- J. A. Coch-Frugoni, *Gazz. Chim. Ital.*, 1957, **87**, 403.
- P. Job, *Ann. Chim. Phys. (Paris)*, 1928, **9**, 113.
- W. C. Vosburgh and G. R. Cooper, *J. Am. Chem. Soc.*, 1941, **63**, 437.
- J. Yoe and A. Jones, *Ind. Eng. Chem., Anal. Ed.* 1944, **16**, 111.
- H. Bent and C. French, *J. Am. Chem. Soc.*, 1941, **63**, 568.
- C. P. Nash, *J. Phys. Chem.*, 1960, **64**, 950.
- L. Sommer, V. Kubáň and J. Havel, *Folia Fac. Sci. Nat. Univ. Purkynianae Brunensis, Chemia* 7, Opus 1, 1970, 25.
- E. Asmus, *Z. Anal. Chem.*, 1961, **183**, 321.

A RAPID SPECTROPHOTOMETRIC METHOD FOR THE DETERMINATION OF CARBON MONOXIDE IN AMBIENT AIR

P. SELVAPATHY and R. PITCHAI

Centre for Environmental Studies, Anna University, Madras 600025, India

T. V. RAMAKRISHNA

Department of Chemistry, Indian Institute of Technology, Madras 600036, India

(Received 6 April 1987. Revised 26 October 1989. Accepted 8 November 1989)

Summary—A sensitive spectrophotometric method for the determination of carbon monoxide is described, based on the reduction of palladium(II) by carbon monoxide. The resulting elemental palladium is reacted with iodate in acidic medium in the presence of chloride, to produce an ICl_2^- species that is readily extracted as an ion-pair with Pyronine-G into benzene. Measurement of the absorbance of the extract at 535 nm permits the determination of carbon monoxide down to $1 \mu\text{l/l}$. in air. The effect of interfering gases is discussed. The method is suitable for determination of carbon monoxide in motor vehicle exhaust gases and ambient air.

The method based on the reaction with iodine pentoxide to produce iodine¹ is the best chemical method for the determination of carbon monoxide in flue gases and exhaust gases. The method is not sufficiently sensitive, however, for determination of carbon monoxide in ambient air. Among other chemical methods, a few colorimetric procedures based on the catalytic effect of palladium(II) on the reducing properties of carbon monoxide have been evaluated for its determination. These include formation of heteropoly molybdenum blue from phosphomolybdic acid,² ferriin from the iron(III)-EDTA complex³ and Crystal Violet from leuco-Crystal Violet.⁴ Another approach proposed by Ciuhandu⁵ and later modified by Levaggi and Feldstein⁶ involves reduction of silver *p*-sulphamoylbenzoate by carbon monoxide to form yellowish-brown colloidal silver. Bell *et al.*⁷ used this method, in conjunction with a silicone rubber membrane as a permeation device, to establish the concentration of carbon monoxide in the range 2–80 $\mu\text{l/l}$. in a polluted atmosphere. The major drawback of these reduction methods is their slowness and hence limited use for field applications.

The reduction of iodate in an acidified chloride medium to produce an anionic iodine chloride complex which is extractable as its ion-associate with cationic dyes has been successfully applied for the spectrophotometric determination of low levels of sulphur dioxide⁸

and hydrogen sulphide.⁹ When this reaction was extended to carbon monoxide, considerable diminution in sensitivity was noticed, even in the presence of palladium(II). Detailed study revealed that in the absence of a mineral acid and chloride, reduction of palladium(II) to elemental palladium is fairly fast when air containing carbon monoxide is drawn through the solution. The elemental palladium formed will then reduce iodate in an acidic chloride solution, to produce the anion that is extractable. Pyronine-G is used as the counter-ion, and the absorbance of the extract is measured at 535 nm. This paper describes the development of the method and its application to determination of carbon monoxide in ambient air and automobile exhaust gases.

EXPERIMENTAL

Apparatus

A Cecil linear read-out grating spectrophotometer, model CE 373, with 10 mm silica cells, was used. Fritted glass bubblers (frit diameter 12 mm, pore-size 90–150 μm , internal diameter of outer tube 22 mm) were used with a suitable suction device for sampling air. Air flow-rates were measured with a wet flowmeter or rotameter. Hamilton gas-tight syringes with Teflon tips were used for drawing known volumes of standard carbon monoxide mixtures.

Reagents

All chemicals used were of analytical grade, and distilled water was used for preparing reagent solutions.

Pure carbon monoxide was prepared by adding formic acid dropwise to concentrated sulphuric acid maintained at about 80°. The liberated gas was passed successively through a trap containing 10% potassium hydroxide solution, and a U-tube containing potassium hydroxide pellets. The purity of the resulting gas was established by using two absorbers in series, one containing acid cuprous chloride solution and the other cuprous chloride- β -naphthol solution.¹⁰

Potassium iodate (0.005%), Pyronine-G (0.05%), sodium chloride (25%), sodium hydroxide (50%) and sodium sulphate (10%) solutions were prepared by dissolving appropriate amounts of the reagents in water. Sulphuric acid (3.75*M*) was prepared by suitable dilution of concentrated sulphuric acid with water.

Potassium tetrabromopalladate(II) solution (0.04%) was prepared by dissolving 0.2 g of palladium(II) sulphate and 0.4 g of potassium bromide in 500 ml of water.

Ammoniacal cuprous chloride solution was prepared by adding 75 g of cuprous chloride to a solution of 15 g of ammonium chloride in 80 ml of water and then adding concentrated ammonia solution until dissolution was complete.¹¹

Benzene, free from thiophene, was used for extractions.

Procedures

Sampling. Up to 20 litres of air is drawn at 300 ml/min through a series of three traps containing 50% sodium hydroxide solution, ammoniacal cuprous chloride solution and dilute sulphuric acid (to remove the escaping ammonia), respectively, and finally through a solution consisting of 5 ml each of the potassium tetrabromopalladate(II) and sodium sulphate solutions and 25 ml of water, contained in a fritted-glass bubbler. This solution should be analysed within 6 hr after sampling.

Determination. The palladium solution, after sampling, is transferred into a 50-ml standard flask containing 3 ml each of the 3.75*M* sulphuric acid and potassium iodate, pyronine-G and sodium chloride solutions, made up to volume with distilled water, and mixed. After 5 min, the solution is transferred into a 125-ml separatory funnel and shaken with 5 ml of

benzene for 15 sec. The organic layer is separated, drained into a test-tube, and treated with about 1 g of anhydrous sodium sulphate to remove traces of water, and the tube is stoppered. The absorbance of the benzene extract is measured at 535 nm in 10-mm cells against a reagent blank carried through the procedure. The concentration of carbon monoxide is established by reference to a calibration graph prepared from the results obtained by injecting 20–400 μ l of pure carbon monoxide into 1 litre of air (freed from reducing gases) as it is drawn at 300 ml/min through 35 ml of the palladium reagent mixture, and following the procedure described above.

RESULTS AND DISCUSSION

Initial studies were made by equilibrating air containing 10 μ l of carbon monoxide for 3 hr with a reagent solution consisting of 5 ml of 0.04% potassium tetrachloropalladate(II) solution and 3 ml each of the potassium iodate and sodium chloride solutions and the 3.75*M* sulphuric acid, in a 500-ml stoppered bottle. After equilibration, the solution was treated with 3 ml of 0.05% pyronine-G solution, made up to 50 ml with water and extracted with 5 ml of benzene. The coloured extract had its absorption maximum at 535 nm but the reaction was very slow.

Direct analysis was then examined. One litre of air (with 500 μ l of carbon monoxide injected into it) was drawn at 300 ml/min through the mixed reagent solution (diluted to 35 ml with water and contained in a fritted-glass bubbler). The absorption solution was then analysed by addition of Pyronine-G, dilution, and extraction with benzene. The low absorbance of the extract at 535 nm indicated that under these conditions the reaction of carbon monoxide is again kinetically slow.

Varying the composition of the sampling solution and (after the sampling was complete) restoring it to that used for the determination, and completing the analysis as in the procedure, showed (Table 1) that at pH 4 the presence of potassium iodate in the sampling solution was not necessary and that the presence of sulphuric acid or sodium chloride caused a decrease in the absorbance. Hence it was decided to add the potassium iodate, sulphuric acid and sodium chloride to the palladate solution after the carbon monoxide sample had been taken.

Table 1. Effect of different parameters affecting sampling of carbon monoxide (CO = 250 μ l/l.)

(1)	Acidity*	0.23M	0.15M	0.1M	0.05M	pH 4.0	pH 5.0	pH 6.0	pH 7.0
	Absorbance	0.02	0.03	0.06	0.08	0.10	0.03	0.02	0.01
(2)	Sodium chloride solution (25%),† ml		3.0		2.0	1.0	0		
	Absorbance		0.10		0.12	0.14	0.20		
(3)	Potassium iodate solution (0.005%),§ ml		3.0		2.0	1.0	0		
	Absorbance		0.20		0.20	0.20	0.20		

*Sampling solution contains 5 ml of 0.04% solution of potassium tetrachloropalladate(II), 3 ml each of 0.005% solution of potassium iodate and 25% solution of sodium chloride and 0–2.1 ml of 3.75M sulphuric acid per 35 ml; pH was adjusted with sodium hydroxide.

†Sampling solution contains 5 ml of 0.04% solution of potassium tetrachloropalladate(II), 3 ml of 0.005% solution of potassium iodate and 0–3 ml of 25% solution of sodium chloride per 35 ml.

§Sampling solution contains 5 ml of 0.04% solution of potassium tetrachloropalladate(II) and 0–3 ml of 0.005% solution of potassium iodate per 35 ml.

Since the presence of chloride was found to affect the results, tetrabromopalladate(II) and palladous sulphate were tested for sampling carbon monoxide (Table 2). Tetrabromopalladate(II) proved superior, and 3 ml of 0.04% tetrabromopalladate(II) solution in 35 ml of the sampling solution was found adequate to provide maximum absorbance. However, this was still only 6% of the absorbance obtained with solutions that were first equilibrated for 3 hr with identical amounts of carbon monoxide and then subjected to colour development. With a view to improving the sensitivity and reducing the analysis time, impinger devices containing the optimal concentration of tetrabromopalladate(II) and packed with glass beads to provide a reagent column height ranging from 15 to 50 cm were tested. In all instances, the results were found to be considerably lower than those obtained with a fritted glass bubbler containing 35 ml of sampling solution. Subsequent studies with the fritted glass bubbler and variation of the volume of the sampling solution from 10 to 35 ml, which provided a solution depth of 22–85 mm above the frit, showed that the absorbance for a fixed amount of carbon monoxide gradually increased with increasing depth of the sampling solution (0.01 absorbance per 6 mm). However, with depths between 72 and 85 mm, *i.e.*, 30–35 ml of sampling solution, there was no marked change in the absorbance. No attempt was made to increase the volume of the sampling solution beyond 35 ml, as larger

volumes would affect subsequent manipulations prior to extraction into benzene.

When 35 ml of the sampling solution was used, a constant and maximum absorbance was obtained for flow-rates of 0.2–0.4 l./min. At higher flow-rates, the shorter contact time resulted in a gradual fall in the results.

The effect of temperature on the determination was examined. One litre of air containing 250 μ l of carbon monoxide was drawn at 300 ml/min through 35 ml of sampling solution maintained at different temperatures. Increasing the temperature from 15° to 45° slightly more than doubled the absorbance, showing that sampling should be done at the same temperature for standards and field samples. Slight variation in sampling temperature, however, is not likely to affect the results seriously, as a temperature change of 1° changes the absorbance by only 0.007, corresponding to 5 μ l/l. carbon monoxide. In practice, it was found that 20 litres of air containing carbon monoxide could be sampled in 1 hr with no variation in temperature during the sampling period. However, a temperature correction of +2% per degree should be applied when the sampling temperature and calibration temperature differ by more than 1°.

There was an appreciable decrease in the absorbance when large volumes of air or oxygen containing 250 μ l of carbon monoxide were drawn through the sampling solution, but not when volumes of nitrogen up to 50 litres, containing 250 μ l of carbon monoxide, were drawn through the solution (Table 3). The effect is clearly due to oxidation. Attempts were made to minimize the solubility of oxygen by adding an indifferent electrolyte to the sampling solution.¹¹ The addition of 5 ml of 10% sodium sulphate

Table 2. Choice of palladium salts (CO = 250 μ l/l.)

Palladium salt	Absorbance
Palladium(II) sulphate	0.16
Potassium tetrachloropalladate(II)	0.20
Potassium tetrabromopalladate(II)	0.36

Table 3. Effect of passage of air, nitrogen and oxygen (CO = 250 μ l)

Volume, l.	Absorbance		
	Air	Nitrogen	Oxygen
0	0.36	0.36	0.36
5	0.32	0.36	0.32
10	0.30	0.36	0.28
15	0.28	0.36	0.24
20	0.26	0.36	0.20
25	0.23	0.36	0.18
50	0.16	0.36	0.10

solution was found to overcome the problem (Table 4).

The results in Table 5 for analysis of samples that were allowed to stand for up to 24 hr after sampling indicated that the analysis should be completed within 6 hr.

Experimental variables which could affect the formation of the ion-pair between the ICl_n^- complex and the Pyronine-G cation were then investigated. They were optimized by using 35 ml of sampling solution containing 5 ml each of the tetrabromopalladate(II) and sodium sulphate solutions, and drawing 1 litre of air, containing 250 μ l of carbon monoxide, through the solution at 300 ml/min. The solution, after addition of all the reagents (in systematically varied amounts), was made up to 50 ml with water and allowed to stand for 5 min before equilibration with 5 ml of benzene to extract the ion-pair.

The optimum acidity for the formation of the anion species was established by varying the hydrogen-ion concentration of the solution from 0.2 to 0.7M in the final volume of 50 ml. A constant and maximum absorbance was obtained when the acidity of the medium was greater than 0.4M.

Similar studies showed that 2 ml of 0.05% Pyronine-G solution and 2.5 ml each of 0.005% potassium iodate solution and 25% sodium chloride were adequate and their presence in higher amounts did not affect the absorbance.

The ion-pair formation was almost instantaneous, and equilibration of the phases for

Table 4. Effect of passage of air (CO = 250 μ l)

Volume of air, l.	Absorbance	
	In absence of Na_2SO_4	In presence of 5 ml of 10% Na_2SO_4 solution
0	0.36	0.36
5	0.32	0.36
10	0.30	0.36
20	0.26	0.36
25	0.23	0.36
50	0.16	0.34

Table 5. Effect of delayed analysis (CO = 250 μ l/l.)

Delay time, hr	0	6	9	12	18	24
Absorbance	0.36	0.36	0.34	0.30	0.24	0.21

about 15 sec was sufficient for its quantitative transfer into benzene. The colour of the extract remained stable for 15 min and then slowly faded.

Benzene, toluene, n-hexane, cyclohexane, carbon tetrachloride, n-butyl acetate, isoamyl acetate and chloroform were tested as extraction solvents, and benzene gave the highest absorbance.

A linear calibration graph was obtained over the concentration range 20–400 ppm v/v carbon monoxide. The slope of the calibration graph was found to be 0.0015 per ppm of CO. This corresponds to a detection limit of 20 μ l of carbon monoxide in a sample volume of 1 litre, or 1 μ l/l. in 20 litres of sample.

The precision of the method was checked by analysis of 10 samples containing 200 μ l of carbon monoxide in a sample volume of 1 litre. The mean recovery was found to be 194 μ l, with a coefficient of variation of 7%.

Interferences

The interference of common air pollutants was examined by drawing 1 litre of air containing known volumes of the test gases along with 250 μ l of carbon monoxide through the reagent solution and then analysing. Sulphur dioxide, hydrogen sulphide, acetylene and formaldehyde in excess of 55 nl, 15 nl, 2 μ l and 20 μ l respectively, interfered seriously, giving positive errors. Nitrogen dioxide, when more than 2.5 μ l was present, caused low recovery. A pre-trap containing a 50% solution of sodium hydroxide eliminated the interference of 250 μ l each of sulphur dioxide, hydrogen sulphide, nitrogen dioxide and formaldehyde. The interference caused by up to 100 μ l of acetylene was eliminated by using a pre-trap containing 20 ml of ammoniacal cuprous chloride solution.¹² However, when a large volume of air was drawn through this solution, some copper(I) was oxidized to copper(II) and hence the capacity to trap acetylene was reduced. Incorporation of about 7 g of hydrazine sulphate was found to keep the copper as copper(I) even when 20 litres of air were drawn through the solution.

Application of the method to field samples

Exhaust gases from automobiles were collected in a gas-collecting bottle by displacement

Table 6. Recovery study and analysis for carbon monoxide in automobile exhaust gases

Sample	Volume of sample used in Pyronine-G method*, ml	Carbon monoxide, $\mu\text{l/l}$.		Percentage of CO in exhaust	
		Added	Found	Pyronine-G method	NDIR analyser
Stratified charge engine	50	—	55	0.11	—
Stratified charge engine	50	125	175	—	—
Stratified charge engine	50	250	300	—	—
Stratified charge engine	100	—	100	0.10	—
Stratified charge engine	100	125	230	—	—
Stratified charge engine	100	250	350	—	—
Scooter (1)—idling	5	—	—	5.0	5.0
Scooter (2)—idling	5	—	—	4.4	4.2
Scooter (3)—idling	5	—	—	8.2	8.0
Scooter (4)—idling	10	—	—	2.5	2.6
Car—idling	25	—	—	0.96	1.0

*All samples were diluted to 1 litre with CO-free air.

of a solution containing 20% sodium sulphate and 5% sulphuric acid.¹¹ The carbon monoxide contents of emissions were monitored with an MEXA-441 infrared on-line analyser while the gas was being collected. Known volumes of the collected gas were introduced into 1 litre of air being drawn at 300 ml/min through three pre-traps, containing 50% sodium hydroxide solution, ammoniacal cuprous chloride solution and dilute sulphuric acid (to remove the escaping ammonia) respectively, and finally through 35 ml of the sampling solution contained in a fritted glass bubbler. The analysis was completed by the recommended procedure. To test for possible interference by unknown gases present in automobile exhaust, the determinations were repeated with known amounts of carbon monoxide introduced along with the exhaust gas into the air stream. The results of these studies are shown in Table 6 which clearly demonstrates the suitability of the method for the analysis of automobile exhausts.

Though for field evaluation the proposed method should be compared with non-dispersive infrared spectroscopy as the reference method, the instrument available was not suited to monitor the levels of carbon monoxide in ambient air. Consequently, the suitability of the method was evaluated by the standard addition technique. Air in the vicinity of a traffic junction was collected in a 100-litre plastic container. A known volume of the collected air was drawn at 300 ml/min through a series of traps as described above and finally through 35 ml of sampling solution contained in a fritted glass bubbler, and analysed by the recommended procedure. The determination was repeated with known amounts of carbon monoxide introduced along with the air sample. The results are shown in Table 7, which clearly demonstrates the suitability of the method for the analysis of ambient air. The results obtained when fixed volumes of air, freed from interfering gases, were drawn through the sampling solution at a traffic junction are also furnished in Table 7.

Table 7. Recovery study and determination of carbon monoxide in ambient air

Volume of sample used, l.	Carbon monoxide, μl		Concentration of CO in air, $\mu\text{l/l}$.
	Added	Found	
10	—	45	4.5
10	100	150	—
10	200	240	—
20	—	95	4.8
20	100	190	—
20	200	305	—
18	—	150	8.4*
18	—	190	10.6†
18	—	90	5.0‡

*Early hours of the morning.

†10 a.m. (peak traffic period).

‡5 p.m. (sea-breeze had set in).

Conclusions

The observations made indicate that during the sampling step palladium(II) is reduced by carbon monoxide to elemental palladium. The colloidal palladium produced reacts with iodate in acid medium in the presence of chloride ions to form an ICl_n^- species which may be ICl_2^- or ICl_4^- . This ion forms with Pyronine-G an ion pair which is readily extracted into benzene for spectrophotometric measurement.

The method developed is useful for the determination of carbon monoxide at levels as low as $1 \mu\text{l/l}$. The calibration graph is linear over the range of 20–400 $\mu\text{l/l}$. of carbon monoxide in a

sample volume of 1 litre. The coefficient of variation is 7% at the 200 $\mu\text{l/l}$. level. The method is suitable for determination of carbon monoxide in motor vehicle exhaust gases and atmospheric air.

REFERENCES

1. M. B. Jacobs, *The Chemical Analysis of Air Pollutants*, pp. 233–244. Interscience, New York, 1960.
2. R. D. Polis, L. B. Berger and H. H. Schrenk, *U.S. Bur. Mines Rept. Invest.*, 1944, 3785.
3. J. L. Lambert and P. A. Hamlin, *Anal. Lett.*, 1971, **4**, 745.
4. J. L. Lambert and R. E. Wiens, *Anal. Chem.*, 1974, **46**, 929.
5. G. Ciuhandu, *Z. Anal. Chem.*, 1958, **161**, 345.
6. D. A. Levaggi and M. Feldstein, *Am. Ind. Hyg. Assoc. J.*, 1964, **25**, 64.
7. R. D. Bell, K. D. Reiszner and P. W. West, *Anal. Chim. Acta*, 1975, **77**, 245.
8. T. V. Ramakrishna and N. Balasubramanian, *Indian J. Chem.*, 1982, **21A**, 217.
9. N. Balasubramanian and T. V. Ramakrishna, *ibid.*, 1983, **22A**, 550.
10. F. J. Welcher (ed.), *Scott's Standard Methods of Chemical Analysis*, 6th Ed., Vol. 2, Part B, pp. 1514–1515. Van Nostrand, New York, 1963.
11. C. N. Sawyer and P. L. McCarty, *Chemistry for Environmental Engineering*, p. 510. McGraw-Hill, New York, 1978.
12. A. I. Vogel, *A Text Book of Quantitative Inorganic Analysis*, 2nd Ed., p. 803. Longmans, London, 1957.

DETERMINATION OF ARSENIC, CADMIUM, LEAD AND SELENIUM IN HIGHLY MINERALIZED WATERS BY GRAPHITE-FURNACE ATOMIC-ABSORPTION SPECTROMETRY

GABOR BOZSAI*

National Institute of Hygiene, H-1966 Budapest, Hungary

GERHARD SCHLEMMER and ZVONIMIR GROBENSKI

Bodenseewerk, Perkin-Elmer & Co. GmbH, D-7770 Überlingen, F.R.G.

(Received 20 July 1989. Revised 14 September 1989. Accepted 20 October 1989)

Summary—A graphite-furnace AAS method using the stabilized-temperature platform furnace (STPF) concept, mixed palladium and magnesium nitrates as chemical modifier and Zeeman background correction has been applied to the direct determination of As, Cd, Pb and Se in highly mineralized waters used for medicinal purposes. These contain 20–40 g/l. concentrations of salts, mainly sodium and magnesium chlorides, bicarbonates and sulphates. The use of a pre-atomization cool-down step to 20° in the graphite-furnace programme reduced the background absorption. Increasing the mass of magnesium nitrate modifier to 5 times that originally proposed improved the analyte peak shape. Under these conditions, no interference was found in analysis of the chloride/bicarbonate type of water, but the sodium and magnesium sulphate type of water had to be diluted, and even then an interference remained. Calibration with matrix-free standard solutions was used, but use of spike recovery is strongly recommended for testing the accuracy. The limits of determination (4.65σ) of the proposed method for undiluted samples are 2.0 $\mu\text{g/l.}$ for As, 0.05 $\mu\text{g/l.}$ for Cd, 1.0 $\mu\text{g/l.}$ for Pb and 1.5 $\mu\text{g/l.}$ for Se.

A direct, automated method without any matrix separation or preconcentration is desirable for the routine analysis of water for trace elements and of highly mineralized water samples. The method should be free from interferences over the concentration range of the concomitant species. For public health protection, the analytical method used should be able to measure 10% of the maximum allowable contaminant level in drinking water.¹ Graphite-furnace atomic-absorption spectrometry (GF-AAS) is one of the few analytical techniques which fulfils these requirements, and is the method most frequently used.

The maximum allowable contaminant levels of arsenic, cadmium, lead and selenium in drinking waters are 50, 5.0, 50 and 10 $\mu\text{g/l.}$ respectively,² so the corresponding required limits of determination for the analytical methods should be 5.0, 0.5, 5.0 and 1.0 $\mu\text{g/l.}$ respectively. It has been proposed³ in the water industry that the limit of determination be defined as 4.65 times the within-batch standard deviation of measure-

ments of the concentration at levels near the blank. Consequently, any proposed method should achieve these limits.

Two highly mineralized Hungarian waters (which we will call mineral waters in this paper) were selected for this study. "Salvus" mineral water contains sodium, bicarbonates and chlorides as the main components and is a natural stomach-pH buffer, whereas "Hunyadi" water contains sodium and magnesium sulphates, and can be taken as a laxative. The concentrations of the major constituents in these mineral waters are summarized in Table 1. The purpose of the present work was to establish methods for the determination of arsenic, cadmium, lead and selenium in these mineral waters by GF-AAS.

The stabilized-temperature platform furnace (STPF) concept introduced by Slavin⁴ has made possible some interference-free graphite-furnace analyses of complex matrices and when used with Zeeman background correction makes possible the direct determination of trace elements in sea-water.^{5,6} However, to the best of our knowledge, the STPF concept has not been

*Author for correspondence.

Table 1. Major constituents of mineral waters examined

Constituent	"Salvus", mg/ml	"Hunyadi", mg/ml
Sodium	5.90	5.20
Calcium	0.007	0.54
Magnesium	0.022	3.24
Chloride	2.40	0.79
Sulphate	0.068	27.0
Bicarbonate	13.4	1.01
Total solids	22.9	39.5

applied to the determination of trace elements in highly mineralized drinking waters.

We have applied the STPF concept (with Zeeman background correction), using either the manufacturer's earlier recommended conditions⁷ or those recently published by Welz *et al.*⁸ In the latter method, a mixed modifier consisting of palladium and magnesium nitrates was recommended for the determination of trace elements in water. This method⁸ was modified to meet the requirements of direct determination of trace elements in highly mineralized waters.

EXPERIMENTAL

Instrumentation

A Perkin-Elmer Zeeman/5000 atomic-absorption spectrometer was used for most of this work, with an HGA-500 graphite furnace and an AS-40 autosampler. The data were evaluated with a Perkin-Elmer Data System 10 using HGA-Graphics software modified by Perkin-Elmer, which allows the simultaneous display and printing of the analyte and background signals. The program has been improved to enable calculation of the background peak

height. The integrated absorbance was used for all calculations of analyte concentrations.

For part of the investigations, a Perkin-Elmer Zeeman/3030 atomic-absorption spectrometer, equipped with an HGA-600 graphite furnace and an AS-60 autosampler, was used. The instrumental conditions are given in Table 2. Tubes coated with pyrolytic graphite (Perkin-Elmer Part No. B010-9322) and solid pyrolytic graphite platforms Perkin-Elmer Part No. B010-9324) were used for all experiments. The sample volume was 20 μ l. A 10- μ l volume of modifier was pipetted on top of the sample.

Reagents

All reagents used were of the highest purity available and at least of analytical-reagent grade. Stock solutions (1000 mg/l.) were prepared from Merck Titrisol materials. All solutions, including diluted samples, were prepared with 0.3% v/v nitric acid (high-purity grade, Merck "Suprapur"). Palladium nitrate and magnesium nitrate chemical modifiers were prepared as previously reported.⁸ We represent the various chemical modifiers by the code shown below. The weight of Pd, Ni or salt quoted is the weight in the 10 μ l of modifier added; palladium and nickel nitrates were used to make the solutions.

200 μ g $\text{NH}_4\text{H}_2\text{PO}_4$ + 10 μ g $\text{Mg}(\text{NO}_3)_2$	$\text{PO}_4\text{Mg}10$
15 μ g Pd + 10 μ g $\text{Mg}(\text{NO}_3)_2$	PdMg10
15 μ g Pd + 50 μ g $\text{Mg}(\text{NO}_3)_2$	PdMg50
20 μ g Ni + 25 μ g $\text{Mg}(\text{NO}_3)_2$	NiMg25
20 μ g Ni	Ni

Table 2. Graphite-furnace temperature programme and instrumental parameters for the determination of As, Cd, Pb and Se in mineral water, with PdMg50 chemical modifier

Step	1	2	3	4	5	6	7
	Temperature, °C						
Temperature, °C	90	110	varied	20	varied	2650	20
Ramp time, sec	1	20	10	1	0	1	1
Hold time, sec	9	20	30	15	6	5	5
Read					ON		
Internal Ar flow, ml/min	300	300	300	300	0	300	300
Element	Temperature, °C		Wavelength, nm	Band-pass, nm	EDL power, W		
	Pyrolysis	Atomization					
Arsenic	1300	2300	193.7	0.7	6		
Cadmium	800	1650	228.8	0.7	5		
Lead	1100	2100	283.3	0.7	8		
Selenium	1000	2300	196.0	2.0*	6		

*0.7 on the Z/3030.

RESULTS AND DISCUSSION

Method improvement

The analyte and background absorbances of "Salvus" water, diluted 1 + 3 and spiked with 1.0 $\mu\text{g/l}$. Cd are shown in Fig. 1a. The conditions used were a pyrolysis temperature of 900°, an atomization temperature of 1600°, and $\text{PO}_4\text{Mg10}$ as chemical modifier.⁷ The large mass of sodium-containing matrix in the atomizer generated a high background absorbance of 2.3, which distorted the analyte absorbance, so these conditions were unsuitable for this type of sample.

Welz *et al.*⁸ recommended the use of the PdMg10 modifier for Cd, with a pyrolysis temperature of 800° and an atomization temperature of 1650°. Figure 1b shows the result obtained by using these conditions. The background absorbance is reduced to 1.5, and an undistorted signal is produced. As the pyrolysis temperature is 100° lower than that in the original conditions, it would appear that the $\text{PO}_4\text{Mg10}$ modifier, used in combination with a matrix containing large amounts of sodium salts, is responsible for the high background absorption. The matrix is less volatile in the presence of the phosphate modifier, as indicated by the greater delay before appearance of the background absorbance (compare Fig. 1a with Fig. 1b). This is in agreement with data

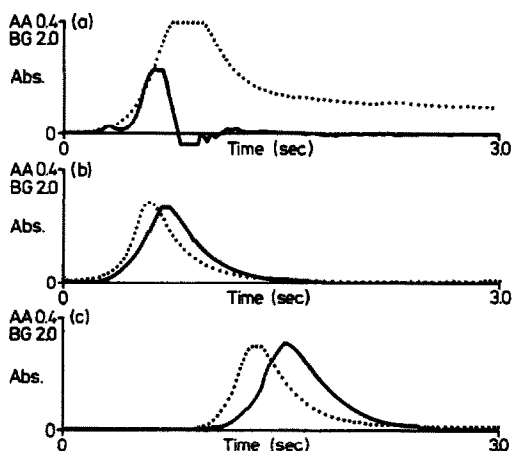


Fig. 1. Direct determination of cadmium in "Salvus" mineral water, diluted 1 + 3 and spiked with 1.0 $\mu\text{g/l}$. Cd. The dotted line is the background signal. (a) $\text{PO}_4\text{Mg10}$ chemical modifier, furnace program⁷ including 900° pyrolysis temperature and 1600° atomization temperature. (b) PdMg10 chemical modifier, furnace program⁸ including 800° pyrolysis temperature and 1650° atomization temperature; $m_0 = 0.73$ pg. (c) PdMg10 chemical modifier, furnace program⁸ with pre-atomization cool-down step, and the same temperatures as for (b); $m_0 = 0.61$ pg.

reported by Yin *et al.*⁹ for the determination of Cd in urine. In Fig. 1b, there is no evidence of spectral interference, although the characteristic mass (m_0) of 0.73 pg/0.004 absorbance .sec is significantly higher than the 0.45 pg/0.0044 absorbance .sec reported by Welz *et al.*⁸ This indicates that there are some residual, unidentified, matrix effects. A pre-atomization cool-down step, as recommended recently by Manning and Slavin¹⁰ and first proposed by Chakrabarti *et al.*,¹¹ was introduced; its effect is shown in Fig. 1c. The background and analyte signals are better separated and the analyte signal appears later. Under these conditions, the characteristic masses are consistent for the standards and spiked "Salvus" mineral water and the m_0 is 0.61 pg/0.0044 absorbance .sec.

The effect of the pre-atomization cool-down step is even more apparent for the determination of selenium in "Hunyadi" water, Fig. 2. Without it, there is a sharp rise in background absorption at the beginning of the atomization cycle (Fig. 2a). When the cool-down step is introduced, this initial background absorption disappears completely (Fig. 2b), but in both cases a pronounced background absorption occurs at the same time as the analyte signal. It is thought that the initial background peak is due to Rayleigh scattering by larger salt particles in the cooler regions at the tube ends. With the pre-atomization cool-down step, the tube is heated more uniformly and the effect of the cool tube ends can be avoided almost completely.¹² However, an interference due to the high-sulphate matrix is still present, indicated by the high characteristic mass of 43 pg/0.0044 absorbance .sec for selenium.

Applying the earlier recommended conditions⁷ for determination of lead in the two

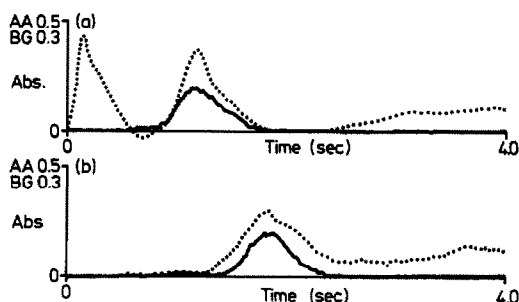


Fig. 2. Direct determination of selenium in "Hunyadi" mineral water diluted 1 + 3 and spiked with 100 $\mu\text{g/l}$. Se. PdMg10 chemical modifier, pyrolysis temperature 1100°, atomization temperature 2100°. The dotted line is the background signal. (a) Without cool-down step, $m_0 = 43$ pg; (b) with pre-atomization cool-down step, $m_0 = 43$ pg.

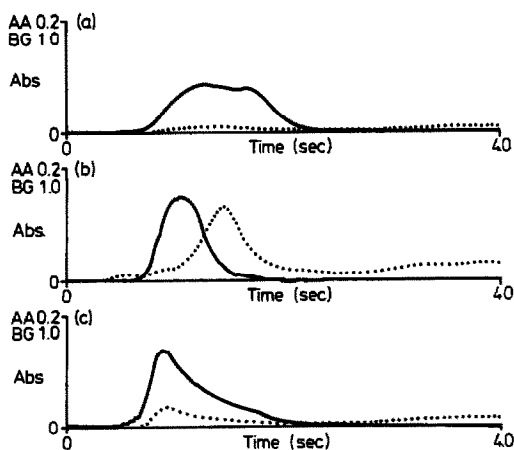


Fig. 3. Direct determination of lead in mineral water samples diluted 1 + 3 and spiked with 20 $\mu\text{g/l}$. Pb. The dotted line is the background signal. PdMg10 chemical modifier, furnace program⁸ including 1000° pyrolysis temperature, 2200° atomization temperature. (a) "Salvus", mass of Mg = 1.7 μg (including modifier), m_0 = 23 pg. (b) "Hunyadi", mass of Mg = 17.8 μg (including modifier), m_0 = 25 pg. (c) "Salvus", mass of Mg = 8.0 μg (including modifier), m_0 = 22 pg.

types of mineral water gave results similar to those for Cd. The method proposed by Welz *et al.*⁸ was also applied, and the results obtained by using 20 μl . of the 1 + 3 diluted samples spiked with 20 $\mu\text{g/l}$. lead, a pyrolysis temperature of 1000° and an atomization temperature of 2200° are shown in Fig. 3. It can be seen that the peak for "Salvus" water (Fig. 3a) is much broader than that for "Hunyadi" (Fig. 3b).

From the different mineral water compositions, it is clear that magnesium is one of the main matrix components in "Hunyadi" but is negligible in "Salvus". The total weight of magnesium in the "Hunyadi" + modifier load is 17.8 μg , but only 1.7 μg for the "Salvus" + modifier load. The amount of magnesium added as modifier to the "Salvus" sample was increased to improve the atomization conditions: a total of 8 μg of magnesium (from sample plus modifier) was found to be sufficient. Figure 3c shows that under these conditions, the peak "Salvus" is much narrower than before (Fig. 3a) and close in shape to that for "Hunyadi" (Fig. 3b). This effect may be explained as due to analyte occlusion within the stable MgO crystal, which decomposes explosively over a narrow temperature range.¹³

With a view to developing a general graphite-furnace program, a pre-atomization cool-down step was applied to the determination of lead. As in the case of cadmium, this increased the temporal separation of the background

and analyte signals. The characteristic mass obtained under the optimized conditions was 20 pg for lead in the matrix-free standard solution, and in "Salvus" water, but the Hunyadi matrix had increased the characteristic mass by approximately 17%.

Nickel has been recommended as a chemical modifier for arsenic determination, and selenium determination,⁷ but memory effects cause difficulty when nickel itself is also to be determined. The use of nickel in the determination of arsenic and selenium in the "Hunyadi" water resulted in poor recoveries. The matrix also produced very high background absorption at a pyrolysis temperature of 900°. The conditions used for Pb and Cd, based on the method of Welz *et al.*⁸ were used with the PdMg50 modifier and a pre-atomization cool-down step, for the determination of As and Se, and gave significantly higher recoveries.

Proposed method

The graphite-furnace programme for the proposed method is presented in Table 2. The pyrolysis and atomization curves for the elements investigated by the proposed method are shown in Figs. 4–7. The curves were established by use of matrix-free standard solutions and the 1 + 3 dilution of mineral waters spiked with 1.0 $\mu\text{g/l}$. Cd, 20 $\mu\text{g/l}$. Pb, 50 $\mu\text{g/l}$. Se and 20 $\mu\text{g/l}$. As. The change in the background absorption is also shown.

The pyrolysis temperature for Cd is critical and the reduction of the background absorption at higher pyrolysis temperatures has to be balanced carefully against the possibility of analyte losses (Fig. 4). There is no pronounced decrease of the background absorbance at the 228.8 nm Cd line when the pyrolysis temperature is varied between 800 and 850° for "Salvus", and 800° is recommended as optimal. This is in good agreement with the conditions proposed for the determination of Cd in complex biological matrices.⁹

From Fig. 5, it is clear that the specific Pb absorbance is not influenced by chloride (curve b) or sulphate (curve c) matrices when the pyrolysis temperature is in the range between 900 and 1300°. The latter temperature is the maximum that can be used for interferent-free standard solutions (curve a) and mineral waters (curves b and c) before loss of analyte occurs. Even at pyrolysis temperatures as low as 900°, the background absorbance is only moderate when palladium is used as chemical modifier. From Fig. 5, it can be seen that the atomization

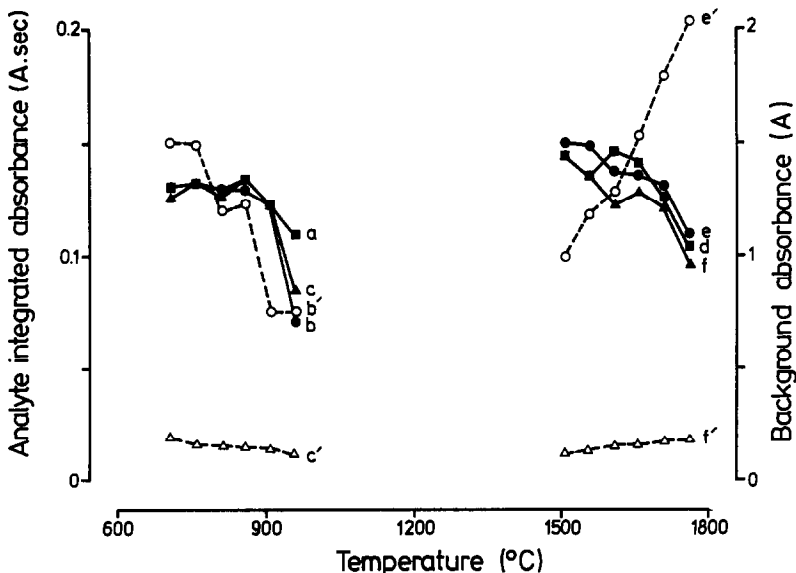


Fig. 4. Optimization of pyrolysis and atomization temperatures for determination of cadmium in mineral waters. PdMg50 chemical modifier, furnace program in Table 3. For the pyrolysis temperature study, an atomization temperature of 1650° was used and for the atomization study a pyrolysis temperature of 800° was used. The dotted line is the background absorption signal. (a) and (d), standard solution; (b) and (e), "Salvus", diluted 1 + 3; (c) and (f), "Hunyadi", diluted 1 + 3; (b') and (e'), "Salvus", diluted 1 + 3; (c') and (f'), "Hunyadi", diluted 1 + 3.

temperature has an influence on the background absorbance. An increase in the atomization temperature from 1900 to 2400° increases the background absorbance by a factor of 3 for the sulphate type mineral water "Hunyadi". A similar effect can be observed for Cd in the

range 1600–1800° in the chloride-bicarbonate type mineral water "Salvus". A pyrolysis temperature of 1100° and atomization temperature of 2100° were found to be optimum for lead, with respect to both analyte and background absorbances.

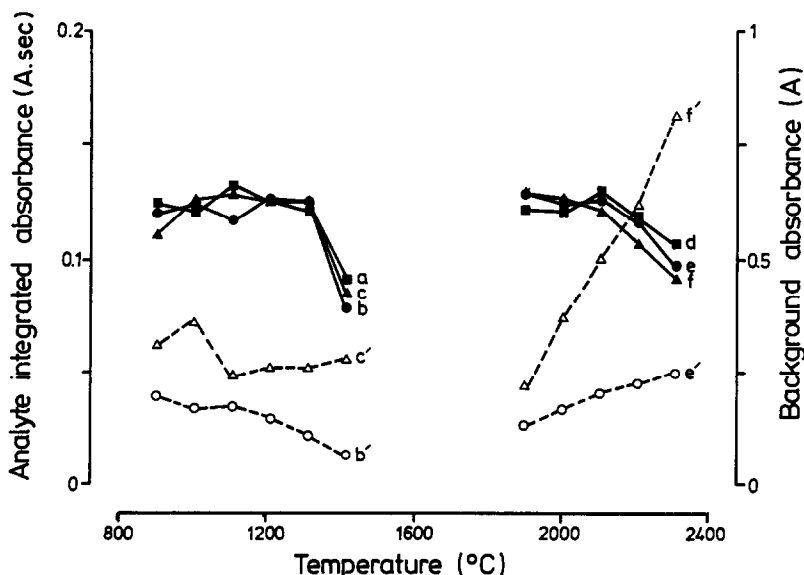


Fig. 5. Optimization of pyrolysis and atomization temperatures for determination of lead in mineral waters. PdMg50 chemical modifier, furnace program in Table 3. For the pyrolysis temperature study, an atomization temperature of 2100° was used, for the atomization study a pyrolysis temperature of 1100° was used. The dotted line is the background absorption signal. (a) and (d), standard solution; (b) and (e), "Salvus", diluted 1 + 3; (c) and (f), "Hunyadi", diluted 1 + 3; (b') and (e'), "Salvus", diluted 1 + 3; (c') and (f'), mineral water "Hunyadi", diluted 1 + 3.

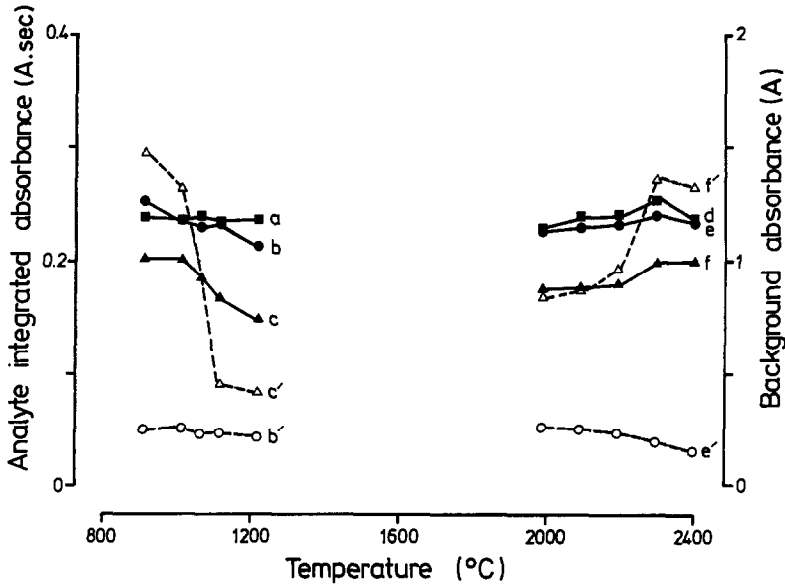


Fig. 6. Optimization of pyrolysis and atomization temperatures for determination of selenium in mineral waters, PdMg50 chemical modifier, furnace program in Table 3. For the pyrolysis temperature study, an atomization temperature of 2300° was used, for the atomization study a pyrolysis temperature of 1000° was used. The dotted line is the background absorption signal. (a) and (d), standard solutions; (b) and (e), "Salvus", diluted 1 + 3; (c) and (f), "Hunyadi", diluted 1 + 3; (b') and (e'), "Salvus", diluted 1 + 3; (c') and (f'), "Hunyadi", diluted 1 + 3.

In contrast to the lead and cadmium pyrolysis curves, for selenium the matrix influences the pyrolysis temperature at which loss of analyte sets in, particularly in the case of the sulphate type mineral water (Fig. 6c). This matrix causes very high background absorption at the 196.0

nm Se line. Even at a pyrolysis temperature as high as 1100°, the background absorbance is still about 1.0, and loss of analyte starts at this temperature. The recommended conditions (pyrolysis at 1000°, atomization at 2300°) for the determination of Se in "Hunyadi" mineral

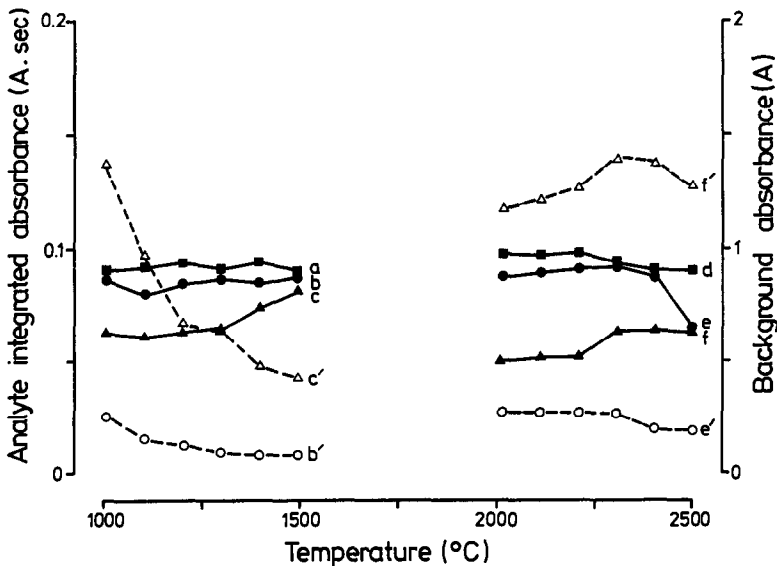


Fig. 7. Optimization of the pyrolysis and atomization temperatures for determination of arsenic in mineral waters, PdMg50 chemical modifier, furnace program in Table 3. For the pyrolysis temperature study, an atomization temperature of 2300° was used, for the atomization study a pyrolysis temperature of 1300° was used. The dotted line is the background absorption signal. (a) and (d), standard solution; (b) and (e), "Salvus", diluted 1 + 3; (c) and (f), "Hunyadi", diluted 1 + 3; (b') and (e'), "Salvus", diluted 1 + 3; (c') and (f'), "Hunyadi", diluted 1 + 3.

Table 3. Comparison of modifiers, pyrolysis and atomization temperatures, recovery and background signal (peak height) obtained from spiked mineral waters by several STPF methods

Element	Sample	Dilution	Method A ⁷		Method B ⁸		Proposed method	
			Recovery, %	Backgrd.	Recovery, %	Backgrd.	Recovery, %	Backgrd.
Cd	Salvus	1 + 1	—*	3.0	—*	3.4	101	1.6
		1 + 2	—	2.8	—	2.3	99	0.8
		1 + 3	—	2.3	101	1.6	102	0.6
	Hunyadi	1 + 1	80	1.4	52	0.4	73	0.3
		1 + 2	88	1.4	60	0.2	81	0.1
		1 + 3	90	1.3	64	0.2	90	0.1
	Modifier		PO ₄ Mg10		PdMg10		PdMg50	
	Pyrolysis/atomization temperature, °C		900/1600		800/1650		800/20†/1650	
Pb	Salvus	1 + 1	—	2.1	91	0.1	98	0.2
		1 + 2	60	1.6	91	0.1	97	0.2
		1 + 3	64	1.5	97	0.1	99	0.2
	Hunyadi	1 + 1	75	1.3	62	0.8	73	0.3
		1 + 2	77	1.3	62	0.8	80	0.5
		1 + 3	80	1.1	69	0.6	83	0.5
	Modifier		PO ₄ Mg10		PdMg10		PdMg50	
	Pyrolysis/atomization temperature, °C		900/1800		1000/2200		1100/20†/2100	
Se	Salvus	1 + 1	89	0.8	99	0.2	99	0.2
		1 + 2	90	0.7	101	0.2	99	0.2
		1 + 3	92	0.7	100	0.2	100	0.2
	Hunyadi	1 + 1	—	2.3	—	2.3	—	2.8
		1 + 2	25	2.0	—	2.1	—	2.1
		1 + 3	25	1.5	69	1.5	83	1.4
	Modifier		NiMg25		PdMg10		PdMg50	
	Pyrolysis/atomization temperature, °C		900/2100		1000/2200		1000/20†/230	
As	Salvus	1 + 1	93	0.1	93	0.4	96	0.1
		1 + 2	95	0.1	97	0.4	98	0.1
		1 + 3	94	0.1	100	0.4	95	0.1
	Hunyadi	1 + 1	21	1.0	—	2.5	68	0.9
		1 + 2	32	0.7	—	2.2	81	0.7
		1 + 3	50	0.6	75	1.8	86	0.6

*—signifies value not calculated, because of high background absorbance.

†Cool-down step.

water can therefore only be a compromise with respect to the analyte and background absorbances.

From Fig. 7, it can be seen that a pyrolysis temperature of 1300° can be used for As, which makes it relatively simple to remove the bulk of the matrix prior to atomization. The recommended atomization temperature is 2300°.

The proposed method was used for the determination of Cd, Pb, Se and As in 1 + 1, 1 + 2 and 1 + 3 diluted mineral water samples spiked with 1.0 µg/l. Cd, 20 µg/l. Pb, 50 µg/l. Se and 20 µg/l. As, respectively. The recovery for a spiked sample was calculated with respect to the absorbance of the matrix-free standard solution. The background absorption was also measured. The results are summarized in Table 3. The recoveries were also calculated by

a method recommended earlier⁷ and one proposed by Welz *et al.*⁸ The results presented are the averages of 5 replicate determinations.

The results in Table 3 show that the conditions recommended here are the most suitable for direct determination of Cd, Pb, Se and As in mineral waters. The recoveries for the "Salvus" samples are >90% for all four elements investigated and the background signals are within the capabilities of the background correction system. There are still some matrix interferences in the case of the "Hunyadi" water, however, the recoveries being lower, and only 83–90% even in the 1 + 3 diluted samples.

The characteristic masses found in this work (As 16 pg, Cd 0.42 pg, Pb 20 pg, Se 23 pg) with PdMg modifier agree with the data published for GF-AAS.¹⁴ The limits of determination

Table 4. Limits of determination (LD) for As, Cd, Pb and Se in water (sample volume 20 μ l, 10 replicates)

Element	Measured LD, μ g/l.			Required LD, μ g/l.
	Undiluted sample	Sample diluted 1 + 1	Sample diluted 1 + 3	
Arsenic	2.0	4.0	8.0	5.0
Cadmium	0.05	0.1	0.2	0.5
Lead	1.0	2.0	4.0	5.0
Selenium	1.5	3.0	6.0	1.0

(taken as 4.65 times the concentration equivalent to the standard deviation of the blank) found for the proposed method are presented in Table 4 and compared with the required limits discussed earlier. The values for undiluted samples in general meet these requirements, except for selenium. The dilution factor must be taken into consideration in calculating the detection limits for the water samples that require dilution.

The mineral waters were analysed for As, Cd, Pb and Se in 1 + 1 dilutions for "Salvus" and 1 + 3 dilutions for "Hunyadi". All the results were below the limits of determination except for As in the "Salvus" sample, which was 16 μ g/l.

CONCLUSIONS

Two significant analytical problems have to be overcome for the direct determination of trace elements in highly mineralized waters by GF-AAS. The limit of determination of the method should meet the requirements given for drinking water quality (0.1–10 μ g/l.), and the interference caused by the high concentration of concomitants, *i.e.*, sodium, magnesium, chlorides and sulphates must be dealt with.

The use of the STPF concept in conjunction with Zeeman background correction has proved useful for this analysis, but the choice of chemical modifier is very important. The addition of $\text{NH}_4\text{H}_2\text{PO}_4$ together with the high mass of sodium-containing matrix generates an extremely high background absorption, which causes interference. Use of nickel as a modifier results in serious contamination of the graphite furnace and significant interferences are observed in the presence of large amounts of sulphate-containing matrices. A mixed palladium nitrate and magnesium nitrate chemical modifier has been found to be the most useful. However, with matrices containing a high level of sulphates, some interferences were

still present, depressing the analyte signal by approximately 17%. The mechanisms and control of these interference effects are under investigation. Presumably use of standard-addition methods instead of matrix-free calibration would improve the performance, but at the cost of inconvenience.

The background absorption was successfully reduced by introducing a pre-atomization cool-down step into the graphite furnace programme. Increasing the amount of magnesium nitrate in the chemical modifier helped to improve the analyte peak shape. Calibration with standard solutions can be used, but optimization of the dilution factor by testing recovery of spikes is strongly recommended.

Except for selenium, the limits of determination obtained are within the required range, provided the dilution of the samples is not greater than 1 + 3.

Acknowledgements—The authors would like to thank Walter Slavin and Glen Carnrick for helpful discussions and Ian Shuttler for constructive comments and assistance with the English.

REFERENCES

1. M. Csanády, *Hidrol. Közl.*, 1978, **58**, 193.
2. Hungarian National Standard, *Drinking Water, Physical and Chemical Quality Criteria*, MSz 450/1–78.
3. R. V. Cheeseman and A. L. Wilson, *Manual on Analytical Quality Control for the Water Industry*, Report No. TR66, Water Research Centre, Medmenham 1978.
4. W. Slavin, D. C. Manning and G. R. Carnrick, *At. Spectrosc.*, 1981, **2**, 137.
5. E. Pruszkowska, G. R. Carnrick and W. Slavin, *Anal. Chem.*, 1983, **55**, 182.
6. Z. Grobowski, R. Lehmann, B. Radziuk and U. Voellkopf, *At. Spectrosc.*, 1984, **5**, 87.
7. *Techniques in Graphite Furnace Atomic Absorption Spectrometry*, Perkin-Elmer, Ridgefield, 1985, Part No. 0993-8150.
8. B. Welz, G. Schlemmer and J. R. Mudakavi, *J. Anal. At. Spectrom.*, 1988, **3**, 695.
9. X. Yin, G. Schlemmer and B. Welz, *Anal. Chem.*, 1987, **59**, 1462.

10. D. C. Manning and W. Slavin, *Spectrochim. Acta*, 1985, **40B**, 461.
11. C. L. Chakrabarti, S. Wu and P. C. Bertels, *ibid.*, 1983, **38B**, 1041.
12. H. Falk, A. Glismann, L. Bergann, G. Minkwitz, M. Schubert and J. Skole, *ibid.*, 1985, **40B**, 533.
13. W. Slavin, personal communication.
14. W. Slavin and G. R. Carnrick, *CRC Crit. Rev. Anal. Chem.*, 1988, **19**, 95.

HOT-INJECTION PROCEDURES FOR THE RAPID ANALYSIS OF BIOLOGICAL SAMPLES BY ELECTROTHERMAL ATOMIC-ABSORPTION SPECTROMETRY

UTTAM K. KUNWAR and DAVID LITTLEJOHN*

Department of Pure & Applied Chemistry, University of Strathclyde, Cathedral Street, Glasgow G1 1XL, U.K.

DAVID J. HALLS

Trace Element Unit, Institute of Biochemistry, Royal Infirmary, Glasgow G4 0SF, U.K.

(Received 23 August 1989. Revised 17 November 1989. Accepted 10 December 1989)

Summary—The combination of palladium/hydrogen matrix-modification and injection of samples into a graphite tube at 120° has allowed the accurate determination of copper, iron, lead and nickel in biological reference materials (urine, milk powder and bovine liver). Palladium modification allowed the use of a standard ashing temperature of 1000° for all four elements. Direct aqueous calibration was applied without the need for standard additions. The total heating cycle, from the start of sample injection, took 45 sec.

Electrothermal atomic-absorption spectrometry (ETAAS) is a well established technique for trace element determinations, but has a number of basic limitations such as (1) matrix interference effects, (2) the need for a range of char temperatures for different elements and (3) a slow rate of sample throughput compared with flame AAS or inductively coupled plasma optical emission spectrometry. Various procedures have been proposed to alleviate matrix interferences in ETAAS and one of the most attractive is matrix modification. Although many different modifiers have been suggested, palladium has shown most promise as a general modifier.¹⁻³ In common with other reagents, addition of palladium(II) to the sample and standard solutions allows the use of higher char temperatures without loss of the more volatile analyte elements. It is therefore possible to remove a greater fraction of the interfering matrix prior to the atomization step. It is thought that thermal stabilization of analyte metals by palladium occurs through formation of intermetallic bonds.^{4,5} This requires the palladium to be in the elemental state early enough in the heating cycle to ensure reaction with the analyte before the tube reaches a temperature at which vaporization would normally occur. To aid reduction of the palladium(II) it has been suggested that

hydrogen should be added to the argon or nitrogen furnace gas.^{6,7} One of the attractive features of modification with palladium is that a char temperature close to 1000° can be used for several elements without analyte loss. At this temperature, many chlorides known to cause matrix interferences begin to vaporize and are flushed from the furnace by the inert gas flow. This suggests that if palladium matrix-modification is used, a standard char temperature could be selected for a number of elements.

The application of shortened atomizer heating programmes has been discussed in a number of recent publications. Omission of the char step has been possible in some biological analyses⁸⁻¹¹ and reductions in the drying time have been achieved by rapid heating of the tube after sample injection.⁸ The facility to inject liquids onto a hot graphite tube is now available with most modern electrothermal atomizers and the advantages of this feature have been illustrated in clinical and water analyses. Apostoli *et al.*¹² heated the electrothermal atomizer tube to 150° before injection of 4-methylpentan-2-one (isobutyl methyl ketone, IBMK) in a solvent extraction procedure for the determination of vanadium in urine. Improvements in precision and a tenfold increase in sensitivity were reported. Hot-injection allowed Knowles¹³ to develop furnace programmes of less than 20 sec for the determination of chromium, copper and

*Author for correspondence.

nickel in water, of chromium and cadmium in urine, and of copper in serum. The accuracy of the procedure was established by analysis of reference materials. The standard-additions technique was required for the analysis of urine and serum. We have recently reported the application of hot-injection for the rapid analysis of water samples by electrothermal AAS.¹⁴ Injection of the water samples onto a graphite tube preheated to 120° and omission of an ashing stage enabled heating programmes of 10 sec (excluding injection time) to be applied for the determination of aluminium, copper and lead. Interferences encountered in the determination of aluminium were removed by addition of palladium as a matrix modifier.

In this study, palladium/hydrogen modification and a hot-injection procedure were combined to develop rapid methods for the determination of copper, iron, lead and nickel in urine, milk powder and bovine liver reference materials. By reference to the literature and from previous experience, a standard char temperature of 1000° was selected and 2 µg of palladium was added as the modifier (10 µl of 200 µg/ml palladium solution). Accurate determination of the analyte elements in the reference materials was achieved by using the standard furnace programme, peak-area measurement and calibration with aqueous solutions.

EXPERIMENTAL

Instrumentation

A Varian SpectrAA-40 atomic absorption spectrometer was used with a GTA-96 graphite furnace and programmable sample dispenser. The system was operated in conjunction with a DS-15 data station and results were printed on an Epson LX-86 printer. The manufacturer's spectrometer parameters were selected for each of the analyte elements. The wavelengths used

for copper, iron, lead and nickel were 324.8, 248.3, 283.3 and 232.0 nm, respectively. The atomizer programme was compiled on the basis of literature information and previous experience, and the results obtained with it served to test the validity of using this previously derived information to design a standard atomization programme for the elements to be determined. Injection at 2 µl/sec (injection rate 3) onto a tube heated to 120° was found to be suitable for each of the samples analysed. Heating the palladium(II) at 300° for 8 sec in the presence of hydrogen was sufficient to convert the modifier into the elemental form. Thereafter, a char temperature of 1000° was selected for all four elements, on the basis that for many analytes thermal stability at this temperature can be achieved with palladium as modifier. In this work, undiluted hydrogen was used during the conditioning step and for the initial char step of the programme given in Table 1. Prior to atomization, the tube was purged with nitrogen (flow-rate 3 l./min) for 5 sec to remove hydrogen from the atomizer. No problems were encountered with this procedure. An atomization temperature of 2300 or 2400° was adopted, without specific optimization. The complete programme details for iron, lead and nickel are given in Table 1. When this programme was applied to the determination of copper, recoveries of approximately 80% were obtained for each of the samples analysed. By replacing the hydrogen flow at stage 2 and the nitrogen purge at stages 3 and 6 with a 3.0-l./min argon flow, recoveries closer to 100% were obtained, as discussed later. The modified programme for copper is given in Table 2. Argon can also be used during measurement of the other elements, and is preferred for general use.

The procedure involved simultaneous injection of 10 µl of the sample or standard solution and 10 µl of the modifier solution. A palladium

Table 1. Atomizer programme for Varian GTA 96 used in analysis of biological standards by hot-injection with Pd modifier

Stage	Temperature, °C	Ramp time, sec	Hold time, sec	Gas flow
1	300	2	6	1.5 l./min H ₂
2	1000	5	10	1.5 l./min H ₂
3	1000	0	5	3.0 l./min N ₂
4	1000	0	2	Gas stop
5	2300 (Pb) 2400 (Fe, Ni)	0	2	Gas stop
6	2600	1	2	3.0 l./min N ₂

Injection volume 10 µl sample + 10 µl modifier (200 µg/ml Pd). Tube temperature 120°. Injection rate 2 µl/sec.

Table 2. Atomizer programme for Varian GTA 96 used in analysis of biological standards for copper by hot-injection with Pd modifier

Stage	Temperature, °C	Ramp time, sec	Hold time, sec	Gas flow
1	300	2	6	1.5 l./min H ₂
2	1000	5	10	3.0 l./min Ar
3	1000	0	5	3.0 l./min Ar
4	1000	0	2	Gas stop
5	2400	0	2	Gas stop
6	2600	1	2	3.0 l./min Ar

Injection volume 10 μ l sample + 10 μ l modifier (200 μ g/ml Pd). Tube temperature 120°. Injection rate 2 μ l/sec.

concentration of 200 μ g/ml was selected, without investigation of the effect of varying it. Although a previous study showed successful use of lower palladium concentrations,¹⁴ it was considered that addition of 2 μ g of palladium would ensure retention of the four elements under study, at temperatures up to at least 1000°.

Reagents

At least four standard solutions were prepared for each analysis, by dilution of 1000 μ g/ml "atomic absorption" stock solutions of copper, iron, lead and nickel (BDH, Poole, U.K.). The palladium modifier (200 μ g/ml) was prepared by dilution of a 1000 μ g/ml palladium solution made with palladium chloride ("Spectrosol" grade, BDH). Distilled water was used for all dilutions. Acids used in the digestion of the bovine liver SRM were of "Aristar" or "AnalaR" grade (BDH).

Preparation of reference materials

The artificial urine reference materials analysed in the study were Lanonorm-metalle 1, 2 and 3 (Behring Institute, Behringwerke AG, Marburg, F.R.G.). They were supplied in freeze-dried form and were reconstituted by dilution with 50 ml of 1% v/v nitric acid. Prior to analysis, the Lanonorm solutions were diluted with distilled water as follows: for copper, Lanonorm 1 undiluted; for lead, Lanonorm 1 undiluted, Lanonorm 2 and 3 diluted 2- and 10-fold, respectively; for nickel, Lanonorm 2 undiluted, Lanonorm 3 diluted 3-fold.

Milk powder reference materials BCR RM 150 and 151 were supplied by the European Community Bureau of Reference. The bovine liver reference material SRM 1577a was supplied by the U.S. National Bureau of Standards. About 1 g of material, accurately weighed, was transferred to a 150-ml tall-form beaker and 20 ml of 50% v/v nitric acid were added. The

beaker was heated gently to minimize frothing and heating was continued until the volume was reduced to about 5 ml. To this solution, 10 ml of a perchloric acid/nitric acid mixture (50 ml of 60% perchloric acid and 250 ml of concentrated nitric acid, both "Aristar" grade) were added. The solution was heated gently until perchloric acid fumes were evolved, then a watch-glass was placed on the beaker and heating was continued until the solution was colourless. After cooling, the solution was diluted to about 30 ml with distilled water, then heated to boiling for 5 min to dissolve all salts. The solution was filtered through a Whatman No. 40 filter paper into a 100-ml standard flask, and the filtrate and washings were diluted to the mark with distilled water. Prior to analysis, the solutions were diluted with distilled water as follows: for copper, BCR RM 150 undiluted, SRM 1577a diluted 100-fold; for iron, BCR RM 150 and 151 diluted 5- and 10-fold, respectively, SRM 1577a, diluted 50-fold; for lead, BCR RM 150 and 151 undiluted. In all analyses, aqueous standard solutions were used for calibration. It was assumed that accurate analysis had been achieved if the analyte concentration found agreed with the certified or recommended value within $\pm 10\%$.

RESULTS AND DISCUSSION

Copper

When the programme given in Table 1 was applied to the determination of copper in the biological reference materials, a recovery of only 80% was achieved. By removal of the hydrogen in stage 2 and use of argon instead of nitrogen (see Table 2) more accurate results were obtained, as given in Table 3. The results of at least five repeat analyses indicated that the precision was better than 3% for the three different materials analysed. Spectral interference of palladium at the 324.8 nm copper line

Table 3. Determination of copper in biological standards at 324.8 nm

Sample	Units	Confidence range	Certified value	Value found*	Recovery, %
Lanonorm 1	$\mu\text{g/l.}$	17.5–24.1	20.8	19.0 ± 0.4	91 ± 2
Milk BCR RM 150	$\mu\text{g/g}$		2.23 ± 0.08	2.1 ± 0.02	94 ± 1
Bovine Liver SRM 1577a	$\mu\text{g/g}$		158 ± 7	169 ± 1	106 ± 1

*Mean \pm standard deviation ($n = 3$, range method).

Table 4. Determination of iron in biological standards at 248.3 nm

Sample	Certified value, $\mu\text{g/g}$	Value found*	Recovery, %
Milk BCR RM 150	11.8 ± 0.6	11.1 ± 0.2	94 ± 2
Milk BCR RM 151	50.1	46.4 ± 0.8	93 ± 2
Bovine Liver SRM 1577A	194 ± 20	177 ± 8	91 ± 4

*Mean \pm standard deviation ($n = 3$, range method).

Table 5. Determination of lead in biological standards at 283.3 nm

Sample	Units	Confidence range	Certified value	Found*	Recovery, %
Lanonorm 1	$\mu\text{g/l.}$	8.5–11.5	10	12.4 ± 0.5	124 ± 5
Lanonorm 2	$\mu\text{g/l.}$	114–138	126	124 ± 4	98 ± 3
Lanonorm 3	$\mu\text{g/l.}$	470–626	548	618 ± 5	113 ± 1
Milk BCR RM 150	$\mu\text{g/g}$		1.00 ± 0.04	1.13 ± 0.06	113 ± 6
Milk BCR RM 151	$\mu\text{g/g}$		2.00 ± 0.03	2.14 ± 0.11	107 ± 6

*Mean \pm standard deviation ($n = 3$, range method).

has been reported by other workers,³ but no problems were encountered in this study.

Iron

The milk powder and bovine liver reference materials were analysed for iron (Table 4). Recovery was in the range 91–94%, and precisions of 2 and 4.5% were obtained for the milk powder and bovine liver, respectively.

Lead

The atomizer programme given in Table 1 was used to determine lead in the three Lanonorm synthetic urine samples and two milk powder reference materials. The results are given in Table 5. Recovery ranged from 98 to 124%. Although the results appear to have a high positive bias, particularly for Lanonorm 1, they are considered reasonable in comparison to those obtained by other procedures used for the direct determination of lead in biological materials, such as ETAAS with probe atomization.¹⁵ The precisions for the lead concentrations found were between 1 and 6%. No significant difference was observed between the shapes of the AAS peaks for the aqueous standards and the Lanonorm samples, suggesting that the components of the urine matrix which remained after the char step did not have a significant influence on lead atomization. A

similar observation was made when analysing the other reference materials.

Nickel

Close to 100% recovery was achieved for the determination of nickel in two of the synthetic urine standards, Lanonorm 2 and 3. The results given in Table 6 shows that precisions of 9 and 1% were obtained for nickel concentrations of 32 and 72 $\mu\text{g/l.}$ respectively.

CONCLUSIONS

It has been shown that it is possible to apply almost the same atomizer programme for the determination of copper, iron, lead and nickel in biological reference materials, without detailed optimization, on the basis of published information and previous experience. The use of matrix modification with palladium and hydrogen allowed the use of a "standard" char temperature of 1000°, after conditioning of the palladium in a hydrogen atmosphere at 300°.

Table 6. Determination of nickel in synthetic urines at 232.0 nm

Sample	Certified value, $\mu\text{g/l.}$	Found,* $\mu\text{g/l.}$	Recovery, %
Lanonorm 2	31.0	32 ± 3	103
Lanonorm 3	71.0	72 ± 1	101

*Mean \pm standard deviation ($n = 3$, range method).

Injection of the standards and samples into a tube at 120° at a rate of 2 μ l/sec provided almost instantaneous drying, which resulted in a comparatively short programme cycle. From the start of sample injection to the end of the cleaning stage, the programme time was 45 sec. This does not include the time required for the autosampler to take up the next volume of sample and modifier, or for cooling of the atomizer tube. Both these operations are out-with the control of the operator, but presumably could be shortened to match the rest of the hot-injection procedure.

The combination of palladium/hydrogen matrix modification and hot-injection has allowed accurate determination of copper in urine, milk powder and bovine liver reference materials, iron in the milk powder and bovine liver, lead in the urine and milk powder, and nickel in the urine reference material, by a method based on calibration with aqueous solutions and peak-area measurement. The relative standard deviations of the results obtained by the proposed method are acceptable for the concentrations determined and there is no indication that the hot-injection procedure has an adverse effect on precision.

The study has demonstrated that it should be possible to achieve rapid, precise and accurate analysis of biological materials by electrothermal AAS with an almost standard furnace programme and aqueous standards, provided

developments in graphite furnace methodology are fully exploited.

Acknowledgements—The authors gratefully acknowledge the loan of the SpectrAA-40 and GTA-96 instrument system by Varian AG, Switzerland, and thank Dr. D. Lowe, Varian Associates, U.K., for his interest in the project. UKK is grateful to the British Council for the award of a study scholarship.

REFERENCES

1. Xiao-quan Shan, Zhe-ming Ni and Li Zhang, *Anal. Chim. Acta*, 1983, **151**, 179.
2. G. Schlemmer and B. Welz, *Spectrochim. Acta*, 1986, **41B**, 1157.
3. B. Welz, G. Schlemmer and J. R. Mudakavi, *J. Anal. At. Spectrom.*, 1987, **2**, 45.
4. Xiao-quan Shan and Dian-xun Wang, *Anal. Chim. Acta*, 1985, **173**, 315.
5. W. Wendl and G. Müller-Vogt, *J. Anal. At. Spectrom.*, 1988, **3**, 63.
6. L. M. Voth-Beach and D. E. Shrader, *ibid.*, 1987, **2**, 45.
7. L. M. Voth-Beach, *Spectroscopy*, 1987, **2**, No. 12, 21.
8. D. J. Halls, *Analyst*, 1984, **109**, 1081.
9. D. J. Halls, C. Mohl and M. Stoepler, *ibid.*, 1987, **112**, 185.
10. D. J. Halls and G. S. Fell, *J. Anal. At. Spectrom.*, 1988, **3**, 105.
11. D. J. Halls, *Anal. Proc.*, 1988, **25**, 232.
12. P. Apostoli, L. Alessio, M. D. Farra and P. L. Fabbri, *J. Anal. At. Spectrom.*, 1988, **3**, 471.
13. M. B. Knowles, *ibid.*, 1989, **4**, 257.
14. U. K. Kunwar, D. Littlejohn and D. J. Halls, *ibid.*, 1989, **4**, 153.
15. O. O. Ajayi and D. Littlejohn, *ibid.*, submitted for publication.

FLUORESCENCE WAVELENGTH, INTENSITY AND LIFETIME FOR MULTIDIMENSIONAL TRANSDUCTION OF SELECTIVE INTERACTIONS OF ACETYLCHOLINE RECEPTOR BY LIPID MEMBRANES

U. J. KRULL, R. S. BROWN, B. D. HOUGHAM, G. MCGIBBON and E. T. VANDENBERG

Chemical Sensors Group, Department of Chemistry, Erindale Campus, University of Toronto,
3359 Mississauga Road North, Mississauga, Ontario, Canada L5L 1C6

(Received 12 May 1989. Revised 19 October 1989. Accepted 25 November 1989)

Summary—Concurrent analysis of the fluorescence intensity, at different emission wavelengths, of lipid vesicles containing acetylcholine receptor (AChR) labelled with a nitrobenzoxadiazole (NBD) moiety shows that selective interactions with the agonist carbamylcholine can be detected reproducibly by a self-calibration method with μM detection limits. Concurrent analysis of the fluorescence intensity and lifetime of the new probe 4-dicyanomethylene-1,2,3,4-tetrahydromethylquinoline (DCQ) shows that general alterations of lipid membrane structure induced by temperature variation in the head-group region of lipid vesicles can be determined. A general approach to detection of selective interactions is introduced by observation of fluorescence intensity and lifetime changes of the probe NBD-phosphatidyl ethanolamine dispersed in lipid membranes containing unlabelled AChR. Detection and differentiation of selective interactions between carbamylcholine and the antagonist α -bungarotoxin are possible by correlation with intensity and lifetime at different emission wavelengths.

Molecular receptor systems are desirable in a biosensing strategy as they exhibit high sensitivity and selectivity, and the formation of receptor-ligand complexes is reversible. Generally, molecular receptors are proteins (found embedded in the cell membrane of many cell types) which detect the presence of certain target molecules, or agonists, in the external environment and mediate some cellular response to the presence of the agonists.¹ Biosensing is possible when the agonist-receptor complexation can be transduced to a measurable signal, as is the case for electrochemical studies of molecular receptors in artificial bilayer lipid membranes.

Natural chemoreception, for processes such as neural communication, operates by using molecular receptors which transduce chemical signals into fast electrochemical events. The rapid response and extreme sensitivity of the gated electrochemical ion translocation provides useful analytical characteristics. However, for *in vitro* use this system is limited by background noise and the inability to distinguish between different agonists. Non-selective binding events and spontaneous ion current transients occurring *in vivo* are filtered and discarded by processing signals from multiple receptor arrays with respect to frequency and amplitude,

in a manner analogous to the combination of hardware and software analysis in chemometric approaches.^{2,3} This technology is in the forefront of research in the area of sensor development, and its state of development sets limits to the analytical potential of biosensors based on electrochemical ion translocation across lipid membranes. However, a chemometric approach is possible when a biosensor is used in the fluorescence mode of transduction, which offers the opportunity for multidimensional analysis based on concurrent observations of intensity, wavelength, polarization and lifetime, as reported by Bright,⁴ Heiftje⁵ and Wolfbeis.⁶ Combination of the information gained from each of these properties can provide sufficient data for identification of selective binding processes and quantitative evaluation of non-selective interferences.⁷

The eventual goal of this research is the adaptation of a molecular receptor fluoroassay for incorporation into a reliable and self-calibrating optode which operates with a chemometric approach. The first step is to establish selective chemistry which can provide multidimensional fluorescence data. Selective interactions resulting in ion gating are common for neurotransmitter receptors, and apparently

involve the opening of conductive "pores" or "channels" in the interior of large protein assemblies when binding of the agonist occurs.¹ Little perturbation of the lipid environment is expected during gating events since large-scale conformational changes of proteins have not been observed in association with "channel" opening, especially in the absence of an electrochemical gradient across the membrane. However, molecular receptors can have specific physical associations with lipids, and may be involved in aggregative events that are related to selective binding of ligands.⁸ This may provide significant perturbation of the lipid membrane and could provide a general transduction mechanism which could be monitored by means of fluorescence from probes located within lipid membranes that support the receptor.

Fluorescence spectroscopy provides high sensitivity, requires only small amounts of fluorescent probe ($\sim 10^{-6}M$) and causes negligible perturbation of lipid membrane environments at mole ratios of $\leq 1:100$. The main objective of using a fluorescent probe in lipid membranes is to garner information about the polarity, microviscosity and phase behaviour of the lipid environment. To study both the steady-state and dynamic physical properties of bilayer lipid membranes 4-dicyanomethylene-1,2,3,4-tetrahydromethylquinoline (DCQ) was prepared (Fig. 1) and used as a probe to determine the polarity, fluidity and phase behavior of artificial membranes, hence indicating how structural changes induced by selective binding events may be transduced.⁹

Acetylcholine receptor (AChR) is the best characterized neurotransmitter receptor with respect to both structure and function. The protein is a dimer in a natural environment, each monomer consisting of five discrete protein subunits which together are arranged to form a cylinder capable of ion conduction through lipid membranes.¹⁰ It operates as a classical ion

gating system, being stimulated by the natural agonist acetylcholine and by many other similar compounds.¹¹ The present report also deals with an investigation of the multidimensional analytical responses derived from perturbations of the lipid membrane by the interactions of acetylcholine receptor with the agonist carbamylcholine and the antagonist α -bungarotoxin (α -BTX). Transduction of selective binding events was monitored by means of the fluorescence intensity and lifetime, obtained from perturbations of the environment of a fluorophore which was either a label for AChR-rich membranes or a label for only the lipids of the membranes. In all the cases examined, the fluorophore and receptor protein were located in bilayer lipid vesicles.

EXPERIMENTAL

Reagents

The fluorescent probe 4-dicyanomethylene-1,2,3,4-tetrahydromethylquinoline (DCQ) was prepared from *N*-methyl-1,2,3,4-tetrahydroquinoline and malononitrile according to a published procedure, and purified.¹² Acetylcholine receptor (AChR) was obtained from *Torpedo californica* (Pacific Biomarine, Venice, CA) and purified according to standard methods,¹³⁻¹⁵ and reconstituted in soybean lecithin (Sigma Chemical Co., St. Louis, MO) in 10mM disodium hydrogen phosphate, pH 7.4, aliquots of which were then stored over liquid nitrogen. The activity of the stock receptor solution was determined by incubation with ¹²⁵I α -bungarotoxin (α -BTX) (ICN Biomedicals Canada Ltd., Montreal) and found to be 1.3 μ mole of toxin sites per litre.¹⁶ The protein concentration was found to be 0.3 mg/ml as described elsewhere,¹⁷ yielding a specific activity of 4.3 nmole of toxin sites per mg. The direct protein labelling used the fluorescent probe 4-[*N*-(iodoacetoxy)ethyl-*N*-methyl]amino-7-nitrobenz-2-oxa-1,3-diazole (IANBD) (Molecular Probes, Eugene, OR). Study of the fluorescence derived directly from lipid membranes was based on the use of *N*-(7-nitrobenz-2-oxa-1,3-diazol-4-yl)dipalmitoyl-L- α -phosphatidyl ethanolamine (NBD-PE) (Molecular Probes). Carbamylcholine was obtained from Sigma, and non-radioactive α -BTX from Miami Serpentarium (Salt Lake City, UT). Solvents were of the highest purity commercially available and were further purified by standard procedures. All water used was purified first by reverse osmosis and then by a

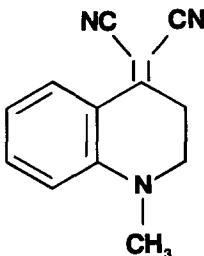


Fig. 1. Structure of the fluorescent probe 4-dicyanomethylene-1,2,3,4-tetrahydromethylquinoline (DCQ).

Millipore system (Milli-Q, Type I reagent grade water system), and had a specific resistivity of not less than 18 M Ω .cm. Dimyristoyl phosphatidyl choline (DMPC) was obtained from Avanti Polar Lipids Inc. (Pelham, AL) and was used without further purification.

Apparatus

The absorption and emission spectra of DCQ were recorded with a Beckman DU-50 spectrophotometer and an SLM 4800 spectrofluorimeter, respectively. The spectrofluorimeter used concave holographic monochromators of 2 nm/mm dispersion and spectra were collected digitally, with a 1-nm bandpass. A GG-21 standard block (Helma, $\phi_r = 0.494$) was used as a standard for relative quantum yield measurements. A constant-temperature sample holder was used, the temperature being monitored with a Fluke 80T-150 probe, which was immersed directly in the sample cell near the irradiation zone. Fluorescence decay times of DCQ were measured by the single-photon counting technique with the PRA system 2000 lifetime apparatus (London, ON, Canada). Fluorescence spectra from vesicles containing AChR were obtained with an in-house assembled fluorescence spectrometer consisting of an atmospheric-pressure nitrogen laser (Model LN 103, PRA) for excitation at 337.1 nm, a Bentham M300 monochromator with SMD 3B stepper-motor controller (Optikon, Waterloo, ON, Canada), a Hamamatsu R928 photomultiplier tube (PMT) (Hamamatsu, Bridgewater, NJ) in a linearity-optimized housing (PRA) operated at -1250 V, and an SR 250 gated integrator/boxcar averager (SRS, Stanford, CA) operated by an IBM PC through an SR 245 interface. A short length of optical cable placed in the laser output carried a small portion of the excitation pulse directly to a second photomultiplier tube for triggering the gated integrator. The PMT output was integrated over 30 nsec, triggered at the beginning of emission. Ten pulses were averaged for each point.

Fluorescence lifetime measurements were obtained with the same in-house assembled fluorescence spectrometer, but with the PMT connected to a LeCroy model 9400 digital storage oscilloscope (DSO) (LeCroy, Chestnut Ridge, NY), which used a 50- Ω input impedance and random interleaved sampling to provide 5×10^9 samples/sec. The DSO and the monochromator driver were controlled through an

IEEE-488 interface by an IBM PC. The fast pulse of the nitrogen laser (300 psec) allowed time-resolved emission decay profiles to be obtained for the fluorescent samples.

The data were read as integral intensity values from the DSO for each bin or time value. This prohibited use of the standard Poisson weighting normally applied in photon-counting systems. To assess the variance of the data, several values were obtained for each bin and a simple standard deviation was calculated. This was used instead of the square root of the count, as a weighting parameter. The lifetimes were deconvoluted by an iterative fit, with use of the weighted least-squares to evaluate "goodness" of the fit. An instrument-response ("lamp") function was obtained by sampling the laser pulse scattered from a non-fluorescent solution. Each iteration involved trapezoidal convolution over the instrument response to obtain a fitted curve for the exponential model being tested, which could be compared with the observed curve. Fit optimization by χ^2 and least-square minimizations were evaluated, the least-square method yielding much better success in achieving convergence of the fit, especially for noisy data.

Final evaluation was made by observing the autocorrelation function. The general inability to achieve a truly flat autocorrelation suggested a poor instrument-response function, indicating that a better profile might be obtained by use of the emission of a standard solution at a wavelength closer to the sample emission.

Procedures

Vesicles containing the phospholipid DMPC and DCQ (molar ratio $\leq 250:1$) in 15mM Tris buffer, pH 7.4, were prepared by sonication for 30 min at 5–10° above the lipid phase transition temperature, with a Model VC250 Sonicator (Sonics and Materials, Inc., Dunbury, CT) set at 40 W and fitted with a microtip. All sonicated solutions were centrifuged (27,000 g for 30 min) to remove insoluble matter. The correction factor for the emission monochromator and phototube of the SLM 4800 was obtained by using quantum counters ($10^{-4}M$ quinine sulphate and $2 \times 10^{-4}M$ 3-aminophthalimide in 0.5M sulfuric acid¹⁸). The fluorescence emission was monitored at right angles to the excitation light-beam. Fluorescence decay curves of DCQ were analyzed over at least a 100-fold range of intensity by iterative deconvolution as previously described.¹⁹

A receptor solution containing AChR and 2 mole% NBD-PE was prepared by addition of the NBD-PE during the reconstitution step in the AChR purification. The appropriate amount of NBD-PE was added to affinity-purified receptor in 2% sodium cholate detergent before dialysis. The sample was centrifuged at 10,900 *g* for 15 min to remove residual NBD-PE solid. IANBD labelling of the AChR was done according to Dunn and Raftery.²⁰ Excess of solid IANBD was added and the solution was stirred on ice and in darkness, for 2 hr. Controls of soybean lecithin and soybean lecithin/bovine serum albumin (BSA) were prepared identically to the AChR/NBD-PE sample. Dry lecithin was suspended as vesicles by evaporation from chloroform followed by addition of 10mM disodium hydrogen phosphate, pH 7.4 and sonication for 2 hr with a probe-tip sonicator. Reagents such as carbamylcholine were added directly to the 1-cm path-length fused-silica cuvettes used in the spectrofluorimeter. All spectral work with AChR was done at room temperature ($21 \pm 1^\circ$). "Poisoning" of the receptor was accomplished by pre-incubation with a minimum threefold excess of α -BTX for at least 2 hr, over ice.

RESULTS AND DISCUSSION

Wavelength and intensity analysis of labelled AChR

The IANBD labelling of the AChR vesicle system was first done to reproduce the fluorescence enhancement experiment of Dunn and Raftery,²⁰ and to establish a chemically selective system for the investigation of multidimensional analytical characterization. The solid water-insoluble fluorophore was added to the crude receptor preparation in aqueous solution. The protein-rich membranes in the crude preparation were then isolated from the bulk tissue by homogenization and centrifugation. The greater solubility of the IANBD in the hydrophobic portion of the lipid membranes than in aqueous medium supports the assumption that most of the probe reaction occurred in the membrane environment. Though many reactions are possible, three predominant labelling schemes are outlined in Fig. 2, depicting covalent fluorophore attachment to nucleophilic sites on the protein, the membrane phospholipids and water.

The fluorescence spectrum obtained from the ANBD-labelled system (Fig. 2) had a broad

peak centered at 570 nm. Addition of the agonist carbamylcholine (carb), which is commonly used to generate an ion-gated response from AChR, caused an asymmetric increase in intensity (greater at the shorter wavelengths), which enabled the application of a multidimensional approach based on wavelength-dependence. Peak areas were obtained from the spectra by integration of the entire peak (500–650 nm), or of the shorter wavelength component (500–550 nm) or by calculation of the ratio of the areas of the shorter and longer wavelength components (500–550 nm)/(550–650 nm). A plot of relative intensity-enhancement *vs.* concentration is shown in Fig. 3. Use of the integrated area of the entire peak yields no spectral information (an analogy is the use of filters placed before a detector) so is not shown. The enhancement of the shorter wavelength region of the peak is much higher, showing the sensitivity available through selective spectral analysis. The intensity enhancement curves show poor reproducibility between trials with the same receptor preparation. This inconsistency could be due to many factors, including changes in the amount and fluorescent yield of fluorophore because of sample inhomogeneity, and variability in biological activity of the receptor from one sample to the next. Other factors, such as instability in the laser source (typical of the nitrogen laser employed) and drift in the photomultiplier, are also possible. The curves in Fig. 4 show the enhancement of the (500–550 nm)/(550–650 nm) peak area ratios, which has much greater reproducibility between samples. The long-wavelength side, which contains a constant component, acts as an internal calibration for the system, compensating for some of the possible variations in intensity mentioned above. To confirm that the observed enhancement was due to selective response of the active receptor, AChR was pre-incubated with the antagonist α -BTX, a highly selective blocker of AChR activity. No fluorescence enhancement was observed for these samples or on the addition of carbamylcholine to ANBD-labelled soybean lecithin vesicles without AChR, confirming that the enhancement was due to receptor-agonist interaction.

Wavelength and intensity analysis by using pure DMPC vesicles with DCQ as probe

DCQ is a fluorescent probe which is extremely sensitive to its environment and provides an example of the potential of fluorescence

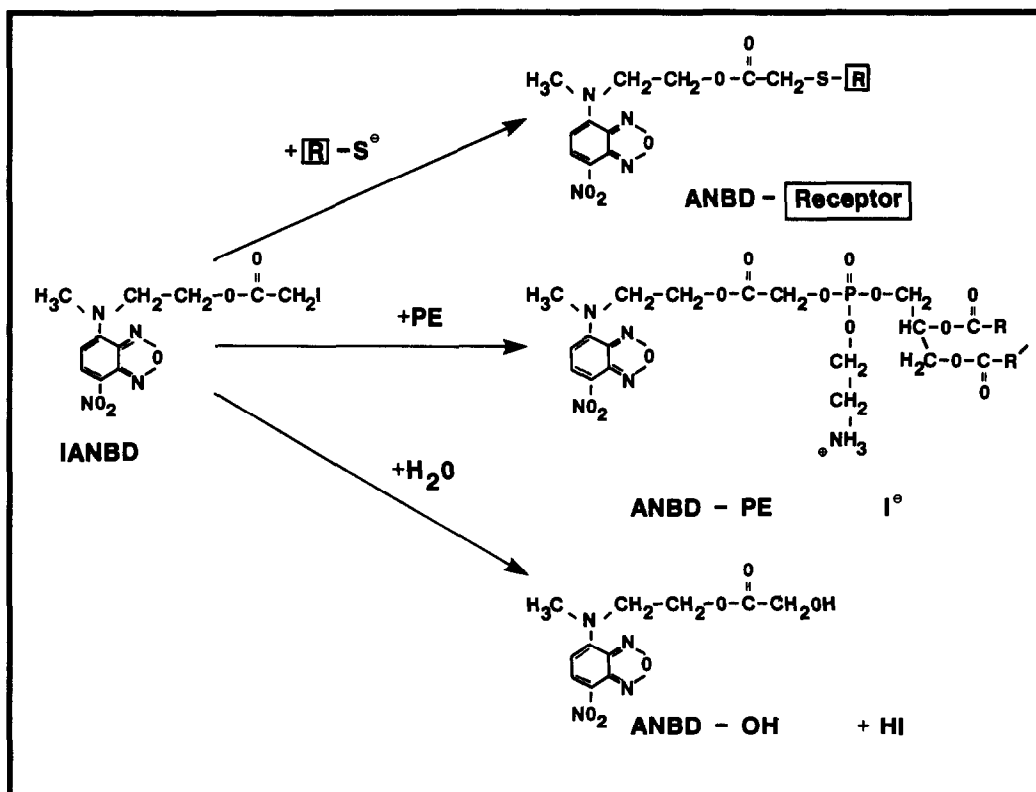


Fig. 2. Major chemical products resulting from the use of IANBD in the labelling of crudely purified AChR.

spectroscopy for observing structural alterations within lipid membranes (in the case of DCQ, by variations in temperature⁹). The absorption and emission spectra of DCQ in DMPC vesicles are shown in Fig. 5. The position of the long-wavelength absorption band at 310 nm is sensitive to solvent polarity and shifts to longer wavelengths when this is increased. This band is the result of an intra-molecular

charge-transfer from the electron lone-pair of the amine nitrogen atom to the antibonding π -state of the cyano group.

The emission spectrum of DCQ also shifts to longer wavelengths with increasing solvent polarity.⁹ This is consistent with the $S_0 \rightarrow S_1$ transition being an intra-molecular charge-transfer transition. Both the fluorescence quantum yield (ϕ_f) and single-term exponential decay time (τ_f)

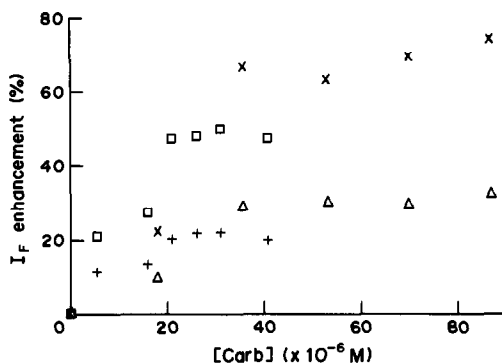


Fig. 3. Concentration-response curves showing relative fluorescence intensity enhancement for AChR interaction with carbamylcholine, based on the integrated responses for two different wavelength windows (two experiments, demonstrating irreproducibility, shown for each window); (\times , \square) 500-550 nm, and (Δ , $+$) 500-650 nm.

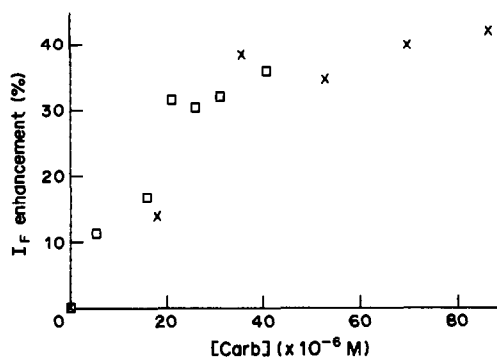


Fig. 4. Concentration-response curves showing reproducibility of relative fluorescence intensity enhancement derived from data shown in Fig. 3. The variability between experiments is largely eliminated by dividing the results from the 500-550 nm wavelength window by the results from the 500-650 nm wavelength window.

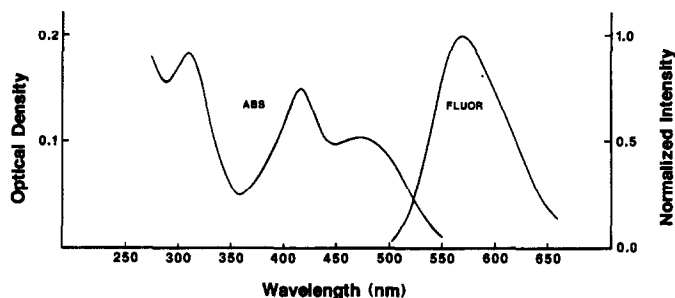


Fig. 5. The absorption and emission spectra of DCQ and DMPC vesicles.

increase with increasing solvent polarity and viscosity. The effect of variation of pH on the absorption spectrum of DCQ⁹ shows that the probe is located in the head-group region of the membrane. The radiative rate constant (k_r) is relatively insensitive to viscosity and polarity, and variation in ϕ_f and τ_f is due to sensitivity of the non-radiative rate constant (k_{nr}) to these parameters. Low values of the fluorescence quantum yield and decay time of DCQ in non-viscous, non-polar hydrocarbon solvents is attributed to very fast non-radiative deactivation of the S_1 state by *trans* \rightleftharpoons *cis* photoisomerization about the ethylenic double bond. Increasing the viscosity (or rigidity) and polarity increases the energy barrier to rotation, and thus increases the probability of emission at the expense of non-radiative deactivation. Decreasing the temperature also increases both the fluorescence quantum yield and decay time. If k_{nr} is the only thermally activated process, it can be expressed in terms of an Arrhenius equation:

$$k_{nr} = A \exp(-E_a/RT) \quad (1)$$

where E_a is an apparent activation energy, representing all processes contributing to the prevention of rotation about the double bond. Combining equation (1) with the familiar relation (2) leads to (3):

$$\phi_f = \frac{k_r}{k_r + k_{nr}} \quad (2)$$

$$\frac{1}{\phi_f} - 1 = \frac{A}{k_r} \exp(-E_a/RT) \quad (3)$$

Thus a change in temperature will result in a linear relationship between $\ln [(1/\phi_f) - 1]$ and $1/T$, and hence a linear relation between $\ln \eta$ and $1/T$,⁹ where η is the viscosity. Thermally induced phase transitions in lipid bilayers affect the molecular mobility of lipids. This should affect the emission quantum yield of the probe, and graphs of $\ln [(1/\phi_f) - 1]$ vs. $1/T$ for DMPC are

shown in Fig. 6. A distinct break point is observed near 22.8°, in agreement with the phase-transition temperature of DMPC when in multilamellar form (23.9°).²¹

Wavelength and intensity analysis: application to AChR in fluorescent vesicles

The use of DCQ in pure DMPC vesicles indicated that structural changes within lipid membranes could be monitored with a fluorescent probe located in the head-group region. However, the use of DCQ in practical experiments is limited since it partitions into lipid membranes from bulk solution and is not permanently located in the membrane (*i.e.*, is extractable). One form of fluorescent probe which has been extensively used in lipid membrane studies is fluorescently labelled lipid, which is incorporated into the membrane in a relatively irreversible manner. The label is placed on the terminus of the lipid head-group so that it remains external to the acyl chain region of the membrane. This helps to limit structural perturbations caused by the presence of the probe. The NBD-PE probe has been used to study phase domain structure in membrane systems by classical spectrofluorometric measurements such as enhancement/self-quenching²² and by

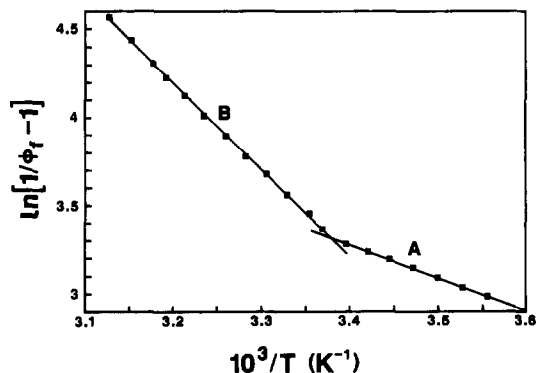


Fig. 6. Effect of temperature on fluorescence quantum yield of DCQ in DMPC vesicles.

the relatively new technique of fluorescence microscopic imaging of lipid monolayers at an air-water interface.²³ Both techniques are possible as a result of the natural tendency of the NBD-PE molecules to become concentrated in the less ordered domains on partitioning between phases in a mixed phase system. In these regions of higher concentration, the fluorescence of the NBD moieties will be self-quenched, causing a reduction in the overall measured intensity. Any changes in the relative domains of phase-structure types will thus result in a change in the overall intensity. Such changes may be proposed for the system under study, as the NBD-PE probe has been shown to indicate perturbation of lipid phase structure by incorporated proteins,²⁴ and by the presence of AChR.²⁵

To investigate the response of a system containing only fluorescently labelled lipid, preparations were made by including fluorescent lipid in the exogenous lipid added to AChR in the detergent phase before reconstitution into vesicles. Fluorescence enhancement was observed on addition of agonist, as shown in Fig. 7. A simplified approach to quantification used a linear approximation of the first few data points for curves as shown in Fig. 7. A linear fit yielded a sensitivity of $40\% \cdot 1. \mu\text{mole}^{-1}$ for carbamylcholine and a limit of detection of 300nM over a dynamic range of $3\mu\text{M}$, with a correlation coefficient of 0.978 for the most sensitive systems studied in this work.²⁶ In addition, it was observed that the fluorescence signal was enhanced by the initial addition of α -BTX at very low concentrations (40% enhancement at 10nM). This indicated an antagonist-associated conformational change which may or may not be similar to the change observed for agonist

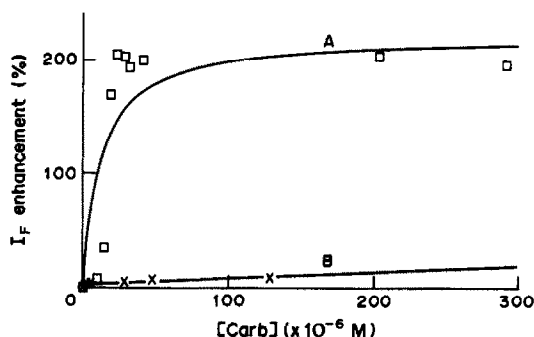


Fig. 7. Concentration-response curve for AChR interaction with carbamylcholine, as determined by enhancement of fluorescence intensity from lipid vesicles containing 2 mole% NBD-PE. Enhancement was measured for a wavelength window of 500–650 nm; A—response curve, B—control in absence of AChR.

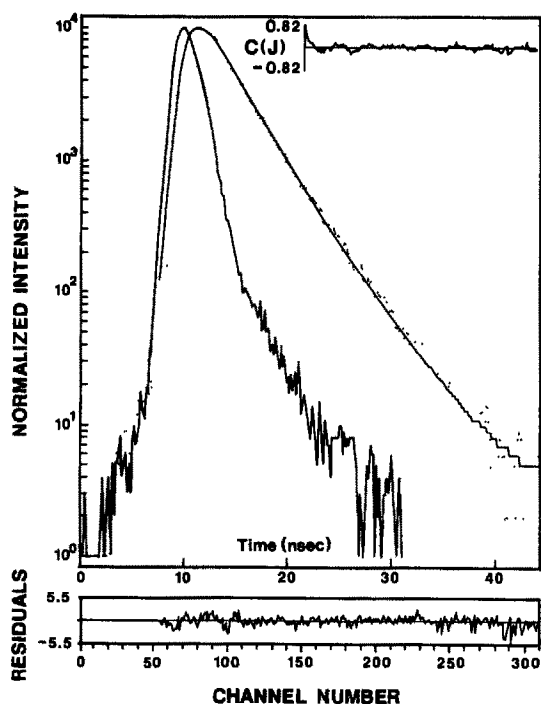


Fig. 8. A typical fluorescence decay curve of DCQ in DMPC at 21.5° . Excitation was at 555 nm and emission was collected over the range 500–650 nm. A double exponential fit provided lifetimes of 2.12 and 3.78 nsec. The points are experimental data and the solid curve is calculated. Also shown are the weighted residuals and their autocorrelation function. The χ^2 value was 1.45.

addition, but which may also permit detection of antagonist. Selectivity in this system was demonstrated by the elimination of the agonist response after pre-incubation with α -BTX. To confirm receptor mediation of the enhancement, controls were run with, pure lipid vesicles, vesicles with another protein (bovine serum albumin) and vesicles containing AChR that had been degraded by extensive sonication. All three controls yielded no fluorescence enhancement.

Fluorescence lifetime analysis for DCQ in pure DMPC vesicles

The use of the steady-state properties of a probe in lipid membranes, such as fluorescence intensity, is based on the assumption that the environment of the probe is homogeneous. However, bilayers are known to be inhomogeneous.²⁷ We have therefore investigated the decay dynamics of DCQ in DMPC over a limited range of temperatures. Figure 8 shows a typical decay curve for DCQ in DMPC vesicles. The decay is clearly non-exponential and can best be described by a double exponential function:

$$I(t) = \alpha_1 \exp(-t/\tau_1) + \alpha_2 \exp(-t/\tau_2) \quad (4)$$

where τ_1 and τ_2 are the average lifetimes and α_1 and α_2 are the pre-exponential factors. Also shown in Fig. 8 are the calculated decay curve, the weighted residual for each decay channel and the autocorrelation function of the residuals. The decay is well described by the double exponential function, as judged from the weighted residuals and their autocorrelation function. At present it is not possible to assign any physical significance to the two individual decay components and further investigations are required if the decay characteristics are to be significantly related to the lipid membrane structure.

The change in quantum yield with alteration in the phase structure of DMPC does not indicate that significant changes occur in the ratios of the pre-exponential factors or the average lifetimes. The pre-exponential factors and mean lifetimes can be treated as a further set of analytical data channels suitable for transduction. Figure 9 shows the lifetime and pre-exponential data as a function of temperature for an excitation wavelength of 360 nm and emission collected at 570 nm. The two lifetime components show a trend to decrease with increasing temperature from 16 to 26°, as would be expected if molecular mobility were a primary factor governing lifetime. There is no clearly defined inflection for either of the two lifetime components which would provide evidence for a phase transition in the range 20–24°. This would indicate that the location and orientation of the probe does not dramatically alter as a function of the phase

transition, and presumably the probe remains in the head-group region of the lipid membrane. The relative contributions to the fluorescence intensity given by the magnitudes of the pre-exponential factors do not clearly identify the structural transition at 20–24°, since they alter linearly over a wider temperature range. It is interesting to note that the relative contributions from the two lifetime components, as determined from the pre-exponential factors, are reversed in the temperature range 20–24°C. The general trends observed in Fig. 9 appear again in Fig. 10, where the lifetime and pre-exponential factors due to excitation at a wavelength of 555 nm are plotted across the entire emission range, but the reversal of the contributions of the two lifetime components to the intensity is more sharply defined in the temperature range 21–24°. Excitation at a longer wavelength would alter the excited-state dipole moment of DCQ, and, as seen, vary the sensitivity of the probe to environmental interactions.

Examination of the data shown in Fig. 9 indicates that τ_1 , τ_2 and α_1 all show a relatively constant decrease as the temperature increases from 17 to 26°. The magnitude of α_2 shows a large and relatively constant increase over the same temperature span. For quantitative analysis, an average lifetime is calculated by

$$\langle \tau \rangle = \left(\frac{\sum \alpha_i \tau_i^2}{\sum \alpha_i \tau_i} \right) \quad (5)$$

Variation of $\langle \tau \rangle$ with temperature is shown in Fig. 11. There is a break point near $21 \pm 1^\circ$ in

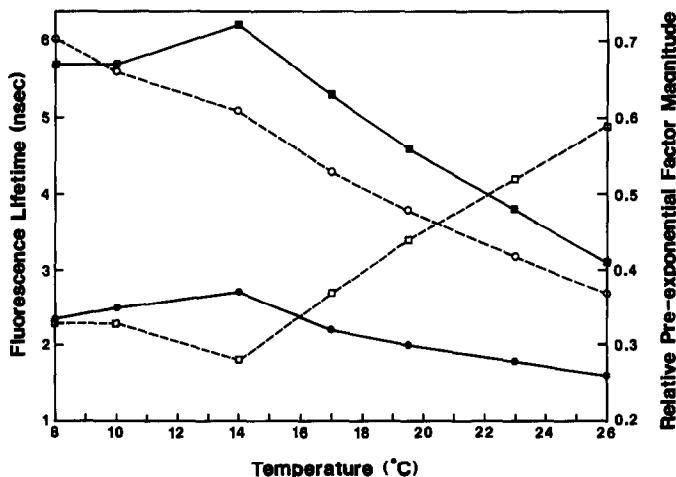


Fig. 9. Effect of temperature on the two lifetime components and the associated relative pre-exponential factors ($\alpha_1 + \alpha_2 = 1$) for DCQ in DMPC. Excitation was at 360 nm and emission was collected at 570 nm. The maximum error was $\pm 10\%$ and the χ^2 value was between 1.2 to 1.5 for all results. τ_1 —●, α_1 —■, τ_2 —○, α_2 —□.

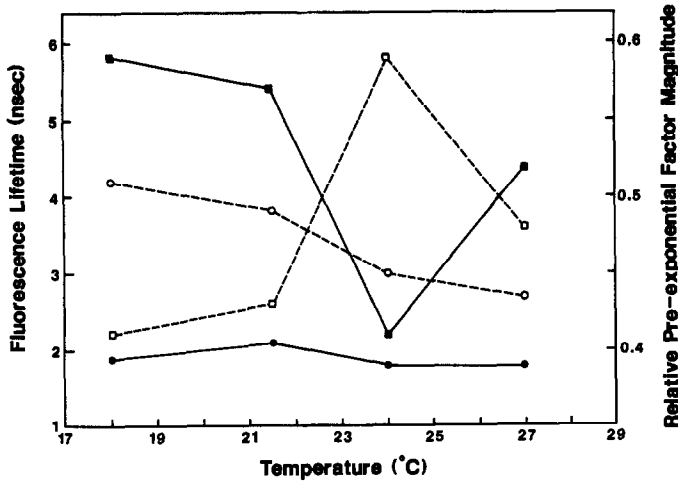


Fig. 10. Temperature-dependence of the lifetime components and pre-exponential factors of DCQ in DMPC as described in Fig. 9, but with excitation at 555 nm and emission collected over the range 500–650 nm.

the plot of $\ln(1/\langle\tau\rangle)$ vs. $1/T$ for DMPC, which agrees with the expected phase transition temperature.

Fluorescence lifetime analysis: application to AChR in fluorescent vesicles

Analysis of the fluorescence lifetime data obtained from NBD-PE in lipid vesicles containing AChR indicated that the decay could be best described by a double exponential function. No physical interpretation of the origin of the two lifetime components can be assigned at present. The dependences of the lifetimes and their associated pre-exponential factors on the wavelength used to study the emission process are shown in Figs. 12 and 13 for the selective interaction of α -BTX with AChR in lipid vesicles. The discrete lifetime components in Figs. 12 and 13, and the average lifetimes compiled in Table 1 do not show significant dependence on

the selective binding event. Substantial variations of the relative pre-exponential factor distribution (and absolute magnitude as shown in Fig. 14) are observed. Considering equation (2) and the relationship

$$\tau_i = \frac{1}{k_r + k_{nr}} \quad (6)$$

it would seem that a relative increase in k_r and an equivalent decrease in k_{nr} could cause fluorescence enhancement with constant mean lifetime. A speculative mechanism for the enhancement would involve an average fluidity

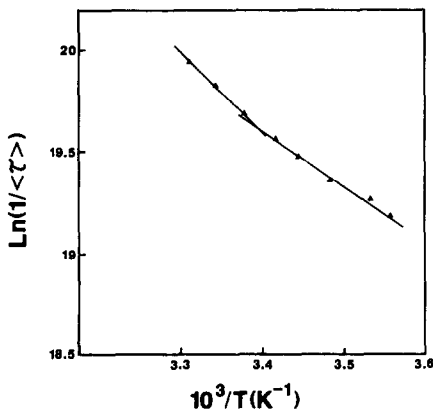


Fig. 11. Temperature-dependence of average fluorescence decay time of DCQ in DMPC.

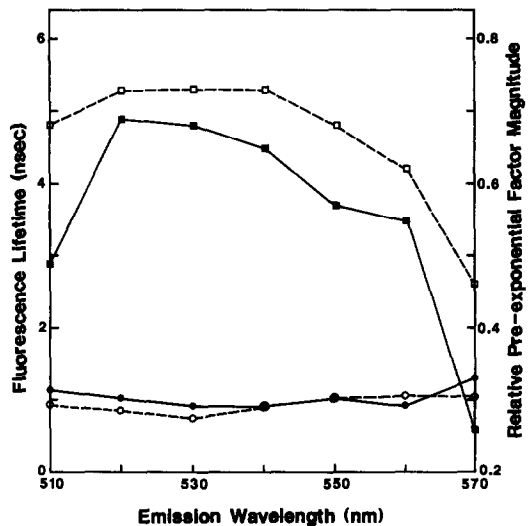


Fig. 12. Change in τ_1 and the relative value of α , (*i.e.*, for $\alpha_1 + \alpha_2 = 1$) for NDB-PE in soybean lecithin vesicles containing AChR, caused by introduction of $1\mu\text{M}$ α -BTX. Before toxin addition: τ_1 —●, α_1 —■. After toxin addition: τ_1 —○, α_1 —□.

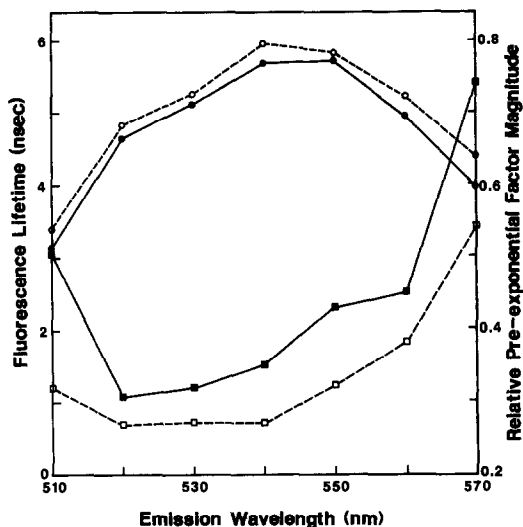


Fig. 13. Change in τ_2 and the relative value of α_2 (i.e., for $\alpha_1 + \alpha_2 = 1$) for NBD-PE in soybean lecithin vesicles containing AChR, caused by introduction of $1\mu\text{M}$ α -BTX. Before toxin addition: τ_2 —●, α_2 —■. After toxin addition: τ_2 —○, α_2 —□.

increase due to selective interaction caused by aggregative events of the protein.²⁸ A general increase in the fluid phase at constant surface pressure would imply that little structural alteration of the environment of the probe would occur, but would result in a general fluorescence enhancement.^{23,24}

The fluorescence enhancement is observed for interaction of AChR with carbamylcholine, but with substantially less sensitivity than for the interaction with α -BTX. Table 2 provides an indication of the utility of the lifetime analysis, showing that the first discrete lifetime is affected by the interaction of carbamylcholine, while the

Table 1. Average lifetime parameters obtained from fluorescence (at various emission wavelengths) of NBD-PE in lipid vesicles for interaction of $1\mu\text{M}$ α -BTX with AChR

Wavelength, nm	$\langle\tau\rangle$ prior to α -BTX addition, nsec	$\langle\tau\rangle$ after α -BTX addition, nsec
510	2.66	2.48
520	3.44	3.54
530	3.97	3.99
540	4.54	4.45
550	4.82	4.50
560	4.19	4.13
570	3.69	3.85

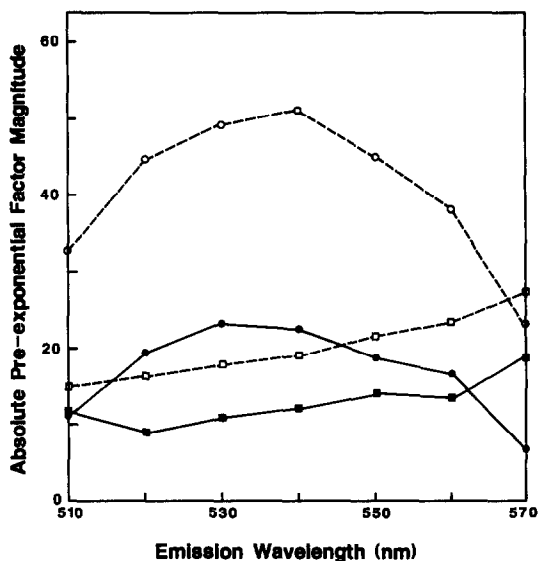


Fig. 14. Changes in the absolute values of the pre-exponential factors (i.e., not normalized to $\alpha_1 + \alpha_2 = 1$) for NBD-PE in soybean lecithin vesicles containing AChR, on introduction of $1\mu\text{M}$ α -BTX. Before toxin addition: α_1 —●, α_2 —■. After toxin addition: α_1 —○, α_2 —□.

other three second-lifetime parameters remain invariant. Consideration of the absolute magnitude of the pre-exponential factors again shows the enhancement effect. This response is different from that caused by interaction with α -BTX, and can be used to distinguish between the agonist and antagonist.

CONCLUSIONS

The results of this work indicate that a fluorescent lipid membrane may be a general transducer of selective binding interactions of proteins that can be embedded within lipid matrices. The fluorescence signal may be acquired in both the wavelength and time domains, and can be used to discriminate between different structural alterations induced in lipid membranes by selective interactions of different types. The origin of the fluorescence enhancement effects caused by AChR binding with carbamylcholine and α -BTX is not clear, and further studies using the technique of fluorescence microscopy are being made in order to observe directly any structural alterations which

Table 2. Lifetime parameters obtained from fluorescence (at 540 nm) of NBD-PE in lipid vesicles for interaction of $100\mu\text{M}$ carbamylcholine (carb) and AChR*

	$\alpha_1(\text{rel})$	$\alpha_1(\text{abs})$	τ_1 , nsec	$\alpha_2(\text{rel})$	$\alpha_2(\text{abs})$	τ_2 , nsec	$\langle\tau\rangle$, nsec
Initial	0.79	38	0.9	0.22	12	7.4	5.63
+ carb	0.82	97	0.5	0.18	23	7.3	5.94

*Maximum error for values quoted is 10%; χ^2 is approximately 1.5.

may be caused by the binding events.²³ Three-dimensional plots involving wavelength, intensity and lifetime may assist in the interpretation of the mechanism of signal generation, and may provide unique mathematical surfaces for qualitative and quantitative studies of selective and non-selective interactions of AChR in lipid membranes.

Acknowledgements—We thank the Natural Sciences and Engineering Research Council of Canada, the Ontario Ministry of the Environment, the Canadian Defense Research Establishment and Imperial Oil Limited for financial support of this work. We are indebted to Dr. A. Safarzadeh-Amiri for technical assistance with the studies of DCQ, and to Professor I. W. J. Still for the gift of the *N*-methyl-1,2,3,4-tetrahydroquinoline.

REFERENCES

1. B. Hille, *Ionic Channels of Excitable Membranes*, Sinauer Associates, Sunderland, Massachusetts, 1984.
2. P. P. C. Graziadei, in *The Ultrastructure of Sensory Organs*, I. Friedmann (ed.), Chap. 4, Elsevier, New York, 1984.
3. M. Thompson, W. H. Dorn, U. J. Krull, J. S. Tauskela, E. T. Vandenberg and H. E. Wong, *Anal. Chim. Acta*, 1986, **180**, 251.
4. F. V. Bright, *Anal. Chem.*, 1988, **60**, 1622.
5. W. A. Wyatt, G. E. Poirier, F. V. Bright and G. M. Heftje, *ibid.*, 1987, **59**, 572.
6. M. J. P. Leiner, M. R. Hubmann and O. S. Wolfbeis, *Anal. Chim. Acta*, 1987, **198**, 13.
7. U. J. Krull, R. Brown, R. F. DeBono and B. D. Hougham, *Talanta*, 1988, **35**, 129.
8. J. L. Tedesco, U. J. Krull and M. Thompson, *Biosensors*, in the press.
9. A. Safarzadeh-Amiri, M. Thompson and U. J. Krull, *J. Photochem. Photobiol.*, in the press.
10. J.-P. Changeux, A. Devillers-Thiéry and P. Chemouilli, *Science*, 1984, **225**, 1335.
11. F. B. Abramson, R. B. Barlow, M. G. Mustafa and R. P. Stephenson, *Brit. J. Pharmacol.* 1969, **37**, 207.
12. P. I. Ittyerah and F. G. Mann, *J. Chem. Soc.*, 1956, 3179.
13. A. Sobel, M. Weber and J.-P. Changeux, *Eur. J. Biochem.*, 1977, **80**, 215.
14. S. Porter and S. C. Froehner, *J. Biol. Chem.*, 1983, **258**, 10034.
15. J. Lindstrom, R. Anholt, B. Einarson, A. Engel, M. Osame and M. Montal, *ibid.*, 1980, **255**, 8340.
16. R. A. Kohanski, J. P. Andrews, P. Wins, M. E. Eldefrawi and G. P. Hess, *Anal. Biochem.*, 1977, **80**, 531.
17. M. A. K. Markwell, S. M. Haas, N. E. Tolbert and L. L. Bieber, *Methods Enzymol.*, 1981, **72**, 296.
18. W. H. Melhuish, in *Accuracy in Spectroscopy and Luminescence Measurements*, R. Mavrodineanu, J. I. Schultz and O. Menis (eds.), pp. 135–150. N.B.S., Washington, D.C., 1973.
19. D. A. Holden, K. Jordan and A. Safarzadeh-Amiri, *Macromolecules*. 1986, **19**, 895.
20. S. M. J. Dunn and M. A. Raftery, *Proc. Natl. Acad. Sci., U.S.A.*, 1982, **79**, 6757.
21. S. Mabrey and J. M. Sturtevant, in *Methods Membrane Biol.*, 1978, **6**, 237.
22. A. E. McGrath, C. G. Morgan and G. K. Radda, *Biochim. Biophys. Acta*, 1976, **426**, 173.
23. W. M. Heckl, *Ph.D. Thesis*, Department of Physics, Technical University of Munich, 1988.
24. W. M. Heckl, M. Losche, H. Scheer and H. Mohwald, *Biochim. Biophys. Acta*, 1985, **810**, 73.
25. U. J. Krull, J. D. Brennan, R. S. Brown and E. T. Vandenberg, *Proc. SPIE—Int. Soc. Opt. Eng.*, Vol. 1067, 1989, in the press.
26. U. J. Krull, R. S. Brown, K. Dyne, B. D. Hougham and E. T. Vandenberg, in *Chemical Sensors and Micro-instrumentation*, R. Murray (ed.), American Chemical Society, Washington, D.C., in the press.
27. L. Davenport, J. R. Knutson and L. Brand, *Faraday Discuss.*, 1986, **81**, 81.
28. W. M. Heckl, B. N. Zaba and H. Moehwald, *Biochim. Biophys. Acta*, 1987, **903**, 166.

DETERMINATION OF CARBARYL AND ITS METABOLITE 1-NAPHTHOL IN COMMERCIAL FORMULATIONS AND BIOLOGICAL FLUIDS

F. GARCIA SANCHEZ and C. CRUCES BLANCO

Department of Analytical Chemistry, Faculty of Sciences, The University, E-29071 Málaga, Spain

(Received 17 January 1989. Revised 6 November 1989. Accepted 14 December 1989)

Summary—A simple and sensitive method for the determination of carbaryl in whole blood and commercial formulations, based on normal, and synchronous first- and second-derivative fluorescence spectra, is presented. Solvent effects on the spectral characteristics of carbaryl solutions and the influences of instrumental parameters are described in detail. Two methods have been developed, with neutral (for carbaryl) and basic (for 1-naphthol) media. Detection limits of 0.9 and 0.7 ng/ml were achieved for carbaryl and 1-naphthol, respectively, with the first-derivative approach.

Carbaryl (1-naphthyl methylcarbamate) is one of the major pesticides used today, owing to its effectiveness against numerous insect pests, along with its relatively short half-life and low plant and mammalian toxicity. Nevertheless, various studies have indicated that carbaryl may cause toxic effects by inhibition of cholinesterase enzyme and by its teratogenic character.^{1–3}

Fluorimetry has attracted much interest as a method for the determination of carbaryl and 1-naphthol, owing to their native fluorescence.⁴ Most procedures involve a separatory technique such as TLC,^{5,6} GC^{7,8} or HPLC,^{9–15} to avoid matrix interferences. In some cases, a prior derivatization is used to obtain greater sensitivity.^{16–18} Spectrophotometric detection has also been widely used as an alternative to spectrofluorimetry,^{19–23} with which it competes in speed and sensitivity.

Determination of carbaryl residues in crops and of the compound in formulations is clearly important.^{24–26} The method of McDermott²⁶ has been recommended for the analysis of formulations, and that of Lawrence and Leduc¹⁶ for crops, water and soil. Both are HPLC methods with photometric detection.

Fluorimetry offers excellent detection limits in the determination of trace amounts of many organic molecules. However, synchronous spectrofluorimetry²⁷ and derivative spectrometry²⁸ are two very valuable techniques for improving sensitivity and reducing interferences. The application of derivative techniques in luminescence spectroscopy was first reported by

Green and O'Haver²⁹ and has been widely extended since.^{30–36}

This paper describes a quick and efficient method for the determination of both carbaryl and 1-naphthol and is a useful alternative to the spectrophotometric method proposed earlier.³⁷

EXPERIMENTAL

Apparatus

All spectra were obtained at room temperature (25°C) over the range 250–600 nm, with a Perkin–Elmer MPF-43A spectrofluorimeter equipped with an Osram XBO 150-W xenon lamp, 1 × 1 cm fused-silica cells, an R-777 Hamamatsu photomultiplier, and a Perkin–Elmer 023 recorder. The derivative spectra were obtained with a Perkin–Elmer model DCSU-2 unit connected to the spectrofluorimeter.

Reagents

Carbaryl and 1-naphthol (purity ≥ 99%) of Pestanal quality were purchased from Riedel–de Haen AG. Stock solutions in ethanol were prepared weekly (1 × 10⁻³ M carbaryl and 1 × 10⁻² M 1-naphthol). The solvents used were analytical-grade ethanol, methanol, butan-1-ol, propan-1-ol, acetone, dimethylformamide and acetonitrile. Demineralized water was used throughout the work.

Analytical procedure

Take appropriate volumes of the carbaryl sample solution (in ethanol) to obtain final

concentrations between 1 and 100 ng/ml. Add 0.5 ml of 0.2M sodium hydroxide (to provide a basic medium) and enough ethanol to give a final concentration of 5% v/v and dilute to volume with demineralized water. Measure the fluorescence intensity at 333 nm with excitation at 285 nm (neutral medium) and at 460 nm with excitation at 330 nm (basic medium) against a solvent blank. Record the synchronous first- and second-derivative spectra with $\Delta\lambda = 50$ nm (neutral medium) or 130 nm (basic medium) with a response-time of 0.3 sec, wavelength increment $\Delta\lambda' = 10$ nm, and a scan speed of 60 nm/min (neutral medium) or 120 nm/min (basic medium). Convert the relative fluorescence intensity (RFI) and the derivative values (expressed in cm) into concentration units by applying the corresponding regression equations or calibration curves.

Extraction procedures

Commercial formulations. An accurately weighed sample containing 0.04 ± 0.01 g of active carbaryl was placed in a 30-ml medium-porosity fritted-glass Buchner funnel, fitted in 250-ml Buchner flask. Ten ml of methanol were added to the funnel, and after 5 min suction was applied until all the liquid was in the flask. This extraction step was repeated twice more in the same way. The contents of the flask were then transferred quantitatively to a 50-ml standard flask and diluted to volume with methanol. Aliquots of this solution were used for the analytical determination.

Blood samples. A white Wistar rat of approximate weight 260 g was anaesthetized with sodium pentobarbital (50 mg), and blood was extracted from the left ventricle with a heparinized syringe and kept in the refrigerator (at 4°) until used.

To 0.25-ml portions of blood sample (in centrifuge tubes) different amounts of a standard ethanolic solution of carbaryl and/or 1-naphthol (200 $\mu\text{g}/\text{ml}$) were added, and the tubes were placed in an ultrasonic bath for 20 sec for haemolysis to take place. Then 2.5 ml of ethyl acetate were added to each tube. The tubes were shaken for 10 min, then centrifuged at 3500 r.p.m. Two ml of the supernatant liquid were transferred to a round-bottomed flask and evaporated to dryness at 40° under reduced pressure. The residue was dissolved with 10 ml of demineralized water, and this solution was analysed as above.

RESULTS AND DISCUSSION

Solvent effects on the spectral data

The effects of solvents on molecular spectra are of interest in analytical spectroscopy because the information they give can be used to increase sensitivity and selectivity. To evaluate these effects, the fluorescence and absorption spectra of carbaryl solutions ($2.5 \times 10^{-5}M$) in solvents of different polarities and hydrogen-bonding capacities were recorded.

The spectral characteristics found are summarized in Table 1. There is a slight bathochromic shift of the fluorescence and absorption maxima when the dielectric constant decreases. As a result, the Stokes shift, $\Delta\lambda$, increases from 52 nm in water to 57 nm in butan-1-ol, but this effect is too small to be significant.

As a general rule, both the relative fluorescence intensity (RFI) and the relative efficiency ($RE = RFI/\epsilon$) increase with solvent polarity except for propan-1-ol and butan-1-ol. The hydrogen-bonding capacity of these two solvents also probably favours the fluorescence emission. This hypothesis agrees well with the behaviour in acetonitrile, which is more polar than dimethylformamide (DMF) but exclusively a hydrogen-bonding acceptor, and gives only half the RFI observed for the DMF solution.

From Table 1, water seems to be the best solvent for the spectrofluorimetric determination of carbaryl, but carbaryl is only slightly soluble in water and is hydrolysed in basic media to its main metabolite 1-naphthol.³⁸ However, examination of use of an aqueous ethanol medium showed that the RFI decreased only slightly with the increase in ethanol content, owing to the decrease in the dielectric constant of the medium (Table 1). A fixed ethanol percentage of 5% v/v was chosen for use.

Fluorescence spectra and effect of experimental variables

Earlier,³⁸ we used the influence of the acidity of the medium on the chemical behaviour of carbaryl and its hydrolysis product 1-naphthol to determine the hydrolysis rate and the ground and excited state pK_a values by spectrophotometry and spectrofluorimetry to establish the best pH values for the determination of carbaryl and 1-naphthol by the two techniques.³⁷ That work shows that it is possible to determine carbaryl spectrofluorimetrically

Table 1. Spectral characteristics of carbaryl in different solvents

Solvent	Dielectric constant	λ_{abs} , nm	λ_{f} , nm	$\Delta\lambda^*$, nm	RFI	$10^3 \times \text{RE}$	$\log \epsilon \dagger$
Water	78.5	278	330	52	138	27.4	3.7
Water/ethanol (50% v/v)	51.5	279	334	55	120	19.8	3.8
Acetonitrile	37.5	279	333	54	60	12.6	3.7
Dimethylformamide	36.7	281	337	56	117	18.0	3.8
Methanol/acetone (50% v/v)	35.1	279	336	57	64	12.0	3.7
Methanol	32.7	278	336	57	56	9.3	3.8
Butanol/DMF (50% v/v)	27.1	281	337	56	101	19.7	3.7
Ethanol	24.5	279	336	57	67	10.3	3.8
Propan-1-ol	20.3	279	336	57	78	10.5	3.9
Butan-1-ol	17.5	280	337	57	85	15.1	3.7

*Stokes shift, $\Delta\lambda = \lambda_{\text{f}} - \lambda_{\text{abs}}$.

† ϵ expressed in $\text{l. mole}^{-1} \cdot \text{cm}^{-1}$.

either as such in neutral medium or as 1-naphtholate in basic medium. The fluorescence spectra of both species are presented in Fig. 1.

The emission spectrum taken at pH 6 has two maxima, at 320 and 333 nm, with excitation at 285 nm. When the 5% v/v ethanol/water solution of carbaryl is treated with 0.2M sodium hydroxide, there is a strong bathochromic shift of the excitation to maximum to 330 nm and of both emission maxima to 460 nm.

Variation of the pH used showed that the hydrolysis takes place instantaneously at room temperature when the pH is higher than the ground state $\text{p}K_{\text{a}}$ value for carbaryl (9.5), and that a small change in pH at this level does not affect the RFI. A $4 \times 10^{-3}M$ sodium hydroxide concentration in the final solution was selected.

A study of the influence of sunlight on the fluorescence intensity of both neutral and basic carbaryl solutions showed that carbaryl is stable for 2 hr when exposed to sunlight but there is a slight decrease in the RFI of basic solutions after 1 hr, in agreement with previous findings.⁴

The onset of self-reversal of fluorescence was examined, and it was found that the response curves were usable over the range 10^{-5} – $10^{-4}M$.

No temperature effects were observed over the range between 10 and 55°, so all measurements were made at $25 \pm 0.5^\circ$.

Optimization of instrumental variables

The use of normal fluorescence spectra for determination of carbaryl in real samples without prior clean-up is generally very difficult, because most co-extracted species would interfere. The suitability of synchronous spectrofluorimetry for the determination was therefore examined. The selectivity of the method can be

improved by using different wavelength scanning intervals ($\Delta\lambda$), and derivative synchronous spectra.³⁹

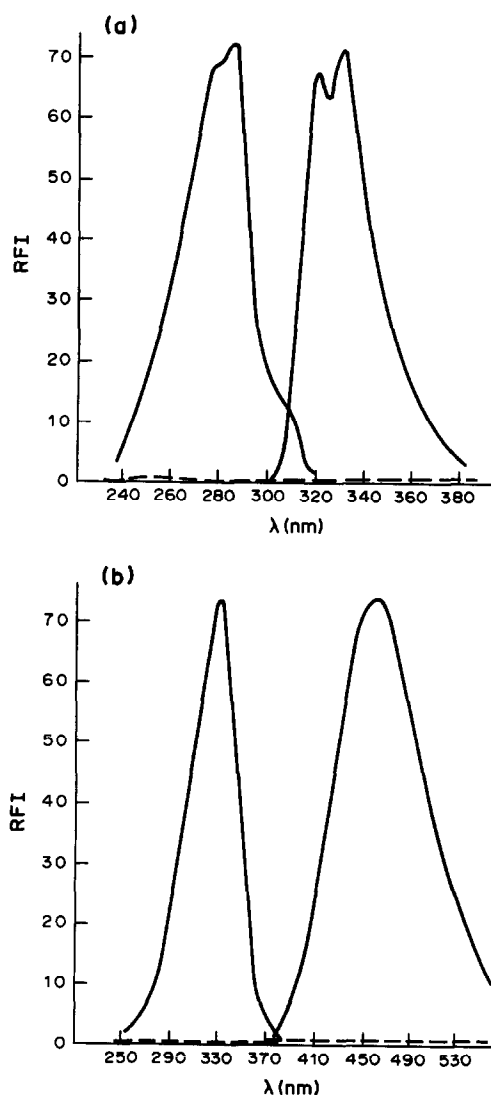


Fig. 1. Excitation and emission spectra of carbaryl in (a) neutral and (b) basic media. Carbaryl concentration 14 $\mu\text{g/ml}$.

To optimize the spectral bandwidth of the synchronous signal, the effect of the wavelength difference between the two monochromators ($\Delta\lambda$) was examined. Various synchronous spectra were recorded with $\Delta\lambda$ varied from 20 to 90 nm (neutral medium) and from 20 to 150 nm (basic medium). As demonstrated earlier,³³ the fluorescence intensity depends strongly on $\Delta\lambda$, and is maximal when $\Delta\lambda$ is equal to the Stokes shift. Hence $\Delta\lambda$ values (*cf.* Fig. 1) of 50 nm (neutral medium) and 130 nm (basic medium) were employed.

The main parameters affecting the shape of the derivative spectra are the scan speed, response time and wavelength increment ($\Delta\lambda'$). The apparatus used gave a choice of three response times and four scan speeds. A combination of 0.3 sec response time, 10 nm $\Delta\lambda'$ and 60 nm/min (neutral medium) or 120 nm/min (basic medium) scan speed was found to be best.

Calibration graphs and statistical analysis

The relationships between the fluorescence intensity, or the peak heights of first and second-derivative synchronous spectra and the carbaryl concentration in neutral and basic media, were found to be linear over the range 1–100 ng/ml. The main characteristics of the calibration graphs are summarized in Table 2. When corrected for the blank, the calibration lines all pass through the origin. The peak-to-trough method of measurement was used for the determination of carbaryl in the derivative mode.

The statistical data for analysis of 11 samples at both the 50 and 10 ng/ml levels in both media by the various methods proposed are also summarized in Table 2. The precision is indi-

cated by the correlation coefficients and the relative standard deviation, and the analytical sensitivity (s_A) is derived from the slopes⁴⁰ and is defined as $s_A = s_s/m$, where s_s is the standard deviation of the analytical signal and m is the slope of the calibration graph.

The linear dynamic range (LDR) varied from 1.9–100 to 5.0–100 ng/ml, and the minimum detectable quantity⁴¹ ($c_L = 3s_b/m$, where s_b is the standard deviation of the blank signal) of 0.6 ng/ml, obtained with the synchronous second-derivative at neutral pH, is particularly low in comparison with the values obtained by the previous spectrophotometric method³⁷ and other methods. The correlation coefficients are larger than 0.99 in all cases, which shows reasonable precision.

It can be deduced from Table 2 that despite the better detection limits obtained in neutral medium, the sensitivity, precision and relative error are much better in basic medium. It is noteworthy that the detection limit, which is a function of the standard deviation of the blank signal, is lower in neutral than in basic medium, whereas the analytical sensitivity, a function of the standard deviation of the analytical signal, is higher.

Analysis of commercial formulations and whole blood samples

The *N*-methyl and *N,N*-dimethylcarbamate insecticides are widely used owing to their effectiveness as pesticides and low mammalian toxicity. Carbaryl in particular has wide use in Spain and numerous commercial formulations are available.

The extraction system used in the present method is based on the one proposed by

Table 2. Statistical treatment of analytical data for carbaryl determination with the methods tested

Method	Slope <i>cm.ml.ng⁻¹</i>	Intercept, <i>cm</i>	Correlation coefficient	Sensitivity, <i>s_A, ng/ml</i>	<i>c_L</i> †, <i>ng/ml</i>	LDR§, <i>ng/ml</i>	Error, %	RSD‡, %
neutral								
A	0.99*	-4.0*	0.9970	0.90	1.5	5.0-100	1.2	1.8
B	0.63	-0.1	0.9994	0.98	0.9	3.0-100	6.9	10.2
C	0.58	+0.2	0.9983	0.91	0.6	1.9-100	6.2	9.3
basic								
A	0.96*	-0.5*	0.9998	0.64	1.1	3.9-100	0.9	1.3
B	0.79	-1.1	0.9997	0.26	0.8	2.5-100	1.7	2.7
C	0.66	+0.2	0.9970	0.23	1.1	3.6-100	1.6	2.3

A, B, C: Normal, synchronous first and synchronous second derivatives.

*Values expressed in (relative fluorescence intensity units).ml.ng⁻¹.

†Limit of detection.

§Linear dynamic range.

‡Relative standard deviation.

Table 3. Application of the normal spectrofluorimetric method to determination of carbaryl in commercial formulations

Formulation*	Neutral pH		Basic pH	
	Found, † %	Recovery, %	Found, † %	Recovery, %
1	4.8 ± 0.4	96 ± 7	4.7 ± 0.1	93 ± 2
2	7.0 ± 0.9	93 ± 1	6.9 ± 0.3	92 ± 4
3	87 ± 1.8	102 ± 2	83 ± 0.8	97 ± 1

*Nominal content: 1—carbaryl 5% (Patatol AC); 2—carbaryl 7.5% (Agres S-7.5); 3—carbaryl 85% (Sevin 85).

†Mean ± standard deviation of 2 extractions and 2 determinations for each.

McDermott,²⁶ which employed 5% methanol in methylene chloride, instead of 10% methanol in chloroform (to avoid the health hazard associated with chloroform).

As indicated by the WHO,⁴² the usual methods employed for carbaryl are based on the colorimetric determination of 1-naphthol.⁴² In 1982 this organization recommended a special investigation to find an easy extraction method applicable with simple equipment in any laboratory.

The results obtained for analysis of some commercial formulations by the proposed direct spectrofluorimetric method are shown in Table 3. The accuracy and precision in terms of the relative standard deviation for duplicate determinations on the solutions from two separate samples compare favourably with those for established methods.^{7,25,26}

Although carbaryl is not very toxic to human beings, there are studies that have indicated that it may be a viral enhancer and a teratogen.³ For this reason accurate and sensitive methods for its determination are needed.

The proposed method has been applied to the determination of carbaryl in samples of whole rat blood spiked with different volumes of standard carbaryl solution and treated as indicated above. The results obtained are given in Table 4 together with the relative standard deviations

for duplicate analyses of each of three extracts from the same sample.

These values demonstrate the applicability of the proposed analytical method to determination of the insecticide in two types of residue analysis, at concentrations relevant to this type of analysis.

Acknowledgement—We thank the Dirección General de Investigación Científica y Técnica (Project PB86-0247) for supporting this study.

REFERENCES

1. R. Elespuru W. Lijinsky and J. K. Setlow, *Nature*, 1974, **247**, 386.
2. M. Uchiyama, *Bull. Environ. Contam. Toxicol.*, 1975, **14**, 589.
3. J. Seifert and J. E. Casida, *Biochem. Pharmacol.*, 1978, **27**, 2611.
4. J. J. Aaron and N. Some, *Analysis*, 1982, **10**, 481.
5. M. Chiba and H. V. Morley, *J. Assoc. Off. Agr. Chem.*, 1964, **47**, 667.
6. G. F. Ernst, S. J. Roder, G. H. Tjan and J. T. A. Jansen, *J. Assoc. Off. Anal. Chem.*, 1975, **58**, 1015.
7. R. J. Argauer, H. Shimanuki and C. Alvarez, *J. Agr. Food Chem.*, 1970, **18**, 688.
8. O. Wueest and W. Meier, *Z. Lebensm.-Unters. Forsch.*, 1983, **177**, 25.
9. B. J. Duck and M. Woolias, *J. Anal. Toxicol.*, 1985, **9**, 177.
10. M. C. Pietrogrande, G. Blo and C. Bigli, *J. Chromatog.*, 1985, **349**, 63.
11. T. D. Spittler, R. A. Marafioti, G. W. Helfman and R. A. Morse, *ibid.*, 1986, **352**, 439.
12. S. Kawai, *Bunseki Kagaku*, 1987, **36**, 574.
13. R. T. Krause, *J. Assoc. Off. Anal. Chem.*, 1980, **63**, 1114.
14. R. T. Krause and E. M. August, *ibid.*, 1983, **66**, 234.
15. M. DeBerardinis Jr. and W. A. Wargin, *J. Chromatog.*, 1982, **246**, 89.
16. J. F. Lawrence and R. Leduc, *J. Assoc. Off. Anal. Chem.*, 1978, **61**, 872.
17. L. K. She, V. A. Th. Brinkman and R. W. Frei, *Anal. Lett.*, 1984, **17**, 915.
18. K.-C. Ting, P. K. Kho, A. S. Musselman, G. A. Root and G. R. Tichelaar, *Bull. Environ. Contam. Toxicol.*, 1984, **33**, 538.
19. K. M. Appaiah, R. Ramakrishna, R. R. Subbarao and O. Kapur, *J. Assoc. Off. Anal. Chem.*, 1982, **65**, 32.
20. P. A. Hargreaves and K. J. Melksham, *Pestic. Sci.*, 1983, **14**, 347.

Table 4. Application of normal spectrofluorimetric method for determination of carbaryl in whole blood samples

Added*, ng/ml	Extraction No.	Found, ng/ml
100	1	107
		95
	2	91
75		89
	1	71
		71
	2	80
		80

*Concentration in the final solution.

21. C. S. P. Sastry, D. Vijaya and K. E. Rao, *Food Chem.*, 1986, **20**, 157.
22. F. J. Bezuidenhout and L. P. Van Dyk, *Bull. Environ. Contam. Toxicol.*, 1981, **26**, 789.
23. M. Kalapanda, R. Ramakrishna, R. S. Kadari and O. Kapur, *J. Assoc. Off. Anal. Chem.*, 1982, **65**, 32.
24. B. M. Colvin, B. S. Engdahl and A. R. Hanks, *ibid.*, 1974, **57**, 648.
25. L. G. Weyer, *ibid.*, 1974, **57**, 778.
26. W. H. McDermott, *ibid.*, 1980, **63**, 650.
27. J. B. F. Lloyd, *Nature Phys. Sci.*, 1971, **231**, 64.
28. P. John and T. Soutar, *Anal. Chem.*, 1976, **48**, 520.
29. G. L. Green and T. C. O'Haver, *ibid.*, 1974, **46**, 2191.
30. T. Vo-Dinh, *Appl. Spectrosc.*, 1982, **36**, 576.
31. J. N. Miller, T. A. Ahmad and A. F. Fell, *Proc. Anal. Div. Chem. Soc.*, 1982, **19**, 37.
32. C. Cruces Blanco and F. García Sánchez, *Anal. Chem.*, 1984, **56**, 2033.
33. S. Rubio, A. Gómez-Hens and M. Valcárcel, *ibid.*, 1985, **57**, 1101.
34. F. García Sánchez and M. Hernández López, *Talanta*, 1986, **33**, 785.
35. S. Rubio, A. Gómez-Hens and M. Valcárcel, *ibid.*, 1986, **33**, 633.
36. F. García Sánchez and C. Cruces Blanco, *Anal. Chem.*, 1988, **60**, 323.
37. *Idem*, *Int. J. Environ. Anal. Chem.*, 1987, **31**, 23.
38. C. Cruces Blanco and F. García Sánchez, *J. Photochem. Photobiol.*, 1988, **42A**, 357.
39. G. I. Romanovskaya, V. M. Pivovarov and A. K. Chibisov, *Zh. Analit. Khim.*, 1987, **42**, 1401.
40. F. García Sánchez, A. Navas and M. Santiago, *Anal. Chim. Acta*, 1985, **167**, 217.
41. *Anal. Chem.*, 1980, **52**, 2242.
42. WHO, *Technical Rept.*, 1982, No. 677.

THREE-DIMENSIONAL SYNCHRONOUS FLUORESCENCE SPECTROMETRY FOR THE ANALYSIS OF THREE-COMPONENT ALKALOID MIXTURES

F. GARCIA SANCHEZ, A. L. RAMOS RUBIO and C. CRUCES BLANCO

Department of Analytical Chemistry, Faculty of Sciences, The University, E-29071 Málaga, Spain

R. SUAUI SUAREZ

Department of Organic Chemistry, Faculty of Sciences, The University, E-29071 Málaga, Spain

(Received 21 April 1987. Revised 28 December 1989. Accepted 4 January 1990)

Summary—A study of a simple and sensitive method for the determination of berberine, luguine and sanguinarine in mixtures by normal and synchronous derivative spectrofluorimetry is described. The influence of solvents and other experimental variables is discussed. A three-dimensional plot of both emission–excitation and synchronous spectra obtained by a new software program provides additional information for optimizing instrumental parameters. Linear, normal and derivative calibration graphs are established in the ng/ml range. A statistical analysis of the results and their application to synthetic and natural samples is given.

Synchronous derivative spectroscopy¹⁻³ offers an elegant approach to the problem of resolving spectral overlap. However, when multicomponent samples with overlapping spectral shapes are analysed, several problems related to pre- and post-filter effects can arise, as recently pointed out.^{4,5}

The information contained in a conventional excitation–emission matrix (EEM) is insufficient for analysis of complex mixtures of such components. However, the additional information, wider scope and cross-dependence of response (λ_{exc} , λ_{em}) that a three-dimensional EEM offers, makes it feasible to detect features that are normally hidden in conventional fluorescence scanning.

Careful observation of the EEM allows optimization of the conditions for obtaining a synchronous excitation matrix (SEM). The software currently offered by the instrument makers does not permit recording of this SEM as a three-dimensional plot. We have therefore developed a program for this purpose, which gives a simple system for optimizing the instrumental parameters affecting synchronous scanning fluorimetry.^{6,7}

Its application to the synchronous derivative approach for analysis of multicomponent samples prevents cross-interferences arising from absorption and/or emission by the other components; this is done by manipulation of the

solvent composition and careful selection of the wavelength increment ($\Delta\lambda_s$).

Alkaloids and other compounds which produce physiological effects in animals are widespread.⁸ The alkaloids berberine, luguine and sanguinarine are structurally related compounds which have overlapping excitation spectra and thus cannot be determined in mixtures by conventional fluorescence spectroscopy, but are amenable to analysis by the derivative technique with the aid of our program.

EXPERIMENTAL

Reagents

Analytical-reagent grade materials and solvents were used unless otherwise indicated. Luguine⁹ and sanguinarine¹⁰ were obtained from the Department of Organic Chemistry, University of Málaga, and were used without further purification.

Standard $1 \times 10^{-3} M$ solutions of the alkaloids were prepared in 1:1 v/v ethanol–dioxan mixture and diluted with the same solvent, as required.

Spectrofluorimeters

A Perkin–Elmer model MPF-43A instrument with an Osram XBO 150-W lamp and an O23 recorder was used for quantitative analysis. The instrument was adjusted daily with a standard

bar of Rhodamine B ($1 \times 10^{-7}M$) to give a reading of 64 units with the sensitivity set at 10 coarse and 7 fine, the slit band-pass at 5 nm, and the temperature at 25°. Derivative spectra were obtained with the Perkin-Elmer Model DCSU-2 differential corrected spectra unit connected to the MPF-43A spectrofluorimeter.

To obtain three-dimensional plots in both the excitation-emission and synchronous spectra modes, a Perkin-Elmer LS-5 spectrofluorimeter was used with a 9.9-W xenon discharge lamp pulsed at line frequency, F/3 Mont-Gillieson type monochromators and 1×1 cm silica cells. For both monochromators the slits were set to give a band-pass of 5 nm. A ratio-recording system with a reference photomultiplier was used. The spectrofluorimeter was computer-controlled through an RS232C serial interface with a Perkin-Elmer Model 3600 Data Station microcomputer. Instrumental control and data collection were achieved with the Perkin-Elmer Computerized Luminescence Software (PECLS-II). For graphical recording an Epson FX-85 printer-plotter was connected to the spectrofluorimeter.

Procedures

Extraction. Roots of *Glaucium flavum* were left to dry for 20 days at room temperature, then triturated. Weighed samples (*ca.* 15 g) were extracted with methanol under reflux. The methanolic extract was evaporated to dryness,

and the residue dissolved in 10% v/v sulphuric acid. The aqueous phase was made alkaline with sodium hydroxide solution and extracted with 50 ml of methylene chloride. The extract was evaporated to dryness and the residue dissolved in 50 ml of 1:1 v/v ethanol/dioxan mixture. This solution was diluted further as required.

Normal (non-derivative) spectrofluorimetry. The fluorescence intensities were measured for alkaloid concentrations between 0.5 and 250 ng/ml in 1:1 v/v ethanol/dioxan. The wavelengths used were λ_{em} 533 nm, λ_{ex} 350 nm for berberine; 440 nm, 340 nm for luguine and 410 nm, 330 nm for sanguinarine.

Synchronous scanning derivative spectrofluorimetry. The samples were the same as for normal spectrofluorimetry. The first and second derivative synchronous spectra were recorded with a derivative wavelength interval ($\Delta\lambda_m$) of 10 nm, a response time of 1.5 sec and a scan-speed of 240 nm/min, with a synchronized difference between λ_{em} and λ_{exc} ($\Delta\lambda_s$) of 98, 47 and 121 nm for berberine, luguine and sanguinarine, respectively. The first and second derivative signals were measured from peak to trough.

RESULTS AND DISCUSSION

Influence of experimental variables

The excitation and emission spectra of the individual alkaloids in 1:1 v/v ethanol/dioxan

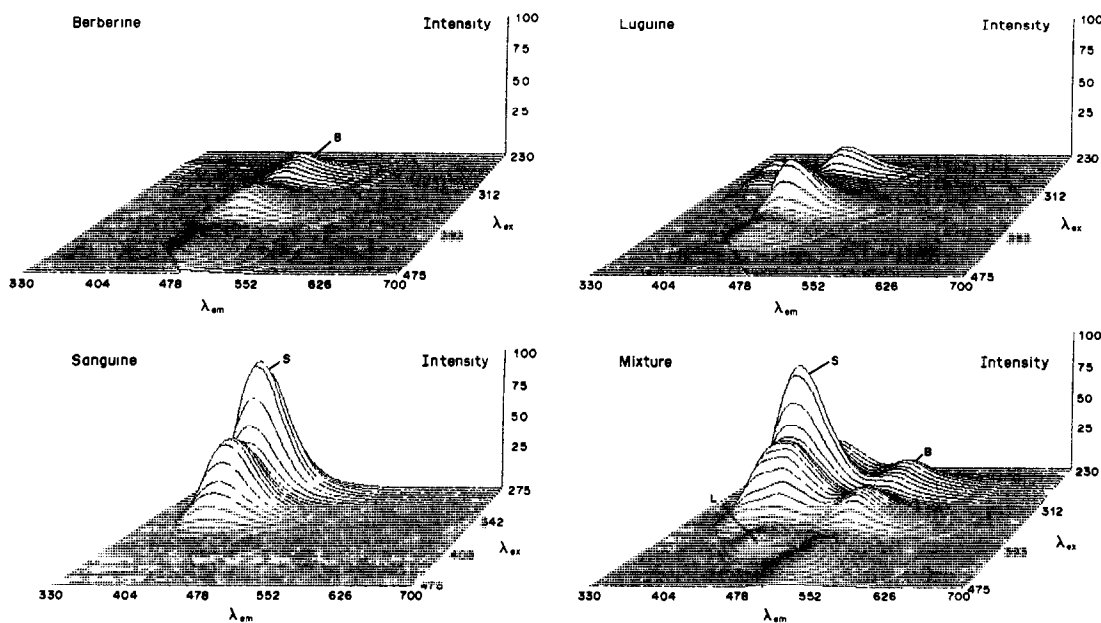


Fig. 1. Three-dimensional emission spectra (EEM) of berberine (B), $1.25 \times 10^{-5}M$; luguine (L), $5 \times 10^{-7}M$; sanguinarine (S), $1.5 \times 10^{-6}M$ and their ternary mixture: 50 scans, excitation wavelength increments 5 nm.

Table 1. Spectral characteristics of several alkaloid/solvent solutions

Compound	Solvent	λ_{abs} , nm	λ_{em} , nm	$D\lambda_s^*$, nm	$\log \epsilon^\dagger$	R.F.I.§, %	R.E.‡, $10^{-5} \text{cm. mole. l}^{-1}$
Berberine	Chloroform	352	525	173	4.26	100	54.1
	Dioxan-ethanol	350	533	183	4.38	91	37.9
	Acetone	349	540	191	4.36	88	38.9
	Ethanol	349	534	185	4.33	82	38.0
	Acetonitrile	345	427	82	4.19	92	59.4
Luguine	Dioxan	342	427	85	4.37	83	35.5
	Dioxan-ethanol	342	440	98	4.40	86	34.4
Sanguinarine	Dioxan-ethanol	325	410	85	4.13	93	68.9
	Acetone	330	420	90	4.11	89	68.5
	Ethanol	327	405	118	4.26	83	46.1
	Acetonitrile	328	540	212	4.33	92	42.6

*Stokes shift, $D\lambda_s = \lambda_{em} - \lambda_{abs}$.

† ϵ expressed in $\text{l. mole}^{-1} \cdot \text{cm}^{-1}$.

§Relative fluorescence intensity.

‡Relative efficiency = $\text{R.F.I.}/\epsilon_{\text{max}}$.

mixture are shown in Fig. 1. Each compound is characterized by three well-resolved excitation maxima and a single emission peak (at 533, 440 and 410 nm for berberine, luguine and sanguinarine, respectively). There is serious overlap of the excitation spectra of the three

alkaloids, which precludes determination of the individual components in mixtures by normal spectrofluorimetry.

To find the most appropriate solvent for simultaneous determination of the three compounds, both the fluorescence and absorption

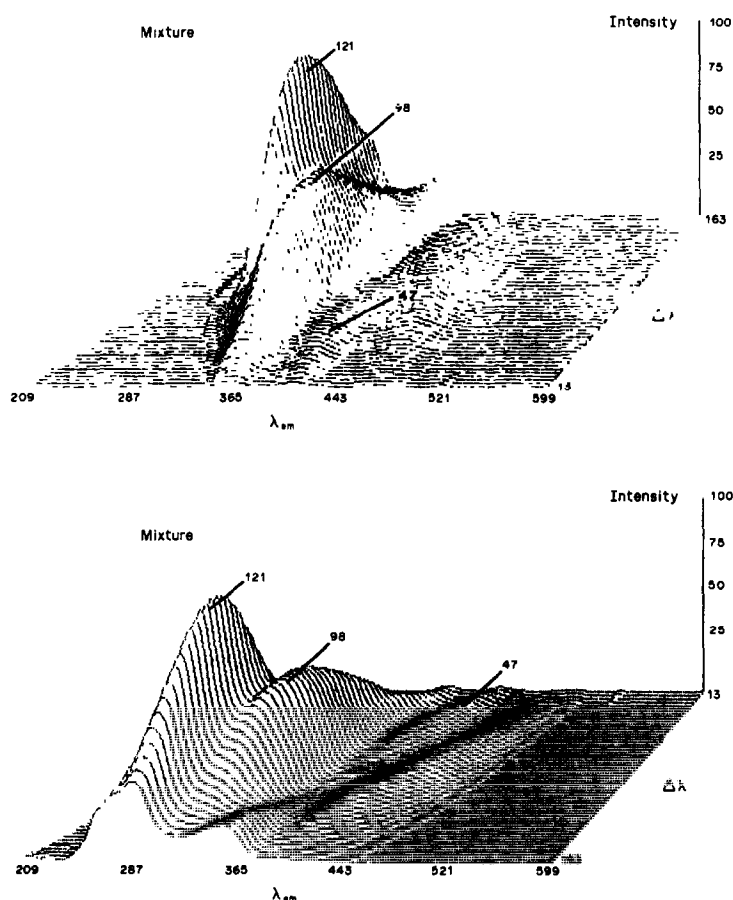


Fig. 2. Three-dimensional synchronous spectra (ESM) of three-component mixture of the alkaloids. Optimum $\Delta\lambda_s$ (89, 47, 121 nm) to determine berberine, luguine and sanguinarine, respectively: 50 scans, excitation wavelength increment 3 nm.

spectra of $1 \times 10^{-5}M$ solutions of the compounds in each solvent tested were obtained. From the results shown in Table 1, it was deduced that the highest relative fluorescence intensities and good Stokes shifts were obtained with ethanol/dioxan mixtures having a medium dielectric constant. The best mixture was found to be 1:1 v/v. The effect of sunlight, temperature and time on the relative fluorescence intensity was examined and indicated that the samples could be left in sunlight and at 25° provided the measurements were made within 3 hr of preparation.

Synchronous scanning derivative spectrofluorimetry

In synchronous scanning spectrofluorimetry, the choice of an appropriate synchronized wavelength difference, $\Delta\lambda_s$, for the determination is critical, especially for quantitative multicomponent analysis. The selection of $\Delta\lambda_s$ is usually empirical^{11,12} and must be made for each component. Generally, the recommended value provides the greatest spectral resolution and minimal half band-width, and avoids Rayleigh scatter. The parameters affect-

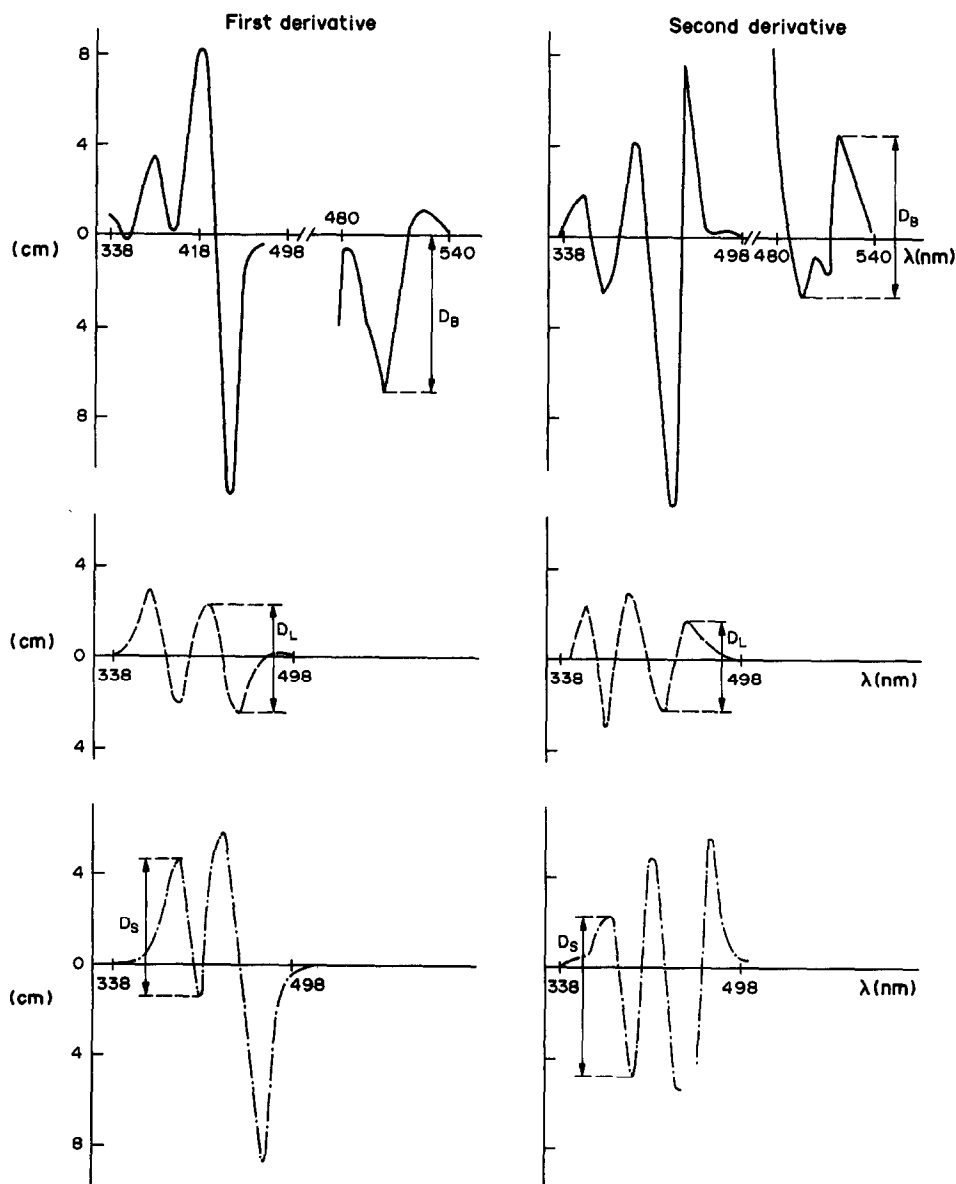


Fig. 3. Synchronous first and second derivatives of ternary mixtures with $\Delta\lambda_s = 98$ nm (—), sensitivity (0.3–3.0), detail (1.0–3.0, scale expansion $\times 5$); $\Delta\lambda_s = 47$ nm (---), sensitivity (0.3–3.0); 121 nm (-·-·-), sensitivity (0.3–3.0).

ing the synchronous spectra are optimized to minimize or eliminate the spectral interference of other compounds present.

A set of sequential scans of the synchronous spectra, with $\Delta\lambda_s$ starting at 13 nm and increasing by 3 nm for each scan (Fig. 2), provides a full picture of the synchronous profile of the mixture. The selection of $\Delta\lambda_s$ values suitable for determination of each component is easily done by simple inspection of the plot (see Fig. 2).

The information in Fig. 1 indicates that the scans should all start from an excitation wavelength of 209 nm, the emission wavelength starting at 222 nm in the first scan and 369 nm in the 50th. The slits should be set to give a band-pass of 5 nm, the scan-speed should be 240 nm/min and the sensitivity factor 0.13.

As indicated in Fig. 2, the appropriate $\Delta\lambda_s$ values for the determination of each component in the ternary mixture are 98, 47 and 121 nm for berberine, luguine and sanguinarine, respectively. It may be emphasized that the program designed to obtain this sequential synchronous scanning avoids the incomplete trial and error search traditionally used for this type of technique.

Despite the advantages of the synchronous technique for separating overlapping bands, it is not sufficient when the interfering spectral band is stronger than that of the analyte. For such cases, the derivative technique can be used to eliminate the interfering band in the synchronous spectrum by recording the synchronous derivative spectrum at a wavelength where only the analyte of interest gives a signal. This signal may be amplified as much as the signal-to-noise ratio permits. This was done for the three synchronous spectra chosen from Fig. 2, with $\Delta\lambda_s = 98, 47$ and 121 nm for berberine, luguine and sanguinarine, respectively, the result being the synchronous derivative spectra in Fig. 3.

Parameters affecting the derivative spectra, such as scan-speed, response time and wavelength range over which the derivative is averaged were selected.^{13,14} A combination of scan-speed 240 nm/min, response time 1.5 sec and wavelength range 10 nm provides the best conditions for good sensitivity and selectivity in determination of the alkaloids.

Peak-height measurements (as vertical distance from peak to trough), were made for different concentrations to establish the calibration graph. The distances D_B , D_L and D_S shown

in Fig. 3 were found to be proportional to the berberine, luguine and sanguinarine concentrations and were the least affected by spectral interferences from the other alkaloids. The $5\times$ magnification clearly shows the otherwise hardly detectable shoulder characteristic of berberine.

Quantitative analysis

To obtain calibration graphs for each alkaloid in ternary mixtures, concentrations in the range between 50 and 250 ng/ml for the species to be determined were introduced into five solutions, with a total constant concentration of 300 ng/ml for the two other alkaloids.

Each calibration graph was repeated five times with solutions containing the same constant total concentration of the other two alkaloids but in different ratios ranging from 1:5 to 5:1. Statistical analysis of the slope and intercept of the regression curves obtained for each case shows a small standard deviation for the slopes, suggesting that no multiplicative interference exists. On the other hand, the intercepts are more affected by the matrix composition, because energy transfer occurs as a consequence of the overlapping spectral profiles. To reduce this problem, the regression equations have been corrected by making the intercepts zero.

The mean regression curves applied for the simultaneous determination of the three alkaloids in ternary mixtures by normal, and synchronous first and second derivative spectrofluorimetry are as follows:

Berberine

$$I_f = (0.134 \pm 0.120) \times [\text{berberine}] + (19.3 \pm 23.9)$$

$$D^1 = (0.035 \pm 0.01) \times [\text{berberine}] - (0.02 \pm 0.43)$$

$$D^2 = (0.026 \pm 0.006) \times [\text{berberine}] + (0.96 \pm 0.52)$$

Luguine

$$I_f = (0.515 \pm 0.334) \times [\text{luguine}] + (23.8 \pm 34.1)$$

$$D^1 = (0.079 \pm 0.002) \times [\text{luguine}] - (0.13 \pm 0.32)$$

$$D^2 = (0.066 \pm 0.002) \times [\text{luguine}] + (0.35 \pm 0.47)$$

Table 2. Application of the methods to synthetic mixtures

Mixture*	Recovery \pm S.D.†, %	
	First derivative	Second derivative
Berberine (B)		
B(250) + L(250) + S(250)	71.4 \pm 0.4	92.0 \pm 2.0
B(50) + L(50) + S(50)	85.8 \pm 2.1	—
B(210) + L(130) + S(90)	87.1 \pm 0.4	123.6 \pm 0.6
Luguine (L)		
B(250) + L(250) + S(250)	94.9 \pm 0.2	95.4 \pm 0.1
B(50) + L(50) + S(50)	104.4 \pm 0.6	106.3 \pm 0.7
B(210) + L(130) + S(90)	90.3 \pm 0.2	101.9 \pm 0.3
Sanguinarine (S)		
B(250) + L(250) + S(250)	70.8 \pm 0.2	79.5 \pm 0.2
B(50) + L(50) + S(50)	74.8 \pm 0.6	88.5 \pm 0.7
B(210) + L(130) + S(90)	70.1 \pm 0.2	82.1 \pm 0.5

*Concentrations (ng/ml) in parentheses.

†Five determinations.

Table 3. Determination of the alkaloids in *Glaucium flavum*

Compound	Alkaloid \pm S.D., mg/g	
	First derivative	Second derivative
Berberine	0.77 \pm 0.03	0.76 \pm 0.04
Luguine	0.77 \pm 0.03	0.80 \pm 0.03
Sanguinarine	0.24 \pm 0.01	0.26 \pm 0.004

Sanguinarine

$$I_r = (0.404 \pm 0.072) \times [\text{sanguinarine}] \\ + (11.4 \pm 15.2)$$

$$D^1 = (0.127 \pm 0.022) \times [\text{sanguinarine}] \\ - (1.9 \pm 3.4)$$

$$D^2 = (0.136 \pm 0.016) \times [\text{sanguinarine}] \\ - (1.1 \pm 2.1)$$

Synthetic mixtures containing the three alkaloids were prepared and measured by the normal, first and second derivative techniques to prove the utility of the regression curves proposed above. The results are shown in Table 2. Serious interferences occurred with the normal spectra, as was expected, but the recovery obtained with the first and second derivatives was much closer to 100%.

From the recoveries in Table 2, the following observations can be made. First, berberine is only accurately determined by the second-derivative method, whereas luguine and sanguinarine can be measured by either the first or second derivative method. Secondly, the best technique for measuring the three alkaloids in the proportions quoted is the second derivative, which gives good recoveries and the smallest R.S.D.

Application of proposed methods to natural samples

To confirm the usefulness of the proposed methods, they were applied to the determination of berberine, luguine and sanguinarine in root extracts of *Glaucium flavum* taken from Misericordia beach (Málaga). The procedure is detailed under "extraction procedure". The results are given in Table 3, and good concordance was obtained between the quantities found by the first and second derivative technique by use of the mean regression curve established for each alkaloid in mixtures.

REFERENCES

1. C. Cruces Blanco and F. García Sánchez, *Anal. Chem.*, 1984, **56**, 2035.
2. F. García Sánchez, A. Navas and M. Santiago, *Anal. Chim. Acta*, 1985, **167**, 217.
3. C. Cruces Blanco and F. García Sánchez, *J. Assoc. Off. Anal. Chem.*, 1986, **69**, 105.
4. H. W. Latz, A. H. Ullman and J. D. Winefordner, *Anal. Chem.*, 1978, **50**, 2148.
5. *Idem, ibid.*, 1980, **52**, 191.
6. J. N. Miller, T. A. Ahmad and A. F. Fell, *Proc. Anal. Div. Chem. Soc.*, 1982, **19**, 37.
7. F. V. Bright and L. B. McGown, *Analyst*, 1986, **111**, 205.
8. K. W. Bentley, *The Alkaloids*, Vol. 1, Interscience, London, 1966.
9. L. Castedo, D. Dominguez, J. M. Saa and R. Suau, *Tetrahedron Lett.*, 1978, **32**, 2923.
10. M. Tomita, Y. Watanabe and M. Fure, *J. Pharm. Soc. Japan*, 1957, **77**, 274.
11. F. García Sánchez, M. Hernández and J. C. Márquez, *Spectrochim. Acta*, 1987, **43A**, 101.
12. C. Gutierrez, S. Rubio, A. Gómez-Hens and M. Valcárcel, *Anal. Chem.*, 1987, **59**, 709.
13. T. Vo-Dinh, *ibid.*, 1978, **50**, 396.
14. J. B. F. Lloyd and I. W. Evett, *ibid.*, 1977, **49**, 1710.

MEASUREMENT OF ^{90}Sr IN ENVIRONMENTAL SAMPLES BY CATION-EXCHANGE AND LIQUID SCINTILLATION COUNTING

HIKARU AMANO and NOBUYUKI YANASE

Department of Environmental Safety Research, Japan Atomic Energy Research Institute, Tokai-mura,
Naka-gun, Ibaraki-ken 319-11, Japan

(Received 21 July 1988. Revised 5 December 1989. Accepted 14 December 1989)

Summary—A new method for the measurement of ^{90}Sr in environmental samples by cation-exchange and liquid scintillation counting is described. Strontium carbonate is purified by precipitation and ion-exchange, weighed for the determination of chemical yield, dissolved in hydrochloric acid and mixed with the liquid scintillator, Aquasol-2. Two channels of a low-background liquid scintillation counter are used to determine ^{90}Sr , ^{90}Y and ^{89}Sr , free from the effects of environmental tritium. The values of ^{90}Sr obtained by this method are in good agreement with those from ordinary ^{90}Y milking and the gas proportional counting method. The concentration of ^{90}Sr in the air at Tokai-mura in Japan has been measured by the new method.

Strontium-90 is one of the most important radionuclides among fission products because of its long half-life and its retention by the body. Several methods for the determination of ^{90}Sr in environmental samples have been reported,¹⁻³ but most of them are time-consuming and tedious. Additionally, if ^{89}Sr , which exists in the air after nuclear detonations as well as in effluents from nuclear facilities, is also present, then two beta-counts are needed to determine both of these radionuclides. It is also difficult to separate strontium chemically from the large quantity of calcium which is inevitably present in environmental samples. Double ion-exchange separations of strontium in biological samples containing gram levels of calcium have been reported.^{3,4} Methods using a single cation-exchange column have also been reported,^{1,5,6} but were not tested for samples containing a large quantity of calcium, so their effectiveness with calcium-rich samples is not clear. The present paper reports separation of strontium from gram levels of calcium with a single cation-exchange column, in routine analysis.

Several methods of measuring the radioactivity of strontium with a liquid scintillation counter (LSC) have been reported.⁷⁻¹² These are categorized as Cerenkov counting methods and liquid scintillation counting methods. The former usually requires two or more measurements for determining ^{89}Sr and ^{90}Sr in the presence of ^{90}Y .^{7,10} Alternatively, three channels of an LSC can be used to determine ^{89}Sr ,

^{90}Sr and ^{90}Y consecutively in the same sample. Piltingsrud and Stencel⁸ determined these nuclides by using liquid scintillation beta-spectroscopy and a spectrum deconvolution program. Shimizu *et al.*¹¹ determined these nuclides by using liquid beta-spectroscopy and Cerenkov counting. In many of these methods the accuracy of the result suffers from the propagation of errors. In addition, it is difficult to eliminate the effect of environmental tritium, which is present in water and interferes with the determination of these nuclides.

For ^{89}Sr , ^{90}Sr and ^{90}Y in environmental samples, measurement in 2 channels of an LSC is proposed here. The concentration of ^{90}Sr in the air at Tokai-mura in Japan has been determined by this method.

EXPERIMENTAL

Reagents

Cation-exchange column. Amberlite CG-120, 100-200 mesh, 25 × 2.0 cm column.

Eluent I. A 1:1 v/v mixture of 2M ammonium acetate and methanol.

Eluent II. Ammonium acetate solution, 2M.

Scintillator. Emulsion type scintillator, Aquasol-2. All chemicals used were of analytical reagent grade.

Radioactivity measurement

Beta activity was measured with an Aloka-LB1 low-background liquid scintillation counter and an anti-coincidence GM-type gas

proportional counter. Gamma activity was measured with a Ge(Li) detector and a multi-channel pulse-height analyser. Two channels of the low-background liquid scintillation counter were used to determine ^{89}Sr and ^{90}Sr in the presence of ^{90}Y .

Procedure

Airborne strontium was continuously collected with a Toyo type HE40-T cellulose (80%)/glass-fibre (20%) filter paper, which was replaced once a week. Thirteen filters were combined and analysed. Each air-particulate sample was ashed completely at 450° . The ash obtained was placed in an 800-ml beaker and a strontium spike was added as carrier. Next, 200 ml of 8M nitric acid were added and the mixture was heated on a hot-plate with occasional stirring. After being allowed to stand for about 1 hr, the mixture was filtered. The residue was heated with 200 ml of 6M hydrochloric acid for 3 hr and the mixture was then filtered. The two filtrates were combined, and any plutonium in the solution was separated by co-precipitation with ferric hydroxide.¹³ The precipitate was separated by centrifugation, then sodium carbonate was added to the supernatant liquid and the resultant precipitate was separated by centrifuging, then dissolved in 5–10 ml of 3M hydrochloric acid. The solution was diluted with water to 30–50 ml and passed through the cation-exchange column, which was then washed with 50 ml of water. The column was then eluted with 600 ml of eluent I at a flow-rate of 2–3 ml/min, followed by 300 ml of eluent II at the same flow-rate. The effluent was reduced to a volume of ~ 50 ml by heating on a water-bath, and ammonium carbonate added to precipitate strontium carbonate. The precipitate was collected in a porosity-4 sintered-glass crucible, dried in an oven at 120° for 2 hr, and weighed to determine the chemical yield. The recovery of strontium was 50–85%. The precipitate was dissolved in 5 ml of 2M hydrochloric acid and the solution was diluted with water to 35 ml, then mixed with 65 ml of Aquasol-2 liquid-scintillator in a 100-ml Teflon vial for the radioactivity measurement with the Aloka LSC-LB1 low-background liquid scintillation counter. Figure 1 shows a flow-sheet for the procedures.

RESULTS AND DISCUSSION

To check the efficiency of the separation, two solutions containing several radioactive nuclides

were used (Table 1). The radioactivities were measured with a Ge(Li) detector and a multi-channel pulse-height analyser. Inactive calcium was used for tests of the elution of calcium.

Elution of strontium

Figures 2 and 3 show the elution curves for solutions containing the fall-out nuclides specified in the figures. The effect of increase in the calcium content is shown in Fig. 2. In all cases calcium was completely eluted with 600 ml of eluent I. The elution of strontium and caesium was affected by the flow-rate. At a flow-rate of 2 ml/min, strontium and caesium were eluted by eluent II (Fig. 2b) but at 3 ml/min, the elution of caesium started before the change from eluent I (Fig. 3). Strontium was completely eluted by 300 ml of eluent II at a flow-rate of 2–3 ml/min.

Capacity of cation-exchange column

The column dimensions were selected to give complete separation of strontium from calcium. It was found that a column 25 cm long and 2 cm in diameter was saturated by 2.44 g of calcium, and a column 17 cm long and 2 cm in diameter by 1.68 g. Therefore the column dimensions should be chosen according to the amount of calcium in the sample. For a 2-cm diameter column, the length in cm should be approximately 10 times the number of grams in the sample loaded.

Figures 2 and 3 show that the volumes of eluate required are 600 ml of I and 200 ml of II for a 17×2 cm column and 600 ml of I and 300 ml of II for a 25×2 cm column.

Liquid scintillation counting

Theory. Figure 4 shows schematically a beta-ray spectrum of ^3H , ^{90}Sr , ^{89}Sr and ^{90}Y in a sample. Two channels of the LSC were used to determine ^{90}Sr , ^{90}Y and ^{89}Sr , the effect of environmental tritium being eliminated by adjusting the lower discrimination level of the LSC. The following equations are used to analyse the data from the two channels.

Channel C:

$$A = X \times E(^{90}\text{Sr}/\text{C}) + Y \times E(^{90}\text{Y}/\text{C}) + Z \times E(^{89}\text{Sr}/\text{C})$$

Channel P:

$$B = X \times E(^{90}\text{Sr}/\text{P}) + Y \times E(^{90}\text{Y}/\text{P}) + Z \times E(^{89}\text{Sr}/\text{P})$$

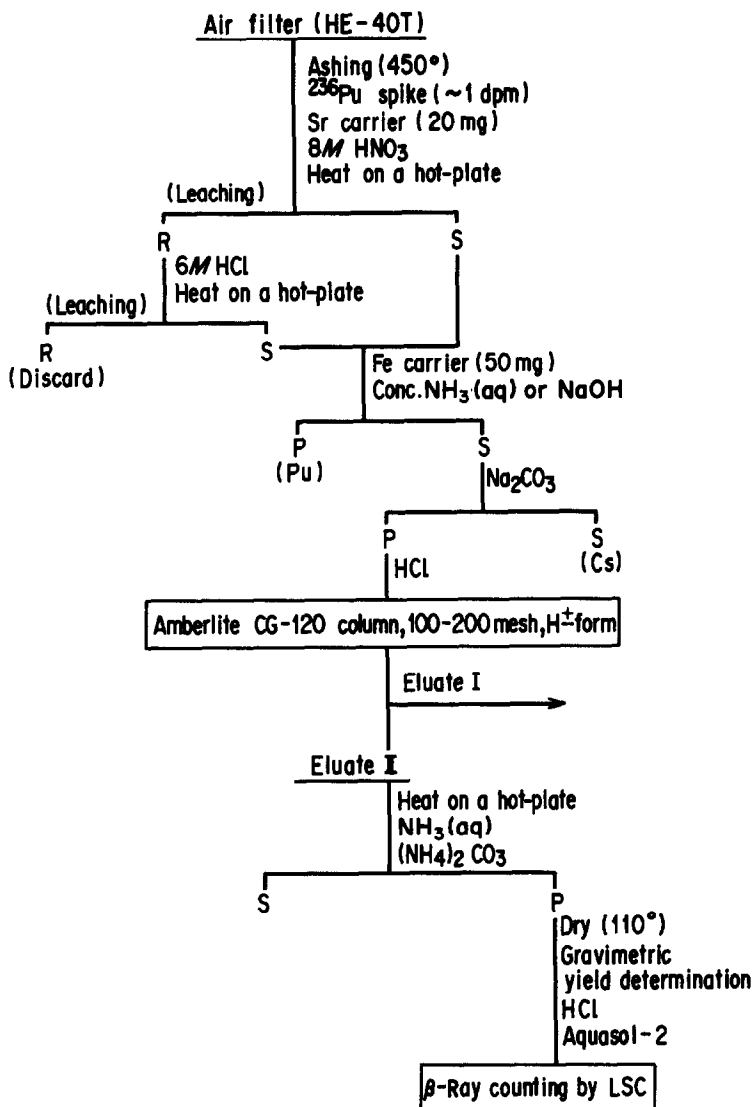


Fig. 1. Analytical procedures for ⁸⁹Sr and ⁹⁰Sr in a dust sample.

where $A = \text{cpm in channel C}$; $B = \text{cpm in channel P}$; $X, Y, Z = \text{activity of } ^{90}\text{Sr}, ^{90}\text{Y}, ^{89}\text{Sr}$ respectively; $E(i/C)$ and $E(i/P) = \text{counting efficiencies for species } i \text{ in channels C and P, respectively.}$

Table 1. Chemical composition and radioactive nuclides in the feed solutions

Solution	Metal ion	Radioactive nuclides	Content, mg
I	Sr ²⁺	⁸⁵ Sr	20
	Cs ⁺	¹³⁷ Cs	20
	Ba ²⁺	¹³³ Ba	20
	Ca ²⁺	—	500–2400
II	Sr ²⁺	⁸⁵ Sr	20
	Cs ⁺	¹³⁷ Cs	20
	Co ²⁺	⁵⁷ Co, ⁶⁰ Co	20
	Y ³⁺	⁸⁸ Y	20
	Mn ²⁺	⁵⁴ Mn	20
	Ce ⁴⁺	¹³⁹ Ce	20

Use of the gross activity and efficiency for ⁹⁰Sr + ⁹⁰Y simplifies these equations to

$$A = X' \times E[(^{90}\text{Sr} + ^{90}\text{Y})/C] + Z \times E(^{89}\text{Sr}/C)$$

$$B = X' \times E[(^{90}\text{Sr} + ^{90}\text{Y})/P] + Z \times E(^{89}\text{Sr}/P)$$

After separation of the strontium, the operative equation is

$$X' = X + Y = X(1 + k)$$

where k is the growth-rate of ⁹⁰Y.

In this case, it is necessary to check the time between separation of the strontium and measurement of the radioactivity for determination of the radioactivities of ⁹⁰Sr and ⁹⁰Y. Furthermore, it is necessary to determine the gross counting efficiency for ⁹⁰Sr + ⁹⁰Y in each channel of the LSC.

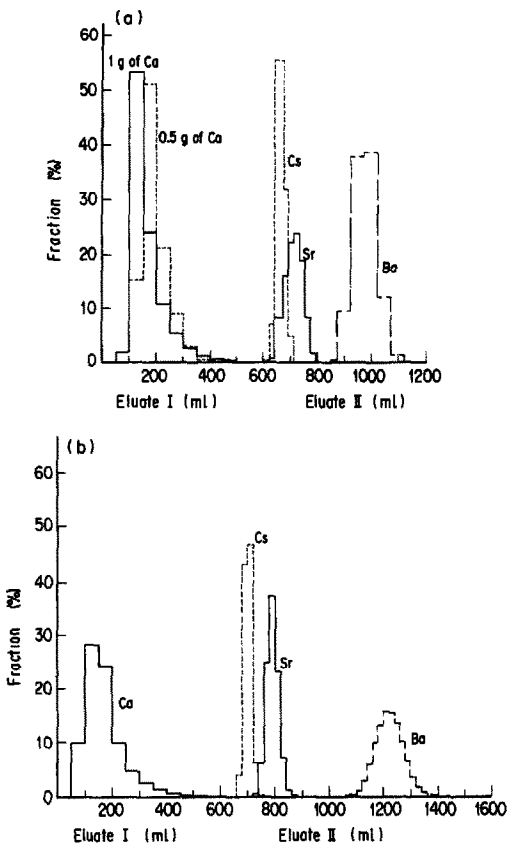


Fig. 2. (a) Elution curves of Ca, Sr, Cs and Ba from a 17×2 cm. Amberlite CG-120 column; the sample contained 0.5 or 1.0 g of Ca, 20 mg of Sr, 20 mg of Cs and carrier-free ^{133}Ba ; elution at 2.0 ml/min with 600 ml of each eluent. (b) Elution curves of Ca, Sr, Cs and Ba from a 25×2 cm. Amberlite CG-120 column; the sample contained 2.4 g of Ca, 20 mg of Sr, 20 mg of Cs and carrier-free ^{133}Ba ; elution at 2.0 ml/min with 600 ml of eluent I and 1000 ml of II.

Standards for calibration with the LSC. To determine the counting efficiency for ^{89}Sr and $^{90}\text{Sr} + ^{90}\text{Y}$ in each channel, several quenching standard samples which had different quenching levels were prepared and added to the standard solution of ^{89}Sr and ^{90}Sr . For these standards ^{90}Sr equilibrated with ^{90}Y was used, with water as the quencher, mixed in various ratios with liquid scintillator Aquasol-2 to give a total volume of 100 ml. Figure 5 shows an example of the relationship between the external ratio (which is the ratio of the count rates of two single-channel analysers set at different discriminator levels, and shows the quenching level) and the efficiency in each channel of the LSC. The effect of environmental tritium is eliminated as already described, to avoid interference with the strontium determination.

The quenching of samples and the background count of the LSC. In the measurement of weak radioactivity with an LSC, the background

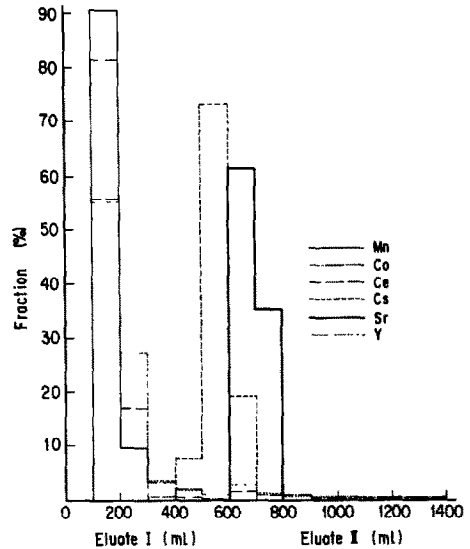


Fig. 3. Elution curves of simulated fall-out solution (20 mg each, of Cs^+ , Sr^{2+} , Y^{3+} , Mn^{2+} , Ce^{4+} , Co^{2+}). Amberlite CG 120 column 25×2 cm, eluted with 600 ml of eluate I and 800 ml of eluate II at 3.0 ml/min.

count and its variation can markedly affect the accuracy of the results, so the relationship between the quenching effect and the background count was examined. Carbon tetrachloride (0.05–2%), water (5–55%) and 2M hydrochloric acid (1–15%, plus 30 mg of strontium carbonate and 0–40% water) were used as quenchers and were mixed with Aquasol-2 to give a total volume of 100 ml. Each quenching level was calibrated by the external ratio method. Figure 6 shows that the background count in each channel of the LSC depends not only on the quenching level of the samples but also on the quencher itself. There was no difference in the C channel background counting rate between all three quenchers as a function of external ratio, but in the P channel water and hydrochloric acid behaved identically, but differed in behaviour from carbon tetrachloride.

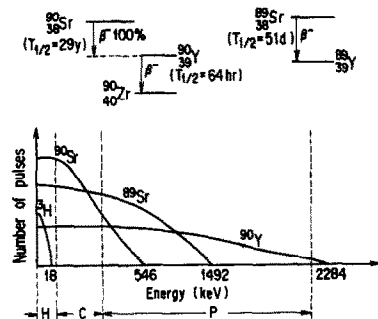


Fig. 4. Abstracts of beta-ray spectrum of ^3H , ^{89}Sr , ^{90}Sr and ^{90}Y in each channel of the LSC.

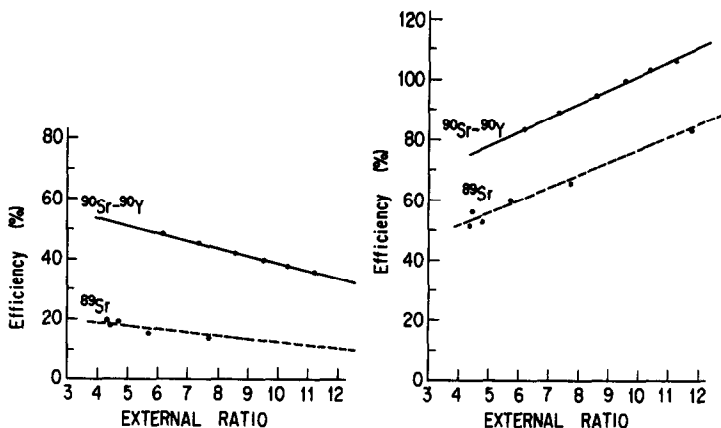


Fig. 5. Relationship between quenching and efficiency in each channel of the LSC. (Left) C channel: gain 1.0, discriminator 350-1000. (Right) P channel: gain 1.0, discriminator 150-1000.

The commercial Teflon vials used for the measurements with the LSC, all have different optical characteristics,¹⁴ so close attention should be paid to background counts.

Simultaneous measurement of ⁹⁰Sr and ⁸⁹Sr with LSC. To check the effectiveness of the simultaneous measurement of ⁹⁰Sr and ⁸⁹Sr by the LSC, several water samples with different activity ratios of ⁹⁰Sr and ⁸⁹Sr were prepared and their activities measured. Very weak radioactivities were used to check the effectiveness with environmental samples. Table 2 shows that this method is very effective for measuring a wide range of concentrations of both ⁸⁹Sr and ⁹⁰Sr.

Comparison between the LSC and milking methods

To check the validity of the method, a comparison between the LSC method and the

ordinary ⁹⁰Y milking plus gas proportional counting method was made. Airborne strontium was collected at Tokai-mura in Japan by continuously passing air through a cellulose/glass fibre filter, which was replaced once a week. The deposits on 13 filters were combined and analysed by the method detailed above. Eluate II was divided into two portions, one being analysed by the LSC method and the other by ⁹⁰Y milking and gas proportional counting. Figure 7 shows the good correlation between the

Table 2. Determination of ⁸⁹Sr and ⁹⁰Sr by LSC

Sample solution	⁸⁹ Sr/ ⁹⁰ Sr	Added activity, dpm	Measured activity, dpm	Yield, %
1	2.3	⁸⁹ Sr 9.5	10.6	112
		⁹⁰ Sr 4.2	4.2	100
2	0.45	⁸⁹ Sr 9.5	9.6	101
		⁹⁰ Sr 21.2	19.0	90
3	0	⁸⁹ Sr 0	DL*	—
		⁹⁰ Sr 21.2	21.0	99
4	∞	⁸⁹ Sr 18.9	19.6	104
		⁹⁰ Sr 0	DL	—

*DL = detection limit.

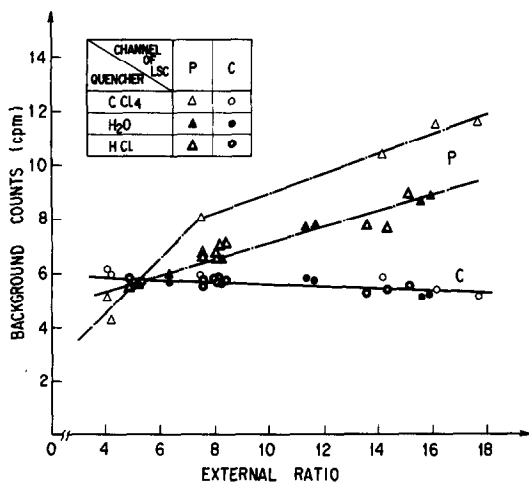


Fig. 6. Relationship between quenching and background counts in each channel of the LSC. C channel: gain 1.0, discriminator 350-1000. P channel: gain 1.0, discriminator 150-1000.

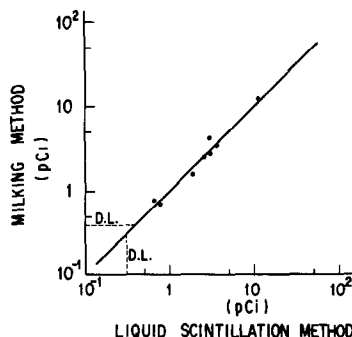


Fig. 7. Comparison of ⁹⁰Sr activities measured by the ordinary milking method and the liquid scintillation method: D.L. = detection limit (3σ).

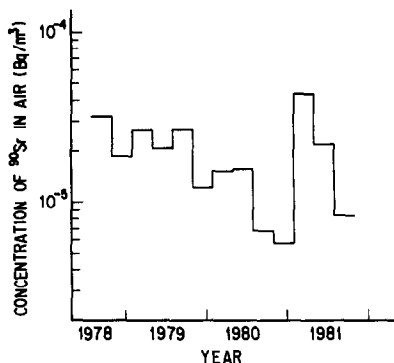


Fig. 8. Concentration of ^{90}Sr in air at Tokai-mura, Japan, over a 3-year period.

Table 3. Analysis of NBS 4353 Rocky Flats Soil

Certified activity of ^{90}Sr , Bq/g	0.00763
Total uncertainty, %	10.2
Activity found, Bq/g	A 0.0073 ₈
	B 0.0083 ₃

results. The results obtained for airborne ^{90}Sr at Tokai-mura, for each three-month period from 1978 and to 1981, are shown in Fig. 8. No ^{89}Sr was detected in any of these samples because of the long storage of the filter samples.

Measurements of standard samples

To check its general applicability, the method was used to analyse an environmental standard sample. Table 3 shows the results, which are in good agreement with the NBS value, the differences (-3% for A and $+9\%$ for B) being within the estimated total uncertainty of the certified value.

Conclusions

The method is very simple, and suitable for the routine analysis of environmental samples.

There is no need to use fuming nitric acid, as in the usual procedures for determination of strontium. It allows simultaneous determination of ^{90}Sr and ^{89}Sr by only one measurement with the LSC, and the chemical procedure is simplified. The ^{90}Y milking procedure is omitted, and ^{90}Sr can be assayed immediately after separation from the other elements, if the counting efficiency curve for the LSC is available. The disadvantage of the method is that the purified strontium is not stored in aqueous solution, which would allow repeated ^{90}Y milking as in the ordinary method.

Acknowledgements—The authors wish to thank Mr. A. Kasai, Dr. K. Sekine and Mr. T. Imai for their assistance in this work.

REFERENCES

1. B. Carmon, *Int. J. Appl. Radiat. Isot.*, 1977, **28**, 435.
2. J. H. Harley (ed.), *Environmental Measurements Laboratory Procedures Manual, HASL-300*, New York, 1980.
3. L. P. Gregory, *Health Phys.*, 1963, **10**, 483.
4. P. J. Brandt and B. Riet, *Anal. Chem.*, 1966, **38**, 1790.
5. H. Tsubota, *Bull. Chem. Soc. Japan*, 1963, **36**, 1545.
6. *Idem, ibid*, 1965, **38**, 159.
7. B. Carmon, *Int. J. Appl. Radiat. Isot.*, 1979, **30**, 97.
8. H. V. Piltingsrud and J. R. Stencel, *Health Phys.*, 1972, **23**, 121.
9. G. S. Uyesugi and A. E. Greenberg, *Int. J. Appl. Radiat. Isot.*, 1965, **16**, 581.
10. S. A. Reynold and J. S. Eldridge, in *Liquid Scintillation Counting—Recent Applications and Development*, C. T. Peng, D. L. Horrocks and E. L. Alpen (eds.), pp. 397–405. Academic Press, New York, 1980.
11. T. Shimizu, N. Hayashi, K. Akutsu, T. Nomura, A. Yamato and M. Iwai, *Hoken Butsuri*, 1985, **20**, 139.
12. J. E. Martin, *J. Appl. Radiat. Isot.*, 1987, **38**, 953.
13. A. Kasai, T. Imai and K. Sekine, *Health Phys.*, 1984, **46**, 214.
14. H. Amano and A. Kasai, *Japan Atomic Energy Research Institute Report, JAERI-M 8578*, 1979.

SYNTHESIS, CHARACTERIZATION AND ANALYTICAL APPLICATION OF A HYDROXAMIC ACID RESIN

RITA MENDEZ and V. N. SIVASANKARA PILLAI*

Department of Applied Chemistry, Cochin University of Science and Technology, Cochin 682022, India

(Received 8 March 1988. Revised 13 December 1989. Accepted 4 January 1990)

Summary—A chelating ion-exchange resin with hydroxamic acid functional groups was synthesized from styrene-maleic acid co-polymer cross-linked with divinylbenzene. A resin prepared from equimolar amounts of styrene and maleic anhydride with 0.75 mole% divinylbenzene gives the best sorption characteristics. The selectivity of the resin for metal ions is copper(II) \gg cobalt(II) $>$ zinc(II) $>$ nickel(II) $>$ manganese(II) $>$ chromium(III) $>$ iron(III) $>$ vanadium(V). Copper(II), chromium(III) and iron(III) in chromium plating baths can be separated by use of the resin and determined spectrophotometrically.

Hydroxamic acids form complexes with various heavy metal ions, particularly iron(III).¹⁻⁴ Polymers bearing hydroxamic acid groups have been used in metal-ion preconcentration and separation.⁵⁻⁹ Most of the research on polyhydroxamic acids has been concentrated on their synthesis, properties and applications. Exceptions to this are found in the work of Winston and co-workers,^{10,11} who studied the spacing of hydroxamic acid units in a polymer and its influence on the affinity for iron(III).

This study deals with the synthesis of a hydroxamic acid resin from a styrene-maleic acid co-polymer cross-linked with divinylbenzene (DVB), and its characteristics. Mixtures of copper(II), nickel(II), iron(III) and vanadium(V), and of chromium(III), copper(II) and iron(III) have been separated on a column of the resin. The resin can also be used for the removal of these ions from wastewater.¹²

EXPERIMENTAL

Apparatus

Metal ion concentrations were determined with a Hitachi 200 spectrophotometer or a Perkin-Elmer Model 2380 flame atomic-absorption spectrometer. Pore volume and pore size were measured by the BET method.

Reagents

Analytical grade reagents were used, and all solutions were made with doubly distilled water. The buffer solutions were prepared by mixing

0.1M ammonium citrate and 1M citric acid, or 0.1M sodium acetate and glacial acetic acid, until the desired pH was attained.

Preparation of the resin

The resin was prepared by a modification of the method of Dhandhukia *et al.*¹³ Maleic anhydride was purified by vacuum sublimation and dissolved in acetone under reflux. The maleic anhydride and styrene were taken in different mole ratios, and mixed with 0.75 mole% divinylbenzene and benzoyl peroxide (0.75% w/w of the styrene-divinylbenzene content). The mixture was heated under reflux on a boiling water-bath and when gelling had taken place (2 hr) the polymer was transferred to a beaker, the acetone was evaporated and the polymer was cured in an oven at 80-100° for 6-8 hr. Similarly, the divinylbenzene content was varied, with constant maleic anhydride-styrene mole ratio (1:1). The dry resin was ground in a mortar and sieved.

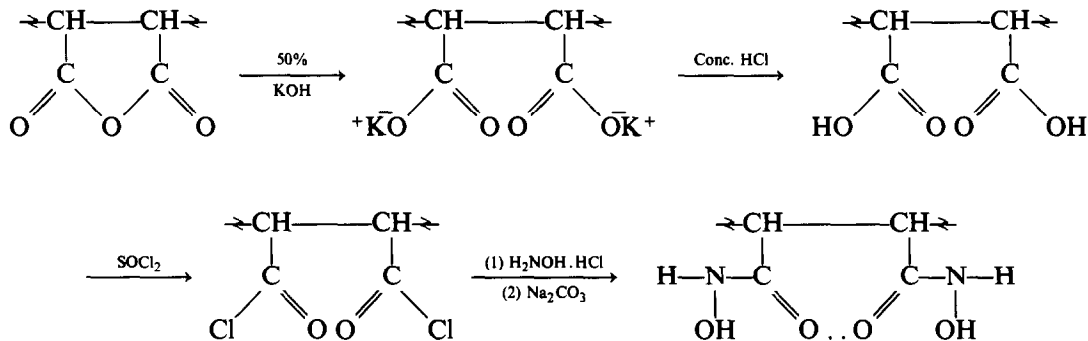
The copolymers were hydrolysed by refluxing with 200 ml of 10M potassium hydroxide for 10 hr, followed by acidification with concentrated hydrochloric acid. The product was washed with water, dried in an oven at 100° for 10 hr, then refluxed with excess of thionyl chloride on a boiling water-bath for 3 hr, with intermittent stirring. The excess of thionyl chloride was distilled off under reduced pressure.

To 1 g of the acid chloride were added 2.1 g of powdered sodium carbonate, 1.4 g of hydroxylammonium chloride, 10 ml of diethyl ether and 2.5 ml of water. The mixture was stirred for 2 hr, then the product was filtered off,

*Author for correspondence.

washed with water until the washings were neutral, then with methanol, and dried in an oven at 80° for 8 hr.

The scheme for the conversion of the copolymer into the hydroxamine acid resin is shown below.



monomer ratios were shaken with 20-ml aliquots of 400 $\mu\text{g/ml}$ solutions of copper(II) (at pH 5) and iron(III) (at pH 2) for 2 hr and the sorption capacities determined. The batch capacities of the resins prepared with varied divinylbenzene content were also determined.

Resin characterization

The resin was characterized by determination of its stability towards acids and alkalis, and its sorption capacity, distribution coefficients and kinetics of sorption.

Stability. The resin was soaked for 24 hr in 0.1M sodium hydroxide, concentrated hydrochloric acid, or 0.1M nitric acid, then filtered off with a sintered-glass funnel, washed with distilled water and dried in an oven at 80° for 8 hr. The resin showed no significant weight loss even after repeated cycles of treatment.

Sorption capacity and distribution coefficients. The batch capacity for copper(II), zinc(II), cobalt(II), nickel(II), manganese(II), chromium(III), iron(III), and vanadium(V) was determined in the pH range 1–7, adjusted with 0.1M hydrochloric acid, sodium hydroxide and ammonium acetate–acetic acid buffer. Portions of the resin (0.1 g) were shaken for 24 hr with 20-ml aliquots of the metal ion solution (400 $\mu\text{g/ml}$).

The distribution coefficients (K_d) were determined by measuring the metal ion concentration in the resin and the aqueous phase after equilibration.

Sorption kinetics. A 0.1-g portion of the resin (100–200 mesh) was shaken for 2 hr with 20 ml of 400 $\mu\text{g/ml}$ metal ion solution (100 $\mu\text{g/ml}$ for vanadium) at the pH for maximum capacity, and the metal ion concentration in the aqueous phase was measured at intervals.

Effect of monomer ratio on batch capacity for copper(II) and iron(III). Portions (0.1 g) of the resins (100–200 mesh) made with different

Column operation

Resin particles (100–200 mesh, 1.5 g) were allowed to swell in the appropriate buffer for 2 hr and then slurry-packed into a glass tube (15.0 \times 0.6 cm) to give a bed volume of 4.2 ml.

The column was conditioned with an appropriate buffer and 1 ml of a mixed metal ion solution was run through the column at a flow-rate of 0.5 ml/min, followed by suitable eluents (Table 1).

Analysis of effluent from a chromium plating plant

The effluent contained chromium(VI), chromium(III), iron(III) and copper(II). To determine the total chromium content and avoid oxidation of the functional groups in the resin, the chromium(VI) was reduced to chromium(III) by addition of sodium metabisulphite solution and boiling off the excess of sulphur dioxide. To reoxidize any iron(II) formed, 2 drops of concentrated nitric acid were added and the mixture was boiled for 5 min. The pH was then adjusted to 3 with 0.1M sodium acetate–acetic acid buffer and the column was conditioned with the same buffer. Then 1 ml of the sample was run through the column at 0.5 ml/min, and the chromium was eluted with 0.1M ammonium citrate–citric acid solution (pH 3), copper with 0.01M hydrochloric acid and iron with 0.2M hydrochloric acid. The eluates were analysed spectrophotometrically.¹⁴

Table 1. Separation of metal ions

Separations achieved	Eluent	Eluate volume, ml	Amount loaded, μg	Amount recovered, μg
1. Cu(II)	0.1M HCl	50	100	100.6
Fe(III)	0.2M HCl	25	100	99.9
2. Ni(II)	0.1M Ammonium citrate-citric acid, pH 5	60	100	97.0
Cu(II)	0.1M HCl	20	100	97.8
3. Ni(II)	0.1M Ammonium citrate-citric acid pH 5	50	50	49.7
Cu(II)	0.1M HCl	20	100	99.3
4. V(V)	0.1M HCl	30	100	96.3
Fe(III)	0.2M HCl	30	100	101.4

RESULTS AND DISCUSSION

The resin reported is porous and typically contains 28% micropores (<20 Å) and 72% mesopores (20–500 Å), and has a pore volume of 0.01 ml/g. It has excellent resistance to concentrated hydrochloric acid, 0.1M nitric acid and 0.1M sodium hydroxide. The nitrogen content of the dry resin was found to be 2.68 mmole/g.

Figure 1 shows that the batch capacity of the resin is maximal for maleic anhydride-styrene ratios >1. The batch capacity for metal ions was found to be maximum when the resin contains 0.75 mole% divinylbenzene.

The K_d values for various metal ions as a function of pH are shown in Fig. 2, and the degree of extraction in Fig. 3. The maximal values of both are high for copper(II) and low for iron(III). This is in contrast to the behaviour of the hydroxamic acid derivative obtained from

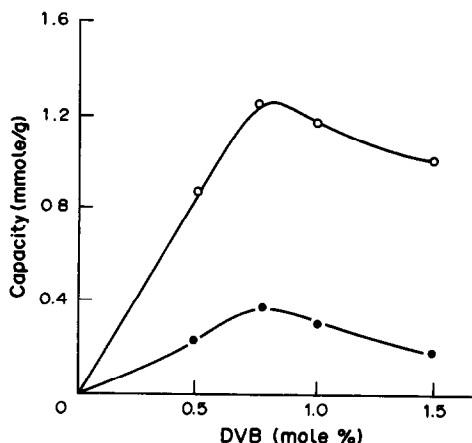


Fig. 1. Effect of varying mole% of DVB in the hydroxamic acid resin on the batch capacity for Cu(II) and Fe(III): 0.1 g of resin; 100–200 mesh size; 20 ml of 400 $\mu\text{g}/\text{ml}$ Cu(II) and Fe(III) solutions; 0.1M ammonium acetate-acetic acid buffer, pH 5; shaking time 2 hr; \circ , Cu(II); \bullet , Fe(III).

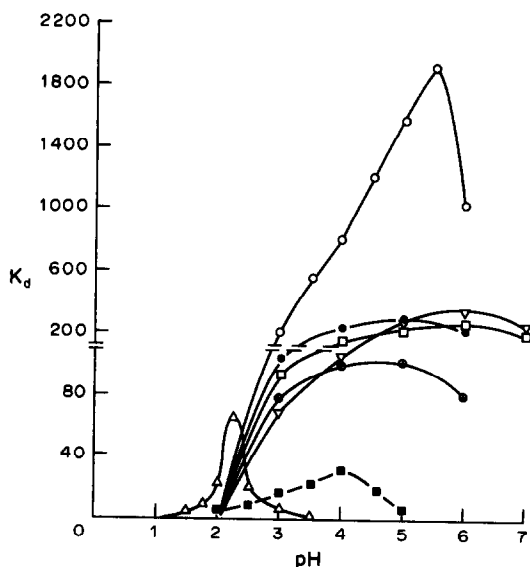


Fig. 2. Distribution coefficient, K_d , for various metal ions at different pH values: 0.1 g of resin; 100–200 mesh size; 20 ml of 400 $\mu\text{g}/\text{ml}$ metal ion solutions; shaking time 2 hr; \circ , Cu(II); \bullet , Ni(II); ∇ , Co(II); \square , Mn(II); \oplus , Cr(III); \triangle , Fe(III); \blacksquare , V(V).

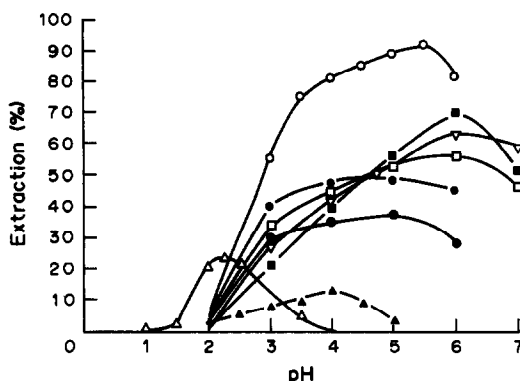


Fig. 3. Effect of pH on the uptake of metal ions by hydroxamic acid resin: 0.1 g of resin; 100–200 mesh size; 20 ml of 400 $\mu\text{g}/\text{ml}$ metal ion solutions; shaking time 2 hr. \circ , Cu(II); \blacksquare , Zn(II); ∇ , Co(II); \square , Mn(II); \bullet , Ni(II); \oplus , Cr(III); \triangle , Fe(III); \blacktriangle , V(V).

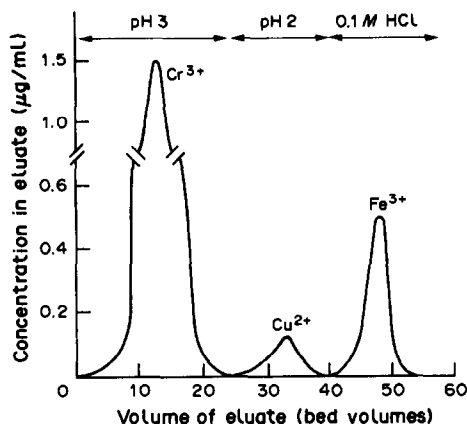


Fig. 4. Separation of Cr(III), Cu(II) and Fe(III) on hydroxamic acid resin from plating bath effluent: 1.5 g of resin; 100–200 mesh size; column 15.0 × 0.6 cm; bed volume 4.2 ml; flow-rate 0.5 ml/min; eluent, pH 3—ammonium citrate–citric acid, pH 2—citric acid.

Table 2. Analysis of a plating bath solution at various dilutions

Plating bath solution	Metal ion	Metal ion found,* µg
1	Cr(III)	43.5 ± 0.3
	Cu(II)	3.96 ± 0.09
	Fe(III)	7.11 ± 0.05
2	Cr(III)	55.8 ± 0.5
	Cu(II)	5.07 ± 0.1
	Fe(III)	8.86 ± 0.05
3	Cr(III)	66.0 ± 0.3
	Cu(II)	6.22 ± 0.03
	Fe(III)	10.54 ± 0.04
4	Cr(III)	90.1 ± 0.2
	Cu(II)	8.09 ± 0.04
	Fe(III)	14.24 ± 0.56

*Mean ± standard deviation of 5 readings.

XAD-4 resin,¹⁵ and of the *N*-hydroxysuccinimide ester of acrylic acid resin,¹⁰ which both have a higher capacity for iron(III) than for copper(II). The hydroxamic acid resins prepared from copolymers of ethylacrylate, acrylic acid and polyacrylonitrile also have a higher affinity for copper(II) than for iron(III).¹⁶ The relative positions of the hydroxamic acid groups in these resins have not been confirmed, but at least a considerable portion of them may be vicinally positioned.

The kinetic studies show that the uptake of various metal ions is fast and the times (min) needed to reach 50% of maximum sorption at the optimum pH are: iron(III), 4; copper(II), 2; nickel(II), 3; cobalt(II), 2; manganese(II), 4; chromium(III), 3 and vanadium(V), 4. The favourable kinetics make the resin suitable for separation of these ions in mixtures by column operation. Table 1 shows the results for separation of selected metal ions from their mixtures.

The chromium plating plant effluent usually contains high concentrations of chromium, copper and iron. Hence it is necessary to dilute the solution before its analysis. Figure 4 shows the separation of copper(II), iron(III) and chromium(III). The separations are clean and the results are reproducible. Some typical values for different dilutions of the same sample are given in Table 2.

Acknowledgement—R.M. is grateful to C.S.I.R., Government of India, for the financial assistance.

REFERENCES

- H. L. Yale, *Chem. Rev.*, 1943, **33**, 209.
- F. Mathis, *Bull. Soc. Chim. France*, 1953, D9.
- J. B. Neilands, *Structure Bonding (Berlin)*, 1966, **1**, 59.
- H. Maehr, *Pure Appl. Chem.*, 1971, **28**, 603.
- J.-P. Cornaz and H. Deuel, *Experientia*, 1954, **10**, 137.
- J.-P. Cornaz, K. Hutschneker and H. Deuel, *Helv. Chim. Acta*, 1957, **40**, 2015.
- H. Deuel and K. Hutschneker, *Chimia*, 1955, **9**, 49.
- F. Vernon and H. Eccles, *Anal. Chim. Acta*, 1975, **77**, 145; 1975, **79**, 229.
- Idem*, *ibid.*, 1976, **82**, 369; 1976, **83**, 187.
- A. Winston and E. T. Mazza, *J. Polym. Sci., Polym. Chem. Ed.*, 1975, **13**, 2019.
- A. Winston and G. R. McLaughlin, *ibid.*, 1976, **14**, 2155.
- V. N. S. Pillai and R. Mendez, *IVth ISAS National Symposium*, University of Burdwan, 1987, p. 19.
- M. M. Dhandhukia, V. K. Indusekhar and K. P. Govindan, *Indian J. Technol.*, 1982, **20**, 203.
- L. Meites, *Handbook of Analytical Chemistry*, p. 6. McGraw-Hill, New York, 1963.
- R. J. Philips and J. S. Fritz, *Anal. Chim. Acta*, 1982, **139**, 237.
- F. Vernon, *Pure Appl. Chem.*, 1982, **54**, 2151.

DETERMINATION OF BROMINE IN ORGANIC COMPOUNDS BY HIGH-PERFORMANCE LIQUID CHROMATOGRAPHY

ARCHANA JAIN, ARCHANA VERMA and KRISHNA K. VERMA*

Department of Chemistry, Rani Durgavati University, Jabalpur 482001, Madhya Pradesh, India

(Received 9 July 1989. Revised 26 September 1989. Accepted 24 October 1989)

Summary—A method is proposed for the determination of bromine in organic compounds (which may also contain chlorine and iodine) by oxygen-flask combustion of the compound followed by pre-column reaction of bromide with acetanilide and 2-iodosobenzoic acid to form 4-bromoacetanilide which is then chromatographed on an ODS column with a mobile phase of methanol:water, 65:35 v/v, detection at 240 nm, and 4-*N*-acetylaminotoluene as internal standard. The method is rapid and precise (RSD \leq 1%), and applicable to a variety of bromine-containing organic compounds; the limit of detection is 0.2 ng of bromine.

The determination of bromine in organic compounds requires (i) conversion of organic bromine into bromide, and (ii) determination of the bromide.¹ The first step involves mineralization of the compound, e.g., by oxygen-flask combustion.² Determination of bromide by titration³⁻⁶ or spectrophotometry based on displacement reactions such as those with mercury(II) chloranilate⁷ or mercury(II) thiocyanate⁸ is neither sensitive nor selective for bromide. A recently published method,⁹ which is based on the anion-exchange reaction of bromide or chloride with excess of solid silver chromate, and polarographic determination of the liberated chromate, should also be applicable to iodide, but cannot be used if the sample contains more than one of these three halides, and is inapplicable to organometallic compounds of metals such as lead, which could yield a precipitate with the chromate liberated. Also, large amounts of phosphate produced by oxidation of phosphorus, if present, may lead to a positive error. 2-Propanol has been used to reduce the effect of co-precipitation in the argentimetric potentiometric titration of bromide and chloride.¹⁰ Oxygen-flask combustion, followed by bromide determination by ion-chromatography with conductivity detection has also been reported.¹¹

Recent developments in pre-column derivatization reactions and high-performance liquid chromatography (HPLC)¹²⁻¹⁷ led us to convert the bromide formed by oxygen-flask combus-

tion of organic bromo-compounds into 4-bromoacetanilide, and to determine this by HPLC.

EXPERIMENTAL

Apparatus

The liquid chromatograph used consisted of a Shimadzu LC-5A pump, an SIL-1A manual loop injector, a Shim-pack ODS column (particle size 5 μ m; 150 \times 6 mm i.d.), an SPD-2A variable wavelength UV detector, and a Shimadzu C-R2AX integrator fitted with a printer-plotter. Peak areas were used for quantification.

Reagents

Acetanilide, 4-*N*-acetylaminotoluene and 4-bromoacetanilide were synthesized and purified by repeated recrystallization.¹⁸ 2-Iodosobenzoic acid was synthesized by the method of Chinard and Hellerman.¹⁹

The mixed reagent solution, prepared by dissolving 100 mg of acetanilide and 150 mg of 2-iodosobenzoic acid in 100 ml of methanol, was filtered through a 0.45- μ m membrane filter. A sulphuric acid solution was made by diluting 1.2 ml of the analytical reagent grade concentrated acid to 100 ml with methanol. A 63:35 v/v mixture of methanol and water was used as the mobile phase.

Standards

All bromo-compounds analysed were of high purity. The internal standard was a

*Author for correspondence.

solution of 5 mg of pure 4-*N*-acetylaminotoluene (*N*-acetyl-4-toluidine) in methanol, diluted to volume in a 50-ml standard flask.

For calibration a standard 30- $\mu\text{g/ml}$ bromide solution was prepared by dissolving 223.1 mg of analytical grade potassium bromide in water and diluting to volume in a 100-ml standard flask, then accurately diluting 5 ml of this solution to 250 ml.

Procedures

Calibration. To portions of the calibration standard ranging from 200 to 1400 μl (6–42 μg of bromide) add 200 μl of internal standard solution, 500 μl of mixed reagent solution and 200 μl of the sulphuric acid solution, dilute the mixture of volume in a 10-ml standard flask with mobile phase, shake the flask well for 1 min, and inject a 10- μl portion into the HPLC column. Set the eluent flow-rate at 1 ml/min (column back pressure approximately 50 kg/cm²) and monitor the eluate with the detector set at 240 nm and a sensitivity of 0.04 absorbance for full scale deflection.

Determination of bromine in organic compounds. Burn a 1–4 mg sample, accurately weighed, in the usual way in a 250-ml Schöniger flask filled with oxygen and containing 10 ml of distilled water, 0.5 ml of 30% hydrogen peroxide and 3 ml of 0.03M sodium hydrogen carbonate. After the combustion, shake the flask for 5–10 min, rinse the stopper and sample holder with about 10 ml of mixed water, and boil the solution gently to decompose the hydrogen peroxide, until the volume is reduced to about 10 ml. Transfer the solution quantitatively to a 25-ml standard flask and dilute to the mark with water. Pipette a 1 or 2 ml portion into a 10-ml standard flask, add 200 μl of internal standard solution, 500 μl of mixed reagent solution and 200 μl of the sulphuric acid solution. Dilute to volume with mobile phase, mix well for 1 min, and chromatograph a 10- μl portion as above.

RESULTS AND DISCUSSION

Several ion-chromatographic methods are available for the determination of bromide. The detection methods include spectrophotometric monitoring at 200–214 nm,^{20–22} indirect photometry at 240 nm by use of eluents containing species such as phthalate²³ which absorb at this wavelength, conductimetry^{24,25} or amperometry.²⁵ Pre-column derivatization reactions are

used to improve chromatographic separation and detection. Thus, conversion of halides into their arylmercury(II) derivatives has been reported for their determination by reversed-phase HPLC and detection at 220 nm.²⁶ In the present work, the pre-column derivatization is based on the oxidation of bromide with 2-iodosobenzoic acid in acid medium to produce bromine which then brominates acetanilide to form 4-bromoacetanilide and bromide. This sequence of oxidation and bromination reactions continues until all the bromide has been

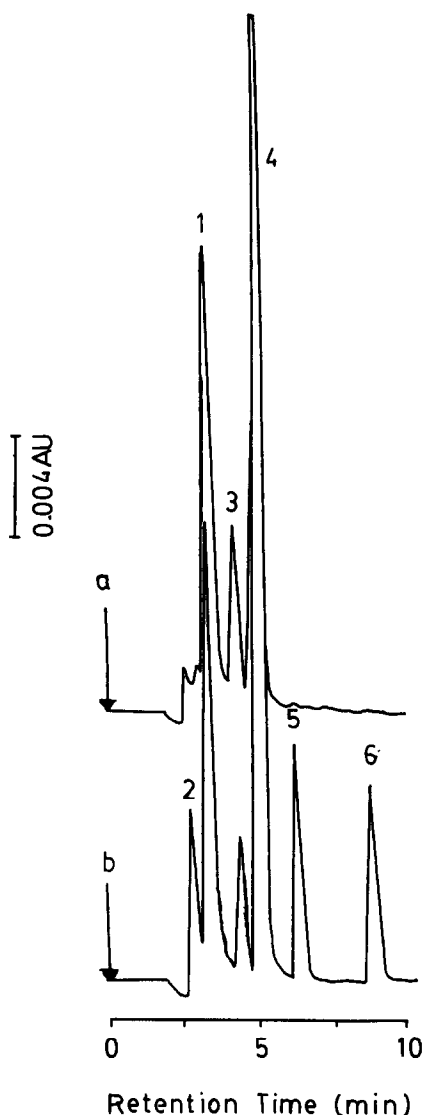


Fig. 1. Chromatogram of (a) reagent blank, and (b) pre-column reacted bromide (31 ng) with the same reagent and mixed with 4-*N*-acetylaminotoluene (51 ng) used as internal standard. Peaks: 1 = 2-iodosobenzoic acid; 2 = 2-iodobenzoic acid; 3 = extraneous matter; 4 = acetanilide; 5 = 4-*N*-acetylaminotoluene; and 6 = 4-bromoacetanilide. Chromatographic condition as in the text.

Table 1. HPLC determination of bromide

Bromide, $\mu\text{g}/100\text{ ml}$		
Taken*	Found ($n = 6$)	RSD, %
60.5 ^a	61.3	0.5
81.4	80.2	0.3
128.1 ^b	129.5	0.4
163.4 ^c	161.7	0.5
208.2	210	0.4
241.6 ^d	237	0.6
276.5	279	0.6
339.2 ^e	336	0.6
365.7 ^f	369	0.8
402.3	406	0.7

*The aliquot injected also contained
(a) 20 μg of trisodium phosphate;
(b) 100 μg of potassium chloride;
(c) 200 μg of sodium nitrate; (d)
10 μg of potassium iodide; (e)
100 μg of lead nitrate; (f) 50 μg of
mercuric chloride.

converted into 4-bromoacetanilide. The acetyl-amino group (in acetanilide) is an *ortho-para* director in electrophilic substitution reactions but its large size causes bromination at the *ortho*-position to be sterically hindered. Acetanilide was selected as the derivatization reagent because its bromination is particularly rapid and yields only 4-bromoacetanilide. In the internal standard, 4-*N*-acetylaminotoluene, the

para-position is already occupied by a methyl group and thus this substance does not undergo bromination. 2-Iodosobenzoic acid is a selective organic oxidizing agent.²⁷⁻²⁹ Its redox potential at 25° and pH 1 is 1.21 V.²⁸

The best chromatographic separation (Fig. 1) was achieved under the conditions recommended, with detection at 240 nm, where most anilides absorb strongly. A calibration graph of peak area for 4-bromoacetanilide *vs.* amount of bromide injected was linear over the range 6–42 ng. A response factor of 0.593 for bromide (as 4-bromoacetanilide) relative to 4-*N*-acetylaminotoluene was calculated from the HPLC peak-area ratios for various concentration ratios of the calibration and internal standards. The percentage of bromine in the sample is calculated from

$$\% \text{ Br} = 59.3 \frac{A_{\text{IS}} D}{A_{\text{IS}} W}$$

where A/A_{IS} is the ratio of the peak areas for 4-bromoacetanilide and the internal standard, C_{IS} the concentration of internal standard, W the weight of sample, and D the dilution factor. Results are given in Table 1 for the analysis of ten standard solutions of bromide, with or without the presence of various ions which may be formed during the oxygen-flask combustion

Table 2. HPLC determination of bromine in organic compounds

Compound	Bromine, %		
	Theory	Found ($n = 5$)	RSD, %
4-Bromoacetanilide	37.33	37.2	0.5
3-Bromobenzoic acid	39.75	39.9	0.5
3-Bromocamphor	34.61	34.5	0.6
5-Bromo-2-chlorobenzoic acid	33.97	33.8	0.7
5-Bromosalicyl-4'-chloroaniline	24.50	24.6	0.6
2-Bromoacetamido-2', 5'-dichloro-benzophenone	20.71	20.7	0.7
2-Bromoacetamido-5-chloro-2'-fluorobenzophenone	21.58	21.7	0.8
5-Bromo-2-iodobenzoic acid	24.46	24.6	0.6

Table 3. Comparison of diverse HPLC methods for bromide determination

Method	Detector	LD*	ULD*	Reference
Liquid chromatography on Zipax SAX column	200 nm	10 ng	5 μg	30
Anion-exchange chromatography	600 nm	15 ng	160 ng	31
Ion-exchange chromatography	190 nm	1 ng/ml	100 ng/ml	32
Anion-exchange chromatography	conductivity	20 ng	—	33
Liquid chromatography on aminopropylsilica	214 nm	1 ng	50 ng	34
Reversed-phase ion-interaction chromatography	205–220 nm	24 ng	—	35
Pre-column derivatization to 4-bromoacetanilide	240 nm	0.2 ng	42 ng	This work

*LD = limit of detection; ULD = upper limit of detection.

of organic compounds and may interfere in other methods for determination of bromide. Large amounts of diverse ions such as phosphate, chloride and nitrate can be tolerated. Other ions which do not interfere when present in up to 50-fold weight ratio to bromide include sulphate, calcium, barium, magnesium, zinc, copper(II) and iron(III). The present method is therefore simple and specific for the determination of bromine in organic compounds (Table 2). The limit of detection is 0.2 ng of bromide injected ($S/N = 2$). A comparison of some HPLC methods with the present one in terms of detection limit and measurement range is given in Table 3.

Acknowledgements—Thanks are due to the Council of Scientific and Industrial Research, New Delhi, for a Research Associateship to A.J., and to the University Grants Commission, New Delhi, for financial assistance to K.K.V.

REFERENCES

1. J. S. Fritz and G. S. Hammond, *Quantitative Organic Analysis*, p. 140. Wiley, New York, 1957.
2. W. Schöniger, *Mikrochim. Acta*, 1955, 123; 1956, 869.
3. L. Mázor, K. M. Pápay and P. Klatsmányi, *Talanta*, 1963, 10, 557.
4. F. W. Cheng, *Microchem. J.*, 1959, 3, 537.
5. S. S. M. Hassan and M. B. Elsayes, *Mikrochim. Acta*, 1972, 115.
6. A. M. El-Wakil and A. B. Farag, *Z. Anal. Chem.*, 1981, 207, 307.
7. I. Lysyi, *Microchem. J.*, 1959, 3, 529.
8. W. J. Kirsten and I. Lindholm-Franzen, *ibid.*, 1980, 25, 240.
9. M. Q. Al-Abachi and E. S. Salih, *Mikrochim. Acta*, 1987 II, 203.
10. A. Pietrogrande, M. Zancato and G. Bontempelli, *Analyst*, 1985, 110, 993.
11. H. Nagashima, K. Kuboyama and K. Ono, *Bunseki Kagaku*, 1985, 34, 381.
12. A. J. Klein, S. G. Morrell, O. H. Hicks and J. W. Worley, *Anal. Chem.*, 1986, 58, 753.
13. K. Akasaka, T. Shuzukim, H. Ohru, H. Meguro. Y. Shindo and H. Takahashi, *Anal. Lett.*, 1987, 20, 1581.
14. K. K. Verma, S. K. Sanghi, A. Jain and D. Gupta, *J. Pharm. Sci.*, 1987, 76, 551.
15. P. J. Whittle and P. J. Rennie, *Analyst*, 1988, 113, 665.
16. B. E. Miller and N. D. Danielson, *Anal. Chem.*, 1988, 60, 622.
17. K. K. Verma, S. K. Sanghi, A. Jain and D. Gupta, *J. Chromatog.*, 1988, 457, 345.
18. B. S. Furniss, A. J. Hannaford, V. Rogers, P. W. G. Smith and A. R. Tatchell (eds.), *Vogel's Textbook of Practical Organic Chemistry*, 4th Ed., p. 684. Longmans, London, 1978.
19. F. P. Chinard and L. Hellerman, *Methods Biochem. Anal.*, 1961, 1, 9.
20. H. J. Cortes, *J. Chromatog.*, 1982, 234, 517.
21. R. S. Bowman, *ibid.*, 1984, 285, 467.
22. J. P. de Kleyn, *Analyst*, 1982, 107, 223.
23. S. A. Wilson and E. S. Yeung, *Anal. Chim. Acta*, 1984, 157, 53.
24. R. M. Cassidy and S. Elchuk, *J. Chromatog. Sci.*, 1983, 21, 454.
25. R. D. Rocklin and E. J. Johnson, *Anal. Chem.*, 1983, 55, 4.
26. P. E. Moss and W. I. Stephen, *Anal. Proc.*, 1985, 22, 5.
27. K. K. Verma and A. K. Gupta, *Talanta*, 1982, 29, 779.
28. K. K. Verma, *ibid.*, 1982, 29, 41.
29. K. K. Verma and A. K. Gulati, *ibid.*, 1983, 30, 279.
30. T. Kamiura, Y. Mori and M. Tanaka, *Anal. Chim. Acta*, 1983, 154, 319.
31. W. Buchberger, *J. Chromatog.*, 1988, 439, 129.
32. N. Ferrer and J. J. Perez, *ibid.*, 1986, 356, 464.
33. M. J. Van Os, J. Slanina, C. L. De Ligny, W. E. Hammers and J. Agterdenbos, *Anal. Chim. Acta*, 1982, 144, 73.
34. C. E. Goewie and E. A. Hogendoorn, *J. Chromatog.*, 1985, 344, 157.
35. W. E. Barber and P. W. Carr, *J. ibid.*, 1984, 316, 211.

COMPUTATIONAL STUDIES OF THE CHIRAL SEPARATIONS OF THREE *N*-acyl-1-aryl-1-AMINOETHANES ON AN (R)-*N*-DINITROBENZOYLPHENYLGLYCINE STATIONARY PHASE

MIRON G. STILL and L. B. ROGERS

Department of Chemistry, University of Georgia, Athens, Georgia 30602, U.S.A.

(Received 21 March 1989. Revised 16 August 1989. Accepted 29 August 1989)

Summary—The chiral chromatographic separations of three *N*-acyl-1-aryl-1-aminoethanes on silica modified with (R)-*N*-dinitrobenzoylphenylglycine-*N'*-propylamide have been modeled by use of molecular mechanics. Formyl groups were substituted for the nitro groups, and a methyl group was tested as a replacement for the propyl group. With the propyl group, the correct elution order was obtained for the two pairs that had the largest α -values, and the third pair had a calculated α -value very close to unity. The relative sizes of the α -values were correctly predicted for all three. Substitution of methyl for propyl gave data that did not agree as well with the experimental values, thereby confirming the important role of the spacer in these separations.

Computational techniques have been used to study recognition mechanisms of chiral stationary phases (CSPs). For instance, Armstrong *et al.* used computer-generated models to examine cyclodextrin phases.¹ Boehm *et al.*² have used statistical mechanics to predict α -values for enantiomeric solutes distributed between a CSP and a non-chiral mobile-phase solute. Their approach also allowed calculations for mixed-solvent phases, and they were able to predict that reversal of the elution order could occur when the solvent ratios are altered. What remains to be done is to test the results of their method against experimental results.

Topiol *et al.*³ utilized semi-empirical and *ab initio* calculations to study the mechanism of separation of enantiomers of *N*-(3,5-dinitrobenzoyl)leucine (DNBL) on an (S)-*N*-(2-naphthyl)alaninate (NNA) stationary phase. The computational results correctly predicted the elution order of enantiomers even though the energies calculated for interaction of (R)- and (S)-DNBL with (S)-NNA differed by less than 1.0 kcal/mole. Furthermore the calculations suggested that the π -functionalities of the species do not serve to differentiate (S)- and (R)-DNBL. Lipkowitz *et al.* have used a molecular mechanics program, MM2, and MNDO (Modified Neglect of Diatomic Overlap) calculations to calculate the relative stabilities of conformers of *N*-dinitrobenzoylphenylglycine-*N'*-methyl-

amide after substituting formyl groups for nitro groups.⁴⁻⁶ MM2 has also been used to study the separation of enantiomers of 2,2,2-trifluoroanthrylethanol (TFAE) by the dinitrobenzoylphenylglycine stationary phase^{7,8} and to study chiral interactions between 2,2,2-trifluoroanthrylethanol and phases synthesized from *N*-*tert*-butyloxycarbonyl-D-valine and *N*-*tert*-butyloxycarbonyl-D-alanine.⁹ Calculations involving these last two phases correctly predicted the elution order of enantiomers of trifluoroanthrylethanol on each phase as well as the relative α -values for each phase, from the differences between the final steric energies.

In the present study the approach taken to minimize the energy of the complexes was different from that⁹ used earlier. Whereas our first study dealt only with the most stable individual complexes and their enthalpies, the present study included the free energies of interaction that were within 2.5 kcal/mole of those of all the docked pairs of the most stable ones. These pairs were first located by using a simplex procedure which treated the two molecules as rigid bodies once the likely orientations had been deduced on the basis of their intermolecular non-bonded energies of interaction.

The previous work examined the chiral recognition mechanisms for a racemic mixture of (R)- and (S)-TFAE on two stationary phases, (BOC-D-alanine and BOC-D-valine). The only

structural difference was that the alkyl group bonded to the chiral carbon atom of the stationary phase molecule was a methyl group for alanine and an isopropyl group for valine. In the present study, the mechanisms of chiral recognition of three enantiomeric pairs by one stationary phase were investigated. This system was experimentally evaluated by Pirkle *et al.*,¹⁰ who resolved three *N*-acyl-1-aryl-1-aminoethanes by using (R)-dinitrobenzoyl-phenylglycine bonded covalently to amino-propyl silica. In all cases the (S) enantiomer was retained longer. The solutes differed from one another more than did the derivatives of alanine and valine used previously.⁹ In one case, a methyl group was replaced by a methoxy group, and, in the other, a naphthyl group was replaced by a phenyl group.

The effect of the dielectric constant of the medium on the relative populations of the conformers of the phenylglycine species was also examined. These calculated values, of course, ignore any specific effects that might result from solvation.

EXPERIMENTAL

Single species

The MM2 program, version 87, by Allinger and Yuh was used.¹¹ All calculations were performed on a VAX 750 or a Microvax II. MM2 was first used for conformational analysis of the stationary phase (without considering the silica), alone, and each of the three solutes alone.

Several approximations were used. Parameters for nitro groups were not currently available; therefore formyl groups were used. Lipkowitz *et al.* had previously used this approximation, as reported above.⁴⁻⁸ This approximation had seemed suitable, but may not have adequately represented the nitro groups. Work by Pirkle suggested that diformyl-benzoylphenylglycine would have a much lower resolving power than the dinitro derivative.¹² Therefore, much lower α -values might be expected to be obtained in the chromatography, and correspondingly smaller calculated differences in the energies of the enantiomeric species. No silanol parameters were available to us, so steric repulsion or attraction interactions between the solute and the silica substrate were not considered. Also, in some calculations a methyl spacer was substituted for the n-propyl chain which was used by Pirkle *et al.*¹⁰ to bond

Table 1. The solutes modeled in Fig. 1, the population of the most stable conformer, the experimental α -value, and the configuration of the longer retained enantiomer

Compound	Ar	Y	Most stable conformer, %	α	Longer retained
I	1-Naphthyl	Methyl	71.2	1.86	S
II	1-Naphthyl	Methoxy	60.0	1.52	S
III	Phenyl	Methyl	89.2	1.15	S

phenylglycine to the silica. No specific solvent effects were taken into account, and a dielectric constant of 4.4 was used for all calculations involving the solutes, in order to approximate the effect of the mobile phase of 10% isopropyl alcohol-90% n-hexane used in the laboratory. Table 1 shows the chromatographic results.¹⁰

Figure 1 shows the basic forms of the solutes used. Dihedral angles for θ and ϕ were examined. In all cases, θ is the angle involving the 1-naphthyl C atom, the chiral C atom, N and H. For solutes I and II, ϕ is the dihedral angle between the carbon atom at position 9 of the naphthyl group, the carbon atom at position 1 of the naphthyl group, the chiral carbon atom, and its hydrogen atom.

Figure 2 shows the basic numbering system for the phenylglycine derivative, and this was maintained throughout the study. The dihedral angles for the methyl derivative were angle 1 for atoms 2, 3, 4, 5 and angle 2 for atoms 3, 4, 6, 7. These values were also used for the n-propyl derivative. In addition, the n-propyl derivative had two other dihedral angles on the n-propyl-amide chain. They were for the H, N, C, C atoms and the N, C, C, C atoms. In all cases, it is assumed that viewing is through the second of the four atoms listed, towards the third atom. A positive value indicates that the fourth atom is situated clockwise from the first. A negative value indicates that the fourth atom is counter-clockwise from the first.

Docked pairs

Only the most stable conformations of the solutes and the stationary phases were used for docking. We first established an arbitrary origin

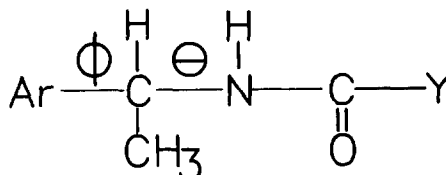


Fig. 1. Structure of solutes examined by Pirkle *et al.*¹⁰

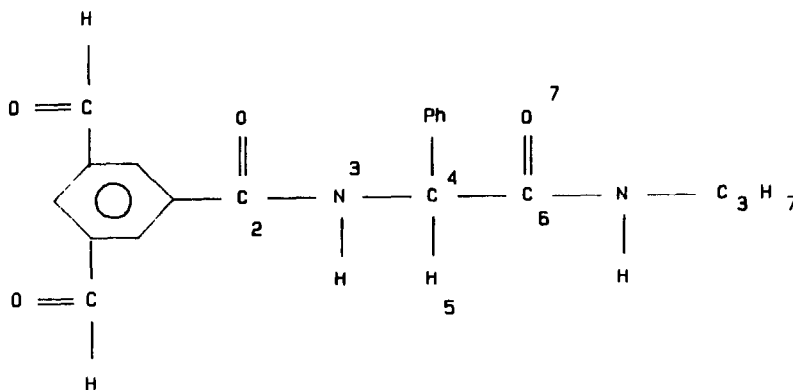


Fig. 2. Structure of (R)-*N*-diformylbenzoylphenylglycine-*N'*-propylamide.

and a standard orientation for each molecule to be docked. Each was then treated as a rigid body. The carbonyl carbon atom of the benzoyl group on the stationary phase was then set at the origin 0, 0, 0. Next, the solute molecule was set at a specific starting distance described by Cartesian coordinates and an orientation described by rotation about the Cartesian axes. The center of the solute molecule was always taken to be the chiral carbon atom. Individual values for each of the variables were selected randomly from different ranges of numbers. The range for the angles of rotation was from 0 to 360°. The ranges for the starting distances (in Å) between the molecules were selected so as to keep the molecules close enough to one another, while also minimizing either interpenetration of the molecules or the chance of an atom from each molecule being assigned to the same location. Thus, the values for the *z* axis ranged from -2.5 to -4.5 Å or from +2.5 to +4.5 Å. This ensured that the solute molecule was safely above or below the stationary phase molecule. The *x* and *y* axes each had ranges from -5.0 to +5.0 Å. These distances corresponded roughly to the length of the phenylglycine molecule up to the point where the spacer group started.

A simplex optimization procedure, which considered only non-bonding interactions and treated the molecules as rigid bodies, was used to locate stable orientations of the solute molecules with respect to the methyl derivative of the stationary phase. Increments of 0.001 Å and 0.001° were used in this procedure. At least 600 different starting orientations for each pair were examined, for which final orientations and energies were collected. Two (or more) of those final orientations were considered to be identical if the difference between the origin for the solute with respect to that for the stationary phase was

less than 0.5 Å on the translation axes *x*, *y*, *z*, and, in addition, the final rotations about axes, R_x , R_y , R_z , were all within 30°.

Intramolecular minimization was then performed only on those orientations for docked pairs having energies that were within 4.0 kcal/mole of those of the most stable one found by the simplex. In all cases a threshold energy value of 1.0×10^{-7} kcal/mole per atom was used to halt calculations. Energies and coordinates for the complexes involving the propyl derivative were obtained by taking the final (minimized) coordinates from complexes involving the methyl derivative, and using them as the initial coordinates for the propyl derivative calculation. For calculations involving the propyl derivative, final structures were again minimized by the simplex routine, which treated the individual molecules as rigid bodies, followed by intramolecular minimization. Sequential use of the simplex followed by intramolecular minimization was repeated until the final steric energies of the complexes differed by less than 0.001 kcal/mole.

The final complexes were then tested to determine whether they were identical. This was done by constraining 3 atoms of the phenylglycine derivative in each file in the following way: (1) one atom was fixed at $x = y = z = 0$, (2) a second atom along one axis ($x = y = 0$), and (3) a third atom in a plane ($x = 0$). The difference between the coordinates of the solutes of the two files was then found and if the average difference in the positions of the solute atoms (calculated from least squares) was at least 3.3 Å, then the complexes were considered different. It should be mentioned that, in all cases, when two files were found to be identical, the average difference for each atom in file one with respect to the same atom in file two was within 1.5 Å,

and no files had an average difference between 1.5 and 3.0 Å. If these values seem high, it should be noted that the minima are expected to be broad, and large changes in the position of a solute chain which does not interact strongly with the stationary phase will increase the values.

Final energies for the docked pairs were used to predict the elution order for the enantiomers as well as the relative α -values for different pairs. When several docked pairs involving the same molecules were similar in energy and population, Boltzmann-weighted averages were calculated by using equation (1).

$$E_{AVG} = \sum_i (P)_i (E_{OR})_i \quad (1)$$

In this case, E_{AVG} is the weighted average energy, (E_{OR}), the energy for a given orientation of the docked pair, and P , the fraction of the population for that orientation, calculated by using a Boltzmann distribution. Lipkowitz *et al.* used a similar equation for calculating TFAE interactions with the diformyl analog of (R)-*N*-dinitrobenzoylphenylglycine-*N'*-methylamide.⁷

We have investigated use of the changes in free energies rather than those in the enthalpies.* In order to calculate the free energies from the weighted averages, equation (2) was used to calculate the entropy change ΔS ,

$$\Delta S = -R \sum_i (P)_i \ln (P)_i \quad (2)$$

where R is 1.99 cal/mole. The free energy change, ΔG , can then be calculated by using equation (3).

$$\Delta G = \Delta E_{AVG} - T\Delta S \quad (3)$$

Effect of dielectric constant. The effect of altering the dielectric constant, on the distribution of stable conformers of (R)-dinitrobenzoylphenylglycine-*N'*-methylamide, was examined by using values of 1.5, 3.1, 4.4 and 6.5 for the dielectric constant. These values correspond, respectively, to a gas phase in the MM2 approximation, and to liquid phases of 5%, 10% and 20% v/v isopropyl alcohol in *n*-hexane. The dielectric constant only partially accounts for solvent effects. Specific inter-

actions, which may alter the stability of complexes, are not included.

RESULTS

Single species

Stable conformations for the solutes (I, II and III) and the relative populations of the (R) enantiomers at a dielectric constant of 4.4 are shown in Tables 2–4. In all cases at least 60% of the population was represented by one conformer. Only the global minima for the individual molecules were used for docking.

Tables 5 and 6 show the stable conformations for the methyl (CSP-methyl) and propyl derivatives (CSP-propyl) of the stationary phase at a dielectric constant of 4.4. Again, only the most stable conformer was used for docking.

The results of changing the dielectric constant (ϵ) are summarized in Table 7. Note that, for a dielectric constant of 1.5, which corresponded to the gas phase, the most stable conformer represented 75% of the population. However,

Table 2. Stable conformers of (R)-*N*-(methylcarbonyl)-1-naphthyl-1-aminoethane I

θ , deg	ϕ , deg	E^* , kcal/mole	Population†, %
47	-22	0.00	71.2
-145	-26	0.75	20.1
-66	-33	2.34	7.3
129	-60	3.31	1.4
107	30	8.53	0.03

*Relative energy differences.

†Relative percentage of population calculated by using $\ln K = -E/RT$ and assuming the entropies of individual conformers are the same.

Table 3. Stable conformers of (R)-*N*-(methoxycarbonyl)-1-naphthyl-aminoethane II

θ , deg	ϕ , deg	E^* , kcal/mole	Population, %
46	-23	0.00	60.0
-146	-30	0.66	19.7
48	-81	0.96	11.7
-66	-33	1.26	7.0
129	-60	2.14	1.6
107	30	7.31	0.0003

*Relative energy difference.

Table 4. Stable conformers of (R)-*N*-(methylcarbonyl)-1-phenyl-1-aminoethane III

θ , deg	ϕ , deg	E^* , kcal/mole	Population, %
45	-31	0.00	89.2
-60	-40	1.35	9.1
-60	129	2.34	1.7

*Relative energy differences.

*The calculated value for a final steric energy (FSE) for a molecule depends on the choice of the parameters for the initial states of the atoms, but the FSE value calculated for a docked pair generally agrees well even when somewhat different sets of parameters are used, which suggests that ΔH values are being calculated.

Table 5. Most stable conformers of (R)-*N*-diformylbenzoyl-phenylglycine-*N'*-methylamide and relative energies and populations at a dielectric constant of 4.4

Conformer	Angles, deg		E^* , kcal/mole	Population, %
	1	2		
1	56	-12	0.00	33.05
2	-39	115	0.26	21.31
3	-57	-114	0.30	19.91
4	42	-9	0.60	12.00
5	52	-97	0.78	8.54
6	172	101	1.16	4.66
7	42	122	2.99	0.21

*Relative energy differences.

Table 6. Most stable conformers, energies and populations of (R)-*N*-diformylbenzoylphenylglycine-*N'*-*n*-propylamide when angles 1 and 2 are -12° and 56°

N,C,C,C	H,N,C,C	E^* , kcal/mole	Population, %
-71	60	0.00	38.87
-60	-63	0.12	31.74
62	63	0.79	10.24
60	-60	0.81	9.90
63	180	0.85	9.25

*Relative energy difference.

under the experimental liquid chromatographic conditions ($\epsilon = 4.4$), this conformer represented only about 20% of the population. Similarly, the most stable conformation at $\epsilon = 4.4$ was calculated to represent 33%, whereas it represented only 8% of the total population at $\epsilon = 1.5$. Note, too, that changing from 5% to 20% isopropyl alcohol (*i.e.*, from $\epsilon = 3.1$ to $\epsilon = 6.5$) can also produce major shifts in the populations, especially for conformers 2-4. Therefore, the choice of dielectric constant critically affects the relative populations of conformers. Hence, all data for docked species were calculated with a dielectric constant of 4.4 to approximate to the experimental conditions as well as possible.

Docked species involving CSP-propyl

Docking studies involving the most stable conformer of CSP-propyl with the most stable conformer of each enantiomer of solutes I, II and III correctly predicted the elution order of all three solutes when the free energies were used, but for only two solutes when the enthalpies were used. Table 8 shows the weighted average changes in enthalpies (ΔH), entropies (ΔS) and free energies (ΔG) for all three solutes. The ΔH and ΔG values were rounded off, which can account for a total rounding-off error of 0.02 kcal/mole in the ΔG value. Table 9 shows the final steric energies (enthalpies) of the individual complexes, used to calculate the weighted average values. The percentage of a given complex in the population is also shown.

Note that the largest difference between the free energy changes, $\Delta(\Delta G)$, was for I (1.05 kcal/mole) and the smallest was for III (0.02 kcal/mole). Thus the relative order of the α -values was also predicted correctly. The results indicate that both I and II would be resolved, but III would have an α -value of 1.00, within experimental error. However, it is important to remember that use of the much stronger dinitrobenzoylphenylglycine in the laboratory tests gave an α -value of only 1.15 for III.

Solute I. The most stable complex of (S)-I/CSP-propyl in Fig. 3a shows the naphthyl ring of (S)-I above the carbonyl group of the phenylglycine and the amino group of the spacer. In this orientation, the phenyl group of the CSP-propyl is below the plane of the paper. This orientation is similar to that of the most stable complex of (S)-TFAE with CSP-methyl proposed by Lipkowitz *et al.*⁷

Figure 3b shows the most stable (R)-I/CSP-propyl complex. In this case, (R)-I is on the same side of the CSP as the phenyl ring bonded

Table 7. Effect of dielectric constant on relative populations of conformers of (R)-*N*-diformylbenzoylphenylglycine-*N'*-methylamide

Conformer	Angles, deg		Population*, %			
	1	2	$\epsilon = 1.5$	$\epsilon = 3.1$	$\epsilon = 4.4$	$\epsilon = 6.5$
1	56	-12	8.00	32.67	33.05	30.41
2	-39	115	75.50	36.77	21.31	7.88
3	-57	-114	0.24	9.21	19.91	30.92
4	42	-9	0.31	6.68	12.00	17.70
5	52	-97	0.68	6.24	8.54	9.98
6	172	101	15.19	8.18	4.66	2.86
7	42	122	0.02	0.24	0.21	0.23

*Calculated by using $E = RT/n\Delta K$.

Table 8. The changes in enthalpies (weighted average energies), ΔH , entropies, ΔS , free energies ΔG and the difference between the free energy changes, $\Delta(\Delta G)$ for solutes I, II and III with CSP-propyl

	ΔH , kcal/mole		ΔS , cal. mole ⁻¹ . deg ⁻¹		$\Delta(\Delta S)$, cal. mole ⁻¹ . deg ⁻¹	ΔG , kcal/mole		$\Delta(\Delta G)^*$, kcal/mole	
	(S)	(R)	(S)	(R)		(S)	(R)		
I	-27.78	-26.83	-0.95	3.94	3.66	0.28	-28.95	-27.90	-1.05
II	-28.07	-28.21	0.14	2.87	1.48	1.39	-28.92	-28.67	-0.25
III	-20.96	-20.87	-0.09	2.74	2.86	-0.12	-21.75	-21.73	-0.02

*For (S) - (R).

Table 9. ΔH values ($-kcal/mole$) and populations (%) for individual complexes with CSP-propyl in decreasing order of stability, the calculated weighted average energies

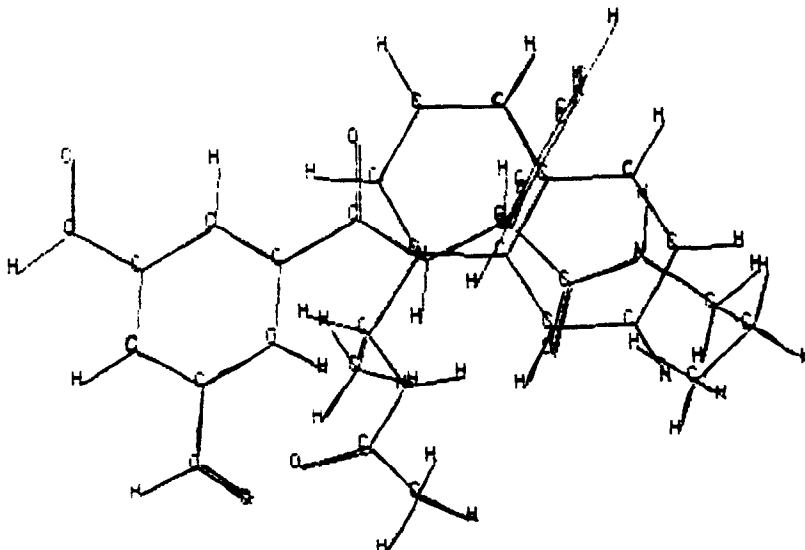
	Solute I				Solute II				Solute III			
	(S)		(R)		(S)		(R)		(S)		(R)	
	ΔH	Popn.	ΔH	Popn.	ΔH	Popn.	ΔH	Popn.	ΔH	Popn.	ΔH	Popn.
	28.14	25.49	27.35	37.98	28.45	45.00	28.50	77.27	21.37	52.43	21.40	57.55
	28.06	22.27	26.85	13.33	28.02	21.77	27.56	15.80	20.94	26.23	20.73	18.56
	27.93	17.88	26.73	16.33	27.99	20.69	26.64	3.34	20.18	7.03	20.15	6.97
	27.49	8.50	26.56	10.01	27.03	4.09	26.32	1.95	20.13	6.46	19.70	3.27
	27.43	7.68	26.26	6.03	27.02	4.02	26.22	1.64	19.63	2.78	19.67	3.10
	27.30	6.17	26.23	5.73	26.82	2.87			19.61	2.68	19.61	2.80
	27.14	4.71	26.11	4.68	26.46	1.56			19.54	2.39	19.60	2.75
	27.12	4.55	26.04	4.16							19.50	2.33
	26.49	1.57	25.53	1.76							19.22	1.45
	26.05	0.75									19.12	1.22
	25.73	0.44										
Mean ΔH	27.78		26.83		28.07		28.21		20.96		20.87	
Mean ΔG	28.95		27.90		28.92		28.67		21.75		21.73	

to the chiral carbon atom of CSP-propyl. The hydrophobic interactions between the naphthyl ring and the diformylphenyl group and the phenyl ring were large.

Solute II. Figure 4a shows the most stable (S) complex. The (S) enantiomer is on the same side of the CSP-propyl as the phenyl ring bonded to the chiral carbon atom of CSP-propyl. The methoxy oxygen atom of (S)-II interacts with the protected amino group of CSP-propyl. Also

the naphthyl ring of (S)-II interacts with both the carbonyl moiety of the protecting group and the phenyl ring bonded to the chiral carbon atom of CSP-propyl. The diformylphenyl group of CSP-propyl interacts with the amino group and the methyl group bonded to the chiral carbon atom of (S)-II.

In the most stable (R) complex, Fig. 4b, (R)-II is on the same side of the CSP-propyl as the phenyl ring bonded to the chiral carbon

Fig. 3a. Most stable orientation of (S)-I/CSP-propyl, $\Delta H = -28.14$ kcal/mole.

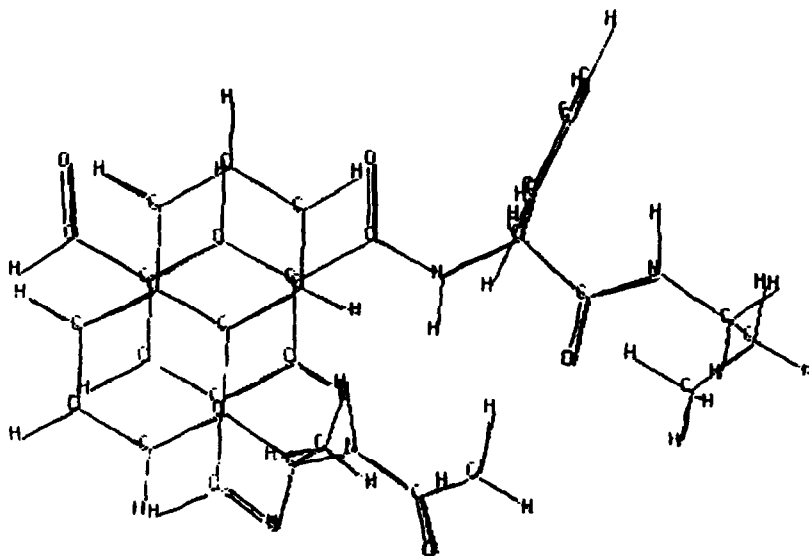


Fig. 3b. Most stable orientation of (R)-I/CSP-propyl, $\Delta H = -27.35$ kcal/mole.

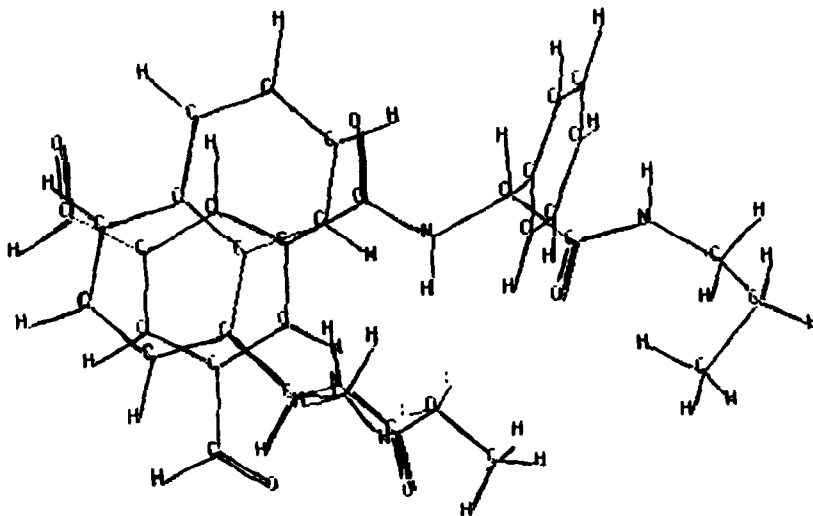


Fig. 4a. Most stable orientation of (S)-II/CSP-propyl, $\Delta H = -28.45$ kcal/mole.

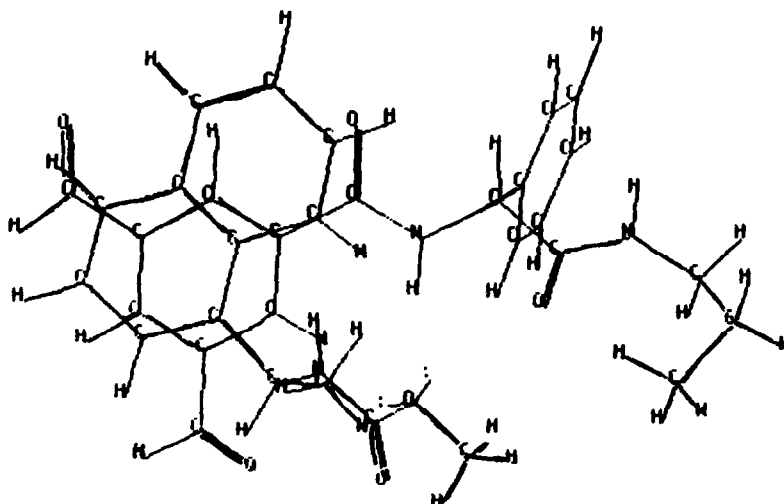


Fig. 4b. Most stable orientation of (R)-II/CSP-propyl, $\Delta H = -28.50$ kcal/mole.

atom. The orientation is similar to that of the most stable (R)-I/CSP-propyl complex. The naphthyl ring of (R)-II interacts with the diformylphenyl ring of CSP-propyl. Also, the oxygen atom of the methoxy group of (R)-II is oriented to interact with the hydrogen atom of the protected amine of CSP-propyl. Table 9 shows the energies of individual complexes of (S)-II and (R)-II with CSP-propyl.

Solute III. In Fig. 5a, the phenyl ring of (S)-III and the diformylphenyl group of CSP-propyl are oriented to interact strongly. (S)-III is able to form a hydrogen bond with the phenyl group of CSP-propyl. Also, the methyl group of (S)-III is able to interact hydrophobically with the phenyl group bonded to the chiral carbon atom of CSP-propyl.

Figure 5b shows the most stable (R) complex. In this particular orientation, (R)-III is on the same side of CSP-propyl as the phenyl ring. The

amino hydrogen atom of (R)-III interacts strongly with the diformylphenyl ring of CSP-propyl. The phenyl group of (R)-III interacts strongly with both the carbonyl of the protecting group and the phenyl ring of CSP-propyl.

Relative stabilities of different orientations

Similar comparisons of the orientations of the most stable complexes of the (S) enantiomers of I, II and III (Figs. 3a, 4a and 5a) revealed that all three of the most stable complexes differed. In two of these three cases, however, similar orientations were found among the stable complexes used.

Table 10 shows that the fourth most stable complex of (S)-II/CSP-propyl and the fifth most stable complex of (S)-III/CSP-propyl were similar to the most stable complex of (S)-I/CSP-propyl.

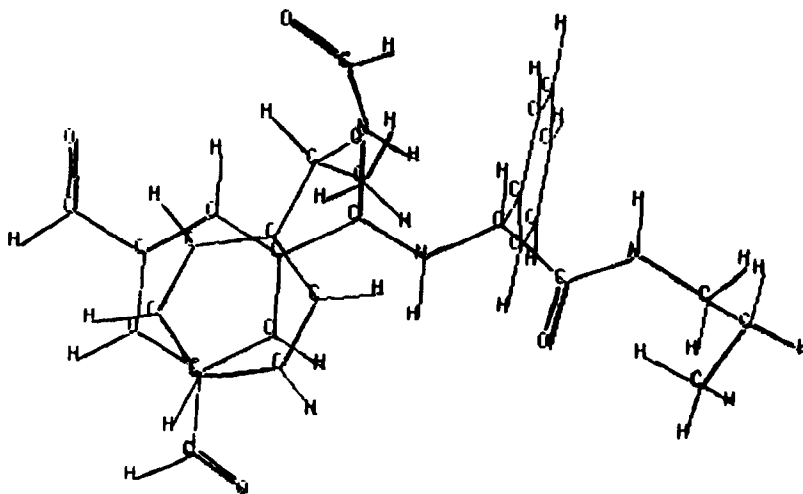


Fig. 5a. Most stable orientation of (S)-III/CSP-propyl, $\Delta H = -21.40$ kcal/mole.

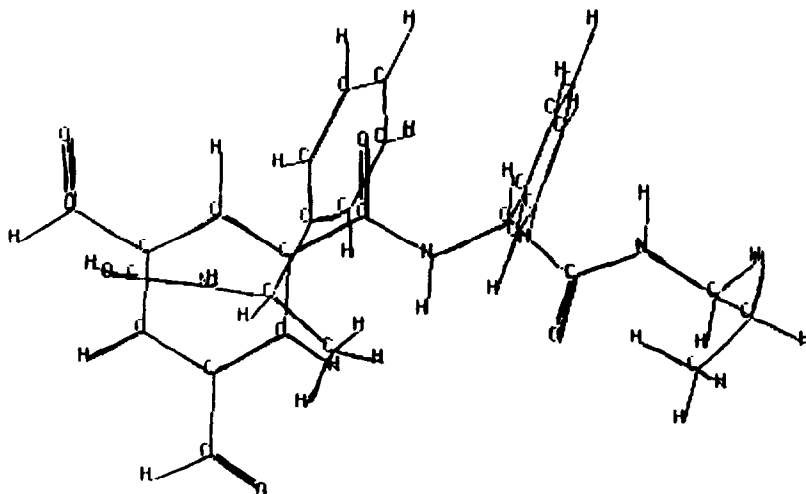


Fig. 5b. Most stable orientation of (R)-III/CSP propyl, $\Delta H = -21.37$ kcal/mole.

Table 10. ΔH values ($-kcal/mole$) of most stable complexes of enantiomers of solutes I, II, and III with CSP-propyl together with the ΔH values and ranks of corresponding complexes of analytes having the same chiral configuration

Most stable solute structure	Corresponding complexes		
	(S)-I	(S)-II	(S)-III
(S)-I (Fig. 3a)	28.14 (1)*	27.02 (5)*	19.61 (6)*
(S)-II (Fig. 4a)	25.22 (-)†	28.45 (1)	20.94 (2)
(S)-III (Fig. 5a)	27.93 (3)	26.82 (6)	27.37 (1)
	(R)-I	(R)-II	(R)-III
(R)-I (Fig. 3b)	27.35 (1)*	28.50 (1)*	20.73 (2)*
(R)-II (Fig. 4b)	27.35 (1)	28.50 (1)	20.73 (2)
(R)-III (Fig. 5b)	26.11 (7)	24.02 (-)†	21.40 (1)

*Number in parentheses represents the ranking in relative stability, with I having the highest stability.

†Not ranked or included in the calculation of weighted average energies.

Also the most stable complex for (S)-II (-28.45 kcal/mole) was similar to the second most stable complex for (S)-III (-20.94 kcal/mole). However, the corresponding complex for (S)-I was calculated to have an energy of -25.22 kcal/mole; thus, this orientation was not used to calculate the weighted average energy for (S)-I complexes.

The orientation of the most stable complex for (S)-III (-27.37 kcal/mole) corresponded to the third most stable orientation for both (S)-I (-27.93 kcal/mole) and (S)-II (-26.32 kcal/mole).

The most stable complexes for the (R) enantiomers of I, II and III (Figs. 3b, 4b and 5b) were all similar. Table 10 shows the most stable complexes of (R)-I (-27.35 kcal/mole) and (R)-II (-28.50 kcal/mole) had the same orientation as the second most stable complex for (R)-III (-20.73 kcal/mole). The most stable complex for (R)-III corresponded to the seventh most stable complex for (R)-I (-26.10 kcal/mole); however, the energy for this orientation was calculated to be only -24.02 kcal/mole when (R)-II was used.

Docked species involving CSP-methyl

In previous work,⁸ a methyl spacer was used to approximate the propyl spacer of

diformylbenzoylphenylglycine. For the solutes we examined, use of a methyl spacer yielded computational results which did not correspond to the experimental data as well as did the data computed by use of a propyl spacer.

In the present study, when a methyl spacer was used, the retention order of only two of the three solutes (I and II) was predicted correctly (Table 11). Furthermore, the calculated elution order for solute III was not only incorrect, but also the α -value was predicted to be larger than that for I or II. Note also that the relative α -values of I and II were predicted to be similar in value, as the absolute values of ΔG were 0.57 and 0.51 kcal/mole, respectively.

Solute I. The most stable complex of (S)-I/CSP-methyl was similar to the most stable complex of (S)-I/CSP-propyl (Fig. 6a). The most stable complex of (R)-I/CSP-methyl (Fig. 6b) has an orientation similar to that of the third most stable (R)-I/CSP-propyl complex. The naphthyl ring of (R)-I interacted with both the diformylphenyl ring and the amino hydrogen atom of CSP-methyl. The amino group of (R)-I also interacted strongly with the phenyl ring bonded to the chiral carbon atom of CSP-methyl.

The size of the spacer group not only affected the calculated elution order and α -values, but

Table 11. The changes in enthalpies (weighted-average energies) (ΔH), entropies (ΔS), free energies (ΔG), and their differences for solutes I, II, and III with CSP-methyl

Solute	ΔH , kcal/mole		$\Delta(\Delta H)$, (S) - (R)	ΔS , cal. mole ⁻¹ . deg ⁻¹		$\Delta(\Delta S)$, (S) - (R)	ΔG , kcal/mole		$\Delta(\Delta G)$, (S) - (R)
	(S)	(R)		(S)	(R)		(S)	(R)	
I	-27.84	-27.18	-0.66	3.12	3.42	-0.30	-28.77	-28.20	-0.57
II	-28.07	-27.70	-0.37	2.37	1.90	0.47	-28.78	-28.27	-0.51
III	-21.50	-22.46	0.96	1.18	0.45	0.73	-21.85	-22.60	0.75

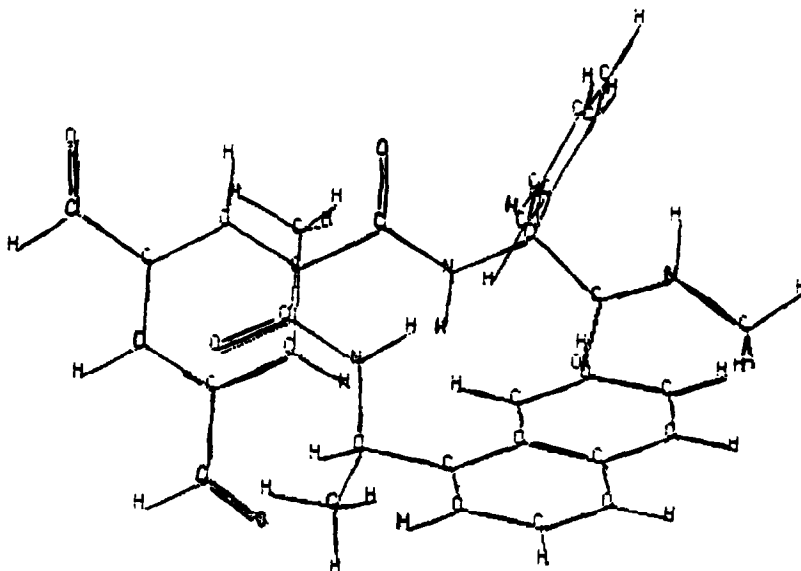


Fig. 6a. Most stable orientation of (S)-I/CSP-methyl, $\Delta H = -28.12$ kcal/mole.

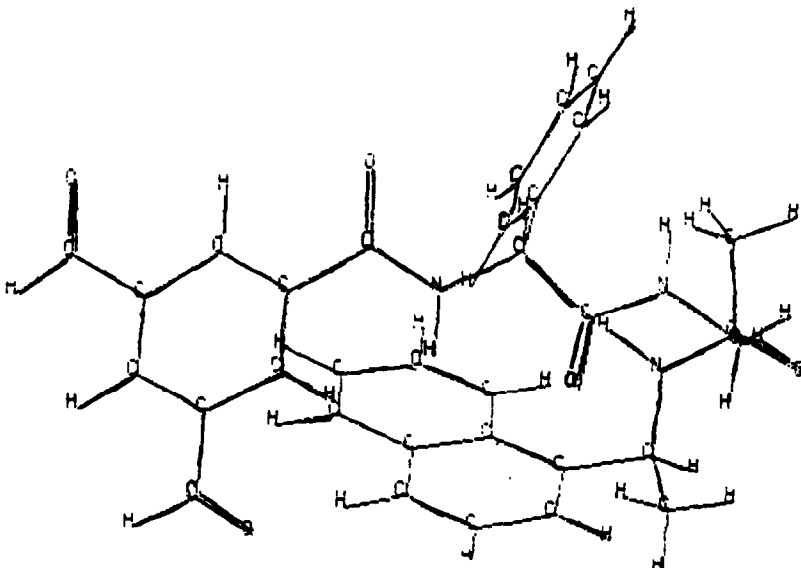


Fig. 6b. Most stable orientation of (R)-I/CSP-methyl, $\Delta H = -27.62$ kcal/mole.

also the mechanistic details. In the most stable complexes involving CSP-methyl, the solute was located near the methyl spacer group. In the complexes involving CSP-propyl, the most stable complexes showed strong interaction with the diformylphenyl ring. For (R)-I, (R)-II and (S)-III, this interaction involved π - π bonding with the aromatic group of the solute. For (S)-I, (S)-II and (R)-III, the diformylphenyl group interacted strongly with the amino group and the methyl group.

Solute II. The most stable (S)-II/CSP-methyl complex (Fig. 7a) shows that the naphthyl ring

of (S)-II on the same side of CSP-methyl as the phenyl ring bonds to the chiral carbon atom of CSP-methyl. The naphthyl ring of (S)-II interacts with both the phenyl ring and both amino hydrogen atoms of CSP-methyl. The methoxy oxygen atom of (S)-II also form a hydrogen bond with the amino hydrogen atom of the spacer group.

Figure 7b shows the most stable (R)-II/CSP-methyl complex. The orientation is similar to that of the most stable (R)-I/CSP-propyl complex.

The free energy changes also predicted that (S)-II would be retained longer than (R)-II. The

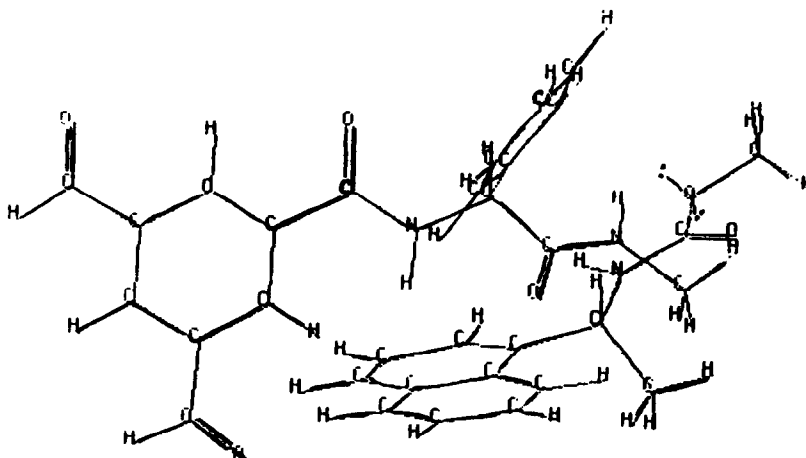


Fig. 7a. Most stable orientation of (S)-II/CSP-methyl, $\Delta H = -28.50$ kcal/mole.

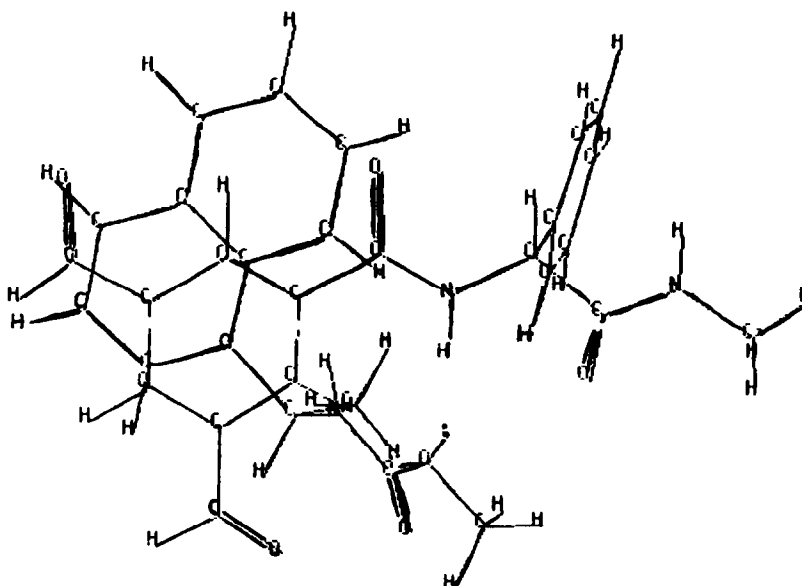


Fig. 7b. Most stable orientation of (R)-II/CSP-methyl, $\Delta H = -28.00$ kcal/mole.

energies for the (S)-II/CSP-methyl complexes were calculated to be -28.78 kcal/mole, compared with -27.27 kcal/mole for the (R)-II/CSP-methyl complexes. Even though (S)-II was predicted to be retained longer than (R)-II, there was an energy difference of 0.51 kcal/mole, which was similar to that for I. This implies that II should have an α -value similar to that of I. It should be mentioned that the (S)-II/CSP-propyl complex similar to the most stable (S)-II/CSP-methyl complex had an energy of -25.96 kcal/mole.

Solute III. The free energy changes contradicted the chromatographic data, as did use of the enthalpies of the most stable complexes.

Figure 8a shows the most stable (S)-III/CSP-methyl complex, where the solute is located on

the same side of the CSP-methyl as the phenyl ring bonded to the chiral carbon atom. The aromatic ring of (S)-III interacts with the diformylphenyl group of CSP-methyl, and amide hydrogen atom and the methyl group of (S)-III interact with the phenyl ring of the CSP-methyl.

Comparison of (R)-III/CSP-propyl and (R)-III/CSP-methyl

Figure 8b shows the most stable complex for (R)-III/CSP-methyl. The aromatic ring of (R)-III interacts with the phenyl ring of CSP-methyl bonded to the chiral carbon atom. The aromatic ring is also in a position to interact with the carbonyl oxygen atom bonded to the spacer chain, and the hydrogen atom of the protected amine. The amino group of (R)-III is also

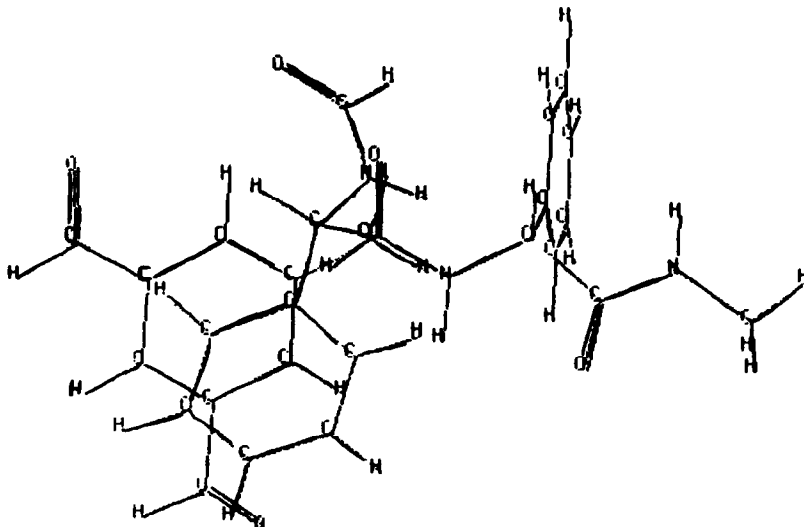


Fig. 8a. Most stable orientation of (S)-III/CSP-methyl, $\Delta H = -21.76$ kcal/mole.

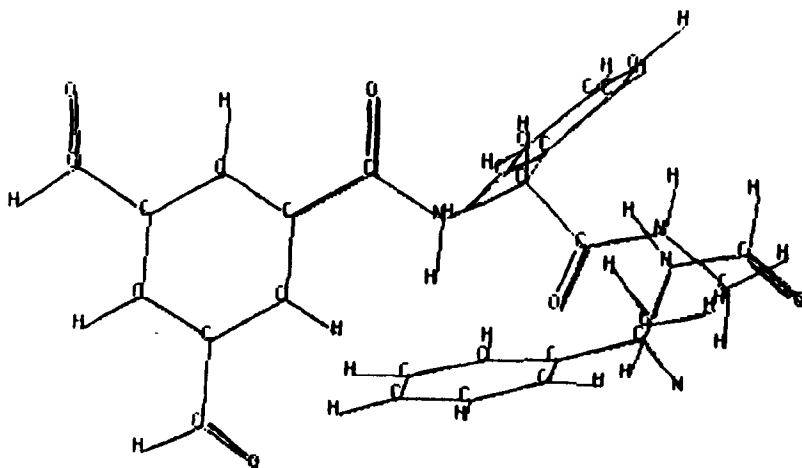


Fig. 8b. Most stable orientation of (R)-III/CSP-methyl, $\Delta H = -22.66$ kcal/mole.

oriented so as to form a hydrogen bond to the phenyl group bonded to the chiral carbon atom of CSP-methyl. The enthalpy change for the similar complex of (R)-III/CSP-propyl was only -19.12 kcal/mole.

There was a large energy difference between the most stable (R)-III/CSP-methyl and (R)-III/CSP-propyl complex with the same orientation. The largest energy difference was for the intermolecular hydrogen bonding and van der Waals interactions. The (R)-III/CSP-methyl complex had an intermolecular interaction energy of -17.14 kcal/mole, whereas the value was -13.01 kcal/mole for the similar (R)-III/CSP-propyl complex (Table 12). The calculated energy of interaction between the amide hydrogen atom of the solutes with the CSPs was -6.53 kcal/mole for the (R)-III/CSP-methyl

complex and only -2.76 kcal/mole for the (R)-III/CSP-propyl complex (Table 13). Similarly, the calculated energy of interaction with the phenyl group in (R)-III/CSP-methyl was -9.85 kcal/mole, compared with -5.62 kcal/mole for (R)-III/CSP-propyl (Table 13), thus these two groups served to stabilize the (R)-III/CSP-methyl complex more than the (R)-III/CSP-propyl complex.

CONCLUSIONS

We have now shown that using only weighted average enthalpy change terms did not always yield results and conclusions agreeing with those based on free energies or with experimental data. Table 9 shows that the weighted average enthalpy change for (S)-II is 0.14 kcal/mole less

Table 12. Comparison of enthalpies (*kcal/mole*) of interaction between individual atoms or small groups of atoms in (R)-III with the entire molecule of CSP-methyl or CSP-propyl

Group or atom	CSP-methyl	CSP-propyl	(CSP-methyl) – (CSP-propyl)
H of amide	–6.53	–2.76	–3.77
Methyl on chiral C	–0.85	–0.34	–0.51
Carbonyl O	–0.49	–0.37	–0.12
Methyl (formyl)	–0.55	–0.45	–0.10
Carbonyl C	–0.65	–0.57	–0.08
H on chiral C	–0.75	–0.82	+0.07
Phenyl	–7.08	–7.18	+0.10
N	–0.25	–0.52	+0.27
Total	–17.15	–13.01	–4.14

Table 13. Comparison of enthalpies (*kcal/mole*) of interaction between individual atoms or small groups of atoms in CSP-methyl or CSP-propyl with the entire molecule (R)-III

Group or atom	CSP-methyl	CSP-propyl	(CSP-methyl) – (CSP-propyl)
Phenyl	–9.85	–5.62	–4.23
Spacer N	–0.42	–0.19	–0.23
H of spacer amide	–0.27	–0.05	–0.22
H of chiral C	–0.55	–0.36	–0.19
H of protected amide	–1.77	–1.61	–0.16
Carbonyl O (DFP)	–0.09	–0.09	–0.00
Carbonyl O (spacer)	–0.27	–0.27	–0.00
Protected N	–0.41	–0.42	+0.01
Diformylphenyl (DFP)	–1.73	–1.74	+0.01
Carbonyl C (DFP)	–0.26	–1.27	+0.01
Carbonyl C (spacer)	–0.36	–0.37	+0.01
Alkyl chain (spacer)	–1.16	–2.02	+0.86
Total	–17.14	–13.01	–4.13

negative than that for (R)-II. This indicates a small α -value, of approximately 1. On the other hand, the calculated free energy change for (S)-II complexes was 0.25 kcal/mole more negative than that for (R)-II, hence (S)-II should be retained longer than (R)-II; this was indeed the case, as shown experimentally, assuming that formyl groups behave qualitatively, but not quantitatively, like nitro groups.

The most stable orientations calculated for each enantiomer were nearly always similar to one of the more stable complexes involving the other solutes. Furthermore, hydrophobic interactions were predicted to be important, especially the interactions involving the phenyl group bonded to the chiral carbon atom of the CSP. Eleven of the twelve most stable complexes showed an orientation in which the solute was on the same side of the CSP as the phenyl group. It should also be pointed out, however, that many of the complexes that were used to calculate changes in free energies did have large interactions involving the carbonyl groups and amino groups. Thus, these groups are important in chiral recognition.

In our previous work, we examined only small structural changes in the (R) group of two amino-acid derivatives.⁹ In the present work, larger changes were made in the solutes and hence provided a more difficult test for MM2. A hydrophobic aromatic group, naphthyl, was used in some calculations whereas a phenyl group, which is smaller and much less hydrophobic, was used in other calculations. Also, a methoxy group, which contains an oxygen atom capable of hydrogen bonding, was present in solute II, whereas I and III contained only a hydrophobic methyl group. Substitution of nitro groups by formyl groups may have produced the relatively small α -value calculated for solute III when CSP-propyl was used. Experimental data have indicated that diformylbenzoylphenylglycine is not as powerful a phase as dinitrobenzoylphenylglycine.¹³

Our work, like that of Topiol *et al.*,³ suggests that small differences in energy between SS and SR complexes appear to be reliable, even though they are usually less than 1 kcal/mole. In addition, we have shown that in our study the structures of the most stable SS and SR

complexes differ for each of the three pairs of enantiomers examined. (This was not true in our first study, involving two pairs of more closely related structures). Furthermore, the present study shows that differences in the weighted-average free energies of different SS and SR complexes for a given enantiomeric pair also lead to predictions in qualitative agreement with experiment. What remains to be done is to start with other conformations of the CSP and of each of the enantiomeric solutes. This is needed because the fraction of the most stable conformer was less than 50% of the total species.

For each enantiomer and each CSP, at least 600 orientations were generated randomly and the non-bonded interactions were minimized. For each pair, between 25 and 50 of the most stable orientations differed in energy from the most stable by not more than 4.0 kcal/mole. Intramolecular minimization of these species further decreased the number of unique orientations to between 5 and 11 for each system. While it cannot be guaranteed that all minima were located for any given system, the technique seems quite adequate. Finally, the present study again demonstrates the importance of the size of the spacer group and shows that use of a smaller group leads to incorrect predictions.

Acknowledgements—We wish to thank N. L. Allinger and Y. H. Yuh for many helpful discussions throughout this study. We also wish to thank J. A. de Haseth for encourage-

ment and interest in this work. Finally we would like to acknowledge financial support of the work by the Department of Basic Energy Science, Department of Energy, Contract Number DE-AS09-76ER-00854. The U.S. Government retains non-exclusive royalty-free license to publish or reproduce the published form of the contribution for the U.S. Government's purposes. M.G.S. also thanks the Department of Chemistry for financial support.

REFERENCES

1. D. W. Armstrong, T. J. Ward, R. D. Armstrong and T. E. Beasley, *Science*, 1986, **232**, 1132.
2. R. E. Boehm, D. E. Martire and D. W. Armstrong, *Anal. Chem.*, 1988, **60**, 522.
3. S. Topiol, M. Sabio, J. Moroz and W. B. Caldwell, *J. Am. Chem. Soc.*, 1988, **110**, 8367, and references therein.
4. K. B. Lipkowitz, J. M. Landwer and T. Darden, *Anal. Chem.*, 1986, **58**, 1611.
5. K. B. Lipkowitz, D. J. Malik and T. Darden, *Tetrahedron Lett.*, 1986, **27**, 1759.
6. K. B. Lipkowitz, D. A. Demeter, C. A. Parish, J. M. Landwer and T. Darden, *J. Comput. Chem.*, 1987, **8**, 753.
7. K. B. Lipkowitz, D. A. Demeter, C. A. Parish and T. Darden, *Anal. Chem.*, 1987, **59**, 1731.
8. K. B. Lipkowitz, D. A. Demeter, R. Zegarra, R. Larter and T. Darden, *J. Am. Chem. Soc.*, 1988, **110**, 3446.
9. M. G. Still and L. B. Rogers, *Talanta*, 1989, **36**, 35.
10. W. H. Pirkle, C. J. Welch and M. H. Hyun, *J. Org. Chem.*, 1983, **48**, 5022.
11. N. L. Allinger and Y. Yuh, to be submitted to the Quantum Chemistry Program Exchange 1988.
12. W. H. Pirkle, M. H. Hyun and B. Banks, *J. Chromatog.*, 1984, **316**, 585.
13. W. H. Pirkle, Personal Communication, December 1988.

SEPARATION OF METAL IONS ON A MODIFIED ALUMINIUM OXIDE

KRYSZYNA BRAJTER✠ and EWA DABEK-ZLOTORZYNSKA

Department of Chemistry, University of Warsaw, Pasteura 1, PL-O2-093 Warsaw, Poland

(Received 6 January 1989. Revised 4 December 1989. Accepted 14 December 1989)

Summary—The possibility of application of a sulpho-derivative of an aromatic organic complexing agent for separation of cations on aluminium oxide has been investigated. Alumina modified with Nitroso-R salt is used for recovery of cobalt from a tap water and for selective separation of palladium from rhodium.

The selective and quantitative separation of metal ions from aqueous solution by a number of materials has been extensively investigated; in particular, chelating agents immobilized on various supports have been recommended for the purpose.¹⁻¹⁰

Recently, porous aluminium oxide has been successfully used in electrochemistry for immobilization of electroactive reagents on electrodes,^{11,12} so it seemed worth trying it as a support for immobilization of complexing reagents for chromatographic separation and preconcentration of metal ions. The following reagents have therefore been examined; tiron, 8-hydroxyquinoline-5-sulphonic acid (HQS), ferron, nitroso-R salt (NRS), Alizarin Red S, Bromopyrogallol Red (BPR) and Xylenol Orange (XO). Separation of some metal ions was obtained, and the alumina modified with NRS was adopted for recovery of cobalt from a tap water and for the selective separation of palladium from rhodium.

EXPERIMENTAL

Apparatus

The atomic-absorption spectrometers used were a Beckman model 1272 with Pye Unicam GRM-1268 graphite furnace atomizer and a Zeiss Jena model AAS-1 with air-acetylene burner. The conditions used for determining the various elements were those recommended by the manufacturers. The pH of solutions was measured with an Elpo model N-517 pH-meter and a Radiometer combined glass/calomel electrode. The flow-rate was regulated with a peristaltic pump.

The columns employed had an internal diameter of 6 mm and were fitted with a stopcock.

Reagents

The alumina used was "acid for column chromatography" with Brockmann activity I, a specific surface area of 186 m²/g, and average pore diameter of 41 Å. It was repeatedly washed with hot water and finally air-dried.

The ligands tested were disodium 1,2-dihydroxybenzene-3,5-disulphonate (tiron), 8-hydroxyquinoline-5-sulphonic acid (HQS), disodium 1-nitroso-2-naphthol-3,6-disulphonate (nitroso-R salt, NRS), 7-iodo-8-hydroxyquinoline-5-sulphonic acid (ferron), sodium 1,2-dihydroxyanthraquinone-3-sulphonate (Alizarin Red S), 3,3'-dibromosulphogallein (Bromopyrogallol Red, BPR) and Xylenol Orange (XO). Their solutions were prepared by dissolving the commercial analytical-grade reagents in water.

A palladium solution was prepared by dissolving PdCl₂ in hydrochloric acid. A platinum solution was prepared by dissolving pure (5N) platinum wire in *aqua regia*, evaporating the solution to dryness, removing nitrate by repeated evaporations with concentrated hydrochloric acid, and finally diluting with dilute hydrochloric acid. A rhodium(III) solution was obtained by dissolving RhCl₃ · 3H₂O in concentrated hydrochloric acid, evaporating the solution to low bulk and diluting to known volume with dilute hydrochloric acid. Other metal ion solutions were prepared by diluting standard solutions (1000 ppm, for atomic-absorption, Merck) as required. All other chemicals were analytical-grade reagents. Twice-distilled water was used. All laboratory glassware and the polyethylene bottles used were thoroughly cleaned by soaking in nitric acid (1 + 9) and then rinsing with twice-distilled water.

Determination of the adsorption isotherms of the ligands

The sorption of the ligands on the alumina was measured under static conditions. A 0.200-g portion of Al_2O_3 was shaken with 20 ml of ligand solution (of various concentrations) at pH 2.0–2.2 for 12 hr. After 24 hr the equilibrium concentration of ligand in the solution was measured by spectrophotometry.

Stability of the modified alumina towards acid and alkali

A 50-ml portion of 0.1M mineral acid or sodium hydroxide was passed through a column containing 0.500 g of the alumina modified with 0.2 mmole of ligand per gram, at a flow-rate of 1.0 ± 0.2 ml/min. The concentration of complexing reagent in the effluent was measured spectrophotometrically.

Retention of metal ions as a function of pH

Samples (0.200 g) of Al_2O_3 modified with NRS (0.1 mmole/g) were mixed with 20 ml of metal ion solution (2×10^{-4} M) adjusted to appropriate pH-values. After equilibrium was reached (24 hr) the residual metal ion concentration was determined by AAS.

Determination of breakthrough capacity

Solutions of cobalt(II) and copper(II) (0.5 $\mu\text{g}/\text{ml}$) at pH 2.0–2.2 were passed through a column of 1.0 g of alumina modified with NRS (0.2 mmole/g) at a flow-rate of 3 ml/min. The breakthrough point was taken as the position at which the metal ion concentration in the eluate was 10% of that in the sample solution.

Separation of Pd(II) and Rh(III)

A 10-ml portion of a solution containing 0.10 mg each of Pd and Rh at pH 2.0–2.2 was passed through a column of 1.0 g of alumina or of modified alumina (NRS 0.2 mmole/g) at a flow-rate of 0.5 ml/min. The column was then washed with 20 ml of a selected eluent and the concentrations of Pd and Rh in the effluent were determined by AAS.

Column separation of Pd(II) from Rh(III) and Pt(IV)

A 5-ml portion of a solution containing a mixture of metal ion chloro-complexes (Pd–Rh, Pd–Pt, Pd–Rh–Pt) at pH 2.0–2.2 was passed through a column of 0.25 g of alumina modified with NRS (0.2 mmole/g) at a flow-rate of 0.5 ml/min. The column was washed with water and the Rh and/or Pt retained were eluted with

20 ml of 1M hydrochloric acid. Palladium was next eluted with 10 ml of 0.02M sodium hydroxide into a 25-ml standard flask, and the solution was diluted to volume. The metal ions were determined by AAS.

Determination of cobalt in tap water

Three litres of tap water, adjusted to pH 2.0–2.2 were passed through a column containing 1.0 g of modified alumina (NRS 0.2 mmole/g, bed height 5 cm, column diameter 6 mm) at a flow-rate of 3 ml/min. The cobalt was eluted with 10 ml of 0.2M sodium hydroxide and determined by AAS.

Determination of palladium in rhodium compounds

A weighed sample of RhCl_3 (Koch Light) was dissolved in 10 ml of concentrated hydrochloric acid, the solution was evaporated to dryness and this step was repeated. The residue was dissolved in 10 ml of 2M hydrochloric acid, and the solution was diluted to volume in a 25-ml standard flask. An H_3RhCl_6 (State Mint) solution (5048 mg/l.) was diluted as required. Aliquots (5 ml) of these solutions were adjusted to pH 2.0–2.2 and introduced into a column of 0.25 g of alumina modified with NRS (0.20 mmole/g). The rhodium retained was eluted with 10 ml of 1M hydrochloric acid. The column was then washed with about 20 ml of water, and palladium was eluted with 10 ml of 0.02M sodium hydroxide and water and made up to volume in a 25-ml standard flask.

RESULTS AND DISCUSSION

Sorption of chelating reagents on the alumina

The adsorption isotherms of the seven chelating agents on the alumina are presented in Fig. 1. It is clear that the size of the reagents has an effect on the adsorption capacity of the alumina. An increase in reagent size decreases the capacity of the alumina for sorption of the reagent.

The sorption capacity was determined at pH 2.0–2.2, at which alumina acts as a cation-exchanger (there is a positive charge on its surface), but in our experiments the reagents are immobilized on the surface of the alumina by sorption rather than exchange.

Figure 2 illustrates the stability of the modified alumina towards mineral acids and an alkali. The degree of resistance to attack is in agreement with the affinity of the anion species for alumina.¹³

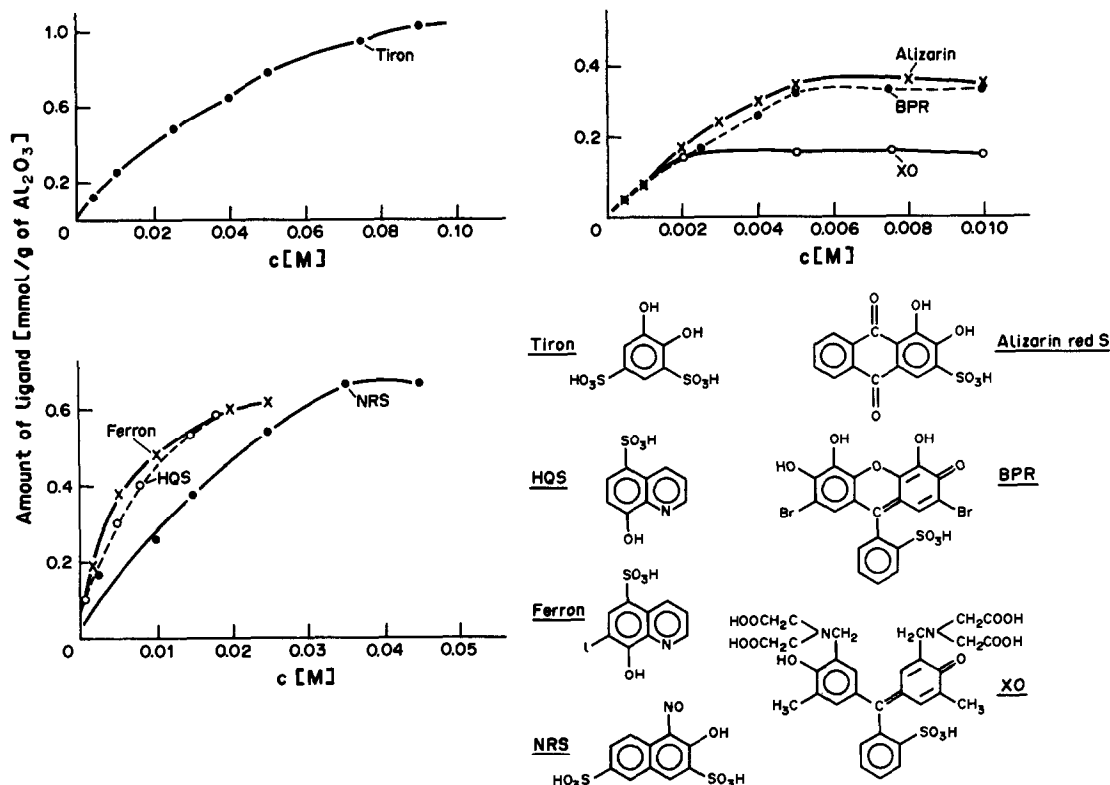


Fig. 1. Adsorption isotherms of ligands.

Retention of metal ions on the modified alumina

NRS was chosen as a representative ligand for further examination of the modified alumina and the separation of some metal ions. The affinity of the metal ions for the modified alumina was measured as a function of pH. Results are presented in Fig. 3. The shape of the curves indicates that the sorption as a function of pH depends on the complexing ability of the ligand immobilized on the alumina. Alumina itself also

acts as a cation-exchanger (in acid medium), but if no complexing ligand is present, metal ions that form insoluble hydroxides will be precipitated. The sorption of metal ions at higher pH is possible only in the presence of a ligand immobilized on the alumina.

There is some differentiation of the retention of metal ions on NRS-Al₂O₃. In acid medium (pH < 2) only Co(II), Cu(II) and Fe(III), which form stable complexes in this medium, are strongly retained on the modified alumina.

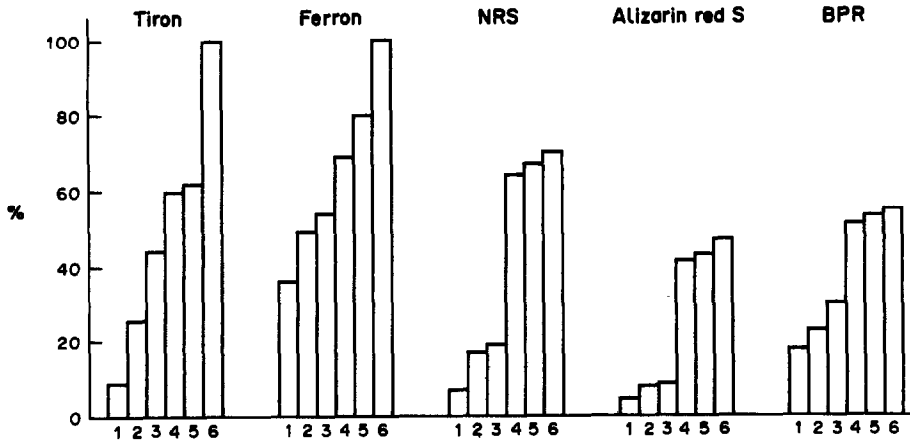


Fig. 2. Release of ligands from modified alumina by 1—HClO₄, 2—HNO₃, 3—HCl, 4—H₂SO₄, 5—H₃PO₄, 6—NaOH.

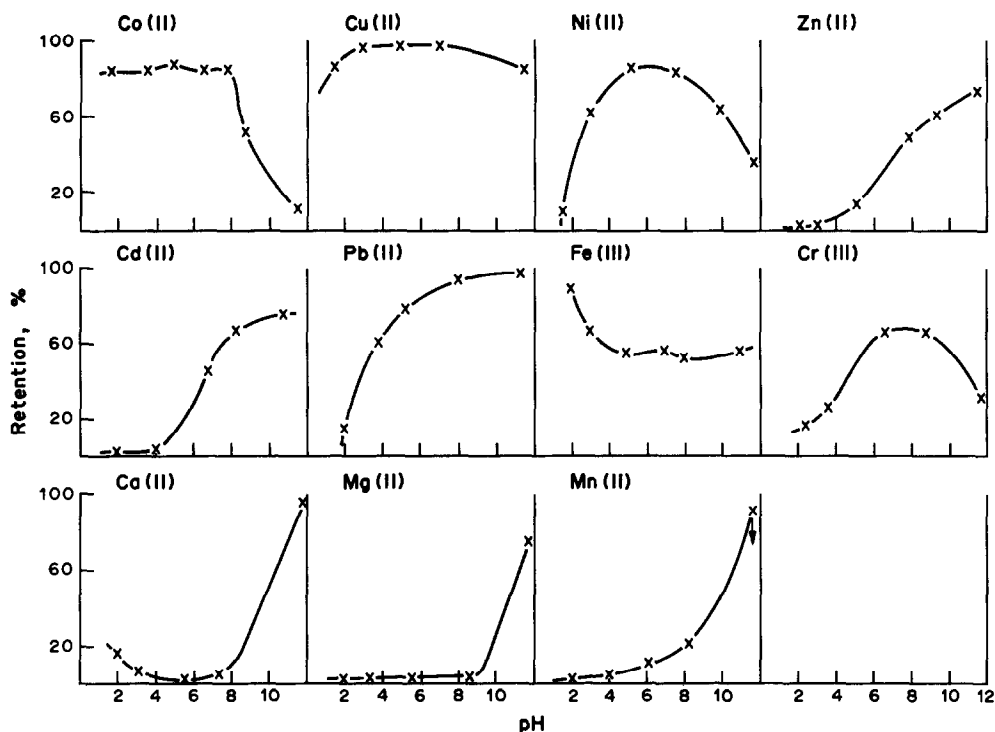


Fig. 3. Retention of metal ions on the NRS-loaded Al_2O_3 , as a function of pH.

Owing to the complexation ability of NRS, cobalt is very strongly retained on NRS- Al_2O_3 at pH 2–8, probably as cobalt(III). At higher pH (8–12), at which the NRS is partly removed from the NRS- Al_2O_3 phase by hydroxide ions, the retention of cobalt is decreased, probably because of insufficient NRS in the alumina phase to form the 3:1 NRS-Co(III) complex.

Cu(II), which forms the stable ML_2 nitroso-R salt complex, is retained over the whole pH range investigated (2–12). The greater retention of Cu(II) than of Co(II) in basic medium (pH > 8) is also probably due to the amount of NRS in the alumina phase being insufficient to form the 3:1 NRS-Co complex, but enough to form the Cu complex.

With sodium hydroxide solution as eluent, cobalt can be separated from copper, and both copper and cobalt from the other metal ions investigated.

Figure 4 shows the retention of platinum metal ions on unmodified and NRS-modified alumina as a function of pH. The modified alumina gives lower retention of Pt(IV), Rh(III) and Ir(IV) chloro-complexes than that on the unmodified alumina, but increased retention of Pd(II), which forms stable red NRS complexes that are strongly sorbed on the modified alumina. This is utilized for the selective

separation of palladium from the other platinum metals.

Preconcentration of Co(II), Cu(II) and Fe(III)

Ni(II), Mn(II), Zn(II), Cd(II), Pb(II) and Cr(III) are not bound to the NRS- Al_2O_3 in acid medium and under dynamic conditions only Co(II), Cu(II) and Fe(III), of the ions tested, are retained on the column. Cobalt(II) and iron(III)

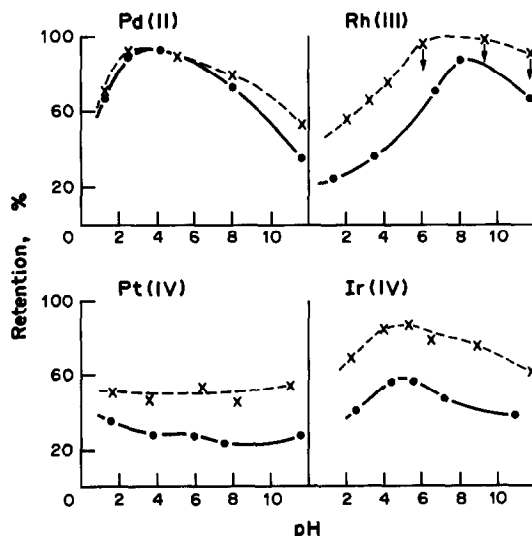


Fig. 4. Retention of platinum metal ions on the unmodified (—x—x—) and NRS-modified alumina (—●—).

can then be eluted together, with 0.2M sodium hydroxide, as their nitroso-R salt complexes; copper(II) is retained on the column and can be eluted with 0.5M nitric acid.

To examine the retention of these three metal ions on an NRS- Al_2O_3 column (1 g, NRS 0.2 mmole/g), 1-litre portions of test solutions of cobalt, copper and iron at 0.1 mg/l. were passed through the column at different flow-rates. At the optimum pH (2.0–2.2) the maximum flow-rate giving quantitative recovery was 3 ml/min. The amount of metal ion retained was determined by elution with 10 ml of the appropriate eluent as above. The preconcentration factor obtained was thus 100. Higher factors can be achieved if the volume of the aqueous sample is larger.

The breakthrough capacity under the given column operating conditions of bed height 5 cm (1.0 g of NRS- Al_2O_3 , NRS 0.2 mmole/g), pH 2.0–2.2, flow-rate 3 ml/min, was evaluated for cobalt and copper, and found to be 1.0 mg of Co(II) and 1.5 mg of Cu(II). From the amount of NRS retained on the alumina bed, the molar ratios of NRS to Co(II) and Cu(II) on the column under the given conditions are 12:1 and 8:1 respectively.

In most of the experiments, the three metal ions were added at 0.1 mg/l. concentration. Quantitative recoveries were also possible when the concentration of each metal ion was as low as 0.005 mg/l.

Effect of some inorganic salts and organic complexants on the retention of Co, Cu and Fe

A 1-litre portion of test solution at pH 2.0–2.2 containing 0.1 mg of Co(II), Cu(II) or Fe(III) and the inorganic test compound at various concentrations was passed through a column containing 1 g of NRS- Al_2O_3 (NRS 0.2 mmole/g) at 3 ml/min. The metal ions were eluted as before. From the results, shown in Table 1, it can be concluded that of the inorganic substances, only the sulphates influence the collection yield for cobalt, even when present at high concentrations. This can be attributed to the high stability of Co-NRS complexes in acid medium. The retention of Co(II) as well Cu(II) and Fe(III) in the presence of sodium or magnesium sulphate is considerably decreased, and this seems to be due to either the sulphate or bisulphate (present in approximately equal proportions at the pH used), presumably by partial removal of NRS from the column (*cf.* Fig. 2). Phosphate had a

Table 1. Effect of inorganic salts on the retention of metal ions on NRS- Al_2O_3

Salt	Amount added, mg/l.	Recovery, %		
		Co	Fe	Cu
NaCl	500	99	96	96
	2000	99	78	94
KCl	1000	99	87	94
	100	99	99	96
Na_2CO_3	200	99	87	96
	1000	99	89	94
MgCl_2	1000	99	90	95
	500	99	94	95
$\text{Ca}(\text{NO}_3)_2$	2000	99	77	94
	500	99	89	96
$\text{Mg}(\text{NO}_3)_2$	2000	99	79	92
	6	99	50	65
Na_2SO_4	100	34	20	0
	10	98	43	60
MgSO_4	100	35	15	0
	10	99	43	90
$(\text{NH}_4)_2\text{HPO}_4$	10			

similar effect on the collection of iron, which was also affected to some extent by nitrate. At low sulphate concentrations, copper(II) was completely retained, but eluted in two fractions, suggesting that part was adsorbed as the Cu-NRS complex and the rest in some other form under these conditions.

The effects of some organic complexing agents are shown in Table 2. EDTA, especially, considerably decreases the retention of iron(III). Cu(II) in the presence of NTA and EDTA is retained quantitatively by NRS- Al_2O_3 , but is partly eluted (12 and 80% respectively) together with cobalt. The retention of copper ions on the unmodified alumina in the presence of NTA and EDTA was also investigated (Table 2). The results show that at pH 2.0–2.2 in the presence of EDTA the copper is retained mainly by

Table 2. Effect of organic substances on the retention of metal ions on NRS- Al_2O_3

Ligand	Concentration	Recovery, %			
		Co	Fe	Cu	
		I*	I*	I*	II*
Na acetate	$1 \times 10^{-5}M$	99	83		97
NaK tartrate	$1 \times 10^{-5}M$	99	97		95
NTA	$1 \times 10^{-5}M$	99	97	12	88
	$2 \times 10^{-5}M$	99	93	14	85
Gly	$1 \times 10^{-5}M$	99	97		96
	$2 \times 10^{-5}M$	99	97	6	92
EDTA	$1 \times 10^{-5}M$	99	32	80	20
	$2 \times 10^{-5}M$	99	24	95	5
Citric acid	$1 \times 10^{-5}M$	99	78	12	88
Humic acid	1 mg/l.	99	99		98
	10 mg/l.	99	99		98
NTA†	$1 \times 10^{-5}M$	0	0	20	0
EDTA†	$1 \times 10^{-5}M$	34	6	80	0

*Eluent: I, 0.2M NaOH; II, 0.5M HNO_3 .

†On unmodified alumina.

Table 3. Recovery of cobalt from tap water

Co added, μg/l.	Co found*, μg/l.	Recovery, %
0	0.43 ± 0.05	
1	1.41 ± 0.04	98
2	2.39 ± 0.06	98

*Mean and 95% confidence limits for four determinations.

sorption of the Cu-EDTA complex rather than by formation of the Cu-NRS complex in the column of modified alumina.

The alumina modified with NRS was used for preconcentration and determination of cobalt in tap water. The results are presented in Table 3. To check the recovery of cobalt(II), a tap water sample spiked with known amounts of Co(II) standard solution was also analysed. The recovery of the cobalt spikes is presented in the table.

Separation of palladium from rhodium and platinum

All three of these platinum metals, when present as chloro-complexes, show some affinity for unmodified alumina (Fig. 3b), as also does iridium, and this affinity is decreased, except for Pd(II), when NRS-modified alumina is used. Table 4 shows the effect of a number of potential eluents at different concentrations for the separation of palladium from rhodium on unmodified and NRS-modified alumina. The rhodium can be eluted with 1M hydrochloric, nitric or perchloric acid without loss of the palladium, which is retained on the column and can be eluted with 0.02M sodium hydroxide. It should be noted, however, that though palladium is completely sorbed on the NRS-Al₂O₃ column, only about 50% of the rhodium and platinum is sorbed. Also, the rhodium on the column cannot be separated from the platinum by selective elution. The method is

Table 4. Elution of palladium and rhodium from modified and unmodified alumina, with different eluents

Eluent	Al ₂ O ₃		Al ₂ O ₃ -NRS	
	Rh	Pd	Rh	Pd
0.02M HCl	60	50	77	0
0.1M HCl	65	90	83	0
0.2M HCl	70	97	90	0
1.0M HCl	99	99	99	0
0.1M HClO ₄	76	37	85	0
1.0M HClO ₄	99	99	99	0
1.0M HNO ₃	99	99	99	0
0.02M NaOH	3	2	50	99

Table 5. Separation of Pd(II) from Rh(III) and Pt(IV) on the alumina modified with NRS

Matrix, mg	Pd, μg	
	Added	Found*
Rh 0.98	120	119 ± 1
Rh 0.98	12.0	11.9 ± 0.2
Rh 0.98	6.0	5.88 ± 0.06
Pt 1.20	120	119 ± 1
Pt 1.20	12.0	11.9 ± 0.05
Pt 1.20, Rh 0.98	6.0	5.82 ± 0.04

*Average and 95% confidence limits of four separate determinations.

Table 6. Determination of palladium in rhodium compounds

Compound	Pd, %	
	After separation*	Direct AAS
RhCl ₃ (Koch Light)	3.82 ± 0.07 × 10 ⁻²	7.20 × 10 ⁻²
H ₃ RhCl ₆ (State Mint)	4.37 ± 0.05 × 10 ⁻²	7.50 × 10 ⁻²

*Mean and 95% confidence limits for four separate determinations.

therefore suitable only for determination of palladium.

Results for the separation of palladium from mixtures with rhodium and/or platinum are given in Table 5, and in Table 6 for the determination of Pd in two rhodium compounds. For comparison, results for the direct AAS determination without separation are given in Table 6. Rhodium increases the AAS analytical signal of palladium by about 80%.¹⁴

REFERENCES

- D. E. Leyden and G. H. Luttrell, *Anal. Chem.*, 1975, **47**, 1612.
- K. Terada, K. Matsumoto and H. Kimura, *Anal. Chim. Acta*, 1983, **153**, 237.
- B. M. Vanderborcht and R. E. Van Grieken, *Anal. Chem.*, 1977, **49**, 311.
- K. Brajter, *J. Chromatog.*, 1974, **102**, 385.
- K. Brajter and E. Dąbek-Złotorzyńska, *Talanta*, 1986, **33**, 149.
- K. Brajter and E. Olbrych-Śleszyńska, *ibid.*, 1983, **30**, 355.
- K. Brajter, E. Olbrych-Śleszyńska and M. Stańkiewicz, *ibid.*, 1988, **35**, 65.
- K. Brajter and E. Dąbek-Złotorzyńska, *Analyst*, 1988, **113**, 1571.
- J. D. Pietrzyk and C. H. Chu, *Anal. Chem.*, 1977, **49**, 860.
- J. D. Pietrzyk, E. P. Kroeff and T. D. Rotsch, *ibid.*, 1978, **50**, 497.
- C. J. Miller and M. Majda, *J. Am. Chem. Soc.*, 1985, **107**, 1419.
- Idem*, *J. Electroanal. Chem.*, 1986, **207**, 49.
- M. J. Fuller, *Chromatog. Rev.*, 1971, **14**, 45.
- K. Stonawska, *Ph.D. Dissertation*, 1981, Warsaw.

SIMULTANEOUS DETERMINATION OF URANIUM AND THORIUM WITH ARSENAZO III BY SECOND-DERIVATIVE SPECTROPHOTOMETRY

ROKURO KURODA, MAYUMI KUROSAKI, YUTAKA HAYASHIBE
and SATOMI ISHIMARU

Laboratory for Analytical Chemistry, Faculty of Engineering, University of Chiba, Yayoi-cho,
Chiba 260, Japan

(Received 14 August 1989. Revised 21 November 1989. Accepted 28 November 1989)

Summary—A derivative spectrophotometric method has been developed for the simultaneous determination of microgram quantities of uranium and thorium with Arsenazo III in hydrochloric acid medium. The second-derivative absorbances of the uranium and thorium Arsenazo III complexes at 679.5 and 684.4 nm are used for their quantification. Uranium and thorium, both in the range 0.1–0.7 $\mu\text{g/ml}$ have been determined simultaneously with good precision. The procedure does not require separation of uranium and thorium, and allows the determination of both metals in the presence of alkaline-earth metals and zirconium, but lanthanides interfere.

Arsenazo III (3,6-bis[(2-arsenophenyl)azo]-4,5-dihydroxy-2,7-naphthalenedisulphonic acid) has been used as a sensitive, selective reagent for uranium, thorium and zirconium in strongly acidic medium.¹ Uranium² and thorium³ can be determined with Arsenazo III in the presence of zirconium if this is masked with oxalic acid. Uranium and thorium interfere mutually, however, so tedious separations are needed before their determination is possible.⁴ These metals are often present together, so it was thought of interest to find whether derivative spectrophotometry with Arsenazo III could be used for their simultaneous determination without a prior separation.

Derivative spectrophotometry is used to eliminate background interference as well as to resolve overlapping absorption bands.⁵ It has been widely used in pharmaceutical analysis, amino-acid and protein analysis, clinical chemistry, environmental analysis *etc.*,⁶ but less often in inorganic analysis.^{7–15}

EXPERIMENTAL

Apparatus

A Hitachi U-3200 double-monochromator double-beam programmable research-grade spectrometer was used, with a non-adjustable iodine-tungsten lamp (50 W) and 20-mm path-length glass cells.

Reagents

A uranium(VI) stock solution (1 mg/ml) was prepared by dissolving $\text{UO}_2(\text{NO}_3)_2 \cdot 6\text{H}_2\text{O}$ (Wako Pure Chemical Industries, Osaka) in 0.1M nitric acid and standardized by an EDTA method using back-titration with thorium. A thorium stock solution (1 mg/ml) was prepared by dissolving $\text{Th}(\text{NO}_3)_4 \cdot 4\text{H}_2\text{O}$ (Wako) in 0.1M nitric acid and standardized by EDTA titration. A 0.1% aqueous solution of Arsenazo III (Kanto Chemical Co., Tokyo) was prepared. All chemicals used were of analytical reagent grade.

Procedures

Color development. Evaporate a mixture of uranium and thorium to dryness. Take up the residue in 5 ml of 8M hydrochloric acid, add 0.7 g of zinc dust and let the mixture stand for 20 min to complete the reduction of uranium(VI) to uranium(IV). Transfer the solution to a 10-ml standard flask, add 1.0 ml of Arsenazo III solution and dilute to the mark with 8M hydrochloric acid.

Spectral measurement. Place a reagent blank solution, prepared as in the procedure, in the sample and reference cells and scan from 750 to 600 nm to set up the baseline. Replace the blank solution in the sample cell with the sample solution and repeat the spectral scan at a scan speed of 120 nm/min with a 2.00-nm band-pass (scale absorbance from –2.000 to 4.000) to

store the whole spectrum on a 3-in. floppy disk. Then record the second-derivative spectrum. Read the derivative amplitudes at 679.5 nm (zero-point wavelength for the thorium complex) and 684.4 nm (zero-point wavelength for the uranium complex) for the determination of uranium and thorium, respectively. For construction of the calibration curve, record the normal and second-derivative spectra for 1–7 μg of uranium or thorium, and plot the derivative amplitudes (measured at the appropriate concentration) *vs.* the metal ion concentration.

RESULTS AND DISCUSSION

The spectrophotometric methods for uranium and thorium with Arsenazo III are superior in sensitivity and selectivity to the other spectrophotometric methods and are widely used for trace determination of these metals. The ordinary absorption spectra of the Arsenazo III complexes of uranium and thorium (Fig. 1) are too similar to allow the spectrophotometric determination of the one metal in the presence of the other.

The first, second and third derivative spectra of the complexes are shown in Fig. 2. The first derivative spectra both show a zero point at

about 665 nm, which tends to shift to shorter wavelength with increasing concentration of uranium and/or thorium, analogously to the absorption maxima of the ordinary spectra, which shift slightly (1–2 nm) to shorter wavelengths with increasing concentration. These trends, which are also reflected in the third-derivative spectra, indicate that the first and third derivatives are not analytically useful. The second-derivative spectra of the complexes, however, each have two zero points, at around 650 and 684 nm for the uranium complex and 648 and 680 nm for the thorium complex. Those at 684.4 and 679.5 nm for the uranium and thorium complexes, respectively, are potentially useful. As can be seen in Fig. 3a, a fixed concentration of the uranium complex has a sufficient and constant amplitude at 679.5 nm (the thorium zero-point wavelength) in the presence of various concentrations of thorium. Similarly, the amplitude at 684.4 nm (the uranium zero-point wavelength) will correspond to the concentration of the thorium complex (Fig. 3b). Thus simultaneous determination of uranium and thorium may be feasible by use of these zero points.

The characteristics of derivative spectra are dependent on the choice of instrument

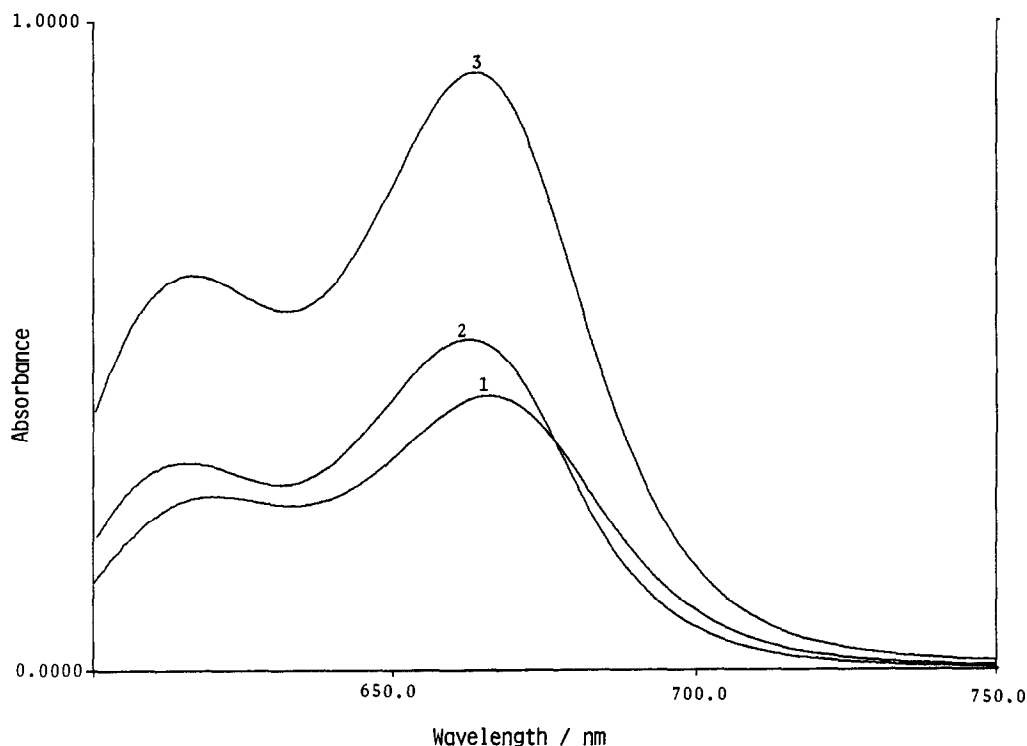


Fig. 1. Normal spectra of Arsenazo III complexes of uranium and thorium in 5.2M HCl. 1, U 0.575 $\mu\text{g}/\text{ml}$; 2, Th 0.585 $\mu\text{g}/\text{ml}$; 3, U 0.575 $\mu\text{g}/\text{ml}$ and Th 0.585 $\mu\text{g}/\text{ml}$.

parameters. These were optimized with respect to reduction of noise levels, stability of the zero points, and sensitivity, as well as the wavelength range used, which is controlled by the memory capacity of the built-in microcomputer. The best results were obtained at a scan speed of 120 nm/min over the range from 750 to 600 nm, with a wavelength interval of 0.5 nm for the differentiation. The spectra were smoothed once, by a weighted moving average technique.

Calibration curves for the determination of uranium and thorium are linear in the range

0–7 $\mu\text{g}/10\text{ ml}$ for uranium and 0–8 $\mu\text{g}/10\text{ ml}$ for thorium.

The results listed in Table 1 show that mixtures containing 0.115–0.575 $\mu\text{g}/\text{ml}$ uranium and 0.117–0.351 $\mu\text{g}/\text{ml}$ thorium can be analysed with a relative error of less than 5%, but the errors are larger for one or both components at concentrations outside these ranges.

The effect of potential interferences on the simultaneous determination procedure was studied, and the results are listed in Table 2. The alkaline-earth metals tested tend to interfere

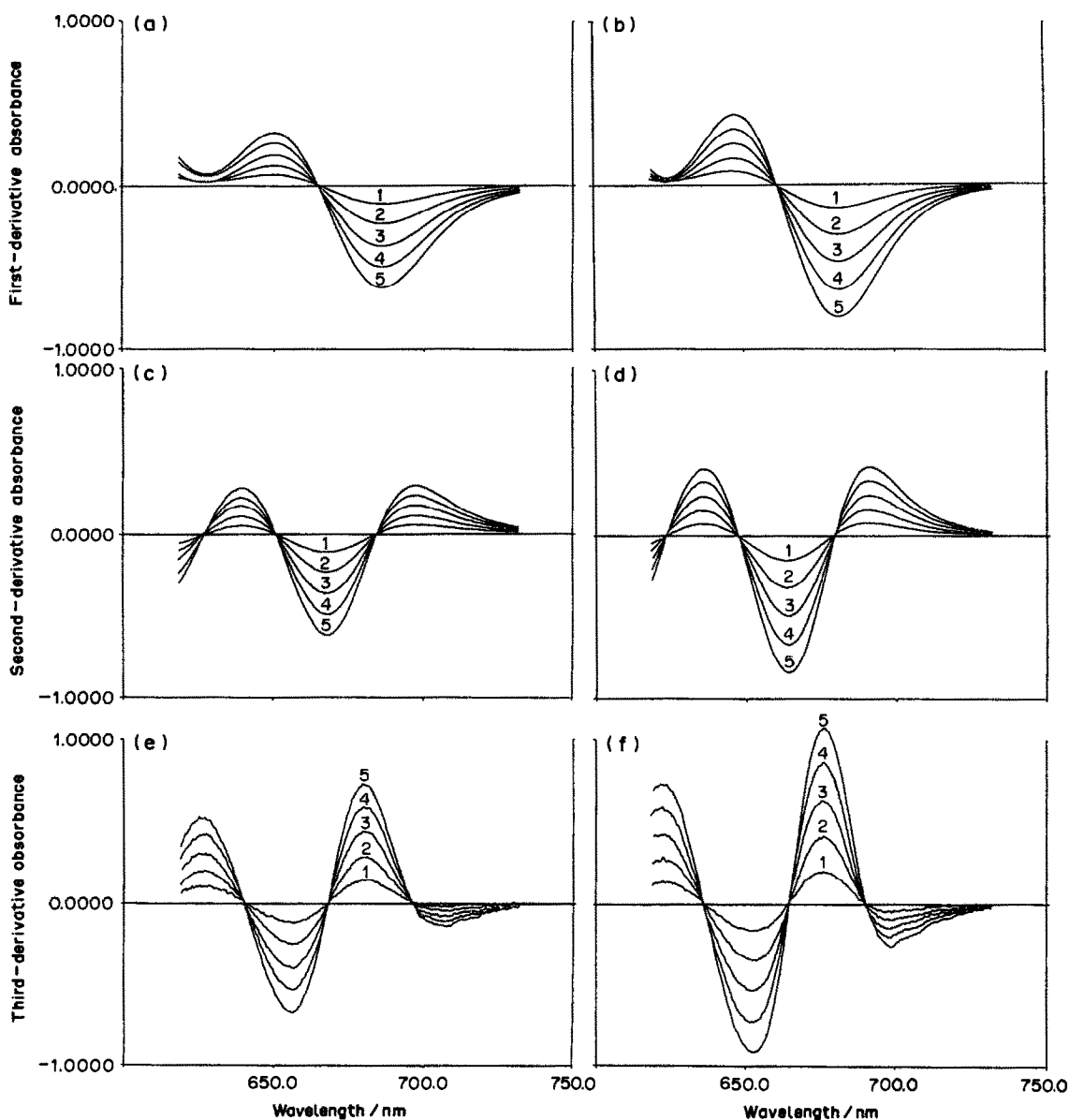


Fig. 2. Derivative spectra of Arsenazo III complexes of uranium and thorium in 5.2M HCl media: (a) first-order (U); (b) first-order (Th); (c) second-order (U); (d) second-order (Th); (e) third-order (U); (f) third-order (Th). [U], $\mu\text{g}/\text{ml}$: 1, 0.115; 2, 0.230; 3, 0.345; 4, 0.470; 5, 0.575. [Th], $\mu\text{g}/\text{ml}$: 1, 0.117; 2, 0.234; 3, 0.351; 4, 0.468; 5, 0.585.

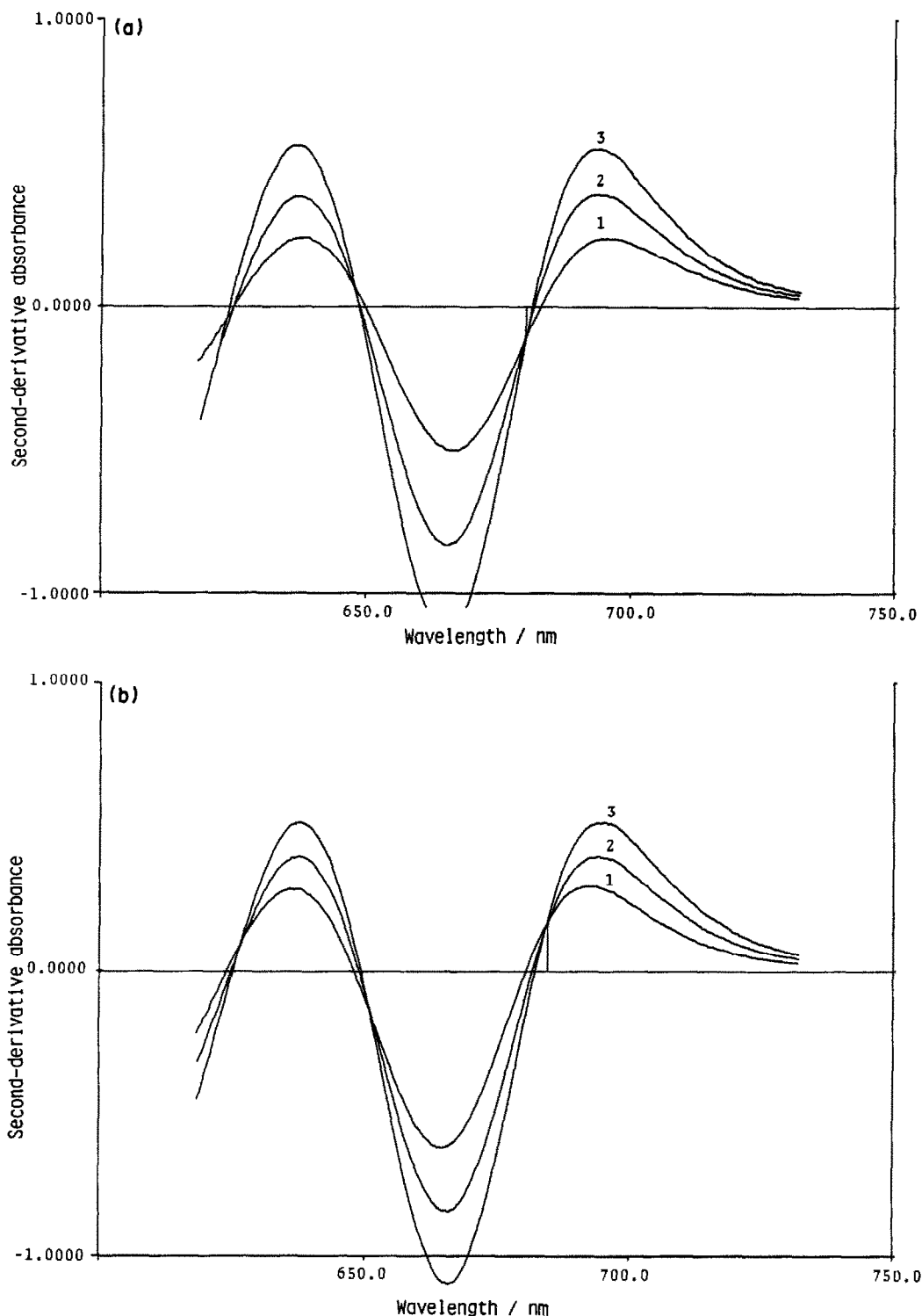


Fig. 3. Second-derivative spectra of mixtures of uranium and thorium Arsenazo III complexes in 5.2M HCl. (a) U, 0.345 $\mu\text{g/ml}$; Th, 0.117 (1); 0.351 (2); 0.585 (3) $\mu\text{g/ml}$. (b) Th, 0.351 $\mu\text{g/ml}$; U, 0.115 (1); 0.345 (2); 0.575 (3) $\mu\text{g/ml}$.

at high concentrations with the determination of 0.2 $\mu\text{g/ml}$ uranium and thorium, but are tolerable at about the 100 $\mu\text{g/ml}$ level. The lanthanides interfere, but are tolerable in 1:1

concentration ratio to uranium and thorium at the 0.4 $\mu\text{g/ml}$ level. Interference by zirconium can be reduced by use of oxalic acid as masking agent, but the tolerance ratio is still only 2:1.

Table 1. Results of quantitative determination of uranium and thorium by second-derivative spectrophotometry

Sample No.	Taken, $\mu\text{g/ml}$		Found, $\mu\text{g/ml}$		Relative error, %	
	U	Th	U	Th	U	Th
1	0.0395	0.0468	0.0324	0.0613	-18	31
2	0.0987	0.0468	0.0925	0.0577	-6.7	23
3	0.197	0.0468	0.181	0.0634	-8.1	36
4	0.494	0.0468	0.484	0.0615	-2.0	31
5	0.691	0.0468	0.685	0.0748	-0.9	60
6	0.115	0.117	0.109	0.118	-5.2	0.8
7	0.345	0.117	0.335	0.115	-2.9	-1.7
8	0.575	0.117	0.588	0.119	2.3	1.7
9	0.115	0.351	0.121	0.357	5.2	1.7
10	0.230	0.351	0.229	0.358	-0.4	2.0
11	0.345	0.351	0.347	0.353	0.6	0.6
12	0.575	0.351	0.580	0.355	0.9	1.1
13	0.0395	0.585	0.0350	0.600	-11	2.6
14	0.0987	0.585	0.109	0.595	10	1.7
15	0.296	0.585	0.276	0.617	-6.8	5.5
16	0.592	0.585	0.552	0.644	-6.8	10
17	0.0395	0.702	0.0342	0.730	-13	4.0
18	0.0987	0.702	0.0911	0.742	-7.7	5.7
19	0.296	0.702	0.271	0.733	-8.4	4.4
20	0.691	0.702	0.624	0.707	-9.7	0.7

Table 2. Effect of foreign species

Taken, $\mu\text{g/ml}$		Foreign ions present, $\mu\text{g/ml}$	Found, $\mu\text{g/ml}$		Relative error, %	
U	Th		U	Th	U	Th
0.197	0.234	Ba 2000	0.163	0.333	-17	42
		80	0.202	0.246	0.6	5.1
		Ca 100	0.211	0.240	7.1	2.6
		80	0.191	0.243	-3.0	3.8
		Mg 2500	0.186	0.269	-5.6	15
		100	0.209	0.238	6.1	1.7
0.394	0.468	Sm 0.8	0.358	0.517	-9.1	10
		0.4	0.376	0.496	-4.6	6.0
		Ce 0.8	0.381	0.508	-3.3	8.5
		0.4	0.397	0.498	0.8	6.4
		La 0.8	0.358	0.528	-9.1	13
		0.4	0.369	0.505	-6.3	7.9
		Y 0.8	0.369	0.490	-6.3	4.8
		0.4	0.374	0.496	-5.0	6.0
0.197	0.234	Zr* 3.8	0.189	0.253	-4.1	8.1
		0.48	0.194	0.240	-1.5	2.6
0.394	0.468	Zr* 4.8	0.385	0.524	-2.3	12
		2.9	0.357	0.494	-9.4	5.6

*With 0.24 g of $\text{H}_2\text{C}_2\text{O}_4 \cdot 2\text{H}_2\text{O}$ in 10 ml of solution.

The precisions (RSD, 5 determinations) are 2.6% for uranium and 1.5% for thorium in a mixture consisting of 0.345 $\mu\text{g/ml}$ uranium and 0.351 $\mu\text{g/ml}$ thorium.

REFERENCES

- Z. Marczenko, *Separation and Spectrophotometric Determination of Elements*, Horwood, Chichester, 1986.
- H. Onishi and Y. Toita, *Bunseki Kagaku*, 1969, **18**, 1134.
- H. Onishi, *ibid.*, 1963, **12**, 1153.
- Idem*, *Photometric Determination of Traces of Metals*, 4th Ed., Part IIB, Wiley, New York, 1989.
- T. Nowicka-Jankowska, K. Górczyńska, A. Michalik and E. Wieteska, in *Wilson and Wilson's Comprehensive Analytical Chemistry*, Vol. XIX, Elsevier, Amsterdam, 1986.
- F. Sanchez Rojas, C. Bosch Ojeda and J. M. Cano Pavón, *Talanta*, 1988, **35**, 753.
- A. Bermejo-Barrera, P. Bermejo-Barrera and F. Bermejo Martinez, *Analyst*, 1985, **110**, 1313.

8. N. Suzuki and R. Kuroda, *ibid.*, 1987, **112**, 1077.
9. S. Kuš and Z. Marzenko, *ibid.*, 1987, **112**, 1503.
10. F. Salinas, A. M. de la Peña and J. A. Murillo, *ibid.*, 1987, **112**, 1391.
11. N. Suzuki and R. Kuroda, *Mikrochim. Acta*, 1987 **II**, 47.
12. H. Ishii and H. Tsuchiai, *Anal. Sci.*, 1987, **3**, 229.
13. J. A. Murillo, J. M. Lemus, A. M. de la Peña and F. Salinas, *Analyst*, 1988, **113**, 1439.
14. A. I. Jiménez, F. Jiménez and J. J. Arias, *ibid.*, 1989, **114**, 93.
15. A. Gallardo Melgarejo, A. Gallardo Céspedes and J. M. Cano Pavón, *ibid.*, 1989, **114**, 109.

SPECTROPHOTOMETRIC DETERMINATION OF EPINEPHRINE AND NOREPINEPHRINE WITH SODIUM PERIODATE

MICHAEL E. EL-KOMMOS, FARDOUS A. MOHAMED and ALAA S. KHEDR

Department of Pharmaceutical Chemistry, Faculty of Pharmacy, Assiut University, Assiut, Egypt

Summary—A simple and accurate spectrophotometric method is described for the determination of epinephrine (EP), norepinephrine (NE) and their bitartrate salts. The method is based on the development of a red colour (λ_{max} 490 nm) with sodium periodate in aqueous alcoholic medium. The colour is stable for at least 1 hr. The molar reacting ratio of EP or NE to periodate is 1:2. The proposed method is particularly suitable for routine analysis of EP and NE injections. The interference due to the sodium metabisulphite normally used as antioxidant can be overcome by addition of acetone. Results for analysis of bulk drugs and injections agree well with those of official methods.

Epinephrine and norepinephrine have numerous pharmacological uses.¹ Techniques employed for the assay of EP, NE and their bitartrate salts in pure and dosage form include non-aqueous titration,² bromometric titration,^{3,4} potentiometric titration,⁵ polarography,^{6,7} spectrophotometry,⁸⁻¹² spectrofluorimetry,¹³⁻¹⁵ and liquid chromatography.¹⁶ The spectrophotometric methods described in this paper depend on the interaction of the two catecholamines with sodium periodate in aqueous alcoholic medium.

EXPERIMENTAL

Apparatus

A Uvidec-320 spectrophotometer (Jasco, Tokyo) and a thermostatically controlled water-bath were used.

Reagents

Sodium periodate solution, 0.2% in water. Standard solutions of EP, NE and their salts, prepared by dissolving 25 mg in 100 ml of 0.1% aqueous sodium metabisulphite solution. Solvents used were analytical grade.

Procedures

Calibration. For each calibration point, pipette 1 ml of working standard into a 10-ml standard flask, add 1 ml of acetone, mix and let stand for 10 min at room temperature, then add 2 ml of sodium periodate solution and mix. For EP, let stand for 5 min, make up to volume with ethanol, mix, and measure the absorbance at 490 nm in 1-cm cells against a reagent blank.

For NE, after adding the periodate heat at $60 \pm 5^\circ$ on a water-bath for 2 min with gentle swirling of the flask, cool to room temperature, then dilute to volume with ethanol, mix and measure the absorbance as for EP.

Analysis of injections. Mix the contents of 10 ampoules and dilute 2 ml of the mixture to volume in a 10-ml standard flask with water. Use 1 ml for the assay as described above. Read the drug content from the calibration graph, or alternatively calculate it by simple proportion from the absorbance of a single standard containing 250 μg of the drug.

RESULTS AND DISCUSSION

EP, NE and their salts were found to react with periodate in aqueous media to form red products which exhibit two absorption peaks, at 302 and 490 nm (Fig. 1). For EP the red colour is developed immediately at room temperature and remains stable for at least 1 hr. Heating the solution causes a marked decrease in absorbance. For NE the maximum colour intensity is attained by heating the mixture on a water-bath at $60 \pm 5^\circ$ for 2 min. The colour is stable for at least 1 hr. In the case of NE, heating the reaction mixture at 50° for 5-10 min, which looks much less critical, gives absorbances that are unstable and less precise.

Maximum colour intensity was obtained with 0.4 mg/ml sodium periodate in the final reaction mixture, which corresponds to addition of 2 ml of 0.2% sodium periodate solution. It was found that in assay of injections, acetone must be added to combine with the common antioxidant

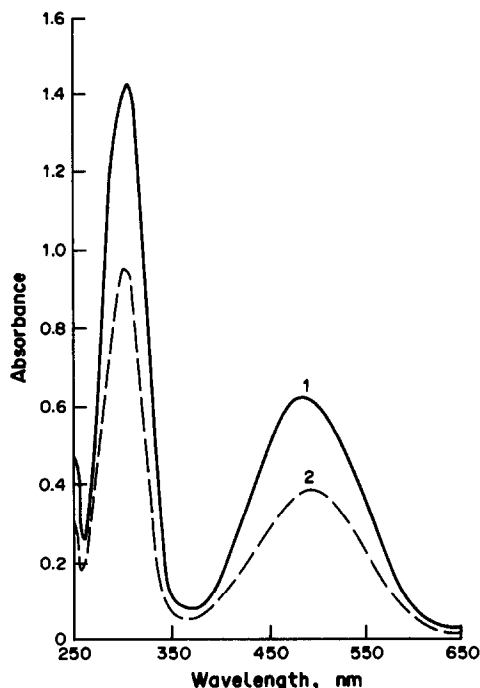


Fig. 1. Absorption spectra of the reaction products of periodate with (—) EP, 25 $\mu\text{g/ml}$ and (---) NE, 30 $\mu\text{g/ml}$.

sodium metabisulphite; the optimum quantity of acetone was found to be 1 ml per 10 ml of the reaction mixture, with a standing time of not less than 10 min for the masking reaction to take place.

Water, methanol, ethanol, 2-propanol, acetonitrile and dimethylsulphoxide were tested as diluents for the reaction mixture for EP, NE and their salts. With the exception of dimethylsulphoxide, all the solvents tested produced a relatively high and stable absorbance. Ethanol was chosen since it gave the highest colour intensity.

The red colour is completely discharged on addition of a few drops of concentrated acids and turns yellow on addition of a few drops of 5M alkali. The effect of pH was therefore studied. Tests with acetate and borate buffers (pH range 2–11) showed that the maximum colour intensity and stability were obtained

Table 1. Apparent molar absorptivities obtained by the periodate, vanadate and Doty methods

Drug	$\epsilon, 10^3 \text{ l. mole}^{-1} \text{ cm}^{-1}$		
	Periodate	Vanadate	Doty
EP	4.56	0.990	2.24
EP bitartrate	4.56	0.990	2.24
NE	3.06	1.375	2.22
NE bitartrate	3.06	1.375	2.22

with borate buffer of pH 7, but this system was still inferior to the ethanol procedure, with regard to colour intensity and stability.

A comparable precision was attained when the procedure was scaled up by a factor of 5.

The molar ratio of periodate to catecholamine was found to be 2:1 by the continuous variation method and shows that two electrons are involved in the oxidation reaction.

The calibration plots are linear over the concentration ranges 5–40 $\mu\text{g/ml}$ for EP base, 10–80 $\mu\text{g/ml}$ for EP bitartrate, 10–60 $\mu\text{g/ml}$ for NE base, and 10–100 $\mu\text{g/ml}$ for NE bitartrate.

An investigation of the absorption intensities of the chromophores obtained from EP and NE with periodate, vanadate,⁵ and the Doty reaction⁸ showed that periodate gives the most intensely coloured chromophore (Table 1).

Application to pure drugs and injections

The method was successfully applied to the determination of bulk EP, NE and their bitartrate salts, and *t*- and *F*-tests showed that there is no significant difference between the results of the proposed and official methods at a probability level of 0.05 (Table 2).

Reaction mechanism

The reaction does not seem to depend on only the catechol function, since pyrocatechol does not form any colour with periodate under the reaction conditions. Catecholamines are oxidized to aminochromes by a large number of oxidizing agents, including silver oxide, lead dioxide, manganese dioxide, mercuric salts,

Table 2. Determination of EP and NE bitartrate in ampoules

Sample	Recovery \pm SD*, %		<i>t</i> †	<i>F</i> ‡
	Periodate method	Official method		
EP powder	99.6 \pm 0.4	99.9 \pm 0.3	1.62	1.85
NE bitartrate	99.7 \pm 0.4	99.9 \pm 0.4	1.86	1.23
EP injection	99.3 \pm 0.9	99.9 \pm 0.6	1.50	2.06
Levarterenol injection	99.4 \pm 1.1	100.0 \pm 1.0	0.78	1.89

*Eight paired determinations for each data point.

†Tabulated value of $t_{14,0.025} = 2.145$.

‡Tabulated value of $F_{7,7,0.05} = 3.79$.

sodium or potassium persulphate, ceric sulphate, Fenton's reagent, hydrogen peroxide, potassium permanganate, potassium ferricyanide, sodium nitrite, iodine, iodic acid, vanadate and potassium iodate. It may therefore be proposed that the colour obtained from the interaction of catecholamines with periodate results from a sequence of reactions analogous to that suggested for aminochrome formation.^{17,18}

REFERENCES

1. Martindale's *Extra Pharmacopoeia*, 26th Ed., N. W. Blacow and A. Wade (eds.), pp. 1-6, 32, 33. Pharmaceutical Society, London, 1972.
2. *United States Pharmacopoeia XX and National Formulary XV*, p. 280. U.S. Pharmacopoeial Convention, Rockville, MD, 1980.
3. M. I. Walsh, A. Abou-Ouf and F. B. Salem, *J. Assoc. Off. Anal. Chem.*, 1982, **65**, 1445.
4. M. I. Walsh and F. B. Salem, *J. Pharm. Belg.*, 1984, **39**, 88.
5. F. B. Salem, *Talanta*, 1987, **34**, 810.
6. J. M. López Fonseca and M. del C. Arredondo, *Analyst*, 1983, **108**, 847.
7. E. Bishop and W. Hussein, *ibid.*, 1984, **109**, 627.
8. J. R. Doty, *Anal. Chem.*, 1948, **20**, 1166.
9. R. B. Salama and S. K. W. Khalil, *J. Pharm. Sci.*, 1974, **63**, 1301.
10. M. I. Walsh, A. A. Abou-Ouf and F. B. Salem, *Indian J. Pharm. Sci.*, 1983, **45**, 223.
11. N. A. El-Rabbat and N. M. Omar, *J. Pharm. Sci.*, 1978, **67**, 779.
12. A. G. Davidson, *J. Pharm. Biomed. Anal.*, 1984, **2**, 45.
13. S. Honda, Y. Araki, M. Takahashi and K. Kakehi, *Anal. Chim. Acta*, 1983, **149**, 297.
14. N. Nohta, A. Mitsui and Y. Ohkura, *ibid.*, 1984, **165**, 171.
15. T. James, *J. Pharm. Sci.*, 1973, **62**, 669.
16. B. Bain and A. J. Collins, *J. Pharm. Pharmacol.*, 1984, **36**, 13.
17. R. A. Heacock, in *Advances in Heterocyclic Chemistry*, A. R. Katritzky, A. J. Boulton and J. M. Lagowski (eds), Vol. 5, pp. 217-224. Academic Press, New York, 1965.
18. R. A. Heacock and W. S. Powell, in *Progress in Medicinal Chemistry*, G. P. Ellis and G. B. West (eds), Vol. 9, p. 291. North-Holland, Amsterdam, 1973.

A SIMPLE SPECTROPHOTOMETRIC METHOD FOR DETERMINATION OF CARBOSULFAN AND PROPOXUR

D. V. NAIDU and P. R. NAIDU*

Department of Chemistry, S.V. University, Tirupati-517 502, India

(Received 3 April 1989. Revised 13 December 1989. Accepted 4 January 1990)

Summary—A new spectrophotometric method for the determination of carbosulfan and propoxur is described, based on coupling their hydrolysis products with diazotized 2-aminobenzophenone to give orange species having an absorption maximum at 465 and 475 nm respectively. Beer's law is obeyed from 0.5 to 10 ppm.

Carbosulfan and propoxur are carbamate insecticides used to combat a wide range of insects. Methods for determining these insecticides are usually based on alkaline hydrolysis followed by coupling the resultant phenols with such compounds as diazotized 3-nitroaniline-4-sulphonic acid,^{1,2} sulphanilic acid,³ 4,4-diaminodiphenylsulphone⁴ or *p*-aminobenzoic acid.⁵ Some other spectrophotometric methods,⁶⁻⁸ and gas chromatographic,^{9,10} high-performance liquid chromatographic,^{11,12} and thin-layer chromatographic^{13,14} methods have also been reported.

A new spectrophotometric method, based on coupling the phenols with diazotized 2-aminobenzophenone is described here.

EXPERIMENTAL

Reagents

All chemicals used were of analytical grade.

Standard solutions of carbosulfan and propoxur (250 µg/ml). Dissolve 125 mg of insecticide in 500 ml of methanol, accurately measured.

2-Aminobenzophenone (ABP) solution, 0.1%. Dissolve 100 mg of 2-aminobenzophenone in the minimum of methanol needed, add 5 ml of concentrated hydrochloric acid and dilute to 100 ml with distilled water.

Sodium nitrite solution, 0.3%.

Sodium hydroxide solution, 0.5M.

Preparation of samples

Formulations. Shake a known amount of well-mixed formulation (equivalent to about 100 mg of the insecticide) with 25 ml of methanol for 5 min and centrifuge the mixture. Filter the supernatant solution, by decantation, into a 100-ml standard flask. Wash the residue four times with 10-ml portions of methanol. Dilute the filtrate and washings to volume with methanol.

Water samples. Adjust the pH of 250 ml of water sample to 4 with 2% sulphuric acid and add 10 g of anhydrous sodium sulphate. Transfer the mixture to a 500-ml separating funnel and extract the insecticides with 150 ml of chloroform. Transfer the chloroform extract into another separating funnel and extract the aqueous phase with 50 ml of chloroform. Wash the combined extracts with 10 ml of 0.1M potassium carbonate to break any emulsion formed during the extraction. Dry the chloroform solution by passing it through 15-20 g of anhydrous sodium sulphate supported on cotton wool in a filter funnel, collect it in a 250-ml standard flask and dilute to the mark with chloroform. Evaporate the chloroform from a known volume of this solution, dissolve the residue in methanol, then develop the colour.

Grain. Take 50 g of sample in a conical flask and shake it with 200 ml of chloroform for 5 min. Decant the solution into a Whatman No. 1 filter paper, and wash the grain in the flask with three 10-ml portions of chloroform. Dilute the combined extract and washings accurately to 250 ml with chloroform. Evaporate the

*Author for correspondence.

Table 1. Characteristics of the method

Compound	Carbosulfan		Propoxur	
	Present work	Rajeswari and Naidu ⁵	Present work	Appaiah <i>et al.</i> ⁴
Concentration range, $\mu\text{g/ml}$	0.5–10	1–10	0.5–10	0.25–5.0
Stability of the coloured species, <i>hr</i>	20	8	24	12
Relative standard deviation, %	0.5	0.8	0.4	0.6
Relative error, %	–0.4	–0.6	–0.2	–0.3

chloroform from a known volume of solution, dissolve the residue in methanol and complete the analysis.

Procedure

Transfer 0.05, 0.1, 0.2, 0.3, 1.0 ml of standard insecticide solution into 25-ml standard flasks. To each flask add 1.5 ml of sodium nitrite solution, 2.0 ml of 2-aminobenzophenone solution and 3.0 ml of sodium hydroxide solution. Mix, and dilute to the mark with distilled water. Measure the absorbance of the orange solution against a reagent blank, and construct a calibration graph. Analyse the samples by the same procedure.

RESULTS AND DISCUSSION

The optimum conditions were established by altering one variable at a time. The absorbance maximum was at 465 nm for carbosulfan and 475 nm for propoxur. Beer's law is obeyed over the range 0.5–10 $\mu\text{g/ml}$ in the final solution for both insecticides. The colour develops instantaneously and remains stable for more than

20 hr. The coupling reaction can be done at room temperature.

The suitability of the proposed method was studied by analysis of ten replicate samples containing 5 ppm of carbosulfan and propoxur. The relative error and relative standard deviation values are given in Table 1.

Formulations containing carbosulfan and propoxur were analysed (7 replicates). For a 25% carbosulfan emulsion the mean \pm standard deviation was $24.6_2 \pm 0.1_4\%$. For a 1% propoxur spray and 4% dust the corresponding values were $0.96 \pm 0.01\%$ and $3.96 \pm 0.02\%$ respectively.

Recovery experiments were performed with known amounts of the compounds added to different samples of water and grains. For water samples a methanol solution of the insecticide was added. Grain samples were spiked by adding a methanol solution of the insecticide to the dry grains and evaporating the solvent.

The results presented in Table 2 show that recovery was in the range 94–98%. The results in Table 3 suggest that the method is applicable for the analysis of field water samples.

Table 2. Recovery of carbosulfan and propoxur from grains and spiked water samples

Sample	Carbosulfan			Propoxur		
	Added, <i>ppm</i>	Recovery, %*		Added, <i>ppm</i>	Recovery, %*	
		Present work	Rajeswari and Naidu ⁵		Present work	Appaiah <i>et al.</i> ⁴
Water	1.0	97.0 \pm 1.6	96.0 \pm 1.6	1.0	98.0 \pm 1.0	97.2 \pm 1.0
	3.0	96.7 \pm 1.0	96.0 \pm 1.2	3.0	98.0 \pm 1.0	97.0 \pm 1.0
	5.0	96.4 \pm 0.8	95.2 \pm 0.8	5.0	96.8 \pm 0.7	96.3 \pm 0.9
	7.0	95.2 \pm 0.6	94.6 \pm 0.7	7.0	96.0 \pm 0.5	95.1 \pm 0.7
Rice	1.0	96.0 \pm 1.6	96.0 \pm 1.6	1.0	97.0 \pm 1.2	96.0 \pm 1.2
	3.0	96.2 \pm 1.1	96.0 \pm 1.2	3.0	97.4 \pm 0.9	96.0 \pm 1.0
	5.0	95.3 \pm 0.7	94.8 \pm 0.8	5.0	96.0 \pm 0.7	95.8 \pm 0.8
	7.0	94.0 \pm 0.5	93.5 \pm 0.6	7.0	95.3 \pm 0.6	94.7 \pm 0.6
Wheat	1.0	96.0 \pm 1.4	95.0 \pm 1.4	1.0	97.0 \pm 1.4	96.0 \pm 1.4
	3.0	94.8 \pm 0.9	94.1 \pm 1.0	3.0	96.5 \pm 1.0	95.6 \pm 1.0
	5.0	94.0 \pm 0.5	93.2 \pm 0.7	5.0	94.7 \pm 0.8	94.7 \pm 0.9
	7.0	93.5 \pm 0.4	92.8 \pm 0.5	7.0	93.8 \pm 0.5	93.0 \pm 0.7

*Each value is an average \pm standard deviation of five determinations.

Table 3. Determination of carbosulfan and propoxur in field water samples

Sample volume, <i>ml</i>	Carbosulfan found, <i>ppm</i>		Propoxur found, <i>ppm</i>	
	Present work	Rajeswari and Naidu ⁵	Present work	Appaiah <i>et al.</i> ⁴
250	0.20	0.20	0.16	0.14
250	0.30	0.29	0.28	0.26

Acknowledgements—The authors are thankful to M/S Rallis India Ltd., Bangalore and M/S Bayer India Ltd., for providing the necessary reference standards of the insecticides.

REFERENCES

1. P. Bracha, *J. Agric. Food Chem.*, 1964, **12**, 461.
2. M. Ramaswamy, *Pestic. Sci.*, 1974, **5**, 383.
3. G. Mukherjee, A. K. Mukherjee and B. R. Roy, *J. Food Sci. Tech.*, 1975, **12**, 96.
4. K. M. Appaiah, O. P. Kapur and K. V. Nagaraja, *J. Assoc. Off. Anal. Chem.*, 1983, **66**, 105.
5. C. V. Rajeswari and P. R. Naidu, *J. Food Sci. Tech.*, 1986, **23**, 101.
6. C. S. P. Sastry and D. Vijaya, *Talanta*, 1987, **34**, 372.
7. C. S. P. Sastry, D. Vijaya and D. S. Mangala, *Analyst*, 1987, **112**, 75.
8. C. S. P. Sastry, D. Vijaya and K. E. Rao, *Food Chem.*, 1986, **20**, 157.
9. H. A. Moye, *J. Agric. Food Chem.*, 1975, **23**, 415.
10. S. Sakaue, *Agric. Biol. Chem.*, 1987, **51**, 1239.
11. H. Jansen, U. A. T. Brinkman and R. W. Frei, *Chromatographia*, 1985, **20**, 453.
12. H. Engelhardt and B. Lillig, *ibid.*, 1986, **21**, 136.
13. A. Ambrus, E. Hargitai, G. Károly, A. Fülöp and J. Lantos, *J. Assoc. Off. Anal. Chem.*, 1981, **64**, 743.
14. K. M. Appaiah, U. C. Nag, J. Puranaik, V. Nagaraja and O. P. Kapur, *Indian Food Packer*, 1984, **38**, 28.

SPECTROPHOTOMETRIC DETERMINATION OF TRACE SULPHATE IN RAIN AND SNOW AFTER PRECONCENTRATION WITH 2-AMINOPERIMIDINE ON A MEMBRANE FILTER

JUNICHI SHIDA, HARUMI SATAKE, NOBUO ONO and TADAMITSU FUJIKURA

Department of Applied Chemistry, Faculty of Engineering, Yamagata University, 4-3-16 Jonan,
Yonezawa-shi, 992 Japan

(Received 9 July 1989. Revised 31 August 1989. Accepted 30 September 1989)

Summary—A simple and precise preconcentration technique, based on collecting a precipitate on a membrane filter and dissolving the filter and precipitate in an organic solvent, has been applied to the spectrophotometric determination of trace sulphate in rain and snow. The sulphate is precipitated with 2-aminoperimidine and the resulting compound is dissolved in nitric acid, made alkaline with sodium hydroxide and then adsorbed on tetradecyldimethylbenzylammonium nitrate. The precipitate is then collected on a membrane filter and both precipitate and filter are dissolved in dimethylsulphoxide (DMSO). The absorbance of the DMSO solution is measured at 550 nm against a reagent blank. The molar absorptivity is $2.1 \times 10^4 \text{ l} \cdot \text{mole}^{-1} \cdot \text{cm}^{-1}$ and the coefficient of variation for six measurements is < 1.5%. The detection limit ($S/N = 3$) is 0.06 μg of sulphate in 5 ml of sample solution.

2-Aminoperimidine sulphate is relatively insoluble in water¹ and the free base was introduced as a reagent for the determination of trace amounts of sulphate by nephelometry^{1,2} and indirect spectrophotometry.³⁻⁶ Subsequently, modified spectrophotometric methods^{7,8} and a ring-oven method⁹ were reported.

When 2-aminoperimidine sulphate is treated with nitric acid, the sulphate is liberated and 2-amino-4,6,9-trinitroperimidine is formed.¹⁰ The product is yellow in acid solution and violet in alkaline solution. We have found that the violet product can be adsorbed on the micellar interface of tetradecyldimethylbenzylammonium nitrate (Zephiramine), which is insoluble in aqueous solution.

Recently, Taguchi *et al.* proposed a simple and fast preconcentration technique,¹¹ based on collecting a precipitate on a membrane filter and dissolving the filter in a small volume of organic solvent. This was applied to the determination of trace phosphorus as phosphomolybdenum blue.

In the present work, this preconcentration technique is coupled to the chemistry involving 2-aminoperimidine sulphate and its nitration, permitting the determination of ng/ml levels of sulphate with satisfactory precision. The detection limit is better, by a factor of ~ 2 , than that

obtained by the conventional ion-chromatographic method.¹²

EXPERIMENTAL

Apparatus

A Hitachi model 228 double-beam spectrophotometer was used to obtain absorption spectra. Absorbance measurements of sample solutions were made with a Hirma model 6B spectrophotometer. Standard 1-cm glass cells were used.

Reagents

All reagents were of analytical grade, and distilled demineralized water was used.

A stock sulphate solution (1000 $\mu\text{g/ml}$) was prepared by dissolving 0.9070 g of dried potassium sulphate in water and diluting the solution accurately to 500 ml; working solutions were freshly prepared by dilution of the stock solution. 2-Aminoperimidine solution ($4.0 \times 10^{-3} M$) was prepared by dissolving 0.106 g of the hydrobromide (Dotite reagent; Wako Pure Chemical Co.) in 100 ml of water at about 40° and cooling to room temperature. The solution can be used for at least 4 days, giving exactly the same calibration graph. Tetradecyldimethylbenzylammonium

chloride dihydrate (Zephiramine; C_{14} DBAN) solution ($5.0 \times 10^{-3} M$) was prepared by dissolving 1.01 g of Zephiramine (Dotite reagent) in 500 ml of water.

Membrane filters and holder

The filter papers used were Millipore membranes [25 mm in diameter, 0.45- μm (type HAWP) and 1.2- μm (type RAWP) pore size]. A Toyo KG-25 filter holder (effective filtration area 1.3 cm^2) was used.

Procedure

A 5-ml portion of sample solution containing up to 15 μg of sulphate, was transferred into a 30-ml beaker and 3 ml of 2-aminoperimidine solution were added. After 5 min, the solution was filtered by suction (0.45- μm membrane filter). The beaker, funnel walls and precipitate were washed with five 10-ml portions of water to remove excess of reagent. The filter and precipitate were transferred into the original 30-ml beaker, and 5 ml of concentrated nitric acid were added. The acid was stirred well to ensure reaction, especially with the precipitate remaining on the beaker wall, and then allowed to stand for 20 min. The solution was transferred into a 100-ml beaker and 4M sodium hydroxide was added until the colour changed from yellow to pink. Another 12.5 ml of 4M sodium hydroxide were added, and the solution was diluted to ~ 50 ml with water. Five ml of Zephiramine solution were added, the solution was mixed well, and the precipitate was collected on a 1.2- μm membrane filter by gentle suction. The beaker, funnel walls and precipitate were washed with two 5-ml portions of 0.01M potassium nitrate. The filter and precipitate were transferred into the original 100-ml beaker, and dissolved in 5 ml of dimethylsulphoxide (DMSO). The absorbance was measured at 550 nm against a reagent blank.

RESULTS AND DISCUSSION

Absorption spectra

Figure 1 shows that 2-amino-4,6,9-trinitroperimidine in acid solution has an absorption maximum at 420 nm and in alkaline solution has two absorption maxima at 462 and 560 nm. The spectrum for a DMSO solution is similar to that for the alkaline solution, and the second peak (at 550 nm) was chosen for use.

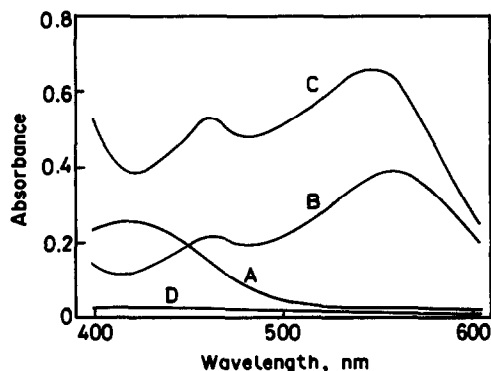


Fig. 1. Absorption spectra of 2-amino-4,6,9-trinitroperimidine: in (A) acid and (B) alkaline aqueous solution, SO_4^{2-} 1.6 ppm; (C) in DMSO, SO_4^{2-} 3 ppm; (D) reagent blank.

Optimum conditions for precipitation of 2-aminoperimidine sulphate

If the unbuffered test solution is in the pH range 5.0–7.0 the precipitation proceeds smoothly.¹ During preliminary investigations the pH of the sample solution was adjusted by addition of hydrochloric acid or sodium hydroxide solution. In the pH range 2–7, blank values were very small, and constant absorbance was obtained for 10 μg of sulphate. Below pH 1, the precipitate was not formed quantitatively. Above pH 7, a yellow precipitate was formed, causing high blank values. The standing time for the formation of 2-aminoperimidine sulphate was 2 min. To ensure complete formation the solution was therefore allowed to stand for 5 min. The effect of sample solution volume was examined by varying it from 5 to 50 ml in the procedure. When 15 μg of sulphate was present, 2, 10 and 25 ml of 2-aminoperimidine solution were required for 5, 25 and 50 ml of sample solution, respectively.

Nitration of 2-aminoperimidine sulphate

Nitric acid⁷⁻⁹ or sodium nitrite⁵ have been used for the nitration of 2-aminoperimidine sulphate, but the products may not be the same. The effect of the nitric acid concentration (7.5M, 11M and concentrated) on the procedure was studied. The volume of each nitric acid solution used was 5 ml. Concentrated nitric acid was found most suitable and the reaction was essentially complete in 20 min at room temperature. When sodium nitrite solution (1%, 5 ml) was used, a lower absorbance was obtained.

Volumes of sodium hydroxide and Zephiramine solutions

The effect of the amounts of 4M sodium hydroxide and $5.0 \times 10^{-3} M$ Zephiramine added

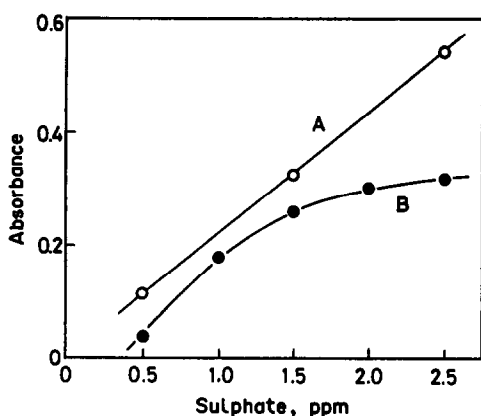


Fig. 2. Effect of different filter pore sizes on the absorbance: (A) 1.2 μm ; (B) 3.0 μm .

after the nitration and neutralization, on the absorption at 550 nm, was investigated. For a sample solution containing 15 μg of sulphate the absorbance increased on addition of up to 11 ml of sodium hydroxide and of up to 5 ml of Zephiramine solution. Further reagent addition did not increase the absorbance.

Filtration

The particle diameter of 2-aminoperimidine sulphate is $>2 \mu\text{m}$ at pH 5.3–5.8 or $<1 \mu\text{m}$ at pH 4.0–4.2.² Therefore a 0.45 μm acetylcellulose membrane filter was used. To remove the small excess of 2-aminoperimidine, the precipitate was washed with water. Washing five times with 10-ml portions of water was sufficient.

On the other hand, for the precipitate of Zephiramine on which the coloured product is adsorbed, nitrocellulose or acetylcellulose membrane filters are suitable because they readily dissolve in DMSO. Although any acetylcellulose membrane filter with pore sizes $<1.2 \mu\text{m}$ can be used, as shown in Fig. 2, 1.2- μm filters are recommended because of their higher

filtration rate. The precipitate should be washed twice with 5-ml portions of 0.01M potassium nitrate to prevent peptization.

Choice of organic solvent

Several water-miscible organic solvents were tested as solvents for the wet membrane filters. DMSO and *N,N*-dimethylformamide (DMF) were suitable for nitrocellulose or acetylcellulose membranes but the colour of 2-amino-4,6,9-trinitroperimidine in DMF decays by 8.4% in 2 hr, whereas it is completely stable in DMSO for at least 4 hr. Therefore, DMSO was used in further work.

Calibration graph, sensitivity and precision

The calibration graph was linear over the range 1.25–15.0 μg of sulphate in 5 ml of DMSO, with absorbance ranging from 0.054 to 0.655. The blank value was negligible (0.01), and the molar absorptivity, as calculated from the slope of the curve, was $2.1 \times 10^4 \text{ l} \cdot \text{mole}^{-1} \cdot \text{cm}^{-1}$. For six measurements at each of five amounts of sulphate, the coefficient of variation were $<1.5\%$. The detection limit (taken as the concentration equivalent to three times the standard deviation of the blank) is about 0.012 $\mu\text{g}/\text{ml}$ in the sample solution.

Effect of other ions

The effects of commonly occurring foreign ions were investigated. At the 1 ppm sulphate level, concentrations of Na^+ , K^+ , Ca^{2+} , Mg^{2+} , Al^{3+} , Fe^{3+} , Fe^{2+} , Pb^{2+} , Zn^{2+} , Cu^{2+} , phosphate and carbonate below 50 ppm did not interfere with the precipitation of 2-aminoperimidine sulphate. These results suggest that the proposed method should be suitable for the determination of sulphate in rain and snow samples.

Table 1. Analysis of rain and snow samples and recovery tests

SO_4^{2-} added, μg	SO_4^{2-} found*, μg	Recovery of added SO_4^{2-} ,	
		μg	%
<i>Rain</i>			
none	5.25 (1.3)	—	—
2.55	7.72 (1.5)	2.47	97
5.10	10.35 (1.0)	5.10	100
7.65	12.75 (1.1)	7.50	98
<i>Snow</i>			
none	5.90 (1.5)	—	—
2.55	8.45 (1.2)	2.55	100
5.10	11.05 (1.1)	5.15	101
7.65	13.47 (1.3)	7.57	99

Sample volume: rain (pH 5.6) 5 ml, snow (pH 4.9) 1 ml.

*Mean of six determinations; value in parentheses is coefficient of variation (%).

Application

The proposed method was applied to the analysis of rain and snow samples collected in Yonezawa-shi. Table 1 shows the results for the original samples and for recovery of known quantities of sulphate added to them. Recovery of the added sulphate was nearly quantitative.

Acknowledgement—The authors are grateful to Professor S. Abe (Yamagata University) for his helpful advice.

REFERENCES

1. W. I. Stephen, *Anal. Chim. Acta*, 1970, **50**, 413.
2. S. Kadowaki, *Kogai To Taisaku*, 1976, **12**, 706.
3. P. A. Jones and W. I. Stephen, *Anal. Chim. Acta*, 1973, **64**, 85.
4. D. T. Burns, J. S. Coy, W. P. Hayes and D. M. Kent, *Mikrochim. Acta*, 1974, 245.
5. A. W. Archer, *Analyst*, 1975, **100**, 755.
6. K. Aihara, M. Kaneko and Y. Wada, *Taiki Osen Gakkaishi*, 1978, **13**, 223.
7. P. K. Dasgupta, L. G. Hanley, Jr. and P. W. West, *Anal. Chem.*, 1978, **50**, 1793.
8. K. Suzuki, K. Ohzeki and T. Kambara, *Anal. Chim. Acta*, 1982, **136**, 435.
9. P. K. Dasgupta and P. W. West, *Mikrochim. Acta*, 1978 **II**, 505.
10. P. K. Dasgupta, A. Nayak, G. R. Newkome and P. W. West, *J. Org. Chem.*, 1979, **44**, 2582.
11. S. Taguchi, E. Ito-oka, K. Masuyama, I. Kasahara and K. Goto, *Talanta*, 1985, **32**, 391.
12. K. Hayakawa, H. Hiraki and M. Miyazaki, *Bunseki Kagaku*, 1985, **34**, T71.

SPECTROPHOTOMETRIC DETERMINATION OF GALLIUM(III) WITH PHENYLFLUORONE IN THE PRESENCE OF HEXADECYLPYRIDINIUM BROMIDE AND PYRIDINE

SATORU SAKURABA

Industrial Research Institute of Aomori Prefecture, Fukuro-machi, Hirosaki-shi, 036 Japan

(Received 26 August 1988. Revised 23 August 1989. Accepted 9 December 1989)

Summary—Phenylfluorone reacts with gallium in the presence of hexadecylpyridinium bromide and pyridine to form a water-soluble chelate with an absorption maximum at 570 nm and constant absorbance in the pH range 4.0–5.5. At this wavelength, Beer's law is obeyed up to $4.3 \times 10^{-6} M$ gallium. The sensitivity is very high and the molar absorptivity is $1.48 \times 10^5 \text{ l. mole}^{-1} \text{ cm}^{-1}$. The chelate has been utilized in the determination of gallium at the μg level. The ratio of gallium to phenylfluorone in the complex is 1:2.

Of the xanthene dyes, 2,3,7-trihydroxy-9-phenyl-6-fluorone (phenylfluorone) has been used for spectrophotometric determination of several metal ions.¹⁻³ Recently it was used in conjunction with cationic surfactants for the spectrophotometric determination of germanium⁴ and titanium.⁵ Phenylfluorone and its metal chelates are soluble in ethanol but the solutions are not stable and turbidity develops. However, when a cationic surfactant and a unidentate ligand such as pyridine or nitrite are also present the turbidity does not appear. We have applied this type of reaction in the determination of cobalt,⁶ nickel,⁷ copper⁸ and zinc.⁹ Gallium reacts with phenylfluorone in the presence of hexadecylpyridinium bromide and pyridine or nitrate to form a water-soluble red chelate. Pyridine is preferred because it gives a molar absorptivity that is nearly 1.5 times that obtained with nitrite.

The spectrophotometric determination of gallium by means of this reaction is described in this communication. For the spectrophotometric determination of gallium Semi-Methylxlenol Blue,¹⁰ Chromazurol S¹¹ and 4-(2-pyridylazo)resorcinol¹² have been used as the chromogenic reagent in aqueous solution, and 2-(2-pyridylazo)-5-monoethylamino-*p*-cresol (PAEAC),¹³ Rhodamine B¹⁴⁻¹⁸ etc.¹⁹ have been used in conjunction with extraction into organic solvents, but the present method is more sensitive than any of those methods. Moreover, it is much simpler than the PAEAC and Rhodamine B methods since no extraction is required.

EXPERIMENTAL

Apparatus

A Hitachi 320 A double-beam recording spectrophotometer and a Hitachi 139 spectrophotometer were used for measuring absorbances, with fused-silica cells of 10 mm path-length. Measurements were made at $25.0 \pm 0.1^\circ$.

A Beckman Expandomatic SS-2 pH meter was used for pH measurement.

Reagents

A standard stock gallium solution was prepared by dissolving 1.00 g of gallium metal (99.999% pure) in 10 ml of concentrated nitric acid. The solution was boiled to expel nitrogen oxides and diluted accurately to 1 litre with water. Working standards were prepared by appropriate dilution.

A standard solution of phenylfluorone (PF) was prepared by dissolving 0.0322 g of the reagent (Merck) in about 50 ml of ethanol containing a few drops of concentrated hydrochloric acid. Then the solution was transferred to a 100-ml standard flask and diluted to volume with ethanol. Working solutions were prepared by appropriate dilution.

Pyridine (Py) solution (2.48M) and $2.0 \times 10^{-2} M$ hexadecylpyridiniumbromide (HPB) solution were prepared by dissolving a suitable amount of the reagent in water.

The pH was adjusted with a buffer solution made by mixing 1M sodium acetate and 1M hydrochloric acid.

All reagents were of guaranteed-reagent grade. Demineralized water was used throughout.

Procedure

Two ml of the buffer solution, 2.5 ml of the HPB solution, 2.5 ml of the pyridine solution and 2.0 ml of the phenylfluorone solution were added to 1 ml of sample solution, in that order. The absorbance was measured at 570 nm against a reagent blank after the solution had stood for 30 min at 25°.

RESULTS AND DISCUSSION

Absorption spectra

Gallium reacts with phenylfluorone to form a red complex in the presence of HPB and pyridine. The absorption spectra of the gallium complex in the four-component system and of the reagent blank at pH 4.8 are shown in Fig. 1. For comparison, the spectra for other combinations of gallium with the reagents at the same pH are also given.

The four-component system shows a pronounced absorption maximum at 570 nm, whereas a less well-defined absorption with a peak at 500 nm appears in the absence of HPB and pyridine. The deep red complex is formed only if both HPB and pyridine are present, and in the absence of either, the absorbance is much smaller than that of the red complex (Fig. 1, curves 4 and 5).

Effect of pH

The effect of pH on the colour development of the complex is shown in Fig. 2. Maximum

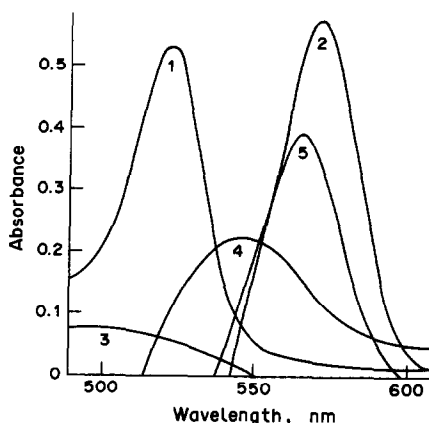


Fig. 1. Absorption spectra of the gallium complex and reagent combinations. (1) HPB-Py-PF, (2) Ga-HPB-Py-PF, (3) Ga-PF, (4) Ga-Py-PF, (5) Ga-HPB-PF. References are water for (1) and reagent blank for (2)–(5). Concentrations of Ga(III), HPB, Py and PF $4 \times 10^{-6}M$, $2.0 \times 10^{-3}M$, $2.48 \times 10^{-1}M$ and $8 \times 10^{-6}M$, respectively.

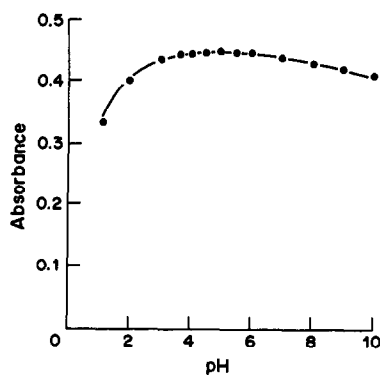


Fig. 2. Effect of pH on absorbance. Ga(III) $2.86 \times 10^{-6}M$, PF $8.0 \times 10^{-6}M$, HPB $2.0 \times 10^{-3}M$, Py $0.248M$.

and practically constant absorbance is obtained over the pH range 4.0–5.5.

Effect of reagent concentrations

The concentrations of the reagents were optimized one at a time, with other conditions constant. Maximum colour formation was obtained with slightly greater than 2-fold molar ratio of phenylfluorone, 300-fold molar ratio of HPB and 3×10^4 -fold molar ratio of pyridine relative to gallium.

Stability of the colour

Full colour development was reached in about 20 min after the reagents were added. The colour, once developed, was very stable and the absorbance remained constant for at least several hours.

Calibration graph

A calibration graph made under the optimum conditions was linear up to $4.3 \times 10^{-6}M$ gallium. The molar absorptivity was 1.48×10^5 l. mole⁻¹. cm⁻¹.

The reproducibility of the method, expressed as the relative standard deviation of the absorbance, was 0.5% for gallium (9 replicates).

Effect of diverse ions

The effect of diverse ions on the determination of 5 μ g of gallium is summarized in Table 1. Aluminium, iron, tin, titanium, cadmium, manganese and vanadium caused some error when present in 1:1 weight ratio to the gallium.

Use of nitrite instead of pyridine completely eliminates the interference of aluminium if fluoride is also present but the sensitivity is reduced: the absorption maximum of the nitrite

Table 1. Influence of various foreign ions on determination of 5 μg of gallium (measured at 570 nm)

Foreign ion	Amount added, μg	Ga found, μg	Error, μg	Foreign ion	Ga added, μg	Ga found, μg	Error, μg
Co^{2+}	50.0	5.0	0.0	Ti^{4+}	5.0	2.3	-2.7
Ni^{2+}	25.0	5.0	0.0	Cd^{2+}	5.0	4.3	-0.7
Cu^{2+}	50.0	5.0	0.0	Mn^{2+}	5.0	3.2	-1.8
Zn^{2+}	25.0	5.0	0.0	V(V)	5.0	5.8	0.8
Pd^{2+}	25.0	5.0	0.0	V(V)*	50.0	5.1	0.1
In^{3+}	10.0	5.0	0.0	Mo(VI)	5.0	5.0	0.0
Fe^{2+}	10.0	5.0	0.0	NO_3^-	50.0	5.0	0.0
Fe^{3+}	5.0	1.6	-3.4	Cl^-	50.0	3.6	-1.6
Fe^{3+*}	100.0	4.8	0.2	F^-	50.0	1.9	-3.1
Al^{3+}	5.0	3.6	-1.4	$\text{F}^- \dagger$	100.0	4.8	-0.2
$\text{Al}^{3+\dagger}$	25.0	5.2	0.2	SO_4^{2-}	50.0	5.1	0.1
Al^{3+*}	100.0	5.2	0.2	PO_4^{3-}	50.0	1.6	-3.4
Sn^{4+}	5.0	7.1	2.1				

*Gallium was separated by ether extraction.

†In the presence of nitrite instead of pyridine, with 0.5 ml of 0.5% sodium fluoride solution added, measurement at 580 nm.

complex is at 580 nm and the molar absorptivity is $1.05 \times 10^5 \text{ l. mole}^{-1} \text{ cm}^{-1}$.

Iron(III) can be masked by reduction with 10% hydroxylamine hydrochloride or 5% ascorbic acid before colour development. If large quantities of iron(III) and aluminium are present, gallium can be separated from them by extraction into diethyl ether from 6–8M hydrochloric acid medium after prior reduction of the iron(III).²⁰ A similar separation can be used when a large quantity of vanadium(V) is present. In both cases the organic phase is washed twice with 6M hydrochloric acid, and gallium is stripped by two extractions with water. This aqueous extract is evaporated to

dryness after addition of a little nitric acid. The residue is dissolved in a small quantity of dilute nitric acid and diluted with water, then the gallium determined as already described.

Composition of the complex

The Benesi and Hildebrand method²² was used to find the composition of the complex. For a GaL_n complex (L = ligand) the following relationship may be derived:

$$a/(A - A') = \{1/(\epsilon_1 - n\epsilon_2)\} + \{K'/(\epsilon_1 - n\epsilon_2)b^n\}$$

where A is the absorbance of the solution measured against the reagent blank, a and b are the initial concentrations of gallium and the reagent respectively, ϵ_1 and ϵ_2 ($\epsilon_2 b = A'$) are the molar absorptivities of the complex and the reagent blank, respectively, at a constant pH value.

The plots of $a/(A - A')$ against $1/b^n$ at 570 nm are shown in Fig. 3. A straight line is obtained for $n = 2$.

When similar plots were made for varied concentrations of pyridine (0.05–0.10M), a straight line was obtained for $n = 2$. Therefore it is concluded that a 1:2:2 complex is formed between gallium, phenylfluorone and pyridine.

It may be considered that this complex is formed in a micelle since the presence of a surfactant such as HPB is important.

Acknowledgements—The author is sincerely grateful to Professor Masao Maruyama of Chuoh University for his kind encouragement, and Professor Kengo Uchida of Hirosaki University for his kind advice and helpful discussions throughout this study.

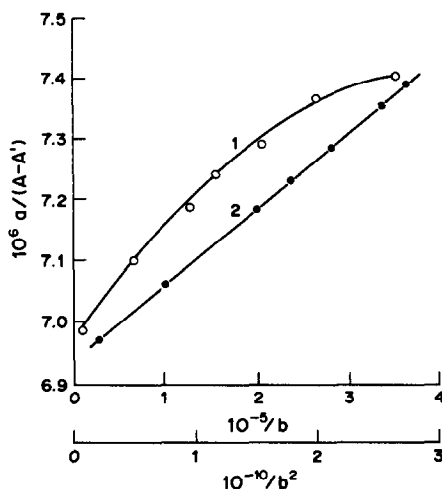


Fig. 3. Relationship between $a/(A - A')$ and $1/b^n$. Concentrations of Ga(III), HPB, Py and PF: $2.0 \times 10^{-6}M$, $2.0 \times 10^{-3}M$, 0.248M and 6.0×10^{-6} – $1.2 \times 10^{-5}M$, respectively. \circ — \circ $n = 1$; \bullet — \bullet $n = 2$; measured at 570 nm.

REFERENCES

1. J. Gillis, J. Hoste and A. Claeys, *Anal. Chim. Acta*, 1947, **1**, 302.
2. E. B. Sandell, *Colorimetric Determination of Traces of Metals*, 3rd Ed., p. 862. Interscience, New York, 1959.
3. C. L. Luke and M. E. Campbell, *Anal. Chem.*, 1956, **28**, 1273.
4. E. M. Donaldson, *Talanta*, 1984, **31**, 997.
5. Wu Quianfeng, *ibid.*, 1985, **32**, 507.
6. S. Sakuraba and M. Kojima, *Nippon Kagaku Kaishi*, 1976, 345.
7. *Idem*, *ibid.*, 1978, 208.
8. *Idem*, *ibid.*, 1980, 209.
9. S. Sakuraba, *Talanta*, 1984, **31**, 840.
10. J. Ueda and T. Kitadani, *Nippon Kagaku Kaishi*, 1982, 1914.
11. L. I. Ganago and N. N. Ishchenko, *Zh. Analit. Khim.*, 1980, **35**, 1718; *Anal. Abstr.*, 1981, **40**, 5B68.
12. K. Hagiwara, M. Nakane, Y. Osumi, E. Ishii and Y. Miyake, *Bunseki Kagaku*, 1961, **10**, 1379.
13. S. Miwa and S. Shibata, *Nagoya Kogyo Gijutsu Shikensho Hokoku*, 1981, **30**, 350; *Chem. Abstr.*, 1982, **96**, 173540m.
14. H. Onishi and E. B. Sandell, *Anal. Chim. Acta*, 1955, **13**, 159.
15. K. Nishimura and T. Imai, *Bunseki Kagaku*, 1964, **13**, 518.
16. F. Culkin and J. P. Riley, *Analyst*, 1958, **83**, 208.
17. Y. Hasegawa, T. Inagake, Y. Karasawa and A. Fujita, *Talanta*, 1983, **30**, 721.
18. G. N. Lypka and A. Chow, *Anal. Chim. Acta*, 1972, **60**, 65.
19. F. J. Barragán de la Rosa, R. Escobar Godoy and J. L. Gómez Ariza, *Talanta*, 1988, **35**, 343.
20. E. B. Sandell, *Colorimetric Determination of Traces of Metals*, 3rd Ed., p. 471. Interscience, New York, 1959.
21. G. H. Morrison and H. Freiser, *Solvent Extraction in Analytical Chemistry*, p. 208. Wiley, Interscience, New York, 1957.
22. H. A. Benesi and J. H. Hildebrand, *J. Am. Chem. Soc.*, 1949, **71**, 2703.

SPECTROPHOTOMETRIC DETERMINATION OF MICROAMOUNTS OF SCANDIUM WITH *o*-CHLOROPHENYLFLUORONE AND CETYLTRIMETHYLAMMONIUM BROMIDE

ZONG-MING LUO and WEI-MING HE

Department of Chemical Engineering, Guangdong Institute of Technology, Guangzhou,
People's Republic of China

(Received 28 September 1988. Revised 15 March 1989. Accepted 14 December 1989)

Summary—The reaction of scandium(III) with *o*-chlorophenylfluorone (*o*-CIPF) in the presence of cetyltrimethylammonium bromide (CTMAB) has been studied. In an acetate buffer at pH 4.4, a red-purple complex is obtained, with maximum absorption at 569 nm and a molar absorptivity of $1.31 \times 10^5 \text{ l. mole}^{-1} \text{ cm}^{-1}$. The composition of the complex is found to be 1:2:2 Sc-*o*-CIPF-CTMAB. Beer's law is obeyed over the range 0–12 $\mu\text{g}/25 \text{ ml}$ scandium. The proposed method has been used for determination of trace scandium in tungsten ores after its prior separation by solvent extraction.

Xylenol Orange and Arsenazo III have been recommended¹ as chromophoric reagents for the spectrophotometric determination of trace amounts of scandium, but as these have poor sensitivity several new methods have been developed.²⁻⁶ Recently it has been proposed⁷ that ternary systems containing scandium, triphenylmethane dyes and cationic surfactants have even greater sensitivity. The derivatives of phenylfluorone⁸ are highly sensitive chromophoric reagents for the spectrophotometric determination of easily hydrolysed high-valence metals, e.g., *o*-chlorophenylfluorone (*o*-CIPF) can be used to determine Mo,⁹ Ta,¹⁰ Al¹¹ and Ga,¹² but there are no reports that it can be used to determine scandium in the presence of surfactants.

In this work, the optimum conditions for the reaction of scandium(III) with *o*-CIPF and cetyltrimethylammonium bromide (CTMAB) have been studied. The spectrophotometric method developed has been used for the determination of scandium in tungsten ores after solvent extraction of scandium.

EXPERIMENTAL

Reagents

All solutions were prepared with analytical-grade chemicals and demineralized distilled water unless otherwise stated.

Standard scandium solution, 5 $\mu\text{g}/\text{ml}$. Dissolve 0.1534 g of pure scandium oxide in 10 ml of

12M hydrochloric acid, bring the solution to the boil to remove some of the acid, then dilute to volume in a 100-ml standard flask. Dilute this solution (1 mg/ml) to 5 $\mu\text{g}/\text{ml}$.

***o*-CIPF solution, $1.0 \times 10^{-3}\text{M}$.** Dissolve 0.0886 g of *o*-CIPF in 125 ml of ethanol and dilute to 250 ml with water.

Acetate buffer solution, 1.0M, pH 4.6. Dissolve 40.5 g of anhydrous sodium acetate in 250 ml of water, adjust the pH to 4.6 with 4M hydrochloric acid and dilute to 500 ml with water.

CTMAB solution, $1.0 \times 10^{-2}\text{M}$.

PMBP solution, $1.0 \times 10^{-2}\text{M}$. Dissolve 1.4 g of 1-phenyl-3-methyl-4-benzoylpyrazol-5-one in 500 ml of benzene.

Sodium diethyldithiocarbamate (DDTC), 20% aqueous solution.

General procedure

Place 1.00 ml of the standard scandium(III) solution in a 25-ml standard flask, add 5 ml of buffer solution, 5 ml of CTMAB solution, 1.5 ml of *o*-CIPF solution, dilute to the mark with water and heat the solution in a water-bath at 70° for 10 min. Cool, and measure the absorbance at 569 nm against a reagent blank in 1-cm cells.

Determination of scandium in tungsten ores

Fuse a 0.5-g sample with 10 g of sodium peroxide in a nickel crucible at 500° for 45 min. Leach the melt with 80 ml of a solution

containing 8 g of sodium carbonate, 2 g of sodium chloride and 2 g of sodium hydroxide, in a 250-ml poly(vinyl fluoride) beaker and warm it for 1 hr. Cool the solution and let it stand overnight. Filter the solution and wash the precipitate with 2% sodium carbonate solution about 10 times. Place the paper in a 250-ml beaker and dissolve the precipitate with 30 ml of hot 6M hydrochloric acid. Transfer the solution to a 100-ml standard flask, dilute to volume with water and mix.

Pipette 20.00 ml of this solution into a 100-ml separatory funnel, add 1 ml of 10% hydroxylamine hydrochloride solution and 1 ml of 20% sulphosalicylic acid solution. Adjust the pH to about 4, add 5 ml of acetate buffer (pH 5.5) and 3 ml of DDTC solution, mix and let stand for 3 min. Then shake the mixture for 1 min with first 15 and then 10 ml of chloroform, discarding the organic phases. Add 20 ml of PMBP solution to the aqueous phase, shake the mixture for 1 min and discard the aqueous phase. Shake the organic phase for 1 min with 10 and 5 ml of 5% hydrochloric acid. Evaporate the combined hydrochloric acid phases on a hot-plate to near dryness. Cool, add 5 ml of 5% v/v hydrochloric acid and heat to take up the residue. Cool and transfer the solution into a 25-ml standard flask. Add 1 drop of 0.1% *p*-nitrophenol solution and 6M ammonia solution until the solution turns yellow. Then add 2% v/v hydrochloric acid dropwise with frequent shaking, until the yellow colour just disappears. Then determine scandium according to the general procedure.

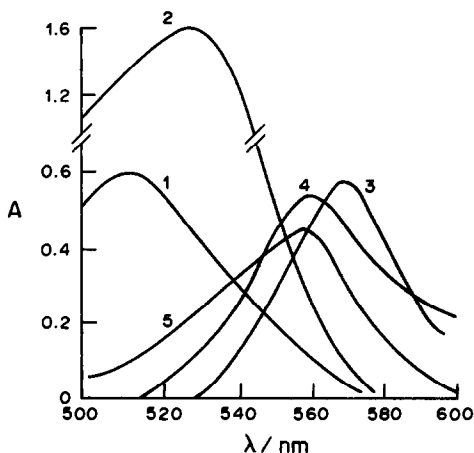


Fig. 1. Absorption spectra: (1) *o*-CIPF and (2) *o*-CIPF-CTMAB, vs. water; (3) Sc-*o*-CIPF-CTMAB, (4) Sc-*o*-HPF-CTMAB, (5) Sc-*o*-NPF-CTMAB, vs. reagent blank. $[Sc] = 4.45 \times 10^{-6}M$, $[o\text{-CIPF}] = [o\text{-HPF}] = [o\text{-NPF}] = 6.0 \times 10^{-3}M$, $[CTMAB] = 2.0 \times 10^{-3}M$.

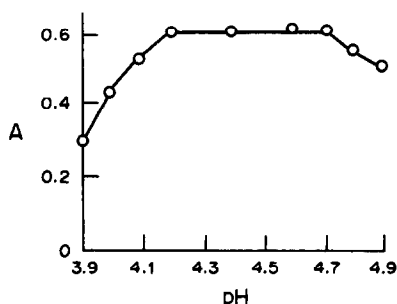


Fig. 2. Effect of pH on the formation of the scandium complex. Absorbance measured at 569 nm against a reagent blank.

RESULTS AND DISCUSSION

Absorption spectra

Figure 1 shows that in the presence of CTMAB the scandium complexes with *o*-chloro (*o*-CIPF), *o*-hydroxy (*o*-HPF) and *o*-nitrophenylfluorone (*o*-NPF) have maximum absorption at 569, 559 and 560 nm with apparent molar absorptivities of 1.31×10^5 , 1.22×10^5 and 1.01×10^5 l.mole⁻¹.cm⁻¹ respectively. The *o*-CIPF complex shows the greatest sensitivity, so was used in the following experiments.

Effect of pH

The effect of pH on the scandium-*o*-CIPF-CTMAB system was studied over the pH range 3.9–4.9. Figure 2 shows that the absorbance is constant and maximal from pH 4.2 to 4.7, so subsequent determinations were performed at pH 4.4.

Acetate buffer is used to maintain the optimum pH and improves the stability of the colour without affecting the absorbance.

Effect of surfactants

The absorbance maximum and apparent molar absorptivity of the binary complex of scandium and *o*-CIPF are 520 nm and 3.60×10^4 l.mole⁻¹.cm⁻¹, respectively. If certain cationic and non-ionic surfactants, for example CTMAB, cetylpyridinium bromide (CPB), Tween-80, Triton X-100 and OP are added as sensitizers to the scandium-*o*-CIPF system, significant bathochromic and hyperchromic shifts are observed. The experimental results are given in Table 1.

The results in Table 1 show that the sensitizing efficiency is greatest for CTMA so this surfactant was chosen as sensitizer.

Table 1. Characteristics of scandium complexes with *o*-CIPF in the presence of surfactants

Surfactant*	λ_{\max} , nm	ϵ , $10^4 \text{ l. mole}^{-1} \text{ cm}^{-1}$
CTMAB	569	13.1
CPB	570	11.3
Tween-80	565	8.33
Triton X-100	565	5.63
OP	570	4.95

*Volume of surfactant added is 3 ml of 0.5% CTMAB or CPB solution, 5 ml of 3% Tween-80 solution, 3 ml of 1% Triton X-100, OP or PVA solution, respectively, in the 25-ml standard flask.

Effect of reagent concentrations

When the general procedure was followed with varied amounts of the reagents, maximum and constant absorbance was obtained with 0.5–2.0 ml of *o*-CIPF solution and 3.0–7.0 ml of CTMAB solution. Therefore, 1.5 and 5.0 ml respectively were selected as the optimal volumes of these reagents.

The addition of ethanol is necessary to stabilize the Sc-*o*-CIPF-CTMAB system. The maximum absorbance is obtained with 2–7% v/v ethanol. A higher level of alcohol than 7% breaks up the micelles.

Effect of temperature

The colour will not develop at room temperature but is completely formed in 10 min at 70°. Once the colour has developed, the absorbance remains constant for at least 24 hr.

Calibration graph and sensitivity

The calibration graph is linear over the range 0–12 $\mu\text{g}/25 \text{ ml}$ scandium. The apparent molar absorptivity calculated from the calibration graph is $1.31 \times 10^5 \text{ l. mole}^{-1} \text{ cm}^{-1}$ at 569 nm.

Composition of the complex

The molar ratio of scandium to *o*-CIPF in the complex was determined by the continuous variations and molar ratio methods and found to be 1:2. The molar ratio of scandium to CTMAB in the complex was established as 1:2 by the Asmus linear method.¹³

Effect of diverse ions

To assess the usefulness of the method, the effect of diverse ions which often accompany scandium was studied. The following μg amounts of the ions were found to give an error of less than $\pm 5\%$ in the determination of 5 μg of scandium: La(III), 2400; Ca(II), Mg(II) and

Ba(II), 2000; Cd(II), 510; Zn(II), 160; lanthanides(III), 140; Pb(II), 65; Co(II), 55; Nb(V), 40; Y(III), 32; Ni(II) and Mo(VI), 25; Bi(III), 23; Ta(V), 18; Be(II), 8. Suitable amounts of certain metal ions that react with *o*-CIPF may be masked by the addition of masking reagents, e.g., 30 μg of Cu(II) by $3.2 \times 10^{-2} M$ thiourea, 8 μg of Fe(III) or 2 μg of Cr(VI) by reduction with $3.5 \times 10^{-2} M$ hydroxylamine hydrochloride, and 20 μg of Cr(III), 8 μg of Th(IV), 6 μg of V(V), 3 μg of Mn(II), 2 μg of Zr(IV) or 1 μg of W(VI) by $1.3 \times 10^{-3} M$ tartaric acid. Under the same conditions, Ga(III) and In(III) form intensely coloured complexes with *o*-CIPF in the presence of CTMAB, and thus interfere in the general procedure. Small amounts of Al(III) and Ti(IV) can be masked with sulphosalicylic acid. Scandium must therefore be separated from these ions if it is to be determined when they are present in the sample.

The tolerance levels of anions and reagents were at least 100 mg of sulphate, 50 mg of nitrate or chloride, 80 mg of hydroxylamine hydrochloride, 60 mg of ascorbic acid, 6 mg of tartaric acid and 1 ml of 30% hydrogen peroxide. Fluoride, oxalate and citrate decrease the reactivity of scandium with *o*-CIPF and therefore must be absent.

Separation of scandium

In addition to the matrix elements such as W, Fe, Mn, Ca and Mg in tungsten ores, Al, Sn, V, U, Nb, Ta and lanthanides may also be present. To eliminate the interference of diverse ions the separation of scandium in the solution prepared from a fused sample is required.

When the sample fused with sodium peroxide is dissolved in water, several elements such as W, Mo, V, Mn and Al form anions and pass into solution; these can be removed by filtering. The precipitate, which contains scandium and other hydroxides, is dissolved in hydrochloric acid and this solution is extracted first with

Table 2. Results for determination of scandium in tungsten ores

Sample	Certified value*	Sc ₂ O ₃ , %	
		Average†	Standard deviation
WO-A	0.0018	0.00178	6.2×10^{-5}
WO-k	0.0039	0.00382	7.6×10^{-5}
WO-l	0.0030	0.00307	6.2×10^{-5}

*Certified value provided by the Guangzhou Research Institute of Non-ferrous Metals.

†Average values of six determinations.

sodium diethyldithiocarbamate to remove Fe, Cu, Ni, Bi, U and Sn *etc.*¹⁴ Scandium and the lanthanides are then extracted with PMBP.^{15,16} Scandium can then be stripped with 0.6M hydrochloric acid.^{16,17} To avoid possible interference by residual traces of aluminium and titanium, which are also extracted into the PMBP organic phase, sulphosalicylic acid is added to mask them.¹⁸ This separation of scandium may also be applied to other ores.^{16,17}

The results for determination of scandium in some tungsten ores by the proposed method are shown in Table 2, and are in reasonable agreement with the certified values.

REFERENCES

1. Z. Marczenko, *Spectrophotometric Determination of Elements*, Chap. 45, Horwood, Chichester, 1976.
2. M. A. H. Hafez, I. M. M. Kenawy and M. A. Kabil, *Anal. Lett.*, 1985, **18**, 2043.
3. G. V. Rathaiah and M. C. Eshwar, *Indian J. Chem.*, 1986, **25A**, 101.
4. I. Mori, Y. Fujita, K. Fujita, A. Usami, H. Kawabe, Y. Koshiyama and T. Tanaka, *Bull. Chem. Soc. Japan*, 1986, **59**, 1623.
5. C. D. Sharma, S. G. Nagarkar and M. C. Eshwar, *ibid.*, 1986, **59**, 1662.
6. Wan-Ru Chen, Jiao-Mai Pan, Chung-Gin Hsu and Sheng-Song Ge, *Mikrochim. Acta*, 1985 **III**, 417.
7. M. Jarosz and Z. Marczenko, *Anal. Chim. Acta*, 1984, **159**, 309.
8. V. A. Nazarenko, V. P. Antonovich and N. A. Veschnikova, *Talanta*, 1987, **34**, 215.
9. Zhen-qing Wang, Quang-hui Xu and Han-xi Shen, *Yankuang Ceshi*, 1986, **5**, 8.
10. Zong-ming Luo and Wei Shen, *ibid.*, 1987, **6**, 210.
11. Zong-ming Luo and Zeng-wen Lin, *ibid.*, 1988, **7**, 104.
12. Ying-lu He, Ying Liu, Jin-duan Zhao, Zhong-yi Zhao and Fu-peng Wang, *Fenxi Huaxue*, 1988, **16**, 341.
13. E. Asmus, *Z. Anal. Chem.*, 1960, **178**, 104.
14. Z. Holzbecher, L. Diviš, M. Král, L. Šůcha and F. Vláčil, *Handbook of Organic Reagents in Inorganic Analysis*, pp. 230-231. Horwood, Chichester, 1976.
15. A. Roy and A. Nag, *J. Inorg. Nucl. Chem.*, 1978, **40**, 331.
16. You-yun Hu, *Fenxi Shiyanshi*, 1985, **4**, No. 12, 57.
17. Jian Shen, *Xiyou Jinshu*, 1987, **11**, 107.
18. D. D. Perrin, *Masking and Demasking of Chemical Reactions*, pp. 42-44. Wiley, New York, 1970.

DETERMINATION OF EQUILIBRIUM PARAMETERS BY MINIMIZATION OF AN EXTENDED SUM OF SQUARES

JAROSŁAW KOSTROWICKI

Institute of Inorganic Chemistry and Technology, Technical University of Gdańsk, 80952 Gdańsk

ADAM LIWO

Institute of Chemistry, University of Gdańsk, 80952 Gdańsk, Poland

(Received 30 June 1988. Revised 28 September 1989. Accepted 20 December 1989)

Summary—A method is proposed for the evaluation of equilibrium parameters from potentiometric data, in which all the sources of random error are taken into account. This means including in the minimized sum the residuals in all the quantities subject to error (titrant volume, emf, parameters of composition of the titrant and titrand, parameters of electrode characteristics, and equilibrium constants known from other experiments). The method of preparation of the solutions is represented by a directed, acyclic graph which allows consideration of the sources of error connected with the composition of the solutions, and avoidance of inconsistency in the composition characteristics. Numerical examples are presented.

The least-squares method is a technique commonly used for the estimation of the parameters which describe chemical equilibrium systems.¹ Usually the sum to be minimized contains only selected measured quantities, because of computational limitations. However, it is not always justified from the statistical point of view.

According to the maximum likelihood principle, in the case of the normal distribution of errors, all the measured quantities should appear in the minimized sum. Neglecting certain terms often causes substantial changes in the parameters determined. In a recent paper² we included in the minimized sum the residuals in emf values and the residuals in the titrant volumes in the case of potentiometry, or the residuals in the absorbances together with the residuals in the composition characteristics in the case of spectrophotometry. Obviously, some other parameters are measured as well and should therefore be included in the sum of squares. In the case of potentiometry, which is considered in this paper, these are:

- (a) the electrode characteristics;
- (b) the measured quantities which describe the composition of all the solutions involved (e.g., the titrant and titrand concentrations and volumes, compositions and amounts of reagents);

- (c) the equilibrium constants and/or other parameters taken from other experiments or from databases.

In previous programs, most of the quantities above are either fixed or treated as additional parameters to be determined, without explicit terms in the sum to be minimized.³⁻⁵

THEORY

In this work the sum to be minimized is expressed by equation (1).

$$\begin{aligned} \phi(\mathbf{x}, \mathbf{y}, \mathbf{E}^\circ, \mathbf{S}, \omega, \mathbf{V}) &= \sum_{i=1}^l \left\{ (1/\sigma_E^i)^2 \right. \\ &\times \sum_{j=1}^{r_i} [\hat{E}_j^i - E(V_j^i, \omega, E_i^\circ, S_i, \mathbf{x}, \mathbf{y})]^2 \\ &+ (1/\sigma_V^i)^2 \sum_{j=1}^{r_i} (\hat{V}_j^i - V_j^i)^2 \\ &+ (1/\sigma_{E_i^\circ} - E_i^\circ)^2 (\hat{E}_i^\circ - E_i^\circ)^2 \\ &\left. + (1/\sigma_{S_i})^2 (\hat{S}_i - S_i)^2 \right\} \\ &+ \sum_{i=1}^u (1/\sigma_\omega)^2 (\hat{\omega}_i - \omega_i)^2 \\ &+ \sum_{i=1}^p \sum_{j=1}^p (W_y)_{ij} (\hat{y}_i - y_i)(\hat{y}_j - y_j) \end{aligned} \quad (1)$$

where $\mathbf{x} = [x_1, x_2, \dots, x_{n_{par}}]^T$ is the vector of the parameters to be determined,

$y = [y_1, y_2, \dots, y_p]^T$ is the vector of the parameters which have been determined from other experiments and for which the variance-covariance matrix (W_y^{-1}) is known (e.g., known equilibrium constants),

$E^\circ = [E_1^\circ, E_2^\circ, \dots, E_t^\circ]^T$ is the vector of the standard emfs of the subsequent titrations,

$S = [S_1, S_2, \dots, S_t]^T$ is the vector of the Nernstian slopes of the subsequent titrations,

$\omega = [\omega_1, \omega_2, \dots, \omega_u]^T$ is the vector of the characteristics of the composition of the titrants and titrands directly measured (described in detail later),

(V_j^i, E_j^i) , $j = 1, 2, \dots, r_i$, $i = 1, 2, \dots, t$ are the j th titrant volume and j th emf in the i th titration.

The σ values are the estimated *a priori* standard deviations of the respective quantities (e.g., on the basis of the apparatus characteristics), t is the number of titrations, r_i is the number of points in the i th titration, u is the number of composition characteristics, p is the number of parameters determined previously, $\hat{}$ indicates the measured quantity.

In the next section we describe in detail the quantities included in the vector ω .

Most of the derivatives required in the minimization have been given in our previous paper.² Of the rest, only the derivatives in the composition characteristics are complicated. Their form and derivation are given in the Appendix.

REPRESENTATION OF THE METHOD OF PREPARATION OF THE SOLUTIONS

The solutions used in the potentiometric titrations result from mixing various *intermediate* solutions, which are in turn formed by dissolving or mixing certain reagents. In general, the *history* of preparing the solutions can be represented by an acyclic *digraph*. Consider the example shown in Fig. 1.

Solution 1, with volume V_{13} and initial concentrations of species given by vector C_1 , and solution 2, with volume V_{23} and initial concentrations given by vector C_2 , were mixed to give solution 3, with a volume found to be w_3 . Then solution 5 was formed analogously from solutions 3 and 4, and solution 6 from solutions 1, 3, and 5. Solution 6 was the one used in the titrations. From the example presented we can see that the vertices of the graph are of three types: *initial*, *intermediate*, and *final*. In the example, the initial vertices are 1, 2, and 4;

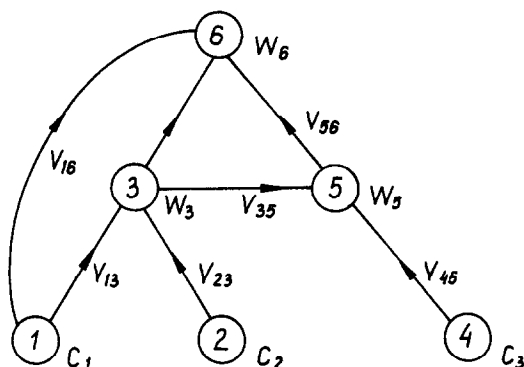


Fig. 1

intermediate are 3 and 5 and the final is vertex 6. The initial vertices need not correspond to solutions; they can also represent solid reagents. In such a case the "concentrations" are simply the percentages of the species.

There are two reasons for introducing the graph. First, particular methods for preparing solutions result in certain relationships between the total concentrations of the final solutions, which cannot therefore be refined independently. Secondly, such a representation of the preparation of the solutions allows the residuals in the quantities which are really measured, to be included in the minimized sum. (It is well known that, from the statistical point of view, the transformation of variables is not always justified.) Consider the example shown in Fig. 2.

Assume that in the system studied, there exist equilibria between a certain base (B) and protons. Assume that solution (reagent) 1 contains BH^+ and H^+ , and that solution (reagent) 2 contains B. Concentrations of these species, together with the volumes of the solutions are subject to error. Thus, the corresponding terms in the minimized sum are given by equation (2).

$$\begin{aligned} \phi' & (T_{BH^+,1}, T_{H^+,1}, T_{B,2}, V_{13}, V_{14}, V_{24}, w_3, w_4) \\ &= (1/\sigma_{BH^+,1})^2 (\hat{T}_{BH^+,1} - T_{BH^+,1})^2 \\ &+ (1/\sigma_{H^+,1})^2 (\hat{T}_{H^+,1} - T_{H^+,1})^2 \\ &+ (1/\sigma_{B,2})^2 (\hat{T}_{B,2} - T_{B,2})^2 \\ &+ (1/\sigma_{V_{13}})^2 (\hat{V}_{13} - V_{13})^2 \\ &+ (1/\sigma_{V_{14}})^2 (\hat{V}_{14} - V_{14})^2 \\ &+ (1/\sigma_{V_{24}})^2 (\hat{V}_{24} - V_{24})^2 \\ &+ (1/\sigma_{w_3})^2 (\hat{w}_3 - w_3)^2 \\ &+ (1/\sigma_{w_4})^2 (\hat{w}_4 - w_4)^2 \end{aligned} \quad (2)$$

where $T_{A,i}$ denotes the total concentration of species A in the i th solution.

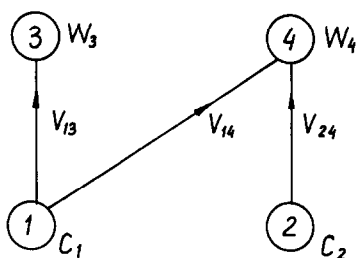


Fig. 2

If the history of preparing the solutions were neglected, these terms would be expressed by equation (3).

$$\begin{aligned} \phi''(T_{\text{BH}^+,3}, T_{\text{H}^+,3}, T_{\text{BH}^+,4}, T_{\text{H}^+,4}, T_{\text{B},4}) &= (1/\sigma_{\text{BH}^+,3})^2 (\hat{T}_{\text{BH}^+,3} - T_{\text{BH}^+,3})^2 \\ &+ (1/\sigma_{\text{H}^+,3})^2 (\hat{T}_{\text{H}^+,3} - T_{\text{H}^+,3})^2 \\ &+ (1/\sigma_{\text{BH}^+,4})^2 (\hat{T}_{\text{BH}^+,4} - T_{\text{BH}^+,4})^2 \\ &+ (1/\sigma_{\text{H}^+,4})^2 (\hat{T}_{\text{H}^+,4} - T_{\text{H}^+,4})^2 \\ &+ (1/\sigma_{\text{B},4})^2 (\hat{T}_{\text{B},4} - T_{\text{B},4})^2 \end{aligned} \quad (3)$$

where

$$\begin{aligned} \hat{T}_{\text{BH}^+,3} &= (\hat{V}_{13}/\hat{w}_3) \hat{T}_{\text{BH}^+,1} \\ \hat{T}_{\text{H}^+,3} &= (\hat{V}_{13}/\hat{w}_3) \hat{T}_{\text{H}^+,1} \\ \hat{T}_{\text{BH}^+,4} &= (\hat{V}_{14}/\hat{w}_4) \hat{T}_{\text{BH}^+,1} \\ \hat{T}_{\text{H}^+,4} &= (\hat{V}_{14}/\hat{w}_4) \hat{T}_{\text{H}^+,1} \\ \hat{T}_{\text{B},4} &= (\hat{V}_{24}/\hat{w}_4) \hat{T}_{\text{B},2} \end{aligned} \quad (4)$$

The "theoretical" values $T_{\text{BH}^+,3}$, $T_{\text{H}^+,3}$, $T_{\text{BH}^+,4}$, and $T_{\text{H}^+,4}$ obtained by the unrestricted minimization of the sum of squares containing equation (3) need not fulfil the equations in (4) (e.g., $T_{\text{BH}^+,3}/T_{\text{H}^+,3} \neq T_{\text{BH}^+,4}/T_{\text{H}^+,4}$). On the other hand, from the way the solutions were prepared it is obvious that these restrictions must also hold for the "theoretical" values.

The violation of the constraints in (4) is not the only deficiency of minimizing the sum containing the terms in (3) instead of that containing the terms in (2). Since the relationships in (4) are not linear, the distribution of error of the transformed quantities is no longer normal. Therefore, use of the least-squares method is no longer justified.

PRACTICAL IMPLEMENTATION

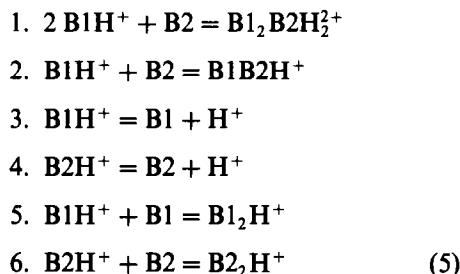
We have modified our previous program STOICHIO,² which used Marquardt's minimization procedure, by incorporating the present approach. The program is designed to

process potentiometric data. Like the original version of STOICHIO, it can also determine unknown stoichiometric coefficients. The program is written in FORTRAN IV and has been implemented on an R-32 computer. A version has also been prepared in FORTRAN 77 and implemented on an IBM PC.

NUMERICAL EXAMPLES

We have performed calculations for a chosen system in various ways, e.g., with or without fixed electrode characteristics, previously determined constants, and solution composition characteristics. The number of terms in the minimized sum also changed from one run to another.

The system was composed of 4-methoxypyridine-*N*-oxide, 2-picoline-*N*-oxide, and protons, in propylene carbonate.⁶ The equilibria are given by (5).



where B1 stands for 4-methoxypyridine-*N*-oxide and B2 for 2-picoline-*N*-oxide.

The constants of equilibria 1 and 2 were to be determined; the remaining equilibrium constants and their variance-covariance matrix were known from other measurements.

Two potentiometric titrations with the use of the glass electrode were performed. The method of preparing the solutions is shown in Fig. 3.

Solution 1 contains B1H^+ (as the perchlorate) with some amount of H^+ , and solution 2 contains B2. Solution 3 was titrated with solution 5, and solution 4 with solution 6.

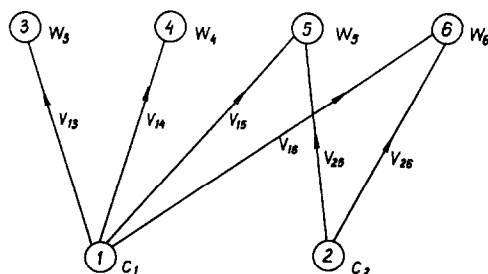


Fig. 3

Table 1. (a) Results of calculations for the 4-MeOPyOHClO₄-2-PicO system

Parameter	Initial*	Run number								
		1†	2§	3	4§	5†	6§	7†	8§	9†
log K ₁	7.0	6.351 (0.061)	diverges	5.5 (25.9)	5.4 (13.6)	6.361 (0.064)	6.378 (0.062)	6.302 (0.073)	4.2 (78.5)	6.295 (0.057)
log K ₂	3.0	3.367 (0.030)	3.339 (0.023)	3.3 (8.7)	3.2 (1.2)	3.395 (0.019)	3.438 (0.074)	3.431 (0.015)	3.3 (1.4)	3.319 (0.018)
log K ₃	-8.627 (0.060)	-8.617 (0.034)	††	-8.8 (14.1)	-9.18 (0.99)	-8.609 (0.035)	f	f	f	f
log K ₄	-10.883 (0.073)	-10.792 (0.060)	f	-10.9 (27.3)	-10.0 (2.0)	-10.716 (0.040)	f	f	f	f
log K ₅	3.120 (0.030)	3.122 (0.014)	f	3.0 (9.1)	3.08 (0.62)	3.124 (0.014)	f	f	f	f
log K ₆	4.146 (0.022)	4.165 (0.030)	f	3.9 (10.0)	4.1 (1.9)	4.177 (0.030)	f	f	f	f
T _{H⁺,1}	0.00 (0.01)	0.009 (0.0056)	f	0.1 (1.2)	f	f	f	f	0.14 (0.12)	0.0219 (0.0025)
V ₁₃	1.000 (0.020)	1.002 (0.012)	f	0.8 (5.6)	f	f	f	f	0.6 (1.2)	1.006 (0.012)
V ₁₄	1.000 (0.020)	1.002 (0.012)	f	0.8 (5.8)	f	f	f	f	0.6 (1.3)	1.006 (0.012)
V ₁₅	1.000 (0.020)	1.000 (0.013)	f	0.9 (5.5)	f	f	f	f	0.6 (1.9)	1.000 (0.014)
V ₁₆	1.000 (0.020)	1.000 (0.013)	f	1.1 (7.0)	f	f	f	f	0.7 (2.0)	1.000 (0.014)
V ₂₅	20.00 (0.40)	19.97 (0.25)	f	20 (154)	f	f	f	f	19 (33)	19.86 (0.22)
V ₂₆	20.00 (0.40)	19.99 (0.25)	f	20 (155)	f	f	f	f	20 (34)	19.91 (0.22)
E ₁ ⁰	1025.3 (2.0)	1025.6 (1.1)	f	1025 (401)	f	f	1028.3 (14.5)	1028.2 (1.1)	f	f
E ₂ ⁰	1025.3 (2.0)	1025.6 (1.1)	f	1025 (403)	f	f	1028.8 (14.5)	1028.2 (1.1)	f	f
S ₁	59.31 (0.20)	59.29 (0.11)	f	59.1 (39.5)	f	f	59.0 (1.5)	59.04 (0.11)	f	f
S ₂	59.31 (0.20)	59.31 (0.11)	f	59.3 (40.3)	f	f	59.0 (1.5)	59.05 (0.11)	f	f
σ _{EMF}	2.0	1.2	2.8	1.1	1.1	1.2	1.3	1.3	1.1	1.2
σ _V	0.01	0.001	0.004	0.001	0.001	0.001	0.001	0.001	0.001	0.001

*In the case of the equilibrium constants determined, the initial estimates are given; for the remaining parameters the values were determined from other experiments (together with the standard deviations). The standard deviations in emf and in V are values resulting from the precision of measurements.

†Run in which all the measured quantities adjusted were included in the minimized sum (with proper values of the standard deviations).

§Run did not converge with the required accuracy in 100 iterations.

†† means the value of the parameter was fixed.

(b) Values of parameters which were never varied in the calculations

Parameter	Value
T _{4MeOPyOH⁺,1}	1.0
T _{2PicO,2}	1.0
W ₂	1000.0
W ₄	1000.0
W ₅	1000.0
W ₆	1000.0
V ₁ ^M (ml)	27.0
V ₂ ^M (ml)	27.0

V^M is the volume of the titrand solution. E^0 , S , and σ_{EMF} values are in mV, σ_V is in ml, T values are molarities, and w and V values are in arbitrary units chosen so that the resulting concentrations in the titrants and the solutions titrated are expressed as molarities.

We chose this system for the following reasons. First, the glass electrode is not so stable in propylene carbonate as in water, and its properties can vary slightly from titration to titration. Secondly, 4-methoxypyridine-*N*-oxide perchlorate always contains traces of either perchloric acid or the free base. Also, errors in the equilibrium constants previously determined should be taken into account.

The results are summarized in Table 1. As shown, when it is assumed that the parameters determined from other measurements are error-free, the program (run 2) gives results that are qualitatively different from those in which certain parameters of this group are adjusted (in run 2 the iteration for the first equilibrium constant diverges). Neglecting information from other measurements (*i.e.* not including in the minimized sum the terms corresponding to parameters previously determined) leads to unreasonably large standard deviations of the equilibrium constants estimated (run 3). In run 1, the minimized sum included all the relevant quantities, with correct values of the elements of the variance-covariance matrix. The equilibrium constants determined in this way had reasonable standard deviations.

To estimate the influence of adjusting certain groups of parameters on the values of the equilibrium constants determined, we performed some additional calculations (runs 4–9). In runs 4 and 5 we adjusted only the equilibrium constants determined from other measurements, in runs 6 and 7 only the electrode characteristics, and in runs 8 and 9 only the composition characteristics. In runs 5, 7, and 9 all the parameters adjusted were included in the minimized sum, while in runs 4, 6, and 8 they were not.

When the parameters determined from other measurements were adjusted without inclusion in the minimized sum, the iterative process did not converge in 100 iterations. Only when the electrode characteristic parameters were adjusted did the equilibrium constants determined have reasonable standard deviations. When all the quantities adjusted were included in the sum, the iterative process converged in a reasonable number of iterations, and the equilibrium constants had small standard deviations. Therefore inclusion of all the quantities adjusted in the minimized sum seems to be essential to obtain reliable parameters.

This conclusion is very important, because the extended sum of squares is the main feature

which distinguishes our method from earlier algorithms which vary the composition and electrode characteristics, but without including them in the minimized sum, *e.g.*, the programs MUCOMP³ and ACBA.⁵ Runs 3, 4, 6, and 8 are very similar to MUCOMP or ACBA computations.

When the results of partial adjustment (runs 5, 7, and 9) are compared with the results of full adjustment (run 1) it seems that varying the equilibrium constants previously determined is essential, because this gives the best agreement with the results obtained when all the parameters subject to error are adjusted.

REFERENCES

1. D. J. Leggett, *Computational Methods for the Determination of Formation Constants*, Plenum Press, New York, 1985.
2. J. Kostrowicki and A. Liwo, *Comput. Chem.*, 1987, 11, 195.
3. M. Wozniak, J. Canonne and G. Nowogrocki, *J. Chem. Soc., Dalton Trans.*, 1981, 2419.
4. D. J. Leggett, *op. cit.*, p. 102.
5. G. Arena, E. Rizzarelli, S. Sammartano and C. Rigano, *Talanta*, 1979, 26, 1.
6. A. Wawrzynów, *Ph. D. Thesis*, University of Gdańsk, 1985.

APPENDIX

For each path in the digraph which leads from vertex number i_s to vertex i_1 through vertices i_{s-1}, \dots, i_2 we can define the product.

$$I(i_1, i_2, \dots, i_s) = (1/w_{i_1}) V_{i_1 i_2} (1/w_{i_2}) \dots \dots V_{i_{s-2} i_{s-1}} (1/w_{i_{s-1}}) V_{i_{s-1} i_s} \quad (\text{A1})$$

The symbol I has the obvious property

$$I(i_1, \dots, i_m, \dots, i_s) = I(i_1, \dots, i_m) I(i_m, \dots, i_s) \quad (\text{A2})$$

Let A denote the set of all initial vertices. Then a concentration in the solution which is represented by any intermediate or final vertex i may be expressed by

$$C_i = \sum_{t \in A} C_t \sum_{\substack{\text{ways from} \\ t \text{ to } i}} I(i, \dots, t) \quad (\text{A3})$$

Let L_{ik} be defined by (A4). Equation (A3) can be then rewritten as (A5).

$$L_{ik} = \sum_{\substack{\text{ways from} \\ k \text{ to } i}} I(i, \dots, k) \quad (\text{A4})$$

$$C_i = \sum_{t \in A} L_{it} C_t \quad (\text{A5})$$

Let us calculate the derivatives $\partial L_{ik}/\partial w_i$.

$$\begin{aligned} \partial L_{ik}/\partial w_j &= \partial/\partial w_j \sum_{\substack{\text{ways from } k \\ \text{to } i \text{ through } j}} I(i, \dots, j, \dots, k) \\ &= \partial/\partial w_j \sum_{\substack{\text{ways from } k \\ \text{to } i \text{ through } j}} I(i, \dots, j) I(j, \dots, K) \\ &= \partial/\partial w_i \left[\sum_{\substack{\text{ways from} \\ j \text{ to } i}} I(i, \dots, j) \right] \\ &\quad \times \left[\sum_{\substack{\text{ways from} \\ k \text{ to } j}} I(j, \dots, k) \right] \\ &= \partial/\partial w_j (L_{ij} L_{jk}) \end{aligned}$$

It can easily be seen that $\partial L_{ij}/\partial w_i = 0$ and $\partial (w_j L_{jk})/\partial w_j = 0$. Therefore:

$$\begin{aligned} \partial L_{ik}/\partial w_j &= L_{ij} \partial L_{jk}/\partial w_j \\ &= L_{ij} \partial [(1/w_j)(w_j L_{jk})]/\partial w_j \\ &= -(1/w_j)^2 w_j L_{ij} L_{jk} \\ &= -L_{ij} L_{jk}/w_j \end{aligned}$$

Hence we immediately obtain the derivatives $\partial C_i/\partial w_j$.

$$\begin{aligned} \partial C_i/\partial w_j &= \sum_{t \in A} C_t \partial L_{it}/\partial w_j \\ &= - \sum_{t \in A} C_t L_{ij} L_{jt}/w_j \end{aligned}$$

$$\begin{aligned} &= -L_{ij}/w_j \sum_{t \in A} C_t L_{jt} \\ &= -L_{ij} C_j/w_j \end{aligned} \tag{A6}$$

Similarly:

$$\begin{aligned} \partial L_{ik}/\partial V_{jl} &= \partial/\partial V_{jl} \sum_{\substack{\text{ways from} \\ k \text{ to } i \text{ through} \\ l \text{ and } j}} I(i, \dots, j, l, \dots, k) \\ &= \partial/\partial V_{jl} \left[\sum_{\substack{\text{ways from} \\ j \text{ to } i}} I(i, \dots, j) \right] \\ &\quad \times w_j^{-1} V_{jl} \left[\sum_{\substack{\text{ways from} \\ k \text{ to } l}} I(l, \dots, k) \right] \\ &= \partial/\partial V_{jl} (L_{ij} V_{jl} L_{lk}/w_j) \\ &= L_{ij} L_{lk}/w_j \end{aligned}$$

and finally

$$\begin{aligned} \partial C_i/\partial V_{jl} &= \sum_{t \in A} C_t \partial L_{it}/\partial V_{jl} \\ &= \sum_{t \in A} C_t L_{ij} L_{lt}/w_j \\ &= L_{ij} C_l/w_j \end{aligned} \tag{A7}$$

Of course:

$$\partial C_i/\partial C_i = L_{ii} \tag{A8}$$

METAL ELECTRODES FOR CONTINUOUS AMPEROMETRIC MEASUREMENT OF FREE HYDROFLUORIC ACID IN ACIDIC SOLUTIONS CONTAINING COMPLEXING IONS

JERRY D. CHRISTIAN, DOUGLAS B. ILLUM and JAMES A. MURPHY

Westinghouse Idaho Nuclear Co., Inc., Box 4000, Idaho Falls, Idaho 83403, U.S.A.

(Received 9 March 1990. Accepted 13 March 1990)

Summary—Titanium-based electrodes have been demonstrated to be useful for measuring free HF concentration in the range 0.01–0.07M at temperatures between 19 and 61°C in acidic, complexed HF solutions, by measurement of the current density resulting when the electrode potential is approximately +0.6 V with respect to an inert electrode. The current density, i , is linearly related to the HF concentration when the solution is adequately stirred to remove diffusion effects at the electrode, and is independent of HNO₃ concentration up to 1.75M. The dependence on the absolute temperature is $\ln i = -A/T + B + C \ln T$, and the activation energy at an absolute temperature T_i is $R(A + T_i C)$, where A , B and C are constants and R is the gas constant. For a Ti–2% Pd electrode, the activation energy for anodic dissolution is found to be 43.7 ± 0.2 kJ/mole at 312 K. The equations relating the current density to HF concentration at different temperatures can be combined to give a single equation for [HF] as a function of both i and T .

A remote, on-line, rapid-response monitor for free HF concentration is required for controlling continuous complexing of excess free HF in the solution produced by dissolving Zircaloy-based nuclear fuel in approximately 10M hydrofluoric acid. Free HF in the solution must be complexed with aluminum nitrate or boric acid to give a narrow residual range of 0.03–0.05M (at 35°) before the solution is transferred to downstream stainless-steel vessels.

Indirect methods have been developed for determining free HF in acidic systems containing complexing metal ions, by simultaneously measuring [H⁺] and [F⁻] with ion-selective electrodes,^{1,2} for which HF-resistant hydrogen-ion electrodes have been developed.¹⁻³ Though useful for laboratory determinations of HF in samples that can be adjusted for ionic strength and compared against standards, this approach cannot be applied to remote, continuous on-line measurements. In addition to the inability to adjust the analyte solution accurately, frequent calibrations are impractical, and ruggedness and long life are essential.

Metals slightly reactive with hydrofluoric acid at process concentrations were investigated as electrode materials that might, when at a positive potential relative to an inert reference electrode, result in anodic dissolution rates and

measured currents that are proportional to the free HF concentration. Criteria for selection of the electrode material were (1) ready availability, (2) that the metal should be sufficiently reactive to produce reasonable limiting anodic currents, but not so reactive that the surface area would change rapidly, requiring frequent calibration or remote-electrode replacement, (3) rapid and constant response to changes in HF concentrations, requiring infrequent calibration, and (4) no response to any strong acids or fluoride complexes present, except for any effects on the free HF concentration.

A number of metals and alloys might be suitable, depending on the HF concentration range and the temperature of interest. For our purposes, pure Ti and a Ti–2% Pd alloy proved to be the best materials and our investigations have been concentrated on them. A summary of early results is reported here. Details and more extensive results, including investigations with other materials, will be reported in a subsequent paper.

EXPERIMENTAL

Reagents

A stock solution of reagent grade hydrofluoric acid was standardized by acid–base

titration (relative standard deviation 0.03%). This and concentrated reagent grade nitric acid were weighed into a standard flask and diluted to volume to prepare HF-HNO₃ solutions. The aluminum nitrate used for complexing the hydrofluoric acid was a 2.2M technical grade solution analyzed by atomic-absorption spectrophotometry (relative standard deviation 2%).

Apparatus

Ti and Ti-2% Pd alloy anodes were prepared by heat-shrinking one layer of 0.238 cm diameter Teflon and two layers of 0.318 cm diameter polyolefin heat-shrink tubing over 0.157 cm diameter metal rods so that only the polished rod ends were exposed to the solution. The cross-sectional areas were determined by photomicrography. The cathode consisted of a 12 cm long, 0.127 cm diameter Hastelloy C-4 metal rod. Pressure fittings were used to connect the rods to wires, which were attached to an adjustable voltage supply. A simple converter circuit was used to measure the current through the electrodes by taking a voltage reading across a resistor.

The solution and electrodes were placed in a capped Teflon bottle immersed in a constant-temperature water-bath. The solution was stirred with a paddle. The temperature of the bath was controlled within 0.1° and measured to 0.1° with an NBS-calibrated thermometer, and was shown by calibration to be within 0.1° of that of the equilibrated experimental solution.

Procedures

A potential of 0.55 V was applied across the anode and the inert cathode. The current changes only slowly with applied voltage if that is at or above this value. For temperature-dependence studies, voltage readings across the resistor were taken by a computer data-acquisition system every 4–5°, with a minimum of 18 readings at each equilibrated temperature. Electrodes were wired so that readings from both types of anode were obtained simultaneously under identical conditions. After measurement of the voltage as a function of increasing temperature from 19 to 61°, the solution was cooled to the mid-range temperature and the measure-

ment was repeated. In this way, constancy of response could be verified. In a few instances, the repeat reading was higher by more than three standard deviations; a slight channeling or shrinkage of the Teflon tubing had occurred, changing the exposed surface area. Data from such experiments were not used. The electrode responses to solutions of 0.03–0.07M hydrofluoric acid were investigated. Nitric acid at 1.75M concentration was normally present to restrict dissociation of HF to less than 0.07%, over the temperature range used. This is typically the concentration of strong acid in the zirconium-fuel solutions after complexation with aluminum nitrate. For measurements at elevated temperatures the HF concentrations were corrected for the measured increase in volume due to expansion. The current densities measured at different temperatures for a given solution were then normalized to a constant HF concentration for correlation of temperature effects.

RESULTS AND DISCUSSION

The current increased with stirring, by a factor of up to 1.5 at 25° and 2.0 at 60°, relative to an unstirred solution, for both the Ti-2% Pd and Ti electrodes, as a result of a mass-transfer limiting process near the electrode. A stirring rate was found, above which the limiting current density did not change, and all measurements were made under those conditions. Freshly prepared electrodes that have been exposed to air have a surface oxide layer that causes the current to increase rapidly for a few minutes and then slowly for ~30 min, before becoming constant. Once conditioned to this state, immersed electrodes with an applied potential give a stable and reproducible response.

The Ti and Ti-2% Pd electrodes provided linear responses to HF concentration over the range 0.03–0.07M. The coefficients of the linear equations for response to 1.75M nitric acid solutions of HF at different temperatures are listed in Table 1. The current densities obtained with Ti electrodes are greater than those with Ti-2% Pd by 8–20%, the difference decreasing as the temperature and HF concentration increase.

When $\ln i$ is plotted against $1/T$, a negative curvature is displayed in all cases, which indicates a dependence of activation energy on temperature. The data of McKaveney and Byrnes⁴ for the *n*-silicon electrode in 0.002 to 0.012M HF showed similar characteristics.†

†The semiconductor, *n*-silicon, is unsuitable for use in continuous monitoring. Its response to HF drifts, necessitating frequent calibration, it is affected by HNO₃, and the sensitivity of material from various sources to HF is widely variable and unpredictable.

Table 1. Coefficients of the equation $i = a[\text{HF}] + b$ (i is current density, mA/cm², and $[\text{HF}]$ is molarity of HF in 1.75M HNO₃)

Electrode	Temperature, °C	a	b	Residual	
				std. devn. of i	r^{2*}
Ti-2% Pd	19.0	24.49	-0.048	0.003	0.9999
	24.9	34.48	-0.065	0.016	0.9992
	29.9	49.05	-0.149	0.028	0.9985
	35.3	68.72	-0.280	0.026	0.9994
	37.2	74.01	-0.219	0.079	0.9949
	40.6	87.59	-0.135	0.069	0.9972
	45.7	114.2	-0.14	0.11	0.9958
	50.7	151.9	-0.46	0.07	0.9991
	56.0	188.5	-0.47	0.20	0.9948
	61.0	222.9	-0.30	0.17	0.9974
Ti	19.0	26.56	0.029	0.009	0.9994
	24.9	36.58	0.040	0.024	0.9983
	29.9	51.94	-0.048	0.048	0.9961
	35.2	72.54	-0.188	0.052	0.9977

*Correlation coefficient. Number of degrees of freedom is ≥ 178 for all cases.

The data were well fitted by the function $\ln i = -A/T + B + C \ln T$. If it is considered that the curvature is imparted by a heat capacity of activation, c^* , that is independent of temperature, the constants are related to the activation energy, E_r^* , at a reference temperature, T_r , and c^* by $A = E_r^*/R - T_r C$ and $C = c^*/R$, where R is the gas constant. Thus, $E_r^* = R(A + T_r C)$ and $-E_r^*/R$ is the tangent, or slope, of the curve at the reference temperature.† T_r is taken here to be at the mid-point of the range of $1/T$, or 311.7 K. Results for the Ti-2% Pd electrode are summarized in Table 2.

The coefficients of the equations are highly correlated; their individual magnitudes may vary considerably, but the overall representation of data remains good, as shown by the

statistical parameters and the derived value of E_{312}^* , 43.7 ± 0.2 kJ/mole for the Ti-2% Pd electrode. Similar treatment of the limited Ti-electrode data yields $E_{300}^* = 43 \pm 1$ kJ/mole for this electrode.

The complete set of Ti-2% Pd data for 1.75M nitric acid medium fitted well to a single equation relating current density, HF concentration and temperature. The linear coefficients a and b from Table 1 were fitted to a quadratic and a linear function of temperature, respectively. The resulting equation, solved for HF concentration, is

$$[\text{HF}] = \frac{i + 0.00871t - 0.0120}{0.0851t^2 - 2.033t + 32.54}$$

where $[\text{HF}]$ is expressed in molarity, i in mA/cm² and t in °C. The residual standard deviation in $[\text{HF}]$ is 0.00088M and the correlation coefficient, r^2 , is 0.9992.

Measurements at 18.1° for 0.050M HF in 0, 1, and 1.75M nitric acid showed the absence of an effect of nitric acid on the current density.

†The E_r^* derived at the mid-point of $1/T$ agrees within ca. 0.5% with the activation energy estimated from a linear fit of $\ln i$ to $1/T$. (Interestingly, E_r^* at the mid-point of the $\ln T$ range agrees with E^* deduced from the linear fit, within 0.02%.)

Table 2. Coefficients of the equation $\ln i = -A/T + B + C \ln T$, and the activation energy E_{312}^* at 311.7 K, for the Ti-2% Pd electrode in HF-1.75M HNO₃ solutions (i is the current density in mA/cm²)

[HF], M	A	B	C	E_{312}^*, \dagger kJ/mole	Residual	
					std. devn. of $\ln i$	r^2
0.0300	12862	186.42	-24.327	43.88 ± 0.15	0.023	0.9988
0.0451	12326	175.21	-22.647	43.79 ± 0.08	0.022	0.9989
0.0500	16624	270.53	-36.401	43.87 ± 0.20	0.029	0.9982
0.0600	15236	240.95	-32.123	43.41 ± 0.15	0.025	0.9985
0.0700	13428	200.26	-26.202	43.73 ± 0.14	0.018	0.9993

†Mean \pm standard deviation. Number of degrees of freedom is ≥ 177 for all cases. Data are over the temperature range 19-61°C.

The HF concentration in the absence of nitric acid was corrected for dissociation and self-complexing to HF_2^- . (Whether HF_2^- contributes to the current is being evaluated; at present, it is ignored in the data correlation for pure HF.) The fact that the pure HF solution results in the same current density as the HF-HNO₃ solution at an equivalent HF concentration shows that the ionic strength of the dilute HF solution is sufficient to conduct the current and that nitric acid does not participate in the electrode response.

The ability to measure HF in an acidic complexed system was tested by titrating a 0.07M HF, 1.75M HNO₃ solution to a final concentration of 0.01M HF with 2.2M Al(NO₃)₃. After each of 10 titrant additions, the HF concentration was measured with the Ti electrode. The free HF concentration was calculated from the composition of the solution by means

of an equilibrium computer program containing the complexing equilibrium constants reported by Hammer.⁵ The measured HF agreed with the calculated concentration within 5% at all points, which indicates the validity of extrapolating the derived equations to 0.01M HF, and is adequate accuracy for the intended application.

REFERENCES

1. J. R. Entwistle, C. J. Weedon and T. J. Hayes, *Chem. Ind. (London)*, 1973, 433.
2. T. Eriksson, *Anal. Chim. Acta*, 1973, **65**, 417.
3. L. J. Warren, *ibid.*, 1971, **53**, 199.
4. J. P. McKaveney and C. J. Byrnes, *Anal. Chem.*, 1970, **42**, 1023.
5. R. R. Hammer, *A Determination of the Stability Constants of a Number of Metal Fluoride Complexes and Their Rates of Formation*, Report ENICO-1004, August 1969. National Technical Information Service, Springfield, Virginia.

DETERMINATION OF SUNSET YELLOW AND TARTRAZINE BY DIFFERENTIAL PULSE POLAROGRAPHY*

F. BECERRO DOMINGUEZ†, F. GONZALEZ DIEGO and J. HERNANDEZ MENDEZ

Departamento de Química Analítica, Nutrición y Bromatología, Universidad de Salamanca,
Salamanca, Spain

(Received 31 January 1989. Revised 7 November 1989. Accepted 13 January 1990)

Summary—A study has been made of the polarographic (DC and DPP) behaviour of the food dyes Sunset Yellow and Tartrazine in acid and alkaline media and in the absence and presence of polyvinylpyrrolidone. Methods are proposed for the determination of both dyes by DPP over a concentration range of 0.1–10 ppm. The methods have been applied to their determination in soft drinks.

Food dyes are usually determined spectrophotometrically¹⁻³ and prior separation is almost always involved.^{2,4} There are several references to electroanalytical determination of food dyes; methods have been proposed for almost all the permitted dyes. Several papers report on determination of the dyes either in isolated form or as mixtures, by differential pulse voltammetry with dropping mercury or solid electrodes, in either batch or flow systems.⁵⁻⁸ The voltammetric (DC and DPP) behaviour of Sunset Yellow and Tartrazine in presence and absence of tetraphenylphosphonium chloride, with glassy carbon⁶ and dropping mercury electrodes,⁹⁻¹¹ is known. The phosphonium compound shifts the waves or peak potentials and modifies the currents. A method is proposed here for the determination of Tartrazine in the presence of other dyes in samples of dandelion and burdock drinks and tablet coatings.

Recently, Barros *et al.*¹² studied the polarographic behaviour of sixteen food dyes and three dyes used in cosmetics, in the presence of gelatin. The presence of gelatin modifies the reduction of Sunset Yellow and Tartrazine. At pH 9.5 the peak current for Tartrazine is completely suppressed. The method can be applied to the determination of Tartrazine in coloured gelatin capsules but not in cosmetic blusher.

In this paper the electroanalytical behaviour of the two dyes in the absence and presence of polyvinylpyrrolidone is described and methods

are proposed for their determination in soft drinks.

EXPERIMENTAL

Apparatus

A Metrohm Polarecord E-506, equipped with an E-505 stand was employed. A three-electrode system was used: a Metrohm EA-1019/1 dropping mercury electrode as working electrode; a home-made saturated calomel electrode as reference and a platinum wire as counter-electrode.

Reagents

Solutions of Sunset Yellow [sodium 1-(4-sulphophenylazo)-2-naphthol-6-sulphonate] and Tartrazine [sodium 5-hydroxy-1-*p*-sulphophenyl-4-(*p*-sulphophenylazo)pyrazol-3-carboxylate] were prepared from the products supplied by Hispanoland S.A. Solutions of polyvinylpyrrolidone K-90 (PVP; Scharlau) were prepared. All chemicals used were of analytical reagent grade.

Procedure

To a suitable amount of dye solution add 10.0 ml of 0.6M Britton-Robinson buffer solution, 1.0 ml of a solution of 1% K-90 PVP, adjust to pH 1.6 and dilute to volume in a 50.0-ml standard flask. Deaerate the solution by passage of nitrogen for 10 min, and polarograph the solution, using the following conditions: temperature, 25°C; mercury column height, 70 cm; drop-time, 2 sec, scan-rate, 4 mV/sec; in DPP, a pulse amplitude of -0.050 V.

*Presented in part at the Tenth Meeting of the Electrochemical Group of the R.S.E.Q., San Sebastián, 1987.

†Author for correspondence.

RESULTS AND DISCUSSION

Polarographic behaviour

With a dropping mercury electrode Sunset Yellow and Tartrazine in 0.12M Britton-Robinson buffer as supporting electrolyte give poorly defined reduction waves with potentials which are a function of pH.

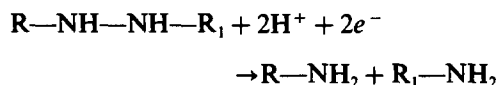
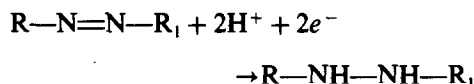
In view of the behaviour of the two dyes, especially the shape of the waves, the following studies were made at pH 1.6 and 10.0.

The polarograms for Sunset Yellow, at pH 1.6 and in the absence of PVP, indicate the presence of adsorption phenomena, and have a very narrow and pronounced maximum which almost completely prevents measurement of the current. At pH 10.0 this phenomenon does not occur. At pH 1.6, the presence of the polymer inhibits appearance of the maximum, though this reappears at high concentrations of the dye. At pH 10.0 the signals are much improved but the current is lower. Figure 1 shows the DPP curves obtained in the absence and presence of PVP.

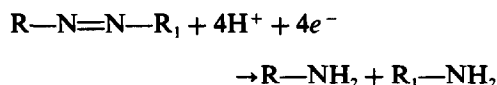
The DPP curves for Tartrazine at both pH values is improved by the presence of PVP and at pH 1.6 the sensitivity is increased but at pH 10.0 the polymer leads to a very pronounced decrease in the DPP peak (Fig. 2).

For both dyes the best results were obtained by use of 0.02% PVP, so this concentration was chosen for later studies.

The mechanism of polarographic reduction of azo-compounds has been known for some time.^{5,13} Both in the absence and presence of PVP, the electrode process must be consistent with the mechanism that postulates a step-wise breakage of the molecule, similar to that occurring in the metabolic processes of these dyes.



At moderate pH values, such as those employed in the present study, the overall process occurs in a single step:



where RNH₂ is sulphanilic acid and R₁NH₂ is 1-amino-2-hydroxy-6-naphthalenesulphonic acid (Sunset Yellow) or 5-hydroxy-1-*p*-sulphophenyl-4-(*p*-sulphophenylazo)-pyrazol-3-carboxylic acid (Tartrazine).

The variation in current with concentration is shown in Fig. 3. For Sunset Yellow at pH 1.6 in the presence of PVP, two well defined zones are observed that are characteristic of adsorption-controlled processes. For low dye concen-

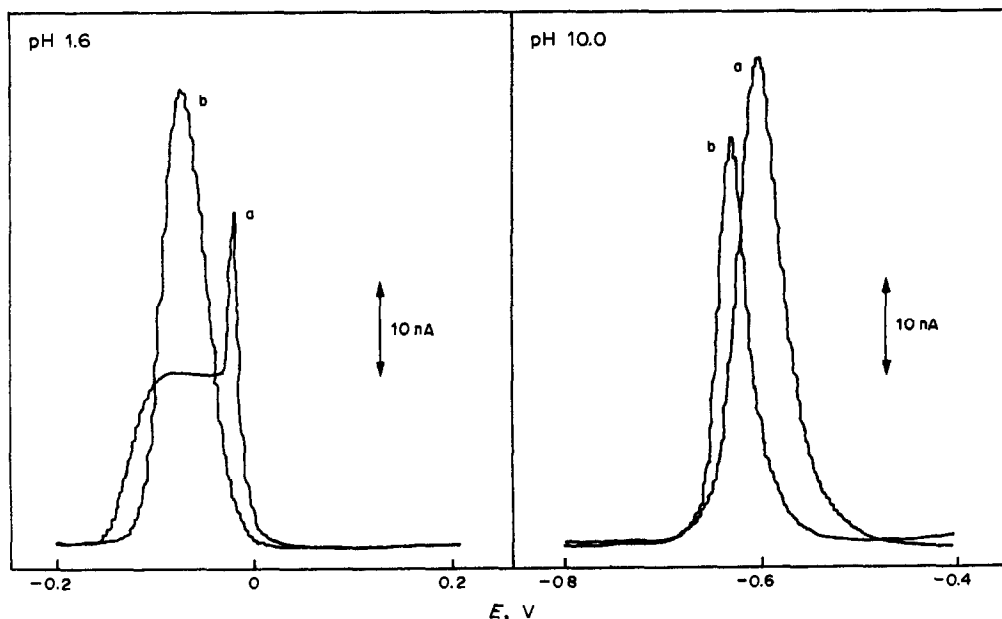


Fig. 1. Voltamperograms (DPP) of solutions of Sunset Yellow in the absence (a) and presence (b) of PVP in 0.12M Britton-Robinson buffer. [Sunset Yellow]: pH 1.6, $1.24 \times 10^{-6}M$; pH 10.0 $3.73 \times 10^{-6}M$.

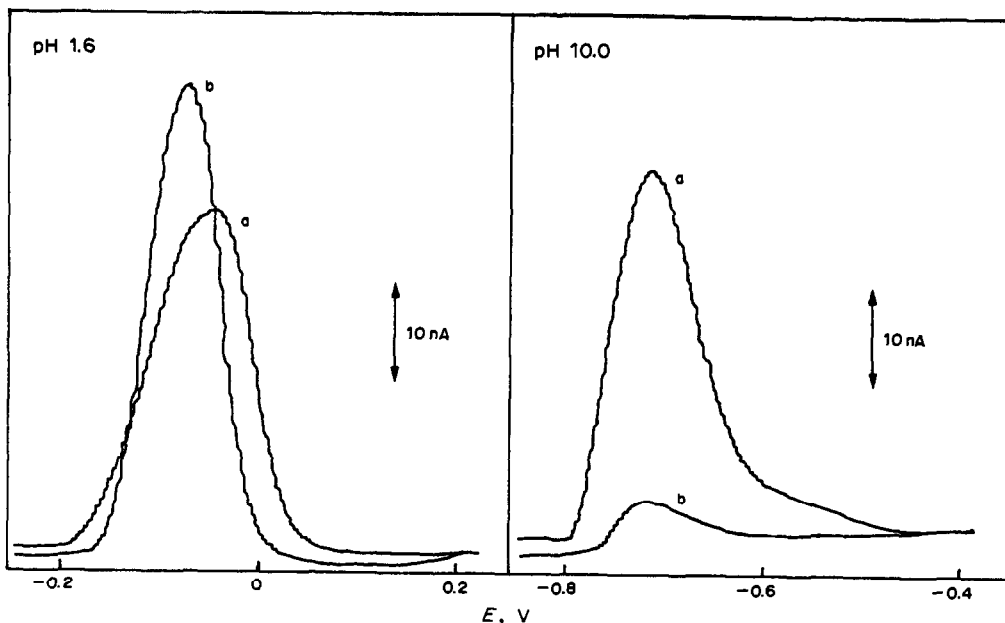


Fig. 2. Voltamperograms (DPP) of solutions of Tartrazine in the absence (a) and presence (b) of PVP in 0.12M Britton-Robinson buffer. [Tartrazine] $2.96 \times 10^{-6}M$.

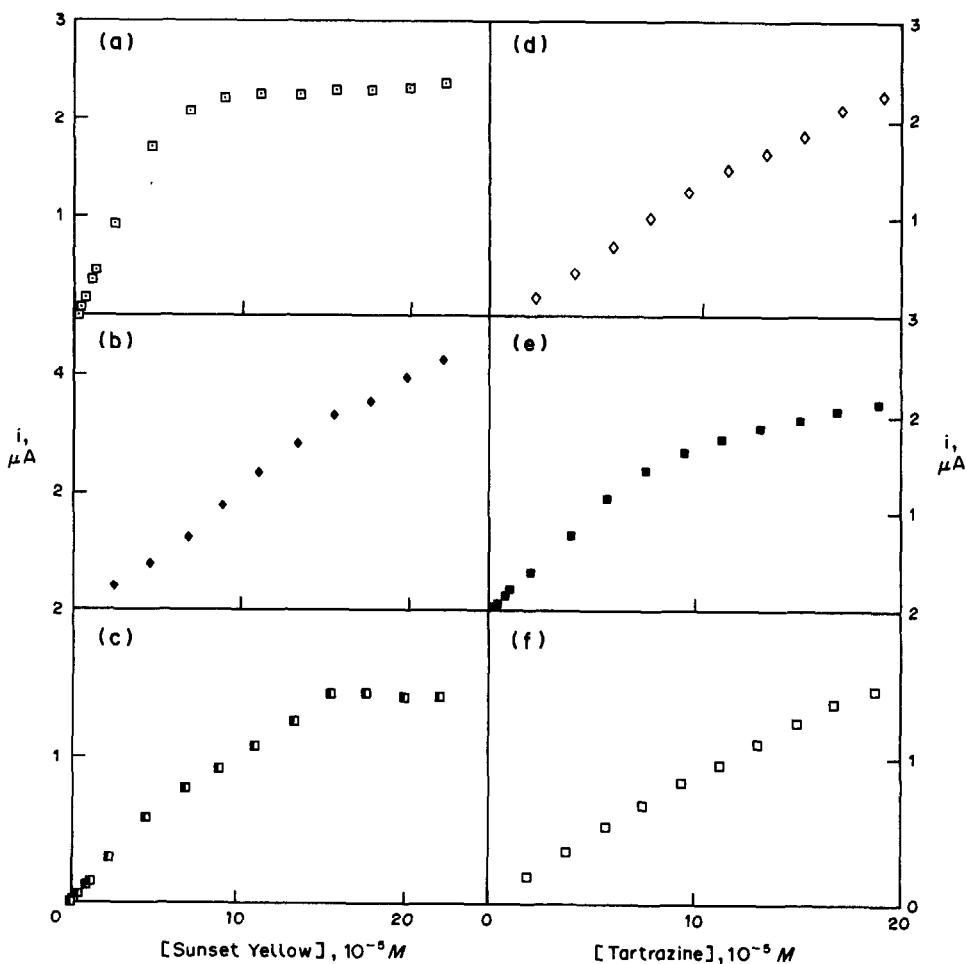


Fig. 3. Differential pulse polarography. Effect of the concentration of dye on peak current. Sunset Yellow: (a) pH 1.6 with PVP; (b) pH 10.0 without PVP, (c) pH 10.0 with PVP. Tartrazine: (d) pH 1.6 without PVP; (e) pH 1.6 with PVP, (f) pH 10.0 without PVP.

Table 1. Calibration data, precision and detection limits*

Dye	pH	Linearity range, M	Slope, $\mu A . l . mole^{-1}$	Intercept, μA	r	Limit of detection, M
Sunset Yellow	1.6	1.6×10^{-8} – 2.2×10^{-5}	4.56×10^4 (± 0.03)	–0.010 (± 0.003)	0.9997 ($n = 22$)	1.3×10^{-8}
	10.0	2.2×10^{-7} – 1.6×10^{-5}	1.34×10^4 (± 0.01)	0.0017 (± 0.0005)	0.9998 ($n = 16$)	4.5×10^{-8}
Tartrazine	1.6	1.9×10^{-7} – 1.9×10^{-5}	1.98×10^4 (± 0.02)	–0.006 (± 0.001)	0.9996 ($b = 19$)	3.0×10^{-8}

*Mercury column height, 70 cm; drop-time, 2 sec, scan-rate, 4 mV/sec; pulse amplitude –0.050 V.

trations, the peak currents are linearly related to the analyte concentrations but at higher concentrations the response is non-linear owing to adsorption phenomena. Something similar occurs at pH 10.0 but the zone controlled by adsorption appears at higher concentrations. At the same pH and in the absence of PVP, although the curve can readily be linearized, it is rather sigmoidal. Tartrazine at pH 1.6 and in the presence of PVP shows more clearly a behaviour typical of adsorption processes. In the other cases, the phenomenon is less pronounced.

Studies of the effect of some of the instrumental parameters point to the same: processes partially controlled by adsorption.

Polarographic determination of Sunset Yellow and Tartrazine

Sunset Yellow can be determined by DPP in the presence of 0.02% PVP at pH 1.6 or 10.0, with 0.12M Britton–Robinson buffer as supporting electrolyte. Tartrazine can also be determined in the presence of PVP at pH 1.6, with the same supporting electrolyte. It should be noted that in the presence of PVP at pH 10.0 Sunset Yellow shows a good polarographic signal, whereas that of Tartrazine is practically zero.

Table 1 shows the data for the concentration ranges used.

Simultaneous determination

To study the applicability of the method, synthetic samples of the two dyes, in different proportions, were analysed. It was observed that at pH 10.0 it is possible to determine Sunset Yellow in the presence of up to 10 times as much Tartrazine. The determination of Tartrazine in the presence of Sunset Yellow was only possible at pH 1.6 and when the Sunset Yellow interferent/Tartrazine ratio was less than 1. In all cases, the recovery was close to 100%.

Determination of Sunset Yellow and Tartrazine in soft drinks

The proposed method was tested for the determination of these dyes in a soft drink and in two orange and lemon juice concentrates. In all cases, 1.0 ml of 1% PVP solution plus a solution of 0.6M Britton–Robinson buffer was added to 1.0 ml of the sample; the pH was modified where necessary and the volume brought accurately to 50.0 ml. Measurement was done by the standard addition method. The content of Sunset Yellow was determined at two pH values and that of Tartrazine only at pH 1.6.

The amounts of Sunset Yellow found were 6.5 ppm in the soft drink (also containing Ponceau Red), 17.8 ppm in the orange concentrate and 7.5 in the lemon concentrate. These values were in agreement with the manufacturer's specifications.

Acknowledgement—This research was supported by the CICYT (Project No. PA86-0113).

REFERENCES

1. J. A. Yeransian, K. G. Sloman and A. K. Foltz, *Anal. Chem.*, 1985, **57**, 278R.
2. H. Zeng, A. Wang, X. Min and C. Fan, *Shipin Yu Fajiao Gongye*, 1983, **4**, 20; *Chem. Abstr.*, 1984, **101**, 71131h.
3. H. Sasak, *Shoukuhin Eiseigaku Zasshi*, 1979, **20**, 93; *Chem. Abstr.*, 1979, **91**, 106687y.
4. R. B. Patel, M. R. Patel, A. A. Patel, A. K. Shah and A. G. Patel, *Analyst*, 1986, **111**, 577.
5. J. P. Hart and W. F. Smyth, *ibid.*, 1980, **105**, 929.
6. A. G. Fogg and D. Bhanot, *ibid.*, 1980, **105**, 868.
7. A. G. Fogg and A. M. Summan, *ibid.*, 1984, **109**, 1029.
8. A. G. Fogg, A. A. Barros and J. O. Cabral, *ibid.*, 1986, **111**, 831.
9. A. G. Fogg and D. Bhanot, *ibid.*, 1980, **105**, 234.
10. A. G. Fogg and K. S. Yoo, *ibid.*, 1979, **104**, 1087.
11. A. A. Barros, *ibid.*, 1987, **112**, 1359.
12. A. A. Barros, J. O. Cabral and A. G. Fogg, *ibid.*, 1988, **113**, 853.
13. T. M. Florence, *J. Electroanal. Chem.*, 1974, **52**, 115.

A SIMPLE SOLID-STATE pH GLASS ELECTRODE

K. L. CHENG and NAILA ASHRAF

Department of Chemistry, University of Missouri-Kansas City,
Kansas City, Missouri 64110, U.S.A.

(Received 24 December 1989. Revised 21 February 1990. Accepted 28 February 1990)

Summary—A modernized version of the Thompson electrode is described. A copper wire is connected to the inner surface of the membrane of a glass electrode with a conductive adhesive resin.

In 1932, Thompson¹ pioneered a glass electrode with a comparatively thick wall and a direct metal connection to the glass, but it was found to be less accurate than the type of electrode that had an internal electrolyte solution. Early patents were also issued on the use of metals and alloys for electrical contact with the glass.^{2,3} Bates⁴ has pointed out that electrodes of this type have not been found as satisfactory as those with inner reference electrodes and have never been widely adopted. Recently, Parr *et al.*⁵ reported a relatively complicated solid-state pH glass electrode that exhibited near Nernstian response (>50 mV/pH). Here we present a simple one with neither an internal solution nor an inner Ag/AgCl reference electrode. A piece of copper wire attached to the inner surface of glass membrane with silver paste (Johnson Matthey conductive adhesive resin, A500H) serves as the reference electrode. A slope of 58.3 mV/pH was obtained for the pH range 1–10. The contact area between the silver paste and the inner glass surface is not important. The time for discharging the electrode potential is

less than 0.1 sec, and that for recharging is 10–20 sec, depending on the pH. This new solid-state pH glass electrode, which behaves in an identical manner to a commercial pH glass electrode could find application as a micro-electrode and in pH measurement at low and high temperature. It is also inexpensive. We have previously stated that the internal solution of an ion-selective electrode is unnecessary; it serves only as a contact between the inner membrane and the reference electrode. Now a piece of copper wire replaces the internal reference electrode.

REFERENCES

1. M. R. Thompson, *Bur. Stds, J. Research*, 1932, **9**, 833.
2. P. A. Kryubov and A. A. Kryubov, *Russian Patent*, 51,509, 31 July, 1937.
3. H. Bender and D. J. Pye, *U.S. Patent*, 2,117,596, 17 May, 1938.
4. R. G. Bates, *Determination of pH*, 2nd Ed., p. 377, Wiley, New York, 1973.
5. R. A. Parr, J. C. Wilson and R. G. Kelly, *Anal. Proc.*, 1986, **23**, 291.

ADSORPTIVE VOLTAMMETRY AND HYDROLYSIS KINETICS OF LOPRAZOLAM MESILATE

J. ARCOS,* J-C. VIRE, A. EL JAMMAL and G. J. PATRIARCHE

Institut de Pharmacie, CP 205/6, Université Libre de Bruxelles, Boulevard du Triomphe,
1050 Bruxelles, Belgium

G. D. CHRISTIAN

Department of Chemistry, BG-10, University of Washington, Seattle, WA 98195, U.S.A.

(Received 3 October 1989. Revised 15 January 1990. Accepted 24 January 1990)

Summary—Loprazolam is determined by square-wave adsorptive stripping voltammetry in 0.04M ammonium chloride at pH 4.0, with an accumulation potential of -0.25 V vs. Ag/AgCl/KCl(s), at which the nitro group is reduced to a hydroxylamine group, with adsorption of the product. Cathodic stripping results in reduction of the azomethine bond of the adsorbed product. With a deposition time of 120 sec the detection limit is 2.5×10^{-10} M. The relative standard deviation is 1.7% for 5×10^{-8} M loprazolam (60 sec deposition). Reversible hydrolysis of the azomethine group occurs in sulfuric or hydrochloric acid. The reaction is initially first-order, followed by an apparent second-order reaction. First-order rate constants and half-lives are reported for 0.1–1 M sulfuric acid and 0.02 M hydrochloric acid media and compared with the values for nitrazepam hydrolysis.

Loprazolam mesilate 6-(2-chlorophenyl)-2,4-dihydro-2-[(4-methyl-1-piperazinyl)methylene]-8-nitro-1H-imidazo[1,2- α]-[1,4-benzodiazepin-1-one methylsulfonate, is a nitro derivative of the imidazobenzodiazepine family and is pharmacologically characterized by a slow absorption rate, low plasma level and slow excretion rate.¹

Adsorptive stripping voltammetry is a powerful electroanalytical technique for trace metal measurements² and trace levels of reducible and oxidable organic compounds such as drugs can also be determined.³ We have previously made an electrochemical study of loprazolam in aqueous and non-aqueous media,⁴ and have now developed a sensitive adsorptive stripping method for determination of this compound. Because of a hydrolysis reaction occurring in acidic media, we have also focused our study on the kinetics of the reaction.

EXPERIMENTAL

Instrumentation

The voltamperograms were recorded with a PAR model 384B Polarographic Analyzer coupled with a PAR 303A Static Mercury Drop

Electrode (medium size drop; area 0.017 cm²) and a Houston "Hiplot" DMP 40 Digital Plotter. All the potentials were referred to the Ag/AgCl/KCl(s) reference electrode and a platinum wire was used as counter-electrode. A PAR 305 stirrer was connected to the PAR 303A instrument. The peak heights were automatically recorded with the "tangent fit" capability of the instrument.

A PAR model 273 potentiostat-galvanostat coupled with the same mercury unit and an IBM XT computer was utilized for cyclic voltammetric measurements.

Reagents

Loprazolam mesilate, generously provided by Roussel (Bruxelles, Belgium) was used without further purification. All other reagents were of analytical grade except ammonium chloride, which was suprapure grade. The supporting electrolyte solution (0.04M ammonium chloride) and the loprazolam mesilate solution for the adsorptive stripping analysis were prepared in doubly-distilled water.

For the hydrolysis study, stock solutions of the compound were prepared in methanol on the day of use. The working solutions for adsorptive stripping measurements did not contain methanol, owing to the low concentrations investigated, but those for the hydrolysis studies contained 20% methanol.

*On leave of absence from Department of Analytical Chemistry, University College of Burgos, APD 231, Burgos, Spain.

Procedure

For adsorptive stripping voltammetry, 10 ml of the supporting electrolyte were deaerated for 12 min. The accumulation potential was then applied to a new mercury drop, the solution being stirred at 400 rpm. A negative-going scan was performed after an equilibration time of 5 sec, with the following parameters: deposition potential (and initial scanning potential), -0.25 V; scan rate, 200 mV/sec; frequency, 100 Hz; pulse amplitude, 20 mV. The same procedure was applied in the presence of the analyte.

RESULTS AND DISCUSSION

Adsorptive stripping voltammetry

Loprazolam exhibits three polarographic reduction waves in methanol/water solution,⁵ successively corresponding to reduction of the nitro group to a hydroxylamine group, reduction of the azomethine group, and reduction of the hydroxylamine group to the amine with reduction of the double bond between the *N*-methylpiperazine and imidazole groups. The reduction products of each wave exhibit adsorption phenomena. In addition, at $\text{pH} < 2.0$, hydrolysis of the azomethine group occurs, resulting in a splitting of the second wave owing to the appearance of a new wave arising from reduction of the benzophenone group formed during hydrolysis. The adsorptive stripping voltammetry is performed at $\text{pH} 4.0$ by adsorbing the hydroxylamine product from the first reduction, and reducing its azomethine group during stripping.

Supporting electrolyte. Acetate, phosphate, carbonate, ammonia and Britton-Robinson buffers, as well as sodium sulfate and perchlorate and ammonium chloride, were investigated as supporting electrolytes. Each medium allows the accumulation of the compound at the electrode surface, since a substantial increase in the response results from imposing a deposition step. However, taking into account the influence of both the pH and the nature of the supporting electrolyte, an ammonium chloride solution ($\text{pH} 4.0$) was selected since it gives rise to a lower background current as well as an enhanced stripping current. A $0.04M$ ammonium chloride concentration was selected, since it had no marked influence on either the intensity or shape of the recorded peak.

Operating parameters. Square-wave voltammetry was selected for further study because it gave ten times the current obtained in the

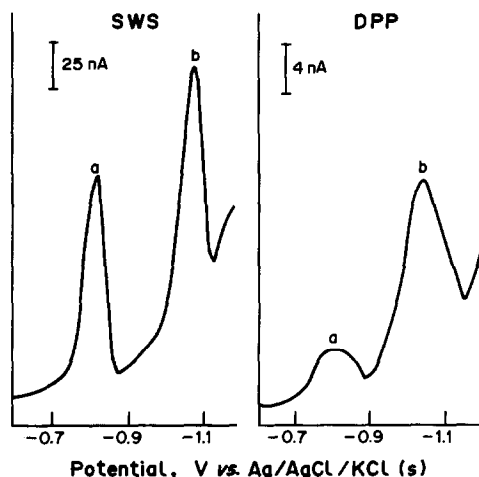


Fig. 1. Comparison of the voltammetric response of SWS and DPS. Loprazolam mesilate; $5.0 \times 10^{-8}M$; supporting electrolyte; $0.04M$ NH_4Cl ; $\text{pH} 4.0$; deposition time, 60 sec; deposition potential; -0.6 V; scan rate, mV/sec; SWS 200; DPS 8; pulse amplitude, SWS and DPS 20 mV; SWS frequency 100 Hz; (a) second peak; (b) third peak.

differential pulse mode (Fig. 1). The background current is also increased, but to a lesser extent.

The voltammetric response is mainly affected by the form and reproducibility of the waves. The peak current increased linearly with drop size and forced convection during the accumulation step also affected the resulting stripping peak current. The best conditions were found to be 400 rpm for a 0.017-cm^2 drop size. The peak height also changed linearly with pulse height up to 20 mV and with frequency up to 100 Hz.

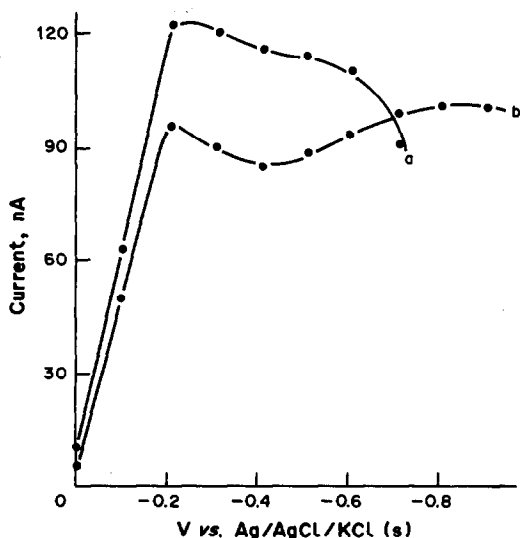


Fig. 2. Influence of the deposition potential on the SWS peak current: loprazolam mesilate; $5.0 \times 10^{-8}M$; supporting electrolyte; $0.04M$ NH_4Cl ; $\text{pH} 4.0$; deposition time; 60 sec; (a) second peak; (b) third peak.

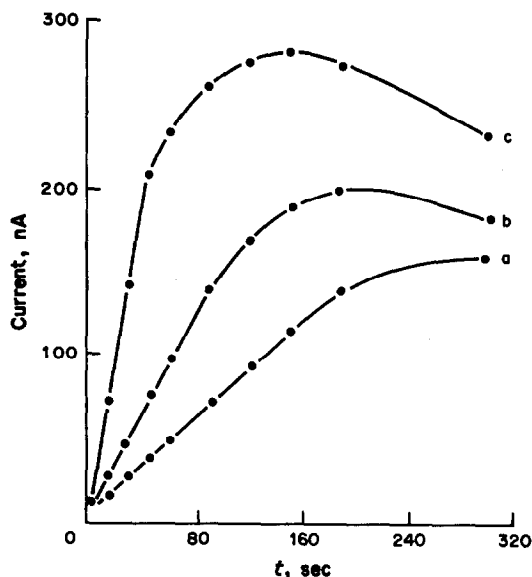


Fig. 3. Effect of the accumulation time on the SWS peak current: for loprazolam mesilate: supporting electrolyte; $0.04M$ NH_4Cl ; pH 4.0; deposition potential, -0.25 V; loprazolam mesilate (a) $2.5 \times 10^{-8}M$; (b) $5.0 \times 10^{-8}M$; (c) $1.0 \times 10^{-7}M$.

The dependence of the adsorptive stripping peak current on the accumulation potential in ammonium chloride is shown in Fig. 2. Accumulation potentials of -0.25 and -0.9 V were selected for determinations based on the second and third peaks, respectively. The proximity of the third peak to the discharge current of the supporting electrolyte, and the very negative potential required, caused poor reproducibility of the measurements and so the second peak was chosen for further studies.

The effect of accumulation time on the peak currents obtained at three different concentrations is shown in Fig. 3. For the lowest concentration, the current increased linearly with accumulation time up to about 180 sec. For the higher concentrations, the range of linear relation to time is decreased. The current

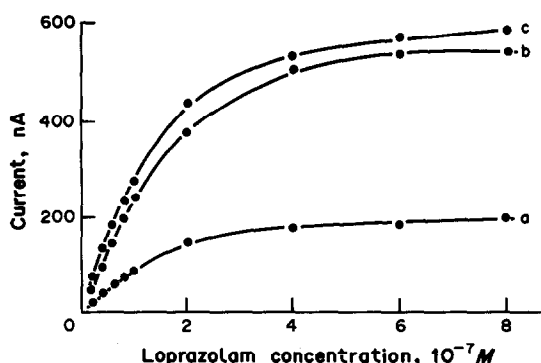


Fig. 4. Calibration plots of loprazolam mesilate: supporting electrolyte; $0.04M$ NH_4Cl ; pH 4.0; deposition potential, -0.25 V; deposition time; (a) 30 sec; (b) 60 sec; (c) 120 sec.

decreases at long accumulation times, a characteristic feature of adsorptive stripping with a stirred solution, since the molecules metastably adsorbed on the electrode surface are in a dynamic interaction with the solution, some being reabsorbed in a more favorable orientation and others being lost to the solution.⁶ This feature, together with the fact that a plateau is observed when the concentration is increased and a constant deposition time is used (Fig. 4), indicates that a monolayer is probably formed. The different levels of the current shown in Fig. 3, where different concentration peak heights are plotted against the deposition time, result from the reorientation of the molecules at the electrode surface.

Figures of merit. Peak currents were plotted against loprazolam concentration for accumulation times of 30, 60 and 120 sec (Fig. 4). Characteristics of these plots are summarized in Table 1. The detection limit was calculated as the concentration equivalent to a signal three times the standard deviation of the blank.

A concentration of $2.5 \times 10^{-10}M$ can be detected if a deposition time of 120 sec is used, which corresponds to 1.44 ng of the compound in 10 ml of solution.

Table 1. Characteristics of the calibration plots for loprazolam mesilate (second reduction peak) with different deposition times: $0.04M$ NH_4Cl ; pH 4.0; square-wave voltammetry; frequency 100 Hz; pulse amplitude 20 mV; scan rate 200 mV/sec

Deposition time, sec	Equation*	r	Linearity range, † M
30	$y = 0.960x + 0.92$	0.999	8.0×10^{-10} – 1.0×10^{-7}
60	$y = 2.50x - 0.32$	0.996	7.5×10^{-10} – 8.0×10^{-8}
120	$y = 4.06x - 0.23$	0.996	2.5×10^{-10} – 8.0×10^{-9}

*Units: y, nA; x, nM; intercept nA.

†The lower limit of the linearity range is the detection limit.

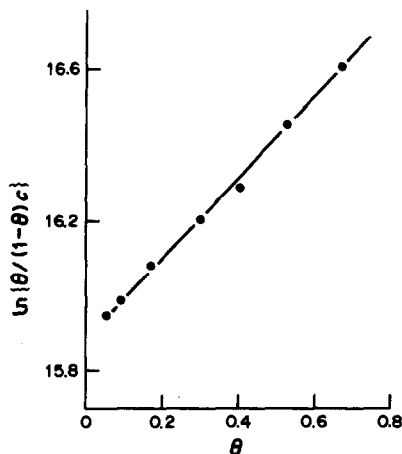


Fig. 5. Loprazolam mesilate adsorption isotherm: supporting electrolyte; $0.04M$ NH_4Cl ; pH 4.0; deposition potential, -0.25 V; deposition time; 120 sec; solution stirred at 400 rpm during the deposition step.

The reproducibility of the adsorption process was evaluated by ten repetitive experiments on a $5 \times 10^{-8}M$ loprazolam solution with a deposition time of 60 sec. The relative standard deviation was 1.7%.

Quantitative measurements. The results of quantitative measurements obtained after pre-concentration have been compared with those obtained without previous accumulation of the compound but with three different potential-time waveforms. These results are summarized in Table 2. The supporting electrolyte was selected with regard to peak current enhancement. Ammonium chloride alone, giving rise to a pH of 4.0, gives the lowest background current in the adsorptive method, whereas the pH 6.5 ammonia buffer used for the polarographic techniques shifts the supporting electrolyte

reduction far enough for a better defined third wave to be recorded.

Comparison of the square-wave peak currents for the second reduction step shows that the application of a 60-sec accumulation period results in only a tenfold increase of the current obtained with the adsorptive technique, and the correspondingly lower detection limit (by a factor of about a hundred) is attributed to the better baseline, allowing measurement of peak currents that are a tenth of these obtained by the same method without accumulation.

Taking into account that for the square-wave potential scan an HMDE was used, and a DME for scanning the differential pulse and the sampled d.c. potentials, the results obtained by the different techniques without preconcentration were compared. The square-wave mode gave a current that was 20 times that for the differential pulse polarograms, but the detection limits were about the same since d.p.p. provides a lower background current. Concentrations higher than the upper limit mentioned in Table 2 gave rise, for both techniques, to a linear relationship up to $1 \times 10^{-4}M$ but with a lower slope, especially when the square-wave mode was used. Uniform linearity up to this concentration level could be obtained only by use of sampled d.c. polarography.

Adsorption isotherms. The loprazolam adsorption isotherm (θ as a function of concentration where θ is the fraction of covered surface estimated from the ratio of the peak area to maximum peak area) was calculated. This was linear up to $8 \times 10^{-8}M$ for 120-sec accumulation time with a stirring rate of 400 rpm. The plots of $\ln [\theta/(1-\theta)c]$ as a function of θ

Table 2. Characteristics of the calibration plots for loprazolam mesilate measured by voltammetric techniques without accumulation step: $0.1M$ NH_4Cl/NH_3 buffer; pH 6.5; 20% methanol; SWV = square-wave voltammetry; DPP = differential pulse polarography; DCP = sampled direct current polarography; frequency of SWV, 100 Hz; pulse amplitude, SWV and DPP, 20 mV; scan rate (mV/sec), SWV, 200; DPP, 5; DCP, 5

Method	Peak/wave	Equation	r	Linearity, M
SWV	1st	$y = 1.37x - 53.1$	0.997	2×10^{-7} – 2×10^{-5}
	2nd	$y = 1.87x - 13.8$	0.998	1×10^{-7} – 1×10^{-5}
	3rd	$y = 1.51x + 19.8$	0.998	1×10^{-7} – 1×10^{-5}
DDP	1st	$y = 0.0750x - 4.28$	0.998	4×10^{-7} – 4×10^{-5}
	2nd	$y = 0.0650x - 1.03$	0.999	4×10^{-7} – 4×10^{-5}
	3rd	$y = 0.0750x + 0.001$	0.999	4×10^{-7} – 4×10^{-5}
DCP	1st	$y = 0.092x - 15.6$	0.998	1×10^{-6} – 1×10^{-4}
	2nd	$y = 0.101x + 12.8$	0.994	1×10^{-6} – 1×10^{-4}
	3rd	$y = 0.152x + 17.3$	0.998	1×10^{-6} – 1×10^{-4}

*Units: y , nA; x , μM ; intercept, nA.

†The lower limit of the range is the detection limit.

Table 3. Kinetic data of hydrolysis reactions in sulfuric and hydrochloric acid media: loprazolam $2 \times 10^{-4}M$, nitrazepam $2 \times 10^{-4}M$; cyclic voltammetry scan rate 200 mV/sec

Acid	Loprazolam		Nitrazepam	
	k, sec^{-1}	$t_{1/2}, \text{min}$	k, sec^{-1}	$t_{1/2}, \text{min}$
H ₂ SO ₄ , 1M	4.7×10^{-4}	24	2.2×10^{-5}	500
H ₂ SO ₄ , 0.25M	3.3×10^{-4}	40	2.8×10^{-5}	410
H ₂ SO ₄ , 0.1M	1.9×10^{-4}	50	2.8×10^{-5}	380
HCl, 0.02M	1.5×10^{-4}	76	2.6×10^{-5}	430

were linear up to $6 \times 10^{-9}M$ (slope = 1.13, intercept = 15.9) indicating a Frumkin-type adsorption.⁷ The validity of this plot at low concentrations under stirring conditions is supported by similar results reported by Zapardiel *et al.* for temazepam.⁸ From the intercept (equal to $\ln \beta$, the adsorption coefficient), β was estimated to be 7.7×10^6 l./mole.

Hydrolysis reaction

As with most of the benzodiazepines, the investigated compound undergoes reversible hydrolysis in acid media. The azomethine reduction wave decreases with time and a wave at a more negative potential increases simultaneously. The kinetics of the reaction was investigated at three sulfuric acid concentrations (0.10, 0.25 and 1.0M), cyclic voltammetry being used to follow the decrease in the azomethine peak with time.

Reaction order. A first-order reaction was observed in each case, as shown by the initial linear portion of a plot of \ln current *vs.* time. All three plots showed eventual curvature, at 10–20 min, which indicated a change in reaction order. The hydrolysis reaction is reversible. When a hydrolyzed solution of loprazolam is neutralized, the polarograms exhibit the features of the initial compound. This means that the hydroxyl group is not eliminated by the hydrolysis reaction and remains in the benzophenone structure, giving rise to an amino-alcohol.

One of the most likely causes of the deviation from first-order kinetics is that the reverse reaction is significant. This is also suggested by the fact that the hydrolysis reactions of benzodiazepines do not go to completion.⁹ Deviation from first-order kinetics can also be explained by postulation of second-order kinetics, and in fact graphs of $1/c$ *vs.* t were linear for 0.10 and 0.25M sulfuric acid media. As the second-order process does not become significant until the reverse reaction has begun, it is probable that the reaction appears to be second-order because

of a combination of the forward and back reactions. The hydrolysis is actually first-order, but the reversibility of the reaction produces second-order kinetics after a short period of time. The reaction then continues under the second-order kinetics until the back-reaction becomes significant and an equilibrium position is reached.

Rate constants. The first-order rate constants for the reaction of loprazolam in the three acid solutions are shown in Table 3. The half-life reported is that which would apply if first-order kinetics were valid for the entire reaction.

Nitrazepam hydrolysis. To assess the influence of the imidazole ring on the hydrolysis reaction, a comparative study of nitrazepam (1,3-dihydro-7-nitro-5-phenyl-2H-1,4-benzodiazapin-2-one) was made. In this case, the appearance of the benzophenone group was monitored since the disappearance of the original reduction peak is complicated by the occurrence of two reduction processes.⁵ A first-order reaction was observed for the entire reaction. The parameters are summarized in Table 3. The two compounds were also studied in hydrochloric acid at pH 1.6, which approximates to conditions in the human stomach.

Though for loprazolam the half-life decreased with increasing acidity, as expected, the reverse was the case for nitrazepam. This unexpected result is similar to that reported by Smyth and Groves⁹ for nitrazepam and other nitrobenzodiazepines. They reported a half-life of 672 min for nitrazepam in 1M hydrochloric acid and 652 min in 0.1M hydrochloric acid.

The loprazolam is hydrolyzed at a much faster rate than nitrazepam. This is attributed to the fact that there is a rigid cycle at the N–C bond of the imidazole ring, making it less stable.^{10,11}

Acknowledgements—The authors are indebted to S. A. Roussel Company and S. A. Produits Roche (Brussels, Belgium) who generously provided the drugs. Thanks are also expressed to the "Fonds National de la Recherche Scientifique" (FNRS Belgium) for help to one of us (G.J.P.),

and to the SPPS (Belgium Politic Research, ARC), Contract No. 86/91-89.

REFERENCES

1. J. Jochemsen, P. A. Van Rijn, T. G. M. Hazelzet, C. J. van Boxtel and D. D. Breimer, *Biopharm. Drug Dispos.*, 1986, **7**, 53.
2. J. Wang, *Stripping Analysis, Principles, Instrumentation and Applications*, VCH, New York, 1985; *Am. Lab.*, 1988, **17**, No. 7, 41.
3. R. Kalvoda and M. Kopanica, *Pure Appl. Chem.*, 1989, **61**, 97.
4. A. El Jammal, J.-M. Kauffmann, J.-C. Viré and G. J. Patriarche, *Pittsburgh Conference*, 6-10 March 1989, Atlanta, Abstract No. 586.
5. J. Arcos, A. El Jammal J.-C. Viré, G. J. Patriarche and G. D. Christian, *Electroanalysis*, 1990, **2**, in the press
6. J.-C. Viré, N. El Maali, G. J. Patriarche and G. D. Christian, *Talanta*, 1988, **35**, 997.
7. S. G. Mairanovskii, *Catalytic and Kinetic Waves in Polarography*, Plenum Press, New York, 1968.
8. A. Zapardiel, J. A. Perez Lopez, E. Bermejo and L. Hernandez, *Z. Anal. Chem.*, 1988, **330**, 707.
9. W. Smyth and J. A. Groves, *Anal. Chim. Acta*, 1981, **134**, 227.
10. J.-C. Viré and G. J. Patriarche, *J. Electroanal. Chem.*, 1986, **214**, 275.
11. J.-C. Viré, G. J. Patriarche and B. Gallo Hermosa, *Anal. Chim. Acta*, 1987, **196**, 205.

A NUMERICAL METHOD OF FINDING POTENTIOMETRIC TITRATION END-POINTS BY USE OF APPROXIMATIVE SPLINE FUNCTIONS

KRZYSZTOF REN

Faculty of Chemistry, A. Mickiewicz University, ul. Grunwaldzka 6, 60-780 Poznań, Poland

(Received 6 April 1988. Revised 6 February 1990. Accepted 14 February 1990)

Summary—A new numerical method of determining potentiometric titration end-points is presented. It consists in calculating the coefficients of approximative spline functions describing the experimental data (e.m.f., volume of titrant added). The end-point (the inflection point of the curve) is determined by calculating zero points of the second derivative of the approximative spline function. This spline function, unlike rational spline functions, is free from oscillations and its course is largely independent of random errors in e.m.f. measurements. The proposed method is useful for direct analysis of titration data and especially as a basis for construction of microcomputer-controlled automatic titrators.

Difficulties in using various methods of determining potentiometric titration end-points have resulted in attempts to develop a method which would be suitable for analysis of any potentiometric titration curve and allow the use of computer techniques for processing the measurements. The fulfilment of this last condition is important in the construction of automatic titrators controlled by microcomputers.

The success of the method depends on the choice of appropriate mathematical tools. A very interesting and useful approach is the use of spline functions.¹ Determination of titration curves by means of spline functions has been attempted several times.²⁻⁵ It is assumed here that the titration end-point coincides with the inflection point of the titration curve, which in most cases appears to be true.⁶

In an earlier method,² the titration curve was described by means of a rational spline function, and the zero points of the second derivative of this function were calculated, and taken as giving inflection points of the curve. This procedure had some disadvantages, however. The rational spline function is constrained to pass through all the points and therefore contains micro-oscillations because of errors in measurement.

As a result of these oscillations, inflection points were also found at places where, according to the stoichiometry of the reaction, they should not occur. Hence it was necessary to introduce an additional calculation stage which

would verify the calculated inflection points so that appropriate titration end-points could be chosen. The value of the first derivative at the inflection points of the spline functions was taken as the criterion for this selection. The inflection point coinciding with the extremum of the first derivative (the highest or lowest, depending on the direction of the titration curve) was accepted as the titration end-point.

When the titration curve has two or more inflection points, corresponding to the titration of more than one component in the solution, the criterion of the minimum or maximum value of the first derivative is insufficient, and this significantly curtails the applicability of the method to the automatic analysis of titration curves of mixtures, *i.e.*, to a fully automatic analysis which does not require any visual interpretation of the titration graph.

A better description, free from the above-mentioned flaws, is ensured by the use of approximative spline functions,¹ which eliminates the oscillations caused by measurement errors (mainly those in the indicator-electrode potential, as discussed elsewhere²).

Approximative spline functions pass between the data points at distances ensuring optimal smoothing of the curve. An example of the difference between curves produced by approximative and rational spline functions is shown in Fig. 1. The inflection points of the titration curve are taken as the zero points of the second derivative of the approximative spline function.



Fig. 1. Examples of the approximative spline function (a) and rational spline function (b) fitted to the same set of points.

THE APPROXIMATIVE SPLINE FUNCTION¹

Let

$\bar{\gamma}$ be a linear operator such that $\bar{\gamma}: S \rightarrow X$, and

γ a linear operator such that $\gamma: S \rightarrow Y$,

where $X, Y, S, (S \in X, S \in Y)$ are linear spaces. If it exists, the spline function s_0 ($s_0 \in S$) which is the solution of

$$\min_{s \in S} [\|\bar{\gamma}(s)\|_X + \rho \|\gamma(s) - f\|_Y] \quad (1)$$

is called the approximative spline function for the function $f \in Y$ in the sense of the operators γ and $\bar{\gamma}$, for a given value of the parameter ρ (a numerical coefficient); f is an element of the set Y . If X, Y are Hilbert spaces, then we can make statements guaranteeing the existence and unicity of the approximative spline function from the definition above.

Existence

The necessary and sufficient condition for the existence of the approximative spline function $s_0 \in S$ for fixed $f \in Y$ and ρ , in the sense of the definition, is that

$$N(\bar{\gamma}) + N(\gamma), \quad [N(a) = \{x \in X: a(x) = 0\}]$$

for the sum of the kernels of operators γ and $\bar{\gamma}$ should be a closed set.

Unicity

The sufficient condition for unicity of the solution of equation (1) is that the intersection of the sets $N(\gamma)$ is an empty set:

$$N(\bar{\gamma}) \cap N(\gamma) = \{0\}$$

Note that the existence and unicity of the spline function that is the solution of (1) do not depend upon the value of ρ .

We will now show what form the solution $s_0 \in S$ takes when particular spaces and operators are selected.

Let

$$X = \left\{ f: f^{(\alpha-1)} \text{ absolutely continuous}; \right.$$

$$\left. \int_a^b |f^{(\alpha)}(t)|^2 dt < \infty \right\}$$

$$Y = R^n, \quad S \equiv X$$

$$\bar{\gamma}: S \rightarrow X \quad \bar{\gamma}(g) = g^{(\alpha)}$$

$$\gamma: S \rightarrow Y \quad \gamma(g) = [g(x_1), g(x_2), \dots, g(x_n)]$$

$$a < x_1 < x_2 < \dots < x_n < b$$

Then $N(\bar{\gamma}) = \Pi_{\alpha-1}$, the space of polynomials of the degree $\alpha - 1$, and $N(\gamma) = \{0\}$. The conditions for solution of the problem (1) given above are fulfilled. The solution of the problem

$$\min_{s \in S} \left\{ \int_a^b [s^{(\alpha)}(t)]^2 dt + \rho \sum [s(x_i) - f(x_i)]^2 \right\} \quad (2)$$

is a polynomial spline function s_0 fulfilling the following conditions:

$$1. \quad s_0 \in \Pi_{2\alpha-1} \langle x_i, x_{i+1} \rangle; i = 1, \dots, n-1$$

$$2. \quad s_0 \in C^{2\alpha-2} \langle a, b \rangle$$

$$3. \quad s_0(x_i) = f(x_i)$$

$$+ \frac{1}{\rho} (-1)^{\alpha} [s_+^{(2\alpha-1)}(x_i) - s_-^{(2\alpha-1)}(x_i)]$$

$$4. \quad s_0^{(j)}(x_1) = s_0^{(j)}(x_n) = 0;$$

$$j = 0, \dots, 2\alpha - 1$$

Condition (3) explains how far the value of $s(x_i)$ differs from the value of $f(x_i)$.

PRACTICAL REALIZATION OF CALCULATIONS

During potentiometric titration a set of data originates in the form of pairs of numbers (V_i, E_i) where V_i is the volume of titrant added and E_i the EMF measured, for the i th point in the titration. In the computational process the spline function will treat the variable V as X and the variable E as Y [in (1)]. It is known that the theoretical titration curve passes near, but not necessarily through, the measurement points, because the data include errors, as discussed above. Thus, the titration curve should pass through points having co-ordinates $(V_i, E_i + \epsilon_i)$ where ϵ_i is the error in measurement E_i . Although the values of the errors ϵ_i are unknown, a mathematical description has to take their existence into account. If the

deviation of the curve from the measurement points is expressed by the so-called root mean square deviation

$$\sum_{i=1}^n \epsilon_i^2 = \sum_{i=1}^n [E_i - s(V_i)]^2 \quad (3)$$

where $s(V)$ is the function describing the titration curve, and the measure of smoothness is

$$\int_{V_1}^{V_n} [s''(V)]^2 dV \quad (4)$$

then we may search for the curve which gives the best compromise between the smoothness (4) and minimization of (3). Mathematical formulation of this problem gives

$$\min_{s \in C^2\langle V_1, V_n \rangle} \left[\int_{V_1}^{V_n} [s''(V)]^2 dV + \sum_{i=1}^n (E_i - s(V_i))^2 \right] \quad (5)$$

where $C^2\langle V_1, V_n \rangle$ denotes the set of all functions that can be twice differentiated continuously in the interval $\langle V_1, V_n \rangle$. For each value of $\rho > 0$ we can, according to (1), obtain a polynomial spline function of the third degree as a solution of this minimization problem.

Numerical solution of (5) proceeds as follows:

$$s(V) = \frac{1}{6} \left\{ e_i \left(\frac{V_{i+1} - V}{h_i} \right) + e_{i+1} \left(\frac{V - V_i}{h_i} \right) + m_i \left[\frac{(V_{i+1} - V)^3}{h_i} \right] - m_i \left(\frac{V_{i+1} - V}{h_i} \right) + m_{i+1} \left[\frac{(V - V_i)^3}{h_i} \right] - m_{i+1} \left(\frac{V - V_i}{h_i} \right) \right\} \quad (6)$$

where

$$h_i = V_{i+1} - V_i; \quad e_i = E_i - \rho p_i; \\ p_i = s''_+(V_i) - s''_-(V_i); \quad m_i = s'(V_i)$$

A significant role in the mathematical description of the measurement points is played by ρ , which controls the course of the spline function. This parameter has great importance in balancing the smoothness against the root mean square deviation. In establishing its value two extreme tendencies have to be taken into account.

(1) If we know that the curve has to pass close to the measurement points (V_i, E_i) , i.e., the errors ϵ_i are small, then greater importance

should be attached to the root mean square deviation, so the value of ρ in (5) should be small.

(2) If we must smooth large oscillations in the data (ϵ_i large), then ρ should be large.

It should be stressed that the numerical value given to ρ depends on the individual set of data (V_i, E_i) . Attempts to use the same value of ρ for all data sets may lead to spline functions that are inappropriate to the problem under consideration.

Several ways are known of establishing appropriate values of ρ ,⁷ but most are based on determination of the values of individual large matrices. This is a time-consuming process requiring a computer with a large memory and is uneconomical for use with a microcomputer. Another method has been suggested,⁸ based on analysis of the components of (5) as a function of the variable ρ . Such an analysis is easy to do on a microcomputer: after evaluating (5) for $\rho = 0.01, 1$ and 100 it is possible to establish a value ρ^* which maximizes the expression

$$\frac{1}{\rho} \sum_{i=1}^n [E_i - s(V_i)]^2 \quad (7)$$

The polynomial spline function calculated for the parameter ρ^* smooths the titration curve and at the same time eliminates points with large measurement errors, provided that they are not too numerous.

DESCRIPTION OF THE PROGRAM

The program used for calculation of titration end-points was designed according to the flow-chart in Fig. 2. Data may be entered from the keyboard, or read directly via the interface from the pH-meter and automatic burette in the case of automatic titrations controlled by a microcomputer. Then spline functions are calculated for three values of ρ (0.01, 1 and 100). Next follows the calculation of the optimal value ρ^* and the coefficients of the corresponding optimal spline function.

The next step is finding all zero points of the second derivative of this spline function and outputting their volume co-ordinates as end-points of the titration. The program also has graphics segments that show the measurement points, plot the spline function and mark the titration end-points. The program allows the value of the spline function to be calculated for any value of V in the interval (V_0, V_n) . A program listing is available on application.

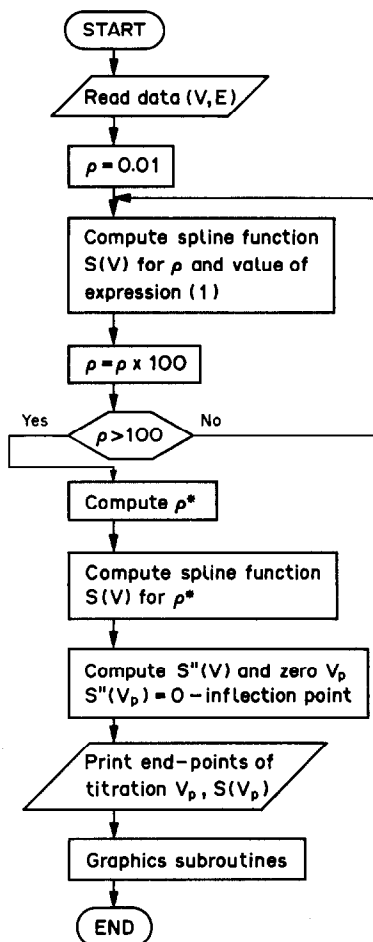


Fig. 2. Flow-chart of the program for calculating potentiometric titration end-points by use of approximative spline functions.

RESULTS

The smoothing properties of the proposed spline function are shown in the titration curve in Fig. 4b. Random measurement errors, even those having relatively large values, should have little effect on the shape of the approximative spline function, provided that the number of error-bearing points is small relative to the total number of points on the titration curve. This is an advantage of the proposed method and the main difference between it and that using rational spline functions.² In the latter case each measurement error resulted in a new inflection point, which later necessitated selection of the true end-point (e.g., from 28 and 22 inflection points for the curves in Figs. 3a and 3b, respectively). On the plot of the titration curve in Fig. 4b, the measurement points with errors have been marked.

Table 1 shows the titration end-points calculated from measurement points ($\Delta V = 0.1$ ml),

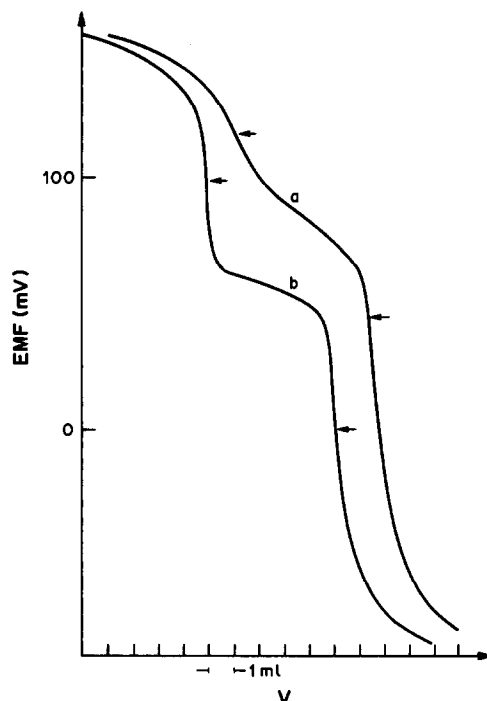


Fig. 3. Complexometric titration curves for pairs of cations titrated with $10^{-2}M$ BADMF (details in Table 3). (a) $10^{-3}M$ $Cu^{2+} + 10^{-3}M$ Zn^{2+} , (b) $10^{-3}M$ $Cu^{2+} + 10^{-3}M$ Mn^{2+} .

for which the experimental EMF has been deliberately loaded with a random error. A significant difference in the results can be observed only in the case of gross errors introduced very close to the theoretical end-point.

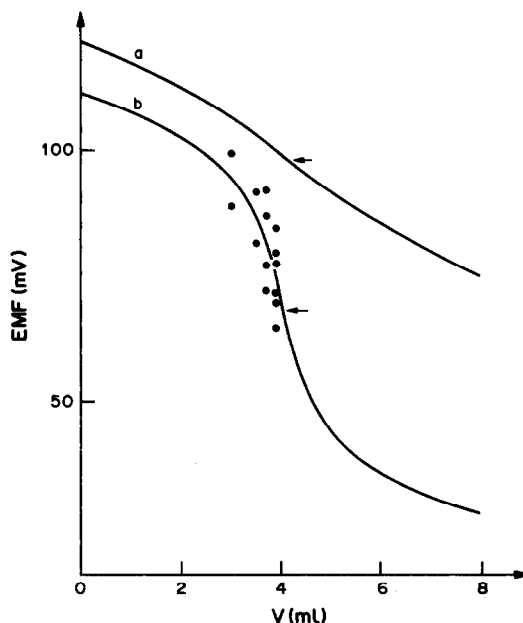


Fig. 4. Curves for the complexometric titration of copper(II) with $10^{-2}M$ BADMF (details in Table 3). (a) $10^{-3}M$ $Cu^{2+} + 10^{-1}M$ Ni^{2+} , (b) $10^{-3}M$ Cu^{2+} .

Table 1. The effect of measurement errors on the calculation of titration end-points (titration of $10^{-3}M$ Cu^{2+} with BADMF at pH 6 with Cu^{2+} -ISE, $\Delta V = 0.1$ ml, theoretical end-point 4 ml)

Volume at which error was introduced, ml	Introduced error in EMF, mV	Calculated end-point, ml
—	—	4.055
3	+5	4.052
3	-5	4.061
3.5	+5	4.037
3.5	-5	4.077
3.7	+5	4.047
3.7	-5	4.074
3.7	+10	4.044
3.7	+10	4.089
3.9	+3	4.071
3.9	-3	4.036
3.9	+5	4.078
3.9	-5	4.014
3.9	+10	4.092
3.9	-10	3.87

Table 2. The effect of the separation of measurement points on the calculation of the end-points for the titration in Table 1

Separation measurement points, ml	Titration end-point, ml
0.1	4.055
0.2	4.057
0.3	4.052
0.4	4.061
0.5	4.072

Table 3. Results for titrations with $10^{-2}M$ BADMF (Cu^{2+} -ISE, pH 6, $\Delta V = 0.1$ ml)

Sample	End-points, ml			
	Theory	Approximative spline	Rational spline	Graphical
$10^{-3}M$ Cu + $10^{-3}M$ Zn*	5, 10	4.95, 10.09	4.93	4.9, 10.7
$10^{-3}M$ Cu + $10^{-3}M$ Mn*	5, 10	5.07, 10.21	10.28	4.0, 10.5
$10^{-3}M$ Cu + $10^{-1}M$ Ni†	4	4.04	4.02	4.3
$10^{-3}M$ Cu†	4	4.05	4.06	4.1

*Figure 3.

†Figure 4.

Table 2 shows end-points calculated for the curve in Fig. 4b, at different separations of the measurement points. The results agree closely, indicating that the spline function is not highly sensitive to the selection of points. It should be stressed that the titration curve in Fig. 4b is moderately symmetrical, like most curves encountered in analytical practice. In the case of titration curves that are less symmetrical about the inflection point, the accuracy of calculations of the end-points will depend more strongly on the distance between the measurement points.

Figure 3 shows curves for the titration of copper in the presence of either zinc or manganese, with benzylamino-*N,N*-di(methane-phosphonic) acid [BADMF].^{9,10} and use of a Crytur 29-17 copper ion-selective electrode as indicator. In spite of distortions of the curves caused by interfering ions, the end-points (Table 3) calculated from the approximative spline function are close to the theoretical values and also to those determined graphically or by means of rational spline functions.² Figure 4

shows the effect of nickel on the titration of copper with BADMF. The end-points are generally accurate (Table 3), except for that determined graphically for the curve distorted by the presence of nickel.

Acknowledgement—The investigations were financially supported by the Ministry of Science, Higher Education and Technology, Project No. MR.I.32.

REFERENCES

1. P.-J. Laurent, *Approximation et optimisation*, Herman, Paris, 1972.
2. K. Ren and A. Ren-Kurc, *Talanta*, 1986, **33**, 641.
3. J. Hăzi, L. Daruházi, O. Pinter and Zs. Szakály, *Microchim. Acta*, 1986 **II**, 379.
4. O. Glatter and H. Greschonig, *ibid.*, 1986 **II**, 389.
5. *Idem*, *ibid.*, 1986 **II**, 401.
6. W. Lund, *Talanta*, 1976, **23**, 619.
7. G. Wahba and S. Wold, *Commun. Stat.*, 1975, **4**, 1.
8. A. Ren-Kurc, *Criterion of Parameter Choice for Approximating Spline Functions in Hilbert Spaces*, *Matematyka Stosowana*, in press.
9. W. Szczepaniak and K. Kuczyński, *Chem. Anal. (Warsaw)*, 1978, **23**, 273.
10. K. Ren, *ibid.*, 1986, **31**, 27.

PLASTIC MEMBRANE ELECTRODES RESPONSIVE TO BETA-BLOCKER DRUGS

ZONG-RANG ZHANG, DAN YI MAO, YI XIN LI and VASILE V. COȘOFREȚ*

Department of Chemistry, Shanghai Teacher's University, 10 Guilin Road, Shanghai,
People's Republic of China

(Received 7 January 1989. Revised 26 January 1990. Accepted 5 February 1990)

Summary—The construction and performance characteristics of ion-selective PVC membrane electrodes for metoprolol, propranolol and timolol are described. The electrodes, based on ion-pair complexes with dinonylnaphthalenesulphonate or with tetra(2-chlorophenyl)borate show near-Nernstian responses down to $10^{-5}M$ drug concentration. Their selectivity relative to various inorganic and organic cations is reported. Direct potentiometry is used to determine beta-blocker drugs both in aqueous solutions and pharmaceutical preparations, with good results.

In recent years, ion-selective membrane electrodes have been used more and more in drug quality control.¹⁻⁶ No pharmacopoeia has yet introduced their use for assays, though this will probably be done in the next few years.

Selinger and Staroscik⁷ have described the behaviour of a PVC potassium ion-selective membrane electrode towards some beta-blocker agents (bambethan, oxprenolol, propranolol), and others have characterized coated-wire electrodes sensitive to propranolol⁸ and acebutolol.⁹

The present paper reports the use of the lipophilic ion-pairs of beta-blockers such as metoprolol, propranolol and timolol with dinonylnaphthalenesulphonate (DNNS) or tetra-(2-chlorophenyl)borate, as the electroactive materials for making beta-blocker responsive plastic membrane electrodes; these have proved useful in pharmaceutical analysis.

The official standard methods for the assay of beta-blockers in pharmaceutical preparations are based on extraction followed by spectrophotometry.¹⁰ Analytical methods based on gas chromatography,^{11,12} HPLC and TLC,¹³⁻¹⁶ and spectrometry¹⁷ have also been developed for assay of beta-blockers in biological samples.

The electrode methods proposed in this paper for assaying beta-blockers in the bulk drug substances as well as in pharmaceutical preparations have the advantages of simplicity, reduced analysis time, and economy.

EXPERIMENTAL

Apparatus

Direct potentiometric measurements on magnetically stirred solutions were performed at room temperature with a pX-meter (Rex, pXSJ-216, Shanghai, China), the beta-blocker selective electrode and a saturated calomel electrode (SCE) (Model 217, Dian Guang, Shanghai, China). The pH measurements were made with a combination glass electrode (Model 231, Dian Guang) and an SCE.

Reagents

All reagents used were of analytical-reagent grade. The beta-blockers used were obtained from the People's Republic of China pharmaceutical industry, and assumed to be pure.

Beta-blocker stock solutions

Metoprolol tartrate and propranolol hydrochloride solutions (0.1M), and timolol maleate (0.01M) were prepared by dissolving the required amounts of the pure substance in water and contained enough acetate buffer to keep the pH (5.0) and ionic strength (0.1M) constant.

Electrode preparation and handling

The PVC membrane electrodes were constructed as described previously¹⁸ (with Aldrich high molecular-weight grade PVC dissolved in tetrahydrofuran) except that the electroactive material used was either dinonylnaphthalenesulphonic acid (DNNS) or tetra(2-chlorophenyl)borate (potassium salt) (ClTPB). The

*Author for correspondence. Present address: Institute of Chemical and Pharmaceutical Research Bucharest, 74351-Sos. Vitan 112, Bucharest-3, Romania.

internal reference solutions were 0.01M solutions of the respective beta-blocker at pH 5.0 (acetate buffer). The DNNS or C1TPB in the PVC membrane was converted into the beta-blocker form by soaking the electrode in a 0.01M solution of the drug for 24 hr. When not in use, the electrodes were stored in air.

Electrode characteristics

The performances of the electrodes were investigated by measuring the e.m.f. values in 10^{-1} – 10^{-6} M metoprolol and/or propranolol and 10^{-2} – 10^{-6} M timolol solutions. Potentials were recorded when stable readings were obtained.

Direct potentiometric measurement of beta-blocker drugs in the $\mu\text{g/ml}$ range

The appropriate drug electrode and an SCE were immersed in the aqueous sample solution (25.0 ml) at pH 5.0 (acetate buffer). After the potential had been brought to equilibrium by stirring, the e.m.f. value was recorded, 2.5 ml of a 0.01M standard solution of the drug were added and the change in reading (accuracy ± 0.1 mV) was recorded and used to calculate the concentration of the drug.

Direct potentiometric measurement of propranolol in tablets

Propranolol tablets were analysed by finely powdering ten tablets from the same lot. A portion of the powder equivalent to about 5 mg of propranolol was transferred to a 50-ml standard flask, 5.0 ml of acetate buffer (pH 5.0) were added and the solution was made up to volume with distilled water. This solution was divided into two 25-ml portions. The indicator and reference electrodes were immersed in the test solution, and after electrode equilibration by stirring, and recording of the e.m.f., 2.5 ml of 0.01M propranolol hydrochloride standard solution (pH 5.0, acetate buffer) were added and the change in e.m.f. was recorded and used to calculate the propranolol content of the tablets.

RESULTS AND DISCUSSION

Membrane materials

Beta-blocker drugs react with DNNS or C1TPB to form stable water-insoluble ion-pairs which are very soluble in the membrane phase. The ion-pairs were obtained *in situ* by soaking DNNS/PVC or C1TPB/PVC membranes in 0.01M drug solution. In all cases *o*-nitrophenyloctyl ether (*o*-NPOE) was used as the plasticizer. Variation of the concentration of electroactive-site carrier in the membrane within the range 2–8% did not produce significant differences in the main characteristics of the electrodes. For further investigations and applications, the membrane compositions used were 5.7% electroactive-site carrier, 63.0% *o*-NPOE and 31.3% PVC (w/w).

Calibration data

The critical response characteristics of these membrane electrodes are summarized in Table 1. Calibrations were done at constant pH and ionic strength, provided by using acetate buffer, pH 5.0. The highest concentrations of metoprolol and propranolol used for calibration were 0.1M, and for timolol 0.01M (its solubility in water is lower than that of metoprolol and propranolol). All the electrodes can be used for drug concentrations down to 10^{-5} M; the low detection limits indicate the feasibility of using them to determine traces of beta-blocker drugs in various samples.

Effect of pH

The effect of pH on the potentials of the electrodes was examined by measuring the e.m.f. of the cells in beta-blocker solutions in which the pH was varied by adding appropriate amounts of hydrochloric acid and/or sodium hydroxide solution. At pH values in the ranges 3.5–7.5, 2.5–7.5 and 2.0–8.0 for the metoprolol, propranolol and timolol electrodes, respectively, no significant changes in the membrane potentials were observed (in all cases, for 10^{-3} M

Table 1. Response characteristics for beta-blocker membrane electrodes

Parameter	Metoprolol electrode		Propranolol electrode		Timolol electrode	
	DNNS	C1TPB	DNNS	C1TPB	DNNS	C1TPB
Slope*, mV/decade	54.0 \pm 0.4	55.6 \pm 0.8	57.4 \pm 0.5	55.4 \pm 1.2	55.2 \pm 0.7	56.6 \pm 0.5
Linear range, M	10^{-1} – 10^{-5}	10^{-1} – 10^{-5}	10^{-1} – 10^{-5}	10^{-1} – 10^{-5}	10^{-2} – 1.5×10^{-5}	10^{-2} – 10^{-5}
Detection limit, M	4.5×10^{-6}	5.6×10^{-6}	4.0×10^{-6}	2.5×10^{-6}	6.3×10^{-6}	4.0×10^{-6}
$\mu\text{g/ml}$	3.1	3.8	1.2	0.7	2.7	1.7

*Mean \pm standard deviation for multiple calibrations in 10^{-2} – 10^{-4} M range.

Table 2. Selectivity coefficients for the beta-blocker membrane electrodes

Interfering species, J	$[BI^+]$ $[J^{z+}]$	Selectivity coefficient					
		Metoprolol electrode		Propranolol electrode		Timolol electrode	
		DNNS	CITPB	DNNS	CITPB	DNNS	CITPB
Alanine	10^{-3}	$<10^{-4}$	$<10^{-4}$	$<10^{-4}$	1.3×10^{-4}	$<10^{-4}$	$<10^{-4}$
Histidine	10^{-3}	1.6×10^{-4}	$<10^{-4}$	$<10^{-4}$	$<10^{-4}$	5×10^{-4}	$<10^{-4}$
Lysine	10^{-3}	$<10^{-4}$	$<10^{-4}$	$<10^{-4}$	$<10^{-4}$	$<10^{-4}$	$<10^{-4}$
Nicotinamide	10^{-3}	$<10^{-4}$	2.5×10^{-4}	3.3×10^{-4}	1.7×10^{-4}	1.7×10^{-4}	2.0×10^{-3}
Caffeine	2×10^{-3}	2.2×10^{-4}	2.2×10^{-4}	1.2×10^{-4}	4.5×10^{-4}	2.4×10^{-4}	4.7×10^{-4}
Vitamin B ₁	10^{-3}	2.4×10^{-3}	4.9×10^{-3}	1.9×10^{-4}	3.8×10^{-4}	8×10^{-3}	1.3×10^{-2}
Vitamin B ₆	10^{-3}	2.2×10^{-3}	4.2×10^{-3}	5.2×10^{-4}	7.5×10^{-4}	2.8×10^{-3}	8.6×10^{-3}
Atropine	10^{-3}	1.4×10^{-1}	5.7×10^{-1}	1.0×10^{-2}	3.1×10^{-2}	4.9×10^{-1}	1.9
Metoprolol	10^{-3}	—	—	3.5×10^{-2}	5.2×10^{-2}	1.9	2.3
Propranolol	10^{-3}	9.1	14.8	—	—	28.4	39.6
Timolol	5×10^{-3}	1.4×10^{-1}	2.4×10^{-1}	1.8×10^{-2}	3.0×10^{-2}	—	—

solution). At pH values >7.5 , the beta-blocker bases are precipitated, and the potentials are shifted towards more negative values.

Selectivity of electrodes

Beta-blocker substances very often have to be determined in pharmaceuticals which also contain various inorganic and organic substances. These matrices constitute a serious problem in various conventional analytical methods and have to be adequately removed before determination of the beta-blocker. The effect of some of these matrices on the response of our electrodes was estimated by the mixed solution method, and the respective selectivity coefficients, $K_{i,j}^{Pot}$, were calculated from the equation:

$$K_{i,j}^{Pot} = (10^{\Delta E/S} - 1)[BI^+]/[J^{z+}]^{1/z} \quad (1)$$

where ΔE is the change in potential in the presence of the interfering ion J^{z+} ; S is the slope of the calibration graph for the beta-blocker primary ion (i) and $[BI^+]$ and $[J^{z+}]$ are the concentrations of the primary and interfering ions, respectively. The selectivity coefficients (Table 2) indicate that the response of all the electrodes is not affected by the presence of amino-acids, nicotinamide, caffeine, or vitamin B₆. The results show that the propranolol elec-

trode has a higher degree of selectivity than either the metoprolol or timolol electrode, because propranolol is more hydrophobic, owing to the naphthalene group in its molecule. The lower selectivity of timolol is related to its higher lipophilicity, due to the morpholino-group in the molecule. Other drug compounds found in commercial beta-blocker formulations (*e.g.*, hydrochlorothiazide, bendrofluazide, spironolactone) do not interfere, since they do not form ion-pairs with DNNS or CITPB. Excipients such as corn-starch, gelatine, sugar, lactose, *etc.*, also do not interfere.

Response time, reproducibility and stability

The electrode response times were measured for beta-blocker solutions of different concentrations. For all the electrodes, the response times were about 3 min for 10^{-6} and $10^{-5}M$ solutions and less than 20 sec for more concentrated solutions.

The reproducibility of the potential readings was better than ± 0.9 mV over the entire range of concentrations but in the first 2–4 days after electrode preparation the absolute potential varied by *ca.* 5–10 mV, necessitating a one-point re-standardization before each run. The potential drift in $10^{-3}M$ solutions was

Table 3. Determination of the beta-blocker drugs in pure solutions by the standard-addition method*

Drug	Taken, mg	Range of concentration of sample solution before std. addition, $\mu g/ml$	Recovery, † %
Metoprolol tartrate	3.42–11.97	137–479	100.0 \pm 1.5
Propranolol hydrochloride	1.48–5.18	59–207	100.2 \pm 1.8
Timolol maleate	1.08–6.48	43–259	100.4 \pm 1.7

*See experimental section.

†Mean recovery \pm std. devn. for 6 determinations over the specified range.

less than ± 0.3 mV/hr. All the electrodes were used continuously for serial calibrations, selectivity coefficient determination and various applications, over a 2-month period, without significant changes in their behaviour.

Analytical applications

All these membrane electrodes proved useful in the determination of the beta-blocker drugs when the standard-addition method was used. Results for measurements of pure drug solutions at 40–480 $\mu\text{g/ml}$ levels are shown in Table 3. In all cases the relative standard deviation was $< 2.0\%$. Propranolol was also determined in tablets with good precision (r.s.d. = 1.1%) and an average recovery of 99.4% ($n = 6$), calculated from the nominal value. Direct single measurements are less precise.

REFERENCES

1. V. V. Coşofreţ, *Ion-Selective Electrode Rev.*, 1980, **2**, 159.
2. *Idem*, *Membrane Electrodes in Drug-Substances Analysis*, Pergamon Press, Oxford, 1982.
3. V. V. Coşofreţ and R. P. Buck, *Ion-Selective Electrode Rev.*, 1984, **6**, 59.
4. Z. Z. Chen, *Huaxue Chuan Gan Qi*, 1985, **5**, 11.
5. Z. Z. Chen and Z. F. Qiu, *Application of Ion-Selective Electrodes in Pharmaceutical Analysis*, Renmin Weisheng Publ. House, Beijing, 1985.
6. Z. R. Zhang and V. V. Coşofreţ, *Ion-Selective Electrode Rev.*, 1989, **11**.
7. K. Selinger and R. Staroscik, *Pharmazie*, 1978, **33**, 208.
8. T. Yamada and H. Freiser, *Anal. Chim. Acta*, 1981, **125**, 179.
9. L. Cunningham and H. Freiser, *ibid.*, 1984, **157**, 157.
10. *United States Pharmacopeia, XX Rev.*, U.S. Convention Inc., Rockville, MD, 1980.
11. L. von Meyer, G. Drasch, G. Kanert and A. Riedl, *Beitr. Gerichtl. Med.*, 1979, **37**, 365.
12. F. Susanto and H. Reinauer, *Z. Anal. Chem.*, 1984, **318**, 425.
13. B. Oosterhuis, M. van der Berg and C.-J. van Boxtel, *J. Chromatog.*, 1981, **226**, 259.
14. H. G. Schulz and R. Zapka, *Z. Anal. Chem.*, 1986, **323**, 162.
15. D. B. Pautler and J. Jusko, *J. Chromatog.*, 1982, **228**, 215.
16. K. U. Buehring and A. Carbe, *ibid.*, 1986, **382**, 215.
17. M. Tkaczyková and L. Šafárik, *Cesk. Farm.*, 1987, **36**, 170.
18. V. V. Coşofreţ and R. P. Buck, *J. Pharm. Biomed. Anal.*, 1985, **3**, 123.

A STUDY OF ELECTRODES USED IN CONTROLLED-POTENTIAL ELECTROLYSIS OF METAL IONS*

ZHOU NAN† and HE CHUN XIANG

Shanghai Research Institute of Materials, SCMI, Shanghai, People's Republic of China

(Received 27 January 1988. Revised 18 November 1989. Accepted 22 January 1990)

Summary—Various electrodes used in controlled-potential electrolysis of metal ions are discussed: (1) a double-junction saturated calomel reference electrode with sodium formate as bridge electrolyte; (2) an auxiliary electrode made by winding platinum wire on a Teflon cylinder; (3) a working electrode made of tantalum gauze. The advantages of the tantalum electrode over a platinum electrode are that the hydrogen overpotential is higher, and the tantalum electrode need not be precoated with copper before deposition of metals such as Bi, Zn and Sn, which tend to form alloys with platinum. The electrode needs pretreatment before use, but this takes only 4 min or less.

Controlled-potential electrolysis (first employed by Haber¹) can be used for both determination and separation. It not only gives selectivity but also maximizes the effective current obtainable. We present here a study of some working, auxiliary and reference electrodes used for the purpose.

EXPERIMENTAL

Reagents

Analytical-reagent grade chemicals were used, and solutions were prepared with distilled water.

Sodium formate solution, 5M.

Sulphuric acid, 1.8M and 9M.

Hydrofluoric acid (1 + 3).

Apparatus

Reference electrode. Take a saturated calomel electrode of double-junction type and fill the upper tube with saturated potassium chloride solution, and the lower sleeve with 5M sodium formate until this solution is in contact with the lower tip of the upper tube. Discard the formate solution in the electrode immediately after use.

Auxiliary electrode. Round the lower 5.5 cm of a Teflon tube (1 cm in diameter and 12.5 cm long, sealed at the bottom) wind a spiral of platinum wire (0.03 cm in diameter, about 40 cm long) and pass the upper end of the wire through

a small hole in the side of the top of the tube, and connect it to a copper wire lead.

Working electrode. Weave tantalum wire (0.2 mm diameter) to form a gauze cylinder 45 mm in height and 45 mm in diameter, with 324 meshes per cm², and stiffen the cylinder at top and bottom with a band of tantalum 2 mm wide and 1 mm thick. Weld it onto a tantalum stem 1 mm in diameter and 140 mm long.

Pretreatment of tantalum electrode. Immerse the electrode in hydrofluoric acid (1 + 3) for 20 sec, then immediately stir it in 1.8M sulphuric acid, finally immerse it in 9M sulphuric acid for 2 min, and rinse it with water.

RESULTS AND DISCUSSION

Reference electrode

The calomel electrode, introduced by Ostwald,² is the most widely used reference electrode. The electrode made with 0.1 or 1M potassium chloride takes longer to prepare than the saturated calomel electrode (SCE), and its conductance is poorer. A calomel electrode made with 3.5M potassium chloride is reported to have a low temperature coefficient and relatively short equilibration time.³ An SCE made with methanol as solvent⁴ offers little practical advantage, and in our experience is readily contaminated if kept in contact with the analyte. Although the SCE is regarded as a "half-bridge", a salt bridge should be incorporated in it to maintain its proper functioning for as long as possible.

*This work was financially supported under the Chinese TDMI Science Foundation, Grant No. 87J51203.

†Author for correspondence. Present address: 99 Handan Road, 200433, Shanghai, People's Republic of China.

Table 1. Ionic conductance λ° at infinite dilution at 25°C (S.cm².mole⁻¹)¹²

Ionic species	λ°
K ⁺	73.52
Cl ⁻	76.34
NH ₄ ⁺	73.4
NO ₃ ⁻	71.44
Na ⁺	50.11
HCOO ⁻	52
$\frac{1}{2}$ SO ₄ ⁻	79.8

KCl,^{5,6} KNO₃,^{5,6} NH₄NO₃,^{5,6} NaNO₃,⁶ (NH₄)₂SO₄,⁵ Na₂SO₄,⁷ and K₂SO₄,^{8,9} have all been suggested for use as bridge electrolytes. The use of a mixture of salts has been found of little advantage.¹⁰

To minimize the liquid-junction potential E'_j the transfer numbers of the oppositely charged ions of the bridge electrolyte should be as close as possible, since¹¹

$$E'_j = [(t_- - t_+)RT/F]\ln(a_2/a_1) \quad (1)$$

where t_- and t_+ are the transfer numbers of the anion and cation of the bridge electrolyte respectively, and a_1 and a_2 are the mean activities of the bridge and external solutions, respectively. The transfer number is the fraction of the total current carried by a given ion, and hence the ratio of the conductance of that ion to the total conductance of all ions present. Of the electrolytes listed above, only KCl and NH₄NO₃ are really suitable (Table 1).

The leakage rate of the bridge solution should be as low as possible, but the flow through the junction should be positive, unimpeded and continuous,¹³ so the bridge electrolyte selected should not interfere with the electroanalytical reaction of interest. This requirement places certain limitations on the use of these two electrolytes: chloride is potentially subject to anodic oxidation to chlorine (which could attack certain anodes), and nitrate is reported to hinder electroreduction of certain ions to the metal, e.g., Ni(II),¹⁴ Sn(IV),¹⁵ Cd(II)^{15,16} and Zn(II).^{15,16} The ammonium ion is also reported to make electroreduction of Sn(IV) to tin incomplete.¹⁷ To the best of our knowledge a universally useful bridge electrolyte is still lacking.

Our study suggests that sodium formate could serve the purpose very well. Its ions satisfy the requirement for equality of transfer numbers better than do those of the other electrolytes proposed (Table 1). Sodium ions will cause no interference, and the formate should have little

if any unfavourable effect. Any carbon dioxide produced by anodic oxidation would have little or no effect on a well buffered solution, and would have limited solubility in acid medium. In general, the ionic strength of a bridge solution should be 5–10 times that of the analyte solution,¹³ so high solubility of the bridge electrolyte is desirable. That of sodium formate is >21M.¹⁸ Moreover, the specific gravity of the 5M solution recommended here (compared to for saturated potassium chloride solution) will ensure adequate flow through the junction.

We recommend loading the electrode with just enough 5M sodium formate solution to make its ionic conductance measurable, and discarding the solution after the electrolysis is complete. For use in fluoride solutions, it is advisable to coat the outer surface of the electrode with a thin film of epoxy resin and to cure this at 100° for 16 hr.¹⁹

Auxiliary electrode

The auxiliary electrode acts as the anode in the electro-deposition of metals. Lead,²⁰ insoluble lead alloys,²¹ mixed oxides of Ti and Ru on a Ti substrate,²² and passivated metals such as iron,²³ nickel²⁴ or steel²⁴ have all been suggested as anode materials. A lead dioxide/titanium anode was reported to be too unstable.²⁵ More attractive are the anodes made of carbon, e.g., graphite,^{26,27} Ceylon graphite,²⁸ and especially glassy carbon,^{29,30} which is highly resistant to chemical attack.

We first examined the use of high-purity glassy carbon in plate form, but found that flaking gradually occurred during the electrolysis. It has been reported³¹ that this happens when the current density reaches 0.02 A/cm², and as a current density as high as 0.04 A/cm² may be required in macro-scale electro-deposition, this material should be used only for microanalysis. Hence for the time being, only platinum seems suitable as a universally applicable anode material. Our method of fabrication of the anode uses it very sparingly (only 1 g was used for making the anode).

Working electrode

The working electrode is the cathode in the electro-deposition of metals. Platinum has long been used as the cathode material. It has some intrinsic drawbacks, however. The hydrogen overpotential is very low, so hydrogen is readily evolved, and this may cause poor adhesion of the deposit. Platinum also tends to form alloys

Table 2. Weight loss of Ta wire under different conditions

Weight loss of Ta wire, mg	Medium	Time of immersion, hr	
		A	B
0.05	HCl(1 + 10)	16	2.5
0.30	HNO ₃ (1 + 9)	49.5	
0.10			105*
0.10	H ₂ SO ₄ (1 + 35)	26.5	
0.05			80*
0.00	H ₂ SO ₄ (1 + 1)	3*	
0.10	HClO ₄ (1 + 9)	46.5	
0.05			3
0.10	HCl/HNO ₃ , 5% v/v each	18	
0.05			3.5
0.05	1M NaOH	40	
2.20			1.5
0.10	1M KOH	21	
0.05	NH ₃ (aq) (1 + 1)	45.5	
0.10	NH ₃ (aq) (1 + 1)†	37	

A—at room temperature; B—at boiling temperature.

*Time in min.

†Containing 6% sodium tartrate.

with various metals, such as Zn,³²⁻³⁴ Sn,^{32,33,35} Bi³³⁻³⁵ and Ga,³⁴ which necessitates its protection by precoating with another metal, such as Cu, Ag or Hg,³³ but a voltaic couple may form between the coating metal and the metal deposited on top of it.³⁶

There has therefore been extensive search for replacements,³⁷⁻⁴⁷ but only mercury has so far been found acceptable. It has a very high hydrogen overpotential, so can be used for deposition of a wide range of metals, but its main use is for separation rather than determination.

Tantalum, first proposed by Brunck,^{48,49} also has a high hydrogen overpotential, 0.39 V,⁵⁰ so a cathode depolarizer is not necessary; it is also cheaper than platinum, an important point in many countries. It can be obtained in high purity by the high-vacuum electron-beam melting technique. We therefore chose it for further examination.

Pretreatment of Ta electrode. Removal of the oxide layer is of paramount importance. Hampson⁵¹ recommended polishing the electrode mechanically, etching it in a mixture of perchloric acid and acetic acid, and finally washing it. Our experiments show, however, that neither acid removes the oxide layer. We decided that a strong complexing agent for tantalum should remove the oxide by formation of a soluble complex. Hydrogen peroxide, oxalic acid and hydrofluoric acid were tested as cleaning agents, but only the last proved useful. Cleaning with a 1 + 3 dilution of concentrated hydrofluoric acid takes only 20 sec, and presumably works by formation of fluoride complexes of tantalum.

The wash solution for removal of the surplus cleaning solution should be used only once, as otherwise the hydrofluoric acid accumulated in it might dissolve some of the metal. We

Table 3. Controlled-potential (E_c) electro-deposition of various metals

Metal	Taken, mg	Found, mg	Medium	E_c , V vs. SCE	i , A
Cu	995.0	994.3	HNO ₃ /H ₂ SO ₄ , each 0.2M	-0.40	
	993.3	993.3			
Bi	104.6	104.0	0.65M HClO ₄	-0.40	≤0.2
	62.7	62.4			
Cd	60.0	60.0	Na ₂ SO ₄ , pH 5	-0.85	
	80.0	79.9			
Ag	100.0	100.1	NaNO ₃ /NaF, pH 5-6	+0.60	≤0.1
Zn	100.0	99.4	Na ₂ SO ₄ , pH 4.7	+0.09	
	100.0	100.3			

selected 1.8M sulphuric acid for the purpose. However, this treatment resulted in uneven depositing metals on the cleaned electrode, and it was concluded that activation of the surface was necessary. It was found that this could be achieved by immersing the cleaned electrode in 9M sulphuric acid for not less than 2 min. The complete three-step pretreatment takes about 4 min. The initial cleaning step with hydrofluoric acid was found to remove about 0.5 mg of material from the electrode, but the weight loss in the other two steps was negligible. Omission of the washing step would increase the loss.

Recommendations for use of the electrode. The pretreated electrode is ready for use and should be used immediately (without being weighed) to ensure the surface is in its active state. The electrolysis is performed, the electrode is dried and weighed, the deposit is dissolved with an acid which does not attack the electrode (Table 2), and the electrode is washed, dried and reweighed. It can then be stored, and pretreated immediately before its next use. This method of operation avoids errors arising from interaction of the electrode with a corrosive electrolyte (such as a hydrofluoric acid/nitric acid medium) before any metal has been deposited.

Applications

Results for some representative determinations are shown in Table 3. The use of a hydrochloric acid medium is not recommended, however, as somewhat lower results are obtained than with a platinum cathode. This will be discussed in a paper on use of the electrode for determination of copper.

Conclusion

Modified working, auxiliary and reference electrodes are proposed for use in controlled-potential electrolysis. The modification include a reduction in the amount of platinum used, which may be of economic importance in many countries.

Acknowledgement—Grateful thanks are due to all members of SRIM's Directorate for permission to publish this paper.

REFERENCES

1. B. Haber, *Z. Elektrochem.*, 1898, 4, 506.
2. W. Ostwald, *Hand und Hilfsbuch zur Ausführung Physikochemische Messungen*, Akad. Verlag, Leipzig, 1893.
3. F. Stráfelda and B. Polej, *Chem. Listy*, 1956, 50, 185; *Collection Czech. Chem. Commun.*, 1956, 21, 1397.
4. B. C. Verma and S. Kumar, *Talanta*, 1977, 24, 694.
5. L. Klein, *Analytische Chemie*, Springer, Berlin, 1984, p. 367.
6. F. G. Kny-Jones, *Analyst*, 1941, 66, 101.
7. A. G. Fogg, in *Ion Selective Electrodes*, E. Pungor (ed.), p. 369. Akadémiai Kiadó, Budapest, 1978.
8. C. N. Reilley and W. W. Porterfield, *Anal. Chem.*, 1956, 28, 443.
9. F. Cassani, *Chim. Ind.*, 1969, 51, 1248.
10. N. P. Finkelstein and E. T. Verdier, *Trans. Faraday Soc.*, 1957, 53, 1618.
11. S. Glasstone, *An Introduction to Electrochemistry*, p. 208. Van Nostrand, New York, 1946.
12. *Idem*, *op. cit.*, pp. 56–57.
13. H. H. Willard, L. L. Merritt, Jr and J. A. Dean, *Instrumental Methods of Analysis*, 5th Ed., p. 571. Van Nostrand, New York, 1974.
14. A. Classen, *Quantitative Analyse durch Elektrolyse*, 6th Ed., p. 188. Springer, Berlin, 1920.
15. A. Schleicher, *Elektroanalytische Schnellmethoden*, pp. 95–115. Enke, Stuttgart, 1947.
16. B. Alfonsi, *Anal. Chim. Acta*, 1958, 19, 569.
17. H. Diehl, *Electroanalytical Analysis with Graded Cathode Potential*, p. 48. Smith Chem. Co., Columbus, Ohio, 1948.
18. A. Seidell, *Solubilities of Inorganic and Metal-Organic Compounds*, 3rd Ed., p. 1165. Vol. 1, Van Nostrand, New York, 1953.
19. A. S. Hallsworth, J. A. Wetherell and D. Deutsch, *Anal. Chem.*, 1976, 48, 1660.
20. S. V. Bleshinskii, *Tr. Inst. Khim. AN Kirgiz. SSR*, 1956, 7, 21.
21. Yu. D. Dunaev, *Nerustvorimy anody iz splavov na ocnove svintsya*, p. 242. Nauka Kazakh. SSR, Alma-ata, 1978.
22. F. Goodridge, K. Lister and R. E. Plimly, *J. Appl. Electrochem.*, 1980, 10, 55.
23. G. Darius, *Dissertation*, University of Aachen, 1922.
24. P. N. Kovalenko, *Ukr. Khim. Zh.*, 1961, 27, 109.
25. D. Gilroy, *J. Appl. Electrochem.*, 1982, 12, 171.
26. T. Holth, *Anal. Chem.*, 1949, 21, 1221.
27. J. Martin and W. Wagner, *Talanta*, 1962, 9, 265.
28. W. M. Schallfeyev and A. P. Bessabotnova, *Zavodsk. Lab.*, 1936, 5, 1311.
29. A. Mizuike, *Bunseki Kagaku*, 1968, 17, 1259.
30. *Idem*, *Bull. Chem. Soc. Japan*, 1969, 42, 253.
31. A. Dodson and V. J. Jennings, *Nature*, 1972, 240, 15.
32. A. Classen, *op. cit.*, p. 62.
33. A. Schleicher, *op. cit.*, p. 43.
34. I. M. Kolthoff and E. B. Sandell, *Textbook of Inorganic Quantitative Analysis*, 3rd Ed., p. 423. Macmillan, New York, 1950.
35. G. Charlot and D. Bezier, *Quantitative Inorganic Analysis*, p. 176. Methuen, London, 1957.
36. B. Alfonsi, *Anal. Chim. Acta*, 1958, 19, 276.
37. H. J. S. Sand and W. M. Smalley, *Chem. News*, 1911, 103, 14.
38. W. Böttger, *Ber. Dtsch. Chem. Ges.*, 1909, 42, 1824.
39. H. Paweck, *Z. Electrochem.*, 1892, 5, 221.
40. H. Paweck and R. Weiner, *Z. Anal. Chem.*, 1927, 72, 225.
41. A. Schleicher and L. Toussaint, *Z. Angew. Chem.*, 1926, 39, 822.
42. D. F. Calhane and C. M. Alber, *Trans. Am. Electrochem. Soc.*, 1933, 63, 173.

43. J. Grünwald, *Oesterr. Chem. Zig.*, 1917, **20**, 128.
44. P. Nicolardot and J. Boudet, *Bull. Soc. Chim. France*, 1918, **23**, 387.
45. L. J. Gurevich and E. Wichers, *Ind. Eng. Chem.*, 1919, **11**, 570.
46. M. Bleesen, *Z. Anal. Chem.*, 1923, **63**, 209.
47. E. Haynes, *Ind. Eng. Chem.*, 1917, **9**, 974.
48. O. Brunck, *Ber. Dtsch. Chem. Ges.*, 1902, **35**, 1871.
49. *Idem*, *Chem. Zig.*, 1912, **36**, 1233.
50. A. Thiel and W. Hammerschmidt, *Z. Anorg. Chem.*, 1923, **132**, 15.
51. N. A. Hampson, *J. Appl. Electrochem.*, 1978, **8**, 563.

FLOW-INJECTION DETERMINATION OF PHOSPHATE WITH A CADMIUM ION-SELECTIVE ELECTRODE

DAVID E. DAVEY, DENNIS E. MULCAHY and GREGORY R. O'CONNELL

School of Chemical Technology, S.A. Institute of Technology, P.O. Box 1, Ingle Farm, South Australia 5098

(Received 9 August 1988. Revised 21 January 1990. Accepted 8 February 1990)

Summary—A flow-injection method is described, in which phosphate standards are introduced into a reagent stream containing Cd^{2+} , resulting in the formation of $\text{Cd}_3(\text{PO}_4)_2$. The associated reduction in free metal concentration is sensed by a cadmium-selective electrode. With the exception of major interference from iodide and moderate interference from bromide and thiocyanate, the system exhibits excellent response to phosphate and selectivity over several common anions in solutions buffered at pH 8.4. A maximum sampling rate of 160/hr is possible for phosphate standards in the concentration range 10^{-5} – $10^{-1}M$ with a $10^{-4}M$ Cd^{2+} reagent stream at a total flow-rate (carrier and reagent stream combined) of 8.4 ml/min.

In a recent review of ion-selective electrodes for phosphate and sulphate determination, Midgley¹ concluded that no potentiometric phosphate sensor yet devised exhibited sufficient stability and selectivity to be considered acceptable in the analysis of complex matrices. Consequently, the development of indirect methods for phosphate determination with existing electrode systems warrants further attention. By adapting these techniques to flow-injection analysis (FIA),² the problem of slow analysis rates normally associated with indirect potentiometry may be overcome.

Coetzee and Gardner³ used a dual-line manifold, with water as carrier merging with a $10^{-5}M$ lead perchlorate reagent stream buffered at pH 8.0 with ammonium acetate. Injected phosphate standards reacted with this solution to form an insoluble lead phosphate, the accompanying reduction in free $[\text{Pb}^{2+}]$ being monitored with a solid-state $\text{PbS}/\text{Ag}_2\text{S}$ membrane electrode. Use of a similar system to determine sulphate and tripolyphosphate, however, revealed a lack of selectivity towards phosphate, and the authors acknowledged that some form of chromatographic separation would be advantageous. An analogous system using a calcium-selective electrode was reported by Alexander and Koopetngarm.⁴ However, although this was highly sensitive to EDTA, tripolyphosphate and pyrophosphate, no detectable response was found for orthophosphate standards at pH 9.4.

It was the objective of the present work to devise a flow-injection system capable of rapid

and selective phosphate determination with a commercially available electrode. Cadmium forms considerably fewer insoluble compounds than lead does; the phosphate $\text{Cd}_3(\text{PO}_4)_2$, with a K_{sp} of 3.6×10^{-29} at 18°,⁵ is one of them. Consequently, an indirect method similar to that of Coetzee and Gardner, but employing a cadmium sensor in place of the lead electrode, has been investigated. Performance criteria have been examined at length. The specificity of the system towards phosphate in the presence of several commonly encountered anions has been assessed, and mechanisms for both phosphate and interferent response are proposed.

EXPERIMENTAL

Apparatus

The FIA manifold (Fig. 1) consisted of a Gilson Minipuls 2 peristaltic pump fitted with Tygon pump tubing, a network of 0.5-mm internal diameter PTFE tubing and polypropylene connectors linking the other system components. This configuration ensured equivalent flow-rates for both the carrier and reagent streams, permitting the combined rate to be varied between 0.9 and 8.4 ml/min. The total reactor volume, V_r (the volume from the carrier/reagent stream confluence point to the detector cell) was calculated to be 250 μl .

The sampling unit, combining a Rheodyne 5041 4-way rotary valve and a Festo DSN-10-40P pneumatic actuator, was activated by a Festo 4447 air pilot valve and two Festo 7768

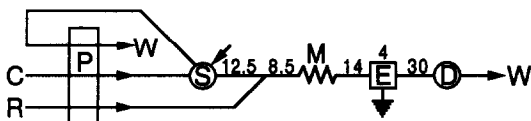


Fig. 1. Flow-injection manifold. (P) Pump, (S) sampling unit, (M) mixing coil(s) (see text), (E) earthing connector, (D) detector cell, (W) solution waste. Tubing lengths given in cm.

240-V coil units. The rotary valve was fitted with lengths of 0.5-mm i.d. PTFE tubing in order to study the effect of sample loop volume, V_s , on electrode response over the range 100–590 μl . A Datum programmable timer (Gammatron, Pooraka, S.A.) was used for controlling all switching sequences. The Perspex detector cell, described elsewhere,⁶ enabled an Orion 94-48A CdS/Ag₂S membrane solid-state electrode to be used, with an Orion 90-02 double-junction reference electrode and an Orion 801A digital pH/mV meter connected to an MFE 2115M variable-scan pen recorder through a home-made offset device.⁷

X-Ray photoelectron spectroscopy was performed with a Perkin-Elmer PHI 5100 ESCA System. The output was fed to a Hewlett Packard LaserJet II laser printer.

Reagents

Analytical grade reagents were used except where noted.

The carrier streams employed were based on two buffer systems. The first, comprising 0.01M ammonium acetate and laboratory-reagent grade ammonia solution,^{3,8} enabled the electrode response to be studied in the pH range 6.6–9.0, where the predominant phosphate species is HPO_4^{2-} . The second, based on 2M solutions of acetic acid and sodium acetate,⁹ covered pH values from 3.6 to 5.4, permitting investigation of the sensor's response to H_2PO_4^- . Electrostatic noise was minimized and the ionic strength adjusted by making all carriers 0.1M with respect to potassium nitrate. Laboratory-reagent grade sodium azide (1 g/l) was added to inhibit mould and microbial growth.

Phosphate stock solutions (0.1M) were prepared by dissolving either potassium hydrogen phosphate or potassium dihydrogen phosphate in the appropriate carrier solution and adjusting the pH accordingly. Stock solutions were similarly prepared from potassium salts for the anion selectivity studies.

Reagent streams consisted of aqueous solutions of cadmium nitrate. Conductivity water

from a Millipore Milli-Q purification system was used throughout.

RESULTS AND DISCUSSION

Effect of pH

At any given pH, the electrode response will be influenced by three major factors: (i) the level of Cd^{2+} in the reagent stream; (ii) the possibility of hydroxide formation given this level of metal ion and the solution pH; (iii) the ability of Cd^{2+} to react with the phosphate species, PO_4^{3-} , HPO_4^{2-} and H_2PO_4^- . The peak-height became irreproducible at pH above 8.5, and the response was found to be most favourable at around pH 8.4, the region where the hydrogen phosphate ion predominates (Fig. 2). Response in this pH region was enhanced by increasing the level of Cd^{2+} in the reagent stream. The irregular response at higher pH may be attributed to blocking of the electrode function by a thin coating of cadmium hydroxide. In contrast, response in the sodium acetate/acetic acid buffers (pH 3.6–5.4), though reproducible, was poor, the reaction between Cd^{2+} and H_2PO_4^- to form $\text{Cd}_3(\text{PO}_4)_2$ being extremely slow. Consequently, all further studies were performed at pH 8.4.

Effect of sample volume and mixing coils

With the 0.1M KNO_3 /0.01M $\text{CH}_3\text{COONH}_4$ / NH_3 carrier at pH 8.4 and a 10^{-5}M Cd^{2+} reagent stream flowing at a combined rate of 3.48 ml/min, five replicate injections of 0.1M phosphate gave an average peak-height which steadily increased from -35.1 to -43.1 mV over the sample volume range 100–590 μl , and the response and baseline-recovery times were doubled in the process. As the aim of the work

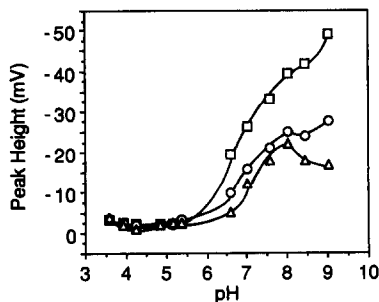


Fig. 2. Effect of pH on response to 0.1M phosphate with (Δ) 10^{-6}M , (\circ) 10^{-5}M and (\square) 10^{-4}M Cd^{2+} reagent streams. Carrier, 0.1M KNO_3 /0.01M $\text{CH}_3\text{COONH}_4$ / NH_3 (pH > 6) or 2M CH_3COOH /2M CH_3COONa (pH < 6); total flow-rate, 1.7 ml/min; sample analysis rate, 20 per hour.

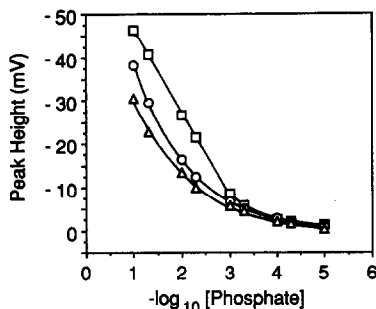


Fig. 3. Calibration curves for phosphate standards injected into (Δ) $10^{-6}M$, (\circ) $10^{-5}M$ and (\square) $10^{-4}M$ Cd^{2+} reagent streams. Carrier, $0.1M$ $KNO_3/0.01M$ CH_3COONH_4/NH_3 (pH 8.4); total flow-rate, 8.4 ml/min; sample analysis rate, 30 per hour.

was to develop a rapid means of phosphate determination, it was decided that the $100\text{-}\mu\text{l}$ loop best suited the situation.

The same manifold, fitted with the $100\text{-}\mu\text{l}$ loop, was used to study the influence of use of mixing coils on the electrode response. It was found that with one 60-cm long coil (aspect ratio¹⁰ = 15.4) fitted, an average peak-height ($n = 5$) of -36.3 mV was recorded. Adding a second coil reduced this to -34.0 mV, identical to the value found when no coil was fitted. The peak broadening was only slightly increased by the addition of each coil; hence, all further tests were done with one coil.

Calibration at pH 8.4

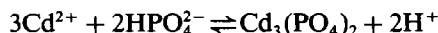
The calibration curves for phosphate standards injected into reagent streams of varying Cd^{2+} concentration (Fig. 3) were perceptibly different from those for ions sensed directly. In direct flow-injection potentiometry, raising the background level of determinand increases the lower limit of Nernstian response, giving rise to inverted peaks when the background concentration of the primary ion exceeds that of the injected standard.⁶ For the indirect system here, however, this lower limit decreased as the level of cadmium in the reagent stream was increased from 10^{-6} to $10^{-4}M$, with little apparent difference between the responses when phosphate standards of $10^{-3}M$ or less were injected.

This trend can be explained in that the electrode will always be responding to a depletion in the level of reagent stream Cd^{2+} by formation of the insoluble phosphate; hence, all peaks recorded are inverted peaks. This also accounts for the relatively high level of phosphate

at which linearity ceased, electrode response always being slower when passing from a solution of higher to one of lower determinand concentration.

Proposed mechanism of phosphate response

The observed slope factor in the linear region of the calibration with $10^{-4}M$ Cd^{2+} reagent stream (-19.0 mV/decade total phosphate) indicated that the product of the reaction was $Cd_3(PO_4)_2$. Evidence that the response arose from an in-stream reaction, rather than at the electrode surface, was obtained by treating the analysis as a flow-injection titration. Considering the reaction to be



equivalence will be reached when

$$3C_s V_s = 2C_r V_r \quad (1)$$

where C_s and C_r are the sample and reagent concentrations, and V_s and V_r are the sample and reactor volumes, respectively.* Růžička and Hansen¹¹ noted that the concentration gradient generated within the sample bolus by an in-stream reaction could best be described in terms of a single-tank reaction model. By selecting a point at a constant height above the baseline on both the rise and fall curves of each peak, they showed that the time between the two points—the equivalence time, t_{eq} —was a function of the flow-rate, Q , and the parameters in equation (1):

$$t_{eq} = \frac{2.303 V_r}{Q} \log \left(\frac{3C_s V_s}{2C_r V_r} \right) \quad (2)$$

This expression will be valid provided (i) V_r is much larger than V_s ; (ii) the sample plug undergoes homogeneous mixing with the reagent; (iii) the flow parameters used in equation (2) are reproducible. Consequently, if V_s and V_r are held constant, the graph of t_{eq} vs. $1/Q$ will be linear for a sample of concentration C_s injected into a system with reagent stream concentration C_r . The slope of this graph, k , will be given by

$$k = 2.303 V_r \log \left(\frac{3C_s V_s}{2C_r V_r} \right) \quad (3)$$

Regression lines were obtained for t_{eq} vs. $1/Q$ for the 10^{-1} and $10^{-3}M$ phosphate standards injected into the three Cd^{2+} systems. Substituting $V_s = 100 \mu\text{l}$ and $V_r = 250 \mu\text{l}$ into equation (3) gave k values that agreed well with the slope factors of the lines for 10^{-4} and $10^{-5}M$ Cd^{2+} (Table 1). This confirms in-stream formation of

*Note that this equation is given incorrectly in reference 11.

Table 1. Application of the single-tank model¹¹ to the determination of phosphates with the manifold in Fig. 1

C_r, M	$C_s = 0.1M$			$C_s = 10^{-3}M$		
	r^2	k_{expt}, ml	k_{calc}, ml	r^2	k_{expt}, ml	k_{calc}, ml
10^{-4}	1.000	1.74	1.83	0.999	0.70	0.68
10^{-5}	0.997	2.45	2.40	0.996	1.28	1.25
10^{-6}	0.992	4.19	2.98	0.885	0.66	1.83

C_r = concentration of Cd^{2+} reagent stream; C_s = concentration of injected phosphate standard; r^2 = coefficient of determination for regressed line; k_{expt} = slope determined experimentally; k_{calc} = slope calculated from equation (3) with $V_s = 100 \mu\text{l}$ and $V_r = 250 \mu\text{l}$.

$\text{Cd}_3(\text{PO}_4)_2$. A departure from linearity, and hence poor correlation between k values, was evident when a $10^{-6}M$ Cd^{2+} reagent stream was used. In this instance, the value of C_r lay outside the region in which the shapes of the rise and fall curves satisfy the requirements for the single-tank model.^{11,12}

Response characteristics

With two notable exceptions, the response characteristics exhibited by the cadmium electrode in the presence of phosphate (Table 2) were similar to those observed in the direct sensing of iodide.⁶ As expected, the response time for the peak maximum, t_R was much smaller than the 99% recovery time, t_{99} , regardless of flow-rate. Again, both t_R and t_{99} decreased when the total flow-rate was increased. However, in the present study, only t_{99} diminished with an increase in the level of Cd^{2+} , t_R increasing slightly. In addition, peak-heights did not always remain constant with increases in flow-rate. The pronounced reduction in H for the $10^{-6}M$ Cd^{2+} system is in accordance with the findings of the single-tank model for that value of C_r .

Table 2. Effect of flow-rate on peak profiles for 0.1M standards injected into (A) $10^{-4}M$ and (B) $10^{-6}M$ $\text{Cd}(\text{NO}_3)_2$ reagent streams; carrier stream 0.1M $\text{KNO}_3/0.01M$ $\text{CH}_3\text{COONH}_4/\text{NH}_3$ (pH 8.4)

Flow-rate, ml/min	t_R , sec	t_{99} , sec	H , mV	r.s.d. of H , % ($n = 4$)
(A)				
0.9	37.7	170.4	-48.3	0.23
1.7	17.9	77.0	-48.4	0.23
3.2	9.2	43.6	-47.8	0.25
8.4	3.7	18.8	-46.1	0.15
(B)				
0.9	33.6	757.5	-43.2	1.55
1.7	15.8	478.5	-40.5	0.99
3.2	8.9	290.3	-36.2	0.89
8.4	3.3	156.8	-31.4	0.41

t_R = response time at peak maximum; t_{99} = recovery time from peak maximum to 1% of peak potential; H = peak-height.

These phenomena appear to be artefacts of the indirect nature of the determination. In direct measurement systems, limitations in the speed and magnitude of response are solely due to the reaction(s) at the electrode membrane. In an indirect system, response is also dependent on the rate of reaction between the injected species and the reagent stream. The reductions found in peak-height and t_R as flow-rate increased would appear to indicate that it is this reaction, and not the response to Cd^{2+} at the electrode, that is the rate-determining factor.

An analysis rate of 160 samples/hr was achieved for phosphate standards in the range 10^{-5} – $10^{-1}M$ injected into the $10^{-4}M$ $\text{Cd}^{2+}/0.01M$ $\text{CH}_3\text{COONH}_4/\text{NH}_3$ system flowing at a combined rate of 8.4 ml/min. Peak-height repeatability and baseline recovery between samples was good throughout, indicating negligible carry-over. This compares well with the performance of the optimized colorimetric system described by Janse *et al.*,¹³ which permitted injection of 180 samples/hr in the concentration range 1.2×10^{-3} – $7.7 \times 10^{-2}M$ phosphate.

Selectivity

The response of the $10^{-4}M$ Cd^{2+} system at pH 8.4 to a number of anions is depicted in Fig. 4; there was no response to fluoride and

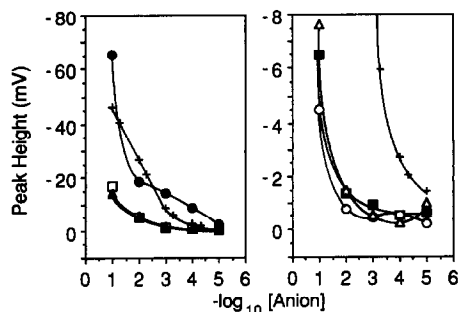


Fig. 4. Calibration curves for (▲) thiocyanate, (△) bicarbonate, (■) sulphate, (□) bromide, (●) iodide, (○) chloride and (+) phosphate standards injected into a $10^{-4}M$ Cd^{2+} reagent stream. Other details as for Fig. 3.

nitrate over the concentration range investigated. Of the anions tested, only bicarbonate would be expected to form a precipitate (CdCO_3) with the cadmium reagent stream¹⁴ and thus give rise to a detectable response. From Fig. 4, however, it appears to constitute a minor interferent in the determination of phosphate by this system, as also do sulphate and chloride.

In contrast, the response towards bromide, thiocyanate and iodide is much greater than that predicted from the solubility of the cadmium salts. Given the presence of silver sulphide in the electrode membrane, this is suspected to be due to some form of direct electrode response rather than any depletion in the level of Cd^{2+} . It is postulated that the Ag_2S at the surface of the membrane undergoes oxidation to Ag_2SO_4 and, as the solubility of this compound is considerably greater than that of AgBr , AgSCN or AgI ,^{5,15} the sulphate is converted into the more insoluble halide or pseudohalide. The oxidation of Ag_2S was invoked by Wilson and Pool to explain the response and stability of their prototype HPO_4^{2-} -selective electrode.¹⁶ As in their studies, X-ray photoelectron spectroscopy (XPS) was employed to confirm the presence of sulphate.

Observations made with the flow system again support this hypothesis. When the 10^{-4}M Cd^{2+} reagent stream was replaced by a 10^{-6}M solution, the response to phosphate was reduced (Fig. 3), yet that to Br^- , SCN^- and I^- was enhanced so much that the bromide and thiocyanate calibration lines almost coincided with that for phosphate. The system became vastly more sensitive towards iodide, the buffered standards giving a linear calibration over the range 10^{-5} – 10^{-1}M I^- , with a slope of -25.8 mV/decade. This may be attributed to some form of mixed potential arising at the electrode membrane. The appearance of "potential overshoot"—a phenomenon where the fall curve of the recorded peak drops to a potential below that of the baseline, then recovers to the original baseline potential—was also noted for the bromide, thiocyanate and iodide standards. Observed by Lewenstam *et al.*¹⁷ in steady state

work with AgX membrane electrodes, such behaviour has been regularly encountered in our studies on the selectivity of AgX/ Ag_2S membrane electrodes in flow-injection environments. It must, therefore, be concluded that only by elimination of Ag_2S from the membrane could a more phosphate-selective system be obtained than that using the cadmium electrode and a 10^{-4}M Cd^{2+} reagent stream. Current studies with home-made membranes are being pursued with this in mind.

Acknowledgements—The authors extend their thanks to the School's Workshop for the construction of the sampling unit and detector cell used in this work, and to the Surface Technology Centre, S.A.I.T., for the provision of XPS data and advice regarding its interpretation. G.R.O'Connell acknowledges financial support from S.A.I.T. and the Australian Government.

REFERENCES

1. D. Midgley, *Ion-Selective Electrode Rev.*, 1986, **8**, 3.
2. J. Růžička and E. H. Hansen, *Anal. Chim. Acta*, 1975, **78**, 145.
3. J. F. Coetzee and C. W. Gardner, Jr., *Anal. Chem.*, 1986, **58**, 608.
4. P. W. Alexander and J. Koopetngarm, *Anal. Chim. Acta*, 1987, **197**, 353.
5. R. C. Weast (ed.), *CRC Handbook of Chemistry and Physics*, 62nd Ed., p.B-242. CRC Press, Boca Raton, 1981.
6. D. E. Davey, D. E. Mulcahy and G. R. O'Connell, *Talanta*, 1990, **37**, 313.
7. D. E. Davey, R. D. Hall, D. E. Mulcahy and G. R. O'Connell, *J. Chem. Educ.*, 1989, **66**, 784.
8. D. Midgley, *Talanta*, 1979, **26**, 261.
9. D. D. Perrin and B. Dempsey, *Buffers for pH and Metal Ion Control*, p. 135. Chapman & Hall, London, 1974.
10. W. E. van der Linden, *Trends Anal. Chem.*, 1982, **1**, 188.
11. J. Růžička and E. H. Hansen, *Flow Injection Analysis*, 1st Ed., pp. 90–97. Wiley, New York, 1981.
12. G. Wang, D. Yu and Y. Sun, *Sensors and Actuators*, 1989, **19**, 41.
13. T. A. H. M. Janse, P. F. A. van der Wiel and G. Kateman, *Anal. Chim. Acta*, 1983, **155**, 89.
14. R. C. Weast (ed.), *op. cit.*, pp. B-85–B-86.
15. E. Högfeldt (ed.), *Stability Constants of Metal-Ion Complexes*, Part A: *Inorganic Ligands*, p. 175. Pergamon Press, Oxford, 1982.
16. A. C. Wilson and K. H. Pool, *Anal. Chim. Acta*, 1979, **109**, 149.
17. A. Lewenstam, A. Hulanicki and T. Sokalski, *Anal. Chem.*, 1987, **59**, 1539.

POTENTIOMETRIC STRIPPING ANALYSIS AUTOMATION

A. CLADERA, J. M. ESTELA and V. CERDA

Department of Chemistry, University of the Balearic Islands, E-07071 Palma de Mallorca, Spain

(Received 21 December 1988. Revised 18 October 1989. Accepted 22 January 1990)

Summary—A semi-automatic system for potentiometric stripping analysis (PSA) based on the use of a potentiostat, a pH-meter with RS232C interface, and a personal computer is described. The appropriate software developed allows automatic control of the pre-electrolysis time, data acquisition and manual or automatic data treatment. Several elements can be determined at ng/ml level.

Potentiometric stripping analysis (PSA) was introduced by Jagner and co-workers¹⁻³ for trace and ultratrace analysis. One of its advantages is that only simple instrumentation is required. Manual application of PSA is tedious in the determination of very low metal levels, since a very long pre-electrolysis step is required. Automatic techniques are therefore very convenient.

Various oxidants have been proposed for stripping the reduced metals. In most applications, mercury(II) is added prior to the pre-electrolysis for *in situ* formation or regeneration of the mercury film on the glassy-carbon electrode, and for the stripping reoxidation of the amalgamated metals. If mercury (II) is to be the predominant oxidant it is necessary to remove dissolved oxygen from the sample.

Jagner and co-workers have therefore used the dissolved oxygen as the stripping agent, but the faster kinetics of this reaction shortens the plateaus in the potentiometric curves and the determination limits are less favourable. To overcome this problem, a microprocessor-based system was developed,⁴ which could take a great number of measurements in a very short time interval, and then present the potentiometric curve on an expanded time scale. The microprocessor also measured the capacitance background, subtracted it from the potentiometric curve for the sample and gave the difference as output at a data-rate suitable for the strip-chart recorder. Anfält and Strandberg have also designed a computerized PSA system.⁵ Mortensen *et al.*⁶ have described a multichannel scanning PSA apparatus.

More recently, a computerized system for flow potentiometric and constant-current stripping analysis was proposed,⁷ which required

two 12-bit D/A converters and a 12-bit A/D converter, to control a peristaltic pump, a sampler and six inlet valves for controlling an autosampler.

Here we report a very simple semi-automatic system for potentiometric stripping analysis, based on the use of standard laboratory instruments. A suitable BASIC program has been developed, which allows experimental data acquisition and manual or automatic data treatment.

EXPERIMENTAL

Apparatus

The components of the automatic stripping potentiometric system were a general purpose potentiostat; an electrolytic cell provided with a reference SCE, a glassy-carbon or a Kemula hanging-drop working electrode and a Pt auxiliary electrode; a Crison 517 potentiometer and a Crison automatic burette, both provided with serial RS-232C interfaces; a personal computer, with a minimum of 16 kbytes of RAM, graphics card, user port or RS-232C interface and home-made card-supported control relays; cassette or diskette storage units.

A Commodore VIC-20 computer was chosen, with its memory expanded by 16 kbytes and implemented with a Superexpander cartridge for graphics. The RS-232C serial interface was simulated through the user port, which was simultaneously used to trigger the control relays by means of optocouplers.

Since the simulated RS-232C serial interface of the VIC-20 computer works at TTL voltage levels (*i.e.*, 5 V), a voltage adapter was needed to interface it to the standard (*i.e.*, 12 V) RS-232C of the Crison potentiometer.⁸

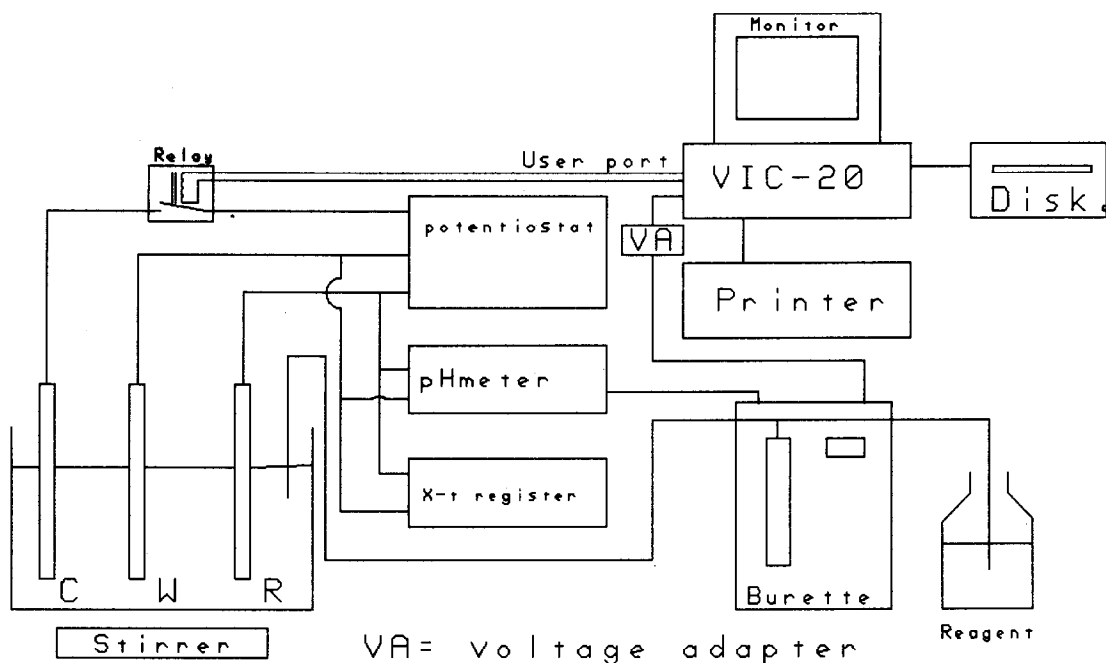


Fig. 1. Block diagram of the automatic potentiometric stripping analysis system.

Figure 1 shows a block diagram of the system.

Chemicals

All chemicals were of analytical grade.

Procedures

Preparation and regeneration of the working electrode surface. The glassy-carbon working electrode was first polished with an abrasive paper. When in constant use, this electrode was manually polished for 1–2 min several times a day. After polishing, the glassy-carbon surface was carefully washed with acetone to remove any trace of grease and fingerprints. When not in use, the working electrode was stored dry.

Precoating with a mercury film. The glassy-carbon working electrode had to be covered with a mercury film thick enough to dissolve all the mercury-soluble metals reduced during the plating period. It was therefore precoated with mercury by holding the electrode at -0.5 V vs. SCE for 10–30 sec in a non-deaerated solution containing 0.1 M hydrochloric acid and 25 mg/l. mercury(II). A stripping curve was registered and a steady baseline established. The plating potential was then changed to -0.60 V and the plating/stripping cycle repeated. This procedure was repeated at -0.70 , -0.80 and -0.90 V. Finally the plating was run for 2 min at -0.9 V,

and after stripping, the working electrode was rinsed with distilled water. If the working electrode was allowed to stand in the precoating solution for long periods of time, calomel formed on the electrode surface.

Analytical procedure. The standard-addition method was used for samples containing 0.05 M hydrochloric acid, 0.5 M sodium chloride and 1 mg/l. mercury(II), previously deaerated by passage of pure nitrogen for 15 min. A nitrogen atmosphere was maintained above the sample surface during the analysis. The sample was plated for 5 min at -0.95 V during the pre-electrolysis period, followed by stripping, data acquisition, etc. Then known volumes of a solution containing lead(II) and cadmium(II) were added from an automatic burette controlled by the computer, the plating/stripping cycle being run after each addition.

Working system

The classic PSA system is controlled by the computer, which starts and stops the pre-electrolysis at preset times. The potentiometer, in parallel with a register, transmits the data to the computer via an RS-232C serial interface. The potential changes are simultaneously monitored throughout the pre-electrolysis and stripping steps.

Program

The BASIC package was split into two programs, owing to the lack of computer memory. As in earlier work,⁸ to control the burette and potentiometer the communication protocol provided by the manufacturer was used. The I/O commands of the user port of the computer were applied to trigger the control relays. The Commodore VIC-20 microcomputer is provided with facilities for these tasks.

Program PSA1 controls the experimental functions, data acquisition and storage, connection and disconnection of the electrodes, addition of the standards, *etc.*

The other program (PSA2) is used for data treatment. It can automatically identify the components of the sample, calculate the length of the plateaus, obtain the calibration curve and provide the sample concentrations.

The data treatment presented a number of problems. The first was automatic location of the plateaus in the potential/time curves for each element to be determined. This was done by means of the first and second derivative curves with respect to time. The potential/time curves have a sudden slope change before and after the plateau, which means a corresponding sign change in the second derivative. The program analyses these sign changes to delimit the actual plateau. The presence of noise introduces additional difficulties since it produces transient sign changes of the second derivative, which do not correspond to true transitions from one element to another.

Two methods were used to deal with the noise. First, when a sign change was detected for the second derivative, a maximum of the first derivative was used to confirm the beginning or the end of a plateau. In this way, small variations of the signal by the background noise could be eliminated from consideration. The second method compared the potential of the detected plateau with a table of potentials for the elements to be determined, and ignored the plateau if the potentials did not match. In this way, good results were obtained even when the signals were noisy.

Once the plateaus were located, the program computed their lengths by means of a linearization of the points corresponding to the plateau and to the zones before and after it.

The first plateau gave additional problems. Once the pre-electrolysis was stopped, the potential rapidly increased until it reached

the potential of the first plateau. If the data acquisition began after the pre-electrolysis was stopped, there were not enough data for calculation of the length of the first plateau. Therefore, the data acquisition had to begin some seconds before the pre-electrolysis was stopped. The points to be considered for linear extrapolation could also be manually chosen.

Finally, the computer automatically computed the concentration of the samples from the plateau lengths obtained by the standard-addition method.

If the automatic procedure fails at any point, or improvement is possible, manual control can be implemented at any time. The overall computerized data treatment may also be overridden and manually performed.

RESULTS AND DISCUSSION

The glassy-carbon electrode, coated with a thin mercury film, and the Kemula hanging-drop electrode both showed an excellent response. The Kemula electrode gives the best and most sensitive behaviour, with least noise, especially when an unstirred solution is used during the stripping step.

However, since constant stirring is needed during the pre-electrolysis to obtain reproducible results, the hanging mercury drop can easily fall. Therefore, the glassy carbon electrode is preferred.

On the other hand, when the standard-addition method is used, the surface of the electrode is very important. Since the automatic procedure performs consecutive deposition/stripping cycles, the concentration of the oxidant [mercury(II)] continuously decreases, an effect which becomes more important with increase in the surface area of the electrode. This induces a deviation from linearity in the standard-addition method, an effect which is more important when the number of additions is increased.

The successive steps in the program are shown in Fig. 2: discrimination of the plateaus, identification of the elements, calculation of the plateau length, and calculation of the plots for the standard-addition method.

Figure 2(a) show the stripping curve for a blank. A little background noise may be observed, identified as such by the program, which points out that there is no element to be determined and directly goes on to obtain the standard-addition plot in order to check its linearity.

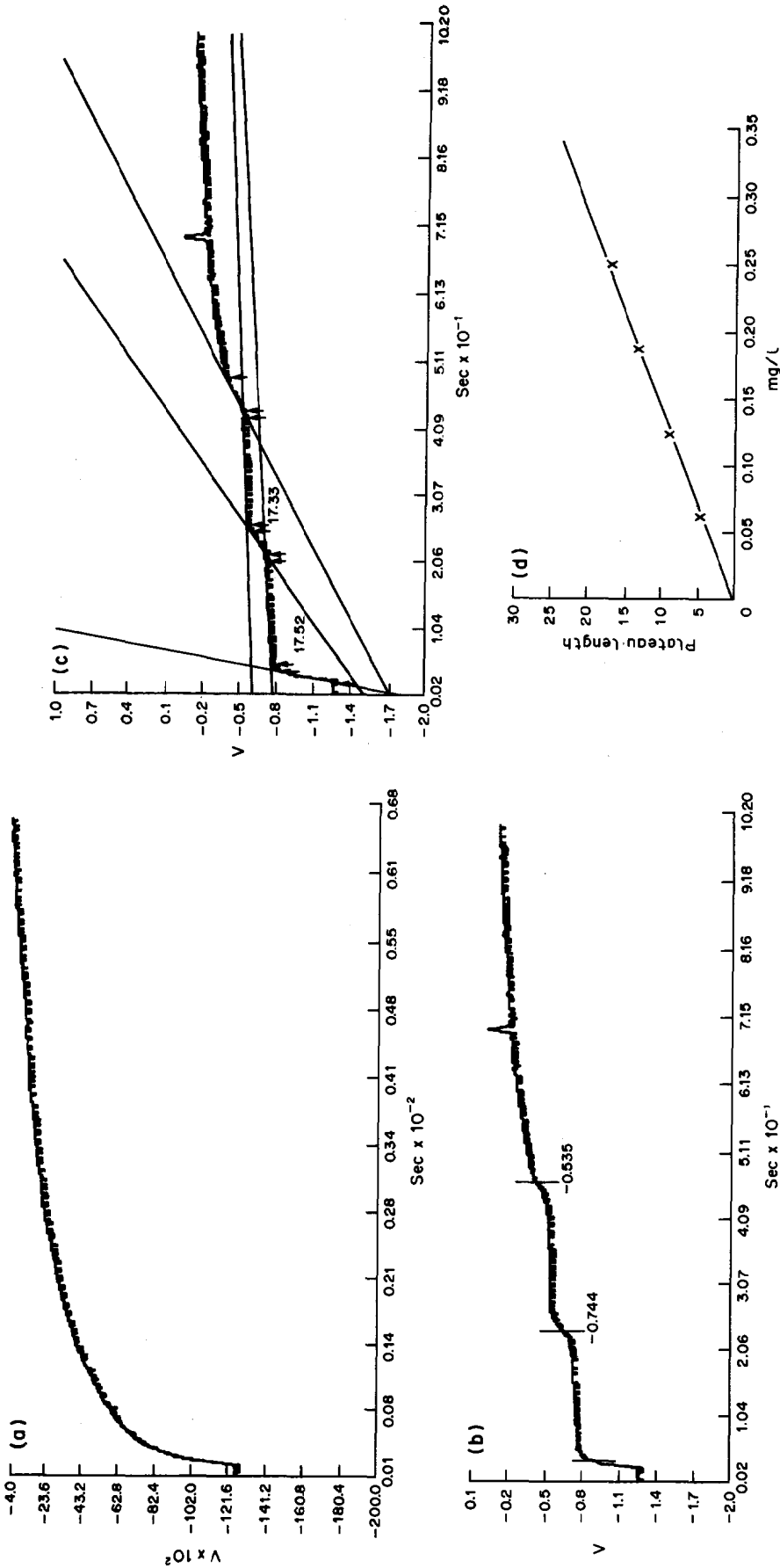


Fig. 2. (a) Anodic stripping curve of a blank constituted by 0.05M HCl, 0.5M NaCl and 1 ppm Hg(II). $E_{\text{pre-dec.}} = -0.95 \text{ V}$, $t = 5 \text{ min}$; (b) the same plus 250 ng/ml Cd and Pb; the location of the plateaus and identification of the elements were done automatically; (c) the same after the automatic calculation of the plateau lengths; (d) overlapping calibration curves automatically obtained for Pb(II) and Cd(II).

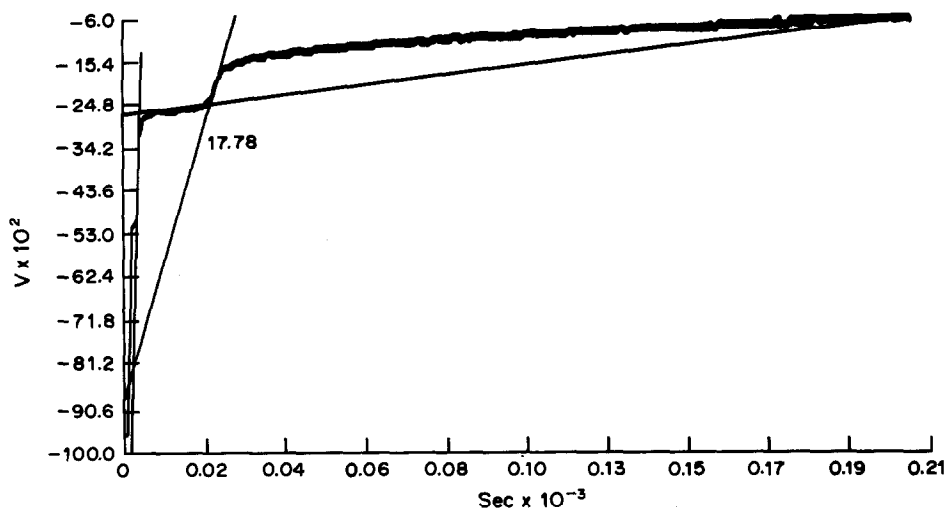


Fig. 3. Determinations of 1 ng/ml Pb under the conditions stated in Fig. 1, with a pre-electrolysis time of 150 min.

Figure 2(b) corresponds to the addition of 250 ng/ml Cd and Pb. The program locates the plateaus for these two elements, shows their corresponding potentials and the beginning and end of each plateau.

Figure 2(c) shows the different linear regressions performed by the program, with the initial and final points marked by arrows. The program computes the intersection points and the length of each plateau. This process is repeated for a second addition and finally [Fig. 2(d)] the program prints out the standard-addition plot and the sample concentration. Since in this case Cd and Pb present similar responses, both calibration lines coincide and the intercepts are zero, since the sample is a blank.

Figure 3 presents an example of the convenience of the automatic system and the program when very low concentration levels have to be determined. It corresponds to the anodic stripping curve of 1 ng/ml lead(II) with a pre-electrolysis time of 150 min. The plateau

for lead can be correctly located and easily measured. In addition, the presence of a cadmium impurity was detected (though not automatically by the program) and could be quantified by the manual method.

Acknowledgement—Thanks are due to the DGIcYT (Spanish Council for Research in Science and Technology) for financial support (PA 86-0033).

REFERENCES

1. D. Jagner and A. Granéli, *Anal. Chim. Acta*, 1976, **83**, 19.
2. D. Jagner, *Anal. Chem.*, 1978, **50**, 1924.
3. *Idem, ibid.*, 1979, **51**, 342.
4. A. Granéli, D. Jagner and M. Josefson, *ibid.*, 1980, **52**, 2220.
5. T. Anfält and M. Strandberg, *Anal. Chim. Acta*, 1978, **103**, 379.
6. J. Mortensen, E. Ouziel, H. J. Skov and L. Kryger, *ibid.*, 1979, **112**, 297.
7. L. Renman, D. Jagner and R. Berglund., *ibid.*, 1986, **188**, 137.
8. J. Maimó, M. Far, J. M. Estela and V. Cerdá, *Quim. Anal. Barcelona*, 1986, **5**, 245.

THE USE OF BF_4^- AS THE SUPPORTING ELECTROLYTE ANION IN VOLTAMMETRIC STUDIES ON CARBON ELECTRODES—A CAUTIONARY NOTE

M. CHANDRASEKARAN, M. NOEL and V. KRISHNAN

Central Electrochemical Research Institute, Karaikudi 623006, Tamilnadu, India

(Received 8 December 1989. Accepted 10 January 1990)

Summary— BF_4^- , a supporting electrolyte anion commonly employed in aprotic as well as protic solvents, is found to give an anodic peak at around +0.8 V *vs.* SCE on glassy carbon electrodes in dimethylformamide media. The voltammetric peak is influenced by the sweep-rate as well as the concentration of BF_4^- . The electrode, when anodically polarized under these conditions, is also found to retard the charge-transfer rate of the ferricyanide/ferrocyanide redox system. Possible mechanisms for formation of a film on the electrode are discussed; possibilities are fluorination of carbon atoms on the electrode surface by reactions such as $\text{C}_{\text{lattice}} + \text{BF}_4^- \rightarrow (\text{C}-\text{F} \dots \text{BF}_3)_{\text{lattice}} + e^-$ or $\text{C}-\text{H}_{\text{lattice}} + \text{BF}_4^- \rightarrow (\text{C}-\text{F} \dots \text{BF}_3)_{\text{lattice}} + \text{H}^+ + 2e^-$. The analytical importance of considering the influence of BF_4^- and other fluoride species on carbon electrodes in the anodic region is emphasized.

Tetrafluoroborate (BF_4^-) anions are assumed to be among the inert species that can be used to obtain wider anodic potential windows in voltammetric investigations in aprotic media.¹⁻⁵ This property, coupled with a weak tendency to form complexes, is responsible for the extensive use of HBF_4 and its salts as supporting electrolytes in such investigations. However, in a recent systematic investigation of the voltammetric behaviour of glassy carbon in an aprotic solvent, a totally unexpected voltammetric response to BF_4^- anion at a potential in the region of +0.8 V *vs.* SCE was observed.⁶ Some experimental details, the possible mechanism involved in this anodic process, and its analytical implications are discussed here, and a cautionary note on the possibility of this wave being misinterpreted as due to another depolarization is sounded.

EXPERIMENTAL

A 5-mm diameter Tokai glassy carbon rod embedded in a glass tube with epoxy resin was used as the working electrode in a conventional "H" type cell with a platinum counter-electrode. A reference SCE was connected to the cell through a Luggin capillary filled with KCl/agar. In a few experiments, a platinum microelectrode was employed for establishing the electrode effect due to the glassy carbon material.

Laboratory-reagent grade dimethylformide (DMF) was freshly distilled before use. The tetra-n-butylammonium salts employed were of analytical reagent grade. The working electrode was polished with successively finer emery papers (ranging from 1/0 to 4/0) to a mirror finish, and washed thoroughly with water, then trichloroethylene and finally with the supporting electrolyte solvent mixture, in which it was then cycled for about 10 min in the potential region of the voltammetric measurements. This treatment was found to give a sufficiently reproducible voltammetric response (± 5 mV variation in peak potential and $\pm 2\%$ in peak current). The reproducibility and active state of the electrode were also tested by recording the voltammetric response to the anthracene/anthracene-radical anion couple in the same media, at regular intervals. All the experiments were done at $25 \pm 1^\circ$.

All other experimental details and the voltammetric instrumentation employed have already been discussed in detail.⁶

RESULTS

Typical background currents at a glassy carbon electrode in 0.1M solutions of tetra-n-butylammonium salts of DMF are shown in Fig. 1. The voltamperograms were recorded under carefully controlled conditions after complete deaeration. The absence of dissolved oxygen

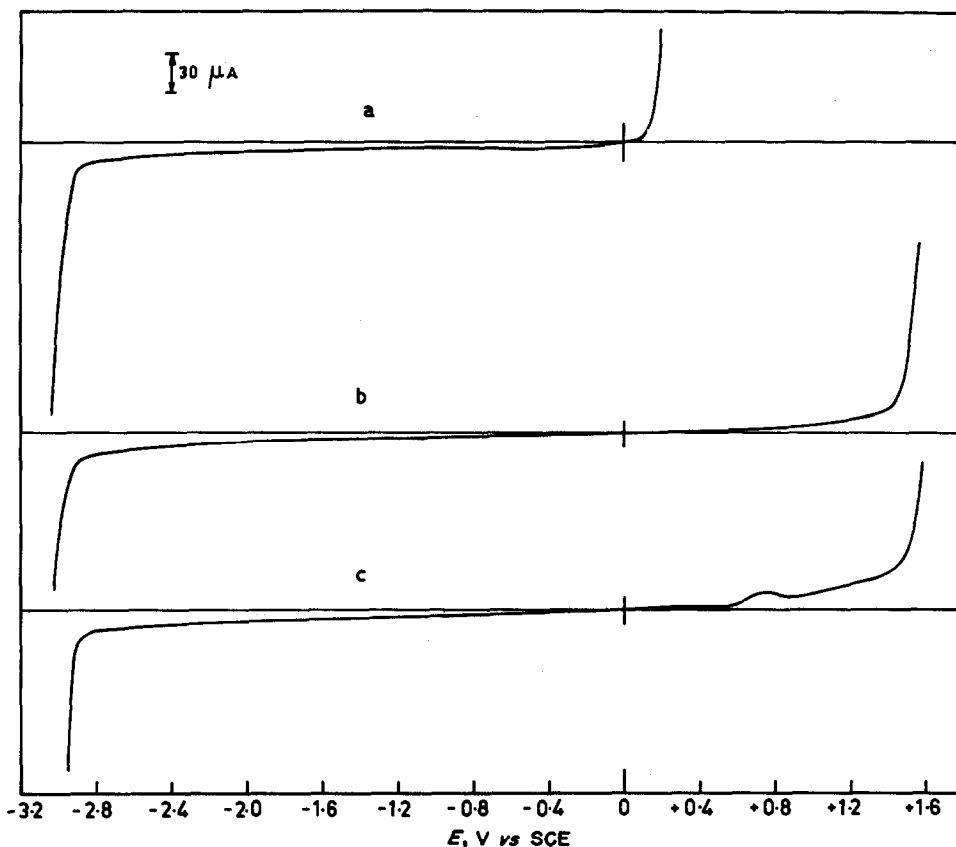


Fig. 1. Potential range of the glassy carbon electrode (GCE) in DMF containing different tetra-alkylammonium supporting electrolytes (0.1M). (a) TBAI, (b) TBAP and (c) TBABF₄. Sweep rate 10 mV/sec.

from the solution is confirmed by the absence of an oxygen/oxygen-radical anion reversible peak at around -0.75 V vs. SCE. The cathodic limit occurred at about the same potential for different tetra-alkylammonium salts. The anodic limit for tetra-*n*-butylammonium iodide (TBAI) was quite low compared to those for tetra-*n*-butylammonium perchlorate (TBAP) and tetrafluoroborate (TBABF₄), as would be expected from the lower oxidation potential for iodide.

The most significant result from the viewpoint of the present investigation was the presence of the anodic peak at around $+0.8$ V, which is substantially lower than the anodic limiting potential of about $+1.6$ V. This anodic peak was thought to be an experimental artifact and every effort was made to eliminate it in order to improve the reproducibility of the systems. The solvent/supporting electrolyte systems were thoroughly purified, the deaeration and moisture removal were carefully repeated, and the electrode was cleaned repeatedly. Some experimental activation procedures (oxidation, reduction, potential cycling)⁷ were also tried on

the glassy carbon electrode. In spite of all these efforts, the appearance of an oxidation peak at around $+0.8$ V was quite consistent.

Final confirmation for this response is due to some specific interaction of glassy carbon with BF₄⁻ anions came from comparison of the background responses of glassy carbon and platinum electrodes in these three solvent/supporting electrolyte systems. The background responses of the platinum electrode were quite similar to those of the glassy carbon electrode except for the absence of the anodic peak at $+0.8$ V for the platinum electrode in TBABF₄ medium.

This wave was investigated further with the glassy carbon electrode. The anodic peak for 0.1M TBABF₄ in DMF increased substantially with sweep rate (Fig. 2), but the peak current did not decrease substantially with successive sweeps. When proper background correction was made, the peak current increased approximately with the square root of the sweep rate. The peak potential was also found to shift anodically with increased sweep rate.

To evaluate the concentration effect, the 0.1M TBAP/DMF system was taken as the back-

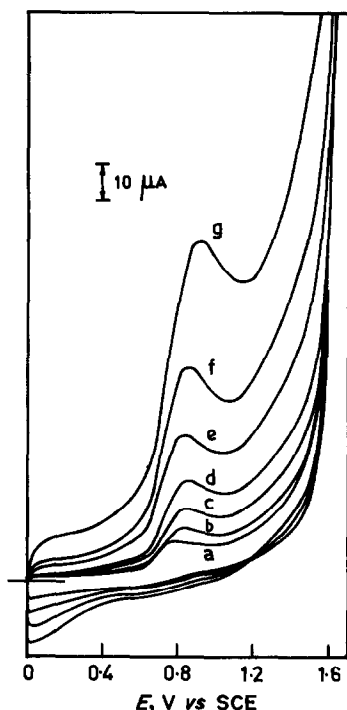


Fig. 2. Cyclic voltamperograms with the GCE in 0.1M TBABF₄/DMF at various sweep rates: (a) 10, (b) 20, (c) 40, (d) 80, (e) 160, (f) 320 and (g) 640 mV/sec.

ground system. The effect of mM concentrations of TBABF₄ on the voltammetric response of the glassy carbon electrode in this medium is presented in Fig. 3. The peak current indeed increased with concentration of BF_4^- , but the $i_p/[\text{BF}_4^-]$ value decreased substantially with increasing $[\text{BF}_4^-]$ and at BF_4^- concentrations $>25\text{mM}$ the peak current became almost independent of BF_4^- concentration.

To see whether the glassy carbon electrode anodically polarized in the BF_4^- medium has a film attached to it, electrodes continuously cycled in the TBABF₄ medium at potentials between 0 and +1.0 V for sufficiently long times were subjected to visual and microscopic examination. The mirror finish of the electrode surface was not affected to any noticeable extent, nor was physical damage observed by microscopic analysis. However, formation of a thin inhibitory film was indirectly confirmed by establishing the effect of this film on a charge-transfer reaction. In aqueous 0.1M potassium chloride medium, the cyclic voltammetric response of a TBABF₄/DMF-treated glassy carbon electrode showed quasi-irreversible behaviour for the ferricyanide/ferricyanide redox couple.⁷ The peak separation, ΔE_p , depended on the duration of potential cycling in the DMF/ BF_4^- medium, but was always greater

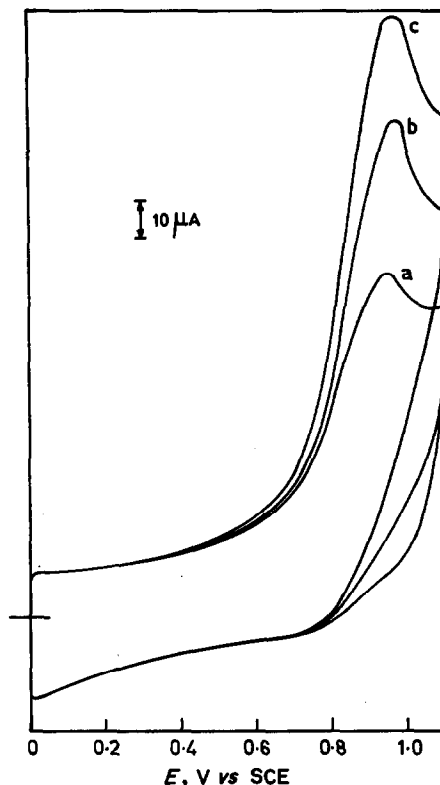


Fig. 3. Effect of BF_4^- concentration on anodic voltammetry with the GCE in 0.1M TBAP/DMF at 320 mV/sec. (a) 5, (b) 10 and (c) 15mM.

than 60 mV and was sometimes 100 mV or more (Fig. 4A). However, a perfectly reversible voltammetric response for the same redox system on the glassy carbon electrode could easily be obtained by polishing the electrode surface with 3/0 and 4/0 emery papers and subjecting it to potential cycling in 0.1M potassium chloride (Fig. 4B).

DISCUSSION

Tetra-alkylammonium tetrafluoroborates and hexafluorophosphates are commonly employed

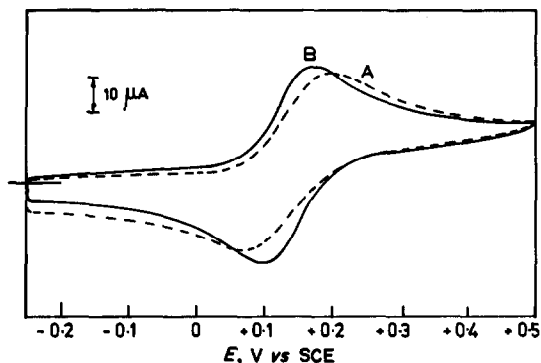
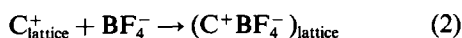
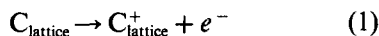


Fig. 4. Cyclic voltamperograms of ferrocyanide (2mM) in 0.1M KCl at 10 mV/sec. (A) with a GCE polarized in TBABF₄/DMF and (B) with a pretreated GCE.

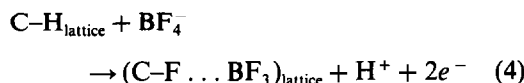
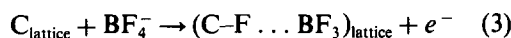
as supporting electrolytes in aprotic solvents to provide a wide potential range for electrochemical studies. However, it is also known that the tetra-alkylammonium cations themselves can be reduced at very negative potentials and the resulting alkyl radicals and trialkylamines can be incorporated in the electrode matrix, especially in the case of porous graphite electrodes.⁸⁻¹¹ In an earlier investigation,⁷ the same type of cathodic process and the resulting inhibitory effect on simple electron transfer was also established for the glassy carbon electrode, but the inhibitory influence of the BF_4^- anion itself is rather surprising.

Graphite is known to form intercalation compounds with anions such as ClO_4^- , F^- and BF_4^- in highly acidic aqueous media.¹²⁻¹⁴ This type of process is linked with the formation of salt-like intercalation compounds between oxidized carbon lattices and the anions.



However, very strongly acidic conditions are required for the formation of such salts and the oxidation potentials encountered in such processes are also much more positive. These types of films also show Nernstian behaviour¹³ and hence are not expected to inhibit charge transfer. This is exactly contradictory to the present observation (Fig. 4). Hence, we assume that in the non-aqueous conditions of the present work, these types of intercalation compounds are not formed on the surface of the glassy carbon electrode.

It should be mentioned that glassy carbon also contains fused benzene ring structures, as do graphite materials, but the former are extremely non-porous because of the method of manufacture, namely the heat-treatment of polymeric materials.^{15,16} The carbon atoms or carbon-hydrogen bonds exposed to the solution side of the interface may be easily fluorinated by an electrochemical oxidation process:



The potential region for this process may be much more negative than the F^-/F_2 redox potential. In this sense, such a process can be compared to the underpotential deposition of metals.¹⁷ This would explain the observation of

the anodic wave at +0.8 V *vs.* SCE although the actual fluorine evolution potential is +2.87 V *vs.* NHE.

In a sense, the formation of a carbon fluoride film proposed here is analogous to formation of graphite fluoride compounds prepared by passing fluorine into a graphite matrix.^{18,19} However, since glassy carbon is quite non-porous, the film formation is confined to the surface region. The electron transfer is generally diffusion-controlled as suggested by the diffusion tail in the voltammetric response (Fig. 1) and the dependence of the peak current on sweep rate (Fig. 2). At constant sweep rate, the $i_p/[\text{BF}_4^-]$ value decreases with increasing $[\text{BF}_4^-]$ (Fig. 3) and hence eventually becomes almost independent of it. The maximum value of the peak current is probably related to the maximum surface area of the electrode available for the surface reaction [equation (3)]. The surface film inhibits the ferricyanide/ferrocyanide redox process (Fig. 4), but this effect can easily be removed by very mild polishing of the electrode surface, which again suggests that film formation is confined to the surface.

CONCLUSIONS

The present work establishes the existence of an electrochemical oxidation process due to BF_4^- at a carbon substrate. A C-F surface film formed by some underpotential process is perhaps responsible for the voltammetric response at around +0.8 V *vs.* SCE in DMF media. Many interesting questions may be asked. Is this process specific to BF_4^- or common to all fluoro-complex anions? Is this process solvent-specific? Can we also observe this process in aqueous solvents? Efforts to answer at least some of these questions are already in progress.

The present communication has the primary objective of pointing out the analytical implications of the results. First, the fact that BF_4^- anions, which are supposed to be inert, can show such a well-defined voltammetric peak in such an easily accessible potential region may be made use of for analytical purposes. Although the plot of i_p *vs.* $[\text{BF}_4^-]$ is non-linear at higher concentrations, a standard graph method may still be used for estimation of BF_4^- at lower concentrations. Secondly, BF_4^- -containing supporting electrolyte/solvent systems should be used with care for the determination of other redox species, especially in the anodic region.

The effect of the surface film in the electron transfer process of interest should be carefully assessed in each case.

REFERENCES

1. M. Fleischmann and D. Pletcher, *Tetrahedron Lett.*, 1968, 6255.
2. G. Sundholm, *J. Electroanal. Chem.*, 1971, **31**, 265.
3. O. Hammerich and V. D. Parker, *J. Am. Chem. Soc.*, 1974, **96**, 4239.
4. M. Gross and J. Jordan, *Pure Appl. Chem.*, 1984, **56**, 1095.
5. S. R. Forsyth and D. Pletcher, *Proc. 1st Internat. Symp. Electrochem. Synth.*, S. Torri (ed.), Elsevier, New York, 1987.
6. M. Chandrasekaran, *Ph.D. Thesis*, Madurai-Kamaraj University, 1989.
7. M. Noel and P. N. Anantharaman, *Analyst*, 1985, **110**, 1095.
8. J. O. Besenhard and H. P. Fritz, *J. Electroanal. Chem.*, 1974, **53**, 329.
9. J. Simonet and H. Lund, *ibid.*, 1977, **75**, 719.
10. G. Bernard, A-M. Martre and J. Simonet, *Electrochim. Acta*, 1980, **25**, 805.
11. E. Kariv-Miller, B. P. Lawin and Z. Vajtner, *J. Electroanal. Chem.*, 1985, **195**, 435.
12. W. Rudorff and V. Hofmann, *Z. Anorg. Allg. Chem.*, 1938, **1**, 238.
13. F. Beck and H. Krohn, *Synth. Met.*, 1986, **14**, 137.
14. F. Beck, H. Krohn and E. Zimmer, *Electrochim. Acta*, 1986, **31**, 371.
15. S. Yamada and H. Sato, *Nature*, 1962, **193**, 261.
16. R. Moy, *Analyst*, 1986, **111**, 883.
17. D. M. Kolb, *Adv. Electrochem. Electrochem. Eng.*, 1978, **11**, 125.
18. Y. Kita, N. Watanabe and Y. Fujii, *J. Am. Chem. Soc.*, 1979, **101**, 3832.
19. N. Watanabe, in *Proc. Workshop Electrochem. Carbon*, Cleveland, OH, September 1983, The Electrochemical Society, Pennington, N.J.

DETERMINATION OF COPPER IN WHITE-METAL BEARING ALLOYS

ZHOU NAN*

Shanghai Research Institute of Materials, Shanghai, MMEI, People's Republic of China

JU ZHAO-QIANG, YU REN-QING, YAO XU-ZHANG and LU ZHI-REN

The Third Factory of Shanghai Reagent Chemicals, Shanghai, People's Republic of China

(Received 18 October 1988. Revised 18 March 1989. Accepted 31 November 1989)

Summary—A method is proposed for the determination of copper in white-metal bearing alloys by direct controlled-potential electrolysis with a tantalum cathode at -0.32 V vs. SCE in a sulphate/bisulphate buffered electrolyte (pH 2) with fluoroboric acid and sodium tartrate as masking agents. Only Bi(III) interferes. Any co-deposited Bi can be corrected for by its spectrophotometric determination with Semi-Xylenol Orange after preconcentration with La(III) as carrier, from an ammoniacal solution containing the redissolved deposit. Any residual Cu(II) in the electrolyte is determined by spectrophotometry with 2,9-dimethyl-1,10-phenanthroline. The standard deviation of this method has been found to be 0.03 mg ($n = 12$) and its relative standard deviation from 0.03 to 0.17%. It has been successfully used for referee analysis and certification of standard reference materials.

The standard methods for the determination of copper in tin- and lead-base alloys are constant-current electrolysis¹⁻⁴ and spectrophotometry with DDTc.⁵ In either case bismuth interferes. The copper may also be determined by iodimetry.^{2,5} A preliminary precipitation of copper from an alkaline tartrate solution is indispensable, however.^{2,5} The spectrophotometric method with hydrobromic acid³ as well as the electrolytic method^{1,3,4} requires the removal of tin and antimony by volatilization as the bromides. It has been reported that the temperature and time of heating during this process should be rigidly controlled, or as much as 25% of the copper may be lost.³ Moreover, it is a time-consuming operation.

We now propose a new method established to meet the requirements of referee analysis and certification of standard reference materials in our laboratory. It is a combination of direct controlled-potential electrolysis with a tantalum cathode and determination of any residual copper by spectrophotometry with 2,9-dimethyl-1,10-phenanthroline. As the bismuth content of alloys of this kind may be as high as 0.2%¹ and under the specified conditions of controlled-potential electrolysis its interference cannot be completely eliminated, a correction for it is incorporated.

EXPERIMENTAL

Apparatus

A controlled-potential electroanalyser, type DJS 52, with a rotating anode (Rex Instruments, Shanghai) was used.

Reagents

Unless otherwise specified, analytical-reagent chemicals and demineralized water were used.

Fluoroboric acid solution, 40%.

Saturated sodium carbonate solution.

o-Cresol Red solution, 0.1%.

Ascorbic acid solution, 4%, freshly prepared.

2,9-Dimethyl-1,10-phenanthroline solution, 0.2% in ethanol.

Lanthanum solution. Dissolve 0.120 g of La_2O_3 of $\geq 99.9\%$ purity in 5 ml of 1M nitric acid (ultrapure grade), transfer the solution to a 50-ml standard flask, dilute to volume and mix. 1 ml Of this solution contains 2 mg of La(III).

DDTC solution. Prepare a 0.2% sodium diethyldithiocarbamate solution just before use.

Copper standard solution A. Dissolve 100.0 mg of electrolytic copper of $\geq 99.9\%$ purity in 20 ml of concentrated hydrochloric acid and several drops of concentrated nitric acid (both ultrapure grade) by gentle warming. Cool the solution, transfer it to a 200-ml standard flask, dilute to volume and mix. 1 ml Of this solution contains 0.500 mg of Cu(II).

*Author for correspondence. Present address: 99 Handan Road, 200433, Shanghai, People's Republic of China.

Copper standard solution B. Prepared just before use by diluting 2.00 ml of standard solution A to volume in a 100-ml standard flask. 1 ml of this solution contains 10 μ g of Cu(II).

Procedures

Sample preparation. Transfer 1 g of the sample, weighed to the nearest 0.1 mg, to a 250-ml beaker. Add 20 ml of concentrated hydrochloric acid and several drops of concentrated nitric acid (both ultrapure grade), and warm gently till dissolution is complete. Cool, add 5 ml of concentrated sulphuric acid and heat to strong fumes. Cool to room temperature. Add successively 10 ml of fluoroboric acid solution, 1.5 g of sodium tartrate, 1 or 2 drops of *o*-Cresol Red indicator solution, and saturated sodium carbonate solution dropwise till the indicator colour changes just from red to yellow. Dilute to *ca.* 70 ml with water.

Controlled-potential electrolysis of copper. The electrodes used are: (1) an SCE reference electrode of double-junction type with 5M sodium formate as the bridge electrolyte, (2) a rotating anode, (3) a tantalum gauze cathode. The use and pretreatment of this cathode has been described elsewhere.⁶ Set the cathode potential at -0.32 V *vs.* SCE. Continue the electrolysis until the electrolytic current no longer decreases. Wash the split cover glasses, the rotating anode and the inner walls of the beaker with a little water. Continue the electrolysis for 5 min. Remove the beaker containing the sample and immediately replace it with one containing *ca.* 100 ml of water, and wash the electrodes in this for 30–60 sec. Repeat this operation once more. Remove the cathode and dip it into ethanol for 30 sec, then dry it to constant weight with hot air from hair-drier. Dissolve the copper in 15 ml of hot ultrapure nitric acid (1 + 3), then wash, dry and reweigh the cathode. Reserve the solution for determination of bismuth as described below. The weight of the deposit is found by difference.

Spectrophotometric determination of residual copper. Transfer the electrolysed sample solution and the washings (the second of which has been evaporated to 50 ml) into a 250-ml standard flask, dilute to volume and mix. Pipette an appropriate aliquot (≤ 25 ml) into a 60-ml separating funnel. Add ultrapure ammonia solution (1 + 1) dropwise until the pH is 5–6, then add 5 ml of ascorbic acid solution and 2.0 ml of 2,9-dimethyl-1,10-phenanthroline solution and mix. Shake the mixture with 10 ml of

chloroform for 1 min. Measure the absorbance of the organic extract at 457 nm *vs.* chloroform as the reference solution,^{7,8} using 2-cm cells. Read the Cu content from a calibration curve prepared with 0.50–3.00 ml of Cu standard solution B treated in the same way as the sample.

Correction for Bi. Transfer the nitric acid solution of the copper deposit in small portions, with vigorous stirring, to a beaker containing 10 ml of ultrapure ammonia solution (1 + 1) and 70 ml of water. Add 5 ml of lanthanum solution and boil gently for 2 or 3 min. Cool to room temperature, filter off the precipitate on a filter paper of medium porosity, wash it with ammonia solution (ultrapure grade, 2 + 98) and redissolve the precipitate with hot nitric acid (ultrapure grade, 1 + 15) added in portions. Concentrate the resulting solution to 3–4 ml. Then determine the bismuth spectrophotometrically with Semi-Xylenol Orange as reported elsewhere.⁹

If a considerable amount of bismuth is present, first dilute the concentrate to volume in a 25-ml standard flask, mix, and use an appropriate aliquot for the determination.

The Cu content of the sample can be calculated from

$$\text{Cu} = 100(a + b - c)/G\%$$

where G = sample weight (g); a = weight of deposit (g); b = amount of residual Cu (g); c = amount of co-deposited Bi (g).

RESULTS AND DISCUSSION

Sample decomposition

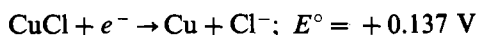
The decomposition technique used is the most efficient available, as discussed elsewhere.¹⁰

Choice of medium for electrolysis

Controlled-potential electrolysis is used, as electrolysis at constant applied voltage or constant current lacks selectivity; we have found that it is impossible to prevent the co-deposition of Sn during electrolysis of Cu by the ASTM procedure¹¹ at constant applied voltage.

Nitric acid is commonly used as the electrolysis medium but has the drawback that nitrous acid is often liberated during the electrolysis, especially in summer, and causes dissolution of freshly deposited copper. The analyte is present in a hydrochloric acid medium after the sample decomposition, but this is unsuitable for

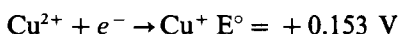
electrolysis, in which the electroreduction of Cu(II) is a two-stage process:



Hence under such conditions Cu(II) is more readily reduced to Cu(I) than Cu(I) is to the metallic state. This is due to the complexation with chloride. Complications may arise because the Cu(I) complexes such as CuCl_2^- and CuCl_3^{2-} can be reoxidized to Cu(II) at the anode unless precautions are taken. Moreover, sufficient anodic depolarizer should be present to prevent the anodic liberation of chlorine.

Therefore sulphuric acid was chosen as the medium because sulphate is not electroactive. The advantages of Ta over Pt as cathodic material have been discussed elsewhere.⁶ The side-reaction of the cathodic reduction of protons to hydrogen is minimized since the overpotential of hydrogen on Ta is considerably higher than that on Pt. Sodium formate⁶ is used as bridge electrolyte for the SCE to avoid contamination of the electrolyte with nitrate or chloride.

Moreover, the electroreduction of Cu(II) in this medium leads straight to the metallic state, because (potentials are taken from Latimer¹²),



On the one hand the reduction of Cu(II) to Cu takes place more readily than that to Cu(I) and on the other, though Cu(I) may be formed as an unstable intermediate, its reduction to Cu goes much more easily than that of Cu(II).

Lead, a major constituent of the sample, will be precipitated as the sulphate in this medium. This does no harm because it settles at the bottom of the beaker and is not disturbed by the rotation of the anode. Under such conditions the conditional electrode potential of Pb(II) would be shifted from -0.113 to -0.359 V,¹³ which is favourable for the electrolytic separation of Cu(II) from Pb(II).

Choice of pH

The analyte solution should be sufficiently acidic to limit the hydrolysis of Sn(IV) (a major component in the solution), otherwise the equilibrium of the system used for masking the tin (see below) would be unfavourably disturbed.

On the other hand too great an acidity would also disturb this system by protonating the ligand used. The optimum pH was found to be *ca.* 2, which is very close to the pK_2 value of sulphuric acid. It is very easy to adjust the system to this value because an equimolar bisulphate/sulphate solution has maximum buffer capacity at this pH and *o*-Cresol Red serves very well as the indicator.¹⁴

Choice of masking agents

Our preliminary experiments revealed that the presence of sodium tartrate and tetrafluoroboric acid does not affect the deposition of Cu and that neither alone can prevent the co-deposition of Sn. The combined use of the two proved effective, however. This may be ascribed to the formation of more stable mixed-ligand complexes. It serves also to prevent the co-deposition of As and Sb, but not Bi. As maskant for Bi(III), EDTA, DPTA, DCTA and NTA were tried, but the deposition of Cu is hindered in each case. Therefore a correction for the co-deposition of Bi is incorporated.

Cathode potential

It was found that the electro-deposition of Cu begins at -0.18 V *vs.* SCE under the chosen conditions. The amount of deposit increases as the cathode potential shifts to more negative values and becomes constant at -0.30 V and below (Table 1). Our preliminary experiments revealed that the co-deposition of Sn begins at -0.36 V under the same conditions. Therefore the cathode potential is set at -0.32 V *vs.* SCE.

Correction for the deposition of Bi

The correction for Bi involves co-precipitation of Bi(III) with La(III) as carrier from an ammoniacal solution to separate it from Cu(II), and subsequent spectrophotometric determination of Bi(III) with Semi-Xylenol Orange⁹ in nitric acid medium (0.18M). This preconcentration technique^{15,16} has been used in our

Table 1. Effect of cathode potential on the deposition of Cu: [added: Cu(II) 67.00 mg; Sn(IV) 1000 mg; 40% HBF₄ 10 ml; sodium tartrate 1.5 g; total volume 80 ml; pH 2]

Cathode potential, V <i>vs.</i> SCE	Cu deposited, mg
-0.18	61.30
-0.25	65.65
-0.30	66.90
-0.34	66.90

laboratory for ten years and is based on the following facts and data: (1) the ionic radii of Bi(III) and La(III) are very similar, 1.20 and 1.15 Å, respectively;¹⁷ (2) bismuth hydroxide is much more insoluble in water than lanthanum hydroxide (their pK_{sp} values are reported to be 36.91 and 19.6 respectively).¹⁸ La(III) is used as carrier because it can be tolerated in considerable amounts in the Bi-SXO spectrophotometric system under the conditions specified.

Successive determination of Cu and Bi

The same sample may be used for determination of Bi. Transfer to a separating-funnel an appropriate aliquot ($f\%$) of the solution reserved for the determination of residual Cu and adjust it to pH 9 with ammonia solution (1 + 1, ultrapure grade). Add 5 ml of freshly prepared 0.2% DDTC solution and shake the mixture with 5 ml of chloroform for 1 min. Repeat this operation till the addition of DDTC gives no turbidity and the extract is colourless. Combine the organic extracts and transfer to a 100-ml beaker containing 10 ml of water. Evaporate the chloroform by heating in a water-bath. Then add 1 ml of perchloric acid (1 + 11) and continue to evaporate to 3–4 ml to decompose the DDTC into carbon dioxide and diethylamine. Finally pipette in $f\%$ of the solution prepared for the bismuth correction, and determine the Bi with Semi-Xylenol Orange.⁹

Application

Volatilization of Sn(IV) as the bromide is easy in the absence of other cations, but is time-consuming in the presence of Cu(II), several repetitions of the volatilization step being needed. This can be explained as follows. Both Sn(IV) and Cu(II) react with bromide to form anionic complexes. During the volatilization these dissociate to form molecular species. The ionic radii of Sn(IV) and Cu(II) are very similar 0.71 and 0.69 Å respectively.¹⁷ Once formed, $CuBr_2$ would precipitate and carry down some

Table 2. Determination of Cu in synthetic samples by the proposed method

Composition of the sample, mg	Cu, mg	
	Taken	Found
Sb 150, Sn 60, Pb 758, Bi 2	30.00	30.05
Sb 50, Sn 898, Bi 2	50.00	49.97
Sb 100, Sn 738, Pb 110, Bi 2	50.00	49.98
Sb 80, Sn 838, Bi 2	80.00	80.03
Sb 110, Sn 688, Pb 100, Bi 2	100.00	100.02

Table 3. Determination of Cu in some SRM samples

Sample		Cu, %	
		Certified value	Proposed method
B.S.	178	4.08	4.08
SRIM	610	5.97	5.96
	615	2.66	2.67

$SnBr_4$. Hence this is by no means a clean-cut and efficient method of separation.

The proposed method is a direct one as it involves no preliminary separation. The controlled-potential electrolysis serves as a means of simultaneous separation and determination of Cu. Its combination with a spectrophotometric finish and correction for Bi eliminates any error, either positive or negative. The accuracy of the method is thus ensured. This has been validated by analysis of some synthetic (Table 2) and SRM samples (Table 3). The standard deviation of this method has been found to be 0.03 mg ($n = 12$) and its RSD from 0.03 to 0.17%. It has been successfully used for referee analysis and certification of standard reference materials.

CONCLUSION

Proposed in this paper is a direct and accurate method for determination of copper in white-metal bearing alloys by controlled-potential electrolysis with a tantalum cathode at -0.32 V vs. SCE in a sulphate/bisulphate buffer of pH 2 in the presence of tetrafluoroboric acid and sodium tartrate. Its combination with a spectrophotometric finish with 2,9-dimethyl-1,10-phenanthroline and correction for co-deposited bismuth eliminates any possible error. The bismuth may also be determined.

REFERENCES

1. ASTM E 57 (1978).
2. JIS H 1501 (1975).
3. ASTM E 87 (1978).
4. ASTM E 46 (1978).
5. JIS H 1503 (1975).
6. Zhou Nan and He Chun-xiang, *Talanta*, 1990, **37**, 677.
7. J. Fries and H. Getrost, *Organic Reagents for Trace Analysis*, p. 133. Merck, Darmstadt, 1975.
8. K. L. Cheng, K. Ueno and T. Imamura, *CRC Handbook of Organic Analytical Reagents*, p. 334. CRC Press, Boca Raton, 1982.
9. Zhou Nan, Yu Ren-qing, Yao Xu-zhang and Lu Zhi-ren, *Talanta*, 1989, **36**, 733.
10. *Idem, ibid.*, 1985, **32**, 1129.
11. ASTM E 478 (1978).
12. W. M. Latimer, *The Oxidation States of the Elements and their Potentials in Aqueous Solutions*, 2nd Ed., p. 342. Prentice-Hall, New York, 1953.

13. G. Millazo and S. Caroli, *Tables of Standard Electrode Potentials*, pp. 22–167. Wiley, New York, 1978.
14. Zhou Nan, Yu Ren-qing, Yao Xu-zhang and Lu Zhi-ren, *Talanta*, 1985, **32**, 1125.
15. Z. Marczenko, *Chem. Anal. (Warsaw)*, 1966, **11**, 347.
16. W. Reichel and B. G. Bleakly, *Anal. Chem.*, 1974, **46**, 59.
17. J. G. Stark and H. G. Wallace, *Chemistry Data Book*, 2nd Ed., pp. 28–29, Murray, London, 1982.
18. S. Kotrlý and L. Šúcha, *Handbook of Chemical Equilibria in Analytical Chemistry*, pp. 212–215. Horwood, Chichester 1985.

AN ATOMIC-EMISSION STUDY OF THE REMOVAL AND RECOVERY OF CHROMIUM FROM SOLUTION BY AN ALGAL BIOMASS (*Chlorella vulgaris*)*

CONSTANTINOS P. PAPPAS, SEAN T. RANDALL and JOSEPH SNEDDON†
Department of Chemistry, University of Lowell, Lowell, MA 01854, U.S.A.

(Received 23 June 1989. Revised 17 August 1989. Accepted 21 August 1989)

Summary—Inductively coupled plasma atomic-emission spectrometry has been used to study the removal of chromium, principally in the hexivalent oxidation state, from solution by an algal biomass, *Chlorella vulgaris*, and its subsequent recovery. Binding of the chromium at the 5–100 µg/ml level was maximal (75%) at pH 3 within 3 min, with 5 mg of algae. Quantitative recovery of chromium was achieved by lowering the pH. The algae could be used four times in removal/recovery cycles before losing their 75% removal efficiency.

The ability of certain phytoplankton and microalgae to bind metal ions has been well documented and there are many reports on the accumulation of metal ions by different species of micro-organisms.¹⁻⁹ When waters containing metal ions are passed through a body of water where algae are growing, the effluent waters often have lower metal ion concentrations than the inflowing waters, and algal growth is often suppressed. Metal ions,¹⁰ cobalt chloride and zinc sulfate,¹¹ and chlorinated waters¹² have all been reported to have a deleterious effect on algal growth. Since favorable environments are needed for the growth and reproduction of algae there are obvious limitations to the removal (and recovery) of low levels of toxic or precious metals by use of living algae. Living micro-organisms primarily accumulate metal ions in solution by adsorbing them on the outer surface of the cell wall. This adsorption process has variously been called bioconcentration, bioaccumulation and biosorption, the last being the most frequently used. Biosorption is independent of biological functions. Thus dead cells may be used for the removal of metal ions from solution under conditions normally toxic to living organisms. Recent work from this laboratory,^{13,14} Darnall and co-workers,^{15,16} and others¹⁷⁻¹⁹ has shown the potential of an algal biomass for the removal and recovery

of metal ions in solution at low concentrations (µg/ml levels). This relatively cheap, simple and rapid method of removing trace and ultratrace metals from solution has potential application in the recovery of precious or important metals,¹³ detection and control of toxic metals in waters,¹⁵ and for the preconcentration of trace metals for determination.¹⁹

In this work a study of the use of *Chlorella vulgaris* for the removal and recovery of chromium, principally in the hexivalent oxidation state, is presented.

EXPERIMENTAL

Instrumentation

A Leeman Labs. Plasma-Spec II (Lowell, MA) inductively coupled plasma atomic-emission spectrometer (ICP-AES) was used with sample introduction by a Hildebrand Grid nebulizer and a variable speed peristaltic pump. The sample uptake rate was 1.5 ml/min in the "slow" position and 3.0 ml/min in the "fast" position. The support gas was argon at a consumption of 10 l./min for the coolant gas and 0.5 ml/min for the injector tube. A detailed description of the ICP-AES characteristics is given elsewhere.²⁰

The pH-meter used was an Orion model 501 Digital Ionanalyzer with an automatically temperature-compensated semimicro combination probe. The precision of the pH measurements

*Presented, in part, at the 40th Pittsburgh Conference in Atlanta, Georgia, 6-10 March 1989.

†Author for correspondence.

was ± 0.01 and of the temperature measurement $\pm 0.1^\circ$.

A Perkin-Elmer Model 570 spectrophotometer and Model 700 infrared spectrometer were used.

Reagents

The algal biomass, *Chlorella vulgaris*, was obtained from Laurel Canyon Herbs Inc. (Emeryville, CA). All other reagents were obtained from Fisher Scientific Co. All pH adjustments were made with 0.5M nitric acid and 0.1M sodium hydroxide. Stock 1000 $\mu\text{g/ml}$ chromium solutions, made from a potassium dichromate certified atomic-absorption standard for Cr(VI) and chromium acetate for Cr(III), were diluted as required, with distilled-demineralized water, and used at pH 0–5.5.

Procedure

The *Chlorella vulgaris* was treated as previously described,¹³ to remove potential contaminants, and killed by heating in an oven at 120° for 6 hr, then cooled to room temperature in a desiccator. This minimized living-cell factors which could adversely affect the experimental reproducibility.

The removal of chromium ions from solution by *Chlorella vulgaris* was examined by the batch method.^{13–16} A known mass of the algae (typically 5 mg) added to a known volume of chromium solution (typically 5.0–10.0 ml) is agitated or stirred gently for a predetermined time. The suspension is then centrifuged at 3000 rpm for 7–10 min and the supernatant liquid analyzed for chromium. The amount of chromium bound by the algae is calculated from the initial and final chromium concentrations in solution. The pH of the chromium solution is adjusted before addition of the algae and measured again afterwards. Previous work^{21,22} had shown that this method gives results comparable to those obtained by direct determination of chromium in the algae. Recent work has shown the potential of a column method in which the metal solution is passed through a column of algae adsorbed on silica gel, and the effluent is analyzed.¹⁷ The ICP-AES measurements were repeated at least three and often five times and the average was taken. Each experiment with the algae was repeated at least twice and more frequently four times.

RESULTS AND DISCUSSION

Determination of chromium by ICP-AES

Use of the following wavelengths was investigated with respect to sensitivity and detection limit for chromium: 205.55 nm (ion), 283.56 nm (ion), 357.87 nm (ion), 360.53 nm (atom), 425.43 nm (atom) and 424.48 nm (atom). Serial dilutions of the 1000 $\mu\text{g/ml}$ chromium stock solution adjusted to pH between 0 and 5.5 (typically 3) were used for the calibration at the six wavelengths. The 283.56 nm line was the most sensitive and the equation of the calibration curve ($Y = a + bX$, where Y is the atomic emission intensity expressed as number of counts, and X is the concentration in $\mu\text{g/ml}$) was $Y = 1.56 \times 10^4 + 4.88 \times 10^4 X$, with a correlation coefficient of 0.999. At this wavelength, the limit of detection was 0.017 $\mu\text{g/ml}$ and the calibration plots was linear up to at least 100 $\mu\text{g/ml}$ (the highest concentration investigated). Short-term precision (~ 15 min) was $\pm 0.5\%$ and long-term precision (several hours) 1.0–2.0% for aqueous solutions. Aqueous solutions were mostly used and some work with magnesium and sodium chloride solutions showed a deterioration in precision by a factor of 1.2–2.0. Salt-to-chromium ratios $> 100:1$ enhanced the chromium signal, but this aspect was not further investigated. Use of another chromium wavelength might give different matrix effects.

Chlorella vulgaris characteristics

The *Chlorella vulgaris* used was obtained commercially and before use was washed in 0.5% v/v nitric acid to remove potential contaminants. The wash solutions were analyzed by ICP-AES and found to contain no detectable chromium, *i.e.*, $< 0.017 \mu\text{g/ml}$. The first acid washing became very light green and the fourth was colorless. Finally the algae were washed with demineralized-distilled water. A very small amount of the algae dissolved in the wash solution. The absorption spectrum of the washings exhibited a broad band with a maximum at 246 nm, but no further work was done on this in this study. The infrared spectra of the heat-killed unwashed, acid-washed and chromium-reacted algae (in nujol mulls) were obtained. The unwashed algae gave a strong band at 3100–3600 cm^{-1} , medium absorption at 1650 cm^{-1} , and weak absorption at 1170 cm^{-1} . The spectrum of the acid-washed algae exhibited similar features, but the 3100–3600 cm^{-1} band

was less intense. The spectrum of the chromium-reacted algae had a very weak band at 1170 cm^{-1} , possibly indicating binding of the chromium by the algae.

Removal of chromium from solution by *Chlorella vulgaris*

The effect of pH between 0 and 5.5 is shown in Fig. 1. In the case of the Cr(VI) solution a maximum binding of approximately 75% occurred at around pH 2.8 with significant decrease in binding at higher and lower pH. When a Cr(III) solution was used the effect of pH between 0 and 5.5 was quite different, with virtually no binding at low pH. Other than in this experiment, the chromium solutions used were in the chromium(VI) oxidation state. Chromium(III) is an essential species in mammals whereas chromium(VI) is considered to be a potentially toxic and severe industrial hazard. Cr(III) solutions are notoriously inert and the hexa-aquo ion is only converted into inner sphere complexes under certain conditions. A control experiment was run in which a series of solutions containing $5\text{ }\mu\text{g/ml}$ of chromium [as Cr(III)] was prepared, with pH adjusted to 0–5.5. Chromium determination before and after the pH adjustment showed that precipitation of the chromium was negligible. Cr(VI) would not be precipitated by pH adjustment. Thus all removal of the chromium from solution by the algae was due to chromium–algae interaction.

The results shown in Fig. 1 for the effect of pH on the binding of the two species of chromium to *Chlorella vulgaris* suggest that a different mechanism of binding may exist for elements in different oxidation states. However, it is possible that the surface groups of the algae will convert Cr(VI) into Cr(III). The removal of

chromium ions from solution will probably occur through two mechanisms: ion-exchange or the formation of coordination compounds. Several authors have proposed these mechanisms^{10,23,24} for various metal ions and strains of algae, but the complexity of the cell surface will lead to a complex mechanism which may be kinetically controlled.

The rate of chromium uptake at pH 3 was investigated with 10 mg of algae in 5.0 ml of $5.0\text{ }\mu\text{g/ml}$ chromium solution, over a period of 1–70 min contact time before centrifugation. Maximal uptake rate was achieved in 3 min.

The effect of algal mass on chromium removal was tested at pH 3 with a contact time of 40 min and 0–100 mg of algae in 5.0 ml of $5.0\text{ }\mu\text{g/ml}$ chromium solution. Removal of chromium was constant at 75% with 5 mg of algae or more. Majidi and Holcombe reported a similar result for the uptake of cadmium by a different algal species.¹⁹ It was observed that at high concentrations, the algae tended to clump together, so the surface area in contact with the chromium could be less than expected, but it is debatable whether this would account for the mass effect just described. The effect of stirring speed was found to be negligible. During this study the suspension of algae in the chromium solution was slowly stirred throughout the exposure time. In earlier experiments, sonication was employed but the results were very variable, which is why the stirring method was used. It might be expected that the larger the mass of algae used, the more efficient the stirring would need to be to ensure adequate contact between the algae cells and the chromium ions. Stirring 10 mg of algae with 5.0 ml of 5–100 $\mu\text{g/ml}$ chromium solution at pH 3 for 40 min gave 75% removal of chromium. As reported for cadmium,¹⁹ the degree of removal appeared to be constant. This shows that the mass of chromium removable by the algae is at least $35\text{ }\mu\text{g}$ per mg of algae. The maximum removable was not examined in this study.

The reproducibility of removal of chromium from 5.0 ml of a $5\text{ }\mu\text{g/ml}$ solution at pH 3 by 10 mg of algae in 30 min was examined (20 replicates). The mean uptake was $1.5\text{ }\mu\text{g}$ per mg of algae (standard deviation $0.07\text{ }\mu\text{g/mg}$) instead of the $1.8\text{ }\mu\text{g/mg}$ (i.e., 75% uptake) achieved in the earlier work. As a single biomass stock was used, with different batches of algae treated in the same manner but prepared at different times, this variation in chromium uptake was attributed to the age of the treated biomass. The

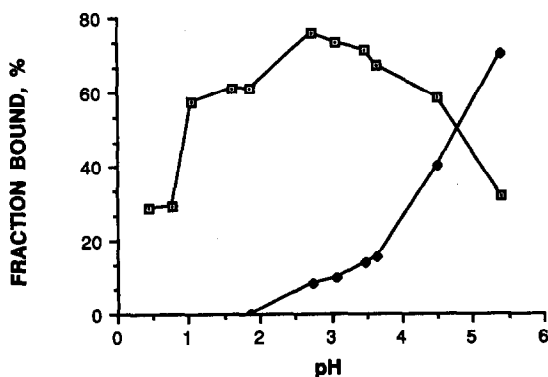


Fig. 1. Effect of pH on the removal of chromium from 5.0 ml of $5.0\text{ }\mu\text{g/ml}$ chromium(VI) [□] and chromium(III) [◆] solutions by 5 mg of *Chlorella vulgaris* in 30 min.

unwashed algae were kept in a refrigerator at -4° to extend their freshness and prevent contamination by the growth of other organisms. Several batches which were used at a later time (the reproducibility study was done about a year after the initial study) showed a reduced binding capacity. A further factor in this decrease could be the extent of cell breakage, as the intercellular material plays an important role in the binding by complexation.

The effect of magnesium or sodium chloride on the removal of chromium by the algae was studied at pH 3, with 10 mg of algae stirred for 30 min in 5.0 ml of 10 $\mu\text{g/ml}$ chromium solution with magnesium and sodium chloride concentrations ranging from 0 to 500 $\mu\text{g/ml}$. These chlorides were selected because they are the most abundant in sea-water. In a magnesium and sodium chloride matrix, the binding efficiency was reduced. At 10 $\mu\text{g/ml}$ salt concentration the uptake of chromium by the algae was only 55% and decreased only slightly at higher concentrations, to 49% at the 500 $\mu\text{g/ml}$ level.

Recovery of chromium taken up by Chlorella vulgaris

Chromium and its compounds are widely used in industry, *e.g.*, in tanning leather, printing, in waterproofing fabrics, corrosion prevention, in paints, in ceramic products, in the manufacture of magnetic tapes, and in the aircraft industry. In certain cases, it may be environmentally desirable or economically feasible to recover this metal from solutions even at relatively low concentrations ($<100 \mu\text{g/ml}$).

Chromium bound to *Chlorella vulgaris* can be recovered by combustion at moderate temperatures, but this has limited potential because the algae are destroyed. Salting out of the chromium from the algae involves the addition of a large concentration ($>100:1$ relative to Cr) of a salt which competes with the chromium for the binding sites of the algae and will displace it. As noted previously, the addition of a relatively small concentration of salt adversely affects the binding of chromium in solution to the algae. The addition of a large amount of salt (typically 10 ml of 5000 $\mu\text{g/ml}$ of sodium chloride) to algae to which chromium had been bound resulted in removal of the chromium into solution. The recovery was determined by ICP-AES and found to be 80%. However, the solution contained the chromium in a salt matrix, from which further separation would be required for its recovery. This aspect was not

pursued in this study. This method has potential for large-scale use if separation of the chromium from the salt matrix is efficient and relatively straightforward. The use of the pH effect was investigated by stirring the chromium-carrying algae for 5 min in a solution at pH 1 and measuring the displaced chromium by ICP-AES. The recovery found was 70%. The *Chlorella vulgaris* could be used four times before the binding efficiency started to decrease below 75%. After a fifth cycle the binding efficiency was only 40% and after a seventh cycle had decreased to 34%. It should be noted that the initial treatment of the *Chlorella vulgaris* will affect the number of times the algae can be recycled, presumably because of changes in the number of active groups.

REFERENCES

1. A. Preston, D. F. Jeffries, J. W. R. Dutton, B. R. Harvey and A. K. Steele, *Environ. Poll.*, 1972, 3, 69.
2. D. R. Trollope and B. Evans, *ibid.*, 1976, 11, 106.
3. W. B. Kerfoot and S. A. Jacobs, *Environ. Sci. Technol.*, 1976, 10, 662.
4. F. Laube, S. J. Ramamoorthy and D. J. Kushner, *Bull. Environ. Contam.*, 1979, 21, 763.
5. D. S. Filip, T. Peters, V. D. Adams and E. J. Middlebrooks, *Water Res.*, 1979, 13, 305.
6. C. L. Brierley, *Sci. American*, 1982, 247, No. 2, p. 42.
7. M. Galun, P. Keller, D. Malki, H. Fieldstein, E. Galun, S. M. Siegal and B. Z. Siegal, *Science*, 1983, 219, 285.
8. A. Les and R. W. Walker, *Water, Air, Soil Pollut.*, 1984, 23, 129.
9. R. J. Kiff and D. R. Little, *Proc. Int. Conf. Heavy Metals in the Environment*, Athens, T. D. Lekkas (ed.), Vol. 1, p. 638. C.E.P. Consultants, Edinburgh, 1985.
10. J. J. Rosko and J. W. Rachin, *Bull. Torrey Bot. Club*, 1977, 104, 26.
11. P. M. Sivalingham, *Japan J. Phycol.*, 1980, 28, 159.
12. J. M. Jouany, P. Vasseur and J. F. Ferard, *Environ. Poll.*, 1982, 27, 206.
13. P. R. Zimnik and J. Sneddon, *Anal. Lett.*, 1988, 21, 1381.
14. J. Sneddon and C. P. Pappas, *Am. Environ. Lab.*, 1990, 2, in the press.
15. D. W. Darnall, B. Greene, M. T. Henzl, J. M. Hosea, R. A. McPherson, J. Sneddon and M. D. Alexander, *Environ. Sci. Technol.*, 1986, 20, 206.
16. D. W. Darnall, B. Greene, M. T. Henzl, R. A. McPherson and M. D. Alexander, *ibid.*, 1986, 20, 687.
17. W. W. Kubiak, J. Wang and D. W. Darnall, *Anal. Chem.*, 1989, 61, 468.
18. C. A. Mahan, V. Majidi and J. A. Holcombe, *ibid.*, 1989, 61, 624.
19. V. Majidi and J. A. Holcombe, *Spectrochim. Acta*, 1988, 43B, 1432.
20. C. P. Pappas, *M.Sc. Thesis*, University of Lowell, 1989.
21. P. G. Mitchell, B. Greene and J. Sneddon, *Mikrochim. Acta*, 1986, I, 101.
22. P. G. Mitchell and J. Sneddon, *Talanta*, 1987, 34, 849.
23. R. H. Crist, K. Oberhoiser, N. Shank and M. Nguyen, *Environ. Sci. Technol.*, 1981, 15, 1212.
24. H. K. Wang and J. M. Wood, *ibid.*, 1984, 18, 106.

RAPID DETERMINATION OF ZINC AND IRON IN FOODS BY FLOW-INJECTION ANALYSIS WITH FLAME ATOMIC-ABSORPTION SPECTROPHOTOMETRY AND SLURRY NEBULIZATION

JOÃO CARLOS DE ANDRADE*

Universidade Estadual de Campinas, Instituto de Química, CP 6154, 13081 Campinas, SP, Brasil

FREDERICK C. STRONG III and NADIR J. MARTIN

Universidade Estadual de Campinas, Faculdade de Engenharia De Alimentos, CP 6121, 13081 Campinas, SP, Brasil

(Received 15 April 1989. Revised 9 August 1989. Accepted 22 August 1989)

Summary—A rapid method of determining zinc and iron in food by flame atomic-absorption spectrophotometry with slurry nebulization into an air-acetylene flame has been developed. A V-groove, clog-free Babington-type nebulizer, coupled to a single-line flow-injection analysis (FIA) system, was employed to introduce the slurry into the spray chamber. Under the FIA conditions described, an injection frequency of 120/hr is possible, with negligible carry-over and memory effects. The calibration graphs were obtained by using various concentrations (up to 0.1 g/ml) of white bean homogenate as standards, rather than solutions. The method has been applied to various kinds of foods, including grains, vegetables, fruits and sausage. Homogenization of semi-prepared samples to form slurries took only 4 min. Relative deviations between results by the slurry and solution methods for both elements averaged 2–3%. Detection limits by the slurry method were 0.3 µg/ml Zn and 0.6 µg/ml Fe.

Bringing samples into a suitable solution form has a number of disadvantages. Dry ashing of animal or vegetable matter is time-consuming, and dissolution of the ash in acid may result in the introduction of impurities. Wet-ashing of organic matter can also result in contamination. On the other hand, conversion of a sample into a slurry that can be directly injected into a flame is rapid and avoids the delay of ashing procedures. Although the samples must be prepared individually, the time required is quite short.

Fry and Denton^{1,2} first introduced a successful clog-free nebulizer for atomic spectroscopy, based on the Babington principle of aerosol generation. This involves a violent disruption of a liquid flowing as a film across a small orifice from which compressed gas emerges at supersonic velocity.³ This type of device, capable of handling high solid-content slurries, has been used for the determination of elements in various complex matrices by atomic-emission spectrometry (AES),^{4–10} but comparatively few such studies have been made by use of flame atomic-absorption spectrophotometry (FAAS).^{1,2,11}

As a peristaltic pump sample-delivery system is usually employed to keep the analyte flow-

rate constant,² a single-line flow-injection analysis (FIA) manifold¹² might be better for sample introduction in a slurry nebulization (SN) procedure, since it would provide the important FIA characteristics, as well as good instrument response.¹³ This simple FIA system consists of one tube through which the carrier stream moves towards the detector. Use of a limited dispersion coefficient ($D \sim 1-2$) will serve to transport the sample in virtually undiluted form to the detector.^{14,15}

This work reports on an FIA/SN/FAAS system employed for the determination of zinc and iron in a variety of foods.

METHOD DEVELOPMENT

Reagents and standard solutions

All chemicals were of analytical grade and distilled demineralized water was used throughout. All solutions, including samples and standards, were stored in high-density polyethylene flasks. The iron and zinc stock standard solutions were prepared by dissolving 1.0000 g of the pure metal in a minimum amount of concentrated hydrochloric acid and diluting to 1 litre. Working solutions were prepared from the stock solutions as required.

*Author for correspondence.

Table 1. Particle sizes in slurries as a function of homogenization time

Homogenization time, min	Particle size, μm					
	Initial slurry		Supernatant liquid*		Residue from decanting*	
	Range	Mean	Range	Mean	Range	Mean
1	4-8	6.7	3-4	3.6	46-62	55
2	4-6	5.0	3-4	3.4	39-62	47
3	4-7	5.3	1-4	2.8	31-39	34
4	3-6	4.2	1-4	2.5	28-50	36
5	3-6	4.5	1-3	2.0	28-52	42

*After a settling period of 30 min.

Preparation of slurries and sample solutions

White beans were chosen as a test sample material and for preparing slurry calibration standards because they have a good consistency for grinding and are stable if properly stored. They were ground in a Tigre hammer mill to pass a 1.8 mm mesh sieve. A Tecnal Model TE 102 tissue homogenizer was used to prepare the slurries. The particle sizes in the slurries were determined with a Nikon microscope, equipped with a graduated scale. All weighings were performed with a precision of ± 0.1 mg.

The sample homogenization procedure was optimized as follows. One-gram portions of white beans were ground and each portion was homogenized in ~ 50 ml of water for a period ranging from 1 to 5 min, then diluted to 100 ml and the suspension was shaken for 1 min. Small portions were then placed on microscope slides and diameters of particles chosen at random were measured with the graduated scale of the ocular micrometer. The suspensions were then allowed to settle for 30 min, the supernatant liquids were decanted from the settled material and the diameters of the particles in the liquid

and the sediment were measured. The results are given in Table 1. Since particles with sizes below $10 \mu\text{m}$ can, in principle, be easily transported through the spray chamber to the flame,^{10,11} a period of homogenization as short as 1 min could have been used. However, as the data show a minimum particle size at 4 min, this period was chosen for use throughout the rest of the work. The larger particles found in the residue after settling for 30 min were probably due to agglomeration. Such large particles were not found in the initial slurry. To avoid settling and agglomeration, samples were always shaken vigorously before their introduction into the FIA system.

Solutions of the test sample were prepared by weighing 3-g samples into porcelain crucibles, heating on a hot plate until no more smoke was evolved, and then heating in a muffle furnace at 450° for 6 hr. After cooling, 0.5 ml of water and 4 ml of hydrochloric acid (1 + 1) were added and the solution was diluted to 100 ml.¹⁶

Instrumentation

The analytical system used (Fig. 1) was based on a single-line FIA manifold,¹² coupled to a

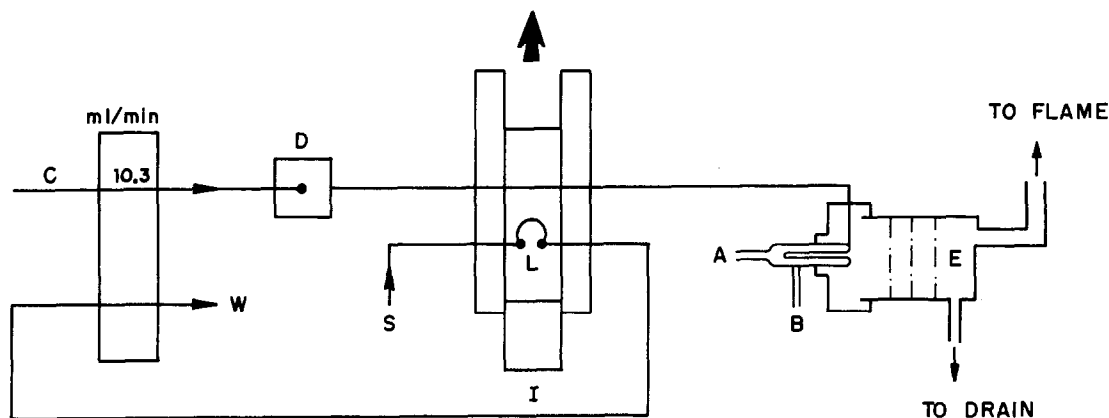


Fig. 1. Single-line FIA manifold used for the FIA/SN/FAAS method. A, Babington nebulizer (details in Fig. 2); B, fuel entrance; C, carrier feed line; D, damper (bore 9 mm, length 40 mm);¹⁷ E, spray chamber with baffles; I, injector (in loading position); L, injection loop (variable volumes); S, sample; W, waste.

premix type spray chamber and a 10-cm three-slot burner, to which the Babington-type nebulizer (Fig. 2) was attached. The nebulizer design was based on the work of Fry and Denton,^{1,2} with some modifications. It was a V-groove type,¹⁸ made of polytetrafluoroethylene (PTFE) and mounted in a glass support. Higher sensitivity was obtained by inserting a second (auxiliary) source of oxidant (air). The V-groove for the flow of sample over the nebulizer orifice (diameter 0.6 mm) had a depth of 1 mm. Additional details and dimensions are given in Figs. 2 and 3.

The sample and FIA carrier (water) were transported by use of a laboratory-made peristaltic pump and Tygon pump tubing (Technicon) to load the FIA injection loop and to keep the flow-rate of the carrier feed-line constant. It was found desirable to use a pulse damper, D, in the carrier line¹⁷ (Fig. 1) to decrease pulsing caused by the pumping.

Polyethylene tubing (i.d. 1.0 mm) was used for the loop and the transmission line (length 60 cm). The sample was injected into the FIA carrier line by means of an acrylic proportional injector.¹⁹ The system can be automated, the injection valve being operated by means of two solenoids, controlled by an electronic sequence timer¹⁷ or by a computer. Flange-free PTFE fittings, with 1/4-28 UNF thread,²⁰ may be employed as connectors to avoid liquid leakage at higher flow-rates.

A Pye-Unicam SP 92A atomic-absorption spectrophotometer was used to measure the Zn and Fe absorption. The transient FIA peaks were recorded on a Pye-Unicam A-25 recorder.

Establishment of operational conditions

A "test slurry" was prepared containing 5 g of homogenized white beans and 2.00 ml of 100 $\mu\text{g/ml}$ Zn solution in 100 ml total volume. Propane was used as fuel since it provides good sensitivity for easily atomized elements such as copper, lead and zinc.²¹ Initially, instrument settings indicated by the manufacturer for the conventional pneumatic nebulizer were used to test the performance of the Babington-type nebulizer. For this, an arbitrary carrier flow-rate of 10.3 ml/min and a sample volume of 560 μl were chosen. The instrument settings were then adjusted to maximize the absorbances, resulting in the conditions shown in Table 2.

Since the literature²¹ suggests use of acetylene for determination of iron, conditions for this flame were also optimized (Table 2). During

development of the method, it was also found desirable to use an acetylene flame for the zinc determination. The flame conditions used were those recommended by the manufacturer (Table 2).

The best FIA carrier flow-rate was determined by injecting 640 μl of the "test slurry" and measuring the changes in absorbance as the carrier flow-rate was varied. The results shown in Fig. 4 are the averages of 10 consecutive injections. The absorbance increased to a maximum at about 10 ml/min and then levelled off. This flow-rate is capable of maintaining a steady transport of fluid over the V-groove orifice, resulting in smooth and reproducible peaks.

With a carrier flow-rate of 10.3 ml/min, the variation in absorbance with volume of sample injected was next examined. The averaged results from 10 consecutive injections, shown in Fig. 5, indicate that sample volumes $\geq 460 \mu\text{l}$ will give a constant signal, comparable to that from continuous nebulization, as indicated in Fig. 6. Slurries containing as much as 11% of suspended solids did not obstruct the FIA transmission line under normal operation. A transport efficiency (ϵ_n)^{22,23} of about 11% was estimated for the slurry nebulization process by comparing the mass of suspension delivered by the peristaltic pump to the spray chamber, with the mass drained from the chamber, in a fixed period of time. This value was obtained from 10 consecutive 30-sec injections of a homogenized slurry containing 5% of suspended solids, with a carrier flow-rate of 10.3 ml/min. Although this method of estimating the transport efficiency is not as accurate as determination of the ratio of amount of analyte entering the flame to amount of analyte aspirated, it was considered adequate for the purpose and had the advantage of not requiring specialized equipment. The results compare well with the average efficiency of pneumatic-type nebulizers. A reliable method of sample introduction for this purpose would be to operate the injection valve with the configuration used for stopped-flow studies.²⁴

Determination of zinc

For convenience and consistency, the FIA system (Fig. 1) was used for analysis of solutions as well as for slurries. At the beginning of all series of absorption measurements, the instrument was set to zero with the FIA carrier. With a flow-rate of 10.3 ml/min and an injection volume of 460 μl , a calibration graph was prepared from 6 aqueous standards containing

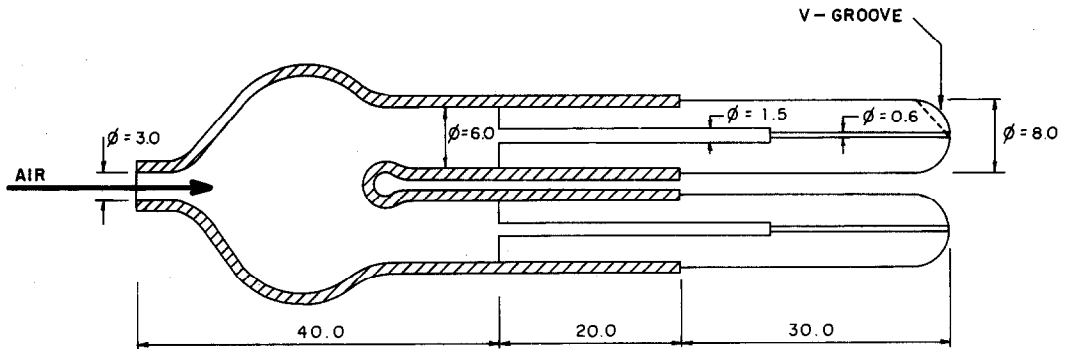


Fig. 2. Babington V-groove type nebulizer and auxiliary air supply (both made of PTFE). Dashed lines represent the glass support. All dimensions in mm.

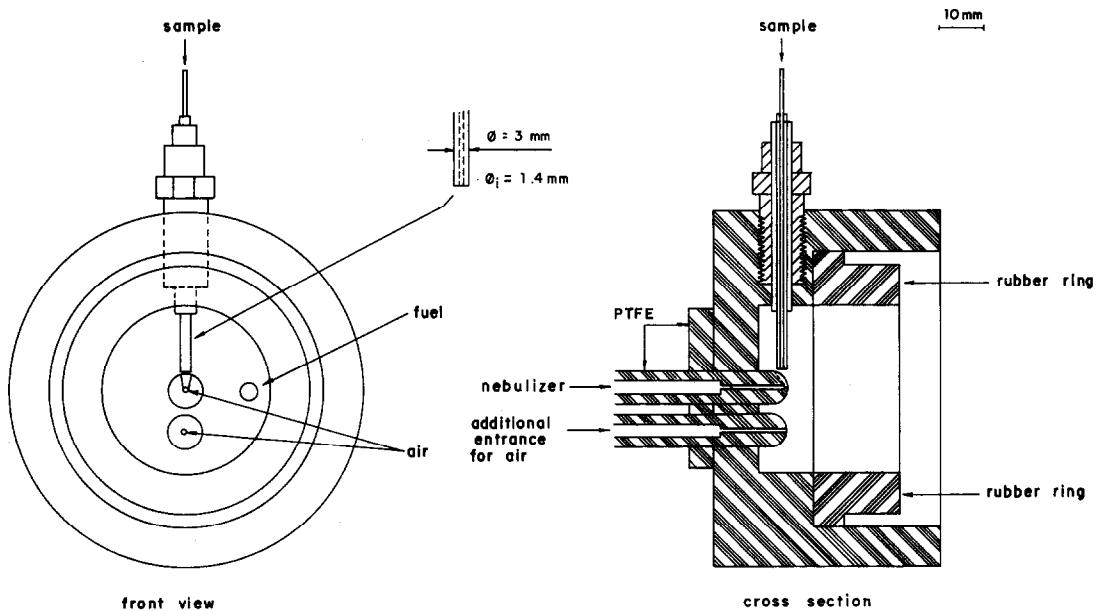


Fig. 3. The Babington-type nebulizer mounting.

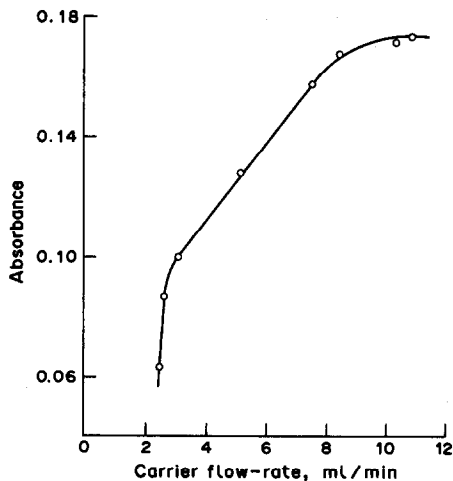


Fig. 4. Effect of FIA carrier flow-rate on analytical signal. Injected volume, 640 μ l. Sample, spiked reference slurry prepared with 5 g (\pm 1 mg) of white beans plus 2.00 ml of 100 μ g/ml Zn solution in 100 ml total volume.

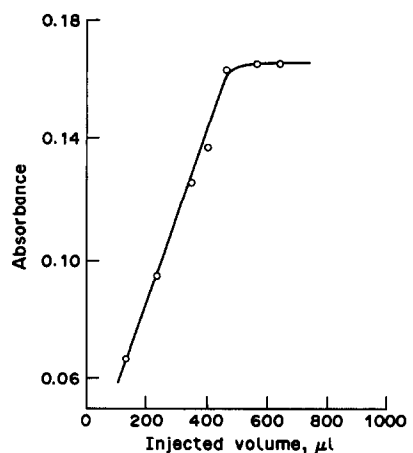


Fig. 5. Effect of injected volume on analytical signal. FIA carrier flow-rate, 10.3 ml/min. Sample as for Fig. 4.

Table 2. Analytical conditions for atomic-absorption analyses

Conditions	Zn	Zn	Fe
<i>Flame system</i>			
Fuel	C ₃ H ₈	C ₂ H ₂	C ₂ H ₂
Fuel flow-rate, ml/min	350	1200	1200
Air flow-rate, l./min	5.0	5.0	5.0
Beam height, cm	0.8	1.0	1.0
<i>Optical system</i>			
Wavelength, nm	213.9	213.9	248.3
Lamp current, mA	7.5	7.5	7.5
Mechanical slit-width, mm	0.4	0.4	0.1
Spectral band-width, mm	2.4	2.4	0.8

0.200–2.00 $\mu\text{g/ml}$ Zn. Six readings for each concentration were averaged. The graph was linear ($A = -0.006 + 0.503C_{\text{Zn}}$, $r = 0.9992$). From the standard deviations of repeated measurements at low analyte concentrations, the detection limit for determining zinc in solution was calculated to be 0.03 $\mu\text{g/ml}$ by the recommended procedure of the Analytical Methods Committee.²⁵ The solution of the test sample was then analysed and found to contain 47.0 $\mu\text{g/ml}$ Zn.

Next, 6 portions of the test sample, ranging from 1 to 10 g, were homogenized in 50 ml of water for 4 min and the slurries were each diluted to 100 ml. From the analysis of a solution of the test sample, the concentrations of zinc in the slurries ranged from 0.470 to 4.70 $\mu\text{g/ml}$.

The air–propane flame was used for these slurries under the same conditions as for solutions, but the resulting calibration graph was

not linear (Fig. 7). Though it is possible to work with non-linear graphs in atomic-absorption methods,²⁶ linear plots are preferred when possible. This non-linearity was attributed to the relatively low temperature of the air–propane flame, which is not high enough to burn the slurry particles completely. Therefore, the experiment was repeated with an air–acetylene flame, which has a higher temperature.²¹ The conditions used were those shown in Table 2; each injection was repeated 5 times and the absorbances were averaged. The resulting plot was linear ($A = 0.003 + 0.0362C_{\text{Zn}}$, $r = 0.9991$) and the detection limit was calculated²⁵ to be 0.3 $\mu\text{g/ml}$ Zn.

Determination of iron

Six iron standards containing 1.000–20.00 $\mu\text{g/ml}$ Fe were prepared. The same volumes and flow-rate as for zinc were used. The flame was air–acetylene, under the conditions given in Table 2. Five measurements for each standard were averaged and gave a linear relation: $A = 0.013 + 0.0420C_{\text{Fe}}$, $r = 0.9994$. The white-bean sample solution prepared for the zinc determination was measured similarly, giving a calculated iron content of 74 $\mu\text{g/ml}$. The detection limit²⁵ was estimated as 0.2 $\mu\text{g/ml}$ Fe.

Six slurries containing 3–7.5 g of ground white beans and 50 ml of water were homogenized for 4 min and diluted to 100 ml. According to the analysis of the solution of the sample, the iron concentrations in the slurries varied from

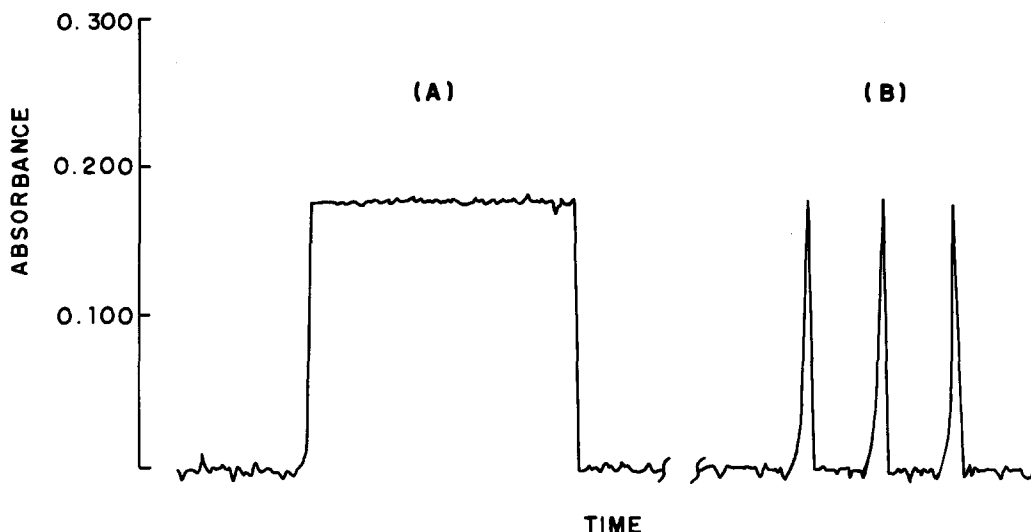


Fig. 6. Recorded profiles of zinc absorbance at a pumping rate of 10.3 ml/min. (A): continuous recording for a period of 10 sec; (B): transient FIA peaks obtained for 3 consecutive injections of 460 μl . Sample as for Fig. 4. Under these FIA conditions an injection frequency of 120 per hr is possible, with negligible carry-over and memory effects.

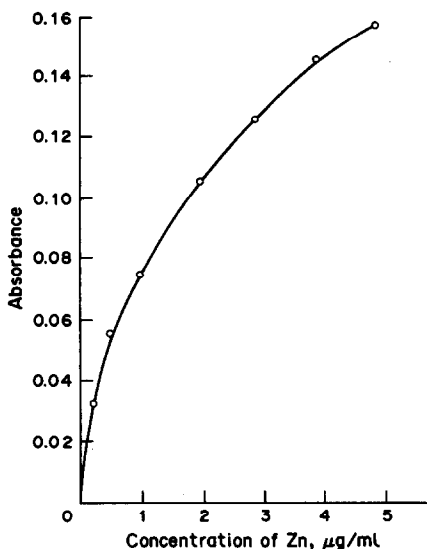


Fig. 7. Non-linear calibration curve for slurries containing zinc; propane-air flame.

2.2 to 5.6 µg/ml. The slurries were injected into the flame under the same conditions as for the standard solutions and the absorbances from 5 readings were averaged. The calibration graph was linear: $A = 0.0009 + 0.0211C_{\text{Fe}}$, $r = 0.9996$. The detection limit was found to be 0.6 µg/ml Fe.

Application of the method

The method was tested by determining the zinc and iron contents of a variety of foods purchased in local markets. The results for analyses of sample solutions and slurries are shown in Table 3. It can be seen that the results for both elements by the slurry method are generally similar to those for the solutions. The average relative deviation between the two methods is about 2% for zinc and 3% for iron. In the case of iron, where acetylene was used for both slurries and solutions, the sensitivity for slurries was half that for solutions, and the detection limit three times as great. For zinc, use of propane for solutions and acetylene for slurries gave a less favourable comparison, with slurries showing a sensitivity of only 7% of that for solutions, and a detection limit ten times greater. However, except for very low concentrations, this difference can be overcome by use of more concentrated slurries.

The generally accepted principle that standards should be as similar to the sample as possible, argues against the use of solution standards for calibration of the slurry nebulization (SN) method, as is the common prac-

tice.^{10,11} As it is impractical to find reference materials with a range of metal ion concentrations, use of varying weights of a slurry material (white beans in this work) for calibration is one approach, justified by the results. Spiked calibration slurries such as the one used for the determination of the FIA parameters could also be employed, by adding known amounts of analyte to a material containing a low concentration of it.

The use of baffles in the spray chamber merits discussion. It is known that particle vaporization in flames and plasmas is a complex process, even for simple solutes.²⁷ Therefore, it is desirable to remove large particles because the solids in the droplets must be burned as well as atomized. As impact with the baffle surface can shatter larger droplets as well as block their passage, the baffles were left in place, although improvements in AES/SN elemental recoveries have been obtained by using a spray chamber free from impact baffles.¹⁰ In the analyses described here, baffles were considered to be of value in reducing background effects caused by light scattering from larger particles. No background correction was employed, as the instrument had no provision for it. However, direct comparison between the data obtained from solution with those obtained by the slurry method indicate that the effects of non-specific absorption from the scattered radiation are negligible, as observed earlier by Fry and co-workers.^{1,11}

PROPOSED METHOD FOR SLURRY ANALYSIS

Sample preparation

A preliminary preparation of samples may be required, depending on the type of food to be analysed: flours and sauces require no preliminary preparation except mixing to ensure homogeneity. Grains, biscuits and bread should be ground in a mill or blender to pass a 1.0–2.0-mm sieve, before storage. Vegetables, fruits and meats should be cut into 0.5-cm cubes after removal of the stems, seeds, skin and bone, then ground in a blender. If not used immediately, all prepared samples should be stored in polyethylene containers at 4°.

Sample standard

Prepare a reference standard from a food such as white beans, that is readily ground and stable. Grind to pass a 1.0–2.0-mm sieve and store.

Table 3. Zinc and iron contents of foods determined by atomic-absorption measurements of solutions of sample ash and of sample slurries*

	Zn content, $\mu\text{g/g}$			Fe content, $\mu\text{g/g}$		
	Solution†	Slurry‡	Sample,§ g	Solution†	Slurry‡	Sample,§ g
Pinto beans	56.8	56	3	170	166	3
Rice (long grain)	37.1	36	3	87	87	3
Cassava flour (raw)	15.8	16	6	37	36	6
Maize meal	14.1	14	6	53	55	3
Maize meal (precooked)	19.9	20	10	16	17	10
Wheat flour	33.4	33	6	29	28	6
French bread	43.2	43	6	58	57	6
Milk crackers	25.3	25	6	51	51	6
Tomato paste (canned)	16.3	16	6	85	84	6
Potatoes (canned)	8.5	9	6	56	57	3
Carrots (canned)	10.4	11	6	48	51	3
Peas (canned)	19.6	20	10	29	29	10
String beans (canned)	12.1	12	6	51	51	6
Sausage (canned)	51.8	49	6	40	39	6
Apples (fresh)	6.3	6	10	13	14	10
Pears (fresh)	8.2	9	10	19	20	10

*All samples injected in triplicate and absorbances averaged.

†Air-propane flame; all samples 3 g.

‡Air-acetylene flame.

§Mass of sample taken for slurry analyses; final volume 100 ml.

Establishment of operational conditions

Prepare a "test slurry" sample by homogenizing 5 g (± 1 mg) of the reference standard in 50 ml of water and diluting to 100 ml. Using the FIA/SN/FAAS system and a sample volume of about 600 μl , set the carrier flow-rate at approximately 10 ml/min. Inject the test sample and record the absorbance. If its maximum is less than 0.2, prepare a new test slurry and increase the ion concentration by doping with a standard solution until the peak absorbance is about 0.4. Then vary, individually, the beam height, slit width, carrier flow-rate and sample volume until maximum absorbance is obtained. Use these conditions in all subsequent analyses.

Analysis of the reference standard

Prepare a series of aqueous standards of the element to be determined. These should cover the range of concentrations expected in the foods to be analysed, when 1–10 g of sample is homogenized to give a volume of 100 ml. Measure the absorbances of the standards with the FIA/SN/FAAS system under the optimized conditions. From the results, plot a calibration graph and/or calculate a regression equation.

Ash a number of 1.000-g samples of the reference standard in porcelain crucibles. Dissolve the ash of one of them in 0.5 ml of water and 4 ml of hydrochloric acid (1 + 1), dilute to volume in a 25-ml standard flask, and measure the absorbance. If this is too high or too low,

make an appropriate change in the final volume of the solution of the other ashed samples. Analyse these and from the average and the calibration graph or regression equation, calculate the content of the element in the reference standard.

Preparation of slurry calibration graph

Knowing the actual element content in the reference standard, homogenize a series of different weighed quantities up to a maximum of 10 g, if necessary, with 50 ml of water, and dilute the slurries to 100 ml. If higher concentrations are needed, the slurry can be doped with a known quantity of the element before dilution. Measure the absorbances with the FIA/SN/FAAS system and prepare a calibration graph and/or calculate a regression equation.

Routine analysis of samples

Homogenize duplicate samples weighing 1, 3 or 10 g (± 1 mg), depending on the metal ion content expected, and dilute the slurries to 100 ml. Using the conditions established above, record the absorbance peaks for the samples injected into the system. If a period of time has elapsed since the calibration was done, it is advisable to inject one standard slurry to verify the calibration. From the calibration and the weight of sample taken, calculate the metal ion content of the food.

Acknowledgements—The authors are glad to acknowledge the assistance of Mr. Edson Massola in machining the nebulizer. NJM is indebted to the Fundação de Amparo à Pesquisa do Estado de São Paulo (FAPESP) for a graduate fellowship. Helpful suggestions by Carol Collins in revising the paper are also acknowledged.

REFERENCES

1. R. C. Fry and M. B. Denton, *Anal. Chem.*, 1977, **49**, 1413.
2. *Idem*, *Appl. Spectrosc.*, 1979, **33**, 393.
3. S. Dresner, *Popular Science*, 1973, May, 102.
4. J. R. Garbarino and H. E. Taylor, *Appl. Spectrosc.*, 1980, **34**, 584.
5. R. Fietkau, M. D. Wichman and R. C. Fry, *ibid.*, 1984, **38**, 118.
6. N. Mohamed, D. L. McCurdy, M. D. Wichman, R. C. Fry and J. E. O'Reilly, *ibid.*, 1985, **39**, 979.
7. D. L. McCurdy, M. D. Wichman and R. C. Fry, *ibid.*, 1985, **39**, 984.
8. M. D. Wichman, R. Fietkau and R. C. Fry, *ibid.*, 1986, **40**, 233.
9. D. L. McCurdy and R. C. Fry, *Anal. Chem.*, 1986, **58**, 3126.
10. S. H. Vien and R. C. Fry, *Appl. Spectrosc.*, 1988, **42**, 381.
11. N. Mohamed and R. C. Fry, *Anal. Chem.*, 1981, **53**, 450.
12. J. Růžička and E. H. Hansen, *Flow Injection Analysis*, 2nd Ed., Wiley, New York, 1988.
13. J. M. H. Appleton and J. F. Tyson, *J. Anal. At. Spectrom.*, 1981, **1**, 63.
14. J. F. Tyson and A. B. Idris, *Analyst*, 1981, **106**, 1125.
15. J. F. Tyson, *ibid.*, 1985, **110**, 419.
16. G. C. Klemm, *J. Assoc. Off. Anal. Chem.*, 1964, **47**, 40.
17. J. C. de Andrade, M. Ferreira, N. Baccan and O. C. Bataglia, *Analyst*, 1988, **113**, 289.
18. R. F. Suddendorf and K. W. Boyer, *Anal. Chem.*, 1978, **50**, 1769.
19. B. F. Reis, E. A. G. Zagatto, A. O. Jacinto, F. J. Krug and H. Bergamin F^o, *Anal. Chim. Acta*, 1980, **119**, 305.
20. J. C. de Andrade and K. E. Collins, *Anal. Chem.*, 1982, **52**, 2398.
21. W. J. Price, *Spectrochemical Analysis by Atomic Absorption*, Wiley-Heyden, Chichester, 1985.
22. R. F. Browner, A. W. Boorn and D. D. Smith, *Anal. Chem.*, 1982, **54**, 1411.
23. R. F. Browner, *Anal. Proc.*, 1984, **21**, 314.
24. J. C. de Andrade, J. C. Rocha, C. Pasquini and N. Baccan, *Analyst*, 1983, **108**, 621.
25. Analytical Methods Committee, *ibid.*, 1987, **112**, 199.
26. H. P. J. Van Dalen and L. de Galan, *ibid.*, 1981, **106**, 695.
27. G. M. Hieftje, R. M. Miller, Y. Pak and E. P. Wittig, *Anal. Chem.*, 1987, **59**, 2861.

DETERMINATION OF FLUORIDE IN SEA-WATER BY MOLECULAR ABSORPTION SPECTROMETRY OF ALUMINIUM MONOFLUORIDE AFTER REMOVAL OF CATION AND ANION INTERFERENCES

M. A. PALACIOS CORVILLO, M. GOMEZ GOMEZ and C. CAMARA RICA

Departamento de Química Analítica, Facultad de Ciencias, Ciudad Universitaria, Universidad
Complutense, Madrid 28040, Spain

(Received 6 January 1989. Revised 18 January 1990. Accepted 5 February 1990)

Summary—Three procedures are proposed for the determination of trace levels of fluoride in sea-water, based on the formation of aluminium monofluoride in an electrothermal graphite furnace, followed by measurement of its molecular absorption at 227.45 nm. They involve the use of dilution, a matrix modifier, or a matrix modifier and an ion-exchange resin, and are all acceptably sensitive and specific for fluoride. Interferences from cations and anions are removed by a simple 20-fold dilution of the sample. At 10-fold sample dilution, chloride interference can be removed by adding 0.3M ammonium nitrate together with 0.01M aluminium + 0.01M strontium as a matrix modifier. The same matrix modifier is valid for use with 5-fold sample dilution and a cation-exchange step to avoid matrix effects from cations and chloride. The detection limit is about 8–10 ng/ml fluoride and the determination limit is 20 ng/ml. The precision of peak-height measurement at 0.2 µg/ml is 5–7%.

Sensitive determination of fluoride is possible by the procedures developed by Tsunoda *et al.*¹ and Dittrich *et al.*,² based on formation of aluminium monofluoride in a graphite furnace, and exploitation of its sharp molecular band near 227.45 nm. This method (the AIF-MA method)² has considerable advantages over the ion-selective electrode (ISE) methods, owing to (i) the small sample volume needed, (ii) the fairly high sensitivity and (iii) its suitability for total fluorine determination, but suffers from matrix ion interference.² Recently we used this technique for the determination of trace levels of fluoride in potable water and sea-water,³ but significant matrix anion and cation interferences were found.

Schweitzer and McCarthy⁴ have shown the usefulness of triphenylantimony dihydroxide (TPSbDH) for the extraction of anions, and Chermette and co-workers have used it for the extraction of halides.^{5,6} Dittrich *et al.*⁷ have used it for extractive separation of fluoride from the matrix, and preconcentration. The fluoride is extracted with TPSbDH in methyl isobutyl ketone (MIBK) and stripped with 0.025M barium hydroxide. The molecular absorption of AIF is then applied for determination of the fluoride. The method is sensitive and specific for fluoride, but when the conditions are optimized

for fluoride, any chloride is also extracted and stripped and thus influences the plasma composition in the furnace.

In this paper, we examine some ways to eliminate the matrix interferences in analysis of sea-water, particularly those due to chloride.

EXPERIMENTAL

Apparatus

A Perkin-Elmer 1100B atomic-absorption spectrophotometer equipped with a deuterium lamp for simultaneous background correction was used for AIF-MA measurements. A programmed furnace (HGA 400), and a pyrolytic graphite furnace with a L'vov platform were used. A platinum hollow-cathode lamp was used as the light-source. The spectral bandpass was 0.07 nm throughout. Argon (200 ml/min flow-rate) was used to purge air from the cuvette.

Reagents

Merck analytical-reagent grade products were used. Standard halide solutions were prepared by dissolving Suprapur NaF, NaCl, NH₄Cl, KBr or KI in distilled water. Solutions for study of metal-ion effects were made from the nitrates.

Cation-exchange column

About 7 g of Amberlite IRA 120 (16–50 mesh) in H⁺-form was soaked in distilled water for 24 hr and then slurry-packed to form a column 10 cm long and 1 cm in diameter. Contaminants were removed from the resin by repeated washing with 0.5M hydrochloric acid at a flow-rate of 5–10 ml/min, followed by washing with distilled water until the effluent was free from chloride. About 50 ml of a 5-fold dilution of sea-water was passed through the column at a flow-rate of 5 ml/min. The eluate was neutralized with ammonia solution (1 + 5) and diluted accurately to 100 ml with distilled water for later analysis. The resin was readily regenerated by passage of 1.0M hydrochloric acid, and this was done after each chromatogram. Care was always taken to avoid drying of the bed.

Procedures

(1) *Matrix-modifier and dilution.* A 20- μ l volume of matrix modifier was placed in the graphite furnace and dried. A 10- μ l volume of suitably diluted sample was then added and dried. The standard-additions method was used for quantification.

(2) *Matrix-modifier and dilution.* A 20- μ l volume of 0.01M Al³⁺ + 0.01M Sr²⁺ + 0.3M NH₄NO₃ solution was placed in the graphite furnace and dried. Then a 10- μ l volume of suitably diluted sample was added to the furnace. Sea-water samples were diluted 10-fold with demineralized water, and the standard-additions method was used. Alternatively, the sea-water was diluted 10-fold with 0.3M NH₄NO₃ matrix modifier solution.

(3) *Cation-exchange and matrix modifier.* A 100-ml sample of a solution made by diluting sea-water 5-fold or 10-fold with demineralized water was loaded into the cation-exchange column at a flow-rate of 5 ml/min. The effluent

was neutralized with ammonia to pH 7. A 20- μ l volume of 0.01M Al³⁺ + 0.01M Sr²⁺ + 0.3M NH₄NO₃ solution was placed in the graphite furnace and dried, then a 10- μ l volume of suitably diluted sea-water was added. The ion-exchange can also be done by shaking 7 g of resin with the diluted sea-water and then removing the resin by filtration. The standard-additions method was used.

RESULTS AND DISCUSSION

Optimization of graphite-furnace conditions

Table 1 shows the vaporization parameters for the atomic-absorption determination of fluoride. The same conditions were used for all three procedures except for the nature of the matrix modifiers added. The stopped-flow gas system gave considerably higher absorbance values and better precision than a miniflow or a high-flow gas purge system. The AlF-MA precision of 5% was improved to 3% by use of a second ashing step with a 2-sec hold time and stopped flow before the vaporization step. Furnace conditions, temperatures, integration times and conditions for AlF radical formation were optimized in earlier work.³

Interferences

Interferences from cations and acid media. It is well established that cations and anions at higher concentrations, and acid media, produce strong interferences when direct analysis is used, and that these effects are decreased by the addition of Sr²⁺ or Ba²⁺ as matrix modifiers. Table 2 shows the magnitude of cation interferences when Sr²⁺ is used as matrix modifier. The serious interference by Ca²⁺ may be attributed to the plasma effect. The saline content in drinking water differs markedly from place to place and interferences from Ca²⁺ in highly saline water can be controlled. Sodium inter-

Table 1. Graphite furnace parameters for the determination of fluoride (all three procedures)

Step	Temperature, °C	Ramp, sec	Hold, sec	Ar flow-rate, ml/min
1 *Application of Al ³⁺ /Sr ²⁺ solution (20 μ l)				310
2 Drying	110	20	30	310
3 Stop and cooling of furnace				
4 Application of F ⁻ solution (10 μ l)				
5 Drying	110	20	30	310
6 Ashing I	700	10	30	310
7 Ashing II	700	0	2	0 stopped flow
8 Vaporization	2400	0	4	0 stopped flow

*Aluminium nitrate and strontium nitrate concentrations both 0.01M.

Integration time: 4 sec.

Measurements of peak height.

Table 2. Interferences

Foreign species	Concentration	Relative signal
none	—	1
Ba ²⁺ , Ni ²⁺ , Zn ²⁺	up to 1000 µg/ml	1
Cd ²⁺ , Co ²⁺ , Cr ³⁺ , Cu ²⁺		
Pb ²⁺ , Mn ²⁺	up to 500 µg/ml	1
Ca ²⁺	up to 30 µg/ml	1
	100 µg/ml	0.6
Fe ²⁺ , K ⁺ , Na ⁺ (as NaNO ₃)	up to 200 µg/ml	1
	1000 µg/ml	0.8
Mg ²⁺	up to 100 µg/ml	1
	1000 µg/ml	0.8
Mn ²⁺	up to 400 µg/ml	1
	1000 µg/ml	0.4
Na ⁺ (as NaOH)	0.01M	0.5
H ₂ SO ₄	0.01M	0.35
	0.1M	0.3
HCl	0.01M	0.8
	0.1M	0.3

Matrix modifier 0.01M aluminium nitrate + 0.01M strontium nitrate; 10 µl of F⁻ solution (0.1 µg/ml F⁻ + x µg/ml interfering cation).

feres more seriously when present as the hydroxide than it does as the nitrate. In acid media, the signal decreases with increasing acid concentration, probably owing to release of hydrogen fluoride by a pyrohydrolysis reaction.

Interferences from anions. Chloride is the most strongly interfering anion in determina-

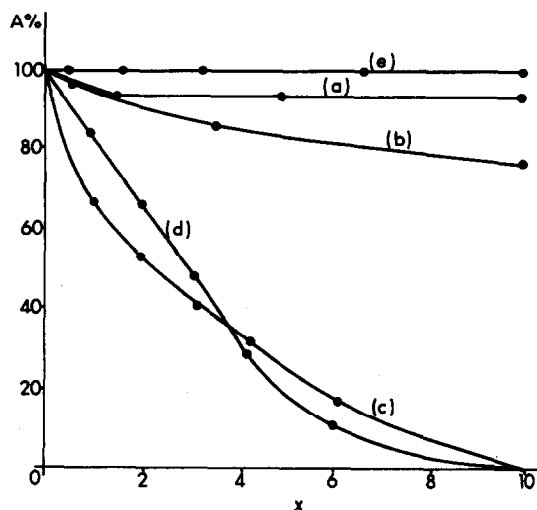
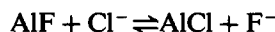


Fig. 1. Interferences with AIF-MA signal by KBr, KI, KCl, NaCl and NH₄Cl. Test solution contains 0.1 µg/ml F⁻ plus different concentrations of interfering ions. Aluminium nitrate and strontium nitrate are 0.01M in test solution. (a) KI interference, abscissa scale 0-10 = 0-5 µg/ml. (b) KBr interference, abscissa scale 0-10 = 0-2000 µg/ml. (c) KCl interference, abscissa scale g/l. (d) NaCl interference, abscissa scale g/l. (e) NH₄Cl interference, abscissa scale g/l. The ordinate shows the absorbance as a fraction of that for a pure NaF solution.

tions of fluoride. Bromide and iodide also interfere. In the presence of a large excess of chloride, interferences may occur in the plasma through the exchange reaction



In the presence of increasing amounts of chloride this reaction results in decreasing AlF concentration. There are literature reports that under some conditions it is possible to determine trace amounts of fluoride in the presence of other halides at levels up to 10⁴-10⁵ times that of the analyte.⁷ Figure 1 shows the interferences caused by KI, KBr, KCl, NaCl and NH₄Cl in determination of fluoride by AlF-MA. At their approximate sea-water concentrations KBr and KI are below the interference level, but KCl and NaCl strongly depress the AlF-MA signal and practically no signal is obtained at chloride levels above 6 g/l., when present as NaCl or KCl, though when the chloride is present as NH₄Cl no interference is noted up to 10 g/l.

Matrix modifier

Sr²⁺ + Ni²⁺ and Sr²⁺ + Fe²⁺ or Ba²⁺ are commonly used as matrix modifiers to (i) reduce volatilization of fluoride in the ashing and vaporization steps, through an immobilization effect; (ii) inhibit the strong thermal hydrolysis of Al³⁺ in the drying and ashing steps and keep the fluoride in the graphite furnace until the AlF formation temperature is reached.^{7,10} The role of Ni²⁺ or Fe²⁺ is to decrease the background.^{1,8}

The effect of LiNO₃ and NH₄NO₃ as matrix modifiers on the removal of chloride interference was tested. These two salts are the matrix modifiers usually used for removal of chloride interference in direct heavy metal determinations in sea-water by a graphite furnace method. When these modifiers are mixed with the sample in the liquid state and the solution is then dried, there will be an intimate mixture of the various salts that can be formed from the ions present, viz. NH₄NO₃, NH₄Cl, LiNO₃, LiCl, NaNO₃, NaCl. These mainly have widely different thermal behaviour, so the effect on the sodium chloride will depend on the relative amounts of the species present, their thermal stability and volatility, boiling points etc. Thus ammonium chloride should be sublimed and thermally dissociated first, closely followed by decomposition of ammonium nitrate, lithium nitrate and sodium nitrate, with lithium chloride and sodium chloride last. It follows that a large

excess of ammonium nitrate will be needed to enhance the elimination of the chloride.

We therefore tested these modifiers for decreasing the interference of sodium chloride in the fluoride determination. The results are given in Table 3.

Chloride concentrations higher than 2 g/l. reduce the signal by 34%, and the $\text{Al}^{3+} + \text{Sr}^{2+}$ matrix modifier does not reduce the background. Thus, fluoride determination in sea-water requires a previous 20-fold dilution to lower the chloride interference. The use of $\text{Al}^{3+} + \text{Sr}^{2+} + \text{Ni}^{2+}$ gave similar results, but the background was slightly lower. With $\text{Al}^{3+} + \text{Ba}^{2+} + \text{Ni}^{2+}$, interference from chloride is marked and is independent of the matrix modifier concentration. $\text{Al}^{3+} + \text{Sr}^{2+} + \text{Li}^+$ does not reduce the chloride interference or background when an ashing temperature of 700° is used. With an ashing temperature of 1350° (the boiling point of LiCl) the background is lowered but the analytical signal is also diminished. This suggests that some fluoride is removed at the same time as the chloride (as LiF, the b.p. of which is variously reported as 1676° ,¹¹ and 1254° ,¹⁰). According to Tsunoda *et al.*¹² strontium should retain fluoride up to the tempera-

ture of AlF formation, but there may be local losses of fluoride as LiF or NaF, for reasons similar to those outlined above for LiNO_3 and NH_4NO_3 as matrix modifiers. The $\text{Al}^{3+} + \text{Sr}^{2+} + \text{NH}_4\text{NO}_3$ matrix modifier removes interference of chloride up to a concentration of 2 g/l. and decreases the background. Determination of fluoride in sea-water is possible with this modifier if the sample is diluted 10-fold. Sodium chloride concentrations higher than 3.3 g/l. interfere even when high NH_4NO_3 concentrations are used. This may be due to the mass action effect already referred to.

Cation-exchange and NH_4NO_3 matrix modifier procedure

As high sodium chloride concentrations may cause incomplete removal of chloride by NH_4Cl volatilization, a cation-exchange resin in H^+ -form was used to remove the sodium, and the effluent was neutralized with ammonia to yield an equivalent amount of ammonium ions. However, it was still found to be necessary to add 0.3M NH_4NO_3 as matrix modifier.

Figure 2 shows how the background decreases and the reproducibility improves when increasing amounts of NH_4NO_3 are added

Table 3. Matrix modifiers used to remove Cl^- interference

Matrix modifier	Cl^- , g/l.	Relative absorbance, %	Background absorbance
0.01M Al^{3+} + 0.01M Sr^{2+}	0	100 ± 5	<0.400
	1	84 ± 5	<0.500
	2	66 ± 7	>1.000
	3	48 ± 10	>2.000
0.01M Al^{3+} + 0.01M Sr^{2+} + 0.005M Ni^{2+}	0	91 ± 6	<0.300
	1	80 ± 6	<0.400
	2	62 ± 9	>1.00
	3	43 ± 9	>2.00
0.01M Al^{3+} + 0.005M Ba^{2+}	0	100 ± 6	<0.400
	1	35 ± 9	<0.400
	2	30 ± 11	<0.800
	3	30 ± 11	>1.00
0.01M Al^{3+} + 0.05M Ba^{2+} + 0.005M Ni^{2+}	0	39 ± 11	<0.400
	1	28 ± 12	<0.600
	2	20 ± 12	<0.800
	3	12 ± 12	>1.00
0.01M Al^{3+} + 0.01M Sr^{2+} + 0.056M LiNO_3 ashing at 710°	0	100 ± 9	<1.00
	1	80 ± 9	<1.00
	2	66 ± 10	<1.00
	3	40 ± 10	>1.00
0.01M Al^{3+} + 0.01M Sr^{2+} + 0.056M LiNO_3 ashing at 1350°	0	20 ± 6	<0.300
	1	15 ± 7	<0.300
	2	6 ± 5	<0.300
	3	6 ± 5	<0.300
0.01M Al^{3+} + 0.01M Sr^{2+} + 0.3M NH_4NO_3	0	100 ± 6	<0.250
	1	100 ± 5	<0.250
	2	100 ± 6	<0.400
	3	70 ± 7	<0.500

A 20- μl volume of matrix modifier solution and 10 μl of 0.1 $\mu\text{g}/\text{ml}$ standard fluoride solution were applied. Five replicate analyses of each sample were run.

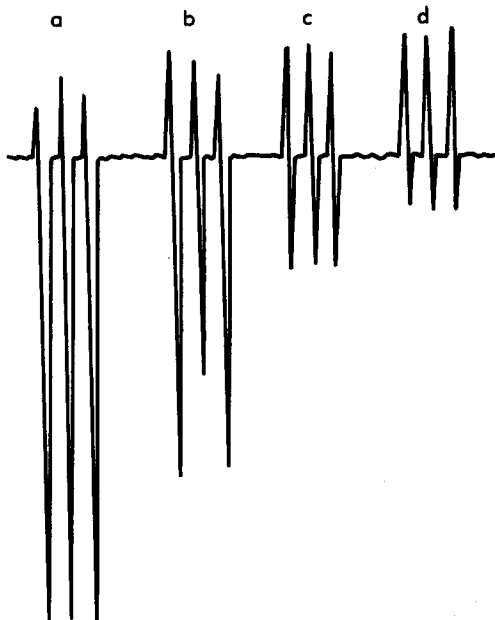


Fig. 2. Effect of increasing amounts of NH_4NO_3 on the AlF signal. Sea-water was diluted after being passed through a cation-exchange resin. (a) No NH_4NO_3 added; (b) $0.28M$ NH_4NO_3 ; (c) $0.56M$ NH_4NO_3 ; (d) $1.0M$ NH_4NO_3 . The signals below the baseline refer to the background.

to a 1:1 sea-water dilution (containing 10 g/l. Cl^-) that has been passed through a cation-exchange resin after dilution. The results were not so satisfactory when a cation-exchange resin in NH_4^+ -form was used.

Determination of F^- in sea-water

The three proposed procedures were applied to artificial and natural sea-waters. To verify the accuracy of the results, artificial sea-waters containing $0.5M$ NaCl , $0.8mM$ KBr , $4mM$ NaHCO_3 , and either $0.5 \mu\text{g/ml}$ (low F^- content) or $1.5 \mu\text{g/ml}$ (high F^- content) fluoride, added as NaF , were prepared.

When procedure 1 was applied, a dilution greater than 20-fold was necessary to lower the chloride content below the maximum acceptable level. Generally, the fluoride content of sea-water is high enough to make use of this dilution possible. The results for artificial sea-water are

in good agreement with the known amount of fluoride added. When procedure 2 was applied, chloride was removed by volatilization as NH_4Cl and determination of fluoride was possible with a 10-fold dilution of the sea-water. Finally, when procedure 3 was applied, metal ions were removed by the cation-exchange column and the determination of fluoride was possible in the presence of 4 g/l. chloride (equivalent to a 5-fold sea-water dilution) provided NH_4NO_3 was added as matrix modifier. The third procedure was applied to a 10-fold dilution of artificial sea-water with F^- content (below the normal content) with enough ammonium chloride added to restore the chloride concentration to 4 g/l. This latter procedure is particularly important because the sensitivity of the determinations is strongly influenced by the condition of the hollow-cathode Pt lamp used as light-source. When the sensitivity becomes low, 10-fold or 20-fold sea-water dilution may reduce the fluoride concentration below the limit of determination.

Table 4 shows the recoveries obtained by application of the three procedures to artificial sea-waters with the same matrix and different fluoride contents. Figure 3 shows the standard-additions plots for 20-fold and 10-fold dilutions of natural sea-water, analysed by the proposed procedures. The detection limits obtained were $8\text{--}10 \text{ ng/ml}$ and the determination limit was 20 ng/ml . The peak height precision for $0.2 \mu\text{g/ml}$ fluoride varied between 5 and 8%, depending on the procedure used.

CONCLUSIONS

The interferences from cations and anions can be removed by a simple 20-fold sample dilution. With 10-fold sample dilution, chloride interference can be removed by adding $0.3M$ NH_4NO_3 , together with $0.01M$ Al^{3+} + $0.01M$ Sr^{2+} as matrix modifier. The same matrix modifier serves with 5-fold sample dilution, if a cation-exchange step is used to replace sodium by ammonium ions.

Table 4. Comparison of total fluoride in natural and artificial sea-water, determined by AlF-MA

Procedure	Artificial sea-water		Natural sea-water (Huelva)
	F^- , $\mu\text{g/ml}$	Recovery, %	F^- , $\mu\text{g/ml}$
1	$1.50 \pm 0.05^*$	100 ± 3	1.30 ± 0.03
2	$1.50 \pm 0.04^*$	100 ± 3	1.31 ± 0.03
3	$0.51 \pm 0.03^\dagger$	102 ± 6	1.30 ± 0.05

*Artificial sea-water with high F^- content.

†Artificial sea-water with low F^- content; 5-fold dilution.

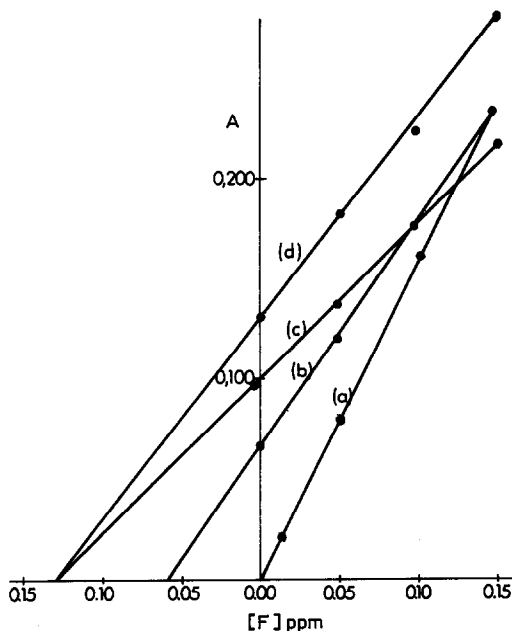


Fig. 3. Working standard-additions curves for determination of fluoride in natural sea-water (Huelva) by AlF-MA. (a) Calibration curve (distilled water); (b) procedure 1, direct 1:20 dilution; (c) procedure 2, 1:10 dilution; (d) procedure 3, 1:10 dilution and cation-exchange.

Acknowledgements—The authors thank Max Gormann for revision of the manuscript, and CAICYT (Project 85/0035) and the International Atomic Energy Agency for financial support.

REFERENCES

1. K. Tsunoda, K. Fujiwara and K. Fuwa, *Anal. Chem.*, 1977, **49**, 2035.
2. K. Dittrich, V. M. Shkinev and B. Ya. Spivakov, *Talanta*, 1985, **32**, 1019.
3. M. Gomez Gomez, M. A. Palacios Corvillo and C. Cámara Rica, *Analyst*, 1988, **113**, 1109.
4. G. K. Schweitzer and S. W. McCarthy, *J. Inorg. Nucl. Chem.*, 1965, **27**, 191.
5. H. Chermette, C. Martelet, D. Sandino and J. Tousset, *ibid.*, 1972, **34**, 1627.
6. M. Ben Alet, H. Chermette, C. Martelet, D. Sandino and J. Tousset, *ibid.*, 1974, **36**, 1859.
7. K. Dittrich, B. Vorberg, J. Funk and V. Beyer, *Spectrochim. Acta*, 1984, **39B**, 349.
8. K. Chiba, K. Tsunoda, H. Haraguchi and K. Fuwa, *Anal. Chem.*, 1980, **52**, 1582.
9. K. Dittrich and P. Meister, *Anal. Chim. Acta*, 1980, **121**, 205.
10. K. Dittrich, *CRC Crit. Rev. Anal. Chem.*, 1986 **16**, 223.
11. R. C. Weast (ed.), *CRC Handbook of Physics and Chemistry*, 67th Ed., CRC Press, Boca Raton, 1986–1987.
12. K. Tsunoda, H. Haraguchi and K. Fuwa, *Spectrochim. Acta*, 1985, **40B**, 1651.

INTERFERENCE FROM IODIDE IN THE DETERMINATION OF TRACE LEVEL SELENIUM

CHRISTINA ERICZON, JEAN PETTERSSON* and ÅKE OLIN

Department of Analytical Chemistry, Uppsala University, P.O. Box 531, S-751 21 Uppsala, Sweden

(Received 20 June 1989. Revised 9 October 1989. Accepted 30 November 1989)

Summary—The rate of the reaction between iodide and selenium(IV) at trace levels to form selenium and iodine has been determined in 1–6*M* hydrochloric acid. The reaction rate increases rapidly with acidity. When hydrochloric acid is added to reduce selenate to selenite prior to the determination of total selenium, some selenium may be lost by reduction to the element if iodide is present. A table of half-lives of the selenite–iodide reaction under various conditions is presented. A method for removal of iodide is suggested.

We have recently investigated the flow of selenium in a garbage incinerator which burns some 250,000 tonnes of household waste annually. One of the sampling points was the flue-gas cooler. The condensate from the cooler was acidic from hydrogen chloride scrubbed from the flue gas and was neutralized to pH 2 with lime as a first step in the purification sequence prior to discharge. When selenium was determined in the partly neutralized condensate by hydride-generation atomic-absorption spectrometry (HGAAS) with a method¹ which had proved adequate for a number of specimens, erratic results were sometimes obtained. The HGAAS technique is subject to a number of well documented interferences in the hydride generation step,^{2,3} but the erratic results were found to be connected with the sample pre-treatment and not the hydride generation.

Selenium must be present in the quadrivalent state to be transformed in solution into selenium hydride, and any hexavalent selenium present must be reduced to the quadrivalent state by boiling with ~4*M* hydrochloric acid. Losses of selenium occurred if the hydrochloric acid concentration in our samples exceeded about 5*M* during addition of the acid needed for the reduction step. A number of tests, to be described in a later section, indicated that the interferent was iodide present at low concentration (10 μ *M*).

Reduction of selenium(IV) by iodide to form elemental selenium and iodine has been used to determine selenium,^{4,5} but the analytical

procedures employ much higher iodide concentrations than those present in our samples. The kinetics of the reaction has been studied at acidities below about 0.1*M*.⁶ Extrapolation of the proposed rate law to the acidities prevalent in the determination of selenium yielded half-lives that were orders of magnitude longer than those observed, thus casting doubt on the nature of the alleged interferent. It was therefore decided to investigate the reaction between low concentrations of selenium(IV) and iodide at high concentrations of hydrochloric acid, the conditions when selenium is determined by HGAAS. Means of inhibiting the interference from iodide were also studied.

EXPERIMENTAL

Apparatus

The kinetic experiments were performed in a water-bath kept at 25°. The selenium determinations were done with HGAAS equipment described elsewhere.¹ Peak heights were evaluated with an integrator (Shimadzu C-R3A). Sample injections were controlled by a laboratory-built timer, which allowed analysis of the reaction mixture at regular intervals.

In a kinetic run, 50 or 100 ml of hydrochloric acid of the appropriate concentration were added to the reaction vessel. After temperature equilibration in the thermostat, iodide was added, followed by selenium(IV). The reaction vessel was connected to the injection valve of the HGAAS apparatus by a short piece of Teflon tubing (i.d. 0.7 mm). The reaction mixture was continuously withdrawn from the reaction

*Author for correspondence.

vessel through the injection loop (0.5 ml) by a peristaltic pump. The pump and the timer were started at the instant of addition of selenium to the reaction vessel. Injections were made into the HGAAS apparatus at regular intervals, and from the results obtained the course of the reaction could be followed. No precautions were taken to exclude air, since separate spectrophotometric experiments showed that air oxidation of iodide was negligible during the short reaction times used in the experiments.

Chemicals

All chemicals were of analytical grade. A standard solution of selenium(IV), 1 g/l., was prepared from an ampoule of selenium dioxide in dilute nitric acid (Merck). Further standards were obtained by dilution. The iodide stock solution was made by dissolving potassium iodide in deaerated distilled water. This solution was prepared at frequent intervals to minimize oxidation by air. Solutions of lower concentration were prepared when needed, by dilution with deaerated distilled water. The silver perchlorate solution was obtained by reacting an excess of silver oxide, prepared from silver nitrate and sodium hydroxide, with standard perchloric acid.

In most of the experiments hydrochloric acid (Merck) was used as received. In the experiments at very low iodide concentration the acid (diluted 1:1) was distilled at normal pressure before use. The middle two-thirds of the distillate was collected. Attempts at chemical removal of any iodide present in the acid, for instance by addition of nitrite and subsequent distillation, failed, very high blanks (compared to the selenium signal) being obtained when the distillate was injected into the single-beam HGAAS apparatus, which had no background correction facility.

Determination of iodide in the flue-gas cooler condensate

An estimate of the iodide concentration in the flue-gas cooler condensate was obtained by first oxidizing the sample with bromine water, destroying the excess of bromine with formic acid, deaerating the solution, then adding a large excess of solid potassium iodide and measuring the absorbance of the solution at 351 nm against a reagent blank (to compensate for any iodine present in the potassium iodide or formed by air oxidation in the test solution). This procedure is a slight modification of a scheme

used in a flow-injection method for the determination of iodide.⁷ Interference from iron and selenium was eliminated by neutralization and subsequent filtration of the sample prior to the iodide determination, removing iron by precipitation and selenium by co-precipitation.⁸ The procedure was checked by analysis of synthetic samples and recovery tests but systematic errors may occur in analysis of condensate samples.

Treatment of the flue-gas cooler condensate with silver perchlorate

The chloride concentration of the sample was about 0.25M, and ~90% of the chloride was precipitated by addition of silver perchlorate and filtered off. No loss of selenium occurred when the filtrate was analysed for total selenium, as opposed to an untreated sample. The precipitation is done with silver perchlorate so that no oxidizing anion is introduced. The concentration of residual chloride should be in the vicinity of that for minimum solubility of silver chloride in a chloride medium; otherwise, silver(I) will interfere with the hydride generation.

The nature of the interference

The condensing water in the flue-gas cooler ridges the combustion gases of mainly hydrogen chloride, other volatiles and fine particles not trapped by the electrostatic precipitators. The condensate will therefore have a complex composition. The loss of the HGAAS signal on acidification of the condensate was due to reduction of Se(IV) to Se, which does not react with tetrahydroborate to form hydrogen selenide. Evidence for this conclusion was furnished by the fact that the selenium could be collected on a 0.45 μm filter and brought into solution again by treatment with bromine water.

The most abundant reducing agent in the flue-gas system is sulphur dioxide, which is known to reduce Se(IV) to Se in strongly acidic medium. However, purging the slightly acidified sample with nitrogen overnight did not remove the interference. This indicates that sulphur dioxide is not the operative reducing agent.

Passing the sample through an anion-exchange column removed the interferent, but a cation-exchanger did not. The interfering anion could be precipitated with Ag^+ (silver perchlorate).

From these experiments it was concluded that iodide was the most plausible cause of the

interference in view of its ability to reduce Se(IV) to Se.

Removal of iodide

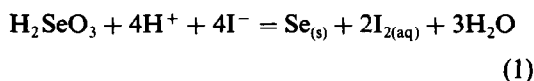
The iodide interference can be eliminated by oxidation of iodide to iodate with bromine. Saturated bromine water was added to a slightly acidic solution containing $5 \times 10^{-4} M$ iodide until the formation of a distinct yellow colour due to excess of bromine. This should not be confused with the colour caused by iodine, which can be obtained as an intermediate. The solution was then allowed to stand for 5 min and the excess of bromine was removed by passage of nitrogen for about 30 min. Equal amounts of selenium(IV) and selenium(VI) were added, and the solution was made $4 M$ in hydrochloric acid. Aliquots of the mixture were transferred to glass tubes which were then heated in a temperature-controlled aluminium block at 120° for 30 min. To some of the samples, enough nitric acid had been added to give a final concentration of $0.01 M$. After cooling, the samples were diluted to have a concentration of $1 M$ hydrochloric acid and the total amount of selenium was measured. The non-reduced samples were also measured. The final concentration of total selenium was $10 \mu\text{g/l}$.

Reagent blanks were carried through all steps and found to be very small or negligible.

RESULTS AND DISCUSSION

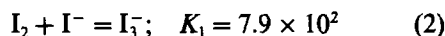
The reaction schemes and kinetic laws describing the reduction of oxo-anions by iodide usually involve many steps and intermediate products, as exemplified by the reaction between iodate and iodide.^{9,10} It was therefore decided to restrict the investigation to an empirical determination of the rate of reaction between selenium(IV) and iodide in hydrochloric acid in the concentration range $1-6 M$. Most experiments were performed at a selenium concentration of about $10^{-7} M$, which is a typical analyte concentration (Se $8 \mu\text{g/l}$.) in the HGAAS method. The iodide concentrations were selected to yield half-lives of less than 40 min, and hence to correspond to conditions in which iodide could interfere in the determination of selenium.

The main stoichiometric reaction is



The reaction is written with $\text{I}_{2(aq)}$ as a product, since the solubility of iodine in water will not be

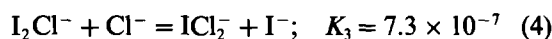
exceeded in the experiments. For convenience $\text{I}_{2(aq)}$ will be denoted by I_2 . The equilibrium constant of reaction (1) can be calculated¹¹ to be 1.05×10^8 . In addition to the reaction



the following equilibria in hydrochloric acid medium must be considered:¹²



and



Chloro complexes of selenium(IV) should also have been included, since weak complexation occurs at hydrochloric acid concentrations exceeding about $4.5 M$,^{13,14} but no equilibrium constants were found for these reactions, so only reactions (1)–(4) could be considered in the equilibrium calculations. As most of our measurements pertain to hydrochloric acid concentrations $\leq 5 M$, omission of the chloride complexes is expected to be of minor importance for the conclusions drawn.

Reaction (1) proceeds to equilibrium⁶ but it is the rate of the forward reaction that is of most interest in connection with interference studies. Moreover a real sample may very well contain components that react with iodine, which would inhibit the reverse reaction and shift the equilibrium of reaction (1) to the right.

An empirical rate law for reaction (1) may be written as

$$R = -d[\text{Se(IV)}]/dt = k_0[\text{Se(IV)}]^a[\text{I}^-]^b[\text{H}^+]^c \quad (5)$$

From measurements with constant iodide and hydrochloric acid concentrations but varying amounts of selenium(IV), it was established that the reaction was first order with respect to selenium. The rate of the reverse reaction was always negligible under the conditions used. This was checked occasionally by leaving the reaction for long times to verify that the selenium(IV) concentration approached zero. The rate constant could therefore be evaluated by fitting the experimental data to the function

$$[\text{Se(IV)}]_t = [\text{Se(IV)}]_0 e^{-kt} \quad (6)$$

where k is the pseudo first-order rate constant, $[\text{Se(IV)}]_t$ the selenium(IV) concentration measured at time t and $[\text{Se(IV)}]_0$ the initial concentration. Figure 1 shows the results of a kinetic experiment and its evaluation. Wall effects were shown to be absent by noting that

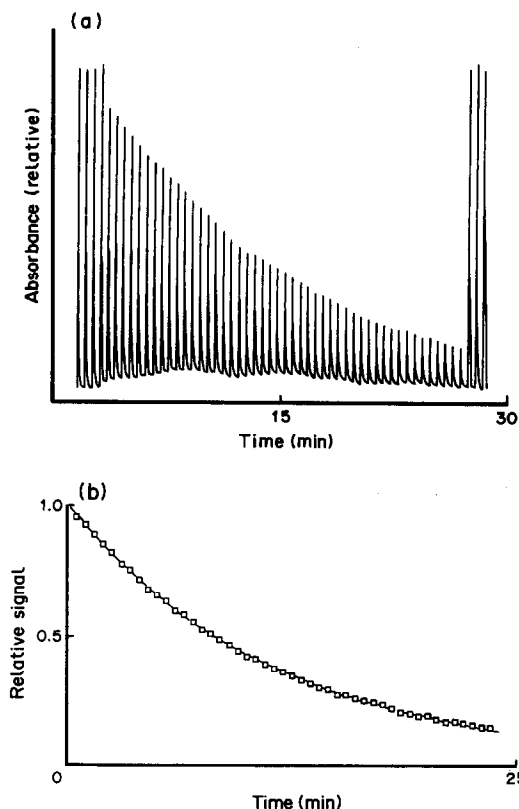


Fig. 1(a) Absorbance peaks from a kinetic run in 2M hydrochloric acid, $[\text{Se(IV)}] = 1 \times 10^{-7} M$ and $[\text{I}^-] = 2 \times 10^{-4} M$. The first four and the last three peaks derive from calibrations made before and after the main experiment. The time interval between peaks is 30 sec. (b) Fit of the first-order rate expression, equation (6), to the experimental data in Fig. 1(a) (squares).

R was not affected by the presence of a piece of glass wool in the reaction vessel.

The main series of measurements was made with 1, 2, 3, 4 and 5M hydrochloric acid. Measurements were also performed with 6M acid medium, but were subject to various difficulties which will be described later. The stoichiometric excess of iodide over selenium(IV) was kept large enough to permit the use of equation (6) for calculating k . At each acid concentration the iodide concentration was varied and the order of reaction with respect to iodide was obtained by plotting the logarithm of the rate constant against $\log [\text{I}^-]$. Straight lines were obtained for each acidity. The order was apparently close to 2 for 3M hydrochloric acid medium but diminished steadily with increasing concentration of hydrochloric acid and/or decreasing iodide concentration. This indicates a complex reaction mechanism. The variation of the order with respect to iodide, n , can be represented by $n = 2.30 - 0.1125C_{\text{HCl}}$, where

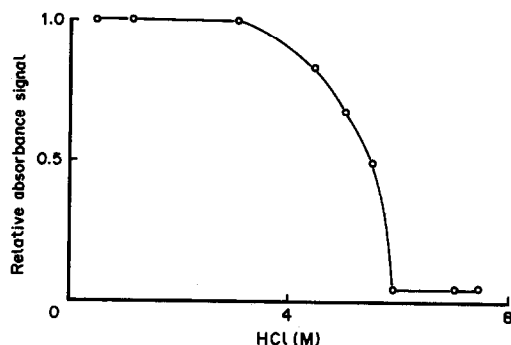


Fig. 2. Relative absorbance signal from a specimen of flue-gas cooler condensate after addition of hydrochloric acid. About 3 min after mixing, the samples were diluted to an acid concentration of about 1M to stop the reaction, and selenium(IV) was determined by the standard procedure.

C_{HCl} is the concentration of hydrochloric acid. For the reaction between iodate and iodide the order with respect to iodide has been found to decrease with iodide concentration.¹⁰ This matter was not pursued further. A reaction order of 2 with respect to iodide might indicate that the reaction rate is determined by a step in which Se(IV) is first reduced to Se(II).

The most striking feature of the reaction between selenite and iodide is its dependence on the hydrochloric acid concentration, as shown in Fig. 2 for a specimen of flue-gas cooler condensate. This dependence was corroborated in the present investigation. The increase in R with concentration of hydrochloric acid is caused mainly by the protons. The influence of chloride appears to be much less than that of the protons. Figure 3 shows that the value of the rate constant diminishes by a factor of only about three on going from 2.4M hydrochloric acid to 2.4M perchloric acid.

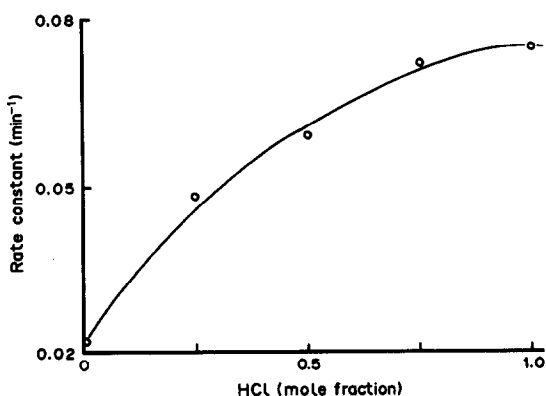


Fig. 3. Variation of the rate constant in mixtures of hydrochloric and perchloric acid. Total acid concentration 2.4M, $[\text{Se(IV)}] = 1 \times 10^{-7} M$, $[\text{I}^-] = 1.2 \times 10^{-4} M$.

Table 1. Corresponding iodide concentrations (rounded values) and half-lives at various concentrations of hydrochloric acid; the iodide concentrations were calculated from equation (7)

$t_{1/2}$, min	[I ⁻], μ M				
	1M HCl	2M HCl	3M HCl	4M HCl	5M HCl
2	2000	460	120	28	6
5	1400	290	74	17	3
10	1000	210	52	12	2
20	720	150	37	8	1
40	520	110	26	6	1

The experimental half-lives fit the equation

$$t_{1/2} = 1.63 \times 10^{-6} [I^-]^{-(2.30 - 0.1125C_{HCl})} \times (y_{\pm} C_{HCl})^{-2.53} \quad (7)$$

where y_{\pm} is the mean molar activity coefficient of hydrochloric acid at the appropriate concentration.¹⁵ The expression covers the following experimental conditions: $5 < t_{1/2} < 40$ min; $1 < C_{HCl} < 5M$; $2 \times 10^{-6} < [I^-] < 1 \times 10^{-3}M$. Table 1 contains the iodide concentrations and half-lives calculated from equation (7) for various concentrations of hydrochloric acid, and illustrates the great dependence of the selenium(IV)-iodide reaction on the hydrochloric acid concentration. This pertains to the rate as well as the equilibrium position of the reaction. Obviously selenium, at trace levels, is readily lost from a solution containing only small amounts of iodide on addition of acid.

Table 2. Removal of interference from iodide by oxidation with bromine; sample A contains no iodide; sample B contains $5 \times 10^{-4}M$ iodide, but is not treated with bromine; sample C is treated with bromine to oxidize the added iodide ($5 \times 10^{-4}M$); the total amount of selenium in the samples is $10 \mu\text{g/l.}$, added as equal amounts of Se(IV) and Se(VI); the reduction is performed in 4M hydrochloric acid at 120° for 30 min

Sample	Non-reduced, recovery of Se(IV), %	Reduced, recovery of total Se, %	Reduced (0.01M HNO ₃ added), recovery of total Se, %
A	100	100	100
B	ND; 9	37; ND	88; 92
C	95; 96	100; 100	100; 100

ND = not detected.

As can be inferred from Table 2, the interference from iodide can be successfully removed by oxidation of iodide to iodate with bromine water (sample C). If this is not done most of the selenium signal is lost (sample B). The addition of 0.01M nitric acid before the reduction step with hydrochloric acid does not seem necessary but it was still used as a precaution. It can also be seen from Table 2 that the reduction of selenium(VI) to selenium(IV) is complete under these conditions.

It must be pointed out that the removal of bromine (or other molecular species) is important when, as in this case, the HGAAS apparatus has no background corrector. Molecular absorbance leads to high and irreproducible blanks. It is possible that this step can

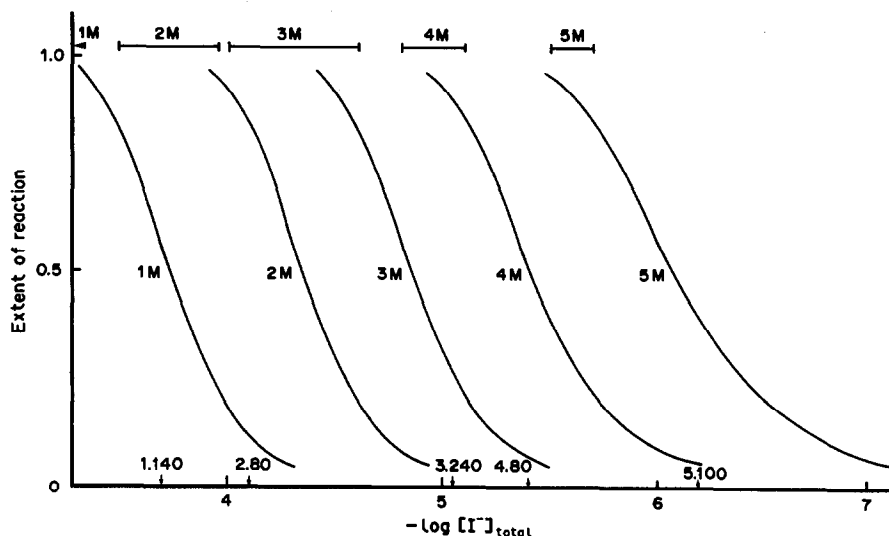


Fig. 4. Calculated extent of reaction at equilibrium for reaction (1) as a function of the logarithm of the total molar concentration of added iodide at selected concentrations of hydrochloric acid. The horizontal bars show the range of iodide concentrations used in the kinetic measurements. The iodide concentrations at which reaction (1) starts with an appreciable rate are marked by vertical arrows. The numbers attached denote the hydrochloric acid concentration and the corresponding half-life (min) estimated from equation (7).

be excluded, or that the interference from iodide can be eliminated simply by adding a larger amount of nitric acid in the reduction step, if a spectrometer with background correction is used. With 0.1M nitric acid, problems with blanks arose when our apparatus was used.

The equilibrium position of reaction (1) was calculated from the equilibrium constants of reactions (1)–(4). Activity coefficients were introduced for the singly charged species, and γ_{\pm} of hydrochloric acid at the appropriate concentration was used. It should be noted that the result of the calculation is greatly dependent on the choice of γ_{\pm} , since the activity coefficient is raised to a power of eight in the equilibrium expression for reaction (1). In Fig. 4 the extent of reduction of selenium(IV) at equilibrium is shown as a function of the logarithm of the total concentration of added iodide. The ranges in iodide concentration used in the kinetic experiments are indicated by horizontal bars. According to the thermodynamic calculations the extent of reaction at equilibrium is 90% or greater for these concentrations. The iodide concentration needed to start reaction (1) was estimated as follows. Iodide was added in increments to solutions of selenium(IV). The decrease in selenium(IV) concentration was measured 1 hr after each addition. When the selenium(IV) concentration had decreased by some 10–20% from its initial value, the corresponding iodide concentration was taken as the concentration needed to start the reaction at an appreciable rate. These concentrations are marked by arrows in Fig. 4 together with the value of $t_{1/2}$ estimated from equation (7). From the curves and experimental results depicted in Fig. 4 we may conclude that the equilibrium calculations and the findings from the kinetic measurements are mutually consistent, although the criterion for the start of the reaction is rather crude.

We have also made measurements for 6M hydrochloric acid medium. These studies failed to yield satisfactory results, mainly because we were unable to prepare stable solutions of selenium(IV) in 6M hydrochloric acid. Since even very low iodide concentrations are expected to reduce selenium(IV) in 6M acid, we tried several methods to remove iodide but obtained high blank values. However, simple distillation of the acid dramatically increased the stability of selenium(IV) in 6M hydrochloric acid and it could be established that addition of only $2 \times 10^{-7}M$ iodide markedly decreased the stability of the selenium(IV). For 5M hydrochloric acid no difference was noted between the results for distilled and undistilled acid.

REFERENCES

1. J. Pettersson, L. Hansson and Å. Olin, *Talanta*, 1986, **33**, 249.
2. F. D. Pierce and H. R. Brown, *Anal. Chem.*, 1977, **49**, 1417.
3. K. Itoh, M. Chikuma and H. Tanaka, *Z. Anal. Chem.*, 1988, **330**, 600.
4. D. F. Boltz and J. A. Howell (eds.), *Colorimetric Determination of Nonmetals*, p. 389. Wiley, New York, 1978.
5. F. F. El-Enany, K. Mahmoud and M. M. Varma, *Anal. Chem.*, 1980, **52**, 1540.
6. J. A. Neptune and E. L. King, *J. Am. Chem. Soc.*, 1953, **75**, 3069.
7. A. Al-Wehaid and A. Townshend, *Anal. Chim. Acta*, 1987, **198**, 45.
8. Y. K. Chau and J. P. Riley, *ibid.*, 1965, **33**, 36.
9. P. Beran and S. Bruckenstein, *J. Phys. Chem.*, 1968, **72**, 3630.
10. A. F. M. Barton, H. N. Cheong and R. E. Smidt, *J. Chem. Soc., Faraday 1*, 1976, 568.
11. W. M. Latimer, *Oxidation Potentials*, 2nd Ed., Prentice-Hall, New York, 1956.
12. D. L. Cason and H. M. Neumann, *J. Am. Chem. Soc.*, 1961, **83**, 1822.
13. A. K. Babko and T. T. Mityureva, *Russ. J. Inorg. Chem.*, 1961, **6**, 213.
14. N. Jordanov and L. Futekov, *Talanta*, 1965, **12**, 371.
15. R. A. Robinson and R. H. Stokes, *Electrolyte Solutions*, p. 491. Butterworths, London, 1959.

USE OF A GC/MS/MS TECHNIQUE IN DETERMINATION OF BIOMARKERS IN REGIONAL PETROLEUM

DING-PING LIN* and NUREDDIN M. ABBAS

Research Institute, King Fahd University of Petroleum and Minerals, Dhahran, Saudi Arabia

(Received 24 March 1989. Revised 12 December 1989. Accepted 3 February 1990)

Summary—The optimum conditions of a GC/MS/MS operation based on the covariant scan of electrostatic-magnetic fields on the trisector double focusing mass spectrometer JMS-HX100 have been searched for and procured. The distribution of C_{29} sterane biomarkers in Arabian Medium crude oil is obtained by utilizing the best acquired parameter settings.

To identify the origin and geological transformation of crude oils, the most direct method is to examine the remnants of the biological material that has undergone diagenesis. Steranes and diasteranes (C_nH_{2n-6}) are groups of biomarkers which are commonly studied¹ in the oil industry, because they are derived from sterols² and their configuration changes during maturation. Thus, the distribution ratios of the major isomers have been used as indicators for source identification³ and migration⁴ and maturation studies.¹

In most petroleum, homologous series of C_{27} , C_{28} and C_{29} steranes predominate. They are often identified by gas chromatography/mass spectrometry (GC/MS), by use of diagnostic fragment ions.⁵ However, as the maturity of the oil increases, the mass fragmentogram becomes much more complex,⁶ making unambiguous identification less likely. Hence, an analytical technique with higher specificity is necessary to resolve the target homologues from the interferences and peak overlaps.

Tandem mass spectrometry (MS/MS) has been shown to be quite specific in petroleum research⁷ and there have been several literature reports of GC/MS/MS of source rocks.⁸⁻¹¹ However, most of the methods employed scanned the accelerating voltage of the mass spectrometer, which changed the ion-source conditions and led to unequal sensitivity for analyte comparison. Some methods used linked scans^{8,11} to monitor apparent mass, instead of using functional scans of both the electrostatic and magnetic fields, giving poorer peak resolution on the chromatograms based on detection of the

metastable transitions (MT). The objectives of the present work are two-fold. First, to test the utility of the present JMA-DA5000 data system (Version 1.07) for GC/linked scans and to optimize the conditions from the technical information available, since the stringent requirements of a fast scanning magnet may pose a problem. Secondly, to apply this technique, if feasible, to the determination of biomarkers and the sterane distribution in Arabian Medium crude oil.

EXPERIMENTAL

Apparatus

A Carlo Erba HR5300 GC was fitted with an HP-1 cross-linked methylsilicone gum capillary column (25 m × 0.2 mm; 0.33 μ m thick coating) directly coupled to the ion-source of the mass spectrometer. A JEOL JMS-HX100 triple-sector E_1BE_2 high-resolution (maximum 100 000 at 10% valley) double-focusing mass spectrometer was used for the constant B/E and B^2/E linked scans.

Procedure

Helium was used as carrier gas at a flow-rate of 1 ml/min. The injector temperature was maintained at 300° and the oven temperature was programmed to rise from 60° to 250° at 32°/min, stay at 250° for 5 min, then rise to 300° at 8°/min, stay there for 5 min and rise at 8°/min to 320°, then remain at this final temperature for 20 min. A complete run took about 45 min. The final temperature selected was close to the maximum allowable for the liquid phase in the column. A 5- μ l sample of crude oil was injected each time, with a split ratio of 100 to 1 after

*Author for correspondence.

40 sec. The scan slope and cycle time for a mass range of m/z 0–800 during B/E calibration were 30 and 15 sec respectively. The actual scan time was 12.6 sec. The scan slope and cycle time of B^2/E calibration were 40 and 20 sec, respectively, with a scan time of 16.8 sec. During the $GC/(B/E)$ and $GC/(B^2/E)$ runs, various accumulation ranges coupled with scan ranges in the accumulation mode were tested by keeping the cycle time to 1 sec and the scan slope time to the same value as that for the calibration. This accumulation mode records the profile of the real-time chromatogram; it does not really accumulate signals during acquisition in these experiments. The single parent/daughter reaction pair was selected according to the reports¹⁻⁶ for other oils, m/z 400.4*/217.2*, which is a typical reaction of $C_{29}H_{52}$ under electron impact (EI). The mass spectrometric conditions were as follows: resolution tuned at 1000; ionization current, 300 μ A; emission current, 390 μ A; filament current, 3.8 A; EI, 70 eV; ion multiplier voltage, -2.5 kV; chamber temperature, 210° at equilibrium; post accelerator voltage, -3.0 kV. The interface temperature was set at 250° and the inlet temperature was maintained at 200°.

RESULTS AND DISCUSSION

Possible causes for the apparent retention time shifts

Table 1 lists the experimental conditions and results for the $GC/(B/E)$ single-reaction monitoring (SRM). The accumulation range was varied from ± 0.1 to ± 0.5 amu and the scan ranges were adjusted from 1 to 10 amu. Only one parameter was varied at a time, to observe

its effects on the appearance of the chromatogram. The retention times of the peaks in each of the SRM chromatograms obtained under these sets of conditions were not exactly consistent. Since this was considered not to be caused by any chromatographic changes, the shifts in retention time had to have originated from the linked scan operation. It appears that there are at least two factors which influence the stability and appearance of the chromatograms. From the data in Table 1 for a constant unit-mass scan time, the narrower the accumulation window (Δm) the higher the signal to noise ratio (S/N) and the peak resolution (R), except for $\Delta m = 0$ at which the data system automatically extended the present mass range to 1 amu. Since there is no peak-dwelling control in the software there is no metastable-peak jumping mechanism to lengthen the acquisition time over the range $217.2^* \pm \Delta m$. Thus, S/N depends on the time spent in the Δm range by the uniform scanning. This phenomenon was even clearer in the $GC/(B^2/E)$ mode where not only was a longer reset time required, but the scan range also had to be made larger to allow enough scan time with 1-sec cycle time. The proportionate time allocated to a given accumulation range in the B^2/E mode is therefore only about a third of that in the B/E mode. This led to lower sensitivity and poorer resolution, with apparently drifted retention times. Further, the 1-sec cycle time appropriate for the capillary column output imposed on the linked scans might be far too short for the magnetic field to have a mass accuracy better than ± 0.1 amu. Broader gate widths allow the isobaric species at around 217.2* in the first field-free region to be picked up by the detector, rendering broader peak

Table 1. Experimental parameters for the $GC/(B/E)$ runs for the metastable transition m/z 400.4* \rightarrow 217.2*, in the Arabian Medium crude oil

Run	$\Delta m, \dagger$ amu	Accumulation range, § amu	Scan range, amu	Scan time, § sec	Remarks
1	0	217–218	212–222	0.22	Fair S/N
2	0.1	217–217	212–222	0.22	Good S/N and R
3	0.2	217–217	212–222	0.22	Fair R
4	0.3	217–217	212–222	0.22	Poor S/N^*
5	0.5	217–218	212–222	0.22	Very poor R
6	0.5	217–218	215–219	0.09	Fair R
7	0.5	217–218	216.7–217.7‡	0.02	Poor S/N and R

† Accumulation range was set from $217.2 - \Delta m$ to $217.2 + \Delta m$ in the parameter page of the program.

‡ Scan range was set to be exactly the same as accumulation range; the latter has to be within the former.

§ Shown in the 'ACM Measurement Condition' page of the program before measurement.

¶ Ion multiplier voltage -1.5 kV.

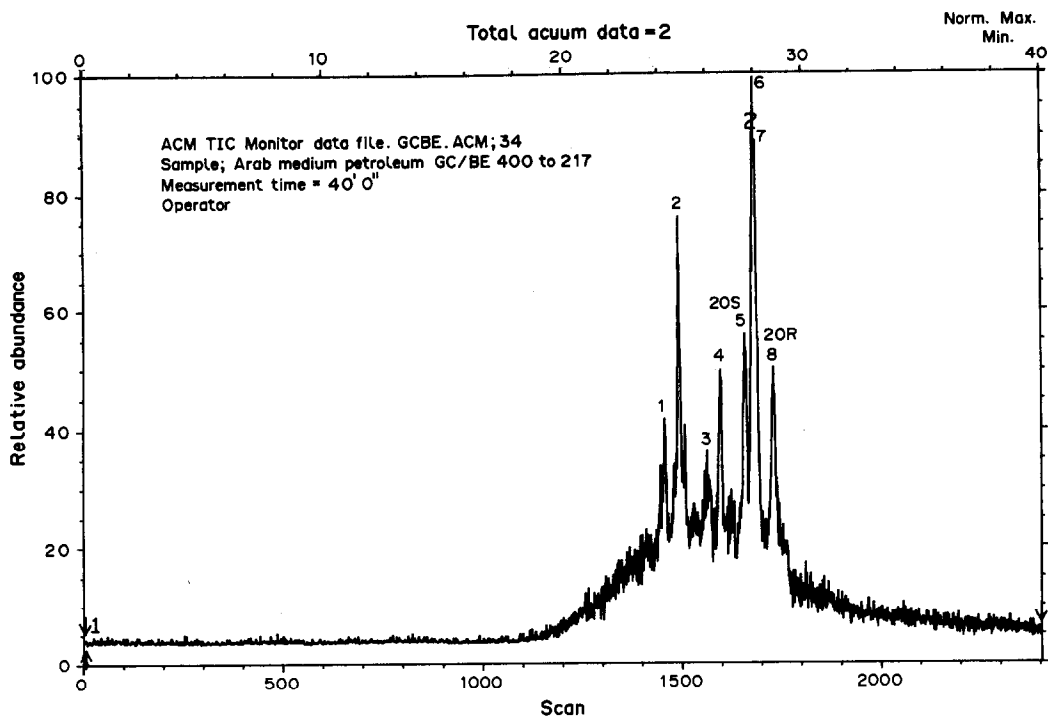


Fig. 1. The best chromatogram obtained by the GC/(B/E) scan for the Arabian Medium crude oil, based on the following experimental parameters: accumulation range 217.1–217.3 amu, scan range 212–222 amu, scan time 0.22 sec, cycle time 1 sec. Note the hump underneath the resolved peaks.

widths and apparent retention time shifts. It is conceivable, however, that to perform single-reaction monitoring, either the *B/E* or *B²/E* linked mode will attain the same goal. Hence, GC/(*B/E*) operation seems to be a better choice than GC/(*B²/E*) with the present set-up. A similar technique with different instrumentation has been applied to the detection of aryl isoprenoids in source rocks and crude oils,¹² and to some hydrocarbons in sediments and fossil algae.¹³ However, depending on the nature of the crude oils, the chemical noise beneath the component GC peaks in the SRM as well as in the multiple-reaction monitored chromatograms is quite obvious, as is evident in Fig. 1.

Maturity of the Arabian crude oils

The best reproducible and resolved reaction chromatograms, with the highest *S/N*, were obtained with parameter set No. 2 in Table 1. These peaks resemble those obtained for the other oils by use of switching the accelerating voltage.⁹ In Fig. 1, they are assigned as follows by comparison with those given in references 1, 6 and 10:

1. 24-Ethyl-13 β (H),17 α (H)-diacholestane (20R) 27%

2. 24-Ethyl-13 β (H),17 α (H)-diacholestane (20S) 72%
3. 24-Ethyl-13 α (H),17 β (H)-diacholestane (20R) 22%
4. 24-Ethyl-13 α (H),17 β (H)-diacholestane (20S) 34%
5. 24-Ethyl-14 α (H),17 α (H)-cholestane (20S) 40%
6. 24-Ethyl-14 β (H),17 β (H)-cholestane (20R) 100%
7. 24-Ethyl-14 β (H),17 β (H)-cholestane (20S) 86%
8. 24-Ethyl-14 α (H),17 α (H)-cholestane (20R) 39%

The most abundant isomers 6 and 7 are formed by geological processes, since no sterols in nature are known which have these configurations.¹ As burial depth and temperature increase, these more stable isomers are transformed from their precursor isomer 8. The extent of maturity in Arabian Medium crude is reflected by the ratio of β -isomers to α -isomers, which is close to 5. On the other hand, isomer 8 correlates directly with one of the most abundant C₂₉ sterols in present day organisms. With increasing maturity of the crude oil, the biologically derived 20R epimer is isomerized to the 20S configuration and the ratio of isomer 5

to isomer 8 is around unity, based on their peak heights. Distinct preference for the 20S isomers of diacholestane over their counterparts also suggests that the petroleum studied here is a stable, mature fossil fuel, which is similar to Arabian Heavy crude ($^{\circ}\text{API} = 27$) in its maturity.¹⁴ Since C_{29} sterane may occur with the α or β configuration of hydrogen at C-5, C-14 and C-17, and as 20S/20R isomers or 24S/24R epimers, mixtures of these may not be completely separated by the GC column used. As maturity increases, the number of these stereoisomers also increases, and their distribution becomes very complex. This degree of maturity is detected by the MS/MS device as an unresolved broad signal for the specific metastable-ion transition, underneath the peaks in Fig. 1.

Acknowledgements—The support of the Research Institute, King Fahd University of Petroleum and Minerals, and permission to publish this work are appreciated. Technical information from both Mr. T. Hara and Mr. T. Oshimi at JEOL was most helpful and we are grateful to both of them.

REFERENCES

1. A. S. Mackenzie, R. L. Patience and J. R. Maxwell, *Geochim. Cosmochim. Acta*, 1980, **44**, 1709.
2. R. P. Philp, *Fossil Fuel Biomarkers, Applications and Spectra*, p. 41. Elsevier, Amsterdam, 1985.
3. W. K. Seifert, R. M. K. Carlson and J. M. Moldowan, in *Adv. Org. Geochem. Proc. Int. Meet.*, 10th 1981, M. Bjoroye (ed.), p. 710. Wiley, Chichester, 1983.
4. W. K. Seifert, J. M. Moldowan and R. W. Jones, *Proc. World Pet. Congr.*, 1979, p. 425, Paper SP 8.
5. R. P. Philp, *Mass Spectrom. Rev.*, 1985, **4**, 1.
6. *Idem*, *Chem. Eng. News*, 1986, **64**, No. 6, 28.
7. D. P. Lin, L. A. Litorja and N. M. Abbas, *Arabian J. Sci. Eng.*, 1988, **13**, 145.
8. J. M. Moldowan, W. K. Seifert and E. J. Gallegos, *Geochim. Cosmochim. Acta*, 1983, **47**, 1531.
9. G. A. Warburton and J. E. Zumberge, *Anal. Chem.*, 1983, **55**, 123.
10. T. Meyer, O. H. J. Christie and P. W. Brooks, *Anal. Chim. Acta*, 1984, **161**, 65.
11. J. M. Moldowan, W. K. Seifert and E. J. Gallegos, *AAPG Bull.*, 1985, **69**, 1255.
12. R. E. Summons and T. G. Powell, *Geochim. Cosmochim. Acta*, 1987, **51**, 57.
13. C. F. Hoffman, C. B. Foster, T. G. Powell and R. E. Summons, *ibid.*, 1987, **51**, 2681.
14. D. P. Lin, L. A. Litorja and N. M. Abbas, *Fuel*, 1989, **68**, 257.

A REVIEW OF pH MEASUREMENT AT HIGH TEMPERATURES

DEREK MIDGLEY

National Power, Technology and Environmental Centre, Kelvin Avenue, Leatherhead,
Surrey KT22 7SE, U.K.

(Received 18 July 1989. Revised 5 February 1990. Accepted 10 February 1990)

Summary—Measurement of pH in aqueous solutions at up to 300° and 150–300 bar is reviewed. Potentiometric membrane electrodes are identified as the sensors giving the most immediate hope of being practical. Zirconia membranes work well above 200° and in alkaline solution, whereas glass membranes are best up to 150° and in acidic solutions. Both membranes are largely free from interferences. Metal–metal oxide electrodes offer poor prospects, deviating from the ideal Nernstian response at all temperatures and being susceptible to interference from many redox and complexing agents, but systems based on iridium oxide have some promise. The hydrogen electrode remains the standard for pH measurement, but its analytical application is limited by the need to know the hydrogen partial pressure. A practical solution to this problem has yet to be found, except in restricted and artificial circumstances. Palladium hydride electrodes may be useful up to about 200°, but in hydrogen-saturated waters revert to being hydrogen electrodes in any case. Non-potentiometric pH measurements with semiconducting oxides have been shown to be possible, but there are many unanswered questions about possible interferences. Considerable extra instrumentation is required, compared with potentiometry. Fibre-optic sensors based on indicator dyes have been investigated at room temperature, and have the great merit of not requiring a reference electrode. They seem, however, prone to many interferences and have an inherently limited working range of ~2 pH. No measurements at high temperature have been reported. Improved reference electrodes for potentiometric systems are still needed, although there have been advances in the design of external pressure-compensated electrodes working at room temperature. The silver–silver chloride system is still the one most favoured. There has been little rigorous work on standard buffer solutions at above 100° and none at above 200°. Neutral and alkaline buffers are especially needed. The establishment of proper pH standards for high-temperature work would make the testing of sensors both speedier and more reliable. Doubtless because of the experimental difficulties involved, few measurements have actually been made at high temperature, and those in a rather restricted range of conditions. In particular, measurements in dilute, poorly buffered, solutions, which provide the most rigorous test of a system's capability, are completely lacking.

Industrial processes have promoted interest in chemical measurements in water at high temperature and pressure for at least 60 years. Although Stene¹ was concerned with the sulphite–cellulose reaction and fat-processing, most interest has come from the electricity supply industry. This arose not only from the operation of steam generators, but particularly from the use of water as a moderator and primary coolant in nuclear reactors for power generation. The work at Oak Ridge,^{2–9} starting in the 1950s, is noteworthy in this respect. Geochemical measurements are also relevant, and have a bearing on hydrothermal energy sources¹⁰ and nuclear waste containment.¹¹ pH is arguably the most important parameter in such conditions, being relevant to the corrosion of metals and the speciation of impurities, dosing chemicals and corrosion products, through hydrolysis or protonation. Table 1 shows

the conditions relevant to power stations, and to some other applications in the energy industries.

In the absence of measurements at high temperatures and pressures, data obtained at below 100° have been extrapolated to more extreme conditions. This involves making assumptions about the thermodynamics of aqueous solutions that are sometimes convenient rather than wholly convincing, although the technique has achieved considerable success. Van Muylder¹² has reviewed potential–pH equilibrium diagrams and the extrapolation methods involved. Inevitably, extrapolated values are less precise than the original data and are prone to systematic errors arising from the assumptions made. Direct measurement would, therefore, be preferable, if it could be made practicable. In power stations, routine measurement of pH is still done on samples cooled to about 25°.

Table 1. High-temperature samples for pH measurement

Sample	Temperature, °C	Pressure, bar	Sources of acidity or basicity	pH range	Comments
PWR* Primary coolant	290–325	155–158	Boric acid	4.2–10.5	H ₂ present
PWR Steam generator	230–285	69	NH ₃	9.0 ± 2	Hydrazine, very low conductivity
AGR† Boiler	150–300	165	NH ₃	9.2 ± 0.1	Hydrazine, very low conductivity
Fossil-fuel heated boiler feed	250–340	166–184	Na ₃ PO ₄ , NaOH, NH ₃	9.2 ± 0.1	Hydrazine, very low conductivity
Hydrothermal energy sources	90–340	1–360	Silica, CaCO ₃	5–8.6‡	Brine and other salts present
Nuclear waste containment	90–260	up to 250	Silica	9–11	Brine and other salts present

*Pressurized water reactor.

†Advanced gas-cooled reactor.

‡Exceptionally down to pH 1.5.

PROBLEMS OF MEASUREMENT AT HIGH TEMPERATURE AND PRESSURE

Whatever the principle of measurement adopted, the sensors will have to meet a common set of requirements that are more stringent than those imposed at ambient temperature.

(1) Resistance to chemical attack: sensors that work at room temperature may be biased, or may fail catastrophically after a short time at high temperatures.

(2) Resistance to thermal (mechanical) stress: apart from the ability of individual components to withstand high temperatures, adjoining components of the sensor must have compatible coefficients of expansion if the sensor is not to break up, either immediately upon a large change of temperature or after a number of temperature cycles.

(3) Calibration: an analytically useful device does not merely respond to changes in pH. It must do so selectively (at least in a given set of conditions) and consistently. Almost all chemical sensors are affected by temperature and, unless operation at constant temperature can be arranged, some form of temperature compensation will be necessary. This requires that variations in the sensor's sensitivity and zero-point should be monotonic and preferably linear. Calibration requires a set of pH standards, the provision of which is itself a major piece of work, especially when a large temperature range is to be covered.

pH SENSORS

Potentiometric devices

In all cases a reference electrode is also required, which brings its own problems (see below). In addition to the general properties

listed above, the ideal potentiometric cell should give a response slope, k , having the Nernstian value of $2.303 RT/F$, where R is the gas constant, T the absolute temperature and F the Faraday constant. A practical cell should at least give a response slope that is a constant proportion of the ideal value over a useful pH range and varies directly with the absolute temperature.

Hydrogen electrode

The hydrogen electrode, Pt/H₂, H_{aq}⁺, is the primary standard for pH measurement.¹³ Its potential is given by

$$E = E^\circ + \frac{k}{2} \log f_{\text{H}_2} - k \text{ pH} \quad (1)$$

The standard potential, E° , is, by convention, 0 mV at all temperatures. f_{H_2} is the fugacity of hydrogen, so the hydrogen electrode is not a simple pH-sensor. At room temperature and pressure, hydrogen is bubbled through the solution and calculation of the fugacity is relatively straightforward, but at high temperatures and pressures this is likely to be less practical. Apparatus^{14–17} has been devised for such purposes, however, including stirred^{9,14} and flow-through cells,^{9,15} as shown in Figs. 1 and 2, respectively. A cell for use up to 1 kbar pressure has been described recently.¹⁷ These are concentration cells, using a second hydrogen electrode to avoid problems with conventional reference electrodes. A system with hydrogen and reference electrodes has been used at high temperatures, with either palladium/silver or PTFE diffusers for the introduction of hydrogen.¹⁸

For closed systems with an overpressure of hydrogen it may be possible to calculate the fugacity, although this becomes less reliable

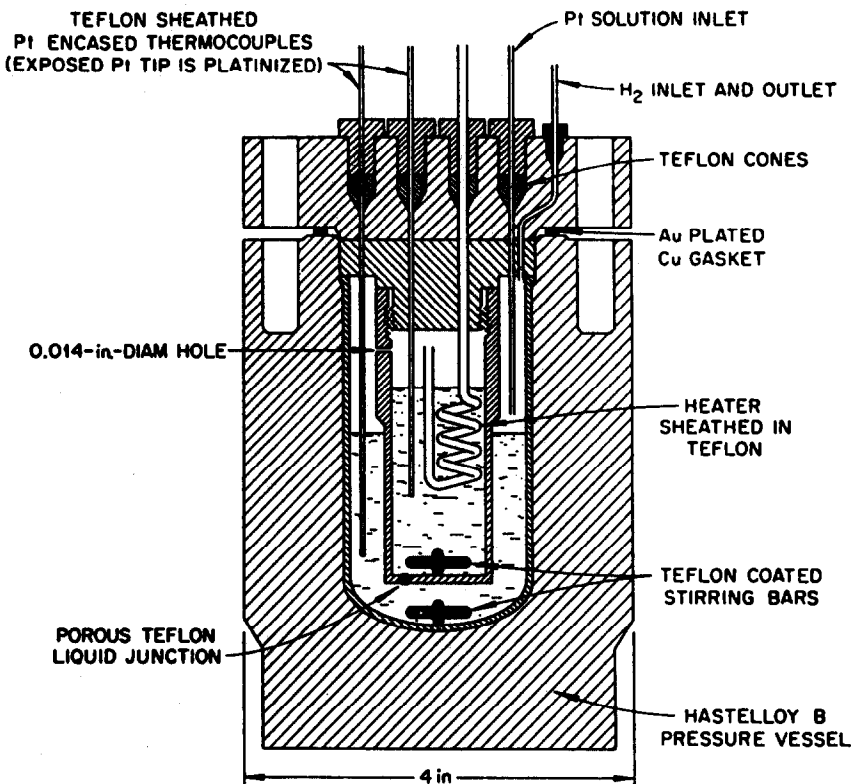


Fig. 1. Cell for pH measurement at high temperatures with stirred solution. Reprinted with permission from R. E. Mesmer, C. F. Baes Jr. and F. H. Sweeton, *J. Phys. Chem.*, 1970, 74, 1937. Copyright 1970, American Chemical Society.

as the total electrolyte concentration increases, because of "salting out" of the hydrogen. In principle, the hydrogen electrode could be combined with a hydrogen-specific sensor so that the $\log f_{\text{H}_2}$ term could be eliminated, but attempts to provide such a system seem not to have been very successful.¹⁸ More than a trace of hydrogen would be required, otherwise the platinum electrode could respond to other redox couples, so the hydrogen electrode can suffer interference from other ions in solution, *e.g.*, Ag^+ , Hg_2^{2+} (which may leak from the reference electrode). The hydrogen may also react directly with dissolved species and disturb the potential at either the sensing electrode or (unless precautions are taken) the reference electrode. If the sample contains volatile substances, passage of hydrogen may change the pH by extracting species such as NH_3 and CO_2 . Nagy and Yonco¹⁹ tried to avoid having to bubble hydrogen through the cell, by using a palladium metal membrane with dry hydrogen on one side. Diffusion through the metal provided the hydrogen fugacity required in equation (1). The responses at temperatures up to 300° , however, were only about 82% of the Nernstian values.

The analytical importance of the hydrogen electrode thus lies in its position as a primary standard rather than as routine tool. Its use in thermodynamic measurements, however, is of the greatest significance. It may also be noted that the deuterium electrode has been used in D_2O up to 225° .⁷

Palladium hydride electrodes

Palladium readily absorbs hydrogen to form first a solid solution (α phase) and then a hydride (β phase); in aqueous solution this may be achieved by electrolysis. Once charged with hydrogen, the electrode will respond to pH in hydrogen-free solutions, with an e.m.f. some 50 mV different from that of a true hydrogen electrode, but only as long as both α and β phases co-exist (*i.e.*, until most of the hydrogen has diffused into the solution). Thus, at constant pH, a plot of e.m.f. *vs.* time elapsed since charging exhibits a plateau between two regions of rapid decrease. To be useful, measurements must be made in this plateau region, the duration of which decreases with temperature. The range of H/Pd atomic ratios in which such behaviour is observed decreases with

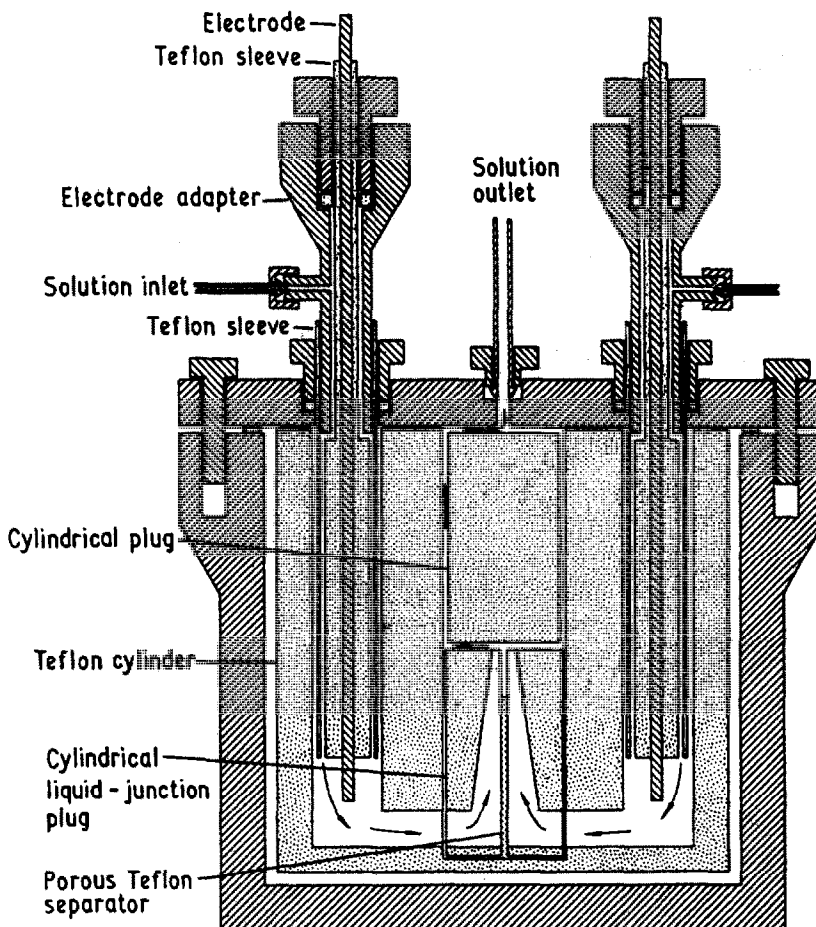


Fig. 2. Flow-through potentiometric cell for pH measurements at high temperature. Reprinted with permission from F. H. Sweeton, R. E. Mesmer and C. F. Baes Jr., *J. Phys. E., Sci. Instr.*, 1973, 6, 165. Copyright 1973, Institute of Physics.

temperature up to about 300°, at which the co-existence of the two phases is thermodynamically impossible (see Fig. 3). Problems may arise before this theoretical limit is reached, because rapid diffusion of hydrogen from the α phase at above about 200° causes irreversible behaviour which manifests itself in sub-Nernstian responses.²⁰ It is claimed that useful measurements can be made up to 250–275°, however. The stability of the e.m.f. in the plateau regions seems to require further investigation; Dobson and Brims²¹ measured the maximum e.m.f. (which occurred after about 1 hr), and Dobson *et al.*²² observed that the e.m.f. slowly changed, whereas Tsuruta and Macdonald²³ and Macdonald *et al.*²⁰ obtained greater stability of the e.m.f., palladized platinum giving more stable results than palladized palladium and especially palladized gold.

The presence of oxygen or reducible ions may cause problems, but published work has not adequately characterized these aspects of per-

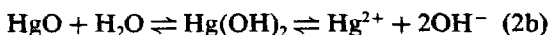
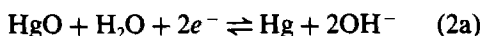
formance. The electrode responds to pressure pulses.²⁴

If the solution contains dissolved hydrogen, the electrode will behave as a hydrogen electrode provided the partial pressure in solution is greater than that in the α -phase, *i.e.*, for hydrogenated solutions there is no point in using it rather than a conventional hydrogen electrode.

Other metals (*e.g.*, nickel, zirconium and titanium) form hydrides that are similar to that of palladium, but too susceptible to corrosion or passivation to be useful.¹⁸

Metal-metal oxide electrodes

A metal in equilibrium with its sparingly soluble oxide (or hydroxide or basic hydroxide) and in contact with an aqueous solution may behave as an electrode of the second kind responsive to pH, *e.g.*, the Hg–HgO electrode.



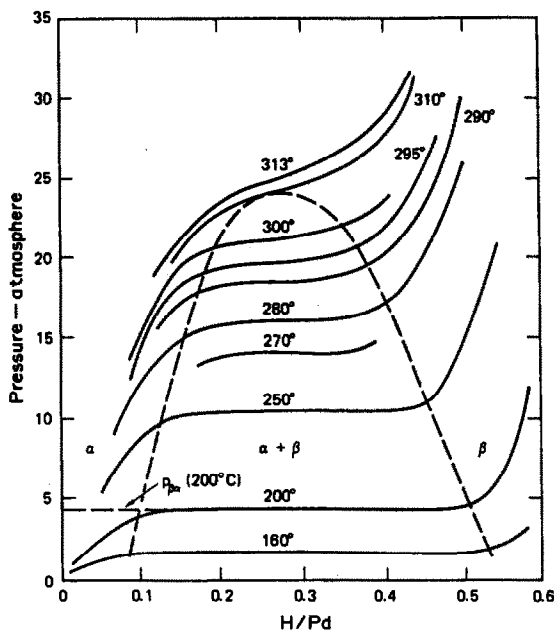


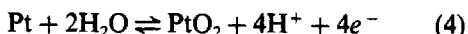
Fig. 3. Phase diagram for the palladium-hydrogen system. Reprinted by permission of the publisher, The Electrochemical Society, Inc., from D. D. Macdonald, P. R. Wentrock and A. C. Scott, *J. Electrochem. Soc.*, 1980, 127, 1745.

The e.m.f. is given by

$$\begin{aligned}
 E &= E^\circ + \frac{k}{2} \log \{ \text{Hg}^{2+} \} \\
 &= E^\circ + \frac{k}{2} \log K_{so} - \frac{k}{2} \log \{ \text{OH}^- \}^2 \\
 &= E^\circ + \frac{k}{2} \log K_{so} - k \log K_w - k \text{ pH} \\
 &= E^{\circ'} - k \text{ pH} \quad (3)
 \end{aligned}$$

where K_{so} is the solubility product of the metal hydroxide and K_w the autoprotolysis constant of water. The Ag-Ag₂O and Tl(Hg)-Tl₂O₃ electrodes are perhaps the only others that fit this type of model.

Many metals do not form thermodynamically well-defined hydroxides, yet some sort of pH response is obtained. The electrode reaction may be summarized as, e.g.,

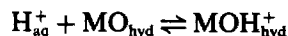


with

$$E = E^\circ_{\text{Pt, PtO}_2} - k \text{ pH} \quad (5)$$

This treatment evades the issue of how the solid and aqueous phases interact. It must be as-

sumed that in many cases the oxide has a hydrated outer layer that acts as an ion-exchanger:



Alternatively, the oxide may be a porous barrier that allows a reaction such as (4) to proceed irreversibly but slowly enough to give reasonably steady electrode potentials. Metals may form more than one oxide (and also non-stoichiometric ones) differing in electronic conduction, ion-exchange and other properties, and the degree of hydration of an oxide may also vary. In consequence of this large number of factors, at the molecular level the mechanism of these electrodes is generally very uncertain, which has consequences for the analytical use of such electrodes.

(i) The standard potential may vary with the mode of preparation of the oxide, e.g., for an electrolytic preparation it may depend on the applied voltage used, or for a thermal one it may depend on the temperature used. It may then vary with age and conditions of use or storage.

(ii) The response may be non-linear (or have a restricted linear range) and the slope may be less than the ideal even in the linear range.

(iii) The electrode may be susceptible to other types of reaction: (a) redox interference from dissolved oxygen, hydrogen or other reagents; (b) complexation of metal ions or dissolution of oxides by complexing agents, which may be as commonplace as Cl⁻ or NH₃; (c) ion-exchange of cations or anions (the same oxide may give exchange with either, depending on the pH); (d) adsorption of ions from solution.

The response range may also be limited by irreversible dissolution of the oxide in sufficiently acidic or alkaline conditions; this range will depend on temperature, and the electrodes that work best at about 25° may be useless at high temperatures.

Because of these many variables, most studies fall far short of an adequate analytical characterization of an electrode's performance, even at room temperature. In consequence, misleading over-optimistic claims for an electrode are often made. The paper by Fog and Buck²⁵ stands as an example of a proper approach to the assessment of electrodes, albeit at room temperature only.

Earlier work (at room temperature) has been reviewed by Ives,²⁶ who concentrated mainly

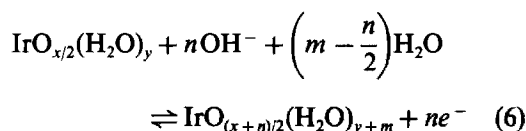
on the Sb–Sb₂O₃ electrode, which remains the only metal oxide electrode of commercial significance. It is, however, subject to interference by oxygen, stirring, and complexing agents. Roychoudhoury and Bonilla²⁷ refer to work showing great irregularities in antimony oxide electrode potentials at temperature of 100–300°. Other systems tried at room temperature in the past include Bi–Bi₂O₃, W–WO₃ and Mo–MoO₃. Dietz and Kreider¹¹ have reviewed more recent work with a view to high-temperature measurements. The attractions of metal oxide electrodes are that fabrication may be straightforward and the impedance is low.

Ag–Ag₂O and Hg–HgO are the most thermodynamically well-defined oxide electrodes, but both are susceptible to halide interferences at low pH and the solubility of Ag₂O is rather high. The physical structure of the Hg–HgO electrode makes it rather delicate, but it has found commercial applications in reference electrodes and it has been shown to work in alkaline solutions up to 250°. A solid-state version, using an HgS/HgO membrane, was tested at room temperature²⁹ and found to give a linear response with 90% of the ideal slope; ammonia interfered severely, however, 1.7 mg/l. giving a pH error of 0.15, which would be a problem in applications to steam generators.

Dobson *et al.*³⁰ investigated Pt–PtO₂, Ir–IrO₂, Zr–ZrO₂ and Rh–Rh₂O₃ electrodes up to 250° and found uncertainties of about 2 mV in E° , non-Nernstian response, response times > 15 min, pressure effects, sensitivity to oxygen and anomalous changes of E° with temperature (going through a minimum in acidic solutions and a maximum in alkaline solutions). Further work with Zr–ZrO₂ electrodes³¹ at room temperature showed a narrow working range (pH 2–6) with thin films, but no response from thick films. The thin film presumably allows a mixed potential to operate at the Zr surface. Note below, however, the more significant development of ZrO₂ membrane electrodes.

Fog and Buck²⁵ surveyed TiO₂, RuO₂, RhO₂, SnO₂, Ta₂O₅, OsO₂, IrO₂ and PtO₂ electrodes at 25°, giving slopes, working pH ranges, redox interferences, other interferences and hysteresis effects for the cycle pH 2 → 12 → 2. The only electrode with a Nernstian response was IrO₂ over the range pH 2–10 and it also had the least redox interference and one of the smaller hysteresis effects (25 mV shift). It did, however, suffer interference from halide ions, especially iodide.

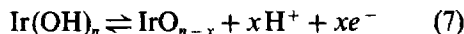
Iridium oxide has been studied more than any oxide except that of antimony, but in different forms, depending on the method of preparation. Thermally prepared IrO₂ on a titanium support³² gave an average response slope of 59 mV/pH at 25°. Sputtered iridium oxide films³³ also gave near-Nernstian responses at room temperature, but the slope was slightly sub-Nernstian at around 100°. These film electrodes changed in response over a period of 4 days after preparation, in which time the standard potential was altered by about –200 mV. A single exposure to water at 200° produced the same effect, but thereafter the electrodes were stable. The standard potential did not correspond to that for Ir–IrO₂ and it was suggested that in these films the reaction is



i.e., it involves a change in the *average* oxidation state, x , of iridium in the oxide phase, and is affected by the extent of hydration. These electrodes suffered some interferences from sodium ions and from oxygen, but none from hydrogen, Fe²⁺, Fe³⁺, Cu²⁺ and Ag⁺.

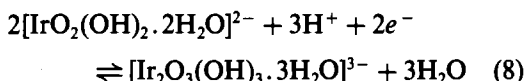
Equation (6) implies that the mechanism is not that of a metal–metal oxide electrode. In further work³⁴ the oxide was sputtered onto non-conducting Al₂O₃ and a Nernstian response was obtained at 156°. At higher temperatures the iridium oxide either broke away from the substrate or dissolved.¹⁸ These sputtered films appear to be unaffected by oxygen.

The anodic iridium oxide film (AIROF) electrode is produced by cycling iridium metal in acid at potentials between –0.25 and 1.25 V *vs.* SCE. The oxide phase builds up irreversibly on the metal but is itself capable of a reversible reaction.



De Rooij and Bergveld³⁵ found a super-Nernstian response of 67.4 mV/pH at 25° and variations of ±2 mV in E° over 100 hr. The electrode's impedance was ~100 Ω. No effect of oxygen was observed. Burke *et al.*³⁶ investigated this electrode further and obtained response slopes (mV/pH at 25°) of 77 in sulphate and phosphate solutions and 72 in chloride solutions over the range pH 2–13. They emphasized that the hydrated nature of the film is an important

factor in the response characteristics, and proposed that the ideal reaction would be



which should give a slope of $1.5k$, *i.e.*, ~ 90 mV/pH at 25° . The hydrated oxide is expected to act as an ion-exchanger, however, with loss of hydroxide. Thus the slope is less than that suggested by equation (8) and depends on other ions in solution.

Kinoshita *et al.*³⁷ found that response slopes were higher for AIROF electrodes formed on monocrystalline iridium (69.7 mV/pH at 25°) than for those formed on the polycrystalline metal (62–68 mV/pH). The electrodes responded about as quickly as glass electrodes in alkaline solution, but at only about a tenth of the rate in acids. Weak complexing agents affected the readings by up to 10 mV at constant pH, and in the presence of redox agents the pH response disappeared. Oxygen caused slow drifts in potential with monocrystalline electrodes and fast changes with polycrystalline ones. The linear response range was pH 2–8.5.

Hitchman and Ramanathan³⁸ showed that the slope at 25° depended on the charge-storage capacity of the AIROF electrode and obtained slopes of 81.9 ± 1.5 mV/pH, which is the nearest approach reported to the ideal value predicted by equation (8). A low rate of drift (8 mV/100 hr) was obtained in pH-6 buffer but the oxide dissolved at pH 12. Redox reagents could swamp the pH response, but dissolved oxygen had only a small effect.

Clearly the iridium oxide electrode provides interesting material for study, but in view of the many factors involved it remains to be seen whether it will be used as a general pH sensor. The dependence of the response slope on the method of preparation and also on the other ions present is a disadvantage and the uncertainty as to the limit of response (in terms of both pH and temperature) needs to be resolved. The other metal oxide systems studied so far have no attractions as practical analytical sensors. Dietz and Kreider¹¹ speculate that alloys of the platinum metals (probably involving iridium) may have better properties than the pure metals, but too little is known to formulate the alloys on a rational basis.

Glass electrodes

The glass membrane electrode is by far the most popular pH sensor and has been so for 40

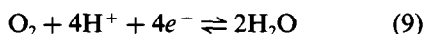
years, in which time its working pH range and mechanical robustness have improved considerably. Its response is ideally Nernstian and independent of redox and complexing interferences. The aqueous filling solution poses problems for work at high temperatures but Krykov and Starostina³⁹ showed that measurements were feasible at 150° if the active part of the electrode could be sealed around the inner reference electrode, leaving only a small air bubble inside. With such an arrangement the solution inside did not boil and the pressures inside and outside the membrane were equalized. As the temperature increases, the increasing solubility of glass reduces the upper limit of linear response. Commercial glass formulations cover low (from -5 to $50 \pm 10^\circ$), standard (5 – 80°) and "high" (20 – 100°) ranges and it may be possible to formulate glasses for higher temperatures. Elimination of the inner aqueous filling solution should also be possible, *e.g.*, Le Peintre⁴⁰ filled glass electrodes with lead amalgam. Dolidze⁴¹ reported an electrode that worked, with a near-theoretical slope factor, at 150° and for short periods at 200° , and suggested that the durability of the glass was better at 300 than at 200° , although no e.m.f. measurements were made at the higher temperature. Baes and Meyer⁴² found that at 148° attack on the glass caused detectable changes in the acidity of acid solutions more dilute than $0.01M$, but that this arose mostly from the stem glass and not the sensitive bulb.

Geothermal studies have prompted research into glass electrodes working in brines at 250° and 250 atm;¹¹ two commercial electrode manufacturers were approached. The first manufacturer's standard electrodes had a "good" performance up to 150° in brines of pH 4–9 and new glass formulations were "excellent" up to 150 or 200° , but deteriorated after 4 hr exposure at 250° , the slope decreasing to about 60% of the theoretical value. This assessment⁴³ was mainly based on survival after exposure to the high temperature solutions; the status of the measurements at 200° is uncertain because of the instability of the solution. The other manufacturer proposed a glass electrode for the same application, using an unflamed glass membrane for greater durability,⁴⁴ but no results with this electrode appear to have been reported or further work on either system to have been done.¹¹ The lack of research (or reported results) on extending the range of the most extensively used pH sensor is surprising, but the zirconia

membrane electrode (below) could be regarded as an equivalent development from a different origin.

Zirconia membrane electrodes

Niedrach⁴⁵ introduced the yttria-stabilized zirconia membrane electrode for measurement of pH at high temperature and this has been taken up by other groups. A recent review⁴⁶ surveys much of the work to date. Zirconia (ZrO_2) stabilized with 8–17% yttria (Y_2O_3) can be made into a membrane which conducts electricity exclusively through movement of the oxide ion. Such membranes are used as oxygen sensors in flue-gas analysers and are available commercially. In aqueous solution the membrane potential is governed by the pH, for reasons not yet established, but presumably related to the ion-exchange properties of zirconia. Writing net reactions such as equation (9) is surely misleading, as the membrane is not an electronic conductor and the e.m.f. is independent of the dissolved oxygen concentration.



These membranes have a high resistance at room temperature (about $10^{11} \Omega$) and are suitable only for high-temperature measurements. It remains to be seen whether other ceramics and dopants will yield less resistive membranes.⁴⁵

There have been various modifications of this sensor in regard to the fraction of yttria in the membrane and the choice of inner reference element. Membranes with 8, 9 and 17% yttria have been tried, but no significant differences have been reported. It has been suggested that trace impurities may hasten the degradation of the membrane.^{47,48} Niedrach⁴⁵ tried Ag–AgCl electrodes in chloride-doped buffer solutions as the inner reference electrode, and also “solid-state” contacts of Cu–Cu₂O or Hg–HgO. The latter is favoured by Hettiarachchi and Macdonald⁴⁹ as being more stable, but this is disputed.⁴⁷ Hettiarachchi *et al.*⁵⁰ also tried Ag–Ag₂O inner elements. Danielson *et al.*⁴⁸ used both silver powder and graphite inner electrodes, but noted that these electrodes required a preliminary autoclaving at 250° before use; they later recommended a Pt–O₂(g) inner reference.⁵¹ In all cases, the slope was less than Nernstian below 200–250° and may be only 30–60% of the theoretical value.⁵² Cycling between temperatures of 300 and 84°

gradually degrades the performance at the lower temperature.⁵²

Comparison with glass electrodes at 95° showed that the slope was 70–80% of the Nernstian value, and that the asymmetry potential (25–50 mV) and irreproducibility (10–30 mV) were several times larger than for the glass electrode.⁵³ Response times were about the same for glass and zirconia electrodes. There was some evidence that the responses were different in acidic and alkaline solutions, but this had been shown more clearly by Tsuruta and Macdonald,⁵⁴ who found that the response was non-linear in acidic solutions and became more so as the temperature decreased. More recently, a good correlation between the hydrogen electrode and the zirconia membrane over the pH range 3–9 at 200–300° has been reported,⁵⁵ in this case the liquid-junction potentials cancel, removing a likely source of error. Neither oxygen^{45,50} nor hydrogen⁵⁰ affects the electrode and no effect from general redox reactions is expected.

Some mechanical difficulties remain with this electrode: the membrane is fragile and may crack and the seals may fail at high temperatures, leading to spurious potentials from the inner reference element. At present, its performance is promising at 200–300° but less so below 200° because of the non-Nernstian response. Its response in acidic solutions also needs further investigation.

Semiconductor devices

Madou *et al.*⁵⁶ measured the flat-band potential of Nb-doped TiO₂ in buffer solutions at 25° and obtained a near-Nernstian response. The potentials depended on the treatment of the oxide (~150 mV difference between acid-etched and alkali-etched material). The measurements are much less convenient than in potentiometry, requiring a frequency-response analyser and a potentiostat. The capacitance, C_s , is measured at a number of imposed potentials and the flat-band potential obtained by extrapolating to zero a plot of $1/C_s^2$ vs. imposed potential. The solution must have a minimum conductivity before plots of this kind can be used accurately: Madou *et al.* suggested ~0.14 mS/cm (corresponding to $10^{-3}m$ potassium chloride) but others propose much higher levels. Hara *et al.*⁵⁷ used such a system up to 150° and found close to Nernstian response. Miyasaka *et al.*⁵⁸ applied it to sour saline environments up to 200°; these solutions contained up to 20% sodium chloride

in equilibrium with up to 4 MPa H₂S or CO₂. Results in the pH range 2.6–3.8 agreed fairly well with calculated values. The pH responses of SrTiO₃ and SiC have also been studied by this means.¹⁸

The ion-selective field-effect transistor (ISFET) has been reviewed by Janata and Huber:⁵⁹ the gate of a conventional field-effect transistor is replaced by a combination of reference electrode, test solution and ion-selective membrane. A change in the composition of the test solution affects the membrane potential, and hence the current passing through the transistor. Usually the system is operated at constant current and the feed-back voltage required to maintain this current is then proportional to the logarithm of the concentration of the ion to which the membrane responds, *i.e.*, the response resembles that of an ion-selective electrode although the measurement is different in character and slightly more elaborate apparatus is required. SiO₂ and Si₃N₄ outer surfaces on an FET confer a pH response but are too soluble for use at high temperatures.¹⁸ Even at room temperature, the encapsulation of ISFETs is a source of trouble, as the adherence of materials such as PVC and silicone rubber breaks down. At high temperatures more problems would be expected.

Measurements with metallic glasses

Lenz and Schultz⁶⁰ proposed the use of corrosion-resistant metallic glasses for pH measurements at high temperatures and tested Fe_{32.5}Ni_{32.5}Cr₁₅B₂₀ glass up to 300°. The glass is charged with hydrogen by electrolysis at a fixed current (*e.g.*, 2 mA) for a fixed time (*e.g.*, 1 min) and the change in resistance is measured. The response appears to be very non-linear, although the only results presented plotted change in resistance at 220° against pH at 25° for only 3 buffer solutions (pH 3.5–7.0).

A number of objections to this technique can be foreseen.

(i) Electrolysis to form hydrogen will change the pH being measured. In a buffer solution this effect may be negligible, but in dilute solutions could lead to considerable bias.

(ii) Electrolysis from alkaline solutions may be inefficient; this pH range needs investigation.

(iii) The technique is by its nature discontinuous. After the 1-min electrolysis and the measurement, there is a delay as the hydrogen diffuses away (approximately 1–2 min).

(iv) The 1-min electrolysis does not produce a plateau in the change of resistance with time. Accurate timing is necessary if the response is to be interpreted precisely.

(v) Interference by redox reagents in solution seems inevitable; such possible effects need investigation.

(vi) The temperature response is unknown. Lenz and Schultz suggest that compensation is possible with a dummy sensor that is not charged with hydrogen, but give no results.

It should be recognized, however, that these are new materials that may have other interesting properties. Lenz and Schultz suggested that pH measurement is possible gravimetrically and by measuring changes in magnetic properties. Other glass formulations were also proposed as being suitable. The main attraction of these materials is their resistance to corrosion, but the bias caused by the electrolysis process itself could limit application of this technique to well-buffered solutions free of redox reagents.

Optical devices

Chemical sensors based on fibre optics have received considerable attention in recent years.⁶¹ Their advantages include easy miniaturization and freedom from electrical interference. Since these sensors are not based on electrochemical methods, there is obviously no need for reference electrodes. The pH sensors generally consist of indicator dyes immobilized on the end of an optical fibre which forms part of an optical cell (coloured, fluorescent and chemiluminescent indicators may be used). These dyes were used in classical colorimetric and spectrophotometric systems many years ago,⁶² but these methods were largely displaced by the glass electrode. The sensors are subject to errors from interference by complexation of the dye with metals, large temperature coefficients and large ionic strength effects. In addition, the pH response is usually linear over a pH range of only about 2 although it may be useful over a longer range if careful calibration is practicable. It appears, therefore, that calibration in terms of operationally defined pH is at least as important as for electrochemical techniques. In very dilute solutions, which have an inherently low buffer capacity, the dissociation of the indicator may provide more protons or hydroxide ions than the sample itself and produce a false reading. These considerations, amongst others, have recently been raised against by Janata,⁶³ who

argued that optical devices are fundamentally less accurate than electrochemical ones for the measurement of pH. Measurements by Edmonds *et al.*⁶⁴ confirm these misgivings.

At high temperatures additional problems are foreseeable, in particular the durability of the dye layer and its encapsulant. An inorganic fluorescent system (uranyl ion in β -alumina) has been suggested,⁶⁵ but mechanical strength was lost rapidly at 100° and above. On general principles, optical sensors appear to offer less versatility than electrochemical ones, but the fact that no reference electrode is involved removes an enormous problem of measurement at high temperature. Any optical device that is durable at high temperatures would be attractive, even if it were confined to well-buffered solutions with a limited pH range.

REFERENCE ELECTRODES

All but the optical sensors require a reference electrode, which may be immersed directly in the test solutions to form (in potentiometric terms) a cell without transfer, or in a separate reference solution connected to the test solution by a liquid junction, in which case it forms a cell with transfer.

Cells without transfer

Macdonald⁶⁶ has listed work on high-temperature (up to 290°) solutions. With a sensing electrode responsive to pH, the reference electrode is almost always of the silver-silver chloride type, but silver-silver bromide,⁶ mercury-mercury(I) sulphate³⁰ and lead-lead sulphate⁶⁷ electrodes have also been proposed. Mercury-mercury(I) chloride electrodes are generally considered unsuitable for use above 80° (depending on pH and the chloride concentration), but Dobson *et al.*⁶⁸ used them successfully up to 200°. Mercury-based electrodes require more care than the silver-silver chloride type and would not normally be favoured. It should also be recognized that, in the event of an accident, mercury-based electrodes create toxic hazards that could spread very quickly, especially at high temperature.

In order to measure the pH with such cells it is necessary for the test solution to contain a known (and preferably constant) activity of the ion to which the reference electrode responds. With an unknown sample this is generally impossible, unless an excess of the ion is deliberately added to the solution. In many appli-

cations this is unacceptable because this ion would affect the process being studied; it also introduces a procedural complication and the problem of calculating activity coefficients. In this arrangement the reference electrode is also open to interference, *e.g.*, from Cl^- with Hg-Hg₂SO₄ electrodes and redox agents with most electrodes (Ag-AgCl electrodes are not suitable for hydrogen-saturated solutions). In order to prevent hydrogen reaching the Ag-AgCl electrode and silver reaching the hydrogen electrode, many cells that are notionally without transference have a diffusive barrier incorporated between the two electrodes; in some cases the solubility of the reference electrode material at high temperatures may be sufficient to create a liquid-junction potential at this barrier and so cause an error in the pH-value obtained.⁶⁸

At sufficiently high pH, AgCl, Hg₂Cl₂, Hg₂SO₄, *etc.* will be converted into Ag₂O or HgO, as noted by Case and Bignold²⁸ for Ag-AgCl electrodes. There will thus always be an upper limit to the pH range measurable in such cells, depending on the concentration of "reference" ion present.

Because of these difficulties, cells without transfer are probably applicable to analytical studies only in special and well-defined circumstances.

Cells with transfer

These cells may be divided into isothermal types, in which the sensing and reference electrodes are at the same temperature, and thermal types, in which the reference electrode is maintained at or near room temperature. The reference electrode is immersed in a solution of known composition containing a relatively high concentration of the ion to which the electrode responds; this arrangement thus introduces a liquid-junction potential between the reference and test solutions.

Calculation of the liquid-junction potential (even with a naively simple model) requires knowledge of the concentrations and mobilities of all the ions in the junction. For analytical purposes this is impractical and a junction must be used that varies as little as possible with the composition of the test solution; this means using concentrated salt solutions (0.1–4M) in the reference side of the junction. Even at room temperature, liquid junctions are a recurrent problem in pH measurement, especially in poorly buffered and poorly conducting

solutions.⁶⁹⁻⁷¹ More tests on such solutions at high temperatures are required.

Thermal cells

Keeping the reference electrode at room temperature largely prevents its degradation by hydrolysis or dissolution. This involves the complication of equipment for cooling and for equalizing the pressures on either side of the junction. The liquid-junction potential also becomes more susceptible to errors, involving the following components.

(i) The diffusion potential arising from differences in concentrations and mobilities on the two sides of the junction.

(ii) The streaming potential arising from mass transfer of a solution through a capillary. It is generally assumed⁶⁶ to be at most a few mV for aqueous solutions at the pressure differentials expected at temperatures up to 300°. For outflow of concentrated electrolyte solution from a pressurized reference electrode the potential should be negligible compared with components (i) and (iii). Influx of dilute test solution would create larger potentials but it is difficult to see how this could be sustained in any practical arrangement. With perfectly efficient pressure equalization this potential should be eliminated.

(iii) The thermal liquid-junction potential produced by the different tendencies of ions to move across a temperature gradient (the Soret effect). A tabulation by Macdonald⁶⁶ shows that for strong acids this is -0.2 ± 0.2 mV/degree, for strong bases ~ 0.5 mV/degree and for alkali-metal chlorides ± 0.03 mV/degree, depending on concentration. In simple cases an empirical correction can be applied.⁷²

(iv) The thermoelectric effect between metallic contacts. This should be negligible compared with the others.

Components (i)–(iii) result in contamination of the test and/or reference solution. Even if the solutes in the test solution do not directly affect the reference element, ingress of test solution or water will dilute the reference solution and thus affect the electrode potential, and ingress into the junction can make it very unstable, as has been observed at room temperature.⁷³ Injection of concentrated salt into the test solution may affect activity coefficients (and hence the pH) or cause corrosion. The prevention of mass transfer by eliminating the pressure differential is the most important factor in reducing these

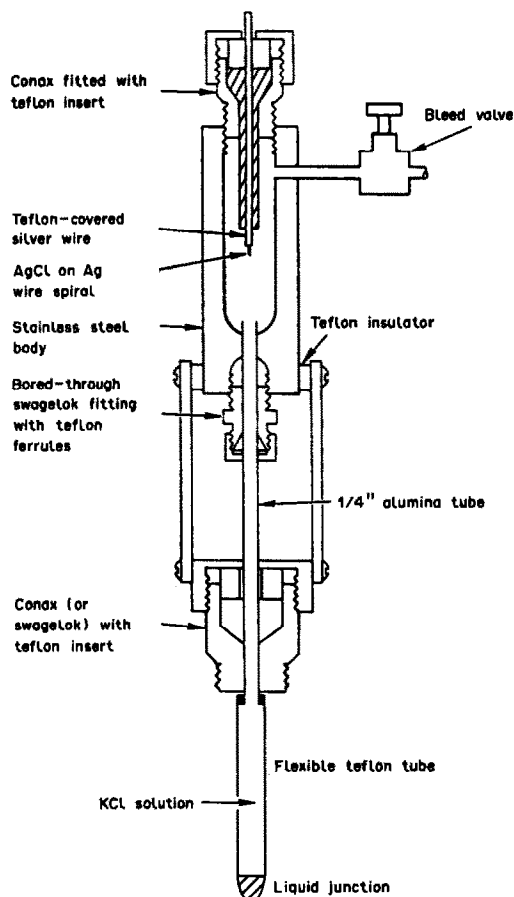


Fig. 4. Pressure-compensating reference electrode for use in high-temperature solutions. Reprinted by permission of the publisher, The Electrochemical Society, Inc., from D. D. Macdonald, P. R. Wentrcck and A. C. Scott, *J. Electrochem. Soc.*, 1980, 127, 1745.

problems, and several designs^{18,20,74-76} have been proposed for pressure-compensating reference electrodes, e.g., that in Fig. 4. Flexible PTFE tubing is used to ensure equality of pressure.

Isothermal cells

Keeping the reference and sensing electrodes at the same temperature eliminates the thermal liquid junction and thermoelectric effects described above, and theoretically the streaming potential also. In practice it is difficult to avoid streaming potentials of some ill-defined sort, especially in stirred or pumped solutions. Hettiarachchi and Macdonald⁷⁷ proposed gelling the reference solution to prevent streaming potentials. Their electrode was stable in two fairly well-buffered solutions at 280°, but apparently only after an initial 400 mV shift on first being taken to high temperatures. From studies at room temperature,^{69,71} gelled electrodes are known to be unsuitable for accurate pH work,

Table 2. NIST standard buffers at high temperature

Buffer	NBS ⁶²		Manning ⁷⁹
	pH (25°)	Max. temp., °C	Max. temp., °C
<i>Primary standards</i>			
KH tartrate (saturated at 25°)	3.557	95	160*†
KH ₂ citrate (0.05 <i>m</i>)	3.776	50	
KH phthalate (0.05 <i>m</i>)	4.008	95	200
KH ₂ PO ₄ (0.025 <i>m</i>) + Na ₂ HPO ₄ (0.025 <i>m</i>)	6.865	95	*§
KH ₂ PO ₄ (0.008695 <i>m</i>) + Na ₂ HPO ₄ (0.03043 <i>m</i>)	7.413	50	§
Borax (0.01 <i>m</i>)	9.180	95	*
NaHCO ₃ (0.025 <i>m</i>) + Na ₂ CO ₃ (0.025 <i>m</i>)	10.012	50	
<i>Secondary standards</i>			
KH ₃ (C ₂ O ₄) ₂ (0.05 <i>m</i>)	1.679	95	120‡
Ca(OH) ₂ (saturated at 25°)	12.454	60	

*See Table 3 for results from cell with transfer. †Decomposes at 170°. ‡Decomposes at 130°C. §Solution stable at 200° but reference electrode decomposed.

because of temperature hysteresis and "memory effects" (from the previous solution tested). Further testing of the high-temperature gelled electrode is required, especially over a number of temperature cycles and in dilute and buffered solutions in succession.

At high temperatures the materials of construction of the body of the reference electrode may be troublesome. Van Osch and Huybregts⁷⁸ preferred zircaloy to PTFE or stainless steel.

BUFFER SOLUTIONS

The National Institute of Standards and Technology (formerly National Bureau of Standards) buffers⁶² have been further studied at above 100° by Manning,⁷⁹ with a hydrogen electrode in a cell without transference. Manning's data for phthalate buffer were corrected for hydrogen pressure and fitted to a function of temperature by Covington *et al.*⁸⁰ The status of the NIST buffers is summarized in Table 2. Manning reported that in neutral and

alkaline solutions, reduction occurred at the Ag–AgCl reference electrode, although this may have been mistaken for Ag₂O formation.

Table 3 summarizes work that is less rigorous in that liquid junctions and/or experimental sensors are involved. Macdonald *et al.*²⁰ calculated the pH of various B(OH)₃–LiOH mixtures from thermodynamic data. Good correlations with e.m.f. values measured with various pH sensors have been obtained up to 200°, but increasing deviations are seen at higher temperatures.²³ Table 4 shows some results for NIST buffers up to 250°, but these are obviously not of the reliability achieved below 100°.

The quantity and quality of data available for temperatures above 100° (and more so above 200°) are very limited. The establishment of good standards is vital for the calibration of cells and intercomparison of data. Further impetus to this work, however, may be lacking unless the sensors and reference electrodes of interest can themselves be improved. Progress is, therefore, likely to be slow and cyclical.

Table 3. Some solutions used in high-temperature pH work*

Composition	pH	Max. temp., °C	Electrochemical cell
B(OH) ₃ (0.001–0.1 <i>M</i>)	5–6	275	Pd hydride—external ref. ^{20,23}
B(OH) ₃ –LiOH mixtures	7–9	275	and
LiOH (0.01–0.1 <i>M</i>)	9.3–10.5	275	ZrO ₂ membrane—external ref. ³⁰
H ₂ SO ₄ (0.005 <i>M</i>)	~2.5	275	
H ₃ PO ₄ (0.01 <i>M</i>)	2.5–3.2	275	ZrO ₂ membrane—external ref. ³⁰
KH ₂ PO ₄ (0.025 <i>M</i>) + Na ₂ HPO ₄ (0.025 <i>M</i>)	5–6.5	240	
HOAc (0.01 <i>M</i>) + NaOAc (0.01 <i>M</i>)	3.8–4.5	250	Pd hydride–Ag/AgCl ²¹
HCl (0.01, 0.1 <i>m</i>)	1–2	250	
KH tartrate (saturated at 25°)	3.5–4.0	150	
HOAc (0.01 <i>m</i>) + NaOAc (0.01 <i>m</i>)	4.7–5.8	250	Differential hydrogen electrode
KH ₂ PO ₄ (0.025 <i>m</i>) + Na ₂ HPO ₄ (0.025 <i>m</i>)	6.9–7.6	250	(<i>vs.</i> Pt/H ₂ in standard HCl) ⁴⁰
Borax (0.01 <i>m</i>)	9.2–8.5	250	

*Older work is cited by Macdonald.⁶⁶

Table 4. pH of some NIST buffers at high temperature

Temperature, °C	100	125	150	175	200	225	250
KH phthalate (0.05 <i>m</i>)*		4.49	4.63	4.78	4.93	5.08	
KH ₂ PO ₄ (0.025 <i>m</i>) + Na ₂ HPO ₄ (0.025 <i>m</i>)†	6.88	6.92	7.04	7.15	7.30	7.45	7.60
Borax (0.01 <i>m</i>)†	8.22	8.75	8.65	8.60	8.56	8.53	8.50

*Measured by Manning,⁷⁹ corrected and fitted to a temperature function by Covington *et al.*⁸⁰ and rounded.

†Measured by Le Peintre⁸⁰ in cell with liquid junction.

Tris(hydroxymethyl)aminomethane is a useful buffer at room temperature and new thermodynamic data⁸¹ for up to 200° should enable pH values to be calculated in the “moderately alkaline” region.

DISCUSSION

Sensors

The hydrogen electrode remains the primary standard but is inconvenient to use and subject to redox interferences. Metal-hydride electrodes appear to offer as many complications as simplifications, compared with the hydrogen electrode itself, and become hydrogen electrodes in hydrogen-saturated solutions.

Metal-metal oxide electrodes offer no advantages of performance, being susceptible to redox and complexation interferences and rarely approaching Nernstian response even in the most favourable circumstances. Iridium oxide electrodes are the only systems to show any promise so far, but there is uncertainty about the mechanism and much remains to be discovered about their performance. The low impedance of these electrodes is an advantage if miniature devices are required.

Membrane electrodes offer convenience in handling and freedom from redox and complexation interference. The two systems at present available are complementary: the glass membranes suffer chemical attack above 150–200° and have alkali errors, while the yttria-stabilized zirconia membranes work best at above 200° and have acid errors. The zirconia membrane electrode is in an early stage of development, roughly equivalent to that of the glass electrode 50 years ago. The membrane's high impedance makes miniaturization difficult.

Semiconductor measurements have been so scanty that assessment is very difficult. The apparatus required is more complicated than for potentiometry, but that would be a secondary matter if the sensor performed well enough.

Optical fibre sensors have the great attraction that a reference electrode is not needed but these devices are affected by many extraneous factors and their performance in poorly buffered solutions is highly dubious. No high-temperature measurements appear to have been demonstrated.

Reference electrodes

In practice, the only question is whether to use a silver-silver chloride reference electrode at the same temperature as the sensor or externally at a constant temperature (with a greater uncertainty about the contribution of the liquid junction). No other reference electrode offers any substantial advantages. The situation is thus much as it has been in studies at room temperature for 80 years, only more extreme. It may be noted that none of the measurements reported so far have been on dilute solutions, so the problems experienced with such solutions at room temperature have yet to be confronted in high-temperature work.

Solutions

Buffer solutions for calibration are required that will suit all temperatures, but particularly for use at above 200° and in the neutral and alkaline pH ranges. Tests on dilute solutions are also necessary to confirm the general feasibility of pH measurements.

Applications

Thermodynamic measurements of protolytic equilibria have been made with the hydrogen electrode for boric⁸² and phosphoric⁹ acids and ammonia⁹ up to 295° and aluminium ion hydrolysis^{9,83} up to 150°. The systems studied by high-temperature pH or conductivity measurements have been reviewed.⁸⁴ The ion product of water is essential to an understanding of these measurements and a good description exists for up to 1000° and 10 kbar.⁸⁵ More recently, the zirconia membrane electrode has been used to study the corrosion of metals at temperatures up

to about 290° either by monitoring the pH^{86,87} or by acting as a "pseudo-reference" electrode in moderately well-buffered solutions.⁸⁸ Most recent work is aimed towards on-line measurements in the reactor coolant of light water reactors¹⁸ and has been concentrated on borate solutions.^{20,23,50} Corrosion by CO₂ in oil and gas wells has led to the development of glass electrodes working at up to 74° and 1000 bar.⁸⁹ Sour environments are even more rigorous (up to 100 bar partial pressure of H₂S or CO₂ in up to 20% sodium chloride at up to 260°) and the Nb-doped rutile semiconductor sensor has been used⁵⁸ for laboratory studies in such conditions. Geochemical use of the measurements may readily be envisaged in both its pure and applied (e.g., geothermal energy,¹⁰ nuclear waste storage¹¹) aspects.

It may be noted that studies have been restricted to temperatures up to 300°, principally because of the properties of PTFE seals and insulators.

CONCLUSIONS

The systems most likely to advance in the immediate future are membrane sensors, whether by development of membranes of zirconia (or similar ceramics) or by improvement of silicate glasses. There have been no recent advances in the appropriate glass technology, probably because of a perceived lack of commercial interest.

The silver-silver chloride reference electrode is still the best available, but its limitations remain, particularly in regard to interference by hydrogen, and new ideas for reference electrodes are worth pursuing. Any improvements in the reference electrode would be doubly valuable in also improving the measurement of redox and corrosion potentials at high temperatures.

Work needs to be done to provide standard pH solutions suitable for use at above 100°, especially above 200° and in neutral and alkaline solutions.

Doubtless because of the need to advance on three fronts at once, no sensor has yet been tested at all thoroughly, particularly in regard to operation in dilute solutions and at varying temperatures. The economics of the energy industries, however, justify continuing effort on high-temperature measurements of pH.

Acknowledgement—Published by permission of National Power.

REFERENCES

1. S. Stene, *Rec. Trav. Chim. Pays-Bas*, 1930, **49**, 1133.
2. M. H. Lietzke and J. V. Vaughen, *J. Am. Chem. Soc.*, 1955, **77**, 876.
3. R. S. Greeley, W. T. Smith, R. W. Stoughton and M. H. Lietzke, *J. Phys. Chem.*, 1960, **64**, 652.
4. R. S. Greeley, W. T. Smith, M. H. Lietzke and R. W. Stoughton, *ibid.*, 1960, **64**, 1445.
5. M. B. Towns, R. S. Greeley and M. H. Lietzke, *ibid.*, 1960, **64**, 1861.
6. M. H. Lietzke and R. W. Soughton, *ibid.*, 1963, **67**, 2573.
7. *Idem*, *ibid.*, 1964, **68**, 3043.
8. M. H. Lietzke, H. B. Hupf and R. W. Stoughton, *ibid.*, 1965, **69**, 2395.
9. R. E. Mesmer, F. H. Sweeton, B. F. Hitch and C. F. Baes, in *High Temperature High Pressure Electrochemistry in Aqueous Solutions*, Intern. Corros. Conf. Ser., NACE-4, p. 365. National Association of Corrosion Engineers, Houston, 1976.
10. H. C. H. Armstead, *Geothermal Energy*, Spon, London, 1978.
11. T. Dietz and K. G. Kreider, *Review of Materials for pH Sensing for Nuclear Waste Containment*, Report NBSIR 85-3237, U.S. Dept. of Commerce, Gaithersburg, 1985 [NTIS PB86-129541].
12. J. Van Muylder, *Rapp. Tech.-Cent. Belge Etude Corros.*, 1979, **136**, No. 249.
13. G. J. Hills and D. J. G. Ives, in *Reference Electrodes, Theory and Practice*, D. J. G. Ives and G. J. Janz (eds.), p. 71. Academic Press, London, 1961.
14. R. E. Mesmer, C. F. Baes, Jr. and F. H. Sweeton, *J. Phys. Chem.*, 1970, **74**, 1937.
15. F. H. Sweeton, R. E. Mesmer and C. F. Baes, Jr., *J. Phys. E, Sci. Instr.*, 1973, **6**, 165.
16. L. Chaudon, H. Coriou, L. Grall and C. Mahieu, *Met. Corros.-Ind.*, 1978, **52**, 389.
17. P. Becker and B. A. Bilal, *Z. Anal. Chem.*, 1984, **317**, 118.
18. EPRI NP-5372, *Probes for Corrosion-related Variables in LWR Coolant*, Electric Power Research Institute, Palo Alto, 1987.
19. Z. Nagy and R. M. Yonco, *J. Electrochem. Soc.*, 1986, **133**, 2232.
20. D. D. Macdonald, P. R. Wentreck and A. C. Scott, *ibid.*, 1980, **127**, 1745.
21. J. V. Dobson and G. Brims, *Electrochim. Acta*, 1987, **32**, 149.
22. J. V. Dobson, M. N. Dagless and H. R. Thirsk, *J. Chem. Soc., Faraday Trans. I*, 1972, **68**, 764.
23. T. Tsuruta and D. D. Macdonald, *J. Electrochem. Soc.*, 1981, **128**, 1199.
24. J. V. Dobson, M. N. Dagless and H. R. Thirsk, *J. Chem. Soc., Faraday Trans. I*, 1972, **68**, 749.
25. A. Fog and R. P. Buck, *Sens. Actuators*, 1984, **5**, 137.
26. D. J. G. Ives, in *Reference Electrodes, Theory and Practice*, D. J. G. Ives and G. J. Janz (eds.), p. 322. Academic Press, London, 1961.
27. R. N. Roychoudhoury and C. F. Bonilla, *J. Electrochem. Soc.*, 1956, **103**, 241.
28. B. Case and G. J. Bignold, *J. Appl. Electrochem.*, 1971, **1**, 141.
29. D. Midgley, *CERL Report TPRD/L/2451/R83*, Central Electricity Research Laboratories, Leatherhead, 1983.

30. J. V. Dobson, P. R. Snodin and H. R. Thirsk, *Electrochim. Acta*, 1976, **21**, 527.
31. M. J. Madou and K. Kinoshita, *ibid.*, 1984, **29**, 411.
32. S. Ardizzone, A. Carugati and S. Trasatti, *J. Electroanal. Chem.*, 1981, **126**, 287.
33. T. Katsube, I. Lauks and J. N. Zemel, *Sens. Actuators*, 1982, **2**, 399.
34. I. Lauks, M. F. Yuen and T. Dietz, *ibid.*, 1983, **4**, 375.
35. N. F. de Rooij and P. Bergveld, in *Monitoring and Vital Parameters during Extracorporeal Circulation*, H. P. Kimmich (ed.), p. 156. Karger, Basel, 1981.
36. L. D. Burke, J. K. Mulcahy and D. P. Whelan, *J. Electroanal. Chem.*, 1984, **163**, 117.
37. E. Kinoshita, F. Ingman, G. Edwall, S. Thulin and S. Glab, *Talanta*, 1986, **33**, 125.
38. M. L. Hitchman and S. Ramanathan, *Analyst*, 1988, **113**, 35.
39. P. A. Kryukov and L. I. Starostina, *Izv. Sibir. Otdel. Akad. Nauk SSSR, Ser. Khim. Nauk*, 1970, No. 3, 27.
40. M. Le Peintre, *Bull. Soc. Fr. Electr.*, 1960, **1**, 584.
41. V. A. Dolidze, in *Ion-selective Electrodes*, E. Pungor and I. Buzás (eds.), p. 57. Elsevier, Amsterdam, 1978.
42. C. F. Baes, Jr. and N. J. Meyer, *Inorg. Chem.*, 1962, **1**, 780.
43. R. M. Taylor and D. M. Phelan, *Report PNL-3593*, Pacific Northwest Laboratory, 1980.
44. D. N. Gray and P. J. Breno, *Report RLO-180-T3*, Pacific Northwest Laboratory, Owens-Illinois, Toledo, 1979.
45. L. W. Niedrach, *J. Electrochem. Soc.*, 1980, **127**, 2122.
46. *Idem*, *Angew. Chem. Int. Ed.*, 1987, **26**, 161.
47. *Idem*, *J. Electrochem. Soc.*, 1985, **133**, 1521.
48. M. J. Danielson, O. H. Koski and J. Myers, *ibid.*, 1985, **132**, 296.
49. S. Hettiarachchi and D. D. Macdonald, *ibid.*, 1984, **131**, 2206.
50. S. Hettiarachchi, P. Kedzierzawski and D. D. Macdonald, *ibid.*, 1985, **132**, 1866.
51. M. J. Danielson, O. H. Koski and J. Myers, *High-level Nuclear Waste Disposal [Proc. Int. Top. Meet.]*, p. 597, 1986.
52. *Idem*, *Mat. Res. Soc. Symp. Proc.*, 1984, **26**, 153.
53. T. S. Light and K. S. Fletcher, *Anal. Chim. Acta*, 1985, **175**, 117.
54. T. Tsuruta and D. D. Macdonald, *J. Electrochem. Soc.*, 1982, **129**, 1221.
55. D. D. Macdonald, S. Hettiarachchi and S. J. Lenhart, *J. Solution Chem.*, 1988, **17**, 719.
56. M. J. Madou, K. Kinoshita and M. C. H. McKubre, *Electrochim. Acta* 1984, **29**, 419.
57. N. Hara, K. Nakajima and K. Sugimoto, *Boshoku Gijutsu*, 1985, **34**, 132; *Chem. Abstr.*, 1986, **105**, 90276h.
58. A. Miyasaka, K. Denpo and H. Ogawa, *ISIJ Intern.*, 1989, **29**, 85.
59. J. Janata and R. J. Huber, *Ion-selective Electrode Rev.*, 1979, **1**, 31.
60. E. Lenz and L. Schultz, *German Patent DE 3315511A1*, 1984.
61. W. R. Seitz, *Anal. Chem.*, 1984, **56**, 16A.
62. R. G. Bates, *Determination of pH, Theory and Practice*, 2nd Ed, Wiley, New York, 1973.
63. J. Janata, *Anal. Chem.*, 1987, **59**, 1351.
64. T. E. Edmonds, N. J. Flatters, C. F. Jones and J. N. Miller, *Talanta*, 1988, **35**, 103.
65. S. M. Angel, *Trans. Geotherm. Resour. Counc.*, 1987, **11**, 155.
66. D. D. Macdonald, *Corrosion*, 1978, **34**, 75.
67. M. Lepeintre, C. Mahieu and J. Monjou, *Compt. Rend.*, 1965, **261**, 3389.
68. J. V. Dobson, R. E. Firman and H. R. Thirsk, *Electrochim. Acta*, 1971, **16**, 793.
69. D. Midgley and K. Torrance, *Analyst*, 1976, **101**, 833.
70. W. Davison and C. Woof, *Anal. Chem.*, 1985, **57**, 2567.
71. D. Midgley, *Atmos. Environ.*, 1987, **21**, 173.
72. W. F. Bogaerts and A. A. Van Haute, *Proc. Intern. Congr. Metal. Corros.*, 1984, **4**, 169.
73. K. Torrance, *CERL Note RD/L/N 102/79*, Central Electricity Research Laboratories, Leatherhead, 1979.
74. M. E. Indig and D. A. Vermilyea, *Corrosion*, 1971, **27**, 312.
75. D. D. Macdonald, A. C. Scott and P. Wentreck, *J. Electrochem. Soc.*, 1979, **126**, 908.
76. M. J. Danielson, *Corrosion*, 1979, **35**, 200.
77. S. Hettiarachchi and D. D. Macdonald, *J. Electrochem. Soc.*, 1987, **134**, 1307.
78. G. A. A. Van Osch and W. M. M. Huybregts, *VGB Kraftwerkstechnik (Engl. Ed.)*, 1980, **60**, 246.
79. G. D. Manning, *J. Chem. Soc., Faraday Trans. I*, 1978, **74**, 2432.
80. A. K. Covington, M. I. A. Ferra and Z. Y. Zou, *Electrochim. Acta*, 1985, **30**, 805.
81. D. A. Palmer and D. Wesolowski, *J. Solution Chem.*, 1987, **16**, 571.
82. R. E. Mesmer, C. F. Baes and F. H. Sweeton, *Inorg. Chem.*, 1972, **11**, 537.
83. R. E. Mesmer and C. F. Baes, *ibid.*, 1971, **10**, 2290.
84. R. E. Mesmer, W. L. Marshall, D. A. Palmer, J. M. Simonson and H. F. Holmes, *J. Solution Chem.*, 1988, **17**, 699.
85. W. L. Marshall and E. U. Franck, *J. Phys. Chem. Ref. Data*, 1981, **10**, 295.
86. L. W. Niedrach and W. H. Stoddard, *Corrosion*, 1985, **41**, 45.
87. D. F. Taylor and C. A. Caramihas, *J. Electrochem. Soc.*, 1982, **129**, 2458.
88. L. W. Niedrach, *ibid.*, 1982, **129**, 1444.
89. M. Bonis and J.-L. Crolet, *Met. Corros.-Ind.*, 1981, **56**, 361.

TRACE MEASUREMENTS OF COLCHICINE BY ADSORPTIVE STRIPPING VOLTAMMETRY

JOSEPH WANG* and MEHMET OZSOZ†

Department of Chemistry, New Mexico State University, Las Cruces, NM 88003, U.S.A.

(Received 13 December 1989. Accepted 30 January 1990)

Summary—A highly sensitive voltammetric method for trace measurements of the alkaloid colchicine is described. The method is based on the controlled adsorptive accumulation of the drug at the hanging mercury drop electrode, followed by voltammetric determination of the surface species. The adsorptive stripping response is evaluated with respect to preconcentration time and potential, solution pH, voltammetric waveform and other variables. With a 10-min preconcentration, a detection limit of $1.3 \times 10^{-10} M$ is obtained. The relative standard deviation (at the $1 \times 10^{-7} M$ level) is 1.1%. Applicability to urine analysis is illustrated.

The plant alkaloid colchicine is known for its effective treatment of acute gouty arthritis.^{1,2} The drug inhibits the migration of leucocytes to inflammatory areas, thus interrupting the inflammatory response that sustains the acute attack. It is also being studied as a potential HIV inhibitor, in connection with the treatment of AIDS.³ Highly sensitive methods are thus essential for the evaluation and administration of colchicine. Various chromatographic^{4,5} and spectrophotometric^{6,7} procedures have been employed for this purpose, as well as for analyses of pharmaceutical preparations. Electrochemistry has not been widely used for measurements of colchicine. The drug produces a single 1-electron polarographic reduction wave⁸ and can be oxidized in two 2-electron steps.⁹ Earlier voltammetric schemes based on these processes yielded detection limits in the micromolar level that were sufficient only for tablet assays.^{8,9}

The present work reports an extremely sensitive voltammetric procedure for trace measurement of colchicine, based on its adsorptive accumulation at the hanging mercury drop electrode. Adsorptive stripping voltammetry has been successfully applied for trace measurements of numerous compounds of pharmaceutical significance.¹⁰ As illustrated in this communication, the reduction behavior of colchicine can be coupled with its strong adsorption on mercury surfaces to yield detection

limits at the subnanomolar level. The characteristics and advantages of the resulting adsorptive stripping scheme are elucidated in the following sections.

EXPERIMENTAL

Apparatus

The equipment used to obtain the voltamperograms, an EG&G PAR Model 264A voltammetric analyzer with an EG&G PAR 303A static mercury drop electrode, has already been described in detail.^{11,12} A medium-size drop (area, 0.015 cm²) was employed. The cell was covered with aluminum foil.

Reagents

All solutions were prepared with doubly distilled water. Stock solutions of colchicine (Sigma) were made up fresh each day and were stored in the dark at 4°. Urine samples were obtained from healthy volunteers.

Procedure

A 10-ml volume of 0.01M sodium hydroxide was added to the cell and deaerated by passage of nitrogen for 8 min. The preconcentration potential (−0.9 V) was applied for a selected time while the solution was stirred at 400 rpm. The stirring was then stopped, and after 15 sec the voltamperogram was recorded by applying a differential pulse scan. The scan was terminated at −1.6 V and the adsorptive stripping cycle was repeated with a new mercury drop.

*Author for correspondence.

†Permanent address: Faculty of Pharmacy, Ege University, Izmir, Turkey.

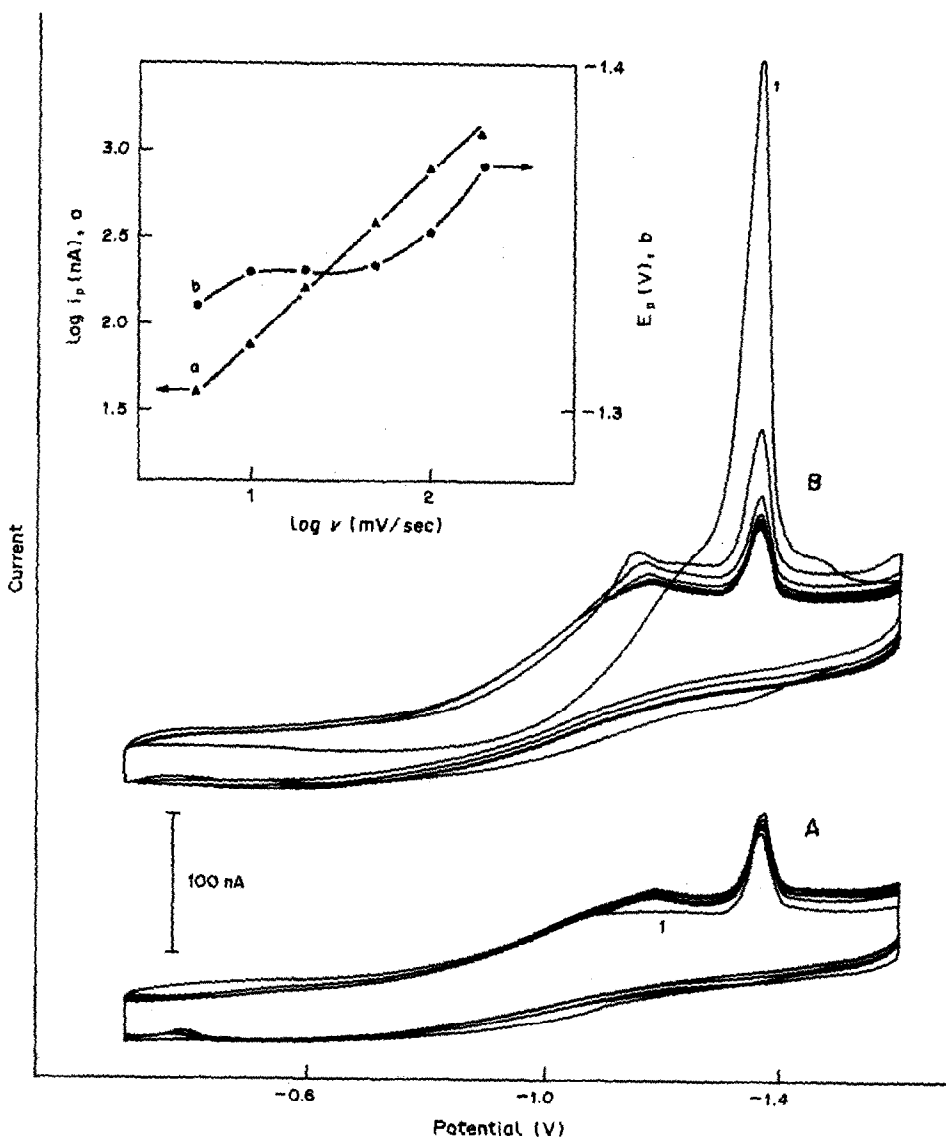


Fig. 1. Repetitive cyclic voltamperograms for $1 \times 10^{-6} M$ colchicine after 0 (A) and 3 (B) min accumulation at -0.9 V. Scan rate, 50 mV/sec. Electrolyte, $0.01 M$ NaOH. Shown also (inset) the dependence of logarithm of the peak current (a) or the peak potential (b) on the logarithm of the potential scan rate.

RESULTS AND DISCUSSION

In Fig. 1, B illustrates repetitive cyclic voltamperograms for $1 \times 10^{-6} M$ colchicine, recorded after preconcentration at -0.9 V for 3 min. A large and well-defined cathodic peak is observed at the first scan (designated as 1), at ca. -1.38 V. No peaks are observed in the anodic branch. Subsequent scans exhibit a rapid diminution of the peak to a stable value representing the response of solution species (as indicated from analogous voltamperograms without accumulation). The large peak shown in B in Fig. 1 represents full surface coverage. Integration of this peak gives a charge of $0.832 \mu C$, which corresponds to surface cover-

age of 5.75×10^{-10} mole/cm². Each colchicine molecule adsorbed thus occupies an area of 0.29 nm². The effects of potential scan rate (v) on the peak current were evaluated for the surface-bound colchicine (Fig. 1, inset). A plot of $\log i_p$ vs. $\log v$ (a) was linear over the 5 – 200 mV/sec range, with a slope of 0.92 (correlation coefficient, 0.999). A slope of 1.00 is expected for an ideal surface reaction. A 40 -mV negative shift in the peak potential was observed upon increasing the scan rate from 5 to 200 mV/sec.

The spontaneous adsorption of colchicine can be used as an effective preconcentration step prior to the voltammetric measurement. In this way, highly sensitive adsorptive stripping

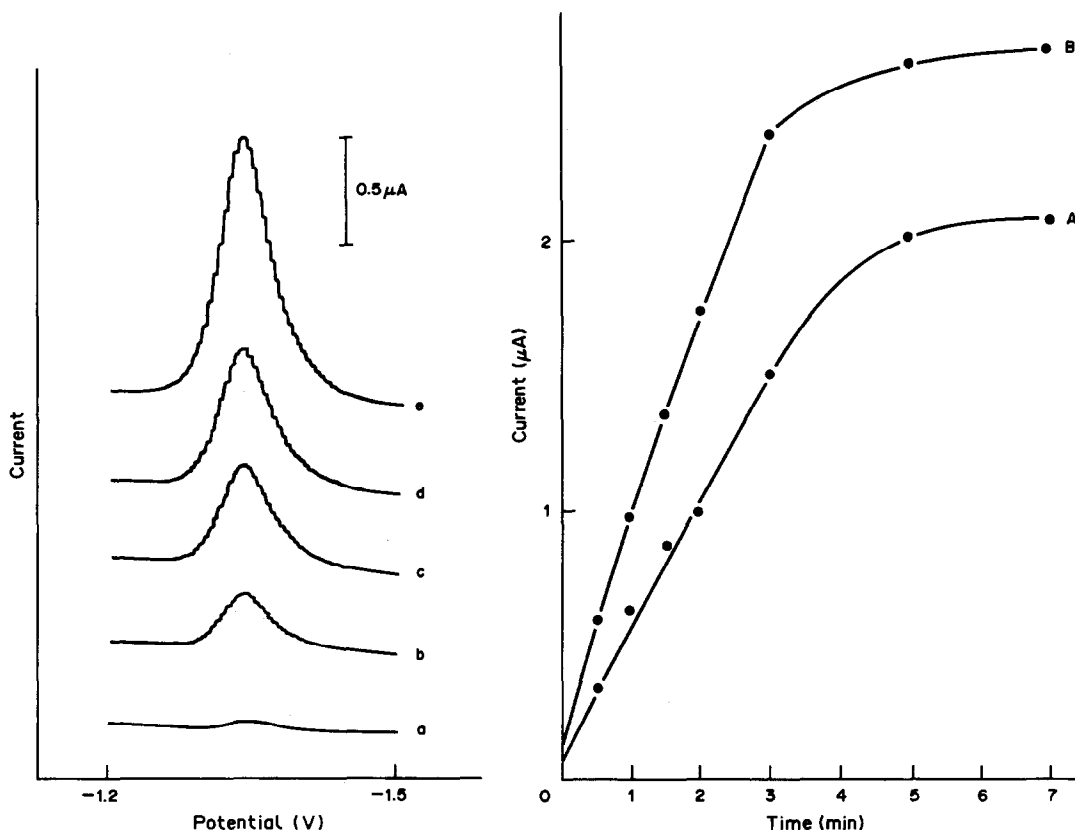


Fig. 2. Effect of pre-concentration period on the voltammetric response for $5 \times 10^{-8} M$ colchicine in $0.01 M$ NaOH solution. Pre-concentration period: (a) 0, (b) 30, (c) 60, (d) 120 and (e) 180 sec. Pre-concentration potential, $-0.90 V$. Differential pulse waveform with $50 mV$ amplitude and $10 mV/sec$ scan rate. Also shown are the resulting current-time plots for $5 \times 10^{-8} M$ (A) and $1 \times 10^{-7} M$ (B) colchicine.

measurements of the drug can be achieved. For example, Fig. 2 shows differential-pulse voltammograms for $5 \times 10^{-8} M$ colchicine after different pre-concentration periods. Quantification at this level is not feasible without pre-concentration (a), but well-defined peaks are observed following pre-concentration (b-e). The peak half-width is $60 mV$. The longer the pre-concentration period, the more colchicine is adsorbed, and the larger the peak current. Also shown in Fig. 2 are plots of peak current vs. pre-concentration time for $5 \times 10^{-8} M$ (A) and $1 \times 10^{-7} M$ (B) colchicine. At both levels the peak current at first increases linearly with time, and then levels off.

The solution pH has a strong effect on the adsorptive stripping response (Fig. 3a). For example, increasing the pH from 10 to 12 results in a sharp increase in the peak; a rapid decrease in the response was observed at $pH > 12$. The dependence of the peak current on the pre-concentration potential was examined over the range from -0.7 to $-1.2 V$ (Fig. 3b). A strong adsorption was observed over the entire range. A pre-

concentration potential of $-0.9 V$ and a pH of 12 offered the best signal-to-background characteristics and were used in most subsequent work.

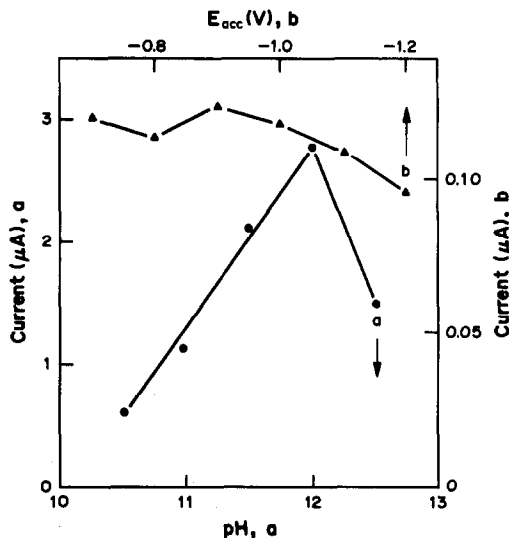


Fig. 3. Effects of the pH (a) and pre-concentration potential (b) on the colchicine peak current. Colchicine concentration, (a) $1 \times 10^{-7} M$ and (b) $2 \times 10^{-7} M$. Pre-concentration period, (a) 120 and (b) 60 sec. Other conditions as for Fig. 2.

Table 1. Effect of pulse amplitude and scan rate upon the adsorptive stripping response of $4 \times 10^{-7}M$ colchicine after 60-sec preconcentration

Scan rate, mV/sec	Amplitude, mV	Peak current, μA	Peak potential, V
2	50	0.95	-1.28
5	50	1.50	-1.30
10	50	2.45	-1.32
10	25	0.95	-1.33
10	50	2.45	-1.32
10	100	2.83	-1.27

Both the differential-pulse and linear-scan stripping modes permitted convenient quantification of submicromolar and nanomolar concentrations. The first of these techniques yielded improved signal-to-background characteristics and was used throughout. As expected, the pulse amplitude and scan rate had a profound effect on the adsorptive stripping peak current and potential (Table 1).

The adsorptive stripping response of colchicine was further characterized with respect to concentration dependence, detection limit and

reproducibility. Figure 4 shows voltamperograms for solutions of increasing colchicine concentration, from 1×10^{-8} to $5 \times 10^{-8}M$ after 120-sec preconcentration. Well-defined peaks are observed. Also shown in Fig. 4 are calibration plots for the $1-10 \times 10^{-8}M$ range, obtained with different preconcentration times. For 30-, 60- and 120-sec preconcentration, the response is linear for the entire range (slopes: 4.4, 8.0 and 13.4 $nA \cdot l \cdot mole^{-1}$ respectively; correlation coefficients, 0.999). The adsorptive accumulation of colchicine results in extremely low detection limits. For example, a well-defined voltammetric peak is obtained for $5 \times 10^{-9}M$ colchicine following a 10 min accumulation (Fig. 5). A detection limit near $1.3 \times 10^{-10}M$ is estimated from the signal-to-noise characteristics ($S/N = 3$) of these data. This value means that in the 10 ml of solution used, 0.5 ng of colchicine can be detected. The high sensitivity is accompanied by good reproducibility of the results. The precision was estimated by 12 successive measurements of $1 \times 10^{-7}M$ colchicine

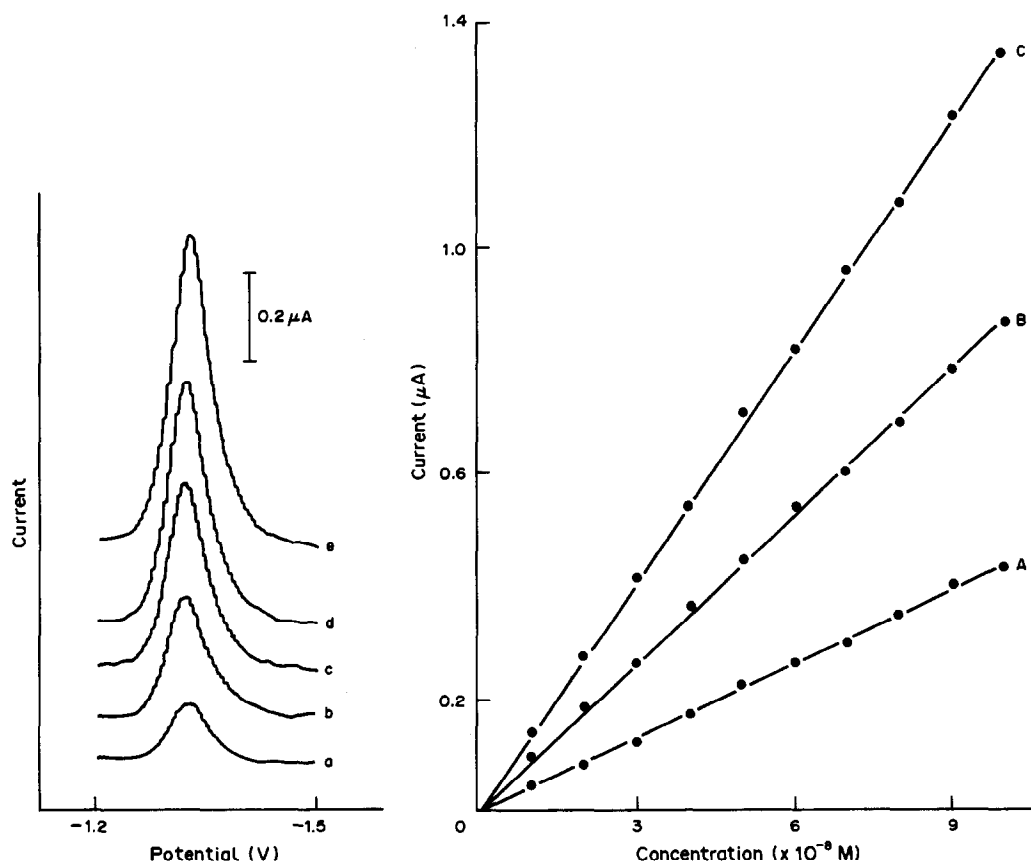


Fig. 4. Voltamperograms obtained for solutions of increasing colchicine concentration, $1-5 \times 10^{-8}M$ (a-e). Preconcentration period, 120 sec. Other conditions as for Fig. 2. Also shown are the resulting calibration plots for different preconcentration times: (A) 30, (B) 60 and (C) 120 sec.

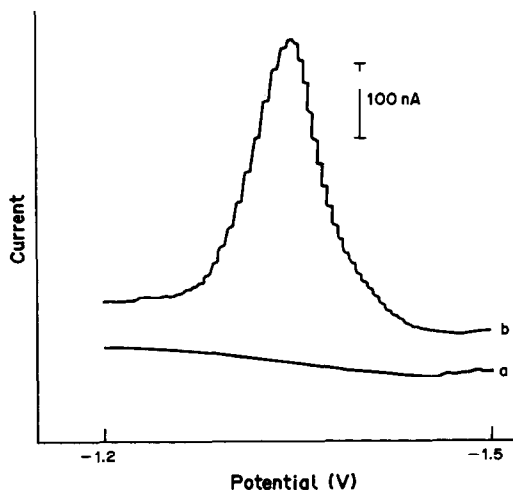


Fig. 5. Voltamperograms for the blank (a) and $5 \times 10^{-9} M$ colchicine (b) solutions, with 10-min pre-concentration. Other conditions as for Fig. 2.

(conditions as for Fig. 2d). The mean peak current was $0.989 \mu A$, range 0.975 – $1.000 \mu A$, and relative standard deviation 1.1%. Such precision, detection limit and linearity offers significant advantages over earlier voltammetric schemes for colchicine,^{8,9} and hold great potential for assays of relevant samples.

Figure 6 illustrates the feasibility of measuring colchicine in urine samples. No sample preparation was used, other than a 1 + 4 dilution with the supporting electrolyte. Urine samples with ascending colchicine concentrations, 1 – $4 \times 10^{-5} M$ (b–d) yielded well-defined peaks, following a very short pre-concentration period. The voltamperogram (a) for a urine blank shows no interfering peaks. Analysis of more complex physiological fluids would require a sample clean-up procedure, commonly used in clinical laboratories. This is particularly the case for blood plasma samples containing strongly adsorbable proteins. Such surface-active materials may affect the adsorptive stripping response of colchicine through competitive coverage. For example, while the presence of dodecyl sodium sulphate (up to 2 ppm) did not alter the $5 \times 10^{-8} M$ colchicine peak, ca. 60% peak depression was observed in the presence of 2 ppm gelatin (60-sec pre-concentration).

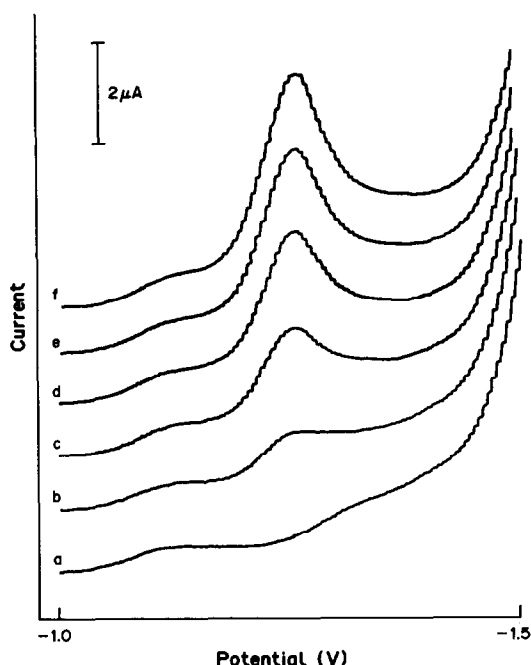


Fig. 6. Voltamperograms for diluted (1 + 4) urine solutions spiked with different levels of colchicine: (a) $0 M$; (b) $1 \times 10^{-5} M$; (c) $2 \times 10^{-5} M$; (d) $3 \times 10^{-5} M$; (e) $4 \times 10^{-5} M$; (f) $5 \times 10^{-5} M$. Pre-concentration for 2 sec. Other conditions as for Fig. 2.

Acknowledgement—This work was generously supported by the National Institutes of Health (Grant No. GM 30913-06).

REFERENCES

- G. Smith, J. M. Bullivant and P. H. Cox, *J. Pharm. Pharmacol.*, 1963, **15**, 92 T.
- D. R. Laurance and P. N. Benaeth, *Clinical Pharmacology*, 5th Ed., Churchill Livingstone, London, 1980.
- R. Baum and R. Dogani, *Chem. Eng. News*, 1989, July 26, 7.
- T. M. Sarg, M. M. El-Domiaty, M. M. Bishr, O. M. Salama and A. R. El-Gindy, *Analyst*, 1989, **114**, 575.
- M. H. Berurier and M. C. Mathis, *Ann. Pharm. Fr.*, 1973, **31**, 457.
- M. S. Karawya and A. M. Diab, *J. Assoc. Off. Anal. Chem.*, 1975, **58**, 1171.
- T. Aray and T. Okuyama, *Anal. Biochem.*, 1975, **69**, 443.
- J. C. Schaar and D. E. Smith, *J. Electroanal. Chem.*, 1979, **100**, 145.
- E. Bishop and W. Hussein, *Analyst*, 1984, **109**, 623.
- J. Wang, in A. J. Bard (ed.), *Electroanalytical Chemistry*, Vol. 16, pp. 1–89. Dekker, New York, 1989.
- J. Wang, D.-B. Luo, P. A. M. Farias and J. S. Mahmoud, *Anal. Chem.*, 1985, **57**, 158.
- J. Wang, M. S. Lin and V. Villa, *Analyst*, 1987, **112**, 1303.

VOLTAMMETRIC DETERMINATION OF LINURON AT A CARBON-PASTE ELECTRODE MODIFIED WITH SEPIOLITE

PEDRO HERNANDEZ, JOSE VICENTE, MARIA GONZALEZ and LUCAS HERNANDEZ
Departamento de Química, Universidad Autónoma de Madrid, Madrid 28049, Spain

(Received 6 February 1989. Revised 16 February 1990. Accepted 27 February 1990)

Summary—The determination of linuron by differential pulse voltammetry with a carbon-paste electrode modified with 20% w/w sepiolite has been studied. The linuron is preconcentrated under open-circuit conditions at pH 2.0. With 0.01M potassium nitrate at pH 1.7 in the measurement cell, a sweep rate of 30 mV/sec and a pulse amplitude of 100 mV, an oxidation wave with a peak potential of 1.2 V is obtained. Under these conditions, determination limits of 75 ng/ml have been obtained, with a relative error of +2.8% and a relative standard deviation of 8.0%. The method has been applied to the direct determination of linuron in river water with no previous separation of the pesticide. Determination in sea-water is not possible, as chloride interferes at high concentration.

The use of magnesium silicates in chromatographic columns or in clean-up systems for the separation and subsequent determination of different pesticides¹ takes advantage of the adsorption capacity of these clay minerals for certain organic compounds.

Carbon-paste electrodes modified with clays can easily be prepared and can be used for the oxidation or reduction of electroactive groups in adsorbed compounds. Such electrodes can be used for the determination of organic compounds which are difficult to determine electrochemically with mercury, carbon or metal electrodes, on account of signals that are difficult to interpret owing to capacitive or residual currents which may mask the analytical signal.

Such modified carbon-paste electrodes have been used for the determination of various organic compounds without prior separation.²⁻⁴

In the present work, the use of an electrode modified with sepiolite (a magnesium silicate) for determination of the organochlorine herbicide linuron, 3-[3,4-(dichlorophenyl)-1-methoxy-1-methylurea], was examined.

Linuron residues have been determined by gas chromatography with electron-capture,⁵⁻⁷ or mass spectral^{8,9} detection, for example in air,¹⁰ and in soya beans by HPLC.¹¹

Various polarographic techniques have been applied to the determination of Linuron.¹² It is now shown that linuron can be directly

adsorbed from aqueous medium onto a carbon-paste electrode modified with sepiolite and then measured by anodic-stripping differential-pulse voltammetry.

EXPERIMENTAL

Apparatus

The electrode was prepared with carbon paste made from spectroscopic grade graphite (particle size <42 μm) and nujol oil (1:1 w/w). Sepiolite previously ground to a particle size of 0.2 μm was added to this under humid conditions. The paste was inserted in a 5-cm length of 1.4-mm bore polyethylene tube to a depth of 0.5 cm, along with a copper wire to achieve direct contact with the mixture. A Metrohm E-506 Polarecord was used for differential pulse (DPV) voltammetry and an Amel 448/A oscillopolarograph coupled to a Hewlett-Packard X-Y recorder for cyclic voltammetry.

Two cells were used: one for preconcentration of linuron from solution and the other, containing the supporting electrolyte, the reference electrode (SCE) and a platinum counter-electrode, for the stripping measurement.

Reagents

Stock solutions of linuron were prepared by dissolving the commercial product (96% pure) in methanol and diluting with water.

Procedure

The modified electrode was placed in the preconcentration cell containing 20.0 ml of a solution of linuron and left under open-circuit conditions for a preselected time. The electrode was then washed with water and transferred to the measurement cell and the DP voltamperogram was recorded between +0.8 and +1.5 V.

RESULTS AND DISCUSSION

Figure 1 shows the cyclic voltammetric behaviour of an electrode modified with 20.0% sepiolite, kept for 5 min in a 50 $\mu\text{g/ml}$ solution of linuron at pH 2, then transferred for measurement to a cell containing 0.01M potassium nitrate adjusted to pH 1.7 with nitric acid.

In the first sweep there is a wave at +1.3 V and in the return sweep two waves appear at (a) 0.45 V and (b) 0.22 V; these are the reduction waves for the oxidation product of linuron.

In the second oxidative sweep two waves appear: (c) at 0.35 V and (d) 0.55 V corresponding to the oxidation steps for waves (a) and (b) respectively, the wave at +1.3 V disappearing in this second cycle.

The other waves decrease in intensity in successive sweeps until a residual current level is reached. This phenomenon provides a method for regenerating the electrode without renewing the surface of the paste electrode.

This behaviour could be accounted for by analogy with what is known of the metabolism of linuron,¹³ that is, by assigning the oxidation wave at 1.3 V to the elimination of the methoxy group (replaced by a hydrogen atom) through the formation of formic acid. The reduction products observed ($E = 0.4$ V) would then be formaldehyde and methanol, which would subsequently be oxidized in a second sweep, and disappear from the surface of the electrode and into the solvent.

In DPV the same kind of behaviour is observed as in cyclic voltammetry (Fig. 2). In this case it is possible to regenerate the electrode with the same efficiency by keeping the electrode polarized at +1.5 V for 2 min.

To establish the most suitable conditions for the determination of linuron, the variables that could affect each of the stages were studied by use of an electrode modified with 10% sepiolite, a 5.0 $\mu\text{g/ml}$ linuron solution, a 6 min preconcentration time, 0.01M potassium nitrate as the supporting electrolyte for the

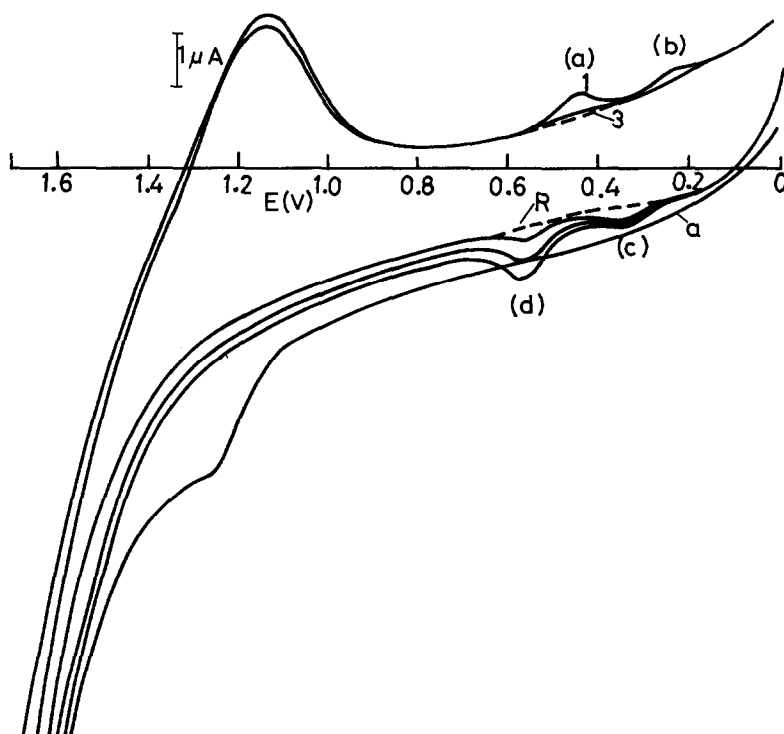


Fig. 1. Multi-sweep cyclic voltamperogram for linuron at 100 mV/sec.

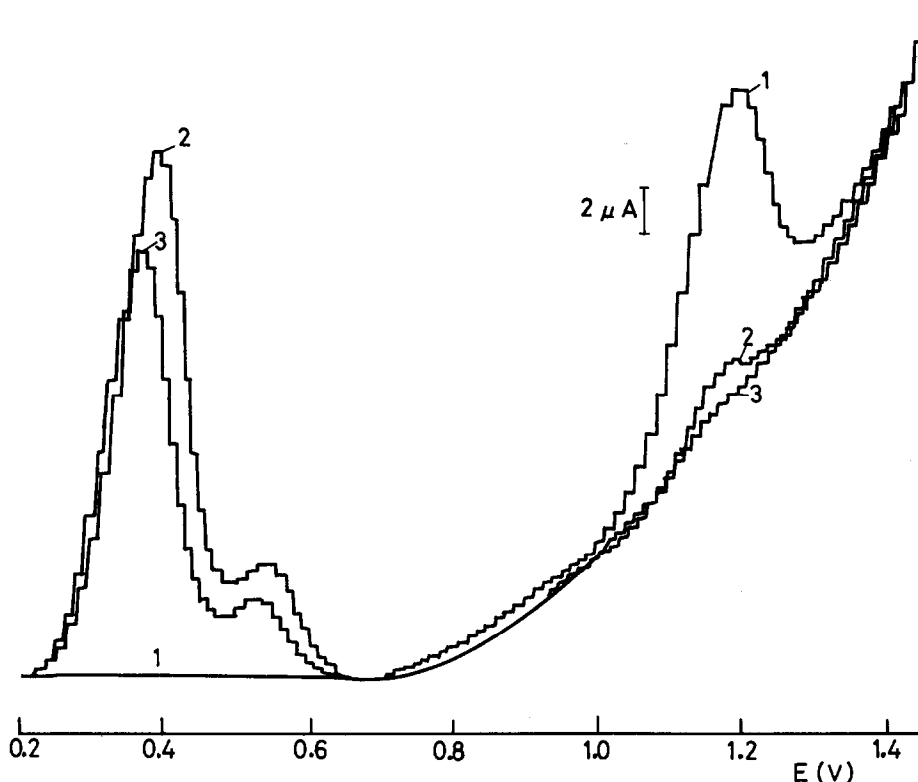


Fig. 2. Differential pulse voltamperogram for linuron, 5.0 µg/ml. (1) First, (2) second and (3) third scan: $v = 30$ mV/sec; $\Delta E = 100$ mV.

DPV, a 30 mV/sec sweep rate and 100 mV pulse amplitude.

When the pH of the sample was varied by addition of nitric acid or potassium hydroxide, with measurement at pH 8 (0.01M phosphate buffer) the highest peak current was reached for accumulation at pH 2 (Fig. 3a). When the pH in the measurement cell was varied, after accumulation at pH 2, the highest peak current was recorded for pH 1.7 (Fig. 3b). In neither of

these modes of measurement did the peak potential (1.2 V) change, indicating that no protons participate in the oxidation of linuron. A variation of the accumulation time (at pH 2.7 with measurement at pH 1.7) showed that for times above 9 min, i_p remained constant (Fig. 4a).

With lower concentrations (0.3 µg/ml) the results pointed to the same kind of behaviour, although a constant i_p was reached at 15 min (Fig. 4b). This confirms that the preconcentration stage is due to adsorption of the analyte onto the electrode, with saturation time increasing as the concentration of the analyte

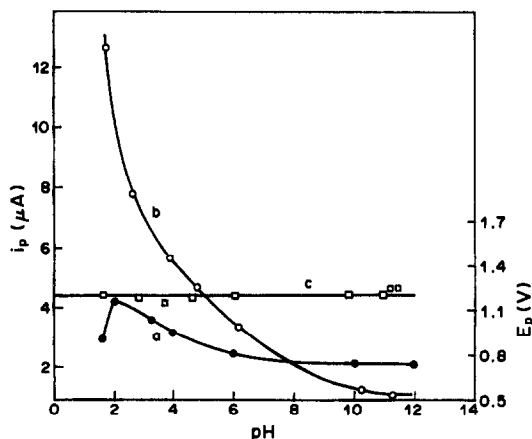


Fig. 3. Influence of pH: (a) i_p in preconcentration cell; (b) i_p measurement cell; (c) E_p .

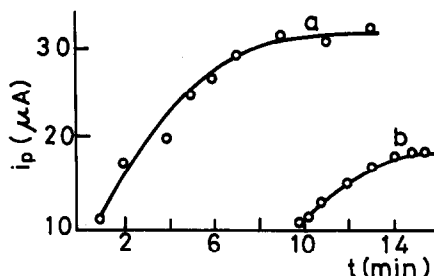


Fig. 4. Influence of accumulation time: (a) 5.0 µg/ml, (b) 0.3 µg/ml linuron.

Table 1. Sensitivity with different compositions

Sepiolite, % w/w	i_p , μA
5.0	1.8
10.0	2.3
20.0	6.9
40.0	No wave

decreases. Varying the proportion of sepiolite showed that maximum i_p was attained with 20% w/w residual currents increasing for higher proportions (Table 1) and i_p decreasing for lower ones.

With the selected pH values and an accumulation time of 6 min, we studied the instrumental parameters with a pulse amplitude (ΔE) of 100 mV (Fig. 5a); i_p increased with sweep rate to a maximum at 30 mV/sec. With a constant sweep rate of 30 mV/sec, i_p varies linearly with $\Delta E = 100$ mV (Fig. 5b).

A study of different electrolytes at a concentration of 0.01M and pH 1.7 (Table 2) showed that of those studied, potassium nitrate and perchlorate gave the largest peak heights, but with the latter, as successive measurements were made i_p decreased until during the fifth measurement the oxidation wave disappeared and it was necessary to replace the electrode by another owing to interference by the perchlorate ion.

A parabolic plot of i_p vs. potassium nitrate concentration was found, with maximum sensitivity at 0.01M, above which exchange of potassium with the sepiolite and a decrease in absorption power was evident.

Figure 6 shows the stripping curves and a calibration plot obtained with an accumulation time of 9 min; it was linear, and could be described by i_p (μA) = 11.7 + 4.12C ($\mu g/ml$) with a correlation coefficient (r) of 0.999. At the

Table 2. Sensitivity with different electrolytes at 0.01M concentration

Electrolyte	i_p , μA
KNO ₃	25.0
KClO ₄	24.6
KCl	15.6
Na ₂ HPO ₄	15.0
CH ₃ COOK	10.1

1 $\mu g/ml$ level, measurement with 5 different electrodes (10 determinations with each) indicated a relative error of +1.7% and a relative

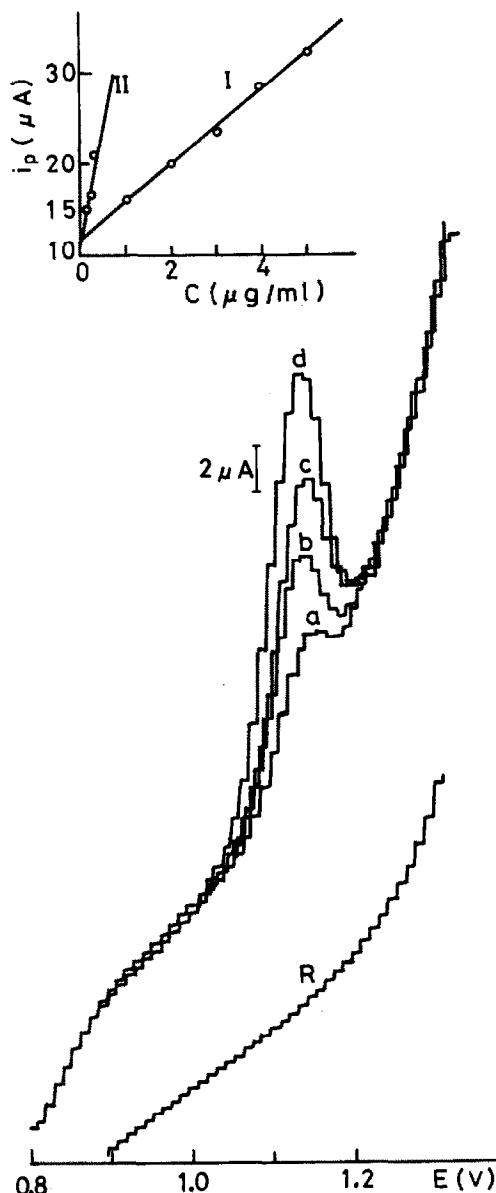


Fig. 6. Calibration voltamperograms and graphs obtained for luron: (I) a, 1.0; b, 2.0; c, 3.0; d, 5 $\mu g/ml$. (II) Below 0.3 $\mu g/ml$. R = residual current.

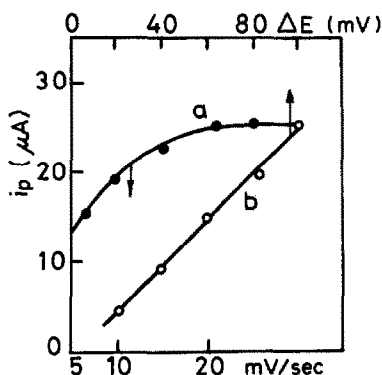


Fig. 5. Influence of (a) scan rate; (b) pulse amplitude, on i_p .

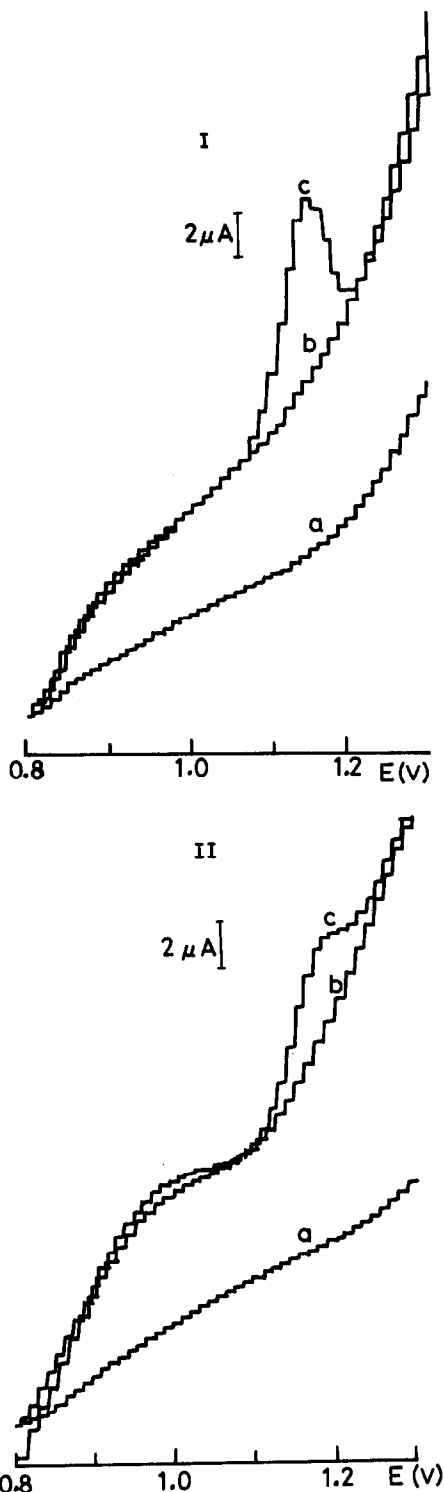


Fig. 7. Determination of linuron in water: I, river; II, sea-water; a, residual current; b, without linuron; c, with addition of 2 µg/ml linuron.

standard deviation of 5.0%. The limit of detection was 0.3 µg/ml. With a view to improving the performance of the method, we also studied

the response of the electrode to concentrations of linuron below 0.3 µg/ml, using an accumulation time of 15 min. The equation for the linear calibration was then $i_p (\mu A) = 11.6 + 27.1C (\mu g/ml)$ with $r = 0.988$.

Under these conditions the relative error was found to be +2.8% for 0.1 µg/ml, with a relative standard deviation of 8.0%; the limit of detection was 75 ng/ml.

The method was employed for the determination of linuron in river water and sea-water with no prior separation step. Samples were acidified to pH 2 and analysed according to the procedure described.

The voltammetric curves are shown in Fig. 7. In this figure, the difference between the two matrices can be seen. Whereas with river water (a) there is a perfectly defined peak, with a large difference between the blank and the sample, the salt concentration of sea-water (b) causes a poorer definition of the voltammetric peak owing to adsorption of the chloride ions present in the matrix. This effect was also observed when potassium chloride was tried as the supporting electrolyte, which is why use of this compound was discarded and replaced by use of the phosphate buffer. The effect of the chloride concentration is to distort the signal to the extent of preventing direct measurement in sea-water.

Interferences

Endosulfan, dinocap, phenol, aniline, nitrobenzene and tetramethin were examined and all found to interfere in the linuron determination. For environmental samples some sort of clean-up or preliminary separation would be necessary, to avoid interferences. On the other hand, the electrode could be used for determination of other pesticides.

Acknowledgement—The authors would like to express their gratitude to the CICYT for support for Project PA 86/0367, under the auspices of which this work was carried out.

REFERENCES

1. K. Beyermann, *Organic Trace Analysis*, Horwood, Chichester, 1984.
2. L. Hernández, P. Hernández, E. Lorenzo and Z. Sosa, *Analyst*, 1988, 113, 621.
3. L. Hernández, P. Hernández and Z. Sosa, *Z. Anal. Chem.*, 1988, 331, 525.
4. L. Hernández, E. González and P. Hernández, *Analyst*, 1988, 113, 1715.

5. V. D. Chmil, *Zh. Analit. Khim.*, 1981, **36**, 1813.
6. L. I. Knyr and V. P. Sukhoparova, *Khim. Selsk. Khoz.*, 1982, No. 8, 60.
7. A. P. Primark, K. V. Krivolutskii and N. F. Biryukova, *ibid.*, 1983, No.2, 58.
8. T. Tamiri and S. Zitrin, *Biomed. Environ. Mass Spectrom.*, 1987, **14**, 39.
9. D. Barcelo, *Chromatographia*, 1988, **25**, 295.
10. A. Gudehn and B. Kolmodin-Hedman, *J. Chromatog.*, 1987, **387**, 421.
11. E. W. Zahnnow, *J. Agric. Food. Chem.*, 1987, **35**, 403.
12. R. J. Hance, *Pestic. Sci.*, 1970, **1**, 112.
13. K. A. Hassall, *The Chemistry of Pesticides*, p. 301. Verlag Chemie, Weinheim, 1982.

AN AMPEROMETRIC ENZYME ELECTRODE FOR THE DETERMINATION OF 3 α -HYDROXYSTEROIDS

MARIA TEODORCZYK* and WILLIAM C. PURDY†

Department of Chemistry, McGill University, 801 Sherbrooke St. W., Montreal, Quebec, Canada H3A 2K6

(Received 5 October 1989. Revised 24 January 1990. Accepted 6 February 1990)

Summary—An enzyme electrode for quantifying the total content of 3 α -hydroxysteroids is described. 3 α -Hydroxysteroid dehydrogenase (E.C. 1.1.1.50) was immobilized on the surface of glassy-carbon and low-temperature isotropic-carbon electrodes by intermolecular cross-linking with bovine serum albumin and glutaraldehyde. The effects of the following factors on the response to androsterone were studied: applied potential, the concentration and pH of the pyrophosphate buffer used, and the NAD concentration. The Michaelis–Menten constant for 3 α -hydroxysteroid dehydrogenase in solution was determined amperometrically with androsterone as substrate ($K_m = 189\mu M$). A preliminary report of the response of the system to serum samples containing a bile acid is presented.

The methods available for the determination of individual steroids in biological fluids are numerous, sensitive and specific. In some situations, however, it is of interest to know the total concentration of groups of steroids. For example, in the diagnosis of adrenocortical or hepatobiliary diseases it is important to know the total content of 3 α -hydroxysteroids in the urine and the total bile acids concentration in the serum.¹⁻³

Several methods for the determination of bile acids are based on the enzymatic reaction between the 3 α -hydroxysteroid and nicotinamide adenine dinucleotide (NAD) in the presence of 3 α -hydroxysteroid dehydrogenase.^{4,5} Very often a combination of HPLC separation with post-column enzymatic reaction and visible,⁶ ultraviolet⁷⁻¹⁰ or fluorescence detection¹¹⁻¹⁵ is used for the assay of bile acids in bile or serum. Because the cofactor of the enzymatic reaction, NAD, can be monitored electrochemically, some attempts have been made to determine serum bile acids amperometrically. Kamada *et al.*¹⁶ used a post-column enzyme reactor with 3 α -hydroxysteroid dehydrogenase immobilized on aminopropyl controlled-pore glass beads. The NADH generated reacted with phenazine methosulfate which, in turn, was oxidized on a glassy-carbon (GC) electrode at +0.10 V. Campanella *et al.*¹⁷ determined cholic acid in human bile by using

a system consisting of 7 α - or 3 α -hydroxysteroid dehydrogenase and peroxidase with NAD; detection was accomplished amperometrically with a Clark oxygen electrode. Albery *et al.*¹⁸ employed a conducting organic salt electrode to oxidize NADH produced in the oxidation of bile acids.

Here we report an extremely easy method for the preparation of an enzyme electrode for the determination of total 3 α -hydroxysteroids. We also describe the optimization of the assay conditions [pH, buffer and cofactor concentration, potential applied to the GC or low-temperature isotropic-carbon (LTIC) electrode], and present some kinetic aspects of the process. Preliminary results for the assay of a bile acid in serum are also included.

EXPERIMENTAL

Reagents

Reagents were purchased from Sigma Chemical Co. (St. Louis, MO) unless otherwise stated. Sodium pyrophosphate buffer solution, 0.1M, was prepared from tetrasodium pyrophosphate and adjusted to the desired pH with concentrated hydrochloric acid. Potassium phosphate buffer, 0.01M, was prepared from potassium monohydrogen and dihydrogen phosphates and adjusted to pH 7.2 with potassium hydroxide.

Glycine, bovine albumin, and glutaraldehyde solutions were prepared at 0.1M, 50 mg/ml, and 2.5% v/v concentrations respectively, in

*Present address: LifeScan Inc., 2443 Wyandotte, Mountain View, CA 94043, U.S.A.

†Author for correspondence.

potassium phosphate buffer. NAD, as the lyophilized free acid, was used as a 12mM solution in demineralized water and neutralized by the addition of solid sodium bicarbonate until effervescence ceased. NADH was used as a 0.1M solution in pyrophosphate buffer. Solid 3 α -hydroxysteroid dehydrogenase (HSD) from *Pseudomonas testosteroni* was reconstituted with potassium phosphate buffer, as needed, and stored at 4° for no longer than 3 days. Triton X-100 was used as a 6.0% v/v solution in pyrophosphate buffer. The 3 α -hydroxysteroids androsterone, tetrahydrocortisone, tetrahydrocortisol, cholic acid and deoxycholic acid were mainly used as 1.5 mg/ml solutions in methanol and stored in tightly sealed vessels at 4°. Calf serum bile acid calibrator was supplied by Sigma Chemical Co. Constant ionic strength in the solutions used in electrochemical experiments was maintained by adding 1.0M sodium chloride.

Apparatus

DC cyclic voltammetry experiments in quiescent solutions were conducted with a Princeton Applied Research Model 273 Potentiostat/Galvanostat connected to a Houston Instruments X-Y recorder. A three-electrode glass cell was fitted with a commercially available aqueous saturated calomel electrode (SCE) and a 1-cm² platinum foil auxiliary electrode. A GC disk electrode (Bioanalytical Systems Inc., West Lafayette, IN) or an LTIC electrode (Carbomedic Inc., Austin, TX) served as the working electrode. The effective areas were found to be 0.067 cm² (GC) and 0.727 cm² (LTIC) by measurement of the anodic potassium hexacyanoferrate(II) cyclic voltamperogram peak ($n = 1$, $D = 6.32 \times 10^{-6}$ cm²/sec) in potassium chloride.¹⁹

Amperometric studies in stirred solution were made with a potentiostat built in this laboratory. A water-jacketed three-electrode cell of 10-ml working volume was used with the GC or LTIC working electrode. Stirring was provided by a magnetic stirring bar. Current-time curves were recorded on a Goerz Metrawatt SE 120 strip-chart recorder.

Spectrophotometry

Spectral studies of the enzyme activity were done with a 1-cm fused-silica cell (kept at 25°) and a Hewlett-Packard 8451A diode array spectrophotometer. The formation of NADH was followed at 340 nm. All experiments were

performed with 3 ml of pyrophosphate buffer solution which was 0.4mM in NAD and enzyme. The reaction was initiated by adding methanolic 3 α -hydroxysteroid solution.

Enzyme immobilization

3 α -Hydroxysteroid dehydrogenase was immobilized directly on the surface of the carbon electrodes by intermolecular cross-linking, much as described by Lubrano and Guilbault.²⁰ Bovine serum albumin, lyophilized enzyme powder, and glutaraldehyde were deposited in that order on the electrode surface. The drying time depended on the electrode area and the ambient temperature (approximately 20 and 60 min for GC and LTIC electrodes, respectively). The enzyme electrode was then conditioned for 30 min in glycine solution to saturate unreacted aldehyde groups. Finally the electrode was washed with phosphate buffer to remove non-immobilized adsorbed enzyme. The electrode was stored in potassium phosphate buffer at 4°. Glassy-carbon electrodes treated as above but without the enzyme were also prepared and are termed GC-BSA electrodes.

Amperometric determination of 3 α -hydroxysteroids

Steady-state current measurements were performed with the enzyme electrodes in pyrophosphate buffer containing NAD, sodium chloride and Triton X-100. Once a constant background current was obtained, steroid samples in methanol were injected and the increase in current was recorded. The performance of the GC enzyme electrode with serum samples was also tested. In addition, the effect of pH, stirring rate and buffer concentration on the response to androsterone samples was studied. The effective Michaelis-Menten constant for androsterone was determined amperometrically, as well as the diffusion coefficient of NADH in the enzyme membrane. The stability of the enzyme electrodes was tested.

RESULTS AND DISCUSSION

Several factors were examined, to determine the optimum conditions for the enzymatic reaction of 3 α -hydroxysteroids. In most cases androsterone was used as the model compound.

Linear-sweep voltammetry

The nicotinamide component of the dehydrogenase enzymes serves as the transient

intermediate carrier of the hydride ion that is enzymatically removed from the substrate molecule by the action of certain dehydrogenases. It is recognized that the electrode process for NAD/NADH is irreversible and that the oxidation of NADH proceeds in one step by a two-electron reaction.^{21,22} The oxidation of NADH was facilitated by phosphate and blocked by Tris buffer.²³ Pyrophosphate buffer was used because the activity of 3 α -HSD is highest in this system.¹⁶

With either the bare GC or LTIC electrode, voltamperograms were run from 400 to 900 mV in buffer only and in buffer with NADH, to determine the effect of pH on the anodic peak current. A pH of 8.90 was optimum for NADH oxidation. To determine the optimum potential for the enzymatic reaction, voltammetric studies were performed with stirred solutions at 25°. Figure 1 shows the results obtained for a bare LTIC electrode with NADH at concentrations from 4 to 80 μ M. For stirred solution with the GC electrode at 600 mV *vs.* SCE (to minimize background current) in 0.03M pyrophosphate buffer (pH 8.90) at constant ionic strength, the following regression equation related the steady-state current i_{ss} (μ A) to the NADH concentration C

$$i_{ss} = 0.158 + 0.263C \quad (1)$$

over the range 2.50–180 μ M (13 data-points). The background current was 0.08 μ A (intercept in μ A, slope in μ A.l. μ mole⁻¹).

Spectrophotometric studies of enzyme activity

The enzymatic oxidation of androsterone at 25° in a 0.03M pyrophosphate buffer of pH 8.90

containing 0.4 μ M NAD was studied to determine the enzyme activity. The increase in absorbance at 340 nm was followed as a function of time for different steroid concentrations. The solid 3 α -hydroxysteroid dehydrogenase was found to have an activity of 17 U/mg.

Controlled-potential studies

Once the 3 α -hydroxysteroid dehydrogenase was immobilized on the surface of the GC or LTIC electrode, controlled-potential studies were initiated in a solution containing pyrophosphate buffer, sodium chloride, NAD, and Triton X-100 (0.48% v/v). The surfactant was found to be necessary when working with 3 α -hydroxysteroids at concentrations greater than 70 μ M. In amperometric experiments this concentration of Triton X-100 was found to stabilize the steroids without inhibiting the enzyme activity.

To optimize the conditions for the amperometric determination of 3 α -hydroxysteroids with an enzyme electrode, the influence of the buffer and cofactor concentrations and the pH were studied. Figure 2 shows the effect of the concentration of pyrophosphate buffer on the steady-state current at a GC-HSD electrode for the oxidation of androsterone. In all subsequent experiments 0.03M pyrophosphate buffer was used. Table 1 presents the results of similar studies for the LTIC-HSD electrode. The effect of NAD concentration on the steady-state current of the GC-HSD electrode and on the androsterone oxidation was also investigated. A 3mM NAD concentration was selected as optimal, as increasing it had virtually no effect on the steady-state current. This NAD

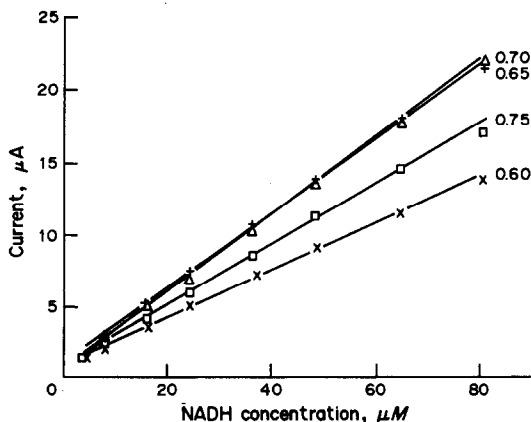


Fig. 1. Response of bare LTIC electrode to fresh NADH in 0.02M pyrophosphate buffer, pH 8.90, at 25°. Applied potential, V: 0.60 (x), 0.65 (Δ), 0.70 (+), 0.75 (\square).

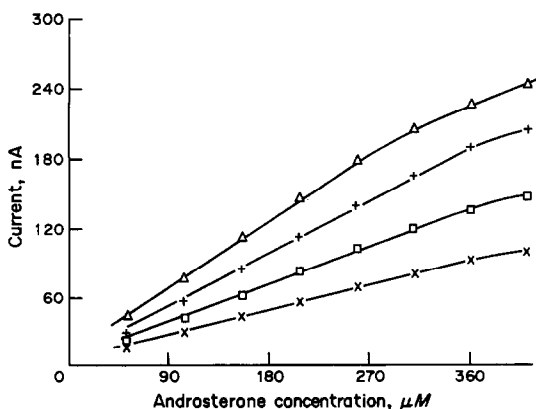


Fig. 2. Effect of pyrophosphate buffer concentration on the response of the GC-HSD enzyme electrode. Conditions: pH 8.90; [NAD] 3mM, 25°; Buffer concentration, M; 0.02 (\square), 0.03 (Δ), 0.04 (+), 0.05 (x).

Table 1. Effect of the concentration of sodium pyrophosphate buffer on the response (i , nA) of the LTIC-HSD electrode at 25° in the presence of 0.48% v/v Triton X-100; androsterone concentration (C) = 50–400 μ M

[Buffer], M	$i = aC + b$		No. of data-points
	a , nA.l. μ mole ⁻¹	b , nA	
0.02	3.69	0.077	9
0.03	3.93	-0.527	8
0.04	3.95	-0.001	9
0.05	3.69	3.05	9

concentration provides pseudo first-order kinetics with respect to the substrate, even at a threefold greater concentration of 3 α -hydroxysteroids.

Effect of pH

The effect of pH on the response of the GC-HSD electrode was investigated over the range 7.5–9.5. Figure 3 shows the optimal range of operation to be pH 8.0–8.5. This pH-dependence of the current, with a maximum at pH 8.0, results from the two-electron oxidation of the steroid and a subsequent oxidation of the reduced form of the cofactor, NAD. Despite these results, a pH of 8.9 was chosen. This was a compromise between the optimum pH for the enzymatic reaction and that for the oxidation of NADH. Furthermore, in defining the activity of the enzyme used, the supplier specified a temperature of 25° and a pH of 8.90. At this pH the steady-state current is about 80% of the response at pH 8.00.

Because of the supplier's recommendations a temperature of 25° was selected for all subsequent measurements. Temperatures higher than 37° are not recommended, because of the possibility of separation of the membrane from the electrode surface.

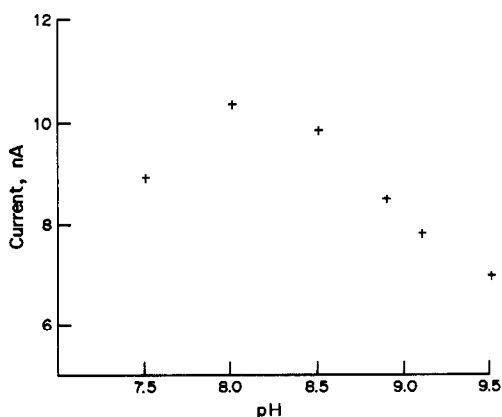


Fig. 3. Effect of pH on the steady-state current for the GC-HSD electrode in 31 μ M androsterone solution containing 0.03M pyrophosphate buffer and 3mM NAD at 25°.

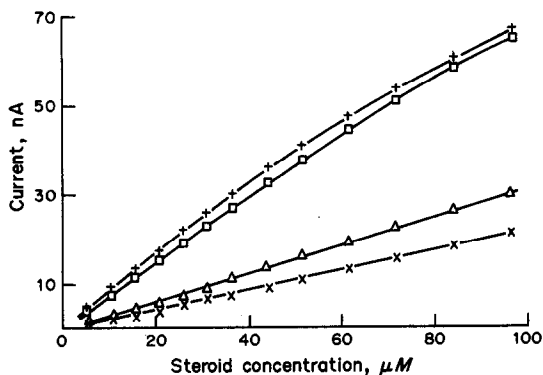


Fig. 4. Calibration curves for GC-HSD electrode: (Δ) androsterone, (\square) tetrahydrocortisol, (+) tetrahydrocortisone, (\times) cholic acid. Conditions as for Fig. 3.

Response of the GC-HSD electrode to 3 α -hydroxysteroids

Figure 4 shows a typical background-corrected steady-state current ($i_{ss} - i_0$) calibration plot for four different 3 α -hydroxysteroids. To minimize background current the GC-HSD electrode was operated potentiostatically at +600 mV vs. SCE. Ranges for linear current response were 5–96 μ M for cholic acid and androsterone, 5–84 μ M for tetrahydrocortisol and 15–70 μ M for tetrahydrocortisone. The background current of the electrolyte in the absence of steroid was $i_0 = 0.1$ nA.

The response of the GC-HSD electrode (nA) to deoxycholic acid (μ M) under the same conditions is described by the equation (7 data-points)

$$i_{ss} = -0.0589 + 0.157C \quad (2)$$

where the intercept is expressed in nA and the slope in nA.l. μ mole⁻¹.

The linear relationship between the steady-state current and the concentration of deoxycholic acid was maintained over the range 3.8–44 μ M. This narrow response range might result from either an inappropriate choice of pH or low affinity of the enzyme for the particular substrate.

At androsterone concentrations up to 350 μ M the response of the GC-HSD electrode was linear, then finally levelled off, with visible precipitation of substrate, at steroid concentrations around 400 μ M. The limit of the linear range is relevant to the determination of bile acids in serum. Levels above 10 μ M are considered to be abnormal and are usually connected with a different type of liver dysfunction.

The response of the GC-HSD electrode to different stirring rates was investigated with four

androsterone solutions varying in concentration from 5.2 to 20.6 μM . The changes in current response never exceeded 9.0%, even when turbulent stirring was used instead of gentle stirring. The electrode had a rapid response time, reaching 95% of the steady-state current in 60–100 sec.

Michaelis–Menten constant determination

Although the LTIC-HSD electrode took over 20 min to reach a stable baseline current and had a significantly shorter lifetime than the GC-HSD electrode, it was used for the amperometric determination of the effective K_m value of the enzyme in solution. If the rate of an enzymatic reaction is controlled by catalysis, K_m may be determined from the following equation of Lineweaver–Burke form.

$$1/i_{ss} = K_m/Ci_{max} + 1/i_{max} \quad (3)$$

where i_{ss} and i_{max} are the currents measured for enzymatic product detection under steady-state and substrate-saturation conditions, respectively. This equation was used by Wilson *et al.*^{24,25} to determine K_m for glucose oxidase at a rotating electrode. In 0.03M pyrophosphate buffer of pH 8.90 with 3mM NAD and 0.48% Triton X-100, K_m for androsterone was found to be 189 μM . Insertion of the appropriate values into equation (3) yielded:

$$1/i_{ss} = 26.14/C + 0.1382 \quad (4)$$

which gave a correlation coefficient of 0.9926 over the androsterone concentration range 25.8–164.7 μM (6 data-points).

A similar experiment performed with the LTIC-HSD electrode permitted the calculation of K_m for the immobilized enzyme. Equation (3) had a slope of 372 and an intercept of 0.416, yielding $K_m = 893 \mu\text{M}$. This value for the immobilized enzyme was several times larger than that for the enzyme in solution. For the same enzyme and substrate, but with a different buffer system and NAD concentration, Pocklington and Jeffery²⁶ reported $K_m = 250 \mu\text{M}$ at 25°, and Bovara *et al.*⁶ found it to be 1.6 μM . Both groups determined K_m spectrophotometrically. Bovara *et al.*, however, did not mention the temperature of the assay, and Pocklington and Jeffery used in their experiments a mixture of sodium phosphate and Tris buffer.¹ The latter was found to be able to block 3 α -HSD action and could cause an increase in the K_m value.²³ Finally, this calculation assumes that the rate of the enzymatic reaction is controlled by catalysis. If

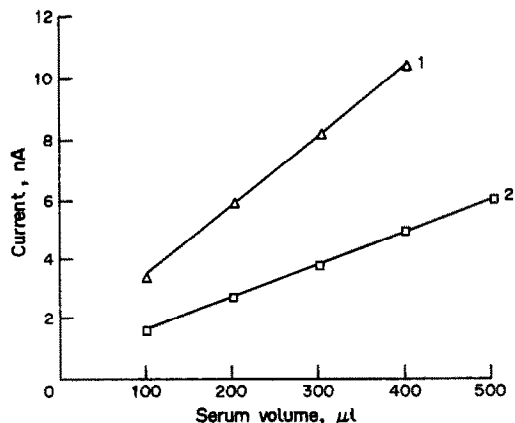


Fig. 5. Response of the GC-HSD (1) and GC-BSA (2) electrodes to serum samples. Steady-state current measured at 600 mV vs. SCE under same conditions as for Fig. 3.

the enzyme loading is sufficiently high for the electrode response to be limited by diffusion, equation (3) does not apply.

Response of the GC-HSD electrode to serum samples

Figure 5 shows the responses of the GC-MSD enzyme electrode and the enzymeless GC-BSA electrode; these studies were conducted with a constant final cell volume. The steady-state currents (corrected for background current) obtained for different volumes of serum samples are shown. The responses of the enzyme electrode were significantly greater than those of the enzymeless electrode, for the same volume of serum sample. Both electrodes required intensive washing after 4 or 5 serum injections, otherwise there was no longer a linear relationship between the steady-state current and the amount of sample injected. This departure from linearity was probably caused by the oxidation of some serum component; the differences between the response of the enzyme and enzymeless electrodes result from the oxidation of 3 α -hydroxysteroids present in the serum. Washing consisted of immersing the electrodes in the same stirred buffer solution for 10–15 min.

The lifetime of the GC-HSD electrode was studied by monitoring the change in slope of the androsterone calibration curves with time. After an initial increase of about 20% in the slope during the first three days, the response was stable from 90 days.

CONCLUSIONS

3 α -Hydroxysteroid dehydrogenase immobilized on the surface of glassy or low-temperature

isotropic carbon provides an easily prepared, stable and sensitive enzyme electrode for the determination of the total 3α -hydroxysteroids content. The NADH produced during the enzymatic reaction is electrochemically oxidized, resulting in a measurable steady-state current. Both electrodes, under optimized conditions of pH, applied potential and buffer concentration, display rapid response, expanded range and stability over a 2–3 month period.

The Michaelis–Menten constants, K_m , for both the free and immobilized enzyme suggest that the affinity of the immobilized 3α -hydroxysteroid dehydrogenase for androsterone is several times lower than that of the free enzyme. The two types of working electrode were used to determine total 3α -hydroxysteroids in serum: the enzyme electrode gave a significantly higher current response for androsterone than that given by the enzymeless electrode.

Acknowledgement—The authors are indebted to the Natural Sciences and Engineering Research Council of Canada for support of this work.

REFERENCES

1. D. Rudman and F. E. Kendall, *J. Clin. Invest.*, 1957 **36**, 530.
2. D. Festi, A. M. Morselli Labate, A. Roda, F. Bazzoli, R. Fraboni, P. Rucci, F. Taroni, R. Aldini, E. Roda and L. Barbara, *Hepatology*, 1983, **3**, 707.
3. S. Skrede, H. E. Solberg, J. P. Blomhoff and E. Gjone, *Clin. Chem.*, 1978, **24**, 1095.
4. G. M. Murphy, B. H. Billing and D. N. Baron, *J. Clin. Path.*, 1970, **23**, 594.
5. J. C. Nicolas, *Anal. Biochem.*, 1980, **103**, 170.
6. R. Bovara, G. Carrea, P. Cremonesi and G. Mazzola, *ibid.*, 1981, **112**, 239.
7. K. Shimada, M. Hagesawa, J. Goto and T. Nambara, *J. Chromatog.*, 1978, **152**, 431.
8. J. Goto, M. Hagesawa, H. Kato and T. Nambara, *Clin. Chim. Acta*, 1978, **87**, 41.
9. N. Parris, *Anal. Biochem.*, 1979, **100**, 260.
10. M. S. Sian and A. J. H. Rains, *Clin. Chim. Acta*, 1979, **98**, 243.
11. T. Kawasaki, K. Maeda and A. Tsuji, *J. Chromatog.*, 1983, **272**, 261.
12. L. J. Kricka, G. K. Wienhausen, J. E. Hinkley and M. De Luca, *Anal. Biochem.*, 1983, **129**, 392.
13. A. Roda, S. Gorotti, S. Ghini, B. Gringolo, G. Carrea and R. Bovara, *Clin. Chem.*, 1984, **30**, 392.
14. M. Hayashi, Y. Imai, Y. Minami, S. Kawata, Y. Matsuzawa, S. Tarui and K. Uchida, *J. Chromatog.* 1985, **338**, 195.
15. M. B. Thompson, P. C. Blair, R. W. Morris, D. A. Neptun, D. F. Deyo and J. A. Popp, *Clin. Chem.*, 1987, **33**, 1856.
16. S. Kamada, M. Maeda, A. Tsuji, Y. Umezawa and T. Kurahashi, *J. Chromatog.*, 1982, **239**, 773.
17. L. Campanella, F. Bartoli, R. Morabito and M. Tomassetti, *Membrane Processes, Proc. Eur.-Jpn. Congr. Membr. Processes*, 1984, 543.
18. W. J. Albery, P. N. Bartlett and A. E. G. Cass, *Phil. Trans. Roy. Soc., B*, 1987, **316**, 107.
19. M. von Stackelberg, M. Pilgrim and V. Toome, *Z. Elektrochem.*, 1953, **57**, 342.
20. G. J. Lubrano and G. G. Guilbault, *Anal. Chim. Acta*, 1978, **97**, 229.
21. R. D. Braun, K. S. V. Santhanam and P. J. Elving, *J. Am. Chem. Soc.*, 1975, **97**, 2591.
22. M. Aizawa, R. W. Coughlin and M. Charles, *Biochim. Biophys. Acta*, 1975, **385**, 362.
23. W. J. Blaedel and R. A. Jenkins, *Anal. Chem.*, 1975, **47**, 1337.
24. F. R. Shu and G. S. Wilson, *ibid.*, 1976, **48**, 1679.
25. R. A. Kamin and G. S. Wilson, *ibid.*, 1980, **52**, 1198.
26. T. Pocklington and J. Jeffery, *Eur. J. Biochem.*, 1968/69, **7**, 63.

SELECTIVE INTERACTIONS OF CONCAVALIN A AT LIPID MEMBRANES ON THE SURFACE OF AN OPTICAL FIBER

ULRICH J. KRULL, R. STEPHEN BROWN, BRUCE D. HOUGHAM and IVAN H. BROCK

Chemical Sensors Group, Department of Chemistry, Erindale College, University of Toronto,
3359 Mississauga Road North, Mississauga, Ontario, Canada L5L 1C6

(Received 12 May 1989. Revised 18 December 1989. Accepted 12 January 1990)

Summary—An optical configuration was developed for sampling fluorescence coupled into an optical fiber from evanescent wave excitation of fluorescent materials at a lipid membrane on a quartz fiber surface. Selective interactions of pyrene-labelled concanavalin A located on a phosphatidyl choline-cholesterol lipid membrane with fluorescein isothiocyanate-labelled dextran in bulk aqueous solution were monitored by the intrinsic fluorescence sensing configuration. Monosialoganglioside, G_{M1} , was employed as a receptor in a phospholipid membrane on an optical fiber for selective measurement of pyrene-labelled concanavalin A in solution. Quantitative measurement was hindered by non-selective adsorption of concanavalin A, but the potential for use of a lipid membrane in a fluorometric biosensor was established.

In development of electrochemical and optical biosensors^{1,2} lipid membranes have great potential as surfaces which can support a wide range of biological materials such as enzymes, antibodies and receptors, in a matrix within which they remain biochemically active. The high degree of biochemical activity, coupled with the extreme thinness of the membrane provides for relatively large and very rapid interfacial response signals. An example is the selective complexation of polysaccharides by the lectin concanavalin A (Con A) at bilayer or monolayer lipid membranes.³ Con A is a globular protein containing saccharide, ion (co-factor) and hydrophobic binding sites,^{4,5} with dimensions about 4.0×3.9 nm, as determined by crystal structure studies.⁶ Con A is non-selectively adsorbed on bilayer and monolayer lipid membranes, and can bind polysaccharides such as dextran or glycogen to form aggregates which tend to alter the physical structure of the lipid matrix within a few tenths of a second.^{3,7}

The selective interactions of Con A at lipid membranes provide an interesting model for testing electrochemical and optical detection. Optical methods such as fluorometry are inherently sensitive and less affected by procedural artifacts than are electrochemical methods, which may suffer from problems such as mixed potentials and charging currents.

In particular, total internal reflectance fluorometry is a sensitive technique for detecting

the presence of biochemical species at a solid-liquid interface. The solution of Maxwell's wave equations for total internal reflection within a waveguide indicates that the exponential decay of the electric field intensity of electromagnetic radiation extends beyond an interface defined by two materials of different refractive index (if the refractive index of the waveguide, n_1 , is greater than that of the external coating, n_2),^{9,10} producing so-called evanescent radiation. Under these conditions the external electric field intensity I , at a distance normal to the surface is given by

$$I = I(\theta) \exp(-2z/d_p) \quad (1)$$

where $I(\theta)$ is the electric field intensity at the interface and d_p is the value of z at which $I = I(\theta)/e$. The value of d_p for a radiation wavelength λ is

$$d_p = \frac{\lambda}{2\pi(n_1^2 \sin^2 \theta - n_2^2)^{1/2}} \quad (2)$$

where θ is the angle of incidence of the totally internally reflected electromagnetic radiation on the interface.

The use of evanescent excitation for an intrinsic optrode configuration, in which a lipid membrane is deposited on the surface of an optical fiber, offers the advantages of mechanical stabilization of the membrane, increased effective path-length for optical excitation (particularly on a multimode optical fiber) and analytical

sampling that is restricted to the chemically selective interface.¹¹

Biochemical interfaces have been studied fluorometrically by evanescent excitation techniques. These investigations have established aspects of quantitative selective binding, and the kinetics and mechanisms of binding processes such as those involving immunochemical systems.¹²⁻¹⁴ Relatively little work has been done at optical wavelengths for investigation of lipid membranes and associated protein-mediated selective interactions. Recent experimental work has confirmed that lipid membranes containing fluorescent lipid species at concentrations of 1-2 mole% can be detected fluorometrically after their deposition on an optical fiber by Langmuir-Blodgett monolayer transfer,¹¹ but the fluorescence intensity is rather low, so the technique may not be suitable for development of transducers based on fluorescent lipid membranes.

This paper reports an investigation of optimization of collection of fluorescence radiation from lipid membranes deposited on quartz optical fibers. The selective complexation of Con A with saccharide residues was chosen to illustrate acquisition of fluorescence signals from a chemically-selective lipid monolayer, the use of a lipid membrane as a structural support for the adsorbed selective protein, and the use of an irreversibly bound receptor site supported in the lipid matrix, in the form of the saccharide residue of a glycolipid for complexation with the lectin.

EXPERIMENTAL

Reagents

The materials used for lipid membrane preparation were egg phosphatidyl choline (EPC), cholesterol (C) (Avanti Biochemicals, Birmingham, AL) and monosialoganglioside from bovine brain, G_{M1} , 95% (Sigma Chemical Co., St. Louis, MO), and were used without further purification. Vesicular solutions of EPC/C were formed by preparing an ethanolic solution of the lipid, evaporating the ethanol to leave a dry film, and suspension of this in an aqueous buffer consisting of 10mM Tris, $10^{-4}M$ calcium chloride and manganese chloride at pH 7.0. The EPC/C molar ratio was selected, and sufficient buffer was added to achieve a total lipid concentration of 1.3 mg/ml. Vesicles of EPC/C/ G_{M1} in molar ratio 5/3/2 were prepared by a similar procedure to give a total lipid concentration of

1.4 mg/ml. Similar solutions of EPC/C and EPC/C/ G_{M1} in hexane were prepared for formation of monolayers on a Langmuir-Blodgett trough (Lauda Model 1974, Sybron Brinkman, Toronto). Before the dip casting the fiber surfaces were treated with a solution consisting of 0.1% v/v octadecyltrichlorosilane (Aldrich Chemical Company, Milwaukee, WI), 80% hexadecane, 12% carbon tetrachloride and 8% chloroform. Pyrene-butyryl concanavalin A, (Py-Con A), and fluorescein isothiocyanate dextran (FITC-dextran, m.w. 4000), were used as received (from Molecular Probes, Eugene, OR) and were dissolved in the aqueous buffer used for the vesicular work. All solvents were reagent grade, and water with a resistivity of at least 18 M Ω .cm was obtained from a Milli-Q cartridge filter system.

Apparatus

Vesicle aggregation induced by selective and non-selective binding events was monitored by measurement of the absorbance at 483 nm of aqueous solutions in a 1-cm path-length fused-silica cuvette with a DU-50 spectrophotometer (Beckmann). Vesicular solutions were dispersed with a Vibra-Cell Model 250 probe-tip sonicator (Sonics and Materials, Inc., Danbury, CT) set at 40 W power, after suspension of the vesicles in aqueous solution and before the experiments were started. Fluorescence from the optical fibers (silica core fibers, 400 μ m, Tasso, Montreal, Canada) was induced by a nitrogen laser (LN 103, Photochemical Research Associates, London ON, Canada), and the emitted radiation was processed by a monochromator (Bentham M300, Optikon, Waterloo, ON, Canada) and photomultiplier tube detector (R928, Hamamatsu). The output from the photomultiplier was passed to a gated-integrator/boxcar averager (Stanford Research Systems) which was operated with a sampling gate width of 40 nsec. The fluorescence acquisition equipment was operated in the two configurations shown in Fig. 1.

Procedures

Vesicle experiments. These experiments were done by standard procedures^{15,16} to establish that lipid membranes containing G_{M1} would be capable of selectively binding Con A. The light-scattering experiments monitored the agglomeration of vesicles caused by cross-linking mediated by the lectin.

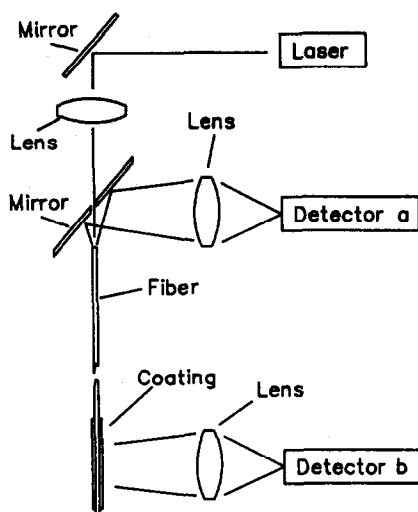


Fig. 1. Experimental optical configuration used for collection of fluorescence from quartz optical fibers by using (a) detector a for end-on detection of radiation coupled into the fiber; (b) detector b for side-on collection of radiation scattered from the fiber.

The vesicular solutions were sonicated for 20 min at room temperature before the experiments were started. Vesicle solution was mixed with an equal volume of Tris buffer containing Con A at 1.3 mg/ml concentration, and the absorbance of the solution was measured periodically for the next 60 min. Solutions were checked for homogeneous suspension of aggregates before each measurement.

Fluorescence experiments. The ability of the equipment to collect fluorescence radiation in the two configurations shown in Fig. 1 was established with a sample consisting of an optical fiber which had been coated with Py-Con A by non-selective adsorption from an aqueous buffered solution containing $10^{-8}M$ Py-Con A. The ends of all the fibers were polished with a rotary sander and a series of successively finer polishing grits.

Non-selective adsorption of Py-Con A was investigated for four fiber surfaces, each 3 cm in length: (a) untreated fiber surfaces exposed by removal of the sheath and cladding with a wire stripper (all fibers were initially cleaned by soaking for 24 hr in Nocromix (Godax, New York), followed by neutralization with sodium hydroxide solution and a water rinse); (b) fiber surfaces which had been coated with a lipid monolayer by Langmuir-Blodgett casting at 7 mm/min from the appropriate lipid mixtures held at a constant surface pressure of 30 mN/m;^{17,18} (c) alkylated surfaces prepared by immersion of the fibers in the silane solution for

60 min, with vigorous agitation every 10 min; (d) alkylated surfaces modified by deposition of a lipid monolayer.¹⁸ The hydrophobic alkylation layer deposited on quartz had been observed to be stable for periods of many months and required no specialized storage. Lipid monolayers deposited on quartz or alkylated quartz tend to change spontaneously with time and were used in these experiments within 24 hr of fabrication.¹⁸ Transfer of deposited lipid monolayers through an air-water interface causes massive structural rearrangement and loss from the surface of the substrate. All lipid-coated samples were therefore handled under aqueous solution. All the fibers were supported in a cuvette containing Py-Con A in buffered aqueous solution. Experimentation was continued in some cases by addition of FITC-dextran as an aqueous solution to the sample cuvette to achieve final polysaccharide solution concentrations of $10^{-6}M$.

RESULTS AND DISCUSSION

The utility of total internal reflection techniques can be understood from equation (2), which indicates that the optical intensity of excitation radiation, and adjustment of penetration depth for sampling near an interface, can be controlled by appropriate selections of excitation wavelength, incident angle and refractive index ratio. Figure 2 provides some examples of theoretical results calculated from equations (1) and (2) for the nitrogen laser source. The experiments described in this work make use of a broad and uncontrolled range of angles of incidence in a multimode distribution at a fixed wavelength (337.1 nm) and a relatively invariant refractive index ratio. The calculations indicate that lipid monolayers (4–5 nm thick), alkylated surfaces coated with lipid monolayers (7–10 nm) and films incorporating lipid monolayers with Con A and dextran (5–20 nm), will all be exposed to relatively high excitation intensities of the laser radiation provided that the refractive index of the organic layers will be in the range 1.45–1.5. While most descriptions of intrinsic mode optrodes have used an evanescent radiation model, it should be noted that films of many biological materials, such as lipids and proteins, have an index of refraction close to that of the quartz optical fibers (approx. 1.5). If the refractive indices of the waveguide and organic layer were identical, internal reflection would not occur at the fiber/coating interface.

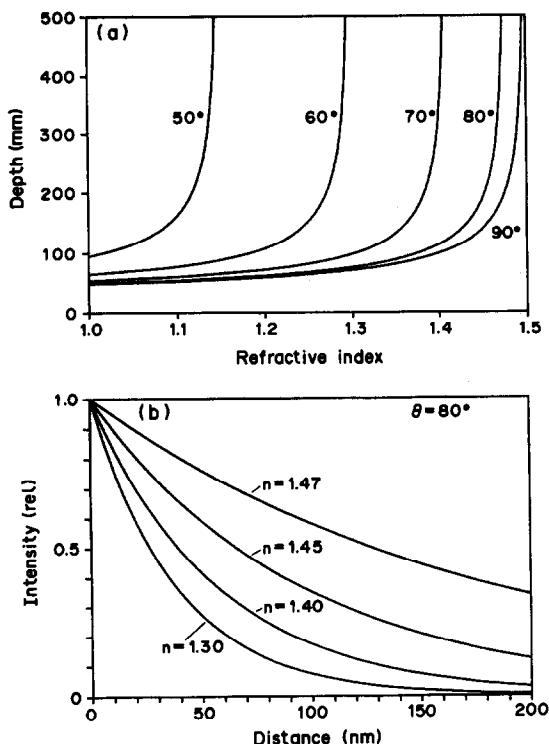


Fig. 2. Calculated relationships of the evanescent field: (a) penetration depth (d_p) and (b) intensity at various distances from a fiber surface for coatings with various indices of refraction, based on equation (2), for a fiber index of refraction of 1.5 and a propagated wavelength of 337 nm.

Optical excitation of the organic layer would be due to the coating acting as a physical extension of the quartz waveguide. Even though the evanescent field would then be propagated beyond the coating/ambient (aqueous solution) interface, there would still be a high degree of surface selectivity and bulk solution interference should be minimal.

The two configurations shown in Fig. 3 highlight the physical phenomena associated with the two collection strategies shown in Fig. 1. The large diameter of the fibers used in this work means that they act as multimode waveguides with respect to optical transmission. A collection strategy where radiation is collected perpendicular to the surface of the fiber (Fig. 3A) would be efficient in a conventional spectrofluorimetric experiment using a standard 1-cm cuvette. The fluorescence generated in a TIRF experiment does scatter perpendicularly to the fiber, but can also couple back into the waveguide under certain conditions. Equation (2) represents the exponential decay of electric field intensity across an interface. A thick (relative to d_p) and homogeneous fluorescent film exposed to such an evanescent wave would emit

radiation at intensities which would decay exponentially with distance from the interface, since fluorescence intensity is proportional to excitation power. This would generate the equivalent of an external component of a new evanescent wave (longer wavelength), which could couple with the waveguide across the refractive index interface to produce a high electric field strength within the waveguide.^{14,19} The presence of such a process could provide for collection of most of the fluorescence by the waveguide, and enable detection to be based on sampling of the fluorescence as shown in Fig. 3B. Evidence has recently appeared indicating that a monolayer lipid membrane or protein film which provides fluorescence in a localized plane can satisfy the conditions of equation (2) and provide significant capture of fluorescence within a waveguide.²⁰

The experimental results indicate a considerable difference in the collection efficiencies of the optical configurations shown in Fig. 1. Observation of fluorescence perpendicular to an optical fiber (Fig. 1b) coated with Py-Con A provided a signal magnitude lower by factors up to 100 than that obtained from coupling the fluorescence into the fiber (Fig. 1a). The efficiency of perpendicular collection was so limited that the distinctive fluorescence profile of the pyrene moiety could not be resolved by the instrumentation used in this work. The same equipment could readily provide a distinctive spectral profile for pyrene when used in the

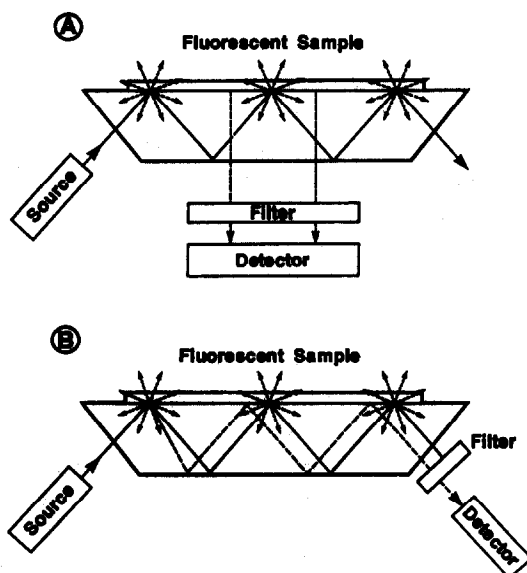


Fig. 3. General strategies for collection of fluorescence from waveguides, showing (A) light-scattering and (B) capture of radiation within the light-guide.

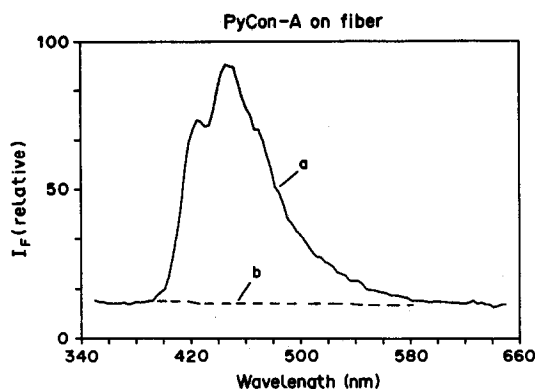


Fig. 4. Fluorescence intensity measurements for pyrene-concanavalin A adsorbed on the surface of a quartz fiber in the end-on fluorescence collection configuration, (a) after adsorption on the fiber surface and (b) background spectrum from the uncoated fiber.

configuration of Fig. 1a, as shown in Fig. 4. Note that the intensity of the nitrogen laser source provided adequate spectral separation of the fluorescence from the excitation radiation, even though the laser wavelength was well removed from the wavelength of maximum absorption by the fluorophore. The efficiency of signal collection by coupling the fluorescence into a fiber does not prove that the effect is necessarily due to the process described by equation (2). If the refractive indices of the fiber and organic film were closely matched, then the coupling of fluorescence into the waveguide would be very efficient. In this case the fluorescence would be produced within the waveguide and would remain in the structure if the propagation angle was greater than the critical angle for total internal reflection.

Concanavalin A as a receptor

Analysis of the adsorption of Py-Con A onto various fiber surfaces indicated no clear preference for non-selective adsorption of the protein by quartz, alkylated quartz or EPC/C-coated fibers. The pH of the solution used in these experiments induces the formation of a quaternary protein structure which takes the form of a tetrameric association of Con A. The complex is physically massive (m.w. $\sim 10^5$) and contains a minimum of 4 hydrophobic binding sites, as well as numerous areas of relatively high polarity. These attributes combine to provide the protein with a capacity to deposit non-selectively onto many different surfaces. Attachment of the protein at significant concentrations to EPC/C membranes was consistent with previous work,³ and the usefulness of the evanescent

radiation technique was clearly indicated by the elimination of extraneous absorption and fluorescence due to Py-Con A in the bulk aqueous solution or on the sample cuvette surfaces, when the system was operated in the configuration shown in Fig. 1a. The Py-Con A on the EPC/C membrane was able to complex FITC-dextran, which was added incrementally directly to the solution in the sample cuvette supporting the optical fiber. A response curve for this experiment is shown in Fig. 5 and analysis of the FITC signal demonstrates selective complexation. The results, collected after the test solution had been incubated for 20 min to allow equilibration of interactions between free Py-Con A and FITC-dextran in the solution, are suitable only for analysis of trends since determination of the amount of Py-Con A and FITC-dextran in dynamic equilibrium on the surface of the fiber was not attempted. The Py-Con A is selectively partitioned onto the surface and its concentration there may be over 100 times that in the bulk solution.³ The concentration-response curve for interaction of Py-Con A with FITC-dextran shows that selective binding occurs (results corrected for bulk solution concentration of FITC-dextran). The non-linear response of low sensitivity at $10^{-6}M$ FITC-dextran may be a result of saturation. Blank experiments using only FITC-dextran indicated that this material was not selectively adsorbed on any of the optical fiber surfaces investigated.

G_{M1} as a receptor

Glycolipids have been extensively investigated as membrane-intrinsic molecular receptors in model membrane studies of lectin-

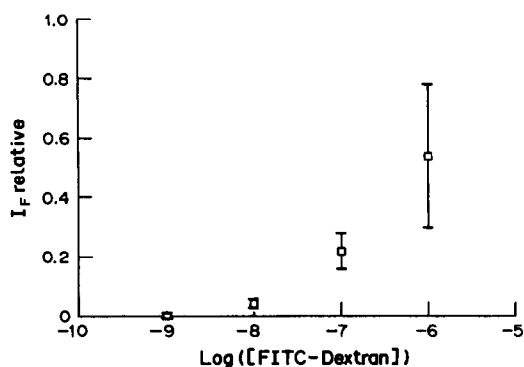


Fig. 5. Concentration-response curve based on increases in relative fluorescence intensity for selective binding of pyrene-concanavalin A (located on a phospholipid-cholesterol monolayer) with fluorescein isothiocyanate dextran.

mediated agglutination.^{15,16} Gangliosides such as G_{M1} have been used in vesicular form and incorporated into PC/C lipid vesicles to provide surfaces coated with saccharide residues suitable for lectin binding. The agglutination of vesicles by lectin has been monitored by observation of changes of light scattering. A series of experiments using vesicular agglutination was done in this work to demonstrate the ability of G_{M1} to act as a receptor for both Con A and pyrene-labelled Con A. The G_{M1} was present at high molar concentrations (20 mole%) in EPC/C vesicles used at room temperature to ensure that glycolipid diffusion could take place on the surface of the membranes. A series of experiments was designed to investigate aggregation or fusion of vesicles with and without G_{M1} in the absence of any protein, in the presence of non-selective protein (bovine serum albumin, BSA), in the presence of Con A (previously associated with vesicle fusion)²¹ and in the presence of Py-Con A. The results of these experiments are summarized in Fig. 6. The trends in light-scattering indicate that little change occurs when BSA is present or when Con A is absent, but some EPC/C vesicle interaction is induced by the presence of the lectin. A greater rate and extent of interaction occurs when G_{M1} is available, and the results confirm that both Con A and pyrene-labelled Con A are selectively complexed by the glycolipid.

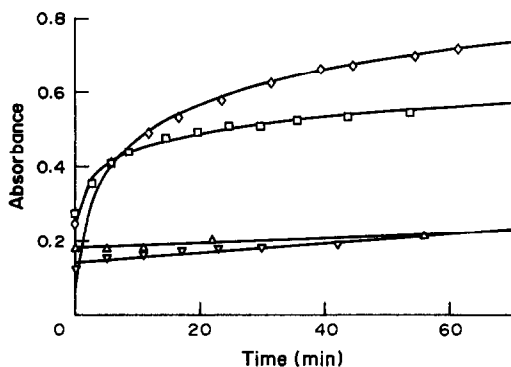


Fig. 6. Lipid vesicle aggregation determined by light-scattering at 455 nm, with monosialoganglioside as a selective binding agent for concanavalin A. (□) Phospholipid-cholesterol vesicles in the presence of concanavalin A or pyrene-concanavalin A; (◇) phospholipid-cholesterol vesicles containing ganglioside in the presence of concanavalin A or pyrene-concanavalin A; (△) lipid vesicles containing the ganglioside G_{M1} ; (▽) lipid vesicles containing the protein BSA in the presence of concanavalin A. Variability between vesicle preparations limits absolute comparisons of reaction rates. The results confirm that the presence of ganglioside assists vesicle aggregation in the presence of Con A.

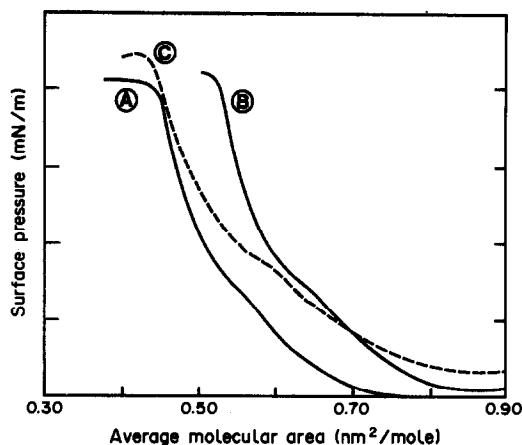


Fig. 7. Pressure-area curves showing results from monolayers of A, 50/50 mole% mixture of phosphatidyl choline and cholesterol; B, 70/30 mol% mixture of phosphatidyl choline and cholesterol; C, 50/30/20 mol% mixture of phosphatidyl choline, cholesterol and ganglioside. Monolayers were transferred to quartz fibers at a constant surface pressure of 30 mN/m.

Lipid membranes of EPC/C containing G_{M1} and devoid of the glycolipid were deposited onto alkylated optical fibers by the Langmuir-Blodgett casting technique, and retained in aqueous solution. Experimental compression curves for these monolayers are shown in Fig. 7, and indicate that differences in physical compressibility and therefore structure are observed for the different membranes. Results for incremental additions of Py-Con A to EPC/C membranes indicated non-selective adsorption of the protein on the membrane. The presence of G_{M1} caused a general trend of enhancement of the pyrene signal relative to that for non-selective adsorption. Quantitative correction for the background signal due to non-selective Py-Con A adsorption on the surfaces could not be done by signal subtraction achieved by use of fibers coated with EPC/C but without G_{M1} . The non-selective binding properties of EPC/C membranes and those containing EPC/C/ G_{M1} were not equivalent because of differences in lateral structure intrinsic to static monolayers (Fig. 7), variations of lateral structure caused by the deposition technique,¹⁸ and differences in the surface free energy, related to the presence of different functional groups at the membrane-solution interface. Chemically selective membranes that employ proteins as binding agents provide a means of improved correction of non-selective adsorption. A reference signal can be derived from a membrane which contains inactivated protein, but is otherwise chemically

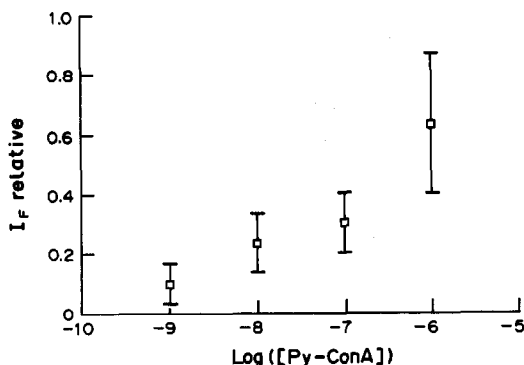


Fig. 8. Concentration-response curve based on relative increases in fluorescence intensity from quartz fibers coated with lipid monolayers containing phosphatidylcholine, cholesterol and ganglioside for selective binding of pyrene-concanavalin A, (results corrected for non-selective adsorption of pyrene-concanavalin A).

identical to the indicator system. It was not possible, however, to denature the G_{MI} used in the present work, to prepare an analogous "inactive" reference membrane. Results for selective Py-Con A adsorption on EPC/C/ G_{MI} membranes are shown in Fig. 8 and represent response trends after a 30-min incubation period, with background correction by estimation of contributions to the analytical signal by non-selective adsorption. The results indicate that the lipid membrane does contain an intrinsic selective receptor, but that the analytical system is not very sensitive or reproducible.

CONCLUSIONS

Chemically-selective lipid membranes can be prepared at the surface of an optical fiber for investigation of binding interactions by monitoring of fluorescence intensity in an intrinsic sensor configuration. The use of Con A as a selective receptor for an analyte resulted in limitation of the analytical reproducibility and sensitivity, owing to non-selective adsorption on the sensing surface. This clearly identifies one of the serious limitations of fiber optic biosensors when used exclusively for fluorescence intensity measurement at a fixed analytical wavelength. The analytical potential of fluorescence lies in the correction of an analytical signal for noise or isolation of the signal from the noise, by use of simultaneous acquisition of data on wavelength, intensity, lifetime and perhaps polarization. A further limitation exposed in this work is that lipid membranes as used here can provide useful matrices for certain receptors (e.g., G_{MI}), but are restricted in scope if the analyte must be fluores-

cently labelled. This is not necessarily the case, since many different biochemical reactions can perturb the structure of lipid membranes, so a fluorescent lipid membrane could be a generic transducer of selective binding events. These aspects will be the subject of a subsequent communication in this journal.

Acknowledgements—The authors wish to thank the Natural Sciences and Engineering Research Council of Canada, the Canadian Defense Research Establishment, the Ontario Ministry of the Environment and Imperial Oil Canada for financial support of this work.

REFERENCES

1. U. J. Krull and M. Thompson, *IEEE Trans. Electron Devices*, 1985, **32**, 1180.
2. U. J. Krull, R. S. Brown, K. Dyne, B. D. Hougham and E. T. Vandenberg, in *Chemical Sensors and Microinstrumentation*, R. Murray (ed.), American Chemical Society, Washington, D.C., in the press.
3. U. J. Krull, R. S. Brown, R. N. Koilpillai, R. Nespolo, A. Safarzadeh-Amiri and E. T. Vandenberg, *Analyst*, 1989, **114**, 33.
4. K. D. Hardman and I. J. Goldstein, in *Immunochemistry of Proteins*, M. Z. Atassi (ed.), Vol. 2, p. 373. Plenum Press, New York, 1977.
5. G. M. Edelman and J. L. Wang, *J. Biol. Chem.*, 1978, **253**, 3016.
6. G. N. Reeke Jr., J. W. Becker and G. M. Edelman, *ibid.*, 1975, **250**, 1525.
7. M. Thompson, H. E. Wong and A. W. Dorn, *Anal. Chim. Acta*, 1987, **200**, 319.
8. M. Thompson, U. J. Krull, L. I. Bendell-Young, I. Lundström and C. Nylander, *ibid.*, 1985, **173**, 129.
9. S. A. Rockhold, R. D. Quinn, R. A. Van Wagenen, J. D. Andrade and M. Reichert, *J. Electroanal. Chem.*, 1983, **150**, 261.
10. M. Reichert, S. Rockhold, R. A. Van Wagenen and J. D. Andrade in *Interfacial Aspects of Biomedical Polymers*, J. D. Andrade, (ed.), Vol. 2, Plenum Press, New York, 1986.
11. U. J. Krull, R. S. Brown, F. R. DeBono and B. D. Hougham, *Talanta*, 1988, **35**, 129.
12. J. D. Andrade, R. A. VanWagenen, D. E. Gregonis, K. Newby and J. N. Lin, *IEEE Trans. Electron Devices*, 1985, **32**, 1175.
13. N. L. Thompson and D. Axelrod, *Biophys. J.*, 1983, **43**, 103.
14. J. F. Place, R. M. Sutherland and C. Daehne, *Biosensors*, 1985, **1**, 321.
15. C. W. M. Grant and M. W. Peters, *Biochim. Biophys. Acta*, 1984, **779**, 403.
16. F. A. Quiocho, *Ann. Rev. Biochem.*, 1986, **55**, 287.
17. W. M. Heckl, M. Thompson and H. Moehwald, *Langmuir*, 1989, **5**, 390.
18. U. J. Krull, J. Brennan, R. S. Brown, G. McGibbon and K. Stewart, *Int. J. Optoelectronics*, 1989, **4**, 133.
19. N. J. Harrick and G. I. Loeb, *Anal. Chem.*, 1973, **45**, 687.
20. P. A. Suci and W. M. Reichert, *Appl. Spectrosc.*, 1988, **42**, 120.
21. J. Van der Bosch and H. M. McConnell, *Proc. Natl. Acad. Sci. USA*, 1975, **72**, 4409.

SIMULTANEOUS DETERMINATION OF SOME RARE-EARTH ELEMENTS BY DERIVATIVE FLUORIMETRY AND USE OF THE KALMAN FILTER

LI JIANJUN and ZENG YUN'E

Department of Chemistry, Wuhan University, 430072 Wuhan, People's Republic of China

CHEN GUANQUAN

The Centre of Analysis and Measurement, Wuhan University, 430072 Wuhan, People's Republic of China

(Received 10 July 1989. Revised 19 November 1989. Accepted 28 November 1989)

Summary—A procedure for the simultaneous determination of dysprosium, europium, samarium and terbium by laser-induced derivative fluorimetry is described. The method is based on the use of $1 \times 10^{-4}M$ hexafluoroacetylacetone (HFA) and $2 \times 10^{-4}M$ tri-*n*-octylphosphine oxide (TOPO) as ligands in aqueous solution at pH 3. The first-derivative and Kalman-filter techniques were used for background correction and reduction of interference. The effects of foreign ions were investigated. The procedure is satisfactory for the simultaneous determination of these four lanthanides.

Because of the similarity of the chemical properties of the lanthanides, the determination of these elements in their mixtures has poor selectivity. Direct spectrophotometric methods are satisfactory for some lanthanides but the sensitivities are very low. Spectrofluorimetric methods can give better results.

Sevchenko and Kuznetsova¹ have investigated the simultaneous determination of dysprosium, europium, samarium and terbium by the use of 1,10-phenanthroline. Alberti and Massucci² have examined the possibility of simultaneous determination of these elements in 0.6M sodium tungstate medium. Unfortunately, both methods are subject to interference from other lanthanides, owing to spectral overlap.

β -Diketones have been widely used for the spectrofluorimetric determination of the lanthanides, especially europium and samarium. Fisher and Winefordner³ have optimized the experimental conditions for spectrofluorimetric determination of europium, samarium and terbium as their hexafluoroacetylacetone-tri-*n*-octylphosphine oxide complexes in non-aqueous solution. However, it is difficult to detect one component with high selectivity in mixed lanthanide samples, owing to overlapping emission bands. Therefore, correction procedures are required.

The derivative technique is becoming increasingly popular in spectrophotometry and spectrofluorimetry.⁴⁻⁶ It can be used to enhance

resolution, to facilitate the detection and location of the wavelengths of poorly resolved components of a complex spectrum, and as a background correction technique to reduce the effect of spectral background interferences.

The Kalman filter is a recursive, linear least-squares digital filtering algorithm. Several applications of this algorithm for improvement of resolution in analytical chemistry have been reported.⁷⁻⁹

In this paper, a highly sensitive laser-induced fluorimetric system coupled with a microcomputer is described, and the laser-induced fluorescence of the derivatives of the ternary complexes formed by Ln(III) (Ln = Dy, Eu, Sm and Tb) with HFA (hexafluoroacetylacetone) and TOPO (tri-*n*-octylphosphine oxide) is reported. This approach combines derivative and Kalman filter techniques, and permits background interferences to be removed from the fluorescence spectra and the four ions to be simultaneously determined.

EXPERIMENTAL

Reagents

The 99.9% pure oxides of the lanthanides and practical grade HFA were obtained from J. T. Baker Chemical Co. Practical grade TOPO was obtained from E. Merck. The HFA and TOPO were used without further purification. Rhodamine 640 was obtained from Exciton Chemical Co. Inc., Dayton, OH.

Stock solutions of the lanthanides were prepared by dissolving their oxides in concentrated hydrochloric acid and diluting with sodium hydroxide solution to obtain 100 ml of 0.01M lanthanide solution with a pH of about 3. The buffer solutions were prepared with sodium acetate, and the pH value was adjusted with hydrochloric acid and sodium hydroxide solution.

Instrumentation

The basic components of the apparatus for the laser-induced derivative fluorimetric system were an Nd:YAG pumped dye laser (Model YG 500/TDL 50, Quantel Co., France), as the excitation light-source, and an Optical Spectra Analyzer (OSA 500 System, B/M Spektronik, FRG) for emission detection. The data were collected and stored in the data terminal WP 2 of the OSA, then transmitted to an IBM PC/XT computer through the serial interface of the OSA and stored on floppy disk for further mathematical processing. A standard fused-silica cell ($4 \times 1 \times 1$ cm) was used in all measurements.

Data processing program

The software used for the transmission was written in assembly language, and the Kalman filter, derivative and the Savitzky-Golay derivative smoothing routines in BASIC. The smoothing routines used a 7-point quadratic smooth.¹⁰

The combination of the first derivatives and Kalman filter techniques is as follows. First, the data stored on floppy disk are smoothed and the first derivative is calculated by the micro-computer for background removal, and used as the measured response for the Kalman filter.

A single iteration with the Kalman filter is used, with an initial guess for the concentration of each component set to 0 and that for the variance set to 0.05. Application of these programs gave the final estimate for the concentration of each component.

RESULTS AND DISCUSSION

Special characteristics

Chelates of dysprosium, europium, samarium and terbium emit luminescence which has the line-spectrum characteristics of the central ions, due to $f-f$ transitions. This luminescence is mainly caused by absorption of radiation by HFA accompanied by subsequent intramolecular energy transfer to the central ion. The complexes have a wide absorption band in the region of 250–360 nm, arising from the $\pi-\pi^*$ transitions of the ligand. Maximum absorption occurs at about 310 nm and so this wavelength is used for excitation.

The emission spectra of Dy(III), Eu(III), Sm(III) and Tb(III) in the HFA-TOPO-Triton X-100 system are shown in Fig. 1. The bands for europium at 610, 589 and 698 nm were assigned to the transitions from the 3D_0 level to the 7F_2 , 7F_1 and 7F_4 levels, respectively, those for samarium at 644, 602, 703 and 571 nm to transitions from the $^4F_{3/2}$ level to the $^6H_{9/2}$, $^6H_{7/2}$, $^6H_{11/2}$ and $^6H_{5/2}$ levels, those for terbium at 484, 544, 580 and 631 nm to the transitions from the 5D level to the 7F_6 , 7F_5 , 7F_4 and 7F_3 levels, and those for dysprosium at 477, 576, and 643 nm to the transitions from the $^4F_{3/2}$ level to the $^6H_{15/2}$, $^6H_{13/2}$ and $^6H_{11/2}$ levels respectively. The strongest emission bands of Dy(III), Eu(III), Sm(III) and Tb(III) were located at 576, 614,

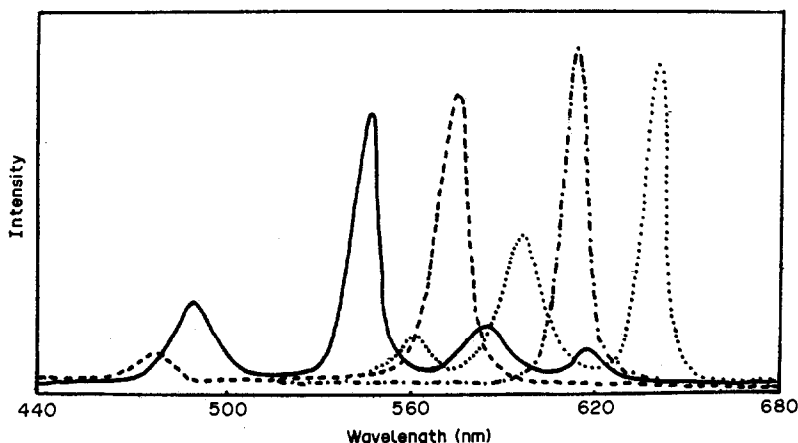


Fig. 1. Emission spectra of $1 \times 10^{-8}M$ Dy(III) (---), $1 \times 10^{-10}M$ Eu(III) (-·-·-), $5 \times 10^{-9}M$ Sm(III) (···), and $5 \times 10^{-10}M$ Tb(III) (—).

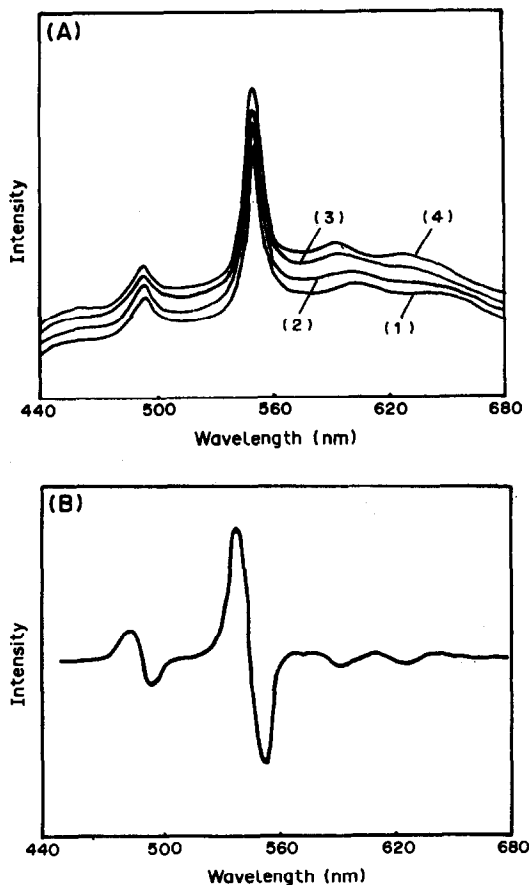


Fig. 2. Spectra of $5 \times 10^{-10} M$ Tb(III) obtained at different times (A), and their first derivatives (B). (1) 0.5 hr; (2) 1.0 hr; (3) 1.5 hr; (4) 2.0 hr.

644 and 544 nm respectively, and it was therefore preferable to use detection at these wavelengths. However, it was difficult to achieve selectivity, because of overlapping. Also, as the dark current of the vidicon is affected by the ambient temperature and hence the time elapsed since the start of measurement, some means of enhancing resolution and removing the background must be used.

Derivative spectra

The major benefits of derivative techniques are expected to lie in the increased resolution of overlapping spectra and correction of background. The spectra of the terbium ion obtained at different times (Fig. 2A) show that there is a significant degree of variability. These spectra show several relatively sharp features, so the background may be removed by the derivative technique. The signal-to-noise ratios of the first-, second- and third-derivative spectra were examined, and it was found that the first-derivative spectrum yields the best results (Fig. 2B), removing most of the variability between the spectra. Figure 3 shows the first derivatives of the emission spectra of dysprosium, europium, samarium and terbium. Although their mutual interference can be reduced to a certain extent, some spectral overlap remains, so the Kalman filter technique

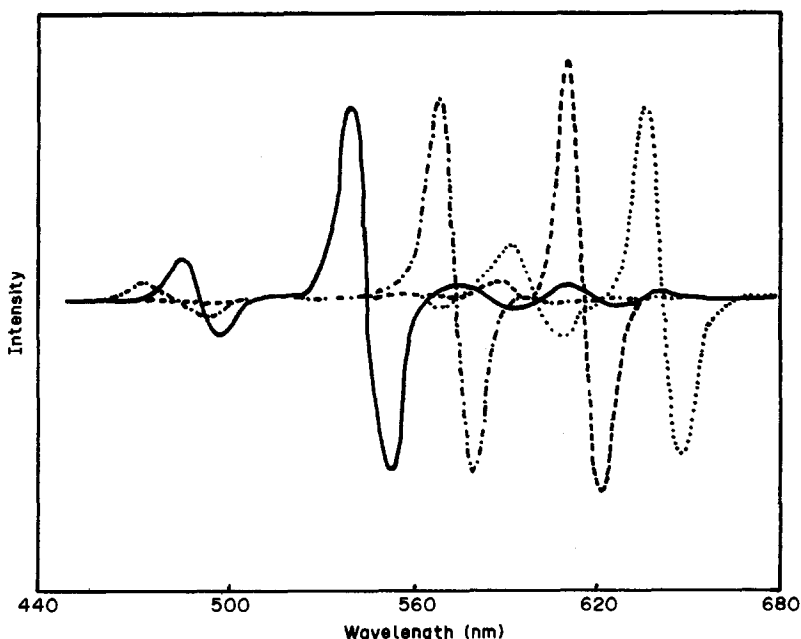


Fig. 3. First-derivatives calculated from the spectra in Fig. 1.

Table 1. Analysis of synthetic samples

Ion	Taken, ng/ml				Found, ng/ml				Relative standard deviation, %			
	No. 1	No. 2	No. 3	No. 4	No. 1	No. 2	No. 3	No. 4	No. 1	No. 2	No. 3	No. 4
Dy(III)	7.0	4.0	5.0	4.5	6.8	4.1	5.1	4.7	0.8	1.1	1.0	0.9
Eu(III)	0.01	0.02	0.04	0.06	0.0104	0.019	0.041	0.061	0.3	0.2	0.1	0.09
Sm(III)	4.0	3.0	2.0	1.0	3.97	2.95	1.92	0.94	0.5	0.8	0.7	1.0
Tb(III)	0.05	0.05	0.10	0.15	0.052	0.051	0.103	0.152	0.3	0.25	0.1	0.1

was used for the simultaneous determination of these four lanthanides.

Quantitative assessment

To assess the performance of the method in the absence of other spectral interferences, mixtures of the four ions were analysed; the results are listed in Table 1. The standard deviations were obtained from the diagonal elements of the covariance matrix. The results show that the combination of derivative spectrometry with the Kalman filter can be used to determine the four ions simultaneously, with higher accuracy and selectivity.

Optimization of experimental conditions

Optimization of the pH and concentrations of HFA, TOPO and Triton X-100 revealed that a correlation might exist among them. However, because of the fairly wide usable ranges of these parameters, each was optimized in turn with the values of the others held constant.

The influence of pH was investigated over the range 2–12, with $1 \times 10^{-4}M$ HFA and $2 \times 10^{-4}M$ TOPO, and maximum fluorescence intensity was obtained for all four complexes at pH 2.5–3.2. An acetic acid–ammonium acetate buffer (pH 3) was selected, and the fluorescence intensities were found to be independent of the buffer concentration. There was adequate buffer capacity at this pH, since nearly neutral metal ion solutions were used.

It was found that TOPO greatly enhanced the fluorescence of the lanthanide–HFA binary mixture, by formation of a ternary complex. The influence of the TOPO concentration on the fluorescence intensities was investigated with $1 \times 10^{-4}M$ HFA, and it was found that the fluorescence intensity increased with increasing TOPO concentration up to $5 \times 10^{-5}M$. Higher concentrations of TOPO had no further effect. The optimal concentration of HFA was taken as in the range 5×10^{-5} – $2 \times 10^{-4}M$.

Effect of foreign ions

The effects of 33 cations and 8 anions on determination of the four lanthanides were

examined, and Table 2 gives the molar tolerance ratios (for a relative error not exceeding $\pm 5\%$).

Calibration graphs and detection limits

Standard solutions containing various concentrations of dysprosium, europium, samarium and terbium were analysed by the proposed method. The relationships between the first-derivative signals and concentrations were linear over the ranges 8×10^{-9} – $5 \times 10^{-6}M$ Dy, 2×10^{-11} – $2 \times 10^{-8}M$ Eu, 5×10^{-10} – $5 \times 10^{-7}M$ Sm and 5×10^{-11} – $5 \times 10^{-8}M$ Tb respectively. The detection limits for dysprosium, europium, samarium and terbium were found to be 5×10^{-10} , 1×10^{-12} , 2×10^{-11} and $2 \times 10^{-12}M$ respectively.

Analysis of simulated mixed lanthanides and yttrium oxide

The technique was applied to the analysis of synthetic samples corresponding to "Nonglan" minerals (relative lanthanide oxide concentrations La₂O₃ 3%, CeO₂ 1%, Pr₂O₃ 1%, Nd₂O₃ 2%, Sm₂O₃ 2%, Eu₂O₃ 0.01%, Gd₂O₃ 7%, Tb₂O₃ 1%, Dy₂O₃ 8%, Ho₂O₃ 2%, Er₂O₃ 6%,

Table 2. Molar tolerance ratios of foreign ion to lanthanide (relative error $\leq 5\%$)

Foreign ion	Dy(III)	Eu(III)	Sm(III)	Tb(III)
La(III)	50	2000	100	2000
Ce(IV)	50	2000	100	2000
Pr(III)	100	2000	100	2000
Nd(III)	50	2000	80	1000
Sm(III)	10	200	—	200
Eu(III)	1.5	—	5	100
Gd(III)	50	2000	50	200
Tb(III)	2.0	100	20	—
Dy(III)	—	1000	100	200
Ho(III)	50	2000	50	1000
Er(III)	50	2000	50	1000
Tm(III)	50	2000	50	1000
Yb(III)	50	2000	50	1000
Lu(III)	50	2000	50	1000
Y(III)	100	1500	200	2000
Sc(III)	30	1500	40	800
Ca(II)	40	1500	50	800
Sr(II)	20	1000	30	1000
Ba(II)	50	1000	50	500
U(VI)	30	1000	50	500
Th(IV)	5	1000	50	800

Table 3. Analysis of a simulated mineral

Element	Taken, ng/ml	Found, ng/ml	RSD, %
Sm	0.2	0.195	0.3
Eu	0.007	0.0069	0.5
Tb	0.1	0.097	0.1
Dy	0.8	0.75	0.9

Table 4. Analysis of yttrium oxide

Element	Found by proposed method, $\mu\text{g/g}$	RSD, %	Found by ICP-AES, $\mu\text{g/g}$
Sm	24.7	0.8	25
Eu	4.87	0.5	5.0
Tb	15.6	0.7	16
Dy	147	1.1	158

Tm₂O₃ 1%, Yb₂O₃ 5%, Lu₂O₃ 1%, Y₂O₃ 60%). The results are listed in Table 3. The results for determination of traces of dysprosium, europium, samarium and terbium in yttrium oxide are listed in Table 4.

CONCLUSIONS

The combined approach described here, based on first-derivative fluorimetry, for background correction, and the Kalman filter, for resolution enhancement, allows for the accurate simultaneous determination of dysprosium, europium, samarium and terbium in their mixtures, without prior separation.

REFERENCES

1. A. N. Sevchenko and V. V. Kuznetsova, *Redkozem. Elementy, Akad. Nauk. SSSR, Inst. Geokhim. i Analit. Khim.*, 1963, 358; *Chem. Abstr.*, 1964, **61**, 2474c.
2. G. Alberti and M. A. Massucci, *Anal. Chem.*, 1966, **38**, 214.
3. R. P. Fisher and J. D. Winefordner, *ibid.*, 1971, **43**, 454.
4. G. L. Green and T. C. O'Haver, *ibid.*, 1974, **46**, 2191.
5. T. C. O'Haver, *Anal. Proc.*, 1982, **19**, 22.
6. J. N. Miller, T. A. Ahmad and A. F. Fell, *ibid.*, 1982, **19**, 37.
7. H. N. J. Poulisse, *Anal. Chim. Acta*, 1979, **112**, 361.
8. S. C. Rutan and S. D. Brown, *Anal. Chem.*, 1983, **55**, 1707.
9. *Idem*, *Anal. Chim. Acta*, 1985, **167**, 23.
10. A. Savitzky and M. J. E. Golay, *Anal. Chem.*, 1964, **36**, 1627.

DETERMINATION OF LANTHANUM, CERIUM, PRASEODYMIUM AND NEODYMIUM IN ALLOY STEELS BY INDUCTIVELY COUPLED PLASMA ATOMIC-EMISSION SPECTROMETRY

ANDRZEJ M. GROSSMAN and JERZY CIBA

Institute of Analytical and General Chemistry, Silesian Technical University, 44-101 Gliwice, Poland

JERZY JURCZYK and WALDEMAR SPIEWOK

Institute of Ferrous Metallurgy, 44-101 Gliwice, Poland

(Received 30 May 1989. Revised 33 October 1989. Accepted 8 December 1989)

Summary—Inductively coupled plasma spectrometry has been applied to the determination of La, Ce, Pr and Nd in alloy steels. Spectral interference by other alloying elements as well as by the lanthanides themselves was studied. The influence of other lanthanides on the Pr and Nd lines could be dealt with by correction equations. It was found that within the range of concentrations corresponding to mild alloy steel, at least one of the lines selected for determining the lanthanides was free from interferences. The detection limits for La, Ce, Pr and Nd in steel were 5×10^{-5} , 1.5×10^{-4} , 1×10^{-4} and $2.4 \times 10^{-4}\%$ respectively. The procedure was tested on standard samples and by the standard-addition method.

Addition of small amounts of rare-earth elements to steel significantly modifies its properties.^{1,2} Colorimetric methods allow the determination of either the total lanthanide content³⁻⁶ or only the cerium.⁷⁻⁹ The individual rare-earth elements can be determined by XRF spectrometry but prior separation from the matrix is required¹⁰⁻¹². Inductively coupled plasma atomic-emission spectrometry (ICP-AES) has been used for the determination of Ce and Y in steels and Nimonic alloys, but Fe, Cr and Zr interfered with the Ce measurement at 418.66 nm.¹³ The technique has also been used for determination of a number of lanthanides in geological samples after precipitation or chromatographic separation.¹⁴⁻¹⁹ A wide range of prominent lines for use in ICP-AES determination of several elements, including La, Ce, Pr and Nd, has been given by Winge *et al.*²⁰ and Bouman has studied the mutual spectral interferences of rare earth elements at chosen lines.²¹ On the basis of the information above we decided to investigate the use of ICP-AES for the direct determination of La, Ce, Pr and Nd in steels.

EXPERIMENTAL

Reagents

Standard solutions of the lanthanides (1 mg/ml) were prepared by dissolving the

“Specpure” oxides (Johnson and Matthey) in concentrated nitric acid. Solutions of matrix components for studying interference effects were made from the metals or suitable salts. All reagents were of analytical grade.

Procedure

The sample of steel turnings (0.5 g) was heated with 10 ml of a 3:1 v/v mixture of concentrated hydrochloric and nitric acids in a covered beaker for 30 min. The solution was evaporated almost to dryness, 10 ml of concentrated perchloric acid were added, and the mixture was heated until white fumes were evolved. The solution was cooled, 15 ml of water were added and the mixture was heated again. The residue was collected on a medium fast filter paper, and washed with 25 ml of 0.1M perchloric acid in small portions, the filtrate and washings being collected in a 50-ml standard flask and diluted to the mark with water. The samples used in the standard-additions method were prepared by the same procedure, with suitable amounts of lanthanide solutions added. Standard samples for calibration curves were prepared by dissolving 0.5 g of “Armco” iron as above, with addition of standard lanthanide solutions to cover the range 0–40 $\mu\text{g/ml}$. Individual series of standards were made for each rare-earth element.

The solvent blank was a 10 g/l. solution of "Armco" iron prepared as above.

RESULTS AND CONCLUSIONS

The choice of line for analysis was based on spectral scans over a range of ± 0.5 nm either side of each of the lines recommended by Winge *et al.*²⁰ (18 lines for La, 13 for Ce, 10 for Pr and 19 for Nd), for solutions of the pure analytes and interferents. This was done to identify the lines which would suffer least from mutual spectral interferences as well as interference from iron (the main constituent of the matrix). On the basis of the results and literature data concerning the influence of other components of the steel matrix,^{22,23} two lines were selected for each lanthanide (Table 1). Calibration graphs were prepared by use of the standards made by addition of the individual elements to the "Armco" iron solution. High correlation coefficients (>0.99997) were obtained for regression analysis of the results, over the range 0–40 μ g/ml. The detection limits C_L were calculated as the concentration equivalent to three times the standard deviation of five measurements of the background signal. As the relative standard deviations of the background (RSDB) were less than 1%, detection limits ($C_{L1\%}$) were calculated for RSDB values assumed to be equal to 1% of the background signal, as recommended by Winge *et al.*,²⁰ for comparison of

Table 1. Apparatus and operating conditions

ICP-ARL 3520B sequential spectrometer				
Incident power		1.18 kW		
Reflected power		10 W		
Coolant argon		11 l./min		
Plasma argon		0.87 l./min		
Nebulizer argon		0.9 l./min		
Liquid uptake rate		2.2 ml/min		
Entrance slit		17 μ m		
Exit slit		20 μ m		
Integration time				
Scanning mode		1 sec		
Analysis mode		5 sec		
Analysis lines				High voltage (arbitrary units)
Line	Identification number	Wavelength, nm	Spectral order	
LaII	4	333.749	2	5
LaII	5	492.179	1	5
CeII	1	413.765	1	9
CeII	4	456.236	1	9
PrII	2	390.844	1	9
PrII	3	440.882	1	9
NdII	3	406.109	1	7
NdII	4	415.608	1	7

Table 2. Coefficients of analytical equations $I = A + BC$ in the concentration range $C = 0-40$ mg/l., and values of detection limits

Line	A	B	Correlation coefficient	C_L mg/l.	$C_{L1\%}$ mg/l.
La 4	18.5	47.2	0.999987	0.005	0.013
La 5	50.6	26.9	0.999976	0.018	0.057
Ce 1	188.3	54.7	0.999971	0.021	0.10
Ce 4	196.6	48.1	0.999971	0.015	0.12
Pr 2	83.4	35.6	0.999984	0.010	0.07
Pr 3	178.5	51.2	0.999981	0.023	0.11
Nd 3	104.3	32.7	0.999980	0.024	0.10
Nd 4	106.1	25.3	0.999989	0.036	0.09

these results with literature data based on this assumption. The values of C_L and $C_{L1\%}$ are gathered in Table 2.

The lines selected for La and Ce determination are free from spectral interference by other lanthanides whereas the lines chosen for Pr and Nd are not, and correction equations must be applied, as shown in Table 3. The coefficients needed are calculated from the concentration-dependence of the interferent signal measured at the wavelength used for determination of the analyte. The corrections were assumed to be additive, and their use resulted in good linearity of calibration graphs prepared from the results for mixtures of the analyte with other lanthanides, even for the 390.844 line for PrII, where the interferences are greatest (Fig. 1).

The influence of other alloying elements on chosen lines of the lanthanides was examined by means of spectral scans of solutions of the interferents (of known concentrations) as well as by measurements of the signals for these elements at the wavelengths used for the lanthanides. The concentrations of these solutions of the alloying elements are given in Table 4, and are those that would be obtained by applying the sample preparation procedure to an iron or steel containing the element at the level also stated in Table 4. These levels are generally the

Table 3. Correction equations for praseodymium and neodymium

Line	Equation
Pr 2	$C = C_m - 0.171C_{Ce} - 0.00121C_{Nd}$
Pr 3	$C = C_m - 0.0373C_{Ce}$
Nd 3	$C = C_m - 0.0217C_{Ce}$
Nd 4	$C = C_m - 0.00956C_{Ce} - 0.0115C_{Pr}$

C = true concentration (mg/l.).

C_m = concentration calculated from analytical curve (mg/l.).

C_{Ce} = concentration of interfering element (mg/l.).

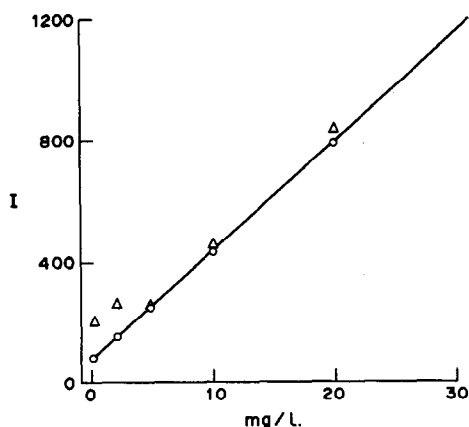


Fig. 1. The effects of correction of Pr signal at 390.844 nm: — calibration curve for pure standard solutions of Pr; Δ measured values for samples with different amounts of other lanthanides; \circ corrected values.

highest used in alloy steels. We assumed that the interference of additives could be considered as negligible (within the range of concentrations examined) if the difference between the signals for the interferent solution and water was lower than that for $C_{L1\%}$. In other cases the critical concentration ratio²⁴ (CCR) was calculated according to

$$CCR = \frac{X_a/C_a}{X_i/C_i}$$

where X_a and X_i are the net signals for the lanthanide and interferent respectively, C_a is the concentration of lanthanide and C_i the concentration of interferent quoted in Table 4. The results are given in Table 4 and show that the greatest interference is caused by V, Zr and Ti, but within the range of concentrations corresponding to low alloy steel and in many cases to

high-alloy steel, at least one line of each lanthanide is free from interference. It is advisable to prepare the lanthanide standards in a solution made from "Armco" iron as the differences caused by the changes in iron content in steel samples with different levels of alloying agents can then be neglected. The data in Table 4 are based on measurements taken with only the highest interferent concentration tested, and corrections for lower concentrations can be calculated by simple proportion from that information, but it must be taken into consideration that any background shift may form part of the measured signal. The method was tested on standard samples with certified cerium contents. Because of lack of certified samples containing all four lanthanides examined, the standard-additions method was applied. Standard samples used in the Polish metallurgical industry were used as the matrix; their composition is given in Table 5. The method used for decomposing the samples resulted in the amount of elements such as W and Nb in solution being considerably lower than that expected from the certified value, the bulk being separated with the silica.

The results obtained are presented in Table 6. Those for Ce are in good agreement with the certified value. The ratios of La, Pr and Nd to Ce found for the standard samples correspond to their ratios in the mischmetall used in production of the standards. Good results were also obtained by the standard-additions method.

On the basis of these results ICP spectrometry may be recommended for rapid precise determination of La, Ce, Pr and Nd in alloy steels.

Table 4. The critical concentration ratios (CCR) for individual interferents and lanthanides

Lanthanide and line, nm	Fe	Cr	Ni	Mn	Co	W	V	Zr	Nb	Ti	Mo	Cu	Al
La 333.749	133,000	54,800	92,000	21,200	19,000	20,300	11,100	2800	—	3900	—	—	—
La 492.179	88,600	7300	—	—	—	—	2600	3780	—	350	—	—	—
Ce 413.765	17,400	11,800	—	28,900	2940	160	2600	1000	530	7300	—	—	—
Ce 456.236	—	20,200	—	—	6600	—	1500	460	3410	1300	—	—	—
Pr 390.844	23,300	13,100	31,100	21,000	1820	—	410	1540	6100	11,200	1000	—	—
Pr 440.882	48,900	26,100	—	—	—	—	97	1660	—	3800	—	—	—
Nd 406.109	11,100	41,400	—	21,200	—	—	1100	1350	1420	—	—	—	—
Nd 415.608	15,100	31,200	—	53,500	1310	—	510	3	5600	3600	—	—	—
Concentrations of the interferents													
Solution, g/l.	10.0	5.2	5.9	5.5	1.0	0.5	1.1	1.0	0.5	1.0	0.2	1.0	1.0
Level in steel, %	100	52	59	55	10	5	11	10	5	10	2	10	10

—Signifies the difference in signal is less than $C_{L1\%}$.

Table 5. IMZ standard samples of steel

Sample	Concentration of alloying agent, %													
	C	Mn	Si	P	S	Cr	Ni	Cu	Mo	V	W	Ti	Zr	Ce
1.7/4*	0.017	0.13	(0.005)	0.013	0.032	0.004	0.012	0.016	0.0017	<0.001	—	<0.001	<0.001	—
1.19/1	0.20	1.00	0.30	0.020	0.017	1.10	0.096	0.11	—	—	—	0.084	—	—
1.25/1	1.48	0.26	0.28	0.018	0.025	0.48	—	—	—	0.29	4.97	—	—	—
1.26/1	0.31	0.48	0.29	0.021	0.009	1.87	4.05	0.14	0.11	—	1.70	—	—	—
1.34/1	0.11	0.84	0.31	0.014	(0.030)	0.73	0.65	(0.05)	0.39	(0.005)	—	—	—	—
1.82	0.10	1.11	0.27	0.017	0.020	0.21	0.085	0.069	0.060	0.101	—	—	(0.0015)	0.02

*“Armco” iron.

Table 6. Determination of lanthanides (%) in standard samples $\pm 95\%$ confidence interval ($n = 3$); quantities in parentheses are amounts added (except for Ce in 1.82, which is the certified value)

Line, nm	Sample				
	1.19/1	1.25/1	1.26/1	1.34/1	1.82
La 333.749	0.198 \pm 0.002	0.049 \pm 0.002	0.000 \pm 0.001	0.098 \pm 0.002	0.012 \pm 0.001
La 492.179	0.197 \pm 0.003 (0.200)	0.049 \pm 0.002 (0.050)	0.000 \pm 0.001 (0.000)	0.098 \pm 0.002 (0.100)	—
La 413.765	0.001 \pm 0.002	0.102 \pm 0.003	0.051 \pm 0.002	0.196 \pm 0.004	0.020 \pm 0.001
Ce 456.236	0.001 \pm 0.002 (0.000)	0.098 \pm 0.003 (0.100)	0.050 \pm 0.002 (0.050)	0.195 \pm 0.003 (0.200)	0.020 \pm 0.001 (0.020 \pm 0.002)
Pr 390.844	0.050 \pm 0.002	0.196 \pm 0.003	0.099 \pm 0.002	0.000 \pm 0.001	0.0002 \pm 0.001*
Pr 440.882	0.049 \pm 0.002 (0.050)	0.199 \pm 0.003 (0.200)	0.099 \pm 0.002 (0.100)	0.001 \pm 0.001 (0.000)	0.003 \pm 0.001*
Nd 406.109	0.098 \pm 0.002	—0.001 \pm 0.001	0.198 \pm 0.003	0.048 \pm 0.002	0.007 \pm 0.002
Nd 415.608	0.098 \pm 0.002 (0.100)	0.000 \pm 0.001 (0.000)	0.198 \pm 0.003 (0.200)	0.048 \pm 0.002 (0.050)	0.006 \pm 0.002 —

*With correction for vanadium.

REFERENCES

- M. Kepka, *Hutn. Listy*, 1977, **32**, 171.
- P. F. Wandby, *Intern. Metals Rev.*, 1978, **23**, 74.
- P. K. Spitsyn and I. G. Surin, *Zh. Analit. Khim.*, 1975, **30**, 284.
- T. I. Romantseva and L. K. Kharitonova, *Zavodsk. Lab.*, 1979, **45**, 495.
- I. G. Surin and P. K. Spitsyn, *ibid.*, 1980, **46**, 886.
- Z. Zhou and Y. Chen, *Fenxi Huaxue*, 1985, **13**, 289.
- L. I. Kharlamova, T. A. Borcheva and W. T. Solomatin, *Zavodsk. Lab.*, 1974, **40**, 1169.
- T. Capalla, J. Jurczyk and K. Szeja, *Pr. Inst. Metal. Zelaza*, 1979, **29**, 59.
- J. Pietrosz and J. Czyz, *Hutn. Listy*, 1978, **33**, 587.
- A. T. Kashuba and C. R. Hines, *Anal. Chem.*, 1971, **43**, 1758.
- J. Jurczyk, I. Sheybal and W. Smolec, *Pr. Inst. Metal. Zelaza*, 1981, **33**, 93.
- T. Sofilić, *Metallurgija (Sisak)*, 1985, **24**, 131.
- V. Rett and I. Hlavaček, *Hutn. Listy*, 1979, **34**, 428.
- J. A. C. Broekaert, F. Leis and K. Laqua, *Spectrochim. Acta*, 1979, **34B**, 73.
- A. Bolton, J. Hwang, A. Vander Voet, *ibid.*, 1983, **38B**, 165.
- I. B. Brenner, E. A. Jones, A. E. Watson and T. W. Steele, *Chem. Geol.*, 1984, **45**, 135.
- R. Aulis, A. Bolton, W. Doherty, A. Vander Voet and P. Wong, *Spectrochim. Acta*, 1985, **40B**, 377.
- S. J. Buchanan and L. S. Dale, *ibid.*, 1986, **41B**, 237.
- H. Iwasaki and H. Haraguchi, *Anal. Chim. Acta*, 1988, **208**, 163.
- R. K. Winge, V. J. Peterson and V. A. Fassel, *Appl. Spectrosc.*, 1979, **33**, 206.
- P. W. J. M. Boumans, J. A. Tielrooy and F. J. M. J. Maessen, *Spectrochim. Acta*, 1988, **43B**, 173.
- A. N. Zaidel, V. K. Prokofev, S. M. Raiskii, V. A. Slavnyi and E. Y. Shreider, *Tables of Spectral Lines*, Plenum Press, New York, 1970.
- H. L. Parson, A. Forster and D. Anderson, *An Atlas of Spectral Interference in ICP Spectroscopy*, Plenum Press, New York, 1980.
- P. W. J. M. Boumans, *Spectrochim. Acta*, 1980, **35B**, 57.

DETERMINATION OF STRONTIUM IN HUMAN SERUM BY INDUCTIVELY COUPLED PLASMA MASS SPECTROMETRY AND NEUTRON ACTIVATION ANALYSIS: A COMPARISON

C. VANDECASTEELE*, H. VANHOE and R. DAMS

Laboratory for Analytical Chemistry, University of Ghent, Institute for Nuclear Sciences,
Proeftuinstraat 86, B-9000 Ghent, Belgium

L. VANBALLENBERGHE, A. WITTOEK and J. VERSIECK

Department of Internal Medicine, Division of Gastroenterology, University Hospital, De Pintelaan 185,
B-9000 Ghent, Belgium

(Received 19 October 1989. Revised 23 January 1990. Accepted 10 February 1990)

Summary—Strontium has been determined in a human serum reference material by ICP-MS and by NAA. By ICP-MS, results for ^{88}Sr and ^{86}Sr in both 10- and 5-fold diluted serum were in good agreement. For ^{88}Sr the precision was better than 3% and the detection limit was 0.05 $\mu\text{g/l}$. under the conditions used. The results were 25.5 $\mu\text{g/l}$. in the liquid serum or 0.281 $\mu\text{g/g}$ in the lyophilized reference material. In the NAA the $^{87\text{m}}\text{Sr}$ produced was radiochemically separated by extraction with oxine in chloroform. The precision was about 10% and the detection limit 0.02–0.05 $\mu\text{g/g}$.

In the course of a systematic study on the determination of trace elements in human serum by inductively coupled plasma-mass spectrometry (ICP-MS)¹ we noticed that strontium can be readily determined with this analytical technique. Knowledge of the strontium concentration in normal human serum is rather limited²⁻⁹ and it is not clear whether it is an essential element or not. Recently, some interest has arisen in the determination of strontium in human serum for forensic purposes.¹⁰ For these reasons, we have developed a method for the determination of strontium in serum by neutron activation analysis (NAA), and now report a comparison of these two entirely independent analytical methods for strontium determination. Most of the analytical results were obtained on the "second-generation" biological reference material (human serum) prepared by Versieck *et al.*¹¹ in this laboratory. The reference material is available in the freeze-dried form to the scientific community.

For ICP-MS, we used material kept in deep frozen form and sample preparation was limited as much as possible in order to avoid contamination or losses of strontium. Sample pretreatment consisted merely of a dilution with 0.14M

nitric acid and addition of indium as an internal standard. Dilution is necessary to avoid blocking the central silica tube of the plasma torch and the pneumatic nebulizer and to reduce the extent of signal suppression by the matrix. In a previous communication we showed that using an indium internal standard corrects for suppression of the analyte signal by easily ionized elements.¹² In addition, it significantly improves the precision of the measurements, as the mass of ^{115}In is close to that of the Sr-isotopes.¹³

For NAA, sample preparation was also kept to a minimum and use was made of the $^{86}\text{Sr}(n, \gamma)^{87\text{m}}\text{Sr}$ reaction. $^{87\text{m}}\text{Sr}$ has a half-life of 2.81 hr and emits 388.4-keV γ -rays in 83.0% of its disintegrations. Separation of $^{87\text{m}}\text{Sr}$ from matrix activities such as ^{24}Na , ^{32}P , ^{38}Cl , ^{82}Br , was achieved by extraction with oxine in chloroform. The determination of strontium was combined with the determination of manganese, copper, and zinc, which has been described earlier.¹⁴

EXPERIMENTAL

ICP-MS

Selection of nuclides. Strontium has four isotopes (abundances in parentheses): ^{84}Sr (0.56%), ^{86}Sr (9.9%), ^{87}Sr (7.0%) and ^{88}Sr (82.6%). Determinations of ^{84}Sr and ^{86}Sr are interfered with by

*Author for correspondence.

^{84}Kr (57%) and ^{86}Kr (17.3%), respectively, from krypton present as impurity in the argon used. Of course this interference can be corrected for by blank subtraction. ^{87}Sr is interfered with by ^{87}Rb (27.8%) which is present at $168\ \mu\text{g/l.}$ in the serum,¹¹ whereas ^{88}Sr is free from isobaric interferences. The obvious choice was thus to use ^{88}Sr , but ^{86}Sr was also used in order to check the absence of interferences. No interferences from polyatomic ions have been reported. Figure 1 gives a spectrum of a serum sample for m/z between 80 and 90.

Instrumentation. A commercially available ICP-MS instrument, the VG PlasmaQuad (VG Elemental, Winsford, U.K.), was used in its standard configuration, with a Meinhard nebulizer and a spray chamber made of borosilicate glass. Details of the operating conditions are given in Table 1. Although strontium was determined by a single-element procedure, it can easily be determined in practice together with several other trace elements.¹

Standards and samples. All solutions were prepared with 0.14M nitric acid obtained by hundredfold dilution, with Millipore MilliQ water, of concentrated nitric acid, purified by sub-boiling distillation.

Two different 100- $\mu\text{g/l.}$ strontium standard solutions were used. The first was prepared by successive dilutions from a 1-g/l. strontium solution prepared by dissolution of solid strontium

nitrate (Merck, Darmstadt, Germany, *p.a.*), the second from a commercial 1-g/l. strontium solution (Fluka A.G., Buchs, Switzerland).

The stoichiometry of the strontium nitrate was checked by heating at different temperatures. Heating at 70 and at 110° yielded no significant difference in weight ($+0.25 \pm 0.43\%$ and $+0.14 \pm 0.35\%$), indicating that no hydration had occurred, since $\text{Sr}(\text{NO}_3)_2 \cdot 4\text{H}_2\text{O}$ loses water at 100°. In addition, the two standards were compared: the ratio of the average count-rate (3 measurements) of ^{88}Sr to that of ^{115}In (100 $\mu\text{g/l.}$ added as internal standard) was 0.828 with a standard deviation of 0.004 for the first standard, and 0.821 with a standard deviation of 0.005 for the second, indicating that there was no significant difference in strontium concentration.

Liquid serum, obtained by defrosting 2.5-ml subsamples of the reference material prepared by Versieck *et al.*¹¹ and stored without prior lyophilization in a polyethylene container in a deep-freezer, was diluted 10-fold or 5-fold. To 2.5 or 5 ml of liquid serum, 2.5 ml of a 1-mg/l. indium solution were added and the solution was diluted accurately with 0.14M nitric acid to obtain 25 ml of a solution with an indium concentration of 100 $\mu\text{g/l.}$ Precleaned polyethylene pipettes and standard flasks were used to prepare the diluted serum samples and all manipulations were done on a clean-bench to

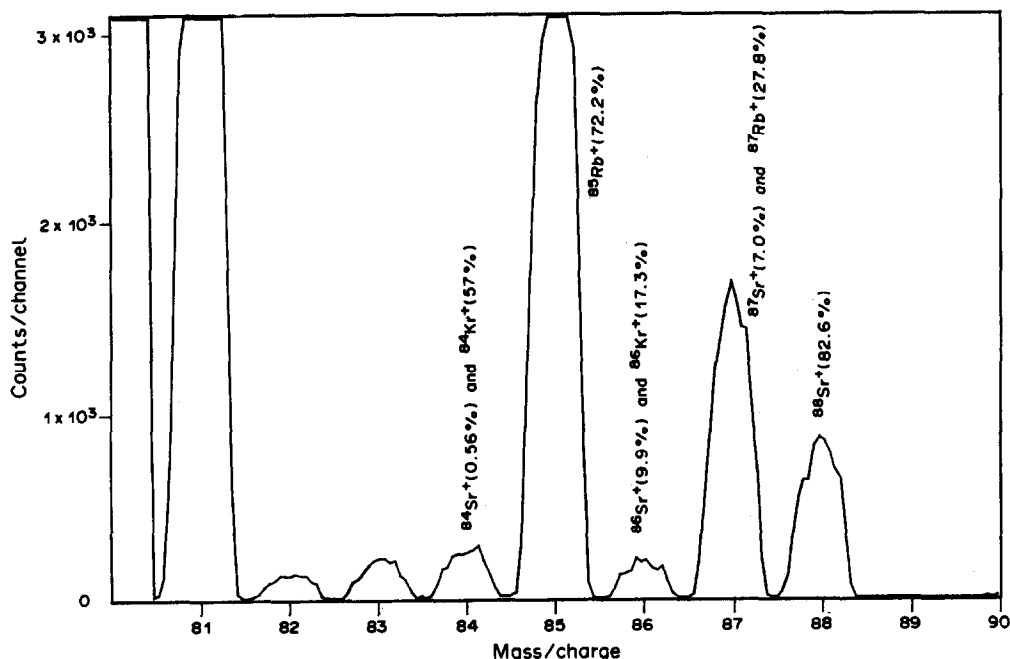


Fig. 1. Mass spectrum of a 5-fold diluted serum sample for m/z between 80 and 90.

avoid contamination. A blank solution was prepared simultaneously.

Measurements. Quantitative analyses were performed by using the scanning mode of data acquisition, with scanning conditions as summarized in Table 1. The following solutions were measured successively: a blank for the samples; two 10-fold diluted serum samples; two 5-fold diluted serum samples; a blank for the standard; a standard.

Each of these solutions was measured three times and between the different solutions the sample introduction system was rinsed with 0.14M nitric acid for 2 min. Such a series of measurements was made in the morning and repeated on the same samples in the afternoon. A similar series of measurements with different samples was made a few months later.

NAA

^{87m}Sr ($t_{1/2} = 2.81$ hr; $E_\gamma = 388.4$ keV) was measured as the analytical indicator for strontium.

Irradiation. A 150–200 mg portion of lyophilized serum (in this case the reference material was used in the form in which it is available to other researchers), packed in polyethylene containers, was irradiated for 3–4 hr in the Thetis reactor of Ghent University at a neutron flux of 1.48×10^{12} cm $^{-2}$ sec $^{-1}$.

Radiochemical separation. The irradiated sample was placed in a 100-ml glass beaker and

Table 2. Recovery of added ^{87m}Sr : all results are expressed in % of total and correspond to mean and standard deviation of 16 measurements

	Recovery, %
Organic extract, obtained at pH 2.1 and 8.5, combined	0.028 \pm 0.078
Organic extract obtained at pH 12.5	98.6 \pm 0.2
Remaining aqueous phase	0.46 \pm 0.23
Wash liquid	0.89 \pm 0.29

weighed. After addition of manganese, copper and zinc carrier solutions,¹⁴ 1 ml of strontium nitrate solution (10 $\mu\text{g/ml}$ Sr) and 5 ml of a 1:1 v/v mixture of concentrated nitric and perchloric acids were added. The solution was heated on a hot-plate fitted with a magnetic stirrer, until nearly dry. The residue was quantitatively transferred to a separatory funnel with 10 ml of 1M perchloric acid. Ten ml of saturated hydrazine sulphate solution were added to reduce manganese. After 2 min, 10 ml of a 0.05M potassium hydrogen phthalate buffer were added. After pH adjustment and successive extraction of copper at pH 2.1 and of manganese and zinc at pH 8.5, the pH was increased to 12.5 by addition of 4M sodium hydroxide. Strontium was then extracted (stirring time 5 min) with two successive 40-ml portions of 1M oxine in chloroform. The organic phase was washed with 0.03M sodium hydroxide and collected in a 150-ml Erlenmeyer flask.

The chemical separation was tested with tracer amounts of ^{87m}Sr . The recoveries are given in Table 2. The overall chemical yield of the strontium was 98.6% with a standard deviation of 0.2%. The excellent reproducibility indicates that recoveries are likely to be the same for the samples and the strontium nitrate standards (see below).

Measurements and standardization. The samples (chloroform phase) were counted for 30 min with an HPGe semiconductor detector (25% relative detection efficiency) 3–5 hr after the irradiation. The ratio of thermal to epithermal neutron fluxes being stable during irradiation, standardization was done by a single-comparator method. For that purpose, the 511-keV activity from ^{64}Cu ($t_{1/2} = 768$ min) induced in a 4-mg copper wire, irradiated as flux monitor together with the sample, was measured 1 day after irradiation. Beforehand, a "k-factor", corresponding to the ratio of the 388.4-keV activity (cpm) of ^{87m}Sr , corrected for decay and saturation and normalized to 1 μg of Sr, to the 511-keV activity of ^{64}Cu ,

Table 1. PlasmaQuad operating conditions

Plasma	
r.f. power:	forward 1.35 kW
	reflected <10 W
gas flows:	plasma 13 l./min
	auxiliary 1 l./min
	nebulizer 0.72 l./min
peristaltic pump:	Gilson Minipuls 2 pumped at 0.9 ml/min
nebulizer:	Meinhard concentric glass nebulizer (type Tr-30-A3)
spray chamber:	double-pass Scott type, water cooled (10°)
Ion sampling	
sampling cone:	nickel, 1.0 mm orifice
skimmer cone:	nickel, 0.75 mm orifice
sampling depth:	10 mm (from load coil)
Vacuum	
expansion stage:	2.3 mbar
intermediate stage:	0.1 μbar
analyser stage:	4.0 nbar
Data acquisition	
quantitative scanning	
sweeps:	120
dwell time:	250 μsec
channels:	2048
mass region:	m/z 80–120
acquisition time:	61 sec

Table 3. Results ($\mu\text{g/l.}$ in liquid serum) obtained by ICP-MS for strontium in the human serum reference material* (mean \pm standard deviation of 6 measurements)

^{88}Sr		^{86}Sr	
10-fold diluted	5-fold diluted	10-fold diluted	5-fold diluted
25.3 ± 0.5	24.8 ± 0.9	25.1 ± 2.7	25.1 ± 1.7
24.9 ± 0.8	25.5 ± 0.8	24.7 ± 2.5	25.2 ± 2.1
26.4 ± 0.5	25.5 ± 0.7	26.8 ± 1.9	25.1 ± 1.3
25.8 ± 0.8	26.1 ± 0.5	25.7 ± 2.0	25.3 ± 1.4
<i>Mean (95% confidence limits)</i>			
25.6 ± 0.4	25.5 ± 0.4	25.6 ± 1.0	25.2 ± 0.6
($n = 24$)	($n = 24$)	($n = 24$)	($n = 24$)
<i>Grand mean (95% confidence limits)</i>			
25.5 ± 0.2	($n = 48$)	25.4 ± 0.6	($n = 48$)

*Values can be recalculated into $\mu\text{g/g}$ dry weight (the form in which the material is available to the scientific community) by multiplying them by 0.011.¹¹

similarly treated, was determined. In the experiments, the irradiated strontium nitrate was radiochemically separated as described above.

RESULTS AND DISCUSSION

ICP-MS

Table 3 gives the results obtained by using ^{88}Sr and ^{86}Sr . Four samples were each analysed 6 times. The precision was, on the average, 2.6 and 2.7% for the analyses based on ^{88}Sr , for 10- and 5-fold diluted serum respectively, and 8.9 and 6.5% for the analyses based on ^{86}Sr , for 10- and 5-fold diluted serum respectively. The mean value obtained for 48 analysed on 8 samples by using ^{88}Sr corresponded to $0.281 \mu\text{g/g}$ with a standard deviation of $0.009 \mu\text{g/g}$ in the freeze-dried reference material; with use of ^{86}Sr it corresponded to $0.279 \mu\text{g/g}$ with a standard deviation of $0.021 \mu\text{g/g}$.

The excellent agreement between the results obtained by using two different isotopes indicates that, as expected, no significant isobaric interferences occur that are not corrected for by blank subtraction. In addition, the agreement between the results obtained on 10- and 5-fold diluted serum indicates that matrix effects, for instance due to the presence of easily ionized elements such as sodium, calcium and potassium, are adequately corrected for by using indium as internal standard.¹²

Table 4. Comparison of calibration with a $100\text{-}\mu\text{g/l.}$ standard and standard addition for the determination of strontium in human serum by ICP-MS; all results are 95% confidence limits, expressed in $\mu\text{g/l.}$ for liquid serum

	Calibration	Standard addition
10-fold diluted	14.4 ± 0.8	13.9 ± 0.4 13.8 ± 0.8
5-fold diluted	13.9 ± 0.6	13.4 ± 0.7 13.4 ± 0.3

A further indication of the adequate correction for matrix effects, achieved by using an indium internal standard, was obtained by applying the method of standard additions. Table 4 lists the results obtained for a normal human serum sample by applying a single standard addition to 10- and 5-fold diluted serum. The results are in good agreement with those obtained by applying the calibration method as described.

As an additional check of the accuracy of the technique, the certified reference material Bovine Liver, NBS 1577a, was analysed for strontium. A value of $0.147 \mu\text{g/g}$ with a standard deviation of $0.005 \mu\text{g/g}$ was obtained, which is in agreement with the certified value ($0.138 \pm 0.003 \mu\text{g/g}$).

The detection limit for 5-fold diluted serum corresponds to *ca.* $0.05 \mu\text{g/l.}$

NAA

For 10 analyses a mean value of $0.244 \mu\text{g/g}$ with a standard deviation of $0.023 \mu\text{g/g}$ was obtained. The relative standard deviation (9.4%) was in good agreement with the value expected from the counting statistics. Indeed, the net area of the $^{87\text{m}}\text{Sr}$ peak was only 200–400 counts and the background area 130–260 counts, corresponding to an average standard deviation of about 10%. The detection limit thus ranges from 0.02 to $0.05 \mu\text{g/g}$. This could obviously be improved using a longer measuring time.

CONCLUSIONS

By ICP-MS, applying ^{88}Sr , a grand mean of $25.54 \mu\text{g/l.}$ with a standard deviation of $0.83 \mu\text{g/l.}$ was found, corresponding to 95% confidence limits of (25.54 ± 0.24) $\mu\text{g/l.}$ This is

equivalent to (0.2809 ± 0.0026) $\mu\text{g/g}$ in the lyophilized material. RNAA yielded 0.244 $\mu\text{g/g}$ with a standard deviation of 0.023 $\mu\text{g/g}$, corresponding to 95% confidence limits of (0.244 ± 0.019) $\mu\text{g/g}$. The ICP-MS results are significantly higher than our results obtained by NAA. However, in view of the rather high statistical uncertainty of the NAA results and the rather complicated chemical separation and standardization, the agreement seems acceptable.

Acknowledgements—Grateful acknowledgment is made to the National Fund for Scientific Research (Belgium) and to the Interuniversity Institute for Nuclear Sciences for financial support.

REFERENCES

1. H. Vanhoe, C. Vandecasteele, J. Versieck and R. Dams, *Anal. Chem.*, 1989, **61**, 1851.
2. D. A. Olchy, R. A. Schmitt and W. F. Bethard, *J. Nucl. Med.*, 1966, **7**, 917.
3. A. A. Alfrey, H. Rudolph and W. R. Smythe, *Kidney Int.*, 1975, **7**, suppl. 2, 85.
4. H. Matusiewicz, *Anal. Chim. Acta*, 1982, **136**, 215.
5. M. Wilhelm, B. Hanewinkel and F. Bläker, *Eur. J. Pediatr.*, 1986, **145**, 372.
6. F. M. Corrigan, J. D. Finlayson, G. Stevenson, G. W. Asferoft and N. I. Ward, *Trace Elements Med.*, 1987, **4**, 117.
7. H. Matusiewicz, *Anal. Chim. Acta*, 1988, **207**, 349.
8. Lin Xilei, D. Van Renterghem, R. Cornelis and L. Mees, *ibid.*, 1988, **211**, 231.
9. O. R. Leeuwenkamp, W. J. F. van der Vijgh, B. C. P. Hüsken, P. Lips and J. C. Netelenbos, *Clin. Chem.*, 1989, **35**, 1911.
10. M. Piette, Ghent University, Personal communication.
11. J. Versieck, L. Vanballenberghe, A. De Kesel, J. Hoste, B. Wallaeyts, J. Vandenhaute, N. Baeck, H. Steyaert, A. R. Byrne and F. W. Sunderman, *Anal. Chim. Acta*, 1988, **204**, 63.
12. C. Vandecasteele, M. Nagels, H. Vanhoe and R. Dams, *ibid.*, 1988, **211**, 91.
13. C. Vandecasteele, H. Vanhoe and F. Vanhaecke, Unpublished results.
14. J. Versieck, A., Speecke, J. Hoste and F. Barbier, *Z. Klin. Chem. Klin. Biochem.*, 1973, **11**, 193.

DEVELOPMENT OF A SLURRY ATOMIZATION METHOD FOR THE DETERMINATION OF CADMIUM IN FOOD SAMPLES BY ELECTROTHERMAL ATOMIZATION ATOMIC-ABSORPTION SPECTROMETRY

SEÁN LYNCH and DAVID LITTLEJOHN

Department of Pure and Applied Chemistry, University of Strathclyde, 295 Cathedral Street,
Glasgow G1 1XL, Scotland, U.K.

(Received 14 December 1988. Revised 20 February 1990. Accepted 27 February 1990)

Summary—Matrix modifiers have been compared for the determination of cadmium in foodstuffs by ETA-AAS with the sample injected in the form of a slurry. Addition of 800 $\mu\text{g/ml}$ Pd stabilized cadmium to a similar extent as did ammonium dihydrogen phosphate, but avoided the increase in background signal associated with the latter. An analytical procedure was developed, based on palladium matrix modification, platform atomization with a pre-atomization cooling step and integrated absorbance measurements. The method allowed the analysis of milk, liver and olive leaf slurries at concentrations up to at least 50 mg/ml by direct calibration with aqueous standards. The accuracy of the analytical results was within 15% and the detection limit for cadmium in analysis of a 50 mg/ml slurry was 10 ng/g.

Various attempts have been made to eliminate the time-consuming sample preparation procedures traditionally associated with the analysis of solid samples by electrothermal atomization atomic-absorption spectrometry (ETA-AAS). Two novel sample introduction methods have been studied. In the first, solid samples¹⁻¹⁰ are weighed on a microbalance and transferred to a furnace. Although, with care, samples may be introduced into a furnace accurately and precisely, the procedure is time-consuming and susceptible to environmental contamination, and calibration is difficult. The second approach used is the introduction of samples as a suspension or a slurry.¹¹⁻²⁸ Although the accuracy and precision of this type of sample-introduction depend on the stability and homogeneity of the slurry, the method has several advantages. Full automation can be achieved by using a stirring device compatible with commercially available autosamplers.²⁸ Chemical modifiers can be added to the slurry diluent, allowing intimate contact with the analyte. Samples may also be injected reproducibly onto the same location within the furnace tube.

Cadmium is a difficult element to determine accurately by use of solid sampling. This is mainly due to the low thermal stability of most cadmium salts, which prevents the thermal removal of interfering matrices prior to atomization, resulting in a loss of analytical sensitivity

and necessitating use of the standard-additions calibration method. Several chemicals which form cadmium compounds of greater thermal stability have been added as modifiers. The most popular is phosphate,^{18,29-34} often as one of its ammonium salts, to form cadmium pyrophosphate. Other modifiers used include ammonium fluoride,³⁵ forming cadmium fluoride, ammonium persulphate³⁶ or thiourea,³⁷ forming cadmium sulphide, selenium,³⁸ forming cadmium selenide, and palladium salts,³⁹ which presumably form an intermetallic species.

In this work ammonium dihydrogen phosphate and palladium nitrate were compared as modifiers for the determination of cadmium in food slurries. Addition of magnesium nitrate with these modifiers was also evaluated.^{40,41} Subsequently, an analytical procedure was developed which used platform atomization with Zeeman background correction. This enabled direct calibration with aqueous standards to be used for the analysis of a range of foodstuffs.

EXPERIMENTAL

Instrumentation

All atomic-absorption measurements were performed with a Perkin-Elmer Zeeman 5000 spectrometer equipped with an HGA 400 furnace programmer and an AS40 autosampler. The Zeeman background correction system

was used throughout this study. Measurements were performed at the 228.8 nm resonance line of cadmium with a spectrometer bandpass of 0.7 nm and use of a hollow-cathode lamp (Cathodeon Ltd., Cambridge, England) operated at 8 mA. Integrated absorbance measurements were made throughout.

Non-grooved pyrolytically coated graphite tubes were used with pyrolytically coated platforms, unless otherwise stated.

Slurry samples (20 μ l) were injected either manually after manual shaking or by using the AS40 autosampler together with the integral magnetic stirring device described previously.²⁸

The tube-wall temperatures over the programmed range of 800–2400° were checked with an Ircon 1100 optical pyrometer. The measured temperatures were within 100° of the programmed temperatures.

Samples

The food samples used in optimization studies (cadmium content not certified) were obtained as finely ground dry powders from the Ministry of Agriculture, Fisheries and Food, Food Analysis Laboratories, Norwich, U.K. The certified reference materials (CRMs) analysed to determine the accuracy of the proposed procedure were (i) Bovine Liver CRM 185, (ii) Milk Powder CRM 150, (iii) Milk Powder CRM 151 and (iv) Olive Leaves CRM 062 (Community Bureau of Reference, Brussels, Belgium).

Preparation of slurries

A 0.1–0.5 g portion of powdered food sample was accurately weighed, appropriate reagents were added to it and the mixture was diluted to 10 or 20 ml with distilled water. Chemical modifiers were added during this preparation, ensuring good mixing with the sample. Addition of 5 mg of antifoaming agent per ml of slurry prevented foaming. Concentrated ammonia solution was added to give a 5% v/v concentration (5 ml per 100 ml of slurry). The suspension was then shaken vigorously for 15 min to achieve thorough dispersion of the milk powder or animal tissue.

Reagents

AnalaR grade reagents (BDH Chemicals Ltd., Poole, England) were used throughout this study unless otherwise stated. Distilled water was used in the preparation of samples and solutions.

Concentrated nitric acid PRONALYSAR grade, (May and Baker Ltd., Dagenham, England).

Concentrated ammonia solution, ARISTAR grade (BDH).

Antifoam B emulsion (Sigma Chemical Company, St. Louis, U.S.A.).

Palladium(II) nitrate solution, 10% w/v (Johnson Matthey PLC, Royston, England).

Cadmium nitrate solution, 1000 mg/l., prepared in 1M nitric acid.

Procedures

Choice of modifier. The major criterion used in selecting a modifier was its ability to produce a more thermally stable cadmium compound from both slurry samples and standards. The thermal stability was determined by making six measurements of the time parameters of the signal, $\tau_{10\%}$ and τ_{peak} , defined as the time required for the atomic-absorption signals to reach 10% of the peak value and the peak absorbance, respectively. An increase in the $\tau_{10\%}$ value indicates an improvement in the thermal stabilization of cadmium, as during the initial stages of the atomization step the temperature of the tube increases with time.

Conditions for direct analysis. Recovery of added cadmium was used as an initial indicator of the accuracy of analysis, and was defined as:

$$\% \text{ Recovery} = \frac{a - b}{c - d} \times 100$$

where a , b , c and d are the mean values of at least three absorbance signals for a , 20 μ l of the slurry sample plus 20 μ l of 2 ng/ml Cd solution, b , 20 μ l of the slurry sample, c , 20 μ l of 2 ng/ml Cd solution, and d , 20 μ l of an appropriate reagent blank mixture. Care was taken to ensure that all atomic absorption measurements were within the linear dynamic range of the instrument response.

Analysis of samples. The certified reference materials (CRMs) were analysed as follows.

(1) Standard solutions containing 0, 1, 2, 3, 4 and 5 ng/ml Cd were atomized in duplicate. Linear least-squares regression analysis was applied to the average of the integrated absorbances.

(2) Samples and appropriate blanks were prepared in triplicate and three aliquots of each were atomized.

(3) The cadmium content of each sample and blank replicate was determined by interpolation from the calibration graph. Sample concentrations were corrected for the blank before calculation of the mean and the 95% confidence interval for the cadmium content in each sample.

RESULTS AND DISCUSSION

Comparison of modifiers

The optimum amount of palladium to be used was determined before different modifiers were compared.

Plots of $\tau_{10\%}$ for a 2 ng/ml Cd solution and a 10 mg/ml kale slurry charred at 500° and atomized at 1800° from the tube wall, are shown in Fig. 1. A palladium concentration of 800 $\mu\text{g/ml}$ in the sample gave an acceptable approach to maximization of the Cd signal and was used in all subsequent investigations. The effects of various modifiers are compared in Table 1 in terms of $\tau_{10\%}$ for samples charred at 700° and atomized from the tube wall at 1800°. The $\text{NH}_4\text{H}_2\text{PO}_4\text{-Mg}(\text{NO}_3)_2$ mixture gives the best performance for the cadmium nitrate solutions. The performances of $\text{NH}_4\text{H}_2\text{PO}_4$ or Pd alone were comparable, but inferior to that of the $\text{NH}_4\text{H}_2\text{PO}_4\text{-Mg}(\text{NO}_3)_2$ mixture.

The corresponding results for the food slurries are rather interesting. The thermal stabilization varies with the type of sample and the type of modifier. Palladium gave significantly better performance than the phosphate-magnesium nitrate mixture for all slurry samples, except the bovine liver, and comparable performance to $\text{NH}_4\text{H}_2\text{PO}_4$ or the Pd-Mg(NO_3)₂ mixture. A combination of 800 $\mu\text{g/ml}$ Pd, 10 mg/ml $\text{NH}_4\text{H}_2\text{PO}_4$ and 10 mg/ml

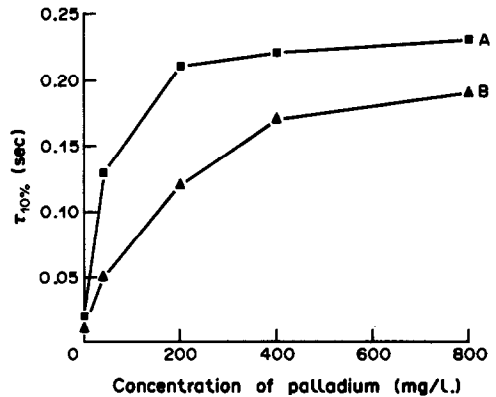


Fig. 1. Influence of palladium concentration on stability of cadmium in terms of the peak-time parameter $\tau_{10\%}$. A, 2 $\mu\text{g/l}$. aqueous solution of cadmium; B, 10 mg/ml kale slurry.

$\text{Mg}(\text{NO}_3)_2$ was examined in an attempt to combine the favourable performance of the $\text{NH}_4\text{H}_2\text{PO}_4\text{-Mg}(\text{NO}_3)_2$ mixture for cadmium nitrate solution with that of Pd for slurry samples, but significant improvement was found only for bovine liver, and the performance was poorer for the milk slurries. Similar trends were observed for the τ_{peak} values.

Char temperature curves for cadmium in aqueous solution and slurries prepared from samples of lettuce, kale, brussels sprouts and fish are shown in Fig. 2 for use of 800 $\mu\text{g/ml}$ Pd as the modifier. The results indicate that with Pd added, the thermal stability of cadmium in slurries is relatively insensitive to differences in the matrix composition. No significant reduction in the cadmium signal was observed for char temperatures up to at least 800° for each of the samples studied. A conservative charring temperature of 750° was chosen for all subsequent studies. Addition of palladium as modifier avoided the high background signal associated with the vaporization of phosphate

Table 1. $\tau_{10\%}$ values obtained for cadmium with different modifiers; samples charred at 700° with wall atomization at 1800° (95% confidence limits in parentheses)

Modifier	$\tau_{10\%}$ values, sec				
	2 ng/ml Cd (aqueous solution)	Slurries (10 mg/ml)			
		Kale	Milk	Fish	Bovine liver
No modifier	<0.01	N.S.	N.S.	N.S.	N.S.
10 mg/ml $\text{NH}_4\text{H}_2\text{PO}_4$	0.14(±0.02)	0.05(±0.02)	0.16(±0.01)	0.13(±0.02)	0.10(±0.02)
10 mg/ml $\text{NH}_4\text{H}_2\text{PO}_4\text{-}$ 10 mg/ml $\text{Mg}(\text{NO}_3)_2$	0.25(±0.04)	0.04(±0.02)	0.09(±0.03)	0.04(±0.03)	0.07(±0.02)
800 mg/l. Pd	0.15(±0.01)	0.09(±0.01)	0.14(±0.01)	0.11(±0.03)	0.07(±0.01)
800 mg/l. Pd- 10 mg/ml $\text{Mg}(\text{NO}_3)_2$	0.10(±0.01)	0.09(±0.02)	0.16(±0.01)	0.13(±0.02)	0.13(±0.02)
800 mg/l. Pd- 10 mg/ml $\text{NH}_4\text{H}_2\text{PO}_4\text{-}$ 10 mg/ml $\text{Mg}(\text{NO}_3)_2$	0.17(±0.03)	0.08(±0.02)	0.10(±0.02)	0.11(±0.01)	0.12(±0.02)

N.S. = No signal.

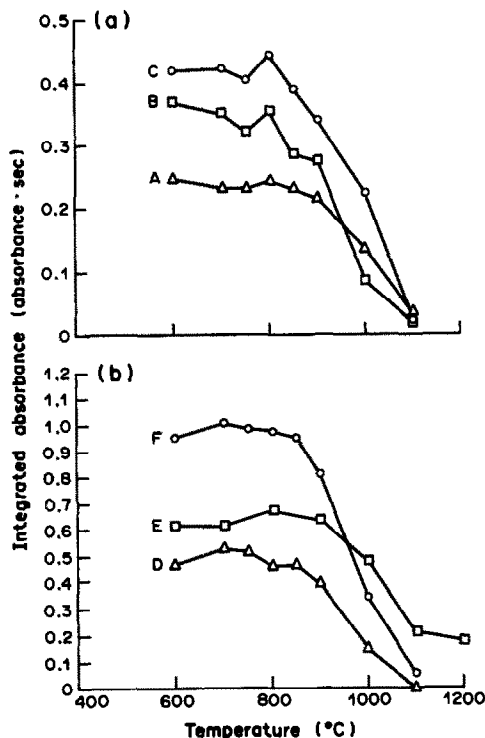


Fig. 2. Graphs of integrated absorbance signal for cadmium as a function of charring temperature. A, 1 ng/ml aqueous solution of cadmium; B, 60 mg/ml brussels sprout slurry; C, 20 mg/ml kale slurry; D, 60 mg/ml fish slurry; E, 40 mg/ml lettuce slurry; F, 20 mg/ml bovine liver slurry; platform atomization at 1700°.

salts in the furnace. The background signals for 20 μ l of 10 mg/ml $\text{NH}_4\text{H}_2\text{PO}_4$, obtained with platform atomization and the temperature programme shown in Table 2, were 1.4 absorbance and 6.0 absorbance · sec for peak height and peak area measurements, respectively. The background signal for 20 μ l of 800 μ g/ml Pd did not deviate significantly from the background measured during atomization of a water blank.

Palladium was therefore selected as a modifier for the determination of cadmium in slurries, on the basis of its comparatively good stabilizing effect and the absence of background signal enhancement when it was vaporized with the analyte.

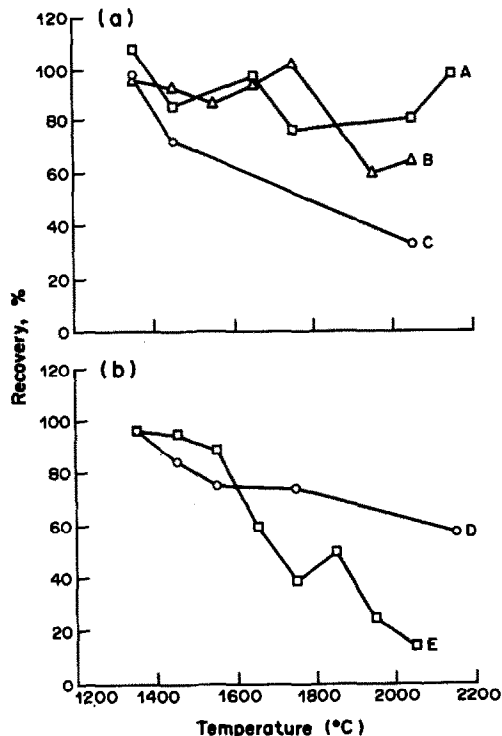


Fig. 3. Recovery of added cadmium at different atomization temperatures. A, 40 mg/ml milk slurry; B and C, 10 and 20 mg/ml bovine liver slurries, respectively; D, 40 mg/ml brussels sprout slurry; E, 40 mg/ml fish slurry. The rest of the temperature programme is as given in Table 2; 20 μ l of 2 ng/ml Cd added to 20 μ l of the slurry in the atomizer tube.

Optimization of atomization stage

The effect of atomization temperature on the recovery of added Cd for slurries prepared from a range of food samples is illustrated in Fig. 3. The recovery of the signal for 20 μ l of 2 ng/ml cadmium solution was used to assess the extent of matrix interferences when the food slurries were analysed with calibration by use of aqueous solutions of cadmium nitrate. A pre-atomization cooling step to room temperature was used to enhance the delay in atomization. An atomization temperature of 1350° allowed recoveries close to 100% to be achieved for the four food samples studied and hence was used for subsequent investigations. Above this temperature there was a general decrease

Table 2. Furnace programme for analysis of samples with platform atomization (nitrogen used throughout)

Step	Temperature, °C	Ramp time, sec	Hold time, sec	Gas flow, ml/min
Dry	300	5	40	300
Pretreat	750	30	20	300
Cool	20	5	20	300
Atomize	1350	0	10	0
Clean	2400	1	2	300

in recovery although the rate of this decline depended markedly on the sample matrix. Comparatively good recoveries of cadmium were achieved over the temperature range 1350–2150° for milk slurries. However, recoveries decreased to 50% at atomization temperatures of approximately 1750, 1950 and 2150° for fish, bovine liver and brussels sprout slurries, respectively.

The general decrease in recovery with increasing atomization temperature may be explained as follows. As the atomization temperature is increased, it takes longer for the tube to achieve the ideal condition of temporal isothermality, if the heating rate is unaltered. Indeed, at high temperature settings cadmium atom production will mostly occur while the tube temperature is still increasing, which results in a shorter atom residence time and lower integrated absorbance compared to measurements made at lower temperatures. As the rate of cadmium atom production was observed to be greater from the food slurries than from an aqueous solution of cadmium nitrate, significant differences in the average cadmium atom residence time can occur for the standard solutions and slurries, when vaporization takes place under non-isothermal conditions. In addition, greater temporal resolution between the atomic absorption and the background signals occurred at lower atomization temperatures. This implies better resolution in the vaporization of the analyte and matrix species and may explain, to some extent, the superior recovery obtained at the relatively low atomization temperature of 1350°.

The effect of slurry concentration on the recovery is shown in Table 3, for a variety of food slurries, and an atomization temperature of 1350°. Recoveries in the range 90–110% were achieved for milk and brussels sprout samples up to the maximum slurry concentration studied, of 100 mg/ml. Similar recoveries were achieved for fish slurries up to a slurry concentration of 60 mg/ml. The high level of

cadmium present in the bovine liver sample prevented the analysis of slurry concentrations above 20 mg/ml. Though the range of slurry concentrations over which close to quantitative recoveries are achieved is impressive, the accuracy and precision of slurry sample deposition into a graphite tube has been shown to deteriorate for some foodstuffs at slurry concentrations above approximately 50 mg/ml.²⁸ Therefore, the highest slurry concentration that can be used for accurate analysis based on the use of aqueous standards may vary for different samples.

Analysis of samples

The furnace conditions optimized for the determination of cadmium in slurry samples by direct calibration with aqueous standards are given in Table 2. A slurry concentration of 40 mg/ml was used for the analysis of the CRMs, except for Bovine Liver CRM 185, as its higher cadmium content required the use of a 10 mg/ml slurry. The cadmium concentrations determined by the proposed method (Table 4) are in close agreement with the certified values, although the 95% confidence limits are generally poorer than those of the certified values.

Good sensitivity was achieved by the proposed method. The cadmium characteristic mass for aqueous solutions was 0.60 pg/0.0044 absorbance.sec and this was within a factor of 2 of the value of 0.35 pg/0.0044 absorbance.sec reported previously⁴² for aqueous solutions. For the food types analysed in this study, the cadmium detection limit (2σ) is 10 ng/g (dry weight), based on a 50 mg/ml slurry.

CONCLUSIONS

Palladium stabilizes cadmium to a similar extent as does the commonly used $\text{NH}_4\text{H}_2\text{PO}_4$ modifier for a variety of food slurries, but gives

Table 3. Recovery as a function of slurry concentration, for platform atomization at 1350° after a cooling step

Slurry concentration, mg/ml	Recovery, %			
	Fish	Milk	Bovine liver	Brussels sprout
10	105	99	96	103
20	107	96	97	100
40	96	108	—	96
60	95	103	—	91
100	82	107	—	92

Table 4. Determination of cadmium in CRMs by the proposed method

Sample	Cadmium concentration, $\mu\text{g/g}$	
	Proposed method*	Certified
Bovine Liver CRM 185	0.30 ± 0.04	0.298 ± 0.025
Milk Powder CRM 150	0.024 ± 0.006	0.0218 ± 0.0014
Milk Powder CRM 151	0.114 ± 0.030	0.101 ± 0.008
Olive Leaves CRM 062	0.106 ± 0.010	0.10 ± 0.02

*Based on triplicate analysis of three specimens of each CRM; results quoted with 95% confidence intervals.

a much lower background signal. A magnesium nitrate-palladium mixture did not give an additional improvement in the thermal stability of cadmium in aqueous solution or food slurries.

The direct determination of cadmium in food slurries was achieved by using palladium matrix modification with platform atomization, a char temperature of 750°, a pre-atomization cooling step and integrated absorbance measurements. Accuracy to within 15% was achieved for the CRMs analysed. Quantitative recoveries were achieved for some slurries up to a concentration of 100 mg/ml, but a maximum slurry concentration of approximately 50 mg/ml is recommended for general use.

REFERENCES

1. F. J. Langmyhr, *Analyst*, 1979, **104**, 993.
2. F. J. Langmyhr and G. Wibetoe, *Prog. Anal. Atom. Spectrosc.*, 1985, **8**, 193.
3. L. Ebdon and W. C. Pearce, *Analyst*, 1982, **107**, 942.
4. U. Völlkopf, Z. Grobowski, R. Tamm and B. Welz, *ibid.*, 1985, **110**, 573.
5. T. M. Rettberg and J. A. Holcombe, *Anal. Chem.*, 1986, **58**, 1462.
6. G. R. Carnrick, B. K. Lumas and W. B. Barnett, *J. Anal. At. Spectrom.*, 1986, **1**, 443.
7. L. Ebdon and E. Hy. Evans, *ibid.*, 1987, **2**, 317.
8. G. Rygh and K. W. Jackson, *ibid.*, 1987, **2**, 397.
9. K. P. Schmidt and H. Falk, *Spectrochim. Acta*, 1987, **42B**, 431.
10. I. Lindberg, E. Lundberg, P. Arkhamman and P. Berggren, *J. Anal. At. Spectrom.*, 1988, **3**, 497.
11. C. W. Fuller, *Analyst*, 1976, **101**, 961.
12. C. W. Fuller and I. Thompson, *ibid.*, 1977, **102**, 141.
13. C. W. Fuller, R. C. Hutton and B. Preston, *ibid.*, 1981, **106**, 913.
14. N. Carrion, Z. A. de Benzo, E. J. Eljuri, F. Ippoliti and D. Flores, *J. Anal. At. Spectrom.*, 1987, **2**, 813.
15. K. W. Jackson and A. P. Newman, *Analyst*, 1983, **108**, 261.
16. D. Littlejohn, S. C. Stephen and J. M. Ottaway, *Anal. Proc.*, 1985, **22**, 376.
17. S. C. Stephen, D. Littlejohn and J. M. Ottaway, *Analyst*, 1985, **110**, 1147.
18. S. C. Stephen, J. M. Ottaway and D. Littlejohn, *Z. Anal. Chem.*, 1987, **328**, 346.
19. L. Ebdon and A. Lechotycki, *Microchem. J.*, 1986, **34**, 340.
20. L. Ebdon and H. G. M. Parry, *J. Anal. At. Spectrom.*, 1987, **2**, 131.
21. *Idem, ibid.*, 1988, **3**, 131.
22. M. W. Hinds and K. W. Jackson, *ibid.*, 1987, **2**, 441.
23. R. Karwowska and K. W. Jackson, *ibid.*, 1987, **2**, 125.
24. D. C. van Loenen and C. A. Weers, in B. Welz (ed.), *Fortschritte in der atomspektrometrischen Spurenanalytik*, Vol. 2, p. 635. VCH, Weinheim, 1986.
25. N. J. Miller-Ihli, *J. Anal. At. Spectrom.*, 1988, **3**, 73.
26. M. Hoening and P. Van Hoeyweghen, *Anal. Chem.*, 1986, **58**, 2614.
27. K. O. Olayinka, S. J. Haswell and R. Grzeskowiak, *J. Anal. At. Spectrom.*, 1986, **1**, 297.
28. S. Lynch and D. Littlejohn, *ibid.*, 1989, **4**, 157.
29. L. T. Wetzel and J. U. Bell, *Clin. Chem.*, 1980, **26**, 1796.
30. H. T. Delves, *At. Spectrosc.*, 1981, **2**, 65.
31. E. Pruszkowska, G. R. Carnrick and W. Slavin, *Anal. Chem.*, 1983, **55**, 182.
32. W. K. Oliver, S. Reeve, K. Hammond and F. B. Basketter, *J. Inst. Water Eng. Sci.*, 1983, **37**, 460.
33. K. S. Subramanian, J.-C. Meranger and J. E. MacKeen, *Anal. Chem.*, 1983, **55**, 1064.
34. A. Rosopoulo and W. Kreuzer, in B. Welz (ed.), *Fortschritte in der atomspektrometrischen Spurenanalytik*, Vol. 2, p. 455. VCH, Weinheim, 1986.
35. K. G. Feitsma, J. P. Franke and R. A. de Zeeuw, *Analyst*, 1984, **109**, 789.
36. K.-R. Sperling, *Z. Anal. Chem.*, 1977, **287**, 23.
37. M. Suzuki and K. Ohta, *Anal. Chem.*, 1982, **54**, 1686.
38. J. Korečková, *7th Czechoslovak Spectroscopic Conference and VIIIth CANAS*, Czechoslovakia, 1984.
39. L. M. Voth-Beach and D. E. Shrader, *Spectroscopy*, 1986, **1**, 49.
40. X. Yin, G. Schlemmer and B. Welz, *Anal. Chem.*, 1987, **59**, 1462.
41. B. Welz, G. Schlemmer and J. R. Mudakavi, *J. Anal. At. Spectrom.*, 1988, **3**, 695.
42. W. Slavin, G. R. Carnrick, D. C. Manning and E. Pruszkowska, *At. Spectrosc.*, 1983, **4**, 69.

EXTRACTION AND SPECIATION OF ARSENIC IN LACUSTRINE SEDIMENTS

WALTER H. FICKLIN

U.S. Geological Survey, Box 25046, Denver Federal Center, Denver, CO 80225, U.S.A.

(Received 21 November 1989. Revised 9 February 1990. Accepted 14 February 1990)

Summary—Arsenic was partially extracted with 4.0M hydrochloric acid, from samples collected at 25-cm intervals in a 350-cm column of sediment at Milltown Reservoir, Montana and from a 60-cm core of sediment collected at the Cheyenne River Embayment of Lake Oahe, South Dakota. The sediment in both reservoirs is highly contaminated with arsenic. The extracted arsenic was separated into As(III) and As(V) on acetate form Dowex 1-X8 ion-exchange resin with 0.12M HCl eluent. Residual arsenic was sequentially extracted with KClO₃ and HCl. Arsenic was determined by graphite-furnace atomic-absorption spectrometry. The analytical results define oxidized and reduced zones in the sediment columns.

The need for an analytical method to determine the concentration of arsenite and arsenate in sedimentary materials became apparent in the study of the mobility and solubility of arsenic species in lacustrine sediments. Studies of arsenic deposition from mine waste and tailings or from natural causes have revealed that changes in the oxidation state of arsenic may occur in the sediment columns of lakes and reservoirs.¹⁻³ The occurrence of both As(III) (arsenite) and As(V) (arsenate) in the interstitial water of the sediment from Milltown Reservoir, Montana,¹ and in the Cheyenne River Embayment of Lake Oahe, South Dakota,³ suggests that measurable concentrations of these two oxidation states should also occur in the solid phase of the sediment, because most of the arsenic in the system is contained in the solid phase. As(III) and As(V) are known to be readily adsorbed onto amorphous hydrous iron oxides⁴ and it is reasonable to assume that this also occurs in environments containing recent depositions of arsenic-bearing sediments.

Determination of As(III) and As(V) concentrations in water has been intensively studied in recent years by Ficklin,⁵ Subramanian and Meranger,⁶ Aggett and Kadwani,⁷ Mok *et al.*⁸ and many others. Lemmo *et al.*⁹ discussed in detail the fate and speciation of arsenical compounds in the aqueous environment. Chemical speciation of arsenic in solid materials requires an extraction in which the reagent does not alter the oxidation state of the arsenic. Iverson *et al.*¹⁰ reported results for speciation of arsenic in sediment contaminated with dimethylarsinite

(DMA) and monomethylarsonate (MMA), although they did not separate the inorganic anions. Moore *et al.*¹ extracted arsenic from highly contaminated sediments at Milltown Reservoir, Montana, with the acetic acid-hydroxylamine reagent of Chester and Hughes¹¹ but did not determine As(III) and As(V) concentrations in the resulting solutions, because of the reducing agent present.

Chao and Zhou¹² used 4.0M hydrochloric acid to determine phase associations of metals in crystalline iron oxides. This reagent and several others were tested in the present study for the stability of arsenate and arsenite upon extraction. Reagents containing hydroxylamine or ascorbic acid reduced all of the As(V) to As(III). The most successful extractions were made with hydrochloric acid, and the 4.0M acid was used because it is standard practice for extraction of iron oxides.

EXPERIMENTAL

Reagents

All reagents were analytical grade or better. The hydrochloric acid used was "J. T. Baker instra-analyzed for trace metals analysis". As(III) solutions were prepared from sodium arsenite (NaAsO₂). As(V) solutions were prepared from sodium dihydrogen arsenate heptahydrate (NaH₂AsO₄·7H₂O). DMA solutions were prepared from sodium cacodylate and MMA solutions from a sample of MMA supplied by Vineland Chemical Co. The ion-exchange resins Dowex 1-×8 and Dowex

50W- \times 8, 100-200 mesh, were obtained from Bio-Rad laboratories, Richmond, CA.

Apparatus

A Perkin-Elmer model 603 atomic-absorption spectrophotometer*, equipped with an HGA 2100 graphite furnace, a deuterium arc background correction system, an electrodeless discharge lamp and pyrolytically coated graphite tubes, was used for all arsenic determinations. Arsenic was stabilized in the graphite furnace by adding 10 μ l of 500 mg/l. nickel solution (nickel nitrate in 1% v/v nitric acid) to 10 μ l of sample in the graphite furnace. A wavelength of 197.2 nm was used instead of the usual 193.7 nm, to reduce the sensitivity because the arsenic in the samples was so abundant. The sample in the tube was dried for 30 sec at 100°, charred for 20 sec at 1100° and atomized for 6 sec at 2700°. Calibration graphs were obtained by use of standards solutions of As(III) in 0.12M acetic acid and of As(V) in 0.12M hydrochloric acid/0.12M acetic acid mixture.

Sample treatment

The samples from Milltown Reservoir, MT, were frozen immediately following collection. The samples originated from a hole about 350 cm deep, made by auger. A sample was collected at each 25-cm interval and was frozen within an hour. The samples from Lake Oahe, SD, were taken from intervals in drill cores and frozen immediately after removal of the interstitial water.

The samples were kept frozen until just before extraction of the arsenic. Each sample was thawed as rapidly as possible in cold water. To minimize the exposure of oxidizable As(III) to the atmosphere, arsenic was extracted from 0.5-0.7 g of wet sediment. The dry weight was calculated from the results obtained by weighing a separate part of each sample wet and again after drying. Samples from Milltown Reservoir were thoroughly homogenized by stirring the contents of the "Ziploc" storage bag with a glass rod. The samples from Lake Oahe were homogenized by kneading the small "Whirlpak" bags used for storage.

The samples were heated with 5.0 ml of 4.0M hydrochloric acid for 30 min at 90° in a water-bath. The extract was allowed to cool and the

volume was adjusted to 5 ml with demineralized water. The arsenic species in this solution were determined after separation by the method of Ficklin,⁵ adapted to the more concentrated acid solution used for the extraction. The method consists of separation of As(III) from As(V) on acetate-form Dowex 1- \times 8(100-200 mesh) ion-exchange resin in a 0.7 \times 15 cm column (glass Econo-Columns from Bio-Rad). The resin in the column was converted into the acetate form by passing 5 ml of 1.0M sodium hydroxide through the column, followed by 10 ml of 1.0M acetic acid.

A 0.3 ml volume of the 4.0M hydrochloric acid extract was then passed through the column, followed by 2.7 ml of 0.12M hydrochloric acid, 3 ml of effluent being collected. Next, 19-24 ml of 0.12M hydrochloric acid were passed through the column and collected as one 4-ml and three or four 5-ml fractions. All the fractions were analyzed for arsenic. As(III), when present, was found in the 4-ml fraction and As(V) in the second and/or third of the 5-ml fractions. The volume of eluent required for removal of As(V) was variable, but the elution always occurred when the resin had been completely converted from the acetate form into the chloride form. With experience the dark yellow acetate form of the resin could be easily distinguished from the light yellow chloride form. With an estimated dry weight of 0.3 g (the water content of the samples varied from 50 to 75% and 0.5-0.7 g of wet sediment was extracted) and a detection limit of 5 μ g/l. arsenic at 197.2 nm, the minimum concentrations of As(III) and As(V) detectable were 0.33 and 0.42 mg/kg, respectively. However, a practical detection limit of 0.5 mg/kg was used.

Arsenic remaining in the solid residue after the extraction with 4.0M hydrochloric acid was dissolved out by letting this residue stand with 0.5 g of potassium chlorate and 5 ml of concentrated hydrochloric acid for 30 min at room temperature.¹³ Total arsenic was determined by use of the decomposition method of Lichte *et al.*,¹⁴ with arsenic determination by graphite-furnace atomic-absorption spectrometry after appropriate dilution.

Known mixtures of As(III), As(V), DMA and MMA were separated by the proposed method. The DMA and As(III) were eluted in the first 7 ml of effluent. MMA was first found in the second of the 5.0-ml fractions and in each succeeding fraction until all of the resin had been converted into the chloride form. Thus,

*Use of brand names is for descriptive purposes only and does not imply endorsement by the U.S. Geological Survey.

MMA and As(V) were not well separated from each other, but they were separated from DMA and As(III). Separation of DMA from As(III) was accomplished by passing the first 7 ml of effluent through a 0.7×2.0 cm column of Dowex 50W- $\times 8$ H⁺ form resin. The DMA remained on the resin, but As(III) passed through. Likewise, MMA was separated from As(V) by passing the 5.0-ml fractions of effluent through a 0.7×2 cm column of Dowex 1- $\times 8$ acetate-form resin. MMA was eluted with 0.16M acetic acid, and As(V) remained on the resin. No MMA or DMA was found in three samples of Milltown Reservoir sediment or in two samples of Lake Oahe sediment.

RESULTS

The results for extraction of arsenic with 4.0M hydrochloric acid from 13 samples of Milltown, MT, reservoir sediment and from a core of sediment from the Cheyenne River Embayment of Lake Oahe, SD, are presented in Table 1. The total arsenic concentration and the concentration of arsenic remaining in the sediment after extraction with 4.0M hydrochloric acid but released by reaction with potassium

chlorate and concentrated hydrochloric acid are also included. The data suggest that a change from oxidizing to reducing conditions takes place, as reflected by the increase in the proportion of As(III) with increasing depth from the sediment surface. In the oxidizing region almost all the arsenic in the sediment is present as As(V). The total arsenic and extracted As(V) are almost equal at depths of 0-75 cm at Milltown Reservoir and in the first 3 cm of the sediment of Lake Oahe. On the other hand, in the reducing zone some As(V) still has not undergone reduction, although the major part of the extractable arsenic occurs as As(III).

In the reducing zone a large percentage of the arsenic was in a form that was insoluble in hot 4.0M hydrochloric acid but was released by reaction with the potassium chlorate concentrated hydrochloric acid solution recommended by Olade and Fletcher.¹³ Because this chemical treatment is designed to oxidize sulfides, and the non-sulfide arsenic compounds have been removed in the 4.0M hydrochloric acid extraction, the residual arsenic may represent detrital and authigenic sulfide mineral phases.

The recoveries of As(III) and As(V) from spiked samples are presented in Tables 2 and 3,

Table 1. Extraction and speciation of arsenic in Milltown Reservoir, MT, and the Cheyenne River Embayment of Lake Oahe, SD

Sample depth, cm	Extracted		Residual As, mg/kg	Total As, mg/kg
	As(III), mg/kg	As(V), mg/kg		
Milltown Reservoir				
0-25	2.5	113	<0.5	130
25-50	2.6	110	<0.5	100
50-75	1.8	90	<0.5	90
75-100	32	74	24	120
100-125	34	15	70	110
125-150	31	10	40	80
150-175	29	13	190	250
175-200	122	26	400-700*	520-800*
200-225	17	5.2	22	36
225-250	7.0	3.9	12	25
250-275	5.9	3.9	6.0	16
300	48	13	280-620*	370-700*
350	94	20	130-650*	190-520*
Lake Oahe				
0-1	<0.5	10	<0.5	11
1-2	<0.5	12	<0.5	11
2-3	<0.5	15	<0.5	15
3-4	8.0	16	3.3	33
6-8	26	4.0	7.6	40
10-12	45	16	22	90
14-16	12	15	4.8	29
50-52	16	5.9	23	58
52-54	23	4.9	13	35
58-60	12	5.0	74	95

*Range of values found in five repeat determinations.

Table 2. Recovery of As(III) spikes added to samples from Milltown Reservoir

Sample	Depth below surface, cm	As(III) in sample, mg/kg	As(III) added, mg/kg	As(III) found, mg/kg	As(III) recovered, mg/kg
Milltown 1	0-25	2.5	10	12.2	9.7
Milltown 2	25-50	2.6	10	12.1	9.5
Milltown 3	175-200	122	100	230	108
Milltown 4	200-225	17	10	29	12
Milltown 5	300	48	50	100	50

Table 3. Recovery of As(V) spikes added to Milltown Reservoir samples

Sample	Depth below surface, cm	As(V) in sample, mg/kg	As(V) added, mg/kg	As(V) found, mg/kg	As(V) recovered, mg/kg
Milltown 1	0-25	113	100	230	117
Milltown 2	25-50	110	100	220	110
Milltown 3	175-200	26	20	44	18
Milltown 4	200-225	5.2	10	14	8.8
Milltown 5	300	13	20	37	24

respectively. The spiked samples were prepared with an amount of wet sample corresponding to 0.5 g of dry sample. A small volume of As(III) or As(V) solution was added to the sample to increase the concentration of analyte, as shown in Tables 2 and 3 then the proposed procedure was followed to determine recovery of the arsenic added to the sample. The results suggest that As(III) is stable in hot 4.0M hydrochloric acid long enough for it to be separated from As(V).

The precision was estimated from five replicate determinations of As(III) and As(V) for two of the samples and is shown in Table 4.

Five independent analyses of the Milltown Reservoir samples marked with an asterisk in Table 1 yielded arsenic results in the range indicated. The arsenic in these samples may have partially originated as sulfide minerals buried in the reservoir bottom sediment. The developing reducing conditions in the sediment column would therefore have preserved them. The non-uniform results are probably due to inhomogeneity in the samples. However, the concentration of acid-extractable arsenic in these samples was much more uniform for repeat analyses, as indicated in Table 4 for Milltown sample 3 (175-200 cm) with relative

standard deviations of 4.3% for extractable As(III) and 9.6% for As(V), respectively. The conclusion is that some of the arsenic in these sediments was oxidized during transport in the river and the environment, and then reduced in the sediment column, where it was preserved as coatings on grains. Hence the extractable arsenic is evenly distributed in the samples, but the residual arsenic, being present as sulfide mineral grains, is not.

REFERENCES

1. J. N. Moore, W. H. Ficklin and C. Johns, *Environ. Sci. Technol.*, 1988, **22**, 432.
2. J. Aggett and G. A. O'Brien *ibid.*, 1985, **19**, 231.
3. W. H. Ficklin and E. Callender *U.S. Geol. Survey Water Resources Invest. Rep.*, 88-4420, 1988, pp. 217-222.
4. M. L. Pierce and C. B. Moore, *Water Res.*, 1982, **16**, 1247.
5. W. H. Ficklin, *Talanta*, 1983, **30**, 371.
6. K. S. Subramanian, J.-C. Meranger and R. F. McCurdy, *At. Spectrosc.*, 1984, **5**, 192.
7. J. Aggett and R. Kadwani, *Analyst*, 1983, **108**, 1495.
8. W. M. Mok, N. K. Shah and C. M. Wai, *Anal. Chem.*, 1986, **58**, 110.
9. N. V. Lemmo, S.D. Faust, T. Belton and R. Tucker, *J. Environ. Sci. Health, Part A*, 1983, **A18**, 335.
10. D. G. Iverson, M. A. Anderson, T. R. Holm and R. R. Stanforth, *Environ. Sci. Technol.*, 1979, **13**, 1491.
11. R. Chester and M. J. Hughes *Chem. Geol.*, 1967, **2**, 249.
12. T. T. Chao and L. Zhou, *Soil Sci. Soc. Am. J.*, 1983, **47**, 225.
13. M. Olade and W. K. Fletcher *J. Geochem. Expl.*, 1983, **3**, 337.
14. F. E. Lichte, D. W. Golightly and P. J. Lamothe, *U.S. Geol. Survey Bull.*, 1770, 1987 B1-B10.

Table 4. Mean \pm standard deviation for five replicate determinations of As(III) and As(V) in two Milltown Reservoir samples

Sample	As(III), mg/kg	As(V), mg/kg
Milltown 1	2.5 \pm 0.3	113 \pm 11
Milltown 3	122 \pm 5.5	26 \pm 2.5

ION-CHROMATOGRAPHY OF METALS WITH POST-COLUMN ION DISPLACEMENT

CHRISTINE J. BOWLES and LAURENCE W. BADER

Department of Chemistry, University of Saskatchewan, Saskatoon, Sask. Canada S7N 0W0

KENNETH W. JACKSON*

Wadsworth Center for Laboratories and Research, New York State Department of Health, and School of Public Health, State University of New York, Albany, NY 12201-0509, U.S.A.

(Received 25 September 1989. Revised 1 December 1989. Accepted 27 December 1989)

Summary—A post-column reagent mixture of Eriochrome Black T and magnesium-EDTA complex is added to the eluent from an ion-chromatograph. Eluted metal cations displace the magnesium, which then forms a complex with the Eriochrome Black T. The absorbance of this complex is measured at 520 nm. Detection limits for several cations are in the $\mu\text{g/ml}$ range.

Ion-chromatographs commonly use conductivity detection and a suppressor column to remove the background conductivity of eluent ions. For cation determinations, the simplest suppression reaction involves a strong-base anion-exchange resin in its hydroxide form to convert the protons in an acidic eluent into water. Typical mobile phases are dilute mineral acids, but for alkaline-earth metal ion separations the mobile phase should contain a doubly charged ion of high equivalent conductance, such as the ethylenediammonium ion. This acts as a "driving ion" and promotes exchange with the metal ions on the column.¹ Transition metal ions can be eluted in a reasonable time by inclusion of a weak complexing agent, such as tartrate, oxalate or citrate in the mobile phase.² For the determination of alkaline-earth metal ions, a zinc nitrate/nitric acid mixture has been used as eluent, zinc hydroxide being precipitated by use of a hydroxide-form suppressor column.³ A problem with basic suppressor resins is the likelihood of metal hydroxide precipitation, and this has led to other types of eluent/suppressor systems being used. Nordmeyer *et al.*⁴ determined alkaline-earth and bivalent transition-metal cations with barium nitrate, barium chloride or lead nitrate solutions as eluents. The suppressor column was loaded with sulfate ions, to precipitate the eluent cations as their sulfates. A column in hydrogen-ion form was placed between the suppressor and detector

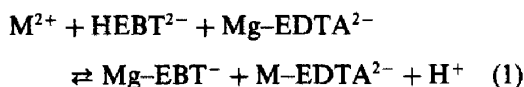
to minimize the effect of pH on the baseline and to increase the sensitivity. A lead nitrate eluent with an iodate suppressor (to precipitate lead iodate) was later used,⁵ and this also allowed barium to be determined. The hydrogen-ion form post-suppressor was replaced by a hydroxide-form column. Overall, the success of suppressed ion-chromatography for cation determinations has been limited. Although the technique is satisfactory for alkali and alkaline-earth metals, many other cations (including those of transition metals) are determined with poor selectivity because of band broadening within the suppressor column. If a low-conductivity mobile phase is used, then its suppression may not be necessary. Sevenich and Fritz⁶ overcame some of the limitations above in use of an unsuppressed system for the determination of 25 metal ions. The eluent contained a mixture of ethylenediammonium and tartrate ions which provided sharper peaks and hence improved selectivity for many cations. However, some metals gave badly tailing peaks due to slow complexing and decomplexing equilibria.

The difficulties of conductivity detection have led to other systems being used, of which ultraviolet-visible molecular absorption spectrometry has been the most common. It is a very suitable detector for flow-through systems, already well established for high-performance liquid chromatography (HPLC). When it is used for cation chromatography, however, post-column derivatization is necessary. A complexing agent, such as 4-(2-pyridylazo)resorcinol

*Author for correspondence.

(PAR), is introduced into the flowing stream after the ion-exchange column,⁷ and the resulting metal complexes absorb light in the visible region of the spectrum. The advantage of PAR over many other chelating agents is the high molar absorptivity of its metal complexes and the wide range of metals that react with it.⁷ This post-column derivatization system has certain disadvantages, however. Although PAR reacts with many cations, each complex has maximum absorption at a different wavelength. The broad absorption bands overlap, allowing all the complexes to be detected at the same wavelength, but this is a compromise, and the sensitivity may not be optimum for all analytes.

A novel derivatization system was introduced by Arguello and Fritz⁸ for the determination of calcium and magnesium ions. The reagent consisted of an equimolar mixture of PAR and zinc-EDTA complex. Analyte ions then displaced zinc from its EDTA complex, which allowed formation of the Zn-PAR complex, which was measured spectrophotometrically. A similar system was described by Yan and Schwedt.⁹ Compromise detection conditions are then not required because the same absorbing species is detected for all ions. In this paper we describe the introduction of a post-column reagent stream containing Eriochrome Black T in its doubly dissociated form (HEBT²⁻) and Mg-EDTA. The following post-column ion-displacement (PCID) reaction (*e.g.*, for a bivalent cation M²⁺) then takes place:



An advantage of this system is that Mg-EDTA is one of the weakest metal-EDTA complexes.¹⁰

Hence, the equilibrium is always strongly to the right, permitting the analyte ion to displace magnesium, which then forms the EBT complex. Detection is by measurement of the increase in absorbance of Mg-EBT⁻ at 520 nm, or the decrease in absorbance of HEBT²⁻ at 610 nm. A possible disadvantage of the earlier Zn-EDTA/PAR system is that some metal-PAR complexes have higher formation constants than that of Zn-PAR.¹⁰ This could prevent the formation of Zn-PAR in the presence of some analytes.

EXPERIMENTAL

Instrumentation

The liquid chromatograph, incorporating PCID, is shown schematically in Fig. 1. A Bio-Rad Model 1330 HPLC pump (Bio-Rad, Mississauga, Ontario, Canada) was used to deliver the mobile phase. Samples were introduced into the mobile phase stream by a Rheodyne Model 7125 injection valve (Bio-Rad), fitted with a 20- μ l sample loop. A Wescan high-speed cation-chromatography column was used (Wescan Instruments, Santa Clara, CA, U.S.A.) and the detector was a Bio-Rad Model 1305A variable wavelength absorbance monitor, fitted with a tungsten lamp as light-source. Chromatograms were recorded on a Fisher Recordall Series 5000 chart recorder. Post-column reagent was pumped by nitrogen pressure from a 1000-ml Nalgene bottle inside a constant-pressure vessel (10 psig; this system was based on that designed by Fritz and Willis).¹¹ The mobile phase and reagent streams were both pumped through 1/16-in. bore stainless-steel tubing. The mixing cell for the two streams was either a "T-piece" or a "Y-piece"

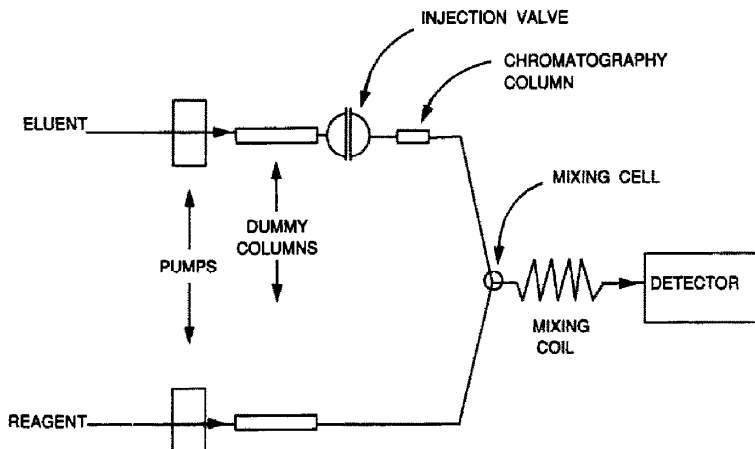


Fig. 1. Schematic diagram of the chromatograph and PCID system.

with 0.5-mm bore channels. These cells were each machined out of a single block of Perspex, drilled to accommodate standard low-pressure stainless-steel or polyethylene fittings. The "T-piece" was used for most of the work described in this paper. Back-pressure was provided in both the mobile phase and reagent streams by inserting dummy columns (50 cm \times 3 mm bore) packed with silica gel. Tygon tubing (0.5 mm bore) was used between the "T-" or "Y-piece" and the detector. The mixing coil was a 2-m length of the same tubing.

Reagents

Throughout the work, reagents of the highest available purity were used. All dilutions were made with glass-distilled water.

Ethylenediamine/tartaric acid (EDA/TA) mobile phase. This contained $1.5 \times 10^{-3}M$ ethylenediamine and $2 \times 10^{-3}M$ tartaric acid, adjusted to pH 4 with nitric acid.

Ammonium α -hydroxyisobutyrate (0.09M) (HIBA) mobile phase. This was prepared by dissolving 9.4 g of α -hydroxyisobutyric acid (Aldrich Chemical Co., Milwaukee, WI 53233) in almost 1000 ml of water and adding 7 ml of concentrated ammonia solution. After adjustment to pH 4 with nitric acid, the solution was made up to 1000 ml with water.

Post-column ion-displacement reagent. This contained $2 \times 10^{-4}M$ Eriochrome Black T and $2 \times 10^{-4}M$ Mg-EDTA, adjusted to pH 10 (for use with EDA/TA mobile phase) or pH 12 (for HIBA mobile phase), with an ammonia/ammonium chloride buffer. This was sufficient to give the mixed stream a pH of 10. The Mg-EDTA solution was prepared by titrating $0.02M$ Mg²⁺ with $0.02M$ EDTA at pH 10 to an Eriochrome Black T end-point, in order to ensure equimolar concentrations of magnesium and EDTA. An indicator-free solution was then made by mixing the appropriate volumes of the components. The titration was repeated whenever a new batch of either component was used.

Metal standard solutions. Appropriate amounts of the pure metal or metal salt were dissolved in nitric acid to produce 1000-mg/l. stock metal solutions. More dilute solutions for injection into the chromatograph were prepared in 1% nitric acid.

Procedure

The flow-rates used were: mobile phase 1.0 ml/min (EDA/TA) or 0.5 ml/min (HIBA);

post-column reagent 0.3 ml/min. The peak areas for the absorbance at 520 nm, and the retention times, were measured.

RESULTS AND DISCUSSION

Applicability of the post-column ion-displacement method

For application to a particular cation, the equilibrium in equation (1) should lie strongly to the right, *i.e.*, the conditional formation constant of the analyte metal-EDTA chelate must be greater than that of Mg-EDTA. Tables of conditional formation constants show this to be the case for most metals.¹⁰ The ion-displacement reaction is unsuitable for some cations, even though the conditional formation constants are high. For example, Cd²⁺ forms a carbonate precipitate, Pb²⁺ a hydroxide precipitate, and Mn²⁺ a green colour, because of oxidation to Mn³⁺ by dissolved oxygen (and formation of a green complex). This complex results in negative absorbance after correction for the blank. This was reflected in a Job plot (at 520 nm) which showed a minimum (the Job plots for all the other metals showed an appropriate maximum).

Optimization of instrumental parameters

Choice of mobile phase. When a cation-exchange column is used, the mobile phase generally includes an acidic anion, often as its ammonium salt. The acids most commonly employed are citric, tartaric and oxalic. As many as 13 metal ions have been separated in 34 min on a strong cation-exchanger with a tartrate mobile phase at pH 2.75.⁹ These acids are often used in conjunction with weak chelating agents, such as ethylenediamine, to enhance the retention properties of the stationary phase. Recently,¹² α -hydroxyisobutyric acid has been shown to give good resolution for several metal species on a cation-exchange column. For the present work, two mobile phases were investigated; ethylenediamine/tartaric acid (EDA/TA) and α -hydroxyisobutyric acid (HIBA).

pH. For the mixed stream, the optimum pH would be that favoring formation of the analyte metal-EDTA complex and the Mg-EBT complex. At pH below 7, EBT forms a red colloid that does not react with metal ions. Therefore, for the mixed stream, a pH of 10 was chosen as a compromise for all the metal ions determined.

The pH of the mobile phase affected the retention of metal ions. The aim was to select the pH which would give the longest retention times in order to obtain the best resolution. For each mobile phase system, the detector response for Mg^{2+} was monitored while the pH was varied, with the reagent concentration and flow-rates kept constant. The mixed stream was maintained at pH 10 by adjusting the reagent pH. The reagent flow-rate was 0.3 ml/min (for the EDA/TA system) or 0.5 ml/min (for HIBA), and the mobile phase flow-rates were 1.0 ml/min (EDA/TA) and 0.5 ml/min (HIBA). The results (Table 1) show that the retention time increased as the pH decreased, until pH 4–5, below which there was little further change in retention time. Hence, pH 4 was chosen as the optimum.

The reagent pH that was needed to maintain the mixed stream at its optimum pH depended on the buffering capacity of the mobile phase. For EDA/TA, the reagent pH was 10, but for HIBA (higher buffering capacity), a reagent pH of 12 was needed.

Reagent concentration. With EBT used alone as reagent, at varied concentration, excess of $4 \times 10^{-2}M$ magnesium solution was injected into the chromatograph. The flow-rates of the EDA/TA mobile phase and reagent were 1.0 and 0.5 ml/min respectively, and the pH conditions were optimum. The absorbance of the resulting Mg–EBT complex (520 nm) increased with increasing reagent concentration and then levelled off at $2 \times 10^{-4}M$ EBT. This EBT concentration was chosen as the optimum.

Flow-rates. Under optimized conditions of pH and reagent concentration, several alkaline earth and transition metal cations were eluted separately to study the effect of flow-rate on retention time. The ion-displacement reaction is fast, so the reagent flow-rate was not critical (provided the 2-m coil was present when HIBA was used). A fast mobile-phase flow-rate is desirable, because it leads to shorter retention times and faster analysis, but this could degrade

Table 1. Effect of mobile-phase pH on the retention time of Mg^{2+}

pH	Retention time, min	
	EDA/TA mobile phase	HIBA mobile phase
6.1	0.9	
6.0		11.0
5.2	1.6	
5.0		11.5
4.0	1.7	12.0
3.5		12.1

Table 2. Retention times of individually chromatographed cations

Cation	Retention time, min	
	EDA/TA mobile phase	HIBA mobile phase
Ca^{2+}	2.8	21.0
Co^{2+}	1.6	9.6
Cu^{2+}	1.1–3.1*	4.4/7.4†
Fe^{2+}	1.7	13.2
Mg^{2+}	1.7	12.0
Ni^{2+}	1.5	9.0
Sr^{2+}	3.4	38.0
Zn^{2+}	1.5	6.6

*Concentration-dependent.

†Double peak.

resolution. With EDA/TA, it was possible to use a high mobile-phase flow-rate (1 ml/min) and resolve the alkaline-earth cations Mg^{2+} , Ca^{2+} and Sr^{2+} , but transition metal cations were not resolved (Table 2). The use of lower flow-rates did not allow transition metal cations to be resolved. The 2-m mixing coil was not required when EDA/TA was used as mobile phase.

The fastest HIBA flow-rate which gave satisfactory resolution was 0.5 ml/min. When various metal cations were eluted individually, they gave the retention times shown in Table 2.

With these optimized flow-rates (1 ml/min for EDA/TA, or 0.5 ml/min for HIBA) the highest detector response was still achieved with the previously optimized EBT reagent concentration ($2 \times 10^{-4}M$), *i.e.*, the optimum reagent concentration is unaffected by change in flow-rate.

Detection limits

Except for Co^{2+} and Fe^{2+} , both mobile phases gave similar detection limits when cations were eluted separately (Table 3). However, the HIBA mobile phase made the detection limit difficult to measure for Cu^{2+} (which gave a double peak). Although the same species

Table 3. Detection limits of individually chromatographed cations

Cation	Detection limit*, mg/l.	
	EDA/TA mobile phase	HIBA mobile phase
Ca^{2+}	1.0	1.0
Co^{2+}	11	2.1
Cu^{2+}	19	
Fe^{2+}	1.0	6.6
Mg^{2+}	0.3	0.5
Ni^{2+}	1.5	1.4
Sr^{2+}	7.6	8.0
Zn^{2+}	2.5	1.6

*Concentration corresponding to 3 times the standard deviation of a blank.

(Mg-EBT) is always measured in the ion-displacement method, metal ions do not all give the same detection limit, because this depends on the extent of the ion-displacement reaction. Also, some metal ions (notably Al^{3+} , Cu^{2+}) "block" EBT by forming particularly stable complexes with it.¹³ The major contribution to noise was the post-column mixing of reagents. Hence, it is highly likely that the lower noise levels associated with the introduction of reagents through a membrane reactor¹⁴ would lead to improved detection limits.

Multielement analysis

The use of EDA/TA was not studied further, because of its limited applicability. All multielement studies were done with HIBA as mobile phase. When mixtures of metal ions were separated, the use of HIBA resulted in alteration of some retention times, presumably because of an interaction on the column or in the eluent. For example, Ni^{2+} and Zn^{2+} were co-eluted at the retention time previously established for Zn^{2+} (Table 2). When Zn^{2+} , Mg^{2+} and Ca^{2+} were present as a mixture, the chromatogram shown in Fig. 2a was obtained. All the peaks were resolved and the calculated separation factor for $\text{Zn}^{2+}/\text{Mg}^{2+}$ was acceptable ($\alpha = 1.33$).

However, when Sr^{2+} was added, the retention times for Mg^{2+} and Ca^{2+} decreased (Fig. 2b), and the separation of Zn^{2+} and Mg^{2+} was poorer ($\alpha = 0.5$). Multielement calibration showed linear response up to at least 9–10 mg/l. for all cations examined (20 μl injection).

A commercial multivitamin tablet was analyzed by dissolving it in 50 ml of (1 + 1) hydrochloric acid, diluting accurately to 250 ml with Millipore water, allowing the insoluble binders to settle, and taking two fractions of supernatant liquid for analysis. (a) A 2-ml portion was diluted to 100 ml with HIBA solution, and (b) a 3-ml portion was diluted to 50 ml. Aliquots (20 μl) were injected into the chromatograph and the chromatograms shown in Fig. 3 were obtained. Table 4 shows the results obtained for multielement calibration, and these show reasonable agreement with the manufacturer's quoted amounts. The results for Ca^{2+} show the poorest agreement, but the narrow precision limits suggest this is due to variability between the tablets.

CONCLUSION

The purpose of this research was to demonstrate the feasibility of PCID for multielement

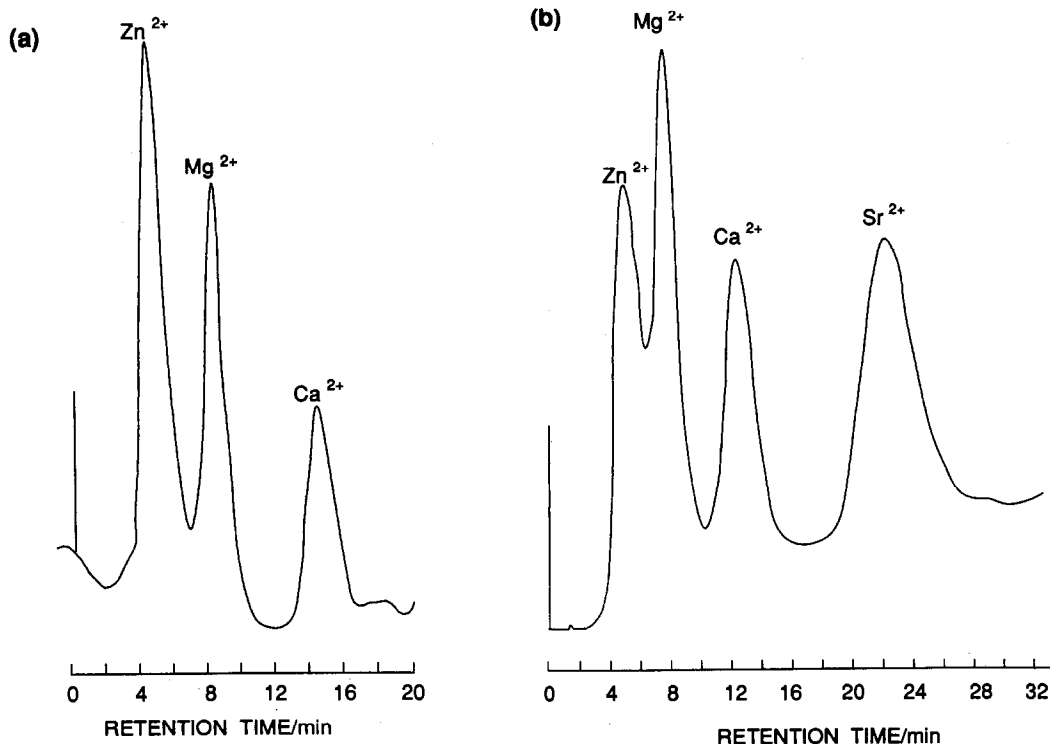


Fig. 2. Typical chromatograms for multielement analysis, with HIBA mobile phase; (a) a mixture of Zn^{2+} , Mg^{2+} and Ca^{2+} ; (b) a mixture of Zn^{2+} , Mg^{2+} , Ca^{2+} and Sr^{2+} .

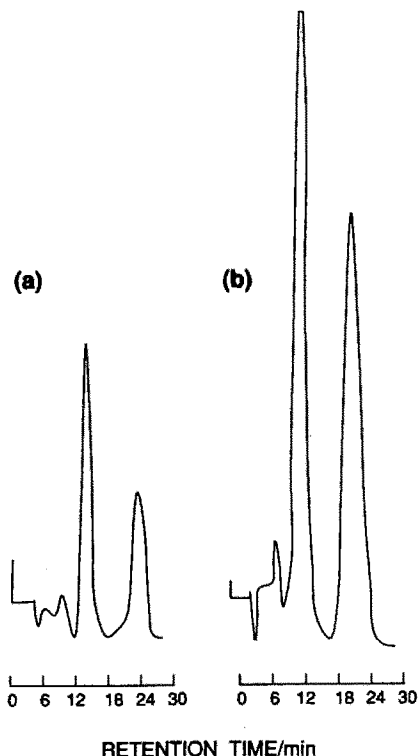


Fig. 3. Chromatograms obtained from two dilutions of a commercial multivitamin tablet. Peaks (from left to right) are Cu^{2+} (negative peak), Zn^{2+} , Mg^{2+} and Ca^{2+} .

determinations. It was possible to determine only about four cations simultaneously, because the chromatographic efficiency was quite low. With this PCID detection system it should be possible to determine more elements simultaneously by use of other stationary phases, such as chemically modified reversed phases. The requirements of the post-column reagent mixture are a metal chelate with a lower formation constant than the corresponding chelates of the analyte metals, together with an indicator that will form a radiation-absorbing complex with the displaced cation. This introduces the possibility of choosing other reagent mixtures for the analysis of various cation mixtures by PCID detection. Atomic spectrometric techniques are most commonly used for trace metal determinations, but multielement analysis requires the high capital expense and

Table 4. Analysis of multivitamin tablets

Cation	Amount found per tablet,*		Manufacturer's
	mg		quoted amount per tablet, mg
Ca^{2+}	158 ± 5	143 ± 2	162
Co^{2+}	ND†		2.6×10^{-4}
Cu^{2+}	NQ‡		2
Mg^{2+}	106 ± 2	100 ± 2	100
Zn^{2+}	18 ± 5	16 ± 3	15

*Precision limits are \pm two standard deviations.

†Not detected.

‡Detected, but not quantified.

high running costs of plasma spectrometers. Although less sensitive, ion-chromatography with PCID would be a lower-priced alternative, with easy automation and providing sequential multielement analysis. An additional advantage for samples such as natural waters could be the ability to detect different oxidation states of a given element.

Acknowledgements—This research was supported by the Natural Sciences and Engineering Research Council of Canada. We are grateful to F. Cantwell for loan of the pressure vessels used in the instrument.

REFERENCES

1. K. Robards, E. Patsalides and S. Dilli, *J. Chromatog.*, 1987, **411**, 1.
2. D. Yan and G. Schwedt, *Z. Anal. Chem.*, 1985, **320**, 325.
3. J. W. Wimberley, *Anal. Chem.*, 1981, **53**, 2137.
4. F. R. Nordmeyer, L. D. Hansen, D. J. Eatough, D. K. Rollins and J. D. Lamb, *ibid.*, 1980, **52**, 852.
5. J. D. Lamb, L. D. Hansen, G. G. Patch and F. R. Nordmeyer, *ibid.*, 1981, **53**, 749.
6. G. J. Sevenich and J. S. Fritz, *ibid.*, 1983, **55**, 12.
7. J. S. Fritz and J. N. Story, *ibid.*, 1974, **46**, 825.
8. M. D. Arguello and J. S. Fritz, *ibid.*, 1977, **49**, 1595.
9. D. Yan and G. Schwedt, *Z. Anal. Chem.*, 1985, **320**, 252.
10. K. L. Cheng, K. Ueno and T. Imamura, *CRC Handbook of Organic Analytical Reagents*, CRC Press, Boca Raton, Florida, 1982.
11. J. S. Fritz and R. B. Willis, *J. Chromatog.*, 1973, **79**, 107.
12. R. M. Cassidy, S. Elchuk and P. K. Dasgupta, *Anal. Chem.*, 1987, **59**, 85.
13. R. Přibil, *Applied Complexometry*, p. 22. Pergamon Press, Oxford, 1982.
14. P. K. Dasgupta, *Approaches to Ionic Chromatography*, in *Ion Chromatography*, J. G. Tarter (ed.), Dekker, New York, 1987.

DETERMINATION OF WATER-SOLUBLE VITAMINS BY LIQUID CHROMATOGRAPHY WITH A PARALLEL DUAL-ELECTRODE ELECTROCHEMICAL DETECTOR

WEIYING HOU and ERKANG WANG*

Laboratory of Electroanalytical Chemistry, Changchun Institute of Applied Chemistry, Chinese Academy of Sciences, Changchun, Jilin 130022, People's Republic of China

(Received 3 August 1989. Revised 28 December 1989. Accepted 4 February 1990)

Summary—A method for the determination of water-soluble vitamins (ascorbic acid, pyridoxine hydrochloride, pyridoxal hydrochloride, pyridoxamine dihydrochloride, *p*-aminobenzoic acid, folic acid) by liquid chromatography, with a parallel dual-electrode electrochemical detector, is described. One electrode was controlled at +0.80 V (*vs.* SCE), the other at +1.20 V (*vs.* SCE). The possibility of interference by eight other water-soluble vitamins (riboflavin, nicotinamide, cyanocobalamin, menadione, dextro calcium pantothenate, thiamine, nicotinic acid, dextro biotin) was studied. These vitamins did not interfere when a parallel dual-electrode detector system was used. The estimation of five of the vitamins was studied in detail. The linear ranges found were 10 ng–1.2 µg for pyridoxine hydrochloride, 2 ng–2 µg for pyridoxal hydrochloride, 10 ng–3 µg for pyridoxamine dihydrochloride, 5–200 ng for folic acid and 0.6–200 ng for *p*-aminobenzoic acid, the limits of detection being 3, 0.6, 1, 2 and 0.06 ng respectively. Application of the technique to the estimation of vitamin B₆ in tablets is illustrated. The results indicate that the vitamin B₆ in these tablets existed in the pyridoxine hydrochloride form and the B₆ content agreed well with liquid chromatography by spectrophotometric analysis.

The separation and estimation of water-soluble vitamins and their analogues by liquid chromatography (LC),¹⁻⁴ electrochemical methods,^{5,6} and LC with electrochemical (LCEC) detection⁷⁻¹² have been reported. We have determined several water-soluble vitamins by LCEC and LC with spectrophotometric detection.¹³⁻¹⁶

LCEC couples the advantages of low detection limits and high selectivity with low cost. The use of dual-electrode detection schemes for LCEC has increased in popularity in recent years.¹⁷ Such systems can be useful for improving selectivity and/or sensitivity. Various dual-electrode detector arrangements have been proposed, of which the series and parallel configurations are the most popular.¹⁸ In the series configuration, changes in the composition of the effluent that are associated with the redox reaction at the upstream electrode are sensed by the downstream electrode. In the parallel configuration, the dual response ratio, obtained by having the two electrodes at different potentials on the slope of the hydrodynamic voltamperogram peak, provides a good estimate of the peak purity. The parallel arrangement also permits the monitoring of both oxidizable

and reducible species in the same sample. The parallel configuration has been widely applied in LCEC detection¹⁹⁻²¹. All dual-electrode detection schemes are based on the redox properties of the eluted compounds.

In the work described here, we studied the consecutive determination of six water-soluble vitamins by LCEC with a parallel dual-electrode detector. Vitamin C has been determined by an LCEC method¹⁰⁻¹² that is the same as the method in this paper.

As a linear concentration range and low detection limit were reported, we have not determined vitamin C again but have concentrated on the determination of pyridoxine hydrochloride, pyridoxal hydrochloride, pyridoxamine dihydrochloride, folic acid and *p*-aminobenzoic acid. The method is simple, rapid, sensitive and selective.

EXPERIMENTAL

Apparatus

The LC system consisted of a Model 510 pump, a U6K injection valve and a Model 481 variable-wavelength detector (Waters Assoc.). The injection volume was 20 µl and the wavelength used was 254 nm. A Nucleosil C₁₈

*Author for correspondence.

(4 mm × 20 cm, 7 μm) column made by the Dalian Institute of Chemical Physics (China) was used, with a Model TL-5A thin-layer electrochemical cell (Bioanalytical Systems Inc., U.S.A.) and a laboratory-made bipotentiostat for amperometric detection.²² A saturated calomel reference electrode (SCE) was employed. The chromatograms were obtained at ambient temperature (20 ± 2°) with a mobile phase flow-rate of 1 ml/min.

Reagents

All chemicals were of analytical reagent grade, unless stated otherwise. The ion-pairing reagent was sodium 1-heptanesulphonate (Aldrich Chemical Co.). All solutions were prepared with doubly distilled water. Riboflavin (vitamin B₂), pyridoxine hydrochloride (PN), pyridoxamine dihydrochloride (PM), nicotinamide (PP), cyanocobalamin (vitamin B₁₂)

menadione (vitamin K₃) and pyridoxal hydrochloride (PL) were biochemical reagent grade. Folic acid, dextro calcium pantothenate, thiamine (vitamin B₁) and nicotinic acid were chemical reagent grade. Dextro biotin (vitamin H) was food reagent grade (Merck). The multi-vitamin tablets were commercially available products (China). Each tablet contained vitamin A [2500 international units (IU)], D₂ (200 IU), E (1 mg), PP (10 mg), B₁ (2 mg), B₂ (1 mg), B₆ (1 mg), C (35 mg) and dextro calcium pantothenate (2 mg).

Procedures

Vitamin B₂ and folic acid were dissolved separately in potassium hydroxide solution and diluted with water to give 1 mg/ml concentration. Dextro biotin was dissolved ultrasonically in a mixture of 4 ml of water and 2 ml of ethanol and then diluted to 1 mg/ml

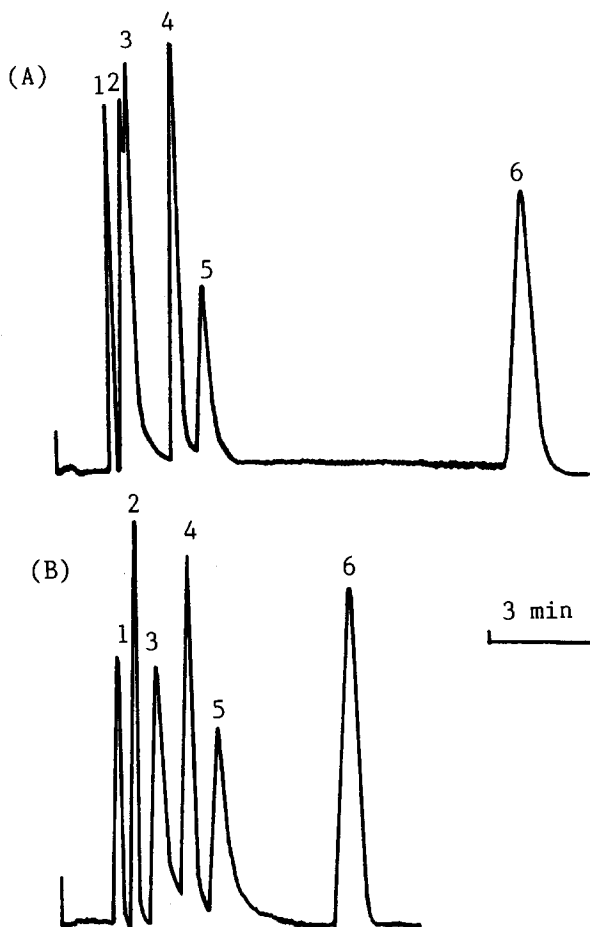


Fig. 1. Chromatograms of six water-soluble vitamins on a Nucleosil C₁₈ column: $\lambda = 254$ nm, flow-rate, 1 ml/min; (1) ascorbic acid, (2) *p*-aminobenzoic acid, (3) pyridoxamine dihydrochloride, (4) pyridoxal hydrochloride, (5) pyridoxine hydrochloride, (6) folic acid. (A) mobile phase, 10% v/v CH₃OH + 0.1M KH₂PO₄, pH 6.5, 0.05 absorbance full scale; (B) mobile phase, 10% v/v CH₃OH + 0.1M KH₂PO₄ (0.1mM sodium 1-heptanesulphonate); pH 6.5, 0.1 absorbance full scale.

concentration with water. All other standard samples were dissolved and diluted to 1 mg/ml concentration with water (vitamin C was dissolved in deaerated water). All standard solutions were stored at 4°. Just before the analysis, an aliquot was taken and diluted to appropriate concentration with the mobile phase.

A multi-vitamin tablet was crushed to a fine powder and dissolved in deaerated water. The solution was filtered through a sintered glass filter (porosity 5–15 μm) and diluted to 50 ml with water.

RESULTS AND DISCUSSION

Separation of six vitamins by liquid chromatography

In our previous papers,^{13–15} it was shown that the separation of PN, PL, PM, folic acid, vitamin C and *p*-aminobenzoic acid (vitamin B_x) was affected by the pH and methanol content of the mobile phase. The effect of the pH and the methanol content of the mobile phase on the separation of the six vitamins on a Nucleosil C₁₈ column was examined with a spectrophotometric detector. When there was no sodium 1-heptanesulphonate in the mobile phase, the peaks of vitamin B_x and PM always overlapped irrespective of the methanol content and pH of the mobile phase [Fig. 1(A)]. When there was

0.1M sodium 1-heptanesulphonate in the mobile phase, the retention time of PM was increased, PM and vitamin B_x were separated and the retention time of folic acid was decreased. A good separation of all six vitamins was achieved in 10% (v/v) methanol + 0.1M KH₂PO₄ (0.1M sodium 1-heptanesulphonate) (pH 6.5) [Fig. 1(B)]. When the sodium 1-heptanesulphonate concentration was increased from 0.1 to 1mM, the retention time of PM increased and that of folic acid decreased. This fact can be explained by a "dynamic ion-exchange" mechanism. The 1-heptanesulphonate ion in the mobile phase was bound to the surface of the stationary phase by the interaction of the heptyl chain and the stationary phase, making the stationary phase an ion-exchanger.

The PM cation underwent ion-exchange and hence its retention time was increased. The folic acid anion was excluded by the 1-heptanesulphonate so its retention time was not decreased.

Electrochemical detection with parallel dual-electrode detector

A parallel dual-electrode system with two different oxidative potentials allows the consecutive detection of six vitamins, vitamin C at +0.80 V and the other five at +1.20 V. Figure 2 shows the chromatograms obtained

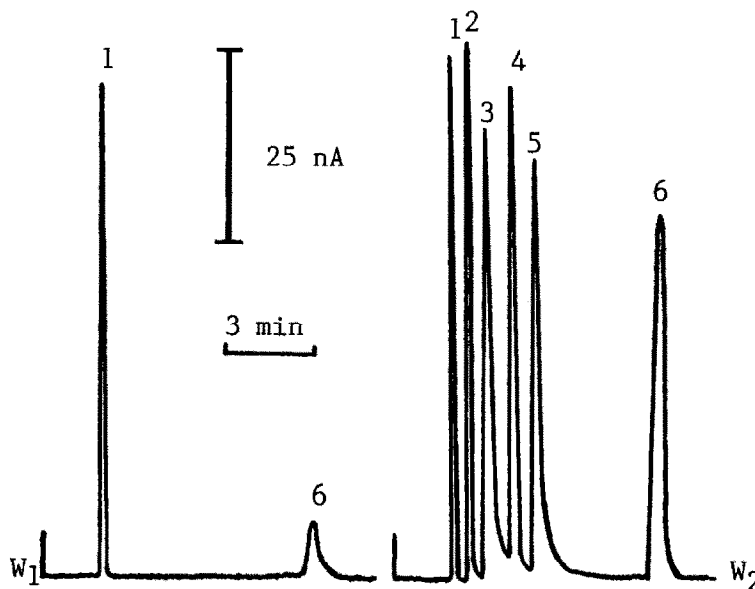


Fig. 2. Chromatograms of six water-soluble vitamins with parallel dual-electrode electrochemical detection: mobile phase, 10% v/v CH₃OH + 0.05M KH₂PO₄ (0.1M sodium 1-heptanesulphonate), pH 6.5; flow-rate, 1 ml/min; 2 $\mu\text{g/ml}$ ascorbic acid (1), 1 $\mu\text{g/ml}$ *p*-aminobenzoic acid (2), 5 $\mu\text{g/ml}$ pyridoxamine dihydrochloride (3) 4 $\mu\text{g/ml}$ pyridoxal hydrochloride (4), 5 $\mu\text{g/ml}$ pyridoxine hydrochloride (5), 10 $\mu\text{g/ml}$ folic acid (6). W₁: working electrode at +0.80 V; W₂: working electrode at +1.20 V.

Table 1. Calibration data (linear regression) and detection limits for the water-soluble vitamins

Vitamin	LR, ng	Slope, nA/ng	r	DL, ng
PN	10–1200	0.58	0.9995	3
PL	2–2000	0.85	0.9994	0.6
PM	10–3000	0.82	0.9993	1
B ₆	0.6–200	10.3	0.9999	0.06
Folic acid	5–200	0.29	0.9999	2

LR = Linear range, r = correlation coefficient, DL = detection limit.

with parallel dual-electrode detection. It can be seen that the detection of the vitamins by LC with a parallel dual-electrode electrochemical detector has high selectivity (Fig. 2, W₁, only vitamin C can be detected) and versatility (Fig. 2, W₂, six vitamins can be detected consecutively). Moreover, the noise is lower at +0.80 V than at +1.20 V and a lower detection limit for vitamin C will be achieved at +0.80 V.

Eight replicate injections of a standard solution containing 20 µg/ml PN, 10 µg/ml PL and PM, 50 µg/ml folic acid and 2 µg/ml *p*-aminobenzoic acid were made, to determine the precision. The coefficient of variation of the peak height was 2.0% for PN and PL, 1.6% for PM, 4.8% for folic acid and 4.6% for *p*-aminobenzoic acid.

Calibration graphs were obtained by use of various concentrations of the standard solutions. The calibration data and detection limits for PN, PL, PM, folic acid and vitamin B₆ are given in Table 1. The calibration graphs are linear and the detection method is sensitive.

The interference of eight other water-soluble vitamins, (PP, H, K₃, B₁₂, B₁, B₂, nicotinic acid and dextro calcium pantothenate) with the electrochemical detection of the six vitamins was examined. All eight vitamins had no effect in the detection of the six vitamins by LC with parallel dual-electrode detection, whereas only dextro calcium pantothenate and vitamin H gave no interference when spectrophotometric detection was used, showing the superior selectivity of the LCEC system.

PN, PM and PL are the three forms of vitamin B₆. Figure 2 shows that all three can be separated and determined by the present method. We examined the form of vitamin B₆ present in the multi-vitamin tablets and determined it by the standard-addition method. The

result indicated that the pyridoxine was present in these tablets. The content found (0.98 mg/tablet) agreed well with the value (0.99 mg/tablet) found by an LC with spectrophotometric method. The relative deviation was 1.0%.

Acknowledgement—The support of the National Natural Science Foundation of China is gratefully acknowledged.

REFERENCES

1. R. B. H. Wills, C. G. Shaw and W. R. Day, *J. Chromatog. Sci.*, 1977, **15**, 262.
2. M. W. Dong, J. Lepore and T. Tarumoto, *J. Chromatog.*, 1988, **442**, 81.
3. R. R. Kwok, W. P. Rose, R. Tabor and T. S. Pattison, *J. Pharm. Sci.*, 1981, **70**, 1014.
4. M. Amin and J. Reusch, *Analyst*, 1987, **112**, 989.
5. J. Lindquist and S. M. Farroha, *ibid.*, 1975, **100**, 377.
6. J. P. Hart, *TrAc*, 1986, **5**, 20.
7. J. Lankelma E. van der Kleijn and M. J. T. Jansen, *J. Chromatog.*, 1980, **182**, 35.
8. K. Kamata, T. Hagiwara, M. Takahashi, S. Uehara, K. Nakayama and K. Akiyama, *ibid.*, 1986, **356**, 326.
9. J. P. Hart and P. J. Hayler, *Anal. Proc.*, 1986, **23**, 439.
10. L. A. Pachla and P. T. Kissinger, *Anal. Chem.*, 1976, **48**, 364.
11. K. Iriyama, M. Yoshiura and T. Iwamoto, *J. Liq. Chromatog.*, 1985, **8**, 333.
12. W. A. Behrens and R. Madere, *Anal. Biochem.*, 1987, **165**, 102.
13. E. Wang and W. Hou, *Microchem. J.*, 1988, **37**, 338.
14. *Idem*, *J. Chromatog.*, 1988, **447**, 256.
15. W. Hou, H. Ji and E. Wang, *Anal. Chim. Acta*, 1990, **230**, 207.
16. W. Hou and E. Wang, *Analyst*, 1990, **115**, 139.
17. D. A. Roston, R. E. Shoup and P. T. Kissinger, *Anal. Chem.*, 1982, **54**, 1417A.
18. C. E. Lunte, P. T. Kissinger and R. E. Shoup, *ibid.*, 1985, **57**, 1541.
19. R. E. Shoup and G. S. Mayer, *ibid.*, 1982, **54**, 1164.
20. D. A. Roston and P. T. Kissinger, *ibid.*, 1981, **53**, 1695.
21. L. D. Hutchins-Kumar, J. Wang and P. Tuzhi, *ibid.*, 1986, **58**, 1019.
22. H. Ji and E. Wang, *Sepu*, 1988, **6**, No. 3, 139.

MICROCOMPUTER-CONTROLLED AUTOMATIC TITRATOR WITH ANALYSIS OF RESULTS BY MEANS OF SPLINE FUNCTIONS

KRZYSZTOF REN

Faculty of Chemistry, A. Mickiewicz University, 60-780 Poznań, Grunwaldzka 6, Poland

(Received 6 April 1988. Revised 6 February 1990. Accepted 14 February 1990)

Summary—A method of controlling an automatic titrator by means of a microcomputer is described. Experimental titration data have been analysed by the use of approximative or rational spline functions.

Previously described methods^{1,2} of determining potentiometric titration end-points by use of rational and approximating spline functions were developed with the intention of applying them to automatic titrators coupled with a microcomputer capable of controlling the titration, calculating the results and presenting them in a form convenient for the user.

The automatic-titration assembly proposed in this paper fulfils two important conditions:

(1) It allows the operator ready interaction with the analytical process and easy adjustment of the assembly for each research problem. This is further facilitated by writing the algorithm for the analytical process in BASIC.

(2) The titration algorithm ensures optimal distribution of the measurement points along the titration curve so that the information is sufficient for formation of a spline function which closely approximates the titration curve. This has increased the accuracy of determining titration end-points and minimizes the analysis time.

The proposed microcomputer-controlled automatic titrator ensures high titration accuracy and also enables the determination of dissociation constants, selectivity coefficients of ion-selective electrodes, construction of calibration curves, and measurement of concentrations by the method of standard additions.

The titration assembly, shown schematically in Fig. 1, consists of a pH-meter, an automatic burette, a microcomputer and an interface. The choice of equipment is optional. In the present instance the following equipment was used: a Mera-Elwro digital pH-meter, type N 517, a Radelkis automatic burette and a Sinclair ZX

Spectrum microcomputer. If cost is an important factor, it may be noted that an 8-bit microcomputer is sufficiently powerful for the calculations required, but a large enough kbyte RAM will be needed.

Interface

The interface should be individually adjusted to the equipment available and provide for two functions: (1) input of the measured potential from the pH-meter to the computer; (2) an output port for controlling the automatic burette by voltage impulses. With the automatic burette used here, one voltage impulse (level TTL) caused addition of 0.002 ml of solution.

Making such an interface is a simple task (e.g., a universal system 8255 can be used). It is also possible to use as an interface a properly programmed parallel port, such as is installed in many microcomputers for interfacing to a printer.

PROGRAM CONTROLLING THE TITRATION

The flow-chart of the program controlling the titration is presented in Fig. 2. The algorithm takes into account various types of titration, even those in which the potential of the electrodes is not stable, e.g., because of difficulties with establishment of equilibria so that there are considerable differences in the times needed for stabilization of the electrode potential at various points of the titration curve.

The program can be divided into two parts. The first is used for controlling the titration, and the second, for analysis of the data, is one of the programs already described^{1,2} for determining potentiometric titration end-points by use of

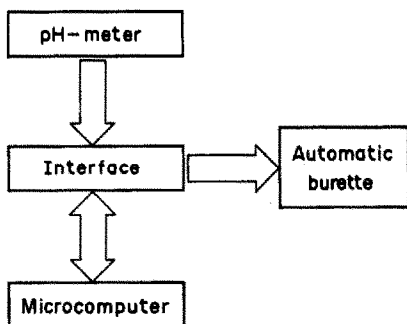


Fig. 1. Block diagram of the automatic titrator.

spline functions. The first part of the program starts by giving the necessary initial values to the variables and determining the total volume of titrant which should be added. This volume may be, for instance, equal to the capacity of the automatic burette or as otherwise determined.

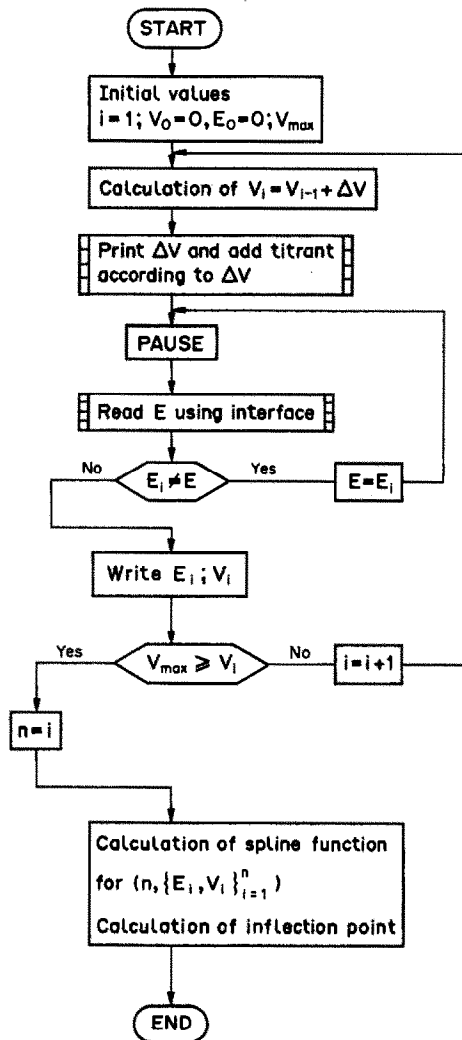


Fig. 2. Flow-chart of the program controlling the potentiometric titration.

Then follows calculation of the incremental volumes of titrant to be added (described below). The calculated increment is converted into the corresponding number of impulses by the microcomputer and transmitting them through the interface to the burette produces the required addition of titrant. After addition of the increment there is a pause (5 sec) assigned in the program, during which the solution is stirred and the electrode potential should reach equilibrium and be stabilized, the potential shown by the pH-meter is read and compared with the previous value stored in the microcomputer memory. If both values agree within a specified limit, it is accepted that the potential of the electrode has stabilized. The program then stores the co-ordinates of this measurement point (E_i, V_i) in appropriate tables in the memory of the computer and repeats the cycle with addition of the next, newly calculated, increment of titrant. If, however, the electrode potential differs from the previously stored value, this potential is stored and the program again introduces a pause to allow for stabilization, and so on. In the case of electrodes with particularly unstable potentials, the program should be supplemented with a condition specifying a maximum overall time for stabilization, after which a new increment will be added even if stabilization has not been reached. Such a situation may occur close to the end-point or at the end of a titration curve where the concentration of the ions to which the electrode is sensitive is low and the electrode potential is less stable.

The titration continues until the volume of titrant determined at the beginning has been added. The coefficients of the spline function are the calculated and the titration end-point is determined.^{1,2}

Calculation of the incremental volume

The accuracy of the titration end-point, which is identified with the inflection point of the spline function^{1,2} formed from the set of measurement points, depends on how far the shape of the spline function differs from that of the real titration curve, the true form of which is not accessible because of random errors. Thus it is important to form the spline function from a set of measurement points containing sufficient information about the titration. Adding small increments, so that the measurement points are closely spaced, leads to accurate results but is very time-consuming and

therefore uneconomical. The optimal procedure should take into account the most advantageous distribution of points on the titration curve, with more information (*i.e.*, more closely spaced points or smaller titrant increments) being concentrated in the parts where the variability of the curve is greatest.

The problem is therefore to find a way of forecasting the further course of the curve from the portion already completed. Two ways of calculating the next titrant increment are presented.

$$a = \frac{(V_{i-2} - V_{i-3})(E_{i-1} - E_{i-3}) - (V_{i-1} - V_{i-3})(E_{i-2} - E_{i-3})}{(E_{i-1}^2 - E_{i-3}^2)(E_{i-2} - E_{i-3}) + (E_{i-2}^2 - E_{i-3}^2)(E_{i-1} - E_{i-3})}$$

$$b = \frac{(E_{i-1}^2 - E_{i-3}^2)(V_{i-3} - V_{i-3})(E_{i-1}^2 - E_{i-3}^2)(V_{i-2} - V_{i-3})}{(E_{i-1}^2 - E_{i-3}^2)(E_{i-2} - E_{i-3}) + (E_{i-2}^2 - E_{i-3}^2)(E_{i-1} - E_{i-3})}$$

$$c = V_{i-3} - aE_{i-3}^2 - bE_{i-3}$$

(1) From the change in gradient ($\Delta E/\Delta V$) in two successive sections of the titration curve. The volume of the i th titrant increment is calculated from the formula:

$$\Delta V_i = V_i - V_{i-1}$$

$$= \left[(V_{i-1} - V_{i-2}) \left(\frac{E_{i-2} - E_{i-3}}{V_{i-2} - V_{i-3}} \right) \right] / \left(\frac{E_{i-1} - E_{i-2}}{V_{i-1} - V_{i-2}} \right)$$

This procedure requires that the first two increments be assigned arbitrarily, and it should be stressed that the distribution of the measurement points on the curve will depend on the two volumes.

Figure 3 shows the distribution of the measurement points calculated in this way for the potentiometric titration of copper with benzylamino-*N,N*-di(methanephosphonic) acid

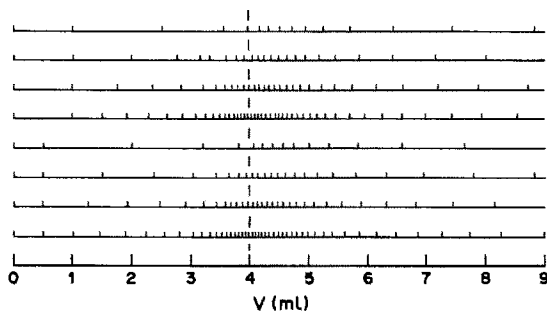


Fig. 3. Distribution of measurement points on the V -axis when titrant increments are calculated from changes of $\Delta E/\Delta V$. Titration of Cu^{2+} with BADMF at pH 6. Crytur 29-17 electrode.

(BADMF),³ with detection by copper-sensitive electrode (Crytur 29-17).

The spacing of the points clearly depends on the choice of the two initial increments. There is some asymmetry in the distribution of the measurement points about the end-point, but in practice this has no effect on the result of the titration.

(2) By extrapolating the existing curve as a parabola. The coefficients of the equation of the parabola which fits the last three measurement points at any time, are calculated from:

The next value of the total volume of titrant is calculated from the equation of the parabola:

$$V = aE^2 + bE + c$$

for $E_i = E_{i-1} + E_{i-1} - E_{i-2}$. This procedure produces more or less regular spacing of the points on the titration curve, but requires imposition of a limiting range for the increment volume if excessive congestion or scattering of points is to be avoided. The spacing of subsequent points again depends on the volumes assigned to the first two increments, which should be determined according to the predicted total volume of titrant to be added, *e.g.*, $0.1 V_{\text{max}}$. Figure 4 illustrates the distribution of points on the curve when ΔV is calculated in this way (with $0.1 \leq \Delta V \leq 1$ ml) for the same titration as in Fig. 3. The distribution of the points is more symmetrical near the end-point than in Fig. 3 and method (2) is undoubtedly better, although more complicated mathematically.

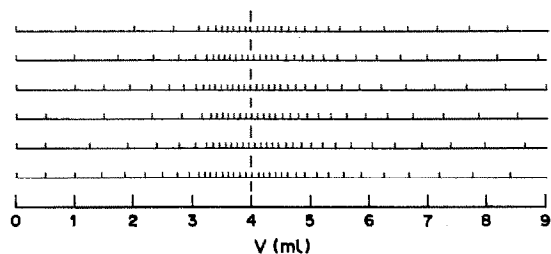


Fig. 4. Distribution of measurement points on the V -axis when increments are calculated by parabolic extrapolation. Other details as for Fig. 3.

Table 1. Results for titrations of Cu, and the dependence of titration time on the two initial increments and the method of calculating successive increments

ΔV_1 , ml	ΔV_2 , ml	Gradient method		Parabola method ($0.1 \leq \Delta V \leq 1$ ml)	
		End-point, ml	Time, sec	End-point, ml	Time, sec
0.5	0.5	4.060	305	4.047	245
0.5	0.75	4.063	205	4.046	225
0.5	1	4.064	160	4.043	210
1	0.5	4.061	320	4.043	240
1	0.75	4.063	200	4.044	225
1	1	4.063	160	4.042	165

Both ways of calculating ΔV significantly shorten the titration time without reducing the accuracy. This is illustrated by the results in Table 1 for titration of copper with BADMF. The dependence of the titration time on the size of the two initial increments is shown. Titration with equal increments of 0.1 ml took 500 sec and the result was 4.049 ml.

REFERENCES

1. K. Ren and A. Ren-Kurc, *Talanta*, 1986, **33**, 641.
2. K. Ren, *ibid.*, 1990, **37**, 667.
3. *Idem*, *Chem. Anal. (Warsaw)*, 1986, **31**, 37.

PROMOTING EFFECT OF IODIDE ON THE HEXACYANOMANGANATE(IV)–ARSENIC(III) REDOX REACTION, FOR KINETIC DETERMINATION OF IODIDE

GUILLERMO LOPEZ-CUETO*

División de Química Analítica, Facultad de Ciencias, Universidad de Alicante,
Apdo. 99, 03080-Alicante, Spain

CARLOS UBIDE

Departamento de Química Aplicada, Facultad de Química, Universidad del País Vasco,
Apdo. 1072, 20080-San Sebastián, Spain

(Received 12 June 1989. Revised 11 September 1989. Accepted 13 October 1989)

Summary—The rate of the reaction between hexacyanomanganate(IV) and arsenic(III) in an acid medium is strongly accelerated by iodide. The reaction kinetics indicates that the iodide activity decreases throughout the reaction, probably because manganese(IV) oxidizes iodide to iodate (an inactive form). This behaviour is defined as *promotion*, rather than catalysis, and this rate-modifying effect has been used to determine iodide by a kinetic method. A linear calibration plot was obtained by a two-point fixed-time procedure. A detection limit of 0.2 ng/ml, a quantification limit of 0.6 ng/ml and relative standard deviations of 5.5 and 13% for the 6.7 and 0.6 ng/ml levels respectively have been found. Positive kinetic interferences from osmium(VIII) and iodate have been observed, and copper(II), silver(I) and mercury(II) inhibit the iodide activity by precipitation. The method has been applied to determination of iodide in sodium arsenite (reagent grade) and table salt. The method has been validated by recovery experiments.

Some of the well-known methods for the trace-level determination of iodide are based on its catalytic activity in a number of redox reactions. The indicator reaction most widely used is probably the oxidation of arsenic(III) with cerium(IV),^{1,2} but other indicator reactions have been proposed and reviewed.^{3–5}

The catalytic effect of iodide on the Mn(III)–As(III) reaction has been known⁶ for some time and the reaction has been used for the kinetic determination of organically bound iodine in rat thyroid⁷ and for the catalytic titration of silver(I), mercury(II) and palladium(II).⁸

Hexacyanomanganate(IV) is produced in acid solution by disproportionation of hexacyanomanganate(III)^{9,10} [$\text{Mn}(\text{H}_2\text{O})_6^{2+}$ and $(\text{CN})_2$ are also produced]. The reaction is quite fast at room temperature and the hexacyanomanganate(IV) slowly decomposes to yield $\text{Mn}(\text{H}_2\text{O})_6^{2+}$, $(\text{CN})_2$ and HCN.¹⁰ The reaction between hexacyanomanganate(IV) and arsenic(III) is slow in acid solution and its kinetics and mechanism have been studied.¹¹ We have found that iodide notably accelerates the

reaction rate. In this paper, the effect of iodide on the hexacyanomanganate(IV)–arsenic(III) reaction has been studied and a method developed for the kinetic determination of iodide.

EXPERIMENTAL

Reagents

Potassium hexacyanomanganate(III). Prepared either by the procedure previously reported¹⁰ or according to the faster method of Lower and Fernelius.¹² Analysis by the methods previously reported¹³ indicated a content of at least 98.5%.

Hexacyanomanganate(IV) solution (2.60×10^{-3} M). Prepared by dissolving 0.0427 g of $\text{K}_3\text{Mn}(\text{CN})_6$ in a dark 25-ml standard flask containing 1.0 g of sodium nitrate and some 0.1 M sulphuric acid previously cooled to 0° [the sodium nitrate prevents precipitation of manganese(IV) oxide by hydrolysis and lowers the freezing point of the solution]. The solution is diluted to volume with 0.1 M sulphuric acid. Before use, the solution must be kept at ~0° for about 1 hr to allow the Mn(III) disproportionation reaction to proceed to completion. The Mn(IV) solution thus obtained can be used for a period of 6–8 hr if kept at ~0°.

*Author for correspondence.

Arsenic(III) solution (0.173 M). Prepared by dissolving 1.14 g of NaAsO_2 and 14.7 g of sodium nitrate in some water and enough sulphuric acid to give a final concentration of 0.86 M, and diluting to 50 ml with water. The arsenic(III) solution was often found to contain iodide as an impurity. To avoid the effect of this, 5 mg of $\text{K}_3\text{Mn}(\text{CN})_6$ [initial Mn(III) concentration, $3 \times 10^{-4} \text{ M}$] were added to the solution, previously heated to 50° ; in these conditions iodide is oxidized to an inactive form, probably iodate, and the excess of oxidant decomposes at this temperature in about 90 min.¹⁰ The solution is ready for use when cooled to room temperature.

Standard iodide solution (10^{-2} M). Prepared by dissolving 0.830 g of potassium iodide in 500 ml of water, standardized against 10^{-2} M silver nitrate, and stored in a polyethylene bottle in the refrigerator. Working solutions were prepared before use and kept in polyethylene flasks. Analytical reagent grade potassium iodide can be used without standardization if it is dried at $110\text{--}120^\circ$ for at least 2 hr.

All chemicals were of analytical-reagent grade (Merck, except sulphuric acid, which was Riedel-de-Haën) and doubly distilled water was used throughout.

Apparatus

A Varian 634-S spectrophotometer (coupled with a Radiometer REC80 Servograph recorder) and a Shimadzu UV-260 spectrophotometer, both with 1.0-cm path-length fused-silica cells and constant-temperature cell-holders were used. The cell compartment was kept at constant temperature ($\pm 0.2^\circ$) by circulating water from a thermostat.

Volumes less than 0.5 ml were added with Brand Transferpettor micropipettes.

Procedures

Kinetic measurements. Solutions were prepared in dark 250-ml standard flasks by mixing the required amounts of solid sodium arsenite (0.65–6.5 g), solid sodium nitrate (0–53.1 g) to adjust the ionic strength and 0.06–0.75 M sulphuric acid, and finally adding 0.1–2.5 ml of 10^{-5} M potassium iodide (when the promoting effect was being studied) and water up to 220–230 ml. The resulting solution was kept in a thermostatic bath for 30 min; the required amount of $\text{K}_3\text{Mn}(\text{CN})_6$ was then added with stirring and the volume was quickly adjusted with water to 250 ml. The solution was stirred

again and transferred to a spectrophotometric cell. For the kinetic curve, the absorbance at 387 nm [where the $\text{Mn}(\text{CN})_6^{2-}$ shows an absorption maximum] was recorded, with water as reference.

Iodide determination. A 1.5 ml volume of the arsenic(III) solution, up to 1.00 ml of the iodide sample and water to adjust the final volume to 2.5 ml were placed in a 1-cm cuvette. The Teflon lid was put on, the cell was shaken, and left to stand for 10 min in the controlled-temperature cell-holder of the spectrophotometer. The absorbance was set to zero, then the cuvette was taken out, 100 μl of the hexacyanomanganate(IV) solution were added carefully to avoid mixing, the lid was put on and the cell inverted two or three times (this point was taken as zero time), and the absorbance was measured after 1 and 5 min. The difference between the reciprocals was then used to read the iodide concentration from a calibration plot prepared in the same way.

Iodide determination in sodium arsenite samples. The procedure was the same as before, but 1.5 ml of arsenic(III) solution (sample plus reagent) without previous oxidizing treatment with $\text{K}_3\text{Mn}(\text{CN})_6$ was used. Instead of the iodide sample, 1.00 ml of water was added.

Iodide determination in table salt samples. A suitable amount between 0.03 and 0.15 g of table salt was accurately weighed, dissolved in water and diluted to volume in a 100-ml standard flask with water. A 0.5-ml portion was accurately measured into the cuvette and treated as for determination of iodide in sodium arsenite. The maximum chloride concentration reached in these conditions (about $5 \times 10^{-3} \text{ M}$) does not interfere with the iodide determination.

RESULTS AND DISCUSSION

Reaction kinetics

The hexacyanomanganate(IV)–arsenic(III) redox reaction proceeds slowly, with pseudo first-order kinetics.¹¹ In the presence of iodide, however, a remarkable accelerating effect is observed; moreover, the first-order kinetics with respect to the $\text{Mn}(\text{CN})_6^{2-}$ species is followed only initially. Plots of $\ln A$ vs. t tend to be linear during the first stages of the reaction and the value of the initial slope seems to be independent of the initial Mn(IV) concentration (Fig. 1). If this concentration is low enough, a linear section that confirms initial first-order kinetics can clearly be seen. Once the initial

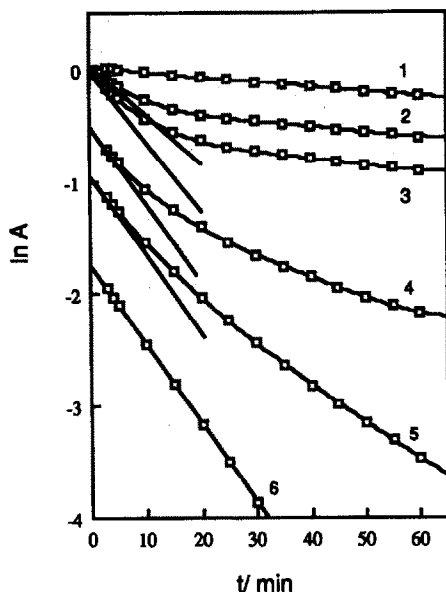


Fig. 1. Plots of $\ln A$ vs. time for the reaction between hexacyanomanganate(IV) and arsenic(III). $\text{As(III)} = 0.1M$; $\text{H}^+ = 0.16M$, ionic strength = 2.0; temperature = 30° . Mn(IV) , curves (1), (2) and (3) $2.5 \times 10^{-4}M$; curve (4) $1.5 \times 10^{-4}M$; curve (5) $1.0 \times 10^{-4}M$; curve (6) $0.5 \times 10^{-4}M$. Iodide, curve (1) 0; curve (2) $2.02 \times 10^{-8}M$; curves (3), (4), (5) and (6), $3.03 \times 10^{-8}M$.

first-order period is complete, curvature appears and the slope decreases. After a certain interval of time, straight lines are obtained again and pseudo first-order kinetics is followed, but the rate constant (the slope) is now lower than that for the initial reaction. The value of the second rate constant does not depend on the initial Mn(IV) or iodide concentrations.

The accelerating effect of iodide could be interpreted as a catalytic one, as the $\text{I}^-/\text{I}^0/\text{I}^+$ catalytic cycle has been reported for some other reactions between arsenic(III) and oxidizing substances such as Ce(IV) .¹⁴ However, the deviation from initial pseudo first-order kinetics when iodide is present seems to indicate that the catalytic action of iodide involves a more complex mechanism.

The slope of the last straight section of the $\ln A$ vs. t plots (Fig. 1) is essentially independent of the iodide concentration, and is practically equal to that obtained from the reaction in the absence of iodide. On the other hand, the period in which the initial first-order kinetics is obeyed decreases as the Mn(CN)_6^{2-} concentration increases. These facts may be explained as due to a side-reaction of iodide in which it is converted into a catalytically inactive species. We think that this deactivation would consist of the oxidation of the catalyst to an oxidation state

higher than I^+ , probably I(V) (iodate). Thus, the decrease of the slope of the plots could reflect the conversion of the catalyst into its inactive form. The oxidation of iodide to iodate would be due to a slow reaction with the hexacyanomanganate(IV), and this would be the reason why the lower the concentration of Mn(CN)_6^{2-} , the slower the deactivation reaction. Similar behaviour has also been observed when iodide catalyses the cerium(IV)–arsenic(III) reaction, where the iodide is continuously oxidized to iodate by the Ce(IV) ,¹⁴ the extent of this reaction being dependant on the relative amounts of the reagents as well as on the experimental conditions. However, the deactivation of iodide during the Ce(IV) – As(III) reaction is much slower than during the Mn(CN)_6^{2-} – As(III) reaction, so the effect on the kinetics of the catalysed Ce(IV) – As(III) reaction is almost negligible.

According to Martell,¹⁵ this kind of behaviour in which the catalyst does not remain unaltered at the end of each reaction cycle (that is, the rate modifying effect is transient in nature), is better defined as *promotion*. A few examples of promoted reactions have been considered from an analytical point of view. Dutt and Mottola¹⁶ have applied some promoting effects on the tris(1,10-phenanthroline)iron(II)–chromium(VI) reaction to the kinetic determination of antimony(III), vanadium(IV), arsenic(III), molybdenum(VI), hexacyanoferrate(III), oxalic acid and citric acid. Milovanović and Protolipač¹⁷ have developed a kinetic method for the determination of sodium thiobarbitone, based on the promoting effect of this anaesthetic on the copper(II)-catalysed Pyrocatechol Violet–hydrogen peroxide reaction. Piemont *et al.*¹⁸ reported a promoting effect of titanium(III) on the oxidation of iodide by hydrogen peroxide, which can be used for the kinetic determination of titanium; the reaction is also promoted by iron(II).¹⁹ More recently, Thompsen and Mottola²⁰ have shown that the accelerating effect of glutaraldehyde on the oxidation of *p*-phenylenediamine by hydrogen peroxide to give Bandrowski's base^{21,22} is actually a promoting effect. The behaviour in iodide on the hexacyanomanganate(IV)–arsenic(III) reaction is similar to the previously reported promoting effects, so iodide must be considered as a *promoter* rather than a catalyst.

Calibration

Kinetic determination measurements are usually performed under pseudo zero-order

conditions, which requires the reaction to be no more than 5% complete. Pseudo zero-order conditions are difficult to attain in the hexacyanomanganate(IV)–arsenic(III) reaction when iodide is present, because a rapid change in the apparent reaction order takes place owing to deactivation of iodide. Thus, when the *initial rate* method was applied, a non-linear relationship between initial rates and iodide concentrations was found. When the more time-consuming *rate constant* method was tried and the pseudo first-order rate constant was measured from the initial slope of the $\ln A$ vs. t plots, the calibration was again non-linear. It was observed that there was a linear relationship between the value of D (defined as the difference between the reciprocals of the absorbance values measured at 5 min and at 1 min; $D = 1/A_5 - 1/A_1$) and the iodide concentration, C_1 , according to the general equation:

$$D = D_0 + KC_1$$

where D_0 is the difference that corresponds to the reaction in the absence of iodide. This two-point *fixed-time* method may be considered as the most suitable for iodide determination, and so it has been used to select the optimum conditions.

Optimization

The conditions selected should achieve the maximum signal/background ratio. In a cata-

lytic method, signal and background values are obtained from the overall and uncatalysed reactions respectively. The two-point *fixed-time* method was used to examine the effects of the experimental conditions on the D/D_0 ratio. These effects may be directly visualized if both $\log D$ and $\log D_0$ are plotted vs. the appropriate variable in the study. Obviously, better conditions will be achieved for larger $\log D - \log D_0$ values (Fig. 2). High ionic strength, low Mn(IV) concentrations and low temperatures increase the D/D_0 ratio, which has a maximum value at about $0.4M$ $[H^+]$. Neither the As(III) concentration nor the Mn(II) concentration seem to exert a significant influence. According to these results the experimental conditions selected as optimal were: Mn(IV), $10^{-4}M$; As(III), $0.1M$; H^+ , $0.4M$; ionic strength, 2.5; temperature, 20° .

Concentrations of Mn(IV) lower than $10^{-4}M$ result in too low a value for the initial absorbance, and temperatures lower than 20° can result in condensation of water on the outside of the cell, necessitating a continuous purge of the cell compartment with dry air or nitrogen.

Under the optimum conditions a linear calibration graph over the range 0.6–17.6 ng/ml iodide was obtained and the equation of the regression line was found to be:

$$D = (0.052 \pm 0.006) + (0.108 \pm 0.001)C_1$$

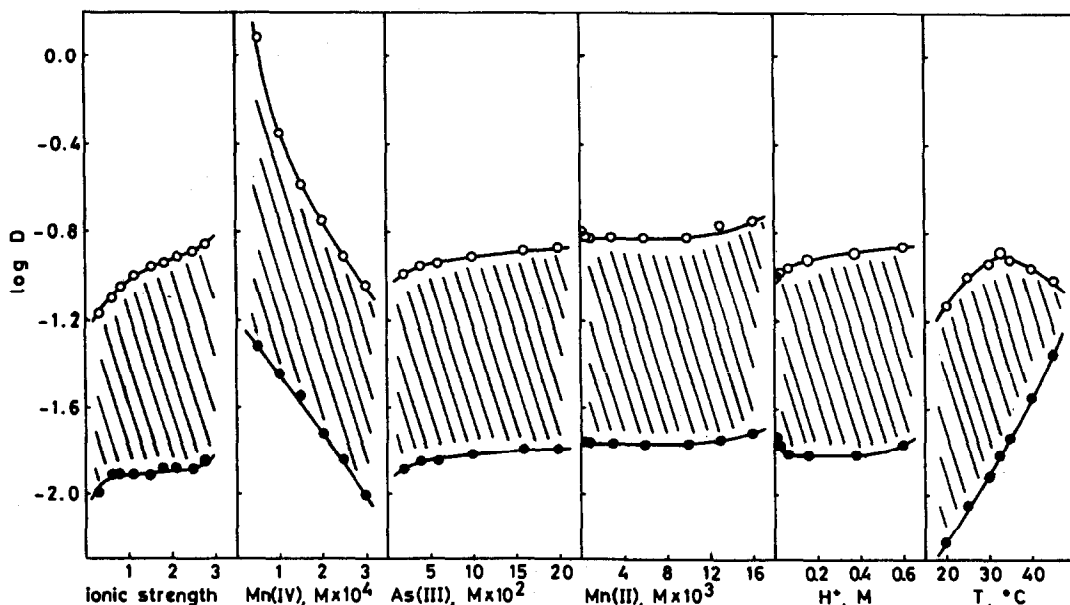


Fig. 2. Optimization. ●: Iodide not added. ○: I^- , $3.03 \times 10^{-8}M$ [except for Mn(II) as the variable, when I^- was $4.04 \times 10^{-8}M$]. Except when the variable under study: Mn(IV), $2.5 \times 10^{-4}M$; As(III), $0.1M$; H^+ , $0.16M$; ionic strength, 2.0; temperature, 30° .

where the errors in both the intercept and the slope are given as the standard deviations estimated from the regression analysis.

From the standard deviation of the background signal, the detection and quantification limits²³ were estimated to be 0.2 and 0.6 ng/ml respectively. Some possibilities of improving the precision and the limit of detection of the method can be suggested. If the initial Mn(IV) concentration is reduced, pseudo first-order reaction kinetics can easily be obtained and the initial-rate and the rate-constant methods will probably give linear calibration plots (long path-length cells will have to be used to obtain sufficiently high absorbance values). The relative standard deviations calculated at the 6.7 and 0.6 ng/ml levels were 5.5 and 13% respectively (10 replicates).

Effect of foreign ions

The study of interferent ions is summarized in Table 1. When present in excess of the specified amount, chloride, bromide, thiocyanate, oxalate, thiosulphate, sulphite, nitrite, iron(II) and tin(II) interfere by acting as reductants for hexacyanomanganate(IV); chlorate and bromate act as oxidants for arsenic(III) and Cu(II), Ag(I) and Hg(II) act as inhibitors for iodide. Only the interferences from osmium(VIII) and iodate are kinetic in nature.

The effect of iodate deserves some extra comment. When iodide is not present, no modifying effect is observed from iodate if it is added just before the determination, but interference is produced if iodate is allowed to stand together with arsenic(III) for a certain period of time. This is probably due to the reduction of iodate to an active form, *i.e.*, I^- , I or I^+ , that will probably take part in the reaction mechanism and so modify the reaction rate. When iodide is

present, the interference level of iodate is that indicated in Table 1, and this will probably be due to the $IO_3^- - I^-$ interaction to generate I or I^+ as the active species.

Application

The proposed method has been applied to the determination of iodide in sodium arsenite (analytical grade) and table salt. The iodide content of the first is important because arsenic(III) is used as a reagent in the indicator reaction, and the blank value will depend on the iodide impurity in the reagents used; the iodide content in table salt is important for dietary and health reasons.

The results of the iodide determination and the data obtained from the recovery studies are shown in Table 2. It should be noted that the iodide content in sodium arsenite samples depended on the batch number [for instance, a sodium arsenite sample from the same supplier as that labelled (1) in Table 2, but from a different batch number was found to contain no detectable iodide].

CONCLUSIONS

The accelerating effect of iodide in this system is *promotion* and not catalysis, and is useful for the trace level determination of iodide. The limit of detection of the method is probably the lowest reported so far for a kinetic method of determination of iodide,²⁴ an advantage which probably outweighs the consideration that conservation of the Mn(IV) solution needs some care.

Interferences are similar to those in the Ce(IV)-As(III) reaction,¹⁴ but seem to be less serious because the tolerated amounts of interferent ions are usually higher.

Table 1. Interferences in the determination of 0.5 ng/ml iodide ($4 \times 10^{-9} M$)

Tolerated concentrations of interferent species, <i>M</i>	Species assayed
10^{-1} *	ClO_4^- , PO_4^{3-} , SO_4^{2-} , acetate, tartrate, citrate
10^{-2}	Cl^- , F^- , ClO_3^-
10^{-4} †	Br^- , BrO_3^- , Sb(III), Ni(II), Co(II), Fe(III), Cr(III), Cr(VI), W(VI), V(V), Mo(VI)
10^{-5}	Cu(II)
10^{-6}	SCN^- , $C_2O_4^{2-}$, SO_3^{2-} , NO_2^- , Fe(II), Sn(II), Ag(I)
10^{-7}	$S_2O_3^{2-}$
10^{-8}	Os(VIII)
10^{-9}	Hg(II), IO_3^- ‡

*Maximum level tested for anions.

†Maximum level tested for cations.

‡See comment in text about the interference of iodate.

Table 2. Determination of iodide in sodium arsenite (analytical reagent grade) and in table salt samples (Standard deviations are given in parentheses); four replicates

Sample	Iodide content		Iodine, ng/ml			Recovery, %	
	In sample μg/g	In aliquot, ng/ml	Added	Found		Mean	Range
				Found	Recovered		
NaAsO ₂ (1)	0.14	1.8 (0.1)	2.4	4.7 (0.2)	2.9 (0.2)	121	118–134
NaAsO ₂ (2)	0.19	2.5 (0.2)	2.4	4.7 (0.1)	2.2 (0.2)	92	85–97
Iodized table salt (1)	76	4.4 (0.1)	2.4	6.8 (0.1)	2.4 (0.1)	99	96–103
Iodized table salt (2)	81	4.9 (0.8)	2.4	7.5 (0.2)	2.6 (0.8)	108	105–115
Marine table salt	1.1	0.31 (0.07)	2.4	2.9 (0.1)	2.6 (0.1)	109	107–115

The new method has been applied to the determination of iodide in reagents (analytical grade) and table salt. In the first case, methods with a limit of detection as low as possible are needed. In the second case (and especially with non-iodized table salt), the tolerance of the method towards chloride ions is high enough for matrix matching by addition of chloride to the standards²⁵ or use of the standard-additions method not to be necessary.

REFERENCES

1. E. B. Sandell and I. M. Kolthoff, *J. Am. Chem. Soc.*, 1934, **56**, 1426.
2. *Idem*, *Mikrochim. Acta*, 1937, 9.
3. N. M. Ushakova and I. F. Dolmanova, *J. Anal. Chem. USSR*, 1983, **38**, 1158.
4. M. Kopanica and V. Stará, in C. L. Wilson and D. W. Wilson, *Comprehensive Analytical Chemistry*, Vol. XVIII, p. 199. Elsevier, Amsterdam, 1983.
5. D. Pérez-Bendito and M. Silva, *Kinetic Methods in Analytical Chemistry*, p. 62. Horwood, Chichester, 1988.
6. R. Lang, *Z. Anorg. Allg. Chem.*, 1926, **152**, 206.
7. W. Boguth and W. Schaeg, *Mikrochim. Acta*, 1967, 658.
8. N. Kiba and M. Furosawa, *Anal. Chim. Acta*, 1978, **98**, 343.
9. G. Trageser and H. H. Eysel, *Inorg. Chim. Acta*, 1978, **26**, L56.
10. G. López-Cueto and C. Ubide, *Can. J. Chem.*, 1986, **64**, 2301.
11. *Idem, ibid.*, 1988, **6**, 2855.
12. J. A. Lower and W. C. Fernelius, *Inorg. Syn.*, 1946, **2**, 213.
13. G. López-Cueto, A. Alonso-Mateos, C. Ubide and G. del Campo-Martínez, *Talanta*, 1988, **35**, 795.
14. P. A. Rodríguez and H. L. Pardue, *Anal. Chem.*, 1969, **41**, 1369.
15. A. E. Martell, *Pure Appl. Chem.*, 1968, **17**, 129.
16. V. V. S. Eswara Dutt and H. A. Mottola, *Anal. Chem.*, 1974, **46**, 1090.
17. G. A. Milovanović and M. J. Protolipač, *Glas. Hem. Drus. Beograd*, 1981, **46**, 685.
18. E. Piemont, J. L. Leibenguth and J. P. Schwing, *Bull. Soc. Chim. France*, 1979, 254.
19. *Idem*, *Compt. Rend.*, 1979, **288C**, 533.
20. J. C. Thompsen and H. A. Mottola, *Anal. Chem.*, 1984, **56**, 2834.
21. E. Bandrowski, *Ber.*, 1894, **27**, 480.
22. O. D. Shapilov, *J. Anal. Chem. USSR*, 1980, **35**, 1429.
23. T. Cairns and W. M. Rogers, *Anal. Chem.*, 1983, **55**, 54A.
24. Reference 5, pp. 64 and 67.
25. M. C. Gutiérrez, A. Gómez-Hens and D. Pérez-Bendito, *Analyst*, 1989, **114**, 89.

A SPECTROPHOTOMETRIC STUDY OF THE DETERMINATION OF GOLD WITH PHENOTHIAZINE

I. NĚMCOVÁ and P. RYCHLOVSKÝ

Department of Analytical Chemistry, Charles University, Albertov 2030, 128 40 Prague 2, Czechoslovakia

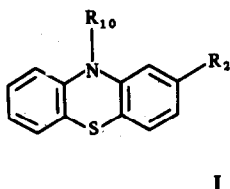
E. KLESZCZEWSKA

Department of Chemistry, Warsaw University, Białystok, Poland

(Received 24 July 1989. Revised 19 January 1990. Accepted 26 February 1990)

Summary—The reaction of Au(III) with phenothiazine has been studied and a reaction mechanism proposed. Optimal conditions for the reaction have been found and a new spectrophotometric method has been developed for determination of Au(III). The method is advantageous in its simplicity and reproducibility. Gold can be determined in the concentration range 2–20 $\mu\text{g/ml}$

Phenothiazine derivatives have been primarily used in spectrophotometric determinations of metals which form complexes or ion-associates with them or oxidize them to coloured (usually red–purple, $\lambda_{\text{max}} = 500\text{--}530\text{ nm}$) cation radicals. The radicals, however, are stable only in concentrated acids, as is the case in the reaction of Au(III) with derivatives with substitution at the heterocyclic nitrogen atom or position 2 (I,b).^{1,2}



(a) $R_2 = \text{H}$, $R_{10} = \text{H}$; (b) $R_2 = \text{H}$, Cl , CF_3 , etc., and $R_{10} = (\text{CH}_2)_2\text{N}(\text{C}_2\text{H}_5)_2$, $(\text{CH}_2)_3\text{N}(\text{CH}_3)_2$, etc.

However, we have found that reaction of Au(III) with unsubstituted phenothiazine (I,a) produces an intensely green product even in weakly acidic media and the product can be utilized for a very simple and sensitive determination of gold. This paper reports a study of the reaction mechanisms and the effect of surfactants on the properties of the reaction product. The use of surfactants permits direct spectrophotometric measurement of the solution, whereas most other spectrophotometric determinations of gold, based usually on the formation of water-insoluble compounds, require extractions with organic solvents.

EXPERIMENTAL

Apparatus

A Pye-Unicam-Philips PU 8800 spectrophotometer was used with 1-cm path-length fused-silica cells. A Radiometer PHM 64 pH-meter was used, calibrated with Radiometer buffers.

Reagents

A 0.005M phenothiazine solution was prepared from the substance triply recrystallized from methanol, by dissolution in 96% ethanol. The purity of the substance was checked by melting point measurement in a Kofler block³ and by TLC with methanol–chloroform (1:1).

A 0.01M HAuCl_4 solution was prepared by dissolving pure gold in several ml of *aqua regia*, adding 0.2 g of sodium chloride, evaporating to dryness on a water-bath and dissolving the residue in 1M hydrochloric acid.

A 0.1M sodium dodecylsulphate (SDS) solution was prepared by dissolving the substance in water.

A Methyl Orange indicator solution was prepared by dissolving 0.05 g of the indicator in 50 ml of ethanol.

The solution pH was adjusted with 0.05M sodium hydroxide or hydrochloric acid.

Procedure

To a measured volume of solution containing not more than 500 μg of gold and diluted with water to ca. 10 ml in a 25-ml standard flask, add 2 drops of Methyl Orange indicator followed by 0.05M sodium hydroxide until the solution has

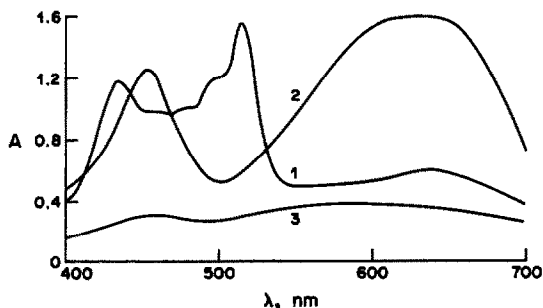


Fig. 1. The absorption spectra of the products of the reaction of Au(III) with phenothiazine at various pH values. 1—pH = 0.50, 2—pH = 5.00, 3—pH = 9.00. $c_{\text{Au(III)}} = 1 \times 10^{-4}M$, $c_{\text{phen}} = 2 \times 10^{-4}M$, $c_{\text{SDS}} = 0.04M$.

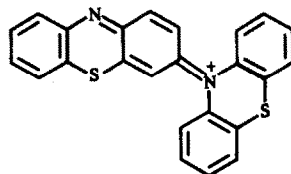
just turned yellow (the colour does not interfere in the determination of gold at 635 nm). Then add 10 ml of 0.1M SDS and 1 ml of 0.005M phenothiazine with continuous stirring, dilute to the mark with distilled water and measure the absorbance at 635 nm against water, 10–20 min after mixing the reactants.

RESULTS AND DISCUSSION

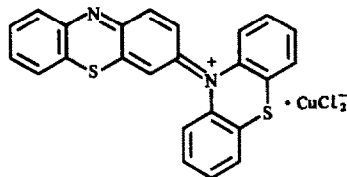
Study of the Au(III) reaction with phenothiazine

The nature of the product of reaction of Au(III) with phenothiazine depends on the acidity of the medium (see Fig. 1). In strongly acidic solutions, a red colour appears and the absorption spectrum (curve 1) indicates that it corresponds to the phenothiazine cation radical.⁴ On decrease in the acidity the absorption curve exhibits two more pronounced maxima at 460 and 635 nm (curve 2); the solution is intensely green. These two maxima were ascribed to the

dimer cation in a study of the properties of phenothiazine.^{4,5}



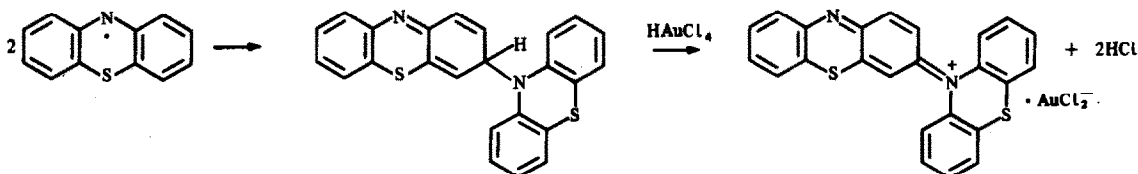
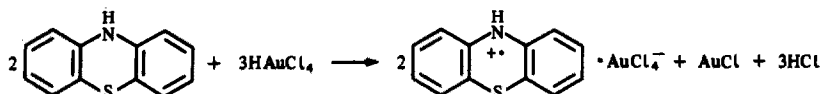
A product with an analogous absorption spectrum was also obtained in the reaction of phenothiazine with cupric chloride; the structure



has been proposed for it.^{6,7}

According to the papers cited, in its reactions with oxidants, phenothiazine is first oxidized to the cation radical, which is converted into the neutral radical in media with low hydrogen-ion concentrations and then dimerizes. A further oxidation leads to the dimer cation (or when CuCl_2 is the oxidant, its ion-associate with the CuCl_2^- formed). The position of the absorption maxima is determined by the conjugated system of the dimer cation, which is not perceptibly affected by association with CuCl_2^- .

As a product with similar properties has been obtained in the reaction of Au(III) with phenothiazine, the appropriate reactions under the given experimental conditions can be expressed in a simplified form (without reaction intermediates) in terms of the following equations (the



oxidation states of the gold are obvious, so are omitted).

The Job method of continuous variations and the molar ratio method yielded the stoichiometric ratio of the product components, Au:phenothiazine = 1:2, confirming the proposed structure.

It is further obvious from Fig. 1 that the absorbance of both the bands decreases on further decrease in the acidity, and a small maximum appears (curve 3), corresponding to phenothiazinone (the wavelengths of the absorption maxima in the ultraviolet region also agree with the literature data for this compound).

Spectrophotometric determination of Au(III)

As phenothiazine and the reaction product are insoluble in water, but phenothiazine is readily soluble in methanol or ethanol, 96% ethanol was first selected as the solvent.

The coloured product appears immediately after the reactants are mixed, but it is insufficiently soluble and separates as a deep green precipitate. As it is well known that the solubility of many organic substances can be increased by the solubilizing properties of surfactant micelles⁸ (the absorption spectra of the solubilized substances are also often altered), the effect of various types of surfactant on the solubility and the absorption spectrum of the product was tested, with cationic carbethoxypentadecyltrimethylammonium bromide, anionic sodium dodecylsulphate and non-ionic Triton X-100. It was found that only sodium dodecylsulphate (SDS) affects the solubility, with increase in the absorbance of the solution. The greatest change in the absorbance is with SDS in the range $5\text{--}10 \times 10^{-3}M$ (see Fig. 2), *i.e.*, in the range of critical micelle concentration of

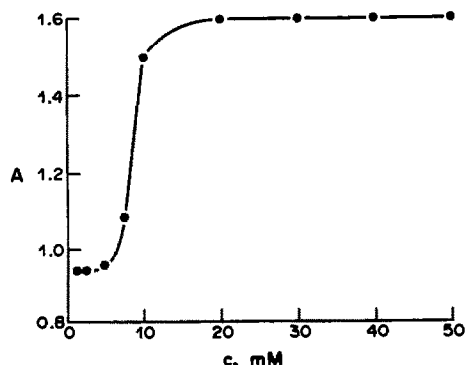


Fig. 2. Dependence of the absorbance on SDS concentration. $\lambda = 635\text{ nm}$, $c_{\text{Au(III)}} = 1 \times 10^{-4}M$, $c_{\text{phen}} = 2 \times 10^{-4}M$, $\text{pH} = 5.0$.

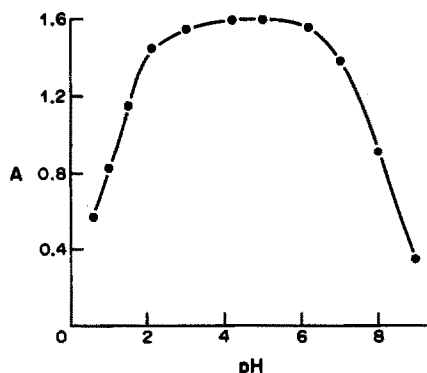


Fig. 3. Dependence of the absorbance on pH. $\lambda = 635\text{ nm}$, $c_{\text{Au(III)}} = 1 \times 10^{-4}M$, $c_{\text{phen}} = 2 \times 10^{-4}M$, $c_{\text{SDS}} = 0.04M$.

SDS.⁹ Constant colour intensity was attained with SDS concentrations higher than $0.02M$. A concentration of $0.04M$ was therefore used for the determination because it gave greater stability of the reaction product.

The optimal pH for the product formation is in the range 3.5–6 (see Fig. 3). Small amounts of $0.05M$ hydrochloric acid or sodium hydroxide can be used for pH adjustment.

A maximum amount of the product is formed at a phenothiazine concentration equal to, or at least twice, that of the gold. We selected a phenothiazine concentration of $2 \times 10^{-4}M$ as the most suitable.

The maximum absorbance is obtained 10 min after the mixing of the components, and is stable for 10 min, then decreases again. This stability period makes it possible to analyse a batch of about 6 samples. Ethanol concentrations higher than 20% v/v decrease the stability of the reaction product (see Fig. 4).

The solution must be continuously stirred during addition of the reactants, as the instantaneous concentrations of the reactants determine the reaction rate and thus also the time required for development of the colour. The reproducibility

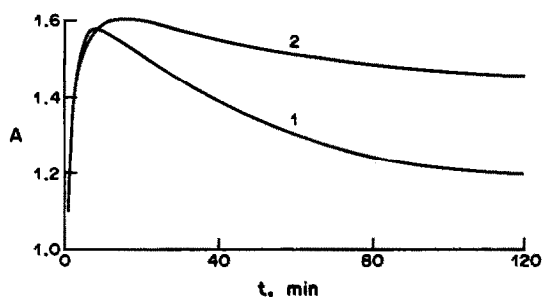


Fig. 4. Influence of ethanol on the time stability of the reaction product. 1— $c_{\text{eth}} = 30\%$, 2—without ethanol. $\lambda = 635\text{ nm}$, $c_{\text{Au(III)}} = 1 \times 10^{-4}M$, $c_{\text{phen}} = 2 \times 10^{-4}M$, $c_{\text{SDS}} = 0.04M$, $\text{pH} = 5.0$.

bility of the determination is improved when this condition is observed.

The measurements were made at 25°; at temperatures lower than 10° the reaction does not occur, and at very high temperatures the solution is decolorized.

Under the optimum conditions for the formation of the coloured complex, the Lambert–Beer law is obeyed from 2.0 to 20 $\mu\text{g/ml}$ Au(III). The relative standard deviation is 2.8% for Au(III) concentrations of less than 4 $\mu\text{g/ml}$ and from 0.5 to 1.5% for higher concentrations.

Ions giving analogous reactions (Cu^{2+} , Hg^{2+} , Ag^+) and strong oxidants (KMnO_4 , $\text{K}_2\text{Cr}_2\text{O}_7$) interfere in the determination when present at a ratio to gold as low as 1:1 w/w. The alkali-metal and alkaline-earth metal ions do not react with phenothiazine. Among the platinum metals, only Pd^{2+} and Pt^{4+} interfere, the former through a complexation reaction and the latter through oxidation of phenothiazine to the cation radical.

For these reasons the method is unsuitable for determination of gold in common alloys, but it is convenient for determination of gold in organic compounds.

Practical application

The method developed has been validated by determination of gold in the pharmaceutical

Tauredon for injections (BYK Gulden, Konstanz). The preparation contains 100 mg of sodium aurothiomaleate, *i.e.*, 46 mg of Au(III) per ml of the solution.

One ml of concentrated hydrochloric acid and 0.5 ml of 30% H_2O_2 were added to 10 μl of the test solution and the mixture was diluted with water to 5 ml, and the excess of H_2O_2 was decomposed by heating. The solution was then allowed to cool, the pH was adjusted and the procedure already described was followed.

Four determinations yielded a mean of 45.78 mg of Au per ml of the solution, *i.e.*, 99.5% of the theoretical content, with a relative standard deviation of 0.5%.

REFERENCES

1. L. Kum-Tatt, *Anal. Chim. Acta*, 1962, **26**, 478.
2. H. S. Gowda and H. Ramappa, *Z. Anal. Chem.*, 1976, **280**, 221.
3. *Čs. lékopis 3*, Avicenum, Prague, 1971.
4. P. Hanson and R. O. C. Norman, *J. Chem. Soc., Perkin Trans. II*, 1973, 264.
5. Y. Tsujino, *Tetrahedron Lett.*, 1968, **21**, 2545.
6. M. V. Diudea and I. A. Silberg, *J. Prakt. Chem.*, 1983, **324**, 769.
7. M. V. Diudea, *Rev. Roum. Chem.*, 1983, **28**, 249.
8. P. H. Elworthy, A. T. Florence and C. B. Farlane, *Solubilization by Surface-Active Agents*, Chapman & Hall, London, 1968.
9. H. J. Corrin and W. D. Harkins, *J. Am. Chem. Soc.*, 1947, **69**, 683.

SOFTWARE SURVEY SECTION

Software package TAL-001/90

PHASE PLANE METHOD FOR LIFETIME DETERMINATION
OF SINGLE AND DOUBLE EXPONENTIAL DECAYS

Contributors: A. Ruperez, L. Ayala and J.J. Laserna, Department of Chemistry, Faculty of Sciences, University of Malaga, 29071, Spain.

Brief description: An observed luminescence (fluorescence or phosphorescence) decay curve can be due to the luminescence or photochemical degradation of the analyte and impurities in the solvents, and decay of the scattered stray radiation from the source. In these cases, the observed decay behaviour is not simply the summation of the sample decay plus the background decay; there is some degree of convolution. In addition, distortions in the data may arise from several factors, including the wavelength-dependence of the excitation profile, the dependence of the response of the detector on the energy of the incident photons, scattered exciting light, etc. This program uses the phase plane method for deconvolution of single and double exponential decays.

In the program, the phase plane method can be used in a 3-parameter or 5-parameter version to calculate lifetimes in single or double exponential decays, respectively. Distortions in the data are also considered. The convoluted observed decay can be expressed as $D(t) = Z(t)E(t) + aE(t)$, where $Z(t)$ corresponds to a single or double exponential, $E(t)$ is the background contribution to the convoluted decay, and $aE(t)$ considers distortions in the experimental data. Depending on whether a single or double decay is being analysed, $D(t)$ can be linearized as a function of 2 or 4 independent variables. After introduction of the experimental luminescence data (intensity vs. time), the program computes the values of the variables at each time, and then by application of standard linear least-squares methods, the best values of the lifetimes, pre-exponential factors and distortion factors can be calculated easily.

Potential users: Spectroscopists.

Fields of interest: Chemical analysis and spectrochemistry.

This application program has been developed in BASIC for the Apple Macintosh Plus computer, to run under Macintosh 5.0. It is available on 3.5-in floppy discs. The memory required is 492K.

Distributed by the contributors [Tel. Spain (34) 52 28 13 00].

Documentation is minimal, but no user training is required. The program has been fully operational for 1 year. The source code is not available, but the contributors are willing to answer user enquiries.

THERMOSONIMETRY OF THE PHASE II/III TRANSITION OF HEXACHLOROETHANE

OLIVER LEE, YOSHIKATA KOGA and ADRIAN P. WADE*

Chemistry Department, University of British Columbia, 2036 Main Mall, Vancouver, B.C.,
Canada V6T 1Y6

(Received 21 November 1989. Revised 11 April 1990. Accepted 28 April 1990)

Summary—A thermosonimetric study has shown that the Phase II/III polymorphic transition of hexachloroethane emits acoustic signals. This solid-solid phase transition is known to occur by a nucleation-growth process during which a nucleus of the new phase, once formed, grows at the expense of the mother phase to form a complete crystal without fracture. Acoustic emissions from a conditioned multi-crystal sample have been used to study the transition. Acoustic activity correlated well with dilatometric measurements. Frequency analysis on waveforms of many hundreds of individual acoustic emissions revealed marked differences between individual signals. Principal-components analysis on 24 signal features revealed a single dispersed cluster with a highly non-uniform distribution of signals. These experiments provided highly reproducible average power spectra. Time-resolved acoustic power spectra were also generated. These additional types of information cannot be obtained by other techniques.

Thermosonimetry (TS) is the study of acoustic emission induced by a change in temperature.¹ It has been mainly applied to thermally-induced phase transitions.¹⁻⁵ Emission of acoustic signals is a phenomenon common to other areas of chemistry.⁶⁻¹⁰ So far, this has been widely overlooked as an analytical tool,^{11,12} and requires further development. Acoustic emission (AE) takes the form of many short-duration signals. These often occur at frequencies that are too high to be detected by the human ear and may require extreme amplification for detection.⁸ Each signal has its own time of occurrence, duration, and frequency and amplitude characteristics. These signals may be analyzed by a wide variety of statistical and mathematical methods, and are almost an ideal data source for development and use of modern chemometric techniques. From a theoretical standpoint their interpretation is a highly complex and possibly intractable problem. Therefore empirical pattern recognition methods have been employed.^{8,11,13-15} These have shown the existence of multiple types of acoustic emission, which may be differentiated on the basis of their frequency and time domain characteristics, and then associated with their different physico-chemical sources (*e.g.*, gas evolution *vs.* crystal fracture).¹¹ New types of information may thus

be obtained from AE measurements. Factors such as the nature of the signal to be detected, the rate at which information is to be collected, and instrumental limitations must all be considered.¹⁶

Thermosonimetric studies of phase transitions

Phase transitions result in a redistribution of matter and energy. This causes transient elastic waves in the matrix. The waveforms captured are a function of the original signal envelope, distance from source to sensor, transmission characteristics of the media, the various combinations of pathways by which the signal may reach the detector, and the impulse and frequency response characteristics of the detector and associated circuitry.¹² The true "transfer function" of the system is not readily quantifiable. Because of these considerations, the waveforms detected are not exact representations of the original signals, and signals obtained during an experiment will certainly not all be identical. Despite these limitations, the waveforms collected have readily identifiable acoustic signatures.¹¹

Perhaps the first study of acoustic emission from a phase transition was the work of Förster, in 1934, on the formation of martensite in steel.¹⁷ Much later, Sawada *et al.*⁵ studied phase transitions of *p*-cresol, liquid crystals and water and found that acoustic activity began at the

*Author for correspondence.

onset of the phase transition and finished on its completion. They suggested that a sudden release of elastic energy owing to volume changes was the most likely source of the emissions.⁵ However, processes other than volume change are also likely to participate in phase transitions. Just a few years before, Reynolds,¹⁸ in his work on the β to α transformation of *p*-dichlorobenzene, reported small audible clicks during the transformation of melt-grown crystals which had been doped with small amounts of *p*-dibromobenzene and attributed the sound to the movement of the interface. There was, however, no report on the final state of the crystal after the transformation nor was an acoustic study carried out. Microfracture processes and release of trapped gases during melting of ice have also been shown to be acoustically active.¹² There are many examples in the materials science literature citing crack formation as a source of acoustic emission in materials undergoing stress.

Other thermosonimetric studies have investigated the polymorphic transformations of temperature standards used in differential thermal analysis,¹ the polymorphic phase transition in calcium iodide,² sodium chloride–cesium chloride and cesium chloride–barium chloride systems,³ and the glass transition in Kōrsor glass samples.⁴ Solid-state processes such as motion of dislocations, propagation of cracks, nucleation of new phases, relaxation processes and discontinuous changes in physical properties (thermal expansion/contraction, elastic modulus, electrical conductivity, *etc.*) may be studied by this technique.³

The Phase II/III transition of hexachloroethane

On cooling, the Phase II/III polymorphic transformation of hexachloroethane proceeds from a phase thought to be monoclinic or triclinic to one that is orthorhombic at a transition temperature (T_{tr}) of 43.6°. ¹⁹ The transformation is termed "mild" because the entropy and structural changes associated with it are small. It occurs through nucleation–growth processes and is thought to be a single crystal–single crystal transformation.^{19–22} This has been confirmed by observations with a polarizing microscope.^{19,23} Nucleation is the rate-determining step and a nucleus, once formed, grows at the expense of the mother phase until it forms an entire crystal. Internal fracturing is not observed as long as the temperature is not more than 20° below the transition temperature.¹⁹ Immobile

microbubbles were reported to form at the phase boundary under certain conditions, though this was not reported to occur for the corresponding heating transition.²³ Furthermore, a twinning plane, if it existed, could be moved by the phase boundary.²³ As is common with polymorphic transformations, hexachloroethane crystals exhibit hysteresis. A metastable/unstable changeover for this transition has also been suggested.²² The kinetics of the transition are fairly well known from dilatometric studies^{19–22} which linked volume changes of the sample with the occurrence of the Phase II/III transition. It is recognized that kinetic studies alone cannot adequately characterize the mechanism of solid–solid phase transitions.²⁴ Further understanding of the underlying mechanism is considered valuable.

The objectives of this present work were (*i*) to show that TS can monitor this transition; (*ii*) to discover the contribution TS can make to understanding nucleation/growth (and if possible obtain characteristic signals from these processes); (*iii*) to see whether TS could verify the presence of the metastable/unstable boundary; (*iv*) to compare the efficacy of TS and dilatometry for studying the same process; (*v*) to evaluate the ability of TS and current apparatus to provide quantitative information for this system. Prior to this work no attempt has been made to capture individual acoustic signals from phase transitions of small organic molecules, nor has analysis of the dominant frequency components of such signals been studied in detail.

EXPERIMENTAL

Reagent

The hexachloroethane was a multi-crystal sample (12.130 g) contained in the dilatometer. This sample had undergone extensive preconditioning to minimize the effects of defects and impurities (which would otherwise strongly influence solid phase heterogeneous kinetics). As a result, reasonably reproducible nucleation and growth rates were realized. A description of the conditioning procedure used is given elsewhere.²¹

Large orthorhombic crystals for the single crystal experiments were prepared by slow recrystallization from a saturated methanol solution over a 1.5 month period. The resulting crystals of various size were initially transparent but exhibited growth lines.

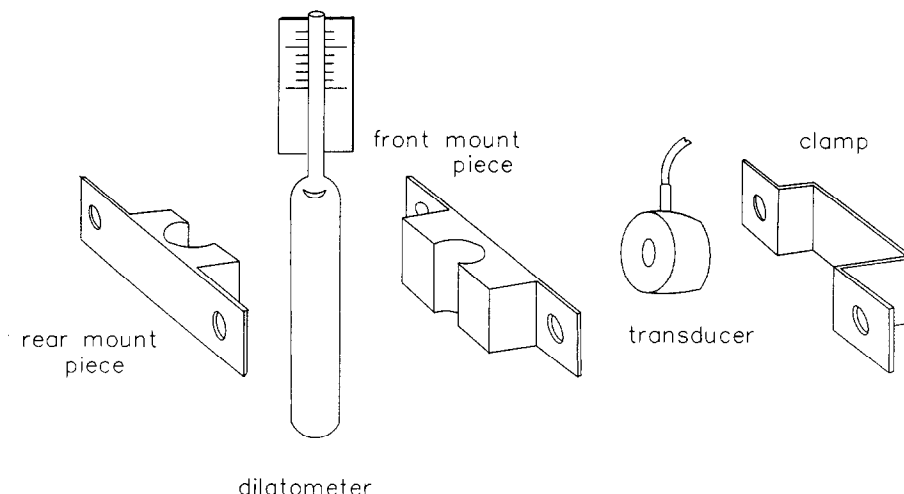


Fig. 1. Exploded schematic diagram of dilatometry apparatus showing mounting of the acoustic transducer.

Apparatus

The first set of experiments used the dilatometric apparatus shown in Fig. 1. A hexachloroethane powder sample was placed in the glass envelope, which was filled with water. As in previous studies with this dilatometer,¹⁹⁻²² changes in the sample volume were monitored by observing the level of the meniscus in the capillary stem. An aluminum mount and clamp arrangement was constructed to attach the acoustic transducer to the side of the dilatometer. Water-baths were used for temperature control and studies on temperature effects. A thin air-tight plastic bag surrounded the submerged portion of the apparatus to keep the transducer's electrical connections dry. A certified mercury partial immersion thermometer (Fisher Scientific, Richmond, B.C.) was placed inside the bag to measure the outer glass temperature of the dilatometer to a precision of 0.02° . The dilatometer-aluminum and aluminum-transducer interfaces were smeared with vacuum grease (Apiezon type M, Fisher Scientific) to enhance acoustic coupling.

In the single-crystal experiments grown crystals were placed directly in a 50 ml Pyrex beaker filled with 10.0 ml of distilled water. The transducer was submerged in the water-bath directly underneath the 50 ml beaker. Acoustic coupling was provided by the water in the bath. Silicone (AutoSealTM, General Electric) was used to seal the transducer electrical connection.

The apparatus shown schematically in Fig. 2a was used for all studies on the sample contained in the dilatometer. The acoustic emissions were detected by means of a broad-band piezoelectric

transducer (Bruel and Kjaer, Naerum, Denmark, type 8312), equipped with an integrated 40 dB preamplifier. This transducer's frequency response is shown in Fig. 3 and the upper frequency limit is estimated to be about 1.2 MHz. Further signal amplification and high-pass filtering (50 kHz–2 MHz) was achieved with a conditioning amplifier (Bruel and Kjaer, type 2638) which had both d.c. "peak detector" and a.c. outputs. The heavily damped d.c. output signal (200 msec decay constant) was sent to a chart recorder to provide signal power *vs.* time plots. Individual signals were acquired from the a.c. output by use of a 100 MHz digital storage oscilloscope (Tektronix, type 2230, Beaverton, OR). This was set to sample at 5 MHz and gave 8-bit resolution by 1024-point recording of each signal. Data acquisition was in triggered mode (using the rising slope of the incoming signal) with the trigger threshold level set just above the level of the background noise. Of the 1024 points collected per signal, 100 were prior to the trigger point. The digitized signals were then transferred to a 40 Mb hard disk on a 12 MHz IBM PC-AT compatible computer (Nora Systems, Vancouver, B.C.) for storage and subsequent data processing. This was achieved via an IEEE-488 bus and GPIB interface board (National Instruments, Austin, TX, model PC-IIA). The data-transfer rate of the Tektronix 2230 allowed a maximum acquisition/storage rate of 30 signals/min. Only a fraction of the acoustic signals generated during a single experiment could be captured by the Tektronix 2230 oscilloscope acquisition system. Typically, however, several hundred acoustic signals were

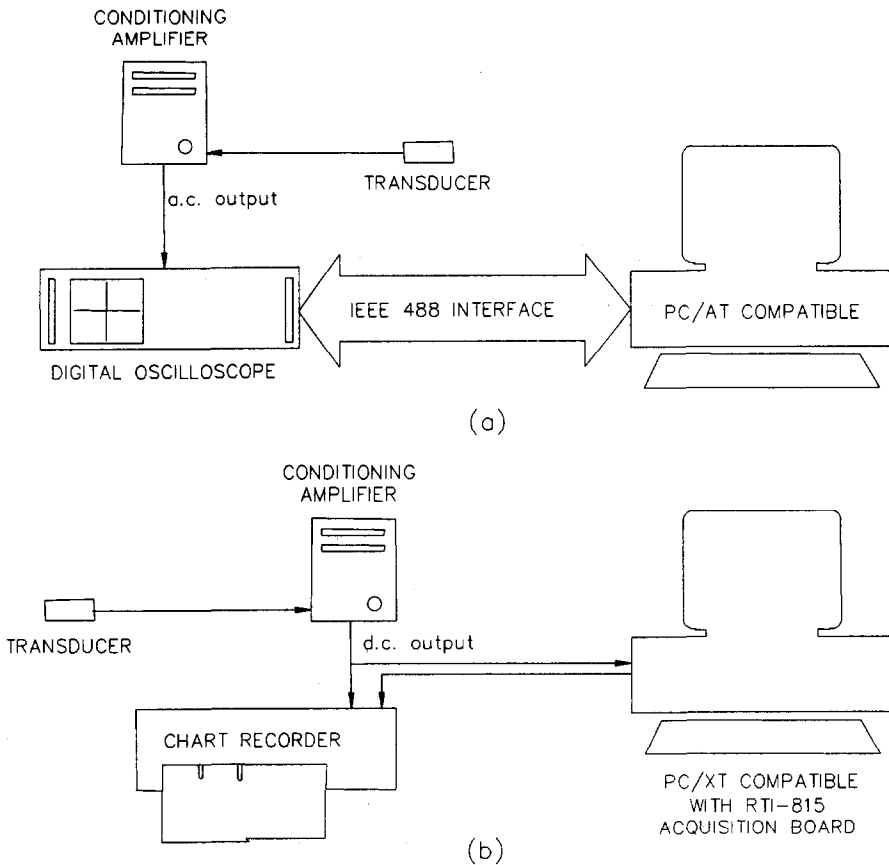


Fig. 2. Schematic diagram of acoustic data acquisition and processing systems: (a) for capture of individual emissions; (b) for simple quantification of RMS acoustic emission.

captured in an identical manner for each experiment, so the data sets obtained are representative.

For the studies involving the recrystallized single crystals, a Tektronix 2430A oscilloscope replaced the Tektronix model 2230. This was set to sample at 2.5 MHz and also gave an 8-bit resolution by 1024-point recording of each

signal. This unit could capture and transfer up to 15 signals/sec.

The apparatus shown in Fig. 2b was used to evaluate the ability of TS to provide quantitative information. The study was conducted on the recrystallized single-crystal samples. The d.c. output from the conditioning amplifier was sampled at 100 Hz with an analogue-to-digital converter board (Analog Devices, Norwood, MA, type RTI-815F) working in direct memory access (DMA) mode.²⁵ This ensured that no peaks were missed. The board was installed in a Compaq Portable PC (Compaq Computer Corp., Houston, TX). Software was written to capture the data and store them on disk. Storage of all 100 values captured per second would result in too large an amount of data being accumulated during an experiment, which might last 15 min. To reduce this, the software first determined the maximum and average value of the readings obtained per 200 msec and only these values were stored. The average readings were continually summed and the updated sum was sent to the second pen on the chart recorder

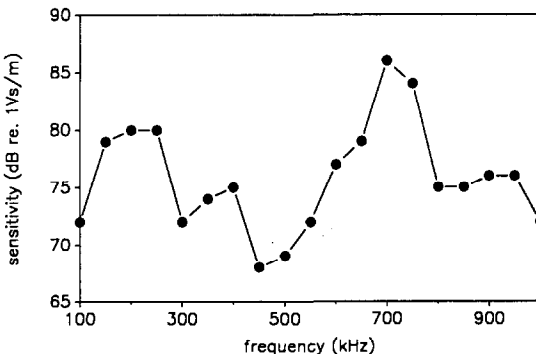


Fig. 3. Frequency response curve for the wide band transducer used in this work (points show calibration frequencies). The sensitivity units are those given in the manufacturer's literature.

via a digital-to-analog converter on the RTI-815F board. Wrap around is included in the software so that an output greater than the upper voltage limit of the recorder reappears on the lower voltage limit.

Method

Phase II/III crystal growth studies. It was decided to study the growth of Phase III from Phase II which occurs on cooling of the sample through the transition temperature. This took advantage of the greater range of temperatures available by supercooling, compared to the equivalent heating experiment. Details regarding the methodology in isolating the growth process have been described previously.¹⁹⁻²² Briefly, the process involved moving the sample between water-baths held at 42.0 and 46.1° until the observed rate of volume change levelled off at a maximum. This is termed "thermal cycling". At this point, the sample crystals are believed to contain both phases in roughly equal proportion and the rate of change of volume (and acoustic emission) may be associated only with growth. Before proceeding further, the sample was placed for about 10 hr in another water-bath held at $T_{tr} = 43.6^\circ$ so that stress accumulated around the phase boundary during transition²⁰ could relax. The sample was then temperature-jumped by rapid transfer from the transition temperature water-bath to a bath set at T_{low} , a temperature lower than T_{tr} . After thermal equilibration (a few minutes), growth of Phase III proceeded and acoustic signals were acquired. The growth of Phase III was allowed to progress by several per cent during the course of each experiment, to ensure capture of an adequate number of signals from the growth. Limiting the amount of growth of Phase III allowed easy restoration of (approximately) the original proportion of Phase II to Phase III: the transition was reversed by heating the sample in a bath set at 46.0°. Series I was conducted at T_{low} values of 39.35, 39.60, 39.95, 40.25, 40.50, 40.65, 40.80, 40.95, 41.11°, in the order listed. Series II used the same temperatures, but in the reverse order.

Nucleation of Phase III. The sample was completely converted into Phase II (high temperature), and then cooled to the transition temperature. Again, it was held at this temperature to allow any stress acquired to dissipate. Following this, the sample was "quenched" to initiate nucleation, by dropping it into a bath at 38.8 or 39.6°. These values were chosen so as to

obtain nucleation rates that differed by approximately one order of magnitude. It was hoped that the first few signals collected would have a dominant contribution from the nucleation process.

Characterization of background noise. In order to characterize the background noise, "blank" experiments were carried out. In these, the dilatometer containing the sample was replaced by one which contained only water. About 200 signals were then collected with the trigger level set just *below* the level of the background noise. These were processed in the same way as the signals from the sample.

Data processing

All data processing algorithms were written in our laboratory in QuickBASIC^R version 4.0 (Microsoft Corp., Redmond, WA). Time-resolved power spectral surfaces were generated with Surfer^R version 3.0 (Golden Software Inc., Golden, CO).

Frequency-intensity-energy analysis. An average power spectrum was calculated for each experiment. This required the generation of power spectra for each signal, by using a fast Fourier transform algorithm, and the averaging of these spectra. Time-resolved average power spectra were generated by averaging spectra from only those signals which occurred within defined time windows. The energy of a signal was taken to be a summation of the intensities of the discrete power spectrum. To obtain an integral of the total energy detected, a cumulative energy plot can be calculated. The cumulative energy at a given time is the sum of the energies of the discrete signals up to and including the energy at that time.

Pattern recognition. Attributes of individual signals were quantified by calculation of numeric descriptors such as peak amplitude, RMS, median frequency *etc.* The distributions of values obtained for all signals from one experiment indicate the (dis)similarity of amplitude, shape, energy and frequency content of the signals. When considered separately or together, the distributions may also indicate the presence of more than one type of signal within each experimental data set. It is presumed that most classes of signal reflect the presence of different types of acoustic event. However, the effects of wave reflections, dispersion, sharp resonances of the vessel or transducer, *etc.*, can obscure real class separations, or (more rarely) cause the experimenter to detect a separation where none

exists. Nevertheless, results from different experiments carried out in the same way with the same apparatus may still be effectively compared by this method, and separate statistical descriptions obtained for each type of signal.

Eleven time-domain and thirteen frequency-domain features were chosen on the basis of previous experience.²⁶ The time-domain features were kurtosis, crest factor, number of zero crossings, and normalized RMS octiles. Frequency-domain features included the most intense frequency component, mean frequency, median frequency, frequency standard deviation, frequency crest and normalized power octiles. These features were calculated for each signal. Principal-components analysis was employed to project these multidimensional data onto a two-dimensional plot with maximum retention of information.

RESULTS AND DISCUSSION

Acoustic activity of the phase transition

In preliminary studies, the temperature of the sample in the dilatometer was scanned between 35 and 50° in both directions. Figures 4a and b show the acoustic traces obtained during heating and cooling, respectively. Both plots provide clear evidence that the transition is highly acoustically active. A dilatometric trace, which depicts the overall rate of the transition, and the integrated acoustic intensity are also plotted in each figure. The following were observed for the cooling experiment: (i) the acoustic activity existed in the form of many short duration (*ca.* 0.2 msec) spikes or bursts; (ii) the onset of acoustic activity coincided with a more rapid decrease in the dilatometric plot (the decreasing background level due to thermal contraction of the water and sample being taken into account); (iii) acoustic activity terminated as the gradient of the dilatometric plot returned to its original values; (iv) all conditions being equal, the acoustic intensity profile was highly reproducible. Analogous statements can be made about the heating experiment. The integrated acoustic intensity plots show the same sigmoidal shape over the course of the phase transition as do the corresponding dilatometric plots. This behavior shows that the acoustic energy emitted is directly proportional to the rate of the phase transition. However, the acoustic emission was less intense during heating than during cooling. For C₂Cl₆, this may be explained in part by the degree of supercooling being much greater than

that of superheating. Phase III nuclei formed on cooling will experience a greater temperature difference from T_{tr} than do Phase II nuclei formed on heating. The higher degree of supercooling results in a faster rate of crystal growth. Thus, from this argument, for phase transformations which have approximately equal acoustic activity per degree, the acoustic energy produced would be expected to be greater on cooling than on heating. That cooling is more acoustically active than heating has been observed experimentally for other phase transitions.^{5,27} Study of other systems is needed to substantiate it as generally applicable. Moreover, kinetic arguments alone do not explain why another rapid phase transition did not give an acoustic signal in the expected frequency range.²⁷

Nucleation studies

The nucleation experiment could be divided into four stages. The first pertained to thermal contraction of the sample and dilatometric liquid, and the second to the induction period, which is equivalent to the inverse of the nucleation rate.¹⁹⁻²² Here, random density fluctuations are believed to occur within the crystal matrix as a critical number of molecules attempt to gain the necessary energy to form a new interface.¹⁸ In the third stage this energy barrier is overcome and nucleation results. This is followed immediately by growth, the fourth stage. Our apparatus was unable to detect any emission from thermal contraction of the sample. However, at the instant of nucleation, stage 3, there may be a rapid release of stress and elastic energy, which quantitatively and qualitatively different enough from the background to be detected acoustically.

In the 38.8° temperature-quench experiment there was no noticeable difference in the power spectra of the first signals as compared to those collected subsequently. However, in the 39.6° experiment, signals Nos. 1 and 2 showed a single high frequency band centered around 630 kHz (Fig. 5). A review of the complete set of signals collected during this experiment revealed occasional occurrences of the 630 kHz component at apparently random time intervals, hinting that the signals with this frequency component might be accompanied by nucleation. A complicating factor is that some signals with this frequency band were also found during Phase III crystal growth (discussed below). Hence, this question of whether nucleation is

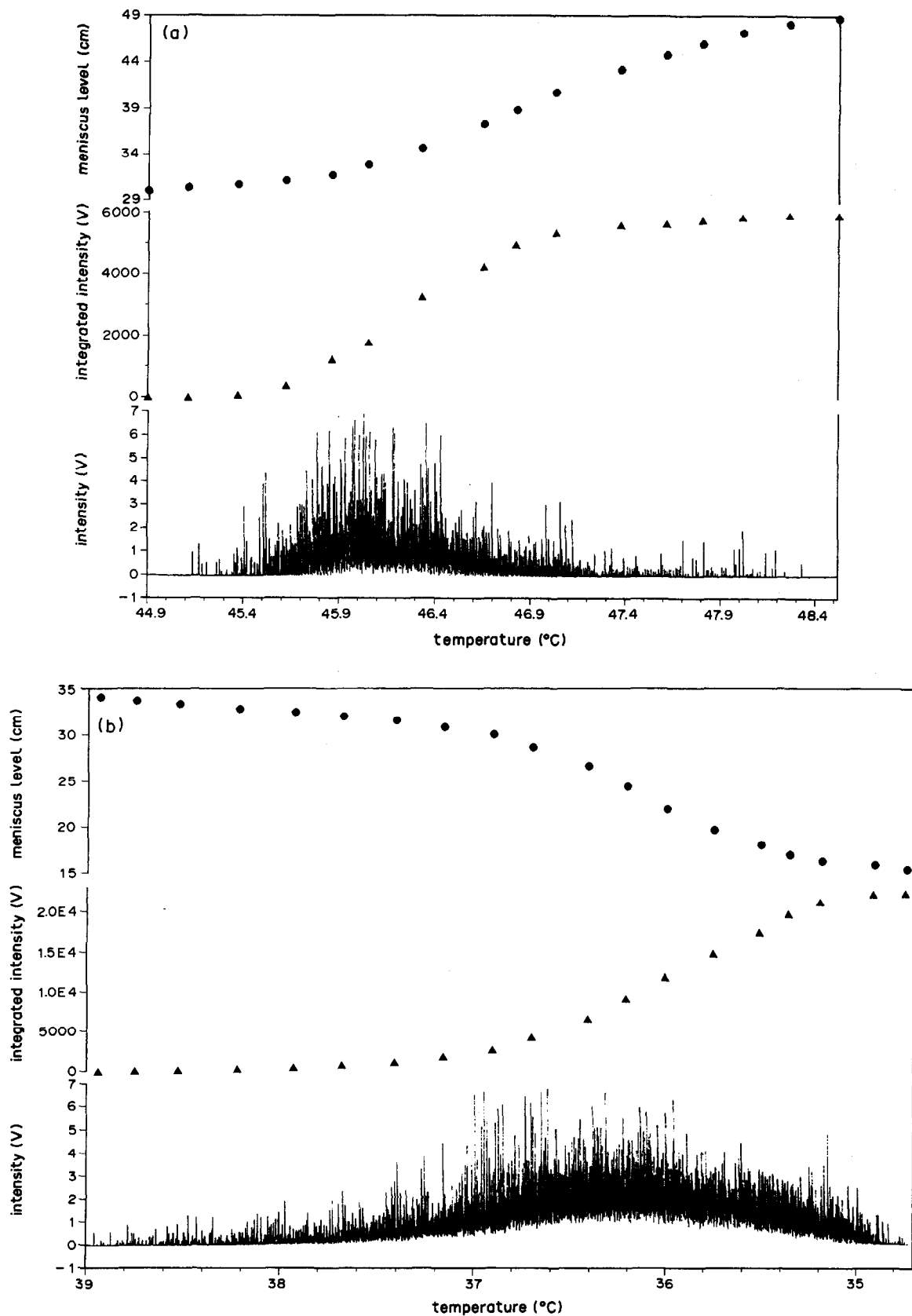


Fig. 4. Acoustic trace, integrated acoustic intensity (solid triangles) and dilatometric (solid circles) plots for C_2Cl_6 : (a) for the transition from Phase III to Phase II, with a scan rate of $0.0035^{\circ}/sec$ and 80 dB total gain; (b) for the transition from Phase II to Phase III, with a scan rate of $0.0034^{\circ}/sec$ and 70 dB total gain.

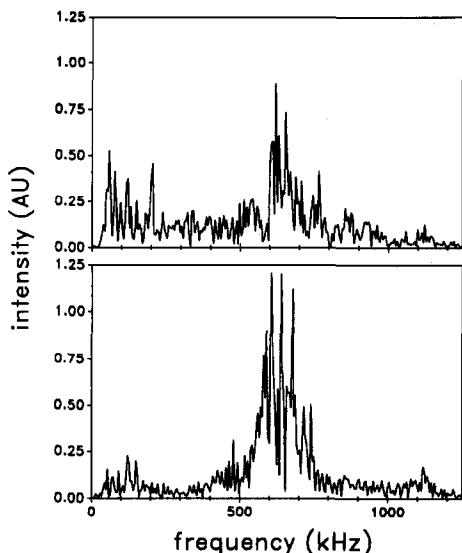


Fig. 5. Power spectra of signals Nos. 1 and 2 from the nucleation experiment in which the temperature was dropped from 43.6 to 39.6°. AU = arbitrary units.

responsible for this higher frequency band could probably only be effectively investigated by using a combination of acoustic emission and video microscopy on single crystal samples. Such a study is planned.

Growth of Phase III from Phase II

Average power spectra have shown the similarity of signals produced by the same mechanism during different chemical processes.¹² As shown in Fig. 3, the transducer used did not possess a flat frequency response over the full spectrum, and this affects the observed magnitudes of the frequency components present in the signals¹² and in the background noise. However, the average power spectra obtained with this transducer are repeatable for a given reaction and apparatus over extended periods and the spectra obtained can show considerable differences. The raw spectra contain contributions from both the analytical signals and the background noise from the apparatus. Since the background noise is readily characterizable, its average power spectrum may be subtracted from that obtained for the signals to obtain a corrected spectrum. A typical average power spectrum is shown in Fig. 6a, the background spectrum obtained during cooling of a blank in Fig. 6b and the background corrected power spectrum in Fig. 6c.

Background noise. Low intensity bands present in the background in the blank experiments were also observed when the transducer

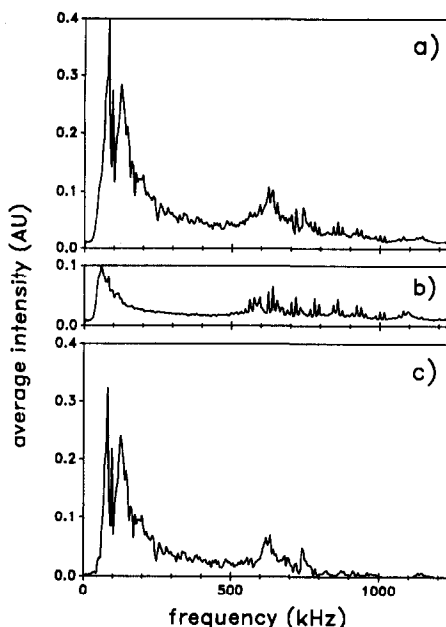


Fig. 6. Average power spectra: (a) growth of Phase III from Phase II of C_2Cl_6 with $\delta T = 2.65^\circ$; (b) background noise; (c) resultant background-subtracted spectrum for the phase transition.

was dismantled from the apparatus, and were therefore due to noise in the transducer/data acquisition system. Background subtraction corrects the observed spectrum for these effects.

Emission spectra obtained. The corrected spectrum shows emission in the frequency ranges of about 50–220 kHz and 600–670 kHz with the former band dominating. It should be noted that the low frequency band appears to extend below the conditioning amplifier's lower band-pass limit of 50 kHz. Though individual signals vary, when the same transducer and supporting electronics are used, the average power spectrum is highly reproducible (correlation coefficients not less than 0.997 between spectra were calculated) and hence is characteristic. Signal variability is indicated by the power spectra for the first 18 signals in this same set, as shown in Fig. 7. It must be recalled that signals can occur anywhere within the sample, and thus signals which occur close to the transducer will be less affected by the transmission characteristics of the media *etc.* than those from further away.

Pattern-recognition studies. Figure 8 plots the integrated acoustic power of the 50–220 kHz emission band against that of the 600–670 kHz band for each of the signals obtained during one experiment on growth of Phase III. This shows the presence of one highly asymmetric cluster of

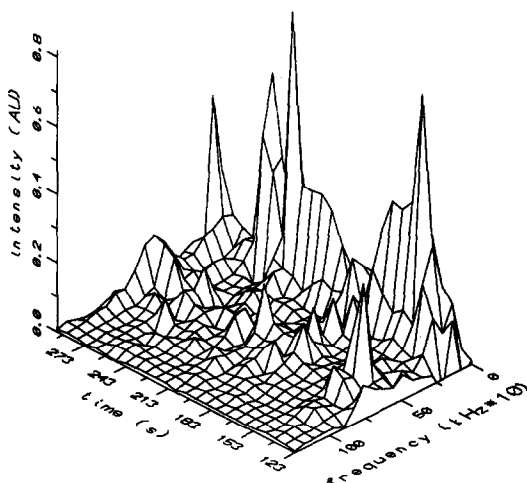


Fig. 7. Time-resolved power spectrum showing variability in first 18 signals collected during the growth of Phase III from Phase II of C_2Cl_6 ($\delta T = 2.65^\circ$).

points: two regions are immediately obvious, a dense core and one (or possibly two) highly dispersed tail(s). This is significant, but is probably insufficient evidence for positively assigning the signals to two different classes (and thus to two physicochemical processes, *i.e.*, growth and nucleation). A principal-components analysis (PCA), employing all the descriptors listed above and the same signal set, also resulted in no absolute separation of the signals into clusters. The greatest loadings were observed for such descriptors as number of zero crossings and for all frequency-based descriptors except the power octiles. A visual scan of the power spectra confirmed this: a number of signals had only the low frequency band; an even smaller number had only the high frequency band; and the rest had varying contributions from both. Hence, PCA could reveal only a single cluster.

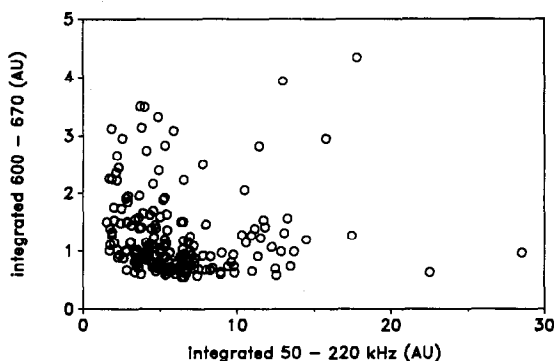


Fig. 8. Scatter plot of the integral of the high frequency band (600–670 kHz) against that of the low frequency band (50–220 kHz) for growth of Phase III ($\delta T = 2.65^\circ$).

Possible acoustic detection of unstable/metastable boundary

Dilatometric studies²² suggested a changeover between the metastable and unstable states since the nucleation process and growth rates behaved differently in the regions above and below about 40.8° (T_0). In terms of acoustic emission characteristics, no qualitative difference was found across this temperature boundary. Again, pattern-recognition studies did not support the existence of two distinct acoustic signatures across T_0 . However, some quantitative differences were apparent. If acoustic activity is sensitive to the growth rate, differences in growth rate should be readily detectable as differences in acoustic activity:

- (i) increase the number of acoustic events; and/or
- (ii) increase the energy content of individual acoustic signals.

As present instrumentation could not reliably count all acoustic events, only the latter effect was determined. An integral of the average power spectrum provides a representative measure of the energy per signal irrespective of the number of signals acquired. Such an energy value was calculated for each growth experiment. The results, shown in Fig. 9, suggest that there may be a peak in the calculated average energy at around 40.65° . A separate plot was generated for each series. This was necessary as the rate (and thus the energy expected) was found to be affected to some extent by the thermal history of the sample.

Above T_0 , the average power increases with the difference from T_r , consistent with the behavior of the growth rate.^{19,20} Below T_0 , the

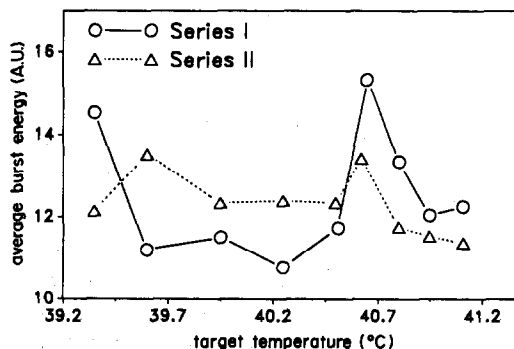


Fig. 9. Mean burst energy vs. temperature attained, in growth of Phase III from Phase II. Series I experiments were obtained in decreasing order of δT and Series II in increasing order of δT .

rates were too fast to be measured by dilatometry. Thus, it was impossible from readings of the meniscus level alone to separate the thermal equilibration process (see references 19 and 20 for details). Acquisition of acoustic signals is possible under such circumstances, however. Thus, the results in Fig. 9 would suggest that the growth rates below T_0 were somehow retarded. The latent heat released during the transition for temperatures just below T_0 may be enough to cause the temperature at the interface to be significantly higher than that of the surroundings, thus retarding the growth rate.

Each point on these plots is obtained by taking the mean of the total acoustic power values for all signals obtained under those experimental conditions. As discussed above, it is known that individual signals are highly variable in form, but that their average properties, such as their average power spectrum (and therefore the area under the average power spectrum), are highly repeatable. In each experiment, the distribution of the power values for individual signals was found not to be Gaussian, but quite broad and asymmetric, with tailing towards high power values. Calculation of median power values yielded a very similar plot to that shown in Fig. 9. That *both* sets of acoustic data suggested a maximum in the integrated acoustic power at close to T_0 is certainly not inconsistent with the hypothesis. Statistically, however, the breadth of the distributions obtained, which is in part due to the many different possible source locations within the sample, does not allow an unequivocal conclusion to be drawn. Further work may therefore be necessary, requiring use of a digitizer which is capable of collecting more signals within the time of an experiment.

Source of acoustic activity

Pattern recognition alone was unable to provide clear evidence for any of the physico-chemical processes thought to underlie this phase transition. However, other observations aid in the interpretation of the acoustic results obtained. Mnyukh observed the growth of Phase III from the Phase II matrix under a polarizing microscope, and found it to be a layering process,²³ *i.e.*, the growth process consisted of two components, creation of a step at the boundary and its lateral movement. Together these result in the net vertical growth. The lateral movement of the step was reportedly

accompanied by density changes ahead of the front. This can be construed as a plastic zone produced as a response to the stress field generated by the step movement.

The elastic wave arising from the release of this stress is suspected to be responsible for the 50–220 kHz spectral band. There are two reasons for this. First, this band is dominant throughout the growth study. Secondly, the frequency range of emission is in the range of acoustically “soft” processes such as bubble emission.^{11,12} Moreover, the movement of the phase boundary must be disjointed. This, which is believed to be true for dislocation movement,²⁸ would seem a necessary requirement for the production of transients, otherwise the movement would only increase the background signal level. In fact, the layered growth may be mechanistically similar to dislocation movement.

The 600–670 kHz band is usually weaker than is shown for the two signals in Fig. 5 even when it is the major component of a signal. It is evidently associated in some manner with the 50–220 kHz band since they are predominantly found together. However, its few isolated occurrences suggest that a separate mechanism may be operating in parallel. As discussed above in connection with the scatter plots of the signals (Fig. 8), it appears unlikely that this could be associated with nucleation. Conditions for the growth study were chosen so that most of the crystals would contain both phases. It is improbable that nucleation would be occurring in a sufficient number of crystals to produce emissions that would convolve with a majority of emissions from growth. One possibility is that the step formation mentioned above is responsible for this high frequency band.

Another possible cause of this band is microfracture. It is likely that microfractures, if any, would form at the Phase II/III interface, which is the weakest place in the crystal.^{23,24} Gross fracture is ruled out since the nature of the sample remained essentially unchanged, despite repeated transition in both directions.

In another set of experiments, a single crystal in a beaker was slowly converted into Phase II and then allowed to cool rapidly at ambient temperature. Profuse fracturing was observed during this experiment, so much so that the crystal became opaque and white. The average power spectrum for the 999 signals obtained is shown in Fig. 10. Multiple bands are evident and the spectrum has much more of a broad

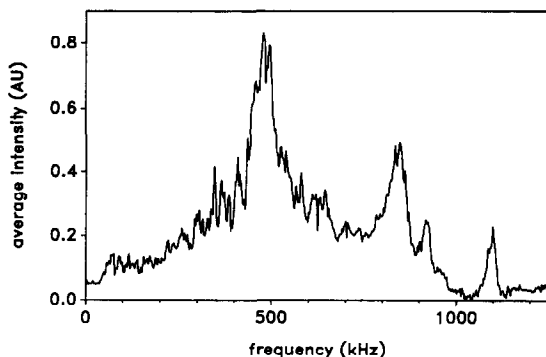


Fig. 10. Average power spectrum when fractures dominate during the growth of Phase III from Phase II.

band character, with the main band at 480 ± 75 kHz and a smaller band at 840 ± 50 kHz. Studies on other chemical systems have indicated that fractures are responsible for broad band spectra and can have a predominant frequency of around 500 kHz.¹² The single crystals studied here gave substantial emission at 200–950 kHz. The band at 1.1 MHz is a known transducer resonance. There was no sign of the 50–220 kHz band most common in the dilatometer studies, which has been assigned to growth. The above results suggest that the sample in the dilatometer did not undergo significant damage due to fracture. Had it been supercooled to the extent where microfractures were caused (thus destroying the integrity of a well conditioned sample), similar emissions would have been detected.

As mentioned above, characteristic nucleation signals cannot be extracted by current data analysis procedures from the data obtained. Perhaps the nucleation process is acoustically inactive, or more likely, is below the detection limits or beyond the frequency band width of our transducer. It has also been argued by Mnyukh²⁴ that nucleation is determined solely by defects which he called "optimum microcavities" and that nucleus formation resulted by molecular relocations from one wall of the cavity to the wall opposite. If this model is correct, then nucleation may not be distinct from growth and hence, from an acoustic perspective, there are no qualitative differences between nucleation and growth. Furthermore, no clear qualitative difference was observed between the acoustic signals for metastable and unstable situations. This, together with the aforementioned inability to distinguish between nucleation and growth, poses a basic question: how small can an event be, yet still be acoustically detectable? This has been partially ad-

ressed by Betteridge *et al.*⁸ More recent work suggests that by use of *nonconventional* sensors, extreme detection limits which approach the noise associated with thermal motions of molecules may be attainable.²⁹

Monitoring the rate of transformation

Studies of whether the signals collected could yield satisfactory quantitative information were conducted with large recrystallized single crystals. An acoustic intensity *vs.* time plot obtained for the Phase II/III transition is shown along with the integrated intensity and calculated cumulative energy in Fig. 11. The cumulative energy correlates favorably with the integrated intensity. Hence, provided an adequate number of signals can be collected and the emission rate is not anomalously greater than the digitizer's ability to collect signals, a cumulative energy plot can effectively be used in place of the integrated intensity. In fact, both these types of plot yield rate information in the same manner as dilatometric plots.

CONCLUSIONS

Physical aspects of the Phase II/III transition of hexachloroethane have been investigated by thermosonimetry. The study was carried out with a well conditioned sample which had shown reasonably reproducible nucleation and growth kinetics. Acoustic emission began at the onset of the phase transition and ceased at its completion. Large amounts of acoustic activity were detected during the transition, and average power spectra were generated. The most prominent acoustic emission bands were at 50–220 and 600–670 kHz. These have been attributed to movement of the phase boundary and (possibly) microfracturing, respectively. Plots of integrated acoustic intensity followed the sigmoidal trend observed in the dilatometry results. The possibility of acoustic detection of the unstable/metastable boundary is suggested. It was not possible to determine different acoustic signatures for nucleation and growth.

Acoustic emission (here in the form of thermosonimetry) is an area of chemistry which has received little attention. Thus studies which reveal where this technique can provide similar information to that obtainable by more established methods are important, and those which show where it provides totally new insights into chemical processes are even more so. Thermosonimetry was able to monitor this

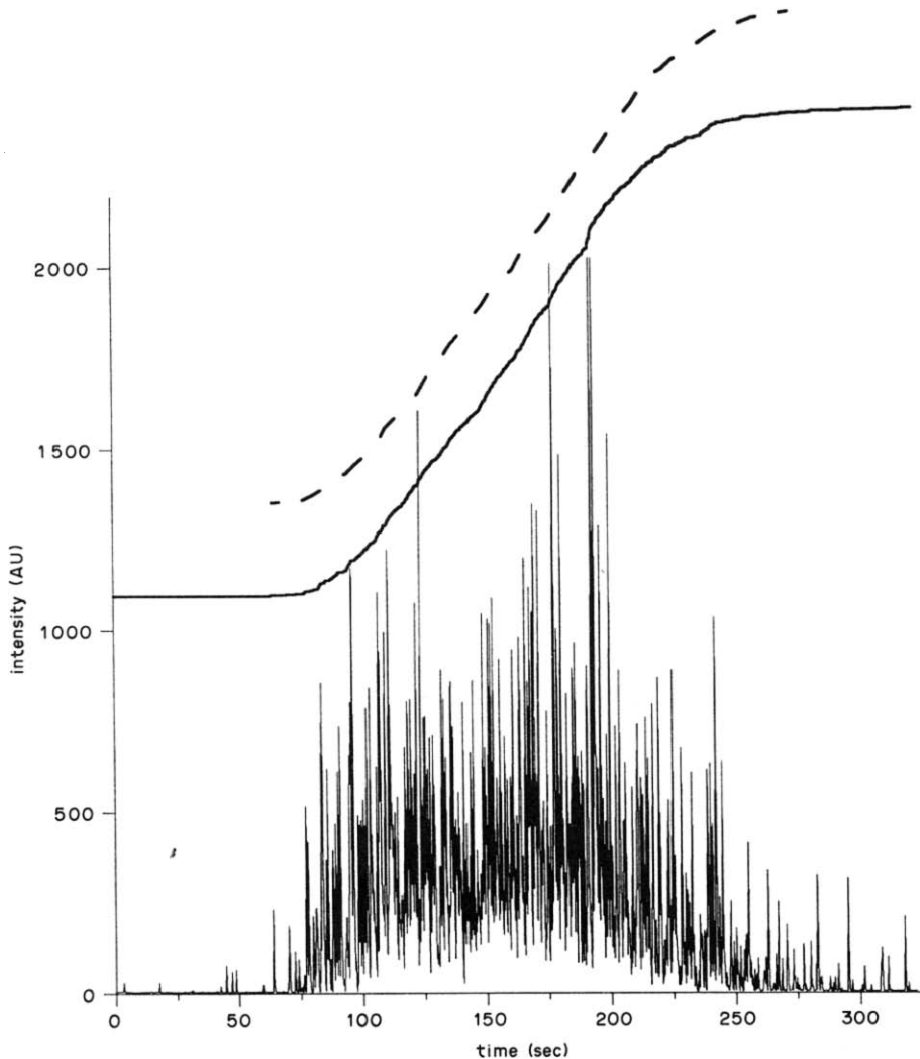


Fig. 11. Acoustic trace, integrated intensity (solid line) and cumulative energy (dashed line) plots from signals obtained during rapid transition from Phase II to Phase III when fracture dominates.

phase transition as effectively as dilatometry and provided new information. However, thermosonimetry and dilatometry must be considered complementary techniques, since some studies require direct measurements of the change in sample volume with time, and other phase transitions may not be so acoustically active. Though the apparatus needed for thermosonimetry is more complex, samples can be studied in any suitable container. The phase transition is directly observable as being comprised of a large number of events at the supramolecular level. The sensitivity of the acoustic monitoring system is high: low intensity acoustic spikes are detected even at the very start and end of the transition, where changes in the slope of the corresponding dilatometric plot are impossible to observe. Thermosonimetry is amenable to automation of the data acquisition

and is not subject to the precision limitations and possible error involved in reading a dilatometer by eye. In addition to providing information about the dynamics of the phase transition, thermosonimetry can also selectively detect the occurrence of adverse phenomena such as cracking.

FURTHER WORK

It is apparent that the acoustic activity from the Phase II/III transition is a direct manifestation of the transition and its intensity is intimately linked to the rate. However, parallel video microscopic evidence from studies on single crystals is needed to confirm the nature and origin of these emissions, which are thought to be predominantly from the layered crystal growth and to a lesser extent, fracture. Together

with a transducer of greater sensitivity and better linearity, this would also establish whether there are, from an acoustic perspective, any qualitative differences between nucleation and growth.

Acknowledgements—The authors acknowledge use of data acquisition and analysis programs written by P. D. Wentzell, D. B. Sibbald, S. J. Vanslyke, D. A. Boyd and K. A. Soulsbury of this group. They also acknowledge support from the Natural Sciences and Engineering Research Council (NSERC) grants 5-80246 and 5-80222. Student support of OL was provided initially by the Institute for Chemical Science and Technology (ICST) grant 5-50886 and subsequently by a G.R.E.A.T. Studentship from the B.C. Science Council and by an NSERC Graduate Research Fellowship.

REFERENCES

- G. M. Clark and R. Garlick, *Thermochim. Acta*, 1979, **34**, 375.
- K. Lonvik, *ibid.*, 1987, **110**, 253.
- K. Lonvik and T. Ostvold, in *Proc. 2nd Intern. Symp. Molten Salts*, J. Braunstein and J. R. Selman (eds.), p. 207, Electrochemical Society, Pennington, NJ, 1981.
- K. Lonvik, in *Proc. 16th Intern. Conf. Thermal Analysis*, Vol. 1, H. G. Wiedemann (ed.), Birkhauser Verlag, Basel, 1980.
- T. Sawada, Y. Gohshi, C. Abe and K. Furuya, *Anal. Chem.*, 1985, **57**, 1743.
- J. A. C. van Ooijen, E. van Tooren and J. Reedijk, *J. Am. Chem. Soc.*, 1978, **100**, 5569.
- T. Sawada, Y. Gohshi, C. Abe and K. Furuya, *Anal. Chem.*, 1985, **57**, 366.
- D. Betteridge, M. T. Joslin and T. Lilley, *ibid.*, 1981, **53**, 1064.
- A. G. Howard and D. A. Greenhalgh, *Anal. Chim. Acta*, 1979, **106**, 361.
- R. M. Belchamber and G. Horlick, *Spectrochim. Acta*, 1982, **37B**, 17.
- R. M. Belchamber, D. Betteridge, M. P. Collins, T. Lilley, C. Z. Marczewski and A. P. Wade, *Anal. Chem.*, 1986, **58**, 1873.
- P. D. Wentzell and A. P. Wade, *ibid.*, 1989, **61**, 2638.
- R. M. Belchamber, D. Betteridge, P. Y. T. Chow, T. J. Sly and A. P. Wade, *Anal. Chim. Acta*, 1983, **150**, 115.
- R. M. Belchamber, D. Betteridge, P. Y. T. Chow, T. Lilley, M. E. A. Cudby and D. G. M. Wood, *J. Acoust. Emiss.*, 1985, **4**, 71.
- R. M. Belchamber, D. Betteridge, M. P. Collins, T. Lilley, C. Z. Marczewski and A. G. Hawkes, in *Acoustic Emission Monitoring and Analysis in Manufacturing*, Vol. PED-14, D. A. Dornfeld (ed.), American Society of Mechanical Engineers, New York, 1983.
- W. Sachse, in *Proc. 9th Intern. Acoustic Emission Symp.*, K. Yamaguchi, I. Kimpara and Y. Higo (eds.), JSNDI, Tokyo, 1988.
- F. Förster and E. Z. Scheil, *Metalkd.*, 1936, **28**, 245.
- P. A. Reynolds, *Acta Crystallogr.* 1977, **A33**, 185.
- Y. Koga and R. M. Miura, *J. Chem. Soc. Faraday Trans. I*, 1978, **74**, 2328.
- Y. Koga, *J. Cryst. Growth*, 1984, **66**, 35.
- Idem*, *Physica*, 1987, **146B**, 408.
- Idem*, in *Advances in Phase Transitions*, J. D. Embury and G. R. Purdy (eds.), pp. 151–153. Pergamon Press, Oxford, 1988.
- N. N. Petropavlov and Yu. V. Mnyukh, in *Kristallizatsiya i fazovye prevrashcheniya*, N. N. Sirota (ed.), p. 4653. Akad. Nauk, S.S.S.R., 1971.
- Yu. V. Mnyukh, *Mol. Cryst. Liq. Cryst.*, 1979, **52**, 163.
- P. D. Wentzell, S. J. Vanslyke and A. P. Wade, *Trends Anal. Chem.*, 1990, **9**, 3.
- P. D. Wentzell, O. Lee and A. P. Wade, Comparison of pattern recognition descriptors for chemical acoustic emission analysis, *J. Chemometrics*, in the press.
- D. B. Sibbald, *M.Sc. Thesis*, University of British Columbia, June, 1990.
- P. P. Gillis, in *ASM STP 505*, pp. 20–29. American Society for Testing and Materials, 1972.
- W. Denk and W. Webb, *Anal. Chem.*, 1989, **61**, 1077A.

EXTRACTION OF AUROCYANIDE ION-PAIRS BY POLY(OXYETHYLENE) EXTRACTANTS

M. D. ADAMS

Mintek, Private Bag X3015, Randburg 2125, South Africa

P. W. WADE and R. D. HANCOCK

University of the Witwatersrand, 1 Jan Smuts Avenue, Johannesburg 2001, South Africa

(Received 18 October 1989. Accepted 24 January 1990)

Summary—Aurocyanide ion-pairs with alkali-metal ions are extracted efficiently into organic phases with the aid of long-chain polyethers. The results of distribution experiments can be rationalized by molecular mechanics calculations. The polyether is shown to co-ordinate to the alkali-metal cation through the ether oxygen atoms, wrapping around the cation in a helical configuration. High extraction efficiencies are obtained with high dielectric-constant solvents, which tend to stabilize the helical polyether-cation complex. The preferential secondary solvation of the aurocyanide anion by the chosen solvents also has an important influence on the extraction efficiency.

The extraction of ions by extractants containing the poly(oxyethylene) functional group is a well known phenomenon. The poly(oxyethylene) extractants may take the form of non-ionic surfactants dissolved in a water-immiscible solvent,^{1,2} or of polyether-based polyurethane foams.^{3,4} Poly(oxyethylene) derivatives have also been used as neutral carriers in ion-selective electrodes.⁵

Several mechanisms have been postulated³ to account for the extraction of ions by polyether-based polyurethane foams. One of the most likely is the so-called "cation-chelation" mechanism,³ in which the cation is co-ordinated to oxygen atoms within a helical structure formed by the poly(oxyethylene) chain, and the co-extracted anion lies outside the helix. Yanagida *et al.*¹ suggest that the helical conformation is energetically favourable for a non-ionic surfactant dissolved in an organic solvent, and propose a similar mechanism for liquid-phase extraction. Some evidence for this type of complexation in the crystalline state is given by Saenger *et al.*,⁶ who present the crystal structure of the RbI complex of 18-hexaoxaicosane, in which the polyether chain wraps smoothly around the Rb⁺ ion in a helical fashion. However, Siddiqui and Wright⁷ suggest that the molecular structures of long-chain poly(oxyethylene)-alkali-metal salt complexes are uncertain. The uncomplexed poly(oxyethylene) chain in the crystalline state⁸ forms a helical structure containing seven units in two turns.

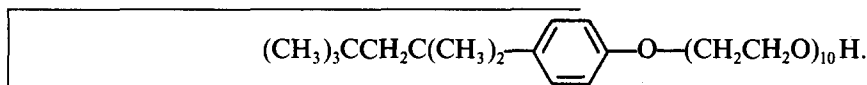
Raman spectroscopic studies⁹ have indicated that the helical structure is maintained to some extent by the uncomplexed chain in aqueous solution. The conformation in organic solutions remains unknown. The solvent extraction of Na⁺AuCl₄⁻ ion-pairs by poly(oxyethylene) derivatives of organic carbonates has been reported by Rollat *et al.*¹⁰ They concluded from infrared spectrophotometric studies that complexation occurs through strong ligand-sodium interactions. The solvent extraction of M⁺Au(CN)₂⁻ ion-pairs by poly(oxyethylene) derivatives has not yet been examined; however, their extraction into solvents such as 1-pentanol¹¹ and tributyl phosphate¹² has been reported. The extraction of aurocyanide by polyether-based polyurethane foam has been discussed briefly by Braun and Farag.¹³

The present work examines the solvent extraction of aurocyanide ion-pairs by poly(oxyethylene) derivatives, and investigates the problem of the mechanism of extraction by liquid-liquid distribution techniques and molecular mechanics calculations. Particular attention is given to the role of coiling of the polyether chain in solvents with different dielectric constants, and the extent to which the possible pre-organization of the chain influences the extraction efficiency.

To quantify the energetics of complexation by molecular mechanics calculations, it is necessary to have some knowledge of the conformations that the uncomplexed polyethers are likely to adopt.

The crystal structure of uncomplexed poly-(oxyethylene) was solved by Takahashi and Tadakoro,¹⁴ and the torsion angles in the O-C-O unit were found to have the conformation t-g-t (*trans-gauche*⁺-*trans*), resulting in a distorted helical conformation for the polyether as a whole.

Baldwin *et al.*¹⁵ performed molecular mechanics calculations on the uncomplexed polyether CH₃O(CH₂CH₂O)₃CH₃, with the MM2 force field. The terminal CH₃O-CH₂-CH₂-O- units were kept in the linear t-t-t (*trans-trans-trans*) conformation, and the ten energetically unique conformations of the central -O-CH₂-CH₂-O unit were investigated. The dielectric constants were varied up to a value of 20, and it was found that for dielectric constants greater than 9.5 there were no differences in the energy calculations. It was found that at very low dielectric constant, the t-t-t conformer has the lowest energy, whereas the t-g-t conformer has the lowest energy at higher dielectric constants,



where the polar contributions to the strain are diminished.

Baldwin *et al.*¹⁵ allowed variation of only three torsion angles. For modelling of the complexation of the polyether with a large metal ion, all the torsion angles in the polyether have to be changed independently. The MM2 force field used in their study considers energetic contributions from all atoms in the molecule; however, if all the atoms in the polyether were considered in the energy minimization, the number of interactions would be too high for practical computation. United-atom force fields have been developed for the consideration of large molecules, and it would be more appropriate to use one of these computational strategies in calculations involving long-chain polyethers.

Fenton *et al.*¹⁶ determined, by X-ray diffraction, a fibre-repeat distance of 8.1 Å for the complex of poly(oxyethylene) with potassium thiocyanate. The structural model consistent with this repeat distance and with other structural features determined by Raman spectroscopy¹⁷ are consistent with a C-C-O-C-C-O unit in the t-t-g-t-g conformation.¹⁸ This results in a helical configuration having an interior channel lined with ether oxygen atoms, and large enough to accommodate a K⁺ ion.¹⁷

Saenger *et al.*⁶ solved the crystal structures of a number of polyethers of different chain length complexed to Rb⁺ and Na⁺. They discovered that helical co-ordination is preferred for long polyethers, and circular co-ordination for short polyethers. Also, whereas O-C-O torsion angles are always *gauche*⁺ or *gauche*⁻, C-C-O-C angles are usually *trans*, but sometimes *gauche*⁺ or *gauche*⁻. The dominant conformer of the C-C-O-C-C-O unit in the large complexed polyethers is t-t-g-t-t-g, as in the K⁺ complex,¹⁸ and this conformer was therefore chosen for the trial structures in the present work.

EXPERIMENTAL

Reagents

The KAu(CN)₂ was from Johnson Matthey. All other reagents were of analytical reagent grade. The soluble poly(oxyethylene) used was the non-ionic surfactant Triton X-100, which has the structure

Liquid-liquid distribution experiments

Twenty ml of 0.1M Triton X-100 solution in benzene, 1-pentanol, or nitrobenzene were agitated for 20 min with 20 ml of aqueous solution initially containing 100 mg/l. Au as well as 0.1M LiCl, KCl or CsCl. This equilibration time was found to be sufficient, in preliminary experiments. The gold concentration in the aqueous phase before and after phase separation was determined by atomic-absorption spectrophotometry (AAS).

Determination of water content

The solubility of water in the pure solvents and in the Triton X-100 solutions was determined by automatic Karl Fischer titration with a Radiometer TTA 80 automatic titration assembly linked to an Apple IIe microcomputer. The titration was checked by comparison of the measured solubility of water in nitrobenzene with that reported in the literature;¹⁴ excellent agreement was obtained.

Molecular mechanics calculations

The force field. The molecular mechanics calculations were implemented with Boyd's version¹⁹ of MOLBLD-3, which was modified to reproduce the united-atom force-field

AMBER.²⁰ AMBER has been used extensively to explain the properties of proteins,²¹ nucleic acids,²² the alkali-metal ion complexes of spherands²³ and, more appropriately to the present application, the alkali-metal ion complexes of 18C6, a cyclic polyether.²⁴ AMBER uses a potential function of the form:

$$E = \sum_{\text{bonds}} k_b (r - r_b)^2 + \sum_{\text{angles } k_a} (\theta - \theta_a)^2 \\ + \sum_{\text{dihedrals } k_d} [1 + \cos(n\phi - \gamma)]/2 \\ + \sum_{\text{non-bonded}} (B_{ij} r_{ij}^{-12} - A_{ij} r_{ij}^{-6} + q_i q_j / \epsilon_{ij} r_{ij})$$

where the "non-bonded" terms are summed over all atom pairs separated by more than three bonds. A "united-atom" approximation²⁵ was used, in which aliphatic CH₂ groups are represented as single atoms. This has the advantage of substantially reducing the number of interactions, and speeding up computer refinement.

The van der Waals terms were input into the modified MOLBLD-3 as 12/6 Lennard-Jones functions, $E_{\text{NB}} = A/r_{ij}^{12} - C/r_{ij}^6$, where the coefficients A and C were derived from group and atomic polarizabilities, effective united-atom atomic numbers, and effective ionic radii by substitution into the Slater-Kirkwood equations as described by Scott and Scheraga.²⁶ The non-bonded parameters for the CH₂ group, the oxygen atom and the K⁺ and Cs⁺ ions were taken from Wipff *et al.*,²⁴ and those for Li⁺ were taken from Kollman *et al.*²³ The ethereal-torsion parameters were taken from Wipff *et al.*,²⁴ and the bond-stretching and angle-bending parameters from Kollman *et al.*²² The partial atomic charge on a complexed oxygen atom was taken²⁴ to be -0.6 . Carbon atoms bonded to the oxygen atom were assigned a compensating charge of $+0.3$ to maintain electrical neutrality of the ligand. The cut-off distance for non-bonded interactions was set at 7 \AA , as recommended by Brooks *et al.*,²⁷ and the electrostatic terms were omitted if the atoms were separated by more than 9 \AA .²⁸ All refinements were terminated when the root mean square shift in co-ordinates was less than 0.2 \AA . The attenuation factor in MOLBLD-3 was set to 9 for all calculations. The structures were generated, and the refined structures were visualized, by means of the molecular modelling package ALCHEMY (Tripos Inc.).

Conformations of uncomplexed polyether in organic solvents. Originally the dielectric constant was set to 1.0 from published data²⁴ for uncomplexed 18C6, but the structure of the polyether became drastically skewed during refinement, owing to the cut-off of the electrostatic interactions at 9 \AA . At a distance of 9.3 \AA , the electrostatic energy between two oxygen atoms is $+3.6 \text{ kcal/mole}$, which is not negligible, since the O-C-O torsion barrier is 3 kcal/mole . The implication is that this cut-off distance is too short, but extension of the cut-off limit is impractical, since the number of non-bonded interactions increases as the square of the number of atoms considered.²⁷

Another option is the approximation of "solvent screening" by use of a dielectric constant proportional to the interatomic distance.²⁷ The preliminary study by Rees²⁹ shows that the internal effective dielectric constant within the non-aqueous environment of proteins increases with charge separation. Warshel³⁰ showed that the effective dielectric constant for short-range ionic interactions in water is considerably smaller than the bulk dielectric constant, and increases roughly linearly with charge separation. This model has been used successfully in molecular dynamics studies of proteins.³¹

Kollman *et al.*²² use a dielectric constant numerically equal to r_{ij} , the interatomic distance (expressed in \AA). It was found that, in the present study, a dielectric constant of 2 led to the same strength of ionic interactions. Vedani and Dunitz²⁸ used a cut-off of about 9.5 \AA and dielectric constants of 1 and r_{ij} in their calculations on native human carbonic anhydrase, and suggested that these dielectric-constant values overweighted the electrostatic terms. The best structural consistency was obtained with a dielectric constant of $4r_{ij}$. Dielectric constants of 1, r_{ij} , 4 and $4r_{ij}$ have been used in work on nucleotides,²² and caused no significant difference in structural reproduction. No cut-off distance was explicitly mentioned in that work, however, and the different dielectric constants were used in different situations, each choice having its own merits. Bovill *et al.*³² maintain that "the assessment of an interatomic dielectric constant is not straightforward", and they used a dielectric constant of 5 to explain structural aspects of some cyclic polyethers.

In conclusion, it seems that at present the values of microscopic dielectric constants are not known with confidence, and a number of different models for the dielectric constant

have been used, each being selected for the situation of interest. In the present investigation, a microscopic dielectric constant of r_{ij} was used for the polyether in the least polar solvent. Since increased polarity of the solvent should quench the effects of partial atomic charges over distance, a microscopic dielectric constant of $4r_{ij}$ was chosen for the most polar solvent.

The ALCHEMY software was used to construct models of the polyether with the formula $\text{CH}_3-(\text{CH}_2-\text{O}-\text{CH}_2)_{12}-\text{CH}_3$, with the C-C-O-C-C-O units in the helical conformations adopted by the ligand in the crystal structure of complexes, and in a linear conformation. For convenience this polyether was used in the calculations, since its behavior should simulate that of Triton X-100.

Energetics of the complexed polyether. Initially, molecular mechanics calculations were performed for Li^+ , K^+ and Cs^+ ions co-ordinated in the cavity of a helical polyether consisting of 24 oxygen units. It was found that although the co-ordinated section of the polyether retained its helical structure, the chain that was not directly co-ordinated to the metal ion had a tendency to unwind partially, and to perform wagging motions that were energetically inconsequential but inhibited refinement. Since calculations on the uncomplexed polyethers in low dielectric-constant solvents had revealed a preference for linear conformation, the ends of the polyether chains were straightened with ALCHEMY, and the structure was re-refined. It was discovered that, depending on where the user decided to linearize the chain, varied results could be obtained. Based on the reasoning that the co-ordination numbers of the metal ions in the refined structures were 11 for Cs^+ , 10 for K^+ and 6 for Li^+ , and that the polyether used in the solution studies had 10 oxygen atoms in its chain, it was decided to use a polyether containing 12 oxygen atoms for the subsequent calculations.

The total amount of water taken into the organic layer when the metal ions were extracted was found to be about one molecule of water per molecule of polyether. Since the errors in these measurements were relatively large, it was decided to omit the modelling of the hydration of the polyether-metal ion complex.

Since the polar solvent is expected to quench the charges on the polyether (with which it directly interacts) but not the metal ion, which is embedded in the polyether, it was decided to use a dielectric constant of $4r_{ij}$ for attenuation of intrapolyether interactions and $2r_{ij}$ for polyether-metal ion interactions.

RESULTS AND DISCUSSION

Solvent extraction of $M^+ \text{Au}(\text{CN})_2^-$ ion-pairs by Triton X-100

Effect of counter-cation and solvent. The extraction efficiencies for various combinations of counter-cations and solvents are shown in Table 1.

It is remarkable that whereas the addition of the polyether to benzene results in only a small increase in the degree of extraction, the addition of Triton X-100 to nitrobenzene results in a marked increase in extraction (up to 99.8% when potassium or caesium are present). The mechanisms involved in the production of this effect can be explained by the results of the molecular mechanics calculations, and will be discussed in detail later.

Effect of the solubility of water in the solvent phase. The case of 1-pentanol is clearly an anomaly, as a comparison between the extractions into the three pure solvents shows (Table 1). Only 1-pentanol displays any marked extraction of gold in the absence of the polyether. The trend towards the minimum with potassium has been described previously,¹¹ and explained in terms of polarization and hydrophobic effects.

Table 1. Degrees of extraction of $M^+ \text{Au}(\text{CN})_2^-$ ion-pairs ($M^+ = \text{Li}^+, \text{K}^+, \text{Cs}^+$) by Triton X-100 dissolved in various solvents

Solvent	ϵ	Degree of extraction, %					
		Li^+		K^+		Cs^+	
		Pure solvent	Solvent plus 0.1M Triton X-100	Pure solvent	Solvent plus 0.1M Triton X-100	Pure solvent	Solvent plus 0.1M Triton X-100
Benzene	2.28	0.0	0.0	2.4	5.8	2.4	9.6
1-Pentanol	13.90	84.9	89.8	66.8	92.3	76.3	92.4
Nitrobenzene	34.82	0.0	77.4	16.8	99.8	19.4	99.8

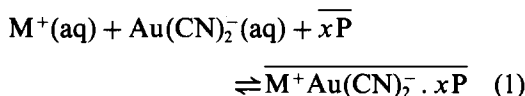
Table 2 shows the results obtained for the solubility of water in both the pure solvents and the polyether-containing solvents.

The fact that the solubility of water in 1-pentanol is more than an order of magnitude higher than that in either benzene or nitrobenzene explains the anomalous properties of 1-pentanol. The extensively hydrogen-bonded hydrated network present in 1-pentanol provides an environment of microdomains, similar to those present in the aqueous phase, that are solvated by the hydrophilic ends of the 1-pentanol molecules. It is also interesting to note that the increase in the solubility of water in 1-pentanol in the presence of 0.1M Triton X-100 is negligible, corresponding to about one water molecule for each polyether chain, eleven oxygen atoms in length. This suggests that the polyether is effectively not hydrated in the solvent phase, for all three solvents studied.

One other point of interest which is evident from Table 1, is the similarity in the efficiencies of extraction of potassium and caesium aurocyanide when the polyether is present. The trend is $\text{Li}^+ < \text{K} \sim \text{Cs}^+$ for all three solvents. Once again, this effect is explicable in the light of the molecular mechanics calculations, and will be discussed in detail in that section.

Effect of cation concentration. The extraction of $\text{M}^+\text{Au}(\text{CN})_2^-$ by the polyether can be thought of as occurring by either of two processes,³ as follows.

(i) Solvation of $\text{M}^+\text{Au}(\text{CN})_2^-$ ion-pairs, similar to that occurring in their extraction by pure solvents such as 1-pentanol¹¹ or TBP:¹²



(the overscore denotes a species in the solvent phase; the polyether is represented as P). The driving force in this instance is the solvation of the entire ion-pair.

Table 2. Solubility of water in the various solvent phases

Solvent	Solubility in pure solvent*		Solubility in solvent plus 0.1M Triton X-100	
	% w/w	100X _w †	% w/w	100X _w †
Benzene	0.072	0.31	0.35	1.50
1-Pentanol	7.5	28.3	8.62	31.59
Nitrobenzene	0.25	1.71	0.41	2.74

*After Marcus and Kertes.³³

†X_w = mole fraction of water in the solvent phase.

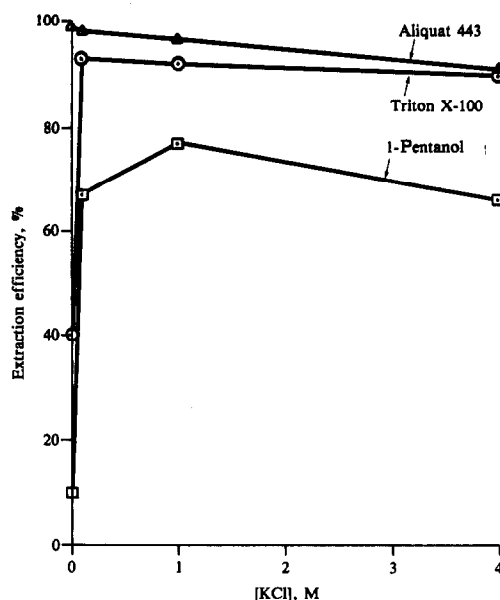
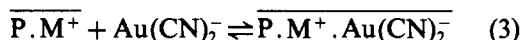
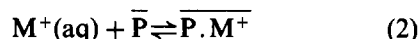


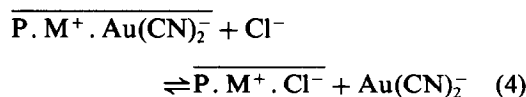
Fig. 1. Effect of KCl concentration on the extraction efficiency of $\text{M}^+\text{Au}(\text{CN})_2^-$ ion-pairs by solutions of a polyether and of a liquid ion-exchanger, and the solvent alone.

(ii) Cation chelation of M^+ by the polyether,³ with concomitant ion-exchange of the anion:



The driving force in this case is the complexation of the cation by one polyether molecule.

The results shown in Fig. 1 shed some light on this aspect. An increase in the concentration of potassium chloride as a background electrolyte should increase the extraction if reactions (1) or (2) are important, and decrease it if the ion-exchange reaction (3) is important, owing to competition with chloride ions at high concentrations:



This type of competition has been found³⁴ to be quite marked in the exchange of Cl^- for $\text{Au}(\text{CN})_2^-$ on a typical anion-exchange resin.

Figure 1 shows that the degree of extraction with a 1-pentanol solution of Aliquat 443, which is the strong-base anion-exchanger methyltri-octylammonium chloride, consistently decreases with increasing potassium chloride concentration. The extraction with 1-pentanol on its own rapidly increases with potassium chloride concentration to a maximum at 1M and then

declines again. The ion-exchange reaction (4) is therefore not a dominant one in this case.

In the presence of the polyether in the 1-pentanol, the situation is somewhat different. The introduction of a small excess (0.1M KCl) of K^+ ions results in a marked increase in the extraction, which is consistent with the formation of complexed cationic sites, reaction (2). At higher K^+ concentrations, the extraction curve closely follows that for Aliquat 443, suggesting that the ion-exchange competition reaction (4) comes into effect at higher ionic strengths.

These results strongly suggest that mechanism (ii), *i.e.*, chelation of the M^+ cations by the polyether, with concomitant ion-exchange of the anion, describes the system more adequately. This is borne out by the molecular mechanics calculations in the following section.

Molecular mechanics calculations

Uncomplexed polyether. Strain energies for various conformations of the uncomplexed polyether are shown in Table 3. The fact that the linear conformation has the lowest strain energy in the solvent of lowest dielectric constant is not surprising, since the *trans* O-C-C-O unit is intuitively expected to have a lower strain energy than the *gauche* or *cis* rotamers. It is in the *trans* condition that the O...O non-bonded and electrostatic interactions are lowest.

What is surprising is that the tight helical conformation has the lowest strain energy in solvents of high dielectric constant, whereas the uncomplexed polyether has the open helical conformation in the crystalline state,⁸ which would be expected to be a low-polarity environment. The cyclic polyether 18C6 crystallizes in the conformation that it adopts in solvents of low polarity,²⁴ in an attempt to minimize intramolecular dipole-dipole interactions,³⁵ and the acyclic polyethers would be expected to do the same. The reason is probably that in the crystalline state the intramolecular dipole-dipole interactions are minimized. As it is, the refined tight helical polyether is seen to have unwound slightly (Fig. 2), although the ratios of the g , \bar{g} , and t angles are still the same as in the metal complexes.

Polyether complexes with alkali-metal ions. Since the process of complexation involves not only attachment of the metal ion to the polyether, but also dehydration of the ions

Table 3. Strain energies of different conformations of uncomplexed poly(oxyethylene) in media of low dielectric constant ($\epsilon = r_{ij}$), high dielectric constant ($\epsilon = 4r_{ij}$) and infinite dielectric constant

C-C-O-C-C-O conformation	Strain energy, kcal/mole		
	$\epsilon = r_{ij}$	$\epsilon = 4r_{ij}$	$\epsilon = \infty$
t-t-t-t-t (linear)	87.9	16.6	-7.4
g-t-g-g-t (tight helical)	92.2	15.0	-21.7
g-t-t-g-t (open helical)	117.8	24.1	-9.1

[reaction (2)] and solvation of the anion, the hydration enthalpies of the metal ions³⁶ were subtracted from the calculated internal energies of the complexes, so that the relative complexation energies of the metal ions could be referred to the same environment. For comparison of the complexation of metal ions in environments of different polarities, it is necessary to subtract the relative energies of the ligands in each solvent. The enthalpy of hydration for the large $Au(CN)_2^-$ anion was assumed to be negligible, and was therefore not included in the calculations. The enthalpies of solvation for $Au(CN)_2^-$ in benzene and in nitrobenzene were calculated by the method of Abraham and Liszi,³⁷⁻³⁹ in which the enthalpy of solvation is considered to be comprised of an electrostatic and a neutral contribution:

$$\Delta H_s^0 = \Delta H_e^0 + \Delta H_n^0 \quad (5)$$

The electrostatic free-energy change component is calculated by means of a modified Born equation,³⁹ in which the distance-dependent dielectric constant is corrected for by the assumption of an ϵ_1 value of 2.0 for the primary solvation shell:

$$\Delta G_e = \frac{Z^2}{2} \left[\left(\frac{1}{\epsilon_1} - 1 \right) \left(\frac{1}{a} - \frac{1}{b} \right) + \left(\frac{1}{\epsilon_0} - 1 \right) \frac{1}{b} \right] \quad (6)$$

where ϵ_0 is the bulk dielectric constant, a is the ionic radius, Z is the ionic charge, and the effective thickness of the local layer is $(b - a) = r$, the radius of the solvent molecule.

The neutral contribution to the free-energy change was calculated from the equation

$$\Delta G_n^0 = ma + c, \quad (7)$$

where the values of m (kcal. mole⁻¹. Å⁻¹) and c (kcal/mole) are³⁷ -3.25 and 9.82 for benzene, and -3.22 (kcal/mole) and 10.19 for nitrobenzene; r is in Å. The ionic radius of $Au(CN)_2^-$ was estimated to be 2.11 Å, on the basis of theoretical calculations and conductivity measurements.

The electrostatic contribution to the entropy change is calculated³⁸ from the equation

$$\Delta S_c^0 = \frac{Z^2}{2} \left[\left(\frac{b-a}{abc_1^2} \right) \frac{\delta \epsilon_1}{\delta T} + \left(\frac{1}{bc_0^2} \right) \frac{\delta \epsilon_0}{\delta T} \right] \quad (8)$$

where the variation of the local dielectric constant with temperature, $\delta \epsilon_1/\delta T$, is set equal to $-0.00160 \text{ deg}^{-1}$ for all solvents.³⁸ The values for the variation of bulk dielectric constant with temperature, $\delta \epsilon_0/\delta T$, are $-0.00199 \text{ deg}^{-1}$ for benzene and -0.180 for nitrobenzene.³⁸

The neutral contribution to the entropy change, $-\Delta S_n^0$, was calculated from the equation³⁸

$$-\Delta S_n^0 = na + d \quad (9)$$

where n is $6.96 \text{ cal. mole}^{-1} \cdot \text{K}^{-1} \cdot \text{\AA}^{-1}$, a is in \AA , and d is $1.2 \text{ cal. mole}^{-1} \cdot \text{K}^{-1}$.

The results of the calculations (Tables 4 and 5) show that in both polar and non-polar media the energy of the Cs^+ complex is slightly lower than that of the K^+ complex. The energies of both the Cs^+ and the K^+ complexes are much lower than that of the Li^+ complex.

Figure 2 shows the lowest energy structures of the free polyether and the Cs^+ complex of the polyether in low- and high-dielectric environments, as determined from the molecular mechanics calculations. The similar structures of the complexed and uncomplexed polyether in a high-dielectric environment, and

Table 4. Strain energies (*kcal/mole*) of metal complexes with poly(oxyethylene) in benzene (low-polarity medium: $\epsilon = r_{ij}$)

	Li^+	K^+	Cs^+
Complex energy	25.7	43.4	53.7
Ligand energy	87.9	87.9	87.9
Enthalpy of complexation	-62.2	-44.5	-34.2
Anion solvation energy	-52.4	-52.4	-52.4
Cation hydration energy	-133.5	-86.1	-75.2
Enthalpy of extraction	18.9	-10.8	-11.4
Extraction, %	0.0	2.4	9.6

Table 5. Strain energies (*kcal/mole*) of metal complexes with poly(oxyethylene) in nitrobenzene (high-polarity medium: $\epsilon = 4r_{ij}$)

	Li^+	K^+	Cs^+
Complex energy	-51.2	-27.8	-20.9
Ligand energy	15.0	15.0	15.0
Enthalpy of complexation	-66.2	-42.8	-35.9
Anion solvation energy	-61.6	-61.6	-61.6
Cation hydration energy	-133.5	-86.1	-75.2
Enthalpy of extraction	5.7	-18.3	-22.3
Extraction, %	77.4	99.8	99.8

the striking modifications that the polyether has to undergo in a low-dielectric environment before it can complex the Cs^+ ion, are immediately obvious. This similarity of ligand conformation before and after complexation has been referred to by Cram *et al.*⁴⁰ as "pre-organization". Ligands with a high degree of pre-organization have more favourable

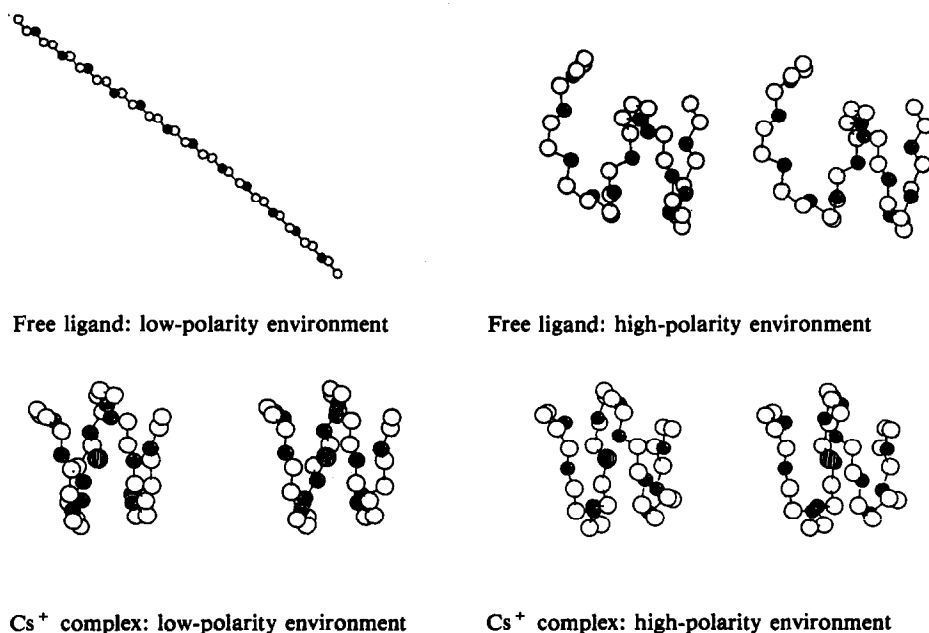


Fig. 2. Stereoscopic representation of minimum-energy structures of $\text{CH}_3(\text{CH}_2\text{OCH}_2)_{12}\text{CH}_3$ and its Cs^+ complex. Dark circles represent oxygen atoms, light circles represent carbon atoms, and shaded circles represent metal ions.

thermodynamics of complexation. This is reflected in the unfavourable (positive) energies of complexation in the low-dielectric solvent (Table 4) compared with the favourable (negative) energies of complexation in the high-dielectric solvent (Table 5). Even in the high-dielectric solvent, the energies of complexation of the cations are less negative than the hydration energies, indicating that the cations would prefer to remain hydrated.

Figure 3 shows the minimum-energy conformations of the Li^+ , K^+ and Cs^+ complexes of the polyether in an environment with a high dielectric constant. A qualitative impression of the relative strain induced by the co-ordinated metal ion can be gained from the amount of distortion the ligand experiences upon complexation. The uncomplexed ligand is most pre-organized with respect to the Cs^+ complex. The K^+ complex shows some distortion of the polyether, and the Li^+ complex is the most distorted, due to the fact that the ligand has to invest a large amount of energy for this ion to form a complex. This investment of energy would detract from the complexation energy, and reduce the proportion of complexed metal in solution.

These results are in accordance with the extraction data, which show that the extraction of the $[\text{Cs}(\text{Triton X-100})]^+$ complex into benzene is greater than that of the K^+ complex, and the extraction of the Li^+ complex is negligible. The extraction of the K^+ and Cs^+ complexes into nitrobenzene is practically complete, whereas there is only about 80% extraction of the Li^+ complex.

The results of the molecular mechanics complexation-energy calculations do not explain the absolute differences in extraction by solvents of differing polarity. There is very little difference between the complexation energies of each of the three metal ions in solvents of high polarity and low polarity (Tables 4 and 5), whereas there is a substantial difference in the extraction efficiencies.

This effect is explained by the comparatively large difference between the calculated solvation energies of $\text{Au}(\text{CN})_2^-$ in nitrobenzene and benzene. It is evident that the preferential extraction of the ion-pair into high-polarity solvents results more from the greater solvation energy of the aurocyanide anion in high-polarity solvents than from the differences in energy of complexation. This conclusion is borne out by the similar dependence of the extraction of

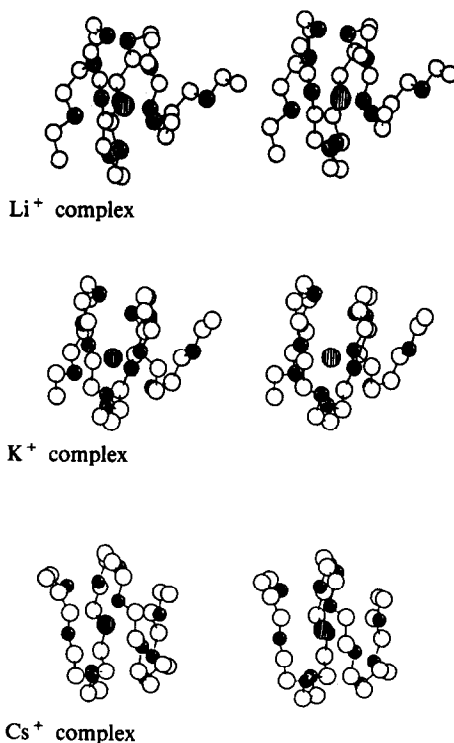


Fig. 3. Stereoscopic representation of minimum-energy structures of the alkali-metal complexes of $\text{CH}_3(\text{CH}_2\text{OCH}_2)_{12}\text{CH}_3$ in a high-dielectric environment. Symbols as for Fig. 2.

$\text{NEt}_4^+\text{Au}(\text{CN})_2^-$ ion-pairs on the dielectric constant of the solvent, an effect that is readily attributable to preferential secondary solvation.⁴⁰ This phenomenon would increase the stability of the complexes in the high-polarity organic solvent, relative to the stability in the low-polarity solvent, by the same amount for each metal. This would explain the much greater extraction of the Li^+ complex into the high-polarity solvent. The small difference in extraction of the K^+ and Cs^+ complexes is explained by the fact that the extraction of these complexes is already at a maximum.

CONCLUSIONS

Aurocyanide ion-pairs are extracted efficiently into organic phases with the aid of long-chain polyethers. The polyether is co-ordinated to the metal ion by the ether oxygen atoms. It wraps around the metal ion in a helical configuration that is stabilized by high dielectric-constant solvents, resulting in higher extraction than into low dielectric-constant solvents.

The results of the distribution experiments can be rationalized in terms of molecular

mechanics calculations. The uncomplexed polyether is more pre-organized with respect to the Cs^+ complex than to the other metal ions, resulting in the preferential complexation of the Cs^+ ion by the polyether, and hence the preferential transport of the $\text{Cs}^+\text{Au}(\text{CN})_2^-$ ion-pair into the organic phase.

The superior extraction of the metal-aurocyanide ion-pair into solvents of high dielectric constant results more from the greater energy of solvation of the aurocyanide anion by high-polarity solvents, than from enhancement of cation complexation by a reduction in intramolecular electrostatic interactions.

Simulation of the ion-pair effect by molecular mechanics calculations is possible, but has not been attempted since it is fraught with complications, such as the fact that the van der Waals parameters of the aurocyanide ion are not known, and would have to be calculated *ab initio*.

Acknowledgement—This paper is published by permission of Mintek.

REFERENCES

1. S. Yanagida, K. Takahashi and M. Okahara, *Bull. Chem. Soc. Japan*, 1977, **50**, 1386.
2. T. Suzuki, N. Murakami and T. Sotobayashi, *ibid.*, 1980, **53**, 1453.
3. R. F. Hamon, A. S. Khan and A. Chow, *Talanta*, 1982, **29**, 313.
4. T. Braun and B. Farag, *Anal. Chim. Acta*, 1978, **99**, 1.
5. R. J. Levins, *Anal. Chem.*, 1971, **43**, 1045.
6. W. Saenger, I. H. Suh and G. Weber, *Isr. J. Chem.*, 1979, **18**, 253.
7. J. A. Siddiqui and P. V. Wright, *Polymer*, 1987, **28**, 5.
8. H. Tadokoro, Y. Chatani, T. Yoshihara, S. Tahara and S. Murahashi, *Makromol. Chem.*, 1964, **73**, 109.
9. J. L. Koenig and A. C. Angood, *J. Polym. Sci., A-2*, 1970, **8**, 1787.
10. A. Rollat, M. Burgard, M. J. F. Leroy, H. S. Park, J. C. Gautier and S. Lecolier, *ISEC '80, International Solvent Extraction Conference*, Liège, Belgium, 12–18 September 1980, paper 80–125.
11. G. J. McDougall, M. D. Adams and R. D. Hancock, *Hydrometallurgy*, 1987, **18**, 125.
12. J. D. Miller, R. Y. Wan, M. B. Mooiman and R. L. Sibrell, *Sep. Sci. Technol.*, 1987, **22**, 487.
13. T. Braun and A. B. Farag, *Anal. Chim. Acta*, 1983, **153**, 319.
14. Y. Takahashi and H. Tadokoro, *Macromolecules*, 1973, **6**, 672.
15. D. T. Baldwin, W. L. Mattice and R. D. Gandour, *J. Comput. Chem.*, 1984, **5**, 241.
16. D. E. Fenton, J. M. Parker and P. V. Wright, *Polymer*, 1973, **14**, 589.
17. B. L. Papke, M. A. Ratner and D. F. Shriver, *J. Phys. Chem. Solids*, 1981, **42**, 493.
18. D. F. Shriver, B. L. Papke, M. A. Ratner, R. Dupon, T. Wong and M. Brodwin, *Solid State Ionics*, 1981, **5**, 83.
19. R. H. Boyd, S. M. Breitling and M. Mansfield, *Am. Inst. Chem. Eng. J.*, 1973, **19**, 1016.
20. S. J. Weiner, P. A. Kollman, D. A. Case, U. C. Singh, C. Ghio, G. Alagona, S. Profeta and P. Weiner, *J. Am. Chem. Soc.*, 1984, **106**, 765.
21. J. M. Blaney, J. K. Weiner, A. Dearing, P. A. Kollman, E. C. Jorgensen, S. J. Oatley, J. M. Burrige and C. C. F. Blake, *ibid.*, 1982, **104**, 6424.
22. P. A. Kollman, P. K. Weiner and A. Dearing, *Biopolymers*, 1981, **20**, 2583.
23. P. A. Kollman, G. Wipff and U. C. Singh, *J. Am. Chem. Soc.*, 1985, **107**, 2212.
24. G. Wipff, P. Weiner and P. A. Kollman, *ibid.*, 1982, **104**, 3249.
25. L. G. Dunfield, A. W. Burgess and H. A. Scheraga, *J. Phys. Chem.*, 1978, **82**, 2609.
26. R. A. Scott and H. A. Scheraga, *J. Chem. Phys.*, 1965, **42**, 2209.
27. B. R. Brooks, R. E. Brucocoleri, B. D. Olafson, D. J. States, S. Swaminathan and M. Karplus, *J. Comput. Chem.*, 1983, **4**, 187.
28. A. Vedani and J. D. Dunitz, *J. Am. Chem. Soc.*, 1985, **107**, 7653.
29. D. Rees, *J. Mol. Biol.*, 1980, **141**, 323.
30. A. Warshel, *J. Phys. Chem.*, 1979, **83**, 1640.
31. J. A. McCammon, P. G. Wolynes and M. Karplus, *Biochemistry*, 1979, **18**, 927.
32. M. S. Bovill, D. J. Chadwick and I. O. Sutherland, *J. Chem. Soc., Perkin Trans.*, 1980, **2**, 1529.
33. Y. Marcus and A. S. Kertes, *Ion Exchange and Solvent Extraction of Metal Complexes*, pp. 932–935. Wiley, New York, 1969.
34. M. D. Adams, G. J. McDougall and R. D. Hancock, *Hydrometallurgy*, 1987, **18**, 139.
35. R. D. Hancock and A. E. Martell, *Comments Inorg. Chem.*, 1988, **6**, 237.
36. F. Franks, *Water: A Comprehensive Treatise*, Vol. 3, p. 55. Plenum Press, New York, 1973.
37. M. H. Abraham and J. Liszi, *J. Chem. Soc., Faraday Trans. I*, 1978, **74**, 1604.
38. *Idem, ibid.*, 1978, **74**, 2858.
39. *Idem, J. Inorg. Nucl. Chem.*, 1981, **43**, 143.
40. D. J. Cram, T. Kaneda, R. C. Helgeson, S. B. Brown, C. B. Knobler, E. Maverick and K. N. Trueblood, *J. Am. Chem. Soc.*, 1985, **107**, 3645.

LIQUID-SOLID EXTRACTION SYSTEM BASED ON TWEEN 40-SALT-H₂O WITHOUT ORGANIC SOLVENTS

LI BUHAI and MENG RIGAN

Department of Chemistry, South-Central College for Nationalities, Wuhan, Hubei, 430074,
People's Republic of China

(Received 15 September 1989. Revised 14 February 1990. Accepted 21 February 1990)

Summary—An aqueous solution of Tween 40 forms liquid and solid phases in the presence of various salts, depending on the Tween 40 concentration, the identity and concentration of the salt, and the solution acidity. The distribution of Zr(IV), U(VI), Fe(III), Pb(II) and some organic photometric reagents between the Tween 40 phase and aqueous phase containing salt was examined. The quantitative extraction, separation and determination of Zr(IV) or U(VI) in the presence of Pb(II) was achieved by controlling the solution acidity in the system. The extraction mechanism has been tentatively studied.

In liquid-liquid extraction with common organic solvents, only neutral species are normally transferred from the hydrophilic to the hydrophobic phase. Therefore the method cannot be applied to the extraction of strongly hydrophilic species, especially those with multiple charges. Also, the solvents are often volatile, flammable (or even explosive) and toxic.

It is known that aqueous solutions of poly(ethylene glycol) (PEG) can separate into two aqueous phases in the presence of certain inorganic salts.^{1,2} This two-phase aqueous system has been applied to the extractive separation of metal ions.^{3,4}

Recently, we found that aqueous solutions of poly(vinylpyrrolidone) (PVP), Tween 80 (polyoxyethylene sorbitan mono-oleate) and other water-soluble polymers form liquid and solid phases on addition of various salts. Under suitable conditions some water-soluble photometric reagents and their complexes with metal ions can be transferred into the solid phases formed by the polymers. Some metal ions can be separated with this system. We have called the system a liquid-solid extraction system.⁵ It has an advantage over the two-phase aqueous system, because it is more convenient (not requiring a separatory funnel) and is more rapid.

In this paper the liquid-solid extraction system based on Tween 40-salt-H₂O is reported.

EXPERIMENTAL

Apparatus

A Shanghai model 721 spectrophotometer was used for photometric measurements. A

Shanghai model pHs-2 pH-meter and a shaking machine were used.

Reagents

An aqueous solution of Tween 40 (polyoxyethylene sorbitan palmitate) was prepared by dissolving 50 ml of Tween 40 in 200 ml of distilled water. Standard 1.0-mg/ml solutions of U(VI), Pb(II) and Fe(III) in 0.15M nitric acid, and Zr(IV) in 10% v/v hydrochloric acid were prepared from UO₂(NO₃)₂·6H₂O, pure lead and iron, and ZrOCl₂·8H₂O respectively. More dilute solutions were prepared by appropriate dilution as required. All other reagents were of analytical grade.

Procedure

Given volumes of Tween 40 aqueous solution, photometric reagent solution and metal ion solution were put into a 25-ml tube fitted with a stopper. The acidity of strongly acidic solutions was adjusted with hydrochloric acid, and in the pH range 1.5-6.5 by use of monochloroacetic acid or acetic acid buffers. The solution was then diluted to 10.0 ml with distilled water, a given weight of solid salt was added and the mixture was shaken for 3 min. After standing for several minutes, the solution separated into liquid and solid phases. The liquid phase was carefully decanted. The Tween 40 solid phase was washed two or three times with 1-2 ml of a saturated solution of the same salt, and the washings were combined with the separated liquid phase. The washed Tween 40 phase was dissolved with distilled water. The photometric

reagent or complex in the dissolved solid or liquid phase was determined spectrophotometrically. The degree of extraction ($E\%$) was calculated as the ratio of the amount of species extracted by the solid phase (Tween 40 phase) to the amount initially added to the system.

The conditions used for determination of the metal ions with arsenazo III as photometric reagent are given in Table 1.

RESULTS AND DISCUSSION

Phase separation conditions for Tween 40 solution

Figure 1 shows the phase diagrams for the system based on Tween 40 and various salts, namely sodium citrate, ammonium sulphate and sodium dihydrogen phosphate. With constant Tween 40 concentration, the salt concentration necessary for phase separation depends on the identity of the salt. Because most metal sulphates are water-soluble, $(\text{NH}_4)_2\text{SO}_4$ is preferred for use in the phase separation. The necessary salt concentration increases as the Tween 40 concentration decreases. The salt concentration necessary also depends on the pH. In the pH range 0.0–2.0 it decreases with increase in pH and remains unchanged when the pH value is further increased. The reason is probably that at low pH the sulphate ion is protonated to HSO_4^- and the salting-out ability is reduced.

Distribution of organic reagents

The distribution of some water-soluble reagents between the Tween 40 and aqueous phases was examined at different pH values from 0.0 to 6.5. The organic reagents chosen, containing different chelating groups, were arsenazo III, Bromopyrogallol Red, Chromazurol S and Xylenol Orange. The $E\%$ values of these reagents were found to be independent of the pH. $E\%$ for the first three reagents was from 95 to 100%, and for the last about 70%. It is possible to use them as extractants and extraction-photometric reagents in this system.

Extraction of metals in the presence of arsenazo III

Effect of pH. Figure 2 presents the dependence of $E\%$ for Zr(IV), U(VI), Fe(III) and

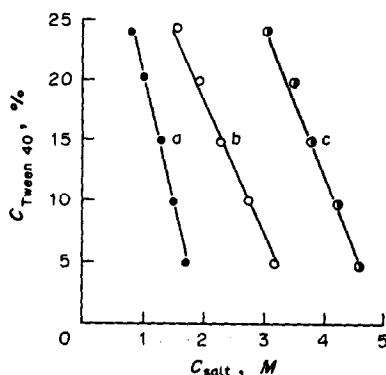


Fig. 1. Phase diagrams of the Tween 40–aqueous salt system: a, $\text{Na}_3\text{C}_6\text{H}_5\text{O}_7$ (pH 6.6–7.2); b, $(\text{NH}_4)_2\text{SO}_4$ (pH 3.8–3.9); c, NaH_2PO_4 (pH 2.9–3.1).

Pb(II) in the Tween 40 phase on the pH value in the presence of arsenazo III. The stability of the complexes of Zr(IV), U(VI) and Fe(III) can be increased by raising the pH from 0.0 to 3.0, so the $E\%$ is correspondingly increased. The $E\%$ for these metals is maximum at pH 3.0, and then decreases with further increase in pH, probably owing to hydrolysis and other side-reactions of the metals at high pH.

In contrast to Zr(IV), U(VI) and Fe(III), for Pb(II) $E\%$ decreases as the pH increases from 0.0 to 3.0, and then increases at higher pH.

Effect of arsenazo III concentration. Figure 3 shows that at fixed pH the degree of formation of the complexes of the metals can be increased by increasing the arsenazo III concentration up to $1.29 \times 10^{-4}M$; the $E\%$ values for Fe(III) and Pb(II) continue to increase, but those of Zr(IV) and U(VI) decrease slightly with further increase in arsenazo III concentration.

Without arsenazo III present, the $E\%$ values for the four metals are all zero. This means that

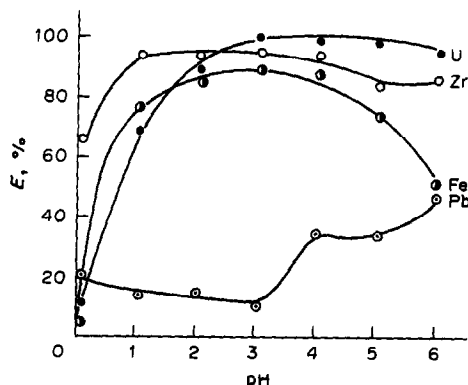


Fig. 2. Relationship between $E\%$ of metals and pH: $C_{\text{Tween 40}} = 12\%$; $C_{\text{arsenazo III}} = 1.29 \times 10^{-4}M$; $C_{(\text{NH}_4)_2\text{SO}_4} = 2.27M$; amount of metals added: Zr, 40 μg ; Pb, 50 μg ; U, 40 μg ; Fe, 20 μg .

Table 1. Spectrophotometric determination of metals

	Zr(IV)	U(VI)	Fe(III)	Pb(II)
Wavelength, nm	624	648	610	646
Acidity	0.1M HCl	pH 2.0	pH 3.5	pH 5.0

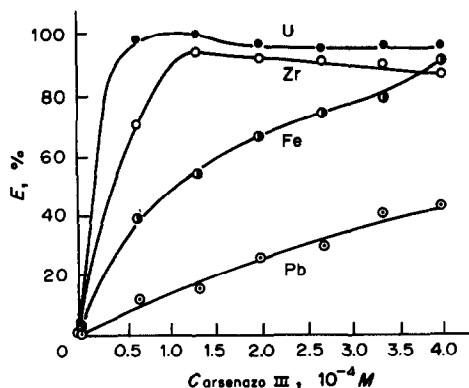


Fig. 3. Effect of arsenazo III concentration on $E\%$ for the metals: extraction acidity, Zr, pH 1.0; Pb, pH 5.0; U and Fe, pH 3.0; other conditions as for Fig. 2.

the uncomplexed metal ions cannot be extracted into the Tween 40 phase.

Effect of $(\text{NH}_4)_2\text{SO}_4$ concentration. When the $(\text{NH}_4)_2\text{SO}_4$ concentration is increased, the $E\%$ of Pb(II) is almost constant, but the values for Zr(IV), U(VI) and Fe(III) increase to a maximum and then decrease, as shown in Fig. 4. As the salt concentration increases, the Tween 40 is salted out and $E\%$ is therefore increased. When the Tween 40 is completely salted out the salt-effect of the excess of ammonium sulphate decreases the stability of the complexes and hence decreases $E\%$.

Recovery tests for quantitative separation

Figure 2 shows that at pH 3.0 the $E\%$ values for Zr(IV) and U(VI) are in the range 96–100%. At the same pH the $E\%$ for Pb(II) is only about 11%, so after the first extraction with arsenazo

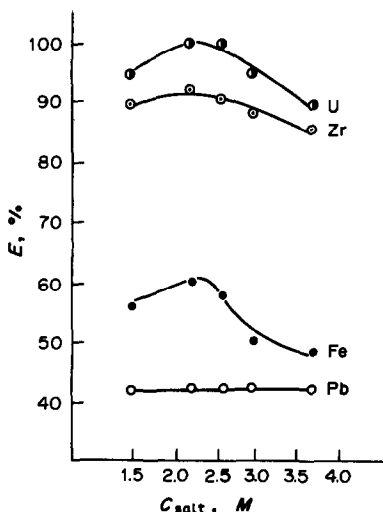


Fig. 4. Relationship between $E\%$ and $C_{(\text{NH}_4)_2\text{SO}_4}$: extraction conditions as for Fig. 3.

Table 2. Recoveries in extractive separation of U(VI) from Pb(II)

U(VI) added, μg	Pb(II) added, μg	U(VI) found, μg	Apparent U(VI) recovery, %	No. of extraction operations
40.0	40.0	39.0	97.5	2
100.0	100.0	101.0	101.0	2
60.0	100.0	60.8	101.3	2
5.0	500	4.6	92	2
5.0	1000	5.3	106	2
5.0	5000	5.4	108	3

III and the Tween 40– $(\text{NH}_4)_2\text{SO}_4$ – H_2O system, Zr(IV) or U(VI) can be quantitatively transferred into the Tween 40 phase, and a large fraction of the Pb(II) remains unextracted. To separate the residual Pb(II), the salted-out Tween 40 phase is dissolved in 10 ml of water, and then salted out with 3.0 g of ammonium sulphate; two or three such operations should result in satisfactory separation of Zr(IV) or U(VI) from Pb(II), as shown in Tables 2 and 3.

Extraction mechanism for Tween 40 phase

Composition of complex of U(VI) with arsenazo III extracted into Tween 40 phase. The continuous-variations and molar-ratio methods were used to determine the composition of the complex, which was found to be 1:1 U(VI):arsenazo III (Figs. 5 and 6).

Effect of cationic and anionic surfactants on $E\%$ for U(VI). To study further the extraction mechanism for the Tween 40 phase, various concentrations of cationic or anionic surfactant were added to the solutions of the extraction system containing the complex of U(VI) with arsenazo III, and the $E\%$ of U(VI) was determined. Figure 7 shows that at pH 3.0 $E\%$ is little affected by the anionic surfactant added (dodecylbenzene sodium sulphonate, DBS) (a in Fig. 7), but is decreased by increasing concentration of cationic surfactant (cetylpyridinium chloride, CPC) (b in Fig. 7). At lower pH (pH 1.0), the situation is quite different. The $E\%$ of U(VI) is decreased by increasing DBS

Table 3. Recoveries for extractive separation of Zr(IV) from Pb(II)

Zr(IV) added, μg	Pb(II) added, μg	Zr(IV) found, μg	Zr(IV) recovery, %	No. of extraction operations
40.0	40.0	39.0	97.5	2
100.0	100.0	94.0	94.0	2
40.0	200.0	40.0	100	2
5.0	500	4.7	94	2
5.0	1000	5.0	100	2
5.0	2500	5.0	100	2

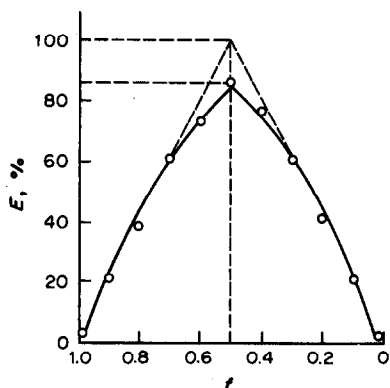


Fig. 5. Job plot. Extraction acidity, pH 3.0.

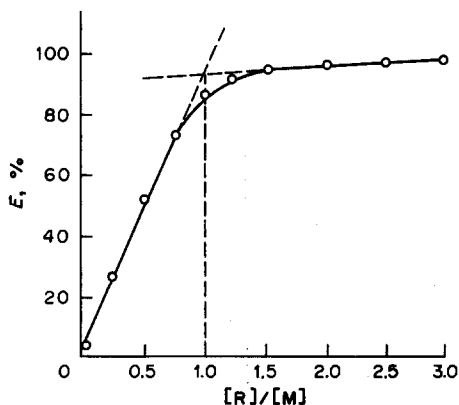


Fig. 6. Molar-ratio plot. Acidity for Fig. 5.

concentration (a' in Fig. 7), but is not affected by CPC (b' in Fig. 7).

As discussed above, U(VI) and arsenazo III form a 1:1 complex, which is extracted into the Tween 40 phase. Arsenazo III is a weak polyacid, H_3L , and there is considerable uncertainty about the values of the dissociation constants. At pH 1.0, however, the dominant species is probably H_2L^- , which would give a positive charge to the 1:1 complex with UO_2^{2+} , for which dodecylbenzene sulphonate might act as counter-ion to give a neutral species. At pH 3.0, however, the dominant species is probably H_3L^{3-} , which would give a negatively charged uranyl complex, which could give a neutral species with a cetylpyridinium counter-ion.

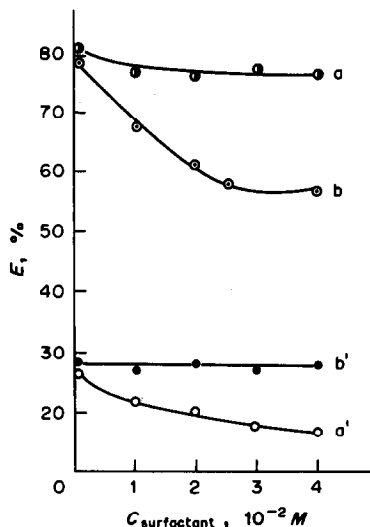


Fig. 7. Effect of cationic and anionic surfactants on $E\%$ of U(VI): a, b, pH 3.0; a' , b' , pH 1.0.

Under both conditions, $E\%$ for U(VI) is decreased, indicating that only the charged complex can be extracted into the Tween 40 solid phase, and not the uncharged species. This mechanism is at present only speculative and requires experimental examination. It is in contrast to that of liquid-liquid extraction systems, in which only uncharged and hydrophobic substances can be extracted from the aqueous phase.

REFERENCES

1. T. I. Zvarova, V. M. Shkinev, B. Ya. Spivakov and Yu. A. Zolotov, *Dokl. Akad. Nauk SSSR*, 1983, **273**, 107.
2. *Idem*, *Mikrochim. Acta*, 1984 **III**, 449.
3. Li Buhai, Sun Xiaomei and Yang Shengcai, *Gaodeng Xuexiao Huaxue Xuebao*, 1989, **3**, 293.
4. Li Buhai, Sun Xiaomei and Wang Shoucheng, *Fenxi Shiyanshi*, 1989, **6**, 10.
5. Li Buhai and Wang Kefu, *Gaodeng Xuexiao Huaxue Xuebao*, 1990, **4**, 1207.
6. B. Buděšínský, *Talanta*, 1969, **16**, 1277.
7. P. K. Spitsyn and V. S. Sharev, *Zh. Analit. Khim.*, 1970, **25**, 1503.
8. S. Kotrlý and L. Šůcha, *Handbook of Chemical Equilibria in Analytical Chemistry*, p. 205. Horwood, Chichester, 1985.

DETERMINATION OF ORTHO- AND PYROPHOSPHATES IN WATERS BY EXTRACTION CHROMATOGRAPHY AND FLOW-INJECTION ANALYSIS

B. YA. SPIVAKOV, T. A. MARYUTINA, L. K. SHPIGUN, V. M. SHKINEV
and YU. A. ZOLOTOV

Vernadsky Institute of Geochemistry and Analytical Chemistry, Academy of Sciences,
V-334 Moscow, U.S.S.R.

E. RUSEVA and I. HAVEZOV

Institute of General and Inorganic Chemistry, Academy of Sciences, 1040 Sofia, Bulgaria

(Received 22 March 1989. Revised 5 February 1990. Accepted 28 March 1990)

Summary—Extraction–chromatographic separation of ortho- and pyrophosphate anions on an inert support modified with an organotin extractant was studied and used for their subsequent determination in a flow-injection system. The proposed FIA manifold includes an extraction–chromatographic mini-column, on which the phosphate anions are separated and preconcentrated, and a post-column spectrophotometric detector. For the determination of orthophosphate, the absorbance of the reduced 12-molybdophosphoric acid is monitored at 660 nm. The sum of ortho- and pyrophosphate can be determined after preliminary hydrolysis of pyrophosphate to orthophosphate in neutral solution at 50° by use of inorganic pyrophosphatase. For a sample volume of 6 ml, the calibration graph is linear within a range of 5.0–100.0 ng/ml P. The limit of detection is 0.3 ng/ml P. The recovery of the ions to be determined is not less than 96%, the relative error is not worse than 4%. The proposed method was used for the analysis of river water samples.

The determination of various phosphorus oxyanions in natural and waste waters is an important analytical problem. The contents of ortho-, pyro- and triphosphates in natural waters are regularly checked to study eutrophication and ecological equilibria in the environment. Their concentrations are most often determined by spectrophotometric methods based on the formation of binary and ternary heteropoly acids and ion-associates,¹ but these procedures are useful for the determination of only orthophosphate anions. The other phosphate anions can be determined after preliminary transformation into orthophosphate. A relatively simple and reliable technique for separation and preconcentration of the oxyanions of phosphorus in combination with a suitable method for determination of phosphorus is still required. Recently, some of the known colour reactions have been used for spectrophotometric detection in the flow-injection determination of phosphorus.^{2,3} Flow-injection analysis is very advantageous owing to its relatively high sample throughput and precision, and readily available instrumentation. Flow-injection systems allowing the speciation of some oxyanions of phosphorus after preliminary separation by HPLC⁴ and

ion-exchange⁵ have been described. Ion-exchange has also been applied for separation of orthophosphate in the simultaneous determination of orthophosphate, silicate and arsenate.⁶

Organotin compounds of the type A_2SnX_2 , where A = octyl or nonyl and X = Cl^- or NO_3^- , quantitatively extract ortho- and pyrophosphate anions.⁷

The present paper describes the extraction–chromatographic separation of ortho- and pyrophosphate anions and its application in the flow-injection determination of phosphorus.

EXPERIMENTAL

Reagents

All chemicals were of analytical-reagent grade. An orthophosphate stock solution (1000 $\mu\text{g/ml P}$) was prepared by dissolving 4.394 g of potassium dihydrogen orthophosphate, preliminarily dried at 80° for 2 hr, in 1 litre of redistilled water. A pyrophosphate stock solution (1000 $\mu\text{g/ml P}$) was prepared by dissolving 7.20 g of sodium pyrophosphate decahydrate in redistilled water. Working solutions (1–100 $\mu\text{g/ml P}$) were prepared by dilution.

Inorganic pyrophosphatase (EC MRE-600) with a molecular weight of 1.2×10^5 was used to hydrolyse pyrophosphate to orthophosphate.⁵ A solution of the enzyme in Tris-HCl buffer (R_4 , pH 8.6), containing $1 \times 10^{-3} M$ magnesium chloride, was prepared.

The molybdenum reagent (R_2) was prepared by dissolving 7 g of ammonium heptamolybdate, $(NH_4)_6Mo_7O_{24} \cdot 4H_2O$, in 1 litre of 0.3M sulphuric acid.

The reducing agent solution (R_3) was made by dissolving 0.4 g of tin(II) chloride and 0.4 g of hydrazine sulphate in 1 litre of 0.3M sulphuric acid.

Apparatus

Electrothermal atomization atomic-absorption spectrometry (ETAAS) measurements were made with a double-beam Perkin-Elmer model 400 atomic-absorption spectrometer equipped with a deuterium lamp background corrector, an HGA-76B graphite furnace and a V-shaped pyrolytic graphite platform.

FIA experiments were performed with a FIAstar 5020-003 microprocessor-controlled flow-injection analyser equipped with a spectrophotometric detector.

Radiometric measurements were performed with an NRQ-603 automatic γ -counter (Tesla, Czechoslovakia).

Procedures

Extraction chromatography support. The extractive chromatographic separation was performed on a support modified with dioctyltin dinitrate, $(C_8H_{16})_2Sn(NO_3)_2$, synthesized as described elsewhere,⁸ dioctyltin dichloride, $(C_8H_{16})_2SnCl_2$, or dinonyltin dichloride, $(C_9H_{18})_2SnCl_2$, as prepared previously.⁹ The supports tested were Polysorb 1 (U.S.S.R.), Chromaton N-AW-HMDS 0.250–0.315 mm (Czechoslovakia), activated carbon (U.S.S.R.) and Spheron 100000 (40–45 μm) (Lachema, Czechoslovakia).

The extractive chromatographic behaviour of ortho- and pyrophosphate anions was studied under dynamic conditions on a glass column (6 mm bore, bed length 30 mm) and on a glass column (2.5 mm bore, bed length 30 mm). Both ends of the second column were plugged with glass wool and the column was mounted in the flow-injection system. The sorption efficiency of the support was estimated by passing 1000 μg of phosphorus through the columns. The phosphorus content in the eluates was measured

either by ETAAS¹⁰ (for the open column), or radiometrically with ^{32}P (for the plugged column).

The organotin compound was applied by shaking a weighed amount of the support with a solution containing the organotin reagent in a minimal volume of diluent for a minimum of 2 hr. The suspension was dried in air, and the dry material was used to pack the columns.

RESULTS AND DISCUSSION

Extractive chromatographic behaviour of ortho- and pyrophosphate

Modification of the support. The larger specific surface and uniform grain size of Chromaton provided some advantages over the other supports studied. It was established that dialkyltin chlorides were well attached to the support surface. Suitable solvents appeared to be chloroform or a mixture of diethyl ether with decanol (which acts as an active additive and improves the solubility of the organotin reagents).¹¹ Decanol, when applied to the support, did not retain either ortho- or pyrophosphate anions. The ratio of reagent to decanol was varied from 1:1 to 1:20. The optimal amount of dialkyltin reagent was found to be 5% of the weight of the support and the ratio of organotin compound to decanol to be 1:2.

Separation. Experiments showed that ortho- and pyrophosphate were sorbed quantitatively on the Chromaton support modified with dialkyltin dichloride. The sorption efficiency was constant for at least 100 sorption/desorption cycles and the columns could be stored for months without any detectable change in sorption capacity.

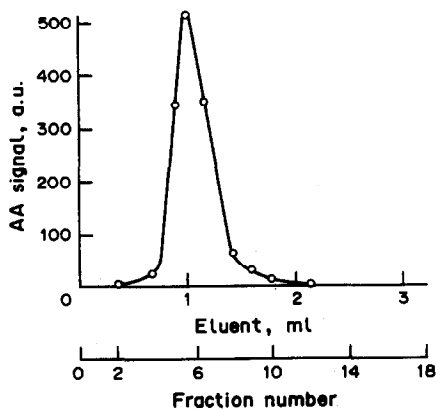


Fig. 1. Elution of orthophosphate with 0.5M HCl from the column containing 100 $\mu g/ml$ P.

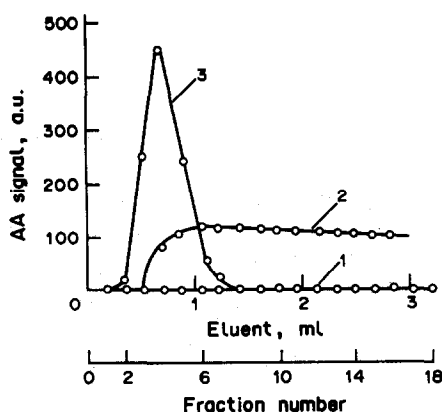


Fig. 2. Elution of pyrophosphate with 0.5M HCl (1), 0.8M HCl (2) and 3M HCl (3) from a column containing 100 $\mu\text{g/ml}$ P.

The elution of sorbed ortho- and pyrophosphate anions with 0.5, 0.8, 1.0 and 3.0M hydrochloric acid was investigated. Figures 1 and 2 show that orthophosphate can be eluted with 0.5M hydrochloric acid (2 ml of the eluent are sufficient) and pyrophosphate with 3.0M hydrochloric acid.

The separation of ortho- and pyrophosphate anions was checked with model mixed solutions which were passed through the column, followed by washing with 2 ml of $1 \times 10^{-3}\text{M}$ hydrochloric acid. Orthophosphate was eluted first with 2 ml of 0.5M hydrochloric acid and the column was again washed with 2 ml of $1 \times 10^{-3}\text{M}$ hydrochloric acid. The eluate and washings were combined and subjected to ETAAS analysis. Pyrophosphate was similarly eluted with 3M hydrochloric acid.

Flow-injection determination of ortho- and pyrophosphate

Manifold for orthophosphate. The manifold is shown in Fig. 3, and comprises two peristaltic pumps which operate in turn, pump I for the preconcentration of phosphate anions on the column, and pump II for the elution and spectrophotometric detection.

For preconcentration the sample solution is mixed with a stream of 0.5M nitric acid, pumped at constant flow-rate through column 3. After a defined sample volume has been pumped, two-way stopcock 2 is turned, first to allow water to flow through the column, and again for passage of 0.5M nitric acid for 60 sec. Pump I is then stopped and pump II started for the elution.

The eluent (300 μl of 0.5M hydrochloric acid/0.5M sodium chloride) is injected into the R_1 stream and pumped through column 3. The eluate is mixed with the streams of reagents R_2 and R_3 . The combined stream proceeds through the reaction coil to form molybdenum blue and the absorbance is monitored at 660 nm. The peak height of the signal is proportional to the concentration of orthophosphate. The peak base-width varies in the range 90–110 sec. The efficiency of the column depends on the flow-rate of the sample, V_0 , at the preconcentration stage, the eluent volume, S_v , and the flow-rate, V_1 , of the carrier stream R_1 (see Fig. 4). The best results were achieved with $S_v = 300 \mu\text{l}$, $V_1 = 0.6 \text{ ml/min}$ and $V_0 = 2.8 \text{ ml/min}$. The optimal conditions for the

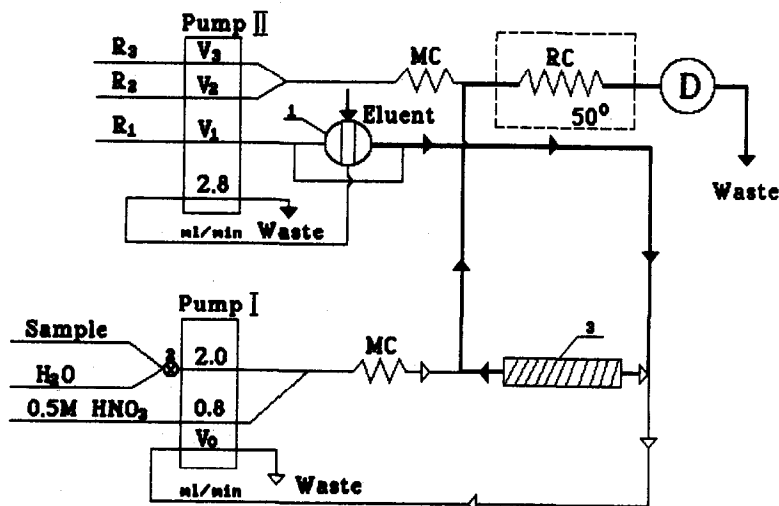


Fig. 3. Manifold of flow-injection system with the extraction chromatography column: 1—injector, 2—two-way stopcock, 3—extraction chromatography column, MC—mixing coil, RC—reaction coils, D—spectrophotometric detector, R_1 —0.5M HNO_3 , R_2 —ammonium molybdate, R_3 —reducing agent.

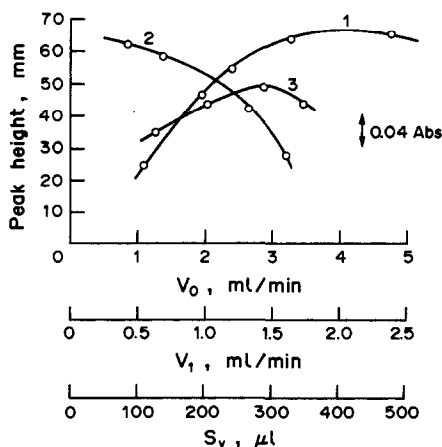


Fig. 4. Peak heights for orthophosphate as function of the eluent volume S_v (1), flow-rate of the carrier stream V_1 (2) and flow-rate of the sample through the column V_0 (3).

formation of 12-molybdophosphoric acid were reagent flow-rate (V_2 and V_3) 0.6 ml/min, reaction coil length 240 cm and temperature 50°.

The signals for orthophosphate recorded under the recommended conditions have maximal height and small half-width. The reproducibility is good and the base line is stable (Fig. 5). For a sample volume of 6 ml, the calibration graph is linear over the range 5.0–100.0 ng/ml P, and the detection limit is 0.3 ng/ml P (3S-criterion).

Silicate, arsenate and several metal cations interfere with the determination of phosphate by the molybdenum blue method,¹² copper(II), nickel(II) and chromium(III) by the colour of the solutions if their concentrations are high, iron(III) by forming a fairly stable phosphate complex and vanadium(V) by forming vanado-molybdophosphate. Chromium(VI) interferes by its oxidative effect. It was established that a 10,000-fold ratio of chromium(III), 5000-fold

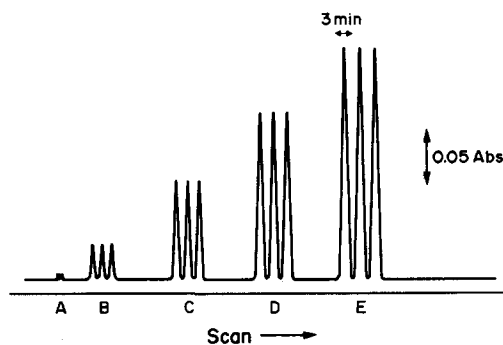


Fig. 5. Flow-injection signals for the determination of orthophosphate. Orthophosphate (ng/ml): A—0; B—10; C—30; D—50; E—70.

ratio of nickel(II) and iron(III), 1000-fold ratio of copper(II), 500-fold ratio of silicon(IV), 200-fold excess of vanadium(V) and chromium(VI) and 3-fold ratio of arsenic(V) do not interfere at the 5–100 ng/ml P level.

The results of recovery studies are given in Table 1. With a sample volume of 6 ml, 12 samples per hour can be analysed. The mean RSD is 3.3%.

Manifold for analysis of ortho- and pyrophosphate mixtures. The manifold for determination of ortho- and pyrophosphate is shown in Fig. 6. The analysis is done in three successive stages.

The first stage is determination of total phosphorus in the injected sample. Hydrolysis of pyrophosphate is catalysed by inorganic pyrophosphatase.⁵ The sample solution is mixed with the enzyme solution stream, R_4 , by means of pump I, pumped through the reaction coil, RC_2 , where the hydrolysis takes place, then mixed with a stream of 1M nitric acid to ensure optimal sorption conditions and pumped through column 3. As soon as the whole sample volume has left this column the two-way stop-cocks 2 and 2' are turned to interrupt the sample

Table 1. Recovery of orthophosphate added to synthetic solutions (sample of volume 6 ml, 6 replicates)

Sample	Concentration of orthophosphate, ng/ml		RSD, %	Recovery, %
	Added	Found		
Redistilled water	5.0	4.8 ± 0.2	4.0	96
	10.0	9.6 ± 0.3	3.0	96
	50.0	49.1 ± 1.4	2.7	98
Redistilled water + Fe(III) + Cu(II) [P]:[Fe]:[Cu] = 1:500:500	50.0	50.9 ± 1.6	3.0	102
Redistilled water + Cr(VI) + Si(IV) [P]:[Cr]:[Si] = 1:100:200	50.0	50.6 ± 1.5	2.8	101

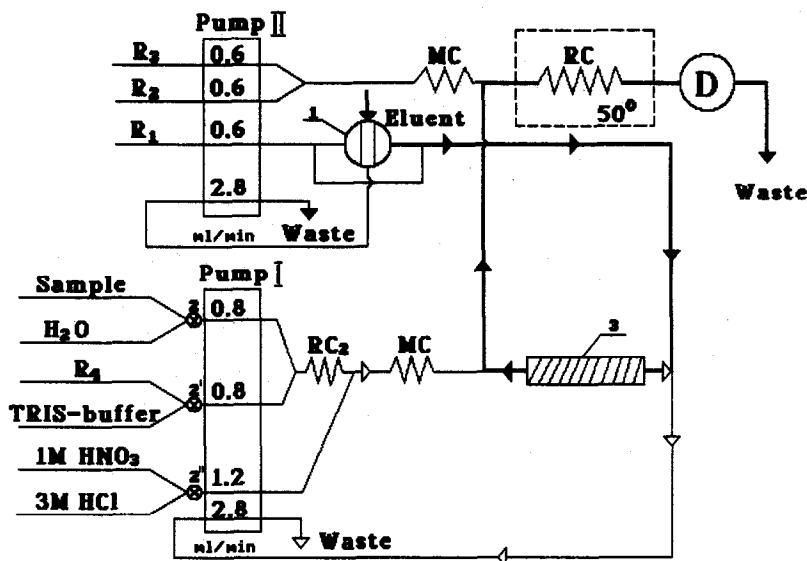


Fig. 6. Multichannel flow-injection system for determination of ortho- and pyrophosphate anions. Symbols as for Fig. 3.

and enzyme streams and let water and Tris-HCl buffer wash the column for 60 sec. Then pump I is stopped and pump II started for elution of the total orthophosphate as already described. The enzymatic hydrolysis is complete with a pyrophosphatase concentration of $6 \times 10^{-9} M$, the calibration plot for pyrophosphate being identical with that for orthophosphate (plotted in terms of phosphorus concentration).

The second stage is determination of the orthophosphate in the sample. The sample solution is mixed with 1M nitric acid and this stream is pumped (by pump I) through column 3. The analysis then proceeds by the same routes as the first stage. In this case both ortho- and pyrophosphate are sorbed but only the orthophosphate is eluted and monitored.

Table 2. Recovery of pyrophosphate added to synthetic solutions containing 30 ng/ml of orthophosphate (sample volume 6 ml, 6 replicates)

Added, ng/ml	Found, ng/ml	RSD, %	Recovery, %
10.0	9.8 ± 0.3	2.8	98
30.0	29.6 ± 0.8	2.6	98
40.0	41.1 ± 1.3	3.0	102
60.0	59.2 ± 1.6	2.6	98

Table 3. Determination of ortho- and pyrophosphate in river water (6 replicates)

Sample	Orthophosphate + pyrophosphate, ng/ml	RSD, %	Orthophosphate, ng/ml	RSD, %
1	11.2 ± 0.4	3.4	9.7 ± 0.3	3.1
2	25.4 ± 0.9	3.6	23.3 ± 0.7	3.0
3	32.0 ± 1.3	4.0	29.1 ± 0.9	3.1
4	14.3 ± 0.5	3.6	12.6 ± 0.5	3.7

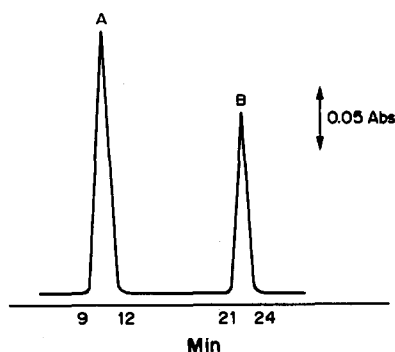


Fig. 7. Elution profile for a mixed solution of orthophosphate and pyrophosphate. A—Total amount of ortho- and pyrophosphate, B—amount of orthophosphate. Sample volume 6 ml, eluent volume 0.3 ml.

The third stage is regeneration of column 3. All three stopcocks are turned to mix the water, Tris-HCl buffer and 3M hydrochloric streams so that this mixture is pumped through column 3 (Fig. 6) by pump I. Figure 2 shows that 2 ml of 3M hydrochloric acid will be sufficient to regenerate the column. Figure 7 illustrates the elution profile for a mixture of ortho- and pyrophosphate. The proposed FIA scheme for consecutive determination of ortho- and pyrophosphate can be completely automated. A more sophisticated micro-processor than the FIAstar 520-003 would enable operation of all the pumps and stopcocks.

The procedure was tested on redistilled water to which known amounts of ortho- and pyrophosphate were added. Quantitative recoveries were obtained (Table 2).

Analysis of river water. Four samples of Moscow river water were analysed by the procedure. The samples were collected in polyethylene bottles and adjusted to pH 2–3 for storage. The water was filtered before analysis (preliminary experiments showed no change in blank values for the anions studied). The results are given in Table 3. The FIA procedure developed can also be applied to the analysis of waste waters. Matrix effects were examined by the standard-addition method (to estimate the multiplicative component of systematic error) and the sample-variation method (to estimate the additive component). For all determinations the deviations between the amounts of phosphate ions found and added were within experimental error. The sample-variation method showed that the results were independent of sample volume ranging from 3 to 30 ml. The data confirmed that systematic errors were absent. In addition, the results for orthophosphate determination in samples 1 and 2 (Table 3) by the FIA method were compared with those obtained by the solvent extraction–spectrophotometric method.¹³ The orthophosphate contents determined by the two tech-

niques (ng/ml) were 9.7 ± 0.3 and 10.1 ± 0.2 respectively for sample 1, and 23.3 ± 0.7 and 25.3 ± 1.0 for sample 2.

The FIA procedure developed can be also used for the analysis of waste waters and other fluids containing various anions and cations.

REFERENCES

1. E. Ruseva, *Izv. Khim.*, 1987, **20**, 504.
2. M. Aoyagi, Y. Yasumasa and A. Nishida, *Anal. Chim. Acta*, 1988, **214**, 229.
3. S. Motomizu, T. Wakimoto and K. Tôei, *Talanta*, 1983, **30**, 333.
4. Y. Baba, N. Yoza and S. Ohashi, *J. Chromatog.*, 1984, **295**, 153.
5. H. Hiranok, Y. Baba, N. Yoza and S. Ohashi, *Anal. Chim. Acta*, 1986, **179**, 209.
6. Y. Narusawa and T. Nashimoto, *Chem. Lett.*, 1987, **7**, 1367.
7. V. M. Shkinev, B. Ya. Spivakov, G. A. Vorob'eva and Yu. A. Zolotov, *Anal. Chim. Acta*, 1985, **167**, 145.
8. V. M. Shkinev, I. Khavezov, B. Ya. Spivakov, S. Mareva, E. Ruseva, Yu. A. Zolotov and N. Iordanov, *Zh. Analit. Khim.*, 1981, **32**, 896.
9. B. Ya. Spivakov, V. M. Shkinev and Yu. A. Zolotov, *ibid.*, 1975, **30**, 2182.
10. E. Ruseva and I. Havezov, *Izv. Khim.*, 1986, **19**, 422.
11. V. M. Shkinev, V. Ya. Rochev, B. Ya. Spivakov, O. P. Kevdin, M. V. Akhmanova and Yu. A. Zolotov, *Koord. Khim.*, 1981, **7**, 1183.
12. W. J. Williams, *Handbook of Anion Determination*, pp. 469–471. Butterworths, London, 1979.
13. S. Motomizu, T. Wakimoto and K. Tôei, *Anal. Chim. Acta*, 1982, **183**, 329.

OBSERVATIONS ON THE DETERMINATION OF OSMIUM BY INDUCTIVELY-COUPLED PLASMA ATOMIC EMISSION SPECTROSCOPY

A. LOPEZ-MOLINERO and J. R. CASTILLO

Department of Analytical Chemistry, University of Zaragoza, 50009 Zaragoza, Spain

J. M. MERMET

Laboratoire des Sciences Analytiques, Université Lyon I, Villeurbanne, France

(Received 16 January 1989. Revised 20 January 1990. Accepted 13 March 1990)

Summary—Osmium tetroxide gives rise to very characteristic atomic emission properties. In acidic samples it gives much higher sensitivity than that given by the lower oxidation states (IV, III, II). However, in alkaline medium (pH 10.5) its atomic emission sharply decreases, and the sensitivity is the same as that for the other oxidation states. It has been shown that there is a direct relation between these characteristics of OsO_4 solutions and pH. With increasing pH the intensity of its atomic emission decreases, the electrode potential of its solutions drops sharply and the molecular absorption of radiation at 193 nm undergoes a hyperchromic and bathochromic shift. The volatility of OsO_4 has also been studied, and found to be minimum at around pH 9.5. This favours its determination at this pH.

Atomic spectroscopy techniques have been used for osmium determination,¹ in particular atomic-emission spectrometry (AES) in flames,^{2,3} electric arcs,⁴ d.c. plasmas,^{5,6} a microwave induced plasma⁷ and inductively coupled plasmas.⁸⁻¹² Atomic-absorption spectrometry (AAS), both with flames and electrothermal atomizers, has also been widely used.¹³⁻²³

The determination by atomic spectrometry is most sensitive with osmium tetroxide. However, because of the volatility (and toxicity) of this compound, its solutions must be handled with great care and, although some authors consider the volatility a factor which increases the sensitivity,⁸ it also produces considerable memory effects when classical nebulizers are used. Compounds containing osmium in lower oxidation states are not volatile, and have received relatively little attention in atomic spectrometry. In alkaline solution OsO_4 loses its volatility, and sensitivity for determination by AAS.¹⁷ Recently Bazan *et al.*^{24,25} have reported an enhancement of ICP signals for osmium when OsO_4 is introduced directly into the plasma.

This work is a study of the volatility of OsO_4 in aqueous solutions and the effect of this on its determination by AES-ICP.

EXPERIMENTAL

Apparatus

A modular inductively coupled argon plasma made up of a 56 MHz generator (Durr, HF "lignes acordées" type) operating at 1.34 kW, with a five-turn induction coil containing a dismountable torch, was used. The observation height was 15 mm above the coil. The radiation was focused on the monochromator (Jobin Yvon model HR-1000, with a Czerny-Turner mounting) equipped with a 2400 lines/mm holographic grating and variable slits, which were set at 50 μm . Coupled to this was a Hamamatsu PM 928R photomultiplier with a Thorn-EMI PM 28B electric supply. The signal was output to a Keithley 480 picoammeter signal amplifier and Linseis Ls-4 chart recorder. Gas feed pressure to the plasma was 3 bar, and the flows of nebulizer gas (0.5 l./min), sheathing gas (0.8 l./min) and outer gas (10 l./min) were controlled by Brooks rotameters. Solutions were introduced into the plasma by a concentric nebulizer (Meinhard type A) mated with a glass spray chamber (Scott-type, dual tube). A SpectraMetric SpectraJet IV plasma DCP, a Perkin-Elmer 551 spectrophotometer with

fused-silica cells of 1.0 and 0.1 cm optical path, a Tacussel TS 40N pH-meter with a glass-SCE combination, a Labovolt magnetic stirrer and a Perkin-Elmer peristaltic pump were used.

Reagents

A 1000 $\mu\text{g/ml}$ standard solution of Os(VIII) was made with osmic acid solution in water, pH = 5.2 (Alfa) and standardized by the Klobbie method²⁶ with the procedure of Gowda *et al.*²⁷ for detecting the end-point.

Standard solutions (1000 $\mu\text{g/ml}$) of Os(IV), Os(III) and Os(II) were prepared by dissolving $(\text{NH}_4)_2(\text{OsBr}_6)$, $\text{Cs}_2\text{Os}(\text{CO})\text{Cl}_5$, and $\text{CsOs}(\text{CO})_3\text{Cl}_3$ (all Johnson-Matthey), in 1M hydrobromic acid for the first compound and demineralized water for the other two.

Solutions of other reagents (Normapur quality) were prepared by dissolution and dilution with demineralized water.

RESULTS AND DISCUSSION

Spectrum of osmium

The emission spectrum of osmium was studied with a 10.47 $\mu\text{g/ml}$ solution of OsO_4 (pH 5.4) over the range 180.0–410.0 nm by use of an ICP plasma under the working conditions detailed above. Table 1 gives the most sensitive emission lines, and the detection limits for each of them, calculated by the Fassel method.²⁸

Study of the "osmium effect"

Various authors have reported that the atomic absorption and emission intensities of aqueous OsO_4 solutions decrease sharply as the pH is increased by addition of sodium hydroxide. Various explanations have been put forward for this. We have shown that the addition of increasing amounts of sodium perchlorate to

a solution of OsO_4 does not reduce the osmium atomic-emission signal; sodium chloride has a greater salt effect and at a concentration of 0.15M results in blockage of the nebulizer and disappearance of the signal. The addition of various reductants, such as NaNO_2 , $\text{Na}_2\text{S}_2\text{O}_3$ and ethanol, to a 1.05 $\mu\text{g/ml}$ solution of OsO_4 also reduces the Os atomic-emission signal. This effect is pronounced for ethanol in alkaline medium (pH 8.5) whereas in acidic medium the same concentration of ethanol does not alter the signal: the effect is smaller with $\text{Na}_2\text{S}_2\text{O}_3$ and even smaller with NaNO_2 .

The addition of perchloric, nitric or hydrochloric acid to an alkaline solution of Os(VIII) restores the Os atomic-emission signal. This recovery is greater with the first two of these acids.

Effect of sodium hydroxide

In view of the effects described above, the ICP atomic-emission of a 1.05 $\mu\text{g/ml}$ OsO_4 solution was studied as a function of pH, along with changes in the electrode potential and molecular absorption spectra. The results are given in Fig. 1, where an inflection point at pH = 7.2 (neutralization point) is seen on the acid-base titration curve, which agrees with the results obtained by Babay *et al.*^{29,30} In the plot of the Os ICP emission, three clearly differentiated zones can be distinguished by their slope, and these correspond to the pH intervals 5.2–6.8, 6.8–9.5 and 9.5–11.4.

Table 1. Characteristics of the most sensitive lines for ICP-AES determination of Os

Wavelength, nm	[Os], $\mu\text{g/ml}$	Detection limit,* $\mu\text{g/ml}$	I_a/I_b †
225.585	0.5	0.3×10^{-3}	49.4
228.226	0.5	0.32×10^{-3}	46.6
233.634	0.5	0.50×10^{-3}	28.3
236.735	0.5	0.80×10^3	18.7
248.633	0.5	0.78×10^{-3}	19.2
290.906	1.0	0.62×10^{-3}	48.6
305.866	1.0	0.76×10^{-3}	39.4
330.156	1.0	1.29×10^{-3}	23.3
315.625	1.0	1.42×10^{-3}	21.1

*Detection limit = $3 \times 0.01 \times [\text{Os}]I_a/I_b$.

†Osmium (I_a) and background intensity (I_b).

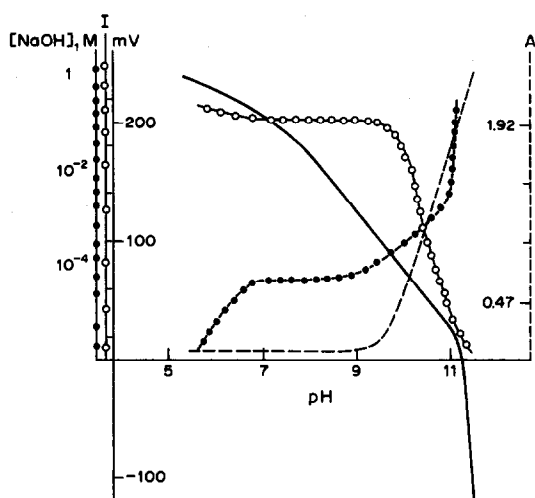


Fig. 1. Effect of NaOH concentration on various characteristics of a 1.05 $\mu\text{g/ml}$ osmium solution (Os present as OsO_4): (●—●—●) pH; (○—○—○) atomic-emission intensity (I) in arbitrary units; (—) electrical potential, mV; (---) absorbance (A) at 193 nm.

These three pH intervals are characterized by a decreasing atomic-emission intensity, whereas the molecular absorption at 193 nm is constant up to pH 9 and then increases. Nevertheless sodium hydroxide concentrations above about 10^{-3} M produce a red shift of the absorption maximum from 193 to 214 nm and also greatly reduce the atomic emission.

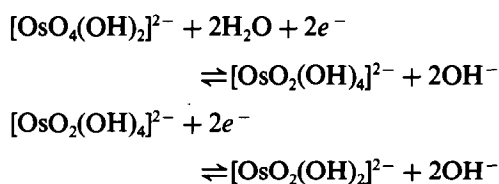
The electrode potential changes fairly slowly with increasing pH up to pH 7, then decreases more rapidly up to pH 11, and very steeply at higher pH.

According to previous experience, OsO_4 behaves as a weak acid, with $\text{p}K_a$ 7.2. The oxidation state VIII is stable up to pH 10 and gives the highest ICP atomic-emission intensity and sensitivity, but at pH above 10.5 the osmium(VIII) signal is sharply reduced as the sodium hydroxide concentration is increased. Moreover the molecular absorption spectrum of OsO_4 solutions have a very important change at pH 10.5.

All this shows that the behaviour of OsO_4 in alkaline solution is not simple, and a key factor is reduction from this oxidation state.

The literature²⁹⁻³² confirms that changes in the behaviour of alkaline osmium tetroxide solutions are due to reduction of Os(VIII), with the simultaneous formation of hydroxy complexes of the reduced forms [principally osmium(IV)], in one or more steps.

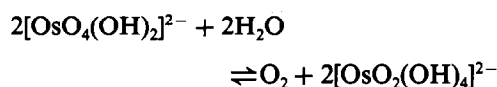
Alekseeva *et al.*³³ propose that this reduction proceeds in two steps with the simultaneous formation of hydroxo complexes of the reduced forms of osmium:



On the other hand, Connery *et al.*³⁴ have studied the nature of the various species present in sodium hydroxide solutions of osmium(VIII), (VI) and (IV) and have characterized three different species, which have a common osmium

core, $[\text{Os}-\text{O}-(\text{OH})]$, along with several coordinating groups (hydroxide groups).

This reduction of osmium(VIII) has been ascribed to oxidation of water according to the equation³⁵



The reduction has also been explained as due to the presence of reducing impurities in the alkaline solution, and the stability of an alkaline solution of OsO_4 , prepared with sodium hydroxide purified electrolytically, has been demonstrated,³⁶ but consideration of the quantitative aspects suggests that the impurities would act only as catalysts.

Volatility of OsO_4

The volatility of osmium solutions, in the form of OsO_4 , was studied as a function of pH in the present work. First, we worked with a discrete sample (15 ml of 10.47 $\mu\text{g}/\text{ml}$ OsO_4 solution) which was placed in a two-necked flask. One neck was connected directly to the injector tube of the torch system. With this configuration the nebulization gas was bubbled through the solution and the OsO_4 volatilized was introduced into the ICP torch. The osmium atomic-emission was recorded. The signal obtained was triangular in shape and could be characterized by its height (h) and base width (w). These two parameters allow determination of the amount of OsO_4 volatilized, on the basis of the peak area, and the rate of volatilization, on the basis of the height, and the time taken to volatilize all the OsO_4 . The results are shown in Table 2.

The second set of experiments was done with a vessel of the type shown in Fig. 2. This permits aqueous solutions of Os to be introduced (and withdrawn) at a regular and constant rate. Inside the vessel the OsO_4 solution is vigorously stirred with a magnetic stirrer, and a tube carries the Ar for nebulization into the flask, where it bubbles through the solution. This further facilitates the liberation of volatile OsO_4 , and carries

Table 2. Characteristics of osmium emission signals for volatilization of 15 ml of 10.50 $\mu\text{g}/\text{ml}$ OsO_4 solution, as a function of pH

pH	3.0	5.0	7.0	8.5	9.5	10.5	11.0	>11.0
Signal area, cm^2	108	103	100	63	51	19	5	0
Relative area, %	100	95	93	58	47	18	5	0
Ratio (h/w)*	0.23	0.11	0.11	0.10	0.08	0.11	0.09	0
Relative ratio (h/w)	100	48	48	43	35	48	39	0

* h = peak-height; w = peak-width.

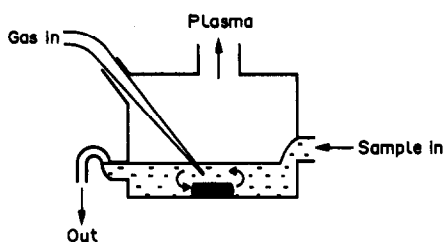


Fig. 2. Diagram of the vessel used to volatilize OsO_4 .

it to the plasma. The system is operated continuously, with a peristaltic pump on both the input and output tubes. The plasma working conditions were as for the first set of experiments, with a solution input of 1.3 ml/min, which is the same as that achieved with pneumatic aspiration, and 1.05 $\mu\text{g/ml}$ solutions of Os were used. The system produces memory effects, and requires long homogenization, washing and signal stabilization periods (20 min). After vigorous stirring, the residual Os solution is collected and its atomic-emission signal in the ICP spectrometer obtained by use of the conventional pneumatic nebulization system with sample aspiration conditions as indicated above.

Figure 3 gives the atomic-emission intensity as a function of the pH (hydrochloric acid was used in the acid zone, up to pH 5.2; above this pH, sodium hydroxide had to be added) for the OsO_4 volatilized from the solution in the flask (curve A). Curve B is the atomic-emission intensity for the Os present in the solution in the flask but not volatilized. In the pH range from 9.0 to 10.4, curve B has a shoulder corresponding to the increase in Os concentration in these solutions, and curve A has a decrease in the signal for volatile Os in the same pH interval, but at pH above 10.4

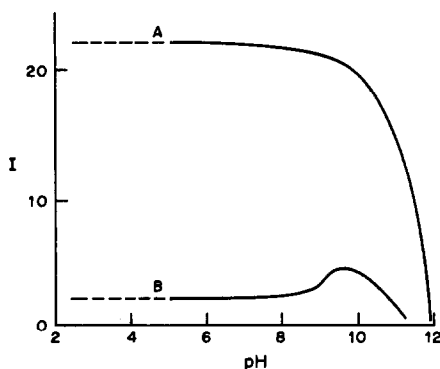


Fig. 3. Atomic-emission intensity (I , arbitrary units) of volatile Os (as OsO_4)—curve A, and of non-volatile Os in a 10 $\mu\text{g/ml}$ solution of OsO_4 —curve B, as a function of pH.

the signal drops sharply for both volatile and involatile Os.

In agreement with the other behaviour listed above, these two zones, the slight decrease in curve A up to pH 9.5 and the steep change from pH 10.5, suggests a change in the osmium species present. It can be proposed that these effects arise from two reactions: first formation of a “salt” of osmic acid, and secondly reduction of Os(VIII). Both reactions diminish the volatility of OsO_4 , but particularly the second.

These considerations lead us to recommend pH 9.5 as the optimum pH for osmium determination by ICP–AES. At this pH the volatility is reduced, decreasing the risk of loss by volatilization, but the system is still very sensitive for osmium.

Various oxidation states of osmium

The molecular absorption spectra for 10 $\mu\text{g/ml}$ solutions of Os in its oxidation states (II), (III) and (IV) were recorded as a function of pH. The atomic-emission intensities of these solutions were also obtained, and are given in Fig. 4. The osmium states (IV, III, II) have much lower atomic-emission intensity than osmium(VIII), but the absorption spectrum of an alkaline solution of osmium(VIII) is identical to that of an alkaline solution of osmium(IV).

The “osmium effect” is observed only for solutions of Os(VIII), the other oxidation states hardly varying in atomic-emission intensity as

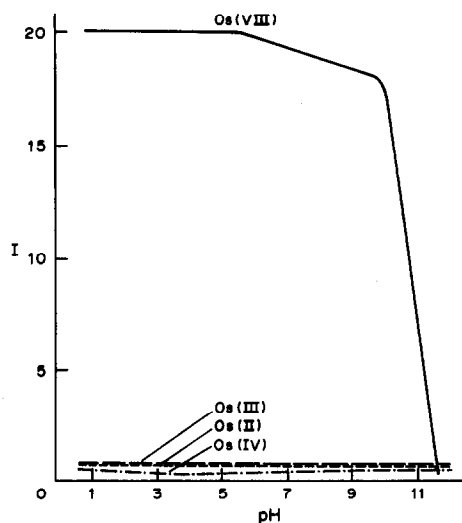


Fig. 4. Atomic-emission intensity (I , arbitrary units) of solutions containing 10 $\mu\text{g/ml}$ Os in various oxidation states (VIII, IV, III and II), as a function of pH.

the pH is changed, and these slight changes are fairly similar.

From the results presented in this work, two possible reasons can be advanced for the "osmium effect" with OsO_4 . The first, is the volatility; that is, the enhancement of the ICP signal would be a consequence of the volatility of this compound whereas the compounds of the other oxidation states are practically non-volatile. The second is the extremely high boiling point of the element and the dynamics of the ICP system. The Os-O bond energy³⁷ of 142 kcal/mole would not be high enough to prevent complete dissociation of OsO_4 in the plasma, but as the compound is already in the gaseous state when it enters the plasma, gaseous osmium atoms will result from the dissociation. When a non-volatile compound (in the solution form) enters the plasma, however, the usual desolvation steps *etc.* will have to precede any dissociation. It is known that the lower oxidation state oxy-compounds can form polymeric species, and all these factors militate against easy dissociation of the molecular species, so the atomic emission taking place during passage of the sample through the observation zone in the plasma will be minimal.

CONCLUSIONS

Osmium gives its maximum atomic-emission signal in an ICP plasma over a wide pH-range when in its oxidation state (VIII). At $\text{pH} > 7$ OsO_4 decreases in volatility and the intensity of the Os atomic-emission spectrum also decreases. A much steeper decrease takes place at above $\text{pH} 10.5$. This lowered volatility of OsO_4 is attributed to (a) the formation of salts of osmic acid and (b) reduction of Os(VIII) to lower oxidation states. The total effect on the atomic-emission intensity is the result of a combination of the effects of pH on the nature and oxidation state of the osmium compounds, together with a difference in dissociation mechanism in the plasma.

Acknowledgement—The authors thank A. Lamotte, at the SCA (CNRS), Lyon (France), where this work was done.

REFERENCES

1. F. E. Beamish, C. H. Lewis and J. C. Van Loon, *Talanta*, 1969, **16**, 1.
2. G. D. Christian and F. J. Feldman, *Anal. Chem.*, 1971, **43**, 611.
3. W. B. Barnett, H. L. Kahn and D. C. Manning, *At. Abs. News.*, 1969, **8**, 25.
4. C. T. Wei, J. Y. Hsieh, C. K. Yu, Y. S. Lu and C. C. Chao, *Fen Hsi Hua Hsueh*, 1980, **8**, 255.
5. A. M. Kurochkina and R. S. Rubinovich, *Zh. Prikl. Spektrosk.*, 1978, **29**, 202.
6. J. F. Chapman, L. S. Dale and R. N. Whitem, *Analyst*, 1973, **98**, 529.
7. S. A. Estes, P. C. Uden and R. M. Barnes, *Anal. Chem.*, 1981, **53**, 1829.
8. K. D. Summerhays, P. J. Lamothe and T. L. Fries, *Appl. Spectrosc.*, 1983, **37**, 25.
9. W. Ge, Y. Gin and J. Li, *Fenxi Huaxue*, 1982, **10**, 300.
10. A. F. Ward, L. F. Marciello, L. Carrara and V. J. Luciano, *Spectrosc. Lett.*, 1980, **13**, 803.
11. G. F. Kirkbright and H. M. Tinsley, *Talanta*, 1979, **26**, 41.
12. R. B. Wemyss and R. H. Scott, *Anal. Chem.*, 1978, **50**, 1694.
13. T. O. Osolinski and N. H. Knight, *Appl. Spectrosc.*, 1968, **22**, 532.
14. K. G. Brodie and P. R. Liddell, *Anal. Chem.*, 1980, **52**, 1059.
15. K. Bächmann, A. Möller, C. Spachidis and C. Zikos, *Z. Anal. Chem.*, 1979, **294**, 337.
16. V. B. L'vov, L. A. Pelieva, E. K. Mandrazhi and S. K. Kalinin, *Zavodsk. Lab.*, 1979, **45**, 1098.
17. R. C. Mallett, S. J. Royal and T. W. Steele, *Anal. Chem.*, 1979, **51**, 1617.
18. G. L. Everett, *Analyst*, 1976, **101**, 348.
19. M. A. Ashy and J. B. Headridge, *ibid.*, 1974, **99**, 285.
20. N. L. Fishkova, *Zh. Analit. Khim.*, 1974, **29**, 2121.
21. J. G. Sen Gupta, *Anal. Chim. Acta*, 1972, **58**, 23.
22. D. F. Makarov, Yu N. Kukushkin and T. A. Eroshevich, *Zh. Analit. Khim.*, 1969, **24**, 1436.
23. B. Welz, *Atomic Absorption Spectrometry*, VCH, Weinheim, 1985.
24. G. P. Russ III, J. M. Bazan and A. R. Date, *Anal. Chem.*, 1987, **59**, 984.
25. J. M. Bazan, *ibid.*, 1987, **59**, 1066.
26. E. A. Klobbie, *Chem. Centralbl.*, 1898, **II**, 65; *J. Chem. Soc.*, 1899, **76**, ii, 184.
27. A. T. Gowda, H. S. Gowda and N. M. M. Gowda, *Analyst*, 1984, **109**, 651.
28. R. K. Winge, V. J. Peterson and V. A. Fassel, *Appl. Spectrosc.*, 1979, **33**, 206.
29. J.-C. Babay, G. Nowogrocki and G. Tridot, *Bull. Soc. Chim. France*, 1967, 2026.
30. *Idem*, *ibid.*, 1967, 2030.
31. L. Meites, *J. Am. Chem. Soc.*, 1957, **79**, 4631.
32. R. E. Cover and L. Meites, *ibid.*, 1961, **83**, 4706.
33. I. I. Alekseeva A. D. Gromova, I. V. Dermeleva and N. A. Khvorostukhina, *Zh. Analit. Khim.*, 1975, **30**, 22.
34. J. G. Connery and R. E. Cover, *Anal. Chem.*, 1968, **40**, 87.
35. M. B. Bardin and V. P. Goncharenko, *Zh. Neorgan. Khim.*, 1970, **15**, 490.
36. P. K. Norkus, G. I. Rozovskii and Yu. Yu. Yankauskas, *Zh. Analit. Khim.*, 1971, **26**, 1561.
37. L. Brewer and G. M. Rosenblatt, *Adv. High. Temp. Sci.*, 1969, **2**, 1.
38. L. O. Atovmyan, V. G. Andrianov and M. A. Porai-Koshits, *Zh. Strukt. Khim.*, 1962, **3**, 685.
39. W. P. Griffith, *J. Chem. Soc.*, A, 1966, 1467.
40. K. A. K. Lott and M. C. A. Symons, *ibid.*, 1960, 973.

AN ANION-SELECTIVE MEMBRANE ELECTRODE BASED ON A MIXTURE OF INSOLUBLE LEAD SALTS

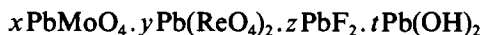
DERREN LEE and K. L. CHENG*

Department of Chemistry, University of Missouri-Kansas City, Kansas City, MO 64110, U.S.A.

(Received 1 September 1989. Revised 21 November 1989. Accepted 27 November 1989)

Summary—The determination of molybdate, tungstate, perrhenate, phosphate, chromate, fluoride and hydroxide with an electrode made of a mixture of lead molybdate, tungstate and perrhenate is described. The sensitivity to the last four of these ions is interpreted in terms of their adsorption and the resultant changes in electrode surface electron density.

A simple precipitation titration of molybdate, tungstate, perrhenate and fluoride with lead was developed by Cheng and Goydish,¹ in which mixed precipitates of lead molybdate, perrhenate and fluoride were formed. Later, Cheng and Chao² reported that an ion-selective electrode (ISE) could be used in the potentiometric titration of molybdate, tungstate, perrhenate and fluoride. Mixed lead compounds were shown to be co-precipitated and the composition of the mixed lead precipitates may be represented as



or, when an excess of fluoride is present, as



the lead then reacts with perrhenate in 1:1 molar ratio.

Usman and Dulari³ reported that a membrane electrode made with lead molybdate bound with paraffin wax was sensitive to molybdate, arsenate, tungstate, and ferricyanide over a limited range of concentrations. The present paper reports our results for determining molybdate, tungstate, chromate, perrhenate, phosphate, fluoride and hydroxide with a membrane electrode made with a mixed precipitate of lead salts. Few ISEs are available for determining these anions; in particular, the LaF_3 single-crystal fluoride electrode is the only one known for fluoride. The lead-molybdate mixture electrode is especially interesting for determining fluoride and phosphate.

EXPERIMENTAL

Preparation of the precipitates

A solution of 1.3 g of sodium molybdate dihydrate, 1.7 g of sodium tungstate dihydrate and 2.7 g of ammonium perrhenate in 100 ml of water was prepared and adjusted to pH 5–6 with ammonia or acetic acid, and a solution of 4.9 g of lead nitrate in 50 ml of water was slowly added, with stirring. The mixture was heated to boiling, then cooled to room temperature. The precipitate was then filtered off, washed with 20 ml of 0.1M acetic acid and 100 ml of water, and dried at 80° overnight. The product was ground and sieved (325 mesh) and the powder used to prepare silicone rubber or paraffin wax or PVC matrix membrane electrodes. A similar technique was used to prepare the individual precipitates (with equivalent amounts of the anion and lead).

Membrane preparation

The methods of membrane preparation and electrode construction were similar to those used by Craggs *et al.*⁴ The master membranes contained 0.4 g of the powdered precipitate plus a solution of 0.17 g of PVC in 6 ml of tetrahydrofuran. We also prepared membranes with silicone rubber and paraffin wax, but these had tiny holes in most cases, so only the PVC membrane type is recommended.

The membrane electrode was conditioned before use by immersing it in water for at least 24 hr and then for at least 1 hr in a solution containing 0.1M of the ion to be sensed.

*Author for correspondence.

EMF measurements

The measurements were made at 22° against a calomel reference electrode, proceeding from low to high concentrations (from 10^{-6} to $0.1M$). If the measurements were made from high to low concentrations, erratic results were obtained owing to a "memory" effect and to the difficulty of removing adsorbed ions from the surface of the electrode membrane.

RESULTS AND DISCUSSION

pH effect

The various electrodes responded most satisfactorily near neutral pH, but the optimum pH ranges for different ions in different matrices and compositions were not the same. Electrodes containing lead molybdate (75%) and lead tungstate (25%) showed optimum pH ranges of 5–6 for a wax matrix and 5–6.5 for the PVC matrix. For the PVC matrix electrode with lead molybdate (34%), lead tungstate (33%) and lead perrhenate (33%), the optimum pH range was 4.5–7.0. Evidently, the EMF measurements depend on the lead salts and matrix used.

Response time

The response time is shorter at high concentrations than at low concentrations and is shorter and more reproducible when the solution is stirred. The greater the amount of lead precipitates contained in the membrane, the shorter the response time.

Electrode calibration

The lead molybdate membrane electrode responded linearly to both molybdate and tungstate in the range 10^{-5} – $0.1M$, but the response time was long (around 2 min). The lead molybdate (75%) plus lead tungstate (25%) membrane electrode responded linearly to both molybdate and tungstate in the ranges 10^{-5} – $0.1M$ MoO_4^{2-} and 10^{-4} – $0.1M$ WO_4^{2-} . Its linear concentration ranges were 10^{-4} – $0.1M$ and 10^{-3} – $0.1M$ for phosphate and fluoride, respectively.

The mixed precipitate electrode of lead molybdate (34%), lead tungstate (33%), and lead perrhenate (33%) showed a linear response for molybdate, tungstate, and phosphate from 10^{-6} to $0.1M$, and from 10^{-4} to $0.1M$ for both perrhenate and fluoride (Figs. 1 and 2). The

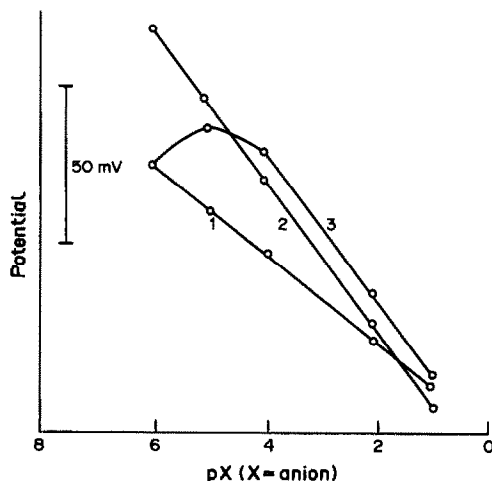


Fig. 1. Calibration curves for (1) molybdate, (2) tungstate and (3) perrhenate with $PbMoO_4$ (34%)– $PbWO_4$ (33%)– $Pb(ReO_4)_2$ (33%)–PVC membrane.

improved sensitivity of mixed precipitates may be attributed to the fact that mixed precipitates are less soluble than their individual components. These electrodes did not respond well to varied concentrations of lead ions, especially when the lead concentration was higher than $10^{-3}M$, forming a white turbidity due to peptization of the mixed lead precipitates.

The chromate response was not useful, because the composition of a chromate solution is a function of pH and concentration,⁵ and the calibration curves were mostly non-linear (Fig. 3). A nearly linear calibration line was obtained at pH 8, with a low response slope (7 mV/decade); this suggests that the electrode responds to chromate in basic solution but that hydroxide ions then interfere.

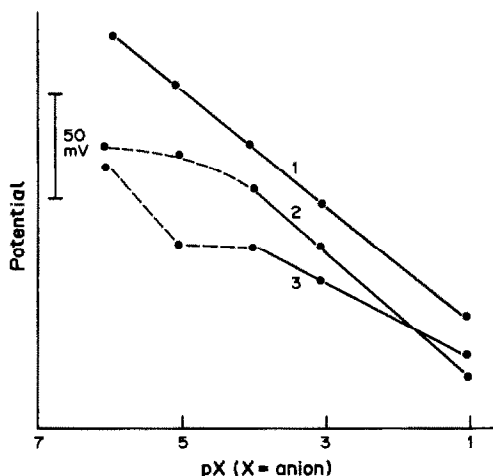


Fig. 2. Calibration curves for (1) phosphate, (2) fluoride and (3) chromate with membrane as in Fig. 1.

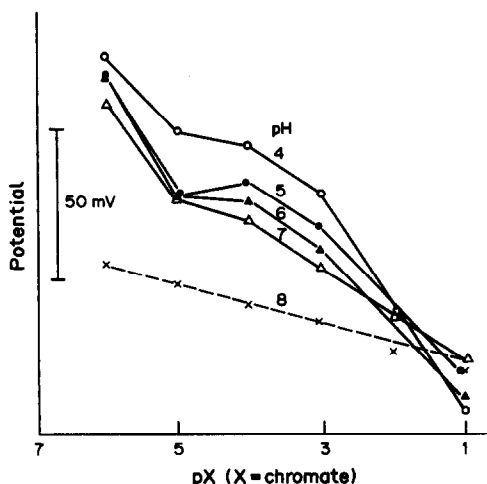


Fig. 3. Effect of pH on measurement of chromate with membrane as in Fig. 1.

Phosphate

Linear responses to phosphate from 10^{-4} to $0.1M$ with various membrane matrices containing phosphate have been reported,⁶⁻⁸ but there is no commercial phosphate electrode, probably because of problems of selectivity, sensitivity and reliability.

We have examined the mixed lead precipitate electrodes for possible response to phosphate and obtained linear calibrations with response times of about 1 min. A linear relationship from 10^{-6} to $0.1M$ phosphate was obtained at pH 6 (Fig. 2) with the mixed precipitate electrode containing 34% $PbMoO_4$, 33% $PbWO_4$, 33% $Pb(ReO_4)$ and PVC. It is noteworthy that this electrode gives a good response slope of 28 mV per decade concentration. This is the first time that a phosphate electrode membrane containing no phosphate within the matrix has been developed. Its behavior can be explained by the capacitor theory.⁹ Its sensitivity down to $10^{-6}M$ phosphate is better than any previously reported.

Fluoride

Fluoride had always been difficult to determine, so the single-crystal LaF_3 electrode was a major breakthrough and has now become the only fluoride sensor known in the field of ion-selective electrodes. However, it is subject to indirect interference by various ions which can form fluoride complexes or precipitates, though some of these effects can be eliminated by use of suitable masking agents. It is necessary to adjust the pH to between 5 and 7 to avoid hydroxide interference or the formation of HF_2^- .

The LaF_3 electrode gives a linear response in the range from 10^{-5} to $0.1M F^-$.

The capacitor theory⁹ emphasizes the importance of surface active sites and adsorption of ions. Consequently, an electrode having no fluoride may serve as a fluoride electrode if the electrode surface has active sites which can adsorb F^- ions. Since lead molybdate, tungstate, phosphate, fluoride and hydroxide are only slightly soluble, an alternative to the capacitor theory would be that the response to these ions depends on the relative solubility products of the membrane and analyte lead salts, although the analyte ion may not itself be present in the membrane formulation. We prefer the capacitor theory. This is the first time a fluoride electrode containing no fluoride within its matrix has been developed. An additional advantage is that the mixed lead precipitate membrane is made of inexpensive polycrystals. It is interesting to note that with the mixed-precipitate electrodes at fluoride concentrations below $10^{-4}M$ in acidic media the potential became more negative, suggesting that the species HF_2^- may play a role (Fig. 4).

Other anions

Most cations and anions do not interfere with the responses for molybdate, phosphate, fluoride and tungstate, but large amounts of anions commonly associated with lead, such as halides and sulphate, will interfere. It is interesting to note that hydroxide ions are also co-precipitated with the lead salts and a linear response to OH^- ions is obtained (Fig. 5). This suggests that the mixed lead precipitate adsorbs

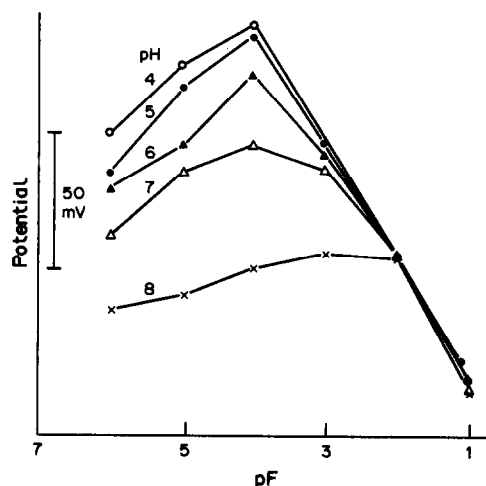


Fig. 4. Effect of pH on measurement of fluoride with membrane as in Fig. 1.

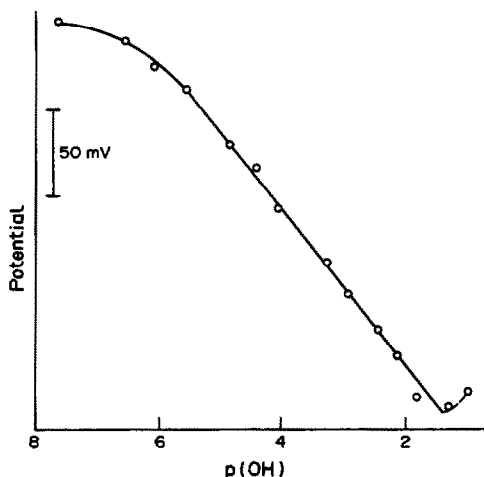


Fig. 5. Calibration curve for hydroxide with PbMoO_4 (75%)- PbWO_4 (25%)-graphite-paraffin wax membrane.

the OH^- ions, causing the electrode membrane to become negatively charged. The optimum pH range is between 7.5 and 12. The tailing below pH 7.5 is probably due to dissociation.

Cleaning the membrane

As is common with solid membranes, it is necessary to clean the electrode surface before making measurements in a solution of lower

concentration than its predecessor, in order to remove strongly adsorbed ions. The cleaning may be done mechanically or chemically. The electrode surface can be cleaned by gentle rubbing with fine emery paper between measurements, but this is unnecessary when going from lower to higher concentrations. In the case of hydroxide determinations, the electrode is rinsed with an acid (such as hydrochloric), then water. Rinsing with water alone is insufficient. Cleaning with fine emery paper is recommended if memory effects are noticed.

REFERENCES

1. K. L. Cheng and B. L. Goydish, *Microchem. J.*, 1968, **13**, 35.
2. K. L. Cheng and E. E. Chao, *Talanta*, 1977, **24**, 247.
3. M. Usman and O. Dulari, *J. Colloid Interface Sci.*, 1982, **86**, 579.
4. A. Craggs, G. J. Moody and J. D. R. Thomas, *J. Chem. Educ.*, 1974, **51**, 541.
5. S.-Y. Tong and K.-A. Li, *Talanta*, 1986, **33**, 775.
6. G. A. Rechnitz, Z. F. Lin and S. B. Zamochnick, *Anal. Lett.*, 1967, **1**, 29.
7. G. G. Guilbault and P. J. Brignac, *Anal. Chem.*, 1969, **41**, 1136.
8. S. A. Glazier and M. A. Arnold, *ibid.*, 1988, **60**, 2540.
9. K. L. Cheng, *Proc. 31st IUPAC Congress, Anal. Div.*, 1987, 173.

PHOTOCHEMICAL DETERMINATION OF THE SOLUBILITY OF OXYGEN IN VARIOUS MEDIA

CHRIS FRANCO and JOHN OLMSTED III*

Department of Chemistry and Biochemistry, California State University, Fullerton, CA 92634, U.S.A.

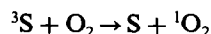
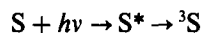
(Received 11 August 1989. Revised 16 February 1990. Accepted 22 February 1990)

Summary—A photochemical method for determining the oxygen concentration in air-saturated non-aqueous solvents has been developed. Solutions containing a sensitizer (Rose Bengal or Methylene Blue) and 1,3-diphenylisobenzofuran (DPIBF) as an oxygen acceptor are irradiated at 546 or 633 nm and the absorbance at 404 nm is monitored. The dissolved oxygen content is found from the change in absorbance and the known 1:1 stoichiometry of addition of singlet oxygen to DPIBF. The solubilities found, accurate to $\pm 6\%$, for oxygen in air-equilibrated solvents, are (mM): acetone, 2.37; acetonitrile, 2.42; dimethylsulfoxide, 0.33; ethanol, 1.94; *N*-methylformamide, 1.31. Measurements on mixed acetone-*N*-methylformamide solvents showed that the solubility of oxygen does not vary with solvent composition in a predictable manner.

The solubility of oxygen in non-aqueous solvent systems is of considerable interest both in photochemistry, where oxygen-quenching of excited states is one of the predominant bimolecular processes, and in electrochemistry, where cathodic production of superoxide anions from dissolved oxygen is an important reduction process. The values cited in compilations of oxygen solubility data^{1,2} and in a recent report of determinations based on a gas chromatographic method³ show significant variation. For dimethylsulfoxide (DMSO), for example, some values cited are nearly twice as large as others.¹

Since we required accurate values for oxygen concentrations in solution for a study of oxygen quenching of luminescence,⁴ we have developed a rapid and straightforward photochemical method for measuring them. It relies on the clean photo-oxygenation reaction of a well-known singlet oxygen acceptor, 1,3-diphenylisobenzofuran (DPIBF).⁵ Though Demas has exploited luminescence quenching reactions for determination of oxygen concentration⁶ and photo-oxygenation reactions for chemical actinometry,⁷ we believe that the use of photo-oxygenation to determine oxygen concentrations has not previously been reported.

In the presence of a suitable sensitizer (*S*; in these determinations, both Rose Bengal and Methylene Blue were used), illumination of an oxygen-containing solution with light in the visible region results in generation of singlet oxygen:



When DPIBF is also present in the solution, the singlet oxygen photo-oxygenates the DPIBF (*D*), leading eventually to oxidation products:



Since DPIBF is the only component of the solution that absorbs radiation of wavelength 404 nm, the progress of this reaction sequence can be readily monitored by measuring the decrease in absorbance at 404 nm. As long as oxygen is present in the system, illumination will result in disappearance of DPIBF. When all the oxygen has been consumed, the reaction sequence stops. The net decrease in absorbance is quantitatively related to the loss of DPIBF and, since the reacting ratio of oxygen and DPIBF is 1:1, the amount of oxygen originally present in the solution can be determined.

*Author for correspondence.

EXPERIMENTAL

Reagents

DPIBF (Aldrich), Rose Bengal (Eastman, 82% certified dye content), and Methylene Blue (Aldrich, certified) were used as received. Spectral grade *N*-methylformamide, dimethylsulfoxide and acetonitrile and HPLC-grade acetone were obtained from Aldrich and used without further purification. Absolute ethanol was obtained from Spectrum.

Apparatus

All absorbance measurements were made with a Beckman DU-7 spectrophotometer. When Rose Bengal was the sensitizer, an Illumination Industries Model LH371Q medium-pressure mercury arc lamp was used as the light-source, with its output filtered through water, a Corning 3-73 yellow glass filter, and an Oriel 546-nm interference filter. For sensitization with Methylene Blue, the output from an LGK 7628 He-Ne laser operated at 6 mW was passed through a defocusing lens so that the light beam filled nearly the full face of the irradiation cell.

Determination of the molar absorptivity of DPIBF

Enough DPIBF to yield a $1.00 \times 10^{-2} M$ solution was weighed into a 10-ml standard flask, solvent was added up to the mark, a small magnetic stirrer bar was added and the solution was stirred, while protected from light, until all the solute had dissolved. At regular intervals during the stirring, 10- μ l aliquots were removed, quantitatively diluted to 3.00 ml, and the absorbances at 404 nm measured. This was continued until complete dissolution of the solid was indicated by no further change in the absorbance, which was then used to compute the molar absorptivity of DPIBF in the solvent used.

Procedure

All measurements were made at room temperature ($25 \pm 2^\circ$). All solvent samples were pre-equilibrated with air by passage of an air stream through them for at least 20 min. A glass cuvette of known volume, fitted with a stopcock, was charged with a weighed amount of DPIBF and a small magnetic stirrer bar (also of known volume). Sufficient stock solution in the test solvent sensitizer to give a final absorbance at 546 nm greater than 1.0 was added by

syringe, then the cuvette was filled by syringe with the solvent of interest to a point well above the stopcock. The sealed cuvette was placed in a cell holder and the contents were mixed by magnetic stirring until the DPIBF was completely dissolved, as indicated by constancy of the absorbance at 404 nm for a 10.0- μ l sample, withdrawn and mixed with 3.00 ml of solvent. The sealed cuvette was then repeatedly irradiated with 546-nm light for constant periods of time (typically 20 sec), the absorbance at 404 nm being measured after each irradiation.

To determine the oxygen concentration of the solution, absorbance *vs.* time plots were prepared (*e.g.*, Fig. 1), from which the total change of absorbance due to irradiation, ΔA , could be found. By use of the molar absorptivity, ΔA was converted into amount of DPIBF consumed, which corresponded to the amount of oxygen present in the solution before the irradiation was started.

RESULTS AND DISCUSSION

The results for five different solvents and a set of mixed *N*-methylformamide-acetone solutions are presented in Table 1. Each value is the mean of 3-5 determinations. The absolute average deviations (AAD) indicate the reproducibility of the determinations; the relative average deviations ranged from 2.5% (DMSO) to 8% (acetone) and were typically 6%. We can judge the accuracy of our method by the results for acetone, for which there is

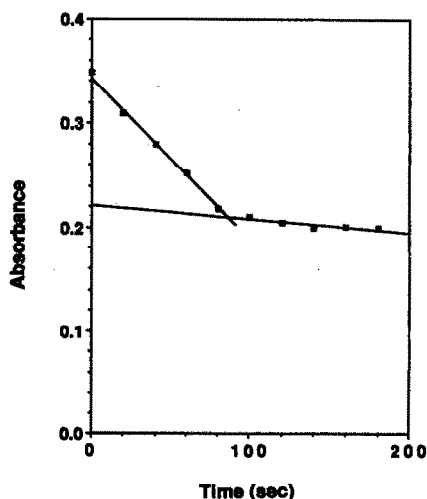


Fig. 1. Plot showing the change of absorbance of diphenylisobenzofuran (at 404 nm) with time of irradiation, for air-saturated acetone containing Rose Bengal as sensitizer. For this irradiation, $\Delta A = 0.132$.

Table 1. Solubilities of oxygen in air-saturated solutions

Solvent	This work			References
	Solubility, $10^{-3}M$	Absolute average deviation, $10^{-3}M$	Literature values, $10^{-3}M$	
Acetone	2.37	0.19	1.89-2.42	1
			2.40	2
			2.3	3
Acetonitrile	2.42	0.14	1.70	3
Dimethylsulfoxide	0.33	0.008	0.32-0.58	1
			0.44	3
Ethanol	1.94	0.09	2.0	1, 8, 9
<i>N</i> -methylformamide	1.31	0.04	—	
3:1 NMF:acetone*	0.79	0.05	—	
1:1 NMF:acetone*	0.82	0.05	—	
1:3 NMF:acetone*	1.76	0.11	—	

*Mole ratio.

agreement among four independent literature values that the solubility of oxygen in acetone saturated with air is $2.35 \pm 0.05 \times 10^{-3}M$ at 25° . Our value, $2.37 \pm 0.19 \times 10^{-3}M$, is in excellent agreement with this consensus value. We obtained the same value with either Methylene Blue or Rose Bengal as sensitizer.

Ethanol provides a second benchmark for judging our method. The consensus value as evaluated by Battino¹ has been verified by Tokunaga⁸ and most recently by Lühring and Schumpe,⁹ all of whom find a concentration of $2.0 \pm 0.05 \times 10^{-3}M$ in an air-saturated solution. Our measurements with Methylene Blue as sensitizer gave $1.94 \pm 0.09 \times 10^{-3}M$. Measurements with Rose Bengal gave a value 15% lower, but the stoichiometry of consumption of DPBIF by oxygen is not 1:1 for this combination of sensitizer and solvent. It has been shown that Rose Bengal sensitizes production of superoxide anions as well as singlet oxygen,¹⁰ and in a protic solvent such as ethanol, the superoxide is destroyed by proton abstraction from the solvent.¹¹

For dimethylsulfoxide, the reported values cover a relatively wide range (we have converted values for equilibrium with pure oxygen at 1 atm pressure into values for equilibrium with air, for purposes of comparison): $3.23 \times 10^{-4}M$,¹² $4.4 \times 10^{-4}M$,^{3,13} $4.64 \times 10^{-4}M$,¹⁴ and $5.80 \times 10^{-4}M$.¹⁵ Our result, $3.28 \pm 0.08 \times 10^{-4}M$, is in excellent agreement with the lowest of these values but is not compatible with the others. For this solvent, Methylene Blue is not a suitable sensitizer; irradiation causes decomposition of the sensitizer, accompanied by generation of a gaseous product, indicating complex photochemistry.

In the case of acetonitrile, only one previous determination seems to have been made, Achord and Hussey³ reported a value of $1.7 \times 10^{-3}M$, significantly lower than our value of $2.42 \pm 0.14 \times 10^{-3}M$. We also obtained a lower value than theirs for dimethylsulfoxide, indicating that the discrepancy, which falls well outside the reported uncertainties in the experiments, is not due to a systematic error. As was the case for acetone, our solubility determinations for acetonitrile gave the same results with either sensitizer.

Errors in our determinations could arise from incomplete saturation with air, incorrect molar absorptivities, oxygen desorbed from the cell walls, photodegradation of DPIBF by competing reactions, or competing photoreactions with oxygen. Since the solvent samples were likely to be air-saturated as received, and air was bubbled through them for 20 min, lack of saturation is unlikely. The molar absorptivities of DPIBF in each solvent were independently determined. Though they differed slightly from solvent to solvent, all values were about $2.2 \times 10^4 \text{ l. mole}^{-1} \text{ cm}^{-1}$, which is of the same order as that reported for DPIBF in dimethylformamide (2.8×10^4 at $\lambda_{\text{max}} = 415 \text{ nm}$).¹⁶ The initial absorbances of the solutions prepared for irradiation were also found to be consistent with the independently determined molar absorptivities.

We have found evidence for either desorption of oxygen or a competing photoreaction in dimethylsulfoxide and *N*-methylformamide, where the plots of absorbance *vs.* irradiation time showed a small but distinct downward slope after the consumption of oxygen was apparently complete. Irradiation of argon-saturated solutions under identical conditions

also yielded slowly decreasing absorbances, with the same slopes. Since this slow consumption of DPIBF occurs with only two of the four solvents we believe that it is due to a solvent-dependent competing photodegradation reaction rather than to desorption of oxygen from the cell walls, which should be the same for all the solvents tested. In any case, we have corrected our results for this slow process by extrapolating the final slope to zero time and measuring ΔA from the initial absorbance to the intercept.

For two of the solvent-sensitizer combinations, our observations indicate that competitive reactions involving oxygen are involved: Methylene Blue-dimethylsulfoxide and Rose Bengal-ethanol. Comparison measurements with different sensitizers provide a sensitive way of identifying the presence of such complications.

Mixed solvent systems are frequently attractive for studies of photophysical processes, as they afford an easy way to adjust solvent properties (viscosity, dielectric constant) as well as substrate solubility. There are virtually no data available on the solubility of oxygen in mixed solvents other than water-alcohol mixtures. We have chosen to look at the *N*-methylformamide-acetone system, which yields an extremely wide range of dielectric constants. A consideration of the thermodynamics of ternary mixtures of a gas and two liquids shows that the Henry's law constants (H) may be expected to follow a logarithmic equation:¹⁷

$$\ln H_{\text{mix}} = x_1 \ln H_1 + x_3 \ln H_3 - \Delta G_E/RT \quad (1)$$

where ΔG_E is the molar excess Gibbs free energy of the solvent mixture containing the two solvents 1 and 3 in mole fractions x_1 and x_3 , and H_i is the Henry's law constant for the i th solvent system, relating mole fraction of dissolved gas, x_2 , to gas pressure p_2 :

$$p_2 = x_2 H_i$$

Figure 2 shows the logarithms of the Henry's law constants obtained from our measurements, *vs.* mole fraction of solvent. Also shown is the solubility curve calculated from the logarithmic equation by using excess Gibbs energies from the literature.¹⁸ It is clear that the oxygen solubility relationship is more complicated than the

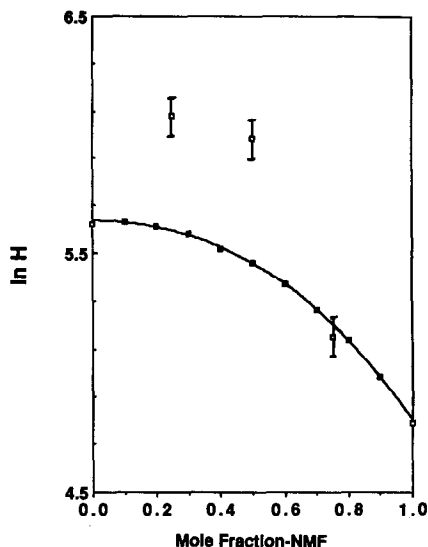


Fig. 2. Variation of the Henry's law constant H with solvent composition for oxygen in acetone-*N*-methylformamide mixed solvent. Open squares are experimental data points (error bars indicate average absolute deviations), the solid line is computed from the thermodynamics [the solid squares were calculated by using equation (1)].

logarithmic equation predicts. The shape of the observed variations is similar to that computed from the excess free energies of mixing, but the magnitude of variation at high acetone concentrations is much larger than predicted. While this behavior may appear anomalous, similar observations of solubilities that exhibit maxima or minima at intermediate solvent compositions have been reported, *e.g.*, acetylene dissolved in acetone-hexane mixtures.¹⁷ Our observation of such deviations from simple expectation emphasizes the necessity of determining experimental solubilities for work associated with the oxygen contents of mixed solvent systems.

The solubility of oxygen in an acetone-rich mixed solvent is sufficiently lower than the oxygen content of the pure solvents for bubble formation to be observed on mixing of the two components, if equilibration is rapid enough. For a 1:1 mole ratio solution, 0.026 ml of gas should be liberated per ml of solvent. We have looked for evidence of bubble formation in freshly-mixed acetone-*N*-methylformamide solutions, both stirred and unstirred, with and without boiling chips present to provide nucleation centers. No bubbles were observed. As our solubility determinations are consistently reproducible, we attribute the lack of bubble formation to slow equilibration between the gas and liquid phases after mixing of these solvents.

Acknowledgements—Support for this research was provided by the Department Associations Council of the Associated Students, California State University, Fullerton. Most of the experiments were done by Mr. Franco in an undergraduate research project.

REFERENCES

1. R. Battino (ed.), *Solubility Data Series*, Vol. 7, *Oxygen and Ozone*, Pergamon Press, Oxford, 1981.
2. S. L. Murov, *Handbook of Photochemistry*, p. 89. Dekker, New York, 1973.
3. C. L. Hussey and C. L. Achord, *Anal. Chem.*, 1980, **52**, 601.
4. C. J. Timpson, C. C. Carter and J. Olmsted III, *J. Phys. Chem.*, 1989, **93**, 4116.
5. J. Olmsted III and T. Akashah, *J. Am. Chem. Soc.*, 1973, **95**, 6211.
6. J. R. Bacon and J. N. Demas, *Anal. Chem.*, 1987, **59**, 2780.
7. J. N. Demas, R. P. McBride and E. W. Harris, *J. Phys. Chem.*, 1976, **80**, 2248.
8. J. Tokunaga, *J. Chem. Eng. Data*, 1975, **20**, 41.
9. P. Lühring and A. Schumpe, *ibid.*, 1989, **34**, 250.
10. V. S. Srinivasan, D. Podolski, N. J. Westrick and D. C. Neckers, *J. Am. Chem. Soc.*, 1978, **100**, 6513.
11. D. T. Sawyer and M. J. Gibian, *Tetrahedron*, 1979, **35**, 1471.
12. J. H. Dymond, *J. Phys. Chem.*, 1967, **71**, 1829.
13. E. L. Johnson, K. H. Pool and R. E. Hamm, *Anal. Chem.*, 1966, **38**, 183.
14. W. R. Baird and R. T. Foley, *J. Chem. Eng. Data*, 1972, **17**, 355.
15. N. V. Chaendo, G. I. Sukhova, N. K. Naumendo and I. A. Kedrinskii, *Russ. J. Phys. Chem.*, 1979, **53**, 1133.
16. A. Zweig, G. Metzler, A. Maurer and B. G. Roberts, *J. Am. Chem. Soc.*, 1967, **89**, 4091.
17. J. H. Hildebrand, J. M. Prausnitz and R. L. Scott, *Regular and Related Solutions*, p. 131. Van Nostrand Reinhold, New York, 1970.
18. U. Seyffert, K. Francke and K. Quitsch, *Z. Phys. Chem. (Leipzig)*, 1974, **255**, 969.

SYNTHESIS AND RESPONSE OF NEW MICROSENSOR COATINGS—II*

ACRIDINIUM BETAINES AND ANIONIC SURFACTANTS

ALAN R. KATRITZKY,§ RICK J. OFFERMAN, JOSE M. AURRECOECHEA and G. PAUL SAVAGE

Department of Chemistry, University of Florida, Gainesville, FL 32611, U.S.A.

(Received 13 December 1989. Revised 5 March 1990. Accepted 8 March 1990)

Summary—Four acridinium betaines and two ionic surfactants were synthesized, and evaluated as chemical microsensor coatings by exposure to vapors of chloroethyl ethyl sulfide (CEES) and dimethyl methylphosphonate (DMMP). Two of the acridinium betaines showed selective and reversible responses (of 9.8 and 6.8 kHz) as SAW (surface acoustic wave) coatings in the detection of CEES vapor: there appears to be a connection between the long alkyl chain (C-12 and C-14) in the acridinium molecules and the response. Response times were generally less than 30 sec but desorption was significantly slower. The ionic surfactant coatings show small SAW changes (> 0.5 kHz) in response to DMMP vapor, and somewhat greater responses (20- and 68-fold), as chemiresistors, to CEES vapor. In each case the response occurred within 3 min, with return nearly to baseline levels within 6 min of cessation of exposure to the vapor. The responses were reproducible within $\pm 5\%$.

Chemical microsensors are devices which utilize a thin coating of an organic or inorganic film to give a selective and sensitive response to an analyte. A number of such sensors exist, including surface acoustic wave (SAW), chemiresistor and optical waveguide devices.^{1,2} Our interests lie in preparing novel organic compounds as coatings for SAW delay lines and chemiresistor devices. These compounds are screened for their potential as sensitive and selective coatings for the detection of a variety of vapors (for a review see Katritzky and Offerman³).

Both chemiresistor and SAW devices are manufactured from piezoelectric quartz crystals and have an interdigitated electrode array lithographically fabricated on the crystal surface.^{4,5} The response of a chemiresistor device is a change in the resistance of a thin film coating between the interdigitated electrodes on its surface (monitored by an electrometer) on exposure to a vapor. In an SAW device a frequency counter is used to monitor changes in the resonant frequency of the device when exposed to a vapor.⁴⁻⁸ This change is related to the mass uptake of the vapor by the coating. SAW devices are similar to piezoelectric quartz crystal sensors,^{9,10} but are more sensitive (owing to their

higher operating frequencies), smaller, easier to coat and more rugged. Whereas for a chemiresistor device only resistance measurements can be made, for an SAW device resistance and frequency measurements can be made simultaneously with the appropriate electronics.⁶

Various compounds have been employed as coatings for SAW and other piezoelectric devices.^{3,11} Many of these materials have not been adequately characterized in the literature, so it is difficult to use the literature to predict their selectivity. To date, no systematic approach has been taken for identification or development of new microsensor coatings, and the selection of coatings for SAW devices appears to be based primarily on the solubility of the analyte in them.¹²⁻¹⁴ There are few reports on selective coatings for use in chemiresistor devices.^{5,6}

Currently we are interested in identifying film coatings for two types of chemical microsensors—chemiresistors and SAW devices—for the detection of dimethyl methylphosphonate (DMMP) and chloroethyl ethyl sulfide (CEES). Our interest in the detection of DMMP is its usefulness as a model compound (simulant) for work on other phosphonate esters. The phosphonate ester group is found in a number of pesticides and its detection at low levels is an important industrial and environmental

*Part I—A. R. Katritzky and R. J. Offerman, *Langmuir*, 1989, 5, 1987.

§Author for correspondence.

problem. The examination of CEES reflects the importance of the detection of the sulfide group at low levels in the environment. In addition, DMMP is a non-toxic simulant for phosphonate nerve-gas agents, and CEES, though toxic, is a relatively safe simulant for mustard-gas type agents. Water vapor was chosen for interference studies as (in the form of humidity) it could pose a problem in the detection of either DMMP or CEES in ambient air.

Previous work¹⁰ in our laboratory has shown that a number of pyridinium compounds (pyridine 1-oxides, pyridinium salts and pyridinium betaines) show utility as coatings for microsensors in the detection of CEES and DMMP. We have therefore extended the investigation to acridinium betaines as sensor coatings. These compounds are similar to the pyridinium betaines but with the quaternary nitrogen shielded by a bulkier hydrocarbon group. We envisaged that the additional hydrocarbon mass around the ionic site would reduce the interference of water vapor.

A number of methods are available to apply coatings to microsensor devices and the selection of a particular coating technique can greatly influence the choice of a coating, and vice versa. Coating techniques can include sublimation,¹⁵ spin coating,¹⁵ spray coating⁶ and the Langmuir-Blodgett (L-B) technique.^{5,15-17} By the L-B technique the coating can be applied in ordered monolayers,¹⁶ but sophisticated equipment is required. For this study we used spray coating, as this method is fast, versatile, and reproducible.

Inadequate characterization of coating materials has been a problem which has plagued studies of microsensor coatings in the past. Each of the coatings used in this work was characterized by elemental analysis and ¹H and ¹³C NMR spectroscopy.

EXPERIMENTAL

Apparatus

Melting points were uncorrected and were taken on a Thomas-Hoover melting point apparatus. The ¹H NMR spectra were recorded with a Varian EM 360 L (60 MHz) NMR spectrometer or a JEOL FX-100 (100 MHz) NMR spectrometer with tetramethylsilane (TMS) as the internal standard. The ¹³C NMR spectra were recorded with a JEOL FX-100 (25 MHz) NMR spectrometer or a Varian XL-200 (50 MHz) NMR spectrometer with

CDCl₃ (δ 77.0) as the internal reference. Reagent grade chemicals were used, without further purification.

Synthesis of coating materials

Schemes 1 and 2 show the synthetic routes used, for carbazoles and acridinium betaines,¹⁸⁻²⁰ respectively.

Preparation of 1-(4-aminophenyl)carbazole, 6. 1-(*p*-Nitrophenyl)carbazole, **4**, was prepared by a literature procedure²¹ by stirring 4.50 g (27 mmole) of carbazole and 0.80 g of sodium hydride (32 mmole) in 44 ml of nitrobenzene at 60° for 7 hr, cooling, filtering off the precipitate and recrystallizing it from water, to obtain 2.76 g (36%) yield: m.p. 210–212° (lit.²¹ 210°); ¹H NMR (CDCl₃) δ 8.60 (d, 2 H, *J* = 9 Hz), 8.30–8.00 (m, 2 H), 7.85 (d, 2 H, *J* = 9 Hz), 7.60–7.20 (m, 2 H); ¹³C NMR (CDCl₃) δ 145.8, 143.8, 139.8, 126.7, 126.4, 125.4, 124.1, 121.2, 120.6, 109.6.

The nitro compound **4** (0.93 g, 3 mmole) was reduced by heating under reflux with iron filings (3.7 g) and concentrated hydrochloric acid (2.3 ml) in 23 ml of 95% ethanol for 4 hr. The mixture was filtered hot, with celite, the resulting solid being washed with absolute ethanol and the washings added to the filtrate. The filtrate was alkalized with saturated aqueous sodium carbonate solution and the precipitate was collected and washed with absolute ethanol. The product was dried and partitioned between diethyl ether and water. The ether extract was dried with anhydrous magnesium sulfate and the solvent removed to yield 0.75 g (90%) of **6** as a resin: ¹H NMR (CDCl₃) δ 8.40–8.10 (m, 2 H), 7.50–7.10 (m, 8 H), 6.70 (d, 2 H, *J* = 9 Hz), 3.5 (br, NH₂).

Preparation of 2-carbazol-1-yl-5-aminopyridine, 7. This was prepared by a modification of the literature procedure.²¹ Carbazole (5.5 g, 33 mmole) was added to a stirred suspension of sodium hydride (0.98 g, 39 mmole) in dry dimethylformamide (DMF) at room temperature. After the evolution of gas had ceased and the reaction mixture had cooled to room temperature, 2-chloro-5-nitropyridine (5.23 g, 33 mmole) was added in portions. The resulting dark solution was stirred at room temperature for 2 hr and then poured onto ice. The solid was collected by filtration, washed with water and diethyl ether and recrystallized from benzene to give 5.4 g (57%) of **5**: m.p. 185–188°; ¹H NMR (CDCl₃) δ 9.50 (d, 1 H, *J* = 3 Hz), 8.55 (dd, 1 H, *J* = 9 Hz, *J* = 3 Hz), 8.30–7.20 (m, 9 H);

^{13}C NMR (CDCl_3) δ 155.8, 145.4, 130.6, 133.3, 128.3, 126.7, 125.3, 122.6, 120.3, 116.5, 112.1. $\text{C}_{17}\text{H}_{11}\text{N}_3\text{O}_2$ requires C, 70.58%; H, 3.80%; N, 14.53%; found: C, 70.3%; H, 3.75%; N, 14.4%.

The nitro compound **5** (2.00 g, 7 mmole) was reduced as described for **4**, with 8.0 g of iron filings, 5.0 ml of concentrated hydrochloric acid and 50 ml of 95% ethanol, with heating for 4 hr. This resulted in 1.80 g (100%) of the product, which was crystallized from a 1:1% mixture of benzene and hexanes: m.p. 153–154°; ^1H NMR (CDCl_3) δ 8.40–8.00 (m, 3 H), 7.90–7.20 (m, 7 H), 7.00 (dd, 1 H, $J = 10$ Hz, $J = 3$ Hz), 3.6 (br, NH_2); ^{13}C NMR (CDCl_3) δ 142.1, 141.8, 140.1, 136.2, 125.9, 123.8, 123.5, 120.1, 110.5. Anal. $\text{C}_{17}\text{H}_{13}\text{N}_3$ requires C, 78.76; H, 5.01; N, 16.21; found: C, 78.44; H, 5.19; N, 15.84.

Preparation of acridinium betaines, **12**.^{18–20}

Compounds **12a** and **12b** were prepared as follows. Triethylamine (3 eq.) and the amine (1 eq.) were added to a suspension of the xanthylium perchlorate, **11** (1 eq.) in dichloromethane. The mixture was stirred at room temperature for 3 hr. Glacial acetic acid (3 eq.) was added to the solution and the stirring was continued for 22 hr. The organic phase was separated, washed with saturated sodium chloride solution, and dried over anhydrous magnesium sulphate, and the solvent was evaporated. The residue was stirred with diethyl ether and the resulting solid collected by filtration.

Compounds **12c** and **12d** were prepared by the addition of 3 eq. of triethylamine and 1 eq. of the carbazole to a suspension of 1 eq. of the xanthylium perchlorate **11** in ethanol. The mixture was heated under reflux for 21 hr and the solid collected after cooling. The solid was dissolved in the minimum of a dichloromethane/trifluoroacetic acid mixture (1:1) and the solution extracted three times with water. The organic phase was dried, the solvent removed *in vacuo* and the residue triturated with diethyl ether to yield the acridinium betaines **12c,d**.

Preparation of ionic surfactants, 13. To a mixture of the amine (1 eq.) and tributylamine (2 eq.) in DMF the alkylating agent (3 eq.) was added at room temperature (methyl iodide directly, methyl tosylate as a solution in DMF). An exothermic reaction occurred and the reaction mixture was stirred at room temperature for 7 hr (methyl tosylate) or 12 hr (methyl iodide). The reaction mixture was diluted with diethyl ether and stirred, and the

resulting solid was removed by filtration. The products were $n\text{-(C}_{18}\text{H}_{37})\text{N(CH}_3)_3^+\cdot\text{I}^-$ and $n\text{-(C}_{18}\text{H}_{37})\text{N(CH}_3)_3^+\cdot p\text{-CH}_3\text{C}_6\text{H}_4\text{SO}_3^-$, **13a** and **13b** respectively.

Determination of coating response

Simultaneous chemiresistor and SAW measurements were performed with a dual 52 MHz surface acoustic wave device (Microsensor Systems, Inc., Part SD-52-B) as described in detail previously.^{3,6} The 52 MHz SAW delay line was fabricated from ST-quartz (1.5 × 2 cm slab) with gold interdigitated electrodes (laid down by optical lithography). The electrodes each had 50 fingers 15 μm in width and spaced 45 μm apart, giving a 15- μm gap between the intermeshed fingers of the electrode pair. The acoustic aperture was 4800 μm and the electrode thickness was 760 Å. The center-to-center spacing of the SAW transmitter–receiver electrode pair was 1 cm. The device is shown schematically in Fig. 1.

For coating, the device was placed in a machined Teflon or Nylon housing in which provision had been made for pressure-clip connection to the interdigitated electrodes. The coating materials were spray-coated onto the device with an air brush, with nitrogen as propellant, the coating thickness being monitored by means of the frequency counter until the desired frequency shift of 50 kHz had been achieved (see reference 10 for more details). The test vapors were generated by passing a regulated flow of nitrogen through a vapor bubbler equipped with a gas dispersion tube, at 0°. The vapor pressures of CEES and DMMP can be calculated by using the equation:²²

$$\log P = 2.8808 - \frac{\Phi \Delta T}{T - 0.15 \Delta T}$$

where p = vapor pressure (mmHg) at absolute temperature T , Φ = entropy of vaporization at 760 mmHg (estimated from graphs in reference 22), and ΔT = boiling point (at 760 mmHg) – T .

With this equation, and assuming the ideal gas law holds, the concentrations of DMMP and CEES can be calculated to be 5.2 and 30.7 g/m^3 , respectively. The vapor pressure of water at 0° corresponds to a concentration of 4.8 g/m^3 . These concentrations were checked gravimetrically by sampling the exit vapors. The concentrations were 3 g/m^3 for DMMP, 23 g/m^3 for CEES and 2 g/m^3 for water, in each case a good

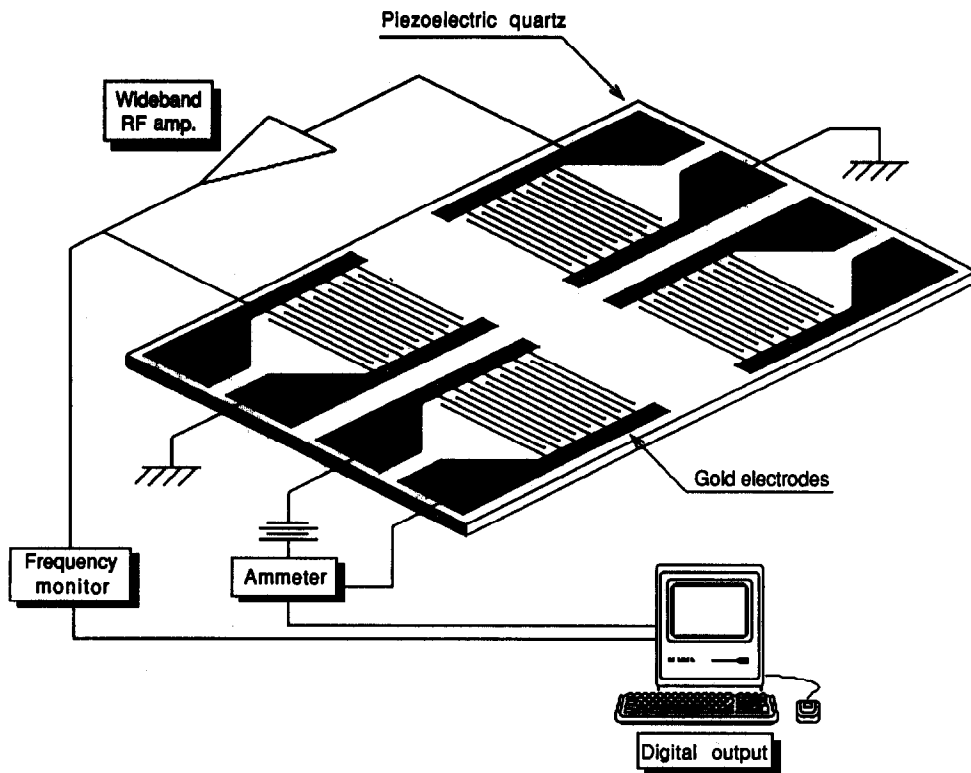


Fig. 1. Dual 52 MHz SAW device used for simultaneous mass and conductivity measurements with computer-controlled data acquisition.

deal less than expected from the vapor pressure calculations.

The resonant frequency was monitored with a Phillips Model PM 6674 universal frequency counter (550 MHz). The conductivity was measured by application of a 1-V bias to either of the two remaining electrodes and measurement of the current with a precision current-to-voltage converter consisting of an operational amplifier and a switch-selectable feedback resistor. A Keithley 617 programmable electrometer was used.

Frequency and resistance measurements were taken at 3–5 sec intervals in the region of the time when the vapor flow was turned on and off, and at 10 sec intervals throughout the remainder of the run. The frequency and resistance measurements were collected and stored by an Apple IIe personal computer with an IEEE-488 interface.

RESULTS AND DISCUSSION

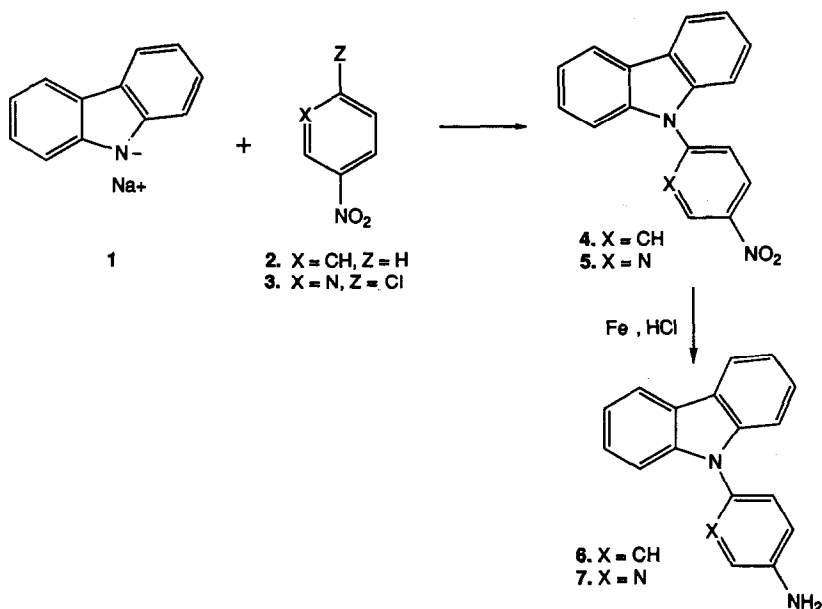
Acridinium betaines

The synthesis of the acridinium betaines (**12**) by reaction of the xanthylium salts (**11**) with the corresponding amine was performed as shown in Scheme 2. The carbazolamines employed

were prepared as shown in Scheme 1 from the sodium salt of carbazole (**1**) and the corresponding nitro compound (**2** and **3**). The 1-substituted carbazole (**4** or **5**) was then reduced with iron and hydrochloric acid to yield the corresponding amine (**6** or **7**).²¹ The pyridine derivatives were characterized by their ¹H NMR spectra and their compositions were confirmed by elemental analysis. The ¹H NMR spectrum of the nitro compound (**5**) displayed a doublet at δ 9.50 ($J = 3.0$ Hz) and a doublet of doublets at δ 8.55 ($J = 9.0$ Hz, $J = 3.0$ Hz) which could be assigned to the pyridine ring H-6 and H-4, respectively. In the corresponding amino compound (**6**) a doublet of doublets at δ 7.00 ($J = 10.0$ Hz, $J = 3.0$ Hz) was assigned to H-4 of the pyridine ring.

The xanthylium salt (**11**) was prepared by sulfonation of *p*-methoxybenzaldehyde and subsequent reaction of the sulfonate with α -tetralone (**10**).²⁰ Reaction of the xanthylium salts with the amine resulted in formation of the acridinium betaines in yields ranging from 30 to 80% (Table 1).

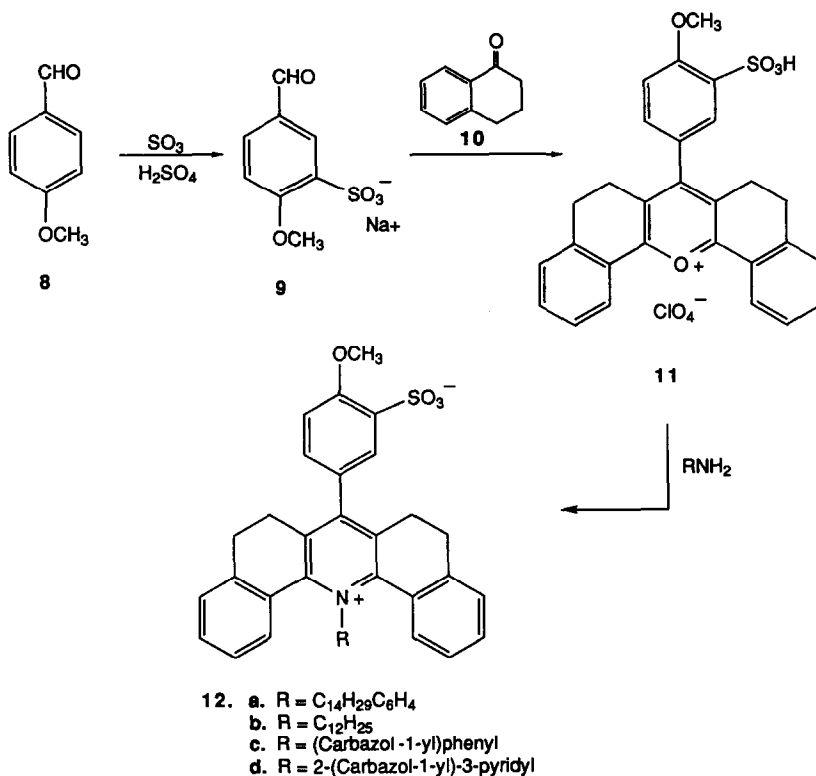
The acridinium betaines (**12a,b**) were prepared by reaction of the amine and the xanthylium salt at room temperature in methylene chloride according to a known procedure.² The betaines

Scheme 1. Synthesis of *N*-substituted carbazoles

Scheme 1.

(12c,d) were prepared by heating equimolar amounts of the amine, the xanthylium salt and three equivalents of triethylamine under reflux

in absolute ethanol. The betaine structures were confirmed with the aid of ^1H and ^{13}C NMR data (with the exception of 12d, which was too



Scheme 2. Synthesis of acridinium betaines

Table 1. Characteristics of acridinium betaines (12) and ionic surfactants (13)

Cpd.	Yield, %	Crystal form	Crystallization solvent	m.p., °C	Formula	Required, %			Found, %		
						C	H	N	C	H	N
12a	80	Micro	EtOH/H ₂ O	204–214	C ₄₈ H ₅₅ NSO ₄ ·2H ₂ O	74.03	7.71	1.80	74.2	7.48	2.27
12b	79	Yellow powder	Diethyl ether	169–171	C ₄₀ H ₄₇ NSO ₄ ·2H ₂ O	71.32	7.57	2.08	71.7	7.21	2.05
12c	30	Yellow powder	EtOH/H ₂ O	348(dec.)	C ₄₆ H ₅₄ N ₂ SO ₄ ·2.5H ₂ O	73.09	5.26	3.71	73.2	4.85	3.67
12d	30	Yellow prisms	EtOH/H ₂ O	> 350(dec.)	C ₄₅ H ₅₃ N ₃ SO ₄ ·2H ₂ O	72.27	4.67	5.90	72.4	4.69	5.54
13a	61	Needles	EtOH	238–241*	C ₂₁ H ₄₆ NI	57.39	10.55	3.19	57.4	10.55	3.16
13b	41	Plates	EtOH	223–225	C ₂₈ H ₅₃ NSO ₃	69.51	11.04	2.90	69.5	11.24	2.86

*Literature²⁴ melting point 237–238.5°.

insoluble for useful spectra to be obtained) and by elemental analysis (Table 1). The ¹H NMR spectra of the betaines exhibited a broad singlet, δ 3.9–4.1, corresponding to integration for the three protons and of the methoxy group. The remaining resonances in the aromatic or alkyl region showed the requisite integral signals and could be assigned to either the *N*-side-chain or to the acridinium group (Table 2). The ¹³C NMR spectra of the adducts (Table 3) were complex but the requisite number of carbon signals were seen for each compound.

Ionic surfactants

Two quaternary ammonium salts (13) were prepared from octadecylamine for use as micro-sensor coatings. Methylation of octadecylamine with methyl iodide in DMF in the presence of tributylamine gave the methiodide (13a); the melting point agreed with that reported in the literature.²⁴ A similar method provided the *p*-toluenesulfonate (13b), characterized by ¹H and ¹³C NMR data (Tables 2 and 3). Doublets at δ 7.85 and 7.20, each giving integration for 2 H (*J* = 8 Hz), were attributed to the phenyl resonances. Multiplets at δ 3.4–3.3 and 1.60–0.80, with integration for 11 H and 35 H, and a singlet for 3 H were assignable to the quaternary

ammonium group, the adjacent methylene group, and the remaining alkyl protons, respectively.

Responses of coatings to vapors

Each of the coatings was spray coated onto an SAW delay line until a 50 kHz shift in the resonant frequency of the device was achieved. This frequency shift was used simply to ensure that the coatings had comparable film thicknesses, but could also be used to calculate the mass per unit area of the coating film.⁸ Simultaneous SAW and chemiresistor measurements were then made while the device was exposed to DMMP, CEES, and water vapors. The vapors were generated by using a gas dispersion tube, with nitrogen as carrier gas. Flow-rates over the device were monitored with a flowmeter and were nominally 5 ml/min. The system was first purged with nitrogen for 5 min to establish a baseline, then exposed to the vapor stream for 40 min and finally purged with nitrogen for 50–60 min.

Table 4 summarizes the frequency shifts in the resonant frequency of the device and the factor by which the resistance of the coating changed. Each of the coatings gave baseline resistances in the 100–200 GΩ range. SAW responses were

Table 2. ¹H NMR data for compounds 12 and 13*

Cpd.	Aromatic region	Aliphatic region
12a	7.95–7.85 (bs, 6 H), 7.7–6.5 (m, 14 H)	4.9–4.3 (bs, 1 H), 3.90 (s, 3 H), 3.1–2.3 (m, 10 H) 1.90–0.70 (m, 27 H)
12b	8.3–8.0 (bs, 1 H), 7.9–7.1 (m, 8 H),	5.7–5.3 (m, 2 H), 4.1 (s, 3 H), 3.3–2.4 (m, 8 H), 1.6–0.7 (m, 23 H)
12c†	8.5–6.9 (m, 23 H)	3.9 (bs, 3 H), 2.7 (m, 8 H)
12d	§	
13a	None	3.8–3.4 (m, 11 H), 2.0–0.9 (m, 35 H)
13b	7.85 (d, 2 H, <i>J</i> = 8 Hz), 7.20 (d, 2 H, <i>J</i> = 8 Hz)	3.3 (m, 11 H), 2.3 (s, 3 H), 1.6–0.8 (m, 35 H)

*CDCl₃ as solvent, TMS as reference.

†CDCl₃/F₃CCO₂D as solvent, TMS as reference.

§The NMR spectrum was not obtained, owing to the insolubility of this compound.

Table 3. ^{13}C NMR data for compounds **12** and **13***

Cpd.	Aromatic region	Aliphatic region
12a	158.1, 155.6, 148.2, 146.5, 141.9, 139.3, 138.2, 135.2, 130.6, 130.4, 130.3, 130.2, 130.1, 130.0, 129.7, 129.6, 129.4, 129.3, 129.1, 128.9, 127.9, 127.1, 126.0, 124.6, 112.1	56.1, 35.5, 31.9, 31.2, 29.9, 29.7, 29.4, 29.4, 29.2, 29.2, 29.1, 28.9, 28.8, 28.4, 28.2, 22.7, 14.1
12b	157.6, 155.0, 152.8, 140.5, 137.2, 135.0, 132.5, 130.0, 128.3, 128.1, 128.0, 125.0, 112.5,	64.2, 56.2, 40.0, 31.6, 29.5, 29.1, 28.9, 28.8, 28.3, 28.1, 29.0, 26.1, 25.3, 22.4, 13.9
12c†	159.2, 158.4, 155.5, 148.5, 142.2, 140.7, 140.0, 138.4, 132.5, 131.7, 131.2, 130.7, 130.5, 129.4, 130.2, 129.5, 129.4, 128.4, 126.2, 124.5, 124.0, 120.3, 120.2, 112.7, 108.9	55.9, 28.1, 28.0
12d	§	
13a	None	66.8, 53.5, 31.6, 29.4, 29.2, 29.1, 29.0, 28.9, 25.8, 22.9, 22.4, 13.8
13b	144.5, 138.9, 128.5, 125.7	66.5, 52.9, 31.7, 29.5, 29.1, 29.0, 26.1, 23.0, 22.5, 21.0, 13.8

* CDCl_3 as solvent, CDCl_3 (δ 77.0) as reference.

† $\text{CDCl}_3/\text{F}_3\text{CCO}_2\text{D}$ as solvent, CDCl_3 (δ 77.0) as reference.

§The NMR spectrum was not obtained, owing to the insolubility of this compound.

calculated by subtracting the lowest frequency reached, from the baseline frequency (nominally 52 MHz). Resistance responses were calculated by dividing the baseline resistance by the lowest resistance reached. Resistance changes are therefore "factors" and a response close to unity denotes essentially no change.

The ionic surfactant films showed very small responses for the frequency-based detection of DMMP, CEES or water vapor, but the chemiresistor response was greatest for the detection of CEES with the iodide **13a**, which gave a 53-fold change in resistance. The tosylate salt **13b** also exhibited its largest chemiresistor response on exposure to CEES. Neither coating gave significant responses to DMMP vapor and the responses to water vapor were nearly as great as the responses for CEES vapor.

The acridinium betaines **12** in general exhibited their largest response as SAW coatings in the detection of CEES vapor. As can be seen in Table 4 the largest frequency shifts were given by compounds **12a** and **12b** on exposure to CEES, 9.8 and 6.8 kHz, respectively (see Fig. 2). The response of **12a** to CEES was rapid but

unfortunately not completely reversible. Fifty minutes after the vapor had been removed the device still exhibited a 4 kHz shift. Compound **12d**, which tended to be hygroscopic, showed its greatest response to water vapor, with much smaller responses to CEES and DMMP vapor.

In general it appears that a long alkyl chain is necessary in the acridinium betaines for SAW response to occur with CEES vapor. We have previously reported¹⁰ that the presence of a sulfonate group in an organic coating enhances its interaction with CEES vapor, resulting in large changes in resistivity. At present we are uncertain why these phenomena occur, but they appear to arise only with compounds in which the sulfonate group is attached to a large organic ring system such as the acridinium betaine and not to a smaller moiety, even with a long chain alkyl group, such as in **13b**.

Table 4. Response of acridinium betaines (**12**) and ionic surfactants (**13**) to vapors of DMMP (512 g/m^3), CEES (30.7 g/m^3) and water (4.8 g/m^3)

Cpd.	Resistance change factors			Frequency shift, kHz		
	DMMP	CEES	H_2O	DMMP	CEES	H_2O
12a	2	16	13	1.7	9.8	2.4
12b	0	2	5	1.1	6.8	1.1
12c	3	0	2	1.4	2.2	2.9
12d	3	3	107	0.9	2.7	5.2
13a	3	68	53	0.3	2.4	0.2
13b	4	20	19	0.2	0.6	0.7

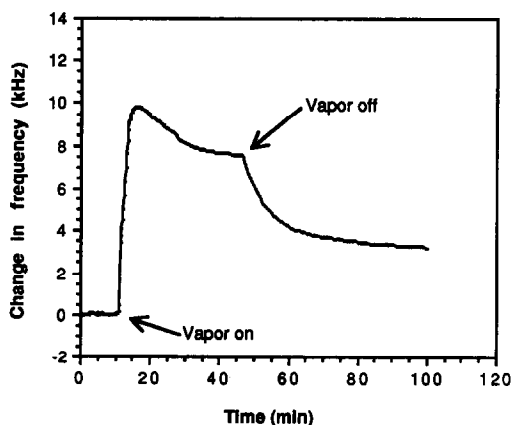


Fig. 2. Frequency change vs. time for response of compound **12a** to CEES vapor.

Unfortunately, there are not yet complete theories to explain the vapor-coating interactions which result in frequency changes in SAW microsensor systems. Frequency changes can be explained, in part, as due to simple sorption (mass loading) of the analyte by the coating material, although a component of the frequency shift is related to the shear modulus of the film.⁸ Thus, the simple solubility of the analyte in the coating, and the hydrogen-bond acceptor/donor natures of the analyte and coating seem to be the most important factors. Various equations defining adsorbate/adsorbent interactions have been developed for the adsorption of organic compounds, by using linear solvation energy relationships (LSERs).¹²⁻¹⁴ These LSERs are dependent on three indexes: π^* , an index of solvent polarity/polarizability, the α -scale of hydrogen-bond donor acidities, and the β -scale of hydrogen-bond acceptor basicities.¹³ This approach, when applicable, has a great deal of potential for determining which features are desirable in a coating for it to interact with (adsorb) a given vapor.

The effect of various vapors and gases (generally $\text{NO}_2/\text{N}_2\text{O}_4$) on the conductivity of thin films has been studied for some time.²⁵⁻³³ In most of these cases the thin film was a metal oxide or a phthalocyanine metal complex. The latter, in the crystalline state, can exhibit pseudo one-dimensional metallic conductivity or semi-conductivity.³² These conjugated organic films (electron donors) form reversible charge-transfer complexes with $\text{NO}_2/\text{N}_2\text{O}_4$ (electron acceptor), which leads to chemisorption, with facile production of ionized states and charge carriers.²⁸

More recently, polypyrrole has been used as a chemiresistor coating for the detection of H_2S and $\text{NO}_2/\text{N}_2\text{O}_4$,³³ but it was remarked that the chemical composition and structural characteristics of such polymeric materials are not well defined. Indeed, coating materials are often poorly characterized and hence it is not surprising to find that an understanding of the surface chemistry, particularly in terms of conductance mechanisms and gas absorption sites, is more or less non-existent.³³

We have recently examined a range of well characterized organic coatings to build a data-base of chemiresistor and SAW responses.³⁴⁻³⁶ These data will be used in a principal-components analysis to determine desirable features in a coating (for maximum

response), and hence shed some light on the mechanisms causing that response.

REFERENCES

1. J. Janata and R. J. Huber (eds.), *Solid State Chemical Sensors*, Academic Press, Orlando, 1985.
2. D. Schuetzle and R. Hammerle (eds.), *Fundamentals and Applications of Chemical Sensors*, American Chemical Society, Washington, DC, 1984.
3. A. R. Katritzky and R. J. Offerman, *CRC Crit. Rev. Anal. Chem.*, 1989, **21**, 83.
4. A. W. Barendsz, C. A. Van Beest and P. P. M. M. Wittgen, *Proc. 1981 Sci. Conf. Chem. Defense Research*, pp. 35-41. ARCSL-SP-83026, June 1983.
5. H. Wohltjen, W. R. Barger, A. W. Snow and N. L. Jarvis, *IEEE Trans. Elect. Dev.*, 1985, **ED-32**, 1170.
6. A. W. Snow, W. R. Barger, M. Klusty, H. Wohltjen and N. L. Jarvis, *Langmuir*, 1986, **2**, 513.
7. W. R. Barger, H. Wohltjen, A. W. Snow, J. Lint and N. L. Jarvis, in *Fundamentals and Applications of Chemical Sensors*, D. Schuetzle and R. Hammerle (eds.), pp. 155-165. American Chemical Society, Washington, DC, 1986.
8. H. Wohltjen, *Sens. Actuators*, 1984, **5**, 307.
9. J. Hlavay and G. G. Guilbault, *Anal. Chem.*, 1977, **49**, 1890.
10. A. R. Katritzky, R. J. Offerman and S. Wang, *Langmuir*, 1989, **5**, 1087.
11. W. R. King, Jr., *Anal. Chem.*, 1964, **36**, 1735.
12. R. W. Taft, M. H. Abraham, R. M. Doherty and M. J. Kamlet, *J. Am. Chem. Soc.*, 1985, **107**, 3105.
13. R. W. Taft, T. Gramstad and M. J. Kamlet, *J. Org. Chem.*, 1982, **47**, 4557.
14. R. W. Taft, M. H. Abraham, R. M. Doherty and M. J. Kamlet, *Nature*, 1985, **313**, 384.
15. A. W. Snow and N. L. Jarvis, *J. Am. Chem. Soc.*, 1984, **106**, 4706.
16. *Thin Solid Films*, 1983, **99**, No. 3.
17. G. L. Gaines, Jr., *Insoluble Monolayers at Liquid-Gas Interfaces*. Wiley-Interscience, New York, 1966.
18. A. R. Katritzky and C. W. Marson, *Angew. Chem. Int. Ed. Eng.*, 1984, **23**, 420.
19. A. R. Katritzky, *Tetrahedron*, 1980, **36**, 679.
20. A. R. Katritzky and Y. K. Yang, *J. Chem. Soc. Perkin Trans. II*, 1984, 885.
21. G. de Montmollin and M. de Montmollin, *Helv. Chim. Acta*, 1923, **6**, 94.
22. R. C. Weast (ed.), *CRC Handbook of Chemistry and Physics*, 57th Ed., p. D-176. CRC Press, Boca Raton, 1975.
23. A. R. Katritzky, J. M. Lloyd and R. C. Patel, *J. Chem. Soc., Perkin Trans. I*, 1982, 117.
24. H. L. Pickering and C. A. Kraus, *J. Am. Chem. Soc.*, 1949, **71**, 3288.
25. J. Kaufhold and K. Hauffe, *Ber. Bunsenges. Physik. Chem.*, 1965, **69**, 168.
26. B. Rosenburg, T. N. Misra and R. Switzer, *Nature*, 1968, **217**, 423.
27. Th. G. J. van Oirschot, D. van Leeuwen and J. Medema, *J. Electroanal. Chem. Interfac. Electrochem.*, 1972, **37**, 373.
28. R. L. van Ewyk, A. V. Chadwick and J. D. Wright, *J. Chem. Soc. Faraday Trans. 1*, 1980, **76**, 2194.
29. *Idem, ibid.*, 1981, **77**, 73.

30. C. L. Honeybourne and R. J. Ewen, *J. Phys. Chem. Solids*, 1983, **44**, 223.
31. *Idem, ibid.*, 1983, **44**, 833.
32. C. L. Honeybourne, R. J. Ewen and C. A. S. Hill, *J. Chem. Soc. Faraday Trans. 1*, 1984, **80**, 851.
33. J. J. Miasik, A. Hooper and B. C. Tofield, *ibid.*, 1986, **82**, 1117.
34. A. R. Katritzky, G. P. Savage, J. N. Lam and M. Pilarska, *Chem. Scripta*, 1989, **29**, 197.
35. A. R. Katritzky, G. P. Savage, Z. Dega-Szafran and M. Pilarska, *ibid.*, 1989, **29**, 235.
36. A. R. Katritzky, G. P. Savage and M. Pilarska, *ibid.*, 1990, **29**, in the press.

SYNTHESIS OF NEW MICROSENSOR COATINGS AND THEIR RESPONSE TO VAPORS—III*

ARYLPHOSPHONIC ACIDS, SALTS AND ESTERS

ALAN R. KATRITZKY,§ G. PAUL SAVAGE, RICK J. OFFERMAN and BOGUSLAW PILARSKI

Department of Chemistry, University of Florida, Gainesville, FL 32611, U.S.A.

(Received 13 December 1989. Revised 5 March 1990. Accepted 8 March 1990)

Summary—Phosphonic acids, phosphonate esters and cyclohexylammonium phosphonates, spray-coated onto surface acoustic wave (SAW) devices, were exposed to vapors of chloroethyl ethyl sulfide (CEES), dimethyl methylphosphonate (DMMP), and water. Changes in the resonance frequency of the device or the resistance of the coating were collected by computer-controlled data acquisition. Two of the esters showed major reversible and selective response to CEES, and one of the acids showed similar behavior with DMMP.

In continuation of the work of this laboratory¹⁻⁵ in the relatively new field of chemical micro-sensors, we have used a surface acoustic wave (SAW) device equipped with the necessary electronics for simultaneous resistance and frequency measurement,⁶ to explore the use of further novel organic compounds that may be suitable coatings for the sensitive and selective detection of chloroethyl ethyl sulfide (CEES, a simulant of mustard gas), and dimethyl methylphosphonate (DMMP, a nerve agent simulant). The investigation clearly has important implications for industrial pesticide monitoring and military defense.

Previous work in our laboratory on microsensor coatings was focused on utilizing pyridinium compounds (pyridine 1-oxides,² pyridinium salts,² and pyridinium^{1,2} and acridinium betaines¹), and met with some success. As mentioned previously,¹ the mass uptake on the surface of the device seems to be associated with the solubility of the test vapor in the coating material,⁷⁻¹⁰ so phosphonate esters and phosphonic acids are promising candidates for such coatings, as the solubility of DMMP in such materials is expected to be high. For the same reason it was envisaged that such coatings would show good discrimination between DMMP and a given interferent (*e.g.*, water). To that end we prepared a number of phenyl-

phosphonate esters, the corresponding acids (if stable), and their cyclohexylammonium salts, together with some diethyl benzylphosphonates and benzylphosphonic acids. These compounds, along with various commercially available benzyl- and phenylphosphonic acid derivatives which were also tested, are shown in Fig. 1.

The methods routinely used to apply coatings to microsensor devices were reviewed in Part II of this series,¹ and the spray coating method⁶ was used in the present work, as described earlier.

EXPERIMENTAL

Simultaneous chemiresistor and SAW measurements were performed during exposure of the device to DMMP, CEES and water vapors, in turn. The dual 52 MHz surface acoustic wave apparatus used (Microsensor Systems, Inc.), has been described in detail previously.^{2,3} The experimental arrangements were the same as those described in Part II.¹ Test vapors were generated as before, by passing a regulated flow of nitrogen through the pure test liquid at 0° in a vapor bubbler equipped with a gas dispersion tube. The flow-rate over the device was controlled by a flowmeter and was found to be 7.5 ml/min by use of a bubble meter. The absolute concentrations of the test vapor were not determined, but the conditions used were constant for successive runs.¹

Initially the system was purged with nitrogen for 5 min to establish a baseline curve. The

*Part II—A. R. Katritzky, R. J. Offerman, J. M. Aurrecochea and G. P. Savage, *Talanta*, 1990, 37, 911.

§Author to whom correspondence should be addressed.

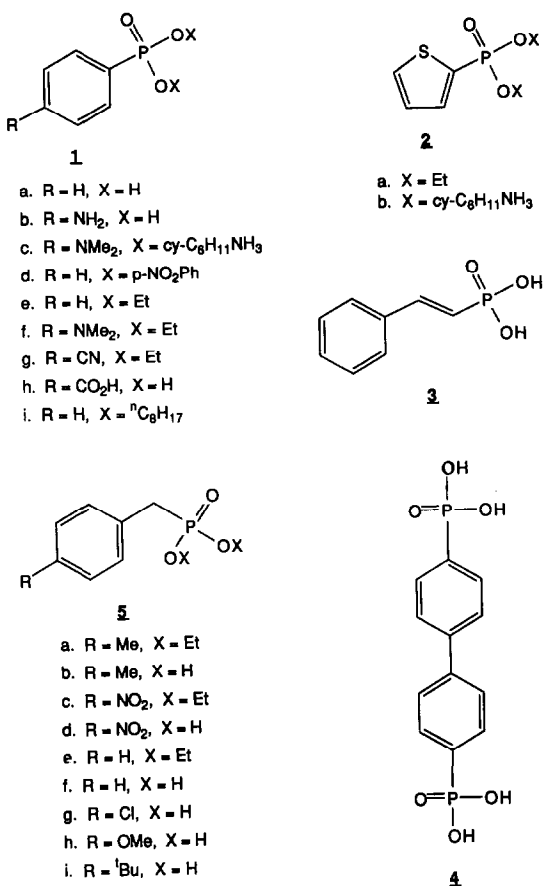


Fig. 1. The formulae of the compounds tested as coatings (for references and data see Table 1).

device was then exposed to the vapor for 40 min, followed by a nitrogen purge for 50–60 min. If a response was irreversible, the SAW device was cleaned and recoated before exposure to the next test vapor.

The SAW devices used were rinsed with acetone between runs, followed by ultrasonic cleaning for 10 min in spectroscopic grade 2-propanol.

All compounds, including those commercially obtained, were characterized by their ¹H-NMR and ¹³C-NMR spectra, and by melting points for the solids. Correct elemental analyses were obtained for all the novel compounds synthesized.

RESULTS AND DISCUSSION

The responses are recorded in Table 1. The frequency shift was calculated as the difference between the lowest frequency recorded during exposure to a vapor and the initial (baseline) frequency. Resistance changes (resistance factors) were the ratios of the initial (baseline) resistance to the lowest resistance recorded during exposure to a vapor. Thus, a resistance factor close to unity denotes essentially no change. Values marked with an asterisk indicate responses that were irreversible. Results were reproducible to within $\pm 5\%$.

Table 1. Response of aryl phosphonic acids and aryl phosphonate esters on exposure to test vapor

Cpd.	Coating mass, kHz	Resistance change factor						Frequency shift, kHz				Compound characterization		
		DMMP			CEES			H ₂ O			m.p. or b.p.		Lit.	
		DMMP	CEES	H ₂ O	DMMP	CEES	H ₂ O	DMMP	CEES	H ₂ O	°C or °C/mmHg	Ref.	Source†	
1a	55	1.0	1.0	142.3	0.1	0.0	24.9	162–164	162.5–163	11	A			
1b	47	1.0	1.8	2.4	0.0	15.1	2.9	205–208/1	185–187/0.3	Aldrich	A			
1c	47	5.5	32.6	3.5 × 10 ⁵	0.0	1.4	32.5	264 (dec)	—	—	B			
1d	58	1.0	1.0	25.5	0.0	2.9	0.0	99–100	99–101	Alfa	C			
1e	49	1.0	2.2	67.0	0.0	22.7	0.5	130–134/3	121–123/2	Alfa	C			
1f	52	2.7	10.5	2.0	21.1	77.5	13.7	201–205/4‡	—	—	B			
1g	48	5.5	2.4	12.8	0.0	5.3	3.9	31–33	31–33	12	B			
1h	54	32.5	3.8	24.2	1.1	2.6	1.5	>300	>300	11	B			
2a	47	1.0	103*	1.2	0.0	65.6	0.0	136–139/4	106–110/0.2	12	B			
2b	47	40.5	4.9	§	16.2	2.8	40.7*	280 (dec)‡	—	—	B			
3	51	10.7	6.1	3.3	33.2	3.9	3.4	154–156	154.5–155	13	B			
4	52	3.9	1.0	17.2	0.9	0.5	2.7	254–258‡	192–193	11	B			
5a	47	1.0	1.0	1.0	0.0	21.0	1.5	142–144/3	130–133/2	14	B			
5b	54	609*	4.1	1.0	74.3	0.4	0.0	185–187	185–186	14	B			
5c	51	3.0	6.1	3.7	0.0	24.5	1.6	184–188/4	148–153/0.1	15	B			
5d	48	321*	4.7	84.1	75.5*	0.0	3.9	234–236	232–234	15	B			
5e	55	65.0	144*	9.1	8.2	0.4	0.3	162–166/16	160–164/15	15	B			
5f	53	1.0	1.6	1.0	0.0	7.0	0.1	172–174	173–175	15	B			
5g	49	165*	1.0	31.7	3.1	0.0	0.1	165–166	302–306°F	16	B			
5h	52	1.0	3.3	1.0	1.3	0.5	0.3	204–205	204–206	17	B			
5i	54	0.4	14.7	3.6	0.3	0.5	0.0	193–194‡	—	—	B			

*Irreversible response.

†A = Aldrich; B = preparation by A. R. Katritzky and B. Pilarski; C = Alfa.

‡Correct G and H values obtained.

§Resistance went irreversibly to zero.

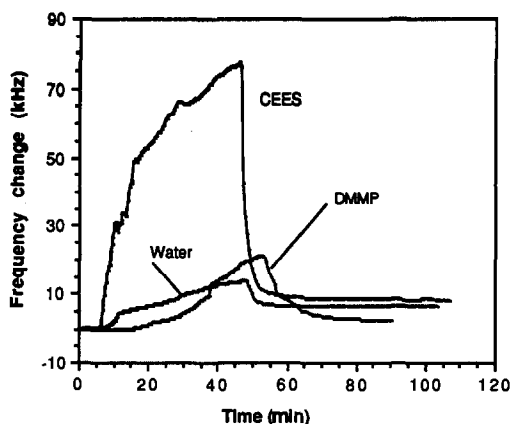


Fig. 2. Frequency response of diethyl 4-dimethylaminophenylphosphonate (**1f**) as a function of time, for vapor exposure (vapor on at 5.4 min, off at 45.8 min).

Diethyl 4-dimethylaminophenylphosphonate (**1f**) gave the largest frequency shift, of 77.5 kHz, on exposure to CEES, and showed satisfactory discrimination, with shifts of only 13.7 and 21.1 kHz for water and DMMP, respectively. Diethyl 2-thienylphosphonate (**2a**) also showed a large response to CEES vapor (65.6 kHz), and excellent selectivity with negligible responses to either water or DMMP.

Figure 2 shows the change in frequency response with time, for diethyl 4-dimethylaminophenylphosphonate (**1f**) exposed to CEES, DMMP and water. The frequency change occurs rapidly on exposure to CEES vapor and even more rapidly returns to almost baseline level when the vapor flow is replaced by a CEES-free gas-stream. The response to DMMP or water vapor is slower. Repeated exposure of **1f** to CEES vapor did not result in saturation, and return to baseline frequency

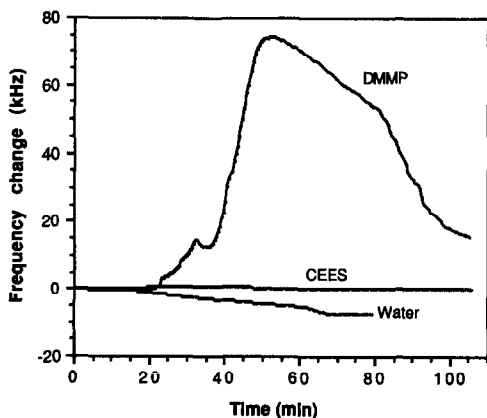


Fig. 3. Frequency response of 4-methylbenzylphosphonic acid (**5b**) as a function of time, for vapor exposure (vapor on at 5.2 min, off at 45.6 min).

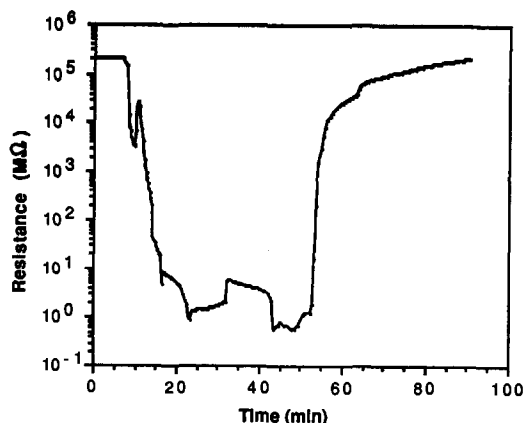


Fig. 4. Chemiresistor response of bis(cyclohexylammonium) 4-dimethylaminophenylphosphonate (**1c**) as a function of time, for exposure to water vapor (vapor on at 5.6 min, off at 45.1 min).

was practically complete on cessation of the exposure.

The greatest reversible frequency response to DMMP vapor was obtained with 4-methylbenzylphosphonic acid (**5b**) (74 kHz, Fig. 3). This coating also showed excellent discrimination, with little or no response to water or CEES vapors. The styrylphosphonic acid **3** also gave a good response to DMMP vapor (33 kHz) with good discrimination against water (3 kHz) and CEES (4 kHz).

None of the phenylphosphonic acids or esters gave exceptional responses as chemiresistors. Diethyl 2-thienylphosphonate (**2a**) gave a significant, though irreversible, chemiresistor response to CEES. The benzylphosphonic acids **5b**, **5d**, and **5g** gave large but irreversible resistance responses to DMMP. Diethyl benzylphosphonate (**5e**) exhibited a large reversible chemiresistance response (65 fold) to DMMP, and a still larger but irreversible response to CEES.

It was not surprising that with many of the salts there was a large irreversible increase in conductivity on exposure to water vapor, as these salts are somewhat hygroscopic. It is interesting that the bis(cyclohexylammonium) 4-dimethylaminophenylphosphonate (**1c**) gave a large (from 200 G Ω to 560 k Ω) reversible response to water vapor (Fig. 4). This means that such a coating on a chemiresistor device essentially constitutes a chemical switch for the detection of water vapor. This has potential application in such areas as humidity control.

It is not feasible to test a given coating with all the possible interferents it may come in

contact with, and it is unlikely that a coating could be found that would be totally selective for a given vapor. Nevertheless, this is not a limiting factor for microsensors. An array of sensors with different selective coatings, coupled with a pattern-recognition algorithm, should be able to detect and quantify a given analyte in a mixture of several vapors. Crucial to this goal is the discovery of coatings that show at least some selectivity of response to different vapors.

All the diethyl phosphonates tested in this work are non-volatile, photochemically stable compounds. Heating the esters under reflux in concentrated hydrochloric acid for 24 hr resulted in minimal hydrolysis. The acids are also stable and have an indefinite shelf-life under ambient conditions, but the salts are generally slightly hygroscopic. Thermal stability is indicated by the generally high melting or boiling points, without decomposition. Thus, as chemical microsensor coatings, diethyl 4-dimethylaminophenylphosphonate (**1f**) and diethyl 2-thienylphosphonate (**2a**) appear to be excellent candidates for CEES detection, as does 4-methylbenzylphosphonic acid (**5b**) for DMMP detection.

Acknowledgements—We acknowledge the helpful advice given by H. Dupont Durst in this work and the support of the U.S. Army, Chemical Research, Development and Engineering Center at Aberdeen Proving Ground, Maryland.

REFERENCES

1. A. R. Katritzky, R. J. Offerman, J. M. Aurrecoechea and G. P. Savage, *Talanta*, 1990, **37**, 911 and references therein.
2. A. R. Katritzky, R. J. Offerman and Z. Wang, *Langmuir*, 1989, **5**, 1087.
3. A. R. Katritzky, G. P. Savage, J. N. Lam and M. Pilarska, *Chem. Scripta*, 1989, **29**, 197.
4. A. R. Katritzky, G. P. Savage, Z. Dega-Szafran and M. Pilarska, *ibid.*, 1989, **29**, 235.
5. A. R. Katritzky, G. P. Savage and M. Pilarska, *ibid.*, 1990, **29**, in the press.
6. A. W. Snow, W. R. Barger, M. Klusty, H. Wohltjen and N. L. Jarvis, *Langmuir*, 1986, **2**, 513.
7. M. J. Kamlet, R. M. Doherty, M. H. Abraham and R. W. Taft, *Proc. 1984 Sci. Conf. Chem. Defense Res.*, CRDC-SP-85006, June 1985, pp. 601–606.
8. R. W. Taft, M. H. Abraham, R. M. Doherty and M. J. Kamlet, *J. Am. Chem. Soc.*, 1985, **107**, 3105.
9. R. W. Taft, T. Gramstad and M. J. Kamlet, *J. Org. Chem.*, 1982, **47**, 4557.
10. R. W. Taft, M. H. Abraham, R. M. Doherty and M. J. Kamlet, *Nature*, 1985, **313**, 384.
11. G. O. Doak and L. D. Freedman, *J. Am. Chem. Soc.*, 1951, **73**, 5658.
12. P. Tavs, *Chem. Ber.*, 1970, **103**, 2428.
13. G. M. Kosolapoff and W. F. Huber, *J. Am. Chem. Soc.*, 1946, **68**, 2540.
14. B. P. Lugovkin and B. A. Arbuzov, *Izvest. Akad. Nauk S.S.S.R., Otdel Khim. Nauk*, 1950, 56; *Chem. Abstr.*, 1950, **44**, 7256e.
15. F. Kagan, R. D. Birkenmeyer and R. E. Strube, *J. Am. Chem. Soc.*, 1959, **81**, 3026.
16. W. Jensen and J. O. Clayton, *U.S. Patent 2,795,609*; *Chem. Abstr.* 1957, **51**, 16535c.
17. A. Williams, R. A. Naylor and S. G. Collyer, *J. Chem. Soc. Perkin Trans. II*, 1973, 25.

COLORIMETRIC DETERMINATION OF LIPID HYDROPEROXIDES IN OILS AND FATS WITH MICROPEROXIDASE

IKUKO AKAZA* and NAOMI AOTA

Kanazawa Women's College, Suemachi, Kanazawa, Ishikawa, 920-13, Japan

(Received 16 August 1989. Revised 9 March 1990. Accepted 14 March 1990)

Summary—The use of the peroxidase-like activity of microperoxidase for the colorimetric determination of lipid hydroperoxides in oils and fats has been investigated. The principle of the determination is that 4-aminoantipyrine and *N,N*-diethylaniline are coupled oxidatively by the hydroperoxides through the action of microperoxidase, yielding a violet colour with maximum absorbance at 554 nm. The response of the microperoxidase system is enhanced by the presence of acetonitrile. The method has been successfully applied to the determination of methyl linoleate hydroperoxide, *tert*-butyl hydroperoxide and the hydroperoxides in oil and fat samples (soybean oil, linseed oil, olive oil, salad oil, butter and lard). The results agreed closely with those obtained by the iodometric method. The proposed method permitted the determination of the hydroperoxides at 0.5–0.05 μ mole levels, with the same sensitivity regardless of sample type tested, with satisfactory reproducibility compared with that obtained by the conventional assay methods.

Recently, much attention has been paid to lipid peroxides in the food and clinical fields, because of their deleterious effects on humans. The oxidation of lipids proceeds by a free-radical chain mechanism to give lipid hydroperoxides as primary products, and these in turn produce many secondary products. Therefore, determination of the hydroperoxides is important for obtaining information relating to the lipid oxidation.

The peroxide value (PV) determined by iodometric titration^{1,2} or its extension,³⁻⁶ the thio-barbituric acid method,⁷ and other methods,⁸⁻¹⁴ is used for evaluating the extent of oxidation of lipids or for determination of fatty-acid, lipid and organic hydroperoxides. For specificity, the use of an enzyme or a substance having enzymatic action is attractive, and a few enzymatic assays using cyclo-oxygenase,¹⁵ glutathione peroxidase¹⁶ and horseradish peroxidase (HRP)¹⁷ have been described for fatty-acid or lipid hydroperoxides. Haeme compounds such as haemoglobin, haematin and cytochrome C, which bear a structural and catalytic resemblance to HRP, have also been used.^{10,18-20} Microperoxidase (MP), a homologue in the peroxidase series, has also been used.¹¹

Although many of these methods have particular advantages, they also have limitations in

practical use for analysis of oils and fats. For example, because the reaction rate is measured, there are some difficulties with sensitivity and measurement of several samples at the same time. We have therefore aimed at establishing a colorimetric method which is generally applicable, accurate and adequately sensitive for determination of hydroperoxides in oils and fats, and have based it on the enzymatic activity of MP. MP is the pepsin digest of cytochrome C, acts as a peroxidase and has a molecular weight of only 1900.²¹ MP has been used as a catalyst for the chemiluminescence determination of hydrogen peroxide²² and of lipid hydroperoxides,¹¹ and seems reasonably stable. It has not hitherto been applied for the colorimetric determination of lipid hydroperoxides. The colour-producing system chosen was the oxidative coupling of *N,N*-diethylaniline (DEA) with 4-aminoantipyrine (4-AA)²³ as the hydrogen-donor. A novel aspect is the use of acetonitrile to enhance the performance of the method.

EXPERIMENTAL

Materials

All chemicals used were of analytical grade or the purest grade available and used as received.

Microperoxidase (MP-11) was purchased from Sigma Chemical Co., Ltd. Horseradish peroxidase (E.C. 1.11.1.7), methyl linoleate and

*Author for correspondence.

oil samples were obtained from Wako Pure Chemical Industries, Ltd. *tert*-Butyl hydroperoxide was obtained from Kishida Chemical Co., Ltd.

Preparation of hydroperoxide sample solutions

Methyl linoleate hydroperoxide was prepared from autoxidized methyl linoleate and purified by column chromatography as described by Frankel *et al.*²⁴ A 1.0-ml portion of this product was dissolved in *n*-hexane to give a concentration of 2.38mM. Solutions of *tert*-butyl hydroperoxide and hydrogen peroxide were prepared by diluting the commercial reagents with redistilled water to give concentrations of 4.50 and 0.56mM, respectively. The oil samples were dissolved in ethanol, to give concentrations not exceeding 1% (because of the low solubility of oils in ethanol). Butter and lard samples were analysed as such.

Reagents

MP. MP (2 mg) was dissolved in redistilled water and the solution diluted to 100 ml.

HRP. HRP (20 mg) was dissolved in redistilled water and the solution diluted to 100 ml.

4-AA. A 0.5% solution in redistilled water.

Tris-HCl buffer (pH 7.2). Prepared by mixing 250 ml of 1.2M tris(hydroxymethyl)amino-methane solution with water, adjusting the pH with 0.2M hydrochloric acid, and diluting to 1000 ml with redistilled water.

Methanolic sodium hydroxide solution, 1%.

Standardization of hydroperoxides and hydrogen peroxide

The hydrogen peroxide solution was standardized by iodometric titration catalysed by ammonium molybdate²⁵ and by titration with potassium permanganate.²⁶ The *tert*-butyl hydroperoxide solution was standardized by Pobiner's titanium complex method.⁸ For other hydroperoxide samples, Wheeler's iodometric method² was used. The peroxide values of the oil and fat samples slowly changed with time, but were of the order of 133 (soybean oil), 26 (olive oil), 399 (linseed oil), 116 (salad oil), 0.6 (fresh salad oil), 0.8 (butter) and 10 (lard).

Procedure

Place a known volume of hydroperoxide or oil sample solution or a known weight of fat sample in a 10-ml glass-stoppered centrifuge tube (1-cm diameter, graduated at 0.1-ml intervals). The sample weight should preferably not

exceed 0.01 g for an oil sample or 0.2 g for a fat. Make up to 1.0 ml with ethanol. If the hydroperoxide was dissolved in *n*-hexane, add 1 ml of ethanol. Add 2 ml of methanolic sodium hydroxide solution and shake the tube vigorously for 5 min. Add 0.4 ml of 0.5M sulphuric acid to neutralize the reaction mixture, then 1 ml of Tris buffer, 2 ml of acetonitrile, 1 ml of 4-AA solution, 0.2 ml of DEA and finally the 1 ml of MP solution. Shake the reaction mixture vigorously for 1 min and then incubate it at 37°. After 10 min, measure the absorbance at λ_{\max} (554 nm). If the solution is turbid at this stage, centrifuge it or shake it with 1 ml of *n*-hexane to remove the turbidity. The total volume of the final aqueous phase for measurement of absorbance should be 8.6 ml.

RESULTS AND DISCUSSION

Validation of the determination method for hydroperoxides

The procedure was applied to *tert*-butyl hydroperoxide, methyl linoleate hydroperoxide, lard, butter, soybean oil, olive oil, linseed oil, salad oil and hydrogen peroxide, at various concentrations. The absorbances measured at 554 nm were found to be linearly related to μeq of active oxygen (calculated from the standardization of the hydroperoxide samples), Fig. 1. The values from the different hydroperoxide samples all fall more or less on the same line, so the same calibration plot can be used for all samples. Alternatively a regression equation can

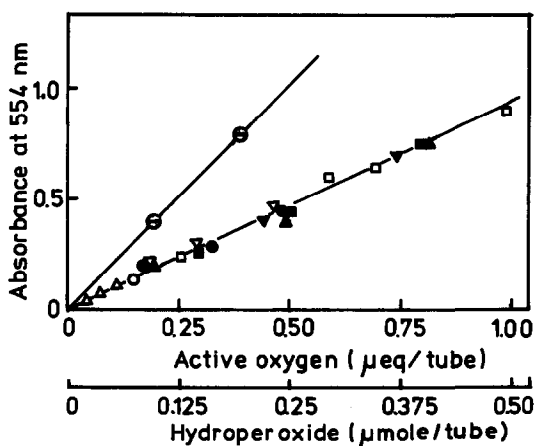


Fig. 1. Relationships between absorbances obtained with different hydroperoxide samples and amounts of active oxygen. Active oxygen (μeq) was converted into hydroperoxide (μmole) in the lower scale: \ominus = hydrogen peroxide; \blacktriangledown = *tert*-butyl hydroperoxide; \blacktriangle = methyl linoleate hydroperoxide; \bullet = soybean oil; \triangle = olive oil; \blacksquare = linseed oil; ∇ = salad oil; \circ = butter; \square = lard.

be used. When methyl linoleate hydroperoxide was used as the standard, the standard deviation of the absorbance, calculated from the deviation of the experimental values from the regression line, was 0.036. Differences in response among various hydroperoxides have sometimes been observed to occur for other methods, where the results were expressed as slopes,⁹ relative rates¹⁷ and relative sensitivities.¹¹ The close similarity of the behaviour of the various hydroperoxide samples in our method makes it very useful for practical analysis. The slope for hydrogen peroxide was about twice that for the hydroperoxides, but the results obtained by the two standardization methods were in agreement, so the difference in slope may be attributable to steric hindrance. Table 1 lists the results obtained by this method and shows the excellent agreement with those obtained by the iodometric method.

Treatment of sample and stability of the coloured product

The lipid sample and the DEA are in the organic phase, while the MP, the buffer solution

Table 1. Determination of hydroperoxides

Sample	Hydroperoxide amount, $\mu\text{eq}/\text{tube}$	
	Iodometric method	Proposed* method
Methyl linoleate hydroperoxide	0.16 ₅	0.16 ₀
	0.49 ₆	0.50 ₆
	0.82 ₇	0.82 ₂
<i>tert</i> -Butyl hydroperoxide	0.45 ₀ †	0.44 ₉
	0.75 ₀ †	0.75 ₀
Soybean oil	0.19 ₉	0.19 ₉
	0.33 ₂	0.32 ₈
	0.53 ₂	0.54 ₈
Olive oil	0.03 ₉	0.03 ₉
	0.06 ₆	0.06 ₆
	0.10 ₅	0.10 ₄
Linseed oil	0.25 ₆	0.25 ₆
	0.51 ₃	0.51 ₃
	0.77 ₀	0.77 ₀
Salad oil	0.17 ₆	0.20 ₆
	0.29 ₅	0.29 ₅
	0.47 ₂	0.46 ₄
Butter	0.14 ₉	0.12 ₈
Lard	0.60 ₀	0.60 ₀
	0.70 ₀	0.69 ₉
	1.00 ₀	1.00 ₀

*Oil samples of less than 0.01 g were used in every case.

†The hydroperoxide was determined by the titanium complex method.

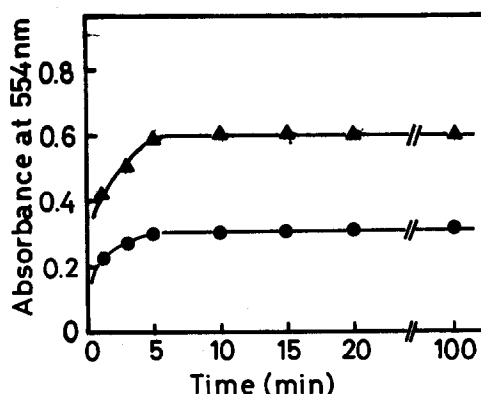


Fig. 2. The colour development and stability of the coloured product: \blacktriangle = methyl linoleate hydroperoxide (active oxygen, 1.94 $\mu\text{eq}/\text{tube}$); \bullet = soybean oil (active oxygen, 0.86 $\mu\text{eq}/\text{tube}$).

and the 4-AA are in the aqueous phase. To avoid the inherent difficulties of using a two-layer reaction system, it was necessary to select a suitable solvent system. In view of the subsequent treatment and the stability of the colour developed, ethanol (which is relatively polar) was chosen as the solvent for the lipid sample. Since it has been reported that methanolic sodium hydroxide solution extracts hydroperoxides from hydrocarbons,⁸ and is also used for esterification of oils and fats, treatment with this reagent was introduced into the procedure, resulting in either a clear homogeneous layer, or an emulsified layer in the case of larger lipid samples with a low level of hydroperoxide. In either case the reaction was facilitated, so the mixture needed to be shaken for only about 1 min, and the rate of the reaction was improved. Figure 2 shows the results obtained in this manner. A constant absorbance at 554 nm is reached after about 5 min and remains stable for at least 100 min at room temperature and under room illumination.

Effect of pH and buffer

The effect of pH and the choice of buffer on the absorbance was studied with methyl linoleate hydroperoxide and the Tris-HCl and phosphate buffers, which have maximum capacity near pH 7, which is commonly employed for enzymes. The optimal choice was Tris-HCl buffer at a pH of about 7.0.

Determination of low level hydroperoxide in oil samples and the effect of antioxidants

Various amounts (up to 0.40 g) of the fresh salad-oil sample were placed in the centrifuge tube directly, and not as a solution in ethanol.

The entire reaction proceeded in the emulsified mixture and the turbidity was finally removed by shaking with *n*-hexane. A good proportionality between the absorbance and the sample weight was observed. The peroxide value of this salad oil was found to be 0.675. Any antioxidant present, such as the tocopherol usually existing in oil samples, may interfere in any analytical method based on redox reactions for the hydroperoxide, unless separated beforehand, *e.g.*, by high-pressure liquid chromatography.¹⁰⁻¹⁴ The influence of antioxidants in the present method was studied with methyl linoleate hydroperoxide and the standard-addition method by use of autoxidized soybean oil and fresh salad oil. The influence on the slope of the calibration line was negligible if the amount of oil sample was restricted to that given in the basic procedure, as shown by lines 1, 2 and 3 in Fig. 3, but the slope was decreased if a relatively large amount of fresh oil (~ 0.2 g) was used (line 4), probably because the antioxidant competes with the hydrogen-donor (the colour-producing reagent) for the active species produced in the enzyme reaction. It is therefore preferable to determine low hydroperoxide contents in oil samples by the standard-addition method, but with small sample volumes to minimize possible interferences.

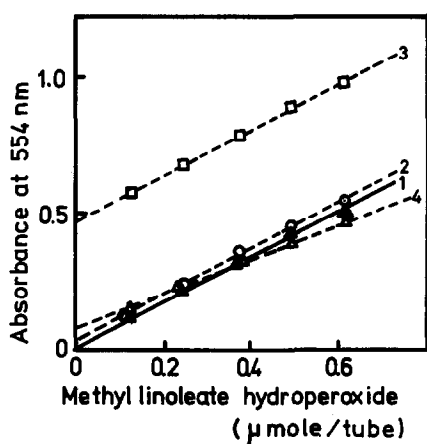


Fig. 3. Influence of antagonistic constituents in oil samples. (1) Calibration line constructed with methyl linoleate hydroperoxide. (2) Fresh salad oil solution in ethanol was added to (1). The oil-ethanol solution (1.00 g/100 ml) was prepared from fresh salad oil (PV 0.780). An aliquot of 1.0 ml of this solution was added to each tube. (3) Autoxidized soybean-ethanol solution was added to (1). The oil-ethanol solution (1.00 g/100 ml) was prepared from soybean oil (PV 133). An aliquot (0.2 ml) of this solution was added to each tube. (4) Fresh salad oil (0.20 g) was added to (1).

Microperoxidase and horseradish peroxidase

The behaviour of the MP in the reaction system was compared with that of the enzyme HRP in the same system in order to examine the similarity of the mechanism of their action. The concentration of HRP used in the experiments was that reported as optimum in other papers. Its enzyme activity was estimated by the guaiacol method²⁷ and found to be 500 units/ml MP resembled HRP in behaviour but gave higher sensitivity. MP seems to give a peroxidase-type reaction.

Stimulation of the MP system acetonitrile

It was found that the formation of colour in the MP reaction system was enhanced by the presence of acetonitrile, which increased both the rate of the reaction and the absorbance. A few spectra were recorded in the range from 340 to 700 nm with hydrogen peroxide and methyl linoleate hydroperoxide, to explore the behaviour of acetonitrile in the MP-catalysed reaction. The spectrum of MP showed an absorption maximum at about 400 nm, but developed an absorption peak at about 470 nm in the presence of hydrogen peroxide. This change was similar to that reported in the case of the enzyme HRP.²⁸ The presence of acetonitrile in the reaction system decreased the absorbance at 470 nm for the complex, simultaneously increasing the absorbance at 400 nm for the free MP. These changes become progressively greater with increasing concentration of acetonitrile, with an isosbestic point.

The effect of acetonitrile in the presence of the hydrogen-donor (the colour-producing reagent) and MP, was examined with hydrogen peroxide and methyl linoleate hydroperoxide. In both cases, the absorbance of the reaction product at 554 nm increased with acetonitrile concentration, in parallel with the increase in absorbance observed at 400 nm in the hydrogen peroxide-acetonitrile-MP system (in the absence of the hydrogen donor) described above. However, the enhancement of the absorbance at 554 nm was not observed when the MP solution was added before the acetonitrile. Similar effects were obtained with HRP instead of the MP.

Even though the phenomenon is still not fully elucidated, according to the literature²⁸⁻³² the role of acetonitrile is probably as follows. The hydroperoxides are known to react with hydrogen-donors to produce superoxide free-

radicals, and these can form relatively inactive complexes with peroxidases. Presumably the acetonitrile, if added first, solvates either the superoxide radicals or the MP, in either case preventing inactivation of the latter. It is reported²⁸ that some other nitrogen compounds, such as ammonia, pyridine, and imidazole, also have a protective action on peroxidases, by preferential occupation of active sites. Further investigation seems needed, however.

CONCLUSION

A new colorimetric method with MP is proposed for the determination of hydroperoxides in oils and fats. The method permits the analysis of oil and fat samples with satisfactory sensitivity and reproducibility. The reactivity of MP seems to be the same towards different hydroperoxides. The performance of the reaction system is enhanced by acetonitrile. This effect may be applicable to other analytical systems using peroxidase. The sensitivity of the MP method would be increased by use of a hydrogen-donor that produces a dye with a higher molar absorptivity.

REFERENCES

1. C. H. Lea, *Proc. Roy. Soc.*, 1931, **108B**, 175.
2. D. H. Wheeler, *Oil and Sheep*, 1932, **9**, 89.
3. T. Takagi, Y. Mitsuno and M. Masumura, *Lipids*, 1978, **13**, 147.
4. T. Asakawa and S. Matsushita, *ibid.*, 1980, **15**, 965.
5. S. Hara, M. Shida and T. Totani, *Yukagaku*, 1988, **37**, 119.
6. U. Fielder, *J. Am. Oil Chem. Soc.*, 1974, **51**, 101.
7. R. O. Sinnhuber, T. C. Yu and T. C. Yu, *Food Res.*, 1958, **23**, 626.
8. H. Pobiner, *Anal. Chem.*, 1961, **33**, 1423.
9. J. Peinado, F. Taribio and D. Pérez-Bendito, *Talanta*, 1986, **33**, 914.
10. T. Miyazawa, K. Yasuda, K. Fujimoto and T. Kaneda, *J. Biochem.*, 1988, **103**, 744.
11. Y. Yamamoto, M. H. Brodsky, J. C. Baker and B. N. Ames, *Anal. Biochem.*, 1987, **160**, 7.
12. K. Asakawa, H. Ohruri and H. Meguro, *Anal. Lett.*, 1988, **21**, 965.
13. M. O. Funk, *Free Radical Biol. Med.*, 1987, **3**, 319.
14. J. Terao, S. S. Shibata and S. Matsushita, *Anal. Biochem.*, 1988, **169**, 415.
15. P. J. Marshall, M. A. Warso and W. E. M. Lands, *ibid.*, 1985, **145**, 192.
16. R. L. Heath and A. L. Tappel, *ibid.*, 1976, **76**, 184.
17. T. Yamaguchi, *Agric. Biol. Chem.*, 1980, **44**, 2747.
18. K. Kikugawa, T. Nakahara, Y. Taniguchi and M. Tanaka, *Lipids*, 1985, **20**, 475.
19. N. Ohishi, H. Ohkawa, A. Mikke, T. Tatano and K. Yagi, *Biochem. Int.*, 1985, **10**, 205.
20. S. S. Shibata, J. Terao and S. Matsushita, *Lipids*, 1986, **21**, 792.
21. N. Feder, *J. Histochem. Cytochem.*, 1970, **18**, 911.
22. B. Olsson, *Anal. Chim. Acta*, 1982, **136**, 113.
23. P. Kabasakalian, S. Kalliney and A. Westcott, *Clin. Chem.*, 1974, **20**, 606.
24. E. N. Frankel, C. D. Evans, D. G. McConnell, E. Selke and H. J. Dutton, *J. Org. Chem.*, 1961, **26**, 4663.
25. I. M. Kolthoff and E. B. Sandell, *Textbook of Quantitative Inorganic Analysis*, 3rd Ed., p. 600. Macmillan, New York, 1952.
26. *Idem, op. cit.*, p. 574.
27. B. Chance and A. C. Maehly, *Methods Enzymol.*, 1955, **2**, 746.
28. B. H. J. Bielski, D. A. Comstock, A. Haber and P. C. Chan, *Biochim. Biophys. Acta*, 1974, **350**, 113.
29. I. Fridovich, *J. Biol. Chem.*, 1963, **238**, 3921.
30. I. Yamazaki and L. H. Piette, *Biochim. Biophys. Acta*, 1963, **77**, 47.
31. H. P. Misra and I. Fridovich, *Anal. Biochem.*, 1977, **79**, 553.
32. T. Odajima and I. Yamazaki, *Biochim. Biophys. Acta*, 1972, **284**, 355.

MODIFICATION OF THE METHYLENE BLUE METHOD FOR SPECTROPHOTOMETRIC SELENIUM DETERMINATION

J. L. BERNAL, M. J. DEL NOZAL, L. DEBAN and F. J. GOMEZ

Department of Analytical Chemistry, Faculty of Sciences, University of Valladolid,
Valladolid, Spain

O. DE URIA, J. M. ESTELA and V. CERDA*

Department of Chemistry, University of the Balearic Isles, E-07071 Palma de Mallorca, Spain

(Received 28 December 1987. Revised 19 December 1989. Accepted 13 March 1990)

Summary—The spectrophotometric method for Se(IV) determination based on its catalytic effect in the reduction of Methylene Blue (MB) by sulphide is modified. The variables that affect the decolorization of MB were taken into account: reagent concentrations, order of addition, mixing and standing times, pH, ionic strength, temperature, solution volume, wavelength, *etc.* The results of this study allowed a decrease of the determination limit and, by selection of the appropriate analytical conditions, choice of optimum linear range according to the selenium content in the sample. The lower limit range is 15–75 $\mu\text{g/l.}$, with 3% relative standard deviation and no systematic errors. Procedures for overcoming several potential interferences were studied. The proposed method was applied to several environmental samples and the results were compared with those obtained by other standard methods.

Increasing interest in environmental and pollution control has promoted development of analytical techniques and methods for the submicrogram range. In this context, one of the most interesting problems is determination of selenium in water and other natural samples.

Selenium is an essential element for animals,¹ and is usually present in very low concentrations in vegetables. Therefore, its addition to fodder is often required, but the necessary quantities lie within a very narrow range, above which the element is very toxic. Hence much effort has been devoted to the development of new methods or modification of old ones for its determination and speciation, as shown in the paper of Robberecht and Van Grieken on selenium determination in waters.²

West and Ramakrishna³ and Goto *et al.*⁴ have proposed a visual method for selenium determination based on its catalytic effect on the reduction of Methylene Blue (MB) by sulphide,⁵ and stated that this catalysed reaction cannot be spectrophotometrically monitored owing to the poor reproducibility of decolorization of the

solution, particularly at very low selenium concentrations. Later, Mesman and Doppelmayr,⁶ in an assessment of alternatives to the 3,3'-diaminobenzidine (DAB) methods,⁷⁻¹⁶ reported that if polychromatic radiation was used instead of monochromatic, a photometric MB method would give good results.

The aim of the present work was to make a thorough study of the parameters involved in the Methylene Blue reaction, in order to find an alternative to the piarselenol method, which is slow, and very pH-dependent. The modified MB method developed as a result allows the use of a spectrophotometer and has been applied to analysis of a fodder corrector and different kinds of waters.

EXPERIMENTAL

Reagents

All reagents were of analytical grade and dissolved in demineralized distilled water.

Selenium(IV) solution (1 mg/l.). Prepared from anhydrous sodium selenite.⁵

Methylene Blue solution, 0.01%.

Sulphide solution. Prepared by dissolving 2.4 g of sodium sulphide 9-hydrate, 2.40 g of anhydrous sodium sulphite and 4 g of sodium

*Author for correspondence.

hydroxide in 100 ml of distilled water, and kept in a dark bottle in the refrigerator.

Disodium EDTA solution (0.25M).

Disodium EDTA-triethanolamine solution.

Prepared by dissolving 25.0 g of EDTA in water, adding 50 ml of triethanolamine, and water to give a final volume of 1 litre. The EDTA concentration is 0.067M.

Procedures

Kinetic Methylene Blue method. To a 5-ml standard spectrophotometric cell, 1.5 ml of formaldehyde solution, 0.4 ml of triethanolamine-EDTA solution, 0.6 ml of 0.01M sulphide solution, V ml ($V < 1.5$) of selenite solution (up to 5 mg/l. Se), $(1.5 - V)$ ml of water and 1.0 ml of 0.001% MB solution were added in that order. The cell was then kept in a thermostat at 15° for 1 min, after which the absorbance was measured at 645 nm against a similar mixture in which the MB was replaced by water.

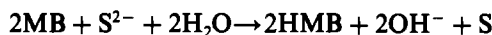
To maximize the reproducibility, it is strongly recommended to follow the times proposed in Table 1, and run the calibration along with the samples.

3,3'-Diaminobenzidine (DAB) method. The procedure recommended by Hoste¹⁵ was used.

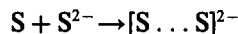
Determination of Se in a fodder corrector. One gram of finely powdered sample was placed in a 250-ml beaker and 10 ml of a 1:1 v/v mixture of concentrated sulphuric and nitric acids were added. This solution was heated, with replacement of acid evaporated, until the mixture was clear. This solution was concentrated to 3 ml, cooled and diluted to 50 ml with demineralized water. The pH was adjusted to 10 with sodium hydroxide and the solution was filtered, and finally diluted accurately to 100 ml with water. The recommended kinetic procedure was applied to 1 ml of this solution.

RESULTS AND DISCUSSION

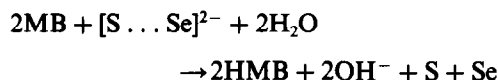
Methylene Blue is reduced by sulphide according to the reaction:



When an excess of sulphide is present, the sulphur obtained is dissolved to give polysulphides:



which in the presence of selenium give selenosulphides $[\text{S} \dots \text{Se}]^{2-}$ and the reaction



takes place. The elemental sulphur and selenium produced dissolve again to give polysulphides or selenosulphides.

The $[\text{S} \dots \text{Se}]^{2-}$ ion reacts more quickly than the S^{2-} ion, and since it is regenerated owing to the excess of sulphide ions in the medium, the catalytic effect of selenium in the reaction is evident. As this effect is caused by elemental selenium, the following reaction is required:



In order to avoid polysulphide formation it is recommended to add sodium sulphite, which is transformed into thiosulphate and does not interfere in the reaction.

From a related paper,¹⁷ several recommendations can be made for use of this reaction, as follows.

The pH should be in the range 8.5–12.

As Fe(III) accelerates the reaction, triethanolamine should be added to avoid this undesirable effect, by masking the Fe(III), which is a very common species in real samples.

Formaldehyde should be added to stabilize the blank.

Table 1. Timetable for the MB method

Starting time	Operation	Final time
—	Take 1.5 ml of 36% HCHO	—
0'00"*	Add 0.4 ml of 0.067M EDTA	0'30"
0'30"	Add 0.6 ml of 0.01M S^{2-}	2'00"
2'00"	Add V ml of SeO_3^{2-} (5 $\mu\text{g}/\text{ml}$ Se)	3'30"
3'30"	Add $(1.5 - V)$ ml of H_2O	5'00"
5'00"	Add 1.0 ml of 0.001% MB	6'00"
6'00"	Stir the mixture	7'00"
7'00"	Let the mixture settle	8'00"
8'00"	Start the recorder	—

Total volume 5 ml; wavelength 645 nm; band-width 10 nm; temperature 15°; pH 10.15

*Start stopwatch.

The large number of interferences, above all copper, should be taken into account.

Absorption spectra

To obtain the absorption spectra of MB under different conditions, much more dilute solutions were used than those proposed in the literature, and a 0.001% MB solution was considered the best.

The absorption spectra obtained at different times have a common maximum at 645 nm (Fig. 1), and this is confirmed by the second derivative curve.

The kinetic curves, Fig. 2, show an induction period before the initial decolorization of the Methylene Blue. The slopes of these curves are independent of the Se concentration, making the induction period and the completion of decolorization equivalent parameters from the analytical point of view, but also making it impossible to use the classic kinetic methods

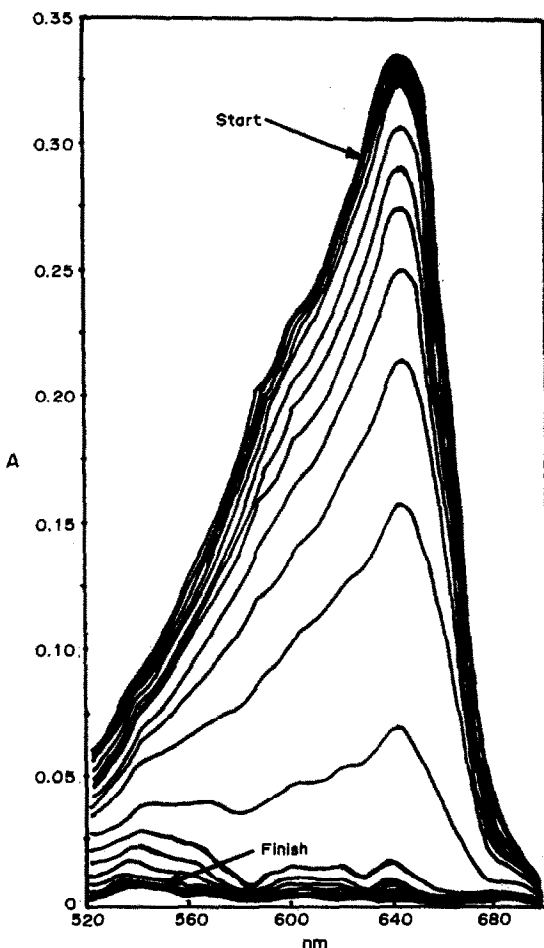


Fig. 1. Absorption spectra of 0.001% Methylene Blue taken at 10-min intervals.

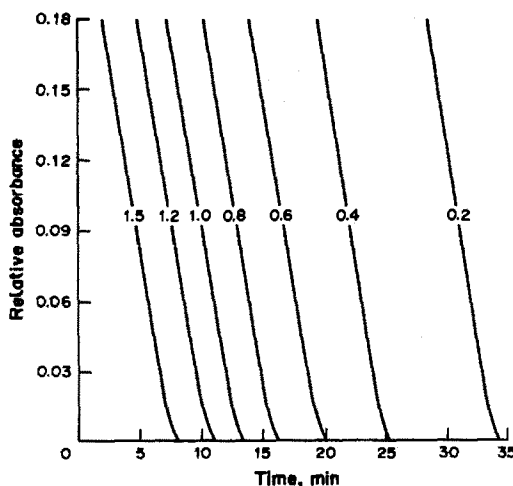


Fig. 2. Kinetic curves of the Methylene Blue reduction.

of analysis (initial slope, fixed time and fixed absorption methods).

Reaction variables

Figure 3 shows the great effect of pH on the kinetics of the reaction, the induction period increasing at pH > 9, especially at pH > 11. The recommended pH of 10.5 can be fixed by use of the proper reagents (EDTA and sulphide solutions), avoiding the need for any additional reagents. As could be expected, the temperature also greatly affects the reaction kinetics (Fig. 3). A room temperature of 20° was selected for further experiments.

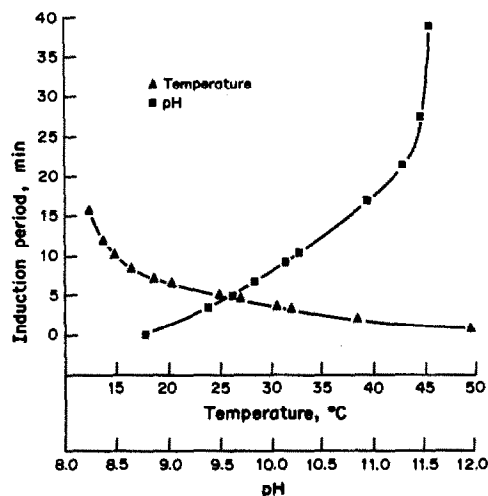


Fig. 3. Effects of pH and temperature (pH 10.5) on the induction period of the MB reduction: 1.5 ml of 36% HCHO + 0.4 ml of 0.067M EDTA in triethanolamine + 0.6 ml of 0.01M S²⁻ + 1 ml of 5- μ g/ml Se + 1 ml of 0.001% MB + up to 0.5 ml of pH modifier (dilute HCl or NaOH) + water to a total volume of 5 ml; wavelength 645 nm.

Formaldehyde not only increases the stability of the blank, as stated elsewhere,³ but also modifies the induction period, which decreases with an increase in formaldehyde content. We selected use of 1.5 ml of 36% formaldehyde solution for a final volume of 5 ml, since this gave the highest sensitivity.

The effect of the EDTA concentration is interesting, the induction period increasing to a maximum and then declining again with increased amount of EDTA.

The amount of sulphide is also of great importance in the kinetics of the reaction; with 0.1 ml of 0.01M sulphide, the induction period is about an hour, whereas with 1.0 ml or more the reaction is almost immediate.

As stated above, the concentration of MB was dramatically decreased, since this modifies not only the induction period, but the shapes and slopes of the kinetic curves as well.

The influence of the concentrations of the reagents (varied one at a time) on the induction period are all represented in Fig. 4. It is clear that there is a complicated interplay of effects.

Different combinations of the order of addition of the reagents were systematically tested. The best results for reproducibility were obtained with HCHO first, then EDTA, S²⁻, Se(IV), and MB last.

Calibration graph

Two very important aspects of the calibration plot have to be taken into account. (1) There is an exponential influence of the selenium concentration on the induction period, and therefore a semi-logarithmic calibration plot has to be used. (2) By an appropriate selection of the analytical parameters, the calibration can cover any desired range from $\mu\text{g/l.}$ to mg/l. We selected for a typical application (analysis of fodder corrector), a 0.2–1.5 $\mu\text{g/ml}$ range.

If a lower pH (9) and a higher HCHO concentration (2 ml of 36% HCHO) are used, a linear relation is achieved over the 0.015–0.075 $\mu\text{g/ml}$ range.

The relative standard deviation (r.s.d.) for 1 $\mu\text{g/ml}$ of Se was 2.8% ($n = 16$).

Foreign ion effects

An exhaustive study of potential interferences was made, with 1-g/l. solutions of the ions. When an interference was evident (induction period >5% different from that for the same solution without the interferent present), the concentration was decreased until the effect was no longer observed. Table 2 gives the results.

A lot of these interferences can be obviated in analysis of "real" samples by adjusting the

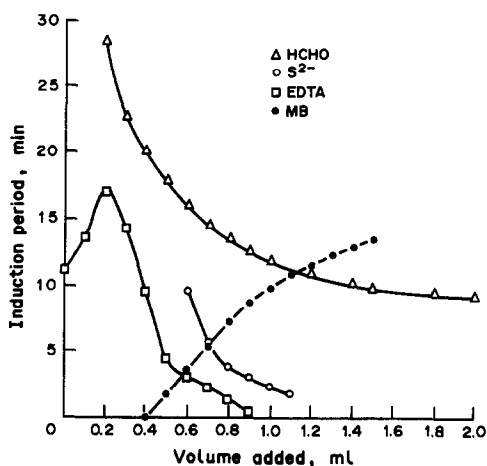


Fig. 4. Influence of formaldehyde, EDTA, sulphide and MB contents on the induction period of the MB reduction, measured at 645 nm.

Variable	0.067M EDTA					
	36% HCHO, ml	in triethanolamine, ml	0.01M S ²⁻ , ml	5- $\mu\text{g/ml}$ Se, ml	0.001% MB, ml	Water, ml
HCHO	V	0.4	0.6	1.0	1.0	2 - V
EDTA	1.5	V	0.6	1.0	1.0	0.9 - V
S ²⁻	1.5	0.4	V	1.0	1.0	1.1 - V
MB	1.5	0.4	0.6	1.0	V	1.5 - V

Table 2. Interferences in determination of 1 $\mu\text{g/ml}$ Se(IV)

Influence	Tolerance ratio to Se, w/w
<i>Positive effect (increased reaction rate)</i>	
Mn(II), Fe(II,III)	10:1
<i>Negative effect</i>	
As(III,V), Sb(III,V), Sn(II,IV), Zn(II)	10:1
<i>Turbidity effect</i>	
Cu(II), Cd(II), Cr(III), Bi(III)	10:1
Ag(I), Hg(I,II), Pb(II), Tl(I)	1:1
<i>Inhibitory effect</i>	
CN ⁻	10:1
IO ₃ ⁻	5:1
NH ₄ ⁺	1:1

pH beforehand to about 10. For example, ammonium ions can be eliminated by heating the sample with sodium hydroxide solution. Therefore, the MB method promises to have adequate selectivity for most likely applications.

APPLICATIONS

Selenium determination in a bird fodder corrector

To confirm its utility, the method was applied to determination of Se(IV) in a bird fodder corrector, the certified mineral composition ($\mu\text{g/g}$) of which was: Se 106, Fe 155, Mn 454, Cu 57.6, Ni 53.0, Co 250 and Zn 122.3.

Appropriate quantities of fodder (*ca.* 1 g) were treated in several ways, such as continued boiling of the sample with (1) water, (2) 2M hydrochloric acid, (3) 2M sodium hydroxide and (4) a 1:1 v/v mixture of concentrated nitric and sulphuric acids. After cooling, the mixtures were filtered (after dilution if necessary) and water was added to the filtrate to give a final volume of 100 ml. The pH values of these extracts were 6, 1, 12 and 0.5, respectively. Appropriate volumes of these solutions were taken and both the proposed MB and the 3,3'-diaminobenzidine methods were applied for determination of Se. The other cations were determined by atomic-absorption spectrometry. The results are given in Table 3. It is evident that the results obtained by the proposed MB method agree with those from the standard

Table 4. Determination of Se in waters

Sample	Se, ng/ml	
	DAB	MB
Fontvella (mineral water)	1.6	1.6
San Narciso (gasified mineral water)	<1	<1
Palma de Mallorca (tap water)	1.3	1.3

3,3'-diaminobenzidine method for a complex matrix, and there is the advantage of saving time and reagents. The best results were obtained with mixed-acid decomposition, with an r.s.d. of 3.8%.

Determination of selenium in waters

The proposed method was also applied to determination of selenium in a number of different waters. Direct application of both the MB and the 3,3'-diaminobenzidine methods gave negative results, and evaporation was required to preconcentrate the sample. The results are shown in Table 4.

Acknowledgement—Thanks are due to the DGICYT (Spanish Council for Research in Science and Technology) for financial support (PA 86-0033).

REFERENCES

1. K. Schwartz and C. M. Foltz, *J. Am. Chem. Soc.*, 1957, **79**, 3292.
2. H. Robberecht and R. Van Grieken, *Talanta*, 1982, **29**, 823.
3. P. W. West and T. V. Ramakrishna, *Anal. Chem.*, 1968, **40**, 966.
4. H. Goto, T. Hirayama and S. Ikeda, *Nippon Kagaku Zasshi*, 1952, **73**, 652.
5. F. Feigl and P. W. West, *Anal. Chem.*, 1947, **19**, 351.
6. B. B. Mesman and H. A. Doppelmayer, *ibid.*, 1971, **43**, 1346.
7. *Standard Methods for the Examination of Water and Wastewater*, 16th Ed., APHA, AWWA, WPCF, Washington, 1985.
8. J. Rossum and P. A. Villarruz, *J. Am. Water Works Assoc.*, 1962, **54**, 746.
9. G. B. Magin, L. L. Thatcher, S. Retting and H. Levine, *ibid.*, 1960, **52**, 1199.
10. J. Hoste and J. Gillis, *Anal. Chim. Acta*, 1955, **12**, 158.
11. K. L. Cheng, *Anal. Chem.*, 1956, **28**, 1738.
12. R. E. Stanton and A. J. McDonald, *Analyst*, 1965, **90**, 497.

Table 3. Determination of Se in a fodder corrector

Sample dissolution medium	Content, $\mu\text{g/g}$					Se*	
	Fe	Mn	Cu	Ni	Co	DAB	MB
Water	11.2	45.0	13	4.2	1.8	106	105
HCl	14.7	45.4	57.6	5.3	2.2	108	108
NaOH	4.2	4.1	2.5	3.0	0.9	107	106
HNO ₃ -H ₂ SO ₄	155	45.2	54.8	5.3	2.5	107	106

*Certified value 106 $\mu\text{g/g}$.

13. E. M. Donaldson, *Talanta*, 1977, **24**, 211.
14. A. Morette and J. P. Divin, *Ann. Pharm.*, 1965, **23**, 169.
15. J. Hoste, *Anal. Chim. Acta*, 1948, **2**, 402.
16. V. Baltensperger and J. Hertz, *ibid.*, 1985, **172**, 49.
17. F. Grases, C. Genestar and R. Forteza, *First International Symposium on Kinetics in Analytical Chemistry*, Córdoba, Spain, 1982.

STUDIES ON THE POLAROGRAPHIC BEHAVIOUR OF ESTAZOLAM

LI QI-LONG and JI GANG

Department of Chemistry, Beijing Normal University, Beijing, 100875, People's Republic of China

(Received 4 October 1989. Revised 29 January 1990. Accepted 26 February 1990)

Summary—In 0.1M $\text{NH}_3\text{-NH}_4\text{Cl}$ buffer (pH 9.2) a sensitive 2-electron reduction wave of estazolam is obtained by single-sweep oscillopolarography. The peak potential is -1.08 V (*vs.* SCE). The peak height is proportional to the concentration of estazolam over the range 1.0×10^{-7} – $9.0 \times 10^{-6}\text{ M}$. The detection limit is $5.0 \times 10^{-8}\text{ M}$. The behaviour of the reduction wave has been studied and applied to the determination of estazolam. The reduction process is irreversible and the wave shows adsorptive characteristics, the behaviour obeying the Frumkin adsorption isotherm. The adsorption coefficient β is 1.16×10^6 l./mole and the interaction factor α is -1.06 . The mechanism of the electrode reaction is discussed.

Estazolam [8-chloro-6-phenyl-4H-*s*-triazol-(4,3-*a*)-(1,4)-benzodiazepine] is a tranquilizer and has hypnotic properties. Its determination by gas chromatography and mass spectrometry has been reported.¹ Jiménez *et al.* have studied the behaviour of estazolam in sampled d.c. and differential pulse polarography.² A linear relationship between current and estazolam concentration in the range 3.4×10^{-7} – $1.0 \times 10^{-4}\text{ M}$ was reported, and a detection limit of $1.7 \times 10^{-7}\text{ M}$, but these methods have not yet been routinely applied to pharmaceutical analysis. In this work the polarographic behaviour of the drug has been further examined, and its determination is described. The present method is simple, convenient and more sensitive, with a detection limit of $5.0 \times 10^{-8}\text{ M}$.

EXPERIMENTAL

Reagents

A stock solution of estazolam ($1.0 \times 10^{-2}\text{ M}$) in methanol was prepared, and kept in the dark and under refrigeration, and was diluted with methanol as required, to give concentrations of 10^{-5} and 10^{-6} M . A 1M $\text{NH}_3\text{-NH}_4\text{Cl}$ stock buffer solution (pH 9.2) was prepared. All reagents were of analytical grade. Water distilled in a fused-silica still was used throughout.

Apparatus

A model Jp-1A single-sweep oscillopolarograph (Chendu Instrumental Factory, China) was used. The conditions for derivative polar-

ography were: drop-time 7 sec; scan rate 250 mV/sec; potential-scan range from -0.80 to -1.30 V . A three-electrode system was used with a dropping mercury working electrode (DME), platinum counter-electrode and a saturated calomel reference electrode. A model 370-8 Electrochemistry System (EG&G, U.S.A.) was used for cyclic voltammetry, with a three-electrode system consisting of a hanging mercury drop electrode (HMDE) as working electrode, an Ag/AgCl (satd. KCl) reference electrode and the platinum counter-electrode. A model 25 pH-meter (Leici Instrumental Factory, Shanghai, China) was used for pH determinations. The electrolytic cell was a 10-ml beaker. All experiments were performed at room temperature, and dissolved oxygen was removed from the solutions.

Procedure

Weigh one tablet and transfer it into a 25-ml standard flask and add 10 ml of methanol, shake the flask for 2 min, and dilute the solution to the mark with distilled water. Transfer 0.2–0.5 ml of the suspension by means of a pipette into a 10-ml standard flask, add 1.0 ml of 1M ammonia/ammonium chloride buffer (pH 9.2) and make up to volume with distilled water. Transfer the solution into the polarographic cell, and remove dissolved oxygen by passage of pure nitrogen. Record the derivative oscillographic polarogram from -0.8 to -1.5 V vs. SCE , without accumulation, and measure the peak height at -1.08 V vs. SCE .

RESULTS AND DISCUSSION

Selection of experimental conditions

Various supporting electrolytes, such as sulphuric acid, sodium hydroxide solution, potassium nitrate solution, and pH-9.2 borax, ammonia/ammonium chloride and Britton-Robinson buffers were tested for use, by single-sweep oscillopolarography; the ammonia buffer system was found to be best, the polarogram of estazolam being well defined and the sensitivity reasonably high. In 0.1M ammonia/ammonium chloride (pH 9.2) buffer the peak potential was -1.08 V *vs.* SCE. The relationship between peak current and concentration of estazolam was linear from 1.0×10^{-7} to 9.0×10^{-6} M. The detection limit was 5.0×10^{-8} M.

Study of polarographic behaviour

Effect of accumulation time. If a process is diffusion-controlled, with no adsorptive accumulation, the peak current will be independent of the accumulation time before scanning. If adsorption occurs, the peak current increases with increasing accumulation time. Figure 1 shows that the peak current for estazolam increased with accumulation time, but limiting current values were reached in 300 and 200 sec for solution of 5×10^{-7} and 1×10^{-6} M estazolam respectively, indicating that adsorption took place.^{3,4}

Effect of scan rate. According to the Randles-Ševčík equation for a diffusion-controlled process, the peak current (I_p) is directly proportional to the square root of the scan rate (\sqrt{v}). For adsorption, however, I_p is proportional to v .

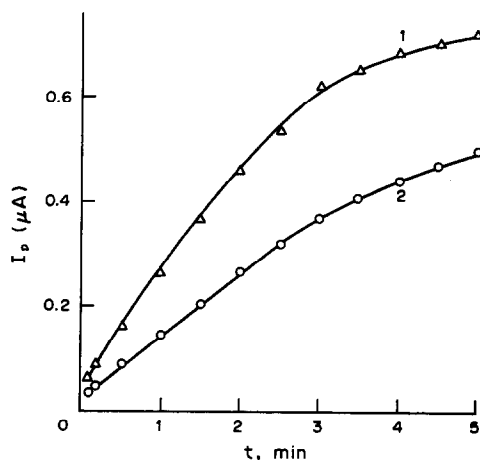


Fig. 1. Effect of accumulation time at -0.80 V: 0.1M NH_3-NH_4Cl , pH 9.2; estazolam concentration, (1) 1.0×10^{-6} M; (2) 5.0×10^{-7} M.

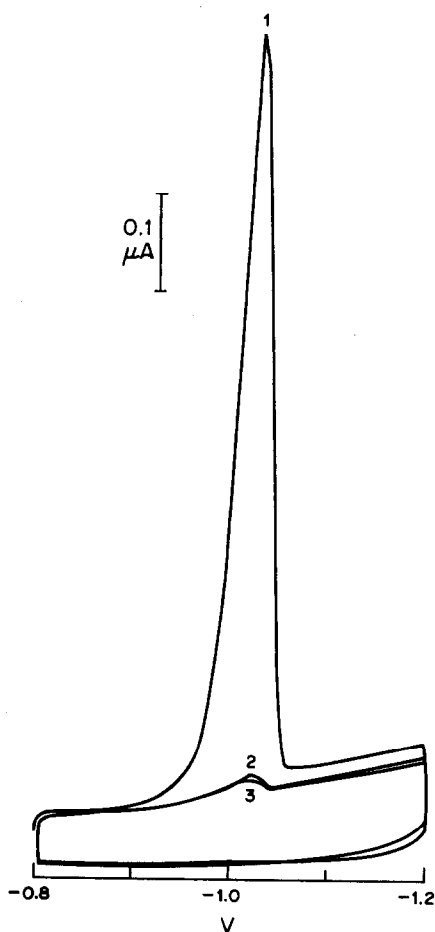


Fig. 2. Repetitive cyclic voltammograms: 0.1M NH_3-NH_4Cl , pH 9.2; 1.0×10^{-6} M estazolam. Accumulation for 3 min at -0.80 V. Scan rate 100 mV/sec.

The peak potential for estazolam became more negative with increasing v , and I_p was a linear function of v for both 5×10^{-7} and 1×10^{-6} M estazolam, again indicating an adsorption process.^{5,6}

Further evidence of an adsorption process was that the presence of a low concentration (0.005%) of gelatin or polyvinyl alcohol strongly depressed the peak current, and that the peak current decreased with temperature increase above 17° .

Repetitive cyclic voltammograms. The repetitive cyclic voltammetry of the system was investigated with a model 370-8 Electrochemistry System with an HMDE. Typical cyclic voltammetric curves are shown in Fig. 2. Estazolam gives a cathodic peak at about -1.04 V (*vs.* Ag/AgCl, satd. KCl). No peak was observed on the anodic branch, indicating irreversibility of the reduction. The reduction peak in the first scan after an accumulation time of 3 min was much higher than that in the second scan.

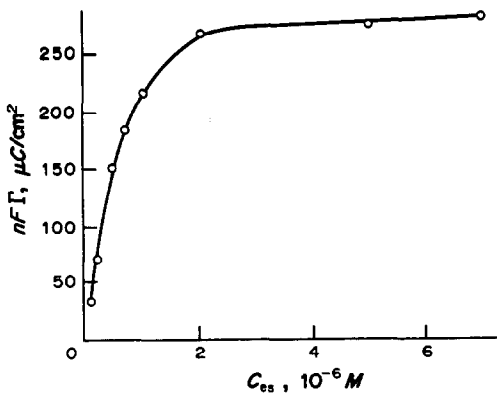


Fig. 3. Plot of $n\Gamma$ vs. C_{es} .

Electron numbers involved in the electro-reduction. Laviron⁷ has proposed that for an irreversible process with adsorption

$$W_{1/2} = 2.44 \frac{RT}{\alpha n F} = \frac{62.5}{\alpha n} \text{ mV (at } 25^\circ)$$

where $W_{1/2}$ is the width at half-height, n is the number of electrons involved in the reduction and α is the transfer coefficient. Duplicate linear sweep polarograms of estazolam gave $W_{1/2}$ values of 47 and 48 mV at 25° , which gives $\alpha n = 1.3$. The number of electrons was determined by constant-potential coulometry. Two 40.0-ml portions of 0.1M ammonia/ammonium chloride buffer, one $1.0 \times 10^{-3}M$ in estazolam and the other $8.0 \times 10^{-4}M$, were electrolysed for

90 min at -1.10 V (vs. SCE), with consumption of 7.38 and 6.34 C, respectively. The values of n thus obtained were 1.9 and 2.05, hence $n = 2$, and α is 0.65.

Determination of the amount adsorbed. After the peak in the linear sweep polarogram, the current decreased to background level, and the area under the peak was determined and the quantity of charge (Q) transferred by reduction was calculated. The amount of estazolam adsorbed per unit area (Γ) was then obtained⁷ from

$$\Gamma = Q/nFA$$

where A is the electrode area. A plot of $n\Gamma$ as a function of estazolam concentration (C_{es}) is shown in Fig. 3. A linear relationship of $\ln[C_{es}(1-\theta)/\theta]$ to θ was found ($\theta = \Gamma/\Gamma_{max}$, where Γ_{max} is the maximum surface coverage), showing that estazolam adsorption satisfies the Frumkin isotherm:⁸

$$\beta C_{es} = \theta \exp[\alpha\theta/(1-\theta)]$$

with adsorption coefficient $\beta = 1.16 \times 10^6$ l./mole and the interaction factor $\alpha = -1.06$.

Like the other triazolobenzodiazepines, estazolam has only one electroactive group. The number of electrons found to be involved in the electrode reaction suggests that the azomethine group is reduced.² The following reduction mechanism for estazolam might be proposed:

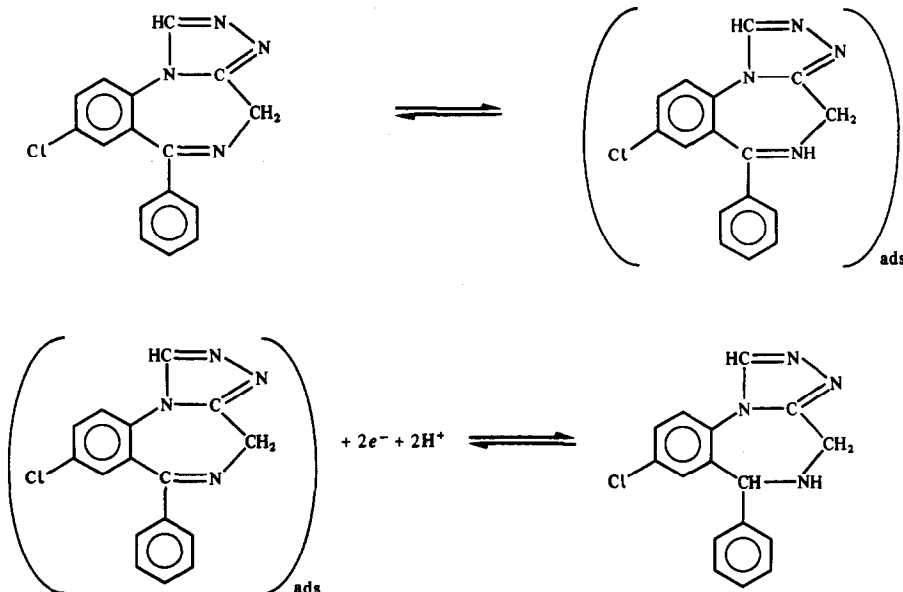


Table 1. Analytical results for estazolam in tablets (mean \pm standard deviation for 6 determinations)

Sample	Estazolam found, mg/tablet	
	This method	Comparison method
1	1.09 \pm 0.02	1.09
2	0.95 \pm 0.03	1.06
3	0.97 \pm 0.01	1.07

Table 2. Recovery experiments

Initial estazolam, μ g	Total found, μ g	Recovery of added estazolam, %
4.48	7.35	97.3
4.72	7.59	97.3
8.96	11.79	96.0
8.96	11.81	96.6

Analysis of tablets

The determination was performed by the standard-addition method. The excipients in the tablets (starch, talc, etc.) did not affect the polarogram. The results of a few analyses of tablets are given in Table 1. The relative standard deviations were about 1–3%. These results

confirm the utility of this proposed method in the determination of estazolam.

In addition, some recovery experiments were done, with addition of 2.95 μ g of estazolam to solutions already analysed for the drug. The results are shown in Table 2.

Acknowledgement—Grateful thanks are due to Dr. Yun Zi-hou for helpful determinations of estazolam by HPLC to provide comparison data.

REFERENCES

1. A. Cailleux, A. Turcant and A. P. Allain, *J. Chromatog. Sci.*, 1981, **19**, 163.
2. R. M. Jiménez, R. M. Alonso, E. Oleaga, F. Vicente and L. Hernandez, *Z. Anal. Chem.*, 1987, **329**, 468.
3. J. Koryta, *Collection Czech. Chem. Commun.*, 1953, **18**, 206.
4. Li Qi-long and Li Song-mei, *Fenxi Ceshi Tongbao*, 1989, **3**, 45.
5. R. A. Osteryoung, G. Lauer and F. C. Anson, *Anal. Chem.*, 1962, **34**, 1833.
6. Li Qi-long and Li Song-mei, *Dianfenxi Huaxue*, 1989, **1**, 65.
7. E. Laviron, *J. Electroanal. Chem.*, 1974, **52**, 355.
8. M. R. Moncelli, L. Nucci, P. Mariani and R. Guidelli, *ibid.*, 1985, **183**, 285.

DETERMINATION OF SILVER IN ALLOYS BY CONTROLLED-POTENTIAL ELECTROLYSIS AT A TANTALUM ELECTRODE

ZHOU NAN*, ZHOU MIN and HE CHUN-XIANG

Shanghai Research Institute of Materials, MMBEI, Shanghai, People's Republic of China

JU ZHAO-QIANG and LIN LI-FEN

The Third Factory of Shanghai Reagent Chemicals, Shanghai, People's Republic of China

(Received 30 October 1989. Revised 7 February 1990. Accepted 22 February 1990)

Summary—A versatile method for the determination of Ag is described. It is based on controlled-potential electrolysis with a tantalum cathode in the presence of lactic acid at pH 2–6. An SCE of double-junction type with sodium formate bridge electrolyte is used as the reference electrode. The role of washing after electrolysis is studied and a novel technique suggested. The standard deviation of the determination is 0.13 mg. A preliminary separation is needed only if W is present. The proposed method has been satisfactorily applied to the analysis of a large number of silver alloys with different compositions.

The most reliable method for the determination of silver in macro amounts is probably controlled-potential electrolysis. A platinum cathode is usually used but has some drawbacks, such as the need for precoating with copper, and the use of tantalum as the cathode material has recently been recommended.¹ It has been satisfactorily used in determination of copper in white-metal bearing alloys.² Here its use is proposed for the determination of silver in alloys of various compositions. Lactic acid is recommended as the complexing agent instead of cyanide.

EXPERIMENTAL

Apparatus

Controlled-potential electroanalyser, type DJS-52 with rotating anode, Rex Instruments, Shanghai. The tantalum cathode was made and pretreated as described earlier.²

Reagents

Analytical-reagent grade chemicals were used unless otherwise specified. Demineralized water should be used throughout.

Nitric acid, chloride-free. Concentrated, and diluted 1 + 3 with water.

Lactic acid, 1 + 1.

Hydrofluoric acid, 40%.

Saturated sodium bicarbonate solution.

Ethanol, 95%.

2,4-Dinitrophenol indicator, saturated aqueous solution.

Methyl Orange indicator solution, 0.1%.

Procedures

General procedure. Transfer a 0.5-g sample (1.0-g for silver metal), weighed to the nearest 0.1 mg, to a 250-ml beaker. Add 10 ml of nitric acid (1 + 3), warm to dissolve the alloy and evaporate the solution nearly to dryness. Cool to room temperature. Add 1 ml of lactic acid (1 + 1) and 10 ml of water, then 1 or 2 drops of 2,4-dinitrophenol indicator and saturated sodium bicarbonate solution dropwise till the appearance of a yellow colour. Dilute to *ca.* 90 ml and add 5 ml of ethanol. Immediately electrolyse with a Ta gauze cathode and SCE reference electrode of double-junction type with 5M sodium formate as salt bridge solution. Gradually adjust the cathode potential to +0.09 V *vs.* SCE, while keeping the electrolysis current at not more than 0.1 A. Wash the split cover glass, the rotating anode and the inner wall of the beaker with a little water. Continue to electrolyse for 10 min. Quickly withdraw the beaker and replace it with another (containing *ca.* 120 ml of water and 1 drop of Methyl Orange indicator) so that the deposited silver is

*Author for correspondence and requests for reprints.
Present address: 99 Handan Lu, 200433, Shanghai,
People's Republic of China.

exposed for the minimum of time. Wash for 30–60 sec. Repeat the washing operation if the wash solution does not turn yellow. Remove the cathode and dip it into ethanol for 30 sec. Dry it in an electric oven at 105° to constant weight. Reweigh it after dissolving the Ag deposit with hot nitric acid (1 + 3) and drying. The difference in weight is the amount of Ag deposited.

Determination of Ag in samples containing graphite. Dissolve the sample by warming with 7 ml of water and 8 ml of concentrated nitric acid. Add 60 ml of water and boil gently for 5 min. Filter off the insoluble material on a close-texture 9-cm filter paper and wash it with hot nitric acid (1 + 3). Evaporate the combined filtrate and washings nearly to dryness, then proceed as in the general procedure above.

Determination of Ag in Ag–Mn alloys. Dissolve the sample by warming with 5 ml of water and 3 ml of concentrated nitric acid. Add 4 or 5 drops of hydrogen peroxide and boil gently to decompose the excess of peroxide. Cool, add lactic acid and follow the general procedure.

Determination of Ag in alloys containing Sn. Transfer the weighed sample to a 250-ml polyethylene beaker, add 2 ml of hydrofluoric acid and nitric acid dropwise to dissolve the sample, with warming in a water-bath if necessary. Cool, add lactic acid and apply the general procedure.

The amount of hydrofluoric acid added may be altered according to the content of Sn in the sample. For samples containing Sn and $\geq 0.8\%$ of Pb, sodium acetate should be used instead of sodium bicarbonate for pH adjustment, to prevent the precipitation of PbF_2 .

In special cases, *e.g.*, in samples containing both Sn and Zr, transfer the weighed sample to a glass beaker, add 3 ml of concentrated nitric acid and 4 ml of sulphuric acid (1 + 1) and heat until white fumes appear. Cool to room temperature, transfer with water to the polyethylene beaker and treat as above.

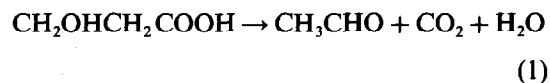
Determination of Ag in Ag–W alloys. Transfer the sample into a small platinum dish, add 2–3 ml of hydrofluoric acid and 5 ml of concentrated nitric acid. Warm to dissolve the sample and evaporate the solution to dryness on a steam-bath. Add 5 ml of ammonia solution and 10 ml of 10% sodium hydroxide solution and stir vigorously to redissolve the silver tungstate. Dilute to 200 ml, add 20 ml of 25% sodium sulphide solution and mix thoroughly. Digest on a steam-bath till the supernatant liquid is

clear. Cool to room temperature, filter off on a close-texture filter paper and wash the precipitate with 2% sodium sulphide solution. Redissolve the precipitate in a few ml of a mixture of hydrogen peroxide and nitric acid, and evaporate the resultant solution nearly to dryness. Then continue as in the general procedure.

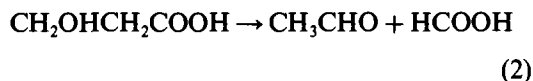
RESULTS AND DISCUSSION

Our preliminary experiments showed that electrolysis of silver in an ammoniacal medium is likely to give low results. To dispense with the use of toxic cyanide in an alkaline medium, some acid media were tested. Perchloric acid medium³ is not always absolutely chloride-free, even after fuming. Nitrous acid⁴ is unsuitable since it catalyses redissolution of deposited silver.⁵ Silver acetate and sulphate are not very soluble in aqueous solutions, and in electrolysis of the sulphate, heavy deposits of silver are likely to be powdery⁶ and Pb(II) and Sn(IV) should be absent. Hence use of sulphuric acid cannot be adopted in a general procedure. Nitric acid is the only choice.

The problem with this medium is the strong tendency for the deposit of silver to be loose. To prevent this a complexing agent may be added. Amines are of little use, however, since they would accelerate the deposition.⁷ Citrate, oxalate and tartrate were found to be unsuitable, but we strongly recommend lactate, though the formation constants of its silver complexes are still lacking. Its special features are that it is readily oxidized after the electrolysis and probably during it as well (at least in part):



and is also readily decomposable:



These oxidation and decomposition products are not harmful in the deposition of silver or the subsequent determinations of the concomitant cations in the analyte solution. Silver lactate is very soluble in water (7.7 g in 100 ml).⁸

The cathode potential at which the electro-deposition of Ag begins depends on the initial concentration. We can only fix that at which it ends. This was determined experimentally. Deposition of 99.4 mg of silver on a Ta (or Pt)

cathode was complete if the final cathode potential was set at +0.09 (or +0.06) V vs. SCE.

The optimum pH for Ag electrolysis was found to be 2–6. The more weakly acidic, the better. To make the background electrolysis current negligible, it is preferable to add just enough acid to dissolve the sample (or to evaporate the excess). In the presence of lactic acid, a clear electrolyte can be obtained at the optimum pH. In the presence of phosphate, *e.g.*, in the analysis of AgCuP brazing alloys, the pH of the electrolyte should be lowered somewhat to avoid precipitation of silver phosphate.

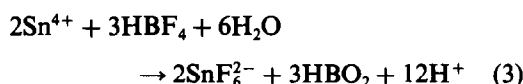
By repeated experiments it was confirmed that at the optimum pH, with lactic acid present, a smooth adherent deposit can be obtained by maintaining the electrolysis current at ≤ 0.1 A.

A general study on controlled-potential electrolysis revealed that some of the analyte ion may be found in the washings (mainly in the first rinse), but not in the electrolysed solution. Hence this residual analyte is not due to incomplete electrolysis, but arises in the washing, which is commonly done by lowering the beaker with the current still on, while rinsing with a stream of water from a wash-bottle.^{9–11} In practice it is hardly possible to wash off immediately all the electrolyte (which is usually acidic) adhering to the cathode, and there is enough time for a small amount of the fresh deposit to be redissolved. Another approach¹² is to siphon off the electrolyte while adding water to maintain the original level of liquid. This is theoretically sound and free from the shortcomings mentioned above, but is time-consuming. We therefore propose rapid withdrawal of the electrolysis beaker with one hand and its prompt replacement with a beaker of wash liquid by the other hand. The thoroughness of the washing is indicated by the colour change of a pH indicator. In this way the amount of the analyte ion in the washings may generally be kept below the level detectable by weighing with an ordinary "fourth-place" balance. It was found that very often no residual silver ion could be detected by AAS at 328.1 nm or spectrophotometrically with 5-[*p*-(dimethylamino)-benzylidene]rhodanine.¹³

It should be noted that ethanol, which is added to prevent the anodic deposition of AgO may itself slowly reduce silver(I) to form a colloidal solution. Therefore the electrolysis should be started immediately at room tem-

perature after addition of the ethanol. Electrolysis at elevated temperatures would be unfavourable since chemical reduction of the silver(I) by both ethanol and lactic acid would be promoted.

For analysis of silver alloys containing tin, hydrofluoric and nitric acids should be added successively for dissolution, to prevent formation of colloidal metastannic acid; 1.2 ml of concentrated hydrofluoric acid suffices to complex 450 mg of tin(IV). Fluoroboric acid was also tried for this purpose as it does not interfere in the electrolysis of silver solutions (Table 1), but it was found that the following reactions take place when tin(IV) is present:



The metaboric acid produced causes trouble by forming insoluble silver metaborate. If both lactic and hydrofluoric acids are present, tin(IV) can be kept in solution at the optimum pH.

A special case is the presence of W(VI). Erratic results were obtained by the general procedure. It was found that the residue from the dissolution and evaporation can only be redissolved with appropriate amounts of ammonia and sodium hydroxide in combination (either alone is of no use, as Ag_2WO_4 is very insoluble in water¹⁴). Electro-deposition of silver in this medium was found to be possible, but co-deposition of tungsten was still significant, presumably owing to adsorption. Hence a preliminary separation of silver from the tungsten (100–400 mg) is indispensable. Precipitation of Ag_2S with sodium sulphide is used for this purpose (Table 1) as Ag_2S is not soluble in alkali-metal sulphide nor polysulphide solutions.¹⁵ Thiourea¹⁶ was also tried as the source of sulphide but unsatisfactory results were obtained.

The effects of diverse ligands and cations are summarized in Table 1. It should be noted that in contrast to electrolysis in nitric or phosphoric acid medium,¹⁷ the presence of nitric, lactic and hydrofluoric acids in a weakly acidic medium makes considerable amounts of Sn(IV) tolerable. This increases the versatility of the proposed method and is of practical significance, for the present trend in industry is the

Table 1. Effects of diverse ligands and cations

Ligand or cation	Added		Ag(I), mg	
	ml	mg	Added	Found
Lactic acid (1 + 1)	1		200.0	200.0
	2		200.0	200.1
40% HF	1.2		65.3	65.4
	3		65.3	65.2
40% HBF ₄ solution	10		73.13	73.09
Cu(II)		424	93.4	93.4
Sb(III, V)		5*	137.4	137.4
Sn(IV)		450*	100.2	100.2
W(VI)		249†	251.0	251.0
		400†	100.0	100.1
Pb(II)/Sn(IV)		450/7.2§	103.0	103.0
Sn(IV)/In(III)		445/15*	77.7	77.6
Sn(IV)/Sb(III, V)		419/2.5*	86.6	86.7
Sn(IV)/Zn(II)		333/165*	85.5	85.3
Sn(IV)/Cu(II)/Ni(II)/Zn(II)		441/100		
		25/4.1*	99.4	99.3

*Plus 1.2 ml of 40% HF.

†After preliminary separation by precipitation with sodium sulphide.

§Plus 10.05 ml of 40% HF and pH adjusted with sodium acetate.

increasing use of Ag-Sn alloys to replace the corresponding traditional ones containing Cd, which is a highly toxic pollutant.

In this determination the cations of gold and the platinum-group metals are the only interferences. Potassium cyanide is used for controlled-potential electrolysis of silver in the presence of Pd(II);¹⁸ attempts to dispense with it were unsuccessful. Separation by precipitation of silver chloride was also unsatisfactory, because of adsorption of the palladium [like that¹⁹ of gold(I)]. No clean-cut separation has yet been found.

Under the specified conditions, silver can be determined with a standard deviation of 0.13 mg ($n = 10$), *i.e.*, with the same precision as with a platinum cathode.

Applications

The proposed method has been successfully applied to the determination of silver in various alloys. Some typical results are shown in Table 2.

The precision and accuracy attained meet the requirements of ordinary routine analysis. Only for referee analysis or standardization of certified reference materials is it necessary to incorporate an AAS or spectrophotometric¹³ finish to determine the residual silver. As already noted, the reagents added in the electrolysis procedure can be readily expelled or decomposed. Hence the solution that has been electrolysed can be analysed for other components in the sample. Thus sequential

Table 2. Determination of Ag in some industrial samples by the proposed method.

Sample	Ag found, %	Total analysis, %
Silver wire	99.95	Known to be ≥ 99.9
Silver graphite alloy	94.50	C 4.45
Ag-Cd alloy	90.36	Cd 9.58
Ag-Cu alloy	76.40	Cu 23.54
Ag-Fe alloy	92.83	Fe 7.13
Ag-In alloy	72.03	In 27.90
Ag-Mg alloy	93.75	Mg 6.21
Ag-Mn alloy	83.62	Mn 17.30
Ag-Ni alloy	59.53	Ni 40.19; Cu 0.20
Ag-Pb alloy	2.88	Pb 97.02; Sb 0.03
Ag-Sn alloy	90.81	Sn 9.10
Ag-W alloy	33.99	W 65.87; Co 0.06
Ag-Zn alloy	70.76	Zn 29.18
Ag-Cu-In alloy	64.35	Cu 20.66; In 14.92
Ag-Cu-P alloy	15.59	Cu 76.98; P 6.38
Ag-Cu-Zn alloy	50.06	Cu 39.57; Zn 10.21
Ag-Cu-Cd-Zn alloy	51.88	Cu 21.44; Cd 17.63; Zn 8.98
Ag-Cu-Zn-Sn-Ni alloy	49.78	Cu 18.88; Zn 20.93; Sn 7.77; Ni 2.58
Ag-Cu-Zn-Ni-Mn-alloy	48.40	Cu 18.68; Zn 19.90; Ni 5.36; Mn 7.66

analysis of a single sample is feasible in many cases.

CONCLUSIONS

A versatile method is proposed for determination of Ag by controlled-potential electrolysis with a Ta cathode and SCE reference electrode of double-junction type with sodium formate as bridge salt, at pH 2–6 in the presence of nitric, lactic and hydrofluoric acids. It is applicable to determination of Ag in alloys, except those containing Au and platinum group elements. The presence of residual Ag in the electrolysed solution is not due to incompleteness of deposition but to inefficient washing. Its amount can be made negligible by using the washing operations suggested, and electrolytes of as low an acidity as possible.

Acknowledgements—Grateful thanks are due to The Chinese TDMI Science Foundation for financial support through Project No. 87J51203. Thanks are also due to all members of SRIM's Directorate for permission to publish this paper, and Dr. Li Yu-juan, technical supervisor of the central laboratories of the Hangzhou Factory of Oxygenerators for checking the experimental section.

REFERENCES

1. Zhou Nan and He Chun-xiang, *Talanta*, 1990, **37**, 677.
2. Zhou Nan, Ju Zhao-qiang, Yu Ren-qing, Yao Xu-zhang and Lu Zhi-ren, *ibid.*, 1990, **37**, 701.
3. B. Alfonsi, *Anal. Chim. Acta*, 1958, **19**, 569.
4. G. Norwitz, *ibid.*, 1951, **5**, 106.
5. A. Cohen, *Rationelle Metallanalyse*, p. 278. Birkhäuser, Basel, 1948.
6. L. Erdely, *Gravimetric Analysis*, Part 2, p. 10. Pergamon Press, Oxford, 1965.
7. P. I. Kravtsova, *Elektrokhimiya*, 1971, **7**, 1565.
8. R. C. Weast and M. J. Astle (eds.), *CRC Handbook of Chemistry and Physics*, 63rd Ed., B 144–145. CRC Press, Boca Raton, 1982.
9. ASTM E 53-86a.
10. ASTM E 75-76, 1984.
11. ASTM E 478-82, 1986.
12. ASTM E 53-48, 1978.
13. Zhou Nan, Zhou Min, He Chun-xiang, Ju Zhao-qiang and Lin Li-fen, *Talanta*, 1990, **37**, 531.
14. S. Kotrlý and L. Šucha, *Handbook of Chemical Equilibria in Analytical Chemistry*, p. 211. Horwood, Chichester, 1985.
15. W. F. Hillebrand, G. E. F. Lundell, H. A. Bright and J. I. Hoffman, *Applied Inorganic Analysis*, 2nd Ed., p. 205. Wiley, New York, 1953.
16. R. Sałoniewicz, *Chim. Anal. Warsaw*, 1964, **9**, 509.
17. G. Norwitz, *Metallurgia*, 1953, **48**, No. 285, 47.
18. K. K. Tsujii, *Eisei Shikensho Kenkyu Hokoku*, 1963, No. 18, 13.
19. K. Beyermann, *Z. Anal. Chem.*, 1964, **200**, 183.

ENHANCEMENT OF THE FLUORESCENCE OF THE BERYLLIUM-MORIN COMPLEX BY NON-IONIC SURFACTANTS

WEI FUSHENG, TEN ENJIANG and WU ZHONGXIANG

China National Environmental Monitoring Centre, Beijing, 100012, People's Republic of China

(Received 20 April 1989. Revised 18 February 1990. Accepted 28 March 1990)

Summary—The effect of surfactants on the fluorescence of the beryllium–morin system has been studied. Non-ionic surfactants strongly enhance the fluorescence intensity of the beryllium complex. The addition of Triton X-100 makes possible the fluorimetric determination of submicrogram quantities of beryllium in feebly acidic media (pH 5.8–6.2, hexamine buffer). The fluorescence is excited at 440 nm and measured at 530 nm. The calibration graph is linear up to 10 ng/ml Be and the detection limit is 0.04 ng/ml. The relative standard deviation is 2.2% for beryllium at 0.5 ng/ml concentration and 0.7% for 5.0 ng/ml. The effects of 25 ions commonly found in water have also been studied; Zn^{2+} and F^{-} give the main interference. The method has been applied to the determination of beryllium in water pollution quality-control samples with satisfactory results.

The reaction with morin¹ has been extensively used for determining submicrogram quantities of beryllium in air,^{2,3} sea-water,⁴ rocks⁵ and other samples, but must be applied in alkaline medium.

In recent years, surfactants have been successfully used for improving existing analytical methods and in developing new ones. In micellar media, the sensitivity and selectivity of numerous reactions are improved and metal complexes are generally more stable than when formed in the absence of surfactants. Although most of the analytical work done with surfactants deals with their application to spectrophotometric methods,⁶ they are now also being applied successfully to fluorimetric methods. Their first application in this area was the determination of aluminium with lumogallion in the presence of the non-ionic surfactant poly(ethylene glycol) monolauryl ether.⁷ Enhancement of the fluorescence of the metal–morin complexes in the presence of surfactants has been extensively studied. It has been found that the fluorescence of the morin complexes of Al,^{8,9} Nb,^{10–12} Ta,¹¹ Pb,¹³ Zn,¹⁴ Zr, Hf, Ga, In and Sb(V)⁹ is enhanced by the use of surfactants. Cationic surfactants strongly enhance the fluorescence of the Nb(V)^{10,11} and Ta(V)¹¹ complexes, e.g., cetyltrimethylammonium bromide (CTAB) gives an 80-fold increase for the Nb–morin complex. The anionic surfactant sodium lauryl sulphate (SLS) strongly enhances

the fluorescence of the Zr, Hf, Al, Ga, In and Sb complexes (by a factor of 3–13).⁹ The non-ionic surfactant Genpol PF-20 (ethylene oxide–propylene oxide condensate) strongly increases the fluorescence of the Al,⁸ Pb¹³ and Zn¹⁴ complexes (by factors of 8, 9 and 75, respectively).

In this paper the influences of various surfactants (non-ionic, cationic, anionic and zwitterionic) on the fluorescence intensity of the beryllium–morin complex are studied and the characteristics of the determination of beryllium with morin in feebly acidic media are discussed.

EXPERIMENTAL

Apparatus

A Hitachi 850 fluorescence spectrophotometer was used with 1-cm silica cells and a 5-nm bandpass for both excitation and emission.

Reagents

All reagents used were of analytical grade. *Morin solution, 0.04% in absolute ethanol.* *Hexamine buffer (pH 6.2).* Dissolve 70 g of hexamine in 250 ml of water, and adjust the pH to 6.2 with 1M hydrochloric acid.

Beryllium stock solution, 100 µg/ml. Dissolve 0.0416 g of BeO in 5 ml of sulphuric acid (1 + 1) and dilute to the mark with water in a 150-ml standard flask. Dilute this appropriately with water to obtain a 0.01 µg/ml working solution.

General procedure

To a solution containing 20 ng of beryllium, add 2.0 ml of buffer, 0.5 ml of ethanolic morin solution and 3.0 ml of aqueous 5% Triton X-100 solution. Dilute to volume in a 25-ml standard flask with water and measure the fluorescence intensity at 530 nm, with excitation at 440 nm.

RESULTS AND DISCUSSION

Effect of different surfactants

Figure 1 shows the excitation and emission spectra of the beryllium–morin and beryllium–morin–Triton X-100 systems. The fluorescence intensity of the beryllium complex was greatly increased by adding Triton X-100, and the excitation and emission maxima occurred at 426 and 550 nm, respectively. In this study, optimum linearity and sensitivity were achieved with 440 and 530 nm as the excitation and emission wavelengths, respectively. The fluorescence spectra of the beryllium complexes in the presence of other surfactants were also studied. The results show that the addition of 0.6% of non-ionic surfactant (Triton X-100, Tween 80 and/or the emulsifier OP) increases the fluorescence intensity of the beryllium complexes (by at least 5-fold, 4.5-fold and 4-fold, respectively), whereas the presence of gelatin or the anionic surfactant SLS causes little increase. In the presence of the zwitterionic surfactant dodecyltrimethylaminoacetic acid (DDMAA) or the cationic surfactant CTAB there is again little increase.

Red-shifts (of about 25 nm) were observed in the fluorescence spectra of the beryllium complexes in the presence of Triton X-100, Tween 80, emulsifier OP, CTAB and DDMAA, but not in the presence of gelatin and SLS.

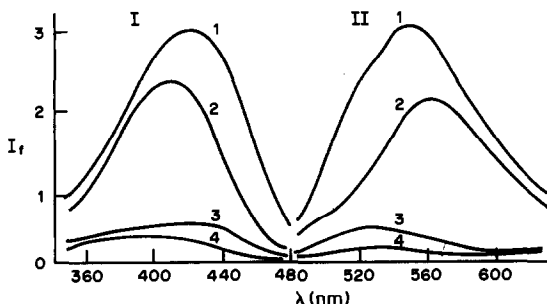


Fig. 1. Excitation (I) and emission (II) spectra: (1) Be–morin–Triton X-100; (2) morin–Triton X-100; (3) Be–morin; (4) morin. Be concentration 1 ng/ml, morin 0.0008%, Triton X-100 0.6%, pH 6.0, room temperature.

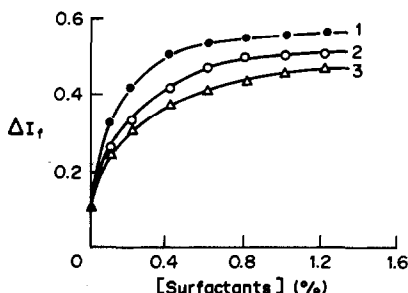


Fig. 2. Effect of non-ionic surfactant concentration: (1) Triton X-100; (2) Tween 80; (3) OP; Be concentration 0.8 ng/ml, morin 0.0008%, pH 6.0, room temperature.

The red-shifts of λ_{em} in the presence of non-ionic surfactants show that the interaction between the beryllium complex and non-ionic surfactants causes the excited state of the complex molecules to change. The beryllium complex molecules may be fixed by the non-ionic micelles, and thus made more rigid and hence the fluorescence quantum yield is raised.

Effect of concentration of non-ionic surfactants

The effect of non-ionic surfactants (Triton X-100, Tween 80 and OP) on the fluorescence intensity of the beryllium complexes is shown in Fig. 2. It was observed that between 0.4% and 1.2% Triton X-100 concentration there was little change in the fluorescence intensity of the beryllium complex. The optimum surfactant concentration was therefore selected as 0.6%.

Effect of pH

In the absence of surfactants the fluorescence of the complex was very weak over the pH range 4.5–9.0. Maximum fluorescence occurred at pH 11.5–12.5, which agrees with the literature.³

The fluorescence intensity of the beryllium complex was strongly enhanced in feebly acidic medium by addition of Triton X-100, but in

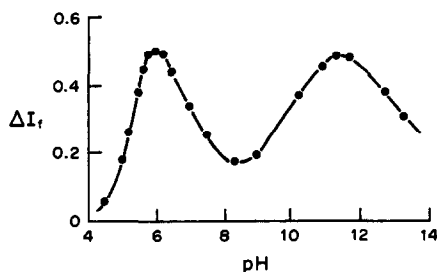


Fig. 3. Effect of pH. Be concentration 0.8 ng/ml, morin 0.0008%, Triton X-100 0.6%, room temperature. (Note: when the pH was less than 8.0, it was adjusted with hexamine buffer; when it was more than 8.0, it was adjusted with borax buffer and 1M NaOH).

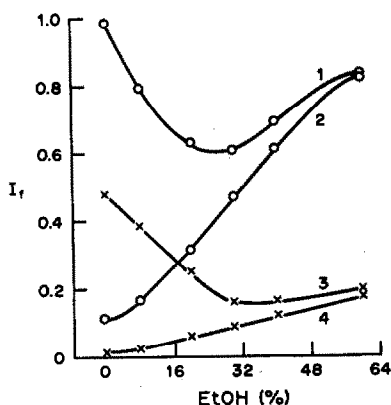


Fig. 4. Effect of ethanol. (1) Be-morin-Triton X-100-ethanol; (2) Be-morin-ethanol; (3) morin-Triton X-100-ethanol; (4) morin-ethanol. Be concentration 0.8 ng/ml, morin 0.0008%, Triton X-100 0.6%, pH 6.0, room temperature.

alkaline medium the fluorescence was practically unaffected by the surfactant.

Effect of morin concentration

When the morin concentration was increased, the fluorescence intensities of the beryllium complex and the morin blank were also increased, but the difference between the two intensities was practically constant over the morin concentration range from 0.00032 to 0.0016%, and 0.0008% was selected as the optimum.

Table I. Effect of co-existing ions on the determination of 20 ng of beryllium in 25 ml of aqueous solution

Co-existing ions	Be found, ng	Relative error, %
10 mg K ⁺	20.4	+2
10 mg Na ⁺	20.0	0
10 mg NO ₃ ⁻	20.6	+3
10 mg Cl ⁻	19.2	-4
10 mg HCO ₃ ⁻	20.3	+1.5
10 mg SO ₄ ²⁻	20.3	+1.5
5 mg As(III)	19.4	-3
0.5 mg Ca ²⁺	18.2	-9
0.5 mg Mg ²⁺	19.8	-1
0.1 mg H ₂ PO ₄ ⁻	18.3	-8.5
10 μg Cr(VI)	19.4	-3
10 μg Cd ²⁺	20.5	+2.5
10 μg Co ²⁺	18.8	-6
10 μg Ni ²⁺	18.8	-6
5 μg V(V)	18.7	-6.5
5 μg La ³⁺	19.5	-2.5
5 μg Mn ²⁺	19.7	-1.5
1 μg Cu ²⁺	18.5	-7.5
1 μg Al ³⁺	21.2	+6
1 μg Pb ²⁺	19.5	-2.5
1 μg Fe ³⁺	19.5	-2.5
1 μg Fe ²⁺	21.8	+9
0.5 μg Zr ⁴⁺	18.1	-9.5
0.1 μg Zn ²⁺	21.0	+5
0.1 μg F ⁻	18.8	-6
1 μg F ⁻	16.6	-17

Table 2. Determination of beryllium in WPCS*

Sample	Result obtained, ng/ml	r.s.d., %	Certified value, ng/ml
WPCS 4	18.9, 17.8, 19.9, 18.4, 18.9, 19.4	3.9	16.1-24.9
WPCS 6	856, 875, 888, 894, 850, 831	2.8	810-978

*WPCS 6 was diluted 100-fold with water.

Effect of ethanol

Figure 4 shows that in the absence of Triton X-100, ethanol enhances the fluorescence of the beryllium complex, by its solvation effect.^{11,15} When Triton X-100 is also present the ethanol may destroy the micelles. The fluorescence intensity of the beryllium complex first decreases as the ethanol concentration increases, but when the ethanol concentration is more than 30% v/v, the solvation effect comes into operation and the intensity increases again.

Effect of temperature

The fluorescence intensities of the beryllium complex and morin increase with decrease in temperature, but the change is small in the temperature range 16-20°. At room temperature, the fluorescence of the beryllium complex and of morin remains almost constant for at least 2 hr.

Analytical characteristics

The calibration graphs obtained in the presence and absence of Triton X-100 were linear up to 10 ng/ml Be in the final solution, but the slope for the reaction in presence of the surfactant was about 5 times that in its absence.

The detection limits found were 0.04 and 0.08 ng/ml in the presence and absence of Triton X-100, respectively, as calculated from $3s/S$ (where s is the standard deviation of the blank and S is the slope of the calibration graph) ($n = 12$).

The precision was studied at two beryllium concentrations, and relative standard deviations (r.s.d.) of 2.2 and 0.7% (11 replicates) were obtained for 0.5 and 5.0 ng/ml Be, respectively.

Interferences

The effects of 25 ions commonly found in water, on the determination of 0.8 ng/ml beryllium were studied. The results are summarized in Table I. Most do not interfere and only Zn²⁺ and F⁻ have a serious effect;

Zn²⁺ increases the fluorescence because of formation of the Zn–morin complex and F⁻ decreases the fluorescence of the beryllium complex because of the formation of beryllium fluoride.

Application

The method has been applied to the determination of beryllium in water pollution control samples (WPCS) (supplied by the U.S. Environmental Protection Agency) without prior separation from the matrix, with satisfactory results. The results are shown in Table 2.

REFERENCES

1. H. L. J. Zermatten, *Prod. Acad. Sci. Amsterdam*, 1933, **36**, 899.
2. J. Walkey, *Am. Ind. Hygiene Assoc. J.*, 1959, **20**, 241.
3. C. W. Sill and C. P. Willis, *Anal. Chem.*, 1959, **31**, 598.
4. M. Y. Ishibashi, W. N. Kasamatsu and C. O. Nishimura, *Bull. Inst. Chem. Research Kyoto Univ.*, 1956, **34**, 210.
5. R. May and F. S. Grimaldi, *Anal. Chem.*, 1961, **33**, 1251.
6. W. L. Hinze, in *Solution Chemistry of Surfactants*, K. L. Mittal (ed.), Vol. 1. Plenum Press, New York, 1979.
7. N. Ishibashi and K. Kina, *Anal. Lett.*, 1972, **5**, 637.
8. J. Medina Escriche, M. De La Guardia Cirugeda and F. Hernandez Hernandez, *Analyst*, 1983, **108**, 1386.
9. W. C. Cui, Z. J. Han and H. M. Shi, *Chem. J. Chinese Univ.*, 1986, **7**, 672.
10. A. Sanz-Medel and J. I. Garcia Alonso, *Anal. Chim. Acta*, 1984, **165**, 159.
11. A. Sanz-Medel, J. I. Garcia Alonso and E. Blanco González, *Anal. Chem.*, 1985, **57**, 1681.
12. A. T. Pilipenko, T. A. Vasilchuk and A. I. Vilkova, *Zh. Analit. Khim.*, 1983, **38**, 855.
13. J. Medina Escriche, F. Hernandez Hernandez, R. Marin and F. J. Lopez, *Analyst*, 1986, **111**, 235.
14. F. Hernandez Hernandez, J. Medina Escriche and M. T. Gasco Andreu, *Talanta*, 1986, **33**, 537.
15. H. G. Wang and L. Y. Li, *Chem. J. Chinese Univ.*, 1987, **8**, 601.

HPLC DETERMINATION OF SOME ANTIBILHARZIAL ANTIMONIALS BY EXTRACTION OF ANTIMONY

NAWAL A. EL-RABBAT, HASSAN H. FARAG, MICHAEL E. EL-KOMMOS and IBRAHIM H. REFAAT
Department of Pharmaceutical Chemistry, Faculty of Pharmacy, University of Assiut, Assiut, Egypt

(Received 10 July 1989. Revised 10 February 1990. Accepted 19 March 1990)

Summary—The antimonial drug (antimony potassium tartrate, antimony piperazine tartrate or antimony lithium thiomaleate) in aqueous solution or biological fluid is treated with sodium diethyldithiocarbamate in the presence of a suitable masking reagent, the pH is adjusted to 9 ± 0.5 , and the antimony complex extracted with *n*-hexane and determined by reversed-phase HPLC with an ODS column and detection at 254 nm. The limits of detection are 20 ng (for antimony potassium tartrate and antimony lithium thiomaleate) and 16 ng (for antimony piperazine tartrate).

A number of workers have reported the use of dithiocarbamates for the precolumn derivatization of lead, mercury(II), cadmium, copper(II), zinc, iron(II), manganese(II), nickel, chromium(III), cobalt(II) and bismuth prior to liquid chromatography.¹⁻⁵ Antimony(III) dithiocarbamates have been determined by thin-layer chromatography,⁶ gas chromatography⁷ and atomic-absorption spectrometry.⁸⁻¹⁰ These AAS methods suffer from interference by copper(II), cadmium, iron(III) and nitrate, which renders them unsuitable for analysis of biological fluids.

The present paper describes the determination of three antibilharzial antimonial drugs (antimony potassium tartrate, antimony piperazine tartrate and antimony lithium thiomaleate) by derivatization with sodium diethyldithiocarbamate (DDTC) and extraction, followed by liquid chromatography. The method offers two main advantages: first, higher sensitivity than AAS⁸⁻¹⁰ or spectrophotometry, which is especially important when dealing with biological fluids; secondly, no interference from copper(II) and iron(III), which are present in biological fluids. However, the method does not differentiate between different forms of antimony or different antimonial drugs. The antimonials investigated are an important class of antibilharzial drugs.^{11,12}

EXPERIMENTAL

Apparatus

A Beckman 112 Solvent Delivery Module connected to a column (25 cm \times 4 mm) packed with Bio-Sip ODS, 5 μ m (Bio-Rad

Laboratories), an LDC Model 1203 UV detector operating at 254 nm, and a Fisher Recordall Series 5000 recorder, were used.

Reagents

Drugs. Pharmaceutical grade antimony potassium tartrate and antimony piperazine tartrate were obtained as gifts from CID Laboratories, Cairo, Egypt. Pharmaceutical grade antimony lithium thiomaleate was obtained as a gift from May & Baker Ltd. (Dagenham, U.K.). DDTC was purchased from Aldrich, and recrystallized from ethanol before use. All other chemicals used were of analytical grade, and all organic solvents were of liquid chromatographic grade (Fisher).

DDTC solution. A freshly prepared 8 mg/ml aqueous solution was used. It was found to be stable for at least 6 hr at 20° and for 24 hr at 4°.

Buffered masking reagent. This solution was 0.5M dipotassium hydrogen phosphate, 0.04M potassium cyanide and 0.02M EDTA disodium salt (adjusted to pH 9.0 ± 0.5).

Stock solutions of drugs. Prepared by dissolving the compounds in distilled demineralized water.

Eluent. An 85:15 v/v mixture of methanol and a buffer solution of 0.05M dipotassium hydrogen phosphate and 0.005M potassium dihydrogen phosphate (pH 8.0-8.5).

Procedure

To 0.5 ml of sample solution add 2.0 ml of the buffered masking reagent and 0.5 ml of DDTC solution, mix well and leave for about 5 min. Add 4 ml of *n*-hexane and equilibrate the

mixture with the aid of a vortex shaker for 1 min or by shaking it manually for 3 min. Leave the mixture for 5–10 min for complete separation of the phases. Inject 20 μ l of the organic layer into the chromatographic system and determine the response as the peak-height for the compound eluted 6 min after injection.

RESULTS AND DISCUSSION

The antimonial drugs investigated have no absorption in the ultraviolet, so cannot be monitored in a chromatographic system equipped with an ultraviolet detector.

Bode¹³ reported that the antimony(III) DDTC chelate can be quantitatively extracted at pH 8.0–9.5 in the presence of EDTA and cyanide as masking reagents. Under these conditions only the bismuth, tellurium and thallium chelates are extracted simultaneously with the antimony(III) chelate. These species should not be present in the bulk drugs or dosage forms examined here, so this system was made the basis of the proposed method.

Optimum conditions for precolumn chelate formation

The pH of the aqueous phase is critical for avoiding the extraction of free diethyldithiocarbamic acid together with the antimony(III) chelate into the organic layer. The free acid has a very similar retention time and molar absorptivity to the chelate under the proposed chromatographic conditions. At pH higher than 8.0, however, the reagent will be almost entirely in the anionic form and hence remain in the aqueous phase.

It was found necessary to recrystallize the DDTC if a steady baseline was to be obtained, since traces of impurities in the commercial product caused a detectable noise. The optimum amount of DDTC for quantitative chelate formation under the chosen conditions was 4 mg (Fig. 1).

To make the method specific for antimony(III), EDTA and potassium cyanide were added to eliminate interferences by other heavy metals or metal parts of the analytical system. The optimum concentrations of EDTA and cyanide were 0.04 and 0.02M respectively.

The chelate is formed almost instantly after mixing of the reaction components and is stable for at least 24 hr at the pH of the buffered masking reagent. Various organic solvents (n-hexane, carbon tetrachloride, chloroform,

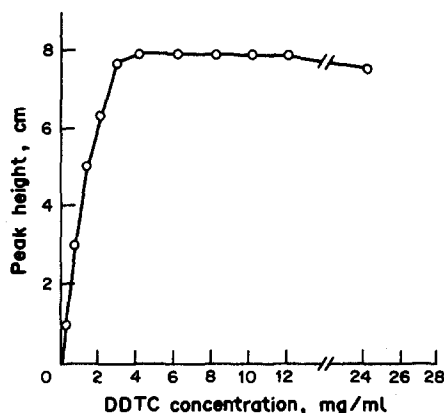


Fig. 1. Effect of DDTC reagent concentration on chelate formation. Concentration of antimony potassium tartrate in the final solution, 12 μ g/ml. Detector sensitivity, 0.064 absorbance for full-scale deflection.

dichloroethane, ethyl acetate and diethyl ether) were tested for the extraction. Quantitative and very rapid extraction was obtained with n-hexane (Table 1).

Optimum chromatographic conditions

Mixtures containing different proportions of methanol and aqueous buffer were tried for the chromatography. Table 2 shows the results; a mobile phase of 85% v/v methanol and 15% buffer was chosen as giving the best compromise between speed and capacity factor. When methanol was replaced by acetonitrile, a distorted chromatogram was obtained. On the other hand, with a mobile phase of 85% methanol in water, strong tailing and irreproducible results were obtained. The optimum pH of the buffer was found to be 8.0–8.5. As an alternative to the phosphate buffer, 0.05M sodium acetate can be used.

Biological applications

Antimonial drugs are usually used parenterally as 3–6% solutions in saline, either daily

Table 1. Effect of extracting solvent and extraction time on Sb chelate extraction (40 μ g of antimony potassium tartrate; detector sensitivity 0.032 absorbance for full-scale deflection)

Solvent	Height of the chelate peak, cm					
	10*	20*	30*	50*	80*	120*
n-Hexane	6.3	8.5	9.7	10.1	10.1	10.1
Carbon tetrachloride	4.1	7.1	8.6	9.3	9.8	9.8
Chloroform	3.9	6.5	8.3	9.0	9.7	9.7
Dichloroethane	3.6	6.3	8.1	9.0	9.6	9.7
Ethyl acetate	3.0	5.9	7.4	8.6	9.3	9.5
Diethyl ether	2.7	5.7	7.3	8.6	9.2	9.4

*Extraction time, sec.

Table 2. Effect of mobile phase composition on Sb chelate retention

Mobile phase composition, % v/v			
Methanol	Aqueous buffer	R_V^* , ml	$K'†$
100	0	6.0	0.00
90	10	7.3	0.22
85	15	9.0	0.33
80	20	11.4	0.90
75	25	14.9	1.48
70	30	18.7	2.11
65	35	23.9	2.96

* R_V = retention volume for chelate peak.

† K' (capacity ratio) = $(R_V - R_0)/R_0$ where R_0 = void volume.

or on alternate days on 5 occasions, or once weekly for 5 weeks. There are no data for the distribution of trivalent antimony compounds in different human organs,¹² probably owing to lack of specific methods. Therefore, authentic samples of the antibilharzial antimonial drugs

investigated were added in appropriate concentration (25 $\mu\text{g/ml}$) to human plasma, blood, and urine as well as to liver and brain homogenates from male 6–8 week old hamsters. Results for the bulk drugs and the spiked biological materials are presented in Table 3. The calibration graphs are linear. The range over which the method can be applied with reasonable precision and accuracy is 5–10 $\mu\text{g/ml}$ in either aqueous solutions or biological specimens. The absence of interference by biological backgrounds is illustrated in Fig. 2. The relative standard deviation did not exceed 1.6%. The limits of detection in aqueous solution or biological fluids are 1 $\mu\text{g/ml}$ for antimony potassium tartrate and antimony lithium thiomaleate, and 0.8 $\mu\text{g/ml}$ for antimony piperazine tartrate in the sample solution (*i.e.*, 20 and 16 ng respectively, in the 20 μl injected).

Table 3. Determination of some antibilharzial antimonials in bulk powder form and in spiked biological materials

Compound	Sample	Linear range,* $\mu\text{g/ml}$	Recovery,† %
Antimony potassium tartrate	Powder	1.0–12.0	100.0
	Plasma	2.0–20.0	102.1
	Blood	1.5–16.0	103.1
	Urine	2.0–20.0	104.4
	Liver homogenate	1.5–25.0	102.9
	Brain homogenate	1.5–25.0	103.1
Antimony piperazine tartrate	Powder	0.8–15.0	100.0
	Plasma	1.0–12.5	100.5
Antimony lithium thiomaleate	Powder	1.0–18.0	100.0
	Plasma	3.0–18.0	102.6

*Concentrations in the final solution injected.

†These values are the means of 6 determinations for a 7.5 $\mu\text{g/ml}$ solution. The standard deviation was 1.6%.

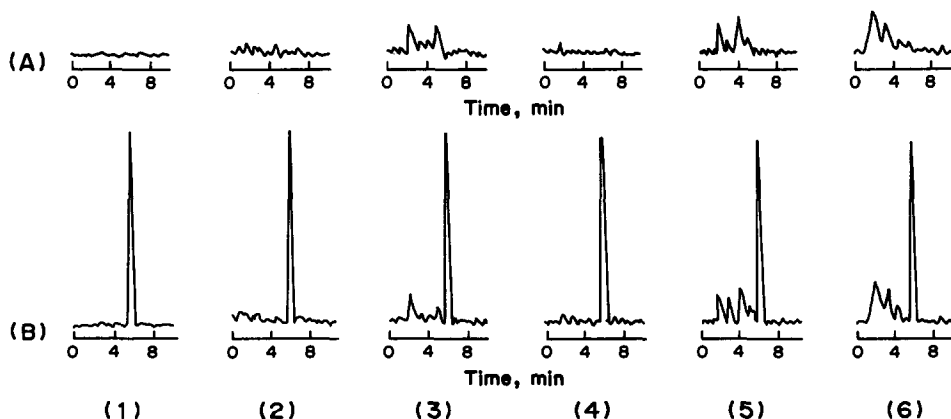


Fig. 2. Chromatograms of Sb(III)-DDTC chelate obtained from the following samples: (1) aqueous solution, (2) plasma, (3) blood, (4) urine, (5) liver homogenate, (6) brain homogenate. (A) Original sample material. (B) Material spiked with antimony potassium tartrate (concentration 10 $\mu\text{g/ml}$ in the final extract). Detector sensitivity, 0.064 absorbance for full-scale deflection.

Individual calibration graphs can be prepared for the compounds assayed, or a single calibration plot can be made for antimony(III), the concentration of which can then be multiplied by an appropriate factor to give the amount of compound assayed. The method is more suitable for analysis of biological samples than of formulations.

REFERENCES

1. G. Schwedt, *Chromatographia*, 1978, **11**, 145.
2. *Idem, ibid.*, 1979, **12**, 289.
3. S. R. Hutchins, P. R. Haddad and S. Dilli, *J. Chromatog.*, 1982, **252**, 185.
4. S. Ichinoki, T. Morita and M. Yamazaki, *J. Liq. Chromatog.*, 1983, **6**, 2079.
5. R. M. Smith and L. E. Yankey, *Analyst*, 1892, **107**, 744.
6. G. Soundararajan and M. Subbaiyan, *Indian J. Chem.*, 1983, **22A**, 311.
7. H. Schneider and N. R. Hubert, *Z. Anal. Chem.*, 1978, **293**, 1115.
8. Y. Nagafuchi, K. Fukamachi and M. Morimoto, *Bunseki Kagaku*, 1977, **26**, 729.
9. S. Hernandez and H. Iturriaga, *An. Quim.*, 1979, **75**, 545.
10. I. Khavezov, E. Ivanova, P. Koehler, N. Iordanov, R. Matchat, K. Reiher, G. Emrich and K. Licht, *Z. Anal. Chem.*, 1987, **326**, 536.
11. D. M. James and H. M. Gilles, *Human Antiparasitic Drugs: Pharmacology and Usage*. Wiley, New York, 1985.
12. L. L. Gustafsson, B. Beermann and Y. A. Abdi, *Handbook of Drugs for Tropical Parasitic Infections*". Taylor & Francis, London, 1987.
13. H. Bode, *Z. Anal. Chem.*, 1954, **143**, 182.

DETERMINATION OF ANTIMONY IN ORES AND RELATED MATERIALS BY CONTINUOUS HYDRIDE-GENERATION ATOMIC-ABSORPTION SPECTROMETRY AFTER SEPARATION BY XANTHATE EXTRACTION*

ELSIE M. DONALDSON

Mineral Sciences Laboratories, Canada Centre for Mineral and Energy Technology, Department of Energy, Mines and Resources, Ottawa, Canada

(Received 7 November 1989. Revised 5 March 1990. Accepted 16 March 1990)

Summary—A continuous hydride-generation atomic-absorption spectrometric method for determining $\sim 0.02 \mu\text{g/g}$ or more of antimony in ores, concentrates, rocks, soils and sediments is described. The method involves the reduction of antimony(V) to antimony(III) by heating with hypophosphorous acid in a 4.5M hydrochloric acid-tartaric acid medium and its separation by filtration, if necessary, from any elemental arsenic, selenium and tellurium produced during the reduction step. Antimony is subsequently separated from iron, lead, zinc, tin and various other elements by a single cyclohexane extraction of its xanthate complex from $\sim 4.5M$ hydrochloric acid/0.2M sulphuric acid in the presence of ascorbic acid as a reductant for iron(III). After the extract is washed, if necessary, with 10% hydrochloric acid-2% thiourea solution to remove co-extracted copper, followed by 4.5M hydrochloric acid to remove residual iron and other elements, antimony(III) in the extract is oxidized to antimony(V) with bromine solution in carbon tetrachloride and stripped into dilute sulphuric acid containing tartaric acid. Following the removal of bromine by evaporation of the solution, antimony(V) is reduced to antimony(III) with potassium iodide in $\sim 3M$ hydrochloric acid and finally determined by hydride-generation atomic-absorption spectrometry at 217.8 nm with sodium borohydride as reductant. Interference from platinum and palladium, which are partly co-extracted as xanthates under the proposed conditions, is eliminated by complexing them with thiosemicarbazide during the iodide reduction step. Interference from gold is avoided by using a 3M hydrochloric acid medium for the hydride-generation step. Under these conditions gold forms a stable iodide complex.

Because of the increasing demand for reference ores and related materials with certified trace element contents, the accurate determination of small amounts of antimony in these materials is of importance in CANMET's Canadian Certified Reference Materials Project (CCRMP). Reliable results for antimony are also essential in other CANMET in-house projects. For these reasons, and to aid in the possible certification of antimony, at the $< 1 \mu\text{g/g}$ -level, in a recent candidate reference tailings sample, UMT-1, the development of a relatively simple and sensitive method for the determination of ng and μg amounts of antimony was undertaken in which the antimony would ultimately be determined by either graphite-furnace (GFAAS) or hydride-generation atomic-absorption spectrometry (HGAAS). Because moderate amounts of hydride-forming elements (arsenic, bismuth and

tin), and those that form insoluble iodides (lead and copper) with the potassium iodide used as reductant, interfere in the hydride method for antimony, and because large amounts of transition-metal and other matrix elements interfere in both methods,¹⁻⁷ the preliminary separation of antimony by a reasonably selective solvent extraction procedure was considered necessary, particularly for very small amounts. Recently, in this laboratory a flame AAS method involving the separation of antimony from matrix elements by a single methyl isobutyl ketone extraction as the iodide from 2M sulphuric acid was developed for the determination of $\sim 5 \mu\text{g/g}$ or more of antimony in ores and related materials.⁸ However, this extraction procedure cannot be used directly for samples containing lead, because of the occlusion of antimony by lead sulphate, and it is not very selective, because copper, bismuth, silver and various other elements are completely co-extracted as iodides

*Crown copyright reserved.

under the same conditions. In earlier work,⁹ a spectrophotometric method was developed for the determination of $\geq 1 \mu\text{g/g}$ of antimony in ores and in copper, molybdenum, nickel, zinc and lead concentrates. This method was based on the measurement of the absorbance of the iodide complex at 331 nm, after the preliminary separation of antimony from copper, zinc, nickel, molybdenum and other elements by collection with an iron-lanthanum mixture from ammoniacal medium, followed by its separation from the iron and lanthanum and from lead, tin, aluminium and other elements by a triple chloroform extraction of the antimony(III) ethyl xanthate complex from $\sim 5M$ hydrochloric acid containing tartaric acid as an auxiliary complexing agent for antimony. Owing to the relatively high selectivity of this extraction procedure, it was considered that xanthate extraction might be very useful in the rapid and direct separation of small amounts of antimony before its determination by GFAAS or HGAAS, particularly if, as found recently for arsenic¹⁰ and tellurium,¹¹ quantitative extraction could be achieved in one extraction step into a solvent of specific gravity < 1 . As shown in these methods,^{10,11} this simplifies and shortens the extraction procedure and facilitates washing of the extract to remove entrained salts and reduce the concentration of some co-extracted elements.

The proposed method involves the reduction of antimony(V), produced during the decomposition step, to antimony(III) by heating with hypophosphorous acid in a $4.5M$ hydrochloric acid-tartaric acid medium, followed by its separation, if necessary, from any elemental arsenic, selenium and/or tellurium formed during the reduction step, by filtration. Antimony is then separated from iron, lead and other matrix elements by a single cyclohexane extraction of its xanthate complex from $4.5M$ hydrochloric acid/ $0.2M$ sulphuric acid containing ascorbic acid as a reductant for iron(III). After washing to remove co-extracted copper and residual iron and other elements, antimony(III) in the extract is oxidized with bromine solution in carbon tetrachloride and stripped into dilute sulphuric acid-tartaric acid solution. The resultant antimony(V) is ultimately reduced to the trivalent state with potassium iodide in $\sim 3M$ hydrochloric acid, in the presence of thiosemicarbazide as a complexing agent for platinum and palladium, and determined by HGAAS with sodium borohydride as reductant. A graphite-

furnace finish, which involved the use of $16M$ nitric acid for stripping purposes and both palladium and thiourea as matrix modifiers, as described earlier for arsenic,¹⁰ was investigated initially, but this work was discontinued because of the low and erratic results obtained for antimony. These were caused by the high sulphate content of the strip solution, resulting from the nitric acid oxidation of the co-extracted excess of xanthate. An advantage of the proposed method over many other HGAAS methods for antimony is that the element is separated from selenium, tellurium and the other hydride-forming elements mentioned above.

EXPERIMENTAL

Apparatus

A Perkin-Elmer model 5000 atomic-absorption spectrometer, equipped with a single-slot 10-cm air-acetylene burner and an antimony hollow-cathode lamp, was used in this work in conjunction with a Varian model VGA-76 automated continuous vapour-generation accessory.¹² These were used under the following conditions and measurements were made in the absorbance mode with deuterium-arc background correction.

Wavelength: 217.8 nm

Lamp current: 20 mA

Spectral band-width: 0.2 nm

Air flowmeter reading: 40 (~ 13 l./min)

Acetylene flowmeter reading: 15 (1.5 l./min)

Integration period for absorbance measurement: 2 sec after ~ 40 sec delay time

Hydrochloric acid ($10M$) uptake rate: ~ 1 ml/min

Sodium borohydride solution uptake rate: ~ 1 ml/min

Sample solution uptake rate: ~ 8 ml/min

Nitrogen flow-rate: ~ 90 ml/min

Reagents

Standard antimony solution, 100 $\mu\text{g/ml}$. Dissolve 0.2669 g of pure potassium antimony tartrate (dried at 105° for 1 hr) in water, add 10 ml of 20% tartaric acid solution and dilute to 1 litre with water. Prepare a 1- $\mu\text{g/ml}$ solution by diluting 5 ml of this stock solution plus 5 ml of 20% tartaric acid solution to 500 ml with water. Prepare this diluted solution fresh as required.

Sodium borohydride solution, 0.6% containing ~0.5% sodium hydroxide. Prepare fresh as required and store in a plastic bottle.

Sulphuric acid (3%)–tartaric acid (0.5%) solution. Dissolve 5 g of tartaric acid in ~900 ml of water, add 30 ml of concentrated sulphuric acid, cool and dilute to ~1 litre with water.

Thiosemicarbazide solution, 2.5% in 4% v/v hydrochloric acid. Dissolve 2.5 g of the reagent (by stirring vigorously) in ~100 ml of water containing 4 ml of concentrated hydrochloric acid, then filter the solution through a Whatman No. 541 filter paper and store it in a plastic bottle. Prepare a fresh solution weekly.

Potassium iodide (10%)–ascorbic acid (2%) solution. Store in a plastic bottle.

Hydrochloric acid, 10M.

Hypophosphorous acid, 20% v/v. Add 40 ml of concentrated hypophosphorous acid, 10 ml of 20% tartaric acid solution, 60 ml of concentrated hydrochloric acid and 4 ml of 50% v/v sulphuric acid to a 250-ml beaker and dilute to ~200 ml with water. Cover the beaker, heat the solution to boiling, and boil it vigorously for ~10 min to reduce any antimony(V) present to antimony(III). Cool the resulting solution to room temperature, transfer it to a 250-ml separating funnel, then add 15 ml of chloroform and ~2.5 ml of 20% potassium ethyl xanthate solution and shake the funnel vigorously for ~2 min. Allow the layers to separate, then drain off and discard the chloroform phase. Repeat the extraction, then wash the aqueous phase twice by shaking it with ~10 ml of chloroform each time. Drain off the chloroform and store the aqueous layer in a 250-ml plastic bottle.

Tartaric acid solution, 20%.

Hydrochloric acid, 12M, containing ~1% v/v formic acid. Add 5 ml of concentrated formic acid to ~500 ml of concentrated hydrochloric acid.

Hydrochloric acid, 4.5M, containing ~1% v/v formic acid. Dilute 385 ml of concentrated hydrochloric acid and 4 ml of concentrated formic acid to 1 litre with water.

Bromine, 20% v/v solution in carbon tetrachloride.

Sulphuric acid, 50% v/v.

Potassium ethyl xanthate solution, 20%. Prepare fresh as required.

Hydrochloric acid (10%)–thiourea (2%) wash solution. Dissolve 2 g of thiourea in 100 ml of 10% v/v hydrochloric acid.

Doubly demineralized water was used throughout and all acids employed were analytical-reagent grade.

Calibration solutions

Prepare 5-, 10-, 15- and 20-ng/ml antimony solutions by adding 0.5, 1, 1.5 and 2 ml, respectively, of 1- μ g/ml standard antimony solution to 100-ml standard flasks, followed by 40 ml of 3% sulphuric acid–0.5% tartaric acid solution, 25 ml of concentrated hydrochloric acid, 4 ml of 2.5% thiosemicarbazide solution and 10 ml of 10% potassium iodide–2% ascorbic acid solution, diluting to volume with water and mixing thoroughly. Prepare a blank calibration solution in a similar manner. These solutions are stable for ~3 days when stored in the dark.

Procedure

Transfer up to 2 g of powdered sample, containing up to ~40 μ g of antimony and not more than ~10 mg of arsenic and ~800 mg of lead, to a 250-ml Teflon beaker, then cover the beaker with a Teflon cover and add ~5 ml of water, 15 ml of concentrated nitric acid and 10 ml of concentrated perchloric acid. Heat the solution until the evolution of oxides of nitrogen ceases, then allow it to cool to room temperature. Remove the cover, wash down the sides of the beaker with water, add 10 ml of concentrated hydrofluoric acid and carefully evaporate the solution to fumes of perchloric acid. Cool, cover the beaker with a Teflon cover (Note 1), add 5 ml of *aqua regia* (Note 2), heat until the evolution of oxides of nitrogen ceases, then remove the cover, wash down the sides of the beaker with water and carefully evaporate the solution to ~3 ml. Cool, add 5 ml each of 20% tartaric acid solution and purified 20% hypophosphorous acid solution, 18 ml of concentrated hydrochloric acid containing 1% formic acid, and 20 ml of water. Cover the beaker with a Teflon cover, heat the solution to boiling and boil it gently for ~10 min (Note 3) to reduce antimony(V) to antimony(III) and to reduce any arsenic, selenium and tellurium present to their elemental states. Run a blank through the whole procedure.

If elemental arsenic, selenium and tellurium are absent, as indicated by the absence of a black precipitate, cool the solution to room temperature (Note 4), then transfer it to a 100-ml plastic standard flask, using 4.5M hydrochloric acid–1% formic acid solution contained in a squeeze-type wash-bottle to wash

the beaker. Dilute to volume with the same solution.

If elemental arsenic, selenium or tellurium is present, filter the solution (Whatman No. 40 paper) (Note 5) into a 100-ml plastic standard flask, using 4.5*M* hydrochloric acid–1% formic acid solution to wash the beaker, paper and precipitate and to dilute the filtrate to volume.

Transfer a 4–50-ml portion of the resulting solution, containing not more than 2 μg of antimony and ~ 5 mg of copper, to a 125-ml separating funnel marked at 50 ml and containing 1 ml of 50% v/v sulphuric acid (Note 6). Depending on the size of the aliquot taken, add 0.5–1.5 g of ascorbic acid (Note 7), dilute the solution to the mark with 4.5*M* hydrochloric acid–1% formic acid solution, stopper and mix thoroughly to dissolve the ascorbic acid, then allow the solution to stand for ~ 15 min to ensure the reduction of most of the iron. Add 15 ml of cyclohexane and 1 ml of freshly prepared 20% potassium ethyl xanthate solution (Note 8) and shake the solution for 2 min. Allow the layers to separate, then drain off and discard the aqueous phase. If copper xanthate is present, as indicated by a yellow precipitate in the aqueous and organic phases, wash the extract by shaking it with 10 ml of 10% hydrochloric acid–2% thiourea solution until the precipitate dissolves, then drain off the acid phase. Wash the extract by shaking it for ~ 30 sec with 5 ml of 4.5*M* hydrochloric acid–1% formic acid solution to remove residual iron. Drain off the acid phase (Note 9), then add 2 ml of 20% bromine solution in carbon tetrachloride to the extract, stopper the funnel and mix thoroughly. Allow the solution to stand for ~ 5 min to ensure the complete oxidation of antimony(III) to antimony(V), then add 5 ml of 3% sulphuric acid–0.5% tartaric acid solution and shake the funnel for ~ 30 sec. Allow the layers to separate, then drain the aqueous phase into a 100-ml Teflon beaker. Wash the stem of the funnel with water and collect the washings in the beaker. Repeat the stripping step once more, then wash the extract with 5 ml of water. Wash the stem of the funnel with water each time and collect these washings in the beaker.

Evaporate the resulting blank and sample solutions until they are colourless, then add 500 μl of concentrated formic acid to destroy any traces of bromine remaining and evaporate the solutions to ~ 3 –5 ml (Note 10). Transfer the blank solution to a 25-ml standard flask

containing 1 ml of 2.5% thiosemicarbazide solution, 6 ml of concentrated hydrochloric acid and 2.5 ml of 10% potassium iodide–2% ascorbic acid solution. Transfer the sample solution to a standard flask of appropriate size (25–100 ml) containing corresponding amounts of the reagents above and of the 3% sulphuric acid–0.5% tartaric acid solution (Note 11). Dilute both solutions to volume with water, mix and let stand for ~ 20 min to ensure the complete reduction of antimony.

Using the blank calibration solution to zero the spectrometer, measure the absorbance generated by the calibration solutions, followed by the blank and sample solution (Note 12), under the conditions described under "Apparatus". Determine the antimony concentration of both solutions by reference to the absorbance values obtained concurrently for the calibration solutions. Calculate the antimony content of the solutions (in ng or μg) and correct the result obtained for the sample solution by subtracting that obtained for the blank solution.

Notes

(1) A watch-glass should not be used, because any hydrofluoric acid not removed in the preceding step will etch the glass and contaminate the solution with antimony from it.

(2) *Aqua regia* is added to ensure that all the antimony is present as antimony(V).⁹

(3) During the reduction step the boiling period should not be prolonged unduly because if the volume of the solution decreases to ~ 45 ml the final hydrochloric acid concentration of the solution, after it is diluted to 100 ml with 4.5*M* hydrochloric acid, may be too high. This can cause incomplete extraction of antimony.

(4) Any white insoluble material (barium and strontium sulphates or lead chloride) does not need to be removed by filtration. The final solution can either be allowed to stand until this material has settled, or it can be removed more quickly, if desired, by centrifuging a suitable portion of the solution. The solution is stable for at least 10 days.

(5) Filtration is not usually necessary if only a small amount of black precipitate is present. As mentioned in Note 4, this can be allowed to settle out or can be removed by centrifugation.

(6) Depending on the amount of antimony present, none or $< 10\%$ will be extracted if the sulphuric acid is omitted. To avoid this source of error it is recommended that a habit be made

of adding the sulphuric acid to the separating funnel before the addition of the sample solution.

(7) About 1.5, 0.75 and 0.5 g of ascorbic acid are recommended for 50-, 25- and ≤ 20 -ml aliquots, respectively, of the sample solution.

(8) Because of the rapid decomposition of xanthate in acidic solutions, xanthate solution should be added to only two solutions at a time, followed by immediate extraction of the complex. For health reasons, all operations involving xanthate should be performed in a fume-hood, and an automatic pipette or one equipped with a suction bulb should be used for dispensing the solution. The aqueous phase after extraction and any remaining xanthate solution should be treated with concentrated nitric acid and boiled to destroy the xanthate before disposal of the solution.¹³

(9) If any salts are still present in the aqueous phase, wash the extract by shaking it with 3 or 4 ml of water, then drain off the aqueous phase.

(10) The solution should not be evaporated to dryness or near dryness, because of the organic material (tartaric acid) present.

(11) For practical reasons, it is recommended that the hydrochloric acid and the thiosemicarbazide (TSC) and potassium iodide solutions required be added to the standard flasks before the addition of the sample solution. The volumes of these solutions and of the additional sulphuric-tartaric acid (H_2SO_4 -HTA) solution required for final sample solution volumes of 25, 50 and 100 ml are as follows:

Final volume, ml	Volume required, ml			
	H_2SO_4 -HTA solution	TSC solution	KI solution	HCl concentrated
25	0	1	2.5	6
50	10	2	5	12.5
100	30	4	10	25

(12) If dilution of the sample solution is necessary, dilute a suitable aliquot with the blank calibration solution.

RESULTS AND DISCUSSION

Separation of antimony by extraction as the xanthate

Previously,^{9,14} it was found that up to at least 500 μg of antimony(III) can be completely extracted as the xanthate in three extractions into chloroform from $\leq 5M$ hydrochloric acid containing tartaric acid as an auxiliary complexing agent for antimony. However, in prelimi-

nary tests to determine whether μg quantities could be quantitatively extracted into cyclohexane in one extraction, as described recently for arsenic¹⁰ and tellurium,¹¹ the extraction of antimony was incomplete and decreased rapidly with an increase in the hydrochloric acid concentration from ~ 2 to $5M$, presumably because of the increased complexing action of chloride. Under these conditions, and at the $5\text{-}\mu g$ level, $< 10\%$ of the antimony present was extracted from 4 to $5M$ hydrochloric acid. Subsequent work showed that considerably more antimony was extracted if a second extraction was performed and, although the reason for this behaviour is not clear, it was thought that it might be caused by the presence of sulphur compounds produced, during the extraction step, by the decomposition of xanthate. This was suggested by further work in which complete extraction of antimony was obtained in one step when some sulphuric acid was present. Tests showed that up to at least 5 μg of antimony can be quantitatively extracted into 15 ml of cyclohexane from 50 to 60 ml of solution $\leq 5M$ in hydrochloric acid and $\sim 0.2\text{--}0.5M$ in sulphuric acid. At hydrochloric acid concentrations $> 5M$ the extraction of antimony is incomplete under these conditions. Consequently, to ensure complete extraction, and to prevent the co-extraction of lead and minimize that of bismuth and tin,¹⁴ a hydrochloric acid concentration of $\sim 4.5M$ was chosen for further work. Some additional tests indicated that toluene can also be used as the solvent but this was not pursued in the present work.

In initial work involving the extraction of antimony under the recommended experimental conditions ($4.5M$ hydrochloric acid- $0.2M$ sulphuric acid), complete extraction was obtained from solutions of various reference materials prepared essentially as described in the proposed method. However, in later work low and erratic results were obtained which were ultimately attributed to the use of a different brand of hydrochloric acid, containing chlorine. This caused the partial oxidation of antimony(III) to antimony(V) when the sample solutions were diluted to 100 ml with $4.5M$ hydrochloric acid after the reduction step. This, in turn, resulted in incomplete extraction of antimony as the xanthate because it is not appreciably extracted in the quinquevalent state.¹⁴ Tests showed that this source of error could be eliminated by dissolving a reductant such as ascorbic acid in the sample solution just before its dilution to

volume with 4.5*M* hydrochloric acid, or by adding formic acid to the 4.5*M* hydrochloric acid to destroy the chlorine present. The use of formic acid is preferable because the solutions obtained are stable for at least 3 weeks. Solutions containing ascorbic acid can only be used for ~2 days because they become progressively brown to black on standing, owing to the decomposition of the reductant. The presence of more than ~2 ml of concentrated perchloric acid during the extraction step is not recommended, because it may interfere with the extraction of antimony. For this reason, the concentration of this acid is regulated in the proposed method by evaporating the sample solution to ~3 ml to remove most of the added perchloric acid, followed by dilution to 100 ml and the use of ≤50 ml of the resultant solution for the extraction step.

Stripping and HGAAS determination of antimony

In recent work involving the determination of arsenic by HGAAS after its separation from matrix elements by extraction as the xanthate,¹⁵ arsenic(III) xanthate in the cyclohexane extract was oxidized with bromine solution in carbon tetrachloride and arsenic(V) was then stripped into water. This was followed by the removal of bromine by heating and evaporation of the solution before the reduction of arsenic(V) with potassium iodide and its ultimate HGAAS measurement. This method was also advantageous for antimony except that dilute sulphuric acid containing tartaric acid was used for stripping to prevent the hydrolysis of antimony(V). The addition of a small amount of concentrated formic acid to the strip solution, after the removal of most of the bromine by evaporation, was also found to be beneficial for eliminating any traces of bromine remaining. Formic acid could probably also be used to advantage for the same purpose in the arsenic method. Similarly to arsenic,¹⁵ the antimony(V) formed during the stripping step is readily reduced to the trivalent state required for the hydride-generation step, by acidifying the solution with hydrochloric acid, and then adding potassium iodide and allowing the solution to stand for ~20 min to ensure complete reduction.⁵ A potassium iodide concentration of ~1% was found to be adequate for the reduction of antimony, and as recommended by other investigators^{12,16} using the same hydride-generation accessory, 10*M* hydrochloric acid

and 0.6% sodium borohydride solutions were used in the acid and borohydride channels of the hydride-generator (a borohydride concentration of 1% was also investigated but this only increased the absorbance by ~6% at the 20 ng/ml antimony level). Under these conditions, the final hydrochloric acid concentration of the sample solution can vary from ~1 to 5*M* without affecting the sensitivity for antimony. At the pumping rates specified, this corresponds to hydrochloric acid concentrations in the range ~1.8–5*M* during the stibine generation step. A final hydrochloric acid concentration of ~3*M* was ultimately chosen for the sample and calibration solutions to eliminate interference from co-extracted gold. At this acidity, moderate amounts of gold do not interfere, because it forms a stable iodide complex. Deuterium-arc background correction is recommended to eliminate positive error from photochemical decomposition products such as iodine, which is formed in the presence of aerial oxygen in the highly acidic sample and calibration solutions on standing. Probably this is carried into the absorption cell and absorbs at the wavelength employed, causing an increase in the signal for antimony. The calibration solutions can be used for up to 3 days if stored in the dark to minimize the formation of iodine.

Reduction of antimony and its separation from arsenic

Previous work involving a study of extraction of ethyl xanthate complexes from hydrochloric acid media¹⁴ showed that antimony must be in the trivalent state for the extraction step, and in the spectrophotometric iodide method mentioned earlier, this reduction was accomplished with sodium metabisulphite in hot 6*M* hydrochloric acid before the separation of antimony by collection with iron-lanthanum mixture and xanthate extraction. Although arsenic is also reduced to arsenic(III) under these conditions and completely co-extracted as the xanthate at the hydrochloric acid concentration (5*M*) used in this earlier work, it does not interfere in the spectrophotometric determination of antimony as the iodide. However, in the case of an HGAAS finish, the large amounts of arsenic present in some ores and concentrates, relative to antimony, could interfere in this method because of depressive gas phase reactions during the atomization stage.¹⁶ Consequently, it was considered that a reductant such as hypophosphorous acid,^{17,18} which reduces antimony to the

tervalent state and arsenic to the elemental state in hot hydrochloric acid media, might be very useful both for the reduction of antimony and for the separation of arsenic from antimony. Tests showed that up to at least 5 mg of arsenic can be readily reduced to the element by boiling for ~10 min with 1 ml of concentrated (~50%) hypophosphorous acid under the acid conditions (4.5M hydrochloric acid) used for the reduction and extraction of antimony. It can then be separated from ng and μg amounts of antimony by filtration. Selenium and tellurium, which are also completely co-extracted as xanthates from 4.5M hydrochloric acid, are also reduced to their elemental states and separated from antimony by this procedure. Purification of the hypophosphorous acid by xanthate extraction under essentially the same conditions (hydrochloric-sulphuric acid medium) used for the extraction of antimony was necessary because of its high antimony content (~280 ng/ml). Boiling of the hypophosphorous acid-hydrochloric acid-sulphuric acid solution was also necessary to reduce the antimony, present in the quinquevalent state in hypophosphorous acid.

Effect of diverse ions

Elements other than arsenic, selenium and tellurium that are completely or almost completely extracted as xanthate under the conditions (4.5M hydrochloric acid) used for the extraction of antimony are gold and palladium. Copper, platinum, molybdenum, bismuth and thallium(III) are partly extracted.¹⁴ Copper can readily be removed from the extract by washing it with 10% v/v hydrochloric acid containing 2% thiourea. The use of 4.5M hydrochloric acid containing thiourea is ineffective because copper forms a strong xanthate complex under these conditions. Thiourea complexes copper more effectively in dilute hydrochloric acid media. Washing with 10% hydrochloric acid containing thiourea, rather than 10M hydrochloric acid-thiourea solution, would also be advantageous for the removal of co-extracted copper in the previously reported GFAAS¹⁰ and HGAAS¹⁵ methods for arsenic. However, as mentioned in those methods, the presence of more than ~5 mg of copper during the extraction step is not recommended because the insoluble yellow cuprous xanthate formed may interfere mechanically with the extraction or with the separation of the layers. Thiosemicarbazide, which was used as a complexing agent for small amounts of copper in recent work involv-

ing the separation of tellurium by xanthate extraction from ~9.5M hydrochloric acid,¹¹ was ineffective under the extraction conditions used in this work. Thallium is not co-extracted in the proposed method because it is reduced to thallium(I) with hypophosphorous acid. This is essentially not extracted from $\geq 0.5\text{M}$ hydrochloric acid.¹⁴

Interference from up to at least 4 $\mu\text{g}/\text{ml}$ of gold during the hydride-generation step is avoided, as mentioned earlier, by adjusting the hydrochloric acid concentration of the final solution to ~3M to allow the formation of a stable gold iodide complex. Interference from up to 2 $\mu\text{g}/\text{ml}$ of platinum and palladium is eliminated by complexation with thiosemicarbazide as described in the HGAAS method for arsenic.¹⁵ Up to 1 $\mu\text{g}/\text{ml}$ of gold, platinum and palladium can be present collectively in the final solution without causing significant error in the result. Up to at least 3 mg of molybdenum, which is ~25% co-extracted as a reddish-purple complex, does not interfere in the extraction of antimony, and relatively large amounts (10 mg) do not interfere in its determination by HGAAS. Similarly, up to at least 5 mg of bismuth and 400 mg of lead do not interfere during the extraction step. At these levels, only ~5 μg of bismuth and ~160 μg of lead were found in the final solution used for the determination of antimony. Some lead may precipitate as the chloride and settle out in the initial solution on standing but this does not cause error in the antimony result.

Iron(III) is partly reduced with hypophosphorous acid¹⁹ under the conditions used for the reduction of antimony, and that remaining must be largely reduced with ascorbic acid before the extraction step or a low result will be obtained for antimony. Residual iron, lead and other elements that may be mechanically entrained in the extract, and small amounts of co-extracted elements are removed or reduced in concentration by washing the extract with 4.5M hydrochloric acid. Under these conditions, and at the 300-mg level, only ~10–30 μg of iron were found in the final solution. Tin is not significantly extracted as the xanthate from 4.5M hydrochloric acid and up to at least 50 mg can be present during the extraction step without causing error in the result.

Applications

Table 1 shows that the mean result obtained for the industrial zinc concentrate is in good

Table 1. Determination of antimony in CCRMP and other reference ores and related materials

Sample*	Antimony, $\mu\text{g/g}$			
	Certified value	This work†	Consensus value 1989‡	Other reported values post-1979
UMT-1 Tailings	—	0.12 \pm 0.01 (6)	—	—
Industrial zinc concentrate-732	—	9.1 \pm 0.4 (4)	—	9.2 ₈ , 8.8
SO-1 Regosolic soil	0.2 [¶]	0.26 \pm 0.02	0.30	0.27, ²⁰ 0.2, ² 0.11 ²¹
SO-2 Podzolic soil	0.1 [¶]	0.13 \pm 0.02	0.11	0.13, ²⁰ 0.1, ² 0.08 ²¹
SO-3 Calcareous C Horizon soil	0.3 [¶]	0.25 \pm 0.01	0.32	0.33, ²⁰ 0.3, ² 0.23 ²¹
SO-4 Chernozemic A Horizon soil	0.7 [¶]	0.56 \pm 0.03	0.71	0.69, ²⁰ 0.4, ² 0.55 ²¹
SY-2 Syenite rock	0.2 ^a	0.35 \pm 0.04	0.25	0.3, ² 0.39 ²¹
SY-3 Syenite rock	0.3 ^a	0.39 \pm 0.00	0.31	0.4, ² 0.44 ²¹
MRG-1 Gabbro	0.4 ^a	0.50 \pm 0.04	0.86	0.68, ²⁰ 0.42 ²¹
FER-1 Iron formation rock	5 ^b	5.1 \pm 0.1	—	—
FER-2 Iron formation rock	0.7 ^b	0.73 \pm 0.02	—	—
FER-3 Iron formation rock	1 ^b	0.96 \pm 0.01	—	—
FER-4 Iron formation rock	3 ^b	1.4 \pm 0.0	—	—
NRCC MESS-1 Marine sediment	0.73 \pm 0.08	0.78 \pm 0.08	—	0.71, ²² 0.67 ²³
NRCC BCSS-1 Marine sediment	0.59 \pm 0.06	0.63 \pm 0.07	—	0.61, ²² 0.47 ²³
NRCC PACS-1 Marine sediment	171 \pm 14	201 \pm 8 (5) 203 \pm 9 ^c	—	195, 206 ²⁴
USGS AGV-1 Andesite	—	4.5 \pm 0.2	4.3	4.8, ²⁵ 3.96, ²⁶ 3.3, ² 4.49, ²⁷ 4.38 ²¹
USGS PCC-1 Peridotite	—	1.5 \pm 0.1	1.28	1.5, ²⁵ 1.1, ² 0.99 ²⁷
USGS DTS-1 Dunite	—	0.66 \pm 0.03	0.5	0.4 ²
NBS 1633a Coal fly ash	6.9 \pm 0.5 ^d	6.2 \pm 0.1	—	6.95, ²⁰ 7.3, ²⁸ 6.5, ² 7.7 ²¹
NBS 1645 River sediment	31 \pm 6 ^d	29.8 \pm 2.2 (4)	—	40, ²⁰ 33.2, 36, ²⁸ 33.6, ²⁶ 32.5, ²¹ 31 ²⁹ 0.36, ²² 0.4 ²⁹
NBS 1646 Estuarine sediment	0.79 \pm 0.16 ^d	0.53 \pm 0.09	—	—
NBS 2704 River sediment	3.79 \pm 0.15	3.8 \pm 0.2 (4)	—	—

*CCRMP reference materials except where indicated otherwise. Except for UMT-1 nominal compositions are given in references 8, 10 and 30. The approximate percentage chemical composition of UMT-1 is 10 Fe, 15 Mg, 4 Ca, 23 Si and 2 Al.

†Mean and standard deviation for 3 values except where indicated otherwise in parentheses.

‡From 1989 compilation of data.³⁰

§Mean value obtained by the author by the iron-lanthanum collection/xanthate extraction/spectrophotometric iodide method.⁹

¶CCRMP value given for information only (not certified).

||Mean value obtained by the author by the iodide extraction/flame AAS method.⁸

^aUsable value.³¹

^bUsable value.³²

^cMean result obtained by direct method (no extraction).

^dMost recent consensus value.³³

agreement with previous results obtained in this laboratory by the iron-lanthanum collection/xanthate extraction/spectrophotometric iodide⁹ and the iodide extraction/flame AAS⁸ methods mentioned previously. Except for FER-4, PACS-1 and NBS 1633a, the results obtained for the CCRMP soils and rocks, for some United States Geological Survey (USGS) rocks and for the National Research Council of Canada (NRCC) and the National Bureau of Standards (NBS) marine and river sediments are also, in most cases, in good agreement with the certified and usable or information-only values and, where applicable, with the 1987 NBS consensus values.³³ They also agree reasonably well with other values obtained within the last decade by a variety of instrumental methods.

Although the result obtained for FER-4 is only about half the reported "usable value",³² it is considered to be much more representative of the true antimony content of this material. The usable value is probably much too high because it is the approximate mean of only 5 results ranging from 1.3 to 7, *viz.* 1.3, 1.4, 3, 4 and 7. The first two of these values were obtained by HGAAS and the last three by neutron activation, direct flame AAS without prior separation of antimony, and X-ray fluorescence, respectively. Of these methods, the last two would not yield accurate results for antimony at the level present in FER-4. Conversely, the certified value for the NRCC marine sediment PACS-1 is probably too low because the results obtained in this work by the proposed method

and by direct HGAAS, without prior separation of the antimony, are in excellent agreement with recent values obtained in the NRCC laboratory by inductively-coupled plasma mass spectrometry with both external calibration and isotope dilution.²⁴ The result obtained for the NBS coal fly ash 1633a is slightly lower than the most recent consensus value but still within the wide range of values (4.2–10.1) reported by other workers.³³ The result obtained for UMT-1, which is currently undergoing certification in the CCRMP, is included for information purposes for other analysts. Each of the individual results obtained for all the reference materials was the mean of 3 or 4 HGAAS runs involving duplicate measurements each time. The antimony concentration was calculated by the linear regression least-squares method from absorbance data obtained for each run with antimony calibration solutions covering the linear response range of 0–20 ng/ml.

The proposed extraction procedure has some definite advantages over various other extraction procedures recently employed for the separation of antimony from matrix elements before its determination by graphite-furnace, flame or hydride-generation AAS. It is considerably more selective than procedures involving the extraction of the ammonium pyrrolidinedithiocarbamate³⁴ and chloro complexes,³⁵ or the extraction of the antimony(III) iodide complex from hydrochloric acid media with methyl isobutyl ketone containing both Alamine 336 (tricaprylyl tertiary amine) and Aliquat 336 (tricaprylyl methyl ammonium chloride)⁶ or tri-octylphosphine oxide.⁷ This is because lead, iron, tin, manganese, chromium, cadmium, cobalt, nickel, bismuth, gallium, indium, silver and zinc are not extracted, or are not significantly extracted, under the conditions used in this work. Contrary to most of these methods, large amounts of iron and lead and moderate amounts of copper do not interfere. A further advantage over methods involving the extraction of the antimony(V) chloro-complex is that it involves the extraction of antimony(III), which is stable in strong hydrochloric acid media. Antimony(V) is notoriously unstable under these conditions and rapidly hydrolyses.³⁶ Although the xanthate extraction step is not necessary for samples of very high antimony content such as PACS-1, it is recommended for most rocks, ores, soils and sediments because high results were obtained for several samples containing from ~1 to

10 $\mu\text{g/g}$ of antimony, when the extraction step was omitted.

In the proposed method, the detection limit, calculated as three times the standard deviation of the reagent blank, based on a 1-g sample taken through the extraction step and a final volume of 25 ml, is ~20 ng of antimony per g of sample. The sensitivity or characteristic concentration is ~0.15 ng of antimony per ml for 0.0044 absorbance. In this work the reagent blank for a 50-ml aliquot of sample solution varied in the range ~40–50 ng of antimony, but this could probably be reduced by using ultra-pure acids. The method is directly applicable to lead concentrates but not to copper or molybdenum concentrates unless antimony is first separated from most of the copper and molybdenum by co-precipitation with iron and lanthanum as described earlier.⁹ The method has been applied to the determination of $\geq 1 \mu\text{g/l}$ quantities of antimony in zinc electrolytes after treatment of a suitable portion of the solution with nitric and perchloric acids. This is followed by evaporation of the solution to ~1–2 ml and the subsequent reduction, extraction and determination of antimony.

REFERENCES

1. A. E. Smith, *Analyst*, 1975, **100**, 300.
2. J. G. Crock and F. E. Lichte, *Anal. Chim. Acta*, 1982, **144**, 223.
3. J. R. Castillo, J. Lanaja, M. C. Martinez and J. Aznarez, *Analyst*, 1982, **107**, 1488.
4. L. H. J. Lajunen, T. Merkkiniemi and H. Hayrynen, *Talanta*, 1984, **31**, 709.
5. K. Petrick and V. Krivan, *Z. Anal. Chem.*, 1987, **327**, 338.
6. J. R. Clark, *J. Anal. At. Spectrom.*, 1986, **1**, 301.
7. N. K. Roy and A. K. Das, *Talanta*, 1988, **35**, 406.
8. E. M. Donaldson and M. Wang, *ibid.*, 1986, **33**, 233.
9. E. M. Donaldson, *ibid.*, 1979, **26**, 999.
10. *Idem*, *ibid.*, 1988, **35**, 47.
11. E. M. Donaldson and M. E. Leaver, *ibid.*, 1990, **37**, 173.
12. B. T. Sturman, *Appl. Spectrosc.*, 1985, **39**, 48.
13. E. M. Donaldson and E. Mark, *Talanta*, 1982, **29**, 663.
14. E. M. Donaldson, *ibid.*, 1976, **23**, 411.
15. E. M. Donaldson and M. E. Leaver, *ibid.*, 1988, **35**, 297.
16. K. Brodie, B. Frary, B. Sturman and L. Voth, *Varian Instruments at Work*, 1983, No. AA-38.
17. B. S. Evans, *Analyst*, 1931, **56**, 171.
18. J. L. Lingane, *Analytical Chemistry of Selected Metallic Elements*, p. 28. Reinhold, New York, 1966.
19. I. M. Kolthoff and R. Belcher, *Volumetric Analysis*, Vol. III, p. 151. Interscience, New York, 1957.
20. E. S. Gladney and D. R. Perrin, *Geostds. Newsl.*, 1981, **5**, 113.
21. S. Terashima, *ibid.*, 1986., **10**, 127.
22. E. de Oliveira, J. W. McLaren and S. S. Berman, *Anal. Chem.*, 1983, **55**, 2047.

23. J. W. McLaren, D. Beauchemin and S. S. Berman, *ibid.*, 1987, **59**, 610.
24. *Idem*, *Spectrochim. Acta*, 1988, **43B**, 413.
25. H. A. van der Sloot and J. Zonderhuis, *Geostds. Newsl.*, 1979, **3**, 185.
26. C. M. Elson, J. Milley and A. Chatt, *Anal. Chim. Acta*, 1982, **142**, 269.
27. H. Niskavaara, J. Virtasolo and L. H. J. Lajunen, *Spectrochim. Acta*, 1985, **40B**, 1219.
28. H. A. van der Sloot, D. Hoede, Th. J. L. Klinkers and H. A. Das, *J. Radioanal. Chem.*, 1982, **71**, 463.
29. K. A. Elrick and A. J. Horowitz, *Varian Instruments at Work*, 1986, No. AA-56.
30. K. Govindaraju, *Geostds. Newsl.*, 1989, **13**, 1.
31. S. Abbey, *Geol. Surv. Canada Paper*, 83-15, 1983.
32. S. Abbey, C. R. McLeod and W. Liang-Guo, *ibid.*, 83-19, 1983.
33. E. S. Gladney, B. T. O'Malley, I. Roelandts and T. E. Gills, *National Bureau of Standards Special Publication*, 260-111, 1987.
34. J. Aznarez, F. Palacios, M. S. Ortega and J. C. Vidal, *Analyst*, 1984, **109**, 123.
35. P. Hannaker and T. C. Hughes, *Anal. Chem.*, 1977, **49**, 1485.
36. E. B. Sandell, *Colorimetric Determination of Traces of Metals*, 3rd Ed., p. 259. Interscience, New York, 1959.

SELECTIVE DETERMINATION OF THEOPHYLLINE IN THE PRESENCE OF CAFFEINE BY SENSITIZED LUMINESCENCE OF EUROPIUM(III)

L. M. PERRY and J. D. WINEFORDNER*

Department of Chemistry, University of Florida, Gainesville, FL 32611, U.S.A.

(Received 13 November 1989. Revised 19 April 1990. Accepted 18 May 1990)

Summary—Theophylline was determined in a mixture with caffeine by room-temperature luminescence. The excitation energy absorbed by the theophylline was transferred to europium(III), which then emitted its characteristic luminescence. The enhanced luminescence emission intensity was quantitatively related to theophylline concentration without interference from caffeine or emission from the sample matrix. A mechanism explaining the observed selectivity is presented. Possible analytical use of the energy-transfer approach for the determination of similarly structured compounds is discussed.

Theophylline (1,3-dimethylxanthine) and caffeine (1,3,7-trimethylxanthine) are two naturally occurring alkaloids of significant interest in biological and medicinal chemistry.¹ Caffeine is a major constituent (1.2%) of coffee beans and is not only a major natural constituent of the American diet, but is also utilized in the production of beverages and pharmaceuticals.² Theophylline, on the other hand, is a minor constituent of plant leaves and is synthesized for use in drugs and pharmaceutical formulations.³ Caffeine and theophylline share several pharmacological actions of therapeutic interest.^{1,2} Both stimulate cardiac muscle and the central nervous system. One of their most important applications is the relaxation of smooth muscle, notably bronchial muscle. Theophylline is the principal drug used for treating acute asthma and most lung disorders. Despite the similarities between these two alkaloids, a significant difference exists in their therapeutic index.^{1,2,4} Caffeine appears to exhibit no obvious toxicity, whereas theophylline at plasma concentrations of 50 $\mu\text{g/ml}$ has been reported to induce severe toxic symptoms and even death. The therapeutic plasma concentration range is 10–20 $\mu\text{g/ml}$. The toxicity of theophylline and its widespread use in medical treatment have prompted numerous investigations for its determination, especially for therapeutic drug monitoring.¹ Because caffeine is normally present as a metabolite of

theophylline in addition to its ingestion from the diet, both compounds are usually present in human samples.

Caffeine and theophylline possess very similar structures and give nearly the same absorption spectra and luminescence spectra.⁵⁻⁷ Since both are generally present in biological samples, their individual determination requires time-consuming separation procedures before analysis and immunoassay techniques can be applied.^{8,9} Spectroscopic determination of theophylline in a mixture has been primarily limited by lack of selectivity.

Earlier, we developed a method for the determination of theophylline by room-temperature luminescence in buffered aqueous solution by energy transfer to trivalent europium.¹⁰ Excitation energy is absorbed by the theophylline and transferred to a europium ion, which then gives luminescence in a spectral region distant from possible matrix interference. The present investigation deals with the application of this methodology to a mixture of theophylline and caffeine, and assessment of the selectivity of the method. The selective association of Eu(III) with theophylline in a mixture of the two alkaloids results in transfer of excitation energy from theophylline to the metal ion, and enhanced luminescence emission from the Eu(III). This approach provides a simple method for trace detection of theophylline in a mixture, without interference for caffeine. A possible mechanism is postulated to explain the observed selectivity of the method.

*Author for correspondence. Research supported by NIH-R01-GM11373-26.

EXPERIMENTAL

Apparatus

A Perkin-Elmer LS-5 luminescence spectrofluorimeter (Perkin-Elmer, Norwalk, CT) interfaced to a model CLS-3600 data station was used in the fluorescence mode for the collection of all room-temperature luminescence spectra and intensity measurements. The excitation and emission slits were both set at 10 nm band pass for all measurements. A 360 nm cut-off filter was placed in front of the emission monochromator in order to minimize second-order scatter. Scanning of the excitation and emission spectra at 120 nm/min and of the resulting peak intensity and wavelength were processor-controlled by the Perkin-Elmer PECLS application program. All measurements for analytical calibration curves and titration experiments involving energy transfer were made by use of the peak excitation wavelengths of the analytes and the peak emission wavelength of europium(III).

Fused-silica cuvettes with a 1-cm path-length were used. The highest precision was obtained by using the same cuvette in the same position in the sample holder in the spectrofluorimeter. The same cuvettes were used in the absorption spectrometer.

A model 8450A diode array spectrophotometer (Hewlett Packard, San Diego, CA) was used from the absorption studies; a Perkin-Elmer Metrion IV pH-meter was used in the preparation of the buffer solutions.

Reagents

Europium(III) nitrate pentahydrate and 1,3-dimethylxanthine (theophylline) (Aldrich Chemical Co., Milwaukee, WI), 1,3,7-trimethylxanthine (caffeine) (Sigma Chemical Co., St. Louis, MO), tris(hydroxymethyl)aminomethane (THAM) and nitric acid (Fisher Scientific Co., Fair Lawn, NJ) were reagent grade and used as received. The buffer solution was prepared with "Nanopure" demineralized water (Barnstead System, Sybron Corp., Boston, MA).

The buffer was prepared by dissolving 2.42 g of THAM in 2 litres of demineralized water and adjusting the pH to 7.5 with 1M nitric acid. Stock solutions (0.001M) of theophylline and caffeine were prepared by dissolution of the analyte and dilution to volume with buffer solution in 100 or 250 ml standard flasks. A europium nitrate solution of twice the final concentration desired was prepared by dis-

solving the appropriate weight of europium(III) nitrate pentahydrate in the buffer solution and dilution to volume with the buffer in 500 or 1000 ml standard flasks. For the titration studies, all analyte solutions, as well as the europium nitrate solution, were 0.001M.

Standard solutions were prepared by dilution of the theophylline stock solutions; the final solutions all contained $7.5 \times 10^{-4}M$ Eu^{3+} . Blank solutions were prepared in standard flasks and consisted of equal volumes of buffer and europium(III) solution.

Procedures

Standard solutions were allowed to equilibrate for specific time periods, before absorbance and fluorescence measurements were made in separate experiments. To ensure equilibration in the titration and fluorescence experiments; after each addition of titrant, the solution was stirred for 2 min (magnetic stirrer) before the luminescence was recorded. The 4-ml volume taken for measurement was returned to the titration beaker, so that no substantial loss of reagents occurred. The emission intensity for each analyte was recorded with the appropriate peak excitation wavelength (300 nm) for the analyte and the peak emission wavelength (615 nm) of europium(III). Rigorous cleaning of the sample cuvette was required before all measurements, except for the titration studies, because of contamination by the analytes and memory effects with europium(III). For cleaning, the cuvette was rinsed once with distilled water, once with 1M nitric acid, thrice with buffer solution, and finally three small portions of the solution to be measured. It was necessary to measure at least two blanks before each analyte measurement to ensure that the sample cuvette was clean. All analyte measurements, except for the luminescence titration experiments, were corrected for the background emission of the blank. Each analyte measurement was made in triplicate, and a minimum of 16 blanks was measured for each analytical curve.

RESULTS AND DISCUSSION

The excitation and emission luminescence spectra of theophylline showed prominent bands at 308 and 320 nm, the latter being the Raman band of water. The luminescence of theophylline occurred at 365 nm, which unfortunately is in a spectral region where serious

spectral interferences would occur in applications. The optimum Eu(III) concentration was found to be $7.5 \times 10^{-4} M$ for theophylline concentrations between 0 and $100 \mu\text{g/ml}$. Of the luminescence excitation peaks (250, 300, 321 and 395 nm) and emission peaks (590 and 615 nm) of these solutions, the combination of excitation at 300 nm and measurement of the emission at 615 nm gave the best analytical figures of merit.

Figure 1 shows the luminescence intensities obtained when successive additions of $0.001 M$ theophylline or caffeine solution or of buffer were made to 10 ml of $0.001 M$ Eu(III) solution. Figure 1 shows that the maximum luminescence signal for theophylline occurs when approximately 1.8 ml of $0.001 M$ theophylline has been added to the titration beaker. This corresponds to a europium(III) concentration of approximately $8.5 \times 10^{-4} M$ when corrected for dilution, and a europium(III)/theophylline molar ratio of 5.5. This procedure provided a working range for the optimum Eu(III) concentration for the determination of theophylline. The luminescence titration curve for caffeine under the same conditions shows only a very small increase in luminescence intensity over a broad region, compared to the blank luminescence emission intensity. The maximum luminescence signal occurs at a europium(III)/caffeine molar ratio of approximately 1. This means that the optimum Eu(III) concentration for determination of this compound should be somewhere around $3.8 \times 10^{-4} M$, which is less than half that required for the sensitized Eu(III)–theophylline system. A 10-ml aliquot of $0.001 M$ Eu(III) was titrated with the buffer solution in order to determine any changes that might be caused by the buffer (blank); a slight decrease in the emission intensity was observed and attributed to dilution of the europium. The results of these experiments suggest that caffeine sensitized the europium luminescence at much lower concentrations of Eu(III) than theophylline does, and with significantly less intensity. Therefore, for a mixture of these two alkaloids in a europium(III) solution of the appropriate concentration, theophylline would be primarily responsible for the observed sensitized emission.

To ascertain the optimum Eu(III) concentration for the determination of theophylline, six series of standard solutions of theophylline were prepared, with Eu(III) concentrations of 2.5×10^{-4} , 5.0×10^{-4} , 7.5×10^{-4} , 10×10^{-4} , 15×10^{-4} , and $25 \times 10^{-4} M$ respectively. The

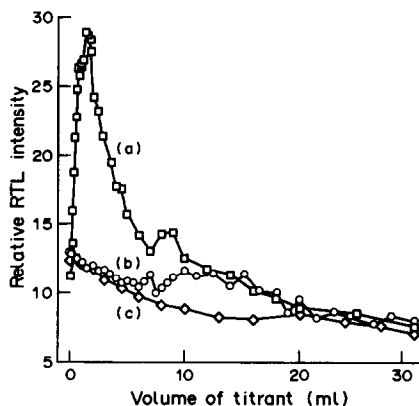


Fig. 1. Comparison of luminescence titration curves for Eu^{3+} with (a) theophylline, (b) caffeine, (c) blank.

sensitized luminescence was found to be maximum and stable when the concentration of Eu(III) was held at $7.5 \times 10^{-4} M$.

A second set of experiments was performed in order to confirm that caffeine, at concentrations between 6 and $60 \mu\text{g/ml}$, would not sensitize the luminescence of $7.5 \times 10^{-4} M$ Eu(III). There was virtually no difference between the luminescence intensity for the blank (buffer only) and the caffeine solution, at any concentration.

The possibility of chemical interactions between theophylline and caffeine in solution was investigated. Each plot in Fig. 2 represents the luminescence observed for caffeine concentrations ranging from 5 to $65 \mu\text{g/ml}$, with three different constant Eu(III) concentrations and $30 \mu\text{g/ml}$ theophylline. It is seen that the sensitized signal intensities for $30 \mu\text{g/ml}$ theophylline depend on the Eu(III) concentration, and are increasingly quenched by increased caffeine concentrations when 10×10^{-4} or $15 \times 10^{-4} M$

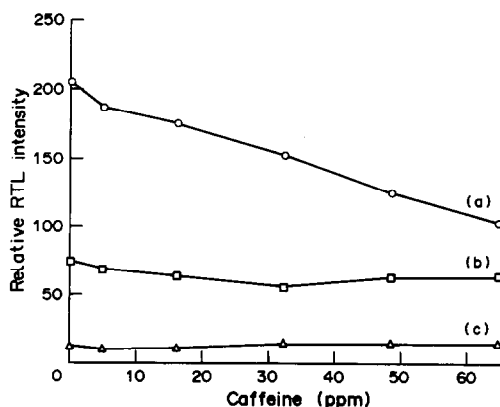


Fig. 2. The effect of increasing caffeine concentration on the theophylline-sensitized Eu(III) luminescence signal intensity. Theophylline concentration was constant at $30 \mu\text{g/ml}$. Plots (a) $15 \times 10^{-4} M$ Eu(III), (b) $10 \times 10^{-4} M$ Eu(III), (c) $7.5 \times 10^{-4} M$ Eu(III).

Eu(III) is used. The plot for the $7.5 \times 10^{-4} M$ Eu(III) system is the least sensitive to caffeine concentration. Triplicate measurements were made for each point and all the relative standard deviations (RSDs) were less than 5%. Each signal was corrected for that of a blank consisting of buffer, caffeine and europium(III) at the appropriate concentrations. This set of experiments confirmed that in this system, caffeine did not sensitize the Eu(III) emission and did not interfere with energy transfer from the theophylline.

The useful linear range, 10–70 $\mu\text{g/ml}$, for the analysis of pure theophylline solutions is shown in Fig. 3 together with that (2–70 $\mu\text{g/ml}$) for theophylline in the presence of 35 $\mu\text{g/ml}$ caffeine, with $7.5 \times 10^{-4} M$ Eu(III) and excitation and emission wavelengths of 300 and 615 nm, respectively. Triplicate measurements were made for each point, and the RSDs for all points were 6% or less. The analytical figures of merit for both analytes are summarized in Table 1. It is evident from Fig. 3 that there is virtually no interference by caffeine in the determination of theophylline. There are two main advantages of the method. First, it is not necessary to separate the theophylline from caffeine, and secondly the useful linear working range for theophylline covers the concentration range for theophylline toxicity.

CONCLUSIONS

The selective determination of theophylline in the presence of caffeine can be accomplished by transfer of the excitation energy of theophylline at 300 nm to Eu(III). The resulting sensitized emission from Eu(III) at 615 nm is far removed

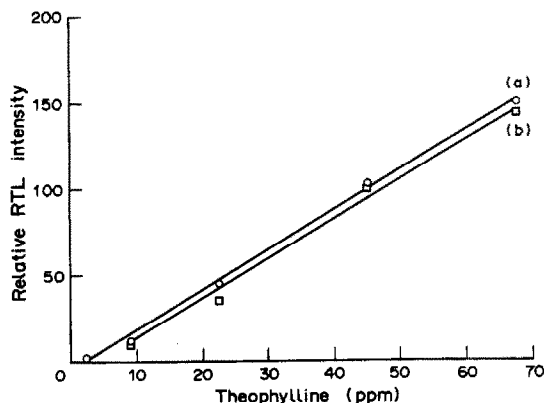


Fig. 3. Working curves for the determination of (a) theophylline + 35 $\mu\text{g/ml}$ caffeine in $7.5 \times 10^{-4} M$ Eu(III), (b) theophylline in $7.5 \times 10^{-4} M$ Eu(III). Instrumental sensitivity is 4 \times greater than in Fig. 2.

Table 1. Characteristics of room-temperature luminescence determination of theophylline in the presence and absence of caffeine, by sensitized Eu(III) emission ($\lambda_{\text{ex}} = 300 \text{ nm}$; $\lambda_{\text{em}} = 615 \text{ nm}$; [Eu(III)], $7.5 \times 10^{-4} M$)

Caffeine present, $\mu\text{g/ml}$	Useful linear range, $\mu\text{g/ml}$	Correlation coefficient	Regression equation*
—	10–70	0.996	$I = 2.4c - 8$
32	2–70	0.996	$I = 2.3c - 6$

* I = luminescence intensity; c = theophylline concentration ($\mu\text{g/ml}$).

from any background radiation of the buffer matrix and possible stray radiation. A linear working range of 2–70 $\mu\text{g/ml}$ is obtained for theophylline in the presence of caffeine. The calibration standards are easily and quickly prepared by addition of the reactants from burets.

The structures of caffeine, theophylline, and THAM are presented in Fig. 4. The spectral properties of caffeine and theophylline are nearly identical and the structures of the two compounds differ only in the substituent attached to one of the nitrogen atoms. It is therefore surprising that the energy transfer method is so highly selective for theophylline. The absorption studies performed in a previous

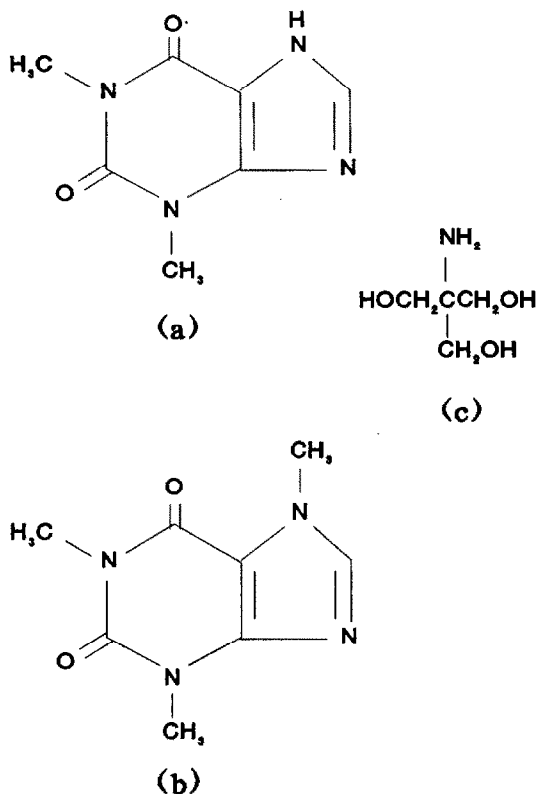


Fig. 4. Structure of (a) theophylline, (b) caffeine, (c) THAM.

investigation showed that no complex is formed between theophylline and the europium ion, (the appropriate absorption spectra of a Eu(III)-theophylline mixture and of theophylline alone are practically the same).¹⁰ It is possible that the buffer, THAM, is coordinated to the europium ion through one of its oxygen atoms, creating an outer sphere that is capable of hydrogen-bonding to theophylline molecules. This interaction could protect the analyte molecule from collisional deactivation by solvent molecules and restrict its molecular motion. Both conditions are needed in luminescence analyses for stabilization of triplet excited states,¹¹ and could promote efficient energy transfer from theophylline to the Eu(III) ion. It is generally accepted that energy transfer from organic molecules to the europium ion occurs from the triplet excited state.^{12,13} Since it is also well known that europium is most strongly bound by charged oxygen donor atoms, as in carboxylate groups,¹³ hydrogen bonding between the buffer and caffeine and theophylline would be expected to occur at a hydroxyl or amino group of the buffer and the carbonyl groups or nitrogen atoms of the alkaloids. If a carbonyl group or the unsubstituted ring nitrogen atom is involved in interactions with the buffer, energy transfer should occur from both alkaloids. Since this was not observed, there must be some other explanation. As already stated, the only structural difference is the replacement of a hydrogen atom by a methyl group on a ring nitrogen atom. Presumably this methyl group could cause steric hindrance preventing interaction of the nitrogen atom with the buffer. It would seem that the selectivity of the theophylline

energy transfer process is associated with the hydrogen-substituted ring nitrogen atom.

Although theophylline was not measured in biological materials in the present work, previous work using energy transfer from tetracyclines to Eu(III) in blood serum showed no significant luminescence background,¹⁴ so determination of theophylline in biological materials should be readily possible by the approach given here.

REFERENCES

1. W. J. Taylor and M. H. Diers Caviness (eds.), *A Textbook for the Clinical Application of Therapeutic Drug Monitoring*, Abbot Laboratories, Irving, Texas, 1986.
2. R. P. Bateh and J. D. Winefordner, *Anal. Lett.*, 1982, **15**, 373.
3. M. Windholz (ed.), *The Merck Index*, 10th Ed., Merck, Rahway, New Jersey, 1983.
4. C. N. Ou, *Am. Assoc. Clin. Chem.*, 1985, **6**, 1.
5. M. M. Andino, C. G. de Lima and J. D. Winefordner, *Spectrochim. Acta*, 1987, **43A**, 427.
6. K. Florey (ed.), *Analytical Profiles of Drug Substances*, Vol. 4, Academic Press, New York, 1975.
7. L. M. Perry, E. Y. Shao and J. D. Winefordner, *Talanta*, 1989, **36**, 1037.
8. S. M. Donahue, C. W. Brown and G. J. Kavarnos, *Am. Biotechnol. Lab.*, 1988, **6**, No. 4, 36.
9. J. F. Wilson, J. Williams, R. W. Marshall, A. Richens, I. C. Dijkuis, A. R. Hartevelde and H. J. de Jong, *Clin. Chem.*, 1985, **31**, 1089.
10. L. M. Perry and J. D. Winefordner, *Anal. Chim. Acta*, 1990, in the press.
11. A. A. Lamola, *Photochem. Photobiol.*, 1968, **8**, 601.
12. A. Heller and E. Wasserman, *J. Chem. Phys.*, 1965, **42**, 949.
13. F. S. Richardson, *Chem. Rev.*, 1982, **82**, 541.
14. L. A. Files, L. Hirschy and J. D. Winefordner, *J. Pharm. Biomed. Anal.*, 1985, **3**, 95.

ENHANCED CHEMILUMINESCENCE DETERMINATION OF α -AMYLASE BY USE OF AMYLOSE LABELLED WITH HORSERADISH PEROXIDASE

L. J. KRICKA, J. M. MARCINKOWSKI and P. WILDING

Department of Pathology and Laboratory Medicine, Hospital of the University of Pennsylvania,
Philadelphia, PA 19104, U.S.A.

S. LEKHAKULA

Department of Biochemistry, Faculty of Medicine, Siriraj Hospital, Mahidol University,
Bangkok 10700, Thailand

(Received 19 January 1990. Revised 24 April 1990. Accepted 30 April 1990)

Summary—An enhanced chemiluminescence method for determining soluble and immobilized α -amylase has been developed, based on use of an insoluble amylose substrate labelled with horseradish peroxidase. Soluble peroxidase-labelled fragments of the substrate, released by the action of α -amylase, are quantified by the peroxidase-catalyzed luminol-peroxide-*p*-iodophenol reaction. The detection limit for α -amylase was 125 fmole (12.5 nM). An insoluble amylopectin labelled with horseradish peroxidase was also effective as a substrate for this type of assay.

Enhanced chemiluminescence methods for the determination of horseradish peroxidase (HRP) labels are widely used in enzyme immunoassay.¹⁻³ This type of method is based on the HRP-catalyzed oxidation of luminol by peroxide in the presence of an enhancer such as *p*-iodophenol. Light emission from this reaction is prolonged and intense, thus simplifying initiation of the reaction and measurement of the light. We have now developed an enhanced chemiluminescence method for determining α -amylase (E.C. 3.2.1.1), an enzyme which has clinical applications in the diagnosis of acute pancreatitis.⁴ The new method entails catalysis by α -amylase of the release of soluble HRP-labelled maltose and glucose molecules from an insoluble HRP-labelled amylose substrate by cleavage of the α -1,4-hemiacetal links. These molecules are separated from the unreacted insoluble substrate and HRP released from them is then determined by use of the luminol-peroxide-*p*-iodophenol reaction.

EXPERIMENTAL

Apparatus

A Berthold Biolumat LB 9500T luminometer (Berthold Analytical Instruments, Nashua, NH) was used to measure the light emission.

Reagents

Amylose (corn), amylopectin (potato), horseradish peroxidase (type VI), cyanogen bromide, polyoxyethylene sorbitan monolaurate (Tween-20), hydrogen peroxide, α -amylase (*Bacillus sp.* type II-A, 2050 units/mg), and α -amylase immobilized on polyacrylamide gel (700 units/g) were purchased from Sigma Chemical Co. (St. Louis, MO). *p*-Iodophenol was obtained from Aldrich (Milwaukee, WI). Luminol was purified by conversion into its sodium salt as described previously.⁵

Preparation of HRP-labelled amylose substrate

Amylose was activated with cyanogen bromide by a procedure previously used for the activation of Sepharose.⁶ Amylose (0.5 g) was suspended in 20 ml of 2M potassium carbonate by vigorous stirring for 5 min. Then 300 μ l of 333 mg/ml cyanogen bromide solution in acetonitrile were added dropwise to the stirred suspension, and the suspension was cooled in an ice-bath and stirred for an additional 5 min. The activated amylose was filtered off with a sintered-glass funnel and washed with 200 ml of cold distilled water and then 200 ml of cold 0.1M potassium pyrophosphate buffer (pH 8). This activated amylose was then added to 5 ml of 0.6 mg/ml HRP solution in the pyrophosphate buffer and stirred overnight at 4°.

The amylose preparation was stored in 5 ml of 0.1M Tris buffer (pH 8.6) at 0–4°. Amylopectin was labelled with HRP by an analogous procedure.

Determination of α -amylase

The HRP-labelled amylose was washed extensively with phosphate-buffered saline (PBS) (0.01M potassium phosphate, 0.120M sodium chloride, pH 7.4) containing 0.5 ml/l. Tween-20 to remove any HRP leached from the substrate. It was then resuspended (50 mg/ml) in 0.1M Tris buffer (pH 8.6). Then a 50- μ l aliquot of the suspension was incubated with 10 μ l of a 0.1 mg/ml solution of α -amylase (205 units/ml, 20 μ M) in 9 g/l. sodium chloride solution, for 15 min at room temperature. The mixture was centrifuged and a 10 μ l volume of the supernatant liquid was tested for HRP by addition of 100 μ l of a chemiluminescence substrate solution. The intensity of the light emission (integrated over 10 sec) was measured between 2 and 20 min after addition of the substrate. The substrate was prepared as follows: sodium luminol (12.5 mg) was dissolved in 50 ml of 0.1M Tris buffer (pH 8.6) and a 3 ml aliquot was mixed with 2 μ l of 30% v/v hydrogen peroxide and 3 μ l of 9 mg/ml *p*-iodophenol solution in dimethylsulfoxide.

Effect of agitation. Dilutions of α -amylase (1 mg/ml) were prepared in 9 g/l. sodium chloride solution and 10 μ l samples assayed as described above except that the reaction mixture was agitated on a Hema-Tek Aliquot Mixer (Miles, Elkhart, IN) during the 15 min incubation at room temperature.

Effect of incubation time. A 10 μ l sample of α -amylase (1 mg/ml, 2050 units/ml) was mixed with 50 μ l of the HRP-labelled amylose substrate. The mixture was incubated for 5 min at room temperature and a 10 μ l sample of the supernatant liquid was assayed for HRP activity as described. The experiment was repeated with different incubation times (15, 30 and 60 min).

Effect of substrate concentration. A 10 μ l sample of α -amylase (1 mg/ml, 2050 units/ml) was mixed with different amounts of HRP-labelled amylose substrate (25, 50, 75 and 100 μ l) and the HRP released was assayed as above.

Stability of HRP-labelled amylose

A sample of HRP-labelled amylose was stored at room temperature for 2 years and its properties as a substrate for α -amylase

were compared with a fresh preparation of the HRP-amylose substrate.

Determination of immobilized α -amylase

A preparation of α -amylase immobilized on polyacrylamide gel (700 units/g) was rehydrated according to the manufacturer's instructions and washed repeatedly to remove any unbound α -amylase. A sample of the immobilized α -amylase suspension (10 μ l) was assayed as described above, to determine whether the immobilized enzyme could also react with the amylose substrate.

RESULTS AND DISCUSSION

Figure 1 shows the release of soluble HRP from the HRP-labelled amylose substrate by the action of α -amylase, as a function of time. Prolonged incubation (>15 min) did not improve the signal and an incubation time of 15 min was used in subsequent assays. Both steps in the determination of α -amylase were performed at pH 7.8 in order to maximize the light emission in the HRP-catalyzed chemiluminescence detection reaction, which has a sharp pH optimum at 7.8.⁷ Previous assays for the *Bacillus* sp. α -amylase with dye-amylose substrates have been performed at pH 7.5, so the assay pH chosen should not affect the α -amylase activity.⁸ The influence of the substrate concentration on the signal and background for the α -amylase assay is shown in Fig. 2. A 50 μ l aliquot of a 50 mg/ml suspension of the substrate was selected for use, as giving the best compromise between reagent economy and signal-to-background ratio. The effect of agitation on the heterogeneous reaction between

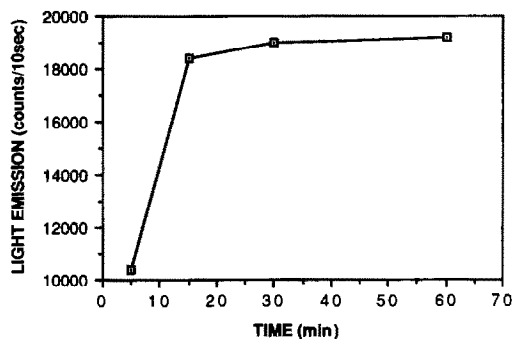


Fig. 1. Kinetics of α -amylase catalysis of release of horseradish peroxidase from horseradish peroxidase-labelled amylose. (200 pmole of α -amylase and 2.5 mg of substrate incubated at room temperature; all points are the means of duplicate determinations).

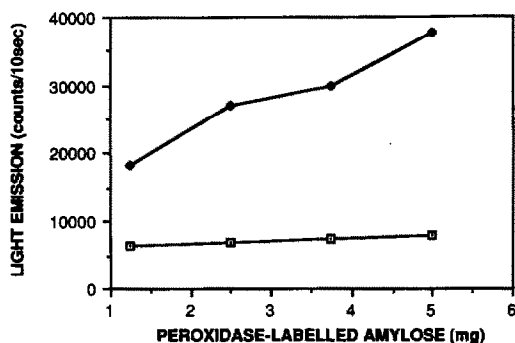


Fig. 2. Effect of concentration of horseradish peroxidase-labelled amylose on signal (◆) and blank (□) in an assay for α -amylase (200 pmole; all points are the means of duplicate determinations).

the soluble α -amylase and the insoluble amylose substrate was investigated. This showed the improvement in signal expected for use of more efficient mixing of the two reactants (Fig. 3).

The stability of the substrate was excellent, as judged by the performance of a fresh preparation compared with that of a preparation which had been stored for 2 years at room temperature. The activity of the stored preparation was still about 50% of that of a fresh preparation of the substrate.

The working range and detection limit of the chemiluminescence assay varied from batch to batch of substrate, presumably owing to differences in the amount of active HRP immobilized, but a dose response up to 200 pmole and a detection limit of 125 femtomole (12.5 nM; signal-to-background ratio = 2) were achieved. Within-batch precision of this manual assay was 15% for 50 pmole ($\equiv 5 \mu\text{M}$) of α -amylase.

In an attempt to increase the assay sensitivity a series of HRP-labelled substrates was prepared with higher HRP:amylose ratios and a higher cyanogen bromide concentration in the activation step. Increasing the amount of HRP bound to the amylose did not produce a significant gain in sensitivity. This was in part due to an increase in the assay background, caused presumably by leaching of unbound enzyme that was trapped in the polymer matrix and not removed in the preliminary washing steps. A major reason for the lack of improvement in sensitivity is the steric hindrance caused by the high density of bound peroxidase molecules. These would hinder the approach of α -amylase to the substrate and decrease the number of soluble fragments formed. Interestingly, it was possible to measure α -amylase immobilized on polyacrylamide gel, by incubating a mixture of the immobilized enzyme with the insoluble sub-

strate. Surprisingly, the kinetics of the release of HRP was similar to that obtained with the soluble enzyme.

HRP-labelled amylopectin was also effective as a substrate for α -amylase (data not shown), but was more difficult to prepare than the HRP-labelled amylose and was not investigated further.

α -Amylase activity can be measured by saccharogenic, amyloclastic and chromogenic methods.⁹ The last of these methods involves the release of soluble dyed-starch from an insoluble dyed-starch substrate.¹⁰ The method presented in this paper is based on the same principle, except that the molecule released is an enzyme. Release of peroxidase molecules from an insoluble elastin substrate by the enzyme elastase has also been described previously, but the peroxidase released was detected colorimetrically.¹¹ The use of an enzyme rather than a chromogenic label offers the potential for amplifying the signal and thus increasing the assay sensitivity since each HRP molecule released catalyzes the chemiluminescent conversion of many luminol molecules. The detection limit for HRP by use of the enhanced chemiluminescence assay is 25 attomoles¹ and it was expected that the detection limit for α -amylase by use of a combination of enhanced chemiluminescence and HRP-labelled amylose would also be in the attomole region. The limited sensitivity of this assay is due to a number of factors. The presence of large HRP molecules on the amylose may restrict the interaction of the enzyme with the substrate and this may account for the minor improvements in assay performance when the HRP:amylose ratio was increased. α -Amylase makes random cuts in the

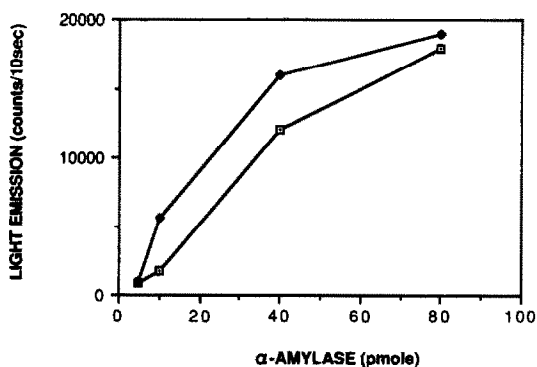


Fig. 3. Effect of mixing on the release of horseradish peroxidase from horseradish peroxidase-labelled amylose by α -amylase (100 pmole) (◆ with mixing, □ without mixing, during incubation of the enzyme and substrate; all points are the means of duplicate determinations).

amylose chain and not all of these lead to the soluble products. Large soluble products, once formed, can compete with the insoluble substrate and this would reduce the overall rate of generation of soluble HRP-labelled products. Inhibition of α -amylase by sugar products formed from starches has been demonstrated and this would also be detrimental to the sensitivity.¹² In biological samples, a further limitation may be destruction of HRP by proteases, although this was not a problem in previous work on the determination of serum bile acids with a steroid dehydrogenase and bioluminescent enzymes co-immobilized on Sepharose.¹³

This preliminary study has demonstrated that the enhanced chemiluminescence assay principle can be extended to include hydrolase enzymes such as α -amylase. Further work is being directed to the investigation of this assay for α -amylase in clinical samples, and the extension of enhanced chemiluminescence assay to other enzyme systems.

Acknowledgement—The financial support of the British Technology Group is gratefully acknowledged. Aspects of this work are the subject of patents which have been assigned to the British Technology Group.

REFERENCES

1. G. H. G. Thorpe and L. J. Kricka, *Methods Enzymol.*, 1986, **133**, 331.
2. L. J. Kricka, G. H. G. Thorpe and T. P. Whitehead, *Eur. Pat.*, 11645, 1983.
3. L. J. Kricka and G. H. G. Thorpe, in *Luminescence Immunoassay and Molecular Applications*, K. Van Dyke and R. Van Dyke (eds.), p. 77. CRC Press, Boca Raton, 1990.
4. H. Song, N. W. Tietz and C. Tan, *Clin. Chem.*, 1970, **16**, 264.
5. R. A. W. Stott and L. J. Kricka, in *Bioluminescence and Chemiluminescence*, J. Scholmerich, R. Andreesen, A. Kapp, M. Ernst and W. G. Woods (eds.), p. 237. Wiley, Chichester, 1987.
6. J. Ford and M. DeLuca, *Anal. Biochem.*, 1981, **110**, 43.
7. G. H. G. Thorpe, L. J. Kricka, S. B. Moseley and T. P. Whitehead, *Clin. Chem.*, 1985, **31**, 1335.
8. P. Mantsala and H. Zalkin, *J. Biol. Chem.*, 1979, **254**, 8540.
9. A. Y. Foo and S. Rosalki, *Ann. Clin. Biochem.*, 1986, **23**, 624.
10. H. R. Rinderknecht, P. Wilding and B. J. Haverback, *Experientia*, 1967, **23**, 805.
11. G. C. Saunders, Z. Svitra and A. Martinez, *Anal. Biochem.*, 1982, **126**, 122.
12. H. W. Leach and T. J. Schoch, *Cereal Chem.*, 1961, **38**, 34.
13. A. Roda, L. J. Kricka, M. DeLuca and A. F. Hofmann, *J. Lipid Res.*, 1982, **23**, 1354.

DETERMINATION OF TRI-*n*-BUTYLTIN IN OYSTERS BY REACTION-GAS CHROMATOGRAPHY OF HYDRIDE DERIVATIVES

JAMES M. HUNGERFORD^{1,*}, KEVIN D. WALKER¹, JAMES D. TORKELSON²,
KURT STEINBRECHER² and MARLEEN M. WEKELL¹

¹Seafood Products Research Center, and ²Science Branch, U.S. Food and Drug Administration, 22201
23rd Dr. S.E., P.O. Box 3012, Bothell, WA 98041-3012, U.S.A.

(Received 12 December 1989. Revised 5 February 1990. Accepted 12 February 1990)

Summary—A reaction-gas chromatography method for determining tri-*n*-butyltin (TBT) as the hydride derivative has been adapted to allow determination of TBT in oysters. The extraction method has been modified to prevent fouling of the hydride formation reactor and the gas chromatography has been made faster by employing a different column and temperature program. The detection limit is 3–6 ng/g in oyster tissue. Apparent recoveries of TBT from oyster tissue at 25 and 125 ng/g levels are 107 and 97%, respectively.

Alkyltins, especially tri-*n*-butyltin (TBT), are used as biocidal preservatives,¹ as disinfectants,¹ and as antifouling agents in marine coatings.^{2,3} Release of TBT from the treated surfaces of ship hulls⁴ is of particular concern because TBT is a general biocide and also because food-chain concentration of TBT has been demonstrated in chinook salmon,⁵ crabs,⁶ mussels⁷ and oysters.⁸ TBT is also toxic to mammalian species, causing both hepatic and cutaneous toxicity and producing (*in vitro*) metabolic and cellular alterations. On the basis of these findings, there is concern that the presence of TBT in shellfish and finfish may pose a threat to human health. In a recent review⁹ it was concluded that the toxicity data are not yet adequate to allow a permissible daily intake of tributyltin to be set. However, since mammalian toxicity has been demonstrated, there is a need for sensitive and rapid analytical methods to screen human foods for TBT, even before tolerance levels are established.

Chromatographic techniques used for determination of TBT include HPLC^{10,11} and, more commonly, gas chromatography, preferably combined with selective detection.¹² These methods can be divided into those in which the extract is injected without prior derivatization of TBT¹³ and those where prior derivatization is used to improve the quality of the separation. In

the derivatization methods, both alkylation¹⁴⁻¹⁷ and hydride formation¹⁸⁻²⁰ have been used to form volatile species which are easily separated.

Sullivan *et al.* have described a reaction-GC method for determining butyltins in salmon by on-line formation of butyltin hydrides.²⁰ A packed reactor containing sodium borohydride was mounted below the injection port of a gas chromatograph. The hydrides formed in the reactor passed directly into the GC capillary column where they were separated prior to detection with a flame-photometric detector (FPD). TBT was extracted from salmon tissue by a modified Bligh and Dyer²¹ procedure.

We have attempted to apply this extraction method to oysters, but without success. TBT and interfering materials were co-eluted, there was pronounced baseline drift and the hydride reactor was fouled so rapidly by the extract that quantitative determination was impossible. Alternative extraction procedures were explored, and the on-line hydride formation-GC method was adapted to allow the determination of TBT in oysters.

EXPERIMENTAL

Reagents

Tri-*n*-butyltin chloride (TBT), di-*n*-butyltin dichloride (DBT), tri-*n*-propyltin chloride (TPrT) and tri-*n*-butyltin hydride were obtained from Alfa (Danvers, MA). Tropolone was purchased from Aldrich (Milwaukee, WI). Stock

*Author for correspondence.

solutions of TBT, DBT, TPrT, and TBT hydride in hexane were prepared at 1.61, 1.47, 1.35 and 1.44 g/l. concentrations respectively. All solvents used were glass-distilled (Omnisolv. EM Science, Cherry Hill, NJ). The sodium borohydride reactor and injection solvent were as described previously.²⁰ Working organotin standard solutions in the range 37.9–757 µg/l. Sn were prepared by dilution of stock solutions in the injection solvent (containing 264 µg/l. Sn, as TPrT, as internal standard) and also by dilution of the stock solutions with a solution of 500 µg/g tropolone and 500 µg/ml TPrT in hexane.

Apparatus

The hydride formation reactor, gas chromatograph and flame photometric detector previously described²⁰ were used. The phenylmethylsilicone capillary column was no longer commercially available, so a more readily available capillary column (Megabore DB-1, 15 m long, 0.53 mm i.d., coated with 100% dimethylsilicone gum, 1.5 µm thick, J&W Scientific, Rancho Cordova, CA) was substituted for it.

Oyster tissue extraction

Oysters (*C. gigas*) were collected from unaffected areas and from one area heavily used by naval and recreational vessels²² in the Northwest Pacific. The ages of the oysters were given by the suppliers. Oyster tissues were separated from the shell, homogenized in stainless-steel micro-blender cups and either extracted immediately or stored at -20°. Organotins were extracted from the oyster tissue by the procedure shown

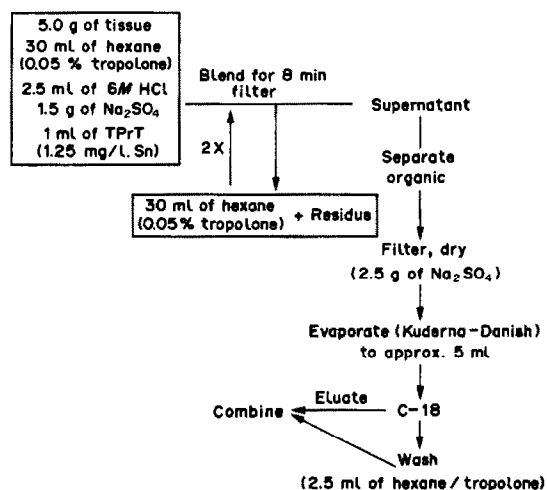


Fig. 1. Diagram of procedure used for extraction of TBT from oyster tissue.

in Fig. 1. For all samples triplicate extractions were made from thoroughly homogenized material. The tissue homogenate (5.0 g) was blended (in the stainless-steel micro-blender cup) with 30 ml of hexane containing 0.05% w/w tropolone, 1.00 ml of 0.66 mg/l. Sn, as TPrT (internal standard), 2.5 ml of 6M hydrochloric acid, and 15 g of sodium sulfate for 8 min (control experiments from which TPrT was omitted confirmed that it was not present in the original sample). The mixture was filtered under suction, with a fast filter paper. The solid residue was blended and filtered twice more, each time with 30 ml of the hexane/tropolone mixture. A final wash was made with a further 30 ml of the tropolone solution. The combined supernatant was transferred to a separatory funnel and the aqueous layer was removed. The organic layer was filtered under gravity through 2.5 g of sodium sulfate in a Schleicher & Schuell "Shark Skin® filter paper into a Kuderna-Danish apparatus (250 ml, 5-ml receiver) and evaporated on a steam-bath (under a Snyder column) to approximately 5 ml. The liquid residue was passed through a C-18 cartridge (Waters Associates, Milford, MA) and the cartridge was washed with 2.5 ml of hexane/tropolone mixture. The eluate and wash were then combined before the determination step.

Spike-and-recovery experiments

The tissues from 20 yearling oysters collected from unaffected areas were combined and homogenized in a blender. Before extraction, 1-ml volumes of tri-n-butyltin chloride and internal standard solutions in hexane/tropolone mixture were pipetted into a micro-blender cup containing 5.0 g of homogenized oyster tissue. Other extraction conditions were identical to those described above. The concentrations of TBT were chosen to yield spike levels of 25 and 125 ng/g Sn; the internal standard (TPrT) level was 500 ng/g Sn. Low levels of TBT were found in the oyster composite; recoveries were determined by subtraction of the average TBT level (determined from 6 replicate extractions) in the unspiked oyster tissue from TBT levels determined (in the same composite) after spiking with TBT. For the 25 and 125 ng/g Sn TBT spike experiments, 5 and 7 replicate extractions, respectively, were done.

Determination

The GC was operated with helium as carrier gas at 10 ml/min and hydrogen at 140 ml/min.

Air supply No. 2 was operated at 170 ml/min. In the one-flame mode, air supply No. 1 was turned off, and in the two-flame mode, was operated at 80 ml/min. After installation of a hydride formation reactor, the GC was conditioned at 250° for 2 hr. The injector and detector were both operated at 250°, and the column temperature program was ramped from 70 to 150° at 10°/min. Under these conditions, the retention times of TPrT and TBT were 4.0 and 7.7 min, respectively. Injections were made as described previously.²⁰ A portion of extract or standard solution (2–4 μ l) was drawn into a PTFE-tipped syringe, followed by 0.5 μ l of air and then 4 μ l of injection solvent. It was found that reproducible results could be obtained with injection times from 1 to 3 sec. This injection was followed by another 10 μ l of injection solvent after a pause of about 3–7 sec. Standards prepared in the hexane/tropolone mixture were just as stable as standards prepared in the injection solvent, and yielded identical responses. All the results reported here were obtained with standards prepared in hexane/tropolone mixture. Quantification was achieved by the internal standard method. To determine TBT, at ng/g Sn levels the peak-area ratios (TBT/TPrT) determined for extracts were used together with the calibration ratio obtained from the standard TBT and internal standard added per gram of oyster tissue.

RESULTS AND DISCUSSION

Oyster tissue extractions

The extraction procedure described here gave recoveries of TBT from oyster tissue that were essentially quantitative (Table 1). With 25 and 125 ng/g Sn TBT spikes, the recoveries averaged 107 and 97%, respectively. The corresponding RSDs were 7 and 5%. Taken together, these data suggest efficient extraction of TBT from oyster tissue with the hexane/hydrochloric acid/tropolone system. A similar extraction system was used with success by Uhler *et al.*¹⁷ in their alkylation procedure for determining TBT in oysters.

Table 1. Recovery of tri-n-butyltin from oyster (*Crassostrea gigas*) tissue

Spike level, Sn, ng/g	25	125
Average recovery, %	107	97
Recovery range, %	88–118	92–108
Number of extractions	5	7
Precision of extraction (RSD), %	7	5

Hydride formation

Extracts obtained from oyster tissue by the extraction procedure of Sullivan *et al.*²⁰ were black, whereas in the present procedure the dark pigments adhered to the silica column in the defatting step of the Sullivan procedure²⁰ and were completely removed from the column when the polar injection solvent was applied, giving nearly transparent solutions. This indicates that the pigments are polar and/or surface-active. The hydride formation reactor is sensitive to the sample matrix. Rapid evaporation of the solvent after injection led to deposition of non-volatile sample-matrix components in the form of a dark, tarry residue on the surface of the reactor, which rendered it useless. The reactor-fouling problem was reduced somewhat by careful choice of extraction and clean-up steps and 15–20 injections of oyster extracts could be made before reactor fouling prevented operation. The residue originated from components of the sample matrix. With pure TBT standards, the reactor could be used for hundreds of injections.

C-18 cartridge clean-up

Hexane/tropolone extracts of oyster tissues could be analyzed directly in many cases. However, there were some oyster samples which yielded broad peaks late in the chromatogram, which were large enough to interfere with integration of the TBT peaks. These were not related to any pigments visible in the extract; many of the extracts producing these peaks were nearly transparent. Attempts to remove the cause of the peaks by loading extracts onto silica columns (followed by elution with the injection solvent) were unsuccessful, indicating that the interfering peaks are not caused by nonpolar components. Later it was found that simply passing the hexane extracts through octadecylsilylated silica (C-18) cartridges was effective in removing the interfering material. Although the C-18 clean-up procedure was very effective in preventing interference by matrix-derived peaks, it did not prevent eventual clogging of the reactor, and had no effect on the reactor's useful lifetime.

Although DBT was well resolved from TPrT and TBT, it could not be reliably quantified, because of the steady deterioration of its response, which occurred despite the retention time remaining constant. Thus, the capillary column could not be the source of the problem.

Even when a standard was injected into a freshly-prepared reactor, before any oyster extracts were injected, the DBT peaks steadily declined. After ten injections, there was no response to DBT. Attempts to stabilize the DBT response by changing the detector gas flows, by use of a different source of sodium borohydride in the reactor, by substituting a different source of hydrogen gas, or by use of standards prepared in the injection solvent, were all unsuccessful. Throughout these experiments, TBT and TPrT were readily detectable even at low concentrations. Comparison of peak areas after injection of tri-*n*-butyltin hydride and tri-*n*-butyltin chloride showed that TBT was being quantitatively converted into the hydride even though the DBT response declined.

Separation and detection

For separating the organotins, the dimethylsilicone column used in this work performed at least as well as the phenylmethylsilicone column used in previous work.²⁰ It was not necessary to use an initial isothermal pause in the temperature program as was required with the previous column, and the final temperature used was 70° lower than that required with the more polar phenylmethyl column. These two changes result in a total temperature program that is 40% shorter than that used before.²⁰ The time saving is further increased because the column oven cools more rapidly between cycles, owing to the lower final temperature.

Retention times were very reproducible, even after injections of over a hundred extracts and standards. When the apparent retention times did eventually change, a clogged reactor and not the capillary column was found to be responsible. Consistent retention times could be regained by replacing the reactor. A chromatogram of a tri-*n*-butyltin chloride standard (and TPrT internal standard) is shown in Fig. 2, and a chromatogram of a naturally contaminated oyster extract is shown in Fig. 3. TBT could be detected by using either the 1-flame or 2-flame modes of the FPD. There was no significant difference in detection limit or linearity. With either detection mode, the detection limit (signal corresponding to 3 times peak-to-peak baseline noise) was 3–6 ng/g Sn in the oyster tissue, depending on the degree of concentration of the final extract. The sensitivity of the FPD for organotins was a function of the purity of the hydrogen gas.

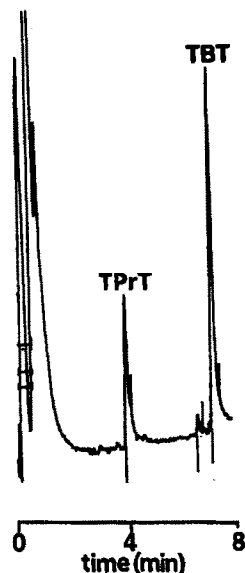


Fig. 2. Chromatogram of the hydrides of TBT and tri-*n*-propyltin (internal standard, TPrT) by the modified reaction-GC method; 4 μ l of standard consisting of TBT at 0.33 μ g/ml Sn level, TPrT at 0.26 μ g/ml Sn, in 0.05% tropolone solution in hexane.

Analysis of oyster meats

TBT levels in oyster tissue from various locations in the Puget Sound area ranged from 15 to 161 ng/g Sn (Table 2). Oysters collected in a bay used for naval and recreational sailing²² were generally higher in TBT than those from unaffected areas. In all but the 4-year old, the oysters collected in the affected area had higher levels of TBT than those from unaffected areas. All the oysters collected from the affected area,

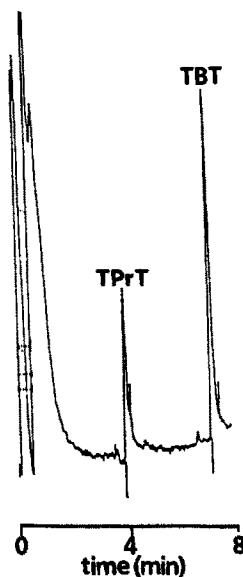


Fig. 3. Chromatogram of an extract. Oyster naturally contaminated with TBT at 161 ng/g Sn level.

Table 2. Levels of tributyltin (TBT) found in oysters from the Puget Sound area

Extract number	TBT (as Sn), ng/g	Comments
1	15	Composite, unaffected area, yearlings
2	30	Composite, unaffected area, yearlings
3	21	Composite, unaffected area, yearlings
4	32	Single oyster, affected area, 4 years old
5	95	Single oyster, affected area, 3 years old
6	98	Single oyster, affected area, 3 years old
7	89	Single oyster, affected area, 3 years old
8	161	Composite, oysters from affected area

including the 4-year old, showed evidence of shell blistering and the oysters used to prepare the 161 ng/g Sn composite showed shell-thickening. Such shell abnormalities have been noted by others to be due to exposure to TBT.²² The oyster samples were collected strictly for method development, rather than regulatory purposes; the results are not intended to support an environmental study.

The most commonly used approach for determining TBT is to alkylate it before analysis. However, procedures based on this approach are time-consuming because the derivatization is performed batchwise. Furthermore, the Grignard reagents used are sensitive to trace amounts of water, and the procedures must be performed with great care.

The on-line hydride-formation method introduced by Sullivan *et al.*²⁰ reduces the number of manual manipulations required for a TBT analysis and was adapted here to answer the need for a rapid and rugged method for determination of TBT in oysters. Substitution of a shorter capillary column and modifications in the temperature program result in a streamlined procedure and a method which is faster than the original method.²⁰ Although the reactor must be replaced after every 15–20 injections, additional reactors are easily fabricated and can be stored in a desiccator until needed. The reaction–GC method is well suited to the determination of TBT in oysters, especially when results must be obtained quickly and the number of samples is small.

Acknowledgements—The authors thank John Sullivan for helpful discussions, Nancy Hill for technical assistance in preparing the manuscript and Robert Stott for collecting the oyster samples.

REFERENCES

1. W. T. Piver, *Environ. Health Perspect.*, 1973, **4**, 61.
2. C. Murray, *Chem. Eng. News*, 1975, **53**, 18.
3. R. Porter and J. B. Miale, *Appl. Biochem. Biotechnol.*, 1984, **9**, 439.
4. K. R. S. Ascher, *Phytoparasitology*, 1985, **13**, 153.
5. J. W. Short and F. P. Thrower, *Mar. Pollut. Bull.*, 1986, **17**, 542.
6. D. W. Evans and R. B. Laughlin, *Chemosphere*, 1984, **13**, 213.
7. R. B. Laughlin, W. French and H. E. Gaurd, *Environ. Sci. Technol.*, 1986, **20**, 884.
8. M. J. Waldock, J. Thain and D. Miller, *Proc. Int. Council Expl. Sea*, 1983, **E**, 52.
9. I. J. Boyer, *Toxicology*, 1989, **55**, 253.
10. I. S. Krull and K. W. Panaro, *Appl. Spectrosc.*, 1985, **39**, 960.
11. K. Ebdon, S. J. Hill and P. Jones, *Analyst*, 1985, **110**, 515.
12. M. D. Müller, L. Reinberg and G. Rippen, *Chemosphere*, 1989, **18**, 2015.
13. S. Morisaki, T. Nagata, T. Ninomiya and S. J. Nakama, *Food Hyg. Soc. Japan*, 1989, **30**, 36.
14. M. D. Müller, *Anal. Chem.*, 1987, **59**, 617.
15. Y. K. Chau, P. T. S. Wong and G. A. Bengert, *ibid.*, 1982, **54**, 246.
16. R. J. Maguire and H. Huneault, *J. Chromatog.* 1981, **209**, 458.
17. A. D. Uhler, M. Clower and G. Miller, unpublished work.
18. Y. Hattori, A. Kobayashi, S. Takemoto, K. Takami, A. Sugimae and M. Nakamoto, *J. Chromatog.*, 1984, **315**, 341.
19. C. L. Matthias, J. M. Belliama and F. E. Brinckman, *Oceans 86 Conference Record*, Vol. 4, pp. 1146–1151. Marine Technology Society, Washington, D.C. 1986.
20. J. J. Sullivan, J. D. Torkelson, M. M. Wekell, T. A. Hollingworth, W. L. Saxton and G. A. Miller, *Anal. Chem.*, 1988, **60**, 626.
21. E. G. Bligh and W. J. Dyer, *Can. J. Biochem. Physiol.*, 1959, **37**, 911.
22. J. M. Cummins, R. R. Bauer, R. H. Reck, W. B. Schmidt and J. R. Yearsley, *Chemical and Biological Survey of Liberty Bay, Washington*, p. 8. U.S. Environmental Protection Agency, Region X, Seattle, WA, 1976.
23. M. J. Waldock and J. E. Thain, *Mar. Pollut. Bull.*, 1983, **14**, 411.

EVALUATION OF "LABILE" METAL IN SEDIMENTS BY ANODIC STRIPPING VOLTAMMETRY

P. A. WALLER and W. F. PICKERING

Chemistry Department, University of Newcastle, N.S.W. 2308, Australia

(Received 7 March 1990. Accepted 11 April 1990)

Summary—A procedure for determining the "labile" metal content of contaminated sediments (in different chemical environments) has been critically examined. The sediments were extracted overnight with different chemical solutions and the suspensions were analysed by differential pulse anodic stripping voltammetry. The extractants used have been recommended for soil/sediment speciation schemes, and by examination of the suspensions directly in the ASV cell, errors due to re-adsorption of released metal ion were minimized. The existence of different chemical forms of metal was signified by changes in peak shape and position or by the appearance of additional peaks. With complexing agents present the peak size was pH-dependent. The limitations of the ASV/suspension analysis technique have been carefully evaluated by using ten different extractants and seventeen sediments. The "lability" results obtained have been compared with the values obtained from a cation-exchanger transfer procedure. For characterizing the lability behaviour of the metal contents of sediments, preliminary extraction into a minimum of four base solutions is advisable, *e.g.*, 0.02M nitric acid (low-pH labile); hydroxylamine in acetic acid (reducing conditions); acetic acid/acetate buffer (weakly sorbed and carbonate-bound) and 0.05M calcium chloride (exchangeable fraction at natural system pH), where the terms in parentheses describe the character of the fraction. The results are critically compared with those obtained by atomic-absorption analysis of the extracts and with those obtained by an earlier ion-exchange fractionation scheme. The advantages and limitations of the ASV systems are discussed.

Only a fraction of the total metal content of sediments tends to be "biologically available" or readily mobilized by changes in the chemical environment. Most analytical schemes for determining these fractions seek to sub-divide the total element content into different reactive fractions¹⁻³ by selective chemical extraction, but opinions differ in respect to the most appropriate reagents and/or the sequence in which they should be used. There is also concern about errors arising from re-adsorption of released metal ions. In most procedures a filtered extract is analysed by a trace technique which measures only the total metal ion concentration in the solution (*i.e.*, the sum of all chemical forms present). If anodic stripping voltammetry (ASV) is used instead of techniques such as atomic-absorption spectrometry or plasma emission, the response is restricted to the levels of hydrated cation and labile complex present in solution. This can be a significantly different value from the total and it has been proposed that "labile" metal ions are more readily "available" than other forms to living matter.

A preliminary study⁴ of the potential value of the ASV approach to "labile metal in sediment" determinations indicated that the procedure was

not only sensitive ($\mu\text{g/g}$ detection levels) but had the capacity to minimize errors arising from re-adsorption of displaced metal ions. The filtration step was omitted, and the suspensions introduced directly into the measuring cell, and loosely bound metal ions then tended to migrate to the mercury drop cathode under the influence of the applied potential. The presence of particulate matter caused some peak distortion, however, and it was recommended that the procedure receive more detailed study with a wider range of extractant solutions and sediment types. In addition, some means of checking the validity of the ASV-labile values was deemed desirable. An analytical procedure based on transfer of labile metal ions to cation-exchangers of different types,^{5,6} followed by back-extraction into EDTA solution, has been developed for this, and measures "lability" at different pH values. The ASV approach is seen as a complementary technique, which allows evaluation of "lability" in different chemical environments.

Model system studies⁷⁻⁹ have indicated that the advantages of using suspensions in the ASV cells outweigh the disadvantages or complications arising from the contact of solid

particles with the Hg electrode. It has been suggested^{10,11} that electrode activation (or passivation) arising from adsorption effects, or abrasion of the film surface by moving particles, can be a problem in ASV studies, and protection of the electrode by a semi-permeable membrane cover has been proposed.¹² In our studies with sediments, the membrane cover had a similar effect to filtration, so we have sought to minimize undesirable effects by replacing the Hg drop after deaeration (*i.e.*, prior to the analytical cycle) or, when using a film electrode, scrubbing the sample with nitrogen before transfer to the cell. Though retention of the solid phase in the analytical system is essential for retrieval of ions loosely sorbed on particle surfaces, the possibility of peak distortions due to adsorption of colloidal particles on the electrode surface cannot be ignored. Fortunately, some guidance is available from publications which describe the effects, on ASV responses, of inorganic particles^{8,13,14} and organic matter.^{7,9,10,15-19} Metal ion interaction with ligands present in the supporting electrolyte solution can also result in changes in peak characteristics, and information on some of these effects is also available.²⁰ Superimposed on the above-mentioned effects are changes associated with the pH of the test systems. With some electrolyte systems, pH effects are small over specified pH regions. For example, in 0.16M acetate buffer, the oxidation currents for deposited copper, cadmium, lead and zinc were found²¹ to be independent of acidity up to pH 7. Variation of peak heights was also found²² to be small over the pH range 4-6 when the acetate buffer was prepared in 0.1M sodium chloride medium. Another study²⁰ confirmed that in acetate base solutions, pH effects were minimal in the pH range 4.5-6.5, but outside this range some distinctive peak changes were observed, particularly for copper.

Others²³ have reported that optimum response for lead, cadmium and copper occurs at pH 5.5, whereas with artificial sea-water systems²⁴ stripping currents reach a maximum at a pH of about 6. Hydrogen evolution can contribute significantly to the baseline current at the zinc stripping potential and zinc determinations can be strongly affected by pH changes.²⁵ In alkaline conditions, two peaks have been observed for copper,^{20,21} the second peak being assigned to either the formation of copper(I) hydroxy species or adsorption of copper(II) hydroxy species. Splitting of the copper peak has also been observed to occur in the presence of chloride ions [and was attributed to formation of copper(I) and copper(II) chloro-complexes²²] and humic acids (attributed to metal humate complex formation).⁹

Some of the variable responses in ASV studies can be readily controlled (*e.g.*, by using similar base solutions and pH values in calibration series), but with sediments present it is difficult to predict (or counteract) effects arising from adsorption of suspended matter on the electrode surface. Standard addition techniques do not provide an answer, since many sediment components (*e.g.*, colloidal hydrous oxides or humic acids) specifically sorb added metal ion,¹³ and electrode protection with a membrane has a similar effect to filtration.⁸ In the present study, the magnitude of the problem has been evaluated by using a large number of polluted sediments and an extensive range of base solutions.

EXPERIMENTAL

Sediment samples

The sediment samples tested were 10-12-cm long segments drawn from the top, middle and bottom of five 60-cm cores taken along a 2-km length of polluted tidal creek. This group of

Table 1. Total element contents of some of the sediment samples

Sediment No.	1	2	3	4	5	6	7	8
Matrix species, %								
SiO ₂	49.0	49.8	53.2	60.8	56.0	52.5	—	49.9
Al	5.0	6.7	6.3	4.3	5.7	6.5	—	8.0
Fe	2.6	3.5	3.2	2.7	3.0	3.2	2.2	3.9
Ca	1.4	0.7	0.9	0.4	0.9	0.6	—	0.6
Mg	0.4	0.7	0.5	0.6	0.7	0.7	—	0.8
Heavy metal ion, µg/g								
Cd	<10	<10	<10	10	<10	<10	<10	<10
Cu	150	130	105	75	125	115	70	145
Pb	750	530	440	265	530	310	170	250
Zn	2390	1565	1550	1050	1025	675	600	590
Suspension pH	6.6	7.5	7.1	6.6	6.7	7.0	7.1	7.2

samples varied greatly in degree of contamination, as shown in Table 1. Suspensions of the creek sediments took over 20 hr to settle and the bed volume in each case was greater than the 10 ml of dry, packed solid initially taken. The increases in volume (3–8 ml) have been attributed to swelling of the "clay" content. Only a few samples yielded clearly defined bands of coarser material (samples 4–6, ~3 ml; 10 and 16, ~5 ml; 11 and 17, ~8 ml). A surface scum formed during initial agitation took over an hour to disperse and was attributed to organic matter since in high pH solutions (*i.e.*, when sodium hydroxide was added) the supernatant liquor was dark brown in colour. The absorption of 270-nm light by these solutions was compared with that for sodium humate standards and the results indicated that the organic levels (expressed as humic acid) ranged between 3% (samples 2 and 4) and 8% (12, 16, and 17). Colloid/clay dispersion increased in high pH systems, and settling was even slower. The silica levels varied between 35 and 74%, values indicative of a high clay content with only moderate amounts of sand present. Also included in the study were two other samples (7 and 9) collected from another polluted estuary.

Standard solutions

Working standards covering the range of individual concentrations encountered in the sediment analysis studies were prepared by diluting aliquots of BDH "AAS Standard Metal Solutions". The most concentrated standard contained 25 $\mu\text{g/ml}$ Zn, 7.5 $\mu\text{g/ml}$ Pb, 1.25 $\mu\text{g/ml}$ Cu and 1.25 $\mu\text{g/ml}$ Cd. This standard was serially diluted, yielding a series in which the most dilute had metal contents of 1 μg of Zn, 300 ng of Pb, 50 ng of Cu and 50 ng of Cd per ml. The standard solutions used for preparation of ASV calibration curves consisted of 4.0 ml of working standard and 4.0 ml of the chemical extractant solution being used in the particular segment of the sediment study.

Chemical extractant solutions

Small amounts of sediment (300 mg) were placed in vials with 30 ml of extracting solution, and the sealed vials were then equilibrated overnight by use of an end-over-end mixing unit. The extractants used in the series of studies were: 0.02M HNO_3 ; 4M CH_3COOH /0.4M $\text{NH}_2\text{OH}\cdot\text{HCl}$; 0.1M $\text{H}_2\text{C}_2\text{O}_4$ /0.18M $(\text{NH}_4)_2\text{C}_2\text{O}_4$ (pH 3); 0.13M CH_3COOH /0.4M CH_3COONa (pH 5); 0.1M $\text{Na}_4\text{P}_2\text{O}_7$ (pH 7);

5 mM EDTA (pH 7); 0.5M NH_4NO_3 ; 0.05M CaCl_2 ; 0.5M NaCl ; 1M MgCl_2 ; distilled water (to leach out soluble salts).

ASV operating conditions

The instrument used for the electroanalytical studies consisted of an Amel control unit, a hanging mercury drop electrode and an X–Y recorder. The mercury drop (medium size) was renewed after deaeration of the cell sample (with nitrogen) and after each test run. Standard solutions were used for finding suitable operating parameters. For the relatively high levels of zinc present, a deposition time of 5 sec was adequate, with a deposition potential of about -1.35 V (*vs.* the Ag/AgCl reference electrode). The deposition step was followed by a short quiescent period before anodic sweep scanning (differential pulse mode) to around -50 mV. For most zinc studies a scan speed of 50 mV/sec and sensitivity settings of 2 or 5 μA full-scale deflection (FSD) were used. With lower zinc levels the scan speed was reduced to 20 mV/sec. In the zinc peak region the baseline sloped (owing to competing electron-transfer processes) and blank runs (*i.e.*, electrolyte only) were used to correct for this effect. With longer deposition periods, peak heights did not increase in direct proportion to deposition time and even with depositions for only 5 sec, the calibration curves occasionally deviated from linearity.

For evaluation of the lower levels of cadmium, copper and lead present, the sediments were re-analysed with a less negative deposition potential (-900 mV), a deposition time of 20 sec, and a scan speed of 20 mV/sec. When there were overlapping peaks, scan speeds of 5 mV/sec were adopted. The cut-off potential was determined by the onset of oxidation of mercury and this varied from -5 to -100 mV, depending on the base solution used.

With the sediment samples, a change in the deposition time (*e.g.*, from 5 to 20 sec) led to much smaller increases in peak size than predicted, *e.g.*, by only 20–50% of the expected value. This was attributed to surface saturation with adsorbed colloids and/or settling of the suspension during the deposition cycle. For reproducible repeat analyses, the cell contents had to be mixed mechanically between each ASV cycle. For both standard solutions and suspensions, the relative standard deviation of repeated scans was $\pm 10\%$, or better, and replicate precision was of the same order.

Table 2. Effect of extractant composition on position of ASV peaks

Extractant solution	Peak position ($-mV$ vs. SRE)				
	Zn	Cd	Pb	Cu	
0.5M NaCl	1010	630	420	170	
1.0M MgCl ₂	1060	710	495	270	
0.05M CaCl ₂	1150	740	540	230	
0.4M NH ₂ OH·HCl	(995)	685	480	235	
Acetate buffer, pH 5	1165	750	560	135	
0.02M HNO ₃	1150	720	510	80	
0.5M NH ₄ NO ₃	1070	655	455	30	
Water*	(a)	1170	740	540	110
	(b)	—	750	550	130
0.1M Na ₄ P ₂ O ₇ ,* pH 7	(a)	nd	785	630	270
	(b)	—	710	575	225
pH 1.5	(a)	1115	740	575	185
	(b)	—	705	540	165
Oxalate buffer,* pH 3	(1075)	640	480	155	
	(b)	—	680	525	195
5mM EDTA,* pH 1.5	(b)	1125	710	525	155
	(b)	—	725	550	180
pH 6.6	(b)	nd	nd	nd	400
	(b)	—	—	—	270
pH 10.6	(b)	nd	nd	nd	485
	(b)	—	—	—	435

*Peak position varied with E_{dep} and pH.

ASV parameters: (a) 5 sec deposition, -1.35 V, 50 mV/sec scan; (b) 20 sec deposition, -0.9 V, 20 mV/sec scan.

nd = none identified. Values in parentheses are estimates.

The peak potential (E_p) for the different elements varied with the electrolyte base solution, as shown in Table 2.

Metal extraction

After overnight mixing, 10-ml aliquots of the sediment suspensions were transferred to the ASV unit measuring cell and stirred with a stream of nitrogen. Settling of solid particle during the metal deposition cycle was minimized by magnetic stirring of the cell contents. Quiet conditions were used for the stripping cycle.

For a selected group of samples, aliquots of the initial suspension were centrifuged, and the supernatant liquid was then transferred to the ASV cell for analysis. Aliquots of most suspensions were also filtered with Whatman No. 50 filter papers (to remove particles $> 1 \mu m$ in diameter) prior to analysis. These phase separations reduced the contribution of sorbed ion species to the peak current size.

Diverse ion effects

When the extractants used were chloride-free, the standard solutions were spiked with various amounts of sodium chloride (up to 0.5M) prior

to ASV analysis, to ascertain whether changes in peak position observed in the sediment studies were attributable to the formation of metal chloro-complexes.

It was also predicted that the structure of the sample ASV peaks could be influenced by iron salts released by some extractants, and to evaluate this effect, standard metal mixtures were spiked with different amounts of iron(III) nitrate solution.

With pyrophosphate or EDTA ions present, the effective stability of the metal complexes formed is pH-dependent, hence with these base solutions standard series analyses were run at two or more different pH values.

In the ASV investigation, seventeen different sediments were studied, and in the discussion sections which follow, similarities in behaviour have been highlighted by bracketing the sample numbers (e.g., 1, 9, 17). In the tabular material, however, only the results obtained with eight of the samples (a highly polluted group) have been listed.

RESULTS AND DISCUSSION

The presence of very fine material and alkali-soluble organic matter in the sediments studied led to some peak distortion and other interference effects, which were found to vary with base solution type and the sample being studied. For discussion purposes the eleven displacing solutions tested have been sub-divided into four major groups (acidic, reducing, neutral salts and metal-complex formers) but each extractant system had some unique responses which warrant special comment.

Low-pH, ASV-labile contents

To evaluate the fraction of the total metal content which may be assigned to human sources and activities, extraction with dilute acid solutions has been widely used. Low-pH extract values also provide an indication of the degree of metal release which might follow exposure of sediments to strong acid leaching (e.g., by an acid spill or through weathering of sulphide minerals present). Dilute acid extractions appear to release metal ions associated with acid-soluble matrix components (e.g., carbonates, amorphous hydrous oxides) as well as promoting displacement from organic acid colloids and surface sites.²

For our ASV study we employed 0.02M nitric acid, as used recently to determine the metal

Table 3. "Low-pH and pH-5 labile" metal content of sediments, $\mu\text{g/g}$

Species	Extractant	Sample No.							
		1	2	3	4	5	6	7	8
Zinc									
	RSO ₃ H	1315	1230	1080	810	850	530	355	415
	HNO ₃	1090	1080	1360	660	700	370	325	300
	RCOOH	1090	930	930	480	635	245	195	245
	Acetate pH 5	980	795	740	495	580	245	205	170
	NH ₂ OH·HCl (a)	(230)	(135)	(115)	(80)	(90)	nd	(60)	nd
Lead									
	NH ₂ OH·HCl	680	420	340	190	360	125	115	175
	HNO ₃	425	250	295	115	175	110	55	80
	RSO ₃ H*	340	215	175	105	125	130	85	125
	Oxalate, pH 3	270	255	275	170	225	135	105	250
	RCOOH*	240	105	80	60	110	60	55	35
	Acetate, pH 5	95	35	15	10	45	15	nd	5
Copper									
	RSO ₃ H*	65	60	35	25	45	75	30	85
	HNO ₃	50	125	70	nd	75	75	30	85
	RCOOH*	25	30	< 10	20	20	20	< 10	15
	NH ₂ OH·HCl	15	10	nd	15	15	15	10	20
	Acetate, pH 5	10	nd	nd	nd	nd	5	nd	nd
	Oxalate, pH 3 (b)	5	nd	nd	5	nd	5	20	5
System Peak									
	(c)	135	190	140	90	100	100	10	140
	HNO ₃	95	130	140	100	220	20	560	95
	Oxalate, pH 3 (d)	120	100	60	70	75	55	10	125
	NH ₂ OH·HCl	nd	25	10	10	10	5	nd	15
	Acetate pH 5								

nd = none detected; (a) NH₂OH·HCl in 4M CH₃COOH, peak reduced by competing reactions; (b) $E_{\text{dep}} = -0.9$ V; (c) not specifically identified, overlaps Cu peak; (d) $E_{\text{dep}} = -1.35$ V.

*Cation-exchanger with functional group specified. Values in parentheses are estimates.

content of some polluted Polish soils.²⁶ When a 300-mg portion of sediment was added to 30 ml of this acid, the system pH ranged from 1.8 to 2.3, which allowed determination of Zn by ASV.

It was predicted that the "low-pH ASV-labile" metal values should be similar to the amount of metal transferred to H⁺-form strong-acid cation-exchangers. This was the case for some copper and lead transfers, but rarely for zinc (Table 3).

In dilute nitric acid solutions the DPASV curves for standard metal solutions had flat baselines in the cadmium, lead and copper region, but with potential values more negative than 1.0 V, the current increased rapidly owing to oxidation processes other than the formation of zinc ions (Fig. 1). With sediment present, baseline effects were accentuated and some shifts in peak positions occurred (cf. Fig. 1). Some peaks broadened and it was concluded that iron species dissolved by the acid were probably responsible for the varied sediment behaviour. Adding an iron(III) salt (50 or

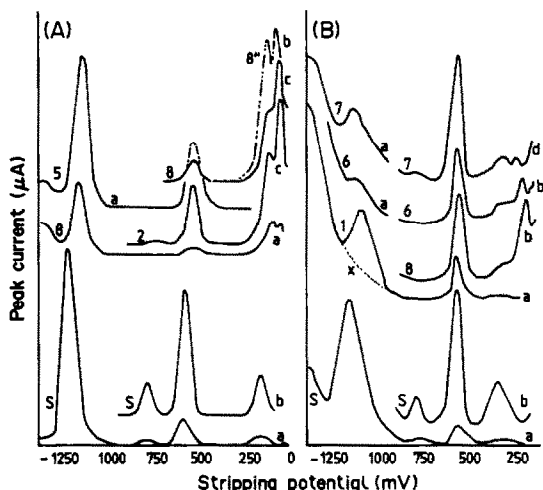


Fig. 1. Typical ASV curves obtained with sediment extracts and either 0.02M HNO₃ (A) or 0.4M NH₂OH·HCl in 4M CH₃COOH (B). Sediment suspensions numbered 1-8; 8* was a filtered solution. The standard solution (S) contained 6.25 $\mu\text{g/ml}$ Zn, 1.88 $\mu\text{g/ml}$ Pb and 0.33 $\mu\text{g/ml}$ Cd and Cu. Extraction solution blank, X. Operating parameters: a, 5 sec at $E_{\text{dep}} = -1.35$ V, 5 μA full-scale deflection (FSD); b, 20 sec at $E_{\text{dep}} = -0.9$ V, 2 μA FSD; c, as for b, but 5 μA FSD; d, as for b, but 1 μA FSD.

Table 4. Cadmium detected in sediment suspensions, $\mu\text{g/g}$

Extractant	Sample No.							
	1	2	3	4	5	6	7	8
Water	2.0	nd	nd	nd	nd	nd	nd	nd
NH_4NO_3	nd	nd	nd	nd	nd	nd	nd	nd
NaCl	2.5	1.5	2.0	5.5	5.0	1.0	nd	nd
Acetate buffer	nd	1.5	1.0	4.0	2.5	nd	3.0	nd
$\text{NH}_2\text{OH}\cdot\text{HCl}$	1.0	1.0	1.0	4.0	2.0	nd	5.0	nd
MgCl_2	2.5	3.0	3.5	9.0	5.0	nd	7.0	nd
HNO_3	3.0	4.0	4.0	10.5	5.5	1.5	7.0	nd

Note: No Cd detected by AAS analysis or transfer to cation-exchanger (values below detection limit).

nd = none detected.

500 μg) to the standard solutions caused the metal peaks to move in an anodic direction (by 100 mV) with some associated small decreases in the size of the cadmium, lead and copper peaks. In the zinc region, the baseline current increased (owing to enhanced levels of depolarizing species). When the added iron was reduced to Fe(II) (*e.g.*, in the presence of hydroxylamine), the peak effects attributed to iron tended to disappear, being replaced by changes arising from the presence of chloride (*cf.* Fig. 1).

With the sediment ASV curves, peak heights were measured from the extrapolated baselines to the peak tops and converted into concentrations with calibration curves. Duplicate analyses, and repeat analyses with different sensitivity settings, were fairly reproducible (*e.g.*, median $\pm 5\%$ of median).

In about 80% of the test studies, filtering the samples with a fine filter paper (Whatman No. 50) prior to ASV analysis reduced the peak size by about 20%, whereas little signal loss was observed for standard solutions. It was concluded in earlier studies^{4,9} that filtering removed labile metal ions loosely bound to particle surfaces, a fraction that is mobilized by the applied potential in ASV analyses of suspensions. When filtered extract test samples were used, the double peaks in the copper region were more clearly resolved, largely because the height of the more anodic peak was reduced by almost half (*cf.* Fig. 1). The second component (present mainly as a shoulder for the suspension systems) was only marginally affected by removal of the solid phase. A shift in peak position to more anodic values (relative to E_p for standards) is often indicative of an adsorption process, and if this generalization applies here, it can be proposed that the more anodic segment of the double peak arises from copper ions sorbed on the surface of positively charged colloids attracted to the mercury drop. Alternatively,

adsorbed metal complexes (*e.g.*, humates) may undergo reversible one- or two-electron changes. Addition of humic acids to acetate base solutions was found⁹ to split the copper peak in a manner similar to that observed for the sediment samples.

The "low-pH labile" values for zinc, lead and copper present in eight of the sediments are summarized in Table 3. The values for cadmium are listed in Table 4. Comparison with the cation-exchange transfer values previously reported (RSO₃H column in Table 6)⁶ showed that the DPASV method yielded smaller labile zinc (and sometimes labile lead) values. This suggests that some sparingly soluble zinc (and lead) compounds were only partially soluble in the dilute acid. Conversely, acid extraction released more copper than did the ion-exchange process, a result which suggests that some of the copper content required oxidation for release to occur (*e.g.*, was present as CuS or Cu metal). The amount of cadmium present in the samples was generally less than the detection limit of the exchanger procedure.

The sloping baseline which preceded the zinc stripping peaks increased in steepness when the deposition potentials were made more negative, or when more nitrate ion was introduced. The source of this current is assumed to be oxidation of sorbed hydrogen gas or ammonium ions (formed by reduction of nitrate in the deposition cycle). Competing processes during the electro-deposition stage may have contributed to the ASV zinc values being lower than the corresponding ion-exchange transfer values.

Low-pH labile reducing conditions

In soils and sediments, significant fractions of the total metal content can be associated with the hydrous oxides of iron, manganese and aluminium and an estimate of the amount associated with the amorphous forms of the

iron and manganese oxides can be obtained through interaction with a reducing agent (e.g., $\text{NH}_2\text{OH}\cdot\text{HCl}$ in 25% acetic acid). When the readily reduced components dissolve, bound metal ions are released. Dissolution of the hydrous oxides also reduces the number of surface-active sites available for re-adsorption of metal ions and eliminates colloidal species, which can interfere with the ASV determinations. When $\text{NH}_2\text{OH}\cdot\text{HCl}$ is used as the reducing agent, these gains can be offset by the effect of the increase in total acidity, the peak shifts induced by the presence of chloride, and the electron-transfer reactions involving hydroxylamine, which occur at high negative electrode potentials. In our study this led to low levels of zinc being detected (0–10% of the total content; cf. Table 3). Typical voltamperograms are shown in Fig. 1.

Conversely, reduction of the oxide phases led to larger amounts of lead being detected (cf. Table 3). With most sediments the levels recorded were around 75% of the total lead content and double the amount released by dilute nitric acid. The enhanced release is consistent with the known high affinity between lead ions and amorphous iron oxide surfaces.

The cadmium values obtained (Table 4) were lower than those found by nitric acid extraction or chloride salt displacement, and were somewhat similar to the acetate buffer results. With all these systems the precision was poor, owing to the very low levels present.

The reliability of the copper values was reduced by the overlapping of the peaks in the appropriate portion of the ASV scan. The more cathodic peak (at -190 mV) fell in the region expected for chloride-rich base solutions. The anodic peak (at -60 mV) was not detected in the standard solution DPASV curves (cf. Fig. 1) and has been assigned to a surface-absorbed species. In most sediment analyses, the copper chloro-complex peak appeared as a shoulder on the larger "sorbed species" peak, and with six samples (2, 6, 13–15, 17) identification of the shoulder was difficult. With some sediments (11, 13–17) extra peaks (broad and flat) were discerned in the region between -330 and -290 mV. These peaks were not present when filtered solutions were used. Filtering (or centrifuging) the sample also decreased the size of the "sorbed species" peak (-60 mV region) which indicates that particulate matter was responsible for this response.

Weak acid (pH 5) ASV-labile

For determination of zinc, cadmium, lead and copper, an acetate buffer of pH 5 has been recommended. Metal ions are converted into acetato-complexes, which are highly labile, and pH effects on the peak size are minimized. Extraction of sediments with pH 5 acetate solutions is reported^{1,2} to release metal ions bound to ion-exchange sites or associated with carbonate minerals. The ASV results obtained with acetate buffer extracts should thus correspond to metal transfer into weak-acid cation-exchangers (i.e., having RCOOH functional groups). Table 3 shows that this happened only occasionally.

The acetate buffer extracted small amounts of zinc from all the sediments, and about a third of the ASV-labile values matched the RCOOH -transfer values (Table 3). Much smaller amounts of lead were displaced and with most sediments the zinc and lead results were similar to (or lower than) those obtained with calcium or magnesium chlorides (Table 5). Release of cadmium was also comparable to the salt-displacement values (see Table 4), but copper release tended to be quite small. As shown by the stripping curves in Fig. 2A, the anodic

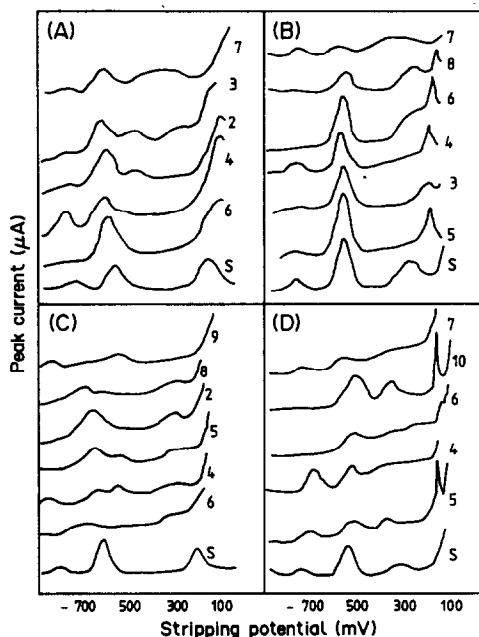


Fig. 2. Typical ASV curves obtained with sediment extracts and different extractants (A), pH 5 acetate buffer; (B), 0.05M CaCl_2 ; (C), 0.5M NH_4NO_3 ; (D), 1M MgCl_2 . Standard solution (S) contained 380 ng/ml Pb, 62 ng/ml Cd and 62 ng/ml Cu. Sediment samples numbered 1–10. Operating parameters: 20 sec at $E_{\text{dep}} -0.9$ V, 1 or 2 μA FSD.

Table 5. "Sediment pH labile" metal content of sediments, $\mu\text{g/g}$

Species	Extractant	Sample No.								
		1	2	3	4	5	6	7	8	
Zinc	CaCl ₂	990	585	650	300	380	140	220	70	
	MgCl ₂	940	390	440	400	430	220	265	115	
	NH ₄ NO ₃	555	315	360	330	325	90	190	75	
	RCOONa*	395	235	210	90	120	75	85	40	
	RSO ₃ Na*	300	90	95	80	120	25	60	20	
	NaCl	185	15	40	35	55	5	20	nd	
	Water	170	10	50	10	15	10	10	<5	
	Na ₄ P ₂ O ₇ , pH 7	(a)	(350)	(440)	(410)	(500)	(380)	(365)	(425)	(180)
Lead	CaCl ₂	240	110	60	55	95	40	20	25	
	NH ₄ NO ₃	40	45	50	30	35	35	30	30	
	MgCl ₂	80	10	10	15	20	10	15	15	
	RSO ₃ Na*	30	15	<20	<20	30	<20	nd	<20	
	NaCl	30	15	25	15	20	10	15	10	
	Water	45	15	10	10	15	10	25	10	
	RCOONa*	45	<20	nd	nd	30	nd	nd	nd	
	Na ₄ P ₂ O ₇	(b)	380	295	220	225	265	140	nd	95
Copper	CaCl ₂	(c)	305	275	160	125	180	115	nd	120
	CaCl ₂	20	10	nd	5	5	10	nd	10	
	NH ₄ NO ₃	5	5	5	5	5	5	nd	5	
	MgCl ₂	30	nd	nd	10	20	10	nd	nd	
	Water	<5	10	5	<5	5	nd	nd	5	
	NaCl	nd	30	nd	nd	nd	nd	nd	nd	
	RSO ₃ Na,RCOONa*	nd	nd	nd	nd	nd	nd	nd	nd	
	Na ₄ P ₂ O ₇	(b)	70	60	70	70	60	70	nd	60
System peak		(c)	5	5	5	5	5	5	nd	5
		(d)								
	MgCl ₂	50	60	70	100	80	10	—	50	
	NaCl	40	30	40	20	55	—	—	—	
	CaCl ₂	35	30	15	20	25	20	—	20	
NH ₄ NO ₃	30	—	—	20	—	—	—	15		

(a) Broad displaced peaks; (b) $E_{\text{dep}} = -1.3 \text{ V}$; (c) $E_{\text{dep}} = -0.9 \text{ V}$; (d) non-identified peak, distinguishable from Cu peak.

nd = none detected. Values in parentheses are estimates.

*Cation-exchanger with functional group specified.

region was characterized by a strongly sloping baseline leading to a "system peak" located 15–35 mV anodic to the copper peak position observed in the standard solution studies. This displacement increased when filtered solutions were used, which implies that an adsorbed soluble electroactive species may be involved.

The presence of particles caused the cadmium and lead peaks to shift in a cathodic direction (by about 30 mV) and with several samples (1, 2, 5, 10, 12, 13, 15) a broad new peak was observed, about 100 mV anodic to the lead peak (*cf.* Fig. 2A). These peaks were not observed when filtered solutions were used and it is believed that they were derived from lead species (*e.g.*, lead humate) sorbed on the mercury electrode.

Filtering the solutions before analysis had little effect on the sizes of copper, cadmium, lead and zinc peaks (<10% reduction). The main exceptions were three of the sediments (2, 9, 12)

which lost 25% of their labile cadmium on filtering; samples 2, 5, 11 lost a similar amount of lead and with five sediments (1, 4, 5, 7, 13) the zinc values for filtered solutions were about 20% lower than the values for the suspensions. These lower results indicate that acetate-complex formation did not fully prevent weak bonding of some metal ions to particle surfaces.

Sediment pH (6–8) ASV-labile values

For displacement of metal ions held by electrostatic attraction (*i.e.*, occupying ion-exchange sites) extraction with a neutral salt solution has been recommended. One popular reagent is 1M magnesium chloride. Others have preferred to use ammonium or sodium acetate, or ammonium nitrate. For displacing copper from soils, 0.05M calcium chloride has been recommended²⁷ and in our ASV study this reagent yielded more clearly defined curves than did the other salts tested (*cf.* Fig. 2). This has

been attributed to the lower ionic strength of the calcium chloride solution and a high affinity between exchange sites and Ca^{2+} . Relative affinity for sites was not the sole controlling factor, however, because displacement effects can be enhanced if the metal ions interact with ligand species in solution (e.g., formation of anionic metal chloro-complexes). Complex formation shows up in ASV studies by causing a peak shift. For example, the presence of excess of chloride ion caused a cathodic shift of about 150 mV in the copper peak position. With all the salt solutions, matrix dissolution should have been minimal and the pH of the sediment suspensions (6.2–7.2) was determined by the slight solubility of the acidic or basic components present.

As shown in Table 5, the greatest degree of lead (and sometimes zinc) release was observed with calcium chloride solutions; least displacement occurred with sodium chloride solutions. In the calcium chloride system much of the ASV signal could be attributed to metal ion loosely bound to particulate matter as filtering or centrifuging prior to analysis led to peaks of much smaller size. With sediments suspended in sodium chloride or magnesium chloride solution, removal of solid had little effect on the ASV peak heights and in the ammonium nitrate systems only the lead peaks displayed any marked change in size when filtered samples were used.

With all the salt suspensions, filtration prior to ASV analysis removed a sharp "system" peak located near the final surge of mercury dissolution current. This system peak has been attributed to electron transfer with a sediment component (e.g., iron humate) absorbed on the mercury drop during the electro-deposition stage.

Typical DPASV curves are shown in Fig. 2. Filtering did not eliminate sloping baselines or increase peak definition. With ammonium nitrate base solution, the baseline slope in the zinc peak region was similar to that found with nitric acid solution (cf. Fig. 1) and this tends to confirm that $\text{NH}_4^+/\text{NO}_3^-$ transitions are a serious competing reaction at potentials more negative than -1 V.

Differences in sediment nature were regularly indicated by the appearance of new peaks, or by peak position shifts (Fig. 2). Only half of the sediments yielded a peak attributable to ion-exchanged copper ions (hence many nd entries in Table 5), but nearly all sediments yielded a

"system" peak located about 100 mV anodic to the copper peak position in standards. In a few cases (mainly with suspensions in calcium chloride solution) there were overlapping peaks in the copper region. When magnesium chloride or ammonium nitrate solution was used as the displacing medium, several sediments (1, 3, 5, 10, 11) gave broad peaks which were located mid-way between the predicted lead and copper peak positions (cf. Fig. 2). These peaks were absent when filtered solutions were used, and hence may reflect adsorption of a colloidal lead species (anodic shift) or a labile-copper surface-complex (cathodic shift). The sloping baselines indicated that sorption of some sediment components (e.g., organic matter) on the electrode occurred in most systems.

The level of electrolyte soluble in distilled water containing suspended sediments was high enough for electrolysis and the aqueous suspensions yielded voltamperograms of similar form to those obtained in the presence of added sodium chloride or ammonium nitrate. The chloride ion level was also sufficient for copper complex formation (as indicated by the peak position). It should be noted, however, that for both the water and salt systems, the levels of copper (and cadmium) present were near the analytical detection limit. Lead values were a little higher and added electrolytes did not significantly increase the recovery of lead. This suggests that the ion-exchangeable fraction was small or non-existent, and that the lead detected was probably present as soluble salts. Little of the zinc content of most sediments was water-soluble (Table 5) but with two sediments (1, 3) significant amounts of zinc were detected. This zinc must have been loosely bound to particles, since the signal disappeared if the solution was filtered.

Extraction with reagents that form metal complexes

Schemes for fractionating the metal content of soils or sediments regularly include procedures for evaluating the amount associated with reducible matrix components such as amorphous iron(III) or manganese(IV) hydrous oxides. The reagents used include acidified hydroxylamine (discussed in an earlier section) and oxalic acid buffer solution (pH 3). For the determination of available lead or copper in soil samples, comparison studies^{28,29} have shown oxalate buffer to be superior to the alternative extractants. The oxalic acid/ammonium oxalate

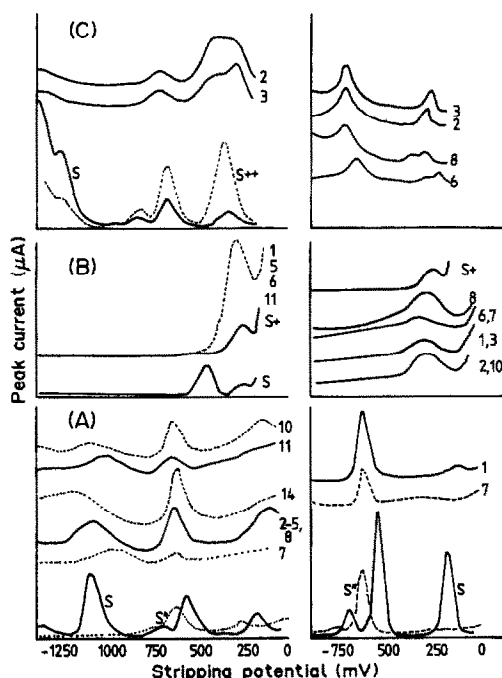


Fig. 3. Typical ASV curves obtained with sediment extracts containing complex-forming reagents: (A), 0.1M $\text{Na}_4\text{P}_2\text{O}_7$ (pH 7); (B), 5mM EDTA (pH 7); (C), oxalate buffer (pH 3). Sediment suspensions numbered 1–14. Standard solutions: A, 8.5 $\mu\text{g}/\text{ml}$ Zn, 2.8 $\mu\text{g}/\text{ml}$ Pb, 0.5 $\mu\text{g}/\text{ml}$ Cu and Cd, pH 9.8 (S), pH 6 (S^+); B, 12.5 $\mu\text{g}/\text{ml}$ Zn, 3.8 $\mu\text{g}/\text{ml}$ Pb, 0.7 $\mu\text{g}/\text{ml}$ Cu and Cd, pH 7 (S); S^+ , 50 μg of Fe added; C, as for B but pH 3.2 (S); S^+ , 500 μg of Fe added. Operating parameters: long scan, 5 sec at -1.35 V; short scan, 20 sec at -0.9 V. Sensitivity settings were 2 μA FSD (except S^+ , 1 μA) for A and B, 5 μA FSD for C.

mixture proved to be an unsuitable base solution for ASV studies, however, owing to the stability of the metal complexes formed, and system-pH effects. When the acidified standard solutions were mixed in equal volume with the buffer, the pH was ~ 2.8 and well separated peaks for each metal ion were obtained (though the zinc peak was superimposed on a sloping baseline). Sediment/buffer mixtures, on the other hand, had a pH of about 3.2 and at this pH the zinc and cadmium peaks were absent and the baseline was no longer flat in the lead and copper peak regions. The metal/oxalate interactions also caused the size and location of the lead and copper peaks to vary with the potential used in the initial electro-deposition stage. For example, the copper levels dropped from about 100 to 5 $\mu\text{g}/\text{g}$ when the deposition potential was changed from -1200 mV to -750 mV. Measurement of copper levels was complicated by the appearance of an overlapping second peak, identified as due to a complex iron species. At pH < 3 (*i.e.*, standard samples)

addition of iron(III) nitrate resulted in a broad enlarged peak in the copper region (*cf.* curve S^{++} in Fig. 3C). With sediment samples containing extracted iron, two distinct peaks could often be discerned (*cf.* Fig. 3C). The cathodic segment was assigned to copper, and the values listed in Table 3 were calculated after partial resolution of the overlap effect. The interfering effect of iron was most marked when the more negative deposition potential was used (*i.e.*, -1.2 V). Filtering the samples before DPASV analysis altered the size and shape of the double peaks.

Linear calibration curves were obtained when standard solutions of iron(III) nitrate were added to oxalate buffer, so the second segment of the overlapping sediment-system peaks could have been used to measure the amount of dissolved iron (shown by AAS analysis to vary between 6 and 12 $\mu\text{g}/\text{g}$).

In most of the sediment/oxalate buffer studies, the lead peaks were clearly defined, but the peak size was influenced by the initial deposition potential (to a lesser extent than for copper). The mean values are recorded in Table 3. The levels detected were somewhat similar to the labile values obtained with 0.02M nitric acid as extractant, a result which suggests that a significant fraction of the lead content of the sediments was associated with the hydrous oxides of iron and manganese (lead is known to have a high affinity for such substrates). Filtering the sediment suspensions prior to ASV analysis yielded lower lead values, which implies that part of the labile lead released during dissolution of the hydrous oxides was resorbed in a loosely bound form onto the solid particles.

In soil studies, solutions containing sodium or potassium pyrophosphate have been used to release organically bound metal ions (*e.g.*, copper).²⁷ Amorphous or crystalline inorganic iron and aluminium species are not attacked³⁰ but at pH 10 the reagent can peptize finely divided amorphous hydrous oxides as well as organic matter.³¹ Dilute sodium pyrophosphate solution (*e.g.*, 0.1M, pH 7) dissolves humic acids and their salts³² and in theory, ASV analysis of pyrophosphate extracts should provide an indication of the amount of labile metal ion associated with organic phases or alkaline-earth metal compounds present in sediments.

In the sediment study, however, it was found that the size, position and shape of the ASV peaks were very sensitive to the pH of the extractant solutions and to the potential applied in

the electro-deposition stage. This variability is illustrated by the bottom two sets of curves in Fig. 3A. The full lines are the results obtained for an acidic standard mixed with pH 10 reagent, yielding base solutions of pH >9.8. The zinc species present at this pH (probably tetrahydroxozincate) was ASV-labile. The dotted lines were obtained by use of standards having a pH of about 6 (the pyrophosphate added had been adjusted to pH 7). In this pH region non-labile zinc pyrophosphate species predominated and no zinc signal was detected. The pH of suspension of sediments in neutral pyrophosphate solution was around 7, and the shape of these curves suggests that there was a mixture of zinc species present. With the sediment extracts the zinc peaks were broad and superimposed on an elevated non-linear baseline, with occasional anodic displacements indicative of adsorbed species.

The zinc content values listed in Table 5 are shown in brackets because they were estimates derived from standard curves which could be in error because of differences in the system and standard pH-values. Peaks attributable to cadmium were noted for three samples (4, 7, 12) with deposition at -1.3 V, but the calculated values were double the total content, an error again attributable to calibration problems.

The effect of deposition potential on sediment lead and copper values is shown in Table 5. For these elements, the value obtained with $E_{\text{dep}} - 0.9$ V was somewhat smaller than that with $E_{\text{dep}} - 1.3$ V, a trend confirmed by changing the deposition potential in 50 mV steps from -900 to -1400 mV. For sediment 1, the lead value gradually increased from 305 to 380 $\mu\text{g/g}$ and the copper values increased from 5 to 80 $\mu\text{g/g}$. With an E_{dep} of -0.9 V only trace levels (5 $\mu\text{g/g}$) of copper were detected in any sample. The copper peaks varied little in size when the solutions were filtered or centrifuged before analysis, but removal of the solid phase led to lower lead results with eight of the sediments tested (1, 4, 7, 11, 12 15–17). Addition of an iron(III) salt to the standards led to enhancement of the peak size.

In view of the many parameters which influenced the peak heights obtained when it was used, pyrophosphate is classed as an unsuitable base solution for DPASV metal determinations.

To isolate the "non-detrital" fraction of the total metal content of soils and sediments, extraction with EDTA solutions has been advo-

cated but analysis of the extracts by ASV has not been proposed, possibly because it has been shown²⁰ that the peak size can vary with EDTA concentration and system pH.

As part of the current investigation, DPASV responses in 5mM EDTA adjusted to pH 7 have been re-examined. As expected, signals for zinc, cadmium and lead were not obtained when the pH of the standard solutions was >6. Well separated peaks for all four metal ions were observed, however, with acidified standards (pH 1.5) since at this pH metal complex formation was minimal. The sediment/EDTA suspensions had pH values between 6.5 and 6.9. In this range only one significant peak appeared on the volt-amperegrams, located in the region where added iron was detected. The baselines were non-linear and elevated (with $E_{\text{dep}} - 900$ mV) and in only two cases (2, 10) were there slight bumps that could be attributed to copper (*cf.* Fig. 3B). The iron peaks were more distinct with $E_{\text{dep}} - 1.35$ V. The full scan shown in Fig. 3B was typical of the response obtained with sediments 1, 5, 6 and 11; with sediment 7 the peak height was half this value, and with sediments 4, 8, 9, 10 the peak was twice as high. Apart from this detection of a soluble iron fraction, ASV analysis of EDTA extracts provided no useful analytical data.

Even interaction of metal ions with chloride ions can cause peaks to change in size and position. Changes with zinc, cadmium and lead tend to be less significant than those for copper. On addition of chloride ions to acetate buffer base, for example, the copper peak becomes asymmetrical, with a steep slope on the anodic side and a shoulder on the cathodic side. This distortion has been attributed²² to overlapping of one-electron and two-electron oxidation processes (*i.e.*, $\text{Cu} + 2\text{Cl}^- \rightarrow \text{CuCl}_2^- + e^-$, or $\text{Cu} + 3\text{Cl}^- \rightarrow \text{CuCl}_3^- + 2e^-$, or $\text{Cu} + 4\text{Cl}^- \rightarrow \text{CuCl}_4^{2-} + 2e^-$).

Splitting of copper peaks was regularly observed when chloride salt extractants were used (*cf.* earlier sections) but in our study the anodic segment has been assigned to electron transfer within an adsorbed species.

Analysis of extracts by both ASV and AAS

The effect of pH on the stability of complexes is far less important when metal extracts are analysed by total content techniques such as atomic-absorption spectrometry (AAS), because both labile and non-labile forms then contribute to the signal. Accordingly, AAS

Table 6. AAS Analysis of sediment extracts, $\mu\text{g/g}$

Species	Extractant	Sediment No.							
		1	2	3	4	5	6	7	8
Zinc	HNO ₃	1850	1500	1500	920	1100	560	390	440
	NH ₂ OH·HCl	2950	1240	1190	—	860	440	460	400
	Oxalate, pH 3	1580	1360	1400	800	950	500	420	400
	Na ₄ P ₂ O ₇	1300	1050	1080	650	760	380	280	300
	CaCl ₂	500	180	270	240	190	30	30	30
Lead	HNO ₃	440	370	240	130	250	90	50	110
	NH ₂ OH·HCl	380	340	200	90	240	70	20	70
	Na ₄ P ₂ O ₇	400	250	430	110	180	80	80	90
	Oxalate, pH 3	130	170	210	100	100	60	60	90
	CaCl ₂	nd	nd	nd	nd	nd	nd	nd	nd
Copper	HNO ₃	90	150	70	65	80	95	30	115
	Oxalate, pH 3	90	40	100	60	80	100	50	110
	Na ₄ P ₂ O ₇	60	60	60	40	50	60	30	70
	NH ₂ OH·HCl	60	50	40	40	50	40	20	60
	CaCl ₂	nd	nd	nd	nd	nd	nd	nd	nd

values should match or exceed ASV values. Where there is little non-labile metal ion present, and some ions are loosely sorbed on particles, the opposite trend can be observed, *i.e.*, the ASV result (for suspensions) can be larger than the AAS value.

With nitric acid extracts, both techniques yielded similar lead and copper levels; for zinc the AAS values were larger than the ASV results (Tables 3, 5 and 6). Iron was dissolved from all sediments in amounts ranging from 3 to 11 mg/g (AAS value only) and in the presence of a reducing agent (*e.g.*, NH₂OH·HCl in acetic acid) these values increased (to 8–15 mg/g). The total amount of zinc detected by AAS in hydroxylamine solutions was less than that found in the nitric acid solutions. The level of zinc detected by ASV was even smaller (<10%), owing to the influence of the reducing agent on the zinc redox process. Lead AAS values were similar with both of these extractants, but in each case the amount found was lower than the ASV values. This suggests that in acid media, displaced lead tends to be re-adsorbed on particles. The hydroxylamine solution released less copper than did nitric acid (based on AAS values), but the AAS readings were larger (by a factor of 2–3) than the corresponding ASV values.

Another example of metal ions tending to be re-adsorbed on sediment components was encountered with calcium chloride solutions. AAS analysis of filtered solutions detected about 10 $\mu\text{g/g}$ copper and lead but after the suspensions had stood for an extended period, no copper or lead was found. ASV analysis of the suspen-

sions, on the other hand, detected 5–20 $\mu\text{g/g}$ copper and up to 240 $\mu\text{g/g}$ lead (Table 5). Zinc AAS values were also very much smaller than the ASV-labile values.

When the ASV readings vary with experimental parameters, *e.g.*, in the presence of oxalate or pyrophosphate ions, comparisons with AAS data have limited significance. As noted earlier, for oxalate solutions there were no zinc peaks and for pyrophosphate solutions the zinc peaks were broad and difficult to quantify. The AAS analyses, on the other hand, yielded zinc values which matched the amount of labile ion transferred⁶ to sulphonic acid group cation-exchangers (RSO₃H).

The ASV readings for lead in oxalate buffer (pH 3.2) were similar in magnitude to the corresponding RSO₃H transfer values. The AAS readings, however, were only about half of these values and it is suspected that some lead was precipitated during a delay before analysis. With pyrophosphate extracts, the AAS results were of similar value to the RSO₃H transfer data but a match with the lead ASV values depended on the electro-deposition potential used. With two sediments (1, 15) the AAS value was similar to the higher value obtained with $E_{\text{dep}} - 1.35$ V, whereas with nine other sediments (2, 4–6, 8–10, 12, 16) the match was with the lower ASV result ($E_{\text{dep}} - 0.9$ V).

Owing to the overlapping of peaks and poor baseline definition, little copper was detected in the presence of oxalate by ASV, and the AAS values were much larger. With pyrophosphate extracts and $E_{\text{dep}} - 1.35$ V, the ASV and AAS values for most sediments were similar, and

both matched the amounts of copper transferred to a strong-acid cation-exchanger (RSO_3H).

Cadmium was not detected in the various solutions by flame AAS, and little was transferred to cation-exchangers, so the ASV approach was the only procedure capable of defining the low levels present.

The role of ASV in metal lability evaluation

Determination of metal ion lability by ASV procedures has been promoted on several grounds, including relative speed and simplicity, selectivity for "labile" species, ability to detect trace levels and retrieve metal ions loosely bound to particles (a fraction that is lost on filtration). Though this study has confirmed part of these claims, it has simultaneously highlighted several limitations of the approach. The most important of these is the effect of adsorbed colloidal matter on the baseline slope, and the appearance of "system" peaks. Filtering before analysis partly overcomes this problem but the fraction loosely bound to particles is then lost, and unless the metal levels are very low, there are few advantages in using the ASV procedures. Competing electrode processes reduce the number of base solutions in which zinc can be determined, and dissolved iron yields peaks which tend to overlap the copper signal.

The validity of the "ASV-labile" data was confirmed for a number of systems by comparison with AAS and cation-exchange transfer results. The precision of the procedure was determined by the variance of the extraction step and the measuring technique.

It was concluded that DPASV analysis of sediment suspensions would be suitable for surveys of labile metal contents, over a limited range of chemical environments. Extractants suitable for such surveys would be 0.02M nitric acid (for low-pH lability); acetic acid/acetate buffer (for pH-5 lability); and 0.05M calcium chloride (for estimating sediment-pH lability).

Acknowledgements—This investigation was supported by the Australian Research Committee and their financial assistance is gratefully acknowledged.

REFERENCES

1. U. Förstner, *Z. Anal. Chem.*, 1983, **316**, 604.
2. W. F. Pickering, *CRC Crit. Rev. Anal. Chem.*, 1981, **12**, 233.
3. *Idem*, *Ore Geol. Rev.*, 1986, **1**, 83.
4. T. U. Aualiitia and W. F. Pickering, *Talanta*, 1988, **35**, 559.
5. A. Beveridge, P. Waller and W. F. Pickering, *ibid.*, 1989, **36**, 535.
6. J. Slavek, P. Waller and W. F. Pickering, *ibid.*, 1990, **37**, 397.
7. T. U. Aualiitia and W. F. Pickering, *Water Res.*, 1986, **20**, 1397.
8. *Idem*, *Talanta*, 1987, **34**, 231.
9. T. Ugapo and W. F. Pickering, *ibid.*, 1985, **32**, 131.
10. R. Ernst, H. E. Allen and K. H. Mancy, *Water Res.*, 1975, **9**, 965.
11. S. A. Wilson, T. C. Huth, R. E. Arndt and R. K. Skogerboe, *Anal. Chem.*, 1980, **52**, 1515.
12. R. B. Smart and E. E. Stewart, *Environ. Sci. Technol.*, 1985, **19**, 137.
13. T. U. Aualiitia and W. F. Pickering, *Water, Air, Soil Pollut.*, 1987, **35**, 171.
14. M. de L. S. Goncalves, L. Sigg and W. Stumm, *Environ. Sci. Technol.*, 1985, **19**, 141.
15. P. Sagberg and W. Lund, *Talanta*, 1982, **29**, 457.
16. P. L. Brezonik, P. A. Brainer and W. Stumm, *Water Res.*, 1976, **10**, 605.
17. G. E. Batley and T. M. Florence, *J. Electroanal. Chem.*, 1974, **55**, 23.
18. Z. Łukaszewski and M. K. Pawlak, *ibid.*, 1979, **103**, 225.
19. A. Beveridge and W. F. Pickering, *Water Res.*, 1984, **18**, 1119.
20. E. A. Schonberger and W. F. Pickering, *Talanta*, 1980, **27**, 11.
21. I. Šinko and J. Doležal, *J. Electroanal. Chem.*, 1970, **25**, 299.
22. M. Pinchin and J. Newham, *Anal. Chim. Acta*, 1977, **90**, 91.
23. V. H. Lewin and M. J. Rowell, *Effluent Water Treat. J.*, 1973, **13**, 273.
24. A. Zurino and M. L. Healy, *Environ. Sci. Technol.*, 1972, **6**, 243.
25. T. R. Copeland and R. K. Skogerboe, *Anal. Chem.*, 1974, **46**, 1257A.
26. J. Opydo, *Water, Air, Soil Pollut.*, 1989, **45**, 43.
27. R. J. McLaren and D. V. Crawford, *J. Soil. Sci.*, 1973, **24**, 172.
28. S. G. Misra and G. Pandey, *Plant, Soil*, 1976, **45**, 693.
29. P. C. Mishra, M. K. Mishra and S. G. Misra, *Indian J. Agr. Sci.*, 1973, **43**, 609.
30. J. A. McKeague, *Can. J. Soil Sci.*, 1967, **47**, 95.
31. C. L. Bascomb, *J. Soil Sci.*, 1968, **19**, 251.
32. J. M. Bremner and H. Lees, *J. Agr. Sci.*, 1949, **39**, 274.

DETERMINATION OF THALLIC AND THALLOUS IONS BY DIFFERENTIAL PULSE ANODIC STRIPPING VOLTAMMETRY WITHOUT PRELIMINARY SEPARATION

ALEKSANDER CISZEWSKI

Institute of General Chemistry, Technical University of Poznań, 60-965 Poznań, Poland

(Received 3 May 1989. Revised 15 January 1990. Accepted 4 April 1990)

Summary—The simultaneous determination of thallic and thallos ions, without preliminary separation, has been achieved by differential pulse anodic stripping voltammetry at a hanging mercury drop electrode. The electrochemical activity of thallic ions in 0.2M EDTA at pH 4.5 ± 0.2 is inhibited by the addition of 0.01% poly(ethyleneglycol) of M.W. 20,000 (PEG 20,000). When the electrolyte also contains ascorbic acid at 0.01M concentration, the sum of thallic and thallos species can be determined.

Speciation analysis has become an important field in analytical chemistry. In the analysis of natural waters, it gives information about the transport, adsorption and precipitation of an element in the water system, and in the analysis of human body fluids allows the observation of bioaccumulation, displacement and excretion of different forms of the element. Furthermore, since different states of an element and its physicochemical forms have different toxicities, speciation analysis is indispensable in many applications such as criminology, environmental pollution or food analysis. Recently, a very interesting speciation scheme was proposed for four metals of prime environmental concern (copper, lead, cadmium and zinc), based on anodic stripping voltammetry (ASV) and a few preliminary speciation steps.¹ ASV (differential pulse or square wave), although the most often used electrochemical technique in speciation measurements, is not free from interferences. Avoiding the interference from surface-active compounds in samples is difficult and often impossible, especially in the cases of trace analysis of such samples as natural waters, blood, plasma, urine, sweat or tears.

Interference by surfactants is a serious problem in all ASV techniques but can sometimes be turned to advantage, as in the technique called electrochemical masking. There are some promising examples of this in stripping analysis for a trace element.¹⁰⁻²³ Although this procedure is not often used in the stripping methods today, electrochemical masking may well turn out to be important for avoiding the serious

problems caused in stripping methods by surface-active compounds accidentally present in the sample and by matrix elements or compounds.

The aims of this work were: (i) to examine the possibility of determining thallium as Tl(I) in the presence of Tl(III) by differential pulse ASV, (ii) to find the conditions for electrochemical masking of thallic or thallos ions and thus to determine Tl(I) in the presence of Tl(III) or vice versa and (iii) to examine the feasibility of this determination in the presence of other metals.

It is well known that thallium commonly exists in either the univalent or trivalent state. Univalent thallium is one of the easiest species to determine by any voltammetric method because the reduction is reversible in most background electrolytes. The ion shows little tendency to hydrolyse, forms only weak complexes, and its reduction is not sensitive to surfactants. The determination of thallium as Tl(I) has been the subject of numerous publications and some of them concern extremely low concentrations.^{24,25} In particular, DPASV has become very useful in this determination because of its high sensitivity.^{26,27} Our knowledge of the electrochemical behaviour of Tl(III) at the mercury electrode is rather poor because the Tl(III) \rightarrow Tl(I) reaction proceeds at this electrode in the positive potential range. Only a few papers deal with the electrochemical behaviour of thallium(III) and none take up the problem of the simultaneous determination of Tl(I) and Tl(III).^{28,29}

EXPERIMENTAL

Apparatus

Anodic stripping voltamperograms were obtained with a Telpod (Poland) pulse polarograph model PP-04, and an Endim (GDR) 620.02 XY recorder. A classical three-electrode system was employed. The hanging mercury-drop electrode (HMDE) was a Radiometer Kemula Equipment E69 model with a drop size corresponding to 3 divisions of the micrometer screw. A platinum wire was used as auxiliary electrode and an SCE as reference. The differential pulse amplitude was 50 mV and the scan-rate was 11.1 mV/sec. During the deposition step, the solutions were stirred by a mechanical stirrer at about 800 r.p.m. Air was purged from all solutions by passage of nitrogen for at least 15 min. All potentials reported are referred to the SCE.

Reagents

Merck EDTA (disodium salt) and ascorbic acid were used. Standard solutions of Tl(I) and Tl(III) were prepared from the nitrates (Merck). The surfactants used were benzyl(di-isobutylphenoxyethoxy)dimethylammonium chloride (Hyamine 1622) (Serva), hexadecyltrimethylammonium bromide (HDTMAB) (Merck), sodium dodecylbenzyl sulphonate (DBS) (POCh), sodium dodecyl sulphate (DS) (Merck), Triton X-100 (Merck) and poly(ethyleneglycols) (PEG) of M.W. 4000 (PEG 4000) (Merck), 6000 (PEG 6000) (BDH), 9000 (PEG 9000) (Fluka), 15,000 (PEG 15,000) (Roth), 20,000 (PEG 20,000) (Fluka).

The background electrolyte was 0.2M EDTA or 0.2M EDTA + 0.01M ascorbic acid, pH 4.5 ± 0.2 . The standard solutions of Tl(I) and Tl(III) with concentrations below 1mM were prepared just before measurement. All solutions were prepared in water which had been triply-distilled in a fused-silica apparatus. Before measurement all solutions were brought to $20 \pm 0.5^\circ$ in a thermostat.

RESULTS AND DISCUSSION

With EDTA solution (0.2M, pH 4.5 ± 0.2) as background electrolyte the stripping peaks for thallium and lead do not coincide, whereas they do for various other electrolytes. Also, Tl(III) forms a very stable EDTA complex whereas Tl(I) forms only a very weak one.

In all anodic stripping techniques, the measured signal is the result of an oxidation

reaction. In the case of thallium, if the electrode potential is negative enough, both thallic and thalious ions will be initially electro-deposited as thallium amalgam. Next, in the stripping step with a linear potential sweep, oxidation of thallium amalgam to thalious ion will occur, $\text{Tl(Hg)} \rightarrow \text{Tl(I)} + \text{Hg}$, giving the signal current which is measured. As this signal is independent of the redox state of thallium present in the original sample, no information is gained regarding speciation of the thallium in the sample. This problem is shown in Fig. 1 where the lines "a" and "b" are calibration curves for thalious and thallic ions, respectively. They differ from each other in slope but cannot be used in practice without prior knowledge about the redox state of thallium present in the solution. The standard addition method may also be risky, e.g., for a tested solution with equal concentrations of thalious and thallic ions, if Tl(I) ions are used as a standard, the result for thallium will be lower than the real value, and if Tl(III) is used as the standard, the result will be higher than the real value.

The only way to resolve these difficulties, apart from preliminary separation of thalious and thallic ions, is by electrochemical masking of one of the redox states of thallium and determination of the other form, followed by changing the experimental conditions to allow determination of total thallium concentration. Taking into account that thalious ions are not affected by surfactants, as mentioned previously,^{19-23,30-34} attempts were made to suppress the electrochemical activity of thallic ions, i.e., to inhibit the reaction $\text{Tl(III)} \rightarrow \text{Tl(I)}$.

In preliminary studies, cationic (Hyamine 1622 and HDTMAB), anionic (DBS and DS) and non-ionic (Triton X-100 and PEG 9000) surfactants were used. All the surfactants tested were capable of inhibiting the reduction

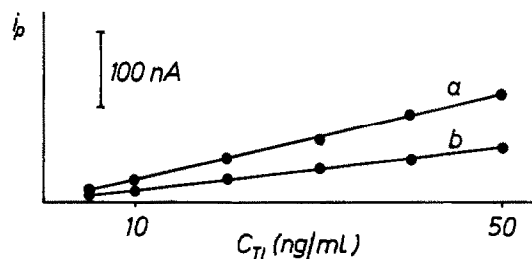


Fig. 1. Dependence of differential pulse anodic stripping peak currents for a, thallic and b, thalious ions. Background electrolyte: 0.2M EDTA, pH 4.5 ± 0.2 . Deposition time 300 sec. Deposition potential -0.800 V. Differential pulse amplitude 50 mV, scan-rate 11.1 mV/sec.

of Tl(III) to Tl(I). The non-ionic surfactants gave the best results (particularly PEG 9000) and were therefore investigated more fully. The next series of experiments was done with poly(ethyleneglycols) of different molecular weights: PEG 4000, PEG 6000, PEG 9000, PEG 15,000 and PEG 20,000. Lower molecular weights were not investigated because of their reported low capability for suppressing the polarographic electrode reactions of many ions.^{33,35-37}

The influence of selected PEGs on the series of reactions $\text{Tl(III)} \rightarrow \text{Tl(I)} \rightarrow \text{Tl(Hg)} \rightarrow \text{Tl(I)}$ is shown in Fig. 2. None of the PEGs examined influences the reactions $\text{Tl(I)} \rightarrow \text{Tl(Hg)} \rightarrow \text{Tl(I)}$, and only the reaction $\text{Tl(III)} \rightarrow \text{Tl(I)}$ is suppressed (Fig. 3). The results obtained are consistent with expectation. The difference in behaviour of thallic and thalious ions is caused by the difference in the stability of their EDTA complexes. Moreover, their ionic potentials (ionic charge divided by the ionic radius) are in good agreement with the data obtained by Loshkarev and Kryukova³⁸ who reported a relationship between the effect of a surfactant on a polarographic wave and the radius and charge of the ion undergoing reduction. The fact that only the electroreduction of thallic ions to thalious ions is affected by PEG allows realization of the aim of this work.

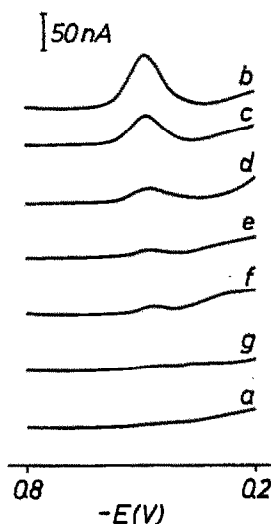


Fig. 2. Influence of poly(ethyleneglycols) of different molecular weights on the peak current for thallic ions: *a*, background electrolyte; *b*, background electrolyte + 50 ng/ml Tl(III); *c-g*, background electrolyte + 50 ng/ml Tl(III) + 0.01% PEG (*c*, PEG 4000; *d*, PEG 6000; *e*, PEG 9000; *f*, PEG 15,000; *g*, PEG 20,000). Conditions of measurement as for Fig. 1.

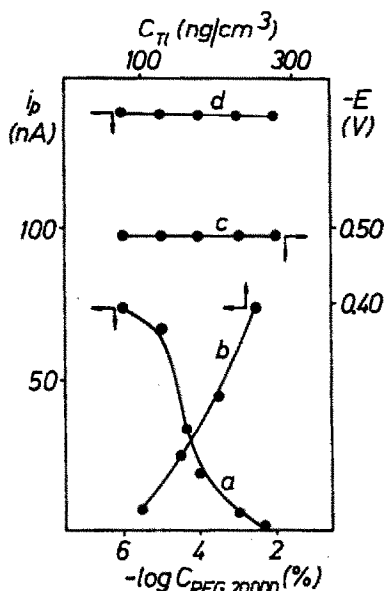


Fig. 3. Variation in the thallium peak in the presence of PEG 20,000: *a*, peak current for 50 ng/ml Tl(III) vs. concentration of PEG 20,000; *b*, peak current vs. concentration for Tl(III) in the presence of 0.01% PEG 20,000; *c*, peak potential for 50 ng/ml Tl(III) vs. concentration of PEG 20,000; *d*, peak current for 50 ng/ml Tl(I) vs. concentration of PEG 20,000.

Conditions of measurement as for Fig. 1.

It can be seen from Fig. 2 that an increase in the molecular weight of the PEG increases the suppression of the $\text{Tl(III)} \rightarrow \text{Tl(I)}$ reaction. The reason is as follows. The standard potential of the electrochemical reaction $\text{Tl(III)-EDTA} \rightarrow \text{Tl(I)}$ is not known, but must be more negative than +1.25 V, which is E_0 for the Tl(III)/Tl(I) couple in non-complexing media.³⁹ The high stability constant of the Tl(III)-EDTA complex is responsible for this shift in potential.⁴⁰ In addition, for an electrochemical reaction to be suppressed, it is necessary for its half-wave potential to lie within the range of adsorption potentials for the surfactant used. In the case of electroreduction of thallic to thalious ions and adsorption of poly(ethyleneglycols), this condition seems to be met. The data reported on the adsorption of PEGs show that the anodic adsorption-desorption peak shifts from about -0.10 V for PEG 4000 to about +0.05 V for PEG 20,000.³⁶ These values, when compared with the literature data for the electroreduction potential of thallic to thalious ions at the mercury electrode (approximately 0 V),⁴¹ allow an explanation of the relationship presented in Fig. 2.

The results presented in Figs. 1-3 allow proposal of the following procedure for simultaneous determination of thallic and thalious

Table 1. Accuracy and precision of the determination of thallic and thalious ions without preliminary separation

Series	Number of tests	Added, ng/ml		Found, ng/ml		Std. devn., ng/ml		Rel. std. devn., %	
		Tl(I)	Tl(III)	Tl(I)	Tl(III)	Tl(I)	Tl(III)	Tl(I)	Tl(III)
I	7	200.0	200.0	203.0	198.0	2.7	4.8	1.3	2.5
II	7	20.0	20.0	20.4	19.6	1.3	0.9	5.5	4.9
III	7	2.0	2.0	2.0	1.8	0.3	0.2	15	11

ions. By introducing the proper amount of PEG 20,000 into a sample having both forms of thallium, and using the correct chosen experimental conditions, it is possible to determine only the thalious ions, by the standard addition method with Tl(I) as standard solution. To determine the total concentration of Tl(III) + Tl(I), from which the concentration of thallic ions can be calculated, it is then necessary to convert Tl(III) into Tl(I). This can be done by using any one of many reductants. In this study, ascorbic acid was chosen, not only for its good reducing properties with respect to thallic ions, but also because the EDTA + ascorbic acid mixture is a very good supporting electrolyte for the determination of thalious ions,⁴² avoiding problems in determination of thallium in the presence of lead, bismuth, copper and titanium.²⁰⁻²³ The change in pH after introduction of ascorbic acid into the test sample does not seem to cause difficulties. Results for the determination of thalious and thallic ions are presented in Fig. 4 and Table 1. Possible interferences by ten ions have been studied. Up to 10,000-fold ratio of Cu(II), Pb(II), Ni(II),

Co(II), Sn(IV), Sb(V), As(V), Zn(II), In(III) or Fe(III) to thallium can be tolerated, making the proposed method suitable for the determination of thallic and thalious ions in such natural samples as waters, body fluids and other materials which can contain relatively large amounts of other ions.

REFERENCES

1. T. M. Florence, *Analyst*, 1986, **111**, 489.
2. J. C. Duinker and C. J. M. Kramer, *Mar. Chem.*, 1977, **5**, 207.
3. S. K. Nilsen and W. Lund, *ibid.*, 1981, **11**, 223.
4. P. Figura and B. McDuffie, *Anal. Chem.*, 1980, **52**, 1433.
5. P. Benes, J. Koc and K. Štulík, *Water Res.*, 1979, **13**, 967.
6. R. J. O'Halloran, *Anal. Chim. Acta*, **140**, 1982, 51.
7. J. Golimowski, P. Valenta and H. W. Nürnberg, *Z. Anal. Chem.*, 1985, **322**, 315.
8. G. E. Batley and T. M. Florence, *J. Electroanal. Chem.*, 1975, **61**, 205.
9. P. L. Buldini, D. Ferri and Q. Zini, *Mikrochim. Acta*, 1980 **1**, 71.
10. R. Neeb and I. Kiehnast, *Naturwissenschaften*, 1970, **57**, 37.
11. N. You and R. Neeb, *Z. Anal. Chem.*, 1983, **314**, 158.
12. *Idem*, *ibid.*, 1983, **314**, 394.
13. J. Georges, *Anal. Chim. Acta*, 1981, **127**, 233.
14. J. Georges and M. Mermet, *ibid.*, 1986, **185**, 363.
15. R. Modolo and O. Vittori, *ibid.*, 1983, **151**, 483.
16. J. L. Guiñón and J. García-Antón, *ibid.*, 1985, **177**, 225.
17. J. Hernández-Méndez, R. Carabias Martínez and J. I. García-García, *ibid.*, 1981, **132**, 47.
18. J. Hernández-Méndez, R. Carabias Martínez and M. E. González López, *ibid.*, 1982, **138**, 47.
19. Z. Łukaszewski, M. K. Pawlak and A. Ciszewski, *Talanta*, 1980, **27**, 181.
20. A. Ciszewski and Z. Łukaszewski, *ibid.*, 1983, **30**, 873.
21. *Idem*, *ibid.*, 1985, **32**, 1101.
22. A. Ciszewski, *ibid.*, 1985, **32**, 1051.
23. *Idem*, *ibid.*, 1988 **35**, 329.
24. G. Calderoni and T. Ferri, *Talanta*, 1982, **29**, 371.
25. J.-M. Kauffmann, Th. Montenez, J. L. Vandenbalck and G. J. Patriarcke, *Mikrochim. Acta*, 1984 **1**, 95.
26. J. E. Bonelli, H. E. Taylor and R. K. Skogerboe, *Anal. Chim. Acta*, 1980, **118**, 243.
27. I. Liem, G. Kaiser, M. Sager and G. Tölg, *ibid.*, 1984, **158**, 179.
28. Kh. Z. Brainina and N. K. Kiva, *Zh. Analit. Khim.*, 1965, **20**, 1306.
29. J. Doležal and E. Hrabánková, *Anal. Lett.*, 1971, **4**, 585.
30. W. Kemula and S. Glodowski, *Roczniki Chem.*, 1962, **36**, 1203.

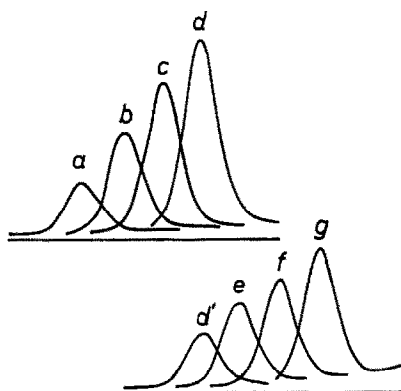


Fig. 4. Determination of thalious and thallic species without preliminary separation. Conditions of measurement as for Fig. 1. a, 0.2M EDTA (pH 4.5) + 20 ng/ml Tl(I) + 20 ng/ml Tl(III) + 0.01% PEG 20,000; peak current is caused only by Tl(I); b, as for a, + 20 ng/ml Tl(I); c, as for b, + 20 ng/ml Tl(I); d, as for c, + 1 ml of 0.2M ascorbic acid; peak current is caused by thallic and thalious ions; d', as for d, deposition time 100 sec; e, as for d', + 40 ng/ml Tl(I); f, as for e, + 40 ng/ml Tl(I); g, as for f + 40 ng/ml Tl(I).

31. J. Kůta, *Z. Anal. Chem.*, 1966, **216**, 242.
32. T. Fujinaga, K. Izutsu and T. Inoue, *Collection Czech. Chem. Commun.*, 1965, **30**, 4202.
33. Z. Łukaszewski, *Talanta*, 1977, **24**, 603.
34. A. Ciszewski and Z. Łukaszewski, *Anal. Chim. Acta*, 1983, **146**, 51.
35. Z. Łukaszewski and M. K. Pawlak, *Chem. Anal. Warsaw*, 1979, **24**, 221.
36. Z. Łukaszewski, *Pol. J. Chem.*, 1981, **55**, 1863.
37. T. Malinski and Z. P. Zagorski, *Hung. Sci. Instrum.*, 1980, **47**, 13.
38. M. A. Loshkarev and A. A. Krjukova, *J. Phys. Chem.*, 1949, **23**, 1457.
39. D. Dobos, *Electrochemical Data*, p. 260. Akadémiai Kiadó, Budapest, 1975.
40. J. Inczédy, *Analytical Applications of Complex Equilibria*, p. 247. Horwood, Chichester, 1976.
41. F. Vydra, K. Štulík and E. Juláková, *Electrochemical Stripping Analysis*, p. 203. Horwood, Chichester, 1976.
42. J. P. Franke, P. M. J. Coenegracht and R. A. De Zeeuw, *Arch. Toxicol.*, 1975, **34**, 137.

ADSORPTION VOLTAMMETRY OF THE COPPER(II) 2-(5-BROMO-2-PYRIDYLAZO)-5-DIETHYLAMINOPHENOL COMPLEX

SHUNITZ TANAKA, KAZUHARU SUGAWARA and MITSUHIKO TAGA

Department of Chemistry, Faculty of Science, Hokkaido University, Nishi-8, Kita-10, Kita-ku,
Sapporo-shi, Hokkaido, 060, Japan

(Received 24 December 1989. Revised 26 March 1990. Accepted 4 April 1990)

Summary—The voltammetric determination of copper(II), based on adsorptive accumulation of the Cu(II)-2-(5-bromo-2-pyridylazo)-5-diethylaminophenol (5-Br-PADAP) complex on a hanging mercury drop electrode, is reported. The complex can be accumulated at the electrode at constant potential in 0.1M ammonium nitrate/ammonia buffer solution, and its reduction wave observed by scanning the potential in the negative direction, in the differential pulse mode. The calibration graph for copper is linear over the range 0.05–0.5 μ M, with accumulation for 5 min at –0.20 V. The adsorption of the complex is discussed and compared with that of copper complexes with several other pyridylazo derivatives.

Stripping voltammetry, a very sensitive method for the determination of many trace metal ions, achieves its low level of detection by combining an accumulation process with a voltage-scanning measurement. However, its application to practical samples is limited by the interferences arising from the sample matrix. In anodic stripping voltammetry (ASV), based on concentration by electrolysis, the formation of intermetallic compounds with co-existing metal ions at the electrode can cause serious error,¹ and the presence of a ligand such as chloride in the sample solution disturbs the stripping wave.² Many attempts have been made to prevent the matrix effect and to concentrate an analyte selectively,³ e.g., selective concentration by the use of chemically modified glassy-carbon⁴ or carbon-paste electrodes⁵ and elimination of matrix effects by the medium-exchange method.⁶ We have reported on use of the kinetic currents produced by a specific reaction with the analyte accumulated at the electrode, to enhance the selectivity and the sensitivity.^{7,8} Another method is the use of adsorptive accumulation on the electrode, which can be applied to many organic substances^{9,10} and also to metal ions when these are converted into adsorbable complexes by reaction with an organic ligand.^{11,12} Adsorptive accumulation is useful to concentrate an analyte selectively for voltammetric analysis or to concentrate the ions of

metals which have too low a solubility in mercury to be concentrated by electrolysis.

In this paper, the adsorption voltammetry of the copper complex with 2-(5-bromo-2-pyridylazo)-5-diethylaminophenol (5-Br-PADAP) was investigated. It is known that copper forms intermetallic compounds with many other metals at the electrode in ASV, and these compounds interfere considerably with the determination of copper. Therefore, it is favourable to determine copper by measuring its reduction current after accumulation without electrolysis. Some adsorptive voltammetric methods for copper have been reported, based on catechol,¹³ 8-hydroxyquinoline¹⁴ and thiourea¹⁵ etc. as the complexing agent. However, the catechol method has the disadvantage that catechol is unstable towards oxidation by dissolved oxygen. The method using 8-hydroxyquinoline is very sensitive, but a more negative potential than –1.0 V, at which Cu(II) is reduced to copper metal, is required to obtain the maximum efficiency of accumulation. 5-Br-PADAP is very stable and is expected to give strong adsorption on the electrode, owing to its hydrophobic properties. The adsorptive power of this reagent has been established by its use in the adsorptive voltammetry of Fe(III)¹⁶ and Bi(III).¹⁷

The copper-5-Br-PADAP complex can be accumulated on the hanging mercury drop

electrode (HMDE) at -0.20 V and the cathodic current can be observed at -0.35 V.

EXPERIMENTAL

Apparatus

A polarographic analyser (PAR 174A) coupled with a PAR 315 electroanalytical controller and an Omnigraphic model 2000H X-Y recorder was used. The working electrode was a Metrohm E-410 HMDE, a glassy-carbon rod was used as the counter-electrode, and a saturated calomel electrode (SCE) with a diaphragm tube containing $1M$ potassium nitrate was used as the reference electrode. All potentials were measured against the SCE, at $25 \pm 0.1^\circ$.

Reagents

A $1 \times 10^{-2}M$ stock solution of Cu(II) was prepared by dissolving copper metal (99.999% pure, Mitsui Chemicals Co.) in 5% v/v nitric acid. A $1 \times 10^{-3}M$ stock solution of 5-Br-PADAP (Dojindo Chemical Laboratories) was prepared in 1:1 v/v ethanol-water mixture. The supporting electrolyte was $0.1M$ ammonium nitrate/ammonia buffer, pH 9.0. Working solutions were prepared by diluting the stock solutions with isopiestic distilled water.

Procedure

The solution was deaerated by passage of pure nitrogen for 5 min. A new mercury drop was set in place and accumulation was conducted for 5 min at -0.2 V, with stirring. After a rest period of 15 sec, voltamperograms were

recorded by scanning the potential in the negative direction, in the differential pulse mode (pulse amplitude 50 mV, pulse repetition time 1 sec, scan-rate 5 mV/sec).

RESULTS AND DISCUSSION

Adsorption voltamperograms of 5-Br-PADAP and the Cu(II)-5-Br-PADAP complex after accumulation for 5 min at -0.20 V from $0.1M$ ammonia buffer (pH 9.0) are shown in Fig. 1. The curve in Fig. 1(a) is the voltamperogram for $1 \times 10^{-6}M$ 5-Br-PADAP after accumulation, and the reduction peak of reagent itself appears at about -0.65 V. This peak is due to the reduction of the azo group, $-N=N-$, in the molecule of 5-Br-PADAP.¹⁶ Since the peak height is increased by increasing the accumulation time, the reagent is evidently adsorbed on the electrode. When $5 \times 10^{-7}M$ Cu(II) was also present, a new reduction peak appeared at about -0.35 V, as shown in Fig. 1(b). This peak current increased in proportion to the concentration of Cu(II) and the accumulation time. It appears that the peak at about -0.35 V is the reduction peak of the Cu(II)-5-Br-PADAP complex adsorbed on the electrode.

The relation between the peak current and the accumulation time is shown in Fig. 2. The peak current increased with increasing accumulation time up to 5 min for both 1 and $5 \times 10^{-7}M$ Cu(II), and was constant for times longer than 5 min, because of the adsorptive equilibrium between the electrode surface and the solution.

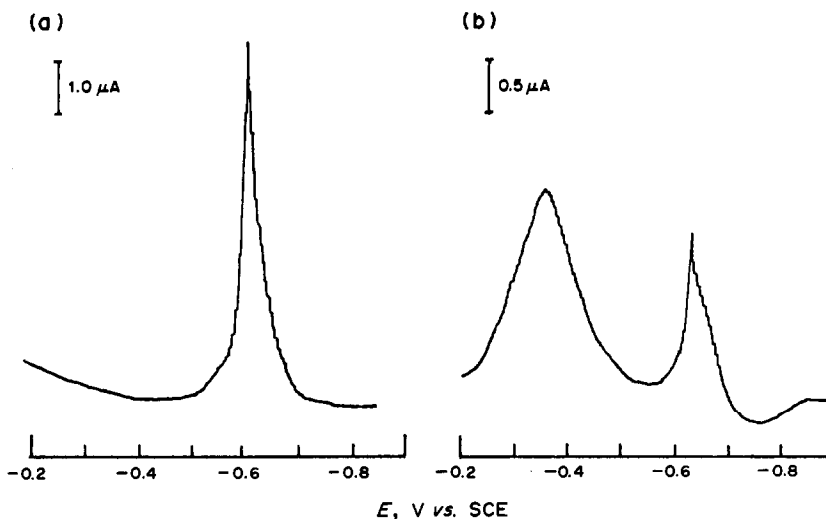


Fig. 1. Voltamperograms of 5-Br-PADAP and Cu(II)-5-Br-PADAP complex. Accumulation for 5 min at -0.20 V in $0.1M$ NH_3/NH_4NO_3 buffer containing (a) $1 \times 10^{-6}M$ 5-Br-PADAP; (b) $1 \times 10^{-6}M$ 5-Br-PADAP + $5 \times 10^{-7}M$ Cu(II). Pulse amplitude 50 mV, pulse repetition time 1 sec, scan-rate 5 mV/sec.

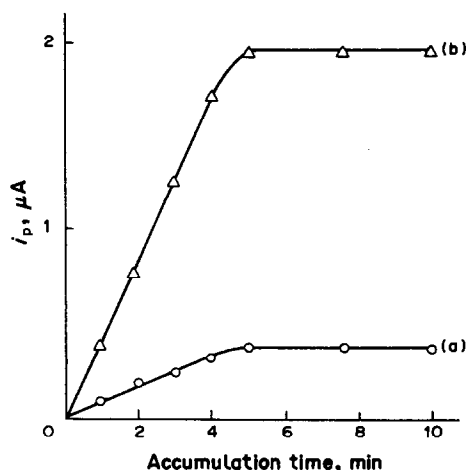


Fig. 2. Dependence of peak current on accumulation time. Accumulation at -0.20 V in $0.1M$ NH_3/NH_4NO_3 buffer containing $1 \times 10^{-6}M$ 5-Br-PADAP and (a) $1 \times 10^{-7}M$ Cu(II), (b) $5 \times 10^{-7}M$ Cu(II).

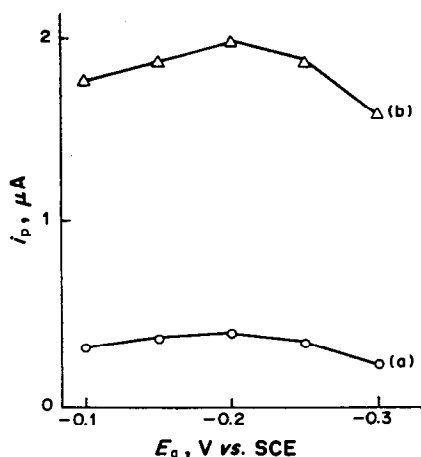


Fig. 4. Dependence of peak current on accumulation potential (E_a). Accumulation for 5 min in $0.1M$ NH_3/NH_4NO_3 buffer containing $1 \times 10^{-6}M$ 5-Br-PADAP and (a) $1 \times 10^{-7}M$ Cu(II), (b) $5 \times 10^{-7}M$ Cu(II).

The relation between peak current and concentration of 5-Br-PADAP is shown in Fig. 3. The peak current for $5 \times 10^{-7}M$ Cu(II) increased linearly with 5-Br-PADAP concentration up to $1 \times 10^{-6}M$, and then levelled off. At the break point ($1 \times 10^{-6}M$) the 5-Br-PADAP concentration is just twice that of the Cu(II). This suggests that the adsorbed species is the 1:2 copper:5-Br-PADAP complex. This was confirmed by changing the concentration of Cu(II) ion, with constant concentration of 5-Br-PADAP.

Figure 4 shows the relation between the peak current and accumulation potential. The copper complex could be accumulated at the electrode over the range from -0.1 to -0.3 V, and gave a well-defined reduction wave. However, the oxidation of mercury at more positive potentials

than -0.1 V and the consequent increase in the base current interfered in the measurement of the reduction current of the copper complex. On the other hand, at more negative potentials than -0.3 V, the peak current decreased sharply because the complex was already reduced at those potentials. Accumulation at -0.2 V was found suitable for obtaining a reproducible peak current. To verify the adsorptive behaviour of 5-Br-PADAP and its Cu(II) complex on the electrode, electrocapillary curves were measured by using a dropping mercury electrode (Fig. 5). Over the potential range from -0.1 to -0.8 V, the drop time in $5 \times 10^{-5}M$ 5-Br-PADAP solution decreased, compared to that with only the supporting electrolyte present. The electrocapillary curve of a solution

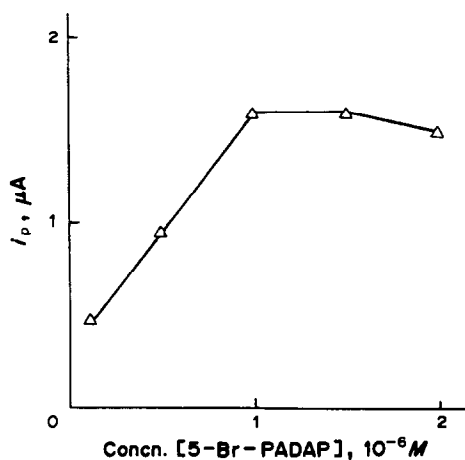


Fig. 3. Effect of 5-Br-PADAP concentration. Accumulation for 5 min at -0.20 V in $0.1M$ NH_3/NH_4NO_3 buffer containing $5 \times 10^{-7}M$ Cu(II).

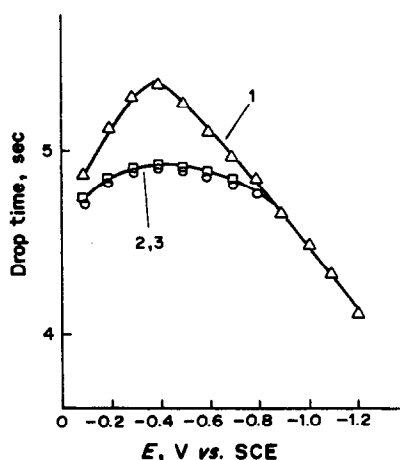
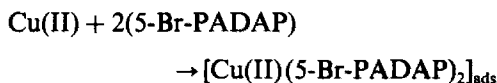
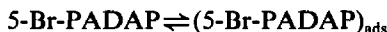


Fig. 5. Electrocapillary curves. 1, $0.1M$ NH_3/NH_4NO_3 buffer; 2, buffer + $5 \times 10^{-5}M$ 5-Br-PADAP; 3, buffer + $5 \times 10^{-5}M$ 5-Br-PADAP + $3 \times 10^{-7}M$ Cu(II).

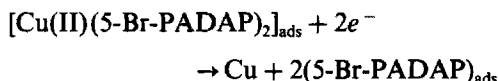
containing 5-Br-PADAP and Cu(II) was similar to that of the reagent itself. This behaviour supports the postulation of adsorption of both the copper complex and the reagent itself on the electrode, over this wide range of potentials. From these results, the accumulation process can be described by



and the reagent is also in adsorptive equilibrium:



The copper complex adsorbed on the electrode was reduced by scanning the potential after accumulation. Since the peak potential at -0.35 V was close to the reduction potential of Cu(II) in the absence of the reagent, it was considered that the Cu(II) in the complex would be reduced:



Adsorption of the copper complex on the electrode is governed by the adsorptive characteristics of the complexing reagent. Therefore, some pyridylazo derivatives similar to 5-Br-PADAP were investigated for the adsorption voltammetry of copper, namely 2-(5-bromo-2-pyridylazo)-5-(*N*-propyl-*N*-sulphopropylamino)phenol sodium salt (5-Br-PAPS), 2-(2-thiazolylazo)-4-methyl-5-sulphomethylamino-benzoic acid (TAMSMB), 2-(5-chloro-2-pyridylazo)-5-diethylaminophenol (5-Cl-PADAP), 1-(2-pyridylazo)-2-naphthol (PAN), 4-(2-pyridylazo)resorcinol (PAR). In the presence of these reagents at $1 \times 10^{-6}M$ concentration accumulation was conducted for 5 min at -0.20 V in $0.1M$ ammonia buffer. The results are shown in Table 1. All these reagents gave a reduction peak at about -0.6 V, due to reduction of the azo group. In the presence of 5-Br-PADAP, 5-Cl-PADAP, PAN and PAR, a well-defined wave for the reduction of the copper complex was observed at about -0.35 V. The magnitudes of the peak currents were in the order 5-Br-PADAP > 5-Cl-PADAP = PAN > PAR. It appears that the peak current for the copper complex increases with increasing hydrophobicity of the reagent. It was confirmed that the copper complexes with reagents containing a hydrophilic sulphonic acid group could not be accumulated on the electrode and hence no

Table 1. Effect of reagent on the reduction peak of copper complex

Reagent	Peak current, μA	Peak potential, V vs. SCE
5-Br-PADAP	2.0	-0.35
5-Br-PAPS	—	—
TAMSMB	—	—
5-Cl-PADAP	1.2	-0.34
PAN	1.2	-0.35
PAR	1.1	-0.35

Accumulation for 5 min at -0.20 V in $0.1M$ ammonia/ammonium nitrate buffer containing $1 \times 10^{-6}M$ reagent and $5 \times 10^{-7}M$ Cu(II).

stripping voltammetry signal would be obtained. 5-Br-PADAP was the best among the pyridylazo derivatives examined for the measurement of Cu(II).

With accumulation for 5 min at -0.2 V in the presence of $1 \times 10^{-6}M$ 5-Br-PADAP, followed by differential pulse voltammetry, the calibration curve was linear over the range 5×10^{-8} – $5 \times 10^{-7}M$ Cu(II), with a correlation coefficient of 0.998. The detection limit for copper, estimated as three times the standard deviation of the blank was $1 \times 10^{-8}M$ with an accumulation time of 5 min. The relative standard deviation for five determinations of $3 \times 10^{-7}M$ Cu(II) was 4.7%.

5-Br-PADAP forms complexes with many metal ions in solution, and these are potential interferents in the method. The influence of several metal ions was investigated by adding them to a solution containing $5 \times 10^{-7}M$ Cu(II) and $1 \times 10^{-6}M$ 5-Br-PADAP and applying the procedure. Ca(II) and Mg(II) at $5 \times 10^{-5}M$ did not interfere; these two ions form 5-Br-PADAP complexes with fairly low stability constants.¹⁸ Fe(III) interfered at concentrations higher than $5 \times 10^{-7}M$ and also interfered in the stripping voltammetry of copper. Bi(III), Ni(II), Pb(II) and Zn(II) at $5 \times 10^{-7}M$ concentration reduced the peak current for copper by about 50%. The stabilities of the 5-Br-PADAP complexes of these metal ions are about the same as or larger than that with copper,¹⁸ and the effect of these ions is due to the competitive consumption of the reagent. The addition of diammonium citrate as a masking agent suppressed the interference of Fe(III) to some extent.

REFERENCES

1. M. S. Shuman and G. P. Woodward, *Anal. Chem.*, 1976, **48**, 1979.
2. T. M. Florence and G. E. Batley, *J. Electroanal. Chem.*, 1977, **75**, 791.

3. J. Wang, *Stripping Analysis*, VCH, Deerfield Beach, 1985.
4. K. Isutsu, T. Nakamura, R. Takizawa and H. Hanawa, *Anal. Chim. Acta*, 1983, **149**, 147.
5. R. P. Baldwin, J. K. Christensen and L. Kryger, *Anal. Chem.*, 1986, **58**, 1790.
6. E. Desimoni, F. Palmisano and L. Sabbatini, *ibid.*, 1980, **52**, 1889.
7. S. Tanaka and H. Yoshida, *J. Electroanal. Chem.*, 1982, **137**, 261.
8. *Idem*, *Talanta*, 1988, **35**, 837.
9. R. Kalvoda, *J. Electroanal. Chem.*, 1984, **180**, 307.
10. N. K. Lam and M. Kopanica, *Anal. Chim. Acta*, 1984, **161**, 315.
11. H. Sawamoto, *J. Electroanal. Chem.*, 1983, **147**, 279.
12. V. Gemme-Colos and R. Neeb, *Z. Anal. Chem.*, 1987, **327**, 547.
13. N. K. Lam, R. Kalvoda and M. Kopanica, *Anal. Chim. Acta*, 1983, **154**, 79.
14. A. Bobrowski, *Talanta*, 1989, **36**, 1123.
15. Ch. Yarnitzky and R. Schreiber-Stanger, *J. Electroanal. Chem.*, 1986, **214**, 65.
16. J. Zhao and W. Jin, *ibid.*, 1989, **267**, 271.
17. *Idem*, *ibid.*, 1989, **256**, 181.
18. S. Shibata, in *Chelates in Analytical Chemistry*, H. A. Flaschka and A. J. Barnard (eds.), Vol. 4, Dekker, New York, 1972.

ADSORPTIVE STRIPPING VOLTAMMETRY DETERMINATION OF MOLYBDENUM(VI) IN WATER AND SOIL

ZAOFAN ZHAO, JIANHONG PEI, XIUJING ZHANG and XINGYAO ZHOU

Chemistry Department, Wuhan University, Wuhan, People's Republic of China

(Received 28 December 1989. Revised 10 March 1990. Accepted 27 March 1990)

Summary—A differential pulse stripping voltammetry method for the trace determination of molybdenum(VI) in water and soil has been developed. In 0.048M oxalic acid and $6 \times 10^{-5}M$ Toluidine Blue (pH 1.8) solution, Mo(V), the reduction product of Mo(VI) in the sample solution, can form a ternary complex, which can be concentrated by adsorption on a static mercury drop electrode at -0.1 V (*vs.* Ag/AgCl). The adsorbed complex gives a well-defined cathodic stripping current peak at -0.30 V, which can be used for determining Mo(VI) in the range 5×10^{-10} – $7 \times 10^{-9}M$, with a detection limit of $1 \times 10^{-10}M$ (4 min accumulation). The method is also selective. Most of the common ions do not interfere but Sn(IV) and large amounts of Cu^{2+} , Ag^+ and Au^{3+} affect the determination.

Special attention has been devoted to the complexes of Mo(VI) in aqueous solution because of their important role in enzymatic redox reactions. It has been shown that Mo(VI) can be reduced polarographically only at $pH < 6$.¹ Electroanalytical methods reported for the determination of Mo(VI) include differential pulse polarography^{2,3} and a voltammetric method based on the formation of mercury molybdate on a mercury electrode.⁴ The detection limits of these methods are about $10^{-7}M$. A polarographic method based on the catalytic reduction of Mo(VI) in the presence of nitrate or perchlorate^{5,6} has a detection limit of $10^{-8}M$ Mo(VI). The molybdenum(VI)–tartaric acid–chlorate and molybdenum(VI)–mandelic acid–chlorate systems^{7,8} are considered to give the most sensitive polarographic methods for Mo(VI). The detection limits are 5×10^{-9} and $1 \times 10^{-9}M$, respectively, but the polarographic waves are ill-defined and subject to many interferences.

Adsorptive stripping voltammetric methods have been developed for various metal ions^{9–11} and these have been reviewed by Wang.¹² Van den Berg¹³ and Fogg and Alonso¹⁴ have developed differential pulse adsorptive stripping voltammetry methods for determining trace Mo(VI), based on accumulation as its 8-hydroxyquinoline complex and 12-molybdophosphoric acid, respectively, at a hanging mercury drop electrode.

This work describes a sensitive and selective differential pulse adsorptive stripping voltam-

metry method for trace Mo(VI). In a weakly acidic oxalic acid–Toluidine Blue system, Mo(V), the reduction product of Mo(VI) in the sample solution, can form an adsorbable electroactive ternary complex. The preconcentration potential is -0.1 V and the cathodic stripping peak current is proportional to the concentration of Mo(VI) over the range 5×10^{-10} – $7 \times 10^{-9}M$ (4 min accumulation). The detection limit is $1 \times 10^{-10}M$. This method has been used to determine trace amounts of Mo(VI) in environmental water and soil samples.

EXPERIMENTAL

Reagents

Oxalic acid solution (0.4M), 0.001M Toluidine Blue and 0.0100M Mo(VI) standard stock solution were prepared. A working Mo(VI) solution was obtained by suitable dilution. All reagents were of analytical grade. Doubly distilled water was used throughout.

Apparatus

An EG&G Princeton Research Model 174A polarographic analyser with a Model 303 hanging mercury drop electrode (HMDE) was used. The three-electrode system included an Ag/AgCl reference electrode and a platinum counter-electrode. The mode used was differential pulse polarography. The pH measurements were made with a Chengdu Instrument Factory PXS-5 digital ion meter.

Procedure

Shake a 6.25-g sample of air-dried soil with 1M ammonium acetate (pH 7) for 15 hr, then filter. Evaporate the filtrate to dryness on a steam-bath. Add 5 ml of nitric acid (1 + 1) to the residue and evaporate to dryness; repeat this addition and evaporation and dissolve the residue in 10 ml of nitric acid (1 + 3). Transfer this solution into a 100-ml standard flask and dilute to volume with water. Water samples can be analysed without pre-treatment.

Transfer a known volume of sample solution into a 10-ml electrolytic cell containing 1.2 ml of 0.4M oxalic acid and 0.6 ml of 0.001M Toluindine Blue. Adjust the pH of the solution to about 1.8 with dilute sulphuric acid and dilute to 10 ml. Deaerate the solution by passage of pure nitrogen for about 10 min and set the potential of the HMDE to -0.1 V to start the preconcentration of Mo(VI) on the electrode. Perform the cathodic stripping in the differential pulse mode after the selected preconcentration time. Use a scan-rate of 5 mV/sec and a pulse amplitude of 50 mV. Measure the peak height at about -0.3 V (*vs.* Ag/AgCl). Repeat the procedure after a standard addition of 10^{-7} M Mo(VI).

RESULTS AND DISCUSSION

Differential pulse polarograms

The pulse polarograms of Mo(VI) in 0.048M oxalic acid/ 6×10^{-5} M Toluindine Blue (pH 1.8) are shown in Fig. 1. Two waves for the reduction of Mo(VI) appear, at -0.08 V (P_1) and -0.30 V (P_2). P_2 was chosen for determination

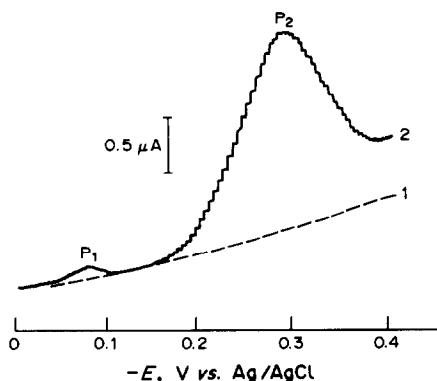


Fig. 1. The differential pulse polarograms: (1) 0.048M oxalic acid and 6×10^{-5} M Toluindine Blue, pH 1.8; (2) 0.048M oxalic acid, 6×10^{-5} M Toluindine Blue and 5×10^{-8} M Mo(VI), pH 1.8. Pulse amplitude: 50 mV, scan rate: 5 mV/sec, preconcentration time: 4 min.

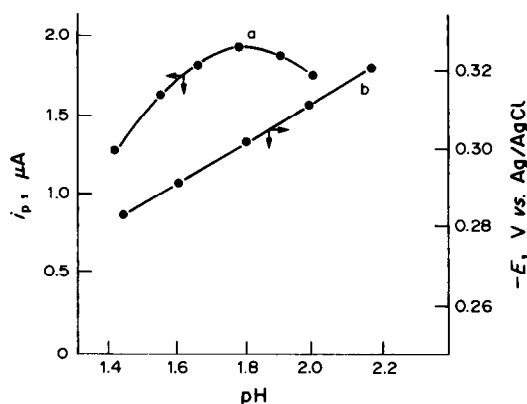


Fig. 2. The effect of pH: (a) on peak height; (b) on the peak potential. Mo(VI) 5×10^{-8} M. All conditions as for Fig. 1.

of Mo(VI) as it has a well-defined shape and greater sensitivity. Under these conditions, the first wave (P_1) corresponds to the one-electron reduction of Mo(VI) to Mo(V), and the second wave (P_2) is caused by the two-electron reduction of the adsorbed ternary complex of Mo(V) with oxalic acid and Toluindine Blue, at -0.30 V.^{15,16}

The effect of pH and concentration of oxalic acid and Toluindine Blue

Both the peak height and peak potential are pH-dependent, as shown in Fig. 2, which implies that hydrogen ions are involved in the electrode process. The optimal pH for the determination is 1.8 ± 0.2 .

Figure 3 shows the effect of the concentrations of Toluindine Blue and oxalic acid on the second wave. The optimal concentrations for determination are $6-8 \times 10^{-5}$ and 0.048M, respectively.

Effect of preconcentration time and potential

For 5×10^{-8} M Mo(VI), the peak height increases with preconcentration time up to 200 sec, and then a plateau is reached (Fig. 4), corresponding to complete coverage of the electrode surface by the adsorbed species.

Figure 5 shows that the best preconcentration potential is about -0.1 V, which is slightly negative relative to P_1 . This implies that the adsorbed species is a complex of Mo(V). The composition of the complex has been found to be Mo(V): $C_2O_4^{2-}$: Toluindine Blue = 1:2:2, by use of the Bent and French method.¹⁷

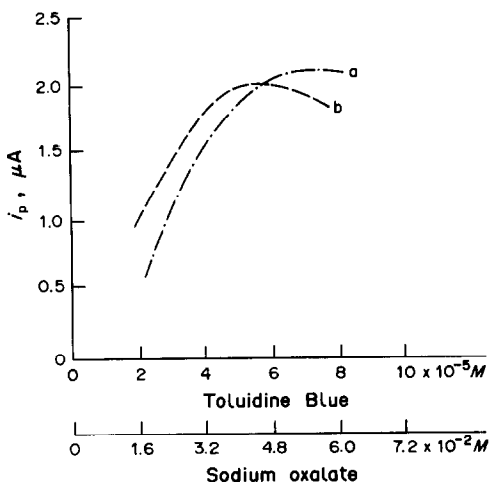


Fig. 3. Effect of concentration of various components on the peak height for $5 \times 10^{-8} M$ Mo(VI). (a) Toluidine Blue; (b) oxalic acid. Pulse amplitude: 50 mV; scan rate: 5 mV/sec, preconcentration potential: -0.1 V; preconcentration time: 4 min.

Effect of instrumental parameters

The peak current is almost unchanged with scan rates from 0.5 to 5 mV/sec so a scan rate of 5 mV/sec was chosen. The peak current increases with the pulse amplitude in the range 10–100 mV and the potential shifts to more positive values. The recommended pulse amplitude is 50 mV, which gives good sensitivity and peak shape.

Calibration graph and limit of detection

Under the optimal conditions described above, with preconcentration at -0.1 V for 4 min the peak height is directly proportional to the Mo(VI) concentration over the range 5×10^{-10} – $7 \times 10^{-9} M$. The calibration plot starts to deviate from linearity when the Mo(VI)

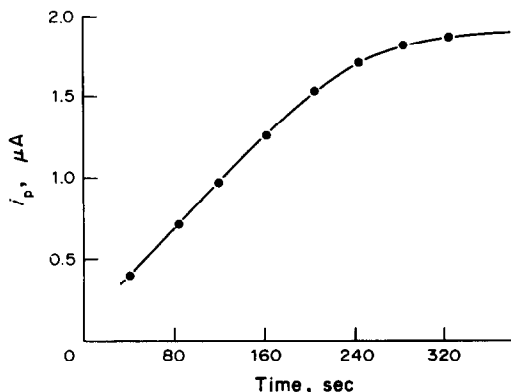


Fig. 4. The relationship between adsorption time and peak height. All conditions as for Fig. 3 except preconcentration time.

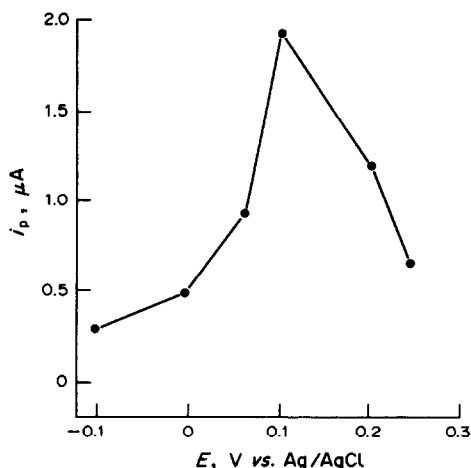


Fig. 5. The relationship between adsorption potential and peak height. All conditions as for Fig. 3 except adsorption potential.

concentration increases further and a plateau is finally reached above $5 \times 10^{-8} M$ Mo(VI). The relative standard deviation for $5 \times 10^{-9} M$ Mo(VI) was 1.3% (7 degrees of freedom). The detection limit calculated as the concentration corresponding to three times the standard deviation of the blank signal was found to be $1 \times 10^{-10} M$.

Interferences

The tolerance for various foreign ions was studied for determination of $1 \times 10^{-8} M$ Mo(VI). It was found that 500-fold molar ratio of Al^{3+} , Mg^{2+} , Zn^{2+} , Fe^{3+} and Mn^{2+} , 100-fold ratio of Pb^{2+} , Ta(V), W(V), Bi^{3+} , Fe^{2+} and Co^{2+} , and 50-fold ratio of Cu^{2+} , Ag^+ and Au^{3+} (to Mo) could be tolerated. Sn(IV) interfered by increasing the peak current.

Surfactants, such as Triton X-100 (0.1 mg/l.), tetramethylammonium bromide ($10^{-5} M$) and sodium dodecylsulphonate ($10^{-5} M$), can lower the peak current significantly.

Determination of trace Mo(VI) in soil and water samples

Table 1 shows the results for determination of Mo(VI) in some soil and water samples; they agree well with the reference values.

Table 1. Determination of Mo(VI) in soil and water

	Soil, $\mu g/g$		Water, ng/ml			
	1	2	1	2	3	4
Found*	1.92	2.60	14.4	7.66	5.07	9.07
Reference value†	1.89	2.52	14.2	7.32	5.02	9.01

*Mean of three determinations.

†Measured by the method of Violanda and Cooke.¹⁸

REFERENCES

1. R. Holtje and R. Geyer, *Z. Anorg. Allgem. Chem.*, 1941, **246**, 258.
2. T. E. Edmonds, *Commun. Soil Sci. Plant Anal.*, 1982, **13**, 1.
3. P. Lanza, D. Ferri and P. L. Buldini, *Analyst*, 1980, **105**, 379.
4. F. Vydra, K. Štulík and E. Juláková, *Electrochemical Stripping Analysis*. p. 252. Horwood, Chichester, 1976.
5. G. D. Christian, J. L. Vandenbalck and G. L. Patriarcho, *Anal. Chim. Acta*, 1979, **108**, 149.
6. T. E. Edmonds, *ibid.*, 1980, **116**, 323.
7. S. Kao and N. Li, *Beijing Daxue Xuebao*, 1963, **4**, 407.
8. C. Dunn, N. Wang and C. Chen, *Fudan Daxue Xuebao*, 1966, **11**, 197.
9. C. M. G. van den Berg and Z. Q. Huang, *J. Electroanal. Chem.*, 1984, **177**, 269.
10. G. Weber, *Z. Anal. Chem.*, 1985, **321**, 217.
11. J. Wang, M. S. Lin and V. Villa, *Analyst*, 1987, **112**, 1303.
12. J. Wang, *Am. Lab.*, 1985, **17**, No. 5, 41.
13. C. M. G. van den Berg, *Anal. Chem.*, 1985, **57**, 1532.
14. A. G. Fogg and R. M. Alonso, *Analyst*, 1988, **113**, 361.
15. Z. Zhao, J. Pei, X. Zhang and X. Zhou, unpublished work.
16. I. M. Kolthoff and I. Hodara, *J. Electroanal. Chem.*, 1963, **5**, 2.
17. H. E. Bent and C. L. French, *J. Am. Chem. Soc.*, 1941, **53**, 568.
18. A. T. Violanda and W. D. Cooke, *Anal. Chem.*, 1964, **36**, 2287.

LIQUID-LIQUID EXTRACTION OF PALLADIUM AND GOLD BY THE SULPHIDE PODAND 1,12-DI-2-THIENYL-2,5,8,11-TETRATHIADODECANE

ELWIRA LACHOWICZ and MALGORZATA CZAPIUK

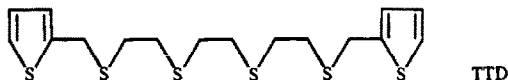
Department of Analytical Chemistry, Warsaw University of Technology, PL-00-664 Warsaw, Poland

(Received 3 March 1989. Revised 21 April 1990. Accepted 3 May 1990)

Summary—The extraction properties of the sulphide podand 1,12-di-2-thienyl-2,5,8,11-tetrathiadodecane (TTD), an open-chain neutral polythioether with six sulphur donor atoms in 1,2-dichloroethane, chloroform and MIBK for Pd and Au in hydrochloric, nitric and perchloric acid media have been examined. The kinetic aspects of the extraction of palladium(II) from hydrochloric acid by TTD and dioctyl sulphide (DOS) were compared. The rate of Pd extraction with TTD is considerably higher than that with DOS, especially with chloroform. Combined use of a reducing agent and TTD enhances the extraction of gold(III) into 1,2-dichloroethane.

Multidentate linear ligands, so-called podands according to the Weber and Vögtle classification,¹ belong together with crown ethers and cryptands to a class of ligands forming host-guest complexes. Podands (being open-chain analogues of cyclic ligands) have the ability to form a spherical wrapping around a metal ion, forming a pseudocavity¹ similar to that possessed by the cyclic compounds. They are much easier to synthesize than the cyclic ligands.

Multi-sulphur podands have an affinity for metal ions classified as "soft" by Pearson.² In a previous work³ the synthesis of a new neutral podand possessing six sulphur donor atoms, 1,12-di-2-thienyl-2,5,8,11-tetrathiadodecane



(TTD) was described, together with its properties for extraction of metal ions. As TTD extracts silver ions highly selectively,³ it has been applied⁴ for the extraction and AAS determination of silver in copper ores and tailings.

The extraction of palladium(II) and gold(III) with various thioethers possessing one or two sulphur atoms has been extensively investigated.⁵⁻⁸ Some thioethers have been utilized commercially for separation of Pd(II),^{9,10} but the slow rate of extraction from hydrochloric acid medium poses a serious problem.^{8,10} The number of publications devoted to extraction of palladium(II) with all-sulphur crown compounds is small. The cyclic thioether 1,4,8,11-

tetrathiacyclotetradecane has been examined as an extraction reagent for, among other metal species, palladium,¹¹⁻¹⁴ and the extraction behaviour of cyclic and acyclic tetrathioethers towards Pd has recently been compared.¹³

The reaction of gold(III) with sulphur-containing reagents often leads to its reduction to gold(I) by the ligand, prior to its complexation. Rhodanine¹⁵ and Michler's thioetone,¹⁶ for instance, simultaneously serve as ligands and reducing agents. Gold has been extracted in Au(III) form by a thioether, but on prolonged contact of the phases (5-20 hr), reduction to Au(I) occurred, resulting in an increased extraction yield.¹⁷ Also, in the combined use of dihexal sulphide and triphenyl phosphite (TPPT)¹⁸ TPPT was said to serve primarily to reduce gold(III) to gold(I).

The aim of the present study was to examine the extraction of palladium and gold with the sulphide podand TTD from various aqueous media. Emphasis was placed on the rate of Pd(II) extraction from hydrochloric acid and on the influence of the preliminary reduction of Au(III) to Au(I) on the gold distribution.

EXPERIMENTAL

Reagents

1,12-Di-2-thienyl-2,5,8,11-tetrathiadodecane (TTD) was synthesized as described previously,³ and used as solutions in 1,2-dichloroethane, chloroform or 4-methylpentanone (MIBK). A

stock 1 mg/ml solution of palladium was prepared by dissolving 0.4165 g of palladium(II) chloride in 5 ml of concentrated hydrochloric acid and diluting to volume with water in a 250-ml standard flask. A stock 1 mg/ml solution of gold was prepared by dissolving 0.2500 g of gold in 8 ml of *aqua regia*, evaporating the solution, taking up the residue with concentrated hydrochloric acid and evaporating the solution almost to dryness (this step being repeated). The final residue was dissolved in 25 ml of 1M hydrochloric acid and diluted to volume with water in a 250-ml volumetric flask. Sodium perchlorate was recrystallized twice from distilled water. Buffer solutions (pH 3–5) were made with 1M acetic acid and 1M sodium acetate. Dioctyl sulphide (DOS, Fluka) solutions in 1,2-dichloroethane or chloroform were prepared.

Other reagents were of analytical purity.

Apparatus

A Pye-Unicam SP90A Series 2 atomic-absorption spectrometer was used for the determination of palladium (at 244.8 nm) and gold (at 242.8 nm) in aqueous (or MIBK) solutions.

Procedure

An aqueous solution containing palladium(II) (5 or 10 $\mu\text{g/ml}$) or gold(III) (10 $\mu\text{g/ml}$) and any other reagents required was prepared. A 10-ml portion of this solution was shaken with 10 ml of TTD solution in 1,2-dichloroethane, chloroform or MIBK, for a given time and then allowed to stand for 15 min. After separation, the aqueous and organic phases were analysed for palladium by atomic-absorption spectrometry.

RESULTS AND DISCUSSION

Extraction of palladium from hydrochloric acid

Because of the inertness of palladium(II) chloride complexes in exchange reactions^{9,18} and the search for ligands having an acceptably high rate of extraction of Pd from hydrochloric acid,⁸ the rate of extraction of Pd with TTD was examined and compared with that obtained with a simple organic sulphide.

As shown by Fig. 1 (curves 1–3) the rate of extraction of Pd with TTD from 1M hydrochloric acid (in which the palladium will be mainly present as PdCl_4^{2-} , which is more inert than PdCl_3^-) is fast and depends to some degree

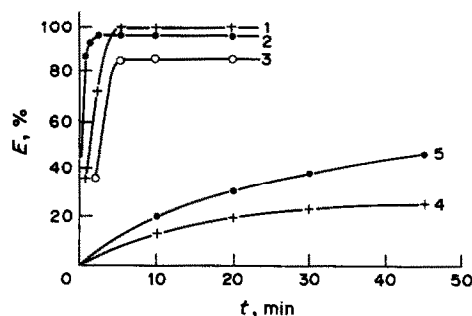


Fig. 1. Rate of extraction of Pd ($9.4 \times 10^{-5}M$) from 1M hydrochloric acid: 1, $1 \times 10^{-3}M$ TTD in 1,2-dichloroethane; 2, $1 \times 10^{-3}M$ TTD in chloroform; 3, $1 \times 10^{-3}M$ TTD in MIBK; 4, $1 \times 10^{-2}M$ DOS in 1,2-dichloroethane; 5, $1 \times 10^{-2}M$ DOS in chloroform.

on the solvent used. Equilibrium is reached most quickly (in 2 min) with a chloroform solution of TTD, but the efficiency of extraction is highest (98%) when 1,2-dichloroethane is used.

The degree of extraction of palladium(II) with $1 \times 10^{-3}M$ TTD in 1,2-dichloroethane or chloroform is independent of the hydrochloric acid concentration in the range 0.1–4M. The shaking time necessary for extraction of Pd from 4M hydrochloric acid is not greater than that needed with 1M hydrochloric acid.

Dioctyl sulphide (DOS) was used as a model simple thioether. It has been utilized on the commercial scale as a selective extractant for Pd.⁹ There are some data on extraction of Pd with DOS and other thioethers possessing one or two sulphur atoms, especially for hydrochloric acid medium. The distribution coefficient (D) is *ca.* 100 for Pd extraction from 1M hydrochloric acid by 0.5M DOS in benzene.²⁰ The value of D increases with decreasing chain length of the organic sulphide.²⁰ In a comparison of dialkyl sulphides²¹ with 1,2-bis(alkylthio)ethanes²² (both 0.1M, in toluene), the extraction of palladium is lower in the case of 1,2-bis(alkylthio)ethanes when the alkyl group has 2 or 4 carbon atoms, but the D value is ten times higher²³ for 1,2-bis(heptylthio)ethane ($D = 2.7 \times 10^4$) than that for diheptylsulphide (both 0.4M, in 1,2-dichloroethane). Increasing the chloride concentration has been reported to affect the rate of equilibration of Pd with 1,2-bis(heptylthio)ethane,²⁴ but detailed kinetic data were not given. The equilibria and kinetics of extraction of Pd by 1,2-bis(*tert*-hexylthio)ethane⁸ and dihexylsulphide²⁵ in toluene have been investigated, and kinetic problems were stressed.

Because of the number of donor sulphur atoms in TTD is greater than that in DOS, the DOS concentration used was made ten times that of the TTD solution examined. The rate of extraction of Pd from 1M hydrochloric acid with $1 \times 10^{-3}M$ TTD was significantly greater than that with $1 \times 10^{-2}M$ DOS (Fig. 1), especially with chloroform as solvent. The high rate of reaction of the typically inert palladium(II) chloride complexes with TTD is an advantage of this multi-sulphur ligand.

To determine the composition of the Pd(II)-TTD complex extracted into 1,2-dichloroethane, the dependence of the degree of extraction (E , %) on the molar concentration ratio of TTD in the organic phase $[TTD]_o$ to the initial concentration of palladium $[Pd]_{in}$ was examined (Fig. 2, curve 1). The fact that the concentration of Pd in the organic phase, $[Pd]_o$, can be greater than the initial TTD concentration, points to the formation of polynuclear complexes. Comparison of curve 1 in Fig. 2, for low TTD concentrations, with the theoretical lines for extraction of 1:1, 2:1 and 3:1 Pd:TTD complexes suggests that all three complexes may be extracted. A loading test in which $[Pd]_{in}$ was varied and $[TTD]_o$ kept constant) was performed for two TTD concentrations. The results show (Fig. 3) that increasing $[Pd]_{in}$ in the aqueous phase increases the Pd:TTD mole ratio in the organic phase up to *ca.* 3 (for $1 \times 10^{-4}M$ TTD). With $1 \times 10^{-3}M$ TTD a precipitate appears during the extraction when $[Pd]_{in}$ exceeds $3 \times 10^{-3}M$, so probably various polynuclear complexes are formed stepwise, depending on the excess of palladium, and their positive

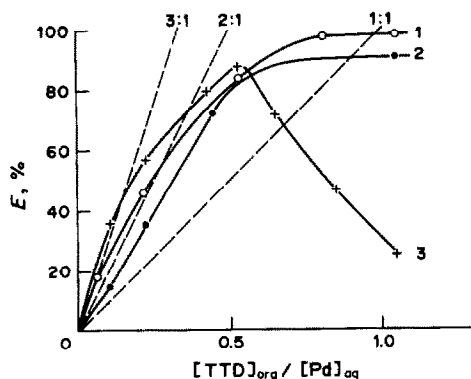


Fig. 2. Dependence of Pd extraction on the initial molar ratio of TTD in the organic phase to Pd in the aqueous phase: 1, 1M HCl, TTD in 1,2-dichloroethane, $9.4 \times 10^{-5}M$ Pd; 2, 1M HClO₄, TTD in MIBK, $4.7 \times 10^{-5}M$ Pd; 3, 1M HNO₃, TTD in MIBK, $4.7 \times 10^{-5}M$ Pd; dashed lines: typical plot for stable 1:1, 2:1 or 3:1 (Me:L) complexes.

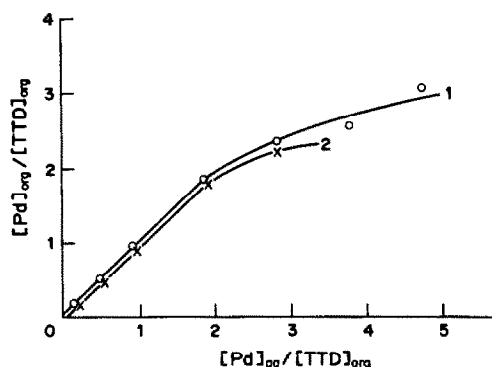


Fig. 3. Results of loading test for Pd: 1, $1 \times 10^{-4}M$ TTD; 2, $1 \times 10^{-3}M$ TTD; solvent 1,2-dichloroethane.

charge is counterbalanced by chloride ions. In the case of silver, examined previously,³ a 1:1 complex (presumably of host-guest type) was formed, but for palladium the composition is far more complicated and a polymeric structure is probable.

Extraction of palladium from perchloric acid or buffered perchlorate medium

Extraction of palladium(II) from perchloric acid attains equilibrium relatively quickly. The shaking times necessary to reach equilibrium are shown in Table 1, along with the values of E , which are independent of perchloric acid concentration in the 0.01–1M range. Curve 2 in Fig. 2 indicates the formation of 2:1 and 1:1 palladium-TTD complexes during the extraction into MIBK.

Extraction from acetate buffer (pH 4.7) containing sodium perchlorate rapidly reaches equilibrium (in 5 min) and the dependence of E on the concentration of sodium perchlorate (Table 2) suggests that the complex extracted is an ion-pair with perchlorate as counter-ion.

Extraction of palladium from nitric acid

The effect of increasing TTD concentration on the extraction of palladium into MIBK from nitric acid is unexpected. The curve reaches a maximum when $[TTD]_o : [Pd]_{in}$ is *ca.* 1:2 for 1M nitric acid (curve 3 in Fig. 2) as well as for 0.25M nitric acid. The first part of the curve is similar to that for the extractions from hydrochloric or perchloric acid, but the decrease at $[TTD]_o > 2.5 \times 10^{-5}M$ is difficult to explain. A similar effect was also observed when chloroform, carbon tetrachloride or toluene were used as solvents (Table 1). In the earlier study³ of separation of silver from nitric acid with TTD

Table 1. Extraction of palladium(II) from perchloric or nitric acid by 2.5×10^{-5} – $1 \times 10^{-3} M$ TTD in various solvents, $C_{Pd} = 4.7 \times 10^{-5} M$

Aqueous phase	TTD in MIBK		TTD in 1,2-dichloroethane		TTD in chloroform	
	$1 \times 10^{-3} M$	$2.5 \times 10^{-5} M$	$1 \times 10^{-3} M$	$2.5 \times 10^{-5} M$	$1 \times 10^{-3} M$	$2.5 \times 10^{-5} M$
<i>E</i> , % 1M HClO ₄	95		99		95	
<i>t</i> , min	2		5		5	
<i>E</i> , % 1M HNO ₃	28	84	30		30	94
<i>t</i> , min	5		16*	96*		
			4†	94†		

t = time necessary to reach equilibrium.

*TTD in CCl₄.

†TTD in toluene.

in MIBK or 1,2-dichloroethane, such an effect did not occur.

The degree of extraction of palladium from nitric acid with TTD in MIBK is almost independent of nitric acid concentration in the range 0.25–3.5M, for both 1×10^{-3} and $2.5 \times 10^{-5} M$ TTD.

Extraction of gold with TTD in 1,2-dichloroethane

Extraction of gold ions with TTD was studied mainly in hydrochloric acid solutions. The influence of the presence of nitric acid was also tested. The degree of extraction of gold(III) from 0.001–1M hydrochloric acid with $1 \times 10^{-3} M$ TTD in 1,2-dichloroethane is constant and equal to 98%. Equilibrium is reached in 3 min. Increasing the concentration of nitric acid in the aqueous phase in the extraction

of gold from $1 \times 10^{-3} M$ hydrochloric acid decreases the value of *E* (Table 3).

Figure 4 shows that the extraction of gold from 0.5M hydrochloric acid is better than from solutions containing nitric acid (curves 1 and 2). Complete separation of gold from 0.5M hydrochloric acid is obtained with $2 \times 10^{-3} M$ TTD solution in 1,2-dichloroethane.

Effect of reduction of gold on its extraction with TTD from hydrochloric acid

Experimental conditions under which the extraction of gold(III) is low (*i.e.*, with a very low TTD concentration, $5 \times 10^{-5} M$) were chosen for examining the effect on *E* of reduction of the gold to gold(I). The influence of the reductant concentration, the distribution of gold between the liquid phases and the amount of metallic gold or insoluble gold(I) species eventually deposited on the funnel walls were all examined.

The reduction was done in two ways: (1) extraction for 3 min, followed by addition of reductant and extraction for 3 min, and

Table 2. The effect of concentration of sodium perchlorate on palladium extraction ($4.75 \times 10^{-5} M$ Pd, pH 4.7, $1 \times 10^{-3} M$ TTD in MIBK)

[NaClO ₄], M	<i>E</i> , %
0	10
5×10^{-5}	22
5×10^{-4}	56
1×10^{-3}	70
2×10^{-3}	82

Table 3. Extraction of gold ($2.0 \times 10^{-5} M$) from nitric acid ($10^{-3} M$ hydrochloric acid also present) by $1 \times 10^{-3} M$ TTD in 1,2-dichloroethane

[HNO ₃], M	<i>E</i> , %
0.04	93
0.1	93
0.5	90
1	85
2	78
3	72

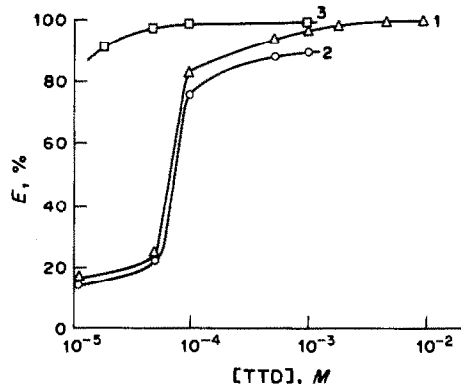


Fig. 4. Dependence of *E* for gold on TTD concentration for extraction from: 1, 0.5M HCl; 2, 1M HNO₃ + $10^{-3} M$ HCl; 3, 0.5M HCl + $2 \times 10^{-3} M$ hydrazine sulphate.

Table 4. Effect of reduction of gold(III) ($2 \times 10^{-3}M$) on its extraction with $5 \times 10^{-5}M$ TTD in 1,2-dichloroethane

Reducing agent and concentration	E, %
none	20
ascorbic acid	
$2.5 \times 10^{-2}M$	92.5
$\times 10^{-3}M$	92.5
hydrazine sulphate	
$2.5 \times 10^{-2}M$	95
$5 \times 10^{-3}M$	98
$2 \times 10^{-3}M$	98
$1 \times 10^{-3}M$	95

(2) addition of a reductant followed by extraction for 3 min. The results obtained by both procedures were consistent, as shown with hydrazine sulphate as model reductant. Procedure (1) was used in further experiments.

Ascorbic acid, hydrazine sulphate (Table 4) and hydroxylammonium chloride were used as reducing agents. The best results were obtained with hydrazine sulphate, as only about 2% of the gold was deposited on the funnel walls. With ascorbic acid about 9% of the gold was found on the funnel walls, and with hydroxylammonium chloride a precipitate was formed at the phase boundary.

The dependence of E on TTD concentration in the presence of hydrazine sulphate was then examined (Fig. 4, curve 3). The extraction in the presence of the reductant was more effective than without it, and almost complete at lower ligand concentrations. In the presence of $2 \times 10^{-3}M$ hydrazine sulphate 100% extraction of gold from $0.5M$ hydrochloric acid was achieved with $1 \times 10^{-3}M$ TTD in 1,2-dichloroethane, and no precipitate was formed on the walls.

Conclusions

Collecting a greater number of S donors in one sulphide podand molecule greatly accelerates the rate of extraction of palladium (introduced as the inert $PdCl_4^{2-}$ complex) in comparison with unidentate sulphides. Probably the fraction of molecular collisions possessing sufficient energy and proper geometry for successful reaction increases considerably.

The best extraction of palladium with $1 \times 10^{-3}M$ TTD was obtained from $0.1-4M$ hydrochloric acid or $0.01-1M$ perchloric acid, with chloroform or 1,2-dichloroethane as solvent, and of gold from $0.5M$ hydrochloric

acid plus $2 \times 10^{-3}M$ hydrazine sulphate, with 1,2-dichloroethane as solvent.

Acknowledgement—This work was supported by the research programme CPBP-01.17.

REFERENCES

1. E. Weber and F. Vögtle, In F. L. Bosche (ed.), *Host-Guest Complex Chemistry*, Vol. I, p. 1. Akademie-Verlag, Berlin, 1982.
2. R. G. Pearson, *J. Am. Chem. Soc.*, 1963, **85**, 3533.
3. E. Lachowicz, A. Krajewski and M. Goliński, *Anal. Chim. Acta*, 1986, **188**, 239.
4. E. Lachowicz, *Analyst*, 1987, **112**, 1623.
5. W. S. Chekushin and W. F. Borbat, *Extraction of Noble Metals with Sulphides and Sulphoxides* (in Russian), Nauka, Moscow, 1984.
6. W. G. Torgov, *Isotopenpraxis*, 1984, **20**, 352.
7. N. G. Vanifatova, I. V. Seryakova and Yu. A. Zolotov, *Extraction of Metals by Neutral Sulphur-containing Compounds* (in Russian), Nauka, Moscow, 1980.
8. T. Baba, M. Ohshima and K. Inoue, *Bull. Chem. Soc. Japan*, 1986, **59**, 1321.
9. J. M. Barnes and J. D. Edwards, *Chem. Ind. London*, 1982, 151.
10. R. I. Edwards, *Proc. Intern. Solvent Extraction Conference, 1977*, p. 24. Can. Inst. Min. Metall., Montreal, 1979.
11. K. Saito, Y. Masuda and E. Sekido, *Anal. Chim. Acta*, 1983, **151**, 447.
12. E. Sekido, K. Saito, Y. Naganuma and H. Kumazaki, *Anal. Sci.*, 1985, **1**, 363.
13. K. Chayama and E. Sekino, *ibid.*, 1987, **3**, 535.
14. M. Oue, K. Kimura and T. Shono, *Anal. Chim. Acta*, 1987, **194**, 293.
15. R. Borissova, *Talanta*, 1975, **22**, 797.
16. A. T. Pilipenko, O. P. Ryabushko and G. M. Matsibura, *Zh. Analit., Khim.*, 1979, **34**, 1088.
17. W. G. Torgov, T. M. Korda and I. G. Yudelevich, *ibid.*, 1978, **33**, 2341.
18. A. Ohki, M. Takagi and K. Ueno, *Anal. Chim. Acta*, 1984, **159**, 245.
19. I. V. Rund, *Inorg. Chem.*, 1974, **13**, 738.
20. V. G. Torgov, V. N. Andrievskii, E. N. Gil'bert, I. L. Kotlyarevskii, V. A. Mikhailov, A. V. Nikolaev, V. A. Pronin and D. D. Trotsenko, *Izv. Sibir. Otd. Akad. Nauk SSSR, Ser. Khim. Nauk*, 1969, No. 5, 148.
21. V. A. Pronin, M. V. Usol'tseva, Z. N. Shastina, B. A. Trofimov and E. P. Vyalykh, *Russ. J. Inorg. Chem.*, 1973, **18**, 1615.
22. V. A. Pronin, M. V. Usol'tseva, Z. N. Shastina, N. K. Gusarova, E. P. Vyalykh, S. V. Amosova and B. A. Trofimov, *ibid.*, 1973, **18**, 1016.
23. V. A. Pronin, M. V. Usol'tseva and S. M. Shostakhovskii, *Izv. Akad. Nauk SSSR, Ser. Khim.*, 1971, 2371.
24. A. V. Nikoleav, V. M. Shul'man, L. M. Gindin, S. V. Larionov, P. L. Artyukhin, L. Ya. Mironova, T. V. Zagorskaya, L. A. Tyuleneva, L. A. Il'ina, I. L. Kotlyarevskii, V. N. Andrievskii and E. A. Startseva, *Izv. Sib. Otd. Akad. Nauk SSSR, Ser. Khim. Nauk*, 1970, No. 4, 60.
25. Y. Baba, T. Eguchi and K. Inoue, *J. Chem. Eng. Japan*, 1986, **19**, 361.

EXTRACTION SPECTROPHOTOMETRIC METHOD FOR DETERMINATION OF ALUMINIUM IN SILICATES

N. L. BANERJEE and B. C. SINHA*

Central Glass and Ceramic Research Institute, Calcutta 700032, India

(Received 22 July 1987. Revised 9 February 1990. Accepted 29 March 1990)

Summary—A simple, rapid and sensitive method has been worked out for spectrophotometric determination of macro and micro amounts of alumina in ceramic raw materials and finished products, including glasses. The method is based on the extraction of aluminum oxinate into chloroform after masking of titanium with chromotropic acid and of iron with ascorbic acid and 1,10-phenanthroline or ferrocyanide at pH 5.2. The absorbance is measured at 385 nm. Interference by Cu, Zn, Cd, Ni and Co, when present, is overcome by stripping them as cyanide complexes by shaking the chloroform extract with potassium cyanide solution. Zr is masked with quinalizarin sulphonic acid and fluoride with BeSO_4 .

Aluminium is present in small amounts in many ceramic raw materials and finished products, and its content has an important effect on the physical and chemical properties of the products. Therefore, rapid and accurate determination of small amounts of aluminium is of importance for evaluation, characterization and quality-control of ceramic raw materials and products.

Spectrophotometric methods are generally used for accurate determination of small amounts of aluminium,¹⁻¹¹ especially those based on the yellow complex of aluminium with 8-hydroxyquinoline (oxine) in chloroform.¹²⁻¹⁵ Various elements can interfere, and of these iron and titanium are invariably present in ceramic raw materials and products. The interference of iron has been prevented by reducing the iron to the bivalent state, and complexing it with 1,10-phenanthroline,⁶ ferrocyanide,¹⁴ bipyridyl¹⁵ or potassium ferricyanide and thioglycolic acid.¹² The attempts made to mask titanium, however, have not been satisfactory so far. Riley¹⁵ therefore preferred to make an empirical correction for the interference of titanium by adding titanium (equivalent to 1% of TiO_2 in the sample) to the standard solutions of aluminium used for constructing the calibration graph. Later, Riley and Williams¹⁶ recommended prior extraction of Ti at pH 4 and of Cu, Co and Zr at pH 10, as their 8-hydroxyquinoline com-

plexes, into chloroform. Both methods are widely quoted in monographs.¹⁷⁻¹⁹ However, Dagnall *et al.*²⁰ obtained low results for aluminium owing to its partial extraction along with titanium as the 8-hydroxyquinoline complexes into chloroform. Further, the methods do not take care of the interference due to Zn and Cd, which are often present in certain glasses and special ceramics. The present communication describes a simple, rapid and sensitive method for determination of micro amounts of aluminium in ceramic raw materials and finished products, including glasses. The method is based on the extraction of aluminium oxinate into chloroform after masking of titanium with chromotropic acid, and of other interfering cations, including Fe, Cu, Zn, Cd, Co, *etc.*

EXPERIMENTAL

Apparatus

A Spectromom model 360 spectrophotometer and a Elico model BI-10 pH-meter were used.

Reagents

Standard aluminium solution, 100 $\mu\text{g}/\text{ml}$. Dissolve 0.1000 gm of Al wire (99.9% purity) in 50 ml of hydrochloric acid (1 + 1) by heating, with a small drop of mercury as catalyst. Decant the solution to remove the mercury, wash the drop of mercury with water by decantation, and dilute the solution and washings to the mark in a 1-litre standard flask. Dilute this solution tenfold to obtain a 10 $\mu\text{g}/\text{ml}$ working solution.

*Present address: 284A, Jodhpur Park, Calcutta 700068, India.

Ascorbic acid solution. A freshly prepared 3% aqueous solution should be used.

Methyl Orange indicator. Dissolve 0.5 g of the sodium salt in 1 litre of water containing 15 ml of 0.1M hydrochloric acid and filter if necessary.

1,10-Phenanthroline monohydrate solution. Dissolve 0.5 g of reagent in 100 ml of water.

Chromotropic acid solution. Dissolve 0.5 g of chromotropic acid in 100 ml of 0.15M sulphuric acid and store in a dark coloured bottle. Use the solution within a week.

8-Hydroxyquinoline solution. Dissolve 2 g of the reagent in 100 ml of 2M acetic acid, add ammonia solution dropwise until a turbidity appears, clarify the solution by addition of a few drops of acetic acid, and keep the solution in an amber bottle.

Ammoniacal potassium cyanide solution. Dissolve 15 g of potassium cyanide in 400 ml of a solution containing 30 g of ammonium chloride and 250 ml of concentrated ammonia solution, and dilute to 500 ml.

Procedures

Preparation of sample solution. Take 0.10–0.50 g of ground and dried ($105 \pm 5^\circ$) sample (containing 0.5–5 mg of Al) in a clean platinum basin and moisten it with a few drops of water. Add 1 ml of concentrated perchloric acid and 15 ml of concentrated hydrofluoric acid and heat on a hot-plate until copious fumes of perchloric acid are evolved. Cool, add 10 ml of concentrated hydrofluoric acid and heat until fumes of perchloric acid appear.* Add 2 ml of concentrated hydrochloric acid and a few ml of water and digest for 10 min on the hot-plate. Cool, transfer the solution quantitatively into a standard flask (100 or 250 ml) and dilute to volume.

Extraction and measurement. Take an aliquot containing up to 0.04 mg of aluminium, in a 100-ml beaker. Add 10 ml of ascorbic acid solution and a drop of Methyl Orange indicator and dilute to 35–40 ml. Add ammonia solution (1 + 4) dropwise until the colour changes to yellow and then a drop of hydrochloric acid (1 + 1). For every 100 μ g of titanium add 2 ml of chromotropic acid solution, and for each

200 μ g of iron 2 ml of 1,10-phenanthroline solution, and then 2.5 ml of the 8-hydroxyquinoline solution, with constant shaking, allowing about 5 min after each addition for the reactions to become complete. Adjust the pH to 5.2 (measured by pH-meter) with dilute hydrochloric acid or ammonia solution. Transfer the solution quantitatively into a 125-ml conical separating funnel marked at 70 ml, dilute to the mark and add 10 ml of chloroform from a pipette. Shake the mixture for about 2 min, and allow the layers to separate. Collect the chloroform layer. If the test solution contains Zn, Cd, Cu, Ni and/or Co, shake the chloroform extract with 50 ml of the ammoniacal potassium cyanide solution in another separating funnel, for 2–3 min, and allow to settle. Transfer some of the chloroform layer into a 1-cm cuvette and measure the absorbance at 385 nm. Prepare a calibration graph covering the range up to 40 μ g of aluminium with standards extracted as just described. Correct all absorbances for a reagent blank treated in the same way.

RESULTS AND DISCUSSION

Preliminary studies confirmed that aluminium can be quantitatively extracted as the oxinate into chloroform from solutions at pH 4.5 and above, as reported by others.²¹ The absorbance is a linear function of aluminium concentration up to 4 μ g/ml in the chloroform layer. Provided the procedure is followed exactly for all samples, standards and the blank, there is no need to separate the chloroform layer quantitatively and dilute it to a fixed volume. We have found that the separation of up to 0.04 mg of aluminium as the oxinate is quantitative in a single extraction with 10 ml of chloroform.

Interferences

During the preliminary study, attempts to separate titanium as its hydroxyquinoline complex by extraction with chloroform at pH 4 yielded low results for aluminium, owing to its partial extraction along with the titanium complex, as reported by Dagnall *et al.*²⁰ Ti, Zr, Fe *etc.* can be extracted as their cupferronates into chloroform²² or *o*-dichlorobenzene²³ from 1M hydrochloric acid. There is no loss of aluminium when *o*-dichlorobenzene is used as the solvent, provided there is an excess of only 2–3 mg of cupferron,²⁴ in agreement with the observations

*Do not heat completely to dryness. If decomposition still seems incomplete, collect and ignite the residue and fuse it with 1 g of sodium carbonate. Dissolve the cooled melt in hydrochloric acid and add the solution to the main solution.

Table 1. Determination of aluminium in solutions containing various amounts of titanium, after masking with chromotropic acid or hydrogen peroxide

Al taken, μg	Ti, μg	Al found, μg	
		Ti masked with 10 mg of chromotropic acid	Ti masked with 10 ml of 3% H_2O_2
10	Nil	10.0	9.9
10	25	10.0	12.6
10	100	10.1	15.8
20	100	19.6	26.5
30	100	29.3	35.5
40	Nil	39.8	—
40	50	40.0	—
40	100	40.7	—
40	150	43.8	—
40	150	40.3*	—

*Masked with 20 mg of chromotropic acid.

of Miller and Chalmers,²³ but an approximate knowledge of the total amounts of Ti, Fe, Zr, V, etc. is then essential for accurate determination of aluminium. Another drawback in use of cupferron is its poor keeping quality, especially in hot climates, as its decomposition gives a

Table 2. Determination of Al in presence of Zn, Cd, Ni, Co and Cu with 4 ml of 8-hydroxyquinoline

Concentration taken, $\mu\text{g/ml}$						
Al	Zn	Cd	Ni	Co	Cu	Absorbance
2	Nil	Nil	Nil	Nil	Nil	0.43
2	5	5	5	Nil	Nil	0.43
2	5	5	5	5	5	0.44
4	10	10	10	10	10	0.82
2	40	20	10	10	30	0.43
4	40	20	10	10	30	0.81

coloured product which is not completely extracted with chloroform or *o*-dichlorobenzene but partially accompanies aluminium oxinate in its subsequent extraction, causing a positive error.

Attempts to mask completely the interfering effect of Ti with common agents such as hydrogen peroxide and tartaric acid²⁴ have not been successful. The results for aluminium are higher in both cases (Table 1) indicating unsatisfactory masking of Ti. We have found that chromotropic acid, which forms a yellow 1:3 Ti-chromotropic acid complex at pH above 5, can

Table 3. Determination of Al_2O_3 in silicates and carbonates

Sample	Al_2O_3 found, %	Mean, %	Certified value, %	Remarks
Optical glass (EDF 653/335)	0.11	0.11	0.15	—
	0.11			
	0.12			
Optical glass (BSC 510/644)	0.66	0.64	0.75	—
	0.65			
	0.62			
Quartz	0.13	0.14	0.12	—
	0.14			
	0.14			
Silica sand	0.25	0.27	0.25	—
	0.27			
	0.25			
Limestone	0.43	0.41	0.39	—
	0.40			
	0.41			
Magnesite	0.14	0.15	0.20	—
	0.15			
	0.15			
Opal glass (NBS 128)	1.75	1.75	1.89	—
	1.69			
	1.81			
Silica brick (NBS 102)	1.87	1.85	1.96	—
	1.75			
	1.93			
Glass frit	1.78	1.73	1.80	ZnO 0.24%, CdO 0.75%, NiO 0.42%, TiO_2 0.16%
	1.72			
	1.70			
Enamel cover coat	3.85	3.77	3.90	ZnO 0.7%, CdO 0.5%, CoO 0.4%
	3.80			
	3.65			

quantitatively mask titanium and the complex is not extracted into chloroform. Two ml of 0.5% chromotropic acid solution can mask up to 100 μg of Ti (Table 1).

Up to 200 μg of iron can conveniently be masked with ascorbic acid and 1,10-phenanthroline. Fluoride forms a strong complex with aluminium and must be removed during decomposition of the sample, by repeated fuming with perchloric or sulphuric acid. Small amounts of fluoride can be masked by the addition of beryllium.²¹

Small amounts of zirconium can be masked with quinalizarin sulphonic acid,¹⁶ but for larger amounts prior separation as $\text{ZrO}(\text{HPO}_4)$ is recommended.²⁵

The interferences of Zn, Cu, Cd, Ni and Co can be successfully eliminated by shaking the chloroform extract of Al-oxinate with ammoniacal potassium cyanide solution,¹⁴ to form cyanide complexes which pass into aqueous phase (Table 2).

The method has been successfully used for determination of alumina in silicate and ceramic raw materials and products, including two standard (NBS) samples. The results (Table 3) compare favourably with the certified or standard values, indicating the accuracy of the method.

Acknowledgement—The authors are thankful to Dr S. Kumar, Director of the Institute, for giving permission to publish the paper.

REFERENCES

- Z. Marczenko, *Separation and Spectrophotometric Determination of Elements*, Horwood, Chichester, 1986.
- E. B. Sandell, *Colorimetric Determination of Traces of Metals*, 3rd Ed., Wiley, New York, 1959.
- A. D. Wilson and G. A. Sergeant, *Analyst*, 1963, **88**, 109.
- F. Alten, H. Weiland and H. Loofman, *Z. Angew. Chem.*, 1933, **46**, 668.
- M. Teitelbaum, *Z. Anal. Chem.*, 1930, **82**, 366.
- E. M. Donaldson, *Talanta*, 1971, **18**, 905.
- A. A. Nemodruk, N. G. Arevedze and G. D. Supatashvili, *Zh. Analit. Khim.*, 1980, **35**, 1511.
- A. Narayanan and D. A. Pantony, *Analyst*, 1981, **106**, 1137, 1145.
- Y-Q. Zhu, L. Zhang and J.-Y. Li, *Talanta*, 1981, **30**, 291.
- A. C. Edwards and M. S. Cresser, *ibid.*, 1983, **30**, 702.
- F. Salinas, A. Muñoz de la Peña and J. A. Murillo, *Analyst*, 1984, **109**, 1135.
- T. Moeller, *Ind. Eng. Chem., Anal. Ed.*, 1943, **15**, 346.
- L. Shapiro and W. W. Brannock, *U.S. Geol. Surv. Bull.*, 1962, 1144A.
- C. H. R. Gentry and L. G. Sherrington, *Analyst*, 1946, **71**, 432.
- J. P. Riley, *Anal. Chim. Acta*, 1958, **19**, 413.
- J. P. Riley and H. P. Williams, *Mikrochim. Acta*, 1959, 804.
- P. G. Jeffery, *Chemical Methods of Rock Analysis*, 1st Ed., Pergamon Press, Oxford, 1970.
- J. A. Maxwell, *Rock and Mineral Analysis*, Interscience, New York, 1968.
- P. G. Jeffery and D. Hutchison, *Chemical Methods of Rock Analysis*, 3rd Ed., Pergamon Press, Oxford, 1981.
- R. M. Dagnall, T. S. West and P. Young, *Analyst*, 1965, **90**, 13.
- T. Kambara and H. Hashitani, *Anal. Chem.*, 1959 **31**, 567.
- J. A. Corbett, *Analyst*, 1953, **78**, 20.
- C. C. Miller and R. A. Chalmers, *ibid.*, 1953, **78**, 686.
- S. Dasgupta, B. C. Sinha and W. S. Rawat, *ibid.*, 1984, **109**, 39.
- B. C. Sinha, S. Dasgupta and S. Kumar, *ibid.*, 1968, **93**, 409.

DETERMINATION OF LEAD BY SELECTIVE CHELATOMETRIC TITRATION WITH HEDTA AFTER SEPARATION AS ITS SULPHATE BY AN IMPROVED METHOD OF PRECIPITATION

ZHOU NAN*

Shanghai Research Institute of Materials, Ministry of Machine-building and Electronics Industries,
Shanghai, People's Republic of China

XU-ZHANG YAO, YUAN-XIANG GU and REN-QING YU

The Third Factory of Shanghai Reagent Chemicals, Shanghai, People's Republic of China

(Received 29 December 1989. Revised 15 March 1990. Accepted 12 April 1990)

Summary—A selective titrimetric determination of Pb after separation by a modified method of precipitation as its sulphate is proposed. Pb(II), present as the perchlorate, is precipitated by gentle boiling in 3.6M H₂SO₄ presaturated with PbSO₄ and free from any extraneous anions. The customary time-consuming evaporation to fumes of sulphuric acid is dispensed with. The precipitate is collected, and dissolved in excess of HEDTA, the surplus of which is back-titrated with Zn(II) at pH 5.0–5.5. Use of Catechol Violet and Xylenol Orange as a mixed indicator gives a sharper end-point. The standard deviation of the proposed method for 60 mg of lead is 0.35 mg. The method has been successfully used to determine Pb in non-ferrous alloys.

Lead is a major component of many important alloys. For its determination in macro amounts, chelatometric titration is doubtless the best choice, but is almost completely non-selective,¹ so a preliminary separation is generally needed. For this purpose, the classical precipitation of lead sulphate is used, but has several drawbacks. It is time-consuming, requiring evaporation to strong fumes of sulphuric acid, and the precipitate must be left standing for a long time or even overnight.² During the evaporation, spattering may occur, especially in the presence of salts in large amounts. After the fuming, the sulphates of certain concomitant cations, e.g., Al(III), Cr(III), Fe(III) and Ni(II), are rendered insoluble and difficult to redissolve. Therefore this separation was discontinued as a standard method³ by ASTM and replaced by dithiocarbamate extraction⁴ into chloroform from an alkaline tartrate-cyanide solution. In the latter method, however, there is the hazard of use of sodium cyanide, and Bi(III), Tl(III) and In(III) interfere.⁵

In this paper a rapid and selective method for the determination of Pb is proposed, based on an improved method of precipitation of

lead sulphate, and a chelatometric finish with HEDTA (*N*-hydroxyethylethylenediamine-*N,N',N'*-triacetic acid), as titrant.

EXPERIMENTAL

Reagents

Analytical-reagent grade chemicals were used unless otherwise specified.

Precipitating solution. To 1000 ml of sulphuric acid (1 + 4) add 0.5 g of lead(II) oxide and boil gently for *ca.* 5 min. Cool to room temperature and let stand for at least 1 hr. Just before use, filter an appropriate amount of the solution through a dry filter paper of fine texture in a dry funnel.

Catechol Violet solution, 0.1% in 50% ethanol. The reagent used should be free from all chromogenic impurities, as tested by TLC.

Xylenol Orange solution, 0.1% in 50% ethanol. The reagent used should be free from all chromogenic impurities, as tested by TLC.

Zn standard solution, 0.02M. Prepare as described earlier.⁶

HEDTA standard solution. Prepared, and standardized with the Zn standard solution, as previously reported.⁶

Saturated sodium bicarbonate solution.

Hexamine solution, 30%. Freshly prepared.

*Author for correspondence. Present address: 99 Handan Road, 200433, Shanghai, People's Republic of China.

Hydrochloric acid (1 + 3).
 Concentrated ammonia solution.
 Concentrated perchloric acid.

General procedure

Take an appropriate amount of the sample, containing 60–150 mg of Pb, weighed to the nearest 0.1 mg, and transfer it to a 250-ml beaker. Add 5–10 ml of concentrated hydrochloric acid and a few drops of concentrated nitric acid. Warm till dissolution is complete. Add 5 ml of perchloric acid and evaporate to *ca.* 2–3 ml. Cool to room temperature. Quantitatively transfer the solution dropwise to a 600-ml beaker containing 70 ml of precipitating solution, rinsing the original beaker thoroughly with precipitating solution from a wash bottle. Dilute to 90 ml with precipitating solution. Boil gently for 2–3 min, cool to room temperature, and filter with a dry filter paper of fine texture in a dry funnel. Wash the filter paper and beaker 3–5 times with precipitating solution from a wash bottle. As soon as the washings have drained completely, spread the filter paper smoothly on the inner wall of the original 600-ml beaker (Note 1).

Add 45 ml (accurately measured) of HEDTA solution (Note 2), then sodium bicarbonate solution dropwise till effervescence ceases, and finally hexamine solution to bring the pH to 5.0–5.5. Boil gently, while tilting the beaker to ensure the precipitate dissolves completely. Cool, add one drop each of the Catechol Violet and Xylenol Orange indicator solutions, and back-titrate with standard Zn solution to the colour change from yellow to violet. Calculate the lead content from $Pb\% = 414.4(V_1f - V_2)/G$ where G is the sample weight (mg) taken, V_1 and V_2 are the volumes of HEDTA and Zn solutions used (ml), and $f = A/B$, (A ml of Zn solution being required for complete reaction with B ml of HEDTA).

Note 1. For samples containing Bi, spread the paper and wash it with 10–15 ml of lukewarm water to dissolve out any co-precipitated Bi(III). Cool to room temperature and adjust the pH carefully to 1.5–2.0 with sodium bicarbonate solution. Add one drop of Catechol Violet solution. A yellow colour indicates the absence of Bi(III). If the solution turns blue, titrate it with HEDTA solution to the colour change through red to yellow. Then add 45 ml of HEDTA solution and continue the titration as described in the general procedure.

Note 2. For samples containing Ba, Sr or Ca, treat the lead sulphate precipitate with HEDTA solution as usual, then add ammonia solution to bring the pH to 9–10. Boil gently till dissolution is complete. Cool to room temperature and adjust the pH to 5.0–5.5 with hydrochloric acid (1 + 3). Then continue the titration as described in the general procedure.

RESULTS AND DISCUSSION

Separation of lead by precipitation as lead sulphate

It has been common practice to precipitate Pb(II) in a medium containing $2.3M^7$ or $0.9M^{3,8}$ or 5% v/v sulphuric acid.⁹ It should be noted, however, that the solubility of lead sulphate is reported to decrease as the concentration of sulphuric acid increases from 0 to 20% and remain minimal over the range 20–60% v/v sulphuric acid.^{10,11} Accordingly we have explored precipitation of Pb(II) at a higher sulphuric acid concentration than any previously reported. Our experiments showed that the optimum range is 3.5–4.4M sulphuric acid. Hence 3.6M is specified in the procedure.

Our study also revealed that perchloric acid is the only common electrolyte that exerts a negligible effect on the solubility of lead sulphate under the specified conditions. Table 1 shows that the method offers some distinct advantages: (1) the drawbacks of the classical method can be completely overcome; (2) fuming the sample with perchloric acid instead of sulphuric makes the separation more selective, since the subsequent precipitation at lower temperature minimizes the co-precipitation of bismuth;¹² (3) the precipitate is readily dissolved for the chelometric finish since it is formed at a temperature much lower than the boiling point of sulphuric acid; (4) the precipitating agent used is free from any extraneous anions which can cause error, such as acetate² or nitrate,¹³ and this ensures complete precipitation of Pb(II). It is also used for washing so that there is no loss of precipitated $PbSO_4$ by dissolution in the wash liquid.

Table 1. Effect of $HClO_4$ on the precipitation of 101.0 mg of Pb as $PbSO_4$

$HClO_4$ added, ml	Pb found, mg
—	101.1*
2	100.9
3	100.9
5	101.1

*Direct titration without separation.

The chelatometric finish

The complexing agent and back-titrant were chosen on the basis of the data summarized in Table 2. As the stability sequence of the metal complexonates in Table 2 is $Pb > Zn > Ca > Sr > Ba$, Zn(II) would be a suitable back-titrant for use at the optimum pH of 5.0–5.5. As the titrant, neither EGTA nor NTA is acceptable, because the conditional formation constants of their Pb-chelates are too small. Those of the Ca-chelates of DCTA and EDTA are quite large ($\log K'_f > 4$), which might cause unfavourable effects in the back-titration. The Ca-chelates of DTPA and HEDTA have much lower $\log K'_f$ values, however, and differences between these values and the corresponding ones for the Zn-chelates are sufficiently large for Zn(II) to readily displace Ca(II) from its DTPA or HEDTA chelate. HEDTA was finally chosen because it is cheaper and is highly soluble in aqueous solutions, even in strong acids.¹⁵

Catechol Violet and Xylenol Orange are used in combination for this determination. The colour change from yellow to violet at the end-point of the back-titration is more distinct. Both have recently been synthesized by us in high purity, free from all chromogenic impurities, as shown by thin-layer chromatography.

Back-titration is used because an excess of HEDTA must be employed to dissolve the $PbSO_4$ precipitate. HEDTA was chosen because it is a much stronger complexing agent than acetate or tartaric acid for Pb(II) and hence more efficient for this purpose. Thus the chemical equilibria of the titration system can be much simplified as the effects of any side-reaction of the complexing agent used for the dissolution are completely excluded. It is not advisable to use acetate or tartaric acid instead: in the latter case lead sulphate would be reprecipitated at the pH used for a direct titration, and in the former the amount of acetate needed would make the end-point indistinct. Moreover, the selective dissolution of lead sulphate in the

presence of barium sulphate is quantitative only under certain conditions.¹⁶

Effects of diverse ions and ligands

If the analyte, after fuming with perchloric acid, is added to the precipitating solution, but not the reverse, only a small amount of Bi(III) will be co-precipitated. It can be readily pre-titrated at pH 2 (Note 1), needing only a few drops of HEDTA solution. Owing to mixed crystal formation, the selective dissolution of $PbSO_4$ in the presence of alkaline-earth metals is not always quantitative at pH 5 with excess of HEDTA (or EDTA),¹⁶ so it is safer to effect complete dissolution at pH 9–10 (Note 2), then back-titrate with Zn(II) at pH 5.0–5.5. The HEDTA-chelates of the alkaline earths will undergo a stoichiometric displacement reaction with Zn(II) during the back-titration. Reprecipitation of alkaline-earth metal sulphates may occur, but this does no harm. Silica, SnO_2 and Sb_2O_3 will be rendered insoluble by fuming with perchloric acid and loss of Pb might occur owing to adsorption. Fortunately, these species can be readily dealt with by volatilization at the evaporation stage, as SiF_4 (or H_2SiF_6), $SnBr_4$ and $SbBr_3$ respectively. When hydrofluoric acid is used, a polytetrafluoroethylene beaker should be employed. The remaining cations do not interfere. Although K^+ , Rb^+ , Cs^+ , if present in large amounts, and Nb(V), Ta(V) and W(VI), will also be rendered insoluble¹⁷ by fuming with perchloric acid, they are rarely, if ever, concomitant with Pb in macro amounts in industrial samples. Even if they were present, it would be easy to separate them by filtration and recover any lead from them prior to precipitating lead sulphate. Hence the proposed method is highly selective with respect to cations. The recovery of $PbSO_4$ is somewhat lower in the presence of some anions in common use, e.g., tartrate, halides and BF_4^- . Hence these should not be used as masking agents in this precipitation system. As already noted, the only exception is perchlorate. Therefore the acids used for sample decomposition should be confined to those which are sufficiently volatile to be subsequently expelled by fuming with perchloric acid.

Applications

The optimum range of determination by the proposed method is 25–150 mg of Pb. The standard deviation has been found to be 0.35 mg for 60 mg of Pb. It has been satisfactorily

Table 2. Conditional formation constants of some complexonates at pH 5*

Cation	K'_f					
	DCTA	DTPA	EDTA	EGTA	HEDTA	NTA
Pb	11.7	9.6	11.4	4.5	10.2	7.0
Zn	10.7	8.7	9.9	4.3	9.2	5.7
Ca	4.5	1.3	4.1	2.5	2.7	1.6
Sr	2.0	0.4	2.0	0	1.5	0.2
Ba	0	-0.5	1.2	-0.1	0.9	0

*Calculated from the data in Ringbom.¹⁴

Table 3. Determination of Pb in some non-ferrous alloys

Nominal composition, %	Pb found, %	
	Proposed method	ASTM method ⁴
Cu 60, Zn 37	2.60	2.57
Cu 85, Sn 6, Zn 3	5.40	5.38
Bi 40, Sn 13, Cd 10	36.16	36.07
Bi 50, Sn 13, Cd 10	27.19	27.01
Bi 50, Sn 13.3, Cd 10	26.77	26.74
Bi 47.5, Sn 12.6, Cd 9.5, In 5	25.09	24.95

used to determine the lead content of non-ferrous alloys. The results for analysis of some industrial samples are shown in Table 3.

CONCLUSION

A selective and pollutant-free method for chelatometric determination of Pb with HEDTA after precipitation as sulphate is proposed. The precipitation conditions are much improved compared with those of the classical method. Owing to its versatility, the proposed method should find many practical applications.

Acknowledgements—Grateful thanks are due to all members of the Directorate of SRIM for permission to publish this paper.

REFERENCES

1. R. Pfübil, *Applied Complexometry*, pp. 153–154. Pergamon Press, Oxford, 1982.
2. *Japanese Industrial Standards*, JIS H 1501–1975.
3. ASTM E 54–80 (1984).
4. ASTM E 478–82 (1986).
5. E. M. Donaldson, *Talanta*, 1976, **23**, 163.
6. N. Zhou, Z. R. Lu, and Y. X. Gu, *ibid.*, 1983, **30**, 851.
7. G. Charlot and D. Bezier, *Quantitative Inorganic Analysis*, p. 456. Methuen, London, 1957.
8. W. F. Hillebrand, G. E. F. Lundell, H. A. Bright and J. I. Hoffman, *Applied Inorganic Analysis*, 2nd Ed., p. 227. Wiley, New York, 1953.
9. K. Študlar and I. Janoušek, *Hutn. Listy*, 1958, **13**, 805.
10. L. Erdey, *Gravimetric Analysis*, Part II, pp. 28–29. Pergamon Press, Oxford, 1965.
11. H. D. Crockford, *J. Am. Chem. Soc.*, 1934, **56**, 2600.
12. A. T. Etheridge, *Analyst*, 1950, **75**, 279.
13. ASTM E 57–60 (1984).
14. A. Ringbom, *Complexation in Analytical Chemistry*, pp. 332–351. Interscience, London, 1963.
15. N. Zhou, R. Q. Yu, X. Z. Yao and Z. R. Lu, *Talanta*, 1985, **32**, 1125.
16. B. C. Sinha and S. K. Roy, *ibid.*, 1975, **22**, 763.
17. G. E. F. Lundell and J. I. Hoffman, *Outlines of Methods of Chemical Analysis*, p. 47. Wiley, New York, 1938.

ANALYTICAL DATA

DISSOCIATION CONSTANTS OF SOME *o,o'*-SUBSTITUTED AZO DYES

KAREL VYTRÁS, JAROMÍR KALOUS and JAROSLAVA ČERNÁ-FRÝBORTOVÁ*

Department of Analytical Chemistry, University of Chemical Technology, 532 10 Pardubice,
Czechoslovakia

(Received 19 June 1989. Revised 10 April 1990. Accepted 4 May 1990)

Summary—The dissociation constants, $pK_a(H_2L^-)$ and $pK_a(HL^{2-})$, were determined spectrophotometrically in aqueous media at ionic strength 0.2 for six *o,o'*-substituted azo dyes, namely C.I. 13900, C.I. 15685, C.I. 18744, C.I. 18760, C.I. 18821 and Calmagite.

Azo dyes substituted in the *o,o'*-positions are an important group of organic dyes as they can be transformed into complexes with metal ions to increase their colour properties. For this purpose, the *o*-substituent is a hydroxyl group and the *o'*-substituent is a hydroxyl, carboxylic or amino group. For determination of the dyes by potentiometric titration based on ion-pair formation,¹ and for numerous applications and detailed studies of the complexing properties of the dyes, it is important that the protolytic equilibria should be known. Unfortunately, such data are mainly available for some *o,o'*-dihydroxy azo dyes which are used as metallochromic indicators² and for only a limited number of other dyes.^{3,4} Therefore, the dissociation equilibria of six industrially important dyes of this group have been studied spectrophotometrically and the corresponding constants are given in this paper.

EXPERIMENTAL

Apparatus

Absorption spectra were obtained with a Specord UV VIS recording spectrophotometer, and other absorbance measurements were made with a Spekol 11 instrument (both Zeiss, Jena). One-cm path-length glass cuvettes were used for all measurements.

Britton-Robinson buffer solutions adjusted to ionic strength 0.2 with sodium perchlorate were used. The pH values were measured with

an OP-211/1 pH-meter (Radelkis, Budapest) equipped with glass and saturated calomel electrodes, and calibrated with the NBS pH standards in the range from 3.557 for potassium hydrogen tartrate to 12.454 for calcium hydroxide.⁵

Dyes

The five azo dyes used in industry as starting compounds in syntheses of metallocomplex dyes, and Calmagite as a comparison model sample, were studied. The samples were obtained from VÚOS (Pardubice-Rybitví), and the C.I. Constitution Number, C.I. Generic Name (or common name if not included in the Colour Index⁶) and chemical constitution are as follows:

(I) C.I. 13900, C.I. Acid Yellow 99, 1-anilino-2-[(2-hydroxy-3-sulpho-5-nitrophenyl)azo]-3-hydroxy-2-buten-1-one, Na salt;

(II) C.I. 15685, C.I. Acid Red 184, 1-[(2-hydroxy-3-sulpho-5-nitrophenyl)azo]-2-naphthol, Na salt;

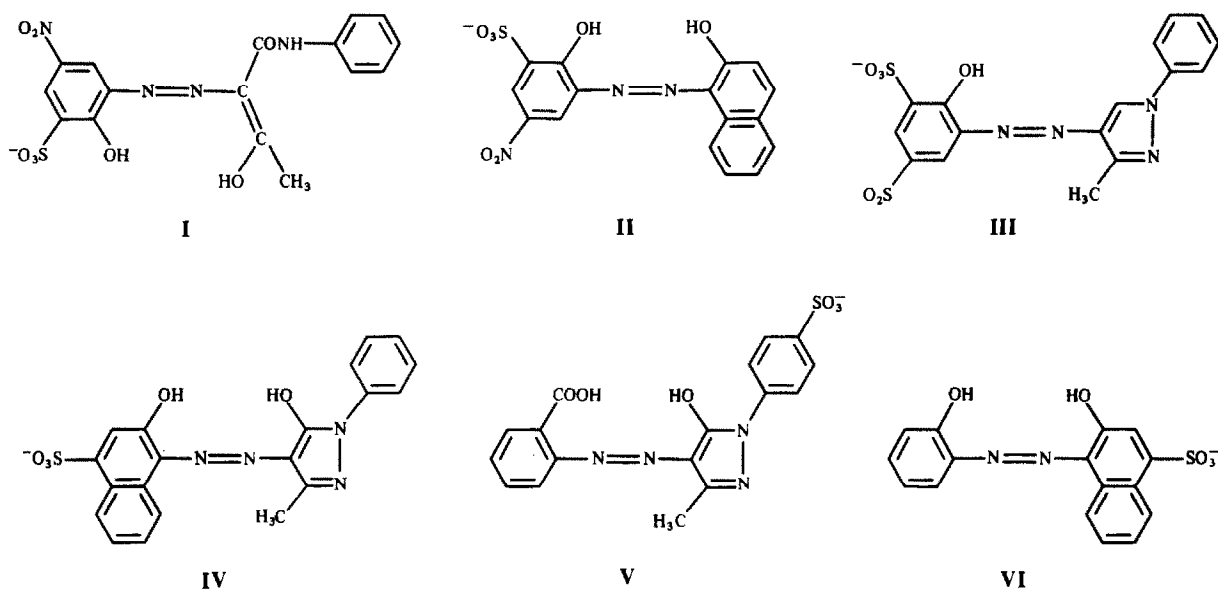
(III) C.I. 18744, C.I. Mordant Orange 29, 4-[(2-hydroxy-3-sulpho-5-nitrophenyl)azo]-1-phenyl-3-methyl-5-pyrazolone, Na salt;

(IV) C.I. 18760, C.I. Mordant Red 7 (Eriochrome Red B), 4-[(2-hydroxy-4-sulphonaphthyl)azo]-1-phenyl-3-methyl-5-pyrazolone, Na salt;

(V) C. I. 18821, C.I. Mordant Yellow 8 (Alizarine Chrome Fast Yellow R), 4-[(2-carboxyphenyl)azo]-1-(4-sulphophenyl)-3-methyl-5-pyrazolone, Na salt;

*Present address: Lachema Corp., 621 33 Brno, Czechoslovakia.

Table 1



(VI) Calmagite, 3-hydroxy-4-[(2-hydroxy-5-methylphenyl)azo]-1-naphthalenesulphonic acid, Na salt.

The formulae are given in Table 1. The purity of the dyes was checked by thin-layer chromatography on 150 × 150-mm Silufol foils (Kavalier, Votice) with 1-propanol + 26% ammonia solution (3:1 v/v) and butyl acetate + acetic acid + water (3:2:1 v/v). No marked colour impurities were found on the chromatograms. Spectrographic examination showed the virtual absence of trace metal impurities.

Procedures

The dyes were dissolved in redistilled water to give *ca.* 10⁻³*M* stock solutions. For spectrophotometric measurements, 5-ml portions of the dye solutions were pipetted into 100-ml standard flasks and diluted to volume with the desired pH buffers. To avoid any decomposition, the spectrophotometric measurements were made immediately after the solution was prepared.

The $pK_a(H_nL)$ values of the particular equilibria $H_nL \rightleftharpoons H_{n-1}L + H^+$ were determined graphically by the customary methods, usually by plotting $\log [A - A(H_nL)]/[A(H_{n-1}L) - A]$ vs. pH,⁷ where *A* is the absorbance measured at a given pH value, and $A(H_nL)$ and $A(H_{n-1}L)$

are the absorbances of the pure forms H_nL and $H_{n-1}L$ at the wavelength used. If either $A(H_nL)$ or $A(H_{n-1}L)$ could not be measured, $pK_a(H_nL)$ was determined by using the formulae^{8,9}

$$\frac{1}{A(H_{n-1}L) - A} = \frac{K_a(H_nL)}{a(H^+)[A(H_{n-1}L) - A(H_nL)]} + \frac{1}{A(H_{n-1}L) - A(H_nL)}$$

or

$$\frac{1}{A - A(H_nL)} = \frac{a(H^+)}{K_a(H_nL)[A(H_{n-1}L) - A(H_nL)]} + \frac{1}{A(H_{n-1}L) - A(H_nL)}$$

where $a(H^+)$ is the hydrogen-ion activity calculated from the pH measurement. For graphical evaluation, $1/[A(H_{n-1}L) - A]$ or $1/[A - A(H_nL)]$ is plotted as the ordinate against $1/a(H^+)$ or $a(H^+)$ as appropriate. In both cases it follows that $K_a(H_nL) = a(H^+)$ when $y = 2/[A(H_nL) - A(H_{n-1}L)]$.

RESULTS AND DISCUSSION

In acidic aqueous dye solutions, the species H_2L^- present can dissociate to form HL^{2-} and L^{3-} species. This model was confirmed by the

Table 2. Dissociation constants of the six *o,o'*-substituted azo dyes at ionic strength 0.2

Dye	$pK_a(H_2L^-)$	$pK_a(HL^{2-})$	Wavelength used <i>nm</i>
I	4.10	13.5	455 (both)
II	4.38	12.5	580 (both)
III	3.63	9.98	500 (both)
IV	5.46	11.44	470 (both)
V	3.26	10.82	430 or 410
VI	7.74	12.5	620 (both)

existence of isobestic points on the absorption spectra measured in the pH regions pertaining to particular protolytic equilibria. The $pK_a(H_2L^-)$ and $pK_a(HL^{2-})$ values were determined, and the results are listed in Table 2. The equilibria for dyes I, III, IV and V are not accompanied by marked colour changes, because although their spectra are markedly different the ion species absorb in the blue region of visible light. The colour changes of dye II are similar to those of Calmagite, but the first is shifted to a lower pH region because of the presence of the electro-negative nitro group.

Only the values for Calmagite could be compared with literature data, namely 7.9 and 12.3,¹⁰ or 8.1 and 12.4,¹¹ for $pK_a(H_2L^-)$ and $pK_a(HL^{2-})$, respectively. As the dye solutions are notoriously unstable in alkaline media the values given in Table 2 can be accepted as in good agreement with these literature values.

For Eriochrome Red B (C.I. 18760), $pK_a = 6.28$ has been reported¹² and ascribed to dissociation of the HL^{2-} form. This value is deemed erroneous, however because the $pK_a(HL^{2-})$ value for this equilibrium is 11.44. From the absorption spectra, the $pK_a(H_2L^-)$ and $pK_a(HL^{2-})$ values given in Table 2 for this dye were determined quite reliably.

REFERENCES

1. K. Vytřas, *Ion-SEL. Electrode Rev.*, 1985, **7**, 77.
2. E. Wänninen, in *Indicators*, E. Bishop (ed.), pp. 231, 237. Pergamon Press, Oxford, 1972.
3. S. Yamamoto, O. Manabe and H. Hiyama, *Kagaku To Kogyo*, 1965, **39**, 13.
4. H. A. Dessouki, A. Ghonium and A. Zaghoul, *J. Soc. Dyers Colour.*, 1987, **103**, 399.
5. R. A. Durst, W. F. Koch and Y. C. Wu, *Ion-SEL. Electrode Rev.*, 1987, **9**, 173.
6. *Colour Index*, 3rd Ed., The Society of Dyers and Colourists, Bradford, 1971.
7. A. Albert and E. P. Serjeant, *Ionization Constants of Acids and Bases*, Methuen, London, 1962.
8. R. S. Stearns and G. W. Wheland, *J. Am. Chem. Soc.*, 1947, **69**, 2025.
9. K. Vytřas and J. Vytřasová, *Chem. Zvesti*, 1974, **28**, 779.
10. B. Kratochvíl, J. Nolan, F. Cantwell and R. Fueton, *Can. J. Chem.*, 1981, **59**, 2539.
11. F. Lindström and H. Diehl, *Anal. Chem.*, 1960, **32**, 1123.
12. E. Hakoila, *Anal. Lett.*, 1970, **3**, 273.

ANNOTATION

CONSIDERATIONS ON THE DIFFERENT OXIDATION STATES OF ANTIMONY, ARSENIC AND SELENIUM IN THE DETERMINATION OF THE ELEMENTS BY HYDRIDE GENERATION-ATOMIC SPECTROMETRY

RAGNAR BYE

University of Oslo, Department of Pharmacy, P.O. Box 1068, 0316 Oslo 3, Norway

(Received 22 August 1989. Revised 13 February 1990. Accepted 16 March 1990)

Determination of antimony, arsenic, selenium and frequently bismuth, germanium, lead, tellurium and tin by hydride generation-atomic absorption spectrometry (HGAAS) has become an established technique. The method is based on the reduction of the elements from a higher oxidation state to the lowest (the hydride form) by a strong reductant such as sodium borohydride. The gaseous hydrides are swept into a spectrometer (ICP, DCP or AA) where the excitation/atomization takes place.

Success in determining the elements by this technique depends on the elements having been brought into one definite (higher) oxidation state before the reduction by borohydride. This is necessary because the ease of reduction to the hydride differs from one oxidation state to another, resulting in different sensitivities in the final excitation/atomization step.

Arsenic and antimony, for instance, may be present in two oxidation states (III and V) in a sample solution, and both forms are reducible by borohydride. However, several authors¹⁻⁴ have observed that the quinquevalent forms usually possess a different (generally lower) sensitivity in the hydride generation process than do the trivalent forms. This can probably be explained by the different rates of reaction. It is therefore desirable to arrange for only *one* oxidation state to be present. Antimony and arsenic in the sample solution are therefore usually reduced to the trivalent state before the borohydride reduction. For this purpose a number of reductants can be applied such as iodide, hydrazine, hydroxylamine and sulphite, the first usually being preferred.²⁻⁴

Selenium(VI), on the other hand, is not reduced at all by borohydride. A prereluction of any Se(VI) in the sample solution to Se(IV) is therefore necessary. This is almost exclusively done by use of hydrochloric acid (*i.e.*, with chloride ions).⁵

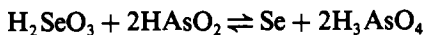
However, when selenium and antimony or arsenic in the *same* solution are to be determined simultaneously as the hydrides, for instance by inductively coupled plasma optical emission spectrometry (ICP-OES), a twofold problem arises. Chloride, which is an effective reductant for selenium(VI), does not reduce antimony(V) and arsenic(V), whereas all the reductants noted above for antimony and arsenic normally reduce selenium(VI) [and selenium(IV) as well] to *elemental* selenium, a fact which has often been overlooked.

When the standard electrode potentials of the actual half-reactions of antimony, arsenic and selenium are examined, it becomes evident that there are no reductants that can reduce antimony, arsenic and selenium simultaneously from their highest to their next lowest stable oxidation states without reduction of the selenium to the elemental state.

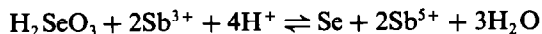
If the three elements are to be determined in the same solution then this problem can be avoided by providing conditions that ensure that antimony and arsenic are in the quinquevalent state before the reduction to the hydride. Any selenium(VI) formed under these oxidizing conditions can be reduced to selenium(IV) by a further treatment with hydrochloric acid, without affecting the antimony(V) and arsenic(V). However, this approach may well affect the

sensitivity for antimony and arsenic adversely.

Although inter-element effects between hydride elements in the gas phase have been well documented,⁶ little attention has been paid to some other reactions that could have resulted in severe interferences and which are therefore undesirable from an analytical point of view:



$$K = 10^{12.5}$$



$$K = 10^{-0.68}$$

Such reactions could result in low results for selenium because of the reduction to the elemental form. In order to examine whether these reactions *could* be a serious problem, two macro-scale experiments were performed, which allowed the occurrence of any reaction to be observed visually.

Sodium selenite ($\equiv 0.2$ g of Se) was dissolved in 200 ml of 2M sulphuric acid and equivalent amounts of sodium arsenite and antimony(III) oxide were added to the selenium solutions. After 4 hr on a boiling water-bath no formation of red elemental selenium could be observed, nor was it observed after 24 hr at ambient temperature. However, after 3 weeks a very faint precipitate of red selenium was detected. Thus, the very slow kinetics of these reactions will prevent problems in real analysis.

REFERENCES

1. J. R. Castillo, J. M. Mir, C. Martinez and M. T. Gomez, *Z. Anal. Chem.*, 1986, **325**, 171.
2. K. Petrick and V. Krivan, *ibid.*, 1987, **327**, 338.
3. H. W. Sinemus, M. Melcher and B. Welz, *Atom. Spectrosc.*, 1982, **2**, 81.
4. P. J. Brooke and W. H. Evans, *Analyst*, 1981, **106**, 514.
5. R. Bye and W. Lund, *Z. Anal. Chem.*, 1988, **332**, 242.
6. J. Dédina, *Anal. Chem.*, 1982, **54**, 2097.

SUPERCRITICAL FLUID EXTRACTION OF VAPOR-DEPOSITED PYRENE FROM CARBONACEOUS COAL STACK ASH

R. F. MAULDIN, J. M. VIENNEAU, E. L. WEHRY* and G. MAMANTOV*

Department of Chemistry, University of Tennessee, Knoxville, TN 37996-1600 U.S.A.

(Received 7 February 1990. Revised 6 April 1990. Accepted 9 April 1990)

Summary—The efficiencies of extraction of vapor-deposited pyrene from a high-carbon coal stack ash by Soxhlet extraction with methanol, ultrasonic extraction with toluene, acid pretreatment and subsequent ultrasonic extraction with toluene, batch extraction with toluene, and supercritical fluid extraction (SFE) are compared. SFE using CO₂ or isobutane yielded extraction recoveries virtually identical with those obtained using ultrasonic or Soxhlet extraction processes. Collection of the SFE extract was performed by expansion into a solvent or onto the head of a gas chromatography (GC) column. No loss of extracted pyrene was observed upon collection of methanol-modified CO₂ SFE by expansion into methanol. Also, no loss of pure CO₂ SFE extract was observed upon collection on the head of a GC column. However, use of a methanol or toluene modifier for CO₂ SFE directly coupled to GC effected complete loss of extracted pyrene.

Polycyclic aromatic hydrocarbons (PAH) are produced in many combustion processes.¹ PAH, released into the atmosphere in the vapor phase, may subsequently be adsorbed onto atmospheric particulate matter. The environmental fate of PAH is important since some PAH have been shown to be carcinogenic and/or mutagenic.²

At present, identification and quantification of PAH sorbed on environmental particulate matter virtually always requires that the PAH be removed from the particulate matter prior to analysis. Techniques used for this purpose³ include conventional Soxhlet extraction,⁴ ultrasonic extraction,⁵ and supercritical fluid extraction (SFE).⁶

It has frequently been observed that conventional extraction techniques produce substantially less than 100% recoveries of adsorbed PAH, especially for adsorbents (such as coal fly ash) that contain significant quantities of carbon.^{7,8} Improved recovery of adsorbed PAH from coal stack ash with ultrasonic extraction has been reported by pretreatment of the sample with HF and/or HCl.⁹ Also, several studies have indicated improved recovery of a variety of compounds from several adsorbents by SFE as compared with traditional extraction methods.¹⁰⁻¹² Additional advantages of SFE

may include a decrease in the number of sample-handling steps and the ease of coupling SFE to other analytical techniques, such as gas chromatography (GC).^{6,13,14}

Herein is reported a comparison of the extraction efficiency of SFE and "traditional" liquid extraction methods, with pyrene (deposited in known quantity from the vapor phase) as the PAH. Coal stack ash was separated by various methods to produce a sample relatively high in carbonaceous particle content. This ash was used as the adsorbent in the present study because it represents an extremely challenging test of any extraction procedure, since carbonaceous particles have been shown to be primarily responsible for strong adsorption of PAH by coal fly ash.⁷

EXPERIMENTAL

Materials

Coal stack ash was obtained from a coal-fired power plant in Lakeland, FL. The bulk coal stack ash contained 5.5% total C, since the coal-fired power plant that produced the ash was not operating efficiently at the time of collection.¹⁵ Merck silica gel (63-200 μm particle size) was obtained from Brinkman, Inc. Pyrene (99 + %) was purchased from Aldrich and used as received. Methanol and toluene (Burdick and Jackson) were used as extraction solvents, supercritical fluid modifiers, and collec-

*Authors to whom all correspondence should be addressed.

tion solvents. Carbon dioxide (SFC grade) and isobutane (instrument grade), equipped with eductor tube and helium headspace, were purchased from Scott Specialty Gases.

Sample preparation

Coal stack ash was mechanically sieved and the 75–124 μm fraction was collected. Separation according to density was used to produce an ash fraction relatively high in bulk carbon content, as described previously.¹⁵ The "carbonaceous" fraction produced in this manner had a bulk elemental carbon content of 36% (Galbraith Laboratories, Knoxville, TN). Further treatment of this "carbonaceous" fraction by elutriation in a stream of nitrogen produced a sub-fraction, having a bulk elemental carbon content of 67%, which was used in this study.

Vapor deposition of pyrene onto the stack ash was used in conjunction with flame ionization detection to measure the quantity of pyrene sorbed by a known amount of the adsorbent, as described by Engelbach *et al.*¹⁶ Coal stack ash was degassed for 24 hr at 250° in a stream of nitrogen before vapor deposition. A surface pyrene concentration of 7.20 mg per g of ash was used for extraction efficiency studies. For studies involving collection of the SFE extract on the head of a gas chromatographic column, a surface concentration of 105 μg of pyrene per g of ash was used. Silica gel was treated similarly to produce a sample containing 122 μg of pyrene per g of silica gel.

SFE apparatus

Only stainless-steel materials were used for construction of the SFE apparatus (shown

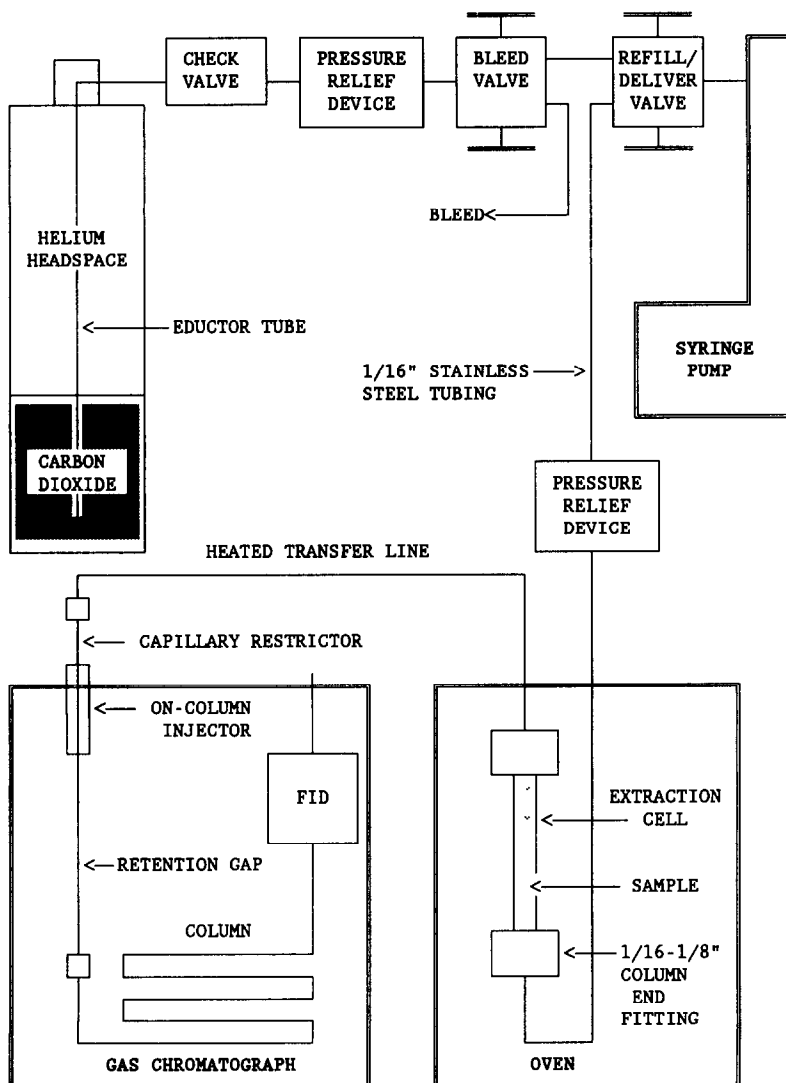


Fig. 1. Schematic diagram of supercritical fluid extraction apparatus.

schematically in Fig. 1). An Isco LC-2600 syringe pump, with a maximum operating pressure of 516 atm, was used to deliver fluids. A check valve, between the cylinder and the pump, prevented contamination of the cylinder. Pressure relief devices from High Pressure Equipment Company were installed in the cylinder-to-pump and the pump-to-cell lines for safety. A Blue M oven, with a maximum operating temperature of 260°, was used to maintain a constant extraction temperature. When higher extraction temperatures were needed, a furnace was used which was constructed by winding nichrome ribbon around a 3-in. Pyrex tube which was then encased in a 4-in. Pyrex tube. The furnace temperature was monitored with an Omega Type K thermocouple.

The extraction cell, also illustrated in Fig. 1, consisted of two Swagelok 1/8–1/16 in. column end fittings with 2.0 μm pore diameter stainless-steel frits. Fittings were placed on each end of a 10 cm piece of 1/8 in. o.d. stainless-steel tubing which housed the sample. A heated transfer line (150°) carried the extract to be collected by expansion of the supercritical fluid from the restrictor into a solvent or onto the head of a gas chromatographic column. Polyimide-coated fused silica capillary tubing (Polymicro Technologies; 25 μm i.d. \times 15 cm long) was used as the restrictor. A Supelco Supeltex M-2A 15% graphite, 85% polyimide ferrule with a 0.4 mm i.d. hole was used to hold the capillary restrictor in place in a 1/16 in. Swagelok stainless-steel union. A 5890A Hewlett Packard gas chromatograph equipped with an on-column injection port and a 10 m long \times 0.53 mm i.d. \times 2.65 μm film thickness analytical column, with 5% phenyl methyl silicone as stationary phase, was used for GC analyses. A 30 cm long \times 0.53 mm i.d. piece of deactivated fused silica tubing, attached between the on-column injection port and the analytical column, served as a "retention gap."

SFE methods

Enough liquid modifier was added to the pump before pressurizing with CO₂ or isobutane, to yield 5% by volume in the modified fluid. The oven temperature was increased linearly to the desired extraction temperature of 250° while the pump was pressurizing the extraction cell to 430 atm for CO₂ systems or 230 atm for isobutane systems. The unusually high extraction temperature of 250° was utilized

in this work since the goal was to increase the efficiency of extraction of adsorbed pyrene, an adsorbate molecule that was expected to be thermally stable at these elevated temperatures. The extract was collected by expansion from the restrictor capillary into 10 ml of toluene for all SFE solvent systems except those modified with methanol, for which methanol was used as the collection solvent. Extracts were quantified by UV-visible absorption spectrophotometry. Alternatively, the extract was collected on the head of a gas chromatographic column by inserting the restrictor through an on-column injection port. The gas chromatographic oven temperature was maintained at 30° during collection of SFE extracts. Gas chromatographic analyses were performed with an initial oven temperature of 30°, followed by a linear increase at 40°/min to 230° (the detector was kept at 325°) for determination of pyrene. Subsequently, extracts were quantified by comparing the pyrene peak height with the peak height for an injection of a standard solution of pyrene. Each sample was repeatedly extracted until the final supercritical fluid extraction removed $\leq 1\%$ of the remaining quantity of adsorbed pyrene. Each sample was then subjected to sonication with toluene in an effort to determine whether any remaining adsorbed pyrene could be extracted.

Traditional extraction methods

In each of the traditional extraction procedures, sample sizes of 10–15 mg were used. For *Soxhlet extractions*, micro-Soxhlet extractors were used with cellulose extraction thimbles. The extraction was continued for 24 hr, with sample exposed to fresh solvent every 15 min. For *ultrasonic extractions*, 15 mg of sample was weighed into a 10 ml standard flask which was then filled to the mark with toluene, and kept in a 125 W Branson ultrasonic cleaner for 2 hr in a water bath at a temperature of 50°. For *exhaustive ultrasonic extraction*, a sample was sonicated for 2 hr at 50° in 50 ml of toluene. The ash was removed from the extract by filtration and then placed in 10 ml of toluene for further sonication. *Batch extractions* were done by placing the sample in a 10 ml standard flask, filling to the mark with toluene, and leaving the sample overnight in the dark. Also, hydrofluoric and hydrochloric acid pretreatment of the ash sample was performed before sonication with toluene, as described elsewhere.⁹

Table 1. Recoveries of adsorbed pyrene observed with SFE and traditional extraction methods

Extraction method	Solvent (volume, ml)	Temperature, °C	Recovery, %
SFE	CO ₂ (260)	250	66
SFE	CO ₂ /Methanol (180)	250	63
SFE	CO ₂ /Toluene (150)	250	66
SFE	Isobutane (100)	250	64
SFE	Isobutane/Methanol (150)	250	68
SFE	Isobutane/Toluene (50)	250	65
Soxhlet	Methanol (10)	60	62
Ultrasonic	Toluene (10)	50	63
Batch	Toluene (10)	25	54
Exhaustive ultrasonic	Toluene (60)	50	65
Acid pretreatment/ultrasonic	Toluene (10)	50	54

RESULTS AND DISCUSSION

SFE study

The efficiencies with which pyrene was extracted from the ash with CO₂, methanol-modified CO₂, toluene-modified CO₂, isobutane, methanol-modified isobutane, and toluene-modified isobutane are compiled in Table 1. The SFE systems studied exhibited virtually identical extraction recoveries. Typically, the 95% confidence intervals for these extractions were *ca.* ±4%. Hence, recoveries in the 62–68% range (Table 1) are statistically equivalent, and the recovery of pyrene from this coal ash sample was remarkably independent of the extraction technique.

Isobutane SFE systems required smaller volumes of solvent (50–100 ml) than did CO₂ systems (150–260 ml) to achieve equal recovery of pyrene; this is probably due to isobutane having a higher solvating power than CO₂ for PAH.¹² It should be noted, however, that essentially the same limiting recovery of adsorbed pyrene was obtained with CO₂ and isobutane. Also, the addition of a polar (methanol) and a nonpolar (toluene) modifier did not significantly increase the extraction efficiency of either CO₂ or isobutane for adsorbed pyrene.

With CO₂ SFE at 250°, the recovery of pyrene decreased from 66 to 51% as the CO₂ pressure was decreased from 430 to 210 atm. Clearly, therefore, use of the higher pressure is essential.

The use of temperatures >250° (to a maximum of 440°) was studied with toluene-modified CO₂ SFE. The use of toluene-modified CO₂ at 250° gave the same extraction efficiency (66%) for adsorbed pyrene as did toluene-modified CO₂ SFE at 440°. Therefore, increasing the extraction temperature of toluene-modified CO₂ from 250 to 440° did not improve recovery of pyrene from the coal stack ash.

Each sample subjected to SFE was subsequently extracted by ultrasonic extraction

with toluene. No detectable pyrene was removed from any of the samples mentioned above except that which had been extracted by CO₂ at 210 atm and 250° (51% recovery of pyrene), from which 3% of the initial quantity of pyrene was extracted by sonication with toluene after SFE.

Collection study

The extraction of vapor-deposited pyrene from silica gel has been shown to be quantitative.¹⁶ Therefore, silica gel loaded with 122 µg of pyrene per g was used to monitor losses of extracted pyrene in the collection of extract by expansion of CO₂ from the capillary restrictor. An 89% recovery of pyrene from silica gel was obtained by CO₂ SFE at 250° and 430 atm with collection onto the head of a gas chromatographic column (held at 30°). Also, an 87% recovery of pyrene from silica gel with CO₂/methanol SFE (250° and 430 atm) was observed with collection into 10 ml of methanol. Therefore, relatively small amounts of extracted pyrene were lost when CO₂ SFE was coupled directly to GC.

On the other hand, liquid-modified CO₂ SFE directly coupled to GC gave complete loss of pyrene extract during collection. Silica gel, coated with 122 µg of pyrene per g, yielded no detectable pyrene by gas chromatographic analysis when the extract from SFE with CO₂ and 5% methanol (45°, 400 atm) was collected on the head of a GC column held at 30°. In another experiment, a sample of the carbonaceous stack ash fraction (105 µg of pyrene per g of ash) was extracted by CO₂/toluene SFE at 65° and 400 atm. When the extract was collected into 10 ml of toluene, a 51% recovery of adsorbed pyrene was observed; when the extract was collected on the head of a gas chromatographic column, no detectable pyrene was observed. For this same stack ash sample, CO₂/methanol SFE at 65° and 400 atm with

with collection into 10 ml of methanol yielded 7% of adsorbed pyrene, while collection on the head of a GC column again gave rise to no detectable pyrene upon gas chromatographic analysis. Therefore, under these experimental conditions, pure CO₂ SFE could be directly coupled to GC without severe losses of extracted pyrene. However, collection of extracts produced by use of CO₂ modified with methanol or toluene, on the head of a gas chromatographic column, led to complete loss of pyrene, despite the use of a "retention gap" before the GC column. Methanol and toluene are liquids at room temperature and pressure, so expansion of a methanol- or toluene-modified CO₂ supercritical fluid from a capillary restrictor produced liquid droplets of methanol or toluene. Subsequently, these liquid droplets impeded concentration of the extract at the head of a GC column. Whether the inapplicability of this technique to SFE systems that employ liquid modifiers is a significant limitation of the procedure remains to be determined.

Traditional liquid extraction methods

Recoveries of pyrene from carbonaceous stack ash particles by liquid extraction methods are listed in Table 1. Soxhlet extraction with 10 ml of methanol yielded 62% recovery of adsorbed pyrene, ultrasonic extraction with toluene yielded 63% recovery and exhaustive ultrasonic extraction with a total of 60 ml of toluene yielded 65%. These recoveries are not statistically different from one another. Therefore, ultrasonic extraction with 10 ml of toluene is virtually an "exhaustive" extraction of the pyrene from this adsorbent.

Batch extraction with toluene was capable of removing 54% of pyrene from the stack ash fraction. Hence, the ultrasonic extraction increased the recovery of adsorbed pyrene from 54 to 63%. Acid treatment prior to ultrasonic extraction with toluene gave rise to 54% recovery. Thus, in contrast to previous observations,⁹ acid pretreatment did not improve recovery of pyrene from coal stack ash by ultrasonic extraction with toluene.

CONCLUSIONS

For pyrene adsorbed on carbonaceous coal ash, supercritical fluid extraction, conventional soxhlet extraction with methanol, and ultrasonic extraction with toluene yielded virtually identical recoveries. The use of modifiers (methanol,

toluene) did not improve recovery of pyrene from the carbon-rich stack ash by the CO₂ and isobutane systems at 250°. Isobutane systems required smaller volumes of solvent than CO₂ systems to yield equal recoveries of adsorbed pyrene. Acid treatment prior to ultrasonic extraction with toluene did not improve recovery of adsorbed pyrene from carbonaceous coal stack ash. Ultrasonic extraction was shown to produce a higher recovery (63%) than batch extraction with toluene (54%). Ultrasonic extraction of pyrene from the carbonaceous stack ash was shown to be as complete as possible even with only 10 ml of toluene.

For collection of an SFE extract on a gas chromatographic column at an oven temperature of 30°, with methanol- and toluene-modified SFE systems there was complete loss of extracted pyrene upon collection, despite the use of a "retention gap" between the on-column injection port and the GC column. Unmodified CO₂ SFE, however, could be successfully coupled to GC without significant losses of extracted pyrene.

Approximately 35% of the pyrene on this stack ash appears "irreversibly" adsorbed. No extraction method that promises to improve the situation has been found. None of the commonly-used extraction methods were capable of removing more than *ca.* 65% of the initially adsorbed quantity of pyrene. SFE did not improve recovery of pyrene from this coal stack ash fraction, though it has been reported to provide improved recoveries of adsorbed PAH from other coal stack ashes.¹¹ Also, acid treatment prior to ultrasonic extraction has been reported to improve recoveries of PAH from coal stack ashes,⁹ yet was not capable of producing improved recovery of adsorbed pyrene from this coal stack ash fraction.

A possible reason for the increased recoveries of PAH from coal stack ash observed by other investigators using SFE and/or acid pretreatment^{9,11} is that the stack ash used by them may have contained $\leq 5\%$ C. Thus, improved recovery of PAH may have been observed for PAH (deposited from solution) on mineral- or iron-rich particles. In this study, however, a stack ash consisting almost solely of carbonaceous particles was used. Also, pyrene was deposited onto the coal stack ash particles from the vapor phase, rather than from a liquid solution. Competition between solvent molecules and PAH for strong adsorption sites when PAH is deposited from a liquid solution might cause the PAH to

be adsorbed on weak adsorption sites, thus enabling higher recoveries of adsorbed PAH. Deposition of the PAH from the vapor phase, however, eliminates such competition; thus, PAH are more likely to be adsorbed on the strongest adsorption sites, which could account for the lower recoveries.

Carbonaceous particles are presumed to be responsible for irreversible adsorption of PAH on coal stack ash,⁷ and an increase in the molecular weight of the PAH often leads to a decrease in efficiency of extraction of PAH from coal stack ash.³ Hence, it is likely that PAH with higher molecular weight than pyrene are likely to be adsorbed irreversibly to an even greater extent than pyrene on coal ashes that contain large proportions of carbonaceous particles.

Acknowledgements—This research was supported by the Office of Health and Environmental Research, U.S. Department of Energy (Contract ASO5-81ER6006). The National Science Foundation is thanked for support of undergraduate research student J. M. Vienneau, of the State University of New York-Fredonia, during the summer of 1989.

REFERENCES

1. M. R. Guerin, in *Polycyclic Hydrocarbons and Cancer*, H. V. Gelboin and P. O. P. Ts'o (eds.), Vol. 1, Chap. 1. Academic Press, New York, 1978.
2. W. Levin, A. W. Wood, P. G. Wislocki, R. L. Chang, J. Kapitulnik, H. D. Mah, H. Yagi, D. M. Jerina and A. H. Conney, in *Polycyclic Hydrocarbons and Cancer*, H. V. Gelboin and P. O. P. Ts'o (eds.), Vol. 1, Chap. 9. Academic Press, New York, 1978.
3. W. H. Griest and J. E. Caton, in *Handbook of Polycyclic Aromatic Hydrocarbons*, A. Bjorseth (ed.), Chap. 3. Dekker, New York, 1983.
4. G. A. Junk and J. J. Richard, *Anal. Chem.*, 1986, **58**, 962.
5. W. H. Griest, B. A. Tomkins and J. R. Caffrey, *ibid.*, 1988, **60**, 2169.
6. S. B. Hawthorne and D. J. Miller, *J. Chromatog.*, 1986, **24**, 258.
7. W. H. Griest and B. A. Tomkins, *Environ. Sci. Technol.*, 1986, **20**, 291.
8. P. A. Soltys, T. Mauney, D. F. S. Natusch and M. R. Schure, *ibid.*, 1986, **20**, 175.
9. C. D. Chriswell, I. Ogawa, M. J. Tschetter and R. Markuszewski, *ibid.*, 1988, **22**, 1506.
10. M. M. Schantz and S. N. Chesler, *J. Chromatog.*, 1986, **363**, 397.
11. S. B. Hawthorne and D. J. Miller, *Anal. Chem.*, 1987, **59**, 1705.
12. B. W. Wright, C. W. Wright, R. W. Gale and R. D. Smith, *ibid.*, 1987, **59**, 38.
13. B. W. Wright, S. R. Frye, D. G. McMinn and R. D. Smith, *ibid.*, 1987, **59**, 640.
14. I. L. Davies, M. W. Raynor, J. P. Kithinji, K. D. Bartle, P. T. Williams and G. E. Andrews, *ibid.*, 1988, **60**, 683A.
15. T. D. J. Dunstan, R. F. Mauldin, Z. Jinxian, A. D. Hipps, E. L. Wehry and G. Mamantov, *Environ. Sci. Technol.*, 1989, **23**, 303.
16. R. J. Engelbach, A. A. Garrison, E. L. Wehry and G. Mamantov, *Anal. Chem.*, 1987, **59**, 2541.

ANALYTICAL UTILITY OF COUPLED TRANSPORT ACROSS A SUPPORTED LIQUID MEMBRANE

SELECTIVE PRECONCENTRATION OF ZINC

JAMES A. COX* and ATUL BHATNAGAR

Department of Chemistry, Miami University, Oxford, OH 45056, U.S.A.

(Received 25 January 1990. Revised 16 April 1990. Accepted 20 April 1990)

Summary—A liquid membrane comprising 5–10% bis(2,4,4-trimethylpentyl)phosphinic acid in dodecane that is supported between an aqueous sample at pH 4.7–6.0 and a 0.1M HCl receiver results in uphill transport of Zn(II) from the sample into the receiver. With 2 ml of receiver, a 5 cm² membrane and 60 min dialysis time, Zn(II) is preconcentrated by a factor of *ca.* 13 when the initial concentration in the sample is in the range 1.5×10^{-7} – 1.5×10^{-4} M. The enrichment factor is directly proportional to time up to 30 min since the transport rate of Zn(II) across the membrane is constant over this period. At longer times the flux is slowed as the system begins to approach equilibrium. The presence of other metals such as Cu(II), Co(II), Ni(II), Cd(II), Pb(II) and Fe(II) does not change the enrichment factor for Zn(II), even when the interferent is at a concentration high enough for the rate of transport (nmole/min) of the interferent and Zn(II) to be about the same. The flux of Zn(II) was about 40 times that of Cu(II) and 100 times that of Co(II) when their concentrations in the sample were equal. The other metal ions examined are not significantly transported.

Coupled transport across supported liquid membranes is an emerging technology for the removal of trace metals from waste streams. The method is also being explored as a means of analytical preconcentration and separation. The procedure is analogous to performing extractions and back-extractions on a continuous basis. The membrane that separates the sample (feed solution) from the receiver (stripping solution) comprises a thin, microporous support that is impregnated with a water-immiscible solvent containing a complexing agent, typically a weak acid. At the sample/membrane interface, the target metal ion reacts to form a neutral complex that partitions into the membrane with the release of protons into the sample. The metal complex diffuses to the membrane/receiver boundary where, assuming that the receiver is acidic relative to the sample, the reverse reaction occurs. A pH gradient serves as the driving force; as long as this gradient exists the transport occurs regardless of the relative concentrations of the target metal ion in the receiver and sample. Hence, "uphill" transport (flux of the target metal ion against its concentration gradient) can occur. If the receiver volume is less than that of the sample, the target metal ions can be preconcentrated.

Bloch¹ and Cussler² described the process above in the early 1970s, but until recently, applications were limited to the removal of target species from water and wastewater. Among the significant reports were studies on the rate of Cu(II) transport across supported liquid membranes (SLMs) that contained oxime mixtures as complexing agents,^{3,4} the recovery of uranium from leach solutions,⁵ and the transport of Pt(IV) from an acidic sample into a basic receiver across an SLM that contained trioctylamine.⁶ Using analogous chemistry, the removal of a variety of target analytes from aqueous samples has been accomplished with liquid surfactant membranes, which were first employed by Li.⁷

Applications related to analytical chemistry have almost exclusively dealt with separation of mixtures of target species. Sakamoto *et al.*⁸ used SLMs containing crown ethers to preconcentrate Li⁺ preferentially to Na⁺. By a related method, Bartsch *et al.* preconcentrated Na⁺ relative to Li⁺ with a chloroform membrane that contained a crown ether.⁹ Here, the organic phase was suspended between the aqueous sample and receiver solutions. Danesi and Rickert separated Co(II) from Ni(II) by preferential transport of the former across an SLM of 0.5M bis(2,4,4-triethylpentyl)phosphinic acid (Cyanex 272) in 67% decalin–33% di-isopropylbenzene.¹⁰

*To whom all correspondence should be addressed.

These experiments employed preconcentration times sufficiently long to allow the systems to approach equilibrium.

When membrane transport methods are used to improve trace determinations of target species, using times that allow an approach to equilibrium is not practical. Unless the receiver volume is on the μl -scale, the time needed is of the order of hours. In addition, the position of equilibrium, and, therefore, the enrichment factors will depend on the sample concentration of the species that provides the driving force. For example, in the case of coupled transport across an SLM that contains a weak acid or weak base as the complexing agent in the membrane, the sample pH will influence the position of equilibrium but not the initial rate of transport across the SLM.¹¹ For these reasons, we used a fixed time kinetic model in our development of Donnan dialysis as an analytical preconcentration method.¹² Here, an ion-exchange membrane is used in conjunction with an ionic strength differential as the driving force; the concentration of the analyte in the receiver after a fixed dialysis time is directly proportional to the initial concentration in the sample as long as the following conditions are observed: the sample volume is much greater than the receiver volume and the dialysis time is much shorter than that needed to approach Donnan equilibrium.¹³

Danesi has shown that the fixed time kinetic model should be suited to coupled transport across an SLM.¹⁴ That is, the flux is predicted to be directly proportional to the concentration of the analyte in the sample. With the restrictions of a large sample volume and a short dialysis time, the sample concentration will be essentially constant.

In a study on the transport of Cu(II) across a membrane that contained a mixture of oximes (LIX 64N, Henkel Corp.), we demonstrated that the fixed time kinetic method was suitable for uphill transport by the proton-coupled mechanism.¹¹ The flux of Cu(II) across the SLM was about the same as that observed for Donnan dialysis when the membranes were about the same in area and thickness.¹⁵ However, further study revealed potential limitations of the liquid membrane method relative to Donnan dialysis. Unlike Donnan dialysis, the proton-coupled transport rate of a target cation across an SLM was changed in the presence of other cations that reacted with the complexing agent in the membrane.^{16,17} Moreover, with

kerosene or dodecane as the liquid and diphenylthiocarbazono as the complexing agent, the flux of Zn(II) was slowed because the complex was coordinatively unsaturated. Addition of an auxiliary ligand, such as thiocyanate or thiosulfate, to the sample alleviated the problem;¹⁷ however, the need to add a reagent to the sample obviates some important potential applications of preconcentration based on membrane transport.

The present study was initiated to determine whether a different choice of immobilized complexing agent could eliminate the need for an auxiliary ligand in the sample. More importantly, the question of whether coupled transport across an SLM could allow simultaneous transport of two cationic species at the same rate as observed for the related single-component samples was addressed.

EXPERIMENTAL

The coupled transport experiments were performed with a simple assembly comprising a sample container, a glass tube closed at one end with Celgard 2400 (Celanese Corp.) microporous polypropylene membrane as the receiver container, and a magnetic stirrer. The sample container was rounded at the bottom to allow reproducible positioning of the magnetic stirring bar. The sample volume was 80.0 ml. The membrane was held with Teflon tape and an O-ring. The receiver volume was 2.0 ml, and the membrane area was 5.0 cm². The membrane characteristics were 38% porosity, 0.02 μm effective pore size and 0.025 mm thickness.

Unless otherwise stated, the liquid phase of the membranes consisted of reagent grade dodecane (Aldrich Chemical Co.) and bis(2,4,4-trimethylpentyl)phosphinic acid, MPPA, available as Cyanex 272 (American Cyanamid Co.), as the mobile carrier. The liquid phase of these membranes consisted of 5–10% by weight MPPA in dodecane.

The supported liquid membranes were prepared by pipetting the liquid phase onto the Celgard 2400 after the receiver cell had been assembled. When saturation was reached, the excess was removed and the cells were placed in contact with aqueous solutions to prevent loss of the organic phase by evaporation. The membranes were cleaned with ethanol and reloaded with organic phase between experiments, even though a single preparation can be used for several trials.¹¹

The HCl was purified by placing reagent grade acid and distilled water in Petri dishes side-by-side inside a closed container (a desiccator is convenient) for 2 weeks. The concentration of HCl in the water was determined by titration of an aliquot. The remainder was subsequently diluted to 0.10M for use as receiver or back-extraction solutions.

The membrane-transport experiments, herein termed mobile-carrier dialysis (MCD), were initiated by contacting the receiver cell with the stirred sample. After a prescribed time, 60 min unless otherwise stated, the receiver solution was removed, and its metal concentration determined by atomic absorption spectrometry (Perkin Elmer 2280 system with either a flame or an HGA-300 furnace). The enrichment factor, EF, is calculated from the expression

$$EF = c_R/c_S \quad (1)$$

where c_R is the concentration of the analyte in the receiver at the end of the timed dialysis and c_S is the initial concentration of the analyte in the sample.

The experiments by which the extraction constants were determined were performed in a 125 ml separatory funnel into which 5 ml of the sample was pipetted. The samples were pH 4.7 acetate buffers that contained 1.0 mg/l. Zn(II) or Cu(II). A 5 ml aliquot of 5% by weight MPPA in dodecane was added by pipet. After agitation, the organic phase was removed, washed with three aliquots of water and back-extracted with 2 ml of 0.1M HCl. The Zn or Cu concentration was determined by atomic absorption spectrometry.

RESULTS AND DISCUSSION

Initial experiments were performed to determine whether uphill transport of Zn(II) occurs across a liquid membrane that contains bis-(2,4,4-trimethylpentyl)phosphinic acid (MPPA). Samples that contained 15.3 μ M Zn(II) at pH 4.7 were dialyzed into 0.1M HCl across an SLM that contained 10% MPPA in dodecane. With sample volumes of 80 ml, receiver volumes of 2 ml and dialysis times of 0.25, 0.50, 1.0 and 2.0 hr, the enrichment factors were 5.7, 11.2, 20.2 and 32.2, respectively. With an initial concentration of 15.3 μ M Zn(II) in the sample, the transport rates were 2.3, 2.3, 2.1 and 1.6 nmole \cdot min⁻¹ \cdot cm⁻² over the first 15, 30, 60 and 120 min, respectively.

Consistent with the prediction by Danesi,¹⁴ as long as the average sample concentration over the period of dialysis is virtually constant, the enrichment factor is directly proportional to the dialysis time; that is, the flux is constant. As detailed below, the relative standard deviation of these experiments is about 9%; therefore, these data demonstrate that the flux is constant for about 30 min under the experimental conditions we employed. Because the EF is independent of the initial concentration of the analyte in the sample, an unknown can be quantified by dividing the concentration of the analyte in the receiver after a prescribed dialysis time by the EF. Alternatively, a linear calibration curve can be prepared for the prescribed dialysis time.

Earlier, we determined the flux of Cu(II) across a well-characterized SLM comprising an oxime mixture (LIX 64N, Henkel Corp.) in kerosene¹¹ and the flux of Zn(II) across an SLM of dithizone in kerosene.¹⁷ In the latter case thiosulfate was included in the sample to overcome the effect of water in unfilled coordination sites on the flux. In both cases the flux of the metal was 1.6 nmole \cdot min⁻¹ \cdot cm⁻² when the membrane support was that (Celgard 2400) used here. The transport rate with MPPA as the complexing agent compares favorably with that observed with these well-characterized systems. Therefore, we selected it for further evaluation as the basis for an analytical preconcentration method.

The reproducibility of the MCD experiments was determined by performing a series of 11 trials with 15.3 μ M Zn(II) in a pH 4.7 buffer as the sample, a 5% MPPA-dodecane SLM, and a 0.10M HCl receiver with dialysis times of 30 min. The average and standard deviation of the EF was 12.8 \pm 1.1. The relative standard deviation, 9%, is comparable to that of Donnan dialysis, 8% when neither temperature nor stirring rate is carefully controlled.¹⁸ Within these limits, variation of the MPPA content of the membrane between 5 and 10% has an insignificant influence on the EF, so in all subsequent experiments the lower amount was used.

Because the pH differential across the membrane is the driving force of the transport, it was of interest to determine the influence of the pH of the sample on the EF. With 0.10M HCl as the receiver, the EF is independent of sample pH over the range 4.7–6.0. This suggests that the transport rate is limited by diffusion across the SLM under these conditions. At pH 3.5, the EF is 15% lower than the limiting value.

Table 1. Effect of the initial concentration in the sample on the EF for Zn(II) across an MPPA-containing SLM

Sample conc., M	EF	n
1.53×10^{-7}	13.0 ± 0.8	4
1.53×10^{-6}	13.6 ± 0.3	3
1.53×10^{-5}	12.8 ± 1.1	11
7.65×10^{-5}	12.5 ± 0.1	3
1.53×10^{-4}	13.1 ± 0.3	5

Sample, 80 ml of Zn(II) solution at pH 4.7; receiver, 2 ml of 0.1M HCl; dialysis time, 30 min; membrane area, 5.0 cm²; membrane composition, 5% MPPA by weight in dodecane.

The hypothesis above that the process is limited by diffusion of the analyte across the membrane is consistent with the independence of EF on the MPPA concentration in the range 5–10%. Moreover, it provides a basis for predicting the influence of stirring rate and temperature on the EF measurements;¹⁸ however, this was not a subject of the present investigation.

For use in analytical preconcentrations it is convenient if the EF is independent of the initial concentration of the analyte in the sample, as discussed above. The data in Table 1 demonstrate that this behavior, which was predicted from the study of flux *vs.* dialysis time, is observed over at least three orders of magnitude of concentration. With a 30 min preconcentration, the average EF \pm standard deviation over the range 0.153–153 μ M was 13.0 ± 0.7 (26 data points).

The EFs for Zn(II) in Table 1 were not changed when other metal ions were present in the sample. The results in Table 2 summarize experiments where Cu(II), Co(II), Ni(II), Fe(II), Cd(II), and Pb(II) were tested as interferents. In each case the test metal concentration was varied up to the tabulated value; higher concentrations were not considered. No influence on the EF for Zn(II) was observed when MPPA in dodecane was the liquid membrane. The only case where an interference was suspected was that with 179 μ M Fe(II) in the sample; however, an *F*-test at the 95% confidence level suggested

Table 2. Influence of other metals on the preconcentration of Zn(II) across an MPPA-containing SLM

Sample component(s)	EF for Zn	n
15.3 μ M Zn(II)	12.8 ± 1.1	11
15.3 μ M Zn(II); 157 μ M Cu(II)	12.9 ± 0.2	3
15.3 μ M Zn(II); 169 μ M Co(II)	12.8 ± 0.6	3
15.3 μ M Zn(II); 170 μ M Ni(II)	12.7 ± 0.6	3
15.3 μ M Zn(II); 179 μ M Fe(II)	13.5 ± 1.4	9
15.3 μ M Zn(II); 89 μ M Cd(II)	13.0 ± 0.5	3
15.3 μ M Zn(II); 48 μ M Pb(II)	12.7 ± 0.3	3

Conditions as for Table 1.

that the difference between the EFs for Zn in the presence and absence of Fe(II) was not statistically significant.

With the general complexing agents diphenylthiocarbazono and diethylammonium dithiocarbamate (DDTC) as the mobile carriers, interference was observed. For example, when the SLM was diphenylthiocarbazono in kerosene, the presence of 1.0 μ M Cu(II) decreased the EF for Zn(II) from 14.6 to 4.3 in a 60 min experiment with an 11.3 cm² Celgard 2400 support.¹⁷ Here, 10mM thiosulfate was included in the sample to accelerate the rate of phase transfer of the Zn(II). In the present study, DDTC was also tested as a general complexing agent. In this case Cu(II) in the sample totally blocked transport of Zn(II), whether thiosulfate was present or not.

The results of the interference study in Table 2 suggested that either MPPA was highly selective for Zn(II) relative to Cu(II), Co(II), Ni(II), Fe(II), Cd(II) and Pb(II) or that our hypothesis that metals would mutually interfere with fluxes during MCD experiments with general complexing agents^{15,17} was incorrect. To interpret the data in Table 2 it was necessary, therefore, to determine the EF-values for the other metals that were tested as interferents. With a 30-min dialysis the respective EF-values for Zn(II), Cu(II), and Co(II) were 13, 0.31, and 0.12. Consistent with a previous report,¹⁹ the flux of Ni(II), as well as the other metals we studied, was significantly lower than that of Co(II).

The results above show that MPPA is selective for Zn(II), so the data in Table 2 do not disprove the hypothesis regarding interferences since the flux of the metals other than Zn across the SLM was small at the concentrations selected. Hence it was necessary to repeat the experiments, with the interferent at a high enough concentration to yield a flux comparable to that for Zn(II) from a 15.3 μ M Zn(II) sample. Of the metals other than Zn(II) tested, Cu(II) showed the fastest transport across the MPPA-containing SLM, so it was selected for these experiments on simultaneous transport.

Table 3 includes a summary of experiments in which the Zn(II) concentration was 15.3 μ M and that of Cu(II) was varied so that its flux across the SLM would be higher or lower than that of the Zn(II), assuming that fluxes calculated from results for single-component samples represent those that occur with mixtures. That the EF of Zn is independent of the concentration of Cu(II)

Table 3. Simultaneous transport of Zn(II) and Cu(II) across an MPPA-containing membrane

Sample		EF	
Zn(II), M	Cu(II), M	Zn	Cu
1.53×10^{-5}	0	12.8	—
0	6.30×10^{-4}	—	0.28
1.53×10^{-5}	6.30×10^{-4}	12.7	0.24
1.53×10^{-5}	1.57×10^{-5}	12.8	—
1.53×10^{-5}	1.57×10^{-3}	12.6	—
1.53×10^{-4}	6.30×10^{-4}	—	0.18

Conditions as for Table 1.

in these cases suggests that, contrary to our previous hypothesis, simultaneous transport can indeed take place across an SLM. This conclusion was supported by fact that the presence of Zn(II) did not markedly decrease the EF for Cu (Table 3). Thus, simultaneous transport with equal fluxes at rates similar to those observed for the single-component systems is possible by the coupled transport mechanism.

The MPPA-dodecane system is highly selective for Zn relative to the other metals in this study. In order to assess whether this selectivity in a membrane transport experiment is transferable to other applications of two-phase systems such as ion-selective electrodes, it is necessary to establish whether phase transfer kinetics or the equilibrium behavior (extraction constant) is responsible. A series of solvent extraction experiments were performed on Zn(II) and on Cu(II) samples with mixing time as a variable. With 1.0 mg/l. Zn as the sample, 98.5% of the metal was extracted in 3 min under conditions listed in the experimental section; this value did not change when the equilibration time was increased to 30 min. The extraction constant was 66. With 1.0 mg/l. Cu as the sample the residual concentration was 0.25 mg/l. Cu at times from 5 to 30 min. Hence, the extraction constant for Cu(II) was 3. The ratio of the extraction constants accounts for the difference in EF-values for these metals, so phase transfer kinetics do not determine the selectivity of this MCD system.

The results of this study suggest that uphill transport across an SLM has more analytical utility than indicated by our previous work with diphenylthiocarbazone as the mobile carrier. Of general importance is the demonstration that

simultaneous transport of two metals can be achieved without the flux of one affecting that of the other. In addition, with MPPA as the mobile carrier the MCD of Zn(II) has the characteristics needed for analytically-useful preconcentrations without the need to include an auxiliary ligand in the sample. These two results are very important for the development of MCD-based water treatment methods as well as for applications to analytical chemistry. The present system will be tried with hollow fiber membranes in order to increase the enrichment factor. The hollow fiber geometry has a more favorable area-to-volume ratio than that of sheet membranes; in comparable Donnan dialysis systems, the efficiency was about 50 times greater when hollow fibers were used.²⁰

REFERENCES

1. R. Bloch, in *Membrane Science and Technology*, J. C. Flinn (ed.), pp. 171–187. Plenum Press, New York, 1970.
2. E. L. Cussler, *AIChE J.*, 1971, **17**, 1300.
3. R. W. Baker, M. E. Tuttle, D. J. Keller and H. K. Lonsdale, *J. Membr. Sci.*, 1977, **2**, 2113.
4. K. H. Lee, D. F. Evans and E. L. Cussler, *AIChE J.*, 1978, **24**, 860.
5. W. C. Babcock, D. T. Friesen and E. D. LaChapelle, *J. Membr. Sci.*, 1986, **26**, 303.
6. T. Nishiki and R. G. Bautista, *AIChE J.*, 1985, **31**, 2093.
7. N. N. Li, *Ind. Eng. Chem. Process Des. Develop.*, 1971, **10**, 215.
8. H. Sakamoto, K. Kimura and T. Shono, *Anal. Chem.*, 1987, **59**, 1513.
9. R. A. Bartsch, W. A. Charewicz and G. S. Heo, *ibid.*, 1982, **54**, 2094.
10. P. R. Danesi and P. G. Rickert, *Solvent Extr. Ion Exch.*, 1986, **4**, 149.
11. J. A. Cox, A. Bhatnagar and R. W. Francis, Jr., *Talanta*, 1986, **33**, 713.
12. G. L. Lundquist, G. Washinger and J. A. Cox, *Anal. Chem.*, 1975, **47**, 319.
13. J. A. Cox and N. Tanaka, *ibid.*, 1985, **57**, 2370.
14. P. R. Danesi, *Sep. Sci. Technol.*, 1984, **19**, 857.
15. J. A. Cox, A. Bhatnagar and S. Al-Shakshir, *Proc. Oak Ridge Model Conf. Waste Management*, Vol. I, Part 3, p. 89, October 1987.
16. J. A. Cox, T. Gray, K. S. Yoon, Y. T. Kim and Z. Twardowski, *Analyst*, 1984, **109**, 1603.
17. J. A. Cox and A. Bhatnagar, *Anal. Chem.*, 1988, **60**, 986.
18. J. A. Cox and J. E. DiNunzio, *ibid.*, 1977, **49**, 1272.
19. P. R. Danesi, L. Riechley-Yinger, G. Mason, L. Kaplan, E. P. Horwitz and H. Diamond, *Solvent Extr. Ion Exch.*, 1985, **3**, 435.
20. J. A. Cox and G. R. Litwinski, *Anal. Chem.*, 1983, **54**, 1640.

DETERMINATION OF THIAMINE BY CONTINUOUS FLOW CHEMILUMINESCENCE MEASUREMENT

NIKOS GREKAS and ANTONY C. CALOKERINOS*

University of Athens, Laboratory of Analytical Chemistry, Panepistimiopolis, Kouponia, 15771 Athens, Greece

(Received 13 February 1990. Accepted 31 March 1990)

Summary—The chemiluminescence produced by oxidation of thiamine by ferricyanide in alkaline medium has been investigated by using a simple continuous flow analyser and a procedure developed for the determination of thiamine hydrochloride or nitrate in the range 2.00×10^{-5} – $5.00 \times 10^{-4} M$ (equivalent to 6.75–169 $\mu\text{g/ml}$ thiamine hydrochloride) with coefficients of variation $< 2\%$. A measurement rate of 112/hr can be obtained. When applied to pharmaceutical formulations, the only interferent among common excipients and coexisting drugs is ascorbic acid. The results obtained for the assay of dosage forms compared well with those obtained by an official method and demonstrated an error $< 4\%$.

There are numerous biological, microbiological and chemical methods which have been employed for the determination of thiamine (vitamin B₁) in a variety of samples.¹ The chemical methods offer great accuracy and speed and thus are widely accepted for routine assays. The chemical method most commonly used involves oxidation of thiamine to thiochrome, which is then measured fluorimetrically. Potassium ferricyanide has been reported as the best oxidizing agent. This procedure is the official U.S.P. method.² The fluorimetric determination of thiamine has been automated by using air-segmented continuous flow³ or flow injection⁴ systems. A kinetic fluorimetric method has also been proposed.⁵

Since thiochrome is a fluorescent compound, it is also a possible chemiluminescence emitter. Chernysh *et al.* were the first to report that during oxidation of thiamine to thiochrome, a bright chemiluminescent radiation appears.⁶ These authors investigated the use of the reaction for the assay of thiamine by a manual chemiluminescence (CL) system.

This work is concerned with the systematic study of the CL generated during oxidation of thiamine with potassium ferricyanide in alkaline medium. A continuous flow-through system is used to develop a simple, fast and sensitive analytical procedure, which has been satisfactorily applied to the assay of the vitamin in pharmaceutical preparations.

EXPERIMENTAL

Apparatus

All measurements were made by using the CL analyser shown in Fig. 1. It consists of two basic units, the detector housing and the flow-through system.

The detector housing contains a spiral glass flow cell situated in front of the photomultiplier tube (PMT) at 90° to the direction of flow in the manifold. The spiral consisted of 3.5 turns of glass tubing (i.d. 2 mm) and its total height was 22 mm (length 90 mm). The distance of the spiral from the PMT was 2 mm and it was backed by a self-adhesive plane mirror 1 mm away from it for maximum light collection by the PMT. High voltage (–670 V) was supplied to the PMT (EMI 9783R, S-5 response) by two Heath Universal Power Supplies (0–500 V) connected in series. The output of the PMT was fed to a current-to-voltage converter (RCA CA 3140 operational amplifier). Damping was provided by inserting an RC circuit between the output of the converter and the recorder (Sargent–Welch, Model XKR).

The reacting solutions were transferred by a Technicon Proportioning Pump III and were mixed at a Y-junction, 20 mm before entering the flow cell. The final solution was carried into the flow cell by a Tygon tube with i.d. 2 mm. Samples were supplied to the manifold by a Technicon Sampler II with a 40-sample capacity.

*To whom correspondence should be addressed.

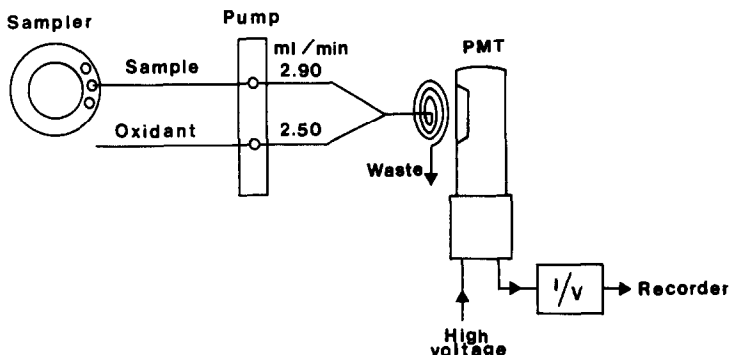


Fig. 1. Schematic diagram of continuous flow CL analyser (not to scale).

Reagents and solutions

Thiamine stock solution (0.0100M) was prepared by dissolving 0.355 g of thiamine hydrochloride monohydrate (Sigma) in water and then diluting to 100 ml final volume. More dilute solutions were prepared by the least possible number of dilution steps. All thiamine solutions were protected from light.

Ferricyanide stock solution (0.100M) was prepared by dissolving 16.5 g of potassium ferricyanide (Merck p.a.) in water and diluting to 500 ml final volume. Ferricyanide working solution (0.0050M) was prepared daily in 2.0M sodium hydroxide by appropriate dilution.

Procedures

Assays of dosage forms. The samples were prepared according to the U.S.P. procedures.²

Measurement procedure. The instrument was set at the optimized conditions shown in Fig. 1 but the sampling needle was kept in the wash position until the base line had been established on the recorder. The sampler was then activated and the analysis proceeded automatically. The calibration graph of emission intensity (I , mV) vs. concentration of thiamine (C , M or $\mu\text{g/ml}$) was constructed and the thiamine content of the samples was determined. Each standard or sample solution was measured three times. Two standards should be included after every 30 measurements.

RESULTS AND DISCUSSION

The oxidation of thiamine in alkaline medium proceeds by two competitive reactions to yield thiochrome and thiamine disulphide (Fig. 2). The latter is a non-fluorescent condensation product of thiamine. Since the best experimental conditions for the fluorimetric method and this

CL method seem to be similar, it is probable that only reaction (a) (Fig. 2) is chemiluminescent. However, this suggestion was not confirmed experimentally.

Previous workers⁶ have shown that potassium ferricyanide is the most suitable oxidant for CL measurement of thiamine. This observation was confirmed by us. Other oxidants operating in alkaline medium such as hypochlorite did not produce measurable CL emission with the analytical system used. When permanganate was introduced into the manifold, the emission intensity was so weak that only $5.0 \times 10^{-4}\text{M}$ thiamine gave a measurable signal. Hydrogen peroxide produced intense emissions but the recorded signals were irreproducible owing to oxygen formation and deterioration of the oxidant under alkaline conditions.

A series of experiments was conducted to establish the optimum analytical conditions for the chemiluminescent oxidation of thiamine by ferricyanide. The parameters studied were reagent and sample flow rate as well as oxidant and alkali concentration.

Effect of flow rate

The effect of flow rate on the emission intensity is shown in Fig. 3. The optimum values for reagent and sample flow rate are 2.50 and 2.90 ml/min, respectively. These flow rates allow the solutions to react for about 0.7 sec before entering the cell, depending on the manifold configuration.

Effect of ferricyanide concentration

The relative CL signals for $1.00 \times 10^{-3}\text{M}$ thiamine were 80.0, 88.0 and 84.0 for 0.0020, 0.0050 and 0.010M ferricyanide, respectively, in 1.0M sodium hydroxide, and 0.0050M ferricyanide is sufficient to oxidize thiamine and generate the most intense radiation. At higher

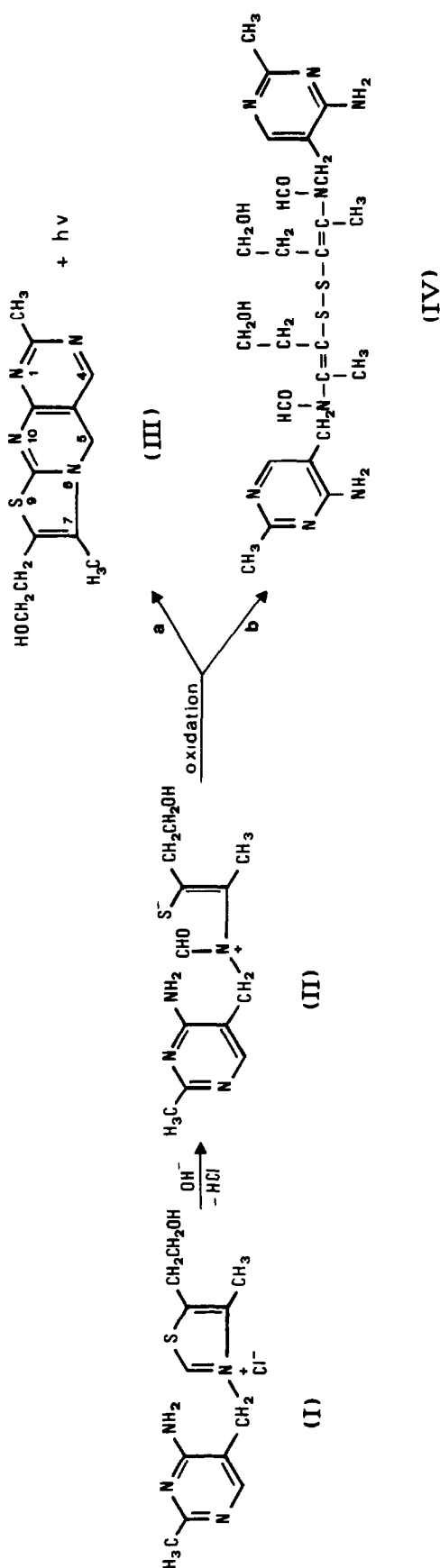


Fig. 2. Reaction pathways in thiamine oxidation.

concentrations the emission intensity decreases slightly. This is probably due either to decomposition of thiochrome or absorption of the radiation from the deeply coloured solution.

Effect of alkali concentration

A study of the effect of 0.50–3.0M sodium hydroxide on the CL intensity demonstrated that 2.0M sodium hydroxide was optimal. The relative CL signals for 1.00 × 10⁻³M thiamine in the presence of 0.0050M ferricyanide were 84.9, 85.0, 100.0 and 90.2 for 0.50, 1.0, 2.0 and 3.0M sodium hydroxide, respectively.

Analytical results

Figure 4 shows a typical recording for a series of thiamine standards. The sampling and wash times were set to 14 and 18 sec, respectively, allowing the introduction of 112 solutions into the manifold per hour. The sampling time is sufficient for the response to reach the value for the steady state. The wash time allows return to the base line between consecutive peaks. The calibration graph is linear in the range 2.00 × 10⁻⁵–5.00 × 10⁻⁴M thiamine nitrate or hydrochloride. The regression equation is $I = (-0.6 \pm 0.1) + (97621 \pm 523)C$; $r = 0.99991$, $n = 8$. The limit of detection (signal-to-noise ratio = 3) was 9.00 × 10⁻⁶M. The correlation coefficients for 6.00 × 10⁻⁵ and 3.00 × 10⁻⁴M thiamine were 1.8 and 0.7%, respectively ($n = 12$). Aqueous solutions of thiamine (hydrochloride and nitrate) were analysed as samples of unknown concentration with a mean relative error of 1.6% (range 0.2–2.1%).

Interference studies

In order to apply the method to the assay of thiamine in dosage forms, the effect of some common excipients and coexisting compounds in pharmaceutical preparations was studied by analysing synthetic sample solutions containing 20.0 and 100.0 µg/ml of thiamine hydrochloride and excess amounts of each potential interferent. The undissolved material, if any, was filtered off before measurement. The results are shown in Tables 1 and 2. Ascorbic acid is the only serious interferent since it reacts with, and therefore consumes, ferricyanide. An attempt was made to reduce its effect by increasing the concentration of oxidant to 0.050M to counterbalance its consumption by ascorbic acid. However, the interference was not eliminated (Table 2). Therefore, the method can not be applied to samples that also contain

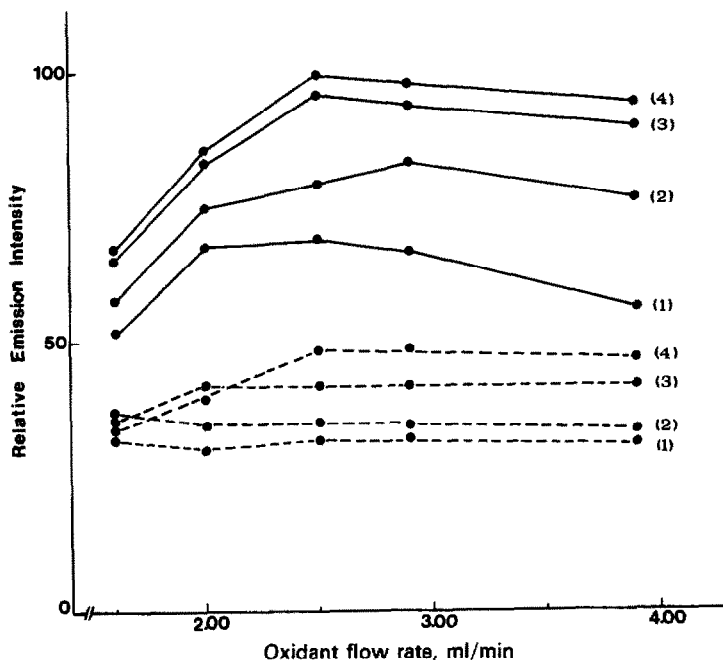


Fig. 3. Effect of oxidant flow rate on the CL intensity from 5.00×10^{-4} (broken line) and $1.00 \times 10^{-4} M$ (solid line) thiamine hydrochloride at (1) 1.60, (2) 2.00, (3) 2.50, and (4) 2.90 ml/min sample flow rate.

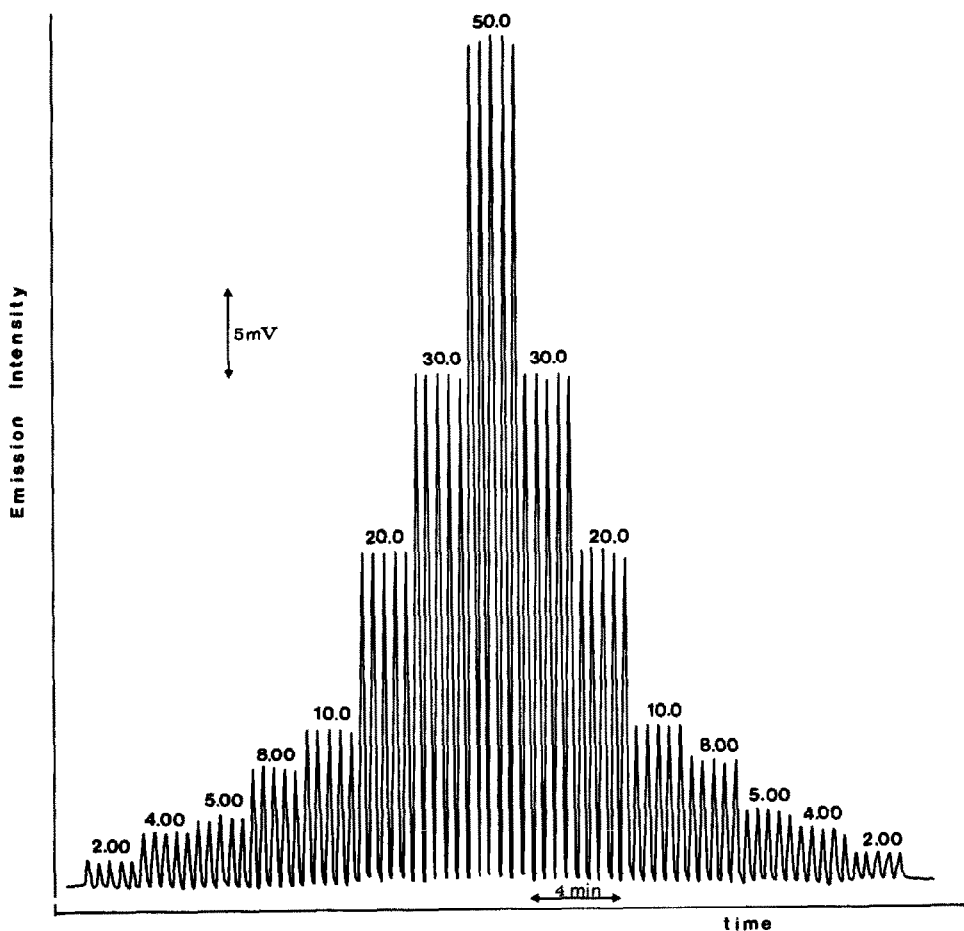


Fig. 4. Typical recorder output for the ferricyanide-thiamine CL reaction under the recommended conditions (the numbers above each set of peaks multiplied by 10^{-5} correspond to the thiamine molarity).

Table 1. Analytical results for two levels of thiamine hydrochloride (A, 20 $\mu\text{g/ml}$; B, 100 $\mu\text{g/ml}$) in solutions containing 10 times as much additive (mean of 3 results)

Additive	Recovery of thiamine, %	
	A	B
Glucose	99.2	102.0
Galactose	101.0	101.6
Lactose	103.5	102.8
Sugar	102.5	103.5
Sorbitol	102.5	98.7
Carbowax*	98.5	98.7
Carbopol†	101.0	103.3
Starch	100.5	98.6
Talc	102.2	98.6
NaCl	102.0	103.2
CaCl ₂	102.0	100.4
CaSO ₄	103.5	100.1
KH ₂ PO ₄	95.0	97.1
EDTA	100.0	102.1
CAHP‡	99.0	100.1
Magnesium stearate	96.0	95.6
Sodium lauryl sulphate	98.0	100.0

*Polyethylene glycol 4000.

†Carboxypolymethylene.

‡Cellulose acetate hydroxyphthalate.

ascorbic acid. Riboflavine interferes since its coloured solution absorbs the emitted radiation. The sensitivity of the method allows extended dilution and, thus, the effect is reduced (Table 2).

Accuracy

The accuracy of the proposed continuous flow CL method was examined by performing recovery experiments on solutions from thiamine formulations (Table 3). A mean recovery of 100.2% (range: 98.0–103.4%) was found. The method was also evaluated by analysing commercial formulations of thiamine. The results were compared with those obtained with the B.P. gravimetric method.⁷ A satisfactory agreement was obtained (Table 4) with a mean relative difference of 2.4% (range: 0.5–3.7%).

CONCLUSIONS

The proposed automated CL method is very simple, accurate and highly selective,

Table 2. Analytical results for thiamine hydrochloride (A, 20 $\mu\text{g/ml}$; B, 100 $\mu\text{g/ml}$) in solutions containing some other vitamins (mean of 3 results)

Vitamin	Concentration ratio (vitamin/thiamine)	Recovery of thiamine, %	
		A	B
Cyanocobalamin	0.2	99.9	98.3
Riboflavine	1	97.8	82.6
Nicotinamide	5	100.6	97.6
Pyridoxine·HCl	5	102.8	101.8
Ascorbic acid	10	0 (16.8)*	9.9 (18.8)*

*Measurement with 0.050M ferricyanide instead of 0.0050M.

Table 3. Recovery experiments for thiamine hydrochloride added to sample solutions of commercial formulations

Formulation	Thiamine·HCl, $\mu\text{g/ml}$			Recovery, % ($n = 3$)
	Initially present	Added	Recovered	
<i>Tablets:</i>				
Benerva	39.1	50.0	50.5	101.0
		100.0	102.6	102.6
<i>Elixirs:</i>				
Becozyme	22.4	50.0	51.4	102.8
		100.0	98.9	98.9
<i>Injections:</i>				
Benerva	29.9	50.0	50.1	100.2
		100.0	98.5	98.5
Multi B	20.6	50.0	49.8	99.6
		100.0	98.2	98.2
Vioneurin 6F	24.3	50.0	50.4	100.8
		100.0	98.7	98.7
Vioneurin F	45.2	50.0	50.7	101.4
		100.0	98.0	98.0
Neurobion	26.9	50.0	51.3	102.6
		100.0	101.7	101.7
Becozyme	21.9	50.0	51.7	103.4
		100.0	98.6	98.6
Triforte	51.3	50.0	49.4	98.8
		100.0	98.1	98.1
			Average	100.2

Table 4. Determination of thiamine hydrochloride in commercial formulations by the proposed method and the official B.P. method

Formulation	Thiamine, mg			Relative difference %
	Claimed*	Found		
		Proposed method \pm sd† ($n = 3$)	Official method	
<i>Tablets:</i>		(mg/tablet)		
Benerva	300	306.0 \pm 3.0	300.2	+1.9
Multi B	15	14.4 \pm 0.2	14.6	-1.4
<i>Injections:</i>		(mg/injection)		
Becozyme	10	10.3 \pm 0.1	10.5	-1.9
Multi B	20	19.7 \pm 0.2	19.0	+3.7
Vioneurin 6F	50	49.8 \pm 0.5	51.6	-3.5
Neurobion	100	107.1 \pm 1.5	106.6	+0.5
Benerva	100	107.6 \pm 1.4	104.3	+3.2
Vioneurin F	250	259.1 \pm 3.1	250.7	+3.3
Triforte	250	258.0 \pm 2.8	253.1	+1.9
			Average	2.4

*Each formulation also contains: Becozyme, elixir (5 ml): 2 mg riboflavine, 20 mg nicotinamide, 2 mg pyridoxine, 3 mg dexpanthenol; injection (2 ml): 4 mg riboflavine, 40 mg nicotinamide, 4 mg pyridoxine, 8 μ g cyanocobalamin, 0.5 mg biotin, 6 mg dexpanthenol; Multi B, injection (2 ml): 6 mg pyridoxine, 5 mg benzyl alcohol; Vioneurin 6F, injection (3 ml): 250 mg pyridoxine, 10 mg cyanocobalamin; Vioneurin F, injection (3 ml): 1 mg cyanocobalamin; Neurobion, injection (3 ml): 100 mg pyridoxine, 1 mg cyanocobalamin; Triforte, injection (3 ml): 1 mg cyanocobalamin, 100 mg pyridoxine.

†sd = standard deviation.

since various accompanying substances do not interfere. Ascorbic acid is the only severe interferent but it is not very commonly found in thiamine formulations, although it could often be present in multivitamin formulations. An additional advantage of the method is that one calibration graph allows the determination of thiamine as either the hydrochloride or the nitrate.

In comparison with the manual CL method,² this method has all the advantages of continuous flow CL methods.⁸ The apparatus is simple compared to fluorescence instruments. In conclusion, CL seems to be a more attractive procedure for the determination of thiamine in pharmaceutical preparations.

REFERENCES

1. R. B. Roy, J. K. Foreman and P. B. Stockwell, in *Topics in Automatic Chemical Analysis*, Horwood, Chichester, 1979.
2. United States Pharmacopeial Convention, *U.S. Pharmacopeia*, XXI Ed., Mack, Easton, PA., 1985.
3. A. J. Khouri and L. J. Cali, *Automation in Anal. Chem., Technicon Symp.*, pp. 22-26. Mediad, White Plains, New York, 1966.
4. B. Karlberg and S. Thelander, *Anal. Chim. Acta*, 1980, **114**, 129.
5. M. A. Ryan and J. D. Ingle, Jr., *Anal. Chem.*, 1980, **52**, 2177.
6. G. P. Chernysh, R. P. Poponina and V. I. Buntushkin, *J. Anal. Chem. USSR*, 1976, **31**, 1475.
7. *British Pharmacopoeia*, H.M. Stationery Office, London, 1980.
8. W. R. Seitz, *CRC Crit. Rev. Anal. Chem.*, 1981, **13**, 1.

FLOW-THROUGH SENSOR FOR THE FLUORIMETRIC DETERMINATION OF CYANIDE

DANHUA CHEN,* M. D. LUQUE DE CASTRO and M. VALCARCEL

Department of Analytical Chemistry, Faculty of Sciences, University of Córdoba, 14004 Córdoba, Spain

(Received 18 December 1989. Revised 23 May 1990. Accepted 31 May 1990)

Summary—A fluorimetric method for the determination of cyanide, based on its reaction with pyridoxal-5-phosphate and the use of an anion-exchange resin (QAE Sephadex) located in the detector flow-cell, is proposed. The merging-zone flow-injection manifold used allows simultaneous injection of the sample and reagent, development of the reaction along the transport system, and retention of the reaction product in the flow-cell. The calibration graph for cyanide is linear over the range from 50 ng/ml to 3.0 µg/ml and the relative standard deviation and sampling frequency are 1.4% (for 2 µg/ml cyanide) and 10 per hr, respectively. The selectivity of the method is much better than that of the conventional fluorimetric and photometric flow-injection methods for cyanide.

Flow-through chemical sensors have roused the interest of analytical chemists in recent years.¹ This type of sensor is made by filling a flow-through cell with a suitable support, usually an ion-exchange resin or controlled-pore glass beads with diameters of about 100 µm. Chemical reaction (and/or physical retention) and optical detection take place at a microzone in the sensor and the analytical signal is obtained as the sample passes through the cell and comes into direct contact with the support. Flow-through sensors can be classified into three groups according to the reaction or retention mechanism used in the flow-cell. (a) Dynamic retention of the analyte,² which is then detected by means of its native absorbance or fluorescence. (b) Permanent immobilization of the reagent or catalyst on the support by chemical binding, such as in the photometric determination of copper,³ the chemiluminescence determination of peroxides^{4,5} and peroxyoxalate,⁶ the fluorescence determination of sodium, potassium and calcium,⁷ and the enzymatic assays for adenosine-5'-triphosphate, creatine phosphokinase and creatine phosphate,⁸ glucose⁹ and ethanol.¹⁰ (c) Transient retention of a reaction product previously formed in the manifold, as in the determination of iron,¹¹ chromium,¹² bismuth¹³ and fluoride.¹⁴ The analytical performance is always improved, relative to that of conventional flow-injection methods, especially as regards sensitivity.

The determination of cyanide is of significance in environmental research and industry. Flow-injection analysis has been applied for this purpose,¹⁵⁻³³ with electrochemical¹⁵⁻²³ and optical²⁴⁻³³ detection. Distillation or gas diffusion separations are generally required to overcome interference problems, however. The chemiluminescence system developed by Yamada and co-workers²⁴⁻²⁶ has the highest sensitivity reported, but its selectivity is limited by intrinsic features of the detection procedure used.²⁴ Spectrophotometric methods²⁷⁻³² for cyanide determination are superior to electrochemical detection as they are subject to fewer memory effects. However, anions with chemical properties similar to those of cyanide, such as iodide, bromide and thiocyanate, interfere seriously with both spectrophotometric²⁷⁻²⁹ and electrochemical¹⁵ methods, although determinations of two or three species in the same sample have been accomplished.³⁰⁻³² In this respect a spectrofluorimetric method developed in our laboratory seems to be better suited to the determination of cyanide.

The present work was aimed at enhancing the sensitivity and selectivity of cyanide determination, by using a flow-through chemical sensor. The determination is based on the reaction of cyanide with pyridoxal-5-phosphate. The oxidation product, 4-pyridoxic acid-5-phosphate,³⁴ resulting from the catalytic action of cyanide in the presence of oxygen, is formed in the flow-injection manifold and led to a flow-through cell filled with an anion-exchange resin, QAE Sephadex. Use of 0.05M

*Permanent address: Department of Chemistry, Wuhan University, Wuhan, People's Republic of China.

hydrochloric acid in the reagent system enhances the sensitivity. The fluorescence signal is much higher than that obtained without the ion-exchanger present and the selectivity is also improved. The interaction between the reaction product, the resin and the hydrochloric acid solution indicates that the signal-enhancing mechanism is completely different from that typical of retention procedures based on flow-through chemical sensors.²⁻¹⁴

EXPERIMENTAL

Reagents

A potassium cyanide solution (1.000 g/l. cyanide) and a 0.005M pyridoxal-5-phosphate solution, (prepared daily by dissolving 0.1326 g of the reagent in 100 ml of 0.25M $H_2PO_4^-/HPO_4^{2-}$ buffer, pH 7.60) were used. All the resins tested were from Sigma.

All reagents were of analytical grade and solutions were prepared with doubly distilled water.

Apparatus

Fluorescence measurements were made with a Kontron SFM 25 spectrofluorimeter equipped with a Radiometer REC 80 recorder. A Gilson Minipuls-2 peristaltic pump, a Rheodyne Teflon double rotary injection-valve system and a fluorescence flow-through cell were used to construct the manifold. The cell (10 μ l inner volume) was blocked with a porous plastic plug and the light-path was filled with QAE Sephadex anion-exchanger, 40–120 μ m bead size (Fig. 1).

Procedure

Cyanide, at a concentration of 0.05–3.0 μ g/ml, and 0.005M pyridoxal-5-phosphate solution are simultaneously injected by the double-valve system (sample volume, 500 μ l) into the manifold shown in Fig. 2C. The reaction occurs in the 500-cm long reactor tube, the product formed being merged with a stream of 0.05M hydrochloric acid before reaching the flow-cell. The fluorescence signal (λ_{ex} 318 nm, λ_{em} 455 nm) yielded by the analyte is corrected by subtraction of the blank signal. The baseline is automatically restored by passage of hydrochloric acid through the flow-cell.

RESULTS AND DISCUSSION

Flow-injection manifold

Three different configurations were tested (Fig. 2). In configuration A, pyridoxal-5-phosphate (Py-5P) was first immobilized on the QAE Sephadex resin in the flow-cell by passing a stream of 0.005M Py-5P through it for 1 hr, but when a cyanide solution was injected into a carrier stream of water, no signal was obtained, irrespective of whether the carrier stream was merged with 0.05M hydrochloric acid or pH 7.6 phosphate buffer. This can be accounted for as follows. First, the bolus of cyanide dwelt in the flow-cell too short a time for formation of a detectable quantity of product. Furthermore, the immobilization of the Py-5P was not permanent and there was not enough reagent for the reaction. Evidently it was necessary for the reaction to take place before the detector was reached. Hence, Py-5P was continuously passed

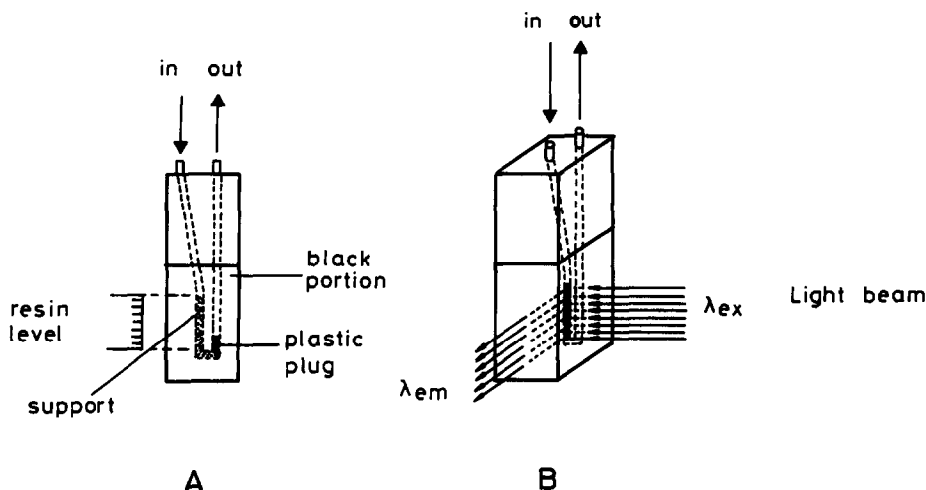


Fig. 1. Fluorescence flow-through cell filled with support: A, front view; B, perspective.

along the main channel as in configuration B. The reaction took place in the reactor, but the signal from the product trapped on the resin was very small and no better than that obtained without the resin. This was because the resin was saturated with the Py-5P (which was continuously passed through it), so the reaction product was difficult to absorb. This led us to design configuration C, where the cyanide and a fixed amount of Py-5P are injected simultaneously. The signal obtained is considerably improved, as the product is formed before it reaches the flow-cell, and is retained on the resin when it gets there. After the maximum signal has been obtained, the hydrochloric acid elutes the product and the baseline is restored. The blank value is obtained by injecting only the reagent.

It is interesting that there are two optimal pH values in the system: one for the derivatization reaction (pH 7.6, phosphate buffer) in reactor L_1 , and the other (pH < 2) for enhancing the fluorescence of the reaction product and eluting it rapidly from the flow-cell.

Choice of support

Various resins were tested under the same experimental conditions (Fig. 3), including anion-exchangers (DEAE Sephadex, Dowex 1 X2-200, QAE Sephadex) and neutral sorbents (XAD-4 and XAD-7). The blank signal was first obtained and then that corresponding to 2.0 $\mu\text{g}/\text{ml}$ cyanide (in triplicate). Conventional flow-injection analysis without a support in the flow-cell was used as a reference to evaluate the support efficiency. Slight differences between

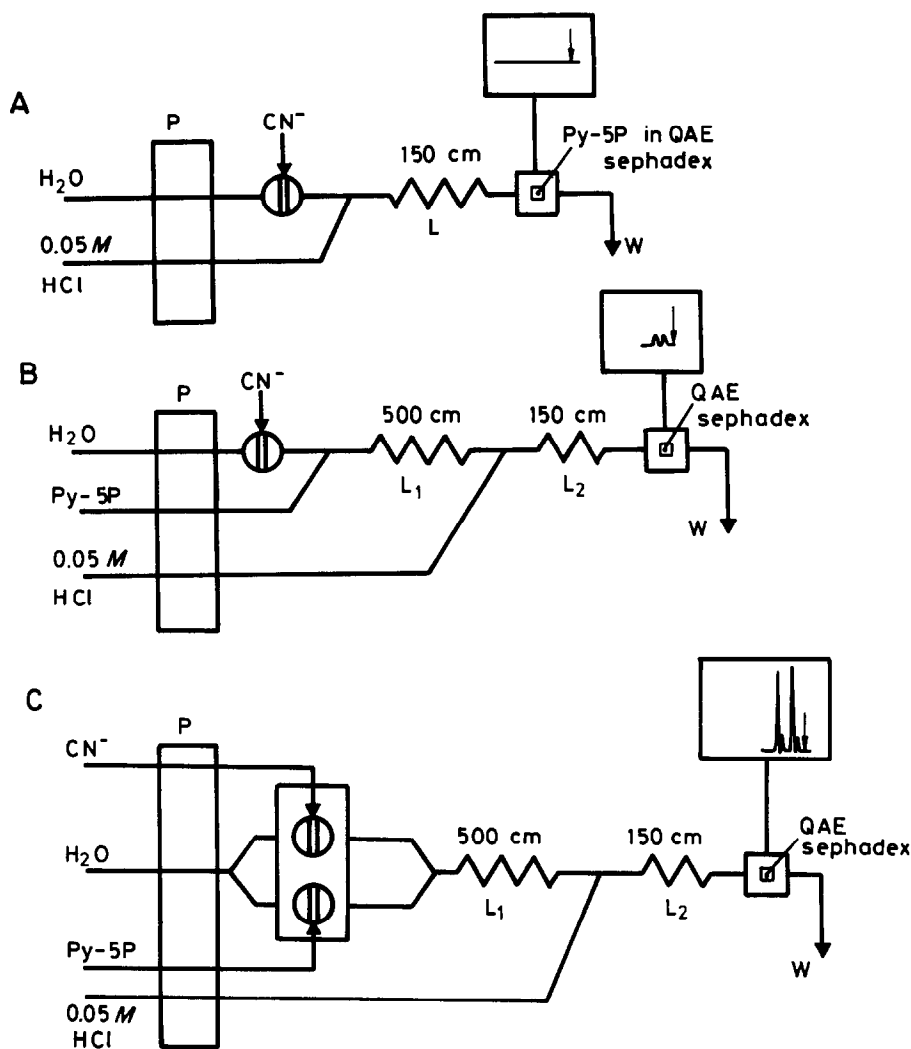


Fig. 2. Configurations tested for the determination of cyanide with a flow-through sensor: P, pump; L, reactors; W, waste.

the blank signal and that yielded by the cyanide solution were observed when XAD-4 and XAD-7 were used, but the signals obtained for cyanide were no better (or were even worse) than the signal obtained without resin. This was because the resin takes up most of the space in the flow-cell, so if it is inactive it reduces the signal intensity for the product in the solution phase. Anion-exchangers proved to be active in retention because the reaction product, 4-pyridoxic acid-5-phosphate, was negatively charged under the working conditions. Among the anion-exchangers, QAE Sephadex was the best both in reproducibility (compared with the other two resins) and in signal intensity (compared with DEAE Sephadex).

Type of carrier

Experiments showed the best carrier for the injections from the double valve to be distilled water, which has no influence on the pH of the chemical reaction. The carrier used in the third channel influenced the signal value, so it was optimized (Fig. 4). Small signals were obtained when only water was used; the signal intensity increased (although the baseline was also raised) when hydrochloric acid/sodium acetate buffer

was used as the carrier. This gave a clue that an acidic medium might favour the retention and detection steps, so different concentrations of hydrochloric acid were tested. The signal intensity increased considerably when dilute hydrochloric acid was used as the medium. The efficiency of elution of the product from the resin increased with increase in acid concentration, and this resulted in inadequate signal enhancement, while higher concentrations were excessive for elution, so the retention was somehow affected. Conventional FIA experiments with water and 0.05M hydrochloric acid as carriers (flow-cell without resin) were also performed to check the influence of the acid on the reaction. The results indicated that the signal was not significantly affected, so the role of the hydrochloric acid in this chemical sensor is to enhance the signal and the elution.

FIA parameters

The following values for certain FIA parameters were selected as a compromise between sensitivity and analytical efficiency: sample loop volumes both 500 μ l; reactor lengths L_1 500 cm, L_2 150 cm; flow-rate 0.5 ml/min in each channel.

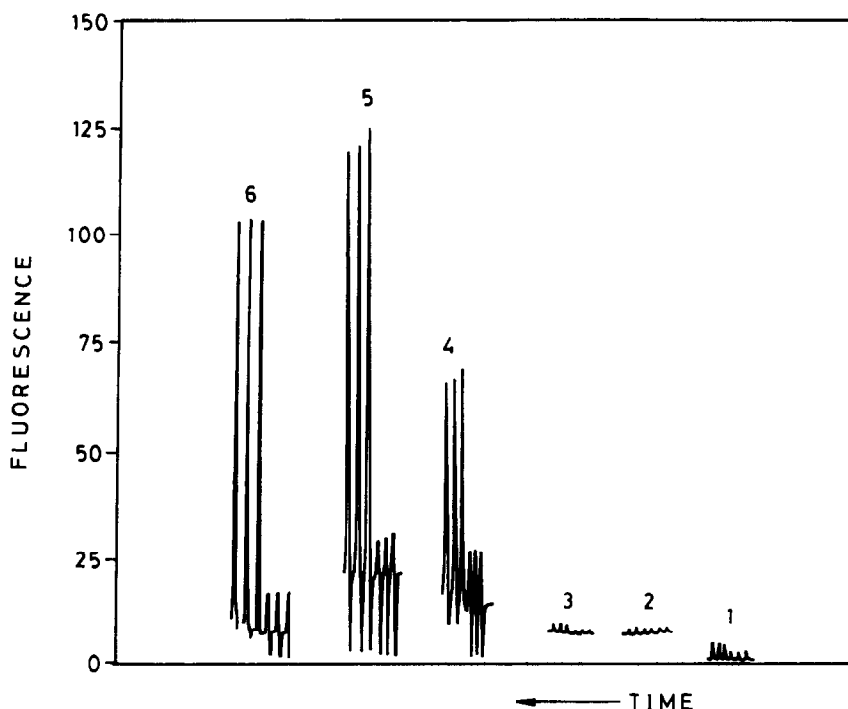


Fig. 3. Behaviour of the different types of resins used for retention of the reaction product of the pyridoxal-5-phosphate/cyanide system. $[\text{Py-5P}] = 5 \times 10^{-3} \text{M}$; $[\text{cyanide}] = 0$ for blank and $2.0 \mu\text{g/ml}$ for analytical signal. (1) Without resin; (2) XAD-4; (3) XAD-7; (4) DEAE Sephadex; (5) Dowex 1(X2-200); (6) QAE Sephadex.

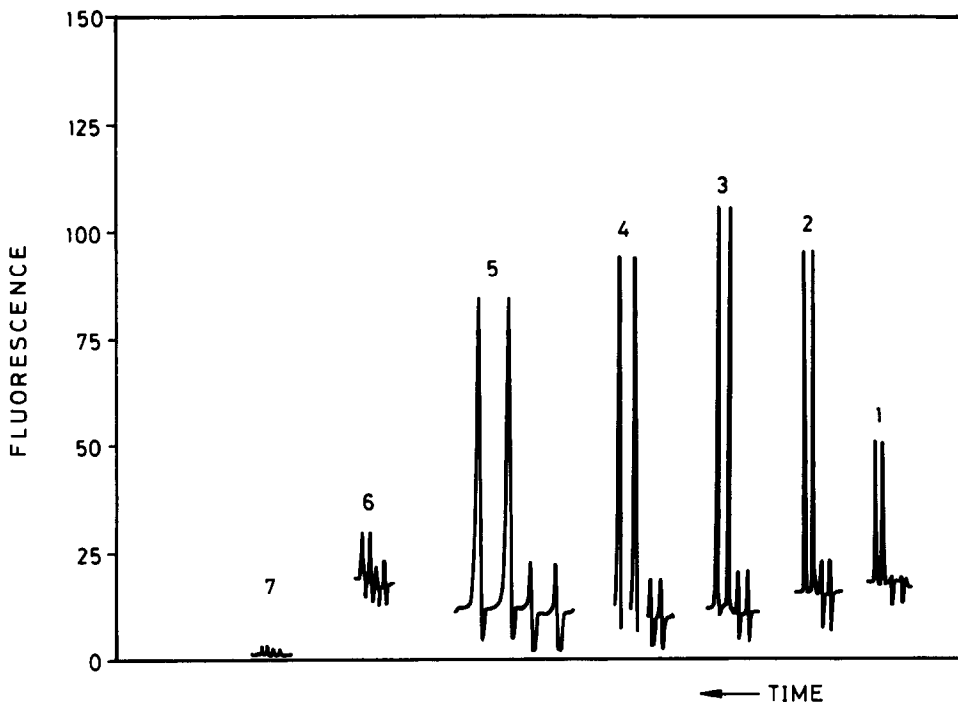


Fig. 4. Influence of the different carriers and/or their concentrations on the analytical signal. $[\text{Py-5P}] = 5 \times 10^{-3} M$; $[\text{cyanide}] = 0$ for blank and $2.0 \mu\text{g/ml}$ for analytical signal. (1) $0.2 M$ HCl; (2) $0.1 M$ HCl; (3) $0.05 M$ HCl; (4) $0.02 M$ HCl; (5) $0.01 M$ HCl; (6) HCl/sodium acetate buffer pH 3.7; (7) H_2O .

Sensitivity enhancement mechanism

The interaction between the reaction product, QAE Sephadex and dilute hydrochloric acid can be inferred from the recordings shown in Fig. 5. When only the reagent in phosphate buffer, or a plug of this buffer, was injected, the signal decreased as the plugs reached the detector, as a result of the change in the pH of the medium, because the baseline was established with the hydrochloric acid stream (the resin was more fluorescent in acid than in basic medium). After the plug of buffer had passed through the flow-cell the baseline was restored, but when the reagent plug passed through the cell, the carrier slightly increased the fluorescence of the retained reagent and a small peak was obtained prior to the elution. When the analyte and the reagent were simultaneously injected, the product formed along reactors L was retained in passing through the flow-cell, but the fluorescence only increased when the hydrochloric acid solution reached the flow-cell and formed the fluorescent product, which was then rapidly eluted.

QAE Sephadex seems to be much more selective towards the reaction product than to pyridoxal-5-phosphate, as the increase in the signal yielded by the reagent blank was only 3.6 times

larger than that obtained without resin, while the signal for the reaction product was 11.5 times more sensitive than that obtained without this support. Furthermore, the resin adsorbed no pyridoxal or its reaction product with cyanide (4-pyridoxolactone), as their maximum signals were obtained over the same interval as without resin, and no further signal increase was obtained on replacing the buffer with the acid solution.

Resin level

Different packing heights of QAE Sephadex resin in the flow-cell were tested. The signal increased with increasing resin level up to the recommended packing. Filling levels above this height had no influence on the signal intensity.

Calibration graph

The calibration graph (triplicate measurements for each point) was linear between 50 ng/ml and $3.0 \mu\text{g/ml}$ cyanide, with a slope of $41.5\% I_f \cdot \text{ml} \cdot \mu\text{g}^{-1}$ and an intercept of $1.9\% I_f$, with a regression coefficient of 0.9991. The relative standard deviation for 11 samples of $2 \mu\text{g/ml}$ cyanide, each injected in triplicate, was 1.4%. The sampling frequency achieved was 10/hr.

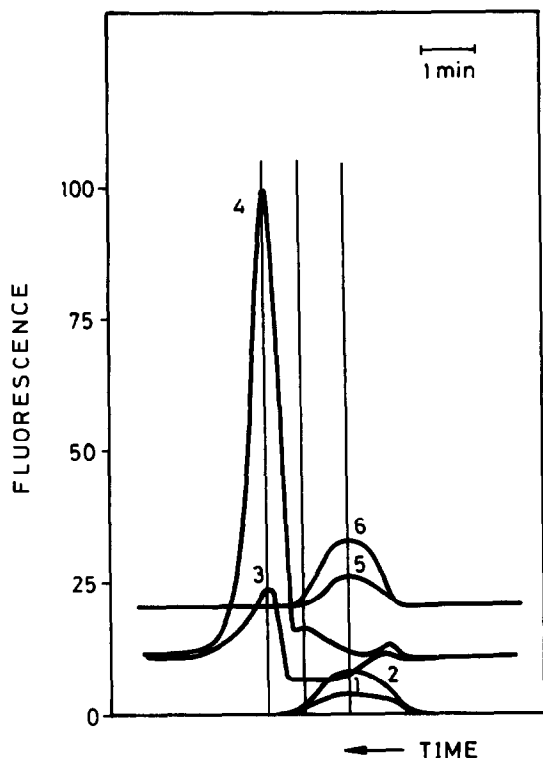


Fig. 5. Recordings obtained in the experiments performed to elucidate the mechanism of development of the analytical signal for the determination of cyanide by using configuration C in Fig. 2. From (1) to (4): [Py-5P] in $\text{H}_2\text{PO}_4^-/\text{HPO}_4^{2-}$ buffer, pH 7.6. Without resin: (1) blank, (2) 2.0 $\mu\text{g}/\text{ml}$ cyanide. With QAE Sephadex: (3) blank, (4) 2.0 $\mu\text{g}/\text{ml}$ cyanide. For (5) and (6), pyridoxal in $\text{H}_2\text{PO}_4^-/\text{HPO}_4^{2-}$ buffer, pH 7.6. With QAE Sephadex: (5) blank; (6) 2.0 $\mu\text{g}/\text{ml}$ cyanide.

Interferences

The influence of 20 cations and anions on the determination of cyanide was studied. The results are summarized in Table 1. The maximum level tolerated was taken as that causing a difference in signal of not larger than $\pm 5\%$. None of the anions and only some of the cations interfere with the determination: Fe(III), Fe(II) and Co(II) interfere seriously by forming complexes with cyanide. The selectivity is greatly improved relative to that of the conventional method³³ or the pyridine-barbituric acid method,²⁸ mainly because of the retention of the reaction product by the resin, and the consequent separation from the matrix.

CONCLUSION

The proposed method increases the sensitivity and selectivity for cyanide determination with flow-through chemical sensors.¹⁵⁻³³ The detection process is completely different from those

Table 1. Interference study

Ion	Proposed method	Ion-to-cyanide weight ratio	
		Conventional FIA methods	
		Fluorimetric ³³	Photometric ²⁸
PO_4^{3-}	400		100
I^-	100	75	1
Cl^-	800		100
Br^-	100	75	1
SCN^-	50	50	<1
CH_3COO^-	800*		100
SO_4^{2-}	400		100
NO_3^-	400		100
Cd(II)	200	35	50
Zn(II)	200	35	50
EDTA^{2-}	400		100
Sr(II)	200	35	
Mn(II)	40†	2	1
Cr(III)	40	100	
Ni(II)	20†	1	<1
Co(II)	1	1	<1
Cu(II)	10	1	<1
Fe(III)	<1	<1	<1
Fe(II)	<1	<1	
S^-	<1		

*Maximum ratio tested.

†In the presence of EDTA^{2-} .

used with flow-through chemical sensors based on analytical systems in which the reaction product is retained on the resin and the matrix is eluted. The signal is greatly increased by use of a hydrochloric acid medium.

Acknowledgements—The authors wish to express their gratitude to CICYT for financial support (Grant No. PA86-0146). One of them (D.C.) is grateful to the Dirección General the Investigación Científica y Técnica for financing his stay in Spain.

REFERENCES

1. M. Valcárcel and M. D. Luque de Castro, *Analyst*, 1990, **115**, 699.
2. K. Yosimura, *Anal. Chem.*, 1987, **59**, 2922.
3. F. Lázaro, M. D. Luque de Castro and M. Valcárcel, *Anal. Chim. Acta*, 1988, **214**, 217.
4. K. Holl and T. A. Nieman, *Anal. Chem.*, 1987, **59**, 869; 1988, **60**, 834.
5. P. van Zoonen, D. A. Kamminga, C. Gooiser, N. H. Velthorst and R. W. Frei, *Anal. Chim. Acta*, 1985, **167**, 249.
6. *Idem*, *Anal. Chem.*, 1986, **58**, 1245.
7. T. C. Turner, J. G. Cummings and W. R. Seitz, *ibid.*, 1989, **61**, 211.
8. P. J. Worsfold and A. Nabi, *Anal. Chim. Acta*, 1986, **179**, 307.
9. J. Růžička and J. Flossdorf, *ibid.*, 1989, **218**, 291.
10. P. Linares, M. D. Luque de Castro and M. Valcárcel, *ibid.*, in the press.
11. F. Lázaro, M. D. Luque de Castro and M. Valcárcel, *ibid.*, 1989, **219**, 231.
12. K. Yosimura, *Analyst*, 1988, **113**, 471.
13. *Idem*, *Bunseki Kagaku*, 1987, **36**, 656.

14. Danhua Chen, M. D. Luque de Castro and M. Valcárcel, *Anal. Chim. Acta*, in the press.
15. B. Pihlar, L. Kosta and B. Hristovski, *Talanta*, 1979, **26**, 805.
16. H. Ma, L. Jin and H. Yan, *Kexue Tongbao*, 1983, **28**, 1145.
17. P. W. Alexander, P. R. Haddad and M. Trojanowicz, *Anal. Chem.*, 1984, **56**, 2417.
18. T. P. Lynch, *Analyst*, 1984, **109**, 421.
19. H. Cui, Z. Zhu and Z. Fang, *Huanjing Huaxue*, 1984, **3**, 48.
20. B. Pihlar and L. Kosta, *Anal. Chim. Acta*, 1980, **114**, 275.
21. C. Ukumoto, M. Nagashima, S. Mizoiri, M. Kazama and K. Akiyama, *Eisei Kagaku*, 1984, **30**, 7.
22. A. G. Fogg and R. M. Alonso, *Analyst*, 1987, **112**, 1071.
23. E. Figuerola, A. Florido, M. Aguilar, J. de Pablo and S. Alegret, *Anal. Chim. Acta*, 1988, **215**, 283.
24. X. Z. Wu, M. Yamada, T. Hobo and S. Suzuki, *Anal. Chem.*, 1989, **61**, 1505.
25. M. Ishii, M. Yamada and S. Suzuki, *Anal. Lett.*, 1986, **19**, 1591.
26. *Idem*, *Bunseki Kagaku*, 1987, **36**, 316; 1986, **35**, 542, 956.
27. Z. Zhu and Z. Fang, *Anal. Chim. Acta*, 1987, **198**, 25.
28. A. Ríos, M. D. Luque de Castro and M. Valcárcel, *Talanta*, 1984, **31**, 673.
29. E. Figuerola, A. Florido, M. Aguilar and J. de Pablo, *Z. Anal. Chem.*, 1988, **331**, 620.
30. A. Tanaka, K. Mashiba and T. Deguchi, *Anal. Chim. Acta*, 1985, **214**, 259.
31. A. Ríos, M. D. Luque de Castro and M. Valcárcel, *Analyst*, 1984, **109**, 1487.
32. J. A. Swileh, *Anal. Chim. Acta*, 1989, **220**, 65.
33. P. Linares, M. D. Luque de Castro and M. Valcárcel, *ibid.*, 1984, **161**, 257.
34. N. Oishi and S. Fukui, *Arch. Biochem. Biophys.*, 1968, **128**, 606.

SOLUTION INTERACTIONS AND SOLID-MATRIX INTERACTIONS IN β -CYCLODEXTRIN SOLID-MATRIX LUMINESCENCE

MARSHA D. RICHMOND and ROBERT J. HURTUBISE*

Chemistry Department, University of Wyoming, Laramie, WY 82071-3838, U.S.A.

(Received 25 January 1990. Revised 14 March 1990. Accepted 19 March 1990)

Summary—A variety of liquid chromatographic, solution fluorescence, and extraction data were obtained in an attempt to correlate solution interactions with solid-matrix interactions for solute- β -cyclodextrin complexes. From the chromatographic data, dissociation constants were calculated for the complexes. Fluorescence spectral characteristics were obtained for sodium chloride, glucose, and β -cyclodextrin solutions of several solutes. In addition, extraction experiments were performed in an attempt to remove the solutes from the β -cyclodextrin solid matrix. Generally, the results revealed that there were no simple correlations between the solution data and solid-matrix luminescence data. However, the extraction results yielded important information related to the solute interactions in the solid matrix.

Cyclodextrins (CDs) are cyclic oligosaccharides comprised of glucose units connected by α -1,4 linkages. The three most commonly used are α -, β -, and γ -cyclodextrins, made up of 6, 7, and 8 glucose units, respectively. The cyclic nature of cyclodextrins gives them the shape of a truncated cone. Cyclodextrins possess a hydrophobic interior cavity and the top and bottom of the cone are lined with hydroxyl groups which provide a hydrophilic exterior environment.¹ The ability of cyclodextrins to sequester or include molecules within their hydrophobic cavity has led to their increasing use in a variety of research projects.²⁻⁶

Cyclodextrins have been used both as a component of the mobile phase and bonded to the stationary phase in chromatography.⁷⁻¹¹ Also, cyclodextrins have been effective in the separation of enantiomeric mixtures,¹² and the formation constants for the inclusion complexes of several compounds have been determined by high performance liquid chromatography (HPLC).¹³ Solution fluorescence has been used to study interactions between CDs and analyte species.¹⁴⁻¹⁷ Patonay *et al.*¹⁸ have employed pyrene as a fluorescent probe to investigate cyclodextrin complexation in the presence of various alcohols. Cline Love and co-workers^{19,20} have used cyclodextrins in the presence of a heavy atom to induce room-temperature

phosphorescence (RTP) from solutions of polyaromatic hydrocarbons (PAHs) and nitrogen heterocycles. Alak *et al.*²¹ demonstrated that filter paper pretreated with cyclodextrin resulted in enhanced RTP signals from the surface. Bello and Hurtubise²² showed that α -cyclodextrin/sodium chloride (α -CD/NaCl) mixtures could be used to analyse mixtures of PAHs at ng levels.

Recently, Richmond and Hurtubise²³ demonstrated that β -CD/NaCl mixtures also induced RTP from a variety of compounds. They reported that unlike α -CD/NaCl mixtures, which showed maximum RTP from the matrix when a saturated solution of α -CD was used in a sample preparation step, the signal intensity from the β -CD/NaCl matrix continued to increase after saturation of the 50:50 methanol/water solvent employed in the sample preparation step. An increase in RTP intensity was found for mixtures containing ten times the amount of β -CD necessary for saturation of the solution. This demonstrated that maximization of the signal required the solid matrix to contain more β -CD than would correspond to saturation of the test solution used to provide effective packing of the dry matrix for optimum RTP signals. This paper presents the results of studies undertaken to obtain better understanding of the relationships among solution interactions of the analyte, the 50:50 MeOH/H₂O solvent, and the 30% β -CD/NaCl mixture used in solid-surface luminescence work.

*To whom all correspondence should be addressed.

EXPERIMENTAL

Instrumental

All fluorescence spectra in solution were obtained with a Fluorlog 2 + 2 spectrofluorometer (Spex Industries, Edison, NJ). The detector was a water-cooled R928 photomultiplier tube (Hamamatsu Corp., Middlesex, NJ). The source was an ozone-free 450-W xenon lamp.

The absorbance values in the determination of unbound analyte on the β -CD/NaCl matrix were obtained with a Hitachi 100-80 spectro-photometer (Sunnyvale, CA).

The liquid chromatographic system employed for the determination of formation constants consisted of a Waters (Milford, MA) Model 6000A pump connected to a Waters U6K injector valve. The detector was a Waters Associate Model 440 fixed wavelength absorbance detector set at 254 nm. The recorder used was an Omniscrite recorder (Houston Instruments, Austin, TX). The column employed was a 10 μ m C_{18} (300 mm \times 3.9 mm) column (Phenomenex, Torrance, CA).

Reagents

Phenanthrene, 4-phenylphenol, and *p*-amino-benzoic acid (PABA) were purchased from Aldrich (Milwaukee, WI) and recrystallized from ethanol prior to use. Benzo(f)quinoline [B(f)Q] and benzo(a)pyrene [B(a)P] were gold-label quality from Aldrich and used as received. The methanol was HPLC grade from Burdick and Jackson (Muskegon, MI), and the water used for the solution fluorescence studies was also obtained from Burdick and Jackson. The diethyl ether employed in the extraction experiments was HPLC grade (99.9%) and purchased from Aldrich. The β -CD was from Aldrich and sodium chloride from J. T. Baker (Phillipsburg, PA). The glucose was A.C.S. reagent grade and was purchased from Aldrich.

Procedures

HPLC. Methanol and water were filtered through a Millipore type FH 0.5 μ m filter. The β -CD was vacuum dried at 0.78 atm pressure and 75° for 8 hr prior to use. The β -CD was then dissolved in purified water, and methanol was added to it. Solutions of 1, 2, 3, and 4mM β -CD in 50:50 v/v MeOH/H₂O were used as mobile phases. The concentration of the samples injected was 1 mg/ml. The void volume was determined by using a methanol solution of potassium nitrite. A flow rate of 1 ml/min

was used in the experiments with PABA, 4-phenylphenol, phenanthrene, and B(f)Q. A flow rate of 2 ml/min for 50:50 MeOH/H₂O and 1.5 ml/min for 4mM β -CD in 50:50 MeOH/H₂O was used for B(a)P.

Solution fluorescence. To obtain solution fluorescence spectra appropriate amounts of β -CD were dissolved in MeOH/H₂O (50:50) to yield 1 and 4mM β -CD solutions. A specific volume of freshly prepared analyte solution was added to the β -CD solution and the mixture brought to known volume with MeOH/H₂O (50:50) to give a 0.1 μ g/ml analyte concentration. The effect of sodium chloride on the solution fluorescence spectrum was determined by examining corresponding β -CD solutions made up with MeOH/H₂O (50:50) saturated with sodium chloride. The effect of glucose was similarly examined with an MeOH/H₂O (50:50) glucose solution containing the same concentration of hydroxyl groups as the β -CD solution, but no sodium chloride.

Ether extraction. Solutions (800 μ g/ml) of PABA, 4-phenylphenol, phenanthrene, B(f)Q and B(a)P were prepared. Five μ l of analyte solution and 0.2 ml of MeOH/H₂O (50:50) were added to each of three test-tubes, the first containing only this solution, the second the solution plus sodium chloride, and the third the solution plus 30% β -CD/NaCl mixture. All three tubes were sonicated, then heated in an oven at 110° for 40 min, removed from the oven, and cooled in a desiccator. The contents of the tubes were then extracted with three 1-ml portions of diethyl ether, each set of extracts being combined in a separate 5-ml standard flask and diluted to volume with diethyl ether. The absorbances were measured and the amounts of analyte present read from a calibration graph prepared by measuring the absorbances of ether solutions of the analytes in the concentration range 0-800 μ g/ml. This allowed determination of unbound analyte on the 30% β -CD/NaCl surface. The experiment with analyte alone was repeated three times.

RESULTS AND DISCUSSION

High performance liquid chromatography (HPLC)

All the compounds except B(a)P showed a decrease in retention with increasing β -CD concentration in the reversed-phase chromatographic system employed. B(a)P was very strongly retained on the C_{18} column and was not

eluted after 6 hr at a flow rate of 2 ml/min with 50:50 MeOH/H₂O, or after 5.5 hr at a flow rate of 1.5 ml/min with 4mM β -CD in 50:50 MeOH/H₂O. This indicated very little interaction between B(a)P and β -CD under the experimental conditions. B(a)P was removed from the column with pure methanol.

Table 1 shows the effect of increasing β -CD concentration on the capacity factors (k') for the four compounds studied. From Table 1, it can be seen that PABA showed essentially no change in k' as the concentration of β -CD increased in the mobile phase. This indicated a rather weak interaction of PABA with β -CD in the 50:50 MeOH/H₂O mobile phase. Because the k' value is so small for PABA in the mobile phase without β -CD, any meaningful correlations with β -CD added to the mobile phase are hard to develop. For example, the change in k' when the β -CD concentration in the mobile phase increases from 0 to 4mM is only 0.11. Obviously, PABA is more strongly attracted to the mobile phase than to the stationary phase or β -CD. This is most likely due to the tendency of the polar PABA molecule to form hydrogen bonds with the MeOH/H₂O mobile phase.

4-Phenylphenol showed the most dramatic change in capacity factor (46%) with increasing β -CD concentration from 0 to 4mM. This is indicative of relatively strong interaction between 4-phenylphenol and β -CD in solution. B(f)Q demonstrated little change in capacity factor with increasing β -CD concentration; however, phenanthrene showed an 18% change in capacity factor with increase from 0 to 4mM β -CD. In general, the results for PABA, B(f)Q, and phenanthrene implied weak interactions between these compounds and β -CD in the mobile phase. B(f)Q and phenanthrene are more bulky than PABA and 4-phenylphenol and would only partially fit into the β -CD cavity.²⁴

The dissociation constants for the β -CD complexes of 4-phenylphenol, phenanthrene, and B(f)Q were obtained by the approach discussed

Table 1. Capacity factors (k') for model compounds with and without β -CD present in the mobile phase

Compounds	50:50 MeOH/H ₂ O				
	0*	1	2	3	4
PABA	0.36	0.29	0.24	0.25	0.25
4-Phenylphenol	8.85	7.79	6.54	5.66	4.81
B(f)Q	14.16	14.57	13.98	13.73	13.17
Phenanthrene	44.86	44.54	42.09	40.20	36.78

*mM β -CD in mobile phase.

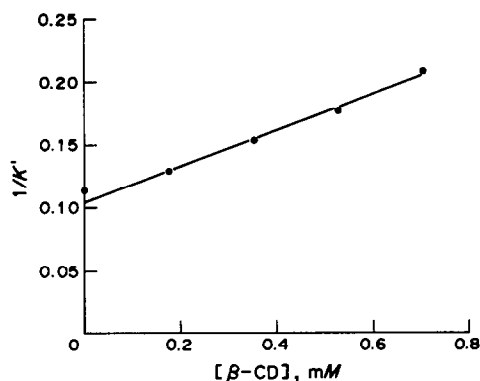


Fig. 1. Change in capacity factor (k') for 4-phenylphenol as a function of the equilibrium concentration of β -CD present in the mobile phase.

by Mohseni and Hurtubise.¹³ Equation (1) shows the relationship between the capacity factor and other parameters:

$$1/k' = 1/k_0 + [(CD)_m]/k_0K_D \quad (1)$$

where k' is the capacity factor in the presence of β -CD, k_0 is the capacity factor with no β -CD present, K_D is the dissociation constant for the inclusion complex and $[(CD)_m]$ is the equilibrium concentration of β -CD. Figure 1 shows a typical graph obtained for 4-phenylphenol. Because of the very small changes in capacity factors for PABA, the accuracy of the data in Table 1 would not permit the determination of a K_D value for PABA.

Table 2 gives the dissociation constants obtained graphically and the formation constants for the model compounds. 4-Phenylphenol showed the largest formation constant, thereby illustrating that a stronger inclusion complex was formed in solution compared to the other three compounds. With use of earlier solid-surface RTF and RTP relative intensity data for PABA, 4-phenylphenol, B(f)Q and phenanthrene,²³ no simple correlation was found between the RTF and RTP relative intensity values and the dissociation constants of the compounds. In fact, on 30% β -CD/NaCl PABA gave much higher RTF and RTP intensity values than the other three compounds,²³

Table 2. Dissociation constants (K_D) and formation constants (K_f) for β -CD complexes in 50:50 MeOH/H₂O

Compound	K_D	K_f^*
4-Phenylphenol	8.25×10^{-4}	1212
B(f)Q	7.58×10^{-3}	132
Phenanthrene	2.88×10^{-3}	347

* $K_f = 1/K_D$.

but the HPLC data indicated that PABA gave the weakest interaction with β -CD in solution. Several other compounds would have to be investigated to determine if there are correlations between K_D values and solid-surface RTF and RTP intensities. In solution, 1:1 complexes are generally formed between the guest and host (β -CD) molecules.¹ However, in the solid state, it is possible for two or more β -CD molecules to interact with one guest molecule.²⁵ Based on the results in this work and the type of complexes that are formed in solution and in the solid state, it was concluded that the solution chemistry of β -CD and the interactions of the guest and host in the solid state are not related in a simple fashion. Events during the evaporation of the solvent in the sample preparation step would have to be studied to clarify more exactly what is occurring between molecules in the solvent and the molecules in the solid matrix as the solvent is evaporating from the liquid–solid suspension.

The effects of glucose, β -CD and NaCl on the solution fluorescence of model compounds

The effects of β -CD and glucose on the solution fluorescence of PABA, 4-phenylphenol, phenanthrene, and B(f)Q were investigated to see if there were any unique relationships between solution interactions and solid-matrix RTF and RTP. In all of the solutions investigated, the analytical concentration of the solute was the same. In addition, concentrations $>4\text{mM}$ β -CD could not be investigated because β -CD was not soluble in 50:50 MeOH/H₂O at such concentrations. It should be mentioned that in water PABA is 10.5% in zwitterion form.²⁶ However, in 50% ethanol only 0.27% is present as zwitterion.²⁶ Also, the fluorescence excitation and emission spectra of PABA in 50% methanol, in this work, gave no evidence of any ionic species present in solution. Thus, it was concluded that the predominant PABA species in solution was the acid form. 4-Phenylphenol is a very weak acid, and it would not be expected to ionize to any extent in 50% methanol. Our fluorescence data and HPLC data gave no evidence of the anion of 4-phenylphenol in solution.

The excitation and emission spectra of B(f)Q and phenanthrene showed only very slight changes in the presence of β -CD or glucose. However, PABA and 4-phenylphenol showed somewhat greater spectral changes due to the presence of β -CD and glucose. Figure 2 shows

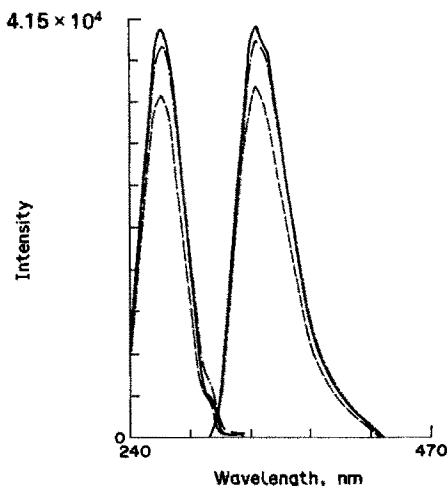


Fig. 2. The effect of β -CD on the solution fluorescence of 4-phenylphenol (0.1 $\mu\text{g/ml}$): (---) no β -CD, (—) 1mM β -CD, and (-·-) 4mM β -CD. The solvent was 50:50 v/v MeOH/H₂O.

the effect of β -CD on the solution fluorescence of 4-phenylphenol. PABA, 4-phenylphenol, and phenanthrene showed little change in fluorescence intensity with the addition of β -CD (0–4mM). B(f)Q showed about a 26% increase in solution fluorescence intensity with the addition of β -CD. PABA, 4-phenylphenol, and B(f)Q showed essentially no change in solution fluorescence intensity with the addition of glucose (0–28mM). Phenanthrene gave about a 13% decrease in fluorescence intensity with the addition of glucose. The concentrations of hydroxyl groups were the same in the respective β -CD and glucose solutions. From the solution spectral shift data and the solution fluorescence intensity data, it was concluded that there were no simple correlations between the solution fluorescence data and the relative magnitude of the solid-matrix luminescence data. This is not surprising given the fact that solution interactions are quite different from solid-matrix interactions.

It has been shown that inorganic salts can influence the formation of β -CD–guest complexes.^{27,28} In this work, the effect of NaCl on the solution fluorescence of the model compounds was studied in the presence of β -CD. With only sodium chloride and no β -CD present in the solvent (50:50 MeOH/H₂O), a small decrease in fluorescence signal was observed for all the compounds. Upon the addition of β -CD to the solutions containing sodium chloride, the same trends were found as when no sodium chloride was present in the solutions. Thus, the presence of sodium chloride had very little effect on the

Table 3. Percentages of analyte extracted with ether under different experimental conditions

Substrate	Compound recovered*, %				
	PABA	4-Phenylphenol	B(f)Q	Phenanthrene	B(a)P
None	91 \pm 0.7	95 \pm 2.0	87 \pm 1.0	92 \pm 0.6	91 \pm 0.7
NaCl	61 \pm 1.0	78 \pm 0.8	70 \pm 1.6	78 \pm 0.2	76 \pm 0.7
30% β -CD/NaCl	0.6 \pm 0.03	0.7 \pm 0.05	0.8 \pm 0.2	0.3 \pm 0.03	0.6 \pm 0.2

*Average results of triplicate runs \pm 95% confidence limits.

solution fluorescence of the model compounds and no correlations could be made with the solid-matrix luminescence. However, NaCl can break intermolecular hydrogen bonds between β -CD molecules in solution, which would prevent the β -CD from aggregating in the solid matrix.²⁹ Also, in the solid state, NaCl can increase the modulus of the solid matrix and enhance the RTF and RTP signals.²⁹

Confirmation of inclusion complex formation with 30% β -CD/NaCl mixture

In order to determine if complex formation occurred with the 30% β -CD/NaCl solid matrix used to induce RTP, the amount of unbound analyte (physically adsorbed analyte) was determined by an ether extraction method described earlier.³⁰ To test the validity of the extraction procedure, two other samples were run simultaneously with the 30% β -CD/NaCl mixture. The efficiency of the procedure is represented in Table 3 by the percentages of analyte extracted with no substrate present. For the compounds, the range of recoveries was from 87 to 95%. The amount of compound adsorbed on the NaCl was also determined. Table 3 shows that a relatively large amount of analyte was extracted from the pure NaCl matrix. However, Table 3 showed that <1% of a given compound was extracted from the 30% β -CD/NaCl mixture. These results indicate that the compounds were not simply adsorbed onto the surface but were held very tightly by the matrix, *i.e.*, included within the β -CD cavity. The ether extraction data show that molecules having dimensions that exceed those of the β -CD cavity, and which exhibit little interaction with β -CD in solution, are none the less held very tightly by the 30% β -CD/NaCl mixture, indicating that more than one β -CD molecule is directly interacting with the analyte within the matrix. Of particular interest are the results obtained for B(a)P, which is a five-membered fused aromatic ring system, with molecular dimensions exceeding those of the β -CD cavity

but is held tightly by the β -CD/NaCl matrix. This is evident since <1% of analyte is extracted from the matrix (Table 3).

CONCLUSIONS

Solution fluorescence of the analyte with β -CD present in MeOH/H₂O (50:50) with and without sodium chloride present showed larger changes in intensity for PABA and 4-phenylphenol compared to B(f)Q and phenanthrene. The formation constant of 4-phenylphenol was the largest for the model compounds studied. Of interest, however, is that well resolved solid-surface luminescence spectra were obtained for the more bulky compounds, B(f)Q and phenanthrene, with 30% β -CD/NaCl.²³ In fact, it has been shown that room-temperature and low-temperature luminescence spectra obtained with the 30% β -CD/NaCl matrix show very good resolution.²³

The most important conclusions were that the solution results offered no clear correlations between the solution interactions of analyte and β -CD and the luminescence intensity observed from the analyte adsorbed on 30% β -CD/NaCl matrix. Also, the results for ether extraction from the solid matrix showed that more than one β -CD molecule was interacting with the analyte in the solid matrix. This correlates with recent crystallographic data which show that in the crystalline state β -CD inclusion complexes prefer an arrangement where there are at least two β -CD molecules per analyte molecule.²⁵

Acknowledgement—Financial support for this project was provided by the Department of Energy, Division of Basic Energy Sciences under Grant DE-FG02-86ER13547.

REFERENCES

1. J. Szejtli, *Cyclodextrins and Their Inclusion Complexes*, Akadémiai Kiadó, Budapest, 1982.
2. A. Buvári and L. Barcza, *J. Incl. Phenom.*, 1989, 7, 313.
3. E. Fenyvesi, *ibid.*, 1988, 6, 537.
4. A. Buvári, J. Szejtli and L. Barcza, *ibid.*, 1983, 1, 151.

5. L. Blyshak, T. M. Rossi, G. Patonay and I. M. Warner, *Anal. Chem.*, 1988, **60**, 2127.
6. F. G. Sanchez, A. L. R. Rubio, C. C. Blanco, M. H. Lopez, J. C. M. Gomez and C. Carnero, *Anal. Chim. Acta*, 1988, **205**, 139.
7. W. L. Hinze, *Sep. Purif. Methods*, 1981, **10**, 159.
8. D. W. Armstrong, F. Nome, L. A. Spino and T. O. Golden, *J. Am. Chem. Soc.*, 1986, **108**, 1418.
9. M. A. Tarr, G. Nelson, G. Patonay and I. M. Warner, *Anal. Lett.*, 1988, **21**, 843.
10. L. Bazant, M. Wurst and E. Smolková-Keulemansová, *J. Chromatog.*, 1988, **445**, 337.
11. J. Snopek, I. Jelinek and E. Smolková-Keulemansová, *ibid.*, 1988, **438**, 211.
12. M. Gazdag, G. Szepesi and L. Huszar, *ibid.*, 1988, **436**, 31.
13. R. M. Mohesni and R. J. Hurtubise, *ibid.*, 1990, **499**, 395.
14. G. Nelson, G. Patonay and I. M. Warner, *Anal. Chem.*, 1988, **60**, 274.
15. *Idem*, *Talanta*, 1989, **36**, 199.
16. *Idem*, *Appl. Spectrosc.*, 1987, **41**, 1235.
17. I. R. Politzer, K. T. Crago, D. L. Kiel and T. Hampton, *Anal. Lett.*, 1989, **22**, 1567.
18. G. Patonay, K. Fowler, A. Shapira, G. Nelson and I. M. Warner, *J. Incl. Phenom.*, 1987, **5**, 717.
19. S. Scypinski and L. J. Cline Love, *Anal. Chem.*, 1984, **56**, 322.
20. R. A. Femia and L. J. Cline Love, *Spectrochim. Acta*, 1986, **42A**, 1239.
21. A. M. Alak, N. Contolini and T. Vo-Dinh, *Anal. Chim. Acta*, 1989, **217**, 171.
22. J. M. Bello and R. J. Hurtubise, *Anal. Chem.*, 1988, **60**, 1285.
23. M. D. Richmond and R. J. Hurtubise, *ibid.*, 1989, **61**, 2643.
24. J. Szejtli, *Cyclodextrin Technology*, pp. 79-185. Kluwer Academic Press, Netherlands, 1988.
25. D. Duchene, *Cyclodextrins and Their Industrial Uses*, pp. 107-130. Editions de Sante, Paris, 1987.
26. B. van de Graff, A. J. Hoefnagel and B. M. Wepster, *J. Org. Chem.*, 1981, **46**, 653.
27. A. Buvári and L. Barcza, *Inorg. Chim. Acta*, 1979, **33**, L179.
28. *Idem*, *J. Incl. Phenom.*, 1989, **7**, 379.
29. S. M. Ramasamy and R. J. Hurtubise, *Anal. Chem.*, 1982, **54**, 2477.
30. J. M. Bello and R. J. Hurtubise, *ibid.*, 1987, **59**, 2395.

SPECTROPHOTOMETRIC DETERMINATION OF TRACE LEVELS OF ATMOSPHERIC AMMONIA BY CONVERSION INTO INDOPHENOL AND EXTRACTION WITH QUATERNARY AMMONIUM SALTS

NORIKO YAMAMOTO, NORIKO KASAHARA and TSUNEO SHIRAI

Department of Applied Chemistry, Faculty of Science and Technology, Keio University, Hiyoshi, Yokohama 223, Japan

(Received 13 February 1990. Revised 18 April 1990. Accepted 2 May 1990)

Summary—Indophenol, produced in proportion to the amount of ammonia present, can be quantitatively extracted into chloroform as an ion-pair with tetradodecylammonium (TDA⁺) bromide and determined by spectrophotometry. The molar absorptivity of the indophenol–TDA⁺ complex is 2.5×10^4 l. mole⁻¹. cm⁻¹ (maximum absorption at 653 nm), which is 25% greater than that for the indophenol–TDA⁺ complex in aqueous medium. This procedure is applicable to determination of $\mu\text{l}/\text{m}^3$ levels of atmospheric ammonia, with 1-hr sampling periods.

Atmospheric concentrations of ammonia are typically under $10 \mu\text{l}/\text{m}^3$ but are subject to rapid temporal variations.^{1–5} The determination of ammonia by the commonly used indophenol procedure is highly reliable, but has limited sensitivity, so sampling periods of several hours are necessary. The sampling frequency is therefore very restricted unless several sampling units are operated in parallel (at staggered starting times) at the same site.^{1,2,5} The present work aimed to develop a sensitive procedure for the analysis of solutions of ammonia, collected by bubblers. The method is based on production of indophenol in alkaline solution by the reaction between phenol, sodium hypochlorite and ammonia, with sodium nitroprusside as catalyst.³

In a previous study, we reported a new solvent-extraction method for indophenol with trioctylmethylammonium (TOMA) as counterion for extraction of the ion-pair into cyclohexane.⁶ Here, we describe the analogous system with tetradodecylammonium (TDA⁺) bromide and chloroform. This method has higher sensitivity than other indophenol methods⁷ and is free from interference by certain gases found in the atmosphere. The method can be applied to the determination of ammonia levels at 1-hr sampling intervals, and is adequate for most applications.

EXPERIMENTAL

Reagents

All reagents were analytical-reagent grade except where otherwise stated. Reagent

solutions were prepared with demineralized water.

Standard ammonia solution (equivalent to 1000 $\mu\text{l}/\text{ml}$ NH_3 at 0° and 760 mmHg). A stock solution was prepared by dissolving 2.948 g of ammonium sulfate, dried at 130° , in 1 litre of water, and further diluted with 3-g/l. boric acid solution as required.

Phenol–sodium nitroprusside solution. Prepared by dissolving 5 g of phenol and 25 mg of sodium nitroprusside in 500 ml of water.

Sodium hypochlorite solution. Enough commercial sodium hypochlorite solution (Wako Pure Chemical Industries, Japan) was dissolved in 500 ml of alkaline buffer solution (consisting of 17.9 g of disodium hydrogen phosphate 12-hydrate and 5.5 g of sodium hydroxide in 500 ml of water) to give an equivalent chlorine (Cl_2) concentration of 0.01M. This concentration was periodically checked.

Tetradodecylammonium bromide (TDAB) solutions. Prepared by dissolution in chloroform, benzene or dichloroethane (purities > 99%).

Apparatus

Spectrophotometric measurements were made with a Hitachi U-2000 or U-100 spectrophotometer with 1-cm and 5-cm cells. The pH was measured with a Toa Denpa pH-meter. Shaking was done with a Taiyo Service Shaker.

Procedure

Indophenol formation.³ To 10 ml of sampling solution (3-g/l. boric acid solution, freshly

prepared daily), containing from 0.2 to 2 μ l of ammonia, 5 ml of phenol solution and 5 ml of hypochlorite solution were added, with mixing after each addition. The color was allowed to develop at 40° for 40 min.

Extraction of the ion-pair. A 20-ml volume of indophenol solution was transferred into a 50-ml centrifuge tube and 2 or 4 ml of 0.04M TDA in chloroform were added and the mixture was shaken for 5 min. After phase separation, the tube was centrifuged for 5 min. The absorbance of the organic phase was measured at 657 nm against chloroform, in 1-cm cells.

Sampling method for atmospheric ammonia.^{3,4} Ammonia was collected in two bubblers in series, each containing 20 ml of 3-g/l. boric acid solution, with a Teflon prefilter, at a flow-rate of 2 l./min. Measurements were performed in duplicate, by use of parallel sampling systems.

The solutions in each bubbler were analysed as described above, and also by a non-extraction method.³

RESULTS AND DISCUSSION

Extraction solvent and absorption spectra

The indophenol-TDA⁺ complex was readily extracted by chloroform, dichloroethane or benzene, and the stability and intensity of the color developed in these solvents, measured at the wavelengths of maximum absorbance, are shown in Fig. 1. Although the color is more stable in dichloroethane and benzene, the absorptivity is greater in chloroform, which is therefore the preferred solvent. The indophenol-TDA⁺ complex in chloroform has an absorption maximum at 653 nm and its molar absorptivity is much higher than that of indo-

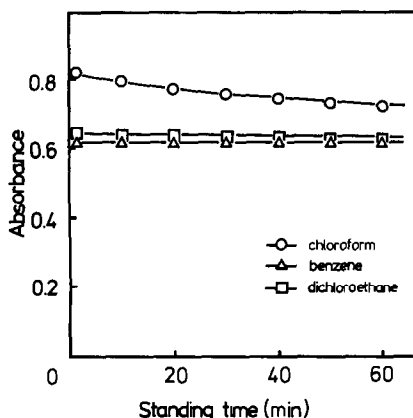


Fig. 1. Color intensity and stability of the indophenol-TDA⁺ complex in various solvents.

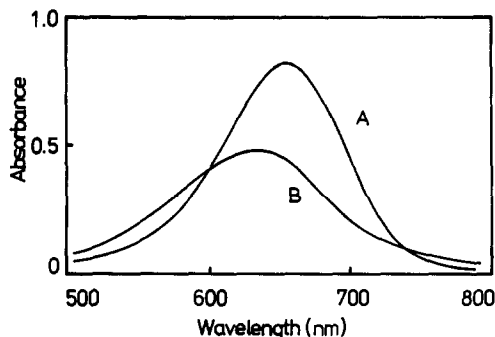


Fig. 2. Absorption spectra of indophenol. A, Indophenol-TDA⁺ complex in chloroform; B, indophenol in aqueous solution.

phenol in aqueous solution (Fig. 2). The conditions for quantitative extraction of the ion-pair with chloroform were examined and absorbance measurements were made within 20 min after the extraction.

Effect of TDA⁺ concentration on the extraction

The effect of varying the TDA⁺ concentration over the range 0.01–0.05M, on the degree of extraction with 4 ml of TDA⁺ solution in chloroform, was examined. The best results were obtained with 0.04–0.05M TDA⁺, as shown in Fig. 3 and 0.04M was selected as the optimal concentration. The extraction was found to be quantitative with shaking for 4 min, so a 5 min shaking time was chosen for use.

Calibration, sensitivity and precision

The calibration graph for ammonia was linear over the range 0–4 μ l (regression coefficient 0.998). The relative standard deviation was 4% for 0.2 μ l of ammonia. The molar absorptivity

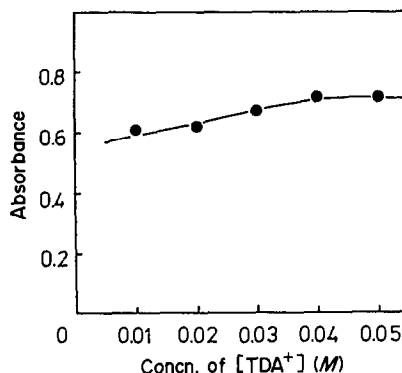


Fig. 3. Effect of TDA⁺ concentration on the extraction of the indophenol-TDA⁺ complex into chloroform. Indophenol solution 20 ml; Organic phase, 4 ml; reference, chloroform.

Table 1. Effect of coexisting SO₂ and NO₂ on absorbance from 2 μl of NH₃ per 20 ml of final solution

Coexisting gas	Concn. of gas,* μl/20 ml	Absorbance
None		0.582
SO ₂	2	0.567
	20	0.580
NO ₂	2	0.597
	20	0.567

*In the final solution measured.

Table 2. Comparison of determination of atmospheric NH₃ in 120 l. of sample by the extraction method and a non-extractive method

Sampling date	Concn. of NH ₃ , μl/m ³	
	Concentration method†	Non-extraction‡
19 Sept. 1989*		
11:30–12:30	11.0 ± 0.3	12.0 ± 0.3
12:30–13:30	10.2 ± 2.4	11.4 ± 2.7
13:30–14:30	8.5 ± 0.1	8.4 ± 1.4
2 Dec. 1989§		
11:30–12:30	2.7 ± 0.5	2.4 ± 0.1
12:30–13:30	3.6 ± 1.1	3.5 ± 0.6
13:30–14:30	4.4 ± 0.3	3.3 ± 0.6
5 Dec 1989§		
11:30–12:30	11.0 ± 1.9	9.5 ± 1.2
12:30–13:30	5.4 ± 0.2	5.6 ± 0.3
13:30–14:30	9.2 ± 0.1	8.8 ± 0.3

*Extractant volume 2 ml.

†1-cm cells.

‡5-cm cells.

§Extractant volume 4 ml.

of the indophenol-TDA⁺ complex in chloroform at 653 nm was 2.5×10^4 l.mole⁻¹.cm⁻¹, which was 25% greater than that of the complex in aqueous solution (2.0×10^4 l.mole⁻¹.cm⁻¹). The sensitivity could be increased further by use of a smaller volume of extractant, e.g., 2 ml.

Effect of foreign substances

Nitrogen dioxide and sulfur dioxide can coexist with ammonia in the atmosphere; their usual concentrations in the urban atmosphere of Yokohama are 10–20 and 30–40 μl/m³ respectively. Although very high concentrations of these gases interfere considerably in the indophenol reaction,³ the usual concentrations of those gases in the atmosphere do not (Table 1).

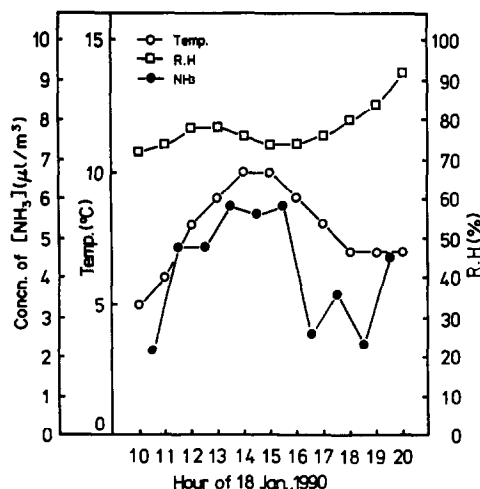


Fig. 4. Diurnal variation of atmospheric ammonia concentration in Yokohama in January 1990.

Determination of ammonia in the atmosphere

The proposed method was applied to the determination of ammonia in the urban atmosphere of Yokohama. Ammonia concentrations in samples collected for 1 hr at 1-hr sampling intervals, were determined as described, with 1-cm cells for absorbance measurements. The results obtained were compared with those from a non-extraction method,³ used with 5-cm cells (Table 2) and found to be satisfactory. The diurnal variation of ammonia concentration, air temperature and relative humidity in January was measured, as shown in Fig. 4. The detection limit for ammonia by use of 2 ml of extractant in the proposed method was $0.6 \mu\text{l/m}^3$, with a sampling volume of 120 litres.

REFERENCES

1. B. R. Appel, S. M. Wall, Y. Tokiwa and M. Haik, *Atmos. Environ.*, 1980, **14**, 549.
2. S. H. Cadle, R. J. Countess and N. A. Kelly, *ibid.*, 1982, **16**, 2501.
3. N. Yamamoto, E. Nakazuka and T. Shirai, *Nippon Kagaku Kaishi*, 1983, 1226.
4. L. M. Hildemann, A. G. Russell and G. R. Cass, *Atmos. Environ.*, 1984, **18**, 1737.
5. N. Yamamoto, N. Kabeya, M. Onodera, S. Takahashi, Y. Komori, E. Nakazuka and T. Shirai, *ibid.*, 1988, **22**, 2621.
6. N. Yamamoto, N. Kabeya, N. Yamaguchi and T. Shirai, *Bunseki Kagaku*, 1989, **38**, 6.
7. M. D. Krom, *Analyst*, 1980, **105**, 305.

DETERMINATION OF THE FLOTATION COLLECTOR ETHYL XANTHATE BY FLOW-INJECTION ANALYSIS

MILOSLAV KOPANICA, VĚRA STARÁ and ANTONÍN TROJÁNEK

UNESCO Laboratory of Environmental Electrochemistry, J. Heyrovský Institute of Physical Chemistry and Electrochemistry, Czechoslovak Academy of Sciences, Dolejškova 3, 18223 Prague 8, Czechoslovakia

(Received 3 July 1989. Revised 1 March 1990. Accepted 28 May 1990)

Summary—A flow-injection method for determination of xanthate with amperometric detection is presented. A composite carbon electrode modified with silica gel is used for detection. Very good reproducibility (1.5% r.s.d.) results from renovation of the electrode surface by three potential scans between measurements. In the analysis of flotation liquor, the interfering effect of metal complexes, formed by leaching of the ore in water, is eliminated by addition of EDTA. The method can be used to determine ethyl xanthate in the concentration range 0.10–10.0 mg/l, with a detection limit of 0.04 mg/l.

For effective control of a flotation process in the ore industry it is necessary to be able to determine the flotation collector potassium ethyl xanthate (PEX) continuously or at least periodically. The polarographic methods are not very suitable owing to their relatively low sensitivity, since the concentration of PEX in the flotation cells ranges from 1 to 10 mg/l. Very low detection limits can be attained by cathodic stripping voltammetry,² but the potential/current response is too complex to be useful for continuous xanthate monitoring. Spectrophotometric methods,³ although sensitive, can be applied only with clear solutions.

Composite carbon-paste electrodes modified with silica gel⁴ are, however, suitable for the voltammetric determination of xanthate in a flow-through system.

EXPERIMENTAL

Reagents

Potassium ethyl xanthate, C₂H₅CSK (PEX) was the product of the ZUPA Company (Yugoslavia). Because of their limited stability, aqueous PEX solutions were freshly prepared daily with doubly distilled water. All reagents were of analytical grade. The carrier solution for the flow-injection analyses was deaerated with helium.

Apparatus

The flow-injection measurements were performed in a system composed of a Spectra-

Physics Model SP 8770 isocratic pump and Rheodyne 7125 injection valve equipped with a 100 μ l sample loop. The voltammetric detector was connected by 0.25-mm bore stainless-steel tubing. The voltammetric (amperometric) measurements were made with a Model PA-4 polarographic analyser (Laboratorní přístroje, Prague, Czechoslovakia) in conjunction with a Model TZ 4100 chart recorder from the same manufacturer.

Flow-through cell. A wall-jet type cell made of "Plexiglas" is shown in Fig. 1. Sample solution is introduced through inlet capillary G onto the carbon-paste disc electrode, 2 mm in diameter, at the tip of the Teflon paste-holder D. The working reference and auxiliary electrodes are placed in the electrolyte contained in the bottom part A of the detector body. The upper part B is fixed to the bottom part, with a rubber gasket between them, by three screws (not shown). It contains openings for the saturated Ag/AgCl reference electrode and the paste-holder housing. The capillary holder E serves two purposes. First, together with the screw F it ensures that the inlet capillary is fixed and sealed, and secondly it ensures constant geometry of the cell. Since the paste electrode is prepared outside the cell, to obtain reproducible results it is necessary to keep the position of the working electrode constant with respect to the inlet capillary. In the arrangement shown in Fig. 1, this is achieved simply by screwing the paste holder down until it touches E.

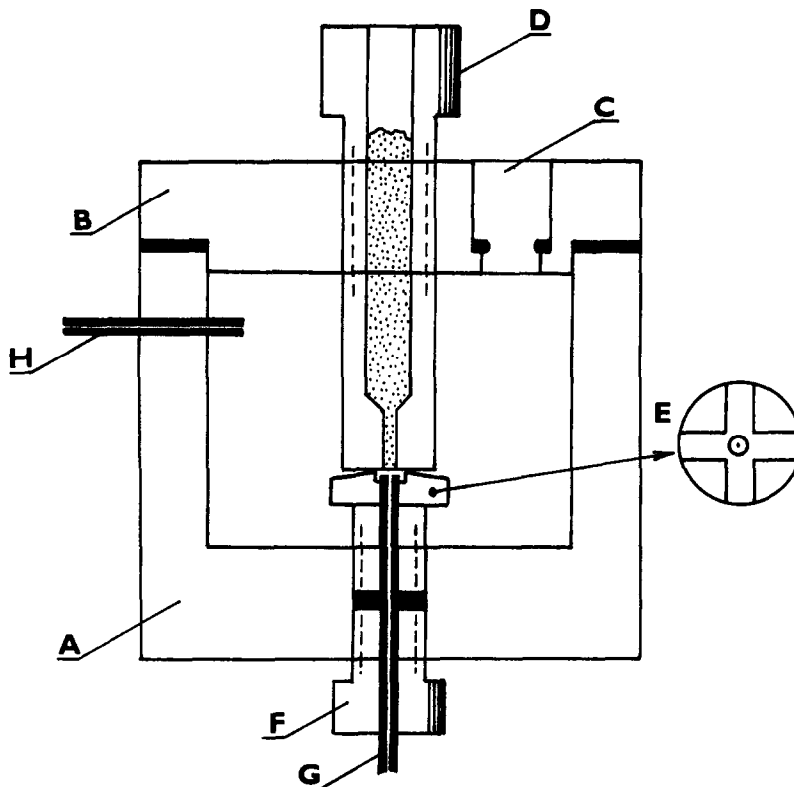


Fig. 1. The flow-through cell. A, B—detector body, C—opening for reference electrode, I—paste holder, E—inlet capillary holder (top view), F—screw, G—inlet capillary, H—stainless-steel outlet capillary, i.d. 0.5 mm (auxiliary electrode).

The modified composite carbon-paste electrode was prepared by mixing a homogenized mixture of graphite and silica gel into melted ceresine and pressing the mixture into the body of the paste holder. The optimum composition (% w/w) was 14 silica gel (30 μm particles), 43 ceresine and 43 graphite (12- μm particles).

The unmodified electrode was prepared similarly, from equal weights of ceresine and graphite.

RESULTS AND DISCUSSION

In slightly acidic (pH 6.6) or neutral media PEX is electrochemically oxidized on graphite electrodes.⁵ The composite carbon-paste electrodes modified with silica gel yield a well developed voltammetric response of sigmoidal shape which can be used for analytical purposes.⁴ In the preliminary experiments, samples containing PEX at a concentration of 5 mg/l. were injected into the 0.1M potassium nitrate carrier solution at a flow-rate of 0.5 ml/min, and the current signal at +0.8 V was recorded. Under these conditions, a sensitive response was obtained with both modified and unmodified

electrodes, the current signal yielded by the unmodified electrode being larger by a factor of ~ 3 . The modified electrode, however, gave better reproducibility. Without mechanical or electrochemical pretreatment, the unmodified electrode gave a response reduced by $\sim 65\%$ on consecutive injection of PEX samples, whereas with the modified electrode the decrease was only $\sim 18\%$. In both cases, the reproducibility of response could be improved by polishing the electrode surface on a piece of card. For the modified electrode an electrochemical procedure was also found to be very effective, and this, owing to its simplicity, was adopted for routine use. The procedure was to apply three potential scans over the range from -0.15 to 0.9 V, and back to -0.15 V, at a scan rate of 0.5 V/sec. With this electrochemical reactivation between successive injections of twenty identical samples, the responses had a relative standard deviation of 1.5% . Mechanical renovation of the modified electrode surface, although effective, was not used, because the successful electrochemical pretreatment was greatly advantageous in the flow-through system.

With flow-rates of 0.2–1.0 ml/min, the response amplitude of the modified electrode was scarcely affected by the flow-rate.

The optimum flow-rate and sample volume were chosen with respect to sample throughput and electrode surface reactivation. Higher flow-rates did not influence the measurement sensitivity substantially. Higher sample volumes (500–1000 μ l) yielded, as expected, a poorly shaped response, and the consequent longer residence time of the sample in the detector (at flow-rates of 0.3–0.6 ml/min) resulted in the formation of more of the reaction product on the electrode surface and thus complicated reactivation of the electrode. Hence, a sample volume of 100 μ l and flow-rate of 0.6 ml/min were used in later experiments.

Figure 2 shows the dependence of the modified electrode response on the applied potential, for a flow-rate of 0.6 ml/min. The shape of the curve is in accordance with previous findings from batch experiments⁴ that for successful amperometric detection of PEX, a potential more positive than +0.7 V must be applied. The hydrodynamic voltamperogram measured under identical conditions but without injection of the PEX samples (background) shows the current obtained at a given detection potential at zero PEX concentration. The salt concentration in the carrier stream has some effect on the response of the modified electrode. For instance, changing the potassium nitrate concentration from 0.01 to 0.3M caused the response to increase by approximately 30%. Thus, to obtain a linear calibration graph, it is necessary to inject samples of approximately the same salt content as that of the carrier.

Procedure and interferences

The following conditions for FIA of xanthate samples can be recommended. Carrier 0.1M potassium nitrate, flow-rate 0.6 ml/min, sample volume 100 μ l, detection potential +0.8 V. Pretreatment before each injection consists of three polarization scans in the range from –0.15 to +0.9 V and back to –0.15 V at the rate of 0.5 V/sec. Under these conditions a linear calibration graph was obtained for 0.1–10 mg/l. PEX, with a slope of 5.8 nA . l . mg⁻¹, and correlation coefficient 0.9998. The procedure permits 20 determinations per hour (with electrode reactivation).

Surprisingly, sulphide ions do not interfere even when present in large excess (100–300-fold

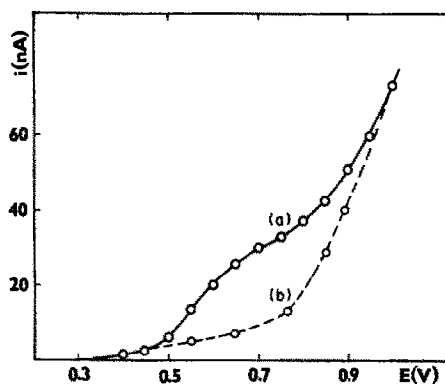


Fig. 2. Hydrodynamic voltamperogram of PEX on the modified composite carbon-paste electrode. Flow-rate 0.6 ml/min, (a) 100 μ l of sample containing 10 mg/l PEX. (b) background (the response corresponding to the measurement at varied detection potential values, without injection of the sample).

ratio to PEX). Interferences from metal ions (e.g. Cu²⁺) that form insoluble compounds with PEX can be eliminated by addition of EDTA.⁴

Determination of PEX in ore samples

To test the proposed method in the analysis of flotation liquor, PEX was determined in ore samples according to the procedure described above. The model samples consisted of suspensions of three kinds of sulphide ores in a tap water, with 10 g of ore in 200 ml of water. The ores were milled to a suitable grain size for the flotation process, and PEX was added to the suspensions to give concentrations in the range 0.1–10 mg/l. After being stirred for 30 min, the suspensions were allowed to settle and an aliquot of the supernatant was taken for analysis. To 5 ml of the sample solution, 4.5 ml of 0.2M potassium nitrate and 0.5 ml of 0.05M EDTA were added and the resulting solution was injected. A linear relationship between PEX concentration and detector response was obtained for all three types of ore, with an average slope of 5.3 nA . l . mg⁻¹. EDTA is added to eliminate the background anodic signal, probably caused by the oxidation of metal complexes formed in water during leaching of the ore.

In routine analysis the flotation liquor is sampled manually and, after a short settling time, analysed as proposed. The FIA principle, however, allows automatic analysis of the flotation liquor in the by-pass used for monitoring the pH of the liquor (on-line measurement).

Table 1. Determination of PEX in model flotation liquor samples

Sample	PEX added, <i>mg/l.</i>	PEX found, † <i>mg/l.</i>	Recovery, %
Sulphide ore I	0.50	0.51	102.0
	1.50	1.45	96.6
	4.50	4.44	98.6
Sulphide ore II	2.50	2.50	100.0
	5.00	5.10	102.0
	8.00	7.95	99.3
Sulphide ore III	0.10	0.09	94.0
	0.40	0.41	102.5
	0.70	0.71	101.4

†Mean of three measurements.

Table 1 summarizes the results of the analysis of the model samples. The recoveries were close to 100%, validating the applicability of the method for the analysis of the flotation liquor. The ore samples used for preparation of the model liquids were two types of iron ore (I, II) and a nickel ore (III) all from Czechoslovakia.

The modified composite carbon electrode, when used for amperometric detection of PEX in FIA, can be regenerated readily by potential scans. In this way, very good reproducibility of response is achieved. The measurement is thus very simple, enabling a high throughput of samples and the possibility of on-line measurement.

REFERENCES

1. J. Leppinen and S. Vahtila, *Talanta*, 1986, **33**, 795.
2. A. Ivaska and J. Leppinen, *ibid.*, 1986, **33**, 801.
3. M. H. Jones and J. T. Woodcock, *Ultraviolet Spectrometry of Flotation Reagent with Special Reference to the Determination of Xanthate in Flotation Liquor*, Institute of Mining Metallurgy, London, 1973.
4. V. Stará and M. Kopanica, *Electroanalysis*, 1989, **1**, 251.
5. M. M. Baizer (ed.), *Organic Chemistry*, pp. 532. Dekker, New York, 1973.

VOLTAMMETRIC DETERMINATION OF PHOSPHONATE ION AS A HETEROPOLY COMPLEX

SADAYUKI HIMENO,* TOSHIYUKI OSAKAI and ATSUYOSHI SAITO

Department of Chemistry, College of Liberal Arts, Kobe University, Kobe 657, Japan

TOSHITAKA HORI

Department of Chemistry, College of Liberal Arts and Sciences, Kyoto University, Kyoto 606, Japan

(Received 30 March 1990. Revised 2 May 1990. Accepted 6 May 1990)

Summary—A simple voltammetric method for the determination of phosphonate ion is described. A 12-molybdodiphosphonate complex is formed in a 50mM Mo(VI)–0.5M HCl–70% (v/v) CH₃CN system containing phosphonate ion. The yellow heteropolyanion undergoes apparent two-step reductions at a glassy carbon electrode. The voltammetric reduction currents depend linearly on the phosphonate concentration in the range 1×10^{-5} – 1×10^{-3} M.

Almost all the methods for the determination of phosphonate ion are based on indirect methods which include oxidation of phosphonate ion to orthophosphate ion.^{1,2} The resultant orthophosphate ion has been determined spectrophotometrically through the formation of a yellow molybdophosphate complex or a mixed-valence blue complex with the use of proper reducing agents.^{3–5} Hirai *et al.* have developed a flow injection system for the determination of phosphonate ion,⁶ in which sodium hydrogen sulphite is used as an oxidizing agent and orthophosphate ion thus formed is determined with the Mo(VI)–Mo(V) reagent method.⁷ Phosphonate ion can also be determined by oxidation with excess standard iodine to orthophosphate ion and titration of excess of iodine with standard reducing agents such as thiosulfate.⁸

In the course of a series of preparative studies of heteropolymolybdates, we have found that phosphonate ion reacts directly with Mo(VI) to form a yellow heteropoly complex with a compositional ratio of Mo/P = 12/2 in acidic solutions containing water-miscible organic solvents such as acetone and acetonitrile. Rosenheim and co-workers have obtained alkali metal salts of a yellow molybdodiphosphonate complex such as $2\text{Na}_2\text{O} \cdot \text{P}_2\text{O}_3 \cdot 12\text{MoO}_3 \cdot 19\text{H}_2\text{O}$ by heating an acidic mixture of MoO₃ and H₃PO₃,⁹ although the chemical properties have not been elucidated so far because of the lack of proper solvents to dissolve it.

The present study has demonstrated that the 12-molybdodiphosphonate complex is stable in aqueous solutions mixed with water-miscible organic solvents. In such aqueous organic media, the 12-molybdodiphosphonate complex is electroreduced to a blue species at the glassy carbon (GC) electrode. The reduction current is found to be linearly dependent on the concentration of phosphonate ion. This work was undertaken to establish a method for the voltammetric determination of phosphonate ion.

EXPERIMENTAL

Apparatus and reagents

Voltammetric measurements were made with a PAR 174-A polarographic analyser. The voltamperograms were recorded on a Yokogawa 3023 X–Y recorder. The working electrode was a glassy carbon rod (GC-30S, Tokai Carbon) mounted in a Teflon tube by means of silicone rubber tubing. The surface area was *ca.* 0.071 cm². A saturated calomel electrode (SCE) was used as the reference and a platinum wire as the counter-electrode. Controlled potential electrolysis (CPE) was done with a Hokuto Denko HA-501 potentiostat. A Hokuto Denko HF-202D coulometer was used for coulometric measurements. IR spectra were recorded on a Hitachi 270-30 spectrophotometer with KBr disks. TG-DTA was performed with a Rigaku Denki 8002-SD thermal analyser.

All the chemicals were of reagent grade and were used as received.

*To whom all correspondence should be addressed.

RESULTS AND DISCUSSION

Identification of the molybdodiphosphonate complex

The molybdodiphosphonate complex was isolated as the tetrabutylammonium ($n\text{-Bu}_4\text{N}^+$) salt by the following procedure. Twelve g of $\text{Na}_2\text{MoO}_4 \cdot 2\text{H}_2\text{O}$ were dissolved in 155 ml of water, and 45 ml of concentrated hydrochloric acid were added, followed by 300 ml of acetonitrile. The solution turned yellow on the addition of 1.0 g of $\text{Na}_2\text{HPO}_3 \cdot 5\text{H}_2\text{O}$. After 1 hr of stirring at room temperature, 15 g of $n\text{-Bu}_4\text{NBr}$ were added. The yellow salt thus precipitated was collected by filtration, washed with water and ethanol, and dried over Drierite in a desiccator. The yield was *ca.* 4 g. Found: Mo, 43.0%; P, 2.25%; C, 20.9%; H, 4.1%; N, 1.7%; H_2O , 3.1%. $\text{H}(n\text{-Bu}_4\text{N})_3(\text{HP})_2\text{Mo}_{12}\text{O}_{42} \cdot 4\text{H}_2\text{O}$ requires Mo, 42.84%; P, 2.30%; C, 21.45%; H, 4.46%; N, 1.56%; H_2O , 2.68%. Molybdenum was determined spectrophotometrically at 390 nm as the complex with 1,2-dihydroxybenzene-3,5-disulfonic acid.¹⁰ Phosphorus was determined by the usual molybdenum-yellow method after oxidation to orthophosphate with perchloric acid.³ The water content of the salt was determined by TGA and by heating at 150°.

Figure 1 shows an IR spectrum of the 12-molybdodiphosphonate complex. The spectrum was characterized by strong bands at 1085, 938, 810 and 525 cm^{-1} . The 1085 cm^{-1} band can be attributed to the PO_3 group.¹¹ Bands in the 1500–1350 cm^{-1} region are due to the Bu_4N^+ unit. The band at 1640 cm^{-1} can be assigned to the water of hydration.

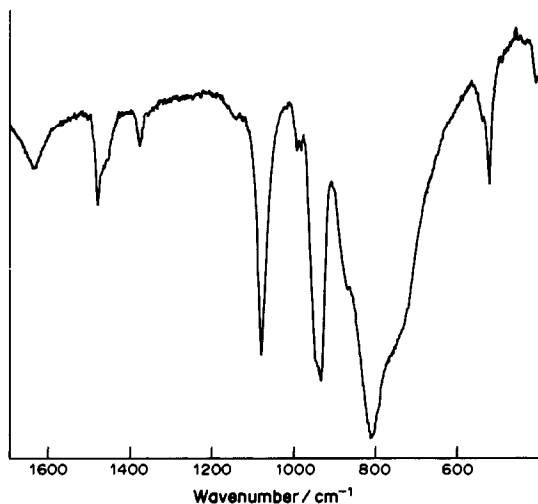


Fig. 1. An IR spectrum of the 12-molybdodiphosphonate complex in a KBr pellet.

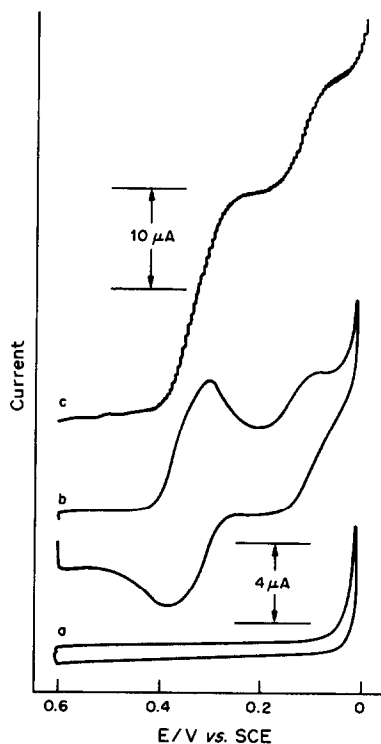


Fig. 2. Cyclic (a,b) and normal pulse (c) voltamperograms of a 10mM Mo(VI)-0.4M HCl-70% (v/v) acetone system in the absence (a) and presence (b) of 1.0mM phosphonate. Scan rate, (a,b), 100 mV/sec; (c) 5 mV/sec. The 4 μA scale is for curves (a,b).

The results of the elemental analysis suggest that the Bu_4N^+ salt contains the same heteropolyanion as that in the Na^+ salt prepared by Rosenheim and co-workers.⁹ This is further confirmed by the IR spectroscopic measurements for both the Bu_4N^+ and Na^+ salts.

Electrochemical characteristics of the 12-molybdodiphosphonate complex in solution

Figure 2 shows cyclic voltamperograms of 10mM Mo(VI) in 0.4M HCl containing 70% (v/v) acetone. The solution was pale yellow owing to the formation of $[\text{Mo}_6\text{O}_{19}]^{2-}$.¹² As shown in curve (a), no reduction waves were observed until the sharp current rise around 0 V, which was due to the reduction of $[\text{Mo}_6\text{O}_{19}]^{2-}$.¹³ On the addition of 1.0mM HPO_3^{2-} , the solution turned from pale yellow to yellow, and an apparent two-step reduction wave appeared with peak-potentials of +0.31 and +0.11 V [curve (b)]. The current increased with time, attaining a constant value around 10 min after the addition of phosphonate ion. After the 10-min current increase period, the yellow species was stable in the solution, as evidenced by no current change. Each reduction current depended

on the square root of the voltage scan rate (20–200 mV/sec), indicating that each step was diffusion-controlled. These voltammetric characteristics indicate the formation of the 12-molybdodiphosphonate complex.

In order to confirm this, a cyclic voltamperogram was taken for a 10mM Mo(VI)–0.4M HCl–70% (v/v) CH₃COCH₃ system containing 0.5mM orthophosphate instead of phosphonate; it is shown in Fig. 3. Three reduction waves of different height were obtained with peak-potentials of +0.340, +0.242 and +0.153 V. As already reported,¹⁴ these waves are due to the reduction of a mixture of α - and β -12-molybdophosphate complexes. From a comparison of Fig. 2 with Fig. 3 it follows that the yellow species responsible for curve (b) of Fig. 2 is not the 12-molybdodiphosphonate anion, but the 12-molybdodiphosphonate anion.

Coulometric analysis of the cyclic voltamperogram in curve (b) of Fig. 2 showed that the first reduction consumed two electrons per HPO₃²⁻ anion added, which means that the reduction consumes four electrons per 12-

molybdodiphosphonate anion. Attempts to apply coulometric analysis to the second wave were unsuccessful because of the overlap with the reduction wave of [Mo₆O₁₉]²⁻. As shown in curve (c), however, the limiting current ratio in normal pulse polarography was 2:1, which suggests that the second wave is due to a two-electron reduction of the 12-molybdodiphosphonate anion.

The first reduction wave in curve (b) of Fig. 2 is somewhat distorted, suggesting that the wave is due to multistep charge-transfers.¹⁵ Therefore, a logarithmic analysis was made of the first normal pulse voltammetric wave shown in curve (c). Plots of log[(i_d - i)/i] vs. E for the first wave yielded two separate straight lines with slopes of 42 and 47 mV. These results suggest that the reduction waves shown in curves (b) and (c) in Fig. 2 are composed of three two-electron transfers, with the first two close together.

Hereafter, the apparent four-electron reduction wave is regarded as the first wave, and is used for the determination of phosphonate ion.

Optimization of formation conditions for the 12-molybdodiphosphonate complex in an Mo(VI)–HCl–CH₃CN system

In order to obtain the limiting conditions for the formation of the 12-molybdodiphosphonate complex, normal pulse voltammetric measurements were made for a series of 50mM Mo(VI)–0.2mM phosphonate–70% (v/v) acetonitrile systems containing various concentrations of HCl (0.08–1.5M).

Curve (a) of Fig. 4 shows the limiting currents of the first wave as a function of the HCl concentration. As can be seen, the complex forms in the 0.15–0.6M HCl concentration range. For comparison, curve (b) shows normal pulse voltammetric second reduction currents in the presence of 0.2mM orthophosphate to illustrate the conditions for formation of 12-molybdodiphosphonate.

The effects of the nature and concentration of organic solvents on the formation of the 12-molybdodiphosphonate complex were studied with 50mM Mo(VI)–0.4M HCl–0.5mM phosphonate solutions containing acetone, acetonitrile, ethanol or 1,4-dioxan. Figure 5 shows the normal pulse voltammetric first reduction currents as a function of the concentration of acetone or acetonitrile as the organic solvent. No voltammetric wave was observed, until at

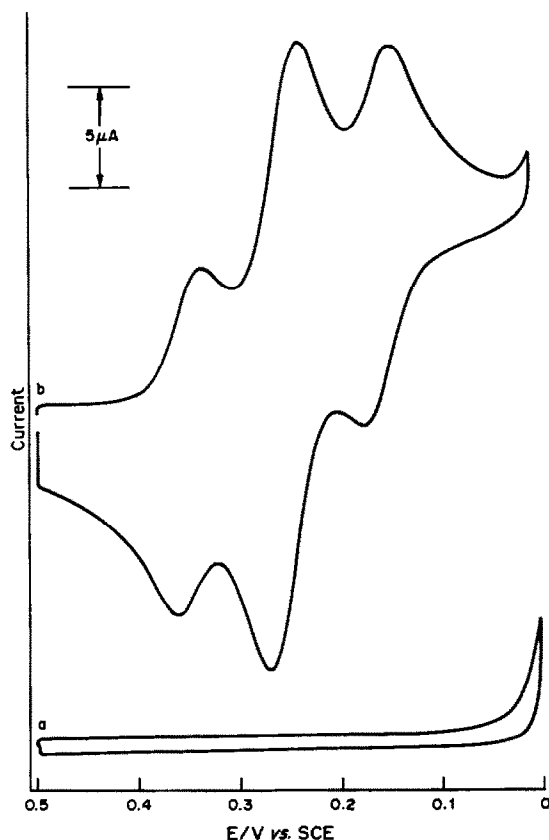


Fig. 3. Cyclic voltamperograms of a 10mM Mo(VI)–0.4M HCl–70% (v/v) acetone system in the absence (a) and presence (b) of 0.5mM orthophosphate. Scan rate, 100 mV/sec.

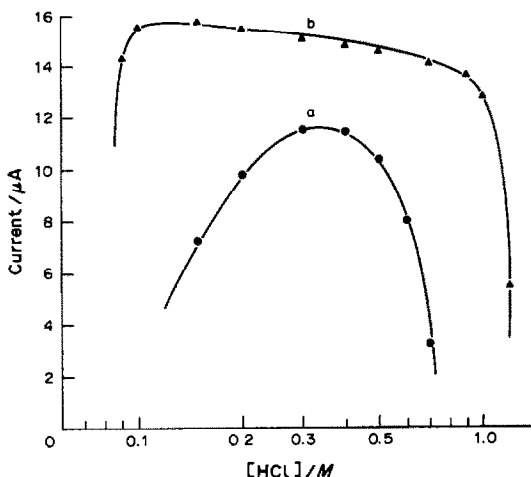


Fig. 4. Normal pulse voltammetric reduction currents for 50mM Mo(VI)-70% v/v acetonitrile systems containing (a) 0.2mM phosphonate; (b) 0.2mM orthophosphate, as a function of the HCl concentration.

least 25% v/v of one of these solvents was present, which indicates that the presence of organic solvent is essential for the formation of the molybdodiphosphonate complex. The voltammetric wave increased in height as the concentration of organic solvent was increased, until two separate phases resulted. In the presence of 1,4-dioxan or ethanol, on the other hand, the voltammetric waves due to the reduction of the 12-molybdodiphosphonate complex were not observed.

The effect of the phosphonate concentration was also investigated. With an increase of the

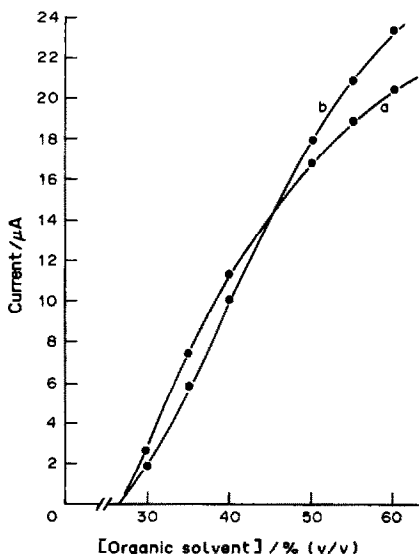


Fig. 5. Effect of concentration of organic solvents on the first normal pulse voltammetric reduction current for a 50mM Mo(VI)-0.4M HCl-0.5mM phosphonate system containing (a) acetone, (b) acetonitrile.

phosphonate concentration while other conditions were kept unchanged, the yellow colour due to the 12-molybdodiphosphonate complex gradually decreased. Simultaneously the cyclic voltamperogram was distorted, with a current decrease. These results suggest decomposition of the 12-molybdodiphosphonate complex. In a previous study,¹⁶ we isolated a colourless 6-molybdopentaphosphonate complex formulated as $\text{Na}_2\text{H}_5[(\text{C}_2\text{H}_5)_4\text{N}]_3(\text{HP})_5\text{Mo}_6\text{O}_{33}$ from an Mo(VI)- H_3PO_3 system containing acetone. The colourless complex is not electrochemically reduced. It is concluded that the 12-molybdodiphosphonate complex is stable only in the presence of a large excess of Mo(VI).

On the basis of these findings, a 50mM Mo(VI)-0.5M HCl-70% (v/v) CH_3CN system was selected as optimum for the voltammetric determination of phosphonate ion. It was found that the normal pulse polarographic limiting currents of the first wave were linearly dependent on the phosphonate concentration in the range 1×10^{-5} - $1 \times 10^{-3}\text{M}$; the calibration line curves downwards at above $1 \times 10^{-3}\text{M}$ under these conditions. An advantage of this method is that removal of dissolved oxygen from the solution is not required because the reduction potentials of the 12-molybdodiphosphonate complex are more positive than those of oxygen.

Thus, the present study has shown that phosphonate ion can be determined directly as a heteropoly complex, without prior oxidation to orthophosphate ion. The proposed voltammetric method is promising for practical uses, *e.g.*, as a detection system for high-performance liquid chromatography.

REFERENCES

1. I. M. Kolthoff, P. J. Elving and E. B. Sandell, *Treatise on Analytical Chemistry*, Part II, Vol. 5, Interscience, New York, 1961.
2. M. Halmann (ed.), *Analytical Chemistry of Phosphorus Compounds*. Interscience, New York, 1972.
3. M. Ishibashi and M. Tabushi, *Bunseki Kagaku*, 1959, **8**, 588.
4. T. R. Hurford and D. F. Boltz, *Anal. Chem.*, 1968, **40**, 379.
5. D. F. Boltz and M. G. Mellon, *ibid.*, 1947, **19**, 873; 1948, **20**, 749.
6. Y. Hirai, N. Yoza and S. Ohashi, *J. Chromatog.*, 1981, **206**, 501.
7. F. Lucena-Conde and L. Prat, *Anal. Chim. Acta*, 1957, **16**, 473.
8. R. A. Keeler, C. J. Anderson and D. Satriana, *Anal. Chem.*, 1954, **26**, 933.

9. A. Rosenheim, W. Weinberg and J. Pinsker, *Z. Anorg. Chem.*, 1914, **84**, 217; A. Rosenheim and M. Schapiro, *ibid.*, 1923, **129**, 196.
10. F. Will, III and J. H. Yoe, *Anal. Chim. Acta*, 1953, **8**, 546.
11. M. Tsuboi, *J. Am. Chem. Soc.*, 1957, **79**, 1351.
12. S. Himeno, N. Ishii, M. Hasegawa, A. Saito and T. Hori, *Inorg. Chim. Acta*, 1987, **131**, L11.
13. T. Osakai, S. Himeno, A. Saito and T. Hori, *J. Electroanal. Chem. Interfacial Electrochem.*, 1990, in the press.
14. S. Himeno, T. Osakai and A. Saito, *Bull. Chem. Soc. Japan*, 1989, **62**, 1335.
15. D. S. Polcyn and I. Shain, *Anal. Chem.*, 1966, **38**, 370.
16. S. Himeno, T. Hori and A. Saito, *Chem. Lett.*, 1989, 633.

POLAROGRAPHIC DETERMINATION OF OSMIUM WITH THE OSMIUM(VIII)-CERIUM(IV)-ARSENIC(III) SYSTEM

JIANG ZHI-LIANG

Laboratory of Instrumental Analysis, Department of Chemistry, Guangxi Normal University, Guilin,
People's Republic of China

LIANG AI-HUI

Department of Qualitative Control, Guilin 3rd Pharmaceutical Factory, Guilin,
People's Republic of China

(Received 19 November 1989. Revised 17 March 1990. Accepted 4 April 1990)

Summary—A highly sensitive and novel polarographic method has been developed for determination of ultratrace amounts of osmium, based on the catalysis of the cerium(IV)-arsenic(III) reaction by osmium(VIII). The reaction rate is monitored by measuring the arsenic(III) with a single-sweep oscillopolarograph. Osmium concentrations from 7.0×10^{-11} to $5.0 \times 10^{-9}M$ can be determined by the initial rate method. The method has been applied to determination of osmium in refined ore and chlorination residues with satisfactory results.

Because osmium ions are easily reduced by mercury, they are rarely determined polarographically.¹⁻³ Catalytic kinetic methods are of very high sensitivity for the determination of osmium.⁴⁻⁸ Recently, iron,⁹ vanadium,¹⁰⁻¹² manganese^{13,14} and silver^{15,16} have been determined by polarographic monitoring of their catalytic reactions. The present study was undertaken to find whether a similar method could be used for osmium. It has been found that the cerium(IV)-arsenic(III)-osmium(VIII) system can be utilized for the purpose. In the present work, single-sweep oscillopolarography was used to monitor the changes in concentration of arsenic(III) by means of the wave at $-0.62V$. A novel and highly sensitive method has thus been developed for the determination of osmium between 7.0×10^{-11} and $5.0 \times 10^{-9}M$. Good results were obtained when the method was applied to the determination of osmium in refined ore and chlorination residues.

EXPERIMENTAL

Reagents

A $0.01M$ cerium(IV) solution in $0.1M$ sulphuric acid, and a $100 \mu g/ml$ arsenic(III) solution are used.

Standard solution of osmium ($10 \mu g/ml$). Weigh out $11.54 mg$ of $(NH_4)_2OsCl_6$ and place it in a 250-ml beaker. Add $50 ml$ of $10M$ sulphuric acid, heat till fumes have evolved for $5 min$, cool, then transfer to a 500-ml standard

flask and dilute to the mark with doubly distilled water. The solution is stable for 40 days. Prepare working solutions by dilution shortly before use.

Apparatus

A model JP-2 oscillopolarograph (Chendu Instrumental Factory) with a three-electrode system (dropping mercury electrode, SCE and platinum electrode) was used, with a 10-ml constant-temperature polarographic cell.¹¹

General procedure

In the polarographic cell, place $0.20 ml$ of $10M$ sulphuric acid, $0.20 ml$ of $100 \mu g/ml$ As(III), $0.50 ml$ of 5% mercuric sulphate solution and 7.0×10^{-13} – 5.0×10^{-11} mole of osmium, then dilute to $9.0 ml$ with water. Keep the temperature of the cell at 25° . After $5 min$ add $1.0 ml$ of $0.01M$ cerium(IV) (also at 25°) and mix. Set the initial scanning potential at $-0.40V$ and the scan in the negative direction. Record the second-derivative of the peak current (I_p'') as a function of time. Plot the slopes of the initial straight-line portion of these curves against osmium concentration to prepare a calibration graph. Run a reagent blank in the same way.

Sample preparation¹⁷

Weigh accurately a 0.1-g sample, mix it with $5 g$ of sodium peroxide and heat at 700° for about $15 min$. Cool, leach the cooled melt with water, transfer the solution into a distillation

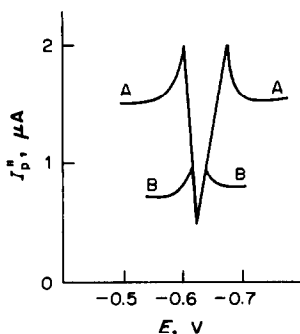


Fig. 1. The second-derivative of the single-sweep oscillographic wave for As(III): A, uncatalysed reaction (reaction time, 4 min); B, catalysed reaction ($2.0 \times 10^{-9}M$ Os, reaction time 4 min).

flask and acidify with 10M sulphuric acid. Add hydrogen peroxide as selective oxidant, and distil the osmium as OsO_4 into dilute sodium hydroxide solution. Acidify the distillate with dilute sulphuric acid, transfer it into a 500-ml standard flask and dilute to the mark with water. Analyse a suitable aliquot as described above, after further dilution if necessary.

RESULTS AND DISCUSSION

Ce(IV)-As(III)-Os(VIII) system

This system has been studied spectrophotometrically by many workers.¹⁸ The system for determination of osmium has high sensitivity and good selectivity, and low blank values. But relatively high concentrations of As(III) are needed in these methods.

It has been found that a sensitive polarographic As(III) wave appears at -0.62 V vs. SCE, and that As(V), Ce(IV), and Ce(III) do not interfere with it. The reaction rate can thus be determined by oscillographic monitoring of the depletion of As(III) (Fig. 1). Os(VIII)

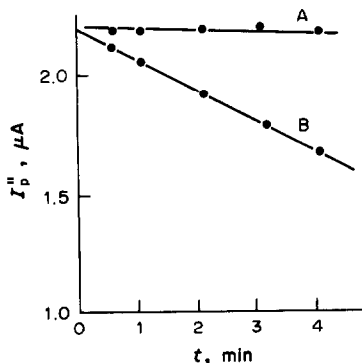


Fig. 2. The second-derivative of the peak current vs. time: A, uncatalysed reaction; B, catalysed reaction ($1.0 \times 10^{-9}M$ Os).

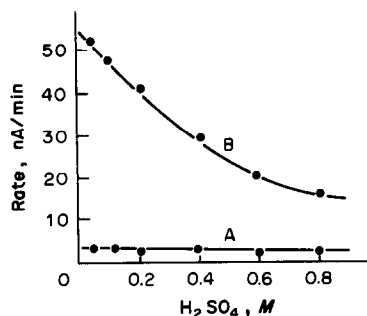


Fig. 3. Variation of initial rate with concentration of H_2SO_4 . A, uncatalysed reaction; B, catalysed reaction ($5.0 \times 10^{-10}M$ Os).

and Os(IV) both have the same catalytic effect on the reaction. Figure 1 shows the second-derivative of the wave for As(III) in the uncatalysed and catalysed reaction systems. Figure 2 shows the second derivative vs. time curve for the catalysed and uncatalysed reactions.

Polarographic character of As(III)

Under the experimental conditions used, the peak current is proportional to As(III) concentration between 0.05 and 5.0 $\mu g/ml$, and is greater than that for the anodic wave. The electrocapillary curve is lower in the presence than in the absence of As(III). The mean temperature coefficient is $-2.5\%/deg$. The wave disappears when poly(vinyl alcohol), cetyltrimethylammonium bromide, Triton X-10 or Triton X-100 is present. These results indicate the adsorptive character of the peak for As(III) at -0.62 V.

Selection of acid

The acids tested were sulphuric, phosphoric, perchloric, nitric and hydrochloric. Sulphuric

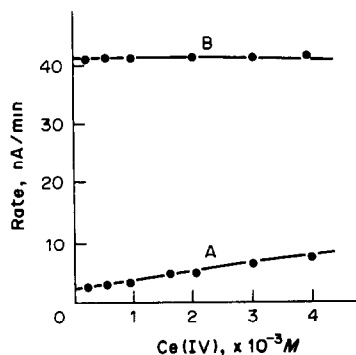


Fig. 4. Variation of initial rate with concentration of Ce(IV). A, uncatalysed reaction; B, catalysed reaction ($5.0 \times 10^{-10}M$ Os).

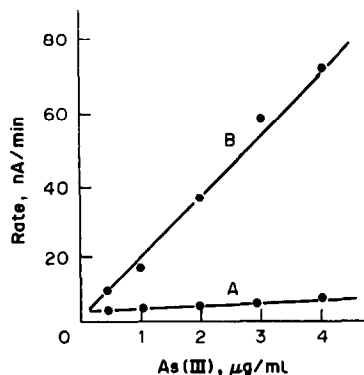


Fig. 5. Variation of initial rate with concentration of As(III). A, uncatalysed reaction; B, catalysed reaction ($5.0 \times 10^{-10} M$ Os).

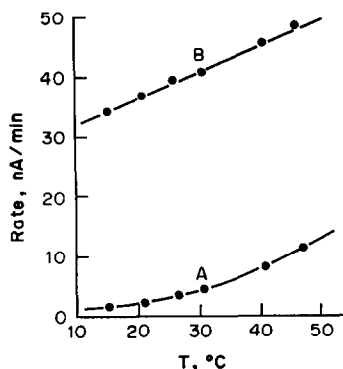


Fig. 6. Effect of temperature. A, uncatalysed reaction; B, catalysed reaction ($5.0 \times 10^{-10} M$ Os).

acid gave a lower blank than the others and was chosen for use. Figure 3 shows that the rates of both the catalysed and uncatalysed reactions decrease with increase in sulphuric acid concentration, but the effect is more pronounced for the catalysed reaction. A concentration of $0.2 M$ sulphuric acid was selected.

Influence of reagent concentrations

The effect of variation of the Ce(IV) concentration on the rate is shown in Fig. 4. The uncatalysed reaction rate increases slowly with Ce(IV) concentration, but that of the catalysed

Table 1. Influence of foreign ions on determination of $5.0 \times 10^{-10} M$ Os

Molar tolerance ratio, (ion)/(Os)	Ion added
1000	Li(I), Be(II), Sr(II), Ba(II), Ca(II), Cd(II), Al(III), Fe(III), Cr(III), Ni(II), Cu(II), Pb(II), Sb(III), Zn(II), V(V), Bi(III), Sn(II), F ⁻ , Br ⁻ , PO ₄ ³⁻ , ClO ₄ ⁻ , Cl ⁻ , CH ₃ OO ⁻
500	Mo(VI), W(VI), Se(IV), Mn(II), Ti(III), Tl(I), Rb(I), La(III), Zr(IV), Co(II)
200	Te(IV), S ₂ O ₈ ²⁻ , IO ₃ ⁻ , IO ₄ ⁻ , SCN ⁻
100	Ag(I), Au(III)
60	I ⁻

reaction rate is not affected. A Ce(IV) concentration of $0.001 M$, which gives a lower blank, was chosen as optimal.

Increasing the As(III) concentration increases the rates of both the catalysed and the uncatalysed reactions (Fig. 5), but the effect on the uncatalysed reaction rate is only slight. An As(III) concentration of $2.0 \mu\text{g/ml}$ ($2.67 \times 10^{-5} M$) was selected.

Influence of temperature

The dependence of the reaction rate on temperature is shown in Fig. 6. A temperature of 25° was selected, to decrease the blank.

Effect of foreign ions

The interference of 40 foreign ions in the system was investigated with $5.0 \times 10^{-10} M$ Os. The results are summarized in Table 1. Other platinum metal ions interfere in the determination when present at substantially higher concentration, but their interference can be eliminated by separation of Os as OsO₄ by distillation under appropriate conditions. Addition of 0.50 ml of 50 mg/ml mercuric sulphate solution was used to prevent the interference of iodide.

Table 2. Analytical results and recovery

Sample	Os added, ng	Os found, ng	Recovery, %	Content, g/ton	
				This method	Spectrophotometric method*
Refined ore	—	1.05	—		
	1.00	2.00	95		
	2.00	2.94	95	5.26×10^3	5.25×10^3
Chlorination residue	—	0.95	—		
	1.00	1.86	91		
	2.00	2.91	98	474	468

*Ce(IV)–As(III)–Os(VIII) system.

Calibration graph

The initial rate method under optimal experimental conditions gave a calibration graph that was linear for osmium between 7.0×10^{-11} and $5.0 \times 10^{-9}M$. The relative standard deviation of the method for $5.0 \times 10^{-10}M$ osmium was 2.4% (11 determinations).

Applications

The results obtained for quintuplicate analysis of two samples are given in Table 2, and are in good agreement with those obtained by the spectrophotometric catalytic method. The recovery of Os added to the samples was also determined, and the results are also given in Table 2.

REFERENCES

1. I. M. Kolthoff and E. P. Parry, *Anal. Chem.*, 1953, **25**, 188.
2. P. Beran, M. Burian and J. Doležal, *Chem. Zvesti*, 1963, **17**, 517.
3. Y. Zhang and Y. Sheng, *Gui-jin-shu*, 1986, **7**, 33.
4. H. Weisz and H. Ludwig, *Anal. Chim. Acta*, 1972, **60**, 385.
5. I. I. Alekseeva, N. K. Ignatova, A. P. Rysev and A. I. Yakshinskii, *Zh. Analit. Khim.*, 1974, **29**, 335.
6. I. N. C. Ling and G. Svehla, *Talanta*, 1984, **31**, 61.
7. E. G. Khomutova, N. A. Khvorostukhina, A. P. Rysev and I. N. Samulenkova, *Zh. Analit. Khim.*, 1985, **40**, 301.
8. A. E. Burgess and J. M. Ottaway, *Talanta*, 1975, **22**, 401.
9. T. Nomura, *J. Electroanal. Chem. Interfac. Electrochem.*, 1981, **124**, 213.
10. Z. Jiang, *Xiyou Jinsu*, 1988, **12**, 310.
11. Z. Jiang and Bi. Lu, *Fenxi Huaxue*, in the press.
12. Z. Jiang and X. Liang, *Ganhan Huanjing Jianche*, 1989, **3**, 25.
13. L. Li, *Fenxi Cheshi Tongbao*, 1988, **7**, 16.
14. Z. Jiang, *Fenxi Huaxue*, in the press.
15. Z. Ma, *Yejin Fenxi*, 1983, **3**, 220.
16. Z. Jiang, *Gui-jin-shu*, in the press.
17. J. Cai and C. Huang, *Gui-jin-shu Fenxi*, Yejin Gongye Chubaxie, Beijing, 1984, pp. 31 and 180.
18. K. B. Yatsimirskii and L. P. Tikhonova, *Talanta*, 1987, **34**, 69.

ANALYTICAL CHARACTERIZATION OF SOME PYRAZOLONES AND THEIR COPOLYMERS WITH SOME VINYL COMPOUNDS

E. IVANOVA, O. TODOROVA, A. TEREENINA and N. JORDANOV

Institute of General and Inorganic Chemistry, Bulgarian Academy of Sciences, BG-1040 Sofia, Bulgaria

G. BORISOV

Central Laboratory of Polymers, Bulgarian Academy of Sciences, BG-1040 Sofia, Bulgaria

(Received 25 May 1989. Revised 15 November 1989. Accepted 16 March 1990)

Summary—Some new pyrazolones have been synthesized and their copolymers with styrene, methylmethacrylate and methacrylic acid prepared. The pyrazolones and their styrene and methylmethacrylate copolymers are insoluble in water but form chelate complexes with some alkaline-earth and transition metal ions. The water-soluble methacrylic acid copolymers do not form complexes with these elements, however, probably because of hydrogen-bonding of the chelating groups to the methacrylic acid carboxyl groups. Special attention was paid to the complexation of Au(III), which was assumed to proceed mainly through the nitrogen atoms of the pyrazolone ring.

Several pyrazolone reagents are known to act as extractants and sorbents with good complexation properties.¹⁻⁴ They react with metal ions either through available chelating groups,^{2,3} or through the nitrogen atoms of the pyrazolone ring,⁵ providing selective or group complexation of metal ions, according to the conditions used.

The polymerization of vinyl derivatives is widely used in the synthesis of ion-exchange resins, since it yields products of uniform structure and high capacity.⁶ Chelating sorbents, however, have rarely been prepared by this procedure, owing to difficulties in the preparation of the monomers and to the complex nature of the polymerization.⁴

The purpose of the present work was the analytical characterization of the reagents 3-methyl-1-phenyl-4-crotonoylpyrazolone-5 (MPCP) and 3-methyl-1-phenyl-4-cinnamoylpyrazolone-5 (MPCyP) and of their copolymers with styrene, methylmethacrylate and methacrylic acid.

EXPERIMENTAL

The pyrazolones were synthesized according to Todorova *et al.*⁷ Their purity was checked by TLC on Merck GF₂₅₄ silica gel plates, with iron(III) chloride as developing agent. The purity and molecular weights of the polymeric products were determined by gel-permeation chromatography on a Waters apparatus

equipped with a WISP 712 automatic injector and either ultrastyrigel columns with pore sizes of 10⁵, 10⁴, 10³ and 500 Å, or a linear ultrahydrogel column. The structural studies were performed on samples in KBr discs or in chloroform solution with a Bruker IFS 113V Fourier transform IR spectrometer. The polymer composition was determined by elemental analysis for nitrogen and titrimetric analysis for carboxylic groups. The analytical characterization of the products involved studies of the pH-dependence, capacity and kinetics of complexation with various metal ions. The metal ion solutions (1 mg/ml) were prepared from Merck "Titrisol" solutions.

Dependence of the distribution coefficients on pH

Extraction studies. A 5-ml portion of solution at fixed pH (adjusted with hydrochloric acid or a buffer solution) containing 10 µg of the analyte element and 1 ml of a 0.05% aqueous solution of the reagent were extracted with 5 ml of methyl isobutyl ketone (MIBK). The concentration of metal ion in the extract was determined by flame atomic-absorption spectrometry (AAS). The degree of extraction *R* was calculated from

$$R = \frac{100D}{D + V_{aq}/V_{org}}$$

where D is the distribution coefficient of the metal ion and V_{org} and V_{aq} are the volumes of the organic and aqueous phases, respectively.

Sorption studies. A 10-mg portion of the sorbent was stirred with 10 ml of an aqueous solution (at fixed pH) containing 50 μg of the analyte element, until equilibrium was reached. The concentration of metal ion (Me) left in solution was determined by flame AAS. The distribution coefficient D was calculated from

$$D = \frac{\text{amount of Me on the sorbent}}{\text{amount of Me in solution}} \times \frac{\text{ml of solution}}{\text{g of dry sorbent}}$$

Sorption capacity

The capacity was determined under the optimum sorption conditions by stirring 10 mg of the sorbent with a solution containing 1 mg of the metal ion until equilibrium was reached, and determining the residual concentration of metal ion in solution by flame AAS.

RESULTS AND DISCUSSION

Characterization of the monomeric and polymeric products

The reaction of 3-methyl-1-phenylpyrazolone-5 with crotonic and cinnamic acid chlorides yielded the compounds MPCP (1) and MPCyP (2) containing a chelating group of β -diketonate type. The copolymerization of MPCP and MPCyP with styrene (St), methylmethacrylate (MMA) or methacrylic acid (MAA) yielded products (3)–(8). The structures are shown in Scheme 1.

In the infrared spectra of the copolymers, the vibrational bands characteristic for the pyrazolone ring (1552 – 1484 cm^{-1}) were preserved, which indicates that the polymerization proceeded through the double bond of the acyl residue of the monomers (1) and (2), without breakage of the pyrazolone ring. The vibrational bands of the carbonyl group (1600 – 1736 cm^{-1}) were also present in the spectra of the copolymers, which signified that the β -diketonate chelating groups were preserved. As a result, the copolymers should exhibit complexation behaviour analogous to that of the monomeric pyrazolones.

The pyrazolone content and weight average molecular weights of the copolymers are presented in Table 1. Clearly, the type of vinyl monomer strongly affects both characteristics.

Table 1. Characteristics of the copolymers

Copolymer	Pyrazolone, %	Weight average molecular weight
MPCP-St (3)	34.4	3.6×10^4
MPCP-MMA (4)	10.5	3.8×10^4
MPCP-MAA (5)	19.7	6.5×10^4
MPCyP-St (6)	42.2	2.8×10^4
MPCyP-MMA (7)	11.2	1.5×10^4
MPCyP-MAA (8)	50.3	5.7×10^4

The products (3), (5), (6) and (8) were obtained in powdered form, (5) and (8) being water-soluble owing to the free carboxylic groups. Products (4) and (7) were obtained in film form. The solids did not swell noticeably in water.

Extraction properties

The extraction curves are shown in Fig. 1. Only the monomeric pyrazolones extracted all the metal ions examined. The polymers extracted only Au(III) to a significant extent. The crotonoyl derivative (MPCP) was more efficient than the cinnamoyl one, and its extraction efficiency was comparable to that of 1-phenyl-3-methyl-4-benzoylpyrazolone-5 (PMBP), which is the most widely used pyrazolone,^{1,2} forming chelate complexes of β -diketonate type with the elements examined. Like PMBP, MPCP gives >95% extraction, but over a narrower pH range. This can be attributed to the MPCP complexes being less stable than those with PMBP, as a result of which hydrolysis prevails over complexation at higher pH values. The lack of extraction by products (5) and (8) can be attributed to blockage of the chelating groups by the free carboxylic groups of MAA, through intramolecular hydrogen bonding. The broad and intense band at 2500 – 3700 cm^{-1} (characteristic of hydrogen bonding) in the infra-

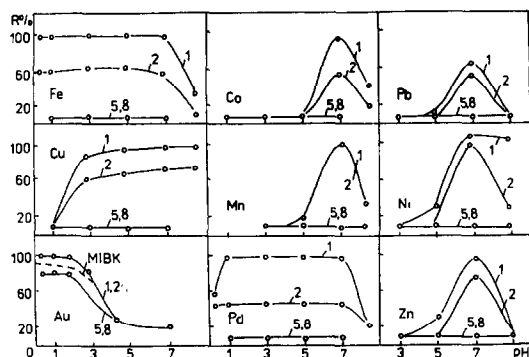
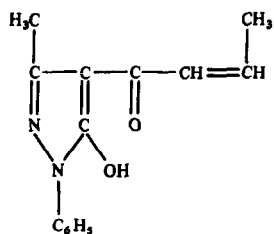
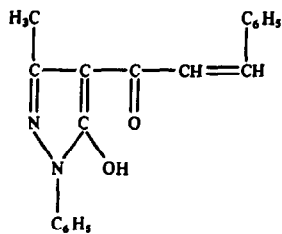


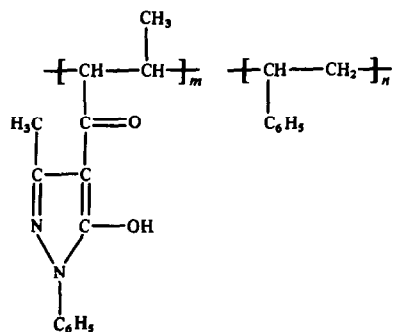
Fig. 1. Extraction curves for use of the pyrazolones MPCP (1), MPCyP (2) and the water-soluble copolymers MPCP-MAA (5) and MPCyP-MAA (8).



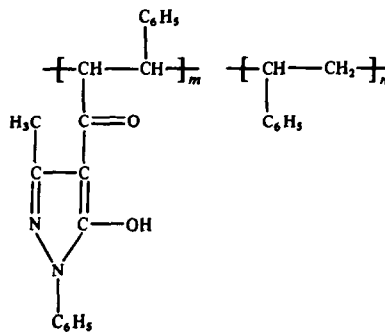
MPCP (1)



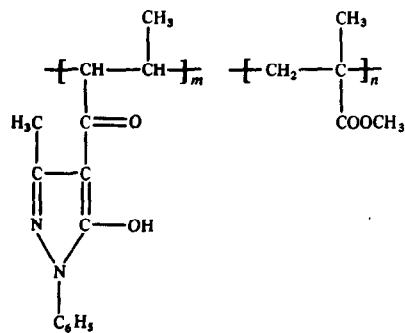
MPCyP (2)



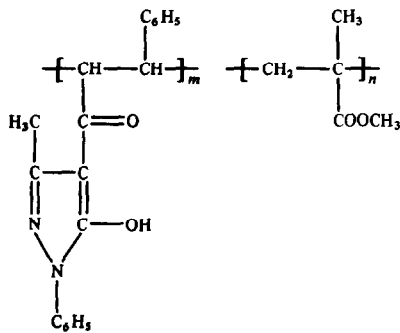
MPCP-St (3)



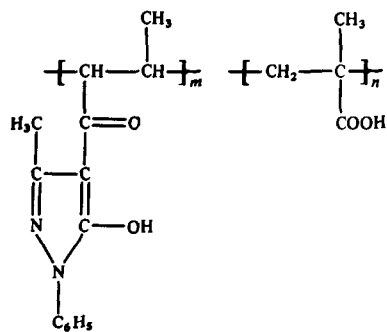
MPCyP-St (6)



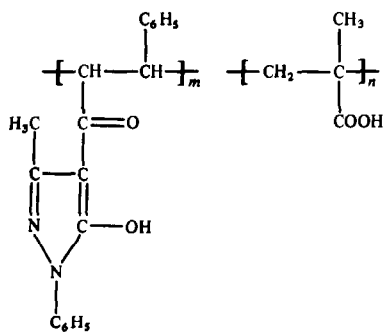
MPCP-MMA (4)



MPCyP-MMA (7)



MPCP-MAA (5)



MPCyP-MAA (8)

Scheme 1

red spectra of these products supports this assumption.

The extraction of Au(III) (see Fig. 1), is assumed to take place by another mechanism. It is known that pyrazolones readily react with Au(III) not through the β -diketonate groups, but through the nitrogen atoms of the pyrazolone ring.^{5,8} On the other hand, Au(III) is extracted from hydrochloric acid medium by organic oxygen-containing solvents (S), *e.g.*, MIBK, as the solvated ion-pair $H^+[(H_2O)_n S_m AuCl_4]^-$.⁹ The greater extraction of Au(III) by the two pyrazolones can be attributed to the co-ordination of these reagents through the nitrogen atoms of the pyrazolone ring to Au(III) by substitution for water molecules in the solvated complex anion. The polymeric reagents (5) and (8) were also co-ordinated to Au(III) (a colour change in the aqueous phase was observed), but their limited solubility in both the acid and the organic phase caused the appearance of a third phase, which contained some of the extracted species (the presence of Au in the third phase was proved qualitatively). The solubility of the two pyrazolones and the polymeric reagents and of the corresponding complexes was lower in *o*-xylene than in MIBK, and a third phase containing the Au(III) complexes was formed in all four cases. This would be in accord with the fact that *o*-xylene would be unable to solvate the $AuCl_4^-$ anion in the same way as MIBK.

Sorption properties of the solid copolymers

The dependences of the sorption efficiency on pH are shown in Fig. 2. Most of the elements tested were quantitatively sorbed from neutral or slightly alkaline medium. Pd(II) was insignificantly sorbed over the whole range examined. Au(III) was quantitatively sorbed between pH 3 and 7.

The sorption efficiency of the copolymers was the same irrespective of the type of vinyl compound and of the form of the sorbent (powder or film).

The sorption capacity of the sorbents was determined for Au(III) and Mg. The expected and experimentally determined values are presented in Table 2. The expected values were

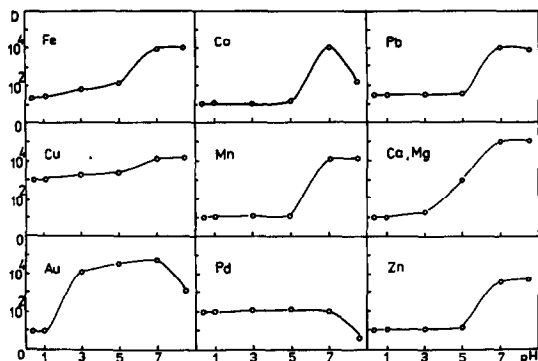


Fig. 2. Sorption curves for use of the solid copolymers. The curves are representative for all these reagents.

calculated on the basis of a stoichiometric reaction between the sorbent and the metal ion, and the content of pyrazolone in the sorbent.

The capacity found was higher than expected, and this is attributed to non-stoichiometric interaction, probably by sorption of metal ions at non-chelating active sites. Partial reduction of Au(III) to Au(I) on the sorbent is also possible. The powdered sorbents had a higher capacity than the film sorbents. This could be attributed both to the lower content of pyrazolone component in the MMA-based copolymers (*cf.* Table 1) and to the lower accessibility of the functional groups in the dense structure of these copolymers. This will only affect the completeness of sorption at high concentrations.

The kinetic studies also showed a difference between the powdered and film sorbents: contact for 3–5 min was sufficient for equilibrium to be reached with the powdered sorbents, whereas for the film sorbents equilibration required 2–3 times longer contact.

Complexation behaviour of the pyrazolones and the copolymers

Comparison of Figs. 1 and 2 reveals that the complexation properties of the pyrazolone monomers are preserved in the solid copolymers, but not in the water-soluble copolymers.

The difference between reagents (1) and (2) is a methyl (1) or phenyl (2) group in the side-chain of the molecule. These substituents affect the chelation properties of the pyrazolones but have no effect on the properties of the solid

Table 2. Sorption capacity, *meq/g*

Species	MPCP-St		MPCP-MMA		MPCyP-St		MPCyP-MMA	
	Expected	Found	Expected	Found	Expected	Found	Expected	Found
Au	0.5	1.0	0.1	0.03	0.5	0.4	0.1	0.02
Mg	0.7	7.3	0.2	1.2	0.7	6.7	0.2	0.4

copolymers. This may be attributed to delocalization of the electron density over the network of the solid copolymers.

The same applies to the complexation with Au(III) taking place through the nitrogen atoms of the pyrazolone ring. The difference in the extraction and sorption behaviour of the reagents towards Au(III) in the acidic range may also be related to the lower electron density of the pyrazolone rings in the structure of the solid copolymer. The increase in the degree of sorption of Au(III) in the pH range 3–7 correlates with the deprotonation of the β -diketonate groups in this pH range, which leads to an increase in the electron density of the pyrazolone ring and thus to an increase in the basicity of the nitrogen atoms. At pH > 7 partial hydrolysis of Au(III) takes place.

CONCLUSIONS

The reagents 3-methyl-1-phenyl-4-crotonoyl-pyrazolone-5 and 3-methyl-1-phenyl-4-cinnamoylpyrazolone-5 react with some transition elements, lead and palladium through chelating groups of β -diketonate type and extract these elements from neutral or slightly alkaline medium. Selective extraction of gold takes place in acidic medium, through co-ordination with the nitrogen atoms of the pyrazolone ring.

The complexation properties of the pyrazolones and their solid copolymers with styrene and methylmethacrylate are analogous. These copolymers may be used for the simultaneous preconcentration of alkaline-earth and transition metals, lead and gold from neutral medium.

The chelating groups of the initial reagents are also preserved in the water-soluble methacrylic acid copolymers, but are blocked by hydrogen bonding to the carboxylic groups of the acid.

REFERENCES

1. E. Ivanova, N. Jordanov, A. Terebenina, S. Mareva and G. Borisov, *Comm. Dept. Chem. Bulg. Acad. Sci.*, 1981, **14**, 167.
2. Yu. A. Zolotov and N. M. Kuz'min, *Ekstraksiya metallov atsilypyrazolonami*, Nauka, Moscow, 1977.
3. O. Todorova, E. Ivanova, A. Terebenina, N. Jordanov, K. Dimitrova and G. Borisov, *Talanta*, 1989, **36**, 817.
4. G. V. Myasoedova and S. B. Savvin, *Khelatobrazuyuchie sorbenty*, Nauka, Moscow, 1984.
5. V. S. Soldatov, S. B. Makarova, A. L. Braulavskaya, L. V. Novizkaya and V. N. Avilina, *Khim. Promysl.*, 1978, **8**, 584.
6. K. M. Saldadze and V. D. Kopylova-Valova, *Kompleksoobrazuyuchie ionity*, Khimiya, Moscow, 1980.
7. O. Todorova, A. Terebenina, I. Gizov, G. Mitov and G. Borisov, *J. Polym. Sci., Polym. Chem. Ed.*, in the press.
9. S. Trofimenko, *Chem. Rev.* 1972, **72**, 497.
10. N. Jordanov and I. Havezov, *Z. Anal. Chem.*, 1969, **244**, 176.

2-IODYLBENZOIC ACID AS AN OXIDIZING AGENT FOR THE DETERMINATION OF CERTAIN THIOXANTHENE DERIVATIVES

A. M. EL-BRASHY

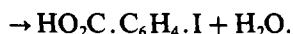
Department of Analytical Chemistry, Faculty of Pharmacy, Mansoura University, Mansoura, Egypt

(Received 30 May 1989. Revised 30 May 1990. Accepted 14 June 1990)

Summary—An indirect titrimetric method is described for the determination of chlorprothixene, methixene and thiothixene. A known and excessive volume of 2-iodylbenzoate is added and after a specified time the surplus is determined iodometrically. The method has been applied to the analysis of pharmaceutical preparations containing these drugs and the results obtained compare favourably with those from the pharmacopoeial methods. The method is simple, accurate and precise.

Thioxanthene derivatives have gradually replaced phenothiazines as neuroleptics.¹ This paper describes the assay of three of them, chlorprothixene, methixene and thiothixene. There are many reports on their identification,² and their determination by precipitation,^{3,4} titrimetry,⁵⁻⁹ colorimetry,¹⁰⁻¹⁴ fluorimetry,^{15,16} polarography,^{17,18} gas chromatography^{19,20} and high-pressure liquid chromatography.^{6,21,22} In the present study, 2-iodylbenzoic acid is used for their determination.

The electrode potentials of the 2-iodylbenzoate/2-iodosobenzoate system at 25° are 1.33, 0.61 and 0.56 V at pH 1, 4 and 7 respectively, whereas those of the 2-iodosobenzoate/2-iodobenzoate system are 1.21, 0.53 and 0.48 V at these pH values. 2-Iodylbenzoate is reduced by a two-electron change to 2-iodosobenzoate, which may undergo a further two-electron change to yield 2-iodobenzoate.²³



2-Iodosobenzoate has been used as a general oxidimetric titrant²⁴ and 2-iodylbenzoate has been used for the determination of isoniazid in the presence of 4-aminosalicylic acid and vitamin C,²³ and for the spectrophotometric determination of paracetamol²⁵ and some phenothiazine derivatives.²⁶

In the present work, 2-iodylbenzoate is used to oxidize chlorprothixene, methixene and

thiothixene to their corresponding sulphones and for their titrimetric determination in pure form or in formulations. The method has the advantage that it is applicable to small amounts of the compounds.

EXPERIMENTAL

Reagent

2-Iodylbenzoic acid was prepared as described by Banerjee *et al.*²⁷ and used as a $5 \times 10^{-3}M$ solution made by dissolving 1.4 g of the acid in about 6 ml of 1M potassium hydroxide and diluting to 1 litre with demineralized water. The solution was standardized iodometrically.

The pure drugs were obtained from several manufacturers. The purity of the chlorprothixene (NF grade), methixene hydrochloride and thiothixene (NF grade) was established by the official methods. Pharmaceutical preparations were obtained from commercial sources and analysed by the recommended official methods.⁶

Procedure

Prepare a 1.0 mg/ml solution of the compound to be studied, in 3M hydrochloric acid (containing 20% v/v acetic acid for chlorprothixene). Add an aliquot of the solution to a known volume of 0.005M 2-iodylbenzoate solution in a glass-stoppered Erlenmeyer flask. Shake the mixture occasionally and after the specified time (10 min for chlorprothixene and thiothixene, 15 min for methixene hydrochloride), add 10 ml of 100 mg/ml potassium iodide solution and titrate the liberated iodine with

0.02M sodium thiosulphate, using starch as indicator. Repeat the experiment without the thioxanthene.

Calculate the amount of drug present from the equation:

$$\text{Amount of drug (mg)} = (V_1 - V_2) MR/4$$

where V_1 and V_2 are the volumes of thiosulphate solution (ml) used in titration of the blank and sample respectively, R is the molecular weight of the drug and M is the molarity of the thiosulphate solution.

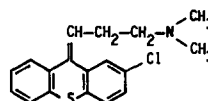
Assay of dosage forms

Extract an accurately weighed amount of the pulverized tablets, equivalent to 100 mg of the drug, with three 20-ml portions of 3M hydrochloric acid (containing 20% v/v acetic acid for taractan tablets). Filter the combined extracts into a 100-ml standard flask and dilute to volume with the solvent used. Transfer an accurately measured volume of this solution, equivalent to 5–12 mg of the drug, into an iodine flask and proceed as described above.

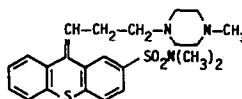
RESULTS AND DISCUSSION

2-Iodylbenzoate (IODB) oxidizes the compounds studied to their corresponding sulphones.

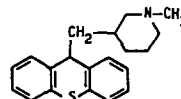
Chlorprothixene



Thiothixene



Methixene



The reaction can be represented by:



and the molar reaction ratio is 1:1. The drugs studied can be determined either in bulk or in tablets (Tables 1 and 2).

Hexa-amminocobalt(III) tricarbonatocobaltate(III) oxidizes chlorprothixene and thiothixene only to their sulphoxides and methixene to its sulphone.⁸ Dibromohydantoin, *N*-bromosuccinimide and *N*-bromophthalimide are reported to act as brominating agents in the titration of the three drugs,⁹ converting the tertiary nitrogen group into an *N*-bromo-derivative and not attacking the ring sulphur atom. The present work adds a new oxidizing

Table 1. Determination of thioxanthene derivatives with 2-iodyl benzoate

Compound	Proposed method		Official method ⁶	
	Taken, mg	Mean recovery, %*	Taken, mg	Mean recovery, %*
Chlorprothixene	3	98.7	100	99.0
	5	99.8	200	98.3
	8	100.7	300	99.8
	10	100.1		
	12	99.3		
	15	99.3		
Mean recovery \pm C.V.†		99.7 \pm 0.7		99.0 \pm 0.8
Methixene hydrochloride	3	100.9	100	100.7‡
	5	99.0	200	101.4
	8	99.5	300	99.2
	10	100.7		
	12	98.8		
	15	99.8		
Mean recovery \pm C.V.†		99.8 \pm 0.9		100.5 \pm 1.1
Thiothixene	3	99.8		
	5	101.0	100	102.2‡
	8	99.8	200	100.1
	10	100.3	300	100.1
	12	98.9		
	15	100.6		
Mean recovery \pm C.V.†		100.1 \pm 0.7		100.8 \pm 1.2

*Results are the average of at least 3 separate experiments.

†C.V. is the coefficient of variation.

‡Non-aqueous titration as for chlorprothixene.⁶

Table 2. Determination of thioxanthene derivatives in their dosage forms

Preparation	Proposed method		Official method ⁶ mean recovery, %*
	Taken, mg	Mean recovery, %*	
Taractan† (5 mg chlorprothixene per tablet)	5	101.4	98.2
	8	98.7	98.6
	10	100.2	98.6
Mean recovery ± C.V.		100.1 ± 1.3	98.5 ± 0.2
Navan‡ (10 mg thiothixene per tablet)	5	100.3	101.1§
	8	100.6	98.9
	10	101.0	99.0
Mean recovery ± C.V.		100.6 ± 0.4	99.7 ± 1.3
Tremaril¶ (5 mg methixene HCl per tablet)	5	100.3	100.0§
	8	99.8	101.4
	10	99.0	102.9
Mean recovery ± C.V.		99.7 ± 0.7	101.4 ± 1.5

*Results are the average of 3 separate experiments.

†Hoffmann La Roche, Switzerland.

‡Pfizer, Inc., Brooklyn, New York.

§Non-aqueous titration as for chlorprothixene.⁶

¶Wander, Berne, Switzerland.

Table 3. Statistical analysis between the proposed and official methods

	Chlorprothixene		Methixene hydrochloride		Thiothixene	
	Proposed	Official	Proposed	Official	Proposed	Official
No. of variates	6	3	6	3	6	3
Mean recovery, %	99.7	99.0	99.8	100.5	100.0	100.8
Variance	0.50	0.58	0.79	1.28	0.53	1.46
<i>Student-t</i>		1.19*		0.99*		1.45*
Variance ratio (<i>F-test</i>)		1.15*		1.61*		2.75*

*The tabulated values at $P = 0.05$ are 2.36 and 5.79 for the *Student-t* and *F-test*, respectively.

agent for conversion of these thioxanthenes into their sulphones.

The results for determination of the pure compounds and analysis of their dosage forms are abridged in Tables 1 and 2 respectively, and are in good agreement with those obtained by the official USP methods.⁶ Statistical analysis²⁸ of the results (Table 3) shows no significant differences in precision and accuracy between the proposed and official⁶ methods. Moreover, the proposed method is simpler than the official⁶ methods, which recommend a non-aqueous titration for chlorprothixene, HPLC for thiothixene and its tablets, and a tedious, lengthy procedure for chlorprothixene tablets. In addition, small amounts (3–15 mg) of the drug can be determined with good results by the proposed procedure.

When the chlorprothixene reaction product was chromatographed on a silica gel plate with 30 mg/ml ammonium acetate solution in methanol–water (100 + 20) mixture it gave only one spot (R_f 0.45), whereas chlorprothixene and chlorprothixene sulfoxide (prepared by oxida-

tion of the former with alkaline permanganate¹⁶), gave spots with R_f values of 0.66 and 0.55 respectively, so the reaction product is not the sulfoxide¹⁶ but presumably the sulphone.

The most striking feature of the reagent is its stability; in the dry form it is stable for many years, and in alkaline aqueous solution is stable for about 2 months and is thus recommended for use in routine analysis in control laboratories.

REFERENCES

1. W. O. Foye, *Principles of Medicinal Chemistry*, p. 218. Lea & Febiger, Philadelphia, 1976.
2. E. G. C. Clarke, *Isolation and Identification of Drugs*, Part I, pp. 49, 258, 349, 414 and 574. Pharmaceutical Press, London, 1978.
3. J. Dobrecky, *Rev. Farm.*, 1972, **114**, 42.
4. S. Tammilehto, *Acta Pharm. Fenn.*, 1979, **88**, 25.
5. O. Adam, *Acta Pol. Pharm.*, 1978, **35**, 63.
6. *The United States Pharmacopoeia XXI*, National Formulary XVI, pp. 207 and 1057. US Pharmacopoeial Convention, Washington, DC, 1985.
7. Y. A. Beltagy, A. S. Issa and M. S. Mahrous, *Talanta*, 1978, **25**, 349.

8. F. Belal, M. I. Walash and F. A. Aly, *Microchem. J.*, 1988, **38**, 295.
9. M. I. Walash, M. Rizk and A. El-Brashy, *Analyst*, 1988, **113**, 1309.
10. Y. A. Beltagy, *Pharmazie*, 1976, **31**, 483.
11. E. S. A. Ibrahim, A. S. Issa, M. A. Abdel-Salam and M. S. Mahrous, *Talanta*, 1983, **30**, 531.
12. M. A. Abdel-Salam, A. S. Issa, M. Mahrous and M. E. Abdel-Hamid, *Anal. Lett.*, 1985, **18**, 1391.
13. M. I. Walash, M. Rizk and A. El-Brashy, *Pharm. Weekblad Sci. Ed.*, 1986, **8**, 234.
14. M. Rizk, M. I. Walash and A. El-Brashy, *Spectrosc. Lett.*, 1988, **21**, 393.
15. L. E. Eiden and J. A. Ruth, *Experientia*, 1978, **34**, 1062.
16. S. A. Tammilehto, *J. Pharm. Pharmacol.*, 1980, **32**, 524.
17. H. Oelschläger and R. Spohn, *Arch. Pharm.*, 1981, **314**, 355.
18. M. I. Walash, M. Rizk, F. Belal and A. El-Brashy, *Microchem. J.*, 1988, **38**, 300.
19. A. Eklund, J. Jonsson and J. Schuberthy, *J. Anal. Toxicol.*, 1983, **7**, 24.
20. M. Krejčí, K. Šlais, D. Kouřilová and M. Vespalcová, *J. Pharm. Biomed. Anal.*, 1984, **2**, 197.
21. A. Po and W. J. Irwin, *J. Pharm. Pharmacol.*, 1979, **31**, 512.
22. B. B. Wheals, *J. Chromatog.*, 1980, **187**, 65.
23. K. K. Verma and A. K. Gulati, *Anal. Chem.*, 1982, **54**, 2550.
24. K. K. Verma and A. K. Gupta, *Talanta*, 1982, **29**, 779.
25. K. K. Verma and A. Jain, *ibid.*, 1985, **32**, 238.
26. S. M. Hassan, F. Belal, F. A. Ibrahim and F. A. Aly, *Anal. Lett.*, 1989, **22**, 1485.
27. A. Banerjee, G. C. Banerjee, S. Bhattacharya, S. Banerjee and H. Samaddar, *J. Indian Chem. Soc.*, 1981, **58**, 605.
28. J. D. Hinchey, *Practical Statistics for Chemical Research*, Methuen, London, 1969.

SPECTROPHOTOMETRIC DETERMINATION OF MOLYBDENUM WITH 7,8-DIHYDROXY-4-METHYLCOUMARIN AND CETYLTRIMETHYLAMMONIUM BROMIDE

M. TAREK M. ZAKI*

Department of Chemistry, Faculty of Science, Ain Shams University, Abbassia, Cairo, Egypt

A. K. ABDEL-KADER and M. M. ABDALLA

Department of Chemistry, Faculty of Science, Azhar University, Nasr City, Cairo, Egypt

(Received 20 April 1989. Revised 14 February 1990. Accepted 17 March 1990)

Summary—The 1:2 complexes formed between molybdenum and 7,8-dihydroxy-4-methylcoumarin in the presence and absence of cetyltrimethylammonium bromide (CTAB) have been studied. The binary complex formed at pH 5.6–6.0 in the absence of CTAB exhibits an absorption maximum at 360 nm with a molar absorptivity of 5.1×10^4 l.mole⁻¹.cm⁻¹. The complex formed at pH 4.8–6.0 in the presence of CTAB has a molar absorptivity of 1.32×10^5 l.mole⁻¹.cm⁻¹ at 400 nm, the wavelength of maximum absorption. Optimum conditions for complex formation were investigated and a rapid, sensitive and relatively selective method for the determination of up to ~70% of Mo in diverse alloys and steels is described. Small amounts of zirconium and tungsten interfere.

The classical spectrophotometric methods for determination of molybdenum, based on its reaction with thiocyanate in the presence of a reducing agent¹ and with toluene-3,4-dithiol,² are not too selective, because they are subject to interference from many other elements. In recent years, various surfactants have been employed to enhance the sensitivity of spectrophotometric methods for molybdenum^{3–18} but many of these methods also lack selectivity because of the use of common unselective chromogenic reagents such as phenylfluorone and its derivatives^{14–17} and flavonols¹⁹ (morin and quercetin). Little attention has been paid to the reaction of the isomeric coumarin-based chromogenic reagents with molybdenum and other metal ions.

Consequently, the present study was undertaken to determine whether 7,8-dihydroxy-4-methylcoumarin (DHMC) might yield greater sensitivity and selectivity in the presence of various surfactants. This paper describes the results of these studies and a new rapid method for the determination of molybdenum in diverse alloys and steels.

EXPERIMENTAL

Reagents

All chemicals used were analytical-reagent grade and doubly distilled water was used throughout.

7,8-Dihydroxy-4-methylcoumarin (DHMC) was synthesized according to Horii's procedure²⁰ and recrystallized from methanol (m.p. 236°). The purity of the reagent was checked by paper chromatography with 1:4 v/v diethyl ether–petroleum ether (b.p. 40–60°) mixture as eluent. A single yellow band was obtained for the pure product and elemental analysis showed that the purity was >99%, (calculated, C 62.50%, H 4.17%; found, C 62.4%, H 4.1%). No changes in the structure of the solid reagent occurred within one year, as shown by infrared, ultraviolet and NMR spectroscopic measurements. A 5×10^{-3} M solution of the reagent was prepared by dissolving 0.3300 g in 85 ml of warm methanol and diluting to 250 ml with water. This solution was stable for more than two weeks.

Molybdenum(VI) solution, 10⁻³M. Prepared by dissolving 1.2359 g of ammonium heptamolybdate tetrahydrate in water and diluting the solution to 1 litre. The solution was standardized complexometrically²¹ and a working solution was prepared by dilution.

*To whom all correspondence should be addressed.

Cetyltrimethylammonium bromide (CTAB) solution, 10⁻²M. Prepared by dissolving 1.822 g of CTAB in warm water and diluting the solution to 500 ml.

Acetate buffer, pH 5.8. Prepared by mixing equal volumes of 0.75M sodium acetate and 0.05M acetic acid. The pH was adjusted by addition of small amounts of concentrated sodium hydroxide solution or glacial acetic acid.

EDTA solution, 0.1M.

Mixed acid solution. Prepared by adding 150 ml of concentrated phosphoric acid and 150 ml of concentrated nitric acid to 700 ml of concentrated perchloric acid, with stirring.

Sulphuric acid, 50% v/v.

Apparatus

A Perkin-Elmer Lambda 3B double-beam spectrophotometer and 1-cm fused-silica cells were used for the absorbance measurements. The pH measurements were made with a Schott Geräte CG 710 pH-meter and an N37A combination glass-calomel electrode.

Determination of molybdenum in alloys and steels

Decompose an accurately weighed amount of sample, containing up to 30 mg of molybdenum, as described in the ASTM procedure for steels,²² by heating gently with 30 ml of the mixed acid solution. Evaporate the solution to fumes of perchloric acid, then add 1.5 ml of concentrated hydrochloric acid and evaporate to fumes again to volatilize chromyl chloride. Repeat the addition of hydrochloric acid and the fuming step until no more red fumes are evolved, then evaporate the solution to *ca.* 15 ml, cool and add 50 ml of water and 70 ml of 50% v/v sulphuric acid. Heat the solution to boiling, then cool it to room temperature in a water-bath and dilute it to volume with water in a 1-litre standard flask. Transfer up to 0.5 ml of this solution to a 25-ml standard flask,

add 0.5 ml of 0.1M EDTA, 2 ml of 5 × 10⁻³M DHMC and 5 ml of 0.01M CTAB and dilute to volume with acetate buffer (pH 5.8). Mix thoroughly, allow the solution to stand for 5 min, then measure the absorbance at 400 nm in 1-cm cells against a similarly prepared reagent blank. Determine the molybdenum concentration by reference to a calibration curve covering the range 0–0.6 µg/ml molybdenum.

RESULTS AND DISCUSSION

Effect of different surfactants

From Table 1, which shows the effect of different types of surfactants on the absorption characteristics of the molybdenum DHMC complex, it is apparent that the anionic and non-ionic surfactants tested were relatively ineffective in sensitizing the complex. However, the cationic surfactants tested resulted in ~2–2.5-fold increases in sensitivity, with bathochromic shifts of ~30–40 nm in the absorption maximum. Because CTAB yielded the greatest increase in sensitivity, it was chosen for further work.

Figure 1 shows the absorption spectra of the molybdenum DHMC complexes formed in the absence (curve III) and presence (curve IV) of CTAB and those of the corresponding reagent blanks (curves I and II, respectively), which do not absorb to any significant extent at the wavelengths of maximum absorption (360 and 400 nm, respectively) of the two complexes. Increasing the ionic strength of the test solutions from 0.2 to 0.4M had no effect on complex formation, and the addition of hydroxylamine hydrochloride or ascorbic acid in 500–700-fold molar ratio to molybdenum did not produce any spectral changes, suggesting that both Mo(VI) and Mo(V) form similar complexes.

Table 1. Effect of surfactants on the absorbance of the molybdenum DHMC complex*

Surfactant	Type	λ_{\max} , nm	Absorbance	ϵ , l.mole ⁻¹ .cm ⁻¹
None	—	360	0.204	5.10 × 10 ⁴
Cetyltrimethylammonium bromide (CTAB)	cationic	400	0.528	1.32 × 10 ⁵
Cetylpyridinium bromide (CPB)	cationic	390	0.416	1.04 × 10 ⁵
Tetradecyldimethylbenzylammonium chloride (Zephiramine)	cationic	400	0.484	1.21 × 10 ⁵
Polyoxyethylene- <i>p</i> - <i>tert</i> -octylphenol (Triton X-100)	non-ionic	360	0.230	5.75 × 10 ⁴
Ethoxylated fatty alcohol (Emulsifier S)	non-ionic	360	0.235	5.87 × 10 ⁴
Sodium lauryl sulphate (SLS)	anionic	360	0.185	4.62 × 10 ⁴
Sodium alkylbenzene sulphonate (SAS)	anionic	360	0.169	4.22 × 10 ⁴

*Taken: 4 × 10⁻⁶M Mo, 4 × 10⁻⁴M DHMC and 2 × 10⁻³M surfactant (1% for non-ionic types) at pH 5.8; 1-cm cells.

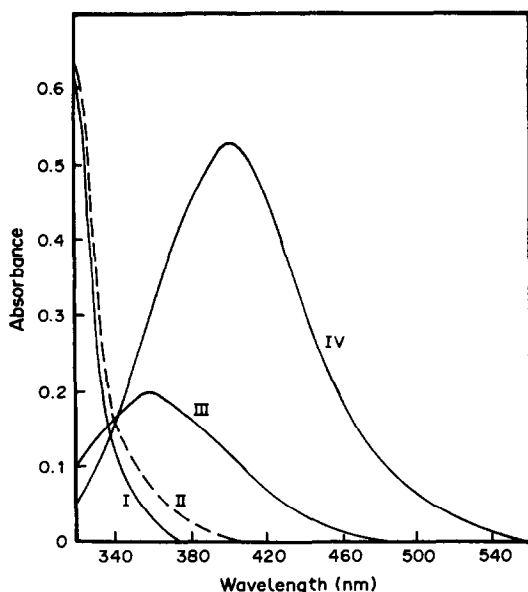


Fig. 1. Absorption spectra of molybdenum DHMC complexes in the presence and absence of CTAB. $[Mo] = 4 \times 10^{-6}M$; $[DHMC] = 4 \times 10^{-4}M$; $[CTAB] = 2 \times 10^{-3}M$; pH = 5.8; 1-cm cells. (I) Reagent blank in the absence of CTAB, vs. buffer solution; (II) reagent blank in the presence of CTAB, vs. CTAB + buffer solution; (III) Mo complex in the absence of CTAB, vs. reagent blank; (IV) Mo complex in the presence of CTAB, vs. reagent blank.

Factors influencing complex formation

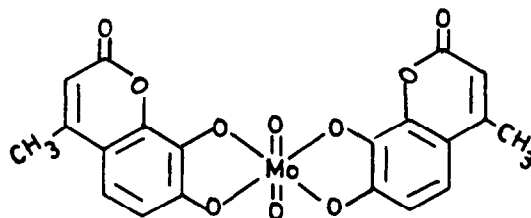
Tests showed that the optimum pH ranges for the molybdenum complexes formed in the absence and presence of CTAB are 5.6–6.0 and 4.8–6.0, respectively. In these tests the pH was controlled by using 0.4M acetate buffers of different pH. The optimum DHMC concentration was found to be $1-5 \times 10^{-4}M$ for both systems and maximum sensitization of the complex occurred at CTAB concentration $> 1 \times 10^{-3}M$. Consequently, a pH of 5.8 and DHMC and CTAB concentrations of 4×10^{-4} and $2 \times 10^{-3}M$, respectively, were chosen for subsequent work.

The critical micelle concentration (CMC) of CTAB under these experimental conditions, as determined by conventional surface tension measurements, was $9.4 \pm 0.2 \times 10^{-4}M$, which is in good agreement with the value ($9.2 \times 10^{-4}M$) reported by Mukherjee and Mysels.²³ The formation of the complexes in the absence and presence of CTAB was instantaneous at room temperature and the absorbances remained constant for up to 90 and 150 min, respectively. Beer's law was obeyed for up to $0.6 \mu\text{g/ml}$ molybdenum both in the absence and presence of CTAB, and the corresponding molar absorptivities were 5.1×10^4

and $1.32 \times 10^5 \text{ l. mole}^{-1} \cdot \text{cm}^{-1}$. The detection limit found was $0.016 \mu\text{g/ml}$ molybdenum.

Stoichiometry of the complexes

The mole-ratio method could not be used to determine the composition of the complexes formed in the absence and presence of CTAB, because the broad dependence of the absorbance on the mole fraction of Mo limited accurate evaluation of the metal to ligand ratio. However, the continuous-variations method indicated a metal to ligand ratio of 1:2 for both complexes. The binary complex formed in the absence of CTAB was retained on an anion-exchanger, indicating that it is negatively charged. Infrared measurements on the solid complex confirmed the presence of both $Mo=O$ and $Mo-O$ bonds.²⁴ On the basis of these data, the following structure is proposed:



Similar structures have been proposed for the formation of molybdate-hydroxamic acid complexes.²⁵⁻²⁷

Effect of diverse ions

Tests showed that up to a 700-fold molar ratio (to Mo) of Co^{2+} , 500-fold ratio of Ba, Cd, La, Mg, Zn, I^- , SCN^- , $S_2O_3^{2-}$, SO_4^{2-} , malonate and oxalate, and 100-fold ratio of Ag, As(V), Ca, Hg^{2+} , Mn^{2+} , Sr, F^- and PO_4^{3-} did not interfere in the determination of $7.5 \mu\text{g}$ of molybdenum.

In the presence of 0.5 ml of 0.1M EDTA as masking agent, up to a 500-fold ratio of Al, 300-fold ratio of Cu^{2+} and Ni^{2+} , 200-fold ratio of Cr^{3+} and Fe^{3+} , a 50-fold ratio of V(V) and 15-fold ratio of Pb^{2+} and Ti^{4+} do not interfere. However, Zr^{4+} and W(VI) interfere seriously and can only be present in 7- and 2-fold ratio to Mo, respectively.

Applications

Table 2 shows that the results obtained by the proposed method for molybdenum in various diverse alloys and low and high alloy steels are in excellent agreement with those obtained by the ASTM method²² involving spectrophotometric measurement of the butyl acetate extract

Table 2. Determination of molybdenum in alloys and steels

Sample	Composition, %	Molybdenum found, %	
		By ASTM method	This work*
Cobalt-chromium alloy	Si 0.2; Mn 0.2; Al 0.1; Fe 0.9; Ni 1.7; Cr 28.2; Co 62.9	5.64	5.64 ± 0.01
Cobalt-chromium-nickel alloy	Si 0.4; Fe 1.5; Ni 14.9; Cr 26.9; Co 50.6	5.39	5.40 ± 0.01
Nickel-chromium alloy	Si 0.4; Mn 1.3; Fe 6.8; Cr 22.0; Ni 63.0	6.12	6.11 ± 0.1
Nickel-chromium-molybdenum alloy	Si 0.4; Mn 0.3; Fe 5.0; W 4.4; Cr 15.4; Ni 57.5	16.85	16.83 ± 0.04
Ferromolybdenum	C 0.2; Si 0.2; Cu 0.1; Fe 27.0	72.23	72.18 ± 0.12
Low alloy steel	C 0.1; Cr 0.1; Cu 0.3; W 0.1; Ti 0.1; Fe 99.0	0.10	0.10 ± 0.00†
Low alloy steel	C 0.4; Mn 0.9; Si 0.3; Ni 0.5; Cr 0.5; Fe 97.0	0.26	0.26 ± 0.00†
Low alloy steel	C 0.1; Mn 0.6; Si 0.5; Cr 1.4; Cu 0.2; Fe 96.6	0.50	0.50 ± 0.00
Low alloy steel	C 0.1; Mn 0.1; Si 1.0; Cr 1.3; Cu 0.2; V 0.4; Ni 0.6; Fe 95.2	0.83	0.83 ± 0.00
High alloy steel	C 1.5; Mn 0.1; Si 0.6; Cr 4.8; Cu 0.1; V 0.9; Fe 90.8	0.95	0.95 ± 0.00
High carbon chromium steel	C 1.6; Si 0.4; Cr 12.1; Fe 84.6	0.97	0.97 ± 0.00
Low carbon chromium steel	C 0.3; Mn 0.1; Si 0.3; V 1.2; Cr 5.2; Fe 91.3	1.42	1.42 ± 0.01
Low carbon molybdenum steel	C 0.6; Si 0.3; W 1.4; Cr 3.9; V 1.1; Fe 84.7	7.86	7.84 ± 0.02

*Mean ± standard deviation of five values.

†Molybdenum separated by α -benzoinoxime extraction.²⁸

of the molybdenum thiocyanate complex. For steels containing <0.5% of molybdenum, the preliminary separation of molybdenum from the matrix elements by chloroform extraction of the α -benzoinoxime complex, as described by Donaldson,²⁸ was necessary. The extract was evaporated to dryness in a water-bath, the residue was treated with 2 ml of concentrated nitric acid to destroy organic material and the solution was evaporated to dryness. The resulting residue was dissolved in the minimum amount of 0.01M hydrochloric acid, 0.5 ml of 0.1M EDTA solution was added and molybdenum was determined as described in the proposed method.

Table 3 shows that the proposed method is more sensitive than many other methods involving the use of surfactants and common chromogenic reagents such as Catechol Violet, and derivatives of gallein and phenylfluorone. It is also more selective than those methods. Methods involving the use of *o*-hydroxyhydroquinonephthalein and salicylfluorone in conjunction with LT-221 and CTAB, respectively, are slightly more sensitive.

Acknowledgements—The authors thank Helwan Engineering Industries, General Metal Co., Delta Steel Mill and Egyptian Iron and Steel Co. (Cairo, Egypt) for providing the alloy and steel samples.

Table 3. Spectrophotometric characteristics of molybdenum complexes in micellar media

Reagent	Surfactant*	λ_{\max} , nm	ϵ , $10^4 \times l.mole^{-1}.cm^{-1}$	Reference
Catechol Violet	CTAB		4.60	3
Pyrocatechol Violet†	DMBAC	560	6.25	4
Pyrocatechol Violet	Zephiramine	690	4.24	5
Gallein	CTAB	618	3.69	6
Dibromogallein	PPOSA	642	10.8	7
Dibromoalazarin Violet	CTAB	635	12.0	10
Sodium 2-bromo-4,5-dihydroxyazobenzene-4'-sulphonate	CTAC	525	6.10	11
<i>o</i> -Hydroxyhydroquinonephthalein	LT-221	520	13.7	12
6,7-Dihydroxy-2-phenylbenzopyrylium chloride	CP	525	7.01	13
Phenylfluorone	Tween 80	536	10.6	14
Phenylfluorone	Triton X-100	520	11.1	15
4,5-Dibromophenylfluorone	CTAB	538	12.0	16
Salicylfluorone	CTAB	530	14.0	17
Thiocyanate	Triton X-100	468	1.70	18
7,8-Dihydroxy-4-methylcoumarin	CTAB	400	13.2	Proposed method

*Dialkylmethylbenzylammonium chloride (DMBAC); poly(propylene oxide)- α -stearyldimethylammonium chloride (PPOSA); cetyltrimethylammonium chloride (CTAC); polyoxyethylene sorbitan monolaurate (LT-221); cetylpyridinium (CP); polyoxyethylene sorbitan mono-oleate (Tween 80). For others see Table 1.

†Extraction procedure.

REFERENCES

- C. E. Crouthamel and C. E. Johnson, *Anal. Chem.*, 1954, **26**, 1284.
- S. H. Allen and M. B. Hamilton, *Anal. Chim. Acta*, 1952, **7**, 483.
- B. W. Bailey, J. E. Chester, R. M. Dagnall and T. S. West, *Talanta*, 1968, **15**, 1359.
- H. Kohara, N. Ishibashi and K. Abe, *Bunseki Kagaku*, 1970, **19**, 48.
- T. C. Chou and S. W. Chang, *Fen Hsi Hua Hsueh*, 1980, **8**, 527; *Chem. Abstr.*, 1981, **95**, 196733v.
- C. L. Leong, *Analyst*, 1970, **95**, 1018.
- K. Liu and R. Yu, *Huaxue Xuebao*, 1987, **45**, 584; *Chem. Abstr.*, 1987, **107**, 146464d.
- L. I. Ganago, L. A. Alinovskaya, I. F. Ivanova and L. V. Kovaleva, *Zh. Analit. Khim.*, 1984, **39**, 251.
- V. I. Nazarova, M. P. Trofimentseva, G. L. Denishchenko, R. K. Chernova and G. M. Beloliptseva, *Otkrytiya, Izobret., Prom. Obratzysy, Tovarnye Znaki*, 1984, **1**, 173; *Chem. Abstr.*, 1984, **100**, 131796v.
- H. Shen, *Huaxue Shiji*, 1981, **4**, 205; *Chem. Abstr.*, 1982, **96**, 115046u.
- Y. Wakamatsu, *Bunseki Kagaku*, 1977, **26**, 470.
- I. Mori, Y. Fujita, Y. Kamata and T. Enkoi, *ibid.*, 1978, **27**, 259.
- G. F. Tansyura and T. G. Plavetskaya, *Zh. Analit. Khim.*, 1985, **40**, 228.
- J. Xu and H. Wang, *Lanzhou Daxue Xuebao, Ziran Kexueban*, 1985, **21**, 128; *Chem. Abstr.*, 1986, **104**, 122113a.
- A. Tie, W. Yu, C. Li, W. Liao, Y. Shi, X. Liao and H. Liu, *Fenxi Huaxue*, 1983, **11**, 839; *Chem. Abstr.*, 1984, **100**, 184933u.
- D. Wang, J. Bai, J. Chen and Q. Pan, *ibid.*, 1984, **12**, 140; *Chem. Abstr.*, 1984, **100**, 167326f.
- H. Shen and Z. Wang, *Gaodeng Xuexiao Huaxue Xuebao*, 1982, **3**, 300; *Chem. Abstr.*, 1983, **98**, 46062y.
- K. Hayashi, A. Yamamoto, Y. Fugimura and S. Ito, *Bunseki Kagaku*, 1980, **29**, T39.
- M. Katyal, *Talanta*, 1968, **15**, 95.
- Z. Horii, *J. Pharm. Soc. Japan*, 1939, **59**, 201.
- T. S. West, in *Complexometry with EDTA and Related Reagents*, 3rd Ed., pp. 196, 197. B.D.H., Poole, 1969.
- 1983 *Annual Book of ASTM Standards, Chemical Analysis of Metals and Metal-Bearing Ores*, Vol. 0.3.05, pp. 564, 565. ASTM, Philadelphia, 1983.
- P. Mukherjee and K. J. Mysels, *Natl. Std. Ref. Data Ser., Natl. Bur. Stds.*, 1971, No. 36, 1.
- M. Cousins and M. L. H. Green, *J. Am. Chem. Soc.*, 1964, **86**, 1567.
- B. Chatterjee, *Coord. Chem. Rev.*, 1978, **26**, 281.
- N. K. Chawdhuri, A. K. Sarkar and J. Das, *Z. Anal. Chem.*, 1971, **254**, 365.
- F. Salinas and M. Jiménez-Arrabal, *Microchem. J.*, 1985, **32**, 383.
- E. M. Donaldson, *Talanta*, 1980, **27**, 79.

COMPLEXOMETRIC TITRATION OF Ti(IV) WITH 2-(5-CHLORO-2-PYRIDYLAZO)-5-DIMETHYLAMINOPHENOL AS INDICATOR

H. J. MARINI, R. I. ANTON and R. A. OLSINA

Departamento de Química Analítica "Dr. Carlos B. Marone", Universidad Nacional de San Luis,
P.O. Box 375, 5700 San Luis, Argentina

(Received June 1989. Revised 15 November 1989. Accepted 2 February 1990)

Summary—A method for determination of titanium by a reverse titration with EDTA in the presence of hydrogen peroxide, with 2-(5-chloro-2-pyridylazo)-5-dimethylaminophenol as indicator, is presented; use of the method for analysis of titanium paints is also described.

Direct methods for complexometric titration of titanium are uncommon, although various means of end-point detection have been developed.¹⁻³ The usual methods are indirect, with back-titration of excess of EDTA with various cations.^{4,5}

It has been shown that most of the indirect back-titration methods which do not use hydrogen peroxide suffer from errors due to the precipitation of hydrous titanium oxide, which begins to form at pH 2.⁶ A possible mechanism for this side-reaction is the initial formation of a titanium-EDTA-oxo (or hydroxo) complex, followed by polymerization through oxygen bridges. This process would continue by the formation of sufficiently large aggregates to produce colloidal hydrous titanium oxide and finally a precipitate. Adding hydrogen peroxide⁷ to a Ti(IV) solution containing EDTA inhibits the precipitation and the solution remains clear during the titration. There is also a stabilizing effect of hydrogen peroxide on the Ti(IV)-EDTA complex by formation of ternary Ti(IV)-hydrogen peroxide-EDTA complexes,⁸ in which hydrogen peroxide displaces the oxo (or hydroxo) group in the Ti(IV)-EDTA complex.

The most frequently used metallochromic indicators are PAN or Calcein,^{9,10} Xylenol Orange,¹¹ Methylthymol Blue and Methylcalcein Blue.⁵ The titrants are EDTA and DCTA; the latter has the advantage of greater selectivity when Nb(V),¹² Ta(V)¹³ and V(V)¹⁴ are present, though the reaction is said to be slower than that with EDTA.⁴ The method has also been combined with a prior separation step to increase its range of application.

In previous work¹⁵ we noted the formation of a ternary complex between 2-(5-chloropyridylazo)-5-dimethylaminophenol (5-CIDMPAP), hydrogen peroxide and Ti(IV) in buffered aqueous ethanol solutions at pH 5.5. This reaction is instantaneous, yielding a 1:2:2 Ti(IV)-hydrogen peroxide-5-CIDMPAP ternary complex. The complex is purple, with maximum absorption at 534 nm; its molar absorptivity is 4.59×10^4 l.mole⁻¹.cm⁻¹. The stability constant is 3.47×10^{13} . The complex remains stable for up to an hour.

In the present work we show the feasibility of using this pyridylazo reagent as indicator in the reverse complexometric determination of Ti(IV), since the stability constant of the complex is considerably lower than that of the ternary Ti(IV)-H₂O₂-EDTA complex (2.51×10^{20}).⁵

EXPERIMENTAL

Reagents

5-CIDMPAP was prepared by coupling *m*-dimethylaminophenol with sodium 5-chloro-2-pyridyldiazotate, according to the method of Shibata *et al.*,¹⁶ and purified by repeated dissolution-precipitation cycles with aqueous ethanol. A 25% solution of the pure material was prepared, and further diluted with ethanol as required. All solutions were kept away from light. A 5×10^{-4} M solution is stable for at least 25 days.

A standard Ti(IV) solution was prepared according to Roseman and Thornton.¹⁷ To obtain reproducible results the solution must be prepared daily.

A 30% hydrogen peroxide solution was prepared by dilution of a "200 volume" solution.

A 0.01M EDTA solution was prepared by dissolving the salt in distilled water, and standardized by potentiometric titration with a standard Cu(II) solution.

A 0.05M acetic acid-ammonium acetate buffer (pH 5.5) was prepared.

Apparatus

Spectrometric titrations were done with special cells built according to Sweetser and Bricker,¹⁸ a Varian spectrophotometer, model 634, and a Metrohm Dosimat F422-P automatic burette.

Procedure

A preliminary titration is needed to establish the volume of strong base required to keep the pH of the titrant solution between 5 and 5.5 near the end-point. For this, place 5.0 ml of 0.01M EDTA, 3 ml of 30% hydrogen peroxide, and 0.4 ml of 0.003M indicator in a 250-ml conical flask. Add 40 ml of buffer solution (pH 5.5) and an equivalent amount of the Ti(IV) solution in sulphuric acid medium and measure the pH near the end-point. Find the volume of 2M sodium hydroxide needed to restore the pH to 5.5.

For the determination place 5.0 ml of 0.01M EDTA, 3 ml of 30% hydrogen peroxide and 0.4 ml of 0.003M indicator in the special cell for spectrometric titrations. Add 40 ml of the buffer and the volume of 2M sodium hydroxide determined as above. Dilute to 100 ml with distilled water and titrate with the sample Ti(IV) solution, monitoring the absorbance at 534 nm.

The end-point can also be detected visually, the colour change being from yellow to violet; the solution must be vigorously stirred throughout the titration.

Analysis of paint

Weigh out a sample of paint containing between 100 and 200 mg of TiO₂ and place it in a 250-ml conical flask. Moisten the sample with a few drops of alcohol, add 40 ml of hydrochloric acid (1 + 1) and boil gently for 5–10 min. Dilute the contents of the flask to 100 ml with hot water, boil for a few minutes, filter (paper), and wash with 100 ml of hot water.

Transfer the insoluble material (TiO₂, silica, silicates) into a 250-ml conical flask. Add 20 ml of concentrated sulphuric acid and 10 g of ammonium sulphate. Mix well, and heat until

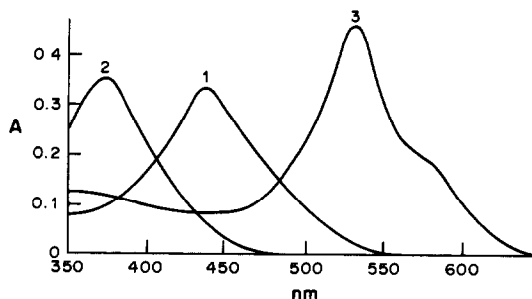


Fig. 1. Spectra of (1) 5-CIDMPAP; (2) Ti(IV)-H₂O₂-EDTA; (3) Ti(IV)-H₂O₂-5-CIDMPAP.

white fumes appear. Cool, dilute to about 100 ml, filter with a sintered glass filter, and wash the residue with 5% v/v sulphuric acid and hot water. Treat the residue with sulphuric acid in the same way and combine the filtrates. Dilute the solution to volume in a standard flask of suitable size and apply the determination procedure.

RESULTS AND DISCUSSION

In the presence of hydrogen peroxide and 5-CIDMPAP, Ti(IV) forms three ternary complex species with compositions varying according to the pH of the medium. In the present work, the complex formed between pH 2.5 and 6.5, which has maximum absorbance at 534 nm, was selected because it has the highest molar absorptivity. Figure 1 shows the spectra of (1) the indicator, (2) the Ti(IV)-H₂O₂-EDTA complex, and (3) the Ti(IV)-H₂O₂-5-CIDMPAP complex.

To determine the optimum pH for the direct titration of Ti(IV), several spectrometric titrations at different pH values (between 1 and 6.5) were performed. From the resulting curves, shown in Fig. 2, a pH of 5.5 was selected for use, as giving the greatest increase in absorbance.

The optimum indicator concentration was similarly selected. Titrations with different concentrations of indicator showed that a final indicator concentration of about 10⁻⁵M is best, giving an adequate absorbance change and very good definition. Higher concentrations render the absorbance measurements practically impossible and lower ones do not define the end-point adequately.

It was not necessary to use a large volume of ethanol to keep the various species in solution, since all the reactants were present at low concentration. It was found experimentally that 0.04% v/v ethanol was enough to keep all species soluble.

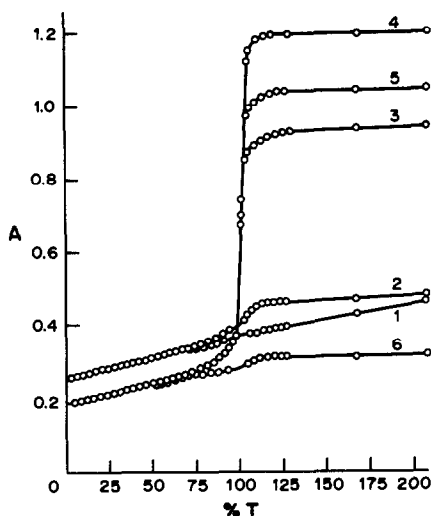


Fig. 2. Effect of pH on the spectrophotometric titration of Ti(IV). (1) pH 1-2; (2) pH 2.5-3; (3) pH 4.5; (4) pH 5.5; (5) pH 6.5; (6) pH 9.

The effect of ionic strength was tested up to 1M concentration of sodium perchlorate, nitrate, chloride, acetate, sulphate or iodide as inert electrolyte, and no difficulties were experienced. When PAN is used as indicator, however, the buffer concentration should be kept as low as possible, because of ionic strength effects on the detection of the end-point.

Table 1 shows the optimal conditions for reverse titration of Ti(IV) with EDTA in the presence of hydrogen peroxide, with Cu(II)-PAN and 5-CIDMPAP as indicators. Table 2 shows the results obtained for Ti(IV) by use of the methods proposed here and the Wilkins procedure.⁹

Use of DCTA as complexing agent gave similar results to those obtained with EDTA, with regard to the titration characteristics.

Under the conditions required for the complexation of Ti(IV) with 5-CIDMPAP and hydrogen peroxide, some other metal ions also give coloured products. Also, the selectivity is poor, as is usual in complexometric methods

Table 2. A comparison of results obtained in the visual titration of Ti(IV), with 5-CIDMPAP as indicator, by the Wilkins method and the present method (6 replicates)

Ti(V) present, mg	Ti(IV) found, mg			
	Present method	Std. devn.	Wilkins method	Std. devn.
0.48	0.47	0.02	0.46	0.02
4.79	4.78	0.02	4.76	0.02
9.58	9.57	0.01	9.56	0.02
23.95	23.94	0.01	23.91	0.02
47.90	47.90	0.01	47.85	0.02
95.80	95.80	0.01	95.70	0.02

using EDTA. However, the interference produced by Nb, Ta and V can be eliminated by using DCTA instead of EDTA. As the aim of the work was to develop a methodology for determination of titanium in samples of diverse composition, use was made of our previously developed method¹⁹ for dealing with the interference of Cd, Co(II), Al, Ni, Mn(II), Pb, Zn, Mo(VI), Cr(VI), U(VI), Ca, Sr, Ba, La and Mg (by extracting them with 8-quinolinol in chloroform at pH 1.5), of Fe(III) (double extraction in the presence of EDTA as masking agent at pH 8.2), and of Zr and Hf (extraction in the presence of oxalate as masking agent at pH 8.2). The methodology thus developed was applied to the determination of Ti(IV) in commercial paints. The results obtained by the procedures given above and by the Wilkins procedure⁹ are given in Table 3.

CONCLUSIONS

5-CIDMPAP gives adequate sensitivity for the determination of Ti(IV) by a reverse visual and photometric titration procedure. The results have a much narrower confidence interval than that found for back-titration procedures such as that of Wilkins. 5-CIDMPAP produces a better contrast at the end-point and greater sensitivity. Further, a low alcohol content is sufficient to keep the indicator and its titanium complex in solution, and the analysis is

Table 1. Experimental parameters for the reaction of Ti(IV) with hydrogen peroxide and EDTA, with Cu(II)-PAN and 5-CIDMPAP as indicator: K_f is 2.51×10^{20} for the 1:1:1 Ti(IV)-H₂O₂-EDTA complex and 6.30×10^{18} for the 1:1 Cu(II)-EDTA complex

Parameter	Ti(IV)-H ₂ O ₂ -5-CIDMPAP	Cu(II)-PAN
pH range	4.5-6.5	4.0-5.0
Optimum pH	5.5	5
Stoichiometry	1:2:2	1:1
λ_{max} , nm	534	550
$\Delta\lambda$, nm	94	75
K_f	3.47×10^{13}	1.00×10^{16}
Molar absorptivity, $l. mole^{-1}. cm^{-1}$	4.59×10^4	2.22×10^4
Colour change at end-point	yellow→purple	yellow→orange red

Table 3. Determination of TiO₂ in paint samples (mean \pm standard deviation of 6 replicates)

Samples	TiO ₂ present, mg	TiO ₂ found, mg			
	Standard method (Ti-H ₂ O ₂)	Spectrophotometric titration		Visual titration	
		This method	Cu-PAN	This method	Wilkins method
1	212.3 \pm 1.7	212.3 \pm 0.01	212.3 \pm 0.019	212.3 \pm 0.013	212.5 \pm 0.019
2	163.4 \pm 1.2	163.4 \pm 0.01	163.4 \pm 0.017	163.4 \pm 0.010	163.5 \pm 0.018
3	158.2 \pm 0.9	158.2 \pm 0.01	158.2 \pm 0.017	158.2 \pm 0.010	158.3 \pm 0.018
4	140.5 \pm 1.2	140.5 \pm 0.01	140.5 \pm 0.018	140.5 \pm 0.011	140.6 \pm 0.019
5	110.9 \pm 1.8	110.9 \pm 0.01	110.9 \pm 0.019	110.9 \pm 0.013	111.0 \pm 0.019
6	90.8 \pm 1.9	90.8 \pm 0.01	90.8 \pm 0.019	90.8 \pm 0.013	90.9 \pm 0.020

unaffected by the presence of up to at least 1M concentrations of the anions of acids likely to be used in decomposition procedures.

REFERENCES

- V. A. Khadev, M. A. Krivosheina and D. Muklamedzhanova, *Tr. Tashkent Gos. Univ.*, 1968, No. 323, 186; *Anal. Abstr.*, 1969, 17, 3390.
- H. Takao and S. Musha, *Bunseki Kagaku*, 1961, 10, 160.
- W. Lieber, *Z. Anal. Chem.*, 1960, 177, 429.
- G. Schwarzenbach and H. Flaschka, *Complexometric Titrations*, 2nd Ed. Methuen, London, 1969.
- R. Přebil, *Applied Complexometry*. Pergamon Press, Oxford, 1982.
- R. L. Pecsok and F. Maverick, *J. Am. Chem. Soc.*, 1954, 76, 358.
- P. B. Sweetser and C. E. Bricker, *Anal. Chem.*, 1954, 26, 442.
- A. K. Babko, *Talanta*, 1968, 15, 721.
- D. H. Wilkins, *Anal. Chim. Acta*, 1959, 20, 113.
- E. Lassner and R. Scharf, *Chemist-Analyst*, 1961, 50, 69.
- B. Bieber and Z. Večeřa, *Collection Czech. Chem. Commun.*, 1961, 26, 2081.
- R. Přebil and V. Veselý, *Hutn. Listy*, 1973, 28, 661.
- E. Lassner and R. Scharf, *Chemist-Analyst*, 1961, 50, 6.
- E. Lassner and R. Püschel, *Mikrochim. Ichnoanal. Acta*, 1963, 950.
- H. J. Marini, R. I. Anton and R. A. Olsina, *Bull. Chem. Soc. Japan*, 1987, 60, 2635.
- S. Shibata and M. Furukawa, *Bunseki Kagaku*, 1974, 23, 1412.
- W. M. Thornton, Jr. and R. Roseman, *Am. J. Sci. (Ser. 5)*, 1930, 20, 14.
- P. B. Sweetser and C. E. Bricker, *Anal. Chem.*, 1954, 26, 195.
- H. J. Marini, R. I. Anton, M. S. Boeris and R. A. Olsina, *Bull. Chem. Soc. Japan*, 1986, 59, 3951.

SPECTROPHOTOMETRIC DETERMINATION OF TRACES OF IRON AFTER EXTRACTION OF Fe(II)-PHENANTHROLINE COMPLEX ON POLYURETHANE FOAM

SWAGATA BHATTACHARYA and S. K. ROY

Analytical Chemistry Division, Central Glass & Ceramic Research Institute, Calcutta 700032, India

A. K. CHAKRABORTY

Department of Chemistry, Jadavpur University, Calcutta 700032, India

(Received 14 August 1989. Revised 5 April 1990. Accepted 2 May 1990)

Summary—A spectrophotometric method for the determination of traces of iron in glass and ceramic materials has been developed. The method involves formation of the Fe(II)-phenanthroline complex at pH 3-4 in aqueous medium, followed by its selective extraction and preconcentration on polyurethane foam from 2.5M perchloric acid and finally elution of the complex with acetone for spectrophotometric measurement at 510 nm. A wide linearity range from 0.05 to 3 µg/ml Fe is obtained with the method. Co, Cu and Ni have no significant effect when they are present in the weight ratios Fe:Co < 1:2, Fe:Cu < 1:10 and Fe:Ni < 1:50. The method yielded satisfactory results when applied to various glass and ceramic samples.

1,10-Phenanthroline has long been established as a reagent for spectrophotometric determination of traces of iron in various materials. Numerous methods have been based on formation of the tris(phenanthroline)iron(II) complex in the pH range 2-9 and its spectrophotometric determination,^{1,2} but suffer interference from various elements. Attempts have been made to extract the ferrous-1,10-phenanthroline complex into various solvents³ in the presence of Cl⁻, Br⁻, I⁻ and ClO₄⁻ ions. Hoste and Gillis⁴ reported a method in which Fe(phen)₃²⁺ was extracted with chloroform at higher pH, in the presence of sodium perchlorate, for the determination of iron at concentrations as low as 0.04 µg/ml. Recently, Hoshi *et al.*⁵ reported the use of chitin, a natural polymer, for extraction and preconcentration of the Fe(II)-phenanthroline complex with tetraphenylborate as counter-ion, in the spectrophotometric determination of iron in water.

During the last decade polyurethane foam⁶⁻¹⁰ has been established in analytical chemistry for the extraction and preconcentration of various inorganic ions, in their determination in environmental samples, and several methods for determination of iron have been based on its use.¹¹⁻¹⁷

The present investigation concerns the use of polyether type polyurethane foam in the extraction and preconcentration of the iron(II)-1,10-phenanthroline complex, from perchloric acid medium, and determination of iron in silicate and other ceramic materials.

EXPERIMENTAL

Reagents

Hydroxylamine hydrochloride solution (10% w/v) and 1,10-phenanthroline solution (0.1% w/v) were used. All reagents were analytical or guaranteed reagent grade. Doubly distilled water was used throughout.

Standard iron solution. Electrolytic iron (0.1 g) was dissolved in a 50-ml beaker by heating with 25 ml of nitric acid (1 + 3). After dissolution, 10 ml of sulphuric acid (1 + 1) were added and the mixture was evaporated on a sand-bath until fumes of sulphur trioxide were evolved. The solution was cooled, 10 ml of concentrated hydrochloric acid were added and the solution was transferred to a 1000-ml standard flask and diluted to the mark with water. Working solutions were prepared by further dilution.

Preparation of foam

The polyurethane foam (commercial "U" foam) was cut into regular shapes and sizes with a cork borer. Each piece was about 2 cm in length and 0.5 cm in diameter, and weighed about 0.01 g. The pieces of foam were soaked in 4*M* hydrochloric acid in a beaker for 24 hr with squeezing at 15-min intervals, then washed thoroughly by squeezing with water in a 50-ml syringe, and finally washed by refluxing with acetone for 6 hr in a Soxhlet apparatus, dried in a desiccator and stored in a plastic container in the dark.

Procedures

Calibration. Iron solutions (1–10 ml) containing 0.5–30 μg of Fe were pipetted into 50-ml glass beakers. A 3-ml volume of 10% hydroxylamine hydrochloride solution was added to each and the pH adjusted to 3–4 by dropwise addition of ammonia solution (1 + 3), followed by addition of 2 ml of 0.1% 1,10-phenanthroline solution and water to make the volume up to 15 ml. The solutions were kept standing for 15 min to develop the colour fully. Perchloric acid (10 ml, 6.5*M*) was added to each beaker, followed by four pieces of foam, which were squeezed manually with a glass plunger every 15 min for 2½ hr. Each set of foams was transferred in turn to a 5-ml glass syringe and the excess of reagents was squeezed out. The foams were then washed by squeezing 4 times with 4 ml of water. Finally the complex was eluted from the foam by squeezing with four 2-ml portions of acetone. Each group of eluates was combined in a 10-ml standard flask and diluted to volume with acetone, added from the same syringe. The absorbance of each solution was measured at 510 nm against a reagent blank similarly prepared, and the calibration graph (absorbance *vs.* μg of Fe) was plotted.

Analysis of samples. The sample (0.2 g) was taken in a Teflon basin and heated on a sand-bath with 2 ml of sulphuric acid (1 + 1) and 5 ml of concentrated hydrofluoric acid until fuming occurred. The basin was cooled, a further 5 ml of hydrofluoric acid were added and the mixture was evaporated and fumed for 30–40 min. The cooled residue was taken up in 2 ml of hydrochloric acid (1 + 1) and the solution was diluted with 10 ml of water and transferred to a 50-ml standard flask and diluted to volume with water. Ten ml of this solution were taken in a 50-ml beaker and evaporated on a water-

bath nearly to dryness; 2 ml of water were added and the determination procedure was applied. The Fe_2O_3 content was calculated from

$$\text{Fe}_2\text{O}_3 = 7.14 \times 10^{-4} A/W \%$$

where *A* is the number of μg of Fe corresponding to the absorbance measured, and the sample weight is *W* g.

RESULTS AND DISCUSSION

It is known from the literature^{3,4} that $\text{Fe}(\text{phen})_3^{2+}$ can be extracted as $\text{Fe}(\text{phen})_3\text{X}_2$ with amyl alcohol and other oxygen-compound organic solvents, where X is Cl^- , Br^- , I^- or ClO_4^- .

During the study it was confirmed that after formation of $\text{Fe}(\text{phen})_3^{2+}$ at pH 3–4, the acidity of the medium can be increased considerably with perchloric acid without affecting the stability of the complex.¹⁹ It was found that the $\text{Fe}(\text{phen})_3^{2+}$ complex can be extracted with polyurethane foam only in the presence of sufficient perchlorate ions, and eluted with acetone.

The wavelength of maximum absorbance (510 nm) reported earlier¹⁹ for the $\text{Fe}(\text{phen})_3^{2+}$ complex in aqueous medium was found to be the same as that for perchloric acid medium (without extraction) and also for the acetone solution obtained from the foam.

Several views¹⁰ have been reported on the mechanism of extraction of ionic species by polyurethane foam. In the present investigation the extraction mechanism was not studied, but it can be expected that the extraction of $\text{Fe}(\text{phen})_3^{2+}$ by polyurethane foam in the presence of perchlorate will be analogous to the extraction by oxygen-compound organic solvents.³

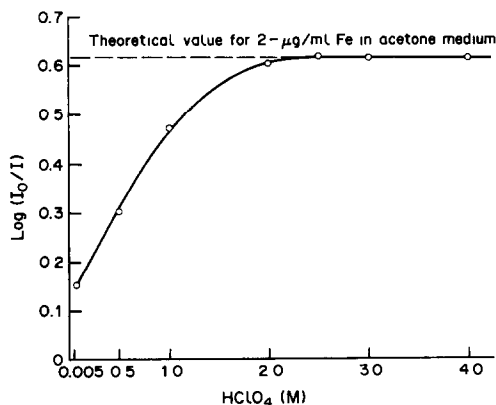


Fig. 1. Effect of HClO_4 concentration on the extraction of $\text{Fe}(\text{phen})_3^{2+}$.

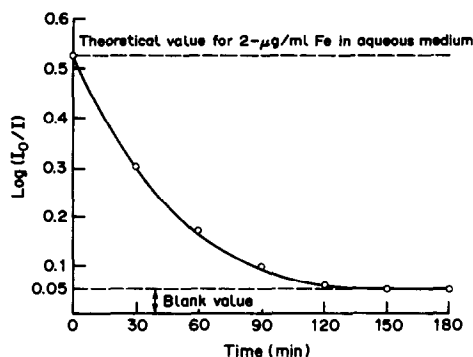


Fig. 2. Effect of equilibration time on the extraction of $\text{Fe}(\text{phen})_3^{2+}$ from $2.5M \text{HClO}_4$.

The extraction of $\text{Fe}(\text{phen})_3^{2+}$ by polyurethane foam was found to be primarily dependent on the concentration of perchloric acid and the equilibration time. The degree of extraction increases with perchloric acid concentration up to $2.5M$ and then remains constant at higher acidity (Fig. 1). Figure 2, which shows the amount of $\text{Fe}(\text{phen})_3^{2+}$ complex remaining in the aqueous

Table 1. Recovery of the Fe-phen complex from foam by elution with four 2-ml portions of acetone

Fe taken, $\mu\text{g/ml}$	Fe found, $\mu\text{g/ml}$
0.10	0.098
	0.099
	0.110
1.0	1.02
	1.00
	0.99
3.0	3.00
	3.04
	2.98

Table 2. Determination of $2.0 \mu\text{g/ml}$ iron in the presence of various ions

Ion	Concentration, $\mu\text{g/ml}$	Fe found, $\mu\text{g/ml}$
Co^{2+}	—	2.0
	2.0	2.0
	4.0	2.0
	6.0	1.8
	10.0	1.2
Cu^{2+}	—	2.0
	2.0	2.0
	10.0	2.0
	20.0	2.0
	40.0	1.5
Ni^{2+}	—	2.0
	2.0	2.0
	10.0	2.0
	25.0	2.0
	50.0	2.05
	100.0	2.0

Table 3. Determination of iron in various materials

Sample	Fe_2O_3 , %	Mean Fe_2O_3 , %	Value obtained by another method ¹⁸
$\text{TiO}_2(1)$	0.010	0.012	0.014
	0.011		
	0.016		
$\text{TiO}_2(2)$	0.013	0.013	0.012
	0.013		
	0.012		
$\text{ZrO}_2(1)$	0.025	0.026	0.030
	0.030		
	0.024		
$\text{ZrO}_2(2)$	0.055	0.054	0.055
	0.055		
	0.052		
Quartz	0.022	0.021	0.022
	0.020		
	0.020		
Opal Glass N.B.S. 91	0.073	0.077	0.08*
	0.083		
	0.075		
Glass	0.0080	0.0081	0.0085
	0.0085		
	0.0080		

*Certified value.

phase, indicates that the extraction is slow and a minimum equilibration time of 150 min is required.

Acetone has frequently been used for stripping complexes from polyurethane foam, and in this study was found suitable for elution of the $\text{Fe}(\text{phen})_3^{2+}$ perchlorate. The molar absorptivity of $\text{Fe}(\text{phen})_3^{2+}$ perchlorate is also slightly higher in acetone medium than in aqueous solution. It was found that four 2-ml portions of acetone would give quantitative stripping of the complex (Table 1). The absorbance of the complex in acetone solutions at 510 nm is stable for at least 24 hr.

The system obey's Beer's law up to $3 \mu\text{g/ml}$ Fe. The lowest concentration that can be reliably measured is $0.05 \mu\text{g/ml}$ Fe.

The effect of various species such as Mn^{2+} , Zn^{2+} , Cd^{2+} , Mo(VI) , Co^{2+} , Cu^{2+} and Ni^{2+} , on the determination of iron was studied. Mn^{2+} , Zn^{2+} , Cd^{2+} and Mo(VI) have no effect on the method when present in concentrations up to $200 \mu\text{g/ml}$, but Co^{2+} , Cu^{2+} and Ni^{2+} can be tolerated only up to 4, 20 and $100 \mu\text{g/ml}$, respectively (Table 2), under the experimental conditions used.

The method has been successfully applied to analysis of several glass and ceramic samples (Table 3).

Acknowledgements—The authors are thankful to Dr. B. K. Sirkar, Director, Central Glass & Ceramic Research Institute, Calcutta 700032, for his kind permission to publish the paper. Thanks are also due to Dr. S. K. Guha, Deputy Director, for his keen interest in the work.

REFERENCES

1. E. B. Sandell, *Colorimetric Determination of Traces of Metals*, 3rd Ed., Interscience, New York, 1959.
2. Z. Marczenko, *Separation and Spectrophotometric Determination of Elements*. Horwood, Chichester, 1986.
3. E. B. Sandell and H. Onishi, *Photometric Determinations of Traces of Metals*, Part I, pp. 281, 684. Wiley, New York, 1978.
4. J. Hoste and J. Gillis, *Mededel. Koninkl. Vlaam. Acad. Wetenschap., Belg.*, 1951, 13, No. 2, 3.
5. S. Hoshi, M. Yamada, S. Inoue and M. Matsubara, *Talanta*, 1989, 36, 606.
6. H. J. M. Bowen, *J. Chem. Soc. A*, 1970, 1082.
7. G. J. Moody and J. D. R. Thomas, *Chromatographic Separation and Extraction with Foamed Plastics and Rubbers*. Dekker, New York, 1982.
8. T. Braun, A. B. Farag and J. Navratil, *Polyurethane Foam Sorbents in Separation Chemistry*. CRC Press, Boca Raton, 1985.
9. T. Braun and A. B. Farag, *Talanta*, 1975, 22, 699.
10. T. Braun, *Z. Anal. Chem.* 1989, 333, 785.
11. M. P. Maloney, G. J. Moody and J. D. R. Thomas, *Analyst*, 1980, 105, 1087.
12. T. Braun, A. B. Farag and M. P. Maloney, *Anal. Chim. Acta*, 1977, 93, 191.
13. A. B. Farag, A. M. El Wakil and M. S. El Shavi, *Ann., Chim. (Roma)*, 1982, 72, 103.
14. T. Braun and A. B. Farag, *Anal. Chim. Acta*, 1978, 98, 133.
15. J. J. Oren, K. M. Gough and H. D. Gesser, *Can. J. Chem.*, 1979, 57, 2032.
16. M. N. Abbas, A. Vertes and T. Braun, *Radiochem. Radioanal. Lett.*, 1982, 54, 17.
17. G. J. Moody, J. D. R. Thomas and M. A. Yarmo, *Anal. Proc.*, 1983, 20, 132.
18. S. Das Gupta, S. Kumar and B. C. Sinha, *Trans. Ind. Ceram. Soc.*, 1965, 24, 66.

SPRAY REAGENTS FOR THE DETECTION OF AMINO-ACIDS ON THIN-LAYER PLATES

B. BASAK and S. LASKAR*

Natural Product Laboratory, Chemistry Department, Burdwan University, Burdwan-713104,
W. Bengal, India

(Received 17 July 1989. Revised 21 February 1990. Accepted 10 May 1990)

Summary—Three spray reagents for the detection of amino-acids on silica-gel thin-layer chromatography plates are reported. The reagents produce various colours, which may be used to identify some of the amino-acids directly, and assist in their detection.

Detection and identification of amino-acids are most important in protein chemistry as these are the building blocks of proteins. Several spray reagents for the selective and non-selective detection of amino-acids on chromatograms have already been described,¹⁻¹⁵ among which ninhydrin is mostly used because of its high sensitivity, but it gives very similar violet colours with all amino-acids except proline and hydroxyproline. The present communication describes three spray reagents which give various colours with the amino-acids and can be used to identify most of them directly on silica-gel thin-layer chromatography plates.

EXPERIMENTAL

Chromatographic plates (20 × 20 cm) were prepared with a 0.1-mm thick layer of silica gel G (Merck) and a Unoplan apparatus (Shandon, London). Standard 1- μ g/ml solutions of the amino-acids (Sigma) were made in 0.01M phosphate buffer (pH 8.0). These solutions were then spotted (repeatedly if necessary) onto the plates with a 25- μ l graduated micropipette. After development with n-propanol/water mixture (70:30 v/v) as mobile phase,⁷ over a distance of 10 cm, the plates were dried, and sprayed as follows. The auxiliary spray reagents used were Merck analytical grade. The ninhydrin was from Sigma.

Reagent I. The plate was sprayed with 12.5-mg/ml oxalic acid solution in ethanol-water

(3:1 v/v) mixture, dried in air and then sprayed with 2.5 mg/ml ninhydrin solution in acetone.

Reagent II. The plate was sprayed with a saturated solution of dithio-oxamide in ethanol, dried in air, and sprayed again with 2.5-mg/ml ninhydrin solution in acetone.

Reagent III. The plate was sprayed with a saturated solution of dithizone in ethanol, dried in air, and then sprayed with 2.5-mg/ml ninhydrin solution in acetone.

All the plates were finally dried in air and then heated for 15 min at 100° in an oven. The observed colours and limits of detection are presented in Table 1.

RESULTS AND DISCUSSION

These new spray reagents give better colour differentiation than ninhydrin alone for amino-acids, but somewhat lower sensitivities. The detection limits range between 0.04 and 0.2 μ g with Reagent I, 0.1 and 0.2 μ g with Reagent II, and 0.08 and 0.2 μ g with Reagent III (Table 1). The reagents are convenient for rapid identification of amino-acids on silica gel TLC plates. Reagents II and III give similar colours, which differ from those produced by Reagent I. This may be because dithio-oxamide and dithizone both contain a thio-amide group, since they are not otherwise similar in structure. It is possible that the colour reactions are of charge-transfer type. In practical applications, two-dimensional chromatography and use of the R_f values would be necessary.

*To whom all correspondence should be addressed.

Table 1. Colour reactions of amino-acids on silica gel thin-layer plates with three spray reagents

Amino-acid	Oxalic acid-ninhydrin		Dithio-oxamide-ninhydrin		Dithizone-ninhydrin	
	Colour observed	Detection limit, μg	Colour observed	Detection limit, μg	Colour observed	Detection limit, μg
Glycine	Orange (Light orange)	0.2	Pinkish violet (Bluish pink)	0.2	Pinkish violet (Light pink)	0.2
Alanine	Orange (Light orange)	0.1	Pinkish violet (Pink)	0.2	Pinkish violet (Light violet)	0.2
Valine	Pinkish orange (Orange)	0.2	Pink (Pink)	0.2	Reddish pink (Light violet)	0.2
Leucine	Reddish pink (Orange)	0.1	Pink (Pink)	0.1	Reddish pink (Light violet)	0.2
Isoleucine	Reddish pink (Orange)	0.1	Pink (Pink)	0.1	Reddish pink (Light pink)	0.1
Serine	Orange (Orange)	0.1	Pinkish violet (Pinkish violet)	0.1	Pinkish violet (Light violet)	0.2
Threonine	Orange (Orange)	0.04	Pinkish violet (Pinkish violet)	0.1	Pinkish violet (Light violet)	0.1
Aspartic acid	Wild lilac (Light rose)	0.1	Violet (Light violet)	0.1	Violet (Violet)	0.2
Asparagine	Light mushroom (Pink)	0.1	Deep cream (Light brown)	0.1	Brown (Light brown)	0.8
Glutamic acid	Orange (Orange)	0.1	Pinkish violet (Pinkish violet)	0.1	Pinkish violet (Light violet)	0.6
Glutamine	Reddish pink (Light orange)	0.1	Light pink (Light pink)	0.1	Pink (Light pink)	0.6
Lysine	Terracotta (Light terracotta)	0.1	Dirty pink (Light pink)	0.1	Reddish pink (Light terracotta)	0.2
Histidine	Greyish orange (Brownish orange)	0.1	Mushroom (Light mushroom)	0.1	Mushroom (Light terracotta)	0.1
Arginine	Light terracotta (Light terracotta)	0.1	Reddish pink (Light terracotta)	0.1	Reddish pink (Light terracotta)	0.1
Phenylalanine	Violet (Pinkish violet)	0.2	Pink (Light orange)	0.1	Reddish pink (Light pink)	0.1
Tyrosine	Pinkish violet (Pinkish violet)	0.1	Orange (Light orange)	0.2	Dirty pink (Pink)	0.1
Tryptophan	Grey (Pinkish violet)	0.2	Pink (Light orange)	0.2	Pinkish violet (Light pink)	0.2
Cysteine	Mushroom (Pink)	0.04	Pinkish silver grey (Light pink)	0.1	Pinkish silver grey (Pinkish silver grey)	0.1
Cystine	Mushroom (Orange)	0.1	Pinkish silver grey (—)	0.2	Pinkish silver grey (Pinkish silver grey)	0.2
Methionine	Brownish violet (Pinkish violet)	0.2	Pink (Light orange)	0.1	Pink (Light orange)	0.1
Proline	Rose red (Light brown)	0.1	Yellowish grey (Lemon yellow)	0.2	Greyish yellow (Yellow ochre)	0.08
Hydroxyproline	Pink (Lemon yellow)	0.05	Grey (Lemon yellow)	0.1	Grey (Lemon yellow)	0.1

*Colours in parentheses were observable before the TLC plates were heated, but not at low concentrations of the amino-acids, *i.e.*, they were not observable when the amino-acid concentration was below the detection limit quoted above.

Acknowledgement—The authors are grateful to I.C.M.R., New Delhi for financial support.

REFERENCES

1. E. Chargaff, C. Levine and C. Green, *J. Biol. Chem.*, 1948, **175**, 67.
2. G. Toennies and J. J. Kolb, *Anal. Chem.*, 1951, **23**, 823.
3. G. Curzon and J. Giltrow, *Nature*, 1953, **172**, 356.
4. R. Consden, A. H. Gordon and A. J. P. Martin, *Biochem. J.*, 1946, **40**, 580.
5. S. R. Dickmann and A. L. Crockett, *J. Biol. Chem.*, 1956, **220**, 957.
6. H. R. Mahler and E. H. Cordes, *Basic Biological Chemistry*, p. 40. Harper & Row, New York, 1968.
7. E. Stahl, *Thin-layer Chromatography: A Laboratory Handbook*, pp. 747–749, 889. Springer, New York, 1969.
8. G. Pataki, *J. Chromatog.*, 1964, **16**, 541.
9. T. Wolski, W. Golkiewicz and A. Rompala, *Chem. Anal. (Warsaw)*, 1980, **25**, 583.
10. W. Distler, *Z. Anal. Chem.*, 1981, **309**, 127.
11. K. Lorentz and B. Flatter, *Anal. Biochem.*, 1970, **38**, 557.
12. G. Devaux and P. Mesnard, *Bull. Soc. Pharm. Bordeaux*, 1971, **110**, 145.
13. S. Laskar and B. Basak, *J. Chromatog.*, 1988, **436**, 341.
14. R. Circo and B. A. Freeman, *Anal. Chem.*, 1963, **35**, 262.
15. E. D. Moffat and R. I. Lytle, *ibid.*, 1959, **31**, 926.

ANALYTICAL DATA

ON THE INFLUENCE OF IONIC STRENGTH ON THE EQUILIBRIUM CONSTANT OF COPPER-MUREXIDE INTERACTION

FARANGIS FAMOORI, SOHEILA HAGHGOO and MOJTABA SHAMSIPUR*

Department of Chemistry, Shiraz University, Shiraz, Iran

(Received 9 January 1990. Revised 7 April 1990. Accepted 28 May 1990)

Summary—The concentration formation constant for the 1:1 complex between copper(II) and murexide in aqueous solutions has been measured as a function of ionic strength by spectrophotometry at 25°. There is an inverse relationship between the K_c values and ionic strength. The formation constant at infinite dilution was found to be 6.16×10^4 . The distance of closest approach for the Cu^{2+} ion was estimated as $4.3 \pm 0.3 \text{ \AA}$.

Any experimental measurement of equilibrium constants for ionic reactions in solution involves the serious problem of activity corrections. A common practice is to make the measurements at a high and constant ionic strength. However, the salts used to keep the ionic strength constant can sometimes participate in the reaction and consequently alter the apparent formation constant. Also, at high concentrations, even in high dielectric constant solvents such as water, there is some ion-pairing, which could compete with the complexation reaction. It would be better (although more difficult) to determine the equilibrium constants at several ionic strengths, and extrapolate the results to zero ionic strength. Another procedure, less effective than the extrapolation method, is to calculate the activity coefficients by use of an appropriate form of the Debye-Hückel equation.

Murexide, the ammonium salt of purpuric acid, is a metallochromic indicator which forms relatively stable complexes with various metal ions in aqueous,¹⁻³ non-aqueous^{4,5} and binary mixed solvents.⁶ The formation constants of these complexes, which have usually been determined spectrophotometrically, are reported as concentration constants. It was of interest to us to study the influence of ionic strength on the metal ion-ligand interactions in order to evaluate the thermodynamic formation constants of

the resulting complexes. In this paper we report the effect of ionic strength on the formation constant of the Cu^{2+} -murexide complex in aqueous solutions at $25 \pm 1^\circ$, studied by a careful spectrophotometric method.

EXPERIMENTAL

Reagent-grade copper nitrate (Fluka), sodium chlorate (Merck) and murexide (Merck) were used without any further purification except for vacuum-drying over phosphorus pentoxide. Triply distilled water was used for the preparation of solutions. The visible spectra were measured with a Beckman DK-2A ratio recording spectrophotometer and the absorbance measurements were made with a Perkin-Elmer 35 digital spectrophotometer at $25 \pm 1^\circ$.

The formation constant of the Cu^{2+} -murexide complex was determined accurately by methods reported previously.^{3,6} Equality of the murexide concentrations in different solutions and of the amounts of metal ions added was ensured by weighing the materials on a semimicro balance. Equilibrium was assumed to be attained if there was no further change in the spectra after several hours. The ionic strengths of the solutions were maintained at the desired levels by addition of sodium chlorate. The errors associated with the K_c values are reported as \pm one standard deviation.

*To whom all correspondence should be addressed.

RESULTS AND DISCUSSION

The spectra of murexide ($2.0 \times 10^{-5}M$) and its copper complex at ionic strength $0.10M$ are shown in Fig. 1. To avoid the effect of competitive binding by buffer ions added for keeping the pH constant, the spectrophotometric measurements were made in the absence of any buffer, at a neutral pH. The stoichiometry of the resulting complex between Cu^{2+} and murexide was determined by the method of continuous variations,⁷ and invariably found to be 1:1. The concentration formation constant K_c was determined at different ionic strengths. The results are shown in Table 1 and Fig. 2. It is seen that the K_c values decrease with increase in ionic strength, I , of the solution. The variation of K_c with I is more or less linear in the range $0.1-0.4M$. At ionic strengths below $0.1M$, the K_c values increase almost exponentially with I . Regressional extrapolation of the results to infinite dilution yields $\log K_{th} = 4.79$. The reported concentration formation constant at an ionic strength of $0.1M$ (KNO_3) and 10° is $\log K_c = 4.36 \pm 0.10$.¹

For the complexation reaction



the thermodynamic equilibrium constant is given by

$$K_{th} = \frac{a_{CuMu^{+}}}{a_{Cu^{2+}} a_{Mu^{-}}} = K_c \frac{\gamma_{CuMu^{+}}}{\gamma_{Cu^{2+}} \gamma_{Mu^{-}}} \quad (2)$$

where the γ values are the activity coefficients of the species involved. Murexide is a bulky ligand that is much larger than the copper ion and, therefore, it seems reasonable to assume about the same ionic radius for the free and complexed

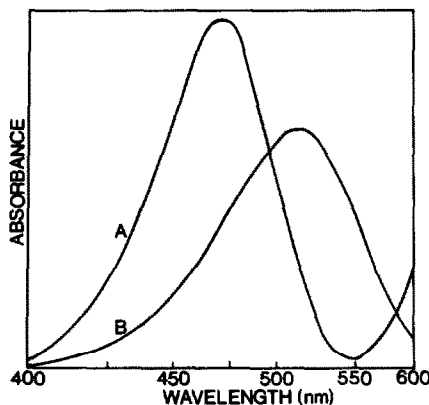


Fig. 1. Visible spectra of murexide (B) and its copper(II) complex (A) at ionic strength $0.10M$.

Table 1. Concentration formation constants of the copper-murexide complex at various ionic strengths

Ionic strength, M	$\log K_c$
0.40	4.08 ± 0.02
0.30	4.17 ± 0.04
0.20	4.24 ± 0.02
0.10	4.35 ± 0.02
0.07	4.39 ± 0.03
0.04	4.47 ± 0.03
0.03	4.51 ± 0.02
0.02	4.55 ± 0.03
0.01	4.61 ± 0.02
0.007	4.64 ± 0.02
0.005	4.66 ± 0.03

ligand in solution. Since murexide and its copper complex both carry a single charge (although of opposite signs), it can be assumed that

$$\gamma_{CuMu^{+}} = \gamma_{Mu^{-}}$$

so the thermodynamic formation constant can be written as

$$K_{th} = \frac{K_c}{\gamma_{Cu^{2+}}} \quad (3)$$

Then, from equation (3) and the exact form of the Debye-Hückel equation⁸

$$-\log \gamma_i = \frac{0.509 Z_i^2 I^{1/2}}{1 + 0.328 r_i I^{1/2}} \quad (4)$$

it is possible to obtain some information about the distance of closest approach, r_i , for the copper ion in solution.

The results given in Table 1 were fitted to equations (3) and (4) and the estimated value for the distance of closest approach of the Cu^{2+} ion was found to be $4.3 \pm 0.3 \text{ \AA}$. A corresponding reported value obtained from a study of copper sulphate solutions is 3.9 \AA .⁹

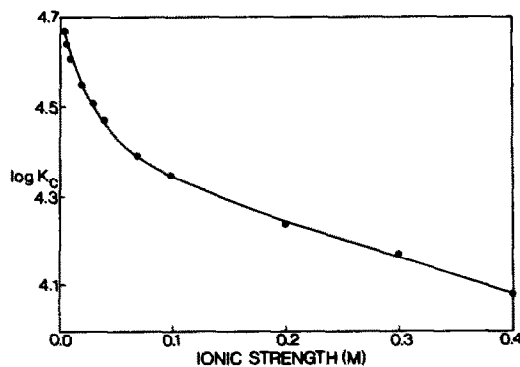


Fig. 2. The value of the concentration formation constant of the Cu^{2+} -murexide complex vs. ionic strength of the solution.

Acknowledgement—The support of this work by the Shiraz University Research Council is gratefully acknowledged.

REFERENCES

1. G. Schwarzenbach and H. Gysling, *Helv. Chim. Acta*, 1949, **32**, 1314.
2. G. Geier, *ibid.*, 1967, **50**, 1879.
3. K. S. Balaji, S. D. Kumar and P. Gupta-Bhaya, *Anal. Chem.*, 1978, **50**, 1972.
4. S. Kashanian, M. B. Gholivand, S. Madaeni, A. Nikrahi and M. Shamsipur, *Polyhedron*, 1988, **7**, 1227.
5. M. Shamsipur, S. Madaeni and S. Kashanian, *Talanta*, 1989, **36**, 773.
6. M. Shamsipur, A. Esmacili and M. K. Amini, *ibid.*, 1989, **36**, 1300.
7. P. Job, *Ann. Chim. (Paris)*, 1928, **9**, 113.
8. P. Debye and E. Hückel, *Phys. Z.*, 1923, **24**, 305.
9. F. E. W. Wetmore and A. R. Gordon, *J. Chem. Phys.*, 1937, **5**, 60.

MECHANISM OF COBALT ATOMIZATION FROM DIFFERENT ATOMIZER SURFACES IN GRAPHITE-FURNACE ATOMIC-ABSORPTION SPECTROMETRY

C. L. CHAKRABARTI* and S. J. CATHUM

Centre for Analytical and Environmental Chemistry, Department of Chemistry, Carleton University,
Ottawa, Ontario, Canada K1S 5B6

(Received 20 December 1989. Revised 26 June 1990. Accepted 4 July 1990)

Summary—The mechanism of cobalt atomization from different atomizer surfaces in graphite-furnace atomic-absorption spectrometry has been investigated. The atomizer surfaces were pyrolytically coated graphite, uncoated electrographite, and glassy carbon. The activation energy of the rate-determining step in the atomization of cobalt (taken as the nitrate in aqueous solution) in a commercial graphite furnace has been determined from a plot of $\log k_r$ vs. $1/T$ (for T values greater than the appearance temperature), where k_r is a first-order rate constant for atom release, and T is the absolute temperature. The activation energy E_a , can be correlated either with the dissociation energy of $\text{CoO}_{(g)}$ or with the heat of sublimation of $\text{Co}_{(g)}$, formed by carbon reduction of $\text{CoO}_{(s)}$, the latter being the product of the thermal decomposition of $\text{Co}(\text{NO}_3)_2$. The mechanism for Co atomization seems to be the same for the pyrolytically coated graphite and the uncoated electrographite surfaces, but different for the glassy carbon surface. The suggested mechanisms are consistent with the chemical reactivity of the three atomizer surfaces, and the physical and thermodynamic properties of cobalt and its chemical compounds in the temperature range involved in the charring and atomization cycle of the graphite furnace.

The mechanisms of atomization in graphite-furnace atomic-absorption spectrometry (GFAAS) have been studied by several authors, who have used different theoretical models based on kinetic,^{1,2} thermodynamic³⁻⁵ or combined kinetic-thermodynamic considerations.⁶ Investigations of the atomization mechanism requires both kinetic and thermodynamic factors to be taken into account.⁷ It is also important to investigate the dependence (if any) of the atomization mechanism on the nature of the atomizer surface. Mechanisms for atom formation and dissipation in GFAAS are of importance in designing more efficient atomizers and in optimizing experimental procedures. Valuable information about the mechanism of atomization in GFAAS can be obtained from the absorbance signal profile.

THEORY

Paveri-Fontana *et al.*⁸ and van den Broek and de Galan⁹ have provided an analytical expression for the number of atoms present in the

analysis volume at any instant t , as a convolution integral of the form:

$$n = \int_0^t S(t')\mathbf{R}(t-t') dt' \quad (1)$$

where $S(t)$ is the rate of atom formation, $\mathbf{R}(t)$ is the rate of atom removal and t' is a variable of integration. $S(t)$ is given by¹⁰

$$S(t) = n_0 k_\infty \exp\left(-\frac{E_a}{RT}\right) \times \exp\left(-\int_0^t k_\infty \exp\left[-\frac{E_a}{RT}\right] dt'\right) \quad (2)$$

where n_0 is the number of analyte atoms initially present, k_∞ the pre-exponential factor, E_a the activation energy, R the gas constant and T the absolute temperature at time t . The rate of atom removal, $\mathbf{R}(t)$, is given^{1,9} by:

$$\mathbf{R}(t) = k_r n \quad (3)$$

where k_r is the temperature-dependent first-order rate constant for the combined rate of atom removal, *i.e.*, by diffusion, expansion and convection; re-adsorption onto the atomizer surface is not considered. If it is assumed that

*Author for correspondence.

the rate of atom removal is much faster than the rate of atom formation, another form of the Smets equation¹ can be obtained from the rate of atom formation [equation (2)] as follows. Assuming that the first-order rate constant k_s for the rate of atom formation is approximated by the Arrhenius law, and that the amount of analyte $\int_t^\infty S(t) dt$ left unatomized at time t is expressed¹⁰ by

$$\int_t^\infty S(t) dt = n_0 \exp\left(-\int_0^t k_\infty \exp\left[-\frac{E_a}{RT}\right] dt\right) \quad (4)$$

then

$$k_s = \frac{S(t)}{\int_t^\infty S(t) dt} = \frac{A}{\int_t^\infty A dt} \quad (5)$$

where $k_s = k_\infty - \exp(-E_a/RT)$ and A and $\int_t^\infty A dt$ are the absorbance and the integrated absorbance, respectively, at time t . Equation (5) is valid if the rate constant for atom removal, k_r , is larger than the rate constant for atom formation, k_s . This condition can be fulfilled in a graphite furnace by using forced convection of inert gas during atomization.^{9,10} This point will be raised again in the Results and Discussion section.

Using transition-state theory, Sturgeon *et al.*⁶ formulated the following expression for the rate constant of atom formation, k_s , and the change in free energy of activation, ΔG^{0*} :

$$k_s = aT \exp\left(-\frac{\Delta G^{0*}}{RT}\right) \quad (6)$$

where $\Delta G^{0*} = \Delta H^{0*} - T\Delta S^{0*}$; ΔH^{0*} and ΔS^{0*} are the enthalpy and entropy of activation, respectively, and a is a constant. Sturgeon *et al.*⁶ assumed that the term containing the linear function of temperature is essentially temperature-independent because of compensating effects from other temperature-dependent terms in the equation. Also, according to transition-state theory, the rate constant of atom formation, k_s , may be formulated by statistical mechanics to yield the expression

$$k_s = bT^m \exp(-E_0/RT) \quad (7)$$

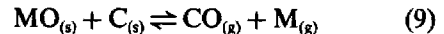
where b and m are constants; the value of m may be deduced from the partition function. E_0 is the molar energy change at absolute zero (assumed to be equal to the activation energy E_a in the Arrhenius law).

Arranging terms and taking the logarithm of both sides of equation (7) yields

$$\log y = -\frac{E_a}{2.303RT} + \log b \quad (8)$$

where $y = k_s/T^m$. Equation (8) indicates that a plot of $\log y$ vs. $1/T$ should be linear with slope $-E_a/2.303R$ and intercept $\log b$.

Earlier investigations⁶ of mechanisms of atom formation in GFAAS showed the importance of the reduction of the metal oxide, MO, according to the equation



This simple equation for atom formation was considered to explain the observed activation energy and the appearance temperature in the graphite furnace for many elements, including cobalt. Sturgeon *et al.*⁶ found an activation energy of 406 kJ/mole for the atomization of cobalt (as the nitrate) and an appearance temperature of 1430 K for cobalt atom formation, and concluded that $\text{Co}(\text{NO}_3)_2$ was first converted into $\text{CoO}_{(s)}$, which was then reduced to $\text{Co}_{(s)}$, followed by sublimation of $\text{Co}_{(s)}$ to $\text{Co}_{(g)}$. Ham and McAllister¹¹ investigated the atomization of Co in a pyrolytically coated graphite tube furnace operating in a vacuum, by using a rapid-scan mass spectrometric detection system, and by thermochemical calculation of the equilibrium in the furnace during atomization. Their calculation showed that the atomization reaction was $\text{Co}_{(s)} \rightarrow \text{Co}_{(g)}$ for both cobalt nitrate and cobalt chloride at the appearance temperature for cobalt. However, Grimley *et al.*¹² reported the dissociation energy of $\text{CoO}_{(g)}$ as 361 kJ/mole from mass spectrometry of $\text{Co}_{(g)}$ and $\text{CoO}_{(g)}$ arising from $\text{CoO}_{(s)}$ in a Knudsen cell between 1578 and 1744 K. Thermochemical calculations by Ham and McAllister¹¹ demonstrated that if more than 5×10^{-11} mole of cobalt was used as the sample $\text{Co}_{(l)}$ would replace $\text{Co}_{(s)}$ at equilibrium above 1880 K, which would result in a heat of atomization of 309 kJ/mole for cobalt, as estimated by using Trouton's rule. These conflicting reports have left the mechanism of cobalt atomization still unresolved. Also, the mechanisms of cobalt atomization from different surfaces in GFAAS need to be investigated.

One objective of this work was to investigate the mechanisms of cobalt atomization from different atomizer surfaces, namely pyrolytically coated graphite, uncoated electrographite, and glassy carbon. The other objective was to investigate how the linearity of Arrhenius plots is

affected by different values for the constant m in equation (7).

EXPERIMENTAL

Apparatus

A Perkin-Elmer model 503 atomic-absorption spectrometer, equipped with a deuterium arc background corrector and a model 76B heated graphite atomizer (HGA) was used. The atomic-absorption spectrometer was modified in our laboratory to allow signals to be registered with a time constant of 20 msec. The graphite furnace was heated with a laboratory-made power supply capable of supplying variable heating rates up to 1 K/msec. The signals were recorded with a model 4094 programmable Nicolet oscilloscope, and the integrated absorbance was obtained by using a software package provided by Nicolet Instrument Corporation. A Perkin-Elmer cobalt hollow-cathode lamp was used at a lamp current of 10 mA. The 240.7 nm line of cobalt was used as the analysis line, with a spectral band-pass of 0.7 nm.

The temperature of the graphite tube inner surface just below the sample injection hole was measured with a model 1100 automatic optical pyrometer (Iron Inc., Niles, IL., USA), the temperature being read off the calibration curve supplied by the manufacturer.

Atomizer tubes

Atomizer tubes fabricated from three different materials were used: pyrolytically coated graphite tubes (Perkin-Elmer, part No. BOO91-504), uncoated electrographite tubes (Perkin-Elmer, part No. 0290-1820), and glassy carbon tubes (Sigri Ringsdorf Werke, GmbH, West Germany). All these tubes had the same dimensions: length 28 mm, outside diameter 8 mm, inside diameter 6 mm.

Reagents

The stock solution of 1000 $\mu\text{g/ml}$ cobalt was prepared by dissolving pure cobalt metal in pure nitric acid (Baker ULTREX) and diluting the solution with ultrapure water obtained direct from a Milli-Q2 water purification system (Millipore Corporation). The test solutions were prepared immediately prior to use, by serial dilution of the stock solution with ultrapure water.

Procedure

Aliquots (10 μl) of the cobalt solution (0.02 $\mu\text{g/ml}$) were used for determining the decompo-

sition and atomization curves. The cobalt sample was atomized in a pyrolytically coated graphite tube, with the furnace used in the gas-interrupt mode.

For determination of the activation energy for cobalt atomization from different atomizer surfaces the furnace was used in the gas-flow mode, with an argon flow-rate of 625 ml/min. Aliquots (10 μl) of the cobalt solution (0.02 $\mu\text{g/ml}$) were deposited in the graphite furnace and atomized with a charring temperature of 1070 K and atomization temperature of 2700 K.

RESULTS AND DISCUSSION

Decomposition and atomization curves

Figure 1 shows the decomposition and atomization curves for cobalt (taken as the nitrate in aqueous solution) atomized from a pyrolytically coated graphite tube. The decomposition curve is defined as that obtained as a function of the charring temperature when the sample is atomized at a constant (optimum) temperature. The atomization curve is defined as that obtained as a function of the atomization temperature when a constant (optimum) charring temperature is used. Each datum point represents the arithmetic mean of three values, corrected for blanks. In Fig. 1, curve A is the decomposition curve and curve B the atomization curve. For the decomposition curve, the sample was dried at 420 K and charred at various temperatures from 670 to 2770 K. The atomization temperature was kept constant at the optimum temperature of 2700 K. For the atomization curve, the charring temperature was kept constant at the optimum charring temperature of 1070 K and the atomization temperature was varied from 1070 to 3170 K. The graphite tube was cleaned after each run by firing at 3170 K. The data for

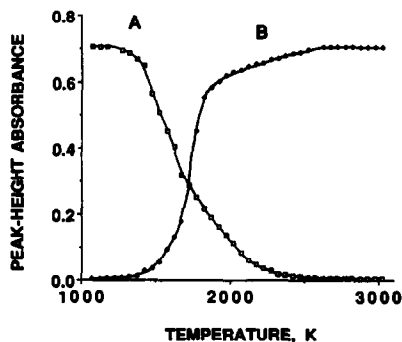


Fig. 1. Decomposition and atomization curves for 0.2 ng of Co (taken as the nitrate in aqueous solution in 1% v/v nitric acid) by atomization from a pyrolytically coated graphite tube. A, decomposition curve; B, atomization curve.

the decomposition curve show that the maximum charring temperature that can be used without noticeable loss is ~ 1100 K. The appearance temperature (defined as the temperature at which the analyte signal is just distinguishable from the baseline) and the optimum atomization temperature (defined as the lowest temperature giving the maximum absorbance) are ~ 1400 and ~ 2700 K, respectively. The decomposition curve (A) can be interpreted as follows. As the charring temperature is increased, the cobalt nitrate is decomposed at about 970 K (not shown in Fig. 1) to form $\text{CoO}_{(g)}$.¹³ A noticeable loss of Co atoms occurs at a charring temperature of ~ 1100 K. In Fig. 1, since there is no significant difference between the temperature in the decomposition curve at which the absorbance starts to decrease, and the appearance temperature in the atomization curve (B), it is reasonable to conclude that the decrease in the absorbance is due to loss of $\text{Co}_{(g)}$ when the $\text{Co}(\text{NO}_3)_2$ is charred at a temperature > 1100 K in the pyrolytically coated graphite tube. Any mechanism for the atomization of $\text{Co}(\text{NO}_3)_2$ must be consistent with these observations in order to be acceptable as satisfactory.

Rate constants for the supply and removal function

The time-dependence of the supply of analyte atoms into and their removal from the graphite furnace has been reported in the literature. Fuller² has proposed a model consisting of a mathematical expression with two exponential terms to describe the release and removal of copper in the Perkin-Elmer model HGA-70 graphite furnace. He concluded that the rate of removal exceeds the rate of atom formation by a factor of 3–20, depending on the atomization temperature. More rigorous studies of supply and removal of analyte atoms during the atomization were published later.^{6,8,9,14,15}

To verify the results reported earlier by others^{2,9} that the value of the rate constant, k_s , for atom formation is less than the value of the rate constant for atom removal, k_r , we will calculate k_s and k_r at each datum point and present the results graphically to show the difference between the two rate constants. It is assumed that k_s is approximated by the Arrhenius law [equation (5)] and that k_r is given⁹ by

$$k_r = k_d + k_e + k_c \quad (10)$$

where k_d , k_e and k_c are first order rate constants for loss by diffusion, expansion and convection, respectively. This assumption is approximately true for the system that we are investigating if we exclude (as we have done) other loss processes. For k_d we have¹⁶

$$k_d = \frac{8D_0}{l^2} \left(\frac{T}{298} \right)^n \quad (11)$$

where D_0 is the diffusion coefficient at STP, T is the absolute temperature, l is the tube length, and the value of n (to be called the gas combination factor) varies from 1.5 to 2.0 for various combination of gases;¹⁷ k_e is given by¹⁶

$$k_e = \alpha/4T \quad (12)$$

where α is the heating rate of the atomizer in K/sec. The value of k_c is expressed by⁹

$$k_c = FT/300MV \quad (13)$$

where F is the flow-rate of the purge gas in ml/min, M is a proportionality constant which depends on the gas flow pattern through the furnace, and V is the analysis volume. Data used in the calculation are given in Table 1. The results are presented in Fig. 2, which shows that k_r is greater than k_s . Under the experimental conditions shown, our results agree with those of van den Broek and de Galan.⁹

Activation energy for atomization of cobalt nitrate

Table 2 summarizes the results for determination of the activation energies for the atomization of cobalt nitrate from the three different surfaces. The standard free energy change at the appearance temperature of 1400 K was calculated by Sturgeon *et al.*⁶ on the assumption that $\text{CoO}_{(g)}$ is the precursor for $\text{Co}_{(g)}$, and was found to be -100 kJ/mole. We may therefore conclude that the reduction of $\text{CoO}_{(g)}$ by $\text{C}_{(s)}$ at the appearance temperature is thermodynamically favorable.

Table 1. Data used in the calculation of the rate constants k_s and k_r *

Activation energy E_a , kJ/mole	387.0
Heating rate α , K/sec	650
Pre-exponential factor k_∞ , sec ⁻¹	2.0×10^7
Gas constant R , J.mole ⁻¹ . K ⁻¹	8.314
Gas combination factor, n	1.89
Tube length l , cm	2.8
Tube volume V , cm ³	0.79
Diffusion coefficient D_0 at 273 K, cm ² /sec	0.097
Proportionality factor, M	90.0
Flow-rate F , ml/min	625.0

*The temperatures used are the same as in Fig. 3.

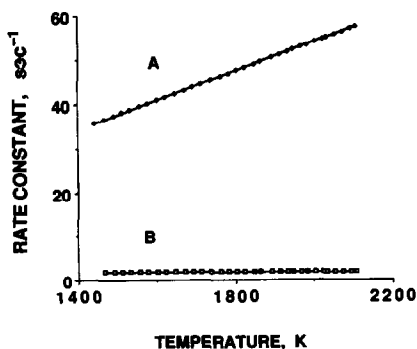


Fig. 2. Rate constants for the supply and loss of Co, as a function of the absolute temperature: A, rate constant k_r for Co atom removal; B, rate constant k_f for Co atom formation.

We have calculated E_a values from the slopes of the Arrhenius plots, drawn by use of the data from the leading edge of the absorbance signal profile (Fig. 3). The slopes were calculated by the least-squares method. The initial linear portion of the slope covers a temperature range of about 340 K. Figure 4 shows that the value of m does not have any discernible effect on the slope of the Arrhenius plots. The effect of the heating rate on E_a for cobalt atomization from a pyrolytically coated graphite tube is presented in Table 3. The heating rate α was determined graphically by using the equation $T = T_0 + \alpha t$, where T is the absolute temperature at time t . No significant effect is seen, which agrees with the experimental observations reported by Sturgeon *et al.*⁶

MECHANISMS OF ATOMIZATION

Table 2 presents a comparison of the activation energies for Co atomization from the three different atomizer surfaces. Since the dimensions of the three atomizer tubes are identical, and the appearance temperatures and the heating rate at the appearance temperatures are not very dissimilar, the activation energies obtained can be compared and interpreted in terms of the mechanisms for atom formation of Co from the different atomizer surfaces.

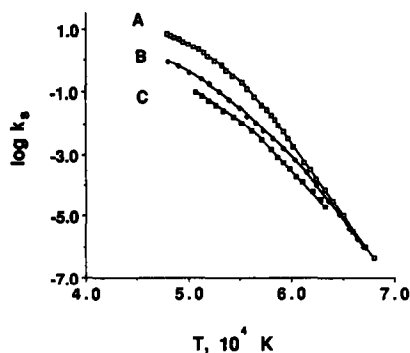


Fig. 3. Arrhenius plots for atomization of 0.2 ng of Co (taken as the nitrate in aqueous solution in 1% v/v nitric acid) in different atomizer tubes: A, pyrolytically coated graphite; B, uncoated electrographite; C, glassy carbon.

In Table 2 there is no significant difference between the activation energies obtained by using the pyrolytically coated graphite surface and the uncoated electrographite surface, but these values are significantly different from the activation energy obtained with the glassy carbon tube. If surface spreading and penetration by the aqueous solution of the sample had played a role in the atomization, then all three E_a values should be appreciably different because significant spreading and penetration would be expected for the uncoated electrographite surface, but not for the pyrolytically coated graphite surface and the glassy carbon

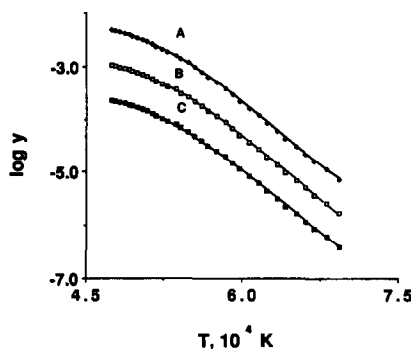


Fig. 4. Arrhenius plots for the atomization of 0.2 ng of Co (taken as the nitrate in aqueous solution in 1% v/v nitric acid) in a pyrolytically coated graphite tube, as a function of m [equation (8)]: A, $m = 1.5$; B, $m = 1.2$; C, $m = 1.0$.

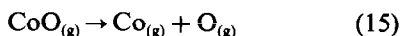
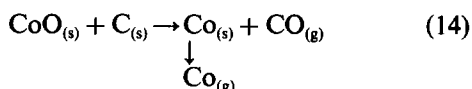
Table 2. Activation energy (\pm standard deviation of four determinations) for atomization of cobalt from different atomizer surfaces

Tube*	Appearance temperature, K	Atomization temperature, K	Heating rate, K/sec	E_a , kJ/mole
PG	1420	2700	650	387 ± 15
UG	1450	2700	800	375 ± 19
GC	1500	2700	850	285 ± 9

*PG, pyrolytically coated graphite tube; UG, uncoated electrographite tube; GC, glassy carbon tube.

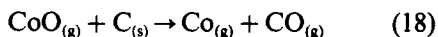
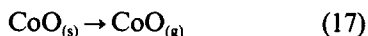
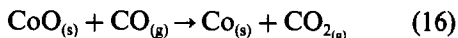
surface. The pyrolytically coated surface is expected to show much less spreading than the uncoated electrographite surface, but no penetration as long as the pyrolytic graphite coating remains intact. The near identity of the E_a values for the pyrolytically coated graphite surface and the uncoated electrographite surface rules out surface spreading and penetration as responsible for the observed difference in the E_a values in the present case. This means that surface spreading and penetration cannot explain the low E_a value for the glassy carbon tube. Perhaps the cause of the observed low E_a value for the glassy carbon tube lies in a different atomization mechanism.

The E_a values (Table 2) for the pyrolytically coated tube and the uncoated electrographite tube may be correlated with either the heat of sublimation of $\text{Co}_{(s)}$, 428.4 kJ/mole, or the heat of dissociation of $\text{CoO}_{(g)}$, 361 kJ/mole (Table 4). Since reduction of $\text{CoO}_{(s)}$ by carbon is thermodynamically favorable at the appearance temperature of 1400 K, identification of E_a by correlating it with the heat of sublimation of $\text{Co}_{(s)}$ is not unreasonable. These two mechanisms are shown below as equations (14) and (15).



The mechanism shown as equation (15) requires the prior formation of $\text{CoO}_{(g)}$ from $\text{CoO}_{(s)}$. Reaction (14) should be kinetically favorable because the $\text{CoO}_{(s)}$ formed by the decomposition of $\text{Co}(\text{NO}_3)_2$ in the charring cycle is in intimate contact with a very large excess of $\text{C}_{(s)}$ (present as the heated graphite tube). Reaction (15) is also kinetically favorable at the high temperature of atomization.

The possibility that any of the following reactions may be an effective pathway for the formation of $\text{Co}_{(g)}$ should also be examined:



Although reaction (16) is thermodynamically favorable, it is kinetically less favorable than the other reactions considered earlier, including reactions (17) and (18). This is because of the very low partial pressure of $\text{CO}_{(g)}$.¹⁸ In order for $\text{Co}_{(g)}$ to reduce $\text{CoO}_{(s)}$, $\text{CO}_{(g)}$ molecules must be

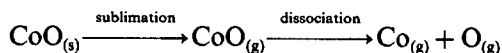
Table 3. Activation energy (\pm standard deviation of four determinations) for atomization of cobalt from a pyrolytically coated graphite tube at different heating rates

Appearance temperature, K	Heating rate,* K/sec	E_a , kJ/mole
1410	580	390 \pm 12
1440	1050	387 \pm 12
1420	2800	405 \pm 16

*At the appearance temperature.

adsorbed onto the condensed-phase $\text{CoO}_{(s)}$. The expected low surface coverage by $\text{CO}_{(g)}$ (because of its very low partial pressure) will cause the reduction of $\text{CoO}_{(s)}$ to be kinetically unfavorable. Reactions (17) and (18) are coupled in the graphite furnace. The dissociation energy of $\text{CoO}_{(g)}$ is so much smaller than the heat of sublimation of $\text{CoO}_{(s)}$ [reaction (17)] that the sublimation of $\text{CoO}_{(s)}$ will occur with the attendant dissociation of $\text{CoO}_{(g)}$ [equation (15)]. It is possible that the small mass of the sample taken allows the sublimation of $\text{CoO}_{(s)}$ to deplete all $\text{CoO}_{(s)}$ to form $\text{CoO}_{(g)}$, for which the dissociation energy is so much lower than the sublimation energy of $\text{CoO}_{(s)}$ that the sublimation of $\text{CoO}_{(s)}$ would result in the dissociation of $\text{CoO}_{(g)}$, the dissociation energy being observed as the activation energy, E_a .

On the basis of the above, it is reasonable to conclude that the more likely mechanism of atomization of $\text{Co}(\text{NO}_3)_2$ in the pyrolytically coated graphite tube or the uncoated electrographite tube is the dissociation of $\text{CoO}_{(g)}$ following the sublimation of $\text{CoO}_{(s)}$.



The E_a value of 380 kJ/mole (Table 2) correlates better with the heat of dissociation of $\text{CoO}_{(g)}$, 361 kJ/mole (Table 4), than the heat of sublimation of $\text{Co}_{(s)}$, 428.4 kJ/mole. However, both mechanisms [equations (14) and (15)] are consistent with the observations made earlier about the decomposition curve in Fig. 1.

The E_a value (285 kJ/mole) of Co atomization for the glassy carbon tube is more difficult to account for, as it does not correlate with any value of the thermochemical properties given in Table 1. By thermochemical calculations Ham and McAllister¹¹ have demonstrated that if more than 5×10^{-11} mole (2.945 ng) of Co is taken, $\text{Co}_{(l)}$ should replace $\text{Co}_{(s)}$ for equilibria at above 1880 K. Since the E_a values for Co atomization were obtained by using 0.2 ng of

Table 4. Physical and thermochemical properties of probable cobalt species

Parameter	Value	Reference
Melting point of Co	1768 K	20
Boiling point of Co	3373 K	13
Melting point of CoO	2208 K	13
Co ₂ O ₃ transformed into Co ₃ O ₄	at 1168 K	13
Co ₃ O ₄ transformed into CoO	at 1223 K	13
Co _(s) → Co _(g)	428.4 kJ/mole	20
Co _{2(g)} → 2 Co _(g)	167 kJ/mole	20
Co _(l) → Co _(g)	370 kJ/mole	21
CoO _(s) → CoO _(g)	510.5 kJ/mole	22
CoO _(g) → Co _(g) + O _(g)	361 kJ/mole	23

Co, the Co atoms should be in the solid state rather than the liquid state. However, for a monolayer distribution of the analyte atoms on the atomizer surface, the energy of interaction between the surface and the analyte atoms may affect the activation energy. It has been reported^{18,19} that glassy carbon is chemically less reactive than graphite, and perhaps pyrolytically coated graphite. If lower chemical reactivity results in a weaker interaction between the glassy carbon surface and the Co atoms on it, and if the measured E_a corresponds to this interaction, then E_a would have a low value. The stronger interaction between Co_(s) and the pyrolytically coated graphite surface or the uncoated electrographite surface should accordingly result in high E_a values. The experimental E_a values (Table 2) are consistent with this.

The E_a value (285 kJ/mole) for Co atomization from the glassy carbon surface can be correlated with the heat of vaporization, 309 kJ/mole, as estimated by Trouton's rule. However, such a correlation would require that the cobalt sample be converted into Co_(l) near the appearance temperature of ~1500 K for atomization from the glassy carbon surface (Table 2). It is possible that cobalt exists as liquid on the tube surface even though its appearance temperature is lower than the melting point, since the latter can be lowered by traces of impurities in the sample. However, it is also possible that the small amount of Co_(s) present can be totally sublimed at a temperature below the melting point of Co_(s). By thermochemical calculations, the mass of cobalt which is atomized at the appearance temperature of 1400 K to give a measurable signal (at the appearance temperature) is found to be approximately 3.7×10^{-5} ng. This small amount of cobalt can be totally sublimed at well below its melting point, which accounts for the appearance temperature for cobalt also being well below its melting point.

Acknowledgements—The authors are grateful to the Natural Sciences and Engineering Research Council of Canada for financial support. One of the authors (Shamil J. Cathum) is grateful to the Government of Iraq for a postgraduate scholarship.

REFERENCES

1. B. Smets, *Spectrochim. Acta*, 1980, **35B**, 33.
2. C. W. Fuller, *Analyst*, 1974, **99**, 739.
3. W. C. Campbell and J. M. Ottaway, *Talanta*, 1974, **21**, 837.
4. W. Frech, E. Lundberg and A. Cedergren, *Prog. Anal. Atom. Spectrom.*, 1985, **8**, 257.
5. C. L. Chakrabarti, S. B. Chang and S. E. Roy, *Spectrochim. Acta*, 1983, **38B**, 447.
6. R. E. Sturgeon, C. L. Chakrabarti and C. H. Langford, *Anal. Chem.*, 1976, **48**, 1792.
7. J. P. Matousek and H. K. J. Powell, *Spectrochim. Acta*, 1988, **43B**, 167.
8. S. L. Paveri-Fontana, G. Tessari and G. Torsi, *Anal. Chem.*, 1974, **46**, 1032.
9. W. M. G. T. van den Broek and L. de Galan, *Anal. Chem.*, 1977, **49**, 2176.
10. W. Frech, N. G. Zhou and E. Lundberg, *Spectrochim. Acta*, 1982, **37B**, 691.
11. N. S. Ham and T. McAllister, *ibid.*, 1988, **43B**, 789.
12. R. T. Grimley, R. P. Burns and M. G. Inghram, *J. Chem. Phys.*, 1966, **45**, 4158.
13. C. Duval, *Inorganic Thermogravimetric Analysis*, 2nd Ed., Elsevier, New York, 1963.
14. G. Torsi and G. Tessari, *Anal. Chem.*, 1975, **47**, 839.
15. G. Tessari and G. Torsi, *ibid.*, 1975, **47**, 842.
16. H. Falk, *CRC Crit. Rev. Anal. Chem.*, 1988, **19**, 29.
17. B. V. L'vov, *Atomic Absorption Spectrochemical Analysis*, Hilger, London, 1970.
18. R. E. Sturgeon and H. Falk, *J. Anal. Atom. Spectrom.*, 1988, **3**, 27.
19. W. Huettner and C. Busche, *Z. Anal. Chem.*, 1986, **323**, 674.
20. R. C. Weast, *Handbook of Chemistry and Physics*, 66th Ed., CRC Press, Boca Raton, 1985–1986.
21. A. F. Trotman-Dickenson, *Comprehensive Inorganic Chemistry*, Vol. 3, p. 1055. Pergamon Press, Oxford, 1973.
22. I. S. Kulikov, *Thermal Dissociation of Chemical Compounds*, p. 106. Israel Program for Scientific Translations, Jerusalem, 1967.
23. M. G. Zhuravleva and G. I. Chufarov, *Tr. Inst. Metall. Akad. Nauk. S.S.S.R. Ural Filial*, 1959, **3**, 63.

DETERMINATION OF 1 ng/l. LEVELS OF MERCURY IN WATER BY ELECTROTHERMAL ATOMIZATION ATOMIC-ABSORPTION SPECTROMETRY AFTER SOLVENT EXTRACTION

A. LE BIHAN* and J. Y. CABON

URA CNRS 322, Université de Bretagne Occidentale, 6, Avenue Le Gorgeu, 29287 Brest Cedex, France

(Received 14 December 1989. Revised 26 June 1990. Accepted 10 July 1990)

Summary—Optimization of the furnace parameters for electrothermal atomization of mercury leads to a characteristic mass of 20 pg in aqueous solution and 30 pg in chloroform extracts (with Zeeman correction). With a single-step solvent extraction from 100 ml of sample, performed in the sampling vessel, and direct injection of 400 μ l of the extract into the furnace, a characteristic concentration of \sim 0.8 ng/l. is reached.

Trace determinations of mercury are currently generally based on the work of Hatch and Ott.¹ The sensitivity of these methods is high but not sufficient for the direct determination of mercury in unpolluted natural waters (at concentrations of a few ng/l.). To reach such low levels it is necessary to preconcentrate the mercury atoms in the cold vapour; the means generally used are amalgamation in a gold trap before determination by atomic-absorption²⁻⁵ or atomic-fluorescence spectrometry⁶ with long-path cells. An alternative is amalgamation in gold⁷ or platinum-coated⁸ furnaces before electrothermal atomic-absorption (AA) spectrometry. In such conditions the characteristic concentration can be decreased by using a larger sample volume.

Trace mercury determination has been reviewed by Drabaek and Iverfeldt,⁹ who emphasize that sampling and storage, and the addition of reagents are critical steps in the determination of ultratrace levels.

To overcome these problems we propose a procedure for determination of mercury in the ng/l. range with sample volumes around 100 ml, by use of only conventional electrothermal AA spectrometers. To reduce the risk of mercury losses (or gains by contamination) the metal is determined in the solvent used for the extraction, which is performed directly in the sampling vessel.

EXPERIMENTAL

Apparatus

Sampling and extraction were performed in 100-ml glass flasks fitted with Teflon stoppers. The AA spectrometer was a Perkin-Elmer Z3030 equipped with an AS-60 automatic sampler in which the plastic cups had been replaced by glass tubes (2.5 cm high). Furnace-wall atomization from pyrolytically graphite-coated graphite tubes was used. The light-source was a Perkin-Elmer EDL working at 5 W; the 253.7 nm line was used.

The solvents and reagents were pipetted with a Gilson Pipetman pneumatic syringe modified to accommodate glass Pasteur pipette tips.

Glassware was used because it allows the elimination of adsorbed mercury by heating.

Reagents

Analytical reagent grade chloroform was washed before use, by shaking it with an equal volume of Millipore MQ ultrapure water, and its mercury level was checked by AAS after evaporation of 250 ml of the washed solvent to low volume in a glass beaker and final evaporation in the furnace. The concentration found was 0.08 pg/ml. Analytical reagent grade sodium diethyldithiocarbamate (DDTC) was used as a 10 mg/ml aqueous solution, purified by extraction with an equal volume of purified chloroform. The pH of this solution was around 9.3 and the complexing capacity did not decrease significantly during three months storage at 20°.

*Author for correspondence.

For calibration a 6 $\mu\text{g/l.}$ mercury diethyldithiocarbamate solution in chloroform was prepared monthly from analytical grade mercuric nitrate and DDTC.

Procedure

One ml of DDTC solution, 1.5 ml of chloroform and a sample volume close to 100 ml are introduced into a 100-ml flask; the exact amount of sample is measured by weighing. At room temperature the solubility of chloroform in water is 5.0 ml/l., the solubility of water in the solvent being negligible (0.8 ml/l.). To prevent contamination from the calomel electrode, the pH of the water sample, which should be between 3 and 9, is not adjusted beforehand but is measured after the extraction. The flask is then shaken for 2 min, and the two phases are separated by centrifugation. The organic phase is transferred to the automatic-sampler cup by pneumatic syringe, and covered with 0.5 ml of ultrapurified water to prevent evaporation of the solvent.

A sample (80 μl) of the organic phase is introduced into the graphite furnace and dried by heating at 80° for 25 sec. When necessitated by a low mercury concentration, multiple injection and drying steps are performed.

Atomization is performed by heating at 700° for 4 sec; the furnace temperature is then lowered to about 30°. Three sec after the beginning of atomization, integration of the signal for 10 sec is started. The nitrogen flow is stopped during the whole of the atomization and measurement steps. A high-temperature clean-out step follows the integration.

Calibration over the 0.7–20 ng/l. mercury concentration range is performed by injecting 5–80 μl of the 6 $\mu\text{g/l.}$ mercury diethyldithiocarbamate chloroform solution into the graphite furnace.

Under these conditions, a single injection of 80 μl of the chloroform extract leads to a characteristic concentration of mercury in the water sample of about 3.8 ng/l. To ensure access to the 1 ng/l. level it is necessary to inject 400 μl of solvent (5 successive injections of 80 μl), the characteristic concentration then being about 0.8 ng/l. when measured in the peak area mode.

RESULTS AND DISCUSSION

Optimized conditions for the AAS measurements

At high atomization temperatures the characteristic mass of mercury, m_0 , is twice as high

when the peak height is measured instead of the peak area. When the atomization temperature is lowered, m_0 decreases when measured in the peak-area mode, but increases if the peak height is used. Thus, the sensitivity is always better when peak areas are measured. Moreover, with the mercury EDL, the integrated noise signal is in the 0.001 sec range for a 10-sec integration time, whereas the maximum absorbance of the noise signal in the peak-height mode is about 0.003.

For a CHCl_3 /DDTC extract of mercury the background absorbance is always below 0.03 and consequently is not increased significantly by the noise signal in the peak-height mode. However, the signal to noise ratio is more than five times better in the peak-area mode than in the peak-height mode, so peak-area measurements are used throughout.

From work by L'vov *et al.*¹⁰ it appears that under fixed experimental conditions m_0 is proportional to D , the diffusion coefficient of the neutral atoms in the gas phase, when the peak area is measured. The diffusion coefficient varies with the temperature:

$$D_T = D_{273}(T/273)^n$$

where T is the absolute temperature and n varies from 1.5 to 1.8.^{11–13}

Thus it appears that the sensitivity is maximum when the temperature is high enough for efficient generation of neutral atoms. In the L'vov experiments, under isothermal conditions with the STPF (stabilized temperature platform furnace) technique, at 1200°, the characteristic mass was $m_0 = 52$ pg of mercury. Also with the STPF technique at 1000°, but in the presence of palladium as matrix modifier,^{14,15} Grobanski *et al.* obtained an m_0 value of 85 pg with a Perkin-Elmer furnace.¹⁶

Under our experimental conditions, with mercuric nitrate solution, the signal is visible when an atomization temperature as low as 200° is reached. Thus operating at low temperatures for the minimum time necessary for efficient transformation of ionic mercury into neutral atoms increases the sensitivity. Although our

Table 1. Furnace parameters for determination of mercury in chloroform extracts (80 μl)

	Drying	Atomization	Clean-out	
Temperature, °C	80	700	30	2500
Ramp time, sec	1	1	1	1
Hold time, sec	24	3	8	4
Integration, sec	—	1	9	—
N ₂ flow, ml/min	300	0	0	300

experiments are not performed by the STPF technique, the delay in the appearance of neutral atoms, at between 500 and 1100°, is so large (more than 3 sec) that the gas and wall thermal equilibria are reached when the neutral atoms are in the furnace atmosphere.¹⁷

The variation of m_0 , for a 10-sec integration time, with temperature during the atomization is represented in Fig. 1 for mercury introduced as mercuric nitrate solution. The values of D are also reported in Fig. 1.

The quasi-constant value of about 30 pg for m_0 from 200 to 500° indicates that the increase in diffusion with temperature is compensated by more efficient atomization. At above 500° and up to 1200°, the variation of m_0 is parallel to the change in diffusion coefficient; diffusion is the governing factor at these temperatures. At above 1200° the increase in characteristic mass is steeper but in this case the gas thermal equilibrium is not reached.

When the temperature of the furnace is lowered from 500 to 30° as soon as the absorption maximum is reached, the diffusion coefficient decreases and the mercury atoms are kept in the optical path by contraction of the gas. Under such conditions the characteristic mass is lowered from 30 to 20 pg.

When the mercury is introduced as its diethyldithiocarbamate complex the minimum temperature for efficient atomization is about 650°. This increase in the atomization temperature is probably due to the stability of the mercury-sulphide compounds resulting from

decomposition of the DDTc. Owing to the lack of precision for the temperature measurements, the atomization temperature is set to a higher value, 700°, a precaution which ensures the efficiency of neutral atom production. The characteristic mass m_0 is 30 pg under these conditions. It should be mentioned that m_0 varies slightly not only from one furnace to another, but also with the number of atomizations performed.

Extraction

Filipelli has shown that mercury and its organo-derivatives are fully extracted into chloroform from sea-water at $\text{pH} \geq 3$, with ammonium pyrrolidinedithiocarbamate (APDC) as the complexing agent.¹⁸ From his results the distribution ratio, P , was estimated to be larger than 3000.¹⁸ To prevent losses of metal, samples are generally stored under acidic conditions; in such a medium, APDC is more stable than DDTc and is generally used as the complexing agent.

In the experimental procedure proposed here, mercury losses are prevented by performing the complexation at the time of sample collection; the extraction is then also done in the same flask. Under such conditions acidification of the sample is not necessary and consequently diethyldithiocarbamate (DDTC) can be used; this is an advantage as DDTC is more stable than APDC in weakly acidic media.

By means of two consecutive extractions with chloroform from the same water sample, the distribution ratio P between water and chloroform has been measured for mercuric ions, and methylmercury and phenylmercury chlorides, with DDTC as the complexing extractant.¹⁵ For aqueous phase pH values between 3 and 9, P is greater than 2500, for all three mercury species. Consequently, the yield is better than 96% for a single-step extraction, if the water to solvent volume ratio is 100. Use of more than one extraction is time-consuming and increases the risk of dilution and contamination errors.

Under our experimental conditions, the reproducibility for the introduction and atomization steps is better than 1.5% (RSD for 10 measurements) for chloroform solutions at the 500 pg mercury level.

The variation in concentration that could result from evaporation from glass tubes open to the air at room temperature is less than 5% during half an hour, in the case of chloroform, and in this case the evaporation can be

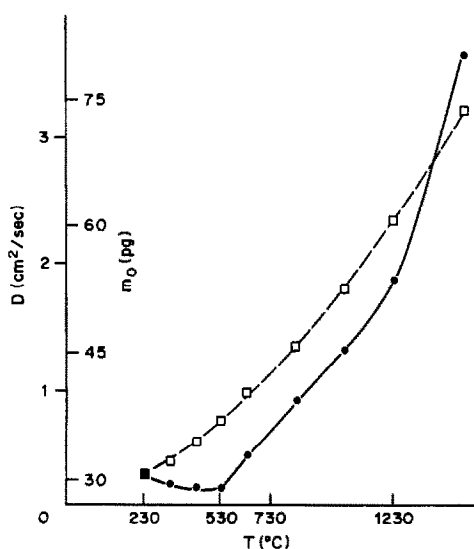


Fig. 1. Characteristic mass and diffusion coefficient of mercury as a function of atomization temperature: (●) characteristic mass (pg); (□) diffusion coefficient (cm²/sec).

suppressed by adding a few drops of water on top of the organic phase. To avoid any hazards associated with chloroform it is possible to extract the mercury complex with freon but in this case the reproducibility of the introduction and atomization steps increases to about 3% (RSD for 10 measurements).

The experimental method described here is the first step towards our goal, the determination of mercury in rain water. In this case, the sample volumes collected are variable and the total mass of mercury collected can be as low as 100 pg or even lower. Under the experimental conditions described the relative standard deviation is 30% for 10 measurements at the 1 ng/l. level of mercury in water; the relative standard deviation decreases to 15% for concentrations around 5 ng/l. The measurement takes only 5 min, and the complete procedure about 10.

CONCLUSION

The determination of mercury in water, at the 1 ng/l. level, requires optimization of the experimental conditions for both the atomic-absorption spectrophotometry and the extraction. A low characteristic mass is achieved by integration of the signal and by choosing an atomization temperature close to 700°; in such conditions the characteristic mass is 30 pg.

When the extraction with DDTC/CHCl₃ is performed directly in the sampling vessel at a sample-to-solvent volume ratio of 100, the characteristic concentration is better than 1 ng/l., with a 30% relative standard deviation. Besides high sensitivity, the advantages of the

procedure are the saving in time and the reduced risks of contamination with or loss of mercury.

REFERENCES

1. W. R. Hatch and W. L. Ott, *Anal. Chem.*, 1968, **40**, 2085.
2. S. J. Long, D. R. Scott and J. R. Thompson, *ibid.*, 1973, **45**, 2227.
3. N. S. Bloom and E. A. Crecelius, *Mar. Chem.*, 1983, **14**, 49.
4. R. Ahmed and M. Stoeppler, in M. Stoeppler and H. W. Dürbek (eds.), *Contributions to Environmental Specimen Banking*, Jül-Spez-349, KFA Jülich, 1986.
5. D. Cossa and J. Noel, *Mar. Chem.*, 1987, **20**, 389.
6. N. Bloom and W. Fitzgerald, *Anal. Chim. Acta*, 1988, **208**, 151.
7. S. H. Lee, K. H. Jung and D. S. Lee, *Talanta*, 1989, **36**, 999.
8. D. C. Baxter and W. Frech, *Anal. Chim. Acta*, 1989, **225**, 175.
9. I. Drabæk and A. Iverfeldt, in *Hazardous Metals in the Environment*, M. Stoeppler (ed.), Chapter 7, Elsevier, Amsterdam, in the press.
10. B. V. L'vov, V. G. Nikolaev, E. A. Norman, L. K. Polzik and M. Mojica, *Spectrochim. Acta*, 1986, **41B**, 1043.
11. F. Fagioli, C. Locatelli, R. Vecchietti and G. Torzi, *J. Anal. Atom. Spectrom.*, 1988, **3**, 159.
12. B. V. L'vov, L. K. Polzik and L. F. Yatsenko, *Talanta*, 1987, **34**, 141.
13. W. M. G. T. van den Broek and L. de Galan, *Anal. Chem.*, 1987, **49**, 2176.
14. X.-Q. Shan and Z.-M. Ni, *Acta Chim. Sin.*, 1979, **37**, 261.
15. G. F. Kirkbright, H.-C. Shan and R. D. Snook, *At. Spectrosc.*, 1980, **1**, 85.
16. Z. Grobowski, W. Erler and U. Voellkopf, *ibid.*, 1985, **6**, 91.
17. C. J. Radmeyer and H. G. C. Human, *J. Anal. Atom. Spectrom.*, 1989, **4**, 393.
18. M. Filipelli, *Analyst*, 1984, **109**, 515.
19. A. Le Bihan and J. Y. Cabon, *Analyst*, 1990, **115**, 126.

INDIRECT DETERMINATION OF CHLORIDE AND CARBONATE BY REVERSED FLOW-INJECTION ANALYSIS COUPLED WITH ATOMIC-ABSORPTION SPECTROMETRY AND IN-LINE PRECONCENTRATION BY PRECIPITATION

FATIMA T. ESMADI

Chemistry Department, Yarmouk University, Irbid, Jordan

MAHER A. KHAROAF and ABDULRAHAMAN S. ATTİYAT*

Chemistry Department, Mu'tah University, Karak, Jordan

(Received 27 October 1989. Revised 30 April 1990. Accepted 25 June 1990)

Summary—Chloride and carbonate are determined indirectly by reversed flow-injection analysis with preconcentration by precipitation. The anions are precipitated in a Tygon tube containing glass beads and connected to an atomic-absorption spectrophotometer, and are then dissolved by suitable reagents. Chloride is precipitated as silver chloride, which is then dissolved with ammonia, sodium thiosulphate or potassium cyanide solution. Carbonate is precipitated as calcium carbonate, which is dissolved with hydrochloric acid. The response of the system has been optimized with respect to concentration, precipitation time, solution flow-rate and other AAS variables. Detection limits are 3×10^{-7} and $5 \times 10^{-7} M$ for chloride and carbonate, respectively, with thiosulphate and hydrochloric acid as the dissolution agents.

Some elements cannot be determined directly by atomic-absorption spectrophotometry (AAS), and various methods have been employed for their indirect determination.¹⁻⁵ Some of these methods involve a precipitation, *e.g.*, chloride has been determined by precipitating it with silver nitrate and determining the silver by AAS after dissolution of the precipitate in ammonia solution.^{6,7} Carbonate has been determined by spectrophotometric,⁸ ion-exchange⁹ or conventional acidimetric titration,¹⁰ but no AAS method has hitherto been reported.

Flow-injection analysis combined with atomic-absorption spectrometry has proved a very versatile method which is simple, has high sample throughput, and offers the possibility of in-line preconcentration, which leads to an increase in sensitivity.¹¹ Injection of the reagent into the sample stream instead of sample injection is called reverse FIA (rFIA) and has been used for cations and anions.¹²⁻¹⁵ In previous work,¹⁶ we described an rFIA technique which used precipitation for a specific time as a preconcentration method for determination of trace amounts of metals. Silver, calcium and iron were precipitated as the chloride, carbonate

and hydroxide, respectively. The precipitates were dissolved in suitable reagents and the cations determined by AAS. This approach enhanced the sensitivity significantly. The present work is an inverse application of the technique, for indirect chloride and carbonate determination by precipitation of silver chloride and calcium carbonate, dissolution of the precipitate and AAS determination of the metal. An AAS method for determination of carbonate is described for the first time.

EXPERIMENTAL

Apparatus

A Perkin-Elmer 372 atomic-absorption spectrometer with appropriate hollow-cathode lamps and a strip chart recorder was used. Teflon tubing (1 mm bore, Beckman Altex) was used in the flow system. Two Rheodyne loop-injection valves were used to introduce either the wash solution or the solvent into the precipitation loop. The mixing coil was 5 cm long and 1 mm in bore. The precipitation loop was a Tygon tube (7 cm long, 2.8 mm bore) filled with 1.9 mm diameter Pyrex glass beads (Thomas Scientific), connected vertically to the injection valve, and to the nebulizer of the atomic-absorption spectrometer by a Teflon tube

*Author for correspondence.

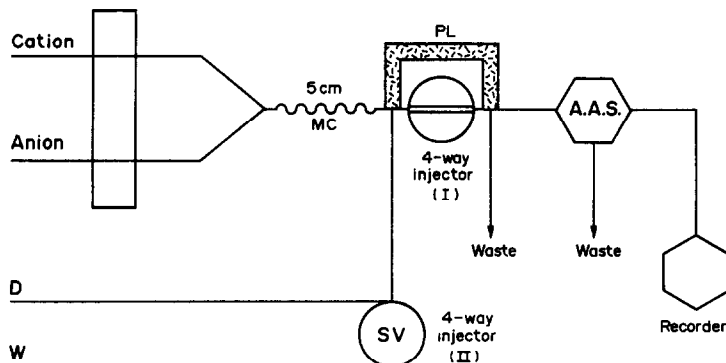


Fig. 1. Analytical manifold for the indirect determination of anions by rFIA-AAS; SV, selecting valve; D, dissolving solution; W, washing stream; MC, mixing coil.

(Fig. 1). The void volume of the precipitation loop was found to be $85 \mu\text{l}$. A four-channel peristaltic pump was used to draw the cation and anion solutions into the precipitation loop and then to waste, and the negative pressure from the nebulizer was used to draw the wash solution and solvent through the precipitation loop to the nebulizer of the AAS instrument. The solvent flow-rate was coarsely controlled by adjusting the nebulizer. The experimental conditions are listed in Table 1.

Reagents

All reagents were of analytical grade. Solutions were prepared in distilled, demineralized water. Standard solutions of silver (as nitrate) and calcium (as chloride) were prepared by appropriate dilution of 1000 ppm Merck stock standards.

Procedure

Standard solutions of either chloride or carbonate and their corresponding precipitating

agents, silver nitrate or calcium chloride, respectively, were passed through the flow system as shown in Fig. 1. The two solutions were mixed in the mixing coil and then pumped to the precipitation loop, where precipitation was allowed to take place for 2 min under the conditions in Table 1, the excess being pumped to waste. The selecting valve (injector II) then allowed passage of wash solution ($1.0 \times 10^{-5} M$ nitric acid for the chloride precipitate, and dimineralized water for the carbonate precipitate) through the precipitation loop, followed by passage of the solvent, which dissolved the precipitate and carried the corresponding cations to the nebulizer. The AAS signal, which was proportional to the cation concentration and hence to the sample anion concentration, was then recorded.

The concentrations of the precipitating agents were $[\text{Ag}^+] 500 \text{ ppm}$ and $[\text{Ca}^{2+}] 300 \text{ ppm}$. The dissolving agent concentrations were varied until the optimum for complete dissolution was found ($4.5 \times 10^{-2} M$ ammonia, $5.0 \times 10^{-3} M$

Table 1. Experimental conditions for the indirect determination of chloride and carbonate

Conditions	Chloride	Carbonate
Hollow-cathode lamp	Silver	Calcium
Lamp current, mA	4	6
Wavelength, nm	328.1	422.7
Type of flame	air-acetylene	air-acetylene
Acetylene flow-rate, l./min	1	1
Air flow, l./min	8	8
Bandwidth, nm	2	2
Recorder output, mV	10	5
Flow-rate of both analyte and precipitant, ml/min	0.90	0.90
Dissolving agent flow-rate, ml/min	4.2	6.2
Washing time, sec	35	23
Dissolution time, sec	33*, 30†, 28‡	17

*Ammonia solution.

†Cyanide solution.

‡Thiosulphate solution.

thiosulphate, $1.5 \times 10^{-3}M$ cyanide and $0.10M$ hydrochloric acid). The precipitation period could be increased up to 30 min to enhance preconcentration. The washing times for silver chloride and calcium carbonate were 35 and 23 sec respectively. Dissolution of silver chloride required 33, 30 and 20 sec with ammonia, cyanide and thiosulphate respectively as dissolving agents when the chloride concentration was $6 \times 10^{-6}M$. Dissolution of calcium carbonate required 17 sec when the carbonate concentration was $6 \times 10^{-6}M$.

RESULTS AND DISCUSSION

Determination of chloride

Indirect chloride determination by AAS involves precipitation with silver.⁶ Precipitation and then dissolution of silver chloride has been used to determine chloride concentration by the rFIA-AAS technique with high sensitivity and low detection limit.¹⁷ We have modified this by incorporating an rFIA system with a continuous precipitation operation. The amount of precipitate produced in a fixed time interval is proportional to the concentration of chloride, under the experimental conditions used. The dissolving agent dissolves the precipitate, and carries the solution to the AA spectrometer, and the signal obtained for silver is proportional to the concentration of chloride in the sample. For a given chloride concentration the signal for silver increased linearly with precipitation time up to 14, 18 and 23 min when the dissolving agents were ammonia, cyanide and thiosulphate, respectively. The signal levels off for longer precipitation times because the dissolving agent becomes saturated. Different times are required by the different dissolving agents owing to the differences in the rates of dissolution. The rate of dissolution will be fastest with the strongest complexing agent, so more precipitate will dissolve in a given dissolution time, enhancing the sensitivity.

To remove the excess of silver ions dilute nitric acid is passed through the precipitation loop before the dissolution, until no signal for silver is obtained. To achieve maximum sensitivity and precision, several other factors were optimized. For a fixed concentration of chloride ($6 \times 10^{-6}M$), a $2.9 \times 10^{-3}M$ concentration of silver solution was found to be the minimum for maximum response. The optimum concentrations of the dissolving agents for complete dissolution of the precipitate were found to be

$0.045M$ for ammonia, $5.0 \times 10^{-3}M$ for thiosulphate and $1.5 \times 10^{-3}M$ for cyanide.

No significant effect of reaction temperature on the AAS signal was found in the range studied ($25-90^\circ$), because the increase in solubility of silver chloride with increase in temperature is counterbalanced by the common-ion effect, if the silver nitrate concentration is high enough, but for convenience all work is done at room temperature.

Changing the flow-rate of both the chloride and silver streams in the range $0.90-4.5$ ml/min increases the signal linearly with increase in the flow-rate. This is expected since the precipitation reaction is fast, and a higher flow-rate results in more precipitate in a given time. A flow-rate of 0.90 ml/min was found to give sufficient sensitivity and reasonable reagent consumption. If more sensitivity is required, the flow-rate can be increased. The signal is also affected by the flow-rate of dissolving agent, increasing exponentially with it, but the best reproducibility was obtained when the flow-rate was 4.2 ml/min.

At constant flow-rates the length of the mixing coil was found to have no significant effect on the signal height, which indicates that all the precipitate is collected and dissolved in the precipitation loop.

Use of precipitation loops longer than 7 cm ($10, 15, 20$ cm) resulted in slightly decreased signal height, owing to broadening of the signal; shorter precipitation loops were difficult to fit into the injection valve. Increasing the bore of the precipitation loops above 2.8 mm (3.0 and 3.5 mm) had no effect on the signal but caused some loss in reproducibility, and longer washing and dissolution times were required (>2 min).

As shown in Fig. 2, the signals obtained for chloride standards when thiosulphate is the dissolving agent are reproducible, and the peak width is 28 sec, so a sampling frequency of 18 /hr can be achieved.

Figure 3 shows calibration curves for chloride determination by use of the three dissolving agents, ammonia, thiosulphate and cyanide, under the optimum conditions. The most reproducible results and lowest detection limit ($3 \times 10^{-7}M$) were obtained with thiosulphate as dissolving agent. Thiosulphate also gave the best sensitivity in the rFIA determination of silver. The linear working range, detection limits and precision are listed in Table 2. The upper limit of linearity is set by saturation of the solvent. The best dissolving agent is the one with

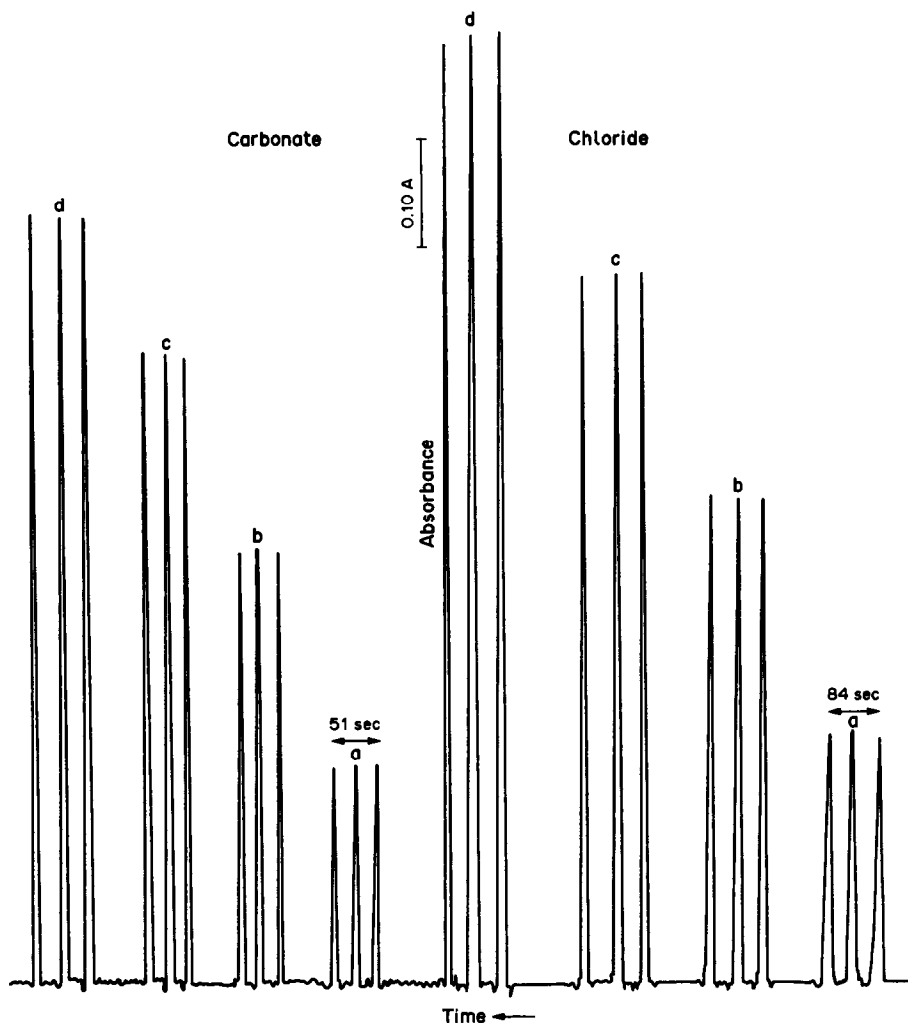


Fig. 2. Response of (a) $2 \times 10^{-6}M$, (b) $4 \times 10^{-6}M$, (c) $6 \times 10^{-6}M$, (d) $8 \times 10^{-6}M$ chloride and carbonate standards. Thiosulphate as dissolving agent for silver chloride.

the highest ability to complex the metal ion, and the highest rate of precipitate dissolution. It was found that thiosulphate gave the fastest dissolution. In previous work¹⁶ it was found that the presence of thiosulphate has no effect on the conventional AAS signal for silver, which indicates that it has no effect on the atomization efficiency.

The method described here has higher sensitivity, lower detection limit and higher sampling frequency than those for a method in which silver chloride was precipitated on a stainless-steel filter.¹⁷ In addition, the precipitation loop is cheap, readily available, and need not be disconnected and washed after use, since the passage of the dissolving agent gives sufficient cleaning.

Determination of carbonate

Carbonate is determined by precipitation as calcium carbonate, which is then dissolved with

$0.10M$ hydrochloric acid. The FIA-AAS signal due to the calcium in this solution is then proportional to the initial concentration of carbonate in the sample. To remove excess of calcium before the dissolution, water is passed through the precipitation loop until the background signal becomes zero. For a fixed concentration of carbonate ($6.0 \times 10^{-6}M$), a $3.0 \times 10^{-3}M$ concentration of calcium was found to be the minimum needed for complete precipitation. The concentration of dissolving agent required for complete dissolution at the optimum cation and anion concentrations was found to be $0.1M$ hydrochloric acid.

As in the chloride determination, the AAS signal height was found to increase linearly with an increase in the flow-rates of the two reactant streams; a flow-rate of 0.90 ml/min was selected for both. For a fixed carbonate concentration the signal height increases exponentially with

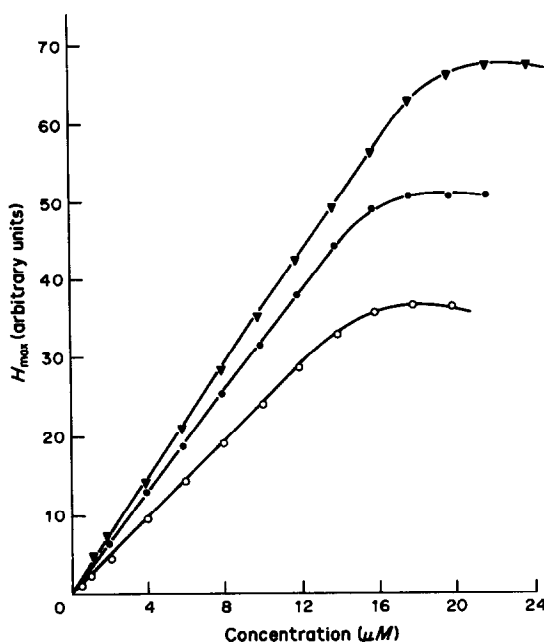


Fig. 3. Calibration curves for chloride determination, with thiosulphate (▼), cyanide (●) and ammonia (○) as dissolving agents, under optimum conditions.

increase in the flow-rate of the dissolving agent but high flow-rates produce irreproducible signals. A flow-rate of 6.2 ml/min was found to give the best reproducibility.

The signal height was found to decrease with increase in temperature in the range 25–90°, and poor reproducibility was obtained at the higher temperatures. This is due to increased solubility of the precipitate in water at higher temperatures, so room temperature is recommended for practical application.

Increasing the mixing coil length from 5 to 20 cm increased the signal height but increasing it further decreased the response. This is believed to be due to the low rate of the precipitation reaction. Increasing the length of the mixing coil increases the time before the mixed solution enters the precipitating loop,

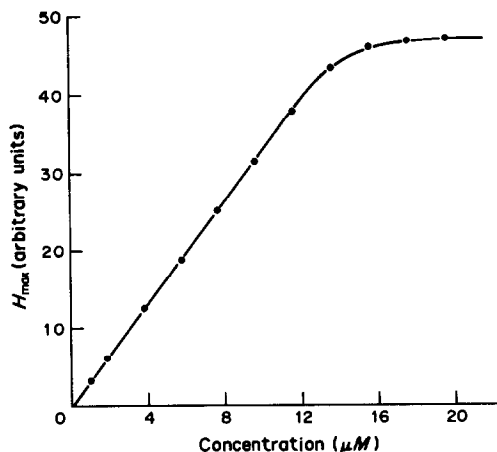


Fig. 4. Calibration curve for carbonate determination under the optimum conditions.

and as this approaches the induction period more calcium carbonate precipitates in the precipitation loop. Increasing the mixing coil length further allows some precipitation to occur in the mixing coil instead of the precipitating loop, and this precipitate will not be dissolved by the dissolving agent, which enters only the loop. This causes a decrease in the signal.

As in the case of chloride determination, the sensitivity decreased when longer precipitation loops were used and the reproducibility became poor if the bore of the precipitation loop was too large. Shorter precipitation loops cannot be fitted easily in the injection valve.

The signals obtained for carbonate standards are shown in Fig. 2. The signals are reproducible and a sampling frequency of 20/hr can be obtained (the peak width is 17 sec).

Figure 4 shows a calibration curve for carbonate determination under the optimum conditions. The linear working range, detection limit and precision are listed in Table 2. The linear upper limit is at 13 μM, then the signal levels off, which is believed to be due to saturation of the solvent.

Table 2. Analytical features of the rFIA-AAS technique for chloride and carbonate determination

Analyte	Dissolving agent	Linear working		
		range, μM	Detection limit,* M	RSD,† %
Chloride	Na ₂ S ₂ O ₃	0.5–16	3 × 10 ⁻⁷	1.4
Chloride	KCN	0.5–16	4 × 10 ⁻⁷	1.0
Chloride	NH ₃	1–14	1 × 10 ⁻⁶	1.7
Carbonate	HCl	1–14	5 × 10 ⁻⁷	2.0

*Detection limit, calculated as the concentration corresponding to three times the standard deviation of the baseline noise.

†Relative standard deviation ($n = 8$) at 6 × 10⁻⁶ M concentration.

Table 3. Effect of other anions on the determination of $6 \times 10^{-6}M$ chloride with thiosulphate as dissolving agent (error < 5%)

Ion	Molar ratio of ion to chloride
PO_4^{3-}	50
F^-	20
SO_4^{2-} , CO_3^{2-}	14
$C_2O_4^{2-}$	6
I^- , Br^- , SCN^-	< 1*

*Error is -16% for $[I^-]$, $[Br^-]$ or $[SCN^-] = 2[Cl^-]$.

Table 4. Effect of other anions on the determination of $6 \times 10^{-6}M$ carbonate

Ion	Molar ratio of ion to carbonate
Br^-	50
BrO_3^- , IO_3^-	25
SO_4^{2-}	10
F^- , $C_2O_4^{2-}$	4
PO_4^{3-}	< 1*

*Error is -12% for $[PO_4^{3-}] = 2[CO_3^{2-}]$.

Recovery and interferences

The recovery, which reflects the precipitation loop efficiency, was determined by allowing a known standard analyte solution to react with the corresponding precipitant for 2 min as described in the procedure. The dissolving agent (thiosulphate for silver chloride and hydrochloric acid for calcium carbonate) was then passed through the precipitating loop for 5 min, collected in a standard flask, and diluted to volume. The cation content of the collected solution was determined by AAS with conventional aspiration. The average recovery in ten determinations was found to be 94% for chloride, with 3.7% relative standard deviation and 92% for carbonate, with 1.6% relative standard deviation.

Tables 3 and 4 show the molar ratios of foreign ions to chloride and carbonate ions

respectively, that cause a relative change in absorbance of around $\pm 5\%$ for $6.0 \times 10^{-6}M$ chloride and carbonate solutions. Both tables indicate that the method is fairly selective. In the chloride method, iodide, bromide and thiocyanate seriously interfere negatively, however, by competitive reaction with silver to produce a precipitate that is less soluble in the dissolving solution than silver chloride is. Phosphate interferes negatively in the carbonate method for the same reason.

Acknowledgement—The authors acknowledge the financial support of Yarmouk University for this project.

REFERENCES

1. G. D. Christian and F. Feldman, *Anal. Chim. Acta*, 1986, **40**, 173.
2. M. Garcia-Vargas, M. Milla and J. A. Pérez-Bustamante, *Analyst*, 1983, **108**, 1417.
3. S. S. Hassan, *Organic Analysis Using Atomic Absorption Spectrometry*, Horwood, Chichester, 1984.
4. W. S. Zaugg and R. J. Knox, *Anal. Chem.*, 1966, **38**, 1759.
5. A. M. Bond and T. A. O'Donnell, *ibid.*, 1968, **40**, 560.
6. U. Westerland-Helmerson, *At. Abs. Newsl.*, 1967, **5**, 97.
7. M. Pinta, *Meth. Phys. Anal.*, 1970, **6**, 268.
8. M. D. Riano, M. Garcia-Vargas and J. A. Munoz Leyva, *Anal. Lett.*, 1988, **21**, 641.
9. D. D. Siemer, *Anal. Chem.*, 1987, **59**, 2439.
10. R. A. Day and A. L. Underwood, *Quantitative Analysis*, 4th Ed., Prentice-Hall, New Jersey, 1980.
11. I. J. Fletcher, *Anal. Chim. Acta*, 1983, **154**, 235.
12. D. T. E. Hunt and D. A. Winhard, *Analyst*, 1986, **111**, 785.
13. J. Marshall and M. Ottaway, *Talanta*, 1983, **30**, 571.
14. P. N. Vijan and R. S. Sadana, *ibid.*, 1980, **27**, 321.
15. K. Sin and M. Taga, *Anal. Chim. Acta*, 1982, **143**, 229.
16. F. Esmadi, M. Kharoaf and A. Attiyat, *Microchem. J.*, 1989, **40**, 277.
17. P. Martínez-Jimenez, M. Callego and M. Valcárcel, *Anal. Chem.*, 1987, **59**, 69.

DETERMINATION OF CHLORAMPHENICOL BY COUPLING A CONTINUOUS REDUCTION SYSTEM TO AN ATOMIC-ABSORPTION SPECTROMETER

R. MONTERO, M. GALLEGO and M. VALCARCEL

Department of Analytical Chemistry, Faculty of Sciences, University of Córdoba, 14004 Córdoba, Spain

(Received 10 January 1990. Revised 8 June 1990. Accepted 14 June 1990)

Summary—A simple method for the determination of chloramphenicol in pure powders, capsules, tablets, oral suspensions and eye ointments, based on its reduction to the amino derivative by a cadmium or zinc column, is reported. Chloramphenicol can be determined in the range 2–30 $\mu\text{g/ml}$, with a relative standard deviation of 1.5% and a sampling frequency of 150/hr. The proposed method has greater simplicity, sensitivity and rapidity than the previously reported batch method.

Chloramphenicol was the first of the broad-spectrum antibiotics and has been determined spectrophotometrically by reaction between its alkaline hydrolysis products and ammonium molybdate,¹ or by formation of their azo-derivatives;² it has also been determined by reaction with cobaltinitrite.³ Other photometric methods used are based on reduction of its nitro group, followed by diazotization and coupling.⁴ Polarography,^{5–7} gas chromatography,⁸ high-performance liquid chromatography,^{9,10} thin-layer chromatography¹¹ and bioluminescence¹² methods have also been reported.

Hassan and Eldesouki¹³ determined chloramphenicol and its esters in pharmaceutical preparations by reduction of the NO_2 group with cadmium in acid medium followed by determination of the cadmium ions produced. However, the reduction involves extensive manipulation, a large amount of cadmium metal (50–100 mg per sample) and boiling for 15–20 min under a carbon dioxide atmosphere (and a blank run under similar conditions). On the other hand, these authors achieved an average recovery of 99.5% and encountered no adverse effects from additives and diluents commonly used in drug formulations, and the results were much better than those afforded by the U.S. Pharmacopeia recommended procedure. The nitro group in organic compounds has also been determined indirectly by atomic-absorption spectrometry¹⁴ by reduction with zinc and ammonium chloride at 95°, followed by reaction with Tollens reagent and determination of the silver produced (after removal of silver chloride by dissolution in ammonia), but

the method is time-consuming and subject to severe interferences.

Flow-injection analysis has been used to develop a large variety of pretreatment procedures¹⁵ for atomic spectrometry. Different types of solid reactors (ion-exchange, enzyme and redox columns) have been employed in conjunction with flow configurations.

This paper reports the joint use of a flow reduction system (including a cadmium or zinc column) and an on-line instrumental set-up to measure the released cadmium or zinc ions by atomic-absorption spectrometry. The method is quite sensitive and permits the determination of chloramphenicol at sampling rates of 150/hr.

EXPERIMENTAL

Apparatus

A Perkin–Elmer 380 atomic-absorption spectrometer equipped with suitable hollow-cathode lamps (zinc or cadmium) and an adjustable nebulizer was connected to a Radiometer REC-80 Servograph recorder. The instrument was operated with deuterium-lamp background correction and the air–acetylene flame was adjusted according to the manufacturer's recommendations. The peristaltic pump was a Gilson Minipuls-2 furnished with poly(vinyl chloride) pumping tubes. The injector consisted of a rotary valve (Tecator Model L 100-1) to which a loop of the required volume was fitted; PTFE tubing (0.5 mm bore) and a selecting valve (Rheodyne Model 5041) were also used. The reduction columns were made by packing a

glass capillary (8.5 cm long, 1.8 mm bore) with cadmium or zinc granules (Merck) of medium size (grain diameter 0.5–1.2 mm).

Sample preparation

Standards. Chloramphenicol solution was prepared by dissolving 1 g of the dried powder (Sigma) in a minimum amount of ethanol and diluting to 1 litre with 1:1 v/v ethanol–water. Chloramphenicol standards in the range 2–30 $\mu\text{g/ml}$ were made by pipetting appropriate volumes of stock solution into 50-ml standard flasks and diluting to the mark with distilled water (the pH was adjusted to 3.7–4.2 with 0.1M hydrochloric acid or sodium hydroxide).

Tablets and capsules. Two or three tablets or the contents of 2 or 3 capsules were placed in a mortar and ground to a fine powder. An amount of powder equivalent to 20–25 mg of pure chloramphenicol was dissolved in 50 ml of ethanol, filtered and diluted to 250 ml with water.

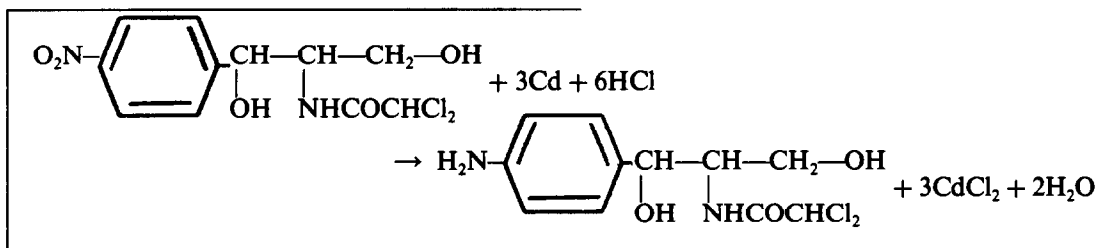
Syrup. The suspension was thoroughly shaken and a 1.5-ml portion was transferred to a 250-ml standard flask. Then 100 ml of ethanol were added, and the mixture was shaken

Recommended procedure

The manifold used is depicted in Fig. 1. A 90- μl water blank at the same pH as the sample was injected first, and then 90 μl of the sample solution (at pH 3.7–4.2), containing 2–30 μg of chloramphenicol per ml, was injected into the water carrier stream. The water blank gave a small peak due to slight dissolution of metal from the reductor column (cadmium or zinc) by the acid medium. The sample gave a higher peak due to the redox reaction (reduction of the nitro group in chloramphenicol and oxidation of the metal). The difference in peak height was proportional to the concentration of drug injected.

RESULTS AND DISCUSSION

The reduction of aromatic nitro-compounds by cadmium or zinc metals is well known.^{13,14} According to Hassan and Eldesouki,¹³ the time required for quantitative reduction of chloramphenicol with cadmium metal in the presence of 0.05M hydrochloric acid is 15–20 min. Six equivalents of cadmium ion are released per mole of chloramphenicol, and the reaction proceeds to completion, yielding the corresponding amine:



vigorously and diluted to the mark with distilled water.

Eye ointment. An accurately weighed portion of ophthalmic ointment¹⁶ equivalent to about 10 mg of pure chloramphenicol was shaken in a separating-funnel with about 50 ml of n-hexane and then extracted with four 20-ml portions of water. The aqueous extracts were combined in a 100-ml standard flask and diluted to volume with ethanol.

The infrared spectrum of the reduction product showed no band from the NO_2 group.¹³ When the process was conducted in a continuous mode, the redox reaction did not reach equilibrium but reproducible timing of the system made this dispensable.

Preliminary studies

The optimum reaction conditions were established by varying each condition one at a time.

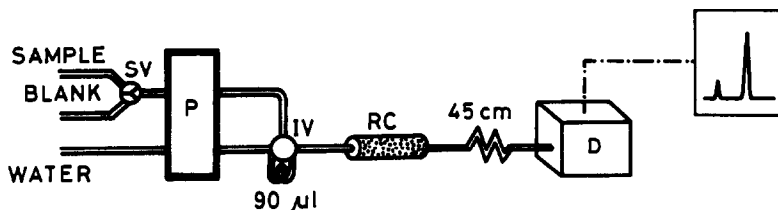


Fig. 1. Manifold and optimum working conditions used in the determination of chloramphenicol. SV, selecting valve; IV, injection valve; RC, reductor column.

Hydrochloric acid was used to adjust the sample pH for the reduction. The absorbance difference between the sample and blank solutions remained constant over the pH ranges 3.7–4.3 and 3.5–4.2 for reduction with zinc and cadmium respectively.

In the batch method, the sample is heated with cadmium metal in 0.05M hydrochloric acid under reflux in a carbon dioxide atmosphere. The influence of temperature on the FIA method was therefore studied over the range 20–70°, but none was found; the measurements are therefore made at room temperature. Since the redox reaction takes place inside a narrow-bore column a carbon dioxide atmosphere is not required, as in the automatic procedure there is efficient shielding against transfer of substances from the atmosphere to the sample and *vice versa*.

The influence of the injected volume on the peak height, at constant carrier flow-rate, was studied over the range 50–150 μ l. The blank and sample signals were dependent on the injected volume, but the difference between them was constant for volumes between 80–130 μ l. With volumes >100 μ l, however, the blank signals fell outside the linear range of the instrument so a volume of 90 μ l was chosen for subsequent experiments.

The effect of the flow-rate was examined in the range 1–5 ml/min and was constant at flow-rates above 2.5 ml/min. A flow-rate of 3.0 ml/min was selected.

The time required for the reduction of chloramphenicol by the cadmium or zinc column was investigated by measuring the amount of metal ion released from different lengths of column (4–8.5 cm, 1.8 mm bore). The signal was not affected by variation in column length in this range, so an 8.5-cm column was selected, which

had a useful life-time of one month under continuous use.

Analytical data

A linear response was observed over the range 2–30 μ g/ml chloramphenicol, with a sensitivity (slope of the absorbance–concentration calibration curve) of 7.6×10^{-3} and 6.8×10^{-3} ml/ μ g for the zinc and cadmium columns, respectively. The detection limits (0.7 and 1.3 μ g/ml for the zinc and cadmium columns, respectively) were calculated as the concentration equivalent to three times the standard deviation of the absorbance for 30 successive injections of the blank. The relative standard deviations for 11 samples each containing 10 μ g/ml chloramphenicol were 1.5 and 1.4% for the zinc and cadmium systems, respectively.

Analysis of pharmaceutical preparations

The proposed method was applied to the determination of chloramphenicol and its palmitate (1 mg of chloramphenicol = 1.738 mg of chloramphenicol palmitate) in various pharmaceutical preparations. The excipients did not interfere. The results of the assays of tablets, capsules, syrup and eye ointment are listed in Table 1. A recovery study was made by adding different amounts of chloramphenicol to each pharmaceutical preparation (Table 2). The average recovery was 99.5 and 99.8% with the zinc and cadmium columns, respectively, with the relative standard deviation ranging between 1.1 and 2.1%.

Advantages of the FIA method over the batch procedure

The proposed automatic method for the determination of chloramphenicol is straightforward and fast, and can be used for direct

Table 1. Determination of chloramphenicol in pharmaceutical preparations

Trade name	Manufacturer*	Nominal amount	Found, mg	
			Zinc method	Cadmium method
Chloromycetin (capsule)	Parke Davis	250 mg/capsule	255 \pm 0.5	256 \pm 0.4
Chemicetina (tablets)	Ifesa	250 mg/tablet	260 \pm 0.6	261 \pm 0.3
Chemicetina† (syrup)	Ifesa	14.4 mg/ml	14.0 \pm 0.2	14.1 \pm 0.1
Oftalmolosa Cusi (ointment)	Cusi	10 mg/ml	10.4 \pm 0.2	10.6 \pm 0.1
Chloramphenicol Oculos (ointment)	Frumtost-Zyma	10 mg/ml	9.6 \pm 0.2	9.7 \pm 0.1

*Spanish.

†The active ingredient is chloramphenicol palmitate (25 mg/ml).

Table 2. Recovery of chloramphenicol added to pharmaceutical preparations

Sample	Spike added	Zinc method		Cadmium method	
		Found, mg	Recovery, %	Found, mg	Recovery, %
Chloromycetin	250 mg/capsule	251.5	100.6	251.0	100.4
Chemicetina	250 mg/tablet	248.5	99.4	250.2	100.1
Chemicetina†	14 mg/ml	14.1	100.7	13.6	97.1
Oftalmolosa Cusi	10 mg/ml	9.9	99.2	10.3	102.8
Chloramphenicol Oculos	10 mg/ml	9.8	98.3	9.8	98.7

*Mean of 7 determinations.

†The active ingredient is chloramphenicol palmitate (25 mg/ml).

assay of formulations. Advantages over its batch counterpart are low sample and reagent consumption; higher sampling frequency; lower cost; no carbon dioxide atmosphere required; higher sensitivity (linear range of 2–30 µg/ml for the FIA technique and 2–15 mg/ml for the batch procedure) and higher precision because there is less sample manipulation.

Acknowledgement—The authors wish to express their gratitude to the CICYT (Project No. PA86-0146) for financial support.

REFERENCES

1. B. Morelli, *J. Pharm. Biomed. Anal.*, 1987, **5**, 577.
2. M. E. Abdel-Hamid and M. A. Abuirjeie, *Analyst*, 1987, **112**, 895.
3. M. S. Mahrous and M. M. Abdel-Khalek, *Talanta*, 1984, **31**, 289.
4. F. Snell and C. Hilton (eds.), *Encyclopedia of Industrial Chemical Analysis*, Vol. 5, Interscience, New York, 1974.
5. K. Kannan, R. Manavalan and A. K. Kelkar, *Indian Drugs*, 1987, **25**, 128.
6. S. Seth and N. R. Bannerjee, *Indian J. Pharm. Sci.*, 1987, **49**, 58.
7. A. Morales, M. I. Toral and P. Richter, *Analyst*, 1984, **109**, 633.
8. P. Fürst, C. Krüger, H.-A. Meemken and W. Groegel, *Dtsch. Lebensm. Rundsch.*, 1988, **84**, 108.
9. M. F. Pochard, G. Burger, M. Chevalier and E. Gleizes, *J. Chromatog.*, 1987, **409**, 315.
10. A. El-Yazigi, A. Yusuf and A. Al-Humaidan, *Clin. Chem.*, 1987, **33**, 1814.
11. E. Soczewinski and M. Matyska, *Farm. Pol.*, 1987, **43**, 73.
12. A. Naveh, I. Potasman, H. Bassan and S. Ulitzur, *J. Appl. Bacteriol.*, 1984, **56**, 457.
13. S. S. M. Hassan and M. H. Eldesouki, *Talanta*, 1979, **26**, 531.
14. T. Mitsui and T. Kojima, *Bunseki Kagaku*, 1977, **26**, 317.
15. J. L. Burguera (ed.), *Flow Injection Atomic Spectroscopy*, Dekker, New York, 1989.
16. *United States Pharmacopeia XXI*, United State Pharmacopeial Convention, Rockville, MD, 1985.

STUDIES ON CATALYTIC FLUORESCENCE FORMATION WITH PEROXIDASE-LIKE METALLOTETRAKIS- (*N*-METHYLPYRIDINIUMYL) PORPHYRINS

YUN-XIANG CI* and FANG WANG

Department of Chemistry, Peking University, Beijing 100871, People's Republic of China

(Received 27 November 1989. Revised 13 March 1990. Accepted 30 March 1990)

Summary—The relative ability of peroxidase-like metallotetrakis(*N*-methylpyridiniumyl)porphyrins [Me-TMPyP, Me = Mn(III), Fe(III), Co(III), Ni(II), Cu(II), and Zn(II)] to catalyse the hydrogen peroxide oxidation of homovanillic acid to a fluorescent dimer has been studied. The complexes of Mn, Fe and Co are effective catalysts in the reaction, but the complexes of Ni, Cu and Zn are not. The catalytic behaviour of Mn-TMPyP, Fe-TMPyP and Co-TMPyP has been compared with that of HRP in both enzymatic and kinetic analysis. The sequence of peroxidase-like catalytic activity is Mn-TMPyP > Co-TMPyP > Fe-TMPyP. The catalytic activity of Mn-TMPyP is 84% of that of HRP. These Me-TMPyP (Me = Mn, Fe, and Co) compounds are good substitutes for HRP in enzymatic analysis. Traces of hydrogen peroxide and glucose can be determined with the Me-TMPyP systems.

Enzymes have been widely used in biochemistry, chemical engineering, and clinical chemistry. However, enzymes are expensive and their solutions are not stable, so the study of potential enzyme mimics is one of the interesting trends in analytical biochemistry. We have found that peroxidase-like metalloporphyrins can catalyse reactions leading to fluorescence^{1,2} and chemiluminescence.³ In this paper, the catalytic behaviour of peroxidase-like metallotetrakis(*N*-methylpyridiniumyl)porphyrins [Me-TMPyP, Me = Mn(III), Fe(III), Co(III), Ni(II), Cu(II), and Zn(II)] on the hydrogen peroxide oxidation of homovanillic acid (HVA) to generate a fluorescent dimer has been studied. The kinetic characteristics of the Me-TMPyP [Me = Mn(III), Fe(III), and Co(III)] catalysed reactions have been compared with those of HRP. The reaction leading to the fluorescent product proceeds as follows:⁴

EXPERIMENTAL

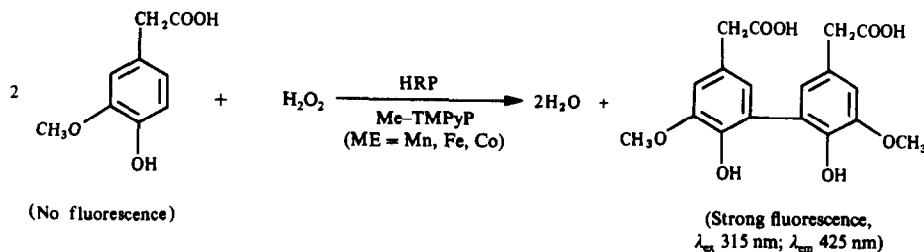
Apparatus

The fluorescence spectra and relative fluorescence intensities were measured with a Hitachi Model 850 Fluorescence Spectrophotometer (with a 10-mm fused-silica cell). The pH was measured with an Orion 811 pH/mV meter.

Reagents

All chemicals were of analytical grade and all aqueous solutions were made up in triply distilled water (prepared by passing doubly distilled water through a column of activated charcoal, adding potassium permanganate to kill bacteria, and distilling in fused-silica apparatus).

HVA (Merck) was dissolved in triply distilled water. Hydrogen peroxide solutions were prepared by dilution of a 30% solution (standard-



*Author for correspondence.

ized by titration with potassium permanganate) with triply distilled water. Tris-HCl and glycine-NaOH buffers (0.05M) were used.

Synthesis of Me-TMPyP

Equal quantities (10 μ mole) of TMPyP and MeCl_2 (Me = Mn, Fe, Cu, or Zn) or $\text{Me}(\text{Ac})_2$ (Me = Co or Ni) were added to a 100-ml flask fitted with a condenser. Triply distilled water, 20 ml, was added and yielded a brown-red transparent solution. The solution was slowly heated under gentle reflux, until the absorption spectrum for porphyrin disappeared completely. Finally, the solution was diluted with triply distilled water to give a fixed concentration. From the spectra obtained for the Me-TMPyP, it can be concluded⁵⁻¹⁰ that the oxidation states were III for Mn, Fe and Co and II for Ni, Cu and Zn in the synthetic complexes.

Procedure

Solutions of HVA, Me-TMPyP and buffer were added to a 5.0-ml standard flask and diluted to about 4.5 ml. The flask was then immersed in a thermostat at $30 \pm 0.5^\circ$. After 5 min, slightly less than 0.5 ml of H_2O_2 solution was added and the mixture was diluted to the mark with triply distilled water. The fluorescence intensity at 425 nm was measured at various time intervals (kinetic method) and when constant (equilibrium method), with excitation at 315 nm.

RESULTS AND DISCUSSION

Spectral characteristics

From the excitation and emission spectra, it was concluded that Mn-TMPyP, Fe-TMPyP and Co-TMPyP catalysed the oxidation while Ni-TMPyP, Cu-TMPyP and Zn-TMPyP did not. The excitation and emission spectra of the Fe-TMPyP system are shown in Fig. 1.

The product has an excitation maximum at 317.5 nm and a fluorescence emission maximum at 423 nm in the Fe-TMPyP system. In the HRP

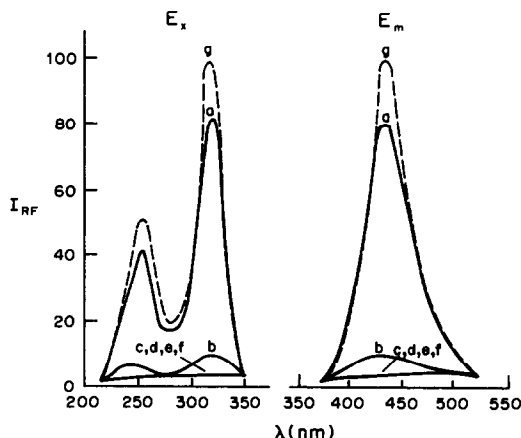


Fig. 1. Fluorescence excitation and emission spectra for the Fe-TMPyP system. pH = 10.00; HVA: $3.0 \times 10^{-5}M$; H_2O_2 : $1.8 \times 10^{-6}M$; Fe-TMPyP, Fe^{3+} , Fe^{2+} , TMPyP: $1.7 \times 10^{-6}M$; HRP: 2.0 $\mu\text{g/ml}$. (a) HVA-Fe-TMPyP- H_2O_2 ; (b) HVA-Fe-TMPyP; (c) HVA- H_2O_2 ; (d) HVA- Fe^{2+} - H_2O_2 ; (e) HVA- Fe^{3+} - H_2O_2 ; (f) HVA-TMPyP- H_2O_2 ; (g) HVA-HRP- H_2O_2 (broken line, pH: 8.50).

system, the emission maximum was at 424 nm, with excitation at 314.0 nm. The emission maxima in the Mn-TMPyP and Co-TMPyP systems were at 424 and 436 nm with excitation at 316.0 and 316.5 nm, respectively, as shown in Table 1.

Effects of reaction variables

The effects of pH, temperature, reaction time, and concentrations of HVA and Me-TMPyP (Me = Mn, Fe, Co) on the fluorescence reaction were studied. The optimal conditions for determination of H_2O_2 are summarized in Table 1. A 0.05M glycine-NaOH buffer solution was used in the tests. The fluorescence intensities of the system and the blank in the absence of H_2O_2 became constant after 1 or 2 min, so the equilibrium method was chosen to determine H_2O_2 . Since the equilibrium fluorescence intensity did not change with temperature in the range $0-35^\circ$, it was measured at room temperature. In the Fe-TMPyP system, 0.50 ml of $3.0 \times 10^{-4}M$ HVA solution, 0.30 ml of $2.8 \times 10^{-5}M$

Table 1. The optimal conditions for determination of H_2O_2 with mimetics of peroxidase

Enzyme	$\lambda_{ex}(\lambda_{em})$, nm	t ,* min	pH	[HVA], M	[Enzyme], M
HRP	314 (424)	3	8.0-8.5	2.7×10^{-4} - 4.8×10^{-4}	2.6×10^{-7} - 7.5×10^{-7}
Mn-TMPyP	316 (424)	2†	9.5-11.0	1.5×10^{-4} - 7.0×10^{-4}	2.3×10^{-6} - 4.5×10^{-6}
Fe-TMPyP	317.5 (423)	1	9.5-10.8	2.7×10^{-5} - 5.5×10^{-5}	1.1×10^{-6} - 2.3×10^{-6}
Co-TMPyP	316.5 (436)	2	11.5-12.0	2.0×10^{-5} - 6.5×10^{-5}	1.7×10^{-6} - 2.3×10^{-6}

*The time when the fluorescence intensity was constant.

Table 2. Comparison of the behaviour of peroxidase-like Me-TMPyP with that of HRP in determination of H_2O_2

Enzyme	Regression equation	Linear range, M	Lowest limit, M	Relative sensitivity
HRP	$I_{RF} = 5.4 \times 10^7 [H_2O_2] + 4.2$	$1.7 \times 10^{-7} - 1.7 \times 10^{-5}$	$1.7 \times 10^{-7} \dagger$	100
Mn-TMPyP	$I_{RF} = 5.0 \times 10^7 [H_2O_2] - 0.2$	$0.0 - 2.4 \times 10^{-6}$	$1.3 \times 10^{-7} *$	94
Fe-TMPyP	$I_{RF} = 4.7 \times 10^7 [H_2O_2] + 1.1$	$0.0 - 3.6 \times 10^{-6}$	$1.1 \times 10^{-7} *$	88
Co-TMPyP	$I_{RF} = 5.0 \times 10^7 [H_2O_2] - 10.3$	$3.0 \times 10^{-7} - 2.0 \times 10^{-6}$	$3.0 \times 10^{-7} \dagger$	94

*Obtained by the method of Hernandez and Escriche.¹¹

†Obtained from the calibration graphs.

Fe-TMPyP solution, and 1.0 ml of pH 10.0 glycine-NaOH buffer were used.

Calibration graphs for H_2O_2

The calibration graphs for H_2O_2 in the Me-TMPyP (Me = Mn, Fe, Co) systems were obtained under the optimal conditions described in Table 1. The linear regression equations and other calibration data are listed in Table 2. The sensitivities of Me-TMPyP for determination of H_2O_2 were compared with that of HRP by comparison of the slopes of the calibration graphs. From Table 2, it can be seen that the sequence of sensitivities is Mn-TMPyP > Co-TMPyP > Fe-TMPyP. With the Fe-TMPyP system the coefficient of variation was 3% ($n = 7$) for the determination of $6.1 \times 10^{-7} M H_2O_2$.

Application

In the determination of glucose in serum by oxidation with oxygen, catalysed by glucose oxidase, H_2O_2 is produced and can be determined by use of the Me-TMPyP systems, e.g., Fe-TMPyP. Typically, 0.20 ml of 1 unit/ml glucose oxidase solution and 1.0 ml of glucose test solution were added to a 5.0-ml flask. After 3 min, 2.5 ml of pH 10.0 glycine-NaOH buffer solution, 0.5 ml of $3.0 \times 10^{-4} M$ HVA and 0.30 ml of $2.8 \times 10^{-5} M$ Fe-TMPyP were added and the mixture was diluted to the mark with triply distilled water. The relative fluorescence intensity was measured after 15 min. The linear range for glucose was 0–8.0 $\mu g/ml$, the correlation coefficient 0.999 ($n = 5$), and the linear regression equation $I_{RF} = 34.5[\text{glucose}] - 3.8$. The lowest limit of determination for glucose by the method of reference 11 was 0.2 $\mu g/ml$. The glucose content in human serum was measured by the standard addition method under these conditions to compensate for any interference from inorganic ions present. The graph obtained in the determination is shown in Fig. 2 and indicates that 89.0 mg/100 ml glucose was present in the sample tested. The sample was

also analysed with the Co-TMPyP system and the glucose content found was 96.5 mg/100 ml. These results agreed within experimental error.

Comparison of catalytic activities of the Me-TMPyP and HRP systems

The experimental results have shown that the complexes of Mn(III), Fe(III) and Co(III) with TMPyP can catalyse the formation of a fluorescent product from the reaction of homovanillic acid with H_2O_2 , whereas the complexes of Ni(II), Cu(II) and Zn(II) can not. It is known that porphyrins have been used as models for corrin ring systems. Many will add groups readily in the axial position, but this is not typical of all. For example, Cu(II) and Ni(II) porphyrins have a low affinity for extra ligands.¹² The complexes of Cu(II) and Ni(II) with TMPyP cannot form mixed-ligand complexes with axially attached ligands such as H_2O_2 and HVA. It is therefore not surprising that Cu-TMPyP and Ni-TMPyP do not catalyse the

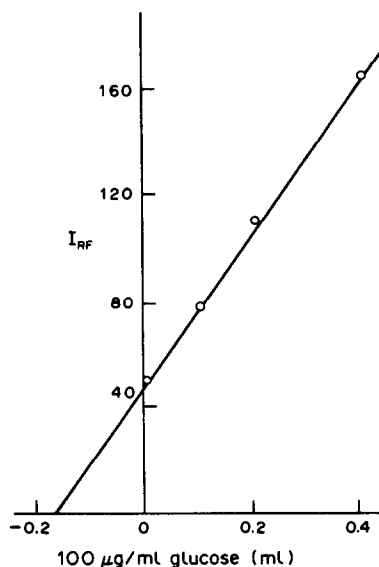


Fig. 2. Determination of glucose in 20 μl of the human serum by Fe-TMPyP, using the method of standard addition.

Table 3. Comparison between the characteristics of peroxidase-like Me-TMPyP and HRP with HVA as substrate

Enzyme	K_m , mM	V_{max} , sec ⁻¹	$[E]$, mM	K_{cat} , 10 ⁻⁷ l. mole ⁻¹ . sec ⁻¹	Relative activity, %*
HRP	0.216	0.567	2.00	2.83	100
Mn-TMPyP	0.366	0.607	2.54	2.39	84
Fe-TMPyP	0.093	0.297	14.7	0.20	7.1
Co-TMPyP	0.460	0.408	17.0	0.24	8.5

*Relative activity means the ratio of K_{cat} of metalloporphyrin to that of HRP.

reaction. Zn(II) porphyrin can add one ligand, giving a square-pyramidal five-coordinate structure,¹² but Zn(II) cannot be further oxidized. Consequently, Zn-TMPyP is ineffective in catalysing the reaction. By contrast, Mn(III), Fe(III) and Co(III) porphyrins can add one or two extra ligands to form a square-pyramidal five-coordinate structure or an octahedral six-coordinate structure. Moreover, these metal ions can be further oxidized, and iron(IV) has been postulated to exist in some porphyrin complexes.¹³ Therefore, the complexes of Mn(III), Fe(III) and Co(III) with TMPyP can catalyse the reaction just as HRP does. From the discussion above, it is clear that the electronic structure and oxidation states of the central metal ions and the affinity of the metalloporphyrin complex for extra ligands determine the catalytic activity of metalloporphyrins as mimetics of peroxidase.

The kinetics of the enzymatic reaction was studied by the initial rate method and the steady-state assumption.¹⁴ It was concluded that the concentration of H₂O₂ was saturating in the test system. The Michaelis–Menten constant K_m and the maximum rate V_{max} were obtained from Lineweaver–Burk plots [$1/V$ vs. $1/(\text{substrate})$],¹⁵ and the transformation constant K_{cat} was obtained from $V_{max} = K_{cat} \times [E]_0$, where $[E]_0$ is the initial concentration of enzyme. The K_{cat} values represent the catalytic activities. The K_m , V_{max} and K_{cat} values for the peroxidase-like Me-TMPyP (M = Mn, Fe, and Co) and HRP systems with HVA as substrate are listed in Table 3. It can be seen that the sequence of catalytic activities of the Me-TMPyP systems is

Mn-TMPyP > Co-TMPyP > Fe-TMPyP. The catalytic activities of all the Me-TMPyP examined were lower than that of HRP. Although the catalytic activity of Fe-TMPyP is low, it is still a useful substitute for HRP in catalysing formation of a fluorescence product from HVA with H₂O₂.

Acknowledgement—This work was supported by the National Natural Science Foundation of China.

REFERENCES

1. Y. X. Ci and F. Wang, *Proc. Chinese 2nd Symposium on Kinetic Analysis*, 1987, p. 1.
2. Y. X. Ci and F. Wang, *Mikrochim. Acta*, 1990, **1**, 63.
3. Y. X. Ci, H. B. He and S. J. Li, *Proc. Chinese 2nd Symposium on Kinetic Analysis*, 1987, p. 7.
4. G. G. Guilbault, P. G. Brignace, Jr. and M. Zimmer, *Anal. Chem.*, 1968, **40**, 190.
5. J. H. Fuhrhop, *Struct. Bonding (Berlin)*, 1974, **18**, 1.
6. K. M. Morehouse and P. Neta, *J. Phys. Chem.*, 1984, **88**, 1575.
7. A. Bettelheim and T. Kuwana, *Anal. Chem.*, 1979, **51**, 2257.
8. D. Dolphin, T. Niem and R. H. Felton, *J. Am. Chem. Soc.*, 1975, **97**, 5288.
9. A. Harriman, M. C. Richoux and P. Neta, *J. Phys. Chem.*, 1983, **87**, 4957.
10. A. Harriman, G. Porter and P. Walters, *J. Chem. Soc., Faraday Trans. 1*, 1983, **79**, 1335.
11. F. H. Hernandez and J. M. Escriche, *Analyst*, 1984, **109**, 1585.
12. M. N. Hughes, *The Inorganic Chemistry of Biological Processes*, Wiley, New York, 1981.
13. G. Simonneaux, W. F. Scholz, C. A. Reed and G. Lang, *Biochim. Biophys. Acta*, 1982, **716**, 1.
14. G. E. Briggs and J. B. S. Haldane, *Biochem. J.*, 1925, **19**, 338.
15. H. Lineweaver and D. Burk, *J. Am. Chem. Soc.*, 1934, **56**, 658.

FLUORIMETRIC DETERMINATION OF INDOLE DERIVATIVES BY FLUOROPHORE GENERATION IN COPPER(II)-SULPHURIC ACID SOLUTION

F. GARCIA SANCHEZ* and C. CARNERO RUIZ

Department of Analytical Chemistry, Faculty of Sciences, University of Málaga, 29071 Málaga, Spain

A. HEREDIA BAYONA

Department of Biochemistry, Faculty of Sciences, University of Málaga, 29071 Málaga, Spain

(Received 22 December 1989. Revised 6 April 1990. Accepted 14 June 1990)

Summary—A spectrofluorimetric procedure for the determination of indole-3-acetic acid, indole-3-propanoic acid and indole-3-butyric acid by derivatization with copper sulphate-sulphuric acid solution has been developed. The optimum reaction conditions, the effect of interferents and the advantages associated with the use of first- and second-derivative synchronous spectrofluorimetry have been studied. The detection limits are 3, 12 and 6 ng/ml for indole-3-acetic, indole-3-propanoic and indole-3-butyric acid, respectively.

Indole-3-acetic acid (IAA) and related compounds are of interest because of their activity as plant growth regulators. The complex nature of the matrix in which indole compounds are required to be determined has led to a number of studies.

These include bioassays¹ and immunoassays,² as well as chromatographic techniques, such as high-performance liquid chromatography.³⁻⁵ Studies involving the use of fluorescent labels include the highly selective and sensitive indole- α -pyrone method⁶ which has been further developed.^{7,8} Another fluorescent label is *o*-phthalaldehyde (OPA) which in concentrated sulphuric acid solutions has been described as a reagent for TLC determination of indole-3-yl acids, including indole-3-acetic acid (IAA), indole-3-propanoic acid (IPA) and indole-3-butyric acid (IBA).^{9,10} Recently, this reagent mixture (OPA-H₂SO₄) was used for developing a synchronous spectrofluorimetric procedure for the determination of IAA, IPA and IBA.¹¹

Most fluorogenic reagents are organic and the use of fluorescent inorganic labels is restricted. Methods based on the chelation of different organic analytes with metal ions have been described.¹²

Ebert¹³ claimed that a fluorescent derivative was produced when IAA was heated with

copper sulphate and concentrated sulphuric acid. This procedure was modified and applied two years later by Rakitin and Povolotskaya¹⁴ and a further qualitative study was performed by Burnett and Audus.¹⁵ However, no further references to this procedure have been found in the literature.

In this paper a systematic study of the experimental variables that affect the reaction between indole compounds and CuSO₄-H₂SO₄ mixtures is presented. The optimum reaction conditions for the fluorimetric determination of IAA, IPA and IBA have been established. In addition, the use of first- and second-derivative synchronous spectrofluorimetry for improving the selectivity and the sensitivity of the proposed methods has been studied.

EXPERIMENTAL

Reagents

Indoles and phenolic compounds were obtained as analytical grade reagents from Sigma. Stock 10mM solutions of these compounds were prepared in absolute ethanol and stored at 4° when not in use. Lower concentrations (100 μ g/ml) were prepared daily by diluting the stock solutions with water.

A 0.5M solution of copper sulphate (Sigma) was prepared. All other chemicals were analytical reagent grade (Merck), and doubly-distilled water was used.

*Author for correspondence.

Apparatus

All fluorescence measurements were obtained with a Perkin-Elmer LS-5 luminescence spectrometer equipped with a 9.9-W xenon discharge lamp pulsed at line frequency and F/3 Monk-Guilleon type monochromators. Standard 1-cm quartz cells were used. The spectrometer was operated in the computer-controlled mode with an RS232C serial interface to a Perkin-Elmer Model 3600 data station. Instrumental control and data collection were achieved with the Perkin-Elmer luminescence software (PECLS II) modified as previously described.¹⁶ An Epson FX-800 printer was used to record spectra.

Procedure

Transfer appropriate volumes to obtain final concentrations between 0.1 and 1.0 $\mu\text{g/ml}$ of each indole solution, into separate standard flasks. Add the appropriate volume of 0.5M copper sulphate, and dilute to the mark with water and chilled concentrated sulphuric acid to obtain the desired final concentrations. Heat the resultant solutions for 5 min in boiling water, cool for 3 min under running water, and let stand for a few minutes in the dark at room temperature. Measure the fluorescence intensity at 475, 526, and 534 nm, with an excitation wavelength of 400, 443, and 400 nm for IAA, IPA and IBA, respectively, against a reagent blank. Record synchronous spectra from 300 to 500 nm against a reagent blank with $\Delta\lambda$ (difference between emission and excitation wavelengths) values of 67, 83, and 134 nm for IAA, IPA, and IBA, respectively.

RESULTS AND DISCUSSION

Experimental variables

To establish the optimum reaction conditions, the parameters that could affect the reaction were studied.

The concentration of sulphuric acid was optimized with a fixed amount of copper sulphate. The sulphuric acid concentrations selected were 8, 10 and 16M for IAA, IPA and IBA, respectively. At these fixed acid concentrations optimum fluorescence intensities were obtained with copper sulphate concentrations of 1.25, 1.25, and 10mM for IAA, IPA and IBA, respectively. These concentrations together with spectral characteristics of the fluorophores obtained are summarized in Table 1.

Table 1. Experimental variables and spectral characteristics of indole compounds

	IAA	IPA	IBA
$[\text{H}_2\text{SO}_4], M$	8	10	16
$[\text{CuSO}_4], mM$	1.25	1.25	10
$\lambda_{\text{exc}}, \text{nm}$	400	443	400
$\lambda_{\text{em}}, \text{nm}$	475	526	534
$\Delta\lambda, \text{nm}$	67	83	134

The effect of sequence of reagent addition was also investigated, but no important differences in the fluorescence signals were observed. The stability of the products obtained was examined and 1 $\mu\text{g/ml}$ of each indole compound gave a constant fluorescence reading at room temperature for at least 70 min. However, after 24 hr the fluorescence of the IAA reaction product had decreased by 22%. The modified software was used to produce three-dimensional synchronous spectra with variable $\Delta\lambda$,¹⁵ and these were used to optimize the wavelength scanning interval ($\Delta\lambda$) for the synchronous determination.

Quantitative analysis

Calibration graphs for IAA, IPA, and IBA were obtained by both the direct and synchronous techniques. To improve the analytical characteristics for an individual determination of IAA, a study by first- and second-derivative synchronous spectrofluorimetry was also performed. Intensities at 386 and 431 nm for first-derivative spectra and at 405 and 454 nm for second-derivative spectra were measured, and each of the calibration graphs obtained showed a linear relationship between intensity and concentration. The correlation coefficients were better than 0.99.

The sensitivity of each method is expressed as the analytical sensitivity, s_m/m , where s_s is the standard deviation of the analytical signal and m is the slope of the calibration graph.¹⁷ The limit of detection is reported as defined by IUPAC.¹⁸ The precision of the methods was determined by analysing nine replicate samples of IAA and IPA; each containing 0.40 $\mu\text{g/ml}$ analyte, and eleven replicate samples of IBA, each containing of 0.60 $\mu\text{g/ml}$. The analytical parameters of the proposed methods are summarized in Table 2, where it is clear that the limit of detection is improved by using the derivative methods.

Interferences

To determine the selectivity of the proposed method, the effect of other compounds on the

Table 2. Analytical parameters of the proposed methods

Compound	Method*	Sensitivity, ng/ml	Limit of detection, ng/ml	Error, %	RSD, %
IAA	Direct	10	12	2.1	2.7
	Synchronous	13	22	2.7	3.6
	D1	18	3	3.1	4.1
	D2	17	3	3.1	4.1
IPA	Direct	13	12	2.6	3.5
	Synchronous	13	13	2.3	3.0
IBA	Direct	20	6	2.2	3.3
	Synchronous	20	13	2.2	3.4

*D1 and D2: first- and second-derivative synchronous scanning.

IAA determination (0.4 $\mu\text{g/ml}$) was investigated. Possible interferent indole compounds tested were: indole-3-methanol (InMe), indole-3-aldehyde (InAl), indole-3-carboxylic acid (InCar) occurring in the IAA catabolism,¹⁹ and 5-hydroxyindole-3-acetic acid (5-OHIAA). Additionally, the interference of two phenolic compounds, 2,4-dichlorophenol (2,4-DCP) and *p*-coumaric acid (PCA) were studied. These compounds are used as co-factors in the indole-3-acetic acid-oxidase assay.¹⁹

The criterion used for interference was a deviation from expectation greater than $\pm 2\sigma$, where σ is the standard deviation found in the reproducibility tests.

The most important interferences are given in Table 3. The results indicate that only for InMe can moderate selectivity be gained by using the synchronous derivative approach.

Table 3. Effect of interferences on the determination of 0.40 $\mu\text{g/ml}$ IAA

Interferent	Ratio to IAA	Recovery, %			
		I	S	D1	D2
InMe	0.25	+	+	+	95
	0.5	+	+	+	108
InAl	1	102	99	103	101
	2	+	+	+	+
InCar	1	+	+	+	+
	0.5	98	99	102	+
5-OHIAA	1	93	—	101	—
	2	—	—	—	—
	1	103	101	100	103
2,4-DCP	3	100	98	101	99
	5	104	102	105	105
	10	+	103	103	107
PCA	1	99	96	96	—
	3	101	100	—	—
	5	105	107	—	—

+ and — indicate values above and below the tolerance criterion. I, direct fluorescence; S, synchronous scan; D1, first-derivative synchronous scan; D2, second-derivative synchronous scan.

CONCLUSIONS

It has been shown that the $\text{CuSO}_4\text{-H}_2\text{SO}_4$ reagent is not very specific. In comparison with the α -pyrone method, the proposed method is less sensitive and selective. However, it has the advantage that dry reaction conditions are not required. Despite its non-specificity, the proposed method could be useful if combined with a preliminary separation.

The proposed method is less sensitive than the $\text{OPA-H}_2\text{SO}_4$ procedure, but more selective since the working wavelengths are more widely separated. The effect of the interferences studied should be viewed in the context that IBA, for example, is rarely found together with other indole compounds. In fact we have applied the proposed method to the determination of IBA in culture medium and obtained satisfactory results.²⁰

Finally, the present work could be used as the basis for a new method to assay IAA oxidase activity. Usually this assay would require high concentration of the substrate (IAA), and as co-factor a phenolic acid which would not interfere. The method proposed here is sensitive enough for use in this assay. It is known that IAA oxidase activity is very low and its measurement normally requires the use of a sensitive radioactive method.²¹ Alternatively, large amounts of plant extract are required if the less sensitive colorimetric method²² is used.

Acknowledgement—We thank the Dirección General de Investigación Científica y Técnica for supporting this study (Project PB86-0247).

REFERENCES

1. R. Sandstedt, *Plant Physiol.*, 1971, **52**, 443.
2. A. Crozier, G. Sandberg, A. M. Monteiro and B. Sundberg, in *Plant Growth Substances*, M. Bopp (ed.), p. 13. Springer-Verlag, Berlin, 1985.

3. M. S. Shiao and Y. Y. Hao, *Bot. Bull. Acad. Sin.*, 1985, **26**, 105.
4. J. Yamada, Y. Sugimoto and K. Horisaka, *Anal. Biochem.*, 1983, **129**, 460.
5. R. Kysilka and M. Wurst, *J. Chromatog.*, 1988, **446**, 315.
6. A. Stoessl and M. A. Venis, *Anal. Biochem.*, 1970, **34**, 344.
7. F. García-Sánchez, A. Heredia and G. Requena, *Anal. Lett.*, 1986, **19**, 1939.
8. C. Sánchez-Roldán, M. A. Quesada, M. I. Bukovac, V. Valpuesta and A. Heredia, *Phytochemistry*, 1988, **27**, 1579.
9. T. C. M. Pastore, E. Nicola and C. G. Lima, *Analyst*, 1984, **109**, 243.
10. T. C. M. Pastore and C. G. Lima, *ibid.*, 1986, **111**, 707.
11. F. García Sánchez, C. Cruces, A. L. Ramos, M. Hernández, J. C. Márquez and C. Carnero, *Anal. Chim. Acta*, 1988, **205**, 149.
12. M. A. Martín, B. Lin and B. Del Castillo, *J. Pharm. Biomed. Anal.*, 1988, **6**, 573.
13. A. V. Ebert, *Phytopathol. Z.*, 1955, **24**, 216.
14. Yu. V. Rakitin and K. L. Povolotskaya, *Fiziol. Rastenii, Akad. Nauk. SSSR*, 1957, **4**, 285; *Chem. Abstr.*, 1957, **51**, 14876d.
15. D. Burnett and L. J. Audus, *Phytochemistry*, 1964, **3**, 395.
16. F. García Sánchez and A. L. Ramos Rubio, *Talanta*, 1987, **34**, 822.
17. A. Navas and F. Sánchez, *Analyst*, 1984, **109**, 1435.
18. G. L. Long and J. D. Winefordner, *Anal. Chem.*, 1983, **55**, 712A.
19. D. M. Reinecke and R. S. Bandurski, in *Plant Hormones and Their Role in Plant Growth and Development*. P. J. Davies (ed.), pp. 24. Martinus Nijhoff, Dordrecht (1987).
20. F. García Sánchez, C. Carnero and A. Heredia, unpublished results.
21. V. Valpuesta and M. J. Bukovac, *J. Plant Growth Regul.*, 1984 **2**, 57.
22. S. A. Gordon and R. P. Weber, *Plant Physiol.*, 1951, **26**, 192.

LINEARIZED MULTIPLE STANDARD ADDITIONS FOR THE POTENTIOMETRIC DETERMINATION OF WEAK ACIDS

CARLO MACCÀ

Department of Inorganic, Organometallic and Analytical Chemistry, University of Padova,
via Marzolo 1, I-35131 Padova, Italy

(Received 12 January 1990. Revised 3 March 1990. Accepted 25 June 1990)

Summary—The feasibility of potentiometric determination of weak monoprotic acids by the multiple standard addition method is examined. A standard solution of pure weak acid is added to the solution containing an unknown amount of the same weak acid, alone or mixed with its conjugate base. The experimental data are processed by Gran-type plots, for which rigorous and approximate equations are obtained. It is shown that weak acids can be determined by multiple standard additions with a precision comparable with that of the usual kinds of potentiometric addition-methods. The validity range of the approximate equations is established. Linear equations similar to those of Hofstee, Scatchard, Lineweaver and Burk, and Scott are also obtained, by which acidity constants can be determined together with equivalence volumes. The effects of systematic and random measurement errors are examined.

Linearized multiple standard addition methods are recommended for potentiometric determination of ionic species for which a selective electrode is available.¹ To a measured volume of the analyte solution of unknown concentration, known volumes of a standard solution of the same ion are added. The e.m.f. of the cell consisting of the ion-selective electrode and a suitable reference electrode is measured after each addition. The experimental data are processed by calculating for each addition the appropriate Gran function (which is identical with that for linearizing the data for the first part of titration of the ion with a suitable reagent²). The plot of the Gran function against the volume added, V , is extrapolated to intercept the V axis is at $-V_e$, where V_e is the equivalence volume.¹⁻³ A Gran function of the same form is used for the potentiometric determination of strong acids by multiple standard additions, when $[H^+]$ is measured with a glass electrode.

The determination of weak monoprotic acids by multiple standard additions has not been considered until now. With weak acids, the analyte (a monofunctional weak acid, HA) is not the species sensed by the pH electrode. A Gran function of the same form as for ionic analytes could still be used for linearizing data from multiple standard addition of weak acids, provided that the ratio between the hydrogen

ion concentration and the total concentration of acid, C_{HA} , is constant. Generally this is not the case, as $[H^+]/C_{HA}$ strongly depends on C_{HA} .⁴

In a previous paper, the principles of linearization methods for potentiometric titrations of monoprotic weak acids have been discussed.⁵ Original (approximate)² and rigorous Gran plots (which require the knowledge of the acid dissociation constant, K_a)^{6,7} have been considered. Other types of linear equations,⁸⁻¹³ which permit both the unknown amount of the analyte and the dissociation constant to be obtained from the titration data, have been examined. Criteria for assessing the linear range of Gran functions have been devised.^{14,15}

This paper examines the possibility of applying a similar approach to the determination of monofunctional weak acids, alone or in mixtures with the conjugate base, by multiple additions of a standard solution of the acid itself.

THEORY

Gran plots

Pure weak acid. Consider multiple standard additions of a weak acid of known concentration C to a given volume V^0 of a solution of the same acid at unknown concentration C^0 . The experimentally controlled variable is the total volume added after each step, V .

Linearized multiple standard additions require the use of an equation that is a linear function of V and has the initial amount of analyte, C^0V^0 , or the equivalence volume, C^0V^0/C , as one of its parameters (the intercept with the abscissa). This equation is obtained by expressing the total amount of analyte (moles), $C^0V^0 + CV$, in terms of the functional dependence, F , on V , the measured variable $[H^+]$ and parameters C^0 , V^0 , C , K_a and K_w .

Substitution of the equilibrium concentrations in the mass-balance equation of the weak acid

$$C^0V^0 + CV = (V^0 + V)([HA] + [A^-])$$

by using the expression for the acid dissociation constant, $K_a = [H^+][A^-]/[HA]$, the electroneutrality condition $[H^+] = [OH^-] + [A^-]$, and the expression for K_w , yields the rigorous equation (1)

$$\begin{aligned} C^0V^0 + CV &= (V^0 + V)[A^-](1 + [H^+]/K_a) \\ &= (V^0 + V)([H^+] - K_w/[H^+]) \\ &\quad \times (1 + [H^+]/K_a) = F \end{aligned} \quad (1)$$

The right-hand side of equation (1) is the required linear function of V . By plotting F against V and extrapolating to $F=0$, $V_e = -C^0V^0/C$ is obtained as the (negative) intercept with the V axis.

The test solution is generally sufficiently acidic for $[OH^-]$ to be negligible in the equations above. Therefore, the simpler equation (2) can be used:

$$F' = (V^0 + V)[H^+](1 + [H^+]/K_a) \quad (2)$$

Further simplifications are possible. Treating $[H^+]/K_a$ as negligible relative to unity yields the Gran function for strong acids. Taking unity as negligible relative to $[H^+]/K_a$ yields the approximate function G :

$$C^0V^0 + CV \approx (V^0 + V)[H^+]^2/K_a = G \quad (3)$$

Equation (1) requires that the actual values of K_a and K_w under the given experimental conditions be known; equations (2) and (3) require only knowledge of K_a . If the electrode is calibrated to measure pH, *i.e.*, the negative logarithm of the hydronium ion activity, $[H^+]$ must be replaced by $10^{-\text{pH}}/y_H$, the activity coefficient, y_H , being calculated from the experimental ionic strength.⁷ More conveniently, the electrode can be calibrated^{16,17} to measure $\log[H^+]$. It can be

seen that the slope of the plot of F and G against V is equal to C : hence, processing multiple-additions data by using equations (1)–(3) can yield the concentrations of both the titrand and titrant solutions, provided that the acid dissociation constant is known.

Omission of the coefficient $1/K_a$ in equation (3) affects neither the linearity nor the value of the intercept V_e , so equation (3) can be reduced to

$$G' = (V^0 + V)[H^+]^2 \quad (4)$$

Moreover, substituting for $[H^+]$ from the response equation of the electrode

$$E = E^* + S \log[H^+]$$

(where E^* is constant at fixed ionic strength and constant temperature) yields

$$G' = (V^0 + V) 10^{-2E^*/S} 10^{2E/S}$$

and omitting the constant term $10^{-2E^*/S}$ permits plotting the equation

$$G'' = (V^0 + V) 10^{2E/S} \quad (5)$$

Equation (5), when applicable, is very advantageous, because it requires neither knowledge of K_a nor accurate calibration of the electrode. Periodical checking of the experimental S value is sufficient, provided that a glass electrode of good quality is employed. Conditions for the validity of the approximate equations are examined in the discussion.

Mixture of a weak acid with its conjugate base (buffer solution). When the solution contains the weak acid HA at initial concentration C^0 and its conjugate base (*e.g.*, the salt NaA) at initial concentration C_b (the total initial concentration of the system is $C^0 + C_b$), the mass balance and the electroneutrality conditions are, respectively

$$(C^0 + C_b)V^0 + CV = (V^0 + V)([HA] + [A^-])$$

$$[Na^+] + [H^+] = [OH^-] + [A^-]$$

By using the equations above, the mass balance of the salt, $C_b V^0 = (V^0 + V)[Na^+]$ and the expressions for the equilibrium constants K_a and K_w , equation (6), representing the total (stoichiometric) amount of acid alone, can be obtained.

$$\begin{aligned} C^0V^0 + CV &= (V^0 + V)([H^+] - K_w/[H^+]) \\ &\quad \times (1 + [H^+]/K_a) + C_b V^0 [H^+]/K_a = F \end{aligned} \quad (6)$$

The rigorous linear function, F , represented by the right-hand side, can be calculated when C_b is known. The intercept, of the plot of F against V , with the abscissa is equal to $-C^0V^0/C$.

A convenient approximate form of equation (6) is obtained by neglecting the first term in the expression for F .

$$G = C_b V^0 [H^+] / K_a \quad (7)$$

Plotting

$$G' = [H^+] \quad (8)$$

against V enables V_e to be found by linear extrapolation. The plot of equation (8) has a slope equal to $K_a C / C_b V^0$; therefore it can yield the value of either C_b or K_a if the other is known. The quantity

$$G'' = 10^{E/S} \quad (9)$$

makes the electrode calibration simpler (see above) and is convenient to use when the determination of C_b or K_a is not required.

Equations (3)–(5) and (7)–(9) are based on similar principles to the (approximate) Gran functions for titrations and other kinds of standard additions⁵ and, therefore, this name will be applied subsequently. [Note, however, that both equations (4) and (8) are different from the Gran function² for the titration of a weak acid with a strong base]. Similarly, equations (1) and (6) will be termed “corrected” or rigorous Gran functions.

Other linear plots

When one of the constants (specifically, K_a or C_b) necessary for calculation of F [equations (1) and (6)] is unknown, and the conditions for validity of equations (3)–(5) or (7)–(9) are not met, linear graphs can still be obtained that allow both the initial amount C^0V^0 of the acid and the other unknown quantity to be calculated. These plots use auxiliary variables as the co-ordinates, that can be calculated from the experimental data and known constants. The relevant equations are obtained by suitable rearrangement of equations (1) or (6) in such a way that the unknown quantities appear only in the intercepts and slopes.

The amount of conjugate base is unknown. Rearrangement of equation (6), using the auxiliary variable

$$\begin{aligned} H &= (V^0 + V) ([H^+] - (OH^-)) \\ &= (V^0 + V) ([H^+] - K_w/[H^+]) \end{aligned} \quad (10)$$

yields

$$\begin{aligned} CV - H (1 + [H^+]/K_a) \\ = -C^0V^0 + C_b V^0 [H^+]/K_a \end{aligned} \quad (11)$$

When K_a is known and C_b is not, the plot of the left-hand side of equation (11), designated W , against $[H^+]$ gives a straight line. The initial amount of the acid, C^0V^0 , is obtained from the intercept $W([H^+] = 0)$ and the amount of base, $C_b V^0$, from the slope.

The dissociation constant is unknown. When K_a is unknown, it is possible to rearrange⁵ equation (6) in three different ways, in order to obtain both C^0V^0 and K_a from the parameters of the linear plots. Three equivalent equations can be written and plots obtained, by interchanging the variables. These equations will be named after the authors of the equations for linearized complexometric⁸ or acid–base⁵ titrations that have the corresponding quantities as the parameters.

The equation for the Hofstee plot⁹ in the general form (for standard additions to a solution containing an unknown amount of acid, C^0V^0 , and a fixed known amount of the conjugate base, $C_b V^0 \geq 0$) is

$$H - CV = C^0V^0 - [H^+](C_b V^0 + H)/K_a \quad (12)$$

where H is given by equation (10). Equation (6) has the form $Y = C^0V^0 - X/K_a$ and the intercept $Y(X = 0)$ of the plot of $Y = H - CV$ against $X \{ = [H^+](C_b V^0 + H) \}$ gives C^0V^0 , and the slope equals $-1/K_a$.

The Scatchard plot¹⁰ is obtained by interchanging the co-ordinates of the Hofstee plot. Therefore, C^0V^0 is given by the intercept $X(Y = 0)$ and the slope is $-K_a$.

The Lineweaver-Burk¹¹ equation, obtained by a different rearrangement of equation (6), has the general form

$$\frac{1}{H - CV} = \frac{1}{C^0V^0} + \frac{[H^+](C_b V^0 + H)}{C^0V^0 K_a (H - CV)} \quad (13)$$

The co-ordinates of the plot are $Y = 1/(H - CV)$ and $X = [H^+](C_b V^0 + H)/(H - CV)$. The initial amount of the acid and the dissociation constant are obtained from the intercepts $Y(X = 0) = 1/C^0V^0$ and $X(Y = 0) = -K_a$, respectively; K_a is also calculated from the slope, $1/C^0V^0 K_a$.

Another rearrangement gives the Scott¹² equation:

$$\begin{aligned} \frac{1}{[H^+](C_b V^0 + H)} &= \frac{1}{C^0V^0 K_a} \\ &+ \frac{H - CV}{C^0V^0 [H^+](C_b V^0 + H)} \end{aligned} \quad (14)$$

The initial amount of the acid is given by the reciprocal of the slope of the plot of

$Y = 1/[H^+](C_b V^0 + H)$ against $X = (H - CV)/[H^+](C_b V^0 + H)$, or directly by the slope of the plot with co-ordinates interchanged (the Mar'yanov¹³ plot).

For $C_b = 0$, the $K_w/[H^+]$ term can usually be neglected in H ; for instance, the equation for the Hofstee plot becomes

$$(V^0 + V)[H^+] - CV = C^0 V^0 - (V^0 + V)[H^+]^2/K_a \quad (12')$$

DISCUSSION

Sensitivity of the addition methods

For evaluation of the methods proposed, it is first necessary to estimate whether the variation of the pH produced by the additions is large enough to yield an acceptable precision. The simplest way to answer this question is the calculation of the variation produced by the addition of an amount of titrant equivalent to a given fraction, say 100%, of the initial amount of the analyte. An estimate of the pH variation can be made by using approximations for the pH of pure acids, equation (15), or of buffer, equation (16).

$$\begin{aligned} \text{pH} &= 0.5(\text{p}K_a - \log C_{\text{HA}}) \\ &= 0.5 \left(\text{p}K_a - \log \frac{C^0 V^0 + CV}{V^0 + V} \right) \quad (15) \end{aligned}$$

$$\begin{aligned} \text{pH} &= \text{p}K_a + \log \frac{C_{\text{NaA}}}{C_{\text{HA}}} \\ &= \text{p}K_a + \log \frac{C_b V^0}{C^0 V^0 + CV} \quad (16) \end{aligned}$$

On addition of enough standard acid to double the acid concentration, (*i.e.*, $CV = C^0 V^0$), the pH is decreased by 0.15 according to equation (15), *i.e.*, the e.m.f. increases by 8.9 mV at 25° (on the assumption that C/C^0 is so large that $V \ll V^0$, and the effect of dilution can be neglected). For the same addition to a buffer solution, a variation of -0.30 pH or $+17.9$ mV is obtained, according to equation (16). These values can be compared with the variations produced in systems in which standard-addition methods are currently used. A decrease of 0.30 p(Ion) is produced by doubling the concentration of a cation, which corresponds to an increase of 17.9 mV for an univalent ion and 8.9 mV for a bivalent ion. Therefore, standard additions of weak acids exhibit a sensitivity similar to that of common standard-addition procedures.

Suitability of the approximate Gran functions

Pure acid. The approximate Gran-type function for standard additions to pure acids, equation (3), is plotted in Fig. 1 for acids of different strengths at various concentrations C^0 , with titrant concentration $C = 10C^0$. The G values have been calculated up to $V = -4V_e$ (the ratio usually recommended¹⁸ for multiple additions).

Linearity is apparently preserved (lines *b-d* in Fig. 1), even when G deviates from the ideal plot F , yielding a large difference between the intercept $V(G = 0)$ and the true value of V_e . Only with rather strong acids or at low concentrations does curvature become apparent (line *e*). Clearly, the absence of curvature in the experimental plot is not a practical diagnostic criterion for the suitability of function G , in contrast to the case of weak-acid titrations.¹⁹ Therefore, the suitability of G [and G' or G'' , equations (4) and (5)] must be evaluated on theoretical grounds. For instance, the extent of the relative deviation of G from F at any value of V can be calculated by using the true value of $[H^+]$ and the equation

$$\frac{G - F}{F} = \frac{(V^0 + V)[H^+]^2}{K_a(C^0 V^0 + CV)} - 1 \quad (17)$$

obtained from equations (1) and (3). [At $\text{pH} < 6$, the corresponding relative deviation of G from F' , equation (2), is $K_a/(K_a + [H^+])$.] It can be observed that the straight lines in Fig. 1

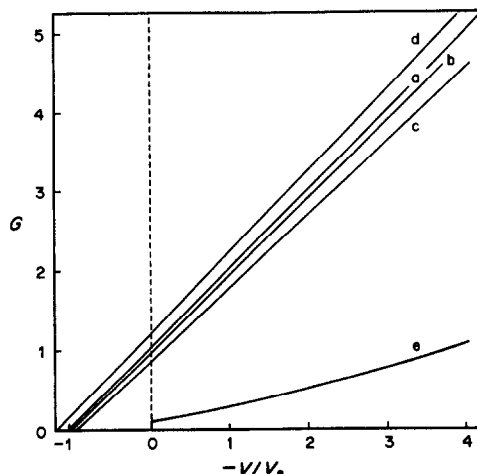


Fig. 1. Plots of G , equation (3), for multiple additions of standard acid at $C = 10C^0$ to pure acid at C^0 . a, $\text{p}K_a = 9.3$, $C^0 = 0.01M$; b, $\text{p}K_a = 4.5$, $C^0 = 0.01M$; c, $\text{p}K_a = 4.5$, $C^0 = 0.001M$ and $\text{p}K_a = 3.5$, $C^0 = 0.01M$; d, $\text{p}K_a = 11.3$, $C^0 = 0.01M$; e, $\text{p}K_a = 2.0$, $C^0 = 0.001M$. The plot of F , equation (1), is practically indistinguishable from *a*. Ordinates are normalized so that the F -plot has unit slope.

are convergent with the ideal linear plot (practically coincident with line *a*) in the region of the intercept on the abscissa. In consequence, the relative deviation of *G* at *V* = 0 is larger than the relative error of *V_e* obtained by extrapolation to *G* = 0. Therefore, the error affecting *V_e* can be conservatively evaluated by calculation of the relative deviation at the initial point (*V* = 0). For instance, the relative deviation of *G* at *V* = 0, and the extrapolation error (based on use of eleven points equally spaced between *V* = 0 and *V* = -4*V_e*) are -0.20 and -0.17% respectively, (plot *a* of Fig. 1), -5.5 and -3.6% (*b*), -16.3% and -11.0% (*c*), +20.0% and +17.6% (*d*).

A simpler, approximate, criterion for suitability follows from the fact that equation (3) is equivalent to the approximate equation (15) for the pH of pure weak acids, as is easily shown. Therefore, the range of validity of the approximate Gran functions, equations (3)–(5), can be deduced from the Flood diagram⁴ of Fig. 2. The area within the outer dotted triangular perimeter corresponds to a relative deviation (*G* = *F*)/*F* smaller than 1%, which is reduced to less than 0.1% in the inner triangle. The examples in Fig. 1 demonstrate the practical validity of this criterion. Only systems lying within the inner triangle in Fig. 2 give plots indistinguishable from *F*, line *a*, as is the case for a 0.01*M* acid with *pK_a* = 9.3.

On the whole, the conditions for suitability of equations (3)–(5) are satisfied only for a few acids of practical interest (those with *pK_a* = 6–11, at relatively high concentrations). Therefore, equations (2) or (12')–(14') must be used in most cases.

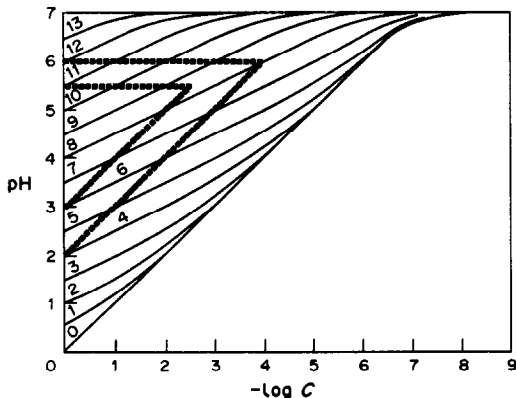


Fig. 2. Flood diagram representing the pH-dependence of pure acid solutions on the logarithm of the concentration. Curves are labelled with the *pK_a* values.

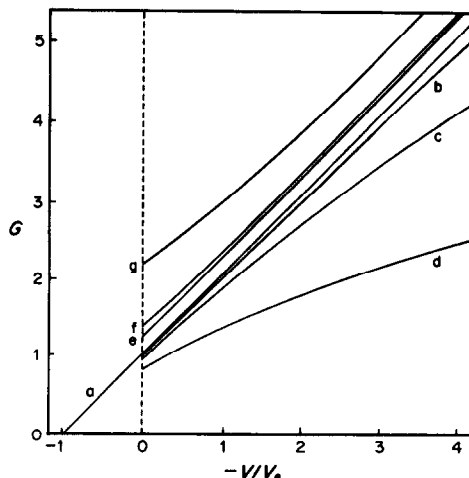


Fig. 3. Plots of *G*, equation (7), for multiple additions of standard acid (*C* = 10*C*⁰) to mixtures of acid (*C*⁰) with base (*C_b*). *a*, *pK_a* = 4.5, *C*⁰ = 0.01*M*, *C_b* = 0.1*M*; *b*, *pK_a* = 4.5, *C*⁰ = 0.01*M*, *C_b* = 0.01*M*; *c*, *pK_a* = 4.5, *C*⁰ = 0.001*M*, *C_b* = 0.001*M*; *d*, *pK_a* = 4.5, *C*⁰ = 0.01*M*, *C_b* = 0.001*M*; *e*, *pK_a* = 11.3, *C*⁰ = 0.01*M*, *C_b* = 0.001*M*, *f*, *pK_a* = 11.3, *C*⁰ = 0.01*M*, *C_b* = 0.01*M*; *g*, *pK_a* = 11.3, *C*⁰ = 0.01*M*, *C_b* = 0.1*M*. The plot of *F*, equation (6), is practically coincident with line *a*. Ordinates are normalized so that the *F*-plot has unit slope.

Buffer solutions. The approximate Gran-type function for standard additions of weak acid to buffer solutions of the same acid, equation (7), is plotted in Fig. 3 for very weak and moderately strong acids at various concentrations and different ratios *C_b*/*C*⁰, with titrant concentration *C* = 10*C*⁰. In contrast to Fig. 1, curvature can be appreciable when deviations of *G* from *F* (curve *a*) are moderate.

The exact extent of the relative deviation of *G* at a given point is calculated by equation (18)

$$\frac{G - F}{F} = \frac{C_b V^0 [H^+]}{K_a (C^0 V^0 + C V)} - 1 \quad (18)$$

on substitution of the value of [H⁺]. Inspection of Fig. 3 shows that deviations must be checked both at the initial point, *V* = 0, and at the maximum value of *V* (typically, -4*V_e*). For instance, for curve *b* in Fig. 3 the relative deviation, which is -0.6% at the initial point, becomes -2.6% at *V* = -4*V_e*. This behaviour must raise some doubt about the suitability of *G* for obtaining an accurate *V_e*, which in fact (on the basis of eleven points equally spaced between *V* = 0 and *V* = -4*V_e*) is affected with an error of +3.7%.

It can also be considered that equation (7) is equivalent to the approximate equation (16) for calculating the pH of buffers, which is valid only

when both $[H^+]$ and $[OH^-]$ are negligible with respect to C_{HA} and C_{NaA} in the rigorous equation²⁰

$$[H^+] = \frac{C_{HA} - [H^+] + [OH^-]}{C_{NaA} + [H^+] - [OH^-]} \quad (19)$$

Qualitatively, equation (7) yields suspect results when the additions make either $[H^+]$ or $[OH^-]$ a fraction of C_{HA} [$= (C^0V^0 + CV)/(V^0 + V)$] or C_{NaA} [$= C_bV^0/(V^0 + V)$] that is larger than the maximum acceptable deviation, for instance 1%. It may be seen from equation (19) that negative deviations appear if $[H^+]$ is larger than $[OH^-]$.

When the conditions of validity of equations (3)–(5) or (7)–(9) are not met, an artifice can be suggested. A sufficient amount of a pure salt of the weak acid is added to bring the composition of the buffer well within the validity range of equations (7)–(9). (It is not necessary that the amount of salt be known exactly.) Multiple additions of the pure weak acid are then made and the titration data are linearized by using equation (8) or (9). This procedure is in some respects similar to that proposed by Johansson²¹ for improving the linearity of Gran plots in titrations of weak acids with strong bases. It is of practical interest only when the amount of salt to be added is not too large, so that the impurities added with it do not appreciably contribute to the titration error. Equation (18) can help in deciding how much weak base must be added to bring the composition of the buffer into the validity range of equations (7)–(9). For instance, the addition of an equal amount of the conjugate base to the moderately weak acid ($pK_a = 4.5$, $C^0 = 0.01M$) of curve *c* in Fig. 1, is ineffective (curve *c*, Fig. 3), whereas the plot of *G* obtained after addition of a tenfold amount of base (not shown) has a relative deviation (from the ideal plot) of only -0.35% at $V = 0$ and -0.6% at $V = -4V_e$ and gives an extrapolation error of $+0.6\%$. The plot obtained by adding a tenfold amount of base to the acid of curve *b* in Fig. 1 is indistinguishable from the ideal plot (deviations $<0.1\%$).

Rigorous linear equations

Effect of error in the acidity constant on corrected Gran plots. Calculation of the rigorous Gran function *F*, equation (1) or (6), from experimental data requires the use of the concentration acidity constant, K_a , at the ionic strength prevailing in the test solution. Since K_a is generally known only with some approxi-

mation, the effect of inaccuracy in the value used must be evaluated.

Plots *b*, *c*, *d* and *e* in Fig. 4 show the effect on the calculated *F* of errors of $+0.3$, $+0.1$, -0.1 and -0.3 , respectively, in the pK_a value for the titration of an acid with $pK_a = 4.5$ at an initial concentration $C^0 = 10^{-3}M$. It may be seen that the slope of the plot of *F* is strongly affected by errors in pK_a , but the curvature is hardly appreciable and would be quite indiscernible for experimental points affected by random errors. The value of the intercept with the abscissa, yielding V_e , is affected to a smaller degree. By least-squares extrapolation through eleven points regularly distributed between $V = 0$ and $V = -4V_e$, errors of -5.3 , -2.2 , 2.6 and 9.5% respectively are obtained.

The error in the intercept decreases with increasing concentration; with increasing pK_a it becomes inappreciable even for moderately high errors in pK_a . Plots for stronger acids become curved, but plots for multiple standard additions of these acids to their buffer mixtures [equation (6)] are still linear and give smaller extrapolation errors, which decrease as the concentration of conjugate base increases. The contrary is true for very weak acids, which yield correct equivalence volumes when titrated alone, and give increasing errors (but still linear plots) in the presence of increasing concentration of conjugate base. On the whole, acceptable results are obtained in a much larger range

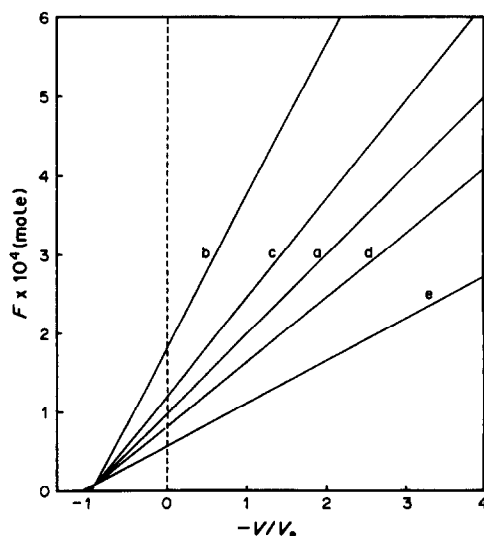


Fig. 4. Plots of *F*, equation (1), for multiple additions of standard acid ($C = 10C^0$) to pure acid ($pK_a = 4.5$, $C^0 = 0.001M$), based on $[H^+]$ values calculated rigorously for: a, $pK_a = 4.5$; b, $pK_a = 4.8$; c, $pK_a = 4.6$; d, $pK_a = 4.4$; e, $pK_a = 4.2$.

by using rigorous Gran functions (1) and (6) with approximate K_a values than by use of the approximate Gran functions (4) and (5) or (8) and (9). Rigorous Gran plots must be preferred (at the small cost of slightly more complex calculations) whenever accurate electrode calibration is possible.

Effect of measurement errors on corrected Gran plots. A statistical analysis⁵ of the methods proposed is beyond the scope of this work. However, qualitative indications of the performance of the addition procedure and of the different forms of the rigorous equation are given below. Only measurement errors in $[H^+]$ are considered, so the importance of careful electrode calibration¹⁶ and e.m.f. measurements is stressed. Of course, the importance of errors in the measured volume V must not be underestimated.

The plots calculated for systematic errors of $\pm 4\%$ in $[H^+]$ (which can result, for instance, from calibration errors of ± 1 mV in the standard e.m.f. of the measuring cell) are shown in Fig. 5 for acids of different strength and concentration. Positive systematic errors yield plots lying higher than the correct line *a*; negative errors yield plots lying lower than *a*.

It is seen that linearity is not affected by a small constant relative error. The pairs of lines labelled *c* are fairly representative of the majority of acids of intermediate strength and concentration, for which pH decreases by

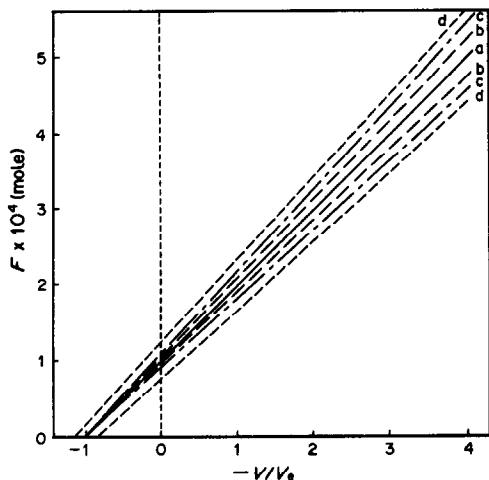


Fig. 5. Plots of F , equation (1), for multiple additions of standard acid ($C = 10C^0$) to pure acid (C^0), calculated with $[H^+]$ affected by a systematic error of $+4\%$ (upper plots) and -4% (lower plots); a, plot using the correct $[H^+]$ value; b, $pK_a = 2.0$, $C^0 = 0.001M$; c, $pK_a = 11.3$, $C^0 = 0.01M$; d, $pK_a = 11.3$, $C^0 = 0.001$. Ordinates are normalized so that plot (a) has unit slope.

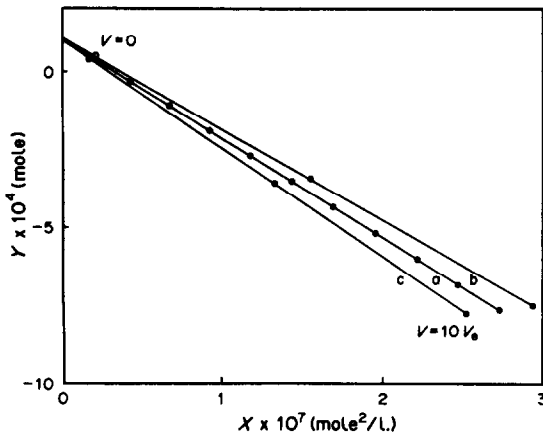


Fig. 6. Hofstee plots [equation (12)] for multiple additions of standard acid ($C = 10C^0$) to 100 ml of pure acid, ($pK_a = 3.5$, $C^0 = 0.001M$) for: a, rigorous $[H^+]$ values; b, $+4\%$ error in $[H^+]$; c, -4% error in $[H^+]$. Co-ordinates are $X = [H^+](C_bV^0 + H)$ and $Y = H - CV$ where H is defined as in equation (10).

0.25–0.30 between $V = 0$ and $V = -4V_e$. The extrapolation error is also moderate for these acids, being smaller than 1.5%. Dilute moderately strong acids, for which the pH decrease is larger, behave still better (lines *b*). Only with dilute very weak acids (lines *d*), which have pH values that are near to 7 and vary little, is the equivalence volume obtained by extrapolation greatly affected by moderate systematic errors in $[H^+]$.

With buffers, results are improved, because a given addition of standard acid causes a variation of pH about twice as large as that for the acids alone (see above).

Effect of measurement errors on the other linear plots. Typical theoretical plots of equations (12)–(14) are represented in Figs. 6–8 respectively (lines labelled *a*). The distribution of points taken at regular volume intervals up to $V = -10V_e$ is also shown. Lines *b* and *c* in the same figures are the corresponding plots calculated with systematic errors of $+4$ and -4% in $[H^+]$, respectively; on these plots, a few points at the same added volumes as nearby points on the theoretical plots *a* are indicated, to show the effect of errors in $[H^+]$ on the co-ordinates of the plots. Random errors not exceeding 1 mV give points lying between these pairs of plots (if errors in volumes are negligible). In this way, a rough indication of the effect of random errors in $[H^+]$ on the precision of the results is obtained. In Figs. 6 and 7, the ordinate is much less affected than the abscissa by errors in $[H^+]$. Therefore, the equations obtained from equations (12) and (13) by interchanging

co-ordinates are superior for least-squares treatment when the volume data are more precise than the e.m.f. data. Weaker acids behave in a similar way; for acids stronger than those considered in these figures, errors in the ordinate and abscissa become comparable. From similar considerations, equation (14) (Fig. 8) is always unsuitable for least-squares treatment.

In Figs. 6 and 7, errors in $[H^+]$ have a very large effect on the slope and, therefore, on the calculated value of the acidity constant derived from it. On the other hand, the linearity is scarcely affected, and the error in the amount of acid calculated from the intercept $Y(X=0)$ is generally moderate, except for dilute very weak acids. For instance, the errors in the V_e value obtained by least-squares extrapolation of lines *b* and *c* of Fig. 6 through eleven points at constant volume increments between $V=0$ and $V=-10V_e$ are 1.6 and -1.5% , respectively whereas the errors in K_a obtained from the slopes are 8.4 and -9.5% , respectively. The errors in V_e obtained by extrapolation of lines *b* and *c* of Fig. 7 through ten points at constant volume increments between $V=-V_e$ and $V=-10V_e$ (the point at $V=0$ is situated far away in the opposite quadrant, with both co-ordinates positive) are -0.5 and 0.5% , respectively, whereas errors in K_a are 8.3 and -9.4% , respectively.

In Fig. 8, errors in $[H^+]$ have a very large effect on the intercept, *i.e.*, again on pK_a , and a small one on the slope, *i.e.*, on the equivalence volume. By extrapolation of eleven points

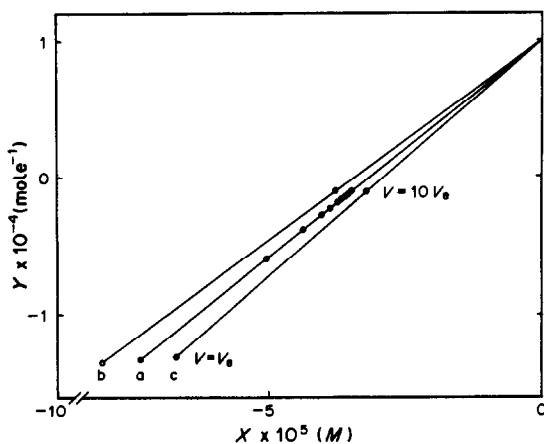


Fig. 7. Lineweaver-Burk plots [equation (13)] for multiple additions of standard acid ($C=10C^0$) to 100 ml of pure acid ($pK_a=4.5$) at $C^0=0.001M$, for: a, rigorous $[H^+]$ values; b, $+4\%$ error in $[H^+]$; c, -4% error in $[H^+]$. Co-ordinates are $X=[H^+](C_bV^0+H)/(H-CV)$ and $Y=(H-CV)$ where H is defined by equation (10).

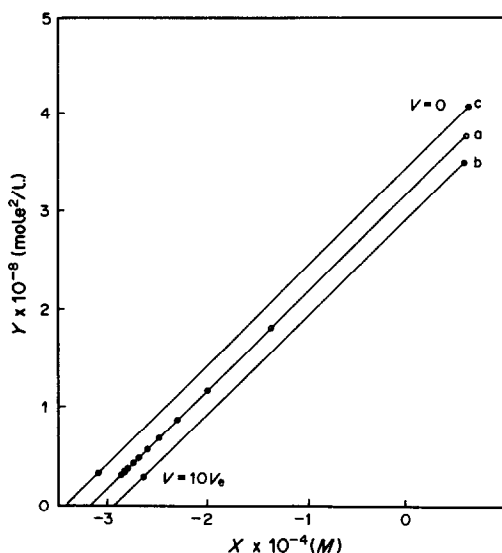


Fig. 8. Scott plots [equation (14)] for multiple additions of standard acid ($C=10C^0$) to 100 ml of pure acid ($pK_a=4.5$, $C^0=0.001M$) for: a, rigorous $[H^+]$ values; b, $+4\%$ error in $[H^+]$; c, -4% error in $[H^+]$. Co-ordinates are $X=(H-CV)/[H^+](C_bV^0+H)$ and $Y=1/[H^+](C_bV^0+H)$, where H is defined by equation (10).

between $V=0$ and $V=10V_e$ on lines *b* and *c*, the errors in V_e are 0.4 and -0.4% , respectively, and the errors in the constant are 7.8 and -8.8% , respectively.

With buffers, the effects of errors in $[H^+]$ are generally smaller, except for buffers made with moderately strong acids.

CONCLUSIONS

Linearized multiple standard addition is not intended as the method of general choice for the analysis of solutions of single weak acids, whether alone or mixed with the conjugate base. However, this method can be of utility in particular cases. For instance, measurements are made in a more acidic pH range than that of the acidic part of a linearized titration of the same sample solution with strong base, and therefore interference from carbon dioxide present in the titrant^{22,23} and/or the test solution (which can be important in titrations of very dilute acids), is largely eliminated. A drawback of the method compared with conventional titrations is that it requires a standard solution of the titrand acid. This, however, once standardized, can be kept for a long time without its efficacy being impaired by carbon dioxide.

When the purpose of the measurements is determination of only the acidity constant, multiple additions to a solution of the

supporting electrolyte are made and rigorous equations are used, with small modifications. These will be discussed, together with experimental results, in a later paper.

REFERENCES

1. M. Mascini, *Ion-Selective Electrode Rev.*, 1980, **2**, 17.
2. G. Gran, *Analyst*, 1952, **77**, 661.
3. A. Liberti and M. Mascini, *Anal. Chem.*, 1969, **41**, 676.
4. H. Flood, *Z. Elektrochem.*, 1940, **46**, 89.
5. C. Maccà, *Z. Anal. Chem.*, 1990, **336**, 29.
6. F. Ingman and E. Still, *Talanta*, 1966, **13**, 1431.
7. D. Midgley and C. McCallum, *ibid.*, 1974, **21**, 723.
8. K. A. Connors, *Binding Constants*, Wiley, New York, 1987.
9. B. H. J. Hofstee, *Science*, 1960, **31**, 39.
10. G. Scatchard, *Ann. N.Y. Acad. Sci.*, 1949, **51**, 660.
11. H. Lineweaver and D. Burk, *J. Am. Chem. Soc.*, 1934, **56**, 658.
12. R. L. Scott, *Rec. Trav. Chim.*, 1956, **75**, 787.
13. B. M. Mar'yanov, *J. Anal. Chem. USSR*, 1975, **30**, 1596.
14. C. Maccà and G. G. Bombi, *Analyst*, 1989, **114**, 463.
15. C. Maccà, *ibid.*, 1989, **114**, 689.
16. L. Pehrsson, F. Ingman and A. Johansson, *Talanta*, 1976, **23**, 769.
17. P. M. May and D. R. Williams, in *Computational Methods for the Determination of Formation Constants*, D. J. Leggett (ed.), p. 37. Plenum Press, New York, 1985.
18. J. Buffle, N. Parthasarthy and D. Monnier, *Anal. Chim. Acta*, 1972, **59**, 427.
19. L. L. Schwartz, *ibid.*, 1989, **225**, 205.
20. G. Charlot, *Les Réactions Chimiques en Solution. L'Analyse Qualitative Minérale*, 6th Ed., p. 29. Masson, Paris, 1969.
21. A. Johansson, *Talanta*, 1975, **22**, 945.
22. C. Maccà, *J. Chem. Educ.*, 1986, **63**, 691.
23. F. J. C. Rossotti and H. Rossotti, *ibid.*, 1965, **42**, 375.

INDIRECT ELECTROCHEMICAL DETECTION OF CATIONS WITH CERIUM(III) IN THE MOBILE PHASE

JULIE WANGSA, MARGARET A. TARGOVE and NEIL D. DANIELSON*
Department of Chemistry, Miami University, Oxford, OH 45056, U.S.A.

(Received 4 December 1989. Revised 28 March 1990. Accepted 3 April 1990)

Summary—Cerium(III) has been used in the mobile phase for indirect electrochemical chromatography of cations. Lithium, sodium, ammonium, and potassium ions have been separated within 4 min and detected with both glassy carbon and Kel-F wax carbon paste electrodes. With a Kel-F wax/graphite electrode at 0.7 V, the detection limit for sodium, ammonium, and potassium ions are 1.5, 1.1, and 2.0 ppm, respectively.

In chromatography indirect detection provides a convenient way to detect analytes that are not easily monitored by other methods.¹ Indirect photometric chromatography (IPC) and indirect fluorescence chromatography (IFC) have been used for the ion exchange separation of organic and inorganic ions.²⁻⁵ However, the majority of the work involves IPC and anion separations.⁶ Although not as well explored, some organic counter-ions⁷⁻¹⁰ have been investigated for IPC of cations. Besides inorganic cations such as copper(II)¹¹ and a cobalt(III) complex,¹² cerium(III) has been used in the mobile phase for indirect detection in ion exchange chromatography. A comparison study¹³ suggests that lower detection limits can be obtained for alkali metal, ammonium, magnesium, and calcium ions by IPC with Ce(III) than with Cu(II). Indirect fluorescence detection for alkali-metal ions has also been developed with Ce(III) as the counter-ion. The detection limits were comparable with those of IPC, but an improvement in selectivity was observed for samples such as urine.¹⁴

As an alternative to IFC, indirect electrochemical chromatography (IEC) should also offer higher selectivity than the photometric methods. Anions such as chloride and nitrate have been detected at < 1 ppm with the electroactive salicylate ion in the mobile phase.¹⁵ In this paper, we examine the potential of Ce(III) as a counter-ion for use in amperometric IEC. To the best of our knowledge, this is the first report of IEC in the oxidative mode for the determi-

nation of cations. Both glassy carbon and Kel-F wax/graphite paste electrodes are compared for the detection of lithium, sodium, ammonium and potassium ions.

EXPERIMENTAL

Chemicals

All solutions were unbuffered and prepared in triply distilled water obtained from a Barnstead Nanopure distillation unit (Sybron/Barnstead Corp., Boston, MA). Cerium(III) was used in the form of its sulfate, and all sample solutions were prepared from the chlorides. All chemicals used were obtained from various sources and were reagent grade or better. Graphite powder (No. 38) purchased from Fisher (Fairlawn, NJ) was found by light microscopy to be approx. 25 μm in grain size. Kel-F [poly(chlorotrifluoroethylene)] wax was obtained from Alltech Associates (Arlington Heights, IL).

Instrumentation

The chromatographic arrangement consisted of a Model SM-909 pump (Anspec, Ann Arbor, MI) with an SSI pulse dampener (Scientific Systems, Inc., State College, PA), a Rheodyne Model 7010 injector (Rheodyne, Berkeley, CA) with a 20 μl sample loop, and a Waters (Milford, MA) Model 460 electrochemical detector. The electrochemical cell was composed of a stainless steel auxiliary electrode, an Ag/AgCl reference electrode, and a glassy carbon or Kel-F wax/graphite carbon paste electrode (CPE). The Kel-F wax CPE¹⁶ was prepared in batches by combining graphite powder (dried at 100°) and the binder in 1:25 weight ratio. The

*Author for correspondence.

required amount of Kel-F wax was weighed into a beaker and heated on a hot plate at low heat until the wax had melted. The graphite powder was added slowly with stirring. The mixture was allowed to cool and then mixed thoroughly with a mortar and pestle. A small amount of paste was then transferred to the flow cell cavity with a spatula and packed by applying pressure with a small brass rod. The electrode surface was flattened by polishing it on smooth white paper. The separations were performed with a 10 cm \times 3.2 mm i.d. ION-210 column (Interaction Chemicals, Mountain View, CA) at room temperature. The peaks were recorded on a Linear Model 1201 (Linear Instruments, Reno, NV) strip chart recorder and quantified by peak height.

RESULTS AND DISCUSSION

In IEC, the current response of the electrochemically active component in the mobile phase is measured at a specific applied potential. During the re-establishment of the ion exchange equilibrium, a decrease in current is expected as the "active" ions in the mobile phase are replaced by the "inactive" analyte ions to maintain electroneutrality. The area of this negative peak is proportional to the concentration of the analyte. In this study, Ce(III) is oxidized to Ce(IV) at a constant potential and the resulting current monitored. The oxidation of Ce(III) to Ce(IV) was observed to take place at 1.0 V but not at 0.5 V. A decrease in fluorescence was noted at 1.0 V, indicating the formation of Ce(IV). Preliminary data obtained with a Nujol CPE showed the IEC determination of Na^+ , NH_4^+ , and K^+ by using Ce(III) was possible. However, only low oxidation potentials (about 0.3 V) could be applied without undue baseline noise.¹⁷ It is surprising that any indirect peaks would be observed at such low potentials, which are certainly not high enough to cause the oxidation of Ce(III). A similar phenomenon has been observed when iodide is used in the mobile phase for the indirect electrochemical detection of anions.¹⁸ To determine the optimum operating potential, a hydrodynamic voltamperogram is generated by injecting 1mM cerium(III) sulfate into the carrier stream of 10mM sodium acetate, pH 4.3. The currents are then measured at various potentials. Figure 1 shows the hydrodynamic voltamperograms obtained with the glassy carbon and Kel-F wax/graphite electrodes. A gradual rise in the current as the

voltage increased to 0.8 V was found for both electrodes. A potential of 0.9 V *vs.* Ag/AgCl or higher must be applied to both electrodes in order to reach the limiting current plateau. However, this potential range resulted in a higher background current and an unstable baseline, especially for the glassy carbon electrode. A comparison of +0.7 and 0.9 V applied potentials was made for both electrodes in subsequent work.

A separation of lithium, sodium, ammonium, and potassium ions was investigated with various mobile phase concentrations of Ce(III) and a flow rate of 1 ml/min. At higher cerium concentrations, such as 1mM, lithium was not retained and was eluted with the void volume. Efforts to increase the retention of lithium by decreasing the cerium concentration to 0.01mM were not successful. Furthermore, the detection limit is poorer with a lower concentration of cerium, because of peak broadening. Figure 2 shows an IEC separation of a mixture containing 6.6 ppm Li^+ , 26.4 ppm Na^+ , 18.2 ppm NH_4^+ , and 39.6 ppm K^+ with detection by a glassy carbon electrode at +0.7 V with 0.1mM Ce(III). Because of the high noise (3 times worse at 0.95 V), the separation was not viable with the glassy carbon electrode at higher potentials. Under the same experimental conditions as for Fig. 2, the separation of the four ions is possible within 4 min with a Kel-F wax CPE for detection (Fig. 3A). Although the baseline is somewhat sloping, the noise is significantly less for this electrode, particularly at 0.9 V (Fig. 3B), than that for the glassy carbon electrode at 0.7 V (Fig. 2). We are uncertain as to why the

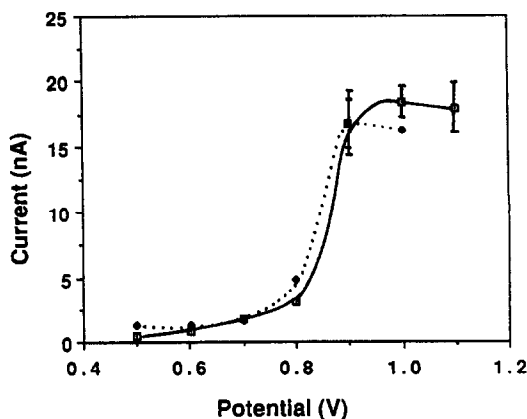


Fig. 1. Hydrodynamic voltamperograms for Ce(III) with the glassy carbon electrode (—□—) and the Kel-F wax CPE (····◆····). Each data point represents at least three repetitive injections of 1mM Ce(III) sulfate. All potentials *vs.* Ag/AgCl.

positive peaks occur. These were observed regardless of the applied potential. The effect is not caused by this particular detector since it was also observed with a different model of detector. We have also carried out indirect electrochemical detection of cations with V(IV) in the reductive mode¹⁹ but did not observe such noise spikes.

Figure 4 depicts the calibration curves for sodium, ammonium, and potassium ions, obtained with the Kel-F wax/graphite electrode. Lithium is not included because it is not as well retained and thus is difficult to quantify. Furthermore, the baseline for lithium has an off-scale positive peak at this particular setting (Fig. 3A). Reproducible calibration plots for sodium, ammonium, and potassium ions could be obtained up to 25, 40 and 50 ppm, respectively. The relative standard deviation (RSD) for these points ranged from 1 to 8%. The calibration data for the ions were similar for the glassy carbon electrode.

Table 1 lists the detection limits for the three ions with both electrodes at +0.7 V and the Kel-F wax CPE at 0.9 V. Since the limit of detection is affected by the magnitude of the noise, the lowest detection limit is observed when the Kel-F wax CPE is used at $E = +0.7$ V. From five peak measurements, the reproducibility of response for the glassy carbon and the

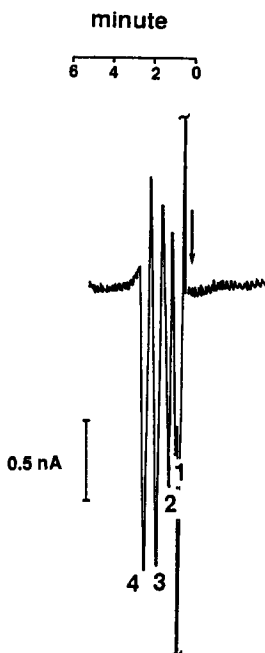


Fig. 2. IEC separation of lithium (1), sodium (2), ammonium (3), and potassium (4) ions, with detection by a glassy carbon electrode at 0.7 V. Mobile phase: 0.1M Ce(III), pH = 4.4. Flow rate: 1 ml/min.

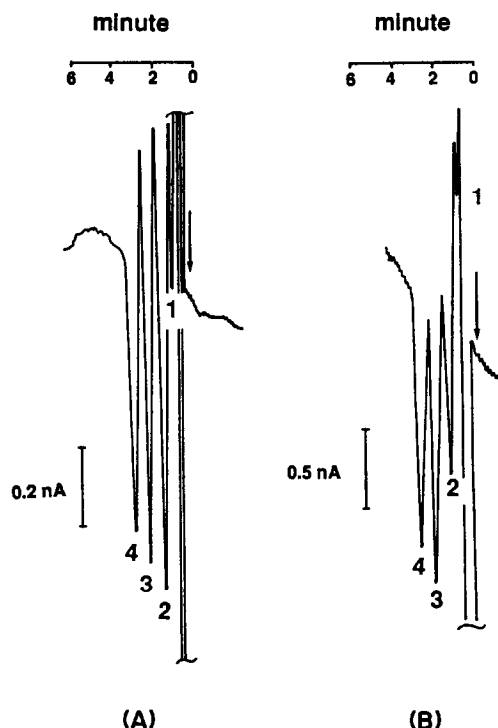


Fig. 3. IEC separation of lithium (1), sodium (2), ammonium (3), and potassium (4) ions; detection with a Kel-F wax CPE at 0.7 V (A) and at 0.9 V (B). Other conditions as for Fig. 2.

Kel-F wax/graphite electrodes at +0.7 V is within 6 and 9.5%, respectively, at the detection limit. The slightly better reproducibility of the glassy carbon electrode is probably due to the "positive" peaks being smaller. The detection limit by IEC, however, is at least a factor of 10 higher than that with the IPC or IFC techniques,¹⁴ but comparable to that for IEC of cations with V(IV).¹⁹

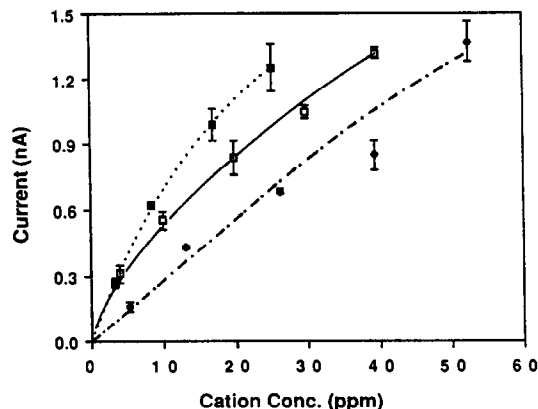


Fig. 4. Calibration curves for sodium (.....■.....), ammonium (—□—), and potassium (—◆—) ions, obtained with the Kel-F wax CPE. Mobile phase and flow rate as for Fig. 2. $E = 0.7$ V. $n = 3$.

Table 1. Comparison of detection limits obtained with the glassy carbon electrode and the Kel-F wax CPE.

Cation	Glassy carbon $E = 0.7 V$	Kel-F wax CPE	
		$E = 0.7 V$	$E = 0.95 V$
Na ⁺ , ppm	1.8	1.5	2.2
NH ₄ ⁺ , ppm	1.6	1.1	1.3
K ⁺ , ppm	2.5	2.0	3.0

A separation of sodium from other constituents of commercial tonic water has been carried out to show the applicability of Ce(III) IEC. This sample would be difficult to analyze by IPC or IFC owing to the strong ultraviolet absorption or fluorescence of quinine. A current peak due to the direct oxidation at 0.5 V of a 150 ppm quinine standard or a diluted tonic water sample injected into an acetate buffer mobile phase was not observed. A large positive peak or system peak²⁰ was seen in the chromatogram for a 1:4 diluted tonic water sample (Fig. 5A). This system peak is probably due to the presence of

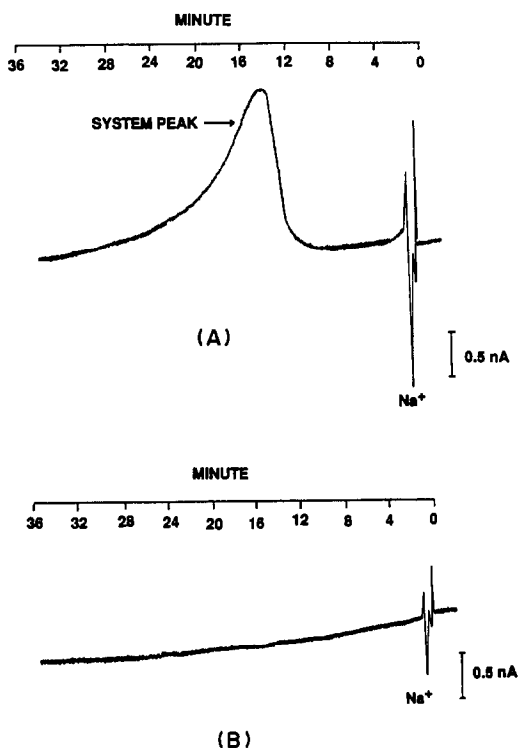


Fig. 5. Chromatograms of the sodium ion in tonic water diluted $\times 4$ (A) and diluted by $\times 10$ (B). Mobile phase and flowrate as in Fig. 2. $E = 0.5 V$.

various components in the tonic water which disturb the distribution of Ce(III) between the mobile and stationary phases. Sample dilution by a factor of 10, as shown in Fig. 5B, permitted the separation and quantification of sodium within 2 min without the appearance of a system peak. The calculated amount of sodium in tonic water (151 ppm) was about 7% higher than the value obtained by flame atomic-absorption spectrometry.

We believe IEC of cations could be optimized further by selecting different more easily oxidized eluents. For example, the possibility of using Sn(II) or an aminophenol as an eluent in the IEC of cations could be explored.

Acknowledgements—We thank Interaction Chemicals, Inc. for the gift of the ion-exchange column and the Waters Chromatography Division for the donation of the electrochemical detector.

REFERENCES

1. H. Small and T. E. Miller, Jr., *Anal. Chem.*, 1982, **54**, 462.
2. E. J. Parkin, *J. Chromatog.*, 1986, **351**, 532.
3. P. G. Rigas and D. J. Pietrzyk, *Anal. Chem.*, 1988, **60**, 454.
4. A. A. Gallo and F. H. Walter, *Anal. Lett.*, 1986, **19**, 979.
5. S. Mho and E. S. Yeung, *Anal. Chem.*, 1985, **57**, 2253.
6. D. T. Gjerde and J. S. Fritz, *Ion Chromatography*, pp. 225–226. Hüthig Verlag, New York, 1987.
7. Z. Iskandarani and T. E. Miller, Jr., *Anal. Chem.*, 1985, **57**, 1591.
8. J. R. Larson and C. D. Pfeiffer, *J. Chromatog.*, 1983, **259**, 519.
9. R. C. L. Foley and P. R. Haddad, *ibid.*, 1986, **366**, 13.
10. P. R. Haddad and R. C. Foley, *Anal. Chem.*, 1989, **61**, 1435.
11. J. R. Larson and C. D. Pfeiffer, *ibid.*, 1983, **55**, 393.
12. C. A. Chang, Q. Wu and C. Sheu, *J. Chromatog.*, 1987, **404**, 282.
13. J. H. Sherman and N. D. Danielson, *Anal. Chem.*, 1987, **59**, 490.
14. *Idem, ibid.*, 1987, **59**, 1483.
15. G. Horvai, J. Fekete, Zs. Niegreis, K. Tóth and E. Pungor, *J. Chromatog.*, 1987, **385**, 25.
16. J. Wangsa and N. D. Danielson, *ibid.*, in press.
17. M. A. Targove, *Ph.D. Dissertation*, Miami University, 1988.
18. P. G. Simonson and D. J. Pietrzyk, *14th Intern. Symp. Column Liquid Chromatography, Boston, 1990*, Abstract No. P236.
19. N. D. Danielson, J. Wangsa, B. T. Jones, J. E. Carlson, *Chromatographia*, 1990, **29**, 139.
20. S. Levin and E. Grushka, *Anal. Chem.*, 1987, **59**, 1157.

SEPARATION OF YTTRIUM AND NEODYMIUM FROM SAMARIUM AND THE HEAVIER LANTHANIDES BY CATION-EXCHANGE CHROMATOGRAPHY WITH HYDROXYETHYLENEDIAMINETRIACETATE IN MONOCHLOROACETATE BUFFER

F. W. E. STRELOW and A. H. VICTOR

Division of Processing and Chemical Manufacturing Technology, CSIR, P.O. Box 395,
Pretoria 0001, South Africa

(Received 15 January 1990. Revised 3 April 1990. Accepted 14 June 1990)

Summary—Trace and mg amounts of yttrium and neodymium are separated from samarium and the heavier lanthanides by elution of the latter with hydroxyethylenediaminetriacetate (HEDTA) in a chloroacetate buffer of pH 2.85 from a column containing 68 ml (20 g) of AG 50W-X4 resin of 200–400 mesh particle size. Yttrium and neodymium (and also praeceodymium, cerium and lanthanum) are retained and can be eluted with 0.01M HEDTA in 0.20M ammonium acetate (pH 6). The separations are reasonably sharp and quantitative: only 3–15 μg of samarium was found in the yttrium fraction and 0.8–3.4 μg of yttrium in the samarium fraction when 4.41 mg of yttrium and 7.12 mg of samarium were present originally. Control of the pH during the column operations is essential because the peak positions are very sensitive to change in pH. The relevant distribution coefficients, elution curves of pairs of elements and results for the analysis of synthetic mixtures are presented. Also included is a method for separating yttrium and the lanthanides from HEDTA and sodium and ammonium ions.

High-pressure liquid chromatography and ion chromatography have become of increasing importance for the determination of lanthanides in rocks and geological materials since the work by Story and Fritz¹ and Elchuk and Cassidy,² mainly because of their relative speed and lower cost compared to that of other methods capable of determining all or most of the lanthanides in one run. A disadvantage of ion chromatography, however, is that yttrium, which has similar properties to the lanthanides and accompanies them through preliminary separations, is generally eluted in the vicinity of dysprosium and holmium and interferes with their determination.

Morton and James,³ and Powell and Burkholder⁴ have shown that at room temperature (25°) hydroxyethylenediaminetriacetate (HEDTA) elutes yttrium somewhere between neodymium and samarium. This behaviour is considerably different from that found with most other eluents used for lanthanide separation. This suggests that quantitative separation of milligram amounts of yttrium from the heavy lanthanides should be possible by use of this reagent. The present paper gives the distribution coefficients for yttrium and some relevant

lanthanides between AG 50W-X4 resin and HEDTA in monochloroacetate buffer solutions and applies the results to quantitative separation of yttrium and neodymium from samarium and the heavy lanthanides.

EXPERIMENTAL

Reagents

All common reagents were of guaranteed reagent quality. Water was distilled and demineralized (Millipore). Trisodium hydroxyethylenediaminetriacetate (HEDTA) of *puriss.* p.a. quality and lanthanide and yttrium oxides of 99.9% purity or better were obtained from Fluka. A 0.100M solution of HEDTA was prepared by dissolving 38.02 g of the reagent in about 500 ml of demineralized water, adjusting the pH to about 5 with 6M hydrochloric acid, and diluting to 1000 ml. Solutions of the lanthanides and yttrium (500 ml, 0.0200M), were made by dissolving the appropriate amount of oxide in nitric acid and making up to volume after the excess of acid had been removed by evaporation on a water-bath. The solutions were standardized by complexometric titration with EDTA at pH 5.5, with Xylenol Orange as

indicator. Working solutions were made by further dilution as required.

The resins used were the strong-acid sulphonated polystyrene cation-exchangers AG50W-X4 and AG50W-X8 (Bio-Rad Laboratories). The 100–200 mesh particle size, ammonium form, resins were used for the determination of distribution coefficients because they contain a smaller amount of fines after drying at 110° and are easier to filter off. Resins of 200–400 mesh particle size were used for column separations because of their better exchange kinetics.

Apparatus

Borosilicate glass tubes (19.8 mm i.d., 430 mm long), fitted with a porosity No. 1 sintered-glass disk and burette tap at the bottom, and a B19 ground-glass socket at the top to hold a dropping funnel as eluent reservoir, were used to make the columns for separation of yttrium and the lanthanides. The tubes were filled with a slurry of AG50W-X4 (200–400 mesh) resin (hydrogen form) until the settled resin reached a mark 260 mm above the disk. This required about 20 g of dry resin. The resin then was transformed into the ammonium form by passage of 1M ammonium chloride until the pH of the eluate was about 4.5. This caused some shrinkage of the resin. Finally the column was equilibrated by passage of 120 ml of a solution made by mixing equal volumes of 0.72M monochloroacetic acid and 0.40M ammonia solution (this is the eluent without the HEDTA, and its pH should be 2.85).

Smaller columns of 16.5 mm i.d. and 400 mm length were used for separation of the lanthanides and yttrium from HEDTA and ammonium ions. These columns were filled to give a bed of 23 ml (5 g of dry resin) of AG50W-X4 resin of 200–400 mesh particle size. The resin was kept in the hydrogen form and washed only with some demineralized water to remove organic decay products.

A Metrohm E512 pH-meter was used for pH measurement, and a Varian Techtron AA-5 atomic-absorption spectrometer for determination of ytterbium, with an acetylene–nitrous oxide flame and 2000 ppm potassium as ionization suppressor. The other lanthanides and yttrium were determined by direct-current plasma emission spectrometry with a Beckman Spectrospan IV instrument.

Distribution coefficients

Portions (2.713 g) of AG50W-X8 resin in the ammonium form ($\equiv 2.500$ g in the hydrogen form), dried at 110°, were equilibrated in a mechanical shaker for 24 hr at 20° with 250 ml of a solution containing 0.2 mmole (10 ml of the 0.02M standard solution) of yttrium or one of the lanthanides in 0.0100M HEDTA/0.20M ammonium monochloroacetate mixture that contained monochloroacetic acid at concentrations ranging from 0 to 1.20M. After equilibration the resin was filtered off and ashed at 900° in a platinum crucible. The ash was washed into a small beaker and dissolved in nitric acid, then the excess of acid was removed by evaporation. The amount of yttrium or lanthanide was determined by complexometric titration with 0.005M EDTA at pH 5.5, with Xylenol Orange as indicator. After measurement of its pH, the filtrate was acidified by addition of 15 ml of 5M hydrochloric acid, passed through a column containing 23 ml (5 g) of AG50W-X4 resin (200–400 mesh, H⁺ form) and rinsed onto the column with 0.2M hydrochloric acid. Ammonium and sodium ions were then eluted with 200 ml of 0.5M nitric acid at a flow-rate of 3.0 ± 0.3 ml/min. Finally the lanthanide retained was eluted with 150 ml of 3.0M hydrochloric acid at a flow-rate of 2.5 ± 0.3 ml/min. After the excess of acid had been removed by evaporation the amount of lanthanide was determined by complexometric titration as described above. Two 10-ml aliquots of the original standard solution were titrated as a control. From the results, the equilibrium distribution coefficients were calculated⁵ and plotted against the measured pH values. Equilibrium distribution coefficients at pH values of 2.0, 2.5, 3.0, 3.5, 4.0 and 5.0 were read from the curves and are presented in Table 1.

Elution curves

Separation of Sm from Y and Nd. A solution containing 6.3 mg of samarium and 4.4 mg of yttrium in 30 ml of ammonium monochloroacetate buffer of pH 2.85 (0.2M CH₂ClCOONH₄ + 0.16M CH₂ClCOOH) was passed through a column containing 86 ml (20 g) of AG50W-X4 resin (200–400 mesh) prepared as described above and equilibrated with 120 ml of the same buffer. The solution was washed into the resin with a few portions of the buffer solution diluted 1:1 with demineralized water and then samarium and yttrium were

Table 1. Cation-exchange distribution coefficients in the 0.01M HEDTA-AG50W-X8 resin system (monochloroacetate buffer)*

Element	Distribution coefficient					
	pH 2.0	pH 2.5	pH 3.0	pH 3.5	pH 4.0	pH 5.0
La	$> 10^4$	2.4×10^3	226	33.5	7.8	0.5
Nd	4.6×10^3	220	22.0	2.8	0.9	0.5
Y	3.8×10^3	216	21.8	2.7	0.8	0.4
Sm	2.6×10^3	90	8.0	1.4	0.6	0.3
Dy	2.3×10^3	84	7.4	1.2	0.6	0.2
Yb	460	24.3	3.0	0.7	0.5	0.3

*For definition of coefficients see Strelow.⁵

eluted with 0.010M HEDTA in the undiluted buffer at a flow-rate of 1.5 ± 0.3 ml/min. Sixty 10-ml fractions were collected with an automatic collector. The concentrations of samarium and yttrium in the fractions were determined by direct-current plasma emission spectrometry at the appropriate wavelength. The experimental elution curve is shown in Fig. 1. An experimental curve for the separation of the Nd-Sm pair was very similar to that in Fig. 1.

Separation of Dy from La. The experiment above was repeated with a solution containing 9.3 mg of Dy and 8.2 mg of La, but the dysprosium was eluted with 350 ml of the HEDTA-monochloroacetate buffer and the lanthanum was then eluted with 0.010M HEDTA in 0.20M ammonium acetate (pH 6.0). The elution curve is shown in Fig. 2.

Separation of Yb from HEDTA, sodium, ammonium and potassium. A solution containing 6.8 mg of ytterbium in 300 ml of HEDTA-monochloroacetate buffer at pH 2.85 (simulating the situation after a separation) was prepared and 50 mg of potassium were added, to

act as a tracer for ammonium ions. Potassium is in fact more strongly sorbed and therefore eluted slightly later than ammonium. The solution was acidified with 20 ml of 5M nitric acid and passed through a column containing 23 ml (5 g) of AG50W-X4 resin (200-400 mesh) as described above. The solution was washed into the resin with 50 ml of 0.2M nitric acid (in small portions) and ammonium and potassium were eluted with 250 ml of 0.50M nitric acid at a flow-rate of 3.0 ± 0.3 ml/min. Finally ytterbium was eluted with 200 ml of 3.0M hydrochloric acid at a flow-rate of 2.5 ± 0.3 ml/min. The eluate was collected in 10-ml fractions from the beginning of the sorption step, and these were analysed for potassium and ytterbium by flame atomic-absorption spectrometry with air-acetylene and nitrous oxide-acetylene flames, respectively, 2000 ppm potassium being added as ionization suppressor in the ytterbium determination. The experimental elution curve is shown in Fig. 3.

Separation of La from HEDTA, sodium and ammonium. A solution containing 5.6 mg of lanthanum in 300 ml of the HEDTA-

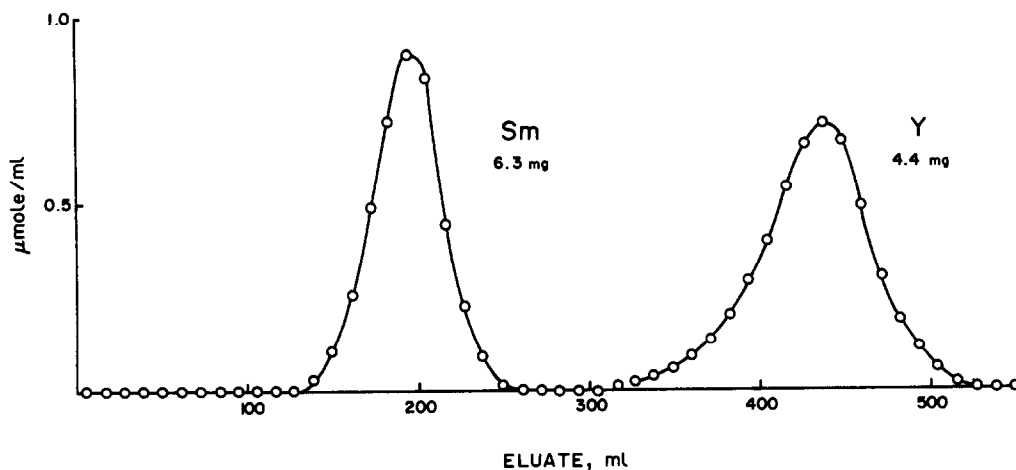


Fig. 1. Elution curve for Sm-Y mixture, with 0.01M HEDTA monochloroacetate buffer (pH 2.85), 86 ml (20 g) of AG50W-X resin, 200-400 mesh (column 260 × 19.8 mm), flow-rate 1.5 ± 0.3 ml/min.

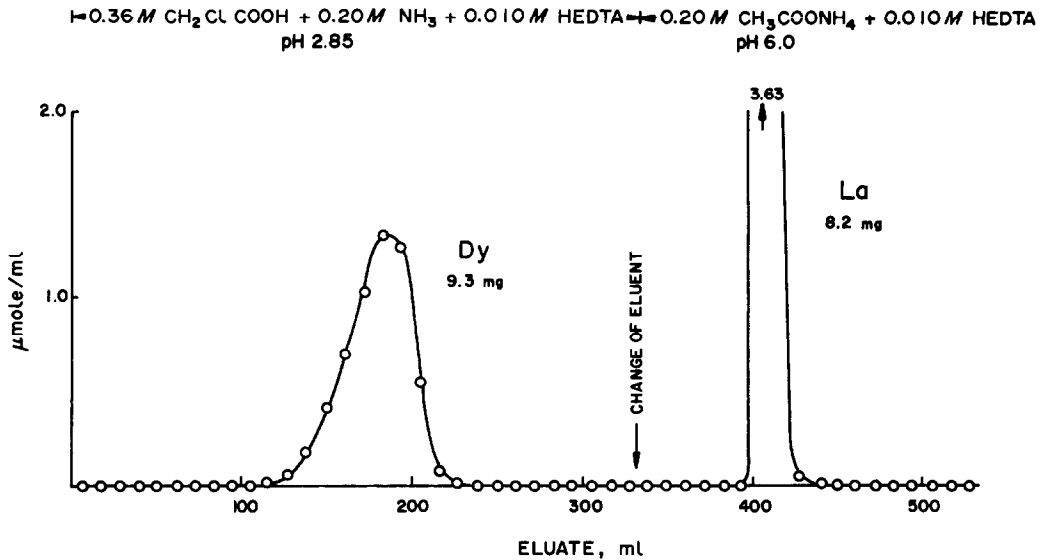


Fig. 2. Elution curve for Dy-La mixture, with HEDTA. Column measurements and flow-rate as for Fig. 1.

monochloroacetate buffer solution was acidified and passed through a 5-g AG50W-X4 resin column as described above. After passage of 400 ml of 0.50M nitric acid, the lanthanum was eluted with 3.0M hydrochloric acid at a flow-rate of 2.5 ± 0.3 ml/min. Direct-current plasma emission spectrometry was used to determine the lanthanum in the 10-ml fractions collected. The experimental curve is shown in Fig. 4. An attempt to elute lanthanum from a column containing 15 ml (5 g) of AG50W-X8 resin showed considerable tailing even with 4M hydrochloric acid as eluent.

Separation of synthetic binary mixtures

Appropriate amounts of standard solutions of yttrium and one other heavy lanthanide (as indicated below in Table 2) were mixed, about 30 ml of monochloroacetate buffer of pH 2.85 ($0.20 M \text{ CH}_2\text{ClCOONH}_4 + 0.16 M \text{ CH}_2\text{ClCOOH}$) were added and the solution was passed carefully, with minimum disturbance of the resin bed, through a column containing 86 ml (20 g of dry resin) of AG50W-X4 resin (200-400 mesh), that had been equilibrated with the monochloroacetate buffer. The solution was

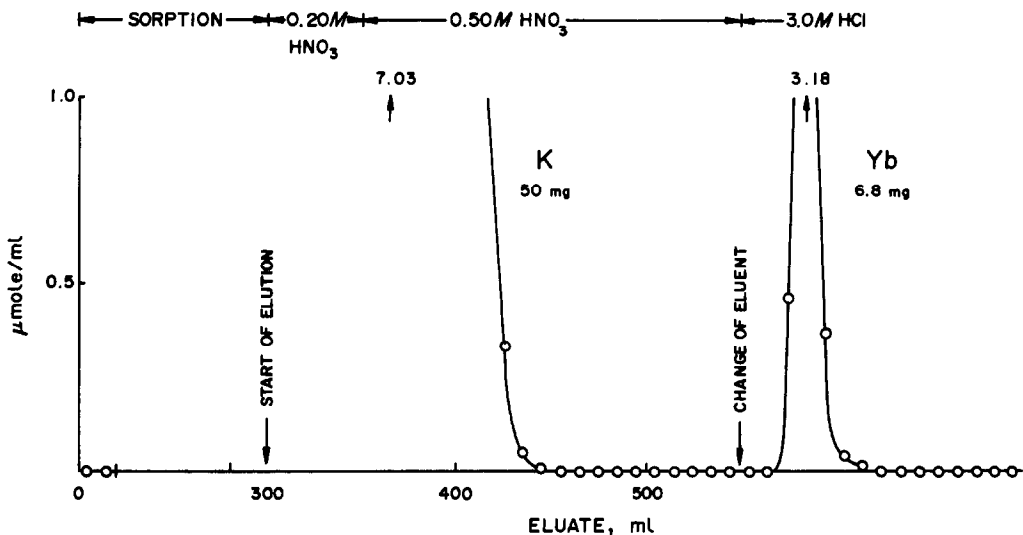


Fig. 3. Separation of Yb from HEDTA, sodium, ammonium and potassium ions: 23 ml (5 g) of AG50W-X4 resin, 200-400 mesh (column 107×16.5 mm), flow-rate 3.0 ± 0.3 ml/min, 2.5 ± 0.3 ml/min for 3.0M HCl.

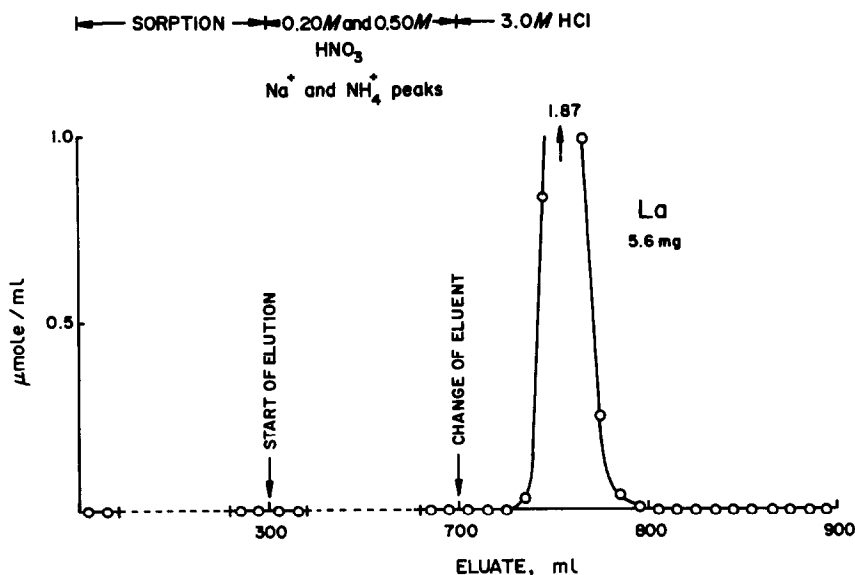


Fig. 4. Separation of La from HEDTA, sodium and ammonium ions. Column measurements and flow-rates as for Fig. 3.

washed into the resin bed with a few small portions of the monochloroacetate buffer solution diluted 1:1 with demineralized water. Then the lanthanide was eluted with 280 ml of monochloroacetate buffer solution containing 0.010M HEDTA (pH 2.85), at a flow-rate of 1.5 ± 0.3 ml/min, followed by elution of the yttrium with 200 ml of 0.20M ammonium acetate containing 0.010M HEDTA (pH 6.0). The two eluates were kept separate and acidified by addition of 20 ml of 5M nitric acid to the first (lanthanide) eluate and 12 ml of the acid to the yttrium eluate.

The acidified eluates were then passed through columns containing 23 ml (5 g of dry resin) of AG50W-X4 resin (200–400 mesh) and washed into the resin with a few small portions of 0.20M nitric acid. Then sodium, ammonium and HEDTA were eluted with 250 ml of 0.50M

nitric acid at a flow-rate of 3.0 ± 0.3 ml/min. These eluates were discarded, and the yttrium or lanthanide was eluted with 150 ml of 3.0M hydrochloric acid at a flow-rate of 2.5 ± 0.3 ml/min. The eluates were evaporated to dryness in small beakers on a water-bath. The salts were redissolved in an appropriate amount of 2.5M nitric acid and finally made up to volume in 0.5M nitric acid, to 50 ml for mg amounts, 25 ml for 100–1000 μ g amounts, and 10 ml for <100 μ g. The elements were then determined by direct-current plasma emission spectrometry and their amounts compared with those found in comparison solutions made by similar dilutions of corresponding amounts of the parent standard solutions. The results are given Table 2.

Because neodymium is very nearly as strongly sorbed as yttrium, it also can be separated from

Table 2. Determination of yttrium in synthetic mixtures

Amount present		Amount found*	
Yttrium	Other element	Yttrium	Other element
4.41 mg	7.12 mg Sm	4.41 ± 0.03 mg	7.05 ± 0.07 mg
4.41 mg	356.0 μ g Sm	4.42 ± 0.02 mg	353.0 ± 4 μ g
4.41 mg	17.8 μ g Sm	4.42 ± 0.02 mg	17.9 ± 0.2 μ g
220.0 μ g	7.12 mg Sm	221 ± 1 μ g	7.06 ± 0.09 mg
11.0 μ g	7.12 mg Sm	11.1 ± 0.2 μ g	7.11 ± 0.09 mg
4.41 mg	7.98 g Dy	4.40 ± 0.03 mg	7.95 ± 0.06 mg
4.41 mg	20.0 μ g Dy	4.42 ± 0.03 mg	19.9 ± 0.2 μ g
11.0 μ g	7.98 mg Dy	10.9 ± 0.2 μ g	8.00 ± 0.06 mg
4.41	8.62 mg Yb	4.41 ± 0.02 mg	8.60 ± 0.04 mg
4.41	21.6 μ g Yb	4.42 ± 0.03 mg	21.5 ± 0.3 μ g
11.0 μ g	8.62 mg Yb	11.0 ± 0.3 μ g	8.64 ± 0.05 mg

*Mean \pm standard deviation of five determinations.

Table 3. Determination of neodymium in synthetic mixtures

Amount present		Amount found*	
Neodymium	Other element	Neodymium	Other element
6.56 mg	7.12 mg Sm	6.58 ± 0.04 mg	7.09 ± 0.07 mg
6.56 mg	17.8 µg Sm	6.55 ± 0.05 mg	17.9 ± 0.3 µg
16.4 µg	7.12 mg Sm	16.3 ± 0.2 µg	7.11 ± 0.08 mg
6.56 mg	7.98 mg Dy	6.57 ± 0.06 mg	7.99 ± 0.05 mg
6.56 mg	20.0 µg Dy	6.54 ± 0.04 mg	20.1 ± 0.3 µg
16.4 µg	7.89 mg Dy	16.5 ± 0.3 µg	7.96 ± 0.6 mg
6.56 mg	8.62 mg Yb	6.55 ± 0.5 mg	8.61 ± 0.03 mg
6.56 mg	21.6 µg Yb	6.56 ± 0.04 mg	21.7 ± 0.2 µg
16.4 µg	8.62 µg Yb	16.3 ± 0.2 µg	8.64 ± 0.04 µg

*Mean ± standard deviation of five determinations.

samarium and other lanthanides by the procedure used for yttrium. Results for analysis of some mixtures are given in Table 3.

DISCUSSION

The method described separates yttrium and neodymium from samarium and the heavier lanthanides. Praeseodymium, cerium and lanthanum are more strongly sorbed than neodymium, and can also be separated from samarium and the heavier lanthanides. This seems to be the only quantitative group separation for lanthanides in which yttrium remains with the cerium group. When anion-exchange in nitric acid-methanol medium is used to separate the cerium group from samarium and the heavier lanthanides,⁶ yttrium accompanies the samarium *etc.* Known elution sequences or stability constants indicate that the same applies to complexing agents such as α -hydroxyisobutyric, lactic or citric acid or the aminopolyacetic acids such as EDTA and DCTA. The method therefore provides a useful preliminary separation before the lanthanides are determined by ion chromatography and avoids the interference of yttrium in the determination of the heavier lanthanides. The light lanthanides and the yttrium can then be easily determined by known ion chromatography methods.

The separations are reasonably sharp and quantitative, even for the most critical element pairs, yttrium-samarium and neodymium-samarium. When 4.41 mg of yttrium and 7.12 mg of samarium were present, only between 3 and 15 µg of samarium was found in the yttrium fraction, and between 0.8 and 3.4 µg of yttrium in the samarium fraction. The elution curve for the samarium-yttrium pair (Fig. 1) shows only a relatively small separation between the peaks. Because the distribution coefficients of yttrium and the lanthanides are very strongly dependent

on pH (see Table 1), rigid control of the pH during the column operation is essential to prevent shifts in the peak positions. When, in a trial run, the column was converted into the ammonium form by passage of an excess of 1M ammonium chloride but not equilibrated with the monochloroacetate buffer (pH 2.85), both samarium and yttrium were more rapidly eluted, presumably because the pH of the eluent was altered by exchange of some hydrogen ions for ammonium ions. Furthermore, when the original sample contains free acid, this should be removed by evaporation if the acid is readily volatile (hydrochloric, nitric) or by ion-exchange if it is not (sulphuric, phosphoric), and the dry salts dissolved in the monochloroacetate buffer before being put on the column. Otherwise shifts to larger elution volumes can occur.

The distribution coefficients in Table 1 were determined with an 8% cross-linked resin. Since column experiments indicated that the exchange kinetics of the HEDTA-lanthanide complexes will be quite slow with this resin, resulting in very wide peaks, and overlapping unless impracticably slow flow-rates are used, it was decided to use a 4% cross-linked resin, which gives faster kinetics. From experience it was known that the distribution coefficients for the 4% cross-linked resin are about 50-60% of the values for the 8% cross-linked resin, so the values in the tables are still usable. Separation factors also tend to become smaller with lower cross-linkage. Although the separation factor for the yttrium-samarium pair decreases from about 2.7 to 2.2 when the 4% cross-linked resin is used, the separation at room temperature is considerably better, with reasonable flow-rates. The resin with the lower cross-linking was also preferred for the separation of the lanthanides from sodium, ammonium and HEDTA, because it provides a much sharper and faster elution of lanthanum and the light lanthanides.

Because, as has been pointed out, the separation between samarium and yttrium or neodymium is rather critical, only small amounts (a few mg) of these elements can be separated with a reasonable safety margin. Lanthanum and cerium are much more strongly sorbed than neodymium, and the distribution coefficients (Table 1) suggest that probably more than 200 mg of these elements can be separated from samarium and the heavier lanthanides without problems. From samarium to dysprosium and holmium the distribution coefficients decrease only very slowly with increasing atomic number (Table 1) and the stability constants of the HEDTA complexes are practically the same.⁷ Thus dysprosium (Fig. 2) and holmium are eluted only slightly ahead of samarium, and the amounts which can be separated from yttrium are probably only slightly

larger (about 20 mg) with a column of the same size. The stabilities of the thulium, ytterbium and lutetium complexes increase and the distribution coefficients decrease at a faster rate and larger amounts of these elements can be separated from yttrium.

REFERENCES

1. J. N. Story and J. S. Fritz, *Talanta*, 1974, **21**, 892.
2. S. Elchuk and R. M. Cassidy, *Anal. Chem.*, 1979, **51**, 1434.
3. J. R. Morton and D. B. James, *J. Inorg. Nucl. Chem.*, 1967, **29**, 2997.
4. J. E. Powell and H. R. Burkholder, *J. Chromatog.*, 1968, **36**, 99.
5. F. W. E. Strelow, *Anal. Chem.*, 1960, **32**, 1185.
6. *Idem, ibid.*, 1980, **52**, 2420.
7. E. J. Wheelwright and F. H. Spedding, *U.S. At. Energy Comm. Rept.*, ISC-637, June 1955.

EQUILIBRIA AND KINETICS OF THE EXTRACTION OF GALLIUM WITH 1-PHENYL-3-METHYL-4-BENZOYL-5-PYRAZOLONE

TSUGIKATSU ODASHIMA, ICHITARO ENDOH* and HAJIME ISHII†

Chemical Research Institute of Non-Aqueous Solutions, Tohoku University, Katahira, Aoba-ku, Sendai, 980 Japan

(Received 17 January 1990. Revised 1 May 1990. Accepted 9 May 1990)

Summary—The equilibria and kinetics of the solvent extraction of gallium(III) from aqueous monochloroacetic acid [HA] media with a benzene solution of 1-phenyl-3-methyl-4-benzoyl-5-pyrazolone [PMBP or HL] has been studied at $25 \pm 0.1^\circ$ and an ionic strength of 0.2. The species extracted was found to be GaL_3 . The value of the acid dissociation constant of PMBP determined spectrophotometrically was 1.17×10^{-4} . The values of the partition coefficient of PMBP and the extraction constant of its gallium complex between an aqueous and a benzene phase were found to be 3.72×10^3 and 2.51×10^4 , respectively. The rate of extraction was first-order with respect to the concentrations of gallium(III) in the aqueous phase and PMBP in the organic phase, inversely first- and second-order with respect to the hydrogen-ion concentration and zero- and first-order with respect to the concentration of monochloroacetate ions. Two mechanisms operate for this extraction, depending on the pH of the aqueous phase, one where the formation of the first complex, GaL^{2+} , between Ga^{3+} and L^- in the region of $\text{pH} < 1.6$ becomes the rate-determining step, and the other where the formation of the first complex between GaA^{2+} and L^- in the region of $\text{pH} 2.0\text{--}2.3$ is the rate-determining step. The rate constant for the first of these reactions was calculated to be $1.62 \times 10^4 \text{ l. mole}^{-1} \text{ sec}^{-1}$, but that for the second could not be determined.

Because 1-phenyl-3-methyl-4-benzoyl-5-pyrazolone [PMBP or HL] is easily prepared by benzoylation of 1-phenyl-3-methyl-5-pyrazolone, is chemically stable and has the ability to extract many "hard" metal ions at relatively low pH, it has been used as a powerful and useful extractant for alkali metals,^{1,2} transition metals,³⁻⁵ lanthanides^{6,7} and actinides,⁸⁻¹⁰ and their extraction equilibria have also been studied.

There is little information, however, on its use for extraction of gallium(III). Gallium is an element of fairly low crustal abundance, and is usually obtained as a by-product in the zinc and aluminium industries. The increasing use of gallium compounds in the electronics industry requires effective separation and/or concentration of gallium.

In the present work the equilibria and kinetics of the extraction of gallium(III) with PMBP have been investigated in detail.

EXPERIMENTAL

Reagents

All reagents were analytical-reagent grade unless stated otherwise. All aqueous solutions were prepared with distilled demineralized water.

PMBP solutions. Prepared by dissolving PMBP (synthesized according to the method of Jensen¹¹) in benzene or 1,4-dioxane.

Standard gallium(III) solution, $5.0 \times 10^{-2} \text{M}$. Prepared by dissolving the required weight of metallic gallium (99.999% pure), with heating, in a sufficient volume of nitric acid (1 + 1) to give an acidity of 0.05M in the final solution. Working solutions were prepared by diluting this solution with water.

Buffer solutions. The following buffers were used, adjusted to the pH required: 0.2M monochloroacetic acid–0.2M sodium monochloroacetate (pH 1.8–3.5), 0.2M acetic acid–0.2M sodium acetate (pH 3.5–6.2) and 0.067M potassium dihydrogen phosphate–0.067M disodium hydrogen phosphate (pH 6.2–8.0).

Apparatus

A Hitachi model 139 spectrophotometer and model 340 automatic recording spectrophoto-

*Present address: Furukawa Technical High School, Kitamachi, Furukawa, Miyagi, 989-61 Japan.

†Author for correspondence.

meter with 10-mm fused-silica cells, a Toa HM-20B pH-meter, an Iwaki KM shaker and a Lauda K-4R thermoelectric water-circulating bath were used. All extractions were performed by shaking the samples in 50-ml separating funnels jacketed to keep the system at constant temperature ($25 \pm 0.1^\circ$) by water circulated from the thermostatic bath.

Procedures

Acid dissociation constant. The acid dissociation constant of PMBP was determined spectrophotometrically¹² in aqueous dioxane solutions of various concentrations (8–40% v/v) at $25 \pm 0.1^\circ$ and an ionic strength of 0.2 (adjusted with sodium perchlorate). Values of pH measured in aqueous dioxane solutions were not corrected, because the logarithmic values of U_H were very small (-0.03 at a dioxane concentration of 40% v/v), where U_H is the conversion factor in the equation proposed by van Uitert and Haas.¹³

Partition of PMBP. A 10-ml portion of an aqueous solution containing acetate or phosphate buffer and sodium perchlorate to keep the ionic strength at 0.2 was placed in a 50-ml separating funnel along with 10 ml of $1.0 \times 10^{-2}M$ PMBP solution in benzene. The funnel was shaken for 30 min and allowed to stand for 15 min for phase separation. A 5-ml portion of the aqueous phase was transferred into a 25-ml standard flask, to which were added 5 ml of 1M sodium hydroxide to convert all the PMBP into its anionic form, L^- , and water to dilute to the mark. The absorbance of this solution was measured at 320 nm against water, the concentration of PMBP being obtained from a calibration graph of L^- prepared by measurement of the absorbances of standard PMBP solutions in 0.2M sodium hydroxide. The equilibrium concentration of PMBP in the organic phase was calculated by difference.

Distribution of gallium. The distribution of gallium between benzene and an aqueous phase was determined as a function of the hydrogen-ion concentration.

A 10-ml portion of an aqueous solution containing 73.9 μg of gallium(III), monochloroacetate buffer and nitric acid to adjust the pH to the required value, and sodium nitrate to keep the ionic strength at 0.2, was placed in a 50-ml separating funnel along with 10 ml of $2.0 \times 10^{-3}M$ PMBP solution in benzene. The funnel was shaken for 80 hr. After phase separation, the equilibrium concentration of gallium

in the aqueous phase was determined spectrophotometrically with Rhodamine B.¹⁴ The equilibrium concentration of gallium in the organic phase was calculated by difference.

Determination of kinetics. The kinetic runs were performed under pseudo first-order conditions, *i.e.*, with a large excess of PMBP.

A 10-ml portion of an aqueous solution containing 73.9 μg of gallium(III) and monochloroacetate buffer and nitric acid to adjust the pH to the required value, and sodium nitrate to keep the ionic strength at 0.2, was placed in a 50-ml separating funnel. After thermal equilibration (for *ca.* 30 min), an equal volume of a benzene solution of PMBP was carefully added. The reaction was begun by shaking. The experiments were performed in the "plateau" region where a further increase in shaking speed had no effect on the rate of extraction. After being shaken for a predetermined time (from 5 to 25 min), the funnel was allowed to stand for 15 min to ensure complete phase separation. The concentration of gallium in the aqueous phase was determined spectrophotometrically with Rhodamine B.¹⁴ The gallium concentration in the organic phase was calculated by difference.

RESULTS AND DISCUSSION

Extraction behaviour

A preliminary experiment suggested that gallium(III) is extracted with PMBP as a 1:3 complex, GaL_3 , from weakly acidic solutions into benzene. A lengthy shaking time was necessary to attain extraction equilibrium, but in the presence of monochloroacetate ions the rate of extraction was almost doubled. The influence of chloride, perchlorate and nitrate ions on the extraction was small, so monochloroacetate buffer and nitric acid were used for pH adjustment, and sodium nitrate was used for keeping the ionic strength constant in the studies on the extraction equilibria and kinetics of gallium(III).

Shaking speed. Figure 1 shows that shaking at more than 317 strokes/min has no effect on the rate of the extraction. A shaking speed of 332 strokes/min (maximum shaking speed of the shaker used) was used for all subsequent experiments.

Shaking time. Figure 2 shows that the rate of extraction is affected by the pH. Even in the presence of monochloroacetate ions shaking for more than 75 hr is necessary to attain extraction equilibrium when the pH is low. Shaking for 80 hr was used in the equilibrium study.

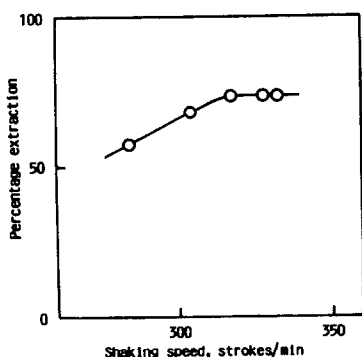


Fig. 1. Influence of shaking speed on the extraction of gallium(III) with PMBP. Ga(III), $1.1 \times 10^{-4} M$; PMBP, $1.0 \times 10^{-2} M$; $V_{aq} = V_{org} = 10$ ml; shaking time, 15 min.

Extraction equilibria

Acid dissociation constant and partition coefficient of PMBP. Although the acid dissociation constant, $K_{a,HL}$, and the partition coefficient, K_D , of PMBP have already been reported,^{15,16} we determined these values for confirmation.

The acid dissociation constant in purely aqueous medium was estimated by extrapolating the plot of apparent $pK_{a,HL}$ values obtained in aqueous 8–40% v/v dioxane solutions *vs.* the dioxane concentration. The value of $pK_{a,HL}$ thus obtained was 3.93, which is nearly the same as the value of 3.94 determined by Sasaki and Koizumi⁵ and close to that of 3.80 in 10% v/v aqueous dioxane determined by Akama *et al.*¹⁶

The distribution ratio, D_L , of PMBP between an aqueous and a benzene phase can be expressed by equation (1) in terms of the acid dissociation constant and partition coefficient:

$$\log D_L = \log K_D + pK_{a,HL} - pH \quad (1)$$

Hence a plot of $\log D_L$ *vs.* pH should give a straight line with a slope of -1 , and the value

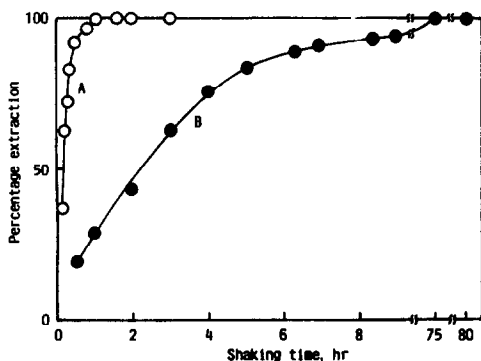


Fig. 2. Influence of shaking time on the extraction of gallium(III) with PMBP. pH—A, 2.1; B, 1.2. Other conditions as for Fig. 1.

of K_D can be calculated from the intercept of this line. Such a relation was experimentally obtained and gave $\log K_D = 3.57$, close to the value (3.67) reported by Sasaki and Koizumi.¹⁵

Distribution of gallium. The overall reaction in the extraction of gallium(III) with PMBP into benzene may be expressed as



where the subscript *org* denotes the organic phase. The extraction constant, K_{ex} , is defined as

$$K_{ex} = \frac{[GaL_{n,org}^{3-n}][H^+]^n}{[Ga^{3+}][HL]_{org}^n} \quad (3)$$

Taking into consideration the complexation of gallium(III) with monochloroacetate ions and assuming that (a) gallium(III) is not appreciably hydrolysed, (b) the formation of intermediate complexes between gallium(III) and PMBP in the aqueous phase is negligible, (c) only one complex, GaL_n^{3-n} , is extracted into benzene and (d) the volume of the organic phase is equal to that of the aqueous phase, the extraction constant, K'_{ex} , called here the apparent extraction constant, is expressed by equation (4), which can be rewritten as equation (5) by using the distribution ratio, D_{Ga} , of gallium(III)

$$K'_{ex} = \frac{[GaL_{n,org}^{3-n}][H^+]^n}{[Ga(III)]_T[HL]_{org}^n} = \alpha K_{ex} \quad (4)$$

$$\log D_{Ga} = \log K'_{ex} + n \log [HL]_{org} + n pH \quad (5)$$

where $[Ga(III)]_T$ denotes the total concentration of gallium(III) not combined with PMBP and α is the mole fraction of gallium(III) ion defined by equation (6) with use of the consecutive formation constants, K_1, K_2, \dots , of the gallium(III)–monochloroacetate complexes:

$$\alpha = \frac{[Ga^{3+}]}{[Ga(III)]_T} = \frac{1}{1 + K_1[A^-] + K_1K_2[A^-]^2 + \dots} \quad (6)$$

Equation (5) implies that the plot of $\log D_{Ga}$ *vs.* pH at constant PMBP concentration is a straight line with a slope of n , and that the value of K'_{ex} can be calculated from the intercept of this line. A linear relationship with a slope of about 3 was obtained experimentally, from which it can be concluded that only GaL_3 is extracted into benzene in this system. The value of $\log K'_{ex}$ was calculated to be 4.40. At pH < 1.6 the formation of gallium(III)–monochloroacetate complexes is negligible, and α can be taken as unity. Therefore, in equation (4) the

value of K_{ex} is practically equal to that of K'_{ex} , *i.e.*, 4.40.

Kinetics of gallium extraction

Rate equation. The rate of extraction of gallium(III) with PMBP into benzene in the presence of an auxiliary complexing agent, monochloroacetate, may be written as

$$\frac{d[\text{Ga(III)}]_T}{dt} = k' [\text{Ga(III)}]_T^a [\text{H}^+]^b [\text{HL}]_{\text{org}}^c [\text{HA}]_T^d \quad (7)$$

where t is the reaction time, k' is the rate constant, $[\text{Ga(III)}]_T$ denotes the total concentration of gallium(III) not combined with PMBP, $[\text{HA}]_T$ denotes the total concentration of the auxiliary complexing agent not combined with gallium(III) and a , b , c and d are the reaction orders with respect to the concentration of the relevant species. When the extractant and the auxiliary complexing agent are present in large excess over gallium(III) and the concentration of hydrogen ion is fixed, *i.e.*, pseudo first-order conditions are used, equation (7) can be written as

$$-\frac{d[\text{Ga(III)}]_T}{dt} = k_{\text{obsd}} [\text{Ga(III)}]_T \quad (8)$$

where k_{obsd} is the observed pseudo first-order rate constant. Integrating equation (8) yields

$$\ln \frac{[\text{Ga(III)}]_{T,t=0}}{[\text{Ga(III)}]_{T,t=t}} = k_{\text{obsd}} t \quad (9)$$

where $[\text{Ga(III)}]_{T,t=0}$ and $[\text{Ga(III)}]_{T,t=t}$ are the total concentrations of gallium(III) not combined with PMBP in the aqueous phase at $t = 0$ and t , respectively.

Reaction order with respect to gallium ion concentration. Equation (9) means that from a plot of $\ln([\text{Ga(III)}]_{T,t=0}/[\text{Ga(III)}]_{T,t=t})$ *vs.* t , we can confirm whether the rate of the extraction is first-order with respect to the concentration of gallium(III) not combined with PMBP. In fact, such plots were all linear and passed through the origin at each pH value from 1.87 to 2.30, as shown in Fig. 3, which indicates that the rate of the extraction is first-order with respect to the concentration of gallium(III) not combined with PMBP, *i.e.*, $a = 1$ in equation (7).

Reaction orders with respect to concentrations of hydrogen ion, extractant and auxiliary complexing agent. From equations (7) and (8), equation (10) can be derived, and rewritten as equation (11).

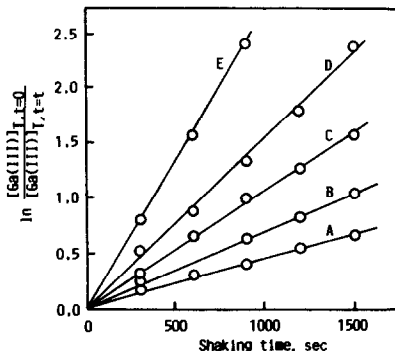


Fig. 3. Plots of $\ln([\text{Ga(III)}]_{T,t=0}/[\text{Ga(III)}]_{T,t=t})$ *vs.* t . Ga(III) , $1.1 \times 10^{-4} M$; PMBP, $1.0 \times 10^{-2} M$; monochloroacetate, $4.0 \times 10^{-2} M$; $V_{\text{aq}} = V_{\text{org}} = 10$ ml; temperature, $25 \pm 0.1^\circ$; ionic strength, 0.2; pH—A, 1.87; B, 2.00; C, 2.08; D, 2.17; E, 2.30. The solid lines were obtained by least-squares treatment of the data.

$$k_{\text{obsd}} = k' [\text{H}^+]^b [\text{HL}]_{\text{org}}^c [\text{HA}]_T^d \quad (10)$$

$$\log k_{\text{obsd}} = \log k' - b \text{pH} + c \log[\text{HL}]_{\text{org}} + d \log[\text{HA}]_T \quad (11)$$

Equation (11) implies the following: (i) when $[\text{HL}]_{\text{org}}$ and $[\text{HA}]_T$ are kept constant, the plot of $\log k_{\text{obsd}}$ *vs.* pH gives a straight line with a slope of $-b$; (ii) when the pH and $[\text{HA}]_T$ are kept constant, the plot of $\log k_{\text{obsd}}$ *vs.* $\log[\text{HL}]_{\text{org}}$ gives a straight line with a slope of c ; (iii) when the pH and $[\text{HL}]_{\text{org}}$ are kept constant, the plot of $\log k_{\text{obsd}}$ *vs.* $\log[\text{HA}]_T$ gives a straight line with a slope of d .

The plot for $\log k_{\text{obsd}}$ *vs.* pH (Fig. 4) has a slope of unity for pH < 1.8 but this increases with pH until it approaches 2 at pH 2.0–2.3, indicating that the reaction order with respect to the hydrogen-ion concentration depends on the pH and in particular is inversely first-order (*i.e.*,

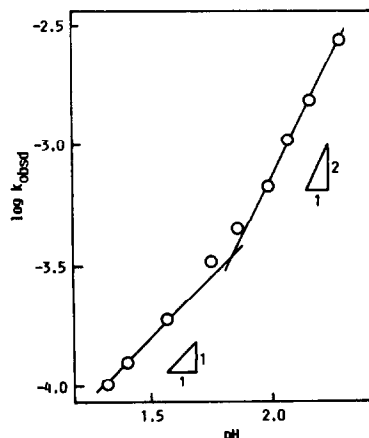


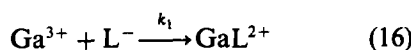
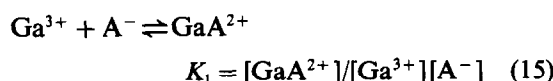
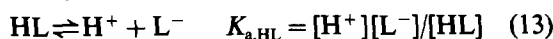
Fig. 4. Plot of $\log k_{\text{obsd}}$ *vs.* pH. Conditions are the same as for Fig. 3.

$b = -1$) in the lower pH region, but inversely second-order (*i.e.*, $b = -2$) in the higher pH region.

In the plot of $\log k_{\text{obsd}}$ vs. $\log[\text{HL}]_{\text{org}}$ the slope was unity at both pH 1.56 and 2.17, showing that the rate is first-order with respect to the extractant concentration, *i.e.*, $c = 1$.

The slope of the $\log k_{\text{obsd}}$ vs. $\log[\text{HA}]_{\text{T}}$ plot was zero at pH 1.33, and unity at pH 2.17, indicating that the rate is independent of the total concentration of the auxiliary complexing agent, *i.e.*, $d = 0$, in the region where the reaction order with respect to the hydrogen-ion concentration is -1 , but is first-order dependent on the monochloroacetate concentration, *i.e.*, $d = 1$, in the region where the reaction order with respect to the hydrogen-ion concentration is -2 .

Rate-determining steps. The major species of gallium(III), the extractant and the auxiliary complexing agent in the aqueous phase under the conditions studied are considered to be Ga^{3+} , GaA^{2+} , HL, L^- , HA and A^- . Taking into consideration the kinetic results described above, however, equations (12)–(17) are involved in the equilibria and reactions in the formation of a GaL^{2+} complex:



where $K_{\text{a,HA}}$ is the acid dissociation constant of monochloroacetic acid and k_1 and k_2 represent the rate constants of the two reaction steps.

Monochloroacetic acid is more than 80% undissociated in the pH region investigated. If it is assumed that the rate-determining step of the extraction system is formation of the GaL^{2+} complex in the aqueous phase [expressed by equation (16) for extraction in the lower pH region and equation (17) for that in the higher pH region), the following equations can be derived as the rate equations:

(i) for $\text{pH} < 1.6$

$$\begin{aligned} -\frac{d[\text{Ga(III)}]_{\text{T}}}{dt} &= k_1[\text{Ga}^{3+}][\text{L}^-] \\ &= k_1 \frac{K_{\text{a,HL}} \alpha [\text{Ga(III)}]_{\text{T}} [\text{HL}]_{\text{org}}}{K_{\text{D}} [\text{H}^+]} \quad (18) \end{aligned}$$

(ii) for $2.0 < \text{pH} < 2.3$

$$\begin{aligned} -\frac{d[\text{Ga(III)}]_{\text{T}}}{dt} &= k_2[\text{GaA}^{2+}][\text{L}^-] \\ &= k_2 \frac{K_1 K_{\text{a,HL}} K_{\text{a,HA}} \alpha [\text{Ga(III)}]_{\text{T}} [\text{HL}]_{\text{org}} [\text{HA}]_{\text{T}}}{K_{\text{D}} [\text{H}^+]^2} \quad (19) \end{aligned}$$

Equations (18) and (19) are consistent with the kinetic experimental results described above in that the rate of the extraction is always first-order with respect to PMBP, inversely first- and second-order with respect to hydrogen ion and zero- and first-order with respect to monochloroacetate.

Hence it can be concluded that there are two mechanisms for the extraction of gallium(III) with PMBP in the presence of monochloroacetic acid, one at $\text{pH} < 1.6$, where formation of GaL^{2+} is the rate-determining step, and the other at $\text{pH} 2.0$ – 2.3 , where the complexation between GaA^{2+} and L^- is the rate-determining step. The first mechanism is first-order dependent on the PMBP concentration and inversely first-order dependent on the hydrogen-ion concentration, and the second is first-order dependent on the concentrations of PMBP and monochloroacetate not combined with gallium(III), and inversely second-order dependent on the hydrogen-ion concentration.

Rate constants. Since the rate constant k_2 cannot be determined because the formation constant, K_1 , of the GaA^{2+} complex is unknown, only the rate constant k_1 was determined.

Since the value of α is regarded as nearly equal to 1 at $\text{pH} < 1.6$, as stated already, equation (20) can be derived from equations (8) and (18):

$$\log k_{\text{obsd}} = \log \frac{k_1 K_{\text{a,HL}}}{K_{\text{D}}} + \text{pH} + \log [\text{HL}]_{\text{org}} \quad (20)$$

which means that the value of k_1 can be calculated from the intercepts of the plots of $\log k_{\text{obsd}}$ vs. pH and $\log k_{\text{obsd}}$ vs. $\log[\text{HL}]_{\text{org}}$. The average of the logarithmic values of k_1 thus obtained gave $k = 1.6 \times 10^4 \text{ l. mole}^{-1} \cdot \text{sec}^{-1}$.

REFERENCES

1. M. Sugiyama, O. Fujino and M. Matsui, *Bunseki Kagaku*, 1984, **33**, 123.
2. S. Umetani, S. Kihara and M. Matsui, *Chem. Lett.*, 1986, 1545.
3. M. K. Chmutova, N. E. Kochetkova and Yu. A. Zlotov, *J. Anal. Chem. USSR*, 1969, **24**, 555.
4. Yu. A. Zolotov and N. T. Sizonenko, *ibid.*, 1970, **25**, 40.
5. Yu. A. Zolotov and L. G. Gavrilova, *J. Inorg. Nucl. Chem.*, 1969, **31**, 3613.

6. A. Roy and K. Nag, *ibid.*, 1978, **40**, 331.
7. E. C. Okafar, *ibid.*, 1980, **42**, 1155.
8. F. T. Coronel, St. Mareva and N. Yordanov, *Talanta*, 1982, **29**, 119.
9. Y. F. Yu and J. J. Tang, *Radiochem. Radioanal. Lett.* 1982, **51**, 103.
10. G. N. Rao and H. C. Arora, *J. Inorg. Nucl. Chem.*, 1977, **39**, 2057.
11. B. S. Jensen, *Acta Chem. Scand.*, 1959, **13**, 1668.
12. G. P. Hildebrand and C. N. Reilly, *Anal. Chem.*, 1957, **29**, 258.
13. L. G. Van Uitert and C. G. Haas, *J. Am. Chem. Soc.*, 1953, **75**, 451.
14. H. Onishi, *Photometric Determination of Traces of Metals*, 4th Ed., Part IIA, p. 578. Wiley, New York, 1986.
15. Y. Sasaki and S. Koizumi, *Abstracts of papers presented at the 34th Annual Meeting of Japan Society for Analytical Chemistry*, Kobe, Japan, 1985, p. 709.
16. Y. Akama, H. Yokota, K. Sato and T. Nakai, *Talanta*, 1986, **33**, 288.

COMPARISON OF SEGMENTORS FOR LIQUID-LIQUID EXTRACTION FLOW-INJECTION ANALYSIS

V. KUBÁŇ,* L.-G. DANIELSSON and F. INGMAN

The Royal Institute of Technology, Department of Analytical Chemistry, S-100 44 Stockholm, Sweden

(Received 10 December 1989. Revised 15 March 1990. Accepted 28 April 1990)

Summary—The segmentation of two immiscible solvents in a continuous liquid-liquid extraction flow system has been studied with a computer-controlled photometric detection system (resolution time ~ 3 msec). The T-shaped segmentors tested were made of fluoroplastic, glass (A4-T fitting) and a modified glass (A8-T fitting). The modified A8-T fitting gave the most repeatable segmentation (rsd $\sim 2\%$).

Liquid-liquid extraction is frequently used as a separation/preconcentration method in flow-injection analysis (FIA).¹⁻⁵ For systems utilizing liquid-liquid extraction FIA, segmentation is of crucial importance. Poor segmentation can adversely affect the sample dispersion, the extraction rate and the phase separation.^{6,7} Poor repeatability of the segmentation can have a detrimental effect on the precision of the signal and may frequently complicate signal processing. Only a small variation in segment length is possible with the currently available segmentors and the repeatability of segmentation is unsatisfactory. Further, the applicability of the segmentors at the high flow-rates and phase flow-rate ratios often sought in connection with preconcentration is limited. In some experiments (especially when it is preferable not to use a phase separator) very precise and repeatable segments are needed. Such segmentation can be accomplished with a pneumatically or electrically actuated loop injector. Very precise and repeatable volumes of one phase can then be introduced into a continuous flow of the other phase.⁸

Several types of segmentor have been described in the literature. Classical T-piece segmentors are made of glass,^{9,10} fluoroplastics^{11,12} or combinations of hydrophobic and hydrophilic materials. Improved glass A8-T and A10-T fittings,^{9,13,14} and fluoroplastic T-pieces with Teflon tubing inserts^{7,11} or enlarged outflow-channel bore^{6,15} are most widely used. Different configurations of Y^{16,17} and W pieces,^{7,18-20} made of glass or fluoroplastic,

and four-way fittings²¹ have also been recommended. Recently a coaxial (falling drop) segmentor has been introduced²² to overcome some of the disadvantages of other types of segmentor. The geometry of the inner capillary system of the T-shape segmentors^{9,23} and the geometry of the confluence chamber of the coaxial segmentors²⁴ have been carefully investigated. Coaxial segmentors seem to offer a more practical and convenient solution to the segmentation problem, as the segmentation repeatability is comparable to that obtained with the loop injector over a wide range of solvent flow-rates.²⁴ Their use does not introduce any additional moving parts into the liquid-liquid extraction FIA system.

In spite of the importance of the segmentation process in liquid-liquid extraction FIA few detailed studies of the factors that govern the segment size and the segmentation reproducibility have been made. Only limited conclusions can be drawn about the advantages and disadvantages of different types of segmentors.²⁴⁻²⁶ Thus there is a need to classify the existing types of segmentors, compare their characteristics and set guidelines for the design of more efficient segmentors.

EXPERIMENTAL

Apparatus

The system used for generating a segmented flow and the measurement procedure for the determination of segment lengths were the same as those described previously.²⁵ A schematic picture of the manifold is shown in Fig. 1. A significant advantage of this system compared to other methods used for the study of segmentation is that the segments are measured in the

*On leave from the Department of Analytical Chemistry, J. E. Purkyně University, Kotlářská 2, CS-61137 Brno, Czechoslovakia.

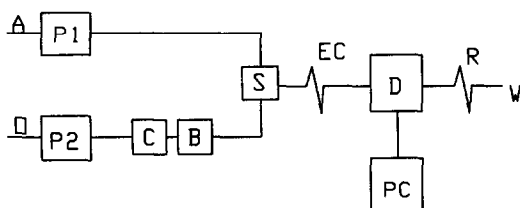


Fig. 1. Liquid-liquid extraction FIA system manifold. P1, P2—either HPLC pumps with pulse dampers and pressure indicators or peristaltic pumps, C—restrictor column, B—displacement bottle, S—segmentor, EC—Teflon equilibrating coil, D—fast reading detector, PC—personal computer, R—restrictor coil, W—waste.

flowing stream and not when the flow has been halted.

A number of different segmentors were tested. Classical T-piece segmentors made of PVDF (polyvinylidene difluoride) with different combinations of the inner diameters of the inlet and outlet channels (0.7/0.7, 0.7/1.2 and 0.7/2.0 mm) as well as a glass A4-T piece (2.0 mm i.d.) with inserts of Teflon or FEP tubing in the inlet and outlet channels were tested. Furthermore, a glass A8-T connector (Technicon) with a platinum inlet capillary and two coaxial inserts of FEP and Teflon tubes (0.7/1.1 and 1.2/2 mm i.d./o.d.) in the outflow channel was also tested. Schematic views of the different segmentors in their normal operating positions are shown in Fig. 2.

Reagents

Chloroform (Merck, analytical grade) saturated with water was used. All solutions were degassed in a Branson 2200 ultrasonic bath before use.

RESULTS AND DISCUSSION

PVDF T-segmentors

The common T-segmentors made of PVDF, oriented so that the aqueous phase flows

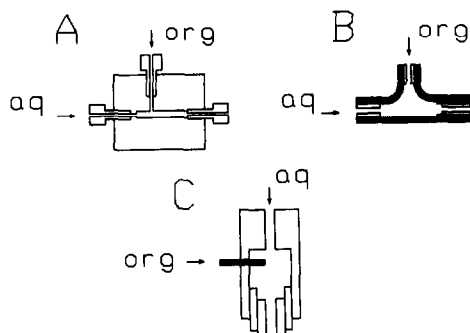


Fig. 2. Different segmentor types tested. A—PVDF T-piece, B—glass A4-T, C—glass A8-T. See text for details.

horizontally through the long axis, generally give the shortest segments and the least repeatable segmentation, compared to the other segmentors (Fig. 3a). This is due to the formation of segments in the extraction coil ("ripple" segmentation mode) and the low precision associated with measurement of short segment lengths. High relative standard deviations (rsd ~ 10%) of the mean segment lengths were obtained for total flow-rates Q_t , ranging from 0.2 to 5 ml/min, with a minimum at $Q_t = 0.5$ –3 ml/min and a flow-rate ratio close to unity. The repeatability decreased rapidly at very low and very high flow-rates (rsd > 20%).

The relative segment length of the organic phase decreased with increasing aqueous phase flow-rate $Q_a = 0.5$ –5 ml/min at a constant organic phase flow-rate for all inner diameters of the outlet tubes. The segment length increases (2, 3 and 5 mm) with increasing outflow channel bore (0.7, 1.2 and 2.0 mm respectively) at low flow-rate of the aqueous phase, $Q_a = 1.5$ ml/min, and constant organic phase flow-rate $Q_o = 0.5$ ml/min.

Rotating the segmentor around the horizontal main axis led to increased segment length and poorer repeatability at low aqueous flow-rates for segmentors with enlarged outlet diameters. The largest effect was obtained when the organic phase was fed from below (180° rotation). Rotating the segmentor so that the aqueous phase flowed vertically gave much longer segments (+50%) for upward flow, whereas downward aqueous flow gave somewhat shorter segments than the horizontal flow orientation did.

The glass A4-T segmentor

The glass T-segmentor with Teflon and FEP tubing inserted into the outflow channel 5 and 15 mm from the T-joint, and oriented so that the aqueous phase flows horizontally along the main axis, gives repeatable segmentation (rsd ~ 5%) over a wide range of aqueous phase flow-rates, $Q_a = 0.2$ –3 ml/min, when the organic phase flow-rate is 0.5 ml/min. The segment length is reduced by up to 30% with increasing flow-rate of the aqueous phase, and reaches a limiting value at $Q_a > 4$ ml/min. The segment length increases with increasing organic phase flow-rate, $Q_o = 0.2$ –1.6 ml/min, at constant flow-rate of the aqueous phase, Q_a . Shorter segments are obtained at higher total flow-rates and constant flow-rate ratio.

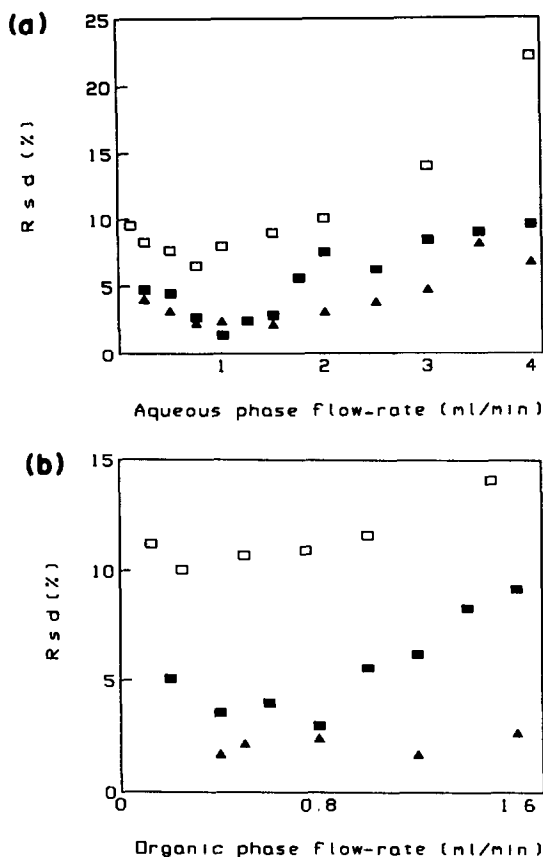


Fig. 3. Repeatability of the organic phase (chloroform) segment length (rsd in %) for different T-pieces. (a) At different aqueous phase flow-rates, $Q_o = 0.5$ ml/min. (b) At different organic phase flow-rates, $Q_a = 1.5$ ml/min. □ PVDF-T; ■ A4-T; ▲ A8-T.

A graph showing the variation in segmentation repeatability under different flow conditions is given in Fig. 3b. The best repeatability is achieved for $Q_a = 1-2$ and $Q_o = 0.25-1.2$ ml/min, respectively, and at a flow-rate ratio of $Q_a/Q_o = 0.7-4$. The segmentation repeatability decreases rapidly at higher flow-rates and flow-rate ratios because of the formation of small droplets at the end of the Teflon tubing insert. The segments are divided into several more or less separate droplets, and double or multiple peaks appear as a result.

The segment length is a linear function of the distance between the Teflon tubing and the confluence point of the T-piece, over the range 3–15 mm, at constant flow-rates of the two phases. In this way, the segment length can easily be varied in the range 3–45 mm. At short distances the segmentation repeatability is drastically reduced owing to a change from “drop” to “ripple” mode of segmentation.

A8-T glass modified fitting

The influence of different aqueous phase flow-rates on the segmentation was tested with a distance of 10 mm between the platinum and Teflon capillaries. This large separation was chosen to prevent any influence of the wetting properties of the Teflon capillaries on the segment formation. The A8-T fitting was oriented so that the aqueous flow was vertical along the main axis, with the platinum capillary protruding horizontally. With increasing aqueous phase flow-rate, Q_a , from 0.2 to 4 ml/min, at constant flow-rate of the organic phase, $Q_o = 0.8, 1.2$ and 1.6 ml/min, there is initially an exponential decrease in the length of the organic segments (Fig. 4). The segment length reaches some limiting value at high aqueous phase flow-rates, $Q_a > 3$ ml/min. This behaviour is especially pronounced for low organic phase flow-rates. The limiting segment length depends primarily on the position of the edge of the inserted Teflon tube and on the total flow-rate Q_t . This behaviour can be explained by the segmentation theory for such a segmentor.²⁴ A basic assumption is that the drop of organic phase forming at the end of the inlet capillary does not make contact with the walls of the confluence cavity. In that case it will be dislodged when the hydrodynamic force exerted on its cross-section by the aqueous flow is large enough to overcome the forces holding the drop on the inlet capillary. However, for non-coaxial segmentors a distortion of the shape of the droplets towards the outlet leads to a premature dislodging of droplets when the forming drop

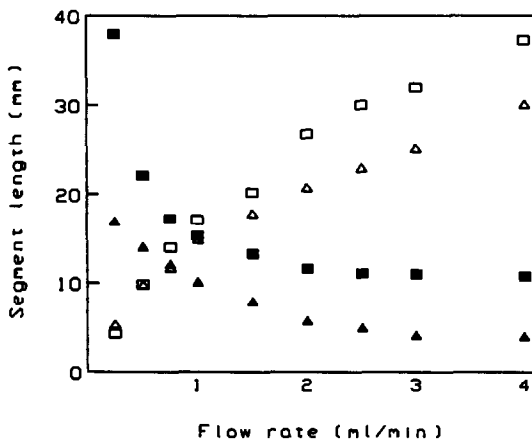


Fig. 4. Influence of the aqueous phase flow-rate (Q_a , ml/min) on the organic (chloroform) and aqueous phase segment lengths for the A8-T segmentor. $Q_o = 0.8$ ml/min, ▲ organic segment; △ aqueous segment. $Q_o = 1.6$ ml/min, ■ organic segment; □ aqueous segment.

makes contact with the hydrophobic insert in the outlet. The basic assumptions are more strictly fulfilled in the case of the glass compartment than in the case of the relatively hydrophobic compartment of the T-segmentor made from Teflon or PVDF.²⁴

The situation changes when a segmentor with a short separation distance (3 or 5 mm) between the capillaries is used. In this case the size of the droplets formed is limited by the volume of the confluence chamber. The segment length is much shorter and only weakly influenced by the flow-rate of the organic phase in the range $Q_o = 0.25\text{--}1.6$ ml/min at constant aqueous flow-rate, $Q_a = 2$ or 4 ml/min. The influence of the total flow-rate Q_t is practically negligible over the flow-rate range studied, $Q_t = 0.8\text{--}7.5$ ml/min, for both Teflon/Pt capillary distances and also for both flow-rate ratios $Q_a/Q_o = 1$ and 2. The segment length is only slightly increased at the lower Q_t values and is practically constant at the higher Q_t values.

The segmentation repeatability is satisfactory (rsd < 10%) over the relatively wide ranges $Q_a = 0.3\text{--}10$ ml/min and $Q_a/Q_o \sim 0.3\text{--}12.5$. The best repeatability (rsd $\sim 1\text{--}3\%$) is achieved in the flow-rate ratio range $Q_a/Q_o = 1\text{--}5$.

A small tilt of the main axis of the A8-T segmentor from its normal vertical orientation does not influence the segment length or the segmentation repeatability, especially not at high aqueous phase flow-rate, Q_a . Less repeatable segmentation with longer segments is obtained for larger tilts ($> 45^\circ$). As with the PVDF-T segmentor, a 180° rotation around the Pt-capillary, resulting in an upward aqueous flow, gives rise to longer segments.

CONCLUSIONS

Of the segmentors tested the PVDF-T gave the least repeatable segmentation. The two segmentors made of glass were similar in performance, with the A8-T superior at high flow-rates. Generally, the A8-T segmentor gives results similar to those for the coaxial segmentor recently presented.²⁴

The T-shape segmentors made of hydrophilic material operate by the wetting and skewing principle at low or moderate flow-rates. The length of the segments is governed by the orientation of the input and output channels and partly by the inner diameter of the output channel (at constant inner diameter of the input channels). When Teflon tube inserts are intro-

duced into all branches of the T-piece, the maximum droplet size is limited by the volume of the compartment formed between the joint and the edge of the Teflon tube in the outflow channel. The segment lengths depend on the total flow rate, Q_t , over a limited range, and decrease with increasing Q_t .

The T-shaped segmentors made of the fluoroplastics are in many cases able to produce small and reproducible segments, provided the geometry of the inner capillary system is optimal. The length of the segments is, however, large compared to the smallest segments obtainable with an A8-T segmentor. Increase in the inner diameter of the outflow channel results in longer segments, a prerequisite being that the organic phase can fill the whole diameter of the channel before the organic segment is dislodged by the aqueous flow. At high phase flow-rate ratios this is not the case and the segments are actually formed in the extraction coil by the "ripple" segmentation process. This type of segmentor works best at low flow-rates and at flow ratios Q_a/Q_o close to unity. At higher flow-rate ratios the repeatability is unsatisfactory. The major advantages of the Teflon T-piece segmentor are that it is inexpensive and readily available.

Although the modified A8-T segmentor functions very well, it cannot be used with standard tubing connectors of the low-pressure HPLC type, which is a drawback in routine work. Serious leakage often occurs at the high pressures needed for membrane-based phase separation.

Acknowledgements—Financial support from the Swedish National Board for Technical Development and the Swedish Institute is gratefully acknowledged.

REFERENCES

1. J. Růžička and E. H. Hansen, *Flow Injection Analysis*, 2nd Ed., pp. 186–196. Wiley, New York, 1988.
2. M. Valcárcel and M. D. Luque de Castro, *Flow Injection Analysis, Principles and Applications*, Ellis Horwood, Chichester, 1987.
3. *Idem*, *J. Chromatog.*, 1987, **393**, 3.
4. B. Karlberg, *Anal. Chim. Acta*, 1988, **214**, 29.
5. *Idem*, *Z. Anal. Chem.*, 1988, **329**, 660.
6. L. Nord, K. Bäckström, L.-G. Danielsson, F. Ingman and B. Karlberg, *Anal. Chim. Acta*, 1987, **194**, 221.
7. T. M. Rossi, D. C. Shelly and I. M. Warner, *Anal. Chem.*, 1982, **54**, 2056.
8. P. K. Dasgupta and W. Lei, *Anal. Chim. Acta*, 1989, **226**, 255.
9. J. Kawase, A. Nakae and M. Yamanaka, *Anal. Chem.*, 1979, **51**, 1640.
10. J. Kawase, *ibid.*, 1980, **52**, 2124.
11. C. A. Lucy and F. F. Cantwell, *ibid.*, 1986, **58**, 2727.

12. L. Nord and B. Karlberg, *Anal. Chim. Acta*, 1983, **145**, 151.
13. B. Karlberg and S. Thelander, *ibid.*, 1978, **98**, 1.
14. P. Martinez-Jimenez, M. Gallego and M. Valcárcel, *ibid.*, 1988, **215**, 233.
15. Y. Sahleström and B. Karlberg, *ibid.*, 1986, **185**, 259.
16. M. Bengtsson and G. Johnsson, *ibid.*, 1984, **158**, 147.
17. A. Farran and J. De Pablo, *ibid.*, 1988, **212**, 123.
18. K. Ogata, K. Taguchi and T. Imanari, *Anal. Chem.*, 1982, **54**, 2127.
19. T. Kato, *Anal. Chim. Acta*, 1985, **175**, 339.
20. V. Kubáň, J. Komárek and D. Čajková, *Collection Czech. Chem. Commun.*, 1989, **54**, 2683.
21. R. H. Atallah, G. D. Christian and S. D. Hartenstein, *Analyst*, 1988, **113**, 463.
22. K. Bäckström and L.-G. Danielsson, *Anal. Chim. Acta*, 1990, **232**, 301.
23. S. Motomizu and M. Oshima, *Analyst*, 1987, **112**, 295.
24. V. Kubáň, L.-G. Danielsson and F. Ingman, *Anal. Chem.*, 1990, **62**, 2026.
25. F. F. Cantwell and J. A. Sweileh, *ibid.*, 1985, **57**, 329.
26. S. Motomizu, M. Onoda and M. Oshima, *Analyst*, 1988, **113**, 743.

EXTRACTION OF GALLIUM(III) AND ALUMINIUM(III) WITH *O,O*-DIALKYLDITHIOPHOSPHORIC ACIDS

IMRE TÓTH* and ERNŐ BRÜCHER

Department of Inorganic and Analytical Chemistry, L. Kossuth University, H-4010 Debrecen, Hungary

ZOLTÁN SZABÓ

Alkaloida Pharmaceutical Works, H-4440 Tiszavasvári, Hungary

(Received 3 October 1989. Revised 18 January 1990. Accepted 25 June 1990)

Summary—The extraction of Ga^{3+} and Al^{3+} with the liquid cation-exchangers di-*n*-butyldithiophosphoric acid (DBTPA) and di-(2-ethylhexyl)dithiophosphoric acid (DETPA) in kerosene, in the presence and absence of alcohols and tri-*n*-butyl phosphate (TBP) has been studied. Both Ga^{3+} and Al^{3+} can be extracted in the form of a neutral complex, MA_3 , but the distribution coefficient of Ga^{3+} is the higher by about two orders of magnitude, which can be the basis of the solvent extraction separation of gallium and aluminium. The differences can be explained by the interaction between the sulphur donor atoms of the extractants and the d^{10} electronic shell of Ga^{3+} as well as by the lower steric hindrance of ligands co-ordinated to Ga^{3+} .

The separation of gallium from aluminium is of practical importance because gallium is often produced from the sodium aluminate liquor of the Bayer process. Laboratory-scale solvent extraction separations have been achieved by the use of Kelex-100 and *o*-dihydroxy derivatives of benzene or naphthalene.¹⁻³

It is known that Al^{3+} and Ga^{3+} are "hard" cations and tend to form complexes of higher stability with oxygen donor ligands than with those of sulphur.⁴ However, some experimental results indicate that Ga^{3+} ($[\text{Ar}]3d^{10}$) has a higher affinity for ligands of charged sulphur donors than does Al^{3+} ($[\text{Ne}]$ electronic structure).^{5,6}

Dialkyldithiophosphoric acids, which are used in various fields of industry (as lubricants, antioxidants, pesticides, *etc.*) have been applied as liquid cation-exchangers for the separation of a number of metal ions.^{7,8} The gallium(III) tris(dialkyldithiophosphate) complexes have also been prepared as solid crystalline compounds in anhydrous benzene.⁹

It has been reported that dibutyldithiophosphoric acid partly extracts Ga^{3+} but not Al^{3+} from acidic solutions, but the study did not investigate extractions from neutral and basic solutions. To obtain more information on the application of dialkyldithiophosphoric acids as non-expensive extractants we have studied

the solvent extraction of Ga^{3+} and Al^{3+} with dibutyldithiophosphoric acid (DBTPA) in a kerosene-*n*-butanol solvent mixture as well as di-(2-ethylhexyl)dithiophosphoric acid (DETPA) in the presence and absence of *n*-octanol or tri-*n*-butyl phosphate (TBP) in kerosene.

EXPERIMENTAL

Gallium nitrate and aluminium nitrate stock solutions were prepared by dissolving gallium (99.999%, Hungarian Aluminium Works, Ajka) and aluminium (*p.a.* Reanal) in dilute nitric acid. The concentrations of the solutions were determined by complexometry.

The dialkyldithiophosphoric acids were prepared and purified by Martin's procedure.¹⁰

The purity of the acids formed was determined by a two-phase acid-base titration and found to be 98.40% for DBTPA, and 90.0% for DETPA.

n-Butanol, *n*-octanol, 2-ethylhexanol, TBP and kerosene were of *puriss.* grade (Reanal), and no further purification was performed.

In the solvent extraction experiments equal volumes (10 ml) of the organic and aqueous phases were shaken together until equilibrium was reached (about 2 min). The initial concentrations of the extractants in the organic phase and of metal ions in the aqueous solution were 0.20 and 0.002*M*, respectively. The ionic strength in the aqueous solution was kept

*Author for correspondence.

constant (1.0M potassium chloride) which resulted in good phase separation.

The equilibrium concentrations of Al^{3+} and Ga^{3+} in the aqueous phase were determined by spectrophotometry (Beckman DB-GT spectrophotometer, 1-cm cells) with Eriochrome Cyanine¹¹ and Malachite Green,¹² respectively. Malachite Green forms a blue-green ion-association complex with GaCl_4^- in 6–6.5M hydrochloric acid, which can be extracted into benzene. The absorption of the organic phase was measured at 634 nm. The calibration curve is linear in the range 0.06–1.00 $\mu\text{g/ml}$ gallium in the benzene phase. The pH of the aqueous phase was measured with a Radelkis 208/1 pH-meter, with a Radiometer GK 2301 combined glass and calomel electrode.

The equilibrium concentration of DBTPA in the organic phase was determined by two-phase acid–base titration.

RESULTS AND DISCUSSION

Distribution ratios of the extractants

The solubility of DETPA in water must be very low, since its distribution ratio (D)¹³ between kerosene and water was found to be $10^{5.4}$.¹⁴ However, DBTPA, which has a lower molecular weight, is more soluble and its solubility was investigated as a function of the initial pH of the aqueous phase at different concen-

trations of n-butanol, with kerosene as diluent. The results (Fig. 1) show that the solubility of DBTPA is relatively low in the presence of 5% v/v n-butanol at $\text{pH} < 11$. In the extraction experiments with DBTPA a 5% v/v n-butanol solution in kerosene was used as the organic solvent.

Extraction of the gallium and aluminium complexes

The results of the solvent extraction experiments are shown in Figs. 2–4, where the logarithms of the distribution ratios ($\log D$) are plotted against the equilibrium pH of the aqueous phase. The extent of the extraction of Ga^{3+} and Al^{3+} significantly depends on the pH of the aqueous solution for both DBTPA and DETPA. The trend of the $\log D$ values can be explained by the competition of metal ions and protons for the extractant at lower pH and by the formation of metal hydroxo-complexes, which decreases the extent of extraction at higher pH values. In the pH interval from about 1.4 to 2.0 the $\log D$ –pH curves for extraction with both DBTPA and DETPA can be regarded as straight lines.

The slope, $n = 3$, can be interpreted as due to extraction of the neutral complexes $\text{Al}(\text{DBTPA})_3$, $\text{Ga}(\text{DBTPA})_3$, $\text{Al}(\text{DETPA})_3$ and $\text{Ga}(\text{DETPA})_3$. The neutral MA_3 complexes are formed in the organic phase according to the equation:

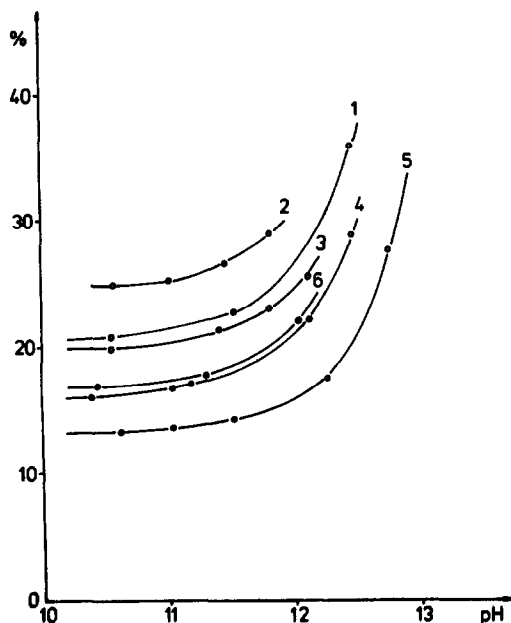


Fig. 1. Fraction of DBTPA in the aqueous phase, as a function of the initial pH in 1M KCl. Concentration of n-butanol (% v/v): (1), 0; (2), 50; (3), 32.5; (4), 10; (5), 5; (6), 2.

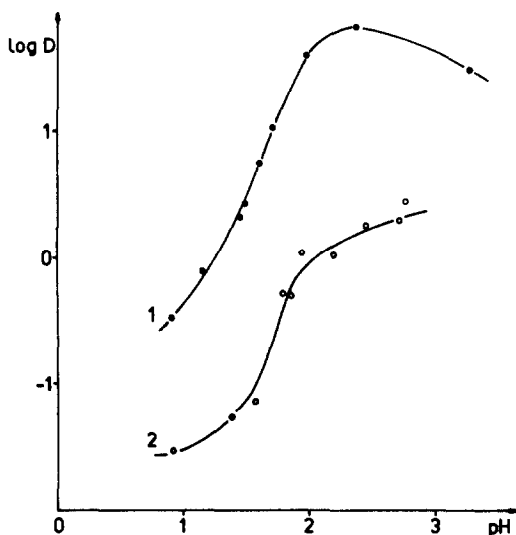


Fig. 2. Extraction of Ga^{3+} (1) and Al^{3+} (2) from 1M KCl with DBTPA in kerosene containing 5% v/v n-butanol.

Dialkyldithiophosphoric acids are present in the organic phase as monomers, HA_{org} , in contrast to the dialkylphosphoric acids, which significantly dimerize.⁸

If the solubility of the extractant in the aqueous solution is low and $[\text{HA}]_{\text{org}} \gg [\text{MA}]_{\text{org}}$, then the logarithm of the distribution ratio can be expressed as¹³

$$\log D = \log K + 3 \log[\text{HA}]_{\text{org}} + 3\text{pH} \quad (2)$$

where K is the extraction equilibrium constant. These conditions are fulfilled in our experiments and the observed slope, $n = 3$ in Figs. 2–4, can be interpreted by means of equation (2).

The presence of *n*-octanol has no effect on the distribution ratios, which are higher for Ga^{3+} than for Al^{3+} (Fig. 3). However, in the presence of TBP the distribution ratios for Ga^{3+} with DETPA are lowered (Fig. 4). The slope of the $\log D$ –pH curve also decreases (to about 2) in the presence of TBP, and the extracted species is

probably an ion-pair, $\text{Ga}(\text{DETPA})_2(\text{TBP})_x^+ \cdot \text{Cl}^-$. A molecule of TBP presumably displaces a DETPA[−] ion from the inner co-ordination sphere of Ga^{3+} and the species $\text{Ga}(\text{DETPA})_2(\text{TBP})_x^+$ [TBP can solvate the species $\text{Ga}(\text{DETPA})_2(\text{TBP})^+$] is not extractable. It can be dissolved in the organic phase as an ion-pair, with a chloride ion neutralizing its charge. The presence of the chloride ion in the organic phase has been detected by qualitative experiments with silver nitrate. The displacement of DETPA by TBP is possible, since even the bidentate co-ordination of dithiophosphate can be blocked by bulky nitrogen bases in complexes such as $\text{Zn}[\text{S}_2\text{P}(\text{OR})_2]_2$.¹⁵

The presence of TBP has practically no effect on the extraction of Al^{3+} (Fig. 4, 2a, 2b). The extraction of $\text{Al}(\text{DETPA})_3$ both into kerosene and mixed kerosene–TBP is proposed.

The pH dependence of the distribution ratios could not be investigated between pH about 4 and 9, since in this range the aqueous phase was unbuffered (the use of a buffer was avoided as this could change the extraction equilibrium by complex formation with Ga^{3+} or Al^{3+}). The values of D for distribution of Ga^{3+} and Al^{3+}

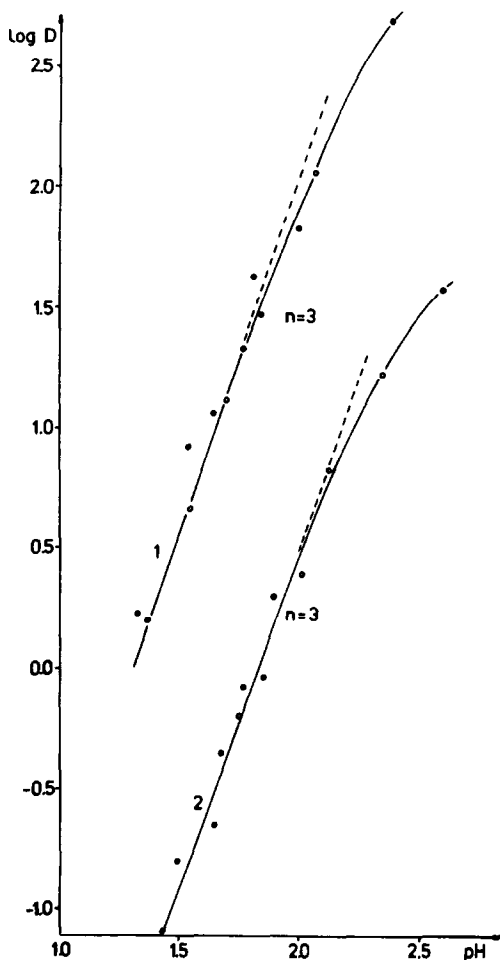


Fig. 3. Extraction of Ga^{3+} (1) and Al^{3+} (2) from 1M KCl by DETPA in kerosene (—●—) and in kerosene containing 2M *n*-octanol (—○—).

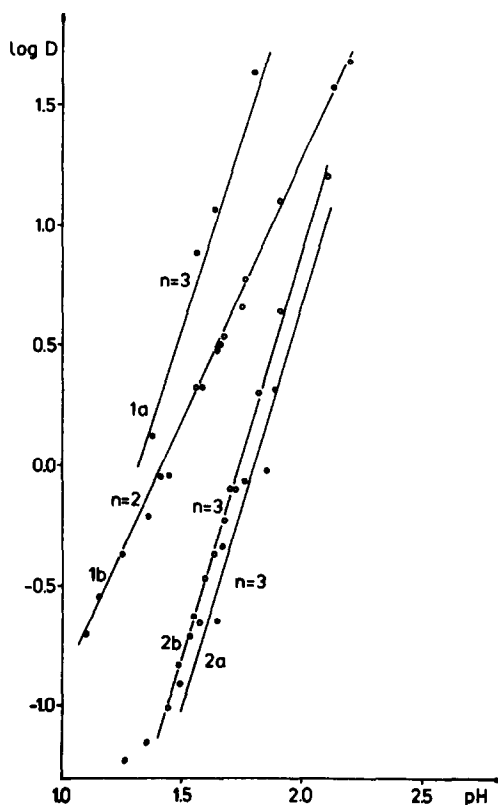


Fig. 4. Extraction of Ga^{3+} (1) and Al^{3+} (2) from 1M KCl by DETPA in kerosene (a; —●—) and in kerosene containing 2M TBP (b; —○—).

between 1M potassium chloride and DETPA in neat kerosene were estimated to be 10^3 and 10^2 , respectively, in the given pH range. At pH values >10.5 there is practically no extraction, probably because of formation of the stable $\text{Al}(\text{OH})_4^-$ and $\text{Ga}(\text{OH})_4^-$ complexes.¹⁶

The chemical bonding and structure of the neutral complex MA_3 have been investigated for some metal ions. Ahmed *et al.* suggested an octahedral geometry and bidentate co-ordination of the ligand in $\text{Ga}[\text{S}_2\text{P}(\text{OR})_2]_3$.⁹ Coggon *et al.* reported the single-crystal structure of $\text{In}[\text{S}_2\text{P}(\text{OC}_2\text{H}_5)_2]_3$ which involves an octahedral co-ordination, with chelating behaviour of the ligand.¹⁷ The same structure is reported for $\text{Fe}[\text{S}_2\text{P}(\text{OPr}')_2]_3$.¹⁸

The structures of dithiophosphates and dithiocarbamates are compared and discussed by Drew *et al.*¹⁸ The M—S bonds are less covalent in dithiophosphates than in dithiocarbamates, because the electron density is diminished by back-donation from the sulphur atom to the $3d$ orbitals of the phosphorus atom. These results suggest that the interaction between the dialkyldithiophosphates and Ga^{3+} as well as Al^{3+} in the MA_3 complexes is predominantly electrostatic. The stability constants cannot be very high since hydroxide ions can very easily displace both DETPA and DBTPA from the complexes. The relatively high values of D can be rationalized as due to the high solubility of the neutral complexes in the organic phase rather than to high stability constants.

In spite of the predominantly electrostatic metal–ligand interaction, the distribution ratios obtained for Ga^{3+} (which is the larger in ionic size) are 1–2 orders of magnitude higher than those for Al^{3+} . The stability of the Ga^{3+} complexes can be higher than that of the Al^{3+} complexes owing to the stronger interaction of Ga^{3+} with the sulphur donor atoms, which is related to the presence of its d^{10} outer electron shell.

CONCLUSIONS

Dibutylidithiophosphoric and di-(2-ethylhexyl)dithiophosphoric acids dissolved in kerosene extract Ga^{3+} and Al^{3+} as non-charged complexes (MA_3) from slightly acidic solutions. At pH 10.5 the extent of extraction is negligible. The distribution ratios are approximately the

same for the extractions with DBTPA and DETPA, but the application of DETPA is more favourable since its solubility in the aqueous phase is lower. The phase separation is fast and complete in the presence of *n*-octanol or TBP, but TBP results in a decrease in the distribution ratios of Ga^{3+} . The D values for Ga^{3+} are higher than those for Al^{3+} by about a factor of 10–100 and thus the two species can be separated by repeated extraction and washing operations. With DETPA the most favourable pH is about 2.5. The chemical bonding between the dialkyldithiophosphate and Ga^{3+} or Al^{3+} is predominantly electrostatic. The higher D values obtained for the extraction of Ga^{3+} are probably due to interaction between the $3d^{10}$ electrons of Ga^{3+} and the empty $3d$ orbitals of the sulphur donor atoms. Another factor could be the smaller steric hindrance between the ligands when co-ordinated to Ga^{3+} , which is larger than Al^{3+} in ionic size.

REFERENCES

1. Yu. I. Tarnopols'kii, V. S. Kuznetsova, V. F. Borbat, *Russ. J. Inorg. Chem.*, 1978, **23**, 77.
2. J. Helgorsky and A. Leveque, *French Patent*, 1979, **2** 397.
3. H. Obi, T. Segava and T. Yotsuyanagi, *Chem. Lett.*, 1989, 547.
4. S. Ahrland, *Structure Bonding (Berlin)*, 1968, **5**, 118.
5. R. Sarin and K. N. Munshi, *J. Inorg. Nucl. Chem.*, 1973, **35**, 201.
6. I. Tóth, L. Zékány and E. Brücher, *Polyhedron*, 1984, **3**, 871.
7. T. H. Handley and J. A. Dean, *Anal. Chem.*, 1962, **34**, 1312.
8. S. Wingefors, *Acta Chem. Scand.*, 1980, **34**, 301, 313; 327.
9. R. Ahmed, G. Srivastava and R. C. Mehrotra, *Inorg. Chim. Acta*, 1985, **97**, 159.
10. T. W. Martin, *J. Am. Chem. Soc.*, 1945, **67**, 1662.
11. F. J. Welcher, *Organic Analytical Reagents*, Vol. 4., p. 355. Van Nostrand, Princeton, 1948.
12. I. Somosi and P. Palovits, private communication, Hungarian Aluminium Works, Ajka, Project Number 4/73-79.
13. T. Sekine and Y. Yasegawa, *Solvent Extraction Chemistry*, p. 100. Dekker, New York, 1977.
14. G. Cote and D. Bauer, *Anal. Chem.*, 1984, **56**, 2153.
15. M. G. B. Drew, M. Hasan, R. J. Hobson and D. A. Rice, *J. Chem. Soc. Dalton Trans.*, 1986, 1161.
16. C. F. Baes, Jr. and R. E. Mesmer, *The Hydrolysis of Cations*, pp. 112, 313. Wiley, New York, 1976.
17. P. Coggon, J. D. Lebedda, A. T. McPhail and R. A. Palmer, *Chem. Commun.*, 1970, 78.
18. M. G. B. Drew, W. A. Hopkins, P. C. H. Mitchell and T. Colclough, *J. Chem. Soc., Dalton Trans.*, 1986, 351.

SOLVENT EXTRACTION OF Fe(III) BY DEHYDRATED CASTOR OIL FATTY ACIDS

O. FATIBELLO-FILHO, M. A. C. BUMBA and J. C. TROFINO

Universidade Federal de São Carlos, Departamento de Química, C.P. 676, CEP 13560, São Carlos, Est.
São Paulo, Brazil

E. A. NEVES

Universidade de São Paulo, Instituto de Química, C.P. 20780, CEP 01498, São Paulo, Est. São Paulo,
Brazil

(Received 13 November 1989. Revised 25 February 1990. Accepted 16 March 1990)

Summary—The effect of temperature on the extraction of Fe(III) by dehydrated castor oil fatty acids (DCOFA) has been studied in the temperature range 283–313 K at 1.0M constant ionic strength (NaClO₄). The temperature dependence of the conditional constant of extraction is given in the form: $\ln K_{\text{ext}} = 31.95 - 12800(1/T)$. Also, it was found that the average thermodynamic parameters, $\Delta H_{\text{ext}}^{\circ}$, $\Delta G_{\text{ext}}^{\circ}$, and $\Delta S_{\text{ext}}^{\circ}$ are 106.5 kJ/mole, 27.3 kJ/mole, and 0.3 kJ.mole⁻¹.K⁻¹, respectively. The extracted species in toluene solution were identified as FeR₃.HR and Fe(OH)R₂, where HR represents the fatty acid used.

The extraction of Fe(III) with carboxylic acids is well documented. It can be extracted with naphthenic acids,^{1–4} Versatic 911 acid (a mixture of mainly monocarboxylic acids containing 9–11 carbon atoms),^{5–9} monocarboxylic acids with short^{10–16} and long chains,^{17–34} mixtures of unsaturated aliphatic monocarboxylic acids,²⁷ salicylic acid³⁵ and metal salts of many fatty acids.^{36–38}

A few studies have reported the equilibrium constants and species for solvent extraction of Fe(III) with carboxylic acids.^{5,9,17,19,31} Only one paper dealing with temperature effects has been published,³⁴ referring to saturated acids.

This paper presents results obtained for extraction with a mixture of the *cis,cis*- and *cis,trans*- isomers of 9,11- and 9,12-octadecadienoic acid. These double-bonded carboxylic acids are found in dehydrated castor oil fatty acids (DCOFA). Extraction studies were performed at controlled temperatures ($\pm 0.1^{\circ}$) and constant 1.0M ionic strength. Graphical methods^{4,7} led to identification of the species extracted into toluene. From the effect of temperature on the extraction, the thermodynamic parameters were evaluated.

EXPERIMENTAL

Reagents

The stock solution of Fe(III) was prepared by dissolving 9.804 g of Fe(NH₄)₂(SO₄)₂·6H₂O

(Mohr salt) in 100 ml of 4.0M perchloric/nitric acid mixture. The working solutions were prepared from stock solutions by dilution. The ionic strength of these solutions was adjusted to 1.0M with sodium perchlorate. All reagents were of analytical grade.

The DCFOA was obtained from Ceralit Indústria e Comércio S/A (Campinas, São Paulo, Brazil) and used without further purification. The average molecular weight of this commercial product was found to be 283.4 by alkalimetric titration, which is very close to the theoretical value 280.3. The iodine value (Wij's method) of 147.0 is consistent with the expected two double bonds. Solutions of the acid mixture were prepared in analytical grade toluene.

Extraction procedure

Both the equilibrium and temperature effect studies were performed as previously described.^{39,40} Equal volumes (15.0 ml) of the toluene solution of DCOFA and the aqueous working solution were introduced into a mixing vessel kept at constant temperature ($\pm 0.1^{\circ}$) by circulation of water from a thermostatic bath.

The concentration of Fe(III) in the aqueous phase after extraction was determined by atomic absorption spectrometry at 248.3 nm (Perkin–Elmer Model 305 instrument). The concentration of Fe(III) in the organic phase was

obtained by difference in order to calculate the distribution ratio, D .

The conditional pH of the working solutions, expressing hydrogen ion concentration instead of activity, was measured with a glass electrode previously standardized with 0.01000M perchloric acid in 0.99M sodium perchlorate, to which a conditional pH of 2.000 was assigned.

RESULTS AND DISCUSSION

For the treatment of the extraction equilibrium data the methodology reported earlier was used.⁴¹ The plots of $\log D$ vs. the conditional pH at different DCOFA concentrations (0.300, 0.600, 1.00 and 1.50M) for a 1.00mM Fe(III) solution of ionic strength 1.0M are linear, with slopes of 2.1, 2.3, 2.3 and 2.4, respectively (Fig. 1). This indicates that an average of 2.3 protons were released per metal ion extracted and an average of 2.3 DCOFA anions was needed to neutralize the charge on each metal ion. On the other hand, considering the average value of pH in the working range (pH = 1.5–3.5) and the instability constant⁴² of 1.52×10^{-12} for FeOH^{2+} , the calculated value of the concentration of this species was $6.7 \times 10^{-4}M$, which leads to the estimate that about 70% of the initial concentration of Fe(III) was hydrolysed. Hence it can be inferred that the fatty acid extracts about 70% of the Fe(III) as FeOH^{2+} and the rest as Fe^{3+} . The experimental value of 2.3 for the slope is in agreement with the calculated value of 2.32 based on the assumption of partial hydrolysis of the iron(III). Although other Fe(III) hydrolysis products exist in this pH range, and their relative concentrations would be pH-dependent, the

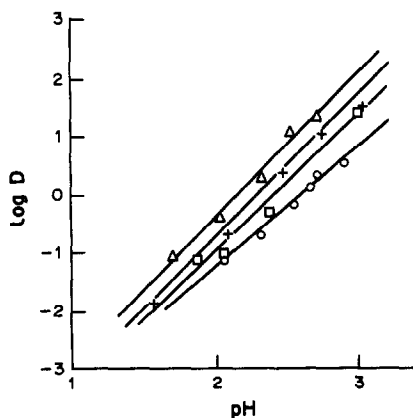


Fig. 1. Effect of pH on extraction of $10^{-3}M$ Fe(III) by DCOFA at different concentrations (\circ : 0.3; \square : 0.6; $+$: 1.0 and \triangle : 1.5M) at 25°.

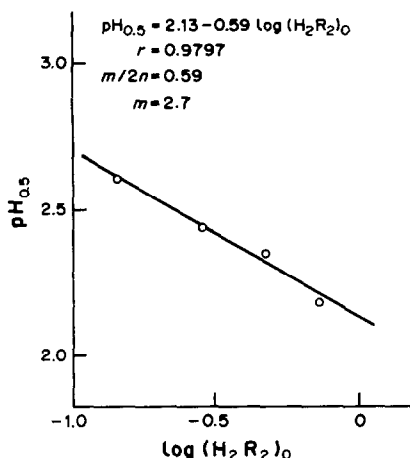


Fig. 2. Relation of $\text{pH}_{0.5}$ and DCOFA dimer concentration for the extraction of $10^{-3}M$ Fe(III) by DCOFA.

hydrolysis is slow and on the time-scale of the experiments is unlikely to proceed beyond FeOH^{2+} .

The $\text{pH}_{0.5}$ (pH at which there is 50% extraction) was determined from the plots of $\log D$ vs. pH. These $\text{pH}_{0.5}$ data, when plotted against $\log[(\text{DCOFA})_2]_0$, exhibited linear behavior with a slope of -0.59 (Fig. 2).

The number of fatty acid monomer molecules involved in the extraction, m , was calculated from the value of -0.59 for the slope, according to the relationship:

$$0.59 = m/2n$$

where n is the number of protons liberated.

The value of 2.7 calculated for m from this equation when $n = 2.3$, implies that each complex molecule extracted is solvated by an average of 0.4 molecule of DCOFA.

If $\log D$ is plotted vs. pH for different metal ion concentrations (1.00, 10.0, 20.0, 30.0 and 40.0mM), all the points lie more or less on the same straight line (Fig. 3), suggesting that the extracted complexes are monomeric.

From the experimental results calculated for n and m , the initial concentrations of Fe^{3+} and FeOH^{2+} and the solvation number ($m - n$), it is concluded that $\text{FeR}_3 \cdot \text{HR}$ and $\text{Fe}(\text{OH})\text{R}_2$ are the predominant species extracted into toluene. Karpacheva *et al.*³¹ investigated the extraction of Fe(III) with a mixture of saturated aliphatic monocarboxylic acids with 7–9 carbon atoms in kerosene and found the extraction equation:

$$\log D = 0.74 + 2.10 \text{ pH}$$

The value of 2.10 for n in this equation is in fair agreement with that reported here.

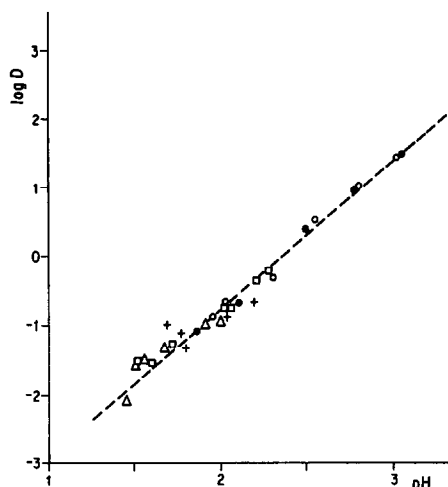


Fig. 3. Effect of pH on extraction of Fe(III) at different concentrations (●, 10^{-3} ; □, 10^{-2} ; △, 2×10^{-2} ; ○, 3×10^{-2} and +, $4 \times 10^{-2} M$) by 1.0M DCOFA.

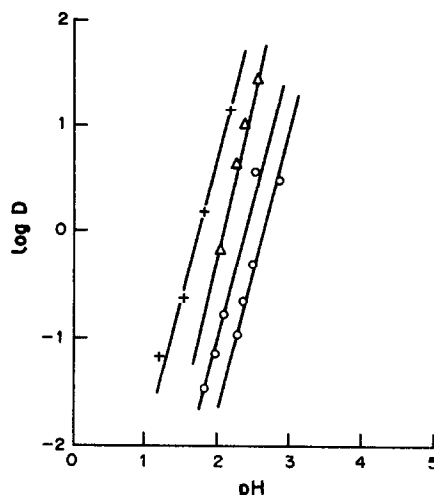


Fig. 4. Effect of temperature on extraction of $10^{-3} M$ Fe(III) by 1.0M DCOFA in the temperature range 283–313 K.

Karpacheva *et al.* proposed that $FeR_3 \cdot HR$ was the main species extracted. Lee and Kim⁵ and Fletcher *et al.*⁷ studied the extraction of Fe(III) by Versatic acid in benzene and found that FeR_3 was the compound extracted. The value of the conditional equilibrium constants obtained in our work (see Table 1) are larger than those obtained by Lee and Kim,⁵ under the same experimental conditions, which indicates that DCOFA has greater extraction power than Versatic acid.

The average thermodynamic parameters ΔH_{ext}° , ΔG_{ext}° and ΔS_{ext}° were determined in the same fashion as reported previously.³⁹

Figure 4 shows the variation of $\log D$ as a function of pH for the extraction of Fe(III) at 283, 298, 303 and 313 K. Values of K_{ext} at these temperatures (Table 1) were determined by using the equation

$$pH_{0.5} = (-1/n) \log K_{ext} - (m/2n) \log [H_2R_2]_0$$

Figure 5 shows the variation of $\ln K_{ext}$ with the inverse of the absolute temperature. The value of H_{ext}° calculated from the slope of this plot is 106.5 kJ/mole. The positive value of ΔH_{ext}°

shows that the extraction of Fe(III) by DCOFA is an endothermic process, indicating that an increase in temperature increases the degree of extraction. In contrast, when Abubakirov *et al.*³⁴ extracted Fe(III) from Al_2O_3 suspensions, a decrease in the extraction efficiency was observed when the temperature was increased from 13 to 60°. However, adsorption on the solid Al_2O_3 may be the cause of this effect.

The following equation was used to calculate K_{ext} within the temperature range studied:

$$\ln K_{ext} = 31.95 - 12800/T$$

The calculated value for K_{ext} at 298 K gives 27.3 kJ/mole for ΔG_{ext}° by use of the standard equation:

$$\Delta G_{ext}^\circ = -RT \ln K_{ext}$$

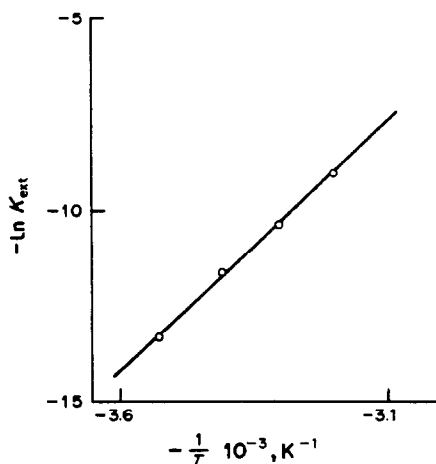


Fig. 5. Variation of $\ln K_{ext}$ with the inverse of absolute temperature.

Table 1. Conditional equilibrium constants for extraction of iron by DCOFA at several temperatures*

T, K	$1/T, 10^{-3} K^{-1}$	$10^6 \times K_{ext}$	$-\ln K_{ext}$
283	3.53	1.9 ± 0.1	13.2
293	3.41	10.2 ± 0.5	11.5
303	3.30	30.4 ± 1.5	10.4
313	3.19	122.6 ± 6.1	9.0

*The error is estimated to be $\pm 5\%$.

The entropy change involved in the extraction can be calculated from:

$$\Delta G_{\text{ext}}^{\circ} = \Delta H_{\text{ext}}^{\circ} - T\Delta S_{\text{ext}}^{\circ}$$

The positive value of $\Delta G_{\text{ext}}^{\circ}$ shows the non-spontaneity of the extraction reaction. However, the extraction is more efficient than that of Cu(II).³⁹ The large positive entropy change ($\Delta S_{\text{ext}}^{\circ} = 266 \text{ cal. mole}^{-1} \cdot \text{K}^{-1}$) is due mainly to the removal of water molecules from the iron(III) aquo-ion in formation of the complex extracted.

A comparison of the present results with those for extraction of uranyl and rare-earth cations will be reported subsequently.

Acknowledgements—The authors gratefully acknowledge the financial support of the CNPq and FAPESP agencies (Brazil).

REFERENCES

- R. A. Alekperov and N. Makov, *Radiokhimiya*, 1968, **10**, 241; *Chem. Abstr.*, 1968, **69**, 32312u.
- R. A. Alekperov, B. I. Kerimova and N. N. Makov, *Uch. Zap. Azerb. Gos. Univ.*, 1967, No. 1, 8; *Chem. Abstr.*, 1968, **69**, 70550c.
- R. A. Alekperov, N. G. Efendieva and S. S. Geibatova, *Azerb. Khim. Zh.*, 1968, No. 5, 96; *Chem. Abstr.*, 1969, **70**, 118643k.
- A. E. Grishchenko, A. M. Berestovoi and I. N. Piskunov, *Izv. Vyssh. Uchebn. Zaved. Tsvetn. Metall.*, 1983, No. 4, 31; *Chem. Abstr.*, 1983, **99**, 143743z.
- D. Lee and S. Kim, *Taehan Kwangsan Hakhoe Chi*, 1977, **14**, 106; *Chem. Abstr.*, 1977, **87**, 204724v.
- S. Sanuki, T. Izaki and H. Majima, *Nippon Kinzoku Gakkaishi*, 1982, **46**, 597; *Chem. Abstr.*, 1982, **97**, 166754b.
- A. W. Fletcher, D. S. Flett and J. C. Wilson, *Bull. Ind. Mining Met.*, 1964, **693**, 765.
- E. L. T. M. Spitzer, J. Raddar and H. M. Muys, *Inst. Mining Met., Trans. Sect., C75*, 1966, **75**, 265; *Chem. Abstr.*, 1967, **66**, 14493m.
- N. M. Rice, *Solv. Extr., Proc. Int. Solvent Extr. Conf.*, 1971, **1**, 483; *Chem. Abstr.*, 1972, **76**, 158969b.
- G. F. Mills and H. B. Whetsel, *J. Am. Chem. Soc.*, 1955, **77**, 4690.
- L. M. Gindin, P. I. Bobikov and A. M. Rozen, *Dokl. Akad. Nauk. SSSR*, 1959, **128**, 295; *Chem. Abstr.*, 1962, **56**, 999a.
- L. M. Gindin, P. I. Bobikov, E. F. Kouba and A. V. Bugaeva, *Russ. J. Inorg. Chem.*, 1960, **5**, 906.
- Idem, ibid.*, 1960, **5**, 1146.
- I. V. Pyatnitskii and V. V. Sukhan, *Ukr. Khim. Zh.*, 1970 **36**, 97; *Chem. Abstr.*, 1970, **72**, 136997z.
- P. Muchl, K. Gloe, C. Fisher, S. Ziegen and H. Hoffmann, *Hydrometallurgy*, 1980, **5**, 161.
- V. V. Sukhan, I. V. Pyatnitskii and A. G. Sakhno, *Zh. Analit. Khim.*, 1973, **28**, 541; *Chem. Abstr.* 1973, **79**, 10420g.
- M. Novák and A. Havel, *J. Inorg. Nucl. Chem.*, 1967, **29**, 531.
- E. M. Kuznetsov and G. A. Tsyganov, *Vestn. Karakalp. Fil. Akad. Nauk. Uz. SSSR*, 1967, No. 1, 40; *Chem. Abstr.*, 1968, **68**, 70425v.
- M. Tanaka, N. Nakasuka and S. Goto, in *Solvent Extraction Chemistry*, D. Dyrssen, J.-O. Liljenzin and J. Rydberg (eds.), p. 154. North-Holland, Amsterdam, 1967.
- C. R. Adams and J. Falbe, *Brennstoff-Chem.*, 1967, **48**, 272; *Chem. Abstr.*, 1967, **67**, 119319j.
- T. Fujinaka, M. Koyama and S. Tsurubo, *Nippon Kagaku Zasshi*, 1963, **84**, 128; *Chem. Abstr.*, 1964, **60**, 3763c.
- F. I. Lobanov, V. P. Gladyshev, A. K. Nurtaeva and N. N. Andreeva, *Russ. J. Inorg. Chem.*, 1981, **26**, 110.
- E. M. Kuznetsov and G. A. Tsyganov, *Vestn. Karakalp. Fil. Akad. Nauk. Uz. SSSR*, 1964, No. 3, 42; *Chem. Abstr.*, 1966, **64**, 8984i.
- Idem, ibid.*, 1965, No. 3, 41; *Chem. Abstr.*, 1966, **65**, 6126f.
- R. Pietsch, *Anal. Chim. Acta*, 1971, **53**, 287.
- A. E. Grishchenko and G. V. Ilyuvieva, *Izv. Vyssh. Uchebn. Zaved., Tsvetn. Metall.*, 1984, **3**, 47; *Chem. Abstr.*, 1984, **101**, 195805a.
- V. B. Tikhomirov, *Dokl. Akad. Nauk. SSSR*, 1961, **139**, 1416; *Chem. Abstr.*, 1962, **57**, 96a.
- E. N. Merkin, M. D. Ivanovskii and V. F. Borbat, *Radiokhimiya*, 1966, **8**, 705; *Chem. Abstr.*, 1967, **66**, 69395n.
- A. K. De and U. S. Ray, *Sepr. Sci.*, 1971, **6**, 25.
- Idem, ibid.*, 1971, **6**, 443.
- S. M. Karpacheva, N. M. Adamskii and V. V. Borisov, *Radiokhimiya*, 1961, **3**, 291; *Chem. Abstr.*, 1962, **56**, 998g.
- G. V. Ilyuvieva, *Tsvetn. Metall.*, 1963, **36**, No. 9, 1; *Chem. Abstr.*, 1964, **60**, 3815f.
- A. A. Goriachev and E. K. Kopkova, *Russ. J. Inorg. Chem.*, 1980, **25**, 747.
- S. A. Abubakirov, R. Kh. Ushvarenko and M. I. Vdovkina, *Tekhnol. Miner. Syr'ya*, 1972, 208; *Chem. Abstr.*, 1976, **85**, 167428m.
- P. D. Pandey and D. C. Rupainwar, *Acta Chim. Acad. Sci. Hung.*, 1982, **110**, 1; *Chem. Abstr.*, 1982, **97**, 188963w.
- A. J. van der Zeeuw, *Hydrometallurgy*, 1977, **2**, 275.
- S. Sanuki, T. Izaki and H. Majima, *Nippon Kinzoku Gakkaishi*, 1982, **46**, 597; *Chem. Abstr.*, 1982, **97**, 166754b.
- P. Muehl, K. Gloe, M. Saradshrow, L. M. Gindin, A. I. Khol'kin and S. N. Ivanova, *Hydrometallurgy*, 1975, **1**, 113.
- O. Fatibello-Filho, J. C. Trofino and E. F. A. Neves, *Anal. Lett.*, 1986, **19**, 1705.
- O. Fatibello-Filho, M. S. Castilho and E. F. A. Neves, *Quim. Nova*, 1987, **10**, 248.
- O. Fatibello-Filho and E. F. A. Neves, *Anal. Lett.*, 1986, **19**, 565.
- K. B. Yatsmirskii and V. P. Vasil'ev, *Instability Constants of Complex Compounds*, p. 46. Bureau Enterprises, New York, 1960.

COMPUTER-ASSISTED SPECTROPHOTOMETRY: MULTICOMPONENT ANALYSIS WITH A DISCRETE FOURIER TRANSFORM

MOHAMED A. KORANY,* MAHMOUD A. ELSAYED, MONA M. BEDAIR
 and HODA MAHGOUB

Department of Pharmaceutical Analytical Chemistry, Faculty of Pharmacy, University of Alexandria,
 Egypt

EZZAT A. KORANY

Institute of Graduate Studies and Research, UNARC, University of Alexandria, Egypt

(Received 6 June 1989. Revised 16 May 1990. Accepted 14 June 1990)

Summary—A computer-assisted method for analysis of multicomponent mixtures by use of conventional absorbance as well as discrete Fourier transform coefficients (combined trigonometric functions) is presented. The program can store absorbance data (A vs. λ), process data by convolution with combined trigonometric functions, apply least-squares analysis and solve the resultant simultaneous linear equations, and display data on screen, printer or plotter.

There have been many attempts to devise methods of computer-assisted spectrophotometry for the analysis of complex systems,¹⁻¹⁷ but none of these has successfully tackled the problem of background interferences.

Absorption curves have been expanded as a finite Fourier series.¹⁸⁻²⁰ If $(n + 1)$ is an odd number, the expansion is

$$f(\lambda) = a_0 + a_1 \cos x + a_2 \cos 2x + \dots + a_{n/2} \cos(n/2)x + b_1 \sin x + b_2 \sin 2x + \dots + b_{n/2} \sin(n/2)x \quad (1)$$

or if $(n + 1)$ is an even number then

$$f(\lambda) = a_0 + a_1 \cos x + a_2 \cos 2x + \dots + a_{(n+1)/2} \cos(n+1)/2x + b_1 \sin x + b_2 \sin 2x + \dots + b_{(n+1)/2} \sin(n+1)/2x \quad (2)$$

The calculation of the coefficients a_1, a_2, a_3, \dots and b_1, b_2, b_3, \dots is simplified since the trigonometric functions are mutually orthogonal.

Any coefficient, t , can be calculated from a set of absorbances, measured at equally spaced wavelengths, by the following summation, in which x takes values from 0 to $2\pi - [2\pi/(n + 1)]$, at intervals of $2\pi/(n + 1)$:

$$t = \sum_{i=0}^n f(\lambda)_i T x_i / \sum_{i=0}^n (T x_i)^2 \quad (3)$$

where T represents cosine or sine.

It has been shown previously,^{18,19} that a correction for linear background absorption can be made by the combination of two trigonometric functions (Table 1). Thus, for discrete measurements at equally spaced wavelengths, the coefficients of $\cos jx$, calculated from $f(\lambda)$ with a linear component $d + mx$ added, are

$$\sum_{i=0}^n [f(\lambda)_i + d + mx_i] \cos jx_i / D = a_j - m/D \quad (4)$$

where D is the denominator of equation (3).

If x is displaced by one interval, *i.e.*, by $2\pi/(n + 1)$, then

$$\sum_{i=0}^n [f(\lambda)_i + d + mx_i] \cos j[x_i + 2\pi/(n + 1)] / D = a'_j + m/D \quad (5)$$

Addition of equations (4) and (5) leads to a sum of two coefficients ($a_j + a'_j$), which is directly proportional to the concentration of the pure compound and is independent of the linear component added to $f(\lambda)$.¹⁹

The two functions, *e.g.*, $\cos x$ and $\cos[x + \pi/(n + 1)]$ or the corresponding sine functions, can be linearly combined to give $T'x$. Thus

$$t' = \sum_{i=0}^n f(\lambda)_i T' x_i / \sum_{i=0}^n (T' x_i)^2 \quad (6)$$

where $T'x_i$ is the combined function and

$$t' = \omega' C \quad (7)$$

*Author for correspondence.

Table 1. Combined trigonometric Fourier functions for $n + 1$ equally spaced points (generated by the computer program)

n (i)	x_i deg	$[\cos x_i +$ $\cos(x_i + 60^\circ)]$	$[\cos 2x_i +$ $\cos 2(x_i + 60^\circ)]$	$[\sin x_i -$ $\sin(x_i + 60^\circ)]$	$[\sin 2x_i -$ $\sin 2(x_i + 60^\circ)]$
0	0	1.5	0.5	-0.866	-0.866
1	60	0	-1.0	0	1.732
2	120	-1.5	0.5	0.866	-0.866
3	180	-1.5	0.5	0.866	-0.866
4	240	0	-1.0	0	1.732
5	300	1.5	0.5	-0.866	-0.866
D		3	3	3	3

n (i)	x_i deg	$[\cos x_i +$ $\cos(x_i + 45^\circ)]$	$[\cos 2x_i +$ $\cos 2(x_i + 45^\circ)]$	$[\sin x_i -$ $\sin(x_i + 45^\circ)]$	$[\sin 2x_i -$ $\sin 2(x_i + 45^\circ)]$
0	0	1.707	1.0	-0.707	-1.0
1	45	0.707	-1.0	-0.293	1.0
2	90	-0.707	-1.0	0.293	1.0
3	135	-1.707	1.0	0.707	-1.0
4	180	-1.707	1.0	0.707	-1.0
5	225	-0.707	-1.0	0.293	1.0
6	270	0.707	-1.0	-0.293	1.0
7	315	1.707	1.0	-0.707	-1.0
D		4	4	4	4

where ω' is $t'(1\%, 1 \text{ cm})$ and C is the concentration.^{18,19}

MULTICOMPONENT SPECTROPHOTOMETRIC ASSAY

In a multicomponent system (provided that each component obeys Beer's law and no interaction exists between the components), the absorbance of the mixture at any wavelength is

$$A_{ij} = C_{i1}\alpha_{1j} + C_{i2}\alpha_{2j} + \dots + C_{in}\alpha_{nj} \quad (8)$$

where A_{ij} is the absorbance of solution i at wavelength j , C_{in} is the concentration of component n in solution i , and α_{nj} is the $A_{1\%}^{1\text{cm}}$ value of component n at wavelength j .

The Fourier coefficient of the mixture at any λ [mean wavelengths $(\lambda_{\text{initial}} + \lambda_{\text{final}})/2$] is given by

$$t'_{ij} = C_{i1}\omega'_{1j} + C_{i2}\omega'_{2j} + \dots + C_{in}\omega'_{nj} \quad (9)$$

where t'_{ij} is the coefficient of the combined trigonometric functions for solution i calculated at the mean wavelength $(\lambda)_j$, C_{in} is the concentration of component n in solution i and ω'_{nj} is $t'(1\%, 1 \text{ cm})$ for component n at mean wavelength $(\lambda)_j$.

THE COMPUTER PROGRAM

The program provides an interactive dialogue to control the data processing of data collected from the spectrophotometer. The program performs the following main tasks.

(A) *Storage of data.* Wavelength and absorbance data for a compound are stored in a sequential named file on magnetic diskette.

(B) *Processing of data.* Data stored in files can be processed as follows:

- (1) Convolute²¹ the absorption data with combined trigonometric Fourier functions and output the results to a file.
- (2) Reduce the number of equations entered to N equations by least squares, and solve for concentrations of N compounds.
- (3) Solve for concentration of N compounds with N equations.

The convolution process can be performed for (a) different numbers of points in a segment, (b) different orders of combined trigonometric functions and (c) different wavelength intervals.

The program outputs the absorption curve convoluted with the combined trigonometric functions. These functions (Table 1), with their respective divisors, are generated by the program according to the number of points entered by the user.

(C) *Display of data.* Data are displayed on screen, printer or plotter. The plotter driver allows data to be scaled to match the dimensions of the plotting area, and specifies the labelling of the axes.

A block diagram of the program is shown in Fig. 1.

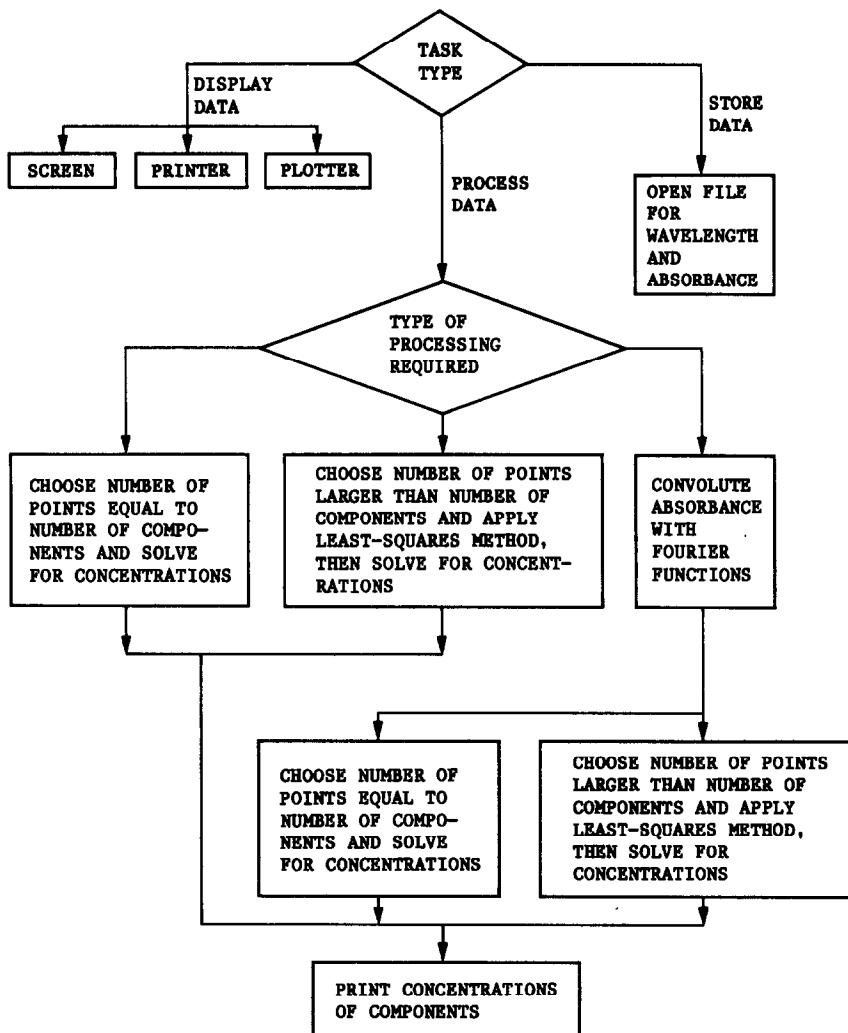


Fig. 1. Functional block diagram of the computer program.

RESULTS AND DISCUSSION

The absorption spectra of the codeine phosphate, phenylephrine hydrochloride, chlorpheniramine maleate and ephedrine hydrochloride are shown in Fig. 2. The methods used to assay these components in a mixture were the Unique Absorbance Method (UAM) and Unique Fourier Function Method (UFFM), and the corresponding least-squares procedures. In UAM four absorbance readings (equal to the number of components) were determined (at different λ values) for each component on its own. Then each mixture was measured at the selected wavelengths.

In UFFM the absorption curves for different components were convoluted (Fig. 2) and the coefficients $t' = (a_1 + a_1')$ were calculated by using 8-point $T' [= \cos x_i + \cos(x_i + 45^\circ)]$ combined trigonometric functions (Table 1) from

λ_{initial} to λ_{final} [268–296 nm (codeine phosphate), 260–288 nm (phenylephrine hydrochloride), 250–278 nm (chlorpheniramine maleate) and 242–270 nm (ephedrine hydrochloride)] at 4-nm intervals.

For the corresponding least-squares methods, the number of coefficients must be greater than the number of components, so for A-LSM (Absorbance Least-Squares Method), 27 absorbances were measured for each component in the region 244–296 nm at 2-nm intervals. For FF-LSM (Fourier Function Least-Squares Method), 19 coefficients were calculated for each component (for 260–296 nm at 2-nm intervals). The results for four synthetic four-component mixtures are given in Table 2. According to the variance-ratio test, all the methods gave F values not exceeding the theoretical value (95% confidence limits). The four methods thus gave equal reproducibility.

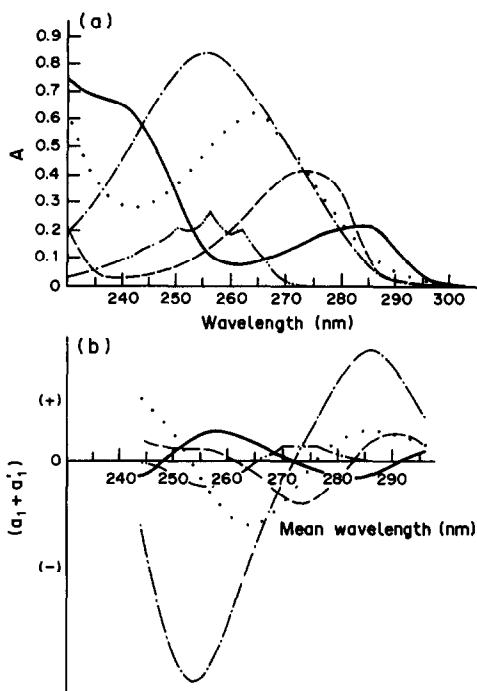


Fig. 2. Absorption curves for 60 $\mu\text{g/ml}$ codeine phosphate (—), 50 $\mu\text{g/ml}$ phenylephrine hydrochloride (---), 30 $\mu\text{g/ml}$ chlorpeniramine maleate (\cdots), 0.30 mg/ml ephedrine hydrochloride (- - -), and propylparaben (- - -) in 0.05M sulphuric acid (a), and the corresponding convoluted curves derived by using 8-point T' [$= \cos x, + \cos(x, + 45^\circ)$] combined trigonometric functions at 4-nm intervals (b).

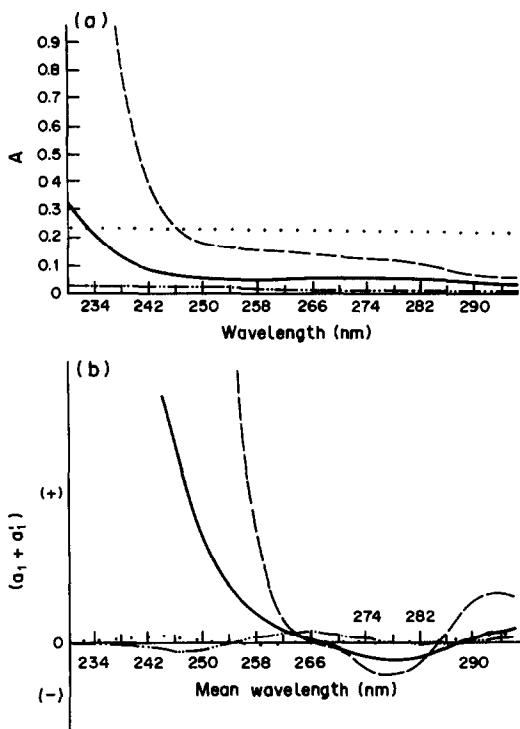


Fig. 3. Absorption curves of 2 mg/ml gum acacia (—), 2 mg/ml gelatin (---), 41 $\mu\text{g/ml}$ barium sulphate (\cdots), 2 $\mu\text{g/ml}$ colouring matter (- - -) in 0.05M sulphuric acid (a), and the corresponding convoluted curves derived therefrom by using 8-point T' [$= \cos x, + \cos(x, + 45^\circ)$] combined trigonometric functions at 4-nm intervals (b).

Table 2. Results for assay of four-component laboratory-made mixtures by the proposed computer-assisted spectrophotometric methods

Mixture*	Recovery, %							
	Codeine phosphate (I)		Phenylephrine hydrochloride (II)		Chlorpeniramine maleate (III)		Ephedrine hydrochloride (IV)	
	UAM	UFFM	UAM	UFFM	UAM	UFFM	UAM	UFFM
1	100.0	99.4	98.6	98.7	98.4	96.8	101.2	100.4
2	101.4	100.5	100.1	99.8	100.1	99.4	100.8	99.1
3	97.8	99.2	99.9	99.7	98.7	97.6	102.6	99.7
4	99.1	98.7	99.6	99.9	99.5	98.4	101.9	101.1
Mean	99.6	99.4	99.5	99.5	99.2	98.0	101.6	100.1
S.D.	1.5	0.8	0.7	0.8	0.8	1.1	0.8	0.9
<i>t</i> -value†		0.23		0.05		1.62		2.55
<i>F</i> -value†		3.98		1.35		2.07		1.19
	A-LSM	FF-LSM	A-LSM	FF-LSM	A-LSM	FF-LSM	A-LSM	FF-LSM
1	100.6	100.8	98.7	98.7	98.0	98.0	101.8	101.3
2	101.3	101.8	99.7	99.7	100.1	100.8	101.2	99.9
3	99.9	99.9	99.5	100.0	98.2	98.2	102.3	102.4
4	100.4	100.6	99.5	100.4	99.3	99.1	101.3	102.0
Mean	100.5	100.8	99.3	99.7	98.9	99.0	101.6	101.4
S.D.	0.6	0.8	0.4	0.7	1.0	1.7	0.5	1.1
<i>t</i> -value	1.2	1.40	0.50	0.30	0.43	0.14	0.05	0.29
<i>F</i> -value	6.8	3.72	2.25	1.18	1.62	2.73	2.45	1.91

*Component concentrations (mg/100 ml) in mixtures 1-4 were I (8,6,6,9); II (6,5,5,6); III (3,2,3,1,9); IV (30,35,30,32).

†The *t*- and *F*-values are calculated with respect to the UAM values. The corresponding theoretical values are 2.44 and 9.28, respectively.

Table 3. Results for assay of a four-component mixture* in the presence of various additives by the proposed computer-assisted spectrophotometric method

Additive	Recovery, %							
	Codeine phosphate (I)		Phenylephrine hydrochloride (II)		Chorpheniramine maleate (III)		Ephedrine hydrochloride (IV)	
	UAM	UFFM	UAM	UFFM	UAM	UFFM	UAM	UFFM
None	100.0 (100.6)	99.4 (100.8)	98.6 (98.7)	98.7 (98.7)	98.4 (98.0)	96.8 (98.0)	101.2 (101.8)	100.4 (101.3)
Carmoisine, 2 μ g/ml	101.1 (102.5)	97.9 (99.4)	101.5 (99.4)	100.4 (99.9)	100.0 (101.0)	96.6 (98.6)	106.1 (106.0)	100.2 (100.2)
Barium sulphate, 41 μ g/ml	150.6 (127.0)	97.3 (98.5)	92.5 (99.2)	100.3 (99.6)	121.63 (130.2)	96.45 (98.2)	97.8 (73.9)	102.0 (100.7)
Gum acacia, 2 mg/ml	114.1 (109.0)	103.5 (101.6)	99.0 (100.8)	100.7 (100.3)	106.2 (107.7)	101.4 (100.0)	103.4 (99.3)	103.8 (100.9)
Gelatine, 2 mg/ml	123.83 (124.6)	110.89 (102.3)	100.49 (94.5)	84.9 (101.1)	111.6 (118.7)	117.8 (98.1)	118.9 (105.2)	55.9 (101.4)

*The mixture contained 80 μ g/ml (I), 60 μ g/ml (II), 30 μ g/ml (III) and 0.30 mg/ml (IV). The figures in parentheses are the assay results obtained by using the same methods with the least-squares approach.

Table 4. Results for assay of a four-component mixture in the presence of a preservative (propylparaben) as the fifth component, by the proposed computer-assisted spectrophotometric methods

Methods	Recovery, %				
	Codeine phosphate (30 μ g/ml)	Phenylephrine hydrochloride (20 μ g/ml)	Chorpheniramine maleate (10 μ g/ml)	Ephedrine hydrochloride (100 μ g/ml)	Propylparaben (10 μ g/ml)
UAM	97.6	99.7	96.1	93.2	100.1
UFFM	112.5	97.7	104.2	99.4	102.7
A-LSM	99.5	97.8	99.1	97.8	99.0
FF-LSM	100.5	101.5	98.3	104.1	98.6

A *t*-test gave 95% confidence that the four methods are of equal accuracy.

To investigate matrix effects and spectral interferences, materials such as colouring matter (carmoisine), barium sulphate, (to form a turbid solution), thickening agents (gum acacia and gelatine) and a preservative (propylparaben) were added. The absorbance spectra of these additives are shown in Fig. 3. Barium sulphate at 41 μ g/ml gives a significant linear spectral interference, whereas carmoisine (2 μ g/ml) gives a negligible interference. Gelatine at 2 mg/ml absorbs strongly at wavelengths shorter than about 246 nm, then has a more or less constant absorbance at longer wavelengths. Therefore special parameters had to be used for the multicomponent analysis when gelatine was present (FF-LSM was used with 15 coefficients calculated over the range 260–288 nm at 2-nm intervals). Gum acacia exhibits less spectral interference than gelatine. The convoluted curves derived by using combined trigonometric functions are shown in Fig. 3.

The results obtained by the proposed computer-assisted spectrophotometric procedure in

the presence of various additives (Table 3), showed that neither UAM nor A-LSM can correct for systematic errors caused by addition of barium sulphate, gum acacia and gelatine. Such errors occurred with codeine phosphate, chlorpheniramine maleate and ephedrine hydrochloride. The other methods allowed correction to be made for matrix effects. The Fourier function least-squares method (FF-LSM) was usually found to be the most accurate.

A different procedure was adopted in the presence of propylparaben preservative, in that the latter (Fig. 2) was treated as a fifth component. The mixture was analysed as before but with an increased number of coefficients determined. Assay results for the five-component mixture are presented in Table 4. The poorest performance was obtained with the UFFM.

REFERENCES

1. S. R. Heller, R. Potenzzone Jr., G. W. A. Milne and Ch. Fisk, *Trends Anal. Chem.*, 1981, 1, 62; *Chem. Abstr.*, 1982, 96, 5709e.
2. H. Gamp, M. Maeder and A. D. Zuberbühler, *Talanta*, 1980, 27, 1037.

3. A. T. Pilipenko, L. I. Savranskii and A. N. Mas'ko, *Zh. Analit. Khim.*, 1985, **40**, 232; *Chem. Abstr.*, 1985, **102**, 142327k.
4. J. Sustek, *Anal. Chem.*, 1974, **46**, 1676.
5. A. T. Pilipenko, L. I. Savranskii, A. N. Mas'ko and V. L. Sheptun, *Dokl. Akad. Nauk SSSR*, 1981, **260**, 377; *Chem. Abstr.*, 1981, **95**, 196844g.
6. W. Yang, *Fenxi Huaxue*, 1985, **13**, 476; *Chem. Abstr.*, 1985, **103**, 152724x.
7. V. Kratochvil, A. Novak and J. Plisek, *Chem. Prum.*, 1978, **28**, 240; *Chem. Abstr.*, 1978, **89**, 164913p.
8. A. F. Vasil'ev and N. L. Aryutkina, *Zavodsk. Lab.*, 1977, **43**, 1330; *Chem. Abstr.*, 1978, **89**, 16009h.
9. N. L. Aryutkina and A. F. Vasil'ev, *ibid.*, 1983, **49**, No. 10, 53; *Chem. Abstr.*, 1983, **99**, 224404s.
10. V. V. Volkov and B. N. Grechushnikov, *Zh. Prikl. Spektrosk.*, 1984, **40**, 264; *Chem. Abstr.*, 1984, **100**, 150403f.
11. B. W. Madsen, D. Herbison-Evans and J. S. Robertson, *J. Pharm. Pharmac.*, 1974, **26**, 629.
12. B. W. Madsen and J. S. Robertson, *ibid.*, 1974, **26**, 682.
13. P. Arnaud, C. Metayer and N. LeGall, *Labo-Pharma-Probl. Tech.*, 1980, **28**, 380.
14. J. Cheng, D. An and R. Wu, *Nanjing Yaoxueyuan Xuebao*, 1985, **16**, No. 2, 74; *Chem. Abstr.*, 1986, **104**, 24252a.
15. T. Tajima and T. Maeda Shimizu Hyoron, 1983, **40**, 139; *Chem. Abstr.*, 1984, **100**, 95865f.
16. A. E. McDowell and H. L. Pardue, *J. Pharm. Sci.*, 1978, **67**, 822.
17. A. E. McDowell, R. S. Harner and H. L. Pardue, *Clin. Chem.*, 1976, **22**, 1862; *Anal. Abstr.*, 1978, **34**, 3D53.
18. M. A. Korany, *Ph.D. Thesis*, University of Alexandria, 1974.
19. A. M. Wahbi, H. Abdine and M. A. Korany, *Pharmazie*, 1978, **33**, 278.
20. I. M. Dubrovkin, *Izv. Sev.-Kavk. Nauchn. Tsentra Vyssh. Shk., Estestv. Nauki*, 1981, No. 1, 57.
21. A. V. Oppenheim and R. W. Schaffer, *Digital Signal Processing*, p. 11 ff. Prentice-Hall, Englewood Cliffs, 1975.

SPECTROPHOTOMETRIC DETERMINATION OF IRON AND COBALT WITH FERROZINE AND DITHIZONE

MARTIN V. DAWSON and SAMUEL J. LYLE

Department of Chemistry, King Fahd University of Petroleum and Minerals, Dhahran 31261, Kingdom of Saudi Arabia

(Received 14 March 1990. Revised 3 June 1990. Accepted 22 June 1990)

Summary—Procedures are described whereby iron (1–50 μg) and cobalt (1–25 μg) are determined spectrophotometrically, iron as iron(II) with the disodium salt of 3-(2-pyridyl)-5,6-bis(4-phenylsulfonic acid)-1,2,4-triazine (Ferrozine) and cobalt as the cobalt(III) dithizonate complex. The reduction to iron(II) prevents interference of iron(III) in the cobalt determination, and both metals can be determined in the same portion of sample solution. Removal of interference by other metal ions is described.

Iron can be determined spectrophotometrically in aqueous solution as the iron(II) complex with the disodium salt of 3-(2-pyridyl)-5,6-bis(4-phenylsulfonic acid)-1,2,4-triazine (Ferrozine).^{1,2} This reagent behaves like 1,10-phenanthroline but is more sensitive by a factor of 2.5 (molar absorptivity $2.79 \times 10^4 \text{ l. mole}^{-1} \times \text{cm}^{-1}$).¹ Cobalt(II) can be extracted into a solution of dithizone in carbon tetrachloride and determined spectrophotometrically as the cobalt(III) dithizonate complex.³ However, dithizone is oxidized by iron(III), and the oxidation products interfere in the determination of cobalt. This interference can be overcome by the addition of fluoride before extraction of the cobalt.³ Alternatively, as shown here, if Ferrozine is added together with hydroxylamine to a mixture of iron(III) and cobalt(II), iron(II) is produced and complexed and not only is the interference of iron(III) in the dithizone extraction prevented, but both metals can be determined in the same portion of sample solution.

EXPERIMENTAL

Reagent grade chemicals were used unless stated otherwise, and all aqueous solutions were prepared in demineralized water. Ferrozine (Aldrich) was used as received; a 0.75 mg/ml solution in water was prepared. Dithizone (B.D.H.) solution ($5 \times 10^{-4} \text{ M}$) in carbon tetrachloride was prepared fresh every few days and stored at 4° in the dark. Metal ion stock solutions were prepared in very dilute nitric acid. A 0.5M sodium acetate/0.1M sodium tartrate mixture adjusted to pH 6.8 ± 0.5 with

acetic acid was used as a buffering and auxiliary masking agent. A 100 mg/ml aqueous hydroxylamine hydrochloride solution was used as the reductant for iron(III).

Before use the buffer and reducing agent solutions were shaken with $5 \times 10^{-4} \text{ M}$ dithizone in carbon tetrachloride to remove extractable metals.

Apparatus

A Bausch & Lomb Spectronic 20 spectrophotometer was used for absorbance measurements, and a Varian Cary-2390 spectrophotometer for taking spectra.

Procedure. Transfer a known volume of solution containing 1–25 μg of cobalt and 1–50 μg of iron into a 25-ml standard flask, add 2 ml of reducing agent, 2 ml of Ferrozine solution and 5 ml of buffer/masking solution and set aside for 10 min to allow development of the iron(II)–Ferrozine complex. Dilute to volume with water, mix and measure the absorbance at 562 nm in a 1-cm cell against a reagent blank. Transfer 10.0 ml of this solution to a separating-funnel, add 10.0 ml of dithizone solution and shake the mixture vigorously for at least 12 min. Collect the organic phase and remove excess of dithizone by shaking the organic phase with 10–15 ml portions of 0.01M ammonia solution for a few seconds each time until the aqueous extract is colourless. Measure the absorbance of the organic phase at 550 nm in a 1-cm cell against a reagent blank prepared by similar treatment of the blank solution from the iron determination.

Table 1. Statistical data from 3 series of replicate measurements on iron and cobalt mixtures (C.V. = coefficient of variation)

Series	Iron, μg	Mean absorbance	C.V., %	Cobalt, μg	Mean absorbance	C.V., %	No. of determinations
1	1.00	0.015	5.4	10.0	0.91	1.0	3
2	15.0	0.329	0.88	4.00	0.330	1.9	5
3	40.0	0.88	1.1	1.00	0.081	6.4	3

Alternatively, for up to 10 μg of cobalt and 20 μg of iron, the initial aqueous solution can be made up to 10.0 ml instead of 25.0 ml, the same volumes of reagents being used. This approach is recommended for low levels of iron (1–5 μg) in the presence of ≥ 15 μg of cobalt.

RESULTS AND DISCUSSION

The calibration graphs obtained by application of the entire procedure to mixtures of iron and cobalt are linear, and that for cobalt is essentially identical with one obtained in the absence of iron in the initial solution, showing that iron(III) is efficiently reduced and the iron(II) complexed. Table 1 gives data on the reproducibility of analysis of mixtures of iron and cobalt at low, medium and high concentrations within the recommended ranges.

The reproducibility is good, except, as would be expected, at the low end of the concentration ranges.

The presence of at least 15 μg of cobalt does not interfere in the determination of iron and up to at least 10 μg of nickel is also without effect (Table 2).

According to Stookey,¹ tests with copper, cobalt, calcium, magnesium, lead, silver, molybdenum, aluminum, nickel, zinc, arsenic, manganese, chromium(VI) and chromium(III) revealed that only iron(II), copper(I) and cobalt(II) form coloured complexes with Ferrozine. The broad absorbance bands centered⁴ at 470 nm for copper and 450–520 nm for cobalt can be expected to cause some inter-

ference in the determination of iron. As the data in Table 2 confirm, however, within the concentration limits specified in the procedure, an error exceeding 5% in the iron determination is likely only for < 5 μg of iron in the presence of ≥ 15 μg of cobalt. This source of error can be eliminated by extracting the cobalt from the aqueous phase with dithizone before measuring the absorbance of the iron complex.

Interference can also be caused by other metal ions which can form complexes with Ferrozine if they are present in sufficient amount to compete with iron(II) for the reagent. Nickel(II) is such an ion; for, example, in the procedure given here the presence of 1500 μg of nickel along with 15 μg of iron will completely prevent formation of the iron–Ferozine complex. However, as shown in Table 2 up to at least 10 μg of nickel will not interfere in the iron determination under the recommended conditions.

Nickel(II) is partially extracted along with cobalt by dithizone in the presence of Ferrozine, however, and even increasing the Ferrozine concentration 10-fold (to $1.2 \times 10^{-4}M$ in the 25 ml of final test solution) will not retain all the nickel in the aqueous phase. Four samples containing 5.00 μg each of cobalt, nickel and iron gave an average absorbance of 0.480 (standard deviation 0.008) when the dithizone extract was measured at 550 nm against carbon tetrachloride (the average absorbance in the absence of nickel was 0.480). More than 6 μg of nickel was found to increase the absorbance unacceptably, however. Fortunately nickel can be removed efficiently³ by the addition of a few mg of 1,10-phenanthroline to the carbon tetrachloride extract and shaking this with an equal volume of 0.01–0.1M hydrochloric acid for about 30 sec; this treatment also removes zinc, cadmium, thallium(I), and lead(II). Removal of the released dithizone, by shaking with 0.01M ammonia solution, as in the procedure, leaves only the cobalt(III) dithizonate in the carbon tetrachloride phase.

The extraction of cobalt(III) dithizonate can be used to improve the reliability of the

Table 2. Effect of cobalt and nickel on iron determination

Iron, μg	Cobalt, μg	Nickel μg	Iron found, μg
1.0	25.0	0.0	1.2
5.0	20.0	0.0	5.4
10.0	15.0	0.0	9.8
15.0	10.0	0.0	15.0
30.0	5.0	0.0	30.3
40.0	2.5	0.0	39.6
5.0	20.0	10.0	5.0
15.0	10.0	10.0	14.8
40.0	2.5	10.0	39.3

determination of low levels of iron ($< 5 \mu\text{g}$) and can also be extended³ for the spectrophotometric determination of cobalt in the presence of nickel and other elements at μg levels as outlined above. The work described here illustrates some advantages derived from the use of two colorimetric reagents in the determination of more than one component in a single sample.

Acknowledgement—The authors acknowledge support from the Chemistry Department, King Fahd University of Petroleum & Minerals.

REFERENCES

1. L. L. Stookey, *Anal. Chem.*, 1970, **42**, 779.
2. M. M. Gibbs, *Water Res.* 1979, **13**, 295.
3. M. V. Dawson and S. J. Lyle, *Talanta*, 1990, **37**, 443.
4. S. K. Kundra, M. Katyal and R. P. Singh, *Anal. Chem.*, 1974, **46**, 1605.

SPECTROPHOTOMETRIC DETERMINATION OF TETRACYCLINES IN PHARMACEUTICAL PREPARATIONS, WITH URANYL ACETATE

U. SAHA, A. K. SEN and T. K. DAS

Central Public Health & Drug Laboratory, 2 Convent Lane, Calcutta 700016, India

S. K. BHOWAL*

Department of Chemistry, Jadavpur University, Calcutta 700032, India

(Received 26 September 1988. Revised 21 June 1990. Accepted 26 June 1990)

Summary—Uranyl acetate is proposed as a reagent for the spectrophotometric determination of the tetracycline group of antibiotics. The reagent forms orange-red 1:1 complexes with the drugs in *N,N*-dimethylformamide medium. The complexes show absorption maxima at 414, 406, 419, 405 and 402 nm for tetracycline hydrochloride (TCH), oxytetracycline hydrochloride (OTCH), chlortetracycline hydrochloride (CTCH), doxycycline hydrochloride (DCH) and methacycline hydrochloride (MCH), respectively. Beer's law is valid over the concentration ranges 0–115, 0–120, 0–125, 0–135 and 0–110 $\mu\text{g/ml}$ for TCH, OTCH, CTCH, DCH and MCH, respectively.

Tetracycline hydrochloride (TCH), oxytetracycline hydrochloride (OTCH), chlortetracycline hydrochloride (CTCH), doxycycline hydrochloride (DCH) and methacycline hydrochloride (MCH) are important members of the tetracycline group of antibiotics, which have found extensive use in current therapy because of their broad spectrum antibacterial properties. Spectrophotometry is the most popular method for determination of these drugs in bulk and in pharmaceutical preparations.^{1–9} Reagents used for this purpose include sodium hydroxide, ferric chloride, thorium nitrate, ammonium vanadate or molybdate, aminophrine, sodium tungstate, cupric chloride and cerium acetate. The ferric chloride method is applicable only in the narrow pH range of 2.0 ± 0.05 and there is interference by phosphate, thiocyanate and fluoride. The other methods also have drawbacks such as narrow Beer's law range, instability of colour, critical reaction and heating times, low sensitivity, multiple reaction steps and multiple pH adjustments. Uranyl nitrate has been used for the determination of OTCH,¹⁰ but the procedure was not widely accepted, owing to the slow colour development. A second method utilizing uranyl nitrate¹¹ is very sensitive to changes in pH and has a very narrow optimum pH range (4–4.5). Also

the complex precipitates in aqueous medium shortly after colour development. Moreover, the method is very insensitive and the solubility of the drug in ethanol (used as a solvent in the method) is very low. Determination of microbiological potency¹² is recognized as an official method for the estimation of tetracycline hydrochloride and its derivatives. The method described here utilizes the colour reaction of tetracyclines with uranyl acetate in dimethylformamide (DMF) medium. The procedure is superior to the earlier methods with respect to stability of the colour, Beer's law range, simplicity, speed and sensitivity. The method has been applied to the determination of various tetracyclines in bulk and in various pharmaceutical preparations. The results obtained are similar to those obtained by the official method.¹²

EXPERIMENTAL

Apparatus

A Shimadzu UV 160 spectrophotometer with matched 1.00-cm fused-silica cells was used.

Reagents

All reagents and solvents were of analytical grade. Uranyl acetate solution was prepared by dissolving 200 mg of the dihydrate in 100 ml of DMF. Test solutions were freshly prepared by dissolving 100 mg of the tetracycline in 100 ml

*Author for correspondence.

of DMF. Laboratory reference standards were used for calibration.

General procedure

Suitable volumes of standard drug solutions (0.25–5.75 ml for TCH, 0.25–6.00 ml for OTCH, 0.25–6.25 ml for CTCH, 0.25–6.75 ml for DCH and 0.25–5.50 ml for MCH) were transferred separately into 50-ml standard flasks, 3.5 ml of reagent solution were added to each, and the solutions were diluted to the mark with DMF and mixed. The absorbances were measured at 414, 406, 419, 405 and 402 nm for TCH, OTCH, CTCH, DCH and MCH, respectively, against a reagent blank.

Capsules and tablets

A quantity of the sample (a mixture of 20 powdered tablets or the contents of the capsules) equivalent to 100 mg of the drug was weighed accurately and transferred into a 100-ml standard flask and shaken with 50 ml of DMF for 10 min. The mixture was then diluted to volume with DMF and filtered. A portion of filtrate (1.5 ml) was transferred into a 50-ml standard flask and the assay was completed as above.

Ointments

An accurately weighed amount, equivalent to 100 mg of the drug, was transferred into a 100-ml conical flask. The drug was extracted with three successive 30-ml portions of warm DMF, which were filtered into a 100-ml standard flask, cooled, and diluted to volume with DMF. The analysis was completed with 1.5 ml of the solution.

Suspensions and syrups

The suspension or syrup was shaken well and an accurately known amount, equivalent to 100 mg of the drug, was transferred into a 100-ml standard flask. The assay was completed as for capsules and tablets.

Injections

An accurately known volume of the injection, equivalent to 100 mg of the drug, was transferred into a 100-ml standard flask and then diluted to volume with DMF. The analysis was completed with 1.5 ml of this solution.

RESULTS AND DISCUSSION

The tetracyclines formed orange-red complexes with uranyl acetate in DMF solution.

Chloroform, benzene, ethanol, methanol and diethyl ether were found unsuitable because of the low solubility of the drugs or their uranium complexes in them. The complexes are also unstable in these solvents. In aqueous medium, the complexes are formed at pH 4.0, but gradually precipitate. In dimethylsulphoxide or formamide medium the colours are less intense than in DMF.

Absorption spectra

The absorption spectra of the TCH, OTCH, CTCH, DCH and MCH complexes have maximum absorbance at 414, 406, 419, 405 and 402 nm respectively, whereas the reagent blank has relatively low absorbance.

Choice of uranium salt and pH

Uranyl acetate has been found to be the most efficient uranium salt for colour formation with the tetracyclines. The phosphate and sulphate are only sparingly soluble in DMF and the reaction of the nitrate with the tetracyclines is too slow (maximum colour intensity obtained only after 96 hr). The acetate is freely soluble in DMF, and the complexes form instantaneously, and are stable for about 7 days, at temperatures in the range 0–100°. For 100 µg of the tetracycline, 100 µg of uranyl acetate is sufficient to produce maximum colour intensity, but addition of more has no adverse effect.

The effect of pH on the colour intensity was studied by addition of hydrochloric acid, ammonia, sodium acetate–acetic acid buffer (pH 4–6) and ammonium chloride–ammonia buffer (pH 8–9), to the DMF solution of the complex, and in all cases there was a drastic reduction of the colour intensity. Hence, a completely non-aqueous DMF environment is required for obtaining the maximum colour intensity.

Beer's law and sensitivity

The complexes obey Beer's law over the concentration ranges shown in Table 1, and the correlation coefficients¹³ were calculated.

Nature of the complex

The composition of the complexes was shown to be 1:1 by Job's method¹⁴ (Fig. 1) and the molar ratio method.¹⁵ From the structures of the tetracyclines investigated, it was deduced that the active groups for complex formation were the same for all. Therefore a representative complex, that formed between uranyl acetate

Table 1. Regression equations for the calibration graphs

Drug	ϵ , $10^4 \text{ l. mole}^{-1} \text{ cm}^{-1}$	Beer's law range, $\mu\text{g/ml}$	λ_{max} , nm	Regression equation	Correlation coefficient
TCH	1.05	0-115	414	$A = 0.0216C + 0.0077$	0.9999
OTCH	0.98	0-120	406	$A = 0.0185C + 0.0060$	0.9998
CTCH	1.04	0-125	419	$A = 0.0198C + 0.0158$	0.9995
DCH	0.95	0-135	405	$A = 0.0196C + 0.0082$	0.9996
MCH	1.07	0-110	402	$A = 0.0222C + 0.0111$	0.9998

* A = absorbance at λ_{max} (1-cm cells), C = concentration ($\mu\text{g/ml}$).

and tetracycline hydrochloride, was isolated. Dimethylformamide solutions of uranyl acetate dihydrate (0.356 g, 10 ml) and excess of TCH (0.465 g, 10 ml) were mixed in a 100-ml conical flask and shaken for 5 min. Diethyl ether (50 ml) was added dropwise to precipitate the orange-red complex (with scratching with a spatula if necessary). The mixture was kept in a refrigerator for about 30 min for the precipitate to settle. The ether layer was then decanted and the complex washed with three small portions of petroleum ether (b.p. 40–60°). The solvent was removed and the complex was repeatedly washed with warm (50–60°) portions of methanol to remove the excess of tetracycline. The complex was then filtered off with a sintered-glass crucible and washed repeatedly with warm methanol. The product was finally dried under vacuum and kept in a desiccator.

The complex is insoluble in water, chloroform, benzene, hydrocarbons, petroleum ether,

diethyl ether, acetone, ethyl acetate and dichloromethane, slightly soluble in methanol and ethanol, and readily soluble in dimethylformamide and dimethylsulphoxide. Acids and bases dissolve the complex and decompose it. The complex does not melt even at 280° and becomes dark at >220°, whereas TCH melts at 210–215°. The solid complex has the empirical formula $\text{UO}_2(\text{C}_{22}\text{H}_{23}\text{N}_2\text{O}_8) \cdot \text{CH}_3\text{COO} \cdot 4\text{H}_2\text{O}$, as ascertained from elemental analysis, infrared spectral data, and thermogravimetric (TG) and differential thermogravimetric (DT) studies. The elemental analysis gave 34.1% C, 3.2% H, 3.6% N and 27.8% U; the formula above requires 34.15% C, 3.79% H, 3.32% N and 28.22% U. The TG curve shows the gradual loss of four molecules of water from about 50 to 180°. The DT curve shows this loss as an endothermic change, which is compatible with the loss of water molecules. The weight loss at 200–300° corresponds to loss of the acetate, and this appears as an exothermic peak in the DT curve, because of the liberation of CO_2 . At above 300° the complex slowly breaks down by decomposition of the tetracycline moiety.

The infrared spectra of the hydrated and dehydrated forms of the complex were recorded. The dehydrated form was obtained by heating the hydrated complex to constant weight at 70° (8.51% loss; the formula requires 8.54%). The spectrum of the hydrated complex could not be fully interpreted, however, owing to the band at 1630–1600 cm^{-1} for the bending mode of water.^{16,17}

Application

Table 2 shows the results obtained for the determination of tetracyclines in bulk form and in various pharmaceutical preparations by the proposed and official methods.¹² The Student t -test and the variance-ratio F -test,¹⁸ show that there is no significant difference between the two methods as regards accuracy and precision.

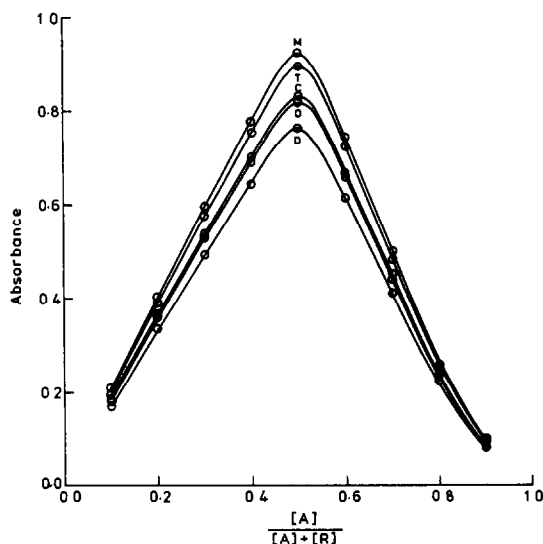


Fig. 1. Continuous variation curves for uranyl acetate complexes of TCH (T), OTCH (O), CTCH (C), DCH (D) and MCH (M) in DMF. $[A] = [\text{drugs}]$ (T, O, C, D and M) $[R] = [\text{uranyl acetate}]$ $[A] = [R] = 2 \times 10^{-4}M$.

Table 2. Determination of tetracyclines by the proposed and official methods

Sample	Found*, %		$t_{\text{calc}} \dagger$	$F_{\text{calc}} \ddagger$
	Proposed method	Official method		
TCH Powder	100.1 ± 0.3	100.1 ± 0.1	0.33	4.27
TCH Capsule	97.8 ± 1.2	98.1 ± 0.9	1.32	1.90
TCH Tablet	99.3 ± 0.5	99.4 ± 0.4	0.78	1.99
TCH Syrup	102.8 ± 0.5	101.6 ± 0.4	1.67	1.49
TCH Injection	97.6 ± 0.8	97.9 ± 0.9	0.85	1.27
TCH Ointment	102.3 ± 0.3	100.6 ± 0.2	0.71	3.16
DCH Powder	101.0 ± 0.3	100.7 ± 0.2	1.98	1.37
DCH Capsule	99.5 ± 0.4	99.6 ± 0.5	1.38	1.33
DCH Syrup	102.3 ± 0.6	102.0 ± 0.5	1.96	1.26
DCH Suspension	101.0 ± 0.4	100.6 ± 0.2	0.27	3.69
OTCH Powder	100.2 ± 0.4	100.1 ± 0.2	0.97	3.06
OTCH Capsules	99.9 ± 0.3	99.9 ± 0.4	0.23	1.03
OTCH Tablet	101.7 ± 0.7	101.5 ± 0.5	0.56	1.91
OTCH Suspension	97.1 ± 0.3	98.8 ± 0.4	0.99	1.89
OTCH Ointment	103.4 ± 0.8	103.0 ± 0.4	0.49	3.96
OTCH Injection	98.8 ± 0.5	99.0 ± 0.4	0.56	1.19
CTCH Powder	100.1 ± 0.5	100.0 ± 0.7	0.40	2.00
CTCH Capsule	102.1 ± 1.1	101.8 ± 1.2	0.74	1.28
CTCH Ointment	102.2 ± 0.6	101.0 ± 0.5	2.20	1.36
MCH Powder	100.0 ± 0.2	100.1 ± 0.2	0.86	1.29
MCH Capsule	97.4 ± 1.0	97.5 ± 0.9	0.61	1.21
MCH Suspension	101.3 ± 0.2	100.1 ± 0.1	1.78	2.15

*Average ± standard deviation of 6 determinations.

†Theoretical value 2.23 ($p = 0.05$).

‡Theoretical value 5.34 ($p = 0.05$).

Interferences

The common excipients lactose, sucrose, glucose, starch, calcium lactate, magnesium stearate, talc, ascorbic acid, sodium ascorbate, carboxymethyl cellulose, gum acacia and guar gum did not interfere with the assays.

Acknowledgements—The authors are grateful to Dr N. N. Chakraborty, Director, and Dr S. K. Moitra, Assistant Director, of the Central Public Health and Drug Laboratory, for laboratory facilities.

REFERENCES

- M. H. Woolford, Jr. and F. S. Chiccarelli, *J. Am. Pharm. Assoc., Sci. Ed.*, 1956, **45**, 400.
- F. Monastero, J. A. Means, T. C. Grenfell and F. H. Hedger, *ibid.*, 1951, **40**, 241.
- T. Sakaguchi and K. Taguchi, *J. Pharm. Bull. Japan*, 1955, **3**, 166, 303.
- N. M. Andel-Khalek and M. S. Mahrous, *Talanta*, 1983, **30**, 792.
- K. Kakemi, T. Uno and T. Miyake, *J. Pharm. Soc. Japan*, 1955, **75**, 970.
- Idem, ibid.*, 1956, **76**, 903.
- D. Vasinović and M. Jelick-Stankov, *Pharmazie*, 1987, **42**, 199.
- U. Saha, *J. Assoc. Off. Anal. Chem.*, 1987, **70**, 686.
- B. Janik and D. Holiat, *Acta Pol. Pharm.*, 1972, **29**, 169.
- A. Fiebig, S. Janicki and H. Wasiak, *Diss. Pharm.*, 1965, **17**, 81.
- Y. K. Agarwal and D. R. Patel, *Indian J. Pharm. Sci.*, 1986, **48**, 92.
- U.S. Pharmacopeia XXth 1980*, Mack, Easton, Pa., 1980.
- Remington's Pharmaceutical Sciences 1985*, 17th Ed., p. 123. Mack, Easton, Pa., 1985.
- P. Job, *Ann. Chim. (Paris)*, 1928, **9**, 113.
- J. H. Yoe and A. L. Jones, *Ind. Eng. Chem., Anal. Ed.*, 1944, **16**, 111.
- L. J. Bellamy, *The Infra-red Spectra of Complex Molecules*, p. 205. Wiley, New York, 1959.
- K. Nakamoto, *Infrared and Raman Spectra of Inorganic and Coordination Compounds*, pp. 231–232, Wiley, New York, 1978.
- L. Saunders and R. Fleming, *Mathematics and Statistics*, 2nd Ed., pp. 192–197. Pharmaceutical Press, London, 1971.

SPECTROPHOTOMETRIC DETERMINATION OF SMALL AMOUNTS OF XYLENOL ORANGE, SEMI-XYLENOL ORANGE AND *o*-CRESOL RED

STANISLAW KICIAK

Department of Physical Chemistry, Institute of Chemistry and Technical Electrochemistry,
Technical University, Poznan, Poland

(Received 30 November 1989. Revised 30 May 1990. Accepted 26 June 1990)

Summary—An extraction method based on the butanol–water system is used in an improved spectrophotometric determination of Xylenol Orange (XO), Semi-Xylenol Orange (SXO) and Cresol Red (CR) in mixtures. Small amounts of SXO in the presence of much greater amounts of XO, and small amounts of XO in the presence of large amounts of SXO can be determined with good accuracy after extractive separation of the compound to be determined, from the bulk of the other components of the mixture.

Commercially produced Xylenol Orange (XO) always contains a certain amount of Semi-Xylenol Orange (SXO) and in some cases small amounts of Cresol Red (CR)¹⁻³ Even well purified synthetic SXO always contains small amounts of XO and CR.^{3,4} The properties of the metal complexes of XO and SXO are appreciably different, so the use of impure SXO or XO as spectrophotometric reagents for determination of metals^{5,6} can lead to errors and poor reproducibility.

The methods described up till now allow relatively exact determination of one of the three dyes (XO, SXO and CR) when its molar fraction in the mixture is not lower than 10%. For accurate determination when the molar fraction of the dye is lower than this, a separation is necessary to remove the bulk of the other dye(s) or the whole of the dye of interest.

In either case a qualitative separation of all three dyes is not necessary, but the whole amount of the dye of interest should be present, accompanied by amounts of the other two dyes that are much lower than those in the initial mixture. As shown in the previous paper,⁴ extractive separation of the three dyes is possible with the butanol–water solvent system. In that work it was adapted for purification of the dyes, *i.e.*, for practically complete removal of the impurities, without regard to any loss of the main compound. In the present work, the most important question is how to remove all or most of the main compound without loss of the impurity to be determined.

In the raffinate from *t* successive extraction steps, the molar ratio of the components of a binary mixture is

$$\frac{(n_1)_t}{(n_2)_t} = \frac{(n_1)_0}{(n_2)_0} \left(\frac{D_2 S + 1}{D_1 S + 1} \right)^t$$

where $(n_i)_0$ and $(n_i)_t$ are the numbers of moles of compound *i* in the aqueous phase (the raffinate) before and after *t* extractions, D_i is the extraction coefficient of compound *i* (defined as the ratio of its concentrations in the organic phase to that in the raffinate, and *S* is the volume ratio of the organic phase to the raffinate.

If compound 1 is the minor component, then $(n_2)_0 \gg (n_1)_0$. Suppose that for exact determination of compound 1 the necessary molar ratio for the desired separation is $n_1/n_2 > 0.2$; then two cases arise. For the first, almost the whole amount of compound should remain in the raffinate, *i.e.*, $(n_1)_t \sim (n_1)_0$, and almost all of the major component (2) should be extracted, *i.e.*, $(n_2)_t \rightarrow 0$, or more exactly, $(n_1)_t/(n_2)_t > 0.2$. For the second case practically all of compound 1 should be extracted, *i.e.*, $(n_1)_t \rightarrow 0$, and almost all of the compound 2 should remain in the raffinate, *i.e.*, $(n_2)_t \sim (n_2)_0$, or more exactly, $[(n_1)_0 - (n_1)_t]/[(n_2)_0 - (n_2)_t] > 0.2$.

Extension of this to a ternary mixture of CR, SXO and XO without significant loss of the compound to be determined is not possible by use of a single extraction system, but requires a combination of extraction and back-extraction processes, so these have been more particularly investigated.

EXPERIMENTAL

Apparatus

All absorption measurements were made with a Zeiss-Jena Specord M40 spectrophotometer with 1-cm cells, and pH measurements were made with a type N 517 pH-meter ("Mera", Poland).

Reagents

Semi-Xylenol Orange (SXO) and Xylenol Orange (XO) were obtained from the Organic Chemistry Department, Technical University of Poznan, and separated and purified as described previously.^{1,3} The purified samples were free from Cresol Red (CR). Any other impurities did not absorb in the visible region of the spectrum, and their content did not exceed 1%.

A commercial sample of CR was recrystallized from ethanol. All other reagents were of analytical grade.

Extraction experiments

The data given in the previous paper⁴ showed that the ratio of the extraction coefficients for CR and SXO was highest in the 1-butanol-water system ($D_{CR}/D_{SXO} = 13.0$) and for SXO and XO in the 1-butanol-0.5M sulphuric acid system ($D_{SXO}/D_{XO} = 26.6$), so these systems were used again. The phases were mutually saturated before use for the extraction experiments.⁴

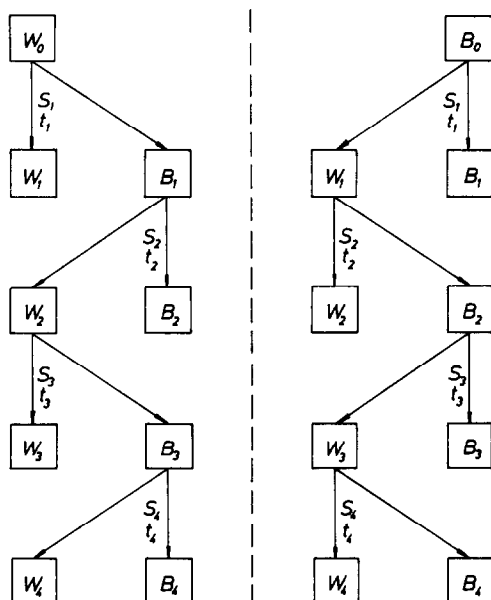


Fig. 1. Scheme for extractive separations. W_t —water solutions, B_t —butanol solutions, S_t —ratio of volume of extractant phase to volume of the solution to be extracted, t_i — number of extraction stages.

Three kinds of mixture were extracted, with XO, SXO or CR as the dominant component. The first kind was dissolved in water, the second in water or in butanol, and the third in butanol. The preliminary experiments consisted of 1-stage or 4-stage extractions with different phase-volume ratios. The next step was to examine t_1 -stage extractions followed by t_2 -stage back-extractions, and if necessary the procedure was continued according to the general scheme exemplified in Fig. 1, and the detailed scheme in Fig. 2 which shows the sequence of operations for sample No. 3 in Table 1, and the symbolism used for denoting the extraction systems.

RESULTS AND DISCUSSION

The preliminary work showed that CR can be relatively easily transferred from aqueous solution into butanol, whereas almost all the XO and the major part of the SXO remain in the aqueous solution. However, the quantitative transfer of the CR requires a relatively large volume of butanol.⁴ However, all the XO and a major part of the SXO in the butanol phase can be transferred back into an aqueous phase with a relatively small volume of water, the CR remaining in the butanol phase, but separation of XO and SXO in this system is much more complicated. It is much simpler to use the butanol-0.5M sulphuric acid system, in which all the CR, accompanied by a large fraction of the SXO, can be transferred from 0.5M sulphuric acid into a relatively small volume of butanol. In back-extraction from butanol into 0.5M sulphuric acid, a major part of the XO is transferred into the aqueous phase, almost all the CR and a major part of the SXO remaining in the butanol phase.⁴

Figure 2 shows that the differences between the results obtained by 1-stage and 4-stage extractions when the extraction coefficients are low ($D_i < 0.4$) are relatively small in comparison with those when the extraction coefficients are high ($D_i > 3$). For example, in extraction of XO from water into butanol ($D_{XO} = 0.19$) when the relative volume of extractant (S_t) is 0.48 or 0.96, the fractions of total XO remaining in the aqueous phase are 0.914 (for $t = 1$) and 0.913 (for $t = 4$) or 0.846 (for $t = 1$) and 0.837 (for $t = 4$) respectively, whereas for back-extraction of XO from butanol into water, the fractions of XO retained in the butanol phase are 0.28 (for $t = 1$) and 0.14 (for $t = 4$) or 0.17 (for $t = 1$)

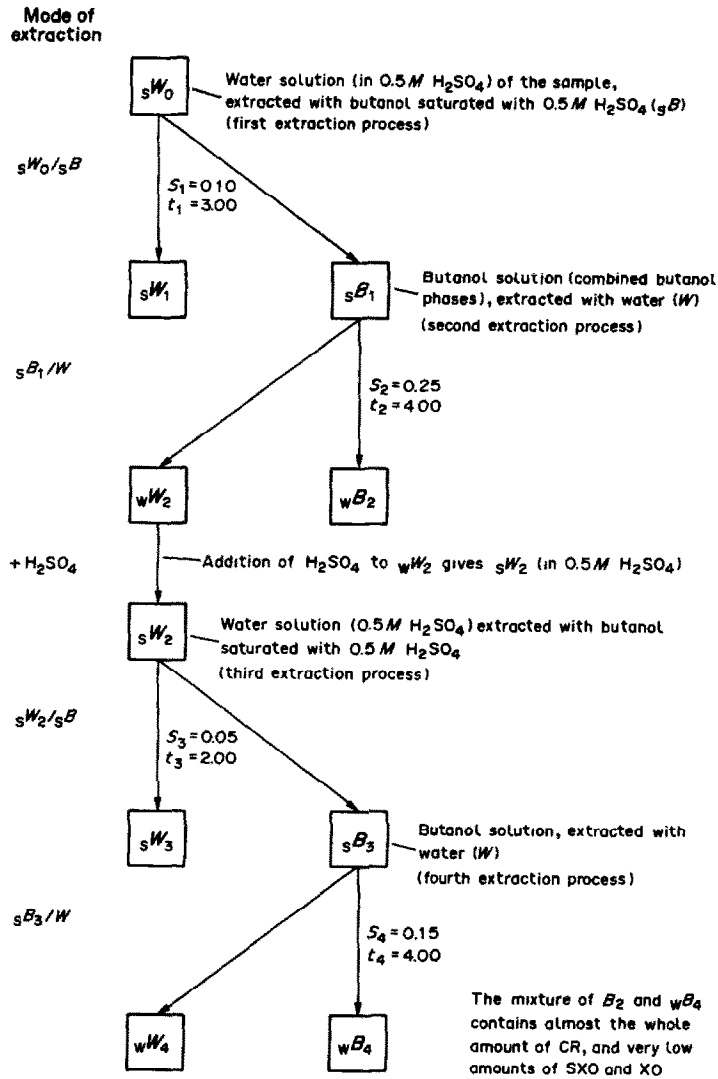


Fig. 2. Scheme for extraction of sample 3 in Table 1.

Fig. 3. Dependence of the molar fraction (X_r) of compound remaining in the raffinate, on the ratio of the total volume of extractant ($v_e/v_s = St$), to the volume of the solution to be extracted (v_s) for 1-stage (●) and 4-stage* (○) extraction processes. Extraction coefficients: 1, 0.0198; 2, 0.198; 3, 0.311; 4, 3.21; 5, 5.26; 6, 44.3. *The same volume as for the 1-stage process but divided into four equal parts.

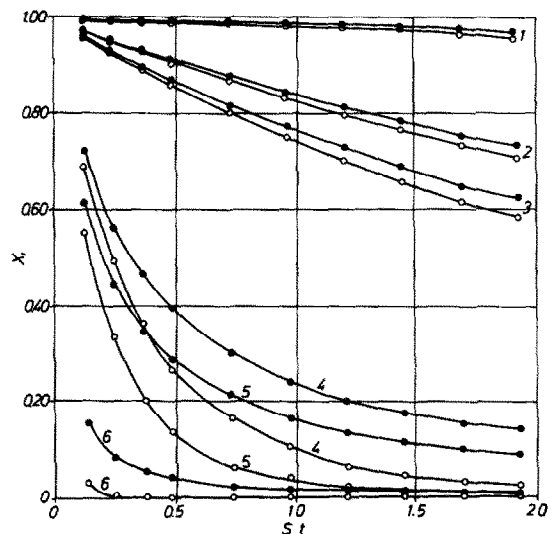


Table 1. Results* for determination of SXO after removal of most of the XO, and for determination of CR after extraction of XO and most of the SXO

No.	Sample			Found in ${}_1W_0$, μmole			Mode of extraction; t_i = number of stages, (S_i) \dagger = volume ratio used for system of phases				Analysed after extraction	
	Taken, μmole			XO \bar{X} (sd)	SXO \bar{X} (sd)	CR \bar{X} (sd)	${}_1W_0/{}_sB$ t_1 (S_1)	${}_sB_1/W$ t_2 (S_2)	${}_sW_2\dagger/{}_sB$ t_3 (S_3)	${}_sB_3/W$ t_4 (S_4)	Phase	Found \bar{X} , μmole (sd)
1	90	10	0	89.1 (1.9)	12.2 (2.8)	—	4 (0.25)	—	—	—	${}_sB_1$	SXO 9.6 (0.8)
2	99	1	0	98.5 (1.8)	2.9 (2.8)	—	6 (0.20)	3 (0.30)	5 (0.10)	—	${}_sB_2$ ${}_sB_3$	SXO 0.94 (0.23)
3	28	70	2	28.1 (1.2)	69.4 (2.2)	1.8 (1.7)	3 (0.10)	4 (0.25)	2 (0.05)	4 (0.15)	${}_wB_2$ ${}_wB_4$	CR 1.87 (0.26)
4	69	30.5	0.5	68.8 (1.5)	30.8 (1.2)	0.2 (1.3)	3 (0.10)	4 (0.25)	2 (0.05)	4 (0.15)	${}_wB_2$ ${}_wB_4$	CR 0.45 (0.16)

*Mean (\bar{X}) and standard deviations (sd) for 5 determinations.

$\dagger S_1 = V_e/V_s$, where V_e = volume of extractant phase, V_s = volume of solution to be extracted.

\ddagger After addition of H_2SO_4 to solution W_2 .

${}_1W_0$ = sample solution in 0.5M H_2SO_4 ; ${}_sB$ = butanol saturated with 0.5M H_2SO_4 ; ${}_wB_1$ = butanol saturated with water.

and 0.040 (for $t = 4$), for $S_i = 0.48$ and 0.96 respectively.

Further improvement of the separation may be achieved by changing the extraction medium. For example if the approximate composition of the mixture is $C_{XO}:C_{SXO}:C_{CR} = 1:10:100$, the mixture should be dissolved in butanol and extracted a few times with small volumes of water. The whole of the XO, part of the SXO and a very small fraction of the CR will be transferred into the aqueous phase. Back-extraction of the dyes into butanol is then possible without addition of acid but needs large

volumes of butanol for quantitative transfer of the SXO. Hence before the back-extraction the combined aqueous extracts should be made 0.5M in sulphuric acid. After back-extraction, the aqueous phase will contain a major part of the XO, a very small part of the SXO and almost no CR, and the butanol extract will contain the major part of the SXO, almost all the CR which was previously in the aqueous phase, and a smaller but not negligible part of the XO. If this butanol solution is extracted with 0.5M sulphuric acid, almost all the CR and the major part of the SXO will remain in the

Table 2. Results* for determination of XO after removal of CR and most of the SXO

No.	Sample			Found in ${}_wB_0$, μmole			Mode of extraction; t_i = number of stages, (S_i) \dagger = volume ratio used for system of phases				XO found, μmole	
	Taken, μmole			XO \bar{X} (sd)	SXO \bar{X} (sd)	CR \bar{X} (sd)	${}_wB_0/W$ t_1 (S_1)	${}_sW_1\dagger/{}_sB$ t_2 (S_2)	${}_sB_2/{}_sW$ t_3 (S_3)	${}_sW_3/{}_sB$ t_4 (S_4)	${}_wB_1$ \bar{X} (sd)	${}_sW_2$ \bar{X} (sd)
1	5	50	45	4.4 (2.3)	49.8 (0.7)	45.6 (0.7)	4 (0.10)	5 (0.20)	4 (0.125)	5 (0.05)	1.58 (0.77)	4.83 (0.51)
2	2	18	80	1.3 (1.1)	18.3 (0.8)	80.3 (0.7)	4 (0.00)	5 (0.20)	5 (0.10)	3 (0.10)	1.68 (0.55)	1.92 (0.49)
3	2	97	1	1.3 (0.9)	96.5 (1.1)	0.3 (1.0)	4 (0.00)	5 (0.20)	4 (0.125)	5 (0.05)	1.45 (1.80)	1.76 (0.55)
4	1	9	90	0.2 (1.4)	9.4 (1.5)	90.5 (1.3)	4 (0.10)	5 (0.20)	5 (0.10)	3 (0.10)	0.85 (0.35)	0.93 (0.42)

*Mean (\bar{X}) and standard deviation (sd) for 5 determinations.

$\dagger S_i = V_e/V_s$, where V_e = volume of extractant phase, V_s = volume of solution to be extracted.

\ddagger After addition of H_2SO_4 to solution W_1 .

Table 3. Results* for determination of SXO in 20 mg of XO reagents after removal of most of the XO and for determination of CR after removal of most of the XO and SXO

No.	Sample of XO	Year of production	Composition, $\mu\text{mole}/100\text{mg}$		Mode of extraction; t_i = number of stages, $(S_i)^\dagger$ = volume ratio used for system of phases						Analysed					
			XO \bar{X} (sd)	SXO \bar{X} (sd)	CR \bar{X} (sd)	$W_0/t_1 B$ (S_1)	${}_1B_1/W$ t_2 (S_2)	$W_2/t_2 B$ t_3 (S_3)	${}_2B_2/W$ t_4 (S_4)	${}_3B_3/W$	Phase	\bar{X} (sd)	\bar{X} (sd)			
1	Merck	1987	97.5 (1.3)	6.8 (1.8)	nd	4 (0.25)	—	—	—	—	—	—	SXO	CR	4.9 (0.8)	nd
1	Merck	1987	97.5 (1.3)	6.8 (1.8)	nd	6 (0.20)	3 (0.30)	5 (0.10)	—	—	—	—	SXO	CR	4.8 (0.28)	nd
2	POCh	1985	104 (1.6)	11.9 (1.2)	nd	4 (0.25)	—	—	—	—	—	—	SXO	CR	11.6 (0.7)	nd
3	POCh	1987	70.5 (1.2)	15.8 (1.3)	2.5 (1.7)	3 (0.10)	4 (0.25)	2 (0.05)	4 (0.15)	4	—	—	SXO§	CR	1.18 (0.23)	15.7 (0.9)

*Mean (\bar{X}) and standard deviation (sd) for 5 determinations.† $S_i = V_c/V_s$ where V_c = volume of extractant phase, V_s = volume of solution to be extracted.‡After addition of H_2SO_4 to solution W_2 .

§Extracted as for sample 3 in Table 1.

nd = Not detectable.

Table 4. Results* for determination of XO after removal of most of the CR and SXO, for samples taken during synthesis of SXO and for determination of CR in initially purified SXO

Sample	Composition (found before extraction), $\mu\text{mole}/100\text{ ml}$				Mode of extraction; t_i = number of stages, (S_i) = volume ratio used for system of phases				Analysed		
	XO \bar{X} (sd)	SXO \bar{X} (sd)	CR \bar{X} (sd)	XO \bar{X} (sd)	B_0/W_1 (S_1)	W_1^\dagger/W_2 (S_2)	B_2/W_3 (S_3)	W_3/W_4 (S_4)	Phases	\bar{X} (sd)	\bar{X} (sd)
Butanol solution of 1-ml sample taken during synthesis of SXO											
1 1 hr after beginning of the synthesis	4.1 (3.9)	45.4 (2.3)	480.5 (3.1)	480.5 (3.1)	4 (0.10)	4 (0.20)	4 (0.20)	3 (0.20)	W_2 W_4	XO 2.9	SXO§ 43.5
2 2 hr after beginning of the synthesis	8.6 (6.1)	85.2 (1.6)	435.0 (2.8)	435.0 (2.8)	4 (0.10)	4 (0.20)	4 (0.20)	3 (0.20)	W_2 W_4	XO 7.7 (0.6)	—
3 3 hr after beginning of the synthesis	14.0 (5.4)	121.2 (1.9)	395 (2.8)	395 (2.8)	4 (0.10)	4 (0.20)	4 (0.20)	3 (0.20)	W_2 W_2	XO 12.6 (0.6)	—
4 Butanol solution of initially purified SXO	46 (1.7)	148 (1.6)	3.1 (2.3)	3.1 (2.3)	4 (0.40)	4 W_1/B (0.30)	2 B_2/W B_2/W (0.05)	—	B_1 B_2	CR 3.8 (0.31)	—

*Mean (\bar{X}) and standard deviation (sd) for 5 determinations.

† $S_1 = V_e/V_s$ where V_e = volume of extractant phase, V_s = volume of solution to be extracted.

‡After addition of H_2SO_4 to solution W_1 , but not for sample 4.

§In W_1 after 8-stage extraction with water at $S_1 = 0.125$.

butanol phase, and the XO be practically quantitatively transferred into the aqueous phase. This aqueous phase can be washed with small amounts of butanol (to remove the rest of the SXO), and then added to the aqueous solution left after the first back-extraction. This combined aqueous solution will contain over 95% of the original amount of XO and only a very little SXO and CR, which makes possible the exact determination of XO in this solution.

The details of the extractions and the results for determination of the small amounts of one of the dyes in the presence of much higher amounts of other two dyes, are collected in Tables 1-4. The results for determination of chosen dyes in specially prepared mixtures of XO, SXO and CR are collected in Tables 1 and 2. Table 3 shows the possibilities for determination of small amounts of SXO and CR in Xylenol Orange reagents.

Table 4 gives results obtained during monitoring of the first 3 hr of an SXO synthesis, and

the results of examination of initially purified SXO.

These results show that simple combinations of extraction and back-extraction processes with different phase volume ratios and neutral and acidic aqueous media make possible the relatively exact determination of very small amounts of one of the three dyes in spite of the presence of much higher amounts of the other two dyes in the original mixture.

REFERENCES

1. M. Murakami, T. Yoshino and S. Harasawa, *Talanta*, 1967, **14**, 1293.
2. R. P. Pantaler and I. V. Pulayeva, *Zh. Analit. Khim.*, 1977, **32**, 2450.
3. S. Kiciak and H. Gontarz, *Talanta*, 1986, **33**, 341.
4. S. Kiciak, *ibid.*, 1989, **36**, 1101.
5. N. F. Kosenko and T. V. Malkova, *Izo. Vyssh. Uchelon. Zavod. Khim. i Khim. Tekhnol.*, 1981, **24**, 54.
6. S. Kiciak, *Talanta*, 1980, **27**, 429.

SPECTROPHOTOMETRIC DETERMINATION OF SOME DITHIOCARBAMATES

ASHOK KUMAR MALIK and A. L. J. RAO

Department of Chemistry, Punjabi University, Patiala 147002, India

(Received 27 February 1990. Revised 18 May 1990. Accepted 22 June 1990)

Summary—A procedure has been developed for the determination of six dithiocarbamates [sodium dimethyldithiocarbamate (dibam), sodium diethyldithiocarbamate (NaDDC), tetramethylthiuram disulphide (thiram), zinc dimethyldithiocarbamate (ziram), sodium *N*-methylpiperazinecarbodithioate and potassium morpholine-4-carbodithioate] in microgram quantities by converting them into selenium dithiocarbamate complexes, which are then extracted into chloroform and measured at 430 nm against a reagent blank. The method is sensitive and can be used for the determination of dithiocarbamates in commercial samples and synthetic mixtures.

Dithiocarbamates and their metal derivatives are widely used as agricultural fungicides on foliage and fruit to control a variety of pests. Various methods have been reported for the determination of dithiocarbamates by the carbon disulphide evolution technique.¹⁻³ Spectrophotometric methods have also been reported for the determination of dithiocarbamates.⁴⁻⁸ As most of these methods are indirect and time-consuming there is a need for a simple, direct and rapid spectrophotometric method. Here we present a simple, sensitive and selective method for the determination of sodium dimethyldithiocarbamate (dibam), sodium diethyldithiocarbamate (NaDCC), tetramethylthiuram disulphide (thiram), zinc dimethyldithiocarbamate (ziram), sodium *N*-methylpiperazinecarbodithioate and potassium morpholine-4-carbodithioate, based on extraction of their selenium complexes into chloroform.

EXPERIMENTAL

Apparatus

A digital pH-meter and an SP-20 Spectronic spectrophotometer were used.

Reagents

Pure ziram and thiram samples were obtained from Wilson Laboratories, Bombay. Sodium dimethyldithiocarbamate and sodium diethyldithiocarbamate were prepared by the method of Klopping and van der Kerk,⁹ and sodium *N*-methylpiperazinecarbodithioate and potassium morpholine-4-carbodithioate by the method

of Marcotrigiano *et al.*¹⁰ The purity of the samples was checked by elemental analysis. Ziram was decomposed with concentrated nitric acid and the zinc content determined by EDTA titration with Eriochrome Black T as indicator.¹¹ Solutions (0.1%) of water-soluble dithiocarbamates were prepared in distilled water and standardized by adding an excess of standard copper(II) solution, buffering with pyridine and titrating the excess of copper with EDTA, using pyrocatechol as indicator.¹² Stock solutions (0.1%) of ziram and thiram were prepared in 0.1M sodium hydroxide, the thiram requiring boiling for 20 min to achieve dissolution, and standardized.¹¹ All solutions were further diluted with distilled water as required.

A 1% solution of sodium selenite (JMC Industrial Chemicals, England) in distilled water was prepared. Stock solutions of substances to be tested for interference were prepared by dissolving suitable salts in water. Synthetic samples were prepared by mixing solutions of the constituents and diluting to give the required composition.

Procedure

A known volume (≤ 1 ml) of sample containing up to 50 μg of the dithiocarbamate was pipetted into a beaker, 2 ml of 1% sodium selenite solution and 1.5 ml of acetic acid-sodium acetate buffer (pH 5.8) were added and the volume was made up to 5 ml with distilled water. This solution was transferred into a separating funnel and shaken with exactly 5 ml of chloroform for 2 min. The organic phase

was transferred into a dry tube containing anhydrous calcium chloride. A second extract obtained with another 5 ml of chloroform had negligible absorbance, so the absorbance of the first extract, measured at 430 nm against a reagent blank, was used for the determination.

RESULTS AND DISCUSSION

The absorption spectra of selenium dithiocarbamate complexes in chloroform were recorded against a reagent blank. The complexes absorb strongly at 430 nm. Maximum absorbance was observed when the pH of the aqueous phase was 5.0–8.0 and 1.5–2.0 ml of 1.0% sodium selenite was used, except for sodium *N*-methylpiperazinecarbodithioate, for which the optimum pH was 4.0–7.0. The complexes were extracted into *n*-butyl acetate, amyl acetate, diethyl ether, butan-2-one, ethyl acetate, isobutyl alcohol, isobutyl methyl ketone and chloroform. Maximum absorbance was obtained with chloroform, hence its selection for use in this method. The absorbance of the complexes remained practically constant for more than 12 hr.

Analytical characteristics

The calibration graphs obtained under the optimum conditions were linear over wide concentration ranges (Table 1). The molar absorptivity, and the relative standard deviation for ten replicate determinations of 50 μg of dithiocarbamate are also given in Table 1.

Interferences

Sample solutions containing 50 μg of dithiocarbamates and various amounts of different anions (as alkali-metal salts) or metal ions were prepared and the general procedure was applied. The following foreign ions in the mg amounts shown in parentheses did not interfere: acetate (2.5), bromide (26), chloride (20), citrate

(36), iodide (25), nitrate (24), oxalate (1) and sulphate (32). EDTA up to 0.1 mg is tolerable, whereas higher amounts decrease the absorbance. Thiosulphate, metabisulphite and orthophosphate interfere strongly. Of the metal ions examined, Pb^{2+} (0.50), Zn^{2+} (0.15), Fe^{3+} (0.04), Bi^{3+} (0.045) and Cd^{2+} (0.42) could be tolerated but Cu^{2+} interfered strongly.

Interferences due to the presence of other dithiocarbamates such as disodium ethylene-bisdithiocarbamate (nabam), manganese ethylenebisdithiocarbamate (maneb), zinc ethylenebisdithiocarbamate (zineb) and sodium *N*-methylanilinecarbodithioate were studied; up to 2 mg of these compounds did not interfere in the determination of 50 μg of the six dithiocarbamates tested, because they do not form complexes with sodium selenite under the conditions used. Nabam, sodium monomethyldithiocarbamate (vapam), sodium dimethyldithiocarbamate, sodium diethyldithiocarbamate and potassium morpholine-4-carbodithioate, if present with ziram or thiram, can be separated by extraction of the ziram or thiram with chloroform; the chloroform can then be removed by evaporation.

Determination of ziram and thiram in synthetic mixtures and commercial samples

Mixtures of ziram or thiram with nabam, zineb and maneb in various proportions were prepared and analysed by the general procedure. Ziram and thiram can also be determined in the presence of water-soluble dithiocarbamates by extraction into chloroform, which is then evaporated to 2 ml on a hot water-bath, the remainder being removed by a gentle current of dry air. The residue is dissolved in 0.1M sodium hydroxide; ziram is soluble in the cold and can be separated from the thiram, which dissolves only on boiling.

Table 1. Absorption characteristics of the selenium dithiocarbamate complexes

Dithiocarbamate	Beer's law range, $\mu\text{g/ml}$	Molar absorptivity, $l.\text{mole}^{-1}.\text{cm}^{-1}$	Relative standard deviation, %
Sodium dimethyldithiocarbamate (dibam)	1–20	60×10^2	0.5
Tetramethylthiuram disulphide (thiram)	0.9–16	1.06×10^4	0.5
Zinc dimethyldithiocarbamate (ziram)	0.8–12	1.59×10^4	0.3
Sodium diethyldithiocarbamate (NaDDC)	1.2–16	5.65×10^3	1.0
Potassium morpholine-4-carbodithioate	1.9–14	4.82×10^3	0.8
Sodium <i>N</i> -methylpiperazinecarbodithioate	2–14	4.75×10^3	0.9

Table 2. Analysis of dilutions of commercial samples of ziram and thiram

Commercial sample	Active ingredient taken, %	Active ingredient found, %	
		Present method	Cullen method ³
Ziram 27% SC	0.100	0.099	0.097
	0.250	0.249	0.247
	0.500	0.498	0.497
	0.800	0.798	0.796
	0.900	0.899	0.898
Ziram 100%	0.100	0.100	—
Thiram 75 w.p.	0.100	0.098	0.096
	0.200	0.197	0.197
	0.400	0.399	0.397
	0.600	0.598	0.598
	0.800	0.799	0.798
Thiram 100%	0.100	0.100	—

The method was applied to the determination of ziram and thiram in commercial samples. Table 2 shows typical results for five dilutions of the stock solutions prepared from "Ziram 27% S.C." and "Thiram 75 W.P." containing inert carrier materials. Pure samples of ziram and thiram were taken for reference. Results obtained by the present method are compared with those obtained by the Cullen method,³ in which the dithiocarbamates were destroyed in acidic solution to give carbon disulphide, which was then reacted with cupric acetate and diethanolamine to form the yellow cupric salt of *N,N*-bis(2-hydroxyethyl)dithiocarbamic acid, which was measured spectrophotometrically.

Comparison of sensitivity

The present method is more sensitive than those of Lowen,¹ Cullen,² Chmiel¹³ and many others reported in the literature. According to Lowen, a minimum of 10 μg of evolved CS_2 can be determined. In the present method, a minimum of 5.0, 4.6, 4.0, 6.0, 9.8 and 10.0 μg of sodium dimethyldithiocarbamate, thiram, ziram, sodium diethyldithiocarbamate, potassium morpholine-4-carbodithioate and sodium *N*-methylpiperazinecarbothioate, respectively,

equivalent to 2.65, 2.91, 1.99, 2.66, 3.68 and 3.84 μg of evolved CS_2 , can be determined.

The wide applicability, simplicity and selectivity of this method make it preferable to others.

Acknowledgement—One of the authors (A.K.M) thanks the Bureau of Police Research and Development, New Delhi, for financial assistance.

REFERENCES

1. D. G. Clarke, H. Baum, E. L. Stanley and W. F. Hester, *Anal. Chem.*, 1951, **23**, 1842.
2. W. K. Lowen, *ibid.*, 1951, **23**, 1846.
3. T. E. Cullen, *ibid.*, 1964, **36**, 221.
4. R. Warren and J. Bontoyan, *J. Assoc. Off. Agric. Chem.* 1965, **48**, 562.
5. W. Fischer, *Z. Anal. Chem.*, 1952, **90**, 137.
6. J. R. Rangaswamy, P. Poornima and S. K. Majumder, *J. Assoc. Off. Anal. Chem.*, 1971, **54**, 1120.
7. W. K. Lowen, *ibid.*, 1953, **36**, 484.
8. R. F. Heuermann, *ibid.*, 1957, **40**, 264.
9. H. L. Klopping and G. J. M. van der Kerk, *Rec. Trav. Chim. Pays Bas.*, 1951, **70**, 949.
10. G. M. Marcotrigiano, G. C. Pallacani, C. Preti and G. Tosi, *Bull. Chem. Soc. Japan*, 1975, **48**, 1018.
11. A. I. Vogel, *A Text Book of Quantitative Inorganic Analysis*, 3rd Ed., p. 433. Longmans, London, 1969.
12. A. L. J. Rao and S. Singh, *Z. Anal. Chem.*, 1974, **270**, 31.
13. Z. Chmiel, *Chem. Anal. (Warsaw)*, 1979, **24**, 505.

BOOK REVIEWS

Multidimensional Chromatography: H. J. CORTES (editor), Dekker, New York, 1990. Pages viii + 378. \$99.75 (U.S. and Canada), \$119.50 (elsewhere).

To the non-specialist the term 'multidimensional chromatography' would probably convey initially the well-known technique of thin-layer chromatography (TLC) in which a secondary separation is developed orthogonally on the same plate. This is just one example of the method and multidimensional TLC is the subject of Chapter 2. What this chapter does and indeed what the book as a whole achieves, is to bring together a wealth of information on the variety, scope and resolving power of multidimensional chromatography. It appears that all the important aspects of the subject are covered somewhere in the volume by contributors who are leading authorities in the field.

As well as addressing the mathematical treatment and theoretical advantages of multidimensional chromatography and thus setting the scene for the rest of the book, Chapter 1 also deals more generally with multidimensional separation methods but only so far as is necessary to place multidimensional chromatography in context within the broader framework of separation methodology as a whole.

Advances in two-dimensional gas chromatography are highlighted in Chapter 3 which emphasizes the practical aspects of the technique and focuses attention on recent developments relating to capillary columns.

Chapter 4 deals with selectivity tuning in capillary gas chromatography (CGC), including multidimensional CGC, while Chapter 5 looks at the applications of multidimensional gas chromatography to process control. This chapter thus complements Chapter 3 and once again there is emphasis on practical aspects.

Instrumentation and applications of on-line multidimensional high-performance liquid chromatography (MD HPLC) are covered in Chapter 6.

In a book in which multidimensional HPLC and multidimensional GC feature strongly, it is fitting that there should be a chapter devoted to on-line coupled HPLC-CGC, a technique which offers a very high degree of resolution of complex mixtures. Transfer techniques for the introduction of the effluent from a liquid chromatography into a capillary gas chromatograph are considered in some detail, as are numerous applications.

Another chapter is concerned with supercritical fluid chromatography (SFC) but it is little surprising to find that the following chapter deals with supercritical fluid extraction (SFE) coupled to SFC, since SFE is not a chromatographic technique. However, perhaps we should not be too pedantic and allow the editor some licence because, after all, SFE is likely to become increasingly important in future separation science.

The final chapter performs a useful function by dealing with some practical points on the assembly and operation of automated equipment.

The book contains 650 references, 150 clear illustrations, mainly line drawings and chromatograms, and 22 tables. It is a useful blend of theoretical principles, details of instrumentation and practical applications. As such it is bound to be a valuable guide and source of information for analytical and industrial chemists, biochemists and pharmaceutical scientists.

A. K. DAVIES

Marine Toxins—Origin, Structure and Molecular Pharmacology: S. HALL and G. STRICHARTZ (editors), ACS, Washington, DC, 1990. Pages xi + 377. \$74.95.

This book developed from a conference on toxins from aquatic and marine environments, held at Woods Hole, Mass., in 1987. However, the submission dates of individual chapters range from May to October 1989 so the work is commendably up-to-date and includes some 1989 references.

In some parts of the world marine toxins are a significant health hazard, and cases of severe and lethal poisoning occur annually from such causes as the consumption of shellfish, contact with jellyfish, and from toxic algae in fresh water. Understanding such events is obviously of medical and scientific interest, and studies on these toxins may help to solve related biochemical and physiological problems, and provide leads for drug development.

The editors are pharmacologists and the 27 chapters, like the preceding conference presumably, are devoted predominantly to molecular pharmacology. Six chapters are concerned with polyether toxins, six with palytoxin, and eight with peptide toxins. Saxitoxins and related molecules are also discussed in several chapters.

For *Talanta* readers the chapters of most interest are those on HPLC (Sullivan), X-ray studies (Van Duyne), and the biosynthesis of saxitoxins and brevetoxins (Shimizu). The HPLC method is comparatively new in this research area, and ion-interaction chromatography on porous polymer columns is found to be most efficient. Examples are given of the application of HPLC to the metabolism of toxins in clams, and in tracing toxins through the food chain. The X-ray chapter gives a detailed account of crystallographic work on the brevetoxins.

BOOK REVIEWS

Standardization Within Analytical Chemistry: P. KIVALO, Akadémiai Kiadó, Budapest, 1989. Pages 155 + 125 (appendices). £23.00.

*This book is about standard methods, not standard solutions, and is not concerned with matters of technique. It is also more about standardization than about analytical chemistry, so "electrical engineering" might be substituted throughout without much affecting the logic of the argument. Kivalo seems to propose that the force of the argument would be different, however, because he sees analytical chemistry as an undervalued discipline, to the extent that he calls for the formation of an International Union of Pure and Applied Analytical Chemistry (an isolationism curiously at odds with the general spirit of the book). I think we should beware of this view, since it may be one of a series of grudges we hold as chemists, scientists, graduates or even citizens, but can this book change it anyway? I doubt if those whom Kivalo seeks to influence will read it, or finish it if they start. The historical background has some interesting aspects and Kivalo puts the arguments for and against standardization very fairly, but his style is too close to that of a standards document for comfort. One or two concrete examples of progress in standardization, with costs and benefits, would have helped. The bad side of standardization is bureaucratic wrangling of the sort that gives rise to terminology that numbs the mind rather than elucidates the meaning; Kivalo hints at the phenomenon, but is not very critical of any specific effects. About half the book is taken up by reproductions of four standards documents which, while of value in themselves, are available elsewhere. This book does provoke thought and eventually I found that I mostly agreed with the author, but the ideas would have been better promoted at essay length.

DEREK MIDGLEY

Drug Formulation: I. RACZ, Wiley, Chichester, 1989. Pages x + 416. £61.00.

The title of the text may prove rather misleading to many, as the bulk of material deals mainly with physicochemical details with little information provided on formulation or the processing methods used in formulation. The first chapter makes reference to pharmaceutical technology, saying that it includes unit operations such as milling, drying and compression to prepare dosage forms such as tablets, capsules and emulsions, but these are then not discussed in any detail.

The book consists of four chapters. The first, covering the principles of preformulation and formulation testing, is rather brief at only 27 pages and including only 21 references. A useful list of tests which may be required in preformulation for different types of dosage forms is included, but as in some other areas of the text there is little or no other detail provided. A reasonable introduction to mathematical and experimental design is given in the limited space devoted to this topic, although further reading would be essential to anyone interested in this area.

The second chapter, approximately one third of the text, with some 349 references, provides a comprehensive cover of chemical stability, including kinetics, decomposition mechanisms and assay methods. However, there is very little included on packaging, or formulation methods such as microencapsulation which may be used to minimize stability problems. Other areas such as the physical stability of emulsions and suspensions have not been mentioned at all.

Physicochemical interactions are covered in some depth in the third chapter. Various combinations of drug-drug, drug-excipient and excipient-excipient interactions have all been included, with many useful examples. Potential advantages such as improved absorption by use of cyclodextrin inclusion complexes have also been given, as well as the numerous disadvantages. Many of the commonly used excipients have been included here but further reading of the many references listed may be required to obtain greater detail. Also included in this chapter is a table of some 14 pages listing expected interactions for i.v. preparations, all with references, which may prove useful for a limited number of readers but is more likely to be of limited value for most.

The final chapter deals with biopharmaceutical aspects of formulation. Again there are a number of sections, including pharmacokinetics, bioavailability, physicochemical factors affecting absorption and one on controlled-release formulations. The physicochemical factors affecting absorption are well covered, with useful examples. The section on controlled release is rather mathematical, with little detail on formulation processes.

The book, rather than being an essential text for either those involved in drug development and manufacturing or those in research or academic areas, should be regarded as a useful reference text. To this end there are many detailed examples and over 1000 references are included.

K. I. CUMMING

Pharmaceutical Thermal Analysis—Techniques and Applications: J. L. FORD and P. TIMMINS, Ellis Horwood, Chichester, 1989. Pages 313. £55.00.

Thermal analysis occupies an important niche in physical and industrial pharmacy and a text devoted to this area is long overdue. The book will be of much interest to those in both industry and academia, each being represented by the joint

BOOK REVIEWS

Standardization Within Analytical Chemistry: P. KIVALO, Akadémiai Kiadó, Budapest, 1989. Pages 155 + 125 (appendices). £23.00.

*This book is about standard methods, not standard solutions, and is not concerned with matters of technique. It is also more about standardization than about analytical chemistry, so "electrical engineering" might be substituted throughout without much affecting the logic of the argument. Kivalo seems to propose that the force of the argument would be different, however, because he sees analytical chemistry as an undervalued discipline, to the extent that he calls for the formation of an International Union of Pure and Applied Analytical Chemistry (an isolationism curiously at odds with the general spirit of the book). I think we should beware of this view, since it may be one of a series of grudges we hold as chemists, scientists, graduates or even citizens, but can this book change it anyway? I doubt if those whom Kivalo seeks to influence will read it, or finish it if they start. The historical background has some interesting aspects and Kivalo puts the arguments for and against standardization very fairly, but his style is too close to that of a standards document for comfort. One or two concrete examples of progress in standardization, with costs and benefits, would have helped. The bad side of standardization is bureaucratic wrangling of the sort that gives rise to terminology that numbs the mind rather than elucidates the meaning; Kivalo hints at the phenomenon, but is not very critical of any specific effects. About half the book is taken up by reproductions of four standards documents which, while of value in themselves, are available elsewhere. This book does provoke thought and eventually I found that I mostly agreed with the author, but the ideas would have been better promoted at essay length.

DEREK MIDGLEY

Drug Formulation: I. RACZ, Wiley, Chichester, 1989. Pages x + 416. £61.00.

The title of the text may prove rather misleading to many, as the bulk of material deals mainly with physicochemical details with little information provided on formulation or the processing methods used in formulation. The first chapter makes reference to pharmaceutical technology, saying that it includes unit operations such as milling, drying and compression to prepare dosage forms such as tablets, capsules and emulsions, but these are then not discussed in any detail.

The book consists of four chapters. The first, covering the principles of preformulation and formulation testing, is rather brief at only 27 pages and including only 21 references. A useful list of tests which may be required in preformulation for different types of dosage forms is included, but as in some other areas of the text there is little or no other detail provided. A reasonable introduction to mathematical and experimental design is given in the limited space devoted to this topic, although further reading would be essential to anyone interested in this area.

The second chapter, approximately one third of the text, with some 349 references, provides a comprehensive cover of chemical stability, including kinetics, decomposition mechanisms and assay methods. However, there is very little included on packaging, or formulation methods such as microencapsulation which may be used to minimize stability problems. Other areas such as the physical stability of emulsions and suspensions have not been mentioned at all.

Physicochemical interactions are covered in some depth in the third chapter. Various combinations of drug-drug, drug-excipient and excipient-excipient interactions have all been included, with many useful examples. Potential advantages such as improved absorption by use of cyclodextrin inclusion complexes have also been given, as well as the numerous disadvantages. Many of the commonly used excipients have been included here but further reading of the many references listed may be required to obtain greater detail. Also included in this chapter is a table of some 14 pages listing expected interactions for i.v. preparations, all with references, which may prove useful for a limited number of readers but is more likely to be of limited value for most.

The final chapter deals with biopharmaceutical aspects of formulation. Again there are a number of sections, including pharmacokinetics, bioavailability, physicochemical factors affecting absorption and one on controlled-release formulations. The physicochemical factors affecting absorption are well covered, with useful examples. The section on controlled release is rather mathematical, with little detail on formulation processes.

The book, rather than being an essential text for either those involved in drug development and manufacturing or those in research or academic areas, should be regarded as a useful reference text. To this end there are many detailed examples and over 1000 references are included.

K. I. CUMMING

Pharmaceutical Thermal Analysis—Techniques and Applications: J. L. FORD and P. TIMMINS, Ellis Horwood, Chichester, 1989. Pages 313. £55.00.

Thermal analysis occupies an important niche in physical and industrial pharmacy and a text devoted to this area is long overdue. The book will be of much interest to those in both industry and academia, each being represented by the joint

BOOK REVIEWS

Standardization Within Analytical Chemistry: P. KIVALO, Akadémiai Kiadó, Budapest, 1989. Pages 155 + 125 (appendices). £23.00.

*This book is about standard methods, not standard solutions, and is not concerned with matters of technique. It is also more about standardization than about analytical chemistry, so "electrical engineering" might be substituted throughout without much affecting the logic of the argument. Kivalo seems to propose that the force of the argument would be different, however, because he sees analytical chemistry as an undervalued discipline, to the extent that he calls for the formation of an International Union of Pure and Applied Analytical Chemistry (an isolationism curiously at odds with the general spirit of the book). I think we should beware of this view, since it may be one of a series of grudges we hold as chemists, scientists, graduates or even citizens, but can this book change it anyway? I doubt if those whom Kivalo seeks to influence will read it, or finish it if they start. The historical background has some interesting aspects and Kivalo puts the arguments for and against standardization very fairly, but his style is too close to that of a standards document for comfort. One or two concrete examples of progress in standardization, with costs and benefits, would have helped. The bad side of standardization is bureaucratic wrangling of the sort that gives rise to terminology that numbs the mind rather than elucidates the meaning; Kivalo hints at the phenomenon, but is not very critical of any specific effects. About half the book is taken up by reproductions of four standards documents which, while of value in themselves, are available elsewhere. This book does provoke thought and eventually I found that I mostly agreed with the author, but the ideas would have been better promoted at essay length.

DEREK MIDGLEY

Drug Formulation: I. RACZ, Wiley, Chichester, 1989. Pages x + 416. £61.00.

The title of the text may prove rather misleading to many, as the bulk of material deals mainly with physicochemical details with little information provided on formulation or the processing methods used in formulation. The first chapter makes reference to pharmaceutical technology, saying that it includes unit operations such as milling, drying and compression to prepare dosage forms such as tablets, capsules and emulsions, but these are then not discussed in any detail.

The book consists of four chapters. The first, covering the principles of preformulation and formulation testing, is rather brief at only 27 pages and including only 21 references. A useful list of tests which may be required in preformulation for different types of dosage forms is included, but as in some other areas of the text there is little or no other detail provided. A reasonable introduction to mathematical and experimental design is given in the limited space devoted to this topic, although further reading would be essential to anyone interested in this area.

The second chapter, approximately one third of the text, with some 349 references, provides a comprehensive cover of chemical stability, including kinetics, decomposition mechanisms and assay methods. However, there is very little included on packaging, or formulation methods such as microencapsulation which may be used to minimize stability problems. Other areas such as the physical stability of emulsions and suspensions have not been mentioned at all.

Physicochemical interactions are covered in some depth in the third chapter. Various combinations of drug-drug, drug-excipient and excipient-excipient interactions have all been included, with many useful examples. Potential advantages such as improved absorption by use of cyclodextrin inclusion complexes have also been given, as well as the numerous disadvantages. Many of the commonly used excipients have been included here but further reading of the many references listed may be required to obtain greater detail. Also included in this chapter is a table of some 14 pages listing expected interactions for i.v. preparations, all with references, which may prove useful for a limited number of readers but is more likely to be of limited value for most.

The final chapter deals with biopharmaceutical aspects of formulation. Again there are a number of sections, including pharmacokinetics, bioavailability, physicochemical factors affecting absorption and one on controlled-release formulations. The physicochemical factors affecting absorption are well covered, with useful examples. The section on controlled release is rather mathematical, with little detail on formulation processes.

The book, rather than being an essential text for either those involved in drug development and manufacturing or those in research or academic areas, should be regarded as a useful reference text. To this end there are many detailed examples and over 1000 references are included.

K. I. CUMMING

Pharmaceutical Thermal Analysis—Techniques and Applications: J. L. FORD and P. TIMMINS, Ellis Horwood, Chichester, 1989. Pages 313. £55.00.

Thermal analysis occupies an important niche in physical and industrial pharmacy and a text devoted to this area is long overdue. The book will be of much interest to those in both industry and academia, each being represented by the joint

BOOK REVIEWS

Standardization Within Analytical Chemistry: P. KIVALO, Akadémiai Kiadó, Budapest, 1989. Pages 155 + 125 (appendices). £23.00.

*This book is about standard methods, not standard solutions, and is not concerned with matters of technique. It is also more about standardization than about analytical chemistry, so "electrical engineering" might be substituted throughout without much affecting the logic of the argument. Kivalo seems to propose that the force of the argument would be different, however, because he sees analytical chemistry as an undervalued discipline, to the extent that he calls for the formation of an International Union of Pure and Applied Analytical Chemistry (an isolationism curiously at odds with the general spirit of the book). I think we should beware of this view, since it may be one of a series of grudges we hold as chemists, scientists, graduates or even citizens, but can this book change it anyway? I doubt if those whom Kivalo seeks to influence will read it, or finish it if they start. The historical background has some interesting aspects and Kivalo puts the arguments for and against standardization very fairly, but his style is too close to that of a standards document for comfort. One or two concrete examples of progress in standardization, with costs and benefits, would have helped. The bad side of standardization is bureaucratic wrangling of the sort that gives rise to terminology that numbs the mind rather than elucidates the meaning; Kivalo hints at the phenomenon, but is not very critical of any specific effects. About half the book is taken up by reproductions of four standards documents which, while of value in themselves, are available elsewhere. This book does provoke thought and eventually I found that I mostly agreed with the author, but the ideas would have been better promoted at essay length.

DEREK MIDGLEY

Drug Formulation: I. RACZ, Wiley, Chichester, 1989. Pages x + 416. £61.00.

The title of the text may prove rather misleading to many, as the bulk of material deals mainly with physicochemical details with little information provided on formulation or the processing methods used in formulation. The first chapter makes reference to pharmaceutical technology, saying that it includes unit operations such as milling, drying and compression to prepare dosage forms such as tablets, capsules and emulsions, but these are then not discussed in any detail.

The book consists of four chapters. The first, covering the principles of preformulation and formulation testing, is rather brief at only 27 pages and including only 21 references. A useful list of tests which may be required in preformulation for different types of dosage forms is included, but as in some other areas of the text there is little or no other detail provided. A reasonable introduction to mathematical and experimental design is given in the limited space devoted to this topic, although further reading would be essential to anyone interested in this area.

The second chapter, approximately one third of the text, with some 349 references, provides a comprehensive cover of chemical stability, including kinetics, decomposition mechanisms and assay methods. However, there is very little included on packaging, or formulation methods such as microencapsulation which may be used to minimize stability problems. Other areas such as the physical stability of emulsions and suspensions have not been mentioned at all.

Physicochemical interactions are covered in some depth in the third chapter. Various combinations of drug-drug, drug-excipient and excipient-excipient interactions have all been included, with many useful examples. Potential advantages such as improved absorption by use of cyclodextrin inclusion complexes have also been given, as well as the numerous disadvantages. Many of the commonly used excipients have been included here but further reading of the many references listed may be required to obtain greater detail. Also included in this chapter is a table of some 14 pages listing expected interactions for i.v. preparations, all with references, which may prove useful for a limited number of readers but is more likely to be of limited value for most.

The final chapter deals with biopharmaceutical aspects of formulation. Again there are a number of sections, including pharmacokinetics, bioavailability, physicochemical factors affecting absorption and one on controlled-release formulations. The physicochemical factors affecting absorption are well covered, with useful examples. The section on controlled release is rather mathematical, with little detail on formulation processes.

The book, rather than being an essential text for either those involved in drug development and manufacturing or those in research or academic areas, should be regarded as a useful reference text. To this end there are many detailed examples and over 1000 references are included.

K. I. CUMMING

Pharmaceutical Thermal Analysis—Techniques and Applications: J. L. FORD and P. TIMMINS, Ellis Horwood, Chichester, 1989. Pages 313. £55.00.

Thermal analysis occupies an important niche in physical and industrial pharmacy and a text devoted to this area is long overdue. The book will be of much interest to those in both industry and academia, each being represented by the joint

BOOK REVIEWS

Computer-Aided Drug Design: THOMAS J. PERUN and C. L. PROPST (editors), Dekker, New York, 1989. Pages xii + 493. \$99.75 (USA and Canada), \$119.50 (elsewhere).

The discovery of drug molecules has been the principal aim of the pharmaceutical industry for many years. Traditional methods of drug discovery have included screening large numbers of synthetic chemicals and natural products, and isolating active components from mixtures used in folk medicine; occasionally serendipity has lent a hand. However, drugs are normally developed as part of an organized effort to treat specific disease states.

This well-produced book is concerned with the methods and applications of advanced computer-based techniques that are used to examine potential medicinal agents, drug receptors, and the possible interactions between them. Contributions from authors in academia and industry, based in the USA and Germany, have been collated to form the 12 chapters of the text.

The methods section covers the topics of computer graphics, molecular mechanics and molecular dynamics, X-ray crystallography, nuclear magnetic resonance and enzyme kinetics. These chapters are easy to read and are descriptive, rather than mathematical, in their treatment of the subject material. In fact, Bragg's law is the only equation given in the chapter on X-ray crystallography. This section of the book is very informative but it would benefit from more details on quantum mechanics and databases of molecular structures.

The applications section, which occupies about half of the book, deals with the modern design of drugs to treat specific disease states. There are chapters on the design of inhibitors of angiotensin-converting enzyme, renin and dihydrofolate reductase. A separate chapter on antiviral drug design includes studies involving rhinovirus, which is responsible for the common cold. Conformational features are emphasized in the final chapters devoted to opioid peptides and cyclopeptides. Much biochemistry is included in this section of the book and the interdisciplinary nature of modern drug design is presented in an extremely competent and professional manner.

Nice features of the book include cross references between chapters, conclusions or summaries at the end of most chapters, extensive references, colour plates and excellent illustrations, including many stereo diagrams. It is to be recommended to the advanced student or to those already involved with drug research who wish to keep abreast of the concepts at the forefront of this technology.

P. J. COX

Handbook of Low Temperature Electronic Spectra of Polycyclic Aromatic Hydrocarbons: L. A. NAKHIMOVSKY, M. LAMOTTE and J. JOUSSOT-DUBIEN, Elsevier, New York, 1989. Pages xiv + 508. U.S.\$ 260.50, Dfl. 495.00.

Chapter 1 summarizes the theory of electronic transitions required for an understanding of some of the facets of Shpolskii spectroscopy, which provides the main theme of the book. This type of spectroscopy was described originally by E. V. Shpolskii and A. A. Il'ina, in 1951. It involves the observation of highly resolved (quasi-line) vibronic spectra of polycyclic aromatic compounds present as metastable supersaturated solid solutions in n-alkanes at low temperatures. Chapter 2 covers aspects of the host-guest interactions which are relevant to choice of the optimum alkane.

Chapter 3 deals with applications of the Shpolskii effect in analysis, particularly with respect to the identification and quantification of polycyclic aromatic compounds by "fingerprinting" from their quasi-line spectra.

Chapter 4 provides an outline description of equipment constructed by the authors to measure Shpolskii spectra. Two monochromators, one before and one after the sample, are used in order to achieve adequate signal-to-noise ratios from the low levels of light transmitted through the solid solutions, and to minimize interference from fluorescence and phosphorescence. Although the best spectra are obtained at 5 K, bandwidths are increased only slightly for samples at 10-20 K, thereby allowing a closed-cycle helium cryostat to be used for routine purposes.

Chapter 5 accounts for over 80% of the book. It treats 2-, 3-, 4-, 5-, 6- and 7-ring systems in five separate sections, each containing a review of relevant spectroscopic data for selected members of the group, and presenting full-page graphs which show 77 K (liquid nitrogen) electronic spectra down to 220 nm, 5 K (liquid helium) absorption spectra in the first $S_1 \leftarrow S_0$ region, and 5 K fluorescence (or phosphorescence) spectra, all recorded with the same equipment, thus ensuring comparability.

There is a total of 360 graphs, presenting data for 118 compounds, although, unexpectedly in view of the title of the book, 28 of these are either quinones or oxygen, nitrogen or sulphur heterocycles. There are over 600 literature citations, covering the period from 1937 to 1987. The presentation is clear, with few typographical errors.

It is unfortunate that the first author's name appears on the outside cover as L. (or I.) Nakhimovsky, and on the frontispiece as L. (or I.) A. Nakhimovsky. This author is L. A. Nakhimovsky. Accuracy should take precedence over artistic styling.

Overall, this book represents a major contribution to the field, and presents a sizeable compilation of spectra, most of them published for the first time, which will serve as reference standards for those involved with the theory and applications of Shpolskii systems.

The text provides stimulating reading.

J. M. BRUCE

BOOK REVIEWS

Computer-Aided Drug Design: THOMAS J. PERUN and C. L. PROPST (editors), Dekker, New York, 1989. Pages xii + 493. \$99.75 (USA and Canada), \$119.50 (elsewhere).

The discovery of drug molecules has been the principal aim of the pharmaceutical industry for many years. Traditional methods of drug discovery have included screening large numbers of synthetic chemicals and natural products, and isolating active components from mixtures used in folk medicine; occasionally serendipity has lent a hand. However, drugs are normally developed as part of an organized effort to treat specific disease states.

This well-produced book is concerned with the methods and applications of advanced computer-based techniques that are used to examine potential medicinal agents, drug receptors, and the possible interactions between them. Contributions from authors in academia and industry, based in the USA and Germany, have been collated to form the 12 chapters of the text.

The methods section covers the topics of computer graphics, molecular mechanics and molecular dynamics, X-ray crystallography, nuclear magnetic resonance and enzyme kinetics. These chapters are easy to read and are descriptive, rather than mathematical, in their treatment of the subject material. In fact, Bragg's law is the only equation given in the chapter on X-ray crystallography. This section of the book is very informative but it would benefit from more details on quantum mechanics and databases of molecular structures.

The applications section, which occupies about half of the book, deals with the modern design of drugs to treat specific disease states. There are chapters on the design of inhibitors of angiotensin-converting enzyme, renin and dihydrofolate reductase. A separate chapter on antiviral drug design includes studies involving rhinovirus, which is responsible for the common cold. Conformational features are emphasized in the final chapters devoted to opioid peptides and cyclopeptides. Much biochemistry is included in this section of the book and the interdisciplinary nature of modern drug design is presented in an extremely competent and professional manner.

Nice features of the book include cross references between chapters, conclusions or summaries at the end of most chapters, extensive references, colour plates and excellent illustrations, including many stereo diagrams. It is to be recommended to the advanced student or to those already involved with drug research who wish to keep abreast of the concepts at the forefront of this technology.

P. J. COX

Handbook of Low Temperature Electronic Spectra of Polycyclic Aromatic Hydrocarbons: L. A. NAKHIMOVSKY, M. LAMOTTE and J. JOUSSOT-DUBIEN, Elsevier, New York, 1989. Pages xiv + 508. U.S.\$ 260.50, Dfl. 495.00.

Chapter 1 summarizes the theory of electronic transitions required for an understanding of some of the facets of Shpolskii spectroscopy, which provides the main theme of the book. This type of spectroscopy was described originally by E. V. Shpolskii and A. A. Il'ina, in 1951. It involves the observation of highly resolved (quasi-line) vibronic spectra of polycyclic aromatic compounds present as metastable supersaturated solid solutions in n-alkanes at low temperatures. Chapter 2 covers aspects of the host-guest interactions which are relevant to choice of the optimum alkane.

Chapter 3 deals with applications of the Shpolskii effect in analysis, particularly with respect to the identification and quantification of polycyclic aromatic compounds by "fingerprinting" from their quasi-line spectra.

Chapter 4 provides an outline description of equipment constructed by the authors to measure Shpolskii spectra. Two monochromators, one before and one after the sample, are used in order to achieve adequate signal-to-noise ratios from the low levels of light transmitted through the solid solutions, and to minimize interference from fluorescence and phosphorescence. Although the best spectra are obtained at 5 K, bandwidths are increased only slightly for samples at 10-20 K, thereby allowing a closed-cycle helium cryostat to be used for routine purposes.

Chapter 5 accounts for over 80% of the book. It treats 2-, 3-, 4-, 5-, 6- and 7-ring systems in five separate sections, each containing a review of relevant spectroscopic data for selected members of the group, and presenting full-page graphs which show 77 K (liquid nitrogen) electronic spectra down to 220 nm, 5 K (liquid helium) absorption spectra in the first $S_1 \leftarrow S_0$ region, and 5 K fluorescence (or phosphorescence) spectra, all recorded with the same equipment, thus ensuring comparability.

There is a total of 360 graphs, presenting data for 118 compounds, although, unexpectedly in view of the title of the book, 28 of these are either quinones or oxygen, nitrogen or sulphur heterocycles. There are over 600 literature citations, covering the period from 1937 to 1987. The presentation is clear, with few typographical errors.

It is unfortunate that the first author's name appears on the outside cover as L. (or I.) Nakhimovsky, and on the frontispiece as L. (or I.) A. Nakhimovsky. This author is L. A. Nakhimovsky. Accuracy should take precedence over artistic styling.

Overall, this book represents a major contribution to the field, and presents a sizeable compilation of spectra, most of them published for the first time, which will serve as reference standards for those involved with the theory and applications of Shpolskii systems.

The text provides stimulating reading.

J. M. BRUCE

BOOK REVIEWS

Preparative-Scale Chromatography. Eli Grushka (editor), Dekker, New York, 1989. Pages xi + 324. Price \$99.75 (USA and Canada); \$119.50 (elsewhere).

This book presents a highly detailed account of factors which either in theory, in practice, or in both, determine or markedly influence chromatographic characteristics and behaviour. The targets of concern are various types of preparative-scale chromatography. The opening chapter by P. Rouchon *et al.* details and explains reasons for the departure of chromatographic behaviour from linearity when larger samples are being separated, by considering what happens to a single component band on a column. Theoretical calculations are excellently supported by experimental findings. D. J. Wilson is concerned with a mathematical consideration of the effect of solvent-solvent interactions on retention-times, on loss of resolution, and on peak-distortion in preparative GC. H. Colin deals with problems of design of preparative columns, including consideration of the effects of particle size, and of column length and diameter on the load a column can carry. K.-P. Hupe and B. Hoffmann deal with scaling-up from analytical to preparative liquid chromatographic columns so that under the conditions selected the sample may be separated in the shortest possible time, with as little solvent as necessary, on as small a column as possible and with recovery of the solutes in minimal volumes. These objectives must be the targets of many chromatographic separations: targets that are often easier to define than to meet in practice. G. Cretier and J. L. Rocca, in considering the optimization of the injection conditions in preparative liquid chromatography (PLC), provide excellent data on column-overloading and solute-separation but conclude that "the optimal injection conditions depend both on the isotherm and on the solubility limit of the sample in the mobile phase" and that trial-and-error is necessary. V. R. Meyer considers the influence of sample-mass and of flow-velocity in PLC by studying separations on fine and coarse grades of silica. C. Dewaele *et al.* continue in similar vein but deal additionally with the effect of column diameter and particle size. J. Newburger *et al.* offer interesting, and surprising, comments and explanation of observations on the sharpening of peaks when closely related compounds are eluted, compared to their elution from columns on which they are individually present. P. Gareil and R. Rosset are concerned with the characterization of strongly non-linear elution peaks in LC. Y. Ito deals in two chapters with the gyrations of coil planet centrifuges and demonstrates their successful use in separating DNP-amino-acids and dipeptides. P. E. Barker and G. Ganetsos supply a valuable survey of the use, and potential use, of semicontinuous chromatographic refining on an industrial scale and predict that industry, which is at present often hesitant to use chromatographic procedures, will shortly be persuaded of both their desirability and practicality, not only for carbohydrate and biotechnological applications but for many other separations. G. Leaver *et al.* describe the production of pure protein (specifically of albumin from animal blood) by ion-exchange chromatography, and H. Schott deals with the isolation of purine oligonucleotides from partial hydrolysates of depyriminated DNA. E. Soczewinski *et al.* describe the migration of zones of dyes in PTLC. In spite of the complexity of some of the detail the authors and editor are to be congratulated on presenting clearly and interestingly matter which is on occasion quite complex. The text is clear and the diagrams excellent and extremely valuable.

K. C. B. WILKIE

Laser Raman Spectrometry—Analytical Applications: H. BARAŃSKA, A. ŁABUDZINSKA and J. TERPIŃSKI, Ellis Horwood, Chichester, 1987. Pages 271. £38.50

Raman spectroscopy is a vibrational technique which is not as widely used in analytical chemistry as it might be. In a number of industrial situations it has proved to be an ideal answer to many problems. Its main advantage is that it can be used for analysis of aqueous solutions. The vibrations which it senses are usually symmetric and relatively easily recognized, and since laser excitation is used it is possible to employ flexible optical systems in which the beam is directed quite precisely. Perhaps some of the disadvantages are that it is not particularly sensitive and that in the past there have been problems with expensive and unreliable equipment. This latter disadvantage is rapidly disappearing and modern instruments using multiple wavelength detection have made Raman spectroscopy a much more user-friendly and available technique. Thus, a good book on basic Raman spectroscopy may be a welcome addition to the analytical chemist's library.

The book by Barańska *et al.* is well written and provides a good fundamental introduction to conventional Raman spectroscopy. It includes, along with standard chapters on the theory of Raman spectroscopy, a very useful short chapter on group theory that helps to make the spectral interpretation of small molecules more understandable to the average chemist or analyst.

The measurement of Raman scattering requires that the instrument is capable of detecting weak signals in the presence of a strong signal at a slightly different wavelength. Normally visible-region lasers are used and consequently the conventional Raman spectrometer includes a large double or triple monochromator and a photon-counting photomultiplier detector. This type of spectroscopy and the many optical arrangements which Raman spectroscopists favour are well

BOOK REVIEWS

Algorithms for Chemists: J. ZUPAN, Wiley, 1989. Pages xv + 290. £39.50.

This book, which is for serious users of the computer, contains 31 algorithms that are suitable for handling experimental data sets. It is based on a course entitled "Introduction to computer methods for chemists" aimed at senior and postgraduate students. No one book can describe all computational procedures of interest to chemists and methods for manipulating data are constantly evolving. In this context the author has decided to concentrate on certain topics to the exclusion of others. For example, algorithms relating to linear regression, elementary statistical analysis and simultaneous equations are omitted. The book has been divided into three parts: "Data", "Preprocessing of Data" and "Data Handling". Algorithms are included in each of these sections but the allocation to subject headings is a little arbitrary.

Part one covers data representation and structure of data files. The algorithms of interest here include generation of random numbers and sorting procedures. The pictorial explanation, of the bubble type complete with rising bubbles, is a nice addition.

In part two, smoothing, peak detection and baseline correction of instrumental data are well presented. The chapter on transformations is of necessity very mathematical and includes geometrical, fast Fourier and Hadamard transformations. Some prior knowledge of these techniques would be desirable and the inclusion of some chemical applications, e.g., crystallographic analysis, would improve the chapter. An algorithm for Simplex optimization is also included in this section and the underlying principles are clearly explained.

Part three bravely attempts to describe a number of demanding data handling techniques. These are clustering of data, pattern recognition, computer handling of chemical structures, fractal forms and processes, and expert systems. The final algorithm relates to spectra simulation by reference to a spectroscopy-based expert system.

It should be noted that the algorithms presented are not suitable for immediate use. Each one is written as an unusual mixture of various computer languages but clear explanations are appended to each instruction line. The reason for this format relates to the course "Introduction to computer methods for chemists" where the students are asked to transform the algorithms into working programs. Most computer-literate chemists will be quite happy with the presentation of the algorithms. However, many chemists want commercial software for data handling, or complete, debugged programs that are suitable for immediate use. In an ideal world chemists should be able to process data in any way they wish and the book will be welcomed by those with the time and ability to aspire to this goal. Professor Zupan should be congratulated on bringing so many different computer software techniques to the attention of chemists.

P. J. Cox

Measurement of Oxygen by Membrane-covered Probes: V. LINEK, V. VACEK, J. SINKULE and P. BENEŠ, Horwood, Chichester, 1988. Pages 330. £45.00.

This book aims at providing a state-of-the-art review on membrane-covered oxygen probes. There is little doubt it will attract the attention of scientists involved in oxygen detection and quantitative determination.

Interesting characteristics of the book result from the practice-oriented presentation and writing. This is obvious from the very beginning of the book, where (Chapter 2) the polarographic determination of oxygen is described with selective comments and hints on the experimental conditions and the possible problems arising in the measurements. The formal descriptions of the probe response during oxygen reduction are sound and reasonably sized in Chapters 3 and 4. The major part of the book, however (Chapters 5-9) is dedicated to the practical implementation of the probe devices, to the analysis of their operational characteristics and to the control of their experimental significance and calibration. It includes several examples where membrane-covered oxygen probes are used for monitoring the progress of reacting systems and for determining kinetic and thermodynamic parameters.

As such, this book is a comprehensive and up to date document, which should be in the hands of any scientist confronted with the monitoring of oxygen.

M. GROSS

Chemical Instrumentation: A Systematic Approach: H. A. STROBEL and W. R. HEINEMAN, 3rd Ed., Wiley, New York, 1989. Pages 1210. £34.85.

This book fills a long-felt need for a basic book on chemical instrumentation. The authors have been successful in condensing material from a wide variety of disciplines. Though other excellent books on instrumental analysis do exist, the present book has a definite edge because it treats the instrumental part in more detail and more authoritatively. The earlier books treated instruments simply by block diagrams and some discussion of the various components. However, with the massive developments in chemical instrumentation such an approach today is perhaps not adequate.

BOOK REVIEWS

Algorithms for Chemists: J. ZUPAN, Wiley, 1989. Pages xv + 290. £39.50.

This book, which is for serious users of the computer, contains 31 algorithms that are suitable for handling experimental data sets. It is based on a course entitled "Introduction to computer methods for chemists" aimed at senior and postgraduate students. No one book can describe all computational procedures of interest to chemists and methods for manipulating data are constantly evolving. In this context the author has decided to concentrate on certain topics to the exclusion of others. For example, algorithms relating to linear regression, elementary statistical analysis and simultaneous equations are omitted. The book has been divided into three parts: "Data", "Preprocessing of Data" and "Data Handling". Algorithms are included in each of these sections but the allocation to subject headings is a little arbitrary.

Part one covers data representation and structure of data files. The algorithms of interest here include generation of random numbers and sorting procedures. The pictorial explanation, of the bubble type complete with rising bubbles, is a nice addition.

In part two, smoothing, peak detection and baseline correction of instrumental data are well presented. The chapter on transformations is of necessity very mathematical and includes geometrical, fast Fourier and Hadamard transformations. Some prior knowledge of these techniques would be desirable and the inclusion of some chemical applications, e.g., crystallographic analysis, would improve the chapter. An algorithm for Simplex optimization is also included in this section and the underlying principles are clearly explained.

Part three bravely attempts to describe a number of demanding data handling techniques. These are clustering of data, pattern recognition, computer handling of chemical structures, fractal forms and processes, and expert systems. The final algorithm relates to spectra simulation by reference to a spectroscopy-based expert system.

It should be noted that the algorithms presented are not suitable for immediate use. Each one is written as an unusual mixture of various computer languages but clear explanations are appended to each instruction line. The reason for this format relates to the course "Introduction to computer methods for chemists" where the students are asked to transform the algorithms into working programs. Most computer-literate chemists will be quite happy with the presentation of the algorithms. However, many chemists want commercial software for data handling, or complete, debugged programs that are suitable for immediate use. In an ideal world chemists should be able to process data in any way they wish and the book will be welcomed by those with the time and ability to aspire to this goal. Professor Zupan should be congratulated on bringing so many different computer software techniques to the attention of chemists.

P. J. Cox

Measurement of Oxygen by Membrane-covered Probes: V. LINEK, V. VACEK, J. SINKULE and P. BENEŠ, Horwood, Chichester, 1988. Pages 330. £45.00.

This book aims at providing a state-of-the-art review on membrane-covered oxygen probes. There is little doubt it will attract the attention of scientists involved in oxygen detection and quantitative determination.

Interesting characteristics of the book result from the practice-oriented presentation and writing. This is obvious from the very beginning of the book, where (Chapter 2) the polarographic determination of oxygen is described with selective comments and hints on the experimental conditions and the possible problems arising in the measurements. The formal descriptions of the probe response during oxygen reduction are sound and reasonably sized in Chapters 3 and 4. The major part of the book, however (Chapters 5-9) is dedicated to the practical implementation of the probe devices, to the analysis of their operational characteristics and to the control of their experimental significance and calibration. It includes several examples where membrane-covered oxygen probes are used for monitoring the progress of reacting systems and for determining kinetic and thermodynamic parameters.

As such, this book is a comprehensive and up to date document, which should be in the hands of any scientist confronted with the monitoring of oxygen.

M. GROSS

Chemical Instrumentation: A Systematic Approach: H. A. STROBEL and W. R. HEINEMAN, 3rd Ed., Wiley, New York, 1989. Pages 1210. £34.85.

This book fills a long-felt need for a basic book on chemical instrumentation. The authors have been successful in condensing material from a wide variety of disciplines. Though other excellent books on instrumental analysis do exist, the present book has a definite edge because it treats the instrumental part in more detail and more authoritatively. The earlier books treated instruments simply by block diagrams and some discussion of the various components. However, with the massive developments in chemical instrumentation such an approach today is perhaps not adequate.

EDITORIAL ANNOUNCEMENT

PROFESSOR I. P. ALIMARIN

With great sadness we announce the death (from a heart attack, on 17 December 1989, at the age of 86) of Professor I P Almarin, Member of the USSR Academy of Sciences, Head of the Analytical Chemistry Division of Moscow University, Senior Scientist of the Vernadsky Institute of Geochemistry and Analytical Chemistry of the USSR Academy of Sciences, and a Regional Editor of *Talanta* since 1962.

BOOK REVIEWS

Computerized Multiple Input Chromatography: M. KALJURAND and E. KÜLLIK, Ellis Horwood, Chichester, 1989. Pages 225. Price £45.00

The authors explore a number of applications of computer control and data interpretation in gas and liquid chromatography. Their principal interest is in correlation chromatography (CC) in which a pseudo-random binary sequence of overlapping injections is coupled with cross-correlation between the sequence and the resulting signal to improve the signal to noise ratio for separations of trace levels of analytes.

They then examine the application of sequential repeated injections to monitor changes in samples with time or conditions, and discuss column switching techniques in which time slices from the first column are fed to a second column. In both cases they emphasize the need to use a computer to control the multiple injections and monitor the results and describe the experimental systems used for injection and column switching.

The overall theme of the book is the application of information theory to these chromatographic processes. Unfortunately the authors often mix techniques and it is often difficult to decide whether CC or repeated injection with fast separations is being used. The applications concentrate on thermal analysis, including pyrolysis of polymers, and trace constituents in environmental samples.

The book was completed in January 1987 but there are few references even to 1986, so that some sections, particularly those referring to computers, are dated. The advantages of the Apple II for control are described but no mention is made of the much more powerful computing ability of the IBM (or its clones). Newer instruments and intelligent integrators would also now routinely incorporate many of the required control facilities.

The book is interesting to read (the matrix algebra can be skipped), but with relatively few applications to real samples other than pyrolysis, its value will be mainly as a general background to chromatography.

R. M. SMITH

Troubleshooting LC Systems: JOHN W. DOLAN and LLOYD R. SNYDER, Humana, New Jersey, 1989. Pages viii + 515. \$65.00 (U.S.), Export \$75.00.

The authors of this text are very well known in the field of liquid chromatography, from their articles and short courses. Professor Snyder has also recently been appointed editor of *J. Chromatography* and so even before opening this book the reader can be assured that its contents will merit consideration.

The book is best described as a reference manual and it is similar in design to those books which describe the function, efficient use and possible faults that may occur in a car or a human body. The three sections of the book attempt to condense the expertise of many practical LC workers into an easy-to-use format.

The first section examines LC difficulties in terms of problem area, primary symptom, secondary symptom and likely cause. This approach is expanded in an extensive problem-isolation table which is essentially a flowchart with 676 rows and 6 column headings. Examples explaining the use of this table are given and whereas many problems can be solved through use of this guide, others, such as specific electronic problems, are considered outside the expertise of most readers. The logic involved in isolating and correcting LC problems is similar to that found in computer-based expert systems such as "The HPLC Doctor". Other basic considerations such as elementary separation theory, preventative procedures and good troubleshooting habits are covered in this section of the book.

Individual LC modules are described in the next section and this occupies about half of the book. Each of the eight chapters here is self-contained and each describes a module, e.g., pumps, columns, detectors etc., in detail. Good use is made of diagrams and photographs, and principles of operation and maintenance are included together with extensive coverage of possible problems and their solutions.

The final section deals mainly with problems associated with separation difficulties. Reasons for band tailing and peak distortion are given and other changes in the appearance of the chromatogram are discussed. Solutions to problems in quantification, gradient elution and sample pretreatment are offered. The index is comprehensive and deals efficiently with the inevitable overlap of subject material.

I checked some of the advice offered on dealing with practical problems, with the chief technician in our HPLC laboratories. The resulting comments were favourable: "That's precisely what I did" or "That's just what I would do". In conclusion, a very useful book for beginners and those on their way to becoming competent in practical LC.

P. J. Cox

Advances in Drug Therapy of Gastrointestinal Ulceration: ANDREW GARNER and BRENDAN J. R. WHITTLE (editors), Wiley, Chichester, 1989. Pages xvi + 306. £40.00.

The 20 chapters in this book are based on the proceedings of the 38th Annual Biological Council Symposium on Drug Action held at the Royal Institution in London on 11-12 April 1988. The topic is presented from a physiological/pharmacological viewpoint with chemistry very much in the background. As the emphasis is not on chemistry the book might be regarded as unsuitable for analytical chemists. However, much analytical effort today is directed towards producing safe and effective drugs and the world's two top selling (i.e., money-making) drugs, ranitidine and cimetidine, are both anti-ulcer drugs. These two histamine H₂-antagonists together with other possible anti-ulcer agents are of much interest to the pharmaceutical industry, where many analytical chemists work.

BOOK REVIEWS

Computerized Multiple Input Chromatography: M. KALJURAND and E. KÜLLIK, Ellis Horwood, Chichester, 1989. Pages 225. Price £45.00

The authors explore a number of applications of computer control and data interpretation in gas and liquid chromatography. Their principal interest is in correlation chromatography (CC) in which a pseudo-random binary sequence of overlapping injections is coupled with cross-correlation between the sequence and the resulting signal to improve the signal to noise ratio for separations of trace levels of analytes.

They then examine the application of sequential repeated injections to monitor changes in samples with time or conditions, and discuss column switching techniques in which time slices from the first column are fed to a second column. In both cases they emphasize the need to use a computer to control the multiple injections and monitor the results and describe the experimental systems used for injection and column switching.

The overall theme of the book is the application of information theory to these chromatographic processes. Unfortunately the authors often mix techniques and it is often difficult to decide whether CC or repeated injection with fast separations is being used. The applications concentrate on thermal analysis, including pyrolysis of polymers, and trace constituents in environmental samples.

The book was completed in January 1987 but there are few references even to 1986, so that some sections, particularly those referring to computers, are dated. The advantages of the Apple II for control are described but no mention is made of the much more powerful computing ability of the IBM (or its clones). Newer instruments and intelligent integrators would also now routinely incorporate many of the required control facilities.

The book is interesting to read (the matrix algebra can be skipped), but with relatively few applications to real samples other than pyrolysis, its value will be mainly as a general background to chromatography.

R. M. SMITH

Troubleshooting LC Systems: JOHN W. DOLAN and LLOYD R. SNYDER, Humana, New Jersey, 1989. Pages viii + 515. \$65.00 (U.S.), Export \$75.00.

The authors of this text are very well known in the field of liquid chromatography, from their articles and short courses. Professor Snyder has also recently been appointed editor of *J. Chromatography* and so even before opening this book the reader can be assured that its contents will merit consideration.

The book is best described as a reference manual and it is similar in design to those books which describe the function, efficient use and possible faults that may occur in a car or a human body. The three sections of the book attempt to condense the expertise of many practical LC workers into an easy-to-use format.

The first section examines LC difficulties in terms of problem area, primary symptom, secondary symptom and likely cause. This approach is expanded in an extensive problem-isolation table which is essentially a flowchart with 676 rows and 6 column headings. Examples explaining the use of this table are given and whereas many problems can be solved through use of this guide, others, such as specific electronic problems, are considered outside the expertise of most readers. The logic involved in isolating and correcting LC problems is similar to that found in computer-based expert systems such as "The HPLC Doctor". Other basic considerations such as elementary separation theory, preventative procedures and good troubleshooting habits are covered in this section of the book.

Individual LC modules are described in the next section and this occupies about half of the book. Each of the eight chapters here is self-contained and each describes a module, e.g., pumps, columns, detectors *etc.*, in detail. Good use is made of diagrams and photographs, and principles of operation and maintenance are included together with extensive coverage of possible problems and their solutions.

The final section deals mainly with problems associated with separation difficulties. Reasons for band tailing and peak distortion are given and other changes in the appearance of the chromatogram are discussed. Solutions to problems in quantification, gradient elution and sample pretreatment are offered. The index is comprehensive and deals efficiently with the inevitable overlap of subject material.

I checked some of the advice offered on dealing with practical problems, with the chief technician in our HPLC laboratories. The resulting comments were favourable: "That's precisely what I did" or "That's just what I would do". In conclusion, a very useful book for beginners and those on their way to becoming competent in practical LC.

P. J. Cox

Advances in Drug Therapy of Gastrointestinal Ulceration: ANDREW GARNER and BRENDAN J. R. WHITTLE (editors), Wiley, Chichester, 1989. Pages xvi + 306. £40.00.

The 20 chapters in this book are based on the proceedings of the 38th Annual Biological Council Symposium on Drug Action held at the Royal Institution in London on 11-12 April 1988. The topic is presented from a physiological/pharmacological viewpoint with chemistry very much in the background. As the emphasis is not on chemistry the book might be regarded as unsuitable for analytical chemists. However, much analytical effort today is directed towards producing safe and effective drugs and the world's two top selling (*i.e.*, money-making) drugs, ranitidine and cimetidine, are both anti-ulcer drugs. These two histamine H₂-antagonists together with other possible anti-ulcer agents are of much interest to the pharmaceutical industry, where many analytical chemists work.

BOOK REVIEWS

Multidimensional Chromatography: H. J. CORTES (editor), Dekker, New York, 1990. Pages viii + 378. \$99.75 (U.S. and Canada), \$119.50 (elsewhere).

To the non-specialist the term 'multidimensional chromatography' would probably convey initially the well-known technique of thin-layer chromatography (TLC) in which a secondary separation is developed orthogonally on the same plate. This is just one example of the method and multidimensional TLC is the subject of Chapter 2. What this chapter does and indeed what the book as a whole achieves, is to bring together a wealth of information on the variety, scope and resolving power of multidimensional chromatography. It appears that all the important aspects of the subject are covered somewhere in the volume by contributors who are leading authorities in the field.

As well as addressing the mathematical treatment and theoretical advantages of multidimensional chromatography and thus setting the scene for the rest of the book, Chapter 1 also deals more generally with multidimensional separation methods but only so far as is necessary to place multidimensional chromatography in context within the broader framework of separation methodology as a whole.

Advances in two-dimensional gas chromatography are highlighted in Chapter 3 which emphasizes the practical aspects of the technique and focuses attention on recent developments relating to capillary columns.

Chapter 4 deals with selectivity tuning in capillary gas chromatography (CGC), including multidimensional CGC, while Chapter 5 looks at the applications of multidimensional gas chromatography to process control. This chapter thus complements Chapter 3 and once again there is emphasis on practical aspects.

Instrumentation and applications of on-line multidimensional high-performance liquid chromatography (MD HPLC) are covered in Chapter 6.

In a book in which multidimensional HPLC and multidimensional GC feature strongly, it is fitting that there should be a chapter devoted to on-line coupled HPLC-CGC, a technique which offers a very high degree of resolution of complex mixtures. Transfer techniques for the introduction of the effluent from a liquid chromatography into a capillary gas chromatograph are considered in some detail, as are numerous applications.

Another chapter is concerned with supercritical fluid chromatography (SFC) but it is little surprising to find that the following chapter deals with supercritical fluid extraction (SFE) coupled to SFC, since SFE is not a chromatographic technique. However, perhaps we should not be too pedantic and allow the editor some licence because, after all, SFE is likely to become increasingly important in future separation science.

The final chapter performs a useful function by dealing with some practical points on the assembly and operation of automated equipment.

The book contains 650 references, 150 clear illustrations, mainly line drawings and chromatograms, and 22 tables. It is a useful blend of theoretical principles, details of instrumentation and practical applications. As such it is bound to be a valuable guide and source of information for analytical and industrial chemists, biochemists and pharmaceutical scientists.

A. K. DAVIES

Marine Toxins—Origin, Structure and Molecular Pharmacology: S. HALL and G. STRICHARTZ (editors), ACS, Washington, DC, 1990. Pages xi + 377. \$74.95.

This book developed from a conference on toxins from aquatic and marine environments, held at Woods Hole, Mass., in 1987. However, the submission dates of individual chapters range from May to October 1989 so the work is commendably up-to-date and includes some 1989 references.

In some parts of the world marine toxins are a significant health hazard, and cases of severe and lethal poisoning occur annually from such causes as the consumption of shellfish, contact with jellyfish, and from toxic algae in fresh water. Understanding such events is obviously of medical and scientific interest, and studies on these toxins may help to solve related biochemical and physiological problems, and provide leads for drug development.

The editors are pharmacologists and the 27 chapters, like the preceding conference presumably, are devoted predominantly to molecular pharmacology. Six chapters are concerned with polyether toxins, six with palytoxin, and eight with peptide toxins. Saxitoxins and related molecules are also discussed in several chapters.

For *Talanta* readers the chapters of most interest are those on HPLC (Sullivan), X-ray studies (Van Duyne), and the biosynthesis of saxitoxins and brevetoxins (Shimizu). The HPLC method is comparatively new in this research area, and ion-interaction chromatography on porous polymer columns is found to be most efficient. Examples are given of the application of HPLC to the metabolism of toxins in clams, and in tracing toxins through the food chain. The X-ray chapter gives a detailed account of crystallographic work on the brevetoxins.

The book has been attractively produced from camera-ready copy and is reasonably priced. Errors appear to be few, the most obvious to this reviewer being those in the saxitoxin formulae on pages 22 and 24. The book is unlikely to be purchased by analytical chemists, but it should find a home in the libraries of all institutions interested in marine metabolites.

R. H. THOMSON

Radioanalytical Chemistry: J. TÖLGYESSY and M. KYRŠ, Ellis Horwood, Chichester, 1989. Volume 1, pages 354. Volume 2, pages 498. £59.95 (each).

These two volumes describe a wide range of methods of analysis in which determinations culminate with measurement of radioactivity, and so are frequently applicable where low limits of detection or non-destructive analyses are required. Provided for an analytical readership, introductory chapters on basic radioactivity and instrumentation, which are frequently included in books in this area, are excluded.

Volume 1 covers (i) Analysis by measurement of natural radioactivity, (ii) Isotope dilution analysis, (iii) Radio-reagent methods, (iv) Radiometric titrations, (v) Radioimmunoassay, and (vi) Radiochemical methods for determination of biological activity of enzymes. Whilst the last two sections are concerned with organic applications, the remainder (in both volumes) are concerned with inorganic analysis. The use of radioactive tracers is a useful means of investigating aspects of alternative methods of analysis, and a chapter on this topic would have been welcome.

Volume 2 covers (i) Activation analysis and (ii) Physical methods based on absorption, scattering and fluorescence, with an additional chapter on automation and a 172 page appendix of radionuclide data and tables of optimum spike/analyte ratios for isotope dilution analysis. The survey of automation of radiochemical methods is timely since this approach is likely to increase in response to reduction of acceptable dose limits. With increasing awareness of radiological and other hazards experienced in the analytical laboratory, it would also have been timely to include some comment (possibly in the introduction) of potential radiation exposure when using the methods described.

Each section concludes with a collection of references, for when comprehensive details of methods are required, and a "Selected" bibliography. The latter occasionally includes manufacturers' literature and material from the 1960's which may be difficult to locate.

Overall, these two volumes provide comprehensive coverage of a variety of radioanalytical methods, some of which have only previously been described in specialized monographs. Whilst the applicability of some of these methods is limited, the overall content is relevant to postgraduate students of analytical chemistry, notwithstanding the apparent age of some apparatus used in illustrations. Examples of applications are very diverse, so most analysts should find something of interest in library copies. For those who subscribe to Kolthoff and Elving's *Treatise on Analytical Chemistry*, most of the subject matter is also covered in the multi-authored Volume 14 (Part 1, 2nd Ed.) which was published by Wiley in 1986.

J. E. WHITLEY

Physical Organic Chemistry, 2nd Ed.: CALVIN D. RITCHIE, Dekker, New York, 1990. Pages x + 357. \$59.75 (U.S. and Canada), \$71.50 (elsewhere).

Probably the first book to carry the title "Physical Organic Chemistry" was by Hammett in 1940. This remained the major text until the first edition of Ingold's *magnum opus* in 1953. This tome spawned Gould's book, which cheekily inverted Ingold's title and presented material with a lighter touch; even today Gould's book is far from passé. Subsequently a number of books in the area have appeared, but few have dominated the market for long.

The second edition of Ritchie's book follows fifteen years after the first, and, as with all second editions, is larger. In the preface, intending readers are counselled darkly against perusing the book at bedtime, and this is true since the text is sited well to the physical side of physical organic chemistry. Much mathematical rigour is included. It is probable that there is a Boltzmann distribution of attitudes such that the majority audience would prefer a more descriptive approach and certainly one that included more background material. Ritchie has apparently gone unashamedly for the minority and one feels that he is almost wilfully shooting to miss the audience target.

Although the author has written a commendable book from his viewpoint, it does not, in contrast to his research papers, read easily.

On selected specified points: ρ_+ appears out of mid-air on page 138 and on page 137 peroxide ion is said, without explanation, to be a good nucleophile (and merits an index entry). The perceptive student may wonder: why peroxide rather than hydroxide, and what is the relationship between them? Yet there is no mention of the alpha effect, which featured in a paper of Ritchie's in 1975. On pages 280–282 a section on solvent isotope effects is devoid of explanation; a potted summary of the papers of Bunton and Shiner in 1961 would provide more help. On page 288 a sterile problem on steric deuterium isotope effects could have been more enticingly posed around a real-life example—several are in the literature, e.g., results from Mislow, Melander and McKenna, again from the 1960s.

It may be wondered how many students will benefit from the last chapter "Transition State Theory and Primary Isotope Effects" in which real chemistry is sparse; indeed a review article would be more appropriate for this material.

It would be interesting to know the rationale of the publishers in charging \$11.75 less for the book in the U.S.A., where salaries are higher, than elsewhere.

D. G. MORRIS

BOOK REVIEWS

Standardization Within Analytical Chemistry: P. KIVALO, Akadémiai Kiadó, Budapest, 1989. Pages 155 + 125 (appendices). £23.00.

*This book is about standard methods, not standard solutions, and is not concerned with matters of technique. It is also more about standardization than about analytical chemistry, so "electrical engineering" might be substituted throughout without much affecting the logic of the argument. Kivalo seems to propose that the force of the argument would be different, however, because he sees analytical chemistry as an undervalued discipline, to the extent that he calls for the formation of an International Union of Pure and Applied Analytical Chemistry (an isolationism curiously at odds with the general spirit of the book). I think we should beware of this view, since it may be one of a series of grudges we hold as chemists, scientists, graduates or even citizens, but can this book change it anyway? I doubt if those whom Kivalo seeks to influence will read it, or finish it if they start. The historical background has some interesting aspects and Kivalo puts the arguments for and against standardization very fairly, but his style is too close to that of a standards document for comfort. One or two concrete examples of progress in standardization, with costs and benefits, would have helped. The bad side of standardization is bureaucratic wrangling of the sort that gives rise to terminology that numbs the mind rather than elucidates the meaning; Kivalo hints at the phenomenon, but is not very critical of any specific effects. About half the book is taken up by reproductions of four standards documents which, while of value in themselves, are available elsewhere. This book does provoke thought and eventually I found that I mostly agreed with the author, but the ideas would have been better promoted at essay length.

DEREK MIDGLEY

Drug Formulation: I. RACZ, Wiley, Chichester, 1989. Pages x + 416. £61.00.

The title of the text may prove rather misleading to many, as the bulk of material deals mainly with physicochemical details with little information provided on formulation or the processing methods used in formulation. The first chapter makes reference to pharmaceutical technology, saying that it includes unit operations such as milling, drying and compression to prepare dosage forms such as tablets, capsules and emulsions, but these are then not discussed in any detail.

The book consists of four chapters. The first, covering the principles of preformulation and formulation testing, is rather brief at only 27 pages and including only 21 references. A useful list of tests which may be required in preformulation for different types of dosage forms is included, but as in some other areas of the text there is little or no other detail provided. A reasonable introduction to mathematical and experimental design is given in the limited space devoted to this topic, although further reading would be essential to anyone interested in this area.

The second chapter, approximately one third of the text, with some 349 references, provides a comprehensive cover of chemical stability, including kinetics, decomposition mechanisms and assay methods. However, there is very little included on packaging, or formulation methods such as microencapsulation which may be used to minimize stability problems. Other areas such as the physical stability of emulsions and suspensions have not been mentioned at all.

Physicochemical interactions are covered in some depth in the third chapter. Various combinations of drug-drug, drug-excipient and excipient-excipient interactions have all been included, with many useful examples. Potential advantages such as improved absorption by use of cyclodextrin inclusion complexes have also been given, as well as the numerous disadvantages. Many of the commonly used excipients have been included here but further reading of the many references listed may be required to obtain greater detail. Also included in this chapter is a table of some 14 pages listing expected interactions for i.v. preparations, all with references, which may prove useful for a limited number of readers but is more likely to be of limited value for most.

The final chapter deals with biopharmaceutical aspects of formulation. Again there are a number of sections, including pharmacokinetics, bioavailability, physicochemical factors affecting absorption and one on controlled-release formulations. The physicochemical factors affecting absorption are well covered, with useful examples. The section on controlled release is rather mathematical, with little detail on formulation processes.

The book, rather than being an essential text for either those involved in drug development and manufacturing or those in research or academic areas, should be regarded as a useful reference text. To this end there are many detailed examples and over 1000 references are included.

K. I. CUMMING

Pharmaceutical Thermal Analysis—Techniques and Applications: J. L. FORD and P. TIMMINS, Ellis Horwood, Chichester, 1989. Pages 313. £55.00.

Thermal analysis occupies an important niche in physical and industrial pharmacy and a text devoted to this area is long overdue. The book will be of much interest to those in both industry and academia, each being represented by the joint

authors, as the role of thermal analysis in the characterization of both pure substances and drug-exipient mixtures is covered extensively in this well-produced text.

The first four chapters of the book are concerned with instrumentation, information obtained from thermal data, instrument optimization, and kinetics (stability). Relevant pharmaceutical examples are given but this section of the book is, in the main, quite general and the techniques described are not confined to studies solely in the pharmaceutical arena. The authors refer the reader to other works for greater details of instrument design.

The remaining ten chapters, which occupy about two-thirds of the text, are each concerned with a particular aspect of pharmaceutical thermal analysis. These chapters cover purity, characterization, solid dispersions, polymeric systems, solid dosage forms, compatibility, semi-solid systems, liposomes, freeze-drying, and miscellaneous examples. Purity determinations based on the van't Hoff equation are given and examples of various possible corrections for the fraction melted are discussed. Characterization of pharmaceutical solids concentrates on the important areas of isomers, polymorphs and solvates. Here, as throughout the book, complementary techniques such as X-ray diffraction and infrared spectroscopy are mentioned. Thermal analysis of urea, cyclodextrins, poly(vinyl pyrrolidone), poly(ethylene glycol) and other carriers in solid dispersions are covered and explained with respect to appropriate phase diagrams. Of particular interest is the role of both DSC and DTA in predicting and examining age-induced changes in these dispersions. The application of thermal methods to polymer characterization, detection of drug-polymer interactions and drug release mechanisms is also described. The characterization of drug excipients and solid dosage forms by thermal analysis is covered and the important area of drug-exipient compatibility is mentioned with suitable reference of the literature. Thermal analysis of fats and waxes, suppositories and pessaries, emulsions, and creams and ointments are all mentioned briefly. The chapter on liposomes is concerned with their potential use as drug delivery systems and their use as model membrane systems to provide a simple model of drug activity. The use of thermal analysis to determine eutectic temperatures of formulations to be freeze-dried, and the subsequent amounts of residual solvent in final products is included. The chapter on miscellaneous applications includes detection of polymorphic changes induced by spray-drying or co-grinding.

Each chapter is followed by a suitable number of references and an index, the latter being a necessary inclusion for the inevitable overlap of subject material. On browsing through the index it was a little disappointing not to come across terms such as shelf-life, X-ray diffraction, infrared spectroscopy, reference materials, automation or computer control. As the subject matter of this field is so extensive, some pharmaceutical examples will be excluded from the text and some specific cases will not have been published by workers in industry. However, the authors are to be commended on bringing together a vast amount of material, scattered through many different literature sources, to produce a reference text that will have a place in every pharmaceutical laboratory engaged in thermal analysis.

P. J. Cox

Field-Flow Fractionation: Analysis of Macromolecules and Particles: JOSEF JANČA, Dekker, New York, 1988. Pages vi + 336.

Field-flow fractionation is a method of separating substances of macromolecular and particulate dimensions. The driving force can be gravitational, centrifugal, thermal, electrical, magnetic, or shear, acting in the direction perpendicular to the flow of the fluid. The technique is similar in many aspects to chromatography but differs in that there is no stationary phase other than the walls of the fluid channel.

Anyone unfamiliar with chromatographic or field-flow techniques will find this book hard to read and digest, partly because of the style of writing and/or translation, and partly because of the author's predilection with minutiae; it is a case of not being able to see the forest for the trees. The review is comprehensive and will be of interest to those active in field-flow fractionation.

J. B. CRAIG

Ion Exchange and Sorption Processes in Hydrometallurgy: M. STREAT and D. NADEN (editors), Wiley, Chichester, 1987. Pages x + 229. £45.00.

This book is Volume 19 in a series of Critical Reports on Applied Chemistry, and was published for the Society of Chemical Industry in the UK. The book contains four chapters: Chapter 1, by the editors Streat and Naden, on the application of ion-exchange to the recovery of uranium, describes the interactions of the uranium recovery flowsheet and the ion-exchange process, the ion-exchange resins and equipment, and process design for continuous ion-exchange. Chapter 2, by McDougall and Fleming, on the extraction of precious metals by activated carbon, describes the manufacture, structure and adsorptive properties of activated carbon, the interaction between it and gold complexes, and its application to gold recovery.

Chapter 3, by Warshawsky, on the extraction of platinum group metals (PGM) by ion-exchange resins, describes the modern approach to PGM recovery and separation, the concentration of PGM by selective polymers, and an integrated ion-exchange and liquid-liquid extraction process. Chapter 4, also by Warshawsky, on chelating ion-exchangers, describes the syntheses and applications of chelating and co-ordinating polymers. This book is a critical and objective review written by experts. It is well-written and illustrated by a mixture of clear and simple diagrams and photographs: there is also an excellent balance between theory and application. Primarily, the book will be of great interest to those involved in the extraction of metals, but it will also be of interest to all those using ion-exchange or sorption processes industrially.

J. B. CRAIG

BOOK REVIEWS

Standardization Within Analytical Chemistry: P. KIVALO, Akadémiai Kiadó, Budapest, 1989. Pages 155 + 125 (appendices). £23.00.

*This book is about standard methods, not standard solutions, and is not concerned with matters of technique. It is also more about standardization than about analytical chemistry, so "electrical engineering" might be substituted throughout without much affecting the logic of the argument. Kivalo seems to propose that the force of the argument would be different, however, because he sees analytical chemistry as an undervalued discipline, to the extent that he calls for the formation of an International Union of Pure and Applied Analytical Chemistry (an isolationism curiously at odds with the general spirit of the book). I think we should beware of this view, since it may be one of a series of grudges we hold as chemists, scientists, graduates or even citizens, but can this book change it anyway? I doubt if those whom Kivalo seeks to influence will read it, or finish it if they start. The historical background has some interesting aspects and Kivalo puts the arguments for and against standardization very fairly, but his style is too close to that of a standards document for comfort. One or two concrete examples of progress in standardization, with costs and benefits, would have helped. The bad side of standardization is bureaucratic wrangling of the sort that gives rise to terminology that numbs the mind rather than elucidates the meaning; Kivalo hints at the phenomenon, but is not very critical of any specific effects. About half the book is taken up by reproductions of four standards documents which, while of value in themselves, are available elsewhere. This book does provoke thought and eventually I found that I mostly agreed with the author, but the ideas would have been better promoted at essay length.

DEREK MIDGLEY

Drug Formulation: I. RACZ, Wiley, Chichester, 1989. Pages x + 416. £61.00.

The title of the text may prove rather misleading to many, as the bulk of material deals mainly with physicochemical details with little information provided on formulation or the processing methods used in formulation. The first chapter makes reference to pharmaceutical technology, saying that it includes unit operations such as milling, drying and compression to prepare dosage forms such as tablets, capsules and emulsions, but these are then not discussed in any detail.

The book consists of four chapters. The first, covering the principles of preformulation and formulation testing, is rather brief at only 27 pages and including only 21 references. A useful list of tests which may be required in preformulation for different types of dosage forms is included, but as in some other areas of the text there is little or no other detail provided. A reasonable introduction to mathematical and experimental design is given in the limited space devoted to this topic, although further reading would be essential to anyone interested in this area.

The second chapter, approximately one third of the text, with some 349 references, provides a comprehensive cover of chemical stability, including kinetics, decomposition mechanisms and assay methods. However, there is very little included on packaging, or formulation methods such as microencapsulation which may be used to minimize stability problems. Other areas such as the physical stability of emulsions and suspensions have not been mentioned at all.

Physicochemical interactions are covered in some depth in the third chapter. Various combinations of drug-drug, drug-excipient and excipient-excipient interactions have all been included, with many useful examples. Potential advantages such as improved absorption by use of cyclodextrin inclusion complexes have also been given, as well as the numerous disadvantages. Many of the commonly used excipients have been included here but further reading of the many references listed may be required to obtain greater detail. Also included in this chapter is a table of some 14 pages listing expected interactions for i.v. preparations, all with references, which may prove useful for a limited number of readers but is more likely to be of limited value for most.

The final chapter deals with biopharmaceutical aspects of formulation. Again there are a number of sections, including pharmacokinetics, bioavailability, physicochemical factors affecting absorption and one on controlled-release formulations. The physicochemical factors affecting absorption are well covered, with useful examples. The section on controlled release is rather mathematical, with little detail on formulation processes.

The book, rather than being an essential text for either those involved in drug development and manufacturing or those in research or academic areas, should be regarded as a useful reference text. To this end there are many detailed examples and over 1000 references are included.

K. I. CUMMING

Pharmaceutical Thermal Analysis—Techniques and Applications: J. L. FORD and P. TIMMINS, Ellis Horwood, Chichester, 1989. Pages 313. £55.00.

Thermal analysis occupies an important niche in physical and industrial pharmacy and a text devoted to this area is long overdue. The book will be of much interest to those in both industry and academia, each being represented by the joint

authors, as the role of thermal analysis in the characterization of both pure substances and drug-exipient mixtures is covered extensively in this well-produced text.

The first four chapters of the book are concerned with instrumentation, information obtained from thermal data, instrument optimization, and kinetics (stability). Relevant pharmaceutical examples are given but this section of the book is, in the main, quite general and the techniques described are not confined to studies solely in the pharmaceutical arena. The authors refer the reader to other works for greater details of instrument design.

The remaining ten chapters, which occupy about two-thirds of the text, are each concerned with a particular aspect of pharmaceutical thermal analysis. These chapters cover purity, characterization, solid dispersions, polymeric systems, solid dosage forms, compatibility, semi-solid systems, liposomes, freeze-drying, and miscellaneous examples. Purity determinations based on the van't Hoff equation are given and examples of various possible corrections for the fraction melted are discussed. Characterization of pharmaceutical solids concentrates on the important areas of isomers, polymorphs and solvates. Here, as throughout the book, complementary techniques such as X-ray diffraction and infrared spectroscopy are mentioned. Thermal analysis of urea, cyclodextrins, poly(vinyl pyrrolidone), poly(ethylene glycol) and other carriers in solid dispersions are covered and explained with respect to appropriate phase diagrams. Of particular interest is the role of both DSC and DTA in predicting and examining age-induced changes in these dispersions. The application of thermal methods to polymer characterization, detection of drug-polymer interactions and drug release mechanisms is also described. The characterization of drug excipients and solid dosage forms by thermal analysis is covered and the important area of drug-exipient compatibility is mentioned with suitable reference of the literature. Thermal analysis of fats and waxes, suppositories and pessaries, emulsions, and creams and ointments are all mentioned briefly. The chapter on liposomes is concerned with their potential use as drug delivery systems and their use as model membrane systems to provide a simple model of drug activity. The use of thermal analysis to determine eutectic temperatures of formulations to be freeze-dried, and the subsequent amounts of residual solvent in final products is included. The chapter on miscellaneous applications includes detection of polymorphic changes induced by spray-drying or co-grinding.

Each chapter is followed by a suitable number of references and an index, the latter being a necessary inclusion for the inevitable overlap of subject material. On browsing through the index it was a little disappointing not to come across terms such as shelf-life, X-ray diffraction, infrared spectroscopy, reference materials, automation or computer control. As the subject matter of this field is so extensive, some pharmaceutical examples will be excluded from the text and some specific cases will not have been published by workers in industry. However, the authors are to be commended on bringing together a vast amount of material, scattered through many different literature sources, to produce a reference text that will have a place in every pharmaceutical laboratory engaged in thermal analysis.

P. J. Cox

Field-Flow Fractionation: Analysis of Macromolecules and Particles: JOSEF JANČA, Dekker, New York, 1988. Pages vi + 336.

Field-flow fractionation is a method of separating substances of macromolecular and particulate dimensions. The driving force can be gravitational, centrifugal, thermal, electrical, magnetic, or shear, acting in the direction perpendicular to the flow of the fluid. The technique is similar in many aspects to chromatography but differs in that there is no stationary phase other than the walls of the fluid channel.

Anyone unfamiliar with chromatographic or field-flow techniques will find this book hard to read and digest, partly because of the style of writing and/or translation, and partly because of the author's predilection with minutiae; it is a case of not being able to see the forest for the trees. The review is comprehensive and will be of interest to those active in field-flow fractionation.

J. B. CRAIG

Ion Exchange and Sorption Processes in Hydrometallurgy: M. STREAT and D. NADEN (editors), Wiley, Chichester, 1987. Pages x + 229. £45.00.

This book is Volume 19 in a series of Critical Reports on Applied Chemistry, and was published for the Society of Chemical Industry in the UK. The book contains four chapters: Chapter 1, by the editors Streat and Naden, on the application of ion-exchange to the recovery of uranium, describes the interactions of the uranium recovery flowsheet and the ion-exchange process, the ion-exchange resins and equipment, and process design for continuous ion-exchange. Chapter 2, by McDougall and Fleming, on the extraction of precious metals by activated carbon, describes the manufacture, structure and adsorptive properties of activated carbon, the interaction between it and gold complexes, and its application to gold recovery.

Chapter 3, by Warshawsky, on the extraction of platinum group metals (PGM) by ion-exchange resins, describes the modern approach to PGM recovery and separation, the concentration of PGM by selective polymers, and an integrated ion-exchange and liquid-liquid extraction process. Chapter 4, also by Warshawsky, on chelating ion-exchangers, describes the syntheses and applications of chelating and co-ordinating polymers. This book is a critical and objective review written by experts. It is well-written and illustrated by a mixture of clear and simple diagrams and photographs: there is also an excellent balance between theory and application. Primarily, the book will be of great interest to those involved in the extraction of metals, but it will also be of interest to all those using ion-exchange or sorption processes industrially.

J. B. CRAIG

BOOK REVIEWS

Preparative-Scale Chromatography. Eli Grushka (editor), Dekker, New York, 1989. Pages xi + 324. Price \$99.75 (USA and Canada); \$119.50 (elsewhere).

This book presents a highly detailed account of factors which either in theory, in practice, or in both, determine or markedly influence chromatographic characteristics and behaviour. The targets of concern are various types of preparative-scale chromatography. The opening chapter by P. Rouchon *et al.* details and explains reasons for the departure of chromatographic behaviour from linearity when larger samples are being separated, by considering what happens to a single component band on a column. Theoretical calculations are excellently supported by experimental findings. D. J. Wilson is concerned with a mathematical consideration of the effect of solvent-solvent interactions on retention-times, on loss of resolution, and on peak-distortion in preparative GC. H. Colin deals with problems of design of preparative columns, including consideration of the effects of particle size, and of column length and diameter on the load a column can carry. K.-P. Hupe and B. Hoffmann deal with scaling-up from analytical to preparative liquid chromatographic columns so that under the conditions selected the sample may be separated in the shortest possible time, with as little solvent as necessary, on as small a column as possible and with recovery of the solutes in minimal volumes. These objectives must be the targets of many chromatographic separations: targets that are often easier to define than to meet in practice. G. Cretier and J. L. Rocca, in considering the optimization of the injection conditions in preparative liquid chromatography (PLC), provide excellent data on column-overloading and solute-separation but conclude that "the optimal injection conditions depend both on the isotherm and on the solubility limit of the sample in the mobile phase" and that trial-and-error is necessary. V. R. Meyer considers the influence of sample-mass and of flow-velocity in PLC by studying separations on fine and coarse grades of silica. C. Dewaele *et al.* continue in similar vein but deal additionally with the effect of column diameter and particle size. J. Newburger *et al.* offer interesting, and surprising, comments and explanation of observations on the sharpening of peaks when closely related compounds are eluted, compared to their elution from columns on which they are individually present. P. Gareil and R. Rosset are concerned with the characterization of strongly non-linear elution peaks in LC. Y. Ito deals in two chapters with the gyrations of coil planet centrifuges and demonstrates their successful use in separating DNP-amino-acids and dipeptides. P. E. Barker and G. Ganetsos supply a valuable survey of the use, and potential use, of semicontinuous chromatographic refining on an industrial scale and predict that industry, which is at present often hesitant to use chromatographic procedures, will shortly be persuaded of both their desirability and practicality, not only for carbohydrate and biotechnological applications but for many other separations. G. Leaver *et al.* describe the production of pure protein (specifically of albumin from animal blood) by ion-exchange chromatography, and H. Schott deals with the isolation of purine oligonucleotides from partial hydrolysates of depyriminated DNA. E. Soczewinski *et al.* describe the migration of zones of dyes in PTLC. In spite of the complexity of some of the detail the authors and editor are to be congratulated on presenting clearly and interestingly matter which is on occasion quite complex. The text is clear and the diagrams excellent and extremely valuable.

K. C. B. WILKIE

Laser Raman Spectrometry—Analytical Applications: H. BARAŃSKA, A. ŁABUDZINSKA and J. TERPIŃSKI, Ellis Horwood, Chichester, 1987. Pages 271. £38.50

Raman spectroscopy is a vibrational technique which is not as widely used in analytical chemistry as it might be. In a number of industrial situations it has proved to be an ideal answer to many problems. Its main advantage is that it can be used for analysis of aqueous solutions. The vibrations which it senses are usually symmetric and relatively easily recognized, and since laser excitation is used it is possible to employ flexible optical systems in which the beam is directed quite precisely. Perhaps some of the disadvantages are that it is not particularly sensitive and that in the past there have been problems with expensive and unreliable equipment. This latter disadvantage is rapidly disappearing and modern instruments using multiple wavelength detection have made Raman spectroscopy a much more user-friendly and available technique. Thus, a good book on basic Raman spectroscopy may be a welcome addition to the analytical chemist's library.

The book by Barańska *et al.* is well written and provides a good fundamental introduction to conventional Raman spectroscopy. It includes, along with standard chapters on the theory of Raman spectroscopy, a very useful short chapter on group theory that helps to make the spectral interpretation of small molecules more understandable to the average chemist or analyst.

The measurement of Raman scattering requires that the instrument is capable of detecting weak signals in the presence of a strong signal at a slightly different wavelength. Normally visible-region lasers are used and consequently the conventional Raman spectrometer includes a large double or triple monochromator and a photon-counting photomultiplier detector. This type of spectroscopy and the many optical arrangements which Raman spectroscopists favour are well

described in this book and had it been published a few years ago this chapter would have been particularly useful. However, perhaps one reason why Raman spectroscopy is becoming an important technique is that more modern methods of detection are now employed. Thus, charge-coupled devices and similar systems are becoming favoured as the detection system. In addition, in order to enhance sensitivity, it is usual to spin the sample to reduce problems with photo-dissociation or absorption. Thus, this book would seem to me to be rather dated in its practical approach and I would have been happier if more attention had been paid to the modern developments of Raman spectroscopy.

Much of the interest of the chemist or analyst is usually centred on the vibrational analysis of particular molecules. In two chapters on organic and inorganic applications, the authors have summarized a number of important areas in a way in which the average reader can appreciate the types of signal to be expected and the value of recording them. The book then finishes with selected applications of Raman spectroscopy, including its use with polymers and bio-polymers, with complex compounds, and in matrix isolation spectroscopy. Perhaps surprisingly, the last chapter in the book is entitled fundamental concepts of spectroscopy and is a summary of much useful information that might well have appeared earlier in the text. There is also an atlas of spectra which may be quite useful to the average user.

Thus, if what is required is a conventional teaching text for Raman spectroscopy, this book is about adequate. Where it fails completely is in discussing newer aspects of Raman spectroscopy and consequently it is not a book to be recommended for teaching purposes to those who are not familiar with modern developments. For example, there has been a very great expansion in resonance Raman spectroscopy, including the detection of the spin and oxidation states of haemoglobin. There has also been considerable interest in surface-enhanced Raman spectroscopy for such purposes as detecting the presence of anti-corrosive layers on metal surfaces. There are many more complicated techniques which have also appeared in the last few years. It is always difficult to know where a book should end, but it seems to me that resonance Raman spectroscopy in particular is now just part of the Raman spectroscopist's armoury. Perhaps this can be best illustrated by saying that 10 or 15 years ago Raman spectroscopists tended to avoid coloured compounds, whereas now, many of the papers appearing in the literature make use of visible-region lasers and coloured compounds in order to obtain the sensitivity, through resonance, needed for the intended application. This would seem to be one of the key areas where analytical applications could be very much extended in the future. Thus, this is a good book to be recommended as a teaching text provided the course is taught by spectroscopists who are able to add a more modern gloss to the course they give. It cannot be recommended as an up-to-date account of Raman spectroscopy.

W. EWEN SMITH

Infrared Spectroscopy: W. O. GEORGE and P. S. MCINTYRE, Wiley, Chichester, 1987. Pages xx + 537. £17.50 (softback), £44.00 (hardback).

Infrared spectroscopy is widely used by preparative chemists in qualitative analysis. It also has very important applications in quantitative analysis, but its use there is more restricted. Thus, in the teaching of analytical chemistry the place of infrared spectroscopy is secure but the depth of understanding that is required is more difficult to assess. Many chemistry courses spend most time on discussing theory, whereas the analytical chemist requires in addition a knowledge of the range of applications possible. Thus, there is need for a book which particularly deals with the analytical applications. The book reviewed here is one such text.

The authors have constructed a text of open-learning type, which is both logical in its approach and easy to read. It covers the background theory, the modern applications of the Fourier transform and the main analytical areas very well. Most of the material that will be required for use in analytical courses is available from the text without reference to other books. Therefore it can be recommended as a good teaching text.

Inevitably there will be drawbacks, since different courses have different requirements. This book has been deliberately constructed so that the amount of theory is limited, and on one issue I do not agree with the authors' approach. They use visible-region spectroscopy to illustrate the basic concept of absorption spectroscopy and switch from that to infrared during the first chapter. They do not discuss the selection rules for visible-region spectroscopy but simply switch to selection rules for infrared. I feel that a straight approach to infrared spectroscopy, particularly since it is not intended to cover the field in any depth, would have been better. However, the infrared theory, when it is reached, is well and clearly written. Fourier transform spectroscopy is likely to play a larger part in the use of infrared in future and the basic technique is well explained, as are the general advantages. Perhaps one slightly disappointing feature is that the applications given later in the book cover more conventional and well established areas where infrared has been used and the full potential of Fourier transform spectroscopy in tackling surface layers, biological cells *etc.*, is neither fully explained nor illustrated and it may be that a revised edition of this book will be required within a relatively short space of time.

Parts of infrared spectroscopy theory appear difficult to some students. For example, the concept of normal vibrations is often not clearly explained. In this book there is an explanation that seems both simple and logical, and in other areas of spectroscopy which cause problems (such as the use of group frequencies) the explanation is again both good and clear. It is a pity therefore that the authors did not put a general index at the back of the book, to make it easier for a student later in his career to dip into the text and consider an individual topic. This deficiency is one which I find strange. During a lecture course a text is approached logically from one chapter to another, but in the laboratory, there is a need to turn to a paragraph or subsection to study a particular point of interest. Another omission which seems unusual is the limited amount of information on small molecules such as metal complexes, where symmetry and the nature of normal vibrations plays a bigger part.

BOOK REVIEWS

Algorithms for Chemists: J. ZUPAN, Wiley, 1989. Pages xv + 290. £39.50.

This book, which is for serious users of the computer, contains 31 algorithms that are suitable for handling experimental data sets. It is based on a course entitled "Introduction to computer methods for chemists" aimed at senior and postgraduate students. No one book can describe all computational procedures of interest to chemists and methods for manipulating data are constantly evolving. In this context the author has decided to concentrate on certain topics to the exclusion of others. For example, algorithms relating to linear regression, elementary statistical analysis and simultaneous equations are omitted. The book has been divided into three parts: "Data", "Preprocessing of Data" and "Data Handling". Algorithms are included in each of these sections but the allocation to subject headings is a little arbitrary.

Part one covers data representation and structure of data files. The algorithms of interest here include generation of random numbers and sorting procedures. The pictorial explanation, of the bubble type complete with rising bubbles, is a nice addition.

In part two, smoothing, peak detection and baseline correction of instrumental data are well presented. The chapter on transformations is of necessity very mathematical and includes geometrical, fast Fourier and Hadamard transformations. Some prior knowledge of these techniques would be desirable and the inclusion of some chemical applications, e.g., crystallographic analysis, would improve the chapter. An algorithm for Simplex optimization is also included in this section and the underlying principles are clearly explained.

Part three bravely attempts to describe a number of demanding data handling techniques. These are clustering of data, pattern recognition, computer handling of chemical structures, fractal forms and processes, and expert systems. The final algorithm relates to spectra simulation by reference to a spectroscopy-based expert system.

It should be noted that the algorithms presented are not suitable for immediate use. Each one is written as an unusual mixture of various computer languages but clear explanations are appended to each instruction line. The reason for this format relates to the course "Introduction to computer methods for chemists" where the students are asked to transform the algorithms into working programs. Most computer-literate chemists will be quite happy with the presentation of the algorithms. However, many chemists want commercial software for data handling, or complete, debugged programs that are suitable for immediate use. In an ideal world chemists should be able to process data in any way they wish and the book will be welcomed by those with the time and ability to aspire to this goal. Professor Zupan should be congratulated on bringing so many different computer software techniques to the attention of chemists.

P. J. Cox

Measurement of Oxygen by Membrane-covered Probes: V. LINEK, V. VACEK, J. SINKULE and P. BENEŠ, Horwood, Chichester, 1988. Pages 330. £45.00.

This book aims at providing a state-of-the-art review on membrane-covered oxygen probes. There is little doubt it will attract the attention of scientists involved in oxygen detection and quantitative determination.

Interesting characteristics of the book result from the practice-oriented presentation and writing. This is obvious from the very beginning of the book, where (Chapter 2) the polarographic determination of oxygen is described with selective comments and hints on the experimental conditions and the possible problems arising in the measurements. The formal descriptions of the probe response during oxygen reduction are sound and reasonably sized in Chapters 3 and 4. The major part of the book, however (Chapters 5-9) is dedicated to the practical implementation of the probe devices, to the analysis of their operational characteristics and to the control of their experimental significance and calibration. It includes several examples where membrane-covered oxygen probes are used for monitoring the progress of reacting systems and for determining kinetic and thermodynamic parameters.

As such, this book is a comprehensive and up to date document, which should be in the hands of any scientist confronted with the monitoring of oxygen.

M. GROSS

Chemical Instrumentation: A Systematic Approach: H. A. STROBEL and W. R. HEINEMAN, 3rd Ed., Wiley, New York, 1989. Pages 1210. £34.85.

This book fills a long-felt need for a basic book on chemical instrumentation. The authors have been successful in condensing material from a wide variety of disciplines. Though other excellent books on instrumental analysis do exist, the present book has a definite edge because it treats the instrumental part in more detail and more authoritatively. The earlier books treated instruments simply by block diagrams and some discussion of the various components. However, with the massive developments in chemical instrumentation such an approach today is perhaps not adequate.

The chapter on basic electronics is one of the most well written chapters. With the increasing use of computers and microprocessors in various disciplines of chemistry, especially analytical chemistry, there is a need for lucid presentation of this topic, especially for the non-specialist. This purpose is more than served by this book. The chapters on basic optics treat it in sufficient detail to be warmly welcomed. Since electromagnetic radiation of various forms is in some way or another associated with many analytical techniques, an in-depth treatment (as in the present book) is essential. In the chapters on basic quantification I found chapter 12 (signal to noise enhancement) most fascinating, since this topic is not usually taught in much detail, though such a need does definitely exist.

The rest of the book deals with the principles, theory, *etc.* of conventional instrumental methods and here I hoped for more detailed treatments. I suppose, however, this may not have been possible if the book was to be kept to a manageable size, and in any case, the title does suggest an emphasis on instrumentation. I was nevertheless surprised that Nuclear Magnetic Resonance Spectrometry was ignored completely. In my view, the authors' contention that NMR may best be left to monographs of organic chemistry seems rather odd. The usefulness of this technique lies not only in structure determination, but also in its use for quantitative analysis. Moreover, structure determination is also an integral part of analytical chemistry.

In conclusion, this book is an outstanding contribution to the field of chemical instrumentation and more than fills its objectives. It should be of interest to the chemist and analyst alike.

PUSHKIN M. QURESHI

BOOK REVIEWS

Computerized Multiple Input Chromatography: M. KALJURAND and E. KÜLLIK, Ellis Horwood, Chichester, 1989. Pages 225. Price £45.00

The authors explore a number of applications of computer control and data interpretation in gas and liquid chromatography. Their principal interest is in correlation chromatography (CC) in which a pseudo-random binary sequence of overlapping injections is coupled with cross-correlation between the sequence and the resulting signal to improve the signal to noise ratio for separations of trace levels of analytes.

They then examine the application of sequential repeated injections to monitor changes in samples with time or conditions, and discuss column switching techniques in which time slices from the first column are fed to a second column. In both cases they emphasize the need to use a computer to control the multiple injections and monitor the results and describe the experimental systems used for injection and column switching.

The overall theme of the book is the application of information theory to these chromatographic processes. Unfortunately the authors often mix techniques and it is often difficult to decide whether CC or repeated injection with fast separations is being used. The applications concentrate on thermal analysis, including pyrolysis of polymers, and trace constituents in environmental samples.

The book was completed in January 1987 but there are few references even to 1986, so that some sections, particularly those referring to computers, are dated. The advantages of the Apple II for control are described but no mention is made of the much more powerful computing ability of the IBM (or its clones). Newer instruments and intelligent integrators would also now routinely incorporate many of the required control facilities.

The book is interesting to read (the matrix algebra can be skipped), but with relatively few applications to real samples other than pyrolysis, its value will be mainly as a general background to chromatography.

R. M. SMITH

Troubleshooting LC Systems: JOHN W. DOLAN and LLOYD R. SNYDER, Humana, New Jersey, 1989. Pages viii + 515. \$65.00 (U.S.), Export \$75.00.

The authors of this text are very well known in the field of liquid chromatography, from their articles and short courses. Professor Snyder has also recently been appointed editor of *J. Chromatography* and so even before opening this book the reader can be assured that its contents will merit consideration.

The book is best described as a reference manual and it is similar in design to those books which describe the function, efficient use and possible faults that may occur in a car or a human body. The three sections of the book attempt to condense the expertise of many practical LC workers into an easy-to-use format.

The first section examines LC difficulties in terms of problem area, primary symptom, secondary symptom and likely cause. This approach is expanded in an extensive problem-isolation table which is essentially a flowchart with 676 rows and 6 column headings. Examples explaining the use of this table are given and whereas many problems can be solved through use of this guide, others, such as specific electronic problems, are considered outside the expertise of most readers. The logic involved in isolating and correcting LC problems is similar to that found in computer-based expert systems such as "The HPLC Doctor". Other basic considerations such as elementary separation theory, preventative procedures and good troubleshooting habits are covered in this section of the book.

Individual LC modules are described in the next section and this occupies about half of the book. Each of the eight chapters here is self-contained and each describes a module, e.g., pumps, columns, detectors etc., in detail. Good use is made of diagrams and photographs, and principles of operation and maintenance are included together with extensive coverage of possible problems and their solutions.

The final section deals mainly with problems associated with separation difficulties. Reasons for band tailing and peak distortion are given and other changes in the appearance of the chromatogram are discussed. Solutions to problems in quantification, gradient elution and sample pretreatment are offered. The index is comprehensive and deals efficiently with the inevitable overlap of subject material.

I checked some of the advice offered on dealing with practical problems, with the chief technician in our HPLC laboratories. The resulting comments were favourable: "That's precisely what I did" or "That's just what I would do". In conclusion, a very useful book for beginners and those on their way to becoming competent in practical LC.

P. J. Cox

Advances in Drug Therapy of Gastrointestinal Ulceration: ANDREW GARNER and BRENDAN J. R. WHITTLE (editors), Wiley, Chichester, 1989. Pages xvi + 306. £40.00.

The 20 chapters in this book are based on the proceedings of the 38th Annual Biological Council Symposium on Drug Action held at the Royal Institution in London on 11-12 April 1988. The topic is presented from a physiological/pharmacological viewpoint with chemistry very much in the background. As the emphasis is not on chemistry the book might be regarded as unsuitable for analytical chemists. However, much analytical effort today is directed towards producing safe and effective drugs and the world's two top selling (i.e., money-making) drugs, ranitidine and cimetidine, are both anti-ulcer drugs. These two histamine H₂-antagonists together with other possible anti-ulcer agents are of much interest to the pharmaceutical industry, where many analytical chemists work.

About half the book deals with peptic ulcer disease and existing therapy. The rest of the book examines possible areas for new drug development. Some chapters such as "Strategies for the Development of Novel Anti-ulcer Drugs" are very readable whereas others such as "Pro-ulcerogenic and Related Lipid Mediators in Gastric Mucosal Damage" are a little more demanding.

Although of great relevance and importance this book can only be recommended for those chemists with more than a passing knowledge of physiology, pharmacology and biochemistry.

P. J. COX

Practical Computing for Experimental Scientists: JOHN D. BEASLEY, OUP, Oxford, 1988. Pages xii + 233. £12.50.

This book is eminently suitable for a beginning postgraduate student or postdoctoral fellow, but any other scientist who has not yet come to terms with the computer revolution would find it most helpful in cutting through the jargon that makes it difficult to start at the beginning in computing. It offers wide-ranging advice on the choice and application of computers for scientific experimentation. Both mainframe and personal computing are discussed, with no assumptions of prior knowledge. The wide variety of topics includes: connecting a computer to experimental equipment, data analysis, graphical and tabular presentation of data, scientific word processing, secure storage of data, transfer of data between computers, telemetry, graphical input, data retrieval, the scientist as programmer, use of spreadsheets, high-level languages, machine assembly language, rounding errors, statistical analysis of data, finite approximations, pseudo-random numbers, talking to a computer expert, choosing a computer, and care and safety. As must be evident from the range of topics, readers cannot expect to gain detailed knowledge of any single one, but they will find much sound advice that is not easy to find in the many more specialized computer books available today.

MARY MASSON

Introduction to Microwave Sample Preparation: Theory and Practice: H. M. KINGSTON and LOIS B. JASSIE (editors), ACS Professional Reference Book, ACS, Washington, D.C., 1988. Pages xxii + 263. Price US \$49.95. Export \$59.95.

The process of wet digestion is a necessary step in most analytical procedures, both classical and instrumental. This book describes a small revolution in wet digestion methods that has taken place since 1975. It aims to provide most of the information required for an analyst to get started in microwave dissolution. The wide range of sample types covered includes geological and metallurgical samples, botanical, biological and food samples, pharmaceuticals, selenium-containing materials, and minerals. Procedures for Kjeldahl nitrogen determination, remote operation, dissolution in radioactive environments, and robotic control are described. Theoretical aspects, and the design of equipment, including vessels, are discussed, and safety guidelines are also included.

MARY MASSON

NOTICES

6th INTERNATIONAL WORKSHOP ON TRACE ELEMENT ANALYTICAL CHEMISTRY IN MEDICINE AND BIOLOGY

24-26 April 1991

Neuherberg, F.R.G.

Gesellschaft für Strahlen- u. Umweltforschung (GSF) and Arbeitsgemeinschaft der
Großforschungseinrichtungen (AGF)

Topics

The main scientific topics on the 6th Workshop will be:

- (I) Trace element analysis
 - (1) ICP-MS (capability for biological material)
 - (2) Methods for the determination of micro-distributions of trace elements in tissues
- (II) Speciation of trace elements
 - (1) Complex compounds of trace elements in tissues and foodstuff
- (III) Techniques for speciation studies
 - (1) The functions of protein fractionation
 - (2) Protein separation techniques (in body fluids and tissues); "state of the art"
 - (3) and their connections to trace element analysis
- (IV) Trace elements in the bio-medical field
 - (1) Trace element deficiency: reason or consequence of diseases?
 - (2) Ambivalence of the essential trace elements (an actual inventory)
 - (3) Transferability of data from animal experiments to man
 - (4) Trace elements in geriatrics

The most important aspect will be to cover different problems within special sessions in order to deal with all new points of view and to initiate fruitful discussions among the participating experts. The invited papers will deal with modern developments and latest scientific findings in these special fields. The Workshop will consist of a number of invited papers on specific problem areas followed by an extended discussion period in which all participants will be invited to take part.

Registration fee for participants

DM 400.—

(before 1 March 1991)

DM 450.—

(after this date)

Venue

The Workshop and the Symposium will be held in the Conference Building (Auditorium) of the

Gesellschaft für Strahlen- und
Umweltforschung (GSF)
Ingolstädter Landstrasse 1
D-8042 Neuherberg near Munich
F.R.G.

Transportation between the U-Bahn-terminal "Kieferngarten" and/or hotels booked and the GSF will be provided.

Accommodation

Hotel reservation will be made through

GSF-Conference Service Section
Ingolstädter Landstrasse 1
D-8042 Neuherberg

You are requested to book hotels together with your final registration which will be included in the Second Circular. Deadline for hotel reservation: 1 March 1991.

Address for correspondence

Gesellschaft für Strahlen- und Umweltforschung mbH
Institut für Ökologische Chemie
AG "Spurenelementanalytik"
PD Dr. P. Schramel
Ingolstädter Landstraße 1
D-8042 Neuherberg
F.R.G.

IUPAC COMMISSION ON CHROMATOGRAPHY AND OTHER ANALYTICAL SEPARATIONS

The Commission structure of the Analytical Chemistry Division of The International Union of Pure and Applied Chemistry (IUPAC) has been better reorganized to reflect the present nature of the discipline. At the IUPAC General Assembly meeting in Lund, Sweden in 1989, a new commission on "Chromatography and Other Analytical Separations" was set up. This commission has taken up the mandate of the previously existing IUPAC working group in chromatography and separations, of the former Commission on "Analytical Reactions, Reagents and Separations", which is now restructured as the Commission on "General Aspects of Analytical Chemistry".

The terms of reference for the new Commission are as follows.

- (a) To develop and publish critical guidelines and recommendations for the operation of analytical separation methods.
- (b) To consider and recommend nomenclature and definition of terms used in analytical methods of separation.

The present Commission structure has three Titular and five Associate members, together with a number of national representatives, although future expansion is envisaged as the work of the Commission expands.

The Commission has a number of on-going projects as well as new ones which are planned. Subjects covered are all forms of chromatography, including interfaced methods, analytical electrophoretic separations, and analytical aspects of extraction.

The Commission is anxious to reflect current and developing activities in analytical separations chemistry, and welcomes input from anyone interested in its activities. The Chairman or the Secretary, whose addresses are listed below, will be happy to respond to such contacts.

Chairman: Professor P. C. UDEN
Department of Chemistry
Lederle Graduate Research Tower
University of Massachusetts
Amherst, MA 01003
U.S.A.
TEL: +1 (413) 545 2293
TELEX: 955491 UNIV MASS AMST
FAX: +1 (413) 545 4490

Secretary: Professor C. A. M. G. CRAMERS
Laboratorium voor Instrumentele Analyse
Faculty of Chemical Engineering
Technische Universiteit Eindhoven
Postbus 513, SH 3.06
5600 MB Eindhoven, The Netherlands
TEL: +31 (40) 473025/24
TELEX: 51163 TUEHV NL
FAX: +31 (40) 442576

SYMPOSIUM ON GAS AND HEADSPACE VAPOUR ANALYSERS AND MONITORS

Cardiff, Wales, 1 March 1991

A Symposium on Gas and Headspace Vapour Analysers and Monitors relating to recent developments for monitoring gases and vapours in workplaces, headspace vapour analysis, control of fermentation processes, and for determining gas components in the clinical and biochemical fields, organized by the Analytical Division of the Royal Society of Chemistry, will be held at the University of Wales College of Cardiff on Friday 1 March 1991.

For further details contact:

Miss P. E. Hutchinson, Secretary
Analytical Division,
Royal Society of Chemistry
Burlington House
London W1V 0BN
England

ELECTROCHEMICAL ANALYSIS

Leipzig, 11–14 September 1991

The annual conference series on analytical chemistry "Analytiktreffen" is organized by the Department of Chemistry of the Karl-Marx University of Leipzig in cooperation with the Chemical Society of the G.D.R. The next conference "Electrochemical Analysis" will take place in Leipzig, G.D.R., 11–14 September 1991. Leading international scientists are invited to give an overview of the following topics, including new developments in theory, instrumentation and application:

- new electrochemical methods, including combinations with non-electrochemical techniques
- electrochemical sensors and biosensors
- computers in electroanalysis
- applications of electrochemical methods for environmental, industrial and clinical analysis.

In addition to the lectures the scientific programme consists of poster sessions.

For further details contact:

Dr H. Emons,
Department of Chemistry
Karl-Marx University
Talstrasse 35
Leipzig—7010
G.D.R.

SUBJECT INDEX

Acetylcholine receptor, Interactions	561
Acids, weak, Determination, potentiometric	1141
Acridinium betaines, as microsensor coatings	911
<i>N</i> -Acyl-1-aryl-1-aminoethanes, chiral separations	599
Additive, Determination in brick mortar	261
Algal biomass, Recovery of Cr from solution	707
Algorithms, for kinetic determinations	233
—, RAMESES, further developments	413
Alkaloids, Analysis of mixtures	579
Aluminium, Determination, fluorimetric	385
—, —, spectrophotometric	1017
Aluminium(III), Extraction	1175
Aluminium oxide, Separation of metal ions	613
Amines, aliphatic, Microgram detection	763
Amino acids, Detection on TLC plates	1105
—, Determination by HPLC	377
Ammonia, atmospheric, Determination, spectrophotometric	1063
—, Interaction with 2,4-dinitrophenylhydrazine	361
α -Amylase, Determination by chemiluminescence	971
Anions, Determination with ISE	901
Antibilharzial antimonials, Determination by HPLC	951
Antioxidants, Determination by HPLC	301
Antimony, Determination by AAS	955, 1029
Approximative spline functions, finding of potentiometric titration end-points	667
Arsenic, Determination by AAS	1029
—, — by electrothermal AAS	545
—, — polarographic	325
—, Extraction and speciation	831
Arylphosphonic acids, salts and esters, as microsensor coatings	921
Atomic absorption spectrometry (AAS), Determination of chloramphenicol	1129
—, —, — of Cr	519
—, —, — of Sb	955
—, —, —, for multielement analysis	119
—, —, —, electrothermal, Atomization of Co	1111
—, —, —, Determination of As, Cd, Pb and Se	545
—, —, —, — of Cd	825
—, —, —, — of Cu, Fe, Pb and Ni	555
—, —, —, — of Hg traces	1119
—, —, —, — of Te	173
—, —, —, Improvement of Smets method	167
—, —, —, Hydride generation, Determination of Sb, As and Fe	1029
— emission spectrometry (AES), for multielement analysis	1
—, —, improved detection with CID	15
—, —, with programmed-scan spectrometer	89, 103
—, —, Inductively coupled plasma (ICP), Determination of La, Ce, Pr and Nd	815
—, —, —, — of Os	895
—, —, —, —, optimized line selection	39
—, —, —, —, Selection of spectral windows	33
—, —, —, —, Updating of vintage spectrometer	157
— fluorescence spectrometry, Screening of polycyclic aromatic hydrocarbons (PAH)	111
Aurocyanide ion-pairs, Extraction	875
Automation, of stripping potentiometry	689
Azo dyes, Dissociation constants	1025
Beryllium-Morin complex, Fluorescence	947
Beta-blocker drugs, Determination by ISE	673
BF ₄ ⁻ , as supporting electrolyte ion for voltammetry	695
Bile salts, Determination by TLC/MS	471
Biomarkers, Determination in petroleum	731
1,3-Bis(hydroxyiminomethylpyridinium)propane dichloride (TMB-4), Determination with Pd(II)	535
Bromine, Determination by HPLC	595
—, — by XRF	185

Cadmium, Determination by electrothermal AAS	545, 825
Carbon monoxide, Determination spectrophotometric	539
Carbaryl, Determination, fluorimetric	573
Carbosulphan, Determination, spectrophotometric	629
Cations, Electrochemical detection with Ce(III)	1151
Cerium, Determination by ICP-AES	815
Cerium(III), Extraction	431
Charge injection device (CID), for AES	1, 15
Chelating polymer, for separation and preconcentration of trace metals	491
Chemiluminescence, Determination of α -amylase	971
—, — of Co	393
—, — of thiamine	1043
Chiral separations, of <i>N</i> -acyl-1-aryl-1-aminoethanes	599
Chloramphenicol, Determination by AAS	1129
Chloride and carbonate, Determination by FIA and AAS	1123
Chlorine, Determination by XRF	185
Chlorobenzoquinones, Determination, spectrophotometric	353
Chromatography, cation-exchange, Separation of Y and Nd	1155
—, gas (GC), Determination of methylmercury	207
—, —, — of tri- <i>n</i> -butyltin	975
—, high-performance liquid (HPLC), Determination of amino acids	377
—, ———, — of antibilharzial antimonials	951
—, ———, — of antioxidants	301
—, ———, — of Br	595
—, ———, — of lanthanide chelates	381
—, ———, — of niridazole	481
—, ———, — of Pt metal oxinates	485
—, ———, — of vitamins	841
—, ——— ion (HPIC), Preconcentration of trace metals	127
—, ion, Determination of metals	835
—, —, — of sulphite	201
—, thin-layer (TLC), of bile salts	471
Chromium, Determination by AAS	519
—, Recovery from solution by algae	707
Cobalt, Atomization	1111
—, Determination by chemiluminescence	393
—, —, spectrophotometric	443, 735, 1189
Colchicine, Determination, voltammetric	783
Concanavalin A, Interactions	801
Copper, Determination by controlled potential electrolysis	701
Copper(II), Determination by adsorption voltammetry	1001
Copper-murexide interaction	1107
Cresol Red, Determination, spectrophotometric	1197
Cyanide, Determination, fluorimetric	1049
β -Cyclodextrin, solid-matrix luminescence	1057
Detection limits, Evaluation in ICP-AES	23
Detector, electrochemical for HPLC	841
Dissociation constants, of azo dyes	1025
Dithiocarbamates, Determination, spectrophotometric	1205
Dysprosium(III), hydrolytic polymerization	357
Electroanalytical techniques, for determination of Th	317
Electrochemical detection of cations	1151
Electrode, carbon-paste, for marcellomycin	213
—, ———, for voltammetry	789
—, enzyme, for 3α -hydroxysteroids	795
—, glassy-carbon, for voltammetry	695
—, ion-selective (ISE), for H ⁺	461
—, ———, for phosphate	683
—, ———, for sulphate	455
—, ———, for Zn	307
—, ———, membrane, for anions	901
—, ———, for beta-blocker drugs	673
—, metal, for free HF	651
—, solid-state glass, for pH	659
Electrolysis, controlled-potential, Determination of Ag	941
—, ———, — of Cu	701
—, ———, — metal ions	677
Elemental analysis, of high-purity solids	363
Epinephrine, Determination, spectrophotometric	625
Equilibrium constant, of Cu-murexide interaction	1107
— parameters, Determination from potentiometric data	645
Erbium, Determination, spectrophotometric	337, 341
Estazolam, Determination, polarographic	937

Ethyl xanthate, Determination by FIA	1067
Europium(III), Extraction	431, 757
—, Luminescence	965
Extraction, of As	831
—, of Au	1011
—, of aurocyanide ion-pairs	875
—, of Co	443
—, of Cu(PCD) ₂	229
—, of Fe(III)	1179
—, of Ga	1163
—, of Ga and Al	1175
—, of La(III), Ce(III), Eu(III), Th(IV) and U(VI)	431
—, of La(III), Eu(III) and Lu(III)	757
—, of Pd	1011
—, of pyrene	1031
—, of Sb	955
—, system, liquid-solid	885
Filter-paper test, for aliphatic amines	763
Flotation techniques, Applications in analysis, Review	275
Flow injection analysis (FIA), Comparison of extraction segmentors	1169
———, Determination of chloride and carbonate	1123
———, — of ethyl xanthate	1067
———, — of iodide and iodine	313
———, — of Pd	329
———, — of phosphates	683, 889
———, — of Zn and Fe	711
Fluorescence, of Be-morin complex	947
— spectrometry, Determination of Ga	193
——, — of indole derivatives	1137
——, derivative, Analysis of alkaloid mixtures	579
——, — Determination of carbaryl and 1-naphthol	573
——, —, — of Ga and Al	385
——, —, — of rare-earth elements	809
Fluoride, Determination by molecular absorption spectrometry	719
Formation constants, calculation by RAMESES II	425
Fractionation, of labile metals	397
Gallium, Determination, fluorimetric	193, 385
—, Extraction	1163, 1175
Gallium(III), Determination, spectrophotometric	637
Gold, Determination spectrophotometric	855
—, Extraction	1011
Hexachloroethane, Thermosonimetry of Phase II/III transition	861
Holmium, Determination, spectrophotometric	341
Hydrofluoric acid, Determination, amperometric	651
Hydrogen peroxide, Determination, titrimetric and spectrophotometric	753
Hydrolytic polymerization, of Dy ³⁺	357
Hydroxamic acid resin, Synthesis and applications	591
3 α -Hydroxysteroids, Determination, amperometric	795
Indole derivatives, Determination, fluorimetric	1137
Iodide, Determination, kinetic	849
—, Interference in Determination of Se	725
— and iodine, Determination by FIA	313
Iron, Determination by FIA	711
—, —, spectrophotometric	1101, 1189
Iron(II), Determination, spectrophotometric	745
Iron(III), Extraction	1179
Kalman filter, Use in fluorimetry	809
Kinetic determinations, error-compensated	233
— stability, of Cu(PCD) ₂	229
Labile metal, Determination by ASV	981
——, Fractionation	397
Lanthanide chelates, Determination by HPLC	381
Lanthanum, Determination by ICP-AES	815
Lead, Determination by electrothermal AAS	545
—, Titration with HEDTA	1021
Linuron, Determination, voltammetric	789
Lipid hydroperoxides, Determination, spectrophotometric	925
Liquid-solid extraction system	885
Loprazolam mesilate, Determination, voltammetric	661

Louis Gordon Memorial Award	No. 11, V
Luminescence, of β -cyclodextrin	1057
Lutetium(III), Extraction	757
Malathion, Determination, spectrophotometric	761
Manganese, Review of spectrophotometric methods	237
Marcellomycin, Behaviour at carbon-paste electrodes	213
Mass spectrometry, elemental analysis of high-purity solids	363
—, ICP, Determination of Sr	819
—, —, — of trace metals	127
—, secondary-ion, of bile salts	471
Matrix, Air, Determination of ammonia	1063
—, —, — of CO	539
—, Alloys, Determination of Ag	941
—, — steels, Determination of La, Ce, Pr and Nd	815
—, Argillites, Determination of Cr	519
—, Biological fluids, Determination of carbaryl and 1-naphthol	573
—, — samples, Determination of Ga and Al	385
—, —, — of metals	555
—, —, —, Multielement analysis	119
—, Brick mortar, Determination of additive	261
—, Commercial formulations, Determination of carbaryl and 1-naphthol	573
—, Copper ores, Determination of Ag	527
—, Dog bile, Determination of bile salts	471
—, Environmental samples, Screening of PAH	111
—, —, —, Determination of ^{90}Sr	585
—, Food, Determination of Cd	825
—, —, — of Zn and Fe	711
—, High-purity solids, Elemental analysis	363
—, Human serum, Determination of Sr	819
—, Lacustrine sediments, Determination of As	831
—, Oils and fats, Determination of lipid hydroperoxides	925
—, Ores, Determination of Sb	955
—, —, — of Te	173
—, Organic compounds, Determination of Br	595
—, Oysters, Determination of tri-n-butyltin	975
—, Peat, Determination of Br, Cl, S and P	185
—, Petroleum, Determination of biomarkers	731
—, Pharmaceutical preparations, Determination of tetra-cyclines	1193
—, —, — of Vitamin C	269
—, Rain and snow, Determination of sulphate	633
—, Rare earths, Determination of Nd and Er	337
—, —, — of Nd, Er and Ho	341
—, Rocks, Determination of elements	135
—, Sea-water, Determination of fluoride	719
—, Sediments, Determination of labile metal	397, 981
—, Silicates, Determination of Al	1017
—, Soil, Determination of Mo(VI)	1007
—, Water, Determination of As, Cd, Pb and Se	545
—, —, — of Ga	193
—, —, — of Hg	1119
—, —, — of Mo(VI)	1007
—, —, — of phosphates	889
—, —, — of Se(IV)	749
—, —, — of sulphite	201
—, White-metal bearings, Determination of Cu	701
Mercury, Determination by electrothermal AAS	1119
Methylmercury, Determination by GC	207
Metals, Ion chromatography of	835
—, Separation by chelating resin	591
— ions, Electrolysis	677
—, —, Separation on aluminium oxide	613
Molecular absorption spectrometry, Determination of fluoride	719
Molybdenum, Determination, spectrophotometric	1091
Molybdenum(VI), Determination, voltammetric	1007
Molybdosilicic acids, reduced, Stability	447
Multicomponent analysis, spectrophotometric	347
—, —, with discrete Fourier transform	1183
Multielement analysis, by AAS	119
—, —, Comparison of NAA with other techniques	135
1-Naphthol, Determination by derivative fluorescence spectrometry	573
Neodymium, Determination by ICP-AES	815
—, —, spectrophotometric	337, 341
Neutron activation analysis (NAA), Comparison with other multielement techniques	135

——, Determination of Sr	819
New microsensors coatings	911, 921
Niridazole, Determination by HPLC	481
Norepinephrine, Determination, spectrophotometric	625
Obituary, I. P. Alimarin	No. 9, V
Optimized line selection in ICP-AES	39
Organic dyes, Sorption by polyurethane foam	407
Ortho- and pyrophosphates, Determination by FIA	889
Orthovanadate, Determination of first protonation constant	741
Osmium, Determination by ICP-AES	895
—, —, polarographic	1077
Oxygen, Determination of solubility	905
Palladium, Determination by FIA	329
—, Extraction	1011
pH, Measurement at high temperatures, a review	767
Phosphate, Determination by FIA	683
Phosphonate, determination, voltammetric	1071
Phosphorus, Determination by XRF	185
Platinum metal oxinates, Separation by HPLC	485
Polarography, Determination of As	325
—, — of estazolam	937
—, — of Os	1077
—, differential pulse (DPP), Determination of Sunset Yellow and tartrazine	655
Polycyclic aromatic hydrocarbons (PAH), rapid screening	111
Polyurethane foam, Extraction of Fe(II) complex	1101
——, Sorption of organic dyes	407
Potentiometry, stripping, Automation of	689
Praseodymium, Determination by ICP-AES	815
Preconcentration, of Zn	1037
Propoxur, Determination, spectrophotometric	629
Protonation constant, of orthovanadate	741
Pyrazolones and vinyl copolymers, analytical characterization	1081
Pyrene, Extraction with supercritical fluid	1031
RAMESES, Algorithm for multiple equilibria	413, 425
Rare-earth elements, Determination by derivative fluorimetry	809
Reagent, for detection of aminoacids on TLC plates	1105
—, 2-Aminoperimidine, for preconcentration of sulphate	633
—, Arsenazo III, for U and Th	619
—, <i>N</i> -Bromimides, for Vitamin C	269
—, 2-(5-Bromo-2-pyridylazo)-5-diethylaminophenol, for Cu(II)	1001
—, <i>o</i> -Chlorophenylfluorone, for Sc	641
—, 7,8-Dihydroxy-4-methylcoumarin, for Mo	1091
—, 5-[<i>p</i> -(Dimethylamino)benzylidene]rhodanine, for Ag	531
—, 5,5-Dimethyl-1,3-cyclohexanedione, for Se	439
—, Diphenylcarbazine, for aliphatic amines	763
—, Dithizone, for Co	443, 1189
—, Ferrozine, for Fe	1189
—, Fluorinated pyrazolones, for La(III), Eu(III) and Lu(III)	757
—, HEDTA, for Pb	1021
—, Heterocyclic dithiophosphates, for Ag	527
—, 8-Hydroxyquinoline, for Pt metals	485
—, 8-Hydroxyquinoline-5-sulphonic acid, for Nd and Er	337
—, 2-Iodibenzoic acid, as oxidant	1087
—, Kojic acid, for lanthanides	341
—, Metallotetrakis(<i>N</i> -methylpyridiniumyl)porphyrins, as fluorescence catalysts	1133
—, Methylene blue, for Se	931
—, Molybdenum, for malathion	761
—, Morpholine, for chlorobenzoquinones	353
—, 1-(<i>p</i> -Nitrophenyl)ethylenediamine- <i>N,N,N',N'</i> -tetra-acetic acid, for lanthanides	381
—, Palladium(II), for TMB-4	535
—, Phenothiazine, for Au	855
—, Phenylfluorone, for Ga	637
—, Piperazine, for chlorobenzoquinones	353
—, Rhodamine B, for Se(IV)	749
—, Sodium periodate, for epinephrines	625
—, Sulphochlorophenolazorhodanine, for Pd	329
—, Thiomorpholine, for chlorobenzoquinones	353
—, 2,4,6-Tri(2'-pyridyl)-1,3,5-triazine, for Fe	745
—, Uranyl acetate, for tetracyclines	1193
Review, Applications of flotation techniques	275
—, pH Measurement at high temperatures	767

—, Spectrophotometric methods for Mn	237
Ronald Belcher Memorial Award	No. 11, V
Salicylic and salicyluric acids, resolution of mixtures	347
Scandium, Determination, spectrophotometric	641
Segmentors, for liquid-liquid extraction FIA	1169
Selective interactions, of acetylcholine receptor	561
—, of concanavalin A	801
— multiplex advantage, with Hadamard transform spectrometer for AES	53
Selenium, Determination at trace level	725
—, — by AAS	1029
—, — by electrothermal AAS	545
—, —, spectrophotometric	931
Selenium(IV), Determination, spectrophotometric	439, 749
Sensor, flow-through, for cyanide	1049
Silver, Determination, by controlled-potential electrolysis	941
—, —, spectrophotometric	527, 531
Smets method, in AAS	167
Software Survey, TAL-006/89 Package	273
—, —, TAL-007/89 Package	273
—, —, TAL-001/90 Package	859
Sorption, of organic dyes by polyurethane foam	407
Speciation, of As	831
Spectral windows, Selection for ICP-AES	33
Spectrometer, Hadamard transform, for multielement AES	53
—, —, theoretical multiplex gain	61
—, programmed-scan, for multielement AES	89
Spectrometer, spectrally segmented photodiode-array, for ICP-AES	23
—, Vidicon, two-dimensional multiple entrance slit	71
Spectrophotometry, computer-assisted, analysis of multi-component mixtures	1183
—, derivative, Determination of U and Th	619
—, ion-exchanger phase, Determination of Co	735
Spline functions, for analysis of titration data	845
Stability, of reduced molybdosilicic acids	447
— constants, of metal complexes	219
Strontium, Determination by ICP-AES and NAA	819
—, — by liquid scintillation counting	585
Sulphate, Determination by ISE	455
—, Determination, spectrophotometric	633
Sulphite, Determination by ion chromatography	201
Sulphoxides, Microdetermination, spectrophotometric	435
Sulphur, Determination by XRF	185
Sunset Yellow, Determination, polarographic	655
Surfactants, anionic, as microsensor coatings	911
Tartrazine, Determination, polarographic	655
Tellurium, Determination by electrothermal AAS	173
Tetracyclines, Determination spectrophotometric	1193
Thallic and thallose ions, Determination by ASV	995
Theophylline, determination by luminescence	965
Theoretical multiplex gain, in UV/VIS Hadamard transform spectrometer	61
Thermosoniometry, of Phase II/III transition of hexachloroethane	861
Thiamine, Determination by chemiluminescence	1043
Thioxanthene derivatives, Determination, titrimetric	1087
Thorium, Determination of traces	317
Thorium(IV), Extraction	431
— and uranium, Determination, spectrophotometric	619
Titanium(IV), Titration, complexometric	1097
Titration, chelatometric, of Pb	1021
—, complexometric, of Ti(IV)	1097
—, oxidimetric, Determination of hydrogen peroxide	753
—, potentiometric, Determination of weak acids	1141
—, —, Detection of end points by approximative spline functions	667
Titration, automatic, with analysis by spline functions	845
Trace metals, Preconcentration by HPLC	127
—, —, Separation and preconcentration	491
Tri-n-butyltin, Determination by reaction-GC	975
Two-dimensional multiple entrance slit, for Vidicon spectrometer	71
Uranium(VI), Extraction	431
Uranium and thorium, Determination, spectrophotometric	619
Vitamin C, Determination, titrimetric	269
Vitamins, Water-soluble, determination by HPLC	841
Voltammetry, Determination of phosphonate ion	1071

—, adsorption, of Cu(II) complex	1001
—, adsorptive stripping, Determination of colchicine	783
—, —, Determination of loprozalam mesilate	661
—, —, — of Mo(VI)	1007
—, anodic stripping, Determination of labile metal	981
—, cyclic, Determination of stability constants	219
—, differential pulse, Determination of linuron	789
—, — anodic stripping, Determination of Tl(III) and Tl(I) ions.	995
X-Ray fluorescence spectrometry (XRF), Determination of Br, Cl, S and P	185
Xylenol Orange, Determination, spectrophotometric	1197
Yttrium and neodymium, Separation from Sm and heavier lanthanides	1155
Zinc, determination by FIA	711
—, Preconcentration	1037

Talanta

The International Journal of Pure and Applied Analytical Chemistry

Editors-in-Chief

PROFESSOR G.D. CHRISTIAN,
Department of Chemistry, BG-10,
University of Washington,
Seattle, WA 98195, U.S.A.

PROFESSOR D. LITTLEJOHN,
Department of Chemistry,
University of Strathclyde,
259 Cathedral Street,
Glasgow G1 1XL,
Scotland, U.K.

Consultant Editor

DR. R.A. CHALMERS, Department of Chemistry, University of Aberdeen, Old Aberdeen, Scotland, U.K.

Assistant Editors

DR. W.A.J. BRYCE, University of Aberdeen, Scotland, U.K.

DR. D. MIDGLEY, National Power, Leatherhead, U.K.

DR. P.J. COX, Robert Gordon's Institute of Technology, Aberdeen, Scotland, U.K.

Computing Editor

DR. MARY R. MASSON, University of Aberdeen, Scotland, U.K.

Book Review Editor

DR. P.J. COX, Robert Gordon's Institute of Technology, Aberdeen, Scotland, U.K.

Technical Editor

MISS C. HIGGINSON

Special Issues Co-ordinator

DR. I.L. MARR, University of Aberdeen, Scotland, U.K.

Editorial Board

Chairman: PROFESSOR J.D. WINEFORDNER

DR. R.A. CHALMERS

PROFESSOR G.D. CHRISTIAN

PROFESSOR D. LITTLEJOHN

DR. I.L. MARR

DR. M.R. MASSON

DR. D. MIDGLEY

Advisory Board

Chairman: PROFESSOR J.D. WINEFORDNER, Gainesville,
Florida, U.S.A.

PROFESSOR G. ACKERMANN, Freiberg, D.D.R.

PROFESSOR I.P. ALIMARIN, Moscow, U.S.S.R.

PROFESSOR A.G. ASUERO, Seville, Spain

PROFESSOR P.R. BONTCHEV, Sofia, Bulgaria

DR. P.W.J.M. BOUMANS, Eindhoven, The Netherlands

(Liaison member for *Spectrochimica Acta B*)

PROFESSOR D.T. BURNS, Belfast, N. Ireland, U.K.

PROFESSOR R.G. COOKS, West Lafayette, Indiana, U.S.A.

PROFESSOR A. CORSINI, Ontario, Canada

PROFESSOR S.R. CROUCH, East Lansing, Michigan, U.S.A.

MRS. E.M. DONALDSON, Ottawa, Canada

PROFESSOR H. FALK, Kleve, F.R.G.

PROFESSOR J.F. FRITZ, Iowa, U.S.A.

PROFESSOR R. GIJBELS, Wilrijk, Belgium

PROFESSOR T. HORI, Kyoto, Japan

PROFESSOR A. HULANICKI, Warsaw, Poland

DR. D.T.E. HUNT, Medmenham, U.K.

PROFESSOR J. INCZÉDY, Veszprém, Hungary

PROFESSOR J.D. INGLE, Corvallis, Oregon, U.S.A.

PROFESSOR A. IVASKA, Åbo, Finland

DR. K. IZUTSU, Matsumoto, Japan

PROFESSOR D. JAGNER, Gothenburg, Sweden

DR. K.-H. KOCH, Dortmund, F.R.G.

DR. H. KRAGTEN, Amsterdam, The Netherlands

DR. L.J. KRICKA, Philadelphia, Pennsylvania, U.S.A.

DR. L. KRYGER, Aarhus, Denmark

PROFESSOR D. MALJKOVIĆ, Zagreb, Yugoslavia

DR. J. MATOUSEK, Kensington, Australia

PROFESSOR M. NOVOTNY, Bloomington, Indiana, U.S.A.

DR. N. OMENETTO, Ispra, Italy

PROFESSOR F. PELLERIN, Chatenay-Malabry, France

DR. M. PESEZ, Villemomble, France

PROFESSOR E. PUNGOR, Budapest, Hungary

PROFESSOR I. ROELANDTS, Liège, Belgium

PROFESSOR L. SOMMER, Brno, Czechoslovakia

DR. B.YA. SPIVAKOV, Moscow, U.S.S.R.

DR. K. ŠTULÍK, Prague, Czechoslovakia

DR. J.D.R. THOMAS, Cardiff, Wales, U.K.

(Liaison member for *Selective Electrode Reviews*)

PROFESSOR M. THOMPSON, Toronto, Canada

PROFESSOR G. TÖLG, Dortmund, F.R.G.

PROFESSOR J.F. TYSON, Amherst, Mass., U.S.A.

PROFESSOR M. VALCARCEL, Córdoba, Spain

PROFESSOR E.L. WEHRY, JR., Knoxville, Tennessee, U.S.A.

DR. B. WELZ, Uberlingen, F.R.G.

The book has been attractively produced from camera-ready copy and is reasonably priced. Errors appear to be few, the most obvious to this reviewer being those in the saxitoxin formulae on pages 22 and 24. The book is unlikely to be purchased by analytical chemists, but it should find a home in the libraries of all institutions interested in marine metabolites.

R. H. THOMSON

Radioanalytical Chemistry: J. TÖLGYESSY and M. KYRŠ, Ellis Horwood, Chichester, 1989. Volume 1, pages 354. Volume 2, pages 498. £59.95 (each).

These two volumes describe a wide range of methods of analysis in which determinations culminate with measurement of radioactivity, and so are frequently applicable where low limits of detection or non-destructive analyses are required. Provided for an analytical readership, introductory chapters on basic radioactivity and instrumentation, which are frequently included in books in this area, are excluded.

Volume 1 covers (i) Analysis by measurement of natural radioactivity, (ii) Isotope dilution analysis, (iii) Radio-reagent methods, (iv) Radiometric titrations, (v) Radioimmunoassay, and (vi) Radiochemical methods for determination of biological activity of enzymes. Whilst the last two sections are concerned with organic applications, the remainder (in both volumes) are concerned with inorganic analysis. The use of radioactive tracers is a useful means of investigating aspects of alternative methods of analysis, and a chapter on this topic would have been welcome.

Volume 2 covers (i) Activation analysis and (ii) Physical methods based on absorption, scattering and fluorescence, with an additional chapter on automation and a 172 page appendix of radionuclide data and tables of optimum spike/analyte ratios for isotope dilution analysis. The survey of automation of radiochemical methods is timely since this approach is likely to increase in response to reduction of acceptable dose limits. With increasing awareness of radiological and other hazards experienced in the analytical laboratory, it would also have been timely to include some comment (possibly in the introduction) of potential radiation exposure when using the methods described.

Each section concludes with a collection of references, for when comprehensive details of methods are required, and a "Selected" bibliography. The latter occasionally includes manufacturers' literature and material from the 1960's which may be difficult to locate.

Overall, these two volumes provide comprehensive coverage of a variety of radioanalytical methods, some of which have only previously been described in specialized monographs. Whilst the applicability of some of these methods is limited, the overall content is relevant to postgraduate students of analytical chemistry, notwithstanding the apparent age of some apparatus used in illustrations. Examples of applications are very diverse, so most analysts should find something of interest in library copies. For those who subscribe to Kolthoff and Elving's *Treatise on Analytical Chemistry*, most of the subject matter is also covered in the multi-authored Volume 14 (Part 1, 2nd Ed.) which was published by Wiley in 1986.

J. E. WHITLEY

Physical Organic Chemistry, 2nd Ed.: CALVIN D. RITCHIE, Dekker, New York, 1990. Pages x + 357. \$59.75 (U.S. and Canada), \$71.50 (elsewhere).

Probably the first book to carry the title "Physical Organic Chemistry" was by Hammett in 1940. This remained the major text until the first edition of Ingold's *magnum opus* in 1953. This tome spawned Gould's book, which cheekily inverted Ingold's title and presented material with a lighter touch; even today Gould's book is far from passé. Subsequently a number of books in the area have appeared, but few have dominated the market for long.

The second edition of Ritchie's book follows fifteen years after the first, and, as with all second editions, is larger. In the preface, intending readers are counselled darkly against perusing the book at bedtime, and this is true since the text is sited well to the physical side of physical organic chemistry. Much mathematical rigour is included. It is probable that there is a Boltzmann distribution of attitudes such that the majority audience would prefer a more descriptive approach and certainly one that included more background material. Ritchie has apparently gone unashamedly for the minority and one feels that he is almost wilfully shooting to miss the audience target.

Although the author has written a commendable book from his viewpoint, it does not, in contrast to his research papers, read easily.

On selected specified points: ρ_+ appears out of mid-air on page 138 and on page 137 peroxide ion is said, without explanation, to be a good nucleophile (and merits an index entry). The perceptive student may wonder: why peroxide rather than hydroxide, and what is the relationship between them? Yet there is no mention of the alpha effect, which featured in a paper of Ritchie's in 1975. On pages 280–282 a section on solvent isotope effects is devoid of explanation; a potted summary of the papers of Bunton and Shiner in 1961 would provide more help. On page 288 a sterile problem on steric deuterium isotope effects could have been more enticingly posed around a real-life example—several are in the literature, e.g., results from Mislow, Melander and McKenna, again from the 1960s.

It may be wondered how many students will benefit from the last chapter "Transition State Theory and Primary Isotope Effects" in which real chemistry is sparse; indeed a review article would be more appropriate for this material.

It would be interesting to know the rationale of the publishers in charging \$11.75 less for the book in the U.S.A., where salaries are higher, than elsewhere.

D. G. MORRIS

The book has been attractively produced from camera-ready copy and is reasonably priced. Errors appear to be few, the most obvious to this reviewer being those in the saxitoxin formulae on pages 22 and 24. The book is unlikely to be purchased by analytical chemists, but it should find a home in the libraries of all institutions interested in marine metabolites.

R. H. THOMSON

Radioanalytical Chemistry: J. TÖLGYESSY and M. KYRŠ, Ellis Horwood, Chichester, 1989. Volume 1, pages 354. Volume 2, pages 498. £59.95 (each).

These two volumes describe a wide range of methods of analysis in which determinations culminate with measurement of radioactivity, and so are frequently applicable where low limits of detection or non-destructive analyses are required. Provided for an analytical readership, introductory chapters on basic radioactivity and instrumentation, which are frequently included in books in this area, are excluded.

Volume 1 covers (i) Analysis by measurement of natural radioactivity, (ii) Isotope dilution analysis, (iii) Radio-reagent methods, (iv) Radiometric titrations, (v) Radioimmunoassay, and (vi) Radiochemical methods for determination of biological activity of enzymes. Whilst the last two sections are concerned with organic applications, the remainder (in both volumes) are concerned with inorganic analysis. The use of radioactive tracers is a useful means of investigating aspects of alternative methods of analysis, and a chapter on this topic would have been welcome.

Volume 2 covers (i) Activation analysis and (ii) Physical methods based on absorption, scattering and fluorescence, with an additional chapter on automation and a 172 page appendix of radionuclide data and tables of optimum spike/analyte ratios for isotope dilution analysis. The survey of automation of radiochemical methods is timely since this approach is likely to increase in response to reduction of acceptable dose limits. With increasing awareness of radiological and other hazards experienced in the analytical laboratory, it would also have been timely to include some comment (possibly in the introduction) of potential radiation exposure when using the methods described.

Each section concludes with a collection of references, for when comprehensive details of methods are required, and a "Selected" bibliography. The latter occasionally includes manufacturers' literature and material from the 1960's which may be difficult to locate.

Overall, these two volumes provide comprehensive coverage of a variety of radioanalytical methods, some of which have only previously been described in specialized monographs. Whilst the applicability of some of these methods is limited, the overall content is relevant to postgraduate students of analytical chemistry, notwithstanding the apparent age of some apparatus used in illustrations. Examples of applications are very diverse, so most analysts should find something of interest in library copies. For those who subscribe to Kolthoff and Elving's *Treatise on Analytical Chemistry*, most of the subject matter is also covered in the multi-authored Volume 14 (Part 1, 2nd Ed.) which was published by Wiley in 1986.

J. E. WHITLEY

Physical Organic Chemistry, 2nd Ed.: CALVIN D. RITCHIE, Dekker, New York, 1990. Pages x + 357. \$59.75 (U.S. and Canada), \$71.50 (elsewhere).

Probably the first book to carry the title "Physical Organic Chemistry" was by Hammett in 1940. This remained the major text until the first edition of Ingold's *magnum opus* in 1953. This tome spawned Gould's book, which cheekily inverted Ingold's title and presented material with a lighter touch; even today Gould's book is far from passé. Subsequently a number of books in the area have appeared, but few have dominated the market for long.

The second edition of Ritchie's book follows fifteen years after the first, and, as with all second editions, is larger. In the preface, intending readers are counselled darkly against perusing the book at bedtime, and this is true since the text is sited well to the physical side of physical organic chemistry. Much mathematical rigour is included. It is probable that there is a Boltzmann distribution of attitudes such that the majority audience would prefer a more descriptive approach and certainly one that included more background material. Ritchie has apparently gone unashamedly for the minority and one feels that he is almost wilfully shooting to miss the audience target.

Although the author has written a commendable book from his viewpoint, it does not, in contrast to his research papers, read easily.

On selected specified points: ρ_+ appears out of mid-air on page 138 and on page 137 peroxide ion is said, without explanation, to be a good nucleophile (and merits an index entry). The perceptive student may wonder: why peroxide rather than hydroxide, and what is the relationship between them? Yet there is no mention of the alpha effect, which featured in a paper of Ritchie's in 1975. On pages 280–282 a section on solvent isotope effects is devoid of explanation; a potted summary of the papers of Bunton and Shiner in 1961 would provide more help. On page 288 a sterile problem on steric deuterium isotope effects could have been more enticingly posed around a real-life example—several are in the literature, e.g., results from Mislow, Melander and McKenna, again from the 1960s.

It may be wondered how many students will benefit from the last chapter "Transition State Theory and Primary Isotope Effects" in which real chemistry is sparse; indeed a review article would be more appropriate for this material.

It would be interesting to know the rationale of the publishers in charging \$11.75 less for the book in the U.S.A., where salaries are higher, than elsewhere.

D. G. MORRIS

authors, as the role of thermal analysis in the characterization of both pure substances and drug-excipient mixtures is covered extensively in this well-produced text.

The first four chapters of the book are concerned with instrumentation, information obtained from thermal data, instrument optimization, and kinetics (stability). Relevant pharmaceutical examples are given but this section of the book is, in the main, quite general and the techniques described are not confined to studies solely in the pharmaceutical arena. The authors refer the reader to other works for greater details of instrument design.

The remaining ten chapters, which occupy about two-thirds of the text, are each concerned with a particular aspect of pharmaceutical thermal analysis. These chapters cover purity, characterization, solid dispersions, polymeric systems, solid dosage forms, compatibility, semi-solid systems, liposomes, freeze-drying, and miscellaneous examples. Purity determinations based on the van't Hoff equation are given and examples of various possible corrections for the fraction melted are discussed. Characterization of pharmaceutical solids concentrates on the important areas of isomers, polymorphs and solvates. Here, as throughout the book, complementary techniques such as X-ray diffraction and infrared spectroscopy are mentioned. Thermal analysis of urea, cyclodextrins, poly(vinyl pyrrolidone), poly(ethylene glycol) and other carriers in solid dispersions are covered and explained with respect to appropriate phase diagrams. Of particular interest is the role of both DSC and DTA in predicting and examining age-induced changes in these dispersions. The application of thermal methods to polymer characterization, detection of drug-polymer interactions and drug release mechanisms is also described. The characterization of drug excipients and solid dosage forms by thermal analysis is covered and the important area of drug-excipient compatibility is mentioned with suitable reference of the literature. Thermal analysis of fats and waxes, suppositories and pessaries, emulsions, and creams and ointments are all mentioned briefly. The chapter on liposomes is concerned with their potential use as drug delivery systems and their use as model membrane systems to provide a simple model of drug activity. The use of thermal analysis to determine eutectic temperatures of formulations to be freeze-dried, and the subsequent amounts of residual solvent in final products is included. The chapter on miscellaneous applications includes detection of polymorphic changes induced by spray-drying or co-grinding.

Each chapter is followed by a suitable number of references and an index, the latter being a necessary inclusion for the inevitable overlap of subject material. On browsing through the index it was a little disappointing not to come across terms such as shelf-life, X-ray diffraction, infrared spectroscopy, reference materials, automation or computer control. As the subject matter of this field is so extensive, some pharmaceutical examples will be excluded from the text and some specific cases will not have been published by workers in industry. However, the authors are to be commended on bringing together a vast amount of material, scattered through many different literature sources, to produce a reference text that will have a place in every pharmaceutical laboratory engaged in thermal analysis.

P. J. Cox

Field-Flow Fractionation: Analysis of Macromolecules and Particles: JOSEF JANČA, Dekker, New York, 1988. Pages vi + 336.

Field-flow fractionation is a method of separating substances of macromolecular and particulate dimensions. The driving force can be gravitational, centrifugal, thermal, electrical, magnetic, or shear, acting in the direction perpendicular to the flow of the fluid. The technique is similar in many aspects to chromatography but differs in that there is no stationary phase other than the walls of the fluid channel.

Anyone unfamiliar with chromatographic or field-flow techniques will find this book hard to read and digest, partly because of the style of writing and/or translation, and partly because of the author's predilection with minutiae; it is a case of not being able to see the forest for the trees. The review is comprehensive and will be of interest to those active in field-flow fractionation.

J. B. CRAIG

Ion Exchange and Sorption Processes in Hydrometallurgy: M. STREAT and D. NADEN (editors), Wiley, Chichester, 1987. Pages x + 229. £45.00.

This book is Volume 19 in a series of Critical Reports on Applied Chemistry, and was published for the Society of Chemical Industry in the UK. The book contains four chapters: Chapter 1, by the editors Streat and Naden, on the application of ion-exchange to the recovery of uranium, describes the interactions of the uranium recovery flowsheet and the ion-exchange process, the ion-exchange resins and equipment, and process design for continuous ion-exchange. Chapter 2, by McDougall and Fleming, on the extraction of precious metals by activated carbon, describes the manufacture, structure and adsorptive properties of activated carbon, the interaction between it and gold complexes, and its application to gold recovery.

Chapter 3, by Warshawsky, on the extraction of platinum group metals (PGM) by ion-exchange resins, describes the modern approach to PGM recovery and separation, the concentration of PGM by selective polymers, and an integrated ion-exchange and liquid-liquid extraction process. Chapter 4, also by Warshawsky, on chelating ion-exchangers, describes the syntheses and applications of chelating and co-ordinating polymers. This book is a critical and objective review written by experts. It is well-written and illustrated by a mixture of clear and simple diagrams and photographs: there is also an excellent balance between theory and application. Primarily, the book will be of great interest to those involved in the extraction of metals, but it will also be of interest to all those using ion-exchange or sorption processes industrially.

J. B. CRAIG

authors, as the role of thermal analysis in the characterization of both pure substances and drug–excipient mixtures is covered extensively in this well-produced text.

The first four chapters of the book are concerned with instrumentation, information obtained from thermal data, instrument optimization, and kinetics (stability). Relevant pharmaceutical examples are given but this section of the book is, in the main, quite general and the techniques described are not confined to studies solely in the pharmaceutical arena. The authors refer the reader to other works for greater details of instrument design.

The remaining ten chapters, which occupy about two-thirds of the text, are each concerned with a particular aspect of pharmaceutical thermal analysis. These chapters cover purity, characterization, solid dispersions, polymeric systems, solid dosage forms, compatibility, semi-solid systems, liposomes, freeze-drying, and miscellaneous examples. Purity determinations based on the van't Hoff equation are given and examples of various possible corrections for the fraction melted are discussed. Characterization of pharmaceutical solids concentrates on the important areas of isomers, polymorphs and solvates. Here, as throughout the book, complementary techniques such as X-ray diffraction and infrared spectroscopy are mentioned. Thermal analysis of urea, cyclodextrins, poly(vinyl pyrrolidone), poly(ethylene glycol) and other carriers in solid dispersions are covered and explained with respect to appropriate phase diagrams. Of particular interest is the role of both DSC and DTA in predicting and examining age-induced changes in these dispersions. The application of thermal methods to polymer characterization, detection of drug–polymer interactions and drug release mechanisms is also described. The characterization of drug excipients and solid dosage forms by thermal analysis is covered and the important area of drug–excipient compatibility is mentioned with suitable reference of the literature. Thermal analysis of fats and waxes, suppositories and pessaries, emulsions, and creams and ointments are all mentioned briefly. The chapter on liposomes is concerned with their potential use as drug delivery systems and their use as model membrane systems to provide a simple model of drug activity. The use of thermal analysis to determine eutectic temperatures of formulations to be freeze-dried, and the subsequent amounts of residual solvent in final products is included. The chapter on miscellaneous applications includes detection of polymorphic changes induced by spray-drying or co-grinding.

Each chapter is followed by a suitable number of references and an index, the latter being a necessary inclusion for the inevitable overlap of subject material. On browsing through the index it was a little disappointing not to come across terms such as shelf-life, X-ray diffraction, infrared spectroscopy, reference materials, automation or computer control. As the subject matter of this field is so extensive, some pharmaceutical examples will be excluded from the text and some specific cases will not have been published by workers in industry. However, the authors are to be commended on bringing together a vast amount of material, scattered through many different literature sources, to produce a reference text that will have a place in every pharmaceutical laboratory engaged in thermal analysis.

P. J. Cox

Field-Flow Fractionation: Analysis of Macromolecules and Particles: JOSEF JANČA, Dekker, New York, 1988. Pages vi + 336.

Field-flow fractionation is a method of separating substances of macromolecular and particulate dimensions. The driving force can be gravitational, centrifugal, thermal, electrical, magnetic, or shear, acting in the direction perpendicular to the flow of the fluid. The technique is similar in many aspects to chromatography but differs in that there is no stationary phase other than the walls of the fluid channel.

Anyone unfamiliar with chromatographic or field-flow techniques will find this book hard to read and digest, partly because of the style of writing and/or translation, and partly because of the author's predilection with minutiae; it is a case of not being able to see the forest for the trees. The review is comprehensive and will be of interest to those active in field-flow fractionation.

J. B. CRAIG

Ion Exchange and Sorption Processes in Hydrometallurgy: M. STREAT and D. NADEN (editors), Wiley, Chichester, 1987. Pages x + 229. £45.00.

This book is Volume 19 in a series of Critical Reports on Applied Chemistry, and was published for the Society of Chemical Industry in the UK. The book contains four chapters: Chapter 1, by the editors Streat and Naden, on the application of ion-exchange to the recovery of uranium, describes the interactions of the uranium recovery flowsheet and the ion-exchange process, the ion-exchange resins and equipment, and process design for continuous ion-exchange. Chapter 2, by McDougall and Fleming, on the extraction of precious metals by activated carbon, describes the manufacture, structure and adsorptive properties of activated carbon, the interaction between it and gold complexes, and its application to gold recovery.

Chapter 3, by Warshawsky, on the extraction of platinum group metals (PGM) by ion-exchange resins, describes the modern approach to PGM recovery and separation, the concentration of PGM by selective polymers, and an integrated ion-exchange and liquid–liquid extraction process. Chapter 4, also by Warshawsky, on chelating ion-exchangers, describes the syntheses and applications of chelating and co-ordinating polymers. This book is a critical and objective review written by experts. It is well-written and illustrated by a mixture of clear and simple diagrams and photographs: there is also an excellent balance between theory and application. Primarily, the book will be of great interest to those involved in the extraction of metals, but it will also be of interest to all those using ion-exchange or sorption processes industrially.

J. B. CRAIG

authors, as the role of thermal analysis in the characterization of both pure substances and drug-exipient mixtures is covered extensively in this well-produced text.

The first four chapters of the book are concerned with instrumentation, information obtained from thermal data, instrument optimization, and kinetics (stability). Relevant pharmaceutical examples are given but this section of the book is, in the main, quite general and the techniques described are not confined to studies solely in the pharmaceutical arena. The authors refer the reader to other works for greater details of instrument design.

The remaining ten chapters, which occupy about two-thirds of the text, are each concerned with a particular aspect of pharmaceutical thermal analysis. These chapters cover purity, characterization, solid dispersions, polymeric systems, solid dosage forms, compatibility, semi-solid systems, liposomes, freeze-drying, and miscellaneous examples. Purity determinations based on the van't Hoff equation are given and examples of various possible corrections for the fraction melted are discussed. Characterization of pharmaceutical solids concentrates on the important areas of isomers, polymorphs and solvates. Here, as throughout the book, complementary techniques such as X-ray diffraction and infrared spectroscopy are mentioned. Thermal analysis of urea, cyclodextrins, poly(vinyl pyrrolidone), poly(ethylene glycol) and other carriers in solid dispersions are covered and explained with respect to appropriate phase diagrams. Of particular interest is the role of both DSC and DTA in predicting and examining age-induced changes in these dispersions. The application of thermal methods to polymer characterization, detection of drug-polymer interactions and drug release mechanisms is also described. The characterization of drug excipients and solid dosage forms by thermal analysis is covered and the important area of drug-exipient compatibility is mentioned with suitable reference of the literature. Thermal analysis of fats and waxes, suppositories and pessaries, emulsions, and creams and ointments are all mentioned briefly. The chapter on liposomes is concerned with their potential use as drug delivery systems and their use as model membrane systems to provide a simple model of drug activity. The use of thermal analysis to determine eutectic temperatures of formulations to be freeze-dried, and the subsequent amounts of residual solvent in final products is included. The chapter on miscellaneous applications includes detection of polymorphic changes induced by spray-drying or co-grinding.

Each chapter is followed by a suitable number of references and an index, the latter being a necessary inclusion for the inevitable overlap of subject material. On browsing through the index it was a little disappointing not to come across terms such as shelf-life, X-ray diffraction, infrared spectroscopy, reference materials, automation or computer control. As the subject matter of this field is so extensive, some pharmaceutical examples will be excluded from the text and some specific cases will not have been published by workers in industry. However, the authors are to be commended on bringing together a vast amount of material, scattered through many different literature sources, to produce a reference text that will have a place in every pharmaceutical laboratory engaged in thermal analysis.

P. J. Cox

Field-Flow Fractionation: Analysis of Macromolecules and Particles: JOSEF JANČA, Dekker, New York, 1988. Pages vi + 336.

Field-flow fractionation is a method of separating substances of macromolecular and particulate dimensions. The driving force can be gravitational, centrifugal, thermal, electrical, magnetic, or shear, acting in the direction perpendicular to the flow of the fluid. The technique is similar in many aspects to chromatography but differs in that there is no stationary phase other than the walls of the fluid channel.

Anyone unfamiliar with chromatographic or field-flow techniques will find this book hard to read and digest, partly because of the style of writing and/or translation, and partly because of the author's predilection with minutiae; it is a case of not being able to see the forest for the trees. The review is comprehensive and will be of interest to those active in field-flow fractionation.

J. B. CRAIG

Ion Exchange and Sorption Processes in Hydrometallurgy: M. STREAT and D. NADEN (editors), Wiley, Chichester, 1987. Pages x + 229. £45.00.

This book is Volume 19 in a series of Critical Reports on Applied Chemistry, and was published for the Society of Chemical Industry in the UK. The book contains four chapters: Chapter 1, by the editors Streat and Naden, on the application of ion-exchange to the recovery of uranium, describes the interactions of the uranium recovery flowsheet and the ion-exchange process, the ion-exchange resins and equipment, and process design for continuous ion-exchange. Chapter 2, by McDougall and Fleming, on the extraction of precious metals by activated carbon, describes the manufacture, structure and adsorptive properties of activated carbon, the interaction between it and gold complexes, and its application to gold recovery.

Chapter 3, by Warshawsky, on the extraction of platinum group metals (PGM) by ion-exchange resins, describes the modern approach to PGM recovery and separation, the concentration of PGM by selective polymers, and an integrated ion-exchange and liquid-liquid extraction process. Chapter 4, also by Warshawsky, on chelating ion-exchangers, describes the syntheses and applications of chelating and co-ordinating polymers. This book is a critical and objective review written by experts. It is well-written and illustrated by a mixture of clear and simple diagrams and photographs: there is also an excellent balance between theory and application. Primarily, the book will be of great interest to those involved in the extraction of metals, but it will also be of interest to all those using ion-exchange or sorption processes industrially.

J. B. CRAIG

authors, as the role of thermal analysis in the characterization of both pure substances and drug-exipient mixtures is covered extensively in this well-produced text.

The first four chapters of the book are concerned with instrumentation, information obtained from thermal data, instrument optimization, and kinetics (stability). Relevant pharmaceutical examples are given but this section of the book is, in the main, quite general and the techniques described are not confined to studies solely in the pharmaceutical arena. The authors refer the reader to other works for greater details of instrument design.

The remaining ten chapters, which occupy about two-thirds of the text, are each concerned with a particular aspect of pharmaceutical thermal analysis. These chapters cover purity, characterization, solid dispersions, polymeric systems, solid dosage forms, compatibility, semi-solid systems, liposomes, freeze-drying, and miscellaneous examples. Purity determinations based on the van't Hoff equation are given and examples of various possible corrections for the fraction melted are discussed. Characterization of pharmaceutical solids concentrates on the important areas of isomers, polymorphs and solvates. Here, as throughout the book, complementary techniques such as X-ray diffraction and infrared spectroscopy are mentioned. Thermal analysis of urea, cyclodextrins, poly(vinyl pyrrolidone), poly(ethylene glycol) and other carriers in solid dispersions are covered and explained with respect to appropriate phase diagrams. Of particular interest is the role of both DSC and DTA in predicting and examining age-induced changes in these dispersions. The application of thermal methods to polymer characterization, detection of drug-polymer interactions and drug release mechanisms is also described. The characterization of drug excipients and solid dosage forms by thermal analysis is covered and the important area of drug-exipient compatibility is mentioned with suitable reference of the literature. Thermal analysis of fats and waxes, suppositories and pessaries, emulsions, and creams and ointments are all mentioned briefly. The chapter on liposomes is concerned with their potential use as drug delivery systems and their use as model membrane systems to provide a simple model of drug activity. The use of thermal analysis to determine eutectic temperatures of formulations to be freeze-dried, and the subsequent amounts of residual solvent in final products is included. The chapter on miscellaneous applications includes detection of polymorphic changes induced by spray-drying or co-grinding.

Each chapter is followed by a suitable number of references and an index, the latter being a necessary inclusion for the inevitable overlap of subject material. On browsing through the index it was a little disappointing not to come across terms such as shelf-life, X-ray diffraction, infrared spectroscopy, reference materials, automation or computer control. As the subject matter of this field is so extensive, some pharmaceutical examples will be excluded from the text and some specific cases will not have been published by workers in industry. However, the authors are to be commended on bringing together a vast amount of material, scattered through many different literature sources, to produce a reference text that will have a place in every pharmaceutical laboratory engaged in thermal analysis.

P. J. Cox

Field-Flow Fractionation: Analysis of Macromolecules and Particles: JOSEF JANČA, Dekker, New York, 1988. Pages vi + 336.

Field-flow fractionation is a method of separating substances of macromolecular and particulate dimensions. The driving force can be gravitational, centrifugal, thermal, electrical, magnetic, or shear, acting in the direction perpendicular to the flow of the fluid. The technique is similar in many aspects to chromatography but differs in that there is no stationary phase other than the walls of the fluid channel.

Anyone unfamiliar with chromatographic or field-flow techniques will find this book hard to read and digest, partly because of the style of writing and/or translation, and partly because of the author's predilection with minutiae; it is a case of not being able to see the forest for the trees. The review is comprehensive and will be of interest to those active in field-flow fractionation.

J. B. CRAIG

Ion Exchange and Sorption Processes in Hydrometallurgy: M. STREAT and D. NADEN (editors), Wiley, Chichester, 1987. Pages x + 229. £45.00.

This book is Volume 19 in a series of Critical Reports on Applied Chemistry, and was published for the Society of Chemical Industry in the UK. The book contains four chapters: Chapter 1, by the editors Streat and Naden, on the application of ion-exchange to the recovery of uranium, describes the interactions of the uranium recovery flowsheet and the ion-exchange process, the ion-exchange resins and equipment, and process design for continuous ion-exchange. Chapter 2, by McDougall and Fleming, on the extraction of precious metals by activated carbon, describes the manufacture, structure and adsorptive properties of activated carbon, the interaction between it and gold complexes, and its application to gold recovery.

Chapter 3, by Warshawsky, on the extraction of platinum group metals (PGM) by ion-exchange resins, describes the modern approach to PGM recovery and separation, the concentration of PGM by selective polymers, and an integrated ion-exchange and liquid-liquid extraction process. Chapter 4, also by Warshawsky, on chelating ion-exchangers, describes the syntheses and applications of chelating and co-ordinating polymers. This book is a critical and objective review written by experts. It is well-written and illustrated by a mixture of clear and simple diagrams and photographs: there is also an excellent balance between theory and application. Primarily, the book will be of great interest to those involved in the extraction of metals, but it will also be of interest to all those using ion-exchange or sorption processes industrially.

J. B. CRAIG

Secondary Ion Mass Spectrometry, SIMS VI: A. BENNINGHOVEN, A. M. HUBER and H. W. WERNER (editors), Wiley, Chichester, 1989. Pages xxxiii + 1078. £75.00.

This substantial book brings together over 200 communications presented at the Sixth International Conference on Secondary Ion Mass Spectrometry held at Versailles, September 1987. The overall quality of the papers is high although individual papers can, by the very nature of the book, be of variable quality and a few are but brief, relatively uninformative, notes. It should be acknowledged, however, that all the papers were refereed and recommendations made to the authors for improvement, although there was no follow-up to this.

The book is particularly valuable in that it gives an overall picture of the current (at the time of presentation) state of the technique and of the developments being pursued in different parts of the world. The 13 sections cover latest developments in the understanding of fundamental phenomena (including the process of atom ejection by ion-beam bombardment of solids; secondary-ion formation during ejection, radiation effects on the mobilization of atoms within the target), in instrumentation (especially for the elementary and isotopic analysis of small quantities) and in applications in many fields (electronics, metallurgy, surfaces, organic materials, biology, medicine, geology).

For workers in this field this book must be considered as virtually essential for keeping up with current developments.

J. R. BACON

Quantitative Bioassay: D. HAWCROFT, T. HECTOR and F. ROWELL, Wiley, Chichester, 1987. Pages xxiii + 300. £11.50 (Softback); £32.50 (Hardback).

The title of this book unfortunately belies the fact that it is concerned predominantly with the principles of immunoassay techniques and their applications. After a short introductory section devoted to general aspects of bioassays ("quantitation of a response following application of a stimulus to a biological system"), the book deals with microbiological (bacterial) assays, then the remaining two thirds are devoted to theoretical aspects of antigen-antibody interactions and to the exploitation of these principles in quantitative radioimmunoassay, enzyme immunoassay and immunofluorescence procedures. The attraction of this style of text, from the teacher's viewpoint, is that it continuously tests the reader's comprehension of the concepts expounded. The text is well laid out, easy to follow and the numerous figures are commendably clear. There is a useful glossary of (immunological) terms, although the reader/student is denied the benefits of an index. Included is a bibliography of practical texts, but users of this book should be warned that newer editions of several of the cited volumes have now been published. The cost is not excessive and this book can be recommended to undergraduate students studying practical aspects of microbiology/immunology.

A. W. THOMSON

Detection and Data Analysis in Size Exclusion Chromatography: THEODORE PROVDER (editor), American Chemical Society, Washington, DC, 1987. Pages ix + 307. \$69.95 (USA and Canada); \$83.95 (elsewhere).

Chemists who fabricate polymers for specific end-uses need to know the structure-property relationships and hence the structures of their polymers. One of the most powerful tools for polymer characterization is size exclusion chromatography, SEC, also known as gel permeation chromatography, GPC, a unique separational technique based on size differences among the solute molecules. This book describes the developments in columns and multiple in-line detectors, which can measure concurrently several parameters, such as refractive index, light scattering, IR and UV absorption, viscosity, mass spectra, to provide information on polymer composition, molecular weight, molecular weight distribution, and chain branching. Simultaneous developments in computer technology for instrument control and data analysis are also described.

This 17-chapter book is divided into three sections: the first deals with separational mechanisms, and presents an excellent overview of SEC, non-size effects in high-performance SEC, preparative SEC, and orthogonal chromatography. The second section deals with detectors: five chapters describe the evaluation of molecular weight distribution, molecular size and shape by use of capillary or membrane viscometers in various configurations. One chapter deals with the determination of functional groups and another describes the application of SEC to the analysis of coal liquids. The third section covers the field of data analysis with chapters on chemometrics, signal analysis, spreading factors, and corrections for instrumental broadening.

The book was developed from an American Chemical Society Symposium on SEC in 1986: the papers are reproduced as they were submitted by the authors and not typeset. On the whole the papers are well written, relatively error-free, and should be of interest to all polymer chemists in the design and characterization field.

J. B. CRAIG

Chemiluminescence and Photochemical Reaction Detection in Chromatography: J. W. BIRKS (editor), VCH, New York, 1989. Pages x + 291. £49.45.

The contents of this excellent book are presented in a style which should ensure that those chromatographers who know little about these detection methods will rapidly acquire enough background knowledge and understanding to appreciate their potential use. Those with difficult selectivity or sensitivity problems will find this book essential reading.

Secondary Ion Mass Spectrometry, SIMS VI: A. BENNINGHOVEN, A. M. HUBER and H. W. WERNER (editors), Wiley, Chichester, 1989. Pages xxxiii + 1078. £75.00.

This substantial book brings together over 200 communications presented at the Sixth International Conference on Secondary Ion Mass Spectrometry held at Versailles, September 1987. The overall quality of the papers is high although individual papers can, by the very nature of the book, be of variable quality and a few are but brief, relatively uninformative, notes. It should be acknowledged, however, that all the papers were refereed and recommendations made to the authors for improvement, although there was no follow-up to this.

The book is particularly valuable in that it gives an overall picture of the current (at the time of presentation) state of the technique and of the developments being pursued in different parts of the world. The 13 sections cover latest developments in the understanding of fundamental phenomena (including the process of atom ejection by ion-beam bombardment of solids; secondary-ion formation during ejection, radiation effects on the mobilization of atoms within the target), in instrumentation (especially for the elementary and isotopic analysis of small quantities) and in applications in many fields (electronics, metallurgy, surfaces, organic materials, biology, medicine, geology).

For workers in this field this book must be considered as virtually essential for keeping up with current developments.

J. R. BACON

Quantitative Bioassay: D. HAWCROFT, T. HECTOR and F. ROWELL, Wiley, Chichester, 1987. Pages xxiii + 300. £11.50 (Softback); £32.50 (Hardback).

The title of this book unfortunately belies the fact that it is concerned predominantly with the principles of immunoassay techniques and their applications. After a short introductory section devoted to general aspects of bioassays ("quantitation of a response following application of a stimulus to a biological system"), the book deals with microbiological (bacterial) assays, then the remaining two thirds are devoted to theoretical aspects of antigen-antibody interactions and to the exploitation of these principles in quantitative radioimmunoassay, enzyme immunoassay and immunofluorescence procedures. The attraction of this style of text, from the teacher's viewpoint, is that it continuously tests the reader's comprehension of the concepts expounded. The text is well laid out, easy to follow and the numerous figures are commendably clear. There is a useful glossary of (immunological) terms, although the reader/student is denied the benefits of an index. Included is a bibliography of practical texts, but users of this book should be warned that newer editions of several of the cited volumes have now been published. The cost is not excessive and this book can be recommended to undergraduate students studying practical aspects of microbiology/immunology.

A. W. THOMSON

Detection and Data Analysis in Size Exclusion Chromatography: THEODORE PROVDER (editor), American Chemical Society, Washington, DC, 1987. Pages ix + 307. \$69.95 (USA and Canada); \$83.95 (elsewhere).

Chemists who fabricate polymers for specific end-uses need to know the structure-property relationships and hence the structures of their polymers. One of the most powerful tools for polymer characterization is size exclusion chromatography, SEC, also known as gel permeation chromatography, GPC, a unique separational technique based on size differences among the solute molecules. This book describes the developments in columns and multiple in-line detectors, which can measure concurrently several parameters, such as refractive index, light scattering, IR and UV absorption, viscosity, mass spectra, to provide information on polymer composition, molecular weight, molecular weight distribution, and chain branching. Simultaneous developments in computer technology for instrument control and data analysis are also described.

This 17-chapter book is divided into three sections: the first deals with separational mechanisms, and presents an excellent overview of SEC, non-size effects in high-performance SEC, preparative SEC, and orthogonal chromatography. The second section deals with detectors: five chapters describe the evaluation of molecular weight distribution, molecular size and shape by use of capillary or membrane viscometers in various configurations. One chapter deals with the determination of functional groups and another describes the application of SEC to the analysis of coal liquids. The third section covers the field of data analysis with chapters on chemometrics, signal analysis, spreading factors, and corrections for instrumental broadening.

The book was developed from an American Chemical Society Symposium on SEC in 1986: the papers are reproduced as they were submitted by the authors and not typeset. On the whole the papers are well written, relatively error-free, and should be of interest to all polymer chemists in the design and characterization field.

J. B. CRAIG

Chemiluminescence and Photochemical Reaction Detection in Chromatography: J. W. BIRKS (editor), VCH, New York, 1989. Pages x + 291. £49.45.

The contents of this excellent book are presented in a style which should ensure that those chromatographers who know little about these detection methods will rapidly acquire enough background knowledge and understanding to appreciate their potential use. Those with difficult selectivity or sensitivity problems will find this book essential reading.

Secondary Ion Mass Spectrometry, SIMS VI: A. BENNINGHOVEN, A. M. HUBER and H. W. WERNER (editors), Wiley, Chichester, 1989. Pages xxxiii + 1078. £75.00.

This substantial book brings together over 200 communications presented at the Sixth International Conference on Secondary Ion Mass Spectrometry held at Versailles, September 1987. The overall quality of the papers is high although individual papers can, by the very nature of the book, be of variable quality and a few are but brief, relatively uninformative, notes. It should be acknowledged, however, that all the papers were refereed and recommendations made to the authors for improvement, although there was no follow-up to this.

The book is particularly valuable in that it gives an overall picture of the current (at the time of presentation) state of the technique and of the developments being pursued in different parts of the world. The 13 sections cover latest developments in the understanding of fundamental phenomena (including the process of atom ejection by ion-beam bombardment of solids; secondary-ion formation during ejection, radiation effects on the mobilization of atoms within the target), in instrumentation (especially for the elementary and isotopic analysis of small quantities) and in applications in many fields (electronics, metallurgy, surfaces, organic materials, biology, medicine, geology).

For workers in this field this book must be considered as virtually essential for keeping up with current developments.

J. R. BACON

Quantitative Bioassay: D. HAWCROFT, T. HECTOR and F. ROWELL, Wiley, Chichester, 1987. Pages xxiii + 300. £11.50 (Softback); £32.50 (Hardback).

The title of this book unfortunately belies the fact that it is concerned predominantly with the principles of immunoassay techniques and their applications. After a short introductory section devoted to general aspects of bioassays ("quantitation of a response following application of a stimulus to a biological system"), the book deals with microbiological (bacterial) assays, then the remaining two thirds are devoted to theoretical aspects of antigen-antibody interactions and to the exploitation of these principles in quantitative radioimmunoassay, enzyme immunoassay and immunofluorescence procedures. The attraction of this style of text, from the teacher's viewpoint, is that it continuously tests the reader's comprehension of the concepts expounded. The text is well laid out, easy to follow and the numerous figures are commendably clear. There is a useful glossary of (immunological) terms, although the reader/student is denied the benefits of an index. Included is a bibliography of practical texts, but users of this book should be warned that newer editions of several of the cited volumes have now been published. The cost is not excessive and this book can be recommended to undergraduate students studying practical aspects of microbiology/immunology.

A. W. THOMSON

Detection and Data Analysis in Size Exclusion Chromatography: THEODORE PROVDER (editor), American Chemical Society, Washington, DC, 1987. Pages ix + 307. \$69.95 (USA and Canada); \$83.95 (elsewhere).

Chemists who fabricate polymers for specific end-uses need to know the structure-property relationships and hence the structures of their polymers. One of the most powerful tools for polymer characterization is size exclusion chromatography, SEC, also known as gel permeation chromatography, GPC, a unique separational technique based on size differences among the solute molecules. This book describes the developments in columns and multiple in-line detectors, which can measure concurrently several parameters, such as refractive index, light scattering, IR and UV absorption, viscosity, mass spectra, to provide information on polymer composition, molecular weight, molecular weight distribution, and chain branching. Simultaneous developments in computer technology for instrument control and data analysis are also described.

This 17-chapter book is divided into three sections: the first deals with separational mechanisms, and presents an excellent overview of SEC, non-size effects in high-performance SEC, preparative SEC, and orthogonal chromatography. The second section deals with detectors: five chapters describe the evaluation of molecular weight distribution, molecular size and shape by use of capillary or membrane viscometers in various configurations. One chapter deals with the determination of functional groups and another describes the application of SEC to the analysis of coal liquids. The third section covers the field of data analysis with chapters on chemometrics, signal analysis, spreading factors, and corrections for instrumental broadening.

The book was developed from an American Chemical Society Symposium on SEC in 1986: the papers are reproduced as they were submitted by the authors and not typeset. On the whole the papers are well written, relatively error-free, and should be of interest to all polymer chemists in the design and characterization field.

J. B. CRAIG

Chemiluminescence and Photochemical Reaction Detection in Chromatography: J. W. BIRKS (editor), VCH, New York, 1989. Pages x + 291. £49.45.

The contents of this excellent book are presented in a style which should ensure that those chromatographers who know little about these detection methods will rapidly acquire enough background knowledge and understanding to appreciate their potential use. Those with difficult selectivity or sensitivity problems will find this book essential reading.

About half the book deals with peptic ulcer disease and existing therapy. The rest of the book examines possible areas for new drug development. Some chapters such as "Strategies for the Development of Novel Anti-ulcer Drugs" are very readable whereas others such as "Pro-ulcerogenic and Related Lipid Mediators in Gastric Mucosal Damage" are a little more demanding.

Although of great relevance and importance this book can only be recommended for those chemists with more than a passing knowledge of physiology, pharmacology and biochemistry.

P. J. Cox

Practical Computing for Experimental Scientists: JOHN D. BEASLEY, OUP, Oxford, 1988. Pages xii + 233. £12.50.

This book is eminently suitable for a beginning postgraduate student or postdoctoral fellow, but any other scientist who has not yet come to terms with the computer revolution would find it most helpful in cutting through the jargon that makes it difficult to start at the beginning in computing. It offers wide-ranging advice on the choice and application of computers for scientific experimentation. Both mainframe and personal computing are discussed, with no assumptions of prior knowledge. The wide variety of topics includes: connecting a computer to experimental equipment, data analysis, graphical and tabular presentation of data, scientific word processing, secure storage of data, transfer of data between computers, telemetry, graphical input, data retrieval, the scientist as programmer, use of spreadsheets, high-level languages, machine assembly language, rounding errors, statistical analysis of data, finite approximations, pseudo-random numbers, talking to a computer expert, choosing a computer, and care and safety. As must be evident from the range of topics, readers cannot expect to gain detailed knowledge of any single one, but they will find much sound advice that is not easy to find in the many more specialized computer books available today.

MARY MASSON

Introduction to Microwave Sample Preparation: Theory and Practice: H. M. KINGSTON and LOIS B. JASSIE (editors), ACS Professional Reference Book, ACS, Washington, D.C., 1988. Pages xxii + 263. Price US \$49.95. Export \$59.95.

The process of wet digestion is a necessary step in most analytical procedures, both classical and instrumental. This book describes a small revolution in wet digestion methods that has taken place since 1975. It aims to provide most of the information required for an analyst to get started in microwave dissolution. The wide range of sample types covered includes geological and metallurgical samples, botanical, biological and food samples, pharmaceuticals, selenium-containing materials, and minerals. Procedures for Kjeldahl nitrogen determination, remote operation, dissolution in radioactive environments, and robotic control are described. Theoretical aspects, and the design of equipment, including vessels, are discussed, and safety guidelines are also included.

MARY MASSON

About half the book deals with peptic ulcer disease and existing therapy. The rest of the book examines possible areas for new drug development. Some chapters such as "Strategies for the Development of Novel Anti-ulcer Drugs" are very readable whereas others such as "Pro-ulcerogenic and Related Lipid Mediators in Gastric Mucosal Damage" are a little more demanding.

Although of great relevance and importance this book can only be recommended for those chemists with more than a passing knowledge of physiology, pharmacology and biochemistry.

P. J. COX

Practical Computing for Experimental Scientists: JOHN D. BEASLEY, OUP, Oxford, 1988. Pages xii + 233. £12.50.

This book is eminently suitable for a beginning postgraduate student or postdoctoral fellow, but any other scientist who has not yet come to terms with the computer revolution would find it most helpful in cutting through the jargon that makes it difficult to start at the beginning in computing. It offers wide-ranging advice on the choice and application of computers for scientific experimentation. Both mainframe and personal computing are discussed, with no assumptions of prior knowledge. The wide variety of topics includes: connecting a computer to experimental equipment, data analysis, graphical and tabular presentation of data, scientific word processing, secure storage of data, transfer of data between computers, telemetry, graphical input, data retrieval, the scientist as programmer, use of spreadsheets, high-level languages, machine assembly language, rounding errors, statistical analysis of data, finite approximations, pseudo-random numbers, talking to a computer expert, choosing a computer, and care and safety. As must be evident from the range of topics, readers cannot expect to gain detailed knowledge of any single one, but they will find much sound advice that is not easy to find in the many more specialized computer books available today.

MARY MASSON

Introduction to Microwave Sample Preparation: Theory and Practice: H. M. KINGSTON and LOIS B. JASSIE (editors), ACS Professional Reference Book, ACS, Washington, D.C., 1988. Pages xxii + 263. Price US \$49.95. Export \$59.95.

The process of wet digestion is a necessary step in most analytical procedures, both classical and instrumental. This book describes a small revolution in wet digestion methods that has taken place since 1975. It aims to provide most of the information required for an analyst to get started in microwave dissolution. The wide range of sample types covered includes geological and metallurgical samples, botanical, biological and food samples, pharmaceuticals, selenium-containing materials, and minerals. Procedures for Kjeldahl nitrogen determination, remote operation, dissolution in radioactive environments, and robotic control are described. Theoretical aspects, and the design of equipment, including vessels, are discussed, and safety guidelines are also included.

MARY MASSON

Secondary Ion Mass Spectrometry, SIMS VI: A. BENNINGHOVEN, A. M. HUBER and H. W. WERNER (editors), Wiley, Chichester, 1989. Pages xxxiii + 1078. £75.00.

This substantial book brings together over 200 communications presented at the Sixth International Conference on Secondary Ion Mass Spectrometry held at Versailles, September 1987. The overall quality of the papers is high although individual papers can, by the very nature of the book, be of variable quality and a few are but brief, relatively uninformative, notes. It should be acknowledged, however, that all the papers were refereed and recommendations made to the authors for improvement, although there was no follow-up to this.

The book is particularly valuable in that it gives an overall picture of the current (at the time of presentation) state of the technique and of the developments being pursued in different parts of the world. The 13 sections cover latest developments in the understanding of fundamental phenomena (including the process of atom ejection by ion-beam bombardment of solids; secondary-ion formation during ejection, radiation effects on the mobilization of atoms within the target), in instrumentation (especially for the elementary and isotopic analysis of small quantities) and in applications in many fields (electronics, metallurgy, surfaces, organic materials, biology, medicine, geology).

For workers in this field this book must be considered as virtually essential for keeping up with current developments.

J. R. BACON

Quantitative Bioassay: D. HAWCROFT, T. HECTOR and F. ROWELL, Wiley, Chichester, 1987. Pages xxiii + 300. £11.50 (Softback); £32.50 (Hardback).

The title of this book unfortunately belies the fact that it is concerned predominantly with the principles of immunoassay techniques and their applications. After a short introductory section devoted to general aspects of bioassays ("quantitation of a response following application of a stimulus to a biological system"), the book deals with microbiological (bacterial) assays, then the remaining two thirds are devoted to theoretical aspects of antigen-antibody interactions and to the exploitation of these principles in quantitative radioimmunoassay, enzyme immunoassay and immunofluorescence procedures. The attraction of this style of text, from the teacher's viewpoint, is that it continuously tests the reader's comprehension of the concepts expounded. The text is well laid out, easy to follow and the numerous figures are commendably clear. There is a useful glossary of (immunological) terms, although the reader/student is denied the benefits of an index. Included is a bibliography of practical texts, but users of this book should be warned that newer editions of several of the cited volumes have now been published. The cost is not excessive and this book can be recommended to undergraduate students studying practical aspects of microbiology/immunology.

A. W. THOMSON

Detection and Data Analysis in Size Exclusion Chromatography: THEODORE PROVDER (editor), American Chemical Society, Washington, DC, 1987. Pages ix + 307. \$69.95 (USA and Canada); \$83.95 (elsewhere).

Chemists who fabricate polymers for specific end-uses need to know the structure-property relationships and hence the structures of their polymers. One of the most powerful tools for polymer characterization is size exclusion chromatography, SEC, also known as gel permeation chromatography, GPC, a unique separational technique based on size differences among the solute molecules. This book describes the developments in columns and multiple in-line detectors, which can measure concurrently several parameters, such as refractive index, light scattering, IR and UV absorption, viscosity, mass spectra, to provide information on polymer composition, molecular weight, molecular weight distribution, and chain branching. Simultaneous developments in computer technology for instrument control and data analysis are also described.

This 17-chapter book is divided into three sections: the first deals with separational mechanisms, and presents an excellent overview of SEC, non-size effects in high-performance SEC, preparative SEC, and orthogonal chromatography. The second section deals with detectors: five chapters describe the evaluation of molecular weight distribution, molecular size and shape by use of capillary or membrane viscometers in various configurations. One chapter deals with the determination of functional groups and another describes the application of SEC to the analysis of coal liquids. The third section covers the field of data analysis with chapters on chemometrics, signal analysis, spreading factors, and corrections for instrumental broadening.

The book was developed from an American Chemical Society Symposium on SEC in 1986: the papers are reproduced as they were submitted by the authors and not typeset. On the whole the papers are well written, relatively error-free, and should be of interest to all polymer chemists in the design and characterization field.

J. B. CRAIG

Chemiluminescence and Photochemical Reaction Detection in Chromatography: J. W. BIRKS (editor), VCH, New York, 1989. Pages x + 291. £49.45.

The contents of this excellent book are presented in a style which should ensure that those chromatographers who know little about these detection methods will rapidly acquire enough background knowledge and understanding to appreciate their potential use. Those with difficult selectivity or sensitivity problems will find this book essential reading.

In the opening chapter the principles of chemiluminescence and photochemical reactions are lucidly presented and their utilization or potential utilization as detectors in Gas Chromatography (GC) and Liquid Chromatography (LC) is discussed. Subsequent chapters give the theory, design (including illustrative diagrams), applications and limitations of each detector associated with a particular reaction.

For GC, chemiluminescence detectors based on the use of active nitrogen, nitric oxide/ozone and nitric oxide/ozone/oxygen are described. These detectors are selective for different types of nitrogen-containing compounds and it is suggested, with some justification, that such detectors will have important applications in industrial, petrochemical, environmental and other fields. For LC, post-column on-line detectors based on the use of, *e.g.*, luminol, lucigen, peroxyoxalate (which gets particular attention), electrochemiluminescence and the luciferin-luciferase bioluminescence reactions are described and discussed. Finally, an extensive but concise review of direct and indirect photochemical reaction detectors for LC is given.

Every chapter in the book is very well referenced, *e.g.*, the chapter on photochemical reaction detectors has more than 300 references. Hence further information on some particular topic of interest can be rapidly acquired.

R. R. MOODY

Environmental Analysis using Chromatography Interfaced with Atomic Spectroscopy: R. HARRISON and S. RAPSOMANIKIS (editors), Ellis Horwood, Chichester, 1989. Pages 370. £59.50.

I have very much enjoyed reading this book which is a very timely addition to the secondary literature on environmental analysis. The two editors have served us well, not just with their own chapters (Sulphur and Mercury, respectively) but especially by prevailing upon an excellent team of experienced workers to collaborate and then by making sure that all the contributions fitted the same style and approach. The result is a book both readable and informative, enriched by considerable detail on the individual methods. If, having started, you do not read this book through to the end, it will be because you have already succumbed to the temptation to try the combined instrumentation methods for yourself in the laboratory!

The book is in two sections with Chapters 1–6 covering the general topics of instrumentation (1: Basic principles, 2: Atomic absorption detectors, 3: Flame photometric detectors, 4: Plasma emission detectors, 5: Atomic fluorescence detectors, and 6: Interfaces between HPLC and FAAS). All chapters are well written, make reference to specific applications and give tabulations of performance data. Chapters 7–12 are devoted to particular elements and compare the applicability and success of different techniques, including details of sample handling and work-up (7: Tin and germanium, 8: Lead, 9: Arsenic and antimony, 10: Mercury, 11: Selenium and 12: Sulphur).

The book is attractively presented (though there should be a prize for anyone who can guess what the cover illustration represents), well referenced, and with very few typographical errors: Table 6.1 seems to have got muddled, and on page 307 the microwave plasma is presumably a helium one, not a medium one!

The authors make the important point that in general, the hardware is not commercially available for the coupled techniques described (except for GC-MIP). However, with this book in one hand and a small tool kit in the other, the do-it-yourself enthusiast will surely have success in these endeavours and be saved the frustration of making too many mistakes. I give this book my strongest recommendation.

I. L. MARR

Problems in Chemistry: HENRY O. DALEY, JR and ROBERT F. O'MALLEY, 2nd Edition, Revised and Expanded, Marcel Dekker, New York, 1988. Pages xvii + 476. \$39.50 (USA and Canada); \$47.25 (elsewhere).

This book, which is designed for American Freshman Chemistry courses, could be a most useful source of exercises for the earlier years of a chemistry course at a British University, in particular a Scottish one or for some advanced school courses.

It consists of nineteen chapters, ranging from units, composition and equations to elementary thermodynamics, chemical equilibrium, electrochemistry and kinetics. Each chapter has a series of carefully worked examples which will be very useful to students. One of the very attractive features of the book is that the data for many of the problems are taken from the chemical literature and the references are quoted. Students can then see that the kind of calculations which they are asked to do are part of the chemist's stock in trade and many will be in continual use in later courses.

While the chapter on chemical bonds gives practice in writing Lewis structures and contains examples of the use of electron-pair repulsion theory, there is no mention of orbitals or electron configurations. The problems in this chapter, although very useful, give a slightly dated look to the book. Certainly, students do need to be able to count electrons and know how they are arranged in the molecule, but they also need to know something about electron configurations and elementary molecular orbital theory. The approach to bonding adopted in the book is a version of valence bond theory grafted on to the pioneering ideas of Lewis.

The appendix B on calculators and computers contains a number of typographical errors and errors in logic and is not at all useful. Nevertheless the book as a whole is a useful addition to the library of any chemistry teacher. The production of the book is up to the high standards which one expects from Marcel Dekker but the price will certainly deter students and even teachers from buying it.

J. H. BINKS

described in this book and had it been published a few years ago this chapter would have been particularly useful. However, perhaps one reason why Raman spectroscopy is becoming an important technique is that more modern methods of detection are now employed. Thus, charge-coupled devices and similar systems are becoming favoured as the detection system. In addition, in order to enhance sensitivity, it is usual to spin the sample to reduce problems with photo-dissociation or absorption. Thus, this book would seem to me to be rather dated in its practical approach and I would have been happier if more attention had been paid to the modern developments of Raman spectroscopy.

Much of the interest of the chemist or analyst is usually centred on the vibrational analysis of particular molecules. In two chapters on organic and inorganic applications, the authors have summarized a number of important areas in a way in which the average reader can appreciate the types of signal to be expected and the value of recording them. The book then finishes with selected applications of Raman spectroscopy, including its use with polymers and bio-polymers, with complex compounds, and in matrix isolation spectroscopy. Perhaps surprisingly, the last chapter in the book is entitled fundamental concepts of spectroscopy and is a summary of much useful information that might well have appeared earlier in the text. There is also an atlas of spectra which may be quite useful to the average user.

Thus, if what is required is a conventional teaching text for Raman spectroscopy, this book is about adequate. Where it fails completely is in discussing newer aspects of Raman spectroscopy and consequently it is not a book to be recommended for teaching purposes to those who are not familiar with modern developments. For example, there has been a very great expansion in resonance Raman spectroscopy, including the detection of the spin and oxidation states of haemoglobin. There has also been considerable interest in surface-enhanced Raman spectroscopy for such purposes as detecting the presence of anti-corrosive layers on metal surfaces. There are many more complicated techniques which have also appeared in the last few years. It is always difficult to know where a book should end, but it seems to me that resonance Raman spectroscopy in particular is now just part of the Raman spectroscopist's armoury. Perhaps this can be best illustrated by saying that 10 or 15 years ago Raman spectroscopists tended to avoid coloured compounds, whereas now, many of the papers appearing in the literature make use of visible-region lasers and coloured compounds in order to obtain the sensitivity, through resonance, needed for the intended application. This would seem to be one of the key areas where analytical applications could be very much extended in the future. Thus, this is a good book to be recommended as a teaching text provided the course is taught by spectroscopists who are able to add a more modern gloss to the course they give. It cannot be recommended as an up-to-date account of Raman spectroscopy.

W. EWEN SMITH

Infrared Spectroscopy: W. O. GEORGE and P. S. MCINTYRE, Wiley, Chichester, 1987. Pages xx + 537. £17.50 (softback), £44.00 (hardback).

Infrared spectroscopy is widely used by preparative chemists in qualitative analysis. It also has very important applications in quantitative analysis, but its use there is more restricted. Thus, in the teaching of analytical chemistry the place of infrared spectroscopy is secure but the depth of understanding that is required is more difficult to assess. Many chemistry courses spend most time on discussing theory, whereas the analytical chemist requires in addition a knowledge of the range of applications possible. Thus, there is need for a book which particularly deals with the analytical applications. The book reviewed here is one such text.

The authors have constructed a text of open-learning type, which is both logical in its approach and easy to read. It covers the background theory, the modern applications of the Fourier transform and the main analytical areas very well. Most of the material that will be required for use in analytical courses is available from the text without reference to other books. Therefore it can be recommended as a good teaching text.

Inevitably there will be drawbacks, since different courses have different requirements. This book has been deliberately constructed so that the amount of theory is limited, and on one issue I do not agree with the authors' approach. They use visible-region spectroscopy to illustrate the basic concept of absorption spectroscopy and switch from that to infrared during the first chapter. They do not discuss the selection rules for visible-region spectroscopy but simply switch to selection rules for infrared. I feel that a straight approach to infrared spectroscopy, particularly since it is not intended to cover the field in any depth, would have been better. However, the infrared theory, when it is reached, is well and clearly written. Fourier transform spectroscopy is likely to play a larger part in the use of infrared in future and the basic technique is well explained, as are the general advantages. Perhaps one slightly disappointing feature is that the applications given later in the book cover more conventional and well established areas where infrared has been used and the full potential of Fourier transform spectroscopy in tackling surface layers, biological cells *etc.*, is neither fully explained nor illustrated and it may be that a revised edition of this book will be required within a relatively short space of time.

Parts of infrared spectroscopy theory appear difficult to some students. For example, the concept of normal vibrations is often not clearly explained. In this book there is an explanation that seems both simple and logical, and in other areas of spectroscopy which cause problems (such as the use of group frequencies) the explanation is again both good and clear. It is a pity therefore that the authors did not put a general index at the back of the book, to make it easier for a student later in his career to dip into the text and consider an individual topic. This deficiency is one which I find strange. During a lecture course a text is approached logically from one chapter to another, but in the laboratory, there is a need to turn to a paragraph or subsection to study a particular point of interest. Another omission which seems unusual is the limited amount of information on small molecules such as metal complexes, where symmetry and the nature of normal vibrations plays a bigger part.

Overall, this is a very useful book which should be seriously considered as a teaching text for courses in infrared spectroscopy, particularly its analytical applications. Clear, logical and correct in its approach, it may save future generations a few headaches experienced by their predecessors.

W. EWEN SMITH

George de Hevesy 1885–1966 Festschrift: G. MARX (editor), Akadémiai Kiadó, Budapest, 1988. Pages iv + 165. £11.50.

This *Festschrift* is a compilation of lectures presented in Budapest in 1986 to celebrate the centenary of the birth of George de Hevesy, who received the Nobel Prize for Chemistry in 1943 for establishing the use of radioactive isotopes for investigating chemical processes. As such, the book contains biographical and scientific contributions from scientists present at the meeting who have personally worked with de Hevesy or in laboratories where he had previously worked, or have been associated with major developments that have followed from his work.

In a lifetime devoted to study of radioactivity and its applications de Hevesy contributed to the discovery of the concept of isotopes, discovered the element hafnium (with D. Coster), established the basis of isotope dilution analysis (with R. Hobbie) and neutron activation analysis (with H. Levi). When suitable isotopic tracers became available he turned his attention to their applications in biochemistry, making further benchmark contributions.

The three biographical contributions include a brief general biography with details of his movement around Europe in response to the political climate, a survey of his activities in Hungary, and a review of his contributions to geochemistry. The last of these (by the author of his definitive biography) includes considerations of the age of the earth, the abundance and distribution of the elements, and the recognition of Sm–Nd decay, which subsequently became the basis of a method of geological dating. The scientific contributions include two from Nobel Laureates (R. L. Mössbauer and K. Siegbahn) and provide accounts of the development of some physical methods related to de Hevesy's discoveries—Mössbauer spectroscopy, neutron spin echo (inelastic neutral scattering) and electron spectroscopy for chemical analysis. Some contributions are in an anecdotal style which illustrates the excitement and problems of scientific research. The text is supported with copies of correspondence (e.g., with Goldschmidt), diagrams of historical apparatus associated with original discoveries, photographs of personalities at the celebration, and a comprehensive list of de Hevesy's 396 publications.

This collection of papers, which is very reasonably priced, should provide interesting reading for the scientific community, and will be of particular interest to those involved with studies using radioactive isotopes or interested in the history of science. (A personal regret is that activation analysis and isotope dilution analysis are not more fully covered.)

J. E. WHITLEY

Petroanalysis '87—Developments in Analytical Chemistry in the Petroleum Industry: G. B. Crump (editor), Wiley, Chichester, 1988. Pages x + 290. £50.00.

This book contains the Proceedings of the Third Petro Analysis Symposium held under the auspices of the (U.K.) Institute of Petroleum and the Royal Society of Chemistry in 1987. It contains 26 papers by 42 authors, most of whom work in the analytical divisions of the major oil companies. The papers show that in the past few years there have been considerable advances in the development of existing techniques and in the use of combinations of techniques to overcome present difficulties in the analyses of crude oils, heavy and light refinery distillates, residuals, waxes, lubricating oils and additives, and corrosion inhibitors, and in environmental monitoring of trace elements in water discharges, and of atmospheric pollution by oil-based drilling fluids. The few papers on laboratory information management systems, fully-automated analyses, and the use of robotics, indicate that developments will continue into the future. Although the papers are written in different styles and in different typefaces, they are well presented, clear, and contain sufficient detail to appeal, and be of interest, to analysts inside and out with the petrochemical industries.

J. B. CRAIG

Handbook of Renal-Independent Cardiac Glycosides: NORBERT RIETBROCK and BARRY G. WOODCOCK, Ellis Horwood, Chichester, 1989. Pages xxi + 328. £54.00.

Much of this book deals with the clinical and pharmacological aspects of cardiac glycosides but some interesting history as well as chemistry and pharmaceuticals is included. The relevance of this text is related to the fact that cardiac glycosides are currently the most important class of drugs used for the therapy of chronic heart failure.

The term "renal-independent" is based on both functional and therapeutic practice. Renal-independent cardiac glycosides such as digitoxin (from the purple foxglove), gitoformate and pengitoxin are contrasted with renal-dependent glycosides such as digoxin and its derivatives.

The first chapter on historical aspects is followed by a chapter on the chemical background. Some very nice structure diagrams are presented that show clearly the steroidal and sugar moieties in these molecules. Basic pharmacodynamic actions relating to cardiac and extra-cardiac effects are then discussed. Aspects of tablet formulation, especially the very low dose of active ingredient required, are detailed in a concise and competent manner. The longest chapter deals with the pharmacokinetics of both natural and semi-synthetic cardiac glycosides. Specifically, digitoxin, gitoformate, pengitoxin and gitoxin are examined by the consideration of results from over 200 literature sources.

The remaining chapters concentrate on clinical details such as toxicity, therapy in the aged, prescribing guidelines and drug interactions. Some interesting case studies are included. A small chapter on drug concentration measurement and drug monitoring is included. This describes results from methods involving radioimmunoassay, bioassay and HPLC in combination with radioimmunoassay. The reader is referred to literature sources for full details of these methods.

A comprehensive index is included and throughout the text many experimental results are clearly presented in graphical form. Those who work in the clinical and pharmaceutical sciences will find this book of much interest.

P. J. COX

George de Hevesy 1885–1966 Festschrift: G. MARX (editor), Akadémiai Kiadó, Budapest, 1988. Pages iv + 165. £11.50.

This *Festschrift* is a compilation of lectures presented in Budapest in 1986 to celebrate the centenary of the birth of George de Hevesy, who received the Nobel Prize for Chemistry in 1943 for establishing the use of radioactive isotopes for investigating chemical processes. As such, the book contains biographical and scientific contributions from scientists present at the meeting who have personally worked with de Hevesy or in laboratories where he had previously worked, or have been associated with major developments that have followed from his work.

In a lifetime devoted to study of radioactivity and its applications de Hevesy contributed to the discovery of the concept of isotopes, discovered the element hafnium (with D. Coster), established the basis of isotope dilution analysis (with R. Hobbie) and neutron activation analysis (with H. Levi). When suitable isotopic tracers became available he turned his attention to their applications in biochemistry, making further benchmark contributions.

The three biographical contributions include a brief general biography with details of his movement around Europe in response to the political climate, a survey of his activities in Hungary, and a review of his contributions to geochemistry. The last of these (by the author of his definitive biography) includes considerations of the age of the earth, the abundance and distribution of the elements, and the recognition of Sm–Nd decay, which subsequently became the basis of a method of geological dating. The scientific contributions include two from Nobel Laureates (R. L. Mössbauer and K. Siegbahn) and provide accounts of the development of some physical methods related to de Hevesy's discoveries—Mössbauer spectroscopy, neutron spin echo (inelastic neutral scattering) and electron spectroscopy for chemical analysis. Some contributions are in an anecdotal style which illustrates the excitement and problems of scientific research. The text is supported with copies of correspondence (e.g., with Goldschmidt), diagrams of historical apparatus associated with original discoveries, photographs of personalities at the celebration, and a comprehensive list of de Hevesy's 396 publications.

This collection of papers, which is very reasonably priced, should provide interesting reading for the scientific community, and will be of particular interest to those involved with studies using radioactive isotopes or interested in the history of science. (A personal regret is that activation analysis and isotope dilution analysis are not more fully covered.)

J. E. WHITLEY

Petroanalysis '87—Developments in Analytical Chemistry in the Petroleum Industry: G. B. Crump (editor), Wiley, Chichester, 1988. Pages x + 290. £50.00.

This book contains the Proceedings of the Third Petro Analysis Symposium held under the auspices of the (U.K.) Institute of Petroleum and the Royal Society of Chemistry in 1987. It contains 26 papers by 42 authors, most of whom work in the analytical divisions of the major oil companies. The papers show that in the past few years there have been considerable advances in the development of existing techniques and in the use of combinations of techniques to overcome present difficulties in the analyses of crude oils, heavy and light refinery distillates, residuals, waxes, lubricating oils and additives, and corrosion inhibitors, and in environmental monitoring of trace elements in water discharges, and of atmospheric pollution by oil-based drilling fluids. The few papers on laboratory information management systems, fully-automated analyses, and the use of robotics, indicate that developments will continue into the future. Although the papers are written in different styles and in different typefaces, they are well presented, clear, and contain sufficient detail to appeal, and be of interest, to analysts inside and out with the petrochemical industries.

J. B. CRAIG

Handbook of Renal-Independent Cardiac Glycosides: NORBERT RIETBROCK and BARRY G. WOODCOCK, Ellis Horwood, Chichester, 1989. Pages xxi + 328. £54.00.

Much of this book deals with the clinical and pharmacological aspects of cardiac glycosides but some interesting history as well as chemistry and pharmaceuticals is included. The relevance of this text is related to the fact that cardiac glycosides are currently the most important class of drugs used for the therapy of chronic heart failure.

The term "renal-independent" is based on both functional and therapeutic practice. Renal-independent cardiac glycosides such as digitoxin (from the purple foxglove), gitoformate and pengitoxin are contrasted with renal-dependent glycosides such as digoxin and its derivatives.

The first chapter on historical aspects is followed by a chapter on the chemical background. Some very nice structure diagrams are presented that show clearly the steroidal and sugar moieties in these molecules. Basic pharmacodynamic actions relating to cardiac and extra-cardiac effects are then discussed. Aspects of tablet formulation, especially the very low dose of active ingredient required, are detailed in a concise and competent manner. The longest chapter deals with the pharmacokinetics of both natural and semi-synthetic cardiac glycosides. Specifically, digitoxin, gitoformate, pengitoxin and gitoxin are examined by the consideration of results from over 200 literature sources.

The remaining chapters concentrate on clinical details such as toxicity, therapy in the aged, prescribing guidelines and drug interactions. Some interesting case studies are included. A small chapter on drug concentration measurement and drug monitoring is included. This describes results from methods involving radioimmunoassay, bioassay and HPLC in combination with radioimmunoassay. The reader is referred to literature sources for full details of these methods.

A comprehensive index is included and throughout the text many experimental results are clearly presented in graphical form. Those who work in the clinical and pharmaceutical sciences will find this book of much interest.

P. J. COX

George de Hevesy 1885–1966 Festschrift: G. MARX (editor), Akadémiai Kiadó, Budapest, 1988. Pages iv + 165. £11.50.

This *Festschrift* is a compilation of lectures presented in Budapest in 1986 to celebrate the centenary of the birth of George de Hevesy, who received the Nobel Prize for Chemistry in 1943 for establishing the use of radioactive isotopes for investigating chemical processes. As such, the book contains biographical and scientific contributions from scientists present at the meeting who have personally worked with de Hevesy or in laboratories where he had previously worked, or have been associated with major developments that have followed from his work.

In a lifetime devoted to study of radioactivity and its applications de Hevesy contributed to the discovery of the concept of isotopes, discovered the element hafnium (with D. Coster), established the basis of isotope dilution analysis (with R. Hobbie) and neutron activation analysis (with H. Levi). When suitable isotopic tracers became available he turned his attention to their applications in biochemistry, making further benchmark contributions.

The three biographical contributions include a brief general biography with details of his movement around Europe in response to the political climate, a survey of his activities in Hungary, and a review of his contributions to geochemistry. The last of these (by the author of his definitive biography) includes considerations of the age of the earth, the abundance and distribution of the elements, and the recognition of Sm–Nd decay, which subsequently became the basis of a method of geological dating. The scientific contributions include two from Nobel Laureates (R. L. Mössbauer and K. Siegbahn) and provide accounts of the development of some physical methods related to de Hevesy's discoveries—Mössbauer spectroscopy, neutron spin echo (inelastic neutral scattering) and electron spectroscopy for chemical analysis. Some contributions are in an anecdotal style which illustrates the excitement and problems of scientific research. The text is supported with copies of correspondence (e.g., with Goldschmidt), diagrams of historical apparatus associated with original discoveries, photographs of personalities at the celebration, and a comprehensive list of de Hevesy's 396 publications.

This collection of papers, which is very reasonably priced, should provide interesting reading for the scientific community, and will be of particular interest to those involved with studies using radioactive isotopes or interested in the history of science. (A personal regret is that activation analysis and isotope dilution analysis are not more fully covered.)

J. E. WHITLEY

Petroanalysis '87—Developments in Analytical Chemistry in the Petroleum Industry: G. B. Crump (editor), Wiley, Chichester, 1988. Pages x + 290. £50.00.

This book contains the Proceedings of the Third Petro Analysis Symposium held under the auspices of the (U.K.) Institute of Petroleum and the Royal Society of Chemistry in 1987. It contains 26 papers by 42 authors, most of whom work in the analytical divisions of the major oil companies. The papers show that in the past few years there have been considerable advances in the development of existing techniques and in the use of combinations of techniques to overcome present difficulties in the analyses of crude oils, heavy and light refinery distillates, residuals, waxes, lubricating oils and additives, and corrosion inhibitors, and in environmental monitoring of trace elements in water discharges, and of atmospheric pollution by oil-based drilling fluids. The few papers on laboratory information management systems, fully-automated analyses, and the use of robotics, indicate that developments will continue into the future. Although the papers are written in different styles and in different typefaces, they are well presented, clear, and contain sufficient detail to appeal, and be of interest, to analysts inside and out with the petrochemical industries.

J. B. CRAIG

Handbook of Renal-Independent Cardiac Glycosides: NORBERT RIETBROCK and BARRY G. WOODCOCK, Ellis Horwood, Chichester, 1989. Pages xxi + 328. £54.00.

Much of this book deals with the clinical and pharmacological aspects of cardiac glycosides but some interesting history as well as chemistry and pharmaceuticals is included. The relevance of this text is related to the fact that cardiac glycosides are currently the most important class of drugs used for the therapy of chronic heart failure.

The term "renal-independent" is based on both functional and therapeutic practice. Renal-independent cardiac glycosides such as digitoxin (from the purple foxglove), gitoformate and pengitoxin are contrasted with renal-dependent glycosides such as digoxin and its derivatives.

The first chapter on historical aspects is followed by a chapter on the chemical background. Some very nice structure diagrams are presented that show clearly the steroidal and sugar moieties in these molecules. Basic pharmacodynamic actions relating to cardiac and extra-cardiac effects are then discussed. Aspects of tablet formulation, especially the very low dose of active ingredient required, are detailed in a concise and competent manner. The longest chapter deals with the pharmacokinetics of both natural and semi-synthetic cardiac glycosides. Specifically, digitoxin, gitoformate, pengitoxin and gitoxin are examined by the consideration of results from over 200 literature sources.

The remaining chapters concentrate on clinical details such as toxicity, therapy in the aged, prescribing guidelines and drug interactions. Some interesting case studies are included. A small chapter on drug concentration measurement and drug monitoring is included. This describes results from methods involving radioimmunoassay, bioassay and HPLC in combination with radioimmunoassay. The reader is referred to literature sources for full details of these methods.

A comprehensive index is included and throughout the text many experimental results are clearly presented in graphical form. Those who work in the clinical and pharmaceutical sciences will find this book of much interest.

P. J. COX

Analytical Chemistry by Open Learning—Polarography and other Voltammetric Methods: TOM RILEY and ARTHUR WATSON, Wiley, Chichester, 1987. Pages xxii + 283.

The authors have taken about 300 pages to explain, at an introductory level, four electroanalytical techniques, classical d.c., normal pulse and differential pulse polarography, and stripping voltammetry, but with more succinctness and greater clarity a book half this size would have sufficed. The concept of open learning is a laudable one but its execution, as judged by this publication, leaves much to be desired. This book is a cross between a story book, a text-book, and one on programmed learning, without the merits of each. There are several obvious errors: for example, the model of the electrical double layer, as portrayed in Fig. 1.3b, is incorrect in several ways; Fig. 4.1a is meant to represent the anodic stripping of copper but displays cathodic stripping. CPZNOSO, p. 213, apparently "gives twice the wavelength of CPZSO". The book does have some good points, but these are diluted too often by repetitious comments on less-important matters.

J. B. CRAIG

Analytical Chemistry by Open Learning—Polarography and other Voltammetric Methods: TOM RILEY and ARTHUR WATSON, Wiley, Chichester, 1987. Pages xxii + 283.

The authors have taken about 300 pages to explain, at an introductory level, four electroanalytical techniques, classical d.c., normal pulse and differential pulse polarography, and stripping voltammetry, but with more succinctness and greater clarity a book half this size would have sufficed. The concept of open learning is a laudable one but its execution, as judged by this publication, leaves much to be desired. This book is a cross between a story book, a text-book, and one on programmed learning, without the merits of each. There are several obvious errors: for example, the model of the electrical double layer, as portrayed in Fig. 1.3b, is incorrect in several ways; Fig. 4.1a is meant to represent the anodic stripping of copper but displays cathodic stripping. CPZNOSO, p. 213, apparently "gives twice the wavelength of CPZSO". The book does have some good points, but these are diluted too often by repetitious comments on less-important matters.

J. B. CRAIG

In the opening chapter the principles of chemiluminescence and photochemical reactions are lucidly presented and their utilization or potential utilization as detectors in Gas Chromatography (GC) and Liquid Chromatography (LC) is discussed. Subsequent chapters give the theory, design (including illustrative diagrams), applications and limitations of each detector associated with a particular reaction.

For GC, chemiluminescence detectors based on the use of active nitrogen, nitric oxide/ozone and nitric oxide/ozone/oxygen are described. These detectors are selective for different types of nitrogen-containing compounds and it is suggested, with some justification, that such detectors will have important applications in industrial, petrochemical, environmental and other fields. For LC, post-column on-line detectors based on the use of, *e.g.*, luminol, lucigen, peroxyoxalate (which gets particular attention), electrochemiluminescence and the luciferin-luciferase bioluminescence reactions are described and discussed. Finally, an extensive but concise review of direct and indirect photochemical reaction detectors for LC is given.

Every chapter in the book is very well referenced, *e.g.*, the chapter on photochemical reaction detectors has more than 300 references. Hence further information on some particular topic of interest can be rapidly acquired.

R. R. MOODY

Environmental Analysis using Chromatography Interfaced with Atomic Spectroscopy: R. HARRISON and S. RAPSOMANIKIS (editors), Ellis Horwood, Chichester, 1989. Pages 370. £59.50.

I have very much enjoyed reading this book which is a very timely addition to the secondary literature on environmental analysis. The two editors have served us well, not just with their own chapters (Sulphur and Mercury, respectively) but especially by prevailing upon an excellent team of experienced workers to collaborate and then by making sure that all the contributions fitted the same style and approach. The result is a book both readable and informative, enriched by considerable detail on the individual methods. If, having started, you do not read this book through to the end, it will be because you have already succumbed to the temptation to try the combined instrumentation methods for yourself in the laboratory!

The book is in two sections with Chapters 1–6 covering the general topics of instrumentation (1: Basic principles, 2: Atomic absorption detectors, 3: Flame photometric detectors, 4: Plasma emission detectors, 5: Atomic fluorescence detectors, and 6: Interfaces between HPLC and FAAS). All chapters are well written, make reference to specific applications and give tabulations of performance data. Chapters 7–12 are devoted to particular elements and compare the applicability and success of different techniques, including details of sample handling and work-up (7: Tin and germanium, 8: Lead, 9: Arsenic and antimony, 10: Mercury, 11: Selenium and 12: Sulphur).

The book is attractively presented (though there should be a prize for anyone who can guess what the cover illustration represents), well referenced, and with very few typographical errors: Table 6.1 seems to have got muddled, and on page 307 the microwave plasma is presumably a helium one, not a medium one!

The authors make the important point that in general, the hardware is not commercially available for the coupled techniques described (except for GC-MIP). However, with this book in one hand and a small tool kit in the other, the do-it-yourself enthusiast will surely have success in these endeavours and be saved the frustration of making too many mistakes. I give this book my strongest recommendation.

I. L. MARR

Problems in Chemistry: HENRY O. DALEY, JR and ROBERT F. O'MALLEY, 2nd Edition, Revised and Expanded, Marcel Dekker, New York, 1988. Pages xvii + 476. \$39.50 (USA and Canada); \$47.25 (elsewhere).

This book, which is designed for American Freshman Chemistry courses, could be a most useful source of exercises for the earlier years of a chemistry course at a British University, in particular a Scottish one or for some advanced school courses.

It consists of nineteen chapters, ranging from units, composition and equations to elementary thermodynamics, chemical equilibrium, electrochemistry and kinetics. Each chapter has a series of carefully worked examples which will be very useful to students. One of the very attractive features of the book is that the data for many of the problems are taken from the chemical literature and the references are quoted. Students can then see that the kind of calculations which they are asked to do are part of the chemist's stock in trade and many will be in continual use in later courses.

While the chapter on chemical bonds gives practice in writing Lewis structures and contains examples of the use of electron-pair repulsion theory, there is no mention of orbitals or electron configurations. The problems in this chapter, although very useful, give a slightly dated look to the book. Certainly, students do need to be able to count electrons and know how they are arranged in the molecule, but they also need to know something about electron configurations and elementary molecular orbital theory. The approach to bonding adopted in the book is a version of valence bond theory grafted on to the pioneering ideas of Lewis.

The appendix B on calculators and computers contains a number of typographical errors and errors in logic and is not at all useful. Nevertheless the book as a whole is a useful addition to the library of any chemistry teacher. The production of the book is up to the high standards which one expects from Marcel Dekker but the price will certainly deter students and even teachers from buying it.

J. H. BINKS

In the opening chapter the principles of chemiluminescence and photochemical reactions are lucidly presented and their utilization or potential utilization as detectors in Gas Chromatography (GC) and Liquid Chromatography (LC) is discussed. Subsequent chapters give the theory, design (including illustrative diagrams), applications and limitations of each detector associated with a particular reaction.

For GC, chemiluminescence detectors based on the use of active nitrogen, nitric oxide/ozone and nitric oxide/ozone/oxygen are described. These detectors are selective for different types of nitrogen-containing compounds and it is suggested, with some justification, that such detectors will have important applications in industrial, petrochemical, environmental and other fields. For LC, post-column on-line detectors based on the use of, *e.g.*, luminol, lucigen, peroxyoxalate (which gets particular attention), electrochemiluminescence and the luciferin-luciferase bioluminescence reactions are described and discussed. Finally, an extensive but concise review of direct and indirect photochemical reaction detectors for LC is given.

Every chapter in the book is very well referenced, *e.g.*, the chapter on photochemical reaction detectors has more than 300 references. Hence further information on some particular topic of interest can be rapidly acquired.

R. R. MOODY

Environmental Analysis using Chromatography Interfaced with Atomic Spectroscopy: R. HARRISON and S. RAPSOMANIKIS (editors), Ellis Horwood, Chichester, 1989. Pages 370. £59.50.

I have very much enjoyed reading this book which is a very timely addition to the secondary literature on environmental analysis. The two editors have served us well, not just with their own chapters (Sulphur and Mercury, respectively) but especially by prevailing upon an excellent team of experienced workers to collaborate and then by making sure that all the contributions fitted the same style and approach. The result is a book both readable and informative, enriched by considerable detail on the individual methods. If, having started, you do not read this book through to the end, it will be because you have already succumbed to the temptation to try the combined instrumentation methods for yourself in the laboratory!

The book is in two sections with Chapters 1–6 covering the general topics of instrumentation (1: Basic principles, 2: Atomic absorption detectors, 3: Flame photometric detectors, 4: Plasma emission detectors, 5: Atomic fluorescence detectors, and 6: Interfaces between HPLC and FAAS). All chapters are well written, make reference to specific applications and give tabulations of performance data. Chapters 7–12 are devoted to particular elements and compare the applicability and success of different techniques, including details of sample handling and work-up (7: Tin and germanium, 8: Lead, 9: Arsenic and antimony, 10: Mercury, 11: Selenium and 12: Sulphur).

The book is attractively presented (though there should be a prize for anyone who can guess what the cover illustration represents), well referenced, and with very few typographical errors: Table 6.1 seems to have got muddled, and on page 307 the microwave plasma is presumably a helium one, not a medium one!

The authors make the important point that in general, the hardware is not commercially available for the coupled techniques described (except for GC-MIP). However, with this book in one hand and a small tool kit in the other, the do-it-yourself enthusiast will surely have success in these endeavours and be saved the frustration of making too many mistakes. I give this book my strongest recommendation.

I. L. MARR

Problems in Chemistry: HENRY O. DALEY, JR and ROBERT F. O'MALLEY, 2nd Edition, Revised and Expanded, Marcel Dekker, New York, 1988. Pages xvii + 476. \$39.50 (USA and Canada); \$47.25 (elsewhere).

This book, which is designed for American Freshman Chemistry courses, could be a most useful source of exercises for the earlier years of a chemistry course at a British University, in particular a Scottish one or for some advanced school courses.

It consists of nineteen chapters, ranging from units, composition and equations to elementary thermodynamics, chemical equilibrium, electrochemistry and kinetics. Each chapter has a series of carefully worked examples which will be very useful to students. One of the very attractive features of the book is that the data for many of the problems are taken from the chemical literature and the references are quoted. Students can then see that the kind of calculations which they are asked to do are part of the chemist's stock in trade and many will be in continual use in later courses.

While the chapter on chemical bonds gives practice in writing Lewis structures and contains examples of the use of electron-pair repulsion theory, there is no mention of orbitals or electron configurations. The problems in this chapter, although very useful, give a slightly dated look to the book. Certainly, students do need to be able to count electrons and know how they are arranged in the molecule, but they also need to know something about electron configurations and elementary molecular orbital theory. The approach to bonding adopted in the book is a version of valence bond theory grafted on to the pioneering ideas of Lewis.

The appendix B on calculators and computers contains a number of typographical errors and errors in logic and is not at all useful. Nevertheless the book as a whole is a useful addition to the library of any chemistry teacher. The production of the book is up to the high standards which one expects from Marcel Dekker but the price will certainly deter students and even teachers from buying it.

J. H. BINKS

LIST OF CONTENTS

JANUARY

MULTIELEMENT SPECTROCHEMICAL ANALYSIS

Editorial	V
Kenneth W. Busch and Marianna A. Busch	VII Foreword
G. R. Sims and M. B. Denton	1 Simultaneous multielement atomic-emission spectrometry with a charge-injection device detector
Robert S. Pomeroy, Jonathan V. Sweedler and M. Bonner Denton	15 Charge-injection device detection for improved performance in atomic-emission spectroscopy
K. R. Brushwyler, N. Furuta and G. M. Hieftje	23 Use of a spectrally segmented photodiode-array spectrometer for inductively coupled plasma atomic-emission spectroscopy. Examination of procedures for the evaluation of detection limits
D. P. Webb and E. D. Salin	33 Selection of spectral windows for plasma atomic-emission spectrometry
D. F. Wirsz and M. W. Blades	39 A factor analysis approach to optimized line selection in inductively coupled plasma atomic-emission spectrometry
David C. Tilotta, Robert C. Fry and William G. Fateley	53 Selective multiplex advantage with an electro-optic Hadamard transform spectrometer for multielemental atomic emission
David C. Tilotta	61 Theoretical multiplex gain in a UV/VIS Hadamard transform spectrometer utilizing a uniformly imperfect encoding mask
Marianna A. Busch, Kenneth W. Busch and Betsy B. Malloy	71 Two-dimensional multiple entrance-slit vidicon spectrometer for simultaneous multielement analysis
Kenneth W. Busch, Marianna A. Busch and Larry D. Benton	89 Design and evaluation of a new programmed-scan spectrometer for multielement determinations by atomic emission
Kenneth W. Busch, Marianna A. Busch and Larry D. Benton	103 Statistical evaluation of the performance of a new programmed-scan monochromator for multielement determinations by atomic emission
A. Mellone, Benjamin W. Smith and J. D. Winefordner	111 Rapid screening of polycyclic aromatic hydrocarbons and fingerprinting of environmental materials by laser-excited fluorescence spectrometry
Nancy J. Miller-Ihli	119 Simultaneous multielement atomic-absorption analysis of biological materials
D. W. Boomer, M. J. Powell and J. Hipfner	127 Characterization and optimization of HPIC for on-line preconcentration of trace metals with detection by ICP-mass spectrometry
G. E. M. Hall, G. F. Bonham-Carter, A. I. MacLaurin and S. B. Ballantyne	135 Comparison of instrumental neutron activation analysis of geological materials with other multielement techniques
Robert I. Botto	157 Updating a vintage ICP atomic-emission spectrometer

FEBRUARY

Yan Xiuping, Lin Tiezheng and Liu Zhijun	167 Improvement of the Smets method in electrothermal atomic-absorption spectrometry
Elsie M. Donaldson and Maureen E. Leaver	173 Determination of tellurium in ores, concentrates and related materials by graphite-furnace atomic-absorption spectrometry after separations by iron collection and xanthate extraction
Marit Andersson and Åke Olin	185 Determination of bromine, chlorine, sulphur and phosphorus in peat by X-ray fluorescence spectrometry combined with single-element and multi-element standard addition

F. Capitán, A. Navalón, J. L. Vilchez and L. F. Capitán-Vallvey	193	Determination of submicrogram amounts of gallium by ion-exchanger fluorimetry. Determination of gallium in natural waters
L. Campanella, M. Majone and R. Pucci	201	Behaviour of different eluents and stabilizing agents in the determination of sulphite in water by ion-chromatography
M. Horvat, A. R. Byrne and K. May	207	A modified method for the determination of methylmercury by gas chromatography
Olivier Chastel, Jean-Michel Kauffmann, Gaston J. Patriarche and Gary D. Christian	213	Electrochemical behavior of marcellomycin at lipid-modified carbon-paste electrodes
Gareth M. Barnard, Terry Boddington, Jan E. Gregor, Leslie D. Pettit and Norman Taylor	219	An investigation into the determination of stability constants of metal complexes by convolution–deconvolution cyclic voltammetry
Masahiko Murakami and Takeo Takada	229	Comparative study of IBMK and DIBK as extraction solvents in strongly acidic media: extraction behaviour and kinetic stability of Cu(PCD) ₂ in these solvents
Jan A. Larsson and Harry L. Pardue	233	Comparison of algorithms for error-compensated kinetic determinations without prior knowledge of reaction orders or rate constants
Barry Chiswell, Guy Rauchle and Mark Pascoe	237	Spectrophotometric methods for the determination of manganese
Stephen L. Law, James H. Newman and Francis L. Ptak	261	Field and laboratory determination of a poly(vinyl/vinylidene chloride) additive in brick mortar
K. Girish Kumar and P. Indrasenan	269	Titrimetric methods for the determination of vitamin C in some pharmaceutical preparations by use of two <i>N</i> -bromimides
Software Survey Section	273	Notebook II V.3.02; Fig. P
<i>Book Reviews</i>	i	
<i>Questionnaire: Software Survey Section</i>	iii	

MARCH

M. Caballero, R. Cela and J. A. Pérez-Bustamante	275	Analytical applications of some flotation techniques—a review
C. Grosset, D. Cantin, A. Villet and J. Alary	301	HPLC analysis of antioxidants
M. J. Rocheleau and W. C. Purdy	307	Investigation of materials for making a carbon-support zinc-selective electrode
David E. Davey, Dennis E. Mulcahy and Gregory R. O'Connell	313	Potentiometric flow-injection determination of iodide and iodine
Gian-Antonio Mazzocchin, Salvatore Daniele and Ligia Maria Moretto	317	Determination of trace amounts of thorium by electroanalytical techniques
E. Barrado, Y. Castrillejo, E. del Real, R. Pardo and P. Sánchez Batanero	325	Indirect polarographic determination of arsenic
Paul M. Shiundu, Peter D. Wentzell and Adrian P. Wade	329	Spectrophotometric determination of palladium with sulfochlorophenol-azorhodanine by flow injection
Shi-Fu Zhou and Nai-Xing Wang	337	Direct spectrophotometric determination of Nd and Er in mixed rare earths with 8-hydroxyquinoline-5-sulphonic acid and cetylpyridinium chloride
Shi-Fu Zhou and Zhong Li	341	Spectrophotometric study and analytical applications of lanthanide–kojic acid complexes. Direct determination of Nd, Ho and Er in mixtures of rare earths

F. Sallnas, J. J. Berzas Nevado and A. Espinosa Mansilla	347	A new spectrophotometric method for quantitative multicomponent analysis resolution of mixtures of salicylic and salicylic acids
U. Muralikrishna, K. Surendra Babu and M. Krishnamurthy	353	A simple spectrophotometric determination of some chlorobenzoquinones with morpholine, thiomorpholine and piperazine
<i>Analytical Data</i> Qinhui Luo, Mengchang Shen, Yi Ding, Xinlu Bao and Anbang Dai	357	Studies on hydrolytic polymerization of rare-earth metal ions—V. Hydrolytic polymerization of Dy ³⁺
<i>Annotation</i> Pushkin M. Qureshi, Sant Bahadur Singh, S. Iqbal, M. Kamoonpuri and I. A. Khan	361	Kinetic evidence for a charge-transfer mechanism in the interaction of ammonia with 2,4-dinitrophenylhydrazine in dimethylsulphoxide
<i>Editorial Announcement</i>	i	
<i>Questionnaire: Software Survey Section</i>	iii	

APRIL

R. Gijbels	363	Elemental analysis of high-purity solids by mass spectrometry
Lawrence E. Welch, William R. LaCourse, David A. Mead, Jr. and Dennis C. Johnson	377	A comparison of pulsed amperometric detection and conductivity detection of underivatized amino-acids in liquid chromatography
Orlando Mulero, David A. Nelson, Vernon S. Archer, Gregory Milkis, James R. Beckett and Howard L. McLean	381	Liquid chromatography of lanthanide chelates of 1-(<i>p</i> -nitrophenyl)ethylenediamine- <i>N,N,N',N'</i> -tetra-acetic acid
J. M. Cano Pavón, A. García de Torres and M. E. Urefía Pozo	385	Simultaneous determination of gallium and aluminium in biological samples by conventional luminescence and derivative synchronous fluorescence spectrometry
Lu Minggang, Lu Xiaohu and Yin Fang	393	A new chemiluminescence system for determination of cobalt
Janece Slavek, Pamela Waller and William F. Pickering	397	Labile metal content of sediments—fractionation scheme based on ion-exchange resins
A. Chow, W. Branagh and J. Chance	407	Sorption of organic dyes by polyurethane foam
B. W. Darvell and V. W.-H. Leung	413	The RAMESES algorithm for multiple equilibria—II. Some further developments
V. W.-H. Leung and B. W. Darvell	425	The RAMESES algorithm for multiple equilibria—III. Acceleration and standardized formation constants (RAMESES II)
A. Jyothi and G. N. Rao	431	Solvent extraction behaviour of lanthanum(III), cerium(III), europium(III), thorium(IV) and uranium(VI) with 3-phenyl-4-benzoyl-5-isoxazolone
W. Ciesielski, W. Jędrzejewski, Z. H. Kudzin and J. Drabowicz	435	Highly sensitive spectrophotometric microdetermination of sulphoxides
Mario E. Bodini, Jorge Pardo and Verónica Arancibia	439	Spectrophotometric determination of selenium(IV) with 5,5-dimethyl-1,3-cyclohexanedione
Martin V. Dawson and Samuel J. Lyle	443	Extraction and spectrophotometric determination of cobalt with dithizone
Jan Migdalski and Zygmunt Kowalski	447	Stability of reduced molybdsilicic acids
<i>Book Reviews</i>	i	
<i>Questionnaire: Software Survey Section</i>	iii	

MAY

P. Luts, J. L. C. Vanhees, J. H. E. Yperman, J. M. A. Mullens and L. C. Van Poucke	455	A new design of lead amalgam/lead sulphate electrode for potentiometric measurement of sulphate
---	-----	---

V. V. Egorov and Ya. F. Lushchik	461	H ⁺ -selective electrodes based on neutral carriers: specific features in behaviour and quantitative description of the electrode response
Jocelyn C. Dunphy and Kenneth L. Busch	471	Thin-layer chromatography/liquid secondary ion mass spectrometry in the determination of major bile salts in dog bile
Nawal A. El-Rabbat, Hassan H. Farag, Michael E. El-Kommos and Ibrahim H. Refaat	481	HPLC determination of niridazole
I. P. Allmarin, E. M. Basova, A. Yu. Malykhin and T. A. Bol'shova	485	Separation of some platinum metal 8-hydroxyquinolates by normal phase high-performance liquid chromatography
C. Kantipuly, S. Katragadda, A. Chow and H. D. Gesser	491	Chelating polymers and related supports for separation and preconcentration of trace metals
E. Klaos and V. Odinet	519	Use of matrix-modifiers in atomic-absorption determination of chromium in argillites
D. Atanassova and A. N. Shishkov	527	Heterocyclic dithiophosphates as analytical reagents. Indirect extraction-spectrophotometric determination of silver in copper concentrates and ores
Zhou Nan, Zhou Min, He Chun-Xiang, Ju Zhao-qiang and Lin Li-fen	531	An improved spectrophotometric method for the determination of silver with 5-[<i>p</i> -(dimethylamino)benzylidene] rhodanine
Z. Korićanac, K. Karžiković-Rajić and B. Stanković	535	Determination of 1,3-bis(4-hydroxyiminomethylpyridinium)-propane dichloride (TMB-4) with Pd(II)
P. Selvapathy, R. Pitchai and T. V. Ramakrishna	539	A rapid spectrophotometric method for the determination of carbon monoxide in ambient air
<i>Book Reviews</i>	i	
<i>Notices</i>	v	
<i>Questionnaire: Software Survey Section</i>	xi	

JUNE

Gabor Bozsai, Gerhard Schlemmer and Zvonimir Grobrenski	545	Determination of arsenic, cadmium, lead and selenium in highly mineralized waters by graphite-furnace atomic-absorption spectrometry
Uttam K. Kunwar, David Littlejohn and David J. Halls	555	Hot-injection procedures for the rapid analysis of biological samples by electrothermal atomic-absorption spectrometry
U. J. Krull, R. S. Brown, B. D. Hougham, G. McGibbon and E. T. Vandenberg	561	Fluorescence wavelength, intensity and lifetime for multidimensional transduction of selective interactions of acetylcholine receptor by lipid membranes
F. Garcia Sanchez and C. Cruces Blanco	573	Determination of carbaryl and its metabolite 1-naphthol in commercial formulations and biological fluids
F. Garcia Sanchez, A. L. Ramos Rubio, C. Cruces Blanco and R. Suau Suarez	579	Three-dimensional synchronous fluorescence spectrometry for the analysis of three-component alkaloid mixtures
Hikaru Amano and Nobuyuki Yanase	585	Measurement of ⁹⁰ Sr in environmental samples by cation-exchange and liquid scintillation counting
Rita Mendez and V. N. Sivasankara Pillai	591	Synthesis, characterization and analytical application of a hydroxamic acid resin
Archana Jain, Archana Verma and Krishna K. Verma	595	Determination of bromine in organic compounds by high-performance liquid chromatography
Miron G. Still and L. B. Rogers	599	Computational studies of the chiral separations of three <i>N</i> -acyl-1-aryl-1-aminoethanes on an (R)- <i>N</i> -dinitrobenzoylphenylglycine stationary phase
Krystyna Brajter* and Ewa Dabek-Zlotorzynska	613	Separation of metal ions on a modified aluminium oxide

Rokuro Kuroda, Mayumi Kurosaki, Yutaka Hayashibe and Satomi Ishimaru	619	Simultaneous determination of uranium and thorium with Arsenazo III by second-derivative spectrophotometry
Michael E. El-Kommos, Fardous A. Mohamed and Alaa S. Khedr	625	Spectrophotometric determination of epinephrine and norepinephrine with sodium periodate
D. V. Naidu and P. R. Naidu	629	A simple spectrophotometric method for determination of carbosulfan and propoxur
Junichi Shida, Harumi Satake, Nobuo Ono and Tadamitsu Fujikura	633	Spectrophotometric determination of trace sulphate in rain and snow after preconcentration with 2-aminoperimidine on a membrane filter
Satoru Sakuraba	637	Spectrophotometric determination of gallium(III) with phenylfluorone in the presence of hexadecylpyridinium bromide and pyridine
Zong-ming Luo and Wei-ming He	641	Spectrophotometric determination of microamounts of scandium with <i>o</i> -chlorophenylfluorone and cetyltrimethylammonium bromide
Jarosl�aw Kostrowicki and Adam Liwo	645	Determination of equilibrium parameters by minimization of an extended sum of squares
Jerry D. Christian, Douglas B. Illum and James A. Murphy	651	Metal electrodes for continuous amperometric measurement of free hydrofluoric acid in acidic solutions containing complexing ions
F. Becerro Dominguez, F. Gonzalez Diego and J. Hernandez Mendez	655	Determination of Sunset Yellow and Tartrazine by differential pulse polarography
K. L. Cheng and Naila Ashraf	659	A simple solid-state pH glass electrode
<i>Book Reviews</i>	i	
<i>Notices</i>	v	
<i>Questionnaire: Software Survey Section</i>	vii	

JULY

J. Arcos, J-C. Vir�e, A. El Jammal, G. J. Patriarche and G. D. Christian	661	Adsorptive voltammetry and hydrolysis kinetics of loprazolam mesilate
Krzysztof Ren	667	A numerical method of finding potentiometric titration end-points by use of approximative spline functions
Zong-Rang Zhang, Dan Yi Mao, Yi Xin Li and Vasile V. Coşofreţ	673	Plastic membrane electrodes responsive to beta-blocker drugs
Zhou Nan and He Chun Xiang	677	A study of electrodes used in controlled-potential electrolysis of metal ions
David E. Davey, Dennis E. Mulcahy and Gregory R. O'Connell	683	Flow-injection determination of phosphate with a cadmium ion-selective electrode
A. Cladera, J. M. Estela and V. Cerd�a	689	Potentiometric stripping analysis automation
M. Chandrasekaran, M. Noel and V. Krishnan	695	The use of BF_4^- as the supporting electrolyte anion in voltammetric studies on carbon electrodes—a cautionary note
Zhou Nan, Ju Zhao-Qiang, Yu Ren-Qing, Yao Xu-Zhang and Lu Zhi-Ren	701	Determination of copper in white-metal bearing alloys
Constantinos P. Pappas, Sean T. Randall and Joseph Sneddon	707	An atomic-emission study of the removal and recovery of chromium from solution by an algal biomass (<i>Chlorella vulgaris</i>)
Jo�o Carlos de Andrade, Frederick C. Strong III and Nadir J. Martin	711	Rapid determination of zinc and iron in foods by flow-injection analysis with flame atomic-absorption spectrophotometry and slurry nebulization

M. A. Palacios Corvillo, M. Gomez Gomez and C. Camara Rica	719	Determination of fluoride in sea-water by molecular absorption spectrometry of aluminium monofluoride after removal of cation and anion interferences
Christina Ericzon, Jean Pettersson and Åke Olin	725	Interference from iodide in the determination of trace level selenium
Ding-Ping Lin and Nureddin M. Abbas	731	Use of a GC/MS/MS technique in determination of biomarkers in regional petroleum
Toshio Nakashima, Kazuhisa Yoshimura and Hirohiko Waki	735	Ion-exchanger phase spectrophotometry for trace cobalt
J. J. Cruywagen and J. B. B. Heyns	741	Spectrophotometric determination of the first protonation constant of orthovanadate
G. S. R. Krishnamurti and P. M. Huang	745	Spectrophotometric determination of Fe(II) with 2,4,6-tri(2'-pyridyl)-1,3,5-triazine in the presence of large quantities of Fe(III) and complexing ions
Liu Shaopu, Zhou Guangming and Huang Zhigui	749	A highly sensitive colour reaction for Se(IV) with the iodide-Rhodamine B-PVA system. Spectrophotometric determination of trace amounts of selenium in water
M. S. Prasada Rao, A. Rama Mohan Rao, Karri V. Ramana and S. R. Sagi	753	Thallimetric oxidations—V. Titrimetric and spectrophotometric determination of hydrogen peroxide
M. I. Saleh, M. Ahmad and H. Darus	757	Solvent extraction of lanthanum(III), europium(III) and lutetium(III) with fluorinated 1-phenyl-3-methyl-4-benzoyl-5-pyrazolones into chloroform
U. Venkatadri Naidu, T. Gangaiah, P. Ramadevi, K. Seshaiiah and G. R. K. Naidu	761	Photometric determination of malathion with molybdenum
Saidul Zafar Qureshi, Syed Taufeeq Ahmad and Seema Haque	763	Filter-paper test for microgram detection of aliphatic amines
<i>Book Reviews</i>	i	
<i>Notice</i>	v	
<i>Questionnaire: Software Survey Section</i>	ix	

AUGUST

Derek Midgley	767	A review of pH measurement at high temperatures
Joseph Wang and Mehmet Ozsoz	783	Trace measurements of colchicine by adsorptive stripping voltammetry
Pedro Hernández, José Vicente, María González and Lucas Hernández	789	Voltammetric determination of linuron at a carbon-paste electrode modified with sepiolite
Maria Teodorczyk and William C. Purdy	795	An amperometric enzyme electrode for the determination of 3 α -hydroxy-steroids
Ulrich J. Krull, R. Stephen Brown, Bruce D. Hougham and Ivan H. Brock	801	Selective interactions of concanavalin A at lipid membranes on the surface of an optical fiber
Li Jianjun, Zeng Yun'e and Chen Guanquan	809	Simultaneous determination of some rare-earth elements by derivative fluorimetry and use of the Kalman filter
Andrzej M. Grossman, Jerzy Cioba, Jerzy Jurczyk and Waldemar Spiewok	815	Determination of lanthanum, cerium, praseodymium and neodymium in alloy steels by inductively coupled plasma atomic-emission spectrometry
C. Vandecasteele, H. Vanhoe, R. Dams, L. Vanballenberghe, A. Wittoek and J. Versieck	819	Determination of strontium in human serum by inductively coupled plasma mass spectrometry and neutron activation analysis: a comparison

Séan Lynch and David Littlejohn	825	Development of a slurry atomization method for the determination of cadmium in food samples by electrothermal atomization atomic-absorption spectrometry
Walter H. Ficklin	831	Extraction and speciation of arsenic in lacustrine sediments
Christine J. Bowles, Laurence W. Bader and Kenneth W. Jackson	835	Ion-chromatography of metals with post-column ion displacement
Weying Hou and Erkang Wang	841	Determination of water-soluble vitamins by liquid chromatography with a parallel dual-electrode electrochemical detector
Krzysztof Ren	845	Microcomputer-controlled automatic titrator with analysis of results by means of spline functions
Guillermo Lopez-Cueto and Carlos Ubide	849	Promoting effect of iodide on the hexacyanomanganate(IV)–arsenic(III) redox reaction, for kinetic determination of iodide
I. Němcová, P. Rychlovský and E. Kleszczewska	855	A spectrophotometric study of the determination of gold with phenothiazine
Software Survey Section	859	Phase plane method for lifetime determination of single and double exponential decays
<i>Questionnaire: Software Survey Section</i>	i	

SEPTEMBER

Obituary	V	
Oliver Lee, Yoshikata Koga and Adrian P. Wade	861	Thermosonimetry of the Phase II/III transition of hexachloroethane
M. D. Adams, P. W. Wade and R. D. Hancock	875	Extraction of aurocyanide ion-pairs by poly(oxyethylene) extractants
Li Buhai and Meng Rigan	885	Liquid–solid extraction system based on Tween 40–salt–H ₂ O without organic solvents
B. Ya. Spivakov, T. A. Maryutina, L. K. Shpigun, V. M. Shkinev, Yu. A. Zolotov, E. Ruseva and I. Havezov	889	Determination of ortho- and pyrophosphates in waters by extraction chromatography and flow-injection analysis
A. Lopez-Moliner, J. R. Castillo and J. M. Mermet	895	Observations on the determination of osmium by inductively-coupled plasma atomic emission spectroscopy
Derren Lee and K. L. Cheng	901	An anion-selective membrane electrode based on a mixture of insoluble lead salts
Chris Franco and John Olmsted III	905	Photochemical determination of the solubility of oxygen in various media
Alan R. Katritzky, Rick J. Offerman, Jose M. Aurrecoechea and G. Paul Savage	911	Synthesis and response of new microsensor coatings—II. Acridinium betaines and anionic surfactants
Alan R. Katritzky, G. Paul Savage, Rick J. Offerman and Boguslaw Pilarski	921	Synthesis of new microsensor coatings and their response to vapors—III. Arylphosphonic acids, salts and esters
Ikuko Akaza and Naomi Aota	925	Colorimetric determination of lipid hydroperoxides in oils and fats with microperoxidase
J. L. Bernal, M. J. del Nozal, L. Debán, F. J. Gómez, O. de Uría, J. M. Estela and V. Cerdá	931	Modification of the Methylene Blue method for spectrophotometric selenium determination
Li Qi-Long and Ji Gang	937	Studies on the polarographic behaviour of estazolam

Zhou Nan, Zhou Min, He Chun-Xiang, Ju Zhao-Qiang and Lin Li-Fen	941	Determination of silver in alloys by controlled-potential electrolysis at a tantalum electrode
Wei Fusheng, Ten Enjiang and Wu Zhongxiang	947	Enhancement of the fluorescence of the beryllium-morin complex by non-ionic surfactants
Nawal A. El-Rabbat, Hassan H. Farag, Michael E. El-Kommos and Ibrahim H. Refaat	951	HPLC determination of some antibilharzial antimonials by extraction of antimony
Notices	i	
Questionnaire: Software Survey Section	v	

OCTOBER

Elsie M. Donaldson	955	Determination of antimony in ores and related materials by continuous hydride-generation atomic-absorption spectrometry after separation by xanthate extraction
L. M. Perry and J. D. Winefordner	965	Selective determination of theophylline in the presence of caffeine by sensitized luminescence of europium(III)
L. J. Kricka, J. M. Marcinkowski, P. Wilding and S. Lekhakula	971	Enhanced chemiluminescence determination of α -amylase by use of amylose labelled with horseradish peroxidase
James M. Hungerford, Kevin D. Walker, James D. Torkelson, Kurt Steinbrecher and Marleen M. Wekell	975	Determination of tri-n-butyltin in oysters by reaction-gas chromatography of hydride derivatives
P. A. Waller and W. F. Pickering	981	Evaluation of "labile" metal in sediments by anodic stripping voltammetry
Aleksander Ciszewski	995	Determination of thallic and thalious ions by differential pulse anodic stripping voltammetry without preliminary separation
Shunitz Tanaka, Kazuharu Sugawara and Mitsuhiro Taka	1001	Adsorption voltammetry of the copper(II) 2-(5-bromo-2-pyridylazo)-5-diethylaminophenol complex
Zaofan Zhao, Jianhong Pei, Xiujing Zhang and Xingyao Zhou	1007	Adsorptive stripping voltammetry determination of molybdenum(VI) in water and soil
Elwira Lachowicz and Małgorzata Czapiuk	1011	Liquid-liquid extraction of palladium and gold by the sulphide podand 1,12-di-2-thienyl-2,5,8,11-tetrathiadodecane
N. L. Banerjee and B. C. Sinha	1017	Extraction spectrophotometric method for determination of aluminium in silicates
Zhou Nan, Xu-Zhang Yao, Yuan-Xiang Gu and Ren-Qing Yu	1021	Determination of lead by selective chelatometric titration with HEDTA after separation as its sulphate by an improved method of precipitation
Analytical Data Karel Vytřas, Jaromír Kalous and Jaroslava Černá-Frýbortová	1025	Dissociation constants of some <i>o,o'</i> -substituted azo dyes
Annotation Ragnar Bye	1029	Considerations on the different oxidation states of antimony, arsenic and selenium in the determination of the elements by hydride generation-atomic spectrometry
Questionnaire: Software Survey Section	i	

NOVEMBER

The Ronald Belcher Memorial Award and The Louis Gordon Memorial Award	V	
---	---	--

R. F. Maukkin, J. M. Vienneau, E. L. Wehry and G. Mamantov	1031	Supercritical fluid extraction of vapor-deposited pyrene from carbonaceous coal stack ash
James A. Cox and Atul Bhatnagar	1037	Analytical utility of coupled transport across a supported liquid membrane. Selective preconcentration of zinc
Nikos Grekas and Antony C. Calokerinos	1043	Determination of thiamine by continuous flow chemiluminescence measurement
Danhua Chen, M. D. Luque de Castro and M. Valcárcel	1049	Flow-through sensor for the fluorimetric determination of cyanide
Marsha D. Richmond and Robert J. Hurtubise	1057	Solution interactions and solid-matrix interactions in β -cyclodextrin solid-matrix luminescence
Noriko Yamamoto, Noriko Kasahara and Tsuneo Shirai	1063	Spectrophotometric determination of trace levels of atmospheric ammonia by conversion into indophenol and extraction with quaternary ammonium salts
Miloslav Kapanica, Věra Stará and Antonín Trojánek	1067	Determination of the flotation collector ethyl xanthate by flow-injection analysis
Sadayuki Himeno, Toshiyuki Osakai, Atsuyoshi Saito and Toshitaka Hori	1071	Voltammetric determination of phosphonate ion as a heteropoly complex
Jiang Zhi-liang and Liang Ai-hui	1077	Polarographic determination of osmium with the osmium(VIII)-cerium(IV)-arsenic(III) system
E. Ivanova, O. Todorova, A. Terebenina, N. Jordanov and G. Borisov	1081	Analytical characterization of some pyrazolones and their copolymers with some vinyl compounds
A. M. El-Brashy	1087	2-Iodylbenzoic acid as an oxidizing agent for the determination of certain thioxanthene derivatives
M. Tarek M. Zaki, A. K. Abdel-Kader and M. M. Abdalla	1091	Spectrophotometric determination of molybdenum with 7,8-dihydroxy-4-methylcoumarin and cetyltrimethylammonium bromide
H. J. Marini, R. I. Anton and R. A. Olsina	1097	Complexometric titration of Ti(IV) with 2-(5-chloro-2-pyridylazo)-5-dimethylaminophenol as indicator
Swagata Bhattacharya, S. K. Roy and A. K. Chakraborty	1101	Spectrophotometric determination of traces of iron after extraction of Fe(II)-phenanthroline complex on polyurethane foam
B. Basak and S. Laskar	1105	Spray reagents for the detection of amino-acids on thin-layer plates
<i>Analytical Data</i>		
Farangis Famoori, Soheila Haghgoo and Mojtaba Shamsipur	1107	On the influence of ionic strength on the equilibrium constant of copper-murexide interaction
<i>Book Reviews</i>		i
<i>Questionnaire: Software Survey Section</i>		vii

DECEMBER

C. L. Chakrabarti and S. J. Cathum	1111	Mechanism of cobalt atomization from different atomizer surfaces in graphite-furnace atomic-absorption spectrometry
A. Le Bihan and J. Y. Cabon	1119	Determination of 1 ng/l. levels of mercury in water by electrothermal atomization atomic-absorption spectrometry after solvent extraction
Fatima T. Esmadi, Maher A. Kharouf and Abdulrahman S. Attiyat	1123	Indirect determination of chloride and carbonate by reversed flow-injection analysis coupled with atomic-absorption spectrometry and in-line preconcentration by precipitation
R. Montero, M. Gallego and M. Valcárcel	1129	Determination of chloramphenicol by coupling a continuous reduction system to an atomic-absorption spectrometer

Yun-Xiang Ci and Fang Wang	1133	Studies on catalytic fluorescence formation with peroxidase-like metallo-tetrakis-(<i>N</i> -methylpyridiniumyl) porphyrins
F. García Sánchez, C. Carnero Ruiz and A. Heredia Bayona	1137	Fluorimetric determination of indole derivatives by fluorophore generation in copper(II)-sulphuric acid solution
Carlo Maccà	1141	Linearized multiple standard additions for the potentiometric determination of weak acids
Julie Wangsa, Margaret A. Targove and Neil D. Danielson	1151	Indirect electrochemical detection of cations with cerium(III) in the mobile phase
F. W. E. Strelow and A. H. Victor	1155	Separation of yttrium and neodymium from samarium and the heavier lanthanides by cation-exchange chromatography with hydroxyethylene-diaminetriacetate in monochloroacetate buffer
Tsugikatsu Odashima, Ichitaro Endoh and Hajime Ishii	1163	Equilibria and kinetics of the extraction of gallium with 1-phenyl-3-methyl-4-benzoyl-5-pyrazolone
V. Kubáň, L.-G. Danielsson and F. Ingman	1169	Comparison of segmentors for liquid-liquid extraction flow-injection analysis
Imre Tóth, Ernő Brúcher and Zoltán Szabó	1175	Extraction of gallium(III) and aluminium(III) with <i>O,O</i> -dialkyldithiophosphoric acids
O. Fatibello-Filho, M. A. C. Bumba, J. C. Trofino and E. A. Neves	1179	Solvent extraction of Fe(III) by dehydrated castor oil fatty acids
Mohamed A. Korany, Mahmoud A. Elsayed, Mona M. Bedair, Hoda Mahgoub and Ezzat A. Korany	1183	Computer-assisted spectrophotometry: multicomponent analysis with a discrete Fourier transform
Martin V. Dawson and Samuel J. Lyle	1189	Spectrophotometric determination of iron and cobalt with Ferrozine and dithizone
U. Saha, A. K. Sen, T. K. Das and S. K. Bhowal	1193	Spectrophotometric determination of tetracyclines in pharmaceutical preparations, with uranyl acetate
Stanislaw Kiciak	1197	Spectrophotometric determination of small amounts of Xylenol Orange, Semi-Xylenol Orange and <i>o</i> -Cresol Red
Ashok Kumar Malik and A. L. J. Rao	1205	Spectrophotometric determination of some dithiocarbamates
<i>Questionnaire: Software Survey Section</i>	i	

Electrophoresis: MAUREEN MELVIN, Chichester, 1987. Pages xxi + 131. £9.95 (flexicover); £28.00 (cloth).

This is a good introduction to the technique of electrophoresis. It describes the various versions of electrophoresis, the types of support media used, the factors affecting mobility, and the types of detectors available. There is a small section on immunoelectrophoresis and another on two-dimensional techniques. The book is written in simple, though at times oversimplified, terms, and is well illustrated, except for Fig. 2.3a which contains several mistakes. Some of the self-assessment questions are rather difficult, but the author's responses are an excellent guide on how they can and should be answered. A cautionary note should have been included warning students that some of the stains used in detection are hazardous to health, for example, ethidium bromide is a mutagen, ninhydrin and ANS are irritants, and dansyl chloride is corrosive.

J. B. CRAIG

Chemical Modeling of Aqueous Systems II: D. C. MELCHIOR and R. L. BASSETT (editors), ACS, Washington, DC, 1990. Pages xvi + 556. \$89.95 (U.S.), \$107.95 (elsewhere).

This book is based on a symposium held in 1988, which sets the limits for references. It consists of 41 chapters by separate authors, the work being almost entirely American in origin. The aqueous systems involved are predominantly natural surface and ground waters, although hydrothermal conditions are covered to some extent. Industrial water systems are not specifically considered. The early chapters are of the greatest generality, discussing activity coefficients in concentrated solutions, the effects of pressure and the solubility of volatile electrolytes. Other sections concentrate on solid/solution equilibria, transport, adsorption effects and the role of organics. Although many of these later chapters refer to specific instances, they are often also exemplary. This book can be recommended to the research worker and graduate student in limnology, oceanography and, to a lesser extent, geochemistry as a very useful, up-to-date and authoritative source of data and ideas, many of which should also be relevant to those concerned with the fate of industrial chemical discharges.

D. MIDGLEY

Steroid Analysis in the Pharmaceutical Industry: S. GÖRÖG (editor), Ellis Horwood, Chichester, 1989. Pages xi + 398. £69.50.

The 25 authors that have contributed to this impressive text are based in various countries, notably Hungary and the U.S.A., and they represent much of the steroid industry. The editorial staff must be congratulated for bringing these authors together and for producing such a comprehensive work.

A short introduction on industrial steroid analysis is followed by an excellent chapter on methods used in steroid analysis. It is certainly worth buying the book just for this chapter, which covers spectroscopic methods, chromatographic analysis, protein binding and electroanalytical methods. The 10 authors who have contributed to the chapter have cited over 800 references and all relevant analytical methods are covered at an introductory level.

The smaller chapter on structure elucidation covers previously mentioned instrumentation, *e.g.*, IR, NMR and GC-MS, and the powerful X-ray crystallographic technique is also briefly mentioned. The remaining chapters deal with analytical control of the production of steroids, analytical control of steroid formulations and determination of steroids in biological media. Analytical aspects of preformulation studies are included and there is a section on health control of workers in steroid hormone production. Many case histories of real analytical problems are given and the practical nature of the book is very evident. Also, as might be expected in a text compiled by different authors, there is some overlap between chapters.

Chromatography, especially HPLC, is of prime importance in steroid analysis and this topic is well covered, not only in the section on chromatographic analysis, but also throughout the book. Thin-layer chromatography is not neglected and although a large number of GLC stationary phases (*e.g.*, silicone oils) have been used in packed columns, the more recent fused-silica capillaries with chemically-bonded phases are now recommended by the authors for routine assay work. Resolving chiral steroids by the use of cyclodextrin and the interfacing of LC with MS is also mentioned.

The book, which contains well over 1200 references, is illustrated with many well-produced spectra and chromatograms. There is much here that will be of great interest to all chemists and pharmacists who work with steroids.

P. J. Cox

Packings and Stationary Phases in Chromatographic Techniques: K. K. UNGER (editor), Dekker, New York, 1990. Pages viii + 835. \$150 (U.S. and Canada), \$180 (elsewhere).

Stationary phases have been the subject of relatively few books in chromatography yet they are the most important part of any separation. This deficiency has been rectified in this compilation edited by Klaus Unger which has brought together materials used in the different areas of chromatography. The book has three main areas. Introductory chapters cover the history of packing materials and a survey of the different types of stationary phases.

The second section is the most important, with broad surveys of stationary phases for the main chromatographic methods. Materials for gas-liquid chromatography are considered by Pörschmann and Engewald. They include gas-solid materials and comparisons of the different liquid phases. Thin-layer chromatography sorbents, including reversed phase, cellulose

Electrophoresis: MAUREEN MELVIN, Chichester, 1987. Pages xxi + 131. £9.95 (flexicover); £28.00 (cloth).

This is a good introduction to the technique of electrophoresis. It describes the various versions of electrophoresis, the types of support media used, the factors affecting mobility, and the types of detectors available. There is a small section on immunoelectrophoresis and another on two-dimensional techniques. The book is written in simple, though at times oversimplified, terms, and is well illustrated, except for Fig. 2.3a which contains several mistakes. Some of the self-assessment questions are rather difficult, but the author's responses are an excellent guide on how they can and should be answered. A cautionary note should have been included warning students that some of the stains used in detection are hazardous to health, for example, ethidium bromide is a mutagen, ninhydrin and ANS are irritants, and dansyl chloride is corrosive.

J. B. CRAIG

Chemical Modeling of Aqueous Systems II: D. C. MELCHIOR and R. L. BASSETT (editors), ACS, Washington, DC, 1990. Pages xvi + 556. \$89.95 (U.S.), \$107.95 (elsewhere).

This book is based on a symposium held in 1988, which sets the limits for references. It consists of 41 chapters by separate authors, the work being almost entirely American in origin. The aqueous systems involved are predominantly natural surface and ground waters, although hydrothermal conditions are covered to some extent. Industrial water systems are not specifically considered. The early chapters are of the greatest generality, discussing activity coefficients in concentrated solutions, the effects of pressure and the solubility of volatile electrolytes. Other sections concentrate on solid/solution equilibria, transport, adsorption effects and the role of organics. Although many of these later chapters refer to specific instances, they are often also exemplary. This book can be recommended to the research worker and graduate student in limnology, oceanography and, to a lesser extent, geochemistry as a very useful, up-to-date and authoritative source of data and ideas, many of which should also be relevant to those concerned with the fate of industrial chemical discharges.

D. MIDGLEY

Steroid Analysis in the Pharmaceutical Industry: S. GÖRÖG (editor), Ellis Horwood, Chichester, 1989. Pages xi + 398. £69.50.

The 25 authors that have contributed to this impressive text are based in various countries, notably Hungary and the U.S.A., and they represent much of the steroid industry. The editorial staff must be congratulated for bringing these authors together and for producing such a comprehensive work.

A short introduction on industrial steroid analysis is followed by an excellent chapter on methods used in steroid analysis. It is certainly worth buying the book just for this chapter, which covers spectroscopic methods, chromatographic analysis, protein binding and electroanalytical methods. The 10 authors who have contributed to the chapter have cited over 800 references and all relevant analytical methods are covered at an introductory level.

The smaller chapter on structure elucidation covers previously mentioned instrumentation, *e.g.*, IR, NMR and GC-MS, and the powerful X-ray crystallographic technique is also briefly mentioned. The remaining chapters deal with analytical control of the production of steroids, analytical control of steroid formulations and determination of steroids in biological media. Analytical aspects of preformulation studies are included and there is a section on health control of workers in steroid hormone production. Many case histories of real analytical problems are given and the practical nature of the book is very evident. Also, as might be expected in a text compiled by different authors, there is some overlap between chapters.

Chromatography, especially HPLC, is of prime importance in steroid analysis and this topic is well covered, not only in the section on chromatographic analysis, but also throughout the book. Thin-layer chromatography is not neglected and although a large number of GLC stationary phases (*e.g.*, silicone oils) have been used in packed columns, the more recent fused-silica capillaries with chemically-bonded phases are now recommended by the authors for routine assay work. Resolving chiral steroids by the use of cyclodextrin and the interfacing of LC with MS is also mentioned.

The book, which contains well over 1200 references, is illustrated with many well-produced spectra and chromatograms. There is much here that will be of great interest to all chemists and pharmacists who work with steroids.

P. J. Cox

Packings and Stationary Phases in Chromatographic Techniques: K. K. UNGER (editor), Dekker, New York, 1990. Pages viii + 835. \$150 (U.S. and Canada), \$180 (elsewhere).

Stationary phases have been the subject of relatively few books in chromatography yet they are the most important part of any separation. This deficiency has been rectified in this compilation edited by Klaus Unger which has brought together materials used in the different areas of chromatography. The book has three main areas. Introductory chapters cover the history of packing materials and a survey of the different types of stationary phases.

The second section is the most important, with broad surveys of stationary phases for the main chromatographic methods. Materials for gas-liquid chromatography are considered by Pörschmann and Engewald. They include gas-solid materials and comparisons of the different liquid phases. Thin-layer chromatography sorbents, including reversed phase, cellulose

Electrophoresis: MAUREEN MELVIN, Chichester, 1987. Pages xxi + 131. £9.95 (flexicover); £28.00 (cloth).

This is a good introduction to the technique of electrophoresis. It describes the various versions of electrophoresis, the types of support media used, the factors affecting mobility, and the types of detectors available. There is a small section on immunoelectrophoresis and another on two-dimensional techniques. The book is written in simple, though at times oversimplified, terms, and is well illustrated, except for Fig. 2.3a which contains several mistakes. Some of the self-assessment questions are rather difficult, but the author's responses are an excellent guide on how they can and should be answered. A cautionary note should have been included warning students that some of the stains used in detection are hazardous to health, for example, ethidium bromide is a mutagen, ninhydrin and ANS are irritants, and dansyl chloride is corrosive.

J. B. CRAIG

Chemical Modeling of Aqueous Systems II: D. C. MELCHIOR and R. L. BASSETT (editors), ACS, Washington, DC, 1990. Pages xvi + 556. \$89.95 (U.S.), \$107.95 (elsewhere).

This book is based on a symposium held in 1988, which sets the limits for references. It consists of 41 chapters by separate authors, the work being almost entirely American in origin. The aqueous systems involved are predominantly natural surface and ground waters, although hydrothermal conditions are covered to some extent. Industrial water systems are not specifically considered. The early chapters are of the greatest generality, discussing activity coefficients in concentrated solutions, the effects of pressure and the solubility of volatile electrolytes. Other sections concentrate on solid/solution equilibria, transport, adsorption effects and the role of organics. Although many of these later chapters refer to specific instances, they are often also exemplary. This book can be recommended to the research worker and graduate student in limnology, oceanography and, to a lesser extent, geochemistry as a very useful, up-to-date and authoritative source of data and ideas, many of which should also be relevant to those concerned with the fate of industrial chemical discharges.

D. MIDGLEY

Steroid Analysis in the Pharmaceutical Industry: S. GÖRÖG (editor), Ellis Horwood, Chichester, 1989. Pages xi + 398. £69.50.

The 25 authors that have contributed to this impressive text are based in various countries, notably Hungary and the U.S.A., and they represent much of the steroid industry. The editorial staff must be congratulated for bringing these authors together and for producing such a comprehensive work.

A short introduction on industrial steroid analysis is followed by an excellent chapter on methods used in steroid analysis. It is certainly worth buying the book just for this chapter, which covers spectroscopic methods, chromatographic analysis, protein binding and electroanalytical methods. The 10 authors who have contributed to the chapter have cited over 800 references and all relevant analytical methods are covered at an introductory level.

The smaller chapter on structure elucidation covers previously mentioned instrumentation, *e.g.*, IR, NMR and GC-MS, and the powerful X-ray crystallographic technique is also briefly mentioned. The remaining chapters deal with analytical control of the production of steroids, analytical control of steroid formulations and determination of steroids in biological media. Analytical aspects of preformulation studies are included and there is a section on health control of workers in steroid hormone production. Many case histories of real analytical problems are given and the practical nature of the book is very evident. Also, as might be expected in a text compiled by different authors, there is some overlap between chapters.

Chromatography, especially HPLC, is of prime importance in steroid analysis and this topic is well covered, not only in the section on chromatographic analysis, but also throughout the book. Thin-layer chromatography is not neglected and although a large number of GLC stationary phases (*e.g.*, silicone oils) have been used in packed columns, the more recent fused-silica capillaries with chemically-bonded phases are now recommended by the authors for routine assay work. Resolving chiral steroids by the use of cyclodextrin and the interfacing of LC with MS is also mentioned.

The book, which contains well over 1200 references, is illustrated with many well-produced spectra and chromatograms. There is much here that will be of great interest to all chemists and pharmacists who work with steroids.

P. J. Cox

Packings and Stationary Phases in Chromatographic Techniques: K. K. UNGER (editor), Dekker, New York, 1990. Pages viii + 835. \$150 (U.S. and Canada), \$180 (elsewhere).

Stationary phases have been the subject of relatively few books in chromatography yet they are the most important part of any separation. This deficiency has been rectified in this compilation edited by Klaus Unger which has brought together materials used in the different areas of chromatography. The book has three main areas. Introductory chapters cover the history of packing materials and a survey of the different types of stationary phases.

The second section is the most important, with broad surveys of stationary phases for the main chromatographic methods. Materials for gas-liquid chromatography are considered by Pörschmann and Engewald. They include gas-solid materials and comparisons of the different liquid phases. Thin-layer chromatography sorbents, including reversed phase, cellulose

Computer-Aided Molecular Design: W. G. RICHARDS (editor), IBC, London, 1989. Pages vii + 266. £95.00.

The advances in both computer technology and theoretical calculations have now reached a stage where a publication detailing current activities in molecular design and modelling will attract much interest. In this large, A4 size, book there are 21 short chapters that are based on talks given at European conferences on computer-aided molecular design. Each chapter is a complete work in its own right and hence the reader can turn directly to a topic of interest without missing any required preamble. A subject index, in very small print, is provided and the chapters range in size from 5 to 22 pages. The book is not formally divided into sections but the advertising literature associated with the text has got it about right when it describes the contents under the headings "Tools", "Drugs", "Protein Structure" and "Materials".

The first section is a collection of 7 dissertations that cover the various techniques used by workers in this field. The opening chapter on "Databases of Molecular Structure" by Peter Murray-Rust includes several examples of different search routines that are available. David White's important chapter on "Molecular Mechanics" includes details of the use of transputers for large scale MM calculations. The use of quantum mechanics, free-energy perturbation, distance geometry and symbolic logic in molecular modelling is also covered and the section is completed by a chapter describing the specific features of an IBM graphics system.

The chapter on "Computer-aided Drug Design" by Garland Marshall is very easy to read and forms a basis for the more subject-specific chapters such as "Theoretical Studies of Groove-binding Drugs with DNA" by Krystyna Zakrzewsk and Richard Lavery. Interactions between drug and receptor are discussed in several chapters, as are three-dimensional comparisons of molecular conformations by computer graphics.

Protein structures receive the widest coverage and the statement that the Brookhaven datafile contains about 300 entries appears in several chapters. The use of nmr as well as X-ray crystallographic data in protein molecular modelling is covered and the technique of dynamic simulated annealing to fold structures is explained. The various techniques used for representing protein structures on display screens are detailed and several representations are shown as black-and-white or colour photographs. Unfortunately no stereo diagrams are included in the book. The chapter on "Antigenic Recognition" by Thornton, Barlow and Edwards emphasizes the potential clinical importance of computer-modelling in predicting possible peptides that might be effective against different strains of viruses.

The final chapters cover computer-modelling of materials of non-biological interest. In particular, attempts to understand the complex chemistry of zeolites by constructing models to emphasize the framework topology and the shapes and sizes of the various channels and cages, are detailed. Modelling of doped material, as used for example in lasers and superconductors, by the specification of an interatomic potential is covered.

Extensive references are given after each chapter and 35 colour plates are included at the end of the book. The photographs clearly demonstrate the versatility of modern computer graphics but no book can do justice to this form of molecular modelling; to observe a model of a macromolecule apparently rotating in three-dimensional space can be literally quite breathtaking.

Because important advances are being made in this broad field it is important to know what computer systems and programs are being used, what progress has been made and what ideas for future study are being presented. The subject matter of the various chapters is dealt with at a level that is not too demanding and the extensive range of subjects covered will enable any reader to find something of interest in this well-produced text. Highly recommended.

P. J. Cox

Electrophoresis: MAUREEN MELVIN, Chichester, 1987. Pages xxi + 131. £9.95 (flexicover); £28.00 (cloth).

This is a good introduction to the technique of electrophoresis. It describes the various versions of electrophoresis, the types of support media used, the factors affecting mobility, and the types of detectors available. There is a small section on immunoelectrophoresis and another on two-dimensional techniques. The book is written in simple, though at times oversimplified, terms, and is well illustrated, except for Fig. 2.3a which contains several mistakes. Some of the self-assessment questions are rather difficult, but the author's responses are an excellent guide on how they can and should be answered. A cautionary note should have been included warning students that some of the stains used in detection are hazardous to health, for example, ethidium bromide is a mutagen, ninhydrin and ANS are irritants, and dansyl chloride is corrosive.

J. B. CRAIG

Chemical Modeling of Aqueous Systems II: D. C. MELCHIOR and R. L. BASSETT (editors), ACS, Washington, DC, 1990. Pages xvi + 556. \$89.95 (U.S.), \$107.95 (elsewhere).

This book is based on a symposium held in 1988, which sets the limits for references. It consists of 41 chapters by separate authors, the work being almost entirely American in origin. The aqueous systems involved are predominantly natural surface and ground waters, although hydrothermal conditions are covered to some extent. Industrial water systems are not specifically considered. The early chapters are of the greatest generality, discussing activity coefficients in concentrated solutions, the effects of pressure and the solubility of volatile electrolytes. Other sections concentrate on solid/solution equilibria, transport, adsorption effects and the role of organics. Although many of these later chapters refer to specific instances, they are often also exemplary. This book can be recommended to the research worker and graduate student in limnology, oceanography and, to a lesser extent, geochemistry as a very useful, up-to-date and authoritative source of data and ideas, many of which should also be relevant to those concerned with the fate of industrial chemical discharges.

D. MIDGLEY

Steroid Analysis in the Pharmaceutical Industry: S. GÖRÖG (editor), Ellis Horwood, Chichester, 1989. Pages xi + 398. £69.50.

The 25 authors that have contributed to this impressive text are based in various countries, notably Hungary and the U.S.A., and they represent much of the steroid industry. The editorial staff must be congratulated for bringing these authors together and for producing such a comprehensive work.

A short introduction on industrial steroid analysis is followed by an excellent chapter on methods used in steroid analysis. It is certainly worth buying the book just for this chapter, which covers spectroscopic methods, chromatographic analysis, protein binding and electroanalytical methods. The 10 authors who have contributed to the chapter have cited over 800 references and all relevant analytical methods are covered at an introductory level.

The smaller chapter on structure elucidation covers previously mentioned instrumentation, *e.g.*, IR, NMR and GC-MS, and the powerful X-ray crystallographic technique is also briefly mentioned. The remaining chapters deal with analytical control of the production of steroids, analytical control of steroid formulations and determination of steroids in biological media. Analytical aspects of preformulation studies are included and there is a section on health control of workers in steroid hormone production. Many case histories of real analytical problems are given and the practical nature of the book is very evident. Also, as might be expected in a text compiled by different authors, there is some overlap between chapters.

Chromatography, especially HPLC, is of prime importance in steroid analysis and this topic is well covered, not only in the section on chromatographic analysis, but also throughout the book. Thin-layer chromatography is not neglected and although a large number of GLC stationary phases (*e.g.*, silicone oils) have been used in packed columns, the more recent fused-silica capillaries with chemically-bonded phases are now recommended by the authors for routine assay work. Resolving chiral steroids by the use of cyclodextrin and the interfacing of LC with MS is also mentioned.

The book, which contains well over 1200 references, is illustrated with many well-produced spectra and chromatograms. There is much here that will be of great interest to all chemists and pharmacists who work with steroids.

P. J. Cox

Packings and Stationary Phases in Chromatographic Techniques: K. K. UNGER (editor), Dekker, New York, 1990. Pages viii + 835. \$150 (U.S. and Canada), \$180 (elsewhere).

Stationary phases have been the subject of relatively few books in chromatography yet they are the most important part of any separation. This deficiency has been rectified in this compilation edited by Klaus Unger which has brought together materials used in the different areas of chromatography. The book has three main areas. Introductory chapters cover the history of packing materials and a survey of the different types of stationary phases.

The second section is the most important, with broad surveys of stationary phases for the main chromatographic methods. Materials for gas-liquid chromatography are considered by Pörschmann and Engewald. They include gas-solid materials and comparisons of the different liquid phases. Thin-layer chromatography sorbents, including reversed phase, cellulose

and polymeric materials, and the different designs of TLC plates are discussed by Hauck and Jost. Unger has included two chapters, a brief introduction to liquid-liquid partition chromatography, and then a comprehensive survey of sorbents for column liquid chromatography, which constitutes the major section of the book. This covers the different materials and their physical, chemical, and chromatographic characterization, and ends with a comprehensive listing of the different commercial materials, which now includes over 300 reversed phase materials.

The last part of the book is a series of shorter chapters on specialized areas of columns with specific interactions (size exclusion chromatography, by Dawkins; donor-acceptor complex chromatography, by Hemetsberger; the related chiral phases, by Pirkle and Pochapsky; ion-exchangers, by Pietrzyk; ligand-exchange phases, by Davankov; affinity chromatography, by Janson and Kristiansen; and packings for ion-pair chromatography, by Persson and Lagerström).

One inevitable comparison for this book is with the earlier work by Unger on porous silica, which for many years was the bible of anyone interested in liquid chromatographic stationary phases. The present work is a different book with different aims, much broader in its outlook. The difference also emphasizes two changes in the intervening 10 years, first a greater recognition of the similarities and relationships of the different forms of chromatography and secondly the much wider range of materials now in use, based not just on silica but also on alumina, carbon or polymeric matrices.

The book however, suffers from a common problem of edited works; many of the chapters were prepared some time ago and often contain no references after 1986; in others updating has taken place but little is included after 1987. The chapter on TLC materials appears to have been completed in 1983, with only 2 later references. Sometimes this gives a dated viewpoint—aluminium-coated capillaries had just been introduced as a novelty, the many recent advances in chiral phases are not included, and there are no references to SFC.

However, overall it will be a useful reference book as an introduction to the topic of stationary phases although it will need to be supplemented by more recent books and reviews, particularly in the specialist areas.

R. M. SMITH

BUDAPEST
17–22 August, 1991.

Preliminary Registration Form

Family name First name
 Profession/Title
 Organization/Institution/Company
 Mailing address
 Country
 Telephone Telex Telefax
 Accompanied by (family member) Name(s)
 I wish to present a poster: in the Section
 with the title

EXHIBITION

A technical exhibition will be held with the Congress. All enquiries regarding participation in the exhibition should be directed to:

INTERPRESS

International Business Service
 H-1075 Budapest, Tanács krt. 9.
 Telephone: + 36 1 120 852
 Telefax: + 36 1 327 765
 Telex: 22 3402 ipr h

CORRESPONDENCE

Please address all correspondence concerning the Congress to:

E. Pungor
 c/o Hungarian Academy of Sciences
 H-1111 BUDAPEST, Gellért tér 4.
 HUNGARY
 Telephone: + 36 1 664 705
 Telefax: + 36 1 853 493
 Telex: 22 3628 anal h

SAC 92 and 150th ANNIVERSARY OF THE LABORATORY OF THE GOVERNMENT CHEMIST

20–26 September, 1992

University of Reading

This International Conference on Analytical Chemistry will be organised by the Analytical Division of the Royal Society of Chemistry, in conjunction with the Laboratory of the Government Chemist. Further details may be obtained from Miss P. E. Hutchinson, Analytical Division, The Royal Society of Chemistry Burlington House, Piccadilly, London W1V 0BN, UK.

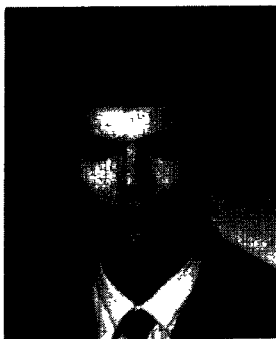
THE RONALD BELCHER MEMORIAL AWARD

The award for 1990 has been divided between three candidates, who will use it for travel in Japan and Europe. The award winners are Dr. Lisa Zeise, Biosource Genetics Corporation, Vacaville, California, Dr. Jonathan V. Sweedler, Stanford University, California, and Dr. Ryszard Kobinski, Warsaw Technical University.

The two winners of the 1988 award made good use of it, Dr. Wentzell travelling to various conferences and research centres in Europe, and Dr. Kolev working with Professor Valcárcel in Córdoba.



Dr. L. Zeise



Dr. R. Kobinski



Dr. J. V. Sweedler

THE LOUIS GORDON MEMORIAL AWARD

The Louis Gordon Memorial Award for 1989 (for the paper judged to be the best written of those appearing in *Talanta* during the year) will be made to Professor H. A. Laitinen, of the University of Florida, for his paper "History of analytical chemistry in the U.S.A." (*Talanta*, 1989, **36**, 1). Professor Laitinen was awarded the twelfth *Talanta* Medal in 1988 (*Talanta*, 1988, **35**, No. 11, I).

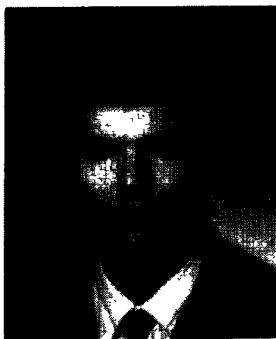
THE RONALD BELCHER MEMORIAL AWARD

The award for 1990 has been divided between three candidates, who will use it for travel in Japan and Europe. The award winners are Dr. Lisa Zeise, Biosource Genetics Corporation, Vacaville, California, Dr. Jonathan V. Sweedler, Stanford University, California, and Dr. Ryszard Kobinski, Warsaw Technical University.

The two winners of the 1988 award made good use of it, Dr. Wentzell travelling to various conferences and research centres in Europe, and Dr. Kolev working with Professor Valcárcel in Córdoba.



Dr. L. Zeise



Dr. R. Kobinski



Dr. J. V. Sweedler

THE LOUIS GORDON MEMORIAL AWARD

The Louis Gordon Memorial Award for 1989 (for the paper judged to be the best written of those appearing in *Talanta* during the year) will be made to Professor H. A. Laitinen, of the University of Florida, for his paper "History of analytical chemistry in the U.S.A." (*Talanta*, 1989, **36**, 1). Professor Laitinen was awarded the twelfth *Talanta* Medal in 1988 (*Talanta*, 1988, **35**, No. 11, I).

NOTICE

FEDERATION OF EUROPEAN CHEMICAL SOCIETIES (FECS)

Working Party on Analytical Chemistry (WPAC)

Chairman: Prof. Dr. Lauri Niinistö (Helsinki)

Secretary: Prof. Dr. R. Kellner (Vienna)

European Analytical Column 13

The Federation of European Chemical Societies (FECS) is a voluntary association of non-profit European chemical societies, founded in 1970 to promote co-operation in important areas of chemical research, development, standardization and education in Europe. Special aspects are treated in "Working Parties", such as the "Working Party on Analytical Chemistry", since 1972.

Thirty-two member societies from 26 European countries (1989): Austria, Belgium, Bulgaria, Czechoslovakia, Cyprus, Denmark, Finland, France, Federal Republic of Germany, German Democratic Republic, Greece, Hungary, Ireland, Italy, Luxembourg, Netherlands, Norway, Poland, Portugal, Soviet Union, Spain, Sweden, Switzerland, Turkey, United Kingdom, Yugoslavia, and 6 observers from China, Egypt, Israel, Japan, Romania and IUPAC take part in the ongoing WPAC activities.

The main aims of the Working Party on Analytical Chemistry of the Federation of European Chemical Societies are to advance research, education and training as well as standardization and accreditation in analytical chemistry. To achieve these goals and promote European co-operation, the WPAC organizes and supports analytical chemistry conferences, symposia, meetings and exchanges, and disseminates information as well as establishing study groups and special projects.

WPAC activities in 1989

1. Annual meeting, 27 August 1989, Wiesbaden (F.R.G.)

The main tasks of the year were the preparations for Euroanalysis VII (26–31 August 1990, Vienna)—2nd circular has appeared (see item 5) and the results of the study groups, "Think tank" (see item 2), "Accreditation systems" (see item 3) and Euroanalysis (see item 4) as well as the topic "Education in AC" (see item 6). WPAC has furthermore supported selected conferences in the field and special international activities (see item 7).

2. WPAC—study group 1, "Think Tank" (Chairman: L. Niinistö)

The report of this study group was presented by the chairman and discussed during the 2nd Symposium on Philosophy and History in Analytical Chemistry, 6–7 October 1989 in Vienna. A summary will appear in the symposium proceedings (see 7.2).

It was agreed that a major goal of WPAC in the future is to help to create and promote a positive modern image of Analytical Chemistry by

- organizing Euroanalysis conferences as state-of-the-art broad spectrum conferences of Analytical Chemistry
- promoting modern education in Analytical Chemistry
- stimulating know-how transfer to Mediterranean and East-European countries.

3. WPAC—study group 2, "Accreditation systems" (Chairman: B. te Nijenhuis)

The report of this study group was also presented (by B. te Nijenhuis) during the 2nd Symposium on Philosophy and History in Analytical Chemistry.

The results of the inquiry made it obvious that in order to make quality assurance by accreditation systems successful, measures have to be set at European educational level to guarantee the standards. The following recommendations have been made.

1. The national societies to watch carefully the preparation and harmonization of requirements and guidelines for quality assurance in Europe, and report to WPAC.
2. To define the skills and expertise of a registered analytical chemist, keeping in mind that certain activities have already been started in some European countries.
3. To define the training and education programmes necessary for the qualification of registered analytical chemist to be obtained and to present these programmes to the organizations and education centres/universities involved.
4. To define a basic analytical curriculum for analytical chemists in general, which may serve also as the scientific base for the "registered analytical chemist" qualification.
5. To instruct the joint WPPA/WPAC Committee of Inquiry on Analytical Chemists to incorporate recommendations 2, 3 and 4 in their activities.
6. To report on the subject at the next WPAC meeting and present the results to all organizations involved, as a firm recommendation of all the European professional societies for analytical chemistry represented in the WPAC.

4. WPAC—study group 3, "Frequency of Euroanalysis conferences" (Chairman: L. Niinistö)

It was proposed to study the possibility of merging Euroanalysis and ISM in 1995 and to have subsequently only one broad spectrum conference on Analytical Chemistry in Europe (but biennially) in co-ordination with CSI.

5. Euroanalysis VII, 26–31 August 1990, Technical University, Vienna

Honorary chairman: H. Malissa.

Chairman: J. F. K. Huber.

Secretary general: M. Grasserbauer.

The scientific programme will strongly emphasize "Problem solving with Analytical Chemistry". The following topics have been announced in the second circular available now from:

Interconvention, Austria Center, A-1150 Vienna

Phone: +43 222-2369-2647

Fax: +43 222-2369-648

(A) *Applications of analytical chemistry*

- 1 Environmental systems and food
- 2 Pharmaceutical and biomedical science
- 3 Biotechnology
- 4 Materials science
- 5 Arts and archaeology

(B) *Methods of analytical chemistry*

- 1 Atomic spectroscopy
- 2 Molecular spectroscopy
- 3 Separation techniques
- 4 Electrochemical methods
- 5 Sensors
- 6 Radiochemical and nuclear techniques
- 7 Thermal analysis
- 8 Local and surface analysis
- 9 Structure analysis of solids
- 10 Immunoassay
- 11 Other methods, such as photometry, kinetic analysis, process analysis, flow-injection analysis

(C) *Special sessions and workshops*

- 1 Sample preparation for inorganic and organic trace analysis
- 2 COBAC V (computer based analytical chemistry)
- 3 Quality assurance in analytical chemistry
- 4 Education and training in analytical chemistry

Important dates:

- | | |
|------------------|--|
| 28 February 1990 | Submission of abstracts to conference secretariat |
| 15 May 1990 | Confirming to authors acceptance and form of presentation |
| 30 June 1990 | Registration at reduced fee and guaranteed room reservation through Austropa |
| July 1990 | Mailing of conference programme (to registered participants only) |

6. WPAC activity—"Education in Analytical Chemistry" (Chairman: R. Kellner)

The aim of this future-oriented activity is to derive guidelines for a modern analytical chemistry curriculum, covering the demands of high-quality thinking in materials sciences, and process and environmental control. In this sense this activity upgrades the results obtained in 1983/84 based on 240 answers from all WPAC-member countries. The final evaluation will be presented in a Special Session (C4) at Euroanalysis VII, including a "hit list" of textbooks and exemplary model curricula. Questionnaires are available from the Secretariat, deadline 30 June 1990.

7. Further WPAC activities in 1989 and the future

- 7.1 It was resolved to continue the joint activities between WPAC (L. Niinistö) and WPPA (W. Henman) as well as WPAC and WPFC (Euro Food Chemistry, 27–29 September 1990, Versailles, and Euroanalysis VII, Vienna). The contacts with IUPAC (G. den Boef) will be strengthened in the fields of standardization and quality assurance, aiming to influence decision-making by legal bodies.
- 7.2. WPAC support has been given to:
 - The 2nd Symposium on Philosophy and History in Analytical Chemistry, 6–7 October 1989, Vienna (Chairman, Prof. H. Malissa, 60 participants, proceedings will appear in *Z. Anal. Chem.*)
 - The 4th Austrian–Hungarian Conference on Recent Advances in IR- and Raman-Spectroscopy, 18–20 April 1990, Veszprem (Hungary), [Chairman, J. Mink (Budapest), 50 lectures for more than 15 countries announced]
 - The XXVII-CSI-Post-Symposium: Speciation of Elements in Environmental and Biological Sciences, 16–18 June 1991, Loen (N) (organizer, Brit Salbu)
 - The 8th International Conference on Fourier Transform Spectroscopy, 1–6 September 1991, Lübeck/Travemünde (Chairmen, E. H. Korte, H. Siesler)
 - Euroanalysis VIII, 5–11 September 1993, Edinburgh, (U.K.) (Chairman, D. T. Burns).
- 7.3 The next meeting of the WPAC is scheduled for Sunday, 26 August 1990, in Vienna, on the occasion of Euroanalysis VII. At this meeting, the venue for Euroanalysis IX in 1995 will be determined, among others. Official bids for venues must be received in the Secretariat by 20 August 1990.

For more information related to WPAC activities please contact the secretary, Prof. Dr. R. Kellner, Institute for Analytical Chemistry, Technical University Vienna, Getreidemarkt 9, A-1060 Wien, Austria. Phone +43-222/58801/48 31 or 4837; Telex 131.000 tvfaw or Telefax +43-222/56 78 13.

NOTICE

FEDERATION OF EUROPEAN CHEMICAL SOCIETIES (FECS)

Working Party on Analytical Chemistry (WPAC)

Chairman: Prof. Dr. Lauri Niinistö (Helsinki)

Secretary: Prof. Dr. R. Kellner (Vienna)

European Analytical Column 13

The Federation of European Chemical Societies (FECS) is a voluntary association of non-profit European chemical societies, founded in 1970 to promote co-operation in important areas of chemical research, development, standardization and education in Europe. Special aspects are treated in "Working Parties", such as the "Working Party on Analytical Chemistry", since 1972.

Thirty-two member societies from 26 European countries (1989): Austria, Belgium, Bulgaria, Czechoslovakia, Cyprus, Denmark, Finland, France, Federal Republic of Germany, German Democratic Republic, Greece, Hungary, Ireland, Italy, Luxembourg, Netherlands, Norway, Poland, Portugal, Soviet Union, Spain, Sweden, Switzerland, Turkey, United Kingdom, Yugoslavia, and 6 observers from China, Egypt, Israel, Japan, Romania and IUPAC take part in the ongoing WPAC activities.

The main aims of the Working Party on Analytical Chemistry of the Federation of European Chemical Societies are to advance research, education and training as well as standardization and accreditation in analytical chemistry. To achieve these goals and promote European co-operation, the WPAC organizes and supports analytical chemistry conferences, symposia, meetings and exchanges, and disseminates information as well as establishing study groups and special projects.

WPAC activities in 1989

1. Annual meeting, 27 August 1989, Wiesbaden (F.R.G.)

The main tasks of the year were the preparations for Euroanalysis VII (26–31 August 1990, Vienna)—2nd circular has appeared (see item 5) and the results of the study groups, "Think tank" (see item 2), "Accreditation systems" (see item 3) and Euroanalysis (see item 4) as well as the topic "Education in AC" (see item 6). WPAC has furthermore supported selected conferences in the field and special international activities (see item 7).

2. WPAC—study group 1, "Think Tank" (Chairman: L. Niinistö)

The report of this study group was presented by the chairman and discussed during the 2nd Symposium on Philosophy and History in Analytical Chemistry, 6–7 October 1989 in Vienna. A summary will appear in the symposium proceedings (see 7.2).

It was agreed that a major goal of WPAC in the future is to help to create and promote a positive modern image of Analytical Chemistry by

- organizing Euroanalysis conferences as state-of-the-art broad spectrum conferences of Analytical Chemistry
- promoting modern education in Analytical Chemistry
- stimulating know-how transfer to Mediterranean and East-European countries.

3. WPAC—study group 2, "Accreditation systems" (Chairman: B. te Nijenhuis)

The report of this study group was also presented (by B. te Nijenhuis) during the 2nd Symposium on Philosophy and History in Analytical Chemistry.

The results of the inquiry made it obvious that in order to make quality assurance by accreditation systems successful, measures have to be set at European educational level to guarantee the standards. The following recommendations have been made.

1. The national societies to watch carefully the preparation and harmonization of requirements and guidelines for quality assurance in Europe, and report to WPAC.
2. To define the skills and expertise of a registered analytical chemist, keeping in mind that certain activities have already been started in some European countries.
3. To define the training and education programmes necessary for the qualification of registered analytical chemist to be obtained and to present these programmes to the organizations and education centres/universities involved.
4. To define a basic analytical curriculum for analytical chemists in general, which may serve also as the scientific base for the "registered analytical chemist" qualification.
5. To instruct the joint WPPA/WPAC Committee of Inquiry on Analytical Chemists to incorporate recommendations 2, 3 and 4 in their activities.
6. To report on the subject at the next WPAC meeting and present the results to all organizations involved, as a firm recommendation of all the European professional societies for analytical chemistry represented in the WPAC.

4. WPAC—study group 3, "Frequency of Euroanalysis conferences" (Chairman: L. Niinistö)

It was proposed to study the possibility of merging Euroanalysis and ISM in 1995 and to have subsequently only one broad spectrum conference on Analytical Chemistry in Europe (but biennially) in co-ordination with CSI.

5. Euroanalysis VII, 26–31 August 1990, Technical University, Vienna

Honorary chairman: H. Malissa.

Chairman: J. F. K. Huber.

Secretary general: M. Grasserbauer.

The scientific programme will strongly emphasize "Problem solving with Analytical Chemistry". The following topics have been announced in the second circular available now from:

Interconvention, Austria Center, A-1150 Vienna

Phone: +43 222-2369-2647

Fax: +43 222-2369-648

(A) *Applications of analytical chemistry*

- 1 Environmental systems and food
- 2 Pharmaceutical and biomedical science
- 3 Biotechnology
- 4 Materials science
- 5 Arts and archaeology

(B) *Methods of analytical chemistry*

- 1 Atomic spectroscopy
- 2 Molecular spectroscopy
- 3 Separation techniques
- 4 Electrochemical methods
- 5 Sensors
- 6 Radiochemical and nuclear techniques
- 7 Thermal analysis
- 8 Local and surface analysis
- 9 Structure analysis of solids
- 10 Immunoassay
- 11 Other methods, such as photometry, kinetic analysis, process analysis, flow-injection analysis

(C) *Special sessions and workshops*

- 1 Sample preparation for inorganic and organic trace analysis
- 2 COBAC V (computer based analytical chemistry)
- 3 Quality assurance in analytical chemistry
- 4 Education and training in analytical chemistry

Important dates:

- | | |
|------------------|--|
| 28 February 1990 | Submission of abstracts to conference secretariat |
| 15 May 1990 | Confirming to authors acceptance and form of presentation |
| 30 June 1990 | Registration at reduced fee and guaranteed room reservation through Austropa |
| July 1990 | Mailing of conference programme (to registered participants only) |

6. WPAC activity—"Education in Analytical Chemistry" (Chairman: R. Kellner)

The aim of this future-oriented activity is to derive guidelines for a modern analytical chemistry curriculum, covering the demands of high-quality thinking in materials sciences, and process and environmental control. In this sense this activity upgrades the results obtained in 1983/84 based on 240 answers from all WPAC-member countries. The final evaluation will be presented in a Special Session (C4) at Euroanalysis VII, including a "hit list" of textbooks and exemplary model curricula. Questionnaires are available from the Secretariat, deadline 30 June 1990.

7. Further WPAC activities in 1989 and the future

- 7.1 It was resolved to continue the joint activities between WPAC (L. Niinistö) and WPPA (W. Henman) as well as WPAC and WPMC (Euro Food Chemistry, 27–29 September 1990, Versailles, and Euroanalysis VII, Vienna). The contacts with IUPAC (G. den Boef) will be strengthened in the fields of standardization and quality assurance, aiming to influence decision-making by legal bodies.
- 7.2. WPAC support has been given to:
 - The 2nd Symposium on Philosophy and History in Analytical Chemistry, 6–7 October 1989, Vienna (Chairman, Prof. H. Malissa, 60 participants, proceedings will appear in *Z. Anal. Chem.*)
 - The 4th Austrian–Hungarian Conference on Recent Advances in IR- and Raman-Spectroscopy, 18–20 April 1990, Veszprem (Hungary), [Chairman, J. Mink (Budapest), 50 lectures for more than 15 countries announced]
 - The XXVII-CSI-Post-Symposium: Speciation of Elements in Environmental and Biological Sciences, 16–18 June 1991, Loen (N) (organizer, Brit Salbu)
 - The 8th International Conference on Fourier Transform Spectroscopy, 1–6 September 1991, Lübeck/Travemünde (Chairmen, E. H. Korte, H. Siesler)
 - Euroanalysis VIII, 5–11 September 1993, Edinburgh, (U.K.) (Chairman, D. T. Burns).
- 7.3 The next meeting of the WPAC is scheduled for Sunday, 26 August 1990, in Vienna, on the occasion of Euroanalysis VII. At this meeting, the venue for Euroanalysis IX in 1995 will be determined, among others. Official bids for venues must be received in the Secretariat by 20 August 1990.

For more information related to WPAC activities please contact the secretary, Prof. Dr. R. Kellner, Institute for Analytical Chemistry, Technical University Vienna, Getreidemarkt 9, A-1060 Wien, Austria. Phone +43-222/58801/48 31 or 4837; Telex 131.000 tvfaw or Telefax +43-222/56 78 13.

NOTICES

1991 EUROPEAN WINTER CONFERENCE ON PLASMA SPECTROCHEMISTRY

14-18 January 1991, Dortmund, Federal Republic of Germany

The "Deutscher Arbeitskreis für Angewandte Spektroskopie" (DAsP) and the "Arbeitskreis für Mikro- und Spurenanalyse der Elemente" (AMSEI) of the "Fachgruppe für Analytische Chemie" in the "Gesellschaft Deutscher Chemiker" (GDCh) are organizing in collaboration with the "Institut für Spektrochemie und angewandte Spektroskopie" (ISAS) in Dortmund, the *1991 Winter Conference on Plasma Spectrochemistry*, 14-18 January 1991. The conference will deal with frontier research in the development, investigation and use of plasma discharges for atomic spectrometric analysis. Inductively coupled plasmas, direct current plasma discharges, microwave discharges and laser plasmas for optical and mass spectrometry will be the main topics. Instrumental developments concerned with sampling devices, and the various modern types of plasma spectrometry, as well as their use for the solution of analytical problems, will be covered.

Keynote lectures will be presented by invited speakers. For the general sessions, contributions are requested for either oral or poster presentations. Discussion panels and contributions from manufacturers, who are invited to take part in the meeting with information booths, will be included in the programme. *Spectrochimica Acta, Part B*, offers to publish the contributions after the usual reviewing procedure.

Conference Organizer: J. A. C. Broekaert, Institut für Spektrochemie und angewandte Spektroskopie (ISAS), Dortmund, F.R.G.

Congress circulars containing further details will be available from:

Gesellschaft Deutscher Chemiker
Abt. Tagungen
Postfach 900 400
D-6000 Frankfurt/Main
F.R.G.

4TH EUROPEAN CONFERENCE ON THE SPECTROSCOPY OF BIOLOGICAL MOLECULES

1-6 September 1991, University of York, England

This major international conference will focus mainly on structural aspects and dynamics of biological and related systems, as determined by Raman and infrared spectroscopic methods. However, it also will provide a critically comparative review of recent progress in this field, as achieved through the application of other methods, particularly NMR, CD, optical absorption and fluorescence, and X-ray crystallography.

Topics to be included: proteins; nucleic acids; membranes; carbohydrates; enzyme mechanisms; protein-nucleic acid interactions; membrane proteins; photobiological systems—including photosynthesis, rhodopsins; virus structure; biomedical applications; new methods—structure and dynamics.

Venue: Located halfway between London and Edinburgh, the 2000-year-old city of York, with its mediaeval centre, magnificent cathedral, and outstanding museums, is surrounded by some of the most beautiful countryside in England. The Yorkshire Moors and Dales are nearby, and the seaside towns of Whitby (home of Captain Cook) and Scarborough only about an hour's drive away. Lots of opportunities for holidays before or after the conference! The conference facilities are excellent on the modern campus of the University: college accommodation will be available for 400 participants.

First Circular: available in early 1990.

Contact: Professor R. E. Hester,
Department of Chemistry,
University of York,
York YO1 5DD
England

Phone: (0904) 432557

Fax: (0904) 410519

E.Mail: REH1@VAXA.YORK.AC.UK

NOTICES

FIFTH INTERNATIONAL SYMPOSIUM ON RESONANCE IONIZATION SPECTROSCOPY (RIS-90)

Varese, Italy, 16-21 September 1990

The Fifth International Symposium on Ionization Spectroscopy and its applications will be held in Varese, Italy, from September 16-21, 1990. This meeting will deal with the analytical and physical aspects of the laser ionization technique, its unique character of isotopic selectivity, and unprecedented sensitivity for ultratrace analysis of atoms and molecules, and its applications in the environmental, biological, medical and nuclear fields. New laser sources, surface analysis and applications in basic physics will also constitute prominent topics of the Meeting.

The technical programme will consist of invited lectures, contributed papers and posters. Limited student attendance will be supported and an RIS short course has also been tentatively planned. There will be a small exhibition of laser-based instrumentation and related material.

The Symposium will be hosted by the Commission of the European Communities, Ispra Site. For further details and information, contact Dr. N. Omenetto, Joint Research Centre, Environment Institute, Chemistry Division, 21020 Ispra (Varese), Italy. Phone: (39) 332-789801. Telex: 380042 EUR I. Telefax (39) 322-789222.

3rd INTERNATIONAL CONGRESS ON TRACE ELEMENTS IN MEDICINE AND BIOLOGY *CHROMIUM AND TRACE ELEMENTS IN ENDOCRINOLOGY*

LES DEUX ALPES (FRANCE)

15-18 January 1991

The topics covered will be:

CHROMIUM

Biology, status and nutritional aspects
Chromium in human diseases

TRACE ELEMENTS IN ENDOCRINOLOGY

Endocrine Systems
Thyroid session
Hormonal mediators of immunity
Diabetes and glucose tolerance
Reproduction and growth
Adrenals and corticosteroid hormones

Poster sessions and trade exhibition

For additional information contact:

Arlette Alcaraz, Laboratoire de Biochimie C, CHRU de Grenoble,
BP 217 X, 38043 Grenoble Cedex, France.
Tel: 76.42.81.21, extension 4465

NOTICES

FIFTH INTERNATIONAL SYMPOSIUM ON RESONANCE IONIZATION SPECTROSCOPY (RIS-90)

Varese, Italy, 16-21 September 1990

The Fifth International Symposium on Ionization Spectroscopy and its applications will be held in Varese, Italy, from September 16-21, 1990. This meeting will deal with the analytical and physical aspects of the laser ionization technique, its unique character of isotopic selectivity, and unprecedented sensitivity for ultratrace analysis of atoms and molecules, and its applications in the environmental, biological, medical and nuclear fields. New laser sources, surface analysis and applications in basic physics will also constitute prominent topics of the Meeting.

The technical programme will consist of invited lectures, contributed papers and posters. Limited student attendance will be supported and an RIS short course has also been tentatively planned. There will be a small exhibition of laser-based instrumentation and related material.

The Symposium will be hosted by the Commission of the European Communities, Ispra Site. For further details and information, contact Dr. N. Omenetto, Joint Research Centre, Environment Institute, Chemistry Division, 21020 Ispra (Varese), Italy. Phone: (39) 332-789801. Telex: 380042 EUR I. Telefax (39) 322-789222.

3rd INTERNATIONAL CONGRESS ON TRACE ELEMENTS IN MEDICINE AND BIOLOGY *CHROMIUM AND TRACE ELEMENTS IN ENDOCRINOLOGY*

LES DEUX ALPES (FRANCE)

15-18 January 1991

The topics covered will be:

CHROMIUM

Biology, status and nutritional aspects
Chromium in human diseases

TRACE ELEMENTS IN ENDOCRINOLOGY

Endocrine Systems
Thyroid session
Hormonal mediators of immunity
Diabetes and glucose tolerance
Reproduction and growth
Adrenals and corticosteroid hormones

Poster sessions and trade exhibition

For additional information contact:

Arlette Alcaraz, Laboratoire de Biochimie C, CHRU de Grenoble,
BP 217 X, 38043 Grenoble Cedex, France.
Tel: 76.42.81.21, extension 4465

EDITORIAL

The new decade brings a new look to *Talanta*! You probably have already noticed the changes to the cover and the inside title pages. As you read on you will see that the print size has been increased and the layout of papers has been altered slightly. The scope of the journal has also been revised, to place a greater emphasis on fundamental studies and novel instrumentation developments. Other refinements are planned and will be announced in future issues.

The editorial production system has been reorganized. After long and valued service, for which we thank them on behalf of contributors and readers, John Majer (25 years) and Iain Marr (24 years) are retiring as Assistant Editors, but Iain will continue his association with the journal by taking responsibility for co-ordination of Special Issues. Bill Bryce, Phil Cox and Derek Midgley will continue as Assistant Editors, and Phil will also act as Book Review Editor. Mary Masson will continue as Computing Editor and in charge of the Software Survey Section. An innovation is the appointment of a Technical Editor, Caroline Higginson. The Advisory Board has been strengthened by the appointment of Dr. Bernhard Welz and Dr. Kosuke Izutsu. We are very pleased that they have agreed to join the Board.

Best regards for 1990.

GARY CHRISTIAN

DAVID LITTLEJOHN

OBITUARY



ACADEMICIAN PROFESSOR

I. P. ALIMARIN
(1903-1989)

On 17 December 1989, Academician Professor Ivan Pavlovich Alimarin—an outstanding scientist in the field of analytical chemistry of our time, an excellent teacher, a kind and feeling friend—passed away.

I. P. Alimarin was born in Moscow on 11 September 1903, and studied in the 1920s at the Moscow Academy of Mining. For many years he investigated the analytical chemistry of gallium, indium, thallium, germanium, rhenium, niobium, tantalum, zirconium and other elements. Many methods developed by him for preconcentration and determination of these elements were absolutely new, and are still applied for analysis of geological and other samples. Special attention was paid by him to micro- and ultramicro-methods of chemical analysis; application of organic reagents, development of methods of preconcentration by co-precipitation, solvent extraction, ion-exchange and partition chromatography; to development of instrumental methods of analysis (spectrophotometric, luminescence, spectroscopic, electrochemical, radiochemical); to theoretical investigation of the mechanism and kinetics of complex-formation reactions in aqueous and non-aqueous solutions. He was passionately devoted to studying the unknown, and was endowed with great creative abilities which characterized his whole life.

In association with his pupils and colleagues, Professor Alimarin published over 800 scientific papers. Monographs, manuals and handbooks by him are widely read and referred to not only by young analysts, but by prominent scientists as well.

He had hundreds of pupils, many of whom became well known scientists; as a teacher he was always attentive to the young, and ready to assist and to support his pupils, who always felt the deepest respect and loyal love in return.

Professor Alimarin played an important role in the organization of scientific research, as he occupied the positions of Vice Academician—Secretary of the Division of Physico-Chemistry and Inorganic Materials of the USSR Academy of Sciences; Chairman of the Scientific Council of Analytical Chemistry of the USSR Academy of Sciences; Editor-in-Chief of the *Russian Journal of Analytical Chemistry (Zhurnal Analiticheskoi Khimii)*, regional editor or member of the Advisory Boards of the international journals *Talanta*, *Journal of Radioanalytical Chemistry*, *Radiochemical and Radioanalytical Letters*. He was also a titular member of the Division of Analytical Chemistry of the International Union of Pure and Applied Chemistry.

I. P. Alimarin was the first Soviet analyst, in the late 1950s, to establish and keep direct contacts with the leading foreign specialists in the field of analytical chemistry. His personal relationships and correspondence with his numerous colleagues from all over the world were always friendly and sometimes deeply emotional; they were kept up by him till the last days of his life.

I. P. Alimarin's contribution to analytical chemistry has been widely recognized and appreciated. He was an Honorary Member of the Division of Analytical Chemistry of the French Society of Industrial Chemistry, of the Society of Analytical Chemistry (now part of the Royal Society of Chemistry), the Japanese Society of Analytical Chemistry and the Chemistry Society of the German Democratic Republic, Foreign Member of the Academy of Finland, and Doctor *honoris causa* of the Budapest Technical University, Göteborg University and the University of Birmingham.

He was awarded the *Talanta* Gold Medal for outstanding achievements in the field of analytical chemistry, the J. Purkyně Gold Medal (Czechoslovakia), the Silver Medal of the Japanese Society of Analytical Chemistry, the Emich Medal (Austria), the Hevesy Medal (Hungary) and the Helsinki University Medal.

The long and fruitful life of this outstanding analytical chemist has come to an end. His students, pupils, colleagues and friends will ever keep the memory of Ivan Pavlovich Alimarin as long as they live.

YU. A. ZOLOTOV and V. K. RUNOV

P E R G A M O N P R E S S
SOFTWARE DESCRIPTION FORM

Title of software program: _____

Type of program: Application Utility Other _____

Category: _____ (ie.) stability constants,
calibration, pattern recognition, optimization)

Developed for (name of computer/s): _____

in (language/s): _____

to run under (operating system): _____

available on: Floppy disk/diskette. Specify:

Size _____ Density _____ Single-sided Dual-sided

Magnetic tape. Specify:

Size _____ Density _____ Character set _____

Hardware required: _____

Memory required: _____ User training required: Yes No

Documentation: None Minimal Self-documenting
 Extensive external documentation

Source code available: Yes No

Stage of development: Design complete Coding complete
 Fully operational Collaboration welcomed

Is program in use? Yes How long? _____ How many sites? _____
 No

Is the contributor available for user inquiries: Yes No

Distributed by: _____

Cost of program: _____

Demonstration disk available? Yes Cost: _____
 No

(continued)

RETURN COMPLETED FORM TO:

Dr. Mary R. Masson
Department of Chemistry
University of Aberdeen
Meston Walk
Old Aberdeen AB9 2UE, Scotland

[This Software Description Form may be photocopied without permission]

Description of what software does [maximum: 200 words]:

Potential users: _____

Field/s of interest: _____

#####

Name of contributor: _____

Institution: _____

Address: _____

Telephone number: _____

#####

Reference No. [Assigned by Journal Editor] _____

[The information below is not for publication.]

Would you like to have your program:

Reviewed? [] Yes [] No [] Not at this time

Marketed and distributed? [] Yes [] No [] Not at this time

[This Software Description Form may be photocopied without permission]

IVth INTERNATIONAL SYMPOSIUM ON
QUANTITATIVE LUMINESCENCE SPECTROMETRY IN
BIOMEDICAL SCIENCES

State University of Ghent, Faculty of Pharmaceutical Sciences, 27–31 May, 1991.

Details from Dr. Willy R. G. Baeyens, Symposium Chairman, State University of Ghent, Pharmaceutical Institute, Harelbekestraat 72, B-9000 Ghent (Belgium); Tel. 32-(0)91-21.89.51 ext. 254, telefax 32-(0)91-21.79.02.

XXVII COLLOQUIUM SPECTROSCOPICUM INTERNATIONALE

9–14 June 1991, Grieg Hall, Bergen, Norway

Organized by the Norwegian Chemical Society

The Organizing Committee cordially invites you to attend the XXVII CSI. This traditional biennial conference in analytical spectroscopy will once again provide a forum for atomic, nuclear and molecular spectroscopists worldwide to encourage personal contact and the exchange of experience.

Participants are invited to submit papers for presentation at the XXVII CSI, dealing with the following topics:

Basic theory and instrumentation of

Atomic spectroscopy (emission, absorption, fluorescence)

Molecular spectroscopy (UV, VIS and IR)

X-Ray spectroscopy

Gamma spectroscopy

Mass spectrometry (inorganic and organic)

Electron spectroscopy

Raman spectroscopy

Mössbauer spectroscopy

Nuclear magnetic resonance spectrometry

Methods of surface analysis and depth profiling

Photoacoustic spectroscopy

Application of spectroscopy in the analysis of

Metals and alloys

Geological materials

Industrial products

Biological samples

Food and agricultural products

Special emphasis will be given to the topics of trace analysis, environmental pollutants and standard reference materials.

The scientific programme will comprise both plenary lectures and parallel sessions of oral presentations. Specific times will be reserved for poster sessions.

PRE- AND POST-SYMPOSIA

In connection with the XXVII CSI the following symposia will be organized:

Presymposia:

I. GRAPHITE ATOMIZER TECHNIQUES IN ANALYTICAL SPECTROSCOPY

6–8 June 1991, Hotel Ullensvang, Lofthus, Norway.

Organized by: Bernhard Welz (West Germany)

Wolfgang Frech (Sweden)

IVth INTERNATIONAL SYMPOSIUM ON
QUANTITATIVE LUMINESCENCE SPECTROMETRY IN
BIOMEDICAL SCIENCES

State University of Ghent, Faculty of Pharmaceutical Sciences, 27–31 May, 1991.

Details from Dr. Willy R. G. Baeyens, Symposium Chairman, State University of Ghent, Pharmaceutical Institute, Harelbekestraat 72, B-9000 Ghent (Belgium); Tel. 32-(0)91-21.89.51 ext. 254, telefax 32-(0)91-21.79.02.

XXVII COLLOQUIUM SPECTROSCOPICUM INTERNATIONALE

9–14 June 1991, Grieg Hall, Bergen, Norway

Organized by the Norwegian Chemical Society

The Organizing Committee cordially invites you to attend the XXVII CSI. This traditional biennial conference in analytical spectroscopy will once again provide a forum for atomic, nuclear and molecular spectroscopists worldwide to encourage personal contact and the exchange of experience.

Participants are invited to submit papers for presentation at the XXVII CSI, dealing with the following topics:

Basic theory and instrumentation of

Atomic spectroscopy (emission, absorption, fluorescence)

Molecular spectroscopy (UV, VIS and IR)

X-Ray spectroscopy

Gamma spectroscopy

Mass spectrometry (inorganic and organic)

Electron spectroscopy

Raman spectroscopy

Mössbauer spectroscopy

Nuclear magnetic resonance spectrometry

Methods of surface analysis and depth profiling

Photoacoustic spectroscopy

Application of spectroscopy in the analysis of

Metals and alloys

Geological materials

Industrial products

Biological samples

Food and agricultural products

Special emphasis will be given to the topics of trace analysis, environmental pollutants and standard reference materials.

The scientific programme will comprise both plenary lectures and parallel sessions of oral presentations. Specific times will be reserved for poster sessions.

PRE- AND POST-SYMPOSIA

In connection with the XXVII CSI the following symposia will be organized:

Presymposia:

I. GRAPHITE ATOMIZER TECHNIQUES IN ANALYTICAL SPECTROSCOPY

6–8 June 1991, Hotel Ullensvang, Lofthus, Norway.

Organized by: Bernhard Welz (West Germany)

Wolfgang Frech (Sweden)

FOREWORD

This special issue of *Talanta* is devoted to recent advances in multielement spectrochemical analysis. The term spectrochemical analysis, as used here, refers to elemental analyses performed by means of optical spectroscopy in the *UV-visible* region of the spectrum. The need for spectroscopic systems with multielement capability arises from the ever increasing demands of technology and materials science and from concern over the environment—areas where survey analyses on previously uncharacterized samples are often important.

Although highly reliable multielement detection systems already exist in the form of conventional spectrographs¹ and direct-reading spectrometers such as that described in 1945 by Dieke and Crosswhite,² these conventional systems are based on relatively old technology and have now reached a stage of nearly optimal development. At the same time, however, increasingly difficult analytical situations call for advanced spectroscopic systems with improved detection limits and the ability to rapidly determine many elements in a variety of sample matrices. To fill the increased demands placed upon spectrochemical techniques, analytical research scientists continue to investigate and evaluate new instrumentation and techniques, many of which are reported for the first time in this issue. For example, the papers by Denton and co-workers in this issue report recent investigations with second-generation image detectors such as charge-transfer devices that offer the opportunity to develop improved spectroscopic systems based on atomic emission and having excellent sensitivity, dynamic range, accuracy, and precision, with the added advantages of flexible multielement, multiwavelength capability.

Multichannel detectors such as vidicon tubes and photodiode arrays have also been evaluated as detection systems for atomic-emission spectroscopy.^{3,4} Although not strictly multielement, the paper by Winefordner *et al.* demonstrates the power of photodiode arrays, while Hieftje and coworkers describe a linear photodiode-array multichannel spectrometer which is configured to monitor simultaneously both the signal and the sideband background. This

instrument offers a distinct advantage over single-channel photomultiplier-based systems because it has the capability to correct for low-frequency fluctuations in background emission. The multiple entrance-slit vidicon spectrometer, reported by Busch *et al.*, can be operated in either a one- or two-dimensional mode, offering maximum flexibility in wavelength selection through the use of movable fiber optic light guides. When configured with an optical multiplexer, this same instrument can be used for programmed scanning, offering the opportunity for extremely rapid acquisition of spectral data.

Another active area of research in spectrochemical analysis involves the use of Fourier and Hadamard transform techniques in multielement determinations. While application of Fourier transform methods to atomic spectroscopy has been explored over the past decade by several research groups,^{5,6} the whole area of Hadamard transform spectroscopy has recently been revitalized by the use of electronically programmable electro-optic encoding masks.^{7,8} In this special issue, papers by Fateley *et al.* and Tilotta report the adaption of a liquid-crystal spatial light modulator Hadamard-transform spectrometer for use in multielement atomic spectrochemical analysis and show how certain features of the multiplex disadvantage generally associated with the application of transform methods to atomic analysis can be circumvented.

The guiding thought behind compiling this issue was not only to provide the reader with a brief summary of some of the current research being conducted in the area of instrumental development, but also to explore some experimental considerations inherent in multielement analysis and to include some actual analytical applications. To cover this range of topics, we sought papers from workers in academe as well as from those in government laboratories and industry. One thing which has emerged from the resulting manuscripts is the importance of statistics in dealing with multielement analysis. This is exemplified by the papers dealing with the selection of spectral lines (Blades *et al.*) and windows (Salin *et al.*), as well as those dealing

with the evaluation of prototype systems (Busch *et al.*) and the comparison of multielement techniques (Hall *et al.*). Another picture which clearly emerges is the diversity of sample types requiring multielement analysis, ranging from biological materials (Miller-Ihli) to trace metals (Boomer *et al.*) and geological samples (Hall *et al.*).

While this issue has pointed out many approaches and solutions to problems in multielement analysis, clearly the "ultimate" system for multielement spectrochemical analysis has yet to be developed. Moreover, given the evolutionary nature of spectrochemical research, multielement instrumentation must continue to change as it takes advantage of new technological developments in other areas. Like the advent of second-generation image detectors, many of the advances which promise to make dramatic improvements in spectrochemical analysis have been made in areas outside spectroscopy.

As new technology is applied to chemical analysis, it should come as no surprise that the early prototype instruments do not match those which have been developed and refined over a long period of time. Therefore, in evaluating emerging technology, it is important not to allow the overwhelming incumbency of existing technology to cause new developments to be dismissed out of hand. Time after time, knowledgeable workers in various disciplines confidently dismissed emerging technology as being inadequate compared with already developed technology. For example, although it may seem strange to us today, it was widely believed at one time that nothing would be able to surpass the prism for high resolution and luminosity. It is also probably safe to assume that pioneers in grating development such as Rowland^{9,10} would be greatly impressed by modern holographic diffraction gratings, made possible by the development of the laser. Likewise, just as the advent of the modern computer has made Fourier transform instruments commonplace in nearly every laboratory, the development of electronically controlled optical modulators has led to the possibility of electronically controlled masks that clearly enhance the ease of implementing Hadamard transform spectroscopy. Nevertheless, in spite of these and many other examples of how new technology and improvements in spectrochemical analysis move forward hand-in-hand, the desire for stasis on the part of the end-users of technology is quite powerful, and it is frequently the end-users themselves who,

having a vested interest in existing technology, fight the hardest against change.

In assessing the current stage of development of multielement spectrochemical techniques, it is worthwhile to consider briefly some of the requirements imposed on multielement analytical systems based on optical spectroscopy. As a result of the great range of concentrations present in many multielement samples, one major problem is to design a detection system having a dynamic range which can match that present in the actual spectrum. Thus, any spectroscopic system proposed for multielement determinations must be capable of detecting weak trace-element lines in the presence of strong major-element lines that arise from the sample matrix. Given modern excitation sources such as the induction-coupled plasma, adequate resolving power is also essential, especially with samples such as ferrous alloys that produce line-rich spectra. Finally, a detailed understanding of the sources of noise in spectroscopic systems is needed for optimizing system operating parameters to provide the necessary detection limits for today's trace analyses.

In developing potential spectroscopic systems for multielement determinations it should also be appreciated that any new technology must be able to fulfill *real* measurement needs if it is to remain viable. This is often the hardest demand for emerging technology to satisfy. In addition, for actual adoption by analytical applications specialists, new systems must possess clear advantages over existing technology. For this reason, it is important for those involved with instrumental development to be aware of the actual performance requirements needed by real-world spectrochemical analysis systems. To fill this need, we have included papers on real-world multielement applications as well as alternative multielement techniques which serve as competing technology. For this reason, we have also included, as the last paper in this collection, an interesting account of the modification and evaluation of an updated induction-coupled plasma atomic-emission spectrometer used in an industrial setting (Botto). For sheer versatility and volume of samples processed, the ICP-AE polychromator remains the practical workhorse of industry, and it is always instructive to review the standards by which any new methodology will be judged.

KENNETH W. BUSCH
MARIANNA A. BUSCH

REFERENCES

1. M. Slavin, *Emission Spectrochemical Analysis*, Wiley, New York, 1971.
2. G. H. Dieke and H. M. Crosswhite, *J. Opt. Soc. Am.*, 1945, **35**, 471.
3. Y. Talmi and K. W. Busch, in *Multichannel Image Detectors*, Y. Talmi (ed.), Chapter 1. American Chemical Society, Washington, DC, 1983.
4. P. M. Epperson, J. V. Sweedler, R. B. Bilhorn, G. R. Sims and M. B. Denton, *Anal. Chem.*, 1988, **60**, 327A.
5. P. R. Griffiths and J. A. deHaseth, *Fourier Transform Infrared Spectrometry*, Chapter 16. Wiley, New York, 1986.
6. K. W. Busch and M. A. Busch, *Multielement Detection Systems for Spectrochemical Analysis*, Chapters 7 and 14. Wiley, New York, 1989.
7. D. Tilotta and W. G. Fateley, *Spectroscopy*, 1988, **3**, 14.
8. K. W. Busch and M. A. Busch, *Multielement Detection Systems for Spectrochemical Analysis*, Chapters 5 and 14. Wiley, New York, 1989.
9. H. A. Rowland, *Phil. Mag.*, 1882, **13**, 469.
10. *Idem*, *J. Astronomy Astrophysics*, 1893, **12**, 129.

II. CHARACTERIZATION OF OIL COMPONENTS BY SPECTROSCOPIC METHODS

6–8 June 1991, Hotel Hardangerfjord, Øystese, Norway.

Organized by: Michael Stöcker (Norway).
Einar Sletten (Norway)
Liv Schou (Norway)

III. MEASUREMENTS OF RADIO-NUCLIDES AFTER THE CHERNOBYL ACCIDENT

6–8 June 1991, Hotel Solstrand, Bergen, Norway.

Organized by: Brit Salbu (Norway)
Eiliv Steinnes (Norway)

Postsymposium:

IV. SPECIATION OF ELEMENTS IN ENVIRONMENTAL AND BIOLOGICAL SCIENCES

17–19 June 1991, Hotel Alexandra, Loen, Norway.

Organized jointly by the Norwegian National Institute of Occupational Health, Nordic Trace Element Society and the IUPAC Commission on Toxicology, Clinical Chemistry Division.

Further information is available from:

XXVII CSI
HSD Congress-Conference
P. O. Box 1721 Nordnes
N-5024 Bergen, Norway
Tel. 47-5-318414, Telex 42607 hsd n, Telefax 47-5-324555

33rd IUPAC CONGRESS

Budapest, Hungary, 17–22 August 1991

The Organizing Committee cordially invites you to attend the 33rd International Congress of the International Union of Pure and Applied Chemistry.

Plenary and keynote lectures will be presented on the following topics:

SECTION I. PERSPECTIVES OF ANALYTICAL CHEMISTRY

- Philosophical aspects of analytical chemistry
- New directions in chromatography
- New directions in spectroscopy
- Possibilities of measurements of single atoms
- Perspective in chemometrics
- Robotics in analytical chemistry
- Environmental analysis
- Trends in nuclear analytical chemistry
- Perspectives of pharmaceutical and biomedical analysis
- Analysis of giant molecules

SECTION II. INORGANIC AND PHYSICAL CHEMISTRY

- Dynamic of elementary reactions
- Unimolecular reactions and energy transfer
- Kinetics of fast reactions in solutions
- Kinetics of radical reactions
- New aspects of coordination chemistry in catalysis and kinetics

AUTHOR INDEX

- Abbas N. M. 731
 Abdalla M. M. 1091
 Abdel-Kader A. K. 1091
 Adams M. D. 875
 Ahmad M. 757
 Ahmad S. T. 763
 Akaza I. 925
 Alary J. 301
 Alimarin I. P. 485
 Amamo H. 585
 Andersson M. 185
 Anton R. I. 1097
 Aota N. 925
 Arancibia V. 439
 Archer V. S. 381
 Arcos J. 661
 Ashraf N. 659
 Atanassova D. 527
 Attiyat A. S. 1123
 Aurrecochea J. M. 911
- Babu K. S. 353
 Bader L. W. 835
 Ballantyne S. B. 135
 Banerjee N. L. 1017
 Bao Xinlu 357
 Barnard G. M. 219
 Barrado E. 325
 Basak B. 1105
 Basova E. M. 485
 Becerro Dominguez F. 655
 Beckett J. R. 381
 Bedair M. M. 1183
 Benton L. D. 89, 103
 Bernal J. L. 931
 Berzas Nevado J. J. 347
 Bhatnagar A. 1037
 Bhattacharya S. 1101
 Bhowal S. K. 1193
 Blades M. W. 39
 Boddington T. 219
 Bodini M. E. 439
 Bol'shova T. A. 485
 Bonham-Carter G. F. 135
 Boomer D. W. 127
 Borisov G. 1081
 Botto R. I. 157
 Bowles C. J. 835
 Bozsai G. 545
 Brajter K. 613
 Branagh W. 407
 Brock I. H. 801
 Brown R. S. 561, 801
 Brücher E. 1175
 Brushwyler K. R. 23
 Bumba M. A. C. 1179
 Busch K. L. 471
 Busch K. W. No. 1, VII, 71, 89, 103
 Busch M. A. No. 1, VII, 71, 89, 103
 Bye R. 1029
 Byrne A. R. 207
- Caballero M. 275
 Cabon J. Y. 1119
 Calokerinos A. C. 1043
 Camara Rica C. 719
 Campanella L. 201
 Cano Pavón J. M. 385
 Cantin D. 301
 Capitán F. 193
 Capitán-Vallvey L. F. 193
- Carlos de Andrade J. 711
 Carnero Ruiz C. 1137
 Castillo J. R. 895
 Castrillejo Y. 325
 Cathum S. J. 1111
 Cela R. 275
 Cerdá V. 689, 931
 Černá-Frýbortová J. 1025
 Chakrabarti C. L. 1111
 Chakraborty A. K. 1101
 Chance J. 407
 Chandrasekaran M. 695
 Chastel O. 213
 Chen Danhua 1049
 Chen Guanquan 809
 Cheng K. L. 659, 901
 Chiswell B. 237
 Chow A. 407, 491
 Christian G. D. 213, 661
 Christian J. D. 651
 Ci Yun-Xiang 1133
 Ciba J. 815
 Ciesielski W. 435
 Ciszewski A. 995
 Cladera A. 689
 Coşofreţ V. V. 673
 Cox J. A. 1037
 Cruces Blanco C. 573, 579
 Cruywagen J. J. 741
 Czapiuk M. 1011
- Dabek-Zlotorzynska E. 613
 Dai Anbang 357
 Dams R. 819
 Daniele S. 317
 Danielson N. D. 1151
 Danielsson L.-G. 1169
 Darus H. 757
 Darvell B. W. 413, 425
 Das T. K. 1193
 Davey D. E. 313, 683
 Dawson M. V. 443, 1189
 Debán L. 931
 del Nozal M. J. 931
 del Real E. 325
 Denton M. B. 1, 15
 Ding Yi 357
 de Uría O. 931
 Donaldson E. M. 173, 955
 Drabowicz J. 435
 Dunphy J. C. 471
- Egorov V. V. 461
 El-Brashy A. M. 1087
 El Jammal A. 661
 El-Kommos M. E. 481, 625, 951
 El-Rabbat N. A. 481, 951
 Elsayed M. A. 1183
 Endoh I. 1163
 Ericson C. 725
 Esmadi F. T. 1123
 Espinosa Mansilla A. 347
 Estela J. M. 689, 931
- Famoori F. 1107
 Farag H. H. 481, 951
 Fateley W. G. 53
 Fatibello-Filho O. 1179
 Ficklin W. H. 831
 Franco C. 905
 Fry R. C. 53
- Fujikura T. 663
 Furuta N. 23
- Gallego M. 1129
 Gangaiah T. 761
 García Sánchez F. 573, 579, 1137
 García de Torres A. 385
 Gesser H. D. 491
 Gijbels R. 363
 Gómez F. J. 931
 Gomez Gomez M. 719
 González M. 789
 González Diego F. 655
 Gregor J. E. 219
 Grekas N. 1043
 Grobenski Z. 545
 Grosset C. 301
 Grossman A. M. 815
 Gu Yuan-Xiang 1021
- Haghgoo S. 1107
 Hall G. E. M. 135
 Halls D. J. 555
 Hancock R. D. 875
 Haque S. 763
 Havezov I. 889
 Hayashibe R. 619
 He Chun-Xiang 531, 677, 941
 He Wei-ming 641
 Heredia Bayona A. 1137
 Hernández L. 789
 Hernández P. 789
 Hernandez Mendez J. 655
 Heyns J. B. B. 741
 Hieftje G. M. 23
 Himeno S. 1071
 Hipfner J. 127
 Hori T. 1071
 Horvat M. 207
 Hou Weiyang 841
 Hougham B. D. 561, 801
 Huang P. M. 745
 Huang Zhigui 749
 Hungerford J. M. 975
 Hurtubise R. J. 1057
- Illum D. B. 651
 Indrasenan P. 269
 Ingman F. 1169
 Ishii H. 1163
 Ishimaru S. 619
 Ivanova E. 1081
- Jackson K. W. 835
 Jain A. 595
 Jędrzejewski W. 435
 Ji Gang 937
 Jiang Zhi-liang 1077
 Johnson D. C. 377
 Jordanov N. 1081
 Ju Zhao-Qiang 531, 701, 941
 Jurczyk J. 815
 Jyothi A. 431
- Kalous J. 1025
 Kamoopuri S. I. M. 361
 Kantipuly C. 491
 Karlijković-Rajić K. 535
 Kasahara N. 1063
 Katragadda S. 491
 Katritzky A. R. 911, 921

- Kauffmann J.-M. 213
 Khan I. A. 361
 Kharoaf M. A. 1123
 Khedr A. S. 625
 Kiciak S. 1197
 Klaos E. 519
 Kleszczewska E. 855
 Koga Y. 861
 Kopianca M. 1067
 Korany E. A. 1183
 Korany M. A. 1183
 Korićanac Z. 535
 Kostrowicki J. 645
 Kowalski Z. 447
 Kricka L. J. 971
 Krishnamurthy M. 353
 Krishnamurti G. S. R. 745
 Krishnan V. 695
 Krull U. J. 561, 801
 Kubán V. 1169
 Kudzin Z. H. 435
 Kumar K. G. 269
 Kunwar U. K. 555
 Kuroda R. 619
 Kurosaki M. 619
- LaCourse W. R. 377
 Lachowicz E. 1011
 Larsson J. A. 233
 Laskar S. 1105
 Law S. L. 261
 Le Bihan A. 1119
 Leaver M. E. 173
 Lee D. 901
 Lee O. 861
 Li Buhia 885
 Lekhakula S. 971
 Leung V. W.-H. 413, 425
 Li Jiangjun 809
 Li Xin Li 673
 Li Qi-Long 937
 Li Zhong 341
 Liang Ai-hui 1077
 Lin Ding-Ping 731
 Lin Li-Fen 531, 941
 Lin Tiezheng 167
 Littlejohn D. 555, 825
 Liu Shaopu 749
 Liu Zhijun 167
 Liwo A. 645
 Lopez-Cueto G. 849
 Lopez-Molinero A. 895
 Lu Minggang 393
 Lu Xiaohu 393
 Lu Zhi-Ren 701
 Lou Qinhui 357
 Lou Zong-ming 641
 Luque de Castro M. D. 1049
 Lushchik Ya. F. 461
 Luts P. 455
 Lyle S. J. 443, 1189
 Lynch S. 825
- MacLaurin A. I. 135
 Maccà C. 1141
 Mahgoub H. 1183
 Majone M. 201
 Malik A. K. 1205
 Malloy B. B. 71
 Malykhin A. Yu. 485
 Mamantov G. 1031
 Mao Dan Yi 673
 Marcinkowski J. M. 971
- Marini H. J. 1097
 Martin N. J. 711
 Maryutina T. A. 889
 Mauldin R. F. 1031
 May K. 207
 Mazzocchin G.-A. 317
 McGibbon G. 561
 McLean H. L. 381
 Mead Jr. D. A. 377
 Mellone A. 111
 Mendez R. 591
 Meng Rigan 885
 Mermet J. M. 895
 Midgley D. 767
 Migdalski J. 447
 Miknis G. 381
 Miller-ihli N. J. 119
 Mohamed F. A. 625
 Montero R. 1129
 Moretto L. M. 317
 Mulcahy D. E. 313, 683
 Mulero O. 381
 Mullens J. M. A. 455
 Murakami M. 229
 Muralikrishna U. 353
 Murphy J. A. 651
- Naidu D. V. 629
 Naidu G. R. K. 761
 Naidu P. R. 629
 Naidu U. V. 761
 Nakashima T. 735
 Navalón A. 193
 Nelson D. A. 381
 Němcová I. 855
 Neves E. A. 1179
 Newman J. H. 261
 Noel M. 695
- O'Connell G. R. 313, 683
 Odashima T. 1163
 Odinets V. 519
 Offerman R. J. 911, 921
 Olin Á. 185, 725
 Olmsted III J. 905
 Olsina R. A. 1097
 Ono N. 633
 Osakai T. 1071
 Ozsoz M. 783
- Palacios Corvillo M. A. 719
 Pappas C. P. 707
 Pardo J. 439
 Pardo R. 325
 Pardue H. L. 233
 Pascoe M. 237
 Patriarche G. J. 213, 661
 Pei Jianhong 1007
 Pérez-Bustamante J. A. 275
 Perry L. M. 965
 Pettersson J. 725
 Pettit L. D. 219
 Pickering W. F. 397, 981
 Pilarski B. 921
 Pillai V. N. S. 591
 Pitchai R. 539
 Pocci R. 201
 Pomeroy R. S. 15
 Powell M. J. 127
 Ptak F. L. 261
 Purdy W. C. 307, 795
- Qureshi P. M. 361
 Qureshi S. Z. 763
- Ramadevi P. 761
 Ramakrishna T. V. 539
 Ramana K. V. 753
 Ramos Rubio A. L. 579
 Randall S. T. 707
 Rao A. L. J. 1205
 Rao A. R. M. 753
 Rao G. N. 431
 Rao M. S. P. 753
 Rauchle G. 237
 Refaat I. H. 481, 951
 Ren K. 667, 845
 Richmond M. D. 1057
 Rocheleau M. J. 307
 Rogers L. B. 599
 Roy S. K. 1101
 Ruseva E. 899
 Rychlovský P. 855
- Sagi S. R. 753
 Saha U. 1193
 Saito A. 1071
 Sakuraba S. 637
 Saleh M. I. 757
 Salin E. D. 33
 Salinas F. 347
 Sánchez Batanero P. 325
 Satake H. 633
 Savage G. P. 911, 921
 Schlemmer G. 545
 Selvapathy P. 539
 Sen A. K. 1193
 Seshaiiah K. 761
 Shamsipur M. 1107
 Shen Mengchang 357
 Shida J. 633
 Shirai T. 1063
 Shishkov A. N. 527
 Shiundu P. M. 329
 Shkinev V. M. 889
 Shpigun L. K. 889
 Sims G. R. I. 1
 Singh S. B. 361
 Sinha B. C. 1017
 Slavek J. 397
 Smith B. W. 111
 Sneddon J. 707
 Spiewok W. 815
 Spivakov B. Ya. 889
 Stanković B. 535
 Stará V. 1067
 Steinbrecher K. 975
 Still M. G. 599
 Strelow F. W. E. 1155
 Strong III F. C. 711
 Suau Suarez R. 579
 Sugawara K. 1001
 Sweedler J. V. 15
 Szabó Z. 1175
- Taga M. 1001
 Takada T. 229
 Tanaka S. 1001
 Targove M. A. 1151
 Taylor N. 219
 Ten Enjiang 947
 Teodorczyk M. 795
 Terebenina A. 1081
 Tilotta D. C. 53, 61
 Todorova O. 1081

Torkelson J. D. 975
Tóth I. 1175
Trofino J. C. 1179
Trojáněk A. 1067

Ubide C. 849
Ureña Pozo M. E. 385

Valcárcel M. 1049, 1129
Vanballenberghe L. 819
Vandecasteele C. 819
Vandenberg E. T. 561
Vanhees J. L. C. 455
Vanhoe H. 819
Van Poucke L. C. 455
Verma A. 595
Verma K. K. 595
Versieck J. 819
Vicente J. 789
Victor A. H. 1155
Vienneau J. M. 1031
Vilchez J. L. 193
Villet A. 301

Viré J.-C. 661
Vytrás K. 1025

Wade A. P. 329, 861
Wade P. W. 875
Waki H. 735
Walker K. D. 975
Waller P. A. 397, 981
Wang Erkang 841
Wang Fang 1133
Wang J. 783
Wang Nai-Xing 337
Wangsa J. 1151
Webb D. P. 33
Wehry E. L. 1031
Wei Fusheng 947
Wekell M. M. 975
Welch L. E. 377
Wentzell P. D. 329
Wilding P. 971
Winefordner J. D. 111, 965
Wirsz D. F. 39

Wittoek A. 819
Wu Zhongxiang 947

Yamamoto N. 1063
Yan Xiuping 167
Yanase N. 585
Yao Xu-Zhang 701, 1021
Yin Fang 393
Yoshimura K. 735
Yperman J. H. E. 455
Yu Ren-Qing 701, 1021

Zaki M. T. M. 1091
Zeng Yun'e 809
Zhang Xiujing 1007
Zhang Zong-Rang 673
Zhao Zaofan 1007
Zhou Guangming 749
Zhou Min 531, 941
Zhou Nan 531, 677, 701, 941, 1021
Zhou Shi-Fu 337, 341
Zhou Xingyao 1007
Zolotov Yu. A. 889